

International Commission on Large Dams



Book of Full Papers

Symposium Hydro Engineering

2nd - 3rd of July 2018 July

Vienna, Austria

26th World Congress **ICOLD 2018** 86th Annual Meeting

1 - 7 JULY, VIENNA www.icoldaustria2018.com



International Commission on Large Dams



Book of Full Papers

Symposium Hydro Engineering

2nd - 3rd of July 2018 July

Vienna, Austria

26th World Congress **ICOLD 2018** 86th Annual Meeting

1 - 7 JULY, VIENNA www.icoldaustria2018.com



EDITOR Gerald Zenz
for Austrian National Committee on Large Dams
Stremayrgasse 10/II
A-8010 Graz, AUSTRIA
E-mail: secretary@atcold.at
<https://www.atcold.at>

LAYOUT Harald Breinhälter

COVER Harald Breinhälter
Tom Sebesta

COVER PHOTO © VERBUND Tourismus

© 2018 Verlag der Technischen Universität Graz
www.ub.tugraz.at/Verlag

ISBN (e-book) 978-3-85125-620-8

DOI 10.3217/978-3-85125-620-8



This work is licensed under a Creative Commons Attribution 4.0 International License.
<https://creativecommons.org/licenses/by-nc-nd/4.0/>

NOTE: The information contained in this publication regarding commercial projects or firms may not be used for advertising or promotional purposes and may not be construed as an endorsement of any product or firm by the Austrian National Committee on Large Dams. The Austrian National Committee on Large Dams accepts no responsibility for the statements made or opinions expressed in this publication.

The author(s) is (are) responsible for obtaining written permission to profile the project or subject matter in their papers from any and all clients, owners or others who commissioned the work. ATCOLD assumes proper permission has been obtained by author(s) and accepts no liability for the author(s) failing to do so.

If a figure, table or photograph has been published previously, it will be necessary for the author(s) either to obtain written approval from the original publisher; or refer clearly to the source of previously published material in the caption of the figure, table or photograph.

SYMPOSIUM HYDRO ENGINEERING - FOREWORD

The ATCOLD Symposium Hydro Engineering will pave the way for presentations and discussions on specific issues of hydraulic structures serving for energy from renewable resources, irrigation, drinking water supply and flood protection. Hydro Engineering requires a wide range of knowledge and expertise. Therefore, many specific disciplines are involved. Research effort is needed to give answers effectively to challenges during project realization, operation and maintenance. Problem solutions should be sustainable and economically feasible in a wide range. To present and discuss specific issues in the field of hydro power production, this Symposium Hydro Engineering focus on the following topics:

- CLIMATE CHANGES RESERVOIR OPERATION
- PERMISSION AND SAFETY ASSESSMENT
- DAM AND FOUNDATION SEALING
- CAVERNS AND POWER WATER WAYS
- STABILITY OF RESERVOIR SLOPES

Additionally, two special seminars will be held about the following topics:

- OROVILLE DAM SPILLWAY INCIDENT
- HIGH STRENGTH STEEL IN HYDRO POWER PLANTS

To allow ICOLD Technical Committee's to present and discuss their work, in parallel to the Symposium Hydro Engineering "Technical Committee Workshops" are organized. Especially Workshops are organized by the following Technical Committees:

- RESETTLEMENT DUE TO RESERVOIRS, EMBANKMENT DAMS AND DAM SAFETY
- JOINT WORKSHOP

A - Committee on Computational Aspects of Analysis & Design of Dams

B - Committee on Seismic Aspects of Dam Design

As green meeting, we provide one printed book of extended abstracts containing, the contents of the contributions and on 2 pages the abstract version of the contributions. Full papers are published electronically and are available for downloading.

We thank all the authors for their efforts and contributions to the Symposium. Based on reviews and authors preferences we selected 240 papers and posters from 55 countries for presentations in parallel sessions and during poster presentations.

We would like to express our deepest gratitude towards all the members of the review panel for their effort, and to the organizing committee members especially - Harald Breinhalter, Josef Schneider, Franz-Georg Pikel, Shervin Shahriari and Edwin Staudacher.



Gerald Zenz

President ATCOLD

ICOLD Vice President – EUROPE



Helmut Knoblauch

Secretary General

ATCOLD

SYMPOSIUM HYDRO ENGINEERING - REVIEWERS

Francesco Amberg

Markus Aufleger

Maria Bartsch

Harald Breinhälter

Horst-Hannes Cerjak

Helmut Czerny

George Darbre

Norbert Enzinger

Martin Fuchs

Reinhold Gerstner

Moshem Ghaemian

Richard Greiner

Sven Jacobs

Helmut Knoblauch

Roman Kohler

Walter Kühner

Leif Lia

Miroslav Marence

Peter Matt

Guido Mazzà

Sophie Messerklinger

Grethe Midttømme

Uwe Müller

Johann Neuner

Sebastian Perzlmaier

Marco Peter

Franz Georg Piki

Reinhard Pohl

Michael Rogers

Burkhard Rüdisser

Josef Schneider

Shervin Shahriari

Edwin Josef Staudacher

Markus Verdianz

Martin Wieland

Gerald Zenz

CONTENTS

TECHNICAL COMMITTEE WORKSHOPS

TECHNICAL COMMITTEE A
COMPUTATIONAL ASPECTS OF ANALYSIS AND DESIGN OF DAMS (2017-20)
TECHNICAL COMMITTEE B
SEISMIC ASPECTS OF DAM DESIGN (2017-20)

SPECIAL SESSION

OROVILLE DAM SPILLWAY INCIDENT

SYMPOSIUM TOPICS

- T1: CLIMATE CHANGES RESERVOIR OPERATION
(Catchment, permafrost, glacier melting, erosion and sedimentation)
- T2: PERMISSION AND SAFETY ASSESSMENT
(Construction and operation of hydraulic structures, inspection & assessment of operating devices)
- T3: DAM AND FOUNDATION SEALING
(Long term behaviour and assessment of uplift distribution)
- T4: CAVERNS AND POWER WATERWAYS
(Design, construction and monitoring, power water way and lining with high strength steel)
- T4.1: SEMINAR HIGH STRENGTH STEEL IN HYDROPOWER PLANTS
- T5: STABILITY OF RESERVOIR SLOPES
(Reservoir operation, avalanches, impulse waves, dam breach)

TECHNICAL COMMITTEE WORKSHOPS

TECHNICAL COMMITTEE A COMPUTATIONAL ASPECTS OF ANALYSIS AND DESIGN OF DAMS (2017-20)

TECHNICAL COMMITTEE B SEISMIC ASPECTS OF DAM DESIGN (2017-20)

1 A	CAPITALIZATION OF BENCHMARK WORKSHOPS RESULTS SINCE BERGAMO 1991 Guido Mazzà (Extended Abstract)	1
2 B	50 YEARS OF COMMITTEE ON SEISMIC ASPECTS OF DAM DESIGN Martin Wieland (Extended Abstract)	3
3 A/B	NUMERICAL METHODS APPLIED AND INTERPRETED FOR SAFE DAM BEHAVIOR Gerald Zenz (Extended Abstract)	5
4 A/B	SEISMIC ASPECTS IN THE DESIGN OF EMBANKMENT AND ROCKFILL DAMS WITH SPECIAL EMPHASIS ON COMPUTATIONAL ASPECTS Camilo Marulanda (Extended Abstract)	7
5 B	COLLAPSE OF AN AGRICULTURAL EARTH-DAM BY RECENT EARTHQUAKE AND ITS RECONSTRUCTION Fumio Tatsuoka (Extended Abstract)	9
6 B	COMPARISON OF MEASURED AND ANALYZED SEISMIC BEHAVIOUR OF ARCH DAM, ROCKFILL DAM, AND GRAVITY DAM IN JAPAN Takashi Sasaki (Extended Abstract)	11
7 A	CURRENT CHALLENGES OF SEISMIC NUMERICAL MODELLING FOR SOME ITALIAN EXPERIENCES Massimo Meghella (Extended Abstract)	13
8 B	QUALIFICATION OF DYNAMIC ANALYSES OF DAMS AND THEIR EQUIPMENT---OUTCOME OF JCOLD-CBFR TECHNICAL EXCHANGE--- Norihisa Matsumoto, Jean-Jacques Fry (Extended Abstract)	15
9 B	OBSERVATIONS OF PERFORMANCE OF EARTHFILL EMBANKMENTS DURING THE M6.6 LAKE GRASSMERE EARTHQUAKE IN 2017 AND THE M7.8 KAIKOURA EARTHQUAKE IN 2016 Trevor Matuschka (Extended Abstract)	17
10 A	LESSONS LEARNED FROM RECENT INTERNATIONAL WORKSHOPS ON SEISMIC NUMERICAL MODELLING FOR CONCRETE DAMS Emmanuel Robbe (Extended Abstract)	19
11 B	SEISMIC HAZARD ANALYSIS OF HARD-ROCK DAM SITES Kofi O. Addo (Extended Abstract)	21

SYMPOSIUM

SPECIAL SESSION “OROVILLE DAM SPILLWAY INCIDENT”

1-ORO	WARNINGS AND THE HUMAN RESPONSE Jason Needham	23
2-ORO	SITUATION DEVELOPMENT, INCIDENT RESPONSE AND PUBLIC SAFETY David Gutierrez, William Croyle	41
3-ORO	FAST-TRACK RECOVERY DESIGN AND CONSTRUCTION TO ADDRESS CRITICAL DAM SAFETY Les Harder	63
4-ORO	ROLLER COMPACTED CONCRETE INFLUENCES ON RECOVERY STRUCTURAL DESIGN FEATURES Michael Rogers	85
5-ORO	GEOLOGICAL AND GEOTECHNICAL INVESTIGATIONS FOR RECOVERY DESIGN FEATURES Mike Gray	101
6-ORO	HYDROLOGIC AND HYDRAULIC ENGINEERING ACTIVITIES TO INFORM OPERATION AND DESIGN Mark Fortner	123
7-ORO	FINDINGS OF THE SPILLWAY INCIDENT FORENSIC INVESTIGATION John France	145

TOPIC 1: CLIMATE CHANGES RESERVOIR OPERATION

T1-1	ID 28 MODELLING THE UNCERTAINTY OF INFLOW TO SHORT-TERM RESERVOIR OPERATION USING FUNCTIONAL EXPANSION-BASED METHOD Duan Chen, Bo Hu	171
T1-2	ID 29 INCREASE EFFICIENCY OF VORTEX SETTLING BASIN IN IMBIBITION OF DAM'S RESERVOIR IN TIME OF FLOODWATER Amin Hajjahmadi, Mojtaba Saneie, Mehdi Azhdari Moghaddam	179
T1-3	ID 34 GROWING NEED FOR STORAGE AS AUSTRALIA TRANSITIONS FROM COAL ENERGY TO RENEWABLES Richard Herweynen, Nick West	199
T1-4	ID 41 CLIMATE EFFECT ASSESSMENT OF THREE GORGES PROJECT Long Xing	211
T1-5	ID 48 DETERMINATION OF CONTROL WATER LEVEL ON SUTAMI AND LAHOR RESERVOIR TO AVOID THE POSSIBILITY OCCURS OVERTOPPING DUE TO PROBABILITY MAXIMUM FLOOD Ulle Mospar Dewanto, Arief Satria Marsudi, Rahmah Dara Lufira	221
T1-6	ID 74 IMPACT OF UPPER YANGTZE CASCADE RESERVOIRS OPERATION ON THREE GORGES RESERVOIR IN IMPOUNDMENT PERIOD Gao Yulei, Wang Hai	231

T1-7	ID 77	STUDY ON THE INFLUENCE OF CLIMATE CHANGE ON THE THREE GORGES RESERVOIR AND ITS COUNTERMEASURES Wang Fangfang, Bao Zhengfeng	241
T1-8	ID 91	A CHANGING FLOW REGIME IN CENTRAL GERMANY: MAGNITUDES, CAUSES AND EFFECTS ON RESERVOIR MANAGEMENT Markus Möller	251
T1-9	ID 94	STUDY ON RISK ANALYSIS FOR FLOOD PREVENTION AND DAM SAFETY BASED ON STOCHASTIC SIMULATION Jie Gao (Extended Abstract)	263
T1-10	ID 95	EROSION AND SEDIMENTATION OF UPSTREAM ASAHAN AND ITS COUNTERMEASURES FOR THE SUSTAINABILITY OF SIRUAR DAM NORTH SUMATERA Muhammad Luckmanul Chakim, Sugik Edi Sartono (Extended Abstract) . 275	
T1-11	ID 107	EVALUATION OF SEDIMENT MANAGEMENT EFFECTIVENESS TO EXTEND THE WLINGI RESERVOIR LIFETIME Zainal Alim	277
T1-12	ID 109	EVALUATION AND MITIGATION OF THE BOGEL RIVER FLOOD Aris Yhadhianto, Ulie Mospar Dewanto	291
T1-13	ID 110	SETTING UP DREDGING AND SPOILBANK MANAGEMENT METHOD TO RECOVERY HYDROPOWER PRODUCTIVITY OF SENGGURUH DAM Aris Yhadhianto, Ulie Mospar Dewanto	301
T1-14	ID 129	NUMERICAL SIMULATION AND EXPERIMENTAL RESEARCH ON REGULAR MECHANISM OF LOCAL CLIMATIC CHANGES AROUND GIANT HYDROPOWER RESERVOIR Yangbing Deng, Jin Xu, Xiaolong Chen, Guanglin Meng, Mi Li	315
T1-15	ID 136	RUNOFF AND SEDIMENT TRANSPORTATION IN UPPER AND MIDDLE REACHES OF JINSHA RIVER Yan Xia, Zhou Yinjun, Jin Zhongwu (Extended Abstract)	327
T1-16	ID 141	STUDY ON THE SEDIMENTATION CHANGES IN THE MANWAN RESERVOIR ON THE LANCANG RIVER Pang Bohui, Li Mengyang, Lu Ji, Chen Hao	329
T1-17	ID 142	ANALYSIS OF KEY INFLUENCING FACTORS FOR THE EVOLUTION OF THE SAND BAR IN THE TRIBUTARIES IN THE XIAOLANGDI RESERVOIR AREA Yuanjian Wang, Enhui Jiang	347
T1-18	ID 164	SEDIMENT MANAGEMENT STRATEGIES FOR HYDROPOWER RESERVOIR IN AGRICULTURAL AREA Azwin Zailti Abdul Razad, Rahsidi Sabri Muda (Extended Abstract)	359
T1-19	ID 167	OBSERVATION AND ESTIMATION METHOD OF SEDIMENT PRODUCTION IN KAMANASHIGAWA BASIN, FUJIKAWA RIVER SYSTEM - TOWARD AN ACCURATE ESTIMATION OF DAM SEDIMENT VOLUME Kunihiro Tomita, Zhengxing Ye, Takashi Hikita, Tetsuya Sumi	361
T1-20	ID 175	EXPERIMENTAL DESIGN OF A TARGETED WATER RELEASE TO FLUSH SAND OUT OF THE BYPASSED REACH OF THE SELVES RIVER Rémi Loire, Loic Grospretre, Hervé Piégay, Jean-René Malavoi, Olivier Ortiz	373
T1-21	ID 186	DAMS AND RESERVOIRS - CLIMATE CHANGE ADAPTATION STRATEGY Hubert Lohr, Felix Froehlich, Marius Herber, Sandra Richter	383

T1-22	ID 195 APPLICATION OF WATER QUALITY INDEXES FOR QUALITY ASSESSMENT OF ZAYANDEHROOD DAM RESERVOIR Masoud Mirmohammad Sadeghi, Niaz Vahdatpour, Ali Basirpour, Zahra Mesmarian, Seyed Reza Roozegar, Zohreh Sheklabadai, Morteza Shahmoradi, Ali Fatehizadeh, Mohammad Ghasemian, Afshin Ebrahimi, Ensiyeh Taheri, Mohammad Mehdi Amin, Forouzan Hemami, Nasim Rafiei (Extended Abstract)	395
T1-23	ID 199 ON THE ESTIMATION OF SEDIMENTATION LEVEL IN IMHA DAM RESERVOIR, KOREA Hongjun Joo, Duckhwan Kim, Hungsoo Kim, Younghye Bae, Jungwook Kim (Extended Abstract)	397
T1-24	ID 203 RESERVOIR OPERATION RULE OF HEPP POSO DAM, INDONESIA Cristina Dwi Yuliningtyas, Rahman Hakim Ardiansyah	399
T1-25	ID 205 ROPES: RESERVOIR OPERATION SIMULATOR FOR ENVIRONMENTAL SUSTAINABILITY Hubert Lohr, Michael Bach, Sandra Richter, Felix Froehlich, Jędrzej Baryla	409
T1-26	ID 207 UNSTEADY STATE APPROACH FOR ESTIMATION OF RESERVOIR SEDIMENTATION Balkrishna Shankar Chavan.....	421
T1-27	ID 211 FINDING BALANCE BETWEEN WATER CONSERVATION, SEDIMENTATION, AND ENERGY IN DAM MANAGEMENT OF SERAYU-BOGOWONTO RIVER BASIN TERRITORY CASE STUDY OF WADASLINTANG AND SEMPOR Vicky Ariyanti, Kisworo Rahayu	435
T1-28	ID 234 A STUDY ON THE VULNERABILITY RANKING USING HYDROLOGICAL SAFETY EVALUATION RESULT OF EXISTING DAMS CONSIDERING CLIMATE CHANGE Jiyeon Park	445
T1-29	ID 236 EXPERIMENTAL STUDY ON BED EROSION DOWNSTREAM FROM A DAM Zhijing Li, Jun Wang (Extended Abstract).....	453
T1-30	ID 241 STUDY ON MECHANISM OF RESERVOIR INDUCED SEISMICITY AND COUNTERPLOTS FOR RESERVOIR OPERATION UNDER EXTREME WEATHER Xinxiang Zeng, Tinggai Chang, Xiao Hu, Lei Yang	455
T1-31	ID 243 IMPACT OF CLIMATE CHANGE ON THREE LARGE RESERVOIRS OPERATION IN CITARUM RIVER – INDONESIA Reni Mayasari, Hari Suprayogi, Harry Muharsyah Sungguh	465
T1-32	ID 263 DETERMINATION OF GERMI CHAY DAM RESERVOIR SEDIMENTATION PROCESS Simin Shahradfar, Shabnam Partovi Azar, Sara Ahmadi Adli (Extended Abstract).....	477
T1-33	ID 265 NUMERICAL SIMULATION OF THE MORPHODYNAMIC CHANGES BY SEDIMENT SUPPLY AT THE DOWNSTREAM OF YOUNGJU DAM Chang-Lae Jang, Ki-Ho Kang, Kwansue Jung	479
T1-34	ID 269 ASSESMENT OF OPERATIONAL PERFORMANCE AND RISKS CONSIDERING THE EFFECT OF CLIMATE CHANGE ON THE TIBETAN PLATEAU Helmut Wenzel, Jia-xiu Yang, Ji Lu, Barbara Theilen-Willige.....	491
T1-35	ID 270 COUNTERMEASURE OF SEDIMENTATION PROBLEM ON WONOGIRI RESERVOIR, INDONESIA Graita Sutadi, Yoga Darmawan Diparindra, Airlangga Mardjono, Nisa Andan Restuti, Duki Malindo.....	503
T1-36	ID 309 CLIMATE CHANGE IMPACT ON SURFACE WATER RESOURCES AND HYDROPOWER GENERATION IN THE DEZ DAM BASIN, IRAN Roya Sadat Mousavi, Mojtaba Ahmadizadeh, Safar Marofi	519

T1-37	ID 317 SEDIMENT MANAGEMENT AT PATRIND HYDRO POWER PROJECT USING OHDS TECHNIQUE Woncheol Park, Kiyong An	533
T1-38	ID 324 ADVANTAGES OF DRY DAM AS FLOOD CONTROL IN JAKARTA'S URBAN AREA Airlangga Mardjono, Agus Safari, Faris Setiawan	545
T1-39	ID 345 GREEN DAM RESERVOIR: A NEXUS CONCEPT FOR SAFE OPERATION AND MAINTENANCE OF DAMS IN IRAN Saied Yousefi, Naser Kheirkhah, Mohamad Rahbari	555
T1-40	ID 369 DAM SAFETY EMERGENCY RESPONSE PLAN : SHARING EXPERIENCE ON ENGAGEMENT WITH LOCAL AGENCIES FOR TNB HYDROPOWER DAM IN MALAYSIA Mohd Sidek Lariyah, Basri Hidayah, Abdul Razad Azwin Zailti, Muda Rahsidi Sabri, Md Said Nur Farazuien, Yalit Mohd Ruzaimi, Kwansue Jung (Extended Abstract)	567
T1-41	ID 471 DEVELOPMENT AND ASSESSMENT OF DAM INFLOW DEFICIT INDEX FOR COPING WITH A DROUGHT Minsung Kwon, Kyung Soo Jun	569
T1-42	ID 507 ADAPTED OPERATION OF TROPICAL GLACIAR RESERVOIRS DUE TO CLIMATE CHANGE Alexander Roland Arch, Anna Hetterich, Eliana Romero, Georg Puchner	581
T1-43	ID 591 STUDY ON SOIL EROSION OF MAHAWELI RIVER UPPER BASIN UNDER CLIMATE CHANGE USING SWAT MODEL D M Thushara Sanjeewa Dissanayake	593
T1-44	ID 625 A USEFUL TECHNOLOGY TO SOLVE OR MITIGATE ARTIFICIAL RESERVOIR SEDIMENTATION Francesco Galante, Luca Masotti, Claudio Fornasari	605
T1-45	ID 631 ASSESSMENT OF TEMPERATURE AND PRECIPITATION CHANGES TREND EFFECTS ON THE DAM INFLOW Mojtaba Noury, Manijeh Ezzati, Behrooz Shaghaghi, Mohammadreza Parhizi, Alireza Shokohi, Atabak Jafari	627
T1-46	ID 650 RAPID SCREENING OF SEDIMENT MANAGEMENT TECHNIQUES FOR MORAGOLLA HPP WITH RESCON-2 Nikolaos Efthymiou, Richard Guimond, Aleksandar Trifkovic, Radovan Miljanovic, Nadun Bulathge	641
T1-47	ID 671 SUSTAINABLE DEVELOPMENT IN HYDROPOWER PROJECT Min Byeong Soo, Hong Young Jin, Nadim Ullah	653
T1-48	ID 719 DCNA - DISASTER COMPETENCE NETWORK AUSTRIA Christian Resch	665

TOPIC 2: PERMISSION AND SAFETY ASSESSMENT

T2-1	ID 17 PERMANENT SAFETY ASSESSMENT OF DAMS, LEVEES, RESERVOIRS, WATERWAYS WITH FIBER OPTIC DISTRIBUTED SENSING Régis Blin, Daniele Inaudi	675
T2-2	ID 21 EXPERIMENTAL INVESTIGATION OF STEPPED SPILLWAY PERFORMANCE OF UPPER CISOKAN DAM IN INDONESIA James Zulfan, Nuryanto Sasmito Slamet	687
T2-3	ID 22 REMOTE INSPECTION OF SMALL DAMS AND LEVEES Bill Sherwood (Extended Abstract)	699

T2-4	ID 25 HOW TO DEAL WITH AGING PRESTRESSED ANCHORS IN DAMS: A NORTH AMERICAN PERSPECTIVE Donald A. Bruce, John S. Wolfhope	701
T2-5	ID 36 DAM SAFETY MONITORING AND PRE-WARNING IN EXTREMELY CONDITIONS Jun Shi Wang, Xing Yun Wu, Qiong Pang, Chang Yan Gu	713
T2-6	ID 111 GROUND VIBRATION CHARACTERISTICS INDUCED BY FLOOD DISCHARGE OF A HIGH DAM: AN EXPERIMENTAL INVESTIGATION Yan Zhang, Guoxin Zhang, Yi Liu, Songhui Li	721
T2-7	ID 119 EXPERIMENTAL STUDY ON THE GLOBAL STABILITY OF THE XIAOWAN ARCH DAM USING A 3D GEO-MECHANICAL MODEL TEST Jian Hua Dong, Lin Zhang, Bao Quan Yang, Jian Ye Chen, Yuan Chen (Extended Abstract)	733
T2-8	ID 121 JUSTIFICATION FOR SELECTION OF A FACTOR OF SAFETY FOR DAMS Thomas Konow, Mathias Strand	735
T2-9	ID 124 DETERMINING ALIGNMENT PATTERN OF TECHNOLOGY STRATEGY WITH POWER PLANTS DEVELOPMENT STRATEGY - CASE STUDY OF KARKHEH DAM Hosseion Boromandfar, Reza Salami, Manouchehr Manteghi	747
T2-10	ID 131 A COMPARISON BETWEEN HYDROSTATIC-TIME-SEASON AND BAYESIAN DYNAMIC LINEAR MODELS FOR MONITORING BEHAVIOR OF DAMS Ianis Gaudot, Luong Ha Nguyen, Benjamin Miquel, James A. Goulet (Extended Abstract)	759
T2-11	ID 145 INCREASE CONCRETE QUALITY IN DAM CONSTRUCTION DURING DESIGN AND EXECUTION PHASE Andreas Zitzenbacher, Massimo Maffezzoli, Stefan Scheuchelbauer	761
T2-12	ID 146 VISUAL DOCUMENTATION AND INSPECTION OF DAM SURFACES USING STATE-OF-THE-ART TOTAL STATIONS Slaven Kalenjuk, Werner Lienhart, Harald Wackenreuther	773
T2-13	ID 158 PARAMETRIC STUDY IN GRAVITY DAMS ANALYZING THE INFLUENCE OF THE FLEXURAL, SHEAR AND ROTATION EFFECTS Iarly Vanderlei da Silveira, Henrique Ataíde Nerys de Castro Filho, Renan Rocha Ribeiro	783
T2-14	ID 162 TIME-SPACE COLLISION ANALYSIS AND ADJUSTMENT METHOD FOR HIGH ARCH DAM SURFACE CONSTRUCTION Chao Hu, Chunju Zhao, Yihong Zhou, Ling Song, Lian Liu	795
T2-15	ID 172 EXTERNAL DEFORMATION MONITORING OF NINETEEN ROCKFILL DAMS USING SATELLITE SAR DATA Hiroyuki Sato, Masafumi Kondo, Toshihide Kobori, Ryotaro Ishikawa, Takashi Sasaki, Wataru Sato, Naruo Mushiake, Takumi Sato, Ken'ichi Honda	807
T2-16	ID 181 BEHAVIOUR OF THE BACKFILLED RIGHT BANK OF THE MAVČIČE DAM Pavel Žvanut, Rudi Brinšek	819
T2-17	ID 189 AIR DEMAND OF BOTTOM OUTLETS: INSIGHTS FROM SCALE MODEL TESTS AND PROTOTYPE MEASUREMENTS Benjamin Hohermuth, Lukas Schmocker, Robert Michael Boes	831
T2-18	ID 215 TECHNICAL STAGE TO PLUG THE LARGE SIZE DIVERSION TUNNEL OF JATIGEDE DAM AT WEST JAVA, REPUBLIC OF INDONESIA, 2017 Anwar Makmur, Dony Faturochman Saefulloh, Tulus Heri Basuki, Rosita Harimukti Rahmawati (Extended Abstract)	843

T2-19	ID 217 AN INTEGRATED GEOPHYSICAL INVESTIGATION FOR THE EARTHEN DAM INSPECTION: ELECTRICAL RESISTIVITY IMAGING, MULTICHANNEL ANALYSIS OF SURFACE WAVE AND GROUND PENETRATING RADAR Noppadol Poomvises, Prateep Pakdeerod, Anchalee Kongsuk (Extended Abstract)	845
T2-20	ID 223 HOW PROBABILISTIC APPROACH CAN IMPROVE CMD DESIGNINGS Ahmad Ghezel Ayagh, Abbas Mohammadian	847
T2-21	ID 227 EFFECT OF DILATANCY ANGLE ON THE RELIABILITY ANALYSIS OF BEARING CAPACITY OF DAM FOUNDATION USING MONTE CARLO SIMULATION Mehraneh Maadi, Ali Noorzad	859
T2-22	ID 230 SPILLWAY HYDRAULIC MODEL TEST OF CIPANUNDAN DAM, WEST JAVA, INDONESIA Airlangga Mardjono, Nisa Andan Restuti, Harvien Mahardika	873
T2-23	ID 237 MAE SUAI DAM SAFETY Pronmongkol Chidchob	881
T2-24	ID 247 SAFETY ASSESSMENT AND MAINTENANCE OF RELIABLE OPERATION OF DAMS IN RUSSIA Evgeniy Bellendir, Elena Filippova, Oleg Buryakov	897
T2-25	ID 251 DAM DEFORMATION MONITORING MODEL AND FORECAST BASED ON PCA-RBF NEURAL NETWORK Chaoning Lin, Tongchun Li, Siyu Chen, Xiaoqing Liu, Siling Liang	903
T2-26	ID 254 SAFETY ASSESSMENT FOR LARGE RESERVOIR CONSTRUCTED FOR DOMESTIC WATER NEAR URBAN AREAS AND A CASE STUDY Hasan Tosun, Turgut Vatantosun	917
T2-27	ID 257 LABORATORY STUDY OF THE EFFECT OF RECYCLED FILLERS FROM COKING AND IRON CONCENTRATE FACTORIES ON THE ROLLER COMPACTED CONCRETE PROPERTIES IN DAMS (RCC DAMS) Jaber Mahmoudi, Faeze Yazdi	929
T2-28	ID 261 OPERATION AND MAINTENANCE OF SABALAN DAM Jamshid Sadrekarimi, Simin Shahradfar, Atusa Mihandoost (Extended Abstract)	945
T2-29	ID 271 RESEARCH OF RESERVOIR EMPTYING DESIGN OF HIGH DAMS IN CHINA Liu Chao, Zhao Quansheng, Zhou Jianping	947
T2-30	ID 275 VISUAL INSPECTION AND ASSESSMENT OF OPERATING DEVICES IN IR. H. DJUANDA DAM – INDONESIA Reni Mayasari, Harry Muharsyah Sungguh, Budi Nugraha	957
T2-31	ID 285 EVENT TREE CONCEPT FOR DESCRIBING THE RELIABILITY OF GATED WEIRS AND SPILLWAYS Markus Aufleger, Barbara Brinkmeier	967
T2-32	ID 291 VEGETATION EFFECT ON RELIABILITY ANALYSIS OF SLOPE STABILITY USING MONTE-CARLO SIMULATION Iman Vaezi, Hesam Saeidi, Ali Noorzad	973
T2-33	ID 296 PERMISSION PROCEDURES OF DAM CONSTRUCTION AND MANAGEMENT IN INDONESIA Cristina Dwi Yuliningtyas, Lolo Wahyu Resdiatmoko, Hari Suprayogi	985
T2-34	ID 304 INTERNAL EROSION RISKS IN RIGHT ABUTMENT OF AHMADBEIGLU STORAGE DAM IN IRAN Mohammadi Arezoo, Bemani Yazdi Ali Asghar	995
T2-35	ID 307 MAIN ECOLOGICAL RISKS FACING THE YANGTZE RIVER BASIN, EXISTING PROTECTIVE MEASURES AND THEIR EFFECTIVENESS Zhu Di, Yang Zhi	1007

T2-36	ID 321 ANALYSIS AND INTERPRETATION OF THE BAIXO SABOR DAM BEHAVIOUR DURING THE FIRST FILLING OF THE RESERVOIR José Piteira Gomes, António Lopes Batista, Domingos Silva Matos	1019
T2-37	ID 331 SCOUR ESTIMATION FOR NAM THEUN 1 SPILLWAY PLUNGE POOL F. Takhtemina, M. P. Bieri, Benno Karl Zuend, S. Martin	1031
T2-38	ID 337 A DEVELOPMENT OF HYDROLOGIC RISK ANALYSIS MODEL FOR SMALL RESERVOIRS BASED ON BAYESIAN NETWORK Jin-Guk Kim, Hyun-Han Kwon, Byoung-Han Choi (Extended Abstract) ..	1043
T2-39	ID 338 EXPERIMENTAL STUDY ON DIRECT SHEAR BETWEEN FRP - CONCRETE IN TERFACE BASED ON DIC Zhang Lei, Lei Dong, Wu Ling Cheng, Yang Yong.....	1045
T2-40	ID 344 COMBINING NUMERICAL AND PHYSICAL MODELS FOR COST EFFECTIVE DESIGN OF IRREGULAR SPILLWAYS Jonas Persson, James Yang, Öyvind Espeseth Lier, Martin J. Eriksson, Carl-Oscar Nilsson	1057
T2-41	ID 347 THE BEHAVIOR OF THE SPILLWAY-STRUCTURE OF THE DJUANDA DAM JATILUHUR INDONESIA Budy Gunady, Harry Muharsyah Sungguh, Mudiwati Rahmatunnisa, Diah Eka Harsani (Extended Abstract).....	1075
T2-42	ID 352 PHYSICAL MODELLING OF THE JIRKOV DAM BELL-MOUTH SPILLWAY Jan Svejkský, Martin Krupka	1077
T2-43	ID 356 STRUCTURAL SAFETY CONTROL OF THE BAIXO SABOR DAM BASED ON AN AUTOMATED DATA ACQUISITION SYSTEM João Gomes Cunha, Juan Mata, Gonzalo Losada	1087
T2-44	ID 372 SEISMIC HAZARD ANALYSIS FOR GAMBIRI DIVERSION DAM Samaneh Soleymani, Abbas Mahdavian, Hamid Bahrami	1099
T2-45	ID 373 IN-DEPTH SAFETY ASSESSMENT OF LARGE RUN-OF-RIVER HYDROPOWER PLANTS IN SWITZERLAND Sven-Peter Teodori, Helmut Stahl	1111
T2-46	ID 381 ASPECTS CONCERNING AGEING OF EMBANKMENT DAMS Ronald Haselsteiner	1125
T2-47	ID 382 PUBLIC SAFETY AROUND DAMS IN BRANTAS RIVER BASIN, INDONESIA Kamsiyah Windianita, Didik Ardianto, Fahmi Hidayat, Raymond Valiant Ruritan, Alfian Rianto, Henda Tri Retnadi - Extended Abstract not available.	
T2-48	ID 406 HYDRAULIC ANALYSIS OF TEMPORARY FLOOD HAZARD TO SUPPORT THE PLANNING OF THE CONSTRUCTION PHASES OF HYDROPOWER PLANT Gašper Rak, Franci Steinman	1135
T2-49	ID 409 THE APPLICATION OF MATURITY MATRIX IN DAMS SAFETY PROGRAM IN BENGAWAN SOLO RIVER BASIN ORGANIZATION (RBO), INDONESIA Agus Jatiwiryono Soemardijo, Antonius Suryono	1151
T2-50	ID 410 FULL WAVE BASED DAMAGE IDENTIFICATION IN DAMS Muyiwa E. Alalade, Frank Wuttke, Tom Lahmer.....	1163
T2-51	ID 414 SELF-PROTECTED UNDERWATER CONCRETE IN REHABILITATION OF HYDRAULIC STRUCTURES Feng Jin, Hu Zhou, Fengliang Li, Peng Wan	1175
T2-52	ID 416 VIBRATIONS IN LARGE DAMS. MONITORING AND MODELLING Sérgio Oliveira, André Alegre	1185
T2-53	ID 422 COMBINED SEEPAGE AND SLOPE STABILITY ANALYSIS OF EARTH DAMS Bakenaz A. Zeidan, M. Shahien, M. Elshemy, M. S. Kirra.....	1197

T2-54	ID 423 IMPROVING MODIFIED ICOLD METHOD WITH LOSS OF LIFE INDEX FOR DAM SAFETY RISK ASSESMENT IN INDONESIA BY USING RASTER METHOD Anto Henrianto, R. Wahyudi, Triweko	1209
T2-55	ID 428 NEAR-FAULT SEISMIC VULNERABILITY OF GRAVITY DAMS Yadollah Yazdani, Mohammad Alembagheri	1221
T2-56	ID 430 EFFECTS OF FOUNDATION FLEXIBILITY ON THE FAILURE PROBABILITY OF KARUN IV ARCH CONCRETE DAM IN SEISMIC CONDITION Farid Miarnaemi, Gholamreza Azizyan, Mohsen Rashki (Extended Abstract)	1231
T2-57	ID 436 UPGRADING THE PERFORMANCE OF POORLY COMPACTED EMBANKMENT DAM FOUNDED ON SOFT CLAY THROUGH ADAPTING SECANT AND STABILITY PILES SYSTEM Ashraf Abdel-hay Elashaal, Alaa Abdalla Abdel-moteleb	1233
T2-58	ID 437 PUBLIC SAFETY AROUND DAMS: SUTAMI DAM EXPERIENCE Didik Ardianto, Raymond Valiant, Alfian Rianto, Fahmi Hidayat, Robert Purba M. Sianipar	1245
T2-59	ID 438 RISK BASED APPROACH AT THE DAM SAFETY ASSESSMENT DURING ITS RECONSTRUCTION Jaromír Řiha, Miroslav Špano	1253
T2-60	ID 446 MASTER PLAN FOR SAFETY OF MAJOR HYDRAULIC STRUCTURES IN EGYPT Khaled Toubar, Pelayo Baztan, Abeer Salamh	1265
T2-61	ID 447 FORMAL INVESTIGATION OF LAHOR DAM, INDONESIA Teguh Winari, Kamsiyah Windianita, Didik Ardianto, Fahmi Hidayat, Raymond Valiant Ruritan (Extended Abstract)	1277
T2-62	ID 459 FLEXIBLE PROTECTION MEASURES FOR ADAPTATION WITH SEA - LEVEL RISE ON THE NILE DELTA Mohamed Ahmed Ali Mohamed Hassan, Ashraf Abdel-hay Elashaal, Mohamed Abdel-Motaleb	1279
T2-63	ID 467 AN INTELLIGENT COOLING CONTROL METHOD AND SYSTEM FOR XILUODU ARCH DAM CONSTRUCTION Peng Lin, Zeyu Ning, Haoyang Peng	1289
T2-64	ID 468 KEY CONSTRUCTION TECHNOLOGY OF 300 M HIGH CORE WALL ROCK-FILL DAM Wu Gao Jian, Fan Peng, Han Xing (Extended Abstract)	1299
T2-65	ID 475 ON-LINE STRUCTURAL HEALTH MONITORING OF REHABILITATED DAMS Amod Gujral, Prateek Mehrotra	1301
T2-66	ID 476 THE OPERATIONAL AND MAINTENANCE OF KEULILING RESERVOIR AS FIRST DAM IN ACEH PROVINCE - INDONESIA Ardiana Junira, Saputra T. Maksal, Mardjono Airlangga	1313
T2-67	ID 481 AN ANALYSIS ON THE BEHAVIORS OF A DAM FOR THE EARTHQUAKE IN SOUTH KOREA Taegeun Lee, Baegun Cho, Gyeongjin Kim, Taekang Yun	1325
T2-68	ID 484 DAM SAFETY REGULATION IN SOUTH AFRICA: 32 YEARS DOWN THE LINE Louis C. Hattingh, Ivor Segers	1337
T2-69	ID 486 BEHAVIOUR OF ASPHALT CONCRETE CORE EMBANKMENT DAMS (ACED) AND SHEAR ZONE DEVELOPMENT Guntram Innerhofer sen., Peter Tschernutter, Adrian Kainrath	1349
T2-70	ID 491 EJEKTOR POWER PLANT - VERTICAL KAPLAN Rudolf Fritsch	1363

T2-71	ID 494 FEATURES OF MONITORING TEMPERATURE OF AN RCC DAM DURING CONSTRUCTION BASED ON DATA MINING Jianwen Pan, Jinting Wang (Extended Abstract)	1391
T2-72	ID 495 RUBBER DAM CONSTRUCTION WITH NAVIGATION LOCKS Paul Oberleitner, Rudolf Fritsch	1393
T2-73	ID 496 EVALUATION OF SLOPE STABILITY CONSIDERING EXISTENCE OF THE SPILLWAY CHANNEL TRENCH AT THE RIGHT AND LEFT ABUTMENTS OF GELEVAR D DAM Kayvan Rahimi, Amir Ali Zad	1405
T2-74	ID 501 ANALYSIS ON THERMAL FIELD EVOLUTION OF WUDONGDE ARCH DAM HaoYang Peng, Peng Lin, Zeyu Ning	1423
T2-75	ID 503 OPERATION OF SMALL AGRICULTURAL DAMS IN BULGARIA - STATE-OF-THE-ART Bogdan R. Nikolov, Dimitar Kisliakov	1435
T2-76	ID 504 COMPARISON OF SELECTED SOFTWARE FOR 3D FLOW MODELING AT THE DAM SPILLWAY Jan Höll, Matouš Holinka, Jiří Hodák	1447
T2-77	ID 506 INVESTIGATION OF THE PROBABILITY OF FAILURE OF A GRAVITY DAM Markus Goldgruber	1459
T2-78	ID 510 CHALLENGES OF DAMS CONSTRUCTION AND MANAGEMENT IN INDONESIA Tri Hartanto (Extended Abstract)	1471
T2-79	ID 512 SEISMIC STABILITY ANALYSIS OF CONCRETE GRAVITY DAM Bakenaz A. Zeidan	1473
T2-80	ID 513 3D BLOCK ERODIBILITY: REAL-TIME MONITORING IN AN UNLINED SPILLWAY CHANNEL Michael F. George, Nicholas Sitar	1491
T2-81	ID 518 KEY NOTES ON QUALITY CONTROL OF ROLLER COMPACTED CONCRETE DAMS Hamed Mahdilou Torkamani	1503
T2-82	ID 545 AN EVALUATION SYSTEM OF HYDROPOWER SUSTAINABLE DEVELOPMENT Chunna Liu (Extended Abstract)	1515
T2-83	ID 556 DAM PROTECTION GATES, ARE WE SOFT ON RISK ? Kenneth Raymond Grubb, Russ Digby, Paul Jones	1517
T2-84	ID 581 HYDRAULIC ASSESSMENT OF TUNNELS Balkrishna Shankar Chavan	1529
T2-85	ID 608 OPERATIONAL MODES MONITORING FOR PREVENTION OF FAILURE OF DAMS WITHIN THE DESIGN ENVELOPE Des Hartford, R. J Rigbey	1551
T2-86	ID 618 STUDY ON THE HARMFUL IMPACT OF SLIT-TYPE ENERGY DISSIPATER WATER WINGS Huang Guobing, Du Lan, Duan Wengang	1563
T2-87	ID 621 SEISMIC ANALYSIS OF MIJARAN EARTH DAM AND OPTIMIZATION OF ITS PARAMETERS USING PSO Seyed Razi Anisheh, Seyed Alireza Anisheh	1577
T2-88	ID 639 REFERENCE PRESSURE CELL, AN EFFECTIVE SOLUTION FOR A CHALLENGING MATTER OF DAM MONITORING Farzin Karimi, Joachim Schneider Glötzl	1587

T2-89	ID 679	THE APPLICATION OF PERFORMANCE ASSESSMENT OF EMBANKMENT DAM MODEL BY USING KNOWLEDGE-BASED SYSTEM	Juliastuti Juliastuti, Widagdo Supardi, Agus Jatiwiryono Soemardijo, Budy Gunady	1599
-------	--------	---	---	-------------

TOPIC 3: DAM AND FOUNDATION SEALING

T3-1	ID 24	REMEDIAL GROUTING OF EXISTING EMBANKMENT DAM FOUNDATIONS: LESSONS LEARNED (AND IGNORED)	Donald A. Bruce, Trent Dreese, Jim Cockburn	1611
T3-2	ID 26	SEEPAGE CUTOFFS FOR DAMS AND LEVEES: LESSONS LEARNED FROM 40 YEARS OF REMEDIAL CONSTRUCTION	Donald A. Bruce	1623
T3-3	ID 31	THE SEEPAGE ANALYSIS OF THE EMBANKMENT DAMS OF A FLOOD RETENTION BASIN IN POLAND	Burcu Ersoy, Ronald Haselsteiner	1635
T3-4	ID 32	GROUT CURTAIN PERFORMANCE PARTICULARITIES IN THE COMPLEX GEOLOGICAL CONDITIONS ENCOUNTERED AT GURA APELOR CLAY CORE ROCKFILL DAM	Adrian Popovici, Dan Stematiu, Eugeniu Marchidanu	1647
T3-5	ID 54	MONITORING AND EVALUATION OF VARIED ANTI-SEEPAGE MEASURES IN DEEP GRAVEL FOUNDATION FOR AN EMBANKMENT DAM - A CASE STUDY	Jun Shi Wang, Qiong Pang, Bing Hai Huang, Hong Wang, Xing Yun Wu	1659
T3-6	ID 79	ASSESSMENT OF HYDRO TASMANIA'S CONCRETE DAMS AND IMPACT OF UPLIFT	Richard Herweynen, Tim Griggs	1667
T3-7	ID 97	RESEARCH AND APPLICATION OF NEW-TYPE MATERIAL IN WUDONGDE AND BAIHETAN 300 M ULTRA-HIGH ARCH DAM - KEY TECH OF CHARACTERISTICS AND APPLICATION ON LOW-HEAT CEMENT CONCRETE	Qixiang Fan, Wenwei Li, Xinyu Li	1677
T3-8	ID 98	REHABILITATION OF THE CENTER HILL EMBANKMENT DAM, TN, USA INCLUDING CONNECTING THE CONCRETE CUT-OFF WALL TO THE EXISTING CONCRETE DAM	Peter Banzhaf	1691
T3-9	ID 151	REMEDIAL GROUTING FOR EMBANKMENT DAM CORE SEALING - 10 YEARS EXPERIENCES	Dong Soon S. Park, Hee-Dae Lim	1703
T3-10	ID 154	THE EFFECT OF THE GROUNDWATER FLOW VELOCITY AND SEDIMENT DISCHARGE ON INTERNAL EROSION OF RIVERS	Fereshteh Noorbakhsh, Mahammad Reza Majdzadeh Tabatabai	1715
T3-11	ID 201	DESIGN OF DEEP SOIL MIXING WALLS AND THEIR ADVANTAGES OVER CONVENTIONAL SEALING FOR EMBANKMENT DAMS	Daniel Kerres, Ronald Haselsteiner	1729
T3-12	ID 216	FIGHTING CRITICAL UPLIFT AT ATATURK DAM	Michel Gavard, Wynfrith Riemer	1741
T3-13	ID 249	WATER TIGHTENING OF RESERVOIR BED AND UPSTREAM FACE OF DAM IN PERSIAN GULF MARTYRS (CHITGAR) LAKE - A CASE STUDY	Ali Emam, Mahdi Zolfagharian, Nima Rashidi, Rouzbeh Radman	1749

T3-14	ID 252 EXPERIENCE ON GROUTING CURTAIN FOR MODERATE HEIGHT-EMBANKMENT DAMS, TURKEY Hasan Tosun	1761
T3-15	ID 274 STUDY ON THE LONG-TERM EFFECT OF INFILTRATION DEFORMATION ON THE DISTRIBUTION OF UPLIFT PRESSURE IN EARTH-ROCK JOINT AREA OF EARTH DAM Zhiyong Mu, Tongchun Li, Zhiwei Niu, Xiaoqing Liu (Extended Abstract)	1773
T3-16	ID 284 ASSESSMENT OF WATER FLOW MEASUREMENT IN A ZONED DAM USING ARTIFICIAL NEURAL NETWORK MODELS Ricardo C. Santos, Juan T. Mata	1775
T3-17	ID 288 APPLICATION OF GEOMEMBRANE AS THE UPSTREAM IMPERVIOUS LAYER OF KAHIR RCC DAM M. Sadri Omshi, Mohsen Jafarbegloo, Hossein Ghiassinezhad, Abbas Mohammadian	1787
T3-18	ID 297 A STUDY ON CAUSE OF PERFORMANCE DEGRADATION OF SEEPAGE MEASURING FACILITY IN OLD DAM Bumlin Cha, Seongho Jang, Junghun Choi	1797
T3-19	ID 298 LONG TERM BEHAVIOR AND PERFORMANCE OF CORE ZONE AGAINST UPLIFT DISTRIBUTION OF MAE NGAD SOMBOON CHON DAM, CHIANG MAI, THAILAND Chatchai Pedugsorn, Kanokwan Chuenuam, Pearasynp Srisawat, Supamitr Krisanamitr	1809
T3-20	ID 300 DAM AND FOUNDATION SEEPAGE CONTROL IMPROVEMENT BY CEMENT-CHEMICAL GROUTING UNDER STORAGE CONDITION OF MAE THI DAM, LAMPHUN, THAILAND Chatchai Pedugsorn, Kanokwan Chuenuam, Pearasynp Srisawat, Supamitr Krisanamitr	1819
T3-21	ID 340 FOUNDATION TREATMENT CHALLENGES FOR EARTH ROCK-FILL DAMS, A CASE STUDY OF ISIMBA HYDRO POWER PROJECT, UGANDA Nicholas Agaba Rugaba, Chad Silas Akita, Isaac Arinaitwe, Harrison Mutikanga	1831
T3-22	ID 342 THIRD REMEDIAL GROUTING CAMPAIGN FOR REINFORCEMENT OF IMPERVIOUS CURTAIN TYPE BATHTUB OF THE CAJON DAM R. Flores Guillén, M. Flores Peñalba, J. Andino Valeriano, C. Iglesias Zúniga	1847
T3-23	ID 351 NECHRANICE DAM - LONG-TERM MONITORING OF SEALING PERFORMANCE AT THE LONGEST EARTH-FILL DAM IN CENTRAL EUROPE Martin Krupka, Jan Svejkský	1857
T3-24	ID 375 SEALING AND FOUNDATION ON A 70 M ALLUVIUM LAYER OF ARKUN DAM Ronald Haselsteiner, Resul Pamuk	1869
T3-25	ID 404 FOUNDATION TREATMENT WITH CUT OFF WALL IN TUGU DAM Ni Made Sumiarsih, Airlangga Mardjono, Nisa Andan Restuti, Ali Cahyadi	1881
T3-26	ID 435 STRENGTHENING AND SEALING OF GOMAL ZAM RCC ARCH-GRAVITY DAM FOUNDATION IN PAKISTAN Eckhard Schnäcker, Chongjiang Du	1891
T3-27	ID 440 CASE HISTORIES OF TAILINGS DAMS WATERPROOFED WITH A BITUMINOUS GEOMEMBRANE (BGM) Bertrand Breul, Jacques Moeglen	1907

- T3-28 ID 452 SEALING PERFORMANCE OF SILVEH EMBANKMENT DAM CUTOFF WALL BASED ON INSTRUMENTATION MEASUREMENTS
Fardin Jafarzadeh, Amir Akbari Garakani, Jafar Maleki, Mehrdad Banikheir, Ramin Raeesi..... 1919
- T3-29 ID 470 FOUNDING AND SEALING DAMS ON VERY WEAK FOUNDATIONS
Wesley Ethiyajeevan Saleira 1931
- T3-30 ID 493 RELIEF DRAINAGES AGAINST HYDRAULIC FAILURE DUE TO UNDERSEEPAGE OF DYKES AND DAMS
Heinz Brandl, Marek Szabo 1943
- T3-31 ID 505 SELECTION OF GROUT CURTAIN IN SPATIAL PLANE BASED ON SET JOINTS AND DIRECTION OF GROUTING GALLERY (GLEVARD DAM, IRAN)
Amir Ali Zad, Kaivan Rahimi, Ali Nabizadeh..... 1955
- T3-32 ID 515 CASE STUDY: ITUANGO HYDROELECTRIC PROJECT-ADDRESSING GEOLOGICAL AND GEOTECHNICAL ISSUES ON THE ROCKFILL-CLAY CORE DAM'S FOUNDATION DESIGN
Maria Cecilia Sierra Bonilla, Juan Esteban Munera Saldarriaga (Extended Abstract)..... 1983
- T3-33 ID 563 COMPARATIVE STUDY ON FOUNDATION TREATMENT TECHNICAL STANDARDS OF HYDROPOWER ENGINEERING BETWEEN CHINA AND AMERICAN
Liu Yaoru, Zhou Haowen, Lv Shuai, Tang Wenzhe..... 1985
- T3-34 ID 613 SEALING WORKS WITH MICROFINE CEMENT AND SYNTHETIC RESIN AT THE CATHALEEN'S FALL DAM, IRELAND
Kurt Kogler, Johann Hechenbichler, Patrick Gabriel, Harry Doherty 1993

TOPIC 4: CAVERNS AND POWER WATER WAYS

- T4-1 ID 35 THE OPERATION AND MAINTENANCE EXPERIENCE OF INDONESIA'S 1ST UNDERGROUND DAM, CASE OF BRIBIN DAM IN KARST CAVE OF GUNUNGSEWU GEOPARK; INDONESIA INSIGHTS ON THE GERMAN-INDONESIAN IWRM PROJECT (2010-2017)
Vicky Ariyanti, Ernowo Ary Fibriyantoro, Shakti Rahadiansyah..... 2005
- T4-2 ID 56 HYDRAULIC DESIGN OF DIVERSION-CUM-DEPLETION TUNNEL
Balkrishna Shankar Chavan..... 2017
- T4-3 ID 113 RESEARCH ON CONTROL MEASURES OF LIMNOPERNA FORTUNEI IN PUMPED STORAGE POWER STATION WATER DELIVERY SYSTEM
Wan Sheng, Liu Xueshan 2031
- T4-4 ID 148 BEHAVIOR ANALYSIS OF THE UNDERGROUND POWERHOUSE BASED ON PRECISE DISPLACEMENT MEASUREMENT
Masayuki Kashiwayanagi, Keisuke Maeda, Norikazu Shimizu..... 2043
- T4-5 ID 178 MODELING TURBULENCE PHENOMENA AND WAVE PROPAGATION IN AYANUNGA HEPP FOREBAY AND ADDUCTION SYSTEM, THROUGH IBER-2D AND ANSYS-3D
Stefano Capillera, Marc Gil Flores, Luca Macchi 2055
- T4-6 ID 179 COMPLEX HYDROGEOLOGICAL RESPONSES DEFY CONSERVATIVE DESIGN OF A PRESSURE TUNNEL - FAILURE OF THE BESAI HEADRACE TUNNEL
Richard Benson, Wynfrith Riemer, M. Iijima..... 2067

T4-7	ID 260 ESTIMATION OF EQUIVALENT PERMEABILITY OF ROCK MASS USING BACK ANALYSIS AND DFN MODEL- CASE STUDY Abbas Kamali bandpey, Ali Alianvari, Mohammed El Tani, Khosru Negintaji, Mohammad Ali Gholami	2081
T4-8	ID 272 OBERVERMUNTWERK II: NUMERICAL MODELING AND DESIGN Christopher Dich, Franz Tschuchnigg	2093
T4-9	ID 299 CONSTRUCTION AND MONITORING OF POWER HOUSE CAVERNS IN CIRATA HIDRO POWER INDONESIA Pangestu Dwipa Airlangga	2105
T4-10	ID 302 LINING CONCEPT TO CONTROL HYDROFRACTURING OF THE POWER WATERWAY OF HPP QUITARACSA IN PERU Wynfrith Riemer, Michael Thiel, Roland Schmidt	2115
T4-11	ID 349 IN-SITU TESTING AND MONITORING OF TUNNELS AND CAVERNS AT A PUMPED-STORAGE POWER PLANT IN THE SWISS ALPS Marcel Hubrig, Andreas Kern, Ursula Rösli, Hans-Jakob Becker, Thomas Trick	2129
T4-12	ID 363 SIPHON INTAKE AS SHPP INTAKE & WATER WAY, A SOLUTION DESIGN FOR SECURING THE LEFT BANK OF WLINGI DAM IN BLITAR, INDONESIA Ulle Mospar Dewanto, Gede Nugroho Ariefianto, Bayu Pramadya, Kurniawan Sakti	2141
T4-13	ID 389 MODIFYING METHOD FOR VORTEX FLOW IN TRIFURCATION IN HYDROPOWER PLANT Yeonju Lee, Waqar Ahmad Khan, Junaid Khan	2155
T4-14	ID 393 HOLLOW CONE VALVE (HCV) IR. H. DJUANDA DAM AND MURI INDONESIA RECORD Angga Prawirakusuma, Joko Mulyono, Dwi Aryani Semadhi Kubontubuh	2167
T4-15	ID 403 THE GROUTABILITY INVESTIGATION OF PUMICE PACKED BEHIND TUNNEL LINING SYSTEM Ghasem Deravi, Ali Akbar Vahedi, Amir Hafezquran	2181
T4-16	ID 412 STATUS AND FUTURE PROSPECTS OF RENEWABLE ENERGY IN SUB-SAHARAN AFRICA Daniel Adu, Jinfeng Zhang, Gao Jing, Lv Suoming	2191
T4-17	ID 427 "THEORY OF EVERYBIM" - WORKFLOW OPTIMIZATION - HYDROPOWER NORWAY Kristoffer Spendrup Bugge	2203
T4-18	ID 449 HIGH PERFORMANCE PRESSURE TUNNEL EXCAVATION AND LINING Alois Vigil, Christian Barwart	2215
T4-19	ID 458 GEOMEMBRANES IN HIGH-PRESSURE TUNNELS AND SHAFTS David A. del Rio, Marco Scarella, Gabriella Vaschetti	2227
T4-20	ID 500 INCREASING POWER OUTPUT AND FLEXIBILITY OF EXISTING HIGH HEAD POWER PLANTS WITH THE HELP OF WATERHAMMER SIMULATIONS Stefan Höller, Helmut Jaberg	2239
T4-21	ID 509 IMPROVEMENT OF INTAKE STRUCTURES WITH NUMERICAL SIMULATION Helmut Benigni, Jürgen Schiffer, Stefan Höller, Helmut Jaberg	2251
T4-22	ID 549 THE IMPACTS OF THE DIFFERENCES BETWEEN CHINESE AND FOREIGN TECHNICAL STANDARDS ON DEVELOPING INTERNATIONAL HYDROPOWER PROJECTS Richun You, Wenzhe Tang, Qingzhen Zhang	2265
T4-23	ID 559 TWO YEAR OF PERFORMANCE OF A PENSTOCK ANCHORED BY PUFOAM Tor Oxhøvd Svalesen, Leif Lia, Stian Løbø Aaker, N. Johnsen, Mattias Kullberg, Guy Harris	2277

T4-24	ID 569	DESIGN OF AERATOR FOR ORIFICE SPILLWAY	Balkrishna Shankar Chavan	2289
-------	--------	--	--	-------------

T4.1: SEMINAR HIGH STRENGTH STEEL IN HYDROPOWER PLANTS

T4.1-1	ID 20	STRAIN MEASUREMENTS AND AXIAL FORCE PREDICTIONS AT THE END OF A STEEL LINED PRESSURE TUNNEL	Andreas Hammer, Paul Bonapace, Harald Unterweger, Alexander Ecker	2301
T4.1-2	ID 23	END OF STEEL LINED PRESSURE TUNNELS - LOAD TRANSFER OF LONGITUDINAL PIPE FORCES	Harald Unterweger, Alexander Ecker, Andreas Hammer, Paul Bonapace	2311
T4.1-3	ID 33	THRUST RINGS FOR TRANSFERRING LONGITUDINAL PIPE FORCES - DEVELOPMENT OF A DESIGN MODEL	Alexander Ecker, Harald Unterweger	2325
T4.1-4	ID 193	A CASE STUDY OF A HIGH STRENGTH STEEL DESIGN: APPLICATION OF DIFFERENT SAFETY CONCEPTS AND THE RESULTING IMPACTS ON A BIFURCATION	Claudia Pollak-Reibenwein, Bettina Neugschwandtner	2337
T4.1-5	ID 279	DESIGN OF STEEL LININGS OF PRESSURE SHAFTS MADE OF HS-STEEL - ULTIMATE LIMIT STATE AND CYCLIC LOAD CONDITIONS	Richard Greiner, Guntram Innerhofer sen., Guntram Innerhofer jun.	2349
T4.1-6	ID 426	ADVANCED DESIGN OF HIGH STRENGTH STEEL-LINED PRESSURE SHAFTS ACCOUNTING FOR FATIGUE CRACK GROWTH	Alexandre Jean Pachoud, Pedro A. Manso, Anton J. Schleiss	2361
T4.1-7	ID 543	EFFECT OF RTE TREATMENT ON TOUGHNESS OF HSS WELD METAL	Horst-Hannes Cerjak, Ozan Caliskanoglug, Norbert Enzinger, Gunter Figner, Milan Pudar (Extended Abstract)	2373
T4.1-8	ID 548	INFLUENCE OF PIPE FABRICATION QUALITY ON LIFETIME OF PENSTOCKS OF PUMPING STORAGE POWER PLANTS	Christian Buzzi, Horst-Hannes Cerjak, Christian Moser	2375
T4.1-9	ID 554	ATOM PROBE INVESTIGATIONS ON TEMPER EMBRITTLEMENT AND REVERSIBLE TEMPER EMBRITTLEMENT IN S 690 STEEL WELD METAL, TO EXPLAIN SUCCESSFUL REHABILITATION OF BRITTLE PENSTOCK WELDS	Horst-Hannes Cerjak, Francisca Mendez Martin (Extended Abstract)	2387

TOPIC 5: STABILITY OF RESERVOIR SLOPES

T5-1	ID 57	SEISMOTECTONIC FEATURES AT RUDBAR LORESTAN DAM SITE IN IRAN AND OBSERVATION OF SLOPE STABILITY DURING IMPOUNDMENT OF THE RESERVOIR	Martin Wieland, Mohammad Hajilari	2389
T5-2	ID 75	EVOLUTION OF STABILITY OF THE VERNAGO RESERVOIR SLOPES UNDER WATER LEVEL VARIATION, DURING SIXTY YEARS OF OPERATIONS	Francesco Federico, Marina Maestri, Chiara Cesali, Martina Cacciotti	2403

T5-3	ID 138 RESEARCH ON STABILITY OF RESERVOIR ACCUMULATIVE BODY SLOPE AND THE IMPACT OF WATER STORAGE Ji Lu, Zheng-gang Zhan, Meng-Xi Wu, Hong-Jie Chen	2415
T5-4	ID 153 DAM UPGRADES USING MECHANICALLY STABILIZED EARTH John E. Sankey, Gary Power	2429
T5-5	ID 180 STUDY OF RESERVOIR RIM SLOPE STABILITY DUE TO OPERATION OF SUSU DAM Ahmad Fadhli Mamat, Rahsidi Sabri Muda, Jimjali Ahmed, Mohd Raihan Taha, Mohd Syazwan MD Rahim (Extended Abstract)	2441
T5-6	ID 192 MONITORING THE SLOPE STABILITY OF RESERVOIRS: AN UPDATE ON THE OBSERVATIONAL METHOD. THE CASE OF A DAM IN PORTUGAL Josep Raventós Fornós, Carles Couso, Maite Garcia, Nadir Plasencia, Elisa Almeida (Extended Abstract)	2443
T5-7	ID 202 COUNTERWEIGHT AS JATIGEDE DAM LANDSLIDE STABILITY COUNTERMEASURE Cristina Dwi Yuliningtyas, Dwi Aryani Semadhi Kubontubuh, Harya Muldianto, Permadi Radityo	2445
T5-8	ID 231 EVALUATION OF SEISMIC PERFORMANCE OF EARTH DAMS DUE TO THE LEVEL OF ITS RESERVOIR USING FINITE ELEMENT METHOD Amin Didari, Mohammad Hassan Saddagh, Zahra Ghadampour	2455
T5-9	ID 244 THREE LARGE RESERVOIRS OPERATION IN THE CASCADE SYSTEM CITARUM RIVER - INDONESIA Hari Suprayogi, Harry Muharsyah Sungguh, Reni Mayasari	2465
T5-10	ID 248 ANALYSIS THE EFFECT OF SOIL PERMEABILITY OF THE UPSTREAM SHELL ON THE DAM STABILITY UNDER RAPID DRAWDOWN (BRADON DAM) Fatima Sharif Fouiti	2477
T5-11	ID 250 EARTH DAMS SAFETY UNDER SEISMIC MOTION USING LIMIT EQUILIBRIUM METHOD AND PHYSICAL MODELING Behrouz Gordan, Azlan Bin Adnan, Ahmad Karbasi, Alireza Naserolmeamar, Sina Jafarirad	2489
T5-12	ID 268 FLOOD WAVE ANALYSIS OF EMBANKMENT DAM FAILURE BY USING 2D MODELS René Dünkner, Michael Berger	2507
T5-13	ID 311 RISK MANAGEMENT FOR THE LAGO BIANCO RESERVOIR IN CASE THE CAMBRENA GLACIER RUPTURES Johannes Maier, Alexandra Beckstein, Georges R. Darbre	2519
T5-14	ID 326 SERVER DESIGN STANDARDS OF RESERVOIR FAILURE ALERT SYSTEM Baeg Lee, Byoung-Han Choi	2535
T5-15	ID 330 SLOPE MONITORING BY DISTRIBUTED FIBER OPTIC SENSING: PROJECT EXAMPLES, RESULTS AND LIMITATIONS Michael Iten, Frank Fischli	2553
T5-16	ID 333 INSAR & PHOTOMONITORING FOR DAMS AND RESERVOIR SLOPES HEALTH & SAFETY MONITORING Benedetta Antonielli, Paolo Caporossi, Paolo Mazzanti, Serena Moretto, Alfredo Rocca	2565
T5-17	ID 365 SLOPE STABILITY ANALYSIS IN GAMBIRI DIVERSION DAM USING NUMERICAL MODELS Samaneh Soleymani, Afshin Hemmati, Hamid Bahrami	2579

T5-18	ID 376	A METHODOLOGY FOR THE MAPPING OF TERRAIN MORPHOLOGY OF DAM BASINS BY MEANS OF SPACEBORNE SAR IMAGES Giovanni Nico, Joao Catalao, Alfredo Pitullo, Catarina Valente (Extended Abstract).....	2591
T5-19	ID 377	MODELLING EARTH-FILLED DAMS: MERGING GBSAR AND TRADITIONAL MEASUREMENTS Giovanni Nico, Marco Corsetti, Alfredo Pitullo, Andrea Di Pasquale	2593
T5-20	ID 395	CRITICAL REVIEW OF DAM BREACH PARAMETERS Ahmed Hussein Soliman, Hesham Mohamed Bekhit, Alaa Mohamed El-Zawahry (Extended Abstract).....	2601
T5-21	ID 425	SLOPES STABILITY IN THE CATCHMENT AREAS AND EFFECT OF LARGE-SCALE ROCKSLIDE DAMMING ON HYDRAULIC PROJECTS SAFETY BY EXAMPLE OF CATCHMENT AREAS OF VAKHSH AND SIANG RIVERS Ruslan Shakirov, Ekaterina Shilina, Alexander Strom, Anatoly Zhirkevich	2603
T5-22	ID 443	INFLUENCES OF WATER LEVEL CHANGES ON THE BEHAVIOUR OF A SLOW MOVING LANDSLIDE Georg Michael Ausweger, Helmut F. Schweiger, Roman Marte.....	2615
T5-23	ID 469	ESTIMATION OF LANDSLIDE INDUCED IMPULSE WAVE IN A CHANNEL TYPE RESERVOIR Qingquan Liu, Yi An, Jiaxiu Yang, Ji Lu (Extended Abstract).....	2627
T5-24	ID 492	FAILURE OF EMBANKMENT DAMS DUE TO OVERTOPPING- EXPERIMENTAL STUDY AND HYDROGRAPH PREDICTION Burkhard Rüdissler, Peter Tschernutter	2629
T5-25	ID 508	A RESERVOIR SYSTEM SIMULATION METHOD TO LESSEN WATER SUPPLY DEFICIT AT DOWNSTREAM POINTS USING A HEURISTIC METHOD Sangho Lee, Youngkyu Jin	2641
T5-26	ID 516	LANDSLIDE DAMS - LONG KNOWN, BUT JET OVERLOOKED, RARE PHENOMENON: POSSIBILITY TO PREVENT DAMAGE Nina Humar, Mitja Brilly, Andrej Kryžanowski (Extended Abstract).....	2653
T5-27	ID 536	GEOLOGY AND GEOTECHNICAL CONDITION FROM GEOLOGICAL MAPPING, CORE DRILLING, AND SEISMIC METHOD AT MASANG II HYDROPOWER PROJECT, WEST SUMATERA, INDONESIA Jodi Prakoso Basuki, Kiki Lukman Nulhakim	2655
T5-28	ID 612	NUMERICAL MODELLING OF ROCK-FALL ON THE CONCRETE ARCH-GRAVITY DAM OF PLACE MOULIN Guido Mazzà, Antonella Frigerio.....	2665
T5-29	ID 617	EXPERIMENTAL STUDY ON OVERTOPPING BREACHING PROCESS OF EARTH DAM AND PEAK DISCHARGE Duan Wengang, Huang Guobing, LiLi.....	2677
T5-30	ID 678	SETTLEMENT OF SOFT ROCKFILL MATERIALS IN MEDIUM-SCALE OEDOMETER Ali Komak Panah, Hamidreza Rahmani.....	2687

COMMISSION INTERNATIONALE
DES GRANDS BARRAGES

VINGT-SIXIÈME CONGRÈS DES
GRANDS BARRAGES
Autriche, juillet 2018

CAPITALIZATION OF BENCHMARK WORKSHOPS RESULTS SINCE BERGAMO 1991

Guido MAZZA'

*Chairman of ICOLD Committee A "Computational Aspects of Analysis and
Design of Dams, RICERCA SUL SISTEMA ENERGETICO RSE S.P.A.*

ITALY

EXTENDED ABSTRACT

Policies on energy and water resources all around the world poses an increasing demand of clean energy and sustainable water resources. These needs require both refurbishment programs of many old dams in those countries where dam construction dates back at the beginning of the industrialization process, such as Europe and USA, and the construction of new infrastructures where the need of water resources and renewable energy is more pressing.

ICOLD in 1988 decided to appoint the Committee *Computational Aspects of Analysis and Design of Dams* with the aim to contribute to the diffusion of computer software in the field of dam engineering and to fill the gap existing between the specialists of mathematical modelling and dam designers, authorities, and managers. As a matter of fact, numerical modelling represents nowadays a key tool for dam engineers to perform efficiently the design making process, the construction stage as well as the whole operational dam life until the possible decommissioning phase. The activities of the Committee have contributed to make fully accepted the numerical models in the engineering practice.

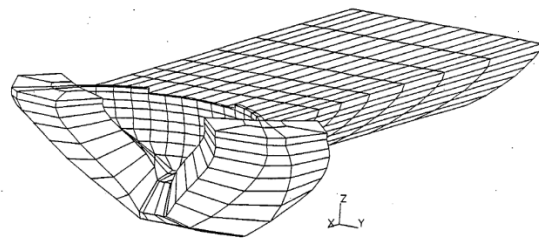
Today and future activities of the Committee are oriented towards:

- ✓ creating a stronger link between the observed dam behavior and the modelling process with the aim to contribute to the preservation and maintenance of existing dams;

- ✓ promoting mathematical modelling improvements to approach safety-related problems that cannot at present be properly analyzed;
- ✓ issuing guidelines to be used for educational purposes in the current practice. The Committee is strongly committed to contribute in the process of a suitable transfer of experience, skill and knowledge across generations.

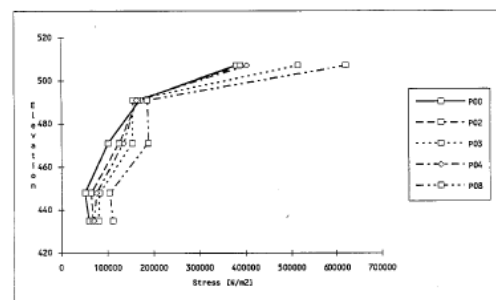
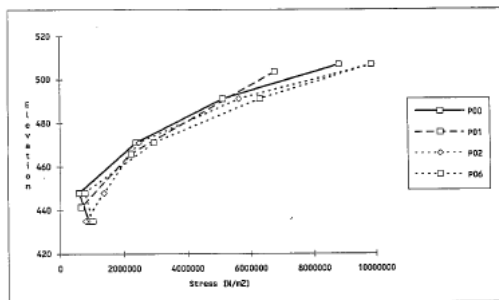
The work done by the Committee during its long activity has given rise to the issuing of three Technical Bulletins (N. 94, *Computer software for dams. Validation*, 1994; N. 122, *Computational procedures for dam engineering*, 2001; N. 155, *Guidelines for use of numerical models in dam engineering*, 2013).

Moreover, the Committee has promoted the organization of benchmark-workshops (BWs), with the aim to guide dam engineers in the correct use of computer programs. The benchmarking program started in Bergamo (Italy) in 1991 and continued up to 2017 with the 14th workshop held in Stockholm.



FLEXIBLE FOUNDATION AND INCOMPRESSIBLE FLUID
MAX ABS PRINCIPAL STRESSES P1 AND THEIR TIME OF OCCURRENCE
CENTRAL CANTILEVER

RIGID FOUNDATION AND COMPRESSIBLE FLUID
MAX ABS PRINCIPAL STRESSES P1 AND THEIR TIME OF OCCURRENCE
CENTRAL CANTILEVER



Bergamo (Italy), 1991-1992. Seismic analysis of Talvacchia dam: the dam seen from the left abutment; the FE model; some results of the seismic analyses

The benchmarking activity represents a reference for the whole dam community, and in particular for young engineers engaged in the challenging task of dam safety assessment and design. To facilitate the accessibility and a critical review of the proceedings related to the 14 BWs held so far, a capitalization activity of the tremendous amount of data at disposal has been recently started.

The preparation of a new Bulletin to provide a synthesis of the BWs results and comments on the progresses achieved on the numerical modelling methods and the strategies to be used to tackle most of the dam engineering problems is foreseen for the end of 2019.

COMMISSION INTERNATIONALE
DES GRANDS BARRAGES

VINGT-SIXIÈME CONGRÈS DES
GRANDS BARRAGES
Autriche, juillet 2018

50 YEARS OF COMMITTEE ON SEISMIC ASPECTS OF DAM DESIGN

Martin WIELAND

*Chairman, ICOLD Committee on Seismic Aspects of Dam Design, POYRY
SWITZERLAND LTD., ZURICH*

SWITZERLAND

EXTENDED ABSTRACT

The Committee on Seismic Aspects of Dam Design is one of ICOLD's oldest technical committees, which at present comprises dam and earthquake experts from 34 different countries from all continents. The Committee was created in 1968 and will celebrate its 50th anniversary in 2018. Guidelines on (i) different seismic hazards affecting storage dams, such as fault movements in the footprint of dams, and reservoir-triggered seismicity, (ii) seismic design criteria, (iii) dynamic analysis of dams, (iv) conceptual guidelines for earthquake-resistant design of dams and design of appurtenant structures, and (v) seismic monitoring and inspection of dams after earthquakes, have been published. These guidelines, listed below, represent the international state-of-the-art in the seismic design, construction and safety assessment of large storage dams, i.e.

Bulletin 52 (1986): Earthquake analysis procedures for dams,

Bulletin 112 (1998): Neotectonics and dams,

Bulletin 113 (1999): Seismic observation of dams,

Bulletin 120 (2001): Design features of dams to resist seismic ground motion,

Bulletin 123 (2002): Earthquake design and evaluation of structures appurtenant to dams,

Bulletin 137 (2011): Reservoirs and seismicity,

Bulletin 148 (2016): Selecting seismic parameters for large dams, and

Bulletin 166 (2016): Inspection of dams following earthquakes

Among these guidelines, Bulletin 137 provides information on reservoir-triggered seismicity (RTS), a hazard unique to large storage dams, which is often a key dam safety argument brought forward by opponents against new dams. For properly designed and constructed dams, RTS is not a new safety concern for dams. However, the publication with the greatest long-term impact on the seismic design and safety assessment of existing dams is Bulletin 148, which includes the concept of two earthquake levels for dams and safety-critical elements, i.e. the Operating Basis Earthquake (OBE) and the Safety Evaluation Earthquake (SEE). The safety-critical elements are the spillway and low level outlets, which are needed to control the reservoir level after the SEE or for lowering for repair works or for increasing the safety of a dam. This is new. Bulletin 120 complements Bulletin 148 as it includes conceptual features for the seismic design of dams, which are extremely important, as it is well known that it will be difficult to have a structure to perform well during an earthquake, when the basic seismic design concepts are not observed.

Dams were the first structures designed against earthquakes, on a worldwide basis, starting in the 1930s. At that time, the ground shaking was the main seismic hazard and was represented by a seismic coefficient of typically 0.1, almost irrespective of the seismic hazard at the dam site, which was often unknown. The seismic analysis was done with the pseudostatic method, ignoring the dynamic characteristics of dams. Because of its simplicity, this method is still in use today, although it has become clear that this method is obsolete following the observations made during the 1971 San Fernando earthquake. The pseudostatic method is also not compatible with current seismic guidelines (Bulletin 148) and, therefore, this obsolete method shall no longer be used for the safety checks of large storage dams. One of the main tasks of the Committee is to promote good practice in dam engineering, which includes the dissemination of the international state-of-the-art. Using the pseudostatic concept, the seismic load case was very seldom the governing one. This has changed by using today's rational concepts for seismic hazard analyses and dynamic analyses of dams. The earthquake load case has become the dominant one for most dams.

Since the formation of the seismic committee, the magnitude 8 Wenchuan earthquake of May 12, 2008 that occurred in Sichuan province, China, was the most important earthquake for dam engineers as it damaged some 1580 dams. Most of them were small earth dams, but also some large dams were damaged. The main lesson from this earthquake was that the seismic hazard is a multi-hazard. Thousands of mass movements occurred in the mountainous epicentral region. Mass movements that can be triggered by strong earthquakes are often ignored or the hazard is assessed using criteria, which are different from those used for the dam body. Based on the past experience, it is obvious that dams are not inherently safe and can be damaged by strong earthquakes. The most vulnerable dams are those, which are poorly constructed and/or designed. Still a lot of work is required in order to ensure that all dams comply with modern seismic safety criteria, which is the main concern of the Committee..

COMMISSION INTERNATIONALE
DES GRANDS BARRAGES

VINGT-SIXIÈME CONGRÈS DES
GRANDS BARRAGES
Autriche, juillet 2018

NUMERICAL METHODS APPLIED AND INTERPRETED FOR SAFE DAM BEHAVIOUR

Gerald ZENZ¹, Edwin STAUDACHER, Shervin SHAHRIARI

¹*Institute of Hydraulic Engineering and Water Resources Management, GRAZ
UNIVERSITY OF TECHNOLOGY*

AUSTRIA

1. INTRODUCTION

Dams are designed to serve in a secure and safe way to our society under any environmental and operational conditions throughout their lifetime. During design and construction models are needed to be set up to account for the safety approach. These models are based on practical experience gained from the performance of existing structures and rely on models we assume for possible failure modes. To set up and apply advanced numerical models and interpret their results a detailed discussion within the engineering community is needed. To show the abilities and the meaningful interpretation of numerical investigations the “Technical Committee on Numerical Analysis and Design of Dams” organizes since 1991 benchmark workshops. These results are published in proceedings and concluded in ICOLD Bulletins. Herein a short summary of the content of investigations and a further step to disseminate the results is undertaken. It is to emphasize the requirement to develop a model about the system behavior of dams based on their foundation, reservoir slopes, catchment area and environment. Numerical models and the interpretation of the gained results are one essential part within this ICOLD network to guarantee for the safe dam operation.

International Benchmark Workshops on Numerical Analysis of Dams are intended to provide an in-depth examination of the computational methods and software used for dam analysis. It is an international forum to share the latest

information regarding state-of-the-art software and techniques available for the analysis of dams' behavior. For the community of Dam Engineers, a possibility is given to discuss on assumptions, results and conclusions drawn by the help of numerical analyses. The Benchmarks are organized by members of the ICOLD "Technical Committee on Computational Aspects of Dam Analysis and Design". During a period now of 29 years the working group is active in discussing computational aspects and concluding the major results in Bulletins. However, the effort is based on the activities of their members, Vice-Chair and especially their Chair as these are from the beginning: Olgierd Zienkiewics, Michele Fanelli, Gabriella Giuseppetti, Alian Carrere, Ignacio Escuder and the current chair Guido Mazza.

The results and outcome of benchmarks workshops result in working group discussions; their work is being published in Bulletins ([1],[2],[3]). These Bulletins aims to offer a support to dam engineers to choose the most suitable computational strategies to cope with the engineering problems under examination in the best possible way having in mind potentialities and possible shortcomings.

REFERENCES

- [1] *ICOLD - Bulletin 94* (1994): "Computer Software for Dams. Validation".
- [2] *ICOLD - Bulletin 122* (2001): "Computational Procedures for Dam Engineering".
- [3] *ICOLD - Bulletin 155* (2013): "Guidelines for use of Numerical Models in Dam Engineering".

COMMISSION INTERNATIONALE
DES GRANDS BARRAGES

VINGT-SIXIÈME CONGRÈS DES
GRANDS BARRAGES
Autriche, juillet 2018

SEISMIC ASPECTS IN THE DESIGN OF EMBANKMENT AND ROCKFILL DAMS

CAMILO MARULANDA

Technical Manager, INGETEC

COLOMBIA

EXTENDED ABSTRACT

Historically, embankment dams have usually performed well during earthquakes. However, earthquakes can undesirably affect embankment dams in different ways. One of the most obvious way is by causing instability or large deformations in the dam, due either to strong shaking, or to increases in pore pressure and resulting decreases in strength (caused by cyclic loading). One of the most well-known cases of liquefaction and instability of a dam during an earthquake, is the Lower San Fernando Dam, where a portion of the embankment liquefied during the 1971 San Fernando earthquake and slid, leaving only about 3 feet of freeboard remaining to contain the reservoir. Dams have also failed due to erosion through cracks caused by an earthquake. Consequently, earthquakes may induce instability in the slopes of the dam, differential settlements and cracks. The assessment of the behavior of an embankment dam under seismic loading typically includes the following aspects:

1. Identifying and characterizing potential sources of earthquake loading, whether known faults or historic seismicity not associated with known faults.
2. Determining the appropriate loadings to apply in the analyses.
3. Determining the properties of the embankment and foundation materials,

4. Analyzing the post-earthquake stability of the embankment, including the evaluation of a possible drastic loss of shear strength.
5. Estimating the extent of deformations resulting from earthquake shaking and reduction in material strengths.
6. Determining the potential for dam failure by the overtopping of deformed embankment, erosion through cracks in the embankment, or other possible failure mechanisms.
7. Evaluating other structures, such as spillway walls adjacent to the embankment, whose failure could cause failure of the embankment dam by allowing overtopping or by creating unfiltered exit points for internal erosion.

The presentation will focus on the different seismic aspects to consider in the design of an embankment dam and some of the available numerical methods to evaluate the different failure mechanisms of a dam under seismic conditions, including, stability of the dam, deformation prediction and liquefaction potential.

COLLAPSE OF AGRICULTURAL EARTH-DAMS BY A RECENT EARTHQUAKE AND ITS RECONSTRUCTION

Fumio TATSUOKA

*Professor Emeritus, UNIVERSITY OF TOKYO and TOKYO UNIVERSITY OF
SCIENCE*

JAPAN

1. COLLAPSE AND RECONSTRUCTION OF IRRIGATION DAMS

A pair of old irrigation dams in Fukushima Prefecture collapsed by the 2011 Great East Japan Earthquake (Fig. 1a). The collapse was due to generally poor soil compaction and the use of inadequate soil type (sandy soil) in the top layer despite homogeneous type of the dam in addition to a prolonged strong seismic motion. The new dams (Fig. 1b) were constructed to be much more stable by the use of adequate type soils, good compaction and an adequate structure.

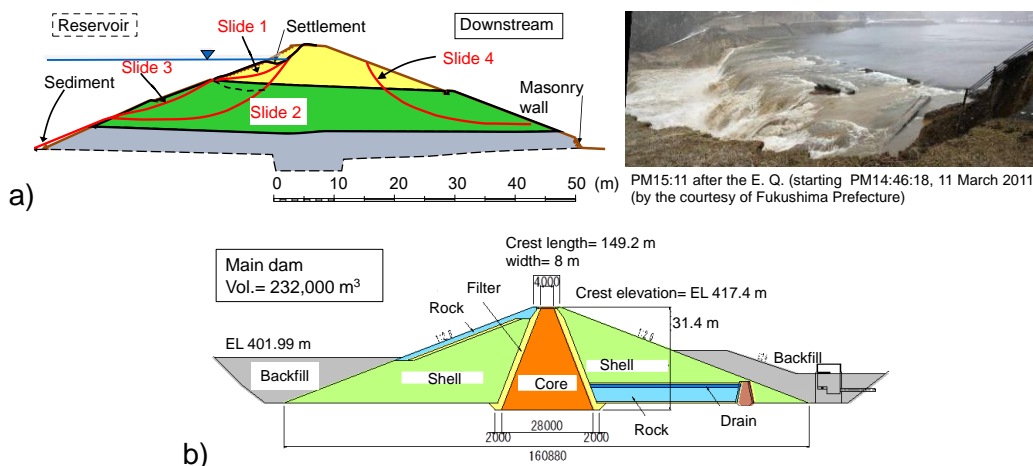


Fig. 1. Fujinuma dam, Fukushima Pref. Japan: a) collapsed; & b) reconstructed.

In soil compaction, the target values of dry density and water content were specified to be equal to the maximum dry density and the optimum water content by Standard Proctor while controlling the degree of saturation to become the optimum degree of saturation (i.e., $S_r = (S_r)_{opt}$) irrespective of variations in the soil type and compaction energy in actual compaction. When $S_r = (S_r)_{opt}$, the highest dry density (so, the highest shear strength and stiffness) and sufficiently low hydraulic conductivity of saturated soil is obtained under any given field condition.

2. STABILITY AND DEFORMATION ANALYSIS

The collapse was successfully simulated by simplified practical analysis incorporating the time histories of undrained stress-strain relation and peak strength of saturated soil that degrade by cyclic undrained loading during an earthquake (Figs. 2a & b). The residual slip evaluated by the Newmark method and the residual deformation outside the slip layer by pseudo-static FEM, both incorporating the time history of response acceleration, were summed up. No slip with very small residual deformation of the new dam by the seismic load by which the old dams collapsed was confirmed by analysis by this method. The effect of compaction on the dam stability is tremendous. Fig. 2c shows the average drained and undrained shear strengths mobilized along the critical slip circles in the top zone of the old and new main dams (as shown in Fig. 2a). With the new dam, the average degree of compaction (Standard Proctor) D_c is equal to 101 %, thus the undrained shear strength at the end of seismic loading is higher than the drained strength while substantially higher than the value at $D_c = 87 %$ of the old dam.

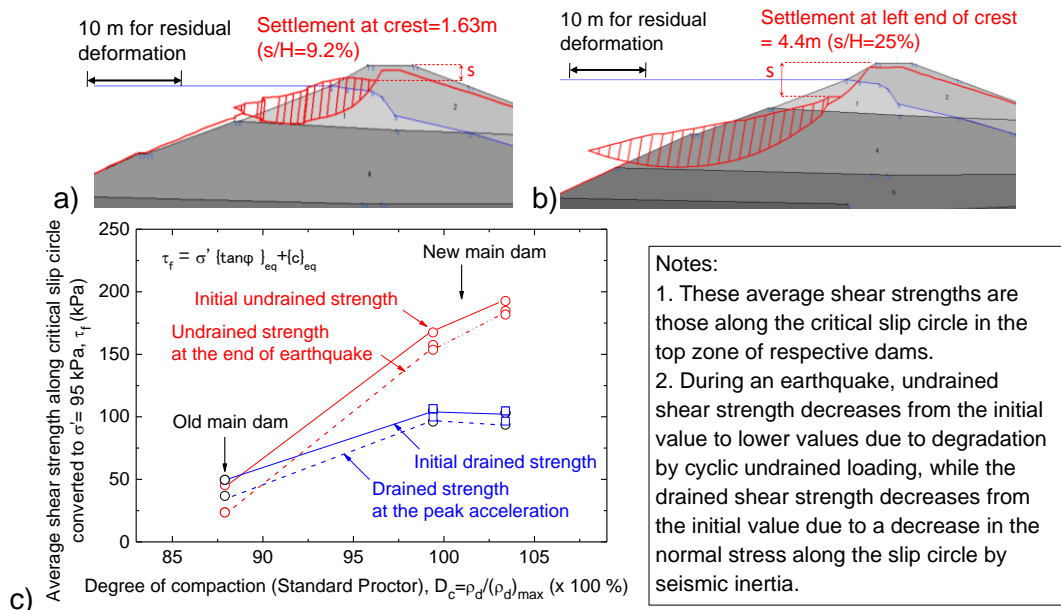


Fig. 2 a) & b) Residual deformation for two critical slip circles by numerical analysis of the old dam; & b) average shear strengths mobilized in the upper zone.

COMMISSION INTERNATIONALE
DES GRANDS BARRAGES

VINGT-SIXIÈME CONGRÈS DES
GRANDS BARRAGES
Autriche, juillet 2018

**COMPARISON OF MEASURED AND ANALYZED SEISMIC BEHAVIOR OF
CONCRETE DAMS AND EMBANKMENT DAM IN JAPAN**

Hiroki SAKAMOTO

Koishiwara Dam Construction Office, JAPAN WATER AGENCY

Hiroyuki SATO and Takashi SASAKI

*National Institute for Land and Infrastructure Management, MINISTRY OF LAND,
INFRASTRUCTURE, TRANSPORT AND TOURISM*

JAPAN

1. INTRODUCTION

Many earthquakes have hit Japan and informative data about seismic behavior has recorded at dams during large earthquakes [1]. The report shows some examples of dynamic analyses of existing dams with efforts in order to reproduce seismic performances exactly. In this abstracts, outlines of an arch dam case and an embankment dam case are briefly explained.

2. CASE OF ARCH DAM [2]

The earthquake record observed at the crest of Yagisawa Dam (dam height of 131m, Fig.1) in Chuetsu Earthquake (Oct.23, 2004) was 656cm/s^2 . In the reproduction analysis, modification of the foundation - reservoir coupling conditions has been conducted as compared with generally used conditions in Japan. By using the modified analysis, reproduced behavior of the dam in the earthquake has higher precision than previous method as shown in Fig. 2.

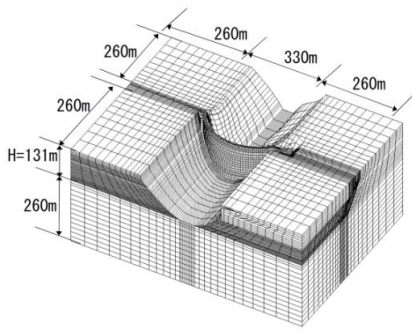


Fig. 1
Analysis Mode

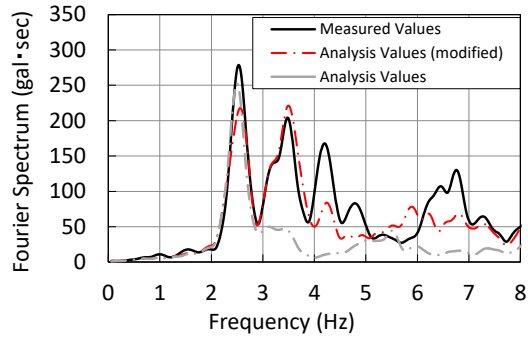


Fig. 2
Fourier Spectrum at Dam Crest
(Upstream-downstream direction)

3. CASE OF EMBANKMENT DAM [3]

Due to the Iwate-Miyagi Nairiku Earthquake in 2008, settlement without sliding deformation was observed at Isawa Dam (ECDR, Fig. 3). The dynamic strength tests for construction materials and deformation analysis using cumulative damage theory were conducted. Through the analysis, the settlement can be reproduced accurately and it is important to consider saturated/unsaturated conditions in dam body for accurate evaluation (see Fig. 4).

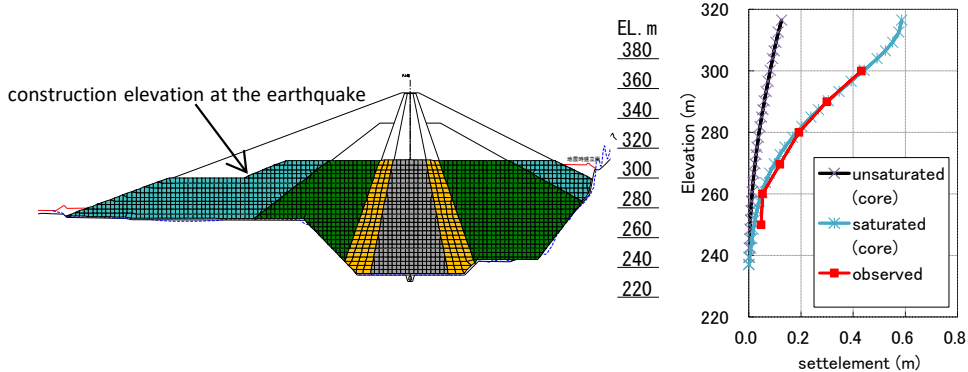


Fig. 3
FEM element

Fig. 4
Vertical distributions of settlements

REFERENCES

- [1] The Japan Commission on Large Dams, Acceleration Records on Dams and Foundations No.3, 2014
- [2] SAKAMOTO. H et al. Three-dimensional behavior properties and reproduction analysis of an arch dam during large-scale earthquake, *ICOLD Congress*, 2018.
- [3] SATO H. et al. Reproduction analysis of settlement of Isawa dam under construction during the 2008 Iwate-Miyagi Earthquake, *ICOLD Congress*, 2012.

COMMISSION INTERNATIONALE
DES GRANDS BARRAGES

VINGT-SIXIÈME CONGRÈS DES
GRANDS BARRAGES
Autriche, juillet 2018

CURRENT CHALLENGES OF SEISMIC NUMERICAL MODELLING FOR DAMS: SOME ITALIAN EXPERIENCES

Massimo MEGHELLA

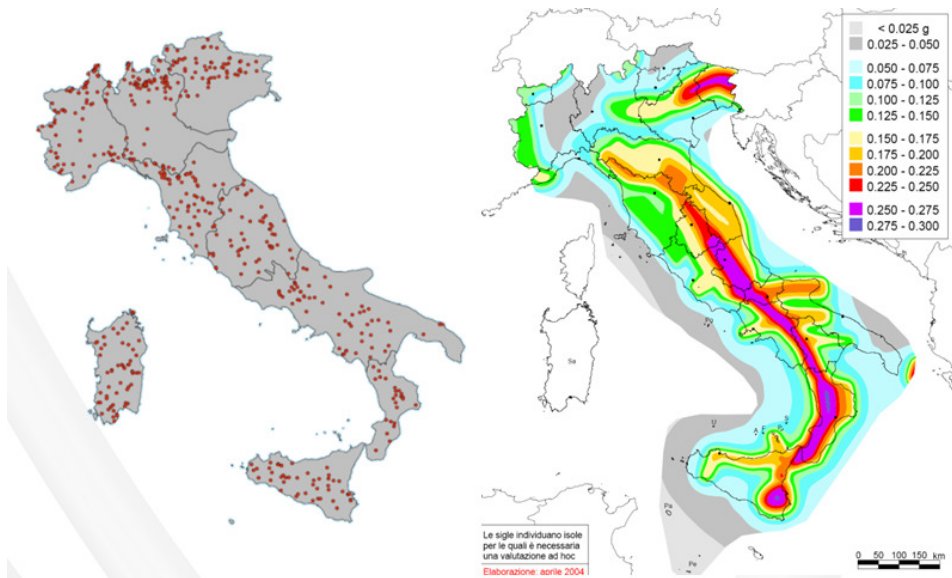
*Member of ICOLD Committee A “Computational Aspects of Analysis and
Design of Dams”.*

*Sustainable Development and Energy Sources Department – Structures,
RICERCA SUL SISTEMA ENERGETICO RSE S.P.A.*

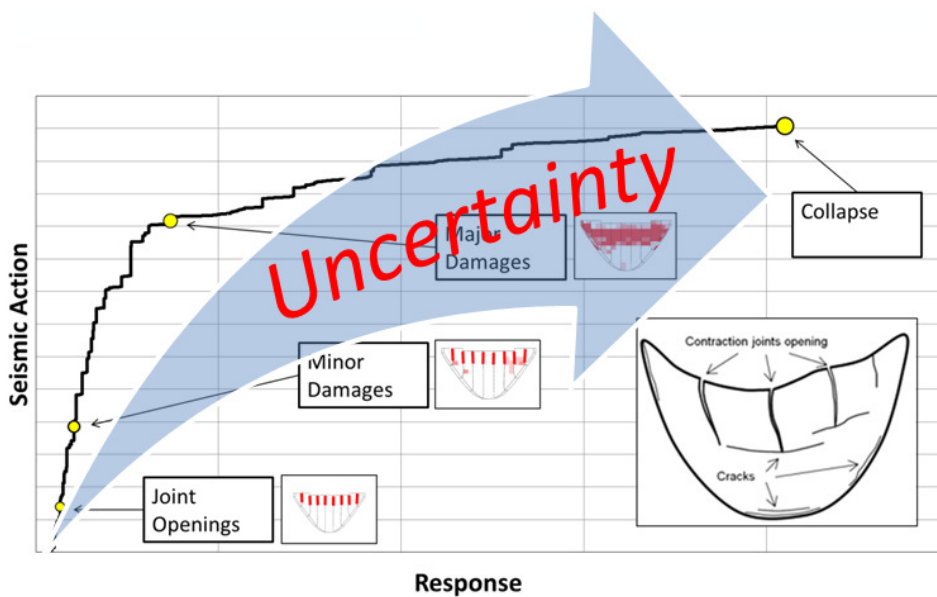
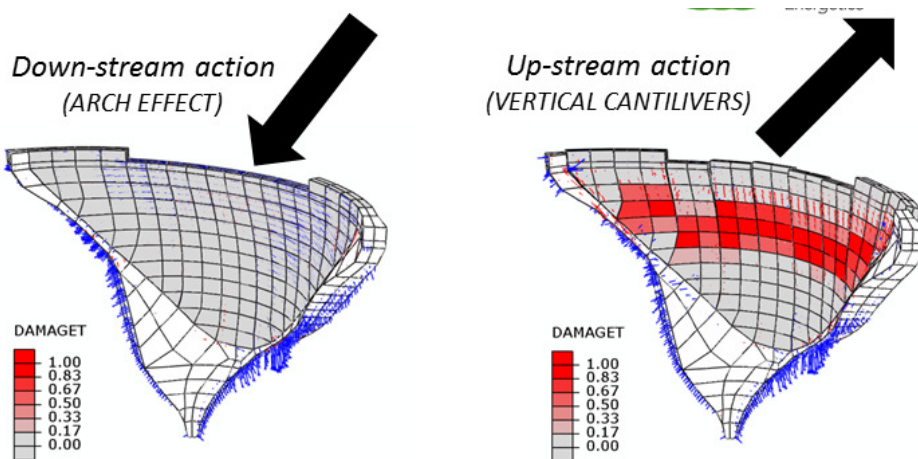
ITALY

EXTENDED ABSTRACT

The dynamic FEM analysis is currently the most effective tool to simulate the seismic response of dams. However, as the seismic forces increase up to the level of intensity typically corresponding to MCE, the complexity of the models and the computation time increase dramatically, having to take into account the non-linear behaviour of both materials and interfaces (joints and pre-existing cracks). At the same time, the overall models uncertainty increases, which in combination with the lack of information on the real response of dams when subjected to strong earthquakes, makes models calibration and subsequent seismic analysis a very challenging, expensive and often impractical task. To cope with that, RSE adopted and further developed, a simplified dynamic method - the Endurance Time Analysis method (ETA) - which allows drastic reductions of the computational effort, to analyze the non-linear response of several large concrete dams in Italy and to obtain their “capacity curves” ranging up to collapse. In such way, even if the overall model uncertainty is still not properly addressed and quantified, the comparison of such curves within the dams portfolio allowed to develop simplified “risk indexes” to rank their relevant seismic risk, so that resource allocation for safety assessment can be definitely optimized.



Italian dam locations (left) and seismic hazard map of Italy (right)



Typical behaviour of arch dams for intensifying seismic actions

COMMISSION INTERNATIONALE
DES GRANDS BARRAGES

VINGT-SIXIÈME CONGRÈS DES
GRANDS BARRAGES
Autriche, juillet 2018

QUALIFICATION OF DYNAMIC ANALYSES OF DAMS AND THEIR EQUIPMENT---OUTCOME OF JCOLD-CFBR TECHNICAL EXCHANGE---

N. MATSUMOTO⁽¹⁾ & J. J. FRY⁽²⁾

(1) Managing director , JAPAN COMMISSION ON LARGE DAMS

(2) Dam expert, Centre d'ingénierie Hydraulique, EDF

JAPAN AND FRANCE

1. JCOLD-CFBR TECHNICAL EXCHANGE

The technical exchange between CFBR and Japan Commission on Large Dams (JCOLD) has been conducted for the qualification of seismic dam analyses in last five years since 2013. The first objective was the comparison between the new French legislation and the current Japanese legislation, discussion about their implementation, the performance of dams under strong motions and the feedback from such performance on dam modeling. The second objective was the validation of dynamic analysis by modeling the performance of some large dams under strong motions earthquakes. The third objective was the calibration of simplified methods according to the large seismic data gathered in Japan. Therefore, the analytical procedure ranges from simplified methods for providing preliminary assessment to sophisticated methods for simulating the nonlinear deformation of dams during large earthquakes. Analyses of appurtenant structures of dams are also included.

2. OUTCOME OF COLLABORATION

CFBR developed own analysis methods and focused on the verification of them through the reproduction simulations of various dam types using the seismic records that were monitored in large dams in Japan. The spillway gates in French dams were roughly assessed for the seismic capability by comparing the dimensional data with ones in Japan. JCOLD provided some cases of the reproduction simulations of the concrete gravity dam, the arch dam and the facing rockfill dams. In addition, state-of-the-art research on the seismic analysis method and material characteristics of a largely deformed rockfill dam due to the seismic impact was introduced. The technical discussion and exchange between CFBR and JCOLD resulted in creative outcomes involving the adequate verification of the methods and finding further technical issues addressed in the future. These results are disseminated to many dam engineers in five workshops and two international symposiums held in French and Japan. An e-book compiling the above technical activity as 36 technical papers will be issued this year as titled "Qualification of Seismic Dam Analyses and their equipment."

The main topics of the book are the following:

- a. Analysis on acceleration data of dams collected by JCOLD
- b. Practical guide for selecting seismic parameters and numerical models
- c. Material properties and performance of embankment dams
- d. Performance and analysis of AFRD and CFRD
- e. Qualification of simplified analysis of embankment dams
- f. Qualification of detailed analysis of embankment
- g. Dynamic modeling, experimental and in-situ results of concrete dams
- h. Effects of radiative boundary conditions and spatial variability of the seismic ground motion
- i. Dynamic behavior of concrete dam : lessons learned from the JCOLD database
- j. Characterization of the dynamic behavior of an arch dam by means of forced vibration tests
- k. Comparison between numerical analyses and seismic records on dams
- l. Simplified analyses for gravity dam
- m. Displacement-Based Seismic Assessment of Concrete Dams
- n. Comparison of design criteria of gates between Japan and France
- o. Analysis of gates compared to field measurements

COMMISSION INTERNATIONALE
DES GRANDS BARRAGES

VINGT-SIXIÈME CONGRÈS DES
GRANDS BARRAGES
Autriche, juillet 2018

OBSERVATIONS OF PERFORMANCE OF EARTHFILL EMBANKMENTS DURING RECENT EARTHQUAKES IN NEW ZEALAND

Trevor MATUSCHKA

Director, ENGINEERING GEOLOGY LIMITED

NEW ZEALAND

1. INTRODUCTION

Many earthfill embankment water storage dams have been constructed near Seddon, New Zealand since 2004 for the purposes of irrigating grapes. They range up to 26m in height. They were subject to very strong earthquake ground motion from earthquakes in 2013 and 2016. Peak horizontal ground accelerations of close to 0.75g were recorded at Seddon during the Mw6.6 Lake Grassmere earthquake (16 August 2013) and the Mw7.8 Kaikoura earthquake (14 November 2016). The performance of eleven water storage dams located near Seddon that were subjected to these two earthquakes is summarized. The embankments were generally designed in accordance with guidelines published by the New Zealand Society on Large Dams (NZSOLD).

2. OBSERVATIONS

Observations of embankment performance are summarized in Table 1. In general, there was minor to no damage to dams that were designed and constructed to modern standards. Some dams were affected more by the Lake Grassmere earthquake. This is explained by this earthquake being closer, even though the Kaikoura earthquake had a much longer duration of strong shaking.

Two dams (F and I) that had deficiencies and were damaged in the 2013 earthquake were repaired and subsequently performed much better in the 2016 earthquake. Seiches were noted in some reservoirs in the 2016 earthquake with heights estimated to be at least 1.2m and in one case overtopped a saddle dam.

Table 1
Summary of observations

Dam ID	H ¹ (m)	Lake Grassmere Earthquake		Kaikoura Earthquake	
		R _{rup} ² (km)	OBSERVATIONS	R _{rup} (km)	OBSERVATIONS
A	17	12.4	Movement of riprap, minor cracks	26	Minor movement of riprap
B	19	14.1	No damage	28	No damage
C	13	14.1	No damage	29	No damage
D	26	17.0	No damage	20	No damage
E	17	13.7	Deformation upstream shoulder, cracks in crest	20	Additional deformation and cracks
F	10	10.7	Deformation upstream shoulder, cracks in crest	22	No damage
G	15	11.4	No damage	22	No damage
H	6	4.1	No damage	20	No damage
I	12	7.0	Deformation of upstream shoulder, cracks in crest	22	Minor cracks
J	8	15.0	No damage	31	No damage
K	11	6.1	Not constructed	21	Minor cracks upstream side dam crest

¹H = embankment height

²R_{rup} = closest distance to fault rupture

3. CONCLUSIONS

Earthfill embankments designed to modern standards and constructed to high standards can withstand very high levels of ground motion with minor damage. Embankments where the earthfill is not properly conditioned and poorly compacted can be expected to deform with the potential for significant longitudinal cracking and some potential for transverse cracking where the abutment profile is irregular or stepped.

COMMISSION INTERNATIONALE
DES GRANDS BARRAGES

VINGT-SIXIÈME CONGRÈS DES
GRANDS BARRAGES
Autriche, juillet 2018

LESSONS LEARNED FROM RECENT INTERNATIONAL WORKSHOPS ON SEISMIC NUMERICAL MODELLING FOR CONCRETE DAMS

Emmanuel ROBBE

Dam specialist, HYDRO ENGINEERING CENTER OF EDF

FRANCE

EXTENDED ABSTRACT

From 2013, the author participated to several workshop dedicated to the safety assessment of concrete dams under earthquakes:

- Several ICOLD benchmark on numerical analyses of arch dam:
 - o Graz 2013 on the fluid-structure interaction effect on arch dam under earthquakes,
 - o Lausanne 2015 on the safety assessment of Luzzzone arch dam following the Swiss guidelines,
 - o Stockholm 2017 with increasing complex numerical analyses on Janeh gravity-arch dam assessment under earthquake
- USSD workshops:
 - o in 2016 for a blind prediction with numerical analyses of the recorded behavior of Monticello arch dam under M4.1 earthquake, 16km away from the dam
 - o in 2017 on the seismic analyses of concrete dams
- Several workshop from 2013 to 2016 during the collaboration between Japanese and French committees on large dams, on seismic behavior of dams.

The presentation will summarize the main lessons learned by the author from these workshops.

First, the numerical modeling of concrete dams under earthquakes will be discussed: from commonly used simplified finite-element models using Westergaard added masses and massless foundations to more complex numerical analyses using advanced soil-fluid-structure interaction with fluid elements and viscous-spring foundation boundaries for example. Comparisons of finite-element analyses with simplified and advanced methods will be presented.

Second, the qualification of numerical methods with earthquake records on dams will be discussed: devices to record and save dam's response under earthquake are now easily available and such data can be used to evaluate and improve numerical tools.

Finally, a software is currently under development by the author to go through the Japanese database of records on dams and foundations. Such a tool might prove very useful to analyze the increasing number of dam's response under earthquake and to evaluate dynamic properties such as eigenfrequencies and damping values during earthquake.

COMMISSION INTERNATIONALE
DES GRANDS BARRAGES

VINGT-SIXIÈME CONGRÈS DES
GRANDS BARRAGES
Autriche, juillet 2018

SEISMIC HAZARD ANALYSIS OF HARD-ROCK DAM SITES

Kofi O. ADDO

*Principal Engineer, British Columbia Hydro & Power Authority, Burnaby
Member, ICOLD Committee on Seismic Aspects of Dam Design*

CANADA

EXTENDED ABSTRACT

Current ground motion models for western North America (WNA) characterize site effects based on scaling with respect to V_{S30} , the time-averaged shear wave velocity (V_S) in the uppermost 30 metres. The upper limit on this V_{S30} -scaling in these models is in the range of 1100 to 1500 m/s and reflects the paucity of earthquake recordings from rock sites with $V_{S30} > 800$ m/s. A review of earthquake recordings on hard-rock shows that shear wave velocity alone does not fully explain observed trends and that another characteristic of the rock, *kappa* (k), a measure of shallow crustal damping, is required to better capture or reproduce the observations in the data. In general, *kappa* decreases as V_{S30} increases but there is no explicit *kappa* scaling in available WNA ground motion models and hence *kappa* is not directly included in seismic hazard analysis

Most hard-rock sites in British Columbia are glaciated and have V_{S30} values higher than 800 m/s, sometimes as much as three times higher. Hence, until such time that the development of these models incorporates data from high V_{S30} sites, seismic hazard analysis for hard-rock sites has to be performed in two stages. First, a seismic hazard analysis is conducted for a reference rock with a known V_{S30} (usually < 800 m/s) and a known inherent *kappa*. Secondly, relative amplifications based on the site-specific V_{S30} and site-specific *kappa* are calculated and applied to the computed reference hazard to derive the site-specific seismic hazard. Figure 1 shows different response spectra (with *kappa* varying from .05 to .01 seconds) for a structure on a hard-rock site that needs to safely resist a $M_w 6.5$

earthquake occurring about 25 km away. If the structure is a concrete dam or supports safety-critical electromechanical equipment sensitive to short period (< 0.2 to 0.3 seconds) shaking, then kappa largely controls the spectral accelerations in this range and the ground motion almost doubles or triples at certain periods. It is therefore imperative that dam owners and their engineers know the values of V_{S30} and κ for their hard-rock dam sites in order to reduce the uncertainty in the ground motion estimates.

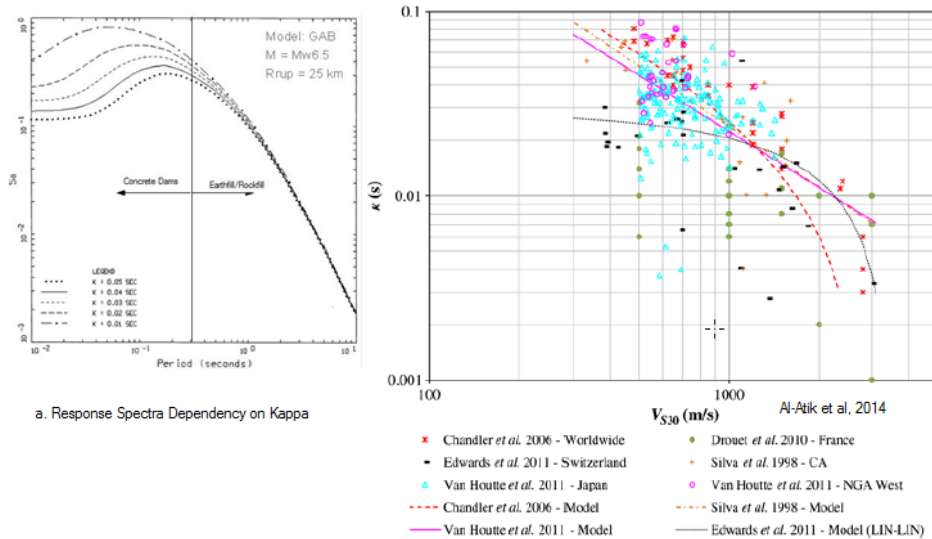


Figure 1 Response Spectra and Shear Wave Velocity Variation with Kappa

At BC Hydro, relative site amplifications based on site-specific properties are calculated and applied to probabilistic seismic hazard based on a reference rock with a V_{S30} of 760 m/s and a kappa of 0.040 seconds. Initial results show that empirical amplifications from field data are generally consistent with analytical amplifications using a hard-rock kappa of 0.015 seconds. The results also show that computed ground motions generally decrease with higher V_{S30} at all frequencies but tend to be significantly underestimated at high frequencies (> 5 Hz) if kappa and its uncertainty are not appropriately considered in the computation of the amplifications. This finding has significant loading implications for high frequency response dams and other safety-critical structures.

Also shown in Figure 1 is an approximate relationship between Kappa and V_{S30} from available global data (Al Atik et al, 2014). Due to the poor correlation, it is preferable to obtain site-specific kappa values rather than rely on its dependency on V_s . To measure kappa, one needs to deploy an energy source powerful enough to excite the top 2-5 km of the earth's crust (which is impractical even if possible) or install strong motion accelerographs (SMAs) and patiently wait for an earthquake to occur. Kappa can then be estimated from the slope of the high frequency (5-20 Hz) portion of the Fourier amplitude spectrum (where it is linear in log-linear space) of an earthquake recording if the event hypocenter is within 50 km or so. Data from the SMAs, if remotely accessible, can also be used to timely inform decision-making on earthquake emergency response planning, further underscoring the importance and urgency of installing SMAs on 'significant' consequence dam sites.

COMMISSION INTERNATIONALE DES GRANDS BARRAGES

VINGT-SIXIÈME CONGRÈS DES GRANDS BARRAGES
Autriche, juillet 2018

DOI 10.3217/978-3-85125-620-8-001



This work licensed under a Creative Commons Attribution 4.0 International License. <https://creativecommons.org/licenses/by-nc-nd/4.0/>

**OROVILLE DAM SPILLWAY INCIDENT - WARNINGS AND THE HUMAN
RESPONSE**

Jason NEEDHAM

Consequence Specialist, UNITED STATES ARMY CORPS OF ENGINEERS
RISK MANAGEMENT CENTER

John SORENSEN

Distinguished Researcher, Retired, OAK RIDGE NATIONAL LABORATORY

Dennis MILETI

Professor Emeritus, UNIVERSITY OF COLORADO, BOULDER

Matthew MURRAY

CALIFORNIA DEPARTMENT OF WATER RESOURCES

UNITED STATES OF AMERICA

COMMISSION INTERNATIONALE
DES GRANDS BARRAGES

VINGT TROISIÈME CONGRÈS
DES GRANDS BARRAGES
L'Autriche, juillet 2018

OROVILLE DAM SPILLWAY INCIDENT — WARNINGS AND THE HUMAN RESPONSE

Jason Needham
Consequence Specialist, United States Army Corps of Engineers Risk
Management Center

Dr. John Sorensen
Distinguished Researcher, Retired, Oak Ridge National Laboratory

Dr. Dennis Mileti
Professor Emeritus, University of Colorado, Boulder

Matthew Murray
California Department of Water Resources

UNITED STATES OF AMERICA

1. INTRODUCTION

Oroville Dam is located on the Feather River in northern California (USA). At 234.7 m (770-ft) tall, this earth embankment is the tallest dam in the United States. With its 4.3 billion m³ (3.5 million acre-feet) of storage, Lake Oroville is the second largest reservoir in California, supplying water to cities as far south as Los Angeles. The Oroville Dam, reservoir (Lake Oroville), and hydropower plant facility is the flagship of the State Water Project (SWP), which is owned and operated by the State of California, Department of Water Resources (DWR).

The 2016-2017 Winter Storms brought record breaking precipitation to the Northern California Sierra mountains including the Feather River watershed. On February 7, 2017, the Oroville Dam's 54.5 m (179-ft) wide Flood Control Outlet (FCO) Spillway chute (Fig. 1) was releasing water to control the Lake Oroville

reservoir level in accordance with the prescribed operations plan. During this operation, the FCO spillway suffered a catastrophic failure of the lower chute area eventually resulting in the loss of approximately 427 m (1400 ft) of the lower chute, including the scour of more than 1.2 million m³ (1.6 million yd³ of soil and rock materials). On February 11, 2017, the Emergency Spillway (Fig. 1) was used for the first time since the project was completed in 1968. During this operation, significant erosion and scour caused by the Emergency Spillway overflow led authorities to fear for the safety of the spillway structures, resulting in the activation of the Emergency Action Plan and evacuation of about 188,000 persons from downstream communities.

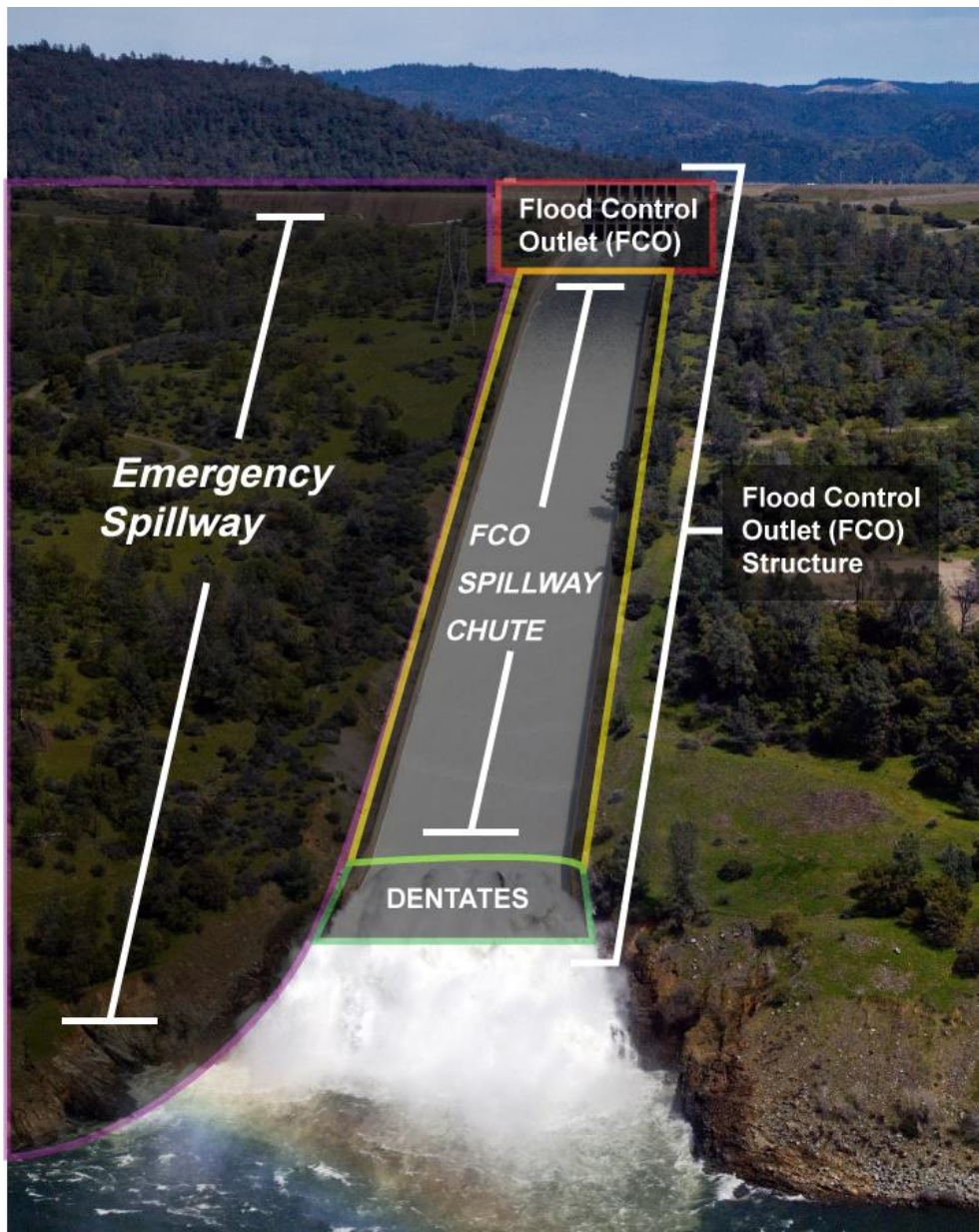


Fig. 1 Flood Control Outlet (FCO) Structure and Emergency Spillway, March 2011

This paper is part of a series developed by the State of California, Department of Water Resources to present the results of warning and evacuation related research, conducted for the United States Army Corp of Engineers (USACE), on the Oroville Dam Spillway Incident. This investigation is part of the USACE effort to collect and analyze data on:

- 1) the timing of the decisions to order public evacuation warnings including the flow of information between engineers and engineering geologists monitoring the hazard and local officials,
- 2) the method and timing of the dissemination of those warnings including the diffusion or warning by various communication channels, and
- 3) the interpretation and response by the public to those warnings, including the timing of protective action decisions.

The findings from this effort will not only provide invaluable lessons learned that can improve emergency management for this type of rare event, but they will also be incorporated into the existing approaches used by USACE and others to better understand evacuations and how their effectiveness impacts the risk associated with flooding downstream from dams and levees.

2. BACKGROUND ON WARNING AND EVACUATION RESEARCH

2.1. PURPOSE OF RESEARCH EFFORT

Decisions within the USACE Dam and Levee Safety Programs follow a risk-informed management process where life safety is paramount. Understanding and making informed decisions related to life safety risk not only requires a clear understanding of the engineering aspects of our flood defense infrastructure, but also the human aspects. To that end, USACE engaged with well-respected social scientists in the areas of warning and evacuation to better understand how flood warnings spread through a community and what causes an individual to delay their decision to take a protective action based on those warnings. This understanding has not only allowed consequence specialists to better assess the existing life safety risk associated with flood defense, but also provide important insights regarding implementing or recommending efficient and effective risk reduction measures.

The research, by Dr. Dennis Mileti and Dr. John Sorensen, both renowned social scientists in the areas of emergency warning and evacuation, covers the warning and protective action initiation timeline, which is composed of three distinct timeframes (illustrated in Fig. 2): warning delay time, warning diffusion time, and protective action initiation time. Their research, which is a culmination of existing social science research on the topic, details the primary factors that influence each

aspect and provide guidance on how to develop inputs to our evacuation modeling tools. Additionally, they developed a facilitator guide that describes how to interview local emergency managers and gain an understanding of the existing evacuation potential in their area in the event of a major flood event.

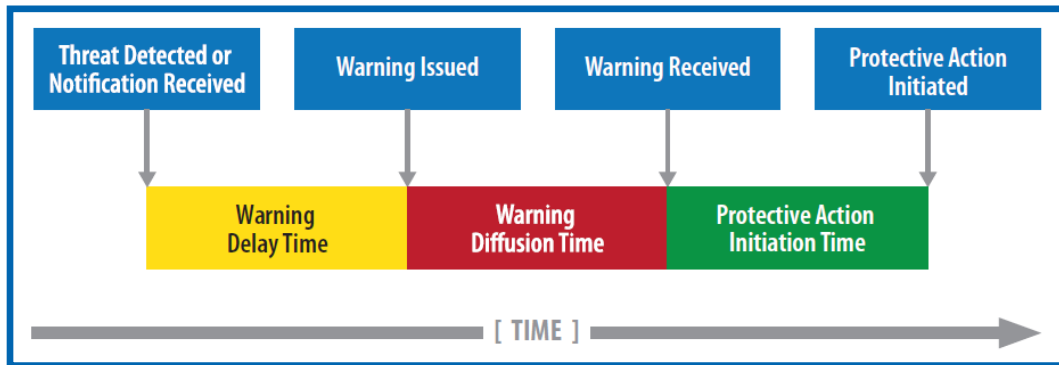


Fig. 2 Warning and Protective Action Initiation Timeline

Finally, and perhaps most importantly, they developed a document titled “A Guide to Public Alerts & Warnings for Dam and Levee Emergencies” [1]. The guidebook’s purpose is to assist those involved with emergency management in issuing more timely and effective public alert and warning messages for flood emergencies. It is based on findings from decades of research on disaster warnings and presents best practices derived from these findings. While the guidebook is targeted toward dam and levee safety emergencies, it can be used to prepare a plan in such a way that allows successful implementation of emergency message communication for a wide range of emergency events.

2.2. LIMITATIONS OF EXISTING RESEARCH

While the previous effort from Drs. Mileti and Sorensen was invaluable in providing a better understanding of the factors that influence the effectiveness of an evacuation, and established the basis for quantitative estimates for analyzing such an event, the research had gaps.

Specifically, they pointed out that research is needed to fill the warning issuance data gap. Due to the scarcity of data on warning issuance times and delays, there is a distinct need to increase the number of data points to gain a better grasp of the problem. Similarly, they stated that warning diffusion and protective action initiation models could be improved by collecting more, recent, and relevant empirical data on which to base the models.

2.3. IMPROVING ON EXISTING RESEARCH

Given the limitations of the previous research, USACE, with the assistance of Drs. Mileti and Sorensen, began monitoring the nation with the goal of gathering the necessary additional information when the next large-scale emergency evacuation inevitably occurred. On February 12, that scenario occurred downstream of Oroville Dam.

3. OROVILLE EVENT OVERVIEW

Based on discussions we had with locals in the Oroville area, it is clear that prior to February 2017, the public generally did not consider the consequences of an uncontrolled release of water from the Oroville Dam or its spillways. The dam was simply part of the landscape of the community that had remained virtually unchanged for nearly 50 years.

3.1. EVENT INITIATION AND EVOLUTION

During the winter of 2016-2017, Northern California experienced its wettest winter in nearly a century. Record inflows from the Feather River into the Oroville Reservoir during the month of January caused employees of the California Department of Water Resources (DWR) to open the main spillway and release water at rates up to 560 m³/s (20,000 ft³/s). The release of water down the spillway was normal procedure during very wet rainy seasons and that rate of flow is far below the designed capacity of the spillway chute and downstream channel.

On the afternoon of February 6, in anticipation of increased inflow from an upcoming storm, the flow from the Flood Control Outlet (FCO) Spillway was increased to 1,550 m³/s (55,000 ft³/s). The following morning, an unusual flow pattern within the FCO Spillway chute caused DWR employees to close the FCO Spillway gates to allow for inspection. The halted water flow revealed a large area of concrete slab failure and foundation erosion beneath the spillway chute.

DWR began consulting with the Federal Energy Regulatory Commission (FERC) and other dam safety agencies the following day. Test flows were released down the damaged FCO Spillway to verify how much flow the spillway chute could bear. This information was important, as the area was still in the middle of a very wet season and it was likely the FCO Spillway would be needed again in the coming months. Further slab failure and foundation erosion within the spillway chute was carefully monitored and an emergency operations center (EOC) was established to oversee the spillway operations.

Even though the Butte County Sheriff's office and others received an electronic message from DWR to inform them that they were investigating the damage at the flood control outlet of Oroville Dam, it was through social media that the Sheriff learned of the hole in the FCO Spillway chute. After the initial communication issues were cleared up, the Sheriff remained in continuous contact with the EOC to ensure that public safety was the top priority. At this point, DWR officials presumed that the remaining storage area within the reservoir was sufficient to capture the expected flood flows from the rainfall during the rest of that week without causing any threat to the dam or the public. It was the goal of the dam operators to avoid using the emergency spillway while the flood flows were contained, but to be prepared in case using the Emergency Spillway became necessary. DWR and the Butte County Sheriff's Office kept the public informed through their respective social media platforms.

On February 9, rainfall in excess of 32.5 cm (12.8 in) over the Feather River Basin caused the inflows into Lake Oroville to exceed 5,380 m³/s (190,000 ft³/s). The peak inflow to the reservoir was significantly higher than originally forecasted. The following morning, dam operators raised flows through the main service spillway to 1,840 m³/s (65,000 ft³/s) and the hole within the spillway chute continued to expand and erode portions of the adjacent mountainside. DWR personnel decided to use the emergency spillway in an effort to minimize the increasing erosion at the main spillway. They reduced flow through the main service spillway to 1,550 m³/s (55,000 ft³/s) and water level within the reservoir continued to rise.

It is important to note that debris deposited in the river downstream of the dam from concrete slab failure and foundation erosion of the FCO Spillway chute raised the tailwater on the Edward Hyatt Power Plant and threatened to flood it out. DWR implemented emergency measures to flood proof the plant with the goal of preserving power and water supply capabilities post event. Without that effort, water supply for the region would have been in jeopardy. Although not an evacuation issue, it was foremost on the minds of the officials during that critical time.

The Emergency Spillway had not been used or tested since the dam was constructed. A large amount of erosion was expected in the Emergency Spillway and DWR employees prepared the face of the mountain by removing brush and trees in the areas where the water was likely to go, trying to limit further impact to the power plant. Due to the erosion concerns on the FCO Spillway chute and higher than anticipated inflows, the water level in Lake Oroville reached the Emergency Spillway crest early in the morning of February 11.

3.2. DETERMINATION OF CRITICAL RISK

On Sunday morning, February 12, after more than 24 hours of water flowing over the Emergency Spillway, work in the EOC was quiet. Water continued to spill over the Emergency Spillway at a rate that posed no direct threat to the downstream communities. Experts remained at the EOC and at the top of the dam communicating with each other by traveling back and forth or through text messaging with spotty cell reception. Later that morning, staff monitoring the situation at the dam noticed deep erosion rills cutting back toward the emergency spillway at a rate and size much larger than anticipated. At approximately 2:00 pm, the erosion began to concern engineering geologists about the safety of the Emergency Spillway.

If the erosion continued and reached the base of the Emergency Spillway, one of the concrete monoliths could be undermined and collapse. Engineers were concerned that a failure of one monolith could result in a domino effect, causing successive collapse of the adjacent monoliths. Engineering geologists estimated that the erosion would reach the base of the Emergency Spillway in two hours. Those monitoring the situation at the top of the dam discussed if the circumstances constituted an emergency declaration, and who had the power to make that decision.

Around the same time, at the Butte County Sheriff's Office, the Sheriff believed the entire incident was nearly complete and decided to head home for the rest of the day. Being unaware of the developing situation at the Emergency Spillway, the Sheriff stopped by the EOC to thank the people for their hard work.

Meanwhile, staff monitoring the Emergency Spillway brought photographs of the advancing erosion to the EOC and showed them to the Incident Commander. The Incident Commander received the photos at approximately 3:00 pm and received a briefing on the developing situation. He asked, "Does the Sheriff know about this?", unaware that the Sheriff had just arrived at the EOC and was standing behind him. Seeing the elevated concern, the Sheriff asked what would happen if the Emergency Spillway were to fail. DWR staff informed him that failure of the Emergency Spillway could result in a 9-10 m (30 ft) wave of water flowing from the breached spillway until the top 9-10 m (30 ft) of Lake Oroville had drained.

3.3. DECISION TO EVACUATE

At 3:30 pm, several dam managers, engineering geologists, and the Butte County Sheriff were discussing how to address the situation developing at the Emergency Spillway. The dam managers decided to allow a flow of 2,830 m³/s (100,000 ft³/s) through the FCO Spillway chute to decrease the water level in the reservoir below the Emergency Spillway crest as quickly as possible. All

acknowledge that this would cause additional erosion along the FCO Spillway chute, but would possibly alleviate the risk that the Emergency Spillway would fail.

During the discussion at the EOC, a DWR dam safety official entered the room and estimated that erosion was moving toward the Emergency Spillway at a rate of approximately 9-10 m (30 ft) per hour. At that moment, the erosion was approximately 9-10 m (30 ft) from the base of the Emergency Spillway. The official recommended an evacuation of the downstream communities in case the Emergency Spillway was to fail. Everyone present began talking loudly amongst themselves until the Sheriff took control of the room. He asked, "Can anyone here give me a reason not to evacuate?" The room went silent. He made the decision to evacuate at approximately 3:50 pm.

An Emergency Action Plan (EAP) had been prepared for Oroville Dam shortly after it was built. An inundation map plan that showed the areas that would be inundated if the entire dam were to fail was included as a part of the EAP. However, a map estimating the flood extents of an Emergency Spillway failure did not exist. The Sheriff, with the assistance of DWR dam safety officials, made a conservative estimate on the areas to evacuate within Butte County based on the available maps. The Sheriff also called the Sheriffs of Yuba and Sutter Counties located downstream. He quickly related that he was evacuating the potential inundation areas along the Feather River within Butte County and that they should do the same in their respective counties.

3.4. COMMUNICATION OF EVACUATION DECISION TO SAFETY OFFICIALS

DWR communicated with a variety of organizations about the situation at Oroville Dam beginning on February 8, 2017. They also distributed the following evacuation decision message to 161 organizational contacts, including safety and emergency managers (159 were reached), on February 12, 2017 at 4:10 pm. That message stated: "This is an evacuation order. Immediate evacuation from the low levels of Oroville and areas downstream is ordered. A hazardous situation is developing with the Oroville Dam auxiliary spillway. Operation of the auxiliary spillway had led to severe erosion that could lead to a failure of the structure. Failure of the auxiliary spillway structure will result in an uncontrolled release of floodwaters from Lake Oroville. In response to this developing situation, DWR is increasing water releases to 100,000 cubic feet per second. Immediate evacuation from low levels of Oroville and areas downstream is ordered. This is NOT A Drill. This is NOT A Drill. This is NOT A Drill."

3.5. CHRONOLOGY OF FIRST PUBLIC EVACUATION MESSAGES

Five first public evacuation messages were subsequently issued to people in different at risk geo-political areas. These were: (1) Butte County, which contains the City of Oroville, (2) the National Weather Service to people in Butte, Sutter, and Yuba Counties, (3) Sutter County, (4) Yuba City, which is the largest city in Sutter County, and (5) Yuba County, which contains the City of Marysville. Fig. 3 illustrates the location of these communities in relation to Oroville Dam. We catalogued first evacuation messages for different subpopulations because their timing was central to our efforts to examine warning decision-making, diffusion, and protective action initiation. The five first public evacuation messages follow.

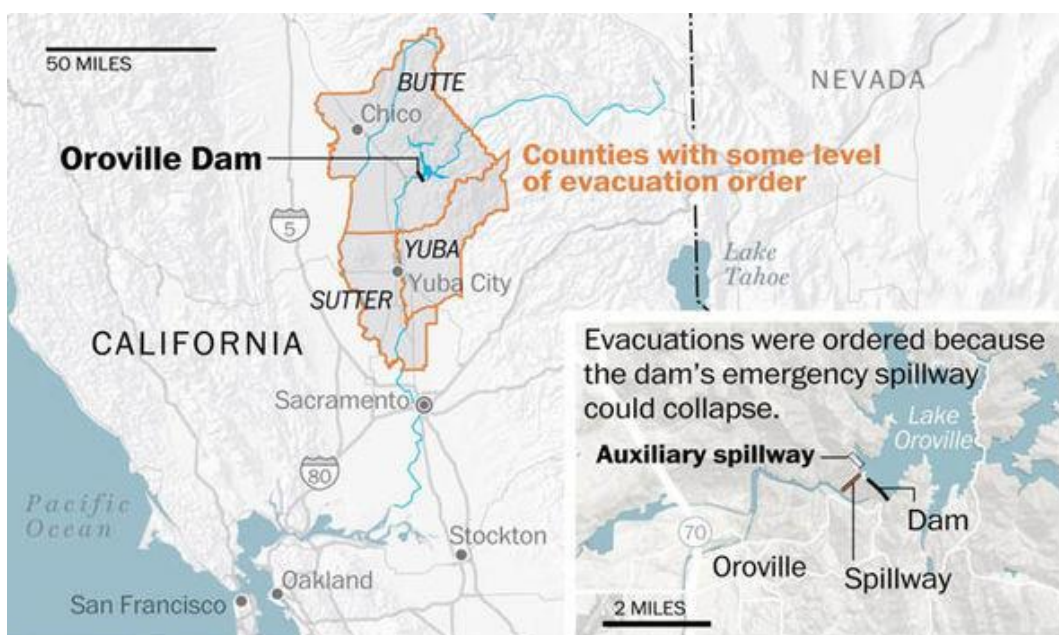


Fig. 3 Areas Receiving Evacuation Orders Downstream of Oroville Dam
(Source: United States Geological Service)

3.5.1. 4:21 pm: Butte County.

The Butte County Sheriff's Office sent the first public evacuation message to the public of Butte County at 4:21 pm on February 12, 2017. It stated the following. "This is an evacuation order. Immediate evacuation from the low levels of Oroville and areas downstream is ordered. A hazardous situation is developing with the Oroville Dam auxiliary spillway. Operation of the auxiliary spillway has led to severe erosion that could lead to a failure of the structure. Failure of the auxiliary spillway structure will result in an uncontrolled release of floodwaters from Lake Oroville. In response to this developing situation, DWR is increasing water releases to 100,000 cubic feet per second. Immediate evacuation from the low levels of

Oroville and areas downstream is ordered. This is NOT A Drill. This is NOT A Drill. This is NOT A Drill.

This message was disseminated using social media, local radio and television, and the Blackboard notification system (described further in Section 4.2.1). The Sheriff also ordered the deputies in Butte County to go to the neighborhoods at risk and announce the evacuation order over the public address system in their police vehicles.

3.5.2. 4:35 pm: All Three Counties at Risk.

The National Weather Service in Sacramento released the following statement at 4:35 pm on February 12, 2017 via Wireless Emergency Alerts (WEA) to everyone in the entire three-county area at risk. “The National Weather Service in Sacramento has issued a Flash Flood Warning for a dam failure in south central Butte County in Northern California. Until 4:15pm PST Monday. At 4:19pm PST, dam operators reported a hazardous situation is developing with the Oroville Dam auxiliary spillway. Operation of the auxiliary spillway has led to severe erosion that could lead to a failure of the structure. Failure of the auxiliary spillway structure will result in an uncontrolled release of floodwaters from Lake Oroville. In response to this developing situation, DWR is increasing water releases to 100,000 cubic feet per second. Immediate evacuation from the low levels of Oroville areas downstream is ordered. From Oroville to Gridley...low level areas around the Feather River will experience rapid river rises. This is not a Drill. This is not a Drill. Repeat this is not a drill. Locations impacted include Oroville, Palermo, Gridley, Thermalito, South Oroville, Oroville Dam, Oroville East and Wyandotte. Turn around, don't drown when encountering flooded roads. Most flood deaths occur in vehicles. Move to higher ground now. Act quickly to protect your life.”

3.5.3. 5:33 pm: Yuba County.

The Yuba County Office of Emergency Services issued the following warning message to people in Yuba County at 5:33 pm on February 12, 2017. “ALERT-ALERT-ALERT — Yes, an evacuation has been ordered. All of Yuba County on the valley floor. The auxiliary spillway is close to failing. Please travel safely. Contact family and friends. Help the elderly. Take only routes to the east, south, or west. DO NOT TRAVEL NORTH TOWARD OROVILLE!!!!” At 5:48 pm, the Marysville Police Department confirmed that a mandatory evacuation for the City of Marysville and Yuba County was in effect. Then at 6:08 pm it was stated that: “Evacuation for Yuba includes Hallwood, Marysville, Olivehurst/Linda and Plumas Lake due to potential failure of Oroville Dam spillway.”

3.5.4. 6:03 pm: Sutter County.

At 6:03 pm on February 12, 2017, the Sutter County Office of Emergency Management issued the following message to people in Sutter County. “Immediate evacuation Live Oak, Yuba City, Nicholas and other communities along Feather River ordered. Evacuate on Highway 99/70 south of Highway 20 west. Do not evacuate north. A partial failure of the Oroville Dam is possible.” The county followed this first evacuation message to people in Sutter County with a subsequent message at 6:17 pm, which declared that the evacuation was ordered (or mandatory). “Immediate evacuation ordered for Live Oak, Yuba City, Nicolaus & all communities Feather River Yuba City basin. Evacuate West on Hwy 20 and/or South on Hwy 99 and Hwy 70 toward Sacramento.”

3.5.5. 6:49 pm: Yuba City.

Another public evacuation message was issued which targeted the people in Yuba City—located in Sutter County. It was distributed at 6:49 pm on February 12, 2017. It was the first message issued by city officials and it followed the mandatory evacuation message distributed by the county. It contained a voluntary evacuation recommendation, and was issued by local Yuba City government. It stated the following. “City of Yuba City strongly recommends an evacuation of all residents immediately. Travel options are as follows. South on Highway 99, West on Highway 20, Highway 99 South to Highway 113, or South on George Washington to Highway 113. Do not travel on Highway 20 or Bridge Street as the bridges are closed. Do not travel North.”

3.6. PUBLIC RESPONSE

At the writing of this paper, response to the public survey that we created to gather information on the response to the warnings described in previous sections was in its final stages. Some preliminary findings are described below, but these may change as the data undergo final analysis. Importantly, the survey was conducted on a representative sample of the entire population in the evacuation zone. Therefore, we have a statistical basis for generalizing the findings for people not in the sample.

3.6.1. Protective Action Initiation Response Rate

Preliminary analysis of public survey responses suggests just under 70% of the population in the targeted evacuation zone actually evacuated. Table 1 lists the reasons why people did not evacuate. The primary reason for non-evacuation (33%) was that even though they were in the evacuation zone, they felt that they would be above the flood elevation. In effect, they felt they were not asked to

evacuate as the evacuation order was targeted to those in “low lying areas”. The next most common responses were that they did not think there would be a flood (19%) or that they were not in an area told to evacuate (14%). Another common response (13%) stated that traffic congestion kept them from evacuating, either they tried and turned around or saw the congestion on the news and stayed home.

Table 1
Reasons for Non-evacuation

NON-EVACUATION REASON	% of NON-EVACUEES
Not in area told to evacuate	14%
Not in low lying area or an area that would flood	33%
Stayed behind to protect my property	10%
Did not think there would be a flood	19%
Stayed behind to do my job	2%
Did not have the resources	6%
Physically unable to evacuate	3%
Other (Mostly traffic congestion related)	13%

3.6.2. Evacuation Timing

Preliminary data analysis suggests that about 10% evacuated prior to the first evacuation order (either due to concerns with the dam or left for other reasons and did not return). Approximately 40% of those that evacuated did so within 30 minutes of the first public evacuation order, which was issued at 4:21 PM on February 12. Approximately 70% evacuated within an hour of the first evacuation order, and 83% evacuated within 2 hours of the first evacuation order.

For those that evacuated, the amount of time they spent on the road was significant. On average, it took 3 hours for people to reach their destination. For context, most evacuees all traveled to destinations that would have normally taken less than 1 hour. Table 2 shows the breakdown of travel times.

Table 2
Evacuation Travel Times

TRAVEL TIME (HOURS)	% of EVACUEES
< ½ hour	14%
½ hour – 1 hour	33%
1-2 hours	10%
2-3 hours	19%
3-4 hours	2%
4-5 hours	6%
5-10 hours	3%
> 10 hours	13%

4. LESSONS LEARNED

The Oroville emergency evacuations provided some new lessons, and reinforced many existing lessons, for emergency managers. The list below is not meant to be exhaustive, but highlights some of the more important ones in the view of the authors. Many of the lessons reinforced by this event are describe by the authors in previous work [1].

4.1. LACK OF INUNDATION MAPS

Perhaps the most important lesson learned, or in this case reinforced, was the value of having inundation maps for a wide range of potential scenarios available for emergency managers at a moment's notice. As described above, the situation on February 12 was relatively calm leading up to the emergency, and nobody was concerned about a potential breach of the Emergency Spillway. Within a couple hours of recognizing erosion that could impact the stability of the Emergency Spillway, local emergency managers were sending out evacuation notices with little understanding of the area at risk. Their only available information was for a complete failure of the main dam embankment, which would have led to flows that would be orders of magnitude higher than were expected from breach of the Emergency Spillway. This short amount of time does not allow even the most experienced hydraulic engineers to model properly the scenario in question. Therefore, it is important to have inundation maps available covering a wide range of potential breach and non-breach scenarios as part of the EAP.

DWR was already aware of the need for additional maps for Oroville and other dams in their portfolio. They were already in the process of creating a library of inundation maps to cover a wider range of breach and non-breach scenarios. If

this emergency had occurred just a few months later, these additional inundation maps would have been available, and the evacuation notice could have been targeted to more specific areas.

4.2. MASS NOTIFICATION SYSTEM

The notification system used by DWR emergency managers, known as Blackboard, and the large notification lists contained therein led to some unforeseen issues and confusion during the incident.

4.2.1. *Blackboard*

Blackboard is an automated mass notification system that has many capabilities, but in this case, was set up by DWR to send messages to a roster of emergency management and response agencies via email and telephone. For telephone messages, it has the capacity to call three phone numbers at a time. It works sequentially through the notification list until all contacts have answered the phone, been left a voicemail, or did not answer after several attempts.

The fact that the system can only call three numbers at a time resulted in a significant delay in disseminating the evacuation notice to those relying on telephone messaging. The initial evacuation message that was sent via Blackboard at 4:10 pm did not reach all of the ~160 contacts on the notification list until 4:44 pm. The follow up message, which indicated that the Emergency Spillway could fail within the next 60 minutes and provided guidance on evacuation routes, was sent at 4:34 pm and was not completely disseminated until 5:10 pm. Because of this delay, many of the emergency management and law enforcement agencies on the notification list found out about the emergency and evacuation via social media prior to learning about it from the official Blackboard notification.

DWR had added various emergency managers to the Blackboard call down list over the years, without understanding the impact that all those additional numbers would have on the efficiency of the system. In that regard, it is important that dam operators or anyone relying on these automated systems to provide important emergency messages understand their limitations and test them regularly.

4.2.2. *Message Specificity and Warning Templates*

Another lesson that was reinforced through the Oroville emergency was the need for emergency messages, especially those ordering protective actions such as evacuations, to be as specific as possible. The initial message that was sent out started with "*This is an evacuation order. Immediate evacuation from the low*

levels of Oroville and areas downstream is ordered." This message went out to all emergency managers downstream of Oroville Dam, which includes the city of Sacramento and surrounding areas about 100 km (70 miles) downstream. Some emergency managers in those areas far downstream interpreted the message to mean they should be preparing to evacuate, when in reality the concern for them potentially being flooded was minimal. Emergency managers in those areas would have been better served if the initial message contained more specific information on the areas downstream from Oroville Dam that should evacuate. Emergency managers downstream but not at risk of flooding could have been preparing to receive evacuees rather than determining if they were really meant to be evacuating their communities.

This re-emphasizes the need for warning templates and examples. Example messages and templates serve a number of significant purposes for an emergency manager. First, it is not reasonable to expect that all emergency managers are familiar with the value of certain content (such as specificity of locations) or wording in messaging, so templates and examples provide an effective starting point. Second, messages cannot be written in advance for every emergency scenario. Message templates provide the capability to create specific event messages much more quickly. Example messages and templates are also useful to avoid hastily written content. Finally, example messages and templates provide emergency managers something to practice and hone their skills on.

4.3. COMMUNICATION ISSUES

A widely recognized issue within the emergency management community is the need for trustworthy means of communication between the various agents during and emergency event. In the case of Oroville, communication between those monitoring the situation from the crest of the dam and the command center was strained due to lack of reception on the mobile phones used by those at the dam site. Calls rarely connected, and text messages were intermittent and lagged. This required those monitoring the site to take pictures and travel to the command center with the information so those managing the situation could have the necessary information. Hardened and redundant communications technologies such as satellite telephones and two-way radios can prevent these kinds of issues and lead to more efficient and effective emergency management.

4.4. LACK OF SLEEP

Admirably, DWR staff were dedicated to understanding and managing the emergency. From the initial discovery of damage on February 7 until the emergency evacuation on February 12 (and beyond), many of the engineers and project staff were on call, either in the local office, at the project, or in the

emergency operations center nearly non-stop. Many of the senior engineers had little to no sleep in the days leading up to the evacuation. A multitude of scientific studies have shown that sleep deprivation makes it difficult to adapt to the unexpected. While the authors of this paper are not questioning the decision-making during the Oroville Dam Incident, emergency managers should take the opportunity to learn from this and implement procedures that require those faced with making potential life and death decisions to get a reasonable amount of sleep during prolonged emergencies such as this.

ACKNOWLEDGEMENTS

We would like to acknowledge the California Department of Water Resources (DWR), the United States Federal Energy Regulatory Commission (FERC), and the local emergency managers in Butte County, Sutter County, Yolo County, and the cities of Marysville and Yuba City for answering all our questions about this emergency. Their open and honest responses provided invaluable information that will be used to better understand the flow of information during an emergency and improve emergency management going forward.

REFERENCES

- [1] MILETI D.S., SORENSEN J.H. A Guide to Public Alerts and Warnings for Dam and Levee Safety Emergencies. *US Army Corps of Engineers, 2015*

COMMISSION INTERNATIONALE DES GRANDS BARRAGES

VINGT-SIXIÈME CONGRÈS DES GRANDS BARRAGES
Autriche, juillet 2018

DOI 10.3217/978-3-85125-620-8-002



This work licensed under a Creative Commons Attribution 4.0 International License. <https://creativecommons.org/licenses/by-nc-nd/4.0/>

**OROVILLE DAM SPILLWAY INCIDENT — SITUATION DEVELOPMENT,
INCIDENT RESPONSE AND PUBLIC SAFETY**

William Croyle

Acting Director (Retired), STATE OF CALIFORNIA, DEPARTMENT OF WATER
RESOURCES

David Gutierrez

Technical Advisor, GEI CONSULTANTS, INC.

Joel Ledesma

Assistant Division Chief, Operations and Maintenance, STATE OF CALIFORNIA,
DEPARTMENT OF WATER RESOURCES

Sharon Tapia

Chief, Division of Safety of Dams, STATE OF CALIFORNIA, DEPARTMENT OF
WATER RESOURCES

Frank L Blackett

Regional Engineer, FEDERAL ENERGY REGULATORY COMMISSION

UNITED STATES OF AMERICA

OROVILLE DAM SPILLWAY INCIDENT — SITUATION DEVELOPMENT,
INCIDENT RESPONSE AND PUBLIC SAFETY

William Croyle

Acting Director (Retired), State of California, Department of Water Resources

David Gutierrez

Technical Advisor, GEI Consultants, Inc.

Joel Ledesma

Assistant Division Chief, Operations and Maintenance, State of California, Department
of Water Resources

Sharon Tapia

Chief, Division of Safety of Dams, State of California, Department of Water Resources

Frank L Blackett

Regional Engineer, Federal Energy Regulatory Commission

UNITED STATES OF AMERICA

1. INTRODUCTION

Oroville Dam is located on the Feather River in northern California (USA). At 234.7 m (770-ft) tall, this earth embankment is the tallest dam in the United States. With its 4.3 billion m³ (3.5 million acre-feet) of storage, Lake Oroville is the second largest reservoir in California, supplying water to cities as far south as Los Angeles. The Oroville Dam, reservoir (Lake Oroville), and hydropower plant facility is the flagship of the State Water Project (SWP), which is owned and operated by the State of California, Department of Water Resources (DWR).

The 2016-2017 Winter Storms brought record breaking precipitation to the Northern California Sierra mountains including the Feather River watershed. On February 7, 2017, the Oroville Dam's 54.5 m (179-ft) wide Flood Control Outlet (FCO) Spillway chute (Fig. 1) was releasing water to control the Lake Oroville reservoir level in accordance with the prescribed operations plan. During this operation, the FCO spillway suffered a catastrophic failure of the lower chute area eventually resulting in the loss of approximately 427 m (1400 ft) of the lower chute, including the scour of more than 1.2 million m³ (1.6 million yd³) of soil and rock materials. On February 11, 2017, the Emergency Spillway (Fig. 1) was used for the first time since the project was completed in 1968. During this operation, significant erosion and scour caused by the Emergency Spillway overflow led authorities to fear for the safety of the spillway structures, resulting in the activation of the Emergency Action Plan and evacuation of about 188,000 persons from downstream communities.

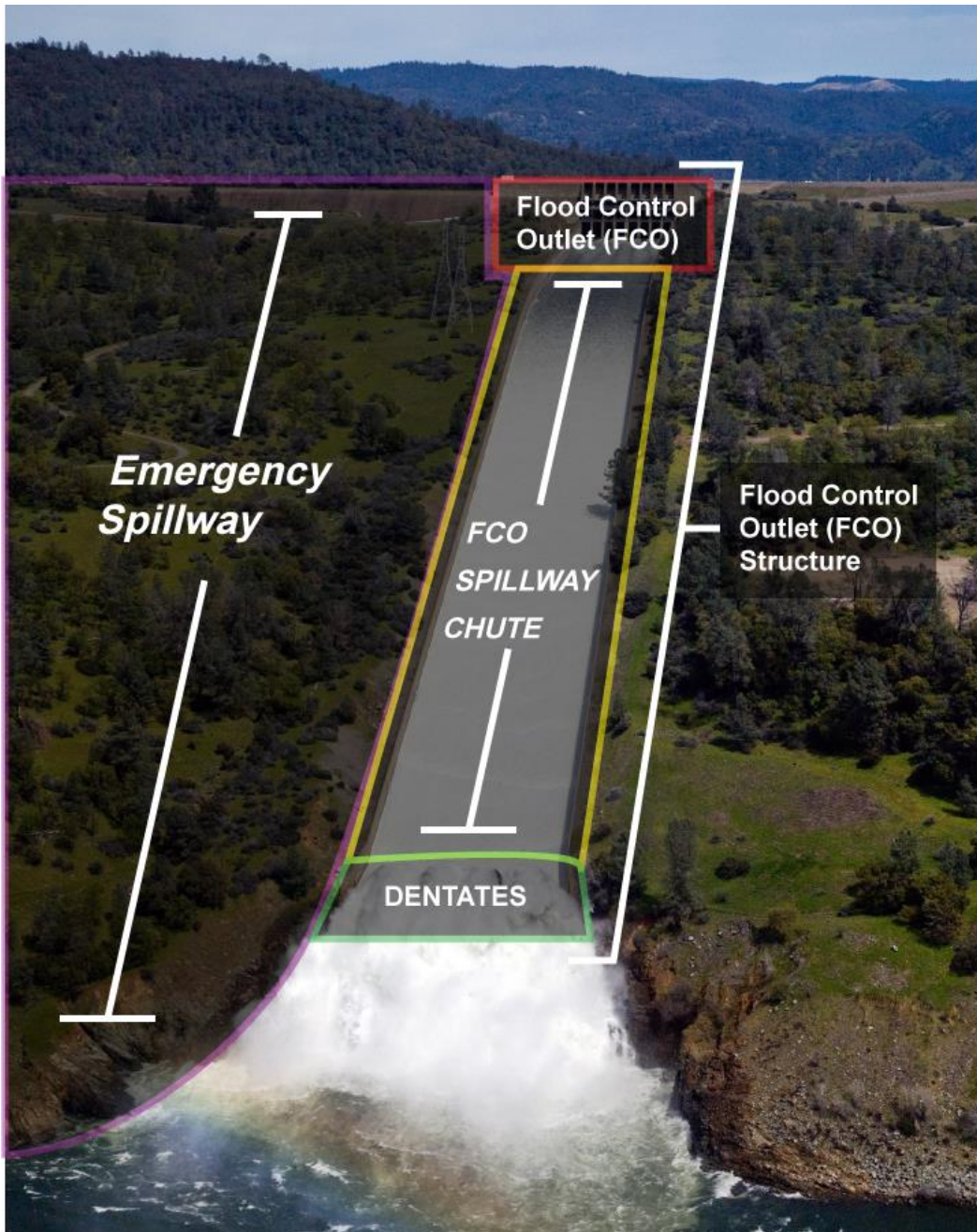


Fig. 1 Flood Control Outlet (FCO) Structure and Emergency Spillway, March 2011

This paper is part of a series to describe the Oroville Dam Spillway Incident Emergency Response and Recovery. This paper focuses on the implementation of the emergency response actions starting on February 7, 2017, and the actions taken in the days and weeks after failure of the concrete in the FCO Spillway chute. It provides detail of the incident as it unfolded, the decisions made to protect the public, the incident command system, and the situation that led to the evacuation.

2. OROVILLE DAM FACILITY

The Oroville Dam facility design was initially proposed in 1953 and was modified a number of times based on new requirements and scaled physical model studies, with construction being complete in 1968.

The Oroville Dam and its major appurtenant facilities consist of a main dam (Oroville Dam), two saddle dams (Bidwell Saddle Dam and Parish Saddle Dam), two spillways (FCO Spillway and Emergency Spillway), the Hyatt Powerplant (Powerplant), and the River Valve Outlet.

The main embankment is a zoned earthfill at 234.7 m (770 ft) high and a crest length of 2110 m (6920 ft). Bidwell Saddle Dam is located at the end of the Bidwell Bar Canyon arm of Lake Oroville and has two embankments. The combined length of the Bidwell Saddle Dam is 409 m (1340 ft) and the maximum embankment height is 14.3 m (47 ft). Parish Camp Saddle Dam is an embankment with a maximum height of 8.2 m (27 ft) and is 79.9 m (260 ft) long.

Oroville Dam's two spillways include a Flood Control Outlet (FCO) structure and an Emergency Spillway. They are configured as two separate structures right (north) of the main dam's right abutment. The function of the FCO structure is to provide flood protection to the downstream communities. Flows are regulated through the FCO structure, thus routing storms and river inflows through the reservoir storage. The FCO structure has three main components: a Flood Control Outlet, a 1310 m (4300 ft) long FCO Spillway chute, and an energy dissipater. The FCO structure was sized to control the "standard project flood" peak inflow of 12460 m³/s (440,000 ft³/s) without using the Emergency Spillway. During the standard project flood routing, the maximum flow through the FCO structure was set at 4248 m³/s (150,000 ft³/s) due to downstream levee capacity. This upper limit of release was set to protect local and downstream urban and agricultural areas from flooding. However, during the estimated Probable Maximum Flood (PMF) events, the FCO structure was designed to release a maximum of 8283 m³/s (296,000 ft³/s). The FCO Spillway chute is a rectangular, reinforced-concrete open-channel chute. The profile of this lined chute closely follows the original natural terrain. This minimized the excavation as well as the disturbances of the underlying rock due to blasting. The FCO Spillway chute was founded on varying degrees of weathered rock. Four dentate structures were placed at the end of the chute to dissipate excess energy. From the end of the dentates, the flow releases into the Feather River.

The purpose of the Emergency Spillway is to discharge extreme floods to prevent overtopping of the Oroville Dam embankment. The Emergency Spillway consists of two sections; an ogee section and a low-sill weir. The ogee section consists of multiple concrete monoliths founded on bedrock with varying heights. The tallest monolith has a height of about 15.9 m (50 ft) from the original ground and excavated into rock. The low-sill weir is a broad-crested concrete weir also founded on rock. The Emergency Spillway was sized such that during a PMF event, the spillway would be able to release a maximum flow of 10,506 m³/s (371,016 ft³/s) when the reservoir elevation is at 297.5 m (917 ft). The natural topography downstream of the Emergency Spillway was designed to convey the Emergency Spillway flows to the river. The area downstream

of the Emergency Spillway was not cleared of vegetation because of the predicted infrequent use of the Emergency Spillway (once in 800 years), and for economic, cultural, and aesthetic reasons. Although the Emergency Spillway was designed to withstand extreme flows, some erosion of the hill slope and debris were expected if the Emergency Spillway was ever engaged. However, the actual weir was not anticipated to be endangered from erosion during flows, based on the original design.

Additional discussion and figures regarding the hydrologic and hydraulic information and data related to Oroville Dam and the Oroville Emergency Response and Recovery are provided in accompanying DWR papers noted earlier, and the references cited.

Two 6.7 m (22 ft) diameter penstock tunnels leading from the reservoir to three reversible pump turbines and three conventional turbines feed the Hyatt Powerplant. The maximum combined release capacity of the Hyatt Powerplant is 479.9 m³/s (16,950 ft³/s). The facility also includes a River Valve Outlet system. The River Valve Outlet is at the lowest elevation that accesses the reservoir with a modest maximum capacity of approximately 122 m³/s (4300 ft³/s). Water from the Hyatt Powerplant and the River Valve Outlet flows into diversion tunnels, which exit near the downstream toe of the dam and into the tailrace, which eventually leads back to the Feather River channel. Normal emergency drawdown of the reservoir is typically through the FCO Spillway and/or the Hyatt Powerplant. The River Valve Outlet is only used when the reservoir level is too low for the Hyatt Powerplant to efficiently operate.

3. CALIFORNIA'S EMERGENCY MANAGEMENT SYSTEM

3.1 CALIFORNIA EMERGENCY MANAGEMENT

California has faced many disasters and emergencies over the years. The State has developed a robust emergency management community and has been a national leader in developing regulations, plans, and policies. DWR is an integral part of California's system and has other responsibilities beyond the SWP, including providing support and technical assistance to local agencies during floods. California's emergency management system works in layers to streamline communication and ensure resources are being delivered to the highest priority emergencies statewide. The following is a brief overview of the emergency management practice that is used during emergency events, such as the Oroville Emergency Response.

3.1.1 *California State Emergency Plan*

The foundation for emergency management in California is the State Emergency Plan (SEP). This plan describes how responses to natural and/or human-caused emergencies should occur in the State. The plan describes: methods for conducting emergency operations, the process for rendering mutual aid, emergency services of government agencies, how resources are mobilized, how the public is informed, and how continuity of government is maintained during an emergency. The SEP also

describes hazard mitigation (actions to reduce risk), as well as preparedness and recovery from disasters. The SEP is compatible with federal emergency planning concepts.

Key elements of the plan are used on a regular basis in response to different incidents and emergencies, such as statewide winter storms, wildfires, and the Oroville Emergency Response. The SEP, through its mutual aid and resource management systems, identified the state agency and department resources to be used to assist local governments in evacuating 188,000 people, providing meals and shelter for almost 10,000 people, and aided the sharing of information and coordination of activities from the field level to state government response.

3.1.2 The Standardized Emergency Management System

The Standardized Emergency Management System (SEMS) (Fig. 2) is the cornerstone of California's emergency response system and the fundamental construct of emergency management. California law requires SEMS for managing multiagency and multijurisdictional responses to emergencies. The system unifies all elements of California's emergency management community into a single integrated system. SEMS incorporates: 1) Incident Command System (ICS) - field-level emergency response system based on management by objectives; 2) Multi/Inter -agency coordination - affected agencies working together to coordinate allocations of resources and emergency response activities; 3) Mutual aid - system for obtaining additional emergency resources from non-affected jurisdictions; and 4) Operational Area Concept - County and its sub-divisions to coordinate damage information, resource requests and emergency response.

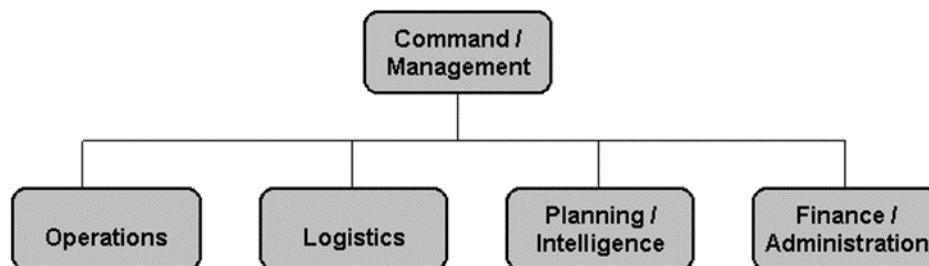


Fig. 2 - SEMS Organization Structure

3.1.3 STATE OPERATIONS CENTER

During major incidents, multiple emergencies can occur simultaneously. It is important that emergency responders communicate and coordinate throughout the various layers of government. At the highest level of emergency coordination in California is the State Operations Center (SOC) that is responsible for coordinating resource requests and resolving priority issues that arise at the regional level. The SOC is also responsible for coordinating with federal agencies. SOC operations are under the management of the California Governor's Office of Emergency Services. SOC responsibilities include, in part: 1) overall state coordinator in the event of simultaneous, multi-regional incidents; 2) monitors and facilitates inter-regional communications and

coordination issues; 3) compiles, authenticates, and makes available summary disaster status information obtained from all sources, in the form of Situation Reports, to the Governor's Office, the legislature, State agency headquarters, media, and others as appropriate; 4) provides necessary coordination with and between established statewide mutual aid systems at the state headquarters level; 5) manages the state government emergency public information; and 6) supports the recovery process and assists State agencies and Regional Emergency Operations Centers (REOC) in developing and coordinating recovery action plans.

During the Oroville Dam Spillway Incident, the SOC and a REOC were activated to the highest level and were critical in addressing local and State agency needs. This system led the State response to assist many local agencies during the mass evacuation of about 188,000 people. It was critical to deploy a number of high-level DWR executives to the SOC to facilitate enhanced communication, situational awareness, and resource priority setting between the DWR Department Operations Center (DOC) and the Governor's Office.

3.1.4 Department of Water Resources Emergency Operations

In addition to many other responsibilities, the Department of Water Resources is responsible for protecting life and property from catastrophic events such as flood, drought, and dam or levee failures. When significant weather events are forecast, DWR is responsible for coordinating local, State, and Federal flood operations. DWR's first layer of emergency coordination is the Department Operation Center (DOC), which is responsible for coordinating all DWR emergencies and communicates directly with the SOC. DWR operates many potential emergency centers, including a State and Federal Flood Operation Center (FOC) to coordinate various flood-related emergencies. DWR's Project Operations Center is responsible for emergencies focused on State Water Project facilities. Similar to the State's Emergency Response plan, DWR and SWP have specific emergency response plans and emergency action plans that focus on their respective responsibilities and facilities.

3.1.5 Public Contract Code Section 10122(b)

In cases of failure or threat to a dam, reservoir, aqueduct, or other water facility or facility appurtenances, DWR has unique emergency construction authority. DWR must expedite processes and, in some cases, immediately implement work. This emergency authority pursuant to Public Contract Code Section 10122(b) is critical to DWR and SWP in safely and efficiently executing its mission.

4. THE OROVILLE DAM SPILLWAY INCIDENT

California receives most of its precipitation and largest storms during the winter months. Thus, large reservoirs, such as Lake Oroville, are needed to provide flood protection in the winter and then water supply for the summer months and carryover in anticipation of drought years. Beginning in January 2017, after 5 years of historic drought, above average rainfall and snowfall occurred throughout most of California.

Major reservoirs were operating based on regulatory flood control curves and were releasing flood flows by design.

Prior to February 7, 2017, DWR had already activated the Joint State-Federal Flood Operations Center (FOC) in Sacramento. This was due to heavy precipitation causing high water conditions in many California streams and rivers, resulting in elevated flood threats throughout California.

By February 7, over 145% of normal precipitation had occurred over the Feather River Basin. A purpose of the Oroville Dam facility is to manage flood flows by routing inflows through the reservoir and the FCO Spillway according to the prescribed operations plan and regulatory requirements. The FCO Spillway began releasing 850 m³/s (30000 ft³/s) on February 3 and then the release was increased to 1416 m³/s (50000 ft³/s) on February 6, 2017.

On February 7, and within standard operating criteria, FCO Spillway release was increased to 1530 m³/s (54000 ft³/s) due to forecasts predicting additional heavy precipitation. After the FCO Spillway flow was increased on February 7, unusual flow patterns and brown water were observed approximately half way down the chute. The FCO Spillway was immediately shut down to observe the chute condition (Fig. 3). Initial assessments of the FCO Spillway chute damage were made and additional technical resources were brought in to evaluate potential mitigation and protective measures that might be implemented. Forecasts were predicting significant reservoir inflows in the coming days. The emergency warranted that DWR activate the Oroville Dam Emergency Action Plan (EAP) to ensure that local, State, and Federal agencies were notified of the current incident.



Fig. 3 – Damage to FCO Spillway chute on February 7, 2017

Over the next hours and days, critical technical and regulatory teams arrived at the facility to assist with the assessment and development of mitigation measures, analyze risks, implement contingency plans, and update local agencies and the media. State and Federal regulatory agencies along with other specialized consultants were some of the first to arrive at the site to engage in these activities.

DWR's Oroville Field Division activated the Oroville Incident Command Team (OICT) in Oroville. The team began field-level emergency response activities, regular communications and coordination with the Project Operations Center (POC), and the DOC. The OICT first organized and developed staffing to assess the FCO Spillway and adjacent facilities, develop risk assessments, develop and implemented immediate mitigation measures, and communicate with partners, local agencies and officials, regulatory agencies, and other State and Federal agencies. The OICT was charged with managing all on-site emergency response activities with support from the DOC and the POC. All DWR resources were made available under a Department declared State Water Project Emergency.

The DOC management team was immediately set up and quickly addressed staffing and operational location questions/concerns. Full activation of the DOC was critical to coordinate, monitor, assess, plan, and respond to the very dynamic conditions at the Oroville Dam facility and the high-water conditions throughout the State. This was important to ensure that all DWR resources were tasked effectively and to ensure the public's safety.

DWR's Acting Director declared a Department Emergency on February 8, 2017, based on internal briefings and field verifications. These briefings provided extensive information regarding the status of the FCO Spillway chute damage, current and anticipated reservoir inflows, forecast reservoir elevations, and downstream infrastructure and potential threats to public safety. This declaration was done to ensure that all DWR resources were made available to respond to and recover from the incident. This declaration was critical to initiating the largest emergency response in DWR's history, and allowed re-tasking of DWR management and staff, consultants and contractors, and the use of emergency contracting for emergency services and resources not currently available.

The POC was also immediately activated in Sacramento to support the Oroville Dam Spillway Incident. The POC, in close coordination with the State Water Project Deputy Director and the DOC, was charged with providing State Water Project system-wide assessments, hydrology forecasts, reservoir routing, assessments of threats and response alternatives, cost forecasting, and executive briefings to DWR directorate and the State Operations Center (SOC). The POC was critical in managing the dynamic environment at the Oroville Dam facilities with close coordination with the Oroville Incident Command Team (OICT).

Figure 4 provides an organization chart for DWR's Emergency Operations Centers and the Incident Command Teams that were activated during the Oroville Emergency.

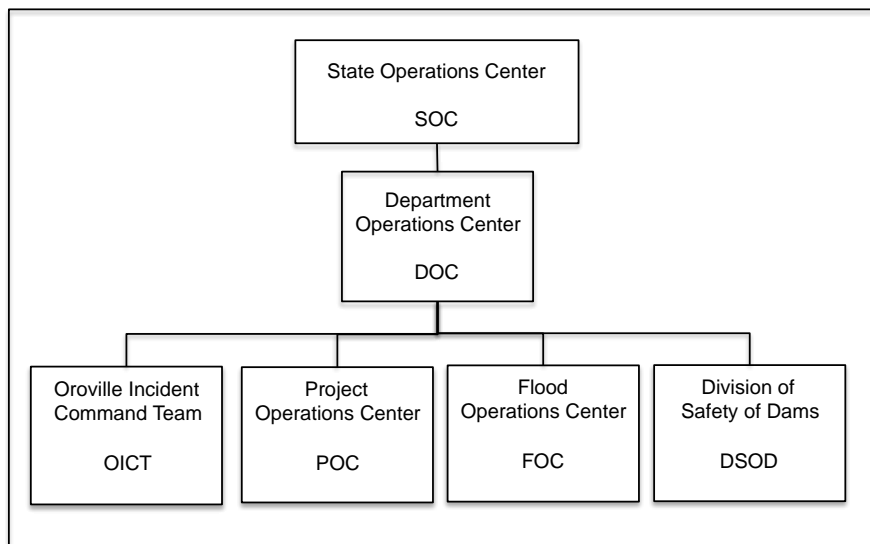


Fig. 4 Emergency Organizations for FCO Spillway Incident

On February 9, 2017, Butte County Sheriff Kory Honea contacted DWR's Acting Director to request direct communication with DWR during the emergency. The Acting Director traveled to Oroville Dam to assess the status of the FCO Spillway chute, related facilities, resource needs, and to ensure that the communication and organization concerns were being properly addressed. The Sheriff met with the Acting Director at the Incident Command Post (ICP) in Oroville and, in a short discussion, the Acting Director and the Sheriff quickly agreed to support each other and their respective missions, with the highest priority being public safety. This understanding and agreement was critical to the outcome of this extremely difficult and dynamic incident.

Organizations that are rarely involved in large emergencies do not have the real-world experience of emergencies, which cannot be fully replicated by training. This resulted in a limited number of experienced DWR staff that could fulfill critical EOC and ICT roles. During this period, it became clear that the ICT needed additional emergency management support, including emergency response personnel and emergency equipment. CalFire is the agency that routinely manages wildfire emergencies throughout the State of California and is very familiar with the incident command system. Therefore, CalFire was contacted at the Director level and was immediately activated to assist DWR in their ICT roles. A CalFire management team ramped up within a few hours and began setting up a CalFire incident command post. It was critical to quickly integrate the experienced CalFire management team into the DWR Oroville ICT to provide formal structure, communication and documentation process, and on-the-job training to existing and rotating DWR Oroville management and staff. Initial challenges included operational space, chain of command and control structure, internal and external communications, and developing a common understanding for the

threats, risks, and potential response actions for a dam safety emergency compared to a wildfire emergency. DWR Executives, Oroville ICT, CalFire, and the Butte County Sheriff met as a team to address situational awareness, identify critical next steps, and lay out a short process to form a Unified Command Team. The Unified Command Team formed between DWR, CalFire, and the Butte County Sheriff was critical to quickly address the chain of command at the local level, reinforcement of the ICT with strong SEMS processes, procedures and roles, and improve internal and external communication with other EOCs, the media, and the public.

Another critical component of the Emergency Management Team was the regulators responsible for overseeing dam owners and the safety of dams. Oroville Dam is regulated by two entities: the State of California Department of Water Resources' Division of Safety of Dams (DSOD) and the Federal Energy Regulatory Commission (FERC). In California, the DSOD takes a prominent role in the regulation and oversight of dams that fall under their jurisdiction. DSOD regulates about 1,250 dams in California and makes regular inspections, construction inspections, and dam re-evaluations. FERC regulates dams associated with the generation of hydroelectric power that are issued a license under their jurisdiction. FERC regulates these dams to assist the licensee in ensuring and promoting dam safety and following Federal dam safety requirements as well as general compliance with license requirements. FERC regulates approximately 2,500 dams throughout the United States and performs regular dam safety inspections, reviews and approves of any new construction or modifications to existing dams, performs construction inspections, and often requires independent consultant reviews of high and significant hazard projects.

State and Federal laws mandate that both the FERC and DSOD play an independent role in dam safety, including during emergency responses such as Oroville. During the emergency, both DSOD and FERC were available on-site 24/7. They participated in briefings, meetings, technical evaluations and other activities to be fully informed of threats, risks and proposed mitigation measures. Many DWR decisions to address the emergency required the regulators to be aware of, consulted with or approve. The regulators maintained authority to allow or disallow proposed actions resulting from those decisions. Even though the regulators were cooperative and collaborative during the emergency, they maintained a high level of independent oversight of DWR. Transparency offered by the DWR and the availability of the regulators allowed the response and recovery process to proceed in an expeditious manner. The regulators therefore played a critical role in the emergency response..

The United States Army Corps of Engineers (USACE) was also added to the Unified Command Team for their expertise in emergency dam repairs and support for decisions on reservoir operations. Their expertise in the development of response alternatives, risk assessments, technical capabilities, and implementation of mitigation measures was critical to the emergency response.

The Unified Command Team proved very effective in addressing response conflicts, improving communication to the media and the public, setting global priorities, and maintaining safety and security. Daily briefings and in-person meetings and frequent telephone conferences were held to ensure that the Unified Command Team maintained common response objectives, threats to the infrastructure, personnel and

the public were verified and understood, action plans were reviewed and a one-team, one-message environment was maintained.

Since February 7, 2017, over 950 DWR staff, working about 190,000 person hours, were activated to support the EOC and ICT response and recovery activities. Communication, command and control, and operational decisions continued to be a challenge and were a priority during the first 30 days or so. These challenges were addressed by: twice-daily status briefings, daily team meetings, written daily action plans, infrastructure condition verification by physical and remote monitoring, twice daily hydrology modeling, daily meetings with cooperators and contractors, and written daily reports submitted to the DOC and SOC.

5. BALANCING RISKS AND DECISIONS

5.1 FACTORS CONSIDERED

As the emergency system was being set up, the FCO Spillway was being assessed, resources were being drawn together, and critical decisions had to be made. After the initial assessment of the FCO Spillway chute damage was made, varying amounts of outflow were throttled through the FCO Spillway to determine what the impact might be on the damaged spillway. Over the next few days, varying test flows were released to assess the impact of the concrete chute failure on the ability to use the FCO Spillway to manage expected reservoir inflows. After considering a number of factors, including increasing reservoir inflows, increasing reservoir elevation, additional precipitation in the long-range forecasts, size and depth of the damaged chute area, inability to access the damage chute area, and no identified temporary repair options or protective measures available, it was decided that the FCO Spillway had to be used to manage reservoir inflows.

5.1.1 Decision Making Protocol

In any emergency, responders are faced with difficult decisions with limited information, assessments, and communication. There were a number of competing factors that made real time decision-making difficult during this emergency. Facing this dynamic incident, the DWR emergency response teams, regulators, consultants, and contractors and their supporting partners had to work together in ways that had not been accomplished in the past. An unfamiliar chain of command, changing command and control structures, critical specialists in remote locations, information and data limitations, safety and security, and the size and scope of the incident were some of the challenges. First and secondary potential impacts or damage to infrastructure and risks were continuously considered and reevaluated throughout the duration of the response to ensure public safety. Some of the early policy directives included transparency and communication with regulators, partners, local officials, responders, the public, and employees.

The DWR SEMS organization structure was the basis for decision-making during this incident. Daily and advance planning needed to consider response

actions, all threats and risks, contingency plans, and mitigation measures. Due to the complexity of the organization, it was critical to remind the team that decisions needed to be made within the organizational structure. Due to the size of the emergency, limited data, competing priorities and/or regional impacts, conflicting recommendations were occasionally passed along to decision makers. These more difficult decisions were elevated up to the POC, DOC, and the Acting Director of DWR. The following sections provide some examples of competing priorities and reasoning for some of the difficult decisions that had to be addressed.

5.1.2 FCO Spillway Chute Condition

The concrete within the FCO Spillway chute was being damaged and displaced with increasing flows and time. Water flowing down the FCO Spillway chute lifted large slabs of concrete, sending them down to the Feather River channel below. Weathered rock and adverse foundation conditions near the original spillway chute failure site were factors in the significant erosion of the underlying foundation rock. As the rock eroded, additional concrete was damaged and displaced. The failure propagated at a rapid pace, both in the upstream and downstream directions. The integrity of the FCO structure at the top of the spillway was critical to the safety of the dam and the potential for an uncontrolled release of the reservoir. Decision makers were also guarding against additional eroded rock in the tailrace, causing backwater affects to the Hyatt Powerplant, and the loss of the transmission line, resulting in the loss of the ability to release water from the reservoir through Hyatt Powerplant.

5.1.3 Emergency Spillway

The Emergency Spillway was intended to protect the dam from overtopping and was not intended to be used during normal flood operations. If ever engaged, the hillside downstream of the control section was expected to experience significant erosion. In addition to surficial soil, further debris such as the trees that covered most of the hillside, would wash into the river channel and would compound issues with downstream structures. Therefore, the use of the Emergency Spillway during this emergency needed to be avoided if possible.

5.1.4 Weather, Forecasts and Modeling

One of the most important aspects of the incident was the long collaborative working relationship DWR has with its mission critical partners. The National Weather Service in Sacramento and the California Nevada River Forecast Center are co-located with DWR at a Joint State Federal Operations Center (JOC) in Sacramento. This is the only location in the nation from which both Federal and State agencies provide weather forecasting, river and reservoir modeling, reservoir operations management, and management of flood emergencies. Working side-by-side 24/7 lays the foundation for a “One Mission, One Message” approach..

During this incident, DWR and its Federal partners at JOC were responsible for monitoring and for analyzing weather forecasts, river and reservoir flood routings,

and modeling of emergency response alternatives. Not only were emergency managers dependent on the weather forecasts, many local levee districts responsible for maintaining levees in the Sacramento Valley were working to assess downstream levee conditions, and to respond to potential levee threats resulting from the extreme weather and releases from the basin's reservoirs. Changing weather forecasts were immediately made available to the OICT, who had to quickly modify decisions due to changing weather conditions.

Having critical weather, modeling, and water managers in the same location and in close communication with the OICT allowed emergency response alternatives to be developed, assessed, vetted by the management team, and implemented in a timely manner.

5.1.5 Hyatt Powerplant

Protection of the Hyatt Powerplant and its connection to the State's electric power grid was one of the most difficult challenges that faced the DWR OICT. The loss of this facility would have been catastrophic to DWR and the Oroville Emergency Response and Recovery. Releasing sufficient water from the reservoir below the FCO Spillway's crest (sill) is virtually impossible without the use of Hyatt Powerplant. This would be critical to allow future repairs to the spillway. Secondly, local and State water supplies for agriculture and 25 million people could potentially be severely impacted for years ahead without the use of the Powerplant. There were two main issues associated with Hyatt Powerplant during the emergency: 1) high flows and debris in the tailrace caused backwater effects that limited the functionality of the Powerplant and caused flooding of the Powerplant; and 2) transmission towers, which secured power lines from the Powerplant, were located adjacent to the FCO Spillway chute and were in danger of collapse due to eroding the rock surrounding the two towers and loss of the tower foundations.

Due to the high water elevation in the Feather River channel from large spillway releases, compounded by the debris building up in the channel, the Powerplant had to be shut down. DWR OICT, pursuant to the facility Emergency Action Plan, and based upon previous experience during high FCO Spillway release events, were aware of potential damage due to backwater flooding of the Powerplant. Therefore, they immediately implemented a number of emergency mitigation measures. Waterproofing measures were continuously reassessed and additional improvements were made on an ongoing basis. These decisions were part of the daily action planning objectives implemented by the Hyatt Powerplant Operations Strike Team. Over time, additional risks were identified as the water elevation continued to increase on the downstream face of the Powerplant. As responder safety and maintaining waterproofing measures at the Powerplant were extremely critical, additional backup power supplies, pumps, and contract resources were stationed at the Powerplant. Around-the-clock monitoring, reassessment of water elevations, and mitigation measures were reported to the OICT Operations Chief.

As a result of these extreme efforts, the Hyatt Powerplant was successfully protected from the unprecedented high backwater caused by the incident.

The six turbines in the Hyatt Powerplant can only produce power when connected to the State's electric power grid. They also must be spinning and generating power in order to release water from the reservoir to the Feather River channel. The assessment of DWR's power lines and towers connecting the Powerplant to the power grid became a high priority since the loss of the power lines would prevent the ability to discharge up to 479.9 m³/s (16500 ft³/s) from the reservoir once the water dropped below the sill of the FCO. Monitoring and assessment teams became aware that continued erosion on the right (north) side of the FCO Spillway chute could compromise at least one of the transmission towers on the right side of the chute. The risk of losing this one tower was increasing and the impact could have resulted in the failure of numerous towers and power lines. This in turn increased the safety risks for responders and the possibility of losing the power grid connection to the powerplant for months, if not years. The OICT Commander ordered additional monitoring and risk assessments of this transmission tower as well as contingency and mitigation plans. It was determined that the tower power lines must be cut, and the tower removed to protect responders, prevent failure of multiple towers, and reduce the threat to the other high-voltage electric power in the area. These actions were approved by the OICT Commander, scheduled into working Actions Plans, coordinated with cooperating partners and the public, and then successfully implemented. Mitigation measures were then necessary to plan, design, and install shoe-fly power lines over the FCO Spillway chute away from the erosion threats. This process was completed with a high level of coordination with OICT Planning, Operations and Logistics teams, the FCO Spillway Strike Team, the Hyatt Powerplant Strike Team, the Emergency Spillway Strike Team, contractors, and the other power utility (Pacific Gas and Electric, PG&E). This work was successfully completed just as sufficient debris was removed from the Feather River channel to allow the water elevation to drop low enough for safe reoperation of the Hyatt Powerplant. This allowed DWR to begin releasing additional water from the reservoir and reduced the need to use the FCO Spillway for the remainder of the 2017 runoff season.

5.1.6 Electric Power Grid Considerations

An additional 230 kV electric power line, which is critical to California's electric power grid, crossed the Oroville Dam facility just downstream of the confluence of the FCO Spillway chute and the Feather River in the area of a large rock debris pile in the river channel. Debris removal was critical to getting the Powerplant back on line, but the use of tall equipment working in proximity to the transmission lines was an extremely high risk. Mitigation alternatives developed and implemented to protect the power lines and the electric power grid, which included flooding the barge and allowing it to sit lower in the water, drawing down the water elevation in the river

channel, removing some of the excavator cabin and roll bar, and adjusting the schedule to move the excavator. These actions were extremely important to preventing a major secondary impact to the utility, the statewide electric power grid, and public safety.

5.2 CRITICAL DECISIONS

There were continuous discussions by technical teams, OICT management, and DWR's Acting Director regarding "what if" scenarios, go/no go criteria for use of the FCO Spillway chute, reservoir inflow and releases, and forecasts of reservoir elevations. DWR's high priorities were responding to public safety, protection of the Hyatt Powerplant and power lines, continued use of the FCO Spillway chute, and avoidance of the use of the Emergency Spillway, if possible. Setting criteria for each of these priorities was very difficult and there was little room for error and little time for decisions. Monitoring and reevaluation of conditions and criteria for decision points was also difficult due to the nature of the changing conditions.

Considering the original weather forecasts, reservoir routing, current FCO Spillway chute and Feather River channel conditions, the expectation was to not allow Lake Oroville to exceed elevation 295.2 m (900 ft) or 0.3 m (1 ft) below the top of the Emergency Spillway crest. Thus, FCO Spillway releases were scheduled at 1,841 m³/s (65,000 ft³/s) February 10 at 1500 hours. DWR and its regulators were very concerned with the erosion of the FCO Spillway chute and the adjacent slopes. The erosion had not stabilized and there was concern that the foundation erosion and the concrete slab failure may migrate up the chute and threaten the operation of the FCO, leaving only the Emergency Spillway to manage the Feather River Basin's large runoff for the remainder of the record-breaking wet season. Due to concerns about additional erosion in and around the FCO Spillway chute and near the power lines and the closest tower, the FCO Spillway release was decreased to 1,559 m³/s (55,000 ft³/s) late on February 10. This spillway release rate was selected to limit the degradation of the FCO Spillway chute, yet prevent the Emergency Spillway from being used.

On February 11, Lake Oroville inflows significantly exceeded the forecast. The storm had unexpectedly stalled over the Feather River Basin watershed, causing a peak inflow of 5,395 m³/s (190,435 ft³/s). This inflow exceeded DWR's original expectations by approximately 850 m³/s (30,000 ft³/s). At this point, greater FCO Spillway releases would be necessary to avoid flow over the Emergency Spillway. However, because of the concerns discussed above, the decision was made not to increase the flows through the FCO. In addition to the FCO Spillway safety concerns at Oroville Dam, downstream levee capacity concerns also played into making this decision. On February 11, water began flowing over the crest of the Emergency Spillway and revised monitoring and contingency plans were quickly developed. Personnel were continually reminded that decisions and actions must stay within the OICT command and control structure for consistency and full cooperation with all those involved with this incident. The OICT and regulatory agencies were also

developing “what if” scenarios and working to reinforce the decision-making processes. Initially, erosion occurring downstream of the Emergency Spillway was within expected levels. . However, on February 12, significant erosion of the rock hillside was noted to be progressing more rapidly than anticipated to the point where it was considered a threat to the Emergency Spillway. This situation prompted an immediate meeting between the Butte County Sheriff, DWR’s Acting Director, OICT management, DSOD, and FERC. Suggestions, such as increasing the FCO Spillway release to 5949 m³/s (210,000 ft³/s) to stop flow over the Emergency Spillway, had to be rejected since that would exceed downstream levee capacities, causing flooding of downstream communities. Based on the best available data, including the FCO Spillway’s current condition, Powerplant flooding potential, the potential for erosion failure of the Emergency Spillway, and continual forecasts, the DWR’s Acting Director agreed to increase FCO Spillway releases to 2832 m³/s (100,000 ft³/s). With the flow through the FCO Spillway increased to 2832 m³/s (100,000 ft³/s) February 12 at 1800 hours, the flow over the Emergency Spillway stopped several hours later.

DWR maintained the FCO Spillway release at 2832 m³/s (100,000 ft³/s until February 16. On February 16, the Lake Oroville water elevation dropped low enough for the Butte County Sheriff to change the mandatory evacuation to an evacuation warning, allowing an estimated 188,000 people to return to their homes and businesses.

Emergency repairs were developed and implemented, using air and ground resources. It was critical to repair the erosion damage below the Emergency Spillway in case it had to be used again. These emergency repairs to the Emergency Spillway consisted of filling erosion voids and armoring the ground surface. However, they were viewed as temporary, based on limited information, planning, and design. Fortunately, the Oroville Emergency Recovery team was onsite 24/7 and was able to collect advance-planning data and information as the damaged area was being backfilled and armored. This response effort was extremely large, yet simple in approach and had no planned stopping point set. DWR Executive management, in close coordination with DSOD and FERC, addressed terminating the Emergency Spillway repairs based on available reservoir storage, forecast, and the amount of completed temporary repair work.

6. COMMUNICATION AND TRANSPARENCY

6.1 COMMUNICATION

As in every emergency, effective and timely communication is critical. DWR faced many challenges in this regard. Communicating technical and nontechnical information relating to changing weather conditions and forecasts, reservoir, dam and spillway conditions, dynamic situational awareness, and associated risks proved to be difficult.

DWR communication resources were limited and had little experience with emergency process and procedures. Under the Unified Command, CalFire brought significant emergency communication resources (people and equipment) and set the processes, procedures, and schedules in place. Call centers, standardized graphics and public messaging were key communication improvements. Integrating DWR and its contractors into the process provided effective on-the-job training. When CalFire demobilized out of the Oroville ICP, they left a much more effective emergency communication team.

Many communication tools and activities were used to inform the responders, partners, other agencies, the media and the public. Global phone lists, written communication plans, set briefing schedules for responders, cooperating partners, the media and the public, public web cameras, daily photographs and drone videos, improved websites and incident websites, radio and television interviews, and live streaming media briefings and public meetings were all used during the Oroville Emergency Response phase. These tools continue to be used and improved during the Emergency Recovery phase.

6.2 TRANSPARENCY

From the beginning, DWR's Acting Director instructed management and staff to be transparent in responding to and recovering from this incident. This proved difficult in the first few days due the changing conditions of the incident, integration of a number of agencies, implementing the command and control organization and magnitude of the emergency and had to be regularly reinforced over time. Due to the size, scope, and public safety concerns of the incident, a number of normal design and regulatory process and procedures had to be modified. DWR took a high intensity, short duration, and no-fail approach to design and implementation of both short-term repairs and long-term recovery actions. This had to be done with DSOD and FERC regulators in the room to facilitate expedited design review and necessary approvals. This is easy to say but was difficult to implement for the processes and procedures that typically take weeks, if not months or years to complete, coupled with limited available staff, location of key specialists, and required third-party oversight. A project of this size, scope, and schedule had never been completed before and required unprecedented commitment by DWR, consultants, DSOD, and FERC, as well as the Independent Board of Consultants and DWR's other partners.

Transparency was also an important concern to the local agencies and the public. DWR took many actions to improve transparency via its communication and outreach procedures. DWR also ensured that the regulatory agencies, the Independent Board of Consultants, the Independent Forensic Team, and the Butte County Sheriff had full access to the facility and its records. Special tours were provided to Federal, State, and local elected officials on a regular basis. Transparency will remain a critical element toward improving communication with regulatory agencies and the public. Dam owners and operators should review their plans, policies, and procedures in advance of an incident to address transparency in such communications.

Transparency was often in conflict with security concerns and the need to protect Critical Energy and Electric Infrastructure Information (CEII). Any time information was held back due to security concerns, there was potential for the public and media to become uncomfortable or alarmed by the lack of full disclosure.

7. EMERGENCY RECOVERY

As is standard practice in emergency management, immediately after the initial incident, DWR began pulling together the Oroville Emergency Recovery (OER) team. It was critical for DWR and its partners to recognize OER had to be quickly mobilized even as conditions and risks to the facility were changing. DWR maintained an emergency management approach during recovery to successfully meet its primary and secondary objectives: an operational FCO Spillway structure by November 1, 2017, and full recovery of the FCO Spillway chute and the Emergency Spillway by January 1, 2019, respectively. Additional discussion and figures regarding various aspects of the Oroville Emergency Recovery efforts are provided in the accompanying DWR papers.

8. LESSONS LEARNED

There have been many valuable lessons learned during this incident. Emergency management systems, policies, and procedures need to be in place and are an essential part of risk reduction programs. Integrating external emergency management partners into the response and recovery efforts under a unified command organization proved very successful. Partnering in advance of an incident with strategic emergency experts would improve response and recovery efforts. It is also critical to have State and Federal emergency management agencies fully onboard and engaged with a project's EAP with annual training as well as functional exercises on a regular basis.

Having facility experts available and on-site during this incident was invaluable. Understanding details of siting, permitting, construction, maintenance,

operations, and management of the facility were critical to assessing risks, mitigations, and potential response actions. Taking a new look at this information is critical to assessing risk and consequences. Fortunately, DWR had immediate access to consultant experts, who were familiar with the facility and the issues of concern. Dam owners should identify critical consultant resources prior to an incident as part of their risk reduction program.

Protection of CEII information is critical for national and economic security, as well as for public health and safety. However, protection of this information will likely be in conflict with efforts to increase communication and transparency. CEII policy review, following policy and third-party education, should reduce this conflict.

Finally, while the Oroville Dam facility is an amazing example of engineering for multiple benefits, this incident is an example of how critical infrastructure can have unanticipated impacts on those benefits and the costs to respond and recover from a major incident. This incident has refocused California on the need to improve infrastructure and ensure its safety and reliability. California has turned the corner on this conversation, and now it is time for action.

SUMMARY

The Oroville Spillway incident was unprecedented in many ways. This “no notice” event brought many difficult challenges and risks that needed to be assessed, verified and mitigated during an historic hydrologic setting. Public safety (responders and the public) has to be the highest priority at all times. The incident required the dam owner, to work side by side with regulators, subject matter experts and contractors in real time to respond and recover from this incident. Maintaining a high level of transparency with the regulators and the public throughout the response and recovery phases allowed decisions and actions to be taken to mitigate or eliminate risks to the public and infrastructure. DWR, FERC, USACE, Cal Fire, and Butte County Sheriff Office quickly and successfully integrated into a unified command organization structure. The California emergency management plans demonstrated that multiple agencies and their contractors could be activated and respond to major catastrophic events in a matter of hours. There are many lessons that can be learned from this event. A new look at infrastructure risk management, security, emergency action plans, emergency training and public education is required. This incident is also an example that large complex infrastructure projects can be designed and constructed in an expedited manner. To repair, replace or improve today’s critical infrastructure in a timely manner, processes to complete projects must be streamlined.

This paper recognizes the hundreds of people who participated in this challenging emergency and in some cases at great personal risk to work for public safety.

REFERENCES

- [1] DILLON, J., ROGER, M., CRADDOCK, T., DRILLER, M., STRAHM, M., FRIESEN, S. Oroville Dam Spillway Incident – Roller Compacted Concrete Influences On Recovery Structural Design Features
- [2] CRADDOCK T., HARDER L., VERIGIN S., KUTTEL J., BROWN D., MIHYAR M., BOYER D. Oroville Dam Spillway Incident – Fast Track Recovery Design to Address Critical Dam Safety.
- [3] NICHOLS, H., GRAY, M., HALL, C., KUTTEL, J., and CRADDOCK, T. Oroville Dam Spillway Incident – Geological and Geotechnical Investigations for Recovery Design Features
- [4] PANDEY, G., FORD, D., CRADDOCK, T., WHITE, M., FORTNER, M., LEAHIGH, J., ANDERSON, M. Oroville Dam Emergency Response and Spillway Restoration – Hydrologic and Hydraulic Engineering Activities to Inform Operation and Design
- [5] Emergency Response Plan 2006 California Department of Water Resources
- [6] California State Emergency Plan 2107, California Governor's Office of Emergency Services
- [7] California Water Code
- [8] Oroville Dam Emergency Action Plan, California Department of Water Resources

KEY WORDS

CHUTE, COMMUNICATION, COMMUNITIES, CONCRETE DAM, CONSTRUCTION, CREST, CORRECTIVE ACTION, DAM, DAM OPERATION, DAMAGE, DEPARTMENT OPERATIONS CENTER, DESIGN, DISCHARGE, EMERGENCY ACTION PLAN, EMERGENCY OPERATIONS CENTER, FLOOD CONTROL, FLOW, FCO SPILLWAY, FORCAST, HYDRAULIC, HYDROLOGY, INFRASTRUCTURE, INCIDENT COMMAND TEAM, INCIDENT COMMAND POST, LEVEE, MAIN SPILLWAY, MITIGATION, OPERATION, OUTLET DISCHARGE, OUTLET STRUCTURE, POWERPLANT, PROTECTIVE MEASURES, PUBLIC SAFETY, RECOVERY, REGULATION, REPAIR, RESERVOIR, RESERVOIR OPERATION, RESPONSE, RUNOFF, SAFETY, SPILLWAY, SADDLE DAM, TRANSPARENCY, UNIFIED COMMAND

COMMISSION INTERNATIONALE DES GRANDS BARRAGES

VINGT-SIXIÈME CONGRÈS DES GRANDS BARRAGES
Autriche, juillet 2018

DOI 10.3217/978-3-85125-620-8-003



This work licensed under a Creative Commons Attribution 4.0 International License. <https://creativecommons.org/licenses/by-nc-nd/4.0/>

**OROVILLE DAM SPILLWAY INCIDENT- FAST-TRACK RECOVERY DESIGN
AND CONSTRUCTION TO ADDRESS CRITICAL DAM SAFETY**

Ted CRADDOCK

Project Manager, STATE OF CALIFORNIA, DEPARTMENT OF WATER
RESOURCES

Leslie HARDER

Deputy Design Branch Chief, HDR ENGINEERING, INC.

Stephen VERIGIN

Deputy Project Manager, GEI CONSULTANTS, INC.

Jeanne KUTTEL

Chief, Division of Engineering, STATE OF CALIFORNIA, DEPARTMENT OF
WATER RESOURCES

Dale BROWN

Deputy Project Manager, STATE OF CALIFORNIA, DEPARTMENT OF WATER
RESOURCES

Mutaz MIHYAR

Oroville Spillway Recovery Program Manager, STATE OF CALIFORNIA,
DEPARTMENT OF WATER RESOURCES, DIVISION OF SAFETY OF DAMS

Douglas BOYER

Chief, Risk-Informed Decision Making Branch, UNITED STATES, FEDERAL
ENERGY REGULATORY COMMISSION

UNITED STATES OF AMERICA

**OROVILLE DAM SPILLWAY INCIDENT- FAST-TRACK RECOVERY DESIGN
AND CONSTRUCTION TO ADDRESS CRITICAL DAM SAFETY***

Ted Craddock
Project Manager, State of California, Department of Water Resources

Leslie Harder
Deputy Design Branch Chief, HDR Engineering, INC.

Stephen Verigin
Deputy Project Manager, GEI Consultants, INC.

Jeanne Kuttel
Chief, Division of Engineering, State of California, Department of Water Resources

Dale Brown
Deputy Project Manager, State of California, Department of Water Resources

Mutaz Mihyar
Oroville Spillway Recovery Program Manager, State of California, Department of Water Resources, Division of Safety of Dams

Douglas Boyer
Chief, Risk-Informed Decision Making Branch, United States, Federal Energy Regulatory Commission

UNITED STATES OF AMERICA

1. INTRODUCTION

Oroville Dam is located on the Feather River in northern California (USA). At 234.7 m (770-ft) tall, this earth embankment is the tallest dam in the United States. With its 4.3 billion m³ (3.5 million acre-feet) of storage, Lake Oroville is the second largest reservoir in California, supplying water to cities as far south as Los Angeles. The Oroville Dam, reservoir (Lake Oroville), and hydropower plant facility is the flagship of the State Water Project (SWP), which is owned and operated by the State of California, Department of Water Resources (DWR).

* *INCIDENT DE DÉVERSEMENT DE BARRAGE D'OROVILLE - CONCEPTION ET CONSTRUCTION DE RÉTABLISSEMENT RAPIDE DE PISTE POUR COMBLER LA SÉCURITÉ DES BARRAGES CRITIQUES*

The 2016-2017 Winter Storms brought record breaking precipitation to the Northern California Sierra mountains including the Feather River watershed. On February 7, 2017, the Oroville Dam's 54.5 m (179-ft) wide Flood Control Outlet (FCO) Spillway chute (Fig. 1) was releasing water to control the Lake Oroville reservoir level in accordance with the prescribed operations plan. During this operation, the FCO spillway suffered a catastrophic failure of the lower chute area eventually resulting in the loss of approximately 427 m (1400 ft) of the lower chute, including the scour of more than 1.2 million m³ (1.6 million yd³) of soil and rock materials. On February 11, 2017, the Emergency Spillway (Fig. 1) was used for the first time since the project was completed in 1968. During this operation, significant erosion and scour caused by the Emergency Spillway overflow led authorities to fear for the safety of the spillway structures, resulting in the activation of the Emergency Action Plan and evacuation of about 188,000 persons from downstream communities.

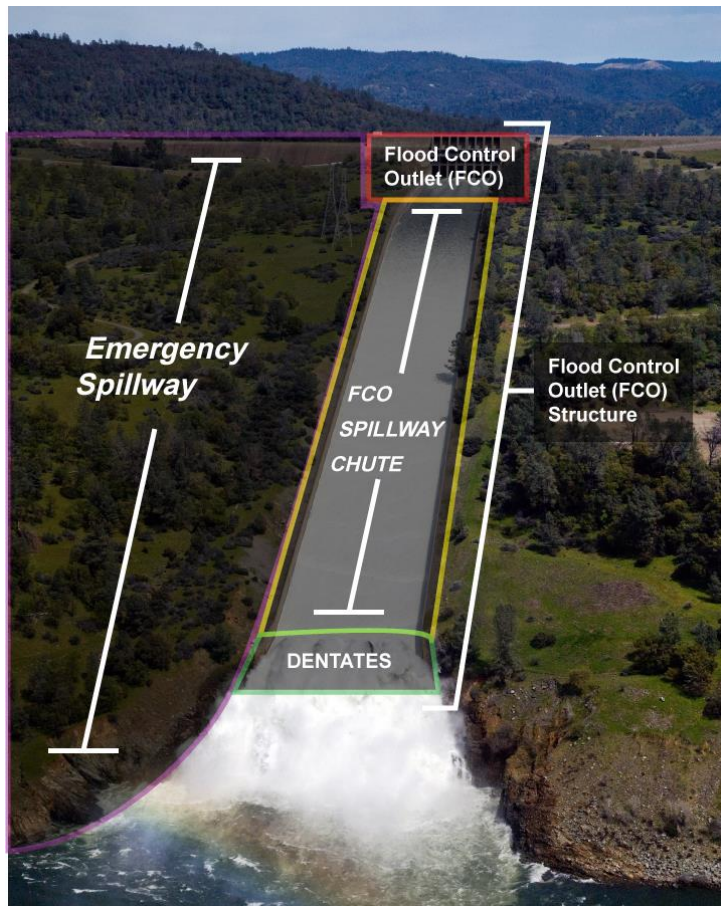


Fig. 1 Flood Control Outlet (FCO) Structure and Emergency Spillway, March 2011

This paper is part of a series developed by the State of California, Department of Water Resources (DWR) to describe the Oroville Spillway Incident Emergency Response and Recovery. This paper focuses on the design and construction processes employed in 2017 to safely allow the dam to pass

expected flood flows during the 2017-2018 Winter Flood Season. The remainder of this paper is organized into the following sections:

- Meeting the Challenges for Spillway Recovery
- Design and Construction Processes
- Regulatory Review
- Reservoir Operations
- Meeting the Schedule
- Lessons Learned

2. MEETING THE CHALLENGES FOR SPILLWAY RECOVERY

2.1. THE CHALLENGES

The management of the Oroville Dam Spillway Incident in February 2017 and in the ensuing months was considered by DWR as the Oroville Emergency Response [1]. The restoration work following this initial effort was known as Oroville Emergency Recovery (OER). The charge for the OER was to restore adequate capacities for the FCO Spillway chute and the Emergency Spillway to safely pass potential flood events during the 2017-2018 Winter Flood Season, and thereafter. This charge presented enormous challenges, including:

- The need to complete repair and replacement designs in only weeks instead of the normal months or years,
- Insufficient qualified DWR staff available,
- Insufficient geologic information,
- The need to operate the damaged FCO Spillway chute through May 2017,
- Limited time for regulatory review and approval of designs,
- Insufficient time to construct complete repairs or replacements,
- Lack of a full understanding as to the causes of the incident, and
- Managing expectations and communicating accurate information to a concerned public and their elected representatives.

2.2. ASSEMBLING THE TEAM

For the Oroville Emergency Recovery, DWR quickly assembled the OER Spillways Task Force devoted to completing the FCO Spillway chute and Emergency Spillway recovery designs, administering construction contracts, and developing a revised reservoir operations plan. The team was composed of several experienced engineers from DWR's Division of Engineering, Project Operations Office, and other units from within DWR. However, there were insufficient staff available from within DWR to perform the necessary engineering work. As a result, DWR contracted with knowledgeable and experienced engineering professionals from a variety of sources including:

- Engineering consulting firms: GEI Consultants, HDR Engineering, Stantec, AECOM, David Ford Consulting Engineers, Northwest Hydraulic Consultants, Lettis Consultants International, Vali Cooper & Associates, and RMA Group.
- United States Army Corps of Engineers and United States Bureau of Reclamation.

In addition to the engineering professionals directly integrated into the OER team, several specialty consultants were added to the OER team to provide specific engineering services:

- Brierley Associates to provide expert peer review evaluations of rock slope stability and planned stabilization of eroded and over-steepened rock slopes along the FCO Spillway chute channel,
- BGC Engineering USA to provide scour evaluations of the rock materials on the Emergency Spillway,
- REVEY Associates, Inc. and EROCK Associates to provide engineering designs and oversight for explosive blasting excavation and demolition, and

Utah State University to provide physical hydraulic modeling for the redesign of the FCO chute. Over 100 individuals were eventually integrated into the OER team, with most initially assigned to work together in spaces provided in the California Natural Resources Building in Sacramento, California. Many members of the team were later relocated, as needed, to Oroville Dam during field investigations and during construction later in 2017. Team members commonly worked 12+ hours each day, 6 to 7 days a week. Key points in the timeline were as follows:

- Oroville Incident and Emergency: initiated February 7, 2017
- OER Design Phase: March – July 2017
- OER Mobilization Phase: April – May 2017
- OER Construction Phase 1: May – November 2017

2.3. PROJECT OBJECTIVES

The original design intent of the FCO Spillway chute was to safely pass flood flows ranging up to about 7390 m³/s (261,000 ft³/s) without using the Emergency Spillway. During larger floods, the Emergency Spillway would also be used to pass flood flows for events up to the Probable Maximum Flood (PMF), a very rare event that had an average recurrence interval commonly on the order of 10,000 years. The total discharge from the FCO Spillway chute and the Emergency Spillway during the PMF event would be about 19000 m³/s (671,000 ft³/s), with the FCO Spillway chute being used to pass flows up to 8500 m³/s (300,000 ft³/s) and the Emergency Spillway being used to pass about 10500 m³/s (371,000 ft³). The purpose of being able to pass the PMF event is to prevent the embankment dam from being overtopped and failing during this extreme design

event. Following the incident, the FCO Spillway lower chute was left badly damaged and the Emergency Spillway was found to be incapable of safely passing even 340 m³/s (12,000 ft³/s).

The mission of OER was to develop and implement measures to:
“Restore the Spillway Capacity to Ensure Public Safety in Advance of the 2017-18 Winter Flood Season.”

It was recognized early on that the full restoration or replacement of the damaged areas would require multiple phases and years, in part because the first design and construction season in 2017 was extremely short – only about 8 months between March 1, 2017 and November 1, 2017, which was the assumed onset of the 2017-2018 Winter Flood Season. Accordingly, the first phase would include structural replacements, modifications, and other remedial measures to rebuild the existing spillway structures to safely pass water flows for the upcoming 2017-2018 Winter Flood Season. Later phases will increase the level of protection incrementally each year until the original design capacities are restored. Later phases are estimated to require as much as 5 to 10 years to complete. The specific design objectives for the 2017 construction season were set as follows:

- The reliable capacity of the relatively undamaged the FCO Spillway upper chute, approximately 488 m (1600 ft) in length between the upstream gated headworks and the main scour hole, would be restored to safely pass a peak discharge flow of 7600 m³/s (270,000 ft³/s).
- The capacity of the damaged FCO Spillway lower chute, approximately 427 m (1400 ft) in length, would be restored to safely pass a peak discharge flow of approximately 2800 m³/s (100,000 ft³/s), and up to 7600 m³/s (270,000 ft³/s) with potential damage.
- The capacity of the Emergency Spillway would be restored to safely pass a limited flow of up to 850 m³/s (30,000 ft³/s) without significant damage to the spillway monoliths and weir, but erosion further downslope would be expected.

These 2017 spillway design objectives are illustrated in Fig. 2 (flows shown in cubic feet per second – cfs).



Fig. 2 2017 Oroville Spillway Recovery design objectives projected onto an aerial view of the damaged spillways at Oroville Dam

2.4. EXPEDITED ALTERNATIVE ANALYSES

On March 6, 2017, less than one month after the beginning of the incident, an all-day alternatives workshop was conducted by DWR at the California Natural Resources Building in Sacramento. The purpose of the workshop was to develop reinforcement and replacement alternatives to restore the FCO Spillway chute and the Emergency Spillway to meet the 2017 design objectives by November 1, 2017. Several restoration concepts were proposed for the FCO Spillway chute and for the Emergency Spillway.

2.4.1. FCO Spillway Chute Alternatives

The FCO Spillway chute is a reinforced-concrete spillway approximately 54.5 m (179 ft) wide and 914 m (3000 ft) long. Alternatives for the relatively undamaged 488 m (1600 ft) long FCO Spillway upper chute above the scour holes included:

- Repair-in-place
- Remove and replace
- Construct new FCO Spillway upper chute

The 427 m (1400 ft) long FCO Spillway lower chute was heavily damaged by the incident. The damage included two deep scour holes as much as 30 m (100 ft) in depth, including a large scoured erosion channel to the left of the FCO Spillway lower chute, and severely distorted, broken concrete walls and invert slabs downstream of the scour holes (see Fig. 2 and 3).



Fig. 3 Aerial view of heavily damaged FCO Spillway lower chute (March 2017)

Alternatives for the heavily damaged FCO Spillway lower chute included:

- Remove, backfill, and replace
- Leave scour holes and erosion channel in place for spillway discharges and only armor sides and bottoms of eroded areas
- Construct bridge/aqueduct across scour holes
- Construct new FCO Spillway chute

These alternatives were further refined and evaluated by OER team in the days following the workshop. Some alternatives were modified or combined with others, while some were eliminated because they did not meet the project objectives, or were simply infeasible. A set of ranking criteria and weighting was developed to evaluate the alternatives. Following the evaluation and ranking of alternatives, the measures recommended for immediate implementation for the FCO Spillway chute were as follows:

- The entire FCO Spillway chute, including both the undamaged upper portion and the heavily damaged lower portion, should be completely removed and replaced with new reinforced-concrete walls and invert slabs constructed to modern spillway design standards.
- The removal and replacement of the upper chute should proceed by completing as much as could be done by November 1, 2017, in time for the 2017-2018 Winter Flood Season, with the remaining portion

of the upper chute replaced the following year, during the 2018 construction season.

- The eroded scour holes in the FCO Spillway lower chute should be filled with roller-compacted concrete (RCC) to restore the eroded spillway rock foundation (see Fig. 4). The damaged concrete chute walls and invert panels in the lower chute should also be removed, and new structural-concrete sections (chute slabs/panels and walls) should be constructed to modern standards for the entire lower chute. If the entire lower chute could not be restored by November 1, 2017, the construction work should be sequenced to defer backfilling of the initial scour hole in order to use the scour hole and the erosion channel to convey spillway discharges from the upper chute to the Feather River.

These measures were accepted by DWR management and an Independent Board of Consultants in mid-March 2017 and designs were initiated immediately. During the design and 2017 (Phase 1) construction phases, the limits for specific measures on both the upper and lower chutes were modified several times as a result of improved understandings of the work involved, various constraints, and what the construction contractors could accomplish during the very abbreviated 2017 construction season. The alternative measures finally adopted for repair and replacement of the upper and lower chutes, during the 2017 and 2018 construction seasons, are illustrated in Fig. 5 and Table 1.

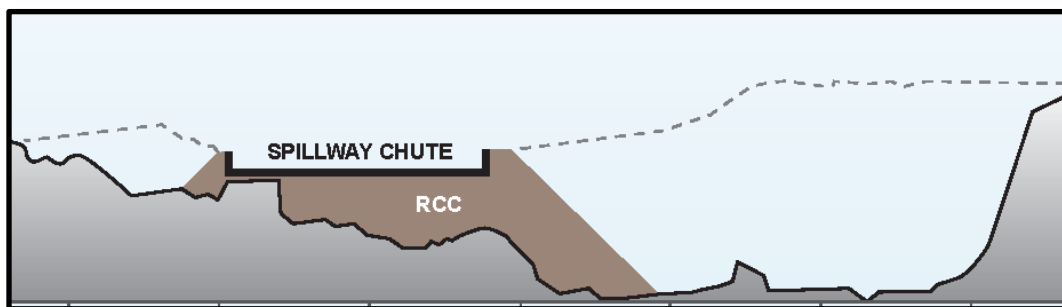


Fig. 4 Conceptual cross section for reconstructing the eroded the FCO Spillway lower chute using Roller Compacted Concrete in 2017

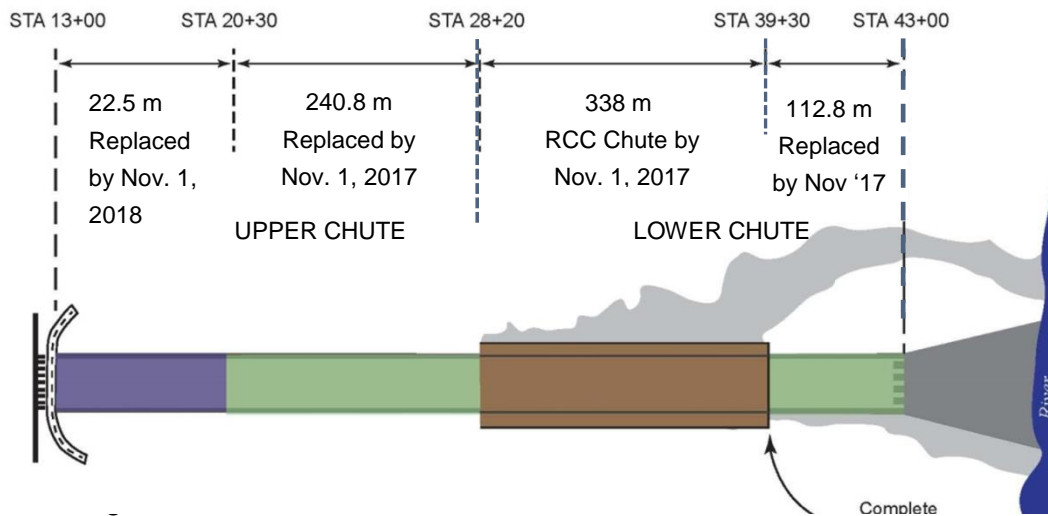


Fig. 5 Plan view of 2017 and 2018 repair/replacement alternative measures for the FCO Spillway chute

Table 1
2017 and 2018 Repair/Replacement Measures for the FCO Spillway chute

FCO Spillway Chute Reach	Stationing (feet)	Length (feet)	Length (meters)	2017 Construction	2018 Construction
Upper Chute	13+00 – 20+30	730	222	Minor repairs	Replacement
	20+30 – 28+20	790	241	Replacement	-
Lower Chute	28+20 – 39+30	1110	338	RCC Backfill	Structural concrete
	39+30 – 43+00	370	113	Replacement	-
Total	13+00 – 43+00	3000	914	Replacement	

2.4.2. Emergency Spillway Alternatives

The Emergency Spillway is an ungated monolith/weir structure that is approximately 527 m (1730 ft) wide at the weir crest. The left 283 m (930 ft) portion consists of concrete-gravity ogee monoliths/weir sections that were keyed into slightly-weathered rock. The structural heights of the monoliths range as high as 27 m (90 ft). The right 244 m (800 ft) portion is a cut section with a small 30 cm (1-ft) high concrete ogee weir. During the Oroville Spillway Incident, there was great concern that rapidly developing head-cutting erosion under a relatively

small discharge of 340 m³/s (12,000 ft³/s) could quickly lead to destabilizing these monoliths/weir sections and result in an uncontrolled release of the reservoir (see Fig. 6). There had also been concern regarding the sliding stability of the larger monoliths during extreme flood events and seismic loadings.



Fig. 6 Aerial view of head-cutting erosion threatening the Emergency Spillway monoliths/weirs during the Feb. 12, 2017 spillway releases

Four alternatives were considered during the initial alternatives analysis phase for the Emergency Spillway. All four alternatives included: a buttress or a rock-anchoring system for the larger monoliths, replacement of the small 30 cm (1-ft) high weir on the right side of the Emergency Spillway, a concrete apron or splash pad for erosion protection over the rock surface for About 100 meters downstream of the monolith/weir sections, and a secant pile wall located at the downstream edge of the concrete apron to protect the apron from undermining by head-cutting erosion. The four alternatives were evaluated and ranked, using the same criteria that were used for the FCO Spillway chute alternatives, and the following measures were selected for the Emergency Spillway:

- An RCC buttress on the downstream side to reinforce the larger monoliths/weir sections (2018)
- A 2 m (6-ft) high concrete wall/weir crest to replace the small 30 cm (1-ft) high weir on the right side of the Emergency Spillway (2017)
- An RCC apron downstream of monoliths/weir sections (2018)
- A secant-pile wall at the downstream edge of the RCC apron (2017)

The selected measures for the Emergency Spillway's monoliths/weir sections are illustrated in Fig. 7. The 2-m-high concrete crest on the right side of the Emergency Spillway and the secant pile wall were to be constructed primarily in the 2017 construction season, but unlike the measures for the FCO Spillway

chute, the completion of these features could extend a few months into the 2017-2018 Winter Flood Season if the FCO Spillway chute measures were completed by November 1, 2017. The RCC buttress and apron would be completed during the 2018 construction season.

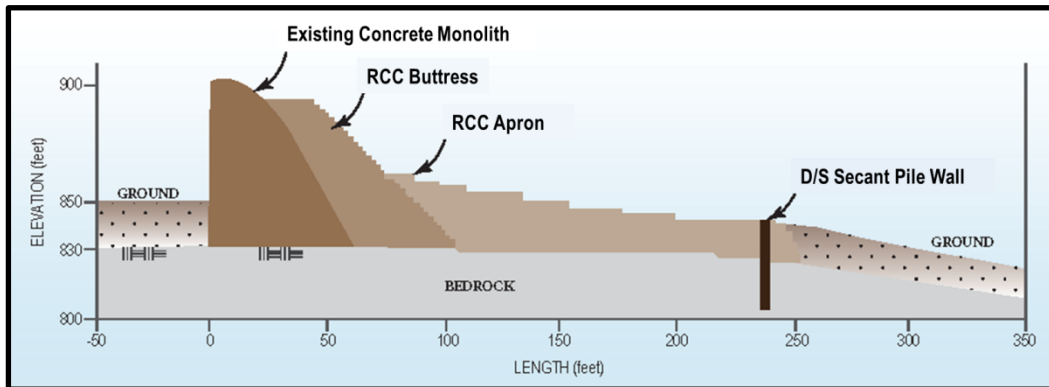


Fig. 7 2017 and 2018 repair/improvement monoliths/weir measures selected for Emergency Spillway

3. DESIGN AND CONSTRUCTION PROCESSES

3.1. CONSTRUCTION CONTRACTING APPROACHES

During the Emergency Response phase, several construction contracts had been awarded by DWR to help manage the emergency, including contracts to temporarily armor the Emergency Spillway and for dredging the Diversion Pool (Feather River) immediately below the FCO Spillway chute and dentates to remove eroded rock and concrete [1]. However, the restoration work under OER could not begin immediately after the incident occurred in February because: (1) the FCO Spillway chute had to be used intermittently between February and May to release the record reservoir inflows to avoid use of the eroded Emergency Spillway, thus preventing any work on this facility until late May; and (2) the designs for the various repair/replacement measures were not yet developed or approved by dam safety regulatory agencies. Yet there was a critical need to start recovery work as soon as possible given the very short 2017 construction season. As a result, DWR proceeded with the following approach:

- An initial construction contract (Specification No. 17-08) was advertised on March 21, 2017, and awarded to Teichert Construction on March 27 for a low-bid amount of \$5.8 million. This first contract was used to construct access roads and staging areas that would be used later for the FCO Spillway chute recovery work. It was also used for the initial excavation work around the upper portions of the scour holes to help stabilize the slopes so that construction work could be safely done beneath the overly steep

and unstable rock slopes. This work was defined by 28 contract drawings and 20 specification sections.

- The Oroville Emergency Recovery contract associated with the spillways (Specification No. 17-09) was advertised on March 31 and awarded to Kiewit Corporation on April 15 for a low-bid amount of \$275 million. This was the main construction contract for completing the work identified to restore the spillway capacities in 2017 and 2018. The Contractor's bid was based on a 30-percent design with 108 contract drawings and 47 specification sections. The purpose for awarding the contract without a completed design was to have a contractor on board to begin mobilization and preliminary work as soon as possible, even though the designs were not completed and the FCO Spillway chute was still being operated intermittently until its final closure on May 19. The contractor was given a Notice to Begin Work on April 20, with 75-percent designs provided on May 18, Final designs provided on June 21, and Revised Final designs provided on July 20. The major elements of work in this contract included:

- Slope stabilization
- Demolition of reinforced-concrete chute walls and slabs
- Foundation excavation
- Foundation cleanup
- Dental and leveling concrete construction
- RCC construction (FCO Spillway chute)
- FCO Spillway chute drains construction
- Structural reinforced-concrete construction
- Chute slab anchors construction
- Crest concrete wall construction (right side of Emergency Spillway)
- RCC buttress and apron construction (Emergency Spillway)
- Secant pile wall construction (Emergency Spillway)

With the approaches described above, it was recognized that the original bid amount would likely increase, possibly by 50 to 100 percent.

A formal, facilitated partnering process was agreed to between DWR and the contractor (Kiewit Construction/Corporation) for the Spillways, Oroville Emergency Recovery contract, as called for in the contract specifications. Following the Award of the Contract, the Partnering Team developed and signed a Partnering Charter on April 24 that laid out project and partnering goals. The Partnering Team had bi-weekly Executive Partnering sessions and quarterly team meetings to help foster a cooperative relationship. Surveys of the Partnering Team members were conducted every two weeks in advance of the Executive Partnering sessions that helped provide a pulse for the project and facilitated information exchanges and issue resolutions.

3.2. DESIGN APPROACHES

3.2.1. *General Design Approach*

Design work was completed by forming multi-disciplined sub-teams assigned to specific design tasks, such as determining slope stabilization methods, excavation depths, foundation objectives and treatments, underdrain designs, structural concrete designs, RCC designs, and secant pile wall designs. Leads and members of the sub-teams were organized beginning on March 6. Eventually, over 100 professionals were involved in developing over 50 design technical memorandums and contract plans and specifications. The work for the preliminary designs was generally completed in Sacramento, with final designs being completed by moving design team members to work on-site in Oroville. This latter work was facilitated by mobilizing over a dozen portable trailers with communication and computer equipment to a large parking area adjacent to the Emergency Spillway. This allowed the design groups to be co-located with the contractor's (Kiewit's) forces and to be on-site as the construction work was being done. This also helped obtain expedited dam safety regulatory approval as the designs were being finalized and the construction work was being completed, as dam safety regulatory staff (FERC, DSOD) were provided temporary office space in the trailers.

3.2.2. *Geologic Investigations*

During the original design, boreholes had been completed along the FCO Spillway chute alignment and along the monoliths/weir sections of the Emergency Spillway. There were also very detailed geologic maps of the FCO Spillway chute and the monolith foundations completed during original construction, but relatively little detailed geologic information was available on the Emergency Spillway area downstream of the monoliths/weir sections. Geologic investigations carried out in 2017 for the OER are described in detail in a companion paper [2]. The 2017 geologic explorations included the use of 10 drill rigs to complete over 104 new borings, install 26 piezometers, and install 15 inclinometers, all by the end of July 2017. In addition, 22 seismic refraction lines were completed, and extensive geologic mapping of exposed rock was carried out at both spillways.

The geologic investigations confirmed that the rock foundation at both spillways consisted generally of amphibolite with varying degrees of weathering. The degree of weathering ranged from intensely weathered or decomposed to fresh, with most of the surface exposures consisting of moderately-weathered rock. There were also numerous shears across both spillways, which significantly contributed to both slope instability and erosion problems. Along the FCO Spillway chute alignment, the vast majority of the intensely-weathered rock was found at the two scour holes, with almost all of this original foundation

material having been eroded out during the 2017 incident. In general, the geologic maps created during original construction were found to be very accurate. The thicknesses of the concrete chute slabs in the FCO Spillway chute, however, were found to be generally much thicker than the nominal 38 cm (15 inch) minimum thickness specified during original design, with thicknesses ranging up to 2.1 m (7 ft) and an average concrete slab thickness on the order of about 1 m (3.5 ft). This larger thickness resulted in additional demolition and excavation in the removal of these concrete slabs, larger thicknesses of new leveling concrete, and deeper underdrains, extending to rock through the leveling concrete beneath the new structural concrete.

3.2.3. *Hydraulic Analyses and Modeling*

Hydrologic and hydraulic analyses, using 1D, 2D, and 3D analytical models and a physical model of the FCO Spillway chute constructed at Utah State University, were used to verify and improve the designs for both spillways. The details of these analyses are presented in a separate companion paper [3].

3.2.4. *FCO Spillway Chute Structural Concrete Designs*

The structural reinforced-concrete designs for new chute wall and slab sections were developed to meet modern spillway design standards and to address any potential areas for improvement identified in the original design. Presented in Table 2 is a list of potential design and/or construction areas for improvement identified by the OER and the Forensic Investigation Team appointed to provide an independent assessment of the potential causative factors that led to the incident. Also shown are the elements included in the new structural-concrete design intended to address these areas for improvement. Fig. 8 illustrates several of these elements.

3.2.5. *Secant Pile Wall/RCC Designs for Emergency Spillway*

During the final design of the interim measures for the Emergency Spillway, designers concluded that a capacity higher than the 850 m³/s (30,000 ft³/s) design objective for the upcoming 2017-2018 Winter Flood Season was needed. This was because it was recognized that a major modification or replacement would eventually be needed in order for the Emergency Spillway to safely pass its original rated design capacity of 10500 m³/s (371,000 ft³/s) for a PMF flood event. Further, it would likely require 5 to 10 years to implement such a major project. Consequently, the interim repairs/upgrades were needed to be able to convey flows that might reasonably be discharged through the Emergency Spillway during the next 5 to 10 years. While not established during the initial alternatives analyses, a target flow of 2800 m³/s (100,000 ft³/s) was later adopted during the final design phase as a design objective for the Emergency Spillway for the next 5 to 10 years.

Table 2

Design Measures Included in New FCO Spillway Chute Structural Concrete to Address Areas of Improvement Identified in the Original Design/Construction

Areas for Improvement Identified in Original Design/Construction	Design Measures in New FCO Spillway Chute Structural Concrete to Address Identified Areas for Improvement
Relatively thin concrete slab at 0.38 m (1.25 ft)	New concrete slab minimum 0.76 m (2.5 ft) thick
Only 1 layer of relatively light steel reinforcement	2 layers of robust steel reinforcement
No waterstops	Waterstops added at each transverse joint
Large variations in slab thickness	Use of thick (~1.5 m [5 ft]) layers of leveling concrete
Corrosion of reinforcing bars	Upper layer of steel reinforcement epoxy coated
Placement of underdrains within concrete slabs	Underdrains placed beneath concrete slabs
Collector pipes drain both underdrain and backfill	Separate collector pipes for underdrain and backfill
Brittle clay underdrain and collector drain pipes	PVC underdrain and collector drain pipes
0.15 m (6 in) I.D. perforated underdrain pipes too small	0.20 m (8 in) I.D. slotted PVC underdrain pipes used
No clean-outs for underdrain system	Clean-outs added for each underdrain pipe
Gravel envelope around drains not filter compatible	Granular filter material around new drain pipes
Presence of untreated erodible rock foundation	Intensely-weathered rock was over-excavated
Presence of untreated shears in rock foundation	Shear zones over-excavated and treated
Less rigorous foundation clean-up	Extremely rigorous foundation clean-up
Insufficient rock anchorage (only ~1.5 m [5 ft] deep)	Deeper rock anchors – 4.6 to 7.6 m (15 to 25 ft) deep
Potential corrosion of rock anchors	Rock anchors epoxy coated
Potential cavitation	Aeration added in Phase 1 spillway section [3]

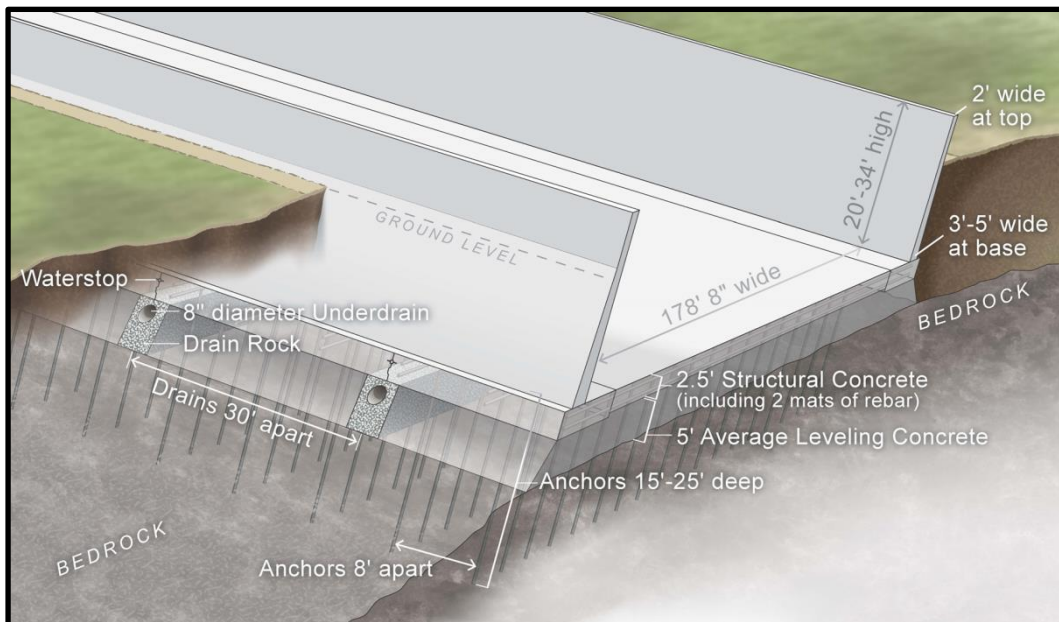
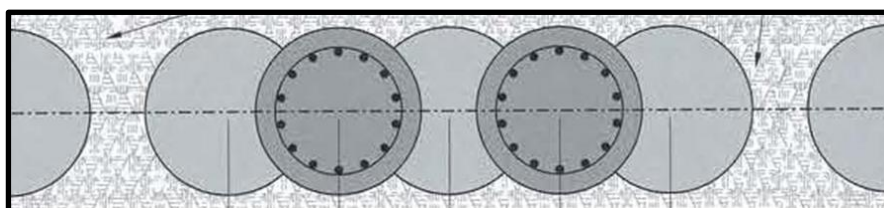


Fig. 8 Design measures included in 2017 structural concrete for FCO Spillway chute

The 3 m (10 ft) thick RCC apron was founded on rock, requiring substantial removal of surface soils, fills, and temporary armoring. The foundations for the RCC buttress and the 2-m-high concrete crest were specified to be of moderately-weathered rock, or better, and to be thoroughly cleaned.

The purpose of the downstream secant pile wall is to support and protect the RCC apron from head-cutting erosion. Using the results of the geologic explorations, an alignment was chosen for the secant pile wall approximately 227 m (746 ft) downstream of the existing monoliths/weir sections. Along this alignment, the depth to slightly weathered or fresh rock is only about 6 m (20 ft) or less. This allows for the bottoms of the piles to be keyed into slightly weathered or fresh rock to depths of at least 4.5 m (15 ft) or more, with total pile depths ranging between 11 and 20 m (35 and 65 ft). As shown in Fig. 9, the piles were designed to be a minimum 91 cm (3 ft) in diameter with centers spaced at 61 cm (2 ft), and to be constructed in 5-pile panels with a 30 cm (1 ft) gap between panels to allow for drainage and to avoid the buildup of groundwater pressure against the wall. Two of the five concrete secant piles in each 5-pile panel were reinforced, while the other three were unreinforced (see Fig. 9). A reinforced concrete grade beam will be constructed across the tops of the piles and anchored back into the RCC apron to a minimum distance of 40 feet (12 meters).

(a)



(b)



Fig. 9

(a) Unreinforced/reinforced pile pattern within 5-pile secant wall panels

(b) Photograph of secant pile wall under construction on Emergency Spillway

4. REGULATORY REVIEW

The declaration of State and Federal Emergencies for the Oroville Dam Spillway Incident greatly facilitated the regulatory permitting process, particularly environmental permitting. However, State and Federal laws also required that the California Division of Safety of Dams (DSOD) and the Federal Energy Regulatory Commission (FERC) review the safety of any dam modifications or repairs, including those for the spillways. Usually, the review and approval process requires months after designs or contract drawings and specifications are submitted for regulatory approval, time that the OER project did not have. The solution to this was to dedicate full-time DSOD and FERC staff to the OER project, both in Sacramento and Oroville. Both agencies were able to commit full-time staff to review the work of OER as it was being developed and implemented in the field. During the foundation excavation and treatments for the chute slabs on the FCO Spillway chute, the final inspection for each slab foundation was approved in the field not only by OER engineers and geologists, but also by an inspector from DSOD and an inspector from FERC, both assigned on-site. The dedication of regulatory staff to the project, while still retaining their independent regulatory function, greatly reduced the time required for regulatory review and approval, typically down to a matter of days or a week for each design review.

State and Federal laws also required that the spillway designs and construction be reviewed by an independent Board of Consultants to provide an independent expert peer review of the work. The members of the Board of Consultants nominated by DWR and approved by DSOD and FERC were:

- John Egbert, P.E.
- Kerry Cato, Ph.D., C.E.G.
- Eric Kollgaard, P.E.

- Faiz Makdisi, Ph.D., P.E., D.GE
- Paul Schweiger, P.E., P.Eng, CFM

The Board of Consultants held their first meeting on March 1-3, 2017, with the Spillway Recovery Team and dam safety regulators. Between March and December 2017, the Board of Consultants met 14 times to review the designs and to inspect construction in the field. The Board of Consultants completed written reports following each meeting, providing comments and recommendations to the Spillway Recovery Team, DSOD, and FERC, which DWR then made available to the media and the general public.

OER also participated in a Risk Assessment Workshop conducted by the United States Army Corps of Engineers in April 2017 and in a Potential Failure Mode Analysis workshop in May 2017 conducted by DWR. These two workshops focused on the safety of the FCO Spillway chute and the Emergency Spillway.

5. LAKE OROVILLE OPERATIONS

Following the 2017 incident, DWR used the damaged FCO Spillway chute intermittently between February and May 19, 2017, to pass reservoir inflows to avoid using the unreliable Emergency Spillway. On May 12, DWR completed a Near-Term Lake Oroville Operations Plan to support the final 2017 closure of the spillway (FCO) gates in the second half of May, and to use the Hyatt Powerplant releases to lower the reservoir to Elevation 214 m (700 ft) by November 1, 2017. The objective of this operations plan was to minimize the likelihood of using either spillway during the rest of the 2017 construction season, and to also minimize the need for using the Emergency Spillway at all during the 2017-2018 Winter Flood Season.

On October 16, 2017, DWR completed a Lake Oroville 2017/2018 Flood Control Season Operations Plan targeted to limit flows on the FCO Spillway chute and to prevent any flow through the Emergency Spillway. The 2017/2018 Plan was based on hydrologic and hydraulic analyses using historical precipitation, snowpack, and reservoir data. It was also developed to balance the competing needs of dam safety versus downstream flood safety. The 2017/2018 Plan incorporates a low initial reservoir elevation target to be held during the Winter Flood Season and uses reservoir set points where increasing releases would be made from the Hyatt Powerplant and the FCO Spillway chute to avoid the use of the Emergency Spillway. The 2017/2018 Plan allows the reservoir to pass the Standard Project Flood without releases on the Emergency Spillway and without a discharge greater than 2800 m³/s (100,000 ft³/s) on the FCO Spillway chute.

6. MEETING THE SCHEDULE

During the height of the 2017 construction season, the contractor (Kiewit) had as many as 750 craft workers on site. During this season, the following work was completed on the FCO Spillway chute before the November 1, 2017, deadline:

- 320,000 m³ (420,000 yd³) of excavation
- 265,000 m³ (347,000 yd³) of RCC construction
- 234 structural-concrete slabs and 78 reinforced-concrete walls constructed
- 32000 m³ (42,000 yd³) of leveling concrete constructed
- 23000 m³ (30,000 yd³) of structural concrete constructed

The progress of the work on the FCO Spillway chute is illustrated in Fig. 10, and the pertinent events for OER are highlighted in Table 3. Final placement of 2017 concrete on the FCO Spillway chute was made on November 1, 2017 (see Fig. 10), thus meeting the most important goal for the project.



Fig. 10 Aerial views of construction on FCO Spillway chute between May and November 2017

Table 3
Pertinent Events in Oroville Emergency Recovery (OER)

2017 Date	No. of Days	Event
Feb. 7	0	Initiation of Oroville Dam Spillway Incident
Feb. 12	5	Emergency declared, downstream areas evacuated
Feb. 23	16	OER Framework adopted
Mar. 1-3	22-24	First meeting of Board of Consultants
Mar. 6	27	OER leads organized, alternatives workshop
Mar. 15	36	Forensic Investigation Team selected

Mar. 27	48	Initial contract (Specification 17-08) awarded to Teichert Construction
Mar. 31	52	30% Design, Advertised Spillways, Spillways, Oroville Emergency Recovery Contract (Specification 17-09)
April 15	67	Spillways, Oroville Emergency Recovery Contract (Specification 17-09) awarded to Kiewit
April 18-20	70-72	USACE Risk Assessment Workshop
April 22	74	First blasting excavation to stabilize over-steepened slopes
May 2-4	84-86	COE Potential Failure Modes Analysis Workshop
May 18	100	75% Design, Plans and Specifications
May 19	101	Final Closure of FCO Gates on FCO for Spring 2017
June 21	134	Final Plans and Specifications issued for Review
July 13	156	DSOD approval of Final Plans and Specifications
July 13	156	First Secant Pile completed
July 15	158	FERC approval of Final Plans and Specifications
July 20	163	Revised Final Plans and Specifications issued
Aug. 17-18	191-192	Final Clean-up/First Placement of RCC in Main Scour Hole
Oct. 16	251	Lake Oroville 2017/2018 Flood Control Season Op. Plan completed
Nov. 1	267	Final concrete placement on FCO Spillway chute Phase 1 Recovery

7. LESSONS LEARNED

The expedited design and construction processes used in the urgent restoration of spillway capacity at Oroville Dam were unprecedented, and were only successful because of the commitment of everyone (owner, consultants, contractors, and regulators) to work together in partnership to ensure that the public was properly protected. Lessons learned during this project included housing all parties in one location, first in Sacramento and then at Oroville. The dedication of regulatory staff full-time to the project team and the timely comments and recommendations from the Board of Consultants were critically important in staying on schedule. The main contractor (Kiewit) maintained an extremely proactive and aggressive schedule throughout the construction period and quickly responded to scheduling issues whenever necessary to overcome the considerable construction challenges associated with the project.

REFERENCES

- [1] CROYLE, W., GUTIERREZ, D., ANDERSEN, M., LEDESMA, J., TAPIA, S., and BLACKETT, F. Oroville Dam Spillway Incident – Situation Development, Incident Response and Public Safety
- [2] NICHOLS, H., GRAY, M., HALL, C., KUTTEL, J., and CRADDOCK, T. Oroville Dam Spillway Incident – Geological and Geotechnical Investigations for Recovery Design Features
- [3] PANDEY, G., FORD, D., CRADDOCK, T., WHITE, M., FORTNER, M., LEAHIGH, J., ANDERSON, M. Oroville Dam Emergency Response and Spillway Restoration – Hydrologic and Hydraulic Engineering Activities to Inform Operation and Design

SUMMARY

Following the February 7, 2017, Oroville Dam Spillway Incident, DWR formed the Oroville Emergency Recovery (OER) team to restore spillway capacity in advance of the 2017-2018 Winter Flood Season. The team worked under considerable pressure during the ongoing incident to quickly develop recovery plans for the two major areas of damage – the Flood Control Spillway and the Emergency Spillway. Using an expedited process that included integral coordination with state and federal dam safety regulators, a recovery design was developed and construction contracts were issued. The 2017 expedited design and construction processes used in the urgent restoration of spillway capacity were unprecedented, and were only successful because of the commitment of everyone involved to work together.

KEYWORDS

analysis, apron, buttress, concrete, construction, dam, design, drainage, emergency spillway, erosion, excavation, flood, flood control, flood storage, foundation treatment, FCO spillway chute, geology, hydraulic model, Oroville Dam, secant pile, reservoir operation, roller compacted concrete, scour protection, spillway, uncontrolled spillway, weathered rock.

COMMISSION INTERNATIONALE DES GRANDS BARRAGES

VINGT-SIXIÈME CONGRÈS DES GRANDS BARRAGES
Autriche, juillet 2018

DOI 10.3217/978-3-85125-620-8-004



This work licensed under a Creative Commons Attribution 4.0 International License.
<https://creativecommons.org/licenses/by-nc-nd/4.0/>

**OROVILLE DAM SPILLWAY INCIDENT- ROLLER COMPACTED CONCRETE
INFLUENCES ON RECOVERY STRUCTURAL DESIGN FEATURES**

Jesse DILLON

Structures Design Lead, STATE OF CALIFORNIA, DEPARTMENT OF WATER
RESOURCES

Michael ROGERS

RCC Design Lead, STANTEC CONSULTING SERVICES, INC.

Ted CRADDOCK

Project Manager, STATE OF CALIFORNIA, DEPARTMENT OF WATER
RESOURCES

Mike DRILLER

Construction Design Lead, STATE OF CALIFORNIA, DEPARTMENT OF
WATER RESOURCES

Mark STRAHM

Engineer - BRYTE SOILS & CONCRETE LAB, STATE OF CALIFORNIA,
DEPARTMENT OF WATER RESOURCES

Steve FRIESEN

Structural Designer, STATE OF CALIFORNIA, DEPARTMENT OF WATER
RESOURCES

UNITED STATES OF AMERICA

COMMISSION
INTERNATIONALE
DES GRANDS BARRAGES

VINGT TROISIÈME CONGRÈS
DES GRANDS BARRAGES
L'Autriche, juillet 2018

**OROVILLE DAM SPILLWAY INCIDENT- ROLLER COMPACTED CONCRETE
INFLUENCES ON RECOVERY STRUCTURAL DESIGN FEATURES*¹**

Jesse Dillon
Structures Design Lead, State of California, Department of Water Resources

Michael Rogers
RCC Design Lead, Stantec Consulting Services, Inc.

Ted Craddock
Project Manager, State of California, Department of Water Resources

Mike Driller
Construction Design Lead, State of California, Department of Water Resources

Mark Strahm
Engineer-Bryte Soils & Concrete Lab, State of California, Department of Water
Resources

Steve Friesen
Structural Designer, State of California, Department of Water Resources

UNITED STATES OF AMERICA

1. INTRODUCTION

Oroville Dam is located on the Feather River in northern California (USA). At 234.7 m (770-ft) tall, this earth embankment is the tallest dam in the United States. With its 4.3 billion m³ (3.5 million acre-feet) of storage, Lake Oroville is the second largest reservoir in California, supplying water to cities as far south as Los Angeles. The Oroville Dam, reservoir (Lake Oroville), and hydropower plant facility is the flagship of the State Water Project (SWP), which is owned and operated by the State of California, Department of Water Resources (DWR).

The 2016-2017 Winter Storms brought record breaking precipitation to the Northern California Sierra mountains including the Feather River watershed. On February 7, 2017, the Oroville Dam's 54.5 m (179-ft) wide Flood Control Outlet (FCO) Spillway chute (Fig. 1) was

* INCIDENT DE DRAINAGE DE BARRAGE D'OROVILLE - INFLUENCES DE BÉTON
COMPACTÉES PAR ROULEAU SUR LES CARACTÉRISTIQUES DE CONCEPTION
STRUCTURALE DE RÉCUPÉRATION

releasing water to control the Lake Oroville reservoir level in accordance with the prescribed operations plan. During this operation, the FCO spillway suffered a catastrophic failure of the lower chute area eventually resulting in the loss of approximately 427 m (1400 ft) of the lower chute, including the scour of more than 1.2 million m³ (1.6 million yd³) of soil and rock materials. On February 11, 2017, the Emergency Spillway (Fig. 1) was used for the first time since the project was completed in 1968. During this operation, significant erosion and scour caused by the Emergency Spillway overflow led authorities to fear for the safety of the spillway structures, resulting in the activation of the Emergency Action Plan and evacuation of about 188,000 persons from downstream communities.



Fig. 1 Flood Control Outlet (FCO) Structure and Emergency Spillway, March 2011

This paper is part of a series developed by the State of California, Department of Water Resources (DWR) to describe the Oroville Dam Spillway Incident - Emergency Response and Recovery. including lessons learned and key design features to allow the Oroville Dam FCO Spillway chute to be able to pass expected annual flood flows by the next wet-year cycle, starting by November 1, 2017. This paper presents the roller-compacted-concrete portion of the reconstructed spillway design that was intended to be used for replacing the eroded foundation of the FCO Spillway chute and as a buttress and apron for the rehabilitated Emergency Spillway. Through a series of design and project management decisions, the

roller-compacted concrete came to play a much more vital role in meeting the project objective of having a completed FCO Spillway chute by the November 1, 2017, deadline. This paper identifies and discusses specific dam safety risks and the evolution of the key structural design features that were developed to meet the project-specific design and public safety requirements, including critical reviews by state and federal regulatory authorities along with the independent Board of Consultants.

2. BACKGROUND

The Oroville Dam Spillway Incident of 2017 was one of the most serious dam safety occurrences in the United States in many years. As the tallest dam in the United States and the keystone of California's State Water Project, Oroville Dam and Lake Oroville stand as a steadfast monument to water resource development in the 20th Century. The Oroville Dam Spillway Incident has provided a testimony to the dedication of emergency response and dam safety professionals who came together to meet the challenges of a rapidly changing situation to assure the safety of the Oroville Dam and the public living downstream. Starting in Oroville, California, this incident will impact the dam safety profession around the world as the details of the incident, response, and recovery become fully known and realized.

The original mission of Oroville Dam and Lake Oroville as part of the California State Water Project (SWP), was originally conceived as the following [1]:

Oroville Dam and its appurtenances comprise a multipurpose project encompassing water conservation, power generation, flood control, recreation, and fish and wildlife enhancement. The Lake stores winter and spring runoff which is released into the Feather River as necessary, to supply project needs. The (United States) Federal Government shared in the cost of the Dam, which provides 750,000 acre-feet of flood control storage. The 15,805-acre surface of the Lake with a 167-mile shoreline provides water-oriented recreational opportunities.

An incident such as this at the Oroville Dam spillways has many facets from beginning to end, along with many lessons learned. Along with others in this series of papers developed for the U.S. Society on Dams [2, 3, 4, 5, 6], this paper presents important technical details from those directly involved in the groundbreaking Herculean effort to recover from the incident in an expedited manner to protect and serve the people of California. With strong leadership from the Oroville Dam owner, the California Department of Water Resources (DWR), the Oroville Emergency Recovery Spillways Task Force pulled in professional resources from industry, including consultants, independent experts, regulators, and contractors to make the seemingly impossible into a reality of success based on pure determination, hard work, commitment, and dedication to the single mission of recovery.

3. KEY RECOVERY STRUCTURAL DESIGN FEATURES

The Oroville Dam Spillway Incident created the need to address many areas of structural rehabilitation to facilitate the reconstruction of damaged or destroyed features of the Flood Control Outlet (FCO) Spillway chute and the Emergency Spillway. As detailed in the related situational development paper [2], the flood damage to both spillways was catastrophic. For the FCO Spillway chute, nearly 40% of the spillway chute was completely destroyed, scouring out an estimated 1.2 million m³ (1.6 million yd³) of material into the downstream Feather River channel, leaving a large hole in the foundation and a cavernous valley of eroded bedrock where once lay one of the largest spillways in the United States.



Fig. 2 Oroville Dam Project Sign

As shown in Fig. 2, the FCO Structure, with eight 10.21 m (33.5 ft) high radial gates, has a capacity of about 8380 m³/s (296,000 ft³/s), which has been restricted to 4200 m³/s (150,000 ft³/s) out of concern for downstream flooding. The FCO Spillway chute is 931 meters (3055 feet) long and 54.6 meters (179 feet) wide, with a steep 4:1 (horizontal:vertical) slope on the lower chute and a large energy-dissipating dentate structure at the terminal end. There is 170 meters (558 feet) of elevation change from the invert of the FCO gates to the normal water surface elevation of the diversion pool - the Feather River below the FCO Spillway chute, which is the tailwater for the powerhouse.

This paper focuses on describing the repair of the FCO Spillway chute, using roller-compacted concrete (RCC), as this work was a large part of the recovery effort during the first year following the 2017 incident. Repair and recovery of the FCO Spillway chute was given the highest priority by DWR management so that the spillway would be available for the next 2017-2018 Winter Flood Season. This led to the rapid development and evaluation of recovery concepts that were constantly evolving and changing based on weekly, if not daily, interactions with the design team professionals, federal and state regulators, and eventually the construction contractor. A critical aspect of all recovery concepts was to determine the maximum work that could be accomplished within the limited timeframe, resulting in an operational FCO Spillway chute by November 1, 2017.

Similarly, the recovery work at the Emergency Spillway was carried forward, considering what could be completed during the 2017 construction season and what work could be deprioritized until 2018. It was determined that a deep secant pile wall should be the highest priority in 2017 to address the serious headcutting observed during the original 2017 incident. Following completion of the secant pile wall, an RCC buttress to the ogee spillway and a large RCC apron would be constructed in 2018. Many of the RCC design features and lessons learned rebuilding the FCO Spillway chute have direct relevance to the upcoming Emergency Spillway work. The RCC mix design and construction processes are anticipated to be the same for both structures.

4. RCC AS A “FILL THE HOLE” SOLUTION AT THE FCO SPILLWAY CHUTE

Immediately following the incident, the Oroville Emergency Recovery (OER) Spillway Task Force was swiftly assembled. The OER Spillway Task Force developed a wide-ranging list of potential recovery approaches for both the FCO Spillway chute and Emergency Spillway. For the FCO Spillway chute, engineers were faced with a spillway chute that was abruptly terminated (by the foundation erosion and chute loss) at about the mid-point of its length, leaving an approximately 30.5 meter (100-foot) deep hole across the full width of the chute and extending beyond with extensive and irregular areas of exposed rock.

An assessment of alternatives to repair the FCO Spillway chute was developed by the OER Spillway Task Force. These alternative concepts were grouped in the following categories:

- “Use the Hole” – These concepts involved developing a long-term stilling basin out of the scoured hole and ending the spillway chute near the location remaining after the incident. It was determined that extensive design and modelling would be needed to assure that such a solution would be suitable for flows up to the spillway design flows anticipated under probable maximum flood (PMF) conditions. A key unknown here was whether the foundation rock would continue to erode under these higher flows and possibly endanger the main dam.
- “Bridge the Hole” – While minimizing the foundation contact and preparation, these concepts involved construction of a reinforced-concrete aqueduct bridge over the chasm to carry flows over the eroded area. Given the lack of precedent for this type of solution on such a large-capacity, high-discharge, high-velocity spillway, it was determined that extensive structural and physical modelling would probably be needed for such a critical structure. These concepts were ultimately deemed to be structurally too intense for the design and construction time available.
- “Fill the Hole” – These concepts centered on replacement of the eroded foundation of the FCO Spillway chute and utilizing the original spillway profile. There were two competing concepts for how this could be achieved:
 - “Fill the Hole with Rock” – This concept involved filling the eroded hole with large boulders and other rock that could be solidified using flowable concrete. This approach was discounted because of the high variability in the available rock on site and unknown imported rock materials. Again, extensive design and modelling seemed to be required for unknown material sources and material properties, including thermal effects.

- “Fill the Hole with RCC” – This concept, shown in Fig. 3, anticipated using horizontal lifts of RCC to fill a portion of the eroded hole sufficient to re-construct the FCO Spillway chute to the original geometry.

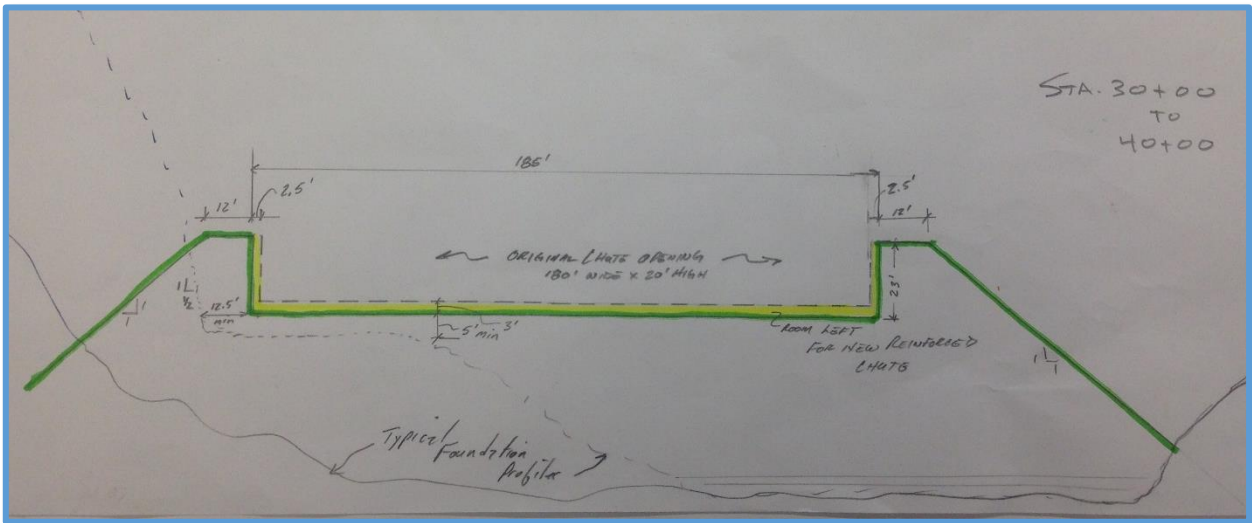


Fig. 3 Initial Sketch of RCC for "Fill the Hole" Solution

The following list of arguments, in support of the “Fill the Hole with RCC” approach, was presented to the OER Spillway Task Force, including regulatory agencies and the independent Board of Consultants for consideration:

1. The recommended alternative would provide the least risk to DWR by reconstructing the damaged portion of the FCO Spillway chute back to the original geometry with the foundation restored using RCC.
2. Reconstructing the FCO Spillway chute to its original geometry would have the least unknowns regarding hydraulic performance, which had already been studied, modeled, and proven through years of service, including:
 - a) the least amount of additional field investigations or hydraulic modelling; and
 - b) the avoidance of further negative impacts on flow patterns and debris in the diversion pool (Feather River) downstream of the spillways.
3. The use of RCC would allow the reuse of scoured rock debris recovered from Feather River as well as rock excavated from the chute foundation as concrete coarse and fine aggregates.
4. Reconstructing the FCO Spillway chute to its original design configuration would have the least environmental impact as no new areas will be permanently impacted.
5. The use of RCC for dams and spillways is mature in the dam engineering profession and construction industry and has been shown to be a highly efficient methodology for accelerated construction as opposed to conventional mass or reinforced concrete.
6. There have been several high-volume RCC projects for dams of this magnitude in the State of California over the last 10 years; thus, this RCC alternative will provide highly-reliable cost estimates and experienced contractors.

7. An assessment of the construction schedule showed that using RCC for foundation replacement would be a feasible solution for reconstruction of a usable FCO Spillway chute by November 1, 2017.
8. Should early storms arise in the fall of 2017, requiring the operation of the FCO Spillway chute before the scheduled completion on November 1st, the RCC should be resistant to scour up to moderate flows – about 1400 m³/s (50,000 ft³/s) or higher under temporary conditions.
9. The completed spillway modification project using RCC would have a positive appearance of a robust and complete solution that restores public confidence in the reliable operation of Oroville Dam.
10. The completed FCO Spillway chute, using RCC, would be a permanent solution capable of a design life of 100 years or more, capable of passing large flows up to the original design value of about 8400 m³/s (296,000 ft³/s)

Based on these initial benefits, the FCO recovery solution, using RCC foundation replacement in the scoured areas, was selected for preliminary design early in the evaluation process. With selection of RCC for the FCO Spillway chute, this decision led to the consideration of RCC for other aspects of the recovery design, including the Emergency Spillway buttress and spillway apron.

5. RCC PRELIMINARY DESIGN SOLUTION

The use of RCC for the FCO Spillway chute reconstruction was initially proposed as shown in Fig. 4, which included a conventional reinforced-concrete slab overlay as well as reinforced-concrete chute walls against RCC. In this initial concept, RCC was envisioned as the primary structural feature for the 6.1 meter (20 foot) high FCO Spillway chute walls with 0.76 meter (2.5 foot) thick reinforced-concrete vertical inside walls that were tied-back into the RCC.

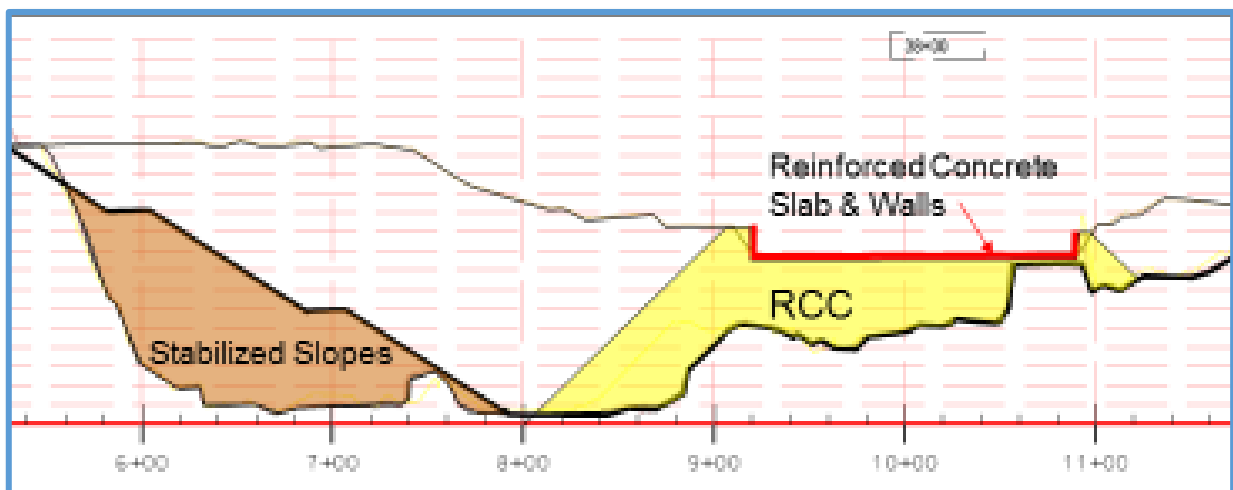


Fig. 4 Preliminary RCC Concept

The constructability of the initial concept envisioned that the RCC chute and walls would be constructed first, then the reinforced-concrete slabs and walls would be placed in sequence later within the same construction season. This concept, developed at the 30-percent design completion, was the basis for the original construction bid.

6. RCC AS FOUNDATION REPLACEMENT

The design process continued, following the initial construction bidding and award, as the overall completion moved forward. As the design progressed towards about 60% complete, a decision was made to modify the RCC portion of the chute to a foundation replacement only, which would provide a similar design approach, using reinforced-concrete for the chute slabs and cantilever retaining walls for the entire FCO Spillway chute. The construction contractor was confident that the RCC foundation replacement could be completed within the necessary timeframe, but indicated that the single-sided reinforced-concrete walls originally envisioned for the RCC portion could not be completed during the 2017 construction season.

As a result, an intermediate design modification of the RCC chute replacement was developed that included RCC as foundation replacement only so that the rebuilt chute would have similar reinforced-concrete slabs and cantilever retaining walls throughout the spillway. This 60% design concept is shown in Fig. 5.

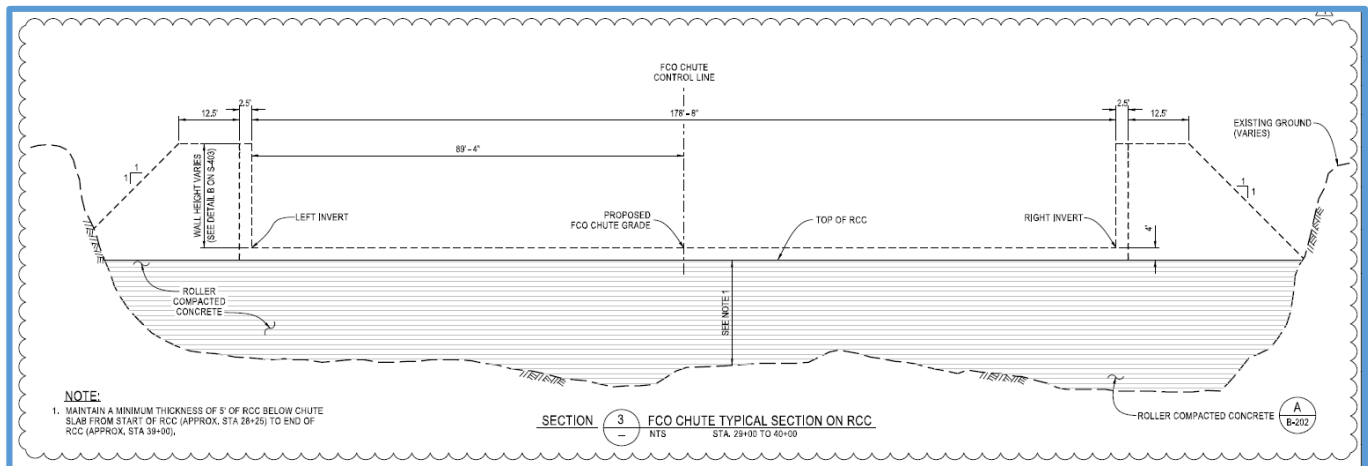


Fig. 5 Intermediate RCC Design Concept (60%)

The advantage of this concept was a simplified RCC construction process without the walls, resulting in a shorter RCC placement schedule. The challenge would be to get the RCC placed in time ahead of the reinforced-concrete work to allow that work to meet the critical November 1st completion date. There was some concern about the early strength of the RCC to allow proper anchoring of the chute slab. Early tests in the RCC Test Fill #1, however, showed that sufficient RCC strength would develop to allow proper anchorages.

7. INTERIM RCC FOUNDATION REPLACEMENT CONCEPT

The design and construction work continued to move together at a fast pace between April 15, 2017, when the construction contract was awarded and the anticipated start of field work on June 1, 2017, following final gate closure of the FCO Structure. During this time, the contractor was evaluating the post-incident condition of the foundation with regard to the clean-up needed for the RCC and conventional concrete work. In this same period, project geologists determined that a considerable volume of rock foundation under the remaining non-eroded FCO Spillway chute was unstable and needed to be removed before foundation clean-up could be started in the deepest upper hole”

In DWR's discussions with the contractor about the scope of work and schedule, it was determined that the November 1, 2017, completion target could not be met with a design concept that included both RCC foundation replacement and conventional reinforced-concrete slabs and walls. Therefore, an Interim RCC Foundation Replacement Concept was developed that restored the RCC walls, though at a lower level to allow up to 2800 m³/s (100,000 ft³/s) as a solution for an interim period only during the 2017-2018 Winter Flood Season. The plan was to shotcrete the inside of the RCC walls for the interim period, then remove the RCC walls in the 2018 construction season to allow completion of the reinforced-concrete slabs and walls as originally designed, as shown in Fig. 6.

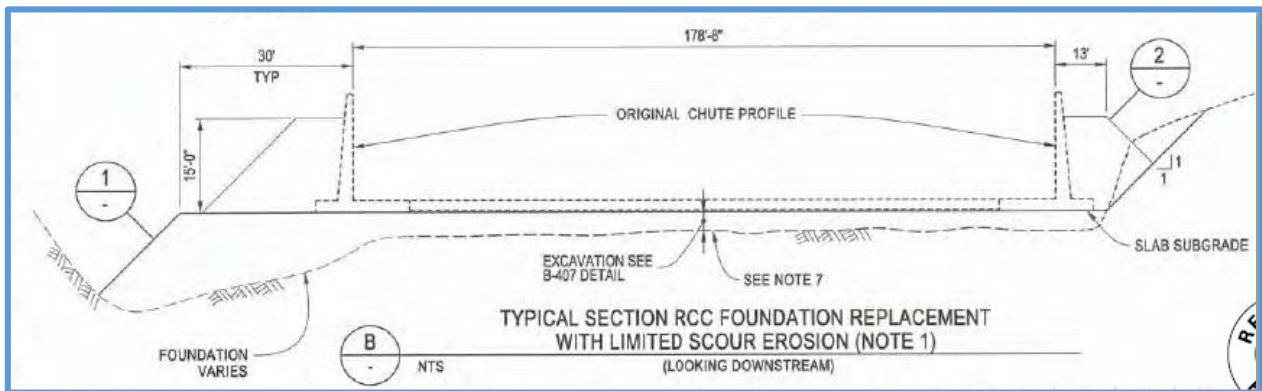


Figure 6 - Interim RCC Foundation Replacement Concept

The characteristics of the Interim RCC Foundation Replacement Concept are provided below:

- RCC is used as the foundation replacement material from Station 28+35 to 39+00.
- A minimum RCC thickness of 1.5 meters (5 feet) perpendicular to the chute slope is provided in the RCC area of the FCO Spillway chute (Sta. 28+35 to 39+00).
- The RCC foundation replacement is placed in horizontal layers below the planned final 4:1 finished grade of the reinforced-concrete spillway chute, creating a roughed-in 4:1 slope for the chute.
- A final 30 cm (12 inch) thick layer of RCC would be placed monolithically on a 4:1 slope using a higher-strength enriched RCC mix to provide a durable surface for the 2017-2018 Winter Flood Season, leaving the final RCC chute surface about 0.91 meter (3 feet) lower than the planned finished reinforced-concrete slab chute grade.
- At the upper end of the RCC (Sta. 28+35), a vertical 0.91-meter (3-foot) step from the FCO Spillway update chute finished reinforced concrete surface to the downstream RCC surface would be used as an aeration ramp with a vertical chimney section at each abutment to allow air to be incorporated into future flows.
- At the lower end of the RCC (Sta. 38+00 to 39+00), a 30.5 meter (100-foot) long transition section would slowly bring the RCC chute surface up flush with the finished FCO Spillway lower chute reinforced-concrete surface.
- Shorter 4.9 meter (16-foot) high RCC walls would be constructed with a similar design as the initial concept - a vertical inside face, 4 meters (12.5 feet) across the top and 1:1 side slopes on the outside faces], which is designed to accommodate a design flow of 2,800 m³/s (100,000 ft³/s).
- A minimum of 6 inches of the inner wall face would be constructed using reinforced shotcrete to provide a durable surface for the 2017-2018 Winter Flood Season.

The Interim RCC Foundation Replacement Concept described above was constructed during the 2017 construction season. As noted above, the Final Design solution for the RCC area of the FCO Spillway chute will include the following modifications during the 2018 construction season:

a. The RCC side walls above the 4:1 chute surface will be removed following the 2017-2018 Winter Flood Season so that new 6.1 meter (20-foot) high reinforced-concrete cantilever retaining walls can be added as the permanent chute walls.

b. Permanent reinforced-concrete slabs will be placed over the RCC, including drainage and anchor design features, for the remaining portions of the chute. Key aspects of this work will include roughening the RCC surface to allow a better connection to the new reinforced concrete.

8. RCC DESIGN

The initial estimated quantity of RCC was about 191,000 m³ (250,000 yd³), based on the initial topographic information from Station 29+00 to 39+00. This estimate was periodically revised during construction to account for changes in the foundation excavation, including the Arena Cut, which laid the upstream foundation area back to about Station 28+00 due to instabilities identified in the FCO Spillway upper chute foundation. Ultimately, the final RCC volume was about 268,000 m³ (350,000 yd³) that was placed during the 2017 construction season.

The technical specification for RCC features were developed based on recently-completed RCC projects in California by members of the OER Spillway Task Force. The project specifications also included technical requirements for crushing on-site rock for the RCC. Key aspects of the project specifications included the following features:

- RCC Mix Design
- Unformed RCC 1:1 Slope for the abutment sides
- Unformed RCC 4:1 Slope for the chute surface

Each of these features of the RCC design are discussed in the following sections.

RCC Mix Design: The intent for the RCC mix design was to use on-site materials for RCC aggregates, primarily rock eroded during the February 2017 incident that were later dredged from the Feather River. These eroded materials had been stockpiled in several areas around the project site. Initial investigations into the RCC mix design commenced shortly after the incident, using the dredged rock. These materials were crushed in several test programs, including preparation of RCC concrete cylinders. The results of these tests showed that an initial sorting process was necessary to remove fine-grained materials (silt, sand and gravel) finer than 1-inch in diameter. This provision was included in the final specification for the RCC Aggregates.

To simplify the preparation of RCC aggregates, the specification was developed using only two types of aggregates: coarse and fine. The coarse aggregate was specified as ASTM C 33, Size Number 357 [8] with a maximum aggregate size of 38 mm (1.5 inches). The fine (sand) aggregate was a custom blend, initially established in the following table. In addition, the sand equivalent value requirement was set to be no less than 35 when tested in accordance with ASTM D 2419.

Table 1
RCC Fine Sand Gradation

Sieve Size	INITIAL SPECIFICATION Percent Finer by Mass	FINAL SPECIFICATION Percent Finer by Mass
9.5 mm (3/8 inch)	100	100
4.75mm (No. 4)	95-100	90-100
2.36 mm (No. 8)	75-95	55-80
1.18 mm (No. 16)	55-80	35-60
600 μ m (No. 30)	35-60	25-45
300 μ m (No. 50)	24-40	15-35
150 μ m (No. 100)	12-28	10-25
75 μ m (No. 200)	8-18	8-18

The design intent of the RCC cementitious materials was to develop a mix that would attain an unconfined compressive strength of about 17 MPa (2,500 lb/in²) at 90 to 120 days, which is expected to give about 27.6 MPa (4,000 lb/in²) at one year. To meet this requirement, a target of 50 percent cement and 50 percent Class F Fly Ash was developed for initial mix design testing. The specification included a range of cement and fly ash components (by weight as shown in the table below) with a target mix at 103 kg of cement and 103 kg of fly ash per cubic meter (175 lb of cement and 175 lb of fly ash per cubic yard) to allow DWR the flexibility to modify the cementitious material content.

Table 2
RCC Material Specification

Location	Batch Proportions - kg/m ³ (lbs/yd ³)			Aggregate Size Range, Percent by Volume of the Total Aggregate	
	Cement	Fly Ash	Water	Group 1 38 mm- 4.75 mm (1.5 in. to 1/4 in.)	Group 2 4.75 mm minus (No. 4 minus)
Gated Spillway Chute	59.3- 118.7 (100-200)	59.3-118.7 (100-200)	112.7-127.5 (190-215)	60-64%	36-40%

RCC Full-Scale Trial Placement: An initial full-scale trial placement was conducted in June 2017 to validate contractor placement means and methods as well as for evaluating the production uniformity of the on-site RCC batch plant. Several key aspects of the construction were tested, including: general placement, Grout Enriched Vibratable RCC (GEVR), forming of 60 cm (2 foot) high steps, and placement of the 1:1 unformed slopes. During this trial placement, the base RCC mix for foundation replacement was finalized as 103/119 kg/m³ (175/200 lb/yd³) of cement/fly ash. The amount of water was tested to produce a VeBe time

of 10 seconds (+/- 4 seconds) when tested in accordance with ASTM C 1170, Procedure B [12]. The trial placement was also used for physical testing as well, including trenching through fresh RCC (anticipated for the installation of foundation drains); installation of contraction joints; installation and testing of foundation anchors; and two types of demolition (blasting and hoe-ram).

Enriched RCC Mix Design: An enriched RCC overlay material was developed for use as a surficial wearing surface on the FCO Spillway chute surface between Stations 28+35 and 39+00, where the RCC would be exposed only for the 2017-2018 Winter Flood Season. This material was required to have an early strength higher than the base mix to allow flows on the FCO Spillway chute as early as November 1, 2017. Based on cylinder testing during the full-scale trial placement, the enriched RCC mix design was established as 178/103 kg/m³ (300/175 lb/yd³) of cement/fly ash, which was expected to produce RCC with an unconfined compressive strength of about 27.6 MPa (4,000 lb/in²) at 28 days and about 41.4 to 51.2 MPa (6,000 to 8,000 lb/in²) at one year.

Unformed RCC 1:1 Slopes: A key factor in the RCC design was construction simplicity in order to provide for timely future recovery at the Oroville Dam's spillways during the 2018 construction season. For the FCO Spillway chute, the outside slopes of the foundation replacement were designed to be unformed at a 1:1 slope (see Fig. 7) in order to expedite and simplify construction. The RCC structural section provides a stable and robust structure against static and dynamic loads, including potential overtopping of walls during the interim 2017-2018 Winter Flood Season (temporary RCC walls are shorter than the permanent reinforced-concrete walls). Unformed 1:1 RCC slopes have been used successfully at other RCC projects, including the foundation replacement shaping blocks at Olivenhain Dam (San Diego, California, 2004). This previous history of RCC construction gave credibility for the mix design to regulatory agencies and the OER's independent Board of Consultants.



Figure 7 Unformed 1:1 Slope of RCC Structure

Unformed RCC 4:1 Slopes: The preponderance of the FCO Spillway chute where RCC is placed as the foundation replacement material will have a spillway chute slope of 4:1. The placement of the final enriched layer of RCC on a 4:1 slope is an innovative method for this project as there are no known occurrences of RCC placement on 4:1 slopes anywhere in the World at the time this spillway design concept was developed. For the base RCC foundation replacement structure, the design intent included placement of RCC in horizontal lifts with a free-form 4:1 slope in the main chute area (see Fig. 8).



Figure 8- Free Form Construction of 4:1 Slope of RCC

As previously discussed, the FCO Spillway chute design included a final 30 cm (12-inch) thick lift of enriched RCC in the main chute placed on the 4:1 slope. A full-scale test program that included placing and compacting RCC on a 4:1 slope was successfully completed as shown in Fig. 9. This trial placement test was critical for confirming the placement procedures using heavy equipment on the steep slope as well as: confirming the placement method (efforts to get a smooth completed surface), the compaction process (number of passes to get required density), and RCC testing. The completed test fill was used to further test different concrete hardening compounds for possible use to further increase the durability of the exposed RCC material during the 2017-2018 Winter Flood Season. Based on the performance of the hardening



Figure 9 - Test Fill #2 for 4:1 Slope Placement

materials during the trial placement, it was decided to apply the hardener only in the area immediately downstream of the aeration ramp on the completed chute.

SUMMARY

In summary, the use of RCC for the foundation replacement provided a robust solution for the Oroville Emergency Recovery – Spillway Task Force. RCC was used to backfill the eroded bedrock chasm within the original damaged FCO Spillway chute area with a high-strength cementitious material, which provided support for the future reinforced-concrete spillway slabs and walls. The RCC was placed within the limited time window to construct an operational FCO Spillway chute for the 2017-2018 Winter Flood Season. Several aspects of this application of RCC were innovative, including the expedited time frame for design and construction; RCC placement on a 4:1 slope with sloping walls; use of an enriched RCC overlay for a robust surface on a high-capacity/high velocity chute spillway; and RCC placement in a challenging rock foundation, using a combination of vibratable RCC with and without mix enrichment with grout.

The RCC solution utilized the reuse of scoured rock debris, and had the least environmental impacts of the alternatives considered. It provided a robust bidding climate as a majority of the construction means and methods were well known in the dam construction industry. It provided a competitive bidding process, which resulted in a low unit bid price. RCC was placed continuously and rapidly to complete the FCO Spillway chute recovery within the limited time frame.

The contractor, Kiewit Corporation, was instrumental in the success of RCC with its commitment to a quality constructed product. The contractor's willingness to experiment and come up with new ways to place RCC on a challenging foundation was instrumental in achieving the desired design intent. The speed of construction, economy of materials (including the reuse of scoured/eroded rock), innovative contractor placement methods, and material adaptability to variable foundation conditions made the use of RCC as foundation replacement in the FCO Spillway chute an ideal solution for Oroville Emergency Recovery.

REFERENCES

- [1] California State Water Project Bulletin 200, State of California Department of Water Resources, 1974
- [2] CROYLE, W., GUTIERREZ, D., ANDERSEN, M., LEDESMA, J., TAPIA, S., and BLACKETT, F. Oroville Dam Spillway Incident – Situation Development, Incident Response and Public Safety “Oroville Dam Spillway Incident – Fast Track
- [3] CRADDOCK T., HARDER L., VERIGIN S., KUTTEL J., BROWN D., MIHYAR M., BOYER D. Oroville Dam Spillway Incident – Fast Track Recovery Design to Address Critical Dam Safety.
- [4] NICHOLS, H., GRAY, M., HALL, C., KUTTEL, J., and CRADDOCK, T. Oroville Dam Spillway Incident – Geological and Geotechnical Investigations for Recovery Design Features
- [5] PANDEY, G., FORD, D., CRADDOCK, T., WHITE, M., FORTNER, M., LEAHIGH, J., ANDERSON, M. Oroville Dam Emergency Response and Spillway Restoration – Hydrologic and Hydraulic Engineering Activities to Inform Operation and Design

- [6] FRANCE, J.W., et al. Independent Forensic Team Report: Oroville Dam spillway incident, United States Society on Dams, January 2018.
- [7] DWR internal memorandum to Tim Wehling by Robert Black, "Oroville Dam Flood Control Spillway - Use of Roller-Compacted Concrete for Backfilling Spillway Voids", dated February 23, 2017.
- [8] American Society for Testing and Materials (ASTM) C33/C33M-16e1 - Standard Specification for Concrete Aggregates
- [9] American Society for Testing and Materials (ASTM) D2419-14 Standard Test Method for Sand Equivalent Value of Soils and Fine Aggregate
- [10] American Society for Testing and Materials (ASTM) C136/C136M-14 Standard Test Method for Sieve Analysis of Fine and Coarse Aggregates
- [11] American Society for Testing and Materials (ASTM) C117-17 Standard Test Method for Materials Finer than 75- μ m (No. 200) Sieve in Mineral Aggregates by Washing
- [12] American Society for Testing and Materials (ASTM) C1170/C1170M-14e1 Standard Test Method for Determining Consistency and Density of Roller-Compacted Concrete Using a Vibrating Table
- [13] American Society for Testing and Materials (ASTM) C1435/C1435M-14 Standard Practice for Molding Roller-Compacted Concrete in Cylinder Molds Using a Vibrating Hammer
- [14] American Society for Testing and Materials (ASTM) C39/C39M-17b Standard Test Method for Compressive Strength of Cylindrical Concrete Specimens
- [15] American Society for Testing and Materials (ASTM) C125-16 Standard Terminology Relating to Concrete and Concrete Aggregates

COMMISSION INTERNATIONALE DES GRANDS BARRAGES

VINGT-SIXIÈME CONGRÈS DES GRANDS BARRAGES
Autriche, juillet 2018

DOI 10.3217/978-3-85125-620-8-005



This work licensed under a Creative Commons Attribution 4.0 International License. <https://creativecommons.org/licenses/by-nc-nd/4.0/>

**OROVILLE DAM SPILLWAY INCIDENT - GEOLOGICAL AND
GEOTECHNICAL INVESTIGATIONS FOR RECOVERY DESIGN FEATURES**

Holly NICHOLS

Lead Geologist - OROVILLE SPILLWAY RECOVERY, CALIFORNIA
DEPARTMENT OF WATER RESOURCES

Michael GRAY

Senior Principal Geologist, LETTIS CONSULTANTS INTERNATIONAL, INC.

Craig HALL

Principal Geotechnical Engineer, GEI CONSULTANTS

Leslie HARDER

Senior Professional Associate, HDR

Ted CRADDOCK

Project Manager, CALIFORNIA DEPARTMENT OF WATER RESOURCES

UNITED STATES OF AMERICA

**OROVILLE DAM SPILLWAY INCIDENT — GEOLOGICAL AND
GEOTECHNICAL INVESTIGATIONS FOR RECOVERY DESIGN FEATURES***

Holly Nichols
Lead Geologist - Oroville Spillway Recovery, California Department of
Water Resources

Michael Gray
Senior Principal Geologist, Lettis Consultants International, Inc.

Craig Hall
Principal Geotechnical Engineer, GEI Consultants

Leslie Harder
Senior Professional Associate, HDR

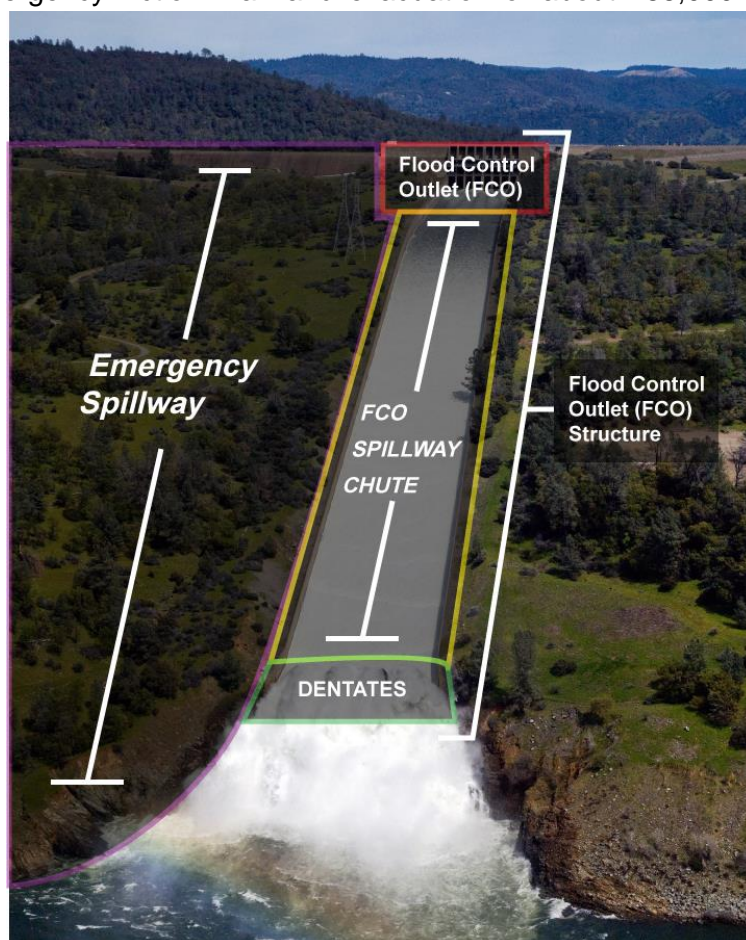
Ted Craddock
Project Manager, California Department of Water Resources

UNITED STATES OF AMERICA

1. INTRODUCTION

Oroville Dam is located on the Feather River in northern California (USA). At 234.7 m (770-ft) tall, this earth embankment is the tallest dam in the United States. With its 4.3 billion m³ (3.5 million acre-feet) of storage, Lake Oroville is the second largest reservoir in California, supplying water to cities as far south as Los Angeles. The Oroville Dam, reservoir (Lake Oroville), and hydropower plant facility is the flagship of the State Water Project (SWP), which is owned and operated by the State of California, Department of Water Resources (DWR).

The 2016-2017 Winter Storms brought record breaking precipitation to the Northern California Sierra Mountains including the Feather River watershed. On February 7, 2017, the Oroville Dam's 54.5 m (179-ft) wide Flood Control Outlet (FCO) Spillway chute (Fig. 1) was releasing water to control the Lake Oroville reservoir level in accordance with the prescribed operations plan. During this operation, the FCO spillway suffered a catastrophic failure of the lower chute area eventually resulting in the loss of approximately 427 m (1400 ft) of the lower chute, including the scour of more than 1.2 million m³ (1.6 million yd³) of soil and rock materials. On February 11, 2017, the Emergency Spillway (Fig. 1) was used for the first time since the project was completed in 1968. During this operation, significant erosion and scour caused by the Emergency Spillway overflow led authorities to fear for the safety of the spillway structures, resulting in the activation of the Emergency Action Plan and evacuation of about 188,000 persons from



downstream communities.

Figure 1 - Flood Control Outlet (FCO) Structure and Emergency Spillway, March 2011

This paper is part of a series developed by the State of California, Department of Water Resources (DWR) to describe the Oroville Dam Spillway Incident - Emergency Response and Recovery. This paper focuses on the geologic conditions known prior to the incident and the subsequent development and execution of a geologic and geotechnical investigation program to support the Oroville Emergency Recovery (OER). The geologic materials at the Oroville Dam site are structurally complex, with numerous cross-cutting shear zones that make predicting ground conditions difficult. It was clear, however, that the geology, in particular the cross-cutting shears, controlled the performance of the FCO Spillway chute and Emergency Spillway during the incident, and controlled the designs developed during the OER phase.

The complex geology, coupled with the urgent time-frame in which to develop and implement a field and laboratory testing program, and then provide useful high-quality subsurface geologic and geotechnical information to the OER design team, was very challenging. Specific challenges ranged from resource management to assessing a wide range of conceptual and then preferred design components, field quality assurance and quality control (QA/QC), expedited data analysis, and interpretations needed to support development of time-critical project designs. These challenges are discussed in the following sections of the paper.

2. GEOLOGY

Oroville Dam is located in the northeastern portion of the Sacramento Valley in northern California in the western Sierra Nevada foothills within the Middle to Late Jurassic arc sequence [4]. The western-most portion of the foothills consist of the Foothills Metamorphic belt, which includes Jurassic-age ophiolitic rocks of the Smartville Complex. The predominant geologic formation where the Oroville Dam and spillways were constructed is an unnamed member of the Smartville Complex, which consists of strongly-foliated green-schist-facies mafic meta-volcanic rocks. The primary mineral assemblage of the on-site rocks consists of actinolite (amphibole) and plagioclase, and is generically referred to as amphibolite.

Site geologic studies completed prior to the dam's construction included regional and site-specific geologic mapping, rock core drilling, packer testing, laboratory shear strength testing, surface geophysics, petrographic studies, exploratory tunnels, and other measures [5, 6]. These studies led to dam and spillway sites that were generally well-characterized, using the standards at the time for design and construction purposes.

The following subsections generally describe the geologic studies completed for design of the original FCO Spillway chute and Emergency Spillway, geologic observations and documentation created during the original construction of Oroville Dam, and geologic investigations performed between the original construction of the FCO Spillway chute and Emergency Spillway and the Oroville Dam Spillway Incident. This background information is presented to illustrate the

detailed geologic and geotechnical information that was relied upon after the incident and during the subsequent development of the exploration program for the OER design efforts.

2.1. GEOLOGIC INVESTIGATIONS PRE-1960S CONSTRUCTION

The Oroville Dam site was well-studied prior to construction in the 1960s. Specifically related to the FCO Spillway chute and Emergency Spillway, 45 rock-core borings were drilled and logged, 11 P-wave surface geophysical profiles were imaged, and geologic mapping of natural outcrops was performed. In addition, 51 bulldozer trenches were excavated to estimate the thickness of overburden that could be removed without blasting and to help determine the rock's excavation characteristics. Most of these explorations were performed along the alignments of the FCO Spillway chute and the Emergency Spillway monolith/weir section.

The initial phase of rock-core borings was laid out along a preliminary FCO Spillway chute alignment that was later abandoned (Fig. 2). This preliminary alignment was also where most of the 51 bulldozer trenches were excavated. The rock-core borings ranged up to 29 m (95 ft) deep and were vertical to inclined. The associated boring logs documented the rock lithology, degree of weathering and fracturing, discontinuities and infilling, and descriptions of other relevant geologic features, and included packer test results and water levels where measured. High-quality photographs of the rock cores were also documented for most of the rock-core borings.

The results of the pre-1960s-construction site geologic studies indicated that un-rippable rock was present at relatively shallow depths – generally about 0.9 to 1.2 m (3 to 4 ft) below the surface [5]. Subsurface rock-core borings and P-wave geophysical lines were used to develop contour maps and profiles showing depths to sound rock. Sound rock included fresh and slightly weathered rock, and might be slightly to moderately fractured. These maps and profiles were used by the engineering geologists and design engineers to help establish the anticipated foundation rock quality at the invert excavations for both the FCO Spillway chute and the Emergency Spillway monolith foundations.

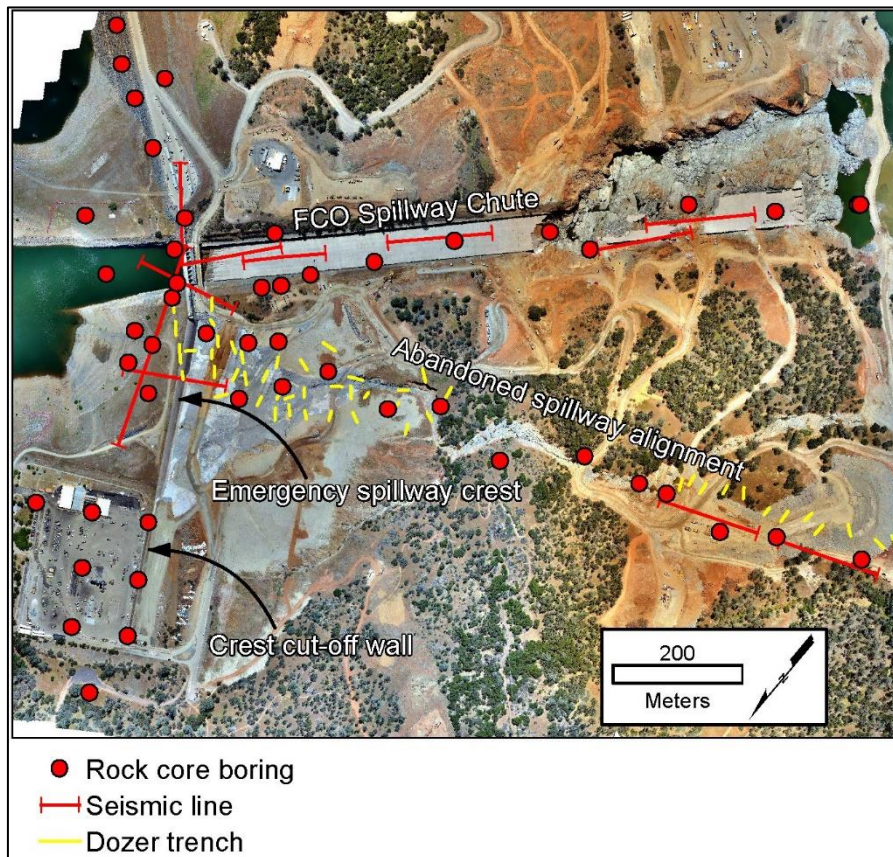


Figure 2 - Geologic explorations prior to original 1960s construction [5].

2.2. GEOLOGIC CONDITIONS DOCUMENTED DURING 1960S CONSTRUCTION

During construction of the FCO Spillway chute, DWR geologists created as-excavated geologic foundation maps (Fig. 3). These maps denoted the general rock weathering at the foundation invert as well as the location of shears and shear zones. Each shear or shear zone greater than 3 cm (0.1 ft) wide was assigned a unique sequential number with a relatively detailed description given in the construction geology documentation. The shear descriptions included the thickness, composition or mineral infilling (e.g., breccia versus clay-filled), and other pertinent information [6].

The Emergency Spillway includes an ungated monolith/weir structure that is approximately 527 m (1730 ft) wide at the weir crest. The left 283 m (930 ft) consists of concrete-gravity ogee monoliths/weir sections that were keyed into slightly-weathered rock. The heights of these monoliths range up to 27 m (90 ft). The right 244 m (800 ft) is in a rock cut with a small 0.3 m (1 ft) high concrete ogee weir. As-excavated foundation geology maps were similarly prepared during original construction to document the foundation rock at each concrete monolith of the Emergency Spillway, as well as the foundation rock conditions in the foundation of the concrete weir.

The detailed as-excavated foundation maps developed during original construction for both spillways were critical pieces of information used by OER to assess the geologic foundation conditions of the FCO Spillway chute where the initial failure occurred, and were used to estimate the headward erosion that could be expected based on the intersection of discontinuities in the foundation. These maps were also used to identify areas downstream of the Emergency Spillway monoliths that might be more susceptible to erosion under high water flows.

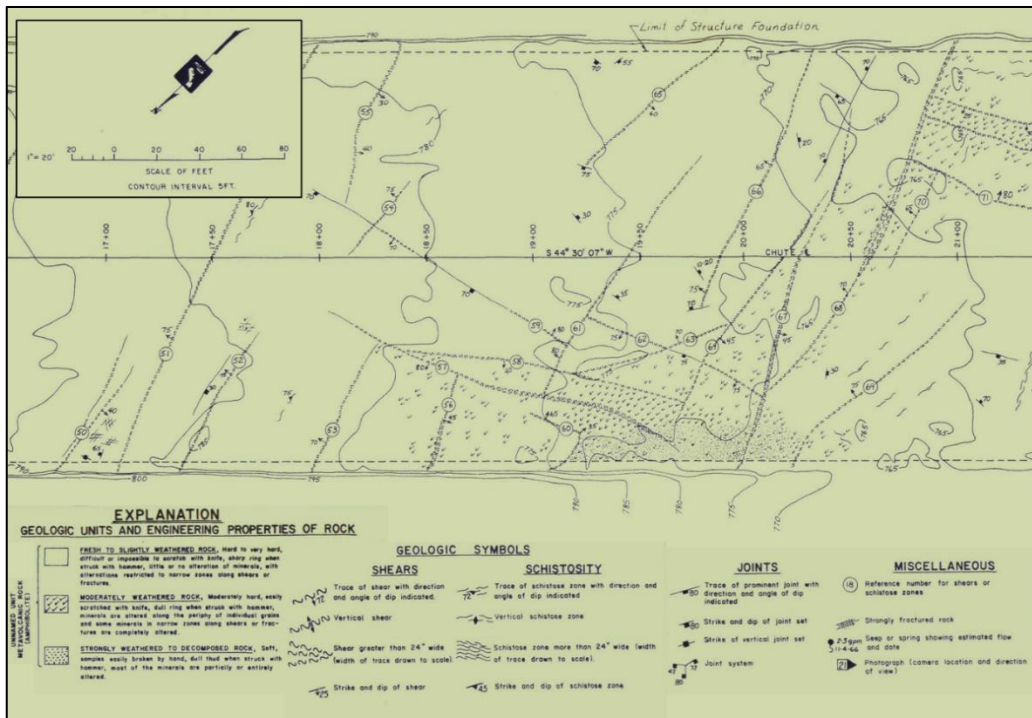


Figure 3 - Example of an as-excavated FCO Spillway chute foundation map [6]

In addition to the foundation geologic mapping during original construction in the 1960s, DWR geologists created foundation maps of areas-which-were and areas-which-were-not fully cleaned up. These clean-up maps documented the presence of fine-grained excavation debris that could remain in place in the FCO Spillway chute foundation. The design specified that the foundation provide at least 50 percent of the rock foundation to be completely cleaned of excavation debris, while the other 50 percent allowed some amount of clean-up debris to be left in place. These fine-grained materials, referred to on the clean-up maps as “compacted clayey fines”, were left in place and have been the source of some confusion. Recent investigations confirm that these materials were sourced from original construction debris.

2.3. GEOLOGIC INVESTIGATIONS SINCE 1960S CONSTRUCTION

Numerous geologic studies have been performed in and around Oroville Dam since original construction in the 1960s. However, only two were located in

or near the FCO Spillway chute and the Emergency Spillway: (1) a landslide investigation was performed in 2004 near the FCO Spillway chute on the lower left slope near the Feather River [7]; and (2) a new boring with downhole shear wave velocity measurements was completed in 2016 downstream of the larger monoliths of the Emergency Spillway [8]. Another such boring was completed on the left abutment of the embankment dam at the same time.

In 2004, slope instability was observed about 30 m (100 ft) to the south of the FCO Spillway dentates. While there was no concern about the stability of the FCO Spillway chute, there was concern that a large block of soil and rock might slide into the Feather River channel, blocking the passage of water flowing from the Hyatt Power Plant. This questionable slope was located in an area where the 1960s dam contractor had wasted soil and rock materials at the completion of dam and spillway construction. Historical aerial photos and topographic maps were examined, and it was determined that the slope instability was localized to within the old waste/spoil areas, which were estimated to be relatively thin (less than about 5 m [16 ft]). Based on the work completed in 2004, DWR geologists concluded that it was highly unlikely a large rock or soil mass would fail and block the river channel. No remediation of the unstable materials was completed in this area.

One rock-core boring was drilled downstream of the Emergency Spillway in September 2016 as recommended by the 2014 Director's Safety Review Board for the Ninth Five Year Part 12D Safety Inspection Report for Oroville Dam [9]. The purpose of this boring was two-fold: (1) to obtain site-specific shear wave velocity (V_{s30}) data for the rock foundation; and (2) to install a piezometer to evaluate potential uplift pressures beneath the Emergency Spillway's concrete monolith structures. Unfortunately, during the Oroville Emergency Response in February 2017, this newly-installed open standpipe piezometer had to be destroyed, as the area was covered with grouted-riprap armoring for added protection prior to and following the initial spill at the Emergency Spillway.

3. DEVELOPMENT OF THE OROVILLE EMERGENCY RECOVERY EXPLORATION PLAN

The damaged FCO Spillway chute was operated intermittently between February 2017 and May 19, 2017 to release water from Lake Oroville. While one team of engineers, geologists, and construction specialists focused on ongoing operations, monitoring, and repairs through the remainder of the 2017 flood season as part of the Oroville Emergency Response phase, a second team of engineers, geologists, and construction specialists began to work on the design for the repairs that would begin in Spring 2017 under Oroville Emergency Recovery. The design work for the Oroville Emergency Recovery phase began in early-March 2017, less than a month after the initial incident. Regardless of the final condition of the structures after the operation of the FCO Spillway chute finally ceased in May 2017,

it was rapidly determined that the foundations of the spillway structures needed to be further explored to better understand the site geologic conditions, provide parameters for the design team (e.g., range of rock shear strength, rock and dowel anchor designs, and filter compatibility), investigate the FCO Spillway chute that would likely remain in place, and to anticipate construction issues (e.g., rippability, areas prone to slope instability, and groundwater conditions interfering with excavations).

3.1. EXPLORATIONS TO UNDERSTAND GENERAL SITE GEOLOGIC CONDITIONS

The Oroville Dam site was one of the most studied dam sites of its time. That said, many of the eroded and scoured areas around both the FCO Spillway chute and the Emergency Spillway exposed fresh geology that clearly indicated the need for additional explorations to better understand and define the geologic site conditions.

The FCO Spillway chute failure initiated in a portion of the chute founded on intensely-weathered to decomposed amphibolite rock (Fig. 4). Within this initial scour hole, the depth of rock scoured out ranged up to 30 m (100 ft). Intermittent spillway discharges resulted in the creation of a large erosion channel leading away from this initial scour hole and running downslope to the left of the damaged FCO Spillway chute (Fig. 4). Within this left erosion channel, the near vertical eroded rock faces were as tall as 60 m (200 ft). The left side of the scour hole and erosion channel generally consisted of a thin veneer of soil or colluvium at the top, about 6.5 to 10 m (20 to 30 ft) of moderately-weathered amphibolite, with slightly-weathered amphibolite below (Fig. 4). There was no intensely weathered to decomposed rock observed in this left channel exposure. The zone of intensely

weathered to decomposed rock previously mapped within the chute itself had been scoured away.

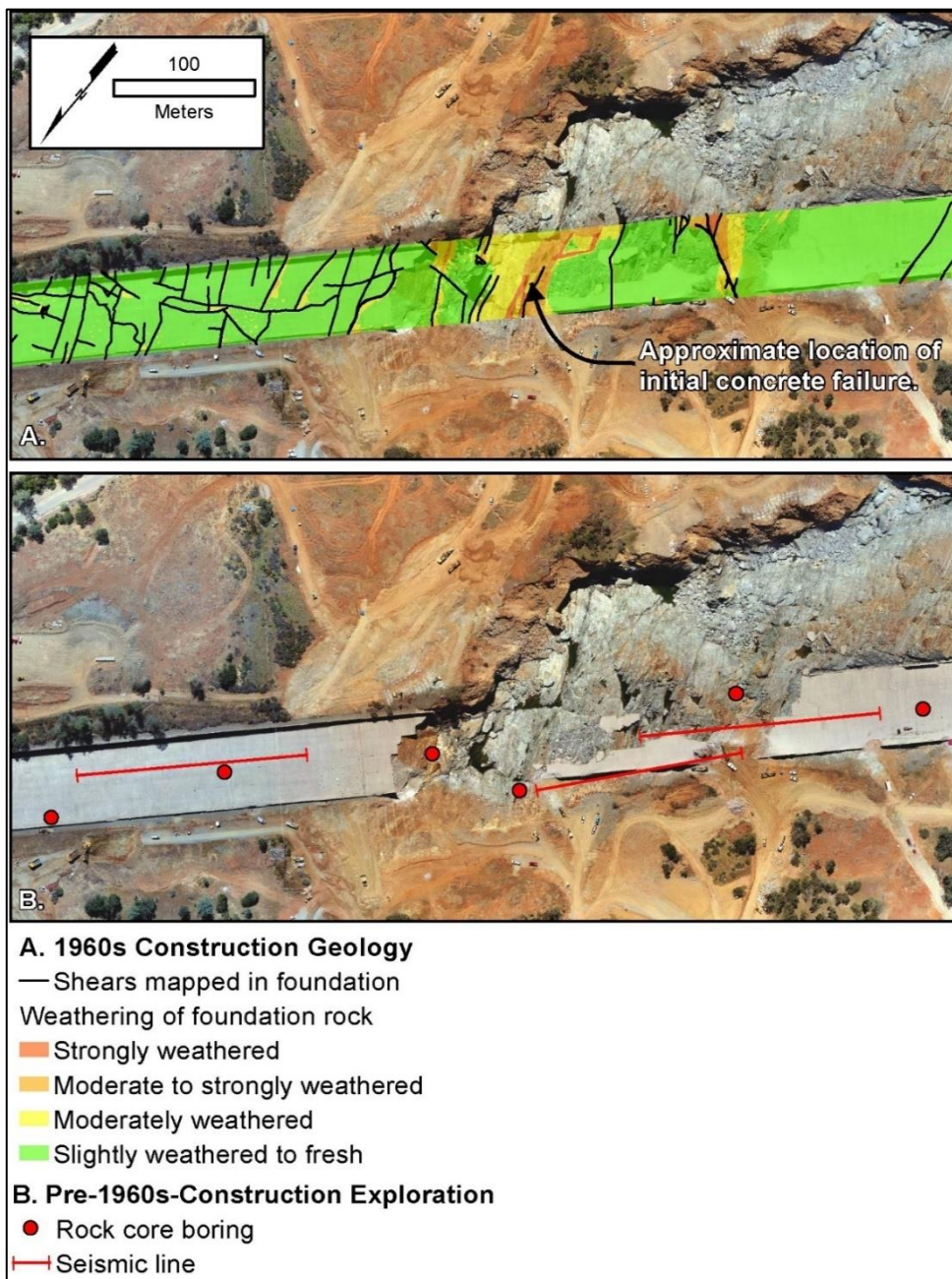


Figure 4
 A. Geologic map of FCO Spillway Chute showing initial concrete failure location [6]. B. Aerial photo showing pre-1960s-construction exploration locations [5].

However, on the right side of the chute’s scour hole, there was an area of intensely-weathered rock that continued to ravel into the scour hole during the Spring 2017 FCO Spillway releases. These disparate exposures raised questions about the continuity of rock weathering and indicated that the presence of cross-

cutting shears could greatly affect the continuity of rock materials. Exploration locations were added to investigate the continuity of similar rock materials.

In the days after the Emergency Spillway flows, between February 10 and 12, 2017, water was observed to be seeping immediately downstream from the Emergency Spillway structure through fractures in the rock with very little head. This led to questions of the efficacy and integrity of the original grout curtain beneath the Emergency Spillway. Exploration locations were added on both sides of the Emergency Spillway to investigate the rock conditions and the hydraulic conductivity of the rock formation.

Figure 5 - Photo of the scour hole and channel forming to the left of the FCO Spillway chute illustrating the geology left behind by erosion and scour. Five drill



rigs are visible in the FCO Spillway chute and one on the right side of the chute).

In erosion gullies created by the flowing water, interpretations based on new reconnaissance-level geologic mapping suggested some larger shears might project back towards the FCO Spillway chute, resulting in unfavorable conditions. These features needed to be explored in detail to assess the overall stability and foundation conditions for the new replacement spillway chute. A series of rock-core borings was added to identify and delineate the continuity of these shears, with inclinometers installed to monitor the stability of the slopes in critical areas.

The examples above are representative of the types of geologic features targeted to investigate the geology of the site. These types of features were explored primarily by drilling borings with further information derived from the

downhole televiewer, surficial geologic mapping, seismic lines, and instrumentation.

3.2. EXPLORATION FOR DESIGN OF OROVILLE EMERGENCY RECOVERY

At the onset of the OER design effort, there were many spillway repair alternatives being examined. Not knowing which design alternative would be selected, the exploration plan accommodated each of the repair alternatives and the issues specific to each alternative. The major design components included repairs or replacement of the FCO Spillway chute, fortifying the Emergency Spillway monolith weirs against potential sliding or over-turning, construction of an erosion cutoff wall downstream from the Emergency Spillway, and erosion protection of the ground surface between the erosion cutoff wall and the Emergency Spillway.

The replacement of the FCO Spillway chute included modifications to the original design features that would bring the chute to current design standards. These modifications included longer chute slab anchors, new underdrains below the slabs (not within them), enhanced underdrain filter designs, and so on. To ensure adequate chute slab anchor lengths, unconfined compressive strength testing was performed on core samples from the foundation rock to accurately calculate the required bond length for anchorage into moderately-weathered or better rock, and for anchorage into intensely-weathered or decomposed rock. Geotechnical borings were also added to collect representative samples of the intensely-weathered to decomposed rock that might be in contact with the chute underdrain materials. These materials were then tested to help design the filters for the underdrain system.

The design criteria for the erosion-resistant cutoff wall within the unlined Emergency Spillway foundation required at least 4.5 m (15 ft) of embedment into the slightly-weathered or better rock. Many rock-core borings were added to the exploration plan to determine the geologic conditions for the proposed erosion-resistant cutoff wall. Several surface P-wave geophysical lines were also performed to examine the variability of rock weathering in the upper 15 m (50 ft). The alignment of the erosion-resistant cutoff wall, which later was designed as a secant pile wall, was adjusted during the design to minimize pile depths based on the geologic conditions encountered.

3.3. FCO SPILLWAY CHUTE EXPLORATION

A major component of the geologic and geotechnical explorations took place within the FCO Spillway chute alignment. As the design process progressed, it became apparent that the reconstruction of the chute would likely take at least two years to complete. Between the two construction seasons, during the Winter Flood Season of 2017-2018, the upstream portion of the original chute nearest the

headworks structure would need to remain in place [3]. However, for the design team and dam safety regulators to be comfortable with this situation, many explorations were performed within the upper chute to better understand the actual thicknesses and quality of the concrete slabs, foundation rock quality, concrete-foundation interface conditions, and so on.

To address design concerns, the chute slab concrete was cored at 68 exploration points within the upper half of the FCO Spillway chute, upslope from the initial scour hole. Of the 68 locations, 24 were additionally cored into the foundation rock to assess foundation rock conditions. Falling-head permeability tests were completed in 18 locations to test the bond between the slab concrete and the foundation rock. Ground-penetrating radar (GPR) was also used to image the concrete and the underlying foundation rock in the upper chute; the results from the GPR imaging were used to guide some of the physical exploration locations. Eight wireless vibrating-wire piezometers were installed in six locations to determine groundwater pore pressures beneath the chute slab during spilling and non-spilling events.

In addition to explorations to address design concerns, DWR performed forensic studies that aimed to address the following potential physical factors raised by the Independent Forensic Team in their preliminary report [10]: 1) thickness of the chute slab above herringbone underdrains; 2) variations in slab thickness, 3) characteristics of weathered foundation rock and intensely-weathered rock; 4) foundation rock bonding with the concrete slab; 5) effects of extended drought impacts on foundation materials; and 6) groundwater pressures exerted on the chute slab.

Four areas of the undamaged concrete-lined FCO Spillway chute were evaluated using saw-cut trenching to examine the foundation conditions and potential physical factors that might have contributed to the damage of the FCO Spillway chute. Each area of the saw-cut concrete chute was carefully lifted away from the surrounding slab concrete to minimize disturbance. Each location was then photographed in detail prior to performing any investigative work. Once the area was thoroughly documented, the gravel surrounding the perforated underdrain pipes (vitrified clay pipes placed during original construction) was hand-picked from around the pipes. Any non-rock materials mantling the foundation rock, such as original excavation debris, were measured, sampled, described, and then cleared off for final geologic mapping of the foundation rock surface.

The findings from the FCO Spillway chute explorations indicated that – where measured – the concrete slab was greater than 18.3 cm (7.2 in) thick above the underdrain pipes; the concrete slab thickness varied from about 38 cm (15 in) to over 2.1 m (7 ft); there were not large extents of intensely-weathered to decomposed rock; there was generally good bonding between the rock and the concrete slab; and groundwater piezometric pressures within the chute's foundation rock were typically below the concrete-foundation interface.

4. EXECUTION OF EXPLORATION PROGRAM

The initial exploration program was outlined by a team of engineers, geologists, and construction specialists between March 6 and 12, 2017. The first drill rigs were mobilized on March 13, 2017, and drilling began on March 14, 2017. The initial exploration program consisted of 60 rock-core borings, 16 seismic lines, 10 inclinometers, and 10 vibrating-wire piezometers. As design efforts progressed and changed, the exploration program was modified to accommodate those design changes. By the end of July 2017, the exploration program had been expanded to 104 rock-core borings (over 2800 m [9180 ft] of rock core), 22 seismic lines, 15 inclinometers, 15 vibrating-wire piezometers, and 11 piezometers (both open standpipe piezometers and observation wells; Fig. 6). In order to successfully execute a large amount of exploration in a short amount of time (about 4 months), an exploration workplan was prepared to establish the project protocols, a wide variety of resources was identified and mobilized, a field QA/QC program was implemented, a team of geologists and geotechnical engineers was stationed in the office to analyze the incoming data, and regular consultations with the design team were held to ensure that design needs were being met.

4.1. EXPLORATION METHODS

Several methods were utilized to explore the subsurface conditions in and around the FCO Spillway chute and the Emergency Spillway, including the following: concrete and rock-core borings, packer and falling head permeability testing, downhole televiewer surveys – optical and acoustic, borehole geophysical suspension logging, grouted-in-place vibrating-wire piezometers (VWPs), open standpipe piezometers, observation wells, inclinometer casings and instrumentation, P-wave surface geophysics, concrete coring, test pits and bulldozer trenches, laboratory testing of rock and soil for index properties and

shear strength data, thin-section petrographic analysis, and x-ray diffraction. These methods are generally described below.

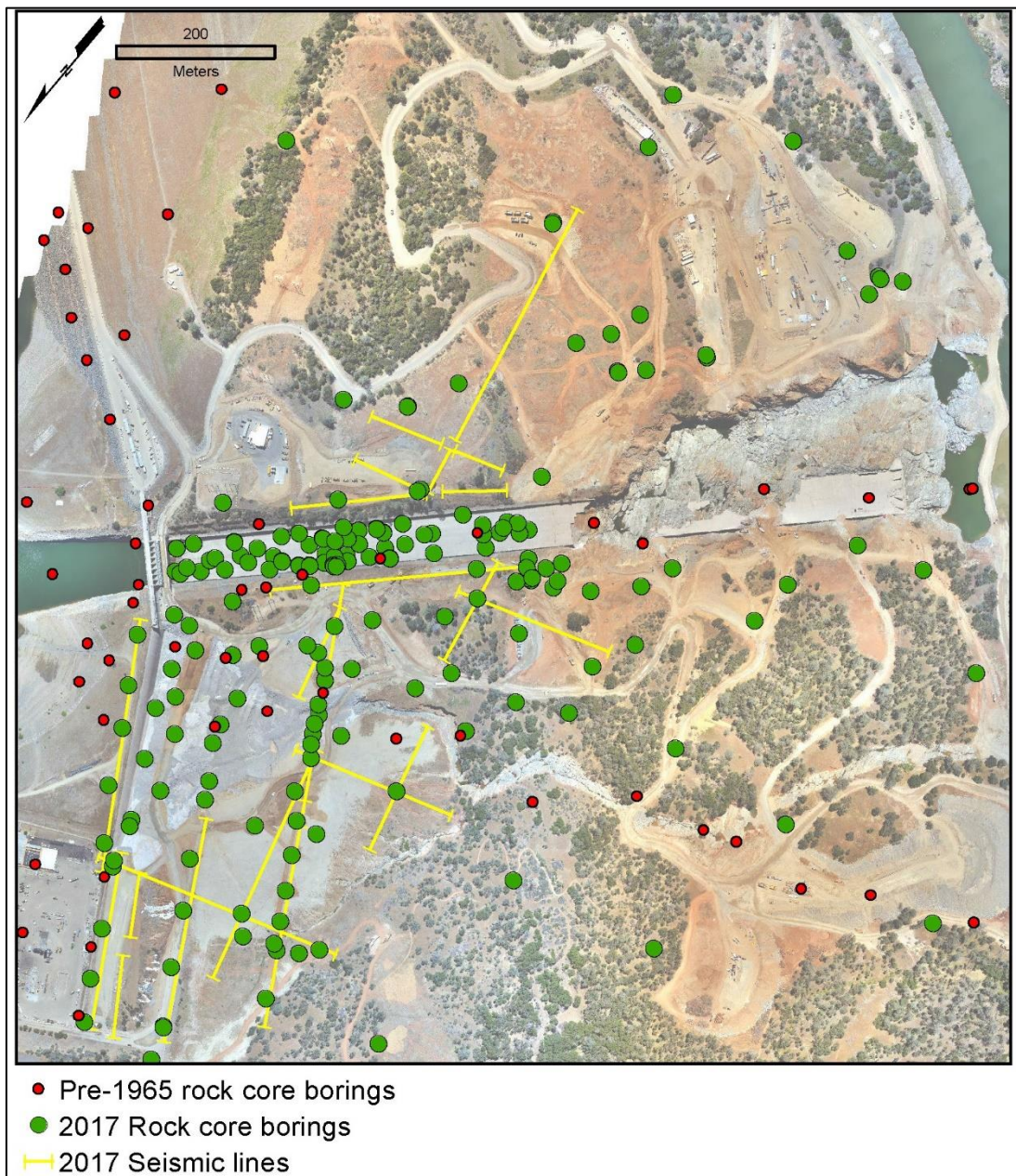


Figure 6 - FCO Spillway Recovery geologic exploration program.

All the rock-core borings were drilled at least 6 m (20 ft) into fresh, un-weathered amphibolite, with drilling depths that ranged up to about 60 m (200 ft). Each boring was logged in accordance with the project procedures, which included the classification of rock lithology, degree of weathering, discontinuities and infilling, Rock Quality Designation (RQD), and descriptions of other relevant geologic features.

The drill rig geologist recorded drilling conditions such as rod drop, water loss and drill chatter, as well as sampling locations, material types, and any occurrences that might have proved informative to characterizing the subsurface conditions. Upon reaching total depth, all drill holes were geophysically logged using either acoustic or optical televiewer, or both, to ensure that the orientation of any discontinuity was documented. Although geophysical logging of nearly every borehole may seem excessive, the decision to geophysically log each boring proved invaluable, considering the time constraints and the need to develop a comprehensive geologic site model to support the range of OER design options being considered. Selected drill holes were additionally logged using suspension P- and S-wave velocity logging techniques to correlate with surficial geophysical results. Upon completion of each drill hole, the borehole was either completed as a VWP, open standpipe piezometer, inclinometer, or it was backfilled with cement-bentonite grout. The ultimate disposition of the borehole completions was developed using a collaborative process with the design team to confirm that the overall purpose of each borehole and the associated design objectives were being accomplished.

Nearly all of the instrumentation (piezometers and inclinometers) was telemetered and viewable on an online dashboard in real time. Six locations within the FCO Spillway chute were completed as grouted VWPs with a data logger and wireless antenna; these data were retrieved manually, rather than through the online dashboard, and the instruments were installed prior to the last controlled spill through the FCO Spillway chute in May 2017.

All drilling work within the FCO Spillway chute began by initially coring through the chute concrete using a 20.3 cm (8 in) diameter thin-walled coring bit. Once the coring reached the concrete-foundation rock interface, select locations were continued using rock-coring methods. Select rock core and hand samples were obtained for shear strength testing and petrographic analysis. Samples of shear gouge and compacted clayey fines from the foundation were analyzed for index properties testing, including mechanical sieve, hydrometer, and Atterberg limits. In addition, select samples were analyzed for clay mineralogy, using x-ray diffraction.

4.2. RESOURCES

Execution of an exploration program of this magnitude is challenging under normal circumstances. In this case, there was very little time for the OER design team to assess the site conditions, review historic construction records, and develop the initial field exploration program. The demand on qualified personnel, including exploration subcontractors and testing laboratories, was unprecedented in magnitude and response. The execution of the initial exploration program, consisting of 60 borings and 16 P-wave surface refraction lines, along with the associated instrumentation, was needed within a very short time-frame to be incorporated into the spillway repair. The exploration program included test

locations within the concrete-lined portion of the FCO Spillway chute, which in turn required special coordination with the OER Incident Command personnel and dam safety regulators, and had to be timed to coincide with short-duration spillway outages. Resources required to perform this work included concrete coring units, rock-coring drill rigs, surface and borehole geophysical testing, engineering geologists, field and office management, instrumentation specialists, and construction support (to build access roads, create drill pads, dig mud pits, etc.). Other required support included environmental scientists, archaeologists, and cultural resource specialists to confirm that the proposed drilling sites, surface geophysical lines, and other work items (e.g., temporary roads and/or equipment staging areas) would not impact documented sensitive areas within the project site.

Ultimately, up to 10 drill rigs, with drilling contractors from three private firms and two federal agencies, were utilized to perform the drilling work. Two geophysical firms were selected to perform the P-wave surface refraction lines. Two geophysical firms performed downhole acoustic and optical televiewer surveys, and P-S suspension logging on select boreholes.

For every drill rig, there was at least one engineering geologist to log the rock core. Experienced engineering geologists logging the rock core were resourced from within DWR, two federal agencies, and several consulting firms. The qualifications of the engineering geologists had to be reviewed and approved by Federal dam safety regulators prior to working on the site. In order to maintain consistency with so many engineering geologists, an exploration work plan was prepared in the days leading up to the initiation of the exploration program. The work plan detailed the logging nomenclature and field procedures defined for the project.

At any given time, there were at least two experienced, on-site engineering geologists coordinating the scheduling and movement of drill rigs, clearing sites with environmental and cultural specialists, scheduling the rotating geology staff, interfacing with the OER Incident Command, holding safety meetings, and all the other typical daily routines for an exploration program (but 10 times as big). There were typically 15 to 20 engineering geologists on site daily during the peak of exploration who were logging rock core, geologically mapping rock exposures, and coordinating drill rig and personnel movements. Many engineering geologists and engineers were in the office, performing real-time data analysis for the design efforts.

4.3. QUALITY ASSURANCE AND QUALITY CONTROL

The drill rig engineering geologists logging the rock core were from several different agencies and consulting firms. To ensure a consistent approach to recording drill hole information, including handling and logging of recovered rock core and performance of borehole testing, a full-time QA/QC Engineering Geologist was assigned to review field logs and recovered rock core throughout

the duration of the field exploration program. The QA/QC function included daily monitoring of drilling activities at each drilling location to confirm compliance with the work plan, performing daily review of borehole logs to ensure completeness and accuracy of the logged conditions, and reviewing the final, completed borehole logs.

The borehole logging QA/QC review used a multi-step approach to oversee the process. The initial step consisted of a QA/QC review that was performed in the field by the on-site QA/QC Engineering Geologist to verify that each drill rig engineering geologist was meeting DWR's borehole logging standards for the project. This review was performed daily at the drill rig, during drilling and sampling. Upon completion of each borehole field log, the QA/QC Engineering Geologist performed an initial field log review to check consistency of logging and completeness of the field log. Then, the borehole log was reviewed and compared to the recovered rock core. If necessary, revisions to the borehole log were made as part of the technical review. The field log was then drafted using Bentley gINT with the QA/QC Engineering Geologist maintaining control over the process until the draft borehole log was accepted as final.

5. CHALLENGES AND LESSONS LEARNED

The geological and geotechnical explorations for the design of OER was a complete success. This success was made possible through the commitment of DWR staff and DWR's key support personnel sourced from the public and private sectors, along with field services organizations. This integrated team truly rose to meet the challenges. One of the major challenges for the geologic and geotechnical design team was the highly variable geologic conditions, which changed significantly both laterally and vertically within short distances. While there was only one geologic rock mass (i.e., amphibolite) truly present across the site, the cross-cutting shears created a patchwork of rock weathering and fracturing conditions. The overall rock mass strength of the amphibolite was controlled by the degree of weathering and the intensity and orientation of discontinuities (e.g., shears and joints) within the rock. The integration of a detailed surface and borehole geophysics program, coupled with extensive rock-core borings, proved invaluable in making proper assessments of foundation rock quality for this project. The surface refraction methods greatly assisted in developing initial interpretations of rock uniformity (horizontal and vertical) and estimates of rock mass strength through correlations to nearby boreholes.

It was critical to this success that the OER design team assembled very early on to discuss geology and geotechnical needs that might arise during the design process. This allowed a relatively small group of geologists, geotechnical engineers, and construction specialists to develop a comprehensive, but adjustable, exploration program to address design needs. As a result, the geologic and geotechnical exploration program provided high-quality results, while

remaining responsive and adaptable to the iterative design process needed to execute the spillway repairs under the very short timeframe.

Active, on-site coordination and QA/QC procedures were critical to the successful implementation of the field exploration program. Although there were daily challenges, the experienced on-site engineering geologists and geotechnical engineers remained flexible and good humored throughout.

The configuration of real-time, accessible instrumentation readings allowed the close monitoring of potential slope instability and changes in groundwater conditions. Placing the instrumentation data in one centralized location that was easily accessible by anyone on the team at any time provided the ability to examine short- and long-term performance trends quickly and remotely. Centralized data storage was essential for time-critical information to be accessible by the design team as needed.

ACKNOWLEDGMENTS

The authors wish to acknowledge many firms and/or entities who assisted with the geologic and geotechnical exploration program: DWR engineering geologists from several divisions, state-wide; Lettis Consultants International, InfraTerra, the United States Bureau of Reclamation, the United States Army Corps of Engineers, Gregg Drilling and Testing, Cascade Drilling, Ruen Drilling, GeoVision Geophysical Services, Gasch Geophysics, NorCal Geophysical (with Terracon), GEI Consultants, Spectrum Petrographics, Cooper Testing Laboratory, Blackburn Consulting, Willamette Geological Service, and Syblon Reid Contractors. Specifically, thank you to Nick Hightower, Bryan Dussell, and Andy Tate, who organized the field teams and were instrumental in successfully executing this enormous exploration program.

REFERENCES

- [1] SAUCEDO G.J., WAGNER D.L. Geologic Map of the Chico Quadrangle, California. *California Geological Survey, Regional Geologic Map No. 7A, 1:250,000 scale*, 1992.
- [2] CROYLE B., GUTIERREZ D., ANDERSEN M., TAPIA S., BLACKETT F. Oroville Dam Spillway Incident – Situation Development, Incident Response, and Public Safety. *ICOLD World Congress Proceedings*, 2018.

- [3] CRADDOCK T., HARDER L., VERIGIN S., KUTTEL J., BROWN D., MIHYAR M., BOYER D. Oroville Dam Spillway Incident – Fast Track Recovery Design to Address Critical Dam Safety. *ICOLD World Congress Proceedings*, 2018.
- [4] SNOW C.A., SHERER H. Terranes of the Western Sierra Nevada Foothills Metamorphic Belt, California: A Critical Review. *International Geology Review*, 2006, Vol. 48.
- [5] O'NEILL A.L., COKE K.J., MARLIAVE E.C. Geologic Report on Preliminary Exploration of the Oroville Dam Site. *California Department of Water Resources, Project Geology Report No. 20-11-05*, 1955.
- [6] HUBER O.L., GROSS D.J., MARLETT J.W. Final Geologic Report, Oroville Dam Spillway. *California Department of Water Resources, Project Geology Report No. C-38 (20-11-26)*, 1970.
- [7] LAMKIN B.L., GLICK F.G. Oroville Dam Spillway, Results of Landslide Evaluation. *California Department of Water Resources, Project Geology Report No. 20-11-35*, 2004.
- [8] DUNBAR S., HOIRUP D., BARRY G.R. Oroville Dam, Emergency Spillway, and Flood Control Outlet, Drill hole and Shear Wave Velocity (Vs) Results. *California Department of Water Resources, Project Geology Report No. 20-11-50*, 2017.
- [9] DAM SAFETY REVIEW BOARD. Oroville Dam, FERC (Federal Energy Regulatory Commission) Project 2100-CA, State Dam No. 1-048, NID No. CA00035, CA00530, & CA83096, Ninth Five-Year Part 12D Safety Inspection Report, 2014 Director's Safety Review Board, December 2014.
- [10] INDEPENDENT FORENSIC TEAM. Oroville Dam Spillway Incident Forensic Investigation Team (IFT), Preliminary Findings Concerning Candidate Physical Factors Potentially Contributing to Damage of the Service and Emergency Spillways at Oroville Dam, Forensic Team memorandum, May 5, 2017.

SUMMARY

Starting on February 7, 2017, a scour hole formed in the concrete-lined Gated Spillway chute at Oroville Dam. Continued intermittent releases between February and May 2017 led to further damage of the Gated Spillway chute and the creation of a large erosion scour channel to the left of the lower chute. During this time, the unlined Emergency Spillway was used for the first time to release reservoir flows. Significant erosion and scour of the weathered rock at the unlined

Emergency Spillway during just two days of limited overflow release resulted in concerns for the Emergency Spillway structures and the evacuation of communities downstream of the dam.

In early March 2017, the Oroville Emergency Recovery (OER) design team was formed to design and implement repairs in order for the Gated Spillway chute and the Emergency Spillway to be able to safely pass reservoir inflows during the following 2017-2018 Winter Flood Season. Within a week, the OER design team had identified a number of potential repair alternatives and the associated geologic and geotechnical data required to develop the designs. This paper provides a background of the geologic conditions known prior to the incident and the subsequent development and execution of the geologic and geotechnical investigation program to support the OER.

The geologic materials at the Oroville Dam site are structurally complex, with numerous cross-cutting shear zones that make predicting ground conditions difficult. The complex geology coupled with the urgent time-frame in which to develop and implement a field investigation and laboratory testing program and then provide useful high-quality subsurface geologic and geotechnical information to the OER design team presented many challenges. These challenges ranged from resource management, to assessing a wide range of conceptual and then preferred design components, to field investigation QA/QC, to expedited data analysis and interpretations needed to properly support development of the time-critical project design.

By the end of the design phase of geologic exploration in July 2017, the exploration program had grown to over 100 rock-core borings, 22 seismic lines, 26 piezometers, 15 inclinometers, 68 concrete cores, trench explorations, thin section petrographic analysis of over 30 rock samples, x-ray diffraction of 6 clayey samples, and geotechnical testing of many more rock and soil samples.

In order to accomplish the exploration program, consistent documentation was achieved by preparing a workplan and having an experienced full-time engineering geologist serve in a QA/QC role to ensure that the workplan was being followed. Results of the explorations were relayed to the OER design team in real time to be incorporated into the engineering design package. The geological and geotechnical exploration program was successful because of dedicated, coherent design and field teams.

Keywords

Oroville Dam, Boring, Emergency Spillway, Chute, Flood Control Outlet, Foundation, Gated Spillway, Geological Investigation, Main Spillway, Monolith, Emergency Spillway.

COMMISSION INTERNATIONALE DES GRANDS BARRAGES

VINGT-SIXIÈME CONGRÈS DES GRANDS BARRAGES
Autriche, juillet 2018

DOI 10.3217/978-3-85125-620-8-006



This work licensed under a Creative Commons Attribution 4.0 International License. <https://creativecommons.org/licenses/by-nc-nd/4.0/>

**OROVILLE DAM SPILLWAY INCIDENT - HYDROLOGIC AND HYDRAULIC
ENGINEERING ACTIVITIES TO INFORM OPERATION AND DESIGN**

Ganesh PANDEY

*Supervising Engineer, STATE OF CALIFORNIA, DEPARTMENT OF WATER
RESOURCES*

David FORD

*Oroville Spillway Restoration Hydrology Team Lead, DAVID FORD
CONSULTING ENGINEERS, INC.*

Ted CRADDOCK

*Oroville Spillways Project Manager, STATE OF CALIFORNIA, DEPARTMENT
OF WATER RESOURCES*

Molly WHITE

*Supervising Engineer, STATE OF CALIFORNIA, DEPARTMENT OF WATER
RESOURCES*

Mark FORTNER

Oroville Spillway Restoration Hydraulic Team Lead, GEI CONSULTANTS, INC.

John LEAHIGH

*Principal Engineer, STATE OF CALIFORNIA, DEPARTMENT OF WATER
RESOURCES*

Mike ANDERSON

*State Climatologist, STATE OF CALIFORNIA, DEPARTMENT OF WATER
RESOURCES*

UNITED STATES OF AMERICA

**OROVILLE DAM SPILLWAY INCIDENT — HYDROLOGIC AND HYDRAULIC
ENGINEERING ACTIVITIES TO INFORM OPERATION AND DESIGN***

Ganesh Pandey
Supervising Engineer, State of California, Department of Water Resources

David FORD
*Oroville Spillway Restoration Hydrology Team Lead, David Ford Consulting
Engineers, Inc.*

Ted Craddock
*Oroville Spillways Project Manager, State of California, Department of
Water Resources*

Molly White
Supervising Engineer, State of California, Department of Water Resources

Mark Fortner
Oroville Spillway Restoration Hydraulic Team Lead, GEI Consultants, Inc.

John Leahigh
Principal Engineer, State of California, Department of Water Resources

Mike Anderson
State Climatologist, State of California, Department of Water Resources

UNITED STATES OF AMERICA

1. INTRODUCTION

Oroville Dam is located on the Feather River in northern California (USA). At 234.7 m (770-ft) tall, this earth embankment is the tallest dam in the United States. With its 4.3 billion m³ (3.5 million acre-feet) of storage, Lake Oroville is the second largest reservoir in California, supplying water to cities as far south as Los Angeles. The Oroville Dam, reservoir (Lake Oroville), and hydropower plant facility is the flagship of the State Water Project (SWP), which is owned and operated by the State of California, Department of Water Resources (DWR).

*OROVILLE BARRAGE RÉPONSE D'URGENCE ET RESTAURATION DE
DÉVERSEMENT - ACTIVITÉS D'INGÉNIERIE HYDROLOGIQUE ET HYDRAULIQUE
POUR INFORMER LE FONCTIONNEMENT ET LA CONCEPTION

The 2016-2017 Winter Storms brought record breaking precipitation to the Northern California Sierra mountains including the Feather River watershed. On February 7, 2017, the Oroville Dam's 54.5 m (179-ft) wide Flood Control Outlet (FCO) Spillway chute (Fig. 1) was releasing water to control the Lake Oroville reservoir level in accordance with the prescribed operations plan. During this operation, the FCO spillway suffered a catastrophic failure of the lower chute area eventually resulting in the loss of approximately 427 m (1400 ft) of the lower chute, including the scour of more than 1.2 million m³ (1.6 million yd³) of soil and rock materials. On February 11, 2017, the Emergency Spillway (Fig. 1) was used for the first time since the project was completed in 1968. During this operation, significant erosion and scour caused by the Emergency Spillway overflow led authorities to fear for the safety of the spillway structures, resulting in the activation of the Emergency Action Plan and evacuation of about 188,000 persons from downstream communities.

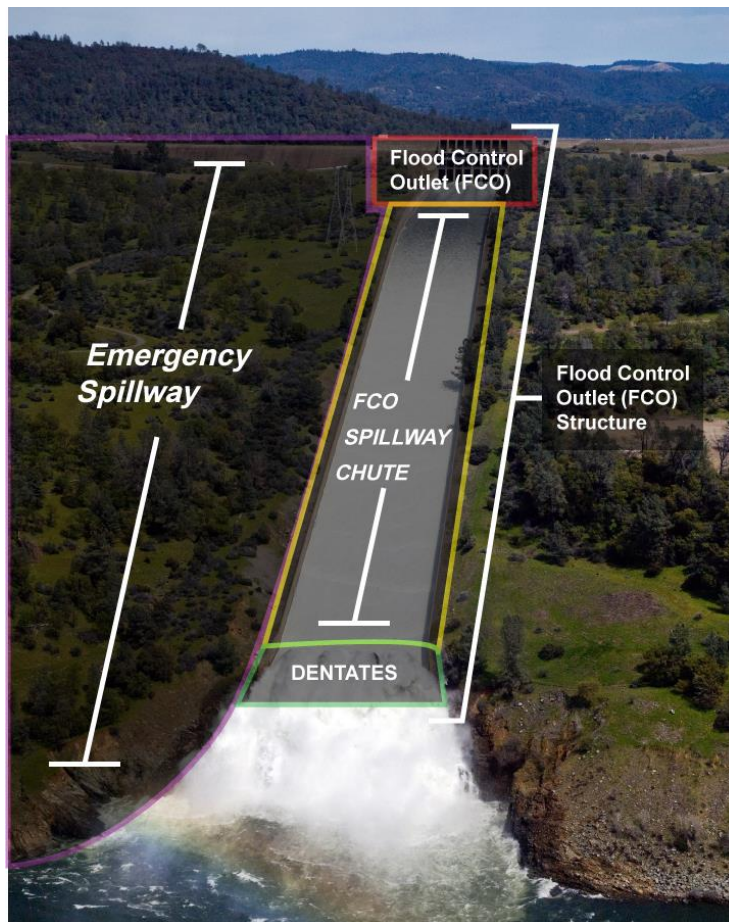


Fig. 1 Flood Control Outlet (FCO) Structure and Emergency Spillway, March 2011

This paper is part of a series developed by the State of California, Department of Water Resources (DWR) to describe the Oroville Dam Spillway Incident Emergency Response and Recovery. This paper focuses on (a) the hydrologic engineering, hydraulic engineering, and reservoir operation analyses completed

during the incident and later as part of the recovery; (b) hydrologic, hydraulic, and operation analysis models and methods used for the analyses; (c) strategies for development, review, and coordinated use of the models and methods by a large team of analysts; and (d) problems faced and solutions found as the models were configured, calibrated, and applied to provide information to design staff and influence interim operation decisions required throughout the response and recovery efforts.

2. PROJECT FEATURES AND HISTORICAL PERFORMANCE

The original design of Oroville Dam, including selection of types and capacities of spillways and placement of the Flood Control Outlet (FCO) Spillway chute and Emergency Spillway relative to the embankment, and the details of a tightly-integrated operation policy, were the result of more than thirteen years of hydrologic and hydraulic (H&H) engineering and operation studies.

An initial design and operation policy was proposed in 1953 and refined in 1955 with results from a scaled physical-model study [2]. To accommodate updated operational requirements by the United States Army Corps of Engineers (USACE), the 1955 design was revised in 1958 and again in 1962. A physical modeling study of the revised spillway concept was carried out in 1962 by the United States Bureau of Reclamation (USBR). To address issues identified then, the FCO Spillway chute and the Emergency Spillway were configured as two separate structures [3].

The Oroville Project consists of the main dam, two saddle dams, a flood control outlet structure, an emergency spillway with concrete weir upstream of an unlined hill slope, and a hydropower plant.

The layout of the spillways is shown in Fig. 2, along with the FCO Spillway chute flow and erosion during the failure incident. The 1310.6 m (4300 ft) long FCO Spillway chute includes an unlined approach channel, a flood control outlet structure, a spillway chute, and an energy dissipater. The outlet structure has eight radial gates each 5.36 m (17 ft 7 in) wide separated by six 1.52 m (5 ft) thick piers and one central 2.44 m (8 ft) thick pier. Finally, the geometry of the outlet structure was optimized using results of 1965 physical modeling studies [4]. The FCO Spillway chute is a rectangular concrete-lined channel with a constant width 54.46 m (178 ft - 8 in). Four reinforced-concrete dentate structures at the end of the chute, the design of which is based on these same 1960s studies, dissipate the water energy. The Emergency Spillway includes an ogee section with multiple concrete monoliths of varying heights and a low-sill, broad-crested weir on natural ground. The area downstream of the Emergency Spillway was not cleared of vegetation because the expected infrequent use did not justify the potential adverse economic and aesthetic impact.



Fig. 2 Photograph of Oroville, showing spillways and main dam embankment

The combined spillway capacity was designed to safely pass the probable maximum flood (PMF). During this event, the design FCO Spillway chute maximum release is 8382 m³/s (296,000 ft³/s), and the design Emergency Spillway discharge is 10506 m³/s (371,016 ft³/s at reservoir pool elevation 279.5 m (917 ft). Integrated design features and operation rules were developed to control a standard project flood (SPF) inflow of 12460 m³/s (440,000 ft³/s) without using the Emergency Spillway, and with the FCO Spillway chute release limited to 4248 m³/s (150,000 ft³/s). This FCO Spillway chute release target was set to protect downstream urban and agricultural areas from potential flooding.

In the 49 years since construction, the FCO Spillway chute has been used 25 of those years and the remaining 24 years the FCO spillway was not operated. Over operational period, the maximum daily release through the FCO Spillway chute equaled or exceeded 2832 m³/s (100,000 ft³/s) four times. Releases have

been at or exceeded 4248 m³/s (150,000 ft³/s twice, in February 1986 and January 1997. Fig. 3 shows the FCO Spillway chute, looking downslope, in February 1986. As predicted during design, flow along the chute appears to be aerated through the development of a boundary layer as well as through the piers of the Flood Control Outlet. DWR maintenance records show no significant cavitation damage through the project history [5]. Any damage patterns were random, not clearly related to a particular flow condition in the FCO Spillway chute.

Prior to the event of 2017, the Emergency Spillway had never been used, so no record of historical performance existed for that facility.



Fig. 3 Photograph of FCO Spillway chute during release of 4248 m³/s (February 21, 1986)

3. HYDRAULIC ENGINEERING, HYDROLOGIC ENGINEERING, AND RESERVOIR OPERATION ANALYSES DURING 2017 INCIDENT

During the 2017 incident, hydrologic and hydraulic engineering and reservoir operation analyses provided information to support decision making by DWR management. Lake Oroville inflow forecasts were made every six hours by DWR staff and the United States National Weather Service (NWS), using conceptual models of watershed hydrology. As snow had accumulated in much of the contributing Feather River Basin watershed, these forecasts included assessments of both runoff from rainfall at lower elevations and snowmelt at higher elevations.

Reservoir behavior and operation with various operation and potential failure scenarios were simulated to predict future pool elevations and timing of potential Emergency Spillway discharge. For this, reservoir conditions were monitored continuously by onsite DWR staff, reported using all available resources, and used as boundary and initial conditions for the models.

Inundation that could result from potential failure of the main dam was predicted and displayed with maps included in the dam's Emergency Action Plan (EAP), which emergency and incident command teams consulted. These inundation maps were augmented with situation-specific maps prepared from near-real-time forecasts as the incident progressed. Both were used to inform local officials regarding the need for evacuation of downstream residents. For inundation mapping, the HEC-RAS [6] and FLO-2D applications [7] were used; maps were created by overlaying computed flood flow depth grids on feature maps with geographic information system (GIS) software. Terrain data and bathymetric data had been collected by DWR in prior years for analysis of downstream floodplain risk and for preparation of the EAP.

Additional hydraulic analyses provided DWR managers with information about potential flow paths along the hill slope downstream of the Emergency Spillway, and with estimates of potential debris and sediment loads in the Feather River downstream. The hill slope was modeled with a 2-D model created with HEC-RAS.

Challenges for analyses during the event in February 2017 included: (1) the need for almost immediate turnaround to provide information critical for decision making; (2) the lack of certainty about near-future inflows to the reservoir due to uncertainty about the weather and watershed response; (3) the lack of certainty about behavior of the never-used Emergency Spillway, with unstable terrain; and (4) the risk of misunderstanding or misinterpreting model results as critical decisions were made. Solutions included: (1) the use of cloud computing, with parallel model runs on multiple servers in the Amazon cloud; (2) analysis with ensemble forecasts, coupled with sensitivity analysis with varying inflow hydrograph properties; (3) constant monitoring and reporting to modelers of observed changes to the spillways so model inputs could be adjusted; and (4) careful communication of results by DWR and consultant subject matter experts.

4. RESERVOIR OPERATION ANALYSES DURING RECOVERY

DWR's Oroville Emergency Recovery (OER) team considered options for restoring the FCO Spillway chute and the Emergency Spillway, and selected the optimal configuration. A consideration in this selection was the way Lake Oroville would be operated to protect public safety prior to, during, and following construction — the reservoir operation plan. Through reservoir operation analysis, alternative schemes were assessed and refined. Once the new spillway

configurations were selected, refinement of the operation policy continued (and continues as this paper is written, as full project restoration is not yet complete), with information for decision making provided by reservoir operation analyses.

The reservoir operation analyses were structured to:

- Assess the flood risk of removing the FCO Spillway chute so it could be reconstructed, and identify or confirm decisions about the timing of this removal and reconstruction. Based in part on this assessment, a decision was made to start construction in May 2017.
- Develop an operations plan for the period of construction in 2017 that did not rely on the FCO Spillway chute and that minimized flood risk during construction. This led to drawing the reservoir down to elevation 213.4 m (700 ft) prior to the Winter Flood Season, using the powerhouse outlets.
- Develop flood operations plan for the 2017-2018 Winter Flood Season to safely manage potential flood inflows with the partially reconstructed FCO Spillway chute, limiting releases through that spillway to 2832 m³/s (100,000 ft³/s). Because of the RCC invert, the maximum flow from the partially reconstructed FCO chute was limited to 2832 m³/s.
- Develop flood operations plan that provides a 2018 construction season window with no reliance on the FCO Spillway chute.
- Develop new flood operations plans for the period following the completely restored FCO Spillway chute.

Flood operations for Lake Oroville and Oroville Dam are prescribed by the USACE, so all analyses were completed in collaboration with USACE staff, and all flood operations plans were submitted to the USACE, Federal Energy Regulatory Commission (FERC), and the State of California, Department of Water Resources, Division of Safety of Dams (DSOD) for their collective review and approval. Although flood protection and dam safety are the overriding operation objectives, operation plans also considered: water quality and environmental flow objectives, the need for water to protect endangered species, the rights of water users, and contractual commitments for water delivery by California's SWP.

The USACE HEC-ResSim application [8] and custom applications developed by DWR were used for the analyses of reservoir operations; the majority of the custom applications are spreadsheet-based. The HEC-ResSim applications were configured to simulate operations with various conditions of the reservoir outlets, including FCO Spillway configurations with reduced capacities. The simulations used various boundary conditions: (a) the historical period of record; (b) forecasts of near-term inflow provided by the NWS; and (c) statistically-derived hydrographs with flood volumes of specified exceedance probability, as developed with the hydrologic engineering analyses described below. The simulations used a daily or sub-daily time step, computing time series of pool elevation and reservoir storage, release through all Oroville Dam outlets, and discharge at downstream locations

to which releases are routed. This information permitted assessment of the flood risk downstream and the risk to the structural integrity of Oroville Dam.

Challenges in reservoir operation analysis for Oroville Dam included: (1) the need for quick turnaround to set guidelines during construction and provide information critical for decision making about recovery; (2) the need for statistical analysis from which reservoir inflow probability information could be derived; (3) the lack of certainty about seasonal and sub-seasonal inflows to the reservoir due to uncertainty about weather; (4) the risk of misunderstanding or misinterpreting model results as critical decisions were made; and (5) the requirement for concurrence by USACE, FERC, and DSOD with changes in Lake Oroville operations. Solutions included: (1) the use of cloud computing, with parallel model runs on multiple servers in the Amazon cloud, and multiple modelers to configure and execute model runs and synthesize results; (2) parallel statistical analysis of reservoir inflow data by hydrologic engineering experts, as described below; (3) analysis with ensemble forecasts, historical period of record, and statistically-based hydrographs; (4) careful communication to decision makers of results by DWR and consultant experts; and (5) continuous collaboration and coordination with reviewers and regulators through in-person meetings, a series of webinars, and technical memorandums for which review and comments were solicited.

The outcome of the reservoir operation analyses was a series of interim operation plans approved by regulators and implemented by DWR. Operation following those plans has been successful thus far, with the initial phase of construction completed in November 2017.

5. HYDROLOGIC ENGINEERING ANALYSIS DURING RECOVERY

Hydrologic engineering analysis during recovery provided information for sizing the restored FCO Spillway chute and for developing the operation plans described above. The analyses included the following:

- Reassessment of the PMF, a design event that fixes the capacity of the spillways and the operational relationship between release capability and reservoir storage.
- Assessment of hydrologic hazard in terms of statistically likely seasonal inflows to the reservoir. Results of this analysis informed decision makers about the schedule of construction and about operation before, during, and following various phases of the construction.

DWR had scheduled the PMF re-analysis for Oroville Dam prior to the February 2017 incident as a part of normal relicensing activities. The PMF update was to account for: (a) enhanced understanding of atmospheric conditions that lead to the probable maximum precipitation (PMP) — the precipitation event that

causes the PMF; (b) improved hydrometeorological monitoring, which yields better information about likely weather and water conditions; (c) improved watershed rainfall-runoff-routing model capabilities, including capabilities to describe watershed properties that influence runoff at greater resolution and with increased accuracy; and (d) changed atmospheric, hydrologic, hydraulic, or operational conditions. Following the 2017 incident, the pace of PMF re-analysis was accelerated. Activities included:

1. Developing a new watershed precipitation-runoff-routing model. In addition to commonly expected features, this model included snow accumulation and melt. The USACE HEC-HMS software application was used for this analysis [9].
2. Calibrating the model with historical events, including events with snow accumulation and melt. Lake Oroville's contributing watershed (the Feather River Basin) permits this, as it is well gauged with stream gauges, rainfall gauges, temperature, wind, and radiation sensors, and snow courses.
3. Selecting final model parameters for analysis of extreme events.
4. Verifying the model using data from precipitation events in addition to those selected for calibration.
5. Updating estimates of the PMP, using guidance from the NWS and DSOD. For this analysis, precipitation boundary conditions were defined by scaling observed storms to have PMP flood volumes.
6. Selecting appropriate initial snowpack and other conditions for application of the PMP storms to the HEC-HMS model.
7. Applying the model to compute PMF inflows.
8. Routing PMF inflows through the reservoir to determine maximum pool elevations and outflows. This was accomplished using the HEC-ResSim software application developed for and used in the reservoir operation analysis described above.

Findings of the PMF study were as follows:

1. The adopted updated PMF inflow hydrograph has a peak flow equal to 21189 m³/s (743,800 ft³/s) and a volume of 3.8 billion m³ (3.1 million acre-feet).
2. Routing the adopted PMF inflow hydrograph with the as-built configuration of the dam and outlets yielded a maximum reservoir pool elevation equal to 280.1 m (919.1 ft) (NGVD29). This maximum reservoir pool does not spill over the dam (crest elevation 281.0 m [922.0 ft]).
3. With the adopted PMF inflow and gate operations, the peak outflow totals 20419 m³/s (721,100 ft³/s).
4. Wind wave setup and runup potential is great — up to 2.0 m (6.7 ft). However, the winds required to produce this extreme event are not likely to occur during large winter storms such as the PMF.

Hydrologic engineering analyses also included seasonal analysis of Lake Oroville inflow volume-frequency. Products included the following:

1. Inflow volume-frequency curves for 1-, 3-, 7-, 15-, and 30-day durations for each month.
2. Hydrographs derived from the monthly frequency curves. These were used to develop inflow hydrographs, which were used as boundary conditions for flood routings with the HEC-ResSim model.
3. Results of flood routings with HEC-ResSim for a set of operation scenarios.
4. Monthly Lake Oroville elevation-frequency analysis information for a variety of design and operation alternatives formulated by DWR.

Challenges in the hydrologic engineering analysis for Oroville Dam included: (1) the need for quick turnaround to provide information critical for decision making about recovery; (2) common difficulties calibrating a precipitation-runoff model and determining appropriate initial and boundary conditions for application with extreme events; (3) the risk of misunderstanding or misinterpreting model results as critical decisions were made; and (4) requirement for concurrence by FERC and DSOD with PMF calculations and conclusions about dam safety based on routing the estimated PMF. Solutions included: (1) the use of cloud computing, with parallel model runs on multiple servers in the Amazon cloud, and multiple modelers to configure and execute model runs and synthesize results; (2) the use of the wealth of hydrometeorological and operational data collected and stored by DWR in the California Data Exchange Center, which is accessible at <http://cdec.water.ca.gov>; (3) careful communication to decision makers of the results by DWR and consultant experts; and (4) continuous collaboration and coordination with reviewers and regulators through in-person meetings, a series of webinars, and technical memorandums for which review and comments were solicited.

6. HYDRAULIC ENGINEERING ANALYSES DURING RECOVERY

Hydraulic engineering analyses were critical to the quick recovery of Oroville Dam's FCO Spillway chute and Emergency Spillway. The analyses completed included the following:

- Simulation of behavior of flow in the FCO Spillway chute to inform decision makers by the DWR design team. This included computation of water surface elevation profiles and hydraulic forces to inform decision makers about chute curvature and alignment, wall heights, and other design properties. It also included assessment of aeration and cross waves in the chute, and evaluation of cavitation potential due to high velocity flow in the chute. Reviews of the original design, maintenance records, and historical performance of the FCO Spillway

were also critical to improve the hydraulic performance of the restored spillway chute.

- Simulation of behavior of flow over the Emergency Spillway's monoliths/weir and down the Emergency Spillway hill slope. Information from this analysis informed designs about the type and extent of protection needed downstream, and methods to increase the factor of safety of the concrete monoliths without adversely impacting the outflow capacity.

The complex hydraulics of the project, the immediate data needs of other teams (structure, geotechnical, and geological), compliance with the current codes and design guidelines, concurrence by regulating agencies (FERC and DSOD), and the available time were some of the challenges faced by the hydraulic engineering team.

To meet the project objectives, the team agreed that: (1) initial hydraulic analyses would be done using simplified one-dimensional (1-D) and two-dimensional (2-D) numerical models, with the resulting data passed to other teams; (2) for selected alternatives, the findings from the simplified 1-D and 2-D models would be verified with three-dimensional (3-D) numerical models; and (3) a 1:50 scaled physical model of the FCO Spillway chute would be developed to validate the findings from the numerical models.

Table 2 summarizes the hydraulic engineering analyses completed and the methods used.

Table 2
Hydraulic Models Used in the Restoration of Oroville Dam's Spillways

Feature Analyzed	Model Type	Modeling Objective
FCO Spillway Chute	1-D models	<ul style="list-style-type: none"> • Determine flow characteristics (flow depth, velocity, drag force, uplift forces, cavitation index, centrifugal forces, boundary layer thickness, and air content) along the spillway chute profile. • Inform design decisions by structural, geotechnical, and geological engineers, and construction managers regarding best design features and methods of construction.

Feature Analyzed	Model Type	Modeling Objective
	3-D (computational fluid dynamics [CFD]) models	<ul style="list-style-type: none"> • Refine/update the results from 1-D models. • Assess conditions for which 1-D or 2-D models were not appropriate.
	1:50 scale physical model	<ul style="list-style-type: none"> • Validate results from 1-D and 3-D models. • Study flow phenomenon for which numerical models were highly uncertain or calibration difficult.
Emergency Spillway	2-D models	<ul style="list-style-type: none"> • Predict depth and velocity of flow on the hill slope downstream of Emergency Spillway to inform design decisions by structural, geotechnical, and geological engineers.
	3-D CFD models	<ul style="list-style-type: none"> • Refine results from 2-D models. • Assess and refine design of roller-compacted concrete (RCC) buttress for the concrete monoliths, which cannot be modeled well with simpler models. • Simulate discharge from ogee crest for multiple buttress alternatives.

6.1. FCO SPILLWAY CHUTE ANALYSIS

Hydraulic analyses of the FCO Spillway chute: (1) led to refinement of the FCO Spillway chute alignment (profile); (2) provided information about depths and velocities along the chute; and (3) provided information necessary to assess the potential for cavitation along the chute as flows reached capacity.

6.1.1. FCO Spillway Chute Profile Analysis

The initial profile of the FCO Spillway chute closely followed the original natural terrain to minimize the excavation as well as the disturbances of the underlying rock due to blasting. This as-built FCO Spillway chute profile has one vertical curve. Modeling led to refinements in this chute profile, with the recommended chute profile curve lengthened and replaced by two curves. The new profile is hydraulically superior to the original as-built chute profile as it

provides a gradual landing of the jet trajectory. In the new chute profile, the elevations of portions of the chute were set 0.6 m (2 ft) above the original elevations, thus reducing the volume of the underlying rock to be removed and reducing construction time.

6.1.2. FCO Spillway Chute Flow Depth and Velocity Analysis

Calculations of the flow depth and velocity along the FCO Spillway chute were done initially with a 1-D model. The calculated velocities and flow depths for selected flows along the FCO Spillway chute are shown in Fig. 4. During the release of 8382 m³/s (296,000 ft³/s), the flow depth changed from 7.5 m (24.6 ft) at the end of the outlet structure to about 3.0 m (9.8 ft) near the dentate structures. The corresponding maximum velocity reached about 52 m/s (170 ft/s) near the dentate structures. The flow on the chute remained uniform flow only when the release was lower than 1415 m³/s (50,000 ft³/s).

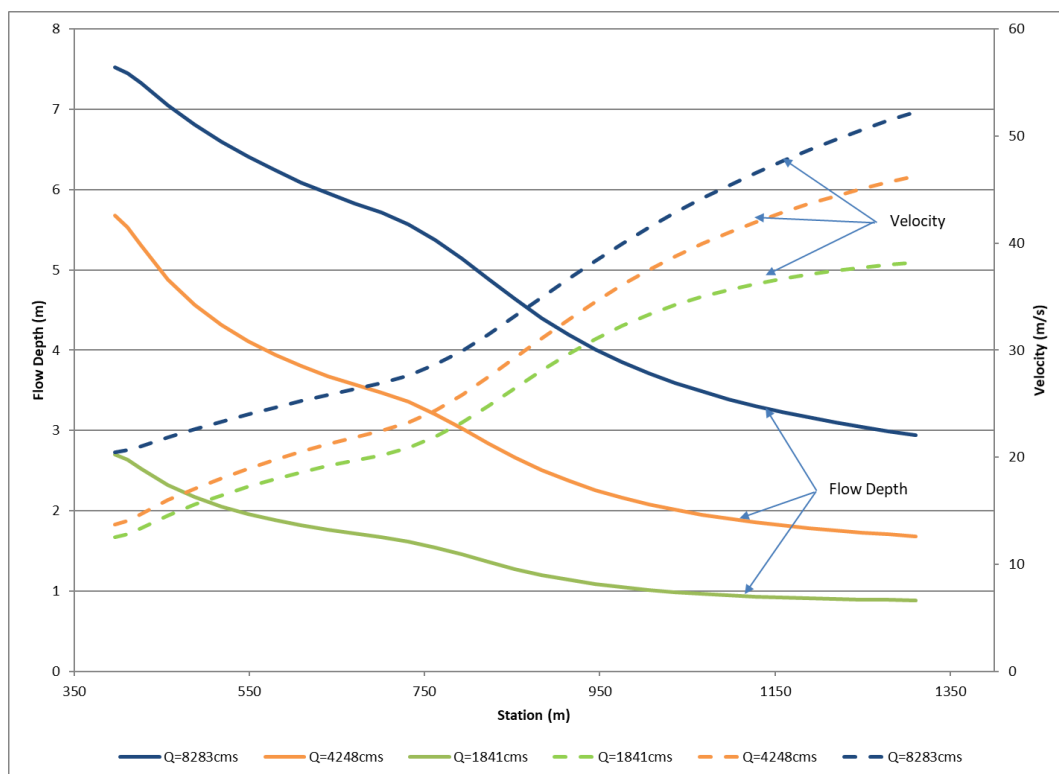


Fig. 4 Variation of flow depth and velocity along Spillway FCO Spillway chute

The 1-D models were used to calculate drag force, uplift due to seepage, centrifugal force at vertical curves, and negative pressures at transverse joints. The resulting chute flow properties were passed to other recovery teams to start their design work. The final wall heights along the chute were determined such that the maximum release of 8382 m³/s (296,000 ft³/s) will be fully contained within the

chute. The wall height was taken as the non-aerated flow depth plus freeboard. The freeboard was calculated using both USACE [10] and USBR [11] guidelines. These guidelines account for flow depths, pier end wave height, slug flow or roll waves, air entrainment, and minimum freeboard above the mean surface elevation. The proposed final wall heights for the FCO Spillway chute are taller than the original wall heights.

6.1.3. Cavitation Index and Air Concentration Analysis

Cavitation along the FCO Spillway chute was a concern, considering the high velocities created by the largest releases. Hydraulic engineering analyses assessed the potential for cavitation. The potential of cavitation damage is measured by a cavitation index (σ), which is a function of pressure and velocity; no cavitation damage is expected when the index exceeds 0.2. If the cavitation index falls below the recommended value of 0.2, cavitation damage can be prevented if air concentration in the flow is about 10% [12, 13], or by using high-strength materials. The proposed FCO Spillway chute was designed as a self-aerating spillway [3, 14], thus avoiding cavitation even with the highest-velocity flows.

Fig. 5 shows the variation of the cavitation index and entrained air concentration computed with a 1-D model developed by DWR. Near the chute failure location, Station 1021 m (3350 ft), for a release of 1841 m³/s (65000 ft³/s), the air concentration is about 25% and the cavitation index is higher than 0.2. This suggests that cavitation was not a significant factor in the failure of the FCO Spillway chute — an assessment that was confirmed by an independent forensic assessment [15]. The entrained air concentration calculation due to self-aeration is very conservative as it neglects the aeration contribution by the outlet structure piers.

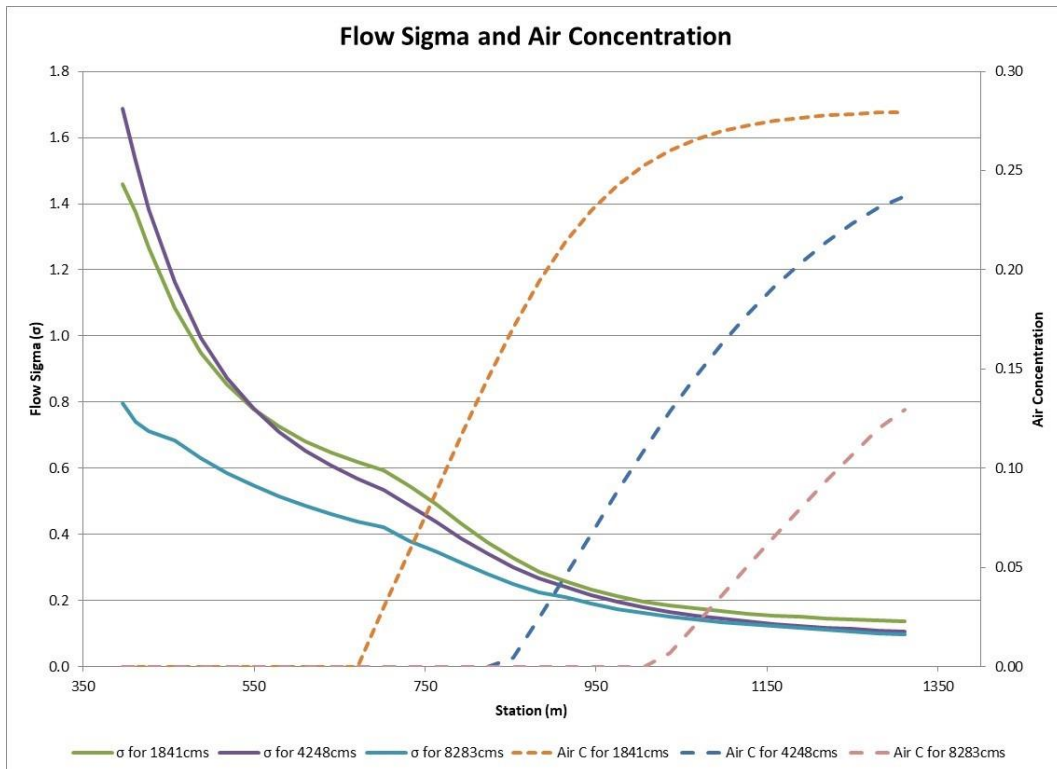


Fig. 5 Variation of cavitation index along the FCO Spillway chute

For a release of 4248 m³/s (150,000 ft³/s), the cavitation index falls below 0.2 near Station 975 m (3200 ft), with a minimum value of 0.11 near the dentate structures. However, the air concentration is about 8%, which is about the minimum air concentration recommended to prevent cavitation damage. This is consistent with the historical performance of the FCO Spillway chute. Past maintenance records show that damage to the chute due to cavitation for flows up to 4248 m³/s (150,000 ft³/s) was negligible [5]. If the initial aeration entrained by the gate piers is considered, the chute should be able to convey flows up to 8382 m³/s (296,000 ft³/s) without cavitation damage.

The need for aerators in the new FCO Spillway chute is still an on-going issue. While model results suggest aerators may reduce potential for chute cavitation, models available are based on certain assumptions not necessarily valid for Oroville Dam. Further, current designs, while efficient for certain flows are less efficient for flows which are larger and/or smaller than the flows. Finally, maintenance of feasible designs is a significant concern. As of December 2017, analysis continues, and no final design decision has been taken regarding aeration.

6.1.4. Model Validation

Measured velocity, flow depth, and air content data along the modified FCO Spillway chute are not yet available to calibrate or verify the models. The model results (velocity and flow depth) from the 1-D model were confirmed by comparing

with results computed with FLOW3D, a commercially available 3-D CFD software application.

6.1.5. *Analysis with Scale Physical Model*

To provide hydraulic engineering information not otherwise available, a 1:50 scale physical model of the FCO Spillway chute, based on Froude number similarity, was built at Utah State University immediately following the spillway chute failure. The model includes the Flood Control Outlet structure, the concrete chute along with energy dissipaters, and part of the Feather River immediately downstream of the terminal end of the chute. This model was used to determine a rating curve of the FCO Spillway structure, to verify flow depth and velocity obtained from numerical models, and to understand flow patterns in the chute in case the spillway construction was not completed in a single construction season.

Initial studies with the physical model were limited to three alternative designs proposed for recovery: a plunge pool alternative, an interim chute, and full restoration of the original concrete chute. Fig. 6 shows the 1:50 scale model of the plunge pool alternative of the FCO Spillway chute; this alternative modified the scour hole created by the spillway failure for use for conveyance and as an energy dissipating device. This alternative was found to be feasible based upon the CFD model runs, but the physical model results showed standing waves on the plunge pool as high as 46 m (150 ft) during a release peak design flow of 8382 m³/s (296,000 ft³/s). Therefore, this alternative was discarded.



Fig. 6 Performance of plunge pool alternative of Oroville Dam's FCO Spillway chute

6.2. ANALYSIS OF EMERGENCY SPILLWAY

To inform design decisions about the damaged hill slope downstream of the Emergency Spillway, a 2-D model of the Emergency Spillway, hill slope downstream, and part of the Feather River was developed using HEC-RAS. Terrain data were available from LiDAR obtained with drone flights by DWR following the spillway failure (and periodically thereafter, as construction progressed). The 2-D model was used to calculate water depth, velocity, and bottom shear for various flow conditions. Results were used by OER to assess the potential for future erosion and scour and to inform designers of remediation features downstream of the Emergency Spillway. Those features included a secant pile wall to prevent head cutting, armoring in key locations, and construction of a concrete apron immediately downstream of the weir.

To assess the need for and to inform designers of modifications to the Emergency Spillway weir, a 3-D CFD model of the weir was developed using FLOW3D. Buttressing of the concrete monoliths was proposed to increase the factor of safety against sliding. The 3-D model showed certain configurations that would reduce the efficiency of the weir, thus reducing capacity of the spillway. This, in turn, would adversely affect the ability of the dam to pass the PMF safely. Analysis with the 3-D model led to modifications to the design. The analysis also yielded information about the flow velocity and bottom shear along the planned protection works downstream of the Emergency Spillway.

7. CONCLUSION

Oroville Dam, the FCO structure, the Emergency Spillway, and the operations plan were designed, developed, and constructed following or exceeding the standard of practice 60 years ago. While the Oroville Project had operated successfully for 49 years, failure of the FCO Spillway chute in 2017 created a need for a new design and an associated operations plan for that design as it was to be constructed in phases. To inform the design and operations, a variety of hydrologic engineering, hydraulic engineering, and reservoir operation analyses were completed during the incident and later as part of the recovery. Conceptual and empirical numerical and physical models were used for the analyses. Analysts encountered problems throughout the analysis, but always found solutions as the models were configured, calibrated, and applied to provide information to design staff and influence interim operation decisions required throughout the response and continuing recovery efforts.

REFERENCES

- [1] United States Army Corps of Engineers (USACE). Oroville Dam and Reservoir report: Reservoir regulation for flood control, August 1970, Sacramento District, Sacramento, CA.
- [2] TRANSTRUM, L.O. Hydraulic modeling studies of the Oroville Dam spillway, Feather River Project, March 1955.
- [3] THAYER, D.P., STROPPINI, E.W. "Hydraulic design for Oroville Dam spillway." Proc., ASCE Hydraulic Conference, Tucson, Arizona, August 25-27, 1965.
- [4] United States Bureau of Reclamation (USBR). Hydraulic modeling studies of the flood control outlet and spillway for Oroville Dam California, Report No. Hyd-510, 1965, Hydraulic Laboratory, Denver, Colorado.
- [5] California Department of Water Resources (DWR). "2008 Oroville Dam spillway inspection and condition assessment," office memorandum, Operation and Maintenance Division, Dam Surveillance Section, April 2008.
- [6] USACE Hydrologic Engineering Center. River Analysis System (HEC-RAS), 2016, Version 5.0.3, Davis, CA.
- [7] FLO-2D Software. FLO-2D, 2014, Nutrioso, AZ.

- [8] USACE Hydrologic Engineering Center. Reservoir System Simulation (HEC-ResSim), 2013, Version 3.1, Davis, CA.
- [9] USACE Hydrologic Engineering Center. Hydrologic Modeling System (HEC-HMS), 2016, Version 4.2, Davis, CA.
- [10] USACE. Hydraulic design of spillways, Engineering Manual 1110-2-1603, Washington, D.C., 1990.
- [11] USBR. Chapter 4: "General spillway design considerations," Design Standards No. 14, Appurtenant structures for dams (spillways and outlet works) design standards, August 2014.
- [12] FALVEY, H.T. Cavitation in chutes and spillways, Water Resources Technical Publications, EM 42, Bureau of Reclamation, Department of Interior, 1990, Denver, CO.
- [13] WILHELMS, S.C., GULLIVER, J.S. "Bubble and waves descriptions of self-aerated spillway flow," J. Hyd. Res., 2005, 43(5) 522-531.
- [14] YOUNGERMAN, J.M. "Volume II, Design Notes," Oroville Dam spillway, Final design, DWR, June 1965.
- [15] FRANCE, J.W., et al. Independent Forensic Team Report: Oroville Dam spillway incident, United States Society on Dams, January 2018.

SUMMARY

During the Oroville Dam Spillway Incident, hydrologic and hydraulic engineering and reservoir operation analyses provided information to support decision making by DWR management. Reservoir inflow forecasts were made almost continuously by DWR staff and the NWS, using conceptual models of Feather River Basin watershed hydrology. Reservoir behavior and operation with various operation and potential failure scenarios were simulated to predict future pool elevations and timing of potential Emergency Spillway discharge.

Inundation that could result from potential failure was predicted and displayed with maps included in Oroville Dam's Emergency Action Plan, which emergency and incident command teams consulted. These maps were augmented with situation-specific maps prepared in near real time as the incident progressed. Additional hydraulic analyses provided DWR managers with information about potential flow paths along the hill slope downstream of the Emergency Spillway, and with estimates of debris and sediment loads in the Feather River downstream.

Challenges for analysis during the event in February 2017 included: (1) the need for almost immediate turnaround to provide information critical for decision

making; (2) the lack of certainty about near-future inflows to Lake Oroville due to uncertainty about the weather; (3) the lack of certainty about behavior of the never-used Emergency Spillway, with unstable terrain; and (4) the risk of misunderstanding or misinterpreting model results as critical decisions were made. Solutions included: (1) the use of cloud computing, with parallel model runs on multiple servers in the Amazon cloud; (2) analysis with ensemble forecasts, coupled with sensitivity analysis with varying inflow hydrograph properties; (3) constant monitoring and reporting to modelers of observed changes to the spillways so model inputs could be adjusted; and (4) careful communication of results by DWR and consultant experts.

KEY WORDS

ANALYSIS, APPURTANANT STRUCTURE, BEHAVIOR, CAVITATION, CHUTE, CONCRETE DAM, CONSTRUCTION, CREST, DAM, DAM OPERATION, DAMAGE, DESIGN, DISCHARGE, ENERGY DISSIPATOR, FAILURE, FLOOD CONTROL, FLOW, FCO SPILLWAY, GAUGE, GEOLOGICAL INVESTIGATION, HYDRAULIC MODEL, HYDROLOGY, MAIN SPILLWAY, MATHEMATICAL MODEL, NUMERICAL MODEL, MODEL, OPEN CHANNEL, OPERATION, OUTLET DISCHARGE, OUTLET STRUCTURE, PERFORMANCE, PHYSICAL MODEL, PLUNGE POOL, POPULATED AREA, POPULATION DISPLACEMENT, PROTECTIVE MEASURES, REGULATION, REPAIR, RESERVOIR, RESERVOIR OPERATION, RUNOFF, SAFETY, SIDE SPILLWAY, SLOPE STABILITY, SPILLWAY

COMMISSION INTERNATIONALE DES GRANDS BARRAGES

VINGT-SIXIÈME CONGRÈS DES GRANDS BARRAGES
Autriche, juillet 2018

DOI 10.3217/978-3-85125-620-8-007



This work licensed under a Creative Commons Attribution 4.0 International License. <https://creativecommons.org/licenses/by-nc-nd/4.0/>

**WHAT HAPPENED AT OROVILLE DAM AND WHY – FINDINGS OF THE
SPILLWAY INCIDENT FORENSIC INVESTIGATION**

John W. FRANCE

Managing Member, JWF CONSULTING LLC, USA

Irfan A. ALVI

President & Chief Engineer, ALVI ASSOCIATES, INC., USA

Peter A. DICKSON

Geotechnical Practice Leader, STANTEC CONSULTING SERVICES, INC., USA

Henry T. FALVEY

President, HENRY T. FALVEY & ASSOCIATES, INC., USA

Stephen J. RIGBEY

Director, SJR CONSULTING, CANADA

John TROJANOWSKI

President, TROJANOWSKI DAM ENGINEERING, LIMITED, USA

UNITED STATES OF AMERICA

WHAT HAPPENED AT OROVILLE DAM AND WHY – FINDINGS OF THE SPILLWAY INCIDENT FORENSIC INVESTIGATION

John W. France, PE, D.GE, D.WRE
Managing Member, JWF Consulting LLC, USA

Irfan A. Alvi, PE
President & Chief Engineer, Alvi Associates, Inc., USA

Peter A. Dickson, PhD, PG
Geotechnical Practice Leader, Stantec Consulting Services, Inc., USA

Henry T. Falvey, Dr.-Ing, Hon.D.WRE
President, Henry T. Falvey & Associates, Inc., USA

Stephen J. Rigbey
Director, SJR Consulting, Canada

John Trojanowski, PE
President, Trojanowski Dam Engineering, Limited, USA

UNITED STATES OF AMERICA

1. INTRODUCTION

On February 7, 2017, the gated service spillway (also known as the Flood Control Outlet or FCO Spillway) at Oroville Dam was being used to release water to control the Lake Oroville level according to the prescribed operations plan. During this operation, the service spillway's concrete chute slab failed, resulting in the loss of spillway chute slab sections and deep erosion of underlying foundation materials. Subsequently, as the damaged service spillway was operated in an attempt to manage multiple risks, the project's free overflow emergency spillway was overtopped for the first time since the project was completed in 1968. Significant erosion and headcutting occurred downstream of the emergency spillway's crest structure, leading authorities to evacuate about 188,000 people from downstream communities.

After the incident, the United States Federal Energy Regulatory Commission (FERC), one of two regulators for Oroville Dam, required the dam's owner, the California Department of Water Resources (DWR), to retain an Independent Forensic Team (IFT) to investigate the Oroville Dam spillway incident and prepare

a report of findings. At the request of DWR, the United States Society on Dams (USSD) and the Association of State Dam Safety Officials (ASDSO) coordinated the assembly of a six-person team, which was approved by FERC. The IFT, composed of the authors of this paper, issued its forensic investigation report on January 5, 2018 [1].

The IFT's work included the review of hundreds of documents covering investigations, design, construction, operations and project reviews, as well as notes taken during the incident. IFT members visited the site, including during forensic investigations made before chute sections were demolished for repairs. The IFT also interviewed more than 75 individuals, conducted two surveys of DWR personnel, and solicited input from the public and DWR employees. Through an iterative process, the IFT applied a mix of fundamental inductive and deductive logic to the assembled information, and provided the resultant evidence, arguments, and findings in its detailed forensic report [1].

The report addressed both the physical factors and the human, organizational, and industry factors that contributed to the Oroville Dam spillway incident. This paper briefly summarizes the IFT's findings and lessons to be learned from this very serious incident. The reader is referred to the full forensic investigation report [1] for more detailed information.

2. PROJECT BACKGROUND

2.1. OROVILLE DAM PROJECT

Oroville Dam is a component of the California State Water Project (SWP), which is the largest state-owned water storage and delivery system in the United States. The Oroville Dam and associated structures were built in the 1960s, with the construction completed in 1968.

The SWP is owned and operated by DWR, which is part of the California Natural Resources Agency and was created in 1956. Oroville Dam is regulated by a separate division within DWR, the Division of Safety of Dams (DSOD), as well as by FERC.

The Oroville Dam facility (see Fig. 1) consists of an embankment dam, a service spillway (also known as the Flood Control Outlet or FCO Spillway), an emergency spillway, the Hyatt Powerplant, and several other appurtenant structures. Oroville Dam is the tallest dam in the United States, at 235 m (770 ft). The design embankment crest is at Elevation 281.0 m (922 ft), and the maximum normal operating pool level is Elevation 274.3 m (900 ft). For reference, the service

spillway gate sill is at Elevation 248.0 m (813.6), and the crest of the emergency spillway overflow structure is at Elevation 274.6 m (901 ft).



Fig. 1

Overview of Oroville Dam facility prior to the February 2017 incident

2.2. SERVICE SPILLWAY

The service spillway is located on the right abutment of the main dam. It consists of an unlined approach channel, a gated headworks structure, and a concrete-lined chute extending to just above the Feather River channel. The headworks structure has a total of eight top-seal radial gates. The upstream sill elevation of the service spillway headworks is at Elevation 248.0 m (813.6 ft) and the tops of the radial gates (in the closed position) are at approximately Elevation 258.2 m (847 ft). The chute downstream of the headworks structure is about 54.6 m (179 ft) wide and just over 914 m (3,000 ft) long, with a drop of about 152 m (500 ft). The first 305 m (1,000 ft) of the service spillway chute downstream of the headworks slopes at about 5²/₃ percent, after which the chute transitions through a vertical curve to a much steeper slope of about 24.5 percent for the last 443.5 m (1,455 ft). Four large, reinforced concrete “dentate” blocks are located at the downstream end of the chute, to disperse the spillway flow and dissipate energy as the flow enters the river.

The service spillway discharge would be 8,382 m³/s (296,000 ft³/s) with Lake Oroville at Elevation 279.5 m (917 ft) and all gates fully open [2].

2.3. EMERGENCY SPILLWAY

The emergency spillway is also located on the right abutment, to the right of the service spillway. The emergency spillway consists of two sections: a 284-m (930-ft) long, concrete, gravity, ogee weir on the left side, and a 244-m (800-ft) long broad-crested, concrete weir on the right side. The crests of both sections are at Elevation 274.6 m (901 ft), which is 0.3 m (1 ft) above the maximum normal operating reservoir level, Elevation 274.3 m (900 ft). The maximum height of the emergency spillway crest structure is about 15.2 m (50 ft) in the ogee weir (left) section. Water flowing over the emergency spillway crest structure would then pass over natural terrain down to the Feather River.

The emergency spillway discharge would be 9,910 m³/s (350,000 ft³/s) with the reservoir at 279.5 m Elevation (917), which corresponds to a depth of flow over the crest weirs of about 4.88 m (16 ft) [2].

2.4. SPILLWAY OPERATION HISTORY

The service spillway gates are operated to control reservoir levels in accordance with the operation plan for the facility. The gates were first operated in 1969, within a year after the project was completed, with a maximum service spillway discharge of almost 2,320 m³/s (82,000 ft³/s) in that year.

Service spillway operations vary from year to year, depending primarily on snowpack in the Feather River Basin. The operating record includes extended periods of time when spillway gate operation was not required, e.g. 1975 through 1979, 1987 through 1992, and 2007 through 2010. Of the 48 years from 1969 through 2016, there were 23 years when the service spillway did not operate, 11 years during which discharges exceeded 1,420 m³/s (50,000 ft³/s), and three years during which discharges exceeded 2,830 m³/s (100,000 ft³/s). The record service spillway discharge was 5,530 m³/s (160,000 ft³/s), in 1997. From 1998 through 2016, spillway discharges exceeded 312 m³/s (11,000 ft³/s) in only three years: about 1,700 m³/s (60,000 ft³/s) in 2005, 2,100 m³/s (74,000 ft³/s) in 2006, and 878 m³/sec (31,000 ft³/s) in 2011.

The emergency spillway was activated for the first time in the project's history during the February 2017 flood event and spillway incident.

2.5. SERVICE SPILLWAY CHUTE DESIGN AND CONSTRUCTION

Understanding the service spillway chute design and construction is critical to understanding the chute slab failure in February 2017.

The nominal service spillway chute slab design thickness was a minimum of 38.1 cm (15 in), although the nominal chute slab thickness as-constructed was significantly greater in many locations. However, as discussed below, the chute slab thickness over the chute's underdrains was much less than 38.1 cm (15 in).

The design included an underdrain system consisting of herringbone drains beneath the chute slab, connected to collector pipes outside of and parallel to the service spillway chute walls. Each herringbone drain was oriented across the spillway with the pipes on either side of the spillway sloping downstream for drainage, from a point beneath the spillway centerline, as shown in Fig. 2. The herringbone drains were spaced at an interval of 7.6 m (25 ft) along the flatter upstream section of the chute and at 6.1 m (20 ft) along the steeper downstream section. When viewed in plan, the pattern of these drains looked like fish bones or herring bones, as shown in Fig. 2, hence the name. Sets of herringbone drains connected to separate collector drain pipes on either side of the chute. The collector drain pipes extended downstream to outfall locations near the tops of the chute walls. To accommodate all of the herringbone drains, there were 12 collector drain pipes on each side of the chute, for a total of 24 collector drain pipes.

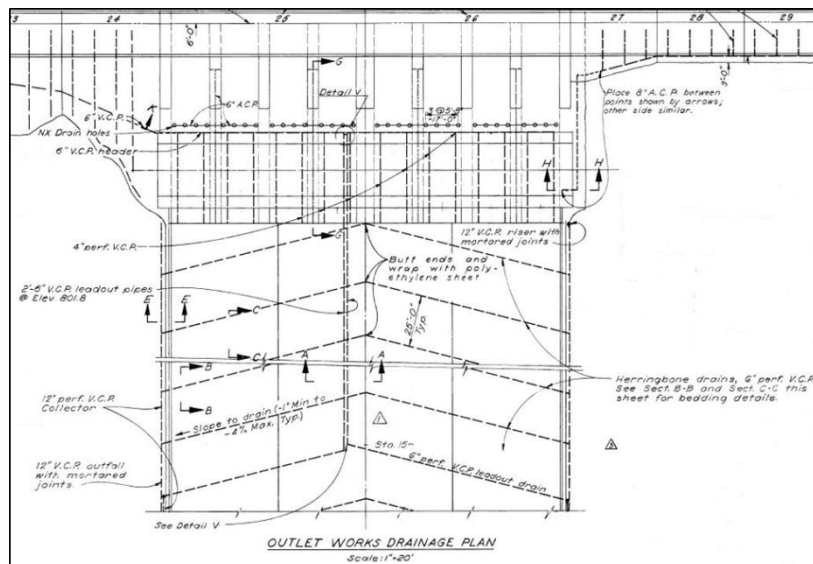


Fig. 2
Plan view of headworks (top) and upper service spillway chute showing herringbone drains and collector pipes

In the original design/bid drawings, the herringbone drains were indicated as 10.2-cm (4-in) diameter perforated vitrified clay pipes (VCPs) surrounded by gravel, and the collector pipes were indicated as 20.3-cm (8-in) and 15.2-cm (6-in)

diameter VCPs. However, construction records indicate that the herringbone drain size was increased to 15.2-cm (6-in) diameter and the collector pipe size was increased to 30.5 cm (12-in) diameter, which is consistent with the as-built drawings and the pipe sizes observed during the post-incident forensic investigations.

In both the design and as-built drawings, the herringbone drains are not located entirely beneath the chute slab, but rather they protrude up into the slab section, as shown in Fig. 3, taken from the as-built drawings. This location of the drain pipes substantially reduced the thickness of the slab immediately above the drains. The drawings noted the slab thickness above the drains as a minimum of 17.8 cm (7 in). From available information, it appears that, in most locations, even when the as-constructed slab thickness increased, the drain pipe locations were maintained near the top of the slab.

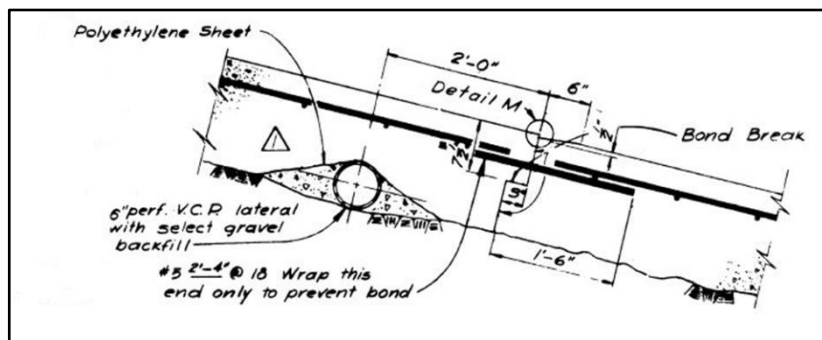


Fig. 3
Herringbone drain VCP pipe protruding into slab section

As designed and constructed, the chute slab included a single layer of reinforcing bars near the top of the slab, as shown in Fig. 4. The reinforcing bars were 15.9 mm (No. 5) bars, spaced at 30.5 cm (12 in) each way.

The chute design also included 35.8 mm (No. 11) anchor bars, spaced at 3 m (10 ft) each way in plan view, to extend 1.5 m (5 ft) minimum into the foundation or 5 ft (1.52 m) minimum into sound rock and to be grouted into the foundation. The anchor bar detail is shown in Fig. 4. From construction records and photographs, it does not appear that anchor lengths were adjusted when “sound rock” was not located at foundation grade, nor when the concrete slab was thicker than 38.1 cm (15 in). Hence, the anchors likely extended a maximum of about 1.5 m (5 ft) into the foundation.

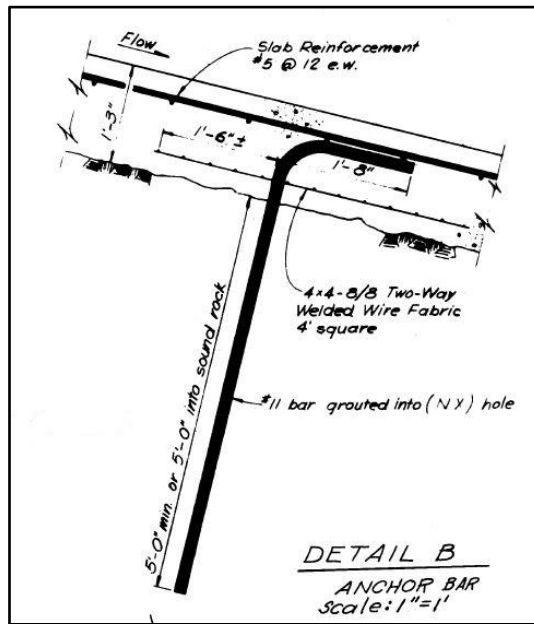


Fig. 4
Typical reinforcing bar and anchor bar configurations

The chute slab included both formed and unformed transverse contraction joints. The as-built drawing details show formed transverse contraction joints including a 19.1-cm (7.5-in) deep key, in which the downstream edge of the upstream slab overlaps the upstream edge of the downstream slab, as shown in Fig. 3.

Construction records and photographs indicate that much of the chute slab was constructed using slip-form methods. Although the as-built drawings show 12.2 m (40 ft) wide by 15.2 m (50 ft) long chute slab panels, it is believed that the slip-forming used to construct the chute concrete allowed the contractor to place more than one 15.2 m (50-ft) long concrete chute slab panel at a time. It is further believed that the contractor created unformed contraction joints by cutting shallow grooves in the freshly placed concrete to initiate a crack at intermediate design joint locations within the slip-form length, rather than stopping the slip-forming operation to construct a formed contraction joint. Formed contraction joints would have been constructed at the ends of the slip-form runs.

The as-built drawings show that all longitudinal contraction joints were to be keyed. The specific key configurations varied for different longitudinal contraction joints.

According to the as-built drawings, all contraction joints were completed with 0.4-cm (1-in) deep by 0.098-cm (0.25-in) wide filler material, placed in a groove formed at the top of the joint, and 15.9 mm (No. 5) dowel bars at 45.7 cm (18-in) spacing were constructed across all of the chute slab formed joints (see Fig. 3). These dowel bars were embedded and bonded for a length of 45.7 cm (18 in) on one side of the joint, and were wrapped to prevent bond for 25.4 cm (10 in) on the

other side. The dowels were shown just below the reinforcement mat near the top of the slab.

Although all formed joints were intended to be keyed, formed joints without keys were observed at a few locations during the post-incident forensic investigations.

Based on the design drawings and specifications, as well as an interview, the design intent was for the chute slab to be founded directly on moderately weathered rock or better, which could not be further removed by heavy-duty power excavating equipment. The excavated surface was to be pressure-washed to remove all mud, debris, and loose or unsound rock fragments. However, the foundation requirements were substantially relaxed during construction. In some places, the prepared foundation appeared to have high points of reasonably sound rock surrounded by areas of what appears to be rock weathered to soil-like material, as shown in Fig. 5. In other locations, the prepared foundation appears to have been almost entirely rock that had weathered to soil-like material, as shown in Fig. 6, which was taken in the area of the initial chute slab failure.



Fig. 5

Example of the clean-up effort for the service spillway chute prior to concrete placement.

The chute slab concrete was specified to have a 28-day compressive strength of 21,000 kPa (3,000 lb/in²), and all concrete cores tested in the post-incident field investigations had compressive strengths higher than the specified strength. Type II cement was used for the concrete, and the coarse aggregate was up to 15.2-cm (6-in) size. While large size coarse aggregate can be beneficial in thicker placements, the 15.2-cm (6-in) maximum size would seem to be too large

for a 38.1-cm (15-in) slab thickness with 7.6-cm (3-in) reinforcing bar cover and 17.8-cm (7-in) drain pipe cover. The construction documentation indicates that some of the large aggregate caused breakage of the herringbone drain pipes as the concrete was being placed.

Although it is believed that broken drain pipes were repaired when they were observed during construction, there may be other locations where pipes were damaged during concrete placement but the damaged pipes were not observed and were not repaired.

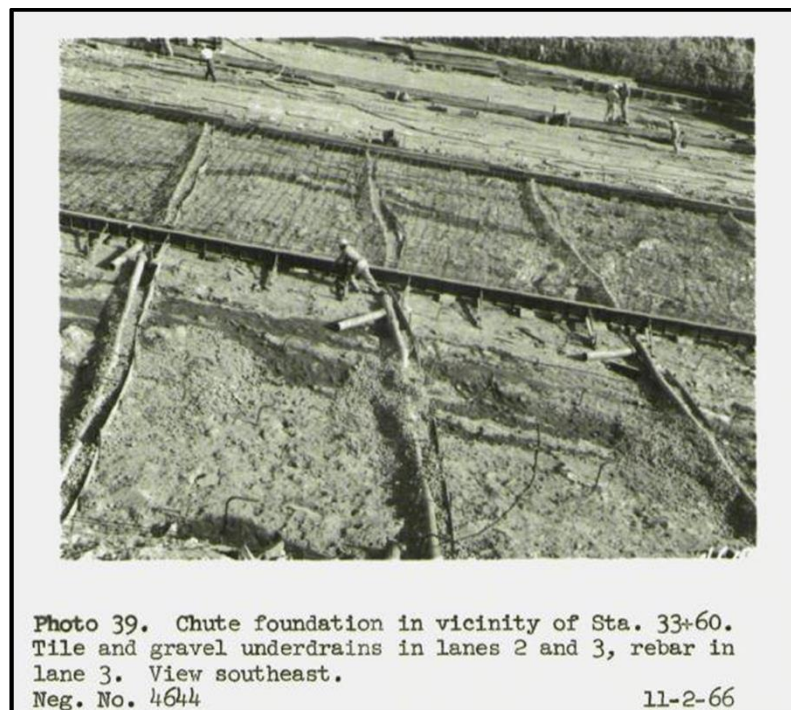


Fig. 6

Foundation preparation in the vicinity of the initial slab failure.
Note what appear to be extensive areas of soil-like materials in the foundation.

2.6. SERVICE SPILLWAY CHUTE SLAB REPAIRS

The service spillway chute slab concrete has been repaired numerous times since the original construction. Documented repair efforts occurred in 1977, 1985, 1997, 2009, and 2013. It is possible that there were other undocumented repair efforts.

The observed spillway chute damage that led to the repairs was caused by various different mechanisms including cracking, removal of joint filler, delamination, and spalling. The cracking occurred predominantly over the herringbone drains. These cracks were first documented in a 1969 report [4], which

indicated that cracks appeared above herringbone drains during slab concrete curing, within one month after concrete placement. These cracks provided pathways for leakage through the slab at times when there was water flowing down the chute.

Over time, joint filler was removed from joints by the high velocity flows in the spillway. Loss of the joint filler would have resulted in increased leakage through joints when water was flowing down the chute.

Spalling occurred almost entirely in delaminated concrete at joints and cracks and at patches from previous repairs, generally in the concrete above the level of the reinforcing steel and dowels. Delamination led to spalling of the slabs near the joints and cracks. The spalling exposed the reinforcing steel in the chute slabs and the dowel bars at the joints to corrosion, leading to reinforcing bar failure (see Fig. 7) when subjected to tension during the winter contraction cycle. Depending on the magnitude and orientation of the spalls, vertical faces that result in stagnation pressures during spillway discharge could have been created.

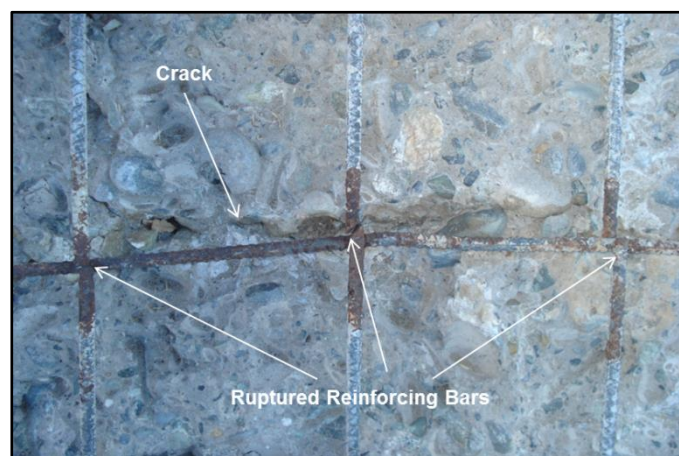


Fig. 7

Corroded and ruptured steel reinforcing bars at a slab crack

The chute repairs were generally shallow, involving removal of damaged concrete and patching of spalls to restore the flow surface. In some cases, the chute repairs also involved replacing the joint filler, reconnecting broken reinforcing bars with couplers, and grouting of cracks. In at least one of the repair efforts, the dowels in some of the formed lateral joints were cut in order to place joint-filler material. Although much of the damage resulted from temperature related stresses, there is no evidence that temperature studies were part of any repair design effort.

Based on reports of repair efforts and interviews with DWR personnel, the IFT understands that spalling both recurred in previously patched areas and occurred in areas that had not exhibited spalling before.

The photograph in Fig. 8 shows a section of the concrete chute slab that was removed during post-incident forensic excavations. Protrusion of the underdrain into the slab section, cracking above the underdrain, repair of the concrete above the reinforcing layer, and recurrence of the cracking are all illustrated in this photograph.



Fig. 8
Section of service spillway chute slab removed
during post-incident forensic investigation

2.7. SERVICE SPILLWAY CHUTE UNDERDRAIN FLOWS

In its first report, DWR's Independent Board of Consultants (BOC), which was convened after the February 2017 incident to provide review and advice for the spillway recovery and repair program, commented that:

“The amount of drain water flowing from the pipe discharge openings along the spillway training walls seems extraordinarily large.” [3]

The IFT concurred. The amount of water that discharged from the chute drains when there was flow in the service spillway was unprecedented in the IFT's experience.

Significant flows from the service spillway chute drain outfalls were observed at the time of the first discharge through the spillway, in 1969, as described in a DWR report and DSOD notes [4, 5, and 6]. The report states that the high flows from the outfalls were related to spillway discharge and that the “high flows from

the spillway drains are mystifying but probably not dangerous as the chute is anchored.” The report also states that “inquiry to the designers regarding this aspect of performance would be in order.” The IFT was not able to locate any documents indicating that the designer(s) were consulted at that time. From the design documents, the IFT is confident that the intent of the chute underdrain system was to collect seepage from groundwater beneath the slab, and not to collect large amounts of leakage from flows in the spillway chute.

Over the life of the project, reports of flows from the spillway chute underdrain outfalls were sporadic and limited. From an evaluation of the available reports, it can be concluded that, when the spillway was discharging, high chute drain flows consistently occurred, and the data indicate that the drain flows increased with increasing spillway chute flow, though not necessarily proportionally. High drain outfall flows were not limited to times when the spillway gates were open. Rather, significant outfall flows were also observed when the gates were closed and the reservoir level was high enough for water to be against the upstream sides of the service spillway gates. In these circumstances, gate leakage resulted in significant flow in the spillway chute.

The IFT agreed with the initial 1969 conclusion that the high drain flows were principally attributable to discharge leakage through the cracks and joints in the service spillway chute slab. This was dramatically demonstrated during post-incident repair work in 2017, when water was observed flowing on the spillway chute from leakage with the gates closed. To facilitate investigation and repair work, sand bags were placed on the spillway chute to direct the leakage flow toward a narrow area near the left chute wall. When the sand bags were placed, drain outfalls on the right side, which had been flowing significantly, stopped flowing, which indicates that the water collected by the drains was not seepage through the foundation, but rather leakage through the slab.

3. CHRONOLOGY OF THE FEBRUARY 2017 SPILLWAY INCIDENT

In January and February 2017, the service spillway experienced its first significant discharges since 2011.

After some limited service spillway discharges earlier in January, the discharges were ramped up beginning on January 30, in response to an approaching large precipitation event. In the first few days of February, discharges were in the range of about 425 to 708 m³/s (15,000 to 25,000 ft³/s). On February 6, 2017, the spillway discharges were increased to between 1,190 and 1,270 m³/s (42,000 and 45,000 ft³/s) and were held in that range until the morning of February 7.

At about 10:10 am on February 7, 2017, on-site DWR personnel noticed a substantial disturbance in the service spillway's flow pattern, while discharges were being ramped up from about 1,200 m³/s (42,500 ft³/s) to about 1,490 m³/s (52,500 ft³/s). On-site DWR personnel contacted DWR headquarters in Sacramento, and an order to close the service spillway gates was issued at about 11:15 am on February 7, 2017. After the gates were fully closed by about 12:25 pm, it was found that a significant section of the service spillway chute slab was missing, and a large erosion hole existed in the foundation in the area where the slab sections were missing, as shown in Fig. 9. This initial erosion hole in the service spillway chute was examined by a climb team on the morning of February 8, 2017.



Fig. 9
Service spillway chute damage observed after gates were closed on February 7

DWR knew that it would need to operate the damaged service spillway because of expected inflow to Lake Oroville; hence, it was decided to begin opening the spillway gates to test the service spillway's capabilities in the damaged condition. The gates were reopened at about 4:00 pm on February 8, 2017, and several different discharge levels were trialed through February 10, while the service spillway chute was observed for additional damage. Spillway discharge reached 1,840 m³/s (65,000 ft³/s) at 3:00 am on February 10, and was held there for about 17 hours. At about 8:00 pm on February 10, the service spillway discharge was reduced to about 1,560 m³/sec (55,000 ft³/s) and maintained at that level through 3:35 pm on February 12.

Meanwhile, inflows to Lake Oroville continued to increase. Sometime between about 7:00 and 8:00 am on February 11, the reservoir level exceeded Elevation 274.6 m (901 ft), and water began flowing over the emergency spillway crest structure for the first time in the facility's history. The reservoir level increased to a maximum level of about Elevation 275.1 m (902.6 ft), about 0.49 m (1.6 ft) above the emergency spillway's crest, at about 3:00 pm on February 12, about 31 hours after the flow over the emergency spillway began. The flow over the

emergency spillway at the peak reservoir level was estimated to be about 354 m³/s (12,500 ft³/s), less than 4 percent of ultimate capacity.

The emergency spillway discharge channelized as it flowed across the natural terrain downstream of the crest structure and caused extensive erosion, with some of the erosion areas headcutting aggressively back toward the emergency spillway crest structure. According to Incident Command notes [7], at 3:44 pm on February 12, an evacuation order was issued for about 188,000 downstream residents, because of the rapidly advancing erosion areas in the emergency spillway's discharge channel.

DWR increased the discharge through the service spillway, beginning at 3:35 pm on February 12, about nine minutes before the evacuation order was issued, according to the Incident Command notes [7]. Service spillway discharge was increased to about 2,830 m³/s (100,000 ft³/s) by about 7:00 pm on February 12 and this discharge level was maintained through 8:00 am on February 16. Discharge over the emergency spillway crest ceased at about 8:00 pm on February 12, about 36 hours after it began and about 5 hours after the flow had peaked.

At about 3:30 pm on February 14, the evacuation order was changed to an evacuation warning, under which residents were allowed to return but were advised to monitor the media and be prepared to evacuate again, if necessary. No further evacuation orders were judged necessary, and the evacuation warning was lifted five weeks after the evacuation order was first issued.

DWR established a target reservoir level at Elevation 259.1 m (850 ft), which is 15.2 m (50 ft) below the normal full-pool level. This target elevation for Lake Oroville was reached on February 20.

The service spillway gates were closed on February 27 to allow for on-site investigations to support remedial actions. After that time, investigations and remedial actions were interrupted occasionally for service spillway releases to manage the reservoir. The service spillway gates were closed for the season on May 19, 2017, so that construction of spillway repairs could begin.

During service spillway operations between February 8 and May 19, 2017, additional spillway chute slab sections were lost and the slab failure and foundation erosion at the service spillway enlarged significantly, as shown in Fig. 10.



Fig. 10
Ultimate damage at the service spillway

4. THE PHYSICS OF WHAT HAPPENED

4.1. SERVICE SPILLWAY

The IFT believes that the service spillway chute failure most likely initiated by the uplift and removal of a section of the chute slab in the vicinity of Sta. 33+50, at about 10:10 am on February 7, 2017. Once the initial section of the chute slab was removed, the underlying moderately to strongly weathered rock and soil-like foundation material beneath the slab at this location (see Fig. 6) was directly exposed to high velocity spillway flow. The high velocity flow rapidly eroded the foundation materials at this location, removed additional chute slab sections in both upstream and downstream directions, and quickly created the large erosion hole that was observed by 12:30 pm on February 7 (see Fig. 9), as flows diminished following spillway gate closure. These findings are based on eyewitness accounts, as well as photographic and videographic records, as explained in detail in the full forensic investigation report [1].

While there are numerous physical factors that contributed to the chute failure, which the IFT studied in detail, the IFT focused on the factors that it believed likely played the most significant roles in the failure of the service spillway chute.

The IFT concluded that the initial uplift and removal of a slab section was most likely caused by water uplift pressure beneath a section of the chute slab, producing an uplift force that exceeded the uplift capacity of that particular section

of slab. The uplift force was a product of both the uplift pressure and the area over which it was applied, and the uplift pressure likely involved transmission of stagnation pressure through the slab to the foundation. The resistance to uplift was provided by a combination of the weight of the slab, the weight of the water above the slab, the uplift resistance provided by the foundation anchor system, the structural interaction of slab panels with adjacent slab panels, and any bond between the concrete slab and the foundation. Once the upstream end of the slab section lifted, creating an offset into the flow, the pressure under the slab rapidly increased due to greater stagnation pressures and produced the sudden failure of the slab.

The initial chute slab failure section could have been small. Once even a small section of slab was removed, the high velocity flow would have quickly attacked the underlying erodible foundation material and would have begun to remove additional sections of the chute slab. Additionally, the edges of the remaining downstream slab adjacent to the removed section would have presented a significant offset into the flow, which would generate high stagnation pressures that could jack out all but the most resistant slab sections. Subsequent downstream slab sections were removed until the flow encountered a slab section with enough resistance to counter these high uplift forces.

The excessive flow into the foundation was mainly due to the high velocity spillway flow injecting water into and through slab surface features, such as open joints, unsealed cracks over the herringbone drains, spalled concrete at either a joint or drain location in either a new or previously repaired area, or some combination of these features that produced offsets into the flow. Localized slab deterioration and repairs existed in the area of the initial slab failure prior to February 7, and these localized areas would have been vulnerable to damage during high velocity spillway flow.

Flows into the foundation would generally increase as flow velocities near the chute surface increased. The chute failure occurred very shortly after the spillway gates were opened more to increase discharge down the spillway chute, which led to higher surface flow velocities, and likely higher injection flows which exceeded drainage capacity and resulted in increased uplift pressures.

Over time, there was likely also some shallow underslab erosion of fines from the weathered rock and some loss of underdrain system effectiveness, which contributed to increased slab uplift forces.

In evaluating the physical factors, it is important to consider why the chute failure happened in 2017 at a spillway discharge of about 1,490 m³/s (52,500 ft³/s), whereas the service spillway chute had not failed previously during higher discharges, most recently a discharge in excess of 1,420 m³/s (70,000 ft³/s) in 2006, and historically discharges as large as about 2,270 m³/s (160,000 ft³/s) in 1997. In other words, what changed from 2006 until 2017 such that the chute slab failure happened in 2017, rather than 2006 or earlier?

There are a number of possibilities for changes that could have occurred during that time period. The IFT believes that some combination of the following factors most likely was involved:

- New chute slab damage and/or deterioration of previous slab repairs, which could have created stagnation pressure and increased flow into the foundation in areas that were already vulnerable because of weak foundation conditions
- Expansion of relatively shallow void(s) under the slab, through foundation soil erosion and/or shrinkage of clayey soils, which would have increased uplift force by increasing the area over which uplift pressure was applied
- Corrosion of the steel reinforcing bars or dowels across concrete cracks or joints, which then failed in tension, resulting in reduced uplift capacity
- Reduction in foundation anchor capacity due to corrosion or reduction in bond length due to erosion, which would have reduced uplift capacity

All of these factors, as well as other less prominent factors and factors eliminated from consideration, are discussed in detail in the full forensic investigation report [1].

Cavitation, groundwater flow/pressure, and seismic loading are physical factors that were suggested by others but were judged by the IFT to not have been significant contributory factors.

The IFT completed calculations that indicated that, for the original service chute, cavitation would be expected only downstream of Sta. 31+00, and there only for extended periods of discharge greater than 2,830 m³/s (100,000 ft³/s). The historical discharges greater than 2,830 m³/s (100,000 ft³/s) were not of sufficient duration to cause significant cavitation damage. This conclusion was supported by observation of chute slab sections remaining in place downstream of Sta. 31+00 after the incident, which did not reveal telltale indicators of incipient cavitation.

The IFT reviewed available information concerning groundwater and geologic conditions in the area of the service spillway. This review led to the conclusion that there was no evidence of large amounts of groundwater flow in the spillway location, and such groundwater flow would not have been expected for the geologic conditions at that location. Therefore, although groundwater flows may have contributed in a very small way to uplift pressures that developed under the chute slabs, it was the IFT's opinion that groundwater was not a significant contributor when compared to water pressure injected through slab joints and cracks when the service spillway was operating.

The IFT completed a review of seismic activity in the vicinity of Oroville Dam over the last 20 years, with a conclusion that no earthquakes stronger than M 4.0 occurred within 160 km (100 mi) of the site in that time period. No ground motions

generated by earthquake events strong enough to conceivably cause damage to large civil structures were recorded by instrumentation at the project within the prior 20 years. Principally for these reasons, the IFT concluded that seismic damage was not a likely contributor to failure of the chute slab.

4.2. EMERGENCY SPILLWAY

The development of the damage to the emergency spillway discharge channel was closely observed during the incident. Photographs and videographic footage, along with eyewitness reports, provide documentation of the development of the emergency spillway damage.

During the incident response, in preparation for the possible use of the emergency spillway, trees had been cleared from the natural hillside downstream of the spillway crest structure before flow over the crest structure occurred. As the emergency spillway discharge flowed over the natural ground downstream of the crest structure, erosion began to occur. Erosion of surficial soil deposits began to develop as expected. However, erosion continued into the underlying weathered bedrock to greater depths than expected. By the afternoon of February 12, concentrated areas of erosion were observed to be rapidly progressing upstream (headcutting) toward the emergency spillway crest structure (see Fig. 11), resulting in the issuance of the evacuation order.



Fig. 11
Emergency spillway headcutting on February 12

The principal physical factor contributing to the damage at the emergency spillway was clearly the presence of significant depths of erodible soil and rock in features orientated to allow rapid headcutting toward the crest control structure. Hillside topography and the presence of infrastructure (roads, transmission towers, etc.) may have concentrated flows and increased erosive forces, facilitating headcut formation. Insufficient energy dissipation at the base of the spillway ogee

crest structure and the absence of erosion protection downstream of the crest structures may have also contributed to the development of the erosion.

5. WHY THE INCIDENT HAPPENED

The February 2017 Oroville Dam spillway incident was the result of interactions of numerous physical and human factors, beginning with the design of the project and continuing during the nearly half-century until the incident. The incident was generally the result of a long-term systemic failure of DWR, regulatory, and general industry practices to recognize and properly address the deficiencies and warning signs which preceded the incident. There was no one root cause, nor can the incident reasonably be “blamed” mainly on any one individual, group, or organization.

5.1. SERVICE SPILLWAY

The conditions that led to the service spillway chute failure have their roots in the original design and construction of the chute, which, combined with the locally poor geologic conditions at the site, resulted in vulnerabilities in the as-built structure. These vulnerabilities were not recognized in various inspections and evaluations that were completed throughout the history of the structure. In fact, warning signs of the vulnerabilities came to be accepted as “normal,” and then generally were not questioned further. Because the seriousness of the vulnerabilities was never recognized, chute slab repair efforts were neither well-conceived nor effective, and likely contributed to the deterioration of chute conditions over time.

As detailed in the forensic investigation report [1], the spillway chute design was generally at the middle of the range of practice for the 1960s for spillway chutes founded on rock. For a structure of the significance of Oroville Dam, the IFT would expect the design to have reflected the best practices of the time, which it did not. The one aspect in which the design was at the very low end of practice of the time was the significant protrusion of the chute underdrains into the slab section. This feature was uncommon and led to the development of extensive cracking over the drains and resulting leakage through the slab at the cracks.

Communication among geologists, designers, and construction managers during the service spillway’s design and construction apparently was poor. This ultimately resulted in a design which was probably more appropriate for a spillway chute on rock foundations rather than one constructed on more variable foundation conditions, including strongly weathered rock, most notably an extensive area of such material at the location of the initial chute slab failure. These conditions

compromised anchor resistance and potentially promoted the formation of shallow voids beneath the slab.

Although the slab cracking and resulting large drain flows were recognized during the first year of project operation, they apparently were judged as non-threatening, and subsequently became accepted as normal. These conditions were reported in many inspections with no further comment. After completion of the project, the detailed geologic information concerning the extent of strongly weathered rock in the right abutment and beneath the service spillway chute was relegated to project records, and the abutment was incorrectly assumed and portrayed as being composed of generally non-erodible rock below a few feet of soil cover.

The seriousness of the weak as-constructed conditions and the lack of repair durability was not recognized during numerous inspections and review processes over the almost 50-year history of the project, including three Potential Failure Mode Analyses (PFMAs) completed between 2004 and 2014. The first two PFMA efforts did not identify any significant potential failure modes (PFMs) related to the service spillway chute. The 2014 PFMA identified the service spillway PFM that initiated in February 2017, but it was judged extremely unlikely and ruled out of further consideration, principally because it was believed that the rock foundation would not headcut enough to fail the headgate structure and result in uncontrolled release of the reservoir.

There is no record of the original design and construction of the service spillway chute having been subsequently reviewed for consistency with more modern design and construction practices or for potential chute failure modes.

Chute slab repairs were neither effective nor durable. Over time, chute flows and temperature variations led to progressive deterioration of the concrete and the corrosion of steel reinforcing bars and anchors, with likely loss of slab strength and anchor capacity.

5.2. EMERGENCY SPILLWAY

Prior to the February 2017 spillway incident, the geology of the right abutment of the dam, including the hillside downstream of the emergency spillway crest structures was fundamentally mischaracterized and misunderstood by DWR, its consultants, DSOD, and FERC. Although geologic data from the time of original design identified the presence of areas of relatively deep strongly weathered rock, over the history of the project DWR's geologists had come to believe that the hillside downstream of the emergency spillway crest structure consisted of shallow soil cover over non-erodible rock, and this was accepted by all others involved, without a critical review of the available information. Hence, the erosion and headcutting that occurred when the free-flow emergency spillway overtopped were not expected.

Once the incident initiated with the failure of the service spillway, DWR attempted to find a "sweet spot" in balancing the risks of operating the service and emergency spillways, with the goal of releasing limited flows down the service spillway to both reduce ongoing service spillway erosion and prevent Hyatt Powerplant flooding, while also not overtopping the emergency spillway weir. These multiple constraints and objectives resulted in very difficult decisions, which were further influenced by a number of changing conditions and differing perceptions and viewpoints. Along the incident management timeline, there were particular points when decisions were made to limit discharge through the service spillway, even though the risks associated with powerplant flooding were clearly diminishing. This ultimately resulted in flow over the emergency spillway weir.

In general, the IFT believes that all decisions during the incident were made with the best of intentions, but in some cases were against the advice of a number of civil engineering and geological personnel. In limiting service spillway discharge to reduce the likelihood of powerplant flooding, the additional dam safety risk associated with the use of the emergency spillway may not have been appropriately considered.

5.3. ORGANIZATIONAL, REGULATORY, AND INDUSTRY FACTORS

The February 2017 Oroville Dam spillway incident can be viewed as a "textbook" case of a major dam incident, in terms of typifying the extent of contribution from human factors, including organizational, regulatory, and industry factors. Through a historical trajectory involving decades of somewhat complex interactions and effects of human and physical factors, numerous warning signs of the spillway chute failure were missed, and many barriers, which were intended to provide "checks and balances," were overcome to eventually produce the spillway chute failure and emergency spillway damage.

The IFT identified a multifaceted array of human factors, additional to those specific to the spillways, which contributed to the incident:

- DWR was significantly overconfident and complacent regarding the integrity of its SWP civil infrastructure. This was not atypical among large dam owners in the United States, and was influenced by a belief that the SWP was designed by the “best of the best” and a lack of prior major incidents at dams owned by DWR. In addition, less attention was generally paid in the United States dam engineering and safety industry to spillways as compared to main dams, which contributed to complacency in managing spillway risks.
- DWR was largely in a mode to react to problems with its civil infrastructure as they arose in the short term, rather than taking preemptive actions to proactively prevent problems. This approach was not atypical among large dam owners in the United States, and was influenced by external and internal pressures to control costs, while focusing on the needs of operations, water delivery, and hydroelectric power production.
- The dam safety culture and program within DWR, although maturing rapidly and on the right path, was still relatively immature at the time of the incident, and was about in the “middle of the pack” as compared to other large dam owners in the United States. DWR had been too reliant on regulators and regulatory processes, including associated periodic inspections and reviews, with the assistance of its numerous consultants. In addition, there was no clear identification of a senior executive within DWR who was responsible for dam safety, and the Chief Dam Safety Engineer, while highly dedicated, was not in a position to best influence either investment or emergency decisions related to dam safety.
- DWR’s information management system was not sufficient to efficiently and effectively handle the very large amount of accumulated information associated with its dams, and thereby ensure that the right information was in the right hands at the right times. This factor was particularly impactful when judgments regarding the quality of the rock at the spillways were being made.
- DWR’s two regulators, FERC and DSOD, like other dam safety regulators in the United States, faced numerous challenges and limitations with respect to maintaining sufficient qualified technical staff to meet workloads, addressing uncertainties when trying to balance the costs imposed on dam owners versus the risks imposed on the public and the environment, and gaining compliance from dam owners with regulatory requirements and expectations.
- DWR, and to some extent its regulators and consultants, also lacked necessary technical expertise in some areas of dam engineering and safety, with expertise generally tending to be stronger for dams than for appurtenant structures. Influencing factors for DWR included excessive organizational pride, organizational insularity, emphasis on electrical and mechanical aspects as compared to civil engineering and geologic aspects, and cost pressures and bureaucratic constraints related to technical staffing. An influencing factor for the United States dam safety industry was that the available technical literature

was not organized as a set of integrated and regularly-updated national guidelines which could readily be found and navigated by engineers and others involved in dam safety.

- Internal relationships within DWR were strained for decades prior to the incident, especially between DWR's Division of Engineering and its Division of Operations and Maintenance. While this strain was not atypical among large dam owners in the United States, it had a negative impact on DWR's decision-making and deployment of technical expertise related to its dams, both during the half-century prior to the incident, as well as during the incident response.

6. LESSONS TO BE LEARNED

In the opinion of the IFT, the following are some of the general lessons to be learned by the broader dam engineering and safety community:

- In order to ensure the safe management of water retention and conveyance structures, dam owners must develop and maintain mature dam safety management programs which are based on a strong "top-down" dam safety culture. There should be one executive specifically charged with the overall responsibility for dam safety, and this executive should be fully aware of dam safety concerns and prioritizations through direct and regular reporting from a designated dam safety professional, to ensure that "the balance is right" in terms of the organization's priorities.
- More frequent physical inspections, primarily based on visual observation, are not always sufficient to properly identify problems, determine risks, and manage dam safety. Some problems can only be identified through records review and/or subsurface investigations or non-destructive testing.
- Periodic comprehensive reviews of original design and construction records and subsequent performance reports are necessary, especially for large and high-hazard dams and their appurtenances. These reviews should be based on complete records and need to be more in-depth than periodic general reviews, such as the current FERC-mandated five-year reviews.
- Appurtenant structures associated with dams, such as spillways, outlet works, power plants, etc., must be given attention by qualified individuals. This attention should be commensurate with the risks that the facilities pose to the public, the environment, and dam owners, including the risks associated with events which may not result in uncontrolled release of reservoirs, but may still result in reduced control of the reservoir or otherwise be highly consequential.
- Shortcomings of the current Potential Failure Mode Analysis (PFMA) processes in dealing with component failures and complex systems must be recognized and addressed. A critical review of these processes in dam safety practice is warranted, comparing their strengths and weaknesses with risk assessment processes used in other industries worldwide and by other Federal

agencies. Evolution of “best practices” in dam safety should continue by supplementing current practice with new approaches, as appropriate, drawing on other industry and international experience and realistically accounting for inherent human fallibility.

- Compliance with regulatory requirements is not always sufficient to manage risk and meet dam owners’ legal and ethical responsibilities.

REFERENCES

- [1] *Independent Forensic Team Report, Oroville Dam Spillway Incident*, France, J.W., Alvi, I.A., Dickson, P.A., Falvey, H.T., Rigbey, S.J., and Trojanowski, J., January 5, 2018.
- [2] *Report on Reservoir Regulation for Flood Control, Oroville Dam and Reservoir*, Department of the Army, Sacramento District, Corps of Engineers, August 1970.
- [3] *Memorandum No. 1 - Orientation Meeting March 1 & 3, Site Visit March 2, and Design Concepts Meeting, March 10, 2017*, Independent Board of Consultants for Oroville Emergency Recovery – Spillways, March 10, 2017.
- [4] *Oroville Dam and Lake, Performance of the Flood Control Outlet during the Storms of January-February 1969*, DWR Division of Design and Construction, March 1969.
- [5] *Inspection of Dam and Reservoir in Approved Status, DSOD Inspection Notes*, J.F. Chaimson and D.L. Christensen, date of inspection: January 29-30, 1969, date of report: February 13, 1969.
- [6] *Inspection of Dam and Reservoir in Approved Status, DSOD Inspection Notes*, J.F. Chaimson and D.L. Christensen, date of inspection: March 5, 1969, date of report: March 10, 1969.
- [7] *Incident Command Notes provided by DWR: typed notes from February 8 through 12, 2017; handwritten notes from February 12 and 13, 2017.*

SUMMARY

The Oroville Dam spillway incident was caused by a long-term systemic failure of practices of DWR, its regulators, and the United States dam safety industry to recognize and address inherent spillway design and construction weaknesses, poor foundation bedrock quality, and deteriorated service spillway chute conditions. The incident cannot reasonably be “blamed” mainly on any one individual, group, or organization.

During service spillway operation on February 7, 2017, water injection through both cracks and joints in the chute slab, and associated transmission of stagnation pressure under the slab, resulted in uplift forces beneath the slab that exceeded the uplift capacity and structural strength of the slab, at a location along the steep section of the chute. The uplifted slab section exposed the underlying poor quality foundation rock at that location to unexpected severe erosion and extreme uplift pressure, resulting in removal of additional slab sections and more foundation erosion.

Responding to the damage to the service spillway chute necessitated difficult risk tradeoffs while Lake Oroville continued to rise. The resulting decisions, made without a full understanding of relative uncertainties and consequences, allowed the reservoir level to rise above the emergency spillway weir crest for the first time in the project’s history, leading to severe and rapid erosion and headcutting downstream of the weir and, ultimately, resulting in an evacuation order for about 188,000 people.

There are a number of lessons to be learned, for both DWR and the broader dam safety community. The question is whether dam owners, regulators, and other dam safety professionals will recognize that many of these lessons are actually *still to be learned*. Although the practice of dam safety has certainly improved since the 1970s, the fact that this incident happened to the owner of the tallest dam in the United States, overseen by a Federal agency, repeatedly evaluated by reputable outside consultants, in a state with a leading dam safety regulatory program, is a wake-up call for everyone in the dam safety community. Challenging current assumptions on what constitutes “best practice” in this industry is overdue.

KEYWORDS

Appurtenant structure, chute, construction, dam, damage, design, drainage, embankment dam, emergency situation, emergency spillway, erosion, flood control, frequency of inspections, gated spillway, geology, internal erosion, Oroville Dam, performance, regulation, scouring, safety of dams, spillway, uncontrolled spillway, uplift, weathered rock

COMMISSION INTERNATIONALE DES GRANDS BARRAGES

VINGT-SIXIÈME CONGRÈS DES GRANDS BARRAGES
Autriche, juillet 2018

DOI 10.3217/978-3-85125-620-8-008



This work licensed under a Creative Commons Attribution 4.0 International License. <https://creativecommons.org/licenses/by-nc-nd/4.0/>

**MODELLING THE UNCERTAINTY OF INFLOW TO SHORT-TERM
RESERVOIR OPERATION USING FUNCTIONAL EXPANSION-BASED
METHOD**

Duan CHEN

*Vice Dean of Trans-boundary River Research Department, CHANGJIANG
RIVER SCIENTIFIC RESEARCH INSTITUTE*

CHINA

Bo HU

*Vice Dean of Water and Soil Conservation Department, CHANGJIANG RIVER
SCIENTIFIC RESEARCH INSTITUTE*

CHINA

COMMISSION INTERNATIONALE
DES GRANDS BARRAGES

VINGT-SIXIÈME CONGRÈS DES
GRANDS BARRAGES
Autriche, juillet 2018

**MODELLING THE UNCERTAINTY OF INFLOW TO SHORT-TERM
RESERVOIR OPERATION USING FUNCTIONAL EXPANSION-BASED
METHOD**

Duan CHEN

*Vice Dean of Trans-boundary River Research Department, CHANGJIANG
RIVER SCIENTIFIC RESEARCH INSTITUTUE*

Bo HU

*Vice Dean of Water and Soil Conservation Department, CHANGJIANG RIVER
SCIENTIFIC RESEARCH INSTITUTUE*

CHINA

1. INTRODUCTION

Single trace of inflow forecast has been commonly used for guiding short-term reservoir operation and provided a better way of managing water resources, compared to traditional rule-based-only operations. However, uncertainty of the inflow information is a major challenge to the operator as the single trace of inflow forecast may deviate far from the reality due to forecast errors. To better represent the uncertainty associated with the inflow forecast, ensemble stream flow prediction ^[1], also called ESP is gradually used to replace the single trace inflow forecast. The ESP is essentially a collection of multiple inflow forecasts that are resulted from multiple runs of weather models. The advantage of the ESP is that the inflow uncertainty under largely variable weather condition e.g., climate change are accounted through different realizations of inflow. However, the usage of the ESP may lead to a high computational cost for optimization of reservoir operation due to uncertainty modeling.

This study use a functional expansion-based method namely Karhunen-Loeve

expansion to model the uncertainty associated with the ESP and demonstrate its high efficiency with a case study.

2. METHODOLOGY

The Karhunen-Loeve (KL) expansion^{[2] [3] [4]} is a representation of a random process as a series expansion involving a complete set of deterministic functions with corresponding random coefficients. Consider a random process of $Q(t)$ and let $\overline{Q(t)}$ be its mean and $C(s,t)=\text{cov}(Q(s), Q(t))$ be its covariance function. The $Q(s)$ and $Q(t)$ are variables at different time step. Then, the KL expansion of $Q(t)$ can be represented by the following function:

$$Q(t) = \overline{Q(t)} + \sum_{k=1}^{\infty} \sqrt{\lambda_k} \psi_k(t) \xi_k \quad [1]$$

where $\{\psi_k, \lambda_k\}_{k=1}^{\infty}$ are the orthogonal eigen-functions and the corresponding eigen-values, obtained as solutions of the equation:

$$\lambda \psi(t) = \int C(s, t) \psi(s) ds \quad [2]$$

Equation (3) is a Fredholm integral equation of the second kind. When applied to a discrete and finite process, this equation takes a much simpler form that can be easily solved. In its discrete form, the covariance matrix $C(s,t)$ is represented as an $N \times N$ matrix, where N is the time steps of the random process. Then the above integral form can be rewritten as $\sum_{s,t=1}^N C(s, t) \psi(s)$ to suit the discrete case. In Eq. [1], $\{\xi_k\}_{k=1}^{\infty}$ is a sequence of uncorrelated random variables (coefficients) with mean of 0 and variance of 1 and are defined as:

$$\xi_k = \frac{1}{\sqrt{\lambda_k}} \int [Q(t) - \overline{Q(t)}] \psi_k(t) dt \quad [3]$$

The form of the KL expansion in Eq.[1] is often approximated by a finite number of discrete terms (e.g., M), for practical implementation. The truncated KL expansion is then written as:

$$Q(t) \approx \overline{Q(t)} + \sum_{k=1}^M \sqrt{\lambda_k} \psi_k(t) \xi_k \quad [4]$$

The number of terms M is determined by the desired accuracy of approximation and strongly depends on the correlation of the random process. The higher the correlation of the random process, the fewer the terms that are required for the approximation^[5]. One approach to roughly determine M is to compare the magnitude of the eigen-values (in descending order) with respect to the first eigen-value and consider the terms with the most significant eigen-values. With the truncated KL expansion, the large number of variables in time-domain is reduced to fewer coefficients in the transformed space (i.e., frequency-domain). The KL expansion has found many applications in science and

engineering and is recognized as one of the most widely used methods for reducing dimension of random processes^{[6] [7] [8] [9]}.

3. CASE STUDY AND RESULTS

The Qinshitan Reservoir is a major hydraulic facility of the Lijiang River basin in the southwest of China. It is located at the upstream of the Gantang River, which is the largest tributary of the Lijiang River. The Qinshitan Reservoir is operated for agricultural irrigation, power generation and domestic water supply for the city of Guilin^[10]. The inflow to the Qinshitan Reservoir is a critical parameter for the operation, however, is associated with large forecast error, particularly in flood season.

For a period of two weeks during flood season, the ESP of inflow (six different forecasts) to the reservoir varied largely in the magnitude (shown in Fig.1). To represent the uncertainty in the ESP, we treat the ESP for the two weeks as six realizations of the random process of $Q(t)$. By following the steps in the section of Methodology, the eigen-value and eigen-funcntion of the $Q(t)$ are calculated. The first ten eigen-values are illustrated in Fig.2.

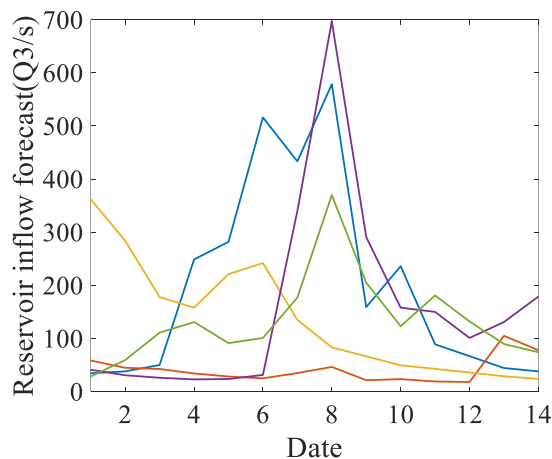


Fig. 1
ESP of Qingshitang Reservoir
de Qingshitang Réservoir

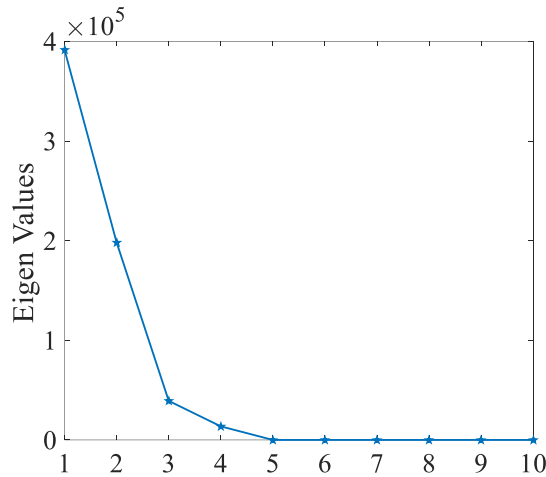


Fig. 2
The First ten Eigen Values of the ESP
Les valeurs de Eigen dix premiers de l'ESP

It is observed from Fig.2 that the first three eigen-value are much larger than the rest, accounting for a large proportion in the sum of eigen-value. According to the KL expansion theory, this result means that significant portion of the random process can be approximately represented by the first three terms (Namely M=3 in this case), and is written in the following:

$$Q(t) = \overline{Q(t)} + \sum_{k=1}^3 \sqrt{\lambda_k} \phi_k(t) \xi_k \quad [5]$$

In the Eq.[5], the average of Q(t) can be easily calculated. The eigen-value and eigen-function for the first three terms are calculated and are deterministic parameters in the equation. Therefore, the uncertainty of the ESP is only determined by three uncorrelated random variables (coefficients) with mean of 0 and variance of 1. In other words, we could use only three variables to approximate the uncertainty that are associated with the ESP of the inflow to the Qinshitan Reservoir.

4. DISCUSSIONS

The KL expansion form of the inflow ESP to the Qinshitan Reservoir (Eq.[5]) results in a great reduction for approximating the ESP uncertainty. This is particular useful for optimization the reservoir operation under uncertainty. In the conventional modeling, Monte Carlo method is used for modeling the uncertainty, which lead to a very high computation cost as thousands or even millions of simulations are carried in each time step. As a comparison, the KL expansion form of the inflow ESP has only three variables and is invariant to the time step. A

high efficiency in optimization of reservoir operation can be achieved, as shown in [11]. However, it is worth mentioning that the representation of the KL expansion is specific to inflow distribution. Different inflow ensembles i.e., the ESP may result in different KL expansion form in which the parameter of M may vary from case to case.

5. CONCLUSIONS

The ensemble inflow and its associated uncertainty can be modeled by a KL representation with only three terms, meaning three variables. This result in a high efficiency in modeling the propagation and optimal control of the inflow uncertainty in reservoir operation, comparing to Monte Carlo method which normally sampling thousand times in each optimization routine.

ACKNOWLEDGEMENT

The authors thank National Natural Science Foundation of Hubei Province (2017CFB613) and open funding of Hunan Provincial Key Laboratory of Key Technology on Hydropower Development(PKLHD201705). The authors would also like to thank Prof. Nathan Gibson and Dr. Veronika Vasylykivska for providing the Matlab code for the Karhunen-Loeve expansion.

REFERENCES

- [1] KIM, S., LIMON, R. A., et al. Integrating Ensemble Forecasts of Precipitation and Streamflow into Decision Support for Reservoir Operations in North Central Texas. In *AGU Fall Meeting Abstracts*, 2016, Feb.
- [2] Kosambi D. D., Statistics in function space, *J. Indian Math. Soc. (N.S.)* 7 (1943), 76–88.
- [3] Karhunen K.K, On linear methods in probability and statistics, *Ann. Acad. Sci. Fennicae. Ser. A. I. Math.-Phys.*, 1947, No. 37, 1–79.
- [4] Williams, M. M. R. (2015). Numerical solution of the Karhunen–Loeve integral equation with examples based on various kernels derived from the Nataf procedure. *Annals of Nuclear Energy*, 76, 19-26.
- [5] XIU, D. (2010). *Numerical methods for stochastic computations: a spectral method approach*. Princeton University Press, 2010.
- [6] Narayanan, M. V., King, M. A., Soares, E. J., Byrne, C. L., Pretorius, P. H., & Wernick, M. N. (1999). Application of the Karhunen-Loeve transform to 4D

- reconstruction of cardiac gated SPECT images. *Nuclear Science, IEEE Transactions on*, 46(4), 1001-1008.
- [7] Phoon, K. K., Huang, S. P., & Quek, S. T. (2002). Implementation of Karhunen–Loève expansion for simulation using a wavelet-Galerkin scheme. *Probabilistic Engineering Mechanics*, 17(3), 293-303.
- [8] Grigoriu, M. (2006). Evaluation of Karhunen–Loève, spectral, and sampling representations for stochastic processes. *Journal of engineering mechanics*, 132(2), 179-189.
- [9] Gibson, N. L., Gifford-Miears, C., Leon, A. S., & Vasylykivska, V. S. (2014). Efficient computation of unsteady flow in complex river systems with uncertain inputs. *International Journal of Computer Mathematics*, 91(4), 781-797.
- [10] Chen, D., Chen, Q., Leon, A. S., and Li R (2016). A Genetic Algorithm Parallel Strategy for Optimizing the Operation of Reservoirs with Multiple Eco-environmental Objectives. *Water Resources Management*, doi: 10.1007/s11269-016-1274-1.
- [11] Chen, D., Leon, A. S., Gibson, N. L. and Hosseini, P (2016). Dimension reduction of decision variables for multi-reservoir operation: A spectral optimization model. *Water Resources Research*. doi:10.1002/2015WR017756.

COMMISSION INTERNATIONALE DES GRANDS BARRAGES

VINGT-SIXIÈME CONGRÈS DES GRANDS BARRAGES
Autriche, juillet 2018

DOI 10.3217/978-3-85125-620-8-009



This work licensed under a Creative Commons Attribution 4.0 International License. <https://creativecommons.org/licenses/by-nc-nd/4.0/>

**INCREASE EFFICIENCY OF VORTEX SETTLING BASIN IN IMBIBITION OF
DAM'S RESERVOIR IN TIME OF FLOODWATER**

Amin HAJIAHAMADI

*Technical Office of Hormozgan Regional water company, PhD Student, SCHOOL
OF CIVIL ENGINEERING, SHAHID BAHONAR UNIVERSITY OF KERMAN*

IRAN

Mojtaba Saneie

*Associate Professor, SOIL CONSERVATION AND WATERSHED
MANAGEMENT RESEARCH INSTITUTE (SCWMRI), Tehran*

IRAN

Mehdi Azhdari Moghadam

*Associate Professor, SCHOOL OF CIVIL ENGINEERING, THE UNIVERSITY OF
SISTAN AND BALUCHESTAN, Zahedan*

IRAN

Increase efficiency of vortex settling basin in imbibition of dam's reservoir in time of Floodwater

Amin Hajiahmadi¹, Mojtaba Saneie², Mehdi Azhdari Moghadam³

1 Technical Office of Hormozgan Regional water company ,PhD Student, School of Civil Engineering, Shahid Bahonar University of Kerman, Iran.

Email:amin.hajiahmadi@yahoo.com

2 Associate Professor, Soil Conservation and Watershed Management Research Institute (SCWMRI), Tehran, Iran.

3 Associate Professor, School of Civil Engineering, The University of Sistan and Baluchestan, Zahedan, Iran.

ABSTRACT

One obstacle of in imbibition of dam's reservoir in time of Floodwater is the Existence of Suspended sediment in floodwater. On the other hand because the lack of water resources in arid regions, providing of water is dependent on imbibition of dams. Thus existence of Suspended sediment in reservoir's water can malfunction in the imbibition programs. Also Entry of this sediments to hydraulic structures can disorder their Performance.

Using vortex settling basins can be suggested as a solution to control the amount of sediments. One of negative point of this basins is settling some part of sediments and not flashing from bottom outlets. In current paper we recommend to use curvature submerge vanes for solving previous problems. The main propose of using this vanes is to adjust and increase the power of vortex flow and to locate the best place for installing curvature submerge vanes in the basin floor. The tests results illustrate that using this vanes with appropriate arrangement can flush out sediments of basin floor, while keeping basins efficiency. The best efficiency is for arrangements which are far away from orifice. More over while increasing Input flow and decreasing radial section of vanes, improves the efficiency of use curvature submerge vanes.

Keywords: Efficiency, Sediment, Settling basin, Submerge Vane, Vortex Flow.

1 Introduction

Since most rivers pass across loose and erodible areas, they always act as the most important factor of transferring eroded materials from the solid crust of the earth. Disregarding incoming sediments to intakes causes the transfer of sediments into water

utilities and their settlement in different parts of the transmission network which will cause many problems. Sediment particles in water at high speeds cause irreparable damages to hydro mechanical parts of the hydroelectric structure such as pumps and turbines. In plants in India, irreparable damage to turbine blades due to sand in water (After two to three thousand hours of operation of turbines) (Ranga Raju *et al.* 1999).

In water transmission, especially in networks where the water is transmitted by gravity, water flow cannot hold sediment particles in the suspended mode because water speed is low and this leads to settlement and accumulation of sediment particles in the channel bed over time. This causes problems such as: A) Accumulation of sediments in the channel and a decrease in the channel free depth and capacity; B) High cost of dredging irrigation canals; C) Erosion of channel walls and aquatic structures; D) Creation of favorable conditions at the floor of canals for growth of plants, and changes in roughness coefficient. These kinds of problems have encouraged many aquatic structure experts to take on appropriate and effective measures from the beginning and avoid the entry of sediments into water transmission and distribution networks as much as possible.

One way is to separate sediments using vortex settling basins. In this type of settlings, vortex flow is used to separate sediment from water flow. This method is a solution for separating solids from liquids at high speeds, unlike classical settling basins in which settling occurs at lower speeds using the gravity force. The vortex created in these basins is generally a Rankine-type vortex consists of a forced vortex in the center of the basin and around the central orifice and a free vortex in the outer section of the central vortex of the basin (Athar *et al.* 2002). In this type of settlings, flow is directed within the basin completely tangentially and exits from the top weir while rotating around the basin. The settling phenomenon and sediment movement towards the washing orifice are occurring by secondary flows. Sediment particles are separated from water with the loss of only a small amount of discharge. Sediment particles entering the basin move along a spiral path towards the basin center (Ziaei 2000). Therefore, in such systems, the extension of the settling path of sediments is several times larger than the basin size.

Among the advantages of this sediment control method compared to other conventional methods like classic settling basin, one can point to reduce water losses, cost-effectiveness, its permanence unlike other settlings, no need for short-term dredging and smaller size (Paul 1991).

Extensive research has been conducted on a vortex settling basin by Vokes and Jenkines (1943), Velioglu (1972), Salakhov (1975), Cecen and Bayazit (1975), Sullivan *et al.* (1978), Curi *et al.* (1979), Mashuri (1981,1986), Svarovski (1981), Ogihara and Sakagouchi (1984), Sanmogantan (1985), Esen (1989), Zhou *et al.* (1989, 1997), Paul *et al.* (1991), Ziaei (2000), Athar *et al.* (2002, 2003) , Keshavarzi and Gheisi (2006) and Niknia *et al.* (2011). By

changing the basin size and shape, these researchers tried to increase its efficiency. Ogihara and Sakaguchi (1984) suggested a plan that differed from other plans in the weir outlet flow. In this basin, they used a Bell-mouth weir within the basin for smooth water transmission. Mashauri (1986) proposed a plan in which inlet and outlet flows were separated by a horizontal vane. Paul (1991) proposed a plan in which a Soleus-shaped vane (deflector) was installed at a distance of one-third of the flow depth in the basin inlet channel. Saneie (1999) studied hydraulic parameters of vortex flow within vortex settling basins. Ziaei (2000) proposed a new model of vortex settling basins that is actually a combination of two inlets for clockwise and anti-clockwise flows. Athar *et al.* (2002) proposed two other models for vortex settling basins. Using experimental models and changing the orifice radius, Chyan and Quang (2010) determined the discharge coefficient C_d for the orifice. In their experiments, Niknia, *et al.* (2011) investigated the flow structure under the deflector and compared it with the flow structure without deflector for counterclockwise inlet flow to vortex basins.

One problem of vortex settling basins is the settlement of part of sediments in the basin floor. More studies are necessary to provide a method to remove or reduce these sediments. At Istanbul University of Technology (IUT), researchers such Cecen and Akmandor (1973), Curi *et al.* (1979) and Cecen and Bayazit (1975) found that the existence of a radial gradient in the floor towards the orifice can lead to better performance of the basin and reduced sediments settled on the floor. Salakhov (1975) proposed two percent increase in the gradient of the basin floor. Paul *et al.* (1991) and Ziaei (2000) suggested that the sediments deposited on the floor can be washed by installing two inlets for the flow and changing the flow from clockwise to counterclockwise and vice versa. To increase the residence time on the floor and increase the sediment washing efficiency in the basin floor, Nguyen (2011) used deflector in different arrangements and by combining one, two and three deflectors.

The present study proposes a plan to solve the problem of sediments being deposited in such basins and investigates the efficiency of vortex settling basins. This plan consists of a batch of curved submerge vanes with different arrangements in vortex settling basins. In fact, the aim of installing curvature submerge vanes in the basin floor is to modify the vortex flow shape and strengthen vortex flow to direct sediments towards the flushing orifice. These submerge vanes were first used to deal with the external erosion of rivers. Moreover, the application of these structures has been developed to control sediments in intakes due to their successful results.

2 Experimental Equipment

2.1. *Experimental Model*

Experimental studies in this research were done at a basin with a height of 96 cm and a diameter of cm. The flow direction in this basin was clockwise. This basin had a weir with a length of 168 cm. The diameter of the inlet opening of the flushing orifice of the vortex sediment basin is 59 mm. Sediments exiting from the basin flushing orifice are entered into a rectangular basin with dimensions of 2×1.5 m and a height of 0.5 m by a tube with a diameter of 17 cm for collection and analysis. Due to the turbulence caused by pumping water from the storage tank, it was necessary to reduce the flow turbulent before the flow enters into the vortex settling basin. So, at the beginning of the inlet channel, the flow smoothing basin was established with dimensions of 2.5 × 2.5 m and a depth of 2 m. The basin inlet channel had a length of 4 meters and a width 42.86 cm and a height of 71 cm.

The vortex settling basin floor had a gradient of 0.1 towards the flushing orifice and also a deflector was installed below the weir, and a diaphragm was placed in the opening of the inlet channel. The deflector structure was installed in horizontal, flat and semicircular forms. To avoid leaving sediment particles on arrival at the basin influenced by the jet outflow, it was installed on top of the weir which increased residence time of the flow containing sediment within the basin and also sediments' spinning. The diaphragm was used in the settling basin to: a) improves the shape and conduction of the jet inflow to the basin; b) create vortex flow and increase the centrifugal force for the removal of suspended sediments in the vortex basin; c) increase the basin hydraulic efficiency and improve the core shape of central air (Keshavarzi and Gheisi 2006).

At the downstream of the vortex settling basin, there were two channels; one for transporting passing water on top of the vortex basin weir and another for transporting the water of a rectangular settling basin after deposition of sediments, both of which had a width of 60 cm and a height of 60 cm.

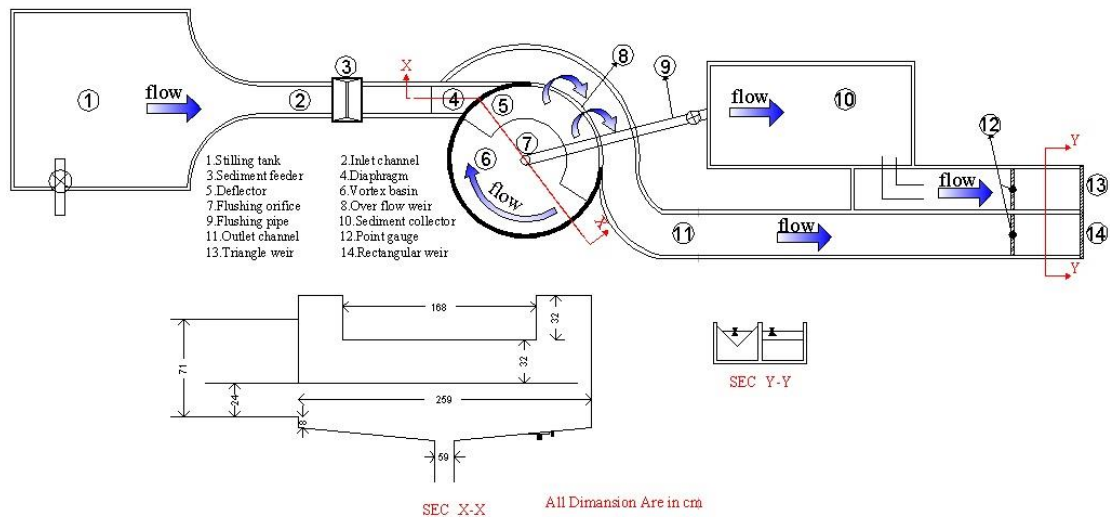


Figure 1 the plan of the experimental model of vortex settling basin

To determine the basin inlet discharge, the discharges of two downstream channels were calculated by measuring their water surface figures using a point Gauge. At the end of these canals, there were two calibrated weirs. The outlet channel weir of the vortex settling basin weir was rectangular and the outlet channel weir of the settling basin was triangular with an angle of 90 degrees.

2.2. Sediment Injection

In experimental models, sediments were injected in such a way that there was the necessary matching between the model and the actual sample. Therefore, the material collected from various parts at the end of the experiments must be equal to the amount of the injected upstream. Moreover, the sediment load should be poured in a suitable place so that it has the opportunity to have a uniform distribution in the flow cross section, and also sediments are entered into the basin in a suspended manner. In their studies, researchers used different grains, some of which are shown in Table 1. Different materials were examined to determine the type of settled material and finally, given issues such as sediment supply, grain size, injection, sampling, collection, drying, density and uniform distribution, sand drift was used. Sediments are made of sand drift with a grain size of $d_{50}=0.22$ mm.

Table 1 Range of sediment size used in previous studies

Authors	Range of sediment size (mm)
Curi et al. (1977)	2.12
Mashauri M-I (1986)	0.375-1.80
Mashauri M-II (1986)	0.1875-0.75
Esen (1989)	0.320-2.7
Mashauri M-III (1986)	0.063-0.25
IPRI (1989)	0.09-0.30
Paul et al. M-I (1991)	0.175
Paul et al. M-II (1991)	0.05-1.00
Paul et al. M-III (1991)	7.64
Athar et al. (2002)	0.055-0.931
Keshavarzi and Gheisi (2006)	0.074-0.3
Niknia et al. (2011)	0.08-2.00

In previous studies, sediment injection was done with different methods. Athar *et al.* (2002) carried out sediment injection by a device composed of a circular-shaped cylinder and sediments lied within it. The device was installed in the floor of the vortex settling basin inlet channel and the sediment injection rate was controlled by a cable. Keshavarzi and Gheisi (2006) performed sediment injection by a device that worked like an hourglass. Niknia *et al.* (2011) mixed sediments with water in a tank and performed sediment injection by obtaining a specific concentration.

The sediment injection device used in this study is seen in Figure 3. For sediment injection, a certain volume of the desired sediment was poured into the injection device tank with a volume 50 liters (funnel-shaped tank) and dry sediment were regularly getting out of the device and poured into the channel by rotating the roller inside it that had three longitudinal grooves. The roller rotation was done by an electric motor that had a controllable revolution. The precision of this control was in revolution per second. This device was placed at a distance of 1.5 m from the upstream channel of the vortex settling basin.

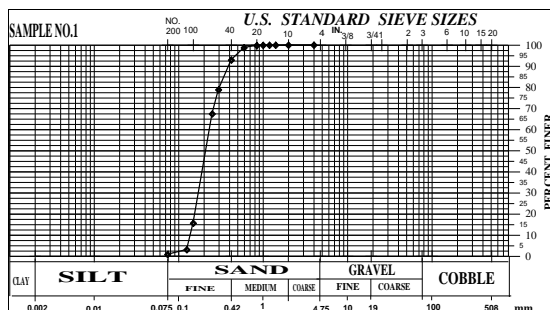


Figure 2 Gradation curve of the injected sediments to the vortex settling basin with $d_{50}=0.22\text{mm}$

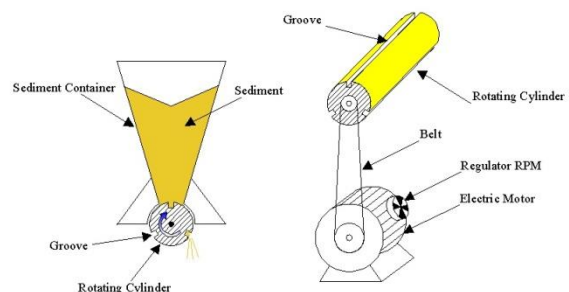


Figure 3 The sediment injection device

2.3. Curvature Submerge Vanes

Submerge vanes are vanes whose effective application in changing flow pattern and bed shear stress in order to control local erosion and change sediment movement pattern has been studied by many researchers. First, Odgaard and Kennedy (1983) and Odgaard and Spoljaric (1986) attempted to design submerge vanes. Then, extensive studies on the application of submerge vanes to avoid bed load entering the intake were done by Barkdoll *et al.* (1999), Nakato and Ogden (1998), Wang *et al.* (1996) and also to control riverine erosion by Odgaard and Wang (1991a, 1991b), Marelius (2001), Voisin and Townsend (2002). According to extensive research on designing these vanes in the mentioned fields, research and theory have been offered on the use of submersibles vanes and also optimal dimensions and arrangements for vortex settling basins.

Vane dimensions were determined based on recommendations by Odgaard and Kennedy (1983) and considering the flow depth ($d= 8$ cm) which is the prolapse of jet flow in the inlet opening of the vortex settling basin. Submerge vanes are galvanized with a rectangular initial shape (Figure 4) and a thickness of 2 mm. Table 2 shows the dimensions of submerge vanes.

Table 2 Dimensions of curvature submerge vanes

Parameter	Height of submerge vane H_v	Length of submerge vane L_v
Recommended by Odgaard and Kennedy (1983)	$0.2 < \frac{H_v}{d} < 0.5$	$3H_v < L_v < 4H_v$
Applied value	$0.5 = \frac{H_v}{d}$	$3H_v = L_v$

The vanes placed on the basin floor are curved. The curvature of any vane is equal to the circular arc laid on its perimeter. Therefore, given the radial distance of vanes from each other, vanes have six different curvatures with radiuses of 27.95, 40.45, 52.95, 65.45, 77.95 and 90.45 cm. Figure 5 shows six different types of vanes with different curvature.

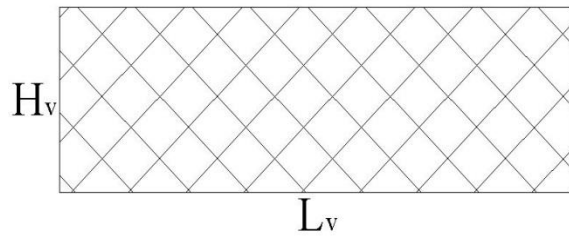


Figure 4 Profile of curvature submerge vanes



Figure 5 Vanes submerge with six types of curvature

To place vanes in the basin floor and achieve the ordered and optimum arrangement, various conditions were considered:

- To evaluate the effect of longitudinal distances of vanes on the vortex basin efficiency, its floor was divided into radial sections with the same angle. The longitudinal distance was examined in three modes with 4, 6 and 8 radial sections with identical angles which were 90, 60 and 45 degrees, respectively. The radial sections are called S4, S6 and S8, as shown in Figure 6.

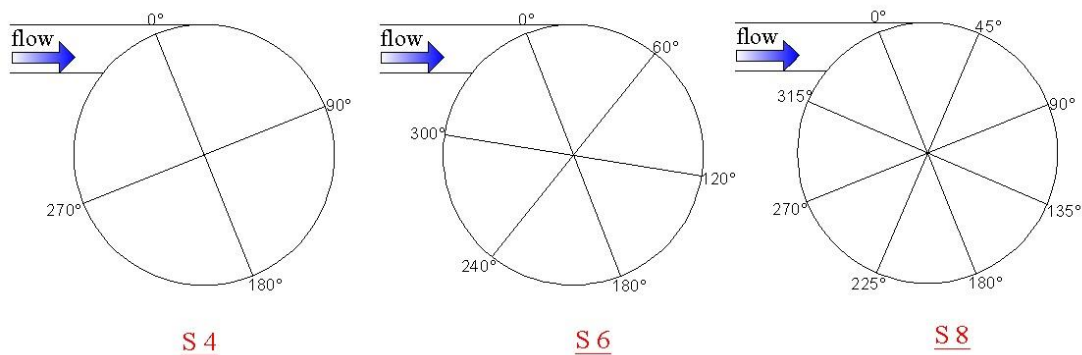


Figure 6 Radial sections of vanes

- To evaluate the radial distance of vanes from the flushing orifice, the basin floor was divided into four equal-interval concentric circles. Figure 7 shows circles with the number of areas intended for them.
- For vanes to affect vortex flow more, another vane was placed between the vanes. The radial distance of vanes from each other considered the constant $\delta_n=3H_v$ (Odgaard and Kennedy 1983).

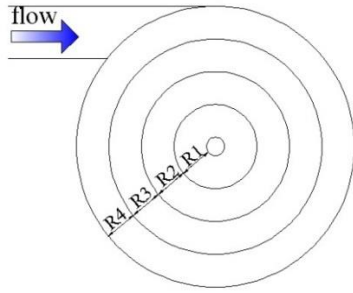


Figure 7 Areas for vane insertion on the basin floor

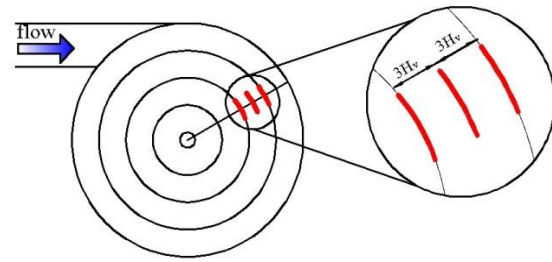


Figure 8 Radial distance of vanes from each other

- Initial tests of sediment injection in the no-vane mode showed that no sediment remains at a distance of the first $\frac{1}{4}$ of the radius around the orifice (area 1) (Figure 9). However, at a distance of the next $\frac{3}{4}$ of the vortex basin radius (areas 2, 3 and 4), most sediments are accumulated. So vane insertion was ignored in area 1. Submerge vanes were inserted in six arrangements. Each arrangement was named according to the vane position area. Since the insertion of several submerge vanes besides each other can affect a larger area, they first were placed separately in the desired radial section in a circle with triplet bunches in areas 2, 3 and 4 called *R2*, *R3*, *R4*, respectively. Then, vane insertions in circles were combined (*R2 3*, *R3 4*, *R2 3 4* arrangements) to broaden the area affected by one. The effect of this widening was investigated on the sediment removal efficiency. The used arrangements are shown in Figure 10.



Figure 9 Initial test of sediment injection in the no-vane mode

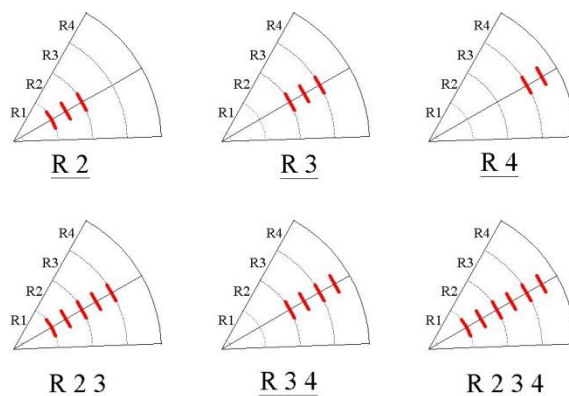


Figure 10 Arrangements of curvature submerge vanes

3 An Experimental Program

In this research, for starting tests, water was entered into the system by pumping. Water flow entered into the vortex settling basin from the inlet channel through the inlet opening under

the diaphragm. Once a steady and constant flow was established in the model, the discharge of the water entering the vortex settling basin was measured by two rectangular and triangular weirs at the end of outlet channels. After flow fixation and discharge adjustment, sediment supply began with a constant discharge for a specified duration (20 minutes). When sediments finished, the pumps were turned off (water inflow to the basin was cut off), the flushing orifice exit valve was closed. Then the sediments within the vortex basin and the sediments exited from the orifice and the weir were separately collected, dried and weighed. This procedure was done for discharges of 45 and 37 l/s and six vane arrangements in three radial sections.

4 Results and Discussion

To calculate the vortex settling basin efficiency, Ziaei (2000) used the sampling method. He gathered samples from the weir outlet and the flushing orifice and then calculated the basin efficiency using sample concentrations. Keshavarzi and Gheisi (2006) and Athar (2000) used another method to calculate the vortex settling basin efficiency. They collected and dried sediment exited from the weir and the flushing orifice and then calculated the vortex settling basin efficiency based on the weight of collecting sediments. After examining methods for determining the vortex settling basin efficiency, it was known that the methods of Keshavarzi and Gheisi (2006) and Atahr (2000) are more accurate. Therefore, the present study used that method.

Sediments in this system are divided into three main categories. The first category is sediments which are transferred out of the basin together with some percent of water from the flushing orifice. The second category is the sediments settled in the vortex basin floor and, over time, they cause dysfunction in the settling performance of the structure. Finally, the third category which consists of a small percent of sediments exited through the vortex weir with water flow. To calculate the vortex settling basin efficiency according to the harvested lab data, parameters η_T , η_O and η_B were used. These parameters were defined as follows:

$$\eta_T = \eta_o + \eta_B \quad (1)$$

$$\eta_o = \frac{W_o}{W_T} \quad (2)$$

$$\eta_B = \frac{W_B}{W_T} \quad (3)$$

Which η_T is total settling efficiency, η_O is the settling efficiency of the orifice, η_B is the settling efficiency of the basin floor, W_T is the total weight of the sediments entering the basin, W_O is

the weight of sediments entering the flushing orifice, and W_B is the weight of sediments on the basin floor.

Also, to show the sediment washing rate of the floor, parameter G' was used:

$$G' = \frac{(\eta'_B - \eta_B)}{\eta'_B} \quad (4)$$

Which G' is sediment washing efficiency of the basin floor, η'_B is settling efficiency of the basin floor without curvature submerge vanes and η_B is settling efficiency of the basin floor with curvature submerge vanes.

First, initial tests were conducted without vanes on the floor with sediment. These tests were done with discharges of 45 and 37 l/s. The two tests were performed as a benchmark for comparing, analyzing, and determining the effectiveness of the modes with and without curvature submerge vanes. In these tests, the total efficiency of the vortex settling basin was obtained 93.66 and 95.76% for discharges of 37 and 45 l/s, respectively. In the presented results, $R0$ and $S0$ represent tests without curvature submerge vanes. $R0$ means without arrangement and $S0$ means without radial sections.

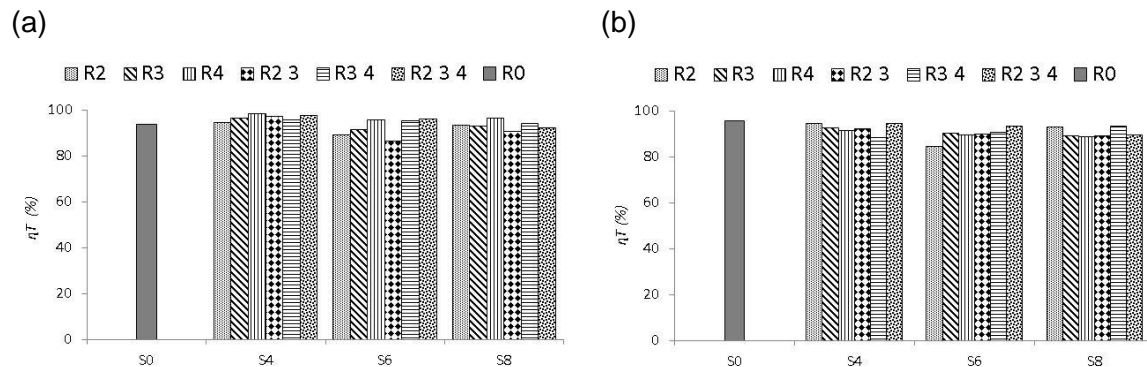


Figure 11 Total efficiency of the vortex settling basin in a) discharge of 37 l/s ,b) discharge of 45 l/s

In Figure 11, according to changes in radial sections of vanes and discharge, it was observed that curvature submerge vanes have a little impact on total efficiency of the vortex settling basin. Overall, for discharge of 37 and 45 l/s, they increased total efficiency of the basin in some arrangements by 0.51-4.68% and decreased it in some arrangements by 0.47-11.45%. The reduction of total efficiency occurred in the discharge of 45 l/s due to the reduction in the efficiency of the basin in the floor. The insertion of submerge vanes in the floor of the vortex settling basin caused significant changes in the share percent of sediments settled in each part of the basin so that these vanes increased the floor efficiency and decreased the orifice efficiency in some arrangements, so these arrangements are not desirable. In some arrangements, the floor efficiency decreased and the orifice efficiency increased. So in these arrangements, the goal which was sediment washing of the basin

floor was realized. This change in the share of settling can be attributed to the vortex flow caused by submerge vanes. These vortices flow move sediments settled on the floor and direct them toward the flushing orifice. As shown in Figures 12 and 13, by holding constant the total efficiency, different modes of arrangements could change the orifice efficiency and the floor efficiency. With these changes, for each R mode, when the orifice efficiency increased compared to its corresponding no-vane mode, the floor efficiency decreased compared to its corresponding no-vane mode.

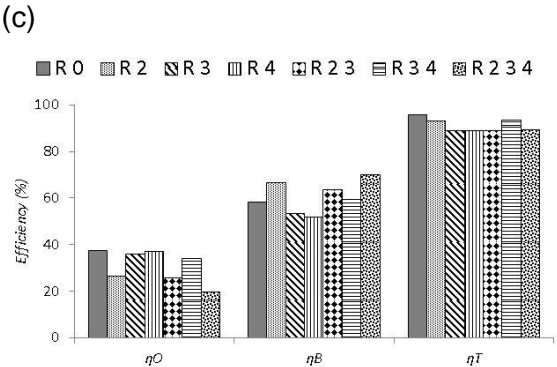
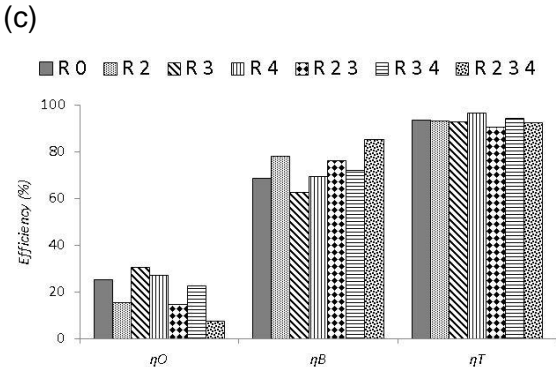
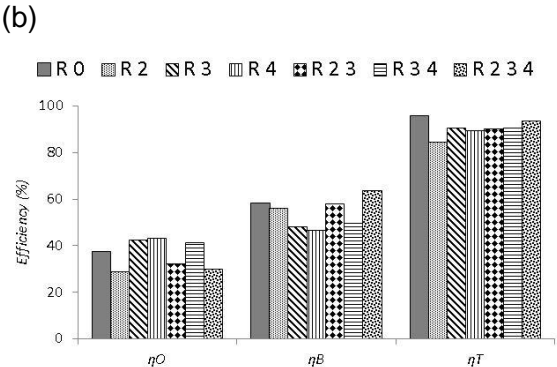
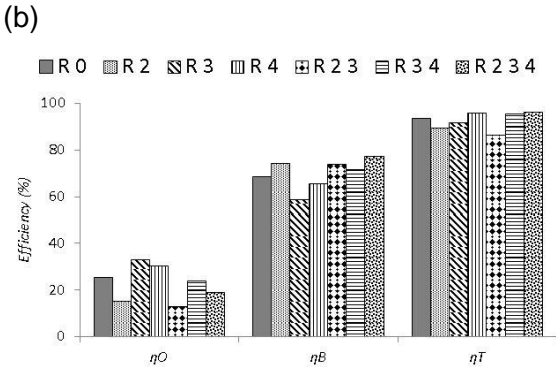
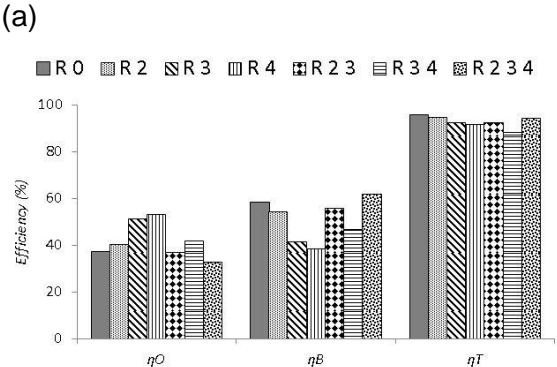
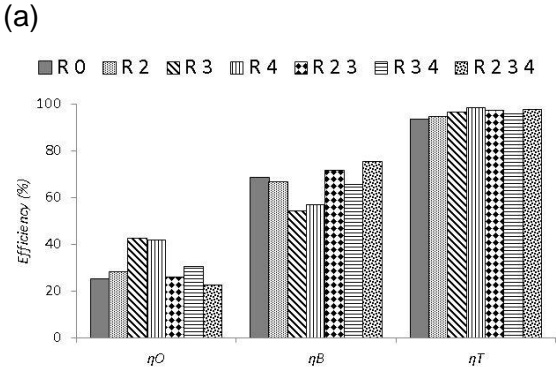


Figure 12 Total, orifice and floor efficiencies in the discharge of 37 l/s (a) S4 mode, (b) S6 mode, (c) S8 mode

Figure 13 Total, orifice and floor efficiencies in the discharge of 45 l/s (a) S4 mode, (b) S6 mode, (c) S8 mode

Efficiency in each part of the vortex settling basin is the weight ratio of the sediment accumulated in that section. Thus, an increase in the orifice efficiency compared to the no-vane mode is desirable but increase in the floor efficiency is not desirable because it means the accumulation of more sediments in this area and the lack of sediment washing of the floor. Thus, as shown in diagrams, R3, R4 and R3 4 arrangements have better efficiency because they reduce the share of sediments settled on the vortex settling basin floor and increase the share of sediments exited from the flushing orifice. In these modes, the floor efficiency reduced and the orifice efficiency increased.

According to no-vane tests, the desirability of such arrangements were somewhat predictable so that most sediments settled on the vortex settling basin floor in no-vane modes are in areas R3 and R4 (Figure 9). So the insertion of vanes in the two areas will increase sediment washing from the floor.

As shown in Figure 14, among R3, R4 and R3 4 arrangements, R3 4 has the lowest efficiency in sediment washing. Curvature submerge vanes in some arrangements decreased sediment washing from the floor. This reduction can be attributed to the impact of vanes in avoiding secondary flows which occur in the vortex settling basin floor towards the orifice.

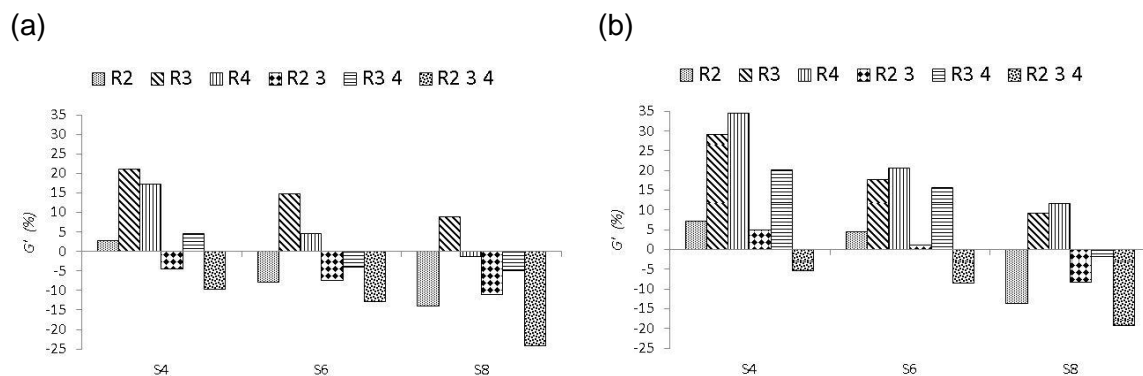


Figure 14: Percent of the floor sediment washing compared to no-vane mode (a) discharge of 37 l/s ,(b) discharge of 45 l/s

This study examined the effect of radial sections in curvature submerge vanes. The vanes were inserted in three modes, with radial sections with angles of 90, 60 and 45 called S4, S6 and S8, respectively. Figures 12 and 13 show the results of changing the number of radial sections of vanes inserted in the floor on the efficiency of each part of the basin. It is

noteworthy that *S0* represents the no-vane mode. According to the results, with an increase in the radial sections of vanes, total efficiency reduced compared to the no-vane test *S0* that among the three modes, minimum orifice efficiency was related to *S8* and maximum orifice efficiency was related to *S4*. The results also show that with an increase in the radial sections of vanes, the orifice efficiency reduced in both discharges and the floor efficiency increased (lower sediment washing from the floor). Among *S4*, *S6* and *S8* modes, *S4* has the best performance. Studying the effect of discharge on the vortex settling basin shows that discharge changes had little impact on the basin total efficiency but changed the share of settling in each part of the vortex settling basin. As seen in Figures 12 and 13, higher discharge (45 l/s) reduced the floor efficiency and increased the orifice efficiency. Lower discharge (37 l/s) reduced sediment washing from the floor.

According to Figure 14, parameter G' was positive in *R3* and *R4* arrangements and both discharges but the reaction of these two arrangements was different in two discharges so that in the discharges of 37 and 45 l/s, *R3* and *R4* showed better reactions, respectively. *R3 4* was somewhat successful in sediment washing from the floor but its value was less than *R3* and *R4* arrangements. As shown in Figure 14, the parameter G' was negative at discharges of 37 and 45 l/s for *R4* and *R3 4*. This decline in sediment washing increased with radial sections of vanes (increased radial sections). Reduced sediment washing (G') at the discharge of 37 l/s occurred for all tests. The reason for reduced sediment washing of the floor at the lower discharge is the reduced vortex strength and the reduced speed because these basins have a better efficiency at high speeds. *S0* when discharge is low, sediments are not affected by vortex flows within the basin and begin to settle on the basin floor. However, according to Figures 12 and 13, reduced orifice efficiency and reduced sediment washing on the basin floor also occur at lower discharges in no-vane modes. *S0*, in this type of basin, with an increase in discharge, vortex strength and thus vanes' efficiency in the basin will increase. Finally, the best cases of sediment removal from the floor occurred at the discharge of 45 l/s at the longitudinal distance of *S4*, and *R3*, *R4* and *R3 4* arrangements. The amounts of increase in sediment removal from the floor at the best cases for *R3*, *R4* and *R3 4* arrangements were 29.12%, 34.49% and 20.15%, respectively. Moreover, these arrangements increased the orifice efficiency in the discharge of 45 l/s by 13.66%, 15.73% and 4.26%, respectively.

Finally This study first introduced previous research on vortex sediment basin and then provided a solution for a problem in vortex sediment basins which is the settlement of some percent of sediments on the basin floor and non-exit from the flushing orifice. The solution presented in this paper is to use curvature submerge vanes to increase vortex power and better conductivity of the floor sediments towards the flushing orifice. It was observed that after inserting curvature submerge vanes in the basin floor, with little change in total

efficiency, one can change the share of the sediments entering the orifice and the sediments settled on the basin floor compared to the no-vane mode. How these vanes work (sedimentation or settling from the floor) depends on their distance from the orifice. At a low radial distance (areas 1 and 2), they increase sedimentation on the floor by preventing the movement of sediments towards the orifice. But at a large radial distance (areas 3 and 4), they remove sediments from the floor by directing the floor sediments towards the flushing orifice so that increased sedimentation on the floor was observed for *R2* and *R2 3*, and *R2 3 4* arrangements and sediment removal was observed on the floor for *R3* and *R4* and *R3 4* arrangements. Also, tests for inserting curvature submerge vanes in three modes of radial sections showed that the lower number of radial sections, the better the settling on the floor will be done. Among the three modes, *S4* (90-degree radial sections) had higher sediment removal efficiency.

5 Acknowledgments

The writers wish to sincerely thank Associate Professor mojtaba saneie for his suggestions during various stages of this study. Financial assistance received for this study from the Soil Conservation and Watershed Management Research Institute is gratefully acknowledged.

Notation

d_{50} = median diameter of sediment grains [mm]

H_v = Height submerged vanes [cm]

L_v = Length submerged vanes [cm]

R = The areas in which vanes are placed [-]

S = number of radial section in which vanes are placed [-]

η_T = Total settling efficiency [-]

η_o = Orifice settling efficiency [-]

η_B = Basin floor settling efficiency [-]

W_T = The total weight of sediments entered to the basin [kg]

W_o = The weight of sediments entered to the flushing orifice [kg]

W_B = The weight of sediments at the floor of basin [kg]

G' = The efficiency of the sediment flushing at the floor [-]

η'_B = The settling efficiency at the floor of the basin without curvature submerged vanes [-]

References

Athar, M. (2000). Study of vortex chamber type extractor. *PhD thesis*. Department of

Engineering, University of Roorkee, India.

- Athar, M., Kothyari, U. C., and Garde, R. J. (2002). Sediment removal efficiency of vortex chamber type sediment extractor. *J. Hydraulic Eng.* 128(12), 1051-1059.
- Athar, M., Kothyari, U. C., and Garde, R. J. (2003). Distribution of sediment concentration in the vortex chamber type sediment extractor. *J. Hydraulic Res.* 41(4), 427-438.
- Barkdoll, B.D., Ettema, R., and Odgaard, J. (1999). Sediment control at lateral diversion: limits and enhancements to vane use. *J Hydraulic Eng.* 125(8), 862-870.
- Cecen, K., and Akmandor, N. (1973). Circular settling basins with horizontal floor. *MAG Rep.* No. 183, TB TAK, Ankara, India.
- Cecen, K., and Bayazit, M. (1975). Some laboratory studies of sediment controlling structures. Proc. 9th Congress of ICID Moscow, Soviet Union, 107-111.
- Chyan, D.J., Quang, T.N. (2010). Discharge Coefficient for a Water Flow through a Bottom Orifice of a Conical Hopper. *J. Irrigation and Drainage Eng.* 136(8), 567-572.
- Curi, K.V., Esen, I.I., Velioglu, S.G. (1979). Vortex type solid liquid separator. *Progress Water Technology.* 7(2), 183-190.
- Esen, I.I. (1989). Solid liquid separation by vortex motion, solid-liquid flow. 1(1), 21-27, 31005, Toulouse, Cedex, France.
- Keshavarzi, A.R., Gheisi, A.R. (2006). Trap efficiency of vortex settling chamber for exclusion of fine suspended sediment particles in irrigation canals. *J Irrigation and Drainage.* 55(4), 419-434.
- Marelius, F. (2001). Experimental investigation of submerged vanes as means of beach protection. *Coastal Eng.* 42(1), 1-16.
- Mashauri, D.A. (1981). Selection of settling basin for sediment removal. *Msc thesis.* Tampere University of Technology, Finland.
- Mashauri, D.A. (1986). Modelling of a vortex settling basin for primary clarification of water. *PhD thesis.* Tampere University of Technology, Finland.
- Nakato, T., Ogden, F.L. (1998). Sediment control at water intakes along sand-bed rivers. *J. Hydraulic Eng.* 124(6), 589-596.
- Nguyen, Q.T. (2011). Effect of deflectors on removal efficiency of a deep-depth vortex chamber sediment extractor. Proc. 12th conference on science & technology Ho chi Minh, Vietnamese, 1-7.
- Niknia, N., Keshavarzi, A.R., Hosseinipour, E.Z. (2011). Improvement the Trap Efficiency of

- Vortex Chamber for Exclusion of Suspended Sediment in Diverted Water. Proc. *World Environmental and Water Resources Congress 2011(ASCE)* California, USA, 4124-4134.
- Odgaard, A.J., Kennedy, J.F. (1983). Bed -river bank protection by submerged vanes. *J. Hydraulic Eng.* 109(8), 1161-1173.
- Odgaard, A.J., Spoljaric, A. (1986). Sediment control by submerged vanes. *J. Hydralic Eng.* 112(2), 1164-1181.
- Odgaard, J., Wang, Y. (1991a). Sediment Management with Submerged Vanes. I: Theory. *J Hydraulic Eng.* 117(3). 267-283.
- Odgaard, J., Wang, Y. (1991b). Sediment management with submerged vanes. II: Applications. *J Hydraulic Eng.* 117(3), 284-302.
- Ogihara, H., Sakaguchi, S. (1984). New system to separate the sediments from the water flow by using the rotating flow. Proc. 4th *Congress of the Asian and Pacific Division. IAHR* Chiang Mai, Thailand, 753-766.
- Paul, T.C., Sayal, S.K., Sakhuja, V.S., Dhillon, G.S. (1991). Vortex-settling basin design considerations. *J. Hydraulic. Eng.* 117(2), 172-189.
- Ranga Raju, K.G., Kothiyari, U.C., Srivastav, S., Saxena, M. (1999). Sediment removal efficiency of settling basins. *J. Irrigation and Drainage Eng.* 125(5), 308-314.
- Salakhov, F.S. (1975). Rational designs and methods of hydraulic calculations of load-controlling water intake structures for mountain rivers. Proc. 9th *Congress of ICID* Moscow, Soviet Union, 151–161.
- Saneie, M. (1999). Experimental Studies on Increasing Sedimentation Efficiency of Vortex Settling Basing. *PhD Thesis*. Department of Agriculture and Natural Resources, University of Islamic Azad, Iran.
- Sanmuganthan, K. (1985). A note on outlet pipe design for circulation chamber silt extractor.” *Rep. No. 87*, Hydraulic Research Wallingford Limited, Wallingford, England.
- Sullivan, R.H., Cohn, M.M., Ure, J.E., Parkinson, F., Galina, G., Boericke, R.R., Kock, C., Zielinki, P. (1978). The swirl primary separator; development and pilot demonstration. *Rep. No. EPA-600/ 2-78-122*, U.S. Environmental Protection Agency, Cincinnati.
- Svarovsky, L. (1981). *Solid–liquid separation*. ed. 2. Butterworth and Co. Ltd., Essex, UK.
- Velioglu, S.G. (1972). Vortex type sedimentation tank. *Msc thesis*. University of Bogasiqi, Turkey.

- Voisin, A., Townsend, R.D. (2002). Model testing of submerged vanes in strongly curved narrow channel bends. *Canadian J. Civil Eng.* 29(1), 37-49.
- Vokes, F.C., Jenkins, S.H. (1943). Experiments with a circular sedimentation tank. *J. ICE.* 19(3), 193.
- Wang, Y., Odgaard, J., Melville, B.W., Jain, S.C. (1996). Sediment control at water intakes. *J. Hydraulic Eng.* 122(6), 353-356.
- Zhou, Z., Hou, J., Tang, Yi. (1997). Flow field measurement of sand funnel and its influence on sediment transport. *Proc. 27th Congress IAHR San Fransisco.*
- Zhou, Z., Wang, C., and Hou, J. (1989). Model study on flushing cone with strong spiral flow. *Proc., 4th Int. Symposium on River Sedimentation, Beijing, 1213–1219.*
- Ziaei, A.N. (2000). Study on the efficiency of vortex settling basin (VSB) by physical modeling. *MSc Thesis.* Department of Agriculture and Natural Resources, University of Shiraz, Iran.

COMMISSION INTERNATIONALE DES GRANDS BARRAGES

VINGT-SIXIÈME CONGRÈS DES GRANDS BARRAGES
Autriche, juillet 2018

DOI 10.3217/978-3-85125-620-8-010



This work licensed under a Creative Commons Attribution 4.0 International License. <https://creativecommons.org/licenses/by-nc-nd/4.0/>

**GROWING NEED FOR STORAGE AS AUSTRALIA TRANSITIONS FROM
COAL ENERGY TO RENEWABLES**

Richard HERWEYNEN

Principal Consultant - Civil, ENTURA

AUSTRALIA

Nick WEST

Senior Hydropower Engineer, ENTURA

AUSTRALIA

COMMISSION INTERNATIONALE
DES GRANDS BARRAGES

VINGT-SIXIÈME CONGRÈS DES
GRANDS BARRAGES
Autriche, juillet 2018

GROWING NEED FOR STORAGE AS AUSTRALIA TRANSITIONS FROM COAL ENERGY TO RENEWABLES

Richard HERWEYNEN
Principal Consultant - Civil, ENTURA

Nick WEST
Senior Hydropower Engineer, ENTURA

AUSTRALIA

1. INTRODUCTION

Climate change is a global problem. On 10 November 2016, Australia ratified the Paris Agreement, committing to achieve a 26 to 28 per cent reduction in greenhouse gas (GHG) emissions below 2005 levels by 2030 [1]. The energy sector accounts for 79 per cent of Australia's emissions and therefore will play a key role in Australia's reduction targets.

As a result, Australia's national electricity market (NEM) is going through a transition as it moves towards low-carbon-emissions generation in response to climate change. This is resulting in new opportunities for existing hydropower generators, leading to potential changes in operating regimes.

2. THE AUSTRALIAN ENERGY MARKET

Australia's electricity system was founded on centralised, carbon-intensive coal-fired generation. Currently, coal-fired generation (both brown and black coal) makes up 78 per cent of electricity generation across Australia's National Electricity Market (NEM). The sector is the single largest contributor to GHG

emissions, and contributes approximately a third of Australia’s total emissions. As coal-fired power stations reach the end of their lives they will be decommissioned. A total of 45 TWh of coal-fired generation is set to retire in Australia.

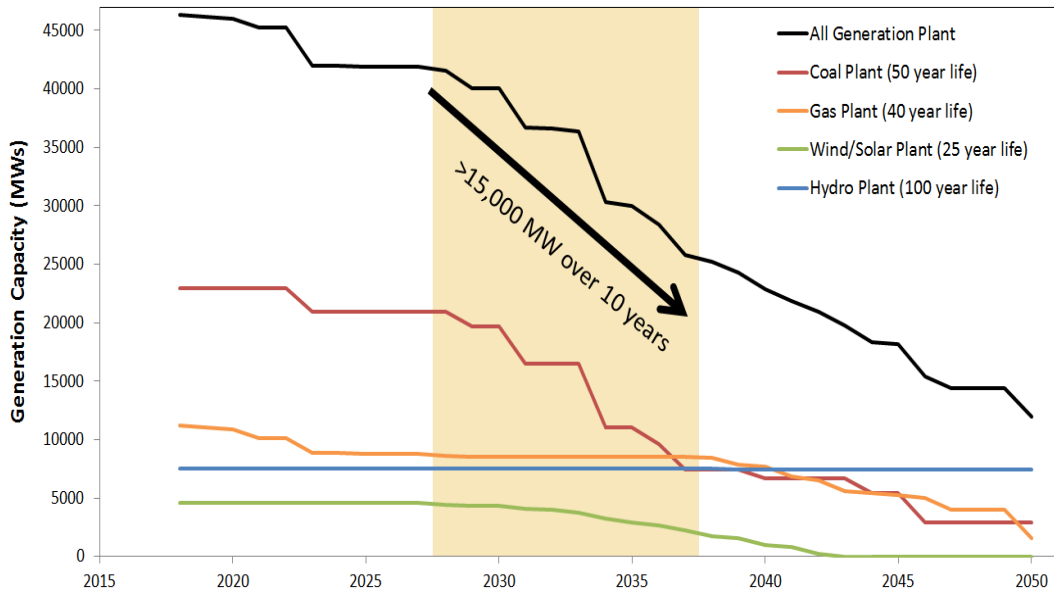


Fig. 1
Expected retirement profile of generation assets in Australia - based on life expectancy [2]

The CSIRO’s Low Emissions Technology Roadmap [1] has identified that the most likely pathway for Australia to meet its commitment to reduction in GHG emissions is to replace the coal-fired generation with renewable energy, mainly wind and solar PV. However, these renewables are highly variable and non-dispatchable. Fig 2 shows the NEM generation mix and how it is likely to transition.

As the proportion of variable renewable energy increases, increased storage is required for supply–demand matching to manage the variability in generation and provide the required system flexibility. Hydropower storage plays an expanding role in integrated power systems internationally and can enable increased use of intermittent renewable energy sources such as wind and solar.

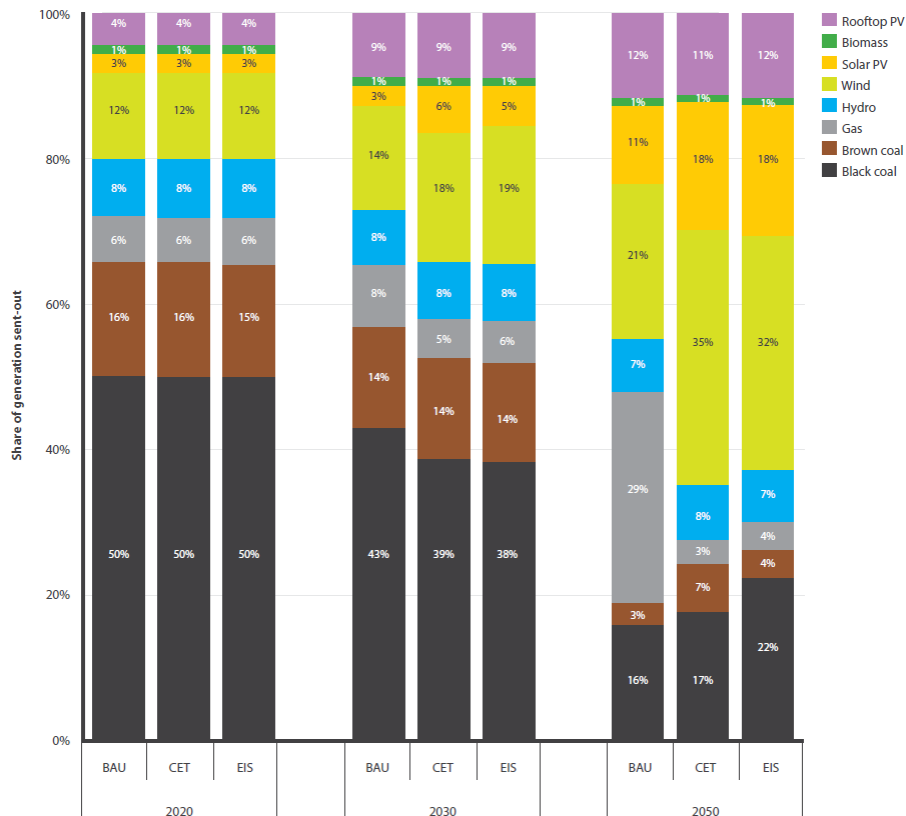


Fig. 2
NEM generation mix, 2020, 2030, 2050 [3]

While moving towards a low carbon future, the challenge is the energy ‘trilemma’ of security, equity (accessibility and affordability) and environmental sustainability. These three factors need to be in balance to ensure a secure power sector that meets the present and future needs of energy consumers while moving towards a lower carbon future.

2.1. THE NEED FOR LARGE-SCALE STORAGE

The rapid growth of renewable energy generation has been driven by two concurrent factors: the falling levelised cost of the energy produced by wind and solar, and the retirement of a number of coal-fired power stations. The recently released Finkel Review [3] notes that by 2035, approximately 68 per cent of the current fleet of Australian coal-generating plants will have reached 50 years of age.

Renewables cannot, on their own, meet the fluctuations in demand that occur throughout the day without some regulation as to when power reaches the grid. Power needs to be dispatchable, which means that energy can be provided upon request. If the sun is not shining or the wind is not blowing, renewable

energy cannot be dispatched unless it has been stored in some way. With increasing proportions of renewable generation in the energy mix, the dispatchability of generation to meet demand becomes more important, as shown in Fig 3. One way of improving the dispatchability of renewables is to add storage in the power system

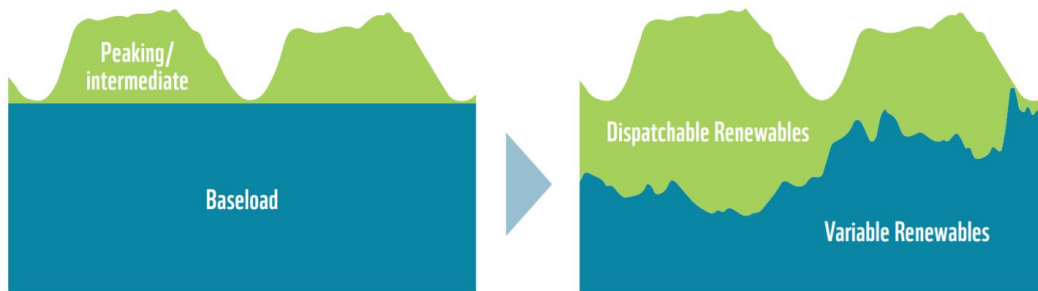


Fig. 3

Comparison of a baseload dominated electricity system (left) and a variable and dispatchable model (right) [4]

There are a number of different types of storage but the two being discussed most widely right now are batteries and pumped storage hydropower. These two technologies are very different and there are some limitations involved in comparing a well-known and established technology, like pumped storage, with one that is new and developing rapidly, like battery technology.

Pumped storage hydropower is based on well-established synchronous generation, providing critical ancillary services to the grid, through the provision of inertia, frequency and voltage support and sufficient fault level support. Battery inverter technologies are still catching up on most of these fronts. The potential for batteries to provide ‘synthetic inertia’ or fast frequency response is high but they rely on system strength to be able to deliver this support. They offer minimal support with fault levels but can still provide some support to system frequency and voltage regulation.

Recent electricity price spikes and a state-wide blackout in the state of South Australia have highlighted the need for reliable power to balance the potential volatility of some renewable power sources.

2.2. HYDRO STORAGE PROJECTS

With an increased amount of renewable energy within the Australian grid, hydro storage has gained increased attention. Whether this be pumped storage hydropower, like the Kidston pumped storage project in Northern Queensland, or better use of existing hydropower storages, like Tasmania’s “Battery of the Nation” concept. Since connecting to Australia’s National Energy Market via the Basslink interconnector in 2006, the flexible hydropower system of the island

state of Tasmania has already acted as a giant 500 MW battery [5] for Australia, because of the volume of water stored.

A brief summary of some of the current hydro storage projects currently being investigated in Australia is given in the following sections.

3. PUMPED STORAGE PROJECTS IN AUSTRALIA

3.1. PUMPED STORAGE HYDROPOWER

As the proportion of renewable energy in an energy market increases, the need grows for the stability and consistency provided by utility-scale energy storage. For example, South Australia needs system-wide storage of 500 MW for a period of 10 hours to improve the flexibility of wind farm operators, according to the Melbourne Energy Institute [6].

At the smaller scale of energy storage, the buzz about various types of batteries continues – but the only storage option with a proven track record at the utility scale is pumped storage hydropower.

Pumped storage hydropower works by pumping the water stored in a lower reservoir into a more elevated reservoir. The water stored at height can be passed through a turbine on its path back to the lower reservoir, creating electricity as and when needed, and making the best use of the water resource without waste.

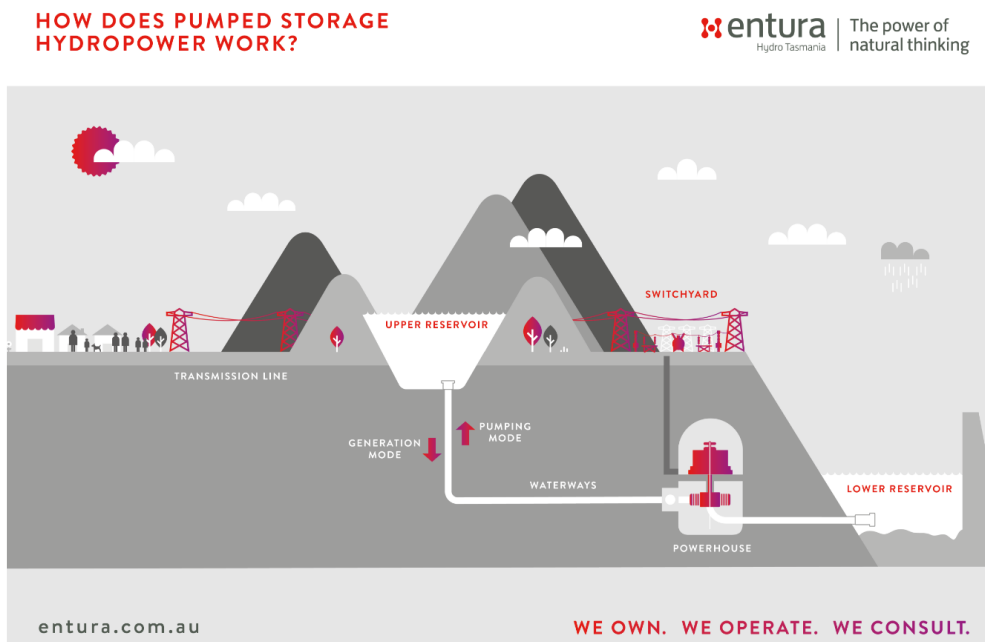


Fig. 3
How pumped storage hydropower works [7]

3.2. EXISTING AUSTRALIAN PUMPED STORAGE

Despite the significant potential and benefits of pumped storage hydro projects, only three projects currently exist in Australia (two in New South Wales and one in Queensland). These projects were built in markets in which thermal sources dominated, where the pumped storage could supplement supply at times of peak demand.

The existing pumped hydro projects in Australia include:

- Tumut 3 Power Station – construction completed in 1963. Installed capacity: 1800 MW (600 MW pumping)
- Shoalhaven Scheme – construction completed in 1977. Installed capacity: 240 MW
- Wivenhoe Power Station – construction completed in 1984. Installed capacity: 500 MW.

3.3. DRIVE TO FIND NEW PUMPED STORAGE PROJECTS

As the proportion of renewable energy in an energy market increases, the need grows for the stability and consistency provided by utility-scale energy storage. A number of high-level studies to identify potential pumped storage hydropower sites have been undertaken using available GIS information. One such study has been undertaken by the Australian National University, which has identified 22 000 potential sites [8], which will need to be further refined. In addition, a number of detailed feasibility studies have recently been completed for two new pumped storage projects in Australia, namely the Kidston Pumped Storage Hydro Project and the Cultana Pumped Hydro Project. A brief summary of these two projects is provided below.

3.4. KIDSTON PUMPED STORAGE HYDRO PROJECT

Genex Power is the developer of the Kidston Energy Hub in the north of the Australian state of Queensland. The site of the proposed development is the disused Kidston Gold Mine near Georgetown. Should the project be developed to its full potential, it will ultimately consist of a 250 MW pumped storage project, collocated with a 270 MW solar PV installation [9]. A 50 MW solar PV project is currently in the final stages of commissioning. A unique aspect of the Kidston Pumped Storage Hydro Project is its use of two existing mine pits as the upper and lower reservoirs.

Given the significant potential water head differential that the pits offer, and the vast quantity of water the pits can hold, the project has been optimised to support 2000 MWh of continuous power generation in a single generation cycle

(250 MW of peaking power generation over an 8-hour period). The power generated will be sold directly into the NEM.

A concrete-lined pressure tunnel will connect the upper reservoir to the underground generation powerhouse. A concrete-lined tailrace tunnel will, in turn, connect the powerhouse to the lower reservoir. A shaft from the surface will connect the underground infrastructure to a surface power control room, which will be connected to a transformer station located on an existing pit bench.

The Kidston Pumped Storage Hydro Project (250 MW) is a closed-loop system, which will involve the transfer of water from the upper reservoir to the lower reservoir. This will ensure minimal environmental impact during operation, on what is an already disturbed former mining site.

3.5. CULTANA PUMPED HYDRO PROJECT

Energy Australia is the developer of a potential seawater pumped storage project on the Eyre Peninsula in South Australia. A lack of freshwater resources in inland South Australia means sites adjacent to the coastline are worthy of consideration for pumped hydro projects. The Cultana site was selected based on the elevation, proximity to the coast, proximity to grid connection and minimal environmental and cultural impacts [10].

There are many precedents for freshwater pumped storage projects globally; however, there is only one international precedent for large-scale seawater pumped storage projects – a 30 MW facility in Okinawa, Japan, which was decommissioned in 2016 [11].

The prefeasibility study for the project considered a capacity envelope of between 100 MW and 250 MW. Below 100 MW it was expected that the fixed costs of large civil construction would be too high to yield a viable project due to lack of economies of scale. Beyond the upper limit of 250 MW there is a risk that the storage capacity would be too large for the South Australian market. The larger the capacity, the lower the expected market revenue per unit of capacity.

Within this range, the proposed 225 MW nameplate capacity of the Cultana Pumped Hydro Project was determined based on the maximum scale that could be achieved while avoiding any significant incremental changes in cost [10].

4. CHANGING USE OF EXISTING HYDRO STORAGES

4.1. EXISTING HYDRO IN AUSTRALIA

The two largest hydro generation companies in Australia are Snowy Hydro and Hydro Tasmania.

Snowy Hydro Limited operates and maintains the Snowy Mountains Scheme in Australia's Southern Alps. Construction started on the scheme on 17 October 1949 and was completed in 1974. On completion, the scheme consisted of seven power stations, 16 major dams, 145 km of interconnected tunnels and 80 km of aqueducts. The company today has 16 power stations, which generate 4500 GWh on average per annum and also has more than 5500 MW of multi-fuel generation capacity across New South Wales, Victoria and South Australia [12].

Hydro Tasmania is Australia's largest generator of renewable energy and largest water manager. Since its inception in 1914, Hydro Tasmania has been a leader in clean energy innovation in Australia - building 54 major dams, 30 hydropower stations with an installed capacity of about 2200 MWh and two major wind farms. Hydro Tasmania produces about 9000 GWh of clean renewable electricity from hydropower every year [13].

4.2. OPPORTUNITY TO OPERATE DIFFERENTLY

The same drivers that are causing the market to explore pumped storage hydropower are also causing existing hydropower energy companies to consider using their existing hydro storage assets differently to meet the growing storage need and/or to modify their assets to meet this new opportunity. This has resulted in two major strategic projects: Snowy 2.0 and the Tasmanian "Battery of the Nation". Both are discussed briefly below.

4.3. SNOWY 2.0

The proposed Snowy 2.0 Pumped Storage Project is currently the subject of a feasibility study. Linking two existing storages, Tantangara (upper) and Talbingo (lower) via 27 km of tunnels and with an installed capacity of 2000 MW, Snowy 2.0 would be one of the largest pumped storage projects in the world and would add about 35% to the installed capacity of the Snowy Mountains Scheme.

One of the most significant aspects of the project is that the volume of the existing storages provides an energy storage capacity of about 350 GWh, or 175 hours of continuous operation at full output – something that is rare amongst pumped storage projects around the world. To put this into context, research by the Australian National University has found that the optimum pumped hydro energy storage contribution is 1525 GW of power capacity with 15-30 hours of energy storage to support a 100% renewable electricity system in Australia [14].

Snowy Hydro, the developers of the Snowy 2.0 project, state that the project will serve the market and consumers by providing dispatchable generation to address supply volatility, as well as fast-start capability and large-scale storage to address intermittency issues.

An investment decision on Snowy 2.0 is expected by the end of 2018. Initial estimates suggest costs in the range of AUD \$3.8 billion to AUD \$4.5 billion.

Assuming the project meets its financial hurdles, it could begin operation in 2024 [15].

4.4. BATTERY OF THE NATION

The ‘Battery of the Nation’ [16] project aims to set a blueprint for how Tasmania's renewable resources could be developed over coming decades. With funding support from the Australian Renewable Energy Agency (ARENA), Hydro Tasmania is investigating future development opportunities through which Tasmania could make a greater contribution to the National Electricity Market (NEM).

With further interconnection to mainland Australia, favourable market settings and a sound development plan, Tasmania could produce significantly more renewable energy and realise the full value of Tasmania's hydropower system.

This initiative, if realised, would lock in full energy security for Tasmania, help give Tasmanians access to the lowest possible power prices and deliver reliable, cost-effective clean energy as the ‘Battery of the Nation’.

The program of works includes:

- ‘future state’ National Electricity Market analysis – investigating and developing a pathway of future development opportunities for Tasmania to make a greater contribution to a future National Electricity Market
- the Hydro Tasmania pumped hydro energy storage project – assessing opportunities for pumped hydro in Tasmania, including potential conversion of existing hydro generators and new installations
- power system improvements – investigating projects that will improve and optimise power generation including options for redesigning the Tarraleah Power Scheme to boost efficiency and improve management of environmental flows through the Gordon Power Station.

5. CONCLUSIONS

This paper has demonstrated the growing importance of storage in Australia's NEM as coal-fired generation is replaced by variable renewables. It has also highlighted the importance of hydro storage and how this can be achieved through either pumped storage hydropower or better utilisation of existing hydropower storages. It is highly probable that the transition to renewables will lead to a change in the way existing hydro storages are operated, not only providing energy but also providing grid reliability and flexibility.

6. REFERENCES

- [1] CAMPEY T., BRUCE S., YANKOS T., HAYWARD J., GRAHAM P., REEDMAN L., BRINSMEAD T., BRINSMEAD T., DEVERELL J. *Low emissions technology roadmap*. CSIRO, Australia, Report No. EP167885, June 2017.
- [2] HYDRO TASMANIA. *Battery of the Nation – analysis of the future National Electricity Market – exploring a vision where Tasmania plays a significantly expanded role in the NEM*. February 2018.
- [3] FINKEL A. *Independent review into the future security of the National Electricity Market – blueprint for the future*. June 2017.
- [4] WWF-AUSTRALIA. *Beyond baseload: 100% renewable energy in Australia*. June 2016.
- [5] BASSLINK. *Operations* <http://www.basslink.com.au/basslink-interconnector/operations/>. Viewed on 6 February 2018.
- [6] HEARPS P., DARGAVILLE R., MCCONNELL D., SANDIFORD M. FORCEY, T. SELIGMAN, P. *Opportunities for pumped hydro energy storage in Australia*. Melbourne Energy Institute. February 2014.
- [7] ENTURA. *Is pumped storage hydro the key to increasing renewables in Australia?* <http://www.entura.com.au/is-pumped-storage-hydro-the-key-to-increasing-renewables-in-australia/>. Viewed on 6 February 2018.
- [8] AUSTRALIAN NATIONAL UNIVERSITY. *ANU finds 22,000 potential pumped hydro sites in Australia*. <http://www.anu.edu.au/news/all-news/anu-finds-22000-potential-pumped-hydro-sites-in-australia>. 21 September 2017.
- [9] GENEX POWER. *The Kidston Pumped Storage Hydro Project (250MW)*. <http://www.genexpower.com.au/the-kidston-pumped-storage-hydro-project-250mw.html>. Viewed on 6 February 2018.
- [10] ENERGY AUSTRALIA. *Cultana Pumped Hydro Project – knowledge sharing report*. September 2017.
- [11] JAPAN UPDATE. *Experimental power plant in Kunigami dismantled*. <http://www.japanupdate.com/2016/07/experimental-power-plant-in-kunigami-dismantled/>, 2016, viewed on 6 February 2018.
- [12] SNOWY HYDRO *Our energy*, <https://www.snowyhydro.com.au/our-energy/>, viewed on 6 February 2018.
- [13] HYDRO TASMANIA *Clean energy*. <https://www.hydro.com.au/clean-energy>. Viewed on 6 February 2018.
- [14] BLAKERS A., LU B., STOCKS M. 100% renewable electricity in Australia. *Energy* 133, 2017, 471–482.
- [15] SNOWY HYDRO. *Snowy 2.0 – feasibility study – summary*. December 2017.
- [16] HYDRO TASMANIA *Battery of the Nation fact sheet*. https://www.hydro.com.au/docs/default-source/clean-energy/battery-of-the-nation/battery-of-the-nation-fact-sheet-november-2017.pdf?sfvrsn=a32d1128_2. November 2017.

COMMISSION INTERNATIONALE DES GRANDS BARRAGES

VINGT-SIXIÈME CONGRÈS DES GRANDS BARRAGES
Autriche, juillet 2018

DOI 10.3217/978-3-85125-620-8-011



This work licensed under a Creative Commons Attribution 4.0 International License.
<https://creativecommons.org/licenses/by-nc-nd/4.0/>

**CLIMATE EFFECT ASSESSMENT OF THREE GORGES PROJECT RICHARD
HERWEYNEN**

Long XING

CHINA THREE GORGES CORPORATION

CHINA

CLIMATE EFFECT ASSESSMENT OF THREE GORGES PROJECT

ABSTRACT

The reservoir was formed by runoff dam, sluice, embankment construction, water conservancy project and weirs water impoundment. The reservoir can be used for water supply, irrigation, power generation, flood control, shipping, tourism and improve the environment, but with the global water resources and energy demand increase, sharp increase in the number and size as well as the reservoir, environmental effects and social impact is gradually being recognized.

The China Three Gorges Project has generated extensive concerns both domestically and abroad.

How to evaluate the climate effect of the Three Gorges water conservancy project scientifically, objectively and quantitatively? Scientists are very concerned about the issue, The assessment of the climate effect of the Three Gorges project is of great significance for the normal operation of the Three Gorges Project and the correct understanding of the Three Gorges Project by the society and the public.

In order to answer this question and to objectively evaluate the climatic effects of Three Gorges project, China Three Gorges Corporation organize relevant experts to carry out research on the climate effect of serious and systematic problems of Three Gorges reservoir. The study yielded a range of objective, scientific conclusions on the climate effects of the project that can be use to develop climate services for informing future decision-making.

Authors:long Xing, unit: China Three Gorges Corporation,

Tel: 8607176763181, fax: 8607176763340,

E-mail: xing_long@ctg.com.cn

KEYWORDS

Climate, Reservoir, Three Gorges Project

1. THE PROJECT

The Three Gorges Water Control Project includes a river-blocking dam, a water reservoir, power generators, navigation structures, and more. It is one of the largest water conservancy projects in the world. The Three Gorges Dam controls a drainage

area of 1 million square kilometers – 55.6 per cent of the total drainage area of the Yangtze River Basin.

Three Gorges Reservoir is able to retain 39.3 billion m³ of water, with a flood control capacity up to 22.15 billion m³. The reservoir feeds the Three Gorges Hydropower Station, which has 34 generator units with an installed capacity of 22.5 million kw and an annual generating capacity of 88.2 billion kwh.

When the Dam's water level is raised to the desired capacity of 175 m, the 632 km² of land flooded in the Three Gorges Reservoir form a man-made lake 600 km long and 1-2 km wide, with a total area up to 1,084 km². In this paper, the Three Gorges Reservoir Area refers to the Yangtze River main stream area from Chongqing city to Yichang city.

2. LOCAL CLIMATE MONITORING SYSTEM IN THE THREE GORGES RESERVOIR AREA

The Three Gorges Reservoir area is complex, and the valley basins are different from each other. There are vertical differences in climate in different regions. In general the valley in the hot summer and warm winter, cool in summer and cool winter mountain, rain, fog wet weight, and has the characteristics of slopes of different climate. The location of the reservoir is unique in the climate, which is one of the non zonal climate types in China, and is also one of the most typical representative of the microclimate in the water body. The climate in the reservoir area is affected by regional weather and climate system changes. At the same time, after the completion of the Three Gorges Dam, the water level will rise and the water area will expand due to impounding. It will cause the change of the thermal properties of the underlying surface and cause the change of the local microclimate in the reservoir area.

In order to fully understand the construction of the Three Gorges Reservoir area before and after the local climate change characteristic, based on the existing business system of meteorological department China, established the "Three Gorges local climate monitoring system", the system includes 1 key local climate monitoring stations, 7 reservoir climate information and security monitoring center station, 50 real-time monitoring of base stations. The realization of real-time monitoring, data acquisition in online and fast delivery, tracking and monitoring the whole process of the impact of climate change caused by three gorge project and meteorological disasters.

3. OBSERVATION AND ANALYSIS OF THE THREE GORGES RESERVOIR

3.1. CHANGE OF METEOROLOGICAL ELEMENTS

Through the analysis of local climate monitoring system, we found that after the Three Gorges Reservoir construction, the average annual precipitation in the reservoir area decreased, but the difference was obvious every month. The precipitation in June and July decreased compared with that before storage, while in August and September, it increased slightly compared with that before storage. The precipitation days of each station in the reservoir area decreased after the storage, but the number of annual rainstorm days increased, the intensity of precipitation in the reservoir area became larger and the frequency of extreme precipitation increased.

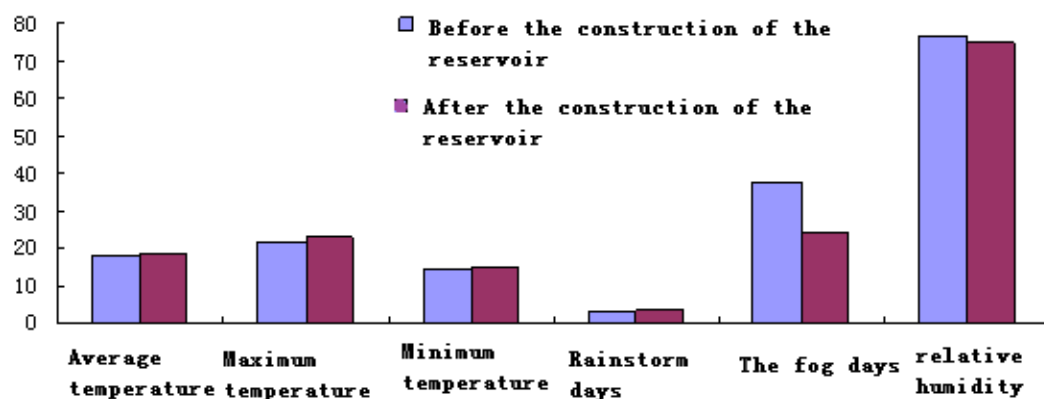


Figure 1: Comparison of annual mean value of meteorological elements

Compared with pre storage, annual mean temperature, maximum temperature and minimum temperature were significantly increased, the average annual temperature of temperature rise in the area between 0.1°C~0.4°C, especially in the seasons of spring and autumn warming significantly, but the change is not obvious in summer temperatures. In addition, after the completion of the reservoir, the annual evaporation amount increased slightly, but the change trend was not significant; the annual relative humidity decreased, the annual fog days decreased, and the change trend was significant.

3.2.

The Three Gorges reservoir has a regulating effect on the local climate after the storage of the Three Gorges reservoir, and the effect of cooling in summer and Warming in winter is obvious

In order to analyze the impact of the Three Gorges Reservoir on the small climate, the near reservoir area and the far reservoir area are divided according to the distance

between the main stream of the Yangtze River. The meteorological stations near the reservoir area (Wushan and Badong) are the representative stations near the reservoir area, and the meteorological stations far away from the reservoir area (Wuxi, Xingshan, Enshi and Jianshi) are the representative stations.

The temperature monitoring number in the near and far reservoir areas is selected and compared with the difference between them. Through the analysis we can see that, The annual variation trend of annual average temperature in the near and far reservoir area is consistent, The annual mean temperature difference between the near and far reservoir areas increased after 2003. the difference is 0.8°C, the average annual temperature difference than 1976-2008 (0.5°C) increased by 0.3°C, It shows that the temperature near the reservoir area is slightly increased after water storage.

time interval	content	Winter temperature difference	Summer temperature difference
After storage	Temperature difference(Near and far reservoir area)	0.9 ^②	0.4 ^②
Pre storage		0.5 ^②	0.5 ^②
change		Increase0.4 ^②	reduce0.1 ^②

Table 1: Comparison of temperature difference between the near and far reservoir area

Further analysis showed that the summer warming in the near reservoir area was smaller than that in the far reservoir area after the impoundment, resulting in a decrease of the average temperature difference between the 0.1°C in summer, indicating that the reservoir had a cooling effect on the waters near the area. In winter, near reservoir area is affected by reservoir, and the increasing range is slightly larger than that in far reservoir area. The average temperature difference between them increases by 0.4°C, indicating that the reservoir has "warming effect" near the water area. As the temperature difference has ruled out the impact of the climate background on the entire reservoir area, we can think that the change of mean temperature difference in near and far reservoir area is caused by local climate effect of reservoir, increasing temperature in winter and cooling in summer.

3.3. THE CHANGE OF PRECIPITATION NEAR THE RESERVOIR AREA IS NOT OBVIOUS COMPARED WITH THE FAR RESERVOIR AREA

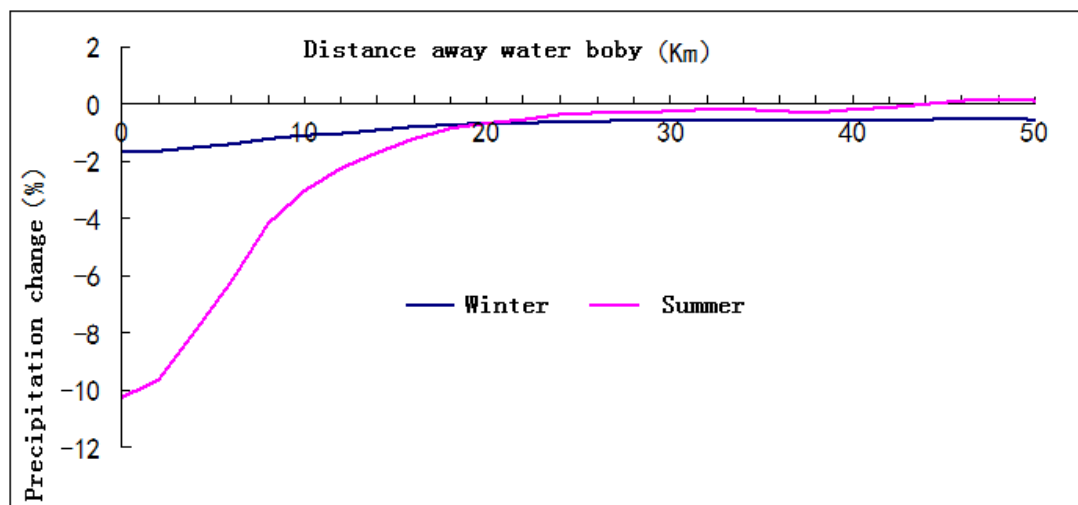
The comparison method of precipitation ratio in two regions(near and far reservoir area) is used. the effects of the removal of large scale changes and to a relatively stable ratio change, found near reservoir area and far reservoir precipitation ratio change trend is not obvious, The fluctuation of precipitation ratio in the years after

storage is in the interdecadal cycle of change, showed that the effect of the impoundment of the Three Gorges Dam on the surrounding of precipitation is not obvious.

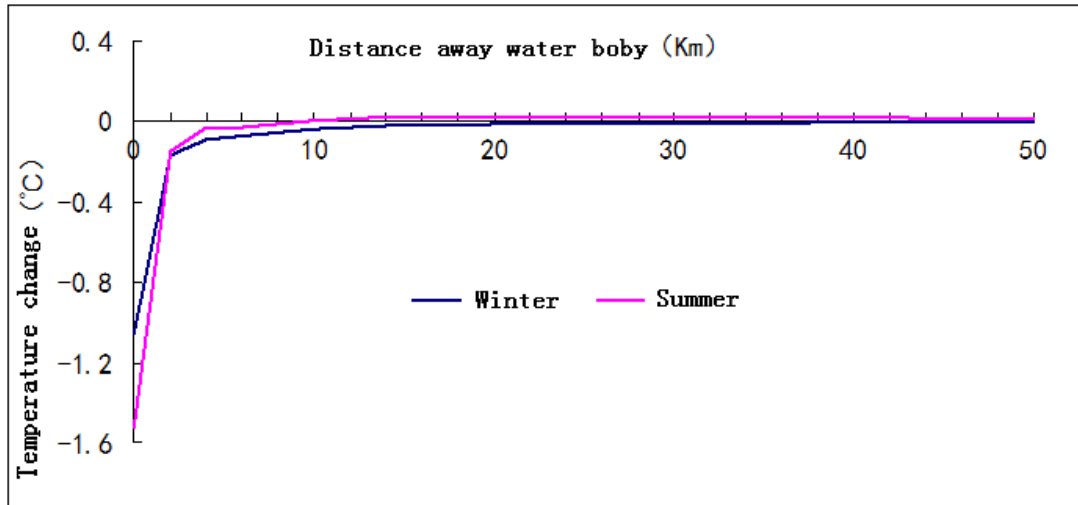
4. NUMERICAL SIMULATION OF THE CLIMATE EFFECT OF THE THREE GORGES RESERVOIR

Regional climate modeling shows that the Reservoir would produce some impact on the neighboring areas climate, But the maximum range of impact is not more than 20km, The Reservoir would noticeably bring down the air temperature above the water surface, by 1°C in the winter, and 1.5°C in the summer, with only 0.1° C for the land surface close to the water.

The water body's evaporative cooling effect would cause the air to sink, and as a result there would be less precipitation. However, the decline in precipitation would be small in winter, a 1 to 2 per cent drop within a 10km radius, and higher in summer, a 10 per cent drop. That 10 per cent would weaken to 3 per cent at a 10km radius and to 1 per cent at a 20 km radius. The numerical model simulation results show that the Three Gorges reservoir, as a typical and very narrow channel reservoir, has a very small impact on the regional climate.



a



b

Figure 2: The scope of the Three Gorges Reservoir's impact on (a) precipitation and (b) temperature in the winter (blue line) and in the summer (red line)

5.

In the last 50 years, the trend of climate change in the Three Gorges area is consistent with the trend of the larger climate change, and the basic climate characteristics of the Three Gorges region have not changed.

In the past 50 years, the Reservoir Area has registered an ascending trend for annual mean temperature, with the largest increase in the last 10 years, though the increase is significantly lower compared with the increase of the Yangtze River Basin. In both the Reservoir Area and the Yangtze River Basin, annual precipitation does vary significantly, but inter-decadal figures do show significant variation. The Reservoir Area saw limited annual rainfall variations from the 1960s to the 1990s, though with significantly reduced rainfall in the last 10 years. Meanwhile, the Yangtze River Basin became abnormally wet in the 1990s, but abnormally dry in other years. In the past 50 years or so, both the Reservoir Area and the Yangtze River Basin witnessed a reduced numbers of rainy days, of annual mean wind speed, and of relative humidity, though the former is on the slower side compared with the latter.

5.1.

Since 1961, the Three Gorges Reservoir area climate warming trend with the global synchronization, the annual average temperature showed an overall warming trend, on average every 10 years increased by 0.08°C, the last 10 years in 1960s compared to an increase of 0.4°C, the annual average temperature change trend and the

southwest region of the upper reaches of the Yangtze River, the Yangtze River and the whole consistent reservoir after this trend in 2004 no significant change.

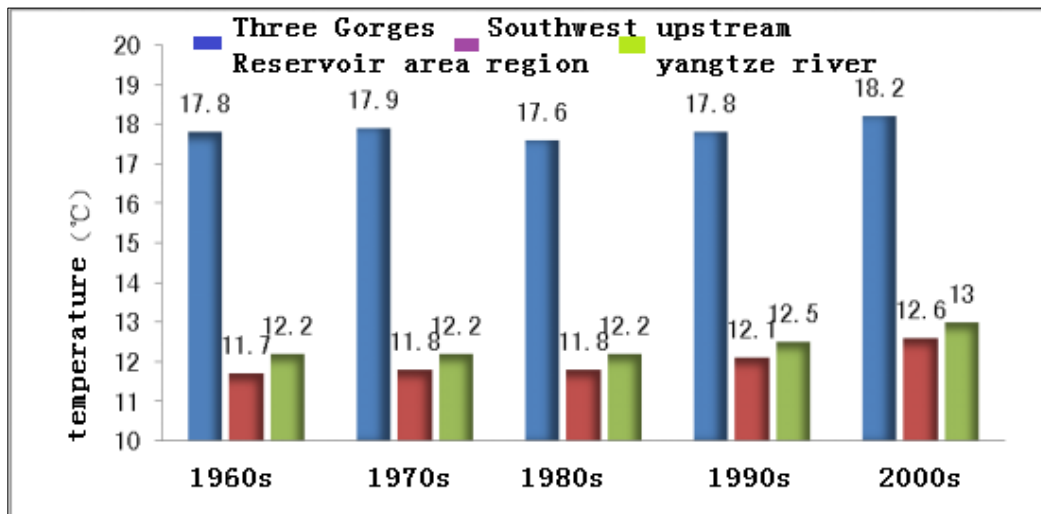


Figure 3: Interdecadal change of average temperature

5.2 Since 1961, the annual precipitation in the Three Gorges Reservoir area has been characterized by annual intergenerational changes. 1970s~1980s is slightly more precipitation. 1960s~1990s precipitation is slightly less; since this century, precipitation has been the least 10 years in the last 50 years. Less rain for nearly 10 years from the beginning of 1999, the annual precipitation increased from more than 1100 mm to more than 1000 mm reduced, reduced by about 10%. The contrast analysis shows that the change of precipitation in the reservoir area before and after the completion of the Three Gorges project is consistent with the trend of the changes in the southwest, the upper reaches of the Yangtze River and the whole Yangtze River Basin.

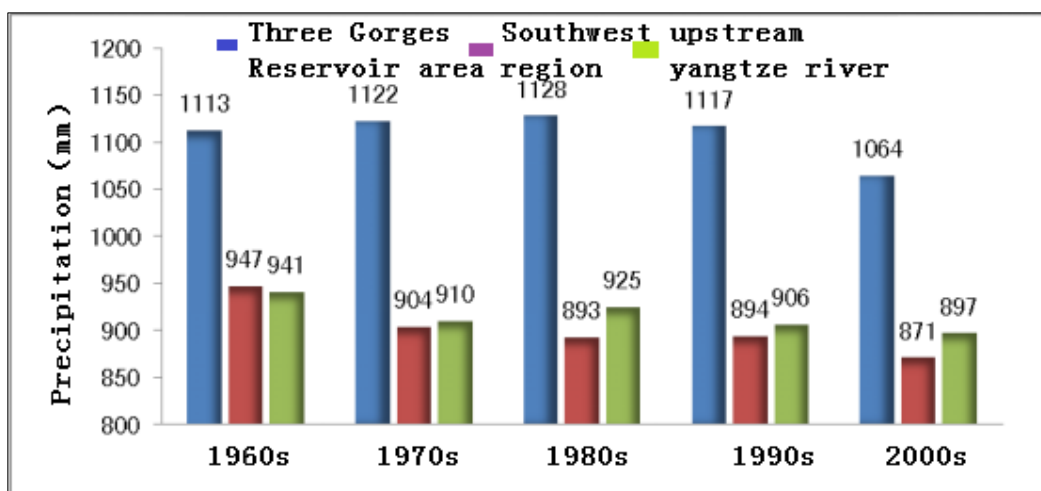


Figure 4: Interdecadal change of average precipitation

6. SUMMARY

After the construction of the Three Gorges reservoir, the average annual precipitation in the reservoir area decreased, but the number of rainstorm days increased, and the precipitation intensity in the reservoir area became larger. Compared with the pre storage, The annual average temperature, the annual average maximum temperature and the minimum temperature increased significantly, and the warming was obvious in spring and autumn. After the completion of the reservoir, the annual evaporation amount increased slightly, but the change trend was not significant, the annual relative humidity decreased, the annual fog days decreased, and the change trend was significant.

Over the past 50 years the average temperature rise, precipitation has interdecadal characteristics. from 1999 the rainy period was less rain, The change of temperature and precipitation is basically the same as that in the southwest and the Yangtze River Basin .After the completion of the Three Gorges reservoir, the temperature in the vicinity of the reservoir area was fine-tuning, warm in winter and cool in summer . After the change of water level, the impoundment only has a slight effect on the climate in some areas, but the influence range is not more than 20 kilometers. There is no obvious change in the climate of the reservoir and surrounding areas.

COMMISSION INTERNATIONALE DES GRANDS BARRAGES

VINGT-SIXIÈME CONGRÈS DES GRANDS BARRAGES
Autriche, juillet 2018

DOI 10.3217/978-3-85125-620-8-012



This work licensed under a Creative Commons Attribution 4.0 International License. <https://creativecommons.org/licenses/by-nc-nd/4.0/>

**DETERMINATION OF CONTROL WATER LEVEL ON SUTAMI AND LAHOR
RESERVOIR TO AVOID THE POSSIBILITY OCCURS OVERTOPPING DUE TO
PROBABILITY MAXIMUM FLOOD**

Ulie Mosphar DEWANTO

Deputy Operational II of JASA TIRTA I PUBLIC CORPORATION

INDONESIA

Arief Satria MARSUDI

Civil Engineering Expert of JASA TIRTA I PUBLIC CORPORATION

INDONESIA

Rahmah Dara LUFIRA

Lecturer in Water Resources Engineering of BRAWIJAYA UNIVERSITY

INDONESIA

COMMISSION INTERNATIONALE
DES GRANDS BARRAGES

VINGT-SIXIÈME CONGRÈS DES
GRANDS BARRAGES
Autriche, juillet 2018

**DETERMINATION OF CONTROL WATER LEVEL
ON SUTAMI AND LAHOR RESERVOIR
TO AVOID THE POSSIBILITY OCCURS OVERTOPPING
DUE TO PROBABILITY MAXIMUM FLOOD**

Ulie Mosphar Dewanto ¹⁾, Arief Satria Marsudi ²⁾, Rahmah Dara Lufira ³⁾

Deputy Operational II of Jasa Tirta I Public Corporation ¹⁾, Civil Engineering
Expert of Jasa Tirta I Public Corporation ²⁾, Lecturer in Water Resources
Engineering of Brawijaya University ³⁾

INDONESIA

1. INTRODUCTION

Sutami Dam and Lahor Dam is located on Malang Regency, Province of Jawa Timur, Indonesia. This study needs to be done considering the extreme weather changes in recent years and the issue of global warming in the last decade that impacted the high intensity of rainfall and the change of land use in the upstream which affects the rise of runoff so that the flood discharge in the river becomes larger. Beside that, Sutami Dam and Lahor Dam at the time of planning (1975) is still designed with 1000 year return period of flood, while the dam safety standard set by the Dam Security Commission is currently the flood discharge of Probability Maximum Flood (PMF).

it is necessary to raise awareness of the possibility of a PMF by evaluating the spillway performance of the PMF discharge that exceeds the initial flood discharge. So that the effort of awareness raising that can be done by the dam operator is by maintaining the Control Water Level (CWL) of the reservoir, so that during the PMF discharge, the reservoir can still reduce the flood and the overtopping can be avoided or the frequency can be reduced minimally. It is an effort to manage the dam safety in the Brantas River Basin.

In the normally calculation of the PMF discharge can only represent the annual value. If this value is applied to the reservoir operation to maintain CWL it will cause a big losses. Because the volume of water that can be utilized must be wasted to maintain the CWL. Probability of PMF discharge is different for every month. Therefore it is necessary to do research to get the value of PMF discharge for each month to get different CWL for each month.

2. METODOLOGY

2.1. DESCRIPTION OF STUDY AREA

Topographic conditions in Malang Regency are dominated by highland or mountainous areas. With such topographical conditions, it is possible to build dams as regulators for water regulator and flood control. There are three dams in the upstream of Brantas River Basin: Sengguruh Dam, Sutami Dam and Lahor Dam, which are interrelated systems. Sengguruh Dam serves as a power plant and sediment controller, so that sediment sediments do not go directly into the Sutami Reservoir. The Sutami and Lahor Reservoirs are interconnected with tunnel, which in the planning of the Lahor Reservoir serves to supply the water needs to the Sutami Reservoir for hydroelectric power plant.

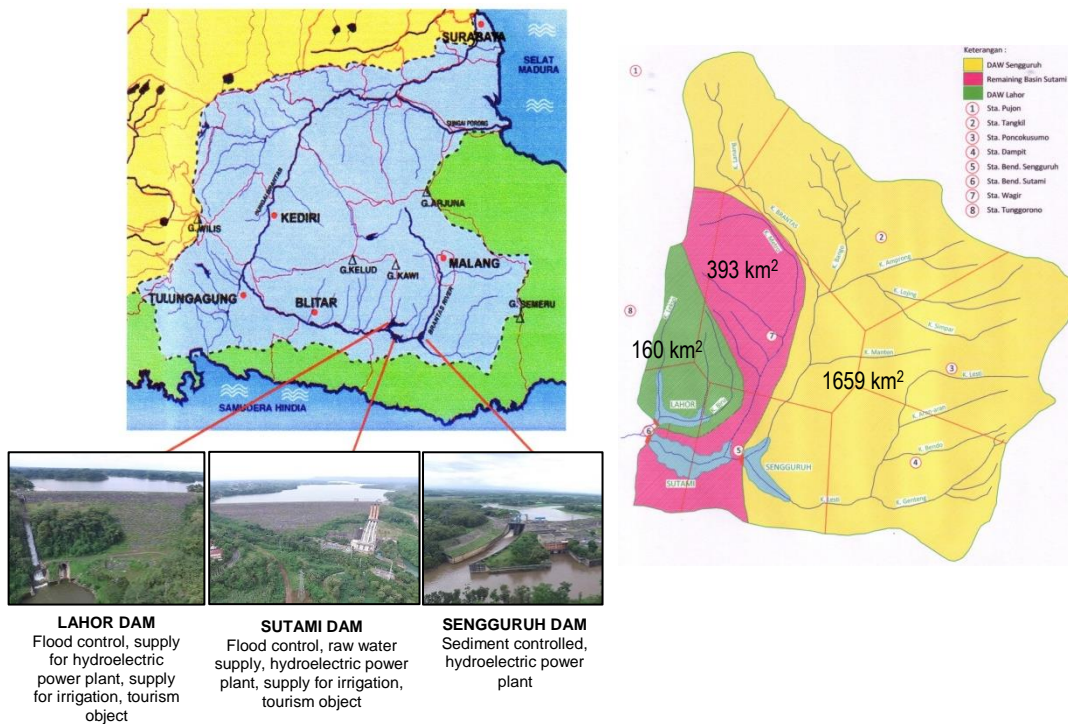


Fig. 1
Dam Location and Chatchment Area Scheme

2.2. STAGES OF ANALYSIS

In the design flood analysis and flood routing analysis there are some related things that affect that is:

- The Sengguruh Dam located on the upstream of the Sutami Dam, resulting in a flood reduction by Sengguruh Reservoir. Beside that the outflow from Hydroelectric Power Plant of Sengguruh also affect the flood discharge into the Sutami Reservoir.
- The connection tunnel between the Lahor Reservoir and Sutami Reservoir affected on flood routing analysis. On the analysis also considered the incoming or outgoing discharge through the tunnel simultaneously by water level difference in both reservoirs. The tunnel gate is located in the Sutami Reservoir, the operation of the tunnel door is rarely done so that the tunnel condition is always open.
- The outflow from hydroelectric Power Plant of Sutami is also taken into flood routing analysis of Sutami - Lahor Dam because the outflow value can reduce the peak flood discharge that occurring.

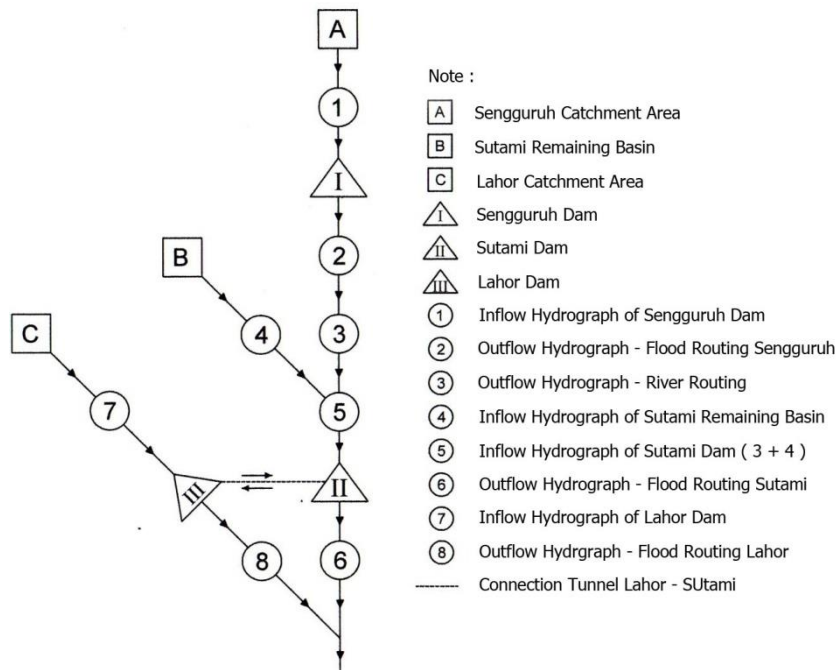


Fig. 2
Chatchment Area System Scheme

Several stages for the completion of this study are hydrological data processing which is principally rainfall design analysis for design flood and flood routing which include; a. Daily maximum rainfall analysis, b. Design rainfall Gumbel type I method, c. Probability Maximum Precipitation (PMP) analysis, d. Frequency distribution match analysis (Chi square & Smirnov Kolmogorov), e. Synthetic unit hydrograph analysis (Nakayasu), f. Design Flood hydrograph analysis, g. Curve reservoir capacity analysis and widespread reservoir (storage

area curve), h. Spillway capacity analysis, flood routing analysis (spillway) and river routing analysis, i. CWL determination as a safe guideline to get flood peak reduction in order to avoid the possibility of overtopping, j. recommendations on maximum water level control at each month as a guideline for reservoir operations related to avoid the possibility occurs overtopping.

3. RESULT AND ANALYSIS

3.3. DESIGN RAINFALL

Based on the value of the maximum daily rainfall monthly and yearly at each point of review calculated the value of PMP rain and the design rain on the re-time of 1000 years with the gumbel type I method as a comparison.

The following is the result of PMP calculations and the annual and monthly of design rainfall are presented in Table 1. The calculation of the synthetic unit hydrograph of Nakayasu method is done with the control point of Sengguruh Dam, Remaining Basin Sutami, and Lahor Dam. The result of the unit hydrograph analysis presented in “Fig 3”.

Table 1
Page margins are as follows

Description	Design Rainfall 1000 years return period (mm/day)			Probability Maximum Precipitation, PMP (mm/day)		
	Sengguruh Dam	R.B Sutami	Lahor Dam	Sengguruh Dam	R.B Sutami	Lahor Dam
Annual	206.58	269.43	305.66	392.72	607.11	710.35
January	108.07	164.29	198.58	192.59	388.67	413.61
February	117.7	113.5	143.32	266.53	283.99	334
March	199.57	228.1	265.57	394.11	489.56	526.17
April	128.57	195.96	208.3	302.87	464.15	447.76
May	88.92	93.07	120.06	267.67	261.75	351.29
June	116.7	95.02	87.28	383.94	228.42	284.35
July	70.09	65.76	79.38	199.44	210.4	260.63
August	75.59	85.36	95.74	221.97	238.19	302.59
September	101.59	109.31	125.19	297.86	322.17	393.69
October	102.37	144.49	181.08	314.03	403.38	494.72
November	178.14	275.72	322.66	358.62	641.31	786.56
December	227.13	229.81	250.35	507.66	546.05	619.61

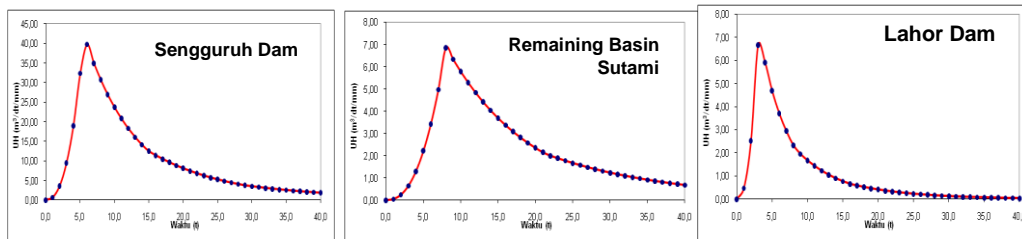


Fig. 3
Synthetic Unit Hydrograph of Nakayasu

Table 2
Runoff Coefficient

Description	1000 years return period			Probability Maximum Precipitation, PMP		
	Sengguruh Dam	R.B Sutami	Lahor Dam	Sengguruh Dam	R.B Sutami	Lahor Dam
Annual	0.61	0.66	0.68	0.71	0.77	0.79
January	0.46	0.56	0.60	0.59	0.71	0.72
February	0.48	0.47	0.53	0.65	0.66	0.69
March	0.60	0.63	0.65	0.72	0.74	0.75
April	0.50	0.60	0.61	0.68	0.74	0.73
May	0.40	0.41	0.48	0.65	0.65	0.70
June	0.48	0.42	0.40	0.71	0.63	0.66
July	0.33	0.30	0.37	0.60	0.61	0.65
August	0.35	0.39	0.42	0.62	0.63	0.68
September	0.44	0.46	0.50	0.67	0.69	0.72
October	0.44	0.53	0.58	0.68	0.72	0.75
November	0.58	0.66	0.69	0.70	0.78	0.80
December	0.63	0.63	0.64	0.75	0.76	0.77

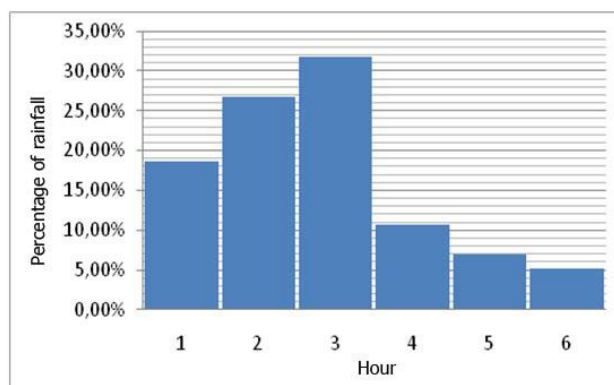


Fig. 4
Hourly Rainfall Distribution Graphic

3.4. FLOOD DESIGN

The following is the peak point of the result from the calculation of flood design of Q1000 th and QPMF (annual and monthly). With the consideration that, the reference of maximum flood is annual maximum, so the maximum monthly flood design needs to be corrected based on the maximum annual flood design with the following results:

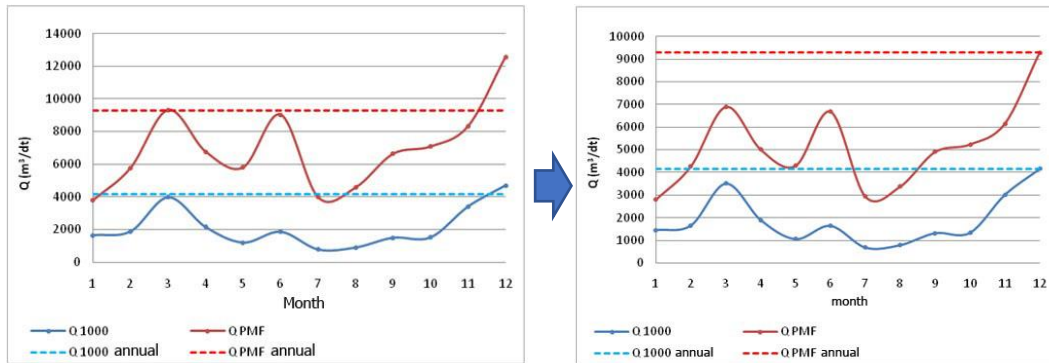


Fig. 5

Maximum Flood Design Annual and Monthly Corrected in Sengguruh Dam

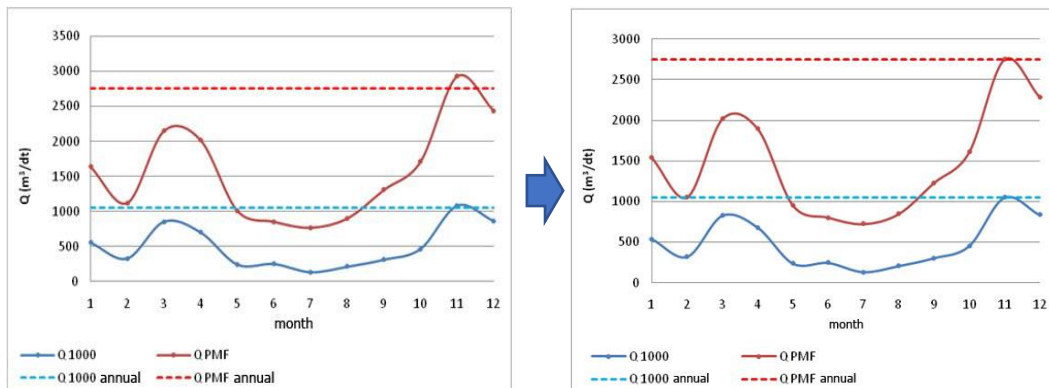


Fig. 6

Max. Flood Design Annual and Monthly Corrected in Remaining Basin Sutami

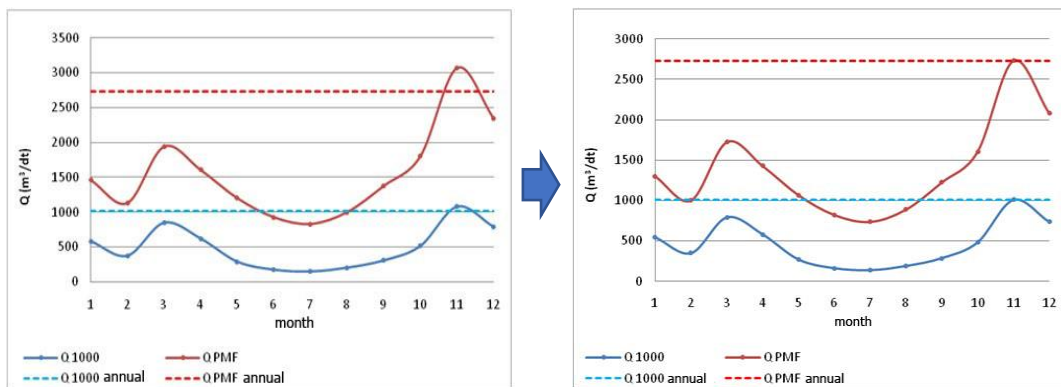


Fig. 7

Maximum Flood Design Annual and Monthly Corrected in Lahor Dam

3.5. FLOOD ROUTING

The result of flood design on Sengguruh Dam then calculated by flood routing in Q1000 th and QPMF to obtain outflow value from Sengguruh Dam (from spillway & turbine). The outflow result from Sengguruh Dam is then used as inflow discharge value for the calculation of river routing (Sengguruh-Sutami). The result value from river routing then combined with flood design from Remaining Basin Sutami to get the inflow value at Sutami Dam. The result of flood design in Lahor Dam then calculated by flood routing to obtain the outflow value at Lahor Dam.

The inflow value of Sutami Dam then calculated by flood routing in Sutami reservoir by considering the in/out discharge from connection tunnel and discharge from hydroelectrical power plant of Sutami. The flood routing also considered the water level on PMF discharge so that the reservoir can still reduce the flood that occurred. Graphical representation of the calculations result can be viewed in “fig 8 and 9”.

In order to obtain safety to manage at Sutami and Lahor Dam on possibility of overtopping caused by PMF discharge in the rainy season, the operation of Sutami and Lahor reservoir need to consider the application of CWL at elevation between +257,00 m to +267.00 m.

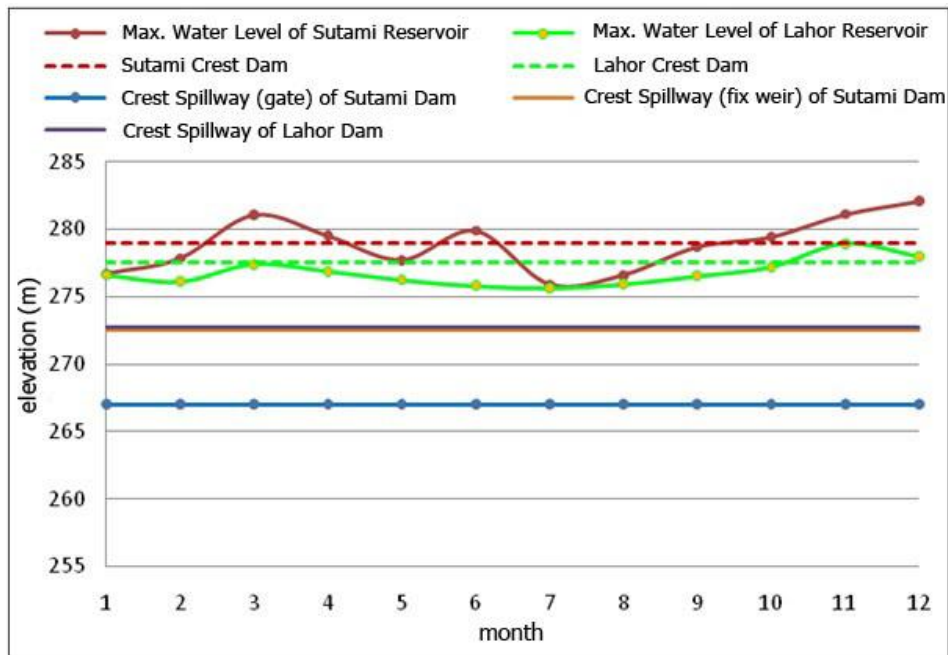


Fig. 8
Water Level Elevation of PMF Discharge

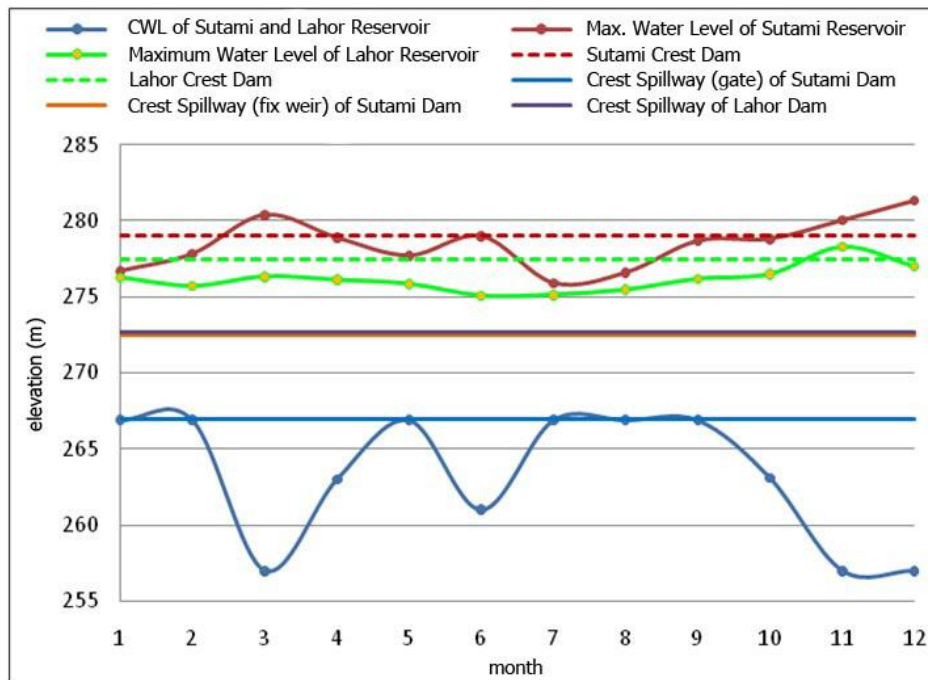


Fig. 9
Water Level Elevation of PMF Discharge with CWL application

3.6. SUMMARY

In hydrology analysis of the annual PMF discharge that potential to occur in the Sutami Dam is very large at 11,629.14 m³/s, where the PMF discharge value is equivalent to $2.31 \times Q_{1000 \text{ years}}$ and with the parapet wall as high as 1 m at the top of the dam and CWL management at elevation between + 257.00 m up to +267.00 m still have 3 times potential of overtopping with water level 3.09 m above the top of the dam. The annual PMF flood discharge that potentially occurs in the Lahor Dam is very large at 2,731.00 m³/s, where the discharge value is equivalent to $2.70 \times Q_{1000 \text{ years}}$ and with the parapet wall as high as 1 m and with CWL management at elevation between +257.00 m up to +267.00 m is not potentially overtopping. The CWL in the Sutami and Lahor reservoirs is difficult to applied because the dams function is to collect water in the rainy season and utilize it during the dry season so that in order to anticipate the possibility of overtopping, emergency spillway is needed to build at the Sutami Dam.

Keyword : Flood Control, Overtopping, Reservoir Operation, Water Level

REFERENCES

- [1] ANONIM. 1976. cara menghitung design flood. jakarta: departemen pekerjaan umum.
- [2] ANONIM. 1986. buku petunjuk perencanaan irigasi, bagian penunjang untuk standar perencanaan irigasi. jakarta: departemen pekerjaan umum.
- [3] CHOW, VEN TE. 1985. hidrolika saluran terbuka. jakarta: erlangga.
- [4] CREAGER, WILLIAM P., JUSTIN, JOEL D., HINDS, JULIAN, CHAND, NEM & BROS. 1995. engineering for dams. new delhi: rorkee.
- [5] FRENCH, RICHARD H. 1986. open channel hydraulics, international student edition. tokyo: mc graw hill.
- [6] HERSFIELD, D.M., 1961. estimating the probable maximum precipitation. amerika: american civil society of civil engineers, journal hydraulics division, vol 87.
- [7] HERSFIELD, D.M., 1965. method for estimating the probable maximum precipitation. amerika: journal american waterwork association, vol 3.
- [8] HUFF, F. A., 1967: time distribution of rainfall in heavy storm. water resources research, american geographical union, vol 3.
- [9] KUMAR, SANTOSH G. 2001. irrigation engineering and hydraulic structure. new delhi: khanna publisher.
- [10] LINSLEY, RAY K., KOHLER, MAX A. & PAULUS, JOSEPH L.H. 1983. hydrology for engineers third edition. tokyo: mc graw hill.
- [11] MCKAY, G. A., 1965: statistical estimating of precipitation extremes for the prioie provinces. canada department of agliculture, pfra engineering brach.
- [12] NOVAK,P., A.I.B.MOFFFAT,C.NALLURI,R.NARAYANAN. 1990. hydraulic structures, first publihed. london : unwin hyman.
- [13] RAUDKIVI, ARVED J. 1979. hydrology, an advanced introduction to hydrological processes and mosdelling. new york: pergamon press.
- [14] SOSRODARSONO, S., TAKEDA, K., 1976. hidrologi untuk pengairan. jakarta: pradnya paramita.
- [15] SOSRODARSONO, SUYONO & TAKEDA, KENSAKU. 1977. bendungan type urugan. jakarta: pradnya paramita.
- [16] SHAHIN, M.M.A. 1976. statistical analysis in hydrology, international courses in hydraulic and sanitary engineering. delft netherlands
- [17] SOEMARTO, CD. 1987. hidrologi teknik. surabaya: usaha nasional.
- [18] SOEWARNO. 1995. hidrologi, aplikasi metode statistik untuk analisa data. bandung: nova.
- [19] SOEWARNO. 2000. hidrologi operasional jilid ke-1. bandung: citra aditya bakti.
- [20] SABAR, HUSNI. 2000. waduk dan tenaga air. bandung: teknik sipil dan lingkungan itb.
- [21] SURIPIN. 2003. sistem drainase perkotaan yang berkelanjutan. yogyakarta: andi.

COMMISSION INTERNATIONALE DES GRANDS BARRAGES

VINGT-SIXIÈME CONGRÈS DES GRANDS BARRAGES

Autriche, juillet 2018

DOI 10.3217/978-3-85125-620-8-013



This work licensed under a Creative Commons Attribution 4.0 International License. <https://creativecommons.org/licenses/by-nc-nd/4.0/>

**IMPACT OF UPPER YANGTZE CASCADE RESERVOIRS OPERATION ON
THREE GORGES RESERVOIR IN IMPOUNDMENT PERIOD**

Gao YULEI

Engineer of CHINA THREE GORGES CORPORATION

CHINA

Wang HAI

Professorate senior engineer of CHINA THREE GORGES CORPORATION

CHINA

IMPACT OF UPPER YANGTZE CASCADE RESERVOIRS OPERATION ON THREE GORGES RESERVOIR IN IMPOUNDMENT PERIOD

Gao Yulei

Engineer of China Three Gorges Corporation, China.

Wang Hai

Professorate senior engineer of China Three Gorges Corporation, China.

1. INTRODUCTION

The Yangtze River is the largest river of China, with a total length of 6300km and a total drainage area of 1.8 million km². The Three Gorges Reservoir (TGR) is the key backbone project for controlling the Yangtze River and developing and utilizing the water resources of the Yangtze River. Its normal storage level is 175 m, flood control level is 145 m, flood control capacity is 22.15 billion m³, and utilizable capacity is 16.5 billion m³, having a huge regulation and storage capacity; the reservoir takes on flood control, power generation, navigation, and other comprehensive utilization tasks. According to the preliminary design diagram, TGR start to impound on October 1 each year and will impound water to 175m by the end of October or November. From January to April of the following year, the water supply dispatch was implemented for the middle and lower reaches to meet the needs of shipping, water supply and ecology. The impoundment of TGR is an important prerequisite for giving full play to its huge water supply benefits.

At present, a large number of reservoirs with large storage capacity and good regulation capacity have been built or will be built in the upper reaches of the Yangtze River. According to the long-term planning, the total regulation capacity of TGR and the upstream controlled reservoirs will approach 100 billion m³ and the total flood control storage will be 50 billion m³. As the upstream reservoirs are gradually put into operation, the regulation of runoff by the cascade reservoirs will become more and more obvious. The regulation of water volume during the year can reach 1/4 of the average annual water discharge of Yichang Station. These cascaded reservoirs are concentrated in the annual water storage from August to October, reducing the amount of storage water in the Three Gorges Reservoir and increasing the risk of failure in water storage of TGR.

In recent years, many scholars have carried out a large amount of research on staging design floods, the comprehensive utilization of the TGR during the storage period, water level and node control water level optimization, and analyzed the flood control risks brought by the optimization plan. Based on the long series of runoff data used in the preliminary design, the long runoff data of TGR from September to October was calculated by considering the impact of reservoir water

storage in upstream reservoirs at different levels. Without reducing the design flood control standards of the Three Gorges Reservoir, a number of water storage schemes are formulated to calculate the full capacity of the Three Gorges Reservoir and seek for a better water storage scheme.

2. NEW SITUATION OF TGR IMPOUNDMENT

2.1. IMPACTS OF UPSTREAM RESERVOIRS ON WATER STORAGE

As of 2017, there are 28 reservoirs in the upper and middle reaches of the Yangtze River that are jointly dispatched, with a total capacity of 57.5 billion m³ and a total flood control storage capacity of 41.5 billion m³. Including TGR, there are 21 reservoirs, with total water demand of 31.87 billion m³, to be large water storage.

In the joint water storage plan approved by the state flood control department in 2017, the flood control reservoir was taken as "sub-reservoirs and gradually water storage". 7 reservoirs started to impound on August 1 ahead of schedule, and the remaining 13 reservoirs began to impound on September 1, partially overlapping the storage time of TGR, drastically reducing the amount of water infused into TGR. In the long term, four large reservoirs of Wudongde, Baihetan, Lianghekou and Shuangjiangkou will also be added on the basis of 2017, and the pressure of water storage will be further increased.

In the 2017 level year, the total storage of upstream reservoirs in September and October is 9.7 billion m³, which is equivalent to 43.9% of the maximum storage capacity of TGR. In the prospective level year, assuming that all four newly added reservoirs begin to impound in September, the total water storage capacity of the upstream reservoirs from September to October is 22.2 billion m³, which is basically the same as that of the Three Gorges Reservoir. Therefore, the impoundment of large-scale upstream reservoirs has a significant impact on runoff in September and October, significantly reducing the inflow into TGR during the impoundment period. The reservoirs have been built and will be built in the upper reaches of the Yangtze River are shown in Figure 1.

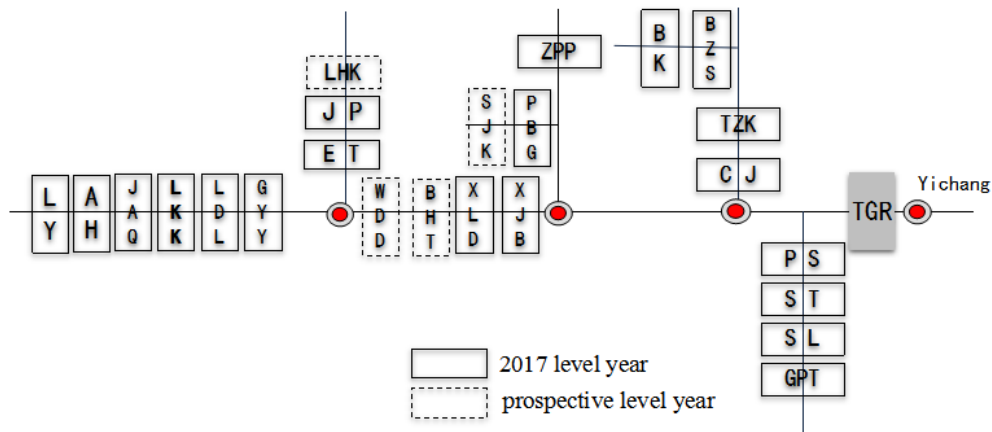


Fig. 1

Large reservoirs in the upper reaches of the Yangtze River

August belongs to the main flood season, relatively abundant water. According to the joint scheduling scheme, seven reservoirs from the beginning of August water storage, and water demand is smaller. Assuming that all of them are fully stocked by the end of August, then they will be controlled by the outbound and inbound balances in September and October. Therefore, the impact of these reservoirs on the runoff in September and October is not calculated during the calculation.

2.2. WATER DEMAND IN DOWNSTREAM AREAS DURING THE IMPOUNDMENT PERIOD

TGR has huge comprehensive benefits such as flood control, power generation, navigation and water resources utilization. With the development of economy and society and the change of the ecological environment, the water demand in the middle and lower reaches of the Yangtze River has changed greatly compared with the initial design, and the water consumption presents an increasing trend. TGR is located at the last stage of the reservoirs with regulatory capacity in the mainstream of the Yangtze River. The impact of upstream reservoirs on the middle and lower reaches is mainly reflected in TGR. Since TGR was put into operation, some new situations and new problems have emerged in the lower reaches. As for the use of water, higher discharge requirements for reservoirs during the storage period have been put forward.

According to the approval requirements of the State flood control department for TGR impoundment program in recent years, the discharge volume of TGR is not less than 10000 m³/s in September and not less than 8000 m³/s in October, To meet the demand of shipping, water supply and ecology .

3. ANALYSIS OF THE INFLUENCE OF UPSTREAM RESERVOIRS ON THE RUNOFF OF TGR DURING THE IMPOUNDMENT PERIOD

3.1 HORIZONTAL YEAR DIVISION

In 2017 level year, 13 reservoirs were selected from the reservoir that has been incorporated into the joint operation, including Guanyinyan, Xiluodu, Xiangjiaba, Zipingpu, Pubugou, Goupi Beach, Silin, Shatuo, Pengshui, Bikou, Baozhusi, Tingzikou and Caojie that impound in September or October.

In the long-term horizon year, 4 large-scale reservoirs, including Wudong, Baihetan, Lianghekou and Shuangjiangkou, will be added on the basis of the 2017 level year, for a total of 17 reservoirs.

3.2 RUNOFF CALCULATION

According to the water storage scheme which has been built and proposed in the upper reaches of the Yangtze River, the amount of water storage needed to be allocated in every ten days is calculated. The long series runoff data of 110 years (1881-1990 years) were calculated by 2017 level year and long-term level year respectively, and the runoff data of Three Gorges dam site under the operation conditions of upstream cascade reservoirs were obtained. Based on the calculated data of long series of runoff, the accumulating rate of TGR and the influence on the downstream are analyzed and compared under different schemes.

The average runoff of the 110-year-long series (1881-1990) of the Three Gorges Dam site in September and October was 122.5 billion m³. The runoff series for the 110-year (1881-1990) Three Gorges Dam site were calculated considering the upstream reservoir construction conditions. In 2017 level year, there are 13 reservoirs operating above TGR, reducing the total runoff of 9.7 billion in September and October. In the prospective level year, there are 17 reservoirs operating above the Three Gorges to reduce the total runoff of 22.2 billion m³. The simulation results show that 75 years is less than the multi-year average of the preliminary design in the 2017 level year, accounting for 68.2%, and 90 years in the prospective level year, accounting for 81.8%.

4. CALCULATION OF THE FULL STORAGE RATE OF TGR

4.1 CALCULATION SCHEME AND CONTROL CONDITION

The initial water storage time of TGR is September 1st, 10, 20 and October 1st, at the initial water level starting from the flood control limit 145m. Considering flood risk and scheduling requirements, the maximum water level at the end of September is controlled at 165m. During the water storage period, the needs of the downstream shipping, production and ecology should be taken into account, so as to minimize the impact of reservoir impoundment on the middle and lower reaches of the Yangtze River. The minimum discharge of TGR is 10000m³/s in September and 8000m³/s in October, and full storage at the end of October.

Impounding from October 1st, the number of non-full storage years are 25 years in 2017 level year and 26 years in prospective level year, and the rate of full storage is 77.3% and 76.4%, respectively. Impounding from September 20, the number of non-full storage years are 12 years in 2017 level year and 18 years in prospective level year, and the rate of full storage is 89.1% and 83.6% respectively. Impounding from September 10, the number of non-full storage years are 6 years in 2017 level year and 15 years in prospective level year, and the rate of full storage is 94.5% and 86.4% respectively. Impounding from September 1st, the number of non-full storage years are 4 years in 2017 level year and 11 years in prospective level year, and the rate of full storage is 96.4% and 90.0% respectively.

In 2017 level year, TGR began to impound from September 10th and reached 90% of the designed rate. In the future level year, due to the large storage capacity of new reservoirs, it was necessary to store water in advance until September 1st, so that the design storage rate of 90% could be achieved. The influence of different level year on the full storage rate of TGR is shown in table 1.

Table 1

The influence of different level year on the full storage rate of TGR

Date	Year of non-full		Full storage rate	
	2017	prospective	2017	prospective
Oct.1st	25	26	77.3%	76.4%
Sep.20	12	18	89.1%	83.6%
Sep.10	6	15	94.5%	86.4%
Sep.1st	4	11	96.4%	90.0%

Based on the calculation and analysis, it is reasonable for TGR to start impounding on September 10 in accordance with the current joint storage of cascade reservoirs in the 2017 level year. Due to the large storage of new large reservoirs in the prospective level year, without considering raising initial water level of impounding, TGR should be further advanced to September 1 to meet the initial design full storage rate.

4.2 THE INFLUENCE OF RAISING INITIAL WATER LEVEL ON THE FULL STORAGE RATE OF TGR.

Since 2008, TGR started for the first time to carry out 175m experimental water storage, according to the principle of “ safety, science, reliable and Gradualism”. In view of the runoff reduction in the impoundment period, the simultaneous storage of the upstream reservoir and the increase of the water demand in the lower reaches, the contradiction between the water storage and the discharge is outstanding. After fully demonstrating the flood control safety and sedimentation of pre-impoundment, the impounding mode of the Three Gorges reservoir has been further studied, and a water storage way to undertake the flood control stage and raise the water level has been put forward. TGR have achieved 175m water target for 8 consecutive years from 2010 to 2017 after further optimizing the storage scheme, and the discharge standard increased from about 5500m³/s to 8000m³/s during October.

Practice in recent years has also shown that storing flood resources and raising the initial water level TGR, were effective measures to improve the full storage rate. Based on the simulated runoff of Three Gorges dam site after the operation of cascade reservoirs in different levels, the storage rate of TGR under different storage levels was calculated.

In the prospective level year, TGR began to store water in September 10th and when the initial water level reached 152m, the full storage rate could reach over 90%. If the water storage started in early September 1st, the storage level from 148m to 152 had little effect on the full storage rate of TGR. The influence of different initial water level on the full storage rate of TGR is shown in table 2.

Table 2

The influence of different initial water level on the full storage rate of TGR

Date	Initial water level	Year of non-full		Full storage rate	
		2017	prospective	2017	prospective
Sep.10	148	6	13	94.5%	88.2%
	150	6	12	94.5%	89.1%
	152	4	10	96.4%	90.9%
	155	4	7	96.4%	93.6%
Sep.1st	148	4	11	96.4%	90.0%
	150	3	11	97.3%	90.0%
	152	3	10	97.3%	90.9%
	155	2	6	98.2%	94.5%

4.3 THE INFLUENCE OF RAISING INITIAL IMPOUNDING WATER LEVEL ON THE DISCHARGE OF TGR DURING IMPOUNDMENT PERIOD.

According to the present situation of scheduling rules, TGR began to impound from September 10th. compared with the 145m water level, if the initial water level of TGR is raised up to 148m, 150m, 152m and 155m respectively, the average discharge can be increased by 350m³/s, 590m³/s, 860m³/s and 1310m³/s during the impoundment period. Since 2010, TGR has been reached to the normal water level of 175m for 8 consecutive years of water. Except for the serious water shortage in early September and low water storage level in 2016, the TGR initial storage level of other years were above 152m. The discharge of TGR during the impoundment period was raised, effectively alleviating the contradiction between reservoir water storage and downstream water use.

5. CONCLUSION

After the operation of the upstream large reservoirs, the runoff of Three Gorges Dam from September to October is 9.7 billion m³ and 22.2 billion m³ less than that of the initial design value respectively, which has a great impact on the impoundment of TGR. In the 2017 level year, that is the status quo year, it is reasonable for TGR to start impounding on September 10 based on the current joint storage of cascade reservoirs in the basin. But the initial water level should be raised to increase the discharge during the impoundment period. In the prospective level year, due to the large storage capacity of new large reservoirs, the impounding time of TGR will need to be arranged on September 1 in advance, in order to reach the designed full storage rate .

The contradiction between the centralized storage and downstream water supply will be further exacerbated after the operation of the constructed and proposed reservoirs in the upper reaches of the Yangtze River . Therefore, the water storage scheme of TGR needs to be optimized continuously. In general, the impounding time of upstream reservoir is earlier than that of TGR. Therefore in the preparation of the annual impounding scheme of TGR, raising up the reservoir initial water level under the premise of ensuring the safety of flood control according to the real-time progress and inflow forecast. The full storage rate of TGR could be increased and the contradiction between reservoir water storage and water supply in the downstream area will be relieved.

6. ACKNOWLEDGEMENTS

This paper has been checked by our corporation and is allowed to be published in the conference.

REFERENCES

- [1] Yangtze Water Resources Committee (1992), *Preliminary Design Report of TGP*.
- [2] Zhou Man & Xu Tao(2014). *Hydropower Generation Journal: Analysis of Multi-goal Optimized Operation of TGP and Its Comprehensive Benefits*, Volume 33, Issue 3, 55-60.
- [3] Xu Jijun(2013). *Research on Essential Technical Issues of Joint Operation of Large-scale Hydropower Station Cluster on the upstream Catchment of the Yangtze River, China Three Gorges, Volume 9, Issue 3,51-56*.

SUMMARY

A large number of reservoirs with large storage capacity have been constructed in Upper reaches of Yangtze River. These reservoirs impound from August to October annually, and store large amounts of water. Thus the Inflow of Three Gorges Reservoir decrease in September and October. In this paper, we analyzed the runoff characteristics of upstream of Yangtze River and the runoff sources of Yichang hydrological station. Then we selected 2017 level year and prospective level year, simulated the runoff of the hydrological station in the upper Yangtze river, and analyzed impact of Upper Yangtze cascade reservoirs operation on Three Gorges Reservoir in impoundment period. The results show that the runoff of tributary and Yichang hydrological station decrease significantly, especially in dry years. Meanwhile, with the increase of the number of upstream reservoirs, the impact increases gradually. We calculated the proportion of the water storage of upper Yangtze cascade reservoirs in impoundment period of Three Gorges Reservoir. The results can be used to optimize the measures of reservoir operation, such as the use of the flood resources at end of flood period and the initial control water level of impoundment.

KEY WORDS

RESERVOIR OPERATION;RESERVOIR CAPACITY;FLOOD STORAGE;THREE GORGES RESERVOIR

COMMISSION INTERNATIONALE DES GRANDS BARRAGES

VINGT-SIXIÈME CONGRÈS DES GRANDS BARRAGES

Autriche, juillet 2018

DOI 10.3217/978-3-85125-620-8-014



This work licensed under a Creative Commons Attribution 4.0 International License.
<https://creativecommons.org/licenses/by-nc-nd/4.0/>

**STUDY ON THE INFLUENCE OF CLIMATE CHANGE ON THE THREE GORGES
RESERVOIR AND ITS COUNTERMEASURES**

Wang FANGFANG

CHINA THREE GORGES CORPORATION, YICHANG

CHINA

Bao ZHENGFENG

CHINA THREE GORGES CORPORATION, YICHANG

CHINA

STUDY ON THE INFLUENCE OF CLIMATE CHANGE ON THE THREE GORGES RESERVOIR AND ITS COUNTERMEASURES

WANG FANGFANG

BAO ZHENGFENG

China Three Gorges Corporation, Yichang, China

CHINA

1. INTRODUCTION

The TGP reservoir is the key project in the Yangtze River basin, with the benefits of flood control, power generation, navigation, water supply etc.. As an important part of the flood control system in the Yangtze River basin and power supply station for power grid security, the TGP reservoir plays an important role in the economic development of the Yangtze River basin and the whole China.

As a critical backbone project for the control of the Yangtze River and harnessing of its water resources, the TGP reservoir is located at Sandouping of Yichang, Hubei Province with a controlled area of $1 \times 10^6 \text{ km}^2$, a normal water level of 175m and an accommodation capacity of 16,500 million m^3 . The project has experienced the stages from the preliminary design, the initial operation to the formal operation. It stored water level to 135m in June 2003 and hence entered the period of power generation. In 2008, the TGP reservoir started 175m experimental storage 5 years ahead of schedule, and firstly stored water level to 175m in 2010. Few years later the reservoir entered the formal operation period in 2016.

The climate change definitely cause the change of precipitation in the basin, which indirectly affects the total runoff and its annual distribution in this area. Corresponding to the obvious change of precipitation in the upper reaches of Yangtze River, the inflow of the TGP reservoir has also been affected, which shows that the inflow has a decreasing trend in the total year, while in the annual distribution, it increased in the dry period and decreased in the flood season and the storage period.

To sum up, with the climate change in the upper reaches of Yangtze River, the hydrologic characteristics of inflow series of the TGP reservoir have changed to a certain extent. It's necessary to make quantitative analysis on the impact of climate change, and deeply research the change regular of precipitation and runoff, and put forward countermeasures from technical aspect and management aspect, to guide the TGP reservoir to give full play to its comprehensive benefits more effectively.

2. THE ORIGINAL DESIGN DISPATCHING RULE OF THE TGP RESERVOIR

The original dispatching rule of the TGP reservoir is designed with the demand in flood control, power generation, shipping, water replenishment etc., based on the historical precipitation characteristics and conditions of water and sediment in the basin. The design scheduling methods in these periods are as follows:

(1) Dispatching rule in flood season

The reservoir is operated at the flood control limit level of 145m during the flood season. In the premise of ensuring dam safety, the flood control compensation in the TGP reservoir improves the flood resistance standard of Jingjiang dike.

(2) Dispatching rule in storage period

The reservoir stores water in the storage period, during which the minimum discharge is not lower than the corresponding flow for smooth downstream shipping, the water level will gradually increase to normal level till the end of October.

(3) Dispatching rule in falling period

The TGP reservoir gradually drops the water level and carries out water supply, drought resistance, shipping and ecological water replenishment for the downstream in falling period. The outflow in the falling period is not less than the guaranteed power output and the corresponding flow of lowest water level for navigable in the downstream. The water level is gradually dropped to limit water level to make preparation for flood season.

3. CLIMATE CHANGE IN THE UPPER REACHES OF YANGTZE RIVER

The mainly influence of climate change on human life is the change of rainfall and temperature. This paper analyzes the climate change in the upper reaches of Yangtze River according to the change of precipitation and temperature, based on 1963~2017 annual climate data.

(1) Precipitation

The annual average precipitation in the basin has been decreasing since 60s. It was more than average value before 80s and less than average after that, and the drop rate is about 17.4mm/10a. As to the annual distribution, it shows that the rainfall has a decreasing trend in spring, autumn and winter, while the precipitation in summer is increasing due to the strong rainfall.

(2) Days and intensity of rainfall

The average annual precipitation days (rainfall more than 0.1mm as a rainy day) in the upper reaches of Yangtze River ranged from 132 to 171 days, showing a decline trend with a rate of 2.9d/10a($\alpha=0.001$). However, it shows that the average daily precipitation intensity is increasing, which increases the probability of flood.

(3) Days and intensity of rainstorm

The average annual rainstorm days (rainfall more than 50mm as a rainstorm day) ranged from 13 to 30 days, showing a slight upward trend. Also, the rainstorm intensity is increasing. The average intensity of rainstorm is greater than the annual value after 80s, and mainly concentrated in the flood season, increasing the probability of rainstorm.

(4) Temperature

The annual average temperature in the Yangtze River basin is on the rise, with an average increase of about 0.14°C every 10 years. The upward trend in the northwest

of basin is more obvious because of its special geological conditions and altitude characters. It is predicted that the overall temperature of the basin is on the rise in the next 50 years under the background of greenhouse gas emissions, and the increase of temperature is about 0.25 ~ 0.41 /10a.

(5) Extreme weather events

The characteristics of extreme precipitation events are demonstrated by spatial distribution and intensity analysis of extreme precipitation events and continuous drought events.

1) Extreme precipitation

The daily maximum precipitation has reached more than 300mm in 2 stations, which are located in the middle of the basin, while the precipitation in most areas is between about 100 mm~300mm. The distribution of the maximum 3-day precipitation was similar to the daily one. Furthermore, the maximum consecutive precipitation time has reached more than 40 days in 5 stations in the southeast area of the basin.

2) Extreme drought

Continuous drought events had occurred more than 10 times in 14 stations in 55 years in the upstream of TGP, and occurred most in Qingshui river(20times), followed by Zunyi(14 times), while the events occurred 3~9 times in other areas.

4. THE INFLUENCE OF CLIMATE CHANGE ON THE TGP RESERVOIR

The influence of climate change on the operation of the TGP reservoir is manifested in two aspects: on the one hand, the change of precipitation and temperature which are caused by climate change, leads to the runoff change and the inflow variation. On the other hand, climate change causes extreme weather and special hydrological events, proposing higher requirements in the emergency dispatching. Therefore, it is necessary to analyze the variation characteristics of inflow and sum up the new requirements for the dispatching in extreme events, so as to lay a foundation for the optimization of the reservoir operation rule in the new environment.

4.1. RUNOFF CHANGE IN THE TGP RESERVOIR

Through analyzing the change trend of annual average inflow in the TGP reservoir based on 1963~2017 years' data, it shows that the overall annual runoff has a downward trend. After comparing the runoff in the trend fitting line, it is found that the measured runoff before 80s is more than the average value, and less than average after that (Fig.1).

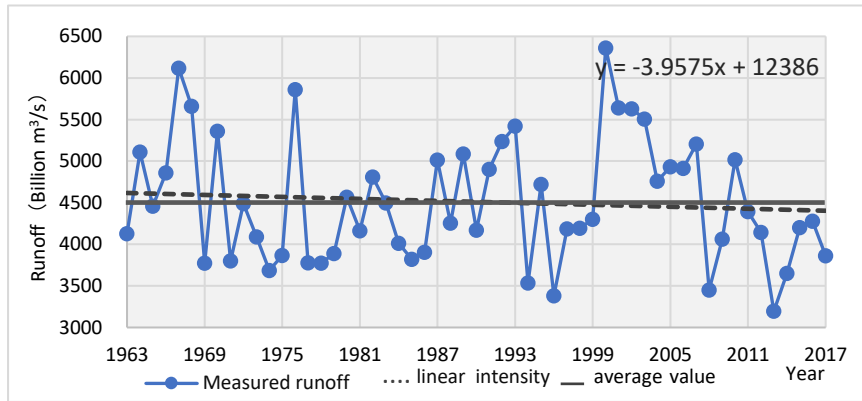


Fig. 1
Annual runoff variation in YiChang Station

The monthly inflow is compared with the time line in 2003, when the TGP reservoir began to store water (Fig.2). According to the figure, it can be seen that the average monthly inflow in the TGP reservoir after 2003 is much less than that before 2003. As to the monthly distribution, it shows that it is slightly more than that before 2003s from January to April in recent years, while the inflow from June to December decreased in varying degrees, and mainly decreased from August to November, when the runoff decreased by 3638 m³/s and 6747 m³/s respectively. It is known that the formation of runoff in flood season and storage period is mostly derived from precipitation, except little runoff in storage period are affected by the discharge from reservoir group in upstream, which can be ignored compared with the influence of the precipitation in storage period.

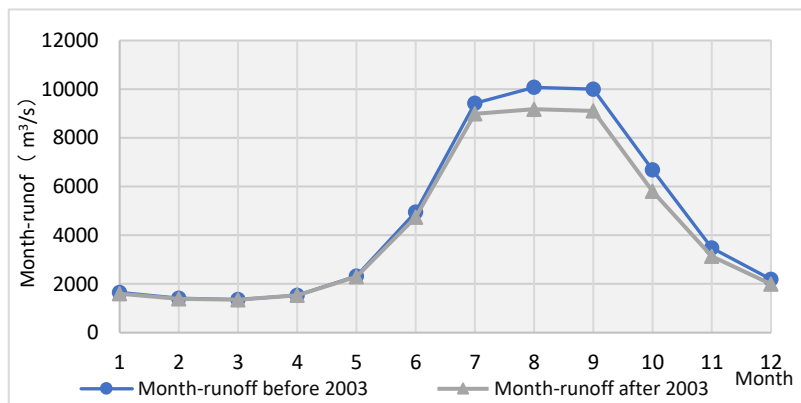


Fig. 2
Monthly runoff before and after 2003 in Yichang station

In the background of runoff decreased, if the TGP reservoir is still operated in the flood limit water level in the flood season, the flood will be almost completely abandoned and unable to be effectively used. From the analysis above, the inflow in the water storage period is obviously decreasing, causing the water for storage is not enough. Therefore, if the reservoir still be operated by the original rule and doesn't store water until October, it will be difficult to fill up the reservoir and the demand for water supply in the lower reaches in dry period will be hard to be guaranteed.

4.2. INCREASES OF EXTREME DROUGHT AND FLOOD

Through summing up the reservoir inflow in recent years, it shows that the extreme dry event occurred 3 times and the extreme precipitation event occurred 1 time in less than 5 years,

(1) In the late September and early October in 2013, the precipitation in the upper reaches of TGP reservoir reduced 30% and 73% respectively compared with the same period in history. In the flood season in 2015, the runoff in the overall upper reaches of Yangtze River are less than 34% and 38% respectively over the average annual runoff in history. The extreme drought occurs again in 2016, the inflow of the TGP reservoir in the early-September is only 11700 m³/s, ranking the least in the data series.

(2) The strong flood occurred in non-flood season in 2017. The heavy rainfall from October 2nd to 4th ranked second in the historical strong flood series. Affected by this, the inflow of the TGP reservoir freshened the maximum record in the same period in history.

Under the same prediction accuracy range, the extreme runoff can increase the forecast flow error which is proportional to the size of flood or drought. Frequent extreme drought and flood bring difficulties to forecast work. With the increase of unforeseeable degree in the forecast dispatching, the flood control operation in super flood will be at greater risk, and the difficulty of water storage work will be increased.

4.3. THE DEMAND IN EMERGENCY SCHEDULING IN THE MID-LOWER REACHES OF THE YANGTZE RIVER

Frequent extreme weather events also has different influence in the middle and lower reaches of the Yangtze River, and mainly manifested in the disaster caused by severe convective weather and extreme strong rainfall. Through the analysis of extreme weather events in the middle and lower reaches of the Yangtze River, this paper demonstrates that the extreme weather events bring great challenges to the coordination of flood control and water storage work, and put forward higher requirements for emergency operation.

During the May in 2011, the precipitation in the middle and lower reaches of the Yangtze River decreased 50% compared with the same period of many years, resulting in the worst drought in 60 years. The water level of some lakes dropped even close to the dead water level. The TGP reservoir increased the discharge by 10000m³/s to ease the drought.

In the flood season in 2015, the tornadoes occurred in the middle and lower reaches of the Yangtze River, resulting in the overturn of "Star of the East". The discharge in the TGP reservoir is gradually reduced by 10000m³/s in 3 hours, and helped to rescue the capsized ship in time.

In 2016, after the heavy sustained precipitation in the middle and lower reaches of the Yangtze River, the water level in the downstream of Yangtze River are almost all over the warning level. In the same period in 2017, the heavy storm occurred again in the middle and lower reaches of the Yangtze River, the water level in some tributary stations have reached the highest in history. The TGP reservoir intercepted water and reduced flood peak timely and effective control of danger.

The cities in the middle and lower reaches of the Yangtze River bear the backbone power of the national economic development. As the key project in the Yangtze River Basin, the emergency assistance of the TGP reservoir plays a crucial role in the city's normal development and the handling of the events. Due to the wide range of the middle and lower reaches of the Yangtze River and the rapid development of the cities along the basin, there are more and more emergencies and hidden dangers, posing higher requirements in the reservoir's emergency dispatching.

5. RESEARCH ON THE COUNTERMEASURES

In view of the influence of climate change on the dispatching of the TGP reservoir, the countermeasures are put forward from the technical and management aspects. Due to the runoff changed in the new climate environment, it is necessary to research on the optimal dispatching mode technically to match with the new runoff conditions. On the other hand, the frequent occurrence of extreme events raises requirements for the emergency response capacity. It is urgent to establish a complete emergency management system and strengthen the reservoir's emergency management ability.

5.1. OPTIMAL SCHEDULING METHOD BASED ON HYDROLOGICAL FORECAST

The change of climate has an adverse effects on the reservoir inflow, which is mainly manifested in inflow decreased in flood season and storage period. Precise flood forecast is an important prerequisite for reservoir operation. Therefore, this paper optimizes the operation mode of the TGP Reservoir during these periods, to ensure the comprehensive benefits such as flood control, shipping, power generation, water supply and ecological environment protection etc..

(1) Utilization of flood resources in flood season

According to the trend that the runoff decreased in flood season and the improved hydrological forecast technology, the TGP reservoir changes the flood control method, and tries to take full use of flood resources rather than defending flood singly. Through the proactively management of flood, realizing the flood resource utilization under the risk controllable. It regulates small-mid-flood by using the limited storage capacity, combines with the short-mid-term hydrological forecast, and give full play to the benefits of the water head with level elevation. In addition, according to the runoff forecasting in late flood season, the reservoir balances flood control and water storage with the method that it intercepts the flood in late flood season to pre-storage with predicted abandoned water, and creates favorable conditions for the water storage after the flood season.

Since the mid-July in 2017, it sustained high temperatures and little rain. According to the inflow forecast, the TGP reservoir reduced the discharge by 3000 m³/s and raised the water level by small and medium flood. It orderly takes the benefit of water head to guarantee the demand of big peak shaving in dry summer.

(2) Optimization of water storage in late flood season

Due to the decrease of natural runoff and the increase of water demand in the downstream in storage period, the full storage ratio of the TGP reservoir with design dispatching mode is low, greatly affecting the navigation and ecological water guarantee during the dry water period. The TGP reservoir optimizes the storage process by moving up the storage time, rising the origin storage level and controlling the water level dynamically combined with the hydrological forecast.

Firstly, the trend of water volume in the storage period is judged according to the long-term prediction, and the water storage scheme can be initially proposed. Also, the impounding strategy is constantly rolling and correcting according to the short-term prediction with high accuracy in the later, is concrete is: when the inflow forecast shows low, storing water in advance appropriately and making full use of the water in late flood season. If the forecast shows low continuity in the storage period, raising the water level in stages in this period, and the water level should be raised in different degrees according to the runoff reduction degree in the forecast. That is to say, the reservoir is regulated with separated methods in wet year, dry year and extreme-dry year ,and the water level in control nodes in the storage period are gradually raised on the basis of the design dispatching regulation, to ensure the completion of water storage tasks at different runoff levels.

Based on the optimization strategies above, the TGP reservoir improves the operation mode with storing water in advance properly and raising the water level in stages according to the runoff forecast. The TGP reservoir has successfully stored to 175m for eight years since 2010(Fig.3). Under the implementation of this optimization method, the TGP reservoir combines the flood control and water storage work. Flood resources in late flood season are fully utilized. The water level elevation in September can increase the water storage capacity, effectively ensuring the reservoir's full filled. Also, the reduced demand for water storage in October can greatly alleviate the impact of water storage on the downstream.

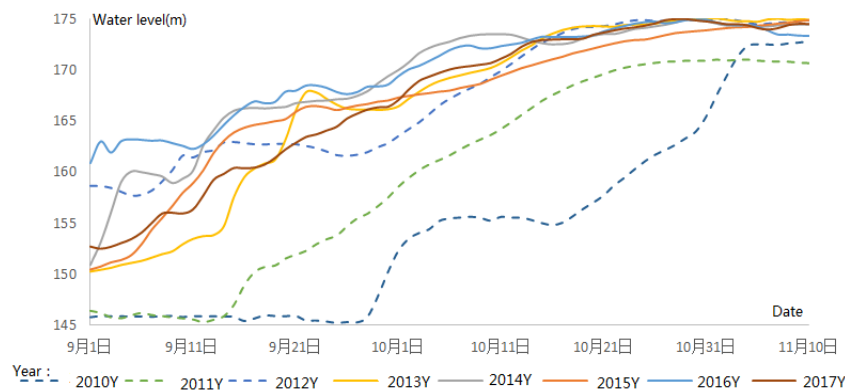


Fig. 3
The storage process of the TGP reservoir from 2010 to 2017

5.2. EMERGENCY DISPATCH MANAGEMENT SYSTEM

As a backbone project in the Yangtze River basin, the TGP reservoir has made many breakthroughs and contributions for emergency assistance. For instance, it

increased power generation to cope with the electricity demand under the ice and snow disaster in 2008. It supplemented freshwater to repulse saline water in dry season in 2014, and rescued the “Star of the East”, who is overthrown by a tornado in 2015. Also, it carried out compensation regulation in flood control for the lower reaches of Yangtze River in 2016 and 2017. With these rich experiences in emergency dispatching, the TGP reservoir has gradually formed a complete emergency response system.

In the emergency dispatching, the TGP reservoir takes the protection of social benefits as the goal, and minimizes the loss with systematic and efficient management method. The main measures are as follow, the reservoir management organization has established a coordination system with flood control department, shipping department, land resources office and other departments, and share the information with each other;

Also, enhancing operation situation analysis and premeditated simulation of accident, to prepare the emergent schemes in advance; Thirdly, building the emergency management system: Distributing the responsibility according to the event types, and forms a complete emergency command mechanism; Also, responding to events in a hierarchical manner, clear the workflow with conferences at different levels, to find the solution to deal with emergency events efficiently. In order to further improve the emergency system, it records the event and summarizes the experience after solving the problem.

Through the emergency dispatching for special events, the TGP reservoir improves its ability to deal with emergencies and brings remarkable social benefits. Also, in the cooperation of public activities, its political and public welfare value is highlighted.

6. SUMMARY AND PROSPECT

This paper focuses on the analysis of reduced precipitation, which is caused by climate change. In view of this, it put forward the optimization scheduling method: utilization of flood resources in later flood season and water level elevation in stages in water storage period based on the hydrological forecast, and the modified scheduling strategy are proved effective and applicable by practice. Furthermore, it sums up the TGP Reservoir’s emergency management measures for disaster events caused by extreme weather, and demonstrates the positive significance of the emergency dispatching system.

Meanwhile, with the construction of the reservoirs in upstream and the accumulation of reservoir operation experience, the accuracy of runoff prediction can be improved based on the information sharing in the basin, so as to coordinate the operation and optimize the storage and discharge structure in reservoir groups. But the operation time of the reservoir in upper reaches is relatively short and the operation experience is not very enough. The joint operation of large reservoir groups in climate change environment needs further study and the optimization potential needs further exploring in the future, so as to better cope with the climate change and greatly play the role of overall coordination in the Yangtze River basin.

ACKNOWLEDGEMENTS

This paper has been checked by our corporation and is allowed to be published in the meeting.

COMMISSION INTERNATIONALE DES GRANDS BARRAGES

VINGT-SIXIÈME CONGRÈS DES GRANDS BARRAGES
Autriche, juillet 2018

DOI 10.3217/978-3-85125-620-8-015



This work licensed under a Creative Commons Attribution 4.0 International License. <https://creativecommons.org/licenses/by-nc-nd/4.0/>

**A CHANGING FLOW REGIME IN CENTRAL GERMANY: MAGNITUDES,
CAUSES AND EFFECTS ON RESERVOIR MANAGEMENT**

Markus MÖLLER

Chief Hydrologist, THÜRINGER FERNWASSERVERSORGUNG, ERFURT

GERMANY

COMMISSION INTERNATIONALE
DES GRANDS BARRAGES

VINGT-SIXIÈME CONGRÈS DES
GRANDS BARRAGES

Autriche, juillet 2018

**A CHANGING FLOW REGIME IN CENTRAL GERMANY: MAGNITUDES,
CAUSES AND EFFECTS ON RESERVOIR MANAGEMENT***

Markus MÖLLER

Chief Hydrologist, THÜRINGER FERNWASSERVERSORGUNG, ERFURT

GERMANY

1. INTRODUCTION

The Harz (10.2 – 11.5 degr. East and 51.5 – 52.0 degr. North) is the main water tower in central Germany. Because of its freshwater endowment, the Harz mountains water resources have been developed since the 16th century to support the mining industry and since the late 19th century for public water supply. Today, nine multi-purpose dams located in the Harz are providing high quality raw water for public water supply. Based on these reservoirs, water treatment and long-distance water transfer schemes have been developed in the 20th century, comprising a total of 1250 km of mains pipe serving more than 3 million people and numerous industries in the five states of Lower-Saxony, Saxony-Anhalt, Saxony, Thuringia and the City State of Bremen. Neustadt dam – a stone masonry dam (H = 33.4 m; L = 127.0 m) – is the Southernmost and smallest of these nine dams and is fulfilling its water supply function since 1905. At present, all safely available water (1.3 MCM) from the dams reservoir is committed in a raw water supply contract and the buyer – the local water company WVN – has requested

* *CHANGEMENT DU REGIME HYDROLOGIQUE EN ALLEMAGNE CENTRALE:
MAGNITUDE, CAUSES ET EFFETS SUR L'EXPLOITATION DU RESERVOIR*

the dam owner and operator Thüringer Fernwasserversorgung to increase water withdrawal in the future. On the other hand, with an already fully committed water budget, any long-term or sudden changes in the dam's inflow regime would have a direct impact on safe yield. Safe yield water withdrawal is constricted by the precipitation and runoff regime of the 5.32 km² catchment area and the total available storage volume of 1.24 MCM. When updating the long-term operational plan of the dam, the owner/operator carried out an analysis of the water balance using historic records. The following questions were guiding the analysis:

- Did significant changes of meteorological parameters and runoff occur in the last 100 years?
- Were these changes gradual or sudden?
- What are the implications for dam operations and which mitigating measures could be put in place?

2. MATERIALS AND METHODS

The location of the dam site and surrounding area is given in Figure 1. Temperature data were taken from Braunlage and Artern met stations (data source: DWD). Precipitation records were taken from three nearby stations (see Figure 1).



Fig. 1.

Location of Neustadt dam and the location of measurements. Artern met station (not depicted) is located 37 km southeast off the dam site

A proxy for the onset and duration of the vegetative season, during which active transpiration does occur, was estimated as the temperature sum above the

5°C threshold. This method (GDD) by Ernst and Loeper is widely used in German agriculture. The commencement of the growing season is set at a daily mean temperature sum of $GDD=200^{\circ}K$ and the annual temperature sum is a proxy for duration and intensity of the growing season. Vegetative development was analysed at Herrmannsacker phenological station, where the day of year (DOY) of the onset of the pine sprouting is being recorded since 1965 (data: DWD).

Flow data is being recorded at the dams inflow gauging station Neustadt 1/Krebsbach ($A_E = 2.96 \text{ km}^2$, records 1912 - 2016, 1 gap year). Furthermore, the state-run stream gauging stations at Ilfeld/Bere ($A_E = 62.5 \text{ km}^2$, 1952 - 2015) and Ellrich/Zorge ($A_E = 42.1 \text{ km}^2$, 1970 - 2015) were also analysed (data: TLUG). All data series were analysed for long-term trends using the package „Trend“, implemented in the R software [1]. Since several studies have indicated that climate and phenological changes might occur suddenly rather than as a long-term gradual trend [2], [3], such a test was also carried out with all long-term data, using the package „Kendall“ in R.

3. RESULTS AND DISCUSSION

3.1. AIR TEMPERATURE AND GROWING SEASON

Recorded annual temperature sums above the 5°C-threshold ($\Sigma GDD_{5^{\circ}C}$) at both Braunlage and Artern meteorological stations showed no clear trend in the first half of the data series, but a steady and significant increase from the late 1980ies onwards (Figure 2). A highly significant breakpoint ($p < 0.0001$) was

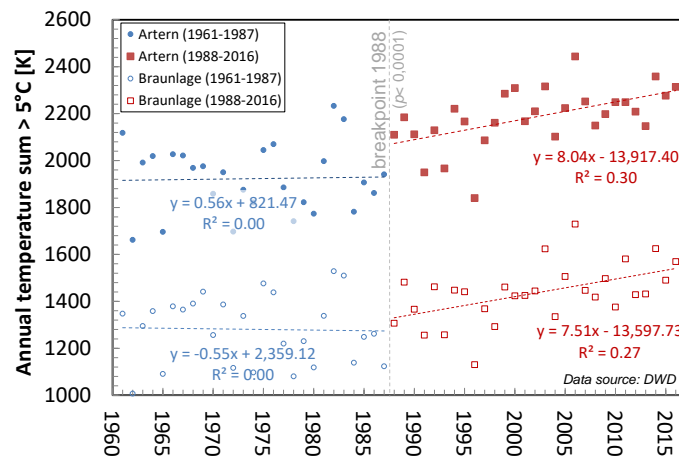


Fig. 2

Annual temperature sum > 5°C at Artern und Braunlage met stations

identified in 1987/88, which is in line with earlier studies in Europe [4]. The day of year (DOY) at which the sum of mean daily temperature had reached the 200°K

mark has moved forward by 17 and 12 days at Artern and Braunlage, respectively, when comparing the 1988-2016 with the 1961-1987 sub-periods. At Herrmannsacker, beginning of pine tree sprouting has been advancing at a rate of 6 days per decade, or with a sudden shift of two and a half weeks starting in the late 1980ies (Figure 3). These results can be directly transferred to the catchment area of Neustadt dam, which has a forest cover of 96 %.

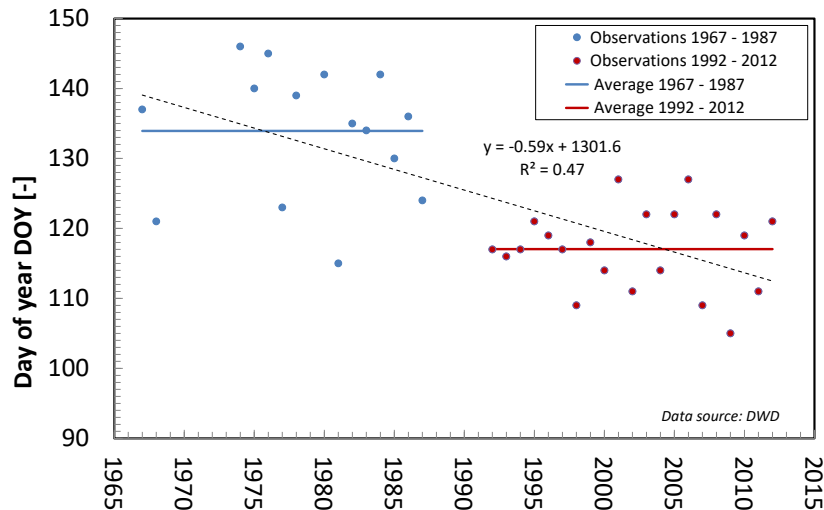


Fig. 3

Trend and breakpoint of the observed commencement of pine tree sprouting (*Picea abies*) at Herrmannsacker

3.2. PRECIPITATION

Precipitation is a key determinant of catchment runoff. At Harztor-Ilfeld-Hufhaus gauging station seasonal long-term trends (1916 - 2016) were weak and statistically not significant, showing small increases in the winter (Nov-Apr) and small decreases during the summer (May-Oct), as shown in Figure 4. Monthly trends for the entire record and sub-periods thereof are given in Table 1 for three precipitation gauging stations in the Southern Harz region. Two of the three stations showed significant linear increases in winter precipitation over the 101 year record length. Comparing annual precipitation for the 1961-1987 and 1988-2016 period revealed a small but significant increase during the latter period for two out of the three stations. A comparison of individual months prior to and after the 1987/88 breakpoint revealed significant decreases in April and June at all stations and, while July, September and October and to some extent also January and February stood out with particularly large increases.

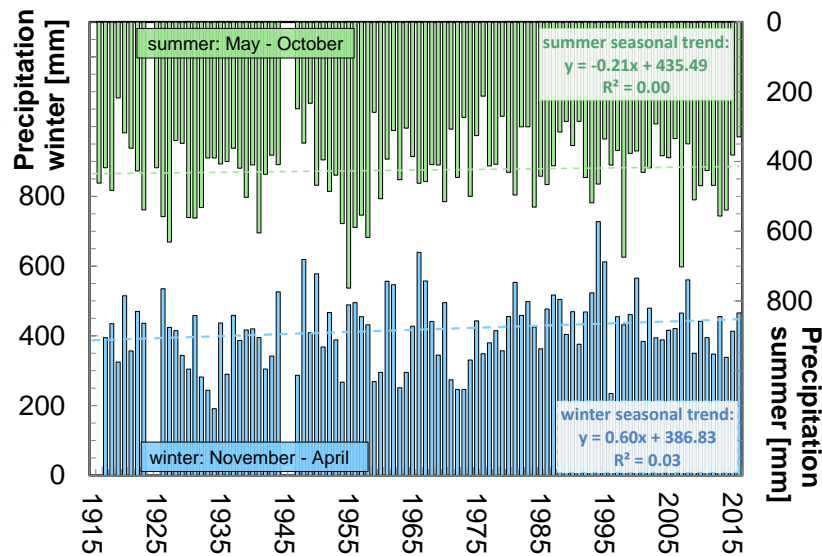


Fig. 4

Precipitation sums at Harztor-Ilfeld-Hufhaus 2,4 km Northwest of Neustadt dam.
Data source: DWD

Table 1

Monthly and seasonal precipitation amounts at gauging stations Harztor-Ilfeld-Hufhaus (3 gap years, GY), Südharz-Hayn (1 GY) and Oberharz-Sorge (3 GY).
Data source: DWD

Station Harztor-Hufhaus	Nov	Dec	Jan	Feb	Mar	Apr	May	Jun	Jul	Aug	Sep	Oct	Wi	Su	Year
Mean 1916-2016 [mm]	74	84	82	61	61	57	65	71	80	76	63	68	419	424	843
Trend 1916-2016 [mm a ⁻¹]	0.2	0.2	0.0	0.0	0.3	-0.1	0.1	0.0	0.0	-0.2	0.1	-0.2	0.4	-0.2	0.1
Breakpoint in year	1938	1976	1980	1934	1938	1986	1949	1993	1957	1970	1983	1942	1979	1958	1991
Mean 1988-2016 [mm]	83	93	82	66	72	48.4	67	64	84	66	73	67	447	420	867
Change from 1988 [%]	17	16	1	13	28	-19	4	-15	6	-17	22	-2	9.7	-1	4
Mean 1961-1987 [mm]	74	84	75	56	65	64.3	71	79	63	70	56	56	420	394	814
Change from 1988 [%]	13	11	10	17	12	-25	-5	-19	33	-6	30	21	6	7	6
Trend 1988-2016 [mm a ⁻¹]	-0.3	-1.1	1.2	-1.5	-1.8	0.19	2.5	-0.4	1.2	0.8	-0.1	0.8	-2.6	3.8	-0.2
Station Südharz-Hayn	Nov	Dec	Jan	Feb	Mar	Apr	May	Jun	Jul	Aug	Sep	Oct	Wi	Su	Year
Mean 1916-2016 [mm]	61	69	66	53	51	52	59	66	70	69	53	56	352	372	725
Trend 1916-2016 [mm a ⁻¹]	0.1	0.2	0.1	0.1	0.3	-0.2	0.2	0.0	0.0	0.0	0.2	-0.1	0.4	0.0	0.4
Breakpoint in year	1938	1953	1980	1932	1954	1973	1947	1991	1963	1970	1992	1942	1936	1974	1991
Mean 1988-2016 [mm]	66	76	69	58	61	44	63	57	72	62	64	55	373	371	747
Change from 1988 [%]	9.7	16	4.98	14	29	-19.9	9	-18	3	-13	33	-2	9	-1	4
Mean 1961-1987 [mm]	63	70	59	48	56	58	63	77	59	63	45	46	359	353	712
Change from 1988 [%]	4	8	16	22	8	-24	0	-26	22	-1	43	19	4	5	4.9
Trend 1988-2016 [mm a ⁻¹]	-0.3	-0.3	1.0	-1.0	-1.1	0.0	1.8	-0.1	0.9	0.0	0.8	0.4	-1.0	3.6	2.7
Station Oberharz-Sorge	Nov	Dec	Jan	Feb	Mar	Apr	May	Jun	Jul	Aug	Sep	Oct	Wi	Su	Year
Mean 1918-2016 [mm]	95	103	104	79	75	66	70	75	86	77	69	78	524	455	980
Trend 1918-2016 [mm a ⁻¹]	0.2	0.5	0.3	0.2	0.5	-0.2	0.2	0.1	0.0	-0.1	0.1	0.0	1.5	0.0	1.5
Breakpoint in year	1962	1953	1980	1987	1965	1986	1992	1950	1967	1970	1992	1942	1979	1992	1991
Mean 1988-2016 [mm]	101	122	120	95	96	56.9	76	67	88	76	75	84	591	466	1057
Change from 1988 [%]	9	28	23	32	47	-19	12	-14	3	-2	14	12	19.6	4	12
Mean 1961-1987 [mm]	102	105	90	65	78	69	71	92	69	69	62	70	510	433	943
Change from 1988 [%]	-1	16	33	46	23	-18	7	-27	27	9.8	21	21	16	8	12
Trend 1988-2016 [mm a ⁻¹]	0.6	0.0	2.0	-0.4	-1.7	0.5	2.1	0.0	1.1	0.5	0.5	0.3	2.0	3.3	5.8

Level of significance of trends and breakpoints: $p > 0,1$ (standard); $p < 0,1$ (*italic*); $p < 0,05$ (**bold**); $p < 0,01$ (**bold italic**)
Color code of changes [%] from 1988: <-30 >-30 >-20 >-10 >-5 >5 >10 >20 >30

3.3. RUNOFF AND RESERVOIR INFLOW

The time series of 105 years streamflow data at Neustadt 1 did show a small but insignificant decrease of seasonal and annual runoff (Table 2), a finding that is in line with observed trends in the Western Harz mountains [5]. At Ilfeld and Ellrich gauging stations, the decreases in summer runoff were significant and at Ellrich, even the decreasing annual runoff trend was statistically significant.

Table 2
Monthly and seasonal runoff totals at stream gauging stations Neustadt 1 (1 GY), Ilfeld (0 GY) and Ellrich (0 GY). Data source: TLUG

<i>Neustadt 1/Krebsbach</i>	Nov	Dec	Jan	Feb	Mar	Apr	May	Jun	Jul	Aug	Sep	Oct	Wi	Su	Year
Mean 1912-2016 [MCM]	0.1	0.2	0.2	0.2	0.2	0.2	0.1	0.1	0.0	0.0	0.0	0.1	1.0	0.3	1.4
Trend 1912-2016 [Tm ³ a ⁻¹]	0.0	0.1	-0.4	-0.2	0.1	-0.5	-0.2	0.0	-0.1	-0.1	0.0	-0.1	-1.5	-0.7	-2.2
Breakpoint in year	1995	1954	1938	1928	2010	1988	1987	1990	1988	1988	1994	1989	1995	1987	1988
Mean 1988-2016 [MCM]	0.1	0.15	0.21	0.16	0.21	0.13	0.07	0.04	0.03	0.02	0.03	0.05	0.97	0.23	1.2
Change after 1988 [%]	-7	-3	1	-6	3	-39	-33	-39	-47	-55	-31	-18	-8	-36	-15
Trend 1988-2016 [Tm ³ a ⁻¹]	-0.7	-2.2	-0.4	-0.6	-7.0	-1.3	0.4	-0.1	0.0	-0.1	-0.2	-0.1	-12	-0.3	-14
<i>Ilfeld/Beere</i>	Nov	Dec	Jan	Feb	Mar	Apr	May	Jun	Jul	Aug	Sep	Oct	Wi	Su	Year
Mean 1952-2015 [MCM]	2.1	3.8	4.5	3.4	4.6	3.9	1.7	1.3	1.0	0.7	0.7	1.2	22	7	29
Trend 1952-2015 [Tm ³ a ⁻¹]	1	1	32	8	8	-23	-4	-8	-7	-7	-3	-3	2	-68	-51
Breakpoint in year	1977	1977	1973	1979	1977	1988	1987	1988	1988	1987	1958	1958	1977	1987	1995
Mean 1988-2015 [MCM]	2.26	3.57	5.0	3.55	4.9	2.85	1.37	0.78	0.62	0.43	0.66	1.08	22	4.95	27.1
Change after 1988 [%]	11	-10	25	10	14	-39	-28	-54	-50	-51	-14	-20	0	-37	-9.6
Trend 1988-2015 [Tm ³ a ⁻¹]	-14	-47	4	-24	-124	-15	16	-2	-4	4	2	0.5	-150	7	-157
<i>Ellrich/Zorge</i>	Nov	Dec	Jan	Feb	Mar	Apr	May	Jun	Jul	Aug	Sep	Oct	Wi	Su	Year
Mean 1970-2015 [MCM]	2.2	3.1	3.8	2.6	3.5	2.7	1.4	1.1	0.8	0.7	0.7	1.2	18	6	24
Trend 1970-2015 [Tm ³ a ⁻¹]	-9	-4	7	-4	-21	-57	-16	-21	-10	-7	-4	-8.5	-128	-77	-248
Breakpoint in year	1997	1998	1980	2003	2008	1995	1986	1987	1988	1988	1993	2000	2000	1986	2000
Mean 1988-2015 [MCM]	2.19	2.92	3.8	2.62	3.51	1.95	1.13	0.68	0.53	0.51	0.68	1.1	17	4.58	21.6
Change after 1988 [%]	0	-13	2	4.9	0	-51	-35	-58	-58	-44	-15	-28	-12	-41	-20
Trend 1988-2015 [Tm ³ a ⁻¹]	-42	-79	-40	-50	-161	-77	-3	-1	-5	-2	-9	-7	-437	-35	-600

Level of significance of trends and breakpoints: $p > 0,1$ (standard); $p < 0,1$ (*italic*); $p < 0,05$ (**bold**); $p < 0,01$ (**bold italic**)
Color codes of changes [%] after 1988:

<-50	>-50	>-40	>-30	>-20	>-10	>-5	>5	>10	>20	>30
------	------	------	------	------	------	-----	----	-----	-----	-----

However, the latter stations record started in 1970 rather than the Neustadt 1911 commencement date, hinting that record length might have impacted the results in some way. The observed long-term changes in seasonal and annual runoff at all three gauging cannot be explained by the long-term trends in precipitation, thus indicating that runoff changes were influenced by other processes. Looking at individual months, we find that at the dams inflow stream gauge Neustadt 1, nine out of twelve months registered significant decreases following the 1987/88 breakpoint (Figure 5). While streamflow in individual months decreased by 50 % or more, seasonal summer inflow decrease was a staggering 36 %, a finding well confirmed at the other two nearby gauging stations of Ilfeld and Ellrich as well as findings in the Eastern part of lower Saxony [6]. Average annual reservoir inflow at Neustadt dam had decreased from 2.56 MCM (1912-1987) to 2.15 MCM (1988-2016). During the 1988-2016 sub-period, March had replaced April as the month with the highest mean runoff as compared to preceding

sub-period ending in 1987, hinting at an earlier and smaller snowpack-melt, which is well in line with the temperature records presented above. However, the statistically significant decrease in March runoff during the most recent period (1988-2016) at two out of the three gauging stations seems to indicate that the runoff shift towards the start of the year is still ongoing (Table 2).

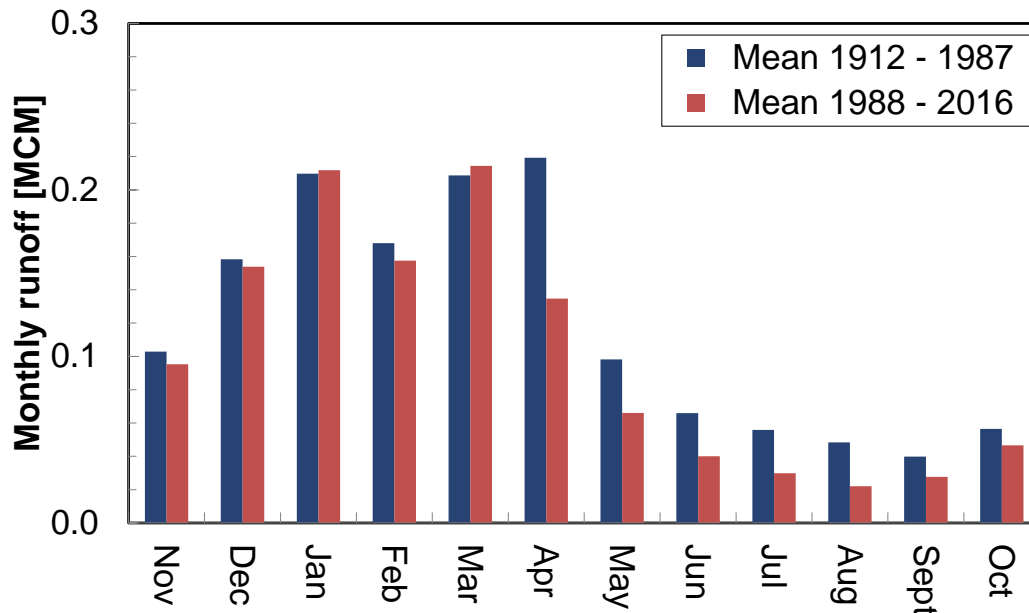


Fig. 5

Changes in mean monthly runoff at Neustadt 1 streamflow gauging station after the 1988 breakpoint

3.4. IMPLICATIONS FOR RESERVOIR MANAGEMENT AND POSSIBLE REMEDIES

With climate projections for the coming decades all pointing towards a strengthening of the trends observed in the last three decades, the dam operators working hypothesis at this point is, that the current changes in runoff regimes are likely to continue into the foreseeable future. This hypothesis must be verified periodically by rigid statistical analyses of measured data. However, there is a residual risk that sudden shifts and breakpoints will only be recognizable in hindsight, when the subsequent time period is long enough, i.e. at least 10 years.

The seasonal partitioning of reservoir inflow flow (winter/summer), as a percentage of mean annual inflow, shifted from a 26/74 ratio during 1912-1987 to a 19/81 ratio after the 1987/88 breakpoint. This increased seasonality and variability has a diminishing effect on safe raw water withdrawals from the reservoir, as has been shown in [7]. Keeping with the current raw water withdrawal RWW_{365} of $3650 \text{ m}^3 \text{ d}^{-1}$ would in turn mean decreasing reliabilities of supply RoS once mean inflow decreases and becomes more variable. Hence it is

recommended to always include RoS in raw water delivery contracts, thus making sure that the residual risk of water deficit periods is well understood and agreed upon in advance.

As these trends and shifts will continue to impact flow volumes and variability in the future, societal demands towards infrastructure, i.e. dams, fulfilling an increased buffering function in the hydrological cycle are also likely to increase. Since some of these dam functions and requirements are contrarian to each other, e.g. flood protection and drinking water supply, it can be expected that dam and reservoir management will become more challenging in the coming decades. Water industry experts are therefore required to plan and prepare possible remedies and solutions well in advance.

At Neustadt dam, one remedial measure includes the calibration and operation of a mid-term reservoir management model (MBM), which helps the operator in determining beginning and duration of hydrological surplus periods, based on current and modelled inflow and actual storage content, during which raw water withdrawals can safely be increased beyond RWW_{365} without compromising RoS [7]. In the future, this model could also be expanded by a module accounting for the water volume occasionally stored in the water catchments snowpack during the winter.

Alternatively, one could consider increasing storage capacity from currently 0.48 of mean annual flow to a higher level. Compared to new dam construction, the incremental costs of dam heightening are usually considered smaller. Nevertheless this approach requires careful economic and hydrologic analysis. It must also be pointed out that it does not solve the problem of decreasing inflows per se but merely increases the useable percentage of that flow.

An alternative solution includes increasing mean annual reservoir inflow by means of a 5.6 km long gravity transfer tunnel tapping into neighbouring streams at higher altitude than the reservoirs full supply level. An initial survey has revealed that the catchment area could thus be tripled. A geological, hydrological and economic scoping study for this investment is scheduled for 2018.

4. CONCLUSIONS

This investigation revealed clear signs of a changing meteorology, hydrology and phenology in the Southern region of one of Germany's most important water towers. The breakpoint identified in 1987/88 and the sudden shifts associated with it are particularly noteworthy. It contradicts the notion that these changes do manifest themselves in a gradual and linear fashion. The evidence suggests an increased duration and intensity of the vegetation season. In the absence of significant aquifers in the catchment area, the considerable decreases in reservoir inflow observed in the last three decades have most likely been caused by increased actual evapotranspiration. Which portion of the increased evapotranspiration has been caused by modified forest management and decreased forest damage due to improved air quality has not been a subject of this

study and can thus not be safely determined at this point. Diminishing reservoir inflow certainly has a negative impact on safe yield, especially if all safe withdrawal is already committed in an existing water delivery contract. The two most prominent adaptation strategies pursued by the dam owner/operator include close monitoring and modelling of the reservoirs short- and long-term water balance combined with exploring additional infrastructural investments aimed at increasing the catchment area and thus reservoir inflow.

REFERENCES

- [1] R DEVELOPMENT CORE TEAM. R: A language and environment for statistical computing. R Foundation for Statistical Computing, Vienna, Austria.
- [2] CHIAUDANI A., BERTI, A., BORIN M., MARIANI L. Piecewise and Strucchange: Test of two methods of changepoint analysis in agroclimatology. COST ACTION 734, 6th Management Committee Meeting and Symposium on Climate Change and Variability - AgroMeteorological Monitoring and Coping Strategies for Agriculture. June 4-6, 2008, Oscarsborg (Norway).
- [3] CHMIELEWSKI F., MÜLLER A., BRUNS E. Climate changes and trends in phenology of fruit trees and field crops in Germany. *Agricultural and Forest Meteorology*, 2004, Vol. 121: 69-78.
- [4] MARIANI L., PARISI S.G., COLA G., FAILLA O. The late 80s breakpoint of European climate and the consequent changes in the spatial distribution of relevant crops. Paper presented at the 16th Italian Congress of Agrometeorology, held 4th-6th June 2013 in Florence, Italy. Online article at: http://agrometeorologia.it/documenti/AIAM2013/93-94_Mariani.pdf
- [5] EGGELSMANN F., Lange A. Wasserwirtschaft im Westharz. Hydrologische Untersuchungen mit Blick auf ein sich veränderndes Klima. 2010. Publication of Harzwasserwerke, Hildesheim.
- [6] FANGMANN A., BELLI A., HABERLANDT U. Trends in streamflow observation series in Lower Saxony. (main text in German). *Hydrologie und Wasserbewirtschaftung*, 2013, Vol. 57-5: p. 196-205.
MÖLLER M., HABERLANDT U., WILLMITZER H., THIELE W. Optimizing reservoir management of the intensively used Neustadt water supply dam. Contribution tot he 85th Annual Meeting of the International Commission on Large Dams, held in Prague, Czech Republic, July 3-7, 2017.

SUMMARY

The Harz is the main water tower in central Germany and its water resources have been developed since the 16th century to support the mining industry and since the 19th century for public water supply. Today, nine multi-purpose dams in the Harz provide high quality raw water for public water supply. Neustadt dam is the Southernmost and smallest of these nine dams and is fulfilling its water supply function since 1905. At present, all safely available water is committed in a raw water supply contract and the buyer – a local water company – has requested to increase the water withdrawal in the future. On the other hand, with a fully committed water balance, any long-term or sudden changes in the dam's inflow regime would have a direct negative impact on safe water withdrawal. In this paper, long-term records from the dam's inflow gauging station, two nearby stream gauges, two met stations, three rain gauges and a phenological station were analysed for any shifts or changes. The investigation revealed significant changes in the flow regime. Firstly, starting in the late 1980s, monthly maximum reservoir inflow shifted from April towards the beginning of the year. Secondly, mean summer runoff had decreased by 35 %, and in some months by up to 55 % in the last 30 years. A breakpoint analysis revealed 1987/88 as a statistically highly significant point in time when these changes occurred, this finding was independently confirmed by data from two nearby gauging stations. The observed changes in the flow regime could not be explained by precipitation data at the site, which showed neither any significant trends nor any breakpoints. This implies a change in the partitioning of precipitation into runoff, evapotranspiration and groundwater recharge. Because of the geological characteristics of the catchment area, both groundwater recharge and subsurface runoff are negligible. The working hypothesis is that a shift of runoff volume towards evapotranspiration has occurred after the 1987/88 breakpoint. This hypothesis is supported by the direct link between measured increases in air temperature and potential evapotranspiration. Furthermore, phenological observations and seasonal temperature sums provide clear evidence of an earlier onset and longer duration of the vegetation season at the site. Going forward, it is expected that future trends and sudden shifts of meteorological and hydrological parameters will potentially increase the demand and expectations of society on dams and their buffering role in the hydrological cycle. However, some of these functions and purposes are contrarian to each other, hence dam management will potentially become more challenging. Finally, several remedial adaptation strategies for dam operators with a fully committed water balance are discussed in general and the two approaches towards increasing safe water withdrawal from Neustadt dam are briefly outlined.

KEY-WORDS - ENGLISH

CLIMATE, HYDROLOGY, FLOW, RESERVOIR OPERATION

MOTS-CLES - FRANCAIS

CLIMAT, HYDROLOGIE, FLOW, EXPLOITATION DU RESERVOIR

COMMISSION INTERNATIONALE DES GRANDS BARRAGES

VINGT-SIXIÈME CONGRÈS DES GRANDS BARRAGES

Autriche, juillet 2018

DOI 10.3217/978-3-85125-620-8-016



This work licensed under a Creative Commons Attribution 4.0 International License. <https://creativecommons.org/licenses/by-nc-nd/4.0/>

**STUDY ON RISK ANALYSIS FOR FLOOD PREVENTION AND DAM SAFETY
BASED ON STOCHASTIC SIMULATION**

Jie GAO

*Senior Engineer of CHINA RENEWABLE ENERGY ENGINEERING INSTITUTE
Master supervisor of CHINA THREE GORGES UNIVERSITY*

CHINA

COMMISSION INTERNATIONALE
DES GRANDS BARRAGES

VINGT-SIXIÈME CONGRÈS DES
GRANDS BARRAGES
Autriche, juillet 2018

STUDY ON RISK ANALYSIS FOR FLOOD PREVENTION AND DAM SAFETY BASED ON STOCHASTIC SIMULATION*

Jie GAO

*Senior Engineer of China Renewable Energy Engineering Institute
Master supervisor of China Three Gorges University*

CHINA

Abstract: Based on stochastic simulation of inflow flood for cascade reservoirs, the P-III distribution of flood peaks, flood regulation and reservoir operation were taken into account. The probabilities of flood overtopping, stage exceeding several critical levels were calculated based on a great number of stochastic samples. Refer to study on acceptable risk analysis, considering climate change, taking four cascade reservoirs as a case study, the procedure of assessment for risk analysis of flood control and dam safety were proposed.

Key words: flood control; hydrology; safety of dams; Risk analysis; risk analysis for dam safety; flood control and dam safety; overtopping risk analysis

1. INTRODUCTION

Public security is closely related to project safety. Both researchers and engineers focus on the analysis, assessment and criterion of project risk. The

* This work is funded by Power Construction Corporation of China (DJ-ZDZX-2016-02)

acceptable risk level frequently serves for decision-making after balancing the cost against benefits from that risk. ALAPR (As low as reasonably practicable) is a widely used acceptable risk criterion which involves unacceptably high risk, generally acceptable risk and negligible risk [1]. The acceptable risk level lies between unacceptably high risk region and generally acceptable risk region, which determines the feasibility. HSE (The Health and Safety Executive) proposed that risk of existing infrastructure is annual fatality risk of 10^{-4} [2]. Concerned with the acceptable risk of dam safety, USBR (United States Bureau of Reclamation) and ANCOLD (Australian National Committee on Large Dams) suggested 10^{-2} and 10^{-3} fatalities/person/year for each dam failure event respectively, while BC Hydro presented the acceptable life and economic risk associated with each dam failure is of 10^{-3} fatalities/person/year and US\$7120/year respectively [3].

Risk depends on probability of failure and loss of hazard. The loss varies with time and place, is closely related to the development of local economy and society, while failure probability can be approached by statistics and simulations. In this article, we focus on dam failure probability. According to analysis on different dam failure modes, flood related problems including flood exceeding control criterion and spillway failure both leading to erosion damage on dams and bank joint, which accounts for one third of overall dam failure events. The dam in United States which were built after 1950s with a height more than 30m is of a failure probability in the range of $1.3 \times 10^{-3} \sim 3.0 \times 10^{-3}$. It indicates [4] the dam failure caused by flood related problems is in the range of $0.43 \times 10^{-3} \sim 1.0 \times 10^{-3}$. Yang et al [4] considered $10^{-3} \sim 10^{-4}$ on the lower side of criterion for dam safety and flood control. Regardless of flood regulation, Xu [5] provided 10^{-5} as risk probability of spillway for high dam. As the technology of design, construction and management for dams and reservoirs improved, dam failure events reduced. In China, from 1990 to 2011, there were 278 dam failed in the overall approximately 98000 dams [6]. It offered a dam failure probability of 2.84×10^{-4} and deduced that probability of flood related risk is 9.47×10^{-5} .

The probability of flood related problems could be attained by numerical simulation as well as statistics. Xu [7] attributed flood-related risk to large flood and failure of spillway, and applied JC method to risk calculation. The P-III and normal distribution were used to describe the uncertainty of flood inflow and initial stage respectively, while triangle and normal distribution were applied to describe the uncertainty of spillways capacity. Based on stochastic simulation approach, Mei et al [8] took both hydrological and hydraulic uncertainty into account, used seasonal AR(1) models to generate a great number of reservoir inflow. The results revealed that flood-related hydrological uncertainty plays the major role in risk analysis compared with any other factors.

Based on stochastic simulation, we researched in the view of: (1) dam safety itself, (2) flood control capability of dam and, (3) flood control for downstream regions provided by dam. The case study is 4 built cascade reservoirs in the Jinsha River, China. Based on statistical parameters obtained from observed 49-year flood peak series of 3 hydrological stations in the study area, climate change is studied and stochastic simulation is adopted to reflect the uncertainty of flood inflow. The calculation and procedure will contribute to

conduct flood related risk analysis for dam safety.

2. METHOD

2.1. STATISTICAL PARAMETERS OF OBSERVATION

According to the drainage characteristic of study area, the representative hydrological stations are selected. Annual maximum discharge in several-year time series are collected and following a P-III frequency distribution curve. The average of annual flood peak (EX), coefficient of variation (Cv) and skewness (Cs) are derived from the fitted P-III frequency curve.

2.2. STOCHASTIC SIMULATION FOR FLOOD PEAKS IN REPRESENTATIVE HYDROLOGICAL STATION

Considering changes in landscape and climate which may lead to nonstationary hydrological regimes, GAMLSS (Generalized Additive Models for Location, Scale, and Shape) model^[10] is introduced to provide a flexible modeling framework for flood peaks and to reveal the trend of flood peaks observed in hydrological stations. For a stationary hydrological series, according to the EX , Cv and Cs deduced in 2.1, followed the sampling method of P-III distribution^[9], a great number of flood peaks for representative hydrological station are generated.

2.3. RESULTS FOR CASCADE RESERVOIRS

According to hydrological analogy method and typical hydrograph, the inflow flood hydrographs for each reservoir are acquired.

2.4. FLOOD REGULATION

Based on water balance principle and regulation requirements, adopted storage-capacity relation of reservoir and stage-discharge relation of spillway, applied trial and error method, the outflow and maximum stage corresponding to each inflow flood are calculated. Therefore, considering the uncertainty of flood inflow, the probability of different stages for each reservoir can be identified.

3. CASE STUDY

Based on the abundant water power resources and mountainous topography in middle reach of the Jinsha River, China, four concrete gravity dams(A, B, C, D) were built for the development and utilization of hydropower resources. The four dams lie among three hydrological stations: Shigu, Jinjiangjie and Panzhihua, making a series of cascade reservoirs. According to feasibility studies, the four dams are all scale first-grade first-class projects with check standard for flood control equals to 5000-year return period.

3.1. PARAMETERS OF REPRESENTATIVE HYDROLOGICAL STATION

Annual flood peaks recorded in the 3 representative hydrological stations during 1957 and 2005 [11] are gained by P-III distribution curve fitting which deduces the best-fitting EX, Cv and Cs for each hydrological station. Results are shown in Table 1.

Table 1
Parameters of curve fitting

Hydrological station	Parameters			Flood peak in different frequency($m^3 \cdot s^{-1}$)		
	EX	Cv	Cs/Cv	0.01%	0.02%	0.2%
Shigu	5140	0.29	4	14600	13900	11500
Jinjiangjie	6710	0.31	4	20200	19200	15800
Panzhihua	7360	0.31	4	22200	21100	17300

3.2. STOCHASTIC SIMULATIONS FOR REPRESENTATIVE HYDROLOGICAL STATION

3.2.1 Climate change

In consideration of climate change, GAMLSS^[12,13] is used to identify the optimum flood distribution^[14], reveals whether time series is stationary or not.

Firstly, three probability distribution functions (PDF) are selected, namely:

- (1)Gumbel distribution
- (2)two parameter LogNormal(LN2)
- (3)two parameter Pearson Type II (P2), Gamma distribution

Secondly, time trend is assumed in the first two moments (the mean value and the standard deviation):

- (1) trends in the mean value (A)
- (2) trends in the standard deviation (B)

Thirdly, three time-trend function are included:

- (1) Stationary, not varied with time (S)
- (2) linear form of a trend (L)
- (3) parabolic form (P)

The Akaike Information Criterion (AIC) is applied to identify the optimum model, which possesses the minimum AIC value.

$$AIC = -2 \ln ML + 2k \quad [1]$$

Where, ML denotes the maximum likelihood, k is the number of fitted parameters.

The results for curve fitting of flood peak at Shigu, Jinjiangjie and Panzihua hydrological stations are as follows^[15]:

Table1 AIC value of Gumbel, Lognormal and Gamma distribution for flood peaks at Shigu, Jinjiangjie and Panzihua hydrological stations

model	Gumbel	LogNo	Gamma	Gumbel	LogNo	Gamma	Gumbel	LogNo	Gamma
	AIC value of Shigu station			AIC value of Jinjiangjie station			AIC value of Panzihua station		
ASBS	<i>930.56</i>	<i>917.18</i>	<i>917.27</i>	<i>910.64</i>	<i>896.04</i>	<i>895.42</i>	900.82	883.69	883.73
ALBS	932.51	919.17	919.27	912.64	897.63	897.08	902.81	885.53	885.53
APBS	933.08	918.53	918.92	912.44	898.02	897.15	<i>900.60</i>	<i>881.19</i>	<i>881.59</i>
ASBL	932.21	919.14	919.24	912.04	898.02	897.34	901.65	885.40	885.65
ALBL	934.20	921.11	921.22	913.72	899.54	898.90	903.25	887.36	887.52
APBL	935.08	920.52	920.90	912.83	899.35	898.33	901.15	883.15	883.42
ASBP	934.14	921.02	920.98	913.87	899.26	899.03	903.48	887.35	887.39
ALBP	936.14	923.01	922.98	915.66	901.18	900.81	904.92	889.25	888.99
APBP	936.72	922.15	922.40	914.83	901.07	900.22	902.90	884.44	884.68

The results indicate that the best curve fitting for flood peaks of Shigu, Jinjiangjie and Panzihua stations are stationary LogNormal, stationary Gamma distribution and nonstationary Lognormal distribution with linear trend of mean value and stationary standard deviation.

The 1st to 3rd reservoirs are located between Shigu and Jinjiangjie. Meanwhile, the 4th reservoir lies between Jinjiangjie and Panzihua, it is much

closer to Jinjiangjie than that to Panzhihua. In the view of watershed scale, the nonstationary impact on flood peak series is not taken into account in this article, and the conventional sampling method for P-III distribution are employed.

3.2.2 Sampling method

(1) Parameters for sampling

$$a_1 = EX \times \left(1 - \frac{2C_v}{C_s}\right) \quad [2]$$

$$a_2 = \frac{2}{EX \times C_v \times C_s} \quad [3]$$

$$a_3 = \frac{4}{C_s^2} \quad [4]$$

$$p = a_3 - n, \text{ where, } n \text{ is an integer and } 0 < p < 1 \quad [5]$$

(2) Three uniform random number $u_1, u_2,$ and u_3 in $[0, 1]$ are generated.

$$(3) a_4 = -\sum_{i=1}^n \ln u_i \quad [6]$$

(4) Three uniform random number $u_{n+1}, u_{n+2},$ and u_{n+3} in $[0, 1]$ are generated.

$$(5) s_1 = u_{n+1}^{\frac{1}{p}}, s_2 = u_{n+2}^{\frac{1}{1-p}} \quad [7]$$

(6) if $s_1 + s_2 \leq 1$,

$$\text{then } t = \frac{s_1}{s_1 + s_2}, x = -t \times \ln u_{n+3}, z' = x + a_4, z = \frac{z'}{a_2} + a_1 \quad [8]$$

Thus, z is a random variable following P-III distribution.

Else if, $s_1 + s_2 > 1$, then return to (4).

40000 samples are generated following the program mentioned above and should be undertaken hypothesis testing to confirm the results.

3.3. FLOOD INFLOW FOR EACH RESERVOIR

The 1st, 2nd and 3rd cascade reservoirs were located between the 1st and 2nd hydrological station, while the 4th reservoir lies between the 2nd and 3rd hydrological station (see Fig 1). Flood peaks of the four cascade reservoirs are calculated by hydrological analogy method based on 40000 flood peak samples of the three hydrological stations and drainage area ratios.

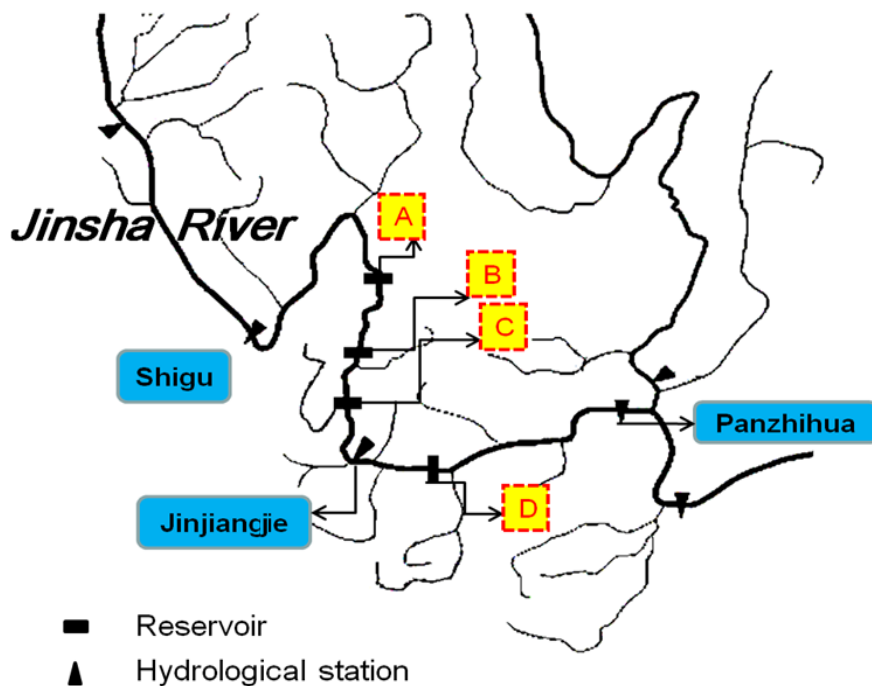


Figure 1 Location of cascade reservoirs and hydrological stations

Among the three hydrological stations, the 2nd hydrological station is the nearest one to all the four reservoirs. From total 49-year observations in 2nd hydrological station, the hydrograph with maximum flood peak and volume is abstracted as typical hydrograph which determine the shape of inflow flood and used to generate 40000 inflow flood processes into each reservoir.

3.4. FLOOD REGULATION AND PROBABILITY STATISTICS

Based on the 40000 inflow flood processes into each reservoir, according to relationships of stage versus capacity, stage versus discharge, following specific regulation, from a certain initial stage (such as normal storage level or full supply level or top level of flood control), 40000 maximum stages for every reservoir are calculated after flood regulation. The probabilities of not exceeding initial stage, exceeding stage of check flood level and overtopping are acquired.

4. RESULT AND ANALYSIS

4.1. RESULTS

The probabilities under several scenarios for each reservoir are calculated

based on 40000 stochastic simulations. The results are shown in Table 3.

Table 3
Probability under different scenario for cascade reservoirs

Reservoir	1st(A)	2nd(B)	3rd(C)	4th(D)
Maximum stage not exceeding the initial stage (top level of flood control or normal storage level)	0.99785	0.99775	0.999175	0.99745
Maximum stage exceeding stage of check criterion for flood control	7.5×10^{-5}	2.0×10^{-4}	5.0×10^{-5}	1.75×10^{-4}
Maximum stage overtopping	2.5×10^{-5}	0	0	5.0×10^{-5}

4.2. ANALYSIS

(1) In the view of dam safety itself, in flood season, dam failure is frequently caused by overtopping. The risk will be unacceptable, if risk probability of overtopping exceeds a certain threshold. According to the statistics of dam failure events between 1950s and 1990s caused by flood related overtopping issues, the threshold or acceptable risk probability will be 1.0×10^{-4} [4]. However, based on the statistics of data after 1990s [6], the critical value decreases to 9.47×10^{-5} that becoming stricter. In the case study, the risk probability of overtopping for 1st to 4th reservoirs are 2.5×10^{-5} , 0, 0, and 5.0×10^{-5} respectively, which are all below the threshold or acceptable risk probability for flood control and satisfy the demands for dam safety.

(2) In the view of flood control capability of dam, when flood of check standard occurs, the spillway works with designed maximum discharge to ensure that stage stops rising and not exceed check flood level. In the case study, the check standard of flood control for all the four reservoirs is with a return period of 5000 years, which means a probability of 2.0×10^{-4} . Based on the statistics of 40000 stochastic simulations, the probabilities of exceeding check flood level for 1st to 4th reservoirs are 7.5×10^{-5} , 2.0×10^{-4} , 5.0×10^{-5} , and 1.75×10^{-4} respectively, which doesn't exceed check standard and satisfy the requirements for flood control capability of dam.

(3) In the view of flood control for downstream regions protected by dam, during flood season, if water level of reservoir maintains lowering than the initial stage, the spillway works to perform flood regulation and reduce outflow comply with the safe and multipurpose requirements of downstream regions. In the case study, the probability not exceeding initial stage is approximately 99.75% for the four reservoirs, which indicates that when flood with a return period less than 400 years occurs, flood regulation works and makes the downstream regions safe and

efficient.

(4)The four reservoirs have similar project scale and flood control standard, and all meet the requirements for flood control. Actually, the procedure will be more applicable for earth and rock-fill dams rather than concrete dams. However, this procedure will contribute to establish a systematical risk assessment method for dam safety.

5. SUMMARY

Based on 40000 stochastic simulations of flood inflow for four reservoirs, the P-III distribution of inflow flood, flood regulation and reservoir operation are taken into account. The probabilities of flood overtopping, stage exceeding several critical levels are calculated based on the 40000 stochastic samples for each cascade. Refer to study on acceptable risk analysis, in the view of dam safety itself, flood control capability of dam and flood control for downstream regions protected by dam, the procedure of assessment for risk analysis of flood control and dam safety are proposed.

References

- [1] XIAO Y., GUO S. L., XIONG L. H., LUO Z. Research review on acceptable risk level for dam safety assessment. *Journal of Safety and Environment*. 2005,5(3): 90-94.(in Chinese)
- [2] DEFRA. *Flood and reservoir safety integration*. Final report. 2002.8.
- [3] SALMON G. M., HARTFORD D. N. D. Risk analysis for dam safety. *International water power and dam construction*. 1995, 47(3): 42-47; 1995, 47(4): 38-39.
- [4] YANG B. Y., WANG R. C., AN Z. G. Risk analysis of flood relief of single reservoir. *Hydrology*. 1999,4: 5-12. (in Chinese)
- [5] XU Z. X., GUO Z. Z. Reliability study on schemes of spillway layout for Ertan hydropower station. *SHUILI XUEBAO*. 1990(3): 48-52. (in Chinese)
- [6] ZHOU X. B., ZHOU J. P., DU X. H., WANG Y. J., LI S. Y. Study on risk acceptance criteria for dams in China. *Journal of hydroelectric engineering*. 2015,34(1):63-72. (in Chinese)
- [7] XU Z. X., GUO Z. Z. Risk calculation for flood releasing of open spillway. *SHUILI XUEBAO*. 1989(4): 51-54. (in Chinese)
- [8] MEI Y. D., TAN G. M. Risk analysis for flood prevention and safety of dam. *Engineering Journal of Wuhan University*. 2002,35(6): 11-15. (in Chinese)
- [9] CHEN Y. F. *Method and application of statistical experiment*. Heilongjiang People's Publishing House: 2000: 46. (in Chinese)
- [10] VILLARINI G., SMITH A. J., SERINALDI F., BALES J., BATES D. P., Witold

- F. K. Flood frequency analysis for nonstationary annual peak records in an urban drainage basin. *Advances in Water Resources*. 2009,32: 1255-1266.
- [11] GAO J. Analysis on flood safety of cascade reservoir based on design flood. *Water power*.2016,42(9): 93-98.(in Chinese)
- [12] STASINOPOULOS D. M., RIGBY R. A. Generalized Additive Models for Location Scale and Shape (GAMLSS) in R. *Journal of Statistical Software*. 2007,23(7): 1-46.
- [13] STASINOPOULOS M., RIGBY B., VOUDOURIS V., HELLER G., FERNANDA D. B. Flexible Regression and Smoothing the GAMLSS packages in R. 2015,7,23.
- [14] STRUPCZEWSKI W. G., FELUCH W. W. System of identification of an optimum flood frequency model with time dependent parameters(IDT). *Integrated approach to environmental data management systems*. Edited by Nilgum B. Harmancioglu, M. Necdet Alpaslan, Sevinc D. Ozkul and Vijay P. Singh. Springer Netherlands,1997. 31: 291-300.
- [15] YE C. Q., CHEN X. H., ZHANG J. M., ZHANG L. J., ZHU A. P. Comparative study on non-stationary flood frequency analysis in different backgrounds of changing environment. *Journal of hydroelectric engineering*. 2014, 33(3): 1-9.(in Chinese)
- [16] FAN Z. W., JIANG S. H. Application of tolerance risk analysis method in decision-making of flood prevention. *SHUILI XUEBAO*. 2005,36(5): 618-623. (in Chinese)

COMMISSION INTERNATIONALE
DES GRANDS BARRAGES

VINGT-SIXIÈME CONGRÈS DES
GRANDS BARRAGES
AUTRICHE, JUILLET 2018

EROSION AND SEDIMENTATION OF UPSTREAM ASAHAN AND ITS COUNTERMEASURES FOR THE SUSTAINABILITY OF SIRUAR DAM NORTH SUMATERA

Muhammad L. CHAKIM¹⁾ Sugik E. SARTONO²⁾

*¹⁾Head of Development Area and Asset Optimization Division, JASA TIRTA I
PUBLIC CORPORATION*

²⁾Chief of Technical Planning Unit, JASA TIRTA I PUBLIC CORPORATION

INDONESIA

1. INTRODUCTION

Asahan River becomes the main source of water flow for Siruar, Siguragura and Tangga Dam. The Siruar dam serves to regulate the stability of the water coming out of Lake Toba to the Asahan River and to supply water to the power station constantly to the Asahan hydroelectric power plant (Asahan I, Siguragura and Tangga power plant). This type of dam is a mass concrete with a height of 39 meters.

Since the changes of land use in the most Asahan catchment area, erosion and sedimentation became problem for the Siruar Dam especially for the operation of Asahan I hydroelectric power plant. Jasa Tirta I as state own enterprise which has authority to manage water resources in Toba Asahan River Basin (given by Government with Presidential Decree No. 2/2014) conducted comprehensive study to identify the rate and sources of sedimentation and the countermeasures as well in 2016 - 2017.

2. DATA COLLECTING METHOD

The primary data taken by topographic survey, bathymetry and also sediment sampling along 14.5 km of upstream Asahan and 5 km of its tributaries which are Bolon and Mandosi River, and water sampling for quality test. In order to get deeper analysis, secondary data also collected through government institutions such as statistical agency, planning and development agency, geophysics and meteorology agency, ministry of public works and ministry of forestry.

3. ANALYSIS AND RESULTS

The study identified that the sediment rate per year is 20.25 ton/ha. The grain sediment analysis also showed that 50% of sediment which settles in river bed is sand. The sources of the sediment were from the lake and from Asahan tributaries which are Bolon and Mandosi river. From the water quality analysis, chlorine has significant parameter for the Asahan water. Asahan River, of which a major part is used by the people around Toba Samosir Regency, is utilized as a place for washing, bathing, industry, and agricultural activity runoff.

THE COUNTERMEASURES OF SEDIMENTATION

Based on the Technical Plans for Rehabilitation of Forest and Land Asahan Barumun Water Catchment Area 2015–2029 by Ministry of Forestry, targets of erosion control in the study area are established to be at least equivalent to the target of erosion control in the Toba Asahan watershed.

Table 1
Proposed Program for Sediment Countermeasure (data processing 2017)

Indicator	Natural Condition	Existing Condition	Target of Sediment Control by Ministry of Forestry	Proposed Target of Study	Projection
The erosion hazard level → light and very light	78,3 %	63%	>50%	>70%	72,8%
Sediment rate per year	11,5 ton/ha	20,25 ton/ha	<20 ton/ha	<15 ton/ha	14,7 ton/ha
Gully plugs = 300 units Check dams = 10 units Strip Vegetation = 160 ha Reforestation = 13.074 ha					

Another approach for sediment control management is dredging works. The analysis showed that dredging works have to be done regularly with estimate volume of 21.000 m³ in order to maintain sedimentation.

4. CONCLUSION

The objective of this study is to identify the rate and sources of sedimentation at Upstream Asahan and the countermeasures as well in order to ensure the sustainability of Siruar Dam and Asahan hydroelectric power plant. From the analysis, the rate of sedimentation reached 20.25 ton/ha/year and 50% which settled in river bed was sand. Changes of land use has important role to speed up the sediment rate, therefore conservation of land, reforestation and civil conservation approach such as check dams, gully plugs have to be done. Another technical approach to maintain deposit sediment in the river is dredging works. The study recommends for regular dredging with estimate volume of 21.000 m³ sediment per year.

COMMISSION INTERNATIONALE DES GRANDS BARRAGES

VINGT-SIXIÈME CONGRÈS DES GRANDS BARRAGES
Autriche, juillet 2018

DOI 10.3217/978-3-85125-620-8-018



This work licensed under a Creative Commons Attribution 4.0 International License. <https://creativecommons.org/licenses/by-nc-nd/4.0/>

**EVALUATION OF SEDIMENT MANAGEMENT EFFECTIVENESS TO EXTEND
THE WLINGI RESERVOIR LIFETIME**

Zainal ALIM

Head of Internal Control Unit, JASA TIRTA I PUBLIC CORPORATION

INDONESIA

COMMISSION INTERNATIONALE
DES GRANDS BARRAGES

VINGT-SIXIÈME CONGRÈS DES
GRANDS BARRAGES
Autriche, juillet 2018

EVALUATION OF SEDIMENT MANAGEMENT EFFECTIVENESS TO EXTEND THE WLINGI RESERVOIR LIFETIME

Zainal ALIM

Head of Internal Control Unit, JASA TIRTA I PUBLIC CORPORATION

INDONESIA

1. ABSTRACT

Wlingi Reservoir is one of the reservoirs in the Brantas River Basin management system. Besides as a flood control, this reservoir has an important role as a supplier of 2 x 27 MW of electrical and serves irrigation area of 15,132 Ha. The reservoir was completed in 1979 and has total storage capacity of 24 million m³, however due to severe sedimentation caused by Mt. Kelud eruption and critical catchment condition, by the year of 2016 its capacity decreased to only 2.55 million m³ or 10.63% of the initial capacity.

To extend the economic lifetime of the reservoir, many efforts have been undertaken, including some preventive activities through conservation in the upstream areas as well as some corrective measurements. Some corrective measurements that have been done are sedimentation dredging (through spoil bank disposal and riverine disposal) and sedimentation flushing. Based on technical and financial aspect, sedimentation flushing is considered more efficient than the other measurements. Based on the technical evaluation, sedimentation flushing can remove approx. 300,000 m³ to 1,2 million m³ sediment per year from reservoir, which is higher than the sedimentation dredging that only remove approx. 100,000 to 350,000 m³ per year. Based on the financial evaluation, sedimentation flushing can save the cost of Rp. 35.85 billion compared to dredging with spoil bank disposal, while dredging with riverine disposal to channel below can save about Rp. 14.96 billion compared to the dredging with spoil bank disposal. Another advantage of sedimentation flushing is the supply of

300,000 m³ up to 1.2 million m³ of sediment per year that may tackle the issue of riverbed degradation at the downstream part of the reservoir, which is currently the riverbed degradation is happened approx. 2 to 8 m caused by rapid illegal sand mining. However flushing implementation should consider the availability of water so it cannot be done every year.

Keywords: Wlingi Dam, flushing, dredging, sedimentation.

2. INTRODUCTION

Wlingi Dam was completed in 1977 with a total catchment area of 2,890 km², located in Blitar, East Java, Indonesia. It has gross reservoir capacity 24.0 million m³ and effective capacity 5.20 million m³. The dam was built as the after bay of Sutami Hydro Electric Power Plant (HEPP) and has benefits:

- Controlling flood discharge from 2,824 - 2,370 m³/sec.
- Providing water for irrigation 17,50 m³/s to Lodagung irrigation area of 15,132 Ha (in Blitar and Tulungagung).
- Generating HEPP with installed capacity 2 x 27 MW, producing energy 164.980 million KWh / year.
- Fisheries and tourism.

Due to its location in the downstream part of Kelud Volcano (one of the most active volcanoes in Java island), cause a huge sediment supply to the reservoir. Combined with land degradation in the upper area of its catchment, sedimentation become the main issue of water resources management in Wlingi dam. To overcome the above issues, some measurements has been conducted such as conservation, dredging, flushing, and preparing sabo dam and check dam in the upstream. Flushing and dredging with riverine disposal that hydraulically pumped the sediment into the downstream of the dam.

The purpose of the study is to know the effectiveness of the management sediment through flushing, dredging with spoil bank disposal, dredging with riverine disposal to channel below. Knowing the effectiveness of this sediment management is expected to increase the lifetime of the reservoir.

3. PROBLEM OF WLINGI DAM AND BRANTAS RIVER MANAGEMENT

SEDIMENTATION

The main problem in managing the reservoir is sedimentation. This problem is a fundamental problem that is almost experienced by all reservoirs in the world. Illegal logging, volcanic activity and land degradation (due to excessive land use exchange) are the main causes of sedimentation.

The Wlingi Reservoir, which was completed in 1979, has a sedimentation rate of 0.81 million m³ per year or 3.34% of reservoir per year, which the Sutami Reservoir, the largest reservoir in the same basin, has a sedimentation rate of 5.07 million m³ per year or 1, 47% of reservoir per year. From the data it appears that the sedimentation rate at Wlingi reservoir is 2.3 times the largest reservoir in the same river basin. The Wlingi Reservoir, built with an initial total storage capacity of approximately 24 million m³, now has only 4.42 million m³ or 18% of its initial storage capacity. This indicates that the sedimentation rate in Wlingi Reservoir is very large. The main cause is the influence of the eruption of Mount Kelud which is still active and is 40 km from Wlingi Reservoir. During the past century, Mount Kelud eruptions occurred in 1901, 1919, 1951, 1966, 1990 and 2014.

Table 1 Wlingi Reservoir Capacity

Years	Gross Storage		Effective Storage		Dead Storage	
	Volume (million m ³)	Percent (%)	Volume (million m ³)	Percent (%)	Volume (million m ³)	Percent (%)
1977	24.00	100.0	5.20	100.0	18.80	100.0
1982	18.32	76.3	NA	NA	NA	NA
1985	14.44	60.2	NA	NA	NA	NA
1988	9.50	39.6	NA	NA	NA	NA
Januari 1990	4.60	19.2	2,20	42.3	2.40	12.8
The eruption of Gn Kelud in February 1990						
Maret 1990	1.60	6.7	NA	NA	NA	NA
1991	4.77	19.9	2.34	45.0	2.43	12.9
1992	2.51	10.5	1.09	21.0	1.42	7.5
1993	1.98	8.3	1.21	23.3	0.77	4.1
1995	4.63	19.3	1.33	25.7	3.29	17.5
1995	4.94	20.6	1.59	30.6	3.35	17.8
1996	5.75	24.0	1.83	35.2	3.92	20.9
2001	3.97	16.6	2.11	40.7	1.86	9.9
2004	4.41	18.4	2.01	38.6	2.41	12.8
2006	4.00	16.7	2.02	38.9	1.98	10.5
2011	4.42	18.4	2.00	38.5	2.42	12.9

Note: 1) The volume reservoir between 1977 and 1996 was obtained from "The Brantas River Rehabilitation Project, Supporting Report 1, Evaluation of River Dredging Works for Wlingi and Lodoyo Reservoirs, December 1996" between 2001 and 2004 based on the HV curve prepared by PJT-1. 2) NA = Not Available. (Source: Jasa Tirta I Public Corporation)

Mount Kelud last eruption was happened in February 2014, but the last eruption has no significant impact on the Wlingi Reservoir. But the eruption of Mount Kelud in February 1990 had a very significant impact on the Wlingi Reservoir. Wlingi Reservoir is fully with sediment. Many efforts have been done as corrective measurements to increase reservoir capacity such as dredging and flushing. It can be recovered to 4.42 million m³ reservoir capacity or 18.4% of the initial capacity of 24.0 million m³.

Total volcanic eruption in 1990 (estimated by the Volcanic Directorate of the Department of Energy and Mineral Resources) was approx. 125 million m³, which 22.3 million m³ of it deposited at Wlingi Reservoir through the Lekso, Semut, Jari, Putih and Kali Abab rivers.

RIVER BED DEGRADATION

Wlingi Dam is located in Brantas River where upper reach occurs sedimentation, but in the middle and lower reach occurs river bed degradation. This degradation occurs due to illegal sand mining. Regularly controlled by the local government in cooperation with Jasa Tirta I Public Corporation, has not been able to reduce the number of people mining sand along Brantas River. The volume of sand mining conducted by 6,280 workers along Brantas River is 2,695,000 m³ / year with details as shown in the Table 2.

Table 2 Volume of Sand Mining Brantas River in 179 Location

Location (City)	Volume of Sand Mining (m ³ /year)			Number of Workers (person / day)
	Manual	Pump	Total	
Sidoarjo	42,500	-	42,500	150
Mojokerto	151,500	111,000	262,500	1,060
Jombang	822,600	168,200	990,800	3,220
Nganjuk	267,100	383,000	650,100	720
Kediri	200,800	135,700	336,500	510
Kediri city	47,900	182,800	230,700	220
Tulungagung	-	183,900	181,900	400
Total	1,532,400	1,164,600	2,695,000	6,280

As a result of excessive illegal sand mining leads to degradation of the river bed. The decrease in the riverbed ranges from 2 - 8 m below the initial river bed. Even at a certain point the river decline reaches 11 m in the area of KB 80. The following illustrates the long section of the river bed at Kali Brantas.

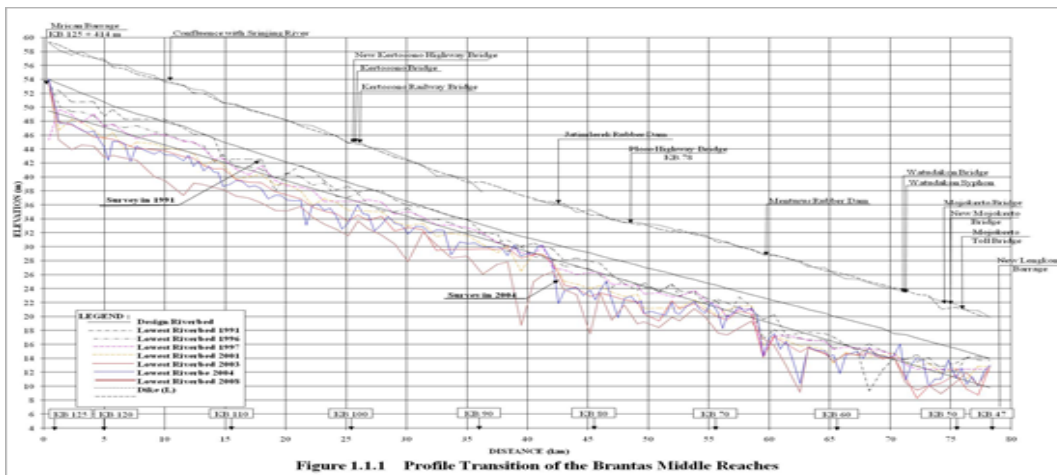


Fig. 1
Long Section of Brantas River

The extreme degradation of riverbed causes the destruction of infrastructure across the river such as the landslide of the embankment, the deformation of the bridge pier, and the decline of the water level which causes the difficulty of water supply for the beneficiaries.



Fig. 2
Damage of Deformation of Bridge Pier and Landslide of Embankment

4. SEDIMENT MANAGEMENT

FLUSHING IMPLEMENTATION

Rainfall, runoff, and river channel erosion provide a continuous supply of sediment that is hydraulically transported in rivers and streams. All reservoirs formed by dams on natural rivers are subject to some degree of sediment inflow and deposition. Because of the very low velocities in reservoirs, they tend to be very efficient sediment traps. Therefore, it is necessary to transfer sediment from reservoir to the downstream of the river. It is expected that flushing can keep the

sediment balance in a river. Flushing carried out at Wlingi Dam during the last 10 years is as in the following table:

Table 3 Flushing at Wlingi Dam

Year	Wlingi Reservoir M3)	Remaks
2008	395,480	
2009	145,514	
2010	561,192	
2011	351,625	
2012	426,481	
2013	269,514	
2014	No flushing	Limited inflow
2015	No flushing	Limited inflow
2016	1,026,500	
2017	787,330	

Source: Jasa Tirta I Public Corporation

Flushing implementation is done by gradually lowering the water level of the reservoir by operating the gate so that water can flow in free flow condition. After a while, the water level is raised again. In order for optimal results, if the discharge is sufficient, this process can be repeated until obtained the planned reservoir profile. Duration for flushing implementation is about 16 - 20 hours with a potential power loss is approx. 969,000 Kwh.

After the completion of flushing, measure of the reservoir profile to calculate the amount of sediment that was flushed and examined the condition of water resources infrastructure in the upstream and downstream of the dam. Technical evaluation conducted to see whether there is damage to water resources infrastructure or not. In the event of damage, calculated how much the damage lost. From the results of several times flushing activities, apparently, no damage to water resources infrastructure.

DREDGING RESERVOIR

In addition to flushing, to increase lifetime of the reservoir is also dredging. Implementation of flushing have to consider inflow while dredging is less concerned inflow. The main obstacle of dredging is limited spoil bank land. Especially recently where high cost of land acquisition of new spoil. If the land acquisition of spoil bank encounters of constraints, then dredging with riverine disposal to channel below is carried out. The dredging of sediments in the Wlingi reservoir over the last 5 years is as shown in the following table.

Table 4 Dredging in Wlingi Dam

Year	Dredging with Spoil Bank Disposal (m3)	Dredging with Riverine Disposal to Channel Below (m3)
2013	150,800	100,031
2014	283,148	110,140
2015	377,384	
2016	100,436	250,475
2017	115,020	

Source: Perum Jasa Tirta I

5. FINANCIAL ANALYSIS OF SEDIMENT MANAGEMENT

5.1 CALCULATION OF FLUSHING AND DREDGING COST

As a basic for evaluation of financial aspects assumed as follows:

- Flushing costs include flushing operational costs, lost potential revenue costs from water services and the cost of losses of electricity production due to discontinued hydropower operations.
- The amount of sediment due to flushing is calculated based on the average of flushing data for 5 years (2009 to 2013, since 2014 and 2015 have no flushing, whereas 2016 and 2017 volumes of sediments are flushed greatly considering 2 years previously not flushing)
- Loss of hydropower production is assumed based on the operating hour loss multiplied by the installed capacity multiplied by 75% ($34,000,000 \times 38 \times 0.75 = 969,000$ kWh)
- Dredging unit price refers to the existing unit price estimate in Wlingi Reservoir, which is Rp 64.100 / m³. Analysis of unit price as attached
- Tariff of water service for hydropower based on tariff which is valid in 2017 at Jasa Tirta I Public Corporation, which is Rp 167 / kWh
- Value of electricity benefit is calculated based on the basic electricity tariff issued by National Electricity Company in 2017 is Rp 1.352 / kWh
- Flushing is assumed not influence to irrigation because the flushing implementation is less than 2 days (38 hours) and not carried out during the dry season.
- During flushing there is no loss due to the temporary interruption of irrigation water supply, domestic and industrial raw water due to the relatively short implementation period.
- Operational cost of flushing based on the existing data in Jasa Tirta Public Corporation is Rp 133.330.000,

Table 5 Flushing Cost Calculation

Discription	Unit	Volume	Unit Price (Rp)	Amount (Rp)
Sediment FLushing = 350,865 m3				
Loss of Water Service Fee	(kWh)	969,000	167.0	161,823,000
Loss of Electricity Service	(kWh)	969,000	1,352	1,310,088,000
Cost of Flushing Implementation	Lump sum	1	133,330,000	133,330,000
Damage of Water Resource Infrastructure				-
Total Cost of Flushing				1,605,241,000

Table 6 Dredging Cost Calculation

Description	Explanation
A. Land Acquisition Cost	
Land acquisition Rp 290,000/m2	
Spoil bank can accommodate sediments 10 m high	
Land Acquisition Cost = $290,000 / 10 = \text{Rp } 29,000 / \text{m}^3$	
Spoilbank Embankment Construction	
For the sediments of 1 m3 the volume of spoil bank embankment is = $1/3 = 0.333 \text{ m}^3$	
Unit price of embankment is Rp 40,930 / m3	Calculation see attachment 1
Spoil bank embankment construction cost = $0.333 \times 40,930 = \text{Rp } 13,630 / \text{m}^3$	
Sediment Dredging Costs	
Sediment dredging cost = Rp 64,100 / m3	Calculation see attachment 2
Dredging with Spoil Bank Disposal Costs = $A + B + C = \text{Rp } 106,730 / \text{m}^3$	
For dredging of 350.865 m3 of sediment cost = $350,865 \times 106,730 = \text{Rp } 37,454,838,750$	
Dredging with Riverine Disposal to Channel Below Costs = C = Rp 64,100 / m3	
For dredging of 350.865 m3 of sediment cost = $350,865 \times 64,100 = \text{Rp } 22,490,446,500$	

From the above table it can be concluded that flushing implementation is more effective than dredging. Flushing can save the cost of Rp. 35.85 billion (Rp 37,454,838,750 – Rp 1,605,241,000) compared to dredging with spoil bank disposal, while dredging with riverine disposal to channel below can save about Rp. 14.96 billion (Rp 37,454,838,750 – Rp 22,490,446,500) compared to the dredging with spoil bank disposal.

5.2 FLUSHING AND DREDGING BALANCE AGAINST RIVER BED DEGRADATION

As described above that in sedimentation upper reach and degradation of river bed are also problem in water resources management. The degradation of river bed along Brantas River is between 2 s / d 8 m. To reduce of river bed degradation some efforts that have been done are:

- Controlling illegal sand mining
- Conducting public awareness on the impact of illegal sand mining
- Implementation of flushing or dredging with riverine disposal to channel below.

Over the past five years, the average sediment that flows to downstream is 350,865 m³/year. While the amount of sediment that can be supply form dredging with riverine disposal to channel below is 250,475 m³/year. If the amount of illegal sand mining along the Brantas River in lower reach of Wlingi dam is 2,470,600 m³/year, and there is no dredging with riverine disposal to channel below, flushing should be done 7 times a year. This is very difficult because the implementation of flushing is depend on the available inflow. Implementation of dredging 2 million m³/year with riverine disposal to channel below in Wlingi Reservoir requires a huge cost. The possible efforts have be done through sustainable public persuasive and constructive actions through controlling the illegal sand mining.

5.CONCLUSION

1. Implementation of flushing is very effective to reduce sediment in the reservoir which has river bed degradation in lower reach. Financially sedimentation flushing can save the cost of Rp. 35.85 billion compared to dredging with spoil bank disposal, while dredging with riverine disposal to channel below can save about Rp. 14.96 billion compared to the dredging with spoil bank disposal. However flushing implementation can not be implemented every year because it must consider the reservoir inflow.
2. If the inflow is not possible to carry out flushing, dredging with riverine disposal to channel below can be done.
3. Although not significant, the implementation of flushing and dredging with riverine disposal to channel below can reduce the river bed degradation occurring in lower reach. To balance the illegal sand mining in downstream it is necessary to flush 7 times a year and it is difficult to achieve. Other efforts to maintain the river bed are the control of illegal sand mining, and public campaign.

6. REFERENCE

- Ministry of Public Works – Nippon Koei Co., Ltd. 2005. *Report on Engineering Studies for the Brantas River and the Bengawan Solo River Basins, Water Resources, Existing Facilities Rehabilitation and Capacity Improvement Project, Jakarta, Indonesia.*
- Jasa Tirta I Public Corporation. 2011. *Report of Sounding Result of Wlingi Dam,*
- Jasa Tirta I Public Corporation. 2014. *Roadmap of Reservoir Sedimentation Management in Brantas River Basin 2015-2019.*
- Tjoek Walujo Subijanto, Ir., CES. 2008. *Adaptation of Water Resources Management Facing Global Climate Change Case Study of Brantas River Basin. Malang: Jasa Tirta I Public Corporation.*

Attachment 1

Unit Price Calculation of Spoil Bank Embankment

No.	Description	Unit	Volume	Unit Price (Rp)	Total (Rp)
I	Preparation				
1	Preparation and Cleaning	ls	1.00	10.00	10.00
2	Mobilization of Heavy Equipments	trip	8.00	1,905.50	15,244.00
3	Preparation Inlet & Outlet Spoil Bank	ls	1.00	1,930.00	1,930.00
II	Spoil Bank Work				
1	Land Cut and Mobilization	m ³	1.00	12,785.00	12,785.00
2	Land Fill, Shape and Spreading of Soil	m ³	1.00	5,983.00	5,983.00
3	Soil Compaction	m ³	1.00	4,106.00	4,106.00
III	Other Job				
1	Final Cleansing	ls	1.00	50.00	50.00
2	Cross Section Measurements	cross	1.00	72.00	72.00
3	Documentation and Reporting	ls	1.00	750.00	750.00
				Total	40,930.00

Attachment 2

Unit Price Calculation of Dredging

No.	Description	Calculation	Total
I	Pruduction per Year		144.000 m ³
II	Cost per Year		
1	Direct Costs		
a.	Operational Fuel	150 × 2.950 × 9.000	3.982.500.000
b.	Operational Lubrication	150 × 70 × 35.000	367.500.000
c.	Freshwater	365 × 5 × 20.000	36.834.900
d.	Dredging allowance	150 × 2380% × 75.000	267.750.000
e.	Food and Beverage	365 × 30 × 45.000	492.750.000
f.	Survey Activities (Progress Sounding)	12 × 35.040.000	420.480.000
g.	Insurance	US\$ 1.936 × 14.000	27.104.000
	Direct Costs Total		5.594.918.900
2	Indirect Costs		
a.	Maintenance/Docking		1.194.637.145
b.	Depreciation		641.979.024
c.	Dredger's Crew Salary		576.000.000
d.	Insurance (H&M)	0,800% × 36.061.945	288.496
	Indirect Costs Total		2.412.904.665
3	Bussiness Cost	14% × 5.594.918.900	783.288.646
	Cost Per Year Total (1 + 2 + 3)		8.791.112.211
III	Unit Cost		
1	For Each Cubic Meter	8.791.112.211 / 144.000 m ³	61.049
2	Minus Paid Tax Deviation	395.454.545 / 144.000 m ³	2.746 - 58.303
3	Added 10% Tax	10% × 58.303 m ³	5.830
Unit Price of Dredging			64.133
Round Off			64.100

Asumptions:

Dredger Work Days	150	per year
Total Days in A Year	365	
Currency Rate US\$	14.000	Rupiah

COMMISSION INTERNATIONALE DES GRANDS BARRAGES

VINGT-SIXIÈME CONGRÈS DES GRANDS BARRAGES
Autriche, juillet 2018

DOI 10.3217/978-3-85125-620-8-019



This work licensed under a Creative Commons Attribution 4.0 International License. <https://creativecommons.org/licenses/by-nc-nd/4.0/>

**EVALUATION AND MITIGATION OF THE BOGEL RIVER FLOOD, BLITAR,
PROVINCE OF EAST JAVA, INDONESIA**

Aris YHADHIANTO
Civil Engineer, JASA TIRTA I PUBLIC CORPORATION
INDONESIA

Ulie Mospar DEWANTO
Deputy of Operational II, JASA TIRTA I PUBLIC CORPORATION
INDONESIA

**EVALUATION AND MITIGATION OF THE BOGEL RIVER FLOOD,
BLITAR, PROVINCE OF EAST JAVA, INDONESIA**

Aris Yhadhianto

Civil Engineer, JASA TIRTA I PUBLIC CORPORATION, INDONESIA

INDONESIA

Ulie Mospar Dewanto

Deputy of Operational II, JASA TIRTA I PUBLIC CORPORATION,

INDONESIA

ABSTRACT

Bogel River located in Sutojayan area, Blitar, Province of East Java. It collected into the Brantas River about ± 1.5 km from the upstream of Lodoyo Dam. It have several subordo river in the upstream there are Kedungpuring River, Kedungunut River, Pijeran River, Kedungriwuk River, and several other subordo river. Seasonal type, Bogel River often overflow and impact of flood in the surrounding area, especially in Sutojayan area. Its because of the land condition in the catchment area already critical / bald and the silting up of the several suborder river in the upstream. Beside that Bogel River system is also used for irrigation. Jasa Tirta I Public Corporation have developed an early warning system and done the handling activities during flood events, although it's not included in working area of the Jasa Tirta I Public Corporation. Mitigation of Bogel River flood until today just partial and emergency activities. So it is necessary for arrange the comprehensive and integrated study and flood mitigation management, supported by the Government and related stake holder. To get the right solution for mitigation the flood of the Bogel River, need a concept in all aspects and stages, so it can give the real benefits and on target. The method used are direct controlling by (a) operating the Lodoyo weir according to Dam Operational Guidelines, Procedures and Work Instructions of Flood Control, (b) arrange the evaluation for historical flood that ever happened, (c) arrange the concept of the proposed for flood mitigation by making the comprehensive study of flood mitigation, short term action 2016, middle term-long term cction, (d) completing the hydrology observation instruments in Bogel River

System. By these integrated flood mitigation concepts in Bogel River will completing the efforts that have been done by Jasa Tirta I Public Corporation, directly and emergency action by participation from all stakeholders according to the authority. By normalitation of the condition and function of the existing water resources infrastructure, the flood control system can be implemented optimally. Of course, the real efforts can be realized so as to built the preparedness for possible flood and reduce the impact that especially for regions and communities in the district Sutojayan, Blitar. It is also become the responsibility of Jasa Tirta I Public Corporation in water resources integrated management.

Keywords : flood, mitigation management, Lodoyo weir, Bogel River

INTRODUCTION

The existence of Bogel River is expected by communities around the watershed to support the needs of water mainly for irrigation. Bogel River watershed with a total area of 54.4 km² is a catchment rivers with a total length of 14.4 km. Bogel River system consists of three main tributaries namely Unut River, Gondang River, and Rau River with a meeting point in the Area / District Sutojayan. Most of area in Bogel watershed is relatively gentle slopes and even tend to be flat and partly is hilly area with 60% of deforested conditions. The shape of the watershed is wide/dilated which have a large flood peaks and short flood peak time, so it could potentially have a high flood peak discharge. The rapid of development with community activities around the watershed, the river's capacity is no longer sufficient to be function as drainage channels. Besides that reducing capacity because of sedimentation, especially in the estuary and the effect of water level fluctuations of Brantas River in the upstream Lodoyo Dam is also a cause which must be anticipated. (Department of Public Works.,2005)

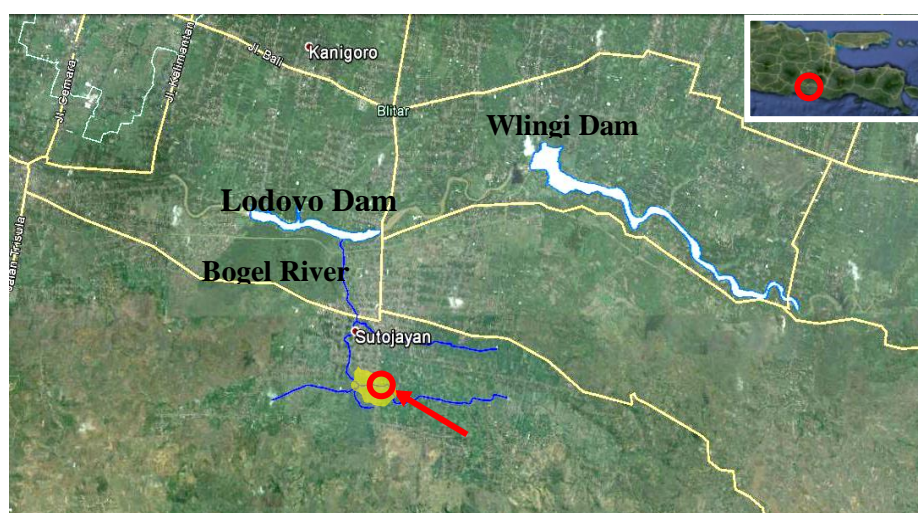


Figure 1. Location map of Bogel River

METHODOLOGY

Discussion in this paper generally consists of two subjects. The first part discusses the flood problem of Bogel River. This is done by studying the secondary data available, the results of previous studies, collecting and analysis of primary data in the field. The second section discusses the planning and solution in order to mitigation and overcome the flood problem of Bogel River. The method used is as follows :

1. Arrange the evaluation for historical flood that ever happened
2. Direct controlling by operating the Lodoyo weir according to Dam Operational Guidelines, Procedures and Work Instructions of Flood Control
3. Arrange the concept of the proposed for flood mitigation that includes :
 - a. Make the comprehensive study of flood mitigation
 - b. Short Term Action 2016
 - c. Middle Term-Long Term Action
4. Completing the hydrology observation instruments in Bogel River System

RESULTS AND DISCUSSION

THE FLOOD PROBLEM OF BOGEL RIVER - SUTOJAYAN

Flood in Sutojayan is a complex problem caused by several factors:

1. Watershed is relatively gentle slopes and even tend to be flat
2. Condition of land in the catchment area is in a critical / deforested so the potential of sedimentation is huge
3. There was silting in most of the tributaries upstream because of erosion and sedimentation
4. Areas that frequent flooding is in the district Sutojayan due to the topography of the area is a basin which is lower than the elevation of the water level of Bogel River
5. The number of irrigation dams in the upstream impede the flow of water during a flood. Moreover, the condition is also full of sediment (sedimented)

Based on the information in the field floods that hit several villages in the district Sutojayan actually a regular puddle on every rainy season. This is because the area in the region is lower than the elevation of the water level of Bogel River, so the drainage can not drain the water into the river.

Historical Events Flood of 2004 that ever happened

1. Chronology Flood of 2004
 - a. Rain drops began on December 2, 2004 at 07.00 am with cumulative rainfall in some places very high: 441 mm Tunggorono, Bhirowo 371 mm, 366 mm Wlingi.

- b. December 3, 2004 at 06.00 am weir Lodoyo provide standby signal III / red for discharge = 1,016 m³ / sec.
- c. The operation of the sluice weir Lodoyo already done on December 2, 2004 beginning at 1:00 am.
- d. The rain did not stop so that the discharge tends to increase steadily even on December 3, 2004 at 08:30 pm at the weir Lodoyo out flow discharge reached 2,115 m³ / sec.
- e. Areas affected by the inundation is under flood water level of Bogel River, so that when water is abundant and several tributaries berms fail then there is a pool of sufficiently high (the highest inundation reached El. 139,87m, while areas were inundated elevation 137.00 - 139.00 m).
- f. Based on the evaluation, the flow capacity of Bogel River in the upstream (15 m³ / s), while in the central part of 20 m³ / s, and upstream tributaries after meeting capacity up to 110 m³ / sec. The estimated calculation of flood discharge reaches + 190 m³ / sec.
(Jasa Tirta I Public Corporation,2005. *Flood Audit Report*)

2. Impact of Fatalities of Flood 2004

There are six (6) people died in the district Sutojayan, Blitar in the event of flooding. (Jasa Tirta I Public Corporation,2005. *Flood Audit Report*)



FIGURE 2. FLOOD 18 JANUARY 2016, WATER LEVEL REACH 30 CM



FIGURE 3. FLOOD 2 FEBRUARY 2016, WATER LEVEL REACH 80 CM

The Evaluation of Flood

1. Flood 2004
 - a. The influence of Lodoyo reservoir water level in the estuary of Bogel River at the time of floods is estimated at El. +138.20 (from the analysis of non-uniform flow for discharge of 2,000 m³/s and water level in the Lodoyo weir is +136.00).
 - b. With the same discharge conditions when the Lodoyo water level was lowered to El. 134.00, so the water level in the estuary Bogel River is +138.05.
 - c. And when the gate fully opened, the discharge of 2,000 m³ / sec, so the Lodoyo water level +131.00 and the water level in the estuary of Bogel River is +138.05.
 - d. Based on these conditions indicate that the water level during a flood in Bogel River not influenced by the water level in Lodoyo Weir, but is determined more by the discharge that passing through the river.
2. Flood dated January 18, 2016 and February 2, 2016
 - a. By two flood events that occurred on January 18, 2016 and February 2, 2016 seen on Flood Hydrograph that during heavy rainfall, water level Bogel River increase up quickly and additions are quite large. Example: In the event of flooding dated January 18, 2016 an increase of water level from +135.5 m to 138.2 m (2.7 m) within 2 hours.
 - b. Effort to reduce the water level of Lodoyo weir already done, but require quite a long time to reduce Bogel River water level. For example on two flood events that take more than 24 hours to reduce the elevation from 1.0-1.5 m.

Table 1. Result of Flood Evaluation 2016

Date	Max. Rainfall (time -mm)	siren sounds (time)	Bogel River Max. Elevation (time-m)	Gate Opened (time) El.min (m)	Gate closed El. Normal (time) Time of Pool (hour)
18/Jan/2016	06.00 pm 142 mm	07.30 pm	09.00 pm +138,25 mm	08.00 pm +131,8 m	10.00 pm (on 19 Jan 2016) 26 hours
2/Feb/2016	02.00 pm 88 mm	04.00 pm	06.00 pm +137,75 mm	04.00 pm +133,2 m	08.00 pm (on 3 Feb 2016) 24 jam

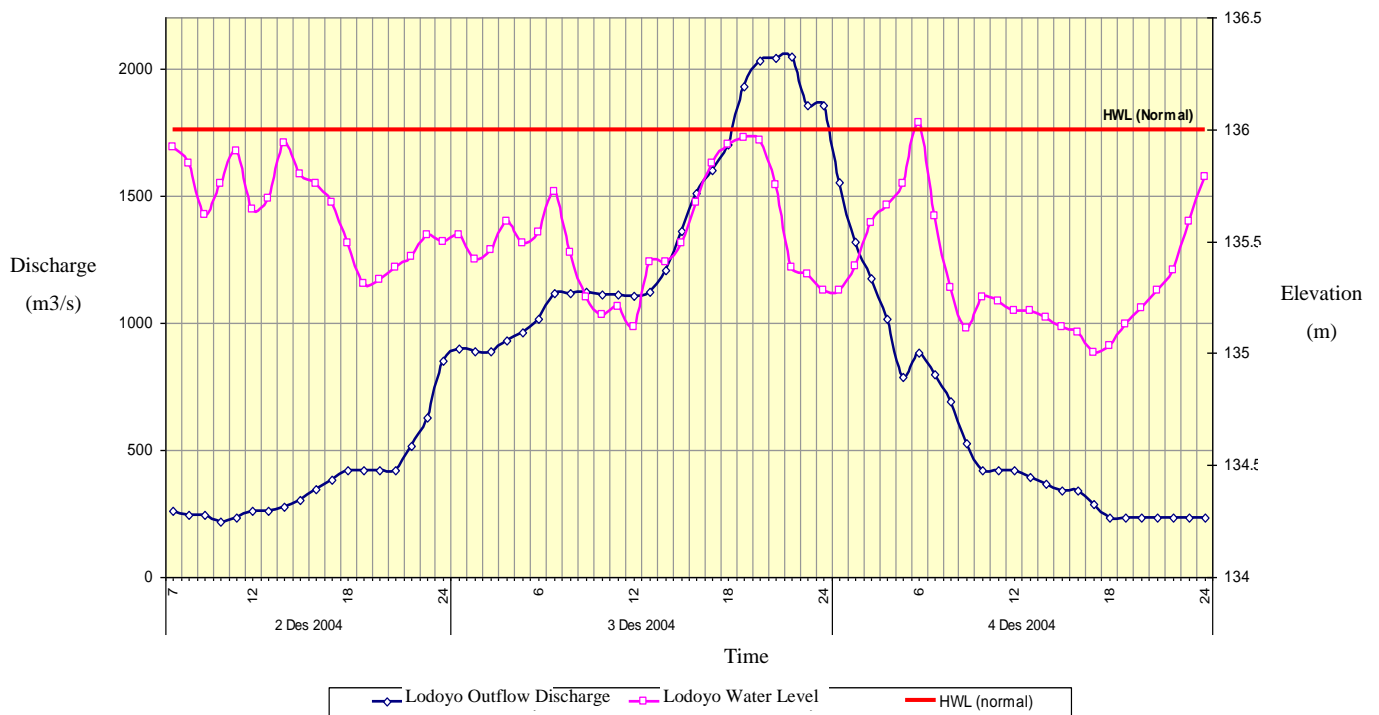


Figure 4. Flood Hydrograph and Water Level of Lodoyo Dam, 2-4 December 2004 (Jasa Tirta I Public Corporation,2005)



Figure 5. Flood Hydrograph Bogel River, 18 January 2016

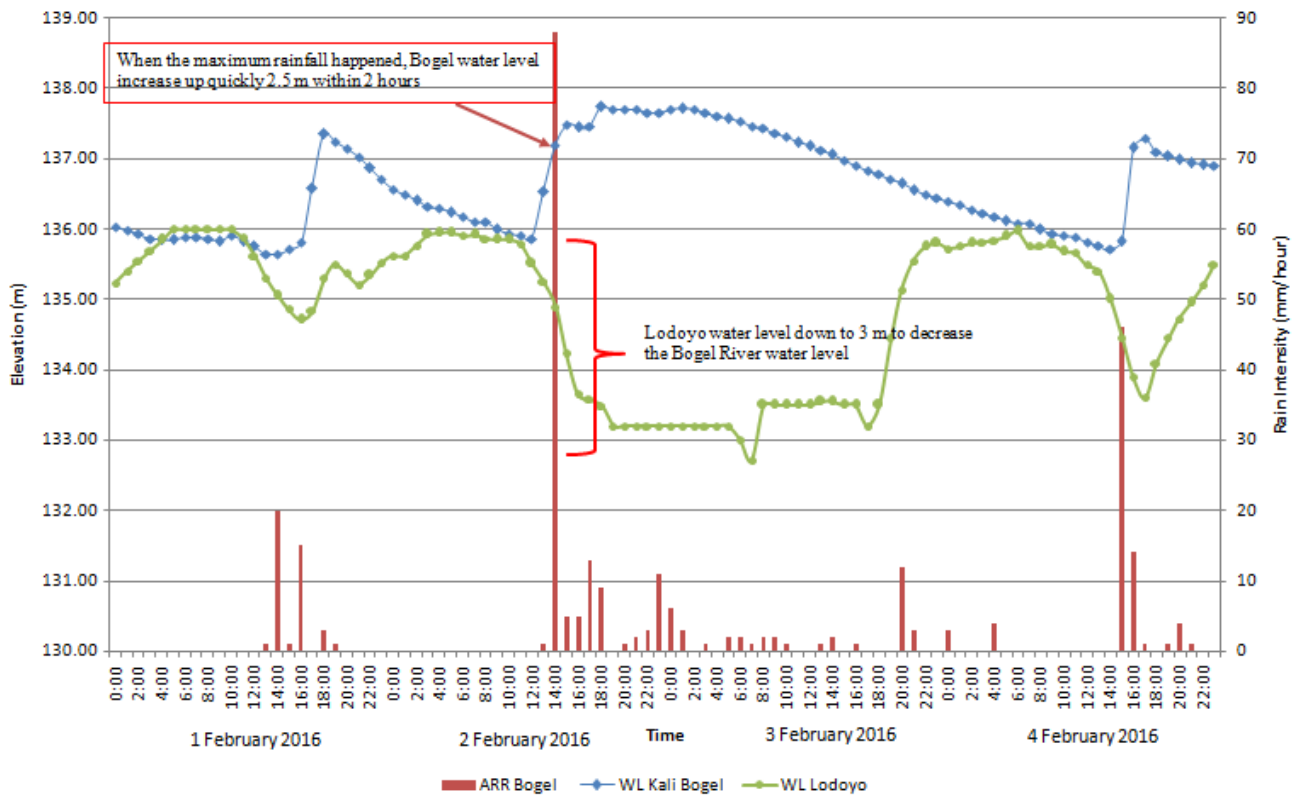


Figure 6. Flood Hydrograph Bogel River, 2 February 2016

The Planning and Solution to Mitigation The Flood Problem of Bogel River
Efforts have been done

1. Jasa Tirta I Public Corporation has doing Bogel River Dredging Works in 2005-2006 by self-managed as follows:
 - a. In 2005 : dredging volume 3,828 m³
 - b. In 2006, Period 1 : dredging volume 25.000 m³
 - c. In 2006, Period 2 : dredging volume 3.925 m³The total length of the river was dredged from Kedung Bunder Bridge-Bacem Bridge 3600 m
2. Drain Outlet Construction Unut - Bogel River in 2005
3. Doing the emergency repair in several times

Efforts to be Proposed

1. Preparation of a comprehensive study of Bogel River flood
2. Short Term Action in 2016
 - a. Emergency repair of Kedungunut river embankment
 - b. Normalization Bogel River start from Gondanglegi Dam until Lodoyo Channel
 - c. Periodically doing the normalization in river upstream :
 - Kedungpuring River, Margomulyo as long as ± 2 km
 - Kedungunut River, Bacem as long as ± 2 km
 - Pijeran River, Pandanarum as long as ± 3 km
 - Kedungriwuk River, Bacem as long as ± 2 km
 - d. Repair of drainage channels in the township
 - e. Overcome the domestic waste Sutojayan which often cause blocking under the bridge.
3. Middle Term-Long Term Action
 - a. To evaluate the function and proposed irrigation dam on the upstream dam to be functioned as long storage.
 - b. Make ponds / retarding basin for the water parking and the water storage tank for the community, because Bogel River is a perennial river / seasonal which is there are some water during the rainy season and dry during the dry season.
 - c. Implement conservation in the upstream of the catchment area to reduce the run-off and erosion.
 - d. Make short cut Bogel River to the downstream of Lodoyo weir (must be studied further).
4. Completing the hydrological observations station on the Bogel watershed
 - a. Increasing the number of AWLR stations in the Bogel watershed
 - b. Increasing the number of ARR stations in the upper of Bogel River, such as in the Mountains Kendeng
 - c. Completion of the Early Warning System, which has been pioneered by Jasa Tirta I Public Corporation to be integrated with other agencies

CONCLUSION AND RECOMMENDATION

Conclusion

1. Jasa Tirta I Public Corporation doing the direct controlling by operating the Lodoyo weir according to Dam Operational Guidelines, Procedures and Work Instructions of Flood Control
2. By this integrated flood mitigation concepts in Bogel River will completing the efforts that have been done by Jasa Tirta I Public Corporation, directly and emergency action by participation from all stakeholders according to the authority.
3. By normalitation of the condition and function of the existing water resources infrastructure, the flood control system can be implemented optimally. Of course, the real efforts can be realized so as to built the preparedness for possible flood and reduce the impact that especially for regions and communities in the district Sutojayan, Blitar. It is also become the responsibility of Jasa Tirta I Public Corporation in water resources integrated management.

Recommendation

Need to do a more study on the conservation action in Bogel watershed so that the management could be done more effectively and efficiently.

Socialization needs to be done at each stage of implementation and involve the community participation

ACKNOWLEDGEMENTS

The authors thank to Jasa Tirta I Public Corporation, the River Basin Organization in Brantas, Bengawan Solo, Jratunseluna, Serayu Bogowonto and Toba Asahan River basins in Indonesia for providing data used in this paper.

REFERENCES

References from report:

Jasa Tirta I Public Corporation,2005. *Flood Audit Report*, Indonesia.

Department of Public Works.,2005.*Final Report: Survey Investigation and Design of Bogel River Repair, Blitar*, Indonesia.

Jasa Tirta I Public Corporation,2015. *Flood Preparedness Guidelines 2015-2016*,

COMMISSION INTERNATIONALE DES GRANDS BARRAGES

VINGT-SIXIÈME CONGRÈS DES GRANDS BARRAGES
Autriche, juillet 2018

DOI 10.3217/978-3-85125-620-8-020



This work licensed under a Creative Commons Attribution 4.0 International License. <https://creativecommons.org/licenses/by-nc-nd/4.0/>

**SETTING UP DREDGING AND SPOILBANK MANAGEMENT METHOD TO
RECOVERY HYDROPOWER PRODUCTIVITY OF SENGGURUH DAM**

Aris YHADHIANTO
Civil Engineer, JASA TIRTA I PUBLIC CORPORATION
INDONESIA

Ulie Mospar DEWANTO
Deputy of Operational II, JASA TIRTA I PUBLIC CORPORATION
INDONESIA

SETTING UP DREDGING AND SPOILBANK MANAGEMENT METHOD TO RECOVERY HYDROPOWER PRODUCTIVITY OF SENGGURUH DAM

Aris Yhadhianto

Civil Engineer, JASA TIRTA I PUBLIC CORPORATION, INDONESIA

INDONESIA

Ulie Mospar Dewanto

Deputy of Operational II, JASA TIRTA I PUBLIC CORPORATION,

INDONESIA

ABSTRACT

Sengguruh dam located in Brantas River watershed, East Java, Indonesia was completed in 1988. The objectives is for generating hydroelectric power plant with installed capacity 2 x 14,5 mW produce of 91 million kWh per year. Located at uppermost of the series dams in Brantas River Basin and therefore is utmost suffered of sedimentation. Also, it prevents sediment comes to the Sutami which is the biggest reservoir at down stream part. The inflow come from two main rivers, namely Brantas River and Lesti River has a catchment area of 1.659 km². The condition currently declining due to the high rate of sedimentation. Based on the echosounding result conducted in 2016, is known that effective capacity has been reduced to 0,6 million m³, or approximately 24% of the initial conditions of 2,5 million m³ and electric generation has been reduced to 68,8 x 10⁶ kWh. The dredging activity has been done routine every year from year of 2001 with an average dredging volume of 300,000 m³/year. Total achievement of the volume of dredging result seems large, but it is not adequate. Based on the present evaluation, particularly in the zone at front of hydropower intake (namely zone 1), was in fact already quite critical because the sediment is getting closer. The zone distance is about 100-200 m with the difference elevation from sediment surface reaching 7-12 m above desired reference base elevations. On contrary, the dredging has been done in the upstream area which is quite far away \pm 1,500-2,000 m from zone 1 due to get close of spoilbank location. In order to sort out the problem and to support President Joko Widodo's Government policy in energy security, the dredging method in 2016 was changed. The innovation and

development of methods to improve its effectiveness are (a) with the combination of 2 dredging types using available dredgers and additional heavy equipment (amphibious excavators) to take out sediment which located at positions could not be done by dredgers (dry-wet excavation), (b) installation of booster pump and floating pipe as support of the dredgers, (c) modification of dredger ladder, (d) management of spoilbank by re-arrange of hauling and reloading cycles, and accelerate sediment material drying by installing vertical-horizontal drainage. By these methods the dredging of sediment can be implemented more effectively and efficiently to ensure high hydropower production, maintain effective storage capacity and prolong age of reservoir with of course considering environmental aspect around the area.

Keywords : dredging, sedimentation, hydropower productivity, Sengguruh Dam

1. INTRODUCTION

Sustainability of the function and lifetime of reservoirs in the world is increasingly threatened today due to the high rate of sedimentation. The conditions of the upstream area which are deteriorating due to devastated watershed and improper land management and ignoring the good aspects of soil and water conservation, has led to increased soil erosion and the rate of sedimentation in the reservoir, thus diminishing the volume of the storage reservoir. The sedimentation of reservoirs in Indonesia today is one of the issues to be a priority in efforts to handle by the government era of President Joko Widodo towards water, food and energy securities.

Management of reservoir sedimentation have a variety of alternative efforts such as: a) an effort to minimize the rate of sediment entering the reservoir through watershed management (conservation, regulation of land use, etc.), and control of sediment into the reservoir with the technical construction in the river (check dams, gully plug, etc.), b) minimize the deposition of sediments in the reservoir by sluicing sediment and venting turbidity density current, and c) remove sediments from reservoirs through flushing and dredging.

Reservoir dredging work is done in many countries like the USA, France, Austria, Switzerland, South Africa, Japan, China, and others. In China, the reservoir dredging routinely performed in many reservoirs such as in the Guanting Reservoir (Yang et al, 2003). In general, the dredging of reservoirs is an expensive effort in order to maintain and restore the reservoir storage capacity, and only considered if the implementation of other alternative measures are not possible or difficult to implement. Dredging the reservoir is limited to removal of sediment that accumulates in front of the intake or for the recovery of the small storage reservoirs (Basson & Rooseboom, 1999). Morris and Fan (1998) give consideration to dredging the reservoir includes four (4) basic components: 1) the sediment that will be dredged (location dredging), 2) dredging equipment, 3) equipment for deliver the dredging materials (eg. pipe for dredging

hydraulically, and 4) dredged material disposal site (riverine disposal into the river below the dam or off-stream disposal/spoil bank).

Sengguruh dam located in Brantas River watershed, East Java, Indonesia was completed in 1988. The location of Sengguruh dam is shown in Figure 1. Sengguruh dam is one of the oldest dams were constructed in accordance with the Brantas River Basin Master Plan for Water Resources Development of the Brantas River Region. The objectives is for generating hydroelectric power plant with installed capacity 2 x 14,5 mW produce of 91 million kWh per year.



Figure 1. Location map of Sengguruh dam
Carte de localisation du barrage de Sengguruh

Located at uppermost of the series dams in Brantas River Basin and therefore is utmost suffered of sedimentation. On the other hands, it prevents sediment comes to the Sutami which is the biggest reservoir and located at down stream part. The inflow come from two main rivers, namely Brantas River and Lesti River has a catchment area of 1.659 km². Condition and sustainability functions of the reservoir currently declining due to the high rate of sedimentation. Based on the echosounding result conducted in 2016, is known that effective capacity has been reduced to 0,6 million m³, or approximately 24% of the initial conditions of 2,5 million m³ and electric generation has been reduced to 68,8 x 10⁶ kWh.

2. METHODOLOGY

Discussion in this paper generally consists of two subjects. The first part discusses the problem of sedimentation in Sengguruh reservoir. The study on sedimentation in Sengguruh reservoir is done by studying the secondary data available, the results of previous studies, collecting and analysis of primary data in the field. The second section discusses the work of sediment dredging in Sengguruh reservoir by explain the current method and development planning to get the best method to doing the dredging operation, there are (a) with the combination of 2 (two) dredging types using available dredgers and additional heavy equipment (amphibious excavators) to take out sediment bank which has become solid and located at positions could not be done by dredgers (dry-wet excavation), (b) installation of booster pump and floating pipe as support of the dredgers, (c) modification of dredger ladder to increase the range of dredger, and (d) management of spoilbank by re-arrange of hauling and reloading cycles, accelerate sediment material drying by installing vertical-horizontal drainage and increase spoilbank capacity. The second discussion includes planning and application method of the dredging work through field studies conducted in Sengguruh reservoir which is conducted at this time.

3. RESULT ANALYSIS AND DISCUSSION

3.1. SEDIMENTATION OF SENGGURUH RESERVOIR

From the results of sediment testing on the soil laboratory in Perum Jasa Tirta 1 there are 6 types of sediment in Sengguruh Reservoir namely loam, silt, silt loam, sand, sandy loam, and loamy sand. Sediment of silt loam type is the most sediment type found in Sengguruh Reservoir

Group	Type	Information
A	[C]	Clay
B	[SaC]	Sandy Clay
C	[SiC]	Silty Clay
D	[SaCL]	Sandy Clay Loam
E	[CL]	Clay Loam
F	[SiCL]	Silty Clay Loam
G	[Sa]	Sand
H	[LSa]	Loamy Sand
I	[SaL]	Sandy Loam
J	[L]	Loam
K	[SiL]	Silt Loam
L	[Si]	Silt

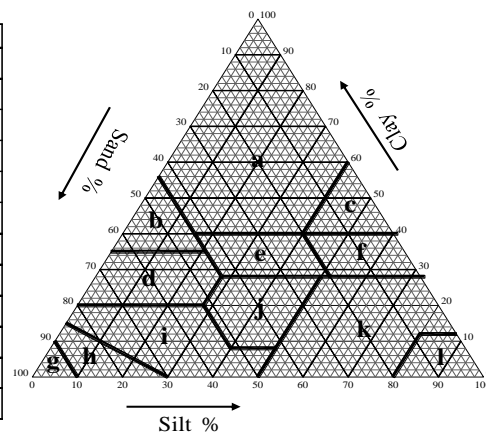


Figure 2. Soil classification of grain size (Sample of passed 2000 sieve)
Classification du sol de la taille des grains (échantillon du tamis 2000 passé)

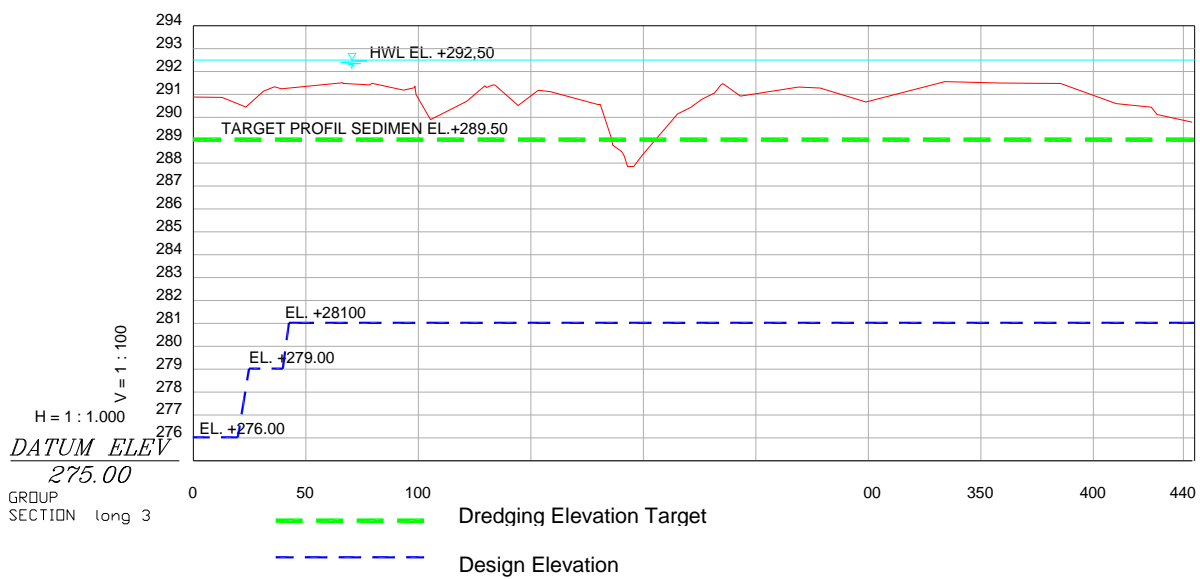
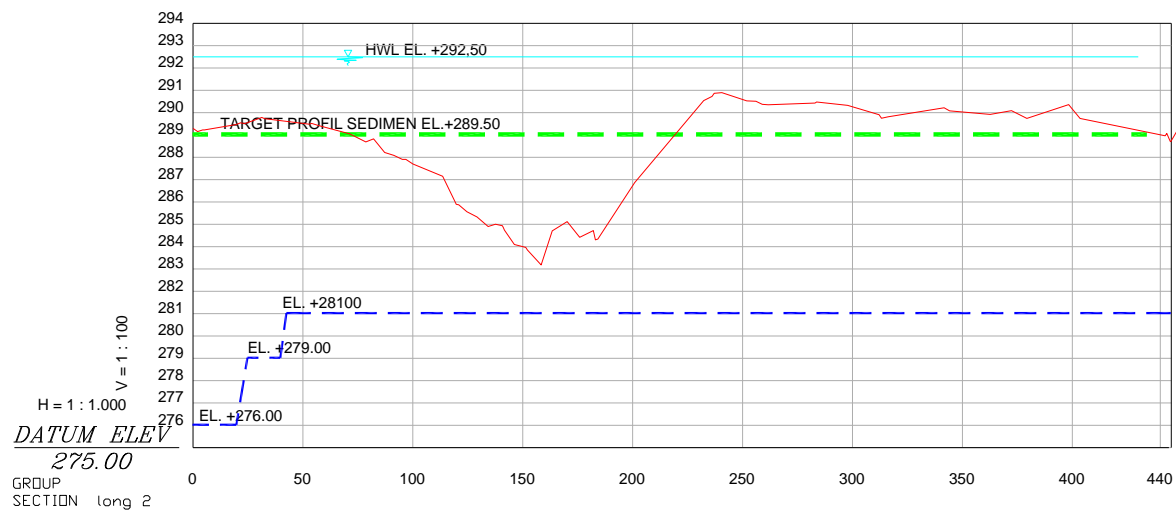
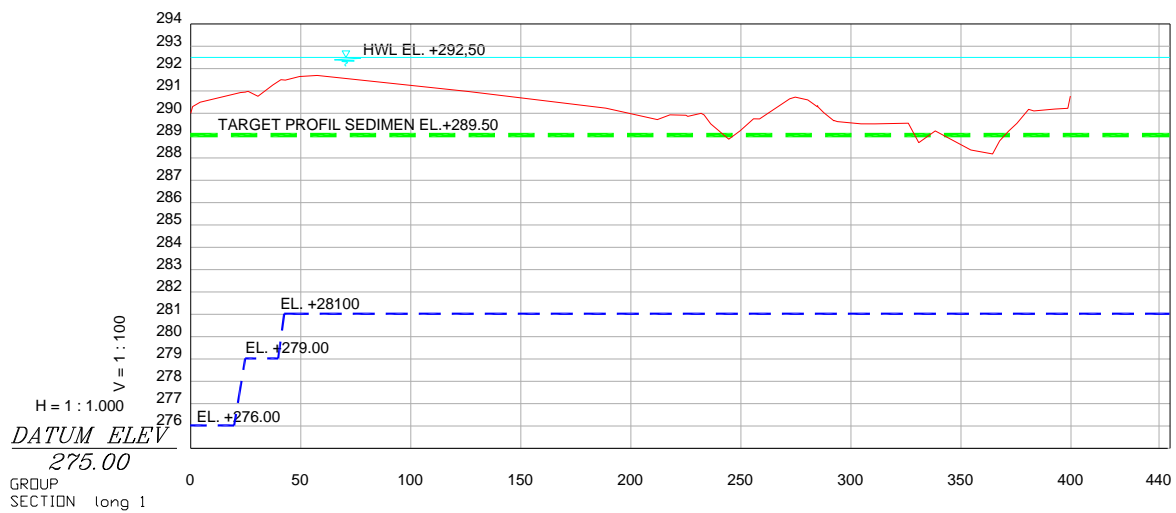
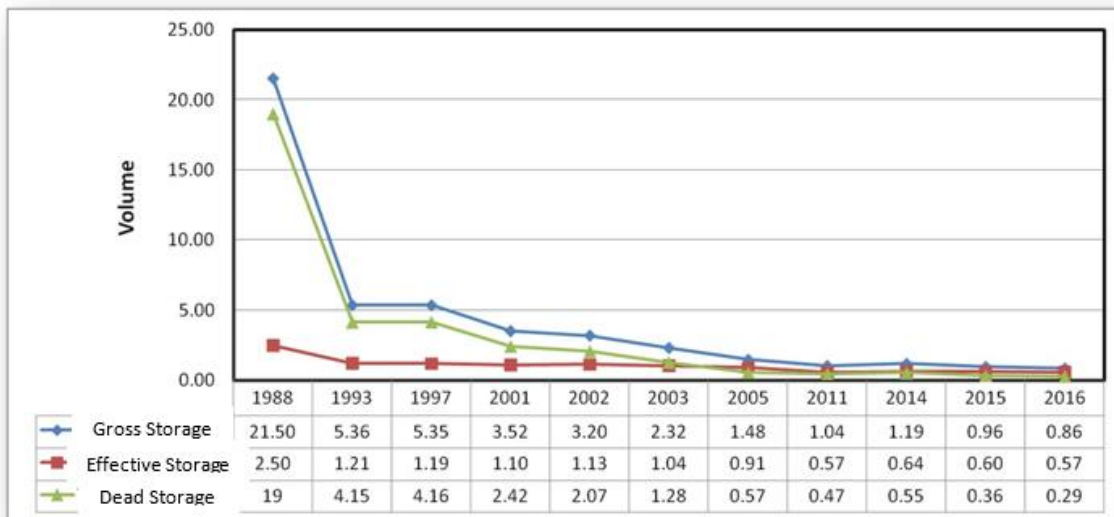


Figure 3. Longitudinal Sedimentation Profile
Profil de sédimentation longitudinale



Figure 4. The condition of Sengguruh reservoir sedimentation
L'état de la sédimentation du réservoir de Sengguruh

Table 1. The historical changes of Sengguruh reservoir storage capacity



3.2. DREDGING WORK ON CURRENT CONDITION

Some control efforts have been made actually, both in stream or off stream, one of them is by sediment dredging. This dredging activity has been done routine every year from year of 2001 with an average dredging volume of 300,000 m³ / year using 2 (units) cutter suction dredger. The location of sediment disposal area (spoilbank) spread out around the reservoir, meanwhile available spoilbank is very limited and provides the new one is very costly. the dredging has been done in the upstream area which is quite far away + 1,500-2,000 m from hydropower intake due to get close of spoilbank location, to get low fuel consumption, to maximize available dredgers production capacity which has

limited operational range (both depth & discharge), and to reduce length of dredging pipelines. Shortly, this condition is not good for keeping high hydropower productivity which affected much of zone 1 condition.



Figure 5. General Plan Dredging Work on Current Condition
Travaux de dragage du plan général sur l'état actuel

3.3. DEVELOPMENT PLANNING OF DREDGING WORK TO RECOVERY HYDROPOWER PRODUCTIVITY

The dredging method in 2016 was changed in order to make the dredging of sediment can be implemented more effectively and efficiently to ensure high hydropower production, maintain effective storage capacity and prolong age of reservoir. The development planning are (a) with the combination of 2 dredging types using available dredgers and additional heavy equipment (amphibious excavators) to take out sediment which located at positions could not be done by dredgers (dry-wet excavation), (b) installation of booster pump and floating pipe as support of the dredgers, (c) modification of dredger ladder, (d) management of spoilbank by re-arrange of hauling and reloading cycles, and accelerate sediment material drying by installing vertical-horizontal drainage.

A. COMBINATION OF 2 DREDGING TYPES USING AVAILABLE DREDGERS AND ADDITIONAL HEAVY EQUIPMENT (AMPHIBIOUS EXCAVATORS)

Seeing the condition of the sediment surface in Sengguruh Dam is not evenly distributed in the entire pool area of the reservoir. In some areas the sediment elevation conditions to the water elevation are shallow enough with a depth of 0.5-1 m whereas deep conditions are found in areas that are the main river channel with a depth of more than 1m. This condition causes the dredger can not reach the shallow areas due to the limited draft of the ship and the minimum reach of the dredger ladder. Overcoming this need to be combined using amphibious excavators because the tool can operate in a wetland area that is not too deep or called dry-wet excavation.

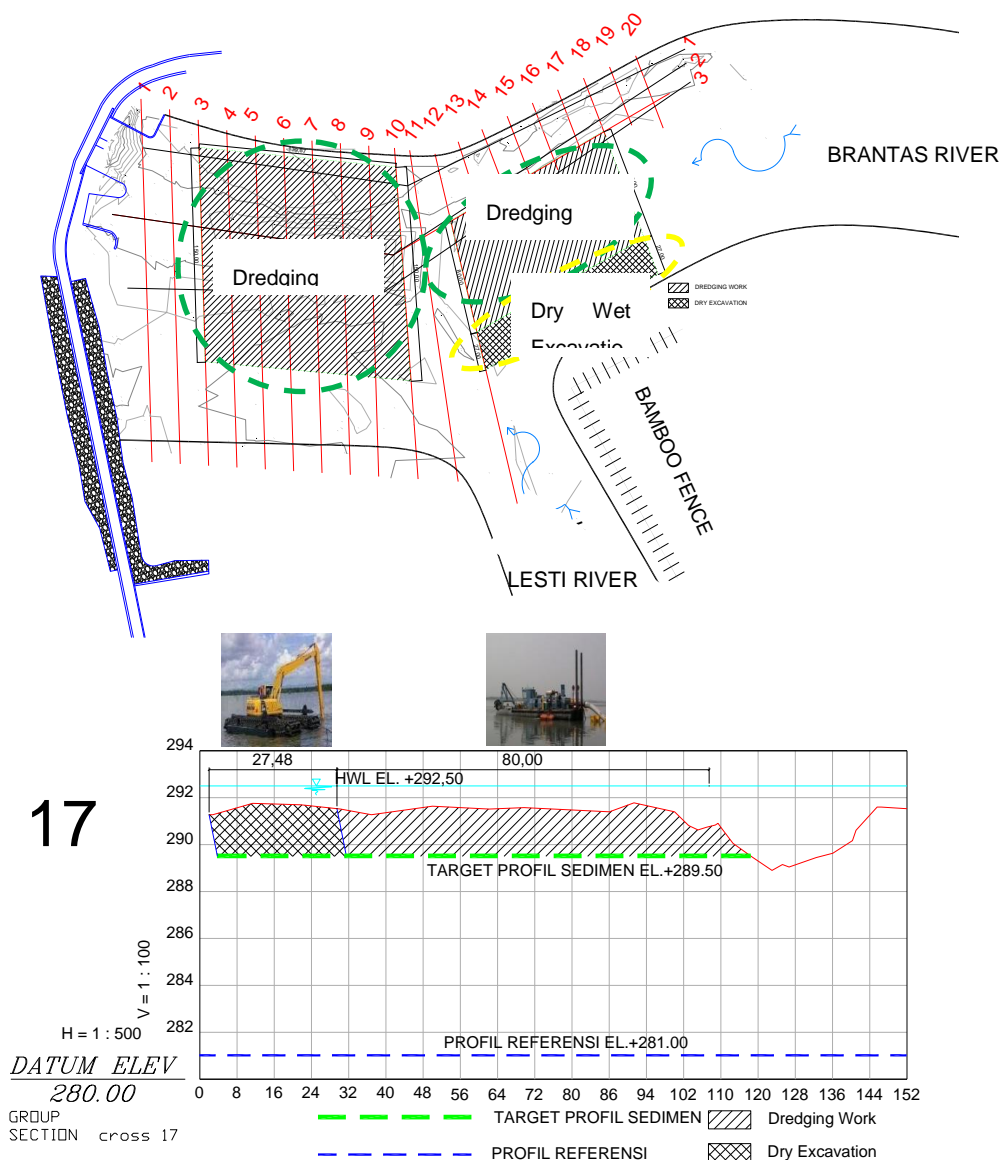
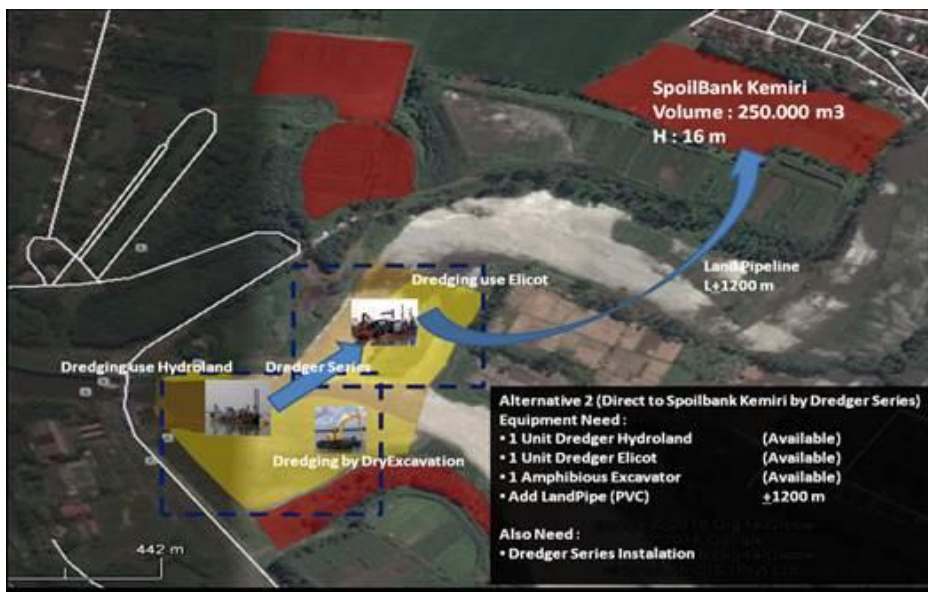
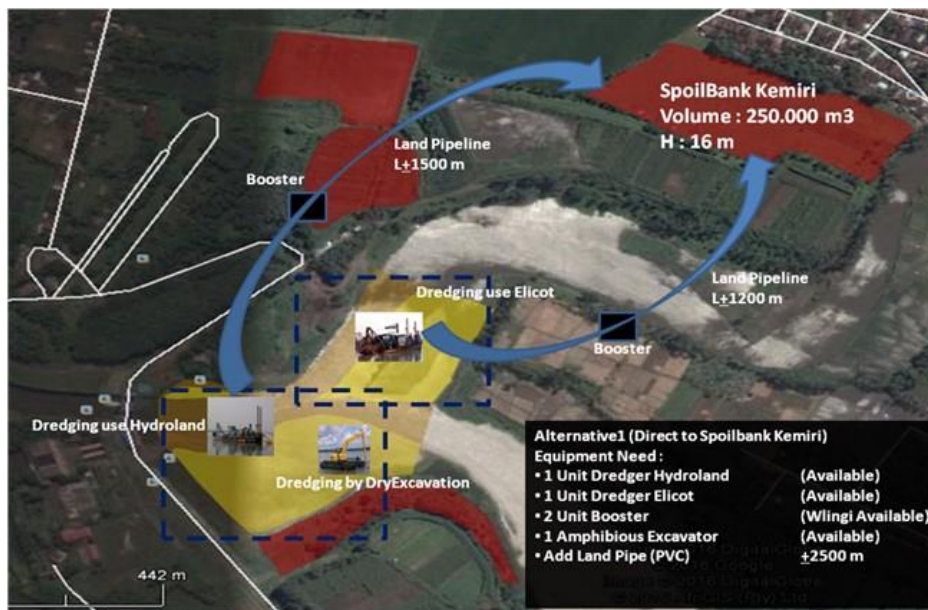


Figure 6. General Plan Dredging Work Combine with Dry Wet Excavation
 Combinaison du travail de dragage du plan général avec l'excavation humide à sec

B. INSTALLATION OF BOOSTER PUMP AND FLOATING PIPE AS SUPPORT OF THE DREDGERS

This method is used in order to support sediment flow from zone 1 near intake to spoilbank area with distance 1500-2000 m at 18 m height. Specifications of existing dredger with type Hydroland and Ellicot are only able to drain sediment optimally at a distance of ± 500 m with a capacity of $\pm 70-100$ m³ / h, so that additional booster is needed, while the previous pipeline using iron pipe and PVC pipe will be replaced by using HDPE floating pipe to be more efficient because of the cheaper material price than the iron pipe and more flexible by using a combination of rubber pipe.



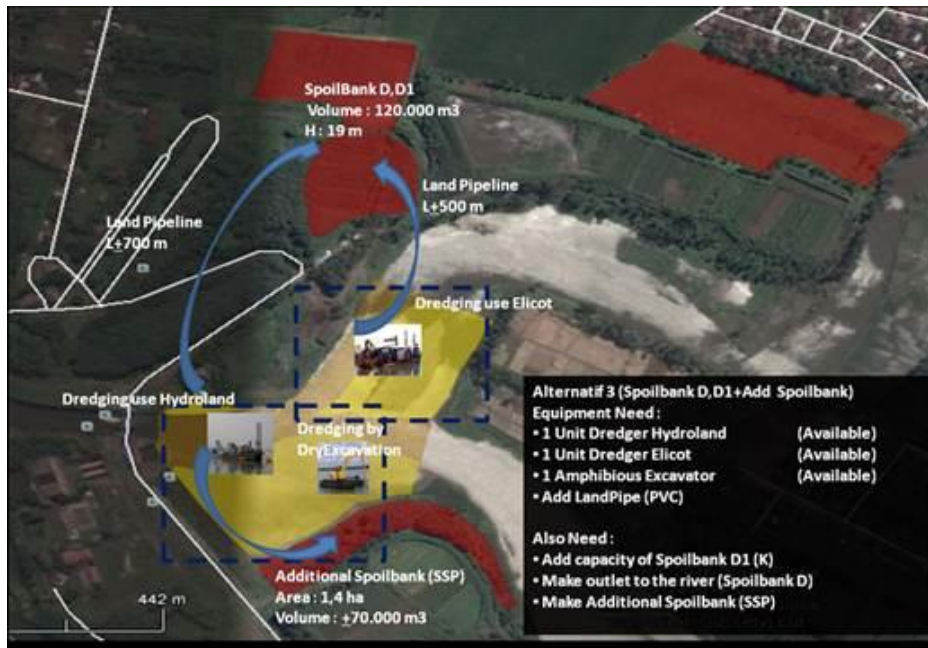


Figure 7. Alternative Scenario of Dredging Work Development Plan in Sengguruh Dam

Scénario alternatif du plan de développement du travail de dragage au barrage de Sengguruh

C. MODIFICATION OF DREDGER LADDER

This is done because the existing dredgers specification is only able to reach the depth of sediment up to ± 5 m, whereas we know that the thickness of the sediment from the surface to the base has reached more than 12 m so that to improve yield and productivity we make modification efforts by extending ladder dredgers become 10-12 m.

D. MANAGEMENT OF SPOILBANK BY RE-ARRANGE OF HAULING AND RELOADING CYCLES

As we already know that the limited availability of land for spoilbank becomes an obstacle in the effort of managing sediment especially to support sediment dredging efforts, because the guarantee of spoilbank availability as a place for the dump material of the dredged sediments greatly influences the volume or the dredging target.

The current condition of existing spoilbank capacity is able to accommodate sediment up to $\pm 200,000$ m³ volume for 1 year period, whereas we have to do annually dredging activities. For that purpose, we made several efforts to maintain the availability of spoilbank by arranging the spoilbank utilization cycle schedule consisting of the hauling schedule (mechanical transfer) and reloading. From the existing spoilbank spoilbank D, D1, and Kemiri we set the maintenance cycle and its use with the aim of all the spoilbank in turn can be used every year.

This arrangement is required because every spoilbank loaded must be dried in advance up to ± 2 years to be reload, and to support the spoilbank drying period acceleration we also make efforts to add technology to the spoilbank construction that is complete with horizontal vertical drain so that the water of the sediment material can immediately flow out so that drying can be faster with an estimated time of 1 year faster. In addition we also make efforts on land acquisition in downstream dam to increase the spoilbank area in the area spoilbank Gampingan.

Table 2. Scheme of Spoilbank Management of Sengguruh Dam

LOCATION	Area (ha)	Distance to Intake	Year											
			2016	Elv.	2017	Elv.	2018	Elv.	2019	Elv.	2020	Elv.		
A. Brantas River														
- Spoilbank I	2.30	750		311	45	45	311	45						
- Spoilbank A	2.92	600		311	60	60	311	60				60	60	
- Spoilbank D	1.45	450	45	311			311	50	50					
- Spoilbank D1	2.50	600	60	309,5	20		309,5			100	100	100		
- Spoilbank Kemiri	3.70	800	200	70	308,5	86	308,5			100	100	100		
- Spoilbank Gampingan	4.50	1.150			180	180	289	180		180			180	
							284							
B. Lesti River														
- Spoilbank C	3.60	850		308,5	100	100	308,5	50		35	15	100	100	
- Spoilbank C1	0.75	750	30	30	308,5	29	308,5			30	30		30	
- Spoilbank B	3.20	400		308,5			308,5	100	100	100				
- Spoilbank B1	1.20	400		308,5	21		308,5			50	50	50		
Built Bamboo Fence (BF) Spoilbank							Repaired							
Built New Spoilbank 2														
TOTAL														
Loading in Spoilbank				305		156		155		185		250		
Spoilbank Half Fill & Ready to use				100		385		330		475		370		
New Land				-		-		-		-		-		
Built Spoilbank (Land Available)				-		180		-		-		-		
Add Spoilbank Capacity (Land Fill)				60		-		-		100		-		
Add Spoilbank Capacity (Bamboo Fence)				-		-		-		-		-		
Hauling Spoilbank				30		205		150		180		160		
Hauling & Add Spoilbank Capacity				-		-		-		-		-		

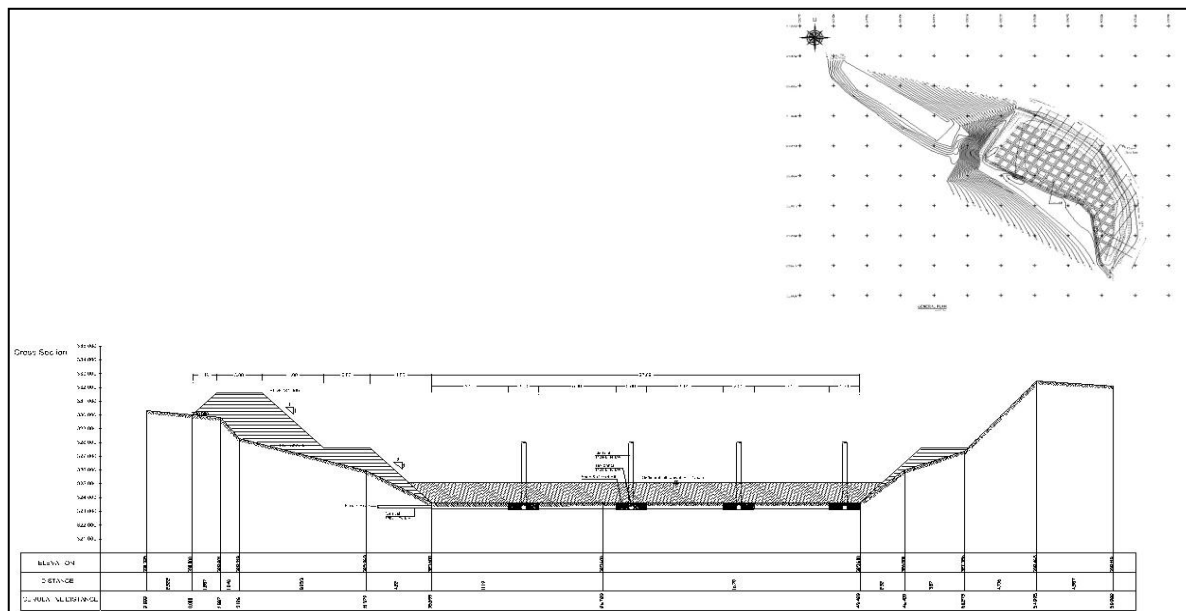


Figure 8. Design of Vertical Horizontal Drainage
Conception de drainage horizontal vertical

4. CONCLUSION AND RECOMMENDATION

4.1. CONCLUSION

Sedimentation is a problem faced by almost all the reservoirs in the world. High sedimentation rate which would threaten the sustainability of the reservoir function and shorten the useful life of the reservoir. Sengguruh reservoir has lost almost 75% of the effective storage since the dam was completed in 1988. To overcome the problem of sedimentation in Sengguruh reservoir some efforts has been conducted sediment management, consist of conservation in the upstream of Brantas River watershed, construction of sediment controlling infrastructure, and sediment dredging. Non-structural efforts such as empowerment and public education have also been carried out. Dredging work in Sengguruh Dam using the dredger has been conducted since 2001. Starting in 2016 the development of dredging work has been done by (a) combination of 2 dredging types using available dredgers and additional heavy equipment (amphibious excavators) to take out sediment which located at positions could not be done by dredgers (dry-wet excavation), (b) installation of booster pump and floating pipe as support of the dredgers, (c) modification of dredger ladder, (d) management of spoilbank by re-arrange of hauling and reloading cycles, and accelerate sediment material drying by installing vertical-horizontal drainage. This dredging method gives the benefit that the dredging of sediment can be implemented more effectively and efficiently to ensure high hydropower production, maintain effective storage capacity and prolong age of reservoir with of course considering environmental aspect around the area. More importantly, it can be done near the hydropower intake because the sediment is increasingly moving forward to the dam.

4.2. RECOMMENDATION

Need to do a more study on the characteristics and processes of sedimentation in Sengguruh reservoir so that the management of sediment through dredging work could be done more effectively and efficiently. Environmental management need to be studied further to minimize the impact.

5. ACKNOWLEDGEMENTS

The authors thank to Jasa Tirta I Public Corporation, the River Basin Organization in Brantas, Bengawan Solo, Jratunseluna, Serayu Bogowonto and Toba Asahan River basins in Indonesia for providing data used in this paper.

6. REFERENCES

Basson, G. R., dan Rooseboom, A., 1999. *Dealing with reservoir sedimentation-dredging*, Water Resources Commission, Pretoria.

Morris, G. L., dan Fan, J., 1998. *Reservoir Sedimentation Handbook: Design and Management of Dams, Reservoir and Watershed for Sustainable Use*, McGraw Hill, New York.

Yang, X., Li, S., dan Zhang, S., 2003. *The sedimentation and dredging of Guanting Reservoir*. *International Journal of Sediment Research*, Vol. 18, No. 2: 130-137.

COMMISSION INTERNATIONALE DES GRANDS BARRAGES

VINGT-SIXIÈME CONGRÈS DES GRANDS BARRAGES
Autriche, juillet 2018

DOI 10.3217/978-3-85125-620-8-021



This work licensed under a Creative Commons Attribution 4.0 International License. <https://creativecommons.org/licenses/by-nc-nd/4.0/>

**NUMERICAL SIMULATION AND EXPERIMENTAL RESEARCH ON REGULAR
MECHANISM OF LOCAL CLIMATIC CHANGES AROUND GIANT
HYDROPOWER RESERVOIR**

Yangbing DENG

XILUODU HYDROPOWER PLANT, CHINA YANGTZE POWER CO., LTD

Jin XU

OVERHAUL AND MAINTENANCE FACTORY,
CHINA YANGTZE POWER CO., LTD

Xiaolong CHEN

XILUODU HYDROPOWER PLANT, CHINA YANGTZE POWER CO., LTD

Guanglin MENG

XILUODU HYDROPOWER PLANT, CHINA YANGTZE POWER CO., LTD

Mi LI

XILUODU HYDROPOWER PLANT, CHINA YANGTZE POWER CO., LTD

CHINA

COMMISSION INTERNATIONALE
DES GRANDS BARRAGES

VINGT-SIXIÈME CONGRÈS DES
GRANDS BARRAGES

Autriche, juillet 2018

**NUMERICAL SIMULATION AND EXPERIMENTAL RESEARCH ON REGULAR
MECHANISM OF LOCAL CLIMATIC CHANGES AROUND GIANT
HYDROPOWER RESERVOIR**

Yangbing Deng^{1,*}, Jin Xu², Xiaolong Chen¹, Guanglin Meng¹, Mi Li¹

1. *Xiluodu Hydropower Plant, CHINA YANGTZE POWER CO.,LTD*
2. *Overhaul and maintenance factory, CHINA YANGTZE POWER CO.,LTD*

CHINA

1. INTRODUCTION

As severe global warming climate comes into effect, the occurrence, frequency and intensity of extreme climate events are increasing rapidly since unbalanced precipitation exists in China's Southwest region. In addition, environmental temperature and humidity significantly affect animals and plants, as well as the stability of the geologic structure^[1-2]. Hydraulic engineering construction plays an important role in water resource allocations, avoiding drought and flood^[3-4]. However, the reservoirs formed by hydraulic engineering structures may affect air temperature and air humidity by changing different evaporation capacity, which could lead to various changes causing extreme climate or disasters^[5-7], such as changes to annual precipitation, annual mean temperature and annual evapotranspiration rate.

Since giant reservoirs could affect local climate over some distance^[8-10], many scholars carried out research topics on quantitative and qualitative analysis of reservoir effects. Their research is mainly based on theory analysis, calculation simulation, prediction or site measured data analysis for giant hydropower

reservoirs:China Three Gorges reservoir,Ertan reservoir,Danjiangkou reservoir etc.^[11-14] The main parameters of annual precipitation and evapotranspiration are different for each location, as the local climate and topography vary.Generally,annual precipitation and annual air temperature increase;annual evapotranspiration rate decreases in summer,but increases in winter in some places.Calculation simulation and experimental research show China Three Gorges reservoir affects air temperature and humidity mainly between 2km upstream and 10km downstream,and nearcirculation could increase air temperature by about 1°C during summer nights, with a 3% humidity difference within 10km of the Three Gorges reservoir^[15-16].

A world-class hydropower station with large reservoir is currently being studied by researchers.It has great water storage capacity,and the local climate is quite complex with the influence of Pacific airflow and Indian airflow in southwest China.Because of actual complex situations and operation data limitations,there are no scholars doing related research for reservoir climate changes in southwest China,especially when the giant reservoir is filled.What's more, local climate around the reservoir is quite different pre and post the hydropower station construction, as well as being affected by reservoir water storage,which could be confirmed clearly by observation of vegetation before and after the reservoir water storage(Figure 1).



a.Before water storage

b.After water storage

Figure 1. Vegetation before and after the reservoir water storage.

2. PHISICAL MODEL

A representative giant reservoir and its surroundings were extracted from the typical hydropower station model in Southwest China that could clarify the reservoir climate changes clearly and representatively.The dam is a double curvature arch dam within maximum height of 285.5m,and results in 600m normal pool level and 540m dead storage level,which provides 12.8 billion m³ of total reservoir volume and 6.5 billion m³ of regulating storage volume(Figure 2).As the hydropower station operates normally,the reservoir will submerge some county districts of

A(Yongshan County),B (Jinyang) and C County (Leibo) etc., as illustrated in Figure 3.

Water depth in the reservoir rises from B County to A County, when the dam comes into effect to store water,and the water depth next to the dam is deepest.The water surface area and water temperature of the reservoir vary from Spring to Winter for various reservoir water levels.



Figure 2. Giant reservoir of the hydropower station in southwest China

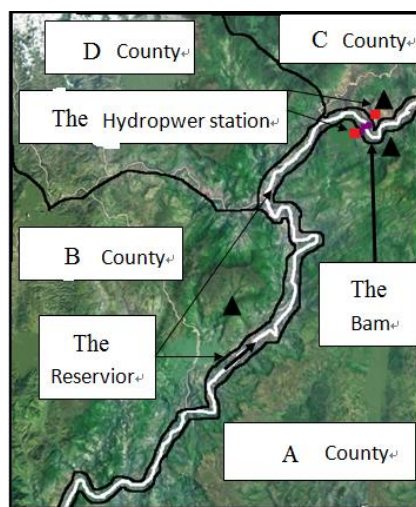


Figure 3. Geographical position of the hydropower station and main reservoir district : ▲stand for measurement points, which could measure air temperature and humidity when reservoir comes into water storage or other conditions

As mentioned in the paper^[17],air humidity would be a specific constant value when, air vapor and water surface evaporation are in dynamic equilibrium. In addition,the vapor medium exchange demonstrates that there exists a law of mutual influence between air humidity and both air temperature and reservoir water temperature.Therefore, there would be significant variations in air temperature and air humidity would around the reservoir,since rainfall and water temperature vary seasonally.

In order to study the mechanism of how reservoir water storage change climate, air temperature and humidity measurements in the district of A County and collection of climate data around the reservoir were promoted carefully in the past six years. The research mainly concentrated on topics of climate changes pre (2011-2013) and post (2013-2016) the reservoir construction, comparative study on water storage rate and air temperature, humidity, etc. Quantitative and qualitative analysis results of the giant reservoir could form laws, which are beneficial to hydropower station design, local vegetation and residents, avoiding extreme disasters in the region.

3. THEORY ANALYSIS

Heat and moisture transfer occurs between the air and the reservoir water surface, according to equation (1). When there is a temperature difference at the reservoir water surface, sensible heat, latent heat and moisture would transfer continuously to approach the equilibrium state^[18].

$$E = S \left[6.1 \exp \left(\frac{L}{273 R_v} * \frac{t}{273+t} \right) - \rho_v R_v (273 + T) \right] \quad (1)$$

Where E represents evaporation capacity of reservoir water surface (Kg). It is determined by surface areas S (m²) and moisture difference value between air moisture concentration and saturated concentration, L for latent heat of water evaporation (KJ/Kg), R_v for specific gas constant of water and vapor, t for reservoir surface water temperature (K), T for air temperature (K) and ρ_v for density of water vapor (Kg/m³).

The air boundary layer transfers sensible heat to the reservoir water surface, when the air temperature of the boundary layer is higher than that of the water surface, and water vapor transfers from the reservoir water surface to the air boundary layer, if its molecular solubility does not reach the saturated solubility of air vapor. Thus, heat and moisture transfer mainly depends on the temperature difference and moisture solubility of the air boundary layer, and the macroscopic computational complexity of the process could be solved by followed equation (2).

$$PE = \frac{0.408 \Delta (R_n - G) + \gamma \frac{900}{T_a + 273} u_2 (e_s - e_a)}{\Delta + \gamma (1 + 0.34 u_2)} \quad (2)$$

Where PE represents possible evaporation amount (mm/d), R_n for surface net radiation [MJ/(m²d)], G for soil heat flux [MJ/(m²d)], T_a for daily mean temperature (K), u₂ for wind velocity at 2m height (m/s), e_s for saturated vapor pressure (kPa), e_a for actual vapor pressure (kPa), Δ for curve slope of saturated vapor pressure (kPa/°C), γ for psychrometric constant (kPa/°C).

Taking everything into account, air temperature and moisture are affected by heat and mass transfer between the air boundary layer and the reservoir water surface, especially during the water storage period the contact area. Based on the above theory analysis, research on climate changes firstly collected related annual and monthly climate data and calculated correlation between climatic elements and time sequences to summarize climate tendency at different times. In order to test the significance of important parameters, the t testing method was taken to verify the average difference of climate elements, pre and post reservoir water storage, and the F testing method was for evaluating the influence of climate change in the above process.

4. THEORY ANALYSIS

Climate changes were analyzed in representative counties around the reservoir. A County was selected for climate trend analysis close to the reservoir, as well as the dam (about 3km from the weather station), B County for the reservoir upstream (about 7km from the weather station). Additionally, A County was also analyzed for the effects of water storage, since it is largely affected by the reservoir. Air temperature, humidity and precipitation were studied comprehensively concerning climate changes, from 1st January 2011 to 31st December 2016. To distinguish the trends of climate change, periods of air temperature and air humidity were analysed as follows: 1st December to 28th February, 1st March to 31st May, 1st June to 31st August, 1st September to 30th November, being winter, spring, summer and autumn respectively, and the main flood season was taken as 1st May to 30th September.

4.1. CLIMATE CHANGES IN A COUNTY

As shown in Figure 4, the air temperature of A County displays some differences before and after water storage, especially in the winter and summer seasons. Compared to the air temperature before water storage, the air temperature after water storage has little temperature difference, which is concentrated between 8.4 °C and 25.2 °C. The maximum temperature difference is 7°C higher than the previous record in winter. What's more, air temperature is essentially the same in the spring and autumn seasons.

Due to the huge specific heat capacity of water, large temperature differences result in summer and winter after water storage. Reservoir water releases heat to the air, causing higher air temperatures than before and vice versa in summer. Air temperature keeps consistent in spring and autumn, since there are no large temperature changes and little heat transfer between air and water. Therefore, there exists a more suitable environmental for people to live and plants to grow.

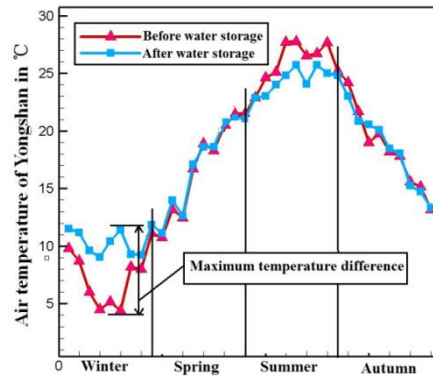


Figure 4. Air temperature comparison of A County pre and post water storage of the reservoir

Figure 5 shows that air humidity in A County rises greatly after water storage. In total, the maximum humidity difference is 25% in spring. Increases in both the evaporation area of the reservoir water surface and the environmental temperature are the main reasons for air humidity increasing. In contrast with other seasons, the air humidity in summer shows little increase because of the high humidity and temperatures in this season, when it is difficult to break air vapor balance.

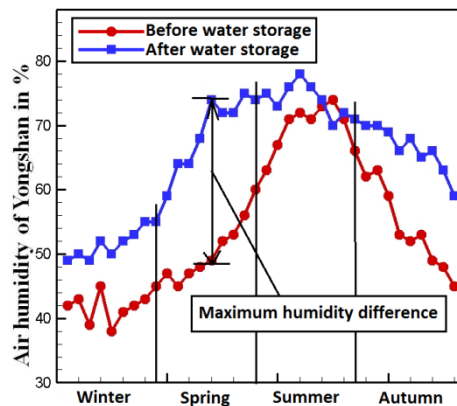


Figure 5. Air humidity comparison of A County pre and post water storage of the reservoir

Precipitation of A County is mainly concentrated between the months of May and September, which have 78% of annual precipitation. As illustrated by the air humidity analysis in Figure 6, air humidity is relatively higher in late spring, summer and early autumn, and could be beneficial in the vapor condensation process. Monthly mean precipitation is above 120mm between June to August, so potential flood disasters should be considered due to extreme weather events.



Figure 6. Monthly mean temperature and precipitation of A County after water storage

After water storage in the reservoir, precipitation of A County increases during all seasons, including during the flood season (Figure 7). Annual precipitation increases nearly 70% than the previously. However, precipitation in winter and spring is often scarce for human consumption and agricultural production, so the reservoir could provide a water source for these.

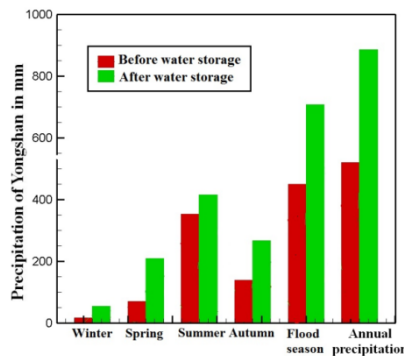


Figure 7. Precipitation comparison of A County pre and post water storage of the reservoir

4.2. CLIMATE CHANGES IN B COUNTY

As shown in Figure 8, air temperature of B County has the same change trend as A County pre and post the water storage of the reservoir, but within smaller changes. For example, maximum temperature difference of B County is 3.8°C in summer, and A County is 7°C in winter. This is because temperature of B County is higher than A County in summer, and the reservoir has less effect on B County air temperature.

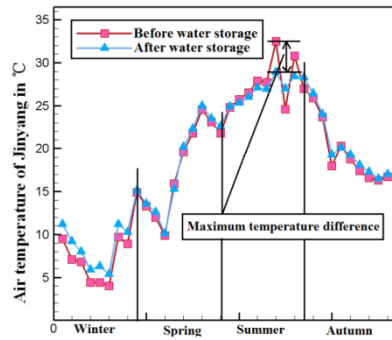


Figure 8. Air temperature comparison of B County pre and post water storage of the reservoir

Figure 9 demonstrates that the air humidity of B County is less affected than for A County. The maximum humidity difference of B County is 18% in spring compared to 25% for A County. Their maximum humidity differences are all in spring, since air temperature in spring keeps median values, with almost the same evaporation.

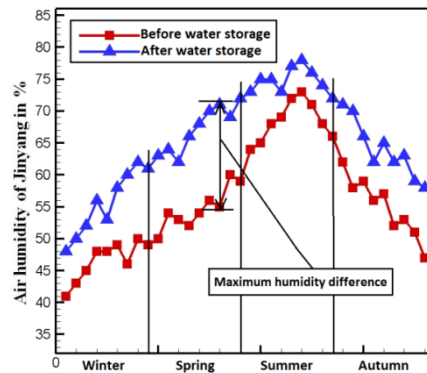


Figure 9. Air humidity comparison of B County pre and post water storage of the reservoir

Precipitation of B County again increases in all seasons, with annual precipitation increases just 31%. Compared to A County, B County has less specific heat capacity of water, lower temperature adjustment and air humidity at a farther distance from the dam.

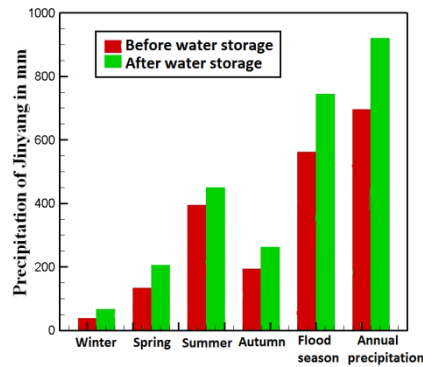


Figure 10. Precipitation comparison of B County pre and post water storage of the reservoir.

REFERENCES

- [1] MORLING K,HERZSPRUNG, P&KAMJUNKE N(2017).Discharge determines production of,decomposition of and quality changes in dissolved organic caron in pre-dams of drinking water reservoir.science of the total environment.Volume577,PP329-339
- [2] WEN ZF,WU SJ,CHEN JL&LU MQ(2017).NDVI indicated long-term interannual changes in vegetation activities and their responses to climatic and anthropogenic factors in the Three Gorges Reservoir Region,China.Science of the Total Environment.Volume 574,pp947-959
- [3] Yasarer LMW&Sturm BSM(2016).Potential impacts of climate change on reservoir services and management approaches.Lake and Reservoir Management, Volume 32,Issue 1,pp13-26.
- [4] Krol MS,Vries MJ, Van Oel PR&Araujo JC(2011).Sustainability of small reservoirs and large scale water availability under current conditions and climate change.Water ResourcesManagement.Volume 25,Issue 12,pp3017-3026.
- [5] IsmailT,HarunS,ZainudinZM&ShahidS(2017).Development of an optimal reservoir pumping operation for adaptation to climate change.KSCE Journal of Civil Engineering.Volume 21,Issue 1,Pp467-476
- [6] Wood SA,Borges H, Puddick J&Biessy L(2017).Contrasting cyanobacterial communities and microcystin concentrations in summers with extreme weather events:insights into potential effects of climate change.Hydrobiologia, Volume 785,Issue 1,pp71-89.

- [7] Eum HI,Vasan A&Simonovic SP(2016).Integrated reservoir management system for flood risk assessment under climate change.Water Resources Management.Volume 26,Issue 13,pp3785-3802.
- [8] Vicente-Serrano SM,Zabalza-Martinez,Borras G,Lopez-Moreno JI, etc. (2017).Effect of reservoirs on streamflow and river regimes in a heavily regulated river basin of Northeast Spain.Citena,Volume149,Issue 3,pp727-741.
- [9] EhapaluK,Tonnol,ReitaluT,AlliksaarT, etc. (2017).Sedimentary carbon forms in relation to climate and phytoplankton biomass in a large shallow,hard-water boreal lake.Journal of Paleolimnology.Volume 57,Issure 1,pp921-938.
- [10] McGloin R,McGowanH&McJannetD(2016).The potential effects of anthropogenic climate change on evaporation from water storage reservoirs within Lockyer Catchment,south-east Queensland,Australia.Marine and Freshwater Research.Volume 67,Issue 10, pp1512-1521.
- [11] Yang G,Guo SL,Li LP&Hong XJ(2016).Multiobjective operatng rules for Danjiangkou Reservoir under climate change.Water Resources Management.Volume 30,Issue 3,pp1183-1202.
- [12] Gebre S,Boissy T&Alfredsen K(2014).Sensitivity to climate change of the thermal structure and ice cover regime of three hydropower reservoirs.Journal of Hydrology,Volume510,pp208-227.
- [13] Chen Guochun(2007).Influence of the reservoir on local climate at Ertan hydropower station on Yalong river.Sichuan Water Power, Volume 26,Issue 2,pp78-81(In Chinese).
- [14] Ma Zhanshan,Zhang Qiang&Qin Yanyan(2010).Numerical simulation and analysis of the effect of Three Gorges reservoir project on the regional climatechange.Resource and Environment in the Yangtze Basin, Volume 19,Issue 9,pp1044-1052(In Chinese).
- [15] Wu Jian,Gao Xuejie,Zhang Dongfeng&Shi Ying(2011).Regional Climate model simulation of the climate effects of the Three Gorges reservoir with specific application to the summer 2006 drought over Sichuang-Chognqing area.Journal of Tropical Meteorology, Volume 27,Issue 1,pp44-52, (In Chinese).
- [16] Zhang Hongtao,Zhu Changhan&ZhangQiang(2004).Numerical modeling of microclimate effects produced by the formation of the Three Gorges reservoir.Resource and Environment in the Yangtze Basin, Volume 13,Issue 2,pp133-137, (In Chinese).
- [17] Wang Na,Sun Xian,Cai Xinling&Wangqi(2010).Characteristics of climate change in ankang reservoir upstream basin before and after impoundment.Meteorological Science and Tech- nology ,Volume 38,Issue 5,pp649-654, (In Chinese).

- [18] Wang Zhihong, Tian Lei, Li Yanchun & Cao Ning (2014). Comparative analysis of climate change in upper basin of Qingtongxia reservoir between impounding before and after. *Ningxia Engineering Technology*, Volume 13, Issue 3, pp241-246, (In Chinese).

SUMMARY

1. Air temperature of A County and B County display some differences pre and post water storage, especially in the winter and summer seasons, with the maximum temperature differences being 7°C and 3.8°C respectively. After water storage in the reservoir, air temperature is more stable than previously. In addition, air temperature effects depend on the distance from the dam to the data measuring points and are more obvious at closer locations.

2. After water storage in the reservoir, air humidity increases largely in the seasons of winter, spring and autumn, with little rise in summer. Air humidity of A County behaves similarly to B County, but the former is more obviously affected than the latter. The maximum air humidity differences are 25% and 18% respectively.

3. Precipitation of A County and B County increase all year round, as well as during the flood season. Annual increases in precipitation are 70% and 31% respectively, and the main precipitation is concentrated during the flood season, which warns that human beings should expect extreme weather events and potential flood disasters in this period.

4. Water storage in the reservoir could increase the specific heat capacity of the water volume and affect air temperature and humidity by the evaporation-condensation process. Air temperature is quite an important factor regarding air humidity, as the transfer of humidity to precipitation is the reason why annual precipitation is mainly concentrated during the flood season, with the need to prevent flood disasters during this period.

COMMISSION INTERNATIONALE
DES GRANDS BARRAGES

VINGT-SIXIÈME CONGRÈS DES
GRANDS BARRAGES
Autriche, juillet 2018

RUNOFF AND SEDIMENT TRANSPORTATION IN UPPER AND MIDDLE REACHES OF JINSHA RIVER

Yan XIA, Zhou YINJUN, Jin ZHONGWU

CHANGJIANG RIVER SCIENTIFIC RESEARCH INSTITUTE, WUHAN

CHINA

EXTENDED ABSTRACT

Jinsha river is the lower stretch of the source region of the Yangtze river, whose runoff mostly delay on the melting of glaciers, and is greatly affected by climate change. Otherwise the hydropower resources is rich in Jinsha basin, and since the Jin Anqiao Hydropower Station has been built in December 2010, several reservoirs have impounded successively. A reservoir group has been formed in middle reach of Jinsha river basin, which plays a huge role in intercepting sediment.

Through statistical analysis of water and sediment data of Zhimenda, Shigu and Panzhihua hydrologic stations in the upper and middle reach of Jinsha river basin, this paper presents the sediment transport characteristics of the reach, including the sediment sources and distribution, the annual variation and annual distribution of sediment load. Then, the method of multiple regression analysis was used to evaluate the sediment trap amount of the reservoir group in the middle stretch.

The calculated results showed that, during year 2001 to 2016, the annual average runoff amount of the Zhimenda station has increased about 24.24% than that of year 1957 to 2000, but the runoff of Shigu and Panzhihua stations haven't changed much. Compared to the annual average sediment discharge of year before 2000, during year 2001 to 2010, the three stations have increased 6.97%, 28.94%, 4.75%, respectively; during year 2011 to 2016, the Zhimenda and Shigu station both increased about 11%, however, the Panzhihua Station decreased

about 88.21%. The sediment trap amount of the reservoir group in the middle reach of Jinsha river is about 2.08×10^8 t during year 2011 to 2016.

REFERENCES

- [1] WANG GUOQING,ZHANG JIANYUN,THOMAS C P ,et al. Identifying contributions of climate change and human activity to changes in runoff using epoch detection and hydrologic simulation. *Journal of Hydrologic Engineering*. 2013,18(11) : 1385 -1392.
- [2] ZHANG XINBAO, WEN ANBANG, WALLONG D E, et al. Effects of large-scale hydropower reservoirs on sediment loads in Upper Yangtze River and its major tributaries. *Journal of Sediment Research*, 2011 (8) : 59 -66.
- [3] YANG X, LU X. Estimate of cumulative sediment trapping by multiple reservoirs in large river basins: An example of the Yangtze River basin. *Geomorphology*, 2014, 227: 49-59.
- [4] ZHOU Y, PERSAND N, WANG H. Scale invariance of daily runoff time series in agricultural watersheds[J]. *Hydrology and Earth System Sciences*, 2006,10:79-91.
- [5] GOCIC M, TAJKOVIC S. Analysis of Changes in Meteorological Variables Using Mann-Kendall and Sen's Slope Estimator Statistical Tests in Serbia. *Global and Planetary Change*, 2013(100) : 172-182.
- [6] XU JIONGXIN. Recent variation in water and sediment in relation with reservoir construction in the upper Changjiang River basin. *Journal of Mountain Science*, 2009, 27(4) : 385-393.
- [7] CHEN SONGSHENG, ZHANG OUYANG, CHEN ZEFANG, et al. Variations of runoff and sediment load of the Jinsha River . *Advances in Water Science*. 2008,19(4) : 475-482.
- [8] YANG, S. L., ZHANG, J., ZHU, J.,etal. Impact of dams onYangtze River sediment supply to the sea and delta wetland response. *Journal of Geophysical Research*. 2005, 110.

COMMISSION INTERNATIONALE DES GRANDS BARRAGES

VINGT-SIXIÈME CONGRÈS DES GRANDS BARRAGES
Autriche, juillet 2018

DOI 10.3217/978-3-85125-620-8-023



This work licensed under a Creative Commons Attribution 4.0 International License. <https://creativecommons.org/licenses/by-nc-nd/4.0/>

**STUDY ON THE SEDIMENTATION CHANGES IN THE MANWAN RESERVOIR
ON THE LANCANG RIVER**

Pang BOHUI

Technology R&D Center, HUANENG LANCANG RIVER HYDROPOWER LTD.

Li MENG YANG

Technology R&D Center, HUANENG LANCANG RIVER HYDROPOWER LTD.

Lu JI

Technology R&D Center, HUANENG LANCANG RIVER HYDROPOWER LTD.

Chen HAO

Technology R&D Center, HUANENG LANCANG RIVER HYDROPOWER LTD.

CHINA

STUDY ON THE SEDIMENTATION CHANGES IN THE MANWAN RESERVOIR ON THE LANCANG RIVER*

Pang Bohui, Li Mengyang*, Lu Ji, Chen Hao

Technology R&D Center, HUANENG LANCANG RIVER HYDROPOWER LTD.

CHINA

1. INTRODUCTION

The Lancang - Mekong River, originating from the Tanggula Mountains in Qinghai-Tibet Plateau of China, flows from north to south successively across Qinghai, Tibet and Yunnan in China, and then Myanmar, Thailand, Laos, Cambodia and Vietnam. It empties into the South China Sea to the west of Ho Chi Minh City of Vietnam. The Lancang River has a river length of 2100km, and a drainage area of $17.4 \times 10^4 \text{km}^2$. 23 cascade hydropower plants have been planned with a total installed capacity of about 32 million kWh. At present, six cascade power plants have been built on mainstream of the middle and lower reaches of the Lancang River, which are successively downstream Gongguoqiao, Xiaowan, Manwan, Dachaoshan, Nuozhadu and Jinghong. And now the Lancang River is the only north-to-south cross-country river that has been totally developed in China. Changes in hydrology and the ecological environment of an international river due to the hydropower development are now drawing more and more attention internationally. One major problem is the sedimentation caused by dams, which have influences not only on the reservoir operation, but also on the migration and transformation of the biogenic substance including carbon and phosphorus in the river. For this reason, it is very important to study the sedimentation problem of the Lancang River due to damming, evaluate and predict the problem scientifically and provide a theoretical foundation and data support for studying the reservoir operation and the ecological environment

**titre de l'article complet*

changes in the transboundary river.

The Manwan HPP is the most typical case of reservoir sedimentation problems of the Lancang River. Its construction was started in 1986 and put into operation in 1993. As the first hydropower plant on the main stream of the Lancang River, it has accumulated lots of measured data on sedimentation over the years. The Manwan HPP stands on the middle reach of the Lancang River, the backwater of which reaches the Xiaowan HPP, and it neighbors the Dachaoshan HPP downstream. Its dam is a concrete gravity dam with a crest length of 418m and a maximum dam height of 132m as well as a crest elevation of 1002.0m. Its normal water level is 994m, total capacity of reservoir is 920 million m³, dead storage capacity is 663 million m³, and the regulating storage capacity is 257 million m³. It is a seasonally regulating reservoir. The annual mean sediment runoff is about 40 million tons, the measured maximum sediment charge is 14.3kg/m³, and the mean sediment charge is 1kg/m³.

The limiting level during the flood season (June - September) for desilting was set for the Xiaowan HPP before it was put into operation, which was 988m. When the Xiaowan HPP was put into operation, the Manwan HPP's operating water level for desilting during the flood season was deactivated. Within 20 years after the Manwan HPP was put into operation, the reservoir was mainly operated in the method of "storing clear and releasing muddy", where the operating water level was lowered prior to and after the flood season every year and the sediment was flushed through the special holes at the bottom of the right and left banks to effectively clear away the mud at the water intake and reduce the regulating capacity loss. In 2010, after the operation commencement of the Xiaowan HPP, its regulating ability as the leading reservoir began to function. To fully exert the power generation capacity of the hydropower plants, the Manwan HPP has been operating at a high water level all year round since then. The change in the operation mode has led to the change in sedimentation in the reservoir.

2. SURVEY OF SEDIMENTATION IN THE MANWAN RESERVOIR

2.1. UNDERWATER TOPOGRAPHIC SURVEY PLAN FOR THE MANWAN RESERVOIR

According to the current situation and characteristics of the reservoir area of the Manwan HPP, the following underwater topographic survey plan shall be implemented: A multi-beam sounding system shall be used to collect the cloud data of underwater high-density points, which consists of a SONIC 2024 high-performance multi-beam sounding instrument from R2Sonic Company of America, Octans fibre-optical rhumbs from France and a Trimble R7 GNSS receiver from America; GPS-RTK real-time positioning technology shall be used for the underwater data collection with the assistance of Hi Target HD27 single beam echo sounder in the shallow area and the total station and the digital echo

sounder shall be used for the data collection where GPS signal is unavailable; For topographic survey on the shore, GPS-RTK shall be the main collecting mode while using the total station as assistance.

Within 2km of the section in front of dam, the survey shall be carried out as per the scale of 1:200 and the reservoir area as per 1:2000.

2.2. CROSS SECTION SURVEY OF RIVERS IN THE RESERVOIR AREA

The latest survey in 2014 covered 72 cross sections of main stream (Fig.1), which were numbered LM09 - LM73, and 8 tributary stream sections of the Gonglang River, numbered LMG01 - LMG04, so the total number were 80 (of which, the A water gauge, B water gauge, lower water gauge and LM73-1 - LM76 for a total of 7 sections were within the warning line of the Xiaowan HPP and were not included in the survey). GPS-RTK real-time dynamic positioning technology shall be used for the layout detection of each end point of the cross section. If the horizontal positioning accuracy is within 3cm and the elevation accuracy is within 3cm, it can be concluded that the end points of the cross section are relatively steady.

(1) Two underwater survey plans shall be prepared for cross section survey: First, use the GPS RTK real-time dynamic positioning technology assisted by the multi-beam sounding system for automatic survey, where the point cloud data of the underwater area scanned by the multi-beam sounding system shall be outputted and the underwater topographic points of the cross section line shall be worked out; Second, use the GPS RTK real-time dynamic positioning technology assisted by the HD27 single beam echo sounder for automatic survey and data collection in addition to collecting plane and 3D data of the measuring points.

A total station or GPS RTK shall be used to record the plane and elevation data of measuring points for the on-shore part of the cross sections.

(2) Before the survey, GPS RTK shall be checked with two or more known points which shall not be put into use before qualification. The measured values are all fixed solutions and information from more than 5 satellites shall be received.

(3) The data collection of measurement points by GPS RTK with the assistant HD27 shall be carried out at the space of 3m. The water depth shall also be collected simultaneously and the navigation procedure shall be activated to follow the cross section reference line.

(4) The allowable control accuracy of the horizontal measuring points shall not be greater than 0.5m away from the cross section lines.

(5) The elevations of the two reference points via the cross section regulation are the same and the calculated distance of the two end points is equal to the accumulated distance of the cross section.

(6) The remark column of the survey results of the cross sections shall indicate the properties of each measuring point (e.g. paddy field, dry land, land type, steep canker, cliff, highway, village, water edge, underwater).

2.3. LONGITUDINAL SECTION SURVEY OF RIVERS IN THE RESERVOIR AREA

Two methods shall be used for the longitudinal section survey of rivers in the reservoir area: First, the polar coordinate method; Second, GPS RTK real-time dynamic positioning method. The GPS RTK real-time dynamic positioning is the major method to be adopted with the polar coordinate method as the supplementary means. All the waterpoints within the reservoir area shall be surveyed in addition to the important feature points on land for data collection at a space of 20m. The main technical requirements for the survey operation are as follows:

(1) Survey Scale: 1:2000.

(2) Survey Coverage: From the Manwan HPP dam site to the warning line of the Xiaowan HPP (from the dam site to LM73), including a main-stream river length of 58km and a branch river length of 3km.

(3) Characteristic positions, such as cross sections, bridges, hydropower plants, tributary inlets, water gauges, and the flow gauging cable way of the hydrometrical station shall be provided with the measuring points and labeled with names. The measuring points shall be densified at the river sections with rapids, drops, river bends and branching based on the principle of controlling the longitudinal change of the river.

(4) The measuring point shall be indicated where it is at a place with a characteristic topography or ground feature. For example, villages, bridges, tributaries (gullies) inlets (left and right banks), rapids, drops, river bends, beaches, and the hydropower plants. Also, the elevations of the characteristic places like the bridge decks and hydropower plants (plant floor, tail water) shall be indicated.

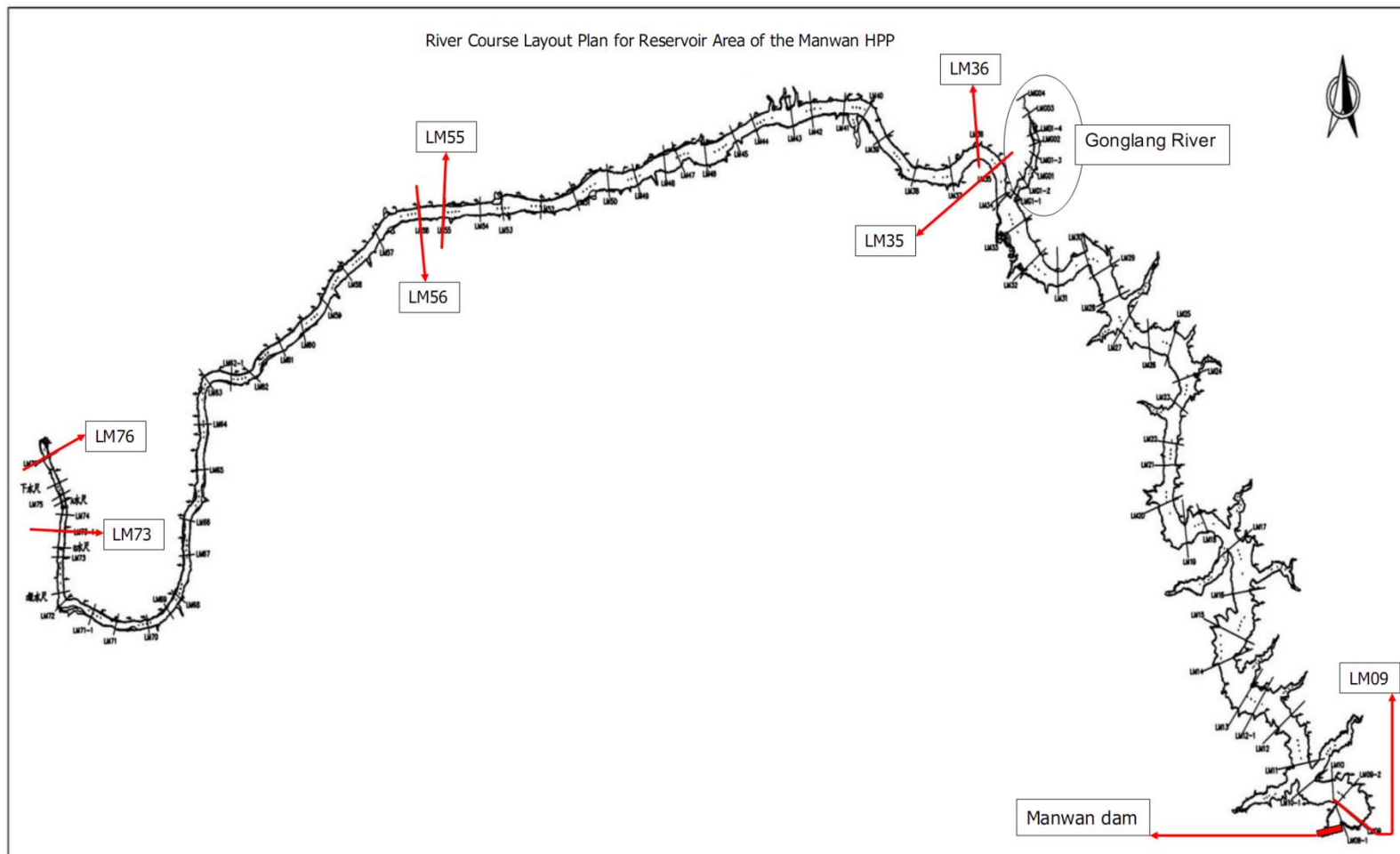


Fig. 1
River Course Layout Plan for Reservoir Area of the Manwan HPP

3. ANALYSIS OF SEDIMENTATION IN THE MANWAN RESERVOIR

3.1. THE SEDIMENTATION FORM OF THE RESERVOIR

The sedimentation analysis shall be based on the section drawings based on the data collected during the surveys in 2005, 2009 and 2014, as shown below:

(1) Fig. 2 is the Main-Stream Talweg Longitudinal Section of the Reservoir, which shows that the sedimentation takes on an obvious delta deposit form, with a front slope gradient of about 2.6‰ and a top slope gradient of about 0.20‰. The sedimentation surface of the delta has been raised year by year and pushed forward to the dam. The head of the delta is about 16.9km from the dam, and the top elevation of the delta is about 983.34m, trending basically the same as in 2009. The reservoir has not reached the balance between scouring and silting.

(2) The Xiaowan HPP was impounded in 2009, thus, based on the relevant data, the yearly average sediment volume to be retained of the Xiaowan Reservoir is 48 million tons (about 32million m³) above the dam site, which greatly relieved the sediment problem of the Manwan HPP. In terms of the lateral distribution of sedimentation of the reservoir, compared with the results in 2009, the sedimentation volume for the whole reservoir is relatively small, the sedimentation volume in the section in front of dam (dam - LM35 section) is more than the back section, with the average sedimentation height of 1.2m and the highest sedimentation height of 6.1m; The sedimentation volume in the section in the middle of the reservoir (LM36 - LM55) is relatively small with the average sedimentation height of 0.5m; The section at the end of the reservoir (LM56 - LM73) generally shows the scouring, which mainly occurred on both sides of the reservoir; For the section conditions, the section in front of the dam (LM09 - LM35) basically shows the horizontal sedimentation, and the section in the middle of the reservoir mainly shows the balance between scouring and silting, the sedimentation volume in the section at the end of reservoir is quite small, and the section near the Xiaowan dam site shows the scouring on both sides.

(3) There are few tributaries in the Manwan Reservoir area, and there is only one bigger tributary – the Gonglang River in the reservoir area. The distance from the mouth of the tributary to the Manwan dam site is about 21km. The upstream area basically shows the scouring, while the scouring volume is quite small. And, as per the scouring sedimentation volume, the Gonglang River has basically reached the balance between the scouring and silting.

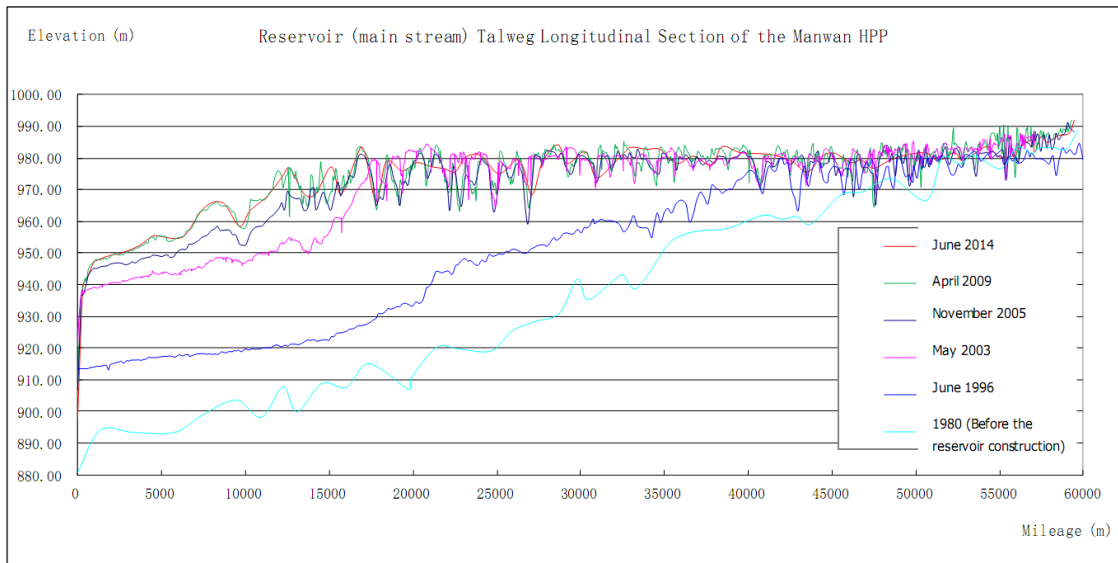


Fig. 2
Talweg Longitudinal Section

3.2. ANALYSIS OF THE SEDIMENT-CAUSED STORAGE CAPACITY LOSS

Now, the storage results calculated and measured by the topographic map before the reservoir construction, in 1996, 2005, 2009 and 2014 have been collected, as well as the results of the cross section survey of the reservoir before the reservoir construction, in 1996, 2000, 2003, 2005, 2009 and 2014, and the method of section is applied to calculate the storages over the years. In order to eliminate the errors caused by the two calculation methods, the storage capacities calculated by the method of section in 2000 and 2003 shall be corrected, and the calculated characteristic capacity and sediment-caused storage capacity loss are shown in Fig.3 and Table 1.

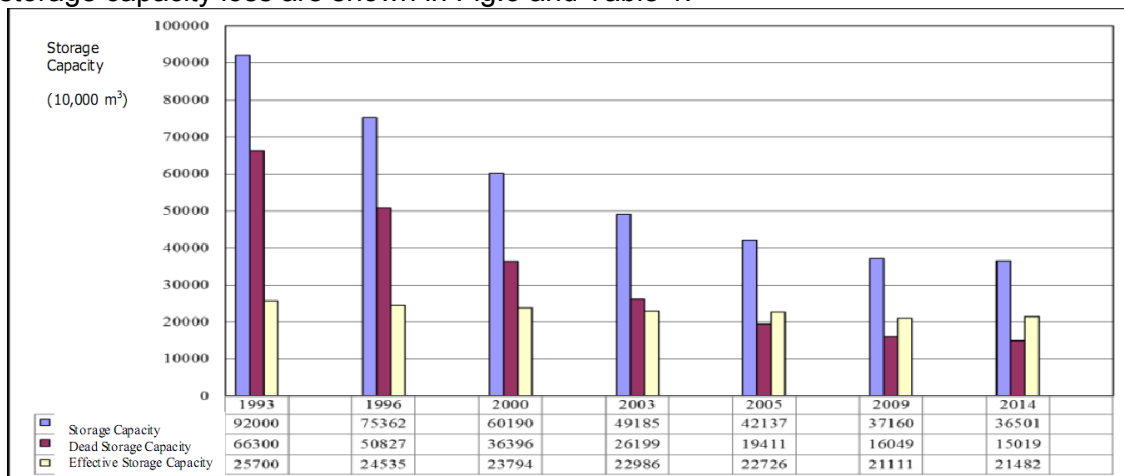


Fig. 3
Characteristic Storage Change in the Manwan Reservoir

Table 1
Characteristic storage of the Manwan reservoir and the sediment-caused storage capacity loss

Project	Before the Reservoir Construction	Impounding after April 1993						
	1993	1996	2000	2003		2005	2009	2014
Storage Below NWL (10,000 m ³)	92000	75362	60190	49185		42137	37160	36501
Sediment-Caused Storage Capacity Loss Below NWL (10,000 m ³) - between the Two Measurements		16638	15172	11005	7048	4977	659	
Rate of Sediment-Caused Storage Capacity Loss below NWL (%)		18.08	34.58	46.54		54.20	59.61	60.33
Dead Storage Capacity (10,000 m ³)	66300	50827	36396	26199		19411	16049	15019
Sediment-Caused Dead Storage Capacity Loss (10,000 m ³) - between the Two Measurements		15473	14431	10197	6788	3362	1030	
Rate of Sediment-Caused Dead Storage Capacity Loss (%)		23.34	45.1	60.48		70.72	75.79	77.35
Effective Storage	25700	24535	23794	22986		22726	21111	21482

Capacity (10,000 m ³)							
Sediment- Caused Effective Storage Capacity Loss (10,000 m ³) - between the Two Measurements		1165	742	807	260	1615	-371
Sediment- Caused Effective Storage Capacity Loss (%)		1.53	7.42	10.56	11.57	17.86	16.41

According to Fig.3, the variation tendency for storage capacity of the Manwan Reservoir is: the storage capacity below NWL, dead storage capacity and effective storage capacity is reduced year by year, the loss ranges for the storage capacity below NWL and dead storage capacity are quite large and basically synchronized, and the loss range for the effective storage is relatively small. Since the Xiaowan HPP was put into operation in 2009, the sedimentation in the Manwan Reservoir area is significantly mitigated.

According to Table 1, since the power plant is put into operation until 2014, the total sedimentation volume below the normal water level - 994m is 554.99 million m³, the residual storage capacity below NWL of the reservoir is 365.01 million m³ and the loss rate for the storage capacity below NWL is about 60.33%; the sedimentation volume below the dead water level - 982m is 512.81 million m³, the residual dead storage capacity is 150.19 million m³, and the loss rate for the dead storage capacity is 77.35%; and the sedimentation volume for the effective storage capacity is 42.18 million m³, the residual effective storage capacity is 214.82 million m³, and the loss rate for the effective storage capacity is about 16.41%.

See Table 2 for the comparison of the measured reservoir sedimentation volume over the years and the predicted sedimentation volume in the initially-set stage.

Table 2
Characteristic storage capacity of the Manwan reservoir and sediment-caused storage capacity loss

	Sedimentation Volume in 5 Years 1998	Sedimentation Volume in 10 Years 2003	Sedimentation Volume in 15 Years 2008	Sedimentation Volume in 20 Years 2013
Predicated Data	1.54	2.99	4.38	5.64
Measured Data	2.43	4.29	5.48	5.55
Difference	0.89	1.30	1.10	-0.09

From the view of the total sedimentation volume, the actual sedimentation of the Manwan Reservoir in the first 15 years of operation is more serious than the result of the original design forecast. This is mainly due to the deviation in the forecast which is based upon the historical hydrological and sediment data and the specified operation and dispatching modes. From the view of the actual sediment volume, affected by human activities, the sediment volume shows a significant increase trend. From 1994 to 2008, the average annual sand volume is 60.49 million tons, but the calculated design value in the preliminary design is only 44 million tons, with an increase of about 50%; According to the operating water level of the Manwan HPP recorded from 1994 to 2009, the average operating water level of the Manwan HPP since its operation during the flood season from June to September is 987.44m, which is 2.44 m higher than the results of the preliminary design.

4. SEDIMENTATION CALCULATION

The sedimentation of the main stream of the reservoir is calculated by the constant flow unbalanced sediment transport method through the program SUSBED_2 provided by Wuhan University of Hydraulic and Electrical Engineering. The WUHEE Zhang Ruijin Formula is adopted as the sediment carrying capacity formula of suspended load.

4.1. CALIBRATION OF SEDIMENTATION PARAMETERS

Before the sedimentation calculation of each scheme, the calibration of sedimentation parameters is carried out firstly. The calculation is carried out based on the terrain data measured in 1996 with year 2000 as the end. The

calculation results and the data measured in 2000 will be compared.

The inflow water level adopted for the sedimentation calculation is the average monthly water level recorded at Jiajiu Station from 1996 to 2000. The average monthly operating water level of the Manwan Reservoir from 1996 to 2000 is adopted as the water level in front of the dam. See Figure 4 for the comparisons between the calculated and the measured sedimentation longitudinal sections in 2000; See Table 3 for the Comparison Between the Calculated and the Measured Sedimentation Volumes.

Table 3
Comparison of the parameter-calibrated sedimentation results

Time	Measured Sedimentation Volume (10,000 m ³)	Calculated Sedimentation Volume (10,000 m ³)
1996 - 2000	13402	13270

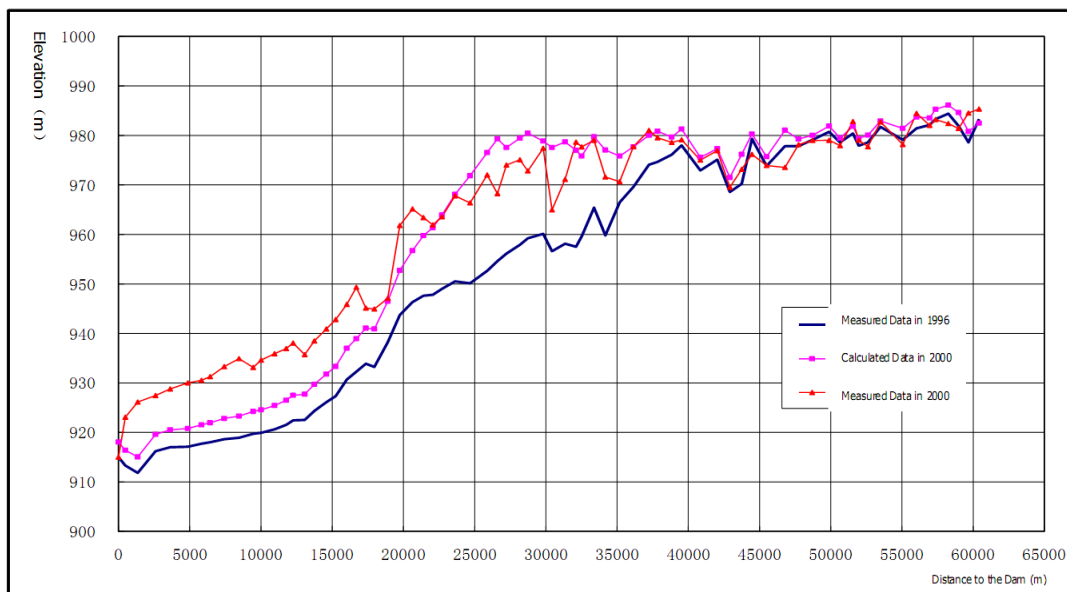


Fig. 4
Comparison of Sedimentation Longitudinal Section of the Reservoir in 2000
(Model Calibration)

According to the calculation of the sedimentation longitudinal section, the sedimentation thalweg point of the section in front of the dam is slightly lower, while that of the section at the tail of the reservoir is slightly higher. From the total sedimentation volume point of view, the measured and the calculated results are almost consistent. On the whole, the calculation can basically reflect the actual sedimentation, but the calculated sedimentation of the tail section is slightly higher than the actual situation. When analyzing the impact on the Xiaowan HPP, it will be safer.

The results of the parameter calibration are as follows: 1) WUHEE Zhang Ruijin formula: m is taken as 1.0; for k value, it is taken as 0.3 for the middle section of reservoir, and 0.2 for the rest sections; 2) Comprehensive Coefficient of Recovery Saturation: It is taken as 1.0 at the scouring condition, and as 0.75 and 0.5 respectively for the two groups of finest suspended sand, and 0.25 for the rest groups.

4.2. CALCULATION FOR THE SEDIMENTATION VERIFICATION

The above-mentioned calibrated parameters are applied to calculate the sedimentation till the time before the flood season in 2003 on the basis of the measured terrain data in 2000. The inflow water level adopted for the sedimentation calculation is the average monthly water level recorded at Jiajiu Station from 2000 to 2002. The average monthly operating water level of the Manwan Reservoir from 2000 to 2002 is adopted as the water level in front of dam. Refer to Table 3 for the sedimentation grain classification and parameter calibration.

See Fig. 5 for comparison between the sedimentation calculation and the calculated longitudinal section in 2003; and see Table 4 for comparison between the calculated sedimentation volume and the measured sedimentation volume.

Table 4
Verification results of the sedimentation volume

Time	Measured Sedimentation Volume (10,000 m ³)	Calculated Sedimentation Volume (10,000 m ³)
2000-2003	11234	11710

According to the verification results, the sedimentation longitudinal section is still slightly lower at the section in front of the dam and slightly higher at the section at the tail of reservoir, and the sedimentation volume is still well consistent with the measured data, which verifies that the calibrated parameters for the calculation is appropriate, and can be used for sedimentation forecast calculation of the reservoir.

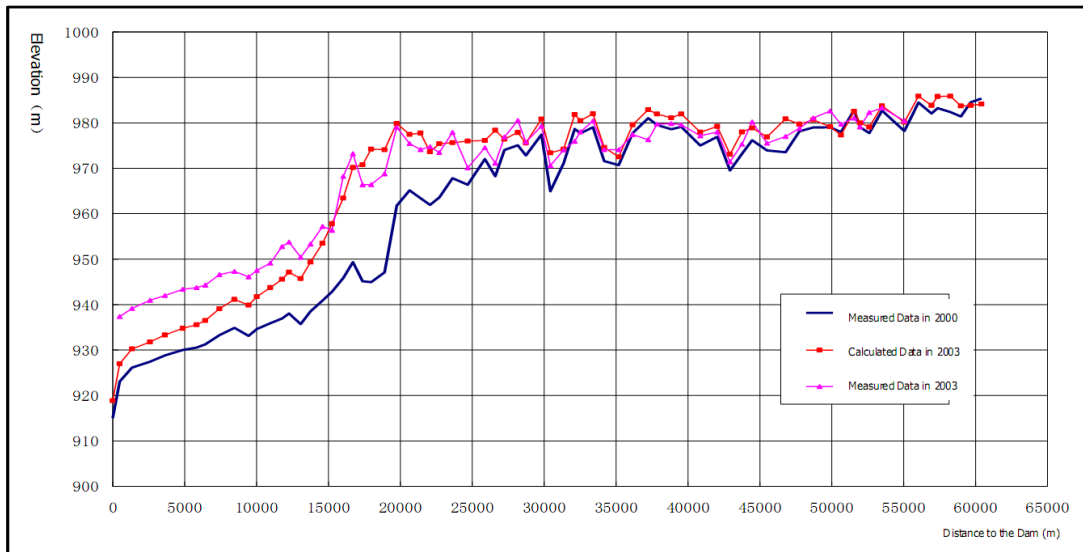


Fig. 5

Comparison of Sedimentation Longitudinal Sections of the Manwan Reservoir in 2003 (model verification)

4.3. SEDIMENTATION FORECAST

4.3.1 CALCULATION DATA AND PARAMETERS FOR SEDIMENTATION

(1) Longitudinal and Cross Sections of the Reservoir Area

The longitudinal and transverse profiles of the reservoir area were surveyed by the Surveying and Mapping Branch of the Kunming Engineering Corporation Limited of Power China from April to May 2014, and the layout of the profiles for scouring and silting calculation of the reservoir is shown in Figure 6, with 71 profiles in total. The section spacing is between 75m--- 1,321m, which can satisfy the calculation requirements. Compared with the measured data in 2009, there are 8 sections less in the end area of the reservoir; and combined the comparison of the calculated results in 2009 and 2014, the scouring and silting in river of the end area of the reservoir changed a little; hence the measured results in 2009 shall be applied for the 8 sections.

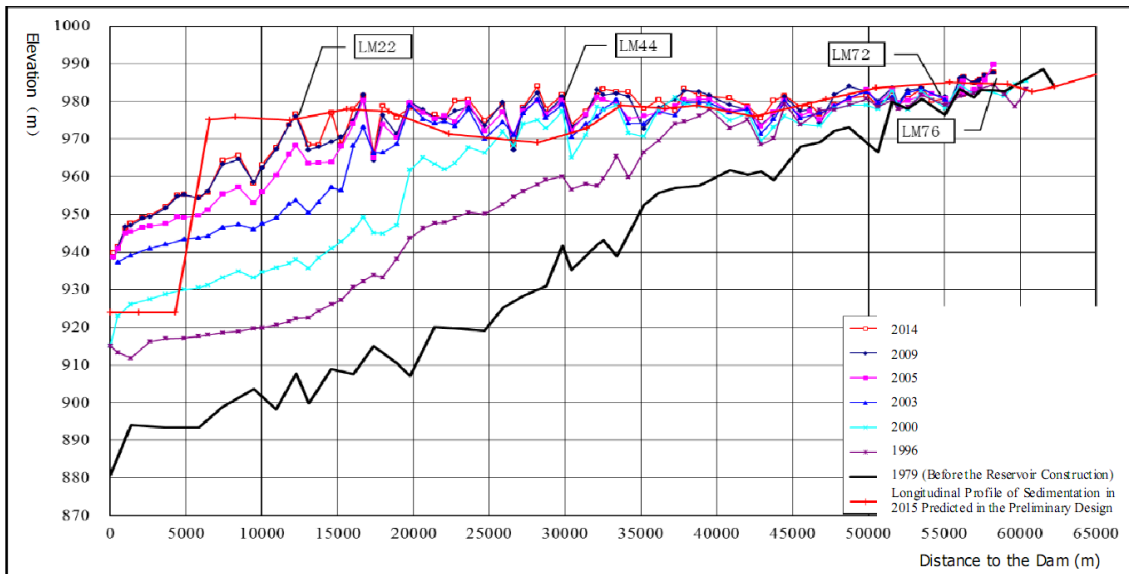


Fig. 6

Longitudinal Section of Sedimentation over the Years for Main Stream of the Manwan Reservoir

(2) The Inflow Flow and Sediment

Considering the impounding and power generation of the Xiaowan HPP since 2009, the Xiaowan HPP has a large sediment ratio, with over year regulating ability; According to the calculation, the sediment retaining ratio of the Xiaowan HPP is up to 95%, and all the outflow sediments are fine wash-load sediments, which is quite hard to be deposited in the Manwan Reservoir area, therefore the inflow sediment volume in the sedimentation calculation is calculated only by applying the sediment volume between the area from the Xiaowan to Manwan areas; Affected by the regulation and storage of the Xiaowan HPP, the inflow water is not natural flow, and the inflow discharge shall be applied with the yearly and monthly inflow discharge of the Manwan dam site after regulation and storage.

(3) Water Level in Front of the Dam

Monthly average water level over the years after runoff regulation

(4) Calculated Parameters

Applied Calibration Results

4.3.2 CALCULATED RESULTS

See Fig. 7 for the longitudinal section of sedimentation, and see Table 5 for reservoir capacity loss.

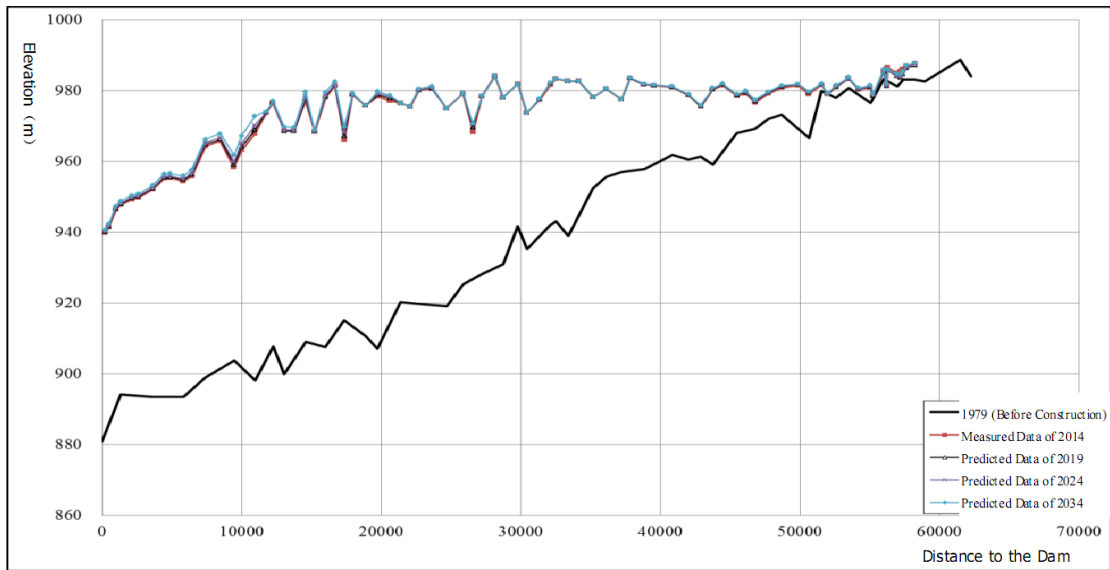


Fig. 7

Longitudinal Section of Sedimentation over the Years for the Manwan Reservoir

According to the calculated results: Affected by the sediment retaining of the Xiaowan HPP, the inflow sediment volume in the Manwan HPP decreased a lot, and it is predicted that the sedimentation volume below the normal water level will be 18.6 million m^3 after 20 years, of which the sediment-caused storage loss rate is 6.17% compared with 2014; The sedimentation volume within the dead storage capacity is 11.32 million m^3 , of which the sediment-caused storage capacity loss rate is 9.63% compared with 2014; and the sedimentation volume of effective storage capacity is 7.29 million m^3 , of which the sediment-caused storage capacity loss rate is 3.97% compared with 2014.

The results of the longitudinal section of the annual sedimentation over the years are shown in Fig.7. Compared with the measured results of the longitudinal section in 2014, the scouring and silting in the Manwan reservoir area changed little, where most sedimentation happened in the section in front of the dam, the scouring and silting in the section in the middle of the dam changed little, while a certain scouring happened in the section at the tail of reservoir due to the clear water discharging of the Xiaowan HPP.

Table 5
Forecast of the Reservoir Storage Capacity Loss for the Reservoir Sedimentation
over the Years

	Project	Results		
Designed Storage Capacity of the Reservoir	Normal Water Level (m)	994		
	Storage below NWL (10,000 m ³)	92000		
	Water Level (m)	982		
	Dead Storage Capacity (10,000 m ³)	66300		
	Adjusted Effective Storage Capacity (10,000 m ³)	25700		
Calculation of the Measured Section in 2014	Normal Water Level (m)	994		
	Storage below NWL (10,000 m ³)	30124		
	Dead Water Level (982m) (m)	982		
	Dead Storage Capacity (10,000 m ³)	11756		
	Effective Storage Capacity (10,000 m ³)	18369		
Sedimentation Forecast	Sedimentation Period (Yrs)	5	10	20
	Residual Storage Capacity below NWL (10,000 m ³)	29655	29185	28264
	Residual Dead Storage Capacity (982m) (10,000 m ³)	11483	11203	10624
	Residual Effective Storage Capacity (10,000 m ³)	18172	17982	17640

Note: The calculated storage capacity of the surveyed sections in 2014 is the main stream storage capacity calculated by the section method, which does not include the storage capacities of tributaries. It satisfies the requirements for storage capacity loss forecast, and has a certain difference with the storage volume calculated by the contour method in 2014.

5. CONCLUSIONS AND SUGGESTIONS

Most sections of the Manwan HPP are covered by the luxuriant vegetation, and the main sources of sediments mainly are: ① The sediment in the upstream flows into the Manwan Reservoir; there are large populations and farmlands around the Gonglang River, thus the water and soil loss is quite serious; ③ Some gullies in the reservoir area are covered by little vegetation, therefore the sediment flows into the main stream through the tributaries and the rainwater.

Sediment of the whole reservoir is mainly deposited below the dead storage capacity. The Xiaowan HPP was impounded in 2009, which greatly

relieved the sediment problem of the Manwan HPP. The storage below NWL, dead storage capacity and effective storage capacity have little change compared with the previous data. The total loss rate of the effective storage capacity below the normal water level - of 994m is 15.21%, and the total loss rate of the storage capacity below the dead water level - elevation: 982m is 77.47%.

Suggestions:

(1) After completion of the Xiaowan Reservoir, the data of the inflow and outflow sediment have been changed fundamentally, the sediment observation and analysis shall be conducted to know the rules for the sediment transport in the Manwan Reservoir, forecast the sediment problem in the reservoir and instruct the operation of the plant.

(2) Regularly (normally 2---3 years) measure the cross section of sedimentation in the main stream and tributaries and the topographic map in the Manwan Reservoir.

(3) Pay attention to the soil and water conservation. Continuously insist on the operation mode of the reservoir - "Storing Clear Water and Releasing Muddy."

ACKNOWLEDGEMENTS

The authors gratefully appreciate the supports from National Natural Science Foundation of China (No.91647000 and No.91647201), and China Postdoctoral Science Foundation (No.2016M602934XB). In addition, the authors would also like to thank Kunming Engineering Corporation and Manwan Hydropower plant, who provided valuable material for this article.

COMMISSION INTERNATIONALE DES GRANDS BARRAGES

VINGT-SIXIÈME CONGRÈS DES GRANDS BARRAGES
Autriche, juillet 2018

DOI 10.3217/978-3-85125-620-8-024



This work licensed under a Creative Commons Attribution 4.0 International License. <https://creativecommons.org/licenses/by-nc-nd/4.0/>

ANALYSIS OF KEY INFLUENCING FACTORS FOR THE EVOLUTION OF THE SAND BAR IN THE TRIBUTARIES IN THE XIAOLANGDI RESERVOIR AREA

Yuanjian WANG

Senior Engineer, YELLOW RIVER INSTITUTE OF HYDRAULIC RESEARCH,
ZHENGZHOU

CHINA

Enhui JIANG

Deputy Dean, YELLOW RIVER INSTITUTE OF HYDRAULIC
RESEARCH, ZHENGZHOU

CHINA

ANALYSIS OF KEY INFLUENCING FACTORS FOR THE EVOLUTION OF THE SAND BAR IN THE TRIBUTARIES IN THE XIAOLANGDI RESERVOIR AREA*

Yuanjian WANG

Senior Engineer, Yellow River Institute of Hydraulic Research, Zhengzhou, China

Enhui JIANG

Deputy Dean, Yellow River Institute of Hydraulic Research, Zhengzhou, China

1. INTRODUCTION

Sand bar is a geomorphologic pattern which is often observed in estuaries and reservoirs. For estuaries, Sand bar alleviates water depth and blocks water and sediment transportation. It is also a threat for navigation (Li, 1997). For reservoirs, San bar blocks river mouth of tributaries, reduces storage volume of reservoirs (Li et al., 1985; Wang and Hu, 2003). Therefore, the research on the evolution of sand bar is valuable for engineering. Separately, the evolution of sand bar in estuaries is influenced by the flow conditions upstream and oceanic dynamic conditions downstream (Hu and Zhang, 2006). And the evolution of sand bar in reservoirs is caused by two ways : the first way usually occurs in a small or median reservoir, the slope in the main channel is mild while in the tributaries is steep. In flood season, the water with sediment and gravel will flow from the source of the tributaries to the main channel and deposit in the river mouth of the tributaries(Qi, 1996); the second way usually occurs in a large reservoir, the slope in the main channel is steep while in the tributaries is mild. In flood season, the water with sediment and gravel will flow form the main channel to the tributaries and deposit in the river mouth of the tributaries (Wang et al., 2011). Because the evolution of sand bar is influenced by many different factors, it is a focus for scientists and engineers. Limited by the complexity of the problem and traditional techniques, former research on sand bar mainly fixed on the influence of a single factor (Shen et al., 1983; Li and Ji, 1988; Yang et al., 2001). With the development of new analysis techniques, now the research turns to be quantitative (Wu et al., 2002) and modelling (Zhang et al., 2003). Accordingly, this paper established a response formula between the height's increment of the sand bar in the tributaries in the Xiaolangdi Reservoir area and a number of influencing factors. Using sensitive analysis, the key factor for the evolution of the sand bar is also found to support the engineering constructions for dealing with sand bar in the reservoir area.

* *titre de l'article complet*

2. STUDY REGION

In this chapter, six main tributaries in the Xiaolangdi area were selected firstly (see figure 1): Dayu River, Zhenshui River, Shijing River, Dongyang River, Xiyang River and Yunxi River.

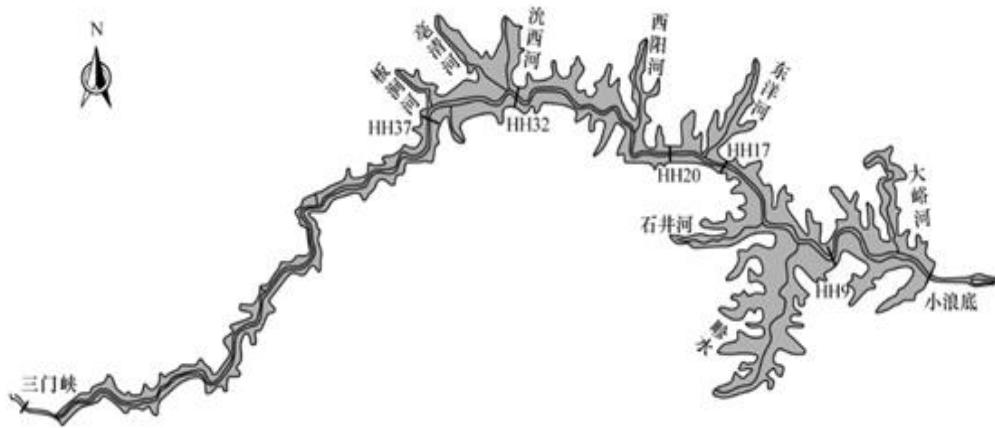


Figure 1. Sketch of Xiaolangdi Reservoir Area

The basic information of six tributaries can be seen in table 1 as follows:

Table 1. Original parameters of tributaries in Xiaolangdi Reservoir Area

name	location	distance from the dam /km	storage volume /10 ⁸ m ³	river length /km	river basin area /km ²	channel gradient /‰	backwater length under the 230m (water level before the dam) conditions/km	backwater length under the 230m (water level before the dam) conditions /km	
Dayu River	Left bank	HH3-HH4	3.9	5.80	55	258	100	9.3	12.3
Dongyang River		HH18- HH19	31.3	3.11	60	571	92	7.9	11.7
Xiyang River		HH23- HH24	41.3	2.35	53	404	106	5.5	9.4
Yunxi River		HH32- HH33	57.6	4.07	72	576	120	4.8	7.2
Zhenshui River	Right bank	HH11- HH12	18	17.67	53.7	431	56	14.5	21.3
Shijiang River		HH13- HH14	22.7	4.80	22	140	120	6.8	10.3

The data series began from 2001 spring and end to 2014 spring. A further analysis on the data showed that Dayu River was too close to the dam of the Xiaolangdi reservoir, the cross-section of that was influenced by the fluctuation of water level before the dam. As a result, the gradient of the main channel of Dayu River changed quickly and sometimes turned negative. Additionally, the phenomenon of sand bar is not significant in the river mouth of Dayu River. As to fix on the evolution of sand bar, we deleted the data series of Dayu River, focus on the other five tributaries.

3. STUDY INDEXES

Using dimensionless parameters, this paper set a multiple regressive formula between the height increment of sand bar and different influencing factors. The form of the formula is as follows:

$$\hat{Y} = K\hat{X}_1^{\alpha_1}\hat{X}_2^{\alpha_2} \dots \hat{X}_n^{\alpha_n} \quad [1]$$

In which \hat{Y} is a dimensionless dependent variable, $\hat{X}_1, \hat{X}_2, \dots, \hat{X}_n$ are dimensionless independent variables, $K, \alpha_1, \alpha_2, \dots, \alpha_n$ are undetermined coefficients.

The research aim is the evolution of sand bar, so the annual height increment of sand bar Δh (m) and annual depositing volume ΔV (m³) are chosen as dependent variables, the dimensionless forms are:

$$\hat{Y}_1 = \frac{\Delta h}{D_{50}}, \hat{Y}_2 = \frac{\Delta V}{D_{50}^3} \quad [2]$$

$$[3]$$

In which D_{50} (m) is the median grain size of bed material load in the river mouth of the tributaries, which is measured every year before flood season.

As the former research, the evolution of sand bar is related to water and sediment conditions, local terrain factors and flow regimes. So the selected independent variables should include all these aspects (See Table 2 and Table 3):

Table 2. Selection I of independent variables for the evolution of sand bars - water and sediment processes

<i>Water and sediment conditions</i>						
<i>factors</i>	Water level condition	Flow Condition I	Flow Condition II	Sediment condition I	Sediment condition II	
	\hat{X}_1	\hat{X}_2	\hat{X}_2^*	\hat{X}_3	\hat{X}_3^*	
<i>Direct Indexes</i>	Averaged water level in flood season H (m)	Averaged inflow of the reservoir in flood season Q (m ³ /s)	Averaged outflow of the reservoir in flood season Q* (m ³ /s)	Averaged sediment flowing into the reservoir in flood season S(kg/m ³)	Averaged sediment flowing out of the reservoir in flood season S*(kg/m ³)	
<i>Dimensionless indexes</i>	$\frac{H}{D_{50}}$	$\frac{Q}{\sqrt{gD_{50}^5}}$	$\frac{Q^*}{\sqrt{gD_{50}^5}}$	$\frac{S}{\gamma/g}$	$\frac{S^*}{\gamma/g}$	

Table 3. Selection II of independent variables for the evolution of sand bars -local terrain and flow regimes

	<i>Local terrain conditions</i>		<i>Local flow regimes</i>		
<i>Factors</i>	Terrain conditions in the tributaries \hat{X}_4		Terrain conditions in the main channel \hat{X}_5	Location of the front of the Delta \hat{X}_6	
<i>Direct indexes</i>	Width of the river mouth of the tributaries B _h (km)	Maximum width of the tributaries B _m (km)	Gradient J _z (1)	Distance from the river mouth to the dam L ₀ (km)	Distance from the front of the delta to the dam L(km)
<i>Dimensionless indexes</i>	$\frac{B_h}{B_m}$		J _z	$\frac{L}{L_0}$	

4. MULTIPLE REGRESSIVE FORMULA

According to the analysis above, using forward and stepwise regressive methods, we got a full regression model (considering all independent variables) and a selecting regression model (Selecting most important independent variables) separately as follows:

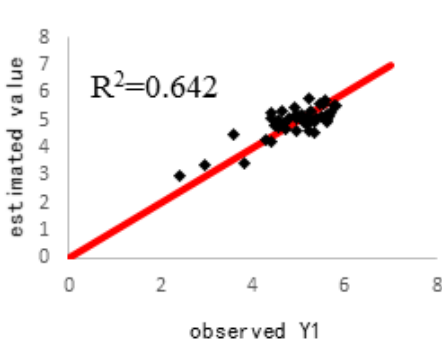
$$\hat{Y}_1 = 0.265\hat{X}_2^{*0.417}\hat{X}_3^{0.415}\hat{X}_3^{*-0.070}\hat{X}_4^{-0.031}\hat{X}_5^{-0.030}\hat{X}_6^{0.951} \quad (R^2=0.642) \quad [4]$$

$$\hat{Y}_1 = 0.0736\hat{X}_1^{0.415}\hat{X}_6^{1.151} \quad (R^2=0.631) \quad [5]$$

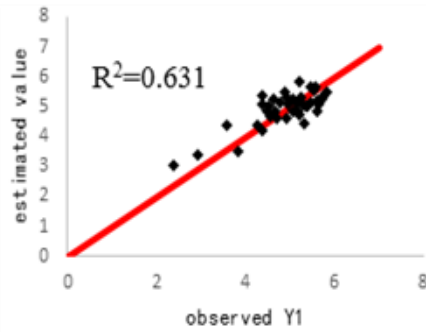
$$\hat{Y}_2 = 185.353\hat{X}_2^{*1.373}\hat{X}_3^{-0.430}\hat{X}_3^{*0.248}\hat{X}_4^{0.317}\hat{X}_5^{0.320}\hat{X}_6^{0.719} \quad (R^2=0.827) \quad [6]$$

$$\hat{Y}_2 = 3.540\hat{X}_2^{*1.428} \quad (R^2=0.801) \quad [7]$$

Figure 2 and figure 3 gave the results of the regression models.

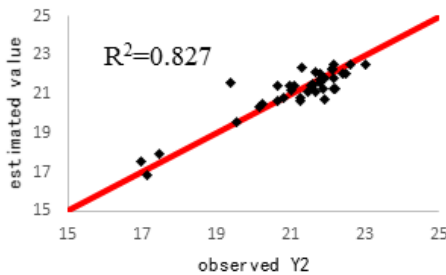


(a) full regression model

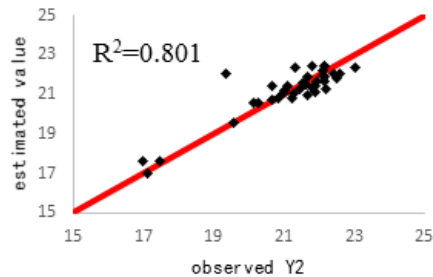


(b) selecting regression model

Figure 2. Multiple regressive result of height increment of sand bars in the tributaries in Xiaolangdi Reservoir Area



(a) full regression model



(b) selecting regression model

Figure 3. Multiple regressive result of annul sedimentation quantity in the tributaries in Xiaolangdi Reservoir Area

Given from fig 2 and fig3, the regressive results agree well with the observed data. The effects of the formula can be accepted. Furthermore, a detailed analysis based on physical meanings should be done:

- (1) The full regression model and selecting regression model of Y_1 : the main influencing factors on Y_1 are outflow discharge (the exponent number is 0.417), sediment concentration flowing into the reservoir (the exponent number is 0.415), sediment concentration flowing out of the reservoir (the exponent number is -0.070), local terrain factor in the tributaries (the exponent number is -0.031), local terrain factor in the main channel (the exponent number is 0.030) and the location of the front of the delta (the exponent number is 0.951). Considering the importance of those factors, the location of the front of the delta, outflow discharge and sediment concentration flowing into the reservoir take the first three places and agree well with the physical meanings. Additionally, although the exponent number of the local terrain factor in the tributaries is small enough, the correlation coefficient of that is significant. So the local terrain factor should also be chosen. Then the final form of the regressive model for Y_1 is shown as follows:

$$\hat{Y}_1 = 0.534\hat{X}_2^{0.4}\hat{X}_3^{0.4}\hat{X}_4^{-0.1}\hat{X}_6 \quad (R^2=0.638) \quad [8]$$

The exponent number and independent variables are all simplified and the results are shown in fig 4.

- (2) The full regression model and selecting regression model of Y_2 : the main influencing factors on Y_2 are outflow discharge (the exponent number is 1.373), sediment concentration flowing into the reservoir (the exponent number is -0.430), sediment concentration flowing out of the reservoir (the exponent number is 0.248), local terrain factor in the tributaries (the exponent number is 0.317), local terrain factor in the main channel (the exponent number is 0.320) and the location of the front of the delta (the exponent number is 0.719). Considering the importance of those factors, outflow discharge, the location of the front of the delta, and sediment concentration flowing into the reservoir take the first three places. Based on the physical meanings, these three factors should all have positive correlations with the depositing volume in the tributaries, while the sediment concentration flowing into the reservoir showed an opposite relation in this model. The physical interpretation is: the sediment flowing into the reservoir area is not equal or positive related to the depositing volume in the reservoir area, because there is a drastic process of the sediment exchange between the channel bed and water flow. Even though clear water flows into the reservoir area, it also may cause a sediment transporting process and a deposition in the river mouth of the tributaries. As a result, the sediment concentration flowing into the reservoir is deleted from the model. Similarly, we can get the final form of the regressive model for Y_2 :

$$\hat{Y}_2 = 85.57\hat{X}_2^{1.4}\hat{X}_4^{0.3}\hat{X}_5^{0.3}\hat{X}_6^{0.7} \quad (R^2=0.820) \quad [9]$$

The exponent number and independent variables are also simplified and the results are shown in fig 5.

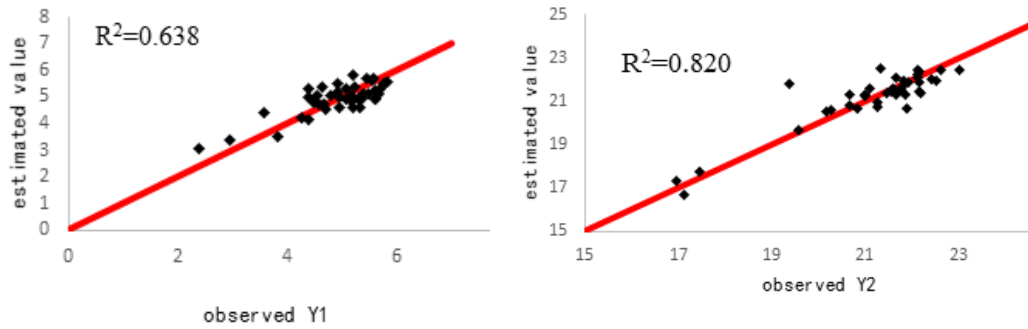


Figure 4. Predictions of final formula of height increment of sand bars (left);

Figure 5. Prediction of final formula of sedimentation quantity (right)

Take the physical expressions of all the variables into equation [8] and [9], we can get the final formula as follows:

$$\Delta h = 0.534 \left(\frac{Q^*}{\sqrt{gD_{50}^5}} \right)^{0.4} \left(\frac{S}{\rho} \right)^{0.4} \left(\frac{B_h}{B_m} \right)^{-0.1} \frac{L}{L_0} \quad (R^2=0.638) \quad [10]$$

$$\Delta V = 85.57 \left(\frac{Q^*}{\sqrt{g}} \right)^{1.4} D_{50}^{-0.5} \left(\frac{B_h}{B_m} \right)^{0.3} J_z^{0.3} \left(\frac{L}{L_0} \right)^{0.7} \quad (R^2=0.820) \quad [11]$$

5. SENSITIVE ANALYSIS

The aim of sensitive analysis are: (1) searching the sensitive factor and using the factor to control the dependent variable; (2) confirming the limitation of the dependent variable.

In this chapter, the annual height increment of sand bar in tributaries and depositing volume in tributaries are two dependent variables. Using the data in Zhenshui River in 2012, we did sensitive analysis in table 4 and table 5:

Table 4. Sensitive analysis of height increment of sand bars in the tributaries (unit: m)

Influencing factors	-20%	-10%	-5%	+5%	+10%	+20%
Outflow discharge	-0.107	-0.052	-0.026	0.025	0.049	0.095
Sediment concentration	-0.107	-0.052	-0.026	0.025	0.049	0.095
Relative width in the river mouth	0.028	0.013	0.006	-0.006	-0.012	-0.023
Distance from the front of delta	-0.252	-0.126	-0.063	0.063	0.126	0.252
Distance from the river mouth	0.315	0.140	0.066	-0.060	-0.114	-0.210

(Note: the mathematic meaning of the sensitive analysis table is: the change for one single factor causes the change of the dependent variable. For example, if the outflow discharge decreases by 20%, then the height of the sand bar will decrease 0.107m).

Table 5. Sensitive analysis of annual sedimentation quantity in the tributaries (unit: $\times 10^6 m^3$)

Influencing factors	-20%	-10%	-5%	+5%	+10%	+20%
Outflow discharge	-3.334	-1.704	-0.861	0.878	1.774	3.613
Grain size of bed material load	1.467	0.672	0.323	-0.299	-0.578	-1.083
Relative width in the river mouth	-0.805	-0.387	-0.190	0.183	0.360	0.699
Distance from the front of delta	-1.797	-0.883	-0.438	0.432	0.857	1.692
Distance from the river mouth	2.101	0.951	0.454	-0.417	-0.802	-1.489
Gradient in the main channel	-0.805	-0.387	-0.190	0.183	0.360	0.699

Given from Table 4 and Table 5, some conclusions can be obtained:

- (1) For the height increment of sand bars in the tributaries, the sensitive order is: Distance from the river mouth to the dam > Distance from the front of delta to the dam > Outflow discharge = Sediment concentration > Relative width in the river mouth;
- (2) For the annual sedimentation quantity in the tributaries, the sensitive order is: Outflow discharge > Distance from the front of delta to the dam > Grain size of bed material load > Gradient in the main channel = Relative width in the river mouth.

6. CONCLUSIONS

Using dimensionless multiple regressive analysis and sensitive analysis, some conclusions can be get:

(1) The evolution of sand bar in the river mouth of those tributaries in Xiaolangdi reservoir area, is related to the water and sediment conditions, local terrain factors in the tributaries and main channel, location of the front of the delta in the reservoir area and others. Among them, the location of the front of the delta is the most sensitive factor;

(2) For engineers, the aim is to limit the evolution of sand bar and utilize the depositing capacity in those tributaries in the reservoir area. According to this paper, these actions are effective: increasing the sediment concentration flowing into the reservoir in flood season, decreasing the grain size of bed material load, increasing the gradient of the main channel, increasing the relative width of the river mouth of those tributaries. Specifically, increasing the relative width of the river mouth is recommended, which can not only limit the evolution of sand bar, but also increase the depositing volume in the tributaries.

ACKNOWLEDGEMENTS

This study was supported financially by the National Science Foundation of China (Grant No.51509102,51679104, and 5153000441).

REFERENCES

Hu Chunhong and Zhang Zhihao (2006). *Evolution and control of estuary sandbar in Yellow River responding to variation of flow-sediment condition*. Journal of Hydraulic Engineering, 37(5): 511-517.

Li Jiufa and Ji Zhong (1988). *The statistical analysis on the sedimentation variations in the south passage of the Changjiang River estuary caused by the flow and sediment conditions*. Journal of Sediment Research, (4): 76-82.

Li Shanzheng, Chen Zongwen and Zhang Qishun (1985). *Sediment problems of Guanting Reservoir*. Journal of Hydraulic Engineering, 16(3): 10-21.

Li Zegang (1997). *Formation and evolution of the bar on Yellow River estuary*. ACTA GEOGRAPHICA SINICA, 52(1): 54-62.

Qi Fudong (1996). *A discussion on the bar sedimentation in Zhexi Reservoir and its controlling measures*. Journal of Hydroelectric Engineering, (7):71-78.

Shen Jinshan, Zhu Zhenmei, Zhang Xinqin (1983). *Origin and evolution of the entrance sandbars in the south passage of the Changjiang River estuary*. OCEANOLOGIA ET LIMNOLOGIA SINICA, 14(6):582-590.

Wang Ting, Chen Shukui, Ma Huaibao and Zhang Junhua (2011). *Distribution of deposition in Xiaolangdi Reservoir*. Journal of Sediment Research, (5): 60-66.

Wang Yangui and Hu Chunhong (2003). *Study on sedimentation and the mouth bar control in Guanting Reservoir*. Journal of Sediment Research, (6): 25-30.

Wu Hualin, Shen Huanting, Hu Hui, Zhang Lili and Huang Qinghui (2002). *GIS supporting study on calculation of the amount of siltation and erosion in mouth bars of the Changjing Estuary*. ACTA OCEANOLOGICA SINICA, 24(2): 84-93.

Yang Shilun, Zhao Qingying, Ding Pingxing and Xie Wenhui (2001). *Seasonal changes in bed level of the passage in the mouth bar area of the Yangtze (Changjiang) River*. Resources and Environment in the Yangtze Basin, 10(3): 258-265.

Zhang Yanjing, Zhang Shiqi and Chen Jinrong.(2003). *Numerical simulation on dredging channel of Guishui River mouth bar of Guanting Reservoir*. Journal of Sediment Research, (1): 45-51.

SUMMARY

Using multiple regression analysis and dimensionless parameters, this paper established a response formula between the height's increment of the sand bar in the tributaries in the Xiaolangdi Reservoir area and a number of influencing factors: water and sediment conditions, terrain factors in the main channel and tributaries and local flow regimes and so on. And also a similar formula between the sedimentation quantity in the tributaries and the influencing factors was obtained. The results show that: the water and sediment conditions, terrain factors, local flow regimes, grain size of bed material were all influencing factors for the evolution of the sand bar. Throughout sensitive analysis, the key factors for the evolution of the sand bar is the flow discharge and local flow regimes. These conclusions will be helpful for the engineering projects to control and limit the evolution of the sand bar in the tributaries in the Xiaolangdi Reservoir area.

COMMISSION INTERNATIONALE
DES GRANDS BARRAGES

VINGT-SIXIÈME CONGRÈS DES
GRANDS BARRAGES
Autriche, juillet 2018

**SEDIMENT MANAGEMENT STRATEGIES FOR HYDROPOWER RESERVOIR
IN AGRICULTURAL AREA**

Azwin Zailti ABDUL RAZAD¹, Rahsidi Sabri MUDA¹
azwin.razad@tnb.com.my

¹*Civil Engineering Unit, TNB Research Sdn Bhd No 1, Lorong Air Hitam,
KAWASAN INSTITUSI PENYELIDIKAN BANGI, 43000 KAJANG,*

MALAYSIA

Jansen Luis ALEXANDER²

²CENTRE OF EXPERTISE, ENERGY VENTURES DIVISION, TENAGA
NASIONAL BERHAD

Lariyah Mohd SIDEK³

³UNIVERSITI TENAGA NASIONAL

Kwansue-JUNG⁴

⁴ INTERNATIONAL WATER RESOURCES RESEARCH INSTITUTE,
CHUNGNAM NATIONAL UNIVERSITY, DAEJON,

REPUBLIC OF KOREA

ABSTRACT

Ringlet reservoir is a multipurpose reservoir that is part of Cameron Highlands – Batang Padang Hydroelectric Scheme. The reservoir has the original design storage of 6.7 million m³, of which 2 million m³ is dead storage and 4.7 million m³ is live storage. The catchment is a famous tourist area with active highland agricultural activities. Changes in land use have been significant since 1960's, showing an increase in agricultural area and reduction of forest cover.

A number of studies were conducted in the past to examine the effects of land use changes on the operation of the hydroelectric scheme. Based on survey and sediment monitoring records, the sedimentation rate has increased by 6 times from original design of 25,000 m³/year (in 1960's) to an average of 139,712 m³/year in 2010, causing a significant reduction of total storage capacity of Ringlet Reservoir from 6.7 million m³ in 1965 to 3.1 million m³ in 2008. Bertam Intake, which is the main power intake is often choked by the sediment built up within the area.

To continue the hydropower operation, various mitigation strategies have been implemented such as development of an Integrated Lake Basin Management Plan for Cameron Highlands' catchment to control sediment production at source. At the same time, sediment in Ringlet Reservoir is continuously removed via dredging. The dredged material is dried temporarily at the designated decantation area and disposed at the selected areas. Dredging is not a sustainable solution, mainly due to larger sediment loads entering the reservoir as compared to capacity of removal. Land availability for disposal area is becoming limited in the future and subsequently increase the total cost of removal. Another strategy considered is construction of two (2) check dams and settling basins at the main inlet rivers into Ringlet Reservoir, namely Habu and Ringlet check dams. Mechanical excavation at the check dams is cheaper than deploying dredger to remove sediment from inside the reservoir.

In conclusion, managing hydropower operation in rapidly changing land use especially in agricultural area is challenging. Rate of reservoir sedimentation in this area can easily exceed the original design, causing the reservoir operators to carefully plan ahead to manage the potential problems. TNB as the responsible manager, has done extensive works to manage and mitigate the sedimentation problem faced at Ringlet Reservoir. Other options such as controlling the reservoir operating regime and operation of the low level outlet can also be considered. There are still other ways to improve the current sediment management practice and they require extra effort to ensure the sustainability of the operation.

COMMISSION INTERNATIONALE DES GRANDS BARRAGES

VINGT-SIXIÈME CONGRÈS DES GRANDS BARRAGES
Autriche, juillet 2018

DOI 10.3217/978-3-85125-620-8-026



This work licensed under a Creative Commons Attribution 4.0 International License. <https://creativecommons.org/licenses/by-nc-nd/4.0/>

**OBSERVATION AND ESTIMATION METHOD OF SEDIMENT PRODUCTION
IN KAMANASHIGAWA BASIN, FUJIKAWA RIVER SYSTEM - TOWARD AN
ACCURATE ESTIMATION OF DAM SEDIMENT VOLUME -**

Kunihiro TOMITA, Zhengxing YE and Takashi HIKITA

CIVIL ENGINEERING AND ECO - TECHNOLOGY
CONSULTANTS CO., LTD.

Tetsuya SUMI

Professor, DISASTER PREVENTION RESEARCH INSTITUTE,
KYOTO UNIVERSITY

JAPAN

COMMISSION INTERNATIONALE
DES GRANDS BARRAGES

VINGT-SIXIÈME CONGRÈS DES
GRANDS BARRAGES
Autriche, juillet 2018

**OBSERVATION AND ESTIMATION METHOD OF SEDIMENT
PRODUCTION IN KAMANASHIGAWA BASIN, FUJIKAWA RIVER SYSTEM
—TOWARD AN ACCURATE ESTIMATION OF DAM SEDIMENT VOLUME—**

Kunihiro TOMITA, Zhengxing YE, Takashi HIKITA

CIVIL ENGINEERING AND ECO-TECHNOLOGY CONSULTANTS CO., LTD.

Tetsuya SUMI

*Professor, DISASTER PREVENTION RESEARCH INSTITUTE, KYOTO
UNIVERSITY*

JAPAN

1. INTRODUCTION

Conventionally, the sediment production and the flowing down situation from the upstream of the river are estimated by aerial photointerpretation or topographic survey etc. The design sediment volume in a dam is usually estimated according to sedimentation results of neighboring dams that have similar watershed condition. And the sediment transport in river channel is not properly measured during the flood event.

In recent years, the observation technology of sediment discharge in the river has greatly improved, so that the bedload can be directly observed by a hydrophone, and the suspended load by a turbidimeter. Additionally, the sediment volume variations in a mountain stream can be estimated from temporal change of riverbed height by satellite SAR (Synthetic Aperture Radar) analysis.

In this paper, using the model of Omukawa River, a branch of Kamanashigawa, Fujikawa River system, we combine the data of sediment discharge obtained by various observation techniques and try to improve the

observation methods for estimating the volume of sediment from the watershed, that will be useful for the sediment management in dam.

2. OUTLINE OF STUDY SITE

2.1. OUTLINE OF STUDY SITE

The study site in Omukawa River is located at the top of the Kofu alluvial fan, left branch of the Kamanashigawa, Fujikawa River system, a rapid river with an average gradient 1/58 and an extension of 16.4 km. The study area corresponds to about 8.3 km of its downstream section (Fig. 1). The upstream area consists of low to middle mountains composed of granite and volcaniclastic materials. Within this river section, about 50 Sabo dams and groundsels exist in the channel.

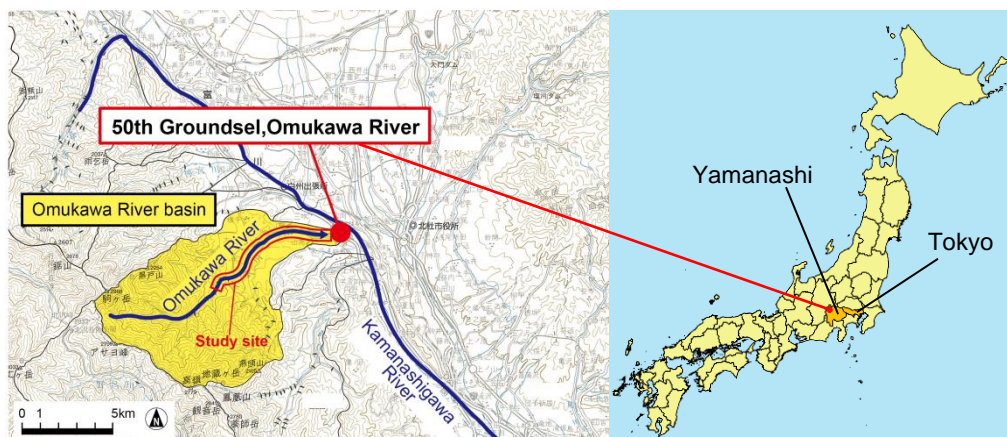


Fig. 1
Sediment discharge observation site map

2.2. IMPLEMENTATION OF SEDIMENT DISCHARGE OBSERVATION

In order to observe the volume of sediment discharge from the mountain stream, sediment discharge measurement is continuously carried out from 2011 by several equipment, such as hydrophone, turbidimeter, water level gauge, suspended load sampler, and a buried sediment trap pit, etc., on the 50th groundsel in Omukawa River. The layout of observation site and a sample of obtained data is shown in Fig. 2 and Fig. 3 respectively. The annual volume of sediment discharge calculated from the observed data is shown in Fig. 4.

The observed results of the hydrophone and sediment trap pit showed that the detectable grain diameter lower limit by hydrophone is about 2 mm, and the volume of sediment measured by the hydrophone is about 2% to 50% of the actual flowing down sediment volume that deposited in trap pit [1], and the ratio depends on the flood conditions such as the season, water depth and so on (Table 1, Fig. 5).

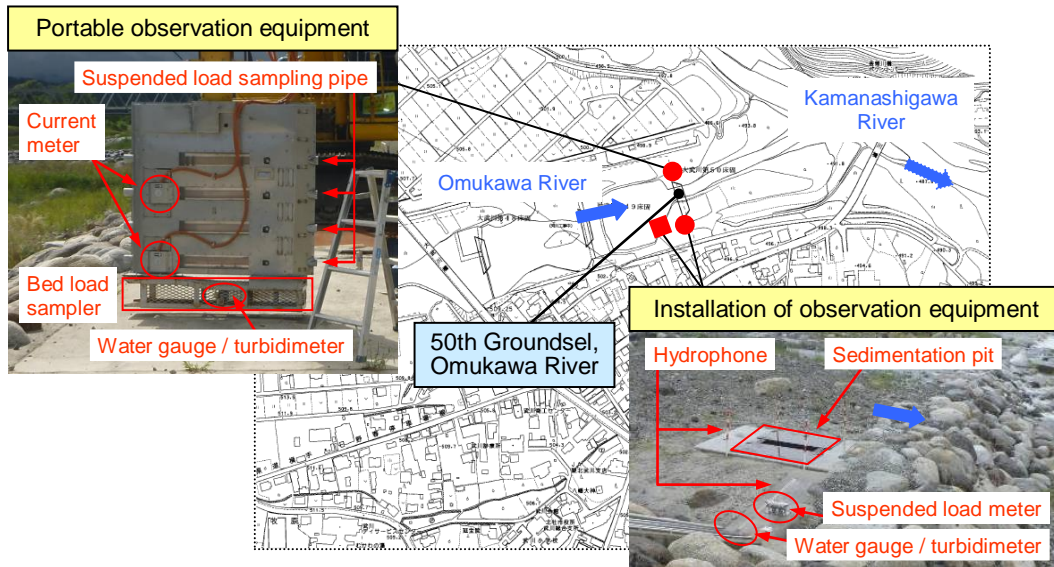


Fig. 2
Observation equipment installed in Omukawa River 50th groundsel

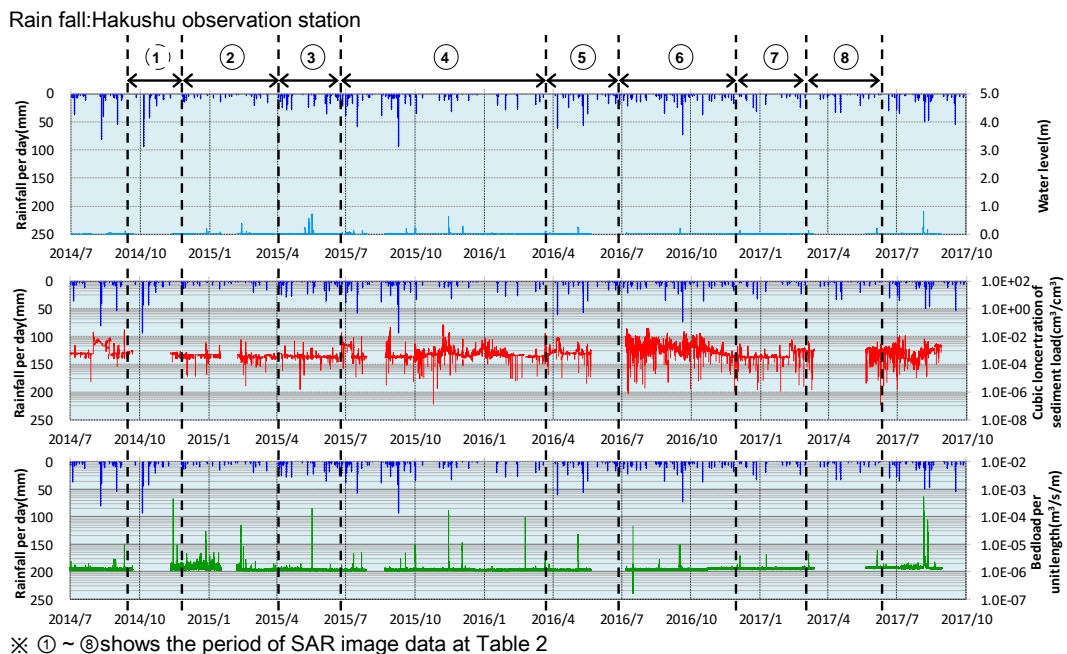


Fig. 3
Observation data from hydrophone, turbidimeter and water level gauge

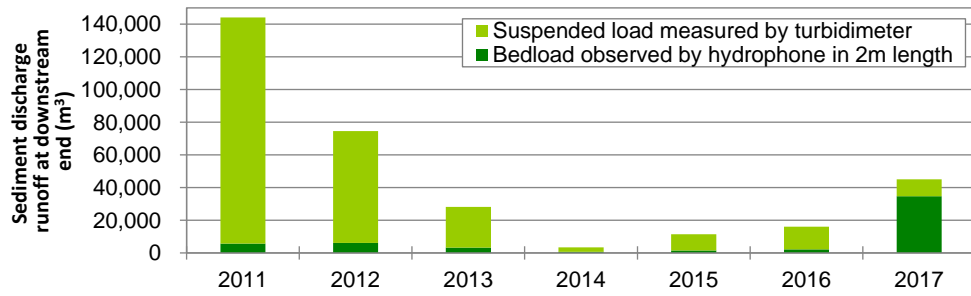


Fig. 4

Annual volume of sediment discharge by observation

Table 1

Sediment volume observed by hydrophone and trap pit

Subject flood	Hydrophone passage sediment discharge volume W_{hd} (kg)	Pit-captured sediment W_{pt} (kg)	Weight ratio W_{hd}/W_{pt} (%)	Pit-captured sediment weight over the lower limit grain diameter			
				W_{p1} ($p1 \geq 1mm$)	W_{p2} ($p2 \geq 2mm$)	W_{p3} ($p3 \geq 3mm$)	W_{p4} ($p4 \geq 4mm$)
① 2013 Typhoon No. 18 (Sep. 16, 2013)	1961	4335.0	45.2%	2688	2298	2124	2037
② 2013 Typhoon No. 26 (Oct. 15-16, 2013)	159	3166.4	5.0%	301.0	79.2	12.7	6.33
③ 2014 Typhoon No. 18 (Oct. 5-6, 2014)	344.5	3322.7	10.4%	697.8	99.7	66.5	49.8
④ 2014 Typhoon No. 19 (Oct. 13-14, 2014)	79.5	3348.3	2.3%	354.9	70.3	30.5	3.0

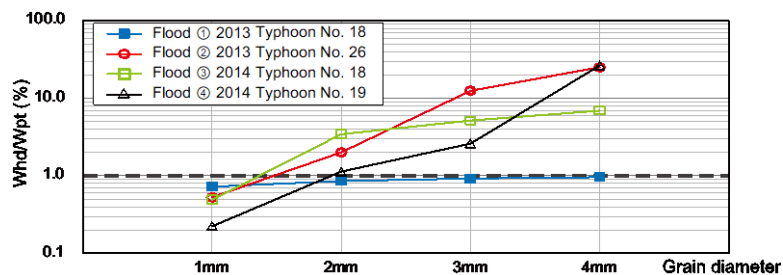


Fig. 5

Ratio of the lower limit grain diameter by hydrophone observation to the measurement in pit sedimentation

2.3. ESTIMATION OF SEDIMENT TRANSPORT BY SAR IMAGE ANALYSIS

2.3.1. SAR image data and analysis period

In the SAR image analysis, a SAR sensor mounted on an artificial satellite sends microwave obliquely to the ground surface and receives backscatter. The image data are obtained by receiving backward scattering from the ground surface. By interference analysis of two observed SAR images next to each other, the ground displacement that occurred during the observation period can be

calculated. Using SAR image interference analysis, it is possible to observe ground surface displacement without being influenced by weather and day or night [2].

Here, we use the following 9 SAR images acquired from the ALOS-2 satellite passing over Japan. Interference SAR image (inSAR) analysis of 8 periods (① ~ ⑧) with pairs next to each other were carried out to obtain river bed fluctuations of about 8 km river section on the upstream of 50th groundsel in Omukawa River (Table 2).

Table 2
Satellite specification and SAR image analysis periods

Items of satellite		No	Analysis period	
			from	to
Satellite	ALOS PASAR-2, SM-1 mode	①	2014/09/19	2014/11/28
		②	2014/11/28	2015/04/03
Running direction	North toward	③	2015/04/03	2015/06/26
		④	2015/06/26	2016/03/18
Survey direction	Right side	⑤	2016/03/18	2016/06/24
		⑥	2016/06/24	2016/11/25
Polarized wave	35.4°HH	⑦	2016/11/25	2017/03/03
		⑧	2017/03/03	2017/06/09

2.3.2. Analysis method

In SAR image analysis, the width of river channel more than 5 times the minimum image resolution (3m) is needed, so that we choose the middle to downstream river section of Omukawa River as a study site, where sediment discharge observation has been carried out at the downstream end since 2011.

In calculating the volume of sediment transport in the river way, the channel was divided into 58 blocks, in order to remove the range of river crossing constructions (e.g., bridges, groundsels etc.) where there is no displacement during floods. Furthermore, each block was subdivided into meshes of 5m squares. The procedure of interference analysis of SAR image was shown in Fig. 6 and Fig. 7.

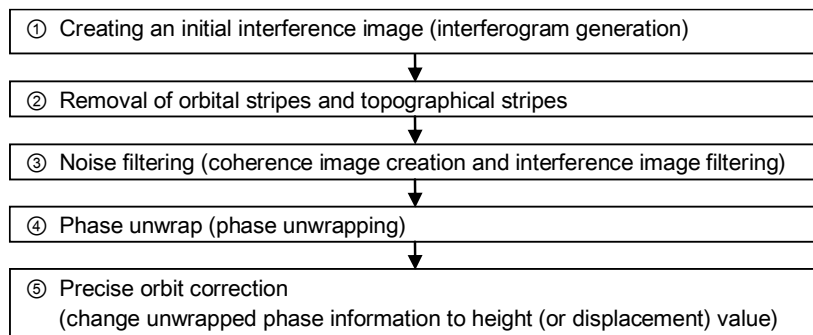


Fig. 6
Procedure of SAR image interference analysis

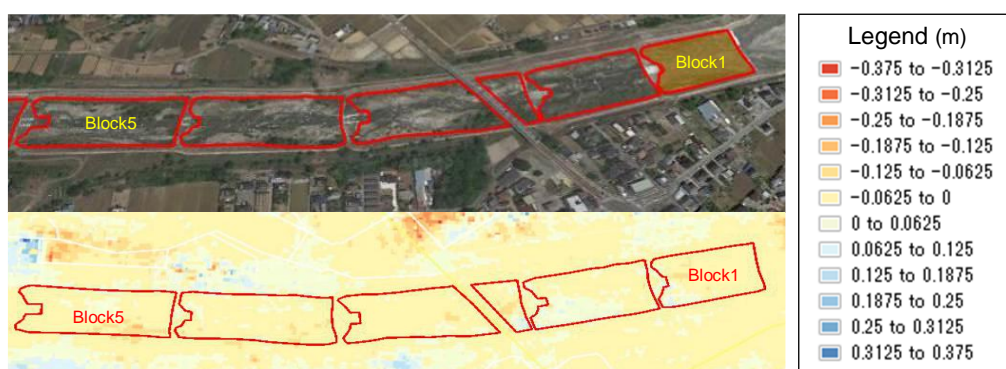


Fig. 7
Image of channel block division and SAR interference analysis

2.3.3. Results of SAR image analysis

Interference analysis on adjacent SAR images by the method shown in Fig. 6 and Fig. 7, the changes in ground height of each mesh occurred between two SAR images is directly obtained. And by each mesh area (s_i) \times average height (Δh_i), the volume change ($\Delta v_i = s_i \times \Delta h_i$) of each mesh is calculated. Then, cumulating the results from each mesh the total volume of sediment transport for each block or the whole section can be calculated.

The vertical sectional view of the riverbed height variation (block average) calculated by the above method is shown in Fig. 8. While, the volume of sediment transport for every analysis period (① to ⑧) is shown in Table 3 and Fig. 9, and the temporal change of sediment volume within the study river section is shown in Fig. 10.

Table 3
Sediment transport volume by inSAR image analysis

No.	Analysis period		Period (Day)	Sediment change volume by inSAR analysis V_s (m^3)
	from	to		
①	2014/09/19	2014/11/28	70	9743.98
②	2014/11/28	2015/04/03	126	-5361.75
③	2015/04/03	2015/06/26	84	1840.07
④	2015/06/26	2016/03/18	266	-21229.55
⑤	2016/03/18	2016/06/24	98	9752.34
⑥	2016/06/24	2016/11/25	154	1599.06
⑦	2016/11/25	2017/03/03	98	-648.32
⑧	2017/03/03	2017/06/09	98	9596.02

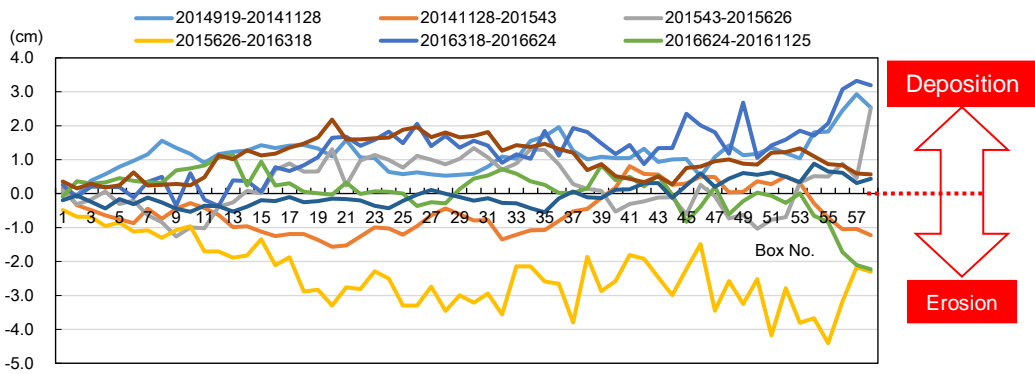


Fig. 8
River bed height variation on longitudinal section during each analysis period

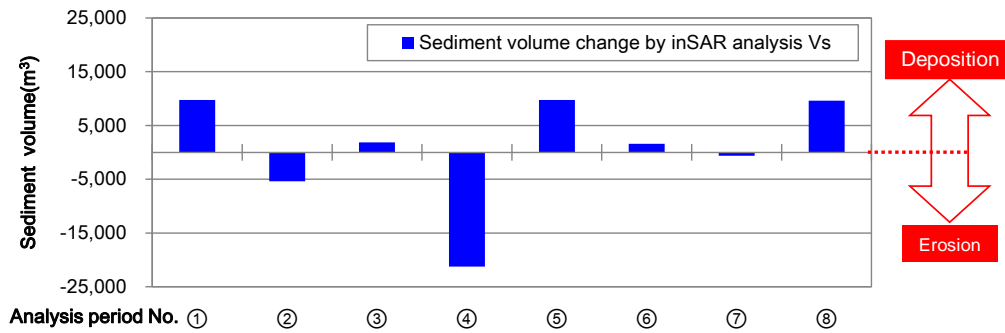


Fig. 9
Sediment transport volume during each analysis period

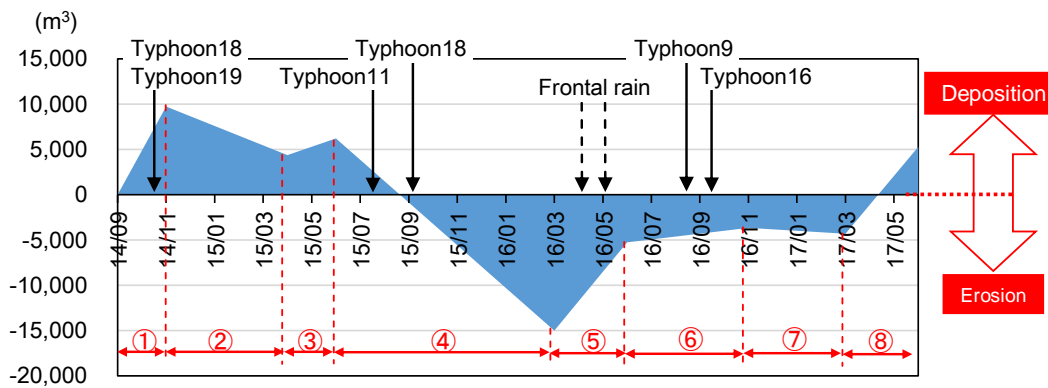


Fig. 10
Sediment temporal change in river channel

From above results, the riverbed rise (deposition) or decrease (erosion) was observed according to the observation target periods. Basically, during the period when large floods (typhoon) occurred, a riverbed rise (deposition)

appeared and if there is no flood in a long term, a tendency of river bed decrease (erosion) is recognized due to the sediment gradually flowing out.

3. RESULTS

3.1. RESULT COMPARISON AND ITS CONSIDERATION

A comparison of transport sediment volume (bedload and suspended load) observed by equipment (hydrophone, turbidimeter, water level gauge etc.) installed at the downstream end in Omukawa River and that calculated from SAR image interference analysis in the same period is shown in Table 4 and Fig. 11.

Table 4
Comparison between results by SAR image analysis and observation

No	Analysis period		Period (Day)	Sediment change in volume by inSAR analysis V_{ss} (m ³)	Sediment discharge observed by hydrophone V_{sH} (m ³)	Event occurred in the period
	from	to				
①	2014/09/19	2014/11/28	70	5846.39	-1469.05	Typhoon18 Typhoon19
②	2014/11/28	2015/04/03	126	-3217.05	-2234.88	
③	2015/04/03	2015/06/26	84	1104.04	-514.11	
④	2015/06/26	2016/03/18	266	-12737.73	-10970.63	Typhoon11 Typhoon18
⑤	2016/03/18	2016/06/24	98	5851.40	-1312.48	
⑥	2016/06/24	2016/11/25	154	959.43	-12317.24	Typhoon9 Typhoon16
⑦	2016/11/25	2017/03/03	98	-388.99	-1458.5	
⑧	2017/03/03	2017/06/09	98	5757.61	-1483.2	

※ Sediment change in volume revised by void ratio of river bed material (0.40)

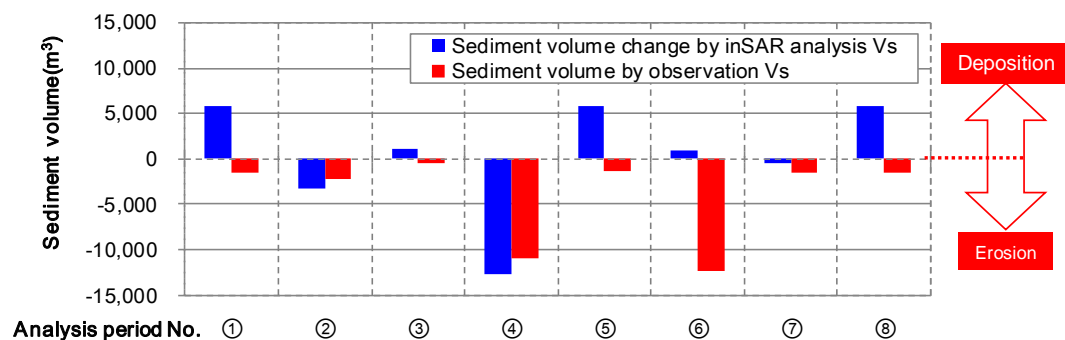


Fig. 11
Comparison between results by inSAR image analysis and observation

During flood period, i.e. ①, ③, ⑤, ⑧, sediment balance within the river section showed positive (deposition). It is presumed that there was abundantly sediment supply from the upstream.

In other hand, during the non-flood period, i.e. ② and ⑦, the balance of sediment within the river section shows negative because the volume of outflow is larger than the inflow. Meanwhile, the period ④ that spans both the flood and non-flood periods, is influenced both by the in-flow during the flood and the outflow in the non-flood season. As the result, the sediment balance showed negative in this case.

Relationship between the sediment volume change in the river section by inSAR analysis and the sediment discharge observed at downstream end by the equipment is shown in Fig. 12. Although the data showed some dispersion, an approximate linear correlation was recognized.

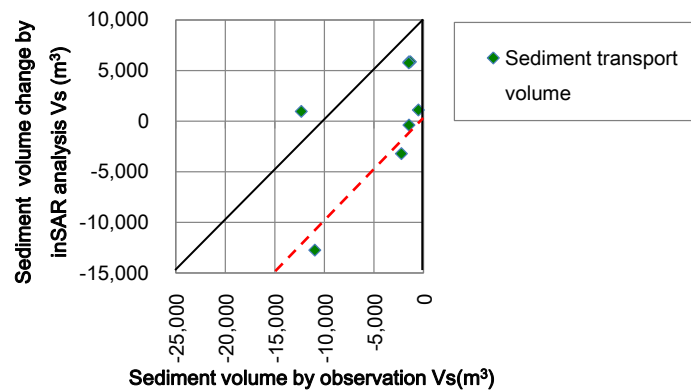


Fig. 12
Relationship between results by SAR image analysis and sediment observation

4. CONCLUSION

In this study, even though it was difficult to precisely analyze and verify the results, because there was limited SAR image data taken in accordance with the flood event (immediately before/after), but the followings can be concluded from the above examination:

1) Combining observation with trap pit can verify the accuracy of sediment observation with hydrophone as well as measure spatio-temporal sediment transport during flood event. By interference analysis of adjacent SAR images, it is possible to capture the change of micro topography in the riverbed.

2) This method can be fully utilized to measure and analyze geomorphologic changes in mountain streams where periodical survey is difficult.

3) In this study, clear correlation between sediment volume obtained by SAR analysis and observed one by hydrophone, turbidimeter, etc. was not be

confirmed due to the limitation of the verifiable data. Moreover, since a hydrophone (length = 2.0 m) is installed at one side near the sidebank of about 72m wide river, it maybe have some difficulties to represent the sediment transport volume calculated by the hydrophone for the entire width of the river.

4) Measurement of topography deformation by interference SAR image analysis is a new technology that rapidly progressed in recent years. In order to obtain accurate data and make precisely analysis, further study and improvement on observation equipment and analysis technique are needed in the future.

ACKNOWLEDGEMENTS

We sincerely thank the staffs in the Fujikawa SABO office, Kanto Rigional Development Bureau, the Ministry of Land, Infrastructure, Transport and Tourism (MLIT), Japan, for their kindly supports in this work.

REFERENCES

- [1] MITUNAGA,T.,MORIYA,T.,UCHIDA,T.,TOMITA,K.,YE, Z. Observation of sediment discharge in the district of Fujikawa Sabo Office. *Journal of the Japan Society of Erosion Control Engineering*, vol.68,No.1, 2015 (In Japanese)
- [2] MIZUNO,M.,KAMIYAMA,J.,EKAWA,M.,SATOU,T.,KANBARA,J.,HAYASHI, S. Method of emergency search for the location of landslide dams using high-resolution single-polarization SAR image interpretation, *Technical Note of NILIM*, No.760,2013 (In Japanese)

SUMMARY

Taking the middle to downstream section of Omukawa River (extension $L = 8.3$ km, gradient $1/58$) as a study site, A comparison between sediment transport obtained by SAR image interference analysis and sediment discharge observed by hydrophone etc. during 2014-2016 period.

The result shows that, although there was data variation, an approximate linear correlation was recognized.

The reason of the difference between two data is assumed that sediment discharge is measured only at the downstream end with a length $L= 2.0$ m, with respect to the river width of 72 m, which is not adequate for representing the entire river cross section.

COMMISSION INTERNATIONALE DES GRANDS BARRAGES

VINGT-SIXIÈME CONGRÈS DES GRANDS BARRAGES
Autriche, juillet 2018

DOI 10.3217/978-3-85125-620-8-027



This work licensed under a Creative Commons Attribution 4.0 International License. <https://creativecommons.org/licenses/by-nc-nd/4.0/>

**EXPERIMENTAL DESIGN OF A TARGETED WATER RELEASE TO FLUSH
SAND OUT OF THE BYPASSED REACH OF THE SELVES RIVER**

Rémi LOIRE

Engineer at the hydro engineering center, EDF

FRANCE

Hervé PIEGAY

Research Director, ENS LYON CNRS UMR5600

FRANCE

Jean-René MALAVOI

Engineer at the hydro engineering center, EDF

FRANCE

Loic Grosprêtre

Engineer, DYNAMIQUE HYDRO

FRANCE

Olivier ORTIZ

Engineer at the Central hydropower production unit, EDF

FRANCE

COMMISSION INTERNATIONALE
DES GRANDS BARRAGES

VINGT-SIXIÈME CONGRÈS DES
GRANDS BARRAGES
Autriche, juillet 2018

**EXPERIMENTAL DESIGN OF A TARGETED WATER RELEASE TO FLUSH
SAND OUT OF THE BYPASSED REACH OF THE SELVES RIVER***

Rémi LOIRE

Engineer at the hydro engineering center, EDF

FRANCE

Hervé PIEGAY

Research Director, ENS LYON CNRS UMR5600

FRANCE

Jean-René MALAVOI

Engineer at the hydro engineering center, EDF

FRANCE

Loic Grosprêtre

Engineer, DYNAMIQUE HYDRO

FRANCE

Olivier ORTIZ

Engineer at the Central hydropower production unit, EDF

FRANCE

* *Dimensionnement de lâchers d'eau expérimentaux pour dessabler le tronçon court-circuité de la rivière Selves*

1. INTRODUCTION

Integrated management of sediment and flows downstream of dams is still relatively rare. In France, we have developed a "morphogenic water release concept" which aims at optimally design the necessary flows/duration of these releases on the basis of "expected results" clearly defined by the stakeholder. The most common "expected results" range from simple surface cleaning of coarse alluvial substrates (low flow/duration releases) to active lateral erosion of meanders (high flow/duration releases) and removal of alluvial vegetation from the medium bed. One of these objectives may concern reducing sand accumulation in downstream reaches that occurs, as a result of reduced bed-mobilizing flows and high sediment load from tributaries.

This is the case of the Selves River (164 km² watershed in the Massif Central - France) downstream of the Maury dam (Fig.1), which creates a reservoir with a 35 million m³ storage capacity. Flow diversion has had a major influence on both average flows and floods. Dam spillovers are infrequent: a single event has occurred since the impoundment of the dam in 1947. The bypassed reach downstream of the dam (approximately 11 km long) is located in a narrow valley with numerous tributaries, which transport large quantities of sand during thunderstorms. Because of flow reduction downstream of the Maury dam, most of this sand accumulates in the riverbed of the bypassed section. This sand accumulation has been noted for several years by both stakeholders and the local hydroelectric company, Electricity of France (EDF). Therefore, it has been decided jointly to implement targeted water releases (i.e., flushing flows) to remove the excess of sand in order to improve fish habitat (refuges and reproduction zones).

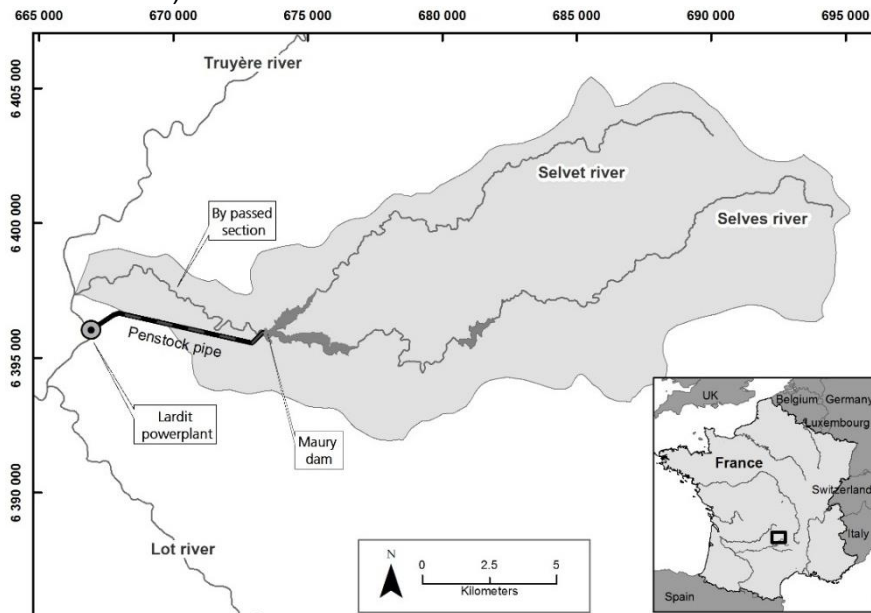


Fig. 1

The Selves River in France and the bypassed reach downstream of the Maury dam.

2. DESIGN OF THE WATER RELEASES

The objective of these experimental releases was to determine the most effective flow rate to remove fine sediments and sand from the river bed. Several flows are tested in order to determine the most efficient flow to entrain sand particles while avoiding the movement of coarser sediments essential to the functioning of the aquatic fauna. These tests will allow us to determine the flow magnitude and duration required for the overall rehabilitation of the bed, and then the frequency, magnitude and duration of the releases to be carried out routinely.

Three water releases of 10, 15 and 20 m³/s were tested, each lasting 4 hours. To meet environmental and safety constraints, the hydrographs were characterized by a progressive ascent to 10 m³/s to limit effects on fish, then a plateau of 1h at the same flow corresponding to an alert wave necessary for the safety of third parties. The target flow rates were then maintained for 4 hours. The transit time of these releases was estimated to be about 2.5 hours. However, we retained a duration of 4 hours to ensure the success of the operation. The releases were conducted on September 6, 13 and 20, 2016.

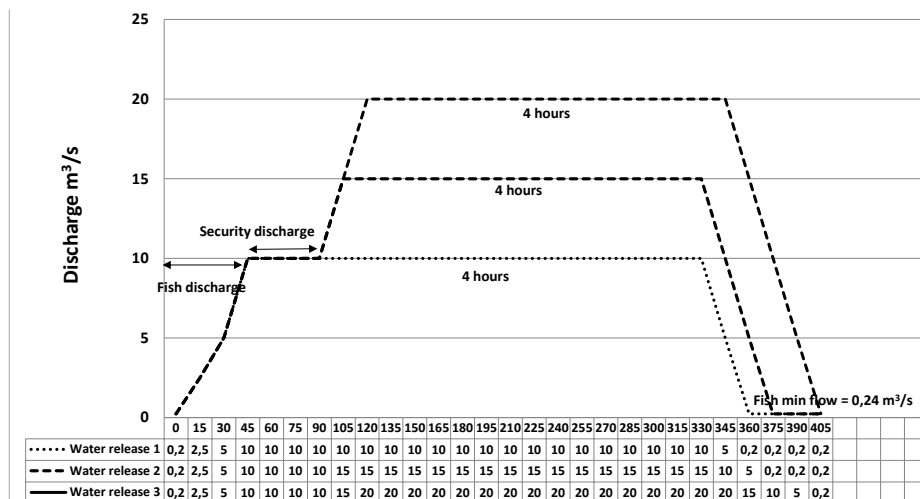


Fig. 2
Hydrographs of the clear-water releases conducted in 2016.

3. MONITORING PROGRAMME

To evaluate the effectiveness of the water releases, an ambitious monitoring programme has been implemented, targeting every major component of the aquatic ecosystem. Two monitoring objectives are targeted : (1) to directly evaluate the effectiveness of the releases (with respect to reduced channel bed clogging) and (2) to evaluate the overall effectiveness of flow restoration measures on biota over a period of at least 3-6 years. This article corresponds to the first phase of the study.

To monitor the efficiency of releases and to avoid environmental degradation, continuous measurements of conductivity, temperature and dissolved oxygen were conducted during the release. Water depth, Suspended Sediment Concentration (SSC) and turbidity were monitored during the releases at two stations. The first station is located immediately downstream of the dam in order to verify the hydrograph and the upstream TSS concentrations. The second station, located in the downstream part of the bypassed reach, serves to verify the diffusion of the hydrograph and of the silt in the bypassed reach.

116 transects spaced at 100-m intervals were surveyed between the Maury dam and the confluence with the Truyère River downstream during the summer preceding the three releases (t0) and in the autumn (t3) to quantify changes before and after the experiments. Within each transect (defined by its bankfull width), water depth, grain size distribution and the fine sediment thickness (silts and sand) were measured.

More detailed transects were also surveyed at 5 stations before the first release (t0), after the first (t1), the second (t2) and the third release (t3). The average station length was 250 m and each of them was composed of about 30 transects. These stations were supposed to be more clogged than the average observed on the river. The parameters measured at these cross-sections are the same as those of the previous protocol. At each of these stations, painted plots and scour chains were installed to determine the size of the sediments mobilized during the various releases.

At Station 4, coloured sand particles were also injected before the first release and before the third release. This method has been already implemented to track the movement of sands in coastal environments (Ingle, 1966) but few studies have used it in rivers (Grosprêtre, 2011). 400 kg of coloured particles (grain size 2-4mm) were placed on a river cross-section (Fig. 3) before each of two releases. Several sediment samples, of approximately 5 kg, were collected after each of the three releases over several hundred meters until the coloured particles disappeared in the samples. The number of sand particles present in each sample was assessed by image analysis. The sand used in each injection had a different color to improve the two releases comparison.

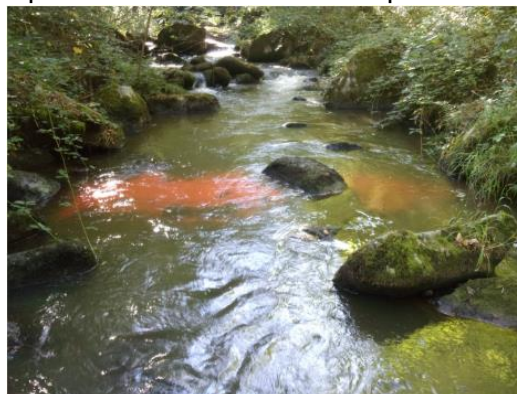


Fig. 3

Photograph of the injection of fluorescent sand tracers on a transect of the Selves River.

4. INITIAL RESULTS

4.1. WATER RELEASES DESIGN

The flow wave of each release was well propagated downstream. The discharge at Maury dam was equal to the flow generated at the downstream reach. On the other hand, the gradual ascent carried out to prevent aquatic fauna impact and ensure the safety alert was not observable at the downstream station. The flow rate quickly rose to the maximum nominal flow rate designed during the tests.

The duration of the hydrograph was sufficient to export the suspended sediment. The SSC was divided by 4, 3 and 2 after the three releases after only 2.5 hours of release, whereas the release has a plateau of 4 hours at maximum flow. During each release, the SSC rates became similar after 1h20 of maximum flow (Fig. 4).

4.2. SUSPENDED SEDIMENT TRANSPORT

The SSC reached 2.1 g/l, 1.6 g/l to 1 g/l respectively for releases of 10,15 and 20 m³/s (Fig.4), which is substantial given the morphological context of the valley. The SSC observed immediately downstream the dam were less than 0.1 g/l during the three releases carried out.

These results illustrate the effectiveness of the releases on the suspended sediments, which primarily come from the wetted channel, starting at only 10 m³/s, as the particle size analysis show silt was infrequent along the cross-sections.

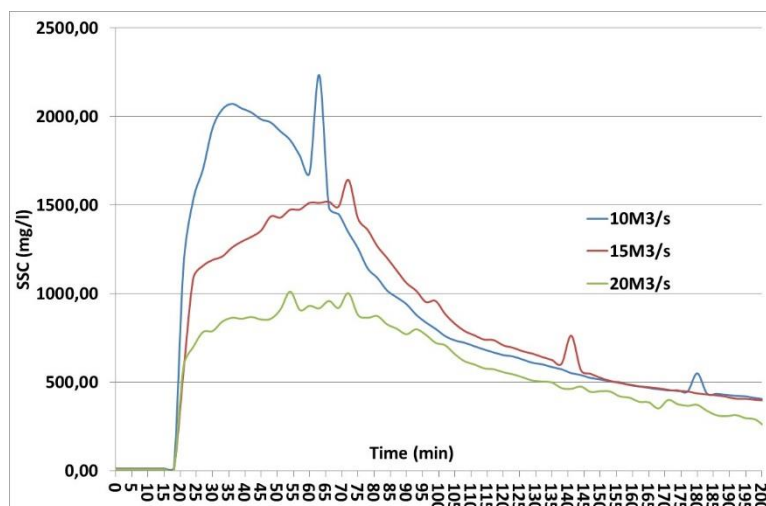


Fig. 4

SSC observed at the downstream station during each water release.

The SSC decreased with each successive release, despite the increased nominal flow rate (10, 15, 20 m³/s). This decline in SSC production has been observed in other studies and is the result of the progressive scouring of fine sediment from the riverbed.

These initial results confirm that regular releases at relatively low flow rates (10 m³/s) and lasting 5 hours could prevent clogging by silts and clays in the Selves River.

4.3. EFFECT ON BEDLOAD TRANSPORT

Fluorescent sand tracers were collected after each release. Their proportion in the sediment samples and the transport distance from the injection point were recorded. The results show a progressive change in mean position, distance travelled by a given fraction of the tracers and maximum distance travelled as a function of flow. The median, average and maximum transport distances have more than doubled between 10 and 15 m³/s, which is not the case between 15 and 20 m³/s. These findings clearly show that release efficiency increases with flow and that there is a relationship between the flow and the distance travelled by the tracers.

The 10 m³/s release mobilized only a few gravels. The second release at 15 m³/s mobilized the same grain size classes with a slightly larger amount of particules entrained. However, these latter were mobilized over short distances. During the last release, fewer plots were set up, but the results show a more damaging transport of coarse particles.

4.4. EFFECT ON HABITAT

The linear survey made it possible to characterize the initial state (t₀) of sand and silt deposits along the Selves and to identify the tributaries contributing the most in fine sediments. It was then possible to measure the evolution between the initial state and the state after the three successive releases. The results are spatially heterogeneous. Both declines and increases in which both variables were observed over the entire length of the bypassed section. In particular, heavily clogged areas near the tributaries have tended to become unclogged and water depth has increased.

Changes in the fine sediment thickness are closely linked to the different geomorphic units. Fine sediment accumulation was non-existent in lotic reaches and in areas where pre-release clogging was already negligible. The most significant changes occurred in glides for which the median values and distribution were considerably reduced and concentrated.

Surveys carried out over the length of the bypassed reach showed that fine sediment thickness has been nearly divided by 3 on average. The proportion of sands and fine gravel remained essentially the same as the 3 releases were not

long enough to allow for significant sediment exports outside the bypassed reach. Fresh sand deposits were observed on the channel banks after the releases, similarly to what it has been shown on the Colorado River [3]. Deposits were also been observed near the wetted channel and in some areas, vegetation has been covered with fines.

Reducing the stock of fine sediments in the river has had a positive impact on water levels and therefore on the habitats available for aquatic fauna.

5. CONCLUSION

The step-by-step design of water releases implemented in the Selves, even if it required considerable human and financial resources, has proven to be a worthwhile strategy. The flow rates were selected in an adequate range and through this process, the optimum flow rate for future operations was identified. We now know that a flow slightly less than or equal to 10 m³/s allows for a significant mobilization of the TSS and that a flow of 15 m³/s allows a much more significant mobilization of the sand fraction. In addition, even if the risk of mobilizing coarser sediments remains relatively low, the cost/benefit of using higher flows does not appear to be worth it. The morphological evolutions observed indicate that in rivers with a high sand load, even modest flows can achieve morphological changes in the active channel.

From an environmental point of view, the various objectives were achieved. There was substantial evacuation of sand and silt in the bypassed section that even exceeded our expectations, thereby improving the quality of available spawning areas. Furthermore, at the upstream station, new habitats are available for aquatic fauna in relation to the increase in water level.

REFERENCES

- [1] INGLE J.C.JR. The movement of beach sand : an analysis using fluorescent grains. *Developments in Sedimentology. Elsevier Publishing Company*, 1966, Nr. 5.
- [2] GROSPRETRE L. Etude et gestion des impacts hydrogéomorphologiques de la périurbanisation. L'exemple du bassin de l'Yzeron dans l'Ouest lyonnais. *PhD thesis*, 2011.
- [3] SCHMIDT J.C., PARNELL R.A., GRAMS P.E., HAZEL J.E., KAPLINSKI M.A., STEVENS L.E. and HOFFNAGLE T.L. The 1996 controlled flood in grand canyon: Flow, sediment transport, and geomorphic change. *Ecological Applications*, 11(3), 657–67. 2001.

SUMMARY

Integrated management of sediment and flows downstream of dams is still relatively rare, including in France. Flow experiments are often necessary to determine appropriate management actions and to verify that environmental objectives (often various) are being met. One of these objectives may concern reducing sand accumulations in downstream reaches that occur as a result of reduced bed-mobilizing flows and high sediment load from tributaries.

This is the case of the Selves River (164 km² watershed in the Massif Central - France) downstream of the Maury dam, which creates a reservoir with a 35 million m³ storage capacity. Flow diversion has a major influence on both average flows and floods. Dam spillovers are infrequent : a single event has occurred since the impoundment of the dam in 1947. The bypassed section downstream of the dam is approximately 11 km long. This section is located in a narrow valley with numerous tributaries, which load large quantities of sand during thunderstorms. Because of flow reduction downstream of the Maury dam, most of this sand accumulates in the riverbed of the bypassed section. This sand accumulation has been documented by both stakeholders and the local hydroelectric company, Electricity of France (EDF), for several years. It has therefore been decided jointly to implement targeted water releases to remove the excess sand in order to improve fish habitat (refuges and reproduction zones).

The first empirical calculations estimated that the displacement rate of the sand would be about 10 m³/s. Implementing a water release at a discharge below this value would risk using water with no significant effect on riverbed morphology. Therefore, 3 operational water release tests (10, 15 and 20 m³/s) were carried out in September 2016 to define the discharge necessary to transport a maximum of sands without mobilizing the coarser elements (gravels and pebbles) necessary to aquatic organisms. The release duration was limited to 5h for each test to minimize environmental impacts and potential problems associated with dam operations.

Suspended sediment monitoring carried out during the releases show a recovery of the stock of fine sediments (clays - silts) present in the bypassed section. At one of the stations, fluorescent particles (2-4 mm) were added prior to releases to observe the distance traveled by the particles as a function of the released discharge. In addition, biological monitoring is underway to elucidate the long-term ecological effects of the releases. The latter two approaches will only be partially discussed here.

The results indicate that the flow rates were selected in the appropriate range for the stated objectives. Furthermore, it was possible to determine the optimum discharge for future releases: a flow rate equal to 10 m³/s allows a significant mobilization of suspended sediments and a flow rate of 15 m³/s allows for substantial mobilization of the sandy elements. Above 15 m³/s, although the risk of mobilizing coarse elements remains relatively low, the cost-benefit ratio of this discharge level does not appear to be advantageous. From an environmental perspective, the different objectives were achieved.

La mise en œuvre d'une gestion environnementale des débits en aval des barrages fait l'objet de plus en plus d'études scientifiques. Ces actions sont encore peu développées en France et des expérimentations sont nécessaires pour les mettre en œuvre car les objectifs sont multiples, tout comme les contextes dans lesquels ils sont conduits et les dimensionnements qui sont appropriés. L'un des problèmes concerne notamment l'ensablement des sections à l'aval de réservoirs lorsque celui-ci influence significativement les débits critiques alors que la charge provient des affluents.

C'est le cas de la Selves (164 km², affluent de la Truyère, dans le Massif Central) à l'aval de la retenue de Maury (volume de l'ordre de 35 millions de m³). L'ouvrage, dont les eaux dérivées sont turbinées à la centrale de Lardit, a une influence majeure sur l'hydrologie moyenne et de crue du cours d'eau. Les déversements sont peu fréquents, une seule occurrence depuis la mise en eau du barrage en 1947. Le constat d'ensablement a été partagé entre les gestionnaires du territoire et EDF depuis plusieurs années. Il a donc été décidé conjointement la mise en œuvre de lâchers de dessablage en aval du barrage de Maury en vue d'améliorer les habitats de refuge et de reproduction pour la population piscicole. Le Tronçon Court-Circuité (TCC) de la Selves en aval du barrage mesure environ 11 km de long. Très encaissé, il reçoit de très nombreux affluents de faibles longueurs et très pentus, qui réagissent principalement aux phénomènes orageux au cours desquels ils transportent d'importantes quantités de sables. Du fait de la réduction des débits en aval de l'ouvrage de Maury, la plus grande partie de ces sables s'accumule dans le lit de la Selves.

Les premiers calculs empiriques ont estimé que le débit de mise en mouvement du sable sur la rivière était d'environ une dizaine de m³/s. En dessous de cette valeur, le risque est d'utiliser de l'eau sans effet notable sur la morphologie. 3 tests opérationnels (10, 15 et 20 m³/s pendant 5h – période courte permettant de préserver les milieux et de limiter les problèmes d'exploitation des ouvrages) ont été réalisés en septembre 2016 pour définir le débit permettant de transporter un maximum de sables sans pour autant mobiliser les éléments plus grossiers (graviers, galets) favorables aux organismes aquatiques. Un suivi physico-chimique de la qualité des eaux a été réalisé pendant toute la durée des lâchers montrant une reprise du stock de sédiments fins (argiles – limons) présents dans le TCC. Sur l'une des stations, des granules (2-4 mm) fluorescentes ont été injectées afin d'observer les distances parcourues par les particules en fonction des débits lâchés. En complément, des mesures biologiques sont mise en œuvre pour suivre les effets sur le milieu à plus long terme.

Les résultats soulignent que les débits ont été choisis dans la bonne gamme et permettent même de déterminer le débit optimum pour les futures opérations : un débit légèrement inférieur ou égal à 10 m³/s permet une mobilisation significative des MES et un débit de 15 m³/s permet une mobilisation bien plus significative des éléments sableux. Au-delà de 15 m³/s, même si les risques de mobilisation d'éléments grossiers restent relativement faibles, le coût/bénéfice de cette gamme de débits n'apparaît pas intéressant. D'un point de vue environnemental, les différents objectifs sont atteints.

COMMISSION INTERNATIONALE DES GRANDS BARRAGES

VINGT-SIXIÈME CONGRÈS DES GRANDS BARRAGES
Autriche, juillet 2018

DOI 10.3217/978-3-85125-620-8-028



This work licensed under a Creative Commons Attribution 4.0 International License. <https://creativecommons.org/licenses/by-nc-nd/4.0/>

DAMS AND RESERVOIRS - CLIMATE CHANGE ADAPTATION STRATEGY

Hubert LOHR

Managing Director, SYDRO CONSULT GMBH

GERMANY

Felix FROEHLICH

Project engineers, SYDRO CONSULT GMBH

GERMANY

Marius HERBER

Project engineers, SYDRO CONSULT GMBH

GERMANY

Sandra RICHTER

Project engineers, SYDRO CONSULT GMBH

GERMANY

COMMISSION INTERNATIONALE
DES GRANDS BARRAGES

VINGT-SIXIÈME CONGRÈS DES
GRANDS BARRAGES
Autriche, juillet 2018

DAMS AND RESERVOIRS - CLIMATE CHANGE ADAPTATION STRATEGY

Hubert LOHR

Managing Director, SYDRO CONSULT GMBH

Felix FROEHLICH

Marius HERBER

Sandra RICHTER

Project engineers, SYDRO CONSULT GMBH

GERMANY

1. INTRODUCTION

The aim of the project is to develop adaptation strategies for dams and reservoirs that take into account shifting precipitation regimes and their resulting discharge and water quality conditions.

For several years, changes in the precipitation regime have been observed in Germany. Rainfall in February to April shifted more into the summer. Although total annual rainfall remained nearly the same, the resulting discharge was less due to higher losses in the summer months. As a consequence, reservoir operators experience difficulties in reaching full supply level in spring in order to fulfill existing and competing uses and requirements over the course of each year. This also impacts on local communities and water suppliers.

The emphasis of this study lies on the early recognition of droughts and corresponding reservoir management. The identification of possible counter

measures if a drought situation becomes more likely is part of the project. The approach will be transferred into a concept for the adaptation of operation rules taking into account competing uses and target conflicts.

The approach uses hydro-meteorological indices to identify the need for counter actions at an early stage. Based on this, necessary individual and site-specific solutions can be worked out for each reservoir. It is envisaged to integrate the course of action identified during the research project into a guideline for Germany. German water authorities and a wide range of reservoir operators from Germany are involved in the research project.

The project ends in spring 2019.

2. DATABASE

Observation data on precipitation, run-off and climate data such as temperature, evaporation or sunshine duration was provided for the project from the participating reservoir operators. The data was collected from monitoring stations located in the study area for the period from 1970 to 2016 with a temporal resolution of one day.

Forecast data on precipitation was obtained from the National Oceanic and Atmospheric Administration (NOAA) [1]. Since May 2011, NOAA issues long-term forecasts of monthly values. This is a relatively short period, so that the data still lack extreme values or extreme events respectively.

NOAA data is given in a grid format with a resolution of approximately 0.94 degrees. In the context of bias correction, it had to be determined with which ground stations (see Fig. 1) and observed values the NOAA data can best be correlated in order to be able to recognize and correct any bias.

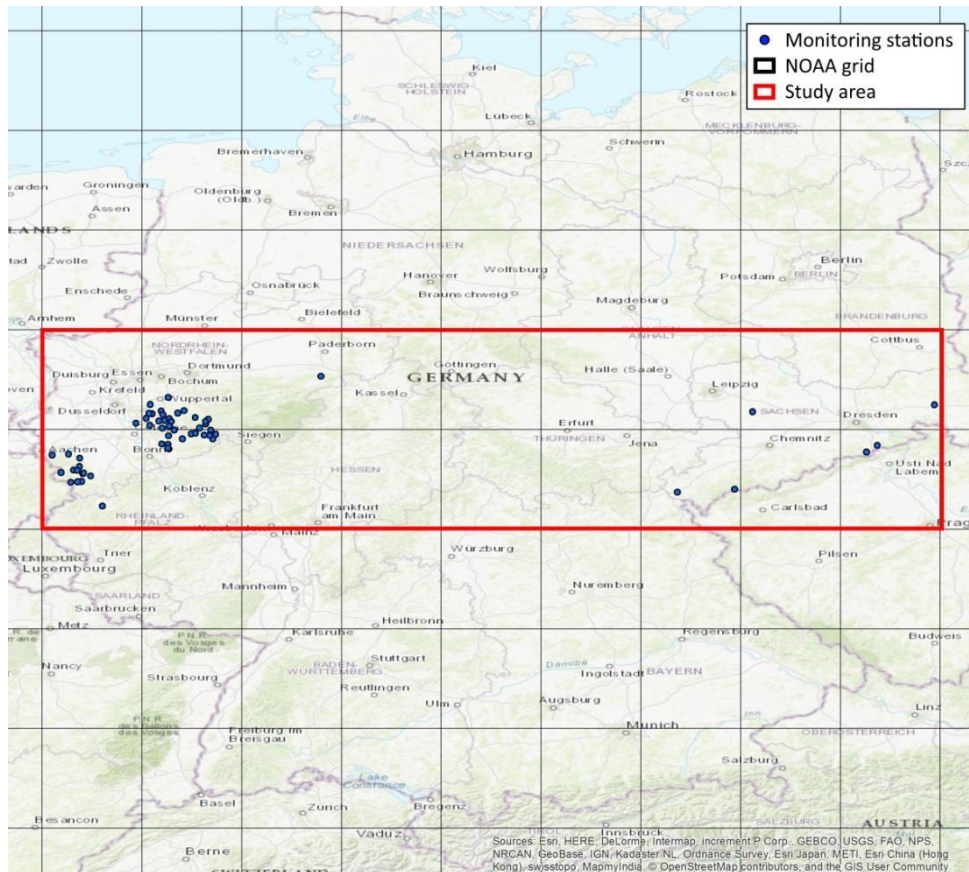


Fig. 1
Relation between study area, monitoring stations and NOAA raster data

3. METHODS

3.1. NOAA FORECAST DATA / BIAS CORRECTION

Bias correction was performed using two different methods: quantile mapping and formation of monthly factors.

The monthly factors were calculated for each calendar month. First, average values for each month were calculated for each observation station and forecast grid over the entire time period for which observed and forecasted datasets are available. This was the time period from 2011 to 2016. Then, the correction factor was calculated for each month by computing the ratio between the observed and the forecasted values. The correction factors are specific to each combination of observation station and forecast grid. Bias corrected forecasts could then be obtained by multiplying each value of the forecasted time series with the appropriate monthly correction factor.

Bias correction using quantile mapping (qmap) was performed according to the method developed by Gudmundsson et. al. [3]. This method entails an empirical adjustment of the distribution of the forecasted values to fit the distribution of the observed values.

The results of using both bias correction methods individually and of using quantile mapping followed by a correction using monthly factor were evaluated using goodness of fit indicators such as the Pearson coefficient, Nash-Sutcliffe efficiency coefficient, bias error, mean absolute error and mean square deviation.

3.2. INDICES

Hydro-meteorological indices play a crucial role in the project. Indices have to be interpreted from the viewpoint of reservoir operation. As indices have differing inertia and apply to different periods, they can be used for predictive operation.

The appropriateness of these indices, the way they should be interpreted and their usefulness regarding early detection of hydrological stress, is tested by conducting hindcast experiments. Indices providing the best skill in hindcast experiments are selected for conducting forecasts. As long as the forecast quality is adequate, this will lead to an enhancement of the current early detection methods.

For a start, the Standardized Precipitation Index (SPI) was used. The SPI is recommended by the World Meteorological Organization for meteorological drought monitoring [2]. The SPI can be calculated for different aggregation periods, e.g. only one month or even up to 60 months.

In order to address uncertainty contained in the forecasts, the SPI is calculated for time periods that extend both into the past as well as into the future, thus consisting of different amounts of observed and forecasted values. The performance of indices calculated with different observed and forecasted aggregation periods was compared with results that used only observed values for computing SPIs. In doing so, it is possible to determine how reliable the SPI computed using forecast data is for different forecast lengths.

In a next step, the Standardized Precipitation Evaporation Index (SPEI) and the Water Supply Index will be tested in terms of their suitability.

4. RESULTS

4.3. BIAS CORRECTION OF FORECAST DATA

Examples for a monitoring station in eastern Germany are shown. The accuracy of the bias-corrected forecast time series was evaluated by means of

the above-mentioned goodness of fit measures (see Table 1). Mean absolute error as well as mean square deviation were significantly improved, the Pearson coefficient only slightly. Looking at the bias error, the perfect value of one is nearly achieved.

Table 1
Error values before / after correction, example eastern Germany

Goodness of fit measure	before correction	factor corrected	qmap corrected	qmap + factor corrected
Pearson coefficient	0.51	0.62	0.54	0.55
Bias error	0.77	1.00	1.01	1.02
Nash Sutcliffe eff. coefficient	0.05	0.39	0.001	0.19
Mean absolute error	29.04	21.87	26.57	24.69
Mean square deviation	37.34	28.78	33.46	31.70

In addition, a qualitative statement can be made using a line graph (see Fig. 2), which maps the graphs for the forecast values before and after bias correction and the observed values. A direct comparison of the original NOAA monthly mean values with the values of the stations showed that amplitudes were not sufficiently reflected. After the bias correction, however, the range of observed values was enhanced and an improved representation of inner-annual patterns was achieved.

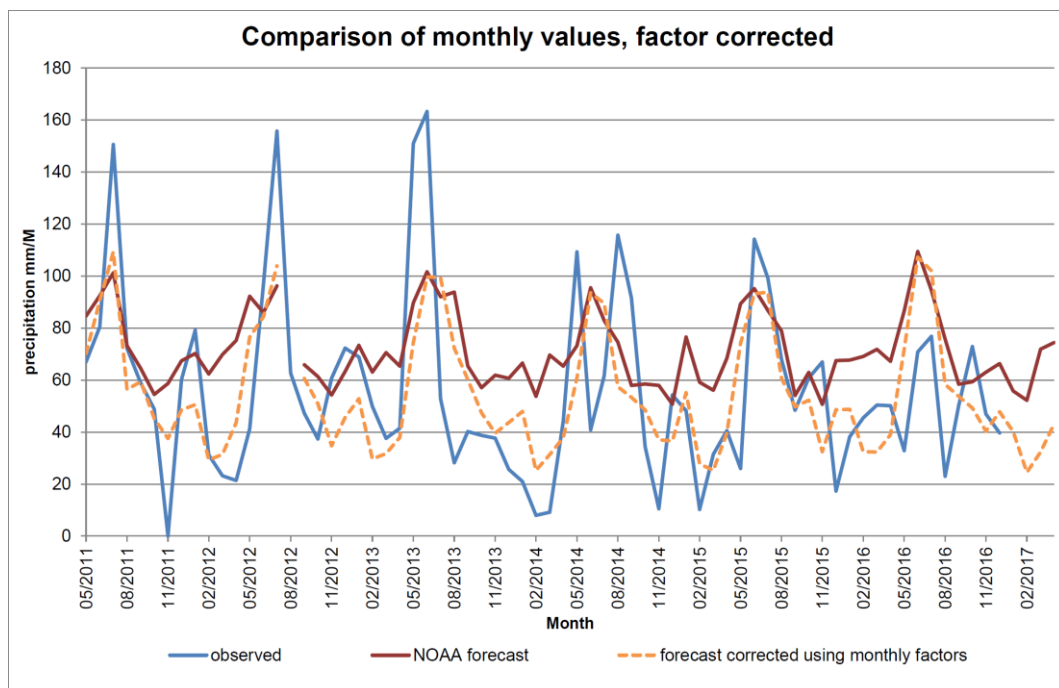


Fig. 2
Comparison of NOAA forecast data before / after factor correction, example eastern Germany

It was found that the quantile mapping method does not produce results that are usable for this study. The reason is that quantile mapping does not take the temporal sequence of values into account, but only adjusts the distribution of values. If, as is the case here, the input time series already contain large differences regarding the temporal sequence of values, quantile mapping can even amplify these differences and produce time series whose goodness of fit parameters are in some cases worse than those of the original time series (see Table 1 and Fig. 3).

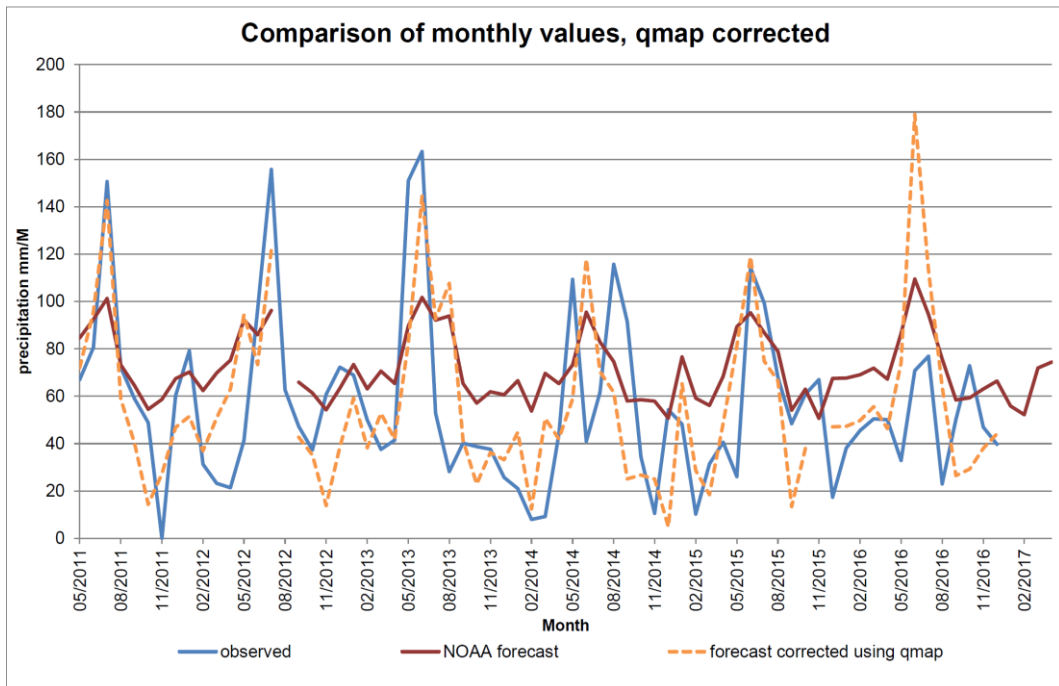


Fig. 3

Comparison of NOAA forecast data before / after qmap correction, example eastern Germany

Performing the bias correction using monthly factors consistently produced better goodness of fit parameters (see Table 1).

Tests using quantile mapping and monthly factors in sequence also produced worse results than using monthly factors alone (see Fig. 4).

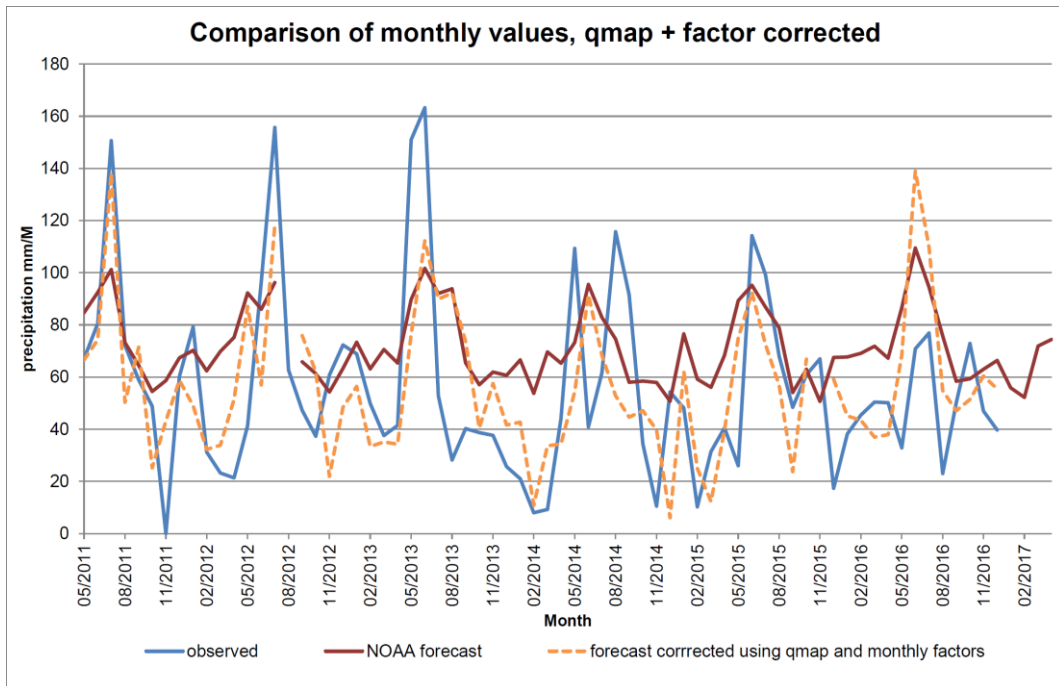


Fig. 4

Comparison of NOAA forecast data before / after qmap and factor correction, example eastern Germany

4.4. INDICES: SPI

Based on observed and bias-corrected forecast data, the SPI was calculated for different aggregation periods. The SPI calculated using only observed data ("certain knowledge") was compared with the SPI obtained by considering different fractions of observed records and NOAA forecasts.

Fig. 5 shows results for a 12-month aggregation period for two ground stations in eastern Germany. The SPI calculated using NOAA forecasts reveals a good fit in comparison to the SPI based on measured data and more significantly exhibits the same tendency for upcoming dry periods.

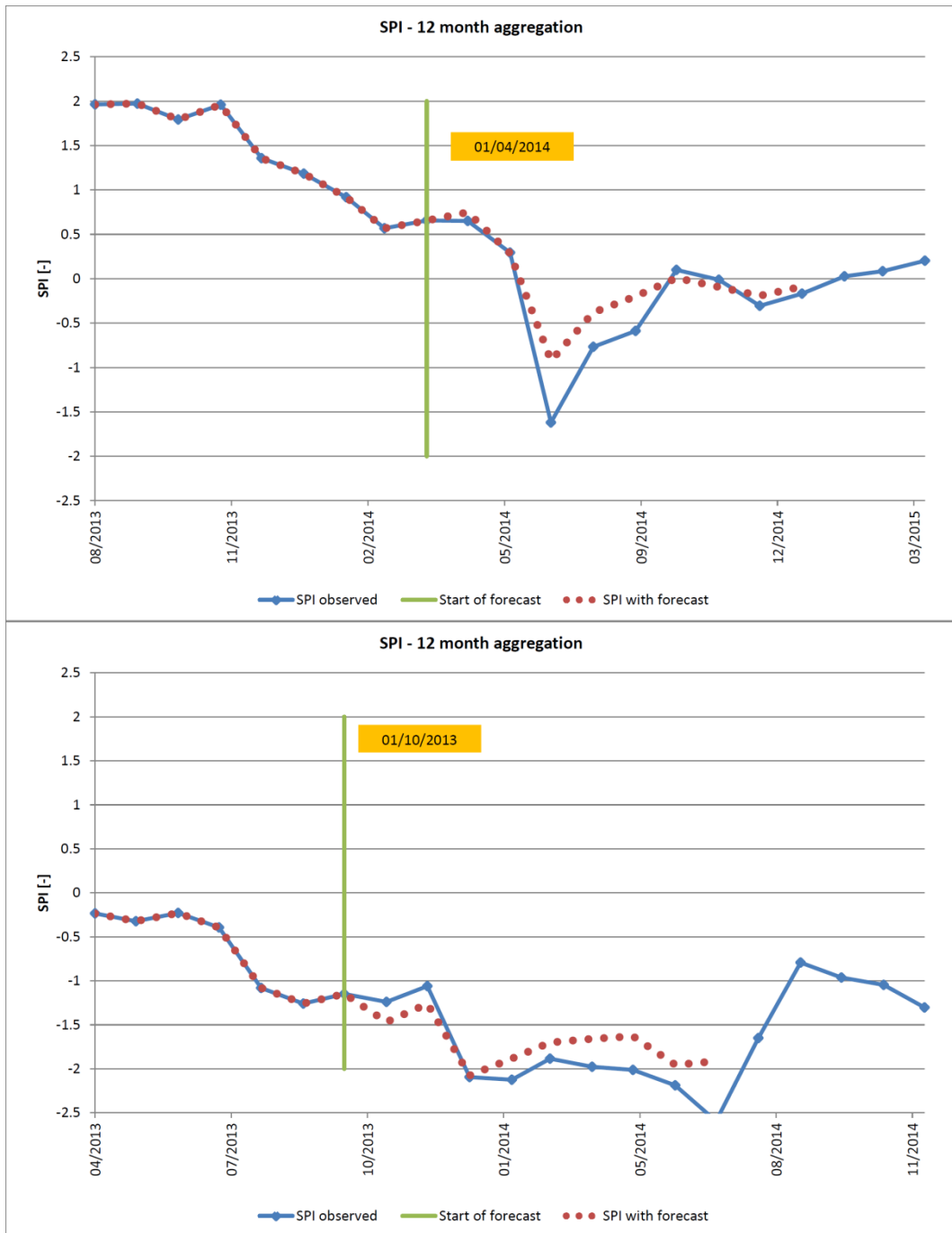


Fig. 5
 SPI calculated with observed / NOAA forecast data, examples from different sites
 in Germany

5. ADJUSTMENT OF OPERATION

Once the SPI (or indices in general) is calculated based on past and forecasted values, it can be used to adjust operation of reservoirs. Adjustment cannot be established in a general way but requires site-specific rules. However, what can be generalized is the way in which the results of indices are introduced. First, site-specific operation rules best suited for intervention must be identified. Second, threshold values for indices must be identified for when intervention should be triggered. Third, the aggregation period is highly dependent on the local situation and needs to be determined for each individual case.

Reservoirs in West-Germany with catchment areas ranging from 250 to 600 km², operated with pool-based rules, could be improved by using a 9 to 12 month aggregation period and a threshold value of -1.5 (SPI + Evaporation based indices). When the index dropped below -1.5, release rules associated with the next lower pool were applied to counter an expected decrease of inflow. This meant a reduction of downstream releases or a different release pattern related to inflow and depending on the time of year and current storage volume. Not surprisingly, not all critical periods could be identified by applying this approach. However, two thirds of critical low flow conditions with corresponding low water levels in the reservoirs could be tackled in a timely way. The approach was used without forecasts prior to 2011 and as of 2011 with forecasts to make full use of the observation period with more than 100 years.

In central Germany, a reservoir with a catchment area of less than 50 km² revealed a different pattern. Only aggregation periods longer than 18 months with a threshold value of -1.0 showed good results. Shorter aggregation periods or lower threshold values were either not consistent enough or started too late to result in counter measures that took effect. In this case, the target operation rules for intervention was water supply provision. Similar to a hedging rule, water provision was subjected to a quota of a rather small percentage as soon as the index dropped below -1.0 to prevent larger reductions later on. In doing so, the reservoir could be mostly kept above a water level that becomes critical from the viewpoint of water quality.

The initial assumption that the size of a catchment area is a reasonable parameter for estimating aggregation periods could not be confirmed. The interplay between climate, the catchment area's geology as an indicator for inertia and the reservoir itself seems more complex. As a result, each reservoir or reservoir system must be individually scrutinized to find the best set of aggregation periods and threshold values.

ACKNOWLEDGEMENTS

The project is funded by the Federal Ministry for the Environment, Nature Conservation, Building and Nuclear Safety (BMUB).

REFERENCES

- [1] NATIONAL OCEANIC AND ATMOSPHERIC ADMINISTRATION (NOAA). <https://www.ncdc.noaa.gov/data-access/model-data/model-datasets/climate-forecast-system-version2-cfsv2#CFSv2%20Operational%20Forecasts>, 2016.
- [2] SVOBODA, MARK; FUCHS, BRIAN. Integrated Drought Management Programme (IDMP), Handbook of Drought Indicators and Indices. *Drought Mitigation Center Faculty Publications*. 117. 2016.
- [3] GUDMUNDSSON, L.; BREMNES, J. B.; HAUGEN, J. E. & ENGENSKAUGEN, T. Technical Note: Down-scaling RCM precipitation to the station scale using statistical transformations - a comparison of methods. *Hydrology and Earth System Sciences*, 2012, 16, 3383-3390, doi:10.5194/hess-16-3383-2012.

SUMMARY

The aim of the project is to develop adaptation strategies for dams and reservoirs that take into account shifting precipitation regimes and their resulting discharge and water quality conditions.

The emphasis of this study lies on the early recognition of droughts and corresponding reservoir management. The approach will be transferred into a concept for the adaptation of operation rules taking into account competing uses and target conflicts.

The approach uses hydro-meteorological indices to identify the need for counter actions at an early stage. Long-term precipitation forecasts from NOAA are bias-corrected for individual ground stations in Germany, for which observed precipitation data is available. The forecasted precipitation values are then used to calculate indices (e.g. Standardized Precipitation Index (SPI)).

Conclusions are that the SPI calculated using forecasted data adequately represents the SPI calculated from observed data. In particular, upcoming dry periods can be detected using the forecasts.

Using the forecasted SPI to adjust reservoir operation rules based on a certain trigger threshold for the SPI in one case lead to reduced critical low flow conditions. In another case, using operation rules adjusted to respond to a certain SPI threshold resulted in fewer occurrences of reservoir water levels below a critical level. These case studies also showed that the SPI aggregation period and the SPI threshold value for triggering adjustments to the operating rules have to be determined individually for each site.

Further steps in the study will involve testing different indices and establishing generalized approaches for integrating index forecasts into reservoir operation.

COMMISSION INTERNATIONALE
DES GRANDS BARRAGES

VINGT-SIXIÈME CONGRÈS DES
GRANDS BARRAGES
Autriche, juillet 2018

APPLICATION OF WATER QUALITY INDEXES FOR QUALITY ASSESSMENT OF ZAYANDEHROOD DAM RESERVOIR

Masoud MIRMOHAMMAD SADEGHI¹, Niaz VAHDATPOUR¹, Ali BASIRPOUR¹,
Zahra MESMARIAN¹, Seyed Reza ROOZEGAR¹, Zohreh SHEKLABADAI¹,
Morteza SHAHMORADI¹, Ali FATEHIZADEH², Mohammad GHASEMIAN², Afshin
EBRAHIMI², Ensiyeh TAHERI², Mohammad Mehdi AMIN², Forouzan HEMAMI²,
Nasim RAFIEI²

¹*Devision of Water and Environment Research,*

²*Environment Research Center and Department of Environmental Health
Engineering, School of Health, ISFAHAN UNIVERSITY OF MEDICAL
SCIENCES, ISFAHAN, IRAN*

1. INTRODUCTION

The storage water in Zayandehrood dam reservoir is supplies drinking water demand of around 5 million peoples and also for agricultural and industrial consumption. The reservoir nominal capacity is 1.5 B m³ and nowadays deceased to less than 200 M m³ due to drought period. The present study aimed to explain the water quality of the reservoir with water quality index (WQI), national sanitation foundation water quality index (NSFWQI) and Carlson's trophic state index (CTSI).

2. MATERIALS AND METHODS

Five points were sampled within dam reservoir form 2016 to 2017. At each point, for bacterial, nutrient, heavy metal, and pesticide analysis, the surface (< 1 m depth) samples were collected and transferred to the laboratory. The other parameters including chlorophyll *a* and physicochemical parameter were measured on site by using CTD (Sea & san Technology: CTD 75M). The WQI, NSFWQI and CTSI were calculated.

3. RESULTS AND DISCUSSION

The pH and EC was relatively stable among and within the stations. Seasonally, high levels of turbidity were observed mainly during the cold weather.

The higher values of COD (sampling point No. 02) indicate water pollution, which is related to wastewater effluents discharged from recreational town. The CTD profiles at sampling point No. 05 for a chlorophyll *a*, temperature, DO, EC and pH were presented in Fig. 2. For other sampling point, the CTD profile was provided but data are not shown.

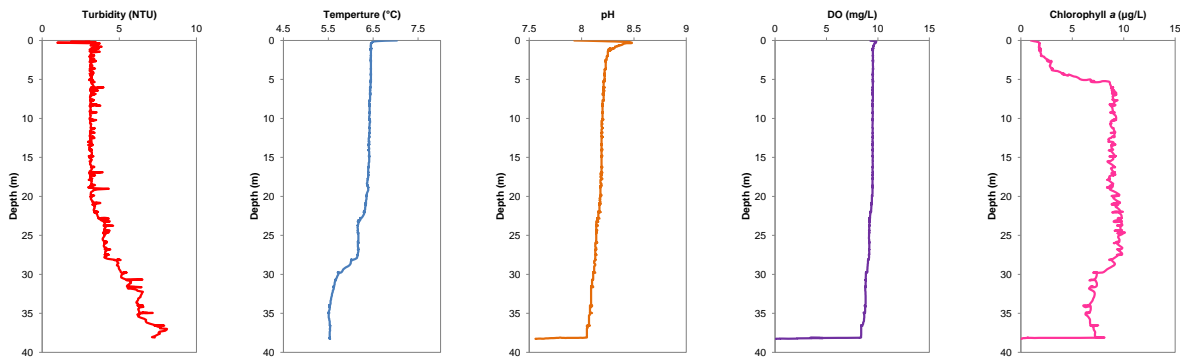


Fig. 1. CTD profiles at sampling point No. 05 (Winter 2016)

As seen in Fig. 2, the increasing of water depth led to decreasing of temperature, DO and pH values. But, the other parameters including turbidity and chlorophyll *a* showed the different pattern and increased. As seen in Fig. 2, at sampling point No. 05 (deepest point), the thermocline was typically at a depth of 25 to 30 m. The separation of the epilimnion from the hypolimnion is fundamental to lake processes because the stratification typically isolates the hypolimnion from sunlight and atmospheric oxygen. Thus, stratification typically separates the nutrient depleted, slightly less saline and algal enriched epilimnion from the oxygen depleted, nutrient enriched and slightly more saline hypolimnion.

Since, the analytical cost involved could be a limiting factor for reservoir quality assessments in developing countries, certain quality indices were used in this study. Fig. 3 shows comparison of WQI evaluations and trophic level for Zayandehrood dam reservoir.

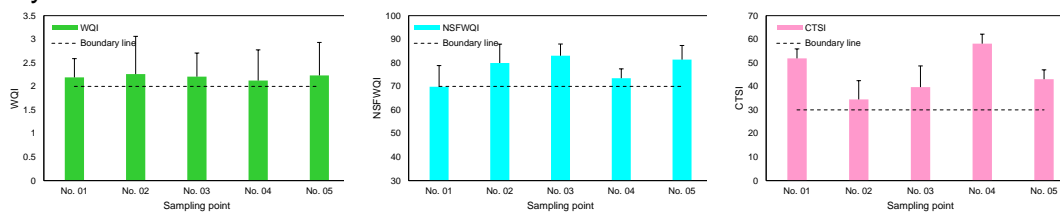


Fig. 2. Variations of WQI, NSFQI and CTSI (2016-2017)

The values of WQI (WQI and NSGWQI) are in good agreement. The results indicated that WQI 2-3, NSFQI from 70-90, while CTSI 35-60 for overall studied period.

4. CONCLUSION

Through WQI, NSFQI and CTSI, it can also be concluded that physicochemical and biological and also trophic characteristic of Zayandehrood dam reservoir water shows sign of well physicochemical and biological characteristic, but mesotrophic (moderately productive) and eutrophic (highly productive) state.

COMMISSION INTERNATIONALE
DES GRANDS BARRAGES

VINGT-SIXIÈME CONGRÈS DES
GRANDS BARRAGES
Autriche, juillet 2018

**ON THE ESTIMATION OF SEDIMENTATION LEVE IN IMHA DAM
RESERVOIR, KOREA**

Hongjun JOO, Duckhwan KIM, Jaewon KWAK, Hungsoo KIM

Department of Civil Engineering, INHA UNIVERSITY

KOREA

This study examined how to determine the optimal sediment level in dam reservoir for efficient plan and operation of dam. Currently, Korea is applying a horizontally accumulated method for sediment level estimation for the safety design of dam and so the method estimated relatively higher level than others. However, the sediment level of dam reservoir should be accurately estimated because it is an important factor in assessing life cycle of a dam. The sediment level in dam reservoir can be determined by SED-2D model linked with RMA-2, horizontally accumulated method, area increment method, and empirical area reduction method. The estimated sediment level from each method was compared with the observed sediment level measured in 2007 in Imha dam reservoir, Korea and then the optimal method was determined. Also, the future sediment level was predicted by each method for the future trend analysis of sediment level. As the results, the most accurate sediment level was estimated by the empirical area reduction method and the future trend of sediment level variation followed the past trend. Therefore, we have found that the empirical area reduction method is a proper one for more accurate estimation of sediment level and it can be validated by the results from a numerical model of SED-2D linked with RMA-2 model.

Table 1 Comparison of the method for sediment level estimation by case

Method for sediment level estimation	Sediment level (El.m)				Remark
	2007	Present (2017)	After 50 years (2067)	After 100 years (2117)	
Observed	110.00	Unobserved	Unobserved	Unobserved	Upstream of dam
RMA-2 & SED-2D model	110.58	111.21	112.43	114.22	
horizontally accumulated method	113.70	114.78	118.53	126.48	
empirical area reduction method	110.25	110.79	111.93	113.50	
area increment method	111.95	112.38	114.35	117.58	

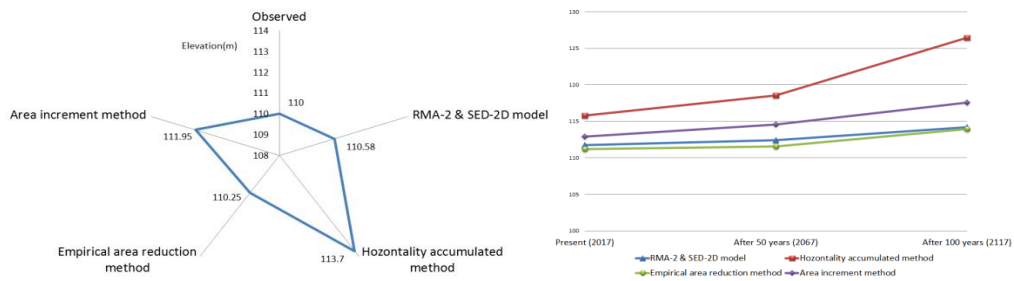


Fig. 1 Trend for the estimated sediment levels by each method

COMMISSION INTERNATIONALE DES GRANDS BARRAGES

VINGT-SIXIÈME CONGRÈS DES GRANDS BARRAGES
Autriche, juillet 2018

DOI 10.3217/978-3-85125-620-8-031



This work licensed under a Creative Commons Attribution 4.0 International License. <https://creativecommons.org/licenses/by-nc-nd/4.0/>

RESERVOIR OPERATION RULE OF HEPP POSO DAM, INDONESIA

Cristina D. YULININGTYAS

Dam Engineer, DAM SAFETY UNIT,
MINISTRY OF PUBLIC WORKS AND HOUSING

INDONESIA

Rahman H. ARDIANSYAH

Dam Engineer, DAM SAFETY UNIT,
MINISTRY OF PUBLIC WORKS AND HOUSING

INDONESIA

RESERVOIR OPERATION RULE OF HEPP POSO DAM, INDONESIA

Cristina D. YULININGTYAS

Dam Engineer, Dam Safety Unit, MINISTRY OF PUBLIC WORKS AND HOUSING

Rahman H. ARDIANSYAH

Dam Engineer, Dam Safety Unit, MINISTRY OF PUBLIC WORKS AND HOUSING

INDONESIA

1. INTRODUCTION

The areas that rapidly increase the electricity demand in Indonesia are South Sulawesi and Central Sulawesi. these regions have potential electric power with Central Sulawesi electrification ratio reached 48.3%. Based on the potential, will be built hydro electric power Poso-1 dam located in the Saojo village, North Pamona, Poso, Central Sulawesi.

This hydropower in addition to serve the needs of the area around the project (Central Sulawesi), are also expected to support the electricity needs throughout Sulawesi, particularly the mining industry spread across South and Southeast Sulawesi.

2. ELECTRICAL SYSTEM IN CENTRAL SULAWESI

Up to the third quarter of 2014, the electrical system of Central Sulawesi Province is supplied by power plant generator centers, diesel and hydropower with total installed capacity is 314 MW with the composition of the plant is still dominated by diesel-fueled HSD amounted to 224.1 MW, or 71 % of total generating capacity, followed by hydropower for 63 MW or 20% of the total generating capacity of 27 MW and a power plant or 9% of total generating capacity. With the completion of construction of 150 kv transmission network Poso-Palu will maximize the evacuation of power from Poso hydropower electricity system, Central Sulawesi.

2.1. Electricity Projection Needs in Central Sulawesi

With the implementation of Special Economic Zones (SEZ) in the Palu city, in the future economy of Central Sulawesi will certainly increase. Almost all sectors of the economy will grow up. In order SEZ can running well, the electricity supply needs to be strengthened in order to support the Government's program. Based on electricity sales data within 5 (five) years and taking into account regional economic growth trends including the regional industry, population growth and increased electrification ratio on future, the projected demand for electricity from 2015 to 2024 can be seen in the following table:

Table 1.
Electricity Projection needs in Central Sulawesi 2015 – 2024

Year	Economic growth (%)	Sale (GWh)	Production (GWh)	Peak load (MW)	Customer
2015	10,90	957	1.081	208	518.509
2016	11,44	1.050	1.229	218	533.401
2017	12,15	1.188	1.382	246	572.185
2018	12,51	1.345	1.613	268	612.940
2019	12,69	1.520	1.805	302	653.976
2020	12,33	1.711	2.016	340	696.067
2021	12,33	1.904	2.229	378	728.451
2022	12,33	2.104	2.454	416	754.118
2023	12,33	2.308	2.677	454	772.538
2024	12,33	2.526	2.918	494	787.202
Growth (%)	12,13	11,4	11,7	10,1	4,8

2.2. Electric Power Development Plan in Central Sulawesi

The generation facilities construction plan in the Central Sulawesi Province regard to potential of local primary energy (hydropower) include the distribution pattern of population. Large hydropower potential of Poso watershed can be developed into a large-scale hydropower up to 575 MW. To meet the electricity needs until 2024, an additional generating capacity was planned about 457 MW with the following details:

Table 2. Development Plant in Central Sulawesi

No	Project	Capacity (MW)	COD
1	Ampana	2x3	2016
2	Buleleng	1,2	2016
3	Palu 3	2x50	2018
4	Tawaeli (Ekspansi)	2x15	2016
5	PLTM Tersebar Sulteng	9,6	2017
6	Luwuk	40	2017
7	PLTM Tersebar Sulteng	15,1	2018
8	PLTM Tersebar Sulteng	10,8	2019
9	PLTM Tersebar Sulteng	14	2020
10	Marana (FTP 2)	20	2022
11	Bora Pulu (FTP 2)	40	2022
12	Tolitoli	2x25	2020/21
13	Poso 1	120	2021/22
Total		457	

Construction of Hydroelectric Power Plant (HEPP) Poso-1 with 4x30 MW capacity will utilize water resources derived from Poso River, with headwaters in the form of Lake Poso.

3. HEPP POSO –1

3.1. Location

Hydroelectric Power Plant Poso-1 (4 x 30 MW Nett) is located in Poso River, administratively located in the District of North Pamona, Poso regency, Central Sulawesi Province. Geographically, the study area is located at position 120 ° 39'07.6 " - 120 ° 39 '35.8" east longitude and 01 ° 39' 49.5 " - 01 ° 40 '23.1" South Latitude.



Figure 1.
Map of HEPP Poso-I, Indonesia

3.2. Purposes of HEPP Poso-I

Poso-1 Dam construction is part of Poso-1 hydroelectric project that serve as a regulating dam through Poso River from Poso Lake in Central Sulawesi Province. The purpose of the construction of Dams Poso-1 (regulating dam) is:

- Regulating water for electric power.
- Water supply in dry season.

3.3. Technical data

- Reservoir
 - Normal water level : +511,7 m
 - Reservoir volume : 1,97 million m³
 - Reservoir area : 148 ha
 - Maximum water level : +512,7 m
- Dam
 - Type : Gravity dam
 - Heigh from deepest foundation : 23,5 m
 - Dam volume : 62.547 m³
 - Crest lenght : 162,2 m
 - Width crest : 12 m
 - Freeboard : 2,3 m
- Hydropower Plant
 - Central Building Type : *Semi Underground*
 - Installed capacity : 4 x 30 MW Nett (MW)
 - Turbine : *Francis Vertical*

Unit	:	2
Surgetank type	:	Surgetank
Dimension (ϕ x L)	:	20x28 (m)
Penstock	:	Steel
Unit	:	1
Lenght	:	300
Dimension (ϕ)	:	6.2
Head	:	55.6
Effective head	:	50
Tailrace	:	Open Channel



Figure 2. Regulating Dam HEPP Poso-I Lay out

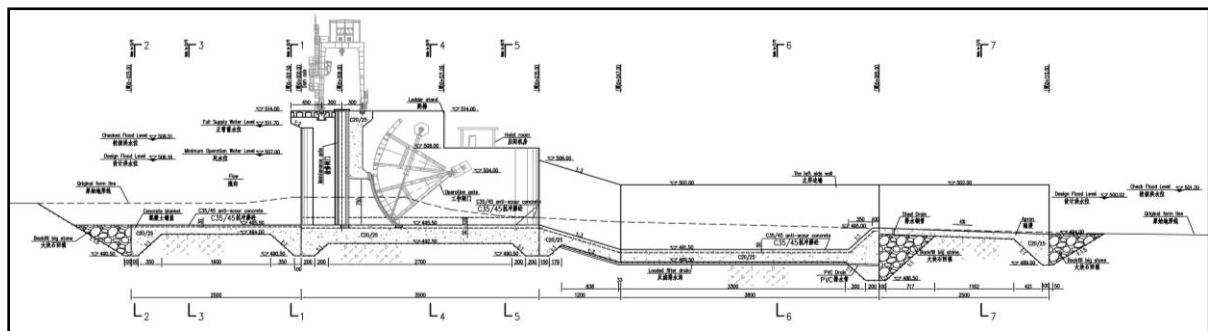


Figure 3.
Dam Cross sections and spillway long section

3.4. Reservoir Operation Rule

a) Poso Lake Water Level

Poso lake water level elevation Data varies from 509.3 m to 512.6 m. Higher elevation is assumed to be very high (flood / flood) and low (dry). To set up the lake, the water will be collected when the water level below the elevation of 511.70 m. When the water level above the elevation of 511.70 m it will be spill out through the gates of the natural capacity of the lake outlet, the highest elevation lakes will follow natural behavior. Because of this, the water level in the lake will not be lower than the existing high data so won't cause environmental impacts. While Minimum Operation Level (MOL) on the dam is setted at elevation of 507 m.

Determining the rule of operation based on the operation of the flow diagram is shown in Figure 5.

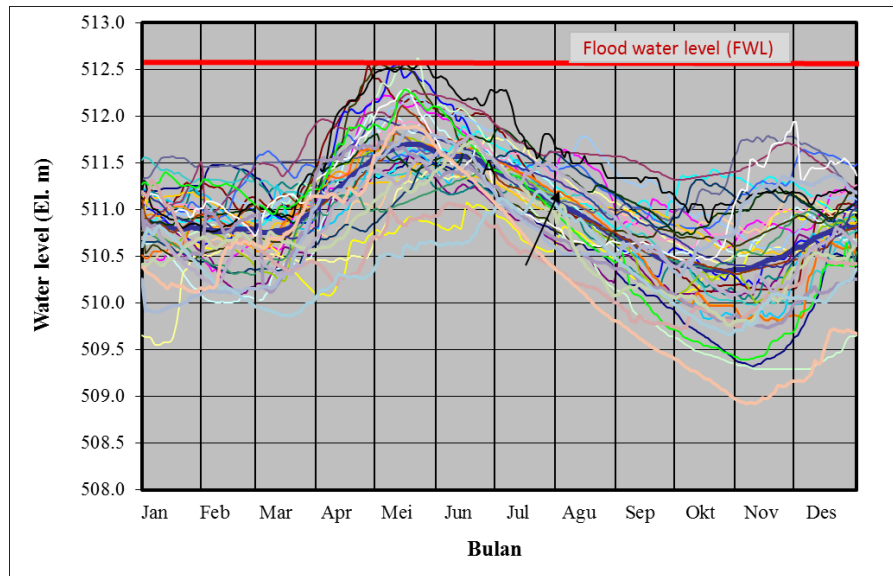


Figure 4. Water level rule chart of Poso Lake

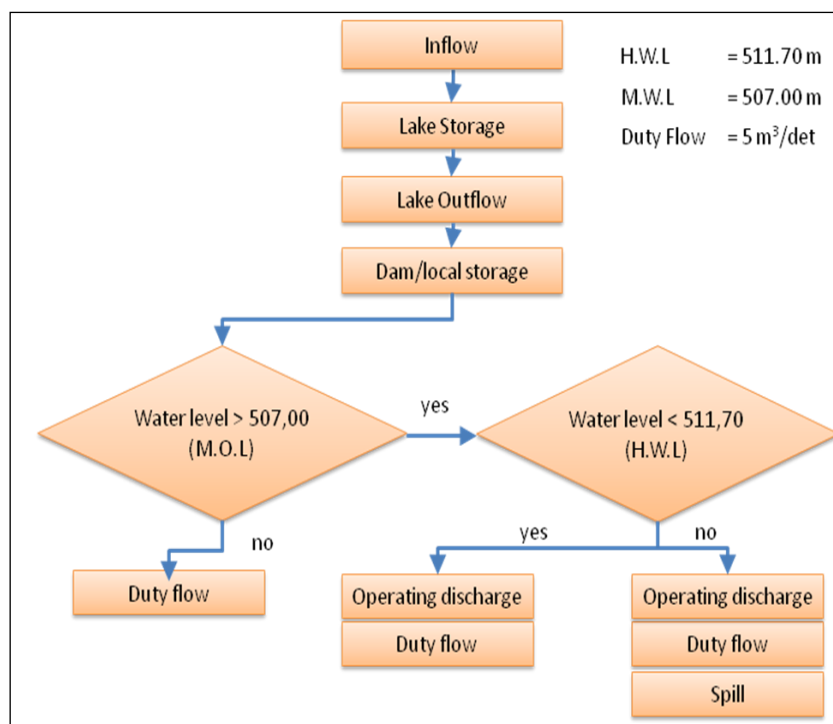


Figure 5. Operation rule chart

Operation rule boundaries without dredging:

- H.W.L = El.+ 511.70 m
- MWL = El.+ 510 m
- Poso lake operation rule using installed capacity of 160 m³ / s

In these conditions the technique things that happen are:

- When lake water level is high, the outflow is controlled by regulating gates.
- When lake water level is low, the outflow is adapted to the cross section of the lake.
- regulating gates will be functioned as a regulator discharge output after passing the peak of the rainy season, so the water reservoir can be utilized as an energy generator with a longer duration.
- The condition of lake water level before the peak of rainy season should be restored as a natural condition for giving the sufficient storage when large discharge into the lake and prevent the overflow above the secure elevation as social impact.

b) Scheme of Operation

Selection of the operating rule is done by making some alternative operating scheme. Alternative schemes operating pattern plan that is chosen is the scheme 2 of the various alternatives available in Table 3, Figures 6 and 7.

Table 3.
Comparison of Daily Averages for Operations Plan

Deskripsi	Skema-1	Skema-	Skema-	Skema-4	Skema-5
<i>Plant discharge capacity (m³/sec)</i>	160	160	160	160	160
<i>Daily rated discharge (m³/sec)</i>	160	93	103	108	113
<i>Minimum operating discharge (m³/sec)</i>	40	40	40	110	113
<i>Duty flow (m³/sec)</i>	5	5	5	5	5
F.W.L (m) untuk Q100					
H.W.L (m)	512.84	512.84	512.84	512.84	512.84
M.O.L (m)	511.7	511.7	511.7	512.02	512.27
<i>Generated Energy (GWH/year)</i>	507	507	507	507	507
<i>Primary energy (GWH/year)</i>	425.0	403.9	410.2	408.7	413.1
<i>Secondary energy (GWH/year)</i>	136.5	317.3	341.4	364.1	376.5
<i>Capacity Factor</i>					

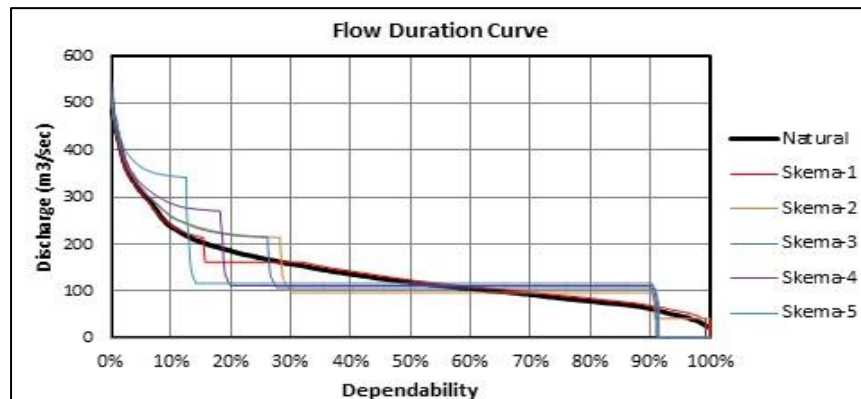


Figure 6.
Dependable Flow

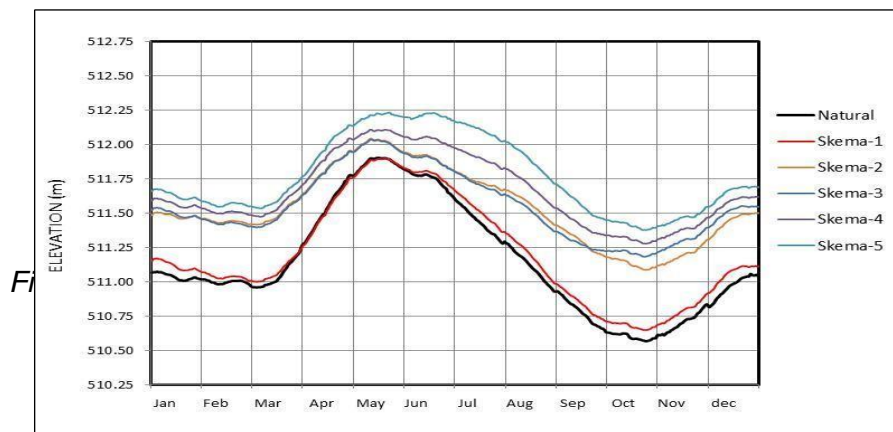


Figure 7.
Water level storage chart for each operation rule alternative

Scheme 2 has advantage that it fits the electricity absorption rules by the State Electricity Company and at dry season is still able to provide electricity at peak hours. Additionally, secure against potential flood in puddles, as well as the primary energy is fulfilled. While the drawbacks in the form of operating at low elevation reservoirs is limited. This scheme has the flexibility to be converted into one scheme in wet years and became scheme 3 when targeted to generate a larger primary energy.

From the simulation shows that:

- High water level during the rainy season can be arranged with a longer duration to be able to meet the flow of water in the dry season.
- Lowest lake water level and lake lowest discharge setted up from October into November.
- With longer dependable discharge duration will be able to increase energy.
- The elevation of annual highest Lake water level average is at 512.01 m and lowest at 510.24 m.

4. CONCLUSION

Based on the results of hydropower potential investigation and analysis in Central Sulawesi shows that:

- The potential for hydropower development in Sulawesi stored is still very large.
- Poso hydropower development can improve the welfare of people especially in the Centre Sulawesi.

5. ACKNOWLEDGEMENT

The authors would like to thank to Dam Safety Unit, Directorate General of Water Resources, Ministry of Public Works and Housing and also Poso-1 HEPP company for the authorization to publish the main result of the present study.

Keywords: Reservoir Operasion Rule, Poso Dam, Hydropower Plant

REFERENCES

- [1] Ministry of Housings and Infrastructures. *Operation and Maintenance Management, Volume 2, Guideline of Dam Operation, Maintenance and Survailance*, 2003.
- [2] PT. Poso Energy Satu Pamona. *Feasibility Study, Poso-1 HEPP Stage 1 (4 x 30 MW) and Regulating Dam*, 2016.
- [3] PT. Poso Energy Satu Pamona. *Detailed Design, Supporting Report – Hydrology, Poso-1 HEPP (4 x 30 MW) and Regulating Dam*, 2016.

COMMISSION INTERNATIONALE DES GRANDS BARRAGES

VINGT-SIXIÈME CONGRÈS DES GRANDS BARRAGES
Autriche, juillet 2018

DOI 10.3217/978-3-85125-620-8-032



This work licensed under a Creative Commons Attribution 4.0 International License. <https://creativecommons.org/licenses/by-nc-nd/4.0/>

**ROPES: RESERVOIR OPERATION SIMULATOR FOR ENVIRONMENTAL
SUSTAINABILITY**

Hubert LOHR

Managing Director, SYDRO CONSULT GMBH

GERMANY

Michael BACH

Project Engineers, SYDRO CONSULT GMBH

GERMANY

Jedrzej BARYLA

Project Engineers, SYDRO CONSULT GMBH

GERMANY

Felix FROEHLICH

Project Engineers, SYDRO CONSULT GMBH

GERMANY

Sandra RICHTER

Project Engineers, SYDRO CONSULT GMBH

GERMANY

COMMISSION INTERNATIONALE
DES GRANDS BARRAGES

VINGT-SIXIEME CONGRES DES
GRANDS BARRAGES
Autriche, juillet 2018

ROPES: RESERVOIR OPERATION SIMULATOR FOR ENVIRONMENTAL SUSTAINABILITY

Hubert LOHR

Managing Director, SYDRO CONSULT GMBH

Michael BACH

Jedrzej BARYLA

Felix FROEHLICH

Sandra RICHTER

Project Engineers, SYDRO CONSULT GMBH

GERMANY

1. BACKGROUND

The construction of dams and reservoirs is experiencing a worldwide renaissance. There are international standards for the construction, the design and the safety of dams. However, similar standards for the subsequent operation of reservoirs do not exist. In contrast to construction, design and safety, the importance of decade-long reservoir operation and its impacts on environmental, economic and social issues is strongly undervalued.

Neglect, inadequate monitoring and data management, a lack of strategies for dealing with competing uses and insufficiently trained personnel lead to enormous problems that translate to failure to meet water usage goals, an inefficient use of resources and considerable environmental impacts. This applies in particular to developing parts of the world such as Africa and South-East Asia.

In contrast, reservoir operation e.g. in Germany is very sophisticated, involving detailed release strategies, risk management, coordinated operating rules for reservoir systems, the use of real-time models to support operation and even the use of scenario simulations to account for climate change and other uncertainties.

2. CURRENT SITUATION

In technologically highly advanced countries such as e.g. Germany it is considered state of the art to model the long-term operation of reservoirs using simulation models, to adjust operation rules to changing boundary conditions on the medium term by looking at scenarios and to react proactively to current events in the short-term.

The practical aspect of reservoir operation is supported by the use of simulation software in which current environmental conditions such as water levels, discharge, precipitation and temperature are recorded and visualized. The necessary operational settings are made based on these observations and the operating rules. In the case of multipurpose reservoirs (e.g. hydropower, flood protection, water supply), the use of simulation tools makes it possible to develop operating rules that are optimized towards catering to all purposes as much as possible and at the same time contain solutions and approaches for dealing with conflict situations. Simulation tools also allow for risk management, coordinated operation and emergency plans to be incorporated into the operating rules.

In other regions such as Africa and South-East Asia, operating reservoirs based on complex operating rules and with the support of simulation tools is the exception. In most cases, operating rules either do not exist or are very simplified [1], [2], [6], [7], [8], [9]. In Ethiopia and Sudan, long and medium term operation is carried out using Excel worksheets [1]. Thus, the complexity of the local conditions, of cause-effect relationships and of target conflicts is hardly considered, if at all. Often, minimum releases for securing downstream ecosystems are not considered as an independent purpose of a reservoir [1], [10], [11], [12]. In Thailand, all reservoirs of the Royal Irrigation Department are operated using a so-called standard rule curve. This rule curve is derived in a simplified manner from precipitation data and reservoir size and provides the desired water level over the course of the year. Usually, this rule curve is not verified for site-specific suitability [2], [3], [8]. In Myanmar, there are currently no guidelines for the operation of reservoirs. Each reservoir operator decides for themselves for example how much residual flow is granted to the downstream water course [4]. In Swaziland, there are reservoirs that do not have rules, monitoring nor qualified personnel [5]. In general, there is a lack of awareness among reservoir operators about the problems that lacking know-how can cause for reservoir operation.

In summary, the following problems can be identified:

- Insufficient data

- Lack of experience with the assessment and evaluation reservoir operation (sustainable vs. not sustainable)
- Lack of tools for assessing the effects of different operating rules
- Lack of strategies for solving conflicts when dealing with conflicting purposes
- Lack of suitable software for simulating reservoir operation both in the planning stages as well as for operational use
- Lack of adequately qualified personnel

This project aims to increase awareness of these problems among reservoir operators and to provide a tool that is suitable for transferring the knowledge necessary to tackle them.

3. PROJECT DESCRIPTION

In this paper, we present an innovative piece of software called the Reservoir Operation Simulator (ROPES), whose purpose is to support classic knowledge transfer (training) regarding reservoir operation.

The simulator is a tool for raising awareness and transferring existing knowledge regarding efficient, sustainable and environmentally friendly reservoir operation to regions where this is lacking and can thus aid in strengthening resource efficiency, reducing environmental strains and improving sustainability.

ROPES can be used to train local reservoir operators regarding reservoir operation while considering different climatological and hydrological conditions and competing uses and goals. Training exercises can cover the following topics:

- Strategies for serving conflicting uses and how to apply them to actual operation
- Impacts of reservoir operation with a focus on the natural environment
- Importance of monitoring and data management
- Integrated reservoir management consisting of catchment, upstream auxiliary dams, water transfers, reservoir water body, dam, operating facilities, power station, water courses
- Risk assessment, emergency planning, reporting
- Comparison of the effects of different operating strategies by simulating and evaluating different scenarios
- Necessity of regularly reevaluating and adjusting operating rules

4. ROPES

Similar to a flight simulator, ROPES mimics the actual control interface for reservoir operation and exposes the trainee to different conditions, in which he must make decisions regarding the operation of the reservoir.

Reservoir operators usually operate the reservoir using a supervisory control and data acquisition (SCADA) system that exposes the variables and controls necessary for supervision and operation of the system in a schematic interface (examples are shown in Fig. 1, Fig. 2, Fig. 3 and Fig. 4).



Fig. 1

Control room of the reservoir operation center of the Ruhrverband in Germany^{*}

^{*} Source: <http://www.ruhrverband.de/fluesse-seen/talsperrensteuerung/>

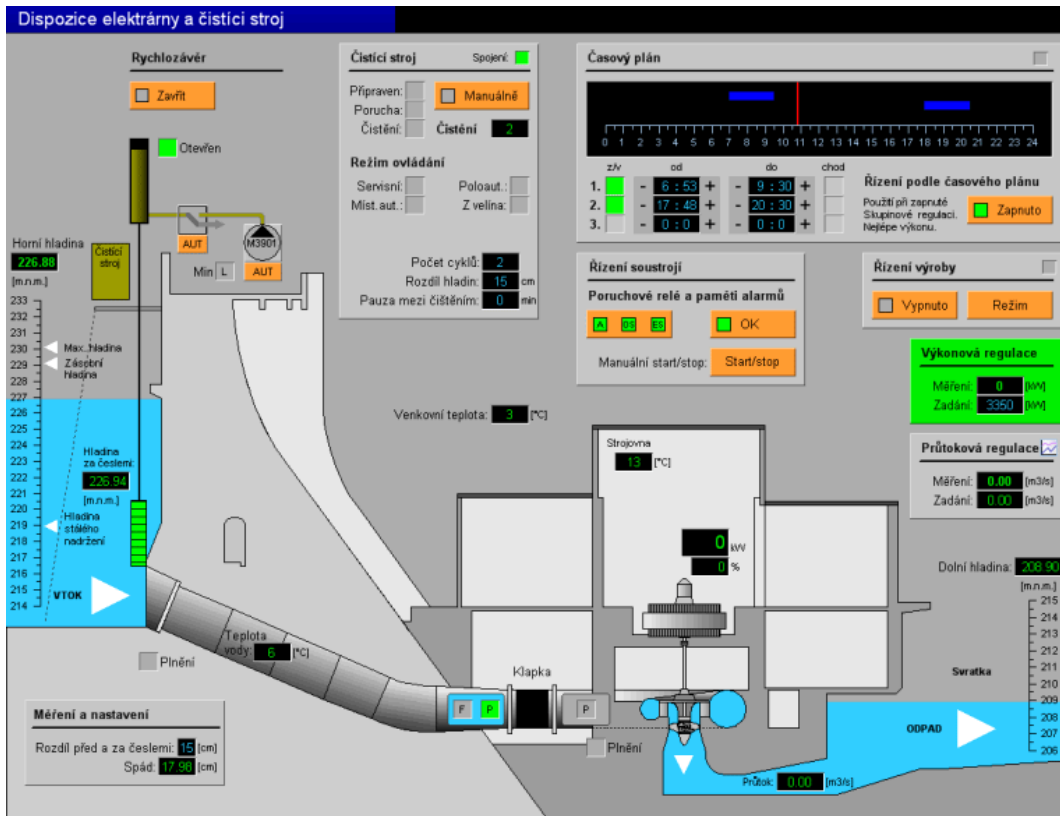


Fig. 2

SCADA interface in a small hydropower plant in Kníničky (source: promotiv.eu)

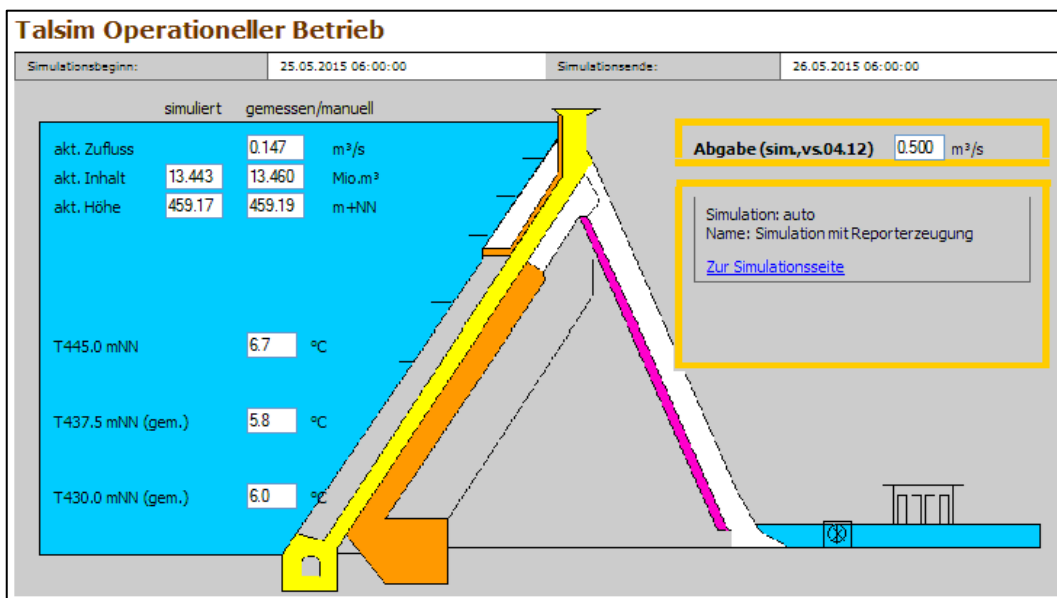


Fig. 3

Interface for the operation of a reservoir in Germany with real-time simulation results

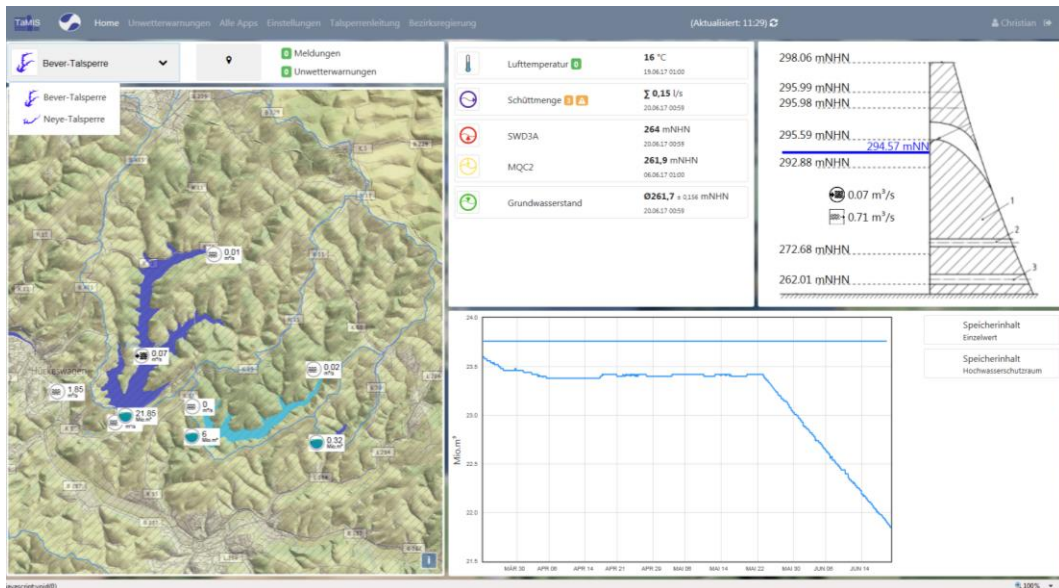


Fig. 4

Web interface of a reservoir monitoring system in Germany (source: fluggs.wupperverband.de)

The ROPES interface is highly customizable and designed to be able to mimic the control interface that the operator uses for actual operation. This also means that the interface visible to the trainee only exposes those variables and controls that he would be able to access during actual operation. So, depending on the system being simulated, the interface may only display a few simple variables such as reservoir water level and the status of the gates. Or, when simulating more complex systems equipped with more monitoring equipment, the displayed variables may also include measurements from across the catchment, as well as other information such as current demand values or even forecasts.

A second interface, only visible to the trainer or supervisor, acts as an administrative interface and allows the trainer to access all variables of the simulated system. With this information, the trainer is able to intervene in the trainee's decision-making while the simulation is still ongoing, if necessary. Ordinarily, however, the second interface is only used to review the trainee's decisions and their effects on the system in the review phase after the simulation has been completed.

4.1. SIMULATION ENGINE

ROPES uses the software Talsim-NG as the backend for running the simulations. Talsim-NG was developed by SYDRO and has been proven and tested as a simulation tool for reservoir operation, rainfall-runoff calculation and flood routing both in planning stages and in real-time operation for more than 15 years.

Talsim-NG has a proven track-record for being able to accurately simulate a wide range of different reservoirs and can consider all important aspects of reservoir operation simulation, including e.g. hydraulic constraints of turbines or other release openings. It also has the ability to accurately compute evaporation and precipitation onto the reservoir surface and incorporates a sophisticated algorithm for calculating the reservoir's water balance, even when multiple variable inflows and outflows are involved. Additionally, the rainfall-runoff and flood routing modules make it possible to simulate not only the reservoir itself, but also catchments and water courses.

Thus, the simulation engine is capable of simulating any existing, planned or fictional reservoir or even entire reservoir systems, including the catchments and water courses upstream and downstream of the reservoirs. It can utilize archived or real-time monitoring data from ground stations or remote sensing as input and can also integrate forecasts into the simulation.

Using Talsim-NG, it is possible to simulate the entire range of possible operating conditions, including exceptional events such as extreme rainfall or failure of control components.

ROPES distinguishes between the internal time step used for the actual simulation by Talsim-NG and the external, or operating time step which is the interval in which results and current conditions are displayed to the trainee and in which the trainee can make inputs.

The internal time step depends on the system being simulated and on the temporal resolution of the input variables.

The operating time step is adjusted to reflect the normal operating interval of the system being simulated. For example, if a reservoir operator usually makes operating decisions once a day, the operating time step is also set to one day. After each operating time step, the simulation is paused in order to await the decisions made by the trainee. The simulator then takes the trainee's decisions as input and calculates the effects of the decisions within the entire system during the next operating time step. Then, the interface is updated to reflect the new system state, and the simulation is paused again to await the trainee's decisions for the next operating time step.

When a simulation scenario includes situations in which the operator receives false or no readings from a malfunctioning instrument, the values displayed in the interface may deviate from the actual values used in the simulation or may be missing entirely from the interface. Similarly, the inputs made by the trainee can be configured to cause unexpected effects in order to simulate malfunctioning controls, e.g. a gate that will not open or close properly.

All decisions made by the trainee as well as all of the system variables, whether visible to the trainee or not, are recorded over the entire course of the simulation and output to result files so that it is possible to review the trainee's decisions and the effects that they had on the system after the simulation has ended.

4.2. SCENARIOS

The scenarios that are simulated using ROPES are designed and predetermined by the trainer. The trainee, on the other hand, does not know what exactly is going to happen during the simulation.

Scenarios can be adjusted to the trainee's level of knowledge and can become more complex or difficult over the course of the training exercise.

There is practically no limit to the kinds of scenarios that can be simulated. For example, scenarios can include different climatological and hydrological conditions and competing uses and goals.

Besides "normal" conditions, scenarios can also include exceptional occurrences such as large flood events, drought periods, the failure of monitoring equipment or malfunctioning controls.

Scenarios can utilize archived or real-time monitoring data from ground stations or remote sensing as forcing data and can also integrate forecasts into the simulation. As the simulation engine also contains a rainfall-runoff module, forcing data for the inflow to the reservoir can consist either of precipitation or of flow time series, or of a combination of both.

4.3. EVALUATION

An important part of the training exercise is the evaluation phase. Using the records from the simulation, all decisions made by the trainee and the effects that they had on the system are reviewed after the simulation has ended. The review process is accompanied by an experienced reservoir operator/expert. Aspects to be reviewed can include the following:

- Were all water supply and/or other demands met?
- Were all constraints on reservoir operation (e.g. maximum discharge, reservoir water levels) adhered to?
- Did the operator deviate from the existing operating rules? If so, could this have been avoided?
- Did the operator make the correct decisions while dealing with emergency situations?

If applicable, a scenario can be simulated again in order to assess the effect of different operating decisions.

5. ROADMAP

Institutions such as the Nile Basin Initiative, the Eastern Nile Technical Regional Office, the Mekong River Commission, the Ethiopian Institute of Water Resources of the Addis Ababa University and the Walailak and Kesetsart

Universities in Thailand have already expressed their interest in conducting a pilot study and aiding in the dissemination of the project's ideas.

Interested parties are invited to contact us at ropes@sydro.de to explore possibilities for cooperation.

REFERENCES

- [1] ENTRO. Roadmap for Coordinated Cascade Dam Operation in the Eastern Nile. Nile Basin Initiative, Eastern Nile Technical Regional Office. 2016. Unpublished document.
- [2] LOHR. Assessment of Water Resources in the Thung Song Area. GIZ, Improved Management of Extreme Events through Eco-system-based Adaption in Watersheds (ECOSWat). Thailand. 2014.
- [3] LOHR. Vulnerability analysis for the river basins of Huai Sai Bat, Tha Di and Trang. GIZ. Improved Management of Extreme Events through Eco-system-based Adaption in Watersheds (ECOSWat). Thailand. 2015.
- [4] SYDRO. Nam Paw Hydro Power Plant. Great Hor Kham. Myanmar. 2016.
- [5] LOHR. Emergency Preparedness Plans for Major Dams in Swaziland. UNDP. 2014.
- [6] SYDRO. Review of Sae-Or Reservoir Plan and Design of Complementary Ecosystem-based Adaptation (EbA) Measures. GIZ, Improved Management of Extreme Events through Eco-system-based Adaption in Watersheds (ECOSWat). Thailand. 2016.
- [7] SYDRO. Yom-Nan Operation & Maintenance Project. GIZ. Thailand.
- [8] LOHR, GFA Consulting-Group. Huai Ta Poe Reservoir Project. GIZ and Royal Irrigation Department. Thailand. 2017.
- [9] LOHR. Water Supply and Demands Management in the Transboundary Kura River Basin. UNDP. Georgia, Azerbaijan. 2017.
- [10] CCES/ADAPT (2013): African Dams Project. An Integrated Water Management Study. Final Stakeholder Report. ETH Zurich, Competence Center Environment and Sustainability (CCES). Zurich, Switzerland.
- [11] EAWAG (2006): Independent Review of the Environmental Impact Assessment for the Merowe Dam Project. EAWAG, Aquatic Research, Kastanienbaum, Switzerland.
- [12] BLACKMORE, D, WHITTINGTON, D. (2008): Opportunities for Cooperative Water Resources Development on the Easter Nile: Risks and Rewards. Report at the request of the Eastern Nile Council of Ministers by the World Bank.

SUMMARY

The use of a reservoir operation simulator for the training of reservoir operators is an innovative, target-oriented and motivational approach towards highlighting the importance of the management and operation of reservoirs.

In this paper, we present the concept of the Reservoir Operation Simulator (ROPES), which uses Talsim-NG as the simulation engine on the backend and a highly customizable SCADA-like interface on the frontend, as a software tool for conducting training exercises for reservoir operators.

COMMISSION INTERNATIONALE DES GRANDS BARRAGES

VINGT-SIXIÈME CONGRÈS DES GRANDS BARRAGES
Autriche, juillet 2018

DOI 10.3217/978-3-85125-620-8-033



This work licensed under a Creative Commons Attribution 4.0 International License. <https://creativecommons.org/licenses/by-nc-nd/4.0/>

**UNSTEADY STATE APPROACH FOR ESTIMATION OF SEDIMENT
TRANSPORT INTO RESERVOIR**

Balkrishna Shankar. CHAVAN

Scientist-D, CENTRAL WATER AND POWER RESEARCH STATION, PUNE

INDIA

COMMISSION INTERNATIONALE
DES GRANDS BARRAGES

VINGT-SIXIÈME CONGRÈS DES
GRANDS BARRAGES

*Autriche,
juillet 2018*

UNSTEADY STATE APPROACH FOR ESTIMATION OF SEDIMENT TRANSPORT INTO RESERVOIR

Balkrishna Shankar. CHAVAN

*Scientist-D, Central Water and Power Research Station, Pune.
India*

1. INTRODUCTION.

Mathematical modeling is based on computation techniques. It has become very popular in the past few decades, mainly due to the increasing availability of more powerful and affordable computing platforms. Much progress has been made, particularly in the fields of sediment transport, water quality, and multidimensional fluid flow and turbulence. Many computer models are now available in the market. Some of the models are in public domain and can be obtained free of charge. Graphical user interfaces, automatic grid generators, geographic information systems, and improved data collection techniques (such as LiDAR, Light Distancing and Ranging) promise to further expedite the use of numerical models as a popular tool for solving river engineering problems.

A. Camenen and Larson (2007)

$$\Phi = 12 \theta^{3/2} e^{(-4.5(\theta_{cr}/\theta))} \quad (1)$$

where

$$\Phi = \frac{q_b}{\sqrt{[g(s-1)d^3]}}$$
$$\theta = \frac{\tau_0}{\rho g(s-1)d}$$

$$\tau_0 = \rho C_D \bar{U}^2 \quad (2)$$

$$C_D = \left[\frac{k}{1 + \ln\left(\frac{z_0}{h}\right)} \right]^2$$

k= Von Karman's constant =0.4

$$k_s = 2.5d_{50}$$

$$z_0 = k_s/30$$

Where:

- θ = Shield's parameter
- θ_{cr} = Critical Shield's parameter
- Φ = Dimensionless transport number
- q_b = Volumetric bed-load transport rate per unit width
- g = acceleration due to gravity
- ρ = density of water
- s = ratio of densities of sediment and water
- d = grain diameter
- C_D = total drag coefficient
- τ_0 = Bed shear stress
- \bar{U} = Depth averaged velocity

B. Engelund and Hansen formula- (1972)- Estimates total sediment load

$$S_t = \frac{0.05UC\tau_c^2\{1+0.5\left(\xi\frac{U_b}{U}\right)^2\}^2}{\rho^2 g^{\frac{5}{2}} \Delta \rho_s^2 d_{50}} \quad (3)$$

where

- C = Chezy's coefficient
- ξ = a coefficient
- τ_c = Bed shear stress due to current, N/m²
- U_b = Amplitude of orbital velocity at the bed
- d_{50} = Grain diameter

C. Ackers and White's (1973) Method – It is based on flume and field data, estimates total sediment load

$$\left(\frac{u_*}{U}\right)^{C_1} \frac{\gamma_f C_T D}{\gamma_s d} = C_2 \left[\frac{F_1}{C_3} - 1 \right]^{C_4} \quad (4)$$

where

$$F_1 = \left[\frac{u_*^{c_1}}{\left[\frac{\Delta\gamma_s d}{\rho_f} \right]} \right] \left[\frac{U}{\sqrt{32 \log\left(\frac{10D}{d}\right)}} \right]^{1-c_1}$$

$$d_* = \frac{d}{\left[\frac{\rho_f v^2}{\Delta\gamma_s} \right]^{\frac{1}{3}}}$$

a. For $1.0 < d_* < 60$

$$C_1 = 1.0 - 0.56 \log d_*$$

$$\log C_2 = 2.86 \log d_* - (\log d_*)^2 - 3.53$$

$$C_3 = \left[\left(\frac{0.23}{d_*^{\frac{1}{2}}} \right) + 0.14 \right]$$

$$C_4 = \left[\left(\frac{9.66}{d_*} \right) + 1.34 \right]$$

b. For $d_* > 60$

$$C_1 = 0.0, C_2 = 0.025, C_3 = 0.17 \text{ and } C_4 = 1.50$$

D. **Meyer-Peter and Muller(1948)** An empirical relation based on a large number of experiments with uniform sediment 3–29 mm, in flumes 20–200 cm bedload transport equation applicable to gravel-bed rivers of coastal British Columbia is the Meyer-Peter & Muller (M-P&M) equation

$$\Phi = 8(\theta - \theta_{cr})^{3/2}$$

(5)

E. **Nielsen(2000)-**

$$\Phi = 12 \theta^{1/2} (\theta - \theta_{cr})$$

(6)

F. **The Bijker Equation:**

Bijker derived the total transport in to two parts, the bed load and suspended load transport. The bed load transport is calculated using the Kalinke-Frinjlink formula in which combined action of wave and current is accounted by a modification of the bed shear stress.

$$S_b = \frac{BDU\sqrt{g}}{c} e^{\left[\frac{-0.27\Delta\gamma_s d}{\gamma\tau_c \left\{ 1 + 0.5 \left(\frac{\xi U_b}{U} \right)^2 \right\}} \right]} \quad (7)$$

G. **Bagnold-Bailard Equation:** Bagnold (1960, 1966) developed an approach to bed load transport prediction that is based on stream power per unit channel width

Average velocity (U) can be given by

$$U = u_c + u_t \quad (8)$$

where u_c = fluid velocity due to current effect (m/s)

u_t = Orbital fluid velocity above the bed at time t (m/s)

assume $u_c = U$, then bed load transport S_b is related to $|U|^{2.5}$

$$S_b(t) = \frac{\tau_0}{\left[1 - \frac{\rho_f}{\rho_s} \right]} \left\{ \frac{e_b}{\tan\alpha} + e_s(1 - e_b) \frac{\bar{u}}{\omega_0} \right\} \quad (9)$$

the suspended load transport S_s is related to $|U|^{3.5}$ and computed from

$$S_s(t) = \frac{\tau_0 U}{\left[1 - \frac{\rho_f}{\rho_s} \right]} \left\{ \frac{e_s}{\tan\alpha} + e_s(1 - e_s) \frac{\bar{u}}{\omega_0} \right\} \quad (10)$$

The Bijker model predicts too small concentration magnitudes and too large fluid velocities in the near bed zone. These results in current related sediment transport rates that are 4 times for small transports (<0.001Kg/ms) and 4 times large transports. The evaluation of sediment transport based on above methods except Bijker and Bagnold is given in table2.

Table:1. Prediction of Sediment by Investigators

S No.	Investigators	Predicted Sediment ton
1.	Camenen and Larson Method	1194604.32
2.	Engelund and Hansen Method	756025.46
3.	Ackers and White's Method	600278.89
4.	Meyer-Peter and Muller Method	445292.83

5.	Neilsen Method	210378.91
	Observed	119607.29

Present Studies:

(A) Proposed Equations for Steady State Flow:

Present studies describe prediction of sediment inflow based on the published data. The catchment area of the basin is 6271 square kilometer. Width of the river at gauging station is 71.4 m. Empirical equation in mathematical form is proposed based on the data sample of 1312 observations collected over span of 20 years.

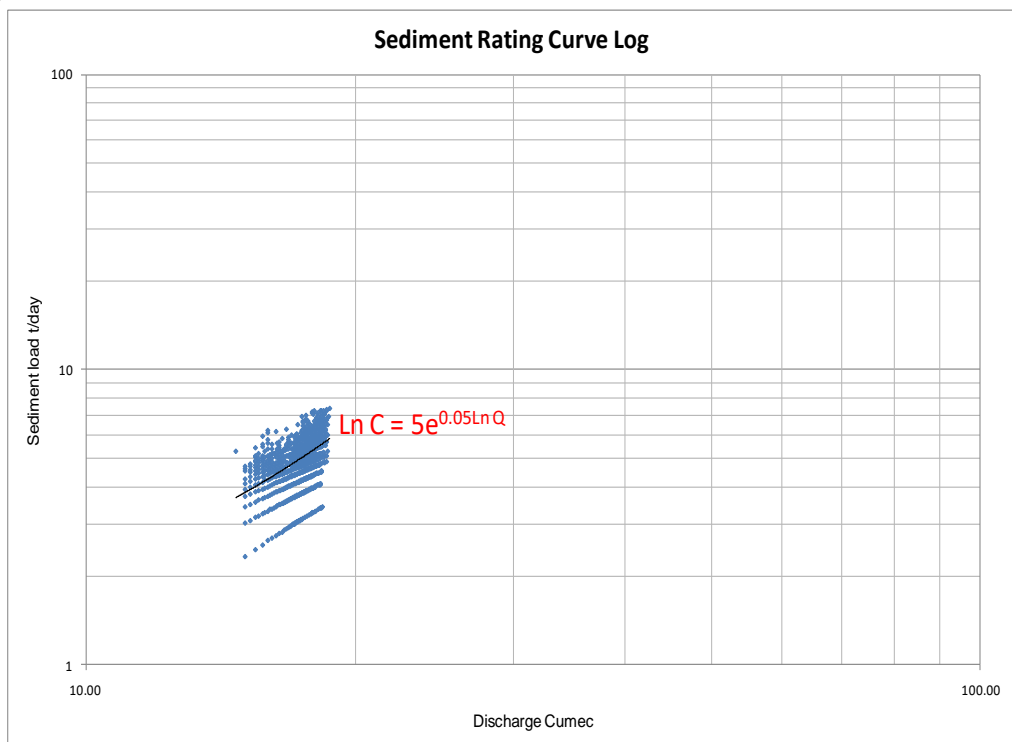


Fig. 1: Variation of Sediment Concentration and discharge (Log plot)

The Correlation coefficient R^2 for the equation (10) is 0.958457, which is shown in Fig. 2.

$$\ln(C) = 5e^{0.05(\ln Q)} \quad (11)$$

Considering the data following power equation is proposed :

$$C = 700Q^{-0.9} \quad (12)$$

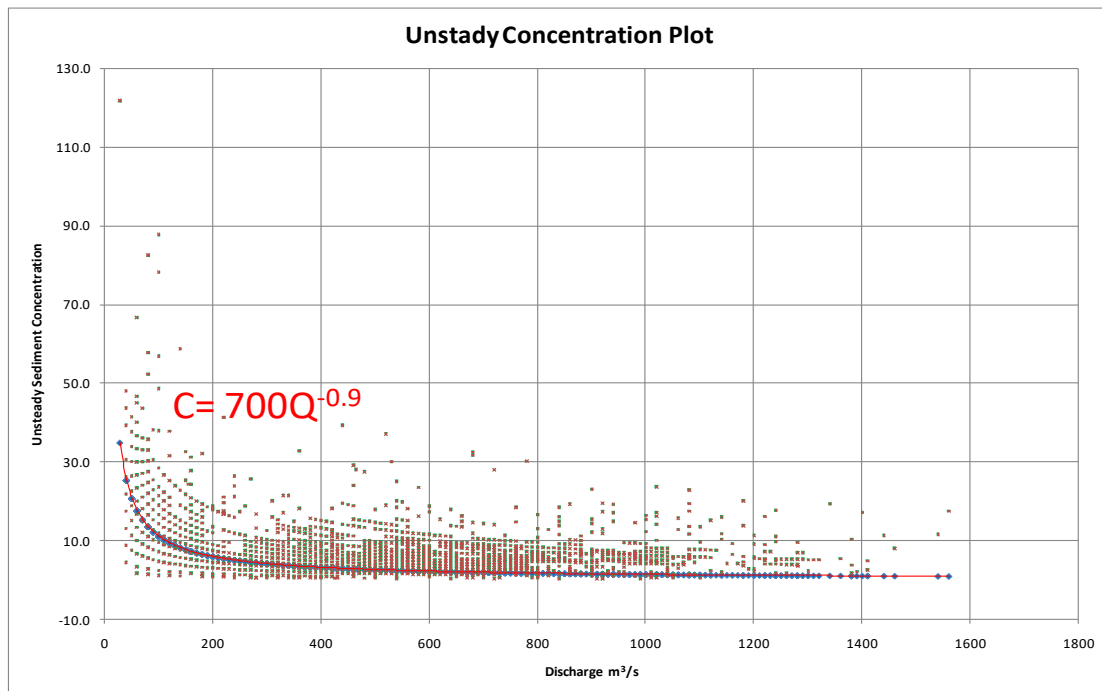


Fig. 2: Variation of Sediment Concentration rate and Discharge

It is hyperbolic curve, underestimates the sediment concentration. Therefore the data was re-analyzed and the proposed quadratic equation is:

$$C = 0.0005Q^2 - 0.2Q + 125 \quad (13)$$

The proposed equation (13) is of second order. It envelops 94 % of the sediment data at one hundred percent band width, it is also seen that 63% of the sediment data at fifty percent band width, which is shown in Fig. 3.

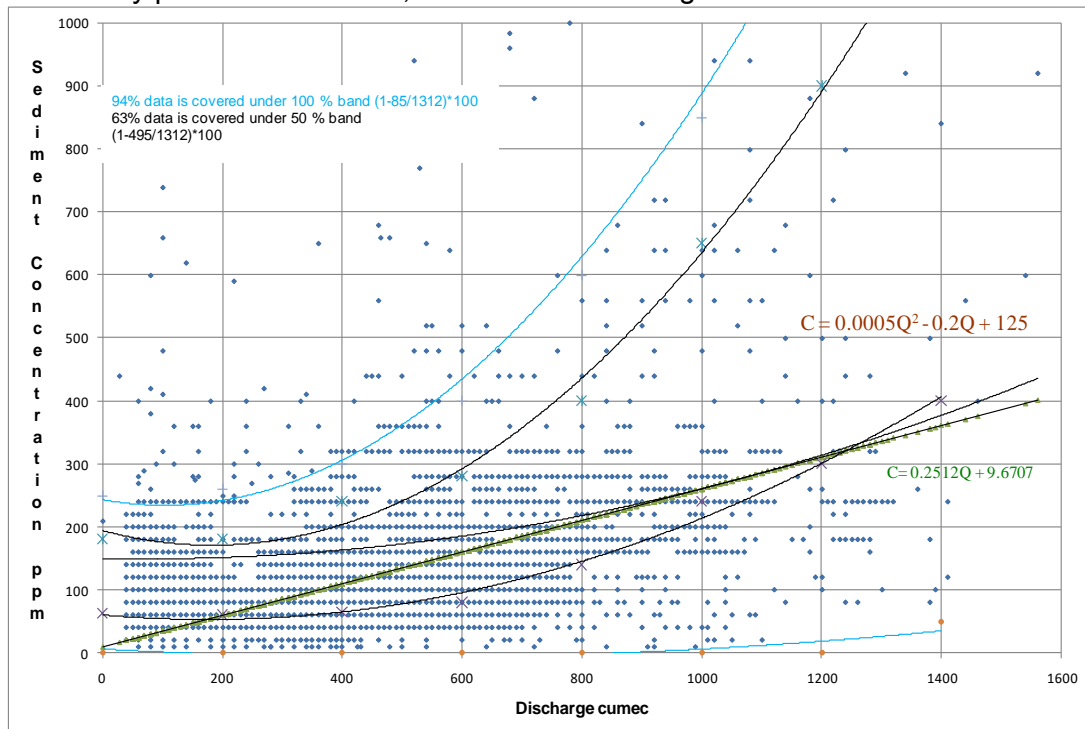


Fig. 3: Variation of Sediment Concentration and Discharge

The proposed equation (13) is of second order. It envelops 94 % of the sediment data at one hundred percent band width, it is also seen that 63% of the sediment data at fifty percent band width, which is shown in Fig. 3. Steady state flow equations which are compared with the observed data are tabulated in table2 given below:

Table:2. Prediction of Sediment for Steady State Flow Equations

S No.	Method/law	Predicted Sediment ton
Present Studies		
Steady State Flow Equations		
1.	Log-log plot $5e^{0.05 \ln Q}$ Method	316959.32
2.	Quadratic $0.0005Q^2 - 0.2Q + 125$ Method	297696.70
3.	Power $700Q^{-0.9}$	127052.40
	Observed	119607.29

(B) Unsteady State Flow Equation:

As in the de St. Venant equations, x represents a boundary attached downstream coordinate. The equation of sediment continuity was first delineated by the Austrian researcher Exner at the beginning of the 20th century, First a one dimensional case is considered Sediment mass balance is expressed in volume form (by dividing the mass balance by ps) below;

$$(1 - \lambda_p) \frac{\partial \eta}{\partial t} = - \frac{\partial q_{bs}}{\partial x} - \frac{\partial q_{bm}}{\partial n} + v_s (\bar{c}_b - E_s) \tag{14}$$

In the above equation (14) λ_p denotes the porosity of the bed deposit q_{bm} and q_{bs} . c_b denotes the volume concentration of suspended sediment, averaged over turbulence, just above the bed. E_s is sediment entrainment into suspension. Bed-load is seen to act as a flux term and suspended sediment as a source/sink term. The bed elevation of a control volume increases if more bed-load is entering than exiting, resulting in net deposition of bed-load. Noting that v_s denotes the volume flux of suspended sediment settling on to the bed and $v_s E$ denotes the volume flux of entrainment of bed sediment into suspension, bed elevation increases due to the net deposition of suspended sediment. If $\bar{c}_b > E_s$. When the length scales of interest are large compared to the relaxation distance $(U/v_s) H$ associated with the settling of suspended sediment, (12) can be rigorously reduced to a simpler form,

$$(1 - \lambda_p) B \frac{\partial \eta}{\partial t} = - \frac{\partial q_t}{\partial x} \tag{15}$$

For the homogeneous unsteady flow neglecting viscous diffusion and including buoyancy effect the rate of change of sediment concentration (ed. Garcia 2007) is:

$$\frac{\partial \bar{C}}{\partial t} = \frac{\partial}{\partial z} \left[\frac{v_t}{\sigma_t} \frac{\partial \bar{C}}{\partial z} \right] + \frac{\partial (w_s \bar{C})}{\partial z} \quad (16)$$

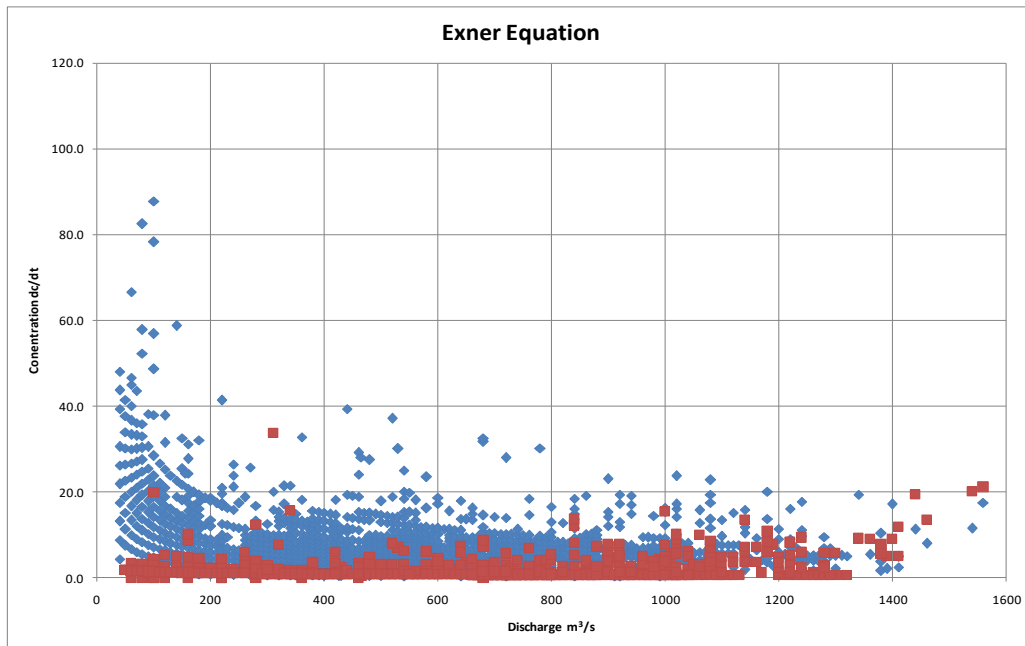


Fig. 4: Variation of Sediment Concentration rate and Discharge,(Exner)

$$\frac{\partial C}{\partial t} = 700 \left(\frac{\partial Q}{\partial x} \frac{dx}{dt} \right)^{-0.9} \quad (17)$$

Since the Exner Equation, Garcia ed.(2007) under estimates sedimentation by 6.19% than observed therefore following best fit equation is proposed.

$$\frac{\partial C}{\partial t} = -5 + 1.35 \left\{ \left(\frac{\partial Q}{\partial x} \frac{dx}{dt} \right)^{0.96} + \left(\frac{\partial Q}{\partial x} \frac{dx}{dt} \right)^{-0.5} - \left(\frac{\partial Q}{\partial x} \frac{dx}{dt} \right)^{-0.25} \right\} \quad (18)$$

This equation precisely predict sedimentation well within 1.7% bandwidth.

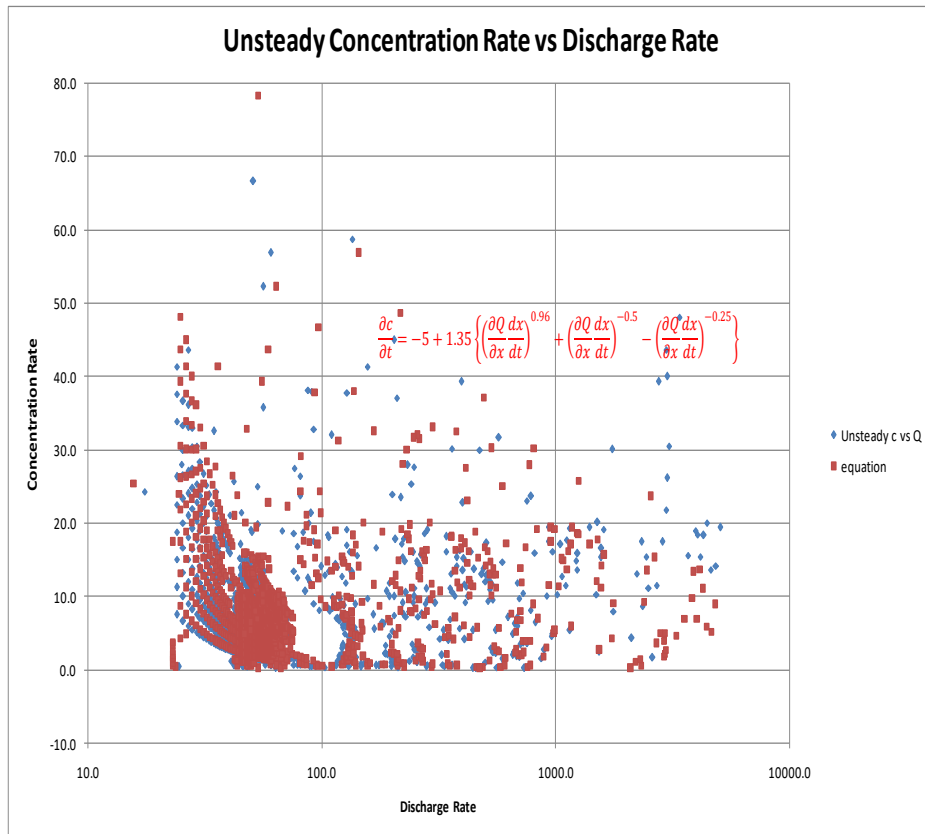


Fig. 5: Unsteady State Observed and Predicted sedimentation
 A graph was plotted for the accuracy of predicted with observed and it was found that total data 1312 covered best within $\pm 5\%$ precisely. The calibration is shown in figure number 6.

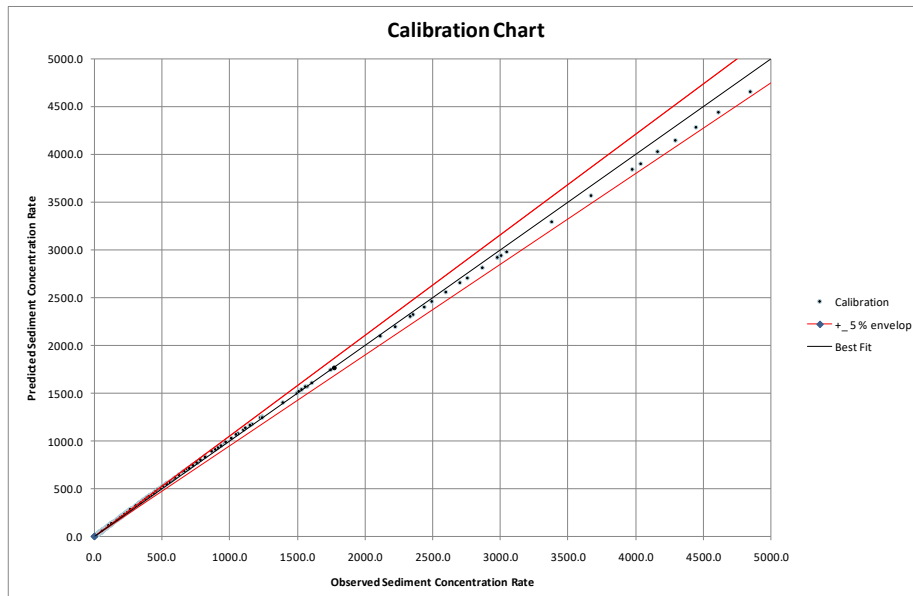


Fig.6: Variation of observed and Predicted data by Equation 18
 The computations made for unsteady flow condition, comparison of quantum and the proposed equation are given in table:3.

Table:3. Prediction of Sediment by Unsteady State Flow Equations

S No.	Investigators	Predicted Sediment ton
Present Studies		
Unsteady State Flow Equations		
1.	Exner $(1 - \lambda_p) \frac{\partial \eta}{\partial t} = - \frac{\partial q_{bs}}{\partial x} - \frac{\partial q_{bm}}{\partial n} + v_s (\bar{c}_b - E_s)$	112200.20
2.	Proposed Unsteady Equation $\frac{\partial c}{\partial t} = -5 + 1.35 \left\{ \left(\frac{\partial Q}{\partial x} \frac{dx}{dt} \right)^{0.96} + \left(\frac{\partial Q}{\partial x} \frac{dx}{dt} \right)^{-0.5} - \left(\frac{\partial Q}{\partial x} \frac{dx}{dt} \right)^{-0.25} \right\}$	120172.6
	Observed	119607.29

Data Analysis and Discussion:

Sediment concentration plays significant role in prediction of sedimentation in the reservoirs.

Table:4. Gist for Prediction of Sediment

S No.	Investigators	Predicted Sediment ton
1.	Camenen and Larson Method	1194604.32
2.	Engelund and Hansen Method	756025.46
3.	Ackers and White's Method	600278.89
4.	Meyer-Peter and Muller Method	445292.83
5.	Neilsen Method	210378.91
Present Studies		
6.	Quadratic $0.0004Q^2 - 0.0025Q + 90$ Method	342617.84
7.	Log-log plot $5e^{0.05 \ln Q}$ Method	316959.32
8.	Power Law $C = 700Q^{-0.9}$	127052.40
9.	Unsteady Exner	112200.20
10.	Unsteady $\frac{\partial c}{\partial t} = -5 + 1.35 \left\{ \left(\frac{\partial Q}{\partial x} \frac{dx}{dt} \right)^{0.96} + \left(\frac{\partial Q}{\partial x} \frac{dx}{dt} \right)^{-0.5} - \left(\frac{\partial Q}{\partial x} \frac{dx}{dt} \right)^{-0.25} \right\}$	120172.6
	Observed	119607.29

Actual sediment deposited in the reservoir and the prediction of sediment by different investigators is tabulated in table 4. This table also includes predicted sediment by empirical equations for steady as well as unsteady flow condition through S. No. 6-10.

Conclusions

From this study to predict the sediment, it can be concluded that:

- Table 1 shows wide variation in results by various methods to predict the sediment in steady state condition flow. Methods/laws are applicable for a region of studies.
- The quadratic equation (13) it is observed that 63% of the sediment data is enveloped at fifty percent band width.
- Equation (13) envelops 94 % of the sediment data at one hundred percent band width,
- Empirical equation (18) shows the prediction for smaller discharges are well within 3%, whereas for the higher discharges it envelops 95% data. The predicted sedimentation is close to the observed quantity.
- Unsteady flow Exner, total sediment estimates lower by 6.19% than observed.
- The equation number 18, has standard error of 3.4%, predicts sediment higher by 6.22% than observed.
- The proposed equation number 18 predicts sedimentation well within 1.7% bandwidth.

References:

- [1] Ackers, P. and White, W. R. (1973) Sediment Transport: New Approach and Analysis, JHD, *Proc. ASCE, Vol. 99, No. HY-11.*
- [2] Bagnold, R A (1956) Flow of Cohesionless Grains in Fluids, Philosophical Trans. RSL No. 964, Vol. 249.
- [3] Garcia, M. H. (2007) Sedimentation Engineering, (ASCE Manual and Reports on Engineering Practice No.110) Chapter 2: Sediment Transport and Morphodynamics by Garcia, M. H, p 70 American Society of Civil Engineers.
- [4] Garcia, M. H. (2007) Sedimentation Engineering, (ASCE Manual and Reports on Engineering Practice No.110) Chapter 16: Turbulence Models for Sediment Transport Engineering by D A Lyn, p 787 American Society of Civil Engineers
- [5] Garde, R. J. (2006) *River Morphology*, New Age International Publishers, New Delhi p-479
- [6] Larry, M. W. (1999) *Hydraulic Design Handbook*. McGraw-Hill Companies, Inc.
- [7] Lawrence, S. H. (1987) "What Are the Impacts of Himalayan Deforestation on the Ganges-Brahmaputra Lowlands and Delta? Assumptions and Facts." *Mountain Research And Development*, Vol. 7, No. 3, Proceedings of the Mohonk Mountain.International Mountain Society.

- [8] Leliavsky, S. (1954) An Introduction to Fluvial Hydraulics, Constable and Co. Ltd. Pp 70-72.
- [9] Meyer-Peter and Muller(1948) Formula for Bed Load Transport, proc. IAHR, 2nd Congress, Stockholm.
- [10] Milliman, J.D., Meade, R.H. (1983) "Worldwide Delivery of River Sediments to Ocean." *Journal of Geology* 91, 1–19. Milliman, J.D., Meade, R.H., (1983) Worldwide Delivery of River Sediments to Ocean." *Journal of Geology* 91, 1-19
- [11] Neilsen, A. F. (2000) Isotope Tracer Demonstration at the Port of Songkhla, Thailand, *Sediment Transport Modelling, WRL* Technical Report No 99/65.
- [12] Ranga Raju, K.G. (1986) Sedimentation of Rivers, Reservoirs and Canals, *International Journal of Fresh Surface Water, vol. III.*
- [13] Shulits, S. (1935) The Schoklitsch Bed Load Formula. Engineering, June.
- [14] Singh, M., Singh, I.B., and Müller, G. (2006) Sediment Characteristics and Transportation Dynamics of the Ganga River, Science Direct. Elsevier B.V. *Geomorphology* 86 (2007) 144–175
- [15] Sonam Choden(2009) Sediment Transport Studies in Punatsangchu River, Bhutan, Division of Water Resources Engineering, Lund University
- [16] Subramanya, K. (2009) *Flow in Open Channels*, Tata McGraw-Hill Education, 548 pages

SUMMARY

Quantitative estimate of sediment transport in alluvial channels is one of the most important task in river engineering for project planning, design, construction, operation and maintenance of hydraulic structures such as river (bridges and training dikes), reservoirs (dams and barrages), lakes and coastal (jetties, berths, breakwaters, dikes, wave absorbers, revetment, seawalls and bulkheads). Even today, numerical models of sediment transport processes are confronted with some difficulties, often of conceptual nature. One of these difficulties is the simulation of unsteady non-uniform sediment transport. This paper describes sediment transport theory in brief, empirical equations proposed by different investigators such as Camenen and Larson, Enaelund and Hansen, Ackers and White's, Meyer-Peter and Muller, Nielsen, Baanold, Biiker, method. Macroscopic concept based on single sediment size has been used for computations. Present research paper is compilation of work carried out by various investigators for steady state and unsteady state flow condition. Published data of Sediment Transport collected over 20 years in Punatsangchhu river basin by Division of Water Resources Engineering, Bhutan is used for analysis. Performance of empirical equations for Bhutan/Indian sub continent is evaluated and presented in a tabular form. New mathematical equations in a log, power and binomial form for steady state flow are compared with various methods as mentioned above. Results obtained by unsteady state equation proposed by author match with observed quantum of sediment. This

equation precisely predicts sedimentation well within 1.7% bandwidth. The variation between predicted by proposed equation and observed sedimentation was accurate initially up to concentration of 2500 mg/l and beyond it within $\pm 5\%$.

COMMISSION INTERNATIONALE DES GRANDS BARRAGES

VINGT-SIXIÈME CONGRÈS DES GRANDS BARRAGES
Autriche, juillet 2018

DOI 10.3217/978-3-85125-620-8-034



This work licensed under a Creative Commons Attribution 4.0 International License. <https://creativecommons.org/licenses/by-nc-nd/4.0/>

**FINDING BALANCE BETWEEN WATER CONSERVATION, SEDIMENTATION
AND ENERGY IN DAM MANAGEMENT OF SERAYU-BOGOWONTO RIVER
BASIN TERRITORY. CASE STUDY OF WADASLINTANG AND SEMPOR**

Vicky ARIYANTI

Technical Planner, INDONESIA COMMISSION ON LARGE DAMS
PhD Candidate, ERASMUS UNIVERSITY ROTTERDAM

INDONESIA

Kisworo RAHAYU

Hydrologist, INDONESIA MINISTRY OF PUBLIC WORKS AND HOUSING,
SERAYU OPAK RBO

INDONESIA

COMMISSION INTERNATIONALE
DES GRANDS BARRAGES

VINGT-SIXIÈME CONGRÈS DES
GRANDS BARRAGES
Autriche, juillet 2018

**FINDING BALANCE BETWEEN WATER CONSERVATION,
SEDIMENTATION, AND ENERGY IN DAM MANAGEMENT OF SERAYU-
BOGOWONTO RIVER BASIN TERRITORY. CASE STUDY OF
WADASLINTANG AND SEMPOR**

Vicky ARIYANTI

*Technical Planner, INDONESIA COMMISSION ON LARGE DAMS
PhD Candidate, ERASMUS UNIVERSITY ROTTERDAM*

Kisworo RAHAYU

*Hydrologist, INDONESIA MINISTRY OF PUBLIC WORKS AND HOUSING,
SERAYU OPAK RBO
INDONESIA*

1. INTRODUCTION

Sedimentation has been the most challenging problem faced by any dams in the world. This condition is worsened by climate change effects. The climate change shifted the rainy season in Java Island to heavier rainfall in a shorter period of time, which forced the upstream farming area produce extra sedimentation to the dams downstream.

The study uses case of two large dams in Serayu-Bogowonto River Basin Territory: Wadaslintang and Sempor. Both are located in mid-stream of the rivers and faced with the different scale of sedimentation problems. For both dams, the sedimentation is worsened due to the rapid changing upstream land use of the catchment (1,2) combined with the impact of climate change (3), which add the probability for landslide and flash floods falling into the reservoirs.

However, the current dams operation managers' work only on the focus of water availability data. They lack the tool to analyze whether the way they manage these dams has a balance point. This paper seeks to find and compare what is considered as 'the balance of water conservation-sedimentation-energy' for both locations using the Nexus approach for water governance (4). The locations are selected based on the existence of data for the bio-ecological

review (5). The result of the review is compared with the periodical data of the dam's operation throughout the last 20 years and the regulation on Indonesian dam management [6].



Fig. 1

Dams in comparison: Wadaslintang (left) and Sempor (right)

2. NEXUS CONCEPTS AND METHODS

3.1. NEXUS CONCEPTS

From the literature review in finding the balance of sedimentation, water conservation, and energy: the Nexus approach came as the highlight. This review is then followed up by a historical review of the approach. The Nexus approach 1st was launched at the 2011 Bonn Conference (6), which addresses the theme of “The Water, Energy, and Food Security (WEF) Nexus – Solutions for the Green Economy.” However, the need for ‘nexus’ has been identified in 2008 at the World Economic Forum annual meeting (7). This approach has been developed since then through serious attempts to make it a simplified tool.

A literature review done by Bassel and Mohtar (2015) identified four main tools used commonly in to address the WEF nexus: WEAP (SEI, 2014), LEAP (SEI, 2013), MuSIASEM (FAO, 2013), and CLEWS (KTH, 2013). Out of which, this paper uses the simplified models of CLEWS and WEAP-LEAP to define the balance of dam management. This paper uses the following data as input: technical data of the reservoir: water for conservation (volume), water balance (discharge versus outcome), and sedimentation (upstream land use, sedimentation rate), while the outputs are categorized as:

- (1) water: drinking water need
- (2) energy: energy production, water for energy generation need
- (3) food: irrigated land, food production, irrigation water need

3.2. METHODS

The methods in defining the balance of the input and output for the tool will be presented by percentage. If the water percentage for the input lower than the output, it shows that the water storage capacity of the dam should be on function,

in order for the dam management to be declared as an effective balance for the WEF nexus. The lower the percentage shows the yield of water using the reservoir storage is high, for example, the number 10% means the yield of 1m³/sec can be for the usage of 10m³/sec. This shows an effective number, but also questions whether the water input is not too low. If the output is lower than input, this means the capacity of the dam is mostly only for storage, which does not represent an effective balance WEF nexus or multi-purpose dam function. For example, for the number 60%, this means 60m³/sec as input is stored, while the output is only 1m³/sec. This condition can mean the reservoir is in filling mode, so the WEF nexus balance is not effective.

Another percentage is used to show the comparison of the sedimentation and volume percentage. Those with higher number show less effective upstream catchment management. For example, the number 50% shows that the volume of the reservoir is no longer in balance, as the age of the dam is half way of its lifetime. The lower the number, the better the condition of the dam.

A better balance is shown when the WEF percentage is between 15-25% (showing effective use of water storage function with water usage) and a better balance for sediment percentage is under 10% (also based on the age of the dam). In the meantime, the dams are hypothesized as in a balance, but we will see what the tool will show.

The data collection methods being used are site visits, secondary data comparison of 'water-energy-food' models and document analysis of published materials. These models are used to seek the balance of sedimentation-water conservation and energy output. A slight adjustment is made to fit the existence of data and the need for the objective of this paper.

As a showcase of the Nexus approach, the multi-purpose reservoirs are included (8) in this paper: Sempor and Wadaslintang Dams. Both dams were built in the 1980's, but data availability constraints in presenting the whole range of time. Thus, the data is using the last ten years data only.

3. RESULTS

The results are found using the data from these dams to test the implementation of the Nexus approach in multipurpose reservoirs. They are based on data collected from different sources and put into the adapted nexus tool specified for the approach in this paper.

3.1. DAM MANAGEMENT

The main research partner for this paper is the dams' operation manager: BBWS Serayu Opak. Site visits were done to the dams' location and their catchment areas to confirm the maps and printed data. The daily operator for both dams is under the BBWS Serayu Opak. However, partnerships of management are done with different aspects of the dam. It is divided based on

the tasks of the institutions and proves the existence of public-private partnership and division of roles in the partnership (table 1).

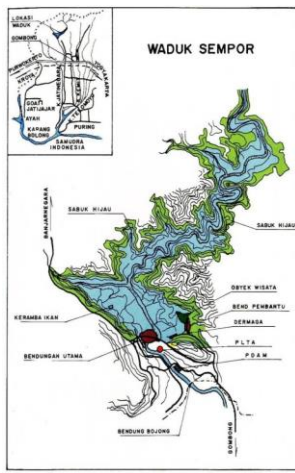
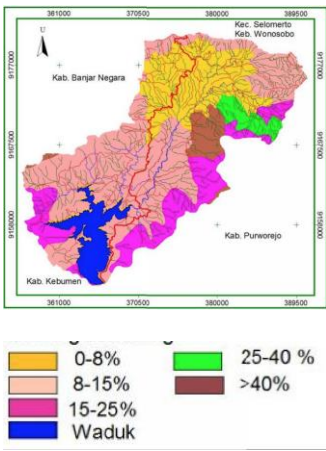
Table 1
Dam Management

Management	
Dam Operation	BBWS Serayu Opak (National Government-Ministry of Public Works and Housing)
Energy Operation	Indonesian Power (Private Company)
Water Supply Operation	PDAM (Local Government Owned Company)
Irrigation Operation	Balai PSDA Probolo (Local Government)
Catchment Management	BPDAS Serayu Opak Progo (National Government-Ministry of Forestry and Environment)

3.2. DAM CONDITION

As a summary, table 2 shows the comparison of the dams' data for the dam catchment and sedimentation condition.

Table 2
Data for catchment and sedimentation for Sempor and Wadaslintang

Data	Sempor	Wadaslintang
Maps of Catchment	<p>Green Belt (9)</p> 	<p>Slope catchment (10)</p> 
Catchment Area	43 km ² (9)	196 km ² (11)
Land use of catchment	42% for agriculture (9)	21% for agriculture, forest, etc.
Sedimentation rate	419,914 m ³ /year (2011) (1)	711,247 m ³ /year (2008) (12)
Catchment slope	25 – 50 ⁰ (1)	5-55 ⁰ (10)

Aside from the change of land use in the upstream catchment, the climate change impacts also cause the change of average precipitation for both dams. These precipitations increase the potential of sedimentation to the dam since the catchment of the dam is not fully forested, and many parts are used as agricultural lands for seasonal cropping pattern (vegetables). The data (figure 2) is showing increased intensities confirming the research on climate change impact to Indonesian island laying below the equator (3): where a higher intensity of rain happens.

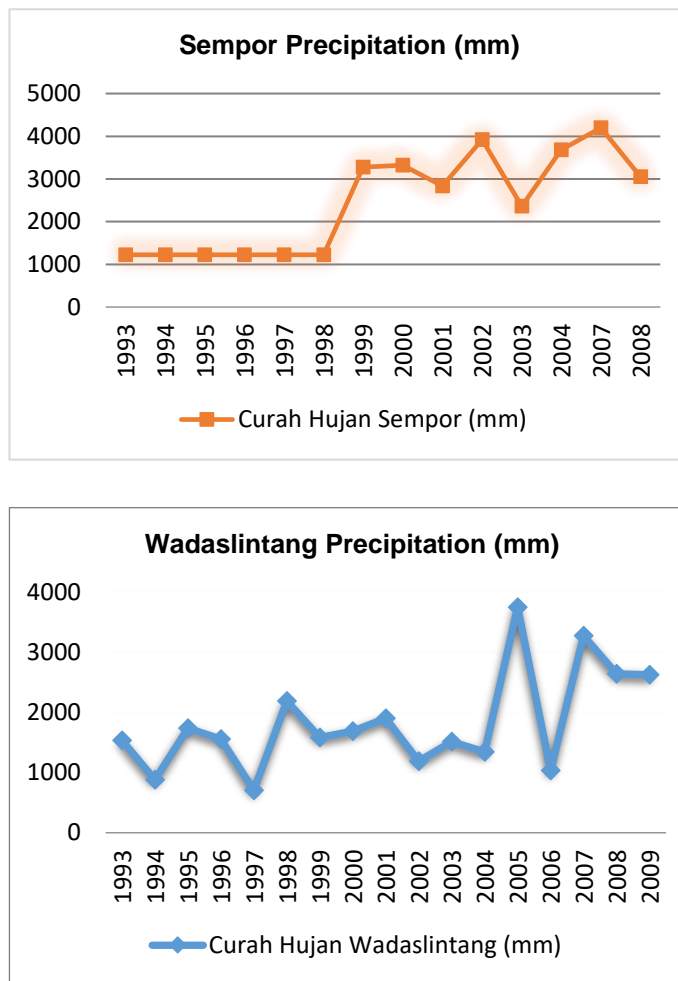


Fig. 2
Precipitation for Sempor and Wadaslintang (1993-2009)

3.3. NEXUS TOOL IMPLEMENTATION AND ANALYSIS

The Nexus tool is used to aggregate and simplify the technical data (see table 3). But, before the data is used, all of them are reduced into average numbers for the last ten years, except for the sedimentation data availability for Sempor, which was last calculated in 1994. The data came from different sources: reports and previous studies. In applying the tool, an adaptation version is made based on the availability of data and the data needed for the models (WEAP-LEAP and CLEWS).

Table 3
Nexus tool implementation in multi-purpose dams

Input		
	Sempor	Wadaslintang
Average discharge (origin)	Average 2.8 m ³ /sec (Rivers: Sampang, Kedungwringin) (1,9)	Average 9.1 m ³ /sec (Rivers: Cingcingguling, Lukulo, Jali, Bogowonto, Bedegolan) (11)
Volume for conservation needs (effective volume)	46,500,000 m ³ (9)	408,000,000 m ³ (11)

Sedimentation	12,04 million m ³ (1994) (1)	27.227 millions m ³ (2008) (12)
Output		
Water:		
Drinking water need	50 l/sec (9)	600 l/sec (2019 SPAM Keburejo) (13)
Food:		
Food production	3 Ton/ha rice (9)	3 Ton/ha (11)
Irrigated field	17,800 ha (9)	33,279 ha (11)
Irrigation need	11.00 m ³ /sec (9)	27 m ³ /sec (10)
Energy:		
Energy production	6,000,000 KWH (9)	92,000,000 KWH (11)
Energy need	3m ³ /sec (9)	24 m ³ /sec (11)
Total water need	14.05 m ³ /sec	51.6 m ³ /sec
Percentage of input vs. output for water	20%	18%
Sedimentation percentage vs. volume effective	26%	7%
WEF vs. sedimentation	77%	264%

The table shows that at the moment both dams are in a balance for effective WEF nexus need and functioning effectively as the percentage is between 10-25%. Meanwhile, for sedimentation, Sempor data is so outdated (1994), which needs to be updated to the current condition, which should be higher than this. However, even so, using this data, the calculation shows the sedimentation in Sempor is much worse than in Wadaslintang. The comparison for WEF and sedimentation also shows that the percentage for Wadaslintang is about three times better, which corresponds to a better balance for Wadaslintang dam management.

Although the data for the dam managers are similar, the condition of Sempor is worse than Wadaslintang. This condition is caused by different the land use of dams' catchment. This paper shows that lack of coordination for catchment management can happen even though both dams are managed by the same institutions, and this may contribute to the sedimentation problem.

This issue can be addressed by introducing and advancing awareness of the water management interrelations to other resources in the river basin level using the Nexus approach. It also recommends the policymakers to make use of the tool for easy visualizations to see these interrelations.

4. CONCLUSION AND RECOMMENDATION

In this paper, the nexus tool is used to give a simple overview of what the approach is about and to showcase that it can be used as a fast assessment towards dam management condition. The results also show that the WEF percentage correlates with the dam effective level of storage and water usage, while the sedimentation percentage correlates with the effective volume of the reservoir. Both percentages are needed to see the whether the balance condition of the dams is met. The case study of Wadaslintang in this paper is proven to be by far in more balance towards the WEF and sedimentation condition than the Sempor.

However, this tool is an over-simplified version of the available tools for the WEF nexus and may need a more precise method to formulate an even comprehensive approach. By means of using a longer time series data and data range rather than using the average data for the input and output may result in better precisions. Also by using an automated source of data will improve the exactness of the results.

5. ACKNOWLEDGEMENT

The authors would like to express their gratitude to BBWS Serayu Opak and INACOLD for their continuous support in the writing process and also the chance to present this paper at ICOLD 2018.

REFERENCES

- [1] Julia H. Significance Scenario Development Check Dam in Reserving The Sedimentation of The Sempor Waduk. *JURNAL ILMU PERTANIAN" AGRIMUM"* 2017;21(1):78-88.
- [2] Kisworo R, Ariyanti RV. Hubungan antara Kemelimpahan Larva Polycentropodidae (Trichoptera) dan Karakteristik Sedimen di Waduk Sempor, Kebumen, Jawa Tengah. *Jurnal Infrastruktur* 2015;1(1 Desember 2015):48-52.
- [3] Case M, Ardiansyah F, Spector E. Climate change in Indonesia: implications for humans and nature. *Climate change in Indonesia: implications for humans and nature* 2007.
- [4] Kurian M, Ardakanian R. *Governing the Nexus*. : Springer; 2015.
- [5] BPPPU. Laporan Teknis Penelitian TA. 2012. Bio-ekologi ikan ekonomis penting untuk penentuan penebaran ikan berbasis budidaya di Waduk Penjalin, Sempor, Sermo dan Wadaslintang, Provinsi Jawa Tengah. 2012.
- [6] www.ooskanews.com. Bonn2011// Bonn Launches Nexus Perspective, Growing demand for water, energy, and food demands resource-efficient economics. 2011; Available at: <https://www.water-energy-food.org/news/2011-11-17-bonn2011-bonn-launches-nexus-perspective/>, 2017.
- [7] Bassel TD, Mohtar RH. Water–energy–food (WEF) Nexus Tool 2.0: guiding integrative resource planning and decision-making, *Water International*, 40:5-6, 748-771, DOI: 10.1080/02508060.2015.1074148. *Water International* 2015;40(5-6):748-771.
- [8] Hülsmann S, Ardakanian R. Advancing a nexus approach to the sustainable management of environmental resources: Capacity development activities of the United Nations University Institute for Integrated Management of Material Fluxes and of Resources (UNU-FLORES). on “Societal Concerns and Capacity Development” organized by UNU-FLORES 2013:69.
- [9] BBWS SO. Bendungan Sempor. 2015.

- [10] Alif Nursoleh. Penentuan Laju Erosi Daerah Tangkapan Hujan (DTH) Waduk Wadaslintang Tahun 2004 Dan 2008 Menggunakan Teknologi Sistem Informasi Geografis (SIG). Semarang: Universitas Negeri Semarang; 2012.
- [11] BBWS SO. Bendungan Wadaslintang. 2015.
- [12] Widyastuti E, Piranti AS, Rahayu, Diana Retna Utarini Suci. Monitoring Status Daya Dukung Perairan Waduk Wadaslintang Bagi Budidaya Keramba Jaring Apung (Monitoring of Carrying Capacity Status Of Wadaslintang Reservoir On Cage Net). Jurnal Manusia dan Lingkungan 2009;16(3):133-140.
- [13] Syarizka D. Pemerintah Siap Bangun Tiga Proyek SPAM Regional Jateng. 2016 21 May 2016.

SUMMARY

Sedimentation has been the most challenging problem that is faced by any dams in the world, which is worsen by climate change effects. The climate change shifted the rainy season in Java Island to heavier rainfall in shorter period, which forced the upstream farming area produce extra sedimentation to the dams downstream.

This paper seeks to compare what is considered as ‘the balance of water conservation-sedimentation-energy’ for both locations using Nexus approach for water governance. The result of the review is compared with the periodical data of the dams operation throughout the last 20 years and the regulation on Indonesian dam management.

This paper shows that Nexus tool can be used to visualize easily the problems of dam management. By introducing the water management interrelations to other resources in the river basin level using the Nexus approach, this will advance the awareness of the policy makers.

Keywords: DAM OPERATION, ECOLOGY, and SEDIMENTATION

6. CLEARANCES AND COPYRIGHT

All necessary permissions and clearance have been obtained by the authors to produce this paper.

COMMISSION INTERNATIONALE DES GRANDS BARRAGES

VINGT-SIXIÈME CONGRÈS DES GRANDS BARRAGES
Autriche, juillet 2018

DOI 10.3217/978-3-85125-620-8-035



This work licensed under a Creative Commons Attribution 4.0 International License. <https://creativecommons.org/licenses/by-nc-nd/4.0/>

**A STUDY ON THE VULNERABILITY RANKING USING HYDROLOGICAL
SAFETY EVALUATION RESULT OF EXISTING DAMS CONSIDERING
CLIMATE CHAGE**

Jiyeon PARK

Researcher of RESEARCH INSTITUTE FOR INFRASTRUCTURE
PERFORMANCE, KISTEC

REPUBLIC OF KOREA (ROK)

**A STUDY ON THE VULNERABILITY RANKING USING
HYDROLOGICAL SAFETY EVALUATION RESULT OF EXISTING DAMS
CONSDERING CLIMATE CHAGE**

Jiyeon Park

Researcher of Research Institute for Infrastructure Performance, KISTEC

REPUBLIC OF KOREA(ROK)

1. INTRODUCTION

In this study, hydrological safety vulnerability assessment on dam facilities were estimated using dams' hydrological safety evaluation result and in-depth inspection assessment result and considering climate change scenario. Hydrological safety assessment of the existing dams was performed by calculating the PMP/PMF using the climate change scenario. Using the results, Multi-Criteria Decision Making was used for vulnerability ranking decision on dams, and assessment scores and weights of hydrological safety evaluation considering climate change were applied as payoff matrix and weight coefficient. In this study, it was evaluated vulnerability ranking that hydrological safety evaluation of existing dam considering climate change.

2. ANALYSIS METHOD

Dam Hydrological safety vulnerability for climate change ranking is calculated using hydrological safety 3 step assessment results and Climate impact factor for future climate results.

Using the results of the existing 4 dams and 3 type method of Multi-Criteria Decision Making (MCDM). Location of 4 target dams was shown in Fig. 1. Three dams belong to the Han river, and one dam belongs to the nakdong river and the 3 target dam type was concrete dams and 1 dam type were fill dam.

2.1. HYDROLOGICAL SAFETY ASSESSMENT

Hydrological dam safety has been currently evaluated depending on freeboard allowance, overflow and downstream hazard without any consideration of types, material and structural conditions. Hydrological safety assessment is made in three steps (MOLTL, 2011), The first step for safety evaluation is to check overflow possibility and freeboard allowance under the consideration of structural type and physical condition obtained from dam inspection results. Fill dam and CFRD(Concrete Faced Rock fill Dam) was applied to a more stable basis than concrete dam because of dam body safety difference when overflow.

If the first step is not satisfied, structural safety evaluation for overflow condition should be carried out as a second step. The evaluation of downstream hazard including human and economical factors is the final step. The final step is assessed to downstream risk with reference to the EAP on the assumption that PMF occurs.

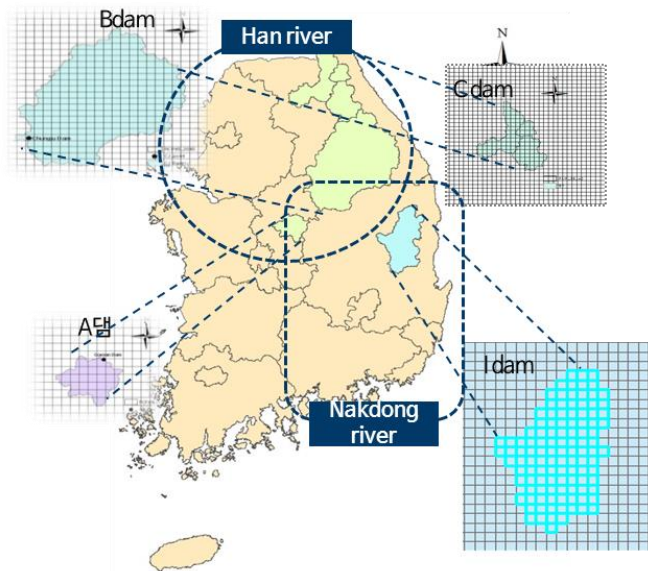


Figure 1 Target dams location

The current hydrologic safety assessment is based on the analysis of the ability to discharge into weir. In this study, To analyze the impacts on climate change, climate change scenarios PMP(RCP 4.5 2040s) were used to assess hydrological safety. And it intends to further assess the factors that may cause a burden on the operation of the target dams in the future.

The factors are criteria 4~6. In order to estimate the long-term variability of climate factors using the data of climate change scenarios,

We used the minimum temperature that can affect monthly maximum rainfall, annual rainfall intensity and dam condition.

Table 1. Hydrological safety evaluation 3 step

Evaluation step	Evaluation contents	Evaluation standard
1 st	Evaluation for freeboard allowance and overflow	Whether or not to secure dam freeboard
2 nd	Evaluation of structural safety for overflow(PMF)	Dam structural stability during overtopping for the PMF
3 rd	Evaluation for downstream hazard(PMF)	Assessment downstream for PMF

Table 2 Long term climate effect factor

Evaluation step	Evaluation contents
1 st	Rate of Monthly maximum rainfall
2 nd	Ratio of rainfall intensity to rainfall
3 rd	Minimum temperature

2.2. MULTI-CRITERIA DECISION MAKING(MCDM)

Multiple-criteria decision-making is a sub-discipline of operations research that explicitly considers multiple criteria in decision-making environments (Triantaphyllou, 2000). Pareto optimal solution is a concept in multi-criteria optimization that allows for the optimization of multiple criteria. MCDM is the process of finding such a Pareto optimal solution (Alternative) on a variety of criteria (Criteria) and shown in Fig. 2(Kim, 2013).

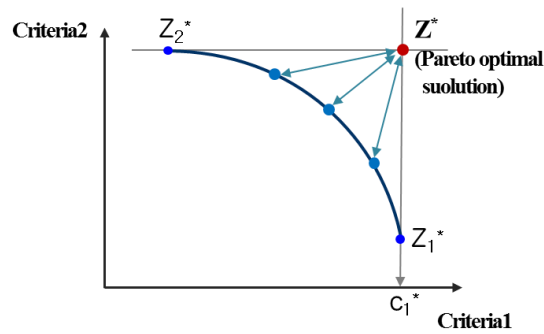


Figure 2 Pareto Optical solution of MCDM

In this study, MCDM was used for vulnerability ranking decision on dams, and assessment scores of each step of the hydrological safety evaluation results which was applied as payoff. It can be available for calculating dams' vulnerability ranking considered dams' hydrological safety.

Compromise Programming(CP), PROMETHEE, VIKOR and TOPSIS, generally used as MCDM technique, were applied to determine the hydrological vulnerability ranking of dams According to each technique, the dam ranking was calculated. In conclusion, the most vulnerable dam and the most safety dam was selected.

3. ANALYSIS RESULTS

In this study, It was ranked using various techniques of MCDM that hydrological safety assessment vulnerability ranking. Criteria of MCDM payoff matrix was shown in Table 3.

Table 3 MCDM criteria

Evaluation contents	Criteria	Evaluation Criteria
Assessment of freeboard for dam type and condition assessment	Criteria1	Lower the vulnerable
Assessment of dam Structural stability during overtopping for the PMF	Criteria2	Lower the vulnerable
Assessment of dam downstream risk	Criteria3	Lower the vulnerable
Rate of Monthly maximum rainfall	Criteria4	Higher the vulnerable
Ratio of rainfall intensity to rainfall	Criteria5	Higher the vulnerable
Minimum temperature	Criteria6	Lower the vulnerable

The target dams were ranked by 6 criteria. The score range of 3 criteria(1~3) is between 1 and 5. And the vulnerability has been evaluated as vulnerable if indicating a lower score for 4 criteria(1~3, 6). If dam has high hydrological safety vulnerability, that ranking is low value (ex: 1 ranking). Table 4 was shown by MCDM payoff matrix. The payoff matrix score in 6 criteria was used as hydrological safety assessment value of recently performed the in-depth inspection and climate change scenario(IPCC AR5).

Table 4 MCDM Payoff Matrix(RCP4.5 2040s)

	Payoff Matrix					
	Criteria1	Criteria2	Criteria3	Criteria4	Criteria5	Criteria6
weight	33	30	19	8	7	3
Dam A	E(1)	B(4)	E(1)	20.8	13.4	-17.3
Dam B	E(1)	A(5)	E(1)	22.9	14.7	-19.1
Dam C	A(5)	A(5)	A(5)	28.5	19.2	-19.8
Dam I	E(1)	E(1)	A(5)	4.1	7.4	-14.9

MCDM result values and ranking were shown in Table 5. MCDM result values were calculated according to various methods. The dams' hydrological safety vulnerability ranking was calculated by using the average value of the ranking to each result values.

Table 5 MCDM values and vulnerability Ranking hydrological safety

	CP	VIKOR	TOSIS	Ranking
Dam A	0.6542	0.8493	0.6342	2
Dam B	0.5737	0.8041	0.5654	3
Dam C	0.0321	0	0.1835	4
Dam I	0.9225	1	0.7957	1

The Vulnerability ranking of hydrological safety in existing dams was shown in Fig. 3. Dam I estimates the highest priority for all techniques, it showed the most vulnerable on hydrological safety. Dam I is considered to be the hydrological assessment most vulnerable.

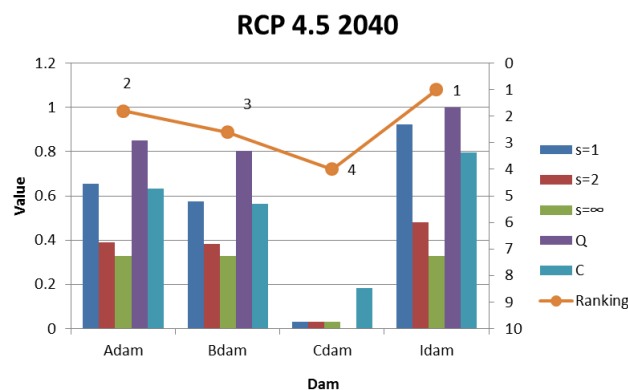


Figure 3 Vulnerability Ranking of hydrological in existing dams

4. CONCLUSION

In this study, Vulnerability Ranking of hydrological safety was ranked using MCDM method in climate change scenario. MCDM technique is difficult the choice of one way due to the differences in the advantages and disadvantages of each method (Min and Song, 2003), However using the results of the various MCDM methods, it is considered to be able to take advantage of prioritization on Vulnerability Ranking for dam hydrological safety. In this study, dam I was calculated as the most vulnerable Dam I. When future peak flooding occurs, it is considered the most vulnerable due to the overflow of dam I. In comparison with other dams, It is considered necessary to take additional actions in the future to secure the remaining capacity of the dam.

ACKNOWLEDGEMENTS

This work is supported by the Korea Agency for Infrastructure Technology Advancement(KAIA) grant funded by the Ministry of Land, Infrastructure and Transport (Grant 18AWMP-B083066-05).

REFERENCES

- [1] Kim, T.H.(2013):Flood Risk Mapping Based on the Fuzzy MCDM by considering Inland River Inundations with Basin Runoff. Ph. D. dissertation, Kyungpook National University, Korea, pp.17-20.
- [2] Min, J.H., and Song, Y.M. (2003): A Comparison of MAUT, AHP and PROMETHEE for Multicriteria Decisions, Proceedings of the Korean Operations and Management Science Society Conference, Nov., pp. 229-232.
- [3] MOLIT, KISTEC(2011).:Specific Guide for In-depth Inspection on dams.
- [4] Triantaphyllou, E. (2000): Multi-Criteria Decision Making: A Comparative Study. Dordrecht, The Netherlands: Kluwer Academic Publishers (now Springer). ISBN 0-7923-6607-7.

SUMMARY

In this study, it was evaluated vulnerability ranking that hydrological safety evaluation of existing dam considering climate change. Using climate change scenario rcp 4.5 2040s.

COMMISSION INTERNATIONALE
DES GRANDS BARRAGES

VINGT-SIXIÈME CONGRÈS DES
GRANDS BARRAGES
Autriche, juillet 2018

EXPERIMENTAL STUDY ON BED EROSION DOWNSTREAM FROM A DAM*

Zhijing LI, Jun WANG

CHANGJIANG RIVER SCIENTIFIC RESEARCH INSTITUTE

CHINA

ABSTRACT

The nature of flow, sediment transport and bed erosion were studied in a laboratory flume using mixed-size sediment under clear water conditions. During each experiment, water depth, bed and water surface elevation, bedload transport and bed state were continuously monitored. Steady inflows were established with an unit discharge of about 0.01 m² s⁻¹ to 0.03 m² s⁻¹. Well sorted gravel and sand were employed to compose four kinds of sediment beds with different gravel/sand contents, i.e., uniform 100% gravel bed, uniform 100% sand bed, and two graded sediment beds respectively with 53% gravel and 47% sand as well as 22% gravel and 78% sand. For different sediment beds, the experiments were conducted under the same discharges, thereby allowing for the role of sediment composition in dictating the bed erosion to be identified. The measured bed elevation for all the twenty runs show that significant degradation is spotted, yet the scour is mainly confined to the upstream part. For a specific sediment sample, the degradation enhanced with the increase of the inlet flow discharge. Under a specific unit-width flow discharge, the degradation for the four sediment samples generally follows the rule that the scour process increases with the increase of sand content in the sediment bed. However, it also exhibits an interesting phenomenon that the maximum scour depth with pure sand is not the largest, instead the case with 78% sand content features the deepest scour. In line with this observation, the scour with pure sand extended considerably farther

**titre de l'article complet*

downstream along the channel than other beds. In fact, bed forms like small dunes were present in cases with pure sand, which were not discerned in other sediment beds. This has important implications for the evaluation of the scour hole evolution, echoing that the sediment bed composition has significant and complicated effects on the scour dimensions below sills, as identified in previous studies.

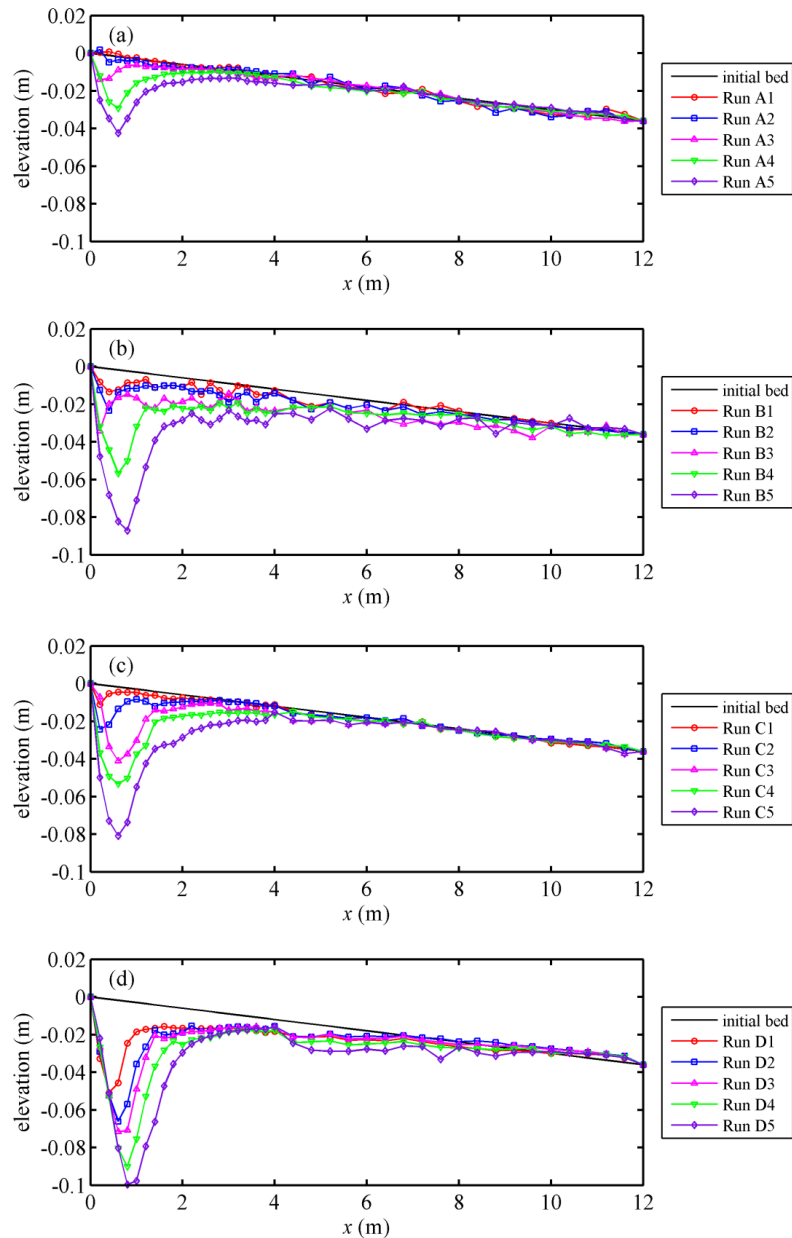


Fig. 1. Cross section averaged final bed elevation in relation to different inflow discharges for (a) uniform 100% gravel bed, (b) uniform 100% sand bed, (c) 53% gravel and 47% sand bed, and (d) 22% gravel and 78% sand bed.

COMMISSION INTERNATIONALE DES GRANDS BARRAGES

VINGT-SIXIÈME CONGRÈS DES GRANDS BARRAGES
Autriche, juillet 2018

DOI 10.3217/978-3-85125-620-8-037



This work licensed under a Creative Commons Attribution 4.0 International License. <https://creativecommons.org/licenses/by-nc-nd/4.0/>

**STUDY ON MECHANISM OF RESERVOIR INDUCED SEISMICITY AND
COUNTERPLOTS FOR RESERVOIR OPERATION UNDER EXTREME
WEATHER**

Xinxiang ZENG

EARTHQUAKE ENGINEERING RESEARCH CENTER, CHINA INSTITUTE OF
WATER RESOURCES AND HYDROPOWER RESEARCH

CHINA

Tinggai CHANG

EARTHQUAKE ENGINEERING RESEARCH CENTER, CHINA INSTITUTE OF
WATER RESOURCES AND HYDROPOWER RESEARCH

CHINA

Xiao HU

EARTHQUAKE ENGINEERING RESEARCH CENTER, CHINA INSTITUTE OF
WATER RESOURCES AND HYDROPOWER RESEARCH

CHINA

Lei YANG

EARTHQUAKE ENGINEERING RESEARCH CENTER, CHINA INSTITUTE OF
WATER RESOURCES AND HYDROPOWER RESEARCH

CHINA

COMMISSION INTERNATIONALE
DES GRANDS BARRAGES

VINGT-SIXIÈME CONGRÈS DES
GRANDS BARRAGES
Autriche, juillet 2018

**STUDY ON MECHANISM OF RESERVOIR INDUCED SEISMICITY AND
COUNTERPLOTS FOR RESERVOIR OPERATION UNDER EXTREME
WEATHER**

Xinxiang ZENG, Tinggai CHANG, Xiao HU, Lei YANG

*Earthquake Engineering Research Center, CHINA INSTITUTE OF WATER
RESOURCES AND HYDROPOWER RESEARCH*

CHINA

1. INTRODUCTION

The odds of extreme weather events increased significantly recently against the backdrop of global climate change, in which China is one of the most affected countries especially for typhoon and rainstorm. The water level will change rapidly if the typhoon or rainstorm occurred in the reservoir region, which is seemed to increase the occurrence probability of Reservoir-Induced Seismic (RIS). The RIS means typically minor earthquake sequence resulting from reservoir impoundment or variation of water level. The damage of RIS may probably be much bigger than that of natural earthquake because its focal depth is very shallow. Therefore, it is necessary to study the mechanism of extreme weather induced RIS events, as well as provide some corresponding countermeasures for reservoir operation management.

Shanxi reservoir is located in the upper stream of Feiyun river (Zhejiang Province, China) with capacity of $18.24 \times 10^8 \text{m}^3$, and the height of the concrete face rockfill dam is 156.8m. Shanxi reservoir region will be affected by typhoon from June to September every year. The impoundment of the reservoir started from May 12th, 2000. And a $M_L 3.5$ seismic events in reservoir region has been recorded in July 28th, 2002^[1]. From that time on, the induced seismic activity has been an issue for the Shanxi reservoir.

Table 1
Details of the seismic catalogue

Year	Frequency	Frequency in different magnitude					Maximum magnitude
		$M_L < 1$	$1 \leq M_L < 2$	$2 \leq M_L < 3$	$3 \leq M_L < 4$	$4 \leq M_L$	
2002	24	0	0	20	4	0	3.9
2003	3	0	3	0	0	0	1.9
2004	0	0	0	0	0	0	/
2005	13	0	10	3	0	0	2.2
2006	1003	321	415	212	42	13	4.6
2007	27	25	2	0	0	0	1.6
2008	20	18	2	0	0	0	1.3
2009	21	19	1	1	0	0	2.8
2010	72	53	18	1	0	0	2.1
2011	46	34	12	0	0	0	1.8
2012	14	14	0	0	0	0	0.9
2013	6	5	1	0	0	0	1.1
2014	4221	3103	889	178	43	8	4.4
2015	334	239	76	18	1	0	3.4
2016	104	73	25	5	1	0	3.9
Total	5908	3904	1454	438	91	21	/

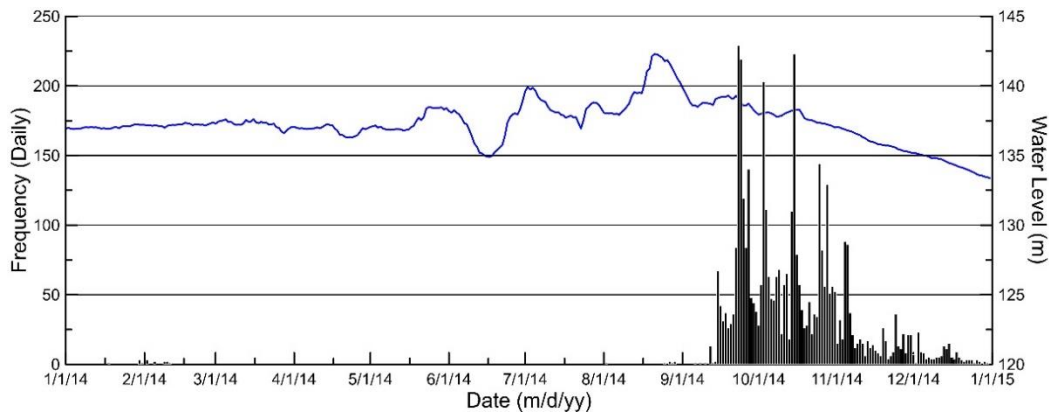


Fig. 2
Daily variations of seismic frequency (bottom bar) in 2014
Blue curve: water level

2.2. SEISMIC MAGNITUDE

Fig. 3 shows that the relationship between water level and seismic magnitude. Combining Table.1, Fig.1 and Fig.3, we recognize that the seismic cluster ② and ④ are much bigger than the other two clusters not only in magnitude but also in frequency. And the seismic activities are mainly weak or micro earthquakes. Actually, more than 99% of the seismic events are smaller than $M_L 4.0$. In addition, the biggest seismic event is $M_L 4.6$ (Feb 9th, 2006), which is right after the water level decreasing dramatically from the first reach of 145+m.

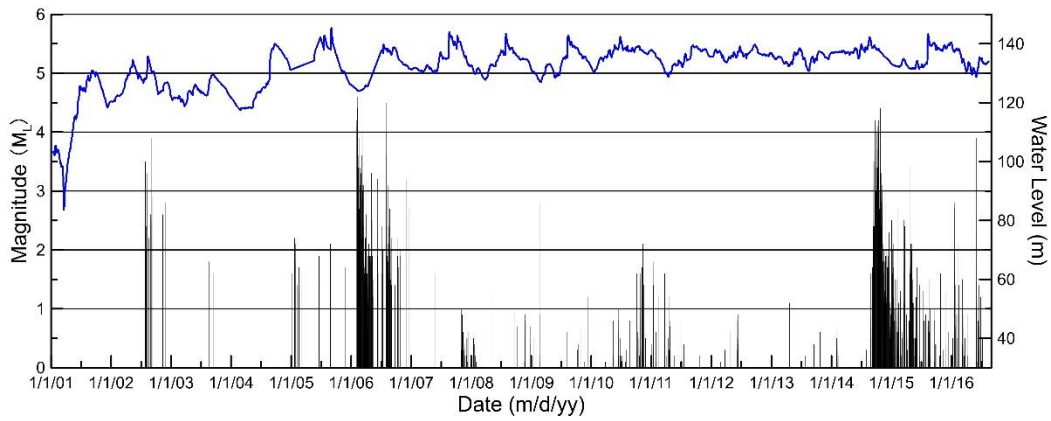


Fig. 3
Time variations of magnitude (bottom vertical line)
Blue curve: water level

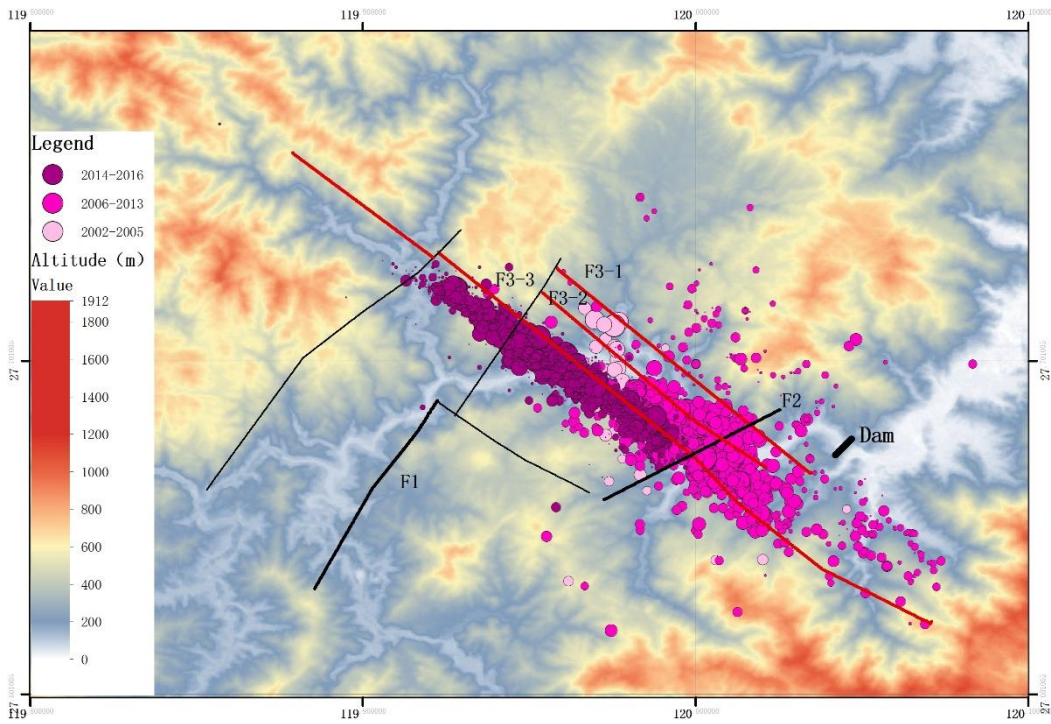


Fig. 4
Spatial distribution of epicenter in Shanxi reservoir region after impoundement
The size of the circle is proportional to the magnitude; F1, Jiangkou-Huixi fault;
F2, Yanshang-Chengken fault; F3, Shuangxi-Jiaoyangxi fault.

2.3. SPATIAL DISTRIBUTION

There are 14 faults developed in research area^[1], in which F1 (Jiangkou-Huixi fault), F2 (Yanshang-Chengken fault) and F3 (Shuangxi-Jiaoyangxi fault) are considered to be the main-controlled-fault^[3]. The fault F3 have 3 branch faults (F3-

1, F3-2 and F3-3) with approximately the same strike of N310° W. As is shown in Fig. 4, the seismic events after the impoundment are mainly distributed in the area near fault F2 and F3. The strike of 2014-2016 comes much more concentrated and closer to that of fault F3 than the 2002~2005 and 2006~2013. In fact, according to the field survey, the permeability of fault F3 is much bigger than that of fault F1 and F2. Furthermore, the permeability order within the 3 branch faults of F3 is F3-3 > F3-2 > F3-1. And the northwest trending faults such as F2 and F3 are parallel tension-shear fault with steep dip^[4]. All the geological conditions mentioned above are beneficial to the infiltration of the increasing reservoir water.

3. DOUBLE-DIFFERENCE LOCATION ALGORITHM

3.1. METHODOLOGY

The source parameters such as hypocenter location and focal depth are key points in the study of earthquake mechanism. The ordinary location methods for these source parameters is very complicate and require accurate earth models. Due to our limited knowledge of structures in the earth, it is scarcely possible to get precise location of single earthquake at a time. The main points of the double-difference location algorithm is reformulate the problem to solve for changes in the distance between pairs of seismic events. By forming differences in this manner, we could steer clear of the travel time errors due to the uncomprehending Earth structure and obtain high resolution results of hypocenter location as well as focal depth^[5].

3.2. RESULTS

In this study, the double-difference location algorithm is used to conduct data processing of 2014 seismic cluster. The processed results are shown in Fig.5, which indicate the spatial distribution of 2014 seismic clusters are much more concentrated along the strike of branch fault F3-3 compared with that shown in Fig.4. Therefore, we consider the branch fault F3-3 is the causative fault of 2014 seismic cluster. Actually, almost all of the seismic events in 2014 are occurred after the typhoon season. We consider the most possibly reason is that there are some hydraulic connections between the raised water and the branch fault F3-3. The water will erode the fault plane, and reduce the effective stress. In case the water level dropped or changed rapidly, the related fault will loss stability and cause earthquake. This point of view is corroborate with the assumption mentioned in Section2.1. Consider the statistical results of seismic activities and the operating experience, we suggest that the changing rate of water level should be controlled in a relative low level (no more than 2m/day).

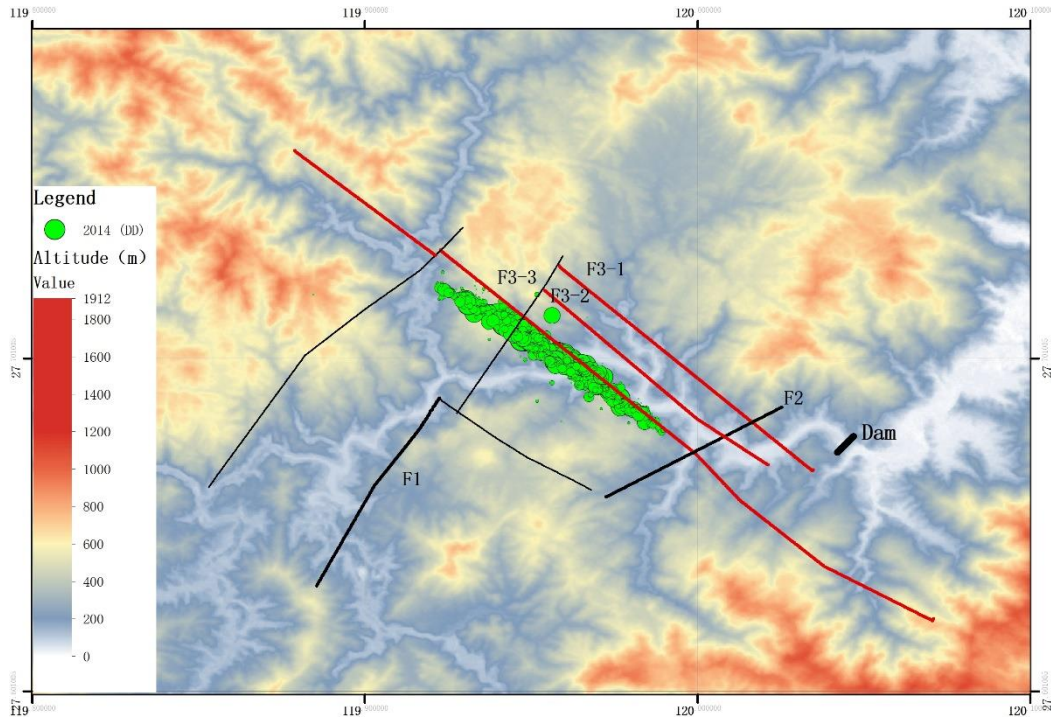


Fig. 5

The results of double-difference location algorithm for 2014 seismic cluster

4. CONCLUSION

Consider the features of seismic activities and geological conditions in Shanxi reservoir, conclusions could be summarized as follows.

1. The seismic frequency of Shanxi reservoir region increases significantly after the impoundment, and the seismic activities shown a periodic change in every 4 years.
2. More than 99% of the seismic events are weak or micro earthquakes, and the maximum magnitude is $M_L 4.6$.
3. The seismic events after the impoundment are mainly distributed in the area near fault F2 and F3.
4. The results of double-difference location algorithm suggest that the branch fault F3-3 is the causative fault of 2014 seismic cluster.
5. The preferably infiltration conditions of fault F3 (steep dip and higher permeability) is the control factor of the seismic activity in Shanxi reservoir.

At last, we suggest that the changing rate of water level in dam operation should be controlled in a relative low level, especially for the water level decreasing rate must be limited to no more than 2m/day.

5. ACKNOWLEDGEMENTS

This study is supported by administration bureau of Shanxi hydro-junction as well as Research Fund of State Key Laboratory of Simulation and Regulation of Water Cycle in River Basin, IWHR (Grant No. 2016TS09). And we also would like to express our gratitude to research fellow Zhong Yuyun in earthquake administration of Zhejiang province for providing us the earthquake catalogue and related data.

REFERENCES

- [1] ZHONG Y.Y., ZHANG F., ZHAO D. Precise Relocation and Seismogenic Structure of the Shanxi Reservoir Earthquake Sequence in Wenzhou , Zhejiang Province (in Chinese). *Journal of Seismological Research*, 2011, Vol.34, No.2.
- [2] ZHONG Y.Y., ZHU X.Y., ZHANGZ.F. Estimation of rock porosity and saturation in the Shanxi reservoir using seismic data (in Chinese). *Earthquake Research in China*, 2016, Vol.32, No.4.
- [3] MA Z.J., ZHONG Y.Y., HAN Y.B., YE J.Q., ZHANG Z.F., LIN S.F., XU M.L., LIU Q.Q. The Tectonic Conditions of Shanxi Reservoir Induced Earthquake in Wenzhou (in Chinese). *Earth Science*, 2016, Vol.41, No.8.
- [4] ZHONG Y.Y., ZHOU X., ZHANG F. On Relation Between Reservoir Water Level Changes and Seismic Activity (in Chinese). *Journal of Geodesy and Geodynamics*, 2013, Vol.33, No.2.
- [5] FELIX WALDHAUSER, WILLIAM L. ELLSWORTH. A Double-Difference Earthquake Location Algorithm: Method and Application to the Northern Hayward Fault, California. *Bulletin of the Seismological Society of America*, 2000, Vol.90, No.6.

SUMMARY

The odds of extreme weather events increased significantly recently against the backdrop of global climate change, in which China is one of the most affected countries especially for typhoon and rainstorm. The water level will change rapidly if the typhoon or rainstorm occurred in the reservoir region, which is seemed to increase the occurrence probability of Reservoir-Induced Seismic (RIS). The RIS means typically minor earthquake sequence resulting from reservoir impoundment or variation of water level. The damage of RIS may probably be much bigger than that of natural earthquake because its focal depth is very shallow. Therefore, it is necessary to study the mechanism of extreme weather induced RIS events, as well as provide some corresponding countermeasures for reservoir operation management.

Shanxi reservoir is located in the upper stream of Feiyun river (Zhejiang Province, China) with capacity of $18.24 \times 10^8 \text{m}^3$, and the height of the concrete face rockfill dam is 156.8m. Shanxi reservoir region will be affected by typhoon from June to September every year. The impoundment of the reservoir started from May 12th, 2000. From that time on, the induced seismic activity has been an issue for the Shanxi reservoir. In this study, a seismic catalogue contains 5908 records are used to study the seismic activity of Shanxi reservoir region ($27^\circ 60' \sim 27^\circ 80'$ N, $119^\circ 80' \sim 120^\circ 10'$ E), which is recorded from July 2002 to July 2016.

Consider the features of seismic activities and geological conditions in Shanxi reservoir, conclusions could be summarized as follows.

1. The seismic frequency of Shanxi reservoir region increases significantly after the impoundment, and the seismic activities shown a periodic change in every 4 years.
2. More than 99% of the seismic events are weak or micro earthquakes, and the maximum magnitude is $M_L 4.6$.
3. The seismic events after the impoundment are mainly distributed in the area near fault F2 and F3.
4. The results of double-difference location algorithm suggest that the branch fault F3-3 is the causative fault of 2014 seismic cluster.
5. The preferably infiltration conditions of fault F3 (steep dip and higher permeability) is the control factor of the seismic activity in Shanxi reservoir.

At last, we suggest that the changing rate of water level in dam operation should be controlled in a relative low level, especially for the water level decreasing rate must be limited to no more than 2m/day.

KEYWORDS

INDUCED SEISMICITY, RESERVOIR OPERATION, WATER LEVEL

COMMISSION INTERNATIONALE DES GRANDS BARRAGES

VINGT-SIXIÈME CONGRÈS DES GRANDS BARRAGES
Autriche, juillet 2018

DOI 10.3217/978-3-85125-620-8-038



This work licensed under a Creative Commons Attribution 4.0 International License. <https://creativecommons.org/licenses/by-nc-nd/4.0/>

**IMPACT OF CLIMATE CHANGE ON THREE LARGE RESERVOIRS
OPERATION IN CITARUM RIVER – INDONESIA**

Hari SUPRAYOGI

Director of River and Coastal, MINISTRY OF PUBLIC WORK AND HOUSING

INDONESIA

Harry M. SUNGGUH

Director II, JASA TIRTA II PUBLIC CORPORATION

INDONESIA

Reni MAYASARI

*Special Expertise Level I of Water Resources Management, JASA TIRTA II
PUBLIC CORPORATION*

INDONESIA

IMPACT OF CLIMATE CHANGE ON THREE LARGE RESERVOIRS OPERATION IN CITARUM RIVER – INDONESIA

Hari SUPRAYOGI

Director of River and Coastal, MINISTRY OF PUBLIC WORK AND HOUSING,
INDONESIA

Harry M. SUNGGUH

Director II, JASA TIRTA II PUBLIC CORPORATION, INDONESIA

Reni MAYASARI

Special Expertise Level I of Water Resources Management, JASA TIRTA II
PUBLIC CORPORATION, INDONESIA

1. INTRODUCTION

Citarum River with a length of ± 270 km has an upstream area that is mostly located in Bandung regency and partly in Garut regency. Citarum River flows from the south then moves towards the West which then turns to the North with the largest estuary in Muara Bendera - Java Sea. The Citarum River area which is the working area of Jasa Tirta II Public Corporation consists not only of the Citarum River basin, but is a unified hydrological system that combines the Citarum River and its surrounding rivers, the result of water resources development based on the thought of Blommestein (1949).

On the Citarum River there are three stair-shaped reservoirs (cascade) with a classification of large dams, namely Saguling, Cirata, and Jatiluhur. These three reservoirs are managed by different institutions, namely Saguling by Saguling Power Generating Unit (UBP) under PT Indonesia Power, Cirata by UBP Cirata under PT PJB where PT Indonesia Power and PT PJB is a subsidiary of PT PLN (Persero) while Jatiluhur is in the management of Public Company (Perum) Jasa Tirta II (PJT-II) under the management control of State Minister of State-Owned Enterprises with related technical department is Ministry of Public Works.

The water resources in the Citarum river is the main source of raw water supply other than the surrounding rivers that are integrated in the Jatiluhur infrastructure system for various purposes, including the need for raw water for drinking water of DKI Jakarta and the district / municipal water supply companies, raw water for industry, irrigation area of 240,000 ha, flood control, hydroelectricity and others. The Citarum cascade reservoir has an installed generation capacity of ± 2000 MW with an annual production of ± 3.7 TWh (3.7×10^9 kWh).

Climate change is already a fact. The doubling of CO₂ emissions (ppm) compared with the Industrial Revolution in the 19th century is defined as a half degree of world temperature rise. This will lead to an increase in half the degree

of global warming for decades to come, due to the inertia of the climate system (Javornik, 2008). The growing awareness of the environment is transformed in the form of global pressure on the use of renewable and environmentally friendly energy sources. Hydropower as one of the environmentally friendly energy sources has an important role in facing the world policy in climate change. On the contrary, hydropower has a dependence on water availability conditions both spatial and time in optimizing its generation, which in this case refers to the operation of the reservoir.

2. CONFIGURATION AND POTENTIAL WATER RESOURCES

The Citarum cascade reservoir operation cannot be separated from the Citarum River Basin system as a whole because the Citarum River has become a hydrological entity through the development of natural resources based on the Blommestein thought that unites the natural resource potential of the Ciujung River (Banten Province) to Kali Rambut (Pemali) (van Blommestein, 1949). This rationale is realized in the development of Citarum River through Jatiluhur Multipurpose Project with the construction of Jatiluhur dam and dam along with irrigation infrastructure so that the Citarum River with the surrounding rivers, from Ciliwung River to Cilalanang River into one hydrological unit as “Fig.1”.

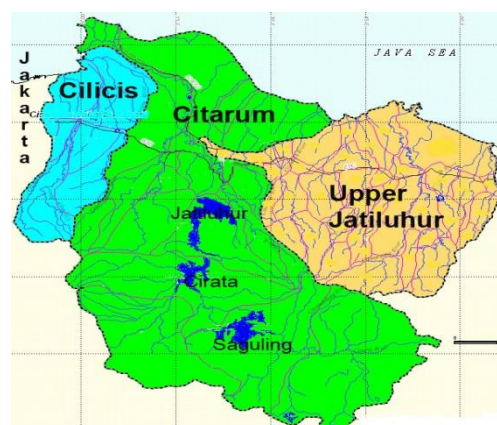


Fig.1

The Citarum River Basin with the surrounding rivers and part of the Ciliwung-Cisadane River Region becomes a hydrological unit.

Extensive infrastructure development with the objective of meeting the water requirement for irrigation of 240,000 ha in the northern plains of West Java as the fulfillment of national food, raw water supply especially for DKI Jakarta in addition to the Regency / Municipal PDAM and industry, electricity generation, fishery, and etc. The development of natural resources in the Citarum River is done by optimizing the availability of water from the surrounding rivers, namely Ciliwung, Bekasi, Cikarang, Ciasem, Cigadung, Cipunegara, and Cilalanang as “Fig.2 “. Citarum cascade reservoir consisting of Saguling, Cirata, and Ir. H.

Djuanda became the main source of supply to meet various water needs downstream of Ir. H. Djuanda dam.

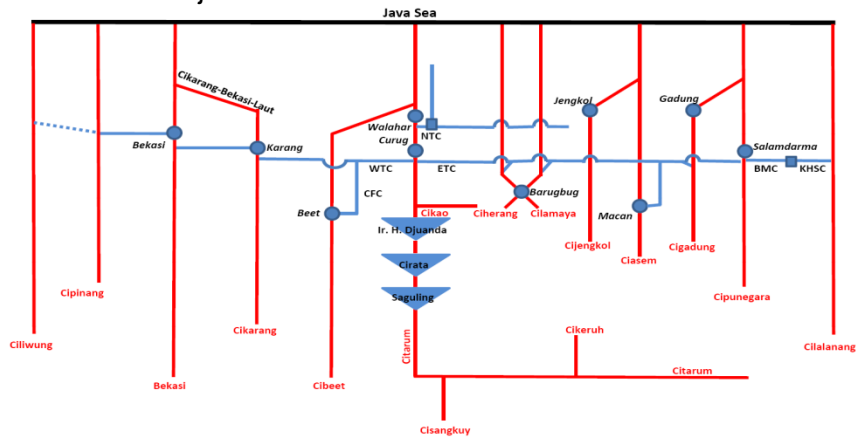


Fig. 2.

Schematic development of water resources in the Citarum River Basin through optimization of water sources from rivers around the Citarum River

The potential of natural resources in WS Citarum can be distinguished into: [1] natural resource potential of Citarum River which is managed through Citarum cascade reservoir operation and, [2] optimization of local water sources through the operation of weirs. With the existence of the three reservoirs in the Citarum River, almost all the potential of natural resources in the Citarum River of $6.0 \times 10^9 \text{ m}^3$ can be used to meet various downstream needs as a by product of electricity generation, because the main priority of Citarum cascade reservoir operation is for the fulfillment the need for water downstream of the Jatiluhur dam. With no reservoirs for local water sources, the potential of natural resources of $6.95 \times 10^9 \text{ m}^3$ can only be used for $1.65 \times 10^9 \text{ m}^3$. The biggest beneficiary is for irrigation by 87% of the total manageable water as “Fig.3”.

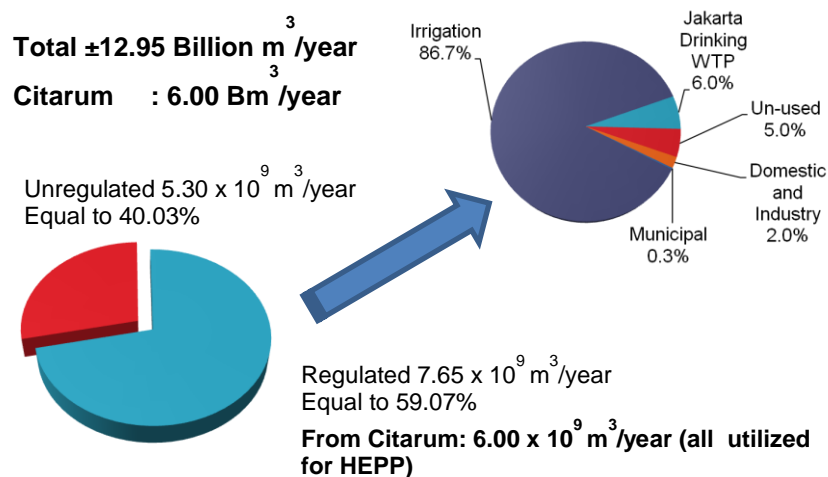


Fig. 3

Configuration of potential and utilization of water resources in Citarum River Basin

3. THE CITARUM RIVER HYDROLOGICAL REGIME.

Indonesia in the tropics in general the main characteristics of the tropical climate is the uniformity of temperature, solar radiation, humidity, wind speed. While the main climate parameter that varies in time and space is rainfall. Factors that control rainfall are (van der Weert, 1994): equatorial double rainy seasons, transfers (monsoons), and local influences. Presents regional variations of rainfall in Indonesia. It is generally seen that seasonal variations are highly visible in Java, Nusa Tenggara, East Timor, and South and Southeast Sulawesi.

Annual runoff depends on rainfall and evapotranspiration. In general, the evapotranspiration in the catchment area is relatively small compared to the existing rainfall, so it is not surprising that the annual rainfall is closely related to runoff (van der Weert, 1994). The runoff component is divided into base flow, interflow and surface runoff. Determination of surface flows for irrigated agricultural areas, mixed gardens, settlements, and plantations is a correlation between soil types, slope and slope length as well as flow management practices.

Citarum River is one of the rivers that have long discharge data. In 1922, the discharge post was installed in Palumbon which was in the upper reaches of Jatiluhur reservoir with an area of 4133 km² of DAS. In January 1944, during the period of independence war, observation data were interrupted and resumed from May 1962 to August 1987 when the station was dismantled because of the flooding of the Cirata dam construction.

Based on the recording of all long-term data in the Citarum River basin using Isohyet method, the mean annual rainfall is estimated to be 2610 mm. From the comparison of precipitation in the pre-independence period (Sep-22 to Aug-29) with after independence (Sep-79 to Aug-86) the annual rainfall is almost 2454 mm / year and 2470 mm / year but the annual flow is increased by 10% from 1137 mm / year to 1261 mm / year (van der Weert, 1994).

In addition, from the observation data of debit at the Palumbon station fluctuations of flow debits between the period before independence (1923-1943) and after independence (1963-1984) were higher. Based on the Citarum cascade reservoir operation data, there is a decrease in annual flow and also higher fluctuations as "Fig.4". Changes from this hydrological regime could be attributed to land use change. Unfortunately, there are no statistics on land use data prior to the independence war that can be used as a comparison. Changes in the hydrological regime include the tendency of seasonal leap, longer dry season, shorter rain time with greater intensity as an indication of climate change as "Fig.5".

Under such conditions, at the operational level of the Citarum cascade reservoir the question arises, "How to treat the reservoir reservoir and Citarum cascade reservoir operation to anticipate the trends?"

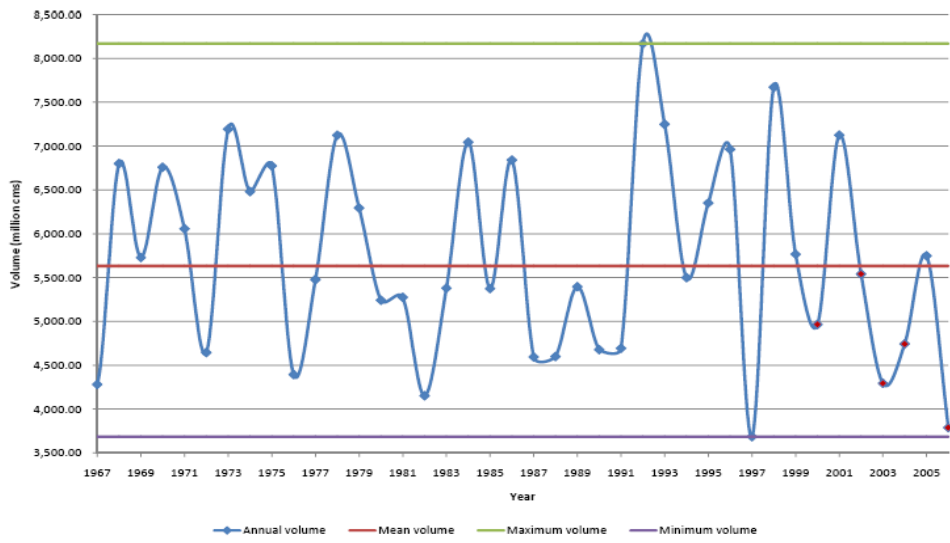


Fig. 4
The annual volume of Citarum during the year 1967-2006.

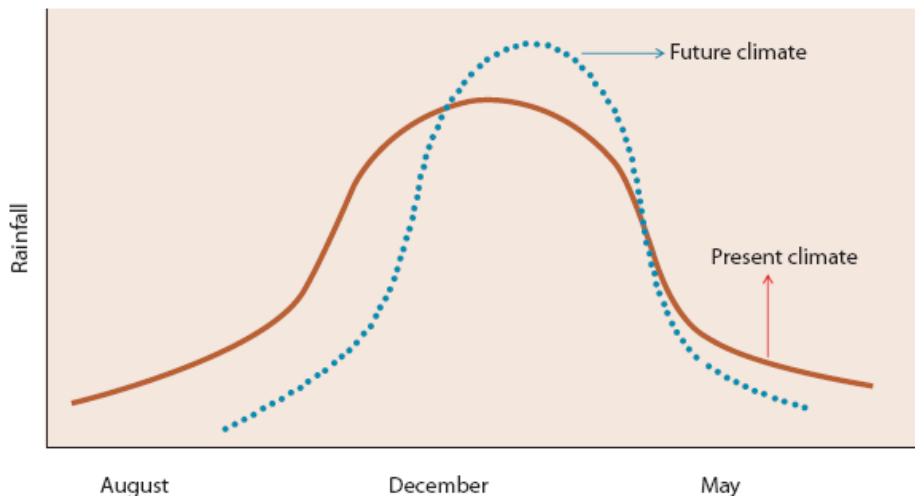


Fig. 5
Trend of rainfall pattern in Java and Bali (source: UNDP Indonesia, 2007)

4. ADAPTATION OF OPERATION PATTERN OF CITARUM CASCADE RESERVOIR

4.1 Operation of Citarum Cascade Reservoir.

The Citarum cascade reservoir has a net capacity of 2.0×10^9 m³, where the net catch is determined from the elevation of the spillway and the minimum elevation of the reservoir (at the Jatiluhur reservoir minimum hydro operation). With annual flow of Citarum in Jatiluhur at $\pm 5.75 \times 10^9$ m³ equivalent to 49% of net capacity, it indicates that this Citarum cascade reservoir is not designed to provide reserve reserves under long drought conditions. The technical data on the Citarum cascade reservoir is presented in as “Table 1”.

Table. 1
Technical Data of Citarum Cascade Reservoir

Name of Dam	Saguling	Cirata	Ir. H. Djuanda
Operational	1985	1988	1967
Specific Reservoirs Data			
Full supply level	643 m	220 m	107 m
Dead storage level	623 m	205 m	56 m [*])
Minimum power level	-	-	75 m
Maximum storage	880×10^6 m ³	$1,973 \times 10^6$ m ³	$2,970 \times 10^6$ m ³
Minimum storage	271×10^6 m ³	$1,177 \times 10^6$ m ³	599×10^6 m ³ ^{**)}
Surface area at max operating level	49 km ²	62 km ²	83 km ² ^{****)}
Hydropower Plant Data			
Tail level (m)	252	103	27.0
Head loss (m)	28.4	4.0	1.0
Spillway characteristics	Gated spillway	Gated spillway	Ungated (ogee) spillway
Installed capacity (max. power, MW)	750	1008	187.5
Number of turbines	4 units	8 units	6 units
Type of turbines	Francis	Francis	Francis
Dam Data			
Type	Rockfill dam with clay core	Rockfill dam with concrete face	Rockfill dam with inclined clay core
Height	99 m	125 m	105
Crest length	301 m	453.5 m	1220 m
Crest elevation	650.20 m	225.0 m	114.5 m

Note: ^{*}) Based on the existing layout of guiding canal in front of hollow jet gates. ^{**)} at El. 49 msl
^{****)} at El. 107 msl.

The annual operation of this Citarum cascade is made by estimating the water requirement, the statistical data of inflows to the three reservoirs with the total energy generated by the system optimized with priority based on the fulfillment of water requirements downstream of the Ir. H. Djuanda Dam. Water needs downstream of the Ir. H. Djuanda reservoir is

primarily for the fulfillment of raw water supply of daily necessities (raw water of DKI Jakarta and districts / cities), irrigation, industry and others.

The water requirement downstream of the Ir. H. Djuanda reservoir is mainly for irrigation covering almost 87% of the total water requirement. Therefore, to determine the water requirement required the classification of irrigation water supply for Jatiluhur Irrigation Area of 240,000 ha by considering data of water availability from local sources, channel capacity and plan and condition of existing cropping pattern. The data is traced from the furthest irrigation area to the water requirement at Bendung Curug as the main building for the various needs downstream of the Ir. H. Djuanda dam by considering also the water loss in the channel and the safety factor.

Water needs downstream of the Jatiluhur dam became one of the inputs in establishing the Citarum cascade reservoir operation. Some of the principles (limits) in determining the operation of the Citarum cascade reservoir are as follows:

- Runoff is avoided.
- Water level elevation at the end of the year is equal to or more than the water level at the beginning of the year.
- The principle of equal-sharing operation, ie the proportion of clean reserves for each reservoir against the total system is constant, ie 18.8% for Saguling, 24.4% for Cirata and 56.8% for Ir. H. Djuanda.

The inflow data for the three reservoirs was statistically determined using data from 1988, the year from which the Citarum cascade reservoir system began to operate fully. From the input data, optimization is done so that the maximum power production with the water requirement is fulfilled with the optimization process done by the Solver program.

In operating the model, the reservoir operation model is conducted sequentially and needs to be continually updated and re-operated to obtain the most accurate forecast data on real conditions and how operational decisions are established for each component of the operation of the reservoir. With many interested parties in the operation of this Citarum cascade reservoir, the Citarum cascade operation is always evaluated and updated monthly through a coordination meeting mechanism within the coordinating team for the operation dam cascade of the Saguling, Cirata and Ir H. Djuanda (TKPBSCJ).

4.2 Economic Value of Water on Citarum Cascade Reservoir Operation.

Climate change is one of the risk factors in the sustainability of the reservoir operation so it should be managed as well as possible through the deepening of climate change and its impact on reservoir operation and management of natural resources as a whole. Climate change, which can lead to changes to the hydrological regime in this case decreasing annual flow may result in a decrease in the production of hydropower generation.

It has also been realized that the day the economic value of water is increasing, and water is not only seen as a social good as it is mentioned in the principle of integrated natural resources management (GWP TAC, 2000). The management of natural resources (= Citarum cascade reservoir operation) is very unique considering the history of Jatiluhur reservoir management is based on the idealism to apply self-reliance in the management of natural resources as a whole, where the utilization of natural resources (water, water and water resources) can be used to fulfill the operational and maintenance of natural resources infrastructure although very limited.

More specifically, the equivalence of the amount of water for power generation for each hydropower unit is affected by the installed capacity and the falling height, $P = f(Q, H)$ with $Q = f(H)$. So for PLTA Saguling, Cirata, and Jatiluhur have their own characteristics of the economic value of water in the generation of electricity. Given the impacts of climate change that require the adaptation of reservoir operations to mitigate the impact, which has little impact on the economic value of hydropower generation, this should also be considered in the Citarum cascade reservoir operation as part of integrated natural resource management.

4.3 Alternative Adaptation and Optimization of Citarum Cascade Reservoir Operation.

The water reservoir in the reservoir contributes about 30% of the world's water availability. If the irregularities caused by climate change that affect the hydrological regime continue to increase, then access to water is decreasing which causes the higher levels of water shortage in the world (Berga, 2008). Adaptation to climate change in the form of initiatives and treatments aimed at reducing human and natural vulnerability in the face of the effects of climate change.

There are several potential handling that can be done, ie in the form of pure technology (eg infrastructure, storage, sea water defense, etc.), behavioral management (water conservation, productivity and water efficiency, changes in food and tourism patterns), management Integrated natural resources, alternative farming practices) to policy (eg, regulatory planning). In the SDA sector, this adaptation strategy can include adding water catchments to rainwater harvesting, conservation, water reuse, irrigation water efficiency to desalinization. Adaptive capacity is the ability of a system to adapt to climate change (including climate variability and hydrological regime change) to reduce potential damage, to take advantage of existing opportunities or to anticipate the consequences. In reservoirs with large capacity, changes in water availability are relatively smaller compared to systems with no small containers or containers. Therefore, reservoir operations on large systems are becoming stronger to changes in water availability, more resistant to the effects of climate change, and shelter acts as a buffer against climate change.

With the down-scaling, in the case of the Citarum cascade reservoir system where the largest reservoir is in the Jatiluhur reservoir, with a proportion of 56.8% of overall capacity, the capacity of the Citarum cascade reservoir adaptation is in

Jatiluhur reservoir. So in the Citarum cascade reservoir operation, Jatiluhur reservoir acts as a buffer against two reservoirs above it. This is contradictory to the principle of operation of reservoirs equal-sharing requiring a balance of clean containment proportions for each constant fixed reservoir and avoiding changes in water level in each reservoir to change drastically from month to month.

Changes in the operating principle of Citarum cascade reservoir will have implications for the economic potential value generated from electricity generation. Therefore, in accordance with the idealism in the management of natural resources in the Citarum River Region unit to achieve independence, the economic value of water must be accommodated in the Citarum cascade reservoir operation. At the present stage, the adaptation of Citarum's cascade reservoir operation to reduce the impact of climate change is done by optimizing the capacity of the container to hold water in the wet season as much as possible in the dry season but by providing space for flood control.

In addition to water availability adaptation, adaptation of water needs through on-demand irrigation management and improved rainwater catchment conditions to improve retention capacity as well as efforts to hold water forever in the area upstream activities such as increasing capacity through the construction of water catchments to rainwater harvesting and water reuse.

CONCLUSION

Climate change is a world problem and one way to reduce the impact of climate change is by using renewable energy sources, such as hydropower. On the contrary, with the influence of climate change, especially on hydrological regimes that are closely linked in reservoir operations, the operation of the reservoir needs to be strengthened by considering these conditions in its operations to reduce its impact. Climate change must be understood as one of the business risks that can result in the decline in electricity production. This should also be considered in terms of operation and management of reservoirs.

The hydrological regime in the Citarum River is changing, as indicated by the higher flow rate fluctuation and the higher coefficient of run-off and the indication of seasonal leap, the longer the dry season, the shorter rain time with the greater intensity requires that adaptation of Citarum cascade reservoir operation to mitigate the impacts of climate change, by optimizing the capacity of containers to hold water in the wet season as much as possible for the needs in the dry season but by providing space for flood control.

The greatest capacity of Ir. H. Djuanda dam reservoirs is the value of adaptation capacity in the Citarum cascade reservoir operation so that in the Citarum cascade reservoir operation, Ir. H. Djuanda reservoir acts as a buffer against two reservoirs above it. Adaptation of water demand through on-demand irrigation management and improved rainwater catchment conditions to increase retention capacity as well as efforts to hold water forever in upstream areas such as increasing capacity through the construction of water catchments up to rainwater harvesting and water reuse.

REFERENCE

- [1] BERGA, LUIS. The role of dams and reservoirs in adapting to climate change. The international journal on Hydropower and dams. 2008.
- [2] BREWSTER, M., F. LING, AND M. CONNARTY. Climate change response from a renewable electricity business. The international journal on Hydropower and dams. 2008.
- [3] IDRUS, H AND E. MURNIATI. Jatiluhur hydropower plant operation and maintenance under severe environmental conditions. The international journal on Hydropower and dams. 2008.
- [4] IDRUS, HERMAN., TJAHJONO, NOOR., WISNU, I GUSTI NGURAH., MURNIATI, E, Operasi waduk kaskade Citarum dalam upaya mengantisipasi dan mengurangi dampak perubahan iklim. Seminar Komite Nasional Indonesia untuk Bendungan Besar. 2009.
- [5] JAVORNIK, LUKA AND Z. STOJIC. The role of renewable hydropower energy in the climate change perspective. The international journal on Hydropower and dams. 2008.
- [6] UNDP INDONESIA. The other half of climate change. Why Indonesia must adapt to protect poorest people. 2007.
- [7] VAN BLOMMESTEIN, PROF. Dr. Ir. W.J. EEN FEDERAAL WELVAARTSPLAN. Voor het westelijk gedeelte van Java. De Ingenieur in Indonesie. 16 Jaargang Nummer 5. Jun 1949.
- [8] VAN DER WEERT, ROB. Hydrological conditions in Indonesia. Delft Hydraulics. 1994.

COMMISSION INTERNATIONALE
DES GRANDS BARRAGES

VINGT-SIXIÈME CONGRÈS DES
GRANDS BARRAGES
Autriche, juillet 2018

DETERMINATION OF GERMİ CHAY DAM RESERVOIR SEDIMENTATION PROCESS

S. SHAHRADFAR

Expert of Dam department, ASHENAB CONSULTING ENGINEERS

SH. PARTOVI AZAR

Expert of Dam department, ASHENAB CONSULTING ENGINEERS

S. AHMADI ADLI

*M.Sc Student of Water Structures Engineering, FACULTY OF AGRICULTURAL
ENGINEERING, TABRIZ UNIVERSITY*

IRAN

1. INTRODUCTION

Prediction of sediment distribution in reservoirs is an important issue for dam designers to determine the reservoir active storage capacity, outlet sill elevation, dam stability, recreational facilities, and backwater conditions. A lot of methods such as physical, mathematical and experimental models are provided in this field. One of the most important experimental methods to study sediment distribution in the reservoir is area reduction method. Several mathematical models for predicting reservoir sedimentation have been developed based on the equations of motion and continuity for water and sediment. Some of these models have additional specific features such as the GSTARS which is developed Molinas and Yang (1986). In this research, GSTARS3 sediment transport model and areareduction method was used to simulate sedimentation processes in Germi Chay dam reservoir. Germi chai dam is a multi-purpose earth-fill dam with central clay core

which has been constructed on Ghermi chai river in the northwest of Iran. Sediment distribution in various reservoir levels is computed and Area-Volume-Height curves for period of 80 years through previously mentioned methods are computed, drawn and compared.

2. DISCUSSION AND CONCLUSION

GSTARS3 sediment transport model was used in this study to predict sediment load from the watershed discharged to reservoir. In order to study the problem and calibrate the models, the results are compared with the experimental method of reducing the level. The results of the experimental method of Area Reduction can be reliable, especially at high reservoir levels. The comparison graphs of Volume-Elevation and Area-Elevation before and after simulation (after a 80-year sedimentation period) are shown in Fig.1 to 2.

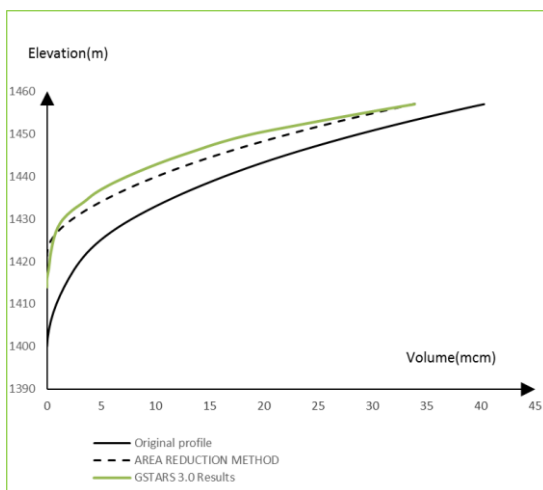


Fig. 1

Volume-Elevation graphs before and after simulation (after a 80-year sedimentation) period

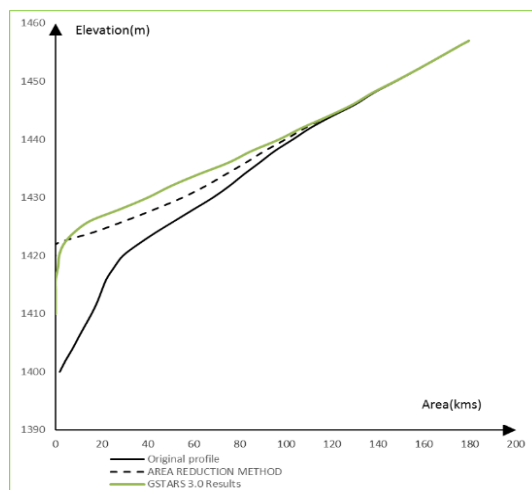


Fig. 2

Area-Elevation graphs before and after simulation (after a 80-year sedimentation) period

According to the research, the Area Reduction Method to estimate the sedimentation in the reservoir of Garmi Chay dam is a priority. Considering that this method can not predict the exact model of sedimentation in the reservoir of the dam such as longitudinal profile, bottom line of reservoir and sedimentation in different sections of the dam reservoir, this is done using the GSTARS3.0 Model.

Comparison of the results of the software in the single-dimensional model and the experimental method of Area Reduction in the low levels of the dam reservoir indicates that the GSTARS 3.0 model is inaccurate near the dam body and transfers a significant amount of sediment input to the outside of the study area.

COMMISSION INTERNATIONALE DES GRANDS BARRAGES

VINGT-SIXIÈME CONGRÈS DES GRANDS BARRAGES
Autriche, juillet 2018

DOI 10.3217/978-3-85125-620-8-040



This work licensed under a Creative Commons Attribution 4.0 International License. <https://creativecommons.org/licenses/by-nc-nd/4.0/>

**NUMERICAL SIMULATION OF THE MORPHODYNAMIC CHANGES BY
SEDIMENT SUPPLY AT THE DOWNSTREAM OF YOUNGJU DAM**

Chang-Lae JANG

DEPARTMENT OF CIVIL ENGINEERING, KOREA NATIONAL UNIVERSITY OF
TRANSPORTATION

KOREA

Ki-Ho KANG

*Head of the Institute of Hydraulic Engineering and Water Resources
Management, K-WATER*

KOREA

Kwanusue JUNG

DEPARTMENT OF CIVIL ENGINEERING, CHUNGNAM NATIONAL
UNIVERSITY

KOREA

COMMISSION INTERNATIONALE
DES GRANDS BARRAGES

VINGT-SIXIÈME CONGRÈS DES
GRANDS BARRAGES
Autriche, juillet 2018

**NUMERICAL SIMULATION OF THE MORPHODYNAMIC CHANGES BY
SEDIMENT SUPPLY AT THE DOWNSTREAM OF YOUNGJU DAM***

Chang-Lae JANG

*Department of Civil Engineering, KOREA NATIONAL UNIVERSITY OF
TRANSPORTATION*

KOREA

Ki-Ho KANG

*Head of the Institute of Hydraulic Engineering and Water Resources
Management, K-WATER*

KOREA

Kwanusue JUNG

Department of Civil Engineering, CHUNGNAM NATIONAL UNIVERSITY

KOREA

1. INTRODUCTION

River restoration can involve various methods, from the management of a riverbed for ecosystem recovery to the positive improvement of river channels and

* *titre de l'article complet*

flood plains. The river restoration methods of which the discharge is controlled by a dam upstream include flexible dam operation for flood control including artificial flooding (Kondolf and Wilcock, 1996), a dam removal that has lost its functions and improvement of sediment transport through sediment supply to the dam downstream (Gaeuman, 2014). River restoration improves the river morphology, or reproduces flood plains to connect the river with the protected lower channel habitats or to increase the flood frequency of the flood plains, increasing the diversity of the habitats (Gaeuman, 2014). For a river where the sediment is trapped by a dam, sediment supply to the river upstream is the most common restoration project (Bunte, 2004). Reduction of the sediment inflow in the river by a dam construction upstream may change the geomorphic features of the river or disturb the ecosystem habitats in the dam downstream, affecting the aquatic ecosystem. Decrease of the sediment supply to a dam downstream lowers the bed elevation, changes the sediment size in the bed, separates gravel from fine sediment to form an armored layer and spreads the layer to the downstream. Sediment can be supplied to a river through various methods, and the specific implementation method is determined by following the major objectives of the sediment supply. Bunte (2004) proposed the sediment supply method of placing pebble piles in a river during a dry season before a flood event, in which the sediment supplied to a river may be immediately swept by a flood to the river downstream. Recently, various methods have been employed in South Korea to improve the river environment in dams downstream. In particular, methods of sediment supply have been prepared to improve the river environment by supplying sediment to dams downstream. In this study, a numerical simulation was conducted to investigate the efficiency of the plans as a preliminary study. The effect of sediment supply was evaluated in the Naeseongcheon Stream under discharge conditions that were dependent on the dam operation.

2. NUMERICAL MODEL

This study used a physical-based morphodynamic model, Nays2DH, developed by Shimizu(Iwasaki et al., 2015). This model solves the two-dimensional depth-averaged flow equations and calculates sediment transport and sediment sorting, and geomorphic changes considering bank erosion and vegetation. This model has been applied in various rivers.

A numerical model is applied to simulate flow field. The governing equations, *i.e.*, the continuity and momentum equations, for water flow are transformed from the Cartesian coordinate system into boundary fitted coordinate system.

Continuity equation:

$$\frac{\partial}{\partial t} \left(\frac{h}{J} \right) + \frac{\partial}{\partial \xi} \left(\frac{hu^\xi}{J} \right) + \frac{\partial}{\partial \eta} \left(\frac{hu^\eta}{J} \right) = 0 \quad (1)$$

Momentum equations in the ξ and η directions:

$$\begin{aligned}
& \frac{\partial u^\xi}{\partial t} + u^\xi \frac{\partial u^\xi}{\partial \xi} + u^\eta \frac{\partial u^\xi}{\partial \eta} + \alpha_1 u^\xi u^\xi + \alpha_2 u^\xi u^\eta + \alpha_3 u^\eta u^\eta \\
& = -g \left[(\xi_x^2 + \xi_y^2) \frac{\partial H}{\partial \xi} (\xi_x \eta_x + \xi_y \eta_y) \frac{\partial H}{\partial \eta} \right] - \frac{C_f u^\xi}{hJ} \sqrt{(\eta_y u^\xi - \xi_y u^\eta)^2 + (-\eta_x u^\xi - \xi_x u^\eta)^2} \\
& + \frac{\partial}{\partial \xi} \left(v_i \xi_r^2 \frac{\partial u^\xi}{\partial \xi} \right) + \frac{\partial}{\partial \eta} \left(v_i \eta_r^2 \frac{\partial u^\xi}{\partial \eta} \right) - \frac{F^\xi}{\rho h}
\end{aligned} \quad (2)$$

$$\begin{aligned}
& \frac{\partial u^\eta}{\partial t} + u^\xi \frac{\partial u^\eta}{\partial \xi} + u^\eta \frac{\partial u^\eta}{\partial \eta} + \alpha_4 u^\xi u^\xi + \alpha_5 u^\xi u^\eta + \alpha_6 u^\eta u^\eta \\
& = -g \left[(\eta_x^2 + \eta_y^2) \frac{\partial H}{\partial \eta} (\xi_x \eta_x + \xi_y \eta_y) \frac{\partial H}{\partial \xi} \right] - \frac{C_f u^\eta}{hJ} \sqrt{(\eta_y u^\xi - \xi_y u^\eta)^2 + (-\eta_x u^\xi - \xi_x u^\eta)^2} \\
& + \frac{\partial}{\partial \xi} \left(v_i \xi_r^2 \frac{\partial u^\eta}{\partial \xi} \right) + \frac{\partial}{\partial \eta} \left(v_i \eta_r^2 \frac{\partial u^\eta}{\partial \eta} \right) - \frac{F^\eta}{\rho h}
\end{aligned} \quad (3)$$

In these equations, ξ and η = the spatial coordinate components in the boundary fitted curvilinear coordinate system; t = the time coordinate in the coordinate system; J = Jacobian of the coordinate transformation given as $J = \tau_x \xi_x \eta_y + \xi_x \tau_y \eta_y + \eta_x \tau_x \xi_y - (\eta_x \xi_x \tau_y + \xi_x \tau_x \eta_y + \tau_x \xi_y \eta_x)$; u^ξ and u^η = contravariant components of the depth-averaged flow velocity in the ξ and η directions, respectively, defined as $u^\xi = \xi_x u + \xi_y v$ and $u^\eta = \eta_x u + \eta_y v$; u and v = the depth averaged velocity components in x and y directions, respectively. The coefficients $\alpha_1 \sim \alpha_6$ are given in Jang and Shimizu (2005).

The morphodynamic module of Nays2DH includes sediment transport, bank erosion, and bed elevation changes. The two-dimensional sediment continuity equation in boundary-fitted coordinate system is as follows:

$$\frac{\partial}{\partial t} \left(\frac{z_b}{J} \right) + \frac{1}{1-\lambda} \left[\frac{\partial}{\partial \xi} \left(\frac{q_b^\xi}{J} \right) + \frac{\partial}{\partial \eta} \left(\frac{q_b^\eta}{J} \right) \right] = 0 \quad (4)$$

where z_b = bed elevation; λ = porosity of the bed material; q_b^ξ and q_b^η = contravariant components of the bedload transport rate per unit width in the ξ and η directions, respectively.

The sediment transport rate in the stream line is calculated using the formula of Ashida and Michiue (1972). As a numerical scheme, the cubic interpolated pseudoparticle (CIP) method is used. The numerical method solves boundary problems while introducing little numerical diffusion, and algorithm implementation is more straightforward than for other high-order upwind. In the non-advection phase, the continuity equation and the non-advection terms in the momentum equations are solved for depth as a Poisson equation. The viscous terms are approximated using the central difference method. Readers are referred to Jang and Shimizu (2005) for more details.

3. APPLICABILITY OF NUMERICAL MODEL

The numerical model was validated by using the experimental result provided by Cui *et al.* (2003) who conducted experiments to investigate how the sediment supplied to a channel as discontinuous pulses were moved to the downstream of the channel. The channel was 45 m long, 0.5 m wide, and 0.7 m deep. The slope was 0.0108, the discharge was 0.009 m³/s, the water depth was 0.0325 m, and the velocity was 0.55 m/s. The sediment pulse, 7.5 cm long and 3.5 cm high, was placed at 8 m away from the inlet of the channel where the sediment was supplied toward the downstream of the channel. The median size of the sediment (D_{50}) was 2.0 mm with the geometric mean of 1.83 mm (Run-2).

Fig. 1 shows the change of the sediment discharge over time. After four minutes of the simulation, a large amount of the sediment was discharged from the sediment pulse. As time passed, the sediment discharge from the pulse decreased. The sediment spread to the downstream of the channel. Alternate bars were developed and migrated to the downstream of the channel. The bars were dissipated at one hour and six minutes. This complies with the experimental results.

Fig. 2 shows the comparison of longitudinal bed changes between numerical and experimental results. At four minutes, the bed elevation at the sediment pulse decreased dramatically, and the sediment was transported to the downstream of the channel (Fig. 2(b)). At 18 minutes, the bed elevation at the sediment pulse decreased and the sediment was gradually diffused to the downstream (Fig. 2(c)). After more time passed, the bed reached an equilibrium state (Figs. 2(d)). The transport and diffusion of the sediment pulse found in the experiment was well simulated numerically.

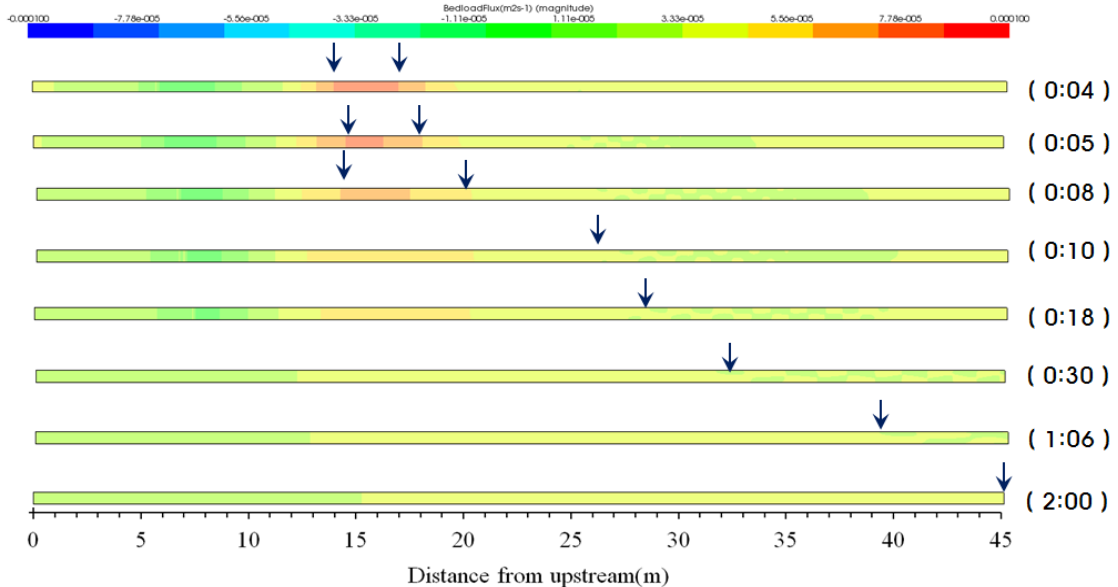


Fig. 1 Numerical results of sediment discharge changes with time for Run-2: The Times are in (hour:min)

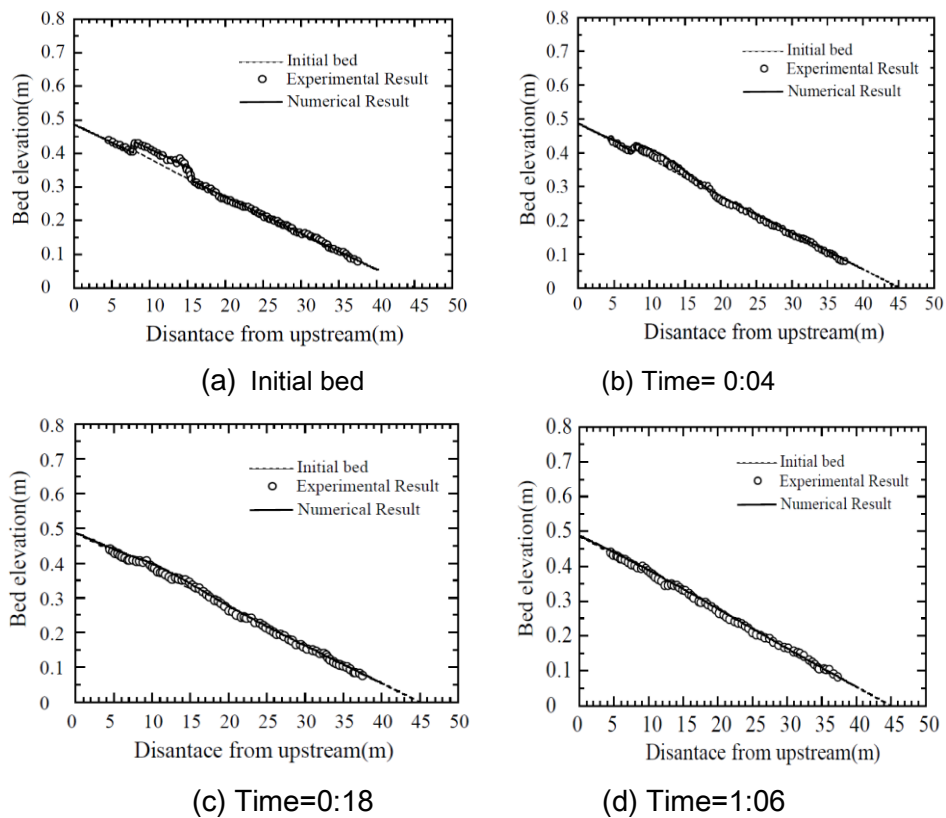


Fig. 2 Comparison of longitudinal bed changes between numerical and experimental results: times are written as (hour:min).

4. ANALYSIS OF RIVER CHANGES BY SEDIMENT SUPPLY IN NAESONGCHEON RIVER DOWNSTREAM OF YOUNGJU DAM

4.1 NUMERICAL CONDITION

To supply sediment effectively for improving the river environments at a dam downstream, the spatial range and location, the sediment supply method, and the quantity and size of the supplied sediment should be determined. Locations of sediment supply are determined as a riffle with a sufficient flow where the tractive force may be easily secured, or as a curved region in which a secondary flow is generated to increase the effect of the sediment supply and improve the river environment.

The numerical model was applied to the Yeongju Dam downstream. The Yeongju Dam is located at the Naeseongcheon River upstream, which is the first tributary of the Nakdong River (Fig. 3). The curved regions, No. 1 and No. 2, were chosen as the sediment supply locations (Fig. 3). Secondary flow at meandering channel is generated in the immediate downstream of Yeongju Dam, No. 1. No. 2

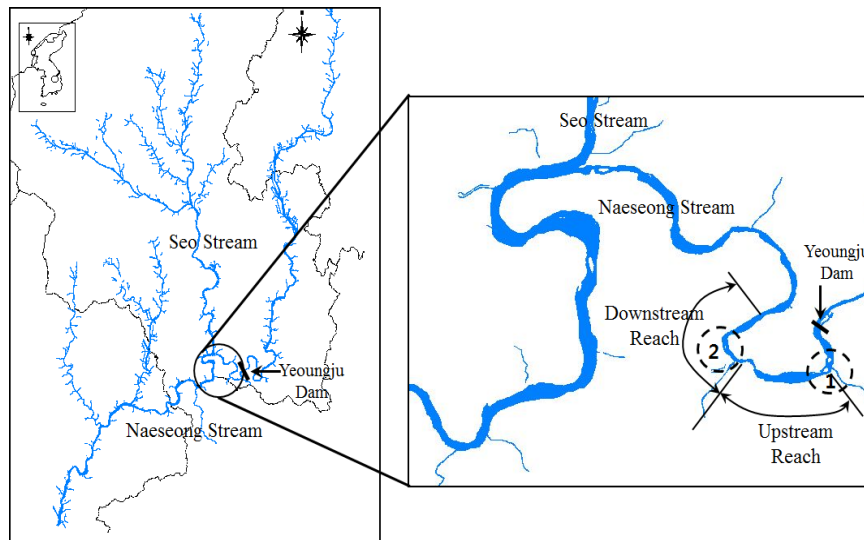


Fig. 3 Location map of study area

is about 1 km downstream from the Yeongju Dam (Fig. 3). At No. 1, the bed slope was 0.0026 and the channel width was 86.5 m. At No. 2, the bed slope was 0.0012 and the width was 112.3 m.

The channel is significantly changed at a bankfull discharge where the water overflows the lower channel and starts to fill the flood plain. Therefore, for the sediment supply to the dam downstream, a bankfull discharge of 9.00 m³/s, calculated using HEC-RAS, was applied to the study reach. In addition, the effect of sediment supply was analyzed at the discharge of 15.13 m³/s, considering the discharge from the dam.

4.2 COMPUTATIONAL CONDITIONS

A two-dimensional numerical model, Nays2DH, was employed to simulate the effect of the sediment supply to the dam downstream. Table 1 shows the hydraulic conditions for the numerical simulation. The length of the river was 10 km, and the bed slope was 0.001. The mean diameter of the sediment was 4.61 mm. The Manning's n value was set to 0.031. The time step for the numerical calculation was 0.01 seconds. Considering the geographic effects of the relatively steep slope and the serpentine flow, the grid size was set to 0.2 m in the flow direction and 0.1 m in the transverse direction. To investigate the channel changes,

Table 1 Parameters for numerical simulation

Case	Discharge (m ³ /s)	Sediment inflow condition	Remarks
Run-1	9.00	Trap efficiency : 98.7%	Bankfull discharge
Run-2	15.13	Trap efficiency : 98.7%	Water supply

the amount of sediment supply was determined by considering the trapped sediment by the dam.

4.3 NUMERICAL RESULTS

Fig. 4 shows the planimetric changes of the bed for Run-2. In the immediate downstream of the dam, the flow focused on the left bank where the bed elevation decreased. The area corresponded to No. 1 where the sediment placed in the dam downstream. The sediment transported to the river downstream. However, as the flow was dispersed in the straight reach, the bed elevation increased. The bed elevation decreased at No. 2. While the bed elevation decreased in the outer part of the curved region downstream, the elevation increased in the inner part of the meandering reach.

Fig. 5 shows the cross-sectional changes at 400 m and 600 m downstream for Run-2. At 400 m downstream, the bed elevation decreased over time. About 10 hours later, the bed elevation decreased at the center of the river and in the right bank (Fig. 5(a)). The bed decreased initially at the center of the channel, and then the bed scoured in the right bank also as the flow focused on the outer part of the curved region (Fig. 5). The sediment was deposited at the center of the river at 600 m.

Fig. 6 and 7 show the comparison results of the bed changes between Run-1 and Run-2. At No. 1 and No. 2, the bed elevation changed over time, and the change was greater in Run-2 than in Run-1. In other words, the change in the bed elevation was greater at a higher discharge. The numerical results showed that the

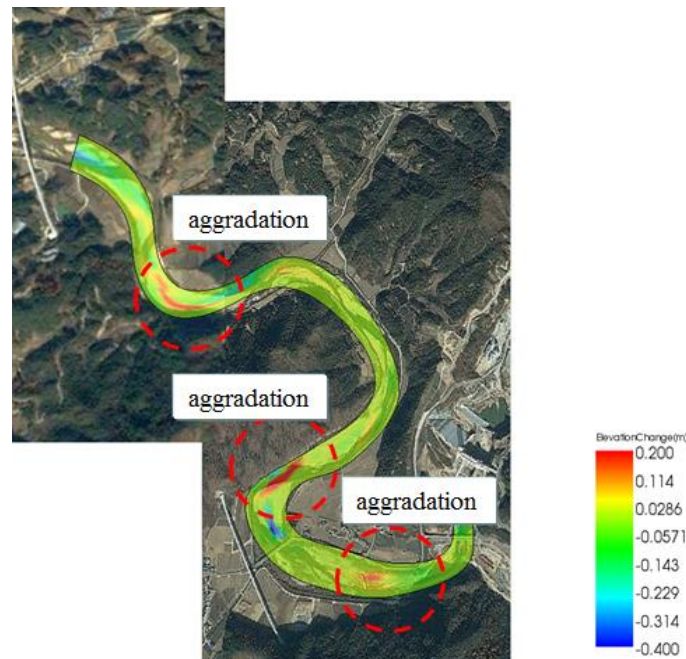
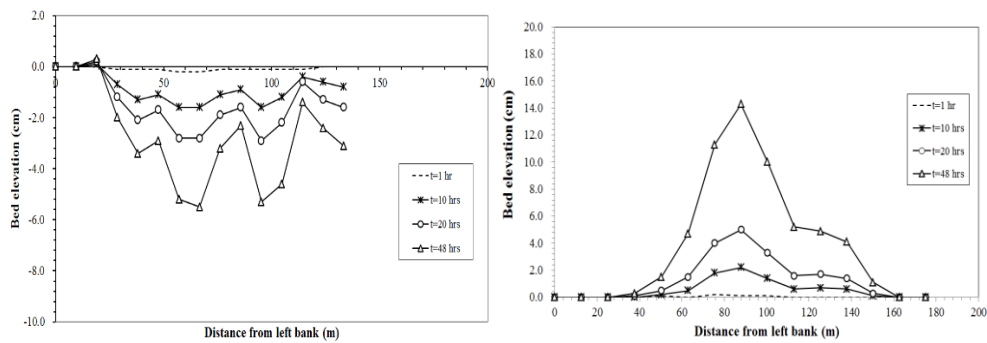


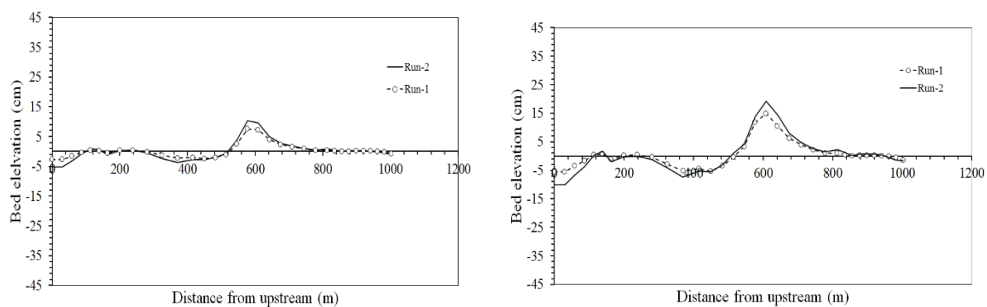
Fig. 4 Planimetric changes for Run-2



(a) At 400m from inlet

(b) At 600m from inlet

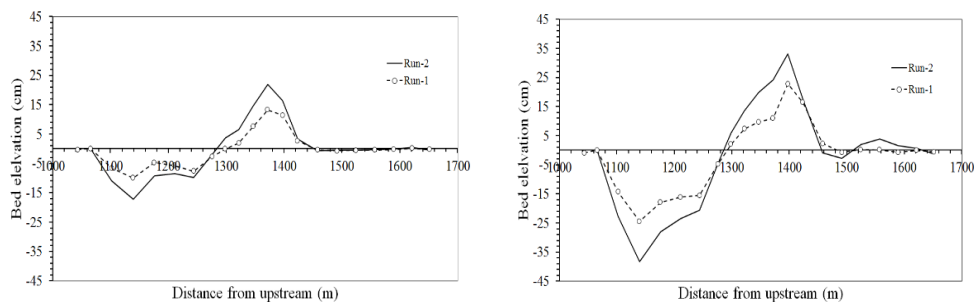
Fig. 5 Cross sectional changes for Run-2



(a) T=20 hrs

(b) T=48hrs

Fig. 6 Bed elevation changes with time for each run in the immediate downstream of the dam



(a) T=20 hrs

(b) T=48hrs

Fig. 7 Bed elevation changes with time for each run at the downstream reach

increasing the discharge from the dam developed the geomorphic diversity of the channel to enhance the effect of the sediment supply on the river in the dam downstream.

Bed Relief Index (BRI) was calculated in order to quantitatively understand the cross-sectional change of the bed. BRI represents the standard deviation at the mean bed elevation. BRI was calculated based on the bed elevation data at

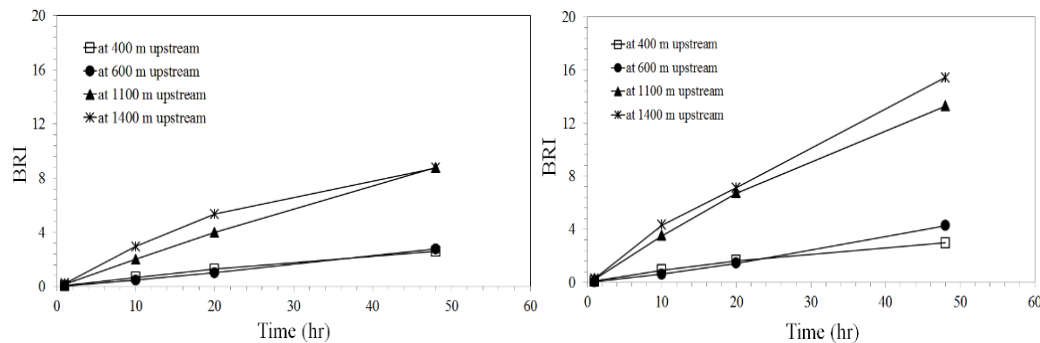
the individual cross-sections, using the following equation (Hoey and Sutherland, 1991):

$$BRI = \frac{\left(\sum_{i=1}^{n-1} \left[\frac{(z_i^2 + z_{i+1}^2)}{2} \right]^{0.50} [x_{i+1} - x_i] \right)}{(x_n - x_1)} \quad (14)$$

where x denotes the transverse distance from the left bank to the i position, and z is the difference between the bed elevation at the i position (z_i) and the mean bed elevation. Fig. 8 shows the change of BRI for each run. BRI increased in both Runs-1 and 2 with time. BRI was great in the areas where the bed scoured and the sediment deposited, indicating that the change in the bed elevation was significant and dynamic. BRI was greater in Run-2 where discharge was 15.13 m³/s than in Run-1 where discharge was 9.00 m³/s. In addition, BRI was greater at the 1,100 m and 1,400 m downstream at No. 2 than at the 400 m and 600 m at No. 1. This showed that a higher discharge enhanced the dynamics of the bed with the sediment supply upstream, and that the river was more dynamic at the 1,400 m downstream at No. 2 than in the immediate downstream of the dam, being affected more by the sediment supply.

5. CONCLUSIONS

In this study, a numerical simulation has been conducted to investigate the efficiency of the plans as a preliminary study. The effect of sediment supply was evaluated in the Naeseongcheon Stream under discharge conditions that were dependent on the dam operation. The sediment supply location candidates determined as a riffle or as a curved region where the secondary flow is formed to effectively perform sediment supply. The bed elevation in the immediate downstream of the dam decreased over time. In addition, as time passed, the sediment pulse scoured and moved to the downstream of the channel, and then deposited at positions where the flow velocity decreased. BRI, representing the dynamics of the bed, increased with time, and was found to be greater in the channel downstream than upstream. In addition, as discharge increased, BRI increased because the higher discharge



(a) Run-1 (b) Run-2
Fig. 8 Bed relief Index (BRI) for each run

had a greater effect on the bed, increasing the dynamics of the river channel.

This study showed that a higher discharge enhanced the dynamics of the bed with the sediment supply upstream, and that the river was more dynamic at the downstream of the channel than in the immediate downstream of the dam, being affected more by the sediment supply. This study has some limitations to a review of the efficiency of the sediment supply method through a numerical simulation. A study on the actual implementation of the sediment supply method should be conducted in future research.

ACKNOWLEDGEMENTS

This research was supported by Basic Science Research Program through the National Research Foundation of Korea(NRF) funded by the Ministry of Education (NRF-2017R1D1A1B03032083).

REFERENCES

- [1] ASHIAD K., MICHUE M. Study on hydraulic resistance and bedload transport rate in alluvial streams, Proc., JSCE, 206, pp. 59-69. 1972
- [2] BUNTE K. Gravel mitigation and augmentation below hydroelectric dams: a geomorphological perspective. Report to the Stream Systems Technology Center, USDA, Forest Service, Rocky Mountain Research Station, Fort Collins, CO. 2004.
- [3] CUI Y., PARKER G., LISLE T.E., GOTT J., HANSLER-BALL M.E., PIZZUTO J.E., ALLMENDINGER N., REED J.M. Sediment pulses in mountain rivers: 1. Experiments, Water Resour. Res., 39(9), 1239, doi:10.1029/2002WR001803. 2003.
- [4] GAEUMAN D. Mitigating downstream effects of dams. In Gravel-Bed Rivers: Processes, Tools, Environments, Church M, Biron P, Roy AG(eds), John Wiley and Sons: Chichester, 563. 2012.
- [5] HOEY T. B., SUTHERLAND A. J. Channel morphology and bedload pulses in braided rivers: A laboratory study. Earth Surf. Process. Landforms. Vol. 16, pp. 447-462. 1991.
- [6] IWASKI T., SHIMIZU Y., KIMURA I. Numerical simulation of bar and bank erosion in a vegetated floodplain: A case study in the Otofuke River, *Advances in Water Resources*, doi:10.1016/j.advwatres.2015.02.001. 2015.
- [7] JANG C.-L., SHIMIZU Y. Numerical simulation of relatively wide, shallow channels with erodible banks. Journal of Hydraulic Engineering, 131(7), pp. 565-575. 2005.

- [8] KONDOLF G.M., WILCOCKP.R. The flushing flow problem: Defining and evaluating objectives. *Water Resour. Res.*, vol. 32, 2589-2599.1996.

COMMISSION INTERNATIONALE DES GRANDS BARRAGES

VINGT-SIXIÈME CONGRÈS DES GRANDS BARRAGES
Autriche, juillet 2018

DOI 10.3217/978-3-85125-620-8-041



This work licensed under a Creative Commons Attribution 4.0 International License. <https://creativecommons.org/licenses/by-nc-nd/4.0/>

**ASSESSMENT OF OPERATIONAL PERFORMANCE AND RISKS
CONSIDERING THE EFFECT OF CLIMATE CHANGE ON THE TIBETAN
PLATEAU**

Helmut WENZEL

*Head of the Monitoring and Asset Management Group, VIENNA UNIVERSITY
OF APPLIED SCIENCES (BOKU)*

AUSTRIA

Jia-xiu YANG

*Deputy general manager of POWERCHINA GUIYANG ENGINEERING
CORPORATION LIMITED*

CHINA

Ji LU

*Head of Engineering Safety Research and Development Dept., Science and
Technology R & D Center, HUANENG LANCANG RIVER HYDROPOWER INC.*

CHINA

Barbara Theilen-Willige

INSTITUTE OF APPLIED GEOSCIENCES, TECHNICAL UNIVERSITY BERLIN
(TUB)

GERMANY

ASSESSMENT OF OPERATIONAL PERFORMANCE AND RISKS CONSIDERING THE EFFECT OF CLIMATE CHANGE ON THE TIBETAN PLATEAU

PROF. DR. HELMUT WENZEL

*Head of the Monitoring and Asset Management Group, VIENNA
UNIVERSITY OF APPLIED SCIENCES (BOKU)*

MR. JIA-XIU YANG

*Deputy general manager of POWERCHINA GUIYANG ENGINEERING
CORPORATION LIMITED*

MR. JI LU

*Head of Engineering Safety Research and Development Dept., Science
and Technology R & D Center, HUANENG LANCANG RIVER HYDROPOWER INC.*

PROF. DR. HABIL.. BARBARA THEILEN-WILLIGE

Institute of Applied Geosciences, TECHNICAL UNIVERSITY BERLIN (TUB)

AUSTRIA, CHINA, GERMANY

1. INTRODUCTION

Reservoirs in mountainous regions are built for many generations to come. Climate change will definitely be a factor of decisive order. In consequence assessing performance and risk of a hydropower plant, it becomes necessary to quantify the impact of climate change. A methodology is proposed which allows the mathematical formulation of changes of performance over time.

2. QUANTIFICATION OF PAST CHANGES AND PREDICTIONS

The archives of LANDSAT, IKONOS, Sentinel and RapidEye images cover a period of 40 years. In case that sufficient satellite images are available, changes within that period can be identified. The following phenomena have been studied:

- Retreat of glaciers and related changes in the creeks
- Indicators for the change in permafrost expressed in debris flow starting at higher elevations
- Changes in shape and volume of natural lakes and ponds
- Changes in vegetation, particularly the lower and upper tree lines
- Changes in vegetation density and character

- Traces of events that happened in the observation period including forming relevant statistics
- Changes in the riverbed and its contributories

The fact that quality and resolution of images has changed over time has to be compensated. Software for change detection is readily available. Nevertheless, plausibility checks are always recommended. Rock falls and all kinds of sliding events receive priority in operational risk assessment.

3. CLIMATE CHANGE, INFLUENCE ON FLOOD AND RAINFALL

Flood risk and, generally speaking, disasters due to natural disasters is constantly increasing. Vulnerability itself tends to change over many areas, due to a range of climatic and non-climatic impacts whose relative importance is site-specific.

Climate-driven changes in future nature-caused disaster frequency are complex, because they depend on the generating mechanism. In many places, for instance, flood risk is likely to grow, due to a combination of anthropogenic and climatic factors. Recent modelling studies show that plausible climate change scenarios project future increases of both amplitude and frequency of natural-disaster events. It is very likely that there will be an almost ubiquitous increase in precipitation intensity in the warming world. Decreasing flood magnitudes, for instance, can be expected in many areas where floods are generated by spring snowmelt. However, global warming may not necessarily reduce snowmelt flooding everywhere.

Several ongoing land-use changes, such as urbanization, deforestation, and reduction of natural storage (floodplains, wetlands), can be regarded as adverse from the viewpoint of safety from nature-caused disasters. Furthermore, human encroachment into unsafe areas has increased the potential for damage. Societies become more exposed, developing disaster-prone areas (maladaptation).

In such a global change, mitigation of the risk disasters calls for a change from reactive to an anticipatory stance.

The warning point is that climate change will perhaps not change the real nature of natural disasters, but their intensity and frequency, thus increasing the risk itself (IPPC,2017).

As a matter of reference, we include the following picture which shows the shows an extreme heavy rainfall event that took place on Aug 15th, 2015 in the area of Eastern Tibet.

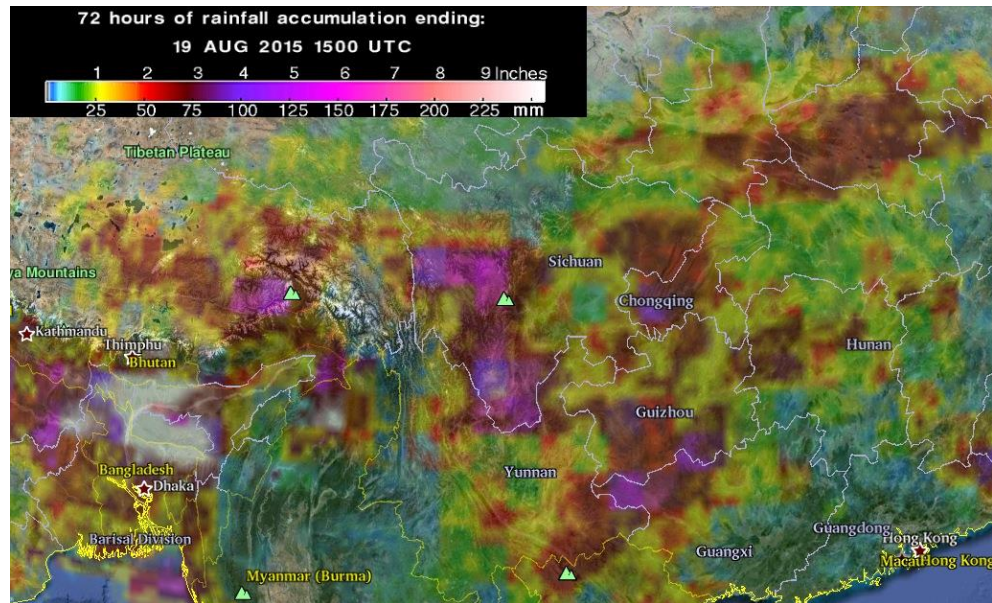


Fig. 1: 72 hours rain event: Extreme heavy rainfall event that took place on Aug 15th, 2015 in the area of Eastern Tibet

4. METHODOLOGY AND APPROACH

The interaction among earth-surface erosion, slope failure, tectonic uplift and the climate is a key issue to understand the processes of mass movements in the study area. The local stress condition is an important factor that may relate to uplift, erosion, deposition, and groundwater fluctuation (Xu, 2014 a and b).

The vertical motion and mechanism in Tibet is very complex: Several geodynamic processes control the complicated uplift pattern in the Tibetan Plateau, including the plate-tectonic movements, glacier isostatic adjustments and the mass loss related to the climate change conditions. The Tibetan Plateau located in central Asia is subject to the northward push from the Indian subcontinent and the collision with Eurasian plate, which results in East-West expulsion and uplift. The uplift rates of most part of the Tibetan Plateau range from 1 mm/yr to 2 mm/yr (Zhang & Jin, 2013). This general uplift also caused local fragmentation into blocks (kilometres or maximally, a few tens of kilometres) of local extent that have subsided and/or uplifted relative to one another. Alluvial deposition of the subsiding blocks contrasts with erosion and formation of gorges in the uplifted blocks. The question arises about the effects of tectonics in a relatively complex setting as drivers for the morphological development and the sedimentary architecture. The study region provides a framework of both regional tectonic uplift overprinted by tectonic movements of more local extent and changing over time.

Climate change will have an influence on precipitations (duration, intensity, frequency, distribution). The following Fig.4 provides an overview of the precipitation distribution during the last decades.

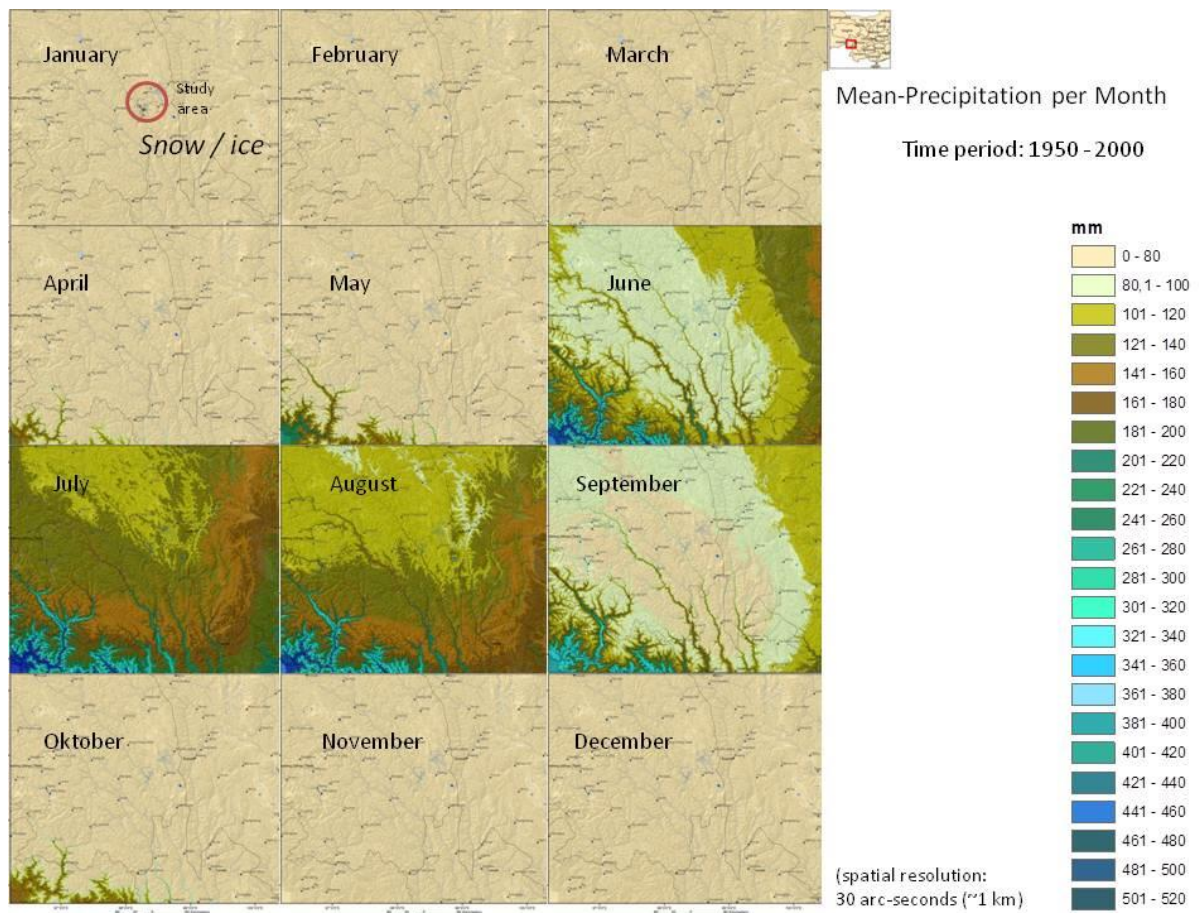


Fig.2: Monthly precipitations during 1950 – 2000 according to WorldClim – Global Climate Data (<http://www.worldclim.org/download>)

Many features in the high mountain environment such as glaciers, permafrost, vegetation or soil are very climate-sensitive and could experience large changes in the future. As a consequence, the potential starting zones for natural hazards, the dynamics of processes, and the areas potentially affected by natural hazards are likely to change as well. Therefore, the high mountains can be seen as a complex system in which various features react to the rising temperatures in different time scales and intensities. The rock glaciers are expected to thaw over the coming years and decades, posing a new threat of landslides in the avalanche starting zone. However, climatic change may be the most direct cause of terrace formation because hydrological dynamic parameters that dominate riverbed sediment aggradation and transportation (e.g., flux and flow velocity) are directly related to climatic conditions (Wang et al.,2008). Another important factor is the wind situation when considering luv and lee-effects of exposed slopes (sun and rain exposition). Therefore, the wind pattern and wind properties have to be monitored.

The monitoring of the seasonal development and changes of the vegetation forms an essential part in the scope of this research study. Although the impact of vegetation on slope stability in mountainous regions are understood and documented, it is difficult to predict how vegetation will impact mass movement processes, such as landslides and mudflows. Vegetation helps to stabilize slope materials by improving the resistance of slopes to both, surficial erosion and mass wasting. Vegetation survival environments are correlated with slope failure-formational environments. Thus, assessments of the spatial distribution of damaged vegetation and its recovery conditions are important for determining susceptible terrain and surface materials to mass movement processes.

The assemblage of trees and other vegetation growing above hillslopes plays an important role in intercepting slope materials and protecting them from the actions of sunshine, wind and rain. Vegetation, including the plant litter (leaves), helps stabilize the slope materials (1) by extensively altering the soil hydrology by reducing water loss and transpiration, intercepting raindrops and dissipating erosive energy and (2) by altering the mechanical and hydrological properties of the soil by affecting the developing root systems. Thus, vegetation improves resistance on slopes to surficial erosion and mass wasting, whereas the removal of slope vegetation tends to accelerate or increase slope failure. Gravity, flowing water, and temperature changes are the main (geomorphic) forces behind mass movement processes. The primary force that acts on mass movement is gravity. However, the substrate, environmental terrain and several additional factors can induce mass movement processes. Among these causative factors, vegetation affects the accumulation of slope material. The thickness of the material strongly affects the relative slope stability by supporting vegetation with stronger roots and influencing the effect of the subsurface on the overland flow. Hence, interactions between vegetation and materials affect mass movement processes (Zhang et al.,2015).

Vegetation requires water, sunshine, nutrients and specific air temperatures. All of these factors are controlled primarily by the local topographical environment and material properties. Elevation influences the air temperature, slope gradient affects the groundwater conditions, slope aspect controls the sunlight duration, and materials provide the nutrients. The topographical conditions influence mass movement processes, such as rockslides, creep and landslides, by affecting the force balance of the surface materials and providing potential energy.

The vegetation in the study area is mainly characterized by a grass, bush and low tree vegetation (Fig.3), whereby the vegetation is concentrated on the river terraces and in those flatter upper parts of the hills smoothed by glacial erosion. In the lower parts of the valleys debris flow, gully erosion, rockfall and landslides are leading to the decrease of vegetation occurrence and density.



Images: HydroChina Guiyang Engineering Corporation (GEC): Prefeasibility Study Report on Rumei Hydropower Station on Lancang River, Tibet Volume IV, Engineering Geology, May 2013

Fig.3: Vegetation in the study area

5. DIGITAL IMAGE PROCESSING

Different satellite data and image processing tools were tested in order to find out whether the satellite data can contribute to the detection of causal factors influencing the susceptibility to slope failure and to seasonal landscape monitoring. For a better overview of seasonal influences multi-temporal analysis of different satellite data has to be carried out, in combination with evaluations of long-term precipitation data, river water and groundwater table measurements in the field and further climate data (precipitation, temperature, wind). Precipitation data and groundwater table data are an important input when dealing with the seasonal influences on mass movements. The different satellite data and the workflow are presented in Fig.4. For the present study mainly Landsat- and RapidEye- images were used. The use of multi-temporal satellite remote sensing data opens up the opportunity for the development of efficient methods for systematic spatiotemporal mapping of landslides over large areas.

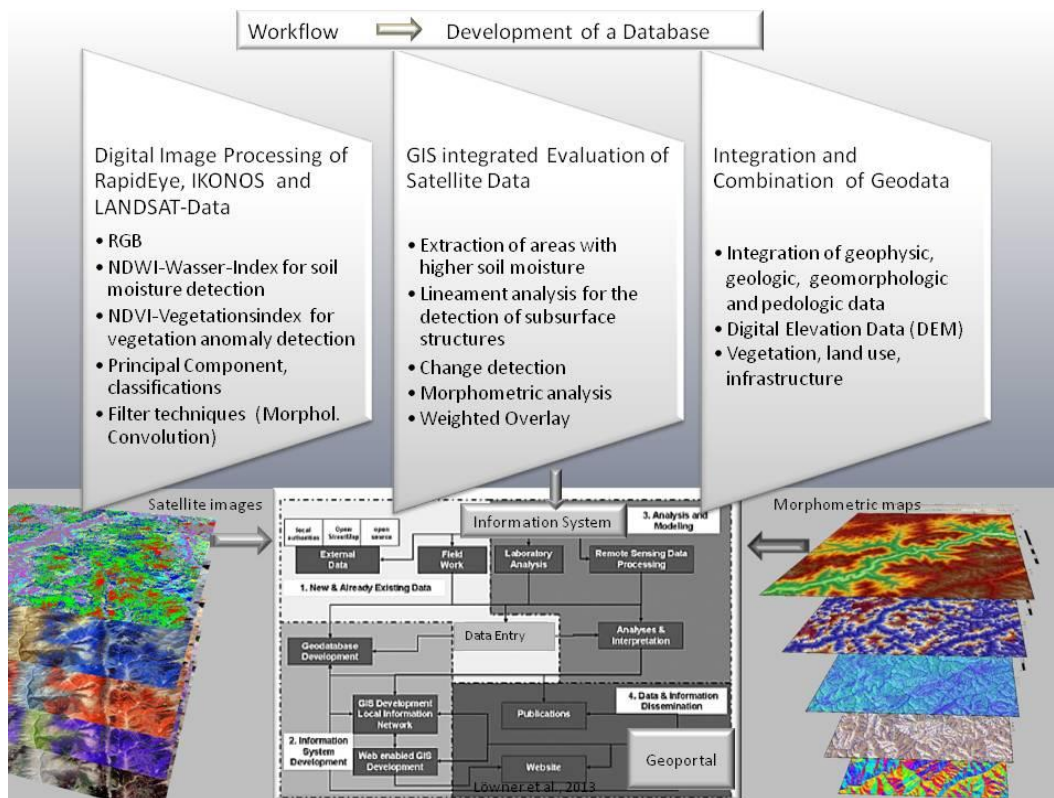


Fig. 4: Data and Workflow

The evaluation of Landsat time series is of special interest. By analysing the landscape development over 40 years environmental changes and future trends become visible. The research is focussed on the detection of the snow cover size and distribution and monitoring of trends (Figs.5 and 6). Unfortunately, many scenes are covered by clouds. This is the reason, why seasonal change detections are not possible for every year. Although cloud covers are a limiting factor for the evaluation of Landsat data, enough data are available to detect seasonal variations and long-term changes. Snow covered areas are classified based on the Landsat-images and then the areas with snow and ice-covers are calculated.

Change Detection of the Environment by Evaluations of Satellite Data available since 1972

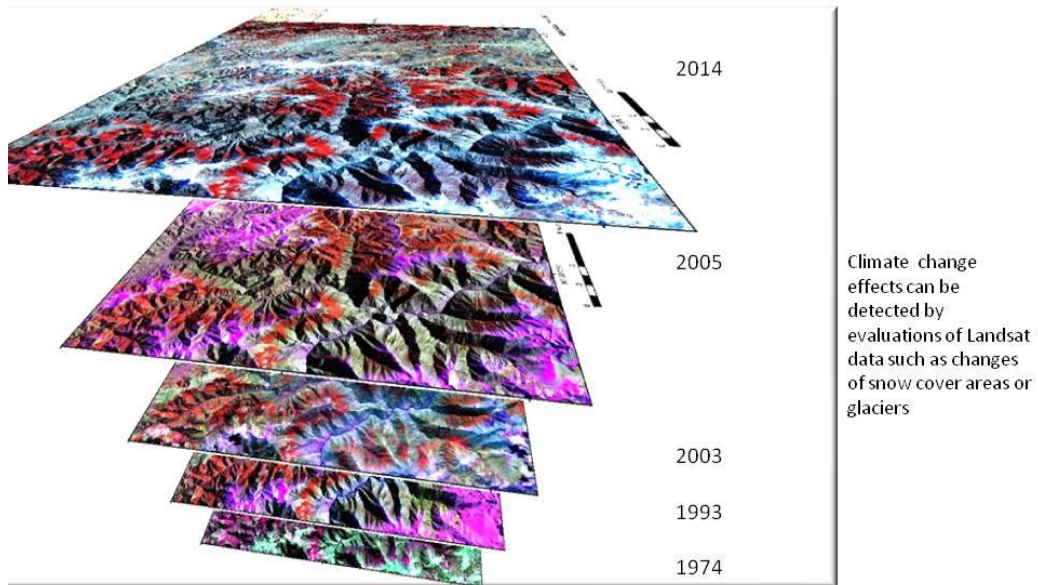


Fig.5 : Evaluation of time series of Landsat-images since 1974

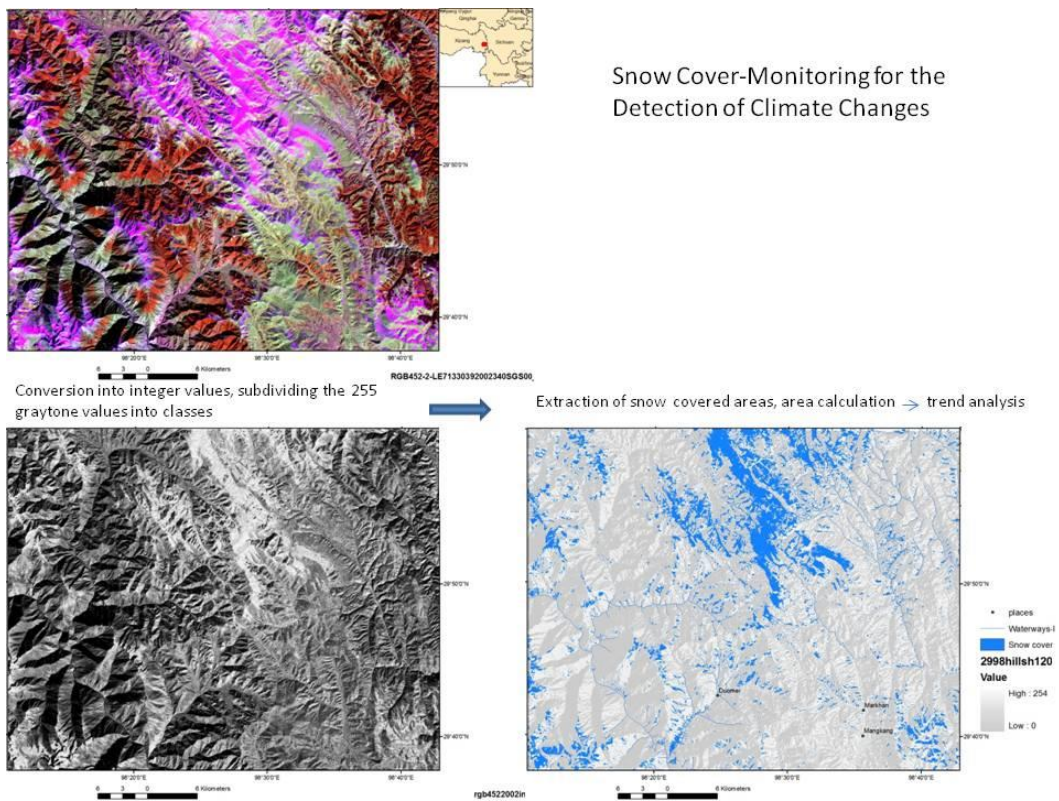


Fig.6: Snow cover detection

6. RISK ASSESSMENT

The methodology implied is oriented at available standards like ISO 31000 on the risk assessment framework and the latest development on risk-based operation in Europe. These approaches follow straightforward strategies consisting of:

- Identification of risks
- Modelling of each individual risk
- Identification of parameters and indicators driving the process
- Monitoring of parameters and indicators
- Periodic determination of changes in parameters and indicators with subsequent adjustment of risk

The entire procedure is organized in loops where the frequency of assessment depends on the magnitude of changes expected.

AKNOWLEDGEMENT

This work was supported by the Huaneng Technology Project (NHKJ15-H1)

REFERENCES

[1] Heller V., Hager W.H. and Minor H.-E. (2009) Landslide generated impulse waves in reservoirs: Basics and computation. Mitteilungen 211. Versuchsanstalt für Wasserbau Hydrologie und Glaziologie (VAW), R. Boes, ETH Zürich.

[2] „Dam building in Tibet increasing earthquake risks” by Yunnan Chen written on the 28.02.2014

[3] Developing Embankment Dam Fragilities For Emergency Modeling and Response, Prashar, Yiadom, Bialek,
<http://ussdams.com/proceedings/2012Proc/431.pdf>

[4] Large-Scale Floods Report: Lessons Learned and Best Practices for Flood Disaster Managers and Policy Makers, by Dr. Ali Chavoshian Prof. Kuniyoshi Takeuchi, 2011

[5] Intergovernmental Panel on Climate Change (IPCC). 2017. IPCC Fifth Assessment Report (AR5) Observed Climate Change Impacts Database, Version 2.01. Palisades, NY: NASA Socioeconomic Data and Applications Center (SEDAC). <https://doi.org/10.7927/H4FT8J0X>.

[6] Zhang, T.Y. & Jin, S.G. (2013): Estimate of glacial isostatic adjustment uplift rate in the Tibetan Plateau from GRACE and GIA models. *Journal of Geodynamics*, Vol.72, December 2013, 59–66, <http://www.sciencedirect.com/science/article/pii/S026437071300077X>

[7] Zhang, H., T. Chi, J. Fan, K. Hu and Yin Ling Pen (2015): Spatial Analysis of Wenchuan Earthquake-Damaged Vegetation in the Mountainous Basins Upstream of Minjiang River and its Applications. *Remote Sens.* 2015, 7(5), 5785-5804; doi: [10.3390/rs70505785](https://doi.org/10.3390/rs70505785)

[8] Xu, Ch. and Xu, X. (2014 a): The spatial distribution pattern of landslides triggered by the 20 April 2013 Lushan earthquake of China and its implication to identification of the seismogenic fault. *Chin. Sci. Bull.* (2014) 59(13):1416–1424

[9] Xu, Ch. (2014 b): Preparation of earthquake-triggered landslide inventory maps using remote sensing and GIS technologies: Principles and case studies. *Geoscience Frontiers*, 1-12, [10.1016/j.gsf.2014.03.004](https://doi.org/10.1016/j.gsf.2014.03.004)

[10] Wang, A., Smith, J.A., Wang, G., Kexin Zhang, Shuyuan Xiang, Demin Liu (2008): Late Quaternary river terrace sequences in the eastern Kunlun Range, northern Tibet: A combined record of climatic change and surface uplift. *Journal of Asian Earth Sciences* 34 (2009) 532–543. DOI [10.1016/j.jseaes.2008.09.003](https://doi.org/10.1016/j.jseaes.2008.09.003)

Corresponding Author:

Helmut Wenzel

helmut.wenzel@boku.ac.at

+43 664 330 2395

COMMISSION INTERNATIONALE DES GRANDS BARRAGES

VINGT-SIXIÈME CONGRÈS DES GRANDS BARRAGES
Autriche, juillet 2018

DOI 10.3217/978-3-85125-620-8-042



This work licensed under a Creative Commons Attribution 4.0 International License. <https://creativecommons.org/licenses/by-nc-nd/4.0/>

**COUNTERMEASURE OF SEDIMENTATION PROBLEM ON WONOGIRI
RESERVOIR, INDONESIA**

Graitia SUTADI

INACOLD

Yoga Darmawan DIPARINDRA

BENGAWAN SOLO RIVER BASIN AUTHORITY, INDONESIAN MINISTRY OF
PUBLIC WORKS AND HOUSING

Airlangga MARDJONO

INDONESIAN DAM CENTRE, INDONESIAN MINISTRY OF PUBLIC WORKS
AND HOUSING

Nisa Andan RESTUTI

INDONESIAN DAM SAFETY UNIT, INDONESIAN MINISTRY OF PUBLIC
WORKS AND HOUSING

Duki MALINDO

BENGAWAN SOLO RIVER BASIN AUTHORITY, INDONESIAN MINISTRY OF
PUBLIC WORKS AND HOUSING

INDONESIA

COMMISSION INTERNATIONALE
DES GRANDS BARRAGES

VINGT-SIXIÈME CONGRÈS DES
GRANDS BARRAGES
Autriche, juillet 2018

**COUNTERMEASURE OF SEDIMENTATION PROBLEM ON WONOGIRI
RESERVOIR, INDONESIA¹⁾**

Graitia SUTADI
INACOLD

Yoga Darmawan DIPARINDRA
*Bengawan Solo River Basin Authority, Indonesian Ministry of Public Works and
Housing*

Airlangga MARDJONO
Indonesian Dam Centre, Indonesian Ministry of Public Works and Housing

Nisa Andan RESTUTI
Indonesian Dam Safety Unit, Indonesian Ministry of Public Works and Housing

Duki MALINDO
*Bengawan Solo River Basin Authority, Indonesian Ministry of Public Works and
Housing*

ABSTRACT

The Wonogiri Dam should continue to contribute to stabilization of people's livelihood as well as improvement of social welfare at least in coming 100 years. This goal will be achieved only in the way to secure and maintain the expected function of the Wonogiri reservoir in terms of flood control, irrigation water, domestic and industrial water supply and hydropower generation.

The Wonogiri reservoir will be separated by closure dike into two reservoirs, namely a Sediment Storage Reservoir with New Gates and a large main Wonogiri Reservoir, and operated independently.

In construction of new dike with saturated soils with soft clay, low bearing capacity and excessive settlement, the ground improvement technique using

deep cement soil mixing is one of the most suitable methods to overcome this problem. The sole purpose of deep cement soil mixing is to improve shear strength of soil by in situ mixing the soil with cement grout.

Keywords: Wonogiri Dam, reservoir, ground improvement, deep cement soil mixing

1) Model Tes Hidraulik Bangunan Pelimpah Bendungan Cipanundan, Jawa Barat, Indonesia

1. BACKGROUND

The Wonogiri Multipurpose Dam was constructed at Upper Solo River basin in 1978-1981. Since impoundment of Wonogiri reservoir on December 29, 1980, the reservoir has been rapidly filled with sediments. The quantity of sedimentation reached 65% of the dead storage on 2013 that mostly from Keduang River as Bengawan Solo's tributary. To mitigate sediment problem in the Wonogiri reservoir, the Master Plan and the Feasibility Study on countermeasures for sedimentation in the Wonogiri Multipurpose dam reservoir were carried out from 2004 to 2007 by JICA for detail design and supporting report by Nippon Koei Co, Ltd and Yachiyo Engineering Co., Ltd until 2010.

1.1. The Location

The Project is located in Wonogiri Regency of Central Java Province in the central region of Java Island approximate 600 km east of the Indonesian Capital city Jakarta.



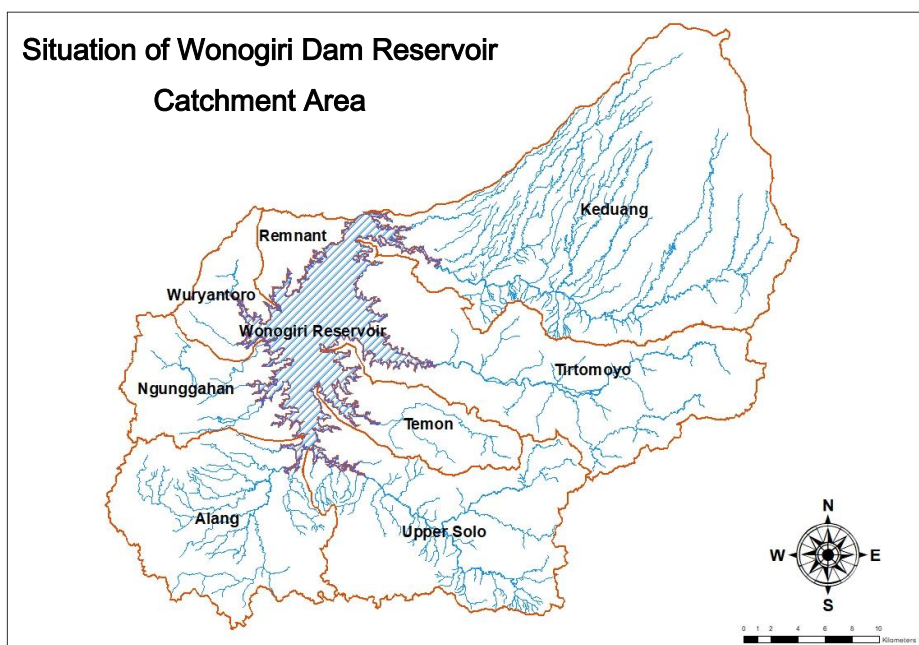
Figure 1.
Indonesian Map, Source: Nippon Koei Report



Figure 2.
 Map showing relative location of Wonogiri Reservoir in Indonesia.
 Source: Nippon Koei Report

1.2. The Problem

The Wonogiri reservoir is fed by 8 main streams of which Keduang is the largest contributing 35 percent of the inflow and sediment.



The sedimentation problem is made worse by the fact that the mouth of Keduang River enters the Wonogiri reservoir is less than 0.5 km from the intake for power plant / irrigation releases. This results in heavy siltation in front of the the intake which needs nearly continuous dredging to keep the reservoir operational, especially in the dry seasons.



Figure 3.
Heavy Siltation requires continues dredging, Source: Nippon Koei staff photo

1.3. The Solution

In order to reduce the amount of siltation that will need to be dredge from in front of the intake, a proposed solution is to divide the reservoir into two parts; a Sediment Reservoir to capture and manage sediment from the Keduang River and a Clear Water Reservoir leading to the intake. The division of the reservoir into two parts is to be accomplished with construction of series of closure dikes between partially submerging islands within the reservoir. A total of three closure dike and an overflow dike (broadcrested overflow spillway) are to be constructed as shown below.

In addition, a new spillway gates shall be constructed at the east bank of Wonogiri Dam closed to the confluence of Keduang River. Sediment trapped in the sediment reservoir will be flushed down through the new spillway gates into the upper solo river during the rainy (flood) seasons.



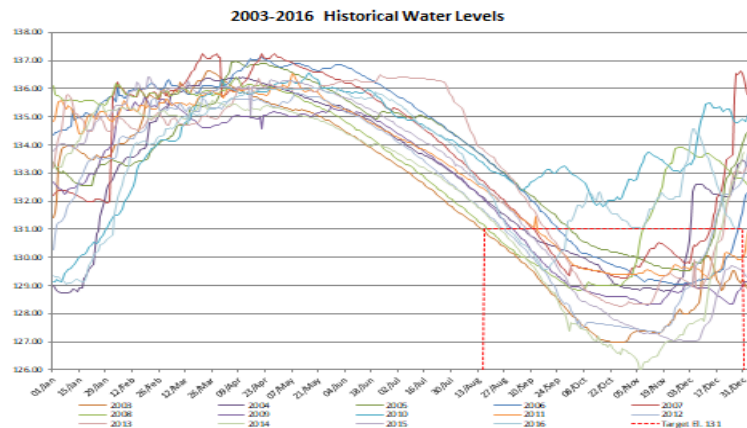
1.4. The Challenges

There are many challenges to be faced in the implementation of projects but right-of-way or resettlement was not an issue here; all of the work will be done within the existing reservoir. That however, leads to the first challenge. The work is to be done inside the reservoir where the water levels fluctuate during the year from the wet to dry seasons. The construction window when it is safe to work within the reservoir is a very limited window.

The second challenge is that the main closure dike is to be constructed on very soft sedimentation deposits that have accumulated over the years to a depth over 20m.

First Challenge – Construction Window

The first challenge, related to the water level, is when can construction start and how long construction can continue until. As seen in the historic fluctuation of water levels below, the timing of drawdown of the reservoir varies over several months.



Fortunately, with close coordination with the Bengawan Solo Water Council representing the various user groups in the basin, the start of a construction window can be controlled by monitoring releases from the reservoir. For the 2017 Construction season the drawdown of the reservoir was very successfully timed to the lower the water levels below Elevation 131.0 to within the exact day (15-Aug-2017) that had been negotiated.

However, the timing of the end of the construction season is not so easily solved as it is dependent on the onset of early rains which induce flash flooding and rapid rising reservoir levels. No amount of “coordination” can control the onset of early rains; therefore, a physical solution is necessary. The two options were considered; using cofferdam against rising waters or raising the base platform for the construction.

Second Challenge – Very Soft Foundation

The second challenge of construction is the soft sediments, which cannot directly support placement of closure dike. The improvement of the soft soils in order to support the weight of the embankment is to be solved with the use of Deep Mixing Soil Improvement (DMSI).

2. DMSI (DEEP MIXING SOIL IMPROVEMENT) – GENERAL

Deep Mixing Soil Improvement (DMSI) is a physical method to form soil-cement columns in soils in order to increase the bearing capacity and / or reduce settlement of soft ground.

Unlike a bored pile where a boring machine excavates a hole, removing the soil which is replaced with reinforcing bar and concrete to form a solid concrete pile, Deep Mixing involves a machine which augurs or drills a mixing blade down a hole and then mixes cement with the soil in-situ, (in place) to form a soil cement columns.

The figure below shows the basic sequence in three steps. In Step 1 - Twin augurs drilling down through the soil until reaching the hard bottom. Then in Step 2- the augurs are rotated back up and at the same time cement slurry is injected from the blades and mixed into the soil. When in Step 3 the augurs are extracted, the remaining column is a mixture of soil and cement. This equipment then moved to the next location and the process repeats.

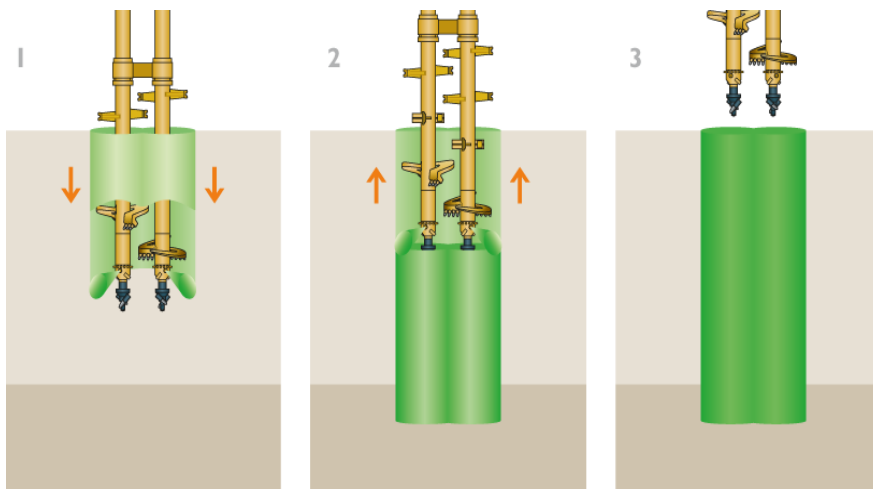


Figure 4.
The Wet DSM method, Source: <http://www.kellerholding.com>



Figure 5.
Wet Soil Deep Soil Mixing Machine, Source: <https://www.liebherr.com>

There are several types of Deep Mixing processes / machines I.e. dry mix vs wet mix, (dry cement injected with air vs cement slurry), single screw vs multi screw, and rotary blade mixing vs jet grouting (soil column for a rotary blade mixing has the same diameter with the blade, whereas, jetting makes a column wider than the diameter of blade). For Wonogiri, a twin-screw rotary blade, wet mix machine, will be used, which is similar to the one shown before.

In addition to the deep soil mixing machine, there is need for support from a slurry batch plant complete with cement silos, water storage tanks, batch mixing systems, storage tanks, and slurry pumps with flowmeters and associated control / monitoring systems.

2.1. DMSI Application at Wonogiri Reservoir Rehabilitation

The Wonogiri reservoir has an annual problem of sedimentation with main river (Keduang) mouth discharging within 0.5 km of the main power /irrigation release intake. Nearly continuous dredging has been required to maintain the operation.

The solution is to divide the reservoir into two; - a sediment reservoir to trap Keduang River sediments and a clear water reservoir leading to the intake. The division of the reservoir will be accomplished with three closure dikes and one overflow dike acting as an overflow spillway. Two of the closure dikes, will be the conventional embankments which is constructed on relatively hard ground, but the main dike, Closure Dike A, is a 700 m long dike, which will be constructed on soft reservoir deposits, up to 20 m thickness or more. This soft deposit of soil is built up of Keduang River sediments over the years can NOT support the weight of conventional embankment without improving the soil strength. Therefore, deep mixing soil improvement, DMSI, is used.

Typical Section of Closure Dike A – Embankment Construction on DMSI Columns

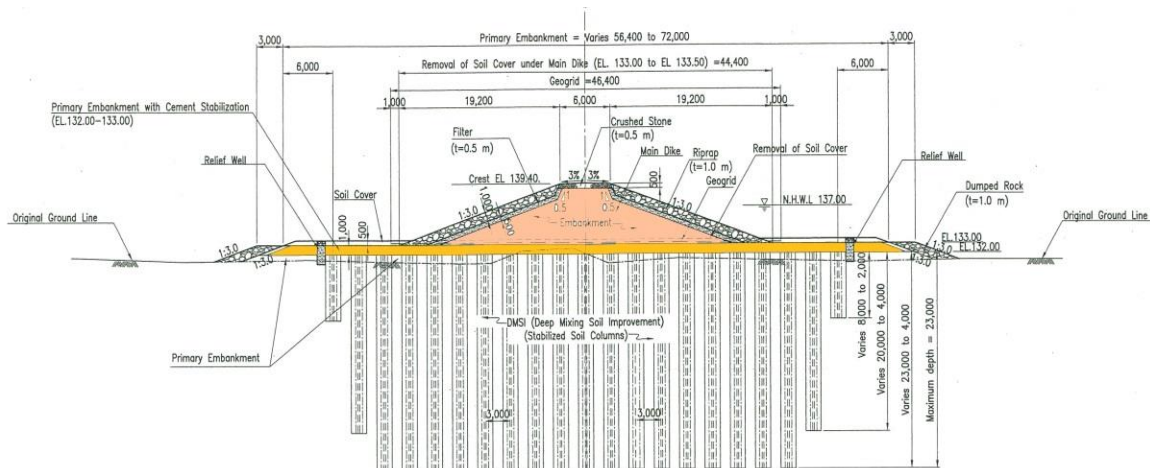


Figure 6.

Typical Section of Closure Dike A – from Bidding Documents of ICB Civil Works – Construction of Closure Dike and Overflow Dike (Package No. 2-1)

2.2. Stage-1. Installation Working Platform, First Construction Season (15-Aug to Dec 2017)

The DMSI equipment including the deep mixing machine and the supporting slurry plant with associated facilities, are heavy and not easily or quickly moved. This becomes a very real problem when the project is being implemented within a reservoir subjected to flash flooding. Therefore, in order to execute the work a working platform is needed that can be made relatively free

from flooding. However, it is not just a question of making the platform at a high level, because the platform is being constructed on unimproved soils. The weight of the platform and equipment must be supported by the unimproved soils before the deep mixing soil improvement can be executed to make the suitable foundation for the closure dike. There is a delicate balance between making the platform high enough for safety against flash floods and low enough such that the total weight of the platform and equipment can be supported by the unimproved soils.

In the case of the Wonogiri reservoir that delicate balance resulted in a platform consisting of two parts. First, primary embankment (varying thickness but approximately 1 m) is placed up to Elevation 132. Second, the primary embankment is overtopped with a constant 1 m thick layer of soil cement up to Elevation 133. The DMSI columns will be drilled through the soil cement. This layer of soil cement not only formed a firm platform but also acts to tie the columns together to limit their horizontal displacements at the tops of the columns.

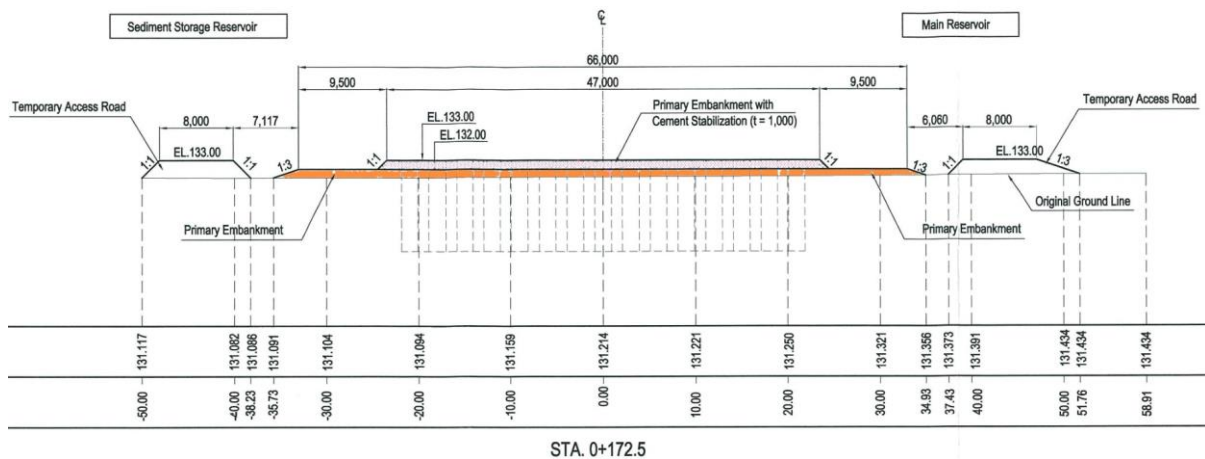


Figure 7.
Typical Section of Primary Embankment and Soil Cement

The average existing ground elevation of the soft reservoir deposits was around Elevation 131 and the construction window was assumed to start when reservoir levels fell below that level. Therefore, the first year construction was to consist of the following steps:

Step 1: After the reservoir level drops the soft deposits were left to dry sufficiently enough to support equipment. Fortunately the construction window corresponds to the normal dry season with strong warm dry winds occur across the reservoir to aid in the drying. While waiting for the drying, clearing and grubbing of the soils was manually executed. When the soils had dried sufficiently to support the load of swamp-track bulldozers the area was then stripped. Since the reservoir deposits were not entirely even, the area was treated by zones corresponding to vary general levels. For the main Closure Dike the area was divided into 7 zones as shown below:

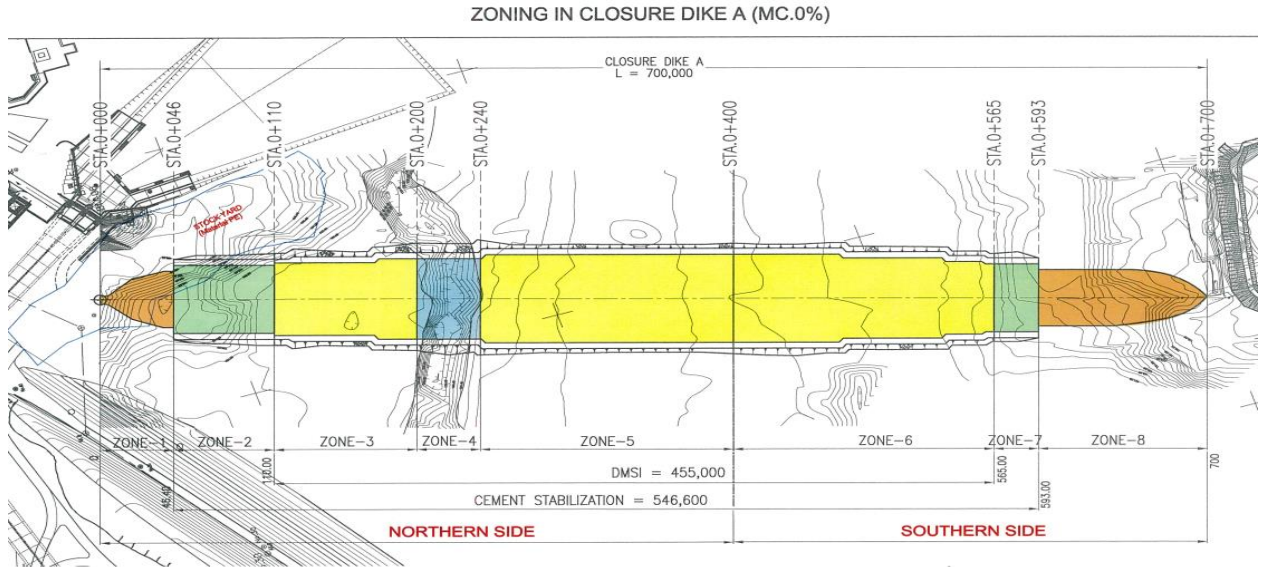


Figure 8.
Seven Zones for Placement of Primary Embankment, Source: Hazma-Ando-Wika JO



Figure 9.
Final inspection of grubbing after stripping and initial compaction

Step 2: After stripping the top of the existing soft reservoir deposit and when the area has dried sufficiently to support trucks and vibratory rollers, the primary embankment was placed and compacted layer by layer up to Elevation 132. (4 layers each 25 cm. each).



Figure 10.
Primary Embankment Placement, Source : Hazama Ando-Wika JO Drone Photo



Figure 11.
Primary Embankment Spreading. Source: Nippon Koei Staff Photo

Step 3: Once the primary embankment was completed the soil cement was placed and compacted layer by layer up to Elevation 132. While the warm-dry winds have been very beneficial during the drying of the exposed reservoir soils to support construction equipment, the same winds become a problem during the mixing and placing of soil cement. Control of the moisture content of the soil

before mixing and preparing the placement area was a crucial step in achieving the desired soil cement.



Figure 12.
Soil Cement Mixing Yard. Source : Hazama Ando-Wika JO Drone photo



Figure 13.
Stabilizer Machine mixing soil cement. Source: Nippon Koei Staff Photo



Figure 14.
**Soil Cement Placement on Primary Embankment. Source :Hazama Ando-Wika
JO Drone**

Step 4: Finally after the soil cement is completed the top layer is covered with soil and the project waits till next year before the DMSI can commence. The soil cover used to prevent the Hexavalent Chromium leaching from cement into the water.

2.3. Stage 2. Deep Mixing Soil Improvement,– Second Construction Season (2018)

After the water level decreased in the second construction season, the start the DMSI works will commence. There are planned for approximately 4,300 columns up to 24 m depth. Each column is a column pair made from twin 1-m screws with 20cm overlap. The column pairs will be placed in sections, with 21 column pairs with 2.2 m Centerlines for section width of 45.8 m. Each section along the axis of dike will be placed at 2.2 m intervals.

As mentioned earlier, the DMSI equipment and support facilities are heavy and not quickly moved. Coupled with the very short construction season of less than 5 month the logistics of completing all the work within a single season is a challenge. Originally, it was planned to use six complete DMSI teams (mixing machines with their cement slurry supply plants) but the Contractor has proposed to utilize 3 DMSI groups working double shifts.

After DMSI works have been completed the tops of the DMSI Columns will be covered with soil again to prevent the Hexavalent Chromium leaching from cement into the water. The Project site will then have to wait until the following year to complete the closure Dike.

2.4. Stage 3. Main Embankment – Third and Final Construction Season

At the beginning of the final construction season, the soil cover over the DMSI columns will be removed, the tops of the DMSI columns will be trimmed smoothly of their excess material and a geotextile GeoGrid will be placed on top of the columns. After which, conventional soil embankment will be built layer by layer until the crest is reached. The embankment will be finished with riprap slope protections and top driving surface for maintenance access.

3. NEW SPILLWAY GATES

Construction of New Spillway Gates (2 fixed rollergates; width = 7.50 m; height = 5.60 m) will serve several function as the following:

1. Sediment materials trapped in the sediment reservoir will be flushed down through the new spillway gates into the upper solo river.
2. New spillway gates will provide additional spillway capacity, which will increase safety against emergency situations (probable maximum floods).
3. This will also provide an opportunity to increase operational water level (NHWL) by 1 meter (from +136 to +137), which will generate 76 millions m³ additional reservoir storage.

4. CONCLUSION

1. Sedimentation become a serious problem to dam reservoir in Indonesia, it will decrease reservoir capacity and also the dam function.
2. Prevent the sedimentation rate is a difficult step due to rapid land development on upper side of the catchment area.
3. It needed a new innovation to restore the capacity of dam reservoir during operation, use proper method such as development of closure dike with DMSI.
4. Operational of the new spillway gates will provide an opportunity to increase normal high water level (NHWL) by 1 m, which will generate 76 millions m³ additional reservoir storage.

5. ACKNOWLEDGEMENT

The authors would like to thank to Bengawan Solo River Basin Authority, Dam Center and Dam Safety Unit, Directorate General of Water

Resources, Ministry of Public Works and Housing for the authorization to publish the main result of the present study. The authors would also like to express the gratitude to Bengawan Solo River Basin Authority as the institution who built the closure dike for having made this fruitful collaboration possible.

REFERENCES

- [1] Ainur Rofiq, Countermeasures for Sedimentation in Wonogiri Multipurpose Dam Reservoir. 2007.
- [2] Cristina Dwi Yuliningtyas, Dwi Aryani Kubontubuh, Design Rehabilitation of Wonogiri Dam, Central Java Province, Indonesia. 2015.
- [3] JICA, Nippon Koei Co. Ltd., Yachiyo Engineering Co. Ltd., Study on Countermeasure for Sedimentation in Wonogiri Multipurpose Dam Reservoir; Final Report. 2007.
- [4] Graitia Sutadi, Sediment Control System for Wonogiri Multipurpose Dam), INACOLD, 2013.

COMMISSION INTERNATIONALE DES GRANDS BARRAGES

VINGT-SIXIÈME CONGRÈS DES GRANDS BARRAGES
Autriche, juillet 2018

DOI 10.3217/978-3-85125-620-8-043



This work licensed under a Creative Commons Attribution 4.0 International License. <https://creativecommons.org/licenses/by-nc-nd/4.0/>

**CLIMATE CHANGE IMPACT ON SURFACE WATER RESOURCES AND
HYDROPOWER GENERATION IN THE DEZ DAM BASIN, IRAN**

Roya Sadat MOUSAVI

*Water Resources Expert, IRAN WATER RESOURCES MANAGEMENT
COMPANY*

IRAN

Mojtaba AHMADIZADEH

*Water Resources Expert, IRAN WATER RESOURCES MANAGEMENT
COMPANY*

IRAN

Safar MAROFI

Professor, BU-ALI SINA UNIVERSITY

IRAN

COMMISSION INTERNATIONALE
DES GRANDS BARRAGES

VINGT-SIXIÈME CONGRÈS DES
GRANDS BARRAGES

Autriche, juillet 2018

**CLIMATE CHANGE IMPACT ON SURFACE WATER RESOURCES AND
HYDROPOWER GENERATION IN THE DEZ DAM BASIN, IRAN¹**

ROYA SADAT MOUSAVI

*¹Water Resources Expert, IRAN WATER RESOURCES MANAGEMENT
COMPANY*

IRAN

MOJTABA AHMADIZADEH

*¹Water Resources Expert, IRAN WATER RESOURCES MANAGEMENT
COMPANY*

IRAN

SAFAR MAROFI

²Professor, BU-ALI SINA UNIVERSITY

IRAN

*¹ ENQUÊTE SUR L'IMPACT DU CHANGEMENT CLIMATIQUE SUR LES
RESSOURCES EN EAU DE SURFACE ET LA GÉNÉRATION D'HYDROÉLECTRICITÉ
DANS LE BASSIN DE DEZ DAM, EN IRAN*

1. INTRODUCTION

Many studies so far have provided evidences in support of climatic changes during the past decades as such variations affected the water balance and caused fluctuations in stream flows at both regional and local (catchment) scales. In Iran many studies support the fact that the climate has experienced variations during recent decades (Dinpashoh et al. 2011; Golian et al. 2015; Marofi et al. 2012; Masih et al. 2011) mostly toward more hot and dry conditions. Also, in recent years anthropogenic global warming and its consequences especially in the arid and semi-arid regions of the world received particular attention as many scholars documented occurrence and dominance of drought, temperature rise and increase in the atmospheric water demand accompanied by reduction of precipitation and runoff (Guo and Shen 2015; Lalika et al. 2015). Also, assessments by IPCC (Intergovernmental Panel on Climate Change) provides means for policymakers to plan for future to adapt to climate change and mitigate its impacts.

Anticipated climatic changes can alter the hydrological behavior such as the amount of discharge or timing of the hydrological regime (Adam et al., 2009; Boyer et al., 2010; Gan et al., 2015). Such alterations can cause socio-economic and environmental consequences. Several studies world-wide predicted that the combination of temperature increase and precipitation change during the present century will result in significant change in runoff (Steele-Dunne et al., 2008; Vezzoli et al., 2015). Also many climate change impact studies have been carried out to investigate the hydrological response to climate change (Pervez and Henebry, 2015; Boyer et al., 2010). For instance it is widely documented that the modeled winter time discharge increase followed by the spring time discharge decrease, which is due to temperature increase; that is the cause to melt snow sooner and remain less snow pack (Arnell and Gosling 2013; Adam et al. 2009 and Boyer et al. 2010). A global scale study on river flow and water temperature changes through forcing by A2 and B1 emission scenarios suggested increase in the seasonality of river flow, i.e. increase in high flows and decrease in low flows for about one-third of the Earth (Van Vliet et al. 2013).

One of the vulnerable industries against climate change is hydropower generation, which completely relies on the amount of precipitation and the stream flow as well as the timing of the flow (Abrishamchi et al., 2012). Based on the IPCC report the potential of hydropower generation is projected to reduce by up to 6%, as a result of climate change (IPCC, 2008). Therefore, it is essential to adapt the water resources management with the future climatic changes (Xu and Singh, 2004). In Iran the climate and hydropower generation changes have been studied by Jahandideh et al. (2015) and Jamali et al. (2013) those focused on Karun and Karkheh river basins, respectively; and they reported reduction of the potential of hydropower generation in both studied basins.

Considering that the freshwater availability is vital in semi-arid and arid basins, it is essential to establish the magnitude of changes in surface water at basin scale. This study is focused on the semi-arid Dez River basin in Iran. Stream flow from this basin is used for hydropower generation, industrial production, irrigation, and domestic water supply. As Dez Basin is not completely developed

yet, it is crucial to assess variations of discharge in this basin, under climate change condition and its impact on hydropower generation. Therefore, this research investigates the changes in hydropower generation in two major hydropower plants in the Dez basin. This assessment provides useful information to modify water resources management strategies with regards to the climate change impact on surface water resources in the Dez Basin.

2. MATERIALS AND METHODS

2.1. STUDY AREA

The Dez Basin is located in the Southwest of Iran ($31^{\circ}35'51'' - 34^{\circ}7'46''$ N and $48^{\circ}9'15'' - 50^{\circ}18'37''$ E) and is the upstream catchment of the great Karun catchment. The basin is comprised of four sub-basins namely Tireh, Marberreh, Sazar and Bakhtiari. The latter is where the Bakhtiari dam is being constructed that its major purpose is to generate electricity. The catchment is located within a mountainous region which provides appropriate head needed for hydro-electric generation. Dez dam is located in the downstream of Bakhtiari and receives two rivers of Sazar and Bakhtiari those join at Tange Panj station which is located just before the lake of Dez Dam. The storage of this reservoir provides water for domestic, agricultural and industrial sectors and also is used to generate electricity.

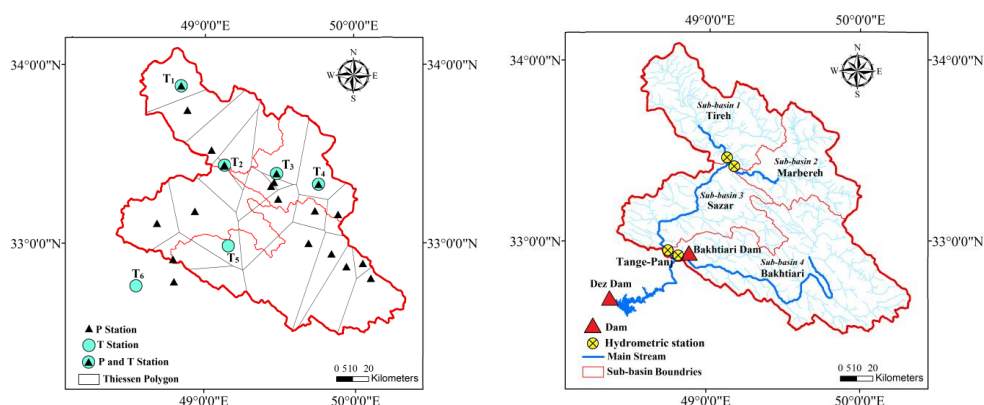


Fig. 1

Study area of the Dez Basin and location of rain gauges, hydrometric and temperature gauging stations

2.2. DATA

Long-term daily temperature (T) and precipitation (P) time-series obtained from I.R. of Iran Meteorological Organization (IRIMO) and Iran Water Resources Management Company (IWRM Co.). To calculate the average T and P in each sub-basin arithmetic mean and Thiessen polygon method applied, respectively.

2.3. GCM-SCENARIO

In order to project the future hydrological condition, two different GCMs were selected (ECHAM5-OM and HadCM3). Description of the applied GCMs is presented in table 1. Also three different SRES emission scenarios (Special Report on Emission Scenarios) of A1B, A2 and B1 were considered to project the future T and P for 2011-2030 (2020's), 2046-2065 (2050's) and 2081-2100 (2080's) time horizons.

Table 1
Description of the Global Climate Models and IPCC-AR4 SRES emission scenarios

Research Centre	GCM	GCM Acronym	Resolution	SRES Scenarios
Max-Planck Institute for Meteorology (Germany)	ECHAM5-OM	ECHAM5	1.9×1.9°	A1B, A2, B1
UK Meteorological Office (UK)	HadCM3	HadCM3	2.5×3.75°	A1B, A2, B1

To downscale T and P under A1B, B1 and A2 SERS scenarios during 2020's, 2050's and 2080's in the study area, the stochastic weather generator of LARS-WG were applied; that generates time-series based on the probability distribution of base period data and correlations between observations. The detailed description of LARS-WG can be found in Semenov (2007).

2.4. HYDROLOGICAL MODELING AND MODEL CALIBRATION AND VALIDATION

The HBV-light, semi-distributed hydrological model is used to simulate the runoff in the Dez basin. This model simulates runoff with temperature, precipitation and evaporation inputs and contains snow routine, soil moisture routine, response function and routing routine. The detailed description of the HBV model structure and routines could be found on Seibert and Vis (2012). Prior to the application of the model it is necessary to calibrate its parameters. This is done through try and error procedure as recommended by Bergstrom (1992).

There are several statistics to identify the efficiency of a model. In this research we examined the goodness of fit with Nash-Sutcliffe measure (R_{eff}), coefficient of determination (R^2) and mean annual difference (M_{diff}).

$$R_{eff} = 1 - \frac{\sum (Q_{Sim}(t) - Q_{Obs}(t))^2}{\sum (Q_{Obs}(t) - \overline{Q_{Obs}})^2} \quad (1)$$

$$R^2 = \frac{(\sum (Q_{Obs} - \overline{Q_{Obs}})(Q_{Sim} - \overline{Q_{Sim}}))^2}{\sum (Q_{Obs} - \overline{Q_{Obs}})^2 \sum (Q_{Sim} - \overline{Q_{Sim}})^2} \quad (2)$$

$$M_{diff} = \frac{\sum (Q_{Obs} - Q_{Sim})}{n} 365 \quad (3)$$

2.5. MODELING TWO RESERVOIRS SYSTEM IN VENSIM

To calculate the hydropower generation, two reservoirs system of Bakhtiari and Dez dam were developed in Vensim by entering the equations of mass balance and power generation, considering the restrictions of operation of the reservoirs and power plants.

$$S_{t+1} = S_t + Q_t - RE_t - RD_t - SPL_t - EVAP_t + ADD_t \quad (4)$$

Where,

S_{t+1} : The reservoir volume at the end of t period (beginning of the t+1 period);
 S_t : The reservoir volume at the beginning of t period; Q_t : Inflow to the reservoir during t period; RE_t : The outflow from the reservoir to generate energy during t period; RD_t : The outflow from the reservoir to meet downstream demand during t period; SPL_t : The spill from the reservoir during t period; $EVAP_t$: Evaporation from the reservoir during t period; ADD_t : The volume of added flow from upstream reservoir during t period.

The power generation is associated to the installed capacity, efficiency, plant factor as well as the inflow and hydraulic head. Equation below shows the power generation which was used to calculate the energy generation.

$$P_t = (\gamma Q_t H_t e_t) 1000 \quad (5)$$

Where,

P_t : Power generated during t period; γ : Water specific weight; Q_t : the inflow to the turbine during t period; H_t : Net hydraulic head on turbine during t period; e_t : The power plant efficiency.

3. RESULTS AND DISCUSSION

3.1. PROJECTED CHANGES IN TEMPERATURE AND PRECIPITATION

Based on the results, three studied scenarios perform in a similar way during the first time horizon and two GCMs and applied scenarios suggest small temperature changes during 2020's. However, temperature increases up to 1.2 and 1.1 °C is projected. While, based on all considered scenarios a significant rise in the average temperature is projected for 2050's and 2080's time horizons; as the average temperature in 2080's is higher than the average of temperature during 2050's. Generally, the B1 scenario suggests slighter temperature increase during 2050's and 2080's; while, scenarios A2 and A1B revealed a higher rise in temperature during these time horizons. HadCM3 revealed higher temperature increase during 2050's, based on scenarios A1B, A2 and B1, respectively. But during 2080's the highest rates of temperature for all the scenarios is suggested by ECHAM5.

Assessing the magnitude of temperature variations from the base period, suggests that the maximum temperature increase is associated to 2080's time horizon under the A2 scenario that shows an average increase of temperature between 3.6 to 4.4 °C in the study area.

In a similar way, average of the projected precipitation for future time horizons based on two GCMs outputs and scenarios A1B, A2 and B1, show that most of the scenarios suggest increasing precipitation amounts compared to the base period. Also projections mostly suggest precipitation decrease in the first time horizon (2020's) for Marbereh.

Studying the percentage of variation of precipitation from the average precipitation amount in base period shows that, the greatest precipitation changes occur in 2080's; that is mostly toward an increase in the amount of precipitation in the study area. Also, based on the projections, the highest precipitation increase is projected for the 2080's time horizon and especially for scenario A2.

Table 2
Percentage of changes in temperature (ΔT) and precipitation (ΔP) under climate change condition

Scenario-Period	GCM1: ECHAM5								GCM2: HadCM3							
	ΔT (%)				ΔP (%)				ΔT (%)				ΔP (%)			
	T ¹	M ²	S ³	B ⁴	T	M	S	B	T	M	S	B	T	M	S	B
A1B- 2020	0	4	3.1	6.4	2.4	-2.5	2.8	1.4	-0.1	3.7	2.8	6	5.9	0.4	7.6	3.8
A1B- 2050	12.5	18.1	15.6	19.5	7.4	-0.1	7.7	3.1	11.3	16.6	14.4	18.1	9	2.8	8.9	6.1
A1B- 2080	28.4	32.3	28	32.3	8	1.4	7.7	4	21.2	27.8	24	28	10.2	5.8	11.2	9.5
A2- 2020	0	3.9	3	6.3	2.3	-3.5	2.9	0.1	0.5	4.4	3.5	6.9	-0.2	-5	0.8	-1.9
A2- 2050	10.1	15.4	13.2	16.9	3.8	-2.1	4	0.7	10.3	15.5	13.3	17	6.7	1.2	7.7	5.2
A2- 2080	27.7	35.5	30.9	35.4	9.2	1.1	10.3	5	26.8	34.3	29.8	34.1	16.8	10.7	18.4	15.9
B1- 2020	0	3.9	3	6.2	4.3	-2	4.9	1.2	-0.2	3.5	2.7	5.8	-1.8	-5.6	-1.2	-2.8
B1- 2050	6.6	11.4	9.6	13	1.2	-6.1	1.7	-2.7	8.3	13.1	11.1	14.6	12	7.4	13.3	10.7
B1- 2080	16.4	22.6	19.5	23.2	3.4	-4.1	3.6	-1.4	13.6	19.1	16.3	19.9	14.3	8.8	16.2	12.6

¹T: TIREH; ²M: MARBEREH; ³S: SAZAR; ⁴B: BAKHTIARI;

3.2. HYDROLOGICAL SIMULATION UNDER CLIMATE CHANGE SCENARIOS

To simulate runoff, First, the HBV model calibration and validation carried out using 12 and 5 years of observed discharge data, respectively. The values of Nash-Suttclif statistics of 0.69, 0.60, 0.61 and 0.6 and R²s of 0.71, 0.61, 0.63 and 0.61 obtained for Tireh, Marbereh, Sazar and Bakhtiari, respectively. After ensuring the efficiency of model, it was applied to simulate discharge under climate change condition with projected T and P time-series as inputs.

The overall changes of the annual flow corresponded to all GCMs and scenarios show that the amount of annual discharge is mostly decreasing in the future; as the reductions are most significant for 2080's time horizon. In Tireh, the greatest reduction of annual flow (19%) is attributed to ECHAM5-B1-2050 and 2080. Similar to Tireh, the reduction of annual flow in Marbereh is more significant in 2080's as it reaches to 26% (ECHAM5-A2-2080). Generally, the amount of annual flow mostly decreases in Sazar. However, some contrasting results obtained, indicating annual flow increase up to 13% (HadCM3-A2-2080). The greatest reductions of annual flow (up to 17% by HadCM3-B1), is corresponded to 2020's time horizon. Also, the greatest reduction of annual flow in Bakhtiari is up to 27% by ECHAM5-B1 in 2080's.

Table 3
Percentage of changes in sub-basins discharge under climate change condition

Scenario- Period	GCM1: ECHAM5-OM				Scenario- Period	GCM2: HadCM3			
	T ¹	M ²	S ³	B ⁴		T	M	S	B
A1B- 2020	-8	2	-5	-7	A1B- 2020	-1	7	0	-14
A1B- 2050	-12	-12	-1	-15	A1B- 2050	-6	-6	0	-8
A1B- 2080	-8	2	-5	-7	A1B- 2080	-9	-9	3	-10
A2- 2020	-8	-1	-6	-8	A2- 2020	-13	-4	-9	-10
A2- 2050	-15	-10	-6	-15	A2- 2050	-11	-5	-1	-10
A2- 2080	-13	-26	2	-20	A2- 2080	2	-5	13	-6
B1- 2020	-4	3	-3	-6	B1- 2020	-17	-6	-12	-11
B1- 2050	-19	-17	-10	-15	B1- 2050	0	6	7	-2
B1- 2080	-19	-20	-7	-21	B1- 2080	2	4	10	-3

¹T: TIREH; ²M: MARBEREH; ³S: SAZAR; ⁴B: BAKHTIARI;

3.3. VARIATION OF THE INFLOW TO DEZ AND BAKHTIARI RESERVOIRS AND HYDROPOWER GENERATION UNDER CLIMATE CHANGE

The amount of annual inflows to the Bakhtiari and Dez reservoirs and percentage of their changes in the future time horizons under climate change condition, compared to the base period and are presented in table 4. Long-term average of the discharges at the outlet of Bakhtiari and Sazar are 5106.88 and 2938.21 Mm³, respectively. Considering that the Bakhtiari Dam is located at the end point of Bakhtiari basin and Dez is located at the downstream of Tange Panj, the inflow to the Bakhtiari reservoir equals to the Bakhtiari basin's discharge and the inflow to the Dez reservoir is the total discharges from upstream basins, that equals to 8045.1 Mm³. Based on the results, variation of the inflow to the Bakhtiari reservoir under climate change, simulated to vary between -1.7% (HadCM3-B1-2050) and -20.8% (ECHAM5-B1-2080). Also the inflow to the Dez reservoir for future time horizons is simulated to decrease by up to 14.3% (ECHAM5-B1-2080) and increase by up to 3.6% (HadCM3-B1-2080).

The potential of hydropower generation for base period and future time horizons is calculated by modeling the two reservoirs systems, using the inflows obtained from previous step (table 4). Based on the results the potential of hydropower generation simulated to decrease between -24.1% (ECHAM5-A1B-2080) and -0.9% (HadCM3-B1-2050) that is in agreement with the reduction of discharges to the Bakhtiari reservoir. On the contrary, the potential of hydropower generation of Dez dam is simulated to slightly increase by up to 2.6% (HadCM3-A1B-2080); while its inflow is projected to decrease for future time horizons.

As mentioned above, in case of Dez reservoir, there are some inconsistencies between the changes caused by climate change in discharge and hydropower generation. While, the results for Bakhtiari reservoir are more compatible. The difference between the responses of two reservoirs in terms of

their potential of hydropower generation could be attributed to different operational rules due to different purposes, as well as the size of the reservoirs and installed capacity of their hydropower plants. To study the reasons to that, time-series of inflow, outflow, spill and the water level in the reservoir for base period were assessed.

About different water utilities, it should be noted that the Dez dam is a multi-purpose dam which provides water for different purposes, in specific time periods, to meet demands. Therefore, the releases from its reservoir are planned and only the part of release or spill, that is not greater than the penstock capacity or turbine capacity, contribute to the power generation. Also, the small capacity of its reservoir (2.7 Bm³) compared to the discharge from draining catchment (8 Bm³) causes considerable spills. Having considered that the whole capacity of its hydropower plant is relatively small compared to its inflow and releases, therefore a significant proportion of the releases or spills does not contribute to the power generation. While, the Bakhtiari reservoir with the capacity of 5.16 Bm³ and average inflow of 5.11 Bm³ can control most of the inflows with negligible spills. Also, large capacity of its hydropower plant does not pose any limit for energy production. Therefore, in case of Bakhtiari, there is a direct relationship between the changes of the rates of inflow and energy generation. Based on the simulations for future time horizons, fewer amounts of inflows and peak flows to the Dez reservoir leads to less losses through spill, which means more water could be saved in the reservoir and used to generate electricity. Considering the reasons explained above, future changes in the potential of hydropower generation, under climate change conditions, are not consonant with the changes in the inflow to the Dez reservoir. Also slight increase in the potential of hydropower generation could be attributed to the changing of the regime of discharges with smaller peaks, leading to fewer spills and remaining more water to produce electricity.

Table 4
Percentage of changes in Inflow (I) and Electricity generation (E) under climate change condition

Scenario-Period	GCM1: ECHAM5-OM				Scenario-Period	GCM2: HadCM3			
	I (B) ¹	E (B)	I (D) ²	E (D)		I (B)	E (B)	I (D)	E (D)
A1B- 2020	-7	-6.8	-4.7	2.4	A1B- 2020	-13.6	-15	-6.8	1.5
A1B- 2050	-14.9	-16.9	-8.3	2.5	A1B- 2050	-8.2	-8.4	-3.5	2.4
A1B- 2080	-19.9	-22.7	-11.5	2.3	A1B- 2080	-10.4	-11.1	-3.7	2.6
A2- 2020	-7.7	-7.6	-5.4	2.4	A2- 2020	-10.1	-10.4	-8.2	2.2
A2- 2050	-14	-16.8	-10	2.4	A2- 2050	-9.5	-10	-4.8	2.5
A2- 2080	-20.5	-23.6	-10.7	2.3	A2- 2080	-6.5	-5.8	2.5	2.2
B1- 2020	-5.9	-5.3	-3.2	2.1	B1- 2020	-10.7	-11	-9.6	2.1
B1- 2050	-15.3	-17.2	-12	2.2	B1- 2050	-1.7	-0.9	3.2	2
B1- 2080	-20.8	-24.1	-14.3	2	B1- 2080	-3.1	-2.1	3.6	1.9

¹B: BAKHTIARI DAM; ²D: DEZ DAM

REFERENCES

- [1] ABRISHAMCHI A., JAMALI S., MADANI K., HADIAN S. Climate Change and Hydropower in Iran's Karkheh River Basin. *World Environmental and Water Resources Congress: Crossing Boundaries*, 2012.
- [2] ADAM J.C., HAMLET A.F., LETTENMAIER D.P. Implications of global climate change for snowmelt hydrology in the twenty-first century. *Hydrol. Process.*, 2009, Nr. 23.
- [3] ARNELL N.W., GOSLING S.N. The impacts of climate change on river flow regimes at the global scale. *Journal of Hydrology*, 2013, Nr. 486.
- [4] BERGSTROM S. The HBV model - its structure and applications. *SMHI Report RH. No. 4. Norrköping*, 1992.
- [5] BOYER C., CHAUMONT D., CHARTIER I., ROY, A.G. Impact of climate change on the hydrology of St. Lawrence tributaries. *Journal of Hydrology*, 2010, Nr. 384.
- [6] Dinpashoh Y., JHAJHARIA D., FAKHERI-FARD A., SINGH V.P., KAHYA, E. Trends in reference crop evapotranspiration over Iran. *J. Hydrol.*, 2011, Nr. 399.
- [7] GAN R., LUO Y., ZUO Q., SUN L. Effects of projected climate change on the glacier and runoff generation in the Naryn River Basin, Central Asia. *J. Hydrol.*, 2015, Nr. 523.
- [8] GOLIAN S., MAZDIYASNI O., AGHAKOUCHAK A. Trends in meteorological and agricultural droughts in Iran. *Theor. Appl. Climatol.*, 2015, Nr. 119.
- [9] GUO Y., SHEN Y. Quantifying water and energy budgets and the impacts of climatic and human factors in the Haihe River Basin, China: 2. Trends and implications to water resources. *J. Hydrol.*, 2015, Nr. 527.
- [10] IPCC, Technical Paper on Clim. Change and Water Rep. *Intergovernmental Panel on Clim. Change, Geneva*, 2008.
- [11] JAHANDIDEH-TEHRANI M., HADDAD O.B., LOAICIGA H.A. Hydropower reservoir management under climate change: The Karoon reservoir system. *Water resour. Manage.*, 2015, Nr. 29.
- [12] JAMALI S., ABRISHAMCHI A., MARINO M. Climate Change Impact Assessment on Hydrology of Karkheh Basin. *ICE – Water Management*, 2013.
- [13] LALIKA M.C., MEIRE P., NGAGA Y.M., CHANG'A L. Understanding watershed dynamics and impacts of climate change and variability in the Pangani River Basin, Tanzania. *Ecohydrol. Hydrobiol.*, 2015, Nr. 15.
- [14] MASIH I., UHLENBROOK S., MASKEY S., SMAKHTIN V. Streamflow trends and climate linkages in the Zagros Mountains, Iran. *Climatic Change*, 2011, Nr. 104.
- [15] MAROFI S., SOLEYMANI S., SALARIJAZI M., MAROFI H. Watershed-wide trend analysis of temperature characteristics in Karun-Dez watershed, southwestern Iran. *Theor Appl Climatol.*, 2012, Nr. 110.
- [16] SEIBERT J., VIS M.J.P. Teaching hydrological modeling with a user-friendly catchment-runoff-model software package. *Hydrol. Earth Syst. Sci.*, 2012, Nr. 16.

- [17] SEMENOV M.A. Development of high-resolution UKCIP02-based climate change scenarios in the UK. *Agric For Meteorol*, 2007, Nr. 144.
- [18] STEELE-DUNNE S., LYNCH P., MCGRATH R., SEMMLER T., WANG S., HANAFIN J., NOLAN P. The impacts of climate change on hydrology in Ireland. *Journal of Hydrology*, 2008, Nr. 356.
- [19] VAN VLIET M.T.H., FRANSSSEN W.H.P., YEARSLEY J.R., LUDWIG F., HADDELAND I. Global river discharge and water temperature under climate change. *Global Environ. Change*, 2013, Nr. 23.
- [20] VEZZOLI R., MERCOGLIANO P., PECORA S., ZOLLO A.L., CACCIAMANI C. Hydrological simulation of Po River (North Italy) discharge under climate change scenarios using the RCM COSMO-CLM. *Science of the Total Environment*, 2015, Nr. 521–522.
- [21] XU C-Y., SINGH V.P. Review on regional water resources assessment models under stationary and changing climate. *Water Resour. Manage.*, 2004, Nr. 18.

4. SUMMARY

Assessment of the impact of climate change on climate and discharge in Dez basin is studied based on the downscaled outputs from two GCMs and three SRES scenarios for three time horizons. The study revealed that the basin experiences a significant temperature rise in mid and late 21st century (up to 4 °C). These changes are accompanied by variations in precipitation that is mostly toward a slight increase in the amount of precipitation. Totally, projections of all the scenarios and GCMs indicate a warmer future and slight to moderate increase in precipitation amount. However, obtained results for precipitation are more anomalous, showing both increase and decrease in the amount of precipitation.

To simulate the future discharge at the outlet of each sub-basin under climate change condition, calibrated HBV hydrologic model was enforced with projected temperature and precipitation time-series. Results mostly suggest reduction of annual discharge in the study area. Most significant reduction of annual flow, compared to the base period, reaches up to 33% in two sub-basins located in the upstream of the basin, namely Tireh and Marberreh; while the greatest reductions of the annual flow of Sazar and Bakhtiari sub-basins reach up to 12 and 15%, respectively.

In this study the future climate and hydrological conditions were investigated to assess the climate change impact on the potential of hydropower generation in Dez basin. Based on the results, climate change has the potential to significantly alter the potential of hydropower generation in the basin. Results showed reduction of inflow and electricity generation in Bakhtiari reservoir. While, for Dez reservoir, reduction of the inflow accompanied by a slight increase in the generated electricity. This contrasting result that obtained for Dez reservoir were assessed and has been attributed to the small size of the reservoir (2.7 Bm³) compared to the basin's discharge (8 Bm³), capacity of hydropower plant, different purposes

and releases of the Dez dam and the flow regime changes in the future which causes less spills due to the lower peaks of floods.

In conclusion, the results showed the reduction of electricity generation at Bakhtiari's power plant, therefore its design seems to be carry-over for future climatic conditions; while based on the findings there is room for further development of Dez power plant.

COMMISSION INTERNATIONALE DES GRANDS BARRAGES

VINGT-SIXIÈME CONGRÈS DES GRANDS BARRAGES
Autriche, juillet 2018

DOI 10.3217/978-3-85125-620-8-044



This work licensed under a Creative Commons Attribution 4.0 International License. <https://creativecommons.org/licenses/by-nc-nd/4.0/>

**SEDIMENTATION MANAGEMENT OF THE PATRIND HYDRO POWER
PROJECT USING OHDS TECHNIQUE**

Woncheol PARK

Vice President, K-WATER

REPUBLIC OF KOREA

Kiyong AN

Senior Manager of Overseas Business Division, K-WATER

REPUBLIC OF KOREA

SEDIMENTATION MANAGEMENT OF THE PATRIND HYDRO POWER PROJECT USING OHDS TECHNIQUE

Woncheol. PARK

Vice President, K-water

Kiyong. AN

Senior Manager of Overseas Business Division, K-water

REPUBLIC OF KOREA

1. INTRODUCTION

Fossil resource depletion and climate change have raised the interest of renewable energy around the world. Among them, the development of hydropower is considered to be an effective way to prepare for electricity shortages.

In the case of Pakistan, the government has already set up the "Policy for Power Generation Projects" (2002) to encourage private participation in the electricity market, in which 16 hydroelectric projects have been proposed as long-term plans. Among them, the Patrind Hydro Power Project has been developed by SHPL and is owned by K-water(Main sponsor).

In general, the development and operation of hydropower generation facilities are greatly influenced by hydrological and topographical conditions. In particular, sedimentation in the upstream of a dam causes reservoir volume reductions and generator abrasions. Therefore, a proper management technique for sedimentation is needed for hydropower plant projects.

The area where the Patrind project is located is highly influenced by sedimentation due to the Himalayas. Therefore, it was necessary to apply a sedimentation management method considering topographic and geological conditions and trap efficiency.

2. PROJECT OUTLINE AND SEDEMENT MANAGEMENT GOALS

2.1. PROJECT OUTLINE

The Patrind project is located in the city of Muzaffarabad and is about 120km northeast of Islamabad, which is capital of Pakistan. As it is a run-of-river type hydropower plant, water is taken from the Kunhar River and then generated by the

plant located on the Zehlum River through a headrace tunnel. The specifications of the plant are as follows.

Table 1.
Specifications of the Patrind Hydropower Project

Weir				Intake	Energy Generation		
Catchment Area	Type	Height	Length	Design Discharge	Turbine Type	Installed Capacity	Annual Generation Energy
2,400 km ²	CGD	43.5m	167.6m	153.7 m ³ /s	Vertical Francis	150MW	641.3GWh

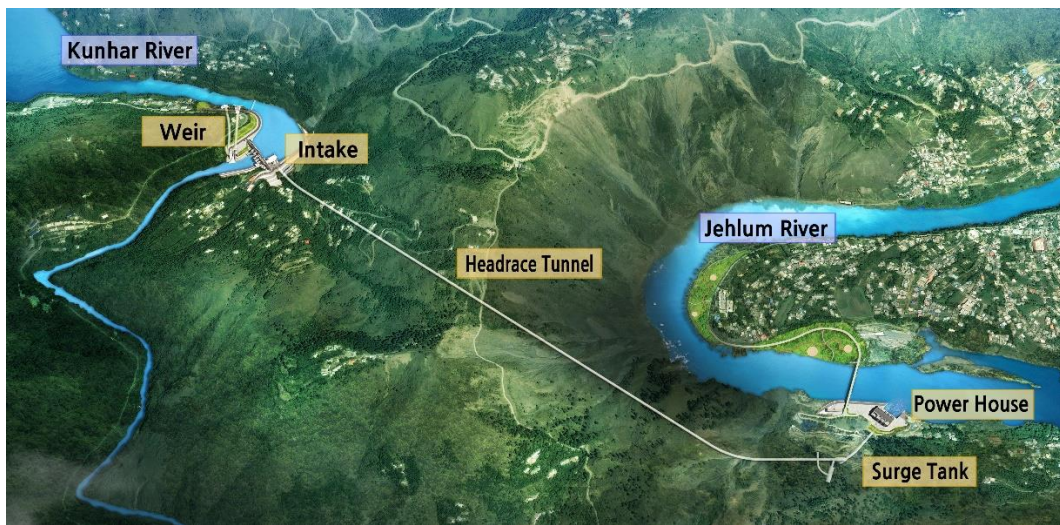


Fig 1.
Bird's-eye View of Patrind Hydropower Project

2.2. SEDIMENT INFLOW STATUS

The project site is directly affected by sedimentation erosion from the Himalayas. In order to check the amount of sediments flowing into weir, we analyzed the discharge and suspended sediment observation data of the Garhi Habibullah station, which is managed by WAPDA (Water and Power Development Authority, Pakistan) and located about 12.3kms upstream of the project site, from 1960 to 2002. The sediment rating curve was made as follows through regression analysis using the observed discharge and suspended sediment amount.

$$Q_{SS} = 0.043 Q^{2.86}$$

Q_{SS} : Suspended sediment load (ton/day), Q : Water flow (m^3/s)

In addition, the results of sieve analysis by discharge conducted by WAPDA allowed for the prediction of the suspended sediment composition flowing into weir.

In the high flow period, the composition ratio of sand was about twice that of the low flow rate due to the high velocity.

Table 2.
Inflow Suspended Sediment Composition

Suspended sediment composition (%)	Clay	Silt	Sand
High flow season(May ~ Aug)	32	52	16
Low flow season(Sep ~ Apr)	21	46	33

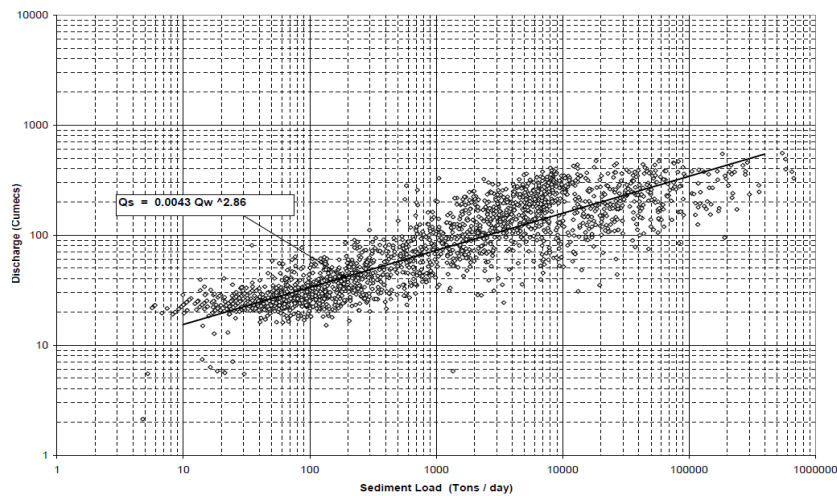


Fig 2.
Suspended Sediment Rating Curve

It was difficult to predict the exact inflow bedload amount due to the lack of observation data. So the bedload was assumed to be about 10% of the suspended sediment. The total amount of sediment flowing into weir was calculated by summing up the bedload and suspended sediment. The amount of sediment was estimated to be 4.4Mt considering the discharge condition during the year.

2.3. SEDIMENT MANAGEMENT GOALS

When the sediments flow in the weir, they have a strong influence on the operation, maintenance, and economics of the hydropower project. Therefore, we set a sediment management goal of preventing 0.2mm or higher of sediments from flowing into the intake.

3. SAND TRAP DESIGN

3.1. DESIGN CHANGE HISTORY OF SAND TRAP

The initial sand trap design was presented in the Feasibility Study prepared in 2007. In that study, the layout included a weir just downstream of the bend of the Kunhar River, with a Power intake in front of the weir on the left side and three underground sandtrap chambers to accomplish goal of sediment management along the headrace tunnel axis.

Table 3.
Specifications of the Sand Trap (Feasibility Study, 2007)

Type	Design Discharge	Chamber		Flushing Tunnel	
		Section	Length	Section	Length
Underground sand trap	153m ³ /s (51×3chamber)	15×17m	180m	3.5×3.5m	407m

In the basic design, however, the location of the weir axis was moved 150m upstream from the proposed location in the Feasibility Study, and a surface sand trap was designed as an alternative instead of an underground type sand trap in the Feasibility Study. This is because the geological properties of the original sand trap site don't have sufficient supporting force for the foundation of the structure. According to a drilling investigation, a clay silt layer is distributed up to 6.0m from the surface. RQD is mostly 0%, even if the values of 10~24.0% are shown, partially.

Table 4.
Specifications of the Sand Trap (Basic Design, 2010)

Type	Design Discharge	Chamber		Flushing Tunnel	
		Section	Length	Type	Section
Open Type	153 m ³ /s (76.5 m ³ × 2 chamber)	23×26.7m	140m	Box Culvert	1.8×2.5m

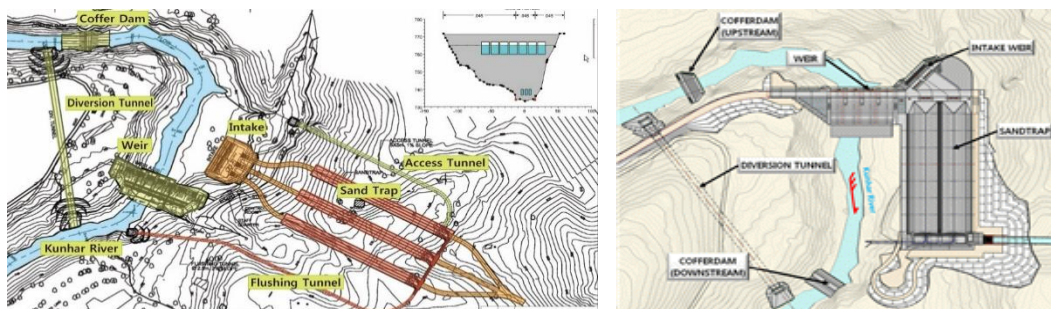


Fig 3.

Project Layout of the Feasibility Study(left) and Basic Design(right)

A numerical analysis(HR Wallingford, 2012) was conducted to review the appropriateness of the modified project layout. For modeling the deposition, a water level of 765m asl, Normal High Water Level, was prescribed at the weir.

Different scenarios were considered for the estimation of annual amount of deposition simulated with the 1D model RESSASS. The results show that the reservoir is likely to be filled in about five years. The average annual amount of sediment deposits is around 2 MT(annual sediment inflow is about 4.2MT) per year.

Several scenarios were considered for the distribution of the sediments near the weir with a 2D modelling system TELEMAC-SYSPHE-HR. The results show that in front of the intake, deposition occurs in all cases up to the elevation of about 760m asl. The invert of the intakes is at 750m asl. During high flows, the model results show a sand bar forming between the intakes and the weir gates, reaching almost the water level surface. These problems led to the consideration of new sediment management methods.

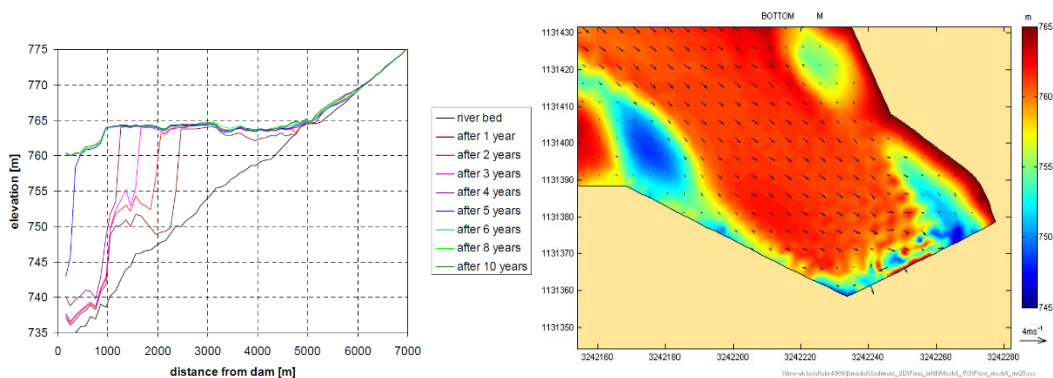


Fig 4. Bed Evolution During Deposition(left) and Deposition after 48days($Q=153\text{m}^3/\text{s}$)(right)

3.2. OHDS TECHNIQUE

Generally, management activities to address reservoir sedimentation may be classified into four broad categories (Morris, 2015). Among them, the Patirind Hydropower Project adopted "Route Sediments" and "Remove and Redistribute Sediment Deposits" to handle inflow sediments. We called adopted method "OHDS technique". This technique was developed by Alam(2014) considering that the flows exceeding the capacity of the intake($153\text{m}^3/\text{s}$) would be diverted through a by-pass tunnel. The area of the reservoir and modified pool(hereafter called MP), between the cofferdam and the weir was conceived as acting as a natural sand trap. As this area has a larger volume than the designed sand traps and considering low velocities than in the sand traps, its efficiency should be higher than that of the artificial sand traps.

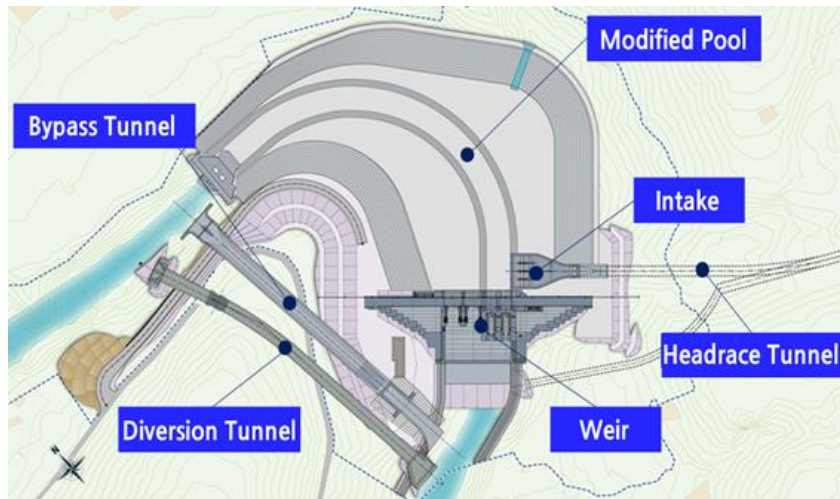


Fig 5.
Layout of the Weir Site(Detail design, 2015)

3.3. NUMERICAL ANALYSIS

3.3.1. *Input data and boundary conditions*

A numerical analysis was carried out to verify sedimentation management performance of the OHDS technique(HR Wallingford, 2014). The long series of water discharges, from 1960 to 2007 has been used in this analysis as input data. The sediment rating curve described in the Feasibility Study was used to define the amount of suspended material. As well, a bypass tunnel and MP were considered. The diameter, length and discharge capacity of the bypass tunnel were 8.5m, 229m, 804m³/s respectively.

The water discharge is split according to the following rule: when discharge is less than 200 m³/s, the bypass tunnel is closed and all water and sediment passes over the coffer dam. When discharge is more than 200 m³/s, the bypass tunnel is opened and the discharge in excess of 153 m³/s, the design discharge rate, flows through the bypass tunnel.

3.3.2. *Analysis results*

First, we analyzed the effects of reducing sedimentation using the bypass tunnel. The results show that any coarse material, gravel fractions > 2.9 mm, will bypass through the tunnel. 47% of the sand material transported by the flow (as average), with diameters from 0.1 to 0.92 mm, will be conveyed towards the MP. The results show that the amount of sand that flows over the cofferdam towards the MP has been fairly constant for all the years (around 0.56Mt)

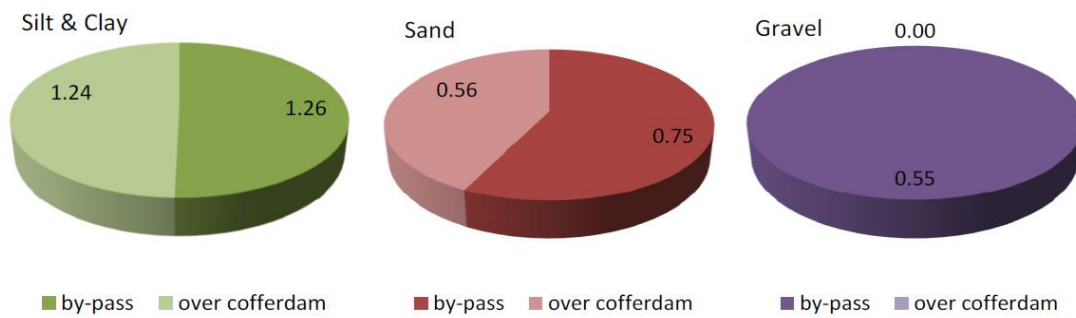


Fig 6.
Average Annual Amount of Sediments(in Mt)

Second, an assessment of the trapping efficiency was presented. MP must meet the velocity standard, 0.2m/s, to function as a sand trap. So a 2D numerical analysis (using TELEMAC) was conducted at a rate of 153 m³/s, the design discharge, and 200 m³/s, the bypass tunnel open condition. The results show that for discharge of 153 m³/s, the flow velocities in the MP do not exceed this limit except locally at the intake. For the discharge of 200 m³/s, there are some areas with velocities greater than 0.2m/s. In most of the MP, however, velocity is still below 0.2m/s. Therefore, the MP can act as a natural sand trap.

3.4. PHYSICAL MODEL INVESTIGATION

3.4.1. Introduction and Basic data

Physical model investigation was conducted to verify the performance of sediment management using the OHDS technique. It is conducted by the Laboratory of Hydraulics, Hydrology and Glaciology(VAW) of the Swiss Federal Institute of Technology Zurich(ETH Zurich). The experiments were separated into hydraulic tests with a fixed bed and sedimentological tests with a movable bed and sediment supply.

The inflow water flow discharge and suspended sediment data collected from 1960 to 2012 were used. The sediment rating curve described in the Feasibility Study was used to define the amount of suspended material. As well, the bed load was assumed to be 15% of the suspended load based on a conservative review.

3.4.2. Physical model construction

In order to choose an appropriate model scale, Froude similarity was applied. This was because for free surface flow, scaling with the Froude law is the most commonly used model that represents the best the general hydraulic phenomena.

Table 5

Scaling Factors Applied to Physical Model Construction

Parameter	Length(m)	Time(s)	Velocity(m/s)	Discharge(m ³ /s)
Scale factors	1 : 45	1 : 6.71 (1:45 ^{1/2})	1 : 6.71 (1:45 ^{1/2})	1 : 13,584 (1:45 ^{5/2})

The suspended sediments are too fine at the model scale of 45 to be reproduced correctly in the model as the scaled down grain diameter would be affected by cohesion. Therefore, the fine sediments are represented by artificial sediment, distorted in density and size having appropriate critical shear velocity according to the Shields curve and appropriate fall velocity. In general, Ground walnut shells are a common material for suspension modeling as they are cohesion-less, easy to mix, produce a homogeneous distribution and have a specific weight smaller than sand (Kantoush 2008, Jenzer 2011). So for the suspended load tests, ground walnut shells were used. The condition of the physical model applied is as follows.

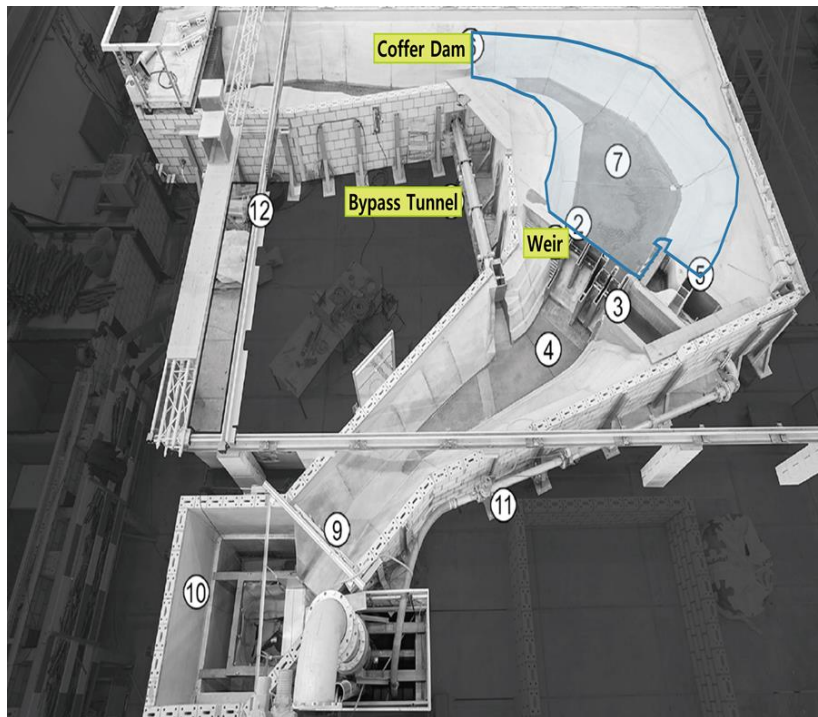


Fig 7.
Bird's-eye View of the Physical Model

3.4.3. Investigation Result

First of all, the flow condition, the water level and the flow velocities in the MP are described for the variant load case. During normal power operation(hereafter called NPO), design discharge $Q=156 \text{ m}^3/\text{s}$, the water surface

is smooth and no waves were observed in the MP. During a high flow condition, discharge starting power shutdown $Q=800 \text{ m}^3/\text{s}$, the flow pattern shows oscillations due to the forming of a vortex in front of the bypass tunnel inlet. The water level in the modified pool is kept at operation reservoir level (765m a.s.l) for NPO and high flow condition. Flow velocities are measured with an Acoustic-Doppler-Velocimetry probe (ADV). During NPO, flow velocities only exceed 0.2m/s in the region of the cofferdam and close to the power intake. In a large region of the MP the vertical velocity fluctuations are smaller than the settling velocity of 2.5 cm/s for grains with $d=0.2 \text{ mm}$ in still water. Therefore, larger grains are expected to settle in the MP during power operation.

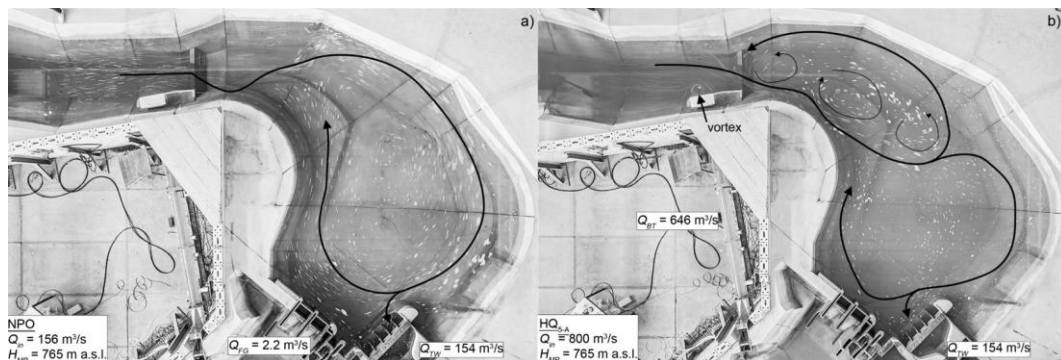


Fig 8.

Top View on the Modified Pool for $Q=156 \text{ m}^3/\text{s}$ (left) and $800 \text{ m}^3/\text{s}$ (right)

Second, a transfer experiment of suspended sediments was conducted for HQ5-A load case, maximum discharge was $748.6 \text{ m}^3/\text{s}$, to identify deposition properties of fine sediment. The following table (Table 8) gives an overview of the deposited and sluiced sediment volumes measured in the model. These results show that all inflow sediment targeted diameters (above 0.2 mm) are deposited through the bypass tunnel and modified pool.

Table 6.
Sediment Balance

Parameter (HQ _{5-A})		Bed load		Suspended load	
		Quantity (m ³)	Ratio (%)	Quantity (m ³)	Ratio (%)
Previous depositions		40,000		150,000	
Inflow	added to the inflow	2,750	100	68,000	100
Deposit	Upper coffer dam	2,750	100	49,220	72
	modified pool	-		11,200	16.5
	Sluiced through the bypass tunnel	500		7,580	10.9
	Power intake			400	0.6

Finally, we conducted a reservoir flushing test to find the optimum condition to remove deposited sediments. The performance of the two flushing tests ($Q =$

150 m³/s and 200 m³/s) were very similar, though the flushed out sediment volume was about 10% higher for Q = 200 m³/s. This means that 85% of the total MP water storage capacity of 687,000 m³ were restored. After the flushing, the deposits in front of the power intake were cleared down to the original bed.

Table 7.
Volume Balance of Flushed Deposits in the MP for Load Case

Load case	MP volume (m ³)	Initial deposit volume (m ³)	Erosion		Residue	
			Volume (m ³)	Percentage of eroded volume	Residual deposits (m ³)	Residual MP volume
Q 150m ³ /s, 1day flushing	687,000	200,000 (100%)	88,000	44%	112,000	84%
Q 200m ³ /s, 1day flushing			96,500	48%	103,500	85%

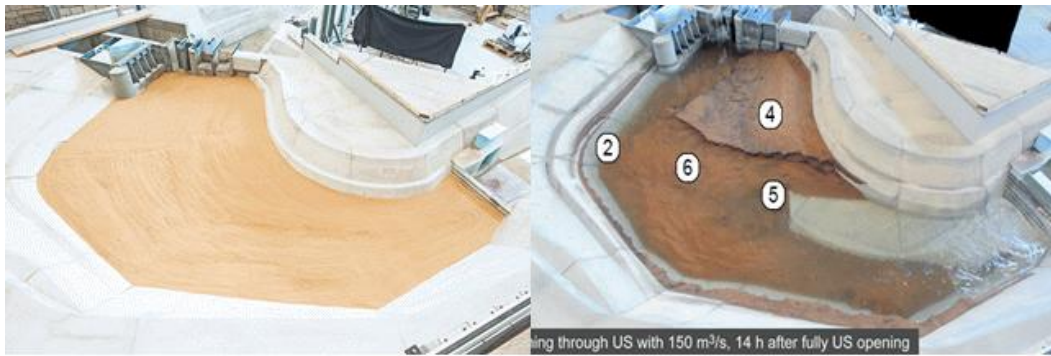


Fig 9.

The Initial Condition(left) and Hydraulic Flushing of Built up deposits with 150 m³/s after 14 Hours of Flushing Through the Fully Opened Underway Spillway Gate

4. CONCLUSION

The area where the Patrind project is located is highly influenced by sedimentation due to eroded soil in the Himalayan Mountains. In order to manage sedimentation effectively, topographic and geological investigations, as well as several numerical analyses and physical model investigations were conducted.

Through this process, the project adopted the OHDS technique, bypass tunnel and natural sand trap(MP), to prevent sediment inflow into the intake. In addition to applying OHDS, stability against sedimentation was further enhanced through turbine coating.

The Patrind Hydropower Plant has been in operation since November, 2017 and hydrological monitoring and flushing effect analyses are scheduled to be conducted at the end of the dry season, March 2018, to confirm OHDS appropriateness.

REFERENCES

- [1] Alam, S. Report on Project Site Visit. Review of the concept of the sediment removal from the power discharge and the proposed modified arrangement, 2014.
- [2] PES, Fichtner. Patrind Hydropower Project Feasibility Study, 2007.
- [3] HR Wallingford. Sedimentation studies at Patrind Hydropower Project, 2012.
- [4] HR Wallingford. Extension of sediment studies at Patrind hydropower project. Assessment of by-pass option, 2014.
- [5] ETH. Patrind Hydropower Project. Physical Model Investigation of the Weir Site. Hydraulic and Sedimentological Tests, 2016.
- [6] Daewoo, Sambu. Pakistan Patrind Hydropower Project. Basic Design Report, 2010.
- [7] Daewoo. Pakistan Patrind Hydropower Project. Detailed Design Report, 2015.
- [8] Morris, G. L. Management Alternatives to Combat Reservoir Sedimentation. In Proceedings of the International Workshop on Sediment Bypass Tunnels, 2015.

COMMISSION INTERNATIONALE DES GRANDS BARRAGES

VINGT-SIXIÈME CONGRÈS DES GRANDS BARRAGES
Autriche, juillet 2018

DOI 10.3217/978-3-85125-620-8-045



This work licensed under a Creative Commons Attribution 4.0 International License. <https://creativecommons.org/licenses/by-nc-nd/4.0/>

**ADVANTAGES OF DRY DAM AS FLOOD CONTROL
IN JAKARTA'S URBAN AREA**

Airlangga MARDJONO

*Head of West Division Dam Centre, MINISTRY OF PUBLIC WORKS AND
PUBLIC HOUSING*

INDONESIA

Agus SAFARI

Chief of Dam Project, CILIWUNG CISADANE RIVER BASIN ORGANIZATION

INDONESIA

Faris SETIAWAN

*Chief of Sukamahi Dam Project, CILIWUNG CISADANE RIVER BASIN
ORGANIZATION*

INDONESIA

COMMISSION INTERNATIONALE
DES GRANDS BARRAGES

VINGT-SIXIÈME CONGRÈS DES
GRANDS BARRAGES

Autriche, juillet 2018

**ADVANTAGES OF DRY DAM AS FLOOD CONTROL
IN JAKARTA'S URBAN AREA**

Airlangga MARDJONO

Head of West Division Dam Centre, Ministry of Public Works and Public Housing

Agus SAFARI

Chief of Dam Project, Ciliwung Cisadane River Basin Organization

Faris SETIAWAN

Chief of Sukamahi Dam Project, Ciliwung Cisadane River Basin Organization

INDONESIA

ABSTRACT

The Ciliwung River Basin population density is roughly about 5100 people per km square. In the last ten years this number has increased rapidly. Ciliwung river basin is located in 2 provinces, West Java Province (Bogor Regency, Bogor City, and Depok City) in the upstream and middle reach and Capital City Jakarta Province (South Jakarta, East Jakarta, Center Jakarta, West Jakarta, and North Jakarta) in the downstream area. The dry dam is one of the alternatives for flood control in the urban area, when the resettlement to be main issues in the urban area.

Keywords: Dry Dam, Flood Control, Small Resettlement

1. BACKGROUND

Jakarta as the Special Capital Region of Indonesia has an area of approximately 661.52 km². Jakarta have a big issues to manage the river, with 'too much water', 'too little water' and 'too dirty water. Too much water, because every year it were hit by the worst flooding. Too little water, because we have varied rainfall distributions from the wettest (> 4,000 mm/year) to the most drought (< 800 mm/year) and very difficult to fulfill a demand of water supply because the population in the Greater Jakarta is rapidly increase, but the quantity and continuity of water supply is very limited. Too dirty water, because many people (mostly the low incomes) live on the river banks even on the middle of the river, the worst thing from the people who live along the river rely on its use for daily necessities including cooking, cleaning and washing, the river is increasingly being used as a place to dispose of trash and inorganic waste materials.

The problem of Jakarta during the rainy season is flooding in several places in the Ciliwung river basin. Based on the masterplan of flood control in Jakarta, planned to be built Ciawi Dam and Sukamahi Dam which will be useful as flood control, this dam is located in the upper Ciliwung river.

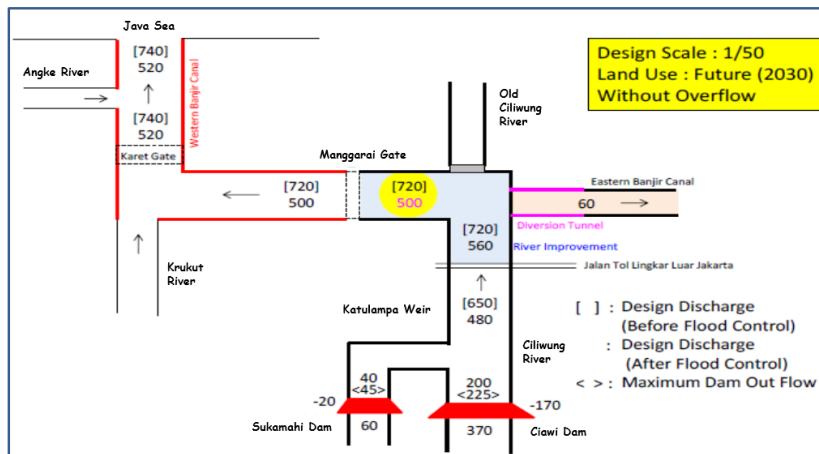


Fig. 1
The Masterplan Of Flood Control In Ciliwung River

Ciawi Dam designed as dry dam, it equipped tunnel without a gate to control the flood. The Dam type is random zone with height 55 meters from bottom fondation, and total volume 6,45 million m³. Sukamahi Dam will be build in Sukabirus river and planned to be build using straight core in the middle, with random zone on shoulder. Sukamahi Dam height 50 meters measured from bottom of the deepest foundation excavation, top Dam elevation + 601 meters with 9 meters width and 198 meters length. Ciawi Dam and Sukamahi Dam are constructed to support flood control system of Jakarta.

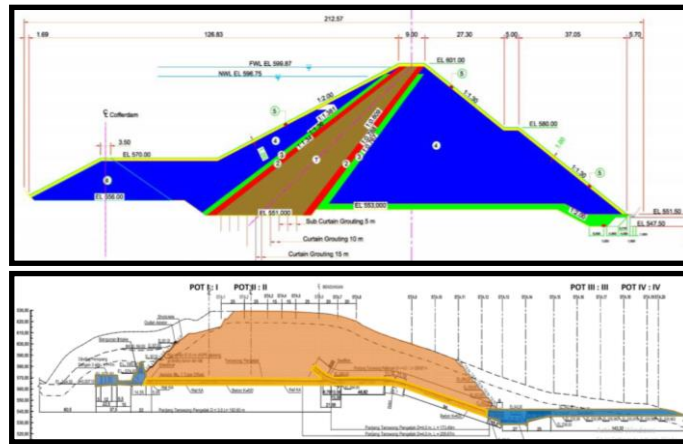


Fig. 2
Typical Detail Design of Sukamahi Dam

Advantages of this type of dam (Dry Dam) are not only the lack of sedimentation in the reservoir, the water quality of the river either upstream or downstream of the natural dam and the supply of the upstream part of the river. Besides, the maintenance of river ecosystem is not disturbed as migration of fish can still go downstream and going home based on previous habit including material condition in all river area.

The main advantage in flood control with dry dam is effective for flood control in the urban area, because with small storage and small resettlement it can delay the peak of flood maximally. The dry dam has a low operating cost and easy to operate because there is no water elevation setting so it can work without door operation. With the above reasons, an engineering operation is performed, which at the beginning of the rainy season, the water level of the reservoir is set to a low elevation so that at the beginning of the flood, the flood discharge flows freely through the tunnel.

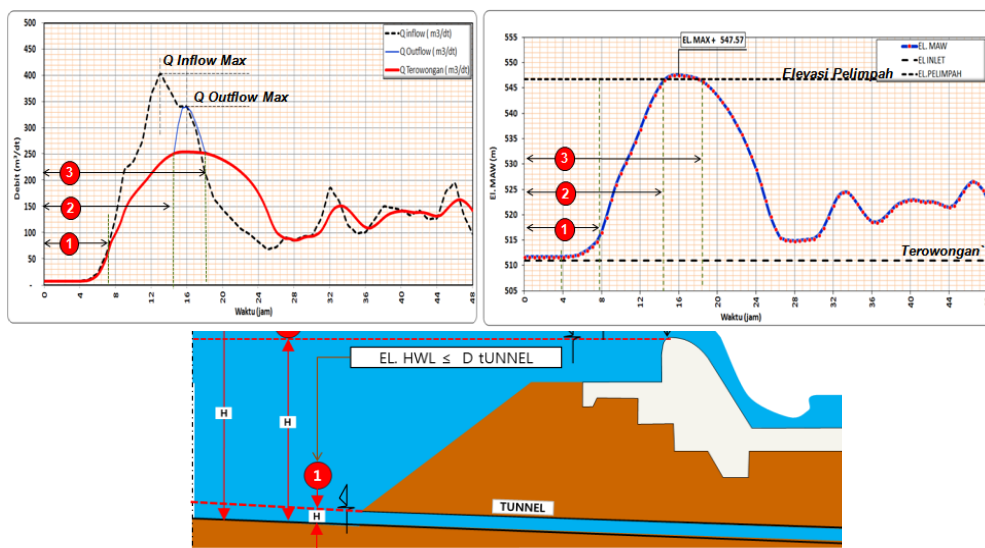


Fig. 3
The Concept of Dry Dam

River Flow Conditions:

a. Condition 1 :

For low flow with discharge is smaller than tunnel capacity, water level in the beginning of tunnel is lower than or as same as the height of tunnel. Water flows with free flow condition inside the tunnel.

b. Condition 2

The flood discharge exceeds the tunnel capacity, water will flow up but the level is still lower than spillway crest elevation. Water flows through the tunnel with pressured condition.

c. Condition 3

The flood discharge exceeds the tunnel capacity, water will flow up and exceeds the spillway crest elevation. Water will flow through the tunnel with pressured condition and overflow through spillway crest.

Considering the need for flood reduction, the concept of control on Ciawi Dam and Sukamahi Dam is as follows:

a. Changing the flow pattern of streams that under existing conditions flow through the natural river channel with the average width of the river bottom 13-15 meters, into a controlled flow by making the dam with the flow of water through the tunnel.

b. As a result of the system, the outflow capacity through the tunnel will be smaller than the natural river, so the water flowing downstream is also smaller.

c. Dam function in the above conditions is to hold the elevation of the rising water surface due to outflow outflow through the tunnel is smaller than inflow discharge.

d. Dam is equipped with spillway, so if the flood discharge happened big enough, the water level of the reservoir rises and the water flows through the spillway. The discharge going downstream of the dam is the total discharge that flows through the tunnel and through the spillway.

2. EXISTING CONDITION OF CILIWUNG RIVER

Water level on Katulampa Weir in the up stream of Ciliwung River currently use as flood reference for the down stream. The limits which are used as the standard of flood early warning are:

Table 1
Katulampa Weir as Flood Alert

Flood Alert	Water Level H (cm)	Discharge Q (m3/s)
Normal	< 80	< 90
Level III	80 - 150	90 - 276
Level II	150 - 200	276 - 442
Level I	> 200	> 442

Based on hourly data from Katulampa AWLR and Cibogo AWLR in period of 2004 – 2013, the history of flood in Ciawi Dam and Sukamahi Dam are:

Table 2
Flood Event in Ciawi Dam and Sukamahi Dam

No	History of Floods	Discharge (m ³ /s)	
		Ciawi	Sukamahi
1	18-Jan-04	73.19	13.12
2	18-Jan-05	119.34	21.39
3	23-Jan-06	100.63	18.03
4	03-Feb-07	360.91	64.68
5	12-Mar-08	125.96	22.57
6	13-Jan-09	117.72	21.1
7	12-Feb-10	218.19	39.1
8	17-Nov-11	78.31	14.03
9	13-Dec-12	103.63	18.57
10	04-Mar-13	253.34	45.4

From the AWLR discharge data, besides the flood event is known, the flood frequency along the year can be studied in Ciawi Dam and Sukamahi Dam. If the discharge in the Katulampa Weir are known, so by using the catchment ratio, the discharge in Ciawi and Sukamahi Dam could be predicted.

Table 3
Flood Frequency in One Year at Ciawi Dam

Discharge (m ³ /s)	jan	Feb	Mar	Apr	May	Jun	Jul	Ags	Sep	Oct	Nov	Dec
Q > 53,17	75	120	36	16	12	0	5	6	7	8	16	16
Q > 163,07	0	8	1	0	0	0	0	0	0	0	0	0
Q > 261,15	0	5	0	0	0	0	0	0	0	0	0	0

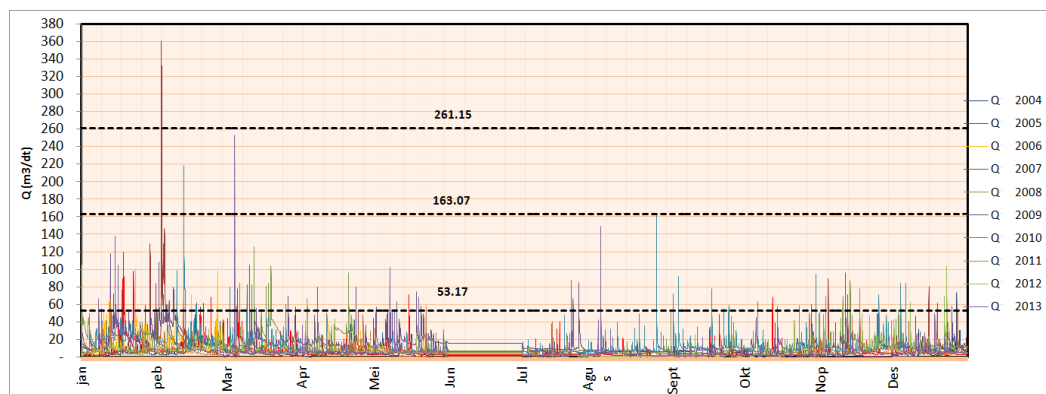


Fig. 4
Flood Frequency in One Year at Ciawi Dam

Table 4
Flood Frequency in One Year at Sukamahi Dam

Discharge (m ³ /s)	Jan	Feb	Mar	Apr	May	Jun	Jul	Ags	Sep	Oct	Nov	Dec
	The Frequency of Occurrence (time)											
Q > 9,5	75	120	36	16	12	0	5	6	7	8	16	16
Q > 29	0	8	1	0	0	0	0	0	0	0	0	0
Q > 46,8	0	5	0	0	0	0	0	0	0	0	0	0

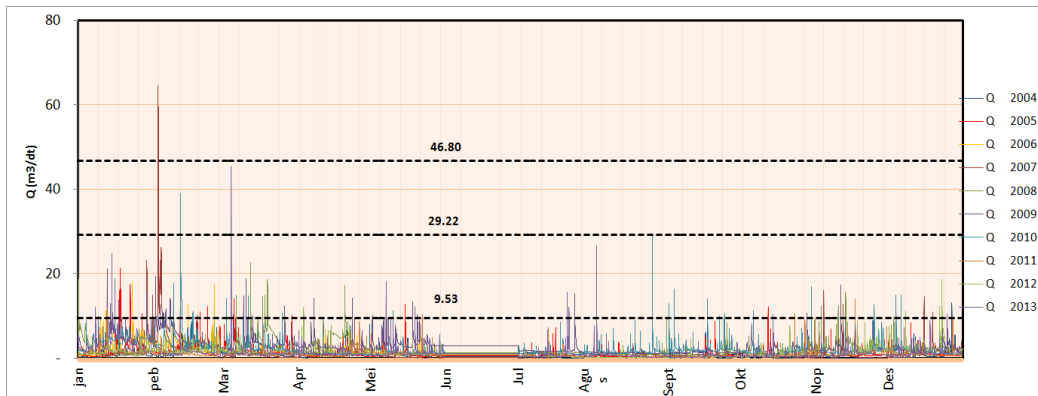


Fig. 5
Flood Frequency in One Year at Sukamahi Dam

From the data above, it can be known that the wet season pattern starts from November to April and dry season is May to October.

3. ANALYSIS OF FLOOD CONTROL IN CIAWI AND SUKAMAH DAM

As stated previously, Ciawi Dam and Sukamahi Dam are planned as flood control measures. To optimize the flood reduction, the reservoir water level should be in low condition, where the water flows freely through tunnel.

Flood routing calculation result for flood return period 2 yr, 5 yr, 10 yr, 20 yr, 25 yr, 50 yr, 100 yr and Q_{PMF} at Ciawi Dam and Sukamahi Dam in fully opened tunnel condition as presented in the next figure.

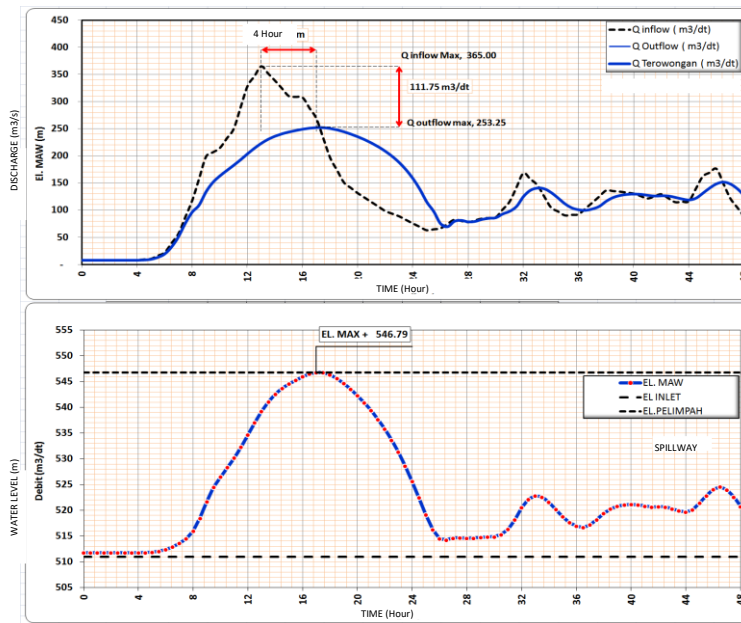


Fig. 6
Flood Discharge Routing of Return Period 50 yr at Ciawi Dam

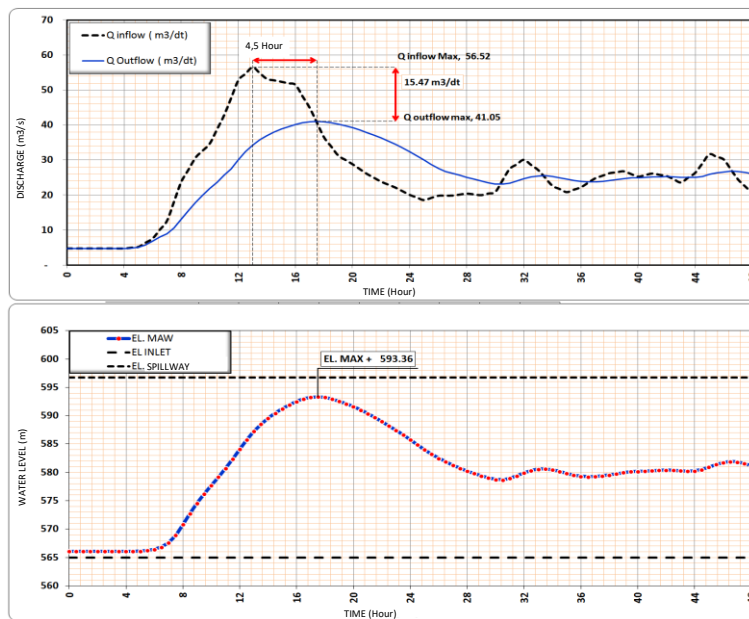


Fig. 7
Flood Discharge Routing of Return Period 50 yr at Sukamahi Dam

Table 5
Summary of Flood Routing through Tunnel in Ciawi and Sukamahi Dam

No	Periode	Ciawi Dam				Sukamahi Dam			
		Inflow	Outflow	Reduction	Defer Time	Inflow	Outflow	Reduction	Defer Time
		(m ³ /s)	(m ³ /s)	(m ³ /s)	Hour	(m ³ /s)	(m ³ /s)	(m ³ /s)	Hour
1	2 th	184,70	162,38	22,33	1,50	30,36	25,75	4,61	3,50
2	5 th	242,87	198,70	44,17	3,00	38,80	31,60	7,20	4,00
3	10 th	281,60	218,48	63,12	3,50	44,42	35,00	9,42	4,00
4	25 th	330,72	239,36	91,36	4,00	51,54	38,73	12,82	4,50
5	50 th	365,00	253,25	111,75	4,00	56,52	41,05	15,47	4,50
6	100 th	403,60	340,42	63,18	3,00	62,12	43,52	18,60	4,50
7	1000 th	524,10	519,33	4,77	0,50	79,60	73,87	5,73	2,00
8	PMF	1,242,96	1,227,04	15,92	-	253,97	250,89	3,08	-

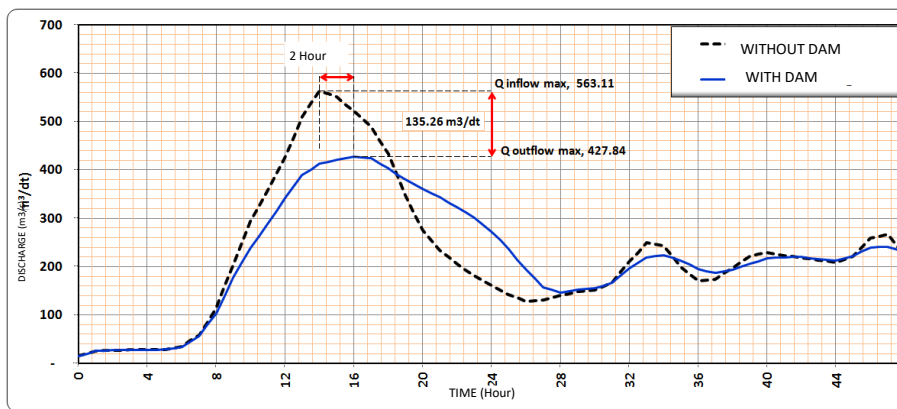


Fig. 8
Change of Discharge in Return Period of 50 year, at Katulampa Weir, due to Ciawi Dam and Sukamahi Dam

From the flood discharge routing for return period of 50 year, with the construction of Ciawi Dam and Sukamahi Dam, the flood discharge in the down stream of Ciliwung River is 577,05 m³/s. If it's deducted by the discharge to East Flood Canal 60,0 m³/s, therefore the discharge at Manggarai gate would be 517,05 m³/s.

The current status of these dam is progressing with site preparation, land acquisition, etc, with schedule of construction commencing in the month of, November, 2017 and plan of completion in 2019.

4. CONCLUSION

This paper can explain the advantages of Dry Dam with single purpose for flood control. Major conclusions are as follows:

- a. The dry dam is one of the alternatives for flood control in the urban area, when the resettlement to be main issues in the urban area.

- b. The dry dam effective for flood control by cutting and defer the peak of flood by:
- existing landscapes and ecosystems have not changed;
 - river morphology and river regime (natural flow) are unchanged;
 - easy to operate;
 - No risk in flood control functions.
- c. The dry dam has a low operating cost because there is no water elevation setting so it can work without door operation.
- d. Ciawi Dam and Sukamahi Dam can delay the flood discharge coming from the river ciliwung to jakarta, so the flood impact in the National Capital of Indonesia can be avoided.

5. ACKNOWLEDGMENTS

This paper was supported by Ciliwung Cisadane River Basin Organization. The author express deep gratitude for the supports.

REFERENCES

- [1] Review Detail Design of Ciawi Dam Report in Bogor Regency of West Java, in 2014, contained the Feasibility Study of Ciawi Dam and Sukamahi Dam.
- [2] Detail Design of Ciawi Dam and Sukamahi Dam, in 2015, including Model Test and Design Certification.
- [3] Certification design of Ciawi Dam and Sukamahi Dam, in 2016.

COMMISSION INTERNATIONALE DES GRANDS BARRAGES

VINGT-SIXIÈME CONGRÈS DES GRANDS BARRAGES
Autriche, juillet 2018

DOI 10.3217/978-3-85125-620-8-046



This work licensed under a Creative Commons Attribution 4.0 International License. <https://creativecommons.org/licenses/by-nc-nd/4.0/>

**GREEN DAM RESERVIUR: A NEXUS CONCEPT FOR SAFE OPERATION
AND MAINTENANCE OF DAMS IN IRAN**

Saied YOUSEFI

*Assistant Professor, UNIVERSITY OF TEHRAN IN IRAN & UNIVERSITY OF
WATERLOO IN CANADA*

IRAN

Naser KHEIRKHAH

*Senior Dam Expert, IRAN WATER AND POWER RESOURCES
DEVELOPMENT COMPANY (IWPCO), TEHRAN*

IRAN

Mohamad RAHBARI

*Directing Head of Small and Medium Dam and Hydropower Plants Projects,
IRAN WATER AND POWER RESOURCES DEVELOPMENT COMPANY
(IWPCO), TEHRAN*

IRAN

COMMISSION INTERNATIONALE
DES GRANDS BARRAGES

VINGT-SIXIÈME CONGRÈS DES
GRANDS BARRAGES
Autriche, juillet 2018

GREEN DAM RESERVIOUR: A NEXUS CONCEPT FOR SAFE OPERATION AND MAINTENANCE OF DAMS IN IRAN

Saied YOUSEFI¹, Naser KHEIRKHAH², Mohamad RAHBARI³

¹ Assistant Professor, UNIVERSITY OF TEHRAN IN IRAN & UNIVERSITY
OF WATERLOO IN CANADA

² *Senior Dam Expert, IRAN WATER AND POWER RESOURCES
DEVELOPMENT COMPANY (IWPCO), TEHRAN, IRAN*

³ *Directing Head of Small and Medium Dam and Hydropower Plants
Projects, IRAN WATER AND POWER RESOURCES DEVELOPMENT
COMPANY (IWPCO), TEHRAN, IRAN*

1. INTRODUCTION

Many dams have been recently constructed in Iran with different purposes, from storing water for agriculture and industrial usages, to household uses for hundreds of years in Persian culture historically. Hydroelectric dams, additionally, act as an alternative to non-renewable energy resources that constitute the majority of the world's energy [1]. Despite enormous benefits of dams, they may have drastic damaging effects on the environment and on the populations that live near dams and thus, have become the subject of great scrutiny, with organizations concerned with environmental health such as Iranian Environmental Organization [2]. In a worldwide perspective, Out of the 38,000 large-scale dams, registered by the International Commission on Large Dams (ICOLD), an international organization that sets the standards for dams, 50 percent of dams are used for irrigation, 18 percent for hydropower, 12 percent for water supply and 10 percent for flood control and the rest for other functions [3]. As such, external effects such as environmental issues are of a huge consideration for any nation.

Water pollution refers to the contamination of a water source by some foreign substance that makes the water unsafe to drink or for use for agriculture and/or industry. This substance could be just about anything, and there are many factors causing water pollution. If the water source is changed in any way by the presence of that substance, then that water should be considered polluted [4].

While hydropower does not cause water or air pollution, it does have an environmental impact: Hydroelectric power plants may harm fish populations, change water temperature and flow (disturbing plants and animals) and force the relocation of people and animals who live near the dam site. Some fish, like salmon, may be prevented from swimming upstream to spawn. Technologies like fish ladders help salmon go up over dams and enter upstream spawning areas, but the presence of hydroelectric dams changes their migration patterns and hurts fish populations. Hydropower plants can also cause low dissolved oxygen levels in the water, which is harmful to river habitats. Reservoirs may also lead to the creation of methane, a harmful greenhouse gas [5].

In this research an environmentally friendly approach for dam construction and maintenance projects in Iran is proposed. The methodology takes into account diverse ranges of environmental issues and categorize them. Afterwards, proper remediation actions are developed to address each category. A brief review of related literature is stated in the next section, followed by Section 3 that presents the methodology development. Finally, Section 4 summarize some concluding remarks.

2. LITERATURE REVIEW

Dams are used for a wide range of purposes including providing drinking water, agricultural water, industrial uses, flood control, and energy generation. The later one began in 1895 when the first dam and hydropower plant was built on the Niagara Falls successfully. The basic of hydropower does not have much changes in 120 years and since then, many efforts have been made to have a fresh look at hydropower to try to make it more environmentally friendly. That's because, while hydro dams provides 85 percent of the world's renewable electricity, it comes with a cost. Along with more commonly known issues such as habitat disruption, recent studies suggest reservoirs created by hydroelectric dams are a significant source of greenhouse gas emissions. That's why many environmentalists argue that other sustainable energy sources have evolved as better alternatives. For example, wind and solar have become cheaper in many countries and they are less risky in climate terms. They can be deployed more quickly, and they have smaller environmental and social footprints [6]. On the other hand, there are many experts believing that hydroelectric dams bring several benefits for societies such as job creation and flood control though it is of course necessary to mitigate their adverse impacts. For example, the US Department of Environment (DOE) develops new

environmental metrics to assess the environmental performance of new hydropower. The peer-reviewed process starts with defining what sustainability means for hydropower, then setting performance measures for different environmental effects, such as fish migration, energy efficiency and greenhouse gas emissions [7].

As a case study, a team from the University of the Philippines Diliman (UPD) has designed a system for the Gaia dam in Philippines that can control or prevent flooding from torrential rains on farms, along rivers and in coastal areas by minimizing and re-routing the flow of water through storm runoff pathways. Its main structural frame consists of gabion cages: wire mesh baskets filled with sturdy columns of recycled concrete cylinders or rocks, which provide stability against the hydrostatic forces pushing through the dam [8]. Like a miniature hydroelectric power plant, the Gaia dam could divert water into the powerhouse where turbines are installed, yet do so less expensively than the concrete dams that are usually used for this purpose. In addition, the dam is designed to release proprietary proteins and enzymes when water passes through its specialized core. Its proteins are designed to help crops absorb soil nutrients and minerals, while its enzymes would gradually dissolve the exoskeletons of insects and other pests that attack the crops, thereby acting as natural fertilizers and pesticides. Thus the Gaia dam has the potential to help in the production of organic crops.

The dams themselves often flood large expanses of forest (creating methane emissions). Also, dams require networks of roads for dam and power grid construction. These roads frequently open a Pandora's Box of environmental problems, including illegal deforestation, mining, poaching, and land speculation. For instance, the 12 dams planned for the Tapajos River in the Brazilian Amazon are projected to increase deforestation by nearly one million hectares, by 2030 [9]. The modern dam explosion and its indirect impacts via road construction into remote frontiers are arguably its worst consequences of all.

2.1. FIXING EXISTING PROBLEMS

Many dams in Iran and worldwide have been constructed in the past when environmental and social impacts were not that much of concern. Recently, endless efforts are being made to retrofit the hydropower projects in the operation phase [11]. Restoring fish passage is a major focus. Many large dams were built without fish ladders and remain an absolute barrier to fish migration. Climate change makes this an even greater concern, because migratory species like salmon and steelhead need access to cold-water spawning habitat above dams as temperatures warm. Adding fish ladders however, exceeds the original construction cost of some large dams. Compromises include trap-and-haul programs, in which fish are collected and transported by tanker truck around dams, and motorized lifts in various configurations.

Dealing with greenhouse gas emissions is another current environmental challenge. Reservoirs may emit substantial amounts of methane, a powerful greenhouse gas, when vegetation and algae decay with changing water levels. Solutions may include controlling erosion in upstream watersheds and managing water elevation more carefully, especially during warm seasons [12].

Reservoirs also trap pollutants left behind by past industrial practices, which flow downstream and concentrate behind dams. These chemicals can accumulate in fish, making them dangerous for people and wildlife, and also, pose a health hazard in drinking water. Removing pollutants trapped in a reservoir presents a huge logistical challenge.

3. METHODOLOGY DEVELOPMENT

This research strives to present an innovative approach called “Green Dam Reservoir” or GDR that helps minimize environmental effects and maximize dam and reservoir green operation in both construction and operation phases. In order to achieve this goal, a framework shown in Figure 1 is proposed. The common polluting sources in a dam reservoir in various aspects are determined using the dam clinic, a concept developed in [13].

Dam clinic, inspired by human clinic, is an innovative approach for dealing with challenges of O&M issues in dams and hydropower plants that are delivered for operation but suffer from some illnesses such as cracks, leakage, low quality, and so on. Although they can generate revenue, these products create great safety concerns and therefore, need to be treated comprehensively. The proposed conceptual model is shown in Figure 2 and Figure 3. More information about the dam clinic can be found in [13]

Once the polluting sources are identified, they will be categorized and each group analyzed. In the implementation phase of the GDR, a specific remediation action is proposed for each group of polluting source (e.g. chemical source, wastewater source, external source). Combination of remediation actions will result in an integrated remediation approach in which upon approval of the dam owner, can be applied in the construction as well as the operation phases of dam projects.

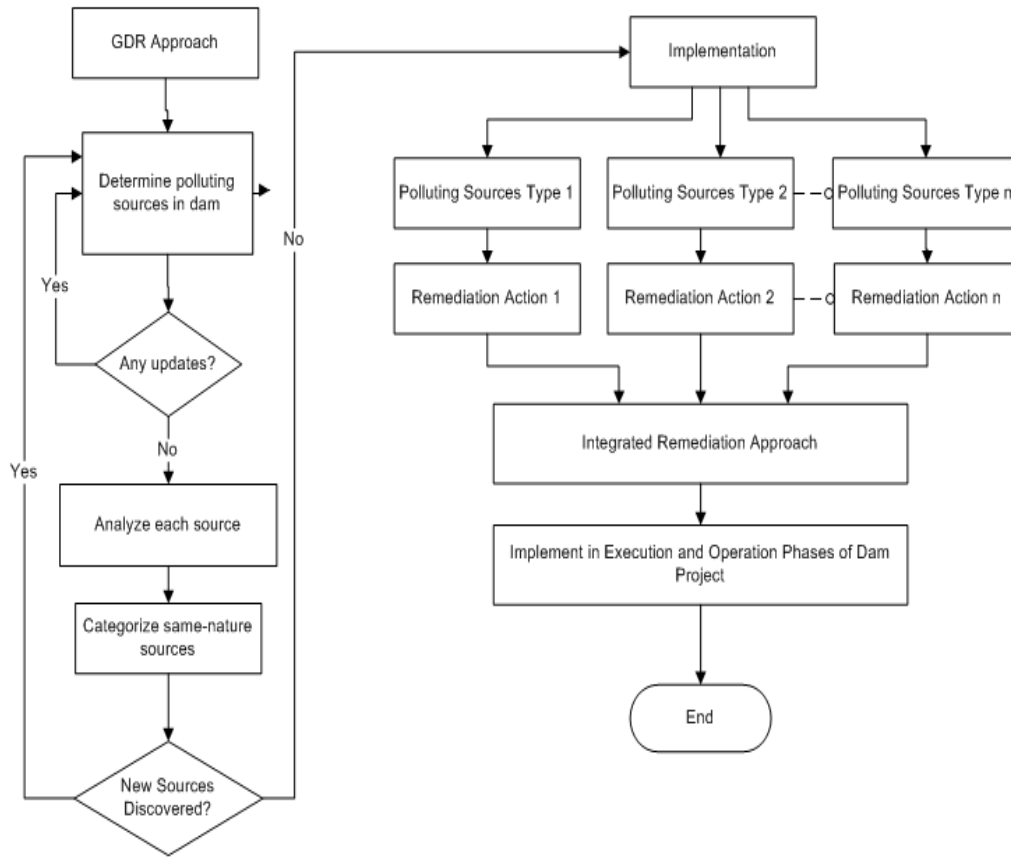


Fig. 1
Green Dam Reservoir (GDR) Procedure

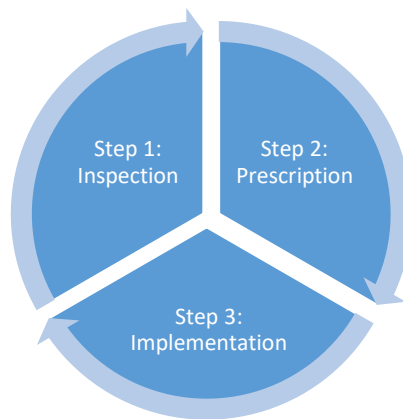


Fig. 2
Dam Clinic Framework [13]

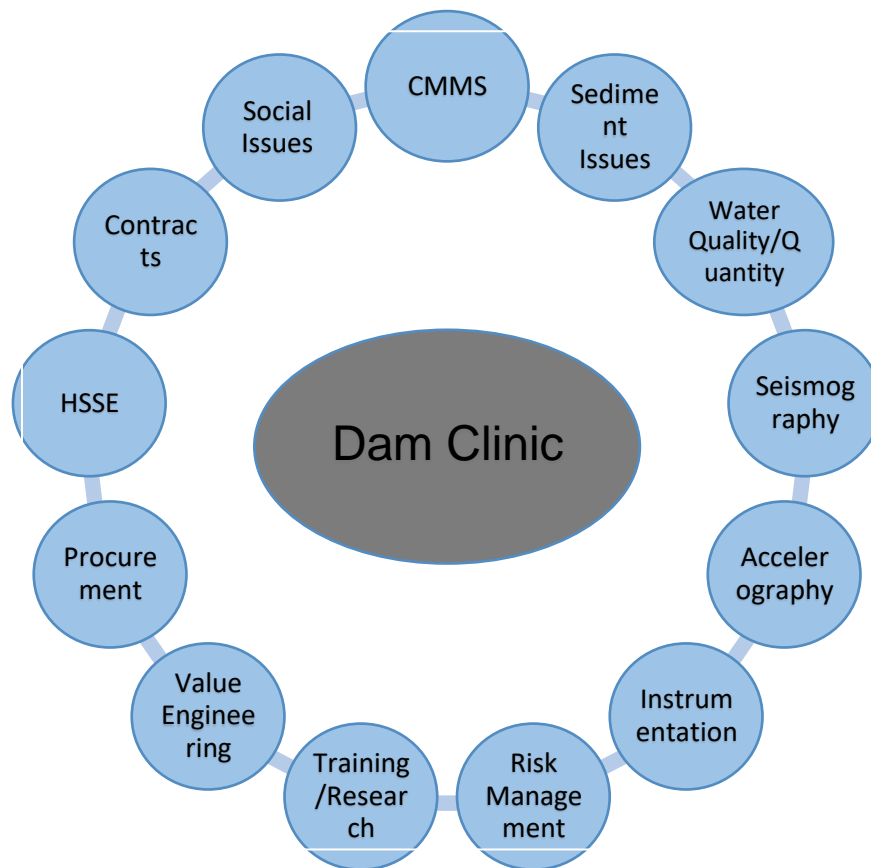


Fig. 3
Various Aspects of Dam Clinic [13]

3.1. ENVIRONMENTAL IMPACT OF LARGE DAMS

According to the guidelines of the International Committee on Large Dams (ICOLD), the damaging environmental effects of dams can be categorized as follows.

1. Physical and Chemical Effects: Creation barrier motion, sedimentation in reservoirs, severe erosion along the river, valve blockage, fog formation and raising the relative humidity, climate changes, ground shaking, increased surface evaporation, rising ground water, changing lands to salinity .

2. Biological Effects: reduce nutrient concentrations downstream of dams, Plankton growth, plant growth, extinction of some species, getting limited fish spawning areas, thermal stratification, production of new species, decline in fish populations, serious changes in water quality, increased opacity of water, Release of toxic substances (pesticides, toxic metals, etc.), increasing the concentration of pollutants in the intake water in periods of water shortage, deterioration of vegetation, Greenhouse gas emissions

3. Health Effects: source of many infectious diseases (such as malaria and blood diseases), creating a favourable environment for oviposition.

4. Economical and Social Effects: increasing urban population, immigration, creation of false jobs, destruction of roads and power transmission lines, lack of access to some of Points of the range, loss of agricultural lands, unemployment, destruction of historical and archaeological sites, destruction of some places with specific topographic.

5. Impacts of Dams on Noise Pollution: increasing volume in the construction phase, disturbing the peace, leaving the nest wildlife, increased risk of loss of animals

6. Effect of Dams on Ecosystems of Aquatic Organisms: increasing of BOD in water (at first), formation of anaerobic degradation environment, formation of dark and funky environment, the exceeding of phytoplankton, growing of macro-flora in the water, increasing plant, increasing evaporation and transpiration, making a barrier to stop fish from passing.

3.2. IDENTIFY SOURCES OF POLLUTION

There are many polluting sources that threat surrounding environment of dam projects. In some cases, the pollution may be extended to the river in the downstream of dam, and in some rare cases, the quality of underground water sources may get affected. There are many types of water pollution because water comes from many sources. Here are a few types of water pollution:

1. Nutrients Pollution

Some wastewater, fertilizers and sewage contain high levels of nutrients. If they end up in water bodies, they encourage algae and weed growth in the water. This will make the water undrinkable, and even clog filters. Too much algae will also use up all the oxygen in the water, and other water organisms in the water will die out of oxygen starvation.

2. Surface water pollution

Surface water includes natural water found on the earth's surface, like rivers, lakes, lagoons and oceans. Hazardous substances coming into contact with this surface water, dissolving or mixing physically with the water can be called surface water pollution.

3. Oxygen Depleting

Water bodies have micro-organisms. These include aerobic and anaerobic organisms. When too much biodegradable matter (things that easily decay) end up in water, it encourages more microorganism growth, and they use up more oxygen in the water. If oxygen is depleted, aerobic organisms die, and anaerobic organisms grow more to produce harmful toxins such as ammonia and sulfides.

4. Ground water pollution

When humans apply pesticides and chemicals to soils, they are washed deep into the ground by rainwater. This gets to underground water, causing pollution underground.

This means when we dig wells and bore holes to get water from underground, it needs to be checked for ground water pollution.

5. Microbiological

In many communities in the world, people drink untreated water (straight from a river or stream). Sometimes there is natural pollution caused by microorganisms like viruses, bacteria and protozoa. This natural pollution can cause fishes and other water life to die. They can also cause serious illness to humans who drink from such waters.

6. Suspended Matter

Some pollutants (substances, particles and chemicals) do not easily dissolve in water. This kind of material is called particulate matter. Some suspended pollutants later settle under the water body. This can harm and even kill aquatic organisms that live at the bottom of water bodies.

7. Chemical Water Pollution

Many industries and farmers work with chemicals that end up in water. This is common with Point-source Pollution. These include chemicals that are used to control weeds, insects and pests. Metals and solvents from industries can pollute water bodies. These are poisonous to many forms of aquatic life and may slow their development, make them infertile and kill them.

8. Oil Spillage

Oil spills usually have only a localized effect on wildlife but can spread for miles. The oil can cause the death to many fish and get stuck to the feathers of seabirds causing them to lose their ability to fly. There are some dam reservoirs that cross oil pipelines and in if the pipeline is broken for any reasons, huge environmental pollution of reservoir water will take place.

3.3. PROPOSE REMEDIATION ACTION

In the previous section, sources of pollution caused by construction and operation of dams are identified and categorized. In this section, a specific remediation action related to each source is proposed, as shown in Table 1. The proposed action should be taken in a right timing by a right team in a right place and should not have the consequences that cause other types of pollution. For example, for dealing with the suspended or particulate matters in the water reservoir, a remediation action may take place to resolve the suspended matter. Such action should not produce the nutrient pollution (First row in Table 1) that needs extra effort to manage. Based on this consideration, there needs an integrated remediation action, as displayed at the end of Figure 1, to make sure that the overall remediation process is effective.

Table 1
Sources of pollution and corresponding remediation action

Sources of Pollution	Effects	Remediation Action
Nutrients, e.g., wastewater, fertilizers and sewage	Develop algae and weed in the water, lack of oxygen in water	1) Prevent Pouring wastes in reservoir, 2) Artificial water turbulence in reservoir, 3) Educate neighbors
Surface water	Polluted water caused by hazardous substances	1) Careful monitoring & controlling, 2) removing hazardous materials along rain waterway to reservoir.
Oxygen Depleting	Growth of more micro-organism and die of more aerobic organisms to produce harmful toxins	More water turbulence in reservoir to enter more air in the water.
Ground water	Pollution of the soil by pesticides and chemicals and then, pollution of underground water	Prevent penetration of pesticides and chemicals into soil by isolating the reservoir
Microbiological	Natural pollution caused by micro-organisms like viruses, bacteria, and protozoa	Prevent direct access for drink of neighboring communities and animals in upstream river
Suspended Matter	They cannot dissolve in water and when settled down in reservoir, kill aquatic organisms that live at the bottom	Design and install gates in the reservoir boundaries to capture substances, particles, and undissolved chemicals
Chemical Water	Wastes produced by farmers and industries pour to the river and causing infertility and killing of many forms of aquatics.	Strict management of point-sources of pollutants (e.g., factories) in the upstream river
Oil Spillage	Widespread life damages to aquatics and dam equipment exposed to water	Displacing the oil pipelines from along the reservoir to another safe place before the reservoir impoundment.

4. CONCLUSIONS

An innovative methodology was developed in this research in order to address environmental threats made by dam construction and maintenance. The methodology is an easy-to-use and logically consistent procedure that can be conveniently applied for under construction and under operation dams and hydropower plants. The owners benefit from using the proposed approach by saving enormous amounts of time and costs for the construction and operation/maintenance activities. There is a great hope that by applying the GDR approach, not only the near-by communities have better life quality but also,

reservoirs operate in safer mode both in physical and technical aspects. This research significantly contributes to the provision of more sustainable operation and maintenance of under operation dams. A new era of dam industry in Iran is recently demanding more focus on the environmental issues. This research is a right attempt in a right direction and in a right timing to address these issues and ultimately, make sure these remarkable national and vital investments have lower damaging effects as well as longer life span for current and next generations.

REFERENCES

- [1] IWPCO: Iran Water and Power Resources Development Company, <http://en.iwpc.ir/default.aspx>
- [2] Mojahedi, S. A. & Attari, J. A Comparative Study of Water Quality Indices for Karun River. World Environmental and Water Resources Congress 2009@ sGreat Rivers, 2009. ASCE, 1-9.
- [3] Pirestani, M. R., Shafaghati, M. & Dehghani, A. A. 2011. Assessment of the Environmental Destructive Effects of Building Dams. World Academy of Science, Engineering and Technology, 5.
- [4] Zafarnejad, F. 2009. The contribution of dams to Iran's desertification. International Journal of Environmental Studies, 66, 327-341.
- [5] Fearnside, M., Ph., 2016, "*Environmental and Social Impacts of Hydroelectric Dams in Brazilian Amazonia: Implications for the Aluminum Industry*", J. of World Development, V. 77: 48-65.
- [6] Q.G. Wang, Y.H. Du, Y. Su, K.Q. Chen, 2012, " *Environmental Impact Post-Assessment of Dam and Reservoir Projects: A Review*", J. of Procedia Environmental Sciences, V. 13: 1439-1443.
- [7] Namy, S. (2007), "Addressing the Social Impacts of Large Hydropower Dams", The Journal of International Policy Solutions, Vol 7. Pp. 22 – 29.
- [8] University of the Philippines Diliman (UPD), (2015). "Engineering a multipurpose, environmentally friendly dam", <https://phys.org/news/2015-03-multipurpose-environmentally-friendly.html>,
- [9] Pringle CM (2001). Hydrologic connectivity and the management of biological reserves: a global perspective Ecol. Appl. 11 981–98.
- [10] Kheirkhah, N., Etaati, H, and Yousefi, S. (2016). "Development of a Novel System for Improvement of Operation and Maintenance Works in Dams and Hydropower Plants in Iran", 84th Annual Meeting of International Commission on Large Dams (ICOLD), May 15-20, Johannesburg, South Africa.
- [12] Sang-Yong Han, Seung-Jun Kwak, Seung-Hoon Yoo, 2008, " Valuing environmental impacts of large dam construction in Korea:An application of choice experiments", J. of Environmental Impact Assessment Review, V. 28 (4–5): 256-266.
- [13] Etaati, H, Kheirkhah, N., and Yousefi, S. (2017). "Dam Clinic: Novel Approach for Effective Operation and Maintenance of Large Dams in Iran", 85th Annual Meeting of International Commission on Large Dams (ICOLD), July 3-7, Prague, Czech Republic.

COMMISSION INTERNATIONALE
DES GRANDS BARRAGES

VINGT-SIXIÈME CONGRÈS DES
GRANDS BARRAGES
Autriche, juillet 2018

DAM SAFETY EMERGENCY RESPONSE PLAN: SHARING EXPERIENCE ON ENGAGEMENT WITH LOCAL AGENCIES FOR TNB HYDROPOWER DAM IN MALAYSIA

Lariyah MOHD SIDEK¹, Hidayah BASRI¹, RAHSIDI Sabri Muda², Azwin
Zailti ABDUL RAZAD², Nur Farazuien MD SAID¹, Mohd Ruzaimi YALIT¹,
KwanSue JUNG³

*¹Department of Civil Engineering, COLLEGE OF ENGINEERING
Sustainable Technology & Environment Group, INSTITUTE FOR ENERGY
INFRASTRUCTURE*

UNIVERSITI TENAGA NASIONAL

²Civil and Engineering Unit, TNB RESEARCH SDN BHD

*³International Water Resources Research Institute, CHUNGNAM NATIONAL
UNIVERSITY*

^{1,2}MALAYSIA

³KOREA

1. INTRODUCTION

Dams are often referred to as monolithic hydraulic structures. Made of adequately impermeable materials, dams are built to create a storage compartment known as reservoir at the upstream to store water for various purposes. These hydraulic structures supply raw water to water treatment plants. In Malaysia, dams contribute to irrigation and flood control mechanisms, on top of its predominant role in generating/ producing hydroelectric energy power source for local consumption.

Despite the aforementioned benefits, dams can also impose risks to the public. In line with current global awareness of water security, the aspect of dam safety has drawn increasing attention from the public as it constitutes the element of a country's national security. The consequences of dam failure may involve substantial downstream injury and property damage as well as catastrophic and long-lasting environmental effects [1]. In Malaysia, Tenaga Nasional Berhad

(TNB) is the owner of most of the larger dams in Malaysia. In fulfilling its corporate responsibility, and also as a responsible dam owner and operator, TNB has embarked a comprehensive research program to study the dam break analysis and assess its impact downstream in terms of social, economic and environmental for all its operating dams since the year 2003.

The dam break simulation results were translated into Emergency Response Plan and quantification of impacts downstream indicating the procedures to be taken in the case of such unfortunate event and the foreseeable loss of all aspects in monetary term. In view of this, TNB has decided to expand the implementation of Emergency Response Plan (ERP) by developing Dam Safety Emergency Response Plan (DSERP) for various TNB power stations to suit both local agencies and TNB station personnel. The DSERP developed to suit the Malaysian Government's management of national disasters, outlined in the Directive No. 20, Policy and Mechanism on National Disaster Management and Relief (In 1997 by National Security Council). The Directive covers all aspects of the management of natural disasters in Malaysia including preparedness, mitigation, response, recovery and rehabilitation.

Potential risks associated with the failure or disruption of these assets could result in significant destruction including loss of life (LOL), massive property damage, and severe long-term consequences [2]. The drill and tabletop exercises prepared the dam personnel in the early detection of the emergency conditions which could endanger the integrity of the dams, provide prescribed procedures for mitigating the emergency condition and timely notification to relevant emergency management agencies. The tabletop exercise helped to ensure timely warning and evacuation of the population at risk by the local agencies. With the SJSIP DSERP manual in place, it will help prevent or minimize the negative impact to the lives and property under the dam failure condition, thus putting corporate image of TNB to greater height.

The implementation of SJSIP DSERP manual through drill and tabletop exercise has successfully highlighted the importance emergency preparedness among dam personnel and also local agencies in minimizing the impact to the society and environment due to dam failure.

REFERENCES

- [1] McClelland, D.M., and Bowles D.S. (2002). Estimating Life Loss For Dam Safety Risk Assessment: A Review And New Approach, IWR Report 02-R-3, Institute For Dam Safety Risk Management Utah State University, Logan.
- [2] Lariyah, M.S, Hidayah, B, Sivadass, T., Rahsidi S.M., Azwin Z.A.R. and Zuraidah, A. (2014). Implementation of Dam Safety Management Program in Malaysia: From Theory to Practice, The 2 nd International Conference on Civil, Offshore & Environmental Engineering A Conference of World Engineering, Science & Technology Congress (ESTCON) 3-5 June 2014 Kuala Lumpur Convention Centre

KEYWORDS: DAM FAILURE, EMERGENCY PLAN, FLOOD WARNING, SAFETY OF DAMS

COMMISSION INTERNATIONALE DES GRANDS BARRAGES

VINGT-SIXIÈME CONGRÈS DES GRANDS BARRAGES
Autriche, juillet 2018

DOI 10.3217/978-3-85125-620-8-048



This work licensed under a Creative Commons Attribution 4.0 International License. <https://creativecommons.org/licenses/by-nc-nd/4.0/>

**DEVELOPMENT AND ASSESSMENT OF DAM INFLOW DEFICIT INDEX FOR
COPING WITH A DROUGHT**

Minsung KWON

Researcher, URBAN RISK MANAGEMENT RESEARCH CENTER,
SEOKYEONG UNIVERSITY

REPUBLIC OF KOREA

Kyung Soo JUN

Professor, GRADUATED SCHOOL OF WATER RESOURCES,
SUNGKYUNKWAN UNIVERSITY

REPUBLIC OF KOREA

COMMISSION INTERNATIONALE
DES GRANDS BARRAGES

VINGT-SIXIÈME CONGRÈS DES
GRANDS BARRAGES
Autriche, juillet 2018

DEVELOPMENT AND ASSESSMENT OF DAM INFLOW DEFICIT INDEX FOR COPING WITH A DROUGHT

Minsung KWON

*Researcher, Urban Risk Management Research Center, SEOKYEONG
UNIVERSITY*

REPUBLIC OF KOREA

Kyung Soo JUN

*Professor, Graduated School of Water Resources, SUNGKYUNKWAN
UNIVERSITY*

REPUBLIC OF KOREA

1. INTRODUCTION

The latest 2014-2015 drought in Korea caused water scarcity of multipurpose dams that supply living and industrial water and led to difficulty with water management. This drought was so severe that it was recorded as an unprecedented event. Drought affects more people than other natural disasters and results in an enormous social, economic and environmental cost ([1]). Sheffield et al. ([2]) expected that frequency and severity of drought would increase due to global climate change. A regional drought is not limited to regional damages, but affecting food and economic matters over wide areas ([3]).

Wilhite and Glantz ([4]) classified drought into meteorological drought, agricultural drought, hydrological drought, and socioeconomic drought. Therefore, Drought indices are estimated using rainfall, evapotranspiration, runoff, soil

moisture, and water supply ability in accordance with study objective. Numerous drought indices had been developed to express droughts which result in various social effects. Typical drought indices are Standardized Precipitation Index (SPI, [5]), Palmer Drought Severity Index (PDSI, [6]), Surface Water Supply Index (SWSI, [7]), Standardized Precipitation Evapotranspiration Index (SPEI, [8]). However, most drought indices are calculated by the lack of amount over the normal phenomenon or the occurrence probability, which has a problem that does not reflect the water supply systems. Modern water use mainly depends on reservoir's water supply system. Therefore, to respond drought in a timely manner and mitigate drought damages, the drought index that considers the dam operation is needed instead of evaluating the shortage of the average or the probability of occurrence.

This study developed Dam Inflow Drought Index (DIDI) considering the criteria for reduction in water supply related to dam operation during a drought. DIDI needs threshold of the cumulative difference between the critical inflow and the observed inflow. In this study, optimal threshold calculated by Receiver Operating Characteristics (ROC) analysis. ROC analysis is commonly used in verification of weather forecast ([9]), but it is also used in verification of drought indices compared with actual drought cases ([10], [11], [12]). The DIDI could be used as the drought monitoring tool that can effectively detect drought of dam basin. Droughts, unlike floods, are characterized by slow progress. Appropriate drought index reflecting the characteristic of water supply system such as the DIDI would contribute to coping with drought and mitigating drought damages.

2. METHOD

Multipurpose dams in Korea have criteria for reduction in water supply during the drought. When using this criterion, we can calculate critical inflow for keeping the criteria by "Eq. [1]."

$$I_{C,i} = AC_i - AC_{i-1} + S_{P,i} \quad [1]$$

where I_C is the critical inflow, AC is the storage of the water supply adjustment criteria, S_P is the amount of the planned water supply, and i is the month.

The difference between the observed inflow and the critical inflow for each month can be calculated by "Eq. [2]," and cumulative the anomalies are calculated by "Eq. [3]." Then the DIDI is calculated by "Eq. [4]."

$$DI_i = I_{O,i} - I_{C,i} \quad [2]$$

$$CDI_i = CDI_{i-1} + DI_i \quad [3]$$

$$CDI_i = CDI / \sigma(CDI) \quad [4]$$

where, DI is the difference in inflows, I_o is the observed inflow, CDI is the cumulative difference in inflows, and $\sigma()$ is standard deviation.

However, when calculating CDI in “Eq. [3],” the upper limit on CDI has to be considered because a considerable amount of inflows that cannot store at the reservoir are not associated with the future water use. In order to determine a threshold, this study calculated “Eq. [3] and [4]” repeatedly with changing the threshold and then conducted Receiver Operating Characteristics (ROC) analysis.

ROC analysis is commonly used in verification of weather forecast, but it is also used in verification of drought indices compared with actual drought cases. This study set ROC model as “Table 1” ROC analysis is separated observed value and prediction value. In this study, the observed value is defined as ‘Water supply’ and the prediction value is defined as ‘DIDI’ in “Table 1” If an actual event occurs and an event predicted in the forecast result, it is expressed as ‘Hit (H).’ Whereas, if an actual event occurs and an event did not predict in the forecast result, it is expressed as ‘Missing (M).’ If an actual event does not occur and an event predicted in the forecast result, it is expressed as ‘False (F).’ On the other hands, if an actual event does not occur and an event did not predict in the forecast result, it is expressed as ‘Negative hit (N).’

Table 1
ROC classification model

		Water supply	
		Reduction	Normal
DIDI	Drought	Hit (H)	False (F)
	Normal	Missing (M)	Negative Hit (N)

The ‘Water supply’ in “Table 1” means that water supply is reduced or normal when dam operation is simulated using the water supply adjustment criteria and historical inflow data. ‘Drought’ in “Table 1” means that DIDI is less than zero and ‘Normal’ of DIDI means that DIDI is equal to or greater than zero. H, F, M, and N with various thresholds can be calculated using ROC classification model in “Table 1.” Then ‘Hit rate (HR)’ and ‘False Alarm Rate (FAR)’ can be estimated by “Eq. [5] and [6].”

$$HR = H/(H + M) \quad [5]$$

$$FAR = F/(F + N) \quad [6]$$

Finally, ROC score has to be calculated to evaluate results of ROC analysis quantitatively. ROC score, which indicates how well the drought index can reproduce actual water shortage, is calculated as the area shown in “Fig. 1.”

The procedure for calculating the DIDI described above is shown in “Fig. 2,” and the optimal DIDI is the DIDI to which the threshold value having the maximum ROC score is applied.

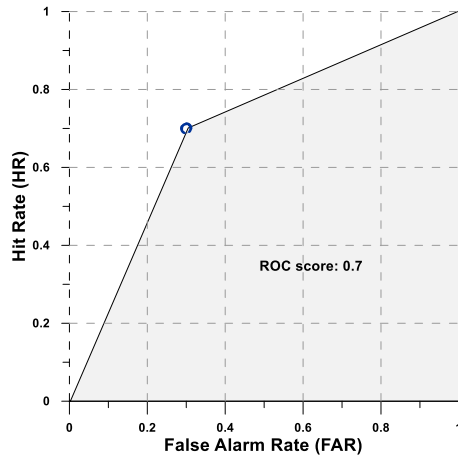


Fig. 1
Description of ROC score

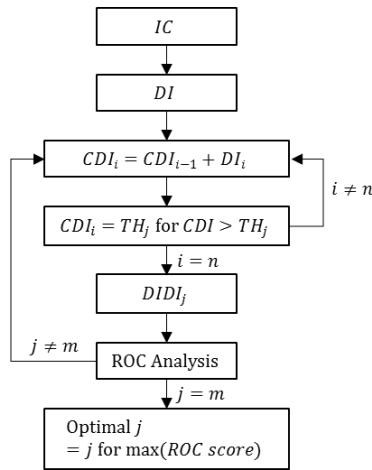


Fig. 2
Procedure for Calculaing DIDI

3. RESULTS AND DISCUSSION

3.1. APPLICATION OF DIDI

This study focused on Chungju Dam in Han River basin. The Chungju Dam, built in the Southern Han River basin which crosses the center of Korean, is the biggest concrete gravity dam in Korea

K-water developed Water Supply Adjustment Criteria (WSAC) to cope with a shortage of water resources in the dam. Drought response strategies of WSAC

is divided into four stages, level1 to level4, according to the degree of water shortage. The critical inflow can be calculated by “Eq. [1],” and “Fig. 3” shows critical inflows of Chungju Dam for each month.

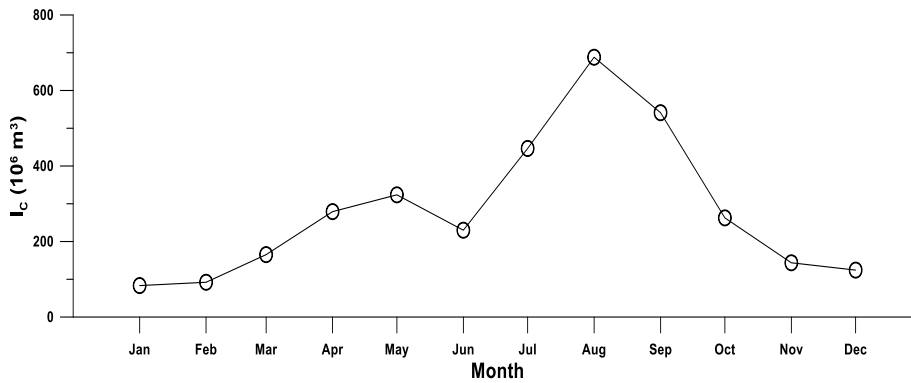


Fig. 3
Critical Inflows of Chungju Dam

“Fig. 4” shows observed monthly inflow of Chungju Dam, and the difference between the observed inflow and the critical inflow can be calculated by “Eq. [2].” “Fig. 5” shows the difference during entire periods. The *CDI* can be calculated by adding up the *DI* of “Fig. 5” in a cumulative manner. However, if the upper limit of the *CDI* is not set, *DI* continuously increases. Therefore, a threshold for *CDI* is needed to estimate optimal *DIDI*.

To determine the threshold of *CDI*, this study performed ROC analysis. Dam operation simulation was implemented from 1987 to 2015 using observed monthly inflow data and volumes of WSAC’s level1. “ A threshold value for maximum ROC score was determined as optimal threshold value, which was $630 \times 10^6 \text{ m}^3$.

“Fig. 6” shows the cumulative difference between the observed inflow and the critical inflow when adapting the optimal threshold. “Fig. 7” shows *DIDI* and the point at which water supply is reduced. This Figure indicates that *DIDI* adequately expresses the water reduction timing of Chungju Dam.

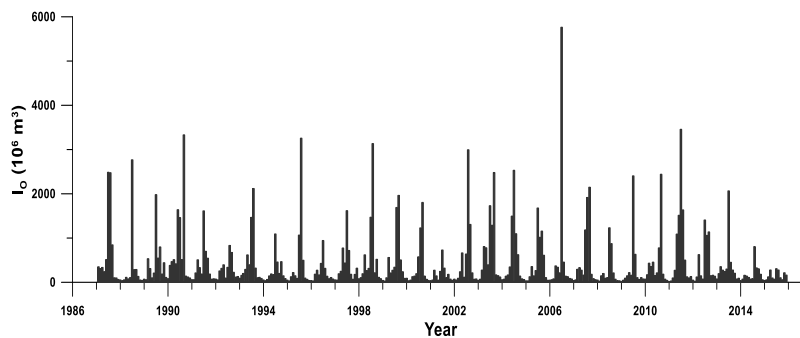


Fig. 4
Observed Monthly Inflows of Chungju Dam

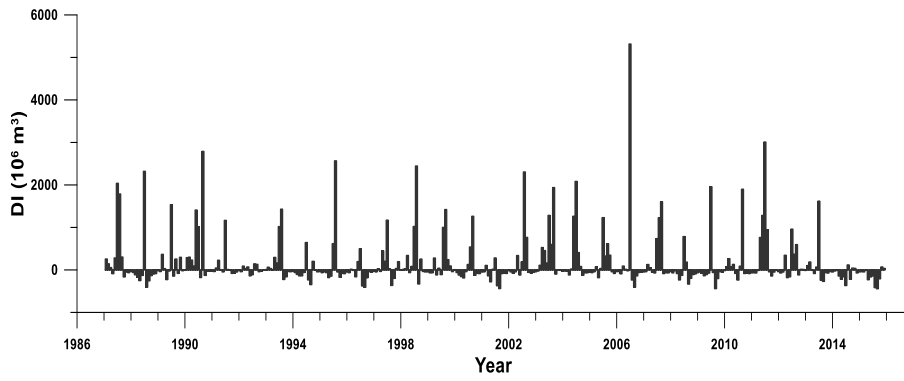


Fig. 5
Difference Between the Observed Inflow and Critical Inflow

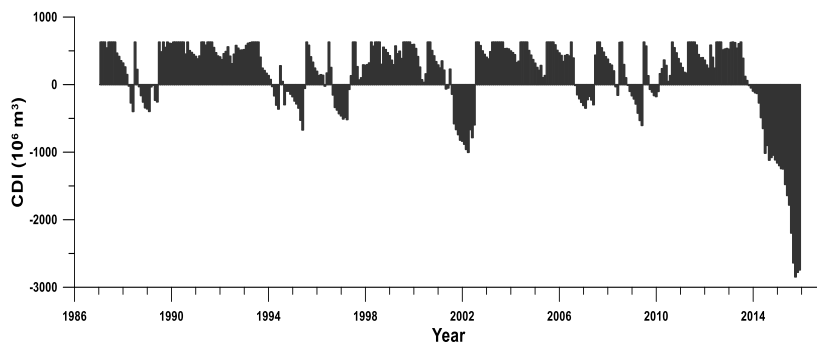


Fig. 6
Cumulative difference between the observed inflow and the critical inflow with the threshold value $630 \times 10^6 \text{ m}^3$.

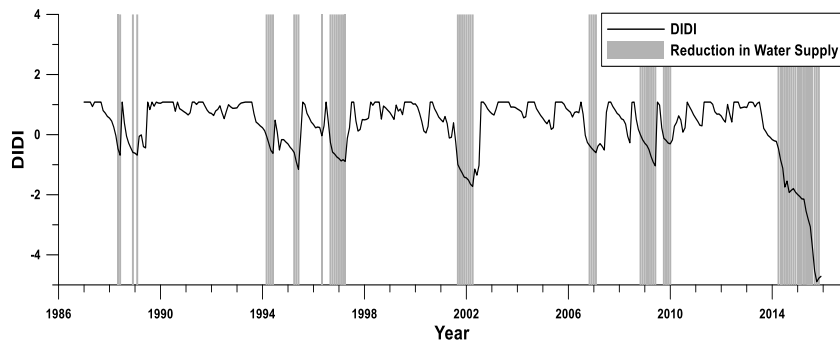


Fig. 7
DIDI and reduction in water supply

3.2. COMPARISON WITH TYPICAL DROUGHT INDICES

This chapter compared DIDI with typical drought indices such as SWSI and SPI. SWSI and SPI are widely used as drought indices. SWSI is calculated by monthly precipitation, snowpack, streamflow, and reservoir storage. Fig. 8 shows DIDI compared with SWSI. SWSI defines -1 or less as drought. The SWSI indicates drought at the time of reduction in water supply adequately, but it can be seen that the drought by SWSI is very common even in the normal water supply condition.

SPI most widely used drought index and it was agreed that using SPI as universal drought index to cope with climate risks at 'The Inter-Regional Workshop on Indices and Early Warning Systems for Drought' held at the University of Nebraska-Lincoln. SPI can calculate simply and easily collect data due to using rainfall only. SPI is calculated by standardizing value of cumulative distribution function (CDF) of Gamma distribution that is estimated using sums of rainfall for a preset period (3 months, 6 months, 12 months, etc.).

"Fig. 9" shows DIDI and SPI of 3, 6, 9, and 12 months. When visually confirmed, DIDI seems to reflect the point of the water supply reductions better. As shown in "Fig. 9," one can see that 6-months and 12-months SPIs that indicate long-term drought are better able to monitor drought than 3-month and 6-month SPIs that show short- and mid-term. In order to evaluate the drought monitoring ability of SWSI and SPI, ROC analysis was also conducted for these. "Table 2" indicates ROC scores of DIDI, SWSI, SPI(3), SPI(6), SPI(9), and SPI(12). ROC score of DIDI was 0.93 which was 0.22 greater than it of SWSI and 0.33, 0.22, 0.16, and 0.17 greater than it of SPI(3), SPI(6), SPI(9), and SPI(12), respectively.

By applying the dam operation and threshold, DIDI was able to express the drought of dam inflow adequately, which indicates that the DIDI is useful for monitoring and responding the drought, and its application would help to mitigate drought damages.

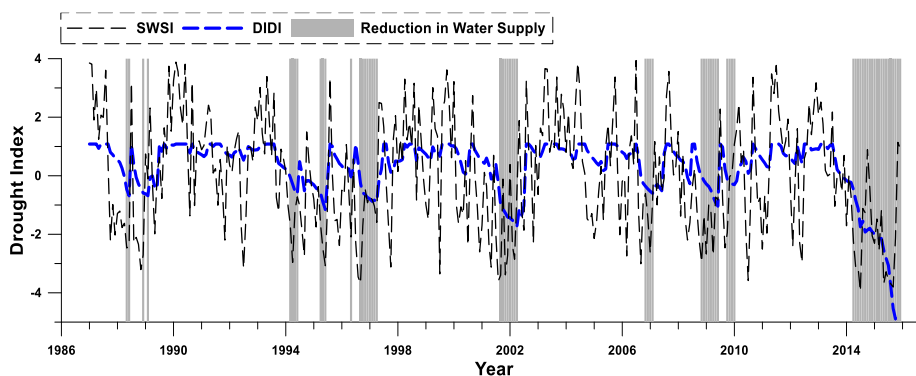


Fig. 8
Comparison with DIDI and SWSI

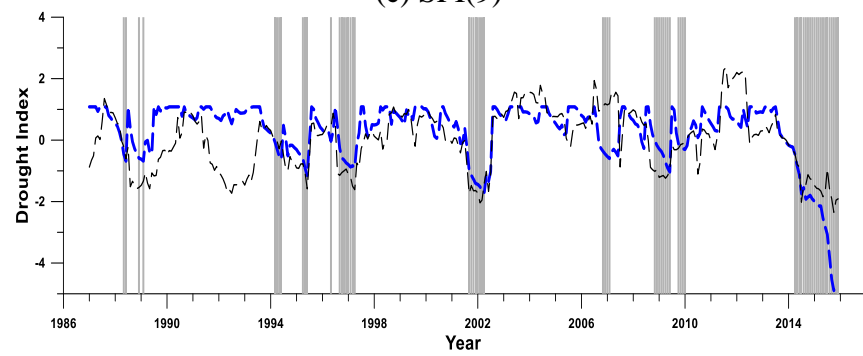
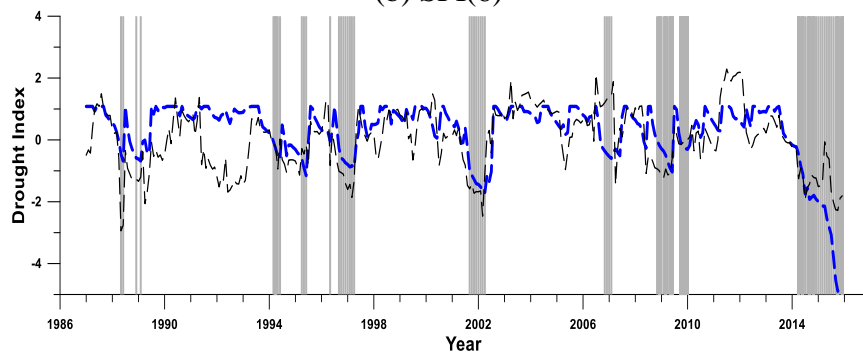
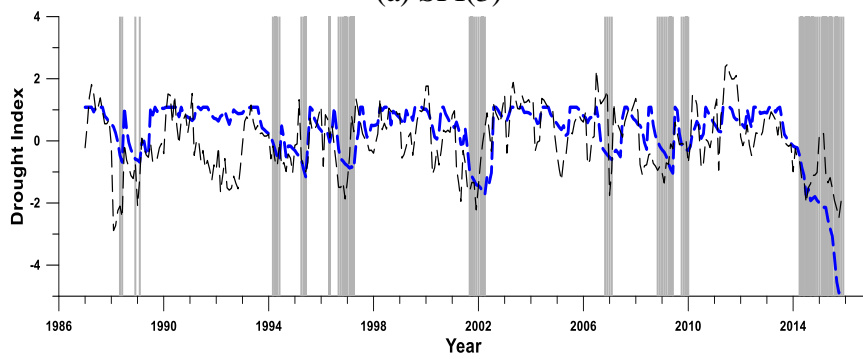
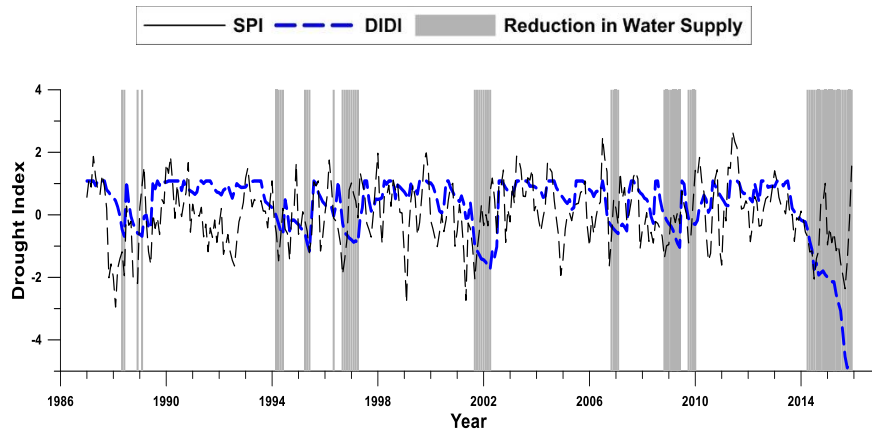


Fig. 9
Comparison with DIDI and SPI

Table 2
Comparison of ROC score

	DIDI	SWSI	SPI(3)	SPI(6)	SPI(9)	SPI(12)
ROC Score	0.93	0.72	0.60	0.71	0.77	0.76

4. CONCLUSIONS

This study developed and evaluated Dam Inflow Drought Index (DIDI) for Chungju Dam in Korea. The DIDI is calculated considering the dam operation. Critical inflows for each month are calculated using the criteria for water supply adjustment. The DIDI can be estimated by dividing the cumulated difference between the observed inflow and critical inflow (CDI) by its standard deviation. Considering the limit of dam storage, the upper limit of CDI has to be determined, and the threshold was estimated by ROC analysis. ROC analysis is implemented using results of the dam operation simulation and DIDI for various thresholds. Optimal threshold of Chungju Dam was calculated as $630 \times 10^6 \text{ m}^3$, DIDI applying the threshold expressed the drought at the time of reduction in water supply adequately. And the DIDI also showed much better performance in monitoring dam droughts than SWSI and short- and long-term SPI (3-, 6-, 9-, and 12-months SPI). The DIDI is useful for monitoring and responding the drought of dam inflow, and its application could help to mitigate drought damages.

REFERENCES

- [1] Wilhite, D.A. (2006). Drought monitoring and early warning: Concepts, progress and future challenges. World Meteorological Organization, 24 pp.
- [2] Sheffield, J., Wood, E.F., and Roderick, M.L. (2012). Little change in global drought over the past 60 years. *Nature*, 491 (7424), 435-438.
- [3] Sternberg, T. (2011). Regional drought has a global impact. *Nature*, 472 (7342), 169-169.
- [4] Wilhite, D.A., and Glantz, M.H. (1985). Understanding: the drought phenomenon: the role of definitions. *Water International*, 10 (3), 111-120.
- [5] McKee, T.B., Doesken, N.J., and Kleist, J. (1993). The relationship of drought frequency and duration to time scales. *Proceedings of the 8th Conference on Applied Climatology*, Boston, MA, USA, 17 (22), 179-183.
- [6] Palmer, W.C. (1965). *Meteorological drought (Vol. 30)*. Washington, DC, USA: US Department of Commerce, 58 pp.

- [7] Shafer, B.A., and Dezman, L.E. (1982). Development of a surface water supply index (SWSI) to assess the severity of drought conditions in snowpack runoff areas. *Proceedings of the Western Snow Conference*, Fort Collins, CO, 50, 164-175.
- [8] Vicente-Serrano, S.M., Beguería, S., and López-Moreno, J.I. (2010). A multiscalar drought index sensitive to global warming: the standardized precipitation evapotranspiration index. *Journal of Climate*, 23 (7), 1696-1718.
- [9] Mason I. (1982). A model for assessment of weather forecasts. *Australian Meteorological Magazine*, 30, 291-303.
- [10] Kim, G. and Lee, J. (2011). Evaluation of drought indices using the drought records. *Journal of Korea Water Resources Association*, 44 (8), 639-652
- [11] Bae, D.H., Son, K.H., and Kim H.A. (2013). Derivation and evaluation of drought threshold level considering hydro-meteorological data on South Korea, *Journal of Korea Water Resources Association*, 46 (3), 287-299.
- [12] Yoo, J.Y., Song, H.Y., Kim, T.-W., and Ahn, J.-H. (2013). Evaluation of short-term drought using daily standardized precipitation index and ROC analysis. *Journal of the Korean Society of Civil Engineers*, 33 (5), 1851-1860.

SUMMARY

This study developed Dam Inflow Drought Index (DIDI) for Chungju Dam in Korea and evaluated the usability of the DIDI by comparing with Surface Water Supply Index (SWSI) and Standardized Precipitation Index (SPI). DIDI is calculated by the cumulative difference between the critical inflow and the observed inflow. The critical inflow means the essential inflow keeping the water supply criteria of the dam. Considering the limit of dam capacity, the upper limit of the cumulative difference has to be determined, and the threshold is estimated by performing Receiver Operating Characteristics (ROC) analysis. The Optimal threshold is determined by a value that represents maximum ROC score. The maximum ROC score of the DIDI was 0.93, and the threshold at this point was $630 \times 10^6 \text{ m}^3$. The maximum ROC score of the DIDI was 0.21 higher than it of SWSI and 0.33, 0.22, 0.16, and 0.17 greater than it of SPI(3), SPI(6), SPI(9), and SPI(12), respectively. DIDI showed much better performance in monitoring dam droughts than SWSI and short-term and long-term SPI. The DIDI is useful for monitoring the dam inflow drought, and its application could help mitigate drought damages.

COMMISSION INTERNATIONALE DES GRANDS BARRAGES

VINGT-SIXIÈME CONGRÈS DES GRANDS BARRAGES
Autriche, juillet 2018

DOI 10.3217/978-3-85125-620-8-049



This work licensed under a Creative Commons Attribution 4.0 International License. <https://creativecommons.org/licenses/by-nc-nd/4.0/>

**ADAPTED OPERATION OF TROPICAL GLACIAR RESERVOIRS DUE TO
CLIMATE CHANGE**

Alexander ARCH

Head of Water-Resources Consulting, PÖYRY PERU S.A.C.

PERU

Anna HETTERICH

Senior Hydraulic Engineer and Project Manager, PÖYRY PERU S.A.C.

PERU

Eliana ROMERO

Senior Hydrologist and Project Manager, PÖYRY PERU S.A.C.

PERU

Georg PUCHNER

Senior Hydraulic Engineer, 2D- Simulation, PÖYRY ENERGY GMBH

AUSTRIA

COMMISSION INTERNATIONALE
DES GRANDS BARRAGES

VINGT-SIXIÈME CONGRÈS DES
GRANDS BARRAGES
Autriche, juillet 2018

ADAPTED OPERATION OF TROPICAL GLACIAR RESERVOIRS DUE TO CLIMATE CHANGE

Dr. Alexander Arch
Head of Water-Resources Consulting,

Anna Hetterich
Senior Hydraulic Engineer and Project Manager,

Eliana Romero
Senior Hydrologist and Project Manager,

PÖYRY PERU S.A.C.

PERU

Georg Puchner
Senior Hydraulic Engineer, 2D- Simulation,
PÖYRY ENERGY GMBH

AUSTRIA

1. INTRODUCTION

Throughout history, there have been a series of catastrophic events in the Cordillera Blanca generated by mudflows coming from glacier reservoirs (see also [1] and [2]). One of the main causes of these events are the detachment of glacial masses that impact at the lagoons located at the base of the glacier, generating waves that produce overflows and in some cases a break of the dam body or the moraine. This omnipresent hazard in the Cordillera Blanca together with the increasing mean temperature due to climate change effects (see [3]), which are most visible in the tropical glacier regions, lead to the necessity to

know the risks and the possible effects when operating reservoirs in this area of Peru. Recent research ([4], [5], [6] and [7]) shows an overall glacier loss of 46% between 1930 and 2016 with an increasing melting rate for the glaciers in the Cordillera Blanca based on climate change effects. In the present paper, the potential risk of ice blocks falling into a reservoir in the Andean region causing an impact wave, overtopping of the dam and provoking a dam break with significant damages downstream is analyzed. Eighteen glacier blocks with danger of detachment due to the melting and retreat of the glacier because of climate effects were identified based on a glaciological hazards analysis. Furthermore, adapted operation of the reservoir, which is located directly downstream of the Huantsán glacier, is presented.

2. INVESTIGATION ENVIRONMENT AND BASIC DATA

The lagoon with a volume of 29 Mio m³ and a maximum depth of 90 m is located at the base of the snowcapped Huantsán glacier on the western slopes of the Cordillera Blanca at an altitude of 4,290 meters. The basin includes the Pariac creek and belongs to the province of Huaraz of the Ancash department (see Fig. 1). The ovoid-shaped reservoir corresponds to a very deep depression of glacier origin. The volume of the former glacier lake was augmented by the construction of an earth dam ($H_{\text{Dam}} = 23$ m) above the former moraine allowing a controlled operation of the lagoon. The 5.5 m wide crest of the dam is located at 4294.5 m.a.s.l. and covered with a concrete slab. The dam has a spillway with a fixed concrete overflow crest at 4290.88 m.a.s.l. and a width of 3.0 m.



Fig. 1

Lagoon and Huantsán glacier (left; view from down- to upstream) and dam & spillway (right)

Lagon et glacier de Huantsán (à gauche - vue de l'amont vers l'aval) et barrage et évacuateur de crue (à droite)

The bottom outlet is located at 4271.00 m.a.s.l. and consists of a pipe running from the intake at the reservoir to the control house at the bottom of the dam. The rocky buttresses surrounding the reservoir correspond to the Chicama Formation (Js-ch), which consists of shales and fine sandstones, forming rather steep slopes, greater than 45 °.

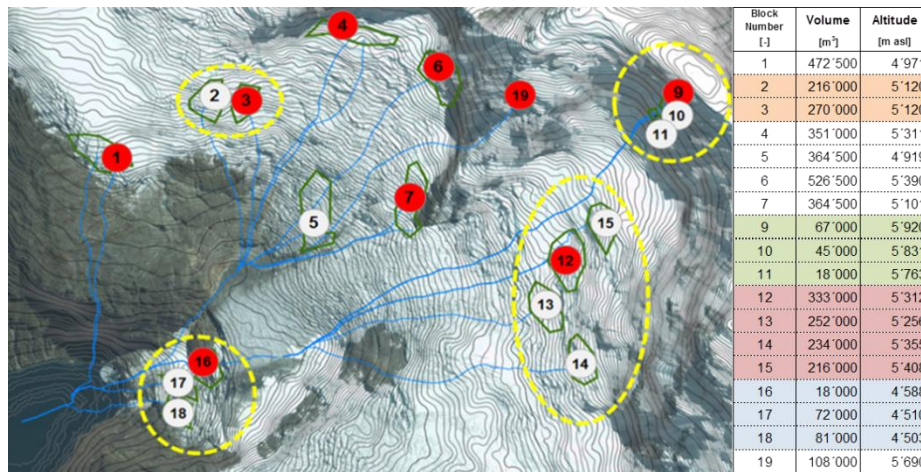


Fig. 2

Identified glacier blocks and their pathways to the lagoon and corresponding volumes (representative blocks for further investigation marked red)
Blocs glaciaires identifiés, leurs voies vers la lagune et les volumes correspondants (blocs représentatifs pour une enquête plus approfondie marqués en rouge)

At the base of the valley propagation of quaternary deposits of morainic origin and some colluvial deposits of little thickness are found. The catchment area is 17.78 km² of which 11.26 km² (63% of the total surface) are snow /ice covered. The average annual precipitation (snow and rain) in the basin is 1070.5 mm/year – high flow season is between December and March.

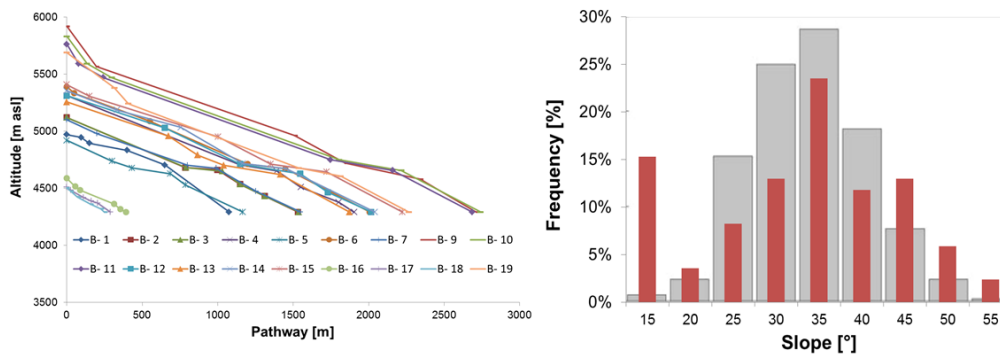


Fig. 3

Sliding paths of the different identified glacier blocks (left) and their slope distribution compared with findings from [9] (grey bars) (right)
Les chemins de glissement des différents blocs glaciaires identifiés (à gauche) et leur distribution de pente par rapport aux résultats de [8] (barres grises) (à droite)

The average annual mean flow rate is 0.87 m³/s with a mean annual yield of 18.0 x 10⁶ m³. In general, the climate in the area of the lagoon is very cold with a very dry atmosphere, but with alternating temperatures during day and night. From June to September the average temperature at the lagoon (4'290 m asl) is below 4°C and the average annual minimum temperature is 0.07°C. July is

usually the coldest month, reaching a monthly average temperature of 3.7°C, with average maximum and minimum monthly means of 11° C and -2.3°C respectively. For the Huantsán glacier, a reduction of the ice masses of 6.4 % was estimated between 1988 and 2008 ([7] and [8]). Due to this reduction of the glacier, the location and corresponding volume of 18 different ice blocks were identified on site (see Fig. 2), which represent a potential risk of detachment. Based on satellite data (ALOS and Sentinel 2b) the mean slopes and topographical conditions were analyzed for these blocks. The determined mean slope for the 18 blocks is 31 ° - maximum slopes reach 65 ° (see Fig. 3). This is also in accordance with the findings from [9], where different glaciers of the Cordillera Blanca were studied with respect of air temperature and slopes. According to the findings from [10], the identified glacier blocks represent a potential threat based on the mean annual temperature, their volumes and the identified slopes (see Fig. 4). Based on these results, the risk of a detachment is eminent and thus consequences of an ice block detachment were analyzed.

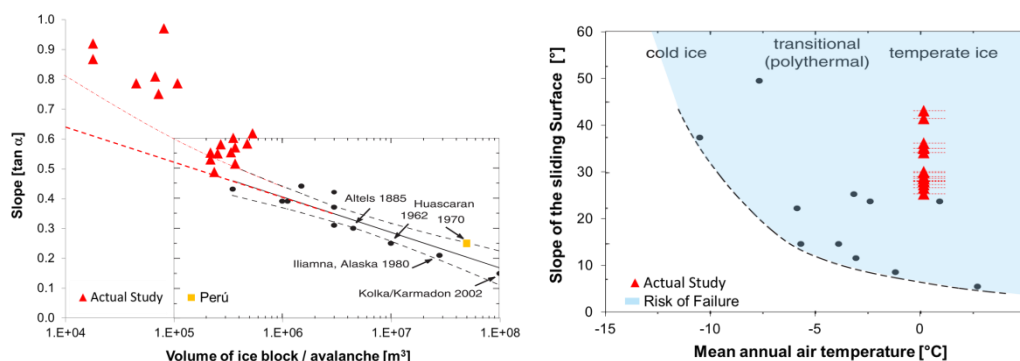


Fig. 4

Relation between average slope and volume of large ice avalanches worldwide (left) & mean annual air temperature to critical slope (right) – comparison of investigation data with findings from [10] (range of temperature from [11])
Relation entre la pente moyenne et le volume des grandes avalanches de glace dans le monde (gauche) & température moyenne de l'air contre la pente critique (droite) - comparaison des resultat de (9) (variété de température de [10])

3. SIMULATION OF THE IMPACTING ICE BLOCKS

3.1. PRESELECTION OF THE SIMULATED ICE BLOCKS

As it can be seen from Fig. 2, some of the identified 18 blocks have similar characteristics in terms of their elevation and fall trajectory. A preliminary analysis based on the methodology described in Chapter 3 of [12] identified the blocks generating the most unfavorable effects. This methodology also was applied to the event occurred in 2010, where a large block of ice and rocks of 450 000 m³

(see [13]) fell from the Hualcan glacier into the reservoir 513. The generated wave height over the natural dam of this event was estimated between 5 and 6 m causing downstream inundations and small damages (see [13] and [14]). According to [13], this event occurred when the reservoir had a free board of 20.0 m. According to the model, the 18 selected blocks generate wave heights above the dam crest between 0 and 45 m. The simulated detachment of an entire group of ice blocks resulted in similar wave heights as for individual blocks. Although block B-16 does not generate an overtopping, this block also was considered in the detailed simulation due to its proximity to the reservoir. Based on this pre-assessment, 6 most important individual blocks were investigated in more detail (Fig. 5 – blocks marked red).

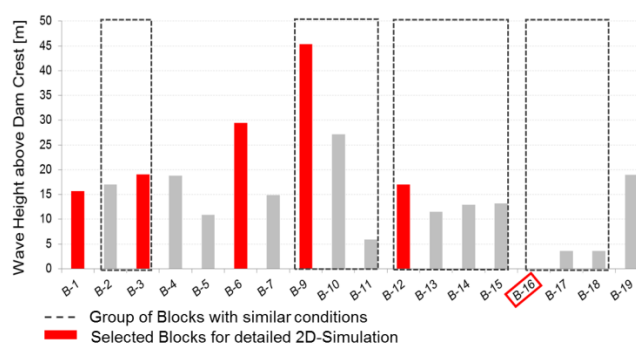


Fig. 5

Wave height above the dam crest applying tool from [12]
Hauteur des vagues au-dessus de crête du barrage avec l'outil selon [11]

3.2. APPLIED MODEL & DETAILED SIMULATION PROCEDURE

For the detailed investigation, a 2D numerical simulation was applied with different scenarios to maintain the operation of the reservoir and at the same time to mitigate the risk of downstream damages due to a glacier block impact and resulting GLOF. The complete process chain of the impact events based on the crated DEM (satellite-, bathymetric- and drone topography) was simulated with a 2-dimensional hydrodynamic model (HYDRO_AS-2D (Hydrotec, Germany)), which is based on the shallow-water equations (depth-averaged) for free surface flow using the Finite-Volume-Discretization. For each selected ice block, (see Fig. 5) the simulation was carried out following a 3-step approach:

- (Step 1) Pre-simulations to model the sliding phase,
- (Step 2) Main simulation to model the impact phase, the wave propagation in the reservoir and the wave run-up at the dam, and
- (Step 3) Iterative simulations to estimate the required reduction of the reservoir water level to prevent overtopping including a variation of the block volumes

Sliding path, impact velocity and impact direction were determined in the pre-simulation (Step 1). To be on the conservative side, the main simulation

(Step 2) starts with a fluid body right before its impact, which has exactly the shape of the ice block as predefined by the glaciologist (in the pre-simulation the sliding fluid body disintegrates somewhat which decreases the impact momentum). The comparison of the results from Step 1 to outcomes from [12] showed minor differences from -9.0 to +5.0% (mean -0.9 %) for the mean impact velocity. Nevertheless, velocities from the pre-simulation (Step 1) are spatially distributed with lower magnitudes at the edges of the impacting fluid body, which decreases the impact momentum. The resulting overtopping wave heights would be in average 22% and the overflow discharges 33% lower. Therefore and to assure a conservative approach, the initial velocity magnitude of the impacting fluid bodies was set constant for the entire fluid body in the main simulations based on the theoretical approach according to Körner [12]. As indicated in Step 3, additional to the 6 base cases, 17 simulations with different ice block volumes maintaining their locations and different reservoir levels were executed to cover the most important conditions and detect the minimal water levels in the reservoir which would prevent overtopping.

3.3. SIMULATION RESULTS

The simulation results show that in five of the six base cases (-a marked red) overtopping occurs when the operational water level is at the actual altitude of 4290.88 m a.s.l.

Table 1
Results of 2D-Simulation
Resultats de la Simulacion 2D

Case	BLOCK B-1					BLOCK B-3				BLOCK B-6				BLOCK B-9			BLOCK B-12				BLOCK B-16				
	a	b	c	d	e	a	b	c	d	a	b	c	d	a	b	c	a	b	c	d	a	b	c		
Block Volume	472,500		220,000		50,000	270,000		150,000		526,500		250,000		67,000		40,000		333,000		200,000		18,000		80,000	[m ³]
Altitude	4,791					5,120				5,390				5,920			5,312				4,588			[m asl]	
Impact Height	500	545	500	520	500	829	835	829	832	1,099	1,149	1,099	1,129	1,629	1,631	1,629	1,021	1,066	1,021	1,041	297	297	305	[m]	
Reduction of FSL	-	45	-	20	-	-	6	-	3	-	50	-	30	-	2	-	-	45	-	20	-	-	8	[m]	
Wave Height	14	-	6	-	-	3	-	1	-	19	3	11	-	1	-	-	12	-	9	-	-	4	-	[m]	
Reservoir Volume	29	7	29	17	29	29	25	29	27	29	5	29	13	29	28	29	29	7	29	17	29	29	24	[Mio. m ³]	

Overtopping heights between 1 and 19 m were obtained based on impact heights between 300 and 1'600 m and volumes between 18'000 and 526'500 m³. Only in one case (B16-a) no overtopping occurred due to the low volume and impact height. To prevent overtopping at the dam, the water level in the lagoon has to be reduced between 2 and 40 m. Correspondingly, the actual water volume of the lagoon (29 Mio.m³) is reduced down to 5 Mio.m³, which represents a reduction of 82 % and would mean to abandon the operation of the lagoon for

any means. Block B-6 a has even such a high impact momentum, that prevention of overtopping through a water level reduction it is not possible at all. For the said scenario only an “optimal” lowest water level could be identified which lead to minimal overtopping, which still is 1'126 m³/s. The required reduction would be 50 m. Any further lowering of the reservoir water level again lead to higher overtopping discharges, as the remaining mass of water in the reservoir is not able to damp the impacting momentum (see Table 1). Overtopping heights with the tool from [12] versus the 2D simulation were in general 1 to 45 m (8 to 98 %) higher (see Table 2). By reducing the impact velocity in the range from 8 to 92 % same results as for the 2D simulation can be obtained. Overtopping volumes from the 2D simulation are in general 2 to 6 times higher. Although the impact of the spillway cannot be represented in the pre-assessment tool from [12], it can be said, that mayor impact heights result in increased differences between the tool and the 2D simulation.

Table 2

Comparison between results of 2D-Simulation and pre-assessment tool from [12]
Comparaison entre les résultats de simulation 2D et l'outil selon [11]

Results / Block Nr.	B1		B3		B6		B9		B12		B16		
	2D ¹⁾	Excel ²⁾	2D ¹⁾	Excel ²⁾	2D ¹⁾	Excel ²⁾	2D ¹⁾	Excel ²⁾	2D ¹⁾	Excel ²⁾	2D ¹⁾	Excel ²⁾	
Maximal Wave Height	-	10	-	11	-	15	-	21	-	10	-	2	[m]
Amplitude of the Wave	-	8	-	9	-	12	-	17	-	8	-	1	[m]
Wave Height upstream of the Dam	21	19	7	23	26	33	4	49	18	21	2	3	[m]
Wave Height over Dam Crest	14	16	3	19	19	29	1	45	12	17	-	-	[m]
Maximal Discharge	9,703	3,383	606	4,332	14,422	6,457	123	10,158	8,334	3,748	-	-	[m ³ /s]
Overtopping Volume	181	41	13	54	321	83	1	136	193	46	-	-	[10 ³ m ³]
Volume at Spillway	58	-	8	-	84	-	3	-	58	-	219	-	[10 ³ m ³]
Impact Velocity	93	92	71	69	105	105	133	133	97	97	61	61	[m/s]
Volume of Ice Block	472,500		270,000		526,500		67,000		333,000		18,000		[m ³]
Altitude of Ice Block	4,791		5,120		5,390		5,920		5,312		4,588		[m asl]
Impact Height	500		829		1,099		1,629		1,021		297		[m]

1) Case 2D: Detailed 2D-Simulation

2) Case Excel: Pre-Assessment based on the Excel-Tool from [11]

4. DISCUSSION OF THE RESULTS

As shown in Fig. 6 (left), overtopping wave heights become more important when the ice block starts to have a significant volume compared to the reservoir volume – threshold for overtopping of the ice block volume is in the order of 50'000 m³ for the investigated situation. Reducing the water level also means to reduce the damping effect of the water mass of the reservoir. As indicated in Fig 7, a reduction of about 40 to 50 meters results to be ineffective regarding the prevention of overtopping. This is also the case, if the volume of the ice block reaches 6 – 10 % of the remaining reservoir volume (Fig. 6 (right)). Of course, not only the block volume and sliding velocity but also the impact location and direction (directly towards the dam or mainly towards a lateral bank) have great

influence on the resulting overtopping heights. To figure out these influences in a first step, the relation of impact momentum (i.e. block mass times sliding velocity) and the required reduction of water level to prevent overtopping were analyzed (Fig. 7).

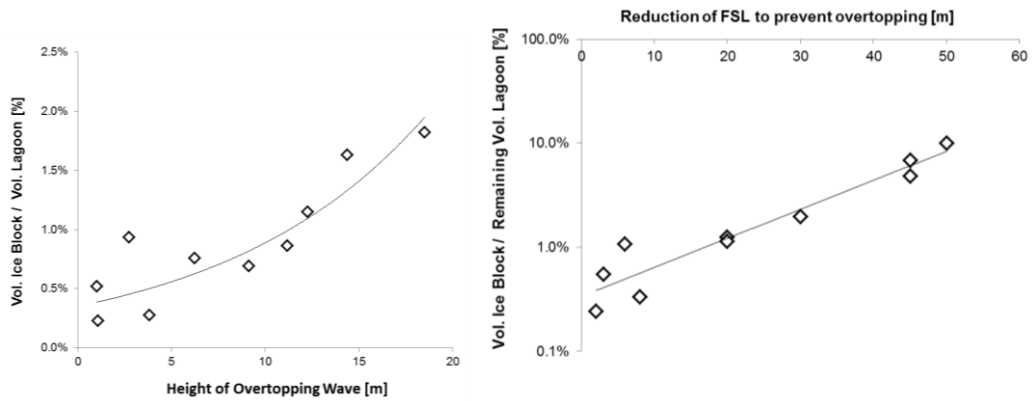


Fig. 6

Relation of ice block to reservoir volume in function of overtopping height (left) and relation of ice block to remaining reservoir volume in function of required reduction of the FSL (right)

Relation entre le bloc de glace et le volume du réservoir en fonction de la hauteur de déversement (à gauche) et la relation entre le bloc de glace et le volume restant du réservoir en fonction de la réduction nécessaire de la FSL (à droite)

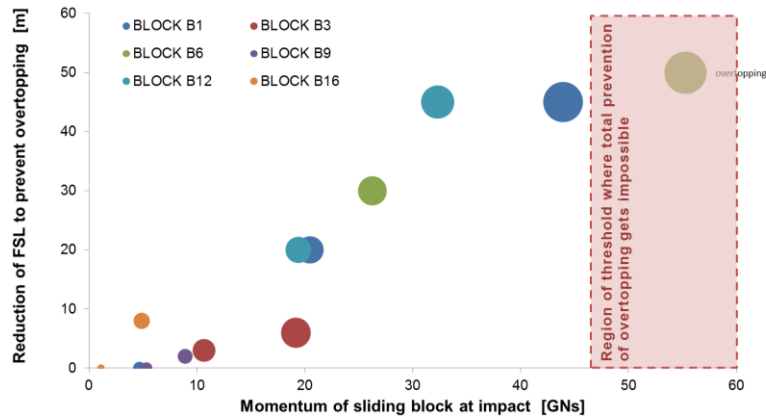


Fig. 7

Analyses of impact momentum and required reduction of reservoir water level to prevent overtopping

Analyses de la dynamique d'impact et de la réduction requise du niveau d'eau du réservoir pour éviter le déversement

From that analysis, it gets clear that some blocks have over-proportional impact in relation to their impact momentum. For instance, blocks B9 (violet dots) and B3 (red dots) do require significantly less reduction for preventing overtopping than other blocks with comparable impact momentum because their impact direction is less critical. Each block is represented by 2 dots (one for each estimated volume). For block B-1 additionally a third dot is drawn to indicate the

maximum block volume which does not lead to overtopping. The size of the points is proportional to the volume of the blocks (maximum is B6-v1 with 526,500 m³ (upper green dot)). Furthermore, prevention of overtopping is impossible for blocks with an impact momentum higher than 45-55 GNs by reducing the reservoir water level. This is at least true for blocks with an impact direction rather straight towards the dam.

SUMMARY

Global warming based on climate change lead to a considerable increase of glacier melting in the sub-tropical region. Most notable the glaciers in the Cordillera Blanca of Peru showed significant reduction of the glacier masses up to 95 % (see [8]). This retreat generates the risk of GLOF due to big ice blocks, which are isolated and fall into the lagoons located at the toe of the glaciers. In the given case 18 ice blocks of the Huantsán glacier with a potential risk of falling into the downstream lagoon were investigated prior identification by the means of site inspections and satellite images. Based on [10] it was shown, that the identified blocks represent a risk of detachment due to the very steep slopes and the high impact heights (up to 1800 m) as well as the mean annual temperature in the area. Based on a pre-assessment applying the excel tool from [12] six ice blocks with the most import potential risk regarding a GLOF event were selected for a detailed 2D simulation. Impact heights between 300 and 1'600 m cause an overtopping of the existing dam with wave heights between 1 and 19 m. For many cases, only a quite drastic reduction of the operational water level, which also would mean to abandon the reservoir, could prevent an overtopping. The technically feasible reduction of the FSL turns out to be approximately 18 m as higher reductions would reach levels below the intake. Even with the initial conditions of the lagoon (without dam), there would be a risk of overflow (wave heights approx. 8 m), as it would be necessary to reduce the level of Lagoon by 35.0 m, far below the level of the former moraine. As there are many other lagoons in the Cordillera Blanca with similar conditions, the risk of a GLOF event in the sub-tropical glaciers becomes more evident taking into consideration the effect of climate change, which already can be observed in the Andean Glaciers in the last decades. To insure the future operation of these reservoirs permanent observation of the glacier by the means of images (satellite and direct photography) might be realized. This also would improve the situation of the still poor database, which nowadays exist in the Andean region with respect of GLOF risk assessment.

ACKNOWLEDGEMENTS

This publication could only be realized with the kind support of the owner ORAZUL PERU who has provided the investigation data. The authors specially want to thanks the team of Richard Rosas (Superintendente de Proceso Hidroeléctrico), which enriched the outcomes based on their experience and the fruitful discusses.

REFERENCES

- [1] M. VUILLE, El cambio climático y los recursos hídricos en los andes tropicales, IDB Technical Note 517, 1-10, (2013)
- [2] CÉSAR A. PORTOCARRERO R., The Glacial Lake Handbook, Technical Report, USAID 2014
- [3] M. CAREY, Living and dying with Glaciers: People's Historical Vulnerability to Avalanches and Outburst Floods in Peru, *Global and Planetary Change* 47 (2005) 122 – 134,
- [4] S. SCHAUWECKER et al, Climate Trends and Glacier Retreat in the Cordillera Blanca, Peru, revisited, *Global and Planetary Change* 119 (2014) 85–97
- [5] M. VUILLE et al, Glacier mass balance variability in the Cordillera Blanca, Peru and its relationship with climate and the large-scale circulation, *Global and Planetary Change* 62 (2008) 14–28
- [6] N. SALZMANN et al, Glacier changes and climate trends derived from multiple sources in the data scarce Cordillera Vilcanota region, southern peruvian Andes
- [7] WALTER SILVERIO AND JEAN-MICHEL JAQUET, Evaluating glacier fluctuations in Cordillera Blanca (Peru), *Arch.Sci.* (2017) 69: 145-162
- [8] AUTORIDAD NACIONAL DEL AGUA DE PERU (ANA), Inventario nacional de glaciares y lagunas, Report July 2014
- [9] A. E. RACOVITEANU, Decadal changes in glacier parameters in the Cordillera Blanca Peru, derived from remote sensing, *Journal of Glaciology*, Vol. 54, no. 186, 2008
- [10] C. HUGGEL et al, An assessment procedure for glacial hazards in the Swiss Alps, *Can. Geotech. J.* 41: 1068–1083 (2004)
- [11] M. VUILLE AND R.S. BRADLEY: Temperature trends in the tropical Andes, *Geophysical Research Letters*, Vol. 27, no. 23, pages 3885-3888, December 1, 2000
- [12] V. HELLER et al, Landslide generated impulse waves in reservoirs - basics and computation, VAW MANUAL 4257, 2009
- [13] D. SCHNEIDER ET AL, Mapping hazards from glacier lake outburst floods based on modelling of process cascades at Lake 513, Carhuaz, Peru, *Adv. Geosci.*, 35, 145–155, 2014

- [14] P. VALDERRAMA Y O. VILCA, Dinamica e implicancias del aluvión de la laguna 513, cordillera blanca, Ancash Perú, Revista de la Asociación Geológica Argentina 69 (3): 400 - 406 (2012)

COMMISSION INTERNATIONALE DES GRANDS BARRAGES

VINGT-SIXIÈME CONGRÈS DES GRANDS BARRAGES
Autriche, juillet 2018

DOI 10.3217/978-3-85125-620-8-050



This work licensed under a Creative Commons Attribution 4.0 International License. <https://creativecommons.org/licenses/by-nc-nd/4.0/>

**STUDY ON SOIL EROSION OF MAHAWELI RIVER UPPER BASIN UNDER
CLIMATE CHANGE USING SWAT MODEL**

D. M. T. S. DISSANAYAKE

Chief Engineer, IRRIGATION DEPARTMENT

SRI LANKA

COMMISSION INTERNATIONALE
DES GRANDS BARRAGES

VINGT-SIXIÈME CONGRÈS DES
GRANDS BARRAGES
Autriche, juillet 2018

STUDY ON SOIL EROSION OF MAHAWELI RIVER UPPER BASIN UNDER CLIMATE CHANGE USING SWAT MODEL^(*)

D. M. T. S. DISSANAYAKE

Chief Engineer, IRRIGATION DEPARTMENT

SRI LANKA

1. INTRODUCTION

Reservoir sedimentation is a world-wide issue. The Mahaweli River Upper Basin (MRUB) in Sri Lanka consists of four major hydro reservoirs namely Kothmale, Victoria, Randenigala and Rantambe in a cascade system (Fig. 1). The total storage capacity of these reservoirs are 1,756.3 million m³, while total power generation potential is 582 MW equalling to 14.8% of installed total capacity of the country by 2014 [1]. The basin area above Victoria reservoir is considered for this soil erosion study. Selected basin area is of 1,865.52 km² where 39.9% of it consists of slopes above 30%. Therefore, the potential for soil erosion is high which can be aggravated by high intensity rainfalls probably due to climate change. Eventually, this would cause sedimentation of reservoirs in the basin. Although, sedimentation cannot be completely avoided rate of sedimentation is very important as it is proportional to the decrease of active storage capacity of a reservoir. When hydropower reservoirs are concerned sedimentation will eventually lead to loss of energy production potential and for Sri Lanka this would be detrimental as the country heavily depends on hydropower.

In addition, the reduction in reservoir capacity may create water scarcity for other users when the demand is high. Further, the loss in capacity of these

^(*) *Étude sur l'érosion de la rivière Mahaweli bassin supérieur en vertu de changements climatiques à l'aide du modèle SWAT*

reservoirs increases the probability of floods as Mahaweli river basin downstream areas are prone to flooding during rainy seasons.

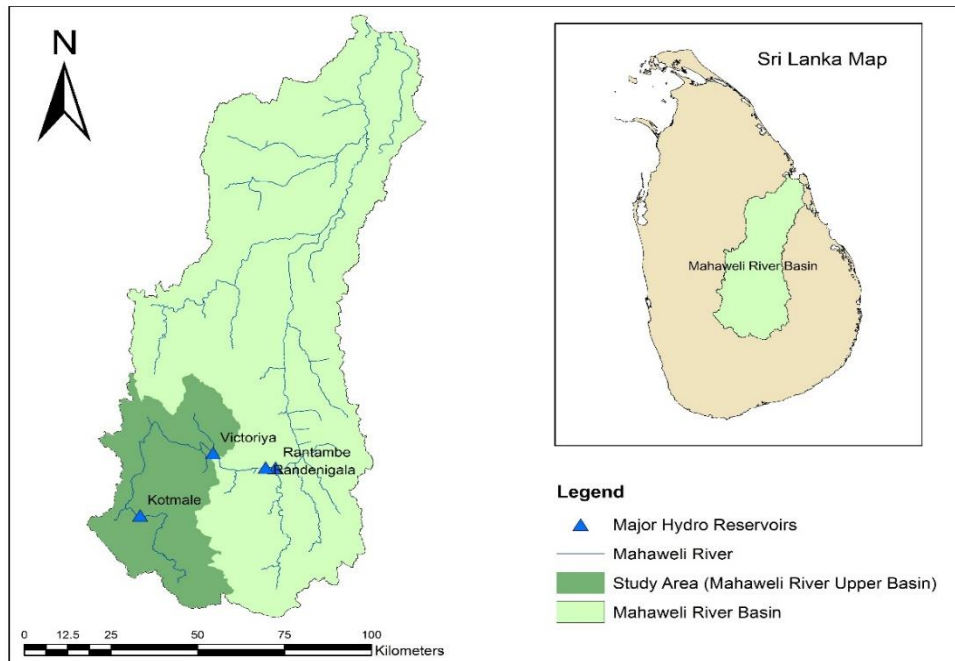


Fig. 1
Mahaweli river basin with major hydro reservoirs

In order to mitigate reservoir sedimentation it is necessary to identify erosion prone areas. Accordingly proper mitigation options has to be planned and executed in order to retard soil erosion. However, reservoir sedimentation analysis need a new approach today due to the influence of climate change. With the climate change it is widely accepted that rainfall intensities are gone up. Intensity of rainfall is a governing factor in soil erosion. Hence, it is important to see the impact of climate change as well, on reservoir sedimentation.

2. LITERATURE REVIEW

2.1 SOIL EROSION PROCESS

The Modified Universal Soil Loss Equation (MUSLE) is widely used around the world to estimate soil erosion [Eq.1]. The SWAT model, which was used for this study and described under methodology, also uses the same equation to calculate erosion outputs (*Sed*) of a basin area [2].

$$Sed = 11.8 \times (Q_{surf} \times q_{peak} \times area_{hru})^{0.56} \times K_{USLE} \times C_{USLE} \times P_{USLE} \times LS_{USLE} \times CFRG \quad [1]$$

Where; Q_{surf}	- Surface runoff volume (mm/ha)
q_{peak}	- Peak runoff rate (m ³ /s)
$area_{hru}$	- Area of hydrologic response unit (ha); defined under methodology
K_{USLE}	- USLE soil erodibility factor
C_{USLE}	- USLE cover and management factor
P_{USLE}	- USLE support practice factor
LS_{USLE}	- USLE topographic factor
$CFRG$	- Coarse fragment factor

As per the MUSLE all other factors except Q_{surf} and q_{peak} are unique characteristics of a basin area. As the same land use and soil map were used throughout the modelling period (1960-2016) of this study, as described under methodology, only Q_{surf} and q_{peak} were the varying parameters. Hence, any increase or decrease in erosion rates during the period considered for the analysis can be attributed to the variability of rainfall.

2.2 TREND ANALYSIS FOR A TIME SERIES

One objective of this study was to check whether climate change has any impact on MRUB soil erosion rate. For finding that time series output of total annual sediment has to be checked for presence of any trend.

The Spearman's rank correlation method is a useful tool for trend analysis of a time series [3]. The Spearman's rank correlation coefficient R_{SP} is defined as follows [Eq. 2].

$$R_{SP} = 1 - \frac{6 \times \sum_{i=1}^n D_i^2}{n(n^2-1)} \quad [2]$$

Where n is the total number of data and D is difference, and i is chronological order number.

$$t_t = R_{SP} \left[\frac{n-2}{1-R_{SP}^2} \right] \quad [3]$$

Where t_t , has Student's t-distribution with $v = n - 2$ degrees of freedom. At a significance level of 5 per cent (two-tailed) and the time series has no trend if;

$$t\{v, 2.5\% \} < t_t < t\{v, 97.5\% \} \quad [4]$$

Accordingly this methodology was applied to check whether sediment yield output time series had got any trend.

3. METHODOLOGY

3.1 MODEL DESCRIPTION

Soil Water Assessment Tool (SWAT) was used as the modelling software for this study. SWAT is a continuous hydrological simulation tool jointly developed by USDA Agricultural Research Service (USDA-ARS) and Texas A&M AgriLife Research. It is GIS-based and simulations can be done at daily time intervals. In addition to hydrological modelling SWAT is capable of calculating the sediment yield of a river basin as well. Accordingly, a SWAT model was developed for the study at a daily time-step for the period 1960 to 2016. Although all the reservoirs in MRUB have been commissioned around 1985, a longer period was taken into account to check any impact from climate change on sediment yield of the basin.

The primary inputs to the model were the basin Digital Elevation Model (DEM), digital land use map, digital soil map, daily rainfall and temperature data of meteorological stations within the study area. A Shuttle Radar Terrain Model (SRTM) downloaded from United States Geological Survey was used as the digital elevation model. The resolution of the model was adjusted to 60m. The elevation of the area varied from 423 m to 2070 m MSL. The land use data were obtained from Land Use Planning Policy Department and digital soil data from Agriculture Department. Daily rainfall data and temperature data were obtained from Meteorological Department.

As no previous land use data maps were available the latest map was used for the total modelling period. In fact, there had not been any significant land use changes in the area and it was a valid reason for using the same map for the whole modelling period. The description of major land use categories are given with the percentages available in the study area (Table 1). It is interesting to note that nearly 20% of the area consists of forests which would least contribute to overall sediment yield.

Daily rainfall data of 11 rain gauge stations located within the area were used. For daily minimum and maximum temperature data four climatic stations, within and around the basin were used. Unavailable climatic data; solar radiation, wind speed and relative humidity were generated by the model itself using a weather generator provided with SWAT [4].

Table 1
Land use categories in the study area

SWAT code	Descriptive Term	% of Catchment Area
URLD	Low density urban	30.14
AGRR	Tea	26.84
FRSE	Forest	19.91
SHRB	Scrub	6.76
RICE	Paddy	6.19

3.2 MODEL SIMULATION

Model development was done using the QGIS QSWAT interface and associated SWAT Editor tool. The model generated the river network based on the DEM where the threshold value selected was 25 km². According to this river network the model delineated 52 sub basins within the study area.

The DEM was categorized into four slope bands as 0-10%, 10-20% and 20-30% and above 30%. During the simulation model created similar sub units with similar hydrological response known as Hydrological Response Units (HRUs). HRUs are areas within the sub basins where slope, land use and soil types are similar. An area threshold of 10% was applied to land use types in order to avoid minor land use types in sub basins to simplify HRU creation. The model was run for the period 1960-2016 in a monthly time step.

4. RESULTS AND DISCUSSION

The model calculated daily sediment yield in the basin area from the beginning of 1960 to the end of 2016. As the rainfall is varying throughout the year the annual series of sediment yields is more appropriate for a trend analysis. The annual totals were plotted for analysis excluding the first and last year of the modeling period to avoid modeling errors due to mass balance (Fig. 2).

It can be observed that highest sediment yield in the basin has been 1,022,717.31 Ton as reported in 2013. The average yield of area for the total period (1961-2015) has been 48.55 Ton/km²/year. However, all the sediments formed due to erosion will not reach the reservoirs as part of it deposits within the catchment itself. On the other hand all the reservoirs have been commissioned around 1985 and soil erosion taken place prior to that time has not contributed to reservoir sedimentation.

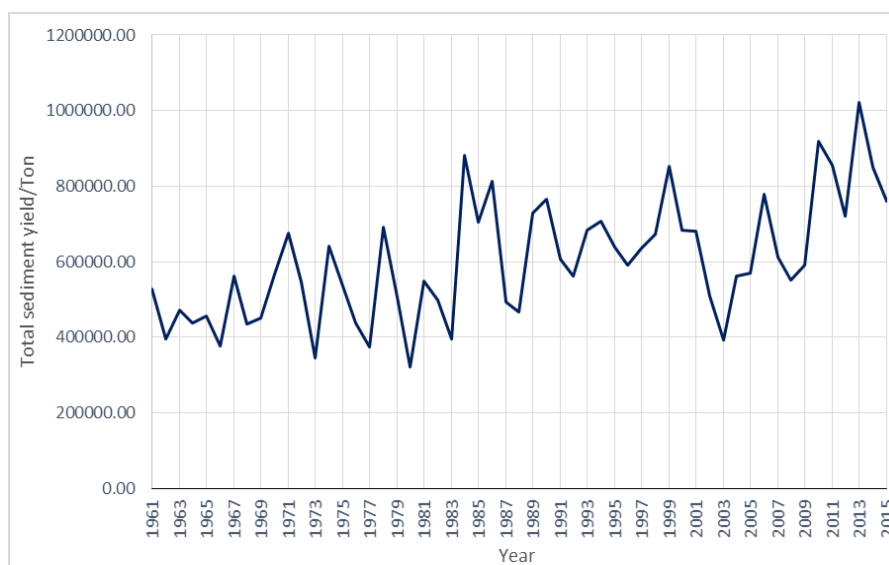


Fig. 2
Annual total sediment yield of study area

If there is an impact of climate change on annual sediment yield during the period 1961-2015 there should be a trend in the time series data. To check whether there is a trend Spearman's Rank-Correlation Method was applied [2]. The results are summarized in Table 2.

Table 2
Parameters for trend analysis calculation

Parameter	Value
Spearman's rank correlation coefficient; (R_{sp})	0.60
For Student's t distribution; (t_t)	5.48
Degree of freedom; $v (= n - 2)$	53
For significance level of 5% ; Upper level value from t distribution	2.01
Lower level value from t distribution	-2.01

If there is no trend in the time series data the value of student's distribution, t_t should be such that; $-2.01 < t_t < 2.01$. As this condition is not satisfied where the calculated value of t_t equals to 5.48 (Table 2) it can be concluded that annual total sediment yield from 1961 to 2015 has a strong increasing trend. Accordingly, sediment yield of the MRUB is influenced by climate change as rainfall and temperature are the only variables during modeling period (1961-2015).

When sub basins are considered soil erosion has a spatial variation (Fig. 3). For finding exact reasons for this variation requires physical inspection of the

catchment in a detailed manner. Therefore, making conclusion on erosion rates of different areas within the study area is beyond the scope of this study.

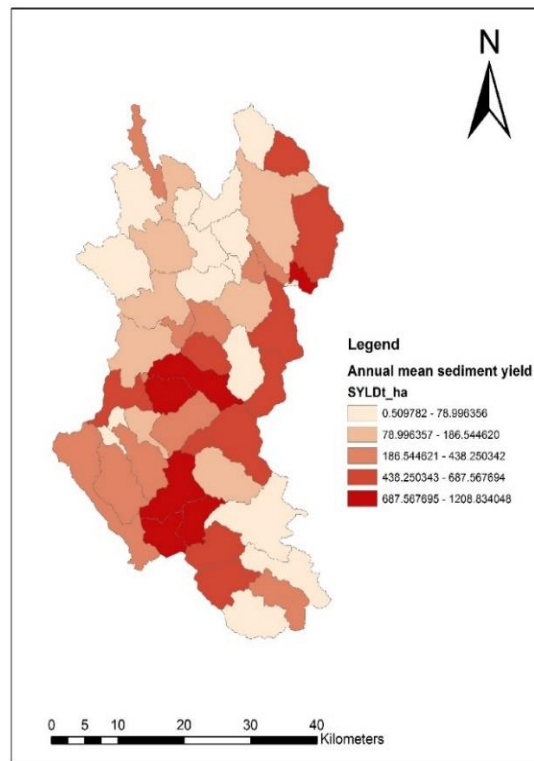


Fig. 3
Annual mean sediment yields of sub basins

5. CONCLUSION & RECOMMEDATIONS

The annual sediment yield rate in the MRUB has an increasing trend during the period from 1961 to 2015. Therefore, it can be concluded that sediment yield rate in MRUB is increasing with climate change posing a risk of rapid reservoir sedimentation. Soil erosion was higher in some of the sub basins within the study area. It is worth finding reasons for this higher erosion rate which is beyond the scope of this study.

Suitable soil conservation methods in agricultural lands and afforestation of bare lands are to be envisaged as measures for erosion mitigation. Further, the future developments within the area, which may take place to cater demands of increasing population, have to be well planned to minimize soil erosion.

ACKNOWLEDGEMENTS

Most of the data used for this study were obtained from World Bank funded Climate Resilience Improvement Project (CRIP) under the Ministry of Irrigation and Water Resources Management. Therefore, the author would like to convey his sincere gratitude to Eng. (Mrs) P.A.A.P.K. Pannala, Deputy Project Director of component I of CRIP for giving the permission to use the data.

REFERENCES

- [1] *Long Term Generation Expansion Plan 2015-2034*, Ceylon Electricity Board, Sri Lanka, September, 2016
- [2] NEITCH S.L. et al. *Soil and water assessment tool, Theoretical documentation, version 2009*. Texas water resources institute, 2011
- [3] DAHMEN E.R., HALL M.J. *Screening of hydrological data: Tests for stationarity and relative consistency*, ILRI, The Netherlands, 1990
- [4] <http://swat.tamu.edu>

SUMMARY

The Mahaweli River Upper Basin (MRUB) in Sri Lanka consists of four major hydro reservoirs namely, Kothmale, Victoria, Randenigala and Rantambe situated in a cascade system. The total storage capacity and power generation capacity of these reservoirs are 1,756.3 million m³ and 582 MW respectively. The catchment above Victoria reservoir was the area selected for this study (1,865.52 km²). As 39.9% of this area consists of slopes above 30% aforementioned reservoirs are facing the risk of sedimentation due to catchment soil erosion. Eventual loss of energy production potential when the storage capacities are reduced would be detrimental as the country heavily depends on hydropower. In addition, the reduction in reservoir capacity may create water scarcity for other users when the demand is high. Further, the loss in capacity of these reservoirs increases the probability of floods as Mahaweli river basin downstream areas are prone to flooding during rainy seasons.

Soil Water Assessment Tool (SWAT) developed by USDA Agricultural Research Service was used as the modelling software for this study. It is GIS-based and a model was developed for the study area at a daily time-step for the period 1960 to 2016. Main inputs to the model were digital elevation model, land-use map, soil map, rainfall and temperature. Unavailable climatic data; solar radiation, wind speed and relative humidity were generated by the model itself.

Although all the reservoirs in the MRUB have been commissioned around 1985 the model analysis was done for a longer period to check any impact from climate change on sediment yield of the area.

It could be observed that highest sediment yield in the MRUB had been 1,022,717.31 Ton as reported in 2013. The average yield for the total period was 48.55 Ton/km²/year. The annual sediment yield rate in the MRUB has an increasing trend. Therefore, it can be concluded that sediment yield rate is increasing with climate change posing a risk of rapid sedimentation of reservoirs. At sub basin level sediment yield indicates a considerable spatial variation.

It is recommended that suitable soil conservation methods in agricultural lands and afforestation of bare lands are to be envisaged as measures for erosion mitigation. Further, the future developments within the area, which may take place to cater demands of increasing population, have to be well planned to minimize soil erosion.

RÉSUMÉ

Le bassin supérieur de la rivière Mahaweli (MRUB) au Sri Lanka se compose de quatre grands réservoirs hydroélectriques, à savoir, de Kothmale, Victoria, Rantambe et Randenigala. Ils sont situés dans un système en cascade. La capacité totale de stockage et la capacité de production d'électricité de ces réservoirs sont 1,756.3 millions de m³ et 582 MW, respectivement. Le bassin versant du réservoir au-dessus de Victoria a été la région sélectionnée pour cette étude (1,865.52 km²). Cependant, 39.9% de cette superficie est constituée de pistes au-dessus de 30%. Par conséquent, ces réservoirs sont confrontés au risque de sédimentation due à l'érosion des sols. Sri Lanka dépend considérablement sur l'hydroélectricité. Diminution de l'énergie hydroélectrique potentiel lorsque les capacités de stockage sont réduits serait préjudiciable. En outre, la réduction de la capacité du réservoir peut créer de la rareté de l'eau pour d'autres utilisateurs lorsque la demande est forte. En aval du bassin de Mahaweli zones sont sujettes aux inondations pendant la saison des pluies. Par conséquent, la diminution du stockage des réservoirs augmente la probabilité d'inondations.

L'outil d'évaluation de l'eau du sol (SWAT) développé par USDA Agricultural Research Service a été utilisé comme le logiciel de modélisation pour cette étude. Elle est basée sur le GIS et un modèle a été élaboré pour la zone d'étude à un pas de temps quotidien pour la période 1960 à 2016. Principaux intrants au modèle ont été modèle d'élévation numérique, modèle d'utilisation des terres, une carte du sol, les précipitations et la température. Les données climatiques comme le rayonnement solaire, la vitesse du vent et de l'humidité relative ont été générées par le modèle lui-même comme non disponible. Bien que tous les réservoirs dans les MRUB ont été construites autour de 1985, d'analyse a été effectuée pour une

période plus longue pour vérifier l'impact du changement climatique sur la production de sédiments de la région.

Il peut être observé que la valeur la plus élevée de production de sédiments ont été 1,022 717.31 tonnes tel que rapporté en 2013. Le rendement moyen pour la période totale était 48.55 tonnes/km²/an. Le taux annuel de sédiments dans l'MRUB a une tendance à la hausse. Par conséquent, on peut conclure que le taux de production de sédiments augmente avec le changement climatique. Par conséquent, il y a un risque de la sédimentation rapide des réservoirs. Dans la production de sédiments sous-bassins montre une variation spatiale considérable.

Il est recommandé que des méthodes de conservation du sol dans les terres agricoles devrait être appliquée pour la réduction de l'érosion. D'autres terres nues doivent être plantées d'arbres. De plus, l'évolution future au sein de la région, qui peut avoir lieu pour répondre aux exigences de l'augmentation de la population, doivent être bien prévues pour minimiser l'érosion du sol.

KEY WORDS

Climate, Erosion, Sedimentation, SWAT, Kothmale, Randenigala, Rantambe, Victoria

COMMISSION INTERNATIONALE DES GRANDS BARRAGES

VINGT-SIXIÈME CONGRÈS DES GRANDS BARRAGES
Autriche, juillet 2018

DOI 10.3217/978-3-85125-620-8-051



This work licensed under a Creative Commons Attribution 4.0 International License. <https://creativecommons.org/licenses/by-nc-nd/4.0/>

**A USEFUL TECHNOLOGY TO SOLVE OR MITIGATE ARTIFICIAL
RESERVOIR SEDIMENTATION**

Francesco GALANTE

Hydraulic Consultant of DRAGFLOW

ITALY

Luca MASOTTI

Sales Manager of DRAGFLOW

ITALY

Claudio FORNASARI

Managing Director of THETIS COSTRUZIONI

ITALY

A USEFUL TECHNOLOGY TO SOLVE OR MITIGATE ARTIFICIAL RESERVOIR SEDIMENTATION

Francesco GALANTE
Hydraulic Consultant of DRAGFLOW

Luca MASOTTI
Sales Manager of DRAGFLOW

Claudio FORNASARI
Managing Director of THETIS COSTRUZIONI

ITALY

KEYWORDS: dam operation, flood storage, grain size distribution, reservoir operation, settlement, siltation;

MOTS CLE: exploitation, réserve de crue, granulométrie, exploitation du réservoir, tassement, alluvionnement

1. RATIONALE

Reduction of sediment flow generated by dam construction leads to erosion on downstream riverbed and on coastal areas; the lack of coarse sediment (sand, gravel) generated channel riverbed deepening and relevant effects on bridge foundation structures, and on other infrastructure affected by water bodies, meanwhile the lack of fine sediment (silt, clay, nutrients) can have serious effects on balance of downstream ecosystems, reducing water turbidity and affecting water temperature.

Loss of reservoir capacity caused by sedimentation can greatly impact reservoir management because it generates a reduction of water availability for several uses (energy generation, irrigation, drinking water). Most recent studies estimated global gross storage capacity at 6,000 km³ and annual reservoir sedimentation rates at 31 km³. According to this growing trend, global reservoir storage capacity will be reduced by 50% on 2100.

Both accumulation of sediments in dams and the lack of these in downstream areas have negative effects on the performance and conditions of the infrastructures, on the coastline stability, already endangered by sea level rise (greenhouse effect), therefore actual handling of these sediments is of paramount importance for long term management of artificial reservoirs.

Several possible solutions can be taken into consideration:

- sediment by-passing into the downstream area;
- drawdown routing involves discharging high flows through the dam during periods of high inflows to allow sediment to be transported through the reservoir minimizing sedimentation;
- drawdown flushing, opposite to sluicing, focuses on scouring and re-suspending deposited sediment and transporting it downstream. It involves the complete emptying of the reservoir through low-level gates;
- turbidity current venting can be done when inflowing water with high sediment concentrations forms a higher density current that flows along the bottom of the reservoir without mixing with the lower density clear waters;
- dredging with specialized equipment to remove the sediments from the dam.

In the last years, sedimentation in artificial reservoirs became more and more important, especially in reservoirs where their catchment basin is affected by important surface erosion rates due to poor vegetation coverage (degradation of the vegetation by human action), or to the presence of heavy rains in very short periods (flash floods).

Climate change has increased the frequency of flash floods, therefore sedimentation in artificial reservoirs is one of the most important challenges of Public/Private Authorities responsible for artificial reservoir management. Sedimentation is really important because there are situations, all around the world, where original reservoir capacity has been dramatically reduced by 30/50%, generating important losses in terms of electricity production, reduction of water for irrigation and human use.

This paper deals with the positive experience happened in an artificial reservoir located in the eastern part of the Italian Alps (Ambiesta reservoir) managed by A2A, that is one of the most important energy supplier in Italy. Few years ago, A2A launched a tender to select a Contractor able to propose a cost-effective technology to remove about 23,000 m³ of sediments settled near the water intake structure located on the right flank of the valley close to the dam, affecting dam bottom outlet, and water intake for hydroelectric purposes.

The tender has been awarded to THETIS COSTRUZIONI & DRAG-FLOW which designed, supplied, installed, tested and managed a dredging system which allowed to complete the activity required by A2A fulfilling contractual time and very stringent environmental constraints established by River Tagliamento Authority. In the following pages the reader will find in detail reference data used to dredging system design, characteristics of the dredging system itself, on site activity and monitoring plan during dredging, and finally the conclusions.

2. REFERENCE DATA & CLIENT REQUIREMENTS

2.1. Environmental data

Ambiesta stream is located in the hydrographic basin of Tagliamento river, 3.5 km far from their confluence, in the eastern part of the Italian Alps (Friuli Venezia Giulia region). Ambiesta dam is a symmetric double curved arch dam, with the following characteristics (Fig. 1):

- Dam height: 58.63 m
- Free board: 2.50 m



Fig. 1
Ambiesta reservoir
Ambiesta reservoir

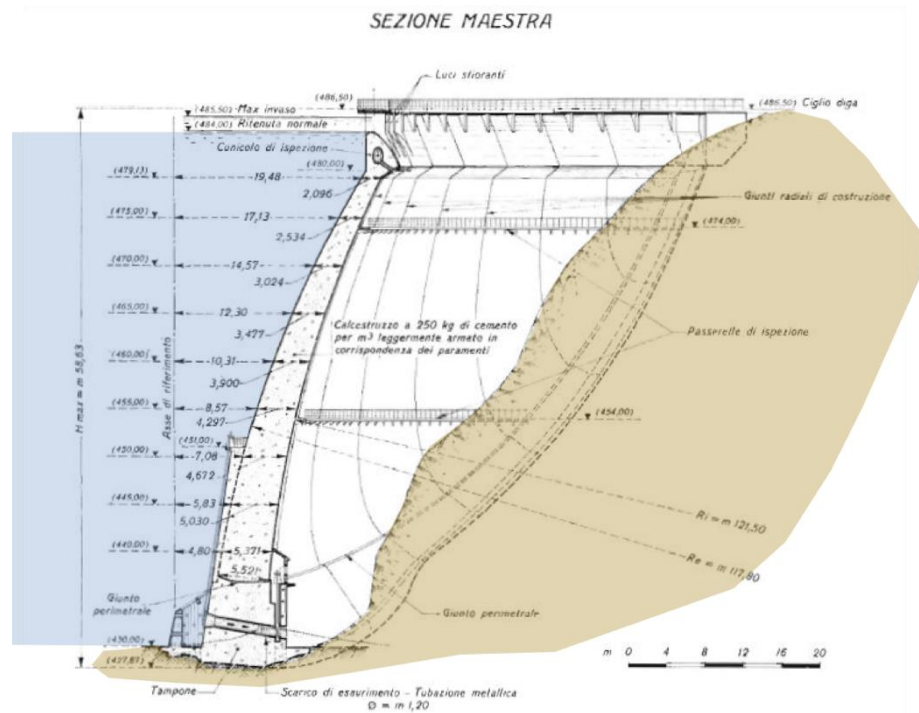


Fig. 2
 Ambiesta dam: typical section
 Ambiesta barrage: section typique

- Normal operating water level: 484 m a.m.s.l.
- Maximum water level: 485.50 m a.m.s.l.
- Dam volume: 28,734 m³ of concrete
- Crest length: 144.64 m
- Dam thickness (at the top): 1.80 m
- Dam thickness (at the toe): 5.52 m

Ambiesta dam (Fig. 2) has been equipped with following ancillary structures:

- Surface outlet on the left side, equipped with gates, with flood discharge of 72 m³/s;
- Surface spillway on the dam body with flood discharge of 120 m³/s;
- Bottom outlet with discharge capacity of 48 m³/s;
- Water intake structure on the right flank of the reservoir, which feeds two different tunnels with a diameter respectively of 4.40 m and 5.15 m, that feed Somplago hydroelectric plant.

The dam has been built in the period 1955 – 57 on behalf of SADE (Società Adriatica di elettricità) and transferred to ENEL (Ente Nazionale per l'Energia Elettrica) on March 1963.

In the following picture we can appreciate the dam shape during construction.



Fig. 3
Ambiesta dam (during construction)
Ambiesta barrage (pendant la construction)

2.1.1. *Area to be dredged*

A2A, the Public Company, responsible for management of Ambiesta reservoir, during the last years has monitored the sedimentation in the reservoir and more in detail sedimentation rate close to the dam structure, through a comparison of several topographic campaigns, to understand the evolution sedimentation phenomenon, and its impact to ancillary structures of the dam (dam bottom outlet and water intake), in terms of efficiency and safety.

On basis of this monitoring, A2A noticed that the quantity of sediments, coming from the rain activity on the surfaces of the catchment basin, reached

an alert level especially nearby bottom outlet intake, and water intake structure as well. Through the comparison of topographic surveys developed along several years, A2A identified the area where the sediments have to be removed, and the total amount of them.

Total area to be dredged (Fig. 4) has a surface of 4,500 m² and is located at a water depth variable between 20 and 36 m, according to the water oscillation in the reservoir. Globally 28,000 m³ have to be removed to assure a correct efficiency of the ancillary structures, and the right safety factor. The thickness of the sediment layer to be removed was variable between 6 and 10 m.

In the following picture we can appreciate the area to be dredged (green area), which affects dam bottom outlet, located on the left side of the dam (axis indicated with red dotted line), water intake on the right side, through which the water is driven to turbine of Somplago power plant (axis indicated with red dotted line), and the ancient cofferdam, concrete made, built at the beginning of the construction activity, to divert stream water to the dam bottom outlet, to kept dry the area where dam foundations have been built.

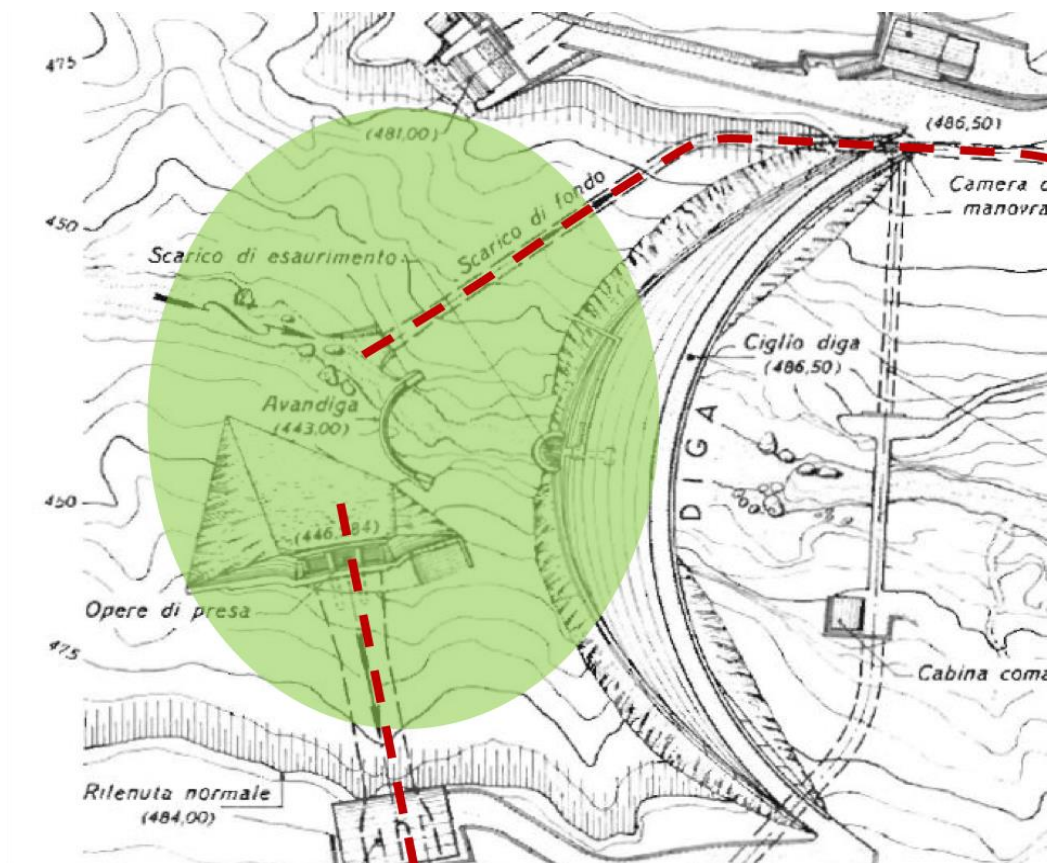


Fig. 4
Area to be dredged
Surface à draguer

As you can imagine, dredging activity has been developed in a quite complicated area from a morphological point of view because of the presence of artificial structures, forcing the submersible pump operator to carefully proceed between existing structures. In Fig. 5 we can appreciate, through an historical photo taken during construction time, the original morphology of the area, with quite big concrete structures (intake screen of the water intake channel) and very steep flanks of the valley.

To correctly design dredging system and determine dredging efficiency of the submersible pump, A2A supplied to the tenderers detailed information on the sediments to be dredged, collected through a field campaign developed all along the reservoir (Fig. 6).

The information used for the project has been related to the sample taken close to the dam. According to the grain size distribution analysis, the sediment to be dredged showed a granular fraction equal to 5%, meanwhile the cohesive fraction reaches 95% (74% silt and 21% clay).

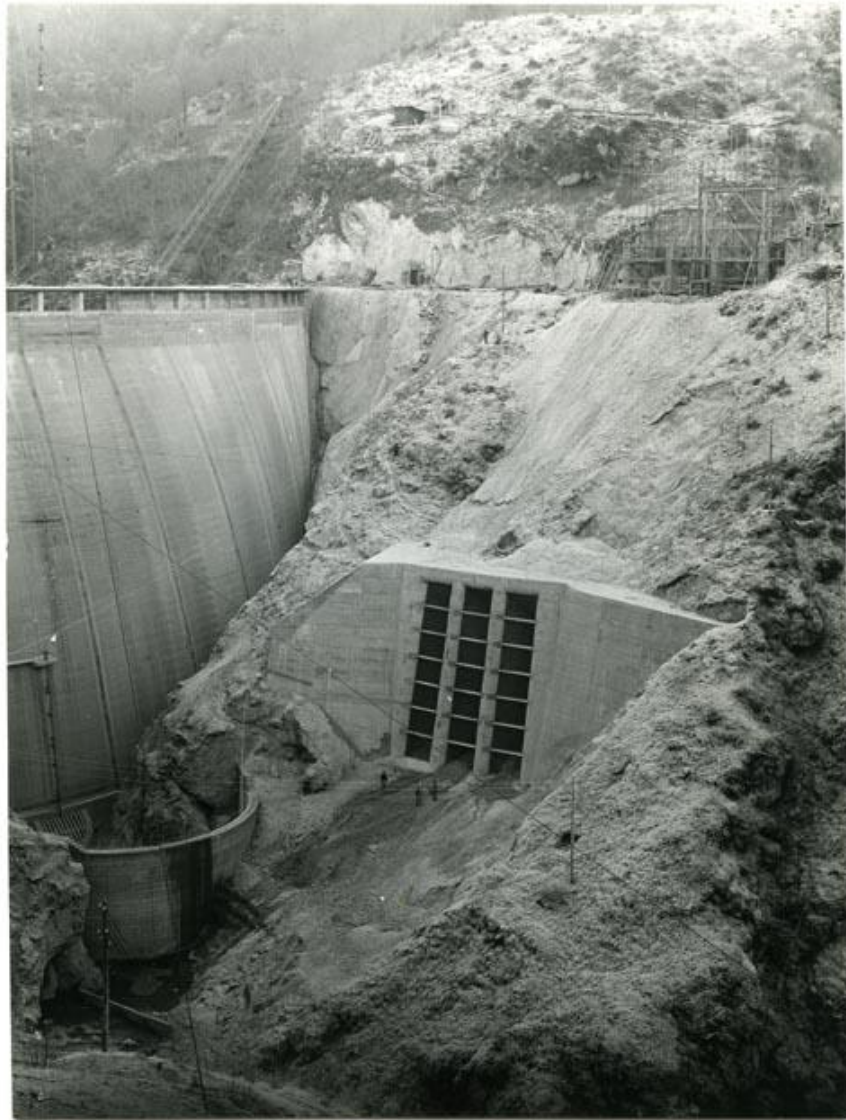


Fig. 5
Dam during construction
Barrage pendant la construction

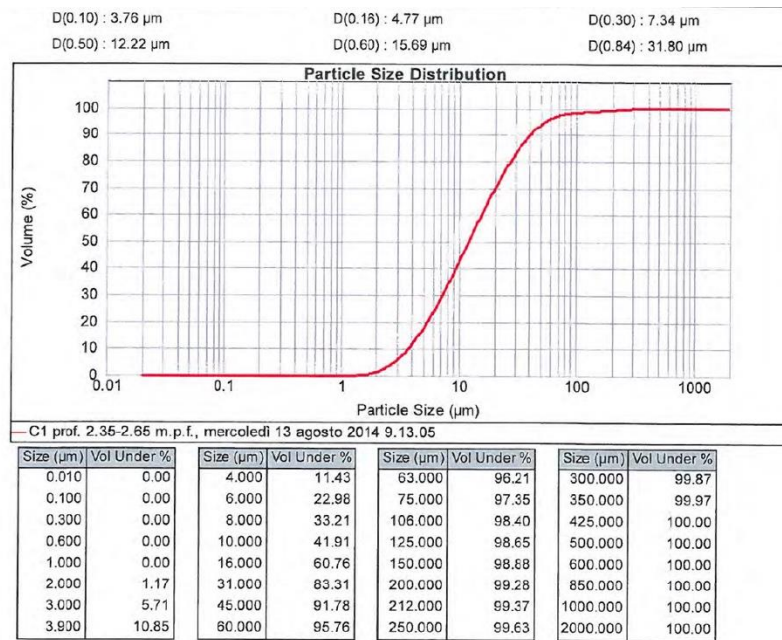


Fig. 6
Sediment particle size distribution
Distribution de la granulométrie du sédiment

2.2. Client requirements

On basis of the management plan of dam operation, and on the environmental constraints, A2A requested to fulfil following design criteria:

- maximum water level variation to be considered inside the reservoir is 9 m, with a water level variation between 475 and 484 m a.m.s.l.; maximum gradient of water level variation can reach 1 m/hour;
- maximum concentration of sediment in the slurry discharged downstream the dam cannot overcome 9 g/l for environmental reasons;
- possible presence of wood debris and large stones on the sediment layer to be dredged has to be considered;
- during dredging activity, the water intake feeding Somplago power plant is in operation discharging 66 m³/s (three Francis turbines), therefore turbidity generated by the dredging pump has to be kept at the minimum;
- during dredging activity, maximum allowed noise level at a distance from dredging pump of 300/400 m cannot overcome 45/50 dB;
- dredging activity of 28,000 m³, including mob - demob activities has to be developed and completed in 100 natural days.

3. PROPOSED SOLUTION

On basis of Client's requirements, and taking into consideration dam location and characteristics, and usual dredging solutions already experimented for similar projects, DRAGFLOW, together with the Contractor THE-TIS COSTRUZIONI decided to propose following technical solution:

- Submersible pump located on a pontoon fully equipped, able to cover all the area to be dredged (4,500 m²);
- Floating pipeline conveying the slurry from the pontoon to the surface outlet located on the left side of the dam, and from this structure downstream the dam;
- To respect environmental constraints (9 g/l), slurry has been mixed with water discharged by the surface outlet of the dam, managing the gates accordingly;
- To check the respect of maximum concentration of sediment in the slurry, three check points have been organized (on the pumping pipeline on the pontoon, just after the confluence of slurry and Ambiesta stream at the toe of the dam itself, and finally at the final confluence between Ambiesta steam and Tagliamento river, 2 km downstream Ambiesta dam);
- Service boat to allow the staff involved in the activity to reach the pontoon and to leave it at the end of the working shift.

3.1. Dredging system

Taking into account the characteristics of the sediment to be dredged, and the total dredging time allowed by the Client A2A, average slurry discharge has been fixed at 500 m³/hour, and it has been mixed with 4 m³/s clear water, taken form the reservoir, and discharged by the surface outlet of the dam located on the left side of the dam, to meet Client's requirements (9 g/l).

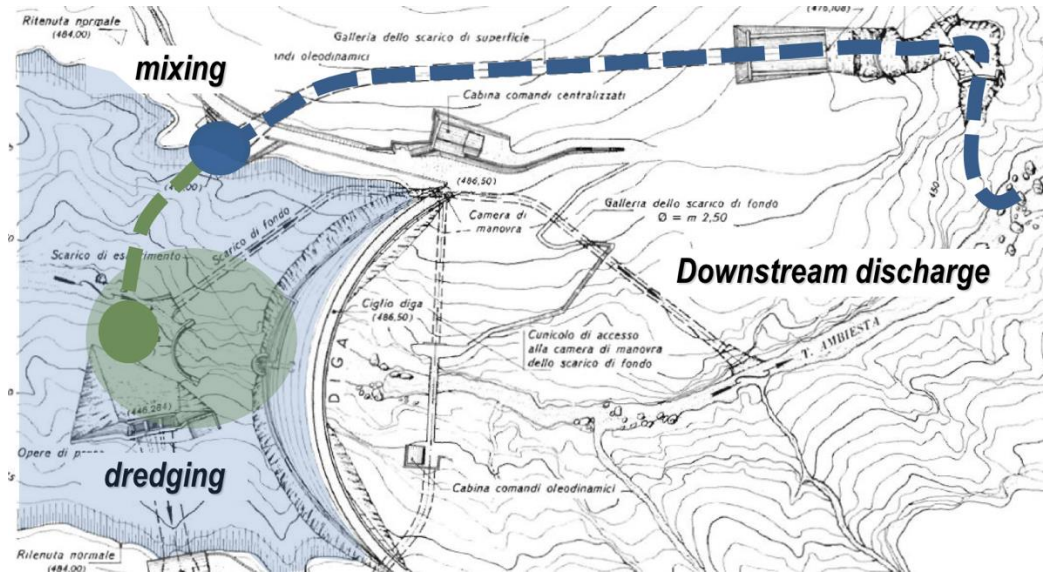


Fig. 7
 Slurry mixing to fulfil environmental requirements
 Mélange du “slurry” pour se conformer aux critères environnementaux

In Fig. 7 you can appreciate the location of the dredging area, and the mixing point where slurry produced by dredging activity has been mixed with fresh water coming from the reservoir to fulfil Client’s environmental requirements. The pump selected for this project has been DRAGFLOW pump HY85/160B; it’s a hydraulic pump with following characteristics (Fig. 8).



Fig. 8
Submersible pump
Pompe submersible

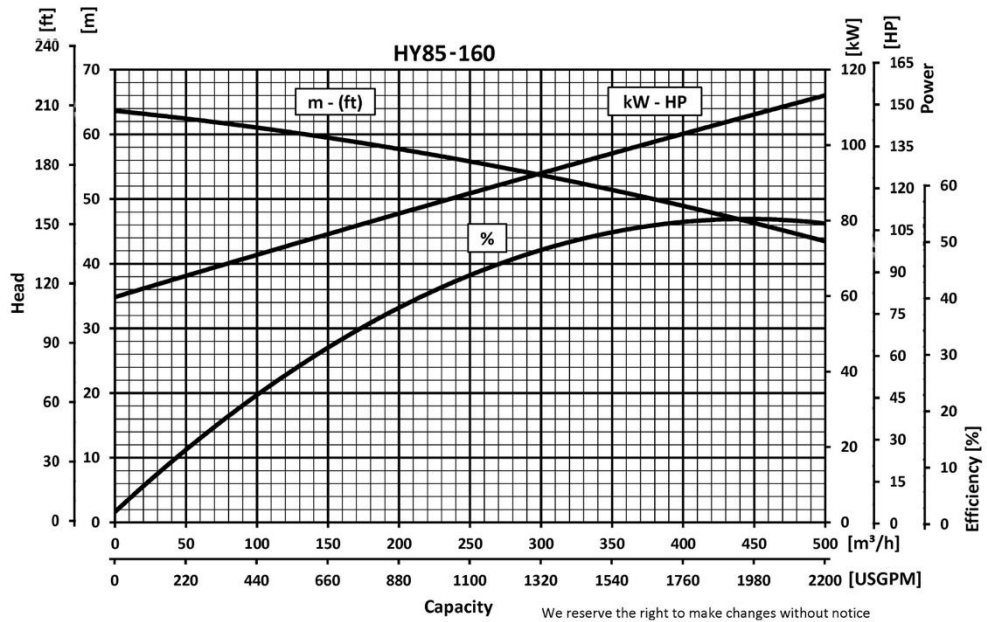


Fig. 9
Submersible pump – working diagram
Pompe submersible – schéma de travail

Since most of the percentage of the sediment to be dredged is cohesive, to assure the correct productivity requested by total project time allowed by A2A, the pump has been coupled to two cutter heads, specifically designed for cohesive materials (Fig. 10).

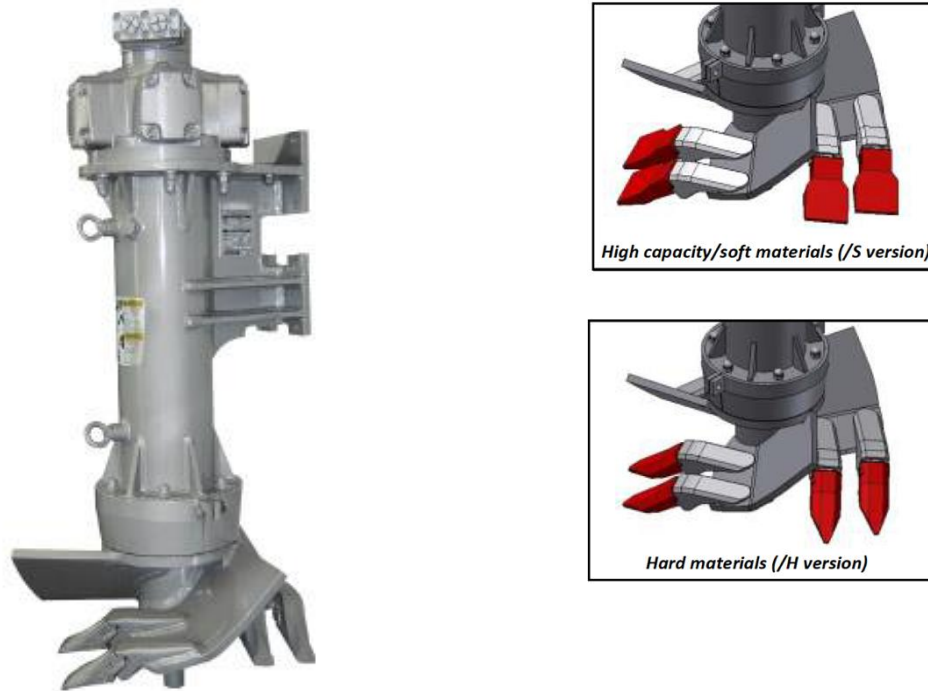


Fig. 10
Cutter heads
Têtes de coupe

In addition to that, according to the request of the Client to minimize the turbidity generated by dredging activity, a special anti-turbidity tool (Fig. 11) has been installed on the submersible pump. This tool allowed to minimize the dispersion of fine sediment around dredging area, avoiding the movement of fine sediment to right side water intake, and the ingestion of fine sediment by turbines installed at Somplago power plant.

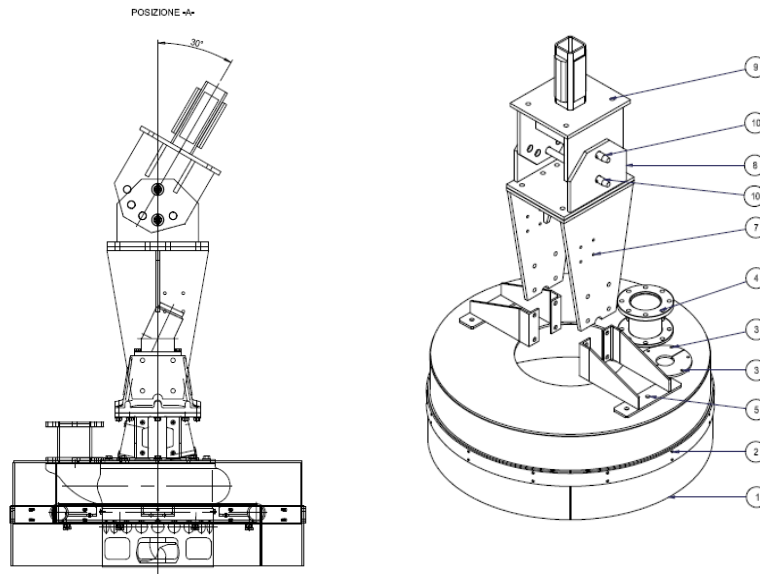


Fig. 11
 Turbidity reduction tool
 Outil de réduction de la turbidité

Submersible pump is managed through a pontoon specifically equipped (Fig. 12 and Fig. 13). DRAGFLOW's pontoons follow a modular design that has been tested over the years in several projects all around the world. The submersible pumps adopted for this project allowed to use very compact pontoon, achieving at the same time quite large working depths requested by A2A.



Fig. 12
 Pontoon
 Ponton



Fig. 13
Pontoon and main operation cabin
Ponton et cabine principale de travail

All DRAGFLOW's pontoons are designed for an easy transportation either by container or by trucks. The pontoons are built with internal reinforcement structures and divided in different compartments. The pontoons follow a catamaran design with a steel tripod and hoist as main movement system for the submersible dredging pump. The pontoon is complete with handrails and skids under the floaters with an integrated high capacity fuel tank.

The pontoon is equipped with 4 mooring winches driven by individual electric motors, each one with cable length of up to several meters. The entire dredging equipment is easily controlled and operated from the central cabin where the operator manages all necessary controls to drive each component of the dredging system with indicators of working depths, current absorption and bathymetric survey system.

3.2. Parameters monitored during dredging activities

During dredging activity, several parameters have been monitored, for both reasons: to be sure that Client's requirements are always fulfilled, especially which ones related to the environment, and to check dredging productivity which has a direct impact on the total duration of the project established by the Client's to 100 natural days.

To do that, the Contractor has to know, during dredging activity, where the submersible pump actually is (x,y,z coordinates), which is the actual water depth where the pump is dredging, in relation with water level in the reservoir, and what is the concentration of sediment in the "slurry".

Summarising, following devices have been installed and continuously monitored:

- GPS installed on board (Fig. 14) of the pontoon to know in every moment real time position of the submersible pump (x,y,z coordinates);
- Sediment concentration device installed on board of the pontoon (on the pumping pipeline) able to continuously record sediment concentration of the “slurry”.

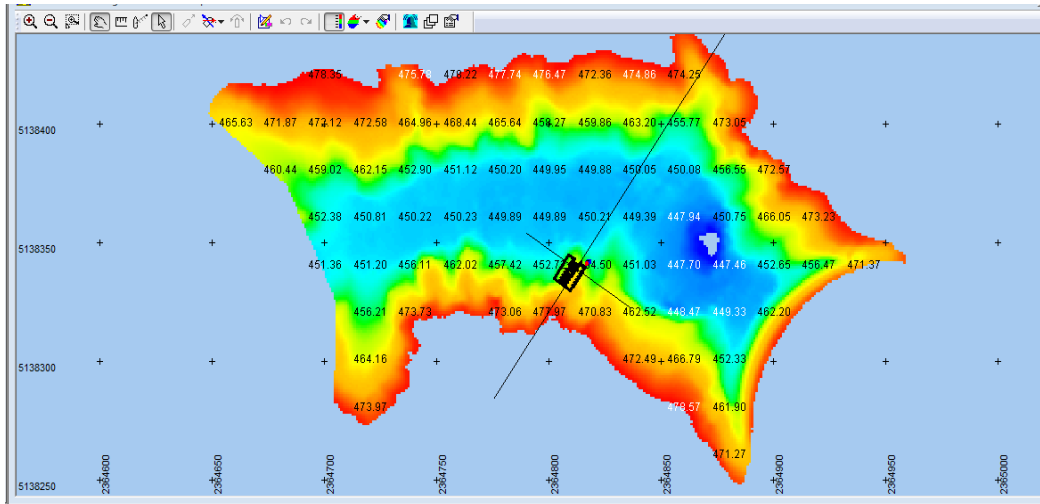


Fig. 14
Dredging pump positioning
Positionnement de la pompe de dragage

GPS coupled with topographic maps of the area to be dredged (Fig. 14) allowed to check every now and then if the dredging thickness required by the Client has been respected.

According to Client's requirement, sediment percentage in the slurry has been continuously checked in three different positions: on board of the pontoon, at the toe of the dam, and at the confluence between Ambiesta stream and Tagliamento river. To correctly understand the location of the dredging activity, the submersible pump productivity, and the new water depths after dredging, the bathymetric survey, done using a multi-beam device (Fig. 15) just before dredging starting, has been compared to a second survey, developed just after dredging activity (Fig. 16).

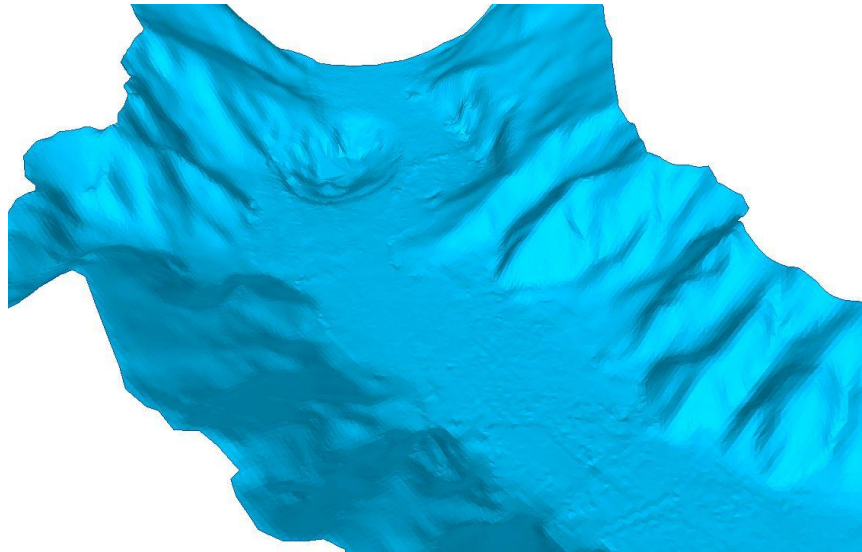


Fig. 15
Multi-beam topographic survey
Relèvement topographique avec le multi-beam

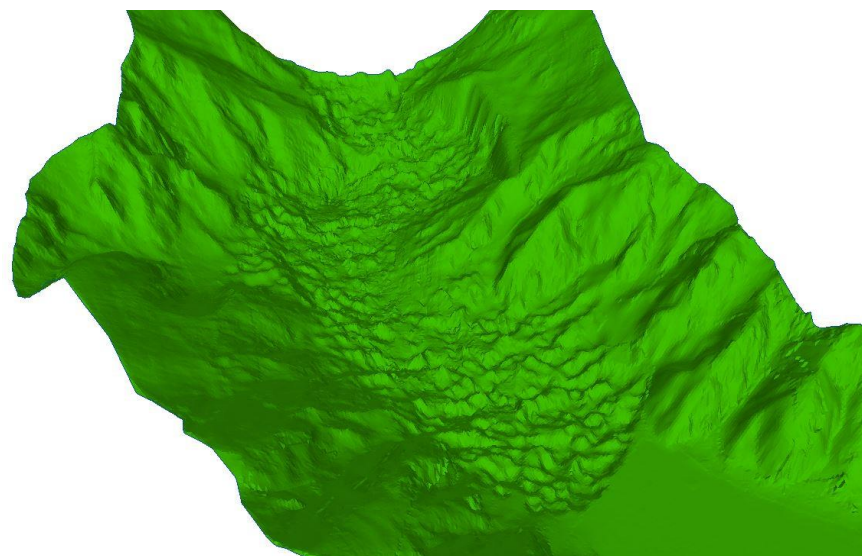


Fig. 16
Multi-beam topographic survey after dredging
Relèvement topographique avec le multi-beam depuis le dragage

From the comparison between two multi – beam surveys, developed just before and just after dredging activity, Client’s Project Manager has been able to check total quantity of the materials actually dredged from the reservoir and the relevant time needed to dredge.

In Fig. 17 we can have a clear picture of the monitoring of the concentration of the sediments in the slurry pumped from the reservoir downstream the dam, till to the confluence between Ambiesta stream and Tagliamento river.

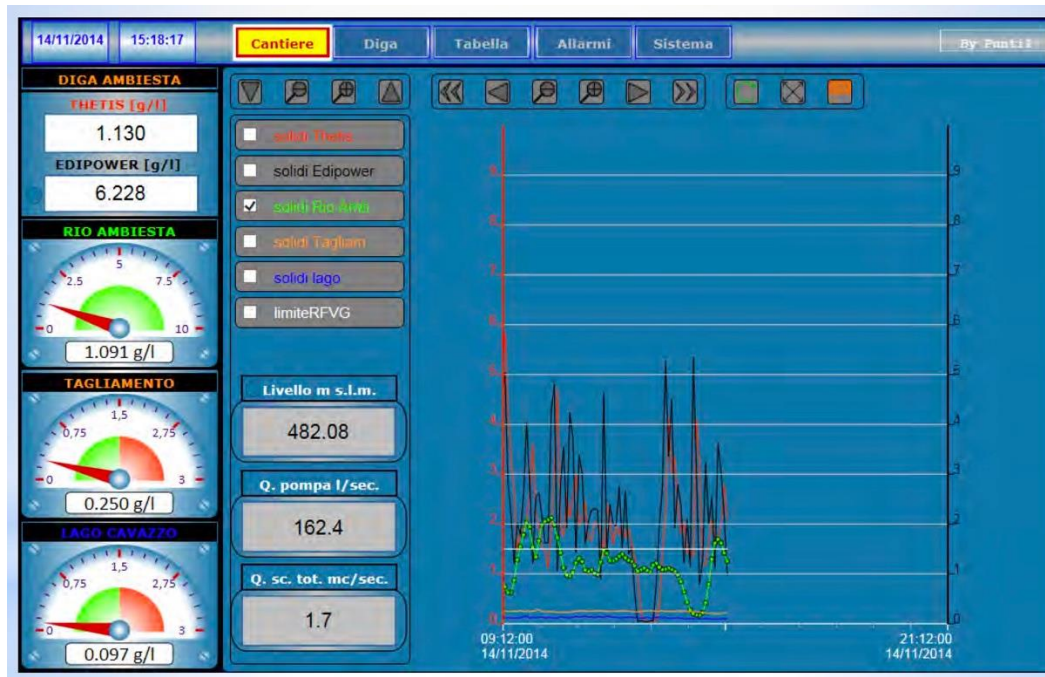


Fig. 17
Slurry concentration monitoring system
Système de monitoring de la concentration du slurry

According to Client's requirements, concentration of the sediments in the slurry has been continuously monitored, giving to the Client and to the Contractor itself, every day, maximum/minimum and average concentration values, through which a simple calculation gave a confirmation of the sediments removed from the bottom of the reservoir calculated using different topographic surveys.

3.3. Productivity rates

Taking into consideration dredging technology, time needed for regular maintenance of the equipment, out of service of some part of the equipment, not constant characteristics of the sediment to be dredged, variable water depth, variable thickness of sediments to be dredged, the dredging productivity, evaluated on daily basis has been the following:

- minimum productivity: 200 m³/day

- average productivity: 400 m³/day
- maximum productivity: 800 m³/day

Dredging activity has been developed along three shifts, therefore 24 hours per day, using the noise reduction tool to avoid any impact on the nearby village.

In the following picture we can appreciate the dredged profile (blue line) compared to the original bed of the reservoir (green line).

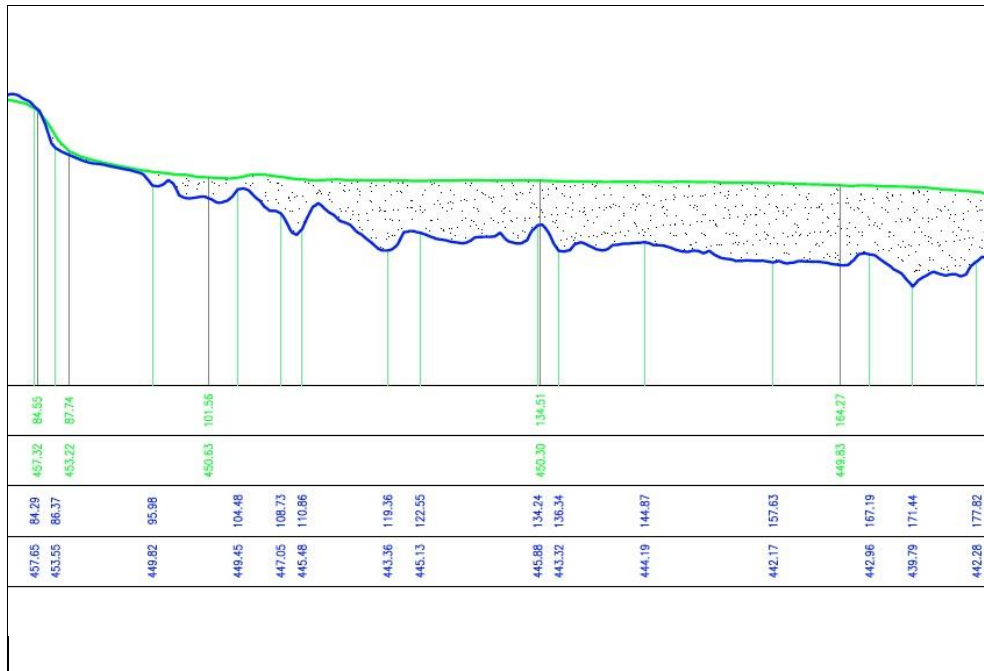


Fig. 18
Dredged profile versus original bed profile
Surface de dragage par rapport au fond original du reservoir

4. CONCLUSIONS

Dredging activity has been concluded fulfilling the total time allowed by the Client, taking into consideration supply and installation of the equipment, preparation of the jobsite area, assembling and testing of the dredging system, maintenance of equipment, and finally the disassembly of the equipment, and the restoration of the jobsite area to the original situation.

Selection of the dredging system demonstrated its validity to fulfil Client's requirements, and maintenance activity was really reduced, demonstrating that DRAGFLOW pumps are really a good and cost-effective solution

for slurry dredging. For security reasons a stock pump has been located at the job site just in case, because the respect of the total time (100 days) was mandatory, but this pump has been never used.

In addition, the high efficiency reached by the dredging system, and the capacity to work 24 hours per day along three shifts, allowed the Contractor to get the bonus made available by the Client.

The system used for the topographic surveys (multi – beam) made at the beginning, in an intermediate time, and at the end of the job, has proven high reliability and a good level of precision. The Client really appreciated the job done by THETIS COSTRUZIONI and DRAGFLOW, their availability to discuss together the best solutions to be proposed to overcome usual small problems that sometimes happen during dredging activity, and their proactive attitude.

REFERENCES

- [1] MOLINO B., MOSCHETTO M.P., SALOMONE M.
L'interrimento dei serbatoi artificiali - I sedimenti: un problema una risorsa
Centro Studi di Economia Applicata all'Ingegneria, 2010 - 2013

SUMMARY

This paper deals with the technology proposed and used to remove sediments settled nearby Ambiesta dam, located in the eastern part of Alps, Friuli Venezia Giulia region, Italy. In the Document many aspects have been detailed starting from design data needed to correctly design a dredging system, Client's requirements, characteristics of dredging system detailing all the components, and finally achieved results. Dredging activity has been developed fulfilling total time established by the Client, and the Contractor got the bonus offered by the Client if the job had been completed on time.

Ce rapport concerne la technologie proposée et utilisée pour enlever les sédiments installés à proximité du barrage d'Ambiesta, situé dans la partie orientale des Alpes, région Friuli Venezia Giulia, Italie. Dans le document de nombreux aspects ont été détaillés à partir des données de conception nécessaires pour concevoir correctement un système de dragage, les exigences du Client, les caractéristiques du système de dragage détaillant tous les composants, et enfin les résultats obtenus. L'activité de dragage a été

développée en respectant le temps total établi par le Client, et le Constructeur a obtenu le bonus offert par le client si le travail avait été achevé à temps.

COMMISSION INTERNATIONALE DES GRANDS BARRAGES

VINGT-SIXIÈME CONGRÈS DES GRANDS BARRAGES
Autriche, juillet 2018

DOI 10.3217/978-3-85125-620-8-052



This work licensed under a Creative Commons Attribution 4.0 International License. <https://creativecommons.org/licenses/by-nc-nd/4.0/>

**ASSESSMENT OF TEMPERATURE AND PRECIPITATION CHANGES TREND
EFFECTS ON THE DAM INFLOW**

Mojtaba NOURY

Research manager, IWRM CO. MINISTRY OF ENERGY

IRAN

Manijeh EZZATI

MSc in water resources Eng

IRAN

Alireza SHOKOHI

Academic member of Imam Khomeini international university

IRAN

COMMISSION INTERNATIONALE
DES GRANDS BARRAGES

VINGT-SIXIÈME CONGRÈS DES
GRANDS BARRAGES
Autriche, juillet 2018

ASSESSMENT OF TEMPERATURE AND PRECIPITATION CHANGES TREND EFFECTS ON THE DAM INFLOW

Mojtaba Noury¹, Manijeh Ezzati², Alireza Shokohi³

*¹Research manager, IWRM Co. ministry of energy, Iran ² MSc in water resources
Eng, ³ Academic member of Imam Khomeini international university*

IRAN

1. INTRODUCTION

The principle of climate change, as a problem, despite of its various angles being discovered worldwide is still discussed by researchers, engineers and managers of related sectors. The importance of climate change issue becomes greatly apparent when this discussion develops issues related to water resource management and flow classification into various sectors of drinking, industry, agriculture and the environment (Cacho et al., 2008). In all of the basins that on its main river, a reservoir dam was constructed, and human factors can thus influence on different parts, the prospect of changing the flow in the basin is a principle. Undoubtedly, the management of two drought and flood issues is one of the priorities of water industry managers, whose short-term and long-term forecasts for making any decision, with respect to the high political, economic and social feedback, are indispensable. Hence, study of climate change and determining its effect on increasing or decreasing the severity of the two phenomena mentioned, as well as basin, along with the explanation of the effect of human factors on the mentioned issues is important. Simultaneously, exploitation of almost all dams constructed on the basin has been increasing (Jalili et al., 2012; Shokoohi and Morovati, 2015). There reported, of course, other analysis that demonstrate the contribution of human factors on the abnormal situation created for the lake through the construction of reservoir dams

is effective and approximately 25 to 40 percent of the principal reasons (Hassanzadeh, 2011).

Since many of the data in the actual situation are skidding and do not have normal distribution, therefore, in order to achieve more appropriate result, it is preferred that nonparametric tests, such as Man-Kendal test, which is one of the most widely used and nonparametric methods, be applied to analyze the time-series process (Fujihara, 2016; Modarres, 2009). In studies by Shokoohi et al. (2014), in order to investigate the occurrence of climate change at the 2nd level of the country, it was concluded that in contrast to the decrease of surface currents, the temperature throughout the country has been increasing. In surveys conducted by Nikghoojaghand Yarmohamadi (2008), to investigate the occurrence of climate change in the Sub-basin of Ziyarat River from Gharehosu basin in Golestan Province, was found that the Mean temperature increased. Shokoohi and Daneshkar arasteh (2008) in surveys conducted to investigate the occurrence of climate change throughout the country, concluded that precipitation in some parts of the country was declining, in some sections stable, and in some others, had an increasing trend, but temperatures throughout the country had an increase of 99%. In the studies of climate change in Mazandaran Province by Jahanbakhsh et al. (2010), based on the Mean annual variation in the 20-year time period (last two decades), showed that there is no significant difference in precipitation levels. Mohamadi (2010), also, analyzed the annual precipitation in Iran using data collected from 1437 synoptic, climatic and rainbow stations during the 40 years of 1964-2003. Results showed that in the time series of the station's Mean and precipitation, there observed no significant increase or decrease trend at 95% and 99% confidence levels. Farokhnia and Morid (2012) studied the trend of precipitation changes using four nonparametric tests of trend analysis in some of the stations in the basin of Urmia Lake and concluded that precipitation in this basin was largely lack of any trend. Khaliili et al. (2013) to declare the relationship between the monthly data trend and flow of SharChay River in western Uremia Lake, concluded that the decreasing trend of the flow in this river could be due to the increase of the climate variable and the dependence of the river discharge on the melting snow. Ababaei et al. (2014) investigated the Taleghan dam under the scenarios of climate change during 2040-2069. In this research, in order to demonstrate the ability of information combination methods with individual simulation methods, finally concluded that the Mean daily flow rate of the dam will decrease and the temperature of the basin will increase. The present study pointed out the uncertainty of many studies and significant contradictions resulting from the use of various models.

2. GENERAL LAYOUT

2.1 MATERIALS AND METHODS

In order to achieve the objectives of the study, the following processes were carried out. The status of the annual water balance of the inflow was analyzed to identify the process. Due to the lack of trend on this scale, the study was conducted on a monthly scale. Afterwards, the total monthly precipitation was investigated to find out the cause of changes in monthly input flow. Considering the lack of trend in the amount of monthly precipitation, attention was paid to the factor of precipitation pattern variation in the region. The best factor that could be taken into account in this snowy area is the monthly temperature and its effects on the precipitation pattern. In other words, the change was in precipitation as snow and thus in the monthly discharge and also in the long-term river discharge pattern of Taleghan river. For this purpose, long-term changes in snow coverage in line with long-term changes of the most influencing and crucial climate parameter, namely temperature, were analyzed. In this regard, Mann-Kendal non-parametric method and non-parametric CUSUM free distribution method was used to determine the beginning time of changes in the precipitation pattern of the region and also the thermal climate of the basin, respectively. To study the statistical accuracy of the analyzes, statistics such as Mean absolute error percentage, Mean absolute deviations and Mean square deviations were applied. Data on precipitation, temperature and inflow of the dam were collected from terrestrial stations and for snow data, satellite images of Terra satellite was used as follows.

2.2 STUDY AREA:

The Taleghan Basin, which is one of the important sub-basins of the Sefid Rud waterfall, is located within the study area of Taleghan Alamut. This basin is located on the southern slopes of the Alborz mountains and in the northwestern part of Iran, 120 kilometers from Tehran. In geographical position, the basin is restricted from the north to the Alamut basin, from the south to Zayaran and Samghabad, from the east to the part of the Karaj basin and from the west to Shahroud Basin.

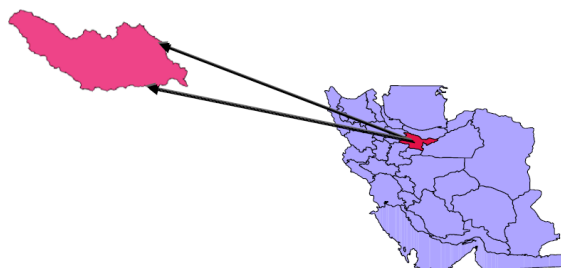


Figure 1: Location of Taleghan Basin

2.3 DATA

In order to study the morphological parameters of hydroxylation, two evaporation stations in the upstream (Joestan station) and downstream of the basin (Zidasht station) and Galinak hydrometric station near the Taleghan dam were used as Table 1 and Fig. 2.

Table 1: Hydrometric meteorological stations of the Taleghan Basin

Name	Digit	latitude	longitude
Zidasht	1931	36-09-29	50-41-46
Joestan	1984	36-11-19	50-53-43
Galinak	1770	36-10-00	50-44-00

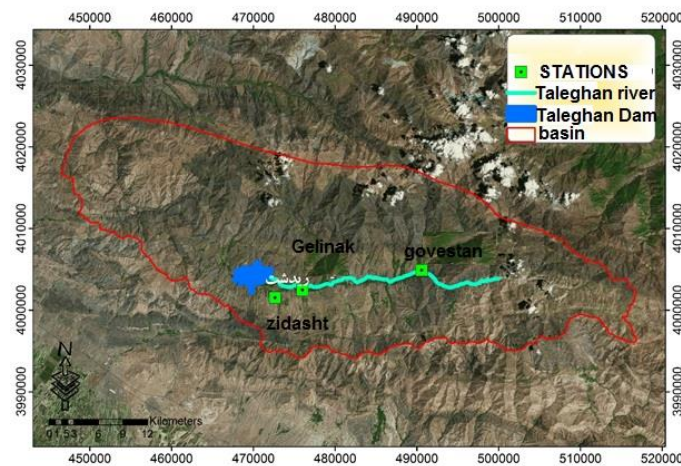


Figure 2: Location of the studied stations and reservoir dam of Taleghan

The time series related to the annual precipitation of the two selected rain-monitoring stations for 1966-2013 was shown in Fig. 3. Also, the summary of their important statistics are given in Table 2. As seen, according to accessible 47-year-old statistics, the annual precipitation of the Zidasht station, which is almost overlooking the Taleghan dam, is about 70 mm less than the Joestan station, at an altitude of about 50 meters. In other statistics, there is a great deal of similarity between the two stations.

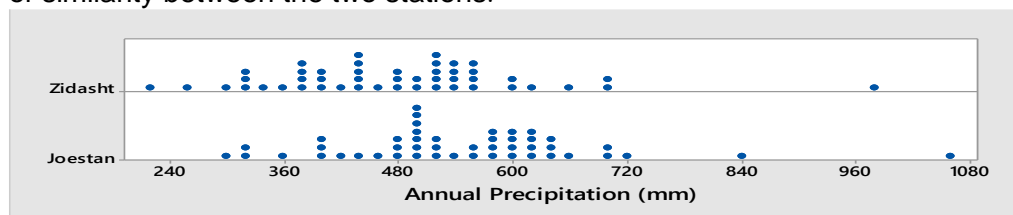


Figure 3: Time series of annual precipitation of Zidasht and Joestan stations related to water during 1966-1967 to 2012-2013

2.4 MANN-KENDAL TEST

The non-parametric Mann-Kendal test, which was presented by Mann in 1945 and then completed by Kendal in 1975, is based on the data rate in a time series. The test is applied to investigate the randomness of the data (the absence of a trend) versus the trend in the hydrological and meteorological time series (Fujihara, 2016; Partal and Kahya, 2005). The advantage of this test is the use of

the data rate in the time series ignoring the value of the variables. Therefore, to the mentioned reason, it can also be used for data with skidding. Meanwhile, it is not required to data with special distribution form (Zhang et al., 2000).

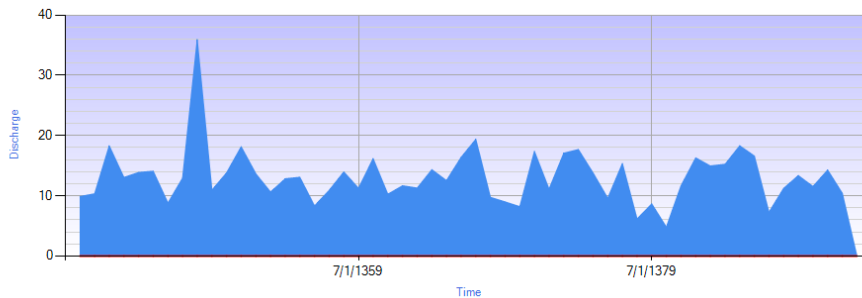


Figure 4: Annual discharge time of the Galinak station (m3 / sec) for the water years from 1961-1962 to 2012-2013

2.4 REMOTE SENSING:

The estimation of snow-covered surfaces, especially in mountainous areas, involves sufficient information and statistics. Today, the use of remote sensing and satellite images in determining the level of snow cover and the same parameters has had a significant improvement. In order to specify the snow cover level, firstly, eight days snow cover achieved by satellite data from 2000 to 2015 were received from NSIDC site in HDF format. And then the Mean snow level was extracted for each month in the GIS environ. The specifications of these data are shown in Table 4.

Table 4: Specifications and spatial accuracy of satellite data

Data date	Product type	Time accuracy (Day)	Spatial accuracy (meter)	Sensor	Satellite
2000-2014 (January, February, March)	10A2	8 Days	500	MADIS	Terra

3. RESULTS

3.1 RESULTS OF METEOROLOGICAL AND HYDROLOGIC VARIABLES TREND TEST

Fig. 5 a shows the annual temperature variation of the Zidasht station in the middle part of the basin. As shown, the annual temperature rise is significant at a 99% probability level and represents an increase of about 4.56 ° C over 1966 to 2012. This means that the studied basin experienced a Mean temperature increase of 12.2 ° C per year. It is interesting to note that the above studies were carried out for the Joestan station in the basin, but practically, as shown in Fig. 5b, due to the steady slope, there is no particular trend at annual temperatures. Indeed, the upper section of the basin shows a constant annual heat scale, and climate change in terms of the thermal system is not probable in this part of the basin.

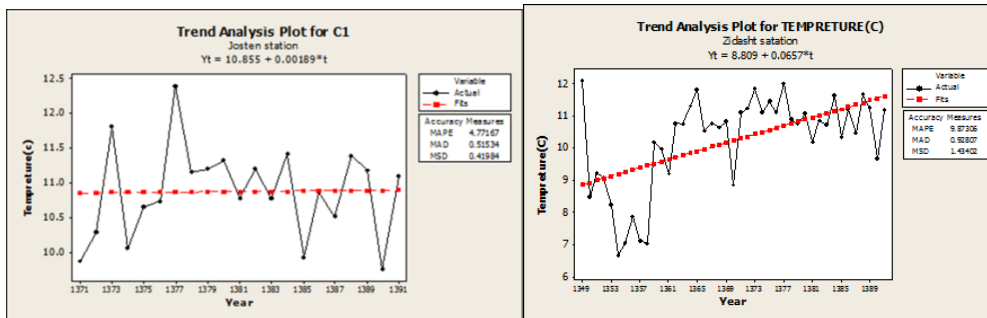


Figure 5: The annual temperature trend in A) Zidasht station, B) Joestan station

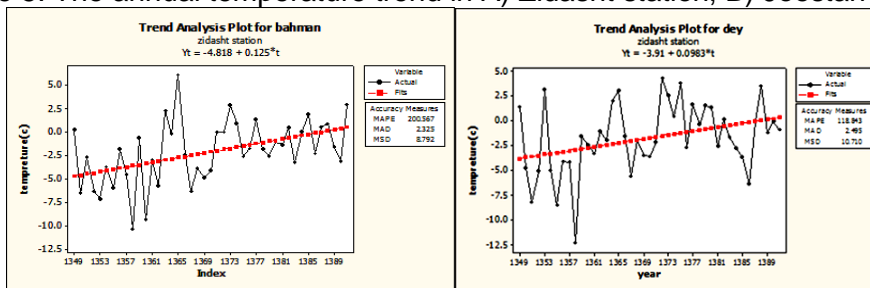


Figure 6: Temperature trend of the Ziadsh station in A) January B) February

Tables 6 and 7 demonstrate the results of trend analysis of precipitation, temperature and runoff variables in monthly and seasonal scales in selected stations.

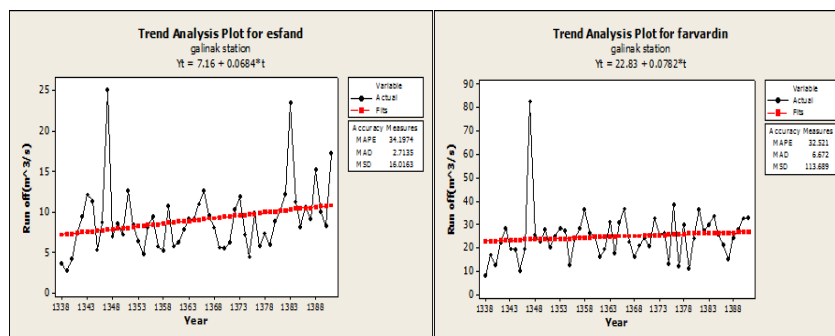
Table 6: Results of the study of precipitation and temperature variables in the monthly and seasonal scale

Month	Result of Temperature series trend test	Station	Result of precipitation series trend test
January	**2.104	Zidasht	-1.11
February	***3.267		0.596
March	**2.637		-1.421

Table 7: Results of runoff trends study in the monthly and seasonal scale

Result of Runoff series trend test	Month	Station
*1.955	January	Galink
1.597	February	
**2.432	March	
**2.328	Mean of winter	
**2.268	April	
-0.88	May	
*-1.805	June	
-0.582	Mean of spring	

(Significant statistics at the probability level of 90%, 95%, and 99% are indicated by symptoms of *, **, and ***).



Figures 7 (a) and (b) show two examples of the process obtained at the Galink hydrometric station.

Table 8 - Snow level (Km2) in the Taleghan dam basin for the years of 2000-2014 by snowflakes

	1379	1380	1381	1382	1383	1384	1385	1386	1387	1388	1389	1390	1391	1392	1393
Jun.	835.0825	788.6875	1161.069	1096.563	1175.125	1023.188	1161.813	1180.188	964.875	737.0825	962.25	1109.75	761.5	891.125	836.3125
Feh	1005.19	1094.94	1085.31	978.94	1139.31	1027.25	994.83	1133.44	971.69	963.06	1050.19	1102.89	819.44	799.88	740.44
March	1048.75	831.6867	491.0833	926.5	386.8333	815.5	893.4167	927.5	732.8333	722.1867	431.5	1051.083	1029.917	782.75	784.5

The results of snow cover the trend in all winter months are presented in Table 9

Table 9: Results for snow cover series-monthly

Results of snow cover series-monthly			Statistical Tests	Station	Factor
March	February	January			
0.792	*-2.177	-0.792	Mann-Kendal	Taleghan area	Snow cover surface

(* Significant statistic at 99% probability level)

Figure 8 was provided to better illustrate the situation shown in Tables 8 and 9, which snow cover changes in the Taleghan basin in February.

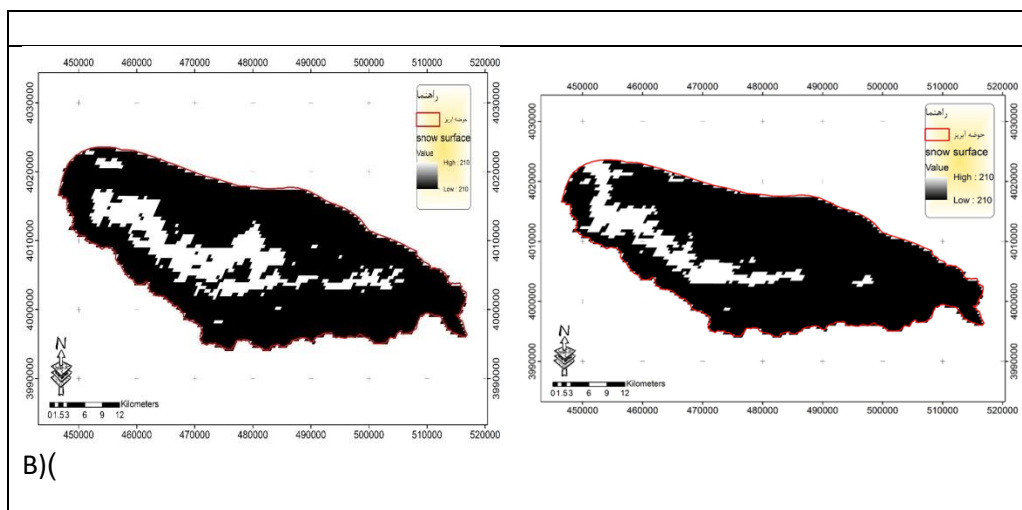


Figure 8 (b): Illustration of snow cover surface in February 2014

4. CONCLUSION

Climate change (temperature and precipitation) affects different parts of the ecosystem of a region such as water resources, plant and animal species, the environment, agriculture and community health. Climate change (global

warming), by shifting precipitation from cold seasons to warm seasons and vice versa, or changing the pattern of seasonal precipitation from snow to rain, obligate all water resource management components to be reviewed. Changing the precipitation pattern, discussed in this study also reduces the snow storm and the displacement of the rivers' regeneration regime. In this way, river basic discharge and dams' adjustment capacity are lowered and the supply and demand balance of the water system is impaired. On the other hand, changes in the precipitation pattern will increase the uncertainty in supplying the plant's water requirements with effective precipitation in the cultivation season. The first effect of these uncertainties is to increase the reliability coefficients used in supplying the water needs of the agricultural sector and thus increasing the need for water extraction. Investigating Taleghan Basin data during 1959-2012, indicates that significant changes have occurred in some of the hydrological parameters of the area. The most important results from the calculations are:

The issue of the effect of temperature change and precipitation pattern on water resources of Taleghan basin is definite.

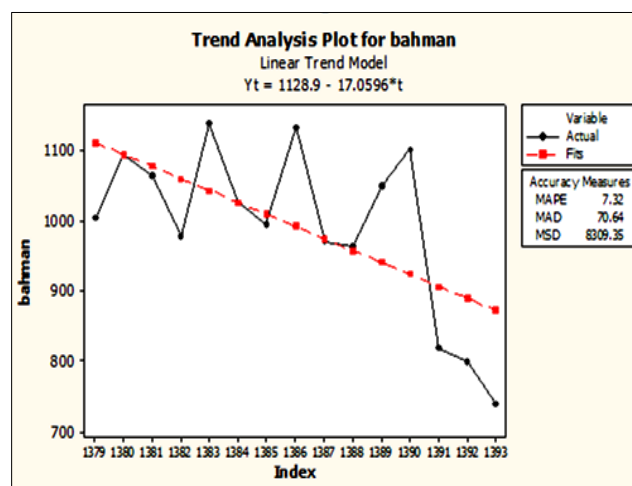


Figure 9: Time series and trend line for snow cover level in Taleghan basin in February

No trend in precipitation series is observed on the annual and monthly scale of precipitation. This confirms other previous researches before referred to in the introduction. Meanwhile, the increasing trend of temperature in the Taleghan basin is in line with the results of the research in other regions of Iran.

Due to the lack of trend in runoff, the annual scale is not a suitable scale for study of hydrological changes in rivers with a snow-rainy regime.

In discharge time series, an incremental trend is observed during the months of March and April (around 7%), and a decreasing trend in May and June (about 10%). This means that the spring runoff has declined sharply, and instead of winter runoff, increased over these periods. This factor stems from the increase in winter temperature, which is due to the decrease in snowfall during recent years, indicating a change in precipitation pattern in the basin and precipitation change from snow to rain.

As changes in the region are actually changes in precipitation pattern from snow to rain, which leads to changing the time of overflowing and dehydration periods as well as floods of Shahroud River, management of Taleghan reservoir dam needs to be reviewed.

The occurrence of changes in the thermal regime in recent year in the study area, and also lack of changes in the flow paths to the dam, reduces or rejects the probability of human intervention in the basin.

5. REFERENCES

- [1] Ababaei, B., Mirzaei, F. & Sohrabi, T. (2014). Assessing climate change impacts on Taleghan reservoir daily inflow using data fusion method. *Water and Irrigation Management* 3(2):12-28. (In Farsi)
- [2] Cacho, O., Hean, R., Ginoga, K. & Wise, R. (2008). Economic potential of land- use change and forestry for carbon sequestration and poverty reduction. Part 1 Australian Centre for International Agricultural Research, Canberra, 99 pages.
- [3] Chiew, F., Siriwardena, L. (2005). *Trend. CRC for catchment hydrology*, 29 pages.
- [4] Farrokhnia, A. & Morid, S. (2014). Assessment of the Effects of Temperature and Precipitation Variations on the Trend of River Flows in Urmia Lake Watershed. *Journal of Water and Wastewater*, 25(3): 86-97. (In Farsi)
- [5] Fujihara, Y., Hosikawa, K., Fujii, H., Kotera, A., Nagano, T., Nagano, T. & Yokoyama, S. (2016). Analysis and attribution of trends in water levels in the Vietnamese Mekong Delta. *Hydrological Processes*, 30: 835-845.
- [6] Hassanzadeh, E., Zarghami, M., Hassanzadeh, Y. (2011). Determining the main factors in declining the Urmia lake level by using system dynamics modeling. *Water Resour Manag* 26(1):129–145
- [7] Jahanbakhsh, S., Hadiani, M., Banafshed, M. & Dinpajouh, Y. (2010). Modeling of Climate change parameters in Mazandaran province. 4th International congress on Islamic worlds geography, Zahedan, Iran. (In Farsi)
- [8] Jalili, S., Kirchner, I., Livingstone, D. & Morid, S. (2012). The influence of large-scale atmospheric circulation weather types on variations in the water level of Lake Urmia, Iran. *Int J Climatol* 32(13):1990–1996
- [9] Kalili, K., Ahmadi, F., Behmanesh, J. & Verdinejad, V. (2013). An Investigation on climate change effect on air temperature and Sharchai River discharge located in the west of Urmia Lake using trend and stationary analysis. *Journal of Irrigation Science and Engineering* 35(4): (In Farsi).
- [10] Kalili K, Nazeri Tahroodi M, Khanmohammadi N (2015) Climate change study in West Azarbaijan province regarding Lake Urmia restoration. *Water and Soil Science* 25(1):223-242. (In Farsi)

- [11] Liang, T.G., Huang, X.D., Wu, C.X., Liu, X.Y., Li, W.L., Guo, Z.G. & Ren, J.Z. (2008). An application of MODIS data to snow cover monitoring in a pastoral area: A case study in Northern Xinjiang, China. *Remote Sensing of Environment*, 112: 1514 – 1526.
- [12] Marcil, G.K., Trudel, M. & Leconte, R. (2016). Using remotely sensed MODIS snow product for the management of reservoirs in a mountainous Canadian watershed. *Water Resources Management*, 30: 2735-2747.
- [13] Modarres, R. & Sarhadi, A. (2009). Precipitation trend analysis of Iran in the last half of the twentieth century. *Journal of Geophysical Research*, 114: 1-9.
- [14] Mohammadi, B. (2010). Analysis of annual precipitation trend in Iran. *Journal of Geography and Environmental Planning*, 22(3): 95-106. (In Farsi)
- [15] Mozafari, M.M., Parhizkari, A., Hoseini Khodadadi, M., Parhizkari, R. (2015). Economic analysis of the effects of climate change induced by greenhouse gas emissions on agricultural productions and available water resources (case study: down lands of the Taleghan Dam). *Journal of Agricultural Economics and Development* 29(1):68-85.
- [16] Nikghoojagh, Y. & Yarmohamadi, M. (2008). Evaluation of climate change and investigation of its influences on surface water resources (Case study: the Ziarat River in Golestan province). 3rd Conference on water resources management, Tabriz Iran. (In Farsi)
- [17] Partal, T. & Kahya, E. (2006). Trend analysis in Turkish precipitation data. *Hydrological Processes* 20(9): 2011-2026.
- [18] Shokoohi, A., Razi, T. & Daneshkar Arasteh, P. (2014). On The Effects of Climate Change and Global Warming on Water Resources in Iran. *International Bulletin of Water Resources & Development (IBWRD)* 2(4): 1-9.
- [19] Shokoohi, A. & Morovati, R. (2015). Basinwide comparison of RDI and SPI within an IWRM framework. *Water resources management* 29:2011-2026.
- [20] Shokoohi, A. & Daneshkar Arasteh, P. (2008). Searching for climate change effects on Iran's climate and surface water resources. 3rd Conference on water resources management, Tabriz Iran. (In Farsi)
- [21] Zhang, X., Vincent, L.A., Hogg, W.D. & Niitsoo, A. (2000). Temperature and precipitation trends in Canada during the 20th century. *Atmosphere – Ocean*, 38(3): 395-429.
- [22] Zhou, X., Xie, H. & Hendrickx, J.M.H. (2005). Static Evaluation of Remotely Sensed Snow-Cover Products with Constraints from Streamflow and SNOTEL Measurements. *Remote Sensing of Environment* 94 (2): 214-231.

6. SUMMARY

The effect of climate change on precipitation, evaporation, and transpiration, surface runoff and extreme hydrological events on the local and regional scale, especially in arid and semi-arid regions of the country, is still a controversial subject. In the present research, the effect of climate change on annual and monthly discharge of Taleghan basin was investigated at the entrance to Taleghan reservoir. To this aim, firstly, the existence of the trend and occurrence of mutation in the meteorological-hydrologic variables was studied on climate change studies using statistical tests. The results of the trend test, while no trends were observed in precipitation, showed an increase in temperature (at a probability level of 99%) and water (at a probability level of 95%) during the winter, especially in the months of February and March. Also, the results of the mutation test showed that the temperature in 1963 was positive at a probability level of 99%. The mountainous state of the basin discusses the theory of increase in the temperature in the winter, snow melting, early runoff, and in other words, early melting of the snow from the spring to winter season. Then, using the remote sensing technique and selecting the Terra satellite, the snow coverage of Taleghan basin during 2000-2014 throughout the winter was investigated. The results indicated a decrease in snow covering level at the probability level of 99% in February. Hence, the effect of climate change on water resources of Taleghan basin, considering all factors such as a significant positive trend in temperature, reducing snow covering, decreasing spring flow and increase of winter flow to the dam were confirmed, although the volume and depth of annual runoff were stabilized. Consequently, it can be argued that climate change in this basin is a change in the precipitation pattern, i.e the change in the type of snowflake to rain as well as seasonal displacement. These studies have shown that according to the existing trend in the amount of annual discharge to the dam reservoir, the effect of human factors on changing the pattern and runoff rate of the basin has not been affected.

Keywords: Climate change, cold climate, flow, Taleghan dam

7. CLEARANCES AND COPYRIGHT

The author(s) is (are) responsible for obtaining written permission to profile the project or subject matter in their papers from any and all clients, owners or others who commissioned the work. ICOLD assumes proper permission has been obtained by author(s) and accepts no liability for the author(s) failing to do so.

COMMISSION INTERNATIONALE DES GRANDS BARRAGES

VINGT-SIXIÈME CONGRÈS DES GRANDS BARRAGES
Autriche, juillet 2018

DOI 10.3217/978-3-85125-620-8-053



This work licensed under a Creative Commons Attribution 4.0 International License. <https://creativecommons.org/licenses/by-nc-nd/4.0/>

**RAPID SCREENING OF SEDIMENT MANAGEMENT TECHNIQUES FOR
MORAGOLLA HPP WITH RESCON-2**

Nikolaos EFTHYMIU

FICHTNER GMBH & CO. KG

GERMANY

Richard GUIMOND

FICHTNER GMBH & CO. KG

GERMANY

Aleksandar TRIFKOVIC

FICHTNER GMBH & CO. KG

GERMANY

Radovan MILJANOVIC

NIPPON KOEI CO. LTD

JAPAN

Nadun BULATHGE

CENTRAL ELECTRICITY BOARD

SRI LANKA

COMMISSION INTERNATIONALE
DES GRANDS BARRAGES

VINGT-SIXIÈME CONGRÈS DES
GRANDS BARRAGES
Autriche, juillet 2018

**RAPID SCREENING OF SEDIMENT MANAGEMENT TECHNIQUES FOR
MORAGOLLA HPP WITH RESCON-2**

NIKOLAOS EFTHYMIIOU, RICHARD GUIMOND, ALEKSANDAR TRIFKOVIC

FICHTNER GMBH & CO. KG

GERMANY

RADOVAN MILJANOVIC

NIPPON KOEI CO. LTD

JAPAN

NADUN BULATHGE

CENTRAL ELECTRICITY BOARD

SRI LANKA

1. INTRODUCTION

The Moragolla Hydro PowerPlant (HPP) project involves the implementation of a Run-of-River Hydropower scheme on the upper reach of Mahaweli River in Sri Lanka. It will be the latest and presumably the last entry in the upper Mahaweli Complex, which is a cascade of five reservoirs serving for hydropower generation and supply of irrigation water.

The reservoir of the Moragolla HPP will be used for daily hydropower peaking and therefore the time path of the active storage can affect significantly the long-

term economic performance of the scheme. Furthermore, the dam owner and operator does not wish the accumulation of sediments in the reservoir, especially since it believes that consolidated sediments would produce H₂S, a detriment to the drinking water quality of the reservoir water.

Numerical simulation indicated that if no sediment management measures are implemented, the reservoir storage will be depleted within approximately 50 years, i.e. the reservoir is non-sustainable. Several sediment management approaches have been developed for handling sedimentation [1], [2]. A preliminary assessment presented below indicated that almost all sediment management techniques can potentially convert the non-sustainable Moragolla reservoir into a sustainable infrastructure for the future generations. The conclusion is however rather generic, since the identification of the best suitable management strategy depends on several other boundary conditions and project development priorities.

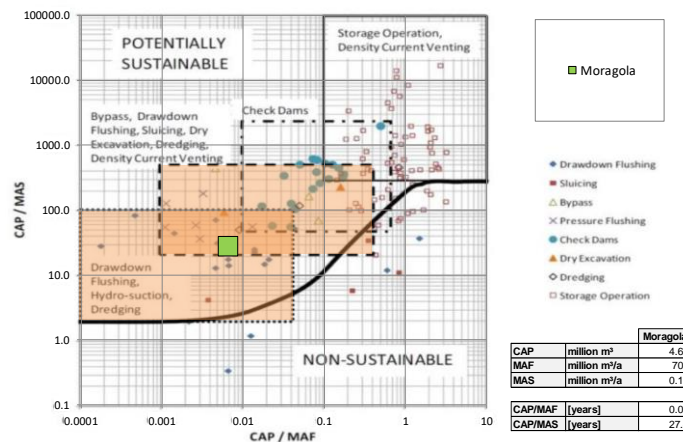


Fig. 1

Preliminary assessment of sediment management options for Moragolla reservoir
(Source of underlying nomograph: [3])

For example, an important constraint is imposed by the fact that in the mid to upper reaches of Mahaweli River lives a fish called Labeo Fisheri which has been put on the IUCN Red List of Threatened Species. Therefore, any risk in terms of too high sediment concentrations that would endanger the habitat of the above-mentioned fish species are rendered as not acceptable.

The objective of the paper is the presentation of the rapid screening for the available state-of-the-art sediment management techniques with purpose of the selection and specification of the optimum solution considering the necessary tailoring onto the project specific boundary conditions.

2. THE MORAGOLLA HPP PROJECT

The envisaged Moragolla Hydropower project will be located in the central Highlands of Sri Lanka, approximately 22 km south of the city of Kandy and 130

km north-east of the capital city of Colombo. The installed capacity of the HPP will be 30.2 MW for the rated head of 69 m and design discharge of 50 m³/s. The expected mean annual energy generation is 100 GWh/a. The project comprises a reservoir inundated by a gravity dam equipped with spillway, bottom outlet and fish ladder, a lateral intake, a low-pressure headrace tunnel, a surge shaft, a steel lined penstock tunnel and a surface powerhouse accommodating two Francis units. The general layout is shown in Fig. 2.

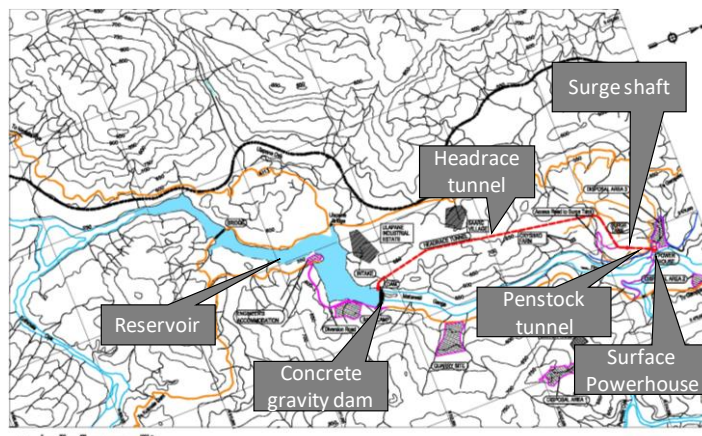


Fig. 2
Project location and general layout

The reservoir will be slightly longer than 3 km with gross storage capacity of 4.66 million m³ at the normal operation water level of 548 masl and active storage of 2.68 million m³. The minimum operating water level will be at 542 masl. The dam will have maximum height of 37 m and length of 236 m. The overflow spillway will be equipped with five radial gates with the ogee crest level at 534 masl. A sand sluice followed by a steel lined conduit embodied in the gravity dam will be installed next to the lateral intake with purpose the removal of sediment deposits. A bottom outlet is also incorporated in the dam body for dam safety reasons. Finally, a micro-hydro power plant will be installed at the dam toe for the exploitation of the hydropower potential of the ecological flow.

The catchment area draining at the Moragolla dam site is 809 km². Upstream of the envisaged Moragolla reservoir is located the Kotmale dam, which inundated the year 1984 a reservoir with gross storage capacity of 177 million m³. The latter regulates the runoff from 562 km², i.e. approximately 70% of the catchment area. It has been calculated that the trap efficiency of Kotmale reservoir is approximately 99.5%. Hence, the regulated part of the catchment will not contribute to the sediment inflow at the envisaged Moragolla reservoir. The unregulated part, i.e. the catchment area excluding Kotmale dam catchment area is 247 km².

The hydrologic analysis concluded that the mean annual flow at the Moragolla dam site will be 22.4 m³/s. The mean annual sediment inflow has been estimated to be 145,000 m³/a. This assessment was based on the specific sediment yield at Kotmale reservoir as calculated from the measured deposits, the trap efficiency and the size of the regulated catchment area. The bulk of sediment

transport occurs in the time period June to November with maximum mean monthly sediment load close to 23,000 m³/month. The sediment inflow at the Moragolla dam site will consist predominantly of silt material, with an important sand content, which will increase with rising river flow. By small discharges i.e.: close to 10 m³/s as observed during the dry season, the sand content will be close to 10-15%. As the discharge increases the sand content can reach up to 30% of the total sediment inflow.

3. RESERVOIR SEDIMENTATION AND COUNTERMEASURES

3.1. METHODOLOGY

The time path of the reservoir storage development has been initially assessed for the no-action scenario with purpose of the determination of the reservoir service lifetime if no sedimentation management measures are implemented. The assessment was performed with one-dimensional simulation with the widely used numerical model HEC-RAS v. 5.03.

The results of the numerical model served in addition for the calibration of the REServoir Conservation - 2 (RESCON- 2) model that was used subsequently for the screening and evaluation of the state-of-the-art sediment management techniques. The RESCON approach was developed and published in 2003 by the World Bank [4] with the purpose to provide a tool that will allow the identification of the technically viable and economically optimal approach for sustainable management of water storage reservoirs. The RESCON approach was recently upgraded by Fichtner for the World Bank Group and the beta version of the RESCON-2 software is now freely available to download at the internet portal of the International Hydropower Association (IHA)*. The improvements incorporated in RESCON-2 can be categorized as follows (5):

- Improved procedure for calculation of the reservoir storage development, allowing allocation of sediment deposits between active and inactive storage as well as partitioning between bedload and suspended load
- Extension of palette of assessed sediment management techniques
- Incorporation of intergenerational equity issues in performed economic appraisal through the concept of declining discount rate
- Climate change analysis allowing the assessment of sediment management as adaptation strategy for increasing the resilience of the infrastructure
- Graphical User Interface (GUI) enhancing the user-friendliness during model setup and result reading

It is pointed out that RESCON-2 serves for a rapid screening and it is not intended to replace detailed studies. The RESCON-2 program is based on

* available at <https://www.hydropower.org/sediment-management/>

empirical methods and therefore sound engineering judgment is required for interpretation of the results. In terms of the Moragolla sedimentation study, the following sediment management techniques were analysed and evaluated.

- No Action (i.e. No sediment management),
- Reduction of sediment inflow by implementing a sediment trap upstream of the reservoir headwaters,
- Deposit removal techniques, including flushing, dredging and trucking and HydroSuction Removal System (HSRS),
- Sediment routing techniques, including sluicing, sediment by-pass and density current venting.

3.2. RESERVOIR LIFETIME FOR THE NO-ACTION SCENARIO

The result of the numerical simulation of sedimentation for the available daily flow time series with duration of 43 years is plotted in Fig. 3 with black points. The black straight lines represent the time-path of the gross and active storage as calculated by RESCON-2. It was concluded that the service lifetime of the reservoir will be approximately 55 years, corresponding to a mean annual storage loss rate of approximately 2%.

The overall good agreement between the results of HEC-RAS and RESCON-2 with regards the gross storage development supports further the application of RESCON-2 for preliminary screening purposes of the available sediment management techniques. Unfortunately, HEC-RAS does not provide the possibility to plot the temporal development of the storage at different pool elevations. This prevented a comparison between the HEC-RAS and RESCON-2 results regarding the allocation of deposits between active and inactive storage respectively. Nonetheless, RESCON-2 indicated that the sedimentation of the active storage pool will commence immediately after the reservoir impoundment due to deltaic deposits at the headwater of the reservoir.

3.3. EVALUATION OF SEDIMENT MANAGEMENT OPTIONS

The assessment of the technical feasibility of the available sediment management techniques and the corresponding temporal development of the reservoir storage has been performed with application of RESCON-2. The specifications of the evaluated sediment management techniques are given in the table below.

The techniques of sediment by-pass and trucking were excluded because they were considered as not economically viable due to very high implementation or annual operation costs. In the case of sediment by-pass, the calculated costs for construction of an approximately 3 km long diversion tunnel were prohibitive for the implementation of this technique. In the case of trucking, the necessary

outages for reservoir emptying and removal of deposits by earthmoving equipment would cause high energy generation loss and accordingly revenue losses that rendered this method also not economically viable. Following table presents analyzed and evaluated management options that could be technically and economically feasible.

Table 1
Specifications of evaluated sediment management techniques

Method	Specifications	
Flushing	water level drawdown	25 m (Pool elevation @ 523 masl)
	Flushing discharge	40 m ³ /s
	Duration	12 hours after water level drawdown
	Frequency	1 flushing event per year
Dredging	Sediment concentration	30%
	deposits removed per dredging event	115000 m ³ / event
	Frequency	Continuous dredging operation
HSRS	Available head	33 m
	Pipeline length & diameter	3000 m & 1 m (one pipe)
Sluicing	water level drawdown	6 m Pool elevation @ 542 masl
	Duration of sluicing	6 months
	Frequency	Annually
Sediment Inflow Reduction	Reduction of sediment inflow	30% of MAS (exclusion of sand and coarse silt)
	Maintenance	Annual sand mining of

RESCON-2 indicated that a hydrosuction removal system as specified in the table above would have a deposit removal capacity of approximately 90,000 m³/a with a continuous slurry discharge release of 2.5 m³/s. The associated water losses would be therefore considerable and would reduce the reservoir firm water yield. Furthermore, the necessary pipeline length of 3 km is marginally at the feasible applicability limits. Therefore, this technique can't be applied the first years of reservoir operation, it is however a method that could be implemented later in the future. When the trap efficiency drop will reduce the annual deposits, a smaller HSR system will be able to maintain the storage in a sustainable manner.

Following the technical feasibility criterion for density current venting that was developed by Morris and Fan (1998), RESCON-2 indicated that the appearance of density currents is plausible. The initial geometry of the reservoir will have as result however the dissipation of the density currents before they arrive at the low-level bottom outlet. Therefore, the venting, i.e. the release of density currents downstream of the reservoir will not be possible, at least the first years of reservoir operation. The progressive propagation of the deltaic deposits downstream will

have as result a steepening of the reservoir invert. Therefore, density current venting might be a feasible option in the future. RESCON-2 indicated that a reduction of the sedimentation by approximately 10% might be possible through density current venting in the future.

RESCON-2 indicated that a standard hydraulic dredger with capacity of 115000 m³/a, which is within the technically feasible limits of dredging in reservoirs, is the only technique that can sustain the active storage at the pre-impoundment levels. The time path of reservoir gross and active storage is plotted in Fig. 3 with the orange line. Dredging however is associated with high operation costs as well as environmental considerations about the disposal of the dredged.

RESCON-2 calculated for flushing a Sediment Balance Ratio (SBR) of 3.1, i.e. the sediment removal capacity of the specified flushing event will be approximately 3 times higher than the expected annual sediment deposits. This indicates that flushing is a technically feasible solution for Moragolla reservoir. The Long-term Capacity Ratio (LTCR) will be 0.64, i.e. 64% of the reservoir gross storage can be preserved sustainably. Its efficiency however drops to 50% with regards to active storage. The time path of reservoir gross and active storage is plotted in Fig. 3 with green lines. Environmental considerations associated with the expected high sediment concentrations downstream of the reservoir that would endanger the fish habitat of Mahaweli River together with the high energy generation losses due to the necessary full water level drawdown had as result that this technique was evaluated as not acceptable.

The unregulated part of the catchment area draining into Moragolla reservoir is mostly forested or covered by tea gardens which are one of the major economic activities in the project region. It was considered therefore, that measures such as reforestation or change of the agricultural practices with purpose the reduction of the surface erosion are not technically feasible. The effect of dispersed check dams in the catchment area on the sediment inflow was not part of this study and has to be investigated more in detail.

The evaluation of the river morphological features indicated that the reach of Mahaweli River extending approximately 2 km upstream of the reservoir headwaters is characterized by pronounced river meandering and sandy river bed. Limited sand mining is already performed by the local communities at this location. Numerical simulations with the one-dimensional model HEC-RAS indicated that the construction of a relatively short check dam with height of approximately 2.5 m would have as result an intensification of the retention of the sand particles in this river reach. A sediment trap at this location can retain annually approximately 60,000 m³ of sediment, corresponding to 40 % of the expected total mean annual sediment inflow into Moragolla reservoir. This can be translated as full retention of the material transported as bedload and retention of the coarsest 20% of the material transported in suspension. The necessary requirement for the above described sediment trap performance is the regular and continuous restoration of its trap efficiency by means of sand mining. The impact of this sediment inflow reduction is that approximately 10% of the gross storage and 50% of the pre-impoundment active storage is preserved sustainably. Except from the sediment inflow reduction an important aspect is that the sediment entering now the reservoir is finer since the coarsest part will be retained in the sediment trap. This has as

result a drop of the trap efficiency of Moragolla reservoir which protects a large part of the active storage.

The construction of the check dam will raise the water level in the river reach extending upstream of this structure by ≈ 2.5 m. Drainage pipes through the check dam will keep the reservoir upstream of the check dam lower during the dry season. The extent of the further inundation upstream of the check dam is expected to be approximately 2 km. If the width of the inundated area need to be confined, two lateral dikes along the river main channel shall be constructed. The necessary sand mining activity will cause an increase of the traffic in the local road network. On the other hand, this activity will reduce the transport distances for supplying sand, and may boost the local economy.

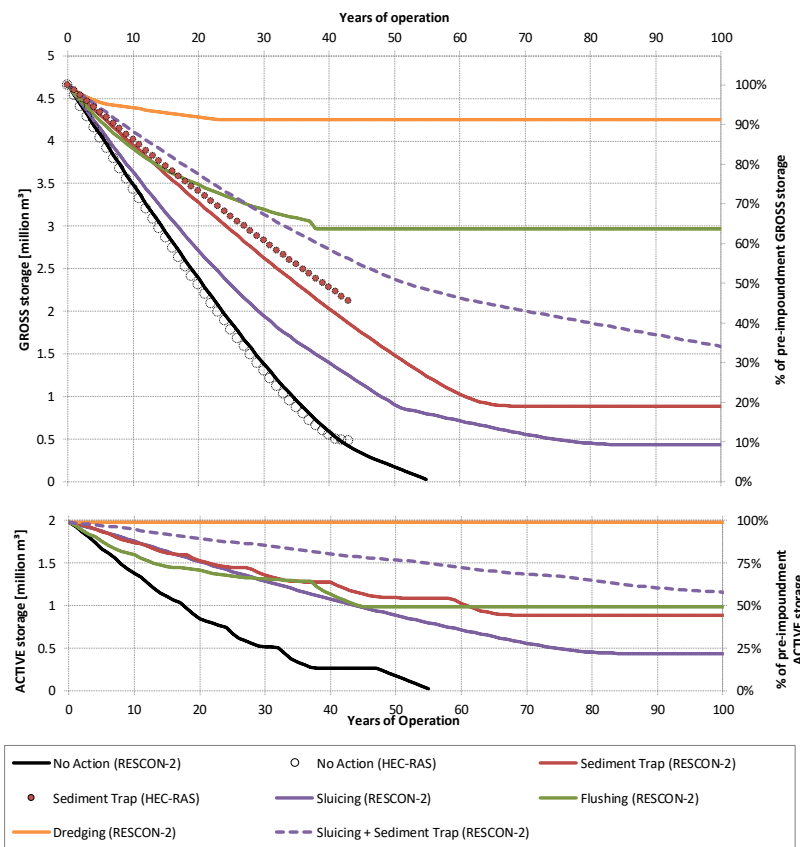


Fig. 3 Storage development for the no-action scenario and the technically feasible sediment management techniques

Sluicing over the spillway crest is technically feasible in Moragolla reservoir as long as a water level drawdown takes place when sediment laden flows enter the reservoir. The prediction of reservoir storage development with RESCON-2 indicated that the first ten years of reservoir operation sluicing will not change substantially the time path of reservoir gross storage because the sediment will be routed into the inactive storage and not out of the reservoir, since it will not be possible to overcome the barrier of the Moragolla dam. Sluicing however, will have as result an alteration of the spatial pattern of deposition in the reservoir which will

be characterized by lower sedimentation rate in the active storage and higher sedimentation rate of the inactive storage compared to the no-action scenario. On the long-term sluicing will be able to sustain only 10% of the gross storage. The impact however on the active storage will be substantially larger, and 25% of the initial active storage will be preserved sustainably. Sluicing however will not trigger the adverse environmental impacts that would follow flushing since the sediment routing will be synchronized with the ambient intra-annual variability of the sediment transport regime of the Mahaweli River. The performance of sluicing is substantially improved if it is combined with the sediment trap upstream of the reservoir. The combination of reduced and finer sediment inflow together with the water level drawdown during the high flow season intensifies the sediment routing out of the reservoir. This has as result a long-term capacity ratio for the active storage of 60%. The time path of the gross and active storage for this combination is plotted in Fig. 3 with dashed line. The detailed specification of the optimum sluicing operational rules will require a detailed assessment of the water, energy generation and revenue losses something that is out of the philosophy and the capabilities of RESCON-2.

Based on the aforementioned results of the technical feasibility assessment, it was concluded that the only two techniques that can be implemented without important environmental disadvantages, are the reduction of sediment inflow through the construction of a sediment trap upstream of the reservoir headwaters and sluicing. Even more, it is concluded that the combination of the two methods will further improve the efficiency of sluicing and will reduce thus the associated energy generation losses providing sufficient space for further optimization.

SUMMARY

The Moragolla Hydro PowerPlant (HPP) project involves the implementation of a daily peaking Run-of-River Hydropower scheme in Sri Lanka. Numerical simulations indicated that the service lifetime of the reservoir will be approximately 50 years if no sediment management is applied, i.e. it will be non-sustainable. Furthermore, the active storage loss will affect the long-term economic performance of the facility. The recently developed software RESCON-2 was used for a rapid screening of the state-of-the-art sediment management techniques. The purpose was the selection and specification of the optimum sediment management solution considering the necessary tailoring onto the project specific boundary conditions that can convert the non-sustainable Moragolla reservoir into a sustainable infrastructure for the future generations.

The economic viability assessment indicated that the costs or the water losses associated with the techniques of hydrosuction removal, sediment by-pass and trucking are prohibitive for their implementation. The technical feasibility assessment indicated that the technique density current venting at the moment is not applicable but it might provide an attractive option for the future. The comparative evaluation of the remaining methods, i.e. flushing, dredging, sluicing

and reduction of sediment inflow through construction of a sediment trap upstream of the reservoir is presented in the table below.

Table 2
Evaluation of technically feasible sediment management techniques

Method	Long-term capacity	Water and energy losses	Env. Impacts	CAPEX	O&M
Flushing	++	-	---	0	-
Dredging	+++	-	---	---	---
Sluicing	+	-	+++	0	-
Sed.trap	++	+++	-	-	+++

The results indicate that dredging is the only method that can sustain the active storage at the pre-impoundment level. It is followed by flushing and the sediment trap that can preserve 50% of the pre-impoundment storage and finally by sluicing that will have as result a long-term active storage capacity ratio of 25%. Dredging and flushing however are excluded because they will increase the sediment concentrations downstream, endangering thus the fish habitat of Mahaweli River. Finally, the combined implementation of sediment trap and sluicing is the optimum solution because it has the best performance below dredging without the adverse environmental impacts. Sluicing can be implemented within a time horizon of 10 -15 years after the impoundment of Moragolla reservoir, while the sediment trap preferably should be in place by the time of the reservoir inundation. Having in mind the above indicated possibilities of the RESCON-2 model for a rapid assessment of different sediment management strategies as well as good agreement of its results with a widely used one-dimensional numerical model we could recommend it for further use in similar applications.

REFERENCES

- [1] ANNANDALE, G.W., MORRIS, G.L., KARKI, P. Extending the Life of Reservoirs: Sustainable Sediment Management for Dams and Run-of-River Hydropower, The World Bank, 2016.
- [2] MORRIS, G.L., FAN, J. Reservoir Sedimentation Handbook, 1998
- [3] ANNANDALE, G.W., Quenching the Thirst: Sustainable Water Supply and Climate Change, 2013
- [4] PALMIERI, A., SHAH F., ANNANDALE, G. W., DINAR A. Reservoir Conservation, Volume I: The RESCON Approach, The World Bank, 2003
- [5] EFTHYMIIOU, N. P., PALT, S., ANNANDALE, G.W., KARKI, P. Reservoir Conservation Model RESCON 2 Beta - Economic and Engineering Evaluation of Alternative Sediment Management Strategies, User Manual, The World Bank & Fichtner, 2017

COMMISSION INTERNATIONALE DES GRANDS BARRAGES

VINGT-SIXIÈME CONGRÈS DES GRANDS BARRAGES
Autriche, juillet 2018

DOI 10.3217/978-3-85125-620-8-054



This work licensed under a Creative Commons Attribution 4.0 International License. <https://creativecommons.org/licenses/by-nc-nd/4.0/>

SUSTAINABLE DEVELOPMENT IN HYDROPOWER PROJECT

Min Byeong SOO

Chief Executive Officer, MIRA POWER LIMITED

PAKISTAN

Hong Young JIN

General Manager (Admin & HR), MIRA POWER LIMITED

PAKISTAN

Nadim ULLAH

Senior Manager (Admin & HR), MIRA POWER LIMITED

PAKISTAN

SUSTAINABLE DEVELOPMENT IN HYDROPOWER PROJECT

Min Byeong Soo
Chief Executive Officer, Mira Power Limited
Pakistan

Hong Young Jin
General Manager (Admin & HR), Mira Power Limited
Pakistan

Nadim Ullah
Senior Manager (Admin & HR), Mira Power Limited
Pakistan

1. INTRODUCTION

Korea Energy (KOEN) is a leading state owned generation company of Republic of Korea which owns and maintains 13.1% (10,329MW) of total generation capacity of Korea.

To comply with KOEN "Vision 2025" regarding adding of green and clean energy to the grid, KOEN acquired Mira Power Limited on mutual benefit basis where Pakistan was facing acute shortage of energy.

Mira Power Limited, a subsidiary of Korea Energy (KOEN) is a special purpose company, setup to design, construct, own, operate and maintain 102 MW Gulpur hydro power plant as shown in Fig. 1 under Government of Pakistan's Policy for Power Generation Projects 2002 as adopted in Azad Jammu & Kashmir, Pakistan. The Project "Gulpur Hydropower" is administratively located in Kotli district, Azad Jammu & Kashmir, Pakistan at latitude 33°27'48.99" and longitude 73°51'48.99", about five Km south of Kotli Town on the Poonch River, a tributary of Jhelum River. The site is about 167 Km from Islamabad and 285 Km from Lahore as shown in Fig. 2.



Fig. 1
Gulpur Hydropower Project Design

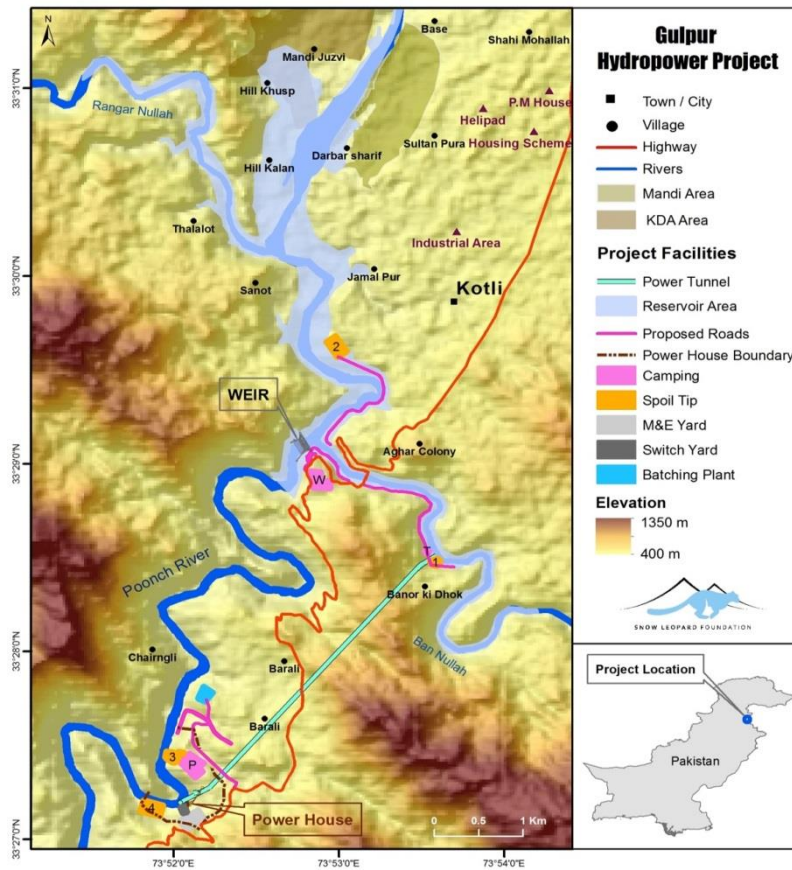


Fig. 2
Gulpur Hydropower Project Location

The Project is being financed by International Finance Corporation (IFC), Asian Development Bank (ADB), Korea Exim Bank (K-Exim), CDC Bank of UK and Multilateral Development Bank of Netherland (FMO). The Project achieved Financial Closing in October 2015 and set to achieve commercial operations by August 2019 with 70% construction already completed. The Project is being constructed by renowned consortium of Korean construction companies i.e. Daelim Industrial and Lotte E&C and many international consultants/technical advisors are collaborating at different levels including Mott McDonalds as technical advisor of Lenders, MWH as Owners Engineer and Multi Consultant (UK) as independent engineer.

Back in 2013 when KOEN decided to invest in Pakistan, the country had a serious power crisis. Everyday millions were being affected by electricity shortage up to six hours in urban areas and twelve hours in rural locations which leads to slowing of productivity and hampering economic growth. KOEN believed at that time that in a country, rich in water resources hydropower can have a significant role in meeting future energy needs.

While acquiring the project KOEN was already very keen to focus on environmental challenges in maintaining the rich ecology and diverse environment specifically in view of already environmental sensitive location where other than rest of the needful almost 128 households were to be resettled/relocated.

The Project is also in compliance with International Finance Corporation (IFC)'s Performance Standards and Asian Development Bank Safeguard Policy Statements. To meet such requirements and to face the prospective challenges from civil society, NGOs, Government and local communities, KOEN facilitated Mira Power to adopt a comprehensive approach of sustainable development.

2. STEPS TOWARDS SUSTAINABLE DEVELOPMENT

To achieve sustainable development plan Mira Power has adopted flawless strategy and devised following best possible plans:

- Biodiversity Action Plan
- Land Acquisition and Resettlement Plan
- Livelihood Restoration and CSR Plan
- Stakeholders Engagement Plan
- Sustainable Mining Plan
- Security Management Plan
- Construction E&S Management Plan
- Health and Safety Plan

The environment portion discussed in already accepted feasibility study was based on Environment Protection Act (EPA) Azad Jammu & Kashmir (AJK) where the biggest challenge was resettlement/ relocation of 128 households, for which Mira Power management was vigorously thinking to change the project design so that to minimize the relocations.

In the meanwhile, after acquisition of the project it was pointed out that the full length of Poonch River has already been declared as National Park by local environmental authorities, which through legislation restricted various forms of species exploration to ensure that the habitat remains pristine and congenial for the indigenous species.

The nomination of this National Park was promoted and/or endorsed by a number of reputable environmental NGOs, including but not limited to International Union for Conservation of Nature (IUCN), WWF, Himalayan Wildlife Foundation, and Snow Leopard Foundation, as they argued that the Poonch river is essential for the global survival of Kashmir Catfish, and presents a unique natural abundance of the Mahaseer fish, an endangered species whose population has been consistently declining all over Himalayan rivers.

The Strategic Environmental Assessment (SEA) of rivers classifies the Pooch River into the most critical category. A total of 37 fish species are associated with the Poonch River. Of these six fish species are listed in International Union for Conservation of Nature (IUCN) Red List with their status as:

1. **Kashmir Catfish** – Critically Endangered,
2. **Golden Mahaseer** – Endangered,
3. Pabdah Catfish – Near Threatened,
4. Butter Catfish – Near Threatened,
5. Common Carp – Vulnerable,
6. Twin-banded Loach – Vulnerable



Golden Mahaseer *Tor Putitora*



Kashmir Cat fish *Glyptothorax kashmirensis*

Fig. 3
Photographs of Golden Mahaseer and Kashmir Catfish

3. KEY ENVIRONMENTAL CHALLENGES FACED BY THE PROJECT

- It was challenging to relocate 128 household in terms of their resettlement and prospective litigation
- Mira Power became aware of National Park notification after submission of initial environmental due diligence and original Environmental Social Impact Assessment (ESIA) to Environmental Protection Agency (EPA) and lenders for approval. Upon knowing of the notification regarding National Park further activity on the project was put on hold due to the new situation emerged with the appearance of critically endangered and endangered fish species within a legally notified area. The situation was pretty much alarming for Mira Power and was requiring immediate strategic interventions with reference to following mandatory requirements:
 - 1) As per AJK Wildlife legislation 'Betterment of the Park' was mandatory to get approved actions and activities normally prohibited in a National Park
 - 2) ADB and IFC in view of declaration of National Park and presence of Endangered Mahaseer and Critically Endangered Kashmir Catfish demanded 'net environmental gain' in biodiversity in Critical Habitat.

4. STRATEGY & IMPLEMENTATION

To cope with the challenging problems Mira Power carried out following key studies/assessments to achieve sustainable development of the project:

- Review of project design
- A critical Habitat assessment study of the entire river in order to establish the actual status of biodiversity and ecological integrity of the river
- A cumulative impact assessment of all projects planned on the river establish that if there is any room for considering the proposed project
- An integrated ecological flow assessment of Gulpur Hydropower project assessing the upstream and downstream response of the project to establish any potential for achieving a net environmental gain and room for betterment of the park
- A Biodiversity Action Plan demonstrating a net environmental gain and a net improvement in the national park

In addition to challenge of relocation of 128 households Mira Power anticipated that the likelihood of achieving a net environmental gain with the original design having 6 kilometers of low flow/dry section with peaking scenarios will be difficult

to achieve. Therefore the location design and layout of project design as shown in Fig. 4 was optimized compared with design of feasibility report whereby the dam was located just downstream of confluence of Bann Nullah and Poonch River and a 3.1 KM tunnel located 1 KM upstream in Bann Nullah from its confluence with Poonch River. The Normal Operating Level (NOL) of the project was changed to be at an elevation of 532 meters from the sea level which was modified from 540 meters in the original plan to reduce environmental and social impacts.

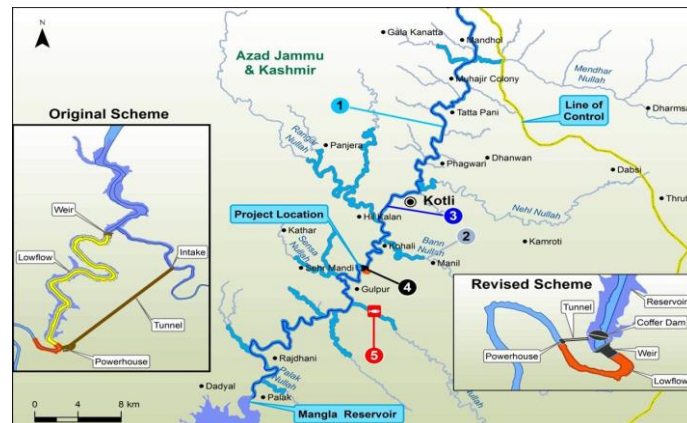


Fig. 4
Change of Project Design

The scheme was changed in order to get following environmental and social benefits:

- Under Feasibility Design, approximately 6.1 km of the River would have experienced the low flows due to operation of the Project while in the revised design only 0.7 km of the River will be affected by these low flows. From an ecological standpoint, the negative impact on the ecological resources of the Poonch River will be much less for the changed design compared with feasibility design.
- During the breeding season, Golden Mahaseer migrates into the tributaries (nullahs) of the Poonch River for spawning including the Bann Nullah and Rangar Nullah as shown in Fig. 5. The construction of a dam, as envisaged in Feasibility Study, at the confluence of Poonch River and the Ban Nullah would disrupt this breeding migration and negatively impact the population of the Golden Mahaseer. Under the new design, the Project facilities will be located about 6 km downstream of Feasibility Study location. The breeding grounds of Golden Mahaseer particularly in the Ban Nullah will not be directly affected by project operations under new scheme.

- The total submerged area (including the present river) will be approximately 320 hectares for design envisaged in Feasibility Report while 292 hectares for the optimized design, therefore, comparatively less terrestrial habitat will be submerged and consequently there will be a lower negative impact on the terrestrial ecology.
- The Resettlement under optimized design is minor in comparison to that for Feasibility Report design.
- For Feasibility Stage design, a new road approximately 1.5 km long was planned to be built from the existing blacktop road to the inlet of the power tunnel in relatively undisturbed pine and scrub forest. For this, vegetation would have to be cleared, and trees cut. For optimized design, a shorter road of 650m length is required.
- The option for peaking mode operations as envisaged in Feasibility Report was discarded to avoid stress on the river ecology downstream of the power house and, therefore, a non-peaking operation of the powerhouse was adopted for the Project in the new design.

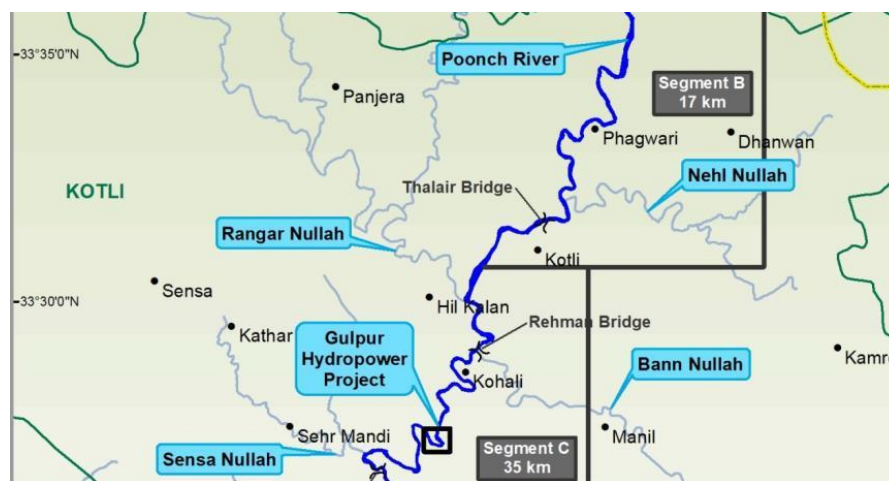


Fig. 5
Tributaries of Poonch River

Based upon changed design the relocation decreased from 128 to almost zero whereas on the basis of above studies/assessments EPA and wildlife departments appreciated Mira Power in terms of efforts towards protection of fish species in National Park specifically Endangered Mahaseer and Critically Endangered Kashmir Catfish and gave approval for:

- Preparation and implementation of Biodiversity Action Plan (BAP) for achieving protection targets of Enhanced Protection Scenario at basin level protection

- Concept of 'net gain' in biodiversity in National Park

The above decisions of the regulators were duly endorsed by the lenders who also advised Mira Power to update the original ESIA and resubmit to EPA and Lenders for public disclosure and approvals from investment committees and Board of directors.

To meet the approvals of regulators and the lenders Mira Power carried out following additional studies/assessments:

- Ecological Flow Assessment- based on revised design option
- Detailed Socioeconomic Surveys
- ESIA Update and Integration
- Climate Change Risk Assessment

All revised reports were resubmitted to Environment Protection Agency (EPA), AJK Fisheries and Wildlife Department (FWD) and lenders for their respective disclosure requirements and approvals. In this process Mira Power successfully managed unprecedented support from the major international NGOs including World Wildlife Fund (WWF), Himalayan Wildlife Foundation (HWF) and International Union for Conservation of Nature (IUCN), regulators including EPA and FWD and other civil society and academic institutions.

To discuss above efforts and potential outcome, a number of video conferences were managed where lenders' experts, Mira Power and various other stakeholders/NGOs participated. Resultantly, subject to following further studies a conditional approval was granted by all lenders based on majority votes:

- Feasibility Assessment for Achieving Net Gain
- Biodiversity Monitoring and Evaluation Plan
- Proposed Ecological Flow Management Plan
- Mahaseer Hatchery Design and Restocking Program
- Proposed Road Map for National Park Management Park (NPMP)

Finally the BAP and ESIA were further updated upon completion of above studies and was requiring an Environmental and Social Management System (ESMS) to implement all the approved plans. The Biodiversity Action Plan (BAP) was developed for the Poonch basin by the project in consultation with all stakeholders. The same is implemented through landmark agreement on a novel concept of public-private-partnership for conservation. An implementing agency, a renowned conservation NGO has been engaged with Government's Fisheries & Wildlife Department to implement the BAP.

A comprehensive BAP has been developed, outlining Pro2 scenario commitments to achieve net positive gain in the ecological values that triggered Critical Habitat classification, namely (a) Kashmir Catfish, (b) Mahaseer fish and

(c) Poonch River Mahaseer National Park conservation objectives. These actions will include, among others:

- 1) Implementing an effective watch and ward system supported by institutional arrangements to reduce illegal and indiscriminate hunting and killing of wildlife (both aquatic and terrestrial) including several bans on non-selective fishing, fishing in tributary breeding grounds, fishing during the breeding season, and sediment mining in ecologically sensitive areas
- 2) Prohibiting removal of vegetation that is important for supporting biodiversity
- 3) Increasing park staff, patrols and mining inspectors
- 4) Limiting areas designated for sediment mining
- 5) Banning of livestock grazing and wood collection in sensitive areas
- 6) Conducting environmental awareness workshops for local communities. The Sponsors will finance supplemental park staff, equipment, facilities, and logistics to close the existing capacity gaps – including the construction of two park management offices and support to the local Fish and Wildlife Department (FWD) on the construction of a hatchery for Mahaseer on the Poonch river. This hatchery is a key component of the actions needed to increase numbers of the Mahaseer in the downstream portion of the Poonch river after the dam is in place as they will be cut off from their breeding grounds upstream. Therefore, success of this hatchery is critical to the success of the BAP actions and will be planned and monitored carefully. In addition, project sponsors will provide technical support to the local FWD by engaging experts in park management and river ecology. Institutional arrangements proposed in the BAP consists of putting in place a protection system for Poonch River Mahaseer National Park partly financed by the project and implemented by an independent organization
- 7) Active support from the local FWD by making available existing staff for protection and assistance in coordination with other government line departments such as police and district administration
- 8) Commitment by the local FWD to provide legal authority to the staff of the independent organization for exercising powers under wildlife legislation
- 9) Oversight and monitoring by the Wildlife Management Board of the local FWD
- 10) Monitoring by an independent third party on a long term basis. These actions, along with development of a strong Poonch River Mahaseer National Park management plan, are expected to lead to net gain on the indicator fish species populations and strengthen and support conservation objectives of the park

The Environmental and Social Management System of Gulpur Hydropower project has been designed in compliance with the requirements of project lenders including IFC and ADB. The requirements of applicable performance standards of IFC and safeguard policy statement, 2009 of ADB are the key documents that

govern the overall framework. Additionally the other documents of IFC and ADB have also been used in shaping up and improving the system.

The construction of Gulpur project is carried out in accordance with the ESMS implementation handbook (Construction) of IFC which is based on the most common method Plan-Do-Check-Act cycle (PDCA). The system is based on following elements as shown below in Fig. 6.

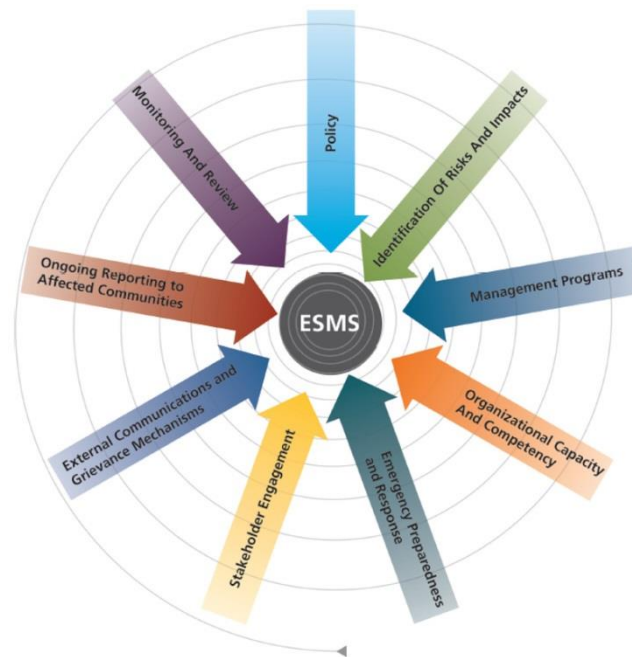


Fig. 6
Gulpur Hydropower Project – ESMS

5. STRATEGIC OUTCOME

After implementation of revised ESIA, land acquisition has been completed without any significant relocation. The initial results after implementation of plans developed for sustainability are very encouraging whereas hatcheries for critically endangered Kashmir Catfish and endangered Golden Mahaseer are under construction whereby a significant 'net gain' in the population of these species is expected. We expect that the concept of net gain implemented for addressing the environmental challenges while developing Gulpur HPP shall be the best solution for various other projects not only on Poonch River rather other rivers as well. This will set an international standard that how development and environmental protection can work together for sustainable development.

COMMISSION INTERNATIONALE DES GRANDS BARRAGES

VINGT-SIXIÈME CONGRÈS DES GRANDS BARRAGES
Autriche, juillet 2018

DOI 10.3217/978-3-85125-620-8-055



This work licensed under a Creative Commons Attribution 4.0 International License. <https://creativecommons.org/licenses/by-nc-nd/4.0/>

DISASTER COMPETENCE NETWORK AUSTRIA

Christian RESCH

*Managing Director DCNA, GRAZ UNIVERSITY OF TECHNOLOGY,
UNIVERSITY OF NATURAL RESOURCES AND LIFE SCIENCES VIENNA*

AUSTRIA

Rainer PRÜLLER

*Managing Director DCNA, GRAZ UNIVERSITY OF TECHNOLOGY,
UNIVERSITY OF NATURAL RESOURCES AND LIFE SCIENCES VIENNA*

AUSTRIA

COMMISSION INTERNATIONALE
DES GRANDS BARRAGES

VINGT-SIXIÈME CONGRÈS DES
GRANDS BARRAGES
Autriche, juillet 2018

DISASTER COMPETENCE NETWORK AUSTRIA

Christian RESCH, Rainer PRÜLLER

*Managing Director DCNA, GRAZ UNIVERSITY OF TECHNOLOGY,
UNIVERSITY OF NATURAL RESOURCES AND LIFE SCIENCES VIENNA*

AUSTRIA

1. INTRODUCTION

The Disaster Competence Network Austria (DCNA) is a cooperation platform of universities and research institutions in the field of security and disaster research. The aim of the initiative is to transfer scientific knowledge into practice, through cooperative research and education activities carried out in collaboration with various stakeholders, as well as the provision of decision-relevant information in the event of a disaster.

2. ABOUT THE ASSOCIATION

The basic idea behind the DCNA initiative is to bundle scientific expertise in Austria in the field of disaster prevention and disaster research. The association acts as a networking platform and coordinating body for scientific institutions, companies and disaster management authorities at all levels. It is organized as a non-profit and open association under university management and distinguishes three different types of memberships. Ordinary members are all Austrian institutions in the field of scientific security and disaster research. Associate members are all Austrian institutions that are interested in DCNA activities and their support, but do not carry out any scientific research themselves. To further

anchor disaster research across multiple institutions, there are strategic partnerships. These can be met with ministries, local authorities and international institutions that will pursue a common goal with DCNA. Meanwhile, the network has been expanded to include major players in disaster management and prevention (**Figure 1**).



Figure 1: Current DCNA members

The common denominator of all participating institutions is disaster prevention and appropriate preparation to potential emergencies. This large clip is drawn by DCNA in order to be equally available to research institutions and academia as well as stakeholders from the public and private sector.

3. ORGANIZATIONAL STRUCTURE

The organizational structure of DCNA includes the Board Members from the founding universities such as Graz University of Technology and University of Natural Resources and Life Sciences Vienna with their rectors holding the Chairmanship. A General Assembly is bringing together all network members and partners once a year. In addition to the management level, the implementation-oriented and scientific activities are carried out in different scientific working groups that are formed by experts from DCNA member organizations. Official meetings of the working groups are scheduled twice a year in spring and autumn for two to three days alternately at one of the various member institutions. A chairperson which is elected coordinates a specific working group. If needed, subgroups or project groups are set up for specific topics and demands. The five working groups within DCNA will be the content of the following sections.

3.1. MASS MOVEMENTS AND EARTHQUAKES

Mass movements are gravitation-related catastrophic events such as landslides, rock-falls or and avalanches. In the Alps, a large number of potential landslides threaten public infrastructure and settlement areas can be detected. The working group therefore devotes itself to the gravitational sources of danger in alpine regions with. As Earthquakes are not very likely to happen in Austria, but

need scientific attention, they are taken into scientific consideration within this working group.

3.2. FLOODS

Flooding is the condition of waters where the water level is significantly above the mean level. In general floods can be predicted in advance, except in the case of flash floods. Risk areas of floods affect both inner and outer Alpine regions in Austria and beyond and are of high likelihood. That is why flooding is to be addressed within a separate working group.

3.3. EXTREME-WEATHER-EVENTS

Under extreme weather events, weather phenomena such as storm, hail, heat and late or extreme frost will be addressed in this group. These occur in hard-to-predict intervals and can only be modeled inaccurately. The main focus of this working group is therefore the prevention of these extreme weather events and its consequences (e.g. Forest fires, droughts...) for public authorities, insurance companies and agricultural decision-makers.

3.4. CRITICAL INFRASTRUCTURE AND INDUSTRIAL HAZARDS

The working group Critical Infrastructure and Industrial Hazards deals with the topics blackout, electricity, communication, traffic, chemical industry or nuclear power plants with their nuclear hazard potential. Process and Plant Safety is of high importance not only because of natural hazards that have high potential to trigger major industrial accidents.

3.5. DISASTER RISK MANAGEMENT

This working group deals with disaster risk assessment, implements needs planning and brings socio-scientific and economic aspects into civil protection. Furthermore, response planning and capacity needs are being addressed. These include among others the risk analysis of technologies, technology-related catastrophic events as well as the modeling of disaster consequences and the appraisal of the extent of damage.

4. RESEARCH AND TECHNOLOGY AREAS

For horizontal linking of the working groups among themselves, research and technology areas are defined. These fields are described in the following chapters.

4.1. MODELING & SIMULATION OF IMPACTS AND PROCESSES

By experimental determination of process-related factors and parameters, including experiments in the laboratory, processes from the five main topics of the DCNA are to be modeled. In the field of gravitational mass movements, the flow behavior is modeled in the laboratory as well as in the field. Interactions between structures and the acting processes are investigated. Hydro-mechanically coupled modeling of profound mass movements in the area of influence of large reservoirs is just as much a topic as the development of geological, climatic and kinematic models in the catchment areas of endangered slope areas. The simulation of impacts includes the analysis and evaluation of temporal and spatial dynamics of mass movements and their effects on infrastructure and populated areas. It is not the simulation of catastrophic events themselves, such as the forces occurring within an avalanche, in the focus of the investigation, but the simulation of the effects of avalanche, for example, the spill of road infrastructure or the destruction of protective forest above permanent settlements.

4.2. STATISTICS & ACTUARIAL SCIENCE

The insurance industry is exposed to the consequences of catastrophic events in most cases, which is why the interest of minimizing damage is an important tool for cost optimization. Due to very well documented claims over a very long time, the quantitative and qualitative data of the insurance companies can be a valuable source for the scientific processing of disasters. On the other hand, the insurance industry benefits from a large network of scientists to gain a greater understanding of the occurrence of disasters based on statistical and mathematical data. This knowledge will then again influence the pricing policy.

4.3. REMOTE SENSING, GEOINFORMATION & NAVIGATION

Remote sensing technologies are imaging techniques that can operate from different carrier platforms. Depending on the spatial and temporal resolution of the

requested data, satellite imagery, aerial photographs, thermal surveys, highly accurate surface models from LiDAR and radar interferometry etc. are available. For example, remote sensing systems for protection forest monitoring with the detection of forest parameters can be used as the planning basis for protection forest management by various evaluation methods. After a catastrophic event, building damage and damage to infrastructure can be detected automatically by remote sensing-based data. In the event of a flood, a real-time detection of the flood stop line can be performed. The harmonization of this data is expediently implemented in a Geographical Information System (GIS). Within this GIS, conclusions can be drawn from the observations using geoinformation methods as well as the documentation of damage events. Navigation as part of this field of technology deals with outdoor and indoor navigation, whereby outdoor navigation part is often seen as a synonym for GPS. However, this would severely restrict research in the field of outdoor navigation, since independent systems, for example Inertial Measurement Systems (IMU) are also be developed using complex filter methods. Indoor navigation plays an important role in the field of robotics, for example. Since satellite-based positioning methods can not be used within buildings, indoor navigation technology has to be used. Autonomous robots in the object exploration of fire in buildings, must be able to navigate and move autonomously with the help of optical and acoustic sensors.

4.4. SENSORS & SENSOR CARRIERS

In order to prevent catastrophes, the establishment of a monitoring network is of crucial importance. Applied to the disaster research carried out within the framework of the DCNA, these are the engineering supervision of large-scale structures and the monitoring of non-slip slopes in the catchment area of infrastructure. Geodetic technologies and methods provide the means to cushion the impending catastrophe very promptly and initiate countermeasures. In this case, Unmanned System (UxS) based carrier platforms such as drones or robots can be used to meet the temporal resolution requirements to the data. Fires or the discharge of hazardous substances can be localized by means of thermal sensors or chemical detectors to be made available to field forces.

4.5. ARTIFICIAL INTELLIGENCE, COMMUNICATION & INFORMATION TECHNOLOGY

This technology group includes the construction of information systems, such as a river information system such as the "Danube River Information Service" as well as the construction and operation of communication technologies in the event of a disaster. Information systems are designed to allow interoperability between civilian and military organizations in disaster management and to provide an interface to government agencies and scientific institutions. Thus, it is possible for experts to assess damage potential and vulnerability.

4.6. RAW MATERIALS, PLANT AND BUILDING MATERIALS RESEARCH

Materials science and engineering is an interdisciplinary field that deals with the research and development of new materials (e.g. lighter, smarter...) to be used for individual protection and safety for first responder organizations for example. Furthermore, research on new materials to be used for collective protection measures such as building structures, are being addressed.

4.7. EDUCATION, TRAINING & OPERATION

DCNA members have the opportunities to get education and training within their research focus as well as trainings out of other DCNA-relevant fields of technology. In addition, DCNA members will be able to participate in large-scale disaster and response training sessions and provide their scientific expertise to the task forces during these test runs. Using the competence map of DCNA, participating institutions and scientists can present their expertise in the field of disaster research and are proposed to the requesting task force in the event of a disaster.

5. MOBILE DCNA-RESEARCHPLATFORM

In the past decade, there have been an increasing number of disasters in Austria, caused for example by floods, mudflows or large-scale gravitational movements. Dealing with these natural phenomena presents massive challenges to the public safety organizations. In the phases of disaster management and recovery, but also in the area of prevention, recent disasters and the increasing complexity of scenarios have shown that response organizations and decision-makers at all administrative levels grow a higher demand of scientific expertise and advice. For this reason, the University of Natural Resources and Life Sciences Vienna and Graz University of Technology have launched the "Disaster Competence Network Austria" to transfer scientific knowledge into practice. With the assistance of acute assignments as well as through cooperative research and educational activities carried out in cooperation with a wide variety of stakeholders, the DCNA platform offers, among other things, the following synergies and added value:

- Contributing to the preservation of human life by avoiding damage caused by disasters and their consequences
- Advisory body of decision-makers in public authorities and organizations at federal and state level

- Close coordination, cooperation and provision of expertise towards thematically related initiatives, such as state crisis and civil protection management
- Establishment of a reliable partner network for national and international research activities by networking and expanding existing structures
- Access to scientific issues initiated directly from the field
- Sharing existing and new infrastructure.

In order to be able to realize these added values, together with the creation of a common organizational structure, the development of the common infrastructure is absolutely necessary. Therefore, a mobile research platform is being developed. The aim of this cooperative project is to establish an infrastructure (analysis laboratory), which enables the researchers and experts of the DCNA network to make their expertise available locally and in real time during disaster events. This system will be modular in its basic technical structure:

- Information and communication modules
- Laboratory and analysis workstations
- basic technical equipment for field operation

With regard to sensors and analytics, the two scientific partners will equip the modules according to their respective scientific strengths. The aim is an integrated overall concept, based on the complementary strengths of the scientific partners and also coordinated with each other in terms of organization. A current focus of the mobile research laboratory will be the monitoring and analysis of gravitational mass movements, e.g. Landslides or potential rock and landslides. With the high-precision measuring systems introduced by the university partners and the selective new acquisitions (terrestrial laser scanners, terrestrial interferometry, drones equipped with multi-sensor systems, engineering geodetic measuring instruments) as a supplement to existing equipment, it will be possible to produce highly precise multi-temporal digital elevation models of affected areas to create and to observe mass movements continuously. Based on these measurement results and deformation controls, model calculations for risk and risk assessment can be carried out at the same time. The analysis of deformations in structures (e.g. piers, buildings, highways, dams...) represents another important application of mobile measurement and analysis units. The planned container systems, which are completed in terms of their equipment to form a complete system, are brought into use as a joint large-scale laboratory. Due to the complementary expertise of both universities, these interdisciplinary missions can increase the measuring and analysis capacities as well as the possibilities for the stationing of scientific staff in the field (number of jobs). The realization of the acquisition of the two container systems planned in the first half of the project requires great know-how about their requirements and design. The fire brigade and the army in particular have been using such systems for many years, and the universities can and do wish to draw on these experiences in the cooperation project. Within the framework of the project, a dedicated section will deal specifically with the technical design of the container systems.

Another section will focus on adapting the existing research infrastructure (contribution of universities to equipment and sensors) and the selectively planned new purchases to the concept of a mobile laboratory. Both specialist groups will cooperate closely with each other in order to develop and implement a technically, ergonomically and organizationally harmonized overall concept. Apart from the deployment scenario of a real loss event, this mobile infrastructure will offer many new opportunities in everyday university life. For the first time, the mobile research infrastructure offers the opportunity to pursue research-relevant issues away from the physical infrastructure and to put them into practice. In addition, a positive effect on the teaching is expected since the students can apply their acquired knowledge in practice. The main advantages of a mobile infrastructure are the following:

- Possibility of monitoring existing critical mass movements within the sphere of influence of settlement areas
- Possibility of effective hazard and risk assessment along infrastructure (railway lines, motorway routes, quarries)
- Increasing understanding of processes and triggering mechanisms by linking to local variables (such as precipitation measurements using weather radar)

Of course, the planned mobile infrastructure should not only be available to the applicants. Organizational integration into the Disaster Competence Network Austria ensures that this infrastructure is subsequently accessible to all users in the field of civil protection and disaster management.

The operation and the further expansion (new thematic emphases in relation to sensor technology and analytics) of the DCNA measuring and analysis laboratory is ensured. The expansion will take place through the integration of further universities.

6. CONCLUSION

The Disaster Competence Network Austria is combining scientific expertise in the field of disaster research and prevention in order to establish a closer cooperation between knowledge carriers and their stakeholders. The aim of the non-profit association is to transfer scientific knowledge into practice through cooperative research and educational activities carried out in conjunction with a wide range of stakeholders, as well as the provision of information and advice to decision-makers in the event of a disaster.

COMMISSION INTERNATIONALE DES GRANDS BARRAGES

VINGT-SIXIÈME CONGRÈS DES GRANDS BARRAGES
Autriche, juillet 2018

DOI 10.3217/978-3-85125-620-8-056



This work licensed under a Creative Commons Attribution 4.0 International License. <https://creativecommons.org/licenses/by-nc-nd/4.0/>

**PERMANENT SAFETY ASSESSMENT OF DAMS, LEVEES, RESERVOIRS,
WATERWAYS WITH FIBER OPTIC DISTRIBUTED SENSING**

Régis BLIN

SMARTEC SA

SWITZERLAND

Daniele INAUDI

SMARTEC SA

SWITZERLAND

COMMISSION INTERNATIONALE
DES GRANDS BARRAGES

VINGT-SIXIÈME CONGRÈS DES
GRANDS BARRAGES
Autriche, juillet 2018

**PERMANENT SAFETY ASSESSMENT OF DAMS, LEVEES,
RESERVOIRS, WATERWAYS WITH FIBER OPTIC DISTRIBUTED SENSING**

Régis BLIN, Daniele INAUDI

SMARTEC SA

SWITZERLAND

1. EARLY DETECTION AS A KEY FOR SAFETY MANAGEMENT

The growing demand of safety awareness, cost effective operations and effective maintenance has rapidly stimulated, in the last decade, the development of smart monitoring techniques capable of detecting early-stage events, thus preventing structures from major failures and leading to a better knowledge of the structure itself. In this publication, the aim is to concentrate on long-term, large-scale field applications on dams, dikes and levees, based on the presented distributed technology and sensors.

2. FIBER OPTIC DISTRIBUTING SENSING

2.1. TECHNOLOGY

The most developed technologies of distributed fiber optic sensors are based on Raman and Brillouin scattering. Both systems make use of a non-linear interaction between the light and the silica material of which a standard optical fiber is made. If light at a known wavelength is launched into a fiber, a very small amount of it is scattered back at every point along the fiber. The scattered light

contains components at wavelengths that are different from the original signal. These shifted components contain information on the local properties of the fiber, in particular its strain and temperature. After an appropriate analysis of those signals, the system can therefore provide a calibrated strain or temperature reading at every meter along the sensing cable, as depicted on Fig. 1.

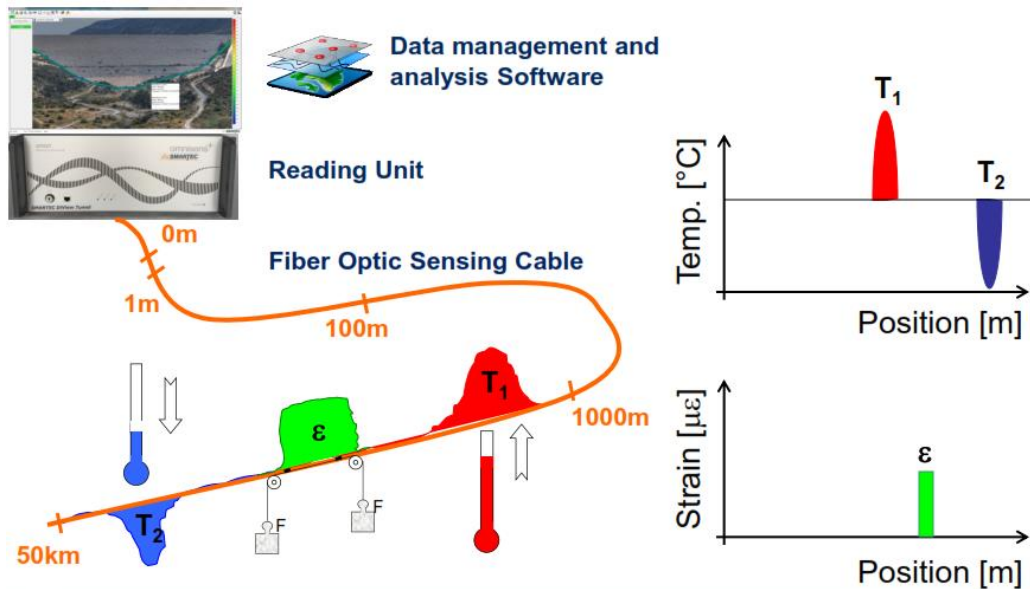


Fig. 1
Fiber Optic Distributed Sensing System

2.2. DATA MANAGEMENT

Direct data analysis based on distributed temperature or strain data has limitations and does not provide real-time data to the operator that often becomes overwhelmed by the amount of data he receives. It is therefore necessary to automate the data management and analysis process. The developed software displays measurement profiles, status maps of temperature or strain, evolution of the structure and events automatically recognized and logged by the monitoring system. All measurements are imported and stored into a single database and data is processed to apply calibrations and select zones of interest. Alarms are generated automatically, based on complex criteria (e.g. for leak detection). The user can then dig-down into raw data for deeper analysis, as shown in Fig. 2.

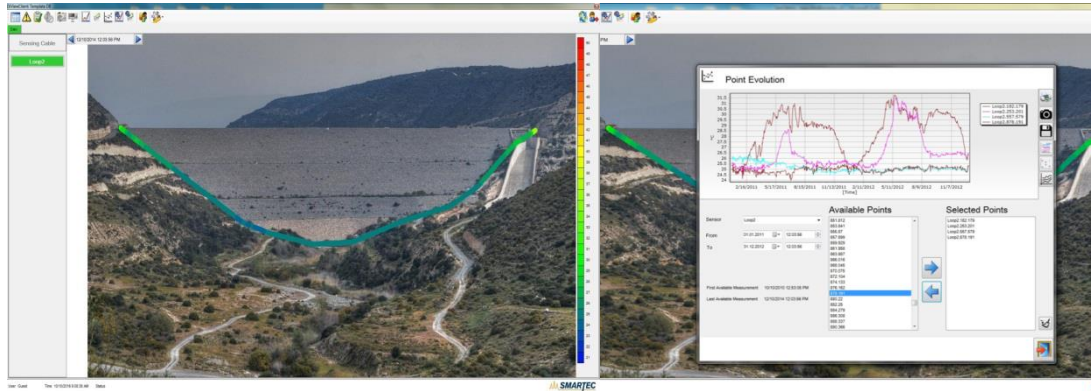


Fig. 2
 Distributed Data - Strain and Temperature - Management and Analysis Software
 Color coding representation (left) - Point evolution display (right)

2.3. BENEFITS

The scale, age and uncertainty of materials in the sometimes huge hydro engineering structures combine a difficult array of parameters for the responsible engineer to navigate when analyzing its structural integrity.

Traditional instrumentation based on localized point sensor is not sufficient to guarantee the detection of early signs of damage and localization of unknown events. Distributed fiber optic sensing allows the early detection, localization and sizing of defects and degradations such as seepages, leakages, settlements, shearing, cracks, abnormal joint movements, intentional tampering and over-flooding.

3. INFILTRATION DETECTION FOR DAMS, DIKES AND RESERVOIRS

A fiber optic distributed system for infiltration detection relies on Raman distributed thermal sensing and can work in two different configurations; the passive and active methods.

The so-called passive method relies on direct detection of temperature anomalies induced by seepage or leak. This method is typically used when a gradient of approximately 5°C between the leaking liquid and the sensing cable can be assured.

The so-called Heat Pulse Method or active method is on the other hand used when the gradient between the liquid and the sensing cable is negligible and smaller than 1°C. In order to ensure a reliable detection of the leak, the self-heating cable is heat up and forced to change its natural temperature. Heating is

provided by flowing electrical current in copper wires of the sensing cable. When forced to change temperature the cable will need a certain time to arrive at a certain temperature, defined as T_{heating} , and as well a certain time to go back in its initial condition. Studying the cooling transient and the value of the maximum temperature reached during the heating phase the analysis software figure out automatically if some events are occurring.



Fig. 3
Sensing cable installation at Grand Ethiopian Renaissance Dam (GERD)

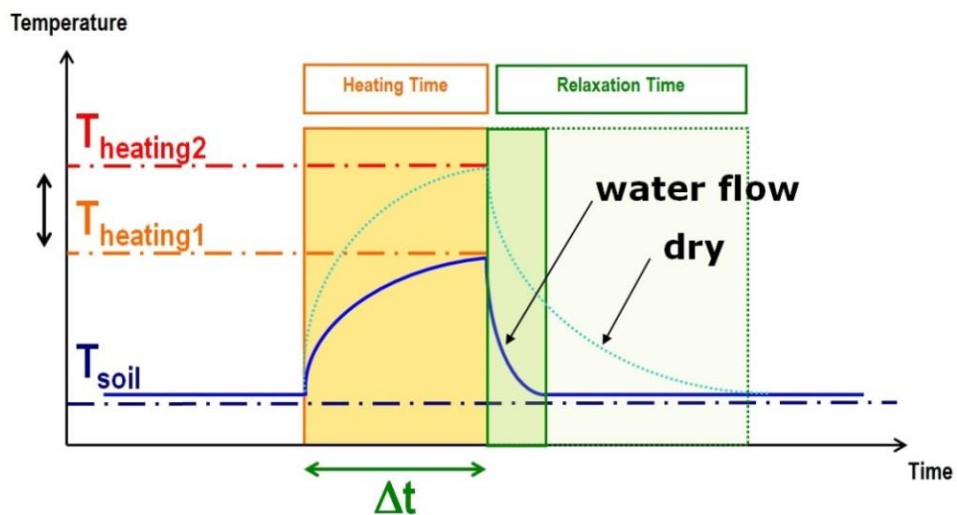


Fig. 4
DiTemp Heat Pulse Method working principle

As an example, a cable surrounded by still water will require more time to heat up, while a cable within flowing water will cool down more quickly.

3.4. APPLICATION: SIAH BISHEH UPPER DAM, IRAN

The Siah Bisheh Pumped-storage Hydroelectric Power Project is the first of this type in Iran. Located 125 km from Tehran it has an installed capacity of 1000 MW. The plant is intended to play a vital role in stabilizing the entire North Iran power grid, ensuring the safe operation of thermal power plants in the surrounding provinces.

The main aims of fiber optic instrumentation are seepage at plinth level and active detection system with Heat Pulse Method technique. Beside this direct detection, the monitoring system can offer an effective analysis of the evolution of the detected anomaly, and a way to define reasonable threshold and trigger alerts if they are overcome. Moreover fiber optic systems are easily integrated with already existing traditional / standard monitoring systems. Distributed sensing offers the unique capacity of locating precisely the event using only few distributed sensors.

Two independent systems are developed to monitor the existing dams. A dedicated control room where the instrumentation rack is located is specifically built on the crest of each dam (Fig. 5).



Fig. 5

Sensing cable installation at the plinth of the upstream face of the upper dam and one monitoring cabinet

The rack contains a display, the DiTemp unit with its accessories, the server PC where the analysis software is installed and the heating module necessary to heat up the cable at scheduled times. All the system is plugged into a network stabilizer and UPS in order to prevent general functionality in case of power failure.

Accuracy and repeatability tests were carried out during implementation phases (Fig. 6 and Fig. 7).

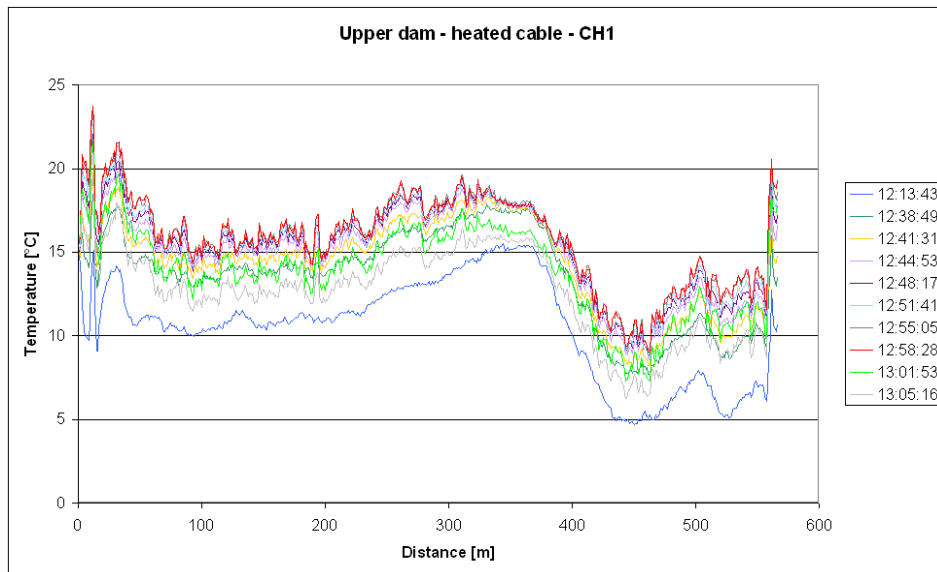


Fig. 6
Absolute temperature measurements during heating

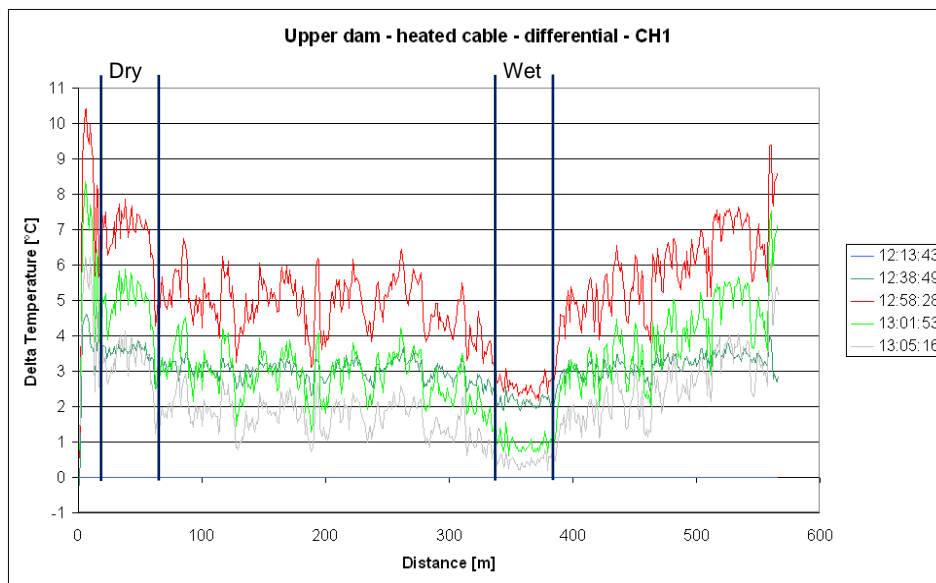


Fig. 7
Differential temperature measurements during heating

It is possible to evince how temperature resolution is about ± 0.2 °C. The initial section showing higher deviation refers in fact to cable section not yet concreted and exposed to the environment. Thanks to the customized visualization and analysis software it is possible to follow in real time any variation in the temperature profiles of the two sensing cable, launching a warning in case of any seepage or leakage.

4. DEFORMATION EARLY WARNING SYSTEMS

A fiber optic distributed system for deformation relies on Brillouin sensing and provides early detection of ground settlements and heaves, local cracks and internal erosion.

4.1. APPLICATION: I-WALL LEVEE – NEW ORLEANS (US)

The iLevees project "Intelligent Flood Protection Monitoring Warning and Response Systems", in the state of Louisiana, has the goal of providing an alerting and monitoring system capable of preventing early stage failure, both in terms of ground instability and seepage. The motivation for the monitoring system is to improve safety awareness, provide sensible information about levees' status and conditions, before, during and after floods, and to avoid the tragic events like the ones that occurred following Hurricane Katrina in 2005. The project had the goal to monitor the levee wall, deformation and shear, and the surrounding soil, movements and water infiltration / seepage.

The particularity of the project was the installation technique adopted for the levee wall integration. In order to provide a good transfer of the acting forces from the wall to the sensor itself a good bonding strength shall be given: to do this it was decided to "cut" a groove all along the installed section, where the sensing cable was deployed and sealed by means of specific episodic resins (Fig. 8).



Fig. 8

Installation of sensor in a groove, on top of the levee wall section and in a trench

For the surrounding soil a more common ground embedding technique was chosen on the base of our previous returns of experience. Sensors are embedded between 0.5 and 1 m below the ground level, after compacting the trench, the sensors are deployed and covered with soft filling material. After this

operation, the trench is back-filled and compacted.

An example of calculated deformation on the sensor placed on the top of the wall section I presented in Fig. 9. Deformation is plotted as a function of position along the wall and as a function of time.

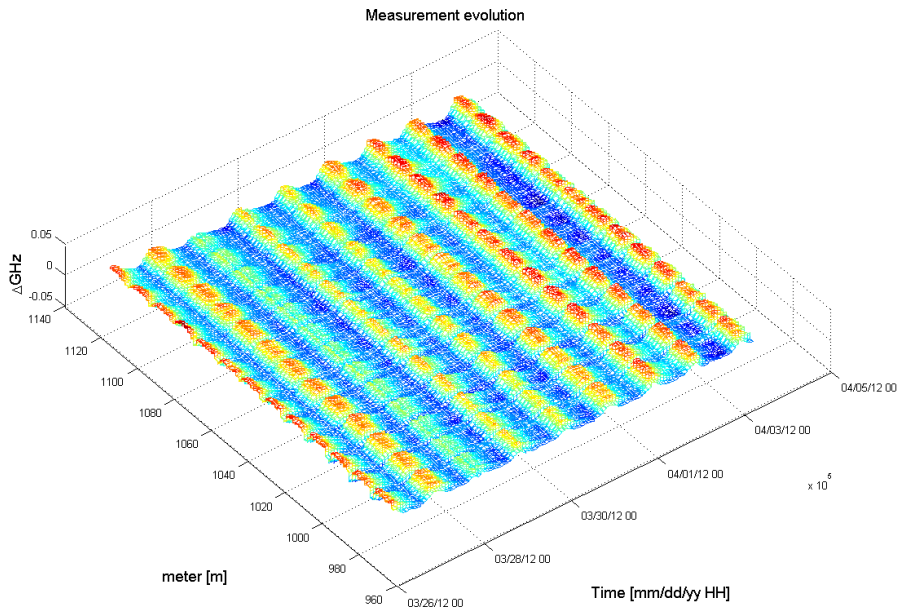


Fig. 9

Recorded deformations on a levee wall as a function of position and time

In the plot it is possible to observe the daily expansion-contraction cycles of the wall due to temperature fluctuations. It is also possible to localize the expansion joints along the levee wall that shows a different behavior. In case of an event along the levee section, a localized deformation peak will appear in the visualization software and would automatically trip an alarm.

4.2. APPLICATION: PENSTOCK MOVEMENT MONITORING PROJECT – NENDAZ (CH)

The penstock of an important mountain dam in the Swiss Alps, is subject to rock mass movements that can influence its mechanical performance (Jordan Papilloud 2015). In order to provide a safe installation, the penstock is made of several pipe sections welded together in order to form a more flexible pipe, thus allowing a higher degree of movement. Nevertheless a deformation monitoring system is necessary to detect any abnormal penstock deformation and penstock curvature. In addition to this, the penstock access tunnel is also affected by concrete cracking due to the water pore pressure and rock movements. A distributed strain monitoring system was selected because of its capability to

monitor long lengths through a single cable, thus simplifying installation and increasing data density. A different installation technique is chosen for the 2 sections: in the penstock, where precise and accurate monitoring under water is required, the sensing cable (flat profile) is directly glued on the internal surface. The steel penstock is sand-blasted to offer a smooth and clean installation surface where 510 m, linear length, of sensing cable is glued along 4 different lines, Fig. 10.



Fig. 10
Strain sensing cable installation inside the penstock

On the other hand, for the access tunnel a mixed installation technique was selected: sensing cable was directly glued on concrete for most of its length, but fixed with stainless steel bracket where wide cracks were already visible and developing; this decision was taken in order to preserve sensor from breaking in case the crack keep developing, Fig. 11. This installation technique allows a precise and accurate monitoring over the whole length of this tunnel of approximately 70 m.



Fig. 11
Strain sensing cable installation on penstock access tunnel

After 3 years of monitoring, the collected results are in line and good agreement with the mathematical predictions and other geo-matic measurements provided by additional monitoring systems installed at site. A typical example of Strain distribution measured in the penstock access tunnel clearly shows the location of open developing cracks, peaks can be seen and easily localized along the sensing cable length, Fig. 12.

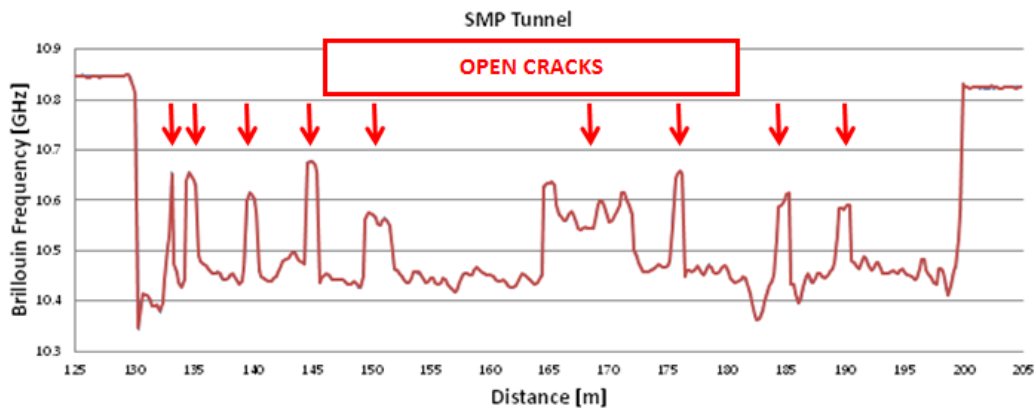


Fig. 12
Strain distribution measured along the penstock access tunnel

5. CONCLUSION

SMARTEC has instrumented more than 20 dams with fiber optic distributed sensing within the last 15 years. The use of distributed fiber optic sensors for the monitoring of civil structures and infrastructures opens new possibilities that have no equivalent in the conventional sensors system. Distributed sensing technologies have been applied on key hydraulic components such as penstock and waterlines.

Fiber optic distributed sensing is a recognized technology in dams engineering and meets today's goals of asset management. It overcomes the limited capability of conventional sensors with reduction of maintenance expenses. Distributed sensing is often combined with fiber optic point sensors (temperature, piezometers) and data communications are fully compatible with plant DCS or SCADA system.

6. REFERENCES

- [1] INAUDI, D., Distributed Fiber Optic Sensors for Dams and Levee Deformation Monitoring, GEG New Orleans, 2015.
- [2] INAUDI, D. and CHURCH, J., Paradigm shifts in monitoring levees and earthen dams: distributed fiber optic monitoring systems, Proceedings, 31st USSD Annual Meeting & Conference, San Diego, California, USA, 2011.
- [3] JORDAN, A and PAPILLOU E., Penstock structural health monitoring, Hydro 2015 Bordeaux, Session 19 Gates and penstock, 2015.

COMMISSION INTERNATIONALE DES GRANDS BARRAGES

VINGT-SIXIÈME CONGRÈS DES GRANDS BARRAGES
Autriche, juillet 2018

DOI 10.3217/978-3-85125-620-8-057



This work licensed under a Creative Commons Attribution 4.0 International License. <https://creativecommons.org/licenses/by-nc-nd/4.0/>

**EXPERIMENTAL INVESTIGATION ON STEPPED SPILLWAY
PERFORMANCE OF UPPER CISOKAN DAM IN INDONESIA**

James ZULFAN

Researcher, MINISTRY OF PUBLIC WORKS AND HOUSING

INDONESIA

Nuryanto S. SLAMET

Phd Candidate, THE UNIVERSITY OF QUEENSLAND

AUSTRALIA

COMMISSION INTERNATIONALE
DES GRANDS BARRAGES

VINGT-SIXIEME CONGRES DES
GRANDS BARRAGES
Autriche, juillet 2018

EXPERIMENTAL INVESTIGATION ON STEPPED SPILLWAY PERFORMANCE OF UPPER CISOKAN DAM IN INDONESIA

¹James ZULFAN & ^{1,2}Nuryanto S. SLAMET

¹*Researcher*, MINISTRY OF PUBLIC WORKS AND HOUSING, INDONESIA

²*Phd Candidate*, THE UNIVERSITY OF QUEENSLAND, AUSTRALIA

1. INTRODUCTION

Nowadays, the stepped spillway design has been widely used in many countries in the world due to the rapid development of RCC (Roller Compacted Concrete) dam which gives both structural and economical benefits. Although this concept existed for 3500 years (Chanson, 2010) the development is still growing from time to time. Peyras et al. (1992) mentioned that this type of spillway would gain economic mean approximately 20% compared to other types, the reason is because the ease of construction and design simplicity. Many studies has been done by several researcher specifically on this type of dam such as Rajaratnam (1990), Rice and Kadavy (1996), Yasuda and Ohtsu (1999), Chanson and Toombes (2002), Boes and Hager (2003), Gonzalez (2005), Takahashi et al. (2006), Hunt and Kadavy (2007, 2008), and Felder and Chanson (2008). Boes and Hager (2003) found that one of the advantages of this design is cheaper construction cost due to the decrease of stilling basin size. However, this concept has not been fully implemented in Indonesia. There are some weir structures that adopt this concept by using stepped shape on its spillway, however, it has not been implemented on dam construction.

Currently, the stepped spillway concept will be applied in Upper Cisokan Dam in Indonesia. The Upper Cisokan Dam is located at West Java Province on Cisokan River. Nevertheless, since this type of spillway is still new and has not been designed in Indonesia before, a physical model test is needed to be done to see the behaviour of the dam. We also found that research to study the pressure on dam spillway using pressure transducer at hydraulic laboratory is still rare. The

aim of this study is to have a proper design of stepped spillway which can be a good reference for further implementation of a stepped spillway. The experiments were conducted inside a hydraulic laboratory and the model covering the upstream reservoir, approach channel upstream apron of the spillway, dam, spillway and appurtenance structures (See Figure 1).

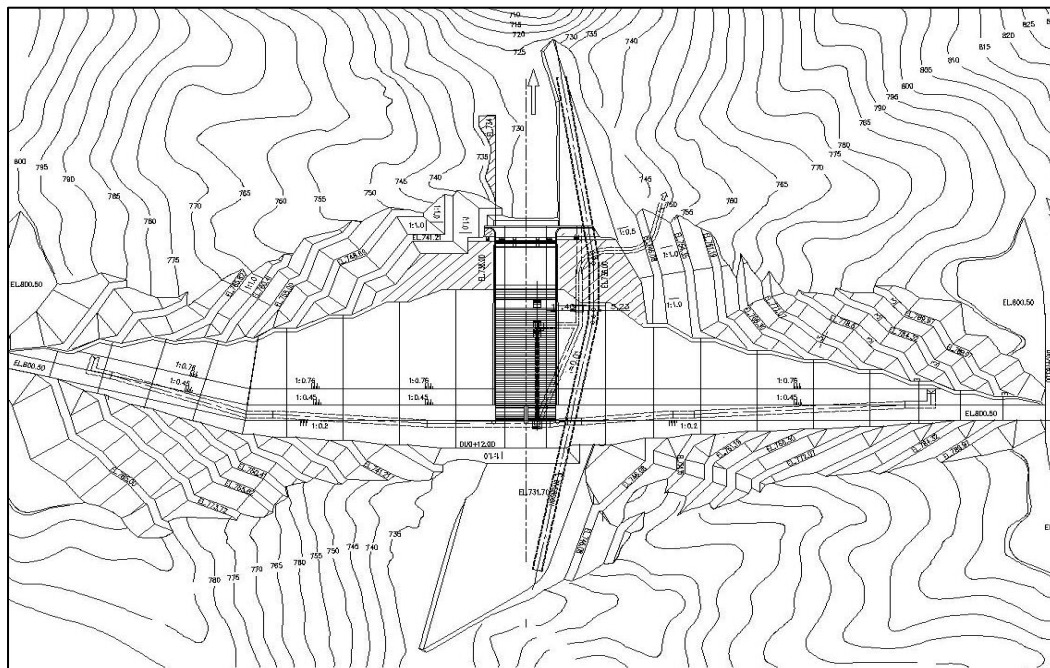


Fig. 1. Plan view of Upper Cisokan Dam

2. EXPERIMENTAL SETUP

The Upper Cisokan Dam spillway model is made as three-dimensional model covering the upstream reservoir, spillway and appurtenance structures (crest, chute channel and energy dissipator), and river in the downstream of the spillway. The experiment conducted at a hydraulic laboratory to observe the water profile, water pressure and scouring. The reservoir model in the upstream reach is made as a fixed bed model; it is constructed using of cement mortar and reproduced based on situation drawings. The reproduce upstream model is up to approximately 300 m upstream of the spillway. In particular for water pressure test, pressure transducers were installed inside the model to indicate the pressure measurement. In this experiment, there will be three scenarios; scenario 1 is the initial design where the downstream riverbed model is reproduced as a movable bed made by sand and left unprotected. Scenario 2 is a condition where the downstream protection material using stone riprap for downstream riverbed protection and arrange with u-shape. Scenario 3 is the condition where the downstream protection material is fully using stone riprap. The length of reach modelled is approximately 440 m downstream of the energy dissipator. The

similarity in shape, dimensions, and roughness of the material in the prototype have closely resembled. It should be noted that the reproduction of shape and dimensions in the model is focussed in the shape and hydraulic measurements that influence the flow pattern and is intended to closely simulate the hydraulic field conditions as can be seen in Table 1. The geometric scale of Cisokan Upper Dam Spillway model is selected to be 1 to $33\frac{1}{3}$.

Table 1
The Dimension of Upper Dam Spillway model

DIMENSION OF STRUCTURES	PROTOTYPE	MODEL
Height of dam	75.5 m	2.265 m
Width of dam crest	6.5 m	0.195 m
Height of spillway crest	71.50 m	2.145 m
Width of spillway crest	10.00 m	0.3 m
Height of end sill	21.2 m	0.636 m
Design discharge PMF	2.70 m	0.081 m
Design discharge 1000 years	300 m ³ /s	46.77 m ³ /s
Design discharge 100 years	185 m ³ /s	28.84 m ³ /s
Debit discharge 2 years	42.7 m ³ /s	6.656 m ³ /s



Fig. 2. Dam model in the hydraulic laboratory

3. EXPERIMENTAL OBSERVATION

3.1. WATER PROFILE ALONG THE SPILLWAY

Test of water surface profiles are conducted along the spillway, started from the crest through the stepped spillway and the energy dissipator using the design discharges. The water flow on stepped chute is known as the nappe, transition, and the skimming regimes (Yasuda 1997; Chanson & Toombes 2002). Based on the results, the flow from the crest spill smoothly and relatively well distributed, for low discharges the flow at the beginning of the steps are splash out of step, while for higher discharges the flow more smoothly over the stepped spillway. Since there are no changes in the upstream condition, the water profile is still the same in all scenario. Figure 3 shows that at the downstream of the center pier the flow is not smooth and splash over due to the rectangular shape of the downstream end of the pier.

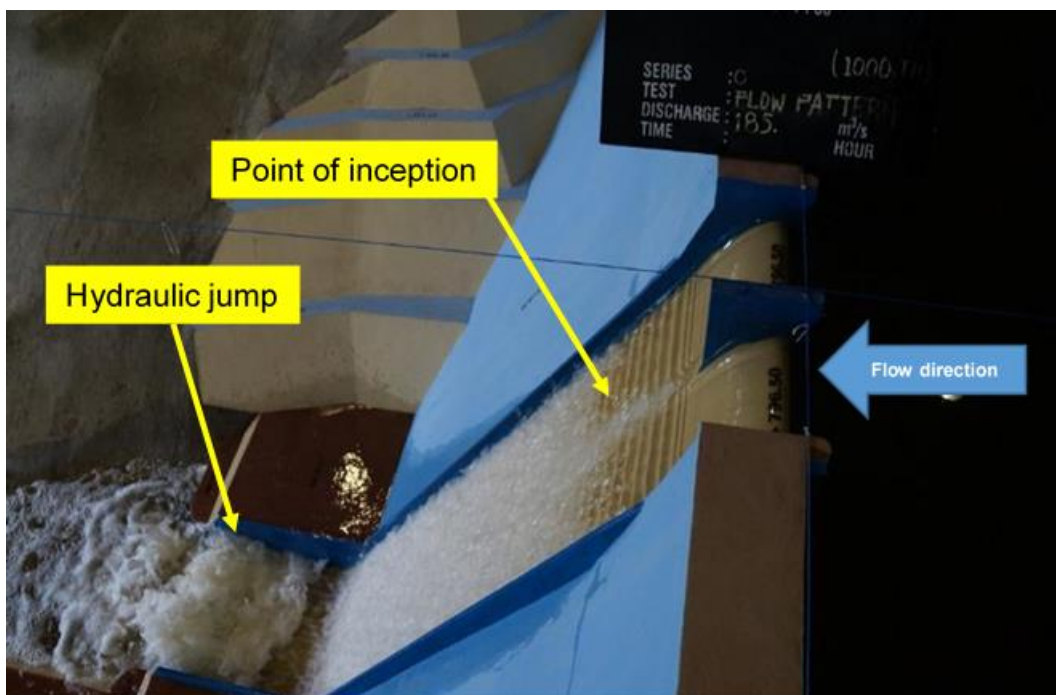


Fig. 3. Upper Cisokan spillway model with discharge $Q_{1000\text{yrs}}$

The inception point occurred and started to shift more downstream in regards of increased discharge from nappe to skimming regime. In particular for high discharge, the hydraulic jump occurred and seemed has not dissipated properly which may cause local scouring at downstream of the dam especially when the downstream area is not protected (see Figure 4).

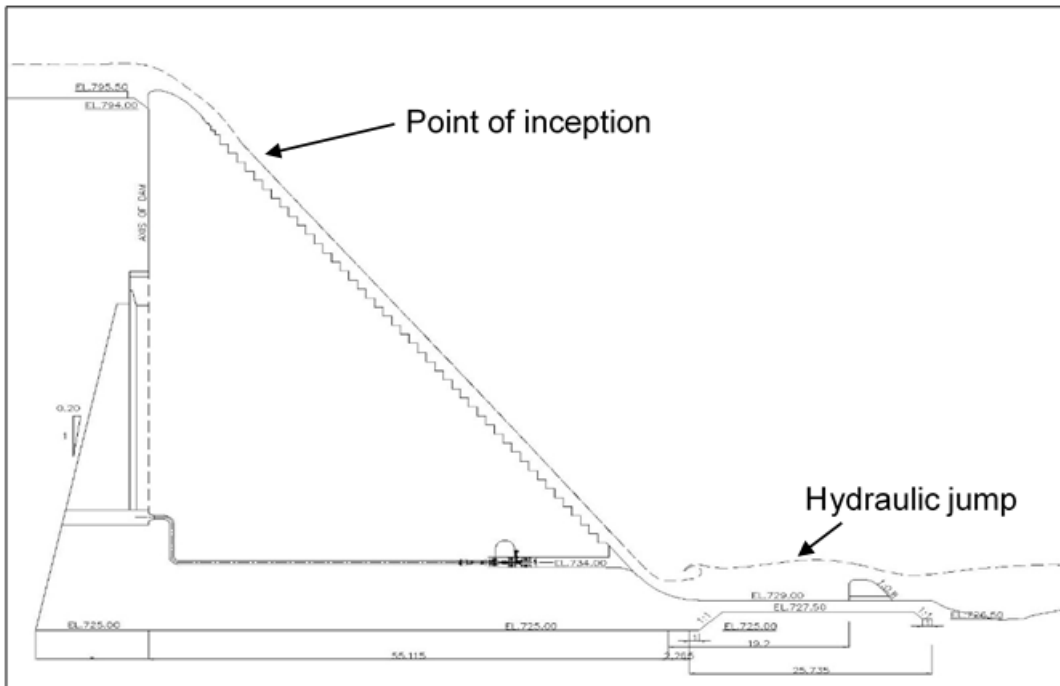


Fig. 4. Water profile with discharge $Q_{1000\text{yrs}}$

3.2. WATER PROFILE ALONG THE SPILLWAY

On this experiment, pressure transducers were installed on spillway to see the pressure characteristic during the observation using various discharges. The location of the transducers can be seen in Figure 5.

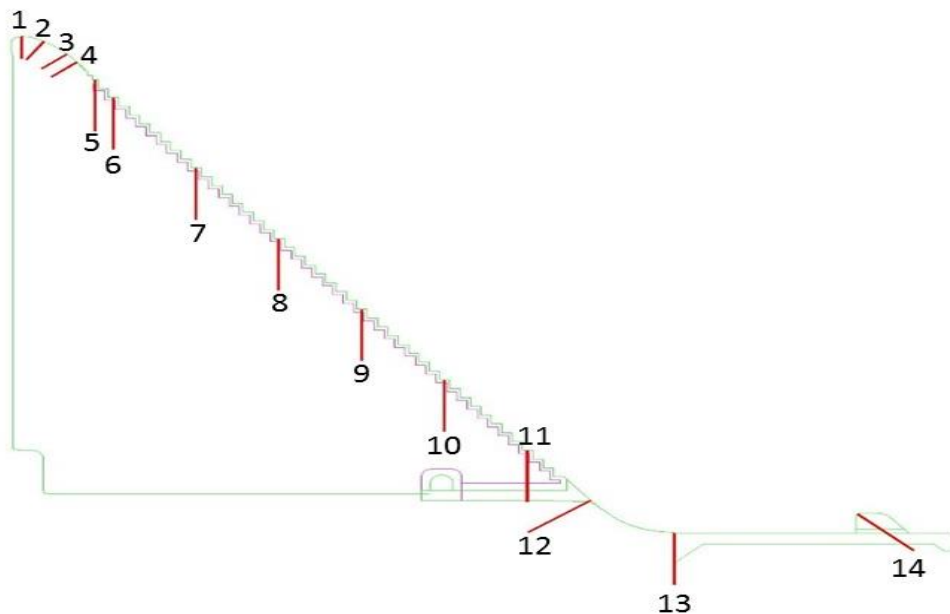


Fig. 5. Section view of pressure transducer layout on dam spillway

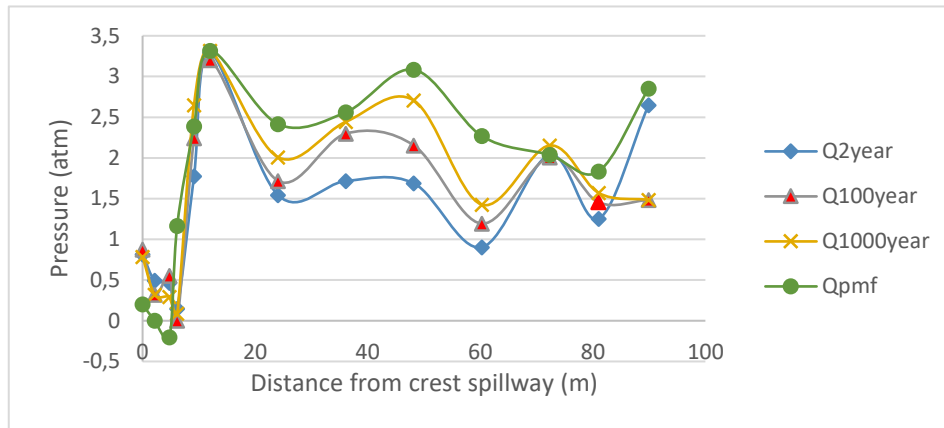


Fig. 6. Pressure distribution on dam spillway

Figure 6 indicates the pressure on each point of the location which described in Figure 5 where the transducers were installed. As can be seen that the pressure is vary along the spillway, some location has higher pressure due to turbulence and impact of the water with the stepped surface. The highest water pressure was shown at point 6 of tranducer location where the point of inception occurred. It is also found that negative pressure also occurred at point 3 of tranducer location where the transition zone from the smooth surface into stepped surface at Q_{pmf} . To avoid cavitation effects from this negative pressure, aerator can be implemented at the spillway to minimize the impacts.

3.3. SCOURING CONDITION

Scouring test were conducted for outflow discharge of period $Q_{100yrs} = 133 \text{ m}^3/\text{s}$ (See figure 7). Three scenarios were conducted, 1st scenario to study existing condition without downstream protection, 2nd and 3rd to study riprap protection.



Fig. 7. 1st scenario without downstream protection



Fig. 8. Upper Cisokan spillway model with discharge of $Q_{100\text{yrs}}$

Based on the experiment, the deepest local scour reaches -3 m measured from elevation El. $+729.00$ m, located at the toe of downstream left and right wing walls as can be seen in Figure 9. This scouring phenomenon may harm the structure, therefore downstream protection is needed.



Fig. 9. Scouring condition at downstream of spillway (Scenario 1)

To minimize the scouring effect at downstream of the spillway, the kinetic energy dissipation needs to be optimized using stone riprap. Considering available material on site, stone riprap protection is recommended to use as downstream protection because there are many stone quarry. Scenario 2 was conducted at the

laboratory, applying stone riprap with the diameter greater than 0,4 meters for downstream protection using U-shape pattern (See Figure 10).

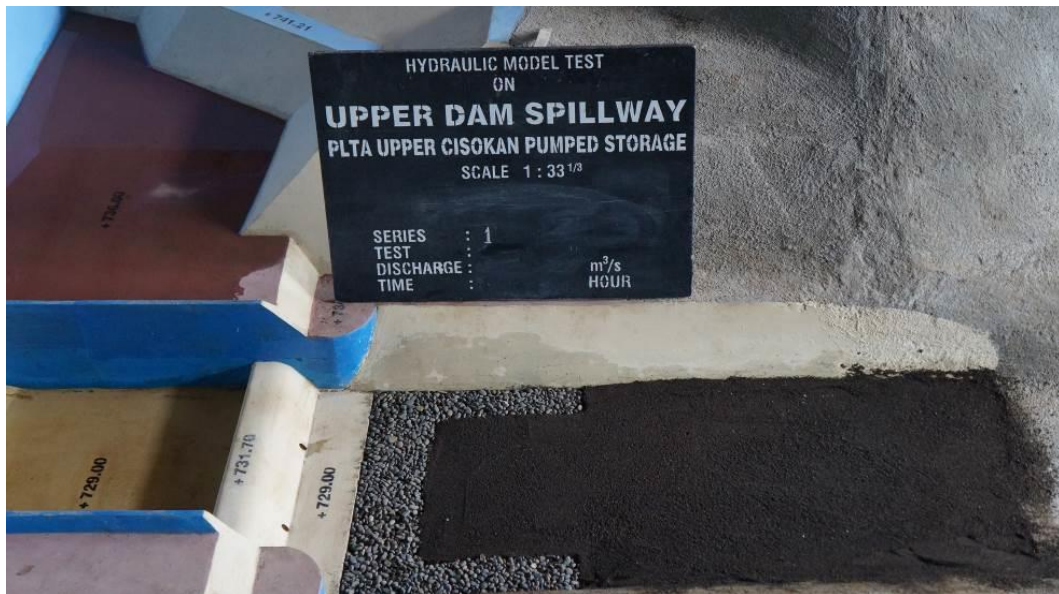


Fig. 10. Stone riprap for downstream protection (Scenario 2)

Various discharges applied to see the impact of the local scouring. According to the simulation results, there is a decline of maximum scouring depth from -3 meters in Scenario 1 to -1,5 meter in Scenario 2 as can be seen in Figure 11. This outcome shows that stone riprap protection is effective to use to reduce the impact of the scouring.



Fig. 11. Scouring condition at downstream of spillway (Scenario 2)

However, to protect and maintain the river bed downstream of the weir, Scenario 3 was applied by using fully stone riprap at downstream of the dam spillway. Based on the simulation, there was no scouring occurs (see Figure 12). Therefore, this condition can be preferred to be used as a final design of the dam in order to have a proper design of stepped spillway. Scouring comparison from 3 scenarios can be seen on Figure 13.



Fig. 12. Scouring condition at downstream of spillway (Scenario 3)

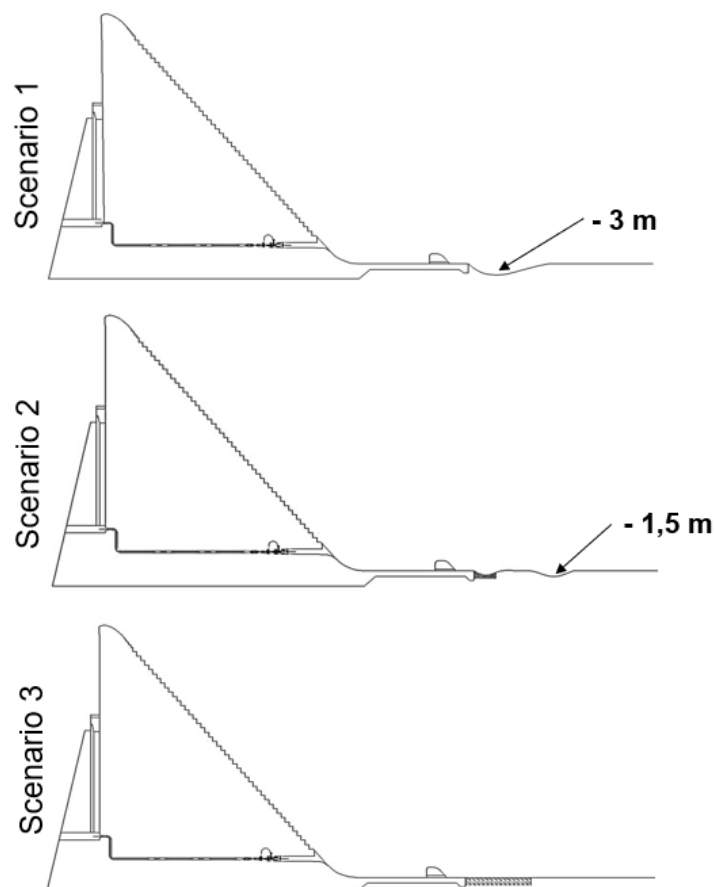


Fig. 13. Scouring comparison from different scenarios

According to the scouring results, scouring condition without downstream protection can be dangerous for the dam structure due to scouring problem. Downstream protection such as riprap can be a good solution for this issues as a transition zone from the massive structure and the river bed.

4. CONCLUSIONS

Upper Cisokan Dam was investigated using hydraulic laboratory experiments using various discharge. Based on the observation, it's known that water profile on stepped spillway at high discharge were dominant by skimming regime and already dissipated from the stepped chute to energy dissipator. Pressure distribution along the dam spillway is vary. It is also found that some negative pressure occurred. Therefore, if needed, aerator can be implemented to avoid cavitation effect. Based on its Froude number, the energy still not fully dissipated by the energy dissipator downstream of the spillway which may cause scouring. Hence, downstream protection such as riprap is needed to minimize the scouring effect. The final simulation shows that the stone riprap protection is effective to use to reduce the depth of the scouring from 3 meters into 0 meters. Ultimately, the stepped spillway can be implemented on the Upper Cisokan Dam after adding some additional treatment such as aerator and riprap protection.

5. ACKNOWLEDGEMENTS

The author also would like to thank Mrs. Yiniarti Eka Kumala for her valuable assistance that helped to improve the quality of this paper. Also for colleagues at Hydraulic Laboratory, Research Center for Water Resources, Ministry of Public Works and Housing for the support and opportunity to conduct dam investigation.

REFERENCES

- [1] Chanson H, Toombes L. Experimental Investigations Of Air Entrainment In Transition And Skimming flows Down A Stepped Chute. *Canadian J Civil Eng.* 29(1):145–156. 2002.
- [2] Chanson H. Forum Article: Hydraulics Of Stepped Spillways. *J Hydraul Eng,* 2000, 126(9): 636—637
- [3] Ohtsu I, Yasuda Y. Characteristics Of Flow Conditions On Stepped Channels. In: Holly Fm, Alsaffar A, Editors. *Proceedings Of 27th Iahr Congress, San Francisco, Usa, D,* 583–588. 1997.

- [4] Peyras, L., Royet, P. and Degoutte, G. 1992. Flow and Energy Dissipation over Stepped Gabion Weirs, *Journal of hydraulic Engineering, A.S.C.E.*, 118 (5):707-717.
- [5] Chanson, H. 1994. Comparison of Energy Dissipation Nappe and Skimming Flow Regime on Stepped Chutes. *Journal of Hydraulic Research, I.A.H.R.*, 32 (2): 213-218.
- [6] Rajaratnam, N. 1990. Skimming Flow in Stepped Spillways. *Journal of Hydraulic Engineering, A.S.C.E.*, 16 (4): 587-591.
- [7] Rice, C. E., and K. C. Kadavy. 1996. Model study of a roller compacted concrete stepped spillway. *J. Hydraul. Eng. ASCE* 122(6): 92-297.
- [8] Yasuda, Y., and I. Ohtsu. 1999. Flow resistance of skimming flow in stepped channels. In *Proc. 28th IAHR Congress, Session B14. International Association for Hydro-Environment Engineering and Research.*
- [9] Chanson, H., and L. Toombes. 2002. Energy dissipation and air entrainment in a stepped storm waterway: An experimental study. *J. Irrig. and Drainage Eng. ASCE* 128(5): 305-315.
- [10] Boes, R. M., and W. H. Hager. 2003a. Two-phase flow characteristics of stepped spillways. *J. Hydraul. Eng. ASCE* 129(9): 661-670.
- [11] Gonzalez, C. A. 2005. An experimental study of free-surface aeration on embankment stepped chutes. PhD diss. Queensland, Australia: University of Queensland, Department of Civil Engineering.
- [12] Takahashi, M., Y. Yasuda, and I. Ohtsu. 2005. Effect of Reynolds number on characteristics of skimming flows in stepped channels. In *Proc. 31st Biennial IAHR Congress, 2880-2889. B. H. Jun, S. I. Lee, I. W. Seo, and G. W. Choi, eds. International Association for Hydro-Environment Engineering and Research.*
- [13] Hunt, S. L., and K. C. Kadavy. 2007. Renwick dam RCC stepped spillway research. In *Proc. ASDSO Annual Meeting, CD-ROM. Lexington, Ky.: Association of State Dam Safety Officials.*
- [14] Hunt, S. L., and K. C. Kadavy. 2008. Velocities and energy dissipation on a flat-sloped stepped spillway. *ASABE Paper No. 084151. St. Joseph, Mich.: ASABE.*
- [15] Felder, S., and H. Chanson. 2008. Turbulence and turbulent length and time scales in skimming flows on a stepped spillway: Dynamic similarity, physical modeling, and scale effects. Queensland, Australia: University of Queensland, Division of Civil Engineering.
- [16] Boes R M, Hager W H. Hydraulic design of stepped spillways. *J Hydraul Eng*, 2003, 129(9): 671—679

COMMISSION INTERNATIONALE
DES GRANDS BARRAGES

VINGT-SIXIÈME CONGRÈS DES
GRANDS BARRAGES
Autriche, juillet 2018

REMOTE INSPECTION OF SMALL DAMS AND LEVEES*

Bill SHERWOOD

Business Development, ASI MARINE, ST. CATHARINES

CANADA

1. INTRODUCTION

Inspections of small dams can present challenges that hinder comprehensive condition assessment. These can include health and safety of personnel, limited access to the inspection area, and water conditions. Each project brings unique complexities, so is important to assess and consider a range of technology and equipment. In this paper, we will review a project where methodology was amended to suit site conditions.

2. METHODS

The original proposed solution to complete this specific dam inspection was to utilize an inspection vessel equipped with sonar systems for data collection. However, as water levels were discovered to be too low for vessel operations, an alternative solution was required. Therefore, a comparative study of technology and equipment suitable for the project was analyzed. In the end, the project involved design and fabrication of an unmanned surface vessel (USV), which was identified as the safest and most adaptable platform for site conditions.

3. RESULTS

The result was an inspection that provided high-resolution georeferenced bathymetry expressed as point cloud data, crack detection, and spall crack size.

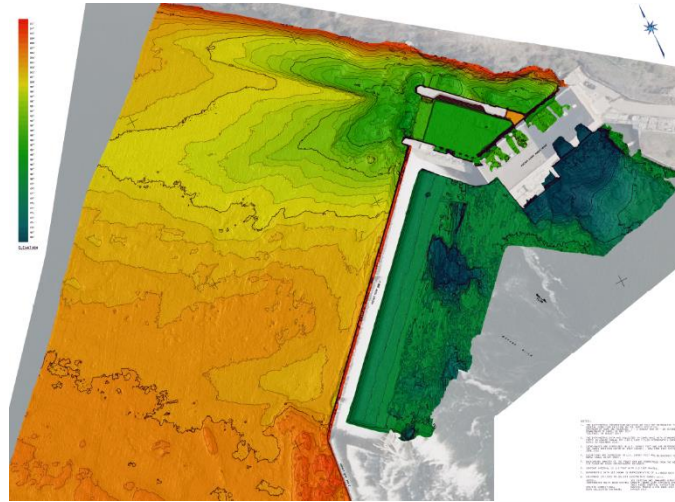


Fig 1. Bathymetric Contour Map of Dam Reservoir and Spillway

4. CONCLUSION

Underwater survey sites can present unique challenges, especially near dams where water level conditions can change dramatically. In the case of unforeseen low water, access to key shallow areas can become impossible using manned vessels or even ROVs, both of which require sufficient draft to maneuver. In the case of personnel on the water, safety is of course the primary concern. Shallow water is still dangerous. Work vessels can strike rocks or become grounded. It only takes about 20 cm of swift moving water to knock someone off their feet. Cold water only adds to the dangers. Additionally, sensors need to be deployed as close as is practicable to the water surface, and ROVs and the underwater portion of the hull of manned boats would partially block the sensor field. This would require additional maneuvering to ensure coverage of shadow areas.

The USV solved these problems firstly by removing most of the danger to human life. Shoreside safety precautions were no less important, but overall the field aspects of this program was far safer and more efficient. Additionally, data collection was done more efficiently and to a higher consistent standard.

COMMISSION INTERNATIONALE DES GRANDS BARRAGES

VINGT-SIXIÈME CONGRÈS DES GRANDS BARRAGES
Autriche, juillet 2018

DOI 10.3217/978-3-85125-620-8-059



This work licensed under a Creative Commons Attribution 4.0 International License. <https://creativecommons.org/licenses/by-nc-nd/4.0/>

**HOW TO DEAL WITH AGING PRESTRESSED ANCHORS IN DAMS: A
NORTH AMERICAN PERSPECTIVE**

Donald A. BRUCE

President, GEOSYSTEMS, L.P.

U.S.A.

John S. WOLFHOPE

Vice President, FREESE AND NICHOLS, INC.

U.S.A.

COMMISSION INTERNATIONALE
DES GRANDS BARRAGES

VINGT-SIXIÈME CONGRÈS DES
GRANDS BARRAGES
Autriche, juillet 2018

HOW TO DEAL WITH AGING PRESTRESSED ANCHORS IN DAMS: A NORTH AMERICAN PERSPECTIVE *

Donald A. Bruce¹ and John S. Wolfhope²

¹ *President, GEOSYSTEMS, L.P.*

² *Vice President, FREESE AND NICHOLS, INC.*

U.S.A.

1. INTRODUCTION

Prestressed rock anchors have been installed in dams throughout the world since 1934. In the U.S., the first installation was in 1964. Since then, well over 400 case histories have been recorded by the authors [1] [2] [3]. Practice has evolved over the years, governed by, and reflected in, successive editions of the Post-Tensioning Institute's "Recommendations" documents. Since 1996, virtually all projects have been completed using what may reliably be referred to as "Permanent" anchor systems (i.e., with PTI Class I Protection) and responsive drilling, water testing, and grouting methodologies. However, older-vintage anchorage systems did not generally include corrosion protection systems which would be acceptable today, and did not generally provide the means to measure residual load or the state of corrosion in-situ. This is a challenge facing dam owners throughout the world, since early anchor technology was largely driven by a limited number of European post-tensioning suppliers operating internationally.

* COMMENT TRAITER LES ANCRAGES PRÉCONTRAINTES DE VIEILLISSEMENT DANS DES BARRAGES :
UNE PERSPECTIVE NORD-AMÉRICAINNE

2. THE EVOLUTION OF CONTEMPORARY PRACTICE

2.1 REFERENCEABLE STANDARD OF CARE

There is no standard, per se, for rock anchoring in the U.S. However, the current governing document is “Recommendations for Prestressed Rock and Soil Anchors,” Fifth Edition, 2014, published by the Post-Tensioning Institute [4]. This document, like its predecessors, was developed by a Committee of industry specialists and practitioners, an equal blend of consultants, contractors, suppliers, and regulators/ clients (Table1). The previous four editions (1980, 1986, 1996 and 2004) were in fact preceded in 1974 by the “Tentative Recommendations” document for the Prestressed Concrete Institute which, as the breakdown of Table 2 clearly illustrates, was principally a marketing and sales tool whose goal was to present illustrated applications to expand sales volumes of prestressing steel.

Table 1
Number and affiliations of ACI/PTI Prestressed Rock
and Soil Anchor Committee members.

ASPECT	1974	1980	1986	1996	2004	2014
Post-Tensioning Suppliers	6 [†]	4*	4*	2*	3*	4
Anchor Contractors	2	2	3	3	3	3*
Consultants	2	None	1	2	2	2
Owners/Regulators	1	2	1	3	3	3
Sponsor Organizations	1	None	0	1	1	2
TOTAL	12	8	9	11	12	14

- * Including the same Chairman from DSI (Post-Tensioning Supplier).
- † Chairman from VSL (Post-Tensioning Supplier).
- Chairman from Schnabel Foundations (Specialty Contractor).

Table 2
Number of pages of major sections of the PTI Recommendations.

ASPECT	1974	1980	1986	1996	2004	2014
Materials	1	2	2	8	10	10
Site Investigation	0	1	1	1	2	2
Design	2	6 ½	6 ½	12+ Appendix on grout/ strand bond	13	13
Corrosion Protection	1	4	5	10	14	15
Construction	7	9	9	10	15	17
Stressing and Testing	1	6	8	17	18	19
Bibliography/References	0	1	1	1 ½	4	3

(continues)

ASPECT	1974	1980	1986	1996	2004	2014
Applications	16	18	0	0	0	0
Recordkeeping	0	1	1	1 ½	1 ½	2
Specifications, Responsibilities and Submittals	0	1	1 ½	2	2	2
Epoxy-Coated Strand	0	0	0	No separate section	10	10
TOTAL PAGES	32	57	41	70	98	109

In this regard, it may be noted that, in the earlier days of practice in the U.S., anchoring was a technique pioneered by the post-tensioning suppliers themselves, subcontracting out to specialty geotechnical contractors the “dirty bits,” i.e., the actual drilling, water testing, tendon placement and grouting processes. This tendency was reversed by the early 1980’s: in the U.S. the geotechnical contractors win the projects, buy the steel and frequently rent the prestressing equipment.

Again it is reiterated that industry operates under a set of “Recommendations” provided by an ad hoc committee of a Trade Association, i.e., the Post-Tensioning Institute. However, for liability reasons, industry treats the Recommendations virtually as a standard, and it is very rare for any significant deviation to be found in Specifications or associated Method Statements. In the authors’ experience, the “Recommendations” constitute excellent, comprehensive and practical guidance, and stand in very favorable comparison with more rigorous European standards and guidelines.

The Recommendations do not provide guidance on the analysis or overall design of an anchored structure (e.g., selection of number and capacity of anchors, their length, spacing and inclination), for that is the responsibility of the Engineer-of-Record, using well established methods of rock mechanics and structural engineering. The Recommendations address the design, construction, testing and performance of individual anchors.

2.2 EVOLUTION OF PRACTICE

This is covered in detail in the papers contained in the References, and only a very brief summary is provided hereunder, insofar as the points have relevance to the assessment of aging anchors.

2.2.1 Design

Excluding, for the moment, the critical issue of corrosion protection, it may be concluded that most key elements of design have been little changed over the years, and so remain as described in Littlejohn and Bruce’s State of the Art Study [5]. It is tacitly assumed that load transfer mechanisms in and around the bond

length are based on uniform bond distribution. Although inaccurate, this is a conservative assumption.

2.2.2 Construction Practices

While most drilling was done in early projects by coring (for fear of somehow damaging the dam, and to extract samples of bedrock in the bond zone), current drilling practice features rotary percussive methods, and especially Down-the-Hole Hammers (DTHH). Grout mix designs, grout blending (in a high speed, colloidal mixer) and placement (always via tremie) have changed only insofar as equipment has improved. Water pressure testing (and pregrouting if necessary) has always been of a high and conscientious standard, and this is of great importance when trying to evaluate the reliability of legacy anchors.

Equally important are the changes to the grouting/stressing sequence:

- (i) Prior to the use of sheathing on the free length of the tendon components, the sequence was:
 - drill, water test (and pregrout and redrill if necessary),
 - place the tendon,
 - grout the bond zone,
 - stress, test and lock-off,
 - grout the free length.
- (ii) After the use of sheathing on the free length of the tendon components, the sequence was:
 - drill, water test (and pregrout and redrill if necessary),
 - place the tendon,
 - grout the tendon completely,
 - stress, test and lock-off,
 - complete underhead grouting.

Most of the early anchors had tendons comprising a multitude (“bundle”) of 6 mm diameter wires (Figure 1). These wires were typically fully bonded to the concrete of the dam by the free length (secondary) grouting after prestressing and lock-off. Thus, such anchors have only grout for corrosion protection and cannot be lift-off tested to establish residual load in the tendon.

2.2.3 Stressing and Testing

Early stressing and testing procedures were surprisingly simple (given the sophistication of the original European post-tensioning specialists), and remained so in the U.S. until the 1996 Recommendations. Thus, it is typical that legacy anchors were quickly stressed to the Test Load in progressive steps, held there for a short period (but without a quantified creep criterion) and then destressed to the lock-off (or “transfer”) load. The benefits of progressive cycle loading, with well-defined criteria for creep and elastic analyses, cannot be exploited when evaluating contemporary records of legacy anchors, while Lift-Off Testing was optional and, in any case, of quite short-term duration (say 48 hours).

2.2.4 Corrosion and Corrosion Protection

References [1] and [2] provide an analysis of the PTI Recommendations to that point (i.e., including the 2004 version) and a summary of over 400 individual case histories. Note that the provisions of the PTI 2014 edition are sensibly the same as in 2004, while the database has recently been further updated [3]. It is extremely important in the context of legacy anchors to gain perspective of contemporary attitudes, and the development of these attitudes with time.

In summary, the anchor grout itself was regarded, during the early decades of practice, as an acceptable barrier to corrosion, for both the bond and free lengths. It was only with the 1996 version of the PTI Recommendations that full-length protection by at least one plastic sheath was required for permanent anchors, i.e., Class I protection, so matching contemporary standards of care in Europe (Figure 1).

3. CHALLENGES TO EVALUATING LEGACY ANCHORS

There are many challenges relating to the design and the construction of such anchors, and to practical/logistical aspects of condition assessment. These challenges are common to dam Owners and Regulators throughout the dam anchor world.

Firstly, it is clear that the majority of dam Owners and their consultants simply did not contemplate at the time of design and construction that long-term monitoring would be advantageous, let alone fundamental to risk management. The general philosophy was that anchors designed and constructed to the standards of the day would not corrode since the steel would be encased in grout, and placed into boreholes whose immediate proximity was pregrouted (to prevent water ingress and to prevent anchor grout loss). The anchor head itself was generally encased in concrete. Further, in acknowledgement that the tendon would naturally suffer long-term stress loss (principally due to relaxation), the post-tensioning specialists selected Lock-Off/Transfer Loads, which included an allowance for these losses, the magnitude and rate of which were well known from structural post-tensioning projects. Such elevated tendon stress levels, while (usually) still within the elastic response range (i.e., $\leq 80\%$ fpu), would however increase the tendency for stress-induced corrosion to be initiated or accelerated under certain conditions. No provisions were made for installing restressable anchor heads.

Secondly, it was exactly these old methods which have now rendered lift-off testing unfeasible: without a developed free length, it is impossible to directly measure the residual load in the tendon, or to determine its distribution within the free length or, of course, the bond length.

Thirdly, it is often the case that the anchor heads are, for all practical purposes, inaccessible for any type of inspection or testing. In some cases, the functional anchor heads could be rendered accessible, but there would be a natural reticence to “probe too deeply” for fear of disturbing the anchor head – not so much from a load holding viewpoint, as the tendon is fully bonded below, but from the corrosion protection viewpoint. This is particularly the case with legacy anchors which do feature a greased and sheathed coating as a bond

breaker to preserve the true free length even when surrounded by grout. In this case, the load is still maintained by the gripping wedges in the head (in the case of strands), or by the lock nut (in the case of bars), and attempts to expose such heads, or indeed to attempt, somehow, a lift-off test, would be inviting trouble.

Fourthly, strain gages or load cells of adequate reliability were simply not available to provide long-term monitoring capability, and indeed are still not available today. Compounding this issue is the stark fact that there is still no completely reliable, calibrated NDT Method that can be used to check the residual load, or the integrity, of wire or strand tendons, fully grouted or otherwise. It may be noted, however, that some recent methods are showing promise for bar tendon assessments.

Fifthly, contemporary construction records may not always be available for review and, even if they are, they may not contain vital pieces of information, the clues to the likely adequacy of the construction details to preventing long-term corrosion. A case in point here would be the static (bleed) and dynamic (pressure filtration coefficient) stability properties of the grouts: if either property were deficient, then bleed pockets would develop, especially in the tightly arranged “bundles” of wires so common in early legacy anchors.

Sixthly, it is not uncommon for Owners to consider somehow exhuming production anchors and then closely examining the tendon for signs of corrosion. Exhumation is feasible if the dam is being deconstructed for decommissioning. This is a relatively rare occurrence and of course is not an option for evaluating legacy anchors in dams required for extended, long-term service. Alternatively, it is technically feasible – if sufficient access exists to allow for the mobilization of a major piece of drilling equipment – to overcore the entire anchor and remove it for inspection. However, this is a very difficult and typically costly option since the drilling method must be precisely colinear with the anchor, and the tendon will not permit the anchor to be removed in convenient “runs,” for example, of 1.5 or 3.0 m. Furthermore, the grout is typically damaged or lost in the drilling process, and the concern will remain if the particular anchor removed is actually representative in its condition of the others, or if any localized corrosion-induced damage will indeed be recognized.

As a final point, it is easy to be critical of the contemporary standards used in the design and construction of legacy anchors. However, at the time of their installation, design lives of 25-30 years were considered satisfactory, whereas some of these installations are now over 50 years old. “Modern” anchors (with Type I Corrosion Protection) are children of the late 1990’s, and a great deal of knowledge has been accumulated since then fuelled, in part, by our current attitudes to risk assessment such as inherent in the Potential Failure Modes Analysis process.

4. KEY FACTORS IN RISK EVALUATION DURING A PORTFOLIO RISK ASSESSMENT PROCESS

In the case where an Owner is responsible for a number of projects dependent for stability on prestressed rock anchors, it is logical and essential to conduct a preliminary screening process to identify and prioritize the most worrisome projects. This is akin to the process first adopted by the U.S. Army

Corps of Engineers in 2005-2006 to allocate a Dam Safety Action Category (DSAC) number (I to VI) to each of its portfolio of over 600 structures. This categorization process then allowed attention to be paid to the “worst first” dams (i.e., DSAC I) in terms of the need for Interim Risk Reduction Measures (IRRM’s) to be emplaced pending the design and construction of Permanent Risk Reduction Measures in the form of Dam Safety Modifications (DSM’s). For the typical dam Owner, the number of dams to be evaluated can be reasonably covered by the same dedicated team, so assuring a very even-handed, and uniform quality of assessment of the portfolio. Such an approach has recently been adopted widely, including as an important example, by the Tennessee Valley Authority.

The Portfolio Risk Assessment process for aging anchors in N. America is a desk study in which the following steps should be taken, in sequence:

Step 1. Determine the date of anchoring, and the edition of the PTI (or ACI) Recommendations under which the anchors were installed. The following risks can be allocated as a “first cut”:

- All anchors installed prior to PTI (1986): High Risk
- Anchors installed 1986-1996 prior to PTI (1996): Moderate Risk
- Anchors installed post-1996 after PTI (1996): Low Risk

It should be noted that practitioners often continue to use an “old” edition of PTI for say 2 years after the “new” edition has been issued. So it would be prudent to amend the “High” category limit from 1986 to 1988, and the “Moderate” category from 1988 to 1998.

Step 2. Beginning with the oldest anchor project in the High Risk Group, very carefully examine all historical records for that project. In particular, the type of tendon (wire, bar, or strand) and the type of corrosion protection (if any, other than cement grout) should be identified. In addition, whether or not a free length actually remains or whether the free length steel is fully bonded to the concrete should be established, together with an understanding of the anchor head protection detail.

Anchors installed with no corrosion protection other than the grout are highest risk, together with anchors whose heads were encased in material other than grout or concrete (e.g., grease, or indeed without any protection). Anchors with no remnant free length, as typified by the multiwire “button head” tendons, cannot have their integrity or residual load measured, even if the heads are accessible.

The source details include the project specifications, the contractor’s method statement and construction records, construction photographs, and any information or observations on post-construction testing or performance.

For High Risk anchors, without sheathing or coating on the free length, a consideration of the intensity and quality of the pregrouting should be conducted. If none were conducted, the risk of long-term corrosion occurring is greater than if intensive pregrouting had been conducted.

Step 3. Beginning with the prioritized list created by Steps 1 and 2, review the original overall anchor design to judge exactly how vital the anchors are to overall stability, and how much overall prestress can be lost (to corrosion, relaxation and creep) before the structure does not meet contemporary standards of care, for sliding and/or overturning, or other loading conditions.

Step 4. Focusing, then, on the “High Risk” list created by Steps 1-3, the Owner/ Regulator must then make a risk-based decision regarding actions to be taken on these projects. Owners with a very low risk tolerance will elect to ignore the legacy anchors and replace them entirely (if space and access permit).

Owners who can tolerate a higher risk may elect for either partial replacement, or indeed for no further post-tensioning at all, and some type of “observation” strategy.

Step 5. Once the “High Risk” projects have been evaluated thus, then the same process can be applied to the “Moderate Risk” projects. Such projects may also afford the possibility of conducting lift-off tests provided the free length is sheathed, the anchor head is accessible, and the field testing will not adversely affect the structural performance of the locking assembly (especially for wedges for strands) or its corrosion integrity.

This process is summarized in the flow diagram (Figure 2) which focuses on high risk legacy anchors. Thus, a project which scores “high-high-high-high-high” in each risk category will have a more urgent need of further action/evaluation, than one which scores, for example, “high-high-high-moderate-low.” This figure only shows the flow path for the highest risk anchors.

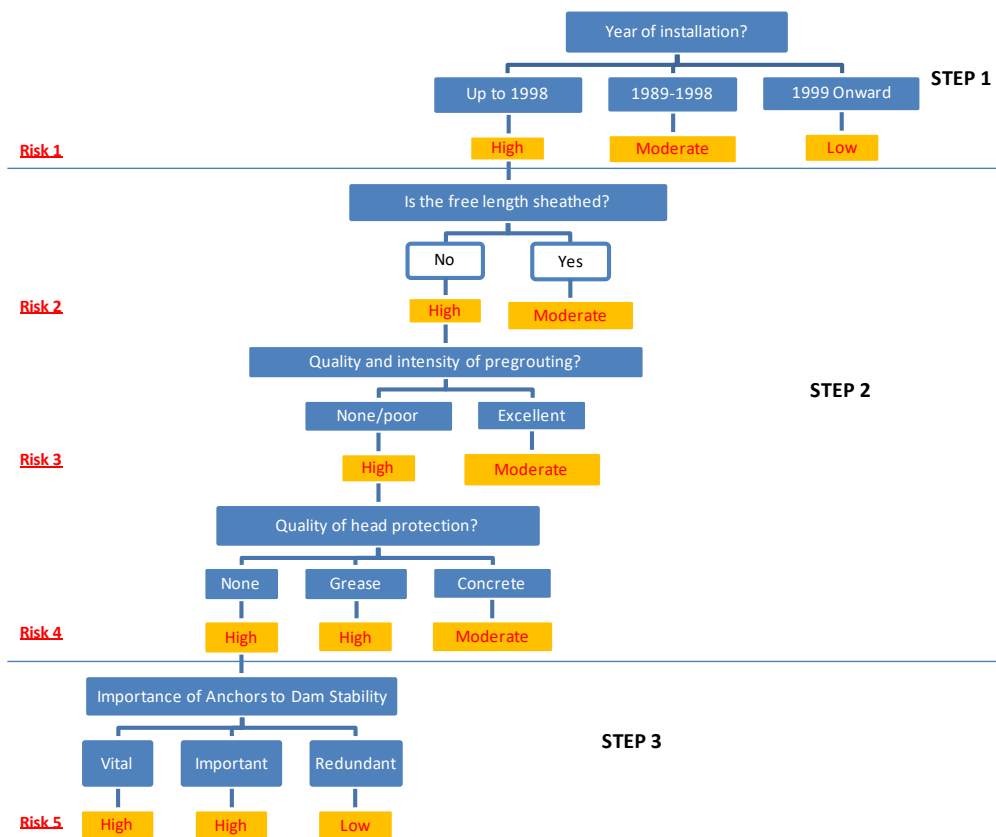


Fig. 2
Flow chart for screening portfolio risk assessment of aging anchors.

REFERENCES

- [1] BRUCE, D.A., AND J. WOLFOPE (2007). “Rock Anchors for North American Dams: The National Research Program Bibliography and Database,” Institution of Civil Engineers, Ground Anchorages and

- Anchored Structures in Service, November 26-27, London, England, U.K., 11 p.
- [2] BRUCE, D.A., AND J. WOLFHOPE (2007). "Rock Anchors for North American Dams: The Development of the National Recommendations (1974-2004)," Institution of Civil Engineers, Ground Anchorages and Anchored Structures in Service, November 26-27, London, England, U.K., 11 p.
- [3] BRUCE, D.A., J.S. WOLFHOPE AND J.D. WULLENWABER. (2013). "Rock Anchors for Dams: A Five-Year Update," 33rd USSD Annual Meeting and Conference, Glendale, AZ, February 11-15, 10 pp.
- [4] POST TENSIONING INSTITUTE (PTI). (2014). "Recommendations for Prestressed Rock and Soil Anchors," Farmington Hills, Michigan, December 8, 109 p.
- [5] LITTLEJOHN, G.S. AND D.A. BRUCE. (1977). "Rock Anchors - State of the Art." Foundation Publications, Essex, England, 50 p. (Previously published in Ground Engineering in 5 parts, 1975-1976.)

SUMMARY

The evolution of practice in the design and construction of prestressed rock anchors for North American dams is described. This provides background to the problem of assessing the reliability of aging anchors, principally those installed prior to 1996. This review is based on the results of a study of over 400 case histories of projects completed since 1964.

L'évolution de la pratique courante en conception et construction avec ancrages précontraints dans le roc pour les barrages nord-américains est décrite dans cet article. Il fournit le contexte du problème d'évaluation de la fiabilité des ancrages en service, majoritairement ceux installés avant 1996. Cette revue s'appuie sur plus de 400 études des cas des projets achevés depuis 1964.

KEYWORDS

Aging, anchorage, concrete dam, inspection, prestressing, risk assessment.

Vieillessement, ancrage, barrage en béton, visite, précontrainte, analyse de risque.

COMMISSION INTERNATIONALE DES GRANDS BARRAGES

VINGT-SIXIÈME CONGRÈS DES GRANDS BARRAGES

Autriche, juillet 2018

DOI 10.3217/978-3-85125-620-8-060



This work licensed under a Creative Commons Attribution 4.0 International License. <https://creativecommons.org/licenses/by-nc-nd/4.0/>

DAM SAFETY MONITORING IN EXTREMELY CONDITIONS

S.J. WANG

NANJING HYDRAULIC RESEARCH INSTITUTE
DAM SAFETY MANAGEMENT CENTER OF THE MINISTRY OF WATER
RESOURCES

CHINA

Y.X. WU

NANJING HYDRAULIC RESEARCH INSTITUTE
DAM SAFETY MANAGEMENT CENTER OF THE MINISTRY OF WATER
RESOURCES

CHINA

Q.PANG

NANJING HYDRAULIC RESEARCH INSTITUTE
DAM SAFETY MANAGEMENT CENTER OF THE MINISTRY OF WATER
RESOURCES

CHINA

Y.C.GU

NANJING HYDRAULIC RESEARCH INSTITUTE
DAM SAFETY MANAGEMENT CENTER OF THE MINISTRY OF WATER
RESOURCES

CHINA

DAM SAFETY MONITORING IN EXTREMELY CONDITIONS

S.J. WANG^{1,2}, Y.X. WU^{1,2}, Q.PANG^{1,2}, Y.C.GU^{1,2},

1. *Nanjing Hydraulic Research Institute*
2. *Dam Safety Management Center of the Ministry of Water Resources*

CHINA

1. INTRODUCTION

With global climate change, extreme events such as floods, rainstorm, typhoon, earthquake are frequent nowadays. Ten floods occurred in Yangtze, Huanghe, Huaihe, Zhujiang, Songhuajiang Rivers and 20 sub-rivers encountered extra-history floods in 2017. There are 27 typhoons in western pacific and 8 numbers landing on China in 2017. There are 8 times of earthquake extra 7 magnitude in the world and 19 times of earthquake extra 5 magnitude in China.

The above extreme events may lead dam incidents or even failure. More than 2000 reservoir dams were damaged following the Wenchuan earthquake of magnitude scale 8 in May 12, 2008. More than 3000 dams breached since 1954 in China. Overtopping, abnormal seepage, structural instability and earthquake are common dam accidents and major unexpected events.

2. EMERGEMCY MONOTROING

Dam safety monitoring following the unexpected events and accidents is essential for emergency action, which prevent or mitigate hazard, emergency inspection, monitoring techniques for the above extreme events and probable accident are studied below.

2.1. PRINCIPLE

Emergency monitoring should be rapid and efficient. The hereinafter should be followed.

(1) A detailed inspection and monitoring plan should be made in advance based on the dam danger type, dam danger consequences and risk degrees. The inspection and monitoring should be combined, and the related monitoring items should be monitored synchronously.

(2) Portable monitoring equipments should be the first selection for emergency monitoring, and the layout of monitoring equipments should be accessible and convenient. The technical performance of monitoring equipments can meet the requirements in extreme conditions. The installation of the instruments should minimize the impact on the safety of the project and avoid aggravating the occurrence of emergencies.

(3) The emergency monitoring methods should be fast, simple, practical, accurate and reliable. The automatic observation should be adopted to improve the efficiency and frequency of the monitoring if it is possible.

(4) The emergency monitoring frequency should be determined by the development speed and degree of the emergency, and the variation of observation values should be monitored. When the degree of emergency became more serious, the monitoring frequency should be increased.

(5) Information of the record should be normative and integrated, including emergency types, emergency degrees, weather conditions, monitoring items, monitoring methods, monitoring frequency, monitoring date, monitoring value, etc. Monitoring data analysis should focus on comparison of historical data and data after the occurrence of events.

2.2. DAM UNEXPECTED EVENT GRADING

Four grades of dam unexpected events are classified according to emergency degree and hazard consequence. The classification standard in China is show in Table 1. When the dam unexpected events grades determined by different standards are inconsistent, whichever is the highest.

Table 1
The classification standard of dam unexpected events

Grade I	Grade II	Grade III	Grade IV
Reservoir water level surpass maximum flood level	Reservoir water level surpass design flood level	Reservoir water level surpass top of level of flood control	Reservoir water level surpass level of flood control
Fatal incidents uncontrolled, probably failure	Fatal incidents but can be controlled	Serious incidents convenient-controlled	Ordinary incidents convenient-controlled

Grade I	Grade II	Grade III	Grade IV
More than 30 death loss	10~30 death loss	3~10 death loss	Less than 3 death loss
Economic loss more than 100millions RMB	Economic loss between 100millions and 50millions RMB	Economic loss between 50millions and 10 millions RMB	Economic loss less than 100millions RMB
Extraordinary serious social and environment impacts	Serious social and environment impacts	Greater social and environment impacts	Ordinary social and environment impacts

2.3. MONITORING ITEM FOR THE UNEXPECTED EVENTS AND ACCIDENTS

2.3.1. OVERTOPPING

Floods, insufficient discharge spillway, malfunction of gates, blocks on spillway may lead dam overtopping. Inspection should be focused on spillway, gates, and unstable slopes around spillway. Unmanned aerial vehicle (UAV) may be applied. Water level, rainfall, inflow and outflow discharge, deformation, seepage pressure and seepage discharge should be monitored, which is shown in Table 2. Spillway pulverization should be monitored during flood discharge.

Operation management problems such as gate and hoist can't work normally and spillway blocking problems resulted from big volume floater and spillway slope instability are major reasons for overtopping and even dam failure of embankment dams. Therefore, according to the weather forecast, when an extra-standard flood occurred, reservoir management department should immediately check that whether the dam, the bank slope close to the dam and the spillway slope have signs of erosion, crack, collapse and slide. Condition of the drainage facilities should also be checked, including whether the gate and the hoist can work normally, whether the spillway is blocked or not. The monitoring items for flood overtopping dam failure mode include water level, rainfalls, inflow and outflow discharge, deformation, seepage pressure, seepage discharge and discharge flood pulverization. Among them, water level, rainfalls, inflow and outflow discharge are the key monitoring items, while deformation and seepage are the important monitoring items, and other monitoring items can be monitored in a synchronized manner according to the actual situation.

Compared with satellite remote sensing and manned aircraft remote sensing, unmanned aerial vehicle(UAV) remote sensing technology has real-time transmission of large-scale image data, which is suitable for emergency inspection under flood condition.

In order to avoid the occurrence of overtopping, the flood water should be released by open the gate in time. But the pulverization caused by the flood discharge will affect the stability of the slopes on both sides of the spillway, so it is necessary to monitor the discharge flood pulverization.

Table 2
Emergency monitoring items for flood overtopping

Number	Monitoring item	Grade			
		I	II	III	IV
1	Inspection	●	●	●	●
2	Water level	●	●	●	●
3	Rainfalls	●	●	●	●
4	Inflow and outflow discharge	●	●	●	●
5	Superficial deformation	●	●	●	○
6	Seepage pressure	●	●	●	○
7	Seepage discharge	●	●	●	○
8	Discharge flood pulverization	○	○	○	○

Notes: ● mandatory item, ○ optional item

2.3.2. ABNORMAL SEEPAGE AND STRUCTURAL INSTABILITY

Abnormal seepage and deformation may occur in dam. Variation of tendency should be more concerned during inspection and monitoring. Monitoring items for corresponding items are shown in table 3. Monitoring data should be analyzed in time.

Table 3
Emergency monitoring items for abnormal seepage and structural instability

Number	Monitoring item	Grade			
		I	II	III	IV
1	Inspection	●	●	●	●
2	Water level	●	●	●	●
3	Rainfalls	●	●	●	●
4	Seepage pressure	●	●	●	●
5	Seepage discharge	●	●	●	●
6	Surface deformation	●	●	●	●
7	Cracks	●	●	●	●
8	Underground water level	●	●	○	○

Notes: ● mandatory item, ○ optional item

2.3.3. EARTHQUAKE

The damages caused by earthquake are related with earthquake magnitude and distance from epicenter. ICOLD bulletin "Inspection of dam following earthquake guidelines" notes that dams around 25km, 50km, 80km, 125km and 200km from earthquake epicenter should be monitored for corresponding earthquake magnitude of 4.0, 5.0, 6.0, 7.0 and 8.0. Little dams are damaged below 4.0. Dams will be damaged seriously if magnitude in more than 7.0. Crack, leakage, structural

deformation and landslide are the major seismic hazards .The monitoring item is shown in table 4.

Table 4
Emergency monitoring items following earthquake

Number	Monitoring item	Grade			
		I	II	III	IV
1	Seismic acceleration	●	●	●	○
2	Inspection	●	●	●	●
3	Upstream and downstream water level	●	●	●	●
4	Rainfalls	●	●	●	●
5	Vertical and horizontal displacement.	●	●	●	●
6	Crack	●	●	●	●
7	Landslide	●	●	●	○
8	Seepage discharge	●	●	●	○
9	Seepage pressure	●	●	●	○

Notes: ● mandatory item, ○ optional item

2.4. MONITORING FREQUENCY FOR DIFFERENT ACCIDENTS

Monitoring frequency are suggested as the table 5 for overtopping, abnormal seepage and structural instability, earthquake.

Table 5
Emergency monitoring frequency for 1 day

Number	Monitoring item	Emergency degree			
		I	II	III	IV
1	Inspection	1	1~2	2~4	2~4
2	Water level	1~2	2~4	4~8	8~24
3	Rainfalls	1~2	2~4	4~8	8~24
4	Inflow and outflow discharge	1~2	2~4	4~8	8~24
5	cracks	1	1~2	2~4	4~8
6	Superficial deformation	1	1~2	2~4	4~8
7	Landslide surface deformation	1	1~2	2~4	4~8
8	Seepage pressure	1~2	2~4	4~8	8~24
9	Seepage discharge	1~2	2~4	4~8	8~24
10	Underground water level	1	1~2	2~4	4~8
11	Discharge flood pulverization	As required	As required	As required	As required
12	Seismic acceleration	Real time	Real time	Real time	Real time

Notes: Emergency degree include four levels namely IV, III, II, I, ranging from low to high according to the degree of urgency and consequence.

3. CONCLUSION

(1) Dam emergency monitoring should be quickly and effectively, and combined with inspection. Emergency monitoring will not only consider increasing the monitoring frequency of existing monitoring facilities, but also consider the addition of temporary monitoring facilities for new dam deficiency. Monitoring data analysis should focus on comparison of historical data and data after the occurrence of unexpected events. Monitoring items are related to dam unexpected events or dam dangers as well as degrees of dam unexpected events.

(2) Inspection should be focused on spillway, gates, and slopes around spillway. Unmanned aerial vehicle (UAV) may be applied. Water level, rainfall, inflow and outflow discharge, deformation, seepage pressure, seepage discharge should be monitored. Spillway pulverization should be monitored during flood discharge.

(3) Variation of tendency should be more concerned during inspection and monitoring for abnormal seepage and structural instability. Monitoring items should be corresponding with dam incidents. Monitoring data should be analyzed in time.

(4) The damages caused by earthquake are related with earthquake magnitude and distance from epicenter. The monitoring item is focused on crack, leakage, structural deformation, landslide and seismic acceleration.

4. ACKNOWLEDGEMENTS

This paper is sponsored by National Key R&D Program of China (grant number 2016YFC0401608) the Nonprofit Industry-Specific Research Project by Chinese Ministry of Water Resources (grant number 201501033) and the International S & T Cooperation Program of China (ISTCP)(grant number 2011DFA72810).

REFERENCES

- [1] SL/Z720-2015 Guidelines for emergency preparedness plan of reservoir dam safety management. *Beijing: China Water & Power Press*, 2015.
- [2] ICOLD (2016), Bulletin 166 inspection of dam following earthquake guidelines.
- [3] Wang SJ, Gu YC. Dam inspection following earthquake, *China Water-Resources*, 2012(6) 35-37.
- [4] Wang SJ, Ni XR, Gu YC, LONG WF. Features of seismic hazard in reservoir dams by the WENCHUAN earthquake, *Twenty-Fourth Congress on Large Dams*, June2-8, 2012 Kyoto, Japan:579-586.

- [5] Gu YC, Wang SJ. Analysis on prediction characteristic of reservoir dam emergent events, 2016(16):10-13.

SUMMARY

Floods, rainstorm, typhoon and earthquake are extreme events nowadays, which may lead dam incidents or even failure. Dam emergency monitoring is an essential non-engineering measure in emergency action for incidents hazard mitigation. The paper analyzes the features of the above extreme events and probable accidents. Emergency inspection procedures, monitoring techniques are presented.

Keywords: DAM EMERGENCY MONITORING, EXTRE EVENT, DAM INCIDENTS.

COMMISSION INTERNATIONALE DES GRANDS BARRAGES

VINGT-SIXIÈME CONGRÈS DES GRANDS BARRAGES
Autriche, juillet 2018

DOI 10.3217/978-3-85125-620-8-061



This work licensed under a Creative Commons Attribution 4.0 International License. <https://creativecommons.org/licenses/by-nc-nd/4.0/>

**GROUND VIBRATION CHARACTERISTICS INDUCED BY FLOOD
DISCHARGE OF A HIGH DAM: AN EXPERIMENTAL INVESTIGATION**

YAN Zhang

Engineer of Department of Structure and Material Engineering,
CHINA INSTITUTE OF WATER RESOURCES AND HYDROPOWER
RESEARCH, STATE KEY LABORATORY OF SIMULATION AND REGULATION
OF WATER CYCLE IN RIVER BASIN

GUOXIN Zhang

Director of Department of Structure and Material Engineering,
CHINA INSTITUTE OF WATER RESOURCES AND HYDROPOWER
RESEARCH, STATE KEY LABORATORY OF SIMULATION AND REGULATION
OF WATER CYCLE IN RIVER BASIN

YI Liu

Deputy director of Department of Structure and Material Engineering,
CHINA INSTITUTE OF WATER RESOURCES AND HYDROPOWER
RESEARCH, STATE KEY LABORATORY OF SIMULATION AND REGULATION
OF WATER CYCLE IN RIVER BASIN

SONGHUI Li

Senior engineer of Department of Structure and Material Engineering,
CHINA INSTITUTE OF WATER RESOURCES AND HYDROPOWER
RESEARCH, STATE KEY LABORATORY OF SIMULATION AND REGULATION
OF WATER CYCLE IN RIVER BASIN

CHINA

COMMISSION INTERNATIONALE
DES GRANDS BARRAGES

VINGT-SIXIÈME CONGRÈS DES
GRANDS BARRAGES
Autriche, juillet 2018

**GROUND VIBRATION CHARACTERISTICS INDUCED BY FLOOD
DISCHARGE OF A HIGH DAM: AN EXPERIMENTAL INVESTIGATION**

YAN ZHANG

*Engineer of Department of Structure and Material Engineering, China Institute of
Water Resources and Hydropower Research, State Key Laboratory of Simulation
and Regulation of Water Cycle in River Basin*

GUOXIN ZHANG

*Director of Department of Structure and Material Engineering, China Institute of
Water Resources and Hydropower Research, State Key Laboratory of Simulation
and Regulation of Water Cycle in River Basin*

YI LIU

*Deputy director of Department of Structure and Material Engineering, China
Institute of Water Resources and Hydropower Research, State Key Laboratory of
Simulation and Regulation of Water Cycle in River Basin*

SONGHUI LI

*Senior engineer of Department of Structure and Material Engineering, China
Institute of Water Resources and Hydropower Research, State Key Laboratory of
Simulation and Regulation of Water Cycle in River Basin*

CHINA

1. INTRODUCTION

As water utilization and demand for hydropower has expanded, the development of high dams containing large reservoirs have increased globally. Due to the high water head of a high dam with a large reservoir, vibrations caused by fluctuating flow loads generated by water energy can be transmitted underground to the surrounding area via the dam's foundations. Due to the "magnifying effect", vibrations can be enhanced when special ground conditions are present, an effect that will increase their impact on the surrounding environment [1]. Vibrations caused by high dam flood discharge, and their effect on the structural safety of surrounding buildings and the environment, as well as on the physical and mental health of the local population, have been recorded [2-4]. Therefore, research on this phenomenon is urgently needed.

Vibrations associated to high dam flood discharge have a close relationship with the hydrodynamic condition and dynamic characteristics of the discharge structures. As the mechanism of fluid-structure coupling vibration is fairly complex, the effective research method to solve the vibration problems induced by high dam flood discharge is to establish a fluid-structure interaction physical model through complete hydroelasticity simulation, and to undertake flood induced vibration tests [5-8].

In this study, by using a bottom-flow energy dissipation hydropower station in China as a case study, approaches to improve the traditional hydroelastic model for ground vibrations induced by flood discharge are proposed. The main factors influencing ground vibration intensity was studied by establishing a correlation system between the dam model and the actual ground in order to provide a theoretical basis to analyze vibrations and damping techniques for high dams.

2. EXPERIMENTAL PRINCIPLES

The hydroelastic experiment simulation of flow-induced vibrations simulates the fluid-structure interaction vibration system combined with "structure - water - foundation - dynamic load". The "dynamic load" input system similarity and the dynamic response similarity of structural systems are simultaneously required for the simulation, which means that the similarity of the hydraulic condition and the structural dynamic condition are simultaneously required [9].

The hydraulic similarity is the similarity of the "dynamic load" input system, and its essence is the similar law of fluctuating pressure in the hydraulic model designed by similar law of gravity. By comparing a series of scale model tests and prototype observations, it was found that the side fluctuating pressure, caused by flow separation or diffusion induced by the dramatic change of integral boundary and flow conditions, was mainly controlled by large-scale and low-frequency vortex motions. The large-scale vortex motion was successfully simulated in the model with a large enough Reynold's number, and fluctuating pressure can be extended

to the prototype according to the similarity law of gravity. This conclusion can be drawn based on water fall model tests under different scales (Fig. 1), and analysis of the prototype observation data from the Ertan hydropower station, Yalong river, China [10] (Fig. 2).

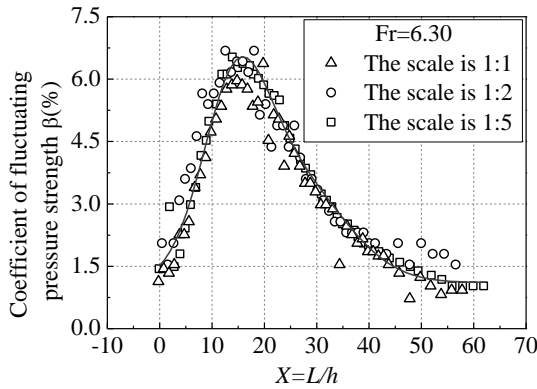


Fig. 1

Strength coefficient distribution of water fall fluctuating pressure

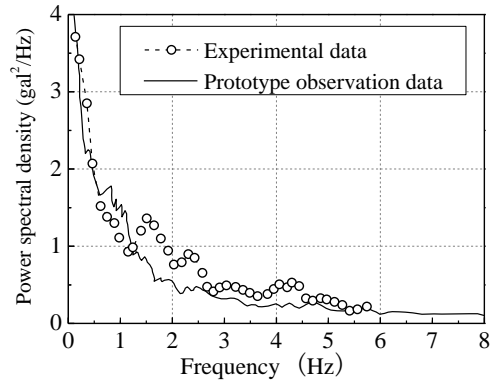


Fig. 2

Comparison between the prototype and model data of the fluctuating pressure frequency of the plunge pool in Ertan hydropower station (convert to prototype by gravity law)

The structural dynamic similarity, including geometric similarity, movement similarity and boundary similarity, refers to the similarity of the dynamic response of the structural system. This similarity is related to the frequency, vibration mode and damping of the structure.

According to the principle that the hydraulic similarity conditions is compatible with the structural dynamic similarity conditions, the hydroelastic model must adhere to the conditions of large density ($\lambda_\rho = 1$), a low elasticity modulus ($\lambda_E = \lambda_L$), an equal damping ratio ($\lambda_\xi = 1$), and an equal Poisson's ratio ($\lambda_\nu = 1$) [11].

3. RESEARCH BACKGROUND

The high concrete gravity dam at Jinsha River, China, was selected to be the study dam for our investigation. This dam has a crest elevation of 384.00 m and a crest length of 909.26 m; the maximum height of the dam is 162.00 m. The dam body consists of 12 surface holes and 10 mid-level outlets which are alternatively arranged and divided into two symmetrical energy dissipation zones by the middle guide wall. This arrangement form is a typical layout for a high dam with energy dissipation via a hydraulic jump.

The minimum and maximum distance between the hydropower station and the nearest urban area downstream is 0.5 km and 2.5 km, respectively. According

to observations, vibrations can be felt on the mountainside area near the county town downstream on the right bank, the vibration was magnified obviously in this region in the propagation process. Geological exploration results from the downstream area showed that the surface and foundation of that area consisted of sand layers and mudstones, respectively. An ancient channel with an average width of about 200 m was identified situated near the right-hand side of the mountain in the main urban area downstream; the maximum thickness of the covering layer over the ancient channel was 80 m. In comparison, the covering layer besides the ancient channel area covering layer of the other urban area had a significantly thinner thickness. The locations of the different regions are shown in Fig. 3.



Fig. 3

Schematic diagram of each region in the hydropower station dam area and the downstream area

4. THE ESTABLISHMENT AND IMPROVEMENT OF HYDROELASTIC MODEL

4.1. THE ESTABLISHMENT OF HYDROELASTIC MODEL

Before making the hydroelastic model, the foundation plain fill was excavated and replaced, reinforcement treatment was undertaken using a C50 concrete foundation (7 m long × 7 m wide × 1.5 m deep); and a vibration isolation channel (0.1 m wide × 1.5 m deep) was created to reduce the influence of background vibration and vibrations caused by the water pump. In addition, in order to prevent background vibrations generated at the convergence between the upstream and downstream sections of the hydroelastic model from being transmitted to the transmission path, the upstream or downstream sections were connected using a rubber belt to form a flexible connection, thereby reducing the influence of external

vibrations on the hydroelastic model. The location of the waterfall was also placed 7 m from the end of the downstream section of the hydroelastic model. Fig. 4 shows the vibration isolation and reduction measures used for our model.



Fig. 4
Vibration isolation and reduction measures of the model

A hydroelastic model of Xiangjiaba hydropower station with energy dissipation via a hydraulic jump was built on the test platform (Fig. 5). The geometry scale of the model was 1:80, and the simulation context included the overflow section of the dam, two stilling pools and a section of its foundation. According to the requirements of the model material property similarity law, synthetic rubber was used as the prototype material. The arrangement of the vibration acceleration measurement points located on the model are shown in Fig. 6.



Fig. 5
The hydroelastic model

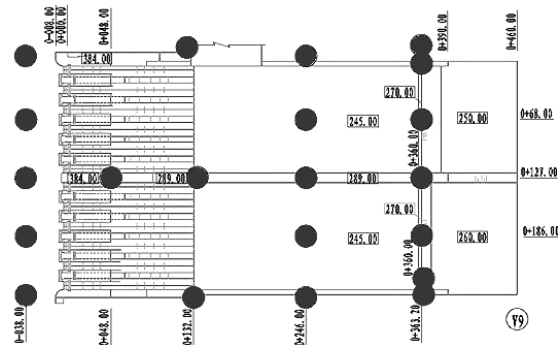


Fig. 6
Arrangement of the vibration acceleration sensor measuring points (the black dots indicating the position of the sensors).

4.2. SIMULATION EFFECT VERIFICATION

Taking the measuring points T9 (Fig. 3) with the largest vibration amplitude as an example, the 13 typical prototype observation conditions were calculated to correspond to the test model. The amplitude comparison between each measuring point of the model structure and T9 is shown in Fig. 6.

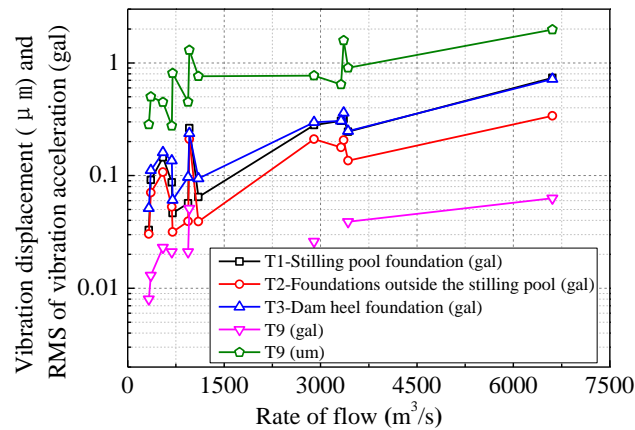


Fig. 6

Vibration comparison between each measuring point of the model structure and the prototype measurement point T9

Results show that the variation trends and patterns of vertical vibrations of each measuring point in the hydroelastic model were basically the same as those at T9. Firstly, the overall vibration intensity increased with an increase of the stilling pool flow; secondly, vibration intensity was sensitive to the route of discharge, with unfavorable routes of discharge resulting in an increase of vibration intensity.

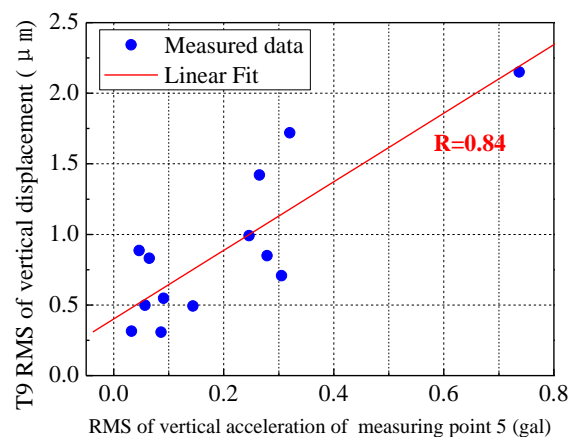


Fig. 7

Vibration correlation between the stilling pool base measurement point of the model and the prototype measurement point T9

Correlation analysis between vibration acceleration of hydroelastic model measuring points and vibration displacement of T9 (Fig. 7) show the coefficients between vibrations of the model stilling pool base and the prototype ground were 0.84. Furthermore, the correlation coefficient between the vertical acceleration of other measuring points in the model and measured vertical displacement, or vertical acceleration of T9, was high (0.71 ~ 0.89). These correlation coefficients indicate that the test results can effectively reflect actual discharge conditions.

5. THE EXPERIMENTAL RESULTS

When model verification effectiveness was undertaken, it was found that the vibration intensity of the downstream area had a close relationship with flood discharge volume and mode, such as the opening way of surface holes and mid-level outlets, the changing of the water level upstream or downstream, etc. Therefore, the influence of these factors on ground vibrations was studied by the principle of controlling a single variable factor. The vibration prediction results of measuring point T9 under the different influencing impact factors of the experiment are shown in Fig. 8 to 12.

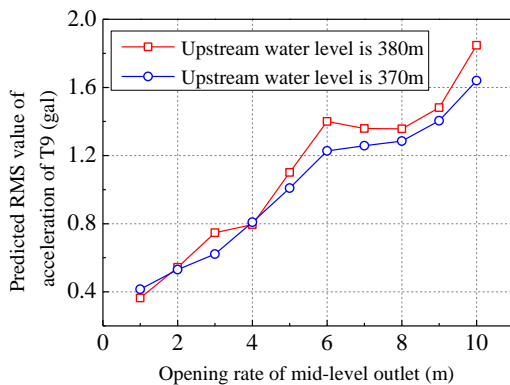


Fig. 8
Prediction results of vertical vibration acceleration of measuring point T9 with mid-level outlet discharge

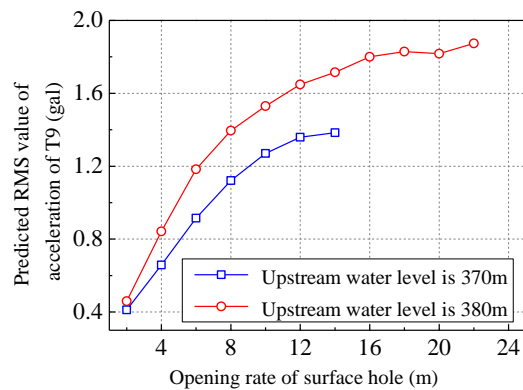


Fig. 9
Prediction results of vertical vibration acceleration of measuring points T9 with surface hole discharge

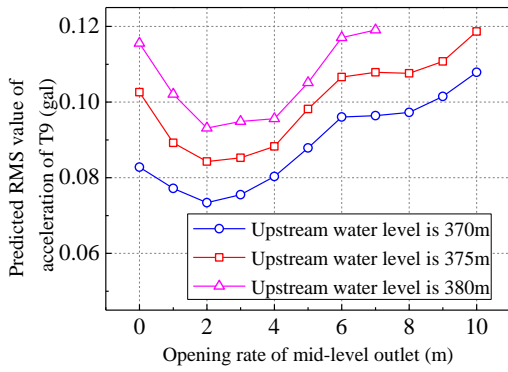


Fig. 10
Prediction results of vertical vibration acceleration of measuring point T9 with discharge from both surface holes and mid-level outlets

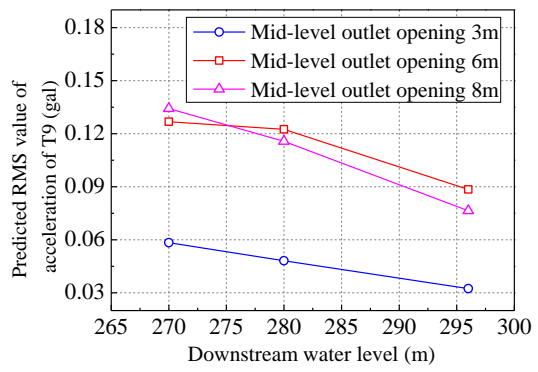


Fig. 11
Prediction results of vertical vibration acceleration of measuring points T9 with different downstream water levels

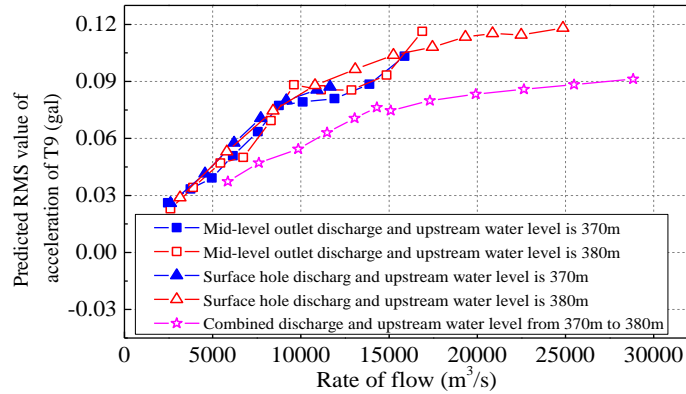


Fig. 12
Comparison of vibration conditions under different discharge modes

It can be seen in Fig.8 to 10 that there was a significant difference between vibration rules under different orifice opening modes. When the surface holes and mid-level outlets were operating, vibrations increased with an increasing in the degree of opening. The mid-level outlets had unfavorable operation ranges from about 5 m to 7 m. A relatively small fluctuating load could be generated at the orifice under both situations. There were no adverse operating conditions when discharging from surface holes, but the increasing range of vibration intensity decreased with a large degree of opening. When discharge occurred at the same time from the surface holes and mid-level outlets, ground vibrations were more sensitive to the degree of opening of the mid-level outlets. The vibration amplitude decreased significantly when the opening degree was between 1 m to 4 m. As can be seen from Fig. 11, the higher the downstream water level, the smaller was the vibration amplitude. While it can be seen from Fig.12 that a higher upstream water level resulted in stronger vibrations, the amplitude growth could be ignored when compared with the flow growth rate. In addition, with the same water flow rate, ground vibration intensity was the strongest when discharge occurred from the

surface holes, followed by ground vibrations generated when discharge occurred from the mid-level outlets; an obvious adverse operating range can be identified. The strength of the vibrations generated with discharge from both the surface holes and mid-level outlets was significantly less than normal operating conditions with the same rate of discharge.

6. RESULTS AND DISCUSSION

The source of vibrations induced by flood discharge from the high dam and the factors affecting vibration intensity were examined based on the combination of a hydroelastic model and prototype observation data. The research findings from our study are:

(1) Before establishing the model, the foundation plain soil at the bottom of the model was reinforced by excavating it and replacing it with concrete, and a vibration isolation channel was set around the foundation. The convergence section between the hydroelastic model and the upstream/downstream sections were connected using a soft rubber belt to form a flexible connection. This adaptation effectively reduced the influence of external vibration sources on the hydroelastic model. Simulated discharge condition results inversed from the experimental model had the same change rule with actual measured ground vibrations, having a high correlation. The prediction results therefore accurately reflected ground vibrations.

(2) The orifice open and upstream and downstream water levels were the major influences on ground vibration intensity, thus controlling these factors and regulating the discharge modes, especially avoiding unfavorable operation ranges for the surface holes and mid-level outlets is beneficial in minimizing ground vibrations.

ACKNOWLEDGEMENTS

This work was supported by the Foundation for the National Natural Science Foundation of China (Grant No. 51709280) and the State Key Laboratory of Simulation and Regulation of Water Cycle in River Basin of China.

REFERENCES

- [1] CUI G.T., MA B. Comprehensive compound method for flow-induced vibration of hydraulic structures. *Advances in Science and Technology of Water Resources*, 2010, 30(1): 1-10.
- [2] SHUMAKOVA E.M., KOTLYAKOV A.V., SHUMAKOV G.V. The effect of vibrations in the Zhigulevskii hydropower structure on soils in the nearby territories of Tolyatti city. *Water Resources*, 2010,37(3): 306-310.
- [3] LIAN J.J. The report of related structures vibration monitoring under bottom outlet discharging condition of Xiluodu Hydropower Station in Jinsha River. *State Key Laboratory of Hydraulic Engineering Simulation and Safety*, 2013.
- [4] Lian J.J., Zhang Y., Liu F., et al. Analysis of the characteristics for ground vibration induced by flood discharge of high dam using cross wavelet transform. *Journal of Renewable and Sustainable Energy*, 2015,7, 1-22.
- [5] CUI G.T., PENG J.L, YUAN X.M, et al. Hydrolastic model study on high arch dam vibration induced by discharge flow. *Journal of Hydraulic Engineering*, 1996, (4):1-9.
- [6] WU Y.H., LI S.Q., XIE S.Z. Dynamic analysis for vibration of dam-water-foundation coupling system during discharge. *Journal of Hydraulic Engineering*, 1996(11): 6-13.
- [7] ZHANG J.W., CUI G.T., Ma B., et al. Time domain identification of excitation source for high arch dam based on discharge flow vibration response. *Journal of Tianjin University*, 2008, 41(9):1124-1129.
- [8] LIAN J.J., CUI G.T., HUANG J.L. Study on flow induced vibration of spillway guide wall. *Journal of Hydraulic Engineering*, 1998(11):34-38.
- [9] LIAN J.J., WANG J.M., GU J.D. Analysis of the similarity law of fluctuating pressures in the hydraulic jump region. *Chinese Science Bulletin*, 2007, 52(15):1832-1839.
- [10] LIU F. Study on characteristics of fluctuating wall-pressure and its similarity law. *Tianjin University*, 2007.
- [11] LIAN J.J, YANG M. Hyderdynamics of high dam. *China Water&Power Press*, 2009.

SUMMARY

Upstream and downstream vibrations generated by large volumes of flood water discharging from a high dam can potentially damage buildings and impact on the normal life of local populations. Modelling vibrations created by overflow conditions has enabled improvements for the traditional physical model, and the establishment of a correlation system by combining the model with prototype observations. In addition, the characteristics of vibration sources, as well as the factors influencing vibration intensities, were investigated. Our results show that establishing a hydroelastic model with vibration isolation and damping measures

can simulate flood discharging conditions and accurately reflect ground vibrations through linear prediction. The vibration energy of the dam orifice was the primary vibration source of ground vibration, followed by the guide wall and stilling pool base slab. Findings from our investigation show that orifice open and upstream and downstream water levels were the major influences on ground vibration intensity, thus controlling these factors and regulating the discharge modes from a high dam will control the intensity of these vibrations.

KEY WORDS

Hydraulic model test, flow fluctuation load, discharge regulation, vibration, Xiangjiaba dam

COMMISSION INTERNATIONALE
DES GRANDS BARRAGES

VINGT-SIXIÈME CONGRÈS DES
GRANDS BARRAGES
Autriche, juillet 2018

EXPERIMENTAL STUDY ON THE GLOBAL STABILITY OF THE XIAOWAN ARCH DAM USING A 3D GEO-MECHANICAL MODEL TEST

J. H. DONG, L. ZHANG, B. Q. YANG, J. Y. CHEN, and Y. CHEN

COLLEGE OF WATER RESOURCES & HYDROPOWER ENGINEERING,
SICHUAN UNIVERSITY, CHENGDU 610065

China

1. INTRODUCTION

This study constructed a three-dimensional (3D) geo-mechanical model for the Xiaowan high arch dam, which simulated the topographical and geological features, the distribution of weak structural planes, the shallow relaxation unloading phenomena, and the dam reinforcement scheme. During the test, traditional model materials were used to simulate the dam body, the concrete reinforcement plug, and the mail rock mass of the abutment and foundation, whereas temperature-analogue materials were used to simulate faults F_{11} , F_{10} , F_5 , F_{12} , F_{19} , and F_{20} . A small specially prepared rhombic block and thin block were used to simulate the shallow layer of the unloading rock body. The failure test was performed using the comprehensive method, which considers both the overloading and strength-reduction techniques.

2. METHODS

The combined overloading and strength reduction methods were applied in this test. The model failure test procedure is as follows. First, the model was pre-loaded and then the normal load level was applied. Afterward, the shear strength of the abutment rock faults, such as F_{11} , F_{10} , and F_5 , were reduced by approximately 20% by heating up the model materials. Finally, the overloading test was implemented until the dam instability caused the destruction of the dam abutment. The loads were applied successively in the following order as factors of the normal working load, P_0 : 1.2, 1.4, 1.6, 1.8, 2.0, 2.2, 2.4, 2.6, 2.8, 3.0, 3.3, and 3.5.

3. RESULTS

The asymmetry of the two-bank terrain and the geological condition of the dam abutments created an asymmetric trend of the displacement of the dam body. In the overloading stage, with an increase in overloading multiples, the displacement of the dam body continuously increased and had an asymmetric trend, which indicates that the displacement of the right arch abutment was slightly larger than that of the left arch abutment.

Under normal working conditions, the surface displacement of the abutments and resistance blocks of both the left and right banks was minimal, and there was no abnormal phenomenon. After K_p was increased to over 3.0, the surface displacements of both abutments increased rapidly and the change amplitude of the displacement curve increased. Furthermore, the measuring points near and around the arch abutment and at the fault outcropped points had abruptly increasing displacement and fluctuating displacement curves.

The primary reasons for the failure of the arch dam and foundation plane are as follows: in the later portion of the overload period, especially when the overloading coefficient K_p was over 3.0, the load born by the arch dam was large, and the geological condition of the two abutments had a large asymmetrical phenomenon. Furthermore, the resistance bodies of the two abutments had inhomogeneous deformation, and the width height of the river valley in the dam area was large. The beam direction effect of the arch dam was large, which caused fissures in the dam body and foundation plane.

Based on the analysis of the experimental data and results, the strength reserve coefficient K_1 is 1.2 and the overloading safety factor K_2 was estimated to be 3.3-3.5, respectively, that is,

$$K_C = K_1 \times K_2 = 1.2 \times (3.3 \sim 3.5) = 3.96 \sim 4.2$$

Thus, the global safety factor K_C for the Xiaowan Arch Dam and foundation should be 3.96-4.2, which meets the present design requirement.

REFERENCES

- [1] J. H. DONG, H. P. XIE AND L. ZHANG, Experimental study on 3D geomechanical model for global stability analysis of Dagangshan double curvature arch dam, *Chin. J. Rock Mech. Eng.* 26 (2007) 2027-2033 (in Chinese).
- [2] D. F. MARTT, A. SHAKOOR AND B. H. GREENE, Austin Dam, Pennsylvania: The sliding failure of a concrete gravity dam, *Environ. Eng. Geosci.* 11 (2005) 61-72.
- [3] E. ITOYA, Y. ZHAO AND Y. O. MARTINS, Stability analysis of a concrete gravity dam and its foundation, *J. Southeast Univ. (English Edition)* 20 (2004) 508-512.
- [4] W. P. FEI, L. ZHANG AND R. ZHANG, Experiment study on a geomechanical model of a high arch dam, *Int. J. Rock Mech. Mining Sci.* 47 (2010) 299-306.

COMMISSION INTERNATIONALE DES GRANDS BARRAGES

VINGT-SIXIÈME CONGRÈS DES GRANDS BARRAGES
Autriche, juillet 2018

DOI 10.3217/978-3-85125-620-8-063



This work licensed under a Creative Commons Attribution 4.0 International License. <https://creativecommons.org/licenses/by-nc-nd/4.0/>

JUSTIFICATION FOR SELECTING A FACTOR OF SAFETY FOR DAMS

Thomas KONOW

Head of Dam Safety, DR. TECHN. OLAV OLSEN

NORWAY

Mathias STRAND

Special Adviser - Advanced Analyses, DR. TECHN. OLAV OLSEN

NORWAY

COMMISSION INTERNATIONALE
DES GRANDS BARRAGES

VINGT-SIXIÈME CONGRÈS DES
GRANDS BARRAGES
Autriche, juillet 2018

JUSTIFICATION FOR SELECTING A FACTOR OF SAFETY FOR DAMS

Thomas Konow

Head of Dam Safety, DR. TECHN. OLAV OLSEN

Mathias Strand

Special Adviser - Advanced Analyses, DR. TECHN. OLAV OLSEN

NORWAY

1. INTRODUCTION

Requirements for stability of concrete dams in the current Norwegian dam safety regulations are based on simplifications, which in many cases are conservative. As a result, rehabilitation works may be carried out on dams that are safe, but does not meet the safety requirements.

Norwegian dams have to meet a minimum safety standard, defined by a Factor of Safety (FoS). It is often assumed that the FoS includes all of the uncertainties in the calculations. However, how these variables affect the FoS are generally not known or not accessible. It is therefore a need to acquire more knowledge on how different assumptions affect the calculations of stability of FoS.

How different parameters affect the dam stability is essential in order to identify which parameters that are most important for stability and sensitivity of the overall dam safety. This knowledge is of particular interest in assessing existing dams. By gaining more knowledge about different parameters, it is possible to reduce the uncertainty connected to these parameters, and thereby reducing the overall uncertainty. This knowledge can thereby be used to reduce the calculated FoS without affecting the safety level of the dam.

In general, a probabilistic analysis would be suitable to identify these type of uncertainties. Due to a very limited budget, we had to use a different approach to the issue. Our selected method and the results from the calculations are described in this paper.

The calculations have been carried out on both concrete gravity dams and masonry dams. For simplicity, this paper only presents the results related to concrete gravity dams with a height > 8 m.

2. REQUIREMENTS FOR DAM SAFETY IN NORWAY

In Norway, dam stability is checked for both overturning and sliding.

Calculation of the sliding resistance require a safety factor of minimum 1.5 against normal design loads. For accident loads a minimum FoS of 1.1 is applied. If cohesion is included, a higher FoS is necessary. However, as this require documentation by testing, the cohesion is generally never included.

Safety against sliding is estimated with the shear friction factor method, where the FoS is generally defined as the following:

$$SF_{sliding} = \frac{\sum F_{horizontal\ capacity}}{\sum H_{horizontal\ load}} = \frac{\sum V \tan(\phi + \alpha)}{\sum H}$$

where ϕ is the fiction angle and α is the inclination of the foundation.

Stability against overturning for concrete gravity dams, is acceptable when calculations show that the resultant force is within the central dam foundation, so that it can be assumed pressure throughout the dam foundation.

To simplify the output of safety against overturning, the FoS is calculated instead of the eccentricity of the resultant force. Safety against overturning thereby defined as:

$$SF_{overturning} = \frac{\sum M_{stab.}}{\sum M_{destab.}}$$

3. METHOD AND ASSUMPTIONS

The calculations has been based on a computing tool for stability control, developed by Dr. Techn. Olav Olsen. To make the calculations more efficient, a

script was developed with the programming language, Python. The script defines changes of different variables, and then generates calculations with these assumptions.

The result of the stability calculation of each parameter is presented graphically, where the resulting FoS is plotted against the varying parameters for each dam height. Variation in the FoS are shown for both sliding and overturning. This paper only presents a sample of the results that have been produced.

The method used, has proven to give a very powerful and flexible tool for estimating stability of all types of concrete dams with different variables. In total, the report has been based on approximately 7000 separate calculations with different variables.

3.1. VARIABLES

Assumptions of for the calculations are shown in the table below. “Initial values” are used to generate dam section as described in the next chapter.

Table 1.
Assumptions used for the computations

Variable	Initial value	Min. value	Max. value	Step for calculations	Comment
Friction angle	40°	35°	60°	1°	
Water level (H_w)	h	$h - 1$ m	h	0.01 m	$h =$ Dam height
Self-weight (kN/m^3):	22	21	24	0.1	
Drainage constant (k)*	1.00	0.50	1.0	0.05	Changes in pore pressure defined by k and dx *.
Drainage position (dx)*	0	$0.1H_w$	$0.5H_w$	$0.1H_w$	

* Both the drainage constant (k) and the drainage position (dx) was changed, - see figure below (i.e. $6 * 11 = 66$ different calculations for each dam height)

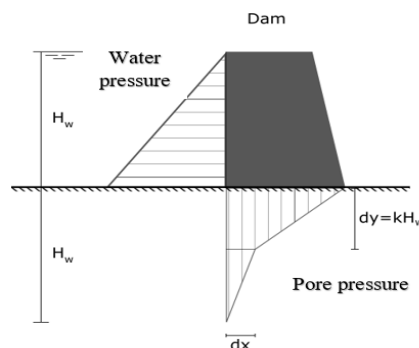


Fig. 1.

Illustration of assumptions to generate pore pressure.

3.2. GENERATION OF DAM SECTION

The dam-sections were generated, satisfying the following requirements:

- Compression throughout the entire foundation (i.e. the resultant force is within the central dam foundation)
- FoS against sliding equal to 1.0.

By changing crest width and downstream slope (see Figure 2) an optimal cross section was found using the “initial values” given in Table 1.

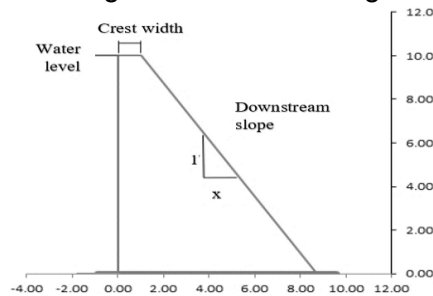


Fig. 2.

Dam section was selected by varying crest width and downstream slope.

It was not possible to generate a cross section that satisfied the assumptions mentioned above. Therefore, the required FoS against sliding was increased from 1.0 to 1.1 as shown in the table below.

Table 2.
Geometry and FoS for dam-sections generated.

Dam height [m]	Crest width [m]	Downstream slope [1:x]	FoS	
			Sliding	Overturing
8	0.81	0.77	1.1	1.5
10	1.01	0.77	1.1	1.5
12	1.21	0.77	1.1	1.5
14	1.41	0.77	1.1	1.5
16	1.61	0.77	1.1	1.5
18	1.82	0.77	1.1	1.5
20	2.02	0.77	1.1	1.5
25	2.52	0.77	1.1	1.5
30	3.03	0.77	1.1	1.5

The above table shows that optimization of the cross sections provided a minimum FoS of 1.1 against sliding and 1.5 against overturning, with the assumptions used. In presentation of the results, the FoS for the initial dam section was normalized. This implies that the computed FoS against sliding was divided by 1.1, while the results against overturning was divided by 1.5.

It can also be noted that when the friction angle was increased to 50°, the FoS against sliding increases to ~1.5, which is the same FoS as for overturning.

4. RESULTS

In this chapter, the results of the calculations with different variables are presented and discussed.

4.1. FRICTION ANGLE (AND ANGLE OF FOUNDATION)

Variation in friction angle is also valid for inclination of the foundation, since horizontal capacity is defined as $\sum V \tan(\phi + \alpha)$ (see chapter 2). The friction angle has no effect on the FoS against overturning.

The computations show that the FoS against sliding is the same for all different dam heights. This implies that friction angles is directly related to FoS, and that the dam height do not influence the results. This means that a change in the friction angle will give the same change of the FoS regardless of the dam height. This can, of course, also be seen directly from the definition of FoS against sliding.

The friction angle will normally be conservative where the friction angle also “includes” possible cohesion and shear capacity due to rock surface roughness. This implies that the corresponding safety factor from friction, should be 1,0. The calculations carried out, also show that a conservative friction angle will result in a high level of safety that is not necessarily reflected in the computed FoS for the dam.

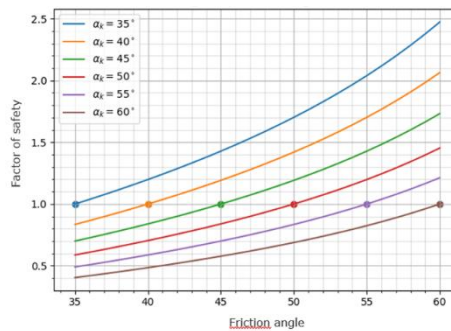


Fig. 3.

Correlation between FoS and friction angle. α_k is the initial friction angle where the different dam sections have a FoS = 1.0.

4.2. WATER LEVEL

How variations in the water level influence the FoS, will identify how sensitive the dam is to changes in flood water level. Changes in design water level can for instance be caused by changes in future flood calculations etc. How much this

affects the safety in relation to different dam heights is calculated and presented graphically in the following figures.

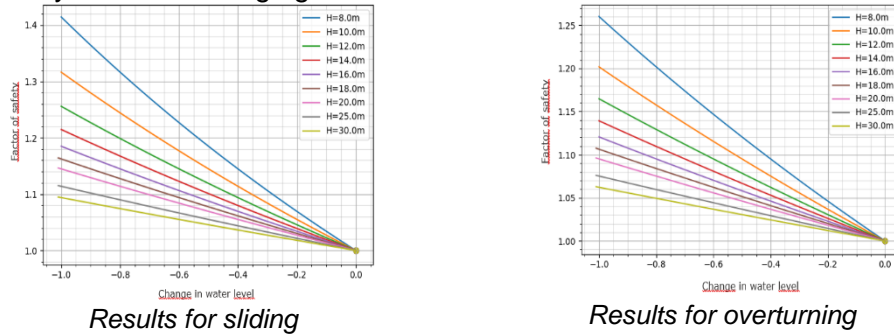


Fig. 1.

Reduced water level (x-axis) vs. FoS for different dam heights (y-axis).

As shown in the above graphs, higher dams are, of course, less sensitive to changes in water levels than lower dams. This is summarized in the following table.

Table 3.
Effects of changes in water level on the FoS for different dam heights.

Change in water level	FoS - Sliding		FoS - Overturning	
	Dam height 8 m	Dam height 30 m	Dam height 8 m	Dam height 30 m
0,2 m	1,07	1,02	1,05	1,01
1,0 m	1,41	1,09	1,26	1,06

The table shows that changes in water levels have more influence on the FoS against sliding than FoS against overturning.

Dam height (i.e. static water pressure) is crucial for how uncertainties in flood calculation and flooding affect stability. When the dam height increases, changes in flood water have little significance for the dam stability.

As uncertainties in floods and operating levels will have different impact on the FoS dependent on the dam height, it is reasonable that these uncertainties are handled in the flood calculations and are not included in the FoS. For instance, a dam dependent on floodgates will have other uncertainties related to flood handling and flood levels than a dam with a free overflow spillway. This implies that the corresponding safety factor from static water pressure, should be 1,0.

4.3. SELF-WEIGHT

The self-weight is essential for the stability of a concrete gravity dam. The calculations carried out show that variations in the self-weight is directly related to the FoS and the dam height does not influence the results.

JCSS, "Probabilistic Model Code", 2015, Table 2.1.1, recommends a coefficient of variation of 0.04 on self-weight. This corresponds to a load factor of 0.96, which imply a reduced self-weight from 24 to 23 kN/m³. The correlation between a load factor of 0,96 and the FoS are shown in the table below.

Table 4.
Correlation between load factor and FoS.

	Load factor	FoS
Sliding	0,96	1,08 (=1/0.93)
Overturning	0,96	1,04 (=1/0.96)

A graphic presentation of the correlation between self-weight and FoS is shown below (blue line = sliding; orange line = overturning).

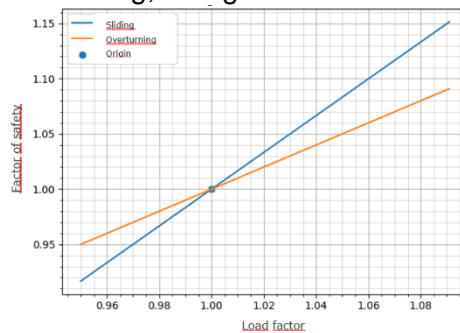


Fig. 5.

Load factor (x-axis) vs. FoS (y-axis) when the friction angle = 40°

The dam geometry also represents an uncertainty, which also can be illustrated by varying the self-weight. However, probabilistic analysis carried out on a gravity dam in Norway indicate that deviations in the geometry do not have a significant effect on the FoS.

4.4. PORE PRESSURE

The pore pressure represents an uncertainty that can be difficult to predict and therefore difficult to quantify in terms of a specific FoS. This would imply that the pore pressure should be subjected to a relatively high FoS to take account of the uncertainty it represents.

In Norway, requirements for stability against overturning assume that the resultant force is within the central dam foundation. Thereby, a linear decreasing pore pressure can be assumed as there is pressure throughout the entire dam foundation. In addition, a check of accident load is required, where the resultant force should be upstream 1/6 of the dam foundation. In this case, full pore pressure can be assumed on the upstream half of the foundation (where there is no pressure on the foundation) and then linearly decreasing to the downstream side. The assumptions for design loads and accident loads are shown in the following figure.

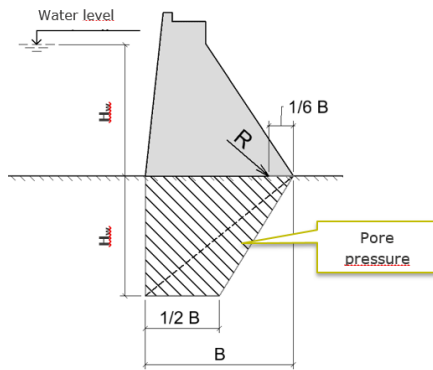


Fig. 6.

Maximum allowable pore pressure assumed for accident loads. Pore pressure distribution for normal design loads is shown as a dotted line.

The criteria for pore pressure distribution provides a logical correlation between the load effects from the dam and the resulting pore pressure for normal design loads. When there is pressure in the entire foundation, the bond between the concrete and the foundation can be assumed to be intact. Thereby, a linearly decreasing pore pressure under the dam will probably be a conservative assumption and generally contribute to a high safety level.

The additional check for accident loads provides an extra safety in case the pore pressure should be greater than assumed for normal design loads.

If the maximum permissible pore pressure for accident loads represents the uncertainty in the pore pressure distribution, the difference of pore pressure between design load situation and accident load situation may be defined as the corresponding load factor. This difference represents an increase in pore pressures of 43%, or a load factor of 1.43. The correlation between the FoS for design loads and accident loads can thus be expressed as shown in the following figure, where FoS = 1 represent a linearly decreasing pore pressure distribution under the dam.

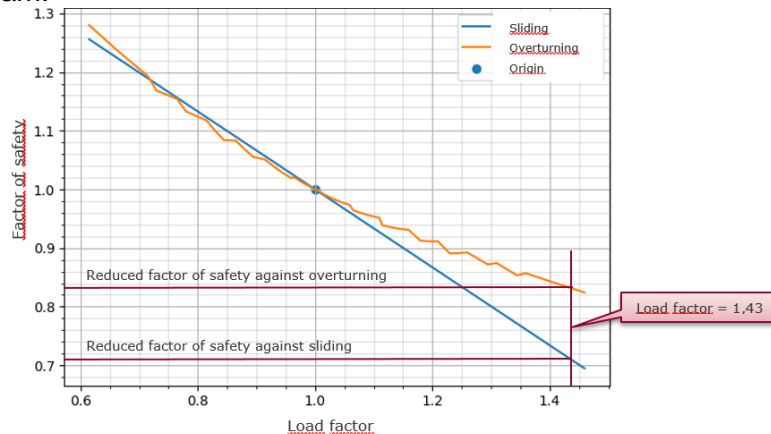


Fig. 7.

Computed correlation between load factor and FoS with changing pore pressure (blue line = sliding; orange line = overturning).

5. SUMMARY AND CONCLUSION

The following table summarizes the suggested FoS for each variable as discussed in this paper. Multiplying the different factors is assumed to represent the overall FoS.

Table 5.
Total FoS as a product of the individual safety factors.

Variable	FoS - Sliding		FoS - Overturning		Reference
	Design	Accident	Design	Accident	
Friction	1,0	1,0	Not relevant		Chapter 4.1
Water level	1,0	1,0	1,0	1,0	Chapter 4.2
Self-weight	1,08	1,08	1,04	1,04	Chapter 4.3
Pore pressure	1,40	1,00	1,20	1,00	Chapter 4.4
SUM	1,51	1,08	1,25	1,04	Overall FoS
Current FoS	1,5	1,1	N.A.*	N.A.*	
* Safety against overturning is defined by position of the resultant					

Elements constituting the total FoS given in the Norwegian dam safety regulations is not publicly available. The factors of safety suggested in the above table can, however, be used to justify the current requirements, but this has not been confirmed by the Norwegian dam safety authority.

How different parameters affect the dam stability is essential when assessing the degree of uncertainty of the calculations. This will make it easier to identify which parameters that are most important for the stability and that influences the uncertainties of the overall dam safety.

By improving the knowledge related to the individual variables, the uncertainties can be reduced and thereby reducing the overall required FoS for the dam in question. This is of particular interest in cases where existing dams do not meet the safety requirements.

It must be underlined that results in this report is valid with the given methodology and assumptions described in chapter **Fehler! Verweisquelle konnte nicht gefunden werden.** and **Fehler! Verweisquelle konnte nicht gefunden werden.**, and a validation of the results is recommended.

6. ACKNOWLEDGEMENTS

We would like to thank EnergiNorge that has supported this project, and thereby made this contribution possible.

7. REFERENCES

This article is based on a study documented in a report by EnergiNorge in Norwegian. When this article was written, the report was not published. The report will in time available on: <https://www.energinorge.no/publikasjoner/>

SUMMARY

The study presented in this paper is part of a larger Norwegian Research and Development project, named “Dam safety in an overall perspective” that is administrated by EnergiNorge. This is a joint project with participants from the Norwegian dam safety sector. One of the objects of this project is to look at alternative approaches to evaluate safety of existing concrete- and masonry dams.

This paper presents a study carried out to identify how different variables affect the estimated safety for dams. To do so, a series of calculations has been carried out to understand how the FoS is affected for a wide range of variables and assumptions.

The calculations have been carried out by combining a computing tool for stability calculations with a script that runs the calculations. This method has proved to produce a very powerful and flexible tool for computing stability with varying assumptions. In total, the report is based on approximately 7000 separate calculations with different variables

The study gives suggestions on how uncertainties related to loads and other assumptions can be represented in the overall FoS. The results can also be used to justify the current practice and safety level applied by the Norwegian dam safety regulations.

COMMISSION INTERNATIONALE DES GRANDS BARRAGES

VINGT-SIXIÈME CONGRÈS DES GRANDS BARRAGES
Autriche, juillet 2018

DOI 10.3217/978-3-85125-620-8-064



This work licensed under a Creative Commons Attribution 4.0 International License. <https://creativecommons.org/licenses/by-nc-nd/4.0/>

**CORRELATION PATTERN OF TECHNOLOGY STRATEGY WITH POWER
PLANTS DEVELOPMENT STRATEGY - CASE STUDY OF HYDRO POWER
PLANT KARKHEH DAM**

H. BOROUMANDFAR

Chief General Engineering of the KARKHEH DAM AND POWER PLANT

IRAN

R. SALAMI

*Assistant Professor, Department of Management and Accounting, ALLAMEH
TABATABAI UNIVERSITY*

IRAN

M. MANTEGHI

Head of the SPACE ORGANIZATION OF THE COUNTRY

IRAN

COMMISSION INTERNATIONALE
DES GRANDS BARRAGES

VINGT-SIXIÈME CONGRÈS DES
GRANDS BARRAGES
Autriche, juillet 2018

**CORRELATION PATTERN OF TECHNOLOGY STRATEGY WITH POWER
PLANTS DEVELOPMENT STRATEGY - CASE STUDY OF HYDRO POWER
PLANT KARKHEH DAM**

H.BOROUMANDFAR

Chief General Engineering of the KARKHEH DAM AND POWER PLANT

R.SALAMI

Assistant Professor, Department of Management and Accounting, *ALLAMEH
TABATABAI UNIVERSITY*

M.MANTEGHI

Head of the SPACE ORGANIZATION OF THE COUNTRY

IRAN

1. INTRODUCTION

Organizations have no choice but to use technology as a strategic resource to achieve their strategic goals, and this means that the concept of strategic alignment of development and technology makes sense. Undoubtedly, the most important component in the progress of organizations in today's world is technology. The lack of a development strategy to manage technology transfer is one of the problems for companies. In this study, first, effective indicators have been identified for development strategy development, and then, by assessing the quality of technology, the strengths and weaknesses of the company in each technology are determined, while specifying the proposed solution of the SWOT analysis (Matrix of Technology) and Grounded theory (Model Alignment) is done briefly.

2. RESEARCH METHODOLOGY

2.1. MAIN HEADING

One of the problems of domestic companies is the lack of a development strategy to manage technology transfer in technology transfer projects. Therefore, this research seeks to provide a method for developing a development strategy in order to identify the technologies that are in line with the needs of the country and provide solutions for the acquisition of the required technologies of the power plants. To this end, effective indicators have been identified for developing a development strategy. By devoting axes to each of the components, a framework for developing a development strategy has been designed. By drawing the technology map based on the external and internal dimension assessment by the quality performance of the technology and the model of the management of the technology requirements, while identifying the technological status of the company in each technology (the strengths and weaknesses), the key technologies of the company, as well as the competitive position of each technology (opportunities And threats) will be identified.

2.2. DETERMINE TECHNICAL CHARACTERISTICS AND MAP THE TECHNOLOGY

To this end, by first examining the contracts concluded between the employer and the manufacturing companies, the quality requirements and technical requirements that directly or indirectly influenced the construction of the power plant were identified. In the next step, a questionnaire was prepared for the first step, and from the 14 experts of the company, the employer was asked to provide an assessment on the weight of each of the demands and technical requirements, based on the questionnaire method [1]. Based on the analysis of the findings, the technical strength of the production capacity was 400 MW, 9; the water in the design reservoir was 100 meters; 7; the ability to manage the mechanical equilibrium system; 5; unit time at 150, 7 rpm; generator voltage 13.8 kV, 5, and the design of the plant's structure according to standard 9 [2]. Then, according to the principles of collective agreement and according to the grading (1-3-5-7-9), provide an assessment of the impact of each of the technical characteristics on the quality requirements and technical requirements of the design and construction of the power plant (Table 2 and 1).

Table 1
 Technical characteristic along with the importance of each one

Technology		Engineering metrics									
List of key requirement	weight	design	Test of better positioning	Test of reservoir changes	Test of the effect of free surface fluid	impact test	speed measurement standard in the direction of the ramp	Structural calculations Corresponding to the instantaneous	Test of torque Created	Test of resistance to movement	Angular variation test of turbine wheel turbine wheel
		And manufacturing laboratory samples	Longitudinal and transverse								
Production capacity of 400 MW	9	3	7								
Having a design tank of 100 meters	9	3	1	9	9				3		3
Mechanical balance Management System	9								9	9	9
Runs at 150 rpm	7					5	9			3	1
The voltage of the generator is 13.8 kV	5					9	5			3	1
Design of the body structure conforming to the standard	9	1	3	3				9			
	Row Score	63	99	10	81	80	88	81	10	11	12
				8					8	7	0
	Relative Weight (%)	7	10	11	9	8	9	9	11	12	13

Table 2
List of matrix technology

List of key requirement	Technology	Engineering metrics												
	weight	Technology required for the technological model	Knowledge of designing and manufacturing laboratory model	Technical calculations conforming to standard	Model Simulation Software	Technical know-how Hydrostatic calculations	Technical know-how Hydrodynamic calculations	Hydrostatic calculations software	Structural Computing Software	Hydrodynamic Computing Software	Tank or Test channel	Isobaric by pass system	Wave Systems Damper	Cavitation tunnel
Design and manufacturing of laboratory samples	%7	9	9	1	9									
Test for better positioning, longitudinal and transverse	%10							9		1				
Reservoir test	%11					3			7	3	3	9	7	
Testing the effect of free surface fluid	%9									1		3		
Water hammer test	%8													9
Measuring instantaneous speed in direction of rotation	%9									9	9	3	1	
Structural calculation conforming to standard	%9			9					9					
Created torque test	%11					3	7			1				
Tensile force test	%12						9		9	9	9	5		
Test of angular variations of flow	%13					7		9		3		3		
	Row Score	%0.63	%0.63	%0.88	%0.63	%1.24	%1.41	%1.14	%1.71	%1.85	%2.91	%2.22	%2.52	%1.58
	Relative Weight	%3	%3	%4	%3	%6	%7	%10	%8	%9	%14	%11	%13	%8

2.3. FINDINGS

To determine the technological capability gap, the collected data was analyzed and the test results confirmed the existence of a technological gap for eight of the technologies. For this purpose, the level of existing capabilities and the level of capabilities required in each technology are specified. Then, the following test was carried out to test the technological capability gap in technologies with different required and existing capabilities [3].

There is no gap between the level of existing and required X technology technology: H0

There is a gap between the existing level of existing and required X technology technology: H1

Measurement of Indicators: For this purpose, a questionnaire was developed in three sections, the internal indicators including the technological gap, the duration of development and the cost of development, were examined in each part of the questionnaire [4]. The output of this step is shown in Table 3.

Table 3
The degree of technological gap in each of the technologies required for power plant design

Technology gap		Technology level of the item need	Available Technology level	Technology Title
Relative amount	Quantitative			
%12	10.16	11.33	1.17	Model simulation software
%5	4.00	11.83	7.83	Hydrostatic calculations software
%10	8.66	12.08	3.42	Structural Computing Software
%18	15.17	16.67	1.50	Hydrodynamic Computing Software
%5	4.17	13.00	8.33	Tank or Test channel
%11	9.23	12.83	2.50	Isobaric by pass system
%20	16.91	18.08	1.17	Wave Systems Damper
%20	16.67	18	1.33	Cavitation tunnel

2.4. DRAW A TECHNOLOGY MAP

In this step, the technology map is taken into account with regard to the component of the importance of technology as the horizontal axis (vector x) and the component of the technological gap as the vertical axis (vector y). Gaining a relatively high value in the component of the importance of technology for a particular technology suggests that the acquisition of this technology by the company is inherently competitive and, in addition to creating opportunity, avoids threats such as dependency on the source. Also, the relative value of the technology gap is considered to be the weak point in the technology [5]. The purpose of drawing up a technology map for the technology of designing and building a power plant in Karkheh Power Generation Company is to show the technological status of the company in each technology (strengths and weaknesses) and identify key technologies and determine the competitive position of each technology in comparison with other technologies. The survey (opportunities and threats) is shown in Figure 1 After determining these; we can adopt a suitable development strategy for the development and acquisition of each technology in the company.

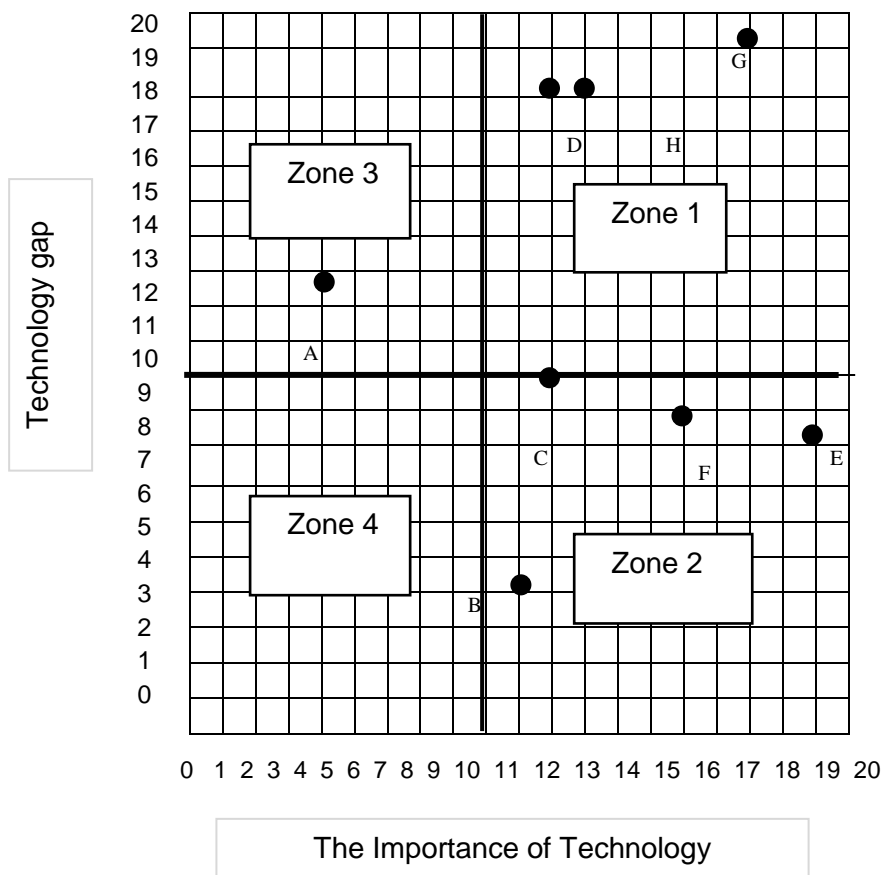


Fig. 1
Technology map area guidance for choosing a development strategy

3. PATTERN COMPILATION ALIGNMENT

3.5. GREDD'S THEORY OF THEORY

In the present study, the theory of grounded theory (granddad theory) is used. One of the techniques of textual data analysis is the grounded theory that is a method of inducing the interpretation of recorded data about the social phenomenon-especially the data from interviews-to build theories about that phenomenon. In general, theories of theory focus on actions and social processes and ask questions about what is happening and how people react. It shows the impact of symbolic interaction and a social psychological approach that focuses on the meaning of human action. Background theory studies begin with open questions, and researchers assume that they may be aware of a small amount of meanings or concepts derived from participant actions. Accordingly, it can be said that, when there is little information about the subject studied and the creation of a respected scholarly theory, the research approach would be appropriate [6]. Using the method of theoretical sampling, 14 managers and experts of Karkheh Power Plant were interviewed. In this study, 14 managers and experts of Karkheh power plant were selected. The statistical sample of the research is reported in the following table in terms of education.

Table 4
Distribution of research samples according to education

Percent	Abundance	Education	Row
%28.57	4	Masters	1
%64.28	9	Masters	2
%7.14	1	P.H.D	3
%100	15	Total	4

The table of Pierre samples discern statistical study based on work histories have been reported.

Table 5
Distribution of statistical samples based on work experience

Percent	Abundance	Education	Row
-	-	Less than a year	1
%21.42	3	One to five years	2
%35.71	5	5 to 10 years	3
%42.85	6	10 Years up	4

The purpose of the coding is to create the relationship between the generated categories (in the open coding step). This practice is usually done based on the paradigm pattern and helps the theorist to make the theorizing process easy. The basis of communication in central coding is the expansion of one of the categories. In central coding, we encounter an organized set of code and initial concepts that results from an accurate and detailed review of articles and interviews in the open coding process. The focus of this phase is on codes and concepts rather than data. The main categorization (such as the idea or event) is defined as a phenomenon, and other categories are related to this major categorization. Cause conditions are events and events that lead to the creation and development of phenomena. The background to a specific set of conditions and intervening conditions refers to a wider set of circumstances in which the phenomenon is located. Action or counteraction strategies refer to actions and responses that occur as a result of the phenomenon, and ultimately-intentionally or unwillingly-these actions and responses to outcomes.

In order to explain the criteria and sub criteria of the process of aligning technology strategy with development strategy, the method of content analysis and theoretical coding technique was used from the data-foundation theory. For this purpose, firstly, using the open coding method, the concepts were classified in the interviews and documents based on the same topics, among which the main categories and subcategories of the process of alignment of the technology strategy with the development strategy were identified. The researcher categorized the title of "criterion" and subcategories related to them as "subclass". Then, in the form of axial coding using the paradigm pattern, the relationship between the criteria and the sub-criteria was established. Therefore, a research model that demonstrates how the criteria of the alignment pattern of technology strategy with the development strategy are related. Figure 4 illustrates the alignment pattern of technology strategy with development strategy. The explanation is that based on the pattern of alignment of the technology strategy with the strategy of development of alignment empowers including the maturity of the communication and the factors of management and exercise of power, strategic planning of technology and organizational architecture compatible with technology, participation factors, human resources (innovation, entrepreneurship, expertise, knowledge) and factors Distinctive merits that lead to the realization of the results of the alignment of the technology strategy with the development strategy.

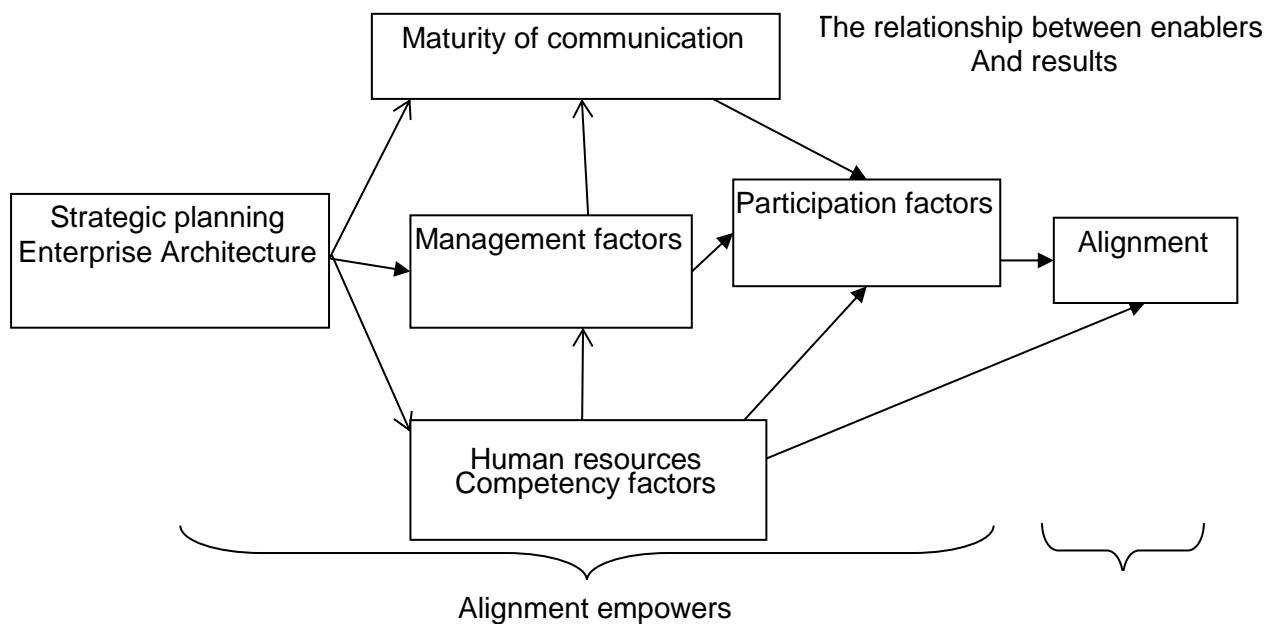


Fig. 2
The Alignment Pattern Of Technology Strategy With Development Strategy

REFERENCES

- [1] ESBATEE, H., "Principles And the house edit Strategy Technology", *Publications industries Defense*, Iran, 2010.
- [2] STOREY, J., EMBERSON, C., GODSELL, J., HARRISON, A. Supply chain management: theory, practice and future challenges, *International journal of operation & production management*, Vol.26, No.7: 754-774, 2006.
- [3] BAGHERI, K., "the missing link in the technology transfer process in the electricity industry", *the first technology management conference in Tehran*, Iran, 2004.
- [4] BERM, A. & VOIGT, K. "Integration of market pull and technology push in the corporate front end of innovation management", *Insights from the German software industry Technovation*, Vol. 29, No. 5: 351-367, 2009.
- [5] SUH, JH, & PARK, SC, "Service-oriented Technology Roamap (SOTRM) using the patent map for R & D strategy of service industry", *Expert system with Applications*, Vol. 36 and No.3: 6754-6772, 2009.
- [6] STRAUSS, A., KURBAN YEN, C., "Basics of research that quality, techniques and procedures produce the desired background Y" *Translation of all we Afshar urethra, the publication of Tehran university*, 2001.

SUMMARY

In this paper, a new approach to developing a strategy of alignment of technology and development strategy using Swat matrix technique and Granddad's theory of theory is introduced as a scientific innovation. For this purpose, development strategy analysis indicators were extracted and then an algorithm was developed for developing a development strategy with technology (proposed model). This model, in addition to determining the technological status of the company in each technology, can identify the key technology of the company and the competitive position of each technology. The basic assumptions of this model are: technology evaluation (identifying the strengths and weaknesses of the company in the field of technology) and improvement through the identification of performance aspirations, comprehensive evaluation and management flexibility. Innovation and features of the proposed model in the domain of 1) designing the proposed model, including: flexibility, ease and simplicity, multi-purpose, obtaining the information, and validity and reliability; and 2) management tool of the proposed model, including the tool for controlling development activities in line with the objectives Strategic and guidance for decision making.

RÉSUMÉ

Dans cet article, une nouvelle approche pour développer une stratégie d'alignement de la technologie et de la stratégie de développement utilisant la technique matricielle Swot et la théorie de la théorie de Granddad est présentée comme une innovation scientifique. A cet effet, des indicateurs d'analyse de stratégie de développement ont été extraits puis un algorithme a été développé pour développer une stratégie de développement avec la technologie (modèle proposé). Ce modèle, en plus de déterminer le statut technologique de l'entreprise dans chaque technologie, permet d'identifier la technologie clé de l'entreprise et la position concurrentielle de chaque technologie. Les hypothèses de base de ce modèle sont: l'évaluation de la technologie (identifier les forces et les faiblesses de l'entreprise dans le domaine de la technologie) et l'amélioration par l'identification des aspirations de performance, l'évaluation complète et la flexibilité de gestion. L'innovation et les caractéristiques du modèle proposé dans le domaine de 1) la conception du modèle proposé, y compris: la flexibilité, la facilité et la simplicité, la polyvalence, l'obtention de l'information, la validité et la fiabilité; et 2) l'outil de gestion du modèle proposé, y compris l'outil de contrôle des activités de développement conformément aux objectifs stratégiques et d'orientation pour la prise de décision.

COMMISSION INTERNATIONALE
DES GRANDS BARRAGES

VINGT-SIXIÈME CONGRÈS DES
GRANDS BARRAGES
Autriche, juillet 2018

A COMPARISON BETWEEN HYDROSTATIC-TIME-SEASON AND BAYESIAN DYNAMIC LINEAR MODELS FOR MONITORING BEHAVIOR OF DAMS*

Ianis GAUDOT¹, Luong Ha NGUYEN², James GOULET³

¹*Postdoc fellow*, ²*Ph.D. student*, ³*Assistant Professor*
POLYTECHNIQUE MONTREAL

Benjamin MIQUEL
Ing., Ph.D., HYDRO-QUEBEC

CANADA

ABSTRACT

Monitoring the long-term behavior of dams is key for addressing safety and serviceability issues. One challenge is to enable the detection of changes in the baseline response of the structure (i.e. anomalies) in real time, while mitigating false alarms.

The most popular data interpretation method for monitoring the long-term behavior of dams is the Hydrostatic-Season-Time model (HST; [1]). The HST performs a regression analysis to decompose a time series into three sub-components related to the hydrostatic effects (H), the thermal effects (S), and the baseline response of the dam (T). The main drawback of HST models, is that they are not dynamic; it means that once the model is built using a training dataset, it stops evolving as new data are collected over time. This is a limitation because the main objective of dam instrumentation/auscultation is to interpret non-stationary (i.e. abnormal) behavior in the baseline response. Moreover, the

* Comparaison entre les modèles Hydrostatique-Saison-Temps et les modèles Bayésiens Linéaires Dynamiques pour le suivi temporel du comportement des barrages

detection of anomalies typically depends on hypothesis testing or threshold-based procedures, which are prone to false alarms.

Bayesian Dynamic Linear Models (BDLMs) are a class of state-space models which are well suited for sequential inference [2]. BDLMs are capable to decompose time series into a set of sub-components, as HST does. In contrast with the HST technique, the behavior of the sub-components can vary with time, without the need to retrain the model. Recent applications have demonstrated the potential of BDLMs to track time-varying baseline responses of civil infrastructures from real dataset [3], and to detect anomalies [4].

This paper compares the HST and BDLMs techniques for the long-term monitoring of dams. This study presents a specific class of BDLMs based on the switching Kalman filter (BDLM-SKF). Two examples of application based on real displacement data recorded on a dam in Canada and simulated data show that BDLM-SKF is robust towards false alarms, and enable to interpret non-stationary time series. One feature of BDLM-SKF is its capacity to interpret the baseline after an anomaly occurs (i.e. when the dam returns to its normal behavior), without retraining the model. In contrast, HST model is prone to false alarms, and is unable to provide information about when an anomaly stops.

This study demonstrates that Bayesian Dynamic Linear models (BDLMs) outperform Hydrostatic-Time-Season (HST) modelling for monitoring the long-term behavior of dams, while providing the same level of interpretability. The main advantages of BDLM over HST model is its ability to interpret non-stationary time series and to detect change in the baseline response of the dam (i.e. anomalies) without being prone to false alarms.

REFERENCE

- [1] WILM G., BEAUJOINT N., 1967. Les méthodes de surveillance des barrages au service de la production hydraulique d'Electricité de France. Problèmes anciens et solutions nouvelles, *IXe Congrès CIGB*, Istanbul, Q34, R30
- [2] WEST M. AND HARRISON P. J., 1997, *Bayesian Forecasting Dynamic Models*. Springer Verlag, 2nd edition
- [3] GOULET J.-A., 2017, Bayesian dynamic linear models for structural health monitoring, *Structural Control and Health Monitoring*, <https://doi.org/10.1002/stc.2035>
- [4] NGUYEN L.H. AND GOULET J.-A., 2018, Anomaly Detection with the Switching Kalman Filter for Structural Health Monitoring, <https://doi.org/10.1002/stc.2136>

COMMISSION INTERNATIONALE DES GRANDS BARRAGES

VINGT-SIXIÈME CONGRÈS DES GRANDS BARRAGES
Autriche, juillet 2018

DOI 10.3217/978-3-85125-620-8-066



This work licensed under a Creative Commons Attribution 4.0 International License. <https://creativecommons.org/licenses/by-nc-nd/4.0/>

INCREASE CONCRETE QUALITY IN DAM CONSTRUCTION DURING DESIGN AND EXECUTION PHASE

Andreas ZITZENBACHER

DOKA GMBH

AUSTRIA

Massimo MAFFEZZOLI

DOKA GMBH

AUSTRIA

Stefan SCHEUCHELBAUER

DOKA GMBH

AUSTRIA

COMMISSION INTERNATIONALE
DES GRANDS BARRAGES

VINGT-SIXIÈME CONGRÈS DES
GRANDS BARRAGES
Autriche, juillet 2018

INCREASE CONCRETE QUALITY IN DAM CONSTRUCTION DURING DESIGN AND EXECUTION PHASE

Andreas ZITZENBACHER, Massimo MAFFEZZOLI, Stefan SCHEUCHELBAUER

Doka GmbH

AUSTRIA

1. INTRODUCTION

The durability and service life of a dam structure is designed in an early stage of the planning phase. In order to achieve the planned target of concrete quality, monitoring during execution is one of the keys of quality management. For instance, in case of mass concrete structures one of the most important aspects is the monitoring of the temperature gradient and appropriate actions on site to avoid cracking and simply guarantee the concrete quality already during construction.

The ambition is to emphasize the importance how to optimize the combination of formwork expertise with superior material technology enabling a well-defined construction sequence between all relevant parties. Resulting in increased quality management and enhanced durability of the designated concrete structure.

2. THE METHOD

2.1. UNDERSTANDING – CONCRETE

Already in the project tendering and work preparation phase, the early strength development of individual concrete mixtures with different performance will be simulated with respective calibration and temperature assumptions. Necessarily, the intended concrete formulations can be re-adjusted.

For this purpose, the early strength development of the intended concrete type is used as a performance indicator that can be planned, measured and controlled with Concremote (=real-time concrete monitoring system). Doka Concremote is used as a method to optimize the construction process and thus significantly increase productivity on the job site resulting in secured cycle time and optimized concrete costs in the execution phase (= 'Concremote Value Engineering Methodology', figure 1).

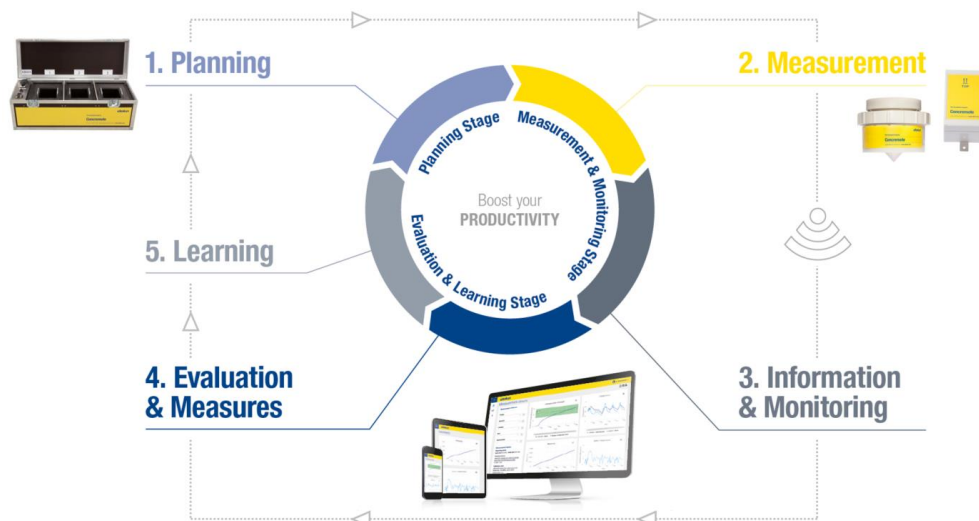


Figure 1: The Concremote Value Engineering Methodology

Ideally a construction company defines a concrete mix portfolio for example to consider ambient temperature changes (e.g. winter, summer, ...) and other influences already before construction. In order to be able to create a portfolio of concrete mix designs a final design strength of specific structure member has to be defined by design engineers. To meet the requirements a wide set of scenarios for possible concrete mix designs are proposed for specific concrete structure ('scenario gaming', figure 2).

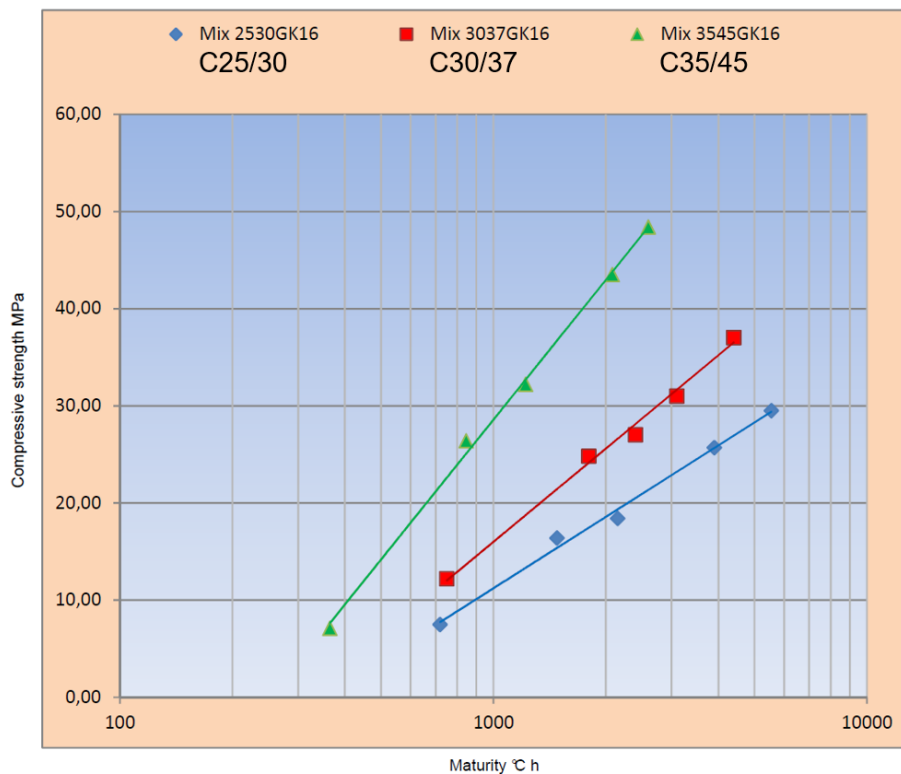


Figure 2: Portfolio of concrete mixtures

Part of the scenario gaming is the temperature simulation, which shows the temperature gradient in various points of critical structural members in a specific pouring section and also the influence to the adjacent building parts (see figure 3).

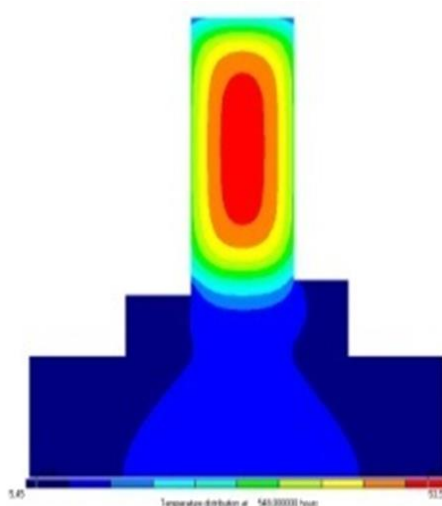


Figure 3: Simulation of the heat of hydration of a structural member

Once the optimized concrete mix portfolio is defined the project can go into the execution phase (transfer to real-time). Before the start of the construction phase each concrete mix design has to be calibrated in order to define correlation between compressive strength and maturity.

By measuring concrete temperature development using Concremote calibration boxes (figure 4), the maturity index of each concrete mixture is uniquely and directly related to its compressive strength and to the other concrete properties.

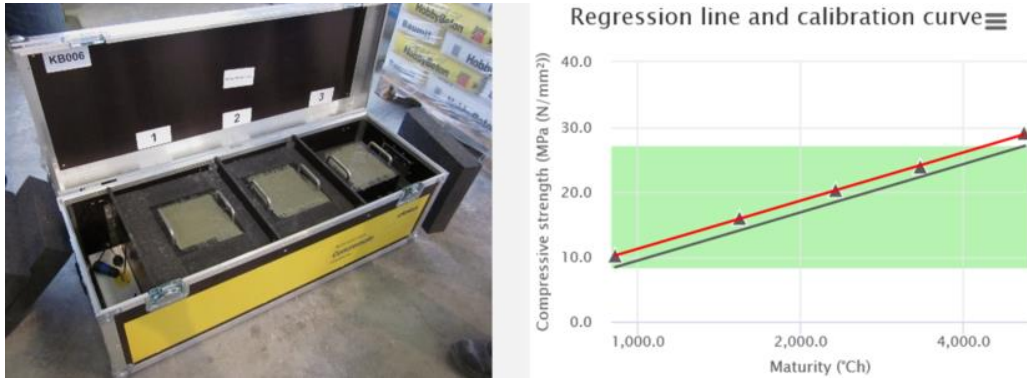


Figure 4: Concremote calibration box, calibration curve in the web portal

In the construction phase, the monitoring of the temperature and strength development by Concremote takes place in each critical concreting section. The reusable devices will be installed before pouring and the result will be monitored with the Concremote web portal (figure 5).

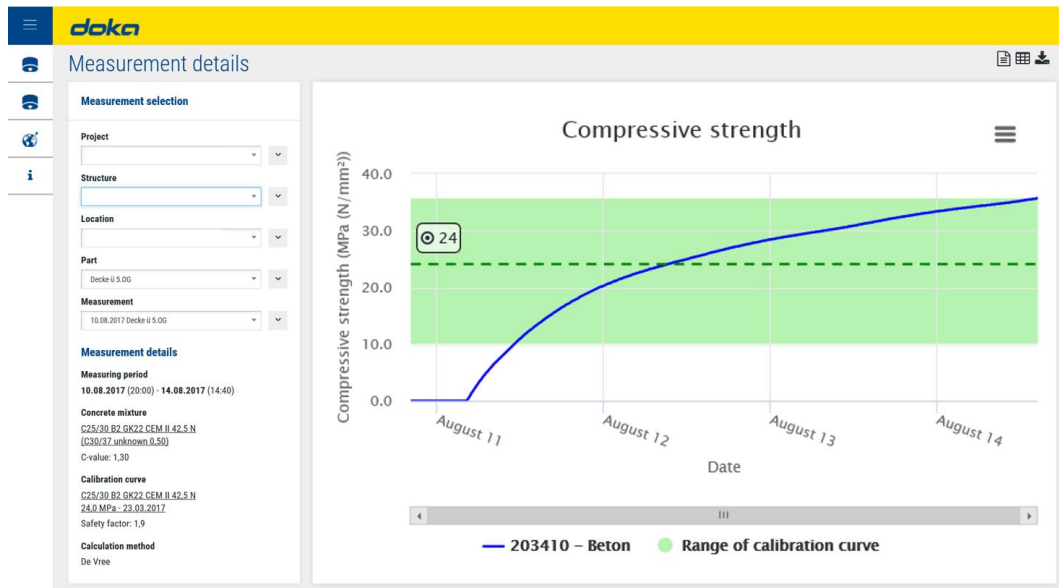


Figure 5: Concremote web portal – Real-time information (e. g. strength)

To enhance the quality of the concrete the curing is monitored and documented. As soon as a certain target value of compressive strength is reached formwork removal takes place. According to that, cycle times and commissioning quantities are reduced and the most optimized curing is obtained at the same time.

For mass concrete, e. g. dam structure, there is also the possibility to monitor the temperature gradient in a 'Delta T' diagram. The difference between core and surface temperature should be limited to enhance the concrete quality (less crack width). Concremote offers the possibility to control other external devices, like heating or cooling equipment. For this purpose, Concremote is able to switch-on and switch-off these devices automatically based on measured data.

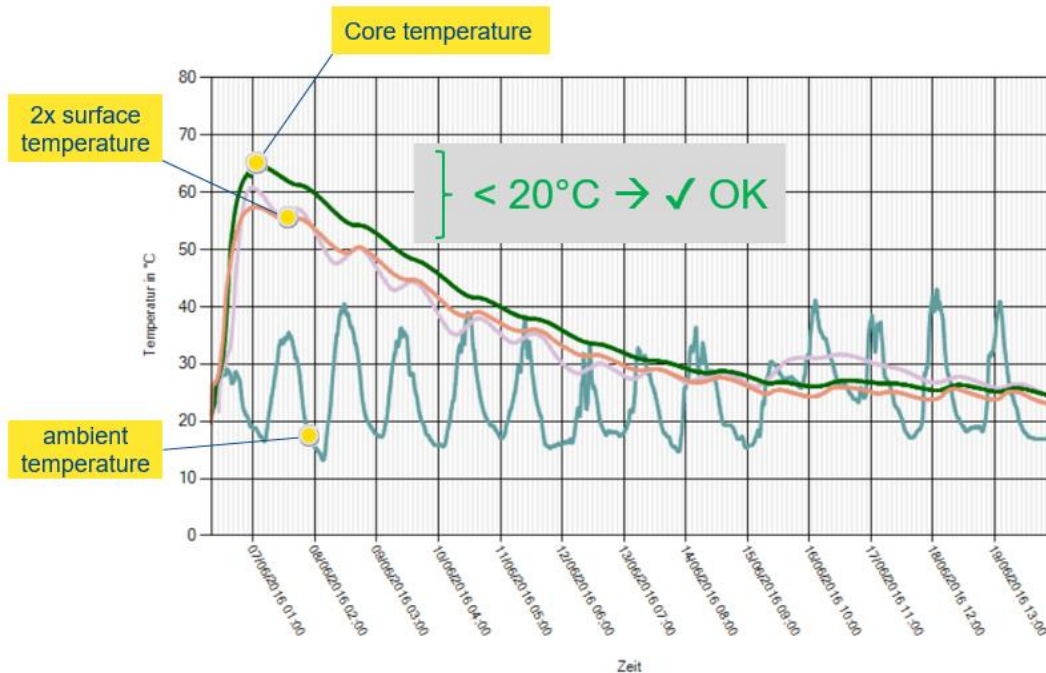


Figure 6: Temperature monitoring of CIP structure

Beside the benefits during design and construction phase, Concremote provides easy access for all stakeholders to the measurement data and a digital backup of all measured data.

In addition to the benefits of the Concremote Value Engineering Methodology, the combination with Doka's formwork expertise will positively impact the durability and the service life of the designated dam construction.

2.2. UNDERSTANDING – FORMWORK

Understanding, the building and job site requirements as well as the clients' intention of the construction method, is one of the main subjects to discuss before talking about an optimized formwork solution. Different to the common procedure on standard projects, the construction method and the corresponding formwork solution for dam constructions shall be defined already in the design phase of a project in order to optimize the processes during execution phase.

The optimized formwork solution can be influenced for example by the geology, the geometry of the structure, the construction method as well as the construction schedule (see figure 7). Vice versa an optimized formwork design can influence the geometry of the structure (e.g. increased block size resulting in less construction and block joints), improve the construction method and speed up the construction schedule resulting in increased productivity and ideally reduced construction costs.

An optimized formwork solution means to meet the right balance between the influencers and the formwork or accordingly align the specifications on both sides in order to meet the project and client expectations and furthermore assure the demanded final quality of the dam structure.



Figure 7: Bykle Dam, Norway – influence of geology and geometry

At the beginning of a planning phase of a project we need to understand two main subjects:

- **What is being built?**
- **How is it being built?**

Understanding - What is being built?

The reason for the question is to analyze the basics of the dam construction and forming the foundation for our future work on the concrete structure (e.g. consultancy, value engineering, ...).

Based on the project's unique requirements ("**what is being built**", figure 8) a tailor-made formwork solution in combination with an optimized construction method between all main structures (e.g. dams, power houses, inlets, outlets, draft tubes or scroll cases) shall be the target of the communication between 'formwork solution provider' and the 'contractor'.

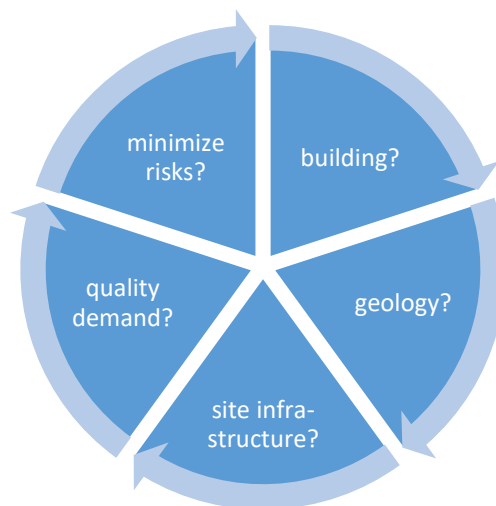


Figure 8: Influencers for optimized formwork solution (what is being built?)

Building: building designs often depend on the geology and surrounding job site conditions. Discussing the given settings in an early phase may result in simplifying the construction process with minor adjustments on the building designs and the pouring sequences.

Geology: type and size of dam structure is influenced by the geology. Most of the time earth and rockwork is influencing the time schedule of an entire project. Keeping the earth and rockwork to a minimum and compensate the mismatch with the concrete structure might be a possibility to save costs and time. Formwork versatility and optimized construction sequences provide the options of financial and time savings.

Site infrastructure: smooth and efficient construction process depend on a workable site infrastructure. Investing in service roads to shorten the paths for material handling or even the investment into an on-site concrete plant is positively impacting the final concrete result.

Quality demand: matching and assuring the exact concrete quality demand can have a major impact on the project budget. Reviewing the demand in an early phase provides the possibility to consider the measures to be taken in the execution phase.

Minimize risks: concrete joints or block joints pear a risk in regards to sealed joints and water tightness. Uncontrolled heat development in mass concrete may cause concrete cracking. In all event it will result in an impact on the project budget for repair works and maintenance. Also it may influence the durability and the service life of the dam structure. Optimize the volume of mass concrete with the corresponding pouring sequence in combination of concrete monitoring equals minimizing risks of unexpected costs.



Figure 9: Wudongde Dam, China

Understand - How is it being built?

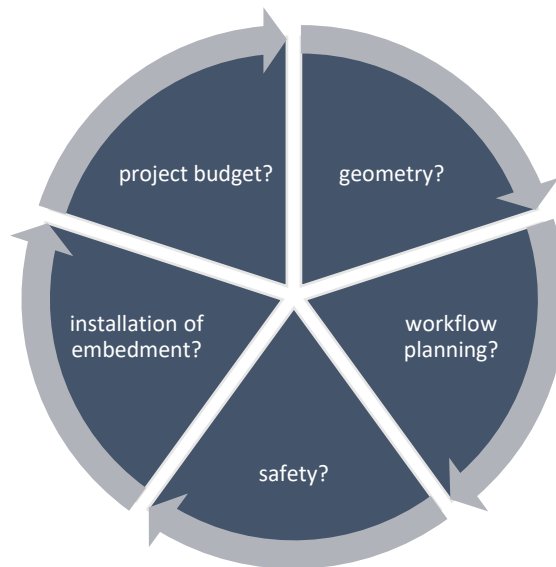


Figure 10: Influencers for optimized formwork solution (how is being built?)

Geometry: fundamental geometric conditions like wall jumps or inclination change in the resulting complexity, as well as the number of pouring sections and sequences, are essential for the selection of the right formwork systems.

Workflow planning: observing cycle times will have a considerable impact on the progress of the entire project. To ensure efficient workflow, detailed planning of system formwork, commissioning quantities, their reuse in additional construction sections within the project and personnel resources will be required for a positive impact on-site (= optimized time schedule).

Safety: developing a project-specific safety concept - from concrete monitoring with real-time measuring values or operating and repositioning formwork to stair towers and safeguards through to emergency planning.

Installation of embedment (reinforcement and water stops): it takes a significant portion of time to install reinforcement and water stops. A specific formwork solution considering any steel inserts or the installation of reinforcement ahead of time is drastically improving the formwork handling resulting in speeding up the time schedule.

Project budget: a solution customized to meet the project's unique requirements saves resources, as well as time and money - due to quality-tested formwork systems and a holistic project solution.

2.3. WHAT DOES IT MEAN IN PRACTICE? (PROJECT PROCEDURE)

The project success does not only depend on selecting the right material. Guidance for the 'big picture' (= products, concrete, logistics and on-site services) from an expert (**Consultant**) can help to enable target oriented processes and assure to meet the demanded result. Consultancy from the very beginning produces a comprehensive solution for the entire production cycle of the dam structure.

Professional coordination (**Project Management**) in all involved processes and along the entire project is the foundation of having an influence on the concrete result. In other words, each individual process needs to be optimized, custom tailored and monitored in order to meet the project specific requirements. Just the sum of all involved processes and the learning of the monitoring is creating and assuring the final concrete result.

To sum up, the 'big picture', considering the influences from the concrete and concrete temperature & strength development in combination with an effective and efficient formwork solution, is providing the possibility to optimize the construction method resulting in increased concrete quality in dam constructions.



Figure 11: Hydro power plant Lehen, Austria

3. ADVANTAGES FOR CONSTRUCTION COMPANIES AND INVESTORS

Amidst the different options in power plant construction, there is one goal at the top of the list: producing energy as quickly as possible. Although the objective is formulated with utmost simplicity, the solutions for getting there are no less challenging.

The combination of formwork experience and concrete expertise of Doka allows the customer a 'scenario gaming' in the design phase of a construction project. During execution phase the 'Concremote Value Engineering Methodology' offers the possibility to use the most economic concrete mixture and to monitor the evolution of the temperature gradients in the concrete. The resulting benefits are a higher productivity during construction, higher concrete quality and financial savings during execution and the service life of a dam structure.



Figure 12: Hydro power plant Muskrat Falls, Canada

REFERENCES

De Vree, R.T.; Tegelaar, R.A. (1998). Gewichtete Reife des Betons – Kontinuierliche, zerstörungsfreie Ermittlung der Betondruckfestigkeit, Beton 48 H. 11, S. 674-678.

Reinisch, A.; Peyerl, M.; Maier, G.; Krispel, S. (2015). Confirmation of Real Time Concrete Strength in Construction Projects, Tagungsband 11th CCC Congress Hainburg.

Saul, A. (1951). Principles underlying the steam curing of concrete at atmospheric pressure, Magazine of Concrete Research H. 6, S. 127-140.

Vereniging Nederlandse Cementindustrie (1984). Gewogen rijpheid, Betoniek 6/20 November/Dezember, S. 1-20.

COMMISSION INTERNATIONALE DES GRANDS BARRAGES

VINGT-SIXIÈME CONGRÈS DES GRANDS BARRAGES
Autriche, juillet 2018

DOI 10.3217/978-3-85125-620-8-067



This work licensed under a Creative Commons Attribution 4.0 International License. <https://creativecommons.org/licenses/by-nc-nd/4.0/>

**VISUAL DOCUMENTATION AND INSPECTION OF DAM SURFACES USING
STATE-OF-THE-ART TOTAL STATIONS**

Slaven KALENJUK

GRAZ UNIVERSITY OF TECHNOLOGY

AUSTRIA

Werner LIENHART

GRAZ UNIVERSITY OF TECHNOLOGY

AUSTRIA

Harald WACKENREUTHER

VERBUND HYDRO POWER GMBH

AUSTRIA

COMMISSION INTERNATIONALE
DES GRANDS BARRAGES

VINGT-SIXIÈME CONGRÈS DES
GRANDS BARRAGES
Autriche, juillet 2018

VISUAL DOCUMENTATION AND INSPECTION OF DAM SURFACES USING STATE-OF-THE-ART TOTAL STATIONS

Slaven Kalenjuk¹, Werner Lienhart¹, Harald Wackenreuther²

¹GRAZ UNIVERSITY OF TECHNOLOGY

²VERBUND HYDRO POWER GMBH

AUSTRIA

1. INTRODUCTION

Dam surveillance is crucial to minimize the risk of a dam failure. The International Commission on Large Dams (ICOLD) proposes guidelines to establish surveillance procedures, including instrumentation of sensors for monitoring and evaluating the data [1]. The overall assessment of dam safety comprises three major pillars: monitoring, visual inspections and checking & testing (Fig. 1). While special tests are due every one to five years, monitoring and visual inspections are required at frequent intervals.

A typical monitoring setup consists of a variety of sensors, each of which complements the other and contributes to the model analysis. The mathematical models also take into account the sensor limitations (e.g. sensitivity, accuracy) and thus give a good estimate on the reliability of the results. By contrast, visual inspections highly depend on the inspector's experience or performance. The resulting report, including photographs, drawings and comments, is subjective and may be incomplete and inaccurate, especially for the long-term documentation and inspection of the concrete surface of a dam's downstream side. Consequently, emerging technologies, as laser scanning and digital imagery, gain more and more attention for addressing these problems. A comprehensive three-dimensional documentation of the dam proved beneficial in deformation monitoring as well as for surface documentation. For this purpose, researchers focused on using Unmanned Aerial Vehicles (UAVs), carrying a Single Lens Reflex (SLR) camera

[2,3], cameras with telescopic lenses [4] and terrestrial laser scanners (TLS) in the past [5].

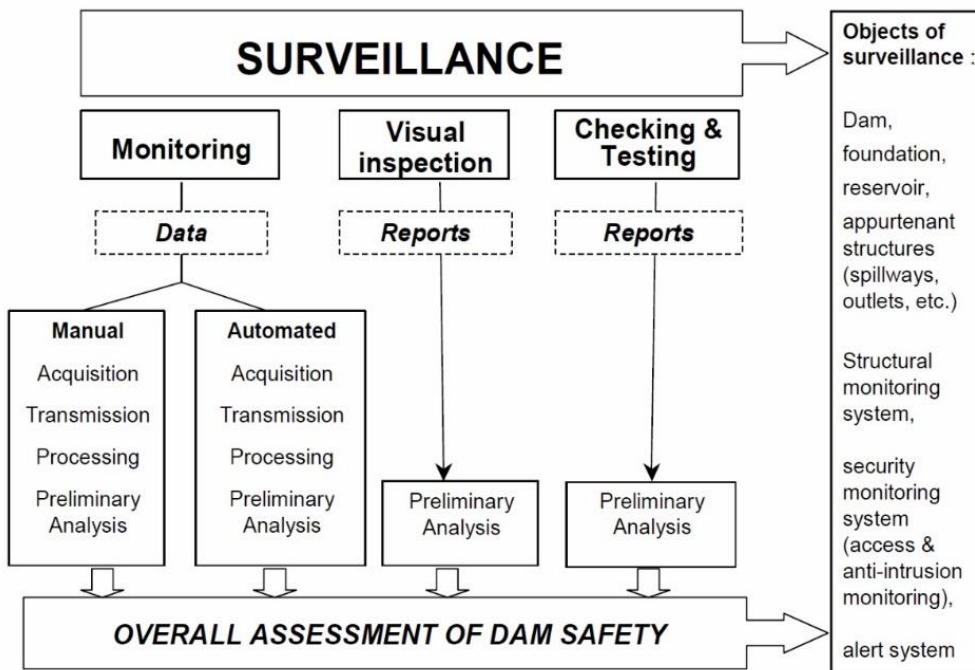


Fig. 1:
Dam surveillance as defined by ICOLD [1, p. 4]

The mentioned technologies imply highly sophisticated data acquisition and processing methods, requiring significant investments of money and time. For this reason, we propose a method, in which we use a sensor commonly used by dam operators in order to accomplish the same as by using UAVs and TLS. The recent developments of total stations (TS) [6] brought scanning and image functionalities, and thus opened up new fields of application such as surface mapping. In this paper, we present an approach for surface documentation and evaluation with modern total stations, which we apply to an Austrian arch dam. We present a workflow to compute a photorealistic three-dimensional model. Additionally, we introduce a novel system concept for automatic on-site detection and mapping of concrete deficiencies with high-resolution. By applying state-of-the-art processing techniques to the scan and image data and by exploiting the hardware features of the hybrid instrument, we demonstrate the potential for a surface monitoring solution. This solution enables merging the two major pillars of dam surveillance, monitoring and visual inspections. The proposed system enables change detection analysis of the dam's surface and hence a novel tool to contribute to an objective overall assessment of dam safety.

2. VISUAL DOCUMENTATION OF DAM SURFACES WITH MODERN TOTAL STATIONS

2.1. DATA ACQUISITION

For geodetic monitoring with total stations, the competent surveyor establishes stable points with known coordinates in the dam's vicinity. These points ensure that observations of multiple epochs and/or setup points are referenced in a common coordinate frame. Regarding modern total stations, which enable scanning and imaging, this is a large benefit over TLS and SLR cameras, as point clouds are registered directly and image orientations are already known and stored when images are captured.

Within a predefined polygonal area, modern TS instruments take images and acquire the scan data autonomously. The scanning resolution is not critical, as the shape of concrete (arch) dams is regular and thus well known.

2.2. DATA PROCESSING

The process of combining geometry and texture content of an object's surface is denoted as surface mapping. The principle workflow for processing the acquired scan and image data to derive a textured 3D photo model is illustrated in Fig. 2.

The processing of the scan data (left box in Fig. 2) implies point cloud registration, filtering, outlier elimination and hole filling procedures. Based on the preprocessed point cloud, we compute a continuous digital representation of the surface with a combined approximation-interpolation method. We partition the data space into voxels, for which we compute characteristic points by averaging the respective points inside. This step provides a simple but effective approximation method and hence noise reduction.

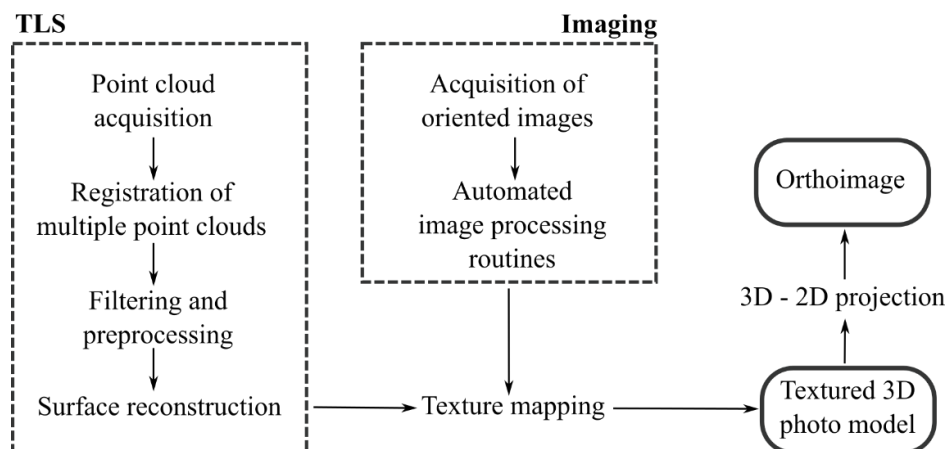


Fig 2:

Workflow to compute 3D photo models from scan and image data of TS

Eventually, we use 3D Delaunay triangulation to compute a triangle mesh, i.e. a set of triangles connecting the denoised point cloud.

Dependent on the properties of the captured images, we apply automated image processing techniques to reduce radiometric differences and thus to obtain a homogenous texture. Due to the knowledge about the orientation of each image, the textures are mapped onto the surface model, which is why this step is called texture mapping. As a result, a photorealistic representation of the dam's surface is obtained, which we then map onto a 2D plane to derive an ortho image with metric information.

2.3. FIELD STUDY AT AN AUSTRIAN ARCH DAM

To validate our approach, we performed practical measurements at the Drossen dam, which is located near Kaprun, Salzburg. It is 112 m high, has a crest length of about 360 m, and is thus one of the largest dams in Austria. Together with the Mooser dam, it impounds the Mooserboden reservoir.

Due to the large object-to-instrument distances (up to 200 m) and the scan range limitations, at least two setup points were required to cover the full dam. In order to speed up the data acquisition, we decided to use two total stations simultaneously set up at P_1 and P_2 (see Fig. 3 left). We used fixed points with known coordinates to reference measurements from both instruments in the national reference system.

We decided to use a Leica Multi Station MS50 and MS60. Both instruments use the same hardware for scanning and imaging. The instrument scans up to 1000 points per second with an accuracy of 2 mm at 100 m distance.



Fig 3:

Measurement site, overview image showing the two concrete dams of the reservoir Mooserboden (left, source: Verbund), illustration of the relevant components of the Multi Station MS60 (right)

The used instruments offer two cameras: the Overview Camera (OVC) and the On-Axis Camera (OAC). The OVC is a wide-angle camera with fixed focus and a large field of view (FOV) located above the telescope (see Fig. 3 right), whereas the OAC has a small FOV but benefits from the telescope's 30× magnification, providing image content rich in detail. Calibration of the OAC [7] gives an angular

resolution of approximately 1.96"/px in horizontal and vertical direction, which corresponds to a spatial resolution of 1 mm at 100 m distance.

Altogether, we acquired point clouds with around 10 million points and 300 OVC photos completely covering the Drossen dam. The fully automatic acquisition of scan and image data took about 4 hours in total.

Fig. 4 displays the final 3D photo model of the Drossen dam.

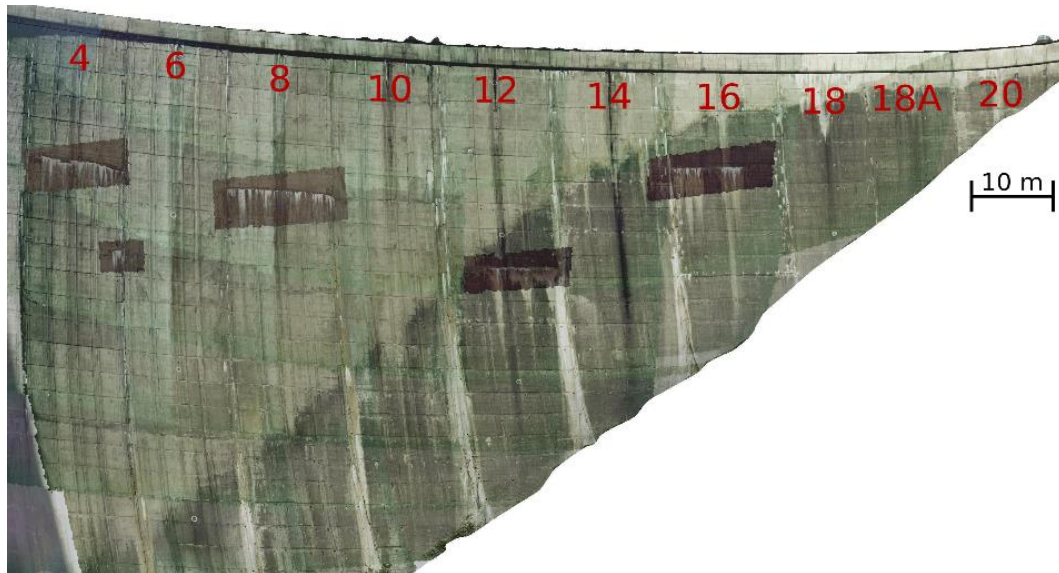


Fig. 4:
Textured 3D photo model of the Drossen dam

Apart from OVC images covering the complete dam, we captured OAC images of selective defects (dark areas of Fig. 4) and used them for texture mapping as well. Hence, large-scale textures and high-resolution textures are combined in one model providing a detailed documentation for areas of interest at relatively low memory capacity and computational cost. For defect regions, we generate ortho images with sequences of overlapping high-resolution OAC photos (see Fig. 5). While easy to handle, ortho images provide a valuable data basis for an objective assessment of the concrete's state. It is now possible to measure on the dam's surface without requiring direct access.



Fig 5:
Ortho image of a defect region on the downstream side of the Drossen dam (block 16), derived from 21 OAC textures (1 pixel corresponds to 2 mm on the surface)

3. SURFACE MONITORING SOLUTION WITH TOTAL STATIONS FOR ENHANCEMENT OF VISUAL INSPECTIONS

3.1. METHODOLOGY

Large dams commonly show concrete deficiencies, which do not necessarily pose a risk to the structure's safety. Some of these deficiencies appear just after construction and do not change over time. Therefore, detection of any visual changes on the dam's surface is crucial. The objective is the development of an algorithm to automatically detect new defects and identify the extent of deterioration of existing ones. In principle, we exploit the spatial information of the TS and use images to derive semantic information for visual change detection. We divide our evaluation into two parts: the on-site detection and acquisition and the change detection analysis, which we perform in a subsequent step (see Fig. 6).

We developed an application to carry out all required work processes (remote control, processing) on-site on a standard laptop. After the user measures the contours of the dam's surface, the instrument starts full dam photo acquisition with the OVC. With image-processing techniques applied to the OVC images, we localize defect regions on the dam (cf. Section 3.2). The known camera model simplifies the combination of image content to spatial information, i.e. horizontal (Hz) and vertical (V) angles.

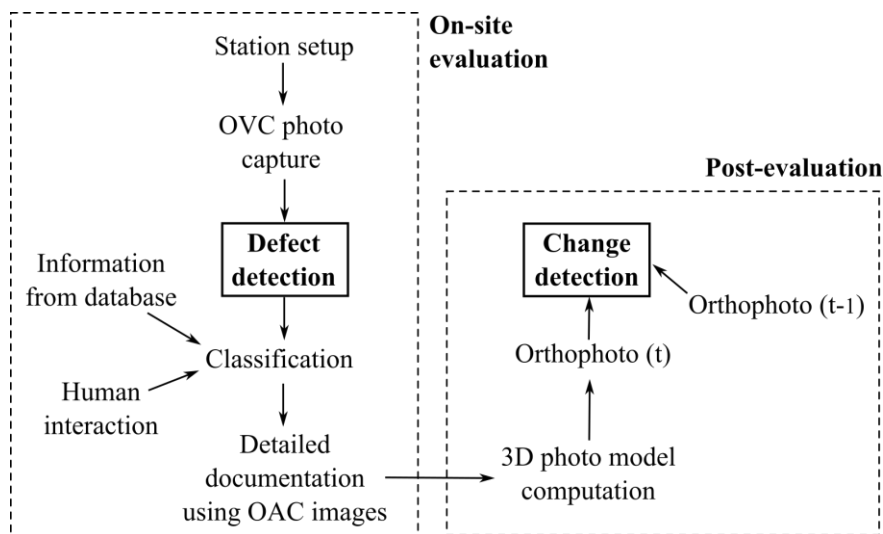


Fig 6:

Operating principle of the proposed surface monitoring solution

Afterwards, the application starts high-resolution scan data and OAC photo acquisition of potential defect regions. At this point, the operator can manually interact in order to minimize the time effort needed for data acquisition. However, to enhance the entire acquisition process, we propose an automatic classification procedure based on foreknowledge. Therefore, we establish a database containing coordinates of true defects as well as mistakenly identified defect regions in the

past surveys. The results of the automatic defect identification is hence dependent on the scope of effort spent on labeling the data (in terms of spatial or semantic information).

3.2. IMAGE-PROCESSING FOR DEFECT DETECTION

In order to formulate an algorithm, which is capable to detect damages on the concrete surface based on OVC photos, knowledge about the visual appearance of defects is necessary. For example, white spots on a concrete surface usually imply sinter formation, which may result from cracking or block joint openings. Wet areas, pop outs and other deficiencies evoke recognizable visual irregularities. Consequently, we analyze the captured OVC photos on these characteristics.

While most researchers focused on detecting cracks from images [8, 9, and 10] in the past, we generalize our analysis to detect any kind of concrete deficiencies on a dam using the captured OVC images. Fig. 7 shows the intermediate results of the algorithm. Detailed information on the procedure can be found in [11]. The algorithm describes potential defects in terms of pixel coordinates of the bounding rectangle (Fig. 7d), which eventually gives the orientation angles for the TS (using the known camera model). This angle values are used to steer the TS and to capture high-resolution images of the potential defect areas. It becomes obvious that the complete data acquisition is automatable by using a modern TS and a database with spatial information on the dam's boundaries and apparent defects.

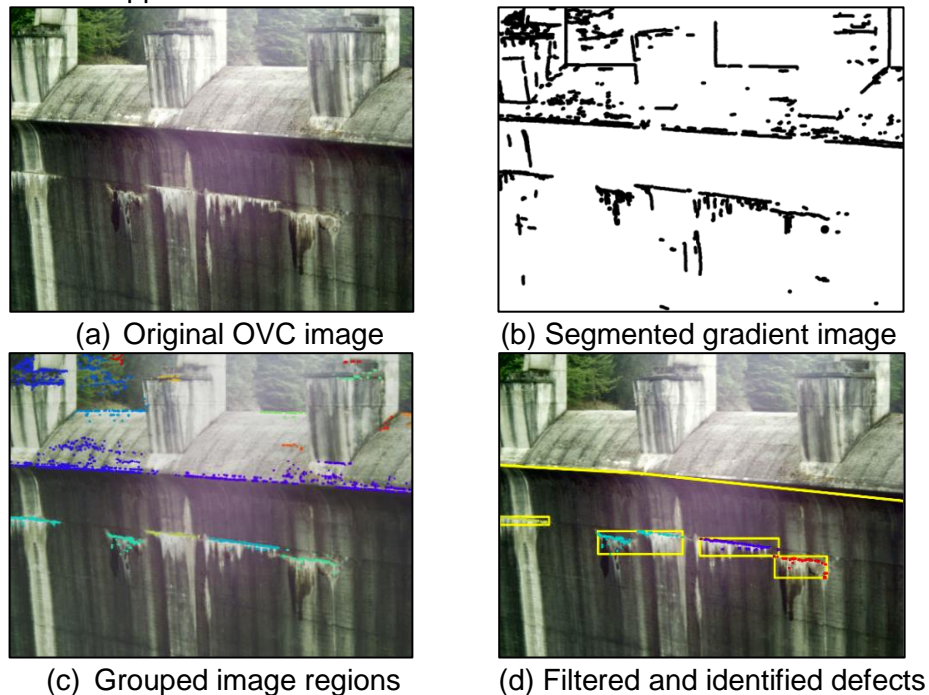


Fig. 7:
Important steps of the defect detection algorithm

3.3. MONITORING VISUAL CHANGES

The detection of visual changes in images is a well-researched topic in the field of remote sensing [12]. Consequently, a wide range of approaches were developed for automatic unsupervised change detection analysis in the past years. However, it turns out that these algorithms are well suited not only for large-scale satellite images but also for high-resolution ortho images of concrete defects.

One approach is to compare the pixel intensities of two images by e.g. differencing, rationing or by image regression [12]. It is simple, easy to implement but is sensitive to the acquisition conditions. Therefore, it is essential to pre-process the data, i.e. to match the images in terms of radiometry and spatial coverage. We adopted the analysis of [12, 13] and focus on gray value differences in the ortho images.

We validated the algorithm by placing shaving foam near a concrete crack to simulate an increase of efflorescence. The approach proved suitable to detect the changes and even to compute the area of change. Nevertheless, changing lighting conditions pose a problem to the algorithm, requiring more investigations for establishing a fully automatic change detection analysis. However, it assists the dam engineer and provides quantities to assess the dam safety objectively.

REFERENCES

- [1] ICOLD. Dam Surveillance Guide. *Technical Report 158, International Commission on Large Dams*. 109p, 2013.
- [2] HENRIQUES M. J., ROQUE D. Unmanned aerial vehicles (UAV) as a support to visual inspections of concrete dams. *Dam World. Portugal, Lisbon*, April 21–24, 2015, 12p, 2015.
- [3] BOAVIDA J., OLIVEIRA A., BERBERAN A. Dam monitoring using combined terrestrial imaging systems, *13th FIG Symposium on Deformation Measurement and Analysis*, LNEC, Lisboa, 2008.+
- [4] CAMP G., CARREAUD P., LANÇON H. Large Structures: Which Solutions for Health Monitoring? *International Archives of the Photogrammetry, Remote Sensing and Spatial Information Sciences. XL-5(W2)*, pp. 137–141, 2013.
- [5] BERBERAN A., PORTELA E.A., BOAVIDA J. Assisted visual inspection of dams as a tool for structural safety control. A case study. *Hydro 2006 – maximizing the benefits of hydropower*, 8p, 2006.
- [6] Leica MS60/TS60, User Manual, Version 1.0. Leica Geosystems, Heerbrugg, Switzerland. 90p, 2016.
- [7] EHRHART M., LIENHART W. Image-based dynamic deformation monitoring of civil engineering structures from long ranges. *Image Processing: Machine Vision Applications VIII*. SPIE 9405. 14p, 2015.

- [8] RABAH M., ELHATTAB A., FAYAD A. Automatic concrete cracks detection and mapping of terrestrial laser scan data. *National Research Institute of Astronomy and Geophysics*. 2(2). pp. 250–255, 2013.
- [9] MOHAN A., POOBAL S. Crack detection using image processing: A critical review and analysis. *Alexandria Engineering Journal*. 12p, 2017.
- [10] VALENÇA J., DIAS-DA-COSTA D., JÚLIO E., ARAÚJO H., COSTA H. Automatic crack monitoring using photogrammetry and image processing. *Measurement*. 46(1). pp. 433–441, 2013.
- [11] KALENJUK S., LIENHART W. Automated Surface Documentation of Large Water Dams Using Image and Scan Data of Modern Total Stations. *FIG Working Week 2017*, 8p, 2017.
- [12] LU D., MAUSEL P., BRONDIZIO E.S., MORAN E. Change Detection Techniques. *International Journal of Remote Sensing*. 25(12). pp. 2365–2407, 2004.
- [13] NIEMEYER I., MARPU P.R., NUSSBAUM S. Change detection using the object features. *IEEE International Geoscience and Remote Sensing Symposium*. pp. 2374–2377, 2007.

SUMMARY

In this paper, we presented a new approach for surface documentation using scan and image data of modern total stations. The proposed method is easy to perform for surveyors and requires less effort in data acquisition and processing compared to other measurement principles (e.g. documentation with UAVs).

The used total stations benefit from classic setup routines providing referenced point clouds and oriented images at the time of measurement. Hence, if stable points with known coordinates exist for referencing the measurements, the surveyor has to perform the time-consuming scanning process only once. It is thus possible to combine geometry acquired at the initial measurement epoch with photos captured at different measurement times to derive textured 3D models and ortho images.

We introduced a novel surface monitoring solution to address the risks related to visual changes on dam surfaces. By applying image-processing techniques to the acquired overview images, we automatically detect concrete deficiencies. With a database containing information from previous surveys, the system identifies newly emerged defects directly on-site. Subsequently, the instrument takes telescope images and scans dense point clouds of selective defects. As a result, the developed system provides multi temporal ortho images with high resolution, which we utilize to detect and to quantify changes on dam surfaces.

Our proposed approach delivers data, which is accurate, complete and objective. However, our system does not intend to replace the human inspector but it aims to provide a valuable data basis to enhance the safety assessment of large concrete dams.

COMMISSION INTERNATIONALE DES GRANDS BARRAGES

VINGT-SIXIÈME CONGRÈS DES GRANDS BARRAGES
Autriche, juillet 2018

DOI 10.3217/978-3-85125-620-8-068



This work licensed under a Creative Commons Attribution 4.0 International License. <https://creativecommons.org/licenses/by-nc-nd/4.0/>

PARAMETRIC STUDY IN GRAVITY DAMS ANALYZING THE INFLUENCE OF FLEXURAL, SHEAR DEFORMATION AND ROTATIONAL INERTIA EFFECTS

Iarly V. da SILVEIRA

Master degree student of the Post-graduate program in Structures and Civil Construction, BRASÍLIA UNIVERSITY

BRAZIL

Henrique A. N. de CASTRO FILHO

Master degree student of the Post-graduate program in Structures and Civil Construction, BRASÍLIA UNIVERSITY

BRAZIL

Renan R. RIBEIRO

Master degree student of the Post-graduate program in Structures and Civil Construction, BRASÍLIA UNIVERSITY

BRAZIL

COMMISSION INTERNATIONALE
DES GRANDS BARRAGES

VINGT-SIXIEME CONGRES DES
GRANDS BARRAGES
Autriche, juillet 2018

**PARAMETRIC STUDY IN GRAVITY DAMS ANALYZING THE
INFLUENCE OF FLEXURAL, SHEAR DEFORMATION AND ROTATIONAL
INERTIA EFFECTS ***

Iarly V. da SILVEIRA

*Master degree student of the Post-graduate program in Structures and Civil
Construction, BRASÍLIA UNIVERSITY*

BRAZIL

Henrique A. N. de CASTRO FILHO

*Master degree student of the Post-graduate program in Structures and Civil
Construction, BRASÍLIA UNIVERSITY*

BRAZIL

Renan R. RIBEIRO

*Master degree student of the Post-graduate program in Structures and Civil
Construction, BRASÍLIA UNIVERSITY*

BRAZIL

*Analyse Paramétrique de l'influence des effets flexuraux, déformation de cisaillement et
de rotation inertielle sur des barrage de poids en béton*

1. INTRODUCTION

Dams have an important economic role, either as reservoirs or to increase the potential energy of water and generate electricity. However, due to the possible rupture; they have a high-risk potential, which imposes more rigorous analyzes and inspections. These structures can cause enormous worries because of the possibility of eventual collapse, with consequences for the environment, destruction of fauna and flora, and loss of human life.

In the literature, there are few researches that contemplate the behavior of the flexion and shear effects of the dam as a result of a simplification adopted on the representation of the problems that involves those structures. Theories of the equation of motion are distinguished, existing theories that include only the bending effect (Euler-Bernoulli theory), bending and rotational inertia (Rayleigh Theory) and bending, rotational inertia and shear deformations (Timoshenko's theory). In general, such effects are more important as less slender the structure is. For plane state structures, the slenderness can be measured as the ratio of its width by length or height

The present study sought to analyze the influence of the consideration of shear effects and rotational inertia as well as to develop a code in the Python language based on the technique of finite differences. For the validation of the results based on the program, the outcomes of a supported beam were compared with those obtained by the Ansys v18 (finite element software).

For simplicity of calculations and numerical modeling, it is assumed that the dam can be modeled as a cantilever beam of variable section, using the hypothesis of plane strain state. Also, the properties of the material are homogeneous, isotropic, linear and elastic.

A parametric analytical study is developed to verify the influence of this consideration on the first five natural frequencies of a beam, admitted by simplification as simply. Then, several models of beams with different boundary conditions and width / length ratios are analyzed. Based on the program developed, it is obtained the results of the first five natural frequencies; then, graphs are drawn illustrating the influence of considering these effects for clamped beams.

The major studies that this article was based on: Anderson [1] studied the transverse motion of beams modeled in the Timoshenko manner for the case of time dependent boundary and normal loads. Clough [2] presents the theoretical dynamic analysis of continuous systems, in which theory this work is based on. Herzog [3] presents an approximate method of calculation using a shell platform and a series of approximations. Silva [5] studied a particular types of non-uniform cantilever beam structures as wedges and cones are vastly used in engineering practice.

2. THEORETICAL EQUATION OF DEEP BEAM NATURAL FREQUENCY

According to Pedroso [4], the vibration equation of a deep beam, with constant properties along its length, considering the flexural, shear deformation, and rotational inertia of the cross-section effects and an applied dynamic distributed load is given by Eq. [1]:

$$EI \cdot \frac{\partial^4 y}{\partial x^4} - \left(q - \bar{m} \cdot \frac{\partial^2 y}{\partial t^2} \right) - J \cdot \frac{\partial^4 y}{\partial x^2 \partial t^2} + \frac{EI}{\gamma} \cdot \frac{\partial^2}{\partial t^2} \left(q - \bar{m} \cdot \frac{\partial^2 y}{\partial t^2} \right) - \frac{J}{\gamma} \cdot \frac{\partial^2}{\partial t^2} \left(q - \bar{m} \cdot \frac{\partial^2 y}{\partial t^2} \right) = 0 \quad [1]$$

Where \bar{m} is the mass by unit length; $\gamma = k' \cdot G \cdot A$, where k' the shear correction factor of the section, A is the section area and G is the transverse elastic modulus of the material; and $q = f(x, t)$ is the dynamic distributed load.

It is useful to state the meaning of each term in the Eq. [1]. The first term (Eq. [2]) represents the basic flexural theory (Euler's beam). The second term (Eq. [3]) represents the consideration of rotational inertia of the cross-section effect. The third term (Eq. [4]) represents the shear deformation effect. The fourth term (Eq. [5]), represents the coupling between the rotational inertia and shear effects.

$$EI \cdot \frac{\partial^4 y}{\partial x^4} - \left(q - \bar{m} \cdot \frac{\partial^2 y}{\partial t^2} \right) \quad [2]$$

$$J \cdot \frac{\partial^4 y}{\partial x^2 \partial t^2} \quad [3]$$

$$\frac{EI}{\gamma} \cdot \frac{\partial^2}{\partial t^2} \left(q - \bar{m} \cdot \frac{\partial^2 y}{\partial t^2} \right) \quad [4]$$

$$\frac{EI}{\gamma} \cdot \frac{\partial^2}{\partial t^2} \left(q - \bar{m} \cdot \frac{\partial^2 y}{\partial t^2} \right) \quad [5]$$

To obtain the mode shape function of free vibration, one can apply the separation of variables procedure to decouple the solution of Eq. [1] into a function of x (mode shape) and t (time-dependent amplitude) [2]. Assuming a harmonic response for the time-dependent amplitude, the application of separation of variables into Eq. [1] written for free vibration, i.e. $q = 0$, yields Eq. [6]:

$$\phi(x)^{IV} - a^4 \cdot \phi(x) + a^4 \cdot r^2 \cdot \phi(x)^{II} + \frac{\bar{m} \cdot \omega^2}{\gamma} \cdot [a^4 \cdot r^2 \cdot \phi(x) + \phi(x)^{II}] = 0 \quad [6]$$

Where $\phi(x)$ is the mode shape; $\phi(x)^i$ denotes the i -th derivative of $\phi(x)$ relative to x ; r is the radius of gyration; and a is a convenient constant defined in Eq. [7]:

$$a = \frac{\bar{m} \cdot \omega^2}{EI} \quad [7]$$

For simplicity it is assumed a mode shape form of a simply supported beam, since analytical solution of Eq. [6] is complex for other support conditions. The

validity of such supposition for gravity dams models will be further assessed. For a simply supported beam, the mode shape has the form [2]:

$$\phi(x) = X \cdot \sin\left(\frac{m \cdot \pi \cdot x}{L}\right) \quad [8]$$

Where L is the length of the beam; $m = 1, 2, 3, \dots$ is a natural number that indicates the vibration mode; and X is a constant for generalization purposes. Substituting Eq. [8] in Eq. [6], one arrives in Eq. [9], after arithmetical manipulations:

$$\left(\frac{m \cdot \pi}{L}\right)^4 - a^4 - a^4 \cdot r^2 \cdot \left(\frac{m \cdot \pi}{L}\right)^2 \cdot \left(1 + \frac{E}{k'G}\right) + a^4 \cdot r^2 \cdot \left(a^4 \cdot r^2 \cdot \frac{E}{k'G}\right) = 0 \quad [9]$$

Following Pedrosa [4], for the first vibration modes the last term of the sum in the left-hand side of Eq. [9] can be disregarded since it can be proven to be very small when compared to the third term. With this consideration, Eq. [9] can be simplified to Eq. [10]:

$$a^4 = \beta^4 \cdot \frac{1}{1+r^2 \cdot \beta^2 \cdot (1+\gamma')} \quad [10]$$

Where the terms β and γ' are defined as:

$$\beta = \frac{m \cdot \pi}{L} \quad [11]$$

$$\gamma' = \frac{E}{k' \cdot G} \quad [12]$$

From Eq. [10] it is possible to define τ as the correction factor for shear deformation and rotational inertia of the cross-section effects:

$$\tau = \frac{1}{1+r^2 \cdot \beta^2 \cdot (1+\gamma')} = \frac{1}{1+r^2 \cdot \beta^2 + r^2 \cdot \beta^2 \cdot \gamma'} \quad [13]$$

With Eq. [7], [10] and [13] one arrives at the Eq. [14]:

$$\omega_m^{f+s+r} = \left(\frac{m \cdot \pi}{L}\right)^2 \cdot \sqrt{\frac{EI}{\bar{m} \cdot L^4} \cdot \tau} \quad [13]$$

With $m = 1, 2, 3, \dots$ defining the vibration mode considered. Eq. [13] defines the natural frequency of a deep beam considering the flexural, shear deformation, and rotational inertia of the cross-section effects. It is interesting to observe the resemblance of Eq. [13] to the classical natural frequencies equation of Euler's beam: the only difference is the correction factor τ .

It is important to note that Eq. [13] is valid for a beam with constant properties along its length and only for its first vibration modes.

3. ANALYTICAL PARAMETRIC ANALYSIS OF SHEAR DEFORMATION AND ROTATIONAL INERTIA OF CROSS-SECTION EFFECTS AND DEVELOPMENT OF A FINITE DIFFERENCE METHOD ALGORITHM

From Eq. [13], making $\tau = 1$ one obtains the classical natural frequencies equation of Euler's beam, which considers only the flexural effect:

$$\omega_m^f = \left(\frac{m \cdot \pi}{L}\right)^2 \cdot \sqrt{\frac{EI}{\bar{m} \cdot L^4}} \quad [14]$$

The division of Eq. [13] by Eq. [14] defines the parametric ratio between these two frequencies:

$$\frac{\omega_m^{f+s+r}}{\omega_m^f} = \sqrt{\frac{1}{1+r^2 \cdot \beta^2 + r^2 \cdot \beta^2 \cdot \gamma'}} \quad [15]$$

To perform the parametric analysis, consider a beam with cross-section height equal to h and Poisson ration ν . Substituting the definitions of Eq. [11] and [12] in Eq. [15], and performing some arithmetic manipulations, one obtains:

$$\frac{\omega_m^{f+s+r}}{\omega_m^f} = \sqrt{\frac{1}{1 + \frac{(m \cdot \pi)^2}{12} \left(\frac{h}{L}\right)^2 + \frac{(m \cdot \pi)^2}{5} \left(\frac{h}{L}\right)^2 \cdot (1 + \nu)}} \quad [16]$$

The ratio h / L is a typical measurement of the importance of considering shear effects in beams. The higher this ratio more the beam behavior approaches to deep beam rather than slender beam.

Due to the complexity of the analytical approach for the dynamic problem of clamped beams, with variable section, based on the theory of Timoshenko, the numerical approach of the problem is justified.

In the present work, it was used the Finite Differences Method (FDM), implemented using the Python programming language, to discretize the general dynamic equation of the Timoshenko beam in free vibration, presented in Eq [6].

The FDM is a method to solve differential equations that is based on the approximation of derivatives by finite differences. The approximation formula is derived from the Taylor series of the derived function. In Eq [6], the differential operators of fourth and second order can be replaced by finite expressions of FDM.

After a mesh convergence study, it was chosen to use a 30-node model in all simulations made in this work.

The first validation of the implemented algorithm was done comparing the analytical results for a typical simply supported beam with constant cross-section, given by the parametric equation presented in Eq. [13], with the numerical results. Considering a typical beam, it is obtained the parametric curves that associate the variation of the h / L ratio, measure of beam depth, to the relation between frequency obtained by Euler's theory and Timoshenko's theory. The results are presented in Figure 1. It is observed a good conformity between the analytical curves and the numerical ones, obtained by the algorithm implemented.

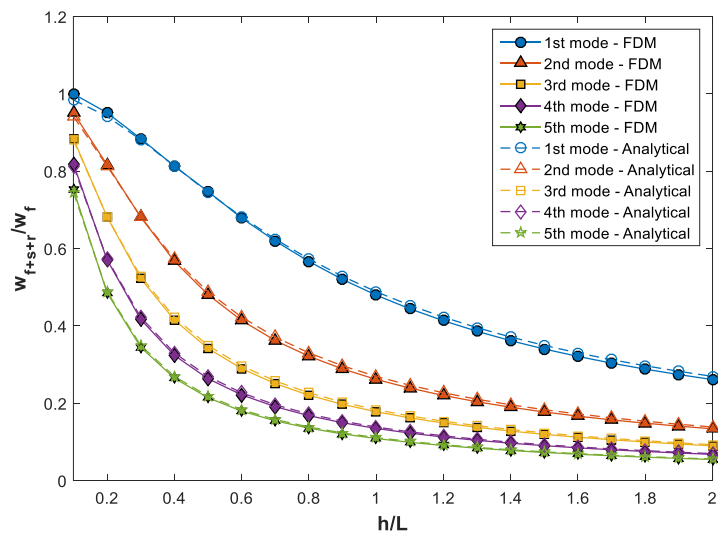


Figure 1: Analytical and numerical results for the ratio between the natural frequencies of Timoshenko and Euler theories, for a simply supported constant cross-section beam.

The analytical results, in general, presents a greater impact of the effects of Timoshenko, denoting that the numerical model implemented produces a more rigid model. However, such behavior is expected from numerical models if compared to analytical results.

In addition, a validation was also made through the comparison with a finite element model developed in Ansys software. In this case, a cantilever beam, with constant section and typical properties, was modeled both in the finite element software and using the FDM algorithm.

It is possible to observe an acceptable approximation between the results, validating the implemented algorithm through the comparison with Ansys, which besides being a consecrated software, uses a stronger formulation (finite elements) than the finite differences.

It is important to note that, as the h / L ratio is increased, making the beam more rigid and the Timoshenko effects more important, the FDM implemented formulation differs more and consistently in all modes from the formulation of finite elements. The results via FDM present visibly more rigid models, with higher natural frequencies, which evidences the difficulty of the implemented modeling to correctly capture the real behavior of the beam.

However, due to the consistency of this increase over all modes, the algorithm is considered as valid for a parametric and qualitative investigation of the effects of Timoshenko on clamped free beams with variable cross-section

4. PARAMETRIC ANALYSIS OF A CANTILVER BEAM WITH VARIABLE CROSS-SECTION

As already presented, the dam dynamic problem can be analyzed, in an initial study, as a cantilever beam with variable cross-section, based on the plane strain state hypothesis. In this section, the FDM algorithm is used to evaluate the impact of shear deformation and rotary inertia consideration on the natural frequencies of a clamped-free beam, representing a dam in plane strain state.

For all analyzes performed, the following properties of the material were used (Table 1):

ρ (kg/m ³)	2400
Young's modulus- E (GPa)	20
Poisson coefficient	0.2

Table 1: Properties of material

First, a beam with constant section is analyzed, to identify only the influence of the shear deformation effects and rotational inertia on the section.

For this, three analyzes are made: two with only one of the effects acting, and a third considering all the effects, including the coupling. The Figures 2, 3 and 4 present the results. The first frequency was not included due to an unexpected behavior, which will be further discussed.

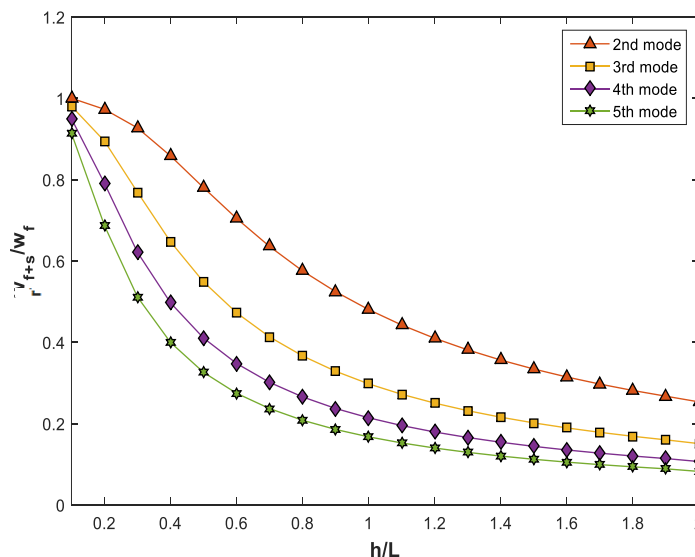


Figure 2: Ratio between the natural frequencies of Timoshenko and Euler theories, for a cantilever beam with constant cross-section, considering only rotary inertia effects.

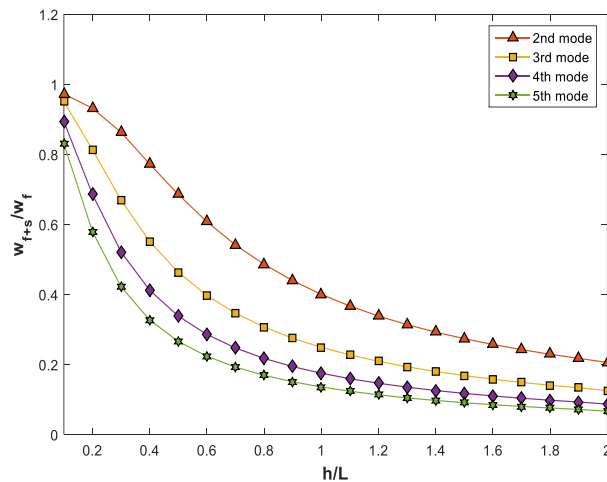


Figure 3: Ratio between the natural frequencies of Timoshenko and Euler theories, for a cantilever beam with constant cross-section, considering only shear deformation effects.

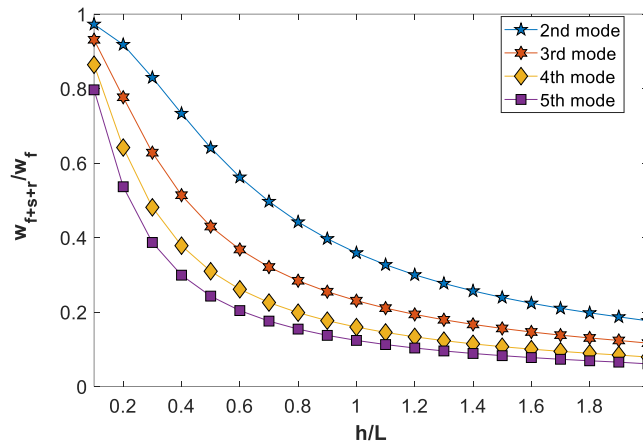


Figure 4: Ratio between the natural frequencies of Timoshenko and Euler theories, for a cantilever beam with constant cross-section, with all effects.

In the analysis, it was noted that the behavior for the first frequency differs from that expected: the consideration of the Timoshenko theory effects made the beam behave more rigid in the first natural frequency, resulting in ratios higher than the unity. Such behavior is contrary to the very nature of considering such effects, which is achieving a more realistic behavior, considering additional effects that induces a more flexible model.

Although the consideration of only the rotational inertia produced values ratios below the unity for the first frequency, the consideration of shear deformation and all effects, including coupling, caused the Timoshenko beam to produce more rigid results. Thus, it was chosen to disregard the analysis of the first frequency which, although it is the most relevant in the dynamic study of structures, could not be well represented by the algorithm developed, either due to the implementation made or by inaccuracies of the Finite Differences Method, since it could not be identify the source of such difference.

The other frequencies, however, presented well-formed and expected behaviors, comparable to results obtained in test models in Ansys. Thus, the analyzes with variable section are also only done for the frequencies of the second to the fifth mode.

For the case of variable cross-section, it is analyzed various relations h/L , being h the height of the base cross-section of the beam (or dam base width in plane strain state) and L the length of the beam (or dam height in plane strain state). The top cross-section height is fixed as half of the base cross-section (Figure 5).

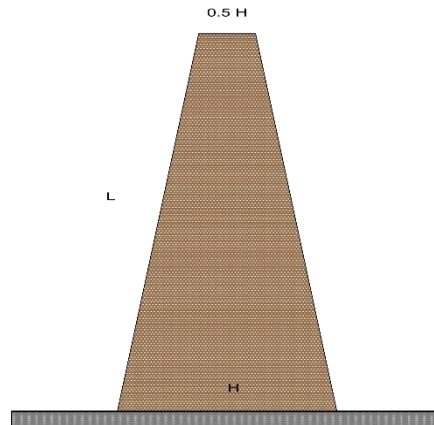


Figure 5: Geometric values used in the variable cross-section study.

The results for the variable cross-section case are presented in the Figure 6.

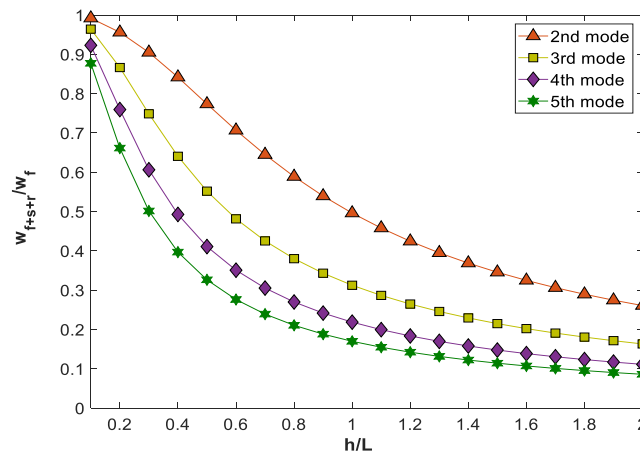


Figure 6: Parametric results for a cantilever beam with variable cross-section.

Comparing the results of variable cross-section with those for constant cross-section, presented in Figure 4, it is observable that the variable cross-section induces higher ratios, i.e. the Timoshenko effects tend to be slightly less present. For the same h / L ratio, the frequency ratios for all modes are higher for a variable cross-section than for the constant cross-section case.

5. CONCLUSION

The aim of this study is to observe the influence of considering the effects of shear deformation and rotational inertia in the dynamic analysis of a dam, modelled as a homogenous clamped beam.

The aim of this study is to observe the influence of considering the effects of shear deformation and rotational inertia in the dynamic analysis of a gravity dam, modelled as a cantilever beam with variable cross-section. This simplified dynamic analysis can serve as a preliminary evaluation of the dam's structural behavior and support additional detailed studies.

A parametric analytical study is developed, based on a simply supported beam model, to obtain first insights on the matter. Sequentially, a numerical analysis using a FDM implementation in Python is presented and used to study the cantilever beam with variable cross-section case.

Various studies are presented aiming to validate the FDM implementation: comparison with the simply supported analytical results and finite element models in Ansys. A satisfactory approximation is observed, appropriate enough for the qualitative and exploratory purpose of this work.

The study of the cantilever beam with variable cross-section presented an unexpected behavior for the first frequency. The consideration of Timoshenko theory induced a more rigid model than Euler theory, which is not acceptable, since the introduction of shear deformation and rotary inertia adds flexibility to the model. The source of this behavior could not be tracked, and it is supposed to arise from the implementation or numerical error of the formulation used. Even though the first mode is of most interest in the dynamic analysis of structure, the analysis was carried on with the second to fifth modes, since their consistent behavior still permits the objective of an exploratory and qualitative evaluation regarding the Timoshenko effects on plane strain dynamic analysis of dams.

5.1. ACKNOWLEDGEMENTS

The authors acknowledge the financial support of FAP-DF, CAPES and CNPq and the technical and infrastructural support of the Post-Graduate Program in Structure and Civil Construction (PECC) – UnB for the development of this work.

REFERENCES

- [1] ANDERSON, G. M. Timoshenko Beam Dynamics. JOURNAL OF APPLIED MECHANICS, 1971.
- [2] Clough, R. W., Penzien, Joseph (2003). Structural dynamics (3a. ed.). Berkeley: Computers & Structures, Inc.
- [3] Herzog, M. A .M.(1999). Practical dam analysis. London.
- [4] PEDROSO L. J. Dinâmica de Vigas Profundas – Publicação didática. Faculdade de Tecnologia da Universidade de Brasília, Brasília, 2003.
- [5] Silva, C. J., Daqaq, F. D. Nonlinear flexural response of a slender cantilever beam of constant thickness and linearly-varying width to a primary resonance excitation. Journal of Sound and Vibration, 2016.

COMMISSION INTERNATIONALE DES GRANDS BARRAGES

VINGT-SIXIÈME CONGRÈS DES GRANDS BARRAGES
Autriche, juillet 2018

DOI 10.3217/978-3-85125-620-8-069



This work licensed under a Creative Commons Attribution 4.0 International License. <https://creativecommons.org/licenses/by-nc-nd/4.0/>

**TIME-SPACE COLLISION ANALYSIS AND ADJUSTMENT METHOD FOR
HIGH ARCH DAM SURFACE CONSTRUCTION**

Chao HU

CONSTRUCTION DEPARTMENT, CHINA RENEWABLE ENERGY
ENGINEERING INSTITUTE, BEIJING, 100120
COLLEGE OF HYDRAULIC & ENVIRONMENTAL ENGINEERING, CHINA
THREE GORGES UNIVERSITY, YICHANG, HUBEI 443002

CHINA

Chunju ZHAO

COLLEGE OF HYDRAULIC & ENVIRONMENTAL ENGINEERING, CHINA
THREE GORGES UNIVERSITY, YICHANG, HUBEI 443002

CHINA

Yihong ZHOU

COLLEGE OF HYDRAULIC & ENVIRONMENTAL ENGINEERING, CHINA
THREE GORGES UNIVERSITY, YICHANG, HUBEI 443002

CHINA

Ling SONG

COLLEGE OF HYDRAULIC & ENVIRONMENTAL ENGINEERING, CHINA
THREE GORGES UNIVERSITY, YICHANG, HUBEI 443002

CHINA

COMMISSION INTERNATIONALE
DES GRANDS BARRAGES

VINGT-SIXIÈME CONGRÈS DES
GRANDS BARRAGES
Autriche, juillet 2018

TIME-SPACE COLLISION ANALYSIS AND ADJUSTMENT METHOD FOR HIGH ARCH DAM SURFACE CONSTRUCTION

CHAO HU^{1,2}, CHUNJU ZHAO², YIHONG ZHOU², LING SONG²

1. *Construction Department, China Renewable Energy Engineering Institute, Beijing, 100120*
2. *College of Hydraulic & Environmental Engineering, China Three Gorges University, Yichang, Hubei 443002*

CHINA

1. INTRODUCTION

The high arch dams are usually located in the narrow valley with steep terrain. The construction space of the storehouse is limited, the construction process is complicated, the construction methods are complex and the operations cross each other. Which makes difficult to layout construction equipment, reduce work efficiency, and even generate security risks. Therefore, how to scientifically formulate construction plans, avoid collisions and rework, and achieve efficient and safe construction of storehouse are the focuses by all parties.

According to the research [1-3], the rationality plan is directly relate to the successful implementation of the construction process. In the research about construction of time-space collisions, Hu Zhenzhong [4-6] integrated BIM and 4D technology to build structural collisions and security collision detection system. Wu Hao [7] integrated GNSS/GIS to guide cable cranes safety monitoring platform to achieve the cable crane safety operation analysis. Li Xuefeng[8] etl built cable machine and tower crane operation anti-collision system for Long Kai Kou hydropower. Xiao Zhihuai [9] combine GPS, rotating decoder and high-speed data acquisition card technology to design a dam building equipment anti-collision system. Wu Binping [10] cable machine analysis the selection of randomness and uncertainty of cable cranes, based on the edge of the limited criteria and space collisions to simulation cable cranes for arch dam. Wang Renchao [11] using spatial analysis and collision identification technology proposed a variety of

construction conditions of cable casting interference and joint simulation of the rules. Ren [12] proposed a mobile crane real-time anti-collision system.

In order to analysis the time-space collision in the process of pouring of the storehouse. It is necessary to figure out the basic construction procedure and activities logical relationship, then to simulate and analyze the plan implementation process, and find out the origin of collision and propose adjustment method to avoid collisions and improve construction efficiency [13-16].

To solve the above problems, the time-space evolution model of storehouse entities is established. Then analyzes the mechanism, classification and effect of the collision of storehouse construction entity. The time-space collision simulation and detection analysis model for the storehouse based on the pouring behavior simulation model were established. The results shows that this model can provide a scientific basis for the analysis and optimization of storehouse.

2. TIME-SPACE EVOLUTION MODEL OF STOREHOUSE CONSTRUCTION

In the construction of high arch dam, efficient construction machinery is usually apply to complete the work. Since there are many contents works on the storehouse surface, different types of construction machinery are required to cooperate with each other. However, the operation modes and efficiency of different machines are different. Therefore, it is necessary to establish the time-space evolution model of different mechanical surface activities to analyze the construction state such as operating status and running trajectory and so on.

The entity in the storehouse can abstract as a mass point, and its trajectory changes with time in the three-dimensional Euclidean space [17-18] is a spatial curve. The point trajectory is divide along the curve according to a certain time step Δt . Based on the trajectory of the point in the coordinate system, the point begins to move along the space curve from point P_t at the time t and arrives at the point P_{t+1} at time $t+1$, $r(s_t)$ and $r(s_{t+1})$ are the arc lengths of the curves at P_t and P_{t+1} , respectively. As shown in Fig.1, the velocity and acceleration of the point moving along the curve can express as:

$$v(t)=ds(t)/dt \quad [1]$$

$$a(t)=dv(t)/dt=d^2s(t)/dt^2+(ds(t)/dt)^2 \quad [2]$$

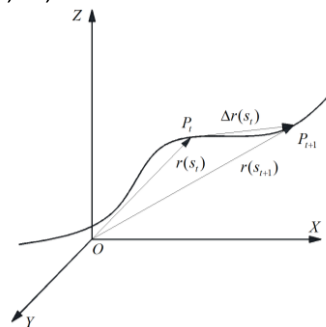


Fig. 1
Time-space path diagram

According to the above description, the time-space evolution model of construction entity in the construction space can describe by motion equations, motion trajectories, velocities and accelerations and so on. By establishing the construction space coordinate system, the entity position transformation can express as a single-valued continuous function of time t:

$$P(t)=[x(t) \ y(t) \ z(t)] \quad [3]$$

The rotation angle around the x-axis, y-axis, or z-axis is express as:

$$O(t)=[ox(t) \ oy(t) \ oz(t)] \quad [4]$$

In order to express the construction entity's translation and rotation in virtual environment, the vector $r(t)=[p(t) \ o(t)]^T$ is defined to represent the position and direction of the entity at a certain moment. When the construction entity moves, the time is from t_1 to t_2 , its direction and position changes from $r(t_1)$ to $r(t_2)$. Through the above matrix transformation operation, the three-dimensional spatial movement characteristics of the entity in the construction space can describe.

3. CONSTRUCTION COLLISION DETECTION AND ANALYSIS

3.1. COLLISION CLASSIFICATION AND EVALUATION INDEXES

According to entities state, all entities can divide into active entities and passive entities. The position of active entity changes constantly with time. The position of passive entity remains stationary. Therefore, the collision can be simplified into two types:1) Collision between active entities;2) Collisions between active and passive entities.

Through the observation and statistical analysis of high arch dam construction process, statistics show that the main types of collisions in construction are show in Table 3.

Table 3
Collision types and description

Collision Type	Explanation
Collision 1	Among cable cranes
Collision 2	Among bucket and surface machine
Collision 3	Between bucket and dam body
Collision 4	Between bucket and temporary structure
Collision 5	Between bucket and other hoists
Collision 6	Among machines in the storehouse
Collision 7	Between machines and dam structure

The collision means that two entities overlap in the same space at the same time. Different degrees of overlap cause different collision effects. Therefore, the degree of overlap can quantify by the indicators with following indexes:

(1) The space area of collision (S_c). Two entities have intersection in space when collisions take place, and the degree of collision can measure intuitively by the calculated area of intersection.

(2) The space ratio of collision (S_r). The space ratio means the ratio between the space area of collision and the original entity, because the entity of Collision gets different damage in the collision, this index can reflect influence extent between the two collisions.

(3) The continuance of collision (D_c). The continuance means the overlap time of two entities in the space, which reflect the influence of working procedure, if the continuance is long, and it maybe influence the project schedule.

(4) The duration ratio of collision (D_s). The duration ratio means the ratio between the continuance and the set time, and determine the adjustment will be necessary or not according to this index.

3.2. CONFLICTS IMPACT ANALYSIS

After the above indicators are analysis, the collision impact to the project can divide into the following types.

(1) Significant Effect. Significant effect usually caused by the breakdown of key equipment during construction. Key equipment cannot work normally, so the construction cannot carry out.

(2) Great Effect. Great effect caused by some troubles of construction equipment due to collision, but it can be solved by analyzing and eliminating the troubles in a certain time, but it may be delay the project schedule more or less as the long solving time.

(3) General Effect. Suspend the construction for a short time because of collision, but some simple processing can solve it, and it influences the project for a short time.

(4) Slight Effect. Collision leads to the put-off of construction date of the following activities, but the normal construction can be assuring by simple adjustment or delay of the process, and it has no effect on the whole schedule.

(5) No Effect. Although there is collision, the degree is subtle and it has no effect on construction entities and schedule.

3.3. COLLISION ADJUSTMENT MECHANISM

The adjustment of collisions can operate by time and space.

1) Time adjustment mechanism

The time adjustment is to change the running time parameters of the entities in the system to make the corresponding trajectories of the entities change to avoid the collision. As shown in Fig.2.

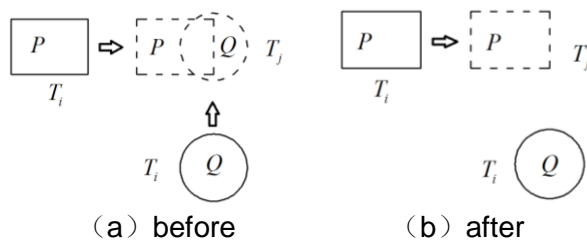


Fig. 2

Diagram of Time Adjustment Method

2) Space adjustment mechanism

Space adjustment is to change the position of entity to avoiding collisions. It obey the following principles: 1) active entity moves priority; 2) spacious entity moves priority.

3.4. CONSTRUCTION COLLISION DETECTION METHOD

In this paper, the bounding box detection method is apply to detect the collision of entities in the virtual scene. Different entities adopt different forms of bounding boxes to satisfy detection accuracy and efficiency in this paper.

Collision detection base on the change of the state of each entity in the storehouse, and the change of the state of the storehouse entity follows a certain rules. The simulation of the storehouse construction process can base on the movement status and movement mode of each entity.

In order to make the construction process efficient and safe to implement, this paper takes the construction process of the storehouses as the main line, simulates the operation of the construction equipment in the pouring activities as the basic unit in the virtual scene, and analyzes the process collision detection and effect in the simulation process. Finally, the simulation results are record to analysis and optimize the construction process. The workflow as shown in Fig.3.

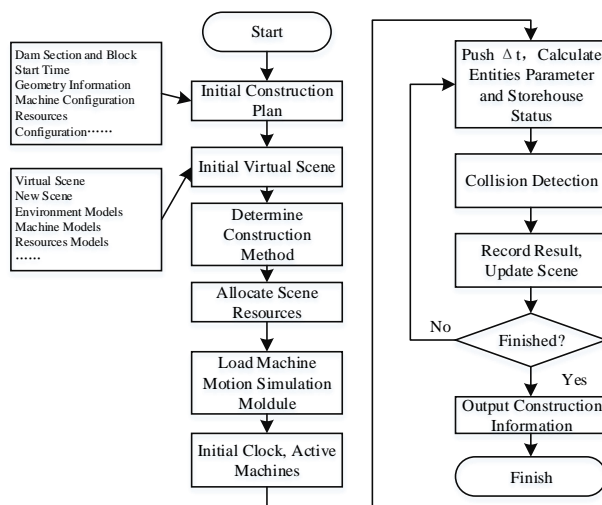


Fig. 3

Simulation process of surface in virtual scene

4. CASE STUDY

A project is located in the southwest of China. The max dam height is 285.5m. The dam body is divide into more than 2000 storehouses. One of a construction storehouse is take to simulate the process. The block located in 7# section layer 38, height 512.0m~518.0m. The volume is 3069 m³, the storehouse area is about 1023 m². In initial plan, five cable cranes, five lateral unloading cars, two scrapers and two vibrators is arrange.

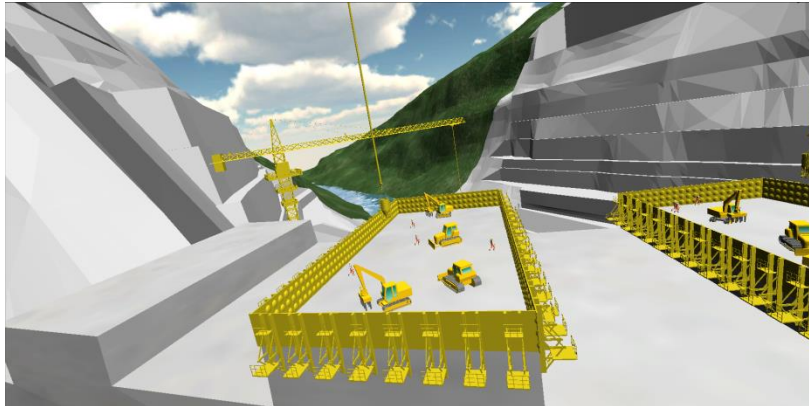


Fig. 3

A construction surface scene

When the cable crane operation speed are $v_1=(7.5\text{m/s},3.5\text{m/s})$, $v_2=(6.5\text{m/s},3.0\text{m/s})$, $v_3=(5.5\text{m/s}, 2.5\text{m/s})$, the best operation path into the storehouse as shown in Figure 7.

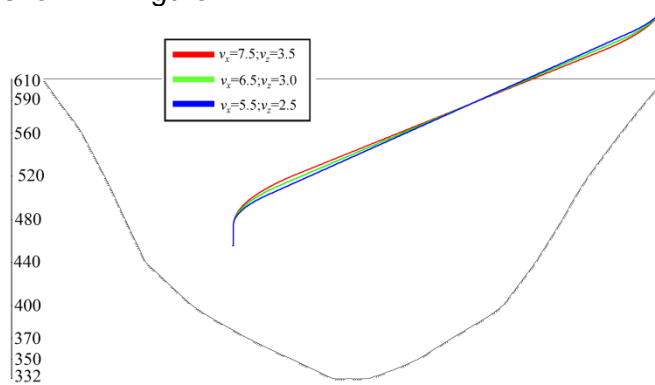


Fig 4

Optimized Cable Crane Path

After deduction of scene simulation, the total pouring time is 26.2h. The operation parameters of every cable crane is count and list in Table 4 (before optimization). In addition, the collision result as shown in Table 5. The statistic results demonstrate that collisions are mainly cause by cable crane, which also reduce the efficiency. By analysis the layout of cable crane, crane 2#~4# are located upward of block, crane 1# and 5# may effect by middle cranes. Thus, a new plan is carry out by reducing the cable crane number, and simulate again. The work time of each cable crane is list in Table 4 (after optimization). The total pouring time reduced to 23.23h.

Table 4.
The Working Time of Cable Cranes Before and After Optimization (Min)

No	Before optimization					After optimization				
	Times	Volume	Working time	Total time	Efficiency	Times	Volume	Working time	Total time	Efficiency
1#	18	162.0	762.08	1572	48.48%	/	/	/	/	/
2#	81	729.0	995.67	1572	63.33%	86	774.0	1079.3	1396	77.31%
3#	83	747.0	959.83	1572	61.06%	89	801.0	1112.9	1396	79.72%
4#	81	729.0	808.67	1572	51.44%	87	783.0	1044.5	1396	74.82%
5#	78	702.0	1008.18	1572	64.13%	79	711.0	890.1	1396	63.76%

Table 5
The Statistics of collision

The type of Collision	Collision Records	Solution
Collision 1	45	Avoid
Collision 2	23	Avoid
Collision 3	0	Null
Collision 4	3	Avoid
Collision 5	0	Null
Collision 6	8	Avoid
Collision 7	19	Avoid

5. CONCLUSION

In this paper, according to the collision problem in high arch dam construction process, the model of time-space evolution model for entities in the storehouse is established first. Then, the type and effect of the collision are analyzed and the collision detection and adjustment mechanism was established. At the same time, a dynamic adjustment and optimization model of the construction scheme was established. At last, a case study is carried out according to a real practice, and the results show that the method proposed in this paper can effectively provide a scientific basis for decision-making of construction projects.

ACKNOWLEDGEMENTS

This research was supported by National Natural Science Foundation of China (SN: 51709156).

REFERENCES

- [1] ZHENG JIAXIANG, YAN SHIQIN, LI XIANG, ET AL. CONSTRUCTION SCHEME AND PROGRESS OF 300 M HIGH ARCH DAM [J]. HYDROPOWER STATION DESIGN, 2013, 12(4): 1-3.
- [2] WANG RENKUN. REVIEW OF CONSTRUCTION ACHIEVEMENTS AND TECHNOLOGICAL DEVELOPMENT OF SUPER-HIGH ARCH DAM IN CHINA [J]. ADVANCES IN SCIENCE AND TECHNOLOGY OF WATER RESOURCES, 2015, 35(5): 13-19.
- [3] WANG AILING, DENG ZHENGANG. DEVELOPMENT AND CHALLENGES OF SUPER HIGH DAMS IN CHINA AND OTHER COUNTRIES [J]. WATER POWER, 2015, 41(2): 45-47.
- [4] HU ZHENZHONG, ZHANG JIANPING, ZHANG XIN. CONSTRUCTION COLLISION DETECTION FOR SITE ENTITIES BASED ON 4-D TIME-SPACE MODEL [J]. JOURNAL OF TSINGHUA UNIVERSITY (SCIENCE & TECHNOLOGY), 2010, 50(6): 820-825.
- [5] ZHANG J P, HU Z Z. BIM- AND 4D-BASED INTEGRATED SOLUTION OF ANALYSIS AND MANAGEMENT FOR COLLISIONS AND STRUCTURAL SAFETY PROBLEMS DURING CONSTRUCTION: 1. PRINCIPLES AND METHODOLOGIES [J]. AUTOMATION IN CONSTRUCTION, 2011, 20(2): 155-166.
- [6] HU Z, ZHANG J. BIM AND 4D BASED INTEGRATED SOLUTION OF ANALYSIS AND MANAGEMENT FOR COLLISIONS AND STRUCTURAL SAFETY PROBLEMS DURING CONSTRUCTION: 2. DEVELOPMENT AND SITE TRIALS [J]. AUTOMATION IN CONSTRUCTION, 2011, 20(2): 167-180.
- [7] WU HAO, TAO JING, LIN DAN. RESEARCH OF CABLE CRANE SAFETY MONITORING PLATFORM IN LARGE HYDROPOWER STATION HOISTING CONSTRUCTION [J]. JOURNAL OF WUHAN UNIVERSITY OF TECHNOLOGY, 2012, 34(10): 127-131.
- [8] LI XUEFENG, XU YIQUN, GAO CHUNHUI, ET AL. DESIGN, DEVELOPMENT AND APPLICATION OF ANTI-COLLISION SYSTEM IN THE CONSTRUCTION OF LONGKAIKOU HYDROPOWER STATION [J]. WATER POWER, 2013, 39(2): 57-60. (IN CHINESE)
- [9] XIAO ZHIHUI, HU YONGJIAN, CHEN JIA, ET AL ANTI-COLLISION SYSTEM FOR DAM CONSTRUCTION EQUIPMENT [J]. ENGINEERING JOURNAL OF WUHAN UNIVERSITY, 2013, 46(6): 815-818. (IN CHINESE)

- [10] WU BINPING, REN BINGYU, ZHONG DENGHUA. RESEARCH FOR CONSTRUCTION SIMULATION FOR ARCH DAM BASED ON MARGIN-PRIORITY PRINCIPAL AND SPATIAL COLLISIONS [J]. JOURNAL OF SYSTEM SIMULATION, 2013, 25(7): 1560-1567. (IN CHINESE)
- [11] WANG RENCHAO, WANG CHENXU. RESEARCH ON INTERFERENCE AND UNION PROBLEM OF CABLE MACHINE IN CONCRETE-DAM POURING SIMULATION [J]. JOURNAL OF WATER RESOURCES & WATER ENGINEERING, 2015, 26(2): 195-199. (IN CHINESE)
- [12] REN W, WU Z. REAL-TIME ANTICOLLISION SYSTEM FOR MOBILE CRANES DURING LIFT OPERATIONS [J]. JOURNAL OF COMPUTING IN CIVIL ENGINEERING, 2015, 29(04014100).
- [13] LI QINGBIN, SHI JIE. DAM CONSTRUCTION 4.0 [J]. JOURNAL OF HYDROELECTRIC ENGINEERING, 2015, 34(8): 1-6. DOI: 10.11660/SLFDXB.20150801. (IN CHINESE)
- [14] ZHONG DENGHUA, WANG FEI, WU BINPING, ET AL. FROM DIGITAL DAM TOWARD SMART DAM [J]. JOURNAL OF HYDROELECTRIC ENGINEERING, 2015, 34(10): 1-13. DOI: 10.11660/SLFDXB.20151001. (IN CHINESE)
- [15] CUI G, WANG X, KWON D. A FRAMEWORK OF BOUNDARY COLLISION DATA AGGREGATION INTO NEIGHBOURHOODS [J]. ACCIDENT ANALYSIS & PREVENTION, 2015, 83: 1-17.
- [16] GOERLANDT F, MONTEWKA J, KUZMIN V, ET AL. A RISK-INFORMED SHIP COLLISION ALERT SYSTEM: FRAMEWORK AND APPLICATION [J]. SAFETY SCIENCE, 2015, 77(1): 182-204.
- [17] SAURIN T A. SAFETY INSPECTIONS IN CONSTRUCTION SITES: A SYSTEMS THINKING PERSPECTIVE [J]. ACCIDENT ANALYSIS & PREVENTION, 2016, 93: 240-250.
- [18] BUDGAGA W, MALENSEK M, PALLICKARA S, ET AL. PREDICTIVE ANALYTICS USING STATISTICAL, LEARNING, AND ENSEMBLE METHODS TO SUPPORT REAL-TIME EXPLORATION OF DISCRETE EVENT SIMULATIONS [J]. FUTURE GENERATION COMPUTER SYSTEMS, 2016, 56: 360-374.
- [19] SUGIMOTO Y, SEKI H, SAMO T, ET AL. 4D CAD-BASED EVALUATION SYSTEM FOR CRANE DEPLOYMENT PLANS IN CONSTRUCTION OF NUCLEAR POWER PLANTS [J]. AUTOMATION IN CONSTRUCTION, 2016, 71: 87-98.
- [20] VAHDATIKHAKI F, HAMMAD A. DYNAMIC EQUIPMENT WORKSPACE GENERATION FOR IMPROVING EARTHWORK SAFETY USING REAL-TIME LOCATION SYSTEM [J]. ADVANCED ENGINEERING INFORMATICS, 2015, 29(3): 459-4

SUMMARY

To resolve the time-space conflicts in pouring concrete of high arch dams, this paper first analyzes the state transition of construction entities in a three-dimensional space, and develops a time-space evolution model and description method of the entities. Then, the transition process examines generation and classification of the conflicts and their effect is examined and a mechanism of space-time adjustment to the pouring procedure is established. Finally, a conflict detection mechanism is construct by simulations of concrete pouring. We have achieved simulations of the pouring procedure in the virtual scene and developed an optimization model for dynamically adjusting the construction scheme. Application to a practical case of concrete pouring shows that this method can provide detailed data for a pouring procedure before its implementation and hence it would help analyze the feasibility and security of a construction scheme.

Keywords: high arch dam; construction process; collision detection; collision adjustment; pouring

COMMISSION INTERNATIONALE DES GRANDS BARRAGES

VINGT-SIXIÈME CONGRÈS DES GRANDS BARRAGES
Autriche, juillet 2018

DOI 10.3217/978-3-85125-620-8-070



This work licensed under a Creative Commons Attribution 4.0 International License. <https://creativecommons.org/licenses/by-nc-nd/4.0/>

**EXTERNAL DEFORMATION MONITORING OF NINETEEN ROCKFILL DAMS
USING SATELLITE SAR DATA**

Hiroyuki SATO

Senior Researcher, HYDRAULIC STRUCTURE DIVISION, RIVER DEPT.

Masafumi KONDO

Head, HYDRAULIC STRUCTURE DIVISION, RIVER DEPARTMENT

Toshihide KOBORI and Ryotaro ISHIKAWA

Researcher, HYDRAULIC STRUCTURE DIVISION, RIVER DEPARTMENT

Takashi SASAKI

Research Coordinator for River Structures, RIVER DEPARTMENT

NATIONAL INSTITUTE FOR LAND AND INFRASTRUCTURE MANAGEMENT

Wataru SATO

Manager, DISASTER PREVENTION AND MITIGATION DEPARTMENT

Naruo MUSHIAKE

Manager, REMOTE SENSING GROUP, GEOSPATIAL TECHNOLOGY DEPT.

Takumi SATO

Senior Engineer, DISASTER PREVENTION AND MITIGATION DEPARTMENT

Ken'ichi HONDA

Engineer, REMOTE SENSING GROUP, GEOSPATIAL TECHNOLOGY DEPT.

KOKUSAI KOGYO CO., LTD.

JAPAN

COMMISSION INTERNATIONALE
DES GRANDS BARRAGES

VINGT-SIXIÈME CONGRÈS DES
GRANDS BARRAGES
Autriche, juillet 2018

**EXTERNAL DEFORMATION MONITORING OF NINETEEN ROCKFILL DAMS
USING SATELLITE SAR DATA**

Hiroyuki SATO

Senior Researcher, Hydraulic Structure Division, River Department,

Masafumi KONDO

Head, ditto,

Toshihide KOBORI

Researcher, ditto

Ryotaro ISHIKAWA

Researcher, ditto,

Takashi SASAKI

Research Coordinator for River Structures, River Department,

NATIONAL INSTITUTE FOR LAND AND INFRASTRUCTURE MANAGEMENT

Wataru SATO

Manager, Disaster Prevention and Mitigation Department,

Naruo MUSHIAKE

Manager, Remote Sensing Group, Geospatial Technology Department,

Takumi SATO

Senior Engineer, Disaster Prevention and Mitigation Department,

Ken'ichi HONDA

Engineer, Remote Sensing Group, Geospatial Technology Department,

KOKUSAI KOGYO CO., LTD.

Japan

1. INTRODUCTION

Satellite SAR (Synthetic Aperture Radar) is one of remote sensing technologies which makes it possible to measure distributions of ground surface deformations over a wide area, and it has been commonly used to evaluate crustal displacement due to earthquakes and volcanic activity, as well as landslides.

Recently, researches on external deformation measurements for dams using satellite SAR data have been conducted [1] to [8]. For the purpose of technological development to contribute to the rationalization and efficiency of dam deformation measurements, the authors have already shown the external deformations of five rockfill dams using satellite SAR data [6]. The authors have found that the satellite SAR produced external deformation measurements which were with an accuracy of about 5 mm when compared with the external deformation measurements obtained by GPS or electro-optical survey.

This paper reports on the results of external deformation monitoring of nineteen rockfill dams in Japan using satellite SAR data. The external deformation of dams for about two years by satellite SAR was measured and compared with other existing geodetic measurements such as GPS or electro-optical survey.

2. EXTERNAL DEFORMATION MONITORING OF NINETEEN ROCKFILL DAMS USING SATELLITE SAR DATA

2.1. OUTLINE OF NINETEEN ROCKFILL DAMS AND SATELLITE SAR DATA FOR STUDY

Fig. 1 shows the locations of the dams for study. Table 1 shows main specifications of nineteen rockfill dams and observational data of satellite SAR for study. In Table 1, ASC and DSC mean ascending and descending orbits of satellite SAR shown in Fig. 2, respectively. A total of 135 scenes of SAR data was used.

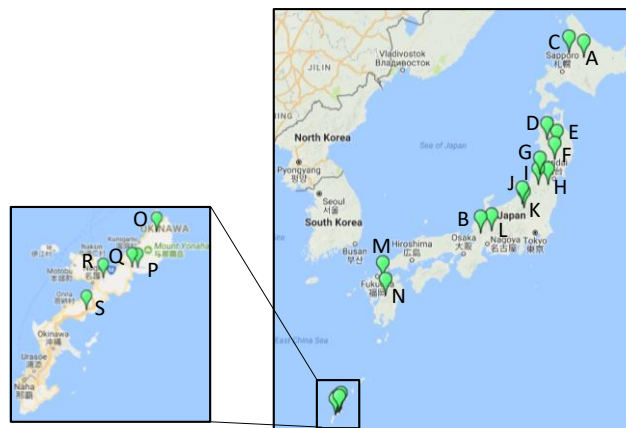


Fig. 1
Locations of Nineteen Dams for Study

Table 1
Main Specifications of Dams and Observational Data for Study

Name of dam	Height(m)	Crest length(m)	Orbit of satellite SAR	Numbers of data used	Observation day (year/month/day)					
A	78.5(*1)	595(*1)	ASC	6	2015/7/30	2015/8/13	2015/11/5	2016/5/5	2016/6/16	2016/7/28
B	161	427.1	DSC	6	2014/8/24	2015/9/20	2015/11/29	2016/3/6	2016/6/12	2016/8/21
C	41.2	440	ASC	5	2015/5/23	2015/6/6	2015/10/24	2015/11/7	2016/6/4	
D	89.9	786	ASC	6	2015/4/7	2015/5/19	2015/6/16	2015/7/28	2015/9/8	2016/6/28
E	52.5(*1)	210(*1)	ASC	6	2014/9/4	2014/10/16	2015/5/28	2015/8/6	2015/10/29	2016/5/26
F	127	723	ASC	6	2015/4/7	2015/5/19	2015/6/16	2015/7/28	2015/9/8	2016/6/28
G	112	510	ASC	5	2014/9/9	2015/6/2	2015/8/11	2015/11/3	2016/5/31	
H	90	565	ASC	8	2014/10/21	2014/12/16	2015/2/10	2015/3/10	2015/6/30	2015/8/25
I	66	348.2	ASC	5	2015/11/17	2016/6/14				
J	119.5	419.5	DSC	6	2014/9/9	2015/6/2	2015/8/11	2015/11/3	2016/5/31	
K	158	520	DSC	6	2014/10/28	2014/11/11	2015/6/23	2015/9/15	2015/11/24	2016/6/7
L	127.5	366	DSC	10	2014/10/9	2015/5/7	2015/5/21	2015/6/4	2015/6/18	2015/7/2
M	83	420	DSC	7	2015/7/16	2015/10/22	2016/4/21	2015/7/14		
N	35	244	DSC	7	2014/9/30	2014/10/14	2014/11/25	2015/10/13	2016/4/12	2016/7/5
O	35(*1)	330(*1)	DSC	8	2016/9/13					
P	91.7	260	ASC	8	2014/10/24	2015/2/27	2015/5/22	2015/6/5	2015/9/11	2015/11/6
Q	66	445	ASC	15	2016/2/12	2016/6/3				
R	66.5	198	DSC	15	2015/2/9	2015/2/23	2015/9/7	2015/9/21	2015/11/30	2016/3/7
S	37	500	DSC	6	2016/4/18	2016/5/2	2016/5/16	2016/6/13	2016/6/27	2016/7/11
					2016/7/25	2016/8/8	2016/9/5			
					2014/10/11	2014/12/20	2015/4/25	2015/7/18	2016/1/2	2016/4/9
					2016/5/21	2016/7/16				
					2014/10/11	2014/12/20	2015/4/25	2015/7/18	2016/1/2	2016/4/9
					2016/5/21	2016/7/16				
					2014/9/26	2015/4/10	2015/7/3	2015/12/18	2016/3/25	2016/5/6
					2016/7/1					
					2014/9/27	2015/4/11	2015/7/4	2015/12/19	2016/3/26	2016/5/7
					2016/7/2					
					2015/2/28	2015/3/28	2015/9/26	2015/12/5	2016/3/12	2016/6/18

ASC : Ascending, DSC : Descending
*1 : Rockfill dam part of combined dam

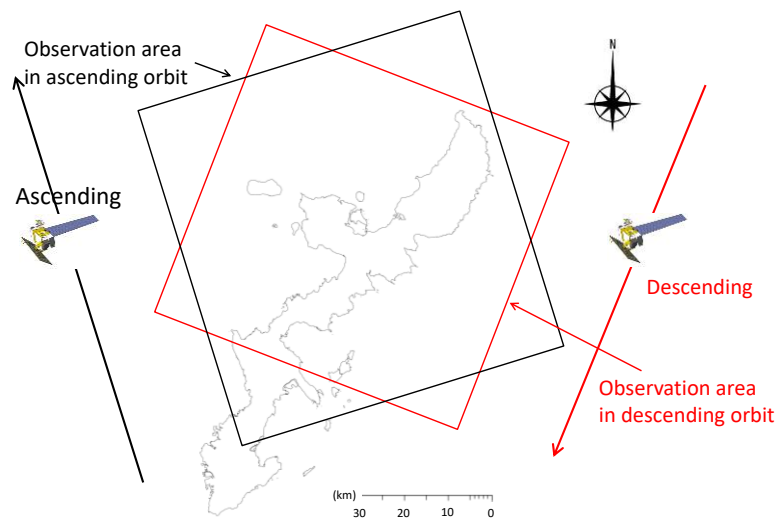


Fig. 2
Ascending and Descending Orbits and Observation Areas

In this paper, we used satellite SAR data obtained by Advanced Land Observing Satellite 2 (ALOS-2) with a Phased Array L-band SAR (PALSAR) sensor (hereinafter referred to as "ALOS-2") [9]. ALOS-2 was launched by Japan Aerospace Exploration Agency (JAXA) in January 2014 and is currently operated. The wavelength and the spatial resolution of the ALOS-2 are 23.6 cm and about 3 m, respectively.

In addition to SAR data, 2 m Digital Elevation Models (DEM) of study areas by Laser Profiler (LP) were used as initial dam body shapes to improve external deformation accuracy.

2.2. EXTERNAL DEFORMATION MONITORING USING SATELLITE SAR DATA

Fig. 3 shows external deformations of nineteen rockfill dams by satellite SAR in the line-of-sight direction from the first SAR observation to the last SAR observation day shown in Table 1. The red arrows in Fig. 3 show the observation directions of the ALOS-2. From the results of preliminary examinations, the multi-look [10], [11] for noise reduction of SAR data was set at 2 x 2 pixels (a spatial resolution of about 5m) in this paper, and the distributions of external deformations in Fig. 3 are expressed with a spatial resolution of about 5 m. Negative values in Fig. 3 mean that the dam surface deforms away from the satellite and it is almost the same direction of settlement of the dam. In the case of Dam N in Fig. 3, which showed a relatively large amount of external deformation, it was clarified with electro-optical survey after the Kumamoto earthquake in April 2016 that there had been settlement of several centimeters due to the earthquake, and earthquake-induced settlement was well measured by satellite SAR.

In order to evaluate the accuracy of satellite SAR based external deformation monitoring, Fig. 4 shows root mean square error (RMSE) distributions at existing GPS or electro-optical survey measurement points. RMSE is calculated using Eq. [1].

$$RMSE = \sqrt{\frac{1}{n} \sum_{i=1}^n (u_{SAR} - u_0)^2} \quad [1]$$

Where n is the number of satellite SAR data, u_{SAR} is the external deformation measured by satellite SAR, and u_0 is the external deformation measured by GPS or electro-optical survey, respectively. If GPS data has been obtained, RMSE in Eq. [1] is calculated from the differences of external deformations between SAR and GPS measurement values at the GPS measurement points. If no GPS data has been obtained, external deformations by electro-optical survey at the SAR observation days were estimated by linear interpolation of two electro-optical survey data and RMSE was calculated from the differences of external deformations between SAR and electro-optical survey at the electro-optical measurement points.

Most RMSE values show less than 5 mm in Fig. 4 and it means that external deformations by satellite SAR have good accuracy by comparing to GPS or electro-optical survey.

Fig. 5 shows the comparisons of temporal changes of external deformations by SAR and GPS/electro-optical survey at the existing geodetic measurement points on the crests in the maximum cross sections of nineteen studied dams. Although there were small variations among the results between

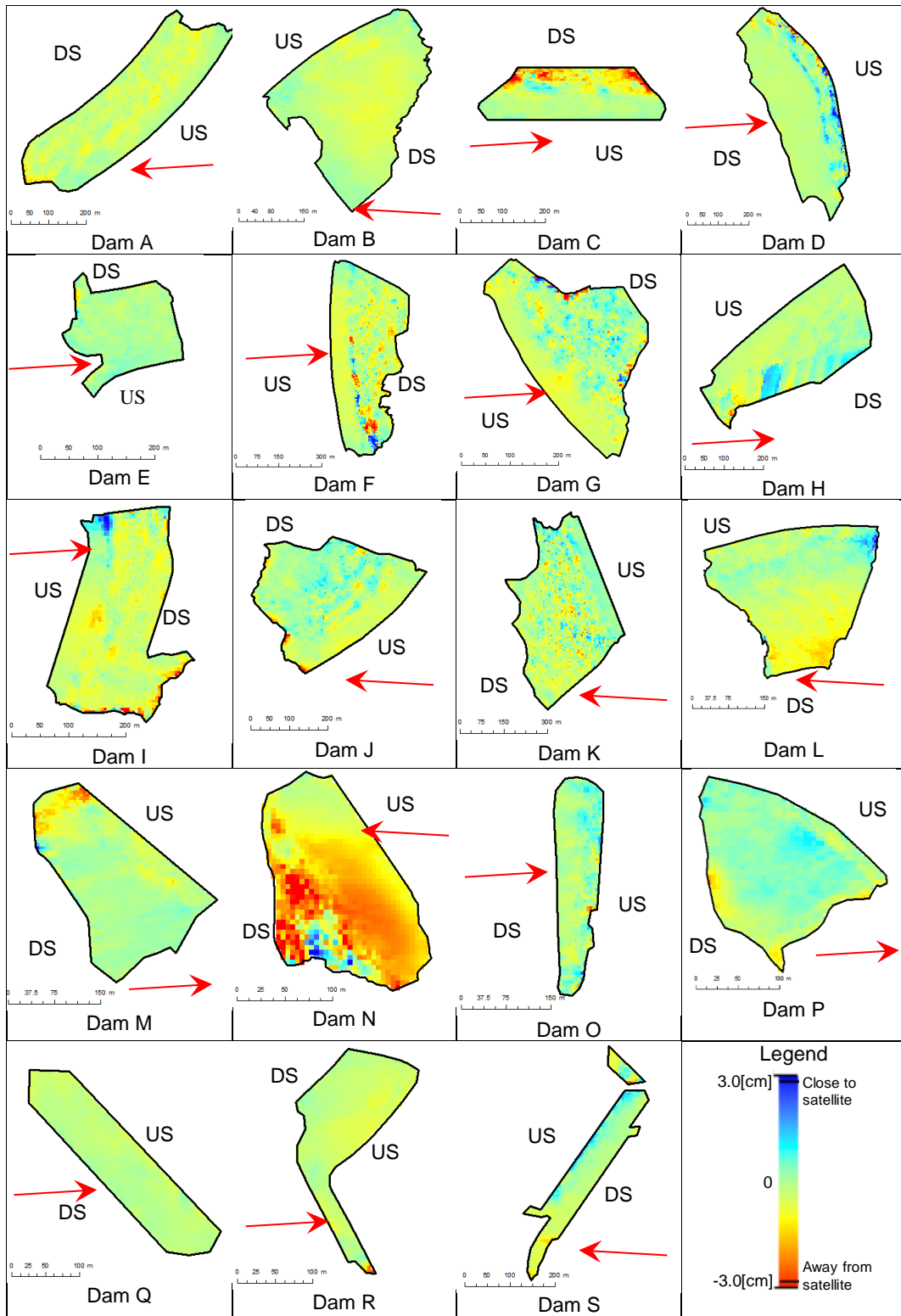
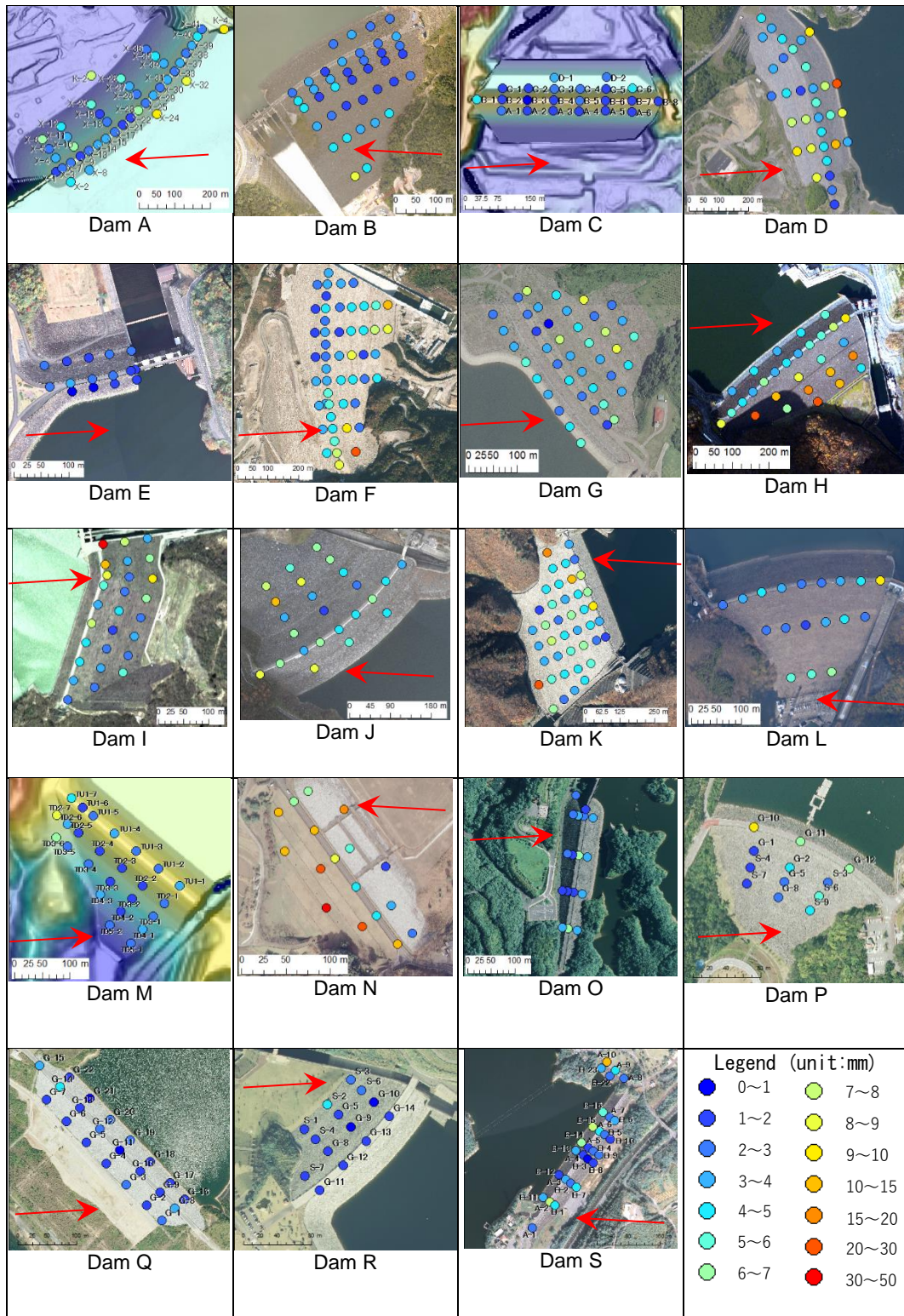


Fig. 3
 External deformations of nineteen rockfill dams using satellite SAR data



Red arrows show line of sight directions of ALOS-2.

Fig. 4
RMSE of external deformations between SAR and GPS/electro-optical survey at existing geodetic points

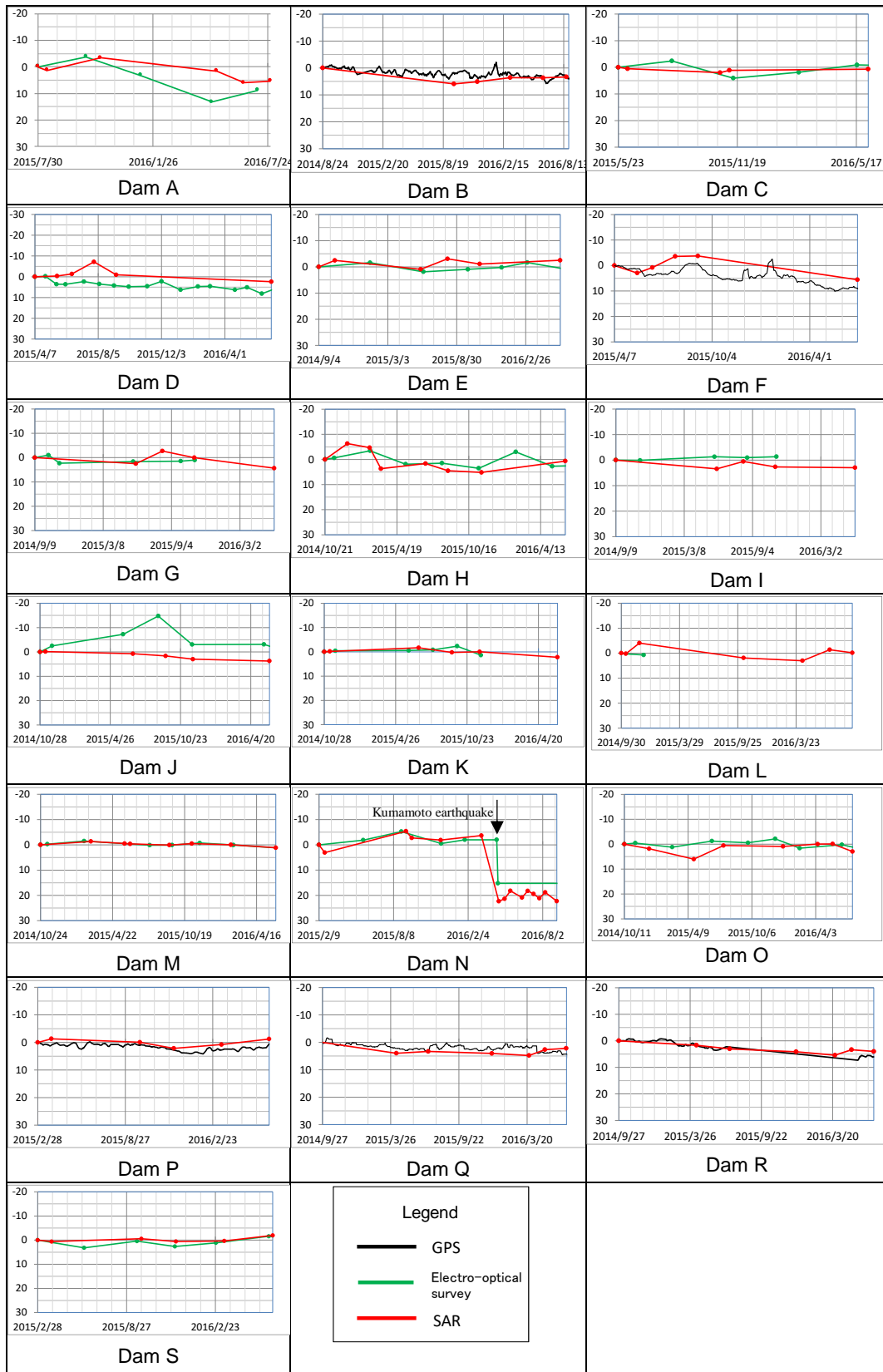


Fig. 5

Comparisons of external deformations between SAR and GPS/electro-optical survey at crests of maximum cross sections

SAR and GPS/electro-optical survey, the results of satellite SAR based external deformation measurements agreed well with the results by GPS or electro-optical survey. In the case of Dam N in Fig. 5, which showed a relatively large and sudden settlement by the Kumamoto earthquake in April 2016, earthquake-induced settlement was well measured by satellite SAR.

Table 2 shows the average RMSE on upstream, crest and downstream surfaces and all existing geodetic points of nineteen rockfill dams. Although there are some variations among the results of RMSEs in Table 2, more than half of the average RMSEs are less than 5 mm and most values are less than 10 mm. On the other hand, several RMSEs in Table 2 show more than 10 mm and the RMSE of the downstream surface of Dam N shows more than 20 mm. It is well known that deterioration in accuracy of SAR based deformation measurements occurs when ground surface is covered with vegetation [10]. Because downstream surface of Dam N has been covered with vegetation, it leads to the relatively large RMSE of downstream surface of Dam N. Table 2 shows that external deformation monitoring using satellite SAR data is generally accurate, but we must pay attention to factors that cause reduction of the accuracy such as ground surface vegetation.

Table 2
RMSE of external deformations between SAR and GPS/electro-optical survey on upstream, crest and downstream surfaces

Name of dam	Height(m)	Crest length(m)	Orbit of satellite SAR	Numbers of data used	RMSE (mm)			
					All	Upstream surface	Crest	Downstream surface
A	78.5(*1)	595(*1)	ASC	6	4.4	7.5	3.2	4.4
B	161	427.1	DSC	6	3.2	2.8	2.9	3.4
C	41.2	440	ASC	5	2.3	1.7	2.1	2.8
D	89.9	786	ASC	6	7.3	11.8	4.1	6.0
E	52.5(*1)	210(*1)	ASC	6	2.2	1.4	2.5	2.2
F	127	723	ASC	6	6.0	3.3	4.6	7.4
G	112	510	ASC	5	4.6	4.2	2.9	5.2
H	90	565	ASC	8	10.2	4.3	5.9	14.5
I	66	348.2	ASC	5	7.9	-	11.4	4.6
J	119.5	419.5	DSC	6	6.3	6.5	5.5	6.7
K	158	520	DSC	10	6.9	-	6.0	7.0
L	127.5	366	DSC	7	4.4	-	4.6	4.2
M	83	420	ASC	8	3.3	-	3.1	3.4
N	35	244	DSC	15	14.7	7.4	8.9	23.8
O	35(*1)	330(*1)	ASC	8	3.4	3.6	4.4	2.3
P	91.7	260	ASC	8	4.6	-	7.5	3.1
Q	66	445	ASC	7	2.1	1.7	2.5	1.9
R	66.5	198	ASC	7	2.0	-	1.5	2.1
S	37	500	DSC	6	4.3	5.0	3.8	3.1

*1 : Rockfill dam part of combined dam.

"-" means no existing geodetic measurement data has been obtained.

3. CONCLUSION

With the aim of carrying out a development of satellite SAR-based external deformation measurement of rockfill dams, this paper focused on nineteen rockfill dams in Japan. A total of 135 scenes of satellite SAR data was used over a period of nearly two years from late 2014 to early 2016 for study. External deformations of nineteen rockfill dams were measured by satellite SAR and compared with existing GPS or electro-optical survey data. The average RMSE of nineteen rockfill dams between SAR and existing geodetic measurements was about 5 mm. As earthquake induced settlement up to several centimeters was also well measured by satellite SAR data, satellite SAR data is useful both in normal times and after earthquakes. In order to conduct accurate external deformation measurements using satellite SAR data, it is important for us to pay attention to factors that cause reduction of the accuracy such as ground surface vegetation.

Because we find that the satellite SAR based external deformation measurement of rockfill dams is accurate and useful, we will continue our research to put our research results into practical use.

ACKNOWLEDGEMENTS

This research has been supported by the Strategic Innovation Promotion Program (SIP) of the Cabinet Office, Government of Japan. We would like to thank to dam management offices in Japan which provided valuable data for our research.

REFERENCES

- [1] EMADARI L., MOTAGH M., HAGHIGHI M.H. Characterizing post-construction settlement of the Masjed-Soleyman embankment dam, Southwest Iran, using TerraSAR-X SpotLight radar imagery, *Engineering Structures*, 143, pp.261–273, 2017.
- [2] GRAZANIC G., LIER O., EKSTROM I., LARSEN Y., LAUKNES T.R. Adopting remote sensing dam surveillance, *82nd Annual Meeting of ICOLD*, pp. 688-697, 2014.
- [3] HANSSEN R. Detecting instabilities in dams using satellite radar interferometry, *81st Annual Meeting of ICOLD*, 2013.
- [4] LAZECKY M., BAKON M., PERISSIN D., PAPCO J., GAMSE S. Analysis of dam displacements by spaceborne SAR interferometry, *85th annual meeting of ICOLD*, 2017.

- [5] MILILLO P., BÜRGMANN R., LUNDGREN P., SALZER J., PERISSIN D., FIELDING E., BIONDI F., MILILLO G. Space geodetic monitoring of engineered structures: The ongoing destabilization of the Mosul dam, Iraq. *Scientific Reports*, 6, 37408, 2016.
- [6] SATO H., SASAKI T., KOBORI T., ENOMURA Y., YAMAGUCHI Y., SATO W., MUSHIAKE N., HONDA K., SHIMIZU N. External Deformation Monitoring of Five Rockfill Dams in the Same Radar Satellite Data, *84th annual meeting of ICOLD*, 2016.
- [7] SATO H., SASAKI T., KONDO M., KOBORI T., ONODERA A., YAMAGUCHI Y., YOSHIKAWA K., SANGO D., MORITA Y. Deformation monitoring of rockfill dams in normal times and after earthquakes using satellite SAR data, *85th annual meeting of ICOLD*, 2017.
- [8] WANG T., PERISSIN D., ROCCA F., Liao M.S. Three Gorges Dam stability monitoring with time-series InSAR image analysis, *Science China Earth Sciences*, Vol. 54, No. 5, pp. 720-732, 2011.
- [9] Japan Aerospace Exploration Agency (JAXA), Advanced Land Observing Satellite 2 (ALOS-2), <http://global.jaxa.jp/projects/sat/alos2/>.
- [10] Geospatial Information Authority of Japan (GSI). Synthetic Aperture Radar Interferometry, <http://vldb.gsi.go.jp/sokuchi/sar/index-e.html>.
- [11] BERARDIO P., FORNARO G., LANARI R. and SANSOSTI E. A New Algorithm for Surface deformation Monitoring Based on Small Baseline Differential SAR Interferograms, *IEEE transaction on geoscience and remote sensing*, Vol. 40, No. 11, pp.2375-2383, 2002.

SUMMARY

It is important to develop a new method of effective and efficient monitoring of dams such as external deformation measurement of embankment dams. External deformations of nineteen rockfill dams in Japan using satellite SAR data were measured in about two years, and the results of external deformations using SAR data were compared with those by GPS or electro-optical survey data. We found that the results of external deformations using satellite SAR data agreed well with those by existing geodetic data and the average error of the external deformations between SAR and existing measurements was about five millimeters. Although external deformation monitoring of rockfill dams using satellite SAR data is generally accurate, it is important to pay attention to factors that cause reduction of the accuracy of satellite SAR based deformation monitoring such as ground surface vegetation.

COMMISSION INTERNATIONALE DES GRANDS BARRAGES

VINGT-SIXIÈME CONGRÈS DES GRANDS BARRAGES
Autriche, juillet 2018

DOI 10.3217/978-3-85125-620-8-071



This work licensed under a Creative Commons Attribution 4.0 International License. <https://creativecommons.org/licenses/by-nc-nd/4.0/>

BEHAVIOUR OF THE BACKFILLED RIGHT BANK OF THE MAVČIČE DAM

Pavel ŽVANUT

Head of the Project Team for Dams, SLOVENIAN NATIONAL BUILDING AND
CIVIL ENGINEERING INSTITUTE

SLOVENIA

Rudi BRINŠEK

Supervising Engineer, SEL - HYDROELECTRIC POWER GENERATION
COMPANY LTD

SLOVENIA

COMMISSION INTERNATIONALE
DES GRANDS BARRAGES

VINGT-SIXIÈME CONGRÈS DES
GRANDS BARRAGES
Autriche, juillet 2018

BEHAVIOUR OF THE BACKFILLED RIGHT BANK OF THE MAVČIČE DAM

Pavel ŽVANUT

*Head of the Project Team for Dams, SLOVENIAN NATIONAL BUILDING AND
CIVIL ENGINEERING INSTITUTE*

Rudi BRINŠEK

*Supervising Engineer, SEL - HYDROELECTRIC POWER GENERATION
COMPANY LTD*

SLOVENIA

1. INTRODUCTION

The Mavčiče concrete gravity dam, part of the corresponding hydro-power plant, was built on the Sava River, in central Slovenia (see Fig. 1), in 1986. It has a maximum structural height of 38.5 m, and the dam crest has a length of 149 m. The concrete dam structure consists of an erection bay, a machine hall, and two spillways, followed by an embankment dam (see Fig. 2). The total capacity of both spillways, which are closed by radial gates with flaps, is 3,200 m³/s. The reservoir, which contains 10.7 hm³ of water, has a length of 7.0 km and the surface area of 1.0 km², whereas the catchment area of the reservoir is 1,480 km² [1, 2].

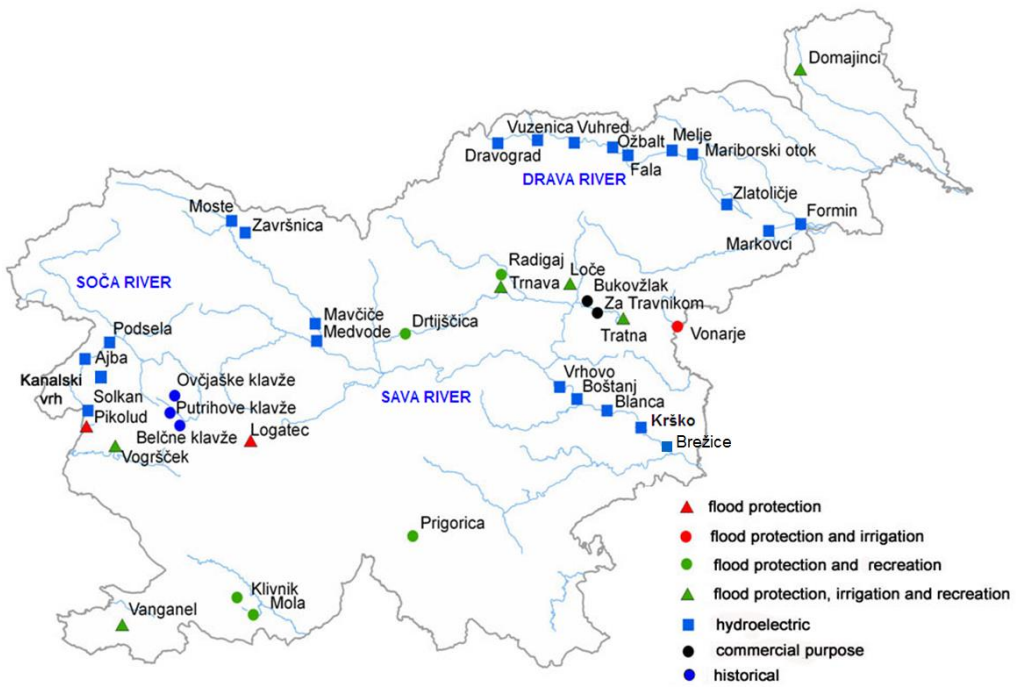


Fig.1
The locations of large dams in Slovenia

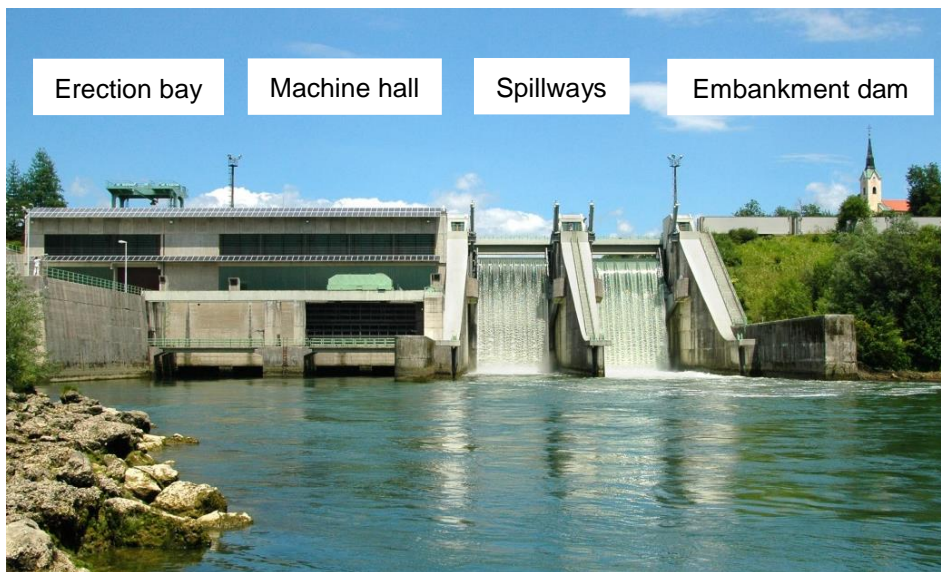


Fig. 2
View of the Mavčiče Dam

2. FOUNDATION OF THE DAM

Most of the Mavčiče Dam is founded on permeable Quaternary conglomerate bedrock, so that a cut-off grout curtain had to be constructed to a depth of up to 60 m below the ground surface, i.e. up to 296 - 302 m above sea level, where a layer of impermeable Oligocene marine clay occurs. The foundation of the machine hall is, for instance, at the altitude of 309.50 m. However, the erection bay, which is located on the right bank of the dam, is founded on a layer of gravel backfill, up to about 25 m thick, which lies on top of the conglomerate bedrock. The upper courtyard, which is located behind the erection bay, has an altitude of 348.00 m, whereas the lower courtyard, which lies in front of the erection bay, is located 10.75 m lower, i.e. at the altitude of 337.25 m [3]. The foundation of the right portion of the dam is presented in Fig. 3.

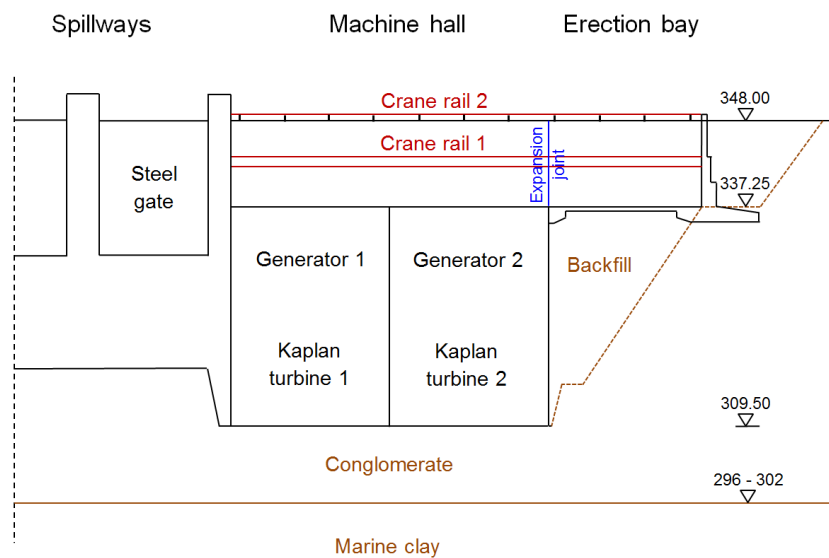


Fig. 3

The foundation of the right portion of the Mavčiče Dam

3. MONITORING SYSTEM OF THE DAM

Long-term manual technical monitoring of the behaviour of the dam began in 1986, at the time of the dam's completion, and included all necessary types of measurements and inspections. In 1999 to 2000 the supplemented monitoring system of the detailed behaviour of the right bank of the dam was established, which included twenty-six points for the vertical displacement measurements. Eighteen of these points (indicated by 1 to 10 and by A to H) were located in the upper courtyard, whereas the other eight points (indicated by 11 to 18) lies in the lower courtyard (see Fig. 4).

Because of the need for more accurate determination of the state of the dam, an automatic measurements of several parameters, mainly hydrostatic and partly hydrodynamic, began in 2003. In 2005 an automated monitoring system for determining the dynamic response of the dam to strong earthquakes, i.e. when the peak ground acceleration exceeds 0.05 g, was established (see Table 1).

Monitoring system of the Mavčiče Dam behaviour includes: deformation measurements (vertical, horizontal and relative displacements, see Fig. 4), visual inspections (structural, geotechnical), groundwater measurements (piezometric levels, uplift pressures, temperatures, specific electrical conductivities) and measurements of external loads on the dam. The latter are carried out in the reservoir, in the stilling basin, in the dam itself (including the inspection gallery and the crest of the dam), as well as on the ground surface about 150 m downstream from the dam [4, 5]. Automatic parameters are shown in Table 2.

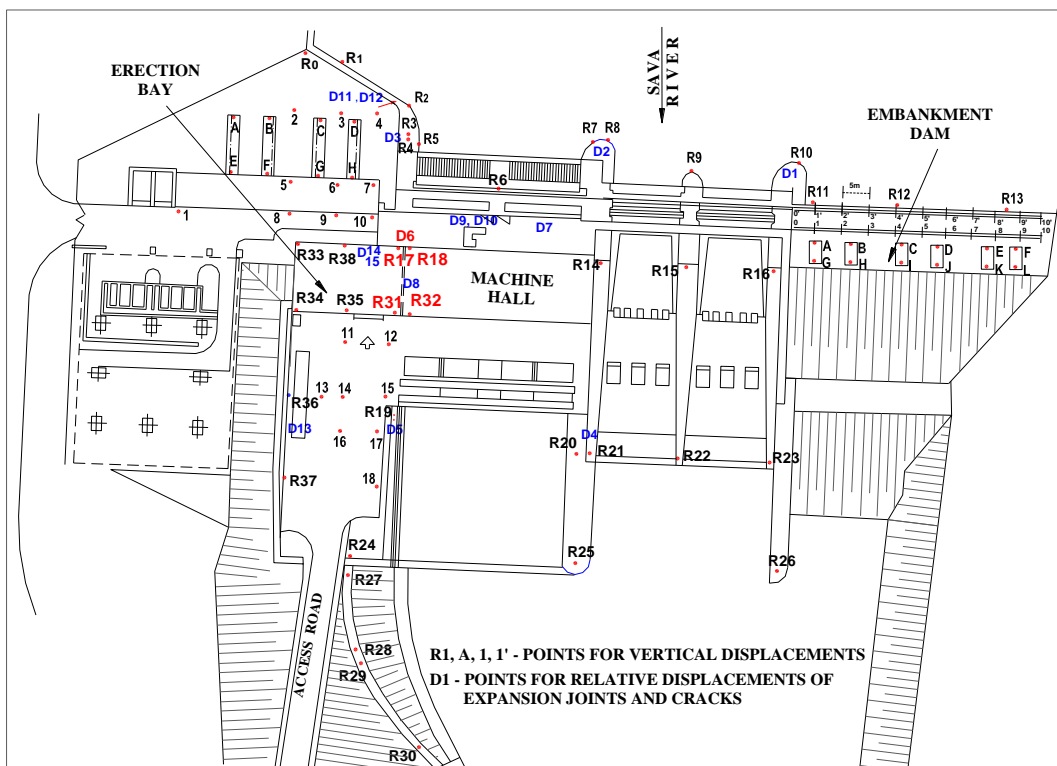


Fig. 4

The monitoring system for measurements of vertical and relative displacements

Table 1

The establishment of the technical monitoring system

Year	Established monitoring activity
1986	Manual measurements and visual inspections
1999 - 2000	Additional deformation measurements (right bank)
2003	Automated measurements (hydrostatic, partly hydrodynamic)
2005	Automated measurements (dynamic - strong earthquakes)

Table 2
Automatic measuring parameters for monitoring the behaviour of the dam

Type	Location	No.	Measuring parameter
Deformation	Expansion joint	1	Displacement (x, y, z)
Groundwater	Uplift pressure caps	4	Uplift pressure
	Side piezometer	6	Piezometric level, temperature, specific electrical conductivity
External loads	Reservoir and stilling basin	1	Water level, temperature, specific electrical conductivity
	Crest of the dam	1	Air temperature, acceleration
	Inspection gallery	1	Air temperature, acceleration
	Dam structure	1	Concrete temperature
	150 m downstream	1	Acceleration

4. RESULTS OF MONITORING, INVESTIGATIONS AND ACTIONS

In general, the results of measurements and visual inspections did not show any abnormalities. However, this was not the case for the erection bay located on the top of the backfilled right bank of the dam, where the results of measurements of vertical displacements showed increasing settlements [6]. By 1999, i.e. over a period of 12 years, these settlements had increased to 22 mm (see Fig. 5). These results were confirmed by measuring the relative displacements of expansion joint D6, located between the erection bay and the machine hall (see Fig. 6).

The results of investigations, by drilling three research boreholes (one in the upper courtyard and two in the erection bay) in 1993, and another six such boreholes (four drilled in the upper courtyard and another two drilled in the lower courtyard) in 1996, indicated that the settlements were the consequence of the secondary consolidation of the backfill, and probable also due to scouring of fine material from the backfill. Due to the resulting differential settlements, the crane rail which connects the erection bay to the machine hall, as well as the crane rail which is located along the crest of the dam, became non-functional, and needed height corrections (see Fig. 7). For this reason rehabilitation works of the backfill and of the substratum of the right bank of the dam were performed between September 1999 and August 2000, using 50 m long grouted boreholes (see Fig. 8). This grouting was performed using a combination of water reactive polyurethane and a cement-bentonite mixture [7]. Measurements performed since then have shown that the settlement rate of the erection bay has slowed down slightly (by 2017, i.e. over the last 17 years, the settlements had increased by up to 8 mm, see Fig. 5), but from the point of view of the operation of the two crane rails the settlement process needed to be stopped.

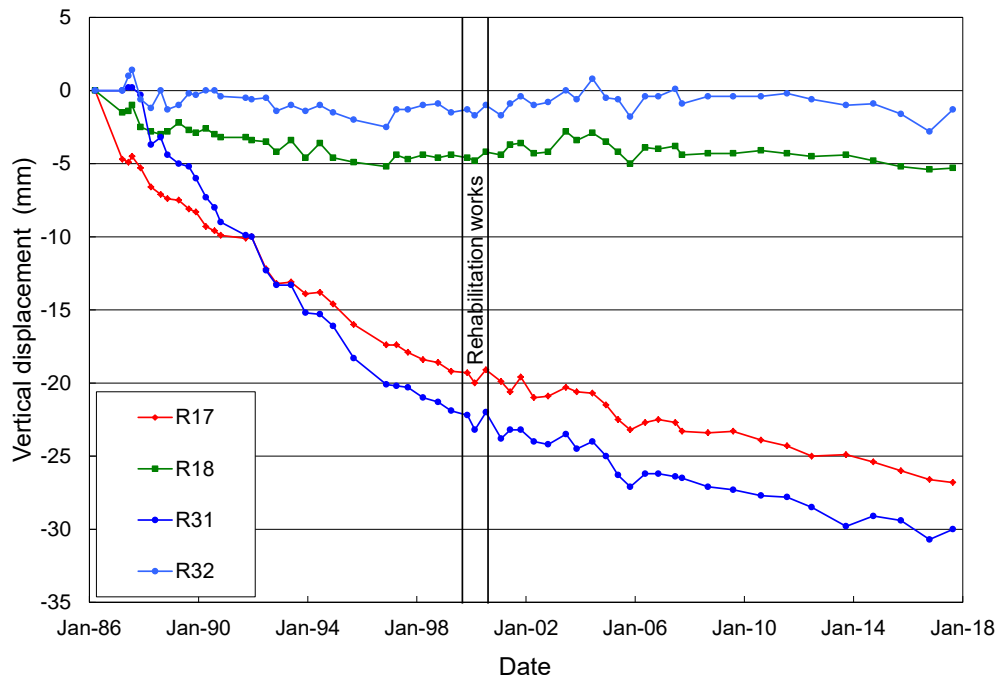


Fig. 5
Vertical displacements of the erection bay

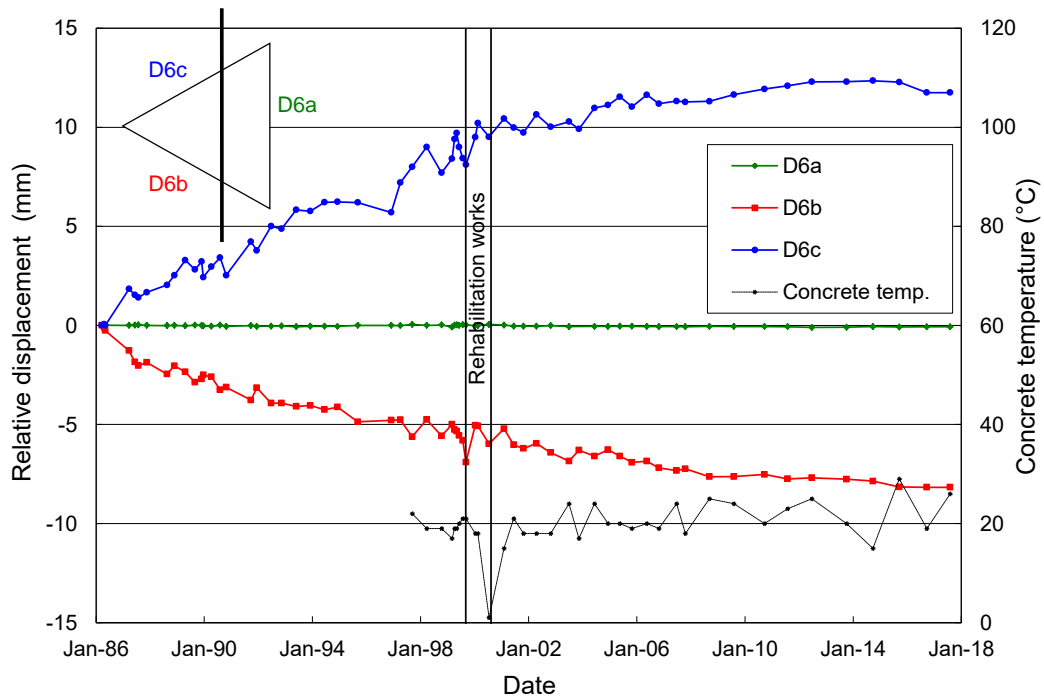


Fig. 6
Relative displacement of expansion joint D6

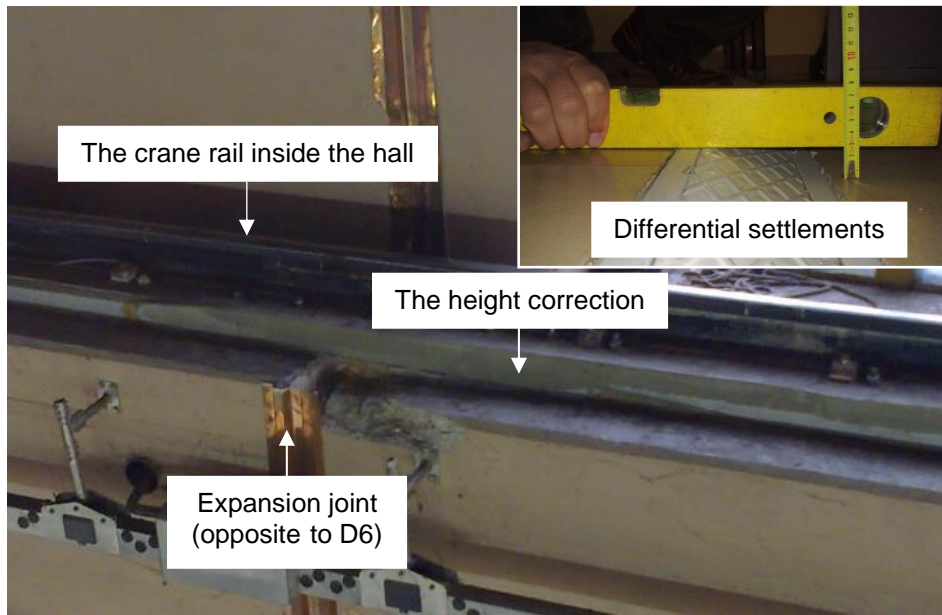


Fig. 7
Height corrections of the crane line inside the erection bay



Fig. 8
Rehabilitation works at the right bank of the dam

The results of the vertical displacement measurements at eight points in the lower courtyard, since the end of rehabilitation works in 2000, showed settlements up to 8 mm, which is similar as in the case of the erection bay. Since 2000, the settlements at ten points in the upper courtyard did not reach 8 mm, whereas at the remaining eight points the settlements reached locally even up to 32 mm.

Additional investigations, involving the drilling of two research boreholes in the upper courtyard, 28.0 m and 30.0 m in depth, as well as appropriate field tests (soil and rock classification, groundwater level, standard penetration test) and laboratory tests (particle size distribution curve, water permeability coefficient) carried out on 21 samples, were performed between November 2015 and March 2016. According to the results of these most recent investigations, the newer settlements were the consequence of additional scouring of fine material from the backfill [8].

5. CONCLUSIONS

In the years following the Mavčiče Dam completion in 1986, the results of measurements of vertical displacements showed increasing settlements of the erection bay at the right bank of the dam, and therefore the differential settlements according to the adjacent machine hall, which resulted to uselessness of both crane rails, which needed height corrections. After investigations, involving the drilling of research boreholes, as well as appropriate field and laboratory tests in 1993 and 1996, the rehabilitation works of the backfill and the substratum of the right bank of the dam were performed in 1999 and 2000. Since even after the rehabilitation works, the settlements of the erection bay continued to increase, additional investigations, involving the drilling of two research boreholes as well as suitable tests (soil and rock classification, groundwater level, standard penetration test, particle size distribution and water permeability coefficient) were carried out in 2015 and 2016. The results of these investigations showed that the settlements measured in the recent years were the outcome of the additional internal erosion of the backfill.

In order to achieve a final solution to the problem of the subsidence of the erection bay, additional rehabilitation works of the backfill and substratum of the right bank of the dam, by grouting the permeable zones, would be needed in order to stop both the scouring of fine material from the backfill, as well as any internal erosion of the cavernous conglomerate at the base of the backfill. The latter concerns the long-term stability of the right bank of the dam with potentially serious results.

REFERENCES

- [1] SLOCOLD. *Slovenian National Committee on Large Dams website*, Slovenia, <http://www.slocold.si/> (in Slovenian), 2018.
- [2] SEL. *Hydroelectric Power Generation Company Ltd website*, Slovenia, <http://www.sel.si> (in Slovenian), 2018.
- [3] ŠTRUCL V. ET AL. Establishment of the technical monitoring system of the Mavčiče Dam. *Report No. 2-710/86*, ZRMK Ljubljana, Slovenia (in Slovenian), 1987.
- [4] BRINŠEK R., ŽVANUT P. Technical and environmental monitoring of the impact areas of the dams managed by Savske Elektrarne Ljubljana Ltd. *Proc. of the Int. Symp.: Dams – Recent experiences on research, design, construction and service*, Skopje, Macedonia, p. 53-62 and CD-ROM, 2011.
- [5] ŽVANUT P., BRINŠEK R. Long-term technical monitoring of the Mavčiče concrete gravity dam. *Proc. of the ICOLD Int. Symp.: Changing Times - Infrastructure Development to Infrastructure Management*, Seattle, WA, USA, p. 2491-2500 and USB flash drive, 2013.
- [6] ŽVANUT P. ET AL. Technical monitoring of the Mavčiče Dam. *Annual reports 1998 - 2017*, ZAG Ljubljana, Slovenia (in Slovenian), 2018.
- [7] ISAKOVIČ S. ET AL. Rehabilitation of Mavčiče Dam at Sava River in Slovenia with extra sealing. *Proc. of the Int. Congress on conservation and rehabilitation of dams: Dam Maintenance and Rehabilitation*, Madrid, Spain, p. 803-809, 2002.
- [8] PROKOP B. ET AL. The control exploration drilling on the right bank of the Mavčiče Dam. *Report No. 8-04-2016*, Proksam Ltd, Vrhnika, Slovenia (in Slovenian), 16 p., 2016.

SUMMARY

The Mavčiče concrete gravity dam, part of the corresponding hydro-power plant, was built on the Sava River, in Slovenia, in 1986. It has a maximum structural height of 38.5 m, and the dam crest has a length of 149 m. The dam structure consists of an erection bay, a machine hall, and two spillways, followed by an embankment dam. Most of the dam is founded on permeable Quaternary conglomerate bedrock, so that a cut-off grout curtain had to be constructed to a depth of up to 60 m below the ground surface, where a layer of impermeable Oligocene marine clay occurs. However, the erection bay, which is located on the right bank of the dam, is founded on a layer of gravel backfill, up to about 25 m thick, which lies on top of the conglomerate bedrock.

Long-term manual technical monitoring of the behaviour of the dam began in 1986, and an automated monitoring system was established between 2003 and 2005. In general, the results of measurements and visual inspections did not show any abnormalities. However, this was not the case for the erection bay located on the top of the backfilled right bank of the dam, where the results of measurements of vertical displacements showed increasing settlements. By 1999, i.e. over a period of 12 years, these settlements had increased to 22 mm.

The results of investigations, by drilling three research boreholes in 1993, and another six such boreholes in 1996, indicated that the settlements were the consequence of the secondary consolidation of the backfill, and probable also due to scouring of fine material from the backfill. Due to the resulting differential settlements, the crane rail which connects the erection bay to the machine hall, as well as the crane rail which is located along the crest of the dam, became non-functional, and needed height corrections. For this reason rehabilitation works of the backfill and of the substratum of the right bank of the dam were performed between September 1999 and August 2000, using 50 m long grouted boreholes. This grouting was performed using a combination of water reactive polyurethane and a cement-bentonite mixture. Measurements performed since then have shown that the settlement rate has slowed down slightly (by 2017, i.e. over the last 17 years, the settlements had increased by up to 8 mm), but from the point of view of the operation of the two crane rails the settlement process needed to be stopped. Additional investigations, involving the drilling of two research boreholes, as well as appropriate laboratory and field measurements, were performed between November 2015 and March 2016. According to the results of these most recent investigations, the newer settlements were the consequence of additional scouring of fine material from the backfill.

In order to achieve a final solution to the problem of the subsidence of the erection bay, additional rehabilitation works of the backfill and substratum of the right bank of the dam, by grouting the permeable zones, would be needed in order to stop both the scouring of fine material from the backfill, as well as any internal erosion of the cavernous conglomerate at the base of the backfill. The latter concerns the long-term stability of the right bank of the dam with potentially serious results.

KEY-WORDS

gravity dam, concrete dam, Mavčiče Dam, behaviour, monitoring, automated monitoring, deformation measurement, groundwater, inspection, piezometer, uplift, water level, seepage, settlement, geotechnical investigation, internal erosion, rehabilitation.

MOTS-CLES

barrage-poids, barrage en béton, Barrage Mavčiče, comportement, auscultation, auscultation automatique, mesure de déformation, eau souterraine, visite, piézomètre, sous-pression, niveau hydraulique, infiltration, tassement, géotechnique, érosion interne, réhabilitation.

COMMISSION INTERNATIONALE DES GRANDS BARRAGES

VINGT-SIXIÈME CONGRÈS DES GRANDS BARRAGES
Autriche, juillet 2018

DOI 10.3217/978-3-85125-620-8-072



This work licensed under a Creative Commons Attribution 4.0 International License. <https://creativecommons.org/licenses/by-nc-nd/4.0/>

AIR DEMAND OF BOTTOM OUTLETS: INSIGHTS FROM SCALE MODEL TESTS AND PROTOTYPE MEASUREMENTS

Benjamin, HOHERMUTH

Doctoral Student, LABORATORY OF HYDRAULICS, HYDROLOGY AND
GLACIOLOGY (VAW), ETH ZURICH

SWITZERLAND

Lukas SCHMOCKER

Research Scientist, SWISS COMPETENCE CENTER FOR ENERGY
RESEARCH – SUPPLY OF ELECTRICITY SCCER-SOE

SWITZERLAND

Robert M. BOES

Director of LABORATORY OF HYDRAULICS, HYDROLOGY AND
GLACIOLOGY (VAW), ETH ZURICH

SWITZERLAND

COMMISSION INTERNATIONALE
DES GRANDS BARRAGES

VINGT-SIXIÈME CONGRÈS DES
GRANDS BARRAGES
Autriche, juillet 2018

AIR DEMAND OF BOTTOM OUTLETS: INSIGHTS FROM SCALE MODEL TESTS AND PROTOTYPE MEASUREMENTS *

Benjamin, HOHERMUTH¹, Lukas SCHMOCKER², Robert M. BOES³

¹ *Doctoral Student*, ³ *Director of Laboratory of Hydraulics, Hydrology and
Glaciology (VAW), ETH ZURICH*, ² *Research Scientist, Swiss Competence
Center for Energy Research – Supply of Electricity SCCER-SoE*

SWITZERLAND

1. INTRODUCTION

Bottom outlets (BOs) are a key safety feature of high-head dams. Their main purpose is the regulation and – if required - a fast drawdown of the reservoir water level in case of floods, structural damage of the dam or maintenance works. Additional purposes include residual flow release, flood diversion or sediment flushing. The large energy heads at the gate lead to a high-speed free-surface flow in the BO tunnel with flow velocities up to some 50 m/s for high dams. These large flow velocities and the high turbulence levels lead to considerable air entrainment and air transport, possibly resulting in negative pressures in the BO. This can cause problems with gate vibrations, cavitation and flow chocking. Sufficient air supply via an aeration chamber can mitigate these problems. Available design equations for the required air demand to prevent excessive negative pressures are based on scale model tests and prototype measurements. Most of these equations express the air demand β as a function of the Froude number at the vena contracta F_c . However, measured and predicted β -values show a large scatter. Some of the scatter can be explained by the different flow patterns. The remaining scatter can be explained with the neglect of crucial parameters in the design equation like the air vent loss coefficient ζ or the tunnel length L . This project aims to investigate the

* *Aération des vidanges de fond: Résultats des essais sur modèle à échelle réduite et des mesures en prototype*

effect of those parameters with small-scale model tests. The employed scale model exceeds most previous model studies in terms of energy head H_E and water discharge Q_w . Nevertheless, scale and model effects still need to be addressed carefully. Detailed prototype data are crucial for the validation and upscaling of model results. Therefore, this project additionally includes air demand measurements at three bottom and one middle outlet(s) in southern Switzerland.

2. SCALE MODEL TESTS

2.1. MODEL SETUP AND INSTRUMENTATION

A physical bottom outlet model was built at the Laboratory of Hydraulics, Hydrology and Glaciology (VAW) at ETH Zurich (Fig. 1a). Two pumps provide a maximum energy head at the gate of $H_E = 30$ m w.c. at a water discharge of $Q_w \approx 600$ l/s. The rectangular sharp-crested gate is 0.2 m wide, 0.25 m high and the downstream tunnel extends to a height of $h_t = 0.3$ m (Fig. 1b). The horizontal BO tunnel has a maximum length of $L = 20.6$ m which can be varied due to detachable elements. The aeration chamber is connected to a circular air vent of diameter $d = 0.15$ m which can be throttled with an orifice plate to vary the loss coefficient ζ of the whole aeration system. A similar air vent is located at the tunnel end to measure the airflow into or out of the tunnel. All channel walls consist of PVC or acrylic glass with a hydraulic roughness of $k = 0.003$ mm.

Q_w is measured with an inductive flow meter with an accuracy of $\pm 0.5\%$ of the measurement value (MV) and ± 0.4 l/s absolute error. The air flow velocity in the air vent $U_{a,o}$ is measured with a thermal anemometer while the air flow velocity at the tunnel end $U_{a,u}$ is measured with a bidirectional vane anemometer. The thermal anemometer has an accuracy of $\pm 2.5\%$ of MV and the vane anemometer has an accuracy of $\pm 1.5\%$ of MV ± 0.2 m/s. From the measured velocity, the air discharges $Q_{a,o}$ and $Q_{a,u}$ are computed assuming a logarithmic velocity profile. The cross section above the air-water mixture is blocked with a gate at the tunnel end. Consequently the air has to be supplied through the second air vent which allows for a precise measurement of $Q_{a,u}$. A total of 40 relative pressure sensors with a measurement range of ± 100 mbar and an accuracy of ± 1 mbar are installed at the invert and the soffit along the tunnel centerline to measure both the water (subscript w) and air pressures (subscript a), respectively.

The following parameters were varied in the model tests: The relative gate opening a/a_{max} was increased from 0.1 to 1 in steps of 0.1. For each a/a_{max} , H_E was varied from 5 to 30 m w.c. in steps of 5 m w.c. and six ζ -values were tested, $\zeta = 0.7, 2.7, 9, 19, 28$ and 57 . All parameter combinations were tested for tunnel lengths of $L = 20.6, 12.6$ and 6.6 m. Combinations of $H_E > 20$ m w.c. and $\zeta > 10$ could not be measured due to strong flow pulsations. Large relative gate openings of $a/a_{max} > 0.8$ led to a drowning of the aeration chamber and were thus excluded from the measurements.

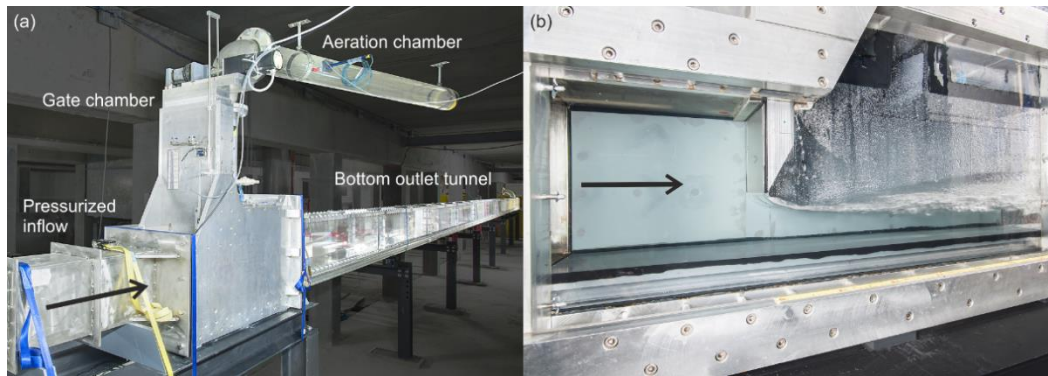


Fig. 1

(a) Physical scale model of a bottom outlet at VAW, (b) gate chamber
 (a) Modèle à échelle réduite d'une vidange de fond à la VAW, (b) chambre de la vanne

2.2. AIR DEMAND IN MODEL TESTS

The air discharge $Q_{a,o}$ through the aeration chamber increases with increasing H_E and attains a maximum for moderate relative gate openings $0.4 \leq a/a_{max} \leq 0.6$ (Fig. 2a). The maximum is shifted towards smaller a/a_{max} for increasing H_E .

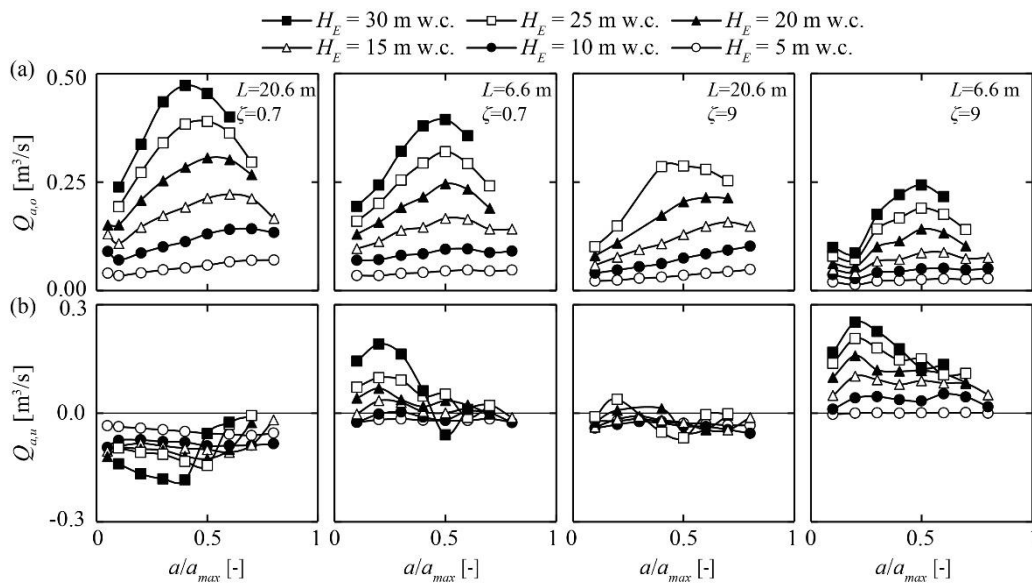


Fig. 2

(a) $Q_{a,o}$ and (b) $Q_{a,u}$ for different values of a/a_{max} , H_E , L and ζ
 (a) $Q_{a,o}$ et (b) $Q_{a,u}$ pour des valeurs différentes de a/a_{max} , H_E , L et ζ

The sudden increase of $Q_{a,o}$ for $a/a_{max} \approx 0.05$ is caused by the transition to spray flow. At large a/a_{max} the air flow rate is decreasing again, especially for large H_E . This is due to the transition to foamy flow with the tunnel almost flowing full at the tunnel end. The reduced cross-sectional area above the air-water mixture for foamy flow allows less air to be dragged along with the flow. $Q_{a,u}$ is negative for moderate a/a_{max} , low ζ value and long tunnel, indicating a net air flow out of the tunnel at the downstream end. For foamy flow conditions $Q_{a,u}$ increases to zero, whereas spray flow leads to a slight decrease of $Q_{a,u}$ (Fig. 2b). An increase in ζ drastically reduces $Q_{a,o}$, while simultaneously increasing $Q_{a,u}$, resulting in a net air flow into the tunnel from the downstream (Fig. 2). The decrease in $Q_{a,o}$ and the increase in $Q_{a,u}$ are even more pronounced for short tunnels as air can enter more easily from the downstream tunnel end.

The minimal air pressure in the gate chamber $p_{a,min}$ depends on $Q_{a,o}$ and ζ . With all other parameters kept constant, an increase in ζ leads to a simultaneous decrease of $Q_{a,o}$ and $p_{a,min}$. The magnitude of decrease of each quantity in turn depends on a/a_{max} , H_E and L .

3. PROTOTYPE MEASUREMENTS

3.1. TEST SITES

The two BOs of the arch dam Malvaglia and the BO and middle outlet (MO) of the arch dam Luzzone in the Canton of Ticino, southern Switzerland were equipped with measurement devices. All outlets are usually operated once a year to flush sediments out of the reservoir. Additionally, a mandatory function test requires the test of small gate openings once a year. All three outlets are equipped with sluice gates. Luzzone features a maximum static head $H_{o,m}$ of 224 m w.c. for the BO and 120 m w.c. for the MO. Malvaglia has two BOs, an old and a new one with $H_{o,m} = 94$ m w.c. and $H_{o,m} = 91$ m w.c., respectively. The new BO was specifically built to flush sediments from the intake vicinity. The old BO features a circular tunnel with a diameter of $d = 4.3$ m, whereas the new BO has a 2 m wide, 2.5 m high horseshoe profile. Both outlet tunnels join a common outlet tunnel ($d = 5.6$ m) to which the spillway is also connected (Fig. 3). The tunnel conjunction is well aerated what leads to effective tunnel lengths of $L = 67$ m and $L = 82$ m for the old and new BO. Up to now only measurements during a function test in Malvaglia could be conducted.

3.2. PROTOTYPE INSTRUMENTATION

The instrumentation applied at Malvaglia Dam and their accuracy are listed in Table 1, and a sketch of the measurement setup is shown in Fig. 3.

The following parameters were measured:

- $Q_{a,o}$: To measure the air flow velocity $U_{a,o}$ in the air vent, vane anemometers were mounted at two locations in the center of the air vent cross section. $Q_{a,o}$ was calculated assuming that the measured velocity $U_{a,o}$ corresponds to 110% of the mean air velocity in the air vent.
- p_a : Absolute pressure sensors were installed in both gate chambers, in the middle of both tunnels and at the tunnel conjunction.
- Air velocity at the end of the outlet tunnel $U_{a,u}$: Bidirectional vane anemometers were installed in the upper half of the tunnel cross section at the end of both tunnels to measure air flowing out of or into the BO tunnel.
- Air temperature T_a : Temperature sensors were installed at two locations in the air vent; in the horizontal part and at the end of the air vent in the new BO.

Additionally, video cameras were installed in both gate chambers and at the tunnel conjunction.

Table 1
Overview on measurement devices and accuracy, symbols refer to Fig. 3

Symbol	Type	Name	Range	Accuracy
U1, U2	unidirectional vane	Höntzsch ZS25-mn120	1.4 - 120 m/s	$\pm (1.5\% \text{ of MV} + 0.6 \text{ m/s})$
U3 - U5	bidirectional vane	Höntzsch ZSR25-mn120	-60 - 60 m/s	$\pm (1.5\% \text{ of MV} + 0.6 \text{ m/s})$
U6, U7	bidirectional vane	Schiltknecht Air	-40 - 40 m/s	$\pm (1.5\% \text{ of MV} + 1 \text{ m/s})$
P1 - P5	absolute pressure sensor	Keller PAA-26 W	mbar	$\pm 2.5 \text{ mbar}$
R	flow direction indicator	VAW-made	0 - 360°	$\pm 2^\circ$
T1, T2	Air temperature	Arthur-Grillo MTA90-P	-30 - 40°C	$\pm (0.25\% \text{ of MV} + 0.15^\circ\text{C})$

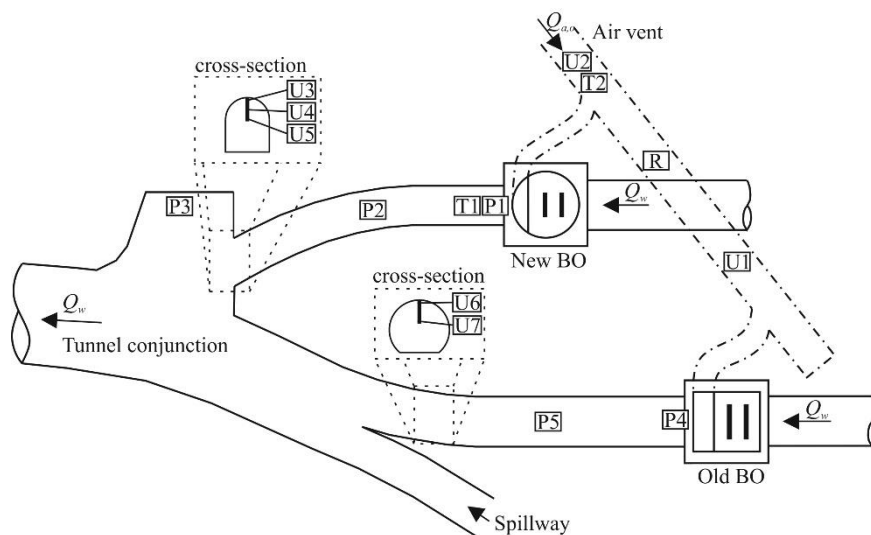


Fig. 3

Sketch of the measurement setup at Malvaglia Dam (not to scale)
Esquisse de la configuration de mesure au barrage Malvaglia (pas à l'échelle)

Two different gate openings were tested for both BOs: $a = 0.05, 0.1$ m for the old BO and $a = 0.1, 0.2$ m for the new BO, respectively. Only one BO was in operation at a time. The reservoir water level varied from 980 to 980.9 m asl. during the test, resulting in an average static pressure head of $H_E = 84.7$ m w.c. for the old BO and $H_E = 81.6$ m w.c for the new BO. An average air temperature T_a of 9°C was used to calculate ρ_a , resulting in $\rho_a = 1.12$ kg/m³ at ~900 m asl. To show the overall trend, the measurements were averaged over 5 s in the following figures. Additionally, the original 10 Hz measurements are shown as thin lines. To calculate characteristic numbers (e.g. β , ζ), the measurement were averaged over the duration of each gate opening. ζ was calculated as $\zeta = 2\Delta p_a / (\rho_a U_{a,o}^2) - 1$, where Δp_a is the air pressure drop in the gate chamber $\Delta p_a = p_a(t=0) - p_a(t)$. The Q_w -values for the calculation of $\beta = Q_{a,o} / Q_w$ were provided by the dam operator.

3.3. RESULTS OF BOTTOM OUTLETS MALVAGLIA

Table 2 summarizes the measurement results and Fig. 4 shows detailed results for the new BO. If only the new BO is in operation, an equal amount of air is supplied through the air vent and the old BO tunnel (U1 and U2 in Fig. 4a). $U_{a,o}$ is slightly higher for $a = 0.1$ m compared to $a = 0.2$ m. This can partly be explained by the transition from spray flow to free-surface flow for $a = 0.2$ m (Fig. 5). The sudden rise in $U_{a,o}$ during the closing of the gate is also caused by a more intense spray formation for $a < 0.1$ m. For spray flow, i.e. $a = 0.1$ m, air is flowing out of the tunnel end, whereas for $a = 0.2$ m air is entering the tunnel from downstream (Fig. 4b). $U_{a,u}$ is significantly lower than the air-water mixture velocity of ~12 m/s (estimated after [1]). The drop of p_a is clearly visible in the gate chamber (P1) and to a lesser extent after half of the tunnel length (P2) (Fig. 4). At P1, more pronounced pressure transients were observed, particularly during gate closure, whereas these transients have already disappeared at P2. No considerable variation in pressure can be observed in the tunnel conjunction (P3), showing that the conjunction is sufficiently aerated from downstream.

Table 2
Overview of the measurement results in Malvaglia

name	Q_w [m ³ /s]	a [m]	a/a_{max} [-]	F_c [-]	$Q_{a,o}$ [m ³ /s]	Δp_a [mbar]	ζ [-]	β [-]
new BO	2.5	0.1	0.08	52	17.7	5.2	2.6	7.1
new BO	5.0	0.2	0.15	36	15.0	3.9	2.8	3.0
new BO	2.5	0.1	0.08	52	17.1	6.3	3.7	6.8
old BO	2.4	0.05	0.03	61	15.2	7.5	5.8	6.3
old BO	5.0	0.1	0.06	43	27.1	23.7	5.8	5.4
old BO	2.4	0.05	0.03	61	11.7	4.5	5.9	4.9

For the old BO no transition to free-surface flow was observed for the larger gate opening $a = 0.1$ m. On the contrary, the old BO showed an even stronger spray formation for $a = 0.1$ m (Fig. 5). Consequently $Q_{a,o}$ increased with increasing a for the old BO.

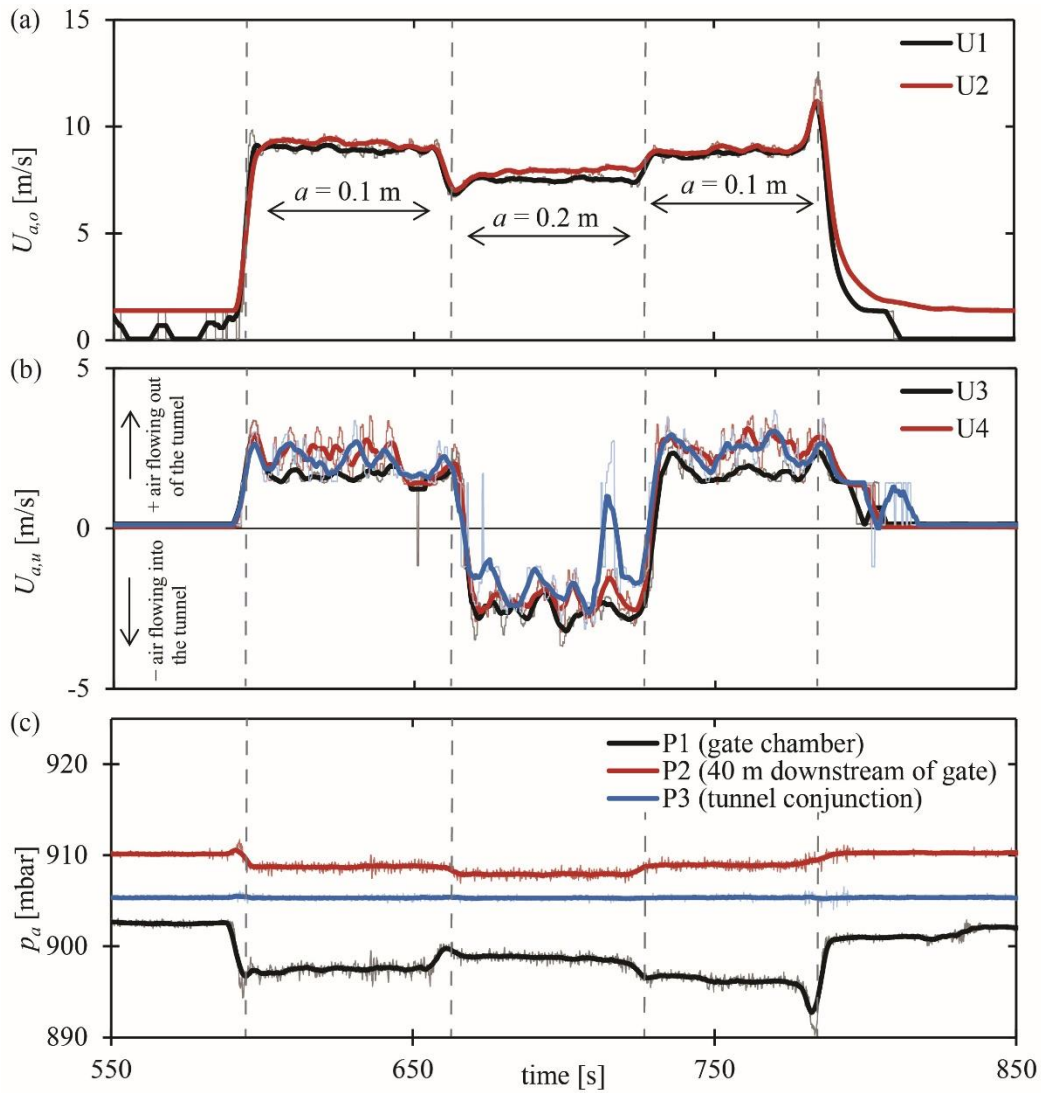


Fig. 4
 Measurements for the new BO (a) $U_{a,o}$, (b) $U_{a,u}$ and (c) p_a at different locations
Valeurs mesurées pour la nouvelle VF (a) $U_{a,o}$, (b) $U_{a,u}$ et (c) p_a aux lieux différents

4. DISCUSSION

Both the model and prototype data demonstrate the significant influence of the flow pattern on $Q_{a,o}$, $Q_{a,u}$ and p_a . The scale model data also clearly show the importance of L and ζ for the aforementioned quantities. The importance of ζ is also supported by the prototype data, i.e. the fact that the new BO exhibits larger β -values than the old BO despite smaller F_c and less intense spray can be attributed to the smaller ζ -value.

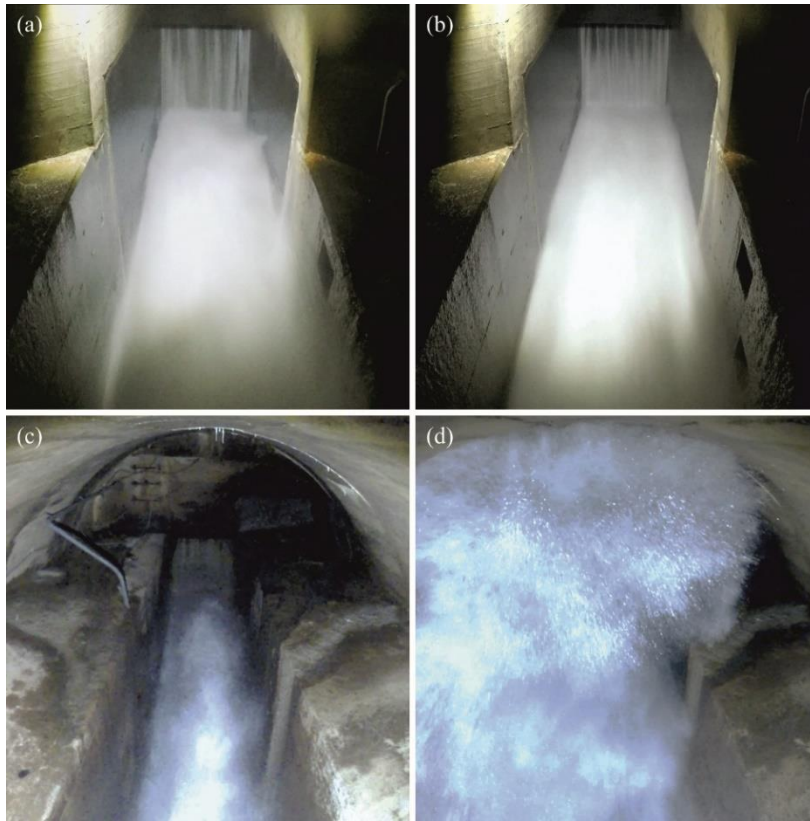


Fig. 5

Bottom outlet sluice gate in operation (a) new BO $a = 0.1$ m, (b) new BO $a = 0.2$ m, (c) old BO $a = 0.05$ m and (d) old BO $a = 0.1$ m.
Vanne de vidanges de fond (VF) en opération (a) nouvelle VF $a = 0.1$ m, (b) nouvelle VF $a = 0.2$ m, (c) vieille VF $a = 0.05$ m and (d) vieille VF $a = 0.1$ m.

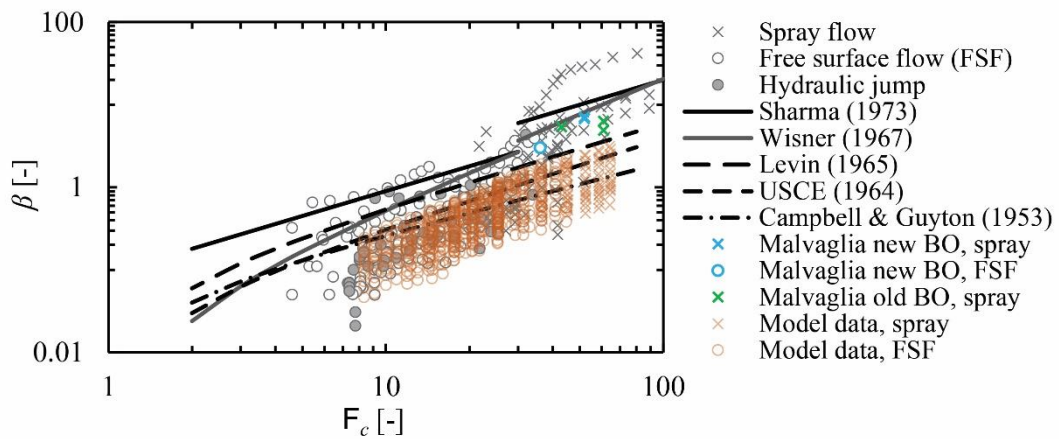


Fig. 6

Comparison of prototype data from literature [2] and design equations with model data and new prototype measurements
Comparaison des mesures en prototype de la littérature [2] et des équations avec des mesures du modèle à échelle réduite et nouvelles mesures en prototype

The new prototype air demand data are moderate to high compared with existing prototype measurements (Fig. 6, [2]). The large scatter in the model data is due to the varying ζ and L . Actually the model data for a given combination of ζ and L is reasonably described by a power law relation $\beta = aF_c^b$, where a , b are dependent on ζ and L . While the model data shows a good agreement with existing prototype data and equations for free-surface flow, the model data tend to underestimate β for spray flow conditions. Indeed the gas Weber number and the Ohnesorge number indicate that the secondary disintegration of droplets is subject to scale effects i.e. the spray is less pronounced in the model. Additionally the model sluice gate has no gate slots which are a main cause for spray formation [8].

5. CONCLUSIONS

A systematic physical scale model study on the air demand of bottom outlets was performed. The results show that the air demand decreases with increasing air vent resistance and decreasing tunnel length. The flow pattern has a decisive influence on the air demand with the maximum air demand occurring for spray flow. The highest air discharge was observed for free-surface flow. New prototype measurements conducted in two bottom outlets in Switzerland support the main findings of the scale model test. Differences were observed for spray flow conditions, where the local gate geometry plays a crucial role.

ACKNOWLEDGEMENTS

The first author is funded by the Swiss National Science Foundation (SNF, Grant No. 163415). The prototype measurements are financed by the Lombardi Engineering Foundation and kindly supported by the dam operator Ofible. The project is embedded in the Swiss Competence Centre for Energy Research – Supply of Electricity (SCCER-SoE).

REFERENCES

- [1] SPEERLI J., HAGER W. H. Air-water flow in bottom outlets. *Canadian Journal of Civil Engineering*, 27, 454–462, 2000.
- [2] HOHERMUTH B. Air demand of high-head bottom outlets. *Proc. 37th IAHR World Congress*, Kuala Lumpur, Malaysia, 2956-2965, 2017.

- [3] SHARMA H.R. Air demand for high head gated conduits. *PhD thesis*, The Norwegian Institute of Technology, Trondheim, 1973.
- [4] WISNER P. Air entrainment in high speed flows. *Proc. 9th ICOLD Congress*, Istanbul, 495-507, 1967.
- [5] LEVIN L. Calcul hydraulique des conduits d'aération des vidanges de fond et dispositifs déversants. *La houille blanche*, No. 2, 121-127 (in French), 1965.
- [6] US CORPS OF ENGINEERS (USCE). Air demand – regulated outlet works. *Hydraulic design criteria*, sheet 050-1/2/3, 211-1/2, 212-1/2, 225-1, 1964.
- [7] CAMPBELL, F.B. AND GUYTON B. Air demand in gated outlet works. *Proc. 5th IAHR Congress*, Minnesota, 529-533, 1953.
- [8] RABBEN, S.L. Untersuchung der Belüftung an Tiefschützen unter besonderer Berücksichtigung von Massstabseffekten. *Mitteilung Nr. 53*, Institut für Wasserbau und Wasserwirtschaft, RWTH Aachen (in German), 1984.

SUMMARY

Bottom outlets (BOs) are a key safety feature of high-head dams. The high-speed free-surface flow in the BO tunnel leads to considerable air entrainment and air transport, resulting in negative pressures in the outlet tunnel. Current knowledge does not allow a coherent design of the air vent needed to mitigate problems due to negative pressures as e.g. gate vibrations and cavitation. Extensive model test conducted in this project showed that: (i) the flow pattern strongly influences the air demand with spray flow resulting in maximal values; (ii) the air demand decreases with increasing air vent loss coefficient, while the air pressure consequently decreases; and (iii) a shorter tunnel length reduces the air demand as air can enter more easily from the downstream end. New prototype data collected in two BOs in Switzerland support these findings.

Des vidanges de fond (VF) sont des structures importantes pour des grands barrages. L'écoulement à surface libre à grande vitesse mène à l'entraînement et transport de l'air résultant en pressions négatives dans le conduit. La connaissance actuelle ne permet pas une conception cohérente du conduit d'aération lequel est pourtant nécessaire pour atténuer les problèmes de vibration des vannes et de cavitation. Des expériences extensifs sur modèle à échelle réduite mènés dans ce projet ont montré le suivant : (i) le régime d'écoulement influence fortement la demande d'air avec un maximum pour le régime « spray », (ii) la demande d'air diminue pour une augmentation du coefficient de perte du conduit d'air tandis que par conséquent la pression diminue et (iii) un conduit plus court diminue la demande d'air parce que l'air peut entrer plus facile par la fin du conduit en aval. Les résultats principaux des essais sur modèle à échelle réduite sont soutenus par des nouveaux essais de prototype.

KEYWORDS

AERATION, BOTTOM OUTLET, FIELD TEST, MALVAGLIA, LUZZONE,
PHYSICAL MODEL,

AERATION, ESSAI EN PLACE, LUZZONE, MALVAGLIA, MODELE
PHYSIQUE, VIDANGE DE FOND

COMMISSION INTERNATIONALE
DES GRANDS BARRAGES

VINGT-SIXIÈME CONGRÈS DES
GRANDS BARRAGES
Autriche, juillet 2018

**TECHNICAL STAGE TO PLUG THE LARGE SIZE DIVERSION TUNNEL OF
JATIGEDE DAM AT WEST JAVA, REPUBLIC OF INDONESIA, 2017**

Email: anwarmakmur@gmail.com; anwarmakmur@gmail.com;
toloose234@gmail.com ; always_rosita@yahoo.com

Anwar MAKMUR IR.,

Sr.Engineering Geologist, at Jatigede dam, West Java

Dony Faturochman SAEFULLOH, ST., MT.,

Head of Dam Planer at Jatigede dam, West Java

Tulus H. Basuki IR.,

Dam Designer at Jatigede Dam, West Java

Rosita. H. ST., MT.,

Hydrologist at Jatigede dam, West java

INDONESIA

1. ABSTRACT

Jatigede Dam is a rock fill dam located on Cimanuk river, West Java province, Republic of Indonesia which is one of Multipurpose dam and second biggest in Indonesia with 114 m height and about 980 Mcm of reservoir volume. To perform the initial filling of the reservoir, the inlet of the diversion tunnel must be closed and followed by plugging work. Systematically, Jatigede Dam diversion structure with a diameter of 10 m, starting from Inlet Diversion Conduit along

61.454 m connected with Tunnel along 546,221m and Outlet tunnel ends at Plunge pool.

There are two types of plugging done that is Primary plugging along the 17,74 m the starting position of the conduit and Main plugging along the 41 m at the core of the dam.

Immediately after closing of closure gate on August 31, 2015, Engineer will confirm the area where is in the right bank of Plunge Pool up to front of Tunnel Outlet is satisfied to use for access and material loading area from above. After closure gate, lining concrete of tunnel at position grout stopper shall be cut by using electric grinder to make groove for fixing of the Steel Galvanized Plate. After the completion of the installation of Steel Galvanized Plate, so Grout Pipes, including Riser Pipes, Backfill pipes, and T-type Socket are installation and fixed firmly by U-bolts at 10 cm center to center at the correct position from Grout Pipe. Drainage pipe is installed at the bottom of tunnel before 1st stage of concrete placing then Shut-off gate, tied with a wire rope of 12 mm diameter, is installed at the upstream end drainage pipe.

Forms are installed and firmly fixed together by using wooden timbers, anchor bars tension bars to avoid displacement or deformation. All supports wooden timbers and anchor bars at upstream of forms for all lift (up to 5th layer of A1 Block) shall be installed and firmly fixed prior to the placing concrete. Cooling pipe was constructed for each Block. All cooling pipes are tested for the leakage under the pressure of 3.5 kg/cm². The cooling water will be continuously provided by pump through the cooling pipes from the time of placing concrete until the concrete temperature comes down to 26oC. The discharge of water shall be controlled not to exceed 50oC of the concrete temperature. If necessary the water temperature shall be controlled by ice.

KEYWORDS

Large Diversion tunnel, Primary plug, Main plug, control the concrete temperature

COMMISSION INTERNATIONALE
DES GRANDS BARRAGES

VINGT-SIXIÈME CONGRÈS DES
GRANDS BARRAGES
Autriche, juillet 2018

**AN INTEGRATED GEOPHYSICAL INVESTIGATION
FOR THE EARTHEN DAM INSPECTION: ELECTRICAL RESISTIVITY
IMAGING, MULTICHANNEL ANALYSIS OF SURFACE WAVE AND
GROUND PENETRATING RADAR**

Noppadol POOMVISES, Prateep PAKDEEROD, Anchalee KONGSUK

*Bureau of Engineering Topographical and Geotechnical Survey,
ROYAL IRRIGATION DEPARTMENT, MINISTRY OF AGRICULTURAL AND
COOPERATIVES,
(e-mail: npoomvises@gmail.com)*

THAILAND

1. ABSTRACT

Royal Irrigation Department (RID) announces that an integrated geophysical investigation can provide useful information for the earthen dam inspection. Nondestructive geophysical techniques; Electrical Resistivity Imaging (ERI), Multichannel Analysis of Surface Wave (MASW), and Ground Penetrating Radar (GPR) have a great potential in identifying subsurface deficiencies and the results are intuitively acceptable.

In relation to these activities, subsurface characteristics of particular interest must be inferred from the physical properties of clay core. Low or high resistivity range means relative moisture in embankment material and implies the homogeneousness of impervious clay core. The shear wave velocity measured by MASW can be numerically converted to undrained shear strength, implying the bearing capacity of compacted clay. The GPR image clearly reveals partial settlement of freeboard zone at the upper part of the old earthen dam as well as the area covered by filled material, if there was any treatment in the past.

Integrated interpretation of the three results together with several field evidences can help verifying the current condition of the old earthen dam. The applicable techniques are applied to twenty six earthen dams of RID for a five-year research project, and finally, exhibit a flowchart for the old earthen dam inspection by using integrated geophysical techniques. Solutions and recommendations from the research lead to big changes in maintenance and/or retreatment program of the RID dams in the present day.

Keywords— Dam inspection, GPR, MASW, Resistivity.

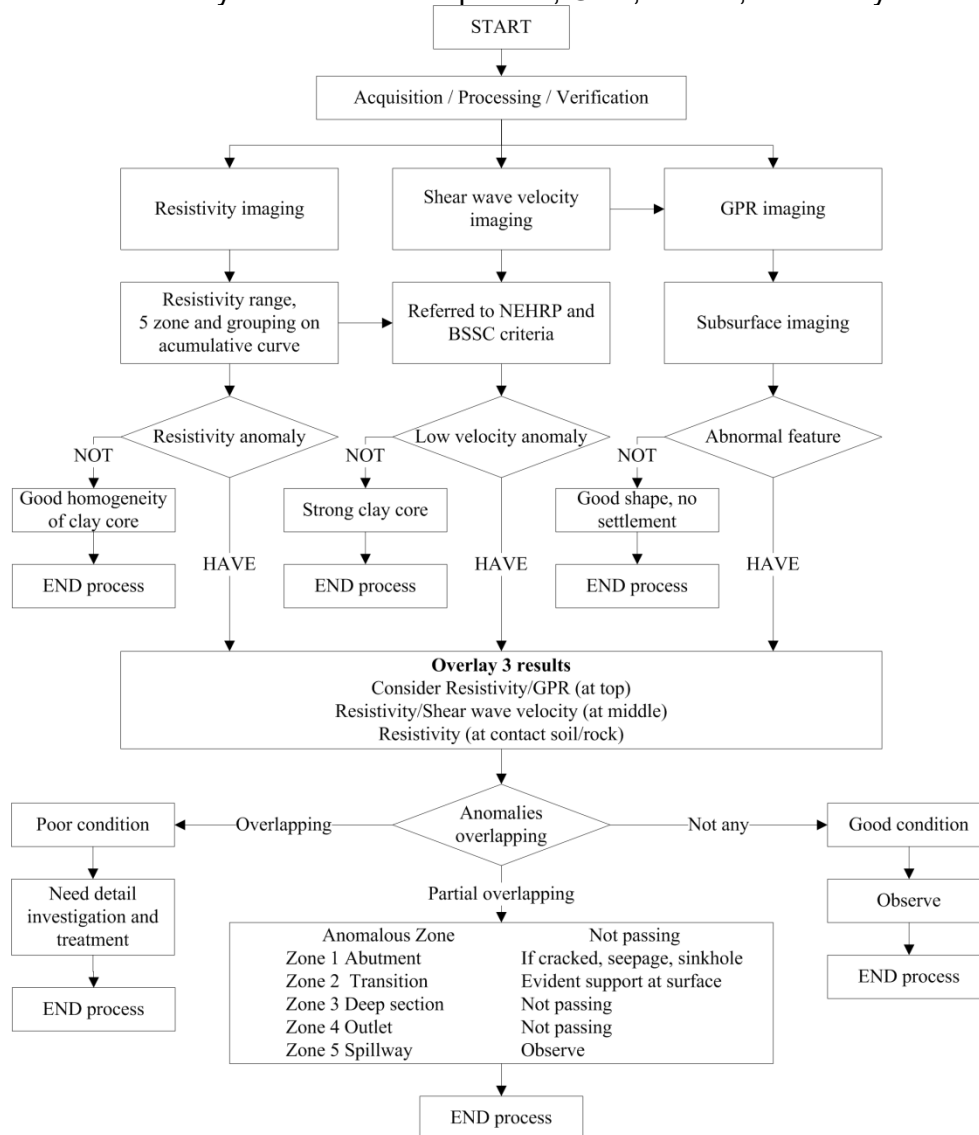


Fig. 1

Flow chart showing criteria of dam inspection, using geophysics. Note: at least resistivity, shear wave velocity and GPR play key technique in this account

COMMISSION INTERNATIONALE DES GRANDS BARRAGES

VINGT-SIXIÈME CONGRÈS DES GRANDS BARRAGES
Autriche, juillet 2018

DOI 10.3217/978-3-85125-620-8-075



This work licensed under a Creative Commons Attribution 4.0 International License. <https://creativecommons.org/licenses/by-nc-nd/4.0/>

HOW A PROBABILISTIC APPROACH CAN IMPROVE CMD DESIGNS

Abbas MOHAMMADIAN

Project Manager, ABFAN CONSULTING ENGINEERS

IRAN

Ahmad Ghezel AYAGH

Managing Director, ABFAN CONSULTING ENGINEERS

IRAN

COMMISSION INTERNATIONALE
DES GRANDS BARRAGES

VINGT-SIXIÈME CONGRÈS DES
GRANDS BARRAGES
Autriche, juillet 2018

HOW A PROBABILISTIC APPROACH CAN IMPROVE CMD DESIGNS

ABBAS MOHAMMADIAN

Project Manager, ABFAN Consulting Engineers

AHMAD GHEZEL AYAGH

Managing Director, ABFAN Consulting Engineers

IRAN

1. INTRODUCTION

The main branches of Cemented Material Dams (CMDs) are shown in Fig.1. Although CMD allows both the construction of admirable gravity dam bodies on weak rock foundations and the employment of low specific materials as aggregates for the dam body, it has more uncertainties than conventional RCC and CVC regarding design. On the other hand, one of the biggest advantages in designing CMDs is the uniform and typical geometry of the dam section, which permits the development of parametric solutions. Therefore, Performance-Based Design (PBD) using a probabilistic approach could be a proper strategy for this type of dam. In this paper, the advantages of this method are described.

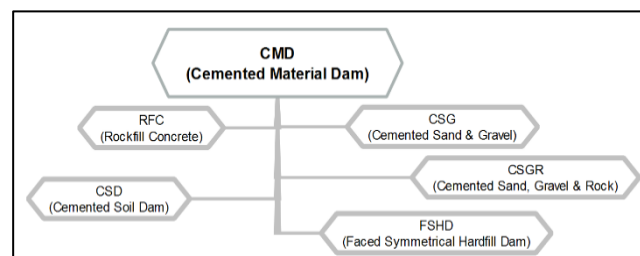


Fig. 1
Cemented Material Dams

Three CMDs, currently being constructed under the supervision of ABFAN consulting engineers in Iran, are used in the case study for the proposed probabilistic approaches. The detailed specification of these dams is presented in the authors' previous papers [1], however, a brief specification of "Dasht-e-Palang" dam which is most referred to in this paper is described for convenience.

"Dasht-e-Palang" is a composite of Gravity and Earthfill dam type, under construction in the south of Iran (Fig.2). The project objective is to provide drinking, industrial and agricultural water:

- Maximum height: 56 m
- CMD part crest length: 350 m. Earthfill part crest length: 680 m
- CMD part crest width: 4 m. Earthfill part crest width: 8 m
- Upstream and downstream slope of the dam body: 0.7 h / 1.0 v
- Hardfill volume: 540,000 m³. CVC volume: 150,000 m³
- Earthfill volume: 950,000 m³

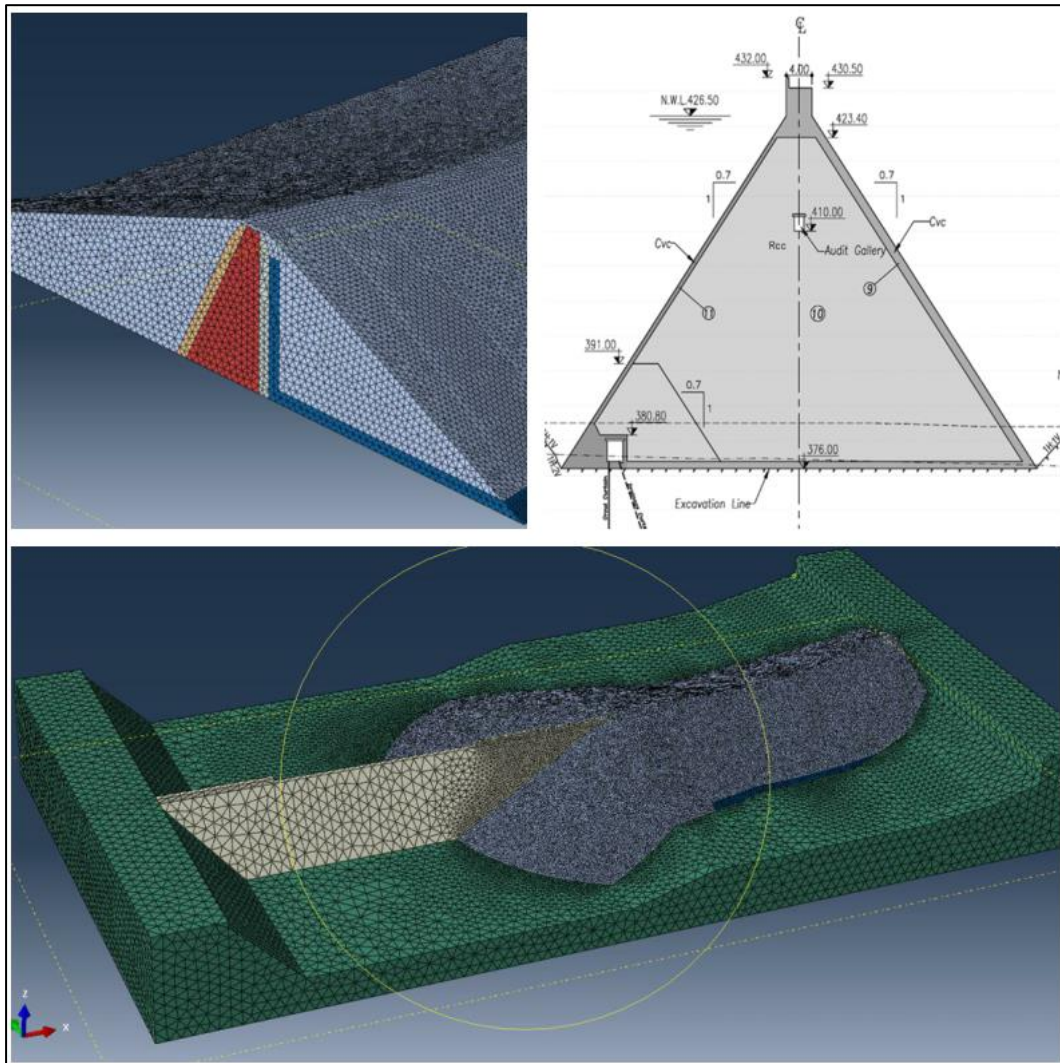


Fig. 2
"Dasht-e-Palang" dam (A composite of CMD & Earthfill)

2. VARIATIONS IN AGGREGATE GRADING'S

One of the most important benefits of CMDs is the ability to adopt raw and even low-quality materials around the dam site [2], which causes unavoidable variations in aggregate grading and the physical properties of Hardfill materials on the other side. Segregations at Hardfill placement are another defect that could occur in this regard. A solution to reduce these variations and mitigate such segregations is dividing the raw materials in two or three stockpiles. Sands and gravels will then be mixed with pre-specified proportions to produce the best fit of aggregate grading compared to the optimum curves. Obviously, this process will lead to the production of some excess aggregates that can be crushed and used again if desirable. Applying the probabilistic method will be of significant help in order to obtain the optimum sieve number of fractions and mixing proportion since the varieties in the samples are unknown. This method can be summarized in the following steps:

- Providing adequate samples of raw materials in the different locations of the borrow area and at different depths of each pit.
- Generating the remaining portions instead of the finer material grading tables.
- Generating a huge series of aggregate grading tables (e.g. more than 10000) based on the probabilistic approach (one may use a numerical method instead of probabilistic distributions to generate a new series).
- Changing the above-mentioned series from the "residue" percentage curves to "finer" percentage curves.
- Selecting the base sieve numbers for aggregate fractioning and the proportion of mixing, γ , in a way that the best fit to the desired curves is obtained with minimum excess materials.

As a case study, the application of this method in the "Kahir" dam project will be discussed:

Riverbed aggregates with MSA=50mm are selected as the raw materials, and the natural grading curves are shown in Fig. 3. The aim is to simplify the construction procedure by reducing the aggregate production process.

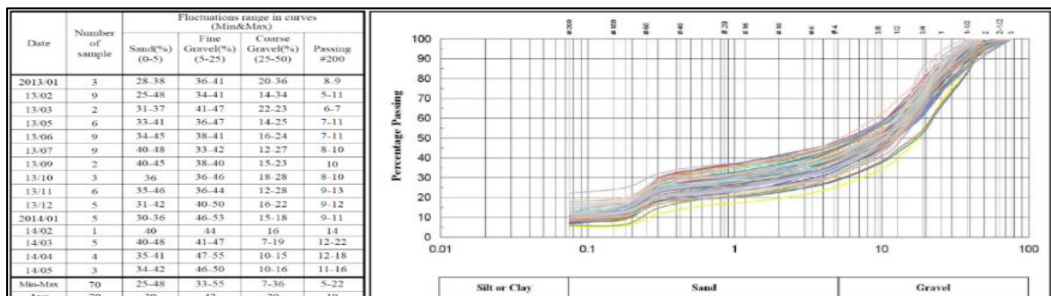


Fig. 3
Grading curves of raw materials

Performing the above-mentioned method, many variants have been studied. Based on the natural grading curves, about 10,000 probabilistic curves have been generated, each subsequently divided in two parts on the selected dividing sieve, e.g. #5, #12 or #25. Afterwards, each division has been mixed with various proportions (25%, 35%, 45% and 55% of the finer portion as shown in Fig. 4). The produced curves have been compared to the desired aggregate curves and the optimum values have been selected in the end. The optimum selection is elaborated as follows:

The total aggregates are separated into fractions by sieve #16 (in other words, we separately have 0-12mm and 12-50mm) with a mixing proportion of 45-55%.

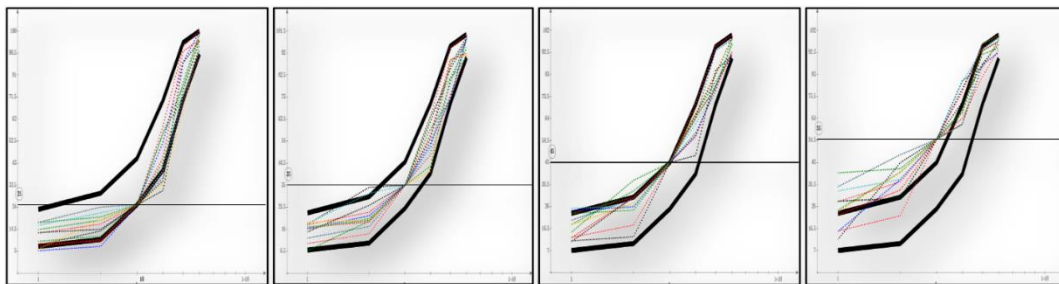


Fig. 4
The grading curves of aggregates for different proportions

3. CMDs FOUNDED ON WEAK ROCKS

CMDs are more compatible with their foundations with respect to RCC and CVC gravity dams, which comes at the price of weaker foundations and hindering the estimation of proper and precise rock engineering parameters (shear strength and modulus of deformation), and also the type of the rock in the basement may varies in each location (Fig. 5 shows the rock lithology profiles in Dasht-e-Palang Dam).

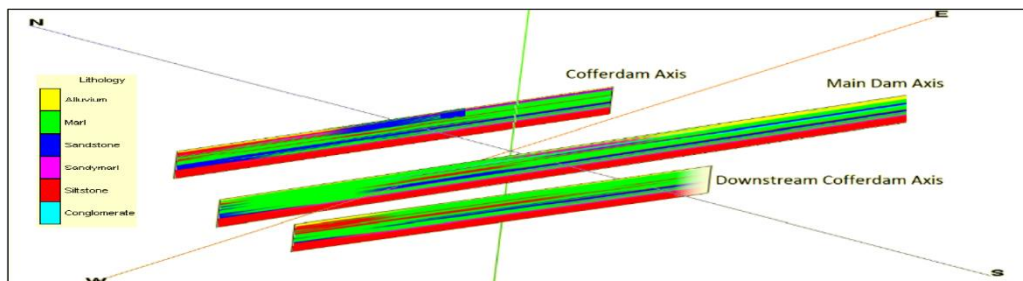


Fig. 5
Different rock properties along the longitudinal axis in Dasht-e-Palang dam

Uncertainties in shear strength parameters will cause uncertainties in the sliding stability of the dam body. Similarly, uncertainties in the rock deformation modulus will cause the stress values in the dam body and foundation to experience variations. Exerting the “minimum” shear strength parameters is a conservative and costly design approach on one hand, and exerting the “mean” values may not be safe on the other. Therefore, studying the stability and stresses in the dam body and foundation would require a huge amount of rigid body stability and finite element analysis, making the final decision-making difficult. This is where applying the probabilistic method comes as a great advantage. In the following, utilizing this method to calculate the sliding stability is described, and its application to determine the modulus of deformation is explained in the next section.

Initially, consider the shear strength parameters of Dasht-e-Palang dam. An evaluation of the rock mechanics parameters based on a vast range of studies is presented in the table shown in Fig. 6 (left). The first step is to perform a stability analysis on different optional pairs of cohesion and friction angle, which will result in a calculable sliding safety factors. Obtaining this data matrix and performing a probabilistic analysis (finding the interpolation of SFs between each node of cohesion and the friction angle), the distribution of SFs can be plotted. In addition, by selecting the minimum desired safety factor, the probability of failure and the adequacy of the dam body geometry will be yielded according to Fig. 6 (right).

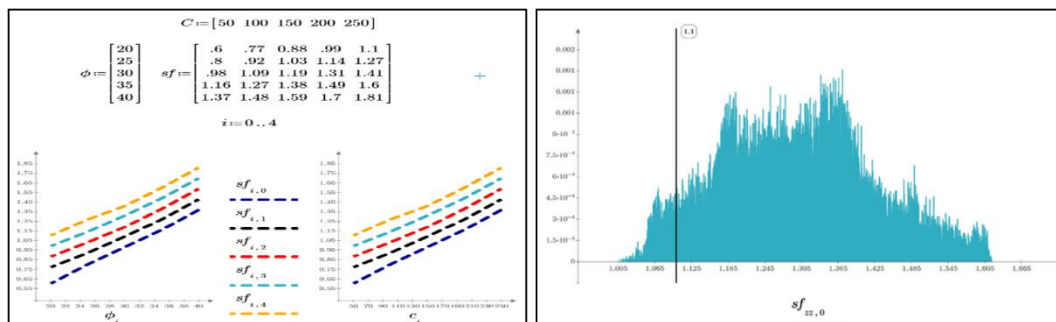


Fig. 6
Safety factors against sliding (left), the distribution of safety factors (right)

4. CONSTRUCTION SIMPLICITY

Even though the construction simplicity of CMDs is a key asset, it could also cause a number of challenges to the prediction of the material behavior, the highly layered dam body amongst them. The bonding between the Hardfill layers is generally less than the RCC layers due to the following reasons:

- The total cement content is low.
- Treatment between successive layers is not necessary.
- There is no need to bedding mortars between layers.
- More segregation occurs compared to RCC.

For example, some cores from the Kahir dam project are demonstrated in Fig. 7. As clearly indicated in this figure, undesirable bonding is observed between the Hardfill layers.

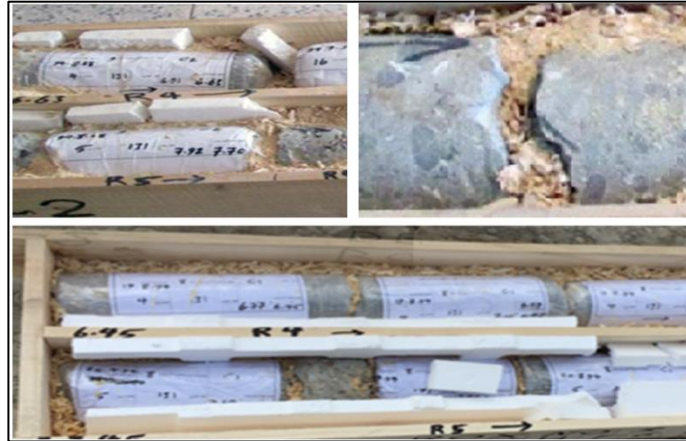


Fig. 7
Core samples from the Kahir Hardfill dam

From the aforementioned facts, we can elicit that the layered behavior of the dam body under loadings (which affects the mass modulus of the dam body deformation) should not be neglected. As also discussed in the next section, the estimation of the modulus of deformation must be sufficiently close to reality in order to give valid stress analysis results. Among the available approaches to overcome this challenge in finite element method, one is to model the layers of the dam body one by one, and considering their interfaces using the appropriate approach [6]. Although this method is more reliable than ignoring the multilayer properties of the materials, performing this complicated method is far more time-consuming and thus impractical, especially in dynamic loads. Two other approaches based on the probabilistic approach are discussed here:

- 1- The strength properties of the CMD layers are reduced in the direction normal to the layers. Employing the mechanics of multilayered or composite materials, we can define an orthogonal material with two different moduli in two perpendicular directions. The parameters which the derived formulas require (the shear and normal stiffness between successive layers) are unknown variables and need large-scale experiments that may not be feasible in regular Hardfill dams. To solve this issue, performing a dilatometry test in the constructed Hardfills will help gather useful data. A set of estimations are also available in rock mechanics [3], including the following equation:

$$E_i := \left(\frac{1}{E_r} + \frac{1}{T_h \cdot K_n} \right)^{-1} \quad [1]$$

Where “ T_h ” and “ K_n ” are the layer thickness and the normal-stiffness, respectively. Assuming the Hardfill layer thicknesses and the normal

stiffness of the layers equal to 30 cm and an estimated value of 13 for K_n , we will have $E_v = 0.3 \cdot E_i$ and $E_h = E_i$.

- 2- A wide range of studies have been done on finding the relationship between the intact modulus (E_i) and the mass modulus (E_m) in rock mechanics [4], most of which apply a reduction factor to E_i in order to obtain E_m . A simple equation proposed by Bieniawski [5] relates the two moduli using RQD as follows:

$$E_m := E_i \cdot \left(10^{0.0186 \cdot RQD - 1.91}\right) \quad [2]$$

Another method is to relate the reduction factor to RMR [4], which could be rewritten in terms of RQD in layered dam bodies.

$$\frac{E_m}{E_i} = \frac{1}{100} \cdot \left(0.0028 \cdot RMR^2 + 0.9 \cdot \frac{RMR}{22.82}\right) \quad [3]$$

The RQDs of Hardfill cores are variable along the dam body, not perfectly precise and containing uncertainties, which makes a probabilistic approach necessary. Exerting RQD distribution of cores will enable us to calculate the modulus of the Hardfill using the relations above. The application of these probabilistic distributions of E to the finite element method will be discussed in the next section. Whereas the stress results in the dam body and foundation are directly dependent on the “modulus ratio” of Hardfill to rock and independent from the single values of E , it is clear that utilizing the same method and data to estimate E in both rock mechanics and dam analysis will result in a better estimation of stress values in the dam body.

5. CHARACTERISTIC COMPRESSIVE STRENGTH

More “variations” occur in the compressive strength and the modulus of elasticity of Hardfill compared to RCC projects, which results in unknown stress distribution in the structure. Determining the characteristic compressive strength for Hardfill dams is of great importance since it plays the main role in the total cement usage of the project. Therefore, a probabilistic approach to determine the optimum compressive strength is proposed in this paper.

All of the stresses in the dam body must be compared to allowable stresses considering various load combinations. A new stress distribution with respect to the load combination is obtained as shown in Fig. 8 (middle) for each value of $E_{(c)}$ or $E_{(Hardfill)}$. By performing finite element analysis for different values of $E_{(Hardfill)}$ and finding the highest compressive stress generated in the structure (and transforming tensile stresses into equivalent compressive stresses), a fitted curve for input $E_{(Hardfill)}$ against the maximum compressive strengths is resulted according to Fig. 8 (left). It is inferred from the figure that each f'_c of the Hardfill material will produce an initially unknown $E_{(Hardfill)}$. Assuming that this relationship is characterized as curve R in Fig. 8 (left), it is clear that the intersection of these two curves may be the desired f'_c , considering the safety factors for the stresses. It is worth noting that

the stress values depend on the ratio of $E_{(Hardfill)}$ to $E_{(rock)}$. However, we will consider the $E_{(rock)}$ values equal to 1 GPa for simplicity.

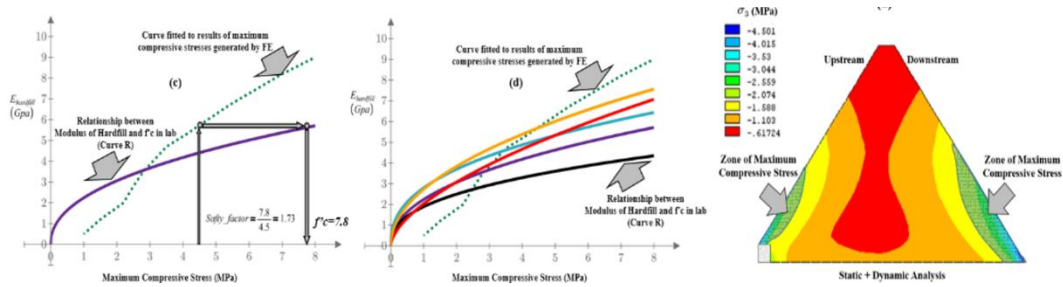


Fig. 8
Modulus of deformation vs. compressive strength

As indicated in Fig. 8 (middle), if a satisfactory fixed curve is not obtained for the relationship between E_c and f'_c of Hardfill, each sample of the Hardfill material may generate a different curve, which in turn yields a different stress safety factor. The challenge is coming up with a way to find a minimum f'_c for Hardfill that also satisfies the allowable safety factors.

The following factors are presumed to affect the output results:

- The relationship between f'_c and E_c in lab tests
- Estimating the modulus of the “Hardfill mass”
(Discussed in the section 4)
- The probabilistic parameters of the rock foundation
(Discussed in the section 3)

The formulae of the probabilistic functions are defined as follows:

$$E_{mass} = f^* \left(f'_c, E_{rock}, \frac{E_m}{E_i} \right) \quad [4]$$

$$\sigma_{max} = g^*(E_{mass}) = g^* \left(f^* \left(f'_c, E_{rock}, \frac{E_m}{E_i} \right) \right) \quad [5]$$

$$\frac{f'_{c_i}}{\sigma_{max_i}} = Safety_factor_i \quad [6]$$

The probabilistic formulation for the relationship between f'_c and E_c can be put this way:

$$E_c := a \cdot f'_c^b \quad [7]$$

Were there enough tests available to relate E to f'_c , we could establish a probabilistic formula instead of a fitting curve with a low coefficient factor. Nevertheless, we are obliged to assume “a” as a random normal distribution (with $\mu=3.5$ and $\sigma=0.5$) and “b” equal to 0.5 based on the vast experiment results in lean RCCs.

Constructing a mathematical model to perform a probabilistic analysis, we will obtain the output in the form of the density distribution of the stress safety factors. To gain the optimum f'_c , we should constantly change f'_c as an input to find a distribution of the stress safety factors with the allowable failure percentage (for example 20% is acceptable for most gravity dams).

Performing the analysis on Dasht-e-Palang dam, the application of the method mentioned above will result in the graphs shown in Fig. 9. Trial and error yields that assuming a normal distribution for f'_c of the samples with a mean of 7 MPa (known as f_{cr}) and a variation coefficient of 30% (i.e. a standard deviation of 2.1 MPa), we will have a f'_c equal to $7 - 0.824 * 2.1 = 5.2$ MPa. Performing tests to determine E in the lab will make a more accurate estimation of f'_c possible.

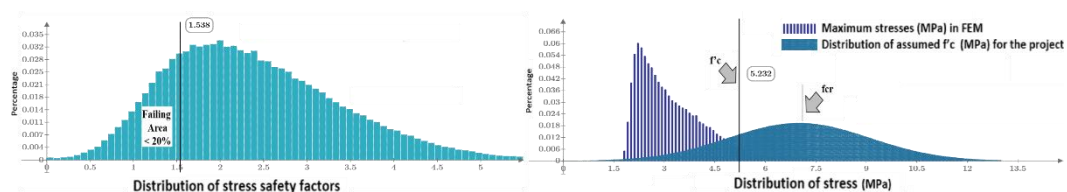


Fig. 9
Dasht-e-Palang dam probabilistic analysis results

6. CONCLUSIONS

CMDs simplify the method of construction at the cost of causing uncertainties in the analysis and design of the dam. Applying an approach based on probabilistic methods with the concept of performance-based design will enable us to overcome these unwanted variations. In this paper, using a probabilistic approach in the designing process of three CMDs (currently under construction) has been described. The main benefits are listed as follows:

- 1- Minimizing the variations of aggregates in the Hardfill using an optimal method for screening and fractioning without any crushing.
- 2- More authentic estimation of the effect of weak rock parameters on the sliding safety factors of the dam body.
- 3- Better estimation of the layered properties of the CMD body.
- 4- Using less cementitious material by optimizing f'_c .

ACKNOWLEDGEMENTS

The authors would like to give special thanks to A.Mohammadi and R.Erami from Bushehr Regional Water Authority (BRWA) for their kind contributions.

REFERENCES

- [1] MOHAMMADIAN A. et al, CMDs on low modulus foundations - four first experiences in Iran. 85th Annual Meeting of International Commission on Large Dams, 2017.
- [2] JAPAN DAM ENGINEERING CENTRE, Engineering Manual for Construction and Quality Control of Trapezoidal CSG Dams, 2007.
- [3] BELL F.G. (Editor), Engineering in Rock Masses, B-Heinemann, 1994, P232.
- [4] GALERA J, ALVAREZ M., BIENIAWSKI Z., Evaluation of deformation modulus of rock masses using RMR, 2007.
- [5] BIENIAWSKY Z. T., Engineering Rock Mass Classifications, John Wiley, New York, 1989.
- [6] MAZLUMI A., GHAEMIAN M., NOORZAD A., Nonlinear Seismic Analysis of RCC Dam Considering Orthotropic Behavior of Layers, International Symposium of ICOLD, 2012.

SUMMARY

Cemented material Dam (CMD) on weak foundation has more challenges than other types of gravity ones. Variations in rock properties in the foundation, natural aggregates and simplicity in construction which results in more inhomogeneities in dam body will cause a lot of uncertainties which is a paradox in design. Performance Based Design using a probabilistic approach may be a proper way in this type of dam.

Using this probabilistic method, uncertainties on estimating the modulus of deformation of foundation is considered, variations in aggregate grading's has been reduced by finding the optimum sieve number of fractions, the layered behavior of dam body which is an inherent specification of CMD's, the relationship between modulus of deformation of Hardfill versus compressive strength and finally finding an optimum characteristic compression of dam body is well defined by a new proposed method in this paper.

KEYWORDS

MATHEMATICAL MODEL, AGGREGATE, FOUNDATION, ROLLER COMPACTED CONCRETE

COMMISSION INTERNATIONALE DES GRANDS BARRAGES

VINGT-SIXIÈME CONGRÈS DES GRANDS BARRAGES
Autriche, juillet 2018

DOI 10.3217/978-3-85125-620-8-076



This work licensed under a Creative Commons Attribution 4.0 International License. <https://creativecommons.org/licenses/by-nc-nd/4.0/>

**EFFECT OF DILATANCY ANGLE ON THE RELIABILITY ANALYSIS OF
BEARING CAPACITY OF DAM FOUNDATION USING MONTE CARLO
SIMULATION**

Mehraneh MAADI

FACULTY OF CIVIL, WATER AND ENVIRONMENTAL ENGINEERING, SHAHID
BEHESHTI UNIVERSITY

IRAN

Ali NOORZAD

FACULTY OF CIVIL, WATER AND ENVIRONMENTAL ENGINEERING, SHAHID
BEHESHTI UNIVERSITY

IRAN

COMMISSION INTERNATIONALE
DES GRANDS BARRAGES

VINGT-SIXIÈME CONGRÈS DES
GRANDS BARRAGES
Autriche, juillet 2018

EFFECT OF DILATANCY ANGLE ON THE RELIABILITY ANALYSIS OF BEARING CAPACITY OF DAM FOUNDATION USING MONTE CARLO SIMULATION

Mehraneh Maadi, Ali Noorzad

*Faculty of Civil, Water and Environmental Engineering, Shahid Beheshti
University*

IRAN

1. INTRODUCTION

Analysis and design of geotechnical structures continue to face many uncertainties, which make it difficult to choose the appropriate design parameters. In the conventional design, engineers are trying to cover the uncertainties involved with a relatively high safety factor. Considering high safety factor leads to construction of conservative design of foundations so that in spite of high cost, due to ignoring the effect of uncertainty, engineering judgment should be very difficult. Selecting geotechnical parameters of soil, due to uncertainties in the field, has always been one of the most challenging issues in geotechnical engineering.

Due to the uncertainties involved, it can be pointed out that considering constant parameters in soil analysis is not reasonable and the best solution to consider uncertainty in the soil is using probabilistic approach. Statistical parameters include the mean, coefficient of variation, and the density function of all parameters. The probabilistic analysis consists of methods that consider the effect of uncertainties on input parameters and determine the response regarding the uncertainty level. Some of these methods can be stated as reliability analysis method.

Reliability analysis method makes it possible to quantify the uncertainties involved in the problem. It also determines safety factor according to the degree

of uncertainty and acceptable risk. Reliability analysis can be considered as an alternative to the definitive methods and makes engineering judgment easier [1].

2. EFFECT OF FLOW RULE ON THE BEARING CAPACITY COEFFICIENTS

Bearing capacity of the soil is the maximum load pressure that soil can tolerate at the moment of the failure. The most common methods used to determine the bearing capacity of foundations are limit methods so that these methods can be divided into three basic types of limit equilibrium method, method of stress characteristic and limit analysis.

Limit analysis method determines the upper and lower collapse load by theory of plasticity. In this method if the upper and lower limit give the same result, then it will be the exact solution of the problem. Researchers investigate foundation bearing capacity using different methods in the literature. One of the famous theories is known as Terzaghi bearing capacity theory. Terzaghi defines ultimate bearing capacity of foundation according to Eq. 1 [2].

$$Q_u = CN_c + qN_q + 0.5B\gamma N_\gamma \quad [1]$$

where N_c, N_q, N_γ are bearing capacity factors which are dimensionless and can be computed by friction angle, ϕ . B is the foundation width, and γ is unit weight. Also in this equation q is surcharge pressure and C is soil cohesion. Michalowski (1997) [3] estimated to calculate bearing capacity of a foundation using the upper bound approach which is applied to determine bearing capacity of a dam foundation on granular soil without surcharge pressure ($C = 0$, $q = 0$). In Michalowski estimation, the substantial influence of the dilatancy angle on limit load was also considered. It is worthy to note that limit theorems are based on rigid-perfectly-plastic behavior that follow the associated flow rule.

It should be noted that the soil used in this paper is coarse; the soil cohesion, therefore, is set zero. Furthermore, surcharge pressure has not been taken into account, i.e. the third term of the bearing capacity equation, qN_q , becomes zero. Accordingly, the bearing capacity equation of Michalowski can be written as below:

$$Q_u = 0.5B\gamma N_\gamma \quad [2]$$

Concerning associated flow rule, the yield function is equal to the potential function [28]. Assuming Mohr-Coulomb yield criterion and associativity, the aforementioned statement renders the equality of yield surface. Although the associated flow rule leads the limit theorems, the theorems based on which limit analysis of stability problems can be well carried out to be developed [29], granular soils often dilates under deviatoric loads in an angle much less than the friction angle. Therefore, it seems to be more or less inaccurate assuming associativity, and non-associated flow rule, instead, should be considered in order to increase the accuracy of the assumptions.

$$T = \sigma \tan \varphi + C \quad [3]$$

Mohr-Coulomb criteria can be modified for non-associated problems as follows [3]

$$T = \sigma \tan \varphi^* + C^* \quad [4]$$

where:

$$\tan \varphi^* = \frac{\sin \varphi \cos \psi}{1 - \sin \psi \sin \varphi} \quad [5]$$

To make a rational and proper judgment to calculate the third term in Eq.1, limit analysis is employed. The advantage of this approach is that a clear distribution weight of the components of the soil, cohesion, and surcharge in bearing capacity formula is considered. N_γ factor for non-associated flow rule is obtained from the perspective of the limit analysis. N_γ factor values are shown in the following table for smooth and rough foundations and for different dilation angles as the part of the friction angle. It is worth re-mentioning that by the use of limit analysis, it is possible to obtain numerically estimated N_γ values, tabled below as the results of Michalovski (1997); the most reasonable curve fits would be achieved in the next step, required for the reliability analysis.

Table 1
 N_γ for smooth foundation (non-associated flow rule)

$(\varphi^* \text{°})$	N_γ		
	$\psi = 0.5\varphi^*$	$\psi = 0.25^\circ$	$\psi = 0$
0	0	0	0
5	0.18	0.18	0.18
10	0.7	0.693	0.683
15	1.894	1.842	1.773
20	4.261	4.028	3.734
25	8.931	8.064	7.058
30	18.309	15.442	12.457
35	37.606	28.798	20.849
40	78.649	52.772	33.306
45	169.436	95.428	50.924
50	379.868	170.386	74.614

Table2
 N_γ for rough foundation (non-associated flow rule)

$(\varphi^* \text{°})$	N_γ		
	$\psi = 0.5\varphi^*$	$\psi = 0.25^\circ$	$\psi = 0$
0	0	0	0
5	0.127	0.127	0.126

10	0.419	0.415	0.413
15	1.027	1.001	0.966
20	2.225	2.107	1.962
25	4.597	4.156	3.646
30	9.353	7.899	6.385
35	19.134	14.667	10.642
40	39.937	26.834	16.958
45	86.045	48.385	25.886
50	192.66	86.4	37.876

As shown in Tables 1 and 2, non-associativity has a negligible effect on N_γ for internal friction angles below 25 degrees but it becomes more significant for larger friction angle. The numerical solutions can approximate N_γ factor for each dilation angle in smooth and rough foundations. Results are given for both rough and smooth footings. for rough footings:

$$N_\gamma = e^{0.66+5.11 \tan \varphi^*} \tan \varphi^* \quad [6]$$

For smooth footings:

$$N_\gamma = e^{5.11 \tan \varphi^*} \tan \varphi^* \quad [7]$$

3. RELIABILITY ANALYSIS METHODS

In reliability analysis, there are three specific categories including analytical, approximate and simulation methods which can be used in different conditions based on their drawbacks and advantages. The analytical methods consider probability density functions of input parameters mathematically defined and the performance function (e.g. safety factor), integrated over input variables; accordingly, probability density function of the performance function can be determined. The drawback of these methods is that they are limited to problems with few numbers of stochastic variables. However, it is possible to assess the probability feature of the problems using ideal mathematical viewpoint. It is worth mentioning that few studies have been done using analytical methods of reliability analysis in view of their mathematical complexity. Jointly Distribution Random Variables (JDRV) approach is the one utilizes mathematical techniques [4-7] by numerical integration in order to find probability distribution function (PDF) of performance function, but it is not able to consider correlation coefficient between stochastic parameters.

However, approximate solutions compute the probability of events with some indicators such as mean value and variance of input stochastic parameters. It should be mentioned that conventional approximate solutions are based on three methods: First Order Reliability Method (FORM) [8], First Order Second Moment (FOSM) [9] and Point Estimation Method (PEM) [10]. Each of them uses several simplifying assumptions for prediction of failure probability that somewhat reduces the accuracy. Furthermore, approximate solutions estimate the mean

and variance of performance function; but they do not provide any information concerning the shape of its PDF. Therefore, the probability of events can be determined merely based on the assumed PDF for performance function by usually using normal distribution function. Recently, most of the reliability analysis, especially in the study of liquefiable soils, have been done using these methods [11-21].

Finally, it is worth noting that simulation methods are somewhat more accurate comparing with the previous ones. By the use of these methods, it is possible to predict the probability of event by simulating stochastic input parameters and implementing in repetitive calculations. The striking feature of these methods is that they can be used in complex mathematical problems, where the closed-form solution of which is not possible [22]. Thanks to the development of computer technology and available personal computer, application of these methods has been increased significantly in engineering problems. Monte Carlo simulation method is one of the most applicable methods, which will be discussed in the next section [1].

4. MONTE CARLO SIMULATION METHOD

In Monte Carlo Simulation (MCS), a mathematical or empirical operator $F(X)$ with the variable X ranging from x_1 to x_n is continuously calculated in which the operator (s) are random or have uncertainty with prescribed probability distributions [22-23]. MCS is actually an accurate reliability analysis method, applicable for collapse problems including slope stability, retaining walls and foundations [24-25]. In the analysis, stochastic values for input parameters are chosen; afterwards, the probability density function of stochastic parameters – which include any shape but normal, log-normal and beta distribution functions are generally implemented based on the characteristics of the stochastic variables, used to obtain the performance function. It is worth mentioning that the current procedure is repeated so far as proper statistical distribution for performance function is obtained enabling the user to determine the mean and standard deviation of performance function and, finally, prediction of the probability of events. Generally, this method consists of four steps as follows [25]:

1. Generating stochastic values for each of stochastic variables according to assigned probability density function.
2. Computing performance function using a proper deterministic method based on generated values in previous step.
3. Repeating steps 1 and 2 for as many times as required.
4. Determining probability distribution function of performance function and calculating the probability of events.

The number of required Monte Carlo trials is dependent on the level of confidence in the solution and the amount of stochastic variables. Based on the statistical theory, Eq. (8) has been recommended for the number of iterations [25]:

$$N = \left(\frac{d^2}{4(1 - \varepsilon)^2} \right)^m \quad [8]$$

where N is the number of Monte Carlo trials, d is the normal standard deviation corresponding to the level of confidence, ε is the desired level of confidence and m is the amount of stochastic variables. Table 3 represents some confidence level (ε) with corresponding standard deviation (Std) with regard to the number of stochastic variables.

Table 3
Standard deviations according to confidence levels

confidence level (ε)	Standard deviation(std)
80%	1.282
90%	1.645
95%	1.96
99%	2.576

To generate random numbers, often probability distribution functions that generate numbers between zero and one are used such as uniform probability distribution function. Then using Eq. 9 these numbers are converted to numbers with standard normal probability distribution.

$$N_1 = \sqrt{-2 \ln R_1} \cos(2\pi R_2) \quad [9]$$

R_1 and R_2 are random numbers generated using uniform distribution and N_1 is an independent random number generated using standard normal distribution. This process will be continued until enough random numbers are generated. The generated random numbers have a mean of zero and a standard deviation of one. To convert numbers with standard normal distribution (N_i) to numbers with the normal distribution having the mean of μ_x and the stress standard deviation of σ_x (X_i), Eq. 10 is applied.

$$N_1 = \sqrt{-2 \ln R_1} \cos(2\pi R_2) \quad [10]$$

$$X_i = \mu_x + N_i \sigma_x \quad [11]$$

In Eq. 10, X_i is a generated random number with normal distribution that is used in the calculation of the performance function and N_i is a random number with standard normal distribution. The presented equations are provided for the case that random numbers are generated independently.

5. CALCULATION OF THE BEARING CAPACITY OF DAM FOUNDATION USING MONTE CARLO SIMULATION METHOD

In this method, the foundation bearing capacity can be analyzed for various performance levels and soil bearing capacity is calculated depending on the desired level of confidence. Probabilistic analysis for bearing capacity of dam

foundations using Monte Carlo simulation and uncertainty parameters is calculated.

Among input variables, the friction angle is considered as random variables and (ψ) , (γ) and (B) are constant. The number of iterations to simulate is set to 200,000 times, also the coefficient of variation of soil friction angle is considered 15% [26, 27].

5.1. NUMERICAL ANALYSIS

In this section, to demonstrate the efficiency of the proposed model to analyze the bearing capacity of foundation, a numerical example is assumed. In the example a foundation with a width of 2 meters and granular soil with the unit weight of 19 kN/m^3 are considered. Also The average of dilation angle (ψ) is assumed to be 6° . In calculating the definitive bearing capacity, the average friction angle is considered 25 degree.

Safety factor in different iterations is calculated and the frequency graph of ultimate bearing capacity is shown in Figures 1 and 2. As can be observed the curve is continuous and follows the log-normal probability distribution function. In Figures 3 and 4 the procedure of calculating allowable bearing capacity with a confidence level of 90% are illustrated.

Ultimate bearing capacity of foundation using Michalowski method is obtained 92.5 kN for smooth foundations and 176 kN for rough foundations.

If the dam foundation with the assumed specifications is analyzed using Monte Carlo method, the cumulative distribution graph of bearing capacity could be as Figures 1 and 2. To select the allowable bearing capacity of foundation, regarding the desired confidence level, cumulative distribution graph of bearing capacity can be selected. it can be concluded that the confidence level required for structures is about 90 to 98%. For example, a confidence level of 90% indicates that 90% of simulated items have more bearing capacity than the allowable bearing capacity. According to Figures 3 and 4 allowable bearing capacity of smooth foundation due to the 90 percent of confidence level equals to 48.2 kN and for rough foundation this value is 95.9 kN.

By comparing the allowable values and ultimate bearing capacity regarding confidence level of 90%, it can be pointed out that safety factors for smooth and rough foundations are obtained 1.92 and 1.83 respectively. According to the above explanation, it can be stated that the method of reliability analysis to calculate the bearing capacity of foundations is more reliable than certain methods, because in addition to reducing construction costs, this method handles the uncertainties that are also quantified.

6. CONCLUSIONS

Reliability analysis methods, which consider uncertainties and estimate the probability of bearing capacity, can facilitate the engineering judgment.

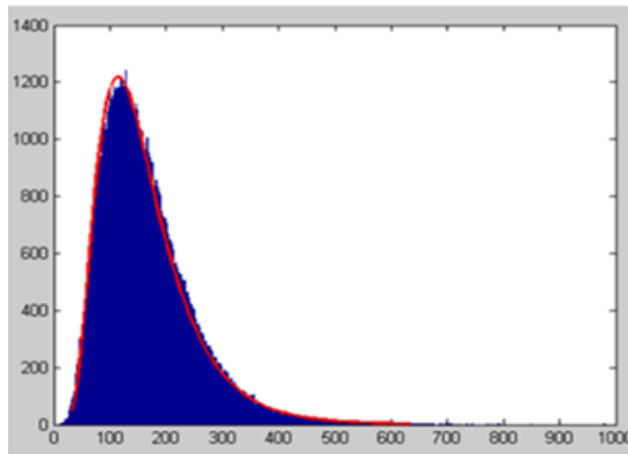


Fig. 1

Frequency diagram of ultimate bearing capacity of smooth foundation

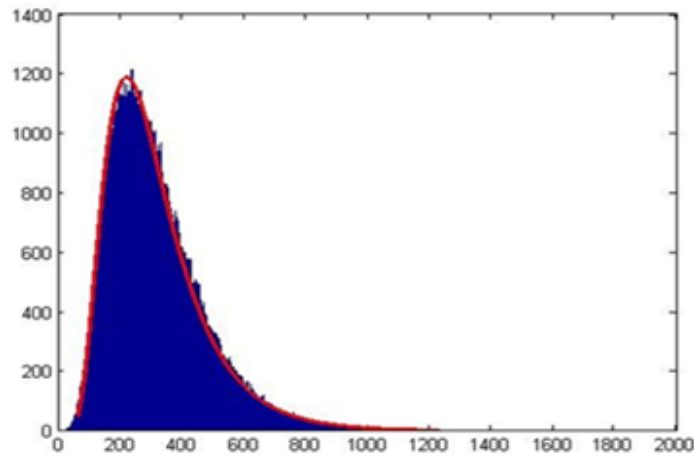


Fig. 2

Frequency diagram of ultimate bearing capacity of rough foundation

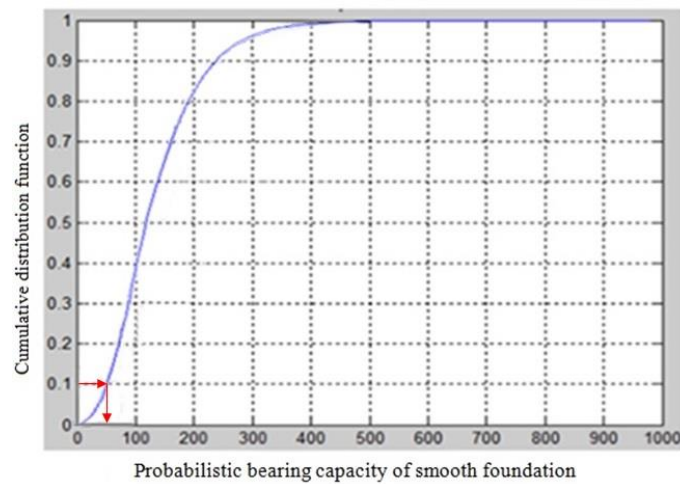


Fig. 3

Probabilistic bearing capacity of smooth foundation

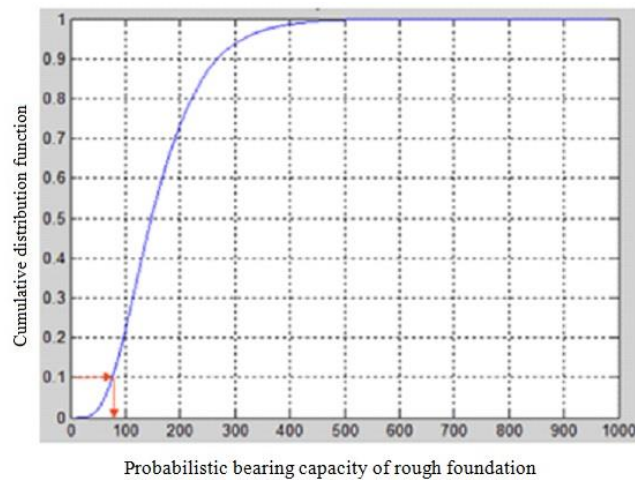


Fig. 4

Probabilistic bearing capacity of rough foundation

In this paper, Monte Carlo's simulation method as one of the reliability analysis methods is used to investigate the influence of the variation of friction angle (φ) on the reliability of dam foundations. In this regard, the performance function is built with Michalowski's equation. In the presented research, based on the results, the following conclusions are drawn:

1. For foundations on granular soils, the probability of failure of foundation is more sensitive to the variation of friction angle of soils, since the COVs of main parameters of bearing capacity like the friction angle (φ) is considered.
2. The proposed probabilistic approach accounts for parameter uncertainty of soil friction angle, and enables bearing capacity to be quantified in the form of a cumulative probability distribution function that provides bearing capacity predictions corresponding to certain reliability levels. This indicates the importance of adopting probabilistic analysis in favor of the factor of safety. It was also shown that the developed probabilistic method can be used to predict bearing capacity of dam foundation for reliability levels of 90% and 95%.
3. The results obtained from Monte Carlo's simulation method and deterministic method indicate that the deterministic method is not reliable enough in comparison to the probabilistic results.
4. A numerical example was given to illustrate the use of Monte Carlo's simulation. The results indicate that the suggested factor of safety of 3 that usually used by available deterministic models is conservative. However, it seems not to be economically beneficial.
5. A substantial influence of the dilatancy angle on N_γ is found and this is a reason for concern. Since the non-associativity of plastic deformation of soils is usually not accounted and especially in high levels of friction angle, is usually an essential phenomenon in soils under applied loads. Taking into account the reliability analysis with non-associativity, one can highlight the aim of the current study.

REFERENCES

- [1] KASEBZADEH, J., NOORZAD, A., & MAHBOUBI, A. R. Reliability Analysis of Liquefaction Utilizing Monte Carlo Simulation Based on Simplified Stress Method. *Journal of Seismology and Earthquake Engineering*, 2015, VOL.17, Nr. 4, 233-248.
- [2] TERZAGHI, K. Theoretical soil mechanics (Vol. 18).1943, New York: John Wiley & Sons.
- [3] MICHALOWSKI, R. An estimate of the influence of soil weight on bearing capacity using limit analysis. *Soils and Foundations*, 1997, Vol. 37, Nr. 4, pr. 57-64.
- [4] JOHARI, A., JAVADI, A. A., MAKIABADI, M. H., & KHODAPARAST, A. R. Reliability assessment of liquefaction potential using the jointly distributed random variables method. *Soil Dynamics and Earthquake Engineering*, 2012, Vol. 38, 81-87.
- [5] JOHARI, A., & KHODAPARAST, A. R. Modelling of probability liquefaction based on standard penetration tests using the jointly distributed random variables method. *Engineering Geology*, 2013, Vol. 158, 1-14.
- [6] JOHARI, A., FAZELI, A., & JAVADI, A. A. An investigation into application of jointly distributed random variables method in reliability assessment of rock slope stability. *Computers and Geotechnics*, 2013, Vol. 47, 42-47.
- [7] Johari, A., & Javadi, A. A.. Reliability assessment of infinite slope stability using the jointly distributed random variables method. *Scientia Iranica*, 2012, Vol.19, Nr. 3, 423-429.
- [8] HASOFER, A.M. AND LIND, N.C. An exact and invariant first-order reliability format. *Journal of the Engineering Mechanics*, 1974, Vol.100, Nr. 1, 111-121.
- [9] ANG, A. H., & TANG, W. H. *Probability concepts in engineering planning and design*.1975, New York: John Wiley & Sons.
- [10] ROSENBLUETH, E. Point estimates for probability moments. *Proceedings of the National Academy of Sciences*, 1975, Vol.72, Nr. 10, 3812-3814.
- [11] HALDAR, A., & TANG, W. H. Probabilistic Evaluation of Liquefaction Potential. *ASCE Journal of the Geotechnical Engineering Division*, 1979, Vol.105, Nr.2, 145-163.
- [12] FARDIS, M.N. & VENEZIANO, D. Probabilistic analysis of deposit liquefaction. *ASCE Journal of Geotechnical and Geoenvironmental Engineering*, 1982, Vol. 108, Nr. 3, 395-417.
- [13] CHAMEAU, J. L., & CLOUGH, G. W. Probabilistic pore pressure analysis for seismic loading. *Journal of Geotechnical Engineering*, 1983, Vol. 109, Nr. 4, 507-524.
- [14] JUANG, C. H., ROSOWSKY, D. V., & TANG, W. H. Reliability-based method for assessing liquefaction potential of soils. *Journal of Geotechnical and Geoenvironmental Engineering*, 1999, Vol. 125, Nr. 8, 684-689.
- [15] JUANG, C. H., YANG, S. H., YUAN, H., & KHOR, E. H. Characterization of the uncertainty of the Robertson and Wride model for liquefaction potential

- evaluation. *Soil Dynamics and Earthquake Engineering*, 2004, Vol. 24(9), 771-780.
- [16] JUANG, C. H., YANG, S. H., & YUAN, H. Model uncertainty of shear wave velocity-based method for liquefaction potential evaluation. *Journal of Geotechnical and Geoenvironmental Engineering*, 2005, Vol. 131, Nr. 10, 1274-1282.
- [17] JUANG, C. H., FANG, S. Y., & KHOR, E. H. First-order reliability method for probabilistic liquefaction triggering analysis using CPT. *Journal of Geotechnical and Geoenvironmental Engineering*, 2006, Vol. 132, Nr. 3, 337-350.
- [18] LEE, Y. F., CHI, Y. Y., LEE, D. H., JUANG, C. H., & WU, J. H. Simplified models for assessing annual liquefaction probability—A case study of the Yuanlin area, Taiwan. *Engineering Geology*, 2007, Vol. 90, Nr. 1, 71-88.
- [19] LEE, Y. F., CHI, Y. Y., JUANG, C. H., & LEE, D. H. Annual probability and return period of soil liquefaction in Yuanlin, Taiwan attributed to Chelungpu Fault and Changhua Fault. *Engineering Geology*, 2010, Vol. 114, Nr. 3, 343-353.
- [20] JHA, S. K., & SUZUKI, K. Liquefaction potential index considering parameter uncertainties. *Engineering Geology*, 2009, Vol. 107, Nr. 1, 55-60.
- [21] JHA, S. K., & SUZUKI, K. Reliability analysis of soil liquefaction based on standard penetration test. *Computers and Geotechnics*, 2009, Vol. 36, Nr. 4, 589-596.
- [22] ANG, A. H., & TANG, W. H. Probability concepts in engineering: emphasis on applications to civil and environmental engineering. 2007, Hoboken: John Wiley & Sons.
- [23] WANG, Y. Uncertain parameter sensitivity in Monte Carlo simulation by sample reassembling. *Computers and Geotechnics*, 2012, Vol. 46, 39-47.
- [24] BAECHER, G. B. & CHRISTIAN, J. T. *Reliability and Statistics in Geotechnical Engineering*. 2003, New Jersey: John Wiley & Sons.
- [25] PHOON, K. Reliability-based design in geotechnical engineering: computations and applications. 2008, London: Taylor & Francis.
- [26] HARR, M. E. *Reliability-based design in civil engineering*. 1996, New York: McGraw-Hill Book Company.
- [27] KULHAWY, F. H. *On the Evaluation of Static Soil Properties*. 1993, New York: McGraw-Hill Book Company.
- [28] DRUCKER, D. C., PRAGER, W., & GREENBERG, H. J. Extended limit design theorems for continuous media. *Quarterly of Applied Mathematics*, 1952, 9(4), 381-389.
- [29] CHEN, W., & LIU, X. L. *Limit analysis in soil mechanics*. 1990, Amsterdam: Elsevier.

SUMMARY

To a great extent, an accurate prediction of the bearing capacity is considered to be a common practice in geotechnical engineering. Analysis and design of geotechnical structures continue to face with many uncertainties which make it difficult to choose the design parameters. Mostly, the uncertainties are pertinent to unreliable deterministic soil characteristics. Use of a deterministic approach for soil specifications may result in either underestimation or overestimation of the soil shear strength in problems dealing with limit loads. Therefore, the traditional deterministic limit load methods, e.g. the conventional limit analysis and slip line methods could not capture a reliable estimation of the bearing capacity. In order to examine the parameters involved in the estimation of bearing capacity of foundations, it is required to take in to account the uncertainty nature of the soil to perform the reliability analysis. In the analysis, the effect of probabilistic input parameters on the limit loads is considered. As a matter of fact, the reliability analysis makes it possible to be able to quantify the uncertainties involved.

In this study, the reliability analysis of the bearing capacity of dam foundations was carried out via Monte Carlo simulation with the focus on the uncertainty associated with the friction angle. To do so, the upper-bound limit analysis was employed assuming the deterministic friction angle. The formulation and the general computational procedure were kept exactly as the one introduced by Michalowski (1997). As it is obvious, the non-associativity of plastic deformation of soils is a significant factor in limit load problems. In the current study, the substantial influence of the dilatancy angle on N_γ was also examined. As a conclusion, appropriate safety factors based on reliability analysis are suggested leading to economical advantage of the design of geotechnical structures.

KEYWORDS

ANALYSIS
DAM
FOUNDATION
PLASTICITY
SAFETYFACTOR

COMMISSION INTERNATIONALE DES GRANDS BARRAGES

VINGT-SIXIÈME CONGRÈS DES GRANDS BARRAGES
Autriche, juillet 2018

DOI 10.3217/978-3-85125-620-8-077



This work licensed under a Creative Commons Attribution 4.0 International License. <https://creativecommons.org/licenses/by-nc-nd/4.0/>

**SPILLWAY HYDRAULIC TEST MODEL OF CIPANUNDAN DAM,
WEST JAVA - INDONESIA**

Airlangga MARDJONO

INDONESIAN DAM CENTRE, INDONESIAN MINISTRY OF PUBLIC WORKS
AND HOUSING

INDONESIA

Nisa Andan RESTUTI

INDONESIAN DAM SAFETY UNIT, INDONESIAN MINISTRY OF PUBLIC
WORKS AND HOUSING

INDONESIA

Harvien MAHARDHIKA

CIMANUK CISANGGARUNG RIVER BASIN AUTHORITY, INDONESIAN
MINISTRY OF PUBLIC WORKS AND HOUSING

INDONESIA

COMMISSION INTERNATIONALE
DES GRANDS BARRAGES

VINGT-SIXIÈME CONGRÈS DES
GRANDS BARRAGES
Autriche, juillet 2018

**SPILLWAY HYDRAULIC TEST MODEL
OF CIPANUNDAN DAM, WEST JAVA - INDONESIA**

Airlangga MARDJONO

Indonesian Dam Centre, Indonesian Ministry of Public Works and Housing

Nisa Andan RESTUTI

Indonesian Dam Safety Unit, Indonesian Ministry of Public Works and Housing

Harvien MAHARDHIKA

*Cimanuk Cisanggarung River Basin Authority, Indonesian Ministry of Public
Works and Housing*

INDONESIA

ABSTRACT

Primary purpose of water resources development in Indonesia is water supply for various needs. Therefore, various efforts are made by the government to solve the problem. One of the efforts in planning phase, is water resources infrastructure development of Cipanundan Dam at Cirebon District .

The physical model spillway of Cipanundan Dam is made on a scale of 1: 20, some scenarios of debit flow based on design flood discharge Q_2 , Q_{25} , Q_{100} , Q_{1000} , and Q_{PMF} . The construction of three dimensional model of Cipanundan Dam is built by using Froude model criteria, because this criteria model is the closest to field condition.

Flow testing on Cipanundan Dam spillway model is expected to provide parameters of hydraulic test results in laboratory that will determine optimal dimensions of the spillway and complementary structure building, so that it can be used as basic work for the next stage.

The results of the hydraulic flow obtained from the test model still needs a further study that is to model the flow condition when it returns to the river and to map scouring pattern in the downstream stilling basin.

Keywords: Cipanundan, test model, hydraulic parameters

1. BACKGROUND

Cipanundan Dam is a dam that is subjected to irrigate the irrigation area in Kabupaten Cirebon and planned to construct soon. Dam reservoir area is located in Cipanundan river valley, at el. +26 m until el.+50 m extended from south to north. Cipanundan Dam axis is located between two hills, stretched along Cipanundan river.

Type of Cipanundan Dam is homogenous soil type, dam height is about 24 m dan dam length is about 511 m. Spillway Cipanundan Dam located on the right toe with overflow type, and stilling basin type is USBR type 2.

2. PURPOSE AND OBJECTIVES

The purposes of the hydraulic test model spillway of Cipanundan Dam are:

- 1) To establish the idea of planning in terms of hydraulic aspects (flow design and sediment transport) by studying and investigating the flow symptoms and parameters that occur.
- 2) To study and verify the layout of spillway designed to obtain hydraulic design properly,
- 3) To determine of optimum type, form and dimension of energy dissipator and appurtenance structure,

The objective of this hydraulic test model spillway of Cipanundan Dam is to provide a refined recommendation based on hydraulic aspect, so that deviations may occur during desgining, it can be eliminated from the test model and will obtain the most optimal hydraulic structures dimension. All of these stages are to guaranty of dam safety and function.

3. PROTOTYPE DATA

Prototype data of Cipanundan Dam are as follows:

a. Main Dam

- Type : Homogeny Embankment
- Crest dam elevation : + 46,80 m
- Crest width : 7,50 m
- Slope : Upstream = 1 : 3,00
Downstream = 1 : 2,50

b. Spillway and Appurtenance Works

■ Spillway works

- Type : Ogee
- Crest dam elevation : + 44,00 m
- Crest width : 17,50 m

■ Transition Channel

- Length : 26,50 m
- Width : hulu = 17,50 m
hilir = 8,50 m
- Elevation : hulu = + 38,00 m
hilir = + 37,25 m
- Basic slope : 0,028302

■ Chute

- Length : 47,65 m
- Width : 8,50 m
- Basic slope : 0,278069

■ Stilling Basin

- Type : USBR Type II
- Length : 30,00 m
- Width : 8,50 m

4. DESIGN FLOOD DISCHARGE

Based on analysis, it is known that the design flood discharge is based on flood routing through reservoir. So for test model Cipanundan Dam, is used the outflow discharge from the debit of Q_2 , Q_{25} , Q_{100} , Q_{1000} , and Q_{PMF} . The design flood discharge data are as follows:

6. SCENARIO OF TESTING

In order to achieved the test model objectives, the test scenario are carried out as follows:

- 1) Testing of spillway weir capacity,
- 2) Investigation to examine the design of spillway structure to follow the designed discharge as expected,
- 3) Investigation to improve and refine spillway structure design and their component,
- 4) Investigation of impacts on dam construction

Based on the test scenario above, to support test program, the model is made with two types of riverbed and riverbank, they are:

- 1) Reservoir model with fixed riverbed and fixed riverbank (Fixed Bed Model), is a model with riverbed and riverbank made from mixed of sand and cement to obtain similarity of roughness,
- 2) Downstream river model with movable riverbed and movable riverbank (Movable Bed Model), is a model with riverbed and riverbank made from loose material fine sand to imitate riverbed and riverbank material in prototype that can be eroded.



Figure 2.
Test Model Of Cipanundan Dam



Figure 3.
Prototipe of Spillway Works, Chute dan Stilling Basin

7. TEST MODEL RESULT

Results from spillway hydraulic test model of Cipanundan Dam are as follows:

- 1) The flow conditions on the transition channel are relatively good and there is no crossing flow,
- 2) The flow conditions on energy dissipator up to Q1000 discharge, still form hydraulic jump,
- 3) The effectiveness of the energy dissipator is functioning optimally

8. CONCLUSION

The results of the hydraulic flow obtained from the test model still needs a further study that is to model the flow condition when it returns to the river and to map scouring pattern in the downstream stilling basin. It is necessary in order that the results of modelling can gain the most optimal condition.

9. ACKNOWLEDGEMENT

The authors would like to thank to Dam Center and Dam Safety Unit, Directorate General of Water Resources, Ministry of Public Works and Housing for the authorization to publish the main result of the present study. The authors would also like to express the gratitude to Dam Safety Unit and Cimanuk Cisanggarung River Basin Authority as the institution who built the dam for having made this fruitful collaboration possible.

REFERENCES

- [1] ADITYA ENGINEERING CONSULTANT. Report for Alternative Spillway Model Test of Cipanundan Dam (Cipanundan II), Indonesia 2016.
- [2] DIRECTORATE OF ENGINEERING. Design of Earthfill Dam Guidance Volume IV: Design of Appurtenance Structure. *Department of Public Works*, Indonesia 1999.

COMMISSION INTERNATIONALE DES GRANDS BARRAGES

VINGT-SIXIÈME CONGRÈS DES GRANDS BARRAGES
Autriche, juillet 2018

DOI 10.3217/978-3-85125-620-8-078



This work licensed under a Creative Commons Attribution 4.0 International License. <https://creativecommons.org/licenses/by-nc-nd/4.0/>

MAE SUAI DAM SAFETY

Pronmongkol CHIDCHOB

ROYAL IRRIGATION DEPARTMENT

THAILAND

Worawut PINTABUTR

SAMART ENGINEERING CONSULTANTS CO.,LTD.

THAILAND

Surachai LAIKARNCHANAPAIBOON

PANYA CONSULTANTS CO.,LTD.

THAILAND

COMMISSION INTERNATIONALE
DES GRANDS BARRAGES

VINGT-SIXIÈME CONGRÈS DES
GRANDS BARRAGES
Autriche, juillet 2018

MAE SUAI DAM SAFETY

1. Mr. Pronmongkol Chidchob, Royal Irrigation Department
2. Mr.Worawut Pintabutr ; Samart Engineering Consultants Co.,Ltd.
3. Mr.Surachai Laikarnchanapaiboon ; Panya Consultants Co.,Ltd.

THAILAND

1. INTRODUCTION

Mae Suai is the second RCC dam in Thailand which is situated in Chaing Rai province, in the northern region as shown in Figure 1. It was constructed on the Mae Suai river during 1999 and 2002 for irrigation. The storage capacity is 73 Million cubic meter. The dam is a composite dam consisting of the RCC dam in the middle part of the dam to be the spillway and the earth dam on the both abutments because of the foundation condition. View of Mae Suai Dam is shown in Figure 2. The maximum height of dam is about 59 m and the crest length is 400 m. The site plan and section of dam as shown in Figure 3. The foundation of the RCC was excavated to the sound rock. Grouting has been done as necessary. The RCC section uses as an overflow spillway. The RCC section is surrounded with the earth dam. The earth dam extends to both sides of the abutment. Core trench has been excavated in the foundation and to the abutments. There are RCC blocks on the crest of earth dam at the downstream side because of earthfill volume and height of spillway's downstream wall reduction.

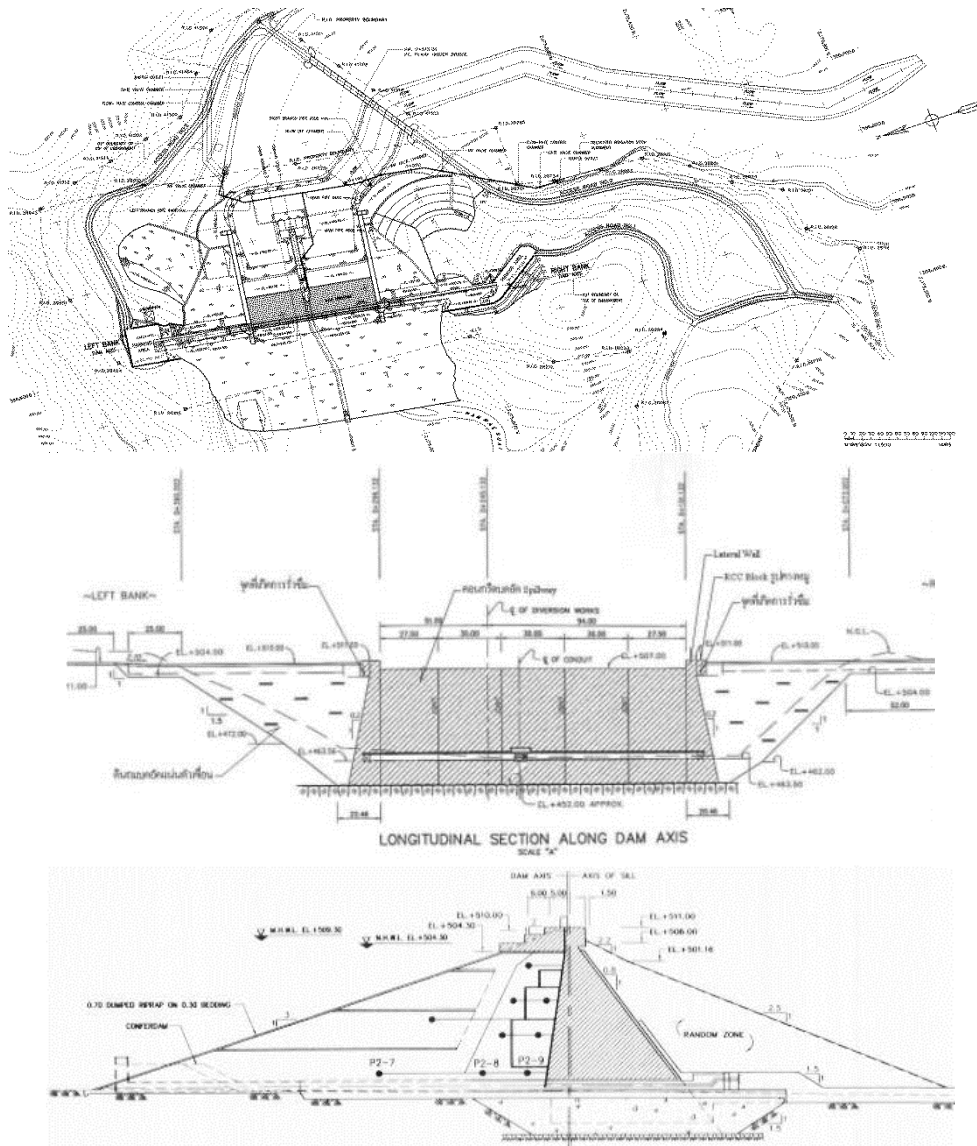


Fig. 3
Site Plan, Longitudinal and Typical Section of Mae Suai Dam

2. DAM CREST SETTLEMENT AND LEAKAGE PROBLEM

The differential settlement between the RCC spillway and the earth dam is occurred causing the cracks and gaps at the RCC blocks. In the first filling, the water overtopped the spillway and flow through the cracks and gaps. The leakage was observed at the downstream crest near the contact area between the RCC part and the earth zone part as shown in Figure 4. They are repaired by the impervious membrane covering at the upstream surface of RCC blocks, the leakage is reducing but stilling. The downstream population worried about the safety of the Mae Suai dam especially in case of earthquake.



Fig. 4

Leakage occurred near the joint between RCC and earth fill, the differential settlement is clearly seen

3. CHIANG RAI EARTHQUAKE AND RESPONSE OF DAM

Fears of an earthquake have deepened after 6.3 magnitude earthquake hit the province in May of 2014. The epicenter to the dam site is 18 km. However, the epicenter of the aftershock is closer to the dam site. Mae Suai Dam is located in the active faults zone as shown in Figure 5. The dam experienced the strong ground motion and the accelerometer at the right abutment recorded the maximum PGA of 0.33g. Fortunately, the seismic force did not affect the Mae Suai Dam. The dam performed well. There is some crack observed in the concrete cover of the RCC block on the crest of the dam. The crack is much

above the maximum water elevation therefore the safety is not to be concerned. Especially, the RCC block that seen some cracks is the part that not related with the stability of the dam.

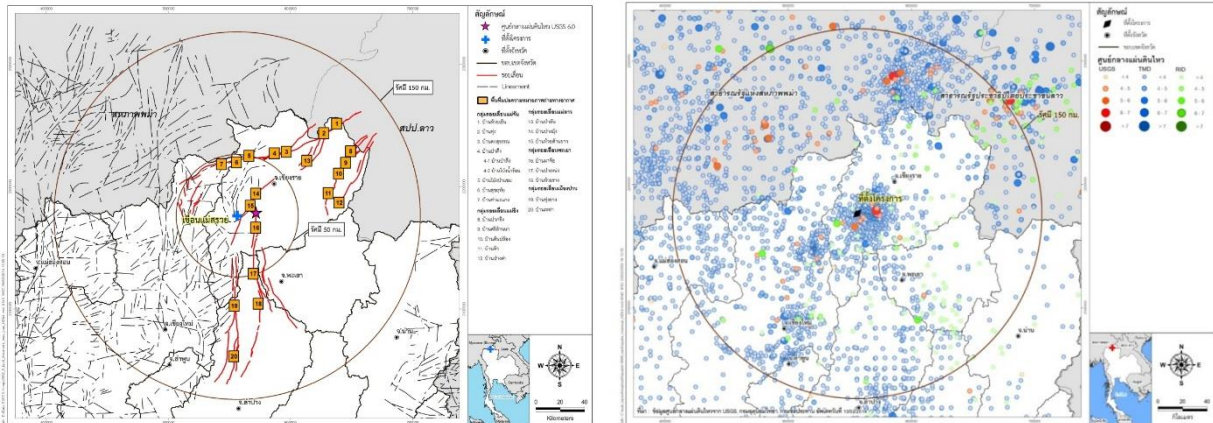


Fig. 5

Active Faults and Earthquake Epicenter near the Dam Site

Even though the dam is performed well according to the engineering evaluation, however the people who lives downstream of the dam are very concerned about the safety of the dam. This is because they thought that the cracks of the concrete covered of the RCC block may lead to the leakage just like what they had experienced before. The concerns became a panic and serious since the community required that the dam shall be removed. Several meetings were set up to discuss about the practical solution and the consensus are to keep the water storage to be lower than 60% until the dam has been fully repaired.

4. EMERGENCY ACTION PLAN

However, people at the dam downstream still worried over the incident. Besides, there was not any study, plan, prevention measures or risk surveillance in terms of surplus discharge and dam break, which caused faster flood and more damage to life and property. Then, the Royal Irrigation Department had studied the dam break of Mae Suai Reservoir Project in terms of surplus discharge, causes of damage of dam and appurtenant structures which may cause flood and flood severity and characteristics, as well as to complete action plan to cope with the dam break.

4.1. FLOOD CONDITIONS AFTER DAM BREAK

The study of flood conditions based on dam break is aimed at applying the result of flood conditions and the flood flow period to the preparation of action plans in case of emergency to cope with situations arising in the event of dam failure. Three dam failure events are identified: flood loading, static loading and earthquake loading.

[1] Flood loading is analyzed to obtain the maximum flood boundary. The study of six case studies found that the most severe flood case that is caused by the failure of mae suai dam in case of the pmf to mae suai reservoir and the 10,000-year return flood in downstream or mae lao river basin areas. Flood conditions of case study are shown in figure 6. The flooded area is about 181 km².

[2] Static Loading is analyzed to determine the flood boundary in case of dam failure by considering that water levels and downstream or Mae Lao River Basin areas are normal and no overflow occurs. The study result revealed that flooded areas are less than the first event. where the reservoir water is at normal high water level. Flood conditions are shown in Figure 7. Flooded areas are about 102 km².

[3] Earthquake Loading is analyzed as a scenario to consider impacts of dam failure in the event of earthquakes and in case of the 10,000-year return flood in downstream or Mae Lao River Basin areas. The study result shows that flooded areas are the same as case 1

4.2. AREAS AFFECTED BY DAM BREAK

The boundary of areas affected by floods due to failure of Mae Suai Dam will change in accordance with characteristics and severity of dam failure in different scenarios. As a result of hydraulics analysis using mathematical models in preparation for flood maps, Mae Suai dam failure is analyzed in various scenarios to study flood conditions, the boundary of affected areas and severity so that damages can be assessed by using flood map data overlapping with area condition data.

The analysis of different case studies indicated that the failure of Mae Suai Dam in case of flood conditions results in the most flooded areas as shown in Figure 8. Affected areas include both banks of the Mae Suai River from the area below Mae Suai Dam to the confluence of the Mae Lao River and both banks of the Mae Lao River from Ban Thung Yao, Si Thoi Sub-district, Mae Suai District to the confluence of the Kok River. The boundary of flooded areas in each area depends on topography and drainage potential of the Mae Suai and Mae Lao Rivers in that period. Flooded areas cover some areas in five districts of Chiang Rai Province – Mae Suai, Mae Lao, Phan, Mueang Chiang Rai and Wiang Chai districts and four municipalities: Wiang Suai, Mae Suai, Mae Lao and Pa Ko Dam sub-district municipalities.

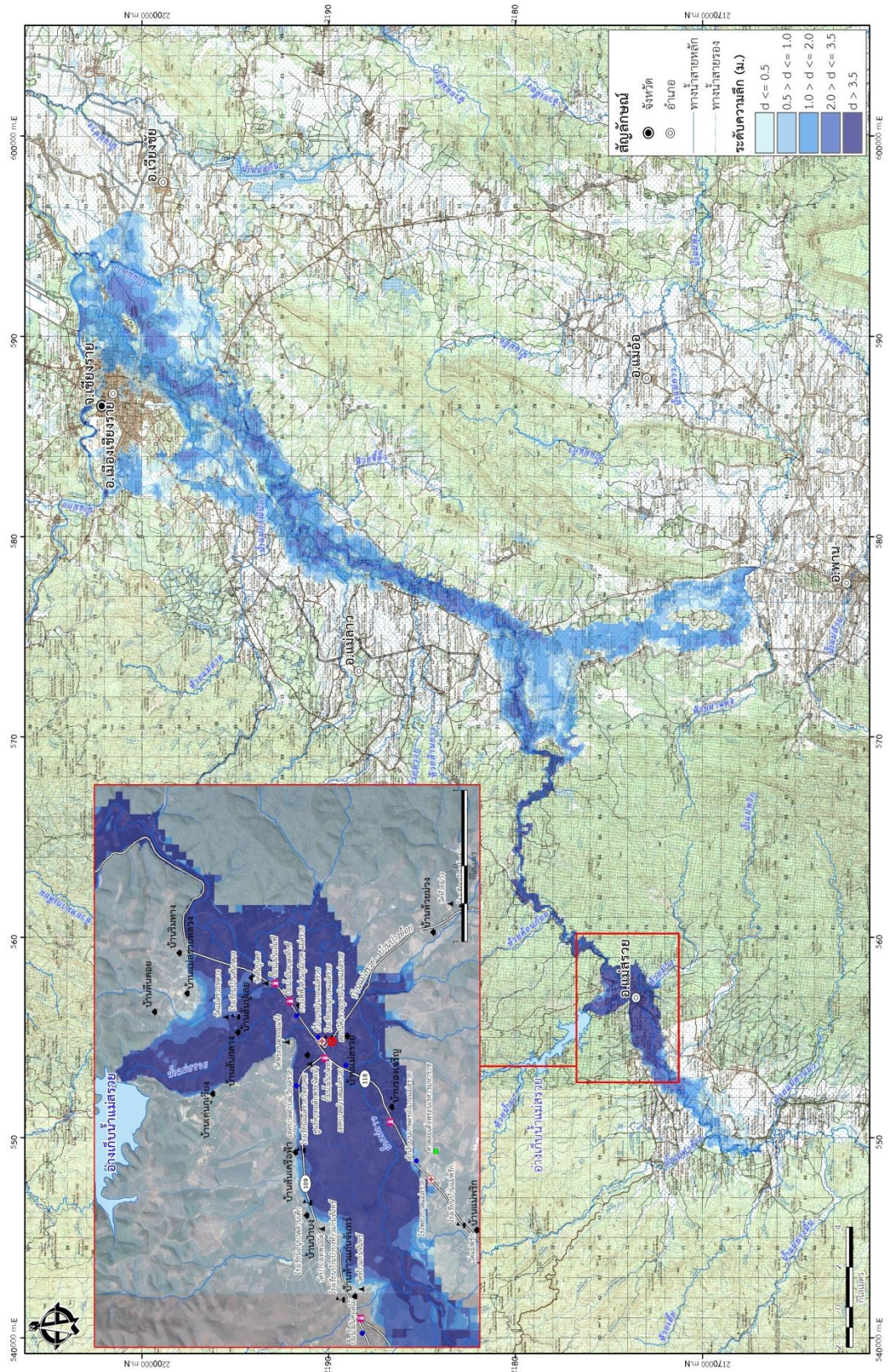


Fig. 6
Flood Map Analysis in Case of PMF Flood and Failure of Mae Suai Dam

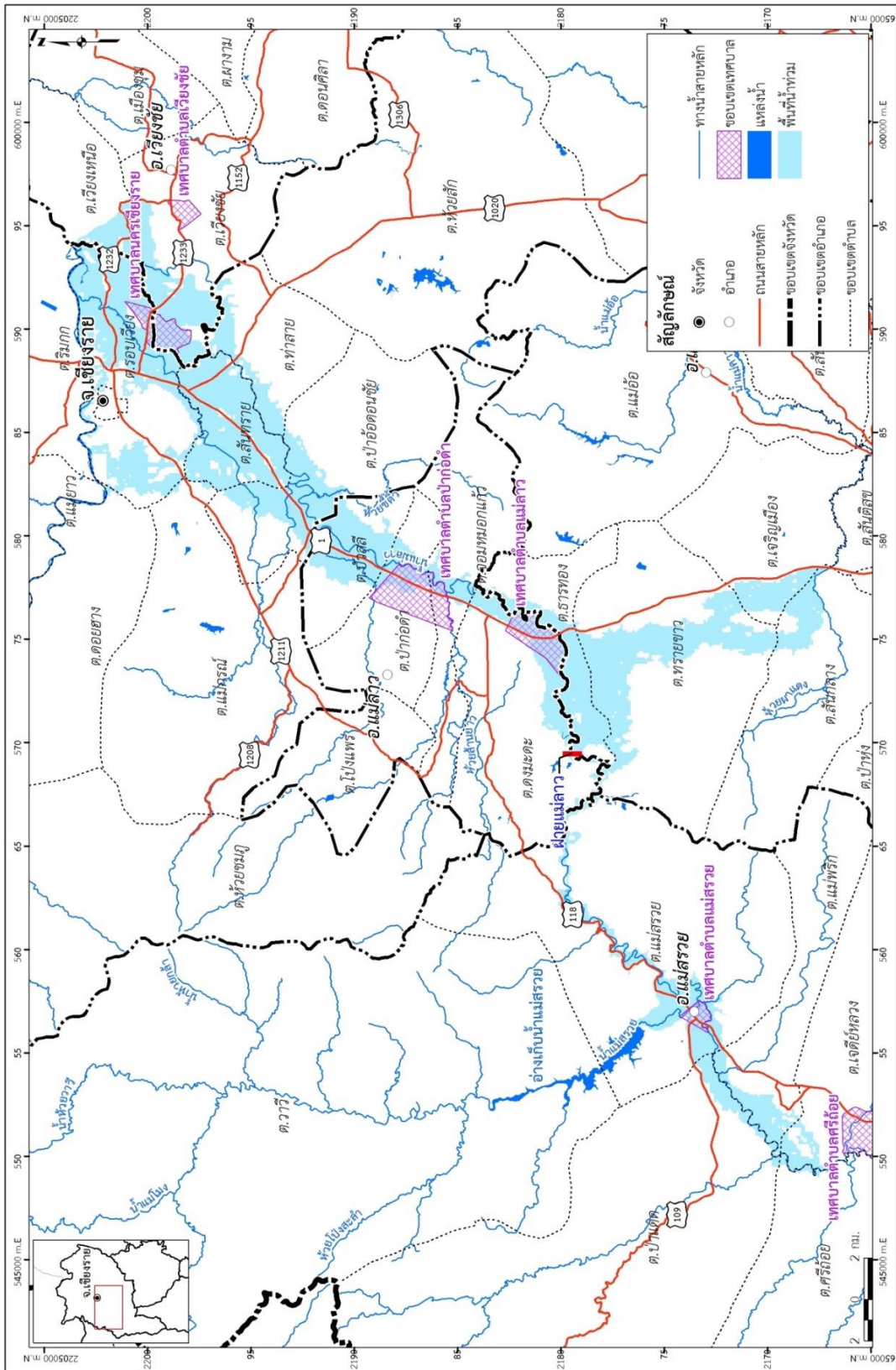


Fig. 8
Flooded Area in Case of Failure of Mae Suai Dam

Areas that may be affected or risk areas due to emergency cases of dams or much drainage from dams include dam downstream areas along both banks of the Mae Suai River in Mae Suai District to the confluence of the Mae Lao River, where floods will also take place. The boundary of risk areas in each event of emergency cases of Mae Suai Dam varies according to flood conditions as a result of the analysis. This depends on the reservoir water volume at that moment, inflow, dam failure types and the existing flood conditions in dam downstream areas prior to the incident. It is summarized as follows:

Zone 1 (downstream of Mae Suai Dam-Ban Rim Thang)

The severity of floods will be very high, especially in Ban Rim Thang, in which Zone 1 ends. There are a mountain pass and a narrow waterway. As a result, flood water levels are very high. Therefore, warning should be issued to people immediately and houses and buildings should not be constructed along the banks because this may cause harm to lives and properties.

Zone 2 (Ban Rim Thang-Mae Lao Weir)

In Zone 2, the severity of floods will be very high because of a narrow mountain pass throughout the area. As a result, the overflow from the Mae Lao River will occur. However, the population in the area is not dense. Warning should be issued to people to evacuate to higher grounds as specified. The wave will take about 2-3 hrs to travel to this area.

Zone 3 (Mae Lao Weir-the confluence of the Mae Kok River)

According to the analysis of all cases, Zone 3 will not face much risk because flood levels will be low or about 0.5-1.0 m. It will take about 4-9 hrs in total for waves to travel. This may not affect people's way of life. It is not necessary to move people to higher grounds. People in such area should monitor the situation closely and cooperate with agencies concerned or seek how to prevent impacts caused by floods.

4.3. ACTION PLAN FOR UNUSUAL CONDITION DAM SAFETY

Generally, when uncommon situations occur, for example, downpour, earthquakes, landslides in reservoirs, the officers in charge of dam maintenance have to examine and evaluate the dam conditions immediately. If unusual conditions or damage of the dams, appurtenant structures or control devices are found, the officers have to report the conditions to the dam safety section to analyze the causes and provide solutions as well as the prevention and monitoring measures intensively. The action plan for the Mae Suai dam safety in unusual conditions can be summarized as follows:

1] In case of downpour or unusual flood; excessive downpour over 200 mm within 24 hours, continuous downpour over 48 hours or flood that causes water levels in reservoirs change rapidly (over 30 cm per hour), the operation approach will be as below:

[1] Analyze and evaluate the volume in the reservoir that will increase from the rainy storm .

[2] Examine the gate control system of the dam and appurtenant structures .

[3] Check the conditions of dam foundation, the seepage of the dam and the possibility of landslides in the reservoir area .

[4] Monitor and examine the abnormality of the dam and appurtenant structures.

[5] In case that the water level in the reservoir cannot be controlled, resulting in rapid overflow over the dam crest and the dam is likely to break down, evacuation of people from the project area should be implemented immediately as well as the notification of related agencies located at the downstream.

2] Earthquakes may impact dams and can cause unusual conditions to the dams. In case of earthquakes, the inspection of the dams and appurtenant structure conditions after the earthquakes is recommended.

Dam conditions and seismic response will be measured by using the dam instruments, such as Survey Monument, Piezometer and Accelerograph, which are already installed.

Normal Level: An earthquake takes place more than 200 km away from the dam and does not certainly cause any effects to the stability of the dam.

Alert Level: An earthquake of magnitude and distance according to ICOLD (1988), or an earthquake which causes ground acceleration at the foundation and is severe enough to cause a few impacts to the dam, occurs) for example, the accelerograph responds the seismic waves of $> 0.02g$ to $<0.2g$, which does not cause damage to the dam.(

Alarm Level: The earthquake generates ground acceleration of $>0.2g$ at the dam foundation or the magnitude and the distance of the earthquake from the dam according to Sadigh)1997('s energy attenuation model causes the ground acceleration of $0.2g$ at the dam foundation, which is serious enough to cause damage to the dam.

3] In case of landslides in a reservoir, the inspection and the evaluation of landslide locations and sizes is recommended, including the massive waves that may cause overflow to the dam crest .Scrap, rock and soil mass which block the water flow should be moved out .It is recommended to inform the dam safety section to evaluate the damage of the dam and appurtenant structures.

5. DAM REHABILITATION

Moreover, Royal irrigation department decided to rehabilitate Mae Suai dam. Repair works shall be able to solve the leakage problem and make the dam to perform well with the future earthquake. The dam rehabilitation will be done in two parts. First, the RCC blocks on the earth dam crest will be removed and replaced by the flexible and vibration resistance structure. The GRS wall with the cutoff sheet pile will be used as shown in Figure 10. GRS wall consists of reinforce gabion. The gabion wall is anchored to the gabion in the opposite side in order to provide additional confining pressure near the slope face and hence

increasing the strength of compacted sand during the earthquake. Hot dipped galvanized steel sheet pile will be placed on both side of the GRS wall. Sheet piles will work as a water tightness barrier. In addition, it designed to minimize lateral movement that may cause from the weight of new GRS wall to the exiting soil below the cut level.

And the second is to build the 3 m diameter tunnel as the additional outlet to control the water level for flood management. The existing outlet diameter is 1.5 m that is small and the maximum discharge is about 30 cms. It is difficult to manage flood because the reservoir volume of Mae Suai Dam is less than the average annual inflow. Adding the new outlet tunnel should be done as shown in Figure 11. The maximum discharge capacity is about 100 cms that less than the capacity of the downstream river.

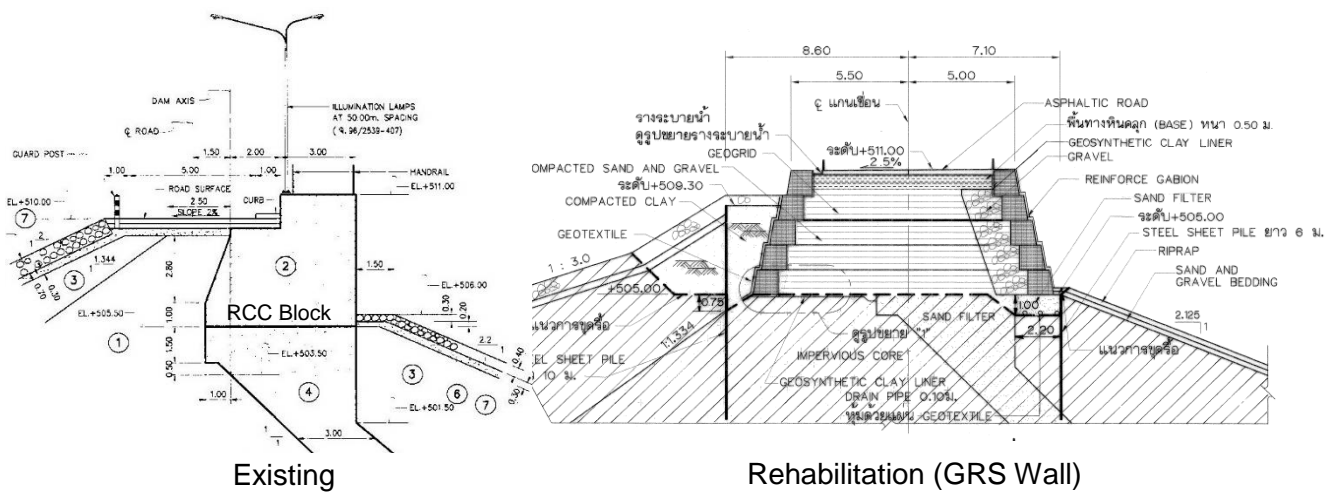


Fig. 10
Dam Crest Rehabilitation Detail

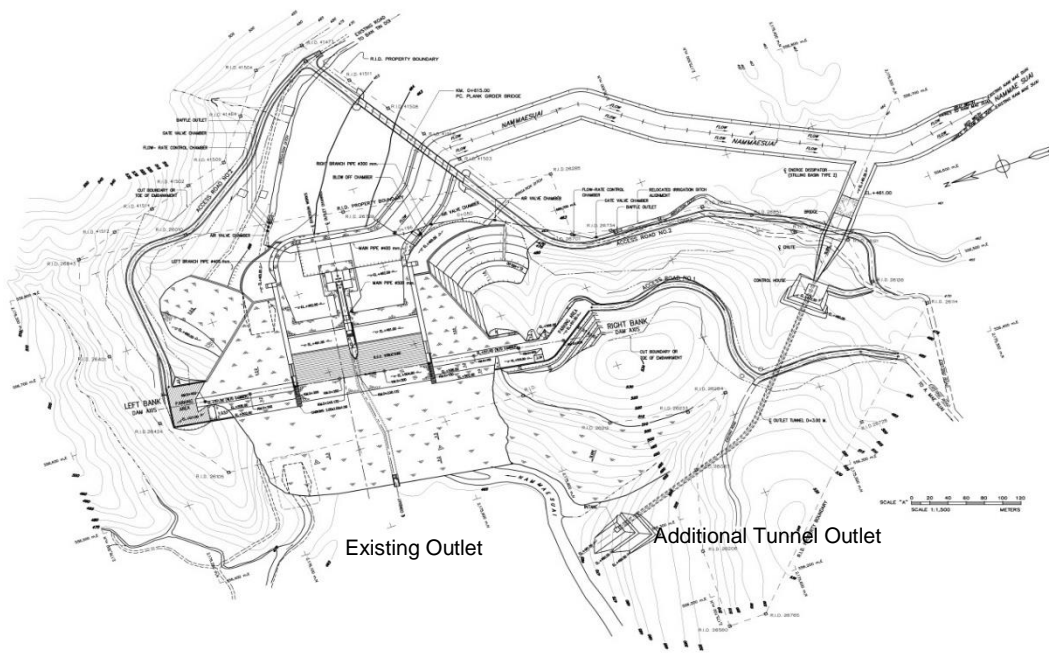


Fig. 11
Additional Outlet Tunnel

6. CONSTRUCTION PROGRESS

The construction of dam rehabilitation started on August 2017. The construction schedule is 20 months so it will be completed on March 2019. The construction is dam crest and spillway rehabilitation that cost is about 100 million baht. In the first part of the schedule, the construction is RCC block and dam crest removal. The photo of construction is shown in Figure 12.



Fig. 12
The Photo of Construction

7. SUMMARY AND KEYWORDS

1] It is not avoidable to have a large differential settlement between the high earth fill zone and rigid rcc or concrete zone, therefore we should avoid having this whenever possible.

2] Even though the leakage occurred but the dam shall be safe since it flows through the rcc material in which suffusion flow might not be able to occur and the leak occurred near the dam crest where hydraulic head is low.

3] Cracks in the rcc crest block due to the earthquake may not be harmful in the engineering point of view. However, for the community who lives downstream, unnecessary worries posted to them.

Therefore, the rigid and brittle rcc crest block will be replaced with the more flexible grs wall.

4] After dam rehabilitation is completed, the mae suai dam reservoir will be full storage.

Keywords: dam, roller compacted concrete dam, leakage, rehabilitation, seismic resistance, emergency plan

8. REFERENCES

- [1] Royal Irrigation Department (RID). (1999) Final design report.
- [2] Royal Irrigation Department (RID). (2014) "Peak ground acceleration, Peak ground velocity, Duration of motion, frequency content of Main shock M6.3 at Phan district, Chiangrai provinces", Bangkok, Thailand.
- [3] Royal Irrigation Department (RID). (2015) Emergency Action Plan of Mae Suai Dam report.
- [4] Royal Irrigation Department (RID). (2015) Conceptual Design of Mae Suai Dam Rehabilitation report.
- [5] Soralump, S., Thongthamachart, C., Jinagoolwipat, M. and Boonpo, A. (2016) "Rehabilitation of leakage and seismic damaged problem of Mae Suai Earth zone composited RCC Dam. *19th Southeast Asian Geotechnical Conference & 2nd AGSSEA Conference (19SEAGC & 2AGSSEA)* Kuala Lumpur 31 May – 3 June 2016

COMMISSION INTERNATIONALE DES GRANDS BARRAGES

VINGT-SIXIÈME CONGRÈS DES GRANDS BARRAGES
Autriche, juillet 2018

DOI 10.3217/978-3-85125-620-8-079



This work licensed under a Creative Commons Attribution 4.0 International License. <https://creativecommons.org/licenses/by-nc-nd/4.0/>

SAFETY ASSESSMENT AND MAINTENANCE OF RELIABLE OPERATION OF DAMS IN RUSSIA

Evgeniy BELLENDIR

CEO, JSC INSTITUTE HYDROPROJECT

RUSSIA

Elena FILIPPOVA

Head of the department "Information and analytical center on the safety of hydraulic structures", JSC VEDENEEV VNIIG

RUSSIA

Oleg BURYAKOV

Research engineer, JSC VEDENEEV VNIIG

RUSSIA

COMMISSION INTERNATIONALE
DES GRANDS BARRAGES

VINGT-SIXIÈME CONGRÈS DES
GRANDS BARRAGES
Autriche, juillet 2018

**SAFETY ASSESSMENT AND MAINTENANCE OF RELIABLE
OPERATION OF DAMS IN RUSSIA**

Evgeniy Bellendir

CEO, JSC INSTITUTE HYDROPROJECT

Elena Filippova

*Head of the department "Information and analytical center on the safety of
hydraulic structures", JSC VEDENEEV VNIIG*

Oleg Buryakov

Research engineer, JSC VEDENEEV VNIIG

RUSSIA

1. INTRODUCTION

The report includes information on the state policy of Russia in the sphere of the safety and reliability of dams, on other laws and standard legal acts and on organization of surveillance of dams.

2. SAFETY MAINTENANCE LEGISLATURE OF RUSSIA

In Russia the maintenance of safety and reliability of hydraulic structures is obligatory to their owners or operators. The control of its quality is a state function implemented by federal executive authorities.

One of the basic laws in the sphere of safety and reliability of hydraulic structures is the Federal Law "On the safety of hydraulic structures" [1], which was adopted 20 years ago. According to this law, maintenance of safety of

hydraulic structures includes development and implementation of measures aimed to prevent possible failure.

The Federal Law “On the safety of hydraulic structures” requires the following documents to be developed by the owners of hydraulic structures:

- hydraulic structure safety declaration — a document, in which the hydraulic structure safety is substantiated and measures concerning its safety control are defined according to its class during the whole life-cycle of the structure from designing to conservation or demolition; the safety of every hydraulic structure, whose failure can lead to an emergency, must be declared;
- hydraulic structures safety criteria—the limiting values of quantitative and qualitative factors of the hydraulic structure condition, representing the allowable failure risk of the structure and being accepted by federal authorities, who are in charge of government supervision of the safety of hydraulic structures;
- the amount of harm that can be done to the life or health of individuals, to the property of individuals or legal persons caused by the failure of the hydraulic structure;
- the plan of measures concerning maintenance and advancement (if needed) of the required level of safety.

These documents undergo public examination, are accepted by hydraulic structures supervision authorities and coordinated with the Ministry of Emergency Situations of Russia regional authorities. When accepting the safety declaration, supervision authority sets its validity period, which cannot exceed five years. On the grounds of the accepted safety declaration, the supervisory authority issues the permission for operation.

According to adopted classification, a hydraulic structure can have one of the following safety levels: normal, reduced, unsatisfactory (low) and dangerous. For hydraulic structures with “normal” safety level, the safety declaration and operation permit are issued for five years. When the safety level is “reduced”, both documents are issued for four years. Hydraulic structures with unsatisfactory safety level both safety declaration and operation permit cannot be issued for the period longer than three years. The exact period is specified by expert commission depending on the circumstances which caused safety reduction. If a hydraulic structure’s safety level is “dangerous”, supervisory authorities do not accept safety declaration and operation permit is not issued. In this case the owner must as soon as possible develop and implement measures aimed to gain an acceptable safety level. For the period of implementation, the design operation mode can be limited and supervisory authorities intensify their control over such structures. Safety declaration must be revised within six months after detection of the following circumstances:

- changes of operating conditions, which influence on the safety of hydraulic structures;
- damages and emergencies;
- changes of emergency management conditions.

Supervisory authorities have the right to withdraw operation permit in case the safety declaration was not submitted on time.

First of all the safety level of hydraulic structure depends on its operational status. According to the Federal Law [1], the owner of hydraulic structures must develop their safety criteria. Diagnostic parameters (settlements, flow rates, hydraulic gradients, etc.) of structures are compared with corresponding safety criteria to identify their operational status. In Russia two levels of safety criteria are used: K1—precautionary level, K2—minimum allowable level.

Under current legislation, the owner of hydraulic structure or its operator (in case the structure is state or municipally owned) must provide financial guarantee of civil liability. Civil liability in case of damages caused by failure of hydraulic structure, except force majeure, is guaranteed by funds of the owner or operator and by insurance. According to the Federal Law, the civil liability risk is subject to compulsory insurance for the whole period of hydraulic structure's construction and operation. The terms and conditions of insurance are regulated by the Federal Law "On Compulsory Insurance of Civil Liability of the Owner of a Hazardous Object for Inflicting Damage as a Result of an Accident at the Hazardous Object" [2].

The financial guarantee is set according to the results of estimation of possible loss suffered by third parties (natural or legal persons or their property) in case the hydraulic structure fails [5]. The estimation, which is fulfilled according to special methodology, is submitted to the supervisory authority called Rostekhnadzor together with the safety declaration. The financial guarantee should be indexed (increased) every year depending on the inflation rate. The process is fulfilled by the owner in accordance with the change of the consumer price index [7].

The safety declaration justify the whole complex of measures aimed to maintain and enhance (if needed) the safety level set by building codes and standards.

The Federal Law [1] stipulates the following responsibilities of the owner:

- To control the parameters of hydraulic structures themselves, natural and technogenic influence, assess the safety of hydraulic structures and if needed, to analyze causes of its decrease;
- To develop safety criteria and specify them timely;
- To inspect the structures regularly;
- To operate the structures according to active codes and standards;
- To develop and implement measures aimed to maintain technically sound state of structures and their safety;
- To develop safety declarations and submit them to supervisory authorities.

Thus, current legislature of Russia covers all the stages of life-cycle of hydraulic structures, including design, construction, operation, closure and demolition. This legislative system includes the assessment of operational safety, ability of the owner to eliminate emergencies and failure risk estimation. The system also includes organization of supervision which is fulfilled by state authorities.

3. CASE STUDY: SAFETY AND RELIABILITY MANAGEMENT SYSTEM OF RUSHYDRO PLC

As a case study let us describe the hydraulic structures' safety and reliability management system used in RusHydro PLC. The goal of this system is to provide the required level of safety and reliability of hydraulic structures throughout their lifecycle in the most cost-effective way. Implementation of the system allowed RusHydro PLC:

To manage the whole set of hydraulic structures operated by the company using evidence-based and cost-effective measures, taking into account contemporary methods;

To use both technical and organizational and if needed, social measures of safety management;

To enter foreign market of design, development and implementation of safety management systems, including non-power hydraulic structures.

Today JSC RusHydro has its own Analytical center for the safety of hydraulic structures and their basic equipment, which help to ensure that the best possible decisions devoted to safety management, reliability and efficiency, are made. The structure of Analytical center includes the Executive office, its branches and research institute.

Major activities of the Analytical center includes:

- Monitoring of hydraulic structures and their equipment;
- State assessment;
- If needed, development of changes to mid-term and long-term production and R&D programs and technical policies;
- The control of compliance with the safety and reliability requirements;
- Taking part in declaration of safety and safety criteria development, drawing up the list of priority measures aimed to support and enhance the safety level within the period between declarations.
- The current activity of Analytical center made it possible:
- To predict the state of hydraulic structures and their equipment and if needed, to develop measures aimed to enhance it;
- To create the hydraulic structures database, this made it possible to compile the experience of state monitoring and to harmonize R&D programs;
- To unify methods of safety assessment and control used by different hydraulic facilities and to develop model solutions;
- To develop uniform format of reporting of the state of hydraulic structures used by their technical managers, uniform requirements and standards of state assessment, certificates and safety criteria.
- To minimize the gap in competencies of the staff of different hydraulic facilities by development of their skills, taking part in monitoring and state assessment, making of annual reports, etc.

SUMMARY

Thus, today in Russia at the governmental level hydraulic structures failure risk management systems are being adopted into theory and practice. These systems make it possible to provide acceptable failure risk with optimal correlation between the costs of failure risk reduction measures and the benefits of hydraulic structures. RusHydro PLC is one of the leaders of hydraulic structures failure risk management systems development and implementation.

REFERENCES

- [1] Federal Law "On the safety of hydraulic structures" No 117-FZ of July 21, 1997.
- [2] Federal Law "On Compulsory Insurance of Civil Liability of the Owner of a Hazardous Object for Inflicting Damage as a Result of an Accident at the Hazardous Object" No 225 of July 27, 2010.
- [3] Government decree "On acceptance of terms of hydraulic structures' safety declaration" No 1303 of November 06, 1998.
- [4] Government Decree "On emergencies classification" No 304 of May 21, 2007.
- [5] Assessment of financial guarantee civil liability procedures, accepted by Government Decree No 876 of December 18, 2001.
- [6] The statute on the Federal supervision in the sphere of the safety of hydraulic structures. Accepted by Government Decree No 1108 of October 27, 2012.
- [7] The procedures of assessment of possible loss, which can be suffered by third parties in case of failure of hydraulic structures. Accepted by EMERCOM on May 18, 2002, No 243.

COMMISSION INTERNATIONALE DES GRANDS BARRAGES

VINGT-SIXIÈME CONGRÈS DES GRANDS BARRAGES
Autriche, juillet 2018

DOI 10.3217/978-3-85125-620-8-080



This work licensed under a Creative Commons Attribution 4.0 International License.
<https://creativecommons.org/licenses/by-nc-nd/4.0/>

DAM DEFORMATION MONITORING MODEL AND FORECAST BASED ON PCA-RBF NEURAL NETWORK

Chaoning LIN

COLLEGE OF WATER RESOURCES AND HYDROPOWER ENGINEERING, HOHAI UNIVERSITY

Tongchun LI

NATIONAL ENGINEERING RESEARCH CENTER OF WATER RESOURCES EFFICIENT UTILIZATION AND ENGINEERING SAFETY, HOHAI UNIVERSITY

Siyu CHEN

COLLEGE OF WATER RESOURCES AND HYDROPOWER ENGINEERING, HOHAI UNIVERSITY

Xiaoqing LIU

COLLEGE OF WATER RESOURCES AND HYDROPOWER ENGINEERING, HOHAI UNIVERSITY

Siling LIANG

COLLEGE OF WATER RESOURCES AND HYDROPOWER ENGINEERING, HOHAI UNIVERSITY

CHINA

COMMISSION INTERNATIONALE
DES GRANDS BARRAGES

VINGT-SIXIÈME CONGRÈS DES
GRANDS BARRAGES

Autriche, juillet 2018

DAM DEFORMATION MONITORING MODEL AND FORECAST BASED ON PCA- RBF NEURAL NETWORK*

Chaoning Lin^a, Tongchun Li^b, Siyu Chen^a, Xiaoqing Liu^a, Siling Liang^a

^a*College of Water Resources and Hydropower Engineering, HOHAI UNIVERSITY*

^b*National Engineering Research Center of Water Resources Efficient Utilization
and Engineering Safety, HOHAI UNIVERSITY*

CHINA

SUMMERY

The safety assessment of a dam requires a wide range of information that is acquired from monitoring systems. Usually, there are many instruments equipped in the dam and its surroundings for monitoring the water level, temperature, deformation and other aspects. The behavior of the dam structure depends on the synergy of multiple factors. It is therefore necessary to detect the significant indicators that have a greater influence on the dam performance. In this paper, a monitoring model based on principal component analysis (PCA) and radial basis function (RBF) neural network is put forward to analyze the displacement trend of the concrete dam. The method of principal component is used to reduce the dimension of the dataset and simplify the multi-correlation of the components. On the basis, the in-situ monitoring displacement and the extracted components is taken as the input of the RBF neural network to build the forecasting model. An example analysis based on the proposed monitoring model is performed on a prototype concrete dam, and the results show that the proposed model is reasonable and practical.

Keywords: Gravity dam; Monitoring; Numerical model; Safety

1. INTRODUCTION

Dam safety assessment has received much attention since the end of the last century. The safety assessment of a gravity dam requires a wide range of information that is acquired from monitoring systems. Usually, there are many instruments equipped in the dam and its surroundings for monitoring the water level, temperature, deformation and other aspects. Now, with the progress of monitoring technology, the current measurement technology has advantages of high precision, good stability and strong sensitivity. But the response of dam structural behavior is the result of multi-factor synergies. So it's necessary to extract the main factors, which influence the dam performance, and in the meantime analyze their development trend.

The positive analysis models are a fundamental component of dam safety systems. They provide an estimate of dam response faced with a given load combination. Then the calculated value can be compared with the actual measurements to draw conclusions about dam safety. The statistical models based on monitoring data have been used for decades for this purpose since 1955. In particular, the hydrostatic-season-time models are fully implemented in engineering practice.

In recent years, powerful tools such as neural networks are used by some scholars to analyze the observed data for interpreting the complex systems. But the multicollinearity issue among the components will influence the generalization ability and prediction accuracy of the model.

In this paper, a monitoring model based on principal component analysis (PCA) and radial basis function (RBF) neural network is put forward to analyze the displacement trend of the concrete dam. The principal components of the displacement monitoring data of the dam is extracted and reconstructed by PCA. On the basis, the method of the RBF neural network is used to predict the displacement trend of dam body.

2. PCA-RBF NEURAL NETWORK

During the operation period, usually, there's a large amount of dam monitoring data accumulated, including displacement, temperature, water level and so on. The large amount monitoring data provides a good basis to analyze the dam behavior and is very important in the diagnosis. But massive data can also be a problem for analysis. It's necessary to separate the useful information from observation and find out the main factors that affect the dam performance.

The PCA is used to reduce the dimensionality of m components including hydraulic components, temperature components and irreversible components. Then the

measured displacements and the n extracted principal components ($n < m$) are trained in the RBF neural network to make predictions. The main steps are shown in Fig. 1.

2.1. PRINCIPAL COMPONENT ANALYSIS

All Generally, there are many related variables involved during the process, and too many input variables will increase the complexity of the calculation. PCA is a kind of analytic method that can transform massive factors into some concentrate ones (principal components). The new principal components are the linear combination of the original variables, which can reflect the information of the original data to the greatest extent. The main steps are as follow:

(1) If there are a variables and each one has b groups of data, a two-dimensional matrix $(X_{ij})_{a \times b}$ can be formed. Then the matrix $(X_{ij})_{a \times b}$ can be standardized to matrix $(X'_{ij})_{a \times b}$;

(2) Calculate the correlation coefficient matrix $(R_{ij})_{b \times b}$ of the standardized matrix $(X'_{ij})_{a \times b}$;

(3) Calculate the eigenvalues λ_i ($i=1,2,\dots,p$) and corresponding eigenvectors l_i ($i=1,2,\dots,p$) of the correlation coefficient matrix $(R_{ij})_{b \times b}$. Arrange p eigenvalues λ_i from the largest one to the smallest one;

(4) Calculate the variance contribution rate and the accumulated variance contribution rate of each principal component;

(5) Select the principal components according to the accumulated variance contribution rate.

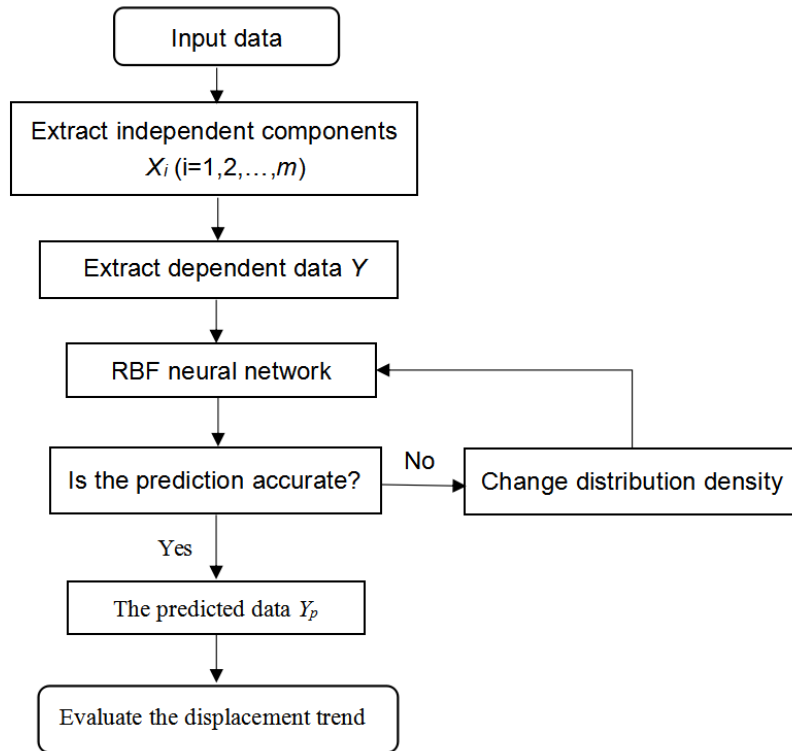


Fig. 1

Process of PCA-RBF neural network

2.2. RBF NEURAL NETWORK

RBF neural network is a kind of three-layer feedforward neural network, including input layer, hidden layer and output layer. The network uses radial basis function as the "base" of the hidden element. By this method, the input vector can be directly mapped to the hidden layer. The transformation from the input layer to the hidden layer is nonlinear mapping, and the transformation from the hidden layer to the input layer is linear mapping. The network is nonlinearly mapped from the input layer to the output layer, but the output layer is linear to the adjustable parameters. Thus, the weights of the network can be directly solved from the linear equations, which can effectively improve the learning efficiency of the network and avoid falling into the local minimum.

Generally, Gaussian function is chosen as the activation function of the hidden layer, and the output of the each hidden layer is:

$$a_{ij} = \exp\left(-\|c_j - x_i\|^2 / 2\sigma_j^2\right), \quad j = 1, 2, \dots, N \quad [1]$$

where c_j is the central value of the Gaussian function corresponding to the j hidden layer unit; σ_j is the central width of the Gaussian function corresponding to the j hidden layer unit; N is the number of the total nodes of the hidden layer.

3. ENGINEERING APPLICATION

3.1. BACKGROUND

A hydropower station is located in Cambodia, and the water-retaining structure is a RCC gravity dam. The crest elevation of the dam is 153.00m, the bottom elevation is 41.00m, the maximum dam height is 112.00m, and the width of the crest is 6.0m. There is a folding point located upstream at 145.00m elevation with the slope of 1:0.75.

This RCC gravity dam has 10 sections from the left bank to the right bank. In order to monitoring the horizontal displacements of the dam foundation, six reversed pendulums (numbered IP1~IP6) were installed symmetrically at abutment sections (at EL153m, EL120m, and EL88m). Two reversed pendulums (numbered IP7~IP8) were installed at riverbed sections (at EL43m and EL60m).

In this section, the monitoring data of IP4 from September 2, 2014 to December 7, 2017 is analyzed as an example: the 126 groups of data from September 2, 2014 to June 24, 2017 are set as the training sample and the 21 groups of data from July 7, 2017 to December 7, 2017 are set as the testing samples.

3.2. SELECTION OF PRINCIPAL COMPONENT

The main components of the displacement at the measuring points can be identified as a linear combination of three effects: the hydraulic component $\delta_H(t)$, the temperature component $\delta_T(t)$ and the irreversible component $\delta_\theta(t)$.

$$\delta = \delta_H(t) + \delta_T(t) + \delta_\theta(t) \quad [2]$$

The hydraulic component $\delta_H(t)$ is related to the types of concrete dam. In this example, three factors are selected as: $X_1 = H - H_0$, $X_2 = H^2 - H_0^2$ and $X_3 = H^3 - H_0^3$.

H_0 represents the water level of the initial monitoring day and H represents the water level of the current monitoring day.

The multicycle simple chord factor is chosen as the temperature component $\delta_T(t)$:

$$X_4 = \sin \frac{\pi t}{365} - \sin \frac{\pi t_0}{365} \quad , \quad X_5 = \cos \frac{\pi t}{365} - \cos \frac{\pi t_0}{365} \quad , \quad X_6 = \sin \frac{2\pi t}{365} - \sin \frac{2\pi t_0}{365} \quad ,$$

$$X_7 = \cos \frac{2\pi t}{365} - \cos \frac{2\pi t_0}{365} .$$

t_0 represents the initial monitoring day and t represents the current monitoring day.

There are four factors selected as the irreversible components $\delta_\theta(t)$: $X_8 = \theta - \theta_0$, $X_9 = \ln \theta - \ln \theta_0$, $X_{10} = \frac{\theta - \theta_0}{\theta - \theta_0 + 1}$, $X_{11} = 1 - e^{-(\theta - \theta_0)}$.

θ_0 is $t_0 / 100$ and θ is $t / 100$.

The above-mentioned 11 components are analyzed by PCA, and the results are shown in Table 1 and Table 2.

Table 1
The eigenvalue and contribution rate of the components

Component	Eigenvalue λ_i	Variance contribution rate/%	Cumulative variance contribution rate /%
1	4.429	40.264	40.264
2	2.852	25.923	66.187
3	1.223	11.121	77.308
4	0.907	8.250	85.558
5	0.733	6.666	92.224
6	0.577	5.241	97.465
7	0.237	2.151	99.616
8	0.202	0.181	99.797
9	0.015	0.132	99.929
10	0.007	0.067	99.996
11	0.000	0.004	100.000

Table 2
Load coefficients of the principal components

Component	X_1	X_2	X_3	X_4	X_5	X_6	X_7	X_8	X_9	X_{10}	X_{11}
Y_1	0.670	0.650	0.663	0.499	0.085	0.460	0.292	0.736	0.822	0.835	0.806
Y_2	0.715	0.737	0.720	0.162	0.154	0.372	0.298	0.434	0.535	0.527	0.498
Y_3	0.055	0.057	0.029	0.133	0.682	0.368	0.747	0.091	0.074	0.073	0.142
Y_4	0.045	0.075	0.107	0.529	0.615	0.378	0.278	0.026	0.065	0.067	0.033
Y_5	0.019	0.005	0.016	0.639	0.311	0.252	0.240	0.295	0.109	0.050	0.068

According to the results, the variance contribution rates of the principal component Y_1 , Y_2 , Y_3 , Y_4 and Y_5 are 40.264%, 25.9234%, 11.121%, 8.250% and 6.666% respectively. The cumulative variance contribution rate of the first five principal components is 92.224%. It is shown that the former five principal components can reflect more than 90% of information from the original 11 components. Therefore, the first five principal components are selected as the input variables of the model. The expressions of the five principal components are as follows:

$$Y_1 = -0.670X_1 - 0.650X_2 - 0.663X_3 + 0.499X_4 - 0.085X_5 + 0.460X_6 + 0.292X_7 + 0.736X_8 + 0.822X_9 + 0.835X_{10} + 0.806X_{11} \quad [3]$$

$$Y_2 = 0.715X_1 + 0.737X_2 + 0.720X_3 + 0.162X_4 - 0.154X_5 - 0.372X_6 - 0.298X_7 + 0.434X_8 + 0.535X_9 + 0.527X_{10} + 0.498X_{11} \quad [4]$$

$$Y_3 = 0.055X_1 + 0.057X_2 + 0.029X_3 - 0.133X_4 + 0.682X_5 - 0.368X_6 + 0.747X_7 - 0.091X_8 + 0.074X_9 + 0.073X_{10} + 0.142X_{11} \quad [5]$$

$$Y_4 = 0.045X_1 + 0.075X_2 + 0.107X_3 + 0.529X_4 + 0.615X_5 + 0.378X_6 - 0.278X_7 - 0.026X_8 - 0.065X_9 - 0.067X_{10} - 0.033X_{11} \quad [6]$$

$$Y_5 = -0.019X_1 - 0.005X_2 + 0.016X_3 - 0.639X_4 + 0.311X_5 + 0.252X_6 - 0.240X_7 + 0.295X_8 + 0.109X_9 + 0.050X_{10} - 0.068X_{11} \quad [7]$$

3.3. RBF NEURAL NETWORK

RBF neural network was created and the calling format is:

$$net = newrb(P, T, spread) \quad [8]$$

where P is the input item, T is the output item, and spread is the distribution density of radial basis functions.

Five principal components are selected as the input items of the neural network:

$$P = (Y_1, Y_2, Y_3, Y_4, Y_5)^T \quad [9]$$

The displacements prediction data are chosen as the output item of the neural network, that is:

$$T = (y_p)^T \quad [10]$$

3.4. COMPARISON

In order to verify the prediction effect, the PCA-RBF neural network model is compared with the multivariate regression analysis statistical model in this section. The above-mentioned 126 sets of data are used as the sample, and the multivariate regression function is shown as follow:

$$Y_s = 0.449 + 0.157X_1 + 0.002X_2 + 3.49e-05X_3 + 0.227X_4 - 0.092X_5 - 0.354X_6 + 0.191X_7 + 0.15X_8 + 0.147X_9 - 0.919X_{10} - 0.812X_{11} \quad [11]$$

The training and prediction results of the two models are shown in Fig. 2. The determination coefficient (R²), mean-square error (RMSE) and mean absolute deviation (MAE) are defined as (12) ~ (14), where $y_s(i)$ is prediction value and $y(i)$ is measured value. The results are listed in Table 3, and the comparison results of the residuals is shown in Fig. 2.

$$R^2 = \frac{[\sum_{i=1}^N (y_s(i) - \bar{y}_s)(y(i) - \bar{y})]^2}{\sum_{i=1}^N (y_s(i) - \bar{y}_s)^2 \sum_{i=1}^N (y(i) - \bar{y})^2} \quad [12]$$

It is shown in Fig. 2 that the displacement prediction line of the PCA-RBF neural network model is more close to the measured displacement line, and the prediction effect is better than that of the statistical model.

As shown in Table 3, the RMSE and MAE of PCA-RBF neural network at training stage are 0.288 and 0.201 respectively, and are 0.702 and 0.548 at the prediction stage respectively, which are all smaller than those of statistical models. The R2 of the PCA-RBF neural network model at the training stage and the prediction stage are 0.959 and 0.910 respectively, which are both larger than those of the statistical models. In addition, with the comparison of the residual results of Fig. 3, the prediction effect of the PCA-RBF neural network model is more accurate.

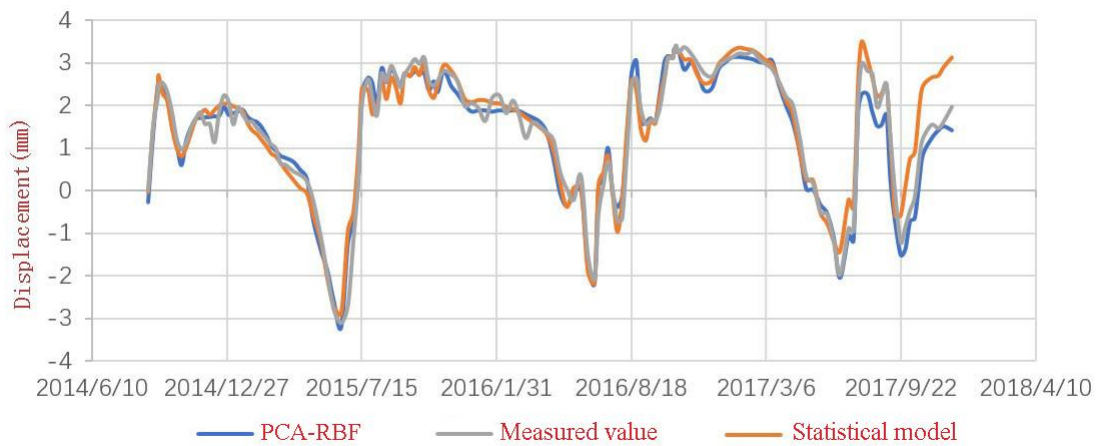


Fig. 2

Comparison of training and prediction effect

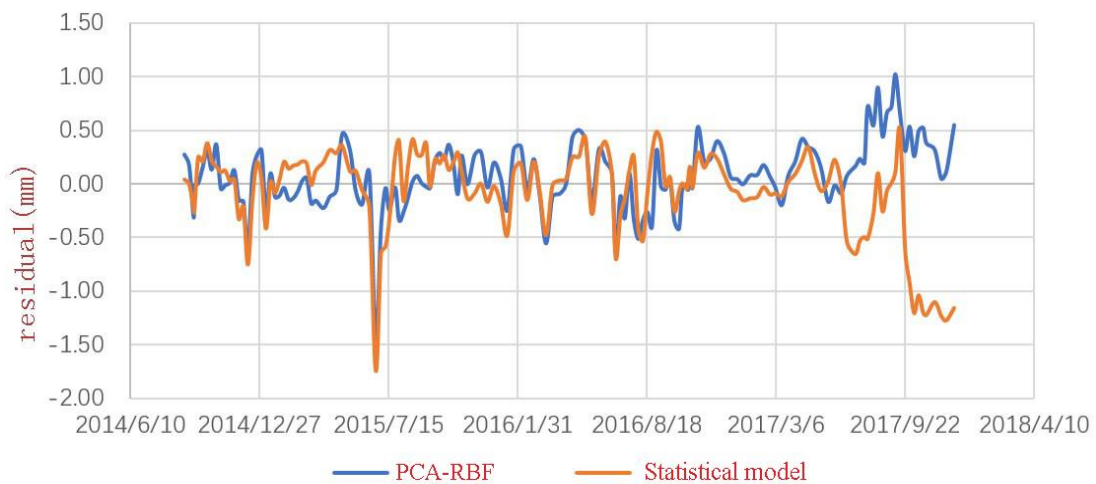


Fig. 3

Comparison of the residual

Table 3
Evaluation of the related parameters

Stage	Model	R ²	RMSE/mm	MAE/mm
Training	PCA-RBF	0.959	0.288	0.201
	Statistical	0.958	0.293	0.209
Prediction	PCA-RBF	0.910	0.702	0.548
	Statistical	0.869	0.827	0.696

4. CONCLUSION

In this paper, a monitoring model based on the principal component analysis (PCA) and radial basis function (RBF) neural network is put forward to predict the displacement trend of the concrete dam. And an example analysis based on the proposed model is performed on a prototype concrete dam. The conclusions are as follows:

(1) The PCA-RBF prediction model reduces the data redundancy and eliminates the multiple correlations among the components. And this model can predict the displacement trend of the concrete dam well.

(2) Compared with the statistical model, the PCA-RBF neural network model has higher prediction accuracy for the displacement trend of concrete dam, and can be applied in practical projects.

ACKNOWLEDGMENTS

This research has been greatly supported by the National Key Research and Development Plan (Grant No. 2016YFC0401601), Postgraduate Research & Practice Innovation Program of Jiangsu Province (KYCX17_0436) and the Fundamental Research Funds for the Central Universities (2017B623X14).

REFERENCES

- [1] Kim Y S , Kim B T . Prediction of relative crest settlement of concrete-faced rockfill dams analyzed using an artificial neural network model . *Computers and Geotechnics* , 2008 , 35 : 313—322 .
- [2] Su HZ, Wen ZP, Chen ZX, et al. Dam safety prediction model considering chaotic characteristics in prototype monitoring data series. *Structural Health Monitoring*, 2016, 15(6):639-649.
- [3] Salazar F, Morán R, Toledo M Á, et al. Data-based models for the prediction of dam behavior: a review and some methodological considerations. *Archives of Computational Methods in Engineering*, 2017, 24(1):1-21.
- [4] Salazar F, Toledo M Á, Oñate E, et al. Interpretation of dam deformation and leakage with boosted regression trees. *Engineering Structures*, 2016, 119:230-251.
- [5] Bonaldi P, Fanelli M, Giuseppetti G. Displacement forecasting for concrete dams. *International Water Power and Dam Construction*, 1977, 29 (9):42-50.
- [6] Mata J. Interpretation of concrete dam behaviour with artificial neural network and multiple linear regression models. *Engineering Structures*, 2011, 33(3): 903-910.
- [7] Zhang Xiuli, Yang Yanze. Hydraulic design manual (Eleventh volume, hydraulic safety monitoring). Beijing: China Water & Power Press, 2013.
- [8] Yang Jie, Zhan Jun, Zhang Ji, etc. MATLAB neural network in 30 cases. Beijing: Publishing House of Electronics Industry, 2014.
- [9] Wu Zhongru. Safety monitoring Theory & Its Application of Hydraulic Structure. Beijing: Higher Education Press, 2003.
- [10] Tonini D. Observed behavior of several leakier arch dams. *Journal of Power Division*, 1956 ,82(12):135-139.
- [11] Cheng L, Zheng DJ. *Two online dam safety monitoring models based on the process of extracting environmental effect*. *Advances in Engineering Software* 2013, 57(1):48-56.
- [12] Anitaa, Rajesh S, Sushabhan C, et al. Wireless disaster monitoring and management system for dams. *Procedia Computer Science*, 2015, 48:381-386.
- [13] Fanelli M. Control of dam displacements. *Energia Elettrica*, 1975;52:125–39.
- [14] Bonaldi P, Fanelli M, Giuseppetti G. Displacement forecasting for concrete dams. *International Water Power and Dam Construction*, 1977, 29 (9):42-50.
- [15] Su HZ, Wu ZH. Identification model for dam behavior based on wavelet network. *Computer-Aided Civil and Infrastructure Engineering*, 2007, 22: 438-448.

- [16] Kao CY, Loh CH. Monitoring of long-term static deformation data of Fei-Tsui arch dam using artificial neural network-based approaches. *Structural Control and Health Monitoring*, 2013, 20(3): 282-303.
- [17] Ranković V, Grujović N, Divac D, et al. Development of support vector regression identification model for prediction of dam structural behaviour. *Structural Safety*, 2014, 48(48):33-39.
- [18] Mata J, Castro A T D, Costa J S D. Constructing statistical models for arch dam deformation. *Structural Control & Health Monitoring*, 2014, 21(3):423-437.
- [19] A.De Sortis, P.Paoliani. Statistical analysis and structural identification in concrete dam monitoring. *Engineering Structures*, 2007, 29(1): 110-120.
- [20] Gu CS, Su HZ. Current status and prospects of long-term service and risk assessment of concrete dams. *Advances in Science and Technology of Water Resources*, 2015, 35(5):1-12.

COMMISSION INTERNATIONALE DES GRANDS BARRAGES

VINGT-SIXIÈME CONGRÈS DES GRANDS BARRAGES
Autriche, juillet 2018

DOI 10.3217/978-3-85125-620-8-081



This work licensed under a Creative Commons Attribution 4.0 International License. <https://creativecommons.org/licenses/by-nc-nd/4.0/>

**SAFETY ASSESSMENT FOR LARGE RESERVOIR CONSTRUCTED FOR
DOMESTIC WATER NEAR URBAN AREAS AND A CASE STUDY**

Hasan TOSUN

Professor, ENGINEERING FACULTY, ESKİSEHİR OSMANGAZI UNIVERSITY

TURKEY

COMMISSION INTERNATIONALE
DES GRANDS BARRAGES

VINGT-SIXIÈME CONGRÈS DES
GRANDS BARRAGES
Autriche, juillet 2018

SAFETY ASSESSMENT FOR LARGE RESERVOIR CONSTRUCTED FOR DOMESTIC WATER NEAR URBAN AREAS AND A CASE STUDY

Hasan TOSUN

Professor, Engineering Faculty, ESKİŞEHİR OSMANGAZI UNIVERSITY

TURKEY

1. INTRODUCTION

Increasing demand for water results to construct large reservoirs in or near urban areas. Same situation can be resulted by extending settlement area around reservoirs, which were constructed many years ago. Therefore, dams with large reservoirs, which are located in or near urban areas, have a high-risk potential for downstream life and property. In other words, a problem on public safety can raise up for people and live life on downstream for urban areas.

Safety assessment is a most significant concept for large reservoir, especially constructed in or near urban area. It is clear that there are mainly two important factors acting on total risk for dam structures. These are (1) the seismic hazard rating of dam site and (2) the risk rating of the dam and appurtenant structures. The seismic hazard of a dam site can be based on the peak ground acceleration. This value derived from the defined design earthquake produces the main seismic loads. For a preliminary study, the existing map of seismic zones can be used to estimate the seismic hazard of a dam site. The risk rating of the dam should be based on the capacity of the reservoir, the height of the dam, the evacuation requirements, and the potential downstream damages. In general, the seismic and risk ratings are evaluated separately for ICOLD method. However, BUREAU method combined these two factors to define the total risk factor for dam structure.

In the study six dams, namely Alacatlı Kutlu Aktas, Balçova, Gordes, Guzelhisar, Tahtalı and Urkmez dams in Kucuk Menderes and Gediz basins, were considered. These dams are mainly utilized for providing domestic water of Izmir Metropolitan Area. In 2017, The water demand was totally 225 million cubic meter for this area. The 42.3 percent of this demand was provided by surface water, which are impounded in the reservoirs of dams mentioned above while others provided by groundwater resources. This paper deals with an evaluation of seismic

hazard and local site effects for large dams and evaluates six large dams, which have a height from river bed between 20.3 m and 89.0 m in the Kucuk Menderes and Gediz basins (Table 1).

Table 1. Physical properties of dams considered for this study.

No	Dam	Basin	Height from river bed (m)	Completed Year	Volume of embankment (hm ³)	Volume of reservoir (hm ³)
1	A.Kutlu Aktaş	K.Menderes	15.3	1997	0.28	16.61
2	Balcova	K.Menderes	63.4	1980	1.11	7.76
3	Gordes	Gediz	82.9	2010	4.54	448.46
4	Guzelhisar	Gediz	89.0	1982	3.21	158.00
5	Tahtali	K.Menderes	54.4	1999	3.37	306.65
6	Urkmez	K.Menderes	32.0	1990	0.98	7.92

2. MATERIALS AND METHODS

For this study seismic study has been carried out by deterministic and probabilistic seismic hazard analyses. The deterministic seismic hazard analysis (DSHA) considers a seismic scenario that includes a four-step process. It is a very simple procedure and gives rational solutions for large dams because it provides a straightforward framework for the evaluation of the worst ground motions. The probabilistic seismic hazard analysis (PSHA), which is widely used for dam sites, considers uncertainties in size, location and recurrence rate of earthquakes. For the seismic hazard analysis of each dam site, all possible seismic sources were identified and their potential was evaluated in detail, as based on the guidelines given by [1] and the unified seismic hazard modeling for Mediterranean region introduced by [2]. Four separate predictive relationships for horizontal peak ground acceleration were used for this study [3,4,5 and 6].

Some institutions have defined some earthquake levels for dynamic analysis of dam structures. In this study, earthquake definitions given by FEMA were considered for seismic hazard analyses [7]. The Operating Basis Earthquake (OBE), which was defined by means of the probabilistic methods mentioned above, is the earthquake that produces the ground motions at the site that can reasonably be expected to occur within the service life of the project. MDE is normally characterized by a level of motion equal to that expected at the dam site from the occurrence of deterministically evaluated MCE. Safety Evaluation Earthquake (SEE) is the level of shaking for which damage can be accepted but for which there should be no uncontrolled release of water from the reservoir. Author states that most of large dams in Turkey were analyzed by using these definitions in past. ICOLD [8] also some earthquake definitions for dynamic analysis of dams. Author mentions these definitions more detail on their research [9].

Some methods are used to quantify the total risk factor of a dam. One of them considers the seismic hazard of the dam site and the risk rating of the structure separately [10]. According to this method, the seismic hazard of the dam site regardless of type of dam, can be classified into four groups from low to extreme. This is a quick way for rating the seismic hazard. The hazard class of a dam site obtained from this method provides a preliminary indication of seismic evaluation

requirements. Other one is Bureau method, which considers various risk factors and weighting points to quantify the total risk factor (TRF) of any dam [11]. In this methods the TRF depends on the dam type, age, size, downstream risk and vulnerability, which depends on the seismic hazard of the site.

For all analyses throughout this study, the peak ground acceleration was determined by two methods discussed above, only the results obtained by DSHA. All procedures mentioned above can be executed by the DAMHA program that is working on the basis of geographic information system (GIS). For total risk of dams, two different methods mentioned above are used for all dams considered for this study.

3. ANALYSES AND RESULTS

Dam designers in Turkey believe the fact that embankment dams, which are well compacted according to the specification, are suitable type for regions having high seismic activity. Whereas it is a well-known fact that strong ground shaking can result to instability on embankment and loss of strength at the foundations. Additionally, active faults, which are very close to the foundation of dams, have the potential to cause damaging displacement of the structure.

Most of the existing dams considered for this study are under near source effect [12]. ICOLD defined the near-field motion, which is ground motion recorded in the vicinity of a fault [8]. In this specification, a correlation between radius of near field area and earthquake magnitude is suggested as based on the cases on West United States. Author established limits of near-field motion for the investigation area. According to this model, the maximum magnitude of the earthquakes ranges from 5.7 to 6.7 and the minimal distance to fault segment is between 1.1 and 3.1 km for five dams (Table 2). The last one, namely Alacati Kutlu Aktas dam, is not under near field motion with minimal distance to fault segment is 10.1 km. The 83.3 percent of dams considered for this study has a minimal distance, which is less than 3.1 km to an active fault. In other word, all dams with exception of Alacati Kutlu Aktas dam, are not far away 10 km to active faults.

Table 2. The results of deterministic seismic hazard analyses

No	Dam	Deterministic Method *			
		Maximum earthquake M_{max}	Minimum distance, R_{min}	Mean PGA + 50 %	Mean PGA + 84 %
1	A.Kutlu Aktas	6.1	10.1	0.116	0.189
2	Balcova	6.1	2.4	0.288	0.450
3	Gordes	6.7	1.1	0.442	0.702
4	Guzelhisar	6.7	3.1	0.409	0.642
5	Tahtali	5.7	1.9	0.277	0.431
6	Urkmez	5.7	1.7	0.310	0.482

The results of the DSHA are given in table 2. In this table, M_{max} is the maximum earthquake magnitude in M_w and R_{min} is the minimum distance to fault

segment. Mean PGA + 50% and Mean PGA + 84% are mean peak ground acceleration at the 50th percentile and Mean Peak Ground Acceleration at the 84th percentile, respectively.

A detailed study was performed to identify all possible seismic sources for the seismic hazard analyses of the dam sites, as based on the macro seismotectonic model of Turkey. The National Disaster Organization and other Institutes prepared the map for general use. But it was modified by the author and his co-workers to use for dam projects at the Earthquake Research Center in Osmangazi University. Local geological features and seismic history were also taken into account to quantify the rate of seismic activity in dam sites. As a result of detailed evaluation, total area covering all basins was separated into four seismic zones. These seismic zones and historical earthquakes are given in Fig. 1. These zones including faults and earthquakes occurred in the basin along last 100 years. The number of earthquakes having a magnitude on the basis of surface wave (M_s), which is greater than 4.0, is 1455. The numbers of earthquakes with M_s that are greater than 6.0 are 34 for dam sites. There is no earthquake having a magnitude greater than 7.0 in the basin.

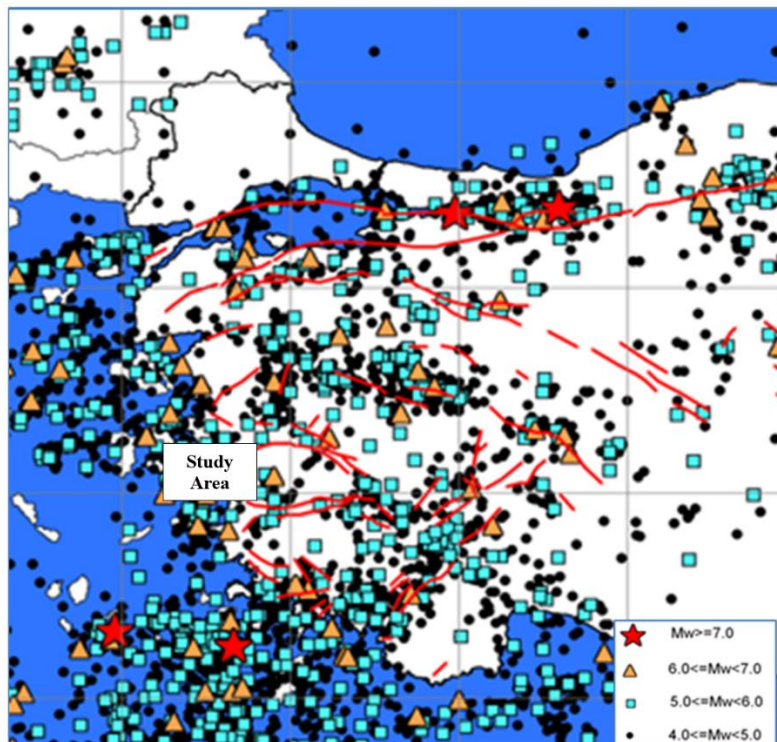


Fig. 1. Energy sources and earthquakes in west Anatolia region of Turkey.

The deterministic analyses indicate that peak ground acceleration (PGA) changes within a wide range. The PGA values ranges from 0.116g to 0.442g for the mean Peak Ground Acceleration at the 50th percentile and from 0.189g to 0.702g for the mean Peak Ground Acceleration at the 84th percentile given in table 2. According to the updated DSI guidelines, the PGA values at the 84th percentile should be taken into account for five dams analyzed throughout the study, when considered deterministic approach (DSI, 2012). For only Alacati Kutlu Aktas dam, the PGA values at the 84th percentile should be considered Table 3 shows the summary of DSI seismic guidelines for dynamic analyses.

Table 3. Selection of Design Earthquake as based on risk classification [13]

Hazard Analysis		Deterministic Method	Probabilistic Method
Class	Hazard Ratio		
I	Low	50 %	$T_R = 224$ years (*)
II	Moderate	50 %	$T_R = 475$ years
III	High	84 %	$T_R = 975$ years
IV	Very high	84 %	$T_R = 2475$ years

(*) T_R = Return time

The seismic hazard analyses were performed for six dams throughout this study. The results with total risk of each dam are given table 4. All dams with exception of Alacati Kutlu Aktas dam are identified in class of IV with extremely high hazard rating. One dam site have moderate hazard rating and are identified as hazard class of II. ICOLD [10] state that if the PGA value is greater than 0.25 g and the energy source is closer than 10 km from the dam site, it is classified as hazard class IV with hazard rating of extreme. For eleven dams, the distance from dam site to active faults, which are given on updated seismic maps, ranges from 1.1 km to 3.1 km. The large dams of basins, which are under the influence of the near-field motion, have been constructed to very close to active segments of the horst-graben fault system in west Anatolia, which were determined after 2013.

Table 4. Total risk of dams considered for this study.

No	Dam	Hazard Analysis		Total Risk (ICOLD,1989)			Total Risk (Bureau, 2003)		
		Class	Hazard Ratio	Risk factor	Risk class	Risk ratio	Risk factor	Risk class	Risk ratio
1	A.K. Aktaş	II	Moderate	30	III	High	163.4	III	High
2	Balcova	IV	Very high	34	IV	Very high	187.6	III	High
3	Gordes	IV	Very high	36	IV	Very high	155.6	III	High
4	Guzelhisar	IV	Very high	36	IV	Very high	158.3	III	High
5	Tahtali	IV	Very high	36	IV	Very high	186.6	III	High
6	Urkmez	IV	Very high	32	IV	Very high	188.5	III	High

Throughout this study, two methods have been considered to quantify the total risk for dam structures. In DSI guidelines, total risk factor depends to reservoir capacity, height, evacuation requirement and potential hazard (DSI, 2012). According to DSI Guidelines all dams are categorized in III and IV risk classes with high and very high risk rating. Following Bureau's method, all large dams are classified in risk class III, a high-risk rating. In Bureau method, the values of the TRF range from 96.5 to 208.6. This means that there is no dam having a risk classes of I and II for all dams considered for this study. Author thinks that the solution obtained from Bureau method is more rational than that of the DSI guidelines.

4. DISCUSSIONS

There are six large dams located in Izmir Metropolitan Area for providing domestic water. Four of them are located on the turbidities of Kucuk Menderes river while other two were constructed in Gediz basin. The earthquake safety and total risk of these dams are evaluated more detail as given below.

Alacati Kutlu Aktas Dam is a earthfill dam 15.3-m high with a total embankment volume of 280 000 m³. It is located on Hirsiz river in Kucuk Menderes basin. Its construction was finished in 1997. When the reservoir is at operation stage with maximum water level, the facility approximately will impound 16.60 hm³ of water with a reservoir surface area of 2.55 km². It is mainly designed to provide domestic water with annual capacity of 3.0 hm³. The side slopes of main embankment is 3.0H:1V for upstream and 2.5H:1V for downstream (H=horizontal and V=vertical) (Fig. 2). On the section there is a central impervious zone, which is composed of impervious clay and a transition section of sand, gravel and small-sized crushed rock was designed over rockfill materials (Figure 2). The shell fill in downstream and upstream parts is composed of semi-pervious clayey material. The alluvium on river bed was removed before beginning the construction of the main embankment. The seismic hazard analyses performed throughout this study indicates that this dam is less critical dam within the Izmir Metropolitan Area. It will be subjected to a peak ground acceleration of 0.116 g by an earthquake of 6.1 magnitude and it is only 10.1 km far away from an active fault given in new seismotectonic map of Turkey in 2013. Its TRF value is 163.4 and it is identified as risk class of III. The 21-years old embankment is in excellent condition.

Balcova dam is a rockfill dam on Ilica River in the Izmir Metropolitan Area. It has a 63.4 m height from river bed. When the reservoir is at maximum capacity, the facility impounds 7.76 hm³ of water with a reservoir surface area of 0.69 km². Its construction was finished in 1980. It was designed to provide domestic water with annual capacity of 12 hm³. The crest length is 231 m and the side slopes of main embankment is 3.5H:1V for upstream and 3.0H:1V for downstream (H=horizontal and V=vertical) (Fig. 3). On the section there is a central impervious core, which is composed of compacted impervious clay and a transition section of sandy and gravelly aggregates was designed between the core and semi-pervious soils. The alluvium on river bed, which is composed of different size of river bed material, was removed before beginning the construction of the main embankment. According to the seismic hazard analyses of this study, it will be subjected to a peak ground acceleration of 0.288g by an earthquake of 6.1 magnitude and its embankment is only 2.4 km far away from an active fault given in new seismotectonic map of Turkey in 2014. Its TRF value is 187.6, and it is identified as risk class of III. This 37-year old earthfill embankment is in excellent condition, but it cannot meet current seismic design standards. Additionally, it is under near-field motion. Therefore, its seismic upgrade should be provided soon.

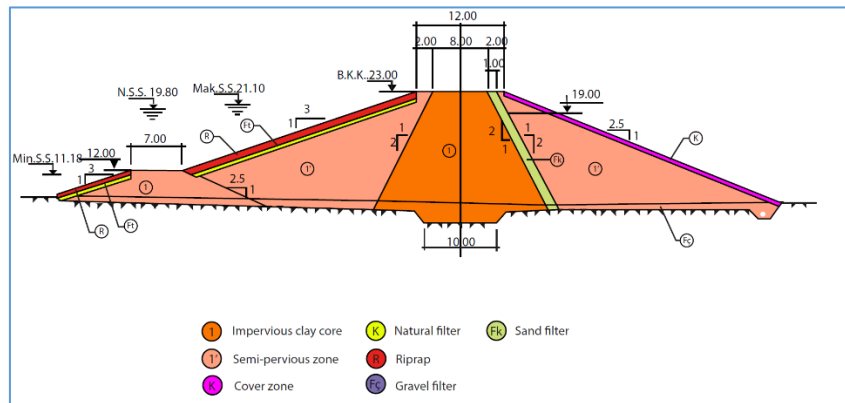


Fig. 2. The maximum cross-section of embankment of A.Kutlu Aktas dam [14]



Fig. 3. A general view from Balcova dam.

The Gordes dam is a concrete faced rockfill dam with a 82.9-m height from river bed. It was located on the Gordes River near Golmarmara County. When the reservoir is at maximum capacity, the facility impounds 448.46 hm³ of water with a reservoir surface area of 14.06 km². Its construction was finished in 2010. It was designed to irrigate land of 14 890 ha land and to provide drinking water for İzmir city. The main embankment consists of crushed rock and transition zone to concrete face. The upstream and downstream fills are large-sized crushed rocks at which the most durable and high strengthened ones are located on the outer part of the shell. The crest width is 10 m and the side slopes of main embankment is 1.5H:1V for upstream and 1.4H:1V for downstream (H=horizontal and V=vertical). According to the seismic hazard analyses of this study, it will be subjected to a peak ground acceleration of 0.442 g by an earthquake of 6.7 magnitude. [9] introduce more detail information about its earthquake safety and total risk.

Güzelhisar dam is a rockfill dam 89-m high with a total embankment volume of 3 210 000 m³. It is located on the Guzelhisar River in Gediz basin. Its construction was finished in 1982. When the reservoir is at operation stage with

maximum water level, the facility approximately will impound 158.00 hm³ of water with a reservoir surface area of 5.8 km². It was mainly designed to provide industrial water for a national chemistry company. The crest width is 10 m and the side slopes of main embankment is 2.5H:1V for upstream and 2.0H:1V for downstream (H=horizontal and V=vertical). On the section there is a central impervious core, which is composed of compacted low-plasticity clay and a transition section of sand, gravel and small-sized crushed rock was designed between the core and rockfill materials for downstream part. The downstream shells are composed of large-sized crushed rocks. The alluvium on river bed, which is composed of mixtures of fine to large size grains, was removed before beginning the construction of the main embankment. The seismic hazard analyses performed throughout this study indicates that Guzelhisar dam is one of the most critical dams within the basin. Detail assessment about its earthquake safety and total risk are introduced by [9].

Tahtalı dam is a rockfill dam on Tahtalı River near Gumuldur County in the Izmir Metropolitan Area. It has a 54.4 m height from river bed. When the reservoir is at maximum capacity, the facility impounds 306.6 hm³ of water in its reservoir. Its construction was finished in 1999. It was designed to provide domestic water with an active volume of 287 hm³. Fig.4 shows a general view from Tahtali dam. On the section there is a central impervious core, which is composed of compacted impervious clay and a transition section of sandy and gravelly aggregates was designed between the core and semi-pervious soils. The alluvium on clay core was removed before beginning the construction of the main embankment. A low-strength concrete wall was constructed for providing impermeability in dense alluvial soil. According to the seismic hazard analyses of this study, it will be subjected to a peak ground acceleration of 0.277g by an earthquake of 5.7 magnitude and its embankment is only 1.9 km far away from an active fault given in the updated seismo-tectonic map of Turkey. Its TRF value is 188.6 and it is identified as risk class of III. It is at second place after Gordes dam when regarding the total capacity of reservoir and one of the most critical dams in Izmir Metropolitan Area. This 19-year old earthfill embankment is in excellent condition, but it cannot meet current seismic design standards. Additionally, it is under near-field motion. Therefore, its seismic upgrade should be provided soon



Fig.4. A general view from Tahtali dam

Urkmez dam is a earthfill dam on Urkmez River near Seferihisar County. It has a 32.0 m height from river bed. When the reservoir is at maximum capacity, the facility impounds 7.92 hm³ of water with a reservoir surface area of 0.61 km². Its construction was finished in 1991. It was designed to provide water for irrigation of 370 ha and drinking water with annual capacity of 0.78 hm³. The crest length is 428 m and the side slopes of main embankment is 3.0H:1V for upstream and 2.5H:1V for downstream (H=horizontal and V=vertical). On the section there is a central impervious core, which is composed of compacted impervious clay and a transition section of sandy and gravelly aggregates was designed between the core and pervious coarse grained soils. The alluvium under clayey impervious core, which is composed of different size of river bed material, was removed before beginning the construction of the main embankment According to the seismic hazard analyses of this study, it will be subjected to a peak ground acceleration of 0.310 g by an earthquake of 5.7 magnitude and its embankment is 1.7 km far away from an active fault given in the updated seismo-tectonic map of Turkey. Its TRF value is 188.5, and it is identified as risk class of III. This 37-year old earthfill embankment is in excellent condition, but it cannot meet current seismic design standards. It will be under near-field motion during earthquake. Therefore, its seismic upgrade should be provided soon.

5. CONCLUSIONS

For the large dams within the Izmir Metropolitan Area, the seismic hazard rating of the dam site and the risk rating of the complete structures were determined and possible modes of failure were estimated. This paper summarizes the seismic hazard and total risk analyses of six large dams, which are located on two basins in Turkey, as based on a preliminary study. The study identified that five of them are under near source effect. As a result of this study, 83.3 percent of dams has extremely high of risk class while others are classified in high risk class. Therefore, detail seismic hazard analyses should be performed for these structures as based on the updated seismic data and design code under circumstances of the study of a national safety program for dam. In other words, these dams must be re-analyzed by selecting appropriate seismic parameters. Rehabilitation design and construction measures, if necessary, may follow after in cases where the dams are found deficient seismically.

REFERENCES

1. Fraser, WA and Howard, JK (2002). *Guidelines for Use of the Consequence-Hazard matrix and Selection of Ground Motion Parameters*: Technical Publication, Department of Water Resources, Division of Safety of Dams.
2. Jiminez, MJ, Giardini, D and Grünthal, G (2001). *Unified Seismic Hazard Modelling throughout the Mediterranean Region*. Bolettino di Geofisica

- Teorica ed Applicata, Vol.42, N.1-2, Mar-Jun., 3-18.
3. Campbell, KW (1981). *Near-Source Attenuation of Peak Horizontal Acceleration*: Bulletin Seism. Soc. Am., V.71, N.6, 2039-2070.
 4. Boore, DM, Joyner, WB. and Fumal, TE (1993). *Estimation of response spectra and peak accelerations from Western North American earthquakes*. An interim report. Open file report 93-509.U.S.G.S.
 5. Boore, DM., Joyner, WB. and Fumal, TE (1997). *Equation for Estimating Horizontal Response Spectra and Peak Acceleration from Western North American Earthquakes*. A Summary of recent Work. Sesimological Reseach Letters, V.68, N.1, January /February, 128-153.
 6. Gülkan, P and Kalkan,E (2002). *Attenuation modeling of recent earthquakes in Turkey*. Journal of Seismology, 6(3), 397-409.
 7. FEMA (2005). *Federal Guidelines for Dam Safety—Earthquake Analyses and Design of Dams*.
 8. ICOLD (2016). *Selecting Seismic Parameters for Large Dams-Guidelines*. ICOLD, Bulletin 148.
 9. Bureau, GJ (2003). *Dams and Appurtenant Facilities in Earthquake Engineering Handbook edited by Chenh, W.F and Scawthorn,C*. CRS press, Bora Raton 26.1-26.47.
 10. Tosun, H and Tosun,V (2017) Total risk and seismic hazard analyses of large dams in northwest Anatolia, Turkey. 85th Annual Meeting of International Commission on Large Dams, July 3-7, Prague.
 11. ICOLD (1989). *Selecting Parameters for Large Dams-Guidelines and Recommendations*. ICOLD Committee on Seismic Aspects of Large Dams, Bulletin 72.
 12. MTA (2013) Scale 1/1.125.000 Turkey Live Fault Map. General Directorate of Mineral Research and Exploration. Special publications series, Ankara, Turkey
 13. DSİ (2012). *Selection of Seismic Parameters for Dam Design*. State Hydraulic Works, Ankara, 29 p (in Turkish).
 14. DSİ (2016). *Dams of Turkey*. TR-COLD, Ankara, 602 p.

SUMMARY

Large reservoirs, which are located in or near urban areas, pose a high-risk potential for downstream life and property. Safety assessment requires for existing dams having large reservoirs built in the settlement area. There are some metropolitan provinces, which are under threatening of earthquakes. One of them is Izmir Metropolitan Area with five million people. Major earthquakes with the potential of threatening life and property occur frequently here. There are six large dams for providing domestic water for Izmir province. These are namely Alacatlı Kutlu Aktas, Balcova, Gordes, Guzelhisar, Tahtalı and Urkmez dams. The investigation area is structurally cut by numerous faults, which are resulted by horst-graben system in west Anatolia. The seismic hazard analyses have indicated that peak ground acceleration changes within a wide range (0.116 g and 0.442 g) for the six dam sites of this area. This study indicates that most of these large dams have high-risk class in the metropolitan area.

Key words: Dam, seismic hazard, total risk

COMMISSION INTERNATIONALE DES GRANDS BARRAGES

VINGT-SIXIÈME CONGRÈS DES GRANDS BARRAGES
Autriche, juillet 2018

DOI 10.3217/978-3-85125-620-8-082



This work licensed under a Creative Commons Attribution 4.0 International License. <https://creativecommons.org/licenses/by-nc-nd/4.0/>

**LABORATORY STUDY OF THE EFFECT OF RECYCLED FILLERS FROM
COKING AND IRON CONCENTRATE FACTORIES ON THE ROLLER
COMPACTED CONCRETE PROPERTIES IN DAMS**

Jaber MAHMOUDI

*MSc of water structure engineering, Laboratory manager and QC at MANA
CONSTRUCTION COMPANY*

IRAN

Faeze YAZDI

*MSc Of civil engineering, Supervisor of Civil and Chief Technical Officer of
BARSOO ENGINEERING CO.*

IRAN

**LABORATORY STUDY OF THE EFFECT OF RECYCLED FILLERS
FROM COKING AND IRON CONCENTRATE FACTORIES ON THE ROLLER
COMPACTED CONCRETE PROPERTIES IN DAMS***

Jaber Mahmoudi

*MSc of water structure engineering, Laboratory manager and QC at Mana
Construction Company*

Faeze Yazdi

*MSc Of civil engineering, Supervisor of Civil and Chief Technical Officer of
Barsoo Engineering Co.*

IRAN

ABSTRACT

This study presents mechanical and durability aspects of using different waste fillers including Iron powder, Iron concentrate, Coal and Coke Powder, which cannot be reused at industry process. (samples from different parts of the Jalalabad Iron Ore Concentrate Plant and Zarand Coking Plant, Kerman, Iran) as well as mineral powder filler as a control sample to replace 3% and 6% of coarse and fine natural aggregates content in RCC combination. Absorption, compressive strength, workability and non-segregation of grains investigated for the concrete specimens. The experimental results showed that RCCs of iron ore- powder filler contents with 6% of the weight of coarse and fine natural aggregates had higher values of 28 days compressive strength and minimum 24-hour water absorption about 2.22%. Generally, the fillers of iron ore concentrate factory including iron ore filler and concentrate filler have better results in improving the mechanical and transitional properties of roller concrete, due to rounding of aggregates, comparing by the case of carbonaceous compounds extracted from the coking plant, including Coke and coal fillers. In addition to that, using this type of waste in concrete may has more environmentally efficient, because this helps to remove some parts of wastes and protects the environment.

* *Roller Compacted Concrete Dams (RCC Dams)*

KEYWORDS

Roller Compacted Concrete (RCC), Slump, Mix design, Compression strength, Water absorption

1. INTRODUCTION

In order to achieve economic self-sufficiency, it is important to control the floods and surface water through the construction of dams which considered essential and infrastructural since water supply has always been a fundamental human need for agriculture, industry and drinking water.

In the early 1980s, conventional concrete dam construction methods replaced by the roller compacted concrete method. RCC dams use embankment dams construction's method, which is based on using heavy equipment machinery. Usage of heavy equipment machinery for constructing concrete dams, leads to development of RCC dams which despite the short construction time, they have the reliability of conventional concrete dams. Also, RCC dams are an economical competitive choice over embankment dams. Construction cost of RCC dams is less than conventional concrete dams as well as embankment dams. It is because of material saving, fast construction, less costly spillway, less risk of coffer dam overtopping and shorter and smaller size of diversion conduit [1].

In addition to economic benefits, the RCC is considered as a "green" concrete because the cement consumption in the RCC is lower as the RCC mixtures are normally designed with leaner binder content. Mineral admixtures are used extensively in RCC mixtures. The use of large amounts of mineral admixtures improves durability, reduce adiabatic temperature rise of concrete, construction costs, and gas emission accompanied with the manufacturing of cement clinker. Class F and Class C fly ashes, slag, and natural pozzolan have been used as mineral admixtures in the RCC [2].

Coarse aggregate size has a significant influence on the degree of RCC compaction in small layers and less effect in relatively thicker layers especially when large vibratory rollers are employed. The coarse aggregates with maximum-size diameter greater than 76 mm are seldom used in the RCC manufacturing because they cause problems in the layers spreading and compaction. However, the use of coarse aggregates with maximum-size diameter finer than 75 mm reduces the volume of voids and produces more cohesive mixture [3].

Waste coking and iron ore concentrate plant, which is not reusable, is normally deposit causing obvious environmental problems; so use of these materials effectively in concrete, make them valorized. A mass of small particle also produced due to the process of iron ore concentrate production, which usually does not have the ability to become concentrate, and is deposit. The waste Coke, consisting of non-consumable materials commonly used in particles smaller than 1 cm in diameter, are discharged as waste and disposed of in garbage dumps.

This waste called coal in input materials, and called coke in exhaust materials. Applying the aggregates smaller than 75 microns (sieve NO. #200), if not plastic, can be a useful solution for reducing the free space among fine-aggregates. Typically, the use of about 2 to 8 percent of aggregates smaller than 75 microns in pavement roller concrete is common (ACI 325.9 R) [4].

This study includes three consecutive parts. In the first part, materials and instruments were prepared and initial tests were performed to establish material properties. In the second part, material properties were checked with codes and proper mix design were defined by testing several initial mix designs. In the last part, main specimens were prepared and tests were conducted on 7, 14, 28, 42 and 90 days specimens.

In this research, we used nine mix designs based on 140 kg/m³ cement type-II and Iron ore powder, Iron ore concentrate, Coal Powder and Coke as filler materials passing sieve no. #100 (0.15>) by replacing 3% and 6% of coarse and fine-aggregate content. Finally, the results compared with mineral powder filler as control sample. In order to study the durability and mechanical properties of concrete; maximum density, VB time, compressive strength on 7, 14, 28, 42 and 90 days and 24-hour absorption of specimens on the day 28 were investigated.

2. EXPERIMENTAL PROGRAM

The material properties of the concrete mixture used in this experimental study has given in the following.

2.1. MATERIALS

2.1.1. *Aggregate*

Of 0–6, 6–12 and 12–25 mm grain size aggregate used in this study have been widely used in the civil projects in Kerman for years, provided from Gloomak Region. The aggregate grade was designed as existing between the curves of 2-4-3-A and 2-4-3-B defined in journal No. 55 Iran Standards [5]. The properties of these aggregates are presented in Table 1 and Figure 1, 2. The gradation curves of mixed aggregates consisted of coarse-aggregates (12-25 mm) (33%), fine-aggregates (6-12 mm) (22%) and fine-aggregates passing sieve No. 4 (4.75mm) (45%) compared with the limits set by ACI 207-5R standard, which presented in Figure 3 [6].

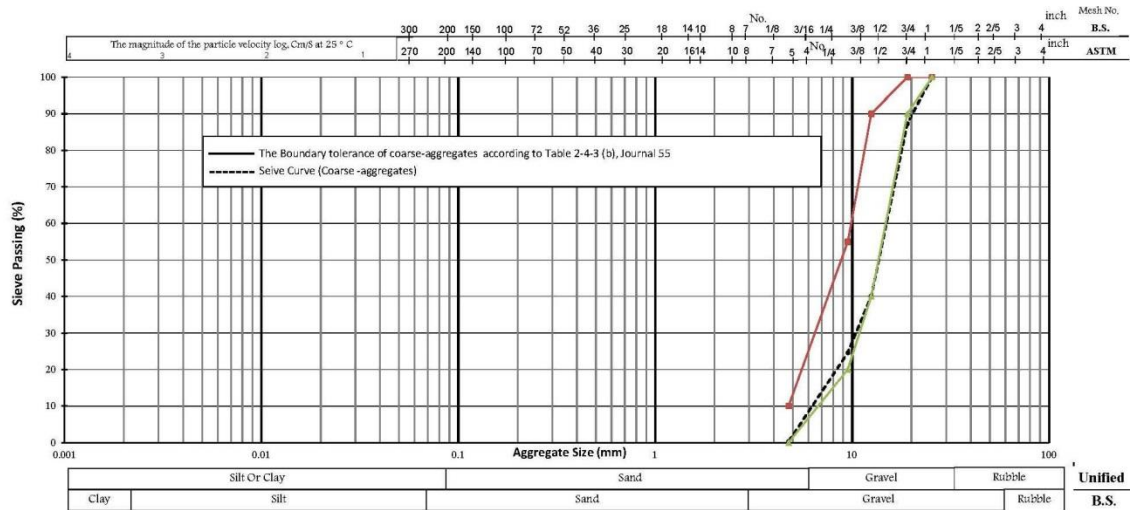


Fig. 1
Particle-Size Analysis of Coarse-aggregates (6-25 mm)

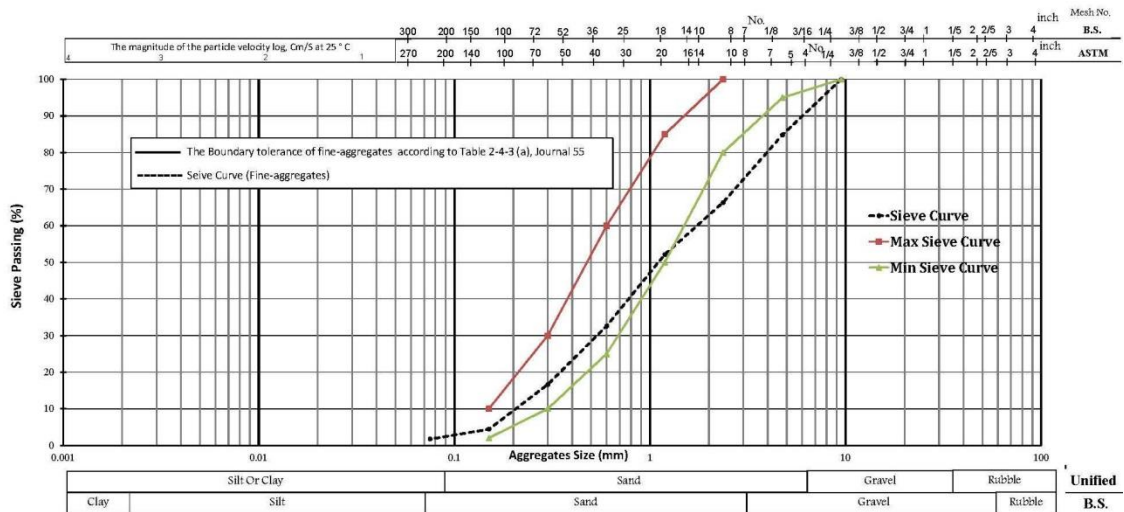


Fig. 2
Particle-Size Analysis of Fine-aggregates (0-6 mm)

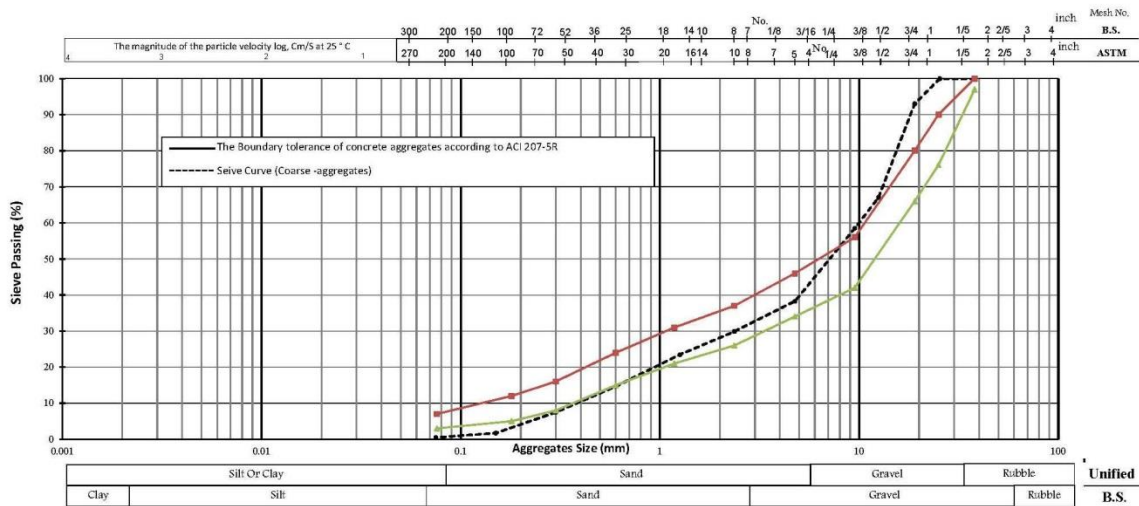


Fig. 3
Particle-Size Analysis of aggregates in Mix Design (0-25 mm)

Table 1. Physical Test results of aggregates

Density & Water absorption			fractions of aggregate	Ductility of aggregate	Prolongation Of aggregate	Lose weight of aggregates by Los Angeles Test			fineness Modulus	Materials
Water absorption %	Real Density (Kg/m ³)	Bulk Density (Kg/m ³)				abrasion %	RPM	Type		
0.8	2654	2703	51	10	18	23	500	B	-	Coarse Aggregates (10-25 mm)
1.1	2641	2712	66	18	12				-	Coarse Aggregates (5-10 mm)
2.0	2580	2720	-	-	-	-	-	-	3.43	Fine Aggregates (0-6 mm)

2.1.2. Cement

CEM – II type of cement in appropriate to Iran Standards used to prepare the concrete mixtures, which physical and chemical characteristics are given in Table 2 [7, 8].

Table 2. Chemical characteristic of cement

Physical characteristics	Value
Water Concentrate %	25
Autoclave %	0.01>
Specific gravity (gr/Cm ³)	3.16
Specific area (m ² /Kg)	316
Setting period (Minutes)	Initial setting: 170
	Final setting: 215
Compressive strength (Lb/in ²)	1 days: 1370
	3 days: 2210
	7 days: 2900
	28 days: 3530

Table 3. Physical characteristic of cement

Chemical characteristics	Value (%)
CaO	62.71
SO ₃	3.06
Cl ⁻	-
C ₃ S	51
C ₂ S	21
C ₃ A	5
Ignition Loss	1.92
Remaining Dissolved	0.42

2.1.3. Water

The water used for mixing the concrete mixtures of the experimental studies was potable and appropriate to the Iran Standards [9]. Water analysis results used in test mixtures gave in Table 4.

Table 4. Analysis results of the water used in test mixtures

Num	Examined Factors		Results		Concrete Standard*
1	PH	Acidity	7.9	-	7
2	EC	Electro Conductivity	1.28 (ds/m)	-	-
3	S.A.R.	Sodium Absorption Ratio	2.32	-	-
			Concentration as ppm	Concentration as meq/L	Concentration as ppm
4	Na ⁺	Sodium	108.1	4.7	-
5	Ca ²⁺	Calcium	96	4.8	-
6	Mg ²⁺	Magnesium	40.8	3.4	200
7	K ⁺	Potassium	0	0	-
8	Cl ⁻	Chloride	287.5	8.1	1000
9	HCO ₃ ⁻	Bi-carbonate	292.8	4.8	-
10	CO ₃ ²⁻	Carbonate	0	0	-
11	SO ₄ ²⁻	Soleplate	0	0	1000
12	TDS	Total dissolved solids	819.2	-	1000
13	TSS	Total Suspended solids	0	-	-
14	THD	Total Hardness	-	410	-
15	Na ₂ O+0.658 K ₂ O	Alkalinity	145.77.	-	600

Description: Section 9 "national building laws" by considering the medium environmental conditions

2.1.4. Filler

Typically, the number of aggregates passing through the sieve #100 called the filler. The filler used in this research is the waste of coke and iron ore concentrates factories with various percentages, which chemical characteristics gave in Table 5.

Table 5. Chemical characteristic of fillers %

	Iron ore Concentrate	Iron ore powder	Coke	Coal
C _{Fixed}	-	-	68.78	47.93
Volatile substances	-	-	9.26	32.65
Moisture	-	-	1.90	0.39
Ash	-	-	20.06	19.04
L.O.I	0.0	4.24	80.39	80.19
K ₂ O	01	0.47	0.85	0.91
SiO ₂	5.69	36.10	7.69	10.21
Fe ₂ O ₃	90.27	35.5	4.80	1.68
Cl	-	0.27	0.30	0.20
Al ₂ O ₃	0.69	5.02	3.77	4.78
TiO ₂	0.13	0.38	0.1	0.17
SO ₃	0.02	0.67	0.51	0.36
MgO	1.46	11.3	0.29	0.30
La&Lu	1>	1>	1>	1>
CaO	1.10	4.9	0.79	0.92
P ₂ O ₅	0.008	0.17	0.02	0.02
Na ₂ O	0.36	0.82	0.49	0.26

Waste Coal is one of the products of Zarand Coal Factory that obtained during the process of coal processing for the production of coke and consumption in iron melting furnaces.

3. IDENTIFICATION AND FORMULATION OF THE RCC MIXTURES

3.1. DETERMINE THE OPTIMUM WATER-CEMENT RATIO

A modify Vebe apparatus, which described in CRD-C 53 [10], used for determining the consistency of RCC. Since RCC mixture with Vebe time between 15 and 20 s has a sufficient workability [11]. The results showed on table 6.

Table 6. Water-cement ratio Results

Specific gravity of fresh concrete gr/Cm ³	Slump mm	Concrete Temp. ° C	Lab. Temp. ° C	VB time S	$\frac{W}{C}$
2.097	None	15.1	19.6	120>	0.35
2.154	None	18.0	19.8	120>	0.45
2.171	None	18.4	19.8	120>	0.55
2.320	0	18.8	19.8	45	0.80
2.395	0	17.7	19.5	15	0.80
2.372	0	18.0	20.4	34	0.7
2.349	0	18.4	20.8	18	0.75
2.365	0	23.2	21.9	18	0.80
2.375	0	20.5	19.6	22	0.75
2.268	0	21.7	19.9	19	0.80

3.2. SPECIMENS

In total, nine different concrete mixtures given in Table 7 prepared. Cylindrical samples used with height of 30 cm (12 in.) and diameter of 15.2 cm (6 in.). Samples made in three layers by vibrating method with Vebe table following the USBR 4906 [12]. Totally 72 specimens were made with 140 kg cement materials per cubic meter. Amount of 3% and 6% of total coarse and fine-aggregate materials were replaced by fillers in different mix design to investigate the effects of different amount of fillers. The results are shown on table 7.

Table 7. Mixing ratio (kg/m³)

$\frac{W}{C}$	Weight of water	Weight of fine-aggr.	Weight of coarse-aggr.	Weight of coarse-aggr.	Type of filler	Weight of filler	Weight of Cement	Specimens No.
0.8	112+34	945	460	690	6% mineral powder	130	140	RCC-1
0.8	112+34	945	460	690	6% iron concentrate	130	140	RCC-2
0.8	112+34	945	460	690	6% coke	130	140	RCC-3
0.8	112+34	945	460	690	3% mineral powder+3% iron concentrate	65 + 65	140	RCC-4
0.8	112+34	945	460	690	3% mineral powder+3% iron powder	65 + 65	140	RCC-5
0.8	112+34	945	460	690	6% iron powder	130	140	RCC-6
0.8	112+34	945	460	690	6% coal powder	130	140	RCC-7
0.8	112+34	945	460	690	3% mineral powder+3% coal	65 + 65	140	RCC-8
0.8	112+34	945	460	690	3% mineral powder+3% coke	65 + 65	140	RCC-9

Compressive strength test, workability test by VB time, water absorption test and compacted concrete density tests were conducted at the ages of 7, 14, 28, 42 and 90 days.

4. EXPERIMENTAL

4.1. VB TIME

A modified Vebe apparatus was used to determine the workability of mix designs. The results showed on table 8.

Table 8. Workability Results

Specific gravity of fresh concrete (gr/Cm ³)	VB Time (sec)	Specimens No.
2.298	18	RCC-1
2.336	18	RCC-2
2.191	105	RCC-3
2.395	15	RCC-4
2.326	16	RCC-5
2.361	38	RCC-6
2.205	40	RCC-7
2.251	36	RCC-8
2.229	36	RCC-9

4.2. 24-HOUR WATER ABSORPTION

24-hour Water absorption test on concrete specimens was performed according to ASTM C642 standard. The results showed in figure 4.

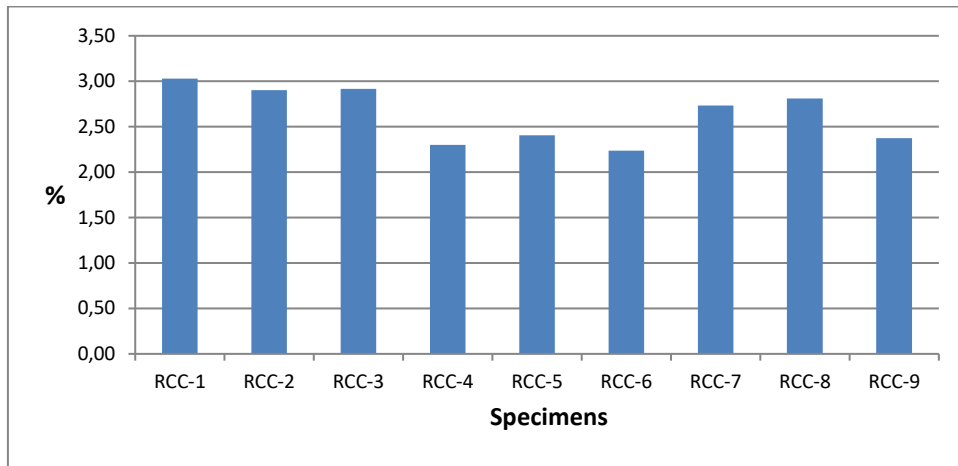


Fig. 4
24-hour water absorption

4.3. WEIGHT OF MASS

The specific density of concrete depends on the specific weight of the sand and the porosity of the roller concrete mass. There are a few air vents in roller concrete, varying between 0.5 and 5%, which reduces the action of compacting. The results showed in figure 5.

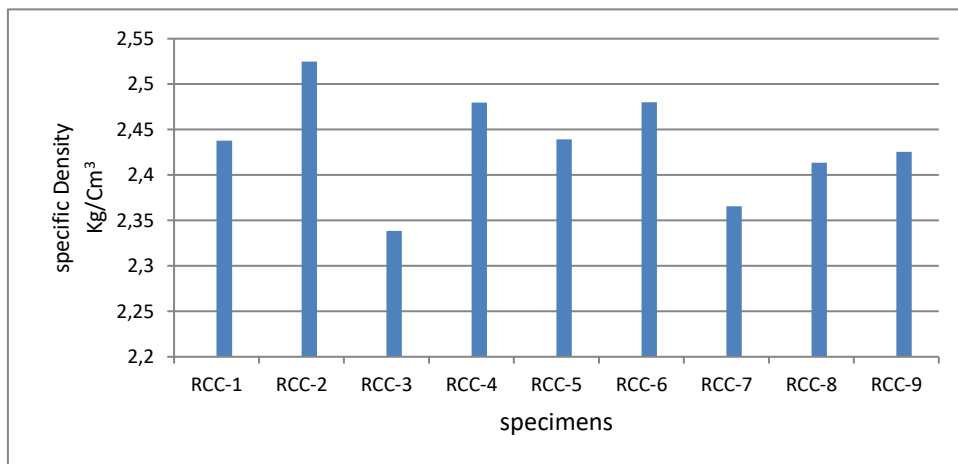


Fig. 5
Specific density of specimens

4.4. CONCRETE COMPRESSIVE STRENGTH

Compressive strengths results of the various mixes for ages of 7, 14, 28, 42 and 90 days presented in Fig. 6 to fig. 8. Comparatively to the reference concrete, at twenty days old, the increase in compressive strength was in the mix design for RCC6 with 6% iron ore powder filler. In a study, Friedin (2005) proved that the high levels of CaO and SO₃ in the ash of wind makes the wind ash have a good cement property and therefore gradually increases the compressive strength [13].

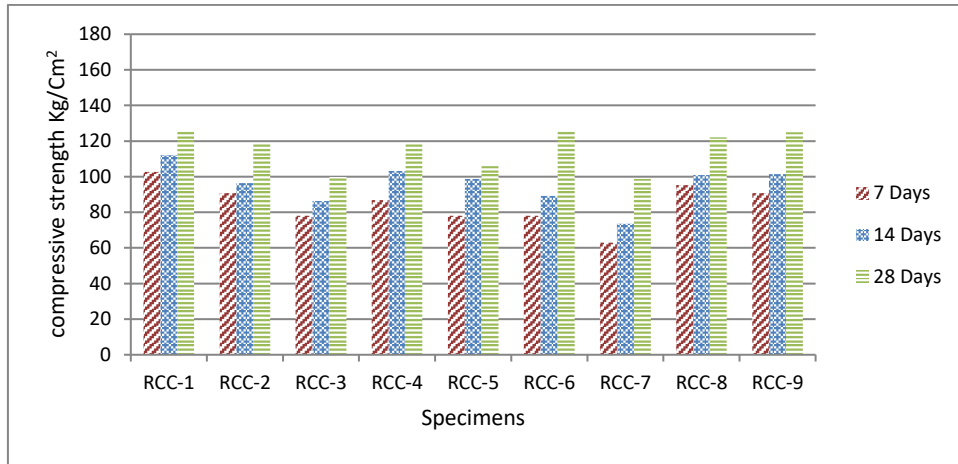


Fig. 6
7, 14, 28-days compressive strength results

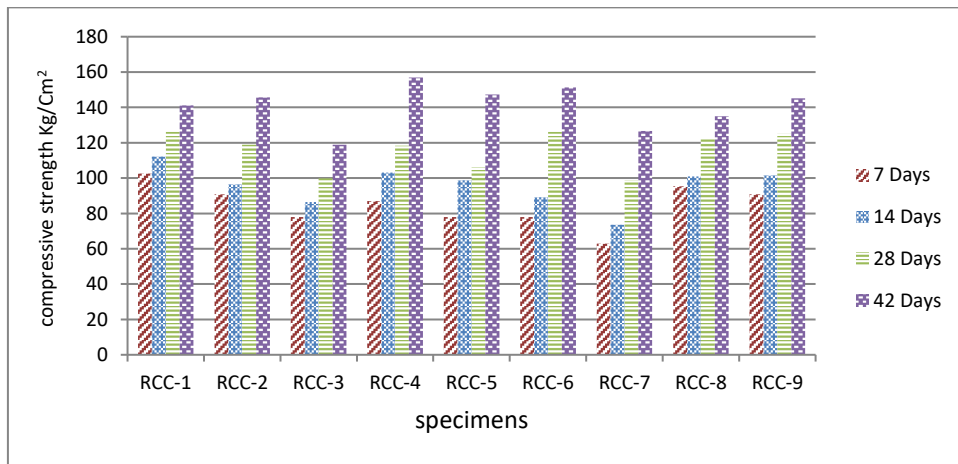


Fig. 7
7, 14, 28, 42-days compressive strength

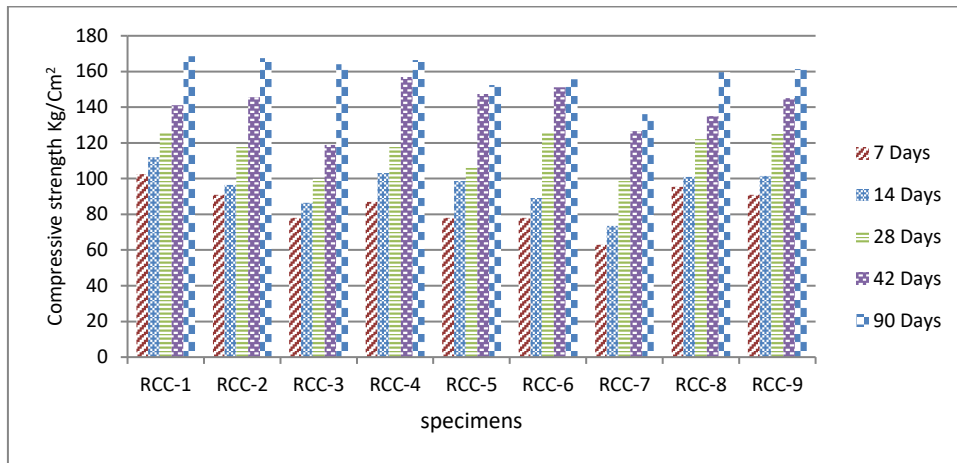


Fig. 8
7, 14, 28, 42, 90-days compressive strength

5. CONCLUSIONS

In this research, different fillers from coking and iron concentrate plants (passing sieve No. #100) made up of 6% of the aggregate's weight, and 3% of the filler along with 3% of the mineral powder filler has been used and investigated. The purpose of this study was to analyze the effect of various fillers on the roller concrete properties, concrete mechanical properties and its permeability. The results indicated a significant change in the mechanical properties and durability of the roller compacted concrete.

1. Using a high water percentage caused the segregation, which prevented by use of fillers to some extent. According to the design and time of VB, the optimal water-cement ratio was obtained in amount of 0.8 .
2. The highest 7-days compressive strength of concrete related to the RCC1 mixing design with the mineral powder filler indicated increasing compressive strength at the early ages.
3. The highest 28-days concrete compressive strength related to the RCC6 mixing design with Iron Ore Powder Filler indicated an increase in the final strength of the concrete at an advanced age by the filler.
4. The lowest compressive strength growth over time (90 days) observed in RCC1 and RCC3 mixing designs made with 6% mineral powder filler and 6% coke filler, which to some extent indicated that these fillers were not very effective in the cement hydration.
5. The best performance of compressive strength up to 28 days is related to the RCC6 mixing design containing 6% Iron Ore Powder Filler, which at the ages has more compressive strength and performance similar to that expected from Pozzolans.

6. The results of 24-hour water absorption of specimens showed that the minimum water absorption related to the RCC6 mixing design with iron ore-powder filler, with amount of 2.24%, which is acceptable and ideal for dam construction projects.
7. The lowest VB time measured in the study related to the RCC4 mixing design with 3% mineral powder filler and 3% iron ore concentrate with amount of 15 seconds.
8. By studying the results of the filler's chemical tests, iron ore powder knew to be close to the pozzolan group type F.

6. ACKNOWLEDGMENT

Funding for this study was provided by MANA Construction Company.

REFERENCES

- [1] USBR 4913. Procedure for water permeability of concrete.
- [2] J.F. Lamond, Significance of Tests and Properties of Concrete and Concrete-Making Materials, 2006, ISBN 0-8031-3367-7, pp. 595–601.
- [3] P.K. Mehta, P.J.M. Monteiro (Concrete: Microstructure, Properties, and Materials), fourth ed., 2014, ISBN 9780071797870.
- [4] American concrete Institute Committee 325.9R. Guide for construction of concrete pavements. *ACI Materials Journal* 2015.
- [5] M. Dehqani pour, 1389, Instructions for implementation of general technical projects on construction works based on the publication No. 55.
- [6] American concrete Institute Committee 207. Roller Compacted Concrete. 207.5R. *ACI Materials Journal* 1998.
- [7] ASTM C114 - 15 Standard Test Methods for Chemical Analysis of Hydraulic Cement.
- [8] Iran national standard, 392, standard methods for physical Analysis of Hydraulic Cement.
- [9] Development and Promotion of National Building Regulations Office, *ninth topic*, 1392.
- [10] CRD-C 53. Test method for consistency of no-slump concrete using the modified Vebe apparatus.
- [11] USBR. Roller compacted concrete, design and construction consideration for hydraulic structures. *Technical Service Center; 2005*.
- [12] USBR 4906. Casting no-slump concrete in cylinder molds using vibratory table
Freidin C. Influence of variability of oil shale fly ash on compressive strength of cementless building compounds. *Constr Build Mater* 2005;19:127–33.

COMMISSION INTERNATIONALE
DES GRANDS BARRAGES

VINGT-SIXIÈME CONGRÈS DES
GRANDS BARRAGES
Autriche, juillet 2018

OPERATION AND MAINTENANCE OF SABALAN DAM

Jamshid SADREKARIMI, Simin SHAHRADFAR, Atusa MIHANDOOST

ASHENAB CONSULTING ENGINEERS, DAM DEPARTMENT, TABRIZ

IRAN

ABSTRACT

Inspection and Monitoring of dams as well as data analysis and interpretation has a critical role in the field of dam safety. Surveillance and Monitoring programs on dams provide information for evaluating the dam`s performance with respect to design intent and expected behavior.

Sabalan dam is an 89 m high rock-fill embankment with central clay core constructed in the north west of Iran and has been operated since 2006.

The dam instrumentation system comprises variety of piezometers, total stress cells, settlement meters and inclinometers that are installed along 5 cross sections. In this paper, instrumentation scheme of Sabalan dam are described. Then the safety of the dam during operation is evaluated through the surveillance reports which have been prepared from records of the whole monitoring system.

The results indicated that the stability of the dam satisfies the safety requirements. The percentage of settlement is within the reasonable range and also stress and pore water pressure graphs indicate safety of the dam. Detailed results of the study are demonstrated through the text.

COMMISSION INTERNATIONALE DES GRANDS BARRAGES

VINGT-SIXIÈME CONGRÈS DES GRANDS BARRAGES

Autriche, juillet 2018

DOI 10.3217/978-3-85125-620-8-084



This work licensed under a Creative Commons Attribution 4.0 International License.

<https://creativecommons.org/licenses/by-nc-nd/4.0/>

RESEARCH OF RESERVOIR EMPTYING DESIGN OF HIGH DAMS IN CHINA

Liu Chao

CHINA RENEWABLE ENERGY ENGINEERING INSTITUTE, BEIJING 100120

CHINA

Zhao Quansheng

CHINA RENEWABLE ENERGY ENGINEERING INSTITUTE, BEIJING 100120

CHINA

Zhou Jianping

POWER CONSTRUCTION COOPERATION OF CHINA, LTD, BEIJING 100048

CHINA

RESEARCH OF RESERVOIR EMPTYING DESIGN OF HIGH DAMS IN CHINA

Liu Chao

China renewable energy engineering institute, Beijing 100120, China

Zhao Quansheng

China renewable energy engineering institute, Beijing 100120, China

Zhou Jianping

Power Construction Cooperation of China, Ltd, Beijing 100048, China

ABSTRACT

Emptying facilities of high dams play an important role for overhauling during operation period and lowering water level in case of emergency so as to reduce risk of the whole projects. Based on summarizing of present design status of reservoir emptying, the key technology problems of lower discharge facilities are analyzed firstly. Secondly, this paper puts forward that characteristics of reservoir and projects as well as hydrologic conditions should all be considered when emptying design to help choosing a reasonable emptying scale and depth. At the last, this paper indicates that the basin cascade dispatching and forewarning, manage systems of dams safety adapting to construction and economic level, as well as dams lifecycle safety management and risk distinction system suited to national conditions, should all be established as soon as possible, in order to minimize risk of basin cascading dams failure.

KEY WORDS

reservoir emptying; lower discharging; underwater overhaul; emergency management; basin cascade

PREFACE

Till 2017, more than 20 super high dams over 200m have been built or were under construction in China, which play an important role in the national economy development. After reservoirs impounding, it not only bring up benefit of flood controlling, irrigation and generating electricity, etc., but also pose a threat to downstream areas. There's no dam failure of large reservoirs occurred in China since 1980s, stood tests of big flood in 1998 and Wenchuan Earthquake in 2008, Ya'an Earthquake and so on. Especially Zipingpu CFRD of 156m height which is only 17km far from the epicenter of Wenchuan Earthquake and Shapai RCC arch

dam of 132m height which is 30km far from that in 2008, were both in good conditions ^[1]. In general, construction, operation and management of large reservoirs and high dams in China are all standard, and keep safety under designed situation ^[2].

However, along with more and more higher dams constructed, people are more and more worried about the losses and influence of public safety, social stability, and economic development coursed by dams' failure. In recent years, some new laws and legislations of security management in China put forward new requirements and research subjects to emergency management when dams suffer extraordinary floods, extremely strong earthquakes, or catastrophic geologic disasters. So, we have to reexamine the emptying design of large reservoirs constructed, summarize the key technology problems of reservoir emptying, and bring out some suggestions about how to improve the ability of emergency.

PRESENT EMPTYING ABILITY OF LARGE RESERVOIRS IN CHINA

Emptying facilities were set up in most of high dams in China to lower water level in case of emergency or dam damage. Table 1 and table 2 shows emptying abilities of primary high earth-rockfill dams and high concrete dams, respectively.

Table 1
Emptying abilities of primary high earth-rockfill dams

Projects	Dam height (m)	Storage capacity ($\times 10^8 m^3$)	Residual head after emptying (m)	Water head emptying ratio (%)	Residual capacity after emptying ($\times 10^8 m^3$)	Storage capacity emptying ratio (%)	Emptying time (d)
Pubugpu	186	50.11	81.4	56.24	1.06	97.88	55
Tianshengqiao I	178	83.3	60.3	66.11	2.31	97.23	78
Shuibuya	233.2	43.12	87.6	62.44	1.97	95.43	43
Tankeng	162	35.2	63.0	61.09	1.625	95.38	48.4
Shuangjiangkou	312	27.32	189.8	39.17	1.69	93.81	30
Malutang II	154	4.85	65.4	57.55	0.37	92.37	14
Houziyan	223.5	6.62	148.7	33.47	0.96	85.50	11.5
Nuozhadu	261.5	217.49	154.8	40.79	33.91	84.41	102
Hongjiadu	179.5	44.97	97.0	45.93	7.42	83.50	38.2
Liyuan	155	7.28	92.7	40.20	1.48	79.66	15
Lianghekou	295	101.5	178.8	39.39	20.78	79.53	87
Dongqing	150	8.824	94.3	37.11	1.91	78.35	17.3
Changheba	240	10.15	146.3	39.06	2.68	73.60	10.8
Quxue	164.2	1.2745	100.2	38.96	0.351	72.46	2.4
Bashan	160	2.93	98.0	38.71	1.5	48.81	10.4

Table 2
Emptying abilities of primary high concrete dams

Projects	Dam height (m)	Storage capacity ($\times 10^8 \text{m}^3$)	Residual head after emptying (m)	Water head emptying ratio (%)	Residual capacity after emptying ($\times 10^8 \text{m}^3$)	Storage capacity emptying ratio (%)	Emptying time (d)
Goupitan	232.5	55.64	500.3	58.41	1.811	96.75	43
Longtan	216.5	272.7	297.6	48.76	16.9	93.80	123
Xiaowan	294.5	146	1090.0	51.81	10.61	92.73	58
Guangzhao	200.5	31.5	646.0	50.77	2.6	91.75	42.5
Wudongde	270	58.86	895.0	31.13	5.604	90.48	62
Laxiwa	250	10.06	2340.8	45.96	1.35	86.58	30
Huangdeng	203	15.49	1549.0	35.53	2.23	85.60	15
Jingping I	305	77.6	1758.9	40.37	14.23	81.66	70
Dagangshan	210	7.42	1051.6	38.24	1.4	81.13	3.7
Xiluodu	285.5	115.7	504.7	34.59	27.74	76.02	30
Ertan	240	57.9	1135.0	27.66	15.26	73.64	7.2
Baihetan	289	190.06	736.3	31.67	51.39	72.96	39
Three Gorges	181	393	145.0	17.54	171.5	56.36	10

The two tables above indicate that, most reservoirs can be discharged more than half water head and 70% capacity which are mainly affected by hydrologic conditions, reservoir topography, dam height and design of emptying facilities. Storage capacities emptying ratios of those reservoirs located in alpine and narrow valleys are usually larger, such as Shuibuya CFRD and Wudongde arch dam. On the other hand, water head emptying ratios of those reservoirs located in wide valleys are usually larger, such as Three Gorges and Bashan dam. Specially, storage capacities emptying ratios of some reservoirs with special topography can reach up to 95%, while water head emptying ratios of those are just about 60%, such as Pubugou, Tianshengqiao I. As most of high dams with 300m height are located in alpine and narrow valleys in southwestern China, it is difficult to emptying the water head of reservoirs. In addition, the emptying time cost varies a great deal for different reservoirs.

KEY TECHNOLOGIES OF LOWER DISCHARGE FACILITIES

The most effective measure to emptying reservoirs is via lower discharge facilities, the key technologies of which are an important breakthrough of emptying design, including enhance emptying ability, shorten emptying time, routine maintenance, hydraulic problems and downstream protection.

ENHANCE EMPTYING ABILITY

Due to technology limitations of sluices and hoists, the intake elevation of emptying facilities cannot be set too low. The water head before the sluice of emptying facilities should not be greater than 120m usually, maximum 160m; otherwise the sluice will bear too large thrust. The water head and capacity been emptied are both limited. So it is very necessary to research the feasibility and rationality of lowering the intake elevation of emptying facilities.

SHORTEN THE EMPTYING TIME

Because of restriction by water thrust on sluice gate, the size of emptying tunnel cannot be designed too large and the discharge flow of it is limited. So the emptying time is too long sometimes to ensure the safety of projects. Such as Lianghekou project, the sluice gate size of emptying tunnel is 8m by 10m, while the water head before the gate reaches 125m, which need 87 days to discharge to designed emptying water level in dry season. So it is necessary to consider hydrologic conditions of both flood season and dry season as well as project investment to research the arrangement and structures of emptying facilities and then shorten the emptying time. The emptying facilities in China are designed considering the requirements of emptying for overhaul under exceptional circumstances in dry season.

ROUTINE MAINTENANCE OF EMPTYING FACILITIES

Usually, the emptying facilities cannot be used until the reservoir water level falls to a very low level. Most of them are rarely used and have very few chances to operate and be maintained. So it should be pay attention to how to make sure the emptying facilities can operate normally at key time. In addition, the intake of emptying facilities should not be set too low because of sediment deposition.

The intake elevation of bottom emptying outlets of Xiaowan arch dam (Fig. 1) is 1080m, which can be partly or must be totally opened when the reservoir water level is lower than 1160m or between 1160m and 1186m, respectively, and cannot be used when the water level is higher than 1186m. Nevertheless, as a multi-year regulating reservoir, the designed dead water level and flood season limited water level are 1166m and 1236m, respectively, much higher than 1186m. So it is obviously that the bottom emptying outlets have almost no chance to operate and be inspected.

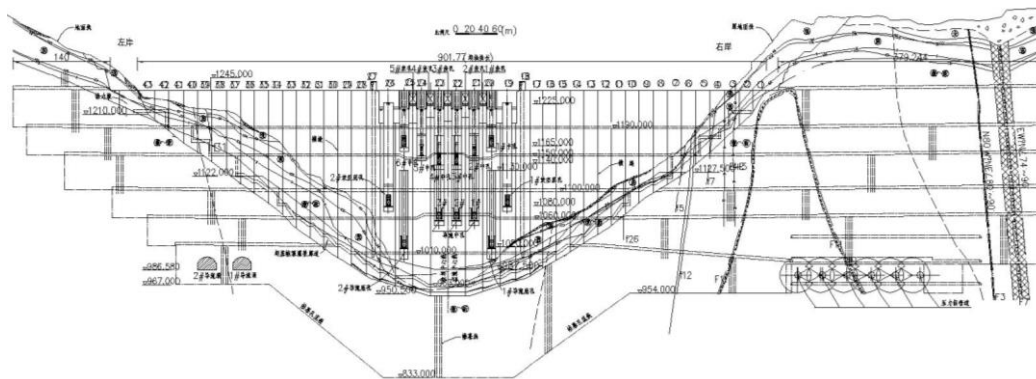


Fig. 1
Upstream vertical unfold view of Xiaowan arch dam

HYDRAULIC PROBLEMS AND DOWNSTREAM AREAS PROTECTION

The elevation of emptying facilities is much lower than any other discharge facilities. So the hydraulic problems such as high water level, high speed flow and cavitation when reservoir emptying, especially emergency emptying, along with energy dissipation and erosion control problems as well as investment should all be took into account. On the other hand, man-made extraordinary flood should not occurred in the downstream areas even if emergency emptying.

SUBJECTS NEED TO BE FURTHER RESEARCHED ABOUT EMPTYING DESIGN OF HIGH DAMS

The emptying requirements and process are much complex and some factors should be considered in the emptying design, including the relationships and requirements of integral safety degree and the water level for overhaul, hydrologic characteristics and downstream area flood control, arrangement conditions and sizes of emptying facilities as well as reservoirs slope stabilities when emptying. Through comprehensive and thematic analysis, a proper emptying ending water level and emptying facilities scale should be chosen to satisfy the dam overhaul requirements, ensure dam safety risk acceptable and prevent dam failures or other secondary disasters.

DAM INTEGRAL SAFETY DEGREE

The water thrust acted on concrete dams can be reduced by lower down the reservoir water level, which is very effective to increase the stabilities of dam foundation and dam abutment. In case of emergency, the first consideration is to enhance the dam integral safety degree as soon as possible, though that may cause excess concrete tensile stress at some local areas.

On the other hand, in case of non-emergency, it's better not to lower down the reservoirs water level too much to avoid excess concrete stress and crack, especially arch dams, to which, the temperature load is a kind of particularly sensitive load. In fact, majority loads of water thrust act on the higher part of arch dams. The total water thrust of Xiaowan arch dam with the height of 294.5m reaches 18 million tons. And half of the thrust act on the top 40m of the dam, while the other half act on the bottom 250m height left. So the integral stability of Xiaowan arch dam is enough safe after discharging to the designed emptying ending water level even if there is still 139.5m water head left.

The safety of embankment contains dam slope stability and seepage stability. When the anti-seepage is damaged, the seepage gradient of dam body behind the anti-seepage can be significantly reduced while the downstream slope stability been increased by lower the reservoirs water level, no matter earth core dam or concrete faced rockfill dam (CFRD).

DAM OVERHAUL CONDITIONS

Foundation galleries are usually set up in concrete dams, especially high dams. So the cracks in the upstream surface of dam body and seepage of dam basement can be handled by grouting in the foundation galleries, without emptying the reservoirs. However, some concrete dams developed cracks penetrating from upstream surface to foundations, which caused dam uplift pressures and leakage increase. In this case, the cracks have to be repaired by emptying the reservoirs instead of grouting only, such as Konbrien arch dam in Austria.

The key problem of embankment dams is overhauling conditions of anti-seepage systems. For earth core dams with foundation galleries, the effects of supplementary grouting under high water head are usually not good if the anti-seepage systems are damaged. So it is need to lower the reservoirs water level to reduce the seepage pressure and velocity in order to achieve good grouting effect. For CFRD, the biggest challenge is how to overhaul the broken seepage system. Clay blanket under the emptying ending water level is designed to protect the anti-seepage systems. But there are still some problems. The leakage position of Baiyun CFRD in Hunan province was just below the clay blanket, so the reservoir has to be emptying and clay blanket be dug out to overhaul the broken concrete face. Some research suggest that do not set clay blanket on the concrete face for convenience of overhaul. In the near future, the dam examine and overhauling may not be limited by the water depth along with the development of intelligent robots and detection technologies in deep water.

COMBINATION OF EMPTYING AND DISCHARGE FACILITIES

Usually, the intakes of emptying facilities are set too low and do not used to discharge flood or silt. Most of them are rarely used and have very few chances to operate and be maintained. So they may not be able to operate in case of emergency. Thus it should be considered to combine the emptying facilities and

routine discharge facilities so as to increase the operating frequency of emptying facilities. Thereby examine their status and repair them if necessary to ensure dams stabilities.

EMERGENCY EMPTYING STANDARD AND MANAGEMENT

(1) Emergency emptying standard

Different from overhauling emptying, extreme disaster at any time of the year must be considered in emergency emptying. Longtan dam for example, two bottom emptying outlets with the size of 5m by 10m were designed to discharge flow of 3210m³/s, 20-year return flood in dry season. However, if it is need to emptying 5-year return flood of the whole year emergently, the flow up to 14400m³/s, 4 more bottom emptying outlets with the same size should be designed, which will increase the investment in great deal. So, it is not economical and reasonable to solve the emergency risk only depending on emptying facilities. It should be deeply researched to choose a proper standard of emergency emptying.

(2) Dam emergency management

In case of extreme disaster or other risk, the reservoirs water level must be lower down rapidly, which may cause man-made extraordinary flood and bank slops stability problems. For example, the maximum discharge flow of Xiluodu arch dam reaches 49000m³/s, which will wreak destruction to downstream banks. Obviously, a professional emergency management institute at the national level should be set to decide whether to empty and discharge to which water level.

So, it is necessary to develop risk assessment mechanism and risk management technology, manage dam safety in case of emergency at the basin cascade and national level, and improve the dam safety management level [3].

SUMMARY

Based on summarizing of present design status of reservoir emptying, the key technology problems of lower discharge facilities are analyzed in this paper, and then some subjects need to be further researched are discussed.

(1) Reservoir emptying is to discharge the reservoir to a proper water level in order to keep the dam stability instead of discharging the entire reservoir.

(2) It is very important and effective to set emptying facilities to lower down the water level in emergency. Characteristics of reservoir and projects as well as hydrologic conditions should all be considered when emptying design to help choosing a reasonable emptying scale and depth.

(3) The key technologies of lower discharge facilities should be further researched in the future to break though the limited factors.

(4) The basin cascade dispatching and forewarning, manage systems of dams safety adapting to construction and economic level, as well as dams lifecycle safety management and risk distinction system suited to national conditions, should all be established and improved in order to minimize risk of basin cascading dams failure.

REFERENCE

- [1] Yan Zhiyong, Wang Bin, Zhou Jianping, et al. Seismic Damage Investigation and Analysis on Large and Medium Sized Hydropower Projects in Wenchuan Earthquake Area, China Water & Power Press, 2009.
- [2] Ministry of Water Resources, State Administration of Work Safety, National Energy Administration, State Electricity Regulatory Commission. General Safety Survey Report of National Large Reservoirs and Dams, 2013.
- [3] Li Lei, Wang Renkun, Sheng Jinbao, et al. Dam risk assessment and management, China Water & Power Press, 2006.

COMMISSION INTERNATIONALE DES GRANDS BARRAGES

VINGT-SIXIÈME CONGRÈS DES GRANDS BARRAGES
Autriche, juillet 2018

DOI 10.3217/978-3-85125-620-8-085



This work licensed under a Creative Commons Attribution 4.0 International License. <https://creativecommons.org/licenses/by-nc-nd/4.0/>

**VISUAL INSPECTION AND ASSESSMENT OF OPERATING DEVICES
IN IR. H. DJUANDA DAM - INDONESIA**

Harry M. SUNGGUH

Director II, JASA TIRTA II PUBLIC CORPORATION

INDONESIA

Reni MAYASARI

*Special Expertise Level I of Water Resources Management, JASA TIRTA II
PUBLIC CORPORATION*

INDONESIA

Budi NUGRAHA

*Special Expertise Level IV of Water Resources & Electric Data Management,
JASA TIRTA II PUBLIC CORPORATION*

INDONESIA

**VISUAL INSPECTION AND ASSESSMENT OF OPERATING DEVICES
IN IR. H. DJUANDA DAM - INDONESIA**

Harry M. SUNGGUH

Director II, JASA TIRTA II PUBLIC CORPORATION, INDONESIA

Reni MAYASARI

Special Expertise Level I of Water Resources Management, JASA TIRTA II
PUBLIC CORPORATION, INDONESIA

Budi NUGRAHA

*Special Expertise Level IV of Water Resources & Electric Data Management,
JASA TIRTA II PUBLIC CORPORATION, INDONESIA*

1. INTRODUCTION

Visual inspection is a visual inspection of ground and water inspection objects, such as dam surfaces, auxiliary buildings, ridges and reservoir cliffs, hydro mechanical equipment, instrumentation and so on. Reservoir Manager Ir. H. Djuanda performs visual inspections twice a year for dams located in his working area, which are around May - June at the time of the high water reservoir and November - December at the time the water level is low.

Visual inspection conducted includes inspection of dam Ir. H. Djuanda in Purwakarta District. The purpose of the visual inspection work is to find out as early as possible about the current state of the field on dams, complementary buildings and facilities for the purpose of encountering unusual things (anomalies) and / or symptoms that may threaten the safety of the dam so that immediate precautions are taken and risk reduction to the safety and safety of dams.

Visual inspection work consists of a series of inspection activities on dam bodies, complementary buildings, hilltop, rim (roving) reservoirs and the surrounding dam environment. Matters inspected during the visual inspection of the dam include cracks, seepage, leaks, basins, springs, burrows, erosion of surface erosion, abrasion scouring, excessive plant growth, top straightness, bulge or slope subsidence or berm, animal burrows of rip-rap quality deterioration as well as other slope protective materials. As for the concrete buildings are examined for cracks, crushing, dissolving, leaking, indication of deterioration of quality or chemical reaction, and or the damage caused by erosion and cavitation, the reliability of construction connections.

Based on the method of implementation, the inspection is divided into two types: visual inspection and underwater inspection. Visual inspection is a visual

inspection of ground and water inspection objects, such as dam surfaces, auxiliary buildings, ridges and reservoir cliffs, hydromechanical equipment and so on. The work of this inspection is a work performed by visual inspection method based on the March 2003 Safety Dam Inspection and Evaluation Guidelines published by the Ministry of Public Works. The steps taken against a finding on the ground during the visual inspection are S I M P L E i,e:

- a. Sketch: Drawing / Sketch that describes a finding in the field.
- b. Investigate: Investigate further on a finding in the field.
- c. Measure: Measuring dimensions of a field findings such as cracks, avalanches, leakage discharge and so on.
- d. Photograph: Take a picture / photo of a finding in the field.
- e. Locate: Marking the location / place of a find in the field is associated with easily recognizable objects such as shear, piezometer, Observation Well and so on.
- f. Engage: Engage experts or engineers who are experienced in visual inspection to be a resource person in consultation every problem that exists.

The tools and materials commonly used in visual inspection at Ir.H.Djuanda Dam include : Four-wheeled vehicles, camera, handy cam, meter tool 50 m and 5 m, stationery, handbags, cranes and steel cages as a means to descend to the bottom of the spillway during Hollow Jet Valve inspection, belt safety (Safe Belt) for Hollowjet Valve inspection, buoy (Life Vest) for Rim Reservoir inspection, boat (Speed Boat) for inspection Rim Reservoir, handheld GPS (Global Positioning Tool).

1.1. DAM IR. H. DJUANDA

Located approximately 100 km southeast of Jakarta and 60 km northwest of Bandung, Ir. H. Djuanda dam is a new urugan dam with clay core, irin (Rock Fill with Inclined Clay Core). It has four saddle dam (saddle dam), namely the saddle dam of Pasir Gombong Barat, Pasir Gombong Timur, Ciganea, and Ubrug. The main spillway shaped tower type of morning glory, which at the bottom also functions as a powerhouse, as "Fig.1".



Fig.1
Ir. H. Djuanda Dam

To assist in the event of a shortage of supply from downstream through the power cord, two irrigation supply channels (hollow jet valve) are available on the eve of +49 m.dpl, see as “Fig 2 and Fig.3”. Based on the result of the year 2000, the volume of TMA +107 m.dpl (normal pool level) of 2.448 million m³ with the puddle area of 81.3 km². The dam was built in 1957 and completed in 1967 on the Citarum River, with a catchment area of 4,500 km², while the catchment area directly to the reservoir after the construction of Saguling and Cirata Dam in the upper reaches 380 km².

Ir. H. Djuanda dam is a multipurpose dam, function as a hydropower plant with installed capacity of 187.5 MW, flood control in Karawang regency and Bekasi district, irrigation for 242,000 hectares of rice field in north coast of West Java, water supply for brackish water fishery cultivation along the west coast of West Java covering an area of 20,000 hectares and tourism.

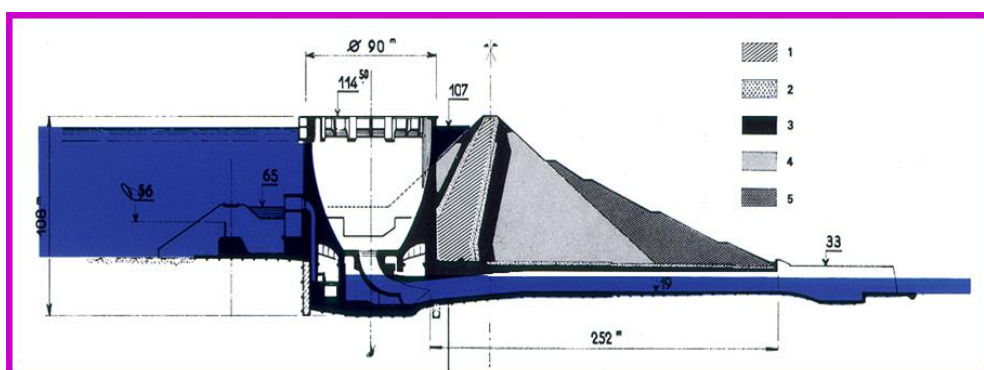


Fig.2
Profile of the main Dam Ir. H. Djuanda

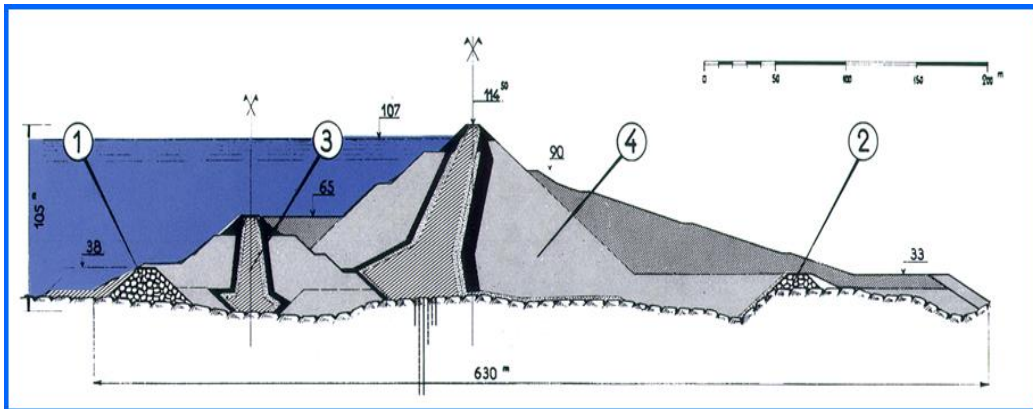


Fig.3
cross Section of the main Dam Ir. H. Djuanda

1.2. PASIR GOMBONG SADDLE DAM

Pasir Gombong saddle dam is a type of Homogenous Earth Fill dam with cover using andesite and some places using chimney drain. Elevation of the saddle hose +114.5 m.dpl. sand dunes sands west of 1950 m long, 19.0 m high maximum and sand dunes sands east of eastern with a length of 400 m, maximum height 15 m.

1.3. CIGANEA SADDLE DAM

The Ciganea saddle dam is a Homogenous Earth Fill type dam similar to the Pasaj Gombong Strip Dam with a cover using andesite rocks and in some places using Chimney Drain. Peak shedd elevation +114.5 m.dpl. the length of this saddle dam is 330 m, the maximum height is 12.5 m.

1.4. UBRUG SADDLE DAM

The Ubrug saddleback is also a Homogenous Earth Fill type dam similar to Pasir Gombong saddle dam with a cover with andesite stone and in some places using Chimney Drain. Peak shed elevation +114.5 m.dpl. The length of this saddle dam is 550 m, the maximum height of 17 m is equipped with an overflow auxiliary. Overflow aids at the Ubrug Saddle Dam has 4 (four) doors with a width of 12.4 m, elevation of overflow floor +102 m.dpl with abundance capacity 2000 m³ / sec.

2. IR H. DJUANDA VISUAL INSPECTION

Based on the results of visual inspection and observation of the dam body and its complementary building, that in general the dam Ir. H. Djuanda relatively good and normal, with the condition of findings in the field, among others:

1. On the hillside there are several rip-rap rock spots happening dislocations, and found grass and shrubs plants growing on the sidelines of rip-rap stones.
2. On the slopes downstream on the sidelines still visible grass and shrubs that grow, the frequency of grass that needs to be reproduced so that the roots of the plant does not penetrate the body of the dam that could be the outlet of water seepage on the lining wall structure and lining paving blocks access road to the dock.
3. Generally the condition of instrumentation in the main dam is relatively good, but on OW5 protective wall made of concrete slab looks damaged and not closed. The accelerometer installed in the Access Gallery of the tool is damaged, the error sign continues and the voltage indicator panel shows 5.4 volts which should be +/- 11 volts. The condition of the surface monument has small damage to the slope (surface monument) which is located at the upper lining of the dam top.
4. Conditions of drainage channels in some places at the foot of the dam and downstream areas appear to be clogged with soil, moss and grass so that the water flow cannot flow smoothly and inundated.
5. Rip-rap conditions are generally good, but need to be weaned and additions around the C2 sliding mark downstream.

3. TOWER MAIN TOWER AND ACCESS GALLERY INSPECTION

Based on visual inspection and observation of the main spillway tower, Access Gallery and its complementary building. In general the condition of the main spillway tower and access gallery is relatively good and normal, with the condition of findings in the field, among others:

- a. The connection between the plates on the bridge ladder has already started to loose due to run out by rust. And at some point bridge paint floor has begun to fade, the handrail and steel rope reinforcement on the right and left side of the bridge looks still pretty good.
- b. There are cracks in the 3 concrete joints under the rails. Found the wild vegetation around joint 9 then on joint 11. Three Dimension Instrument (3D) Joint Apparatus looks rusty start and surface pin is not flat. The 3D Joint Apparatus protective cover is largely unlocked because the lock nut is missing. The sliding mark on the shoulders of the tower must be re-painted because the

paint has begun to fade. Home / Box AWLR (automatic Water Level Recorder) SESAME must be repaired.

- c. The condition of the ladder that is on the wall inside the spillway looks rusty.
- d. The wet location or seepage trace is found in joint G0. The concrete connection is observed by 3 (three) Dimension Joint Apparatus. The condition of the former leakage monitoring tool in joint 0 that is Rive Droite (RD) and Rive Gauche (RG) still looks stagnant due to drainage of seepage see page clogged, If will be measured discharge leakage RD and RG must first pumped. Therefore the measurements of the RD and RG leakage discharges are now done in a new place through two pipes connected directly to the directional pipe steering join 0. The sliding benchmark in the Access Gallery is mostly without a protective cover.
- e. In the ceiling space re-cavitation occurs on the concrete wall that has been done with the addition of using cement. Corrosion section contained in the cooling pipe casing on the staircase entering the ceiling has not been repaired.
- f. In the left sump Pit found cracks in the concrete wall, concrete and concrete floor joints drainage see page (sump pit) left, so the concrete floor is relatively slippery when skipped.
- g. The condition of the right collecting drum space (sump pit) mostly cavitation, moist and wet. The wet location is found almost in all the right (sump pit) areas, so the concrete floor is relatively slippery when skipped.
- h. The condition of the bouchon, the tap (gate valve) to open the waterway has been consumed by corrosion. Condition of concrete wall, and concrete connection experience cavitation, moist and wet. Wet locations and puddles are found only on the side of the baton wall around the entrance hall.
- i. The intake room of the riva pump is inundated about 2 meters deep and needs to be addressed immediately because of mild corrosion.
- j. The old cracks in the majority of concrete are found in the interior walls of the circle and a small part is found in the exterior circle but the condition does not change significantly.
- k. The old vapor that forms the cavity to the right of the tailrace (about 20 m to the left of OW IC748) has been repaired by means of the extraction and compaction of the material.
- l. Elevators contained in the access gallery is not working and severely damaged (high corrosive) as well as around the elevator door area often leaks. The protective cable cover (concrete plate) at the top of the tower is partially cracked.

4. SADDLE DAM INSPECTION

4.1. PASIR GOMBONG BARAT SADDLE DAM

Generally the condition of Pasir Gombong Barat Saddle dam relatively good and normal with visual observation conditions as follows:

- a) Avalanche / sliding in downstream profile 32 and profile 17 handling not entirely.
- b) Some of the stucco slabs are plastered and there are many streaks.
- c) In the downstream area there are many rushes on the drainage especially the lining of the stone pairs.
- d) Water supply to basecamp does not exist.

4.2. PASIR GOMBONG TIMUR SADDLE DAM

Generally, the condition of Pasir Gombong Timur Saddle Dam is relatively good and normal with visual observation conditions as follows:

- 1) The old erosion occurring in the original soil near the R42 and R44 profiles still has not been handled. There is still a wet / muddy area that has not formed a puddle on the original soil to the left of the R46B shear and the wet area around the R42b shear. There is erosion on the hillside to the left of the dam hill slope caused by water abrasion.
- 2) In the downstream of Pasir Gombong Timur saddle dam still found many surface erosion on the original soil.

4.3. CIGANEA SADDLE DAM

In general, the saddle cave dam conditions are relatively normal and normal with visual observation conditions as follows:

- 1) Drainage holes in the hills and downstream of the saddle dam are partially clogged up by soil deposits and garbage.
- 2) Some parts of the lining of the upstream and downstream of the saddle dam are still visible damage to the stone pairs.
- 3) Wild grass and shrubs are seen along the top of the saddle dam, on the sidelines of the ripa-rap of the upstream slope and downstream slope.
- 4) Livestock poultry found in some places on the original soil downstream of the saddle dam.

4.4. UBRUG SADDLE DAM

In general, Ubrug saddle dam conditions are relatively good and normal with visual observation conditions as follows:

- 1) There are cracks along the 11 meters wide 50 cm in 30 between the c.10 -c.11 segment.
- 2) There is still original soil erosion near the downstream drainage next to the emergency spillway.
- 3) The protective building of the instrumentation apparatus in the downstream area of the partially damaged partition (rock pairs on the loose wall) and part of the protective cover is lost.
- 4) Drainage system overgrown with weeds and there is damage to the lining of stone pairs.
- 5) The position of the right collector building is not suitable, the drainage channel is higher than the position of the container tub.
- 6) Grasses and herbaceous plants are still visible in several places on the sidelines of the hill and downstream of the dam, rip-rap hillsides and rafting downstream.

5. RESEVOIRS RIM INSPECTION

In general the condition of the reservoir rim is relatively good and normal with the visual observation conditions as follows:

1. Found water vegetation in the form of water hyacinth in Cimanggu area.
2. There are many patches of illegal floating net cages in the Pasir Gombang Barat, Madang, Kertamanah, Pagadungan - Sukasari, Sukasari - Sodong, Cilendi and Jamaras – Tajur Sindang area.
3. More and more fishing rafts on the edge of the reservoir between the main dam – pasir gombang and Pagadungan area.
4. More and more non-permanent buildings and floating buildings in the puddle area and side of lake reservoir Sukasari, Cidadap, Cimanggu, Bojong, Warung Jeruk, Cilangobar, Sindang, Ciganea - Ubrug area, which is used by the community to trade and as a place of residence that has the potential to produce waste is relatively large.
5. Found erosion and landslides and landslide potential in the right bluff that is wide enough around the outlet Cirata reservoir.

CONCLUSION

Ir. H. Djuanda Dam is one of the largest dams and the first multipurpose dam in Indonesia. The dam with an area of 8,300 ha was built by the French franchise contractor Compagnie francaise d'entreprise in 1957 and completed in 1967, with a water potential of approximately 12.9 billion m³ / year. The capacity of this dam is 2.44 billion m³.

Visual inspection of large dams Ir. H. Djuanda is a routine activity undertaken in the context of monitoring activities on dam safety. Visual inspection is done periodically and continuously to get the latest visual data about the condition of Dam Ir. H. Djuanda. Visual inspection is important because not all changes in the condition and behavior of the dam can be described from the measurement or reading of the instrument. This visual inspection is done twice a year i.e May - June at high water level and November - December when the water level is low.

Visual inspection activities consist of a series of inspection activities on dam bodies, complementary buildings, hilltop, rim (roving) reservoirs and the surrounding dam environment. Matters inspected during the visual inspection of the dam include leakage, basement, springs, evaporator, erosion eruption, surface erosion, scouring, abrasion, excessive plant growth, top straightness, protrusion or subsidence of slopes, animals, deterioration of rip-rap quality as well as other slope protective materials. As for the concrete buildings are examined for cracks, crushing, dissolving, leaking, indication of deterioration of quality or chemical reaction and or damage due to erosion and cavitation, the stability of construction joints.

The method of inspection implementation is divided into 2 types: visual inspection and underwater inspection. Visual inspection is a visual inspection of the ground and water inspection objects, such as dam surfaces, auxiliary buildings, ridges and reservoir cliffs, hydro mechanical equipment and so on.

Based on the results of visual inspection and observation of the dam body, main spillway towers, access galleries, saddle dam bodies, reservoir reefs and complementary buildings that are generally in relatively good condition and normal.

REFERENCE

[1] DIRECTORATE GENERAL OF WATER RESOURCES, Ministry of Public Works, Guidelines for Inspection and Evaluation of Dam Safety, March 2003.

[2] JASA TIRTA II PUBLIC CORPORATION, Report Six Monthly Visual Inspection Dam Ir. H. Djuanda, 2017.

[3] GOVERNMENT REGULATION No.37 Year 2010 on Dams.

[4] JASA TIRTA II PUBLIC CORPORATION, Quality System Document No. 1 / DL / PT / 30.21 applied in Jasa Tirta II Public Corporation on Dam Monitoring and Reporting and Operational Guidance of dam monitoring unit

COMMISSION INTERNATIONALE DES GRANDS BARRAGES

VINGT-SIXIÈME CONGRÈS DES GRANDS BARRAGES
Autriche, juillet 2018

DOI 10.3217/978-3-85125-620-8-086



This work licensed under a Creative Commons Attribution 4.0 International License. <https://creativecommons.org/licenses/by-nc-nd/4.0/>

EVENT TREE CONCEPT FOR DESCRIBING THE RELIABILITY OF GATED WEIRS AND SPILLWAYS

Markus AUFLEGER

Head of the Unit Hydraulic Engineering, UNIVERSITY OF INNSBRUCK

AUSTRIA

Barbara BRINKMEIER

PostDoc at the Unit Hydraulic Engineering, UNIVERSITY OF INNSBRUCK

AUSTRIA

EVENT TREE CONCEPT FOR DESCRIBING THE RELIABILITY OF GATED WEIRS AND SPILLWAYS

Markus AUFLEGER

Head of the Unit Hydraulic Engineering, UNIVERSITY OF INNSBRUCK

Barbara BRINKMEIER

PostDoc at the Unit Hydraulic Engineering, UNIVERSITY OF INNSBRUCK

AUSTRIA

1. INTRODUCTION

The safety and reliability of dams and weirs depend – among other things – on the functionality and reliability of the gates, which are used to control the flow. Various design approaches exist in different countries. In Germany and Austria and numerous other countries, the so called (n-1) – condition has to be met when designing the gates of dams and weirs [1]. This deterministic design concept aims at a safe discharge of the design flood, assuming one gate is out of operation. Typically, the return period of the design flood is of the order of 100 years for weirs and 1.000 to 5.000 years for the spillways of large dams.

In addition to the above mentioned design flood, which has to be discharged through (n-1) gates, typically a much higher ‘check flood’ has to be passed through the weir or spillway in a safe way. In Germany this ‘second design flood’ (or ‘check flood’) has a return period of 1.000 years for large weirs and 10.000 years for large dams, whereby all available openings and outlets can be used for flood discharge. The specific design rules for the safe passage of the ‘check flood’ vary significantly between different countries.

In many cases the (n-1) concept ensures a very robust and safe hydraulic design of weirs and spillways weirs. The probabilistic approach behind this concept is that the coincidence of a blockage of two or more gates with a design flood is very unlikely.

Anyhow, there remains a number of aspects which cannot be taken into account with this very clear and simple (n-1) - approach, among other things

- the number of gates
- the type of gates
- the revision concept
- the steering units (inter alia reliability and type)
- the power supply (inter alia redundancy).

In many cases existing weirs and less frequently existing spillways do not fulfil the (n-1)-criteria. Many of them were carefully investigated and upgraded with additional measures (e.g. additional lifting units). For proofing the reliability of

these structures despite the missing possibility of passing the design flood through (n-1) gates a more sophisticated method using the (n-a)-concept [2] is being used since decades. The parameter 'a' considers both the revision and the malfunction of the gates. Under favourable conditions 'a' can accommodate values lower than 1.0.

The event tree concept presented below can be considered as a base for a future alternative way for determining and proving the reliability of gated weirs and spillways if the (n-1)-criteria cannot be fulfilled. It should be understood as a useful supplement to the very robust (n-1) design method. The event tree concept does not strive to replace any check flood design cases.

2. EVENT TREE CONCEPT

2.1. BASICS

A new design approach, that has the potential to replace respectively to complement the (n-1) condition, was developed at the University of Innsbruck in cooperation with different partners. It is based on the idea, that the required level of safety is determined at the beginning of the design process. For example, it is accepted for weirs, that the maximum operation water level in the reservoir is exceeded with a probability of 0.01 each year (return period of 100 years).

The design has to take into account four variables: the number of gates, the total capacity of the weir respectively the spillway of the dam, the duration of 'critical works', where the gates or their drive systems are under revision and not available for flood discharge, and the probability of the malfunction of one gate. Empirical values for the latter two variables have to be defined carefully. Within the scope of this critical step of the conceptual work for the event tree concept data gained from literature, experiences of the operators and fundamental considerations concerning the overall safety level have to be taken into account.

The present paper will explain the basic design approach in detail. Detailed recommendations for the numerical values of the related variables for the duration of the critical works and the probability of the malfunction of on gate will be given after a period of detailed investigations, comprehensive discussions and sound verifications.

Generally, the event tree concept can be applied for all kind of weirs and spillways with very different gated and not gated openings. Anyhow, within the scope of the present work the presentations, relations and equations are related to gated weirs and spillways with an optional number of gates of the same size and type.

2.2. EVENT TREE

The key of the event tree concept is the consequent presentation of the events, which can happen if a flood approaches a weir or a spillway (Fig. 1). In a first differentiation it has to be checked whether the gate or weir field is blocked due to critical works.

The variable $d_{C,G}$ describes the number of days of 'critical works' per year for one gate. Critical works are defined as works during which an ad hoc opening of a gate would not be possible. Hereby any kind of inspection, revision and replacement works have to be taken into account.

The value $\alpha_{C,G}$ (Eq. 1) shows the probability that one specific gate is being blocked by critical works at any time. If n is the number of gates, consequently p_B describes the probability that one of the n existing gates is being blocked by critical works at any time (Eq. 2.).

It can be ruled out that more than one gate is being blocked by critical works at the same time.

$$\alpha_{C,G} = \frac{d_{C,G} [d]}{365,24 [d]} \quad [-] \quad [1]$$

$$p_B = n \cdot \alpha_{C,G} \quad [-] \quad [2]$$

Within the scope of a second and much more comprehensive differentiation it has to be checked whether it is possible to open every single gate during a flood event. In order to enable this evaluation the probability of a malfunction of one gate has to be defined. Consequently the related statistical parameter p_F describes the fundamental probability that it is not possible to open one gate at any time. In order to allow a much better understanding of this parameter its reciprocal value ' f ' shall be used (Eq. 3). This means that in an estimate, which has to be very much on the safe side, one specific gate has to be considered as not properly working within the scope of each f^{th} gate opening. Gates, where little or no external forces are needed for opening (e.g. flap gates oder rubber dams), will show much higher values of ' f ' compared to other gates like radial gates or even slide gates, where the function of mechanical steering units and a power supply are mandatory for a successful opening.

$$p_F = \frac{1}{f} \quad [-] \quad [3]$$

By using the two newly introduced paramters p_B and p_F a complete event tree in the case of an approaching flood can be set up (Fig. 1). Typically the probabilities of the occurance of two of even three gates not working properly will be very little. Anyhow, for the purpose of a universally applicable approach these very unlikely scenarios shall be kept at that time. The event tree can be set up for an optional number of gates (greater than 1). The example shown below (Fig. 1) shows the potential szenarios for a weir with four gates.

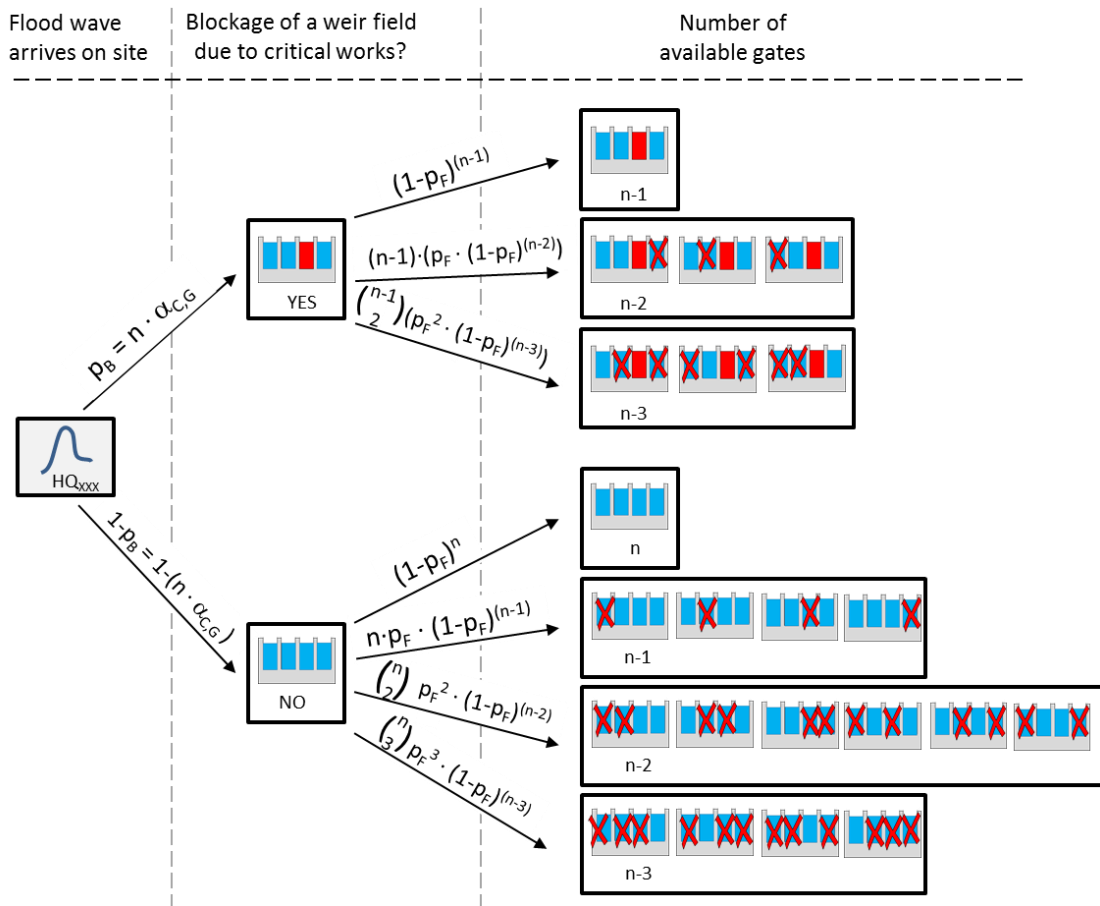


Fig. 1

Event Tree (Example for a weir with four gates and a design flood with a return period of 100 years)

2.3. STATISTICAL DESCRIPTION OF THE FAILURE PROBABILITY

In a next step it is required to determine the probability p_D of a hydraulic respectively hydrological 'failure' by considering all scenarios shown in the set-up of the event tree (see above). Hereby 'failure' is defined as the exceeding of the maximum operation water level in the reservoir. Practically this situation is far away from a structural failure of the concrete structure of the weir or the related embankment dams. The additional freeboard respectively the vertical distance between the maximum water level and the dam crest or the top edge of the sealing element will not be considered directly within the scope of the event tree concept.

To enable a statistical description of the related probability p_D it becomes necessary to determine the return period of the maximal possible flows passing through the weir respectively spillway in all relevant scenarios [Q_n , Q_{n-1} , potentially also Q_{n-2} and Q_{n-3}] defined within the scope of the event tree. This can

be done either by applying site specific flood statistics or simplified statistical approaches based on typical statistical characteristics (e.g. HQ₅₀, HQ₁₀₀, HQ₁₀₀₀). The reciprocal values of these return periods lead to the related probabilities $p(Q_n)$, $p(Q_{n-1})$ etc..

By merging these expressions and relations with the event tree it becomes possible to formulate a simple but long equation for the determination of the 'failure probability' p_D (Eq. 4).

$$\begin{aligned}
 p_D = & (1 - p_B) \cdot (1 - p_F)^n \cdot p(Q_n) & [4] \\
 + & [p_B \cdot (1 - p_F)^{(n-1)} + (1 - p_B) \cdot n \cdot p_F \cdot (1 - p_F)^{(n-1)}] \cdot p(Q_{n-1}) \\
 + & [p_B \cdot (n-1) \cdot p_F \cdot (1 - p_F)^{(n-2)} + (1 - p_B) \cdot \binom{n}{2} \cdot p_F^2 \cdot (1 - p_F)^{(n-2)}] \cdot p(Q_{n-2}) \\
 + & [p_B \cdot \binom{n-1}{2} \cdot p_F^2 \cdot (1 - p_F)^{(n-3)} + (1 - p_B) \cdot \binom{n}{3} \cdot p_F^3 \cdot (1 - p_F)^{(n-3)}] \cdot p(Q_{n-3}) \quad [-]
 \end{aligned}$$

3. OUTLOOK

By referring the above introduced failure probability p_D to the required safety level in the specific load case (e.g. a return period of 100 years for passing the design flood through a weir) it will become possible to determine the required capacity of the weir respectively the spillway. Hereby the site specific conditions (duration of the critical works and the probability of the malfunction of a gate) have to be taken into consideration. This procedure based on the event tree concept enables an adequate determination of the safety level at different sites under very different conditions (e.g. number and type of gates). The biggest challenge for their successful application will be the appropriate determination of suitable input parameters on the safe side.

REFERENCES

- [1] Deutsches Institut für Normung. Normenausschuss Wasserwesen. DIN 19700-13 2004.
- [2] DVWK. DVWK Merkblatt 216, Betrachtungen zur (n-1)-Bedingung an Wehren 1990.

KEYWORDS

SAFETY OF DAMS, GATES

COMMISSION INTERNATIONALE DES GRANDS BARRAGES

VINGT-SIXIÈME CONGRÈS DES GRANDS BARRAGES
Autriche, juillet 2018

DOI 10.3217/978-3-85125-620-8-087



This work licensed under a Creative Commons Attribution 4.0 International License. <https://creativecommons.org/licenses/by-nc-nd/4.0/>

**VEGETATION EFFECT ON RELIABILITY ANALYSIS OF SLOPE STABILITY
USING MONTE CARLO SIMULATION**

Iman VAEZI

Geotechnical Engineer, PEY AB AZMA CONSULTING ENGINEERS
IRANIAN COMMITTEE ON LARGE DAMS

IRAN

Hesam SAEIDI

Data analyst, PEY AB AZMA CONSULTING ENGINEERS

IRAN

Ali NOOZAD

Faculty member, Faculty of Civil, Water and Environmental Engineering,
SHAHID BEHESHTI UNIVERSITY
IRANIAN COMMITTEE ON LARGE DAMS

IRAN

COMMISSION INTERNATIONALE
DES GRANDS BARRAGES

VINGT-SIXIÈME CONGRÈS DES
GRANDS BARRAGES
Autriche, juillet 2018

VEGETATION EFFECT ON RELIABILITY ANALYSIS OF SLOPE STABILITY USING MONTE CARLO SIMULATION

Iman VAEZI^{1,4}, Hesam SAEIDI², Ali NOOZAD^{3,4}

1. *Geotechnical Engineer*, PEY AB AZMA CONSULTING ENGINEERS
2. *Data analyst*, PEY AB AZMA CONSULTING ENGINEERS
3. *Faculty member, Faculty of Civil, Water and Environmental Engineering*, SHAHID BEHESHTI UNIVERSITY
4. IRANIAN COMMITTEE ON LARGE DAMS

IRAN

1. INTRODUCTION

The necessity of dam construction is *prima facie* principle in arid or semiarid regions. As an inevitable consequence in dam construction, unnatural slopes around dam body and reservoir are formed and usually devoid of vegetation. Failures of those slopes can have a significant cost. Translational failure is defined as linear movement along a bedding plane or a soil layer lying near to the surface. Such movements are normally fairly shallow and parallel to the surface [1].

Vegetation surely affects hydrological and mechanical properties of slopes related to slope stability and shallow landslide triggering. The most important and general problem is a shallow seated instability of a slope [2]. Based on the complexity of soil-plant mechanical interactions, the quantification of root mechanical reinforcement remains a challenge. On the other hand, considering the failure mode and uncertainty in geotechnical and vegetation parameters, it seems that using probability theory in slope analysis is inescapable. The aim of this study is evaluation of increased shallow landslide resistance of a slope due to vegetation considering uncertainty of related parameters. With reliability analysis it is possible to quantify the uncertainties involved in the problem and to determine safety factor according to the degree of uncertainty and acceptable risk.

2. UNCERTAINTY AND RISK

In contrast with some engineering fields dealing with man-made materials, geotechnical engineers deal with geometries and materials provided by nature. These natural conditions are unknown to the designer and should be inferred from limited and costly observations. The principal uncertainties have to do with the accuracy and completeness with which subsurface conditions are known and with the resistances that the materials will be able to mobilize. The uncertainties in geotechnical engineering are largely inductive: starting from limited observations, judgment, knowledge of geology and ecology, and statistical reasoning are employed to infer the behavior of a poorly-defined universe [3].

In engineering contexts, risk is commonly defined as the product of probability and consequence, or expressed another way, risk is taken as the expectation of adverse outcome. Risk assessment provides proper opportunity to experts with considering uncertain data related to slope safety decisions, to evaluate qualitative and quantitative assessment of slope safety. Hence, experts finally take appropriate economical and practical decisions. Quantitative risk assessment includes risk analysis, risk assessment and management. Risk management is consideration of the risk analysis along with risk control that threatens safety. Risk control is one of important parts of safety management, which includes review of alternatives in dealing with risks such as risk mitigation, risk acceptance and risk avoidance[4,5].

3. VEGETATION EFFECT

To assess the safety of a slope to prevent human casualties and economic losses, it is necessary to find out the ways in which soil and vegetation interact. The most important and general problem is a shallow seated instability of a slope, that is at depth of around 0.5-2 m below the ground surface and that this is in fact the most widespread form of slope failure particularly in embankments [2]. Depending on the potential slip surface, the factor of safety (FOS) varied from 2.8-3.7 and 1.8-2.0 for unrooted soil. When the mean value of the FOS increased significantly for surface depth of 0.3m, albeit as distance progresses to a depth of 1.2m these benefits diminish [6]. The stability of slopes is governed by the load, which is the driving force that causes failure, and the resistance, which is the strength of the soil-root system [7]. Based on Coppin and Richards (1990), main influences of vegetation on the stability of the slope segment are from enhanced soil cohesion due to soil reinforcement by roots and tensile root force acting at the base of the slip plane [8]. The FOS for a slope may be calculated using the infinite slope model [1] by Eq. 1.

$$FOS = \frac{c + (\gamma z - \gamma_w h) \cos^2 \beta \tan \phi}{\gamma z \sin \beta \cos \beta} \quad [1]$$

Where c: cohesion of the soil (kN/m²); z: depth to shear plane (m); h: height of ground water level above shear plane (m); γ : density of soil (kN/m³); γ_w : density of water (kN/m³); β : slope angle (°) and φ : angle of friction (°). The modified equation for translational failure on an infinite slope taking the effects of vegetation into account is defined by Eq. 2.

$$FOS = \frac{(c_R) + \{[(\gamma z - \gamma_w h) + W] \cos^2 \beta + T \sin \theta\} \tan \varphi + T \cos \theta}{[(\gamma z + W) \sin \beta + D] \cos \beta} \quad [2]$$

Eq. 2 incorporates four additional variables defined as: c_R : the enhanced shear resistance due to roots (kN/m²); T: tensile root force acting at the base of the shear plane (kN/m), W: surcharge of the vegetation (kN/m²) and D: wind loading parallel to the slope (kN/m).

to ascertain these variables, a set of experimental studies were carried out [7]. The values of parameters are selected based on that experiment and worst case scenario demonstrated in Table 1.

Table 1. Values of variables

Parameter	γ	γ_w	Z*	h	W	D	φ	c	c_R	T
Value	11	9.81	0.1-0.5	0.5	0	0	16	10	10	5

* Maximum depth of roots of grass and forbs is usually no greater than 0.5 [9].

Employing Eq.1 and 2 for reliability analysis, several assumptions are made. The weight of the surface vegetation and its subsequent normal force on the soil are quantified as W, the surcharge. This surcharge is included in the calculation primarily due to the plausibly high force exerted on soils by trees, in this paper W has been assumed to be zero as the surcharge exerted by grass is likely to be very small and of little consequence. The tensile root force for the grass is selected based on literature [10]. The wind loading force, D, is chiefly concerned with the effect of 'wind throw'. In the case of grass, the surface area upon which wind can act is small in comparison to trees, additionally grasses tend to be flexible and unlikely to transfer a great deal of force to the roots. The angle between roots and slip plane, θ , has been taken to be equal to that of the slope angle, β , as it was assumed that roots had grown in a gravitonic manner.

4. RELIABILITY AND MONTE-CARLO SIMULATION

Reliability analysis deals with the relation between the loads a system should carry and its ability to carry those loads. Both the loads and the resistance may be uncertain, so the result of their interaction is also uncertain. Reliability analysis of a system means evaluating the probability of satisfactory performance of that system under specified conditions and given time. The engineering design is to create a balanced relation between optimization of maximum safety and minimum

cost. Any method in design satisfying both aspects is very precious. These methods are identified as techniques for determining the reliability of system.

Today, it is common to express reliability in the form of a reliability index, which can be related to a probability of failure. The reliability index β provides a more meaningful measure of stability than the FOS. Geotechnical engineers have long recognized that FOS has little physical meaning and that the choice of a satisfactory value is fraught with difficulty. Conversely, the reliability index describes safety by a number of standard deviations (i.e. the amount of uncertainty in the calculated value of FOS) separating the best estimate of FOS from its defined failure value, that is to say 1.0. It is a more explicit approach.

β is the number of standard deviations by which the expected value of the factor of safety is away from the unsatisfactory performance condition, or the factor of safety equaling one. Obviously larger reliability index indicates the higher confidence of slope safety [11,12]. The reliability index can be computed by Eq. 3.

$$\beta = \frac{m_{FOS} - L}{\sigma_{FOS}} \quad [3]$$

where m_{FOS} is the mean factor of safety, L is a limit state value usually equal to 1 and σ_{FOS} is the standard deviation of the factor of safety [13].

To determine the reliability index β , Monte Carlo simulation can be employed. Monte Carlo simulation is a method for iteratively evaluating both stochastic and deterministic systems using randomly generated points to cover the range of values that enter into a calculation. It is just one of many methods for analyzing uncertainty propagation where the goal is to determine how random variation, lack of knowledge, or error affects the sensitivity, performance, or reliability of the system being modelled. To perform such a study, the data analyst generates a random value represented by a probability density function, for each uncertain variable and performs the calculations necessary to yield a solution for that set of values. This gives one sample of the process. The trials are repeated many times, giving many samples of the process. Once a large number of runs have been completed, it is possible to study the output statistically and to obtain values of means, variances, probabilities of various percentiles, and other statistical parameters. Considering safety factor, repeating process continues until a distribution of factors of safety sufficient to define the probability of failure. Regarding to this, the probability of failure and reliability index is calculated [11,14].

5. ANALYSIS

Employing Monte Carlo simulation, a Python code is developed to evaluate the vegetation effect on slope stability. Discrete values of each variable interacting with slope stability are randomly selected from its probability distribution. Those distributions are depicted in Fig. 1 and 2. Using a set of such discrete values, a value of the performance function FOS is then obtained. This process is repeated

many times. The accuracy of the results increases as the number of simulations is increased. Application of Monte Carlo simulation in geotechnical engineering and its extension to correlated variables has been demonstrated by Nguyen and Chowdhury [15,16].

Such uncertainties have systematic components. Systematic uncertainty includes statistical error in the mean due to insufficient number of tests or observations (small sample size) and bias in measurement methods. Over relatively short distances, the value of a geotechnical parameter may vary far more from the mean value than it does if averaged over relatively long distances. Thus, estimating the standard deviation of a geotechnical parameter requires careful analysis of data. Therefore, in this paper the Monte Carlo method was adopted to evaluate the stabilizing effect of vegetation in order to improve the economic efficiency as well as conserving environment.

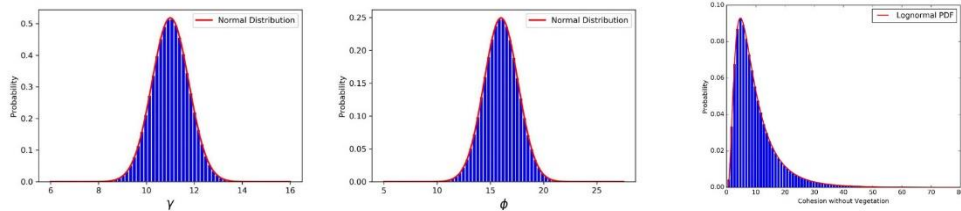


Figure 1. Probability distribution functions for parameters in unrooted system

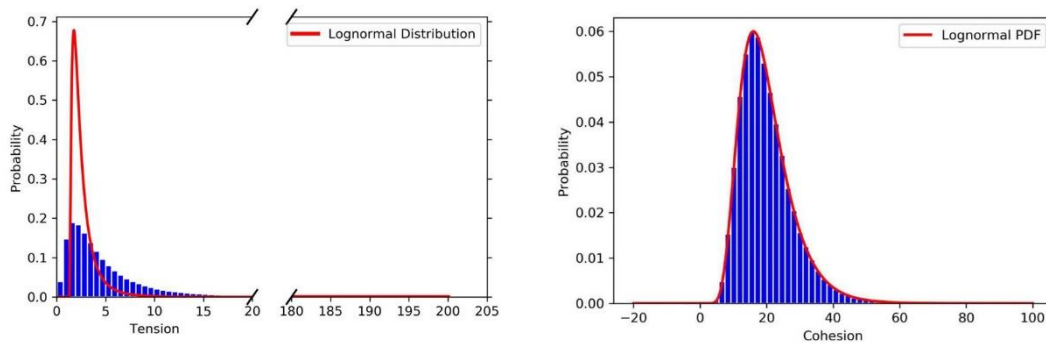


Figure 2. Probability distribution functions for additional parameters in rooted system (T and c_R)

Depend on the desired level of confidence in the solution, as well as the number of variables being considered, the number of required Monte Carlo trials is calculated from Eq. 4.

$$N = \left[\frac{d^2}{4(1-\varepsilon)^2} \right]^z \quad [4]$$

Where N is number of Monte Carlo trials, ε is the desired level of confidence (0 to 100%) expressed in decimal form, d is the normal standard deviation corresponding to the level of confidence illustrated in Fig. 3 and z is number of variables [17]. The standard deviation is considered 1.645 (with the level of

confidence equal to 90%), subsequently the number of Monte Carlo trials will be about 20000000 for 4 variables (i.e. T , c , ϕ and λ).

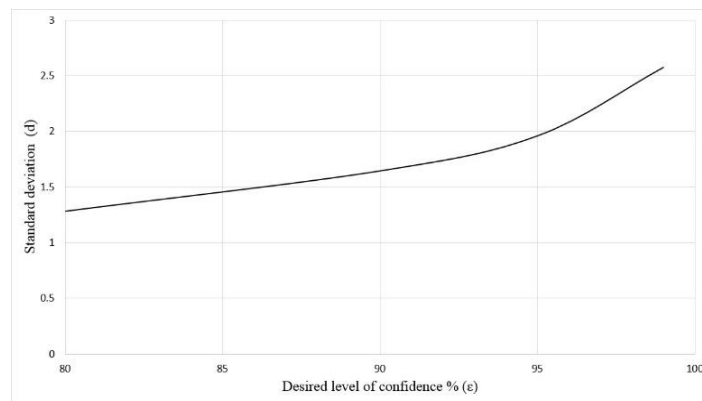


Figure 3. Standard deviations versus confidence levels

6. RESULTS AND CONCLUSION

Probability density function (PDF) and cumulative distribution function (CDF) diagram are plotted for without vegetation slope in Fig. 4 and 5.

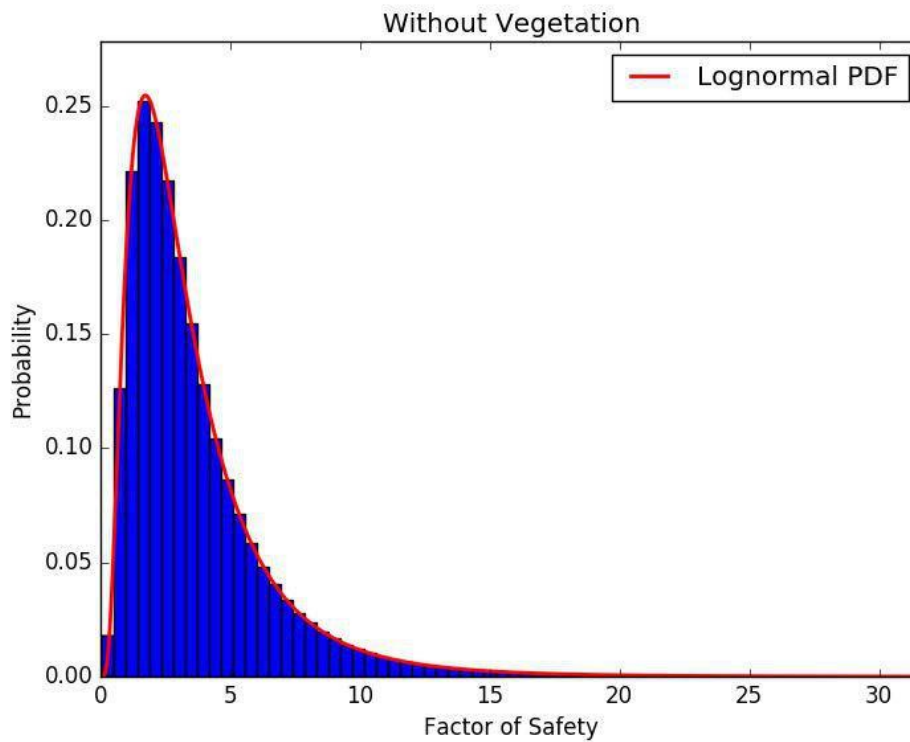


Figure 4. Probability density function of FOS for slope without vegetation

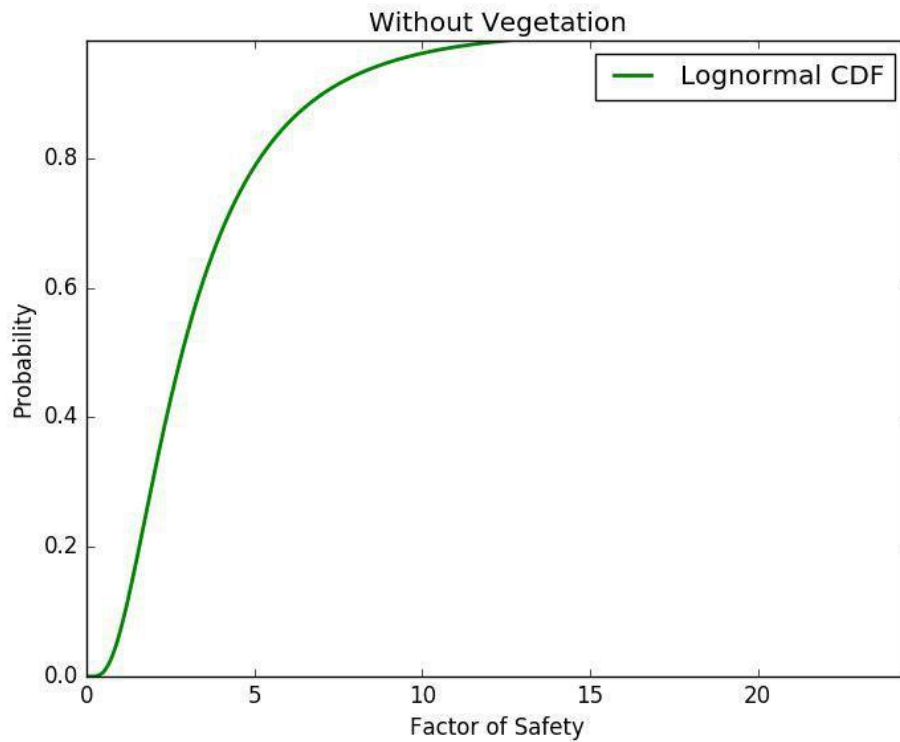


Figure 5. Cumulative distribution function of FOS for slope without vegetation

From these figures, it is observed that there is a chance for instability. For better illustration, failure probability is depicted in Fig. 6.

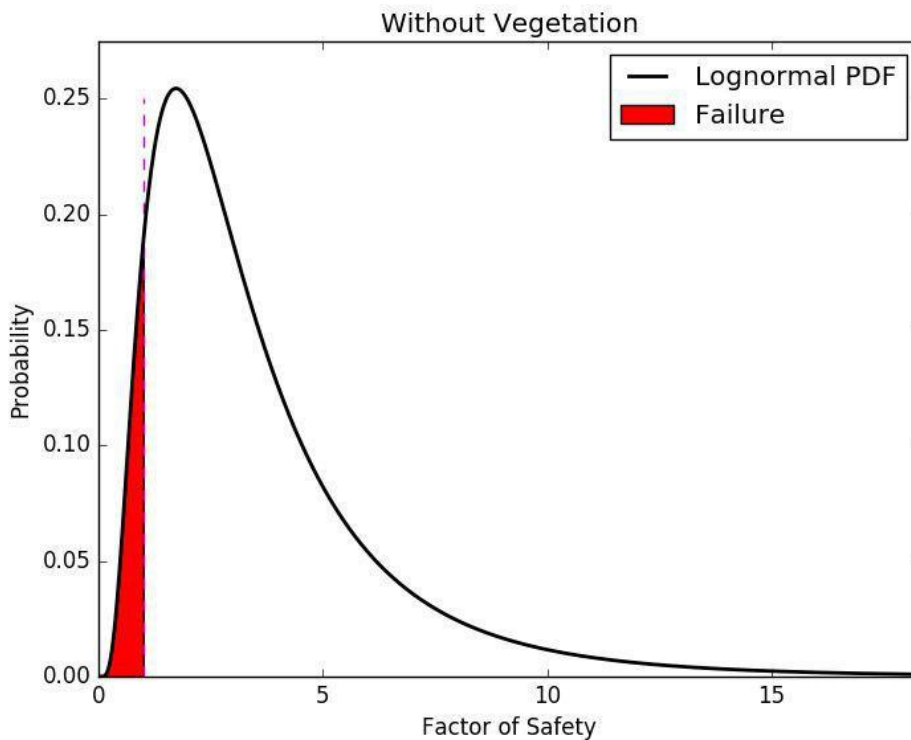


Figure 6. Probability density function of FOS considering failure

Correspondingly, PDF and CDF diagram of SOF in slope with vegetation are plotted in Fig. 7 and 8. Nevertheless, in contrast with the former diagrams the probability of failure is zero. It is demonstrated that vegetation has a stabilizing effect.

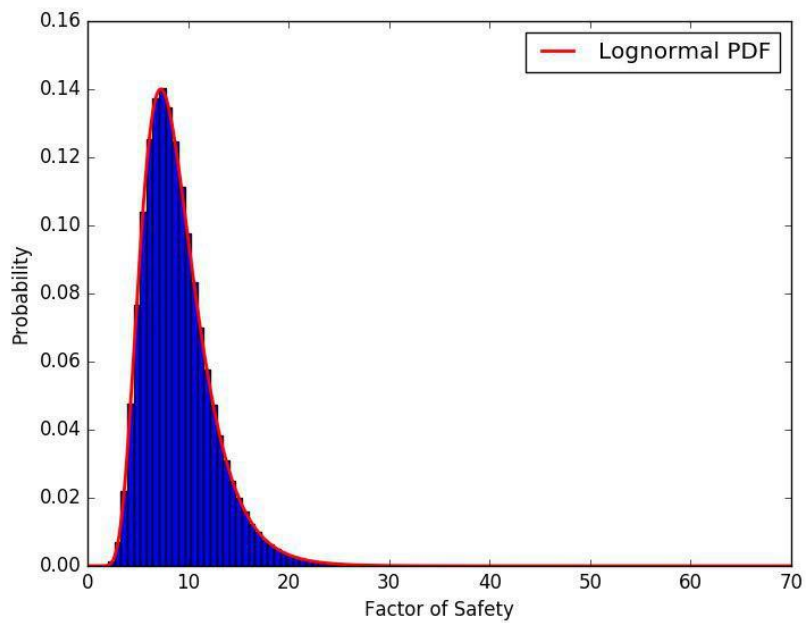


Figure 7. Probability density function of FOS for slope with vegetation

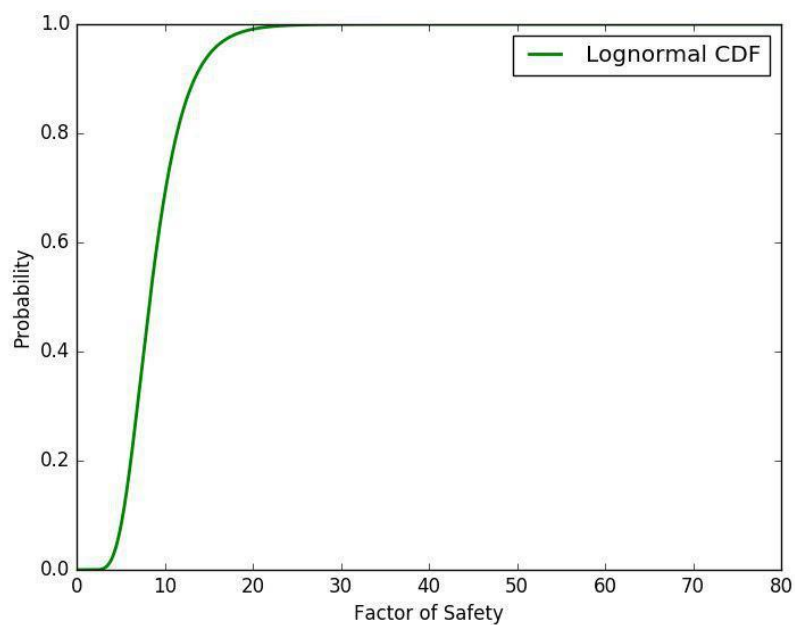


Figure 8. Cumulative distribution function of FOS for slope with vegetation

Comparing these diagrams, it is conspicuous that taking vegetation into account, FOS is significantly increases in the latter case.

For instance, the probability of FOS more than 5 is about 20% in slope without vegetation, yet, that is more than 90% in slope with vegetation. This is a substantial increase.

Based on PDF diagrams, the amount of m_{FOS} and σ_{FOS} are ascertained for both with and without vegetation system. Using these values, the reliability indexes against instability are as Table 2. There is a significant increase in the reliability index.

Table 2. Reliability index for both systems

System	m_{FOS}	σ_{FOS}	β
Without vegetation	2.841	2.027	0.907
With vegetation	8.372	1.440	5.166

Considering geotechnical uncertainty, the aim of this paper is to investigate the reliability of relationship between vegetation and slope stability in order to assess its benefits. A probabilistic analysis approach (Monte Carlo method) based on limit equilibrium employing Python programming was developed using random samples for each parameter generated. The overall results indicate that vegetation roots have a considerable stabilizing effect on the slope, limited to the rooting depth. It is appeared that through a matrix of tensile fibers, enhanced soil cohesion has a significant effect on slope stabilizing and the shallower the location of the sliding plane, the bigger the impact of vegetation.

REFERENCES

1. Whitlow R (2001) *Basic Soil Mechanics*. Prentice Hall,
2. Freer R (1991) *Bio-engineering: the use of vegetation in civil engineering*. Construction and Building Materials 5 (1):23-26
3. Baecher GB, Christian JT (2005) *Reliability and statistics in geotechnical engineering*. John Wiley & Sons,
4. Fell R, Hartford D Landslide risk assessment. In: Landslide risk assessment, *Proceedings of the international workshop on landslide risk assessment*, edited by: Cruden, D. and Fell, 1997. pp 51-110
5. Horrey P, Grocott G Quantitative Risk Assessment Methods for Determining Slope Instability Risk. In: Engineering and Development in Hazardous Terrain: *New Zealand Geotechnical Society 2001 Symposium*, Christchurch, August 2001, 2001. Institution of Professional Engineers New Zealand, p 119
6. Danjon F, Barker DH, Drexhage M, Stokes A (2007) Using three-dimensional plant root architecture in models of shallow-slope stability. *Annals of Botany* 101 (8):1281-1293
7. Hytiris N, Fraser M, Mickovski SB (2015) Enhancing slope stability with vegetation. *International Journal of GEOMATE* 9:1477-1482
8. Coppin NJ, Richards IG (1990) Use of vegetation in civil engineering. Construction Industry *Research and Information Association* London
9. Wu TH (2007) Root reinforcement: analyses and experiments. *Eco-and ground bio-engineering: the use of vegetation to improve slope stability*:21-30

10. Hengchaovanich D Vetiver system for slope stabilization. In: *Proceedings of 3rd International Vetiver Conference*, 2003. pp 301-309
11. COE UA (2006) Reliability analysis and risk assessment for seepage and slope stability failure modes for embankment dams. *Engineering Technical Letter* No 1110-2 561
12. Wolff TF Probabilistic slope stability in theory and practice. In: *Uncertainty in the geologic environment: From theory to practice*, 1996. ASCE, pp 419-433
13. Elkateb T, Chalaturnyk R, Robertson PK (2003) An overview of soil heterogeneity: quantification and implications on geotechnical field problems. *Canadian Geotechnical Journal* 40 (1):1-15
14. Kim H-S, Major G, Ross-Brown D Application of Monte Carlo techniques to slope stability analyses. In: *19th US Symposium on Rock Mechanics (USRMS)*, 1978. American Rock Mechanics Association,
15. Nguyen V, Chowdhury R Probabilistic study of spoil pile stability in strip coal mines—two techniques compared. In: *International Journal of Rock Mechanics and Mining Sciences & Geomechanics Abstracts*, 1984. vol 6. Elsevier, pp 303-312
16. Nguyen V, Chowdhury R (1985) Simulation for risk analysis with correlated variables. *Geotechnique* 35 (1):47-58
17. Greco VR (1996) Efficient Monte Carlo technique for locating critical slip surface. *Journal of Geotechnical Engineering* 122 (7):517-525

SUMMARY

Landslide and lateral spreading may have severe impact on natural and man-made environment and there is a global concern about their prevention and mitigation. The resistance level of a slope against landslide depends on the materials and the properties it of which is composed. In this paper, enhanced shallow landslide resistance of a slope due to vegetation is investigated. Considering the failure modes and uncertainty in geotechnical parameters, it seems that using probability theory in slope stability is inevitable. Regarding the effect of vegetation phenomenon in diminishing the probability of failure and increasing the stability of reservoir slopes, it is necessary to evaluate slope safety level by conducting reliability analysis. Employing Monte Carlo simulation, a python code is developed and the effect of vegetation is investigated by limit equilibrium analyses. The results demonstrate that vegetation roots have a significant stabilizing effect on the slope, limited to the rooting depth. The reliability index substantially increases due to vegetation.

Keywords: Slope stability, Vegetation, Statistical method

COMMISSION INTERNATIONALE DES GRANDS BARRAGES

VINGT-SIXIÈME CONGRÈS DES GRANDS BARRAGES
Autriche, juillet 2018

DOI 10.3217/978-3-85125-620-8-088



This work licensed under a Creative Commons Attribution 4.0 International License. <https://creativecommons.org/licenses/by-nc-nd/4.0/>

**PERMISSION PROCEDURES OF DAM CONSTRUCTION AND
MANAGEMENT IN INDONESIA**

Cristina D. YULININGTYAS

Dam Engineer, Dam Safety Unit,
MINISTRY OF PUBLIC WORKS AND HOUSING

INDONESIA

Hari SUPRAYOGI

Director of Rivers and Coastals,
MINISTRY OF PUBLIC WORKS AND HOUSING
Head of INACOLD

INDONESIA

Lolo W. RESDIATMOKO

Head of Surveillance Section, Dam Safety Unit,
MINISTRY OF PUBLIC WORKS AND HOUSING

INDONESIA

PERMISSION PROCEDURES OF DAM CONSTRUCTION AND MANAGEMENT IN INDONESIA

Cristina D. YULININGTYAS

Dam Engineer, Dam Safety Unit,
MINISTRY OF PUBLIC WORKS AND HOUSING

INDONESIA

Hari SUPRAYOGI

Director of Rivers and Coastals,
MINISTRY OF PUBLIC WORKS AND HOUSING
Head of INACOLD

INDONESIA

Lolo W. RESDIATMOKO

Head of Surveillance Section, Dam Safety Unit,
MINISTRY OF PUBLIC WORKS AND HOUSING

INDONESIA

1. INTRODUCTION

The Republic of Indonesia is the largest archipelago country in the world about 13,466 large and small islands. Indonesia is straddling along the equator, situated between the continents of Asia and Australia and between the Pacific and the Indian Oceans. Lies between 95° - 141° East Longitude and 6° North to 11° South Latitude.

Currently, the number of watersheds in Indonesia is 131 river basins. This amount consist of 5 across the country, 29 across the province, 29 national strategic, 53 across districts, and 15 cities watersheds spreading around the country that more than 5,800 rivers, 500 natural lakes and 214 dams. Indonesia has 2 (two) seasons : dry and rainy seasons. Dry usually occurs from June to September and the rest is rainy season. The average annual precipitation varies 1,5000 mm in eastern region to 2,600 mm in the west.

Indonesia is the country that has huge water availability, it is about 3,909.6 billion m³/year about 2530 km³ (no. 5th water resources in the world). Although Indonesia include 10 water-rich country, but because of the season variations and spatial imbalances in water availability, requires good management of water resources availability specially in dry season such as constructing dam. Beside having many benefits, dams construction also keep potential hazards that can endanger the lives at the downstream. The dams failure can cause major flooding and damage in the downstream area.

In accordance with Minister Regulation No. 27 / PRT / M / 2015 on Dams, dam safety role is intended to realize the orderly development and utilization of dams so be worthy of a technical or non-technical aspects from the design, construction, operation, decommissioning stages in order to prevent or reduce the potential failure risk of the dams construction with criterias are as follow:

- a. Dam with 15 (fifteen) meters height or more, measured from the deepest foundation;
- b. Dam with 10 (ten) meters height up to 15 (fifteen) meters, measured from the deepest foundation with the following provisions:
 - 1) The length of the dam crest at least 500 (five hundred) meters;
 - 2) The capacity of the reservoir at least 500,000 (five hundred thousand) cubic meters; or
 - 3) Maximum flood discharge at least 1,000 (one thousand) cubic meters per second; or
- c. Dams with special difficulty on the foundation or dams designed with new technology and / or dams that have high hazard classification.

2. DAM DEVELOPMENT IN INDONESIA

Many dams in Indonesia are very old. It was built before Mid 80's, some dams were even built before 1950, during the colonial time. Based on Minister Regulation No. 27 / PRT / M / 2015 on Dams, Indonesia has 214 dams are categorized as large dam until 2017. The latest dams that are on going in 2017/2018 are:

1. Bener Dam, Yogyakarta
2. Semantok Dam, East Java
3. Temef Dam, East Nusa Tenggara
4. Tigadihaji Dam, South Sumatera
5. Pamukkulu Dam, South Sulawesi
6. Margatiga Dam, Lampung
7. Sidan Dam, Bali

These dams are constructing specially for irrigation purpose, while for fulfill the national electricity demand, Indonesia has prepared 33 new dams integrated with National Hydroelectric which is expected to produce electricity of 2,300 MW by the State Owned Enterprise or private. And all dams development must go through the process of certification or approval in accordance with Minister Regulation No. 27 / PRT / M / 2015 on Dams.

3. DAM SAFETY APPROVAL PROCEDURE

3.1. GENERAL

In order to minimize the risk of dams development, each stages of Dam and reservoir construction and operation should be implemented based on dam safety conception of and the rules of dams safety contained in various norms, standards, guidelines and manuals to improve the usefulness of the source function water resources, water preservation, control of water damage, and the safety functions of tailing.

Dam safety concept in Indonesia was adopted by dam safety concept from Swiss Dam. The idea of dam safety concept is best provided when due consideration is given to the following tenets:

- a. Structural safety, safety against structural, hydraulic, and seepage failure;
- b. Operation, maintenance and monitoring; and
- c. Emergency action plan.

In order to review the safety of the dams, the dams construction in Indonesia must obtain a license or approval, including:

1. Design.
This permission / approval is intended to obtain technical design aspect. In this process also can be obtained the construction approval if the documents requirement attached.
2. The construction in preparation for reservoir initial impounding.
3. The reservoir initial impounding in preparation for the dam operation.
4. Decommissioning of the dam functions.

This permission / approval is filed if dams have been completed its life time.

3.2. DAM SAFETY ORGANIZATION

As stated in Ministerial Regulation Number 72/PRT/1997, in order to carry out the dam safety, Minister of Public Works and Housing was assisted by dam safety organization consisting of Dam Safety Commission and Dam Safety Unit.

Dam Safety Commission (DSC) provides recommendation and suggestion to the minister in charge of dam safety activities and responsible to the minister. The tasks of dam safety commission are as follow:

- a. Giving the recommendation about dam safety to the minister in every phase of dam development such as design, construction, operation, rehabilitation, and dam closure.
- b. Evaluating Dam Safety Unit activities in order to suggest to the minister
- c. Preparing the accountability report to the minister

Dam safety commission member consists of representative of government and state-owned company as the owner of the dam, professional association and another government agency related to dam appointed by minister. The chairman of dam safety commission is Director General of Water Resources.

Based on structural organization, Dam Safety Unit is under Directorate General of Water Resources, Ministry of Public Work and Housing. The main duty of dam safety unit is to provide support about dam safety to DSC.

The tasks of Dam Safety Unit are as follow:

Provide guidance to technical regulations field of dam safety. Providing permit approval process and dam safety to all elements of the owners of their dams and reservoirs.

Implement programming and budget, regulations, guidelines and technical guidance to dam safety and performance evaluation.

Carry out periodic inspections, inspections extraordinary / special dam inspection and evaluation of data.

3.3. DAM SAFETY LISENCE

There are some steps to do to have dam safety license in every phase of dam development. After the construction finished, there are another dam safety license for rehabilitation or removal of the dam. As mentioned above, that the member of DSC come from various institution based on their competency. So, the discussion about dam safety could be as detailed as could be for making sure the dam is safe.

Here the explanation about the process of dam safety license. In figure 4, dam safety license start with sending application from the dam owner to the Minister c.q. Director General of Water Resources as the chairman of Dam Safety Commission. The report about dam should be sent to DSU to have first assessment. After that, the DSC, DSU and dam owner inspect the dam site and discussed it.

After inspection, the DSU reviewing the inspection result whether the reports are appropriate or not. If everything is going fine, then DSU, DSC, dam owner, consultant and/or contractor will take DSC technical meeting. In this meeting, it discussed about dam safety based on regulation, standard, guideline and manual in technical consideration.

After the dam owner complete the suggestion at the technical meeting, then the process continue to plenum meeting. The DSC members who attend the plenum meeting vary from some other institution, such as environmental, electricity, and geological agency, which are related to dam safety. If all the process is finished, the DSC would give recommendation to the minister. Then the minister will issue the license of dam safety. The documents which are sent to dam safety unit in order to get dam safety license in every phase of dam development and management will be brief explained below.

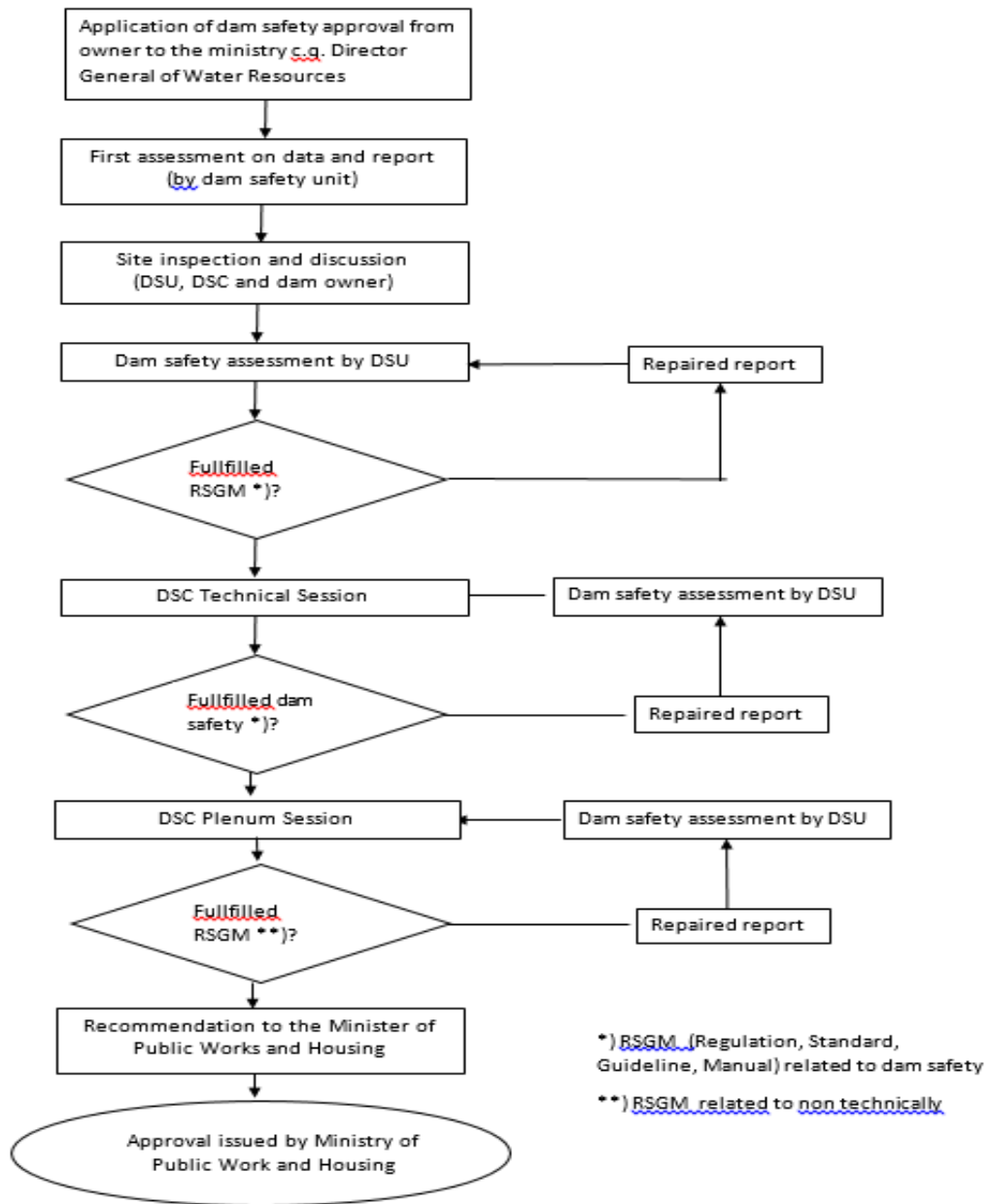


Figure 1.
Dam Safety License Flowchart

3.3.1. Design

The documents should be sent to Dam Safety Unit in this phase are:

A. Administrative requirements

- 1) License of water uses
- 2) Environmental license
- 3) Land Acquisition and Resettlement Action Plan Report
- 4) The location of dam should be stipulated in Urban Land Use and Spatial Plan

B. Technical requirements

- 1) Feasibility study documents, which are contain of: main report, executive summary report, and another report which is support the feasibility study.
- 2) Detail design documents, which are contain of: main report, criteria design, executive summary report, design note, design calculation, survey and investigation, hydrological report, model test report, construction method report, technical specification, operation and maintenance plan, budget plan, design drawing, etc.
- 3) Detail design review (if available)
- 4) Photos of dam location, borrow area and quarry area.

3.3.2. *Impounding*

The documents should be sent to Dam Safety Unit in this phase are:

- 1) Technical geology report based on the result of foundation excavation and additional investigation (if available)
- 2) Foundation treatment report
- 3) Alteration design report, including any judgment why the design should be changed (if available)
- 4) Quality control report, including test
- 5) The result of hydro mechanical equipment test in factory or in site, and also dry and wet test report
- 6) Project completion report. If the reports in number 1) to 5) are included in this report, so they didn't need to submit separately.
- 7) Surveillance program report include the result of instrumentation reading along the construction
- 8) Emergency action plan, flood warning system and the socialization to the downstream population
- 9) Impounding plan
- 10) Operation and maintenance organization include training for the operator
- 11) As built drawing
- 12) Construction photos

3.3.3. *Operation*

The documents should be sent to Dam Safety Unit in this phase are:

- 1) Result of instrumentation reading from construction until the latest reading
- 2) Dam behavior analysis based on instrumentation reading in number 1) and also inspection result in dam, reservoir and its vicinity, and appurtenance structure
- 3) Operation and maintenance manual which is has been adjusted based on the actual condition
- 4) Hydro mechanical operation report
- 5) Incidents and accidents report, such as earthquake, sliding, excess seepage, etc.
- 6) Executive summary report from impounding
- 7) Photos

3.3.4. *Dam Closure*

The documents should be sent to Dam Safety Unit in this phase are:

- 1) Detail planning about termination, demolition of dam (if needed), including environment restoration, and safety of the environment. If the dam body and its appurtenance structure didn't demolished, so maintenance and monitoring plan should be prepared include the operational organization.
- 2) Stability analysis for dam which is not demolished
- 3) Detail investigation about consequences or impact about dam removal for hydrology condition and hydraulically at the dam site
- 4) Environmental impact
- 5) Drawing
- 6) Photos

4. CONCLUSION

Approval of the construction and management of dams in Indonesia is divided into four phases, namely the approval of design and construction, the initial charge, operation, and closure dam. This is intended to minimize the risk of dam failure and function in accordance with the purpose of development as well as to ensure the safety of the dam.

5. ACKNOWLEDGEMENT

The authors would like to thank to Dam Safety Unit, Directorate General of Water Resources, Ministry of Public Works and Housing and INACOLD for the authorization to publish the main result of the present study.

KEYWORDS

Dam, Dam Failue, Safety of Dam safety commission.

REFERENCES

- [1] Ministry of Public Works and Housing. *Minister of Public Works and Housing Regulation no. 27/PRT/M/2015 about Dam*, 2015.
- [2] C.D. Yuliningtyas. Approval procedure of dam development and management in Indonesia. *Proceeding of 85th ICOLD Symposium*. 2016.
- [3] R.H. Ardiansyah and A. Zubaidi. Dam Safety Management in Indonesia. *APG-EADC Symposium*. 2016.

COMMISSION INTERNATIONALE DES GRANDS BARRAGES

VINGT-SIXIÈME CONGRÈS DES GRANDS BARRAGES
Autriche, juillet 2018

DOI 10.3217/978-3-85125-620-8-089



This work licensed under a Creative Commons Attribution 4.0 International License. <https://creativecommons.org/licenses/by-nc-nd/4.0/>

**INTERNAL EROSION RISKS IN RIGHT ABUTMENT OF AHMADBEIGLU
STORAGE DAM IN IRAN**

Mohammadi. AREZOO

Senior Geotechnical Engineer
POOYAB CONSULTING ENGINEERS

IRAN

Bemani Yazdi. ALI ASGHAR

Head of Geotechnic and Dam Design Department
POOYAB CONSULTING ENGINEERS

IRAN

COMMISSION INTERNATIONALE
DES GRANDS BARRAGES

VINGT-SIXIÈME CONGRÈS DES
GRANDS BARRAGES
Autriche, juillet 2018

INTERNAL EROSION RISKS IN RIGHT ABUTMENT OF AHMADBEIGLU STORAGE DAM IN IRAN

Mohammadi. AREZOO

Senior Geotechnical Engineer
POOYAB CONSULTING ENGINEERS

Bemani Yazdi. ALI ASGHAR
Head of Geotechnic and Dam Design Department
POOYAB CONSULTING ENGINEERS

IRAN

1. INTRODUCTION

The Ahmadbeiglu Storage Dam site is located in Ardebil province (northwest of Iran) on the Meshginchay River. The main objective of the Ahmadbeiglu Storage Dam construction is to store for supplying water needed for agriculture, environmental and partially supply Meshginshahr domestic water demand.

Ahmadbeiglu Dam site is located at the upstream of several villages with more than 1000 population and failure of this dam will result in loss of human life, extensive property damage to homes and other structures, thus, ahmadbeiglu Dam is high risk.

In the spring of 2017, during the excavation of clay core foundation in the right abutment from elevation 980 m, seepage through this abutment observed. Since foundation behavior, especially soil foundations can significantly affect the stability of this kind of dams and internal erosion /piping through the soil foundation or along dam body-foundation is one of the leading causes of

embankment failure, a technical team organized to evaluate the internal erosion potential and risks.

The potential of internal erosion through soil foundation can't be completely modeled or analyzed, the probability of this phenomena occurrence were evaluated by using the soil foundation strata, sealing method of dam and foundation, the results of dam and foundation analyses in different loading conditions (in this paper, the analysis is limited to static loading condition), evaluation of hydraulic gradient and finally the dam and foundation behavior after reservoir filling.

2. DAM AND DAM SITE DESCRIPTION

According to the geological studies, the right abutment of this dam is composed of two parts in terms of lithology. The upper part is weathered tuff in form of layered soils including clay, clayed sand and silty sand and then covered with variable thickness of fine-grained alluvial terraces (the thickness is between 3m and 20 m). The lower part is pyroxene andesite rock that is completely weathered and then moderate weathered pyroxene andesite. The foundation in left abutment is low to moderate weathering pyroxene andesite and consists of alluvial deposits of maximum 8.0 m thick in the middle of the valley.

As it previously mentioned, the right abutment is critical due to its strata. Thus, in this paper, the right abutment is our subject. In order to determine the soil foundation strata, permeability and density of the soils, ground water table and finally geotechnical parameters for dam design, geotechnical investigation including field and laboratory tests in 6 boreholes and 7 test pits in this abutment was performed in the feasibility and detail design studies.

According to the Unified Soil Classification System (USCS), and results of field and laboratory tests on the samples of the right abutment, the foundation soil is often in CL classification, soils with classification of SC, CH, SC-SM, SP-SM and SM have been observed as layer between soils with CL classification. The right abutment strata has been presented in Fig. 1.

The fine grained soils of the right abutment is considered as dense and very dense soils based on the results of Standard Penetration Test (SPT), Since the No. of SPT tests (N) are more than 30 and 50.

In order to determine the permeability coefficient of right abutment fine-grained material, lefrance tests were performed in one-meter stage with maximum 2.0 m intervals by using constant and falling head method. Corresponding to the results of lefrance tests, the average permeability coefficient of soils is $1.0e-6$ cm/s and the variation of permeability coefficient is very low. Based on the lefrance tests, the right abutment fine-grained soils have been classified as low to very low permeable soils.

The maximum hydraulic gradient is 25 degree toward to the Meshginchay River. The ground water level has been presented in Fig.1.

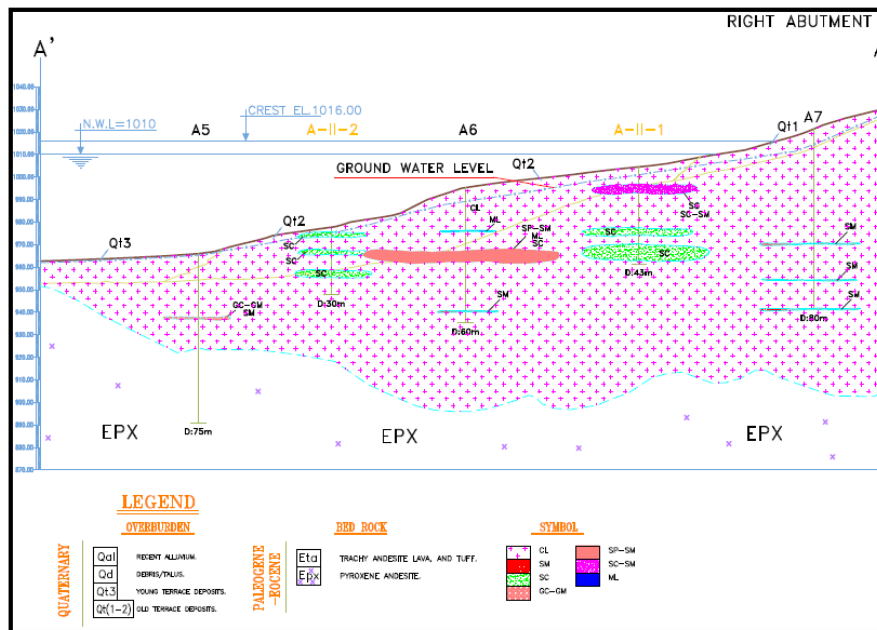


Fig.1.
The right abutment strata along dam axis

By considering the geological and geotechnical investigations and analyses of laboratory and field test, the right abutment strata, the alluvial terrace under clay core foundation in right abutment must be removed and replaced by a key trench as sealing element since the fine grained material of this abutment is generally classified as low to very low permeable material.

Ahmadbeiglu Dam and cofferdam are both earth fill with vertical clay core. Minimum, normal and maximum water levels in the reservoir are levels 971.5 m, 1010.0 m and 1013.3 m, respectively. The total reservoir volume is 27.4 Mm³. The dam crest is 10 m wide and 528 m long at elevation 1016 m. The maximum dam height is 58 m from riverbed and 65 m from foundation. The upstream slope is 2.5 H to 1.0 V from dam crest to elevation of 991 m, which corresponds to the stabilizing berm with 10 m width, then, continue with the same slope to natural ground. The downstream slope is 2.0 H to 1.0 V. The upstream and downstream slopes of cofferdam are 2.5 H to 1.0 V and 2.0 H to 1.0 V, respectively.

3. INTERNAL EROSION RISK ANALYSIS METHODOLOGY

The internal erosion risk analysis in right abutment of Ahmadbeiglu earth fill dam has been carried out in accordance with the methods of “Dam Safety Risk Analysis Best Practices, 2009”. In this paper, the risk analysis is limited to evaluation of internal erosion in normal operation and the other loading condition (flood and seismic loading) has not been considered.

The risk analysis process consists of a) Identification of failure modes b) Estimation of probability of dam failure due to each failure modes c) Dam failure

consequence d) Risk prioritization and risk control. It should be noted that, in this analysis, only life loss has been considered as dam failure consequence.

The probability of dam failure due to internal erosion has been determined based on event tree methods. In this method, all failure modes due to internal erosion are broken down in two four phases; initiation of erosion, continuation of erosion, progression of erosion and detection and finally breach. Thus, the probability of dam failure has been obtained by using below equation [1];

$$P_F = P_{\text{Load}} \times P_{\text{Initiation}} \times P_{\text{Continuation}} \times P_{\text{Progression}} \times P_{\text{Detection}} \times P_{\text{Breac}} \quad [1]$$

3.1. IDENTIFICATION OF FAILURE MODE

The failure of embankment dams by internal erosion or piping has been evaluated in three different modes including piping through embankment, piping through foundation and piping from embankment nto foundation.

3.1.1. *Assessment Of The Probability Of Dam Failure Due To Internal Erosion Through Soil Foundation (PF1)*

In order to evaluate the internal erosion through soil foundation, determination of soil classification and existence of continues layer in dam foundation is the first step. As it was mentation, in feasibility and detail design study, the foundation soil is classified as CL, SC, CH and layers of SC-SM, SM and GC-GM. In this stage, three bore hole which are located in upstream, axis and downstream of dam body has been drilled for determining of the soil classification, existence of continues layered soil and also permeability of the soil.

According to the results of field and laboratory tests, the foundation soil is often in CL classification; soils with classification of SC, SM, and ML have been observed as layer between soils with CL classification and these layers are approximately continues layer. In addition, the plasticity index (PI) of these layer is less than 7.0 ($PI < 7$). Thus, internal erosion in soil foundation with continues cohesionless layer may initiate and progress due to backward erosion or suffusion (erosion of fine soils into adjacent coarse soils). The evaluation of internal erosion has been presented as following;

3.1.1.1. *Initiation of backward erosion*

In order to estimate the initiation of internal erosion by backward, the following issues have been evaluated;

- Estimation of heave occurrence probability at the toe of the embankment dam when reservoir is at normal level;

The probability of heave occurrence should be considered in areas of a thinner confining layer with a distance of 2 x dam height at downstream of dam toe. In order to estimate the probability of heave occurrence, the hydraulic gradient at toe of dam and critical hydraulic gradient should be determined. The hydraulic gradient at toe of dam can be calculated by using piezometers reading or results of seepage analysis and the critical hydraulic gradient are calculated by Terzaghi equation (1960). The gradient at the toe of dam in right abutment has been obtained from the results of seepage modeling ($i = 0.4$) and the critical gradient is equal to 0.9. The probability of heave occurrence has been estimated as 0.01 by using the judgment probability table and hydraulic gradient at the dam toe.

- Estimation of backward erosion occurrence probability with heave occurrence

The initiation of backward erosion is depended on the hydraulic gradient under the main part of dam. The other factors are particle size distribution/uniformity coefficient, permeability of the soil and the geometry of dam and foundation. According to the results of seepage analysis, the gradient is 0.4 and the uniformity coefficient is more than 6 ($C_u > 6$), thus, the probability of backward erosion with heave occurrence is estimated as 0.1.

- Estimation of backward erosion occurrence probability without heave occurrence

For this purpose, the main factors are average hydraulic gradient, uniformity coefficient and permeability of continues layer. By considering the gradient equal to 0.4 and $C_u > 6$, the probability of backward erosion without heave occurrence is estimated 0.02.

From the results of the above assessment, the probability of initiation of backward is estimated 0.0208.

3.1.1.1.1. Continuation of backward erosion

In order to evaluate the continuation of backward erosion, the filtered or unfiltered exit should be assessed. In Ahmadbeiglu Storage Dam, the exit point of seepage is unfiltered but a blanket drain and toe drain system is present. In this dam, a low permeability layer is existent between blanket drain and erodible layer. By considering the mentioned condition and using probability judgment tables, the probability of erosion continuation is estimated 0.25.

3.1.1.1.2. Progression of backward erosion

In order to assess the probability of erosion progression, the following issues have been considered;

- Probability of the forming a roof of a pipe (PR); the roof of a pipe can be formed by layers of soil in the foundation which are cohesive or have high fines content. The erodible soil in foundation has been classified as SM, ML and SC with fine content more than 15%, thus, the probability of forming a roof of a pipe has been calculated as 0.7.

- Probability for no limitation of the flow (PL); the flow limitation can be performed by zoning within the dam, cutoff wall or other sealing elements in dams or foundation. In Ahmadbeiglu dam, the sealing element in right abutment is key trench. Therefore, the probability of no limitation has been considered as 0.01.

Thus, the probability of progression of erosion through the layered foundation has been calculated as $7e-3$ ($PP = P_R \times P_L$).

3.1.1.1.3. Probability of detection, intervention and repair fail

Determination of water level at the downstream of dam by using readout of observation well and open standpipe piezometer during construction show that the water level is normal. For more safe, four open standpipe piezometers in the downstream shell and right abutment and eight observation wells in downstream of dam body and right abutment have been installed in this stage besides the other instrumentations of dam body and foundation. By considering the installed instruments in dam body and foundation in right abutment and frequency of inspection (weekly or every two weeks), it is likely that the intervention on dam and right abutment would be successful. The probability of the intervention and repair not to be successful is considered unlikely ($P=0.1$).

3.1.1.1.4. Probability of breach in the layered soil foundation

Dam breach could be occurred by the following mechanisms in this dam;

- Breach by instability of downstream slope; since there is a blanket drain in downstream and downstream shell is free-drain material, so, the pore pressure will dissipate and the probability of breach by instability of downstream slope is estimated 0.02.

- Breach by sinkhole development; for this purpose, the loss of freeboard due to the settlement of embankment induced by the loss of foundation material should be determined. Since the settlement of dam is less than 1% dam height (according to the stress-strain analysis results), and freeboard is equal to 6 m, the freeboard at the time of failure is calculated 5 m, so breach by sinkhole develop is estimated 0.01.

The probability of breach in layered soil foundation due to the above mechanisms and engineering judgments has been estimated as 0.03.

3.1.1.2. Initiation of erosion by suffusion/internal instability in a cohesionless layer of foundation

Suffusion, or internal instability, involves the erosion of finer particles from the matrix of coarser soils, under the seepage gradient in the soil. For assessing the suffusion/internal erosion of soils, the particle size distribution and hydraulic gradient are the main factors. By using Fell and Wan (2004) method, and considering the particle size for D15 (0.08mm), D60 (0.3mm), D90 (0.8mm), the erosion initiation by internal instability is not possible in right abutment.

3.1.2. Assessment of the probability of dam failure due to internal erosion from embankment into foundation (PF2)

3.1.2.1. Initiation of erosion from embankment into foundation

In order to assess the erosion initiation from embankment into foundation, the existence of a coarse layer in the base or sides of key trench, initiation of scour or initiation of core material erosion by hydraulic fracture due to arching in a narrow key trench should be evaluated.

The probability of existence of a coarse layer in the base of key trench has been estimated as 0.5, by using the geology studies, mapping and photographs taken during construction. According to the results of laboratory tests on samples of the fine borrow area (clay core material), the material is not susceptible to erosion. The results of seepage analysis in a section located in right abutment showed that the maximum hydraulic gradient in the core-foundation contact is 1.4 that is less than allowable value. Therefore, the probability of initiation of scour in core-foundation contact in spite of existence of coarse layer and unfiltered exit is estimated as 0.01.

In addition, according to the results of static stress-strain analysis, occurrence of hydraulic fracture due to arching in key trench with slope 2H: 1V is very unlikely ($p=0.005$). However, the probability of initiation of erosion from embankment into foundation has been calculated 0.01.

3.1.2.2. Continuation of erosion from embankment into foundation

In order to evaluate the probability of erosion continuation from embankment into foundation, the presence of filter/transition zone in downstream of core or filtered and unfiltered exit should be determined.

As previously mentioned, the exit point in Ahmadbeiglu dam is unfiltered but there is a very low permeable layer between erodible layer and blanket drain. Also, there is a filter in downstream of clay core which the D15 filter ranges between 0.2 to 0.7 mm. According to reference [5] for some, excessive and continuing erosion, D15 filter should be between 0.7 to 5, 7 to 12 and 12 to 33

mm, respectively. By considering the mentioned factors, the probability for continuing for erosion has been estimated as 0.01.

3.1.2.3. Progression of erosion from embankment into foundation

For assessing the progression of erosion from embankment into foundation, the possibility of forming roof of the piping path and restriction of the flow in piping path in upstream of dam should be determined;

- *Probability of forming the roof of the piping path (P_R);*

For progression of erosion from embankment into foundation by forming a roof of a pipe path, the core material and erodible layer of soil foundation must be capable of forming and holding the roof of a pipe. The fine content of core/soil foundation (% passing sieve #200, 0.075mm), the plasticity of the soils and the saturation of the soil are the most important factors in forming a roof. According to the grading curve of core material, the fine content of core material is between 30 to 85 % , the average plasticity index is 23 and the fine content of erodible layer of foundation is >15 %. Therefore, by using the reference table and the material characteristic, the probability of forming a roof has been calculated as 0.9.

- *Probability for no limitation of the flow (P_L);*

In this dam there is a filter and transition zone with fine content < 5% that cannot support a roof in upstream side of core, and also, the hydraulic gradient in upstream side of core is less than 1.0, thus, the probability of no limitation of flow is estimated as 0.01.

However, by considering the results of above assessment, the probability of progression of erosion from embankment into soil foundation is obtained 0.009 ($P=P_R \times P_L$).

3.1.2.4. Breach in the embankment or from embankment into foundation due to erosion

In order to assess the probability of breach in the embankment or from embankment into foundation due to erosion, the following aspects should be evaluated;

- *Breach by instability of downstream slope;*

For this purpose, the pore pressure rising or dissipation in downstream shell should be evaluated. In this dam, there is a filter and transition zone in downstream of core, the downstream slope is 2H: 1 V, and the fine content of downstream shell is < 8 %. Thus, the probability of breach by instability of downstream slope has been estimated as 0.02.

- *Breach by sinkhole development;*

The probability of breach by sinkhole development is estimated as 0.01 since the clay core material is well graded and the plasticity indices are low to medium, therefore, the core material is not susceptible to form a large void in dam and finally form a sinkhole.

The probability of breach in embankment or from embankment into foundation due to erosion has been calculated as 0.03 by using the results of above assessment.

Finally, the probability of dam failure by erosion from embankment into layered soil foundation is 1.35×10^{-8} .

3.1.3. *Assessment of the probability of dam failure due to internal erosion through embankment (PF3)*

3.1.3.1. *Initiation of piping through embankment*

According to the results of laboratory tests on samples of fine borrow areas, especially clay size fraction and plasticity index, the probability of erosion initiation by backward or suffusion through embankment is negligible. But, erosion can initiate by concentrate leakage in low stressed zones which may be caused by differential settlement and arching or high permeability zone due to poor compaction. According to the static stress-strain analysis of Ahmadbeiglu dam, evaluation of arching and hydraulic fracturing, and construction quality, the probability of erosion occurrence in this dam is estimated as 0.02.

3.1.3.2. *Continuation of piping through embankment*

As it was mentioned, a protective filter in downstream of clay core is present with D15 between 0.2 and 0.7 mm. According reference [5], the probability of continuing erosion has been considered as 0.01.

The probability of progression, failure to detect, breach is the same as for erosion from embankment into foundation. Therefore, the probability of failure due to erosion through embankment has been estimated as 5.4×10^{-9} .

4. CONCLUSION

According to the geology and geotechnical studies, the results of field and laboratory tests and the dam site investigation, the right abutment of this dam site has been considered as layered soil foundation and the internal erosion was the most important factor in dam failure. In order to assess the probability of dam failure due to erosion, three failure modes have been evaluated as failure by erosion through layered soil foundation, erosion from embankment into soil foundation and erosion through embankment.

All failure modes have been assessed (reservoir is considered to be in normal level) and the probability of their occurrence have determined. In order to categorize the internal erosion risk, f-N event chart has been used. On the f-N

chart, f and N represent the annualized failure probability and the estimated life loss associated with an individual failure mode, respectively. The f - N chart has been presented in Fig.3.

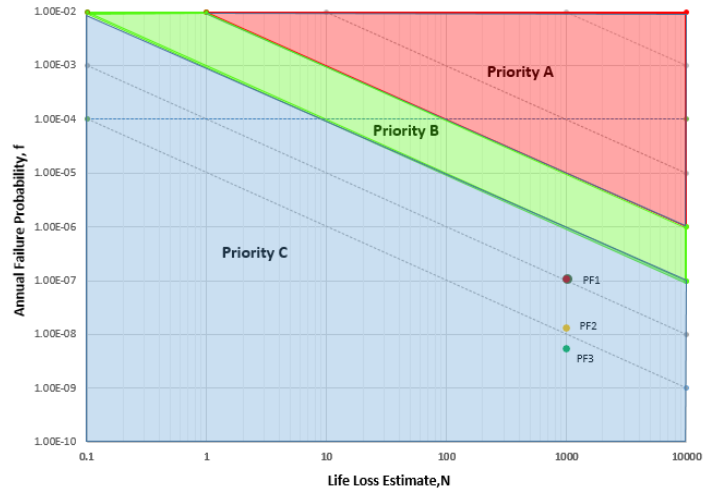


Fig. 3.
The f - N diagram of risk analysis results

Where;

Priority A- Justification to take expedited action to reduce risk

Priority B- Justification to take action to reduce risk

Priority C- Diminishing justification to take action to reduce risk

As it can be seen, the most critical risk comes from erosion through layered soil foundation (PF1), but all the risks of dam failure by erosion in right abutment of Ahmadbeiglu dam is in Priority C that indicate a reduced justification for risk reduction action related to these failure modes.

For increase safety, in addition to the instruments of dam body and foundation in right abutment, instruments such open standpipe piezometers (at the downstream of clay core and foundation) for checking pore water pressure in foundation and downstream of clay core and observation wells (at the downstream of dam body and right abutment) for evaluation ground water level at the downstream and right abutment have been installed.

ACKNOWLEDGEMENTS

The authors appreciate the cooperation of the Ardebil Regional Water Authority and Pooyab Consulting Engineers. The authors would also like to acknowledge Engineer Nosratollah Mostofi, the head of geology department of Pooyab Consulting Engineer, for providing of geological information of Ahmadbeiglu Storage Dam Site.

REFERENCES

- [1] Fell, R., Mac. Gregor, P., Stapledon, D. and Bell, G. Geotechnical engineering of dams, *Balkema, Leiden (in press)*, 2004.
- [2] Fell, R., Wan, C.F. and Foster, M., Methods for estimating the probability of failure of embankment dams by internal erosion and piping – piping through the embankment”, *UNICIV Report No. R-428, the University of New South Wales, Sydney, Australia*, 2004.
- [3] Sherard, J.L., Sinkholes in dams of coarse, broadly graded soils, 13th Int. Congress on Large Dams, *New Delhi. Q47, R2, 325-334. International Commission on Large Dams, Paris*, 1979.
- [4] Sun, B.C.B., Internal stability of clayey to silty sands”, *PhD Thesis, Department of Civil Engineering, University of Michigan*, 1989.
- [5] U.S. Department of Interior, Bureau of Reclamation (Reclamation), Dam safety risk analysis best practices, *Version 1.3. Technical Service Center, Denver, Colorado*, 2009.

COMMISSION INTERNATIONALE DES GRANDS BARRAGES

VINGT-SIXIÈME CONGRÈS DES GRANDS BARRAGES
Autriche, juillet 2018

DOI 10.3217/978-3-85125-620-8-090



This work licensed under a Creative Commons Attribution 4.0 International License. <https://creativecommons.org/licenses/by-nc-nd/4.0/>

**MAIN ECOLOGICAL RISKS FACING THE YANGTZE RIVER BASIN,
EXISTING PROTECTIVE MEASURES AND THEIR EFFECTIVENESS**

Zhu DI

KEY LABORATORY OF HYDROECOLOGICAL EFFECTS AND ECOLOGICAL
RESTORATION, MWR, INSTITUTE OF HYDROECOLOGY, MWR & CAS

CHINA

Yang ZHI

KEY LABORATORY OF HYDROECOLOGICAL EFFECTS AND ECOLOGICAL
RESTORATION, MWR, INSTITUTE OF HYDROECOLOGY, MWR & CAS

CHINA

COMMISSION INTERNATIONALE
DES GRANDS BARRAGES

VINGT-SIXIÈME CONGRÈS DES
GRANDS BARRAGES
Autriche, juillet 2018

MAIN ECOLOGICAL RISKS FACING THE YANGTZE RIVER BASIN, EXISTING PROTECTIVE MEASURES AND THEIR EFFECTIVENESS

ZHU DI & YANG ZHI

*Key Laboratory of Hydroecological Effects and Ecological Restoration, MWR,
INSTITUTE OF HYDROECOLOGY, MWR & CAS
CHINA*

1. INTRODUCTION

The Yangtze River flows for 6,300 kilometers. It is the third longest river in the world. The Yangtze River Basin is a world hot spot of biodiversity, inhabited by over 400 fish species, of which some 350 are freshwater fish and up to 156 are endemic fish (Cao, 2011). Human activities such as water engineering and reclamation have led to changes in the aquatic inhabit, which then affect the reproduction and multiplication of aquatic organisms; the destruction of aquatic communities in turn affects the environment that humans depend on for survival. At present, the major hydroecological risks facing the Yangtze River Basin include decline in aquatic biodiversity, partial loss of biological habitats, water pollution, and reduction in river connectivity.

2. DECLINING AQUATIC BIODIVERSITY

2.1. REDUCTION IN SPECIES NUMBER

The Yangtze River is a wide diversity of unique species, when flooding occurs, provides us with abundant aquatic organisms. Flooding may be a disaster

for human beings, but it provides us with precious hydropower. Dams and sluices are extensively built in the middle and lower reaches to control flooding; and tens of thousands of dams are built to meet the excessive demand for hydropower. Besides, excessive demand has given rise to overfishing in open waters. As a result, the pristine Yangtze River ecosystem was damaged. Many species are threatened with extinction and biodiversity faces an unprecedented crisis. The middle and lower reaches was once abundant in *Lipotes vexillifer*, *Neophocaena phocaenoides*, *Tenuulosa reevesii*, *Lucpobrama macrocephalus*, and *Longjaw grenadier ancho*. Today, *Lipotes vexillifer* and *Lucpobrama macrocephalus* are hard to find. *Tenuulosa reevesii* has dropped significantly since the 1970s, falling to a record low in the early 1980s. Few *Longjaw grenadier ancho*, once the main fishing target, has been spotted in recent years (Li Sifa 2001). *Neophocaena phocaenoides* resources are being exhausted from about 2,700 in 1991 to about 550 in 2015 (*Bulletin of Fishery Ecology in the Yangtze River Basin (Trial)*, 2015). Compared with the 1970s, fish species of Dongting Lake and Poyang Lake decreased by 33.7% and 32.6%, and the proportion of migratory fish decreased by 47.1% and 53.6%. In 1970's, 336 and 310 bird species once lived around Dongting Lake and Poyang Lake, but surveys conducted in recent years showed that only 70-80 species have survived. Since the 1990s, the number of endangered species has seen a dramatic increase.

2.2. SHRINKING POPULATION

Yangtze River Basin is the most important producing area of freshwater fish in China (Yu, 1988a). The fish catches reached 450,000,000kg in 1954, accounting for 72% of the total national freshwater catches. It dropped to over 200,000 tons in the early 1980s, accounting for only about 60%. In recent years, it has maintained about 100,000,000 kg.

The production of semi-migratory fish of black carps, grass carps, silver carps, and bighead carps in rivers and lakes also dropped significantly. In 1964-1965, the annual average egg-laying amount of the Four Major Chinese Carps in the mainstream of the Yangtze River reached 115 billion. In 1981, it fell by 85% to 17 billion (Liu and He, 1992, Survey Groups of the Four Major Chinese Carps' Spawning Sites in the Yangtze River, 1982).

The natural fishery yield of Dongting Lake and Poyang Lake once reached a record high of 55,000,000kg. In 2015, it dropped to 28,000 tons in Dongting Lake and to 25,000 tons in Poyang Lake. The proportion of the Four Major Chinese Carps decreased from 21.0% to 6.61% and from 12.7% to 3.1% in Dongting Lake and Poyang Lake.

2.3. MINIATURIZATION AND HIGH MORTALITY AMONG INDIVIDUALS

In the 1970s, the average weight of two grass gudgeon species living in the Three Gorges Reservoir was about 500g (Ding, 1987). In 2000, the average weight of the two gudgeon species dropped to 276g and 208g, respectively (Chen et al., 2002). During 2005-2006, the average weight of two gudgeon species dropped further to 131g and 171g (Wu et al., 2007). The average ages of the Four Family Carps were 2.34, 2.10, 2.13, and 1.77 years. Compared with the data of the 1970s, fishery catches size was down significantly, and most of them were medium or small-sized young fish (Chen et al., 2002).

In Poyang Lake, small-sized commercial fish are on a general rise, and individuals tend to be younger and smaller. In 2007, there were about 12 major commercial fish species in the survey, those lake-inhabiting species such as carps, crucian carps, yellow-head catfish, and catfish are the main fishing targets, accounting for 71.3% -77.26% of the catches. The majority were 1-2 years old, accounting for 76% of the total catches.

2.4. DEGRADATION OF GERMLASM RESOURCES

In freshwater aquaculture, population blend has led to the degradation of germplasm resources. As a result, over fishing, breeding parents generally tend to be small-sized. Typical examples include silver crucian carps "giving only one times birth" to multiply and germplasm degradation among *Eriocheir sinensis* due to germplasm blend. Moreover, these degraded germplasm resources face the ecological risk of hybridization when they meet natural populations in the Yangtze River. As is the case with invading alien species, so far no relevant mechanism for assessing ecological risk is available in the country.

3. PARTIAL LOSS OF ENVIRONMENTAL CONDITIONS IN HABITATS

For many reasons, wetland degradation in the Yangtze River Basin has been severe for over half a century, and wetlands as important habitats of fish and waterfowl are gradually losing their environmental conditions. According to statistics, more than 1/3 of the lake areas, up to 130km², in the middle and lower Yangtze River have been reclaimed since 1949. More specifically, Dongting Lake dropped sharply from 43.50 km² to the current 26.25 km²; Poyang Lake decreased from 52km² in 1949 to the current 29.33 km². Apart from this, almost all riverine wetlands in the middle and lower Yangtze River have been reclaimed, and about 12.13 km² of wetland has been affected.

Changes have occurred in fish composition and structures after the impoundment of the Three Gorges Reservoir. In 1997-2002, 127 fish species were commonly spotted. In 2005-2006, 108 fish species were surveyed. In 2017, only 71 fish species were discovered, accounting for only 31%-33% of the endemic fish at the upper Yangtze River. Some rapid-loving fish, such as *Coreius*

guichenoti, *Rhinogobio cylindricus*, and *Rhinogobio ventralis*, migrated from the still-water sections of the reservoir area to the flowing-water river sections of the upper reaches of the river indication of the shrinking habitat space and an indirect cause of population reduction among these fish (Wu Qiang et al., 2007).SHRINKING POPULATION

4. INCREASED WATER POLLUTION AND LAKE EUTROPHICATION

According to statistics, sewage discharge in the Yangtze River Basin has risen from 12.7 billion m³ in the early 1980s to the current level of 15 billion m³, accounting for about 40% of the national total. Urban sewage treatment is inefficient, and a large amount of untreated sewage is discharged into various water bodies, causing varying pollution. The middle and lower reaches of the Yangtze River, 4,000 lakes here are larger than 0.5km². Five most famous freshwater lakes are located in the economic development zone in China. 5.6% are oligotrophic, 44.4% are mesotrophic, and 50% are eutrophic. More than half of them, especially those in suburban areas, have been affected by eutrophication. Taihu, Chaohu, and Dianchi Lakes are typical heavily polluted lakes (*China Environmental Quality Report*, 2011). For a vast majority of the lakes in the Yangtze River, sluices and embankments separate them from rivers. Poyang and Dongting Lakes are the only large lakes that are still linking to the River.

5. REDUCED RIVER AND LAKE CONNECTIVITY

Today, it has a lake area of about 15,200km² in Yangtze River, which accounts for 1/5 of the national area. Historically, more than 100 lakes larger than 10km² originally connected with rivers. Since the 1950s, due to massive construction of water conservancy projects and artificial reclamation, the longitudinal, horizontal, and vertical connectivity of the river systems in the Yangtze River Basin has been, in varying degrees, damaged.

5.1. RECLAMATION AND SLUICES AFFECTED RIVER-LAKE CONNECTIVITY

For a vast majority of the lakes in the Yangtze River, sluices and embankments separate them from rivers. Poyang and Dongting Lakes are the only large lakes that are still linking to the River

Table 1 Factors Affecting the Connectivity between Lakes -Rivers in the Middle and Lower Yangtze River

Lake Name	Year of Blocking	Reason for Blocking	Lake Name	Year of Blocking	Reason for Blocking
East Lake	1930	Reclamation	Wang Lake	1975	Embankment
Caisang Lake	958	Reclamation and Embankment	Chihu Lake	1983	Embankment
Taibai Lake	1942	Embankment	Saihu Lake	1983	Embankment
Datong Lake	1951	Reclamation and Embankment	Junshan Lake	1959	Sluice
Huanggai Lake	1959	Embankment	Wuchang Lake	1959	Sluice
Honghu Lake	1955	Embankment	Huangda Lake	Late 50s	Sluice
Xiliang Lake	1935	Sluice	Shengjin Lake	1962	Sluice
Zhangdu Lake	1954	Sluice	Chaohu Lake	1959	Sluice
Daye Lake	1970	Sluice	Gucheng Lake	1971	Sluice

5.2. THE DAMS AFFECTS THE UPPER STREAM-DOWNSTREAM CONNECTIVITY

Dozens of migratory species, such as *Coreius heterodon*, *Coreius guichenoti*, *Leptobotia elongata*, migrate to the middle and upper reaches to lay drifting spawn. Most of their spawning grounds are distributed in the upstream, and their eggs drift dozens or even hundreds of kilometers to the lower reaches for fattening. Another good example is the typical river-lake migratory species of "four major Chinese carps". By 2005, 45,694 reservoirs of various types had been built in the Yangtze River Basin. Dam construction obstructs the migration routes and blocks the migration passageway between the feeding zone and reproduction zone, preventing fish from effectively completing their life history and often resulting in serious decline in resources for these fish species. If these fish do not have spawning grounds in the main channel below the dam, the effects can be very serious and even lead to their extinction.

5.3. LOSS OF LONGITUDINAL AND VERTICAL RIVER CONNECTIVITY

An integrated river ecosystem includes riverways, floodplains, deep pools, shoal patches, and tributaries. During the flood season, fish follow the flow and swim to bottomland to spawn, forage, and avoid hazards. Reservoirs and Dams

cut off the link between rivers and bottomland or floodplains, limits the horizontal spread of water flow, and results in decrease in horizontal river connectivity and habitat loss for aquatic organisms. In addition, transforming rivers into channels and cutting off curves have completely changed the basic landform of meandering rivers, and the pattern in which rapid and slow flows alternate disappeared. The regular geometric changes on the cross-section also altered the pattern in which deep pools and shoal patches alternate. As the habitats heterogeneity was reduced, aquatic ecosystems were changed and biological diversity was reduced accordingly. This is embodied by shrinking areas of riverside vegetation and plants, reduced biodiversity in micro-habitats, altered spawning conditions for fish, changes in the habitats of birds, amphibians, and insects, or disappearance of shelters, which may lead to reduced populations and the extinction of some species.

6. EXISTING PROTECTIVE MEASURES FOR AQUATIC ECOSYSTEMS

6.1. LAWS AND REGULATIONS

By 2005, 9 laws on the protection of the ecological environment and 15 laws on the protection of natural resources has enacted, and more than 660 regulations and local laws have enacted and passed. Seven fish species in the Yangtze River Basin are under national-level protection, the first-class protected animals Dabry's sturgeon, Chinese sturgeon, and Chinese paddlefish; the second-class protected animals huchobleekeri, Chinese high fin banded shark, trachidermusfasciatus, and anguillamarmorata (Law of the People's Republic of China on the Protection of Wildlife, 1989); 69 fish species are included in the China Species Red List at or above the endangered level; aquatic animals listed under first-class protection include Yangtze River Dolphin, finless porpoise, and bank beaver, giant salamander etc. are under second-class protection.

6.2. CONSERVATION AREAS AND ACHIEVEMENTS

By 2004, 561 nature reserves have been established in the Yangtze River Basin, covering a total area of $32.88 \times 10^4 \text{ km}^2$, accounting for 18.3% of the Basin area. Among them, 59 are state-level with an area of $22.89 \times 10^4 \text{ km}^2$; 202 are provincial-level with an area of $6.44 \times 10^4 \text{ km}^2$; 59 are aremunicipal-level with an area of $1.74 \times 10^4 \text{ km}^2$; 241 are county-level nature reserves with an area of $1.81 \times 10^4 \text{ km}^2$. Nature reserves are distributed along the upper reaches and the mainstream as well as at the mouths. So far, a network of diverse nature

reserves with a rational layout and complete functions has taken shape in the Yangtze River Basin.

In order to effectively protect and make rational use of aquatic germplasm resources and promote the sustainable development of fishery, the Ministry of Agriculture has selected a number of fishing and breeding areas as well as major growth and breeding areas such as spawning grounds, feeding grounds, overwintering fields and migration routes as protected areas of aquatic germplasm resources. Until 2017, there are 228 national conservation areas of aquatic germplasm resources in the Yangtze River Basin.

6.3. ARTIFICIAL BREEDING AND RELEASE

As Artificial breeding and release is an important measure to mitigate the adverse impact of water engineering on aquatic resources, breeding and release stations are often correspondingly planned while the hydropower stations is under construction. In response to the decline in fishery resources, the Ministry of Agriculture organized long-term, systematic release activities mainly in the middle and lower reaches of the Yangtze River. The released offspring seeds are normally provided by local fishery production organizations. Among them, seed multiplication and stock seed farms of aquatic germplasm resources play a significant role. According to incomplete statistics, the Yangtze River Basin has 26 stock seed farms and seed multiplication farms.

6.4. RESTRICTIONS ON FISHING

Restricting fishing is the core of fishery resources management on the Yangtze River. The policy was released by the Ministry of Agriculture since 2002. The enforcement scope of the policy of closed fishing season on the Yangtze River sections in 10 provinces (cities) with a total length of more than 8,100 km. Specifically, the mainstream, the tributaries, the Poyang and Dongting Lake areas. During the closed fishing season (February 1 to April 30 above Gezhou Dam; April 1 to June 30 below Gezhou Dam), all the fishing activities are banned.

According to the research results of Shi Weigang et al. (2005), after the implementation of the fishing ban, species diversity index increased significantly and stabilized in the Anhui and Jiangsu sections from 2001 to 2004. The CPUE (catch per unit of effort) in some sections of the river increased significantly, the CPUE of *Coilia ectenes* rebounded, and resource degradation was stopped. The ecological effects of the spring ban on the protection of fishery resources in the middle and lower reaches of the Yangtze River are noticeable, and the interspecific structure of the fishery resources was improved to a certain extent after the implementation of the spring ban.

6.5. FISH PASS STRUCTURES

In 1958, China designed its first fishpass at Qililong Power Station on the Fuchun River. In 1960, the first newly opened fishpass was built near Xingkai Lake and it has a total length of 70m and a width of 11m, and initial operations were successful (Song Dejing et al., 2008). The construction of Yangtang Fishpass in 1980 has taken the design and research on fish pass structures in China's fish collection system. For example, according to statistics gathered in 1982, the total number of fish that passed through the fishpass was 759,325 (77d, 1464h), and 571,143 (77d, 1415d) passed through the fish collection system in the plant, accounting for 75% of the total number of fish that passed through (Wang and Guo, 2006).

With the further development of water conservancy and hydropower projects in China since 2000, more attention was given to the research on the restoration of fish migration routes. A number of fish pass structures are under construction or have been completed, such as the Shangzhuang Reservoir Fishpass in Beijing, the Xinglong Fishpass on the Hanjiang River, the Pengshui Hydropower Station Fishpass on the Wujiang River, the fishpass on the Pearl River and Shiquan River (Hu et al., 2008). According to incomplete statistics, China has built more than 40 fishpasses in various types of water conservancy projects, most of which are built on low water head dams.

7. CONCLUSION AND SUGGESTIONS

The development of the Yangtze River Economic Belt, supported chiefly by the Yangtze River golden waterway, is in full swing. This will undoubtedly place the maintenance of the Yangtze River's biodiversity and the protection of the water environment under unprecedented pressure. We need to analyze the current crisis from a historical perspective because biodiversity in today's Yangtze River system is not inherent but a product of evolution. The subtropical monsoon climate is the basis of the unique biota of the Yangtze River, and the East Asian monsoon climate is the result of the uplifting of the Qinghai-Tibet Plateau, at least it strengthens the monsoon. These major climatic and geological events are important basis for the evolution of biodiversity. They reveal the uniqueness and ecological needs of the ichthyofauna, as well as how species diversity is maintained. The knowledge of the historical contributing factors to species diversity is essential to understanding why human activities have led to a significant loss of biodiversity in water systems. We need to understand the space-time continuity (eg, connectivity of rivers and lakes) and the integrity of ecological processes (eg, hydrological processes, temperature processes) needed by each species to accomplish life histories. Accurate prediction of what species are endangered is hard to come by, not to mention saving them. Our target goal is to rehabilitate or re-naturalize damaged ecosystems, which, though

basically impossible in large rivers, is still worth the effort because it at least delays or reverses the decline of some aquatic animals or the danger of extinction facing them (Xie Ping, 2017).

REFERENCES

- [1] China Freshwater Fish Farming Experience Summarizing Committee. China Freshwater Fish Farming Science. Science Press, 1973.
- [2] Investigation Group of the Spawning Grounds of the Four Major Chinese Carps in the Yangtze River. Investigation into the Spawning Grounds of the Four Major Chinese Carps after the Closure of the Gezhouba Project [J]. Journal of Fisheries of China, 1982, 6(4):287-305.
- [3] Ding Ruihua. Analysis of Fishery Environment and Fishery Development in the Three Gorges Reservoir Area. Chengdu: Sichuan Science and Technology Press, 1987.
- [4] Chen Daqing, Duan Xinbin, Liu Shaoping, et al. Changes in Fishery Resources in the Yangtze River and Management Strategies [J]. Acta Hydrobiologica Sinica, 2002, 26 (6): 685-690.
- [5] Xie Ping. 2017. Biodiversity Crisis in the Yangtze River: Water Conservancy Projects are the Leading Cause and Overfishing is the Accomplice. Journal of Lake Sciences, 29(6):1279-1299, DOI 10.18307/2017.0601
- [6] Ministry of Environmental Protection of the People's Republic of China. 2006-2010 China Environmental Quality Report [M]. China Environmental Science Press, 2011.
- [7] Chen Kaiqi, Chang Zhongnong, Cao Xiaohong, et al. Status and Prospection of Fish Pass Construction in China [J]. Journal of Hydraulic Engineering, 2012, 43 (2): 182-188.
- [8] Guo Jian, Rui Jianliang. Question and Suggestion on Fishway Construction in China: Lesson Learned from the Operation of Yangtang Lock Fishway [J]. Water Power, 2010, 36 (4): 8-10.
- [9] Shi Weigang, Liu Kai, Zhang Mingying, et al. Changes of Biodiversity of Fishery Species in the Lower Reaches of the Yangtze River During the Spring Closed Season (2001-2004) [J]. Journal of Lake Science, 2005, 17 (2): 169-175.
- [10] Song Dejing, Jiang Hui, Guan Changtao, et al. Design of A Fishway for Lao Long Kou Hydro-Junction Project [J]. Marine Fisheries Research, 2008, 29 (1): 92-97.
- [11] Wang Xingyong, Guo Jun. Research on and Construction of Fishpasses Abroad [J]. Journal of China Institute of Water Resources and Hydropower Research, 2005, 3 (3): 222-228.
- [12] Hu Wangbin, Han Deju, Chang Jianbo. Restoration of Fish Migration Practice of Foreign Countries and Strategies of China. Seminar on Promotion of New Technologies in Water Conservancy and Hydropower

SUMMARY

The Yangtze River flows for 6,300 kilometers. It is the third longest river in the world. The Yangtze River Basin is a world hot spot of biodiversity, inhabited by over 400 fish species, of which some 350 are freshwater fish and up to 156 are endemic fish. Increasing human activity in the Yangtze River Basin has led to changes in the habitats that aquatic organisms inhabit, which then affect the reproduction and multiplication of aquatic organisms; the destruction of aquatic communities in turn affects the environment that humans depend on for survival.

The major hydroecological problems and risks facing the Yangtze River Basin today include decline in aquatic biodiversity, partial loss of environmental conditions in biological habitats, aggravation of water pollution, and reduction in river connectivity. The decline in biodiversity is reflected mainly in decrease in species number, shrinking of population, miniaturization and high mortality rate among individuals, and degeneration of germplasm resources. The main reasons leading to the decline in biodiversity include reclamations, sluices, or embankments that reduce the connectivity of rivers and lakes; the construction of reservoirs across rivers lowers upstream-downstream connectivity; embankments turn rivers into channels, resulting in loss of vertical connectivity.

In the face of the hydroecological problems and risks prevalent in the Yangtze River Basin, China has, over the years, enacted 9 laws concerning ecological improvement and environmental protection, 15 laws for the protection of natural resources, and over 660 regulations at all levels of government. In addition, efforts at natural conservation have been redoubled, such as promoting the development of protected areas and taking measures like artificial fecundation, release of fish, restricting fishing, and construction of fish pass facilities. However, as development projects in the Yangtze River Basin continue to grow, existing measures may not be able to delay or reverse ecological recession and more time is needed to test them.

KEY WORDS

Yangtze River Basin, water conservancy projects, ecological risks, ecological problems, protection measures

8. CLEARANCES AND COPYRIGHT

The author(s) is (are) responsible for obtaining written permission to profile the project or subject matter in their papers from any and all clients, owners or others who commissioned the work. ICOLD assumes proper permission has been obtained by author(s) and accepts no liability for the author(s) failing to do so.

If a figure, table or photograph has been published previously, it will be necessary for the author(s) either to obtain written approval from the original publisher; or refer clearly to the source of previously published material in the caption of the figure, table or photograph.

COMMISSION INTERNATIONALE DES GRANDS BARRAGES

VINGT-SIXIÈME CONGRÈS DES GRANDS BARRAGES
Autriche, juillet 2018

DOI 10.3217/978-3-85125-620-8-091



This work licensed under a Creative Commons Attribution 4.0 International License. <https://creativecommons.org/licenses/by-nc-nd/4.0/>

**ANALYSIS AND INTERPRETATION OF THE BAIXO SABOR DAM'S
BEHAVIOUR DURING THE FIRST FILLING OF THE RESERVOIR**

José PITEIRA GOMES

LNEC – NATIONAL LABORATORY FOR CIVIL ENGINEERING, LISBON

PORTUGAL

António L. BATISTA

LNEC – NATIONAL LABORATORY FOR CIVIL ENGINEERING, LISBON

PORTUGAL

D. SILVA MATOS

EDP GESTÃO DA PRODUÇÃO DE ENERGIA S.A., OPORTO

PORTUGAL

COMMISSION INTERNATIONALE
DES GRANDS BARRAGES

VINGT-SIXIÈME CONGRÈS DES
GRANDS BARRAGES
Autriche, juillet 2018

ANALYSIS AND INTERPRETATION OF THE BAIXO SABOR DAM'S BEHAVIOUR DURING THE FIRST FILLING OF THE RESERVOIR

José PITEIRA GOMES ¹, António L. BATISTA ¹, D. SILVA MATOS ²

¹ LNEC – National Laboratory for Civil Engineering, Lisbon

² EDP Gestão da Produção de Energia S.A., Oporto

PORTUGAL

1. INTRODUCTION

The failure of dams with large reservoirs can be the cause of catastrophic accidents with very important losses of human lives and of material and environmental assets. For these reasons, the safety control of these constructions is regulated and followed by national authorities, considering the structural, hydraulic-operational and environmental aspects. In Portugal, the national authority is technically helped, with the dams that involve major risks, by the National Laboratory for Civil Engineering (LNEC).

The structural safety control of dams begins in the design phase and ends only with its decommissioning. This control is based on regular inspections and on the comparison between monitoring data, obtained through the instrumentation installed according to the monitoring plan (defined during the design phase and updated during the dam's lifetime), and results of models, usually numerical ones, considering the most important characteristics of the structures, such as the geometry and the material properties, and the main actions.

The first filling of the reservoir, as a load test for the real operational conditions of the dam-foundation-reservoir system, requires special monitoring. The safety control activities during this period are very important not only to avoid accidents and incidents, but also to acquire knowledge about the structural

behaviour of the dam which will be a reference during its lifetime. The safety regulations of almost all developed countries determine special monitoring programmes during this particular phase.

This paper presents some relevant results of the structural safety activities performed during the first filling of the reservoir of Baixo Sabor dam. After a brief description of the dam and its construction, the monitoring system, the monitoring plan during the first filling of the reservoir and some important results of tests carried out for the characterization of the material rheological properties are presented. The interpretation of the monitoring results is based on their comparison with results of a numerical model that simulates the structural behaviour of the dam and its foundation.

2. BRIEF DESCRIPTION OF THE DAM

2.1. BAIXO SABOR HYDROELECTRIC SCHEME

The Baixo Sabor hydroelectric scheme, in which the dam is integrated, is located on the Sabor river, in the north eastern part of Portugal. The scheme was designed and built by EDP Produção [1], and has been operated by this company.

The scheme mainly consists of the dam, the underground powerhouse, excavated in the rock mass of the right bank, which includes the water intakes and the headrace tunnels upstream, as well as the tailrace tunnels downstream. The total installed power capacity is 171 MW, using two reversible units.

The rock mass, on which the scheme was built, is of a good quality granite. However, it showed heterogeneous characteristics along the dam insertion surface as well as in the underground structures.

2.2. DAM CHARACTERISTICS

The dam is a double curvature thick arch dam (Fig. 1) with 123.00 m high and a crest development and thickness of 505 m and 6.00 m, respectively. The crest and the normal water level (NWL) are at elevations 236.00 m and 234.00 m, respectively. The structure is divided into 32 blocks with approximately 15 m width near the right and the left banks and with 17 m width in the central blocks. The blocks are separated by vertical contraction joints, which were grouted to obtain a monolithic structure, after forced cooling of the concrete blocks. The dam has six horizontal inspection galleries spaced 20.00m in elevation. The reservoir volume is of about 1095 hm³ for the NWL [2].



Fig. 1

Aerial view of Baixo Sabor dam after the first filling of the reservoir

2.3. DAM CONCRETE

The dam has a total concrete volume of, approximately, 670,000 m³. The 32 blocks were cast in 2.0 m height layers. The placement of concrete began in 2011 and ended in 2013.

The cementitious materials were Portland cement CEM I 42.5R and a class F fly ash. The fine and the coarse aggregates were granitic, obtained by crushing the rock from a quarry located on the right bank of the river, upstream. The concrete mixtures presented in Table 1 correspond to the concretes most used in the dam.

Table 1
Dam concrete compositions

Constituents (kg/m ³)	Face concrete	Core concrete
Cement I 42.5R	130	110
Fly ash	130	110
Fine aggregate 0/4.75 mm	637	640
Coarse aggregate 4.75/150 mm	1293	1414
Admixture	1.04	0.88
Water	133	124

For the dominant dam's concrete, the following BaP creep law was adjusted, considering the results of a set of "in situ" and laboratory tests [3],

$$J(t, t_0) = \frac{1}{40.0} \left(1 + 3.2(t_0^{-0.35} + 0.05)(t - t_0)^{0.12} \right) \quad (\text{GPa}^{-1}) \quad [1]$$

which is represented in Fig. 2 for three ages of loading, as well as the corresponding relaxation curves obtained through numerical inversion. Mention must be made to the fact that the concrete presents low creep rates for high loading ages.

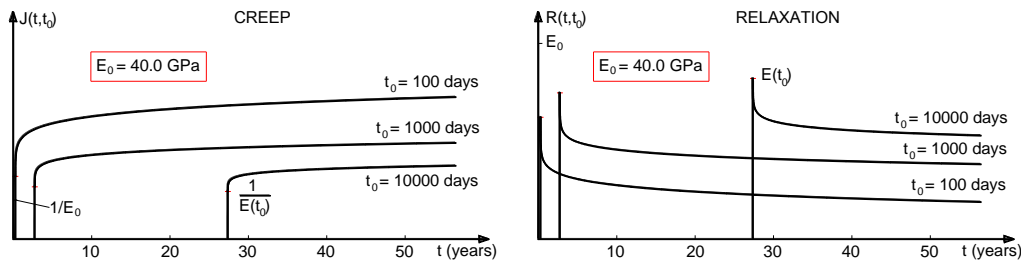


Fig. 2

Creep and relaxation curves of the dominant dam's concrete

2.4. MONITORING SYSTEM

The dam monitoring system allows the evaluation of the actions and the determination of the thermal, structural and hydraulic responses [4], by measuring (in brackets the total number of measurement instruments are indicated): i) the upstream and downstream levels, by staff gauges and water level recorders; ii) air temperatures, in an automatic weather station; iii) uplifts, by means of a piezometer network (41) installed in the drainage gallery; iv) horizontal displacements, by coordimeter bases installed at the intersection of the 5 plumb lines with the inspection galleries; v) horizontal displacements by 3 traverses on galleries; vi) vertical displacements, by precision geometric levelling on the crest and on 4 galleries; vii) vertical and horizontal displacements of the rock mass foundation, by rod extensometers (16) installed also in the drainage gallery; viii) joint movements, using electrical resistance devices for measuring the movement of joints (152) and three-dimensional baselines (103); ix) temperatures in the dam's body, by electrical resistance thermometers (52), by devices for measuring the movement of joints, by strain meters and stress meters; x) strains, by groups of one, five or nine Carlson strain meters (265); xi) stress, by stress meters (10); xii) water pressures in the concrete, by pressure cells (6); and xiii) discharged and infiltrated flows, by foundation drains (216) and measuring weirs (18). The dam is also equipped with 3 creep cells, for evaluation of the concrete deformability over time, a GNSS system to measure displacements (4 antennas, 1 reference station and 3 stations on the crest), a seismic monitoring system (6 triaxial accelerometers, 3 near the foundation and 3 on the upper central zone) and a dynamic response monitoring system (20 accelerometers installed on the upper galleries).

3. ANALYSIS AND INTERPRETATION OF THE STRUCTURAL BEHAVIOUR

3.1. STRUCTURAL MODEL

The dam behaviour was analyzed and interpreted on the basis of the monitoring results and of a continuous structural model (because no significant movement variations were observed in the contraction joints during the first filling). The structure of the dam was approximated by a set of supposedly continuous and homogeneous blocks, considering 30 monthly construction stages, with a rheologic behaviour of the concrete characterized by expression (1) and by Poisson ratio $\nu_c=0.2$. The rock mass foundation was divided in 7 zones of different deformability, as a function of the results obtained from the geomechanical characterization [2] and “in situ” seismic tomography tests [5]. The Poisson ratio was assumed with a value of $\nu_f=0.2$ for all the zones. No time effects on the foundation behaviour have been considered.

The finite element mesh (Fig. 3) has a total of 14854 nodal points for 2795 isoparametric cubic 20 nodes finite elements (1067 elements of the dam’s body and 1728 elements of the rock mass foundation). The dam’s body has 3 elements across the thickness. The spans and the shapes of the surface spillway were explicitly represented in the finite element mesh.

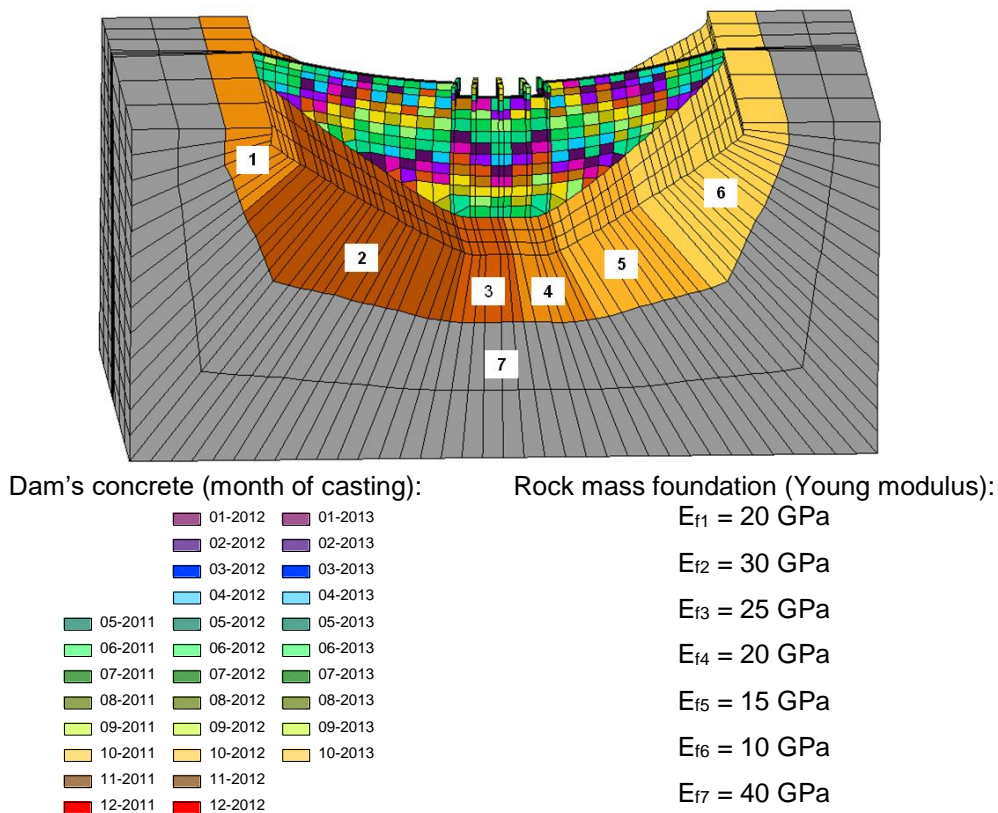


Fig. 3

Dam-foundation finite element mesh considered in structural analysis

3.2. ACTIONS VARIATION DURING THE FIRST FILLING OF THE RESERVOIR

The specific monitoring plan for the first filling of the reservoir defined a set of stages at which the filling was suspended to do general observation campaigns and to perform the dam's behaviour evaluation [6]. The first filling of the reservoir began in December 2013, was interrupted in 3 main intermediate filling stages (FS1, FS2 and FS3, at water levels 180 m, 206 m and 224 m, respectively) and in 2 stabilization levels (SL1 and SL2, at water levels 216 m and 231 m, respectively), and was completed in April 2016 (FS4), when the NWL reached an elevation of 234 m (Fig. 4). The first filling lasted about 28 months.

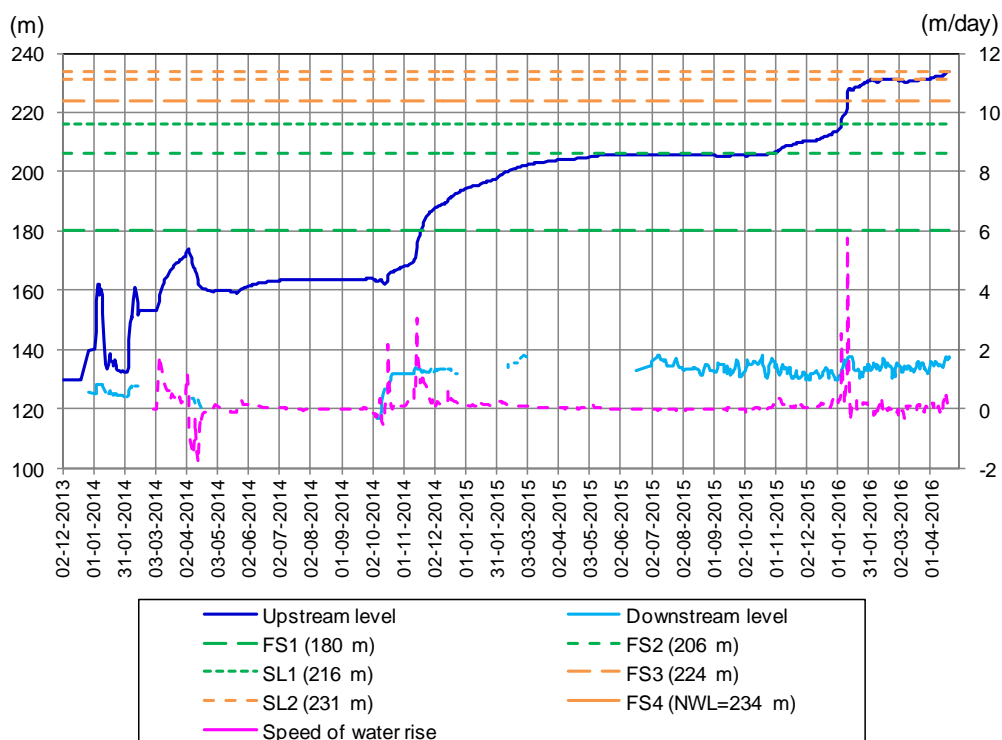


Fig. 4
Water level variation during the first filling of the reservoir

As the uplifts had small variations during the first filling, the water loads were represented only by hydrostatic pressure increments on the upstream surface of the dam, considering $\gamma_w=10 \text{ kN/m}^3$.

The thermal variations in the dam's body were computed from the monitored temperatures in concrete, air and water, considering a numerical procedure to spread the observed values in a set of discrete points to all the mesh nodes of the dam's structure. Fig. 5 represents, as examples, the temperature fields observed in two stages of analysis, August 2014 and December 2015. A linear thermal dilation coefficient was considered for the concrete $\alpha=1.1 \times 10^{-5} / ^\circ\text{C}$.

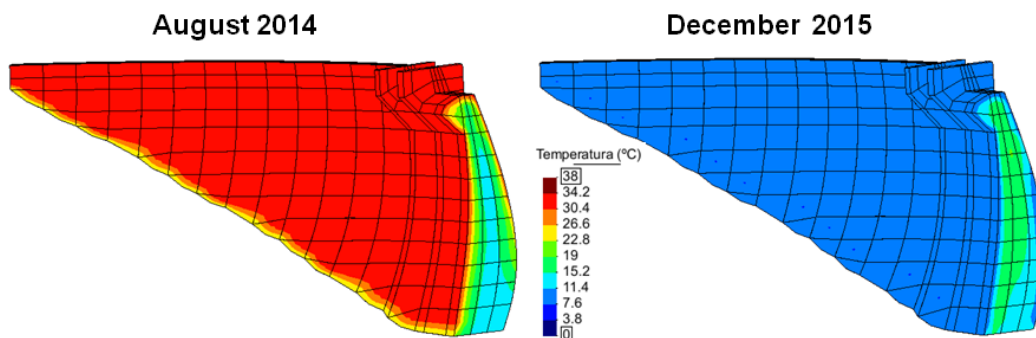


Fig. 5

Temperature fields observed in dam's body in two stages of analysis

The analysis comprises of the first filling period and a subsequent operation period until late January 2017. Actions due to water pressure and thermal variations were discretized fortnightly.

3.3. SOME RELEVANT RESULTS

In Fig. 6 and Fig 7 the horizontal displacements observed over time (from July 2014 to January 2017) for the central plumb-line at elevations 233.10 m and 170.2 m, respectively, and the correspondent computed horizontal displacements, considering the effects of water pressure, thermal variations and creep, are represented. The great influence of the thermal variations on the structural response and the very good agreement obtained between observed and calculated displacements should be pointed out. Concerning the displacements values measured and computed in other points of the dam, good adjustments were also obtained.

Fig. 8 shows the displacements measured and computed on the subvertical rod extensometer EF9, located downstream on the bottom of the central block 17-18 at 116.3 m elevation, from July 2014 to January 2017. In this case the agreement is not so good. The global shape of the displacements evolution over time is similar, but the monitored displacements are about twice the calculated ones. On most rod extensometers the adjustment achieved was better, but in some of them the adjustment was of the same type.

For the data of other types of monitoring devices good agreements were also obtained, demonstrating the good performance of the dam and the adequacy of the models considered for the analysis and interpretation of the observed behaviour.

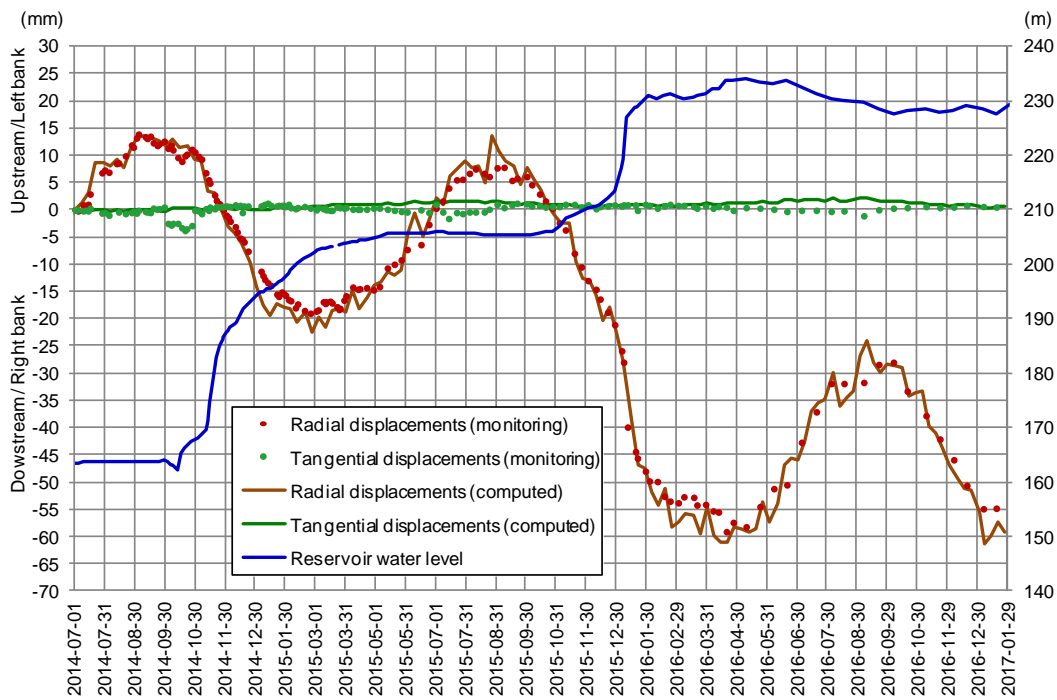


Fig. 6

Central block 17-18 horizontal displacements at 233.1 m elevation, measured on the plumb line and computed from July 2014 to January 2017

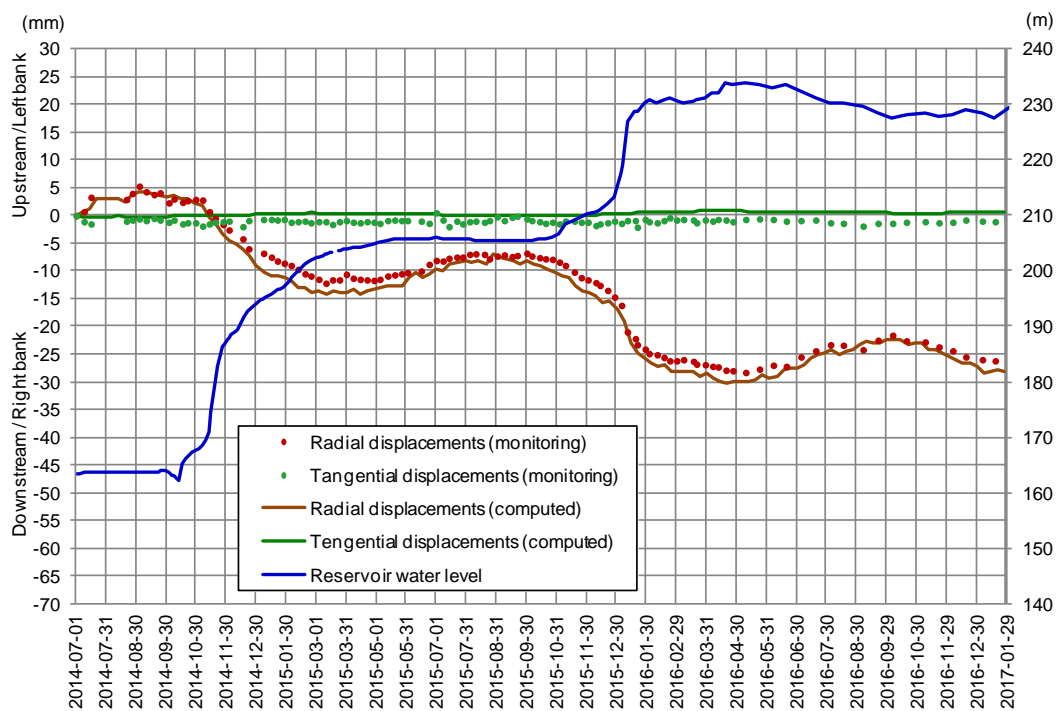


Fig. 7

Central block 17-18 horizontal displacements at 170.2 m elevation, measured on the plumb line and computed from July 2014 to January 2017

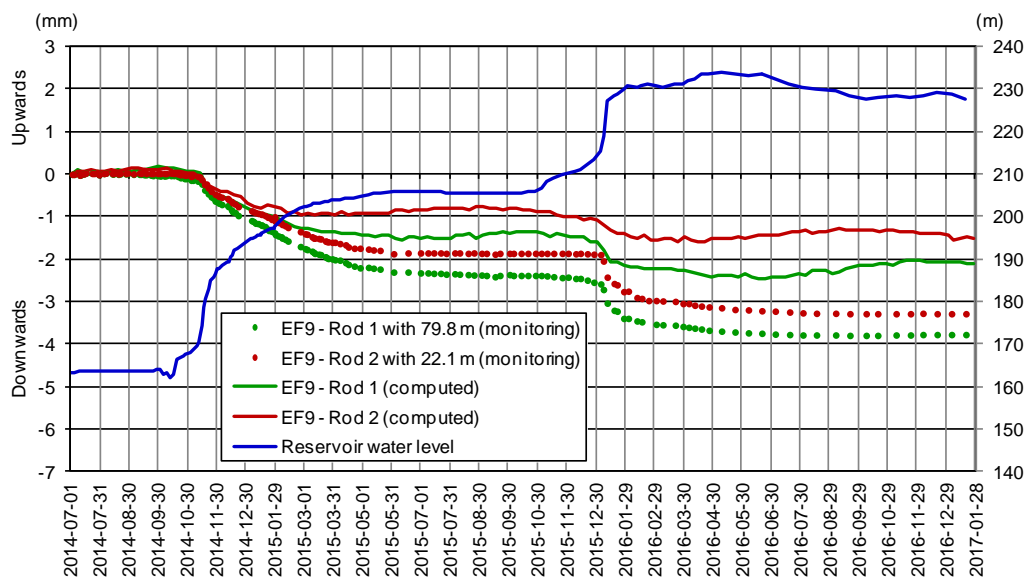


Fig. 8

Displacements measured and computed on the subvertical rod extensometer EF9, located downstream on the bottom of the central block 17-18 at 116.3 m elevation, from July 2014 to January 2017

4. CONCLUSIONS

The mathematical methodologies used to analyse and interpret the structural behaviour of the Baixo Sabor dam during the first filling of the reservoir have proven to be adequate for the intended purposes, in particular regarding to the consideration of both the instantaneous and the differed effects of the main loads, namely the hydrostatic pressure and the temperature variations. Mention should be done to the suitable evaluation of the deformability characteristics of the dam's concrete and of the rock mass foundation, as well as the thermal variations in the dam's body, that allowed a good adjustment between the monitoring data and the structural model results.

The adequate planning of the first filling of the reservoir and the results of both the inspections and the behaviour analysis and interpretation made it possible to carry out a proper monitoring and safety control of the dam during this critical period. The overall results obtained show the good performance of the dam and constitute a reference state for the observation and safety control of the dam over time.

REFERENCES

- [1] EDP. Baixo Sabor Hydroelectric Scheme. Design. Upstream dam (in Portuguese). Internal document, Oporto, 2005.
- [2] MIRANDA M.P., SILVA MATOS D., PIMENTEL R., GOMES A. The Baixo Sabor upstream and downstream dams. Relevant design and construction features. First Dam World Conference, Maceió, Brazil, 2012.
- [3] LNEC. Upstream dam of Baixo Sabor Hydroelectric Scheme. Installation of creep cells and early age tests (in Portuguese). Report 311/2014 – DBB/NO, Lisbon, 2014.
- [4] EDP. Upstream dam of Baixo Sabor Hydroelectric Scheme. Monitoring plan (in Portuguese). Oporto, 2007.
- [5] LNEC. Baixo Sabor Hydroelectric Scheme. Upstream dam. Seismic tomography between the dam foundation holes, after the first filling of the reservoir (in Portuguese). Report 209/2017 – DG/NGEA, Lisbon, 2017.
- [6] EDP. Upstream dam of Baixo Sabor Hydroelectric Scheme. Monitoring plan during the first filling of the reservoir (in Portuguese). Oporto, 2013.

SUMMARY

The first filling of the reservoir, as a real load test, is a crucial stage in the dam's lifetime. During this phase the safety control, based on the continuous monitoring, according to a specific observation plan, is required for the early detection of any abnormal behaviour. The structural modelling is also important to allow a coherent interpretation of the causes-effects relationships.

The paper describes the relevant aspects of the monitoring procedures and of the analysis and interpretation of the Baixo Sabor dam's behaviour, an arch dam with 123 m high and 505 m long at crest (designed, built and operated by EDP Produção), during the first filling of its reservoir (with a volume of about 1095 hm³), which took place between December 2013 and April 2016.

The characterization of the materials' properties (concrete and rock mass foundation) and of the actions and responses during the first filling, as well as the structural model used to simulate the structural behaviour, are presented. This model, developed by LNEC, included a 3D representation of the dam and its rock mass foundation and it was analysed by the finite element method, considering the actions time evolution and the concrete viscoelastic behaviour.

A good agreement between the monitoring results and those obtained through the mathematical modelling was achieved, which confirmed the good performance of the dam and the modelling adequacy during this important stage.

Keywords: Baixo Sabor dam; Arch dam; Reservoir; First filling; Monitoring; Creep; Finite element method; Safety control.

COMMISSION INTERNATIONALE DES GRANDS BARRAGES

VINGT-SIXIÈME CONGRÈS DES GRANDS BARRAGES
Autriche, juillet 2018

DOI 10.3217/978-3-85125-620-8-092



This work licensed under a Creative Commons Attribution 4.0 International License. <https://creativecommons.org/licenses/by-nc-nd/4.0/>

SCOUR ESTIMATION FOR NAM THEUN 1 SPILLWAY PLUNGE POOL

F. TAKHTEMINA

Senior Engineer, PÖYRY ENERGY

THAILAND

M.P. BIERI

Senior Engineer, PÖYRY ENERGY

SWITZERLAND

B. ZÜEND

Senior Engineer, PÖYRY ENERGY

SWITZERLAND

S. MARTIN

Senior Engineer, PÖYRY ENERGY

AND SWITZERLAND

COMMISSION INTERNATIONALE
DES GRANDS BARRAGES

VINGT-SIXIÈME CONGRÈS DES
GRANDS BARRAGES
Autriche, juillet 2018

SCOUR ESTIMATION FOR NAM THEUN 1 SPILLWAY PLUNGE POOL

F. TAKHTEMINA

Senior Engineer, PÖYRY ENERGY

Dr. M.P. BIERI

Senior Engineer, PÖYRY ENERGY

Dr. B. ZÜEND

Senior Engineer, PÖYRY ENERGY

S. Martin

Senior Engineer, PÖYRY ENERGY

THAILAND AND SWITZERLAND

1. INTRODUCTION

Nam Theun 1 (NT1) dam is a 180 m high RCC curved gravity dam situated in Lao PDR. The dam is equipped with four gated spillway bays and a bottom outlet, both terminating at flip buckets as energy dissipaters. To prevent any dam foundation undermining, tailwater level increase and blockage of the draft tube gates as a result of erodible material being deposited at the powerhouse located circa 300 m downstream of the dam, a pre-excavated plunge pool was designed within the river just downstream the spillway and bottom outlet.

This paper describes the step-by-step methodology applied for design and functionality checks of the proposed pre-excavated plunge pool downstream the dam.

2. PLUNGE POOL DESIGN CRITERIA

A pre-excavated plunge pool is proposed for NT1 project in order to prevent uncontrolled progression of the scour towards the dam foundation and the formation of a mound of scoured material at the powerhouse tailrace area. This would cause higher tailwater levels affecting the energy production.

The spillway is designed to safely discharge a Probable Maximum Flood (PMF) of 30,200 m³/s without causing serious damage to the permanent works, whereas the design of the pre-excavated plunge pool focusses on the serviceability of the powerhouse, justifying a 100-year return period as a design basis. For this event the design of the pre-excavated plunge pool shall not allow for any major erosion process by the released water of the spillway and the bottom outlet.

3. SCOURING EVALUATION USING EMPIRICAL FORMULAE

For the hydraulic design of NT1 a theoretical analysis has been coupled with laboratory investigations. The theoretical analysis is based on (semi-) empirical scour depth formulae, the main parameters of which are the duration of the spillway operation, the specific discharge (per meter width) and the head. Other parameters are air entrainment in the jet, the rock characteristics and the tailwater depth. Martins, Chian, Mason and Veronese equation modified by Yildiz and Üzücek have been used to estimate the ultimate scour depth. For NT1 spillway jets, average scour depths in the range of about 45 m to 80 m below tailwater level were achieved for 30-year flood to PMF. Mason and Modified Veronese yielded high range values while Chian and Martins gave lower closer values.

4. PHYSICAL MODEL QUALITATIVE SCOURING TESTS RESULTS

The hydraulic studies of the spillway jets and plunge pool were carried out using 1:80 (overall dam) and 1:60 (partial of three chutes) reduced scale physical models, adopting Froude similarity, built at the Asian Institute of Technology (AIT) in Bangkok, Thailand. The 1:80 overall model reproduces a part of the reservoir and of the dam, the entire spillway (sill, gates, chute, flip buckets), the plunge pool and the powerhouse tailrace together with a downstream river reach for implementing the downstream tailwater condition.

The spillway model, built in PVC and mortar, was designed to accommodate modifications and several alternatives for the flip buckets (varying the lip angle and provision of dents). Erosion in the plunge pool was studied

using a movable bed. With such non-cohesive material good predictive results are expected for the scour depth, but not for its horizontal extents. Therefore the banks were modelled rigid. To minimize the scour depths in the plunge pool, the spillway flip buckets were fitted with dents. The flow patterns for different alternatives of buckets are illustrated Fig.1.



Fig. 1

Hydraulic performance of the flip bucket before and after the modification
($Q=4,200 \text{ m}^3/\text{s}$; “baffle blocks” = dents)

The dents scatter the jet trajectories. This not only favours the energy dissipation but also better regulates the backward currents, thus reducing the maximum scour and the risk of erosion towards the dam toe. The shape and the depth of the scour holes formed by flows from both buckets alternatives are shown in Fig.2.

5. PLUNGE POOL LAYOUT (OUTLINES & DEPTH)

The plunge pool depth design is based on the results of physical model tests and estimates from empirical approaches. Based on this, the excavation level of the plunge pool invert was set at 105.0 m asl which ensures passage of a 100-year flood without any major plunge pool damage.

To be on the safe side, the upstream face of the pre-excavation was designed based on jet trajectory calculations that take into account the considerable effect of the air resistance. In contrast for the downstream side –

potentially affecting the powerhouse tailrace – this influence was omitted, which approximately corresponds to the model test trajectories.

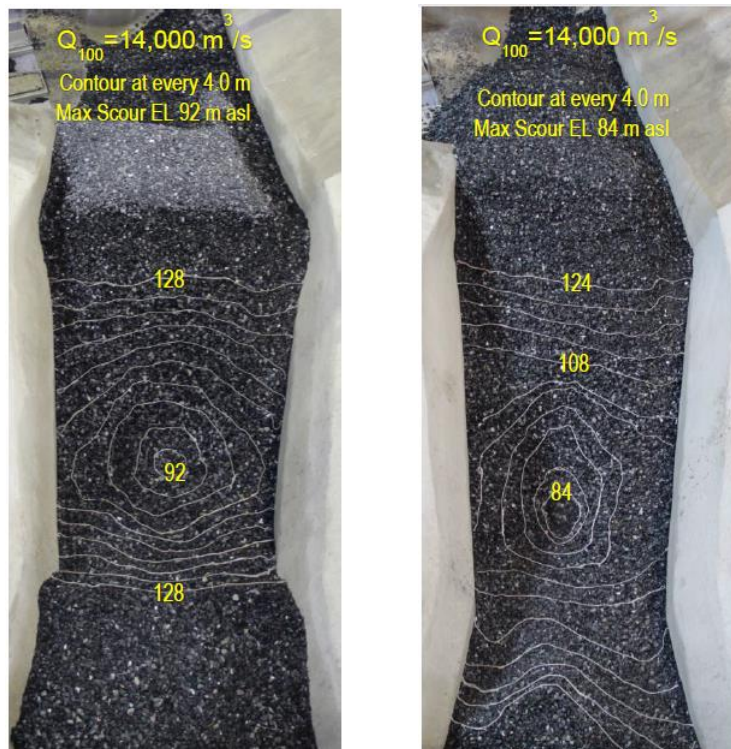


Fig. 2

Scour patterns at plunge pool for flip bucket options with (left) and without (right) dents

The plunge pool forehead general slope including the widths of the berms were such designed to avoid rotational and erosive flow patterns, as e.g. threatening Kariba dam in Zambia. In the framework of the Kariba plunge pool scour mitigation studies, a similar adjustment of the forehead slope was recommended as a countermeasure based on physical and numerical modelling [1]. The layout of the pre-excavated plunge pool of NT1 is shown in Fig.3.

6. JETS CHARACTERISTICS BEFORE AND AFTER IMPACTING THE PLUNGE POOL SURFACE

A parallel method to assess the nature and hence the erosive potential of a plunging jet has been developed by researchers such as Ervine et al. [2] and Castillo [3, 4] which is based on two major processes (see Fig. 4).

First, when travelling through the air the jet develops increasing instability and corresponding turbulent surface disturbances. These gradually reduce the thickness of the solid core of the jet. Beyond the “jet break-up length” L_b the solid

core has vanished. The jet then consists of blobs of water that disintegrate into finer drops. It is considered no more “developing” but “developed”. The decision is made on the parameter L_b/H with H being the jet falling height.



Fig. 3

Pre-excavated plunge pool model together with installed pressure sensors

Second, when the jet – developed or not – plunges into the pool it forms a new core of a thickness B_j , no longer solid this time. This core is gradually reduced by turbulent mixing with the surrounding water. After a distance of $4 B_j$ the core is dissipated. In case the ratio Y/B_j – Y being the pool depth – is larger than 4, the pool is considered “deep”, otherwise “shallow”.

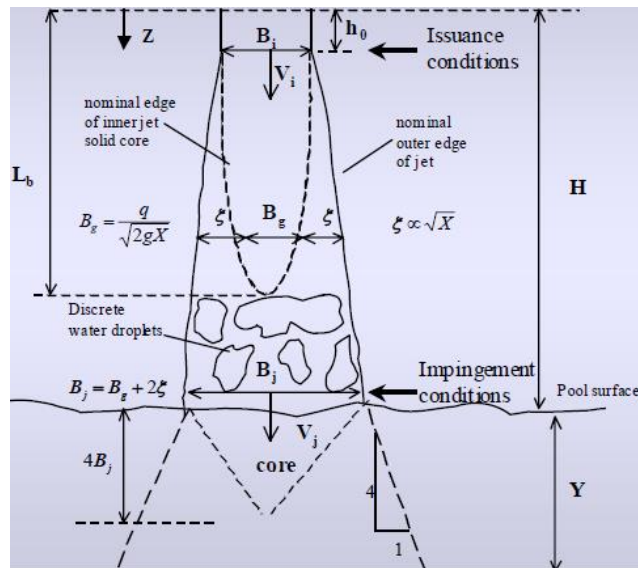


Fig. 4

Impingement jet analysis according to Castillo [4]

Based on these two distinctions Castillo [4] classified four types of jet conditions realized before and after entering the plunge pool:

- a) undeveloped jet $H/L_b < 1$, shallow pool $Y/B_j < 4$
- b) developed jet $H/L_b > 1$, shallow pool $Y/B_j < 4$
- c) undeveloped jet $H/L_b < 1$, deep pool $Y/B_j > 4$
- d) developed jet $H/L_b > 1$, deep pool $Y/B_j > 4$

Applying Castillo's approach [3], the jet break-up length was calculated and it was found that the disintegration occurs before the impact on the plunge pool water surface. Thus, a certain amount of energy will be dissipated in the air. The existence of dents on the buckets shall improve and guarantee the degree of jets' aeration and disintegration. Considering the jet's issuance characteristics, travelling length, falling heights and the tailwater levels at the plunge pool for NT1 case (Table 1), the jets can be classified as type (d) which implies developed (disintegrated) jets condition in the air and a deep pool situation.

Table 1
NT1 spillway design flood jet characteristics at issuance section and before/after impacting the plunge pool surface

Flood	q [m ² /s]	Y [m]	Tu	L _b [m]	H [m]	H/L _b	B _j [m]	Y/B _j
100-year	134.9	55	0.035	95	125	1.3	7.1	7.8

7. PRESSURES REGISTERS AND INTERPRETATION

The pressures at the invert and berms of the pre-excavated plunge pool have been measured by means of low range industrial pressure sensors (10 Hz).

The impact pressures time series on the pre-excavated plunge pool bed and berms for $Q_{100}=14,000$ m³/s are plotted in Fig.6. The flow pattern along the plunge pool area during model test is shown in Fig. 7.

According to Bollaert and Schleiss [5], the scouring process in plunge pools is the result of the interactions of the three phases water, rock and air. Moreover, the highly turbulent nature of the flow and the resulting pressure fluctuations on the water-rock interface and inside rock fissures make appropriate scaling very difficult in hydraulic modelling. Thus, the applicability of Froude-based reduced-scale models is limited and shall only be used as qualitative indication.

The impact of the plunging jets on the proposed pre-excavated plunge pool invert and berms are evaluated using a fixed bed, by measuring the pressures induced by the water jets through electronic transducers. Then, the parameters of the dynamic pressure distribution on the plunge pool surfaces such as mean dynamic pressure (C_p), RMS (root of mean square) (C_p') fluctuation, maximum and minimum peak fluctuations (C_p^+ and C_p^-) were analysed and compared to the values available in literature.

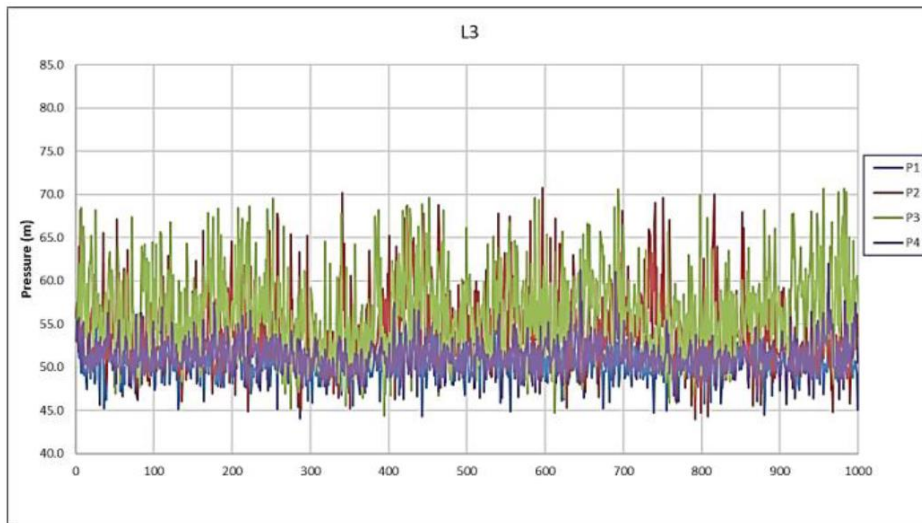


Fig. 6

Measured bed pressures on the pre-excavated plunge pool ($Q_{100}=14,000 \text{ m}^3/\text{s}$)



Fig. 7

Pre-excavated plunge pool in operation ($Q_{100}=14,000 \text{ m}^3/\text{s}$)

The mean, RMS fluctuating and extreme peak dynamic pressure coefficients available in the literature for several different jet and plunge pool conditions are shown in Fig.8 and Fig.9.

The NT1 plunge pool design flood jet processed data is plotted on the relevant graphs. According to the values shown, it can be concluded that the design flood jet is of a developed one while the plunge pool water cushion regarding the corresponding tailwater level was classified as a “Deep Pool”. This confirms the results of the calculations and classifications of the jet already performed in Section 6.

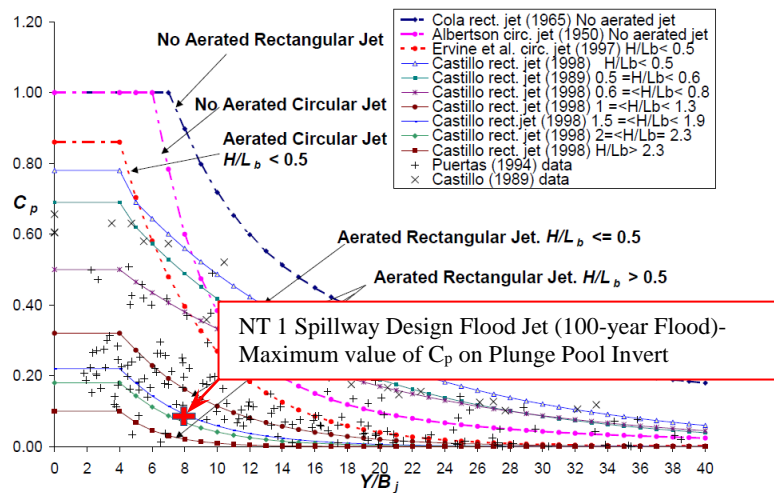


Fig. 8
Mean dynamic pressure coefficient [4]

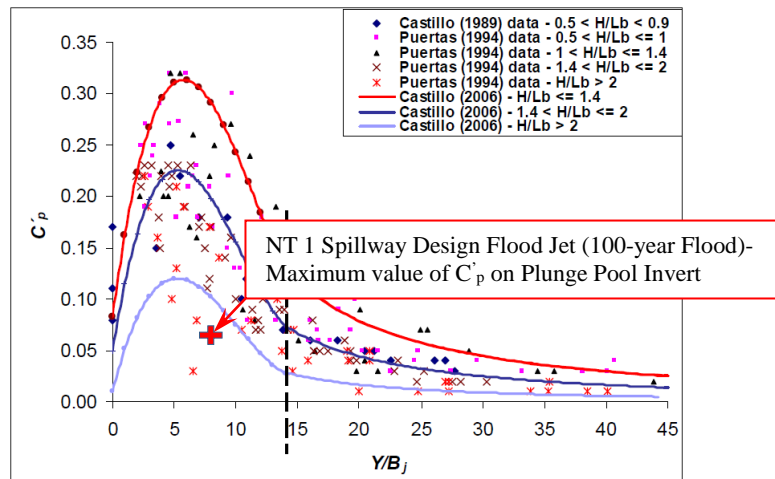


Fig. 9
Fluctuating dynamic pressure (RMS) coefficient for rectangular jet [4]

8. CONCLUSION

A practical methodology for design of NT1 pre-excavated plunge pool has been applied. In the beginning, the ultimate scour depths due to spillway plunging jets are estimated using empirical relationships as well as qualitative scouring tests in physical model. In the next step, the pre-excavated plunge pool was designed for a flood frequency referring to the serviceability of the powerhouse. Then, the dynamic pressures on the plunge pool invert and berms were recorded and the according dynamic pressure coefficients were calculated.

Comparing the range of the pressure coefficients for NT1 plunge pool case with those available in the literature shows that the NT1 proposed pre-excavated plunge pool shall be deep enough to not be eroded in an extensive area deeper than the proposed invert level of 105.0 m asl by its design flood jet.

Also, the calculations show that the spillway jets for all range of floods shall be fully developed before impacting the plunge pool surface which will reduce the erosive power of the plunging jets. Provision of the dents on flip buckets, which are not embedded in the disintegration length relationships, shall further improve the jets disintegration and aeration.

9. REFERENCES

- [1] BOLLAERT, E., DUARTE, R., PFISTER, M., SCHLEISS, A., MAZVIDZA, D. Physical & numerical model study investigating plunge pool scour at Kariba Dam, *24th Congress of CIGB – ICOLD, Kyoto, Japan, 2012*, pp. 241-248.
- [2] ERVINE D.A. Falvey H. R. and Withers W. Pressure fluctuations on plunge pool floors. *J. of Hydraulic Res., IAHR, 1997*, Vol. 35, N°2, pp. 227-279.
- [3] CASTILLO L.G. Pressure characterization of undeveloped and developed jets in shallow and deep pool. *Proceedings of the 32nd IAHR Congress, Venice, 2007*, 2, 645–655.
- [4] CASTILLO L.G. Aerated jets and pressure fluctuation in plunge pools. *Proc.7th International Conference on Hydroscience and Engineering, Philadelphia, 2006*, 1–23.
- [5] BOLLAERT, E., SCHLEISS, A. Scour of rock due to the impact of plunging high velocity jets 1: Experimental results of dynamic pressures at pool bottoms and in one and two dimensional closed end rock joints. *J. Hydraulic Res., 2003*, 41(5), 465–480.

10. SUMMARY & KEYWORDS

Nam Theun 1 is a hydropower plant under construction in Lao PDR, located about 170 km east of Vientiane. The scheme comprises a 177 m high RCC curved gravity dam. The flood release structures including the plunge pool at the dam toe need to be designed to withstand the high dynamic loads and is one of the major hydraulic design issues. In order to reduce the scour depth, the spillway flip buckets will end at different elevations and will be equipped with baffle blocks that will spread the jet and improve its aeration.

In addition, the presumable scour depth and the required pre-excavation are important design parameters both with regard to the powerhouse tailwater conditions, the serviceability of the powerhouse itself and the dam safety. Several

methods were used to estimate the presumable scour depth for different return periods and to design the plunge pool pre-excavation for the 100-year design flood.

At first classical scour formulae were applied. Second a physical model was built at AIT in Bangkok. This was used to investigate further the behaviour of a movable gravel bed, mainly in order to compare the effect of the above mentioned scour reduction measures, as well as to investigate the pressure fluctuations in the pre-excavated area. The pressure data was analysed in terms of the mean dynamic, RMS, maximum and minimum pressure coefficients at the proposed pre-excavation invert and berms. The jet characteristics just before impacting the plunge pool water cushion surface were determined. These results were used to evaluate the residual energy and scouring potential at the plunge pool invert and berms. The chosen approach containing empiric formulae combined with physical model testing allows for a suitable design of the challenging flood evacuation system of the Nam Theun 1 hydropower scheme.

KEYWORDS: EXCAVATION, FLIP BUCKET, HYDRAULIC MODEL TEST, PLUNGE POOL, SCOURING.

Nam Theun 1 est un aménagement hydroélectrique en construction au Lao, situé 170 km à l'est de Vientiane. Il contient un barrage-poids arqué de 177 m d'hauteur. Le système d'évacuation des crues incluent une fosse de dissipation en aval de l'ouvrage qui est dimensionné de façon à résister aux importantes pressions fluctuantes. Son dimensionnement est critique. Afin de mieux distribuer et aérer les jets d'eau ainsi que de réduire la profondeur de l'affouillement, les chutes de l'évacuateur de crue se terminent par des cuillères de dissipation à différentes élévations équipées de dents de dissipation. Par ailleurs, le potentiel d'affouillement et la pré-excavation de la fosse de dissipation sont des variables d'entrée clés influencent les niveaux d'eau et le bon fonctionnement de l'usine à l'aval ainsi que la stabilité du barrage. Plusieurs approches ont été utilisées dans le but d'estimer la profondeur d'affouillement pour des crues de différentes périodes de retour et de dimensionner la pré-excavation correspondant à une crue centennale.

D'abord, des approches empiriques ont été utilisées. Ensuite, un modèle réduit a été construit et exploité au laboratoire AIT de Bangkok dans le but d'étudier l'impact des jets sur un lit mobile avec et sans la mise en œuvre des mesures correctives pour en mesurer l'efficacité et de mesurer les pressions fluctuantes dans la fosse de dissipation. La moyenne dynamique, le RMS ainsi que les coefficients de pression minimum et maximum ont été mesurés sur les bermes et en surfaces de la zone pré-excavée. Les caractéristiques du jet juste avant de pénétrer la surface de la fosse de dissipation ont été étudiées afin d'évaluer l'énergie résiduelle après impact ainsi que le potentiel d'affouillement au pied du barrage. La méthodologie choisie basée sur l'application de formules empiriques combinées avec les résultats obtenus grâce à modèle hydraulique réduit ont permis un dimensionnement hydraulique satisfaisant du très complexe système d'évacuation des crues de l'aménagement de Nam Theun 1.

MOTS CLÉS: FOUILLE, CUILLERE DE DISIPATION, ESSAI SUR MODELE HYDRAULIQUE, BASSIN D'AMORTISSEMENT, AFFOUILLEMENT.

COMMISSION INTERNATIONALE
DES GRANDS BARRAGES

VINGT-SIXIÈME CONGRÈS DES
GRANDS BARRAGES
Autriche, juillet 2018

**A DEVELOPMENT OF HYDROLOGIC RISK ANALYSIS MODEL FOR SMALL
RESERVOIRS BASED ON BAYESIAN NETWORK ***

Jin-Guk KIM¹ , Hyun-Han KWON^{2*} , Byoung-Han CHOI³

*1. Ph.D Course of the Department of Civil Engineering, CHONBUK NATIONAL
UNIVERSITY*

*2. Associate Professor of the Department of Civil Engineering, CHONBUK
NATIONAL UNIVERSITY*

*3. Senior Researcher of the Rural Research Institute, KOREA RURAL
COMMUNITY CORPORATION*

SOUTH KOREA

(Tel: +82-63-270-2426, Fax: +82-63-270-2421, e-mail: kwon@jbnu.ac.kr)

1. ABSTRACT

Typhoon-induced storm surge along with heavy rainfall has been recognized as the most frequently reported hazards for water-related hazards in South Korea. Moreover, it has been widely acknowledged that the frequency and intensity of typhoons (or abnormal low-pressure system) are likely to increase over time due to the potential impact of climate change. There are 14,000 small reservoirs in South Korea and various issues related to the reservoir safety. A hydrologic reservoir risk analysis requires a systematic process to ensure dependency relationships among key hydrologic variables (e.g. precipitation,

* A DEVELOPMENT OF HYDRAULIC-HYDROLOGIC RISK ANALYSIS MODEL FOR
SMALL RESERVOIRS BASED ON BAYESIAN NETWORK

discharge and water surface level). However, the existing reservoir risk approach showed a limitation in assessing the interdependencies across the variables. In this context, this study proposed a Bayesian network based reservoir risk analysis. Based on the basic information of reservoir, various failure modes was first identified and the failure modes are then translated into nodes in the Bayesian network framework. The failure probabilities of the each node were estimated quantitatively by integrating limit state equations, which are composed of a set of random variables. Moreover, we investigated an integrated Bayesian network model to estimate overtopping risk from water surface level rise informed by climate change scenarios. A further discussion on the role of the uncertainty for overall risk is provided. This proposed procedure will help to effectively introduce the risk analysis for reservoirs safety in Korea.

ACKNOWLEDGEMENTS

This research was supported by a grant(17AWMP-B127568-01) from the Water Management Research Program funded by Ministry of Land, Infrastructure and Transport of Korean government.

COMMISSION INTERNATIONALE DES GRANDS BARRAGES

VINGT-SIXIÈME CONGRÈS DES GRANDS BARRAGES
Autriche, juillet 2018

DOI 10.3217/978-3-85125-620-8-094



This work licensed under a Creative Commons Attribution 4.0 International License. <https://creativecommons.org/licenses/by-nc-nd/4.0/>

**EXPERIMENTAL STUDY ON DIRECT SHEAR BETWEEN FRP - CONCRETE
INTERFACE BASED ON DIC**

Zhang LEI

YELLOW RIVER INSTITUTE OF HYDRAULIC RESEARCH, YRCC

CHINA

Lei DONG

HOHAI UNIVERSITY

CHINA

Wu LINGCHENG

YELLOW RIVER WANJIAZHAI WATER MULTI-PURPOSE DAM PROJECT CO.,
LTD

CHINA

YANGYONG

YELLOW RIVER INSTITUTE OF HYDRAULIC RESEARCH, YRCC

CHINA

COMMISSION INTERNATIONALE
DES GRANDS BARRAGES

VINGT-SIXIÈME CONGRÈS DES
GRANDS BARRAGES
Autriche, juillet 2018

EXPERIMENTAL STUDY ON DIRECT SHEAR BETWEEN FRP - CONCRETE INTERFACE BASED ON DIC

ZHANG LEI¹, LEI DONG², WU LINGCHENG³, YANGYONG¹

1. YELLOW RIVER INSTITUTE OF HYDRAULIC RESEARCH, YRCC; 2.
HOHAI UNIVERSITY; 3. YELLOW RIVER WANJIAZHAI WATER MULTI-
PURPOSE DAM PROJECT CO., LTD
CHINA

1. INTRODUCTION

Stress can be transmitted effectively between FRP and concrete, which is the key for FRP-concrete to effectively improve the bearing capacity of the reinforced structure. Numerous tests and engineering projects have shown that the failure of FRP-concrete tends to be caused by the de-bonding of FRP-concrete interface or local failure along the interface of the concrete [1,2]. Consequently, the bond performance of FRP-concrete interface directly determines whether the reinforced structure will succeed. Under most external load conditions, this interface tends to be in the state of shear stress. Currently, there are four types of experimental study to test bond performance of FRP-concrete interface, which is simple-shear test, double-shear test, beam test and corrected beam test. Simple-shear test and double-shear test are most common for their specific and simple stress state. This essay adopts single-shear test to deeply discuss and research on the mechanical property and bond mechanism of FRP-concrete.

Van Gemert [3] researched the bond performance of steel-plate reinforced concrete structure through double-shear test for the first time in 1980. Besides, he presented the values of maximum shearing stress and average shearing stress, and the transmission law of stress distribution and calculation formula of steel plate-concrete interface. Later, based on simple-shear test, Sharma [4] and his fellows focused their research on the influence of the effective bonding length of FRP-concrete interface on the bond strength. When above shear tests measured the stress strain of steel plate or FRP plate, they stuck large quantities of strain gauges on the plate surface alongside the length direction of plate and then read

the value of strain gauges, used to calculate the local average bond shearing stress and local slippage. However, many test outcomes have shown that the constitutive relation of bond slippage derived from above tests cannot demonstrate satisfying law because the material components of concrete and the cracks caused during tests were randomly distributed. Furthermore, when the strain gauges were adopted for measurement, there would be certain difference between the strain values read from the strain gauges at the measurement points and the actual strain values because of the limit on measurement gauge length [5,6]. Therefore, we should find a brand-new measurement method which can accurately measure the overall deformation of FRP plate.

DIC (digital image correlation) was put forward by one Japanese scholar-Yamaguchi [7] and two American scholars-Prof. Peters and Prof. Ranson [8] independently in the 1980s. The research thought of Yamaguchi [7] was to adopt laser beam to irradiate to object surface to form speckles and to measure the peak value of relevant function of light strength before and after the object was deformed. In the meanwhile, he derived the object displacement based on relevant theories, thus achieving the real-time measurement of small deformation in small regions. Prof. Peters and Prof. Ranson [8] used computers and image scanning devices to acquire the speckle diagram before and after the object was deformed. In addition, they found out the extreme value of correlation coefficient through iterative algorithm on the grey field before and after the object was deformed, thus obtaining the displacement field and stress strain field inside the closed regions and then acquiring the deformation field through boundary integral equation.

This experiment measures the surface deformation of FRP plate with the assistance of relevant advanced digital image technologies and can overcome some limitations of above tests quite well, thus eliminating some disadvantages of strain gauges. Besides, this experiment analyzes the stress transmission in different de-bonding stages through careful observations of FRP-concrete de-bonding process, thus establishing the de-bonding law of FRP-concrete interface and providing technical instructions for the disposal of FRP-concrete bonding interface in real hazard elimination and reinforcement projects.

2. DIRECT SHEAR BETWEEN FRP - CONCRETE BONDING INTERFACE BASED ON DIC

2.1. EXPERIMENTAL APPARATUS

All tests are conducted on equipment which is autonomously designed and manufactured. This equipment consists of following parts: upper baseboard with four holes, lower baseboard with eight holes, four pieces of steel bars with screw-thread, two pieces of baffles welded with small steel bars (as clamping chuck for lower pull head connection testing machine), upper pull head and fixture.

2.2. SPECIMENS

(1) concrete sample

Eight pieces of concrete cube specimens are poured in one batch with a strength of C30, a size of 100mm in length, 50mm in breadth and 300mm in height. Grinding papers are used to polish the concrete surface to be measured. In addition, dry cleaning cloth is used to clean the surface.

(2) FRP Plates

Yao Jian [9] and his fellows pointed out that when the breadth ratio between the FRP plate and concrete was equal or higher than one fourth, the de-bonding development process before the specimen damage can hardly be observed. The failure happened all of a sudden with no pre-signs. Therefore, the breadth of FRP plate is set as 20mm. The length of plate is determined by the sum of different bonding length and clamping length in accordance with the testing requirements.

(3) The bond between concrete and FRP plates

The cut concrete specimen and FRP plate are bonded with resin adhesive. The bonding lengths include eight different types: 80mm (Type SS-80), 90mm (Type SS-90), 100mm (Type SS-100), 110mm (Type SS-110), 120mm (Type SS-120), 150mm (Type SS-150), 160mm (Type SS-160) and 180mm (Type SS-180). Stick FRP plate to the concrete surface to be measured with resin adhesive and use rollers to squeeze the bubbles out. Place weight on FRP plate for three days to guarantee that FRP plates are totally stuck with concrete. When the adhesive completely sticks the concrete specimen and FRP plate tightly, install the specimen on the equipment and conduct the test.

2.3. EXPERIMENTAL APPROACH

This experiment adopts optical measurement technique to measure the deformation of FRP plate surface. In order to acquire speckles for optical measurement, two colors-black and white, are sprayed on the surface to be measured respectively. Connect the data line of optical measurement camera with the computer, observe the computer screen, and adjust the height and focal length of camera until the speckles on FRP plate can be clearly seen. Set the photograph frequency as five pics per second. Place the installed testing equipment fixed with FRP plate-concrete specimen on the 10t testing machine. Adopt monotonic loading mode under displacement control, the tensile speed is 0.03mm/min. The model diagram of direct shearing equipment and the diagram of direct shearing equipment are shown in Fig. 1.

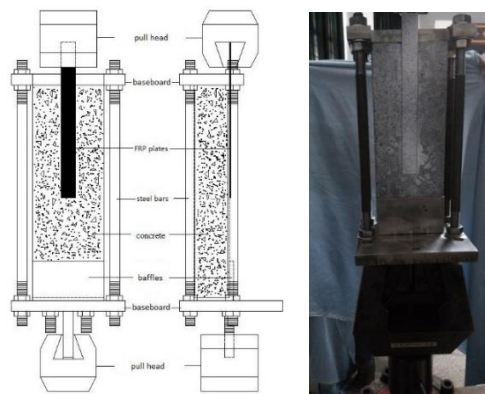


Fig. 1 Direct shear apparatus model

3. EXPERIMENTAL RESULTS AND ANALYSIS

3.1. EXPERIMENTAL RESULTS

(1) Experimental results observed by optical measurement

If we choose to observe the strain of specimen in the vertical direction, we can obviously see the strain distribution of FRP plate at different time. Take the strain distribution of specimen SS-150 at different time for example and analyze the change in strain distribution of FRP plate as shown in Fig. 2.

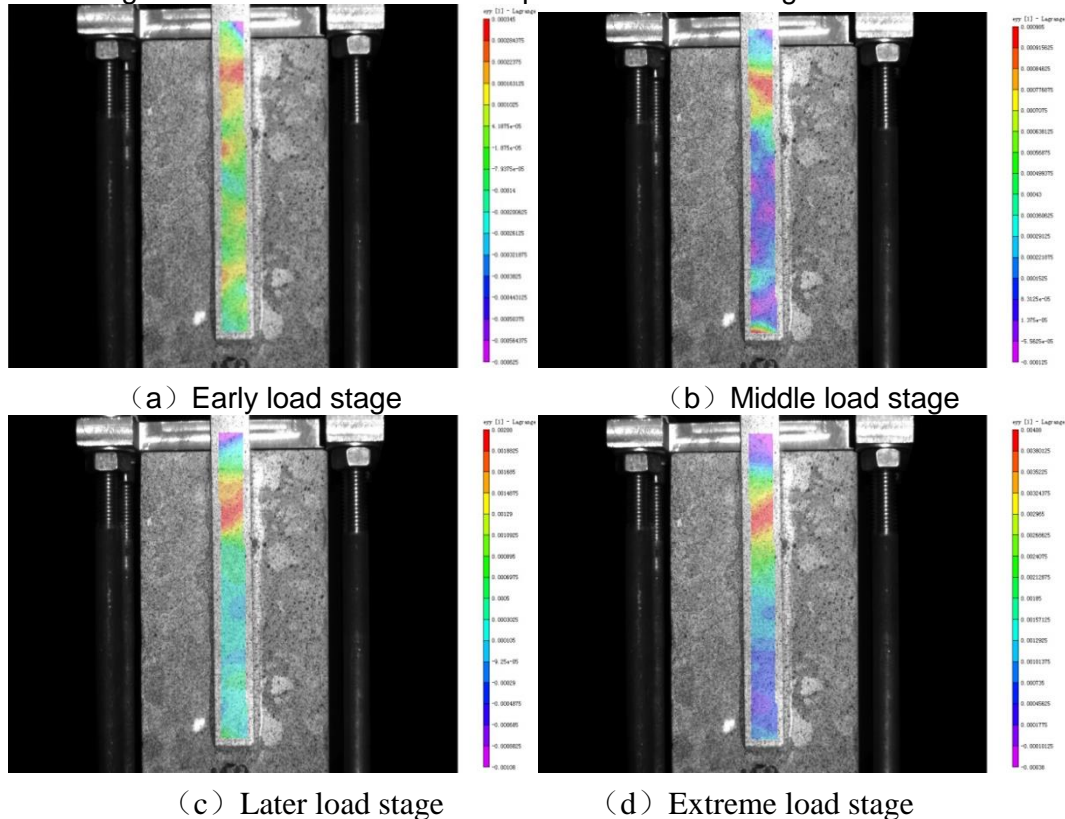


Fig. 2 The strain distribution of the FRP plates at different times in the sample ss-150

The de-bonding of FRP reinforced concrete bonding interface can be divided into following three stages as shown in the Fig. 2:

(1) Early load stage: the strain on each part of FRP plate is very small. The peak value of strain, which is measured in a small region around the load end, which is $\varepsilon_{yy}=0.000345$. As the load increases, when the peak value of strain reaches 0.000985, the strain in its neighboring regions exceeds 0.000779 and the position of peak value of strain basically remains unchanged.

(2) Middle load stage: as the load continues to increase, the peak value of strain ($\varepsilon_{yy}=0.00208$) keeps increasing while its position moves towards the free end of FRP plate. The overall strain of plate increases compared to early load stage. The minimum value of strain is 0.0005 and is measured at the free end of FRP plate. There is very small strain in the regions between the plate center and the free end, ranging from 0.0001 to 0.0003.

(3) Later load stage: the position of peak value ($\epsilon_{yy}=0.00408$) of strain basically remains unchanged compared to middle load stage and the strain of free end only reaches 0.001.

3.2. EXPERIMENTAL DATA ANALYSIS

(1) Load - displacement curve of specimen

The load - displacement curve of specimens can be obtained from the data of the test machine, as shown in fig.3 (for example, specimen ss-120).

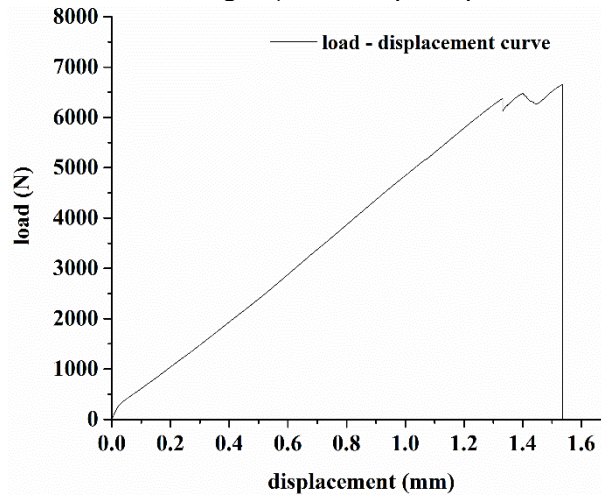


Fig.3 The load-displacement curve of the specimen ss-120

(2) Extreme bearing capacity, slippage of load end and failure mode measured in the test

Collect each specimen according to the extreme capacity of interface (direct shearing strength) as shown in Fig. 4.

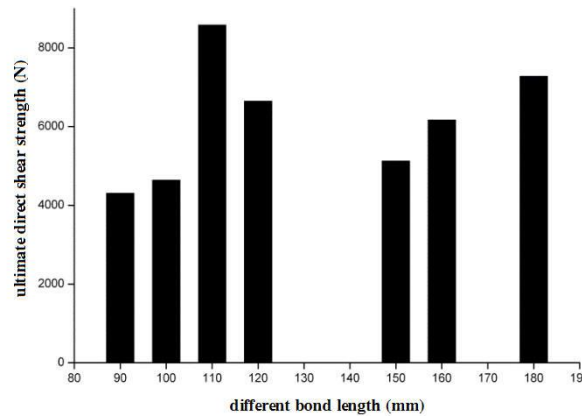


Fig. 4 The ultimate direct shear strength distribution of FRP- concrete specimen with different bond length

We can see from Fig. 4 that except for specimen SS-80, with the bonding length increases, the extreme bearing capacity of interface firstly increases (the bonding length is 110mm) and then demonstrates stable trend. Although the bonding length of specimen SS-80 is only 80mm, its extreme bearing capacity of interface is quite high. It might be that the FRP plate is stuck right at the place with concentrated coarse aggregate and there is relative little mortar in this part. As for

specimen SS-110, its extreme bearing capacity of interface is highest, which can also be attributed to above reason.

(3) Strain distribution of FRP plates surface

Ali-Ahmad [10] and his fellows pointed out that when the test of bonding performance of FRP-concrete was conducted, the FRP plate remains in the elastic range and the strain distribution of FRP plate surface can reflect the strain distribution of FRP-concrete bonding surface quite well. Analyze the data collected by DIC and select the strain distribution of FRP plate alongside the plate length direction of specimen SS-100 and SS-150 at different load time (which means different load stages)-20%, 40%, 80% and 100% of extreme load.

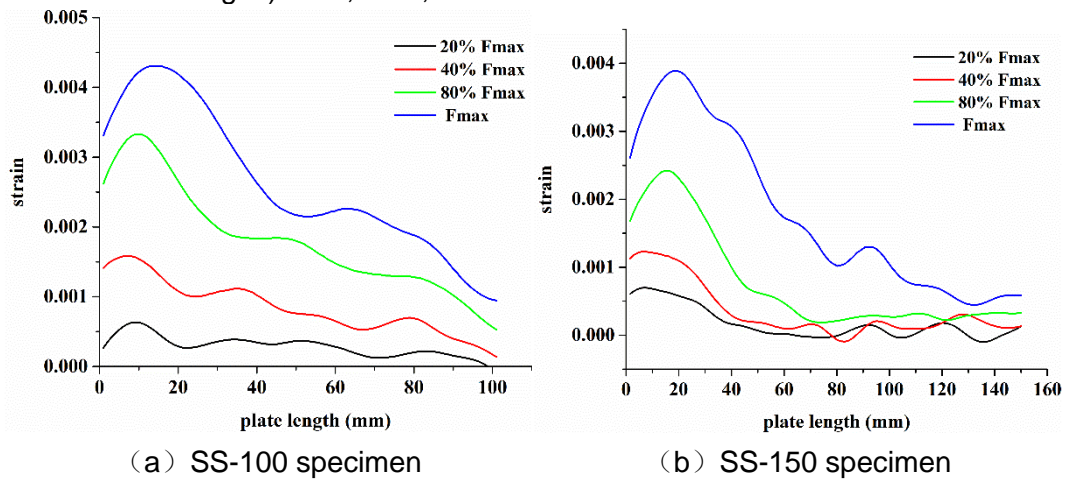


Fig. 5 The strain of FRP plate in different loading moments

We can see from Fig. 5 as follows:

(1) During the stage of 20% to 40% of extreme load, the strain increases obviously except for the region within 40mm from the load end. There is not much increment in strain at other positions on the FRP plate. So we can conclude that the effective bonding length of FRP-concrete is about 100mm or slightly lower than 100mm;

(2) With the external load continues to increase, the overall strain of FRP plate increases and the free end begins to transmit shearing strain stress towards the concrete surface. However, the strain value is relatively smaller compared to other parts.

(3) With the load increases, the strain keeps increasing while the position of peak value of strain moves forward little by little, which indicates that the FRP at original positions of peak value of strain starts de-bonding away from the concrete surface gradually until the external load reaches the maximum shearing stress which the FRP plate and concrete can withstand. When there is no subsequent FRP plate sharing this external load at the free end, the de-bonding failure happens to the specimen.

Collect the strain distribution of each specimen at extreme load as shown in Fig. 6.

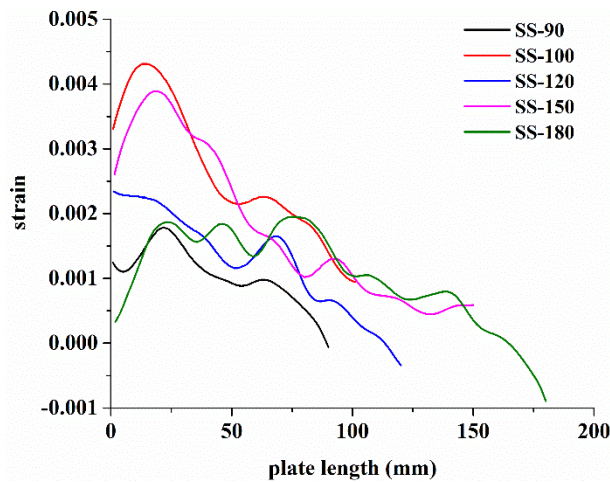


Fig.6 The strain of FRP plates along the plate length at the limit load

We can see from Fig. 6 as follows:

- (1) The strain distribution law of FRP plate of each specimen is consistent.
- (2) The maximum strains of specimen SS-120 and specimen SS-180 are relatively small for influence of clamping chuck of testing machine.
- (3) Apart from some factors that influence the test results, and combined with the analysis of FRP-concrete specimen of each plate length, we can predict that: the maximum strain of each specimen under extreme load increases as the bonding length of FRP plate increases; the strain distribution law curve along the length direction of plate extends outwards as the bonding length of FRP plate increases.

3.3. COMPARISON WITH THE FORMULA OF THE SHEAR BOND STRENGTH MODEL OF CHEN - TENG

The Chen-Teng [13] anti-shear bonding strength equations based on fracture mechanics theories and experimental outcomes are adopted to compare with the testing outcome. Fig. 7 shows the comparison between the ratio of FRP plate stress and its tensile strength σ_{frp} / f_{frp} and the ratio of bonding length of FRP plate and effective bonding length l_{frp} / l_e during de-bonding failure in direct shearing tests.

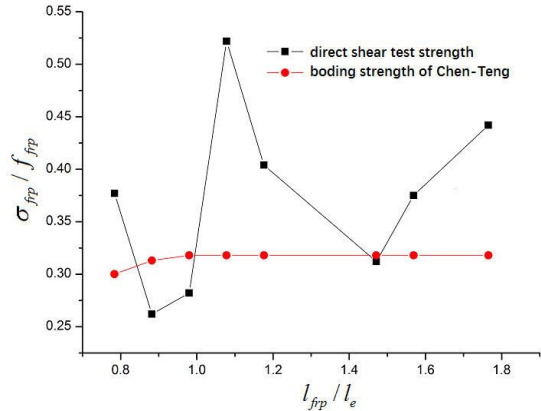


Fig. 7 The bond strength of different bond length in direct shear test We can see from Fig. 7 as follows:

(1) While the bonding length- l_{frp} is equal to 150mm, the testing outcome can agree well with the calculation outcome.

(2) While the bonding length- l_{frp} is equal to 90mm, 100mm and 160mm, the difference rate between the testing outcome and the calculation outcome is about 15%.

(3) While the bonding length- l_{frp} is equal to 80mm, 110mm, 120mm and 180mm, the difference between the testing outcome and the calculation outcome is relatively big and higher than 25%.

3.4. EFFECTIVE BONDING LENGTH OF FRP PLATE - CONCRETE SPECIMEN

Sharma [4] and his fellows put forward the concept of “effective bonding length” based on the results that the bonding strength of FRP-concrete will not keep increasing as the bonding length of FRP plate increases. Chen and Teng[13] put forward the calculation formula for effective bonding length through plenty of tests. The effective bonding length of FRP plate-concrete specimen is roughly estimated through analysis of strain-plate length, and compared with the Chen-Teng effective bonding length.

In the discussion about specimen SS-100 and SS-150 in Chapter 3.2, it has been demonstrated that the effective bonding length of this batch of FRP plates is roughly estimated to be about 100mm. The effective bonding length calculated by Chen-Teng formula is:

$$l_e = \sqrt{\frac{E_{frp} t_{frp}}{\sqrt{f_c}}} = \sqrt{\frac{256000 \times 0.2}{\sqrt{0.76 \times 30}}} \approx 103.5mm$$

On this basis, it is indicated as follows:

(1) The analysis of strain-plate length curve can be estimated the effective bonding length of FRP plate-concrete indeed.

(2) The effective bonding length calculation formula proposed by Chen-Teng is re-verified by amount of analysis.

4. CONCLUSION

The direct shear and de-bonding test of FRP-concrete specimen are conducted by autonomously developed testing equipment. With the assistance of advanced DIC (digital image correlation) technology, the strain distribution on the FRP plate surface of FRP-concrete specimen is accurately measured. Besides, the surface strain distribution law of FRP plate alongside the length direction of plate and the bonding strength of specimen are researched. Furthermore, it reveals the de-bonding failure process of concrete interface and draws following major conclusions:

(1) The shear strain stress of FRP plate and concrete interface is not evenly distributed, the de-bonding starts from the load end and presents itself as brittle failure.

(2) The strain-plate length distribution of FRP plate indirectly reflects the bonded quality of specimen and corresponds to the strength error reflected by the calculation outcome of Chen-Teng formula.

(3) The effective bonding length of FRP plate is estimated by analyzed the surface strain distribution of FRP plate along the length direction. The determination of effective bonding length of FRP plate in project applications means a lot for reducing reinforcement costs and construction work load.

ACKNOWLEDGEMENTS

This work was financially supported by the National Natural Science Foundation of China (51779101, 51209102), and scientific research achievements promotion and transformation demonstration funds of Yellow River Institute of Hydraulic Research (HKYTZJJ-2016-01).

REFERENCES

- [1] McKenna J K, Erki M A. Strengthening of reinforced concrete flexural members using externally applied steel plates and fibre composite sheets-a survey. *Canadian Journal of Civil Engineering*, 1994, 21(1): 16-24.
- [2] Sebastian W M. Significance of midspan debonding failure in FRP-plated concrete beams. *Journal of Structural Engineering*, 2001, 127(7): 792-798.
- [3] Van Gemert D A. Repairing of concrete structures by externally bonded steel plates. *Developments in Civil Engineering*, 1982,5: 519-526.
- [4] Sharma S, Mohamed Ali M, Goldar Detal. Plate-concrete interfacial bond strength of PRP and metallic plated concrete specimens. *Composites ,PartB : Engineering*, 2006, 37(1):54-63.
- [5] Lu Xinzheng. Studies on FRP-Concrete Interface. Tsinghua University, 2004. (in chinese)
- [6] Dai J, Ueda T, Sato Y. Development of the nonlinear bond stress-slip model of fiber reinforced plastics sheet-concrete interfaces with a simple method. *Journal of Composites for Construction, ASCE*, 2005, 9(1):52-62.
- [7] Yamaguchi I. A laser-speckle strain gauge. *Journal of Physics(E)*, 1981, 14(5):1270-1273.
- [8] Peters W H, Ranson W F. Digital Imaging Techniques in Experimental Stress Analysis. *Optical Engineering*, 1982, 21(3):427-431.
- [9] Yao Jian, Teng Jinguang. Experimental study on bond strength between FRP and concrete. *Journal of Building Structures*, 2003, 24 (5):10-18.
- [10] Ali-Ahmad M, Subramaniam K, Ghosn M. Experimental investigation and fracture analysis of debonding between concrete and FRP sheets. *Journal of engineering mechanics*, 2006, 132(9): 914-923.
- [11] Lu X Z, Teng J G, Ye L P, et al. Bond-slip models for FRP sheets/plates bonded to concrete. *Engineering structures*, 2005, 27(6): 920-937. (in chinese)

- [12] YUAN H,WU Z,YOSHIZAWA H. Theoretical solutions on interfacial stress transfer of externally bonded steel/composite laminates. *Journal of Structural Mechanics and Earthquake Engineering,JSCE*,2001,675/1-55,27-39.
- [13] Chen J F, Teng J G. Anchorage strength models for FRP and steel plates bonded to concrete. *Journal of Structural Engineering*, 2001, 127(7): 784-791.

COMMISSION INTERNATIONALE DES GRANDS BARRAGES

VINGT-SIXIÈME CONGRÈS DES GRANDS BARRAGES
Autriche, juillet 2018

DOI 10.3217/978-3-85125-620-8-095



This work licensed under a Creative Commons Attribution 4.0 International License.
<https://creativecommons.org/licenses/by-nc-nd/4.0/>

**COMBINING NUMERICAL AND PHYSICAL MODELS FOR COST EFFECTIVE
DESIGN OF IRREGULAR SPILLWAYS**

Jonas PERSSON

Project Manager, NORCONSULT

SWEDEN

James YANG

Researcher, VATTENFALL R&D

SWEDEN

Öyvind Espeseth LIER,

Vice President Dams, NORCONSULT

SWEDEN

Martin J. ERIKSSON

Project Manager, FORTUM SVERIGE

SWEDEN

Carl-Oscar NILSSON

Dam Safety Manager, UNIPER

SWEDEN

COMMISSION INTERNATIONALE
DES GRANDS BARRAGES

VINGT-SIXIEME CONGRES DES
GRANDS BARRAGES
Autriche, juillet 2018

**COMBINING NUMERICAL AND PHYSICAL MODELS FOR COST
EFFECTIVE DESIGN OF IRREGULAR SPILLWAYS**

Jonas PERSSON
Project Manager, NORCONSULT

James YANG,
Researcher, VATTENFALL R&D

Öyvind Espeseth LIER,
Vice President Dams, NORCONSULT

Martin J. ERIKSSON,
Project Manager, FORTUM SVERIGE

Carl-Oscar NILSSON,
Dam Safety Manager, UNIPER

SWEDEN

1. INTRODUCTION AND BACKGROUND

Regular dam safety evaluations are performed on Swedish dams according to the voluntary Dam-Safety Guidelines (RIDAS). Due to recent revisions, deficiencies in structural and hydraulic performance are routinely discovered leading to dam safety upgrades (Yang *et al.* 2010, 2014). These shortfalls include rock erosion downstream, status of embankment dams, spillway stability and functions of mechanical and electrical systems in addition to spillway discharge capacity (Ygland *et al.* 2012, Bond *et al.* 2014).

Both Långströmmen and Ramsele are among the candidates for spillway upgrade and renewal.

Långströmmen is located on the River Ljusnan in Mid Sweden and was commissioned in 1961. The facility includes more than 2,5 km of embankment dams, owned by the power producer Fortum. The tallest dam sections are placed near the spillway, rising to a height of 29 m. The full retention reservoir level (FRRL) is +279.55 m, with 35 cm of regulation amplitude. Its power plant has two Francis turbines with a gross head of 31.3 m and a turbine flow rate of 100 m³/s. Its annual power production exceeds 250 GWh. dams.

Ramsele hydropower plant, owned by Uniper, is located on Faxälven in Northern Sweden and was commissioned 1958. The dam is a 440 m long buttress dam about 40 m high. The full retention reservoir level (FRRL) is +223.50 m, with 50 cm of regulation amplitude. The power station has three Francis turbines with a total output of about 160 MW, a gross head of 79.2 m. Its annual power production is about 870 GWh.

Figure 1 shows the location of Långströmmen and Ramsele.

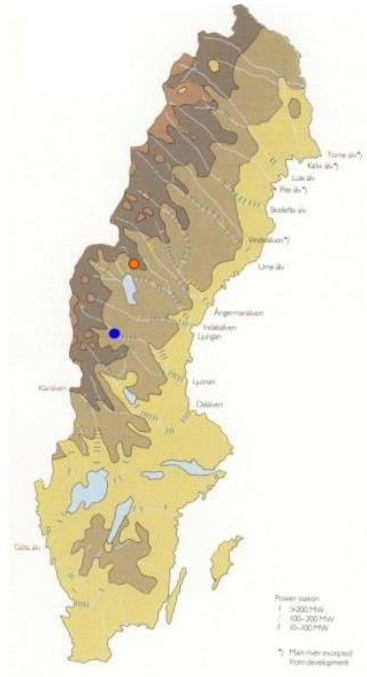


Figure 1. Map of Sweden showing Ramsele (Red) and Långströmmen (Blue)

Fehler! Verweisquelle konnte nicht gefunden werden. and figure 3 show the spillways of Långströmmen and Ramsele dams.



Figure 2: Downstream view of the spillway at Långströmmen prior to dam safety upgrades (Norconsult, 2014).



Figure 3: Aerial photo of Ramsele dam and spillway (Norconsult, 2015).

2. RESULT OF SAFETY EVALUATIONS

The Swedish Guidelines for Design Flood Determination, classify dams into two categories depending on the consequences of a dam failure ().

Table 1: Classifications of dam failure consequences and corresponding design flood.

Design flood category	Class I	Class II
Dam failure consequence category	Loss of human life, damage to vital infrastructure, etc.	Property and infrastructure damage,.
Hydrological modeling technique	Extreme precipitation combined with heavy snowmelt and saturated soils	Frequency analysis
Return period, years	> 10 000	>100

Both Långströmmen and Ramsele are classified as high-hazard dams, or Class I, implying that a 10 000 year flood must be safely passed. Not only does this signify that the floodwaters must be evacuated without exceeding the maximum design water level thereby jeopardizing the structural integrity of the embankment dams.

It also means that the spillways must be designed with energy dissipators and

sufficient downstream riprap to avoid backreaching erosion.

2.1. DISCHARGE CAPACITY

Prior to the dam safety upgrades, the capacity of the spillway at Långströmmen was 1670 m³/s, while the updated design flood was close to 2500 m³/s, an additional 830 m³/s (50 % increase). Due to the very limited active reservoir volume, this leads to a water level increase of 1.8 m above the FRRL, which is 1.45 m above the central moraine core of the embankment dam. For an embankment dam, this is unacceptable.

When the dam was built, in the 1950s, the design flood was about the same as the 100 year-flood, but with today's hydrological methodology the design flood has a return period of about 10 000 years, hence the 50 % increase.

For Ramsele, its existing spillway with a capacity of 800 m³/s, was able to safely handle the updated design flood of 910 m³/s. The additional 110 m³/s results in water levels 50 cm higher than the FRRL to discharge the flood, which still is *under* maximum design water level as the central moraine core of the embankment dam extends another 1,6 meters. This gives the spillway sufficient capacity to evacuate the full volume of the floods, even accounting for wind drag buildup and waves.

2.2. EROSION DOWNSTREAM OF SPILLWAY

At Långströmmen dam, inspections have uncovered damages in the bedrock and concrete adjacent to the rock downstream of the spillway. Diving inspection uncovered that bedrock had been jacked up and washed away during flood episodes downstream the ski jump. Repairs were instigated, but rock erosion at the existing spillway was not handled in the project presented—the focus was on increasing the discharge capacity by adding the new spillway and designing it for safe passage of the design flood.

Downstream of Ramsele's left spillway chute, extensive rock erosion has occurred even though the spillways are rarely used. Before being re-built in 2017, the spillway had no engineered energy-dissipation at all, and the hydraulic conditions were non-favorable. There were reasons for apprehension concerning backward erosion, under the existing spillway chute. As no redundancy exists regarding discharge alternatives, it is of utmost importance that all three gates can be used without limitations regarding rock erosion, at a design flood event.

One outcome from the latest dam safety evaluation was to introduce restrictions regarding usage of the left spillway, since discharge could possibly

threaten the integrity of the dam. Figure 4 shows the eroded area downstream the left spillway chute.



Figure 4 Eroded area (marked red) downstream of the left chute at Ramsele (Norconsult, 2014).

2.3. REHABILITATION OPTIONS

In order to fulfill the design requirements cost-effectively, a number of rehabilitation options were studied in separate feasibility studies for both dam facilities.

2.3.1. *Långströmmen*

The following alternatives were evaluated, with the objective to increase the total discharge capacity (Ygland et al, 2012):

1. Modifications of the existing timber spillway by lowering its threshold
2. A new spillway to the right of embankment 5
3. A new spillway between embankments 4 and 5
4. A new spillway in combination with a siphon spillway
5. An emergency spillway with an erodible dam section
6. An emergency spillway with an automatically regulated flap gate

7. An overflow spillway with a fixed sill
8. An overflow spillway with a fixed sill combined with raise in the impervious cores
9. Modifications of the existing overflow dams.
10. An emergency spillway with Hydroplus fusegates
11. An emergency spillway with Hydroplus combined with raise in the impervious cores

Other factors, such as risks for flooding during construction combined with cofferdams, availability of reservoir for flood regulation during construction including debris and ice, erosion risk in the downstream area, impacts on the dam facility etc were weighed in.

The feasibility study favored construction of a new spillway (alternative 2) as the final option for the dam rehabilitation. The spillway was given a width of 18 m, with a sloping chute of ~80 m, followed by a stilling basin.

2.3.2. *Ramsele*

With a more limited objective of preventing further backward erosion near the dam, the following overreaching approaches were evaluated

- accepting some erosion but stop it from threatening the dam (undermining)
- accepting some erosion but move it to a safe distance from the dam
- introducing energy dissipation structures

Based on the approaches above, the following measures were evaluated:

1. Classic stilling basin
2. Rock reinforcements (rock bolts)
3. Prolongation of the existing spillway chute
4. Cuf-off wall immediately downstream of the existing chute
5. A few different combinations of No. 2 - 4.

The obvious factors that affect the evaluations of the alternatives for Ramsele was cost-efficiency as well as the overall risk reduction and impacts of construction on the existing dam.

The feasibility study recommended the third alternative. The prolongation had a linear slope, covering the entire length of the erosion pit ending with a cut-off wall anchored into bedrock. This construction would achieve both goals of limiting backward erosion threatening the dam body as well as relocating erosion areas to a safe distance from the dam.

3. HYDRAULIC MODEL STUDIES

For both spillways a physical model was constructed to assist in the detailed design of the waterways. The initial design of the models was supported by 2D computational hydraulic models to limit the scope of modeling necessary.

3.4. INITIAL HYDRAULIC MODEL LÅNGSTRÖMMEN:

Prior to detailed design, hydraulic models have been constructed at Vattenfall's hydraulic laboratory in Älvkarleby, Sweden (Yang *et al.* 2015). A 25 m long model, as shown in figure 5, was constructed at a scale of 1:60 with the objective of testing the following:

1. Impact of bathymetric features upstream that creates complex flow patterns during high floods.
2. The new spillway is situated some 350 m from the existing one with a small cross-section. This creates a velocity head that needed examination.
3. The flow behavior in the reservoir (point 1) and the head loss between the existing and new spillways (point 2) impacts the new spillway's threshold and discharge capacity.
4. The energy dissipater design of the new spillway.

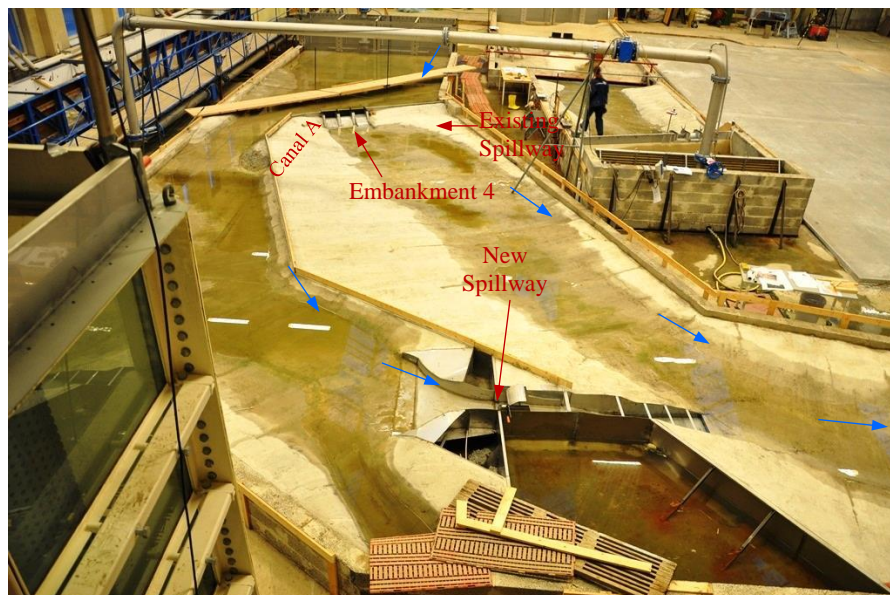


Figure 5: Hydraulic model of Långströmmen dam, scale 1:60

One of the main tasks of the model was to determine the final threshold of the new spillway. The lower the threshold, the higher capacity but also increased velocities downstream which impacts riprap design.

Results from two-dimensional modeling (2D) in the pre-study concluded that the reservoir levels needed to be increased to successfully evacuate the new design flood, since too high velocities would occur otherwise in the channel between the existing spillway and the new one.

In order to achieve acceptable velocities at FRRL, an extensive excavation of the mentioned channel is needed, and it is not likely to get a permit for this with respect to environmental aspects. Figure 6 shows the results from the 2D-modeling: a comparison between FRRL and FRRL+0.75.

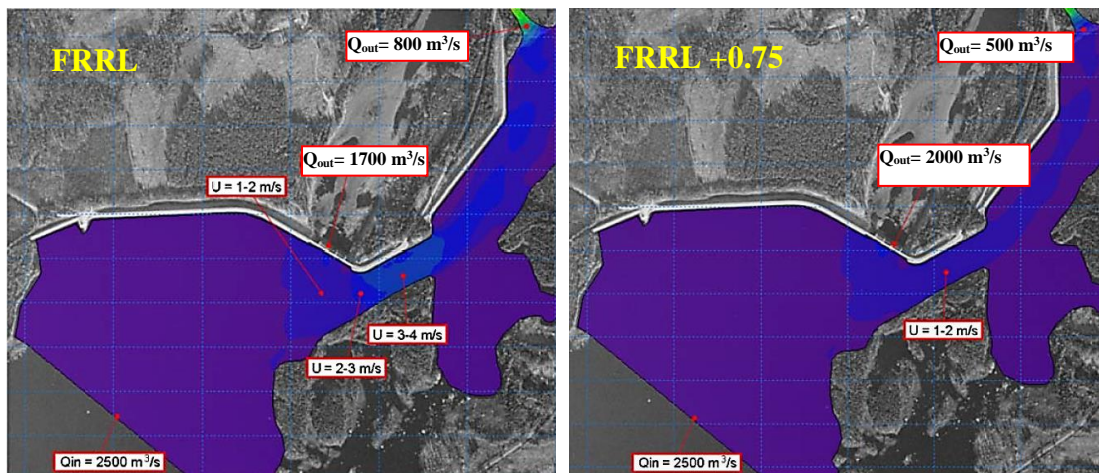


Figure 6: Reservoir flow patterns at FRRL and FRRL+0.75 m

The new spillway is designed with a stilling basin to reduce the risk of erosion in the river bed downstream the spillway and dams. Several configurations of the stilling basin were examined in terms of its floor elevation, end-sill elevation and basin length. Its placement was mainly governed by the hydraulic requirements to produce a stable hydraulic jump. It is also restrained by the geological conditions as it mainly will be excavated from existing bedrock.

Figure 7 shows the final layout of the basin, with a diverging shape downstream and a floor length of 40 m. The length of the sloping chute is about 80 m. The floor is placed at el. +255 m; the end sill is situated 6 m higher. The basin is 30 m wide at its downstream end.

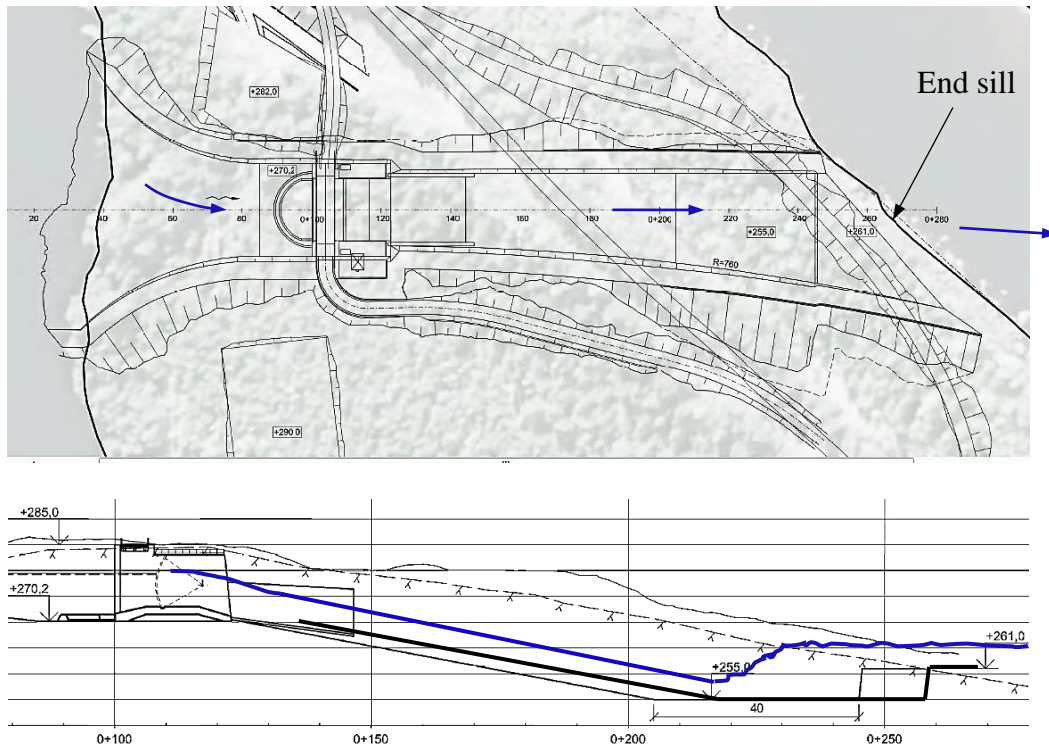


Figure 7. Final design of new spillway's stilling basin

One-dimensional numerical modelling of the river flow showed that the difference between water stages at low and high floods is significant. Therefore, the governing condition for the basin design corresponds to a downstream water level that results from the full discharge through the new spillway, with the existing spillway closed. In figure 8, the energy dissipation is shown at a discharge of $475 \text{ m}^3/\text{s}$ merely from the new spillway.

Due to the low downstream water stage, the end-sill location should be placed as close as possible to the river course. A too large distance would not help hold up the basin water level and form a proper hydraulic jump, as the high-velocity outflow from the basin pushes away the water in the river. The end sill location is, to some extent, limited by the terrain and the rock quality of the river bank.



Figure 8. Energy dissipation at 475 m³/s from the new spillway, with the existing spillway in the closed position.

3.5. REVISED DESIGN DURING CONSTRUCTION

Later, during the construction of Långströmmen, the design needed to be revised due to issues such as poorer rock quality than expected as well as to excavate additional rock from the stilling basin to supply material for the reinforcement of the embankment dams. The well-known fact that CFD has difficulties in correctly modeling the complex flows in a stilling basin led to the construction of a physical models initially.

However, as the physical model no longer existed, Computational Fluid Dynamic-modelling (CFD) was used to evaluate impacts of proposed changes designs. The CFD-model was only used for relative evaluation, by comparing qualitative results from different designs. First, the design preferred in the physical model tests was tested in the CFD-model and later compared with the design motivated by the requested changes in design [9].

Figure 9 and figure 10 show results from the CFD-modeling.

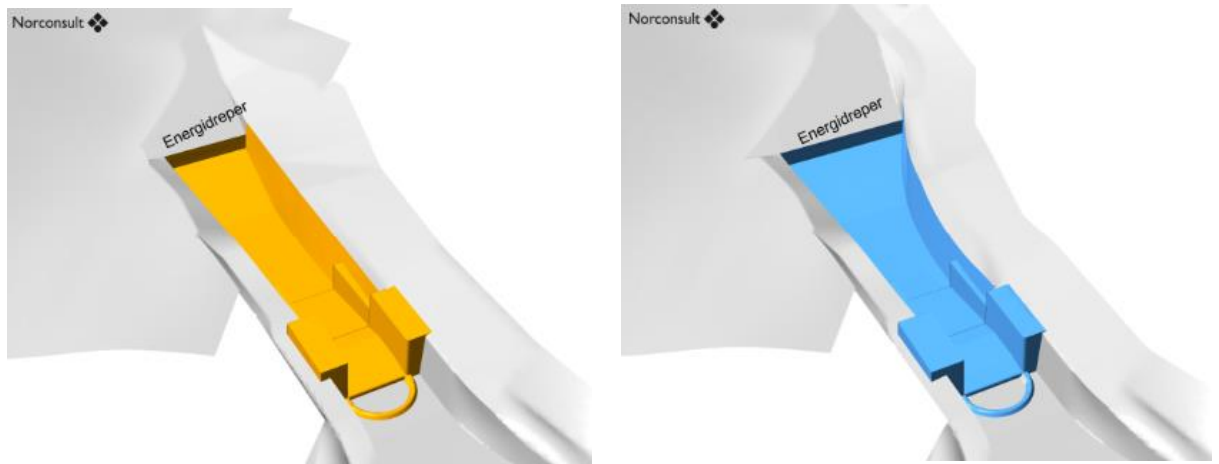


Figure 9: Left: Preferred design of spillway channel / stilling basin. Right: Alternative design, due to request for rock excavation (Norconsult, 2015).

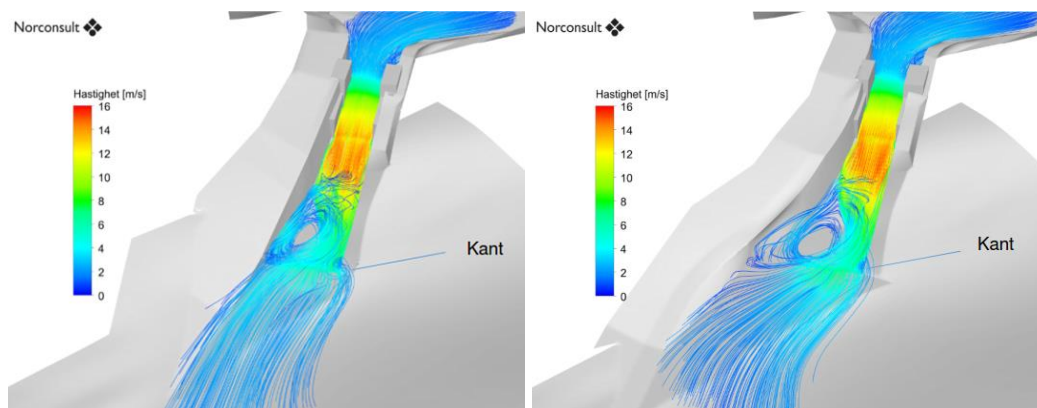


Figure 10: Results from CFD-calculations with preferred design (left) and the alternative design (right), (Norconsult, 2015).

The results show that the alternative design, with a more diverging shape downstream, generates a larger eddy that compresses the jet. This leads to higher velocities and thus, less effective energy dissipation in the stilling basin. However, it was concluded that the increased velocity was acceptable, and the alternative design was approved.

3.6. INITIAL HYDRAULIC MODEL RAMSELE:

Similarly, a physical model was built for Ramsele (Billstein et al. 2016), with the main objective to attain optimal design of the prolonged spillway chute. All three spillway chutes were included in the model, since it was necessary to examine various configurations of gate openings, as well as operation of the left chute, see figure 11 below. It was also of some interest to determine the total discharge capacity of the dam facility.



Figure 11: Hydraulic model of Ramsele dam, scale 1:50, with the proposed prolonged left chute (Vattenfall R&D, 2014)

3.6.1. Spillway Discharge Capacity

The discharge capacity of all three spillways was determined by physical modeling, and was found to agree with the original design values.

3.6.2. Energy dissipation / prevention of rock erosion

The planned design of the prolonged chute was included in the physical model upon which a number of tests were done, including measurements of velocity and wave activity along the slopes at the sides. During the testing phase, an alternative design was proposed: a shorter prolongation with a ski-jump at the end. The design change was chiefly motivated by cost reduction, as the construction length could be decreased by 30% to about 35 m.

This new design was chosen for further testing with a focus on optimizing the ski-jump design – jet throw length, location of the impact zone etc. The updated design flood also demanded for the guide walls to be heightened, and the model tests were used for optimization of this. Figure 12 shows model testing for the left chute, with the final design of the ski-jump.



Figure 12: Ramsele, left spillway – proposed shortened ski jump design (Norconsult, 2016)

4. VERIFICATION OF HYDRAULIC PERFORMANCE IN THE PROTOTYPES

After the completed construction of the planned measures, discharge tests are carried out according to accepted international guidelines. Ramsele has already been completed, and here photogrammetry was performed for the spillway channel before the discharge test, focusing on the area where the jet from the ski-jump plunges. This resulted in a topographic model, and if the procedure is repeated in the future after some discharging has occurred, the models can be compared for evaluating erosion propagation. Figure 13 shows a drone photo from the discharge test.

Upon completion of the last gate structure at Långströmmen, similar tests will be performed here. Aerial filming by drone is to be supplemented with water level measurements in order to verify the downstream water level during

discharge. The readings will be compared to the physical model, and also the fluctuation of the water level.



Figure 13: Drone photo from first discharge test, after completed construction (Norconsult, 2016).

5. CONCLUSION

Both Långströmmen and Ramsele are high-hazard dams where recent dam safety revisions have uncovered deficiencies in their spillway structures. Whether the defects are in spillway capacity or in the structure downstream where scouring can erode the foundations of dam and spillway, one needs to fully understand the forces in play prior to designing the spillway structure. In this, the value provided by physical modelling has been underscored in both projects by findings during the project life.

In Långströmmen, discoveries on site necessitated a revamp of the design. In Ramsele, the discoveries were in the model phase and the design could be adapted parallel to the model tests.

In ideal worlds, the physical models should be kept until the project has been completed successfully. However, as large physical models are costly to keep for extended periods of time, the approach described in the Långströmmen project can be a way forward.

Numerical modeling is already used to enhance physical models in conceptualization by narrowing the scope of modelling. Långströmmen shows a way where CFD can be used to project parameters beyond the scope of the initial physical model.

Acknowledgements

The study of the dam upgrades reported in this paper is performed for power producers Fortum and Uniper, in Sweden. Vattenfall R&D, are acknowledged for their contributions to the hydraulic model tests. The opinions expressed are only those of the authors and do not necessarily represent those of any other individuals or institutions.

References

- [1] YANG, J & ANDREASSON, P. Headward erosion in embankment dams caused by spillway flood discharge. *International Journal Hydropower & Dams*, 2012, issue 6.
- [2] YANG, J & ANDREASSON, P. Headward erosion in embankment dams caused by spillway flood discharge. *International Journal Hydropower & Dams*, 2012, issue 6.
- [3] YANG, J, ANDREASSON, P & CEDERSTRÖM, M, "Experiences from modifications of curved spillway channels in dam rebuilding projects", *International Symposium on Hydraulic Physical Modeling & Field Investigation*, September 2010, Nanjing.
- [4] YANG, J, ASCILA, R & NILSSON, C O. Adding extra spillway discharge capacity, a few dam refurbishment examples in Sweden. *International ICOLD Symposium on Dams in a Global Environmental Challenges*, June 2014, Bali, Indonesia.
- [5] YANG, J, BILLSTEIN, M & HELGESSON, A. Långströmmen dam safety, hydraulic model study 2014. Vattenfall, R&D Laboratories, Report U 14:56, Feb. 2015, Älvkarleby.
- [6] YGLAND, D et al. Långströmmen dam safety, a pre-study (in Swedish). Sweco Infrastructure, Project Report 2157149, Sept. 2012, Stockholm.
- [7] PERSSON J et al. Pre-study Ramsele – waterways downstream of spillways. Norconsult, 2015-05-12.
- [8] BOND, H et al. Ramsele power plant – Dam Safety Evaluation 2014. WSP, 2015-02-25.
- [9] WELDE, A. CFD simulations – New spillway at Långströmmen, 2015-12-15
- [10] BILLSTEIN M et al. Ramsele hydraulic model tests. Vattenfall R&D, 2016-10-05

COMMISSION INTERNATIONALE
DES GRANDS BARRAGES

VINGT-SIXIÈME CONGRÈS DES
GRANDS BARRAGES
Autriche, juillet 2018

THE BEHAVIOR OF THE SPILLWAY-STRUCTURE OF THE DJUANDA DAM JATILUHUR INDONESIA *

Budy GUNADY¹, Harry M. SUNGGUH², Mudyati RAHMATUNNISA³, Diah E.
HARSANI⁴

¹*Manager of Technical and Business Planning of The Business Region IV, JASA
TIRTA II PUBLIC CORPORATION*

²*Director II, JASA TIRTA II PUBLIC CORPORATION*

³*Vice Dean of Postgraduate School, PADJADAJARAN UNIVERSITY*

⁴*Staff of Technical Planning of The Business Region IV, JASA TIRTA II PUBLIC
CORPORATION*

INDONESIA

1. ABSTRACT

Djuanda Dam is the largest dam built in Citarum River, located about 80 km toward southeast from Jakarta the capital city of Indonesia.

Djuanda Dam Jatiluhur is a multipurpose dam with a design-capacity volume of 3 billion m³, and based on the latest bathymetri measurement results has a storage capacity of approximately 2.5 billion m³.

This dam has a concrete cylindrical-shaped spillway called morning glory with a diameter of 90 meters and a height of 105 meters. The maximum capacity of this spillway is 3,000 m³ and also equipped with two irrigation outlets of which capable to release 195 m³/s water on normal water level.

This spillway is integrated with the powerhouse and connected with the access gallery and tailrace tunnel, and make it as the only infrastructure to

* *LE COMPORTEMENT DE LA STRUCTURE DE DÉVERSEMENT DE DJUANDA DAM
JATILUHUR INDONÉSIE*

release water from this dam so that the operation and maintenance of this spillway structure is very important.

The shift of the dam body construction toward the upstream than the planned has shifted the center of gravity of the dam causing the concrete fracture connecting the spillway-structure with the access gallery. This cracks then named as join 0. The water leakage from this cracks are collected and channeled into the drainage channel to monitor the quantity and the quality of leakage. The leakage monitoring activity conducted every two weeks.

There are 37 points of surface marker installed in this morning glory spillway-structure, 3 points placed on the top floor of the morning glory spillway-structure, 3 points on the floor in the powerhouse. While on the wall of the powerhouse is placed 31 points of surface marker, 11 mounted on the inside wall named interior circle, and 20 others mounted on the outside wall named exterior circle. The monitoring activity by measuring the movement of these surface markers conducted every month.

The measurement of the spillway-crest on 14 spillway-windows has conducted twice, on August 2001 and on October 2017.

Based on surface-marker monitoring results, this spillway has experienced movement and the monitoring data record shown the average cumulative settlement is 11 cm, and the largest cumulative settlement reached 15 centimeters at the point of window number 12, with elevation 106,8438 meters above sea level.

The movement of this spillway is influenced by the elevation of the reservoir water level (RWL), when the elevation of the RWL reach the normal elevation the spillway-structure moves down, and vice versa.

The movement of the spillway-structure also impact to the leakage at join 0. The leak is still monitored until now and it shown the largest discharge of 190 ml per second. The water quality of the leakage is monitored and did not indicate it carry the embankment material, visually it looks clear and clean.

COMMISSION INTERNATIONALE DES GRANDS BARRAGES

VINGT-SIXIÈME CONGRÈS DES GRANDS BARRAGES
Autriche, juillet 2018

DOI 10.3217/978-3-85125-620-8-097



This work licensed under a Creative Commons Attribution 4.0 International License. <https://creativecommons.org/licenses/by-nc-nd/4.0/>

PHYSICAL MODELLING OF THE JIRKOV DAM BELL-MOUTH SPILLWAY

Jan SVEJKOVSKÝ

Head of the Department of Dam Monitoring and Safety, POVODÍ OHŘE,
STATE ENTERPRISE

CZECH REPUBLIC

Martin KRUPKA

Department of Water Management Development, POVODÍ OHŘE,
STATE ENTERPRISE

CZECH REPUBLIC

COMMISSION INTERNATIONALE
DES GRANDS BARRAGES

VINGT-SIXIÈME CONGRÈS DES
GRANDS BARRAGES

Autriche, juillet 2018

PHYSICAL MODELLING OF THE JIRKOV DAM BELL-MOUTH SPILLWAY

Jan SVEJKOVSKÝ

*Head of the Department of Dam Monitoring and Safety, POVODÍ OHŘE,
STATE ENTERPRISE*

CZECH REPUBLIC

Martin KRUPKA

*Department of Water Management Development, POVODÍ OHŘE, STATE
ENTERPRISE*

CZECH REPUBLIC

1. INTRODUCTION

Bell-mouth spillways are not a common type of spillways in the Czech Republic. One of the oldest bell-mouth spillways is situated at the Jirkov Dam (Fig. 1). When compared to other spillways of this type, an unusual solution was used for the intake and the circular bottom end of the vertical shaft. The physical model was built in order to clarify the hydraulic conditions during flood flows.

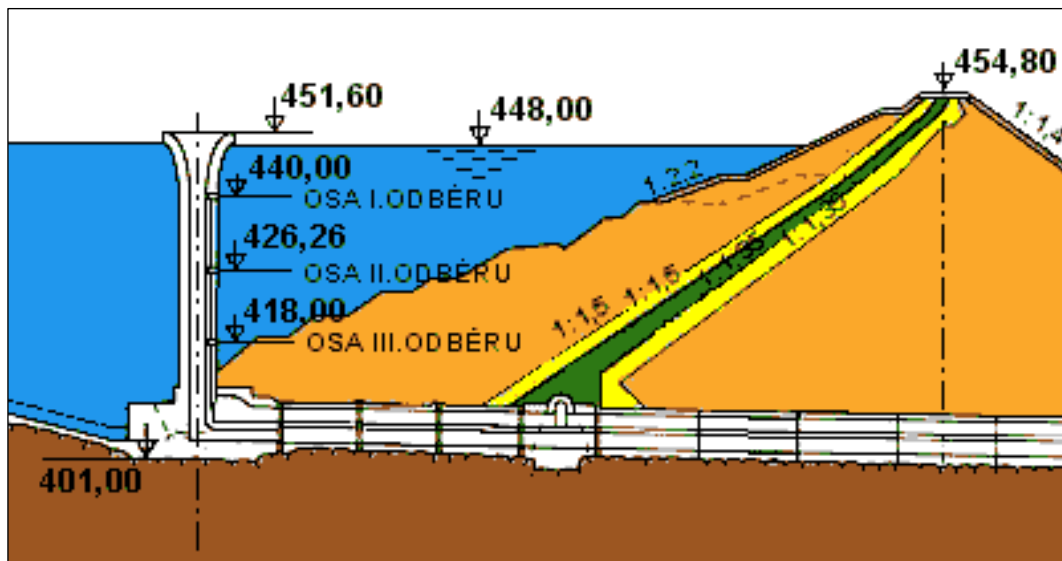


Fig. 1
Cross section of the Jirkov Dam

2. JIRKOV DAM

2.1. DAM

Jirkov Dam is located in the North-west part of the Czech Republic. It was constructed between 1960 and 1965. It is a rockfill dam sealed by the impervious clay core. The dam is equipped with the bell-mouth spillway structure at the upstream toe of the dam that is combined with two bottom outlets and three water abstraction intakes at different levels. Water from the bell-mouth spillway and the bottom outlets is conveyed to the outlet tunnel that ends at the downstream toe of the dam. The upper part of the tunnel structure forms an access to the bottom outlets.

Perpendicular to the tunnel is the injection gallery that goes along the whole dam at the foundations level. In recent years a grout curtain was constructed from the injection gallery in order to seal the seepage that had been observed.

2.2. BELL-MOUTH SPILLWAY

The overflow piers of the Jirkov Dam bell-mouth spillway were constructed rather small in size compared with similar structures at other dams. The piers also force water to rotate in the opposite direction. The water falls to the vertical shaft and then flows to the outlet tunnel via the sharp perpendicular bend that was suspected to limit the capacity of the whole object.

3. RESEARCH ASSIGNMENT

The unusual spillway intake setup led to the research that was carried out by the Civil Engineering Faculty of the Czech Technical University in 2015 and 2016 [1]. The research was ordered by the dam operator Povodí Ohře, state enterprise. The aim of the research was to assess the existing layout and propose optimized design. The research was carried out using the physical model of the bell-mouth spillway that extended from the top of the structure to the end of the spillway tunnel at the downstream toe of the dam.

The physical model was used to derive the rating curve of the spillway and particularly to find the level flow at which the undesirable hydraulic effects occur. It was also used to design and verify suitable modifications to the intake of the bell-mouth spillway, to the bottom end of the vertical shaft and to join of the bottom outlets to the spillway tunnel.

The physical model was built using the Froude similarity, it was considered that gravity and inertial forces are dominant and effect of remaining forces such as kinematic viscosity are small. The model was built in laboratories of the Czech Technical University in Prague, Faculty of Civil Engineering at a 1:20 scale. Setup allowed to measure not only flows, but also vibrations and pulsations. Pressure sensors were used to measure all hydraulic phenomena, which occurred on the model and particularly the dynamic effects of water flow on the structure.

Firstly, the measurements were carried out on the model of the original design and then modifications reflecting the knowledge gained on the modelling of similar bell-mouth spillways were proposed and tested. In particular, the attention focused on the optimization of the shape of overflow piers and the rounded bottom end of the vertical shaft.

3.1. REMOVAL OF OVERFLOW PIERS AT THE SPILLWAY INTAKE

The existing design of the overflow piers (Fig. 2) does not ensure stable spiral inflow to the vertical shaft and sufficient air supply even at low flow rates of 1 in 2 years return period. The inflow into the vertical shaft is strongly affected by the piers and the pressure pulsations were observed. These pulsations generate an unwanted load on the spillway and the shaft structure.



Fig. 2
Model of the original design with 4 overflow piers

In order to improve the hydraulic performance of the existing spillway the overflow piers were removed (Fig. 3).



Fig. 3
Model of the bell-mouth spillway without overflow piers

3.2. IMPROVEMENTS TO THE BOTTOM END OF THE VERTICAL SHAFT

The existing bottom of the vertical shaft has a sharp perpendicular bend (Fig. 4, left). As the water falls vertically to the bottom of the shaft, it forms an aerated turbulent flow cushion that extends downstream to the spillway tunnel. This cushion starts to be significant for 1 in 20 years flow.

The rounded bottom of the vertical shaft was proposed (Fig. 4, right). The model revealed that the aerated cushion has diminished significantly. The energy loss is much smaller and the velocity vector is oriented towards the direction of the outlet tunnel. The aerated cushion at the bottom of the shaft was formed for much higher flow exceeding 1 in 100 years return period.



Fig. 4
 Rounded bottom end of the vertical shaft
 Existing design (Q_{10}) Updated design (Q_{10})

3.3. COMBINED EFFECT OF THE SPILLWAY AND BOTTOM OUTLETS

The physical model allowed testing the effect of combined bell-mouth spillway and two bottom outlets operation. This scenario was tested for the extreme flow of 1 in 1000 years and it was found that the space at the junction of bottom outlets and the spillway tunnel is more aerated, when bottom outlets are in operation (Fig. 5). The use of bottom outlets at extreme flow rates is not recommended based on the model results. These flow rates surcharge the spillway shaft and unfavorably reduce the capacity of the whole hydraulic system.

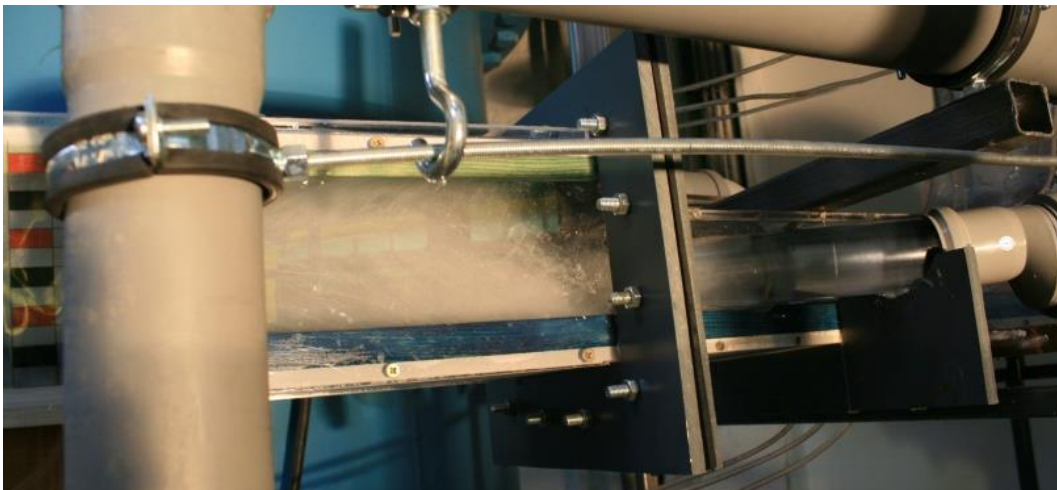


Fig. 5
 Bottom left outlet pipe in operation

3.4. EFFECTS ON SPILLWAY CAPACITY

Rating curve was derived for the existing design (Var 1), on the improved design after the removal of the existing overflow piers (Var 2) and on the improved design with the rounded bottom end of the spillway shaft (Var 3). The comparison of rating curves representing the three modelled cases as well as the existing rating curve that is present in the operating manual can be seen in Fig. 6.

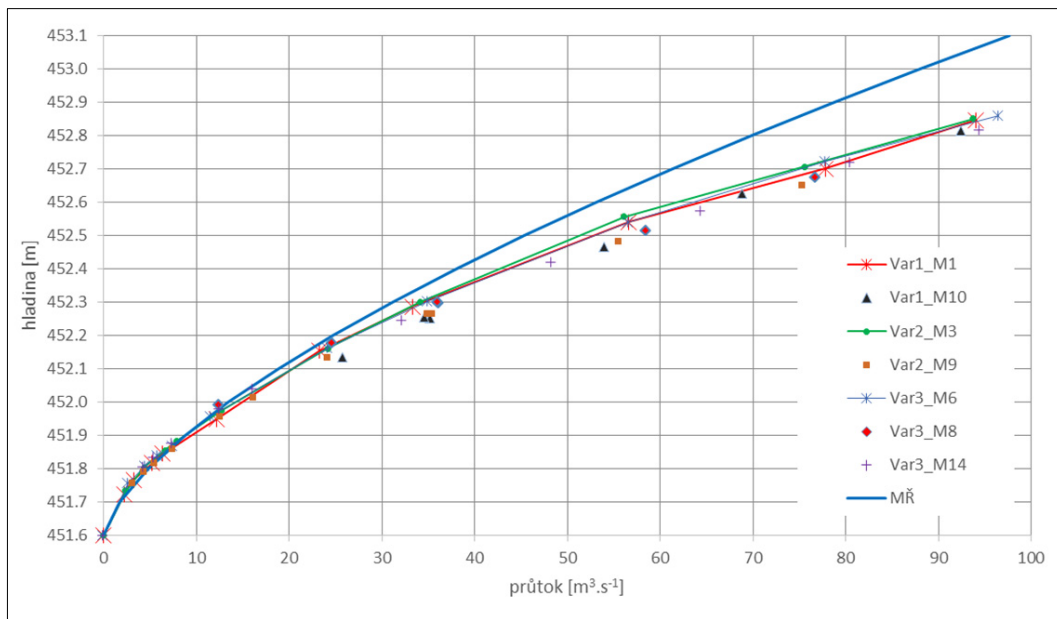


Fig. 6
Rating curve comparison

Curves derived by the physical model do not differ significantly; however, the plot shows the significant difference between the operating manual rating curve (labelled MR) and the models.

As the very small difference between the modelled rating curves suggests, the proposed design improvements do not affect the capacity of the structure significantly. However, it was proved by the physical model that the removal of the overflow piers improve water supply conditions at the vertical shaft and partly eliminate pulsations and decrease the hydraulic load on the structure, while the rounded bottom end of the vertical shaft prevents the existence of the extremely turbulent flow in the spillway tunnel downstream of the bend.

The original capacity of the Jirkov Dam spillway prior the reaching the undesired hydraulic conditions regime was assessed to be $95 \text{ m}^3 \cdot \text{s}^{-1}$, while the improved design capacity is $124,6 \text{ m}^3 \cdot \text{s}^{-1}$. This capacity is higher than 1 in 10 000 years flow which meets the Czech national standards for dam safety.

3.5. FURTHER IMPROVEMENTS OF SPILLWAY INTAKE

When the existing overflow piers were removed, research for a new design was carried out. The aim was to further eliminate the pressure pulsations on the spillway structure while not decreasing the capacity of the spillway.

A design of five-piers based on the similarity with other existing bell-mouth spillways was proposed and tested (Fig. 6). The six piers variant was also considered but it resulted in increase in pressure pulses throughout the tested flow range.



Fig. 7
Model of bell-mouth – designed overflow piers

SUMMARY

This paper presents the hydraulic research of the existing bell-mouth spillway at the Jirkov Dam in the Czech Republic and the improvements proposed to increase the hydraulic performance of the structure.

Proposals comprise the new design of the overflow piers and the rounding of the bottom of the vertical shaft. The improvements were proposed and tested on a physical model by the Czech Technical University in Prague, Faculty of Civil Engineering.

Rating curve was derived for the existing spillway design as well as for the proposed layouts. Proposed layouts showed an improvement, particularly

the capacity of the existing Jirkov Dam spillway prior reaching the undesired hydraulic conditions was assessed to be $95 \text{ m}^3 \cdot \text{s}^{-1}$, while the improved design capacity is $124,6 \text{ m}^3 \cdot \text{s}^{-1}$. This capacity is higher than 1 in 10 000 years flow which meets the Czech national standards for dam safety.

REFERENCES

- [1] SATRAPA, L. ET AL., JIRKOV DAM – DESIGN OF IMPACT SITE OF BELL-MOUTH SPILLWAY – PHYSICAL MODEL, 2015, 2016, CZECH TECHNICAL UNIVERSITY IN PRAG, FACULTY OF HYDROTECHNICS

KEYWORDS

Jirkov Dam, dam, design, spillway

COMMISSION INTERNATIONALE DES GRANDS BARRAGES

VINGT-SIXIÈME CONGRÈS DES GRANDS BARRAGES
Autriche, juillet 2018

DOI 10.3217/978-3-85125-620-8-098



This work licensed under a Creative Commons Attribution 4.0 International License. <https://creativecommons.org/licenses/by-nc-nd/4.0/>

**STRUCTURAL SAFETY CONTROL OF THE BAIXO SABOR DAM BASED ON
AN AUTOMATED DATA ACQUISITION SYSTEM**

João G. CUNHA

DAM ENGINEERING DIVISION, EDP GESTÃO DA PRODUÇÃO DE ENERGIA
SA

PORTUGAL

Juan T. MATA

CONCRETE DAM DEPARTMENT, LABORATÓRIO NACIONAL DE
ENGENHARIA CIVIL

PORTUGAL

Gonzalo L. ORTIZ

PROINTEGA INGENIERIA SL

SPAIN

COMMISSION INTERNATIONALE
DES GRANDS BARRAGES

VINGT-SIXIÈME CONGRÈS DES
GRANDS BARRAGES
Autriche, juillet 2018

STRUCTURAL SAFETY CONTROL OF THE BAIXO SABOR DAM BASED ON AN AUTOMATED DATA ACQUISITION SYSTEM

João G. CUNHA¹, Juan T. MATA², Gonzalo L. Ortiz³

¹ *Dam Engineering Division, EDP Gestão da Produção de Energia SA*

² *Concrete Dam Department, LABORATÓRIO NACIONAL DE
ENGENHARIA CIVIL*

PORTUGAL

³ *Prointega Ingenieria SL*

SPAIN

1. INTRODUCTION

This paper presents the main characteristics of the automated structural monitoring system of Baixo Sabor dam and addresses a proposal for the definition of triggers for the physical quantities measured through the use of an automated data acquisition system (ADAS).

The defined triggers for the physical quantities will be linked to an Internal Early Warning Control System of the dam, allowing the early identification and notification of potential abnormal situations to the entities responsible for the dam safety.

In operation since August 2016, the ADAS of the Baixo Sabor dam defined by EDP allows the measurement of several quantities used for the safety control, analysis and interpretation of the dam behaviour, such as: horizontal and vertical displacements, movements of joints, strains, uplift pressures, foundation displacements, seepage, concrete and air temperatures, and reservoir water level, among others.

The measurements, obtained through the use of the ADAS developed and installed by Prointegra Ingeniería, are sent to the gestBarragens system, which is the LNEC and EDP data processing and management system used for monitoring, diagnosis and safety control of dams.

2. THE BAIXO SABOR DAM

Baixo Sabor is a 123 m high concrete arch dam, 505 m long at the crest, designed, constructed and operated by EDP, located in the northeast of Portugal in Sabor river (a tributary of Douro river). The first filling of its reservoir, with a volume of about 1095 hm³, took place between December 2013 and April 2016.



Fig. 1
Overall view of the Baixo Sabor dam

2.1. THE MONITORING SYSTEM OF THE BAIXO SABOR DAM

In accordance with the best technical practices, the monitoring system of the Baixo Sabor dam aims at the evaluation of the loads, the characterisation of the rheological, thermal and hydraulic properties of the materials, and the evaluation of the dam structural response.

The monitoring system of the Baixo Sabor dam consists of several devices which make it possible to measure quantities such as: concrete and air temperatures, reservoir water level, seepage and leakage, displacements in the dam and in its foundation, joint movements, strains and stresses in the concrete, and pressures, among others [1].

The system used for the measurement of the reservoir water level comprises a high precision pressure meter, which provides a record of the water

height over time, and a level scale. The air temperature and humidity are measured in an automated weather station.

The concrete temperature is measured in 52 electrical resistance thermometers distributed across the dam thickness of several blocks. The location of the thermometers was defined taking into account the set of the others electrical resistance devices (strain gauges, embedded jointmeters and strain gauges) that also allow the measurement of the concrete temperature.

The foundation temperature is measured in 13 temperature sensors distributed in several rod extensometers.

Displacements are measured using an integrated system that includes 5 pendulums, 24 rod extensometers and geodetic observations. The relative movements between blocks are measured by 103 superficial and 152 embedded jointmeters.

The deformation of the concrete is measured with electrical strain gauges arranged in groups, distributed in radial sections, allowing the determination of the stress state through the knowledge of the deformation state and of the deformability law of the concrete. The drained and the infiltrated water are measured in the drainage system which includes 216 drains and 19 weirs. These last devices differentiate the total quantity of water that flows in the drainage gallery in several zones of the dam. The measurement of the uplift pressure in the foundation is performed by a piezometric network that comprises 41 piezometers.

2.2. THE AUTOMATED MONITORING SYSTEM OF THE BAIXO SABOR DAM

A real-time data acquisition system for the auscultation instrumentation (ADAS) has been installed at Baixo Sabor dam, allowing the measurement of the following physical quantities [2]:

- Horizontal movements based on the pendulum method through the use of optical telecoordinometers (4-20mA signal);
- Vertical movements through rod strain meters with position transducer, vibrating wire type;
- Discharges through level gauges with ultrasonic sensors (4-20mA signal);
- Pressures through piezometers with pressure transducers, vibrating wire type;
- Relative movements between blocks through 3D jointmeters with position transducer, vibrating wire type, located in the inspection galleries;
- Relative movements between blocks through 1D jointmeters with resistance transducer, Carlson type, embedded in the concrete dam body;
- Concrete strain through strain meters with resistance strain meter transducers, Carlson type, embedded in the concrete dam body;
- Concrete temperature through thermometers with resistance thermometer transducers, Carlson type.

In addition, the weather station has been integrated into the automated data collection system by communicating the automation server with the station logger.

As a complementary system, a high precision Global Navigation Satellite System (GNSS) has been installed. It allows the displacements measurements of 3 points located at the dam crest, both horizontally and vertically, using an external pillar as reference, allowing to obtain post-process results working every hour, 4 hours and 24 hours. In this last case, a sub-millimeter precision is obtained.

For real-time monitoring and for the analysis of all the information, ADAS auscultation software has been installed, with customised developments for this project. This software allows real-time monitoring of the system, generation of graphs and reports and alarm management, among other functionalities, operating on a multiuser Web environment, allowing several technicians to work on the system at the same time.

The structure of the ADAS is based on industrial decentralised periphery automation, in this case composed of a main box that houses the PLC (Programmable Logic Controller) provided with a touch panel with remote connection, and four secondary boxes, racks, all connected in a ring via optical fibre and secure power supply via batteries. Equipment with galvanic isolation and surge arresters has been placed at strategic points to make the system more robust. The GNSS communicates via optical fibre with the main box, which is connected to the server installed in the control and emergency room where the GNSS and ADAS software is installed.

The touch panel of the main box enables the parameterisation and supervision work on the dam, as well as stopping logs for maintenance work and alarm management. As all the equipment is in the same network, the panel can be remotely accessed from any box, thus allowing the monitoring and parameterisation of the instrumentation from other galleries where there are automation boxes, making these tasks much easier.

The communication between the instrumentation and automation box is performed with multi-wire shielded sheaths from each device to the box, thus avoiding interconnection boxes, all channelled in separate trays of the power supply sheaths, avoiding electromagnetic noise and guaranteeing the quality of the signals.

All the instrumentation is adapted to be able to make a parallel manual reading, allowing data contrast and validation of both systems. The equipment is all standard, allowing easy maintenance and rapid device replacement times. The system is already equipped for an expansion of about 20%.

2.3. MEASURING RANGE OF UPLIFT PRESSURE, MEASURED THROUGH PIEZOMETERS

The automated measurement of uplift pressure is performed through 25 piezometers as presented in Fig. 2.

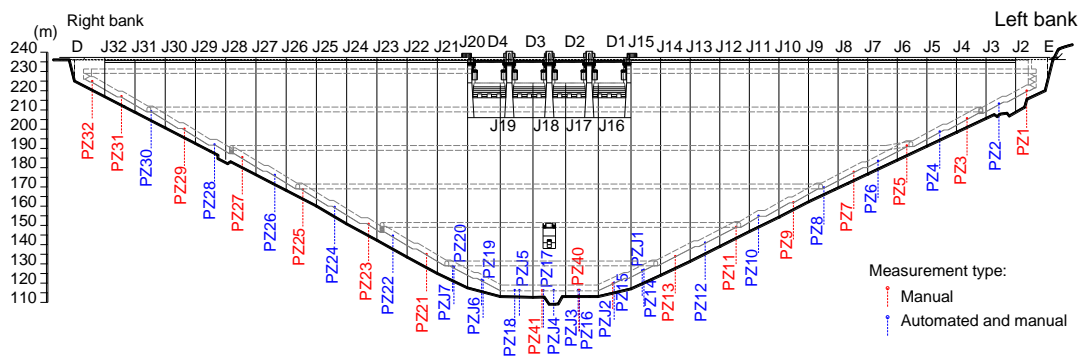


Fig. 2
Location of the piezometers

The automated measurement of the uplift pressure along the dam foundation is performed by vibrating wire piezometers, Geosense VWP-3000, converting fluid pressures on a sensitive diaphragm into a frequency signal and then into a uplift pressure unit (m H₂O), Fig. 3.



Fig. 3
Piezometer with automated readings.

The main features of the vibrating wire piezometers VWP-3000 type, presented in Table 1, are suitable for the environmental conditions and the expected maximum range of the instrument, equal to 70 m H₂O, which is considered adequate.

Table 1
Piezometer VWP-3000 type, main features

Pressure range	0 – 690 kPa
Resolution	0.0255 %FS
Accuracy	0.1%FS
Non-Linearity	<0.5%FS
Temperature range	-20 to 80 °C
Thermal effect	<0.05%FS/°C

The uplift pressure measuring range in terms m H₂O, for the 3 piezometers with more significative measurements, is presented in Table 2.

Table 2
Piezometer measuring range from January 2015 to December 2017

Designation	PZ8 (169m)	PZ12 (138.86m)	PZ14 (126.62m)	PZJ1 (125.9m)
Max (m H ₂ O)	36	19	28	20
Min (m H ₂ O)	13.2	0	1.9	2.7

(elevation of the measurement points is shown in curved brackets)

3. TRIGGER DEFINITION BASED ON THE OBSERVED BEHAVIOUR

The definition of triggers for the uplift pressure measured through use of the piezometers is presented in this work. In order to show the proposed methodology, only the analysis of the uplift pressure measured in the PZ14 (126.6m) is presented. In the case of uplift pressures, the manual measurement was possible since September 2014 (time period more than two years) and the automated measurement was possible since July 2016 (time period less than one year). For these reason, manual measurements were used for the trigger definition. The data analysed corresponds to a period between January 2015 and December 2017, resulting more than 123 observations (manual measurements). The time evolution of the reservoir water level, air temperature and uplift pressure (manual and automated measurements) in the referred PZ14 (126.6m) are presented in Fig. 4. The readings were collected every two weeks for manual measurements and every hour for automated measurements. Among the different loads acting on concrete dams, it is usual to distinguish, as the most important ones for structures in normal operation, the hydrostatic pressure and the air temperature variation, Fig. 4.

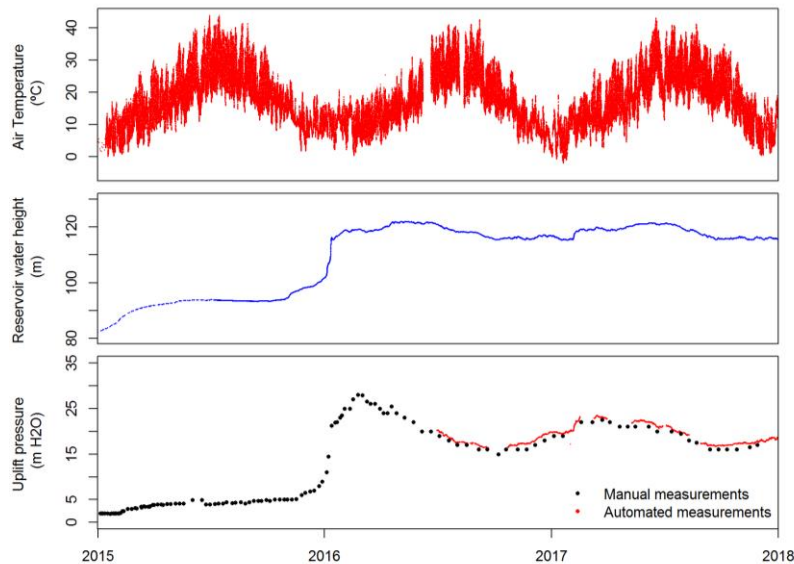


Fig. 4

Uplift pressure in the PZ14 (126.6m), reservoir water level and air temperature along time

The structural response of, for instance, the uplift pressure, is strongly related to the corresponding variation of the reservoir water level. The manual measurements presented in Fig. 4 were used for the computation of the Hydrostatic Season Time (HST) models [3,4,5] presented in this work.

In this case study, the HST model with the best performance for the uplift pressure regarding the manual readings of the piezometer $y^{HST, PZ14 (126.6m)}$ was obtained as the sum of the hydrostatic pressure term $\beta_1 \times h^4$ (where h is the reservoir water level height and can vary between 0 and 123 m) and the temperature terms $\beta_2 \times \cos(d) + \beta_3 \times \sin(d)$ to represent the effect of the annual thermal variation of the temperature (where $d = 2\pi \cdot j/365$ and j represents the number of days between the beginning of the year, January 1, until the date of observation, $0 \leq j \leq 365$). The time effect did not seem to have a significant importance in the period examined by this study. The regression coefficients of the quantitative models obtained are $\beta_1 = 1.342 \times 10^{-7}$, $\beta_2 = 1.2512$ and $\beta_3 = 1.3459$, with $k=-6.049$; being the HST model represented through the Eq. (1).

$$y^{HST, PZ14 (126.6m)} = \beta_1 \times h^4 + \beta_2 \times \cos(d) + \beta_3 \times \sin(d) + k \quad (1)$$

The effects of hydrostatic pressure variation based on the reservoir water level variation, the thermal effect due to temperature variations (considered as a proportional attenuation of the air temperature changes with a phase shift), the residuals* (k), the HST model prediction and the confidence intervals (based on 3 and 6 standard deviation, corresponding to 99.73% and 99.99% confidence levels, respectively) are presented in Fig. 5.

The regression parameter estimates for the HST models, regarding to the uplift pressures, for the piezometers PZ8, PZ12, PZ14 and PZJ1, are presented in Table 3.

Table 3
Regression parameter estimates for the HST models regarding to the uplift pressure obtained through the piezometers

Designation	β_1	β_2	β_3	k	σ (m H2O)
PZ8 (169,0m)	1.107×10^{-7}	1.218	1.305	6.852	2.15
PZ12 (138,9m)	8.504×10^{-8}	-0.084	1.996	-5.774	2.47
PZ14 (126,6m)	1.342×10^{-7}	1.251	1.346	-6.049	1.71
PZJ1 (125,9m)	8.395×10^{-8}	0.941	1.127	-2.111	1.39

* Besides the information related to any possible anomalous phenomena, the residuals contain information related to errors (measurements and model) and other unknown effects.

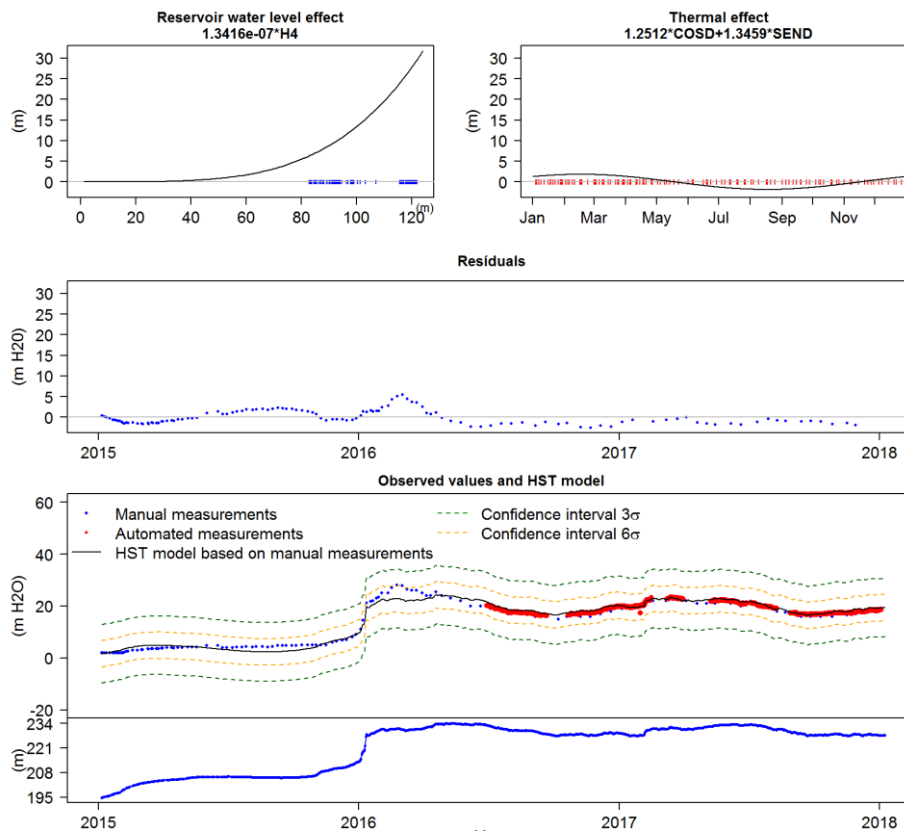


Fig. 5

HST model for the uplift pressure measured in the PZ14 (126.6m), $y^{\text{HST, PZ14 (126.6m)}}$

4. DEFINITION OF TRIGGERS FOR THE AUTOMATED MEASUREMENTS

Currently, the ADAS auscultation software includes a control panel that allows the definition of four different constant triggers (LL, L, H, HH – Low Low, Low, High, High High respectively). Users associated with the dam are notified when any trigger is activated. These messages are sent to ADAS auscultation software, being possible to see the warning in several synoptics that's allows the analysis of the dam behavior in real time (Fig. 6) and sent to the mobile phone of the users.

Based on the analysis of the results:

- The minimum positive value obtained from the confidence interval 6σ was considered for LL and the minimum positive value obtained from the confidence interval 3σ was considered for L;
- The maximum value obtained from the confidence interval 3σ was considered for H and the maximum value obtained from the confidence interval 6σ was considered for HH.
- The value proposed during the design phase (percentages of hydraulic head less than 33,3 %) was considered for.

Despite the use of these triggers, an additional type of trigger will be defined to detect short time variations with more accuracy. Based on the fact that automated measurements are recorded each two hours, the hypothesis that between two consecutive measurements (at time i and time $i-2h$) small variations are expected can be considered adequate. In fact, the use of 3σ as criteria regarding two consecutive automated measurements showed to be adequate, based on the records of manual and automated measurements, (this type of trigger is represented with the black colour in Fig. 7).

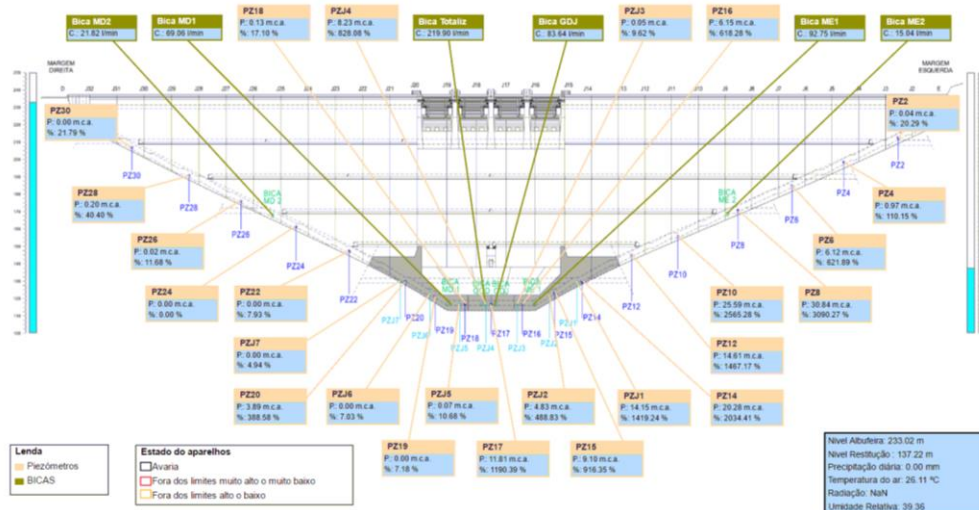


Fig. 6

Synoptic example: Uplift pressures and discharges measured in the Baixo Sabor dam

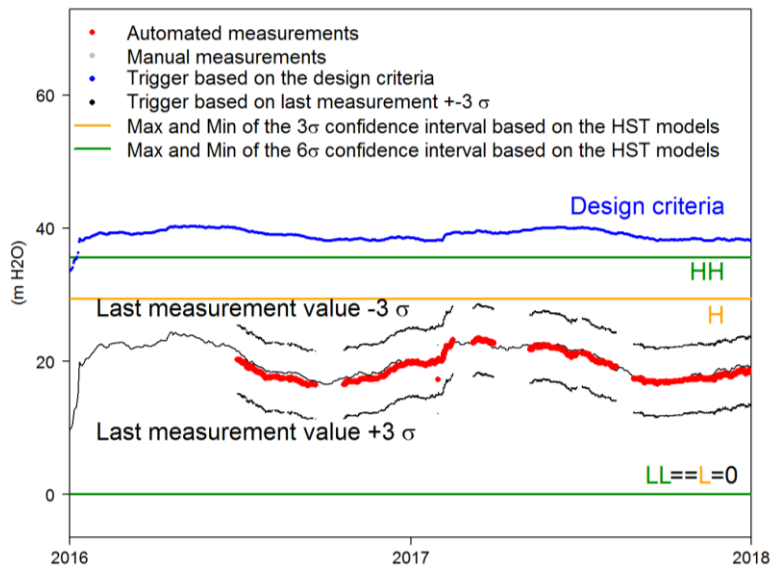


Fig. 7

Triggers used for the assessment of the uplift pressure measured in the piezometer PZ14 (126.6m)

The final results for each trigger are presented in Table 4.

Table 4
Trigger considered for the assessment of the uplift pressure

Designation	LL (mH2O)	L (mH2O)	H (mH2O)	HH (mH2O)	$Abs(\Delta_{(i)-(i-2h)})_{max}$ (mH2O)
PZ8 (169,0m)	0	6.2	39.2	45.7	6.5
PZ12 (138,9m)	0	0	23.1	30.5	7.4
PZ14 (126,6m)	0	0	30.0	35.1	5.1
PZJ1 (125,9m)	0	0	21.7	25.9	4.1

5. FINAL REMARKS

According to the recent trends in automatic monitoring dam systems having in mind the safety control in real time, the ADAS installed in the Baixo Sabor dam includes internal early warning control system allowing early identification and notification of potential situations to the entities responsible for dam safety.

In this work, a methodology to the definition of triggers for the physical quantities observed in automated monitoring systems of the Baixo Sabor dam was presented.

The definition of triggers for the uplift pressures measured on piezometers was performed through the use of HST models and measurement data. The proposed methodology are being used to the definition of the triggers for other physical quantities measured through the automated monitoring system.

Although the importance of physical installation of the systems, it should be noted that the exploitation of ADAS total capacities also involves the incorporation of suitable software for the analysis and validation of the results obtained, based on representative models of the dam behaviour.

So, it can be concluded that the automated monitoring system installed in the Baixo Sabor dam, with internal early warning control system, has a relevant contribution to assure an effective safety control of the dam.

REFERENCES

- [1] LNEC (2013). Barragem de montante do Aproveitamento Hidroelétrico do Baixo Sabor. Revisão do Plano do sistema de recolha automática de dados (in Portuguese). LNEC - Proc. 0403/001/17076; 0401/541/17076. *Technical report 223/2013 – DBB/NO. LNEC*, Portugal. 2013.
- [2] Prointega, Técnicas de soft, EDP. AHBS - Aproveitamento Hidroelétrico do Baixo Sabor. RAD - Recolha Automática de dados de observação. Proyecto y Documentacion (in Portuguese). *Prointega, Técnicas de soft. EDP*, Portugal. 2016.

- [3] MATA J. Interpretation of concrete dam behaviour with artificial neural network and multiple linear regression models. *Engineering Structures. Elsevier*. 48(3):903–910. doi:10.1016/j.engstruct.2010.12.011. 2011.
- [4] LEGER P., LECLERC M.. Hydrostatic, temperature, time-displacement model for concrete dams. *J Eng Mech* 2007;133(3):267–77. 2007.
- [5] ICOLD. Methods of analysis for the prediction and the verification of dam behaviour. *Technical report. Swiss Committee on Dams*. 2003.

COMMISSION INTERNATIONALE DES GRANDS BARRAGES

VINGT-SIXIÈME CONGRÈS DES GRANDS BARRAGES
Autriche, juillet 2018

DOI 10.3217/978-3-85125-620-8-099



This work licensed under a Creative Commons Attribution 4.0 International License. <https://creativecommons.org/licenses/by-nc-nd/4.0/>

SEISMIC HAZARD ANALYSIS FOR GAMBIRI DIVERSION DAM

S. SOLEYMANI

*Expert of Engineering Seismology, TOOSSAB CONSULTATNT ENGINEERING
COMPANY*

IRAN

A. MAHDAVIAN

University professor, UNIVERSITY OF WATER AND POWER TECHNOLOGY

IRAN

H. BAHRAMI

*PhD candidate in Engineering Geology, FERDOWSI UNIVERSITY OF
MASHHAD*

IRAN

SEISMIC HAZARD ANALYSIS FOR GAMBIRI DIVERSION DAM

S.SOLEYMANI¹, A.MAHDAVIAN², H.BAHRAMI³

¹*Expert of Engineering Seismology, TOOSSAB CONSULTANT
ENGINEERING COMPANY*

IRAN

²*University professor, UNIVERSITY OF WATER AND POWER
TECHNOLOGY*

IRAN

³*PhD candidate in Engineering Geology, FERDOWSI UNIVERSITY OF
MASHHAD*

IRAN

1. INTRODUCTION

The Gambiri diversion dam is located at east of Kunar province, near the Asadabad city on the Kunar river, eastern Afghanistan "Fig 1". This project falls within a region of very high seismicity, in the eastern sector of Alpine- Himalaya orogenic belt. In order to estimate the ground motion parameters a comprehensive seismic hazard analysis was performed. This paper gives first a brief overview of the seismo-tectonics of the region and the seismicity. The methodology followed to obtain the peak ground acceleration, response spectra and design accelerograms for different design levels is then described together with selected results.

2. SEISMOTECTONIC SETTING AND HISTORICAL SEISMICITY

As recent deformation continues in the Alpine- Himalaya region, moderate-to-large magnitude, potentially damaging earthquakes are common. Earthquakes in this region will likely cause serious damage, not only from strong ground shaking and faults rupturing the ground surface, but also from liquefaction, lateral spreading and extensive landslide.



Fig. 1

Location of the Gambiri diversion dam site in the eastern Afghanistan.

The data necessary for the seismic hazard analysis were obtained from a survey of the type, location and characteristics of seismic sources, especially faults. Information obtained from earthquake catalogues gave input on the historical seismicity of the region. The catalogues were also used as a basis for probabilistic analyses of earthquake ground motions. The area surveyed for assessing the seismicity comprised a circle with a radius of about 300 km from the site. Epicenters in this region are shown in "Fig 2".

Most of the major faults in the study area follow an NE-SW trend. The Konar- Nari Fault was identified as major active fault. The strongest historical earthquake relevant to the Badakhshan district of northeast Afghanistan is the event of 1832 with an estimated magnitude M_s 7.4. This event can be ascribed to the activity of the central Badakhshan.

3. ESTIMATION OF PEAK GROUND MOTION PARAMETERS

3.1. SEISMICITY PARAMETERS

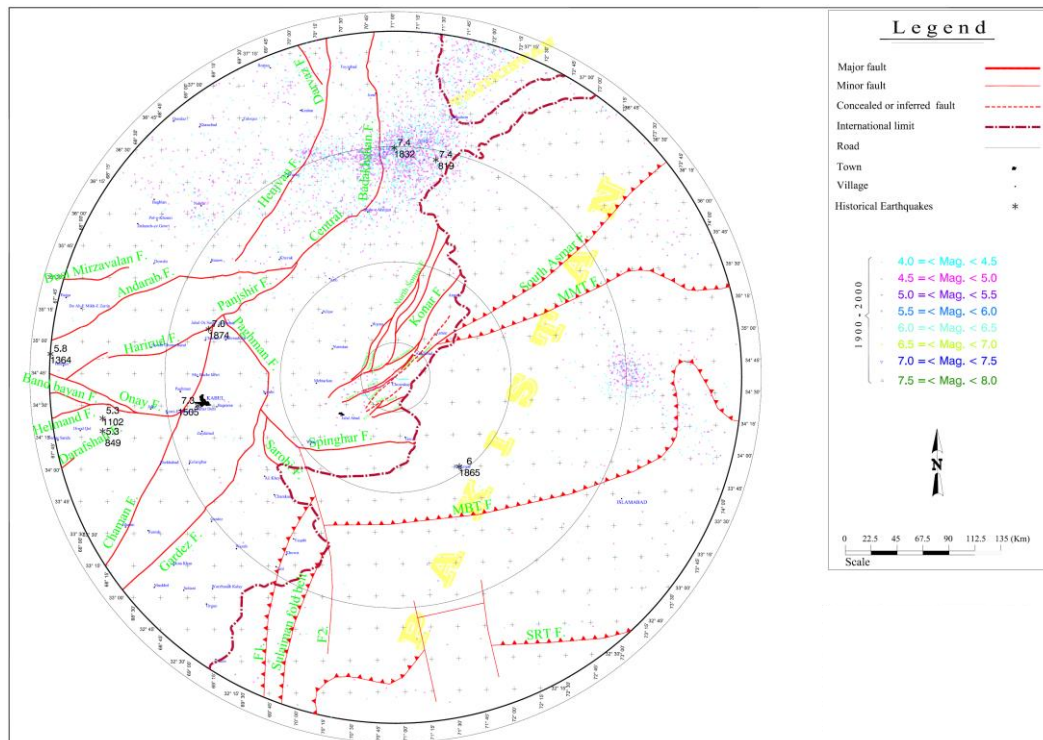


Fig. 2

Location of earthquake epicenters within a radius of 300 km around the site

The estimation of the maximum magnitude (Mmax) and recurrence relationships was performed using by both of the classical approach of Gutenberg & Richter [1] and of the Kijko-Sellevoll method [2].

The advantages of using both of these methods are containing the largest earthquakes and containing data sets which are complete from different thresholds of magnitude upwards. The method can also consider gaps when records in the catalogue are missing and uncertainties in earthquake magnitudes.

3.2. ATTENUATION RELATIONSHIPS

Seismic loads imposed on a dam structure such as power plant by ground motions are usually expressed as peak values of ground acceleration, velocity, and displacement. The peak ground acceleration (PGA) is often used to quantify the seismic hazard for a structure. The values of ground motion parameters (Y) at a site (Include PGA) are estimated by so-called attenuation laws which in their simplest form are expressed as "Eq. [1]".

$$\log Y = \log f_1 (\text{magnitude}) + \log f_2 (\text{distance}) + \dots + \epsilon \quad [1]$$

Attenuation of ground motion depends on many factors such as the fault mechanism, site geological conditions, thickness and type of overburden, etc. The most recent attenuation laws have also taken into account these effects. For

this study the relationships of Campbell & Bozorgnia [3], Ambraseys and Douglas [4], Boore et al. [5] and Mahdavian [6] were used.

3.3. GROUND MOTION DESIGN LEVELS

Four ground motion levels were considered to define the seismic design requirements for the power plant and appurtenant structures. These design levels are partly defined by International Committee of Large Dams [7] and Building and Housing Research Center of Iran [8]. The basic idea is to allow for certain damages during an earthquake of a relatively long return period compared to the lifetime of the structure but not to endanger people's life. The four ground motion levels are defined in following on.

3.3.1. *Operating Basis Level (OBL)*

The Operating Basis earthquake is expected to occur during the lifetime of the dam. The OBE represents the level of ground motion at the dam site which no damage is acceptable. In this study recommended return period of occurring of the OBE is about 150 years.

3.3.2. *Design Basis Level (DBL)*

Ground motions of this level are expected to occur during the lifetime of the power plant. Some minor damage to structures and equipment is accepted but they must remain functional. A PSHA is the most suitable method to establish this level and a return period is about 500 years (usually 475 years).

3.3.3. *Maximum Design Level (MDL)*

This level of ground motions has a low probability of occurrence with a return period of about 1000 years. The dam and appurtenant structures shall be able to resist these ground motions but larger damages are accepted. Safety related devices, such as spillway gates, must remain operational. PSHA is most appropriate to establish values for this ground motion level.

3.3.4. *Maximum Credible Design Level (MCL)*

This level is defined as the largest ground motion that can reasonably be expected at the site from a nearby seismic source or on the basis of the seismic history and tectonics of the region. The DSHA is considered the most appropriate approach to estimate ground motion levels for this scenario. The dam and appurtenant structures may sustain irreparable damage but the uncontrolled release of reservoir water must be prevented. In this study Return Period of occurring of the MCE is more than 2000 years.

For Gambiri diversion dam site, return periods of 200, 500 and 2500 years were considered for the OBL, DBL and MDL respectively and using the 84th percentile of the distribution.

3.4. PROBABILISTIC SEISMIC HAZARD ANALYSIS (PSHA)

PSHA allows the use of multi-valued or continuous events and models to arrive at the required description of the earthquake hazard. Ground motion levels are expressed in terms of probabilistic estimates such as the probability of occurrence of the PGA for a given period of time. The method also allows quantifying the uncertainty of the ground motion parameters. Two models were considered, the seismic point source model and the seismic line source model.

3.4.1. *Seismic Point Source (or Poisson) Model*

This is the oldest approach employing probabilistic tools. The earthquakes are modeled as point sources considering magnitude, epicenter and focal depth. Events are considered independent of each other. The use of this model is advantageous for situations where the identification of faults in an area is difficult and where large and frequent earthquakes have occurred near the site. However, the method cannot consider uncertainties in magnitude and epicentral distance nor does it accept historical earthquakes in the calculations. Since there are numerous large historical earthquakes around the Gambiri diversion dam site, results obtained by this model are believed not to be reliable and they are used for reference purpose only. Calculations were performed using the Gumbel type I distribution function [9].

3.4.2. *Seismic Line Source Model*

This model better fits the many line sources (faults). It can be treated by the well-known software SEISRISK III [10]. Input parameters required include: geometry and location of each seismic source (fault, source zones, including uncertainty), attenuation relationships, and seismicity parameters β and λ (used in the 5 distribution function of the doubly truncated Gutenberg-Richter equation

[1]). The main output obtained from this program is the probability of a ground motion parameter (PGA or spectral acceleration) not being exceeded during a fixed period of time at the site.

For estimating the seismic potential (maximum magnitude) of a fault the Wells & Coppersmith relationship was used which is based on worldwide data [11]. Calculations were carried out for return periods between 100 and 2500 years. In order to obtain a weighted average of the results calculated with the three attenuation laws, a logic tree approach with three branches was applied. Selected results are shown in “Table 1”. The values obtained from the line source model were considerably higher than those derived from the point source model.

Table 1
Values of PGA obtained from PSHA using line source model

Design level	Return period (year)	Dam site	
		Peak ground acceleration (g)	
		horizontal	vertical
OBL (84th percentile)	200	0.30	0.18
DBL (84th percentile)	500	0.394	0.245
MDL (84th percentile)	2500	0.455	0.290
MCL (84th percentile)	Deterministic	0.64	0.53

3.5. DETERMINISTIC SEISMIC HAZARD ANALYSIS (DSHA)

The purpose of the DSHA is to find the worst possible scenario among all the possible seismic sources related to the studied site. The analysis comprises four steps: (1) Identification of the active faults closest to the site, (2) determining the maximum earthquake that could be generated by these faults, (3) selection of appropriate attenuation laws, and (4) determination of the hazard at the site. The maximum values of PGA were calculated for twelve faults or fault segments affecting the dam site using the same attenuation laws as for the PSHA. The distance to the seismic source was taken as the closest distance to the vertical projection of the rupture for Campbell & Bozorgnia [3], Ambraseys and Douglas [4], Boore et al. [5] and Mahdavian [6] laws. A weighted average was calculated using a logic tree approach. The results are given in “Table 2”.

4. ESTIMATION OF RESPONSE SPECTRA

For design and analysis of structures a convenient way to express ground motions is the response spectrum which gives the maximum response

(acceleration, velocity, or displacement) of a simple oscillator to the ground motion.

Table 2
Values of PGA obtained from DSHA (in fractions of g)

Fault name	Distance (km)	M	Dam site			
			horizontal		vertical	
			50%	84%	50%	84%
Harirud	7.8	7.6	0.362	0.580	0.240	0.416
Konar- Nari	1.2	7.3	0.40	0.64	0.312	0.533

The oscillator has the same period of vibration as the fundamental period of the structure. The maximum response is plotted versus the undamped natural period or the natural frequency. Site-specific response spectra are derived from ground motions arising from distinct, well-identified seismic sources in the region considered.

For Gambiri diversion dam site, different methods were chosen to calculate the specific response spectra, namely: (1) probabilistic method using the line source model, (2) deterministic method using active faults in the site area, and (3) statistical method using existing strong motion records. In the following these three methods are briefly described.

4.1. RESPONSE SPECTRA FROM LINE SOURCE MODEL

Some of the attenuation laws used in the PSHA are also frequency dependent. These laws were used to establish so-called Uniform Hazard Spectra or Equal Probability Spectra. On such a spectrum curve each point has an equal probability of exceeding a ground motion parameter (acceleration, velocity, displacement). By means of the logic tree procedure weighted averages of the spectra can be derived.

4.2. RESPONSE SPECTRA FROM DETERMINISTIC MODEL

This model is used for the estimation of the response spectrum for the MCL. The ground motions at a site are estimated deterministically for a selected earthquake scenario. After having determined the earthquake magnitude of a specific seismic source and the closest distance to the site, the site ground motions are estimated using ground motion attenuation laws. The response spectrum is then calculated within a certain range of periods. 50th and 84th percentile values can then also be computed for different damping values.

4.3. RESPONSE SPECTRA FROM STATISTICAL ANALYSIS

In this method, originally proposed by Kimball [12], a suite of strong motion records is statistically treated. These records should originate from earthquakes with similar distances to the rupture source and the magnitude should be of the same order as the target magnitude. Some corrections for differences in site conditions may also be needed. The steps are as follows:

- Selection of suitable strong motion records having magnitudes and distances to the source similar to the target parameters of the earthquake.
- Adjustment of the records for differences in magnitude, distance, faulting mechanism, and other parameters between site-specific conditions and the conditions existing at the site of the record
- Performing a statistical analysis of the adjusted response spectra of the collected records to obtain the target values of the site-specific spectrum. The median (50th percentile) and the median plus one standard deviation (84 percentile) are then selected as DBL and MDL levels respectively. For Gambiri diversion dam sites, site-specific ground motions for distance ranges (about 30 km) similar to the target magnitude were calculated and statistically analyzed. “Fig. 3 and 4” show the horizontal and vertical design response spectra recommended for OBE, DBE, MDE and MCE for this project.

“Fig. 5” shows a comparison between Horizontal components of response spectra estimated by statistical and probabilistic methods with together. The amplitudes of recommended OBE, DBE and MDE response spectra estimated by statistical method are good coordinated with 150, 500 and 1000 year response spectra estimated by probabilistic method respectively.

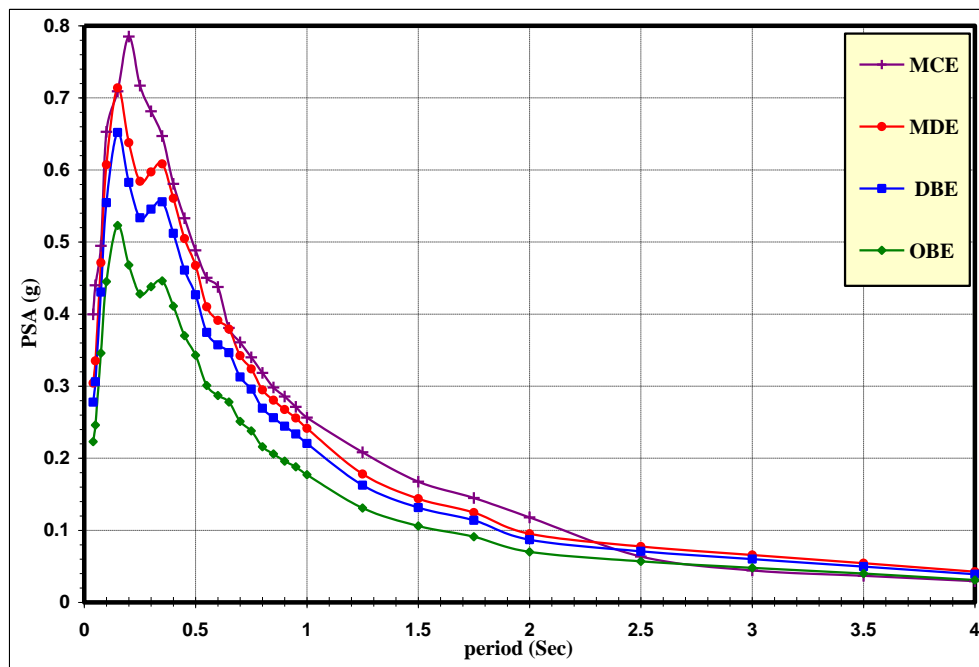


Fig. 3

Response spectra based on statistical processing for horizontal component

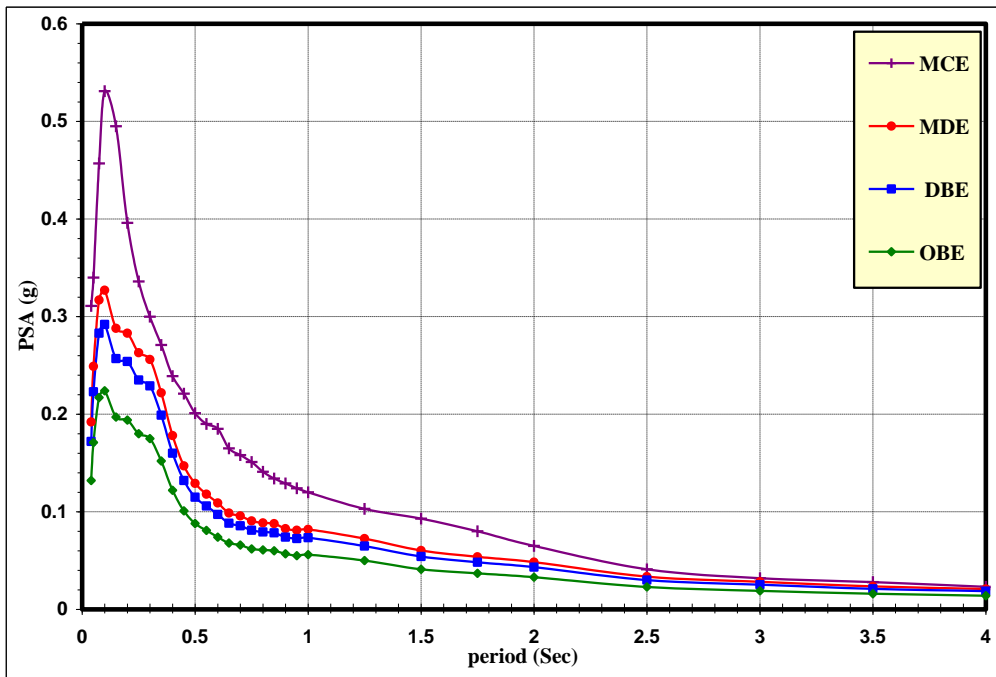


Fig. 4

Response spectra based on statistical processing for vertical component

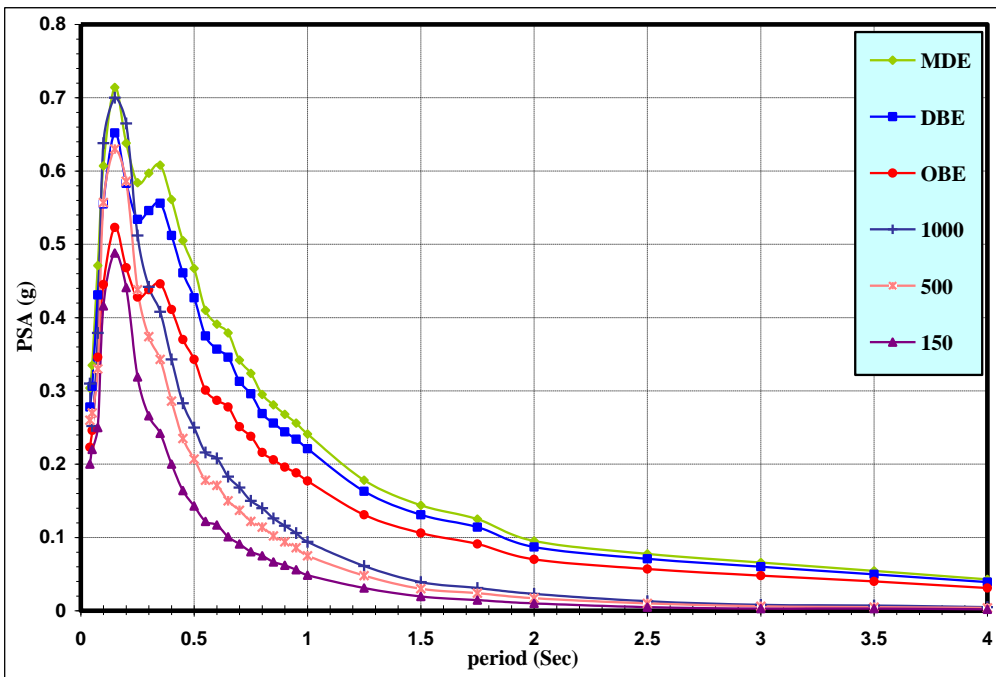


Fig. 5

Comparison between response spectra based on statistical & probabilistic processing for different periods

5. CONCLUSION

The seismic hazard at the Gambiri diversion dam site has been estimated by means of probabilistic and Deterministic methods to obtain the ground motion levels for the design of the dam and appurtenant structures. The dams and relevant structures are designed for the median (84th percentile) of the maximum credible level (MCL). This yields peak ground acceleration of 0.64 g in the horizontal and of 0.53 g in the vertical direction. Response spectra were produced for the design of concrete structures and acceleration-time histories, compatible with the design site-specific response spectrum, for the design of the dams and slopes. The study area has experienced numerous large historical and 20th/21st century earthquakes with M_s between 0.4-7.6. Often earthquakes in this region cannot be related to a mapped surface faulting and they occur between the branches of the major faults. The Konar- Nari fault was considered as the most dominant structure in the deterministic analysis. Smaller faults around the sites are considered non-active or with low seismic potential. Considering that events of surface faulting may be separated by quiescent periods of 3000 to 5000 years, the choice of more conservative ground motion values derived from the Konar- Nari fault is justified.

REFERENCES

- [1] GUTENBERG, B., RICHTER, C. F. Magnitude and Energy of Earthquakes. *Annali di Geofisica*, 1956, 9: 1–15.
- [2] KIJKO A., SELLEVOLL MA. Estimation of earthquake hazard parameters from incomplete data files. Part II. *Incorporation of magnitude heterogeneity Bulletin of the Seismological Society of America*, 1992.
- [3] CAMPBELL, K. W., BOZORGNIA, Y. Updated Near-Source Ground-Motion (Attenuation) Relations for the Horizontal and Vertical Components of Peak Ground Acceleration and Acceleration Response Spectra. *Bulletin of the Seismological Society of America*; 2003; v. 93; no. 1; p. 314-331;
- [4] AMBRASEYS, N., DOUGLAS, N. Equations for the Estimation of Strong Ground Motions from Shallow Crustal Earthquakes Using Data from Europe and the Middle East: Horizontal Peak Ground Acceleration and Spectral Acceleration. *Bulletin of Earthquake Engineering*. 2003, Volume 3, Number 1, 1-53.
- [5] BOORE, D. M., JOYNER, W. B. AND FUMAL, T. E. Equations for Estimating Horizontal Response Spectra and Peak Acceleration from Western North American Earthquakes, A Summary of Recent Work, *Seism. Res. Lett.* 1997, Vol. 68, No. 1, pp. 128-153.
- [6] MAHDAVIAN, A. Empirical evaluation of attenuation relations of peak ground acceleration in the Zagros and central Iran. *First European*

- Conference on Earthquake Engineering and Seismology*, 2006, Geneva, Switzerland, 3-8.
- [7] ICOLD (INTERNATIONAL COMMISSION ON LARGE DAMS),. Selecting Seismic Parameters for Large Dams, Guidelines, *Bulletin 72*, 1989.
 - [8] BUILDING AND HOUSING RESEARCH CENTER OF IRAN., Iranian Code of practice for Seismic Resistant Design of Buildings. *Standard No. 2800*, 3rd edition, *BHRC Publication*, 2008. No. S – 465. ISBN: 978-964-9903-41-5
 - [9] GUMBEL, E. Statistics of Extremes, *Columbia University Press* , New York, USA, 1958.
 - [10] BENDER, B. AND PERKINS, D. M., SEISRISK III: A computer program for seismic hazard estimation, *U.S. Geological Survey Bulletin 1772*, 1987.
 - [11] WELLS, D. L. AND COPPERSMITH, K. J. New Empirical Relationships among Magnitude, Rupture Length, Rupture Width, Rupture Area and Surface Displacement, *Bulletin of the Siesmological Society of America*, 1994, Vol. 84, No. 4, pp. 974-1002.
 - [12] KIMBALL, J.K.. Frisk: Computer Program for Seismic Risk Analysis. *US Geological Survey*, 1983, Open File Report, pp 78-1007.

COMMISSION INTERNATIONALE DES GRANDS BARRAGES

VINGT-SIXIÈME CONGRÈS DES GRANDS BARRAGES
Autriche, juillet 2018

DOI 10.3217/978-3-85125-620-8-100



This work licensed under a Creative Commons Attribution 4.0 International License. <https://creativecommons.org/licenses/by-nc-nd/4.0/>

**IN-DEPTH SAFETY ASSESSMENT OF LARGE RUN-OF-RIVER
HYDROPOWER PLANTS IN SWITZERLAND**

Sven-Peter TEODORI

Dam Engineer, AF-CONSULT SWITZERLAND LTD

SWITZERLAND

Helmut STAHL

Senior Dam Engineer, AF-CONSULT SWITZERLAND LTD

SWITZERLAND

COMMISSION INTERNATIONALE
DES GRANDS BARRAGES

VINGT-SIXIÈME CONGRÈS DES
GRANDS BARRAGES
Autriche, juillet 2018

IN-DEPTH SAFETY ASSESSMENT OF LARGE RUN-OF-RIVER HYDROPOWER PLANTS IN SWITZERLAND

Dr. Sven-Peter TEODORI

Dam Engineer, AF-CONSULT SWITZERLAND LTD

Helmut STAHL

Senior Dam Engineer, AF-CONSULT SWITZERLAND LTD

SWITZERLAND

1. INTRODUCTION AND BACKGROUND

Among the 1200 dams classified in Switzerland, 167 are large dams according to ICOLD standards. The Swiss Federal Office of Energy (SFOE) is entrusted with the overall supervision of the enforcement of the legislation, which comprises the development of the safety concept and dam safety requirements published in form of Guidelines. The SFOE is also entrusted with the direct safety supervision of the 217 largest dams in view of their impounding head, storage capacity and hazard potential for the population in the area downstream of the dam. These are categorized into 124 concrete dams, 66 embankment dams and 27 run-of-river hydropower plants. The latter are deemed to be in the interest of public safety mainly for their relevant storage capacity.

With the new Dam Safety Legislation in Switzerland (2012), large run-of-river hydropower plants along main rivers became subjected to in-depth safety assessments under the direct supervisory authority of the SFOE based on the specific Enforcement Guideline of the Dam Safety Legislation (2015). The Swiss dam safety concept, apart from continuous surveillance, maintenance and emergency planning also entails such periodic in-depth safety assessments. This consists in a review of hydraulic and structural actions (static, flood and seismic)

for all water-retaining structures and safety-critical appurtenant components of such an installation, including lateral embankments or dams within the storage area. Present structural, hydraulic, hydrogeological, geological, steel-structural and process control technology state of all above components require an assessment, as well as implemented surveillance and maintenance practices. If necessary, based on actual scientific and technical state of knowledge, improvements are recommended and may be set into practice.

Two case studies of multi-technical in-depth safety assessments for run-of-river hydropower plants along the Aar river are presented in this paper.

2. LEGAL FRAMEWORK FOR THE IN-DEPTH SAFETY ASSESSMENT OF WATER-RETAINING INSTALLATIONS ALONG THE AAR RIVER

The Aar river with its 295 km is the longest river that both rises and ends entirely in Switzerland by descending 1'845 m from the Swiss Alps to its junction with the Rhine river. There are more than 20 hydropower plants along its course (Fig.1).

The Enforcement Guideline of Dam Safety Legislation specifically referring to the construction and operation of large run-of-river hydropower plants along the Aar river was published in 2015 [1] and covers 11 hydropower plants under the direct supervision of the SFOE.

The scope of the Enforcement Guideline is to clarify and practically-deepen the legislation of water-retaining installations and to supplement the dam safety guidelines [2, 3] specifically for these types of installations in order to accomplish the in-depth safety assessment. The methodology can also be adopted to smaller installations, which are not directly SFOE-supervised but by direct supervision of the cantons.

The in-depth safety assessment end-product is a report which contains multi-technical chapters based on specific qualitative and quantitative evaluations as stepwise presented in the following paragraphs.

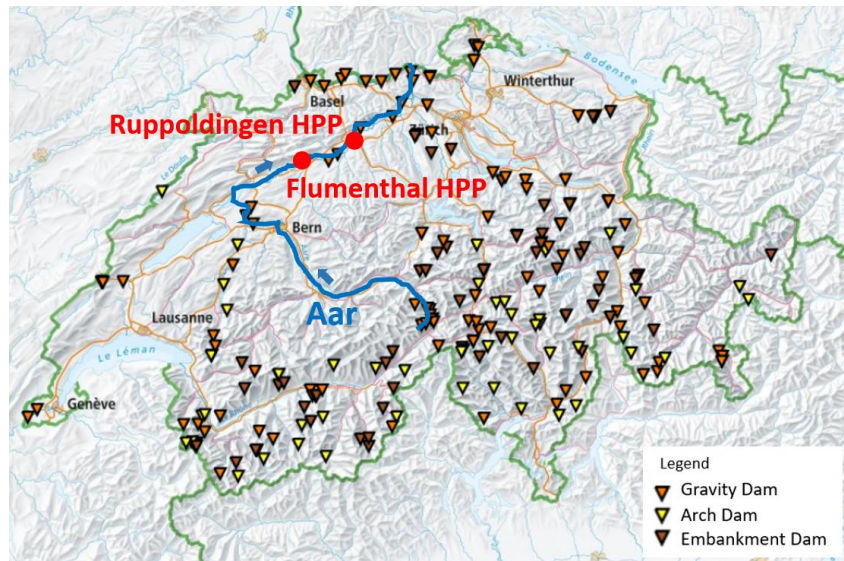


Fig. 1

The Aar river cuts through Switzerland from South to North. The two case studies are highlighted among the 217 SFOE-supervised dams [after 4]

3. CASE STUDIES: FLUMENTHAL AND RUPPOLDINGEN HPPS

Main descriptive features of the two large run-of-river plants case studies are summarized as follows:



Year of Construction	1970
Head water level	426.0 m a.s.l.
Number of turbines	3 Kaplan bulb turbines
Impounding head	9.0 m
Storage capacity	> 500'000 m ³
Capacity	25 MW
Av. annual production	146 GWh
Main water-retaining components	3 radial-gated weirs, each 12.50 m wide 2 piers, each 5.0 m wide Powerhouse (W x L): 46 m x 46 m Left and right abutment guide walls



Year of Construction	2000
Head water level	397.2 m a.s.l.
Number of turbines	2 Kaplan bulb turbines
Impounding head	5.93 m
Storage capacity	2'300 million m ³
Capacity	23 MW
Av. annual production	115 GWh
Main water-retaining components	4 radial-gated weirs, each 14.50 m wide 3 piers, each 4.0 m wide Powerhouse (W x L): 37 m x 62 m Left and right abutment guide walls

3.1. DOCUMENTATION AND ARCHIVES

The plant's operator is responsible to maintain for each plant an archive with below indicated relevant plans and reports. These archives constitute an essential input basis for the in-depth safety assessment.

- Design and as-built plans and information of as-built material's properties based on QA&QC data collected during construction
- Structural, hydrological and hydraulic analyses
- Geotechnical investigations and geological observations
- Plant operational reports
- Annual inspection and monitoring reports
- Reports on maintenance and functional tests of relevant appurtenant structures
- Accident and operating anomalies reports
- Surveillance manuals, O&M manuals and Emergency planning reports

3.2. ASSESSMENT OF ALL WATER-RETAINING AND SAFETY-CRITICAL APPURTENANT STRUCTURES BASED ON EXISTING DOCUMENTATION AND VISUAL INSPECTION

After achieving overview of the plant's relevant documentation, the team of civil, mechanical and electrical engineering experts and a geologist expert perform on-site visual inspections and a present state final qualitative evaluation. In

accordance with the Enforcement Guideline, all water-retaining and safety-critical appurtenant structures of the installation are inspected and evaluated, which include:

- Structural inspection of the weir, powerhouse and gates
- Geological inspection: foundation, lateral embankments or dams and potential slope instabilities within the storage area, natural hazards and groundwater
- State of the monitoring instrumentation and safety-critical appurtenant structures such as drives, control technology, power supply and emergency diesel generators.

3.3. INSTRUMENTATION AND MONITORING PROGRAM

The aim is to assess whether the existing monitoring instrumentation is adequate for the facility. As there are no binding rules on the required type and number of instruments, the judgment is left to an experienced engineer.

For both plants, the deformation monitoring relies mainly on geodetic measurements. It was checked that sufficient monitoring points are available, the points are situated well distributed over the plant and that sufficient fix points are available on both abutments and at appropriate distance from the structures to be monitored. The number of fix points shall guarantee a redundancy in case a fix point is lost e.g. due to construction works. In Ruppoldingen, piezometers are installed under the weir and the powerhouse. As a result of the assessment, it was recommended to consider the installation of additional piezometers in the right abutment to monitor a possible flow around the weir and underlying sheet pile wall through the abutment. In Flumenthal currently no piezometers are available. Based on conservative structural stability calculations, it was assessed whether this state can be further tolerated or the installation of piezometers must be recommended to monitor the uplift pressure for both the weir and the powerhouse.

For both plants, the water level monitoring instruments are assessed as complete, with redundant measurements of the head and tail water levels with both, automatic readings and staff gauges. This is considered as a basic installation for any run-of-river plant.

The instrumentation monitoring is complemented with regular bathymetric surveys which focalize in the downstream area on potential scouring of the weir's stilling basin, in the upstream area on possible sediment depositions. With these surveys and with regular opening of the weir gates for checking its functionality it is ensured that the gates can be opened anytime required.

In addition to the instrumentation array installed, the frequency of the measurements and treatment of the read values was evaluated. It was concluded that the implemented procedures including the back-up of the data is well organized.

3.4. SAFETY-CRITICAL APPURTENANT STRUCTURES AND CONTROL TECHNOLOGY

The aim is to assess the reliability of the weir gate's control technology under unusual and extreme conditions. In a run-of-river plant the functionality of the weir gate is of vital importance to avoid overtopping the weir and overflowing of the river banks upstream of the weir.

This chapter of the safety assessment describes the control technology of the weir gates, which is under normal conditions fully automated to maintain the head water at the concessionary level. In case of failure of the automatic control and concurrent rising of the headwater level, a backup control system is taking over to open the weir and avoid overflowing. As an alternative or if the backup system should fail, the weir can be operated manually from the control room in the powerhouse or from a separate control station at the weir site.

Both plants have a power supply from their own production. In case of failure of the internal power supply, it can be switched to external supply or supply from the emergency diesel generator.

The outcomes from the seismic safety assessment demonstrated that the weir structure and powerhouse, which house the hydraulic system, will remain intact. The hydraulic system is therefore with high probability operable also after an earthquake has occurred. In case of failure of the hydraulic aggregate, in Ruppoldingen a fix installed backup aggregate is available. In both plants, a mobile emergency aggregate with its own diesel generator is available. This allows opening of one gate at the time.

Regular trial runs of the backup systems including moving of the gates with the help of these systems ensures that for both plants, the equipment is well maintained and the personnel is well trained to use the equipment even in emergency situations. The assessment could conclude that sufficient redundancy is available to safely open the weir gates also under unusual and extreme conditions.

3.5. STRUCTURAL SAFETY ASSESSMENT

In this chapter, the safety of all water-retaining structures, i.e. weir, gates and powerhouse are quantitatively assessed. This requires verification of structural stability (sliding, overturning and buoyancy), structural and foundation stress analyses and behavior against reviewed operational and hazard scenarios (load cases). Head and tailwater levels for the same load cases considered at the time of design were updated based on latest hydrological data. The post-earthquake functionality of the gates needs also to be verified.

Hazard scenarios and load cases

In order to start with the structural safety assessment, the specialist engineer defines the operational and hazard scenarios (load cases) according to the Enforcement Guideline: usual, unusual (1000-year return period flood while one weir opening blocked for maintenance) and extreme (probable maximum flood and 5'000-years return period earthquake respectively). Other hazard scenarios to be evaluated either quantitatively or qualitatively are erosion due to high velocity flows, abrasion due to debris transport, impact due to floating debris, sediment deposition on the gates, jamming of gates due to floating debris, rapid water level changes due to rapid closure of the turbines or of the control technology.

Flood safety assessment

The safe passage of a 1000-year return period design flood has to be guaranteed with sufficient freeboard and under the assumption that the gated discharge work of largest capacity is blocked ("n-1 rule"). In this case no damage and no uncontrolled overflow must occur. The "n-1 rule" also applies to side embankments or dams in the vicinity of the installation. For Flumenthal and Ruppoldingen, 1'400 m³/s and 1'550 m³/s are considered respectively.

The probable maximum flood (PMF) must pass the dam without causing it to surpass its critical water level, i.e. level above which stability may be impaired. Overflow and uncritical damages of the installation are allowed. The PMF is evaluated 20% higher than the corresponding 1000-year design flood for each plant.

Seismic safety assessment (SSA)

The seismic evaluation earthquake (SEE) for these large run-of-river installations is assessed on the basis of a 5'000-year return period for all water-retaining and safety-critical appurtenant structures of the installation as evaluated during visual inspection. The main objective of the SSA is to protect the population against loss of life and property damage. To fulfill this goal, the main and sole minimal requirement for the SEE is that no failure with uncontrolled release of water occurs (in accordance to ICOLD 2016 [5]), i.e. non safety-critical damages, such as permanent deformations or structural sliding are allowed if the main objective is fulfilled.

The SSA applies also to the gates, that could suffer partial or total failure with uncontrolled water loss. Their functionality, which has to be rapidly restored after the earthquake, has to be verified. The 1'000-year return period earthquake applies to side embankments or dams in the vicinity of the installation.

Methodology

Major seismic input parameters for SSA are: PGA, duration, site-independent (standard) response spectra and acceleration time-histories. The horizontal PGA in accordance to the SEE return period is derived by means of an empirical intensity-acceleration equation and based on seismic hazard maps (isolines of MSK intensity) published in 1977 [6].

The derived PGA becomes the scaling value of normalized subsoil class-dependent standard response spectral shapes [7] which simultaneously act in the two horizontal and in the vertical directions. Vertical PGA is computed as $2/3$ of horizontal PGA. For Flumenthal and Ruppoldingen, PGA of 0.155 g (duration 13 s) and 0.17 g (duration 14s) are considered respectively.

Geological conditions of riverbeds are usually characterized by a sequence of gravelly, sandy, silty layers above sound bedrock. Therefore, site-dependent response spectra needed to be evaluated at Ruppoldingen HPP (Fig. 2). The presence of a 5.5 m thick fully saturated sand layer above bedrock with averaged granulometric curve with good fit into potential liquefiable sands required evaluation of liquefaction potential based on SPT tests outcomes, available from the geotechnical investigations performed during the construction time (Fig.3).

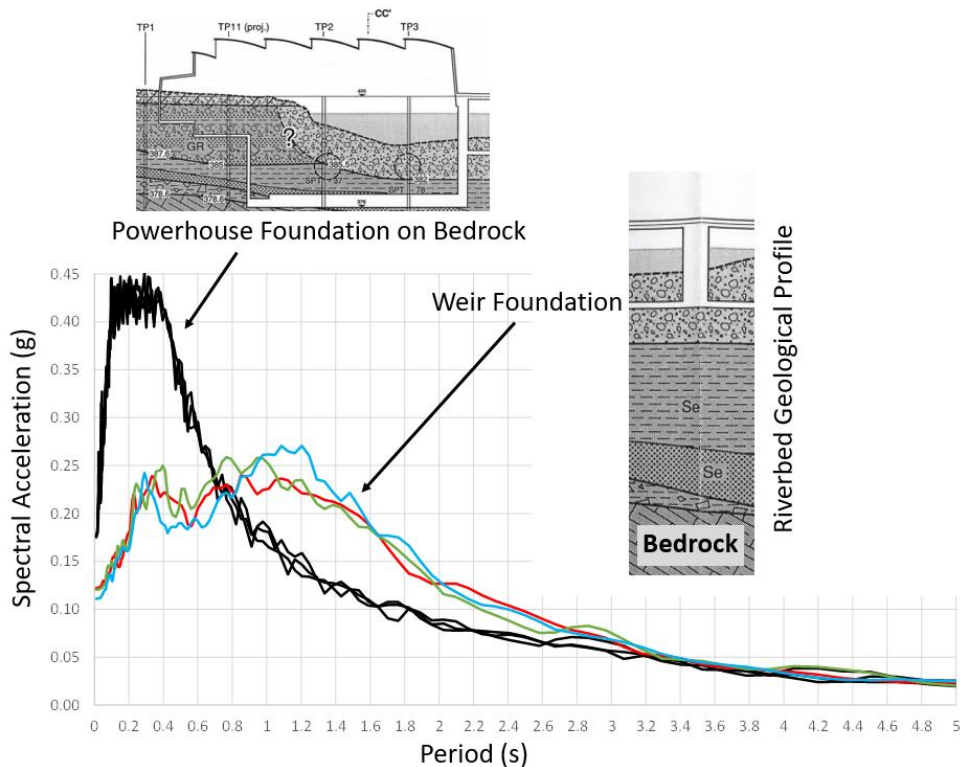


Fig. 2

SSA performed with site-dependent response spectra below weir foundation and below powerhouse foundation on bedrock at Ruppoldingen HPP

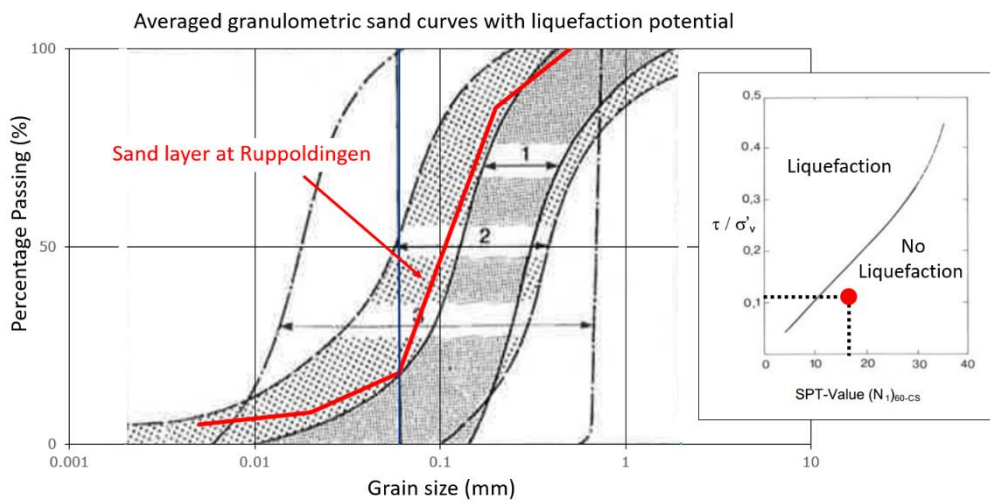


Fig. 3
Liquefaction potential evaluation based on SPT tests at Ruppoldingen HPP
[after 8,9]

Computation procedures for water-retaining structures

The Guidelines require to setup a 3D FE model which includes one pier and a left and right half field of the weir structure and the extended sub-soil. The actions of non-modelled elements such as bridges and gates are implemented in order to consider a realistic dynamic behavior for the SSA. The water-structure inertial interaction is modelled by introducing additional incompressible masses on the structure according to Westergaard's method (Fig. 4). The bedrock mass is neglected, therefore only the soil-structure kinematic interaction is considered in the model. The powerhouse for both HPPs, as a water-retaining structure, is modelled also with a 3D FE model. The radial gates of the weir were manually back-calculated with the updated load cases, thanks to the available steel-structural analyses reports from the original design phase.

Material parameters

The Enforcement Guideline requires as a minimum the static characterization of the structural and geotechnical materials based on laboratory or in-situ tests. These are also accepted if available from the construction time. Required parameters for example would be concrete compression strength, reinforcement density and sub-soil seismic wave velocities.

Structural dynamic characterization of the materials is obtained either from specific dynamic laboratory tests or derived from the static values, e.g. for concrete based on following empirical relationships for the elastic modulus $E_d = 1,25 E_s$, compressive strength $f_{cd} = 1.5 f_{cs}$ and tensile strength $f_{td} = 1,5 f_{ts} \leq 4 \text{ MPa}$. In general, the weir body and the sub-soil are modelled as linear-elastic, isotropic with viscous damping (e.g. 7% for reinforced concrete).

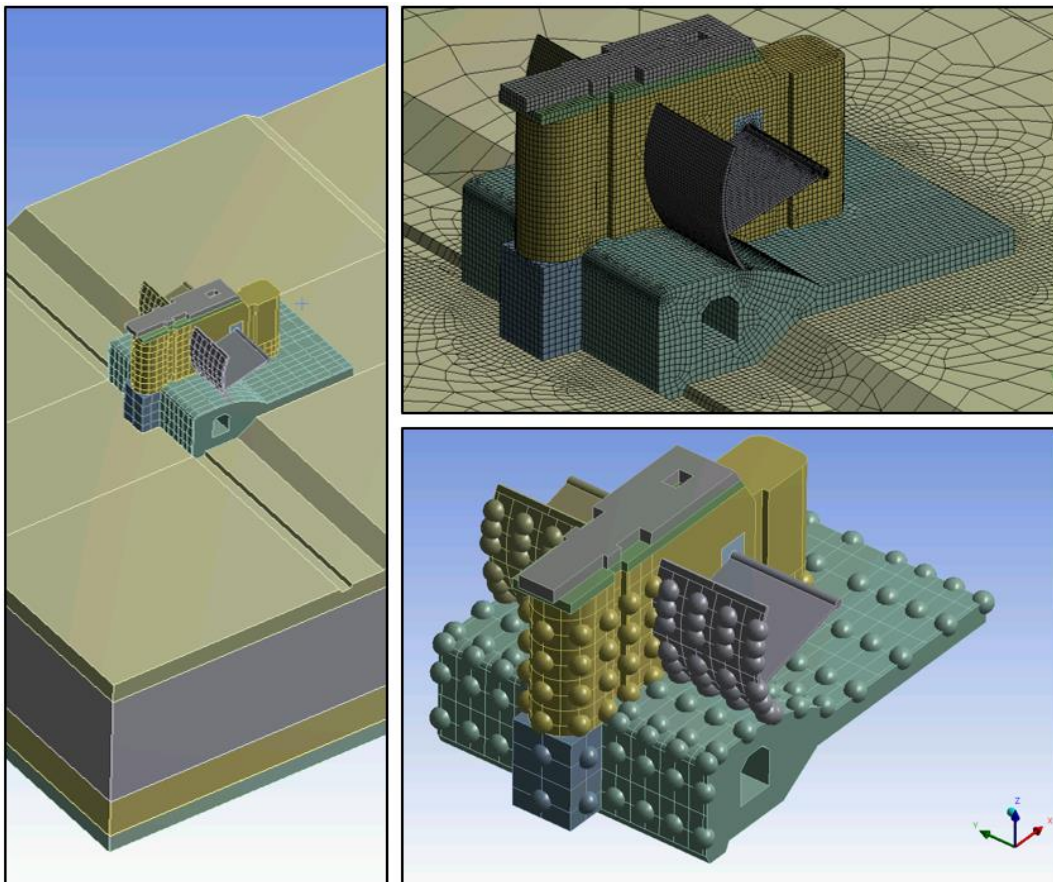


Fig. 4

3D FE numerical model of the weir structure of Ruppoldingen HPP

Final Structural Safety Assessment

The stability, structural and foundation stress and deformation of the weir structure for both HPPs are verified with the updated static and dynamic load cases. The maximal seismic-induced deformation of the pier is considerably smaller than the lateral 30 mm rubber sealed joint between the radial gate and the pillar. Therefore, the post-earthquake functionality of the gates is guaranteed. The radial gate of Flumenthal showed small seismic-induced yield deformations of the flap gates in downstream direction. This would in the worst case lead to a water release due to slight opening of these lateral joints. This however can be recovered within a short time.

The stability analysis of the massive powerhouse structure results in safety factors higher than required.

4. CONCLUDING REMARKS

A multi-technical in-depth safety assessment is performed for large run-of-river hydropower plants along the Aar river, in Switzerland.

The two plants dispose of continuous surveillance (regular function tests of all safety-critical installations and equipment and yearly inspections by external experienced engineer), continuous update of an archive with relevant documents, continuous structural maintenance, adequate monitoring instrumentation and redundant control technology. Further, as all operational and hazardous load cases meet the requirements, it is allowed to conclude that safety of both plants is guaranteed in accordance to the Swiss Dam Legislation.

A team of experts (civil, mechanical and electrical engineers and geologists) can perform straightforwardly a total in-depth safety review of such hydropower plants within a reasonable timeframe.

REFERENCES

- [1] SWISS FEDERAL OFFICE OF ENERGY, Enforcement Guideline of Dam Safety Legislation referred to the construction and operation of hydropower plants along the Aar river under direct SFOE supervision, SFOE Publication, 2015 (in German).
- [2] SWISS FEDERAL OFFICE OF ENERGY, Guidelines for Dam Safety - Part A – Generalities, SFOE Publication, 2015 (in German).
- [3] SWISS FEDERAL OFFICE OF ENERGY, Guidelines for Dam Safety - Part B – High hazard potential as subordination criterion, SFOE Publication, 2014 (in German).
- [4] SWISS FEDERAL OFFICE OF ENERGY, www.bfe.admin.ch
- [5] ICOLD, Selecting seismic parameters for large dams - Guidelines (revision of Bulletin 72), Bulletin 148, Committee on Seismic Aspects of Dam Design, Paris, 2016
- [6] SWISS SEISMOLOGICAL SERVICE, www.seismo.ethz.ch
- [7] EUROCODE 8, Design of structures for earthquake resistance - Part 1: General rules, seismic actions and rules for buildings, DIN EN 1998-1, Germany, 2010
- [8] W.D. L. FINN, Soil dynamics and liquefaction of sand, Proceedings of the International Conference on Microzonation for safer Construction-Research and Application, Seattle, Wash, 1972
- [9] H.B. SEED, I.M. IDRIS, „Ground Motions and Soil Liquefaction during Earthquakes”, Engineering Monograph on Earthquake Criteria, Structural Design and Strong Motion Records”, EERC, 1982

SUMMARY

Among the 1200 dams classified in Switzerland, 167 are large dams according to ICOLD standards. The Swiss Federal Office of Energy (SFOE) is entrusted with the overall supervision of the enforcement of the legislation, which comprises the development of the safety concept and dam safety requirements published in form of Guidelines. The SFOE is also entrusted with the direct safety supervision of the 217 largest dams in view of their impounding head, storage capacity and hazard potential for the population in the area downstream of the dam. These are categorized into 124 concrete dams, 66 embankment dams and 27 run-of-river hydropower plants. The latter are deemed to be in the interest of public safety mainly for their relevant storage capacity.

With the new Dam Safety Legislation in Switzerland (2012), large run-of-river hydropower plants along main rivers became subjected to in-depth safety assessments under the direct supervisory authority of the SFOE based on the specific Enforcement Guideline of the Dam Safety Legislation (2015). The Swiss dam safety concept, apart from continuous surveillance, maintenance and emergency planning also entails such periodic in-depth safety assessments. This consists in a review of hydraulic and structural actions (static, flood and seismic) for all water-retaining structures and safety-critical appurtenant components of such an installation, including lateral embankments or dams within the storage area. Present structural, hydraulic, hydrogeological, geological, steel-structural and process control technology state of all above components require an assessment, as well as implemented surveillance and maintenance practices. If necessary, based on actual scientific and technical state of knowledge, improvements are recommended and may be set into practice.

Two case studies are presented in this paper. The two plants dispose of continuous surveillance (regular function tests of all safety-critical installations and equipment and yearly inspections by external experienced engineer), continuous update of an archive with relevant documents, continuous structural maintenance, adequate monitoring instrumentation and redundant control technology. Further, as all operational and hazardous load cases meet the requirements, it is allowed to conclude that safety of both plants is guaranteed in accordance to the Swiss Dam Legislation. A team of experts (civil, mechanical and electrical engineers and geologists) can perform straightforwardly a total in-depth safety review of such hydropower plants within a reasonable timeframe.

KEYWORDS: Safety of Dams, Run-Of-River Hydropower Plants, Inspection and Assessment

5. CLEARANCES AND COPYRIGHT

The authors have obtained written permission to profile the project or subject matter in this paper from Alpiq Hydro Aare AG - Switzerland on the 11th January 2018.

COMMISSION INTERNATIONALE DES GRANDS BARRAGES

VINGT-SIXIÈME CONGRÈS DES GRANDS BARRAGES
Autriche, juillet 2018

DOI 10.3217/978-3-85125-620-8-101



This work licensed under a Creative Commons Attribution 4.0 International License. <https://creativecommons.org/licenses/by-nc-nd/4.0/>

ASPECTS CONCERNING AGEING OF EMBANKMENT DAMS

Ronald HASELSTEINER

Department Manager Hydraulic Engineering, BJOERNSEN CONSULTING
ENGINEERS

GERMANY

COMMISSION INTERNATIONALE
DES GRANDS BARRAGES

VINGT-SIXIÈME CONGRÈS DES
GRANDS BARRAGES
Autriche, juillet 2018

ASPECTS CONCERNING AGEING OF EMBANKMENT DAMS

Ronald HASELSTEINER

*Department Manager Hydraulic Engineering, BJOERNSEN CONSULTING
ENGINEERS*

GERMANY

1. INTRODUCTION

The process ageing defines the timely change of the behaviour of embankment dams. These changes are caused by biogenic, geogenic, anthropological or climate factors. The ageing processes may occur periodically, temporarily, steadily, or even suddenly. These ageing processes can cause harm and can initiate failure processes and can lead to a total failure.

Different definitions of ageing are available, and were developed within the different engineering faculties. Generally, ageing depicts a deterioration process and, frequently, is treated hand in hand with the long-term behaviour of dam structures.

Particularly, embankment dams, which were designed without safety margin or show design deficits, are sensitive to long-term deterioration effects. Ageing can affect all materials and all parts of embankment dams. Research and science frequently focus on single processes such as the behaviour of dispersive clays, but those single processes are rarely put into an overall context such as life cycle considerations.

Life cycle considerations or management may support risk management approaches as well as may shed light on the obligations of the owner during the different operation periods and life spans of dams (Fig. 1).

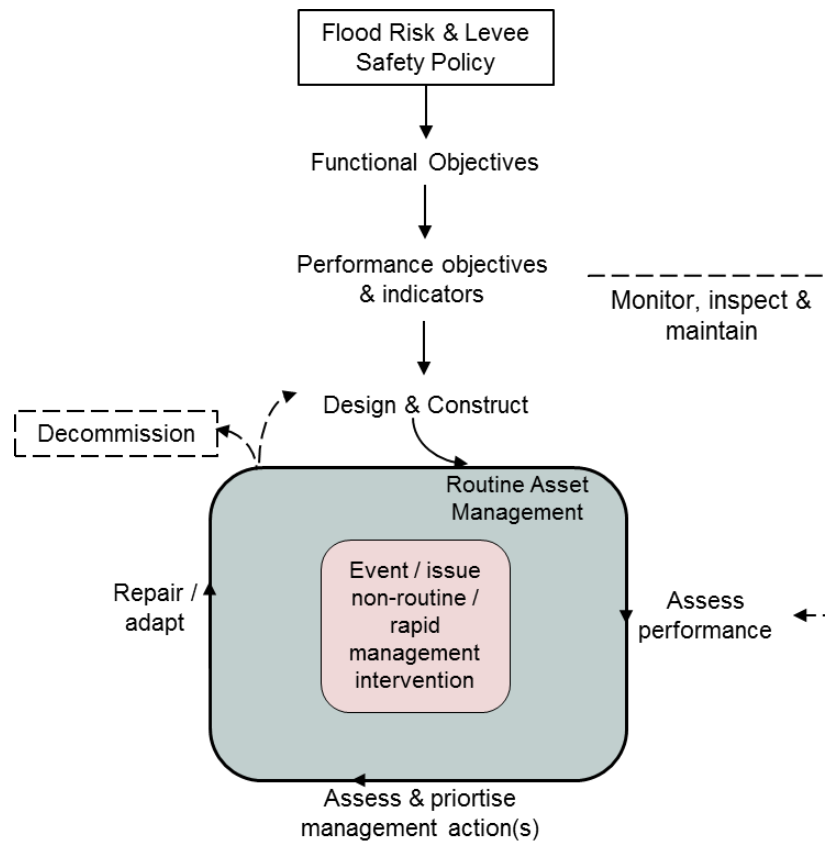


Fig. 1
Life Cycle Management of Levees (according to [1])

2. DEFINITION AND PROCESS CLASSIFICATION

An accurate, general valid definition for the term “ageing” for engineering structures, especially embankments dams, is hard to find in literature. Some authors provide definitions for special applications [2] [4] [5].

The term “ageing” defines the time-dependent alteration of characteristics of structures or materials. In this context the deterioration of characteristics is usually analyzed which leads to a deterioration of the structural behaviour in terms of stability, serviceability, and durability. In contraction to this general approach ageing processes may also lead to an improvement of material characteristics and structural behaviour as discussed in [3], such as the hardening of concrete sealings/barriers and the clogging of cracks in sealings.

A definition is given in the ICOLD bulletin No. 93: *“For the purposes of this therefore, ageing is defined as a class of deterioration associated with time-related changes in the properties of the materials of which the structure and its foundation is constructed. Excluded are the effects if exceptional events. Under*

normal conditions during the operation of structures ageing will usually affect the performance requirements, and then later affect the safety if corrective measures are not taken.“ [4]

A similar definition is used by the USSD: *„The aging of dams, constructed of earth and rockfill material, as defined herein is due to time-related changes in the properties of the materials of which the structure and its foundation are composed.“* [5]

In [6] the term ageing is related to natural processes, whilst damage is considered to be originated in man-made activities. Since also natural events may lead to damage, this distinction may not be valid for all kind of deterioration processes, which have to be considered in the context of embankment dams.

Typical ageing processes for embankment dams are listed below:

- Rooting of sealings/barriers of embankment dams with an increase of permeability
- Rooting of filter elements with a decrease of permeability
- Freezing-thawing-cycles and drying of soils and natural sealings leading to cracks
- Particle breakage by saturation or stresses
- Upcoming woody vegetation close to or on the embankment
- Changing of design fundamentals such as hydrology (climate change) or design risk level which outdates the performance and required safety of the dam
- Sedimentation of reservoirs
- Etc.

3. LIFE CYCLE CONSIDERATIONS

The consideration of life-cycle management of engineering structures is more and more showing practical relevance. Generally, phase models are established as shown in Fig. 1 and Fig. 2.

In practice usually the phases design, construction and operation/maintenance are considered. For supervision and documentation, usually annual reports are prepared on the behalf of the owner [7] [8].

In the context of life cycle management the service life span of dams plays an important role. Life span and ageing interact. The stronger the ageing effects, the shorter the life span of an embankment dam. For embankment dams a life span of 50 to 100 years may be assumed [9].

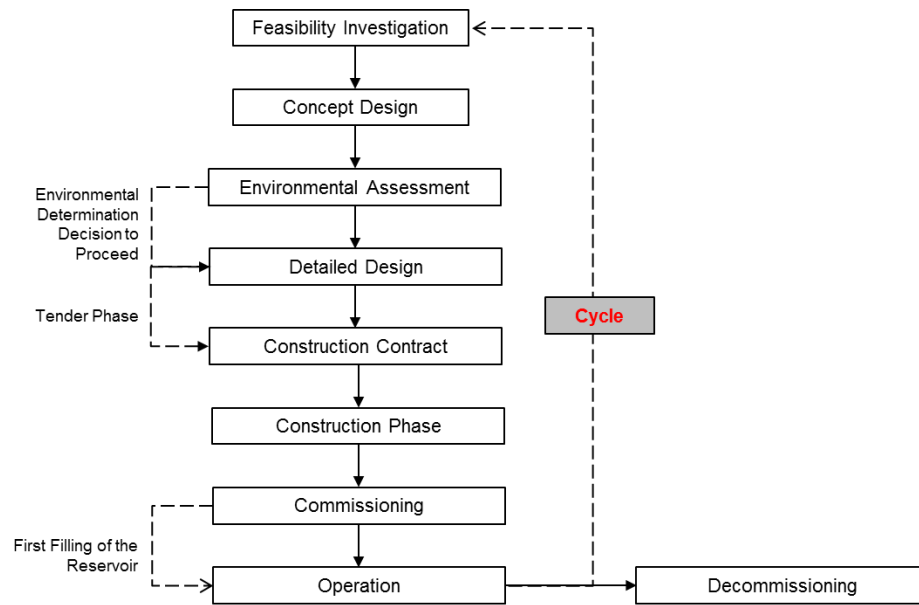


Fig. 2
Life cycle phases for dams

4. LONG-TERM BEHAVIOUR OF EMBANKMENT DAMS

The long-term behaviour of large embankment dams are assessed by analyzing of measurement data derived from the observation of deformation, stresses, pore water pressures, and seepage flow. Changes of material characteristics have to be determined by direct probing and testing in field or in the laboratory.

According to ICOLD Bulletin No. 93 [4] ageing processes and its effects are usually formed by the listed terms:

- Deformation
- Decrease of shear strength
- Pore water pressure increase
- Erosion/suffusion processes
- Surface erosion processes
- Deterioration of construction material characteristics

Especially creeping and consolidation processes contribute to long-term deformations. Embankment and rockfill dams which are constructed according to modern dam construction criteria show a total settlement of less than 1.0 % of the dam height. The long-term settlement are frequently obtained after decades of operation.

The time-dependent deformation may lead to cracking, relocation of stresses or other effects along material borders so that the behaviour under hydraulic load and seepage forces may be affected which may lead to hydrodynamic soil deformation such as suffusion and erosion [10]. The increase of pore water pressures may result from ageing of sealings, drains, filters or changes in the underground.

5. ALTERATION OF MATERIAL BEHAVIOUR

For the construction of embankment dams and levees natural soils, geosynthetics, natural and artificial sealings, concrete, asphalt, etc. are applied as summarized in [11]. All materials are subject to ageing. Corresponding to the type of material and the intensity of the loads and influences ageing is affecting the characteristics more or less strongly. The influencing factors are listed below:

- Freezing and thawing
- Seepage/saturation
- Wind
- UV-radiation
- Heat
- Biological impacts by animals
- Anthropogenic long-term behaviour
- Etc.

These influencing factors need to be assessed for the specific types of materials which are used in embankment dams and levees such as:

- Low permeable soils and natural sealings
- Artificial sealings
- Filter, drains and high permeable soils
- Geosynthetics
- Concrete

The listed materials and the related aspects of ageing are discussed in detail in [12].

6. EFFECTS ON THE DAM BEHAVIOUR AND DESIGN

The process of ageing starts with the construction or with the storing of materials which shall be used for construction. In practice the end of construction (EoC) is usually used as a reference date to determine the ageing period.

In ICOLD bulletin No. 93 [4] the first five years after EoC are not counted for ageing. Therefore, ageing starts five years after EoC according to [4] since all damage that occurs before is considered to be originated in construction shortcomings.

The monitoring and detection of ageing processes are evident in order to assess the dam behaviour correctly. For large embankment dams with permanent reservoirs the measurement of the seepage conditions is of first priority and has to be usually done by the Owner (see [13]). For embankment dams and levees which are only impounded temporarily a continuous surveillance is frequently considered to be not required. For small embankments and small levees frequently no monitoring is conducted [11] [14].

Under favourable conditions the ageing process will not reveal considerable deterioration effects during the life span of the structure. But, e.g., if the embankment dam was designed without safety margin so that with proceeding ageing the limit equilibrium conditions are reached and exceeded. This results in an overload of the system and potential failure. The safety margin should be assessed so that the design requirements are also fulfilled at the end of the service life span of the dam. The dam will subsequently suffer from damages, acceleration of ageing, and finally from failure.

Therefore, a safety margin should be considered to cover ageing effects. This safety margin should be also integrated in the specific technical guideline and codes. Not only material degradation should be integrated but also foreseeable processes, such as sedimentation, an increase of hydraulic loads, etc.

The safety margin should be established by the selection of adequate design parameters such as permeability, shear strength, etc. Generally, for all high risk large embankment dams it is recommended to consider a safety margin and not to design it at "the limit equilibrium border".

In Fig. 3 the effect of ageing on the design approach is shown. Depending on the starting design approach and the influence of ageing the dam may reveal an under or over design during the operation period until the life span is reached. The under design shows an unacceptable risk; the over design requires the utilization of more resources but are welcome in consideration of safety reasons. A conservative design should be applied if the dam's behaviour during the life span shows uncertainties which cannot be assessed reliable.

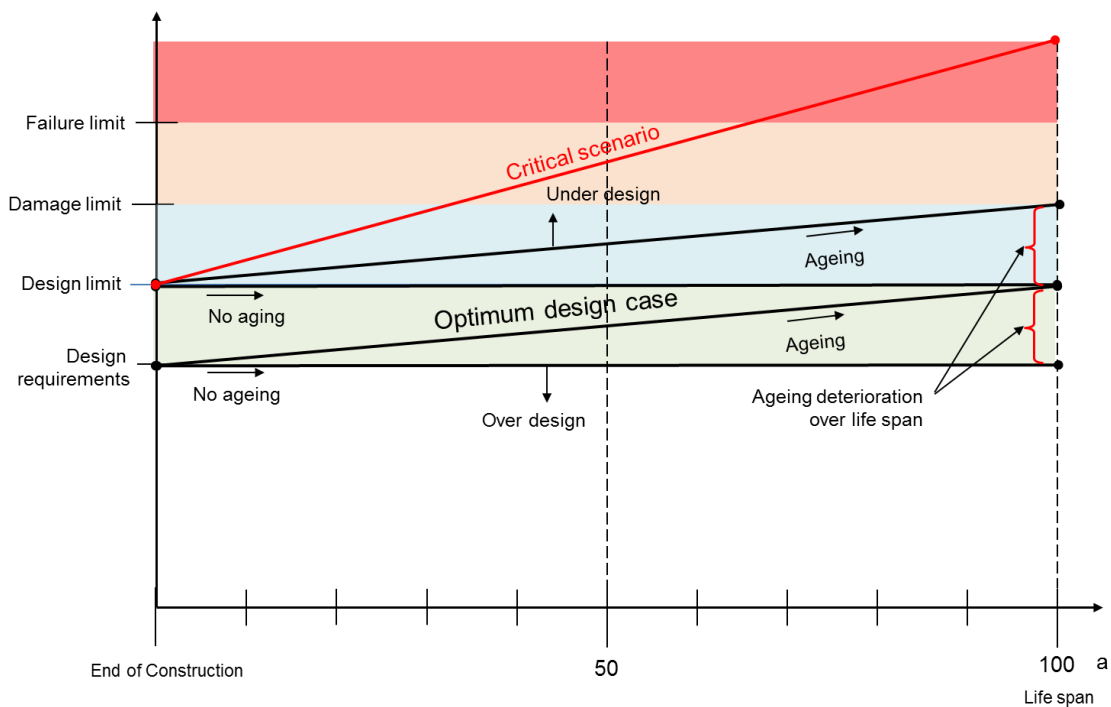


Fig. 3
Effect of ageing during design in consideration of the life span

7. MEASURES

Maintenance works have to be conducted annually. The existing vegetation needs to be controlled and cut according to the design and operation requirements. Small damage has to be refurbished. All ways, roads and access options need to be kept functional in order to guarantee access also in critical situations such as MDE or extreme floods. As soon as the structure does not comply with the engineering standards and codes a need for action exists and the owner is obliged to corresponding measures within a given realization period. This period is not a fixed number but should correspond to the practical periods for the preparation of the detailed dam safety reports which is five to ten years.

Various measures can be taken to upgrade the embankment dam in form of emergency action, partial rehabilitation works or a general upgrade. Rehabilitation works aim on the re-establishment of the former conditions. An upgrade shall improve the performance of the structure [15].

Embankment dams frequently suffer from an inadequate seepage situation, insufficient slope stability or lack of dam height. Therefore, many measures are focussed on the installation of new sealings/barriers and the placement of drains and filters at the downstream toe in order also to stabilize the downstream slope.

For the heightening of a dam frequently little concrete walls are placed in the dam crest if the overall stability allows to do so. The heightening can also be realized by earth-moving techniques which results also in an adaptation of the downstream slope or parts of it.

Upgrading measures may reach from simple earth-moving methods to a complete demolition and reconstruction of the embankment dam. The extent of required works strongly depends on the grade of damage or ageing that occurred. An early detection is favourable in order to minimize the employment of required resources.

REFERENCES

- [1] CIRIA. The International Levee Handbook. Construction industry research and information association (Ciria), *C731, London*, 2013.
- [2] Suarez, N. R. Micromechanical Aspects of Aging in granular Soils. Dissertation, *Virginia Polytechnic Institute and State University, Faculty for Civil and Environmental Engineering*, Blacksburg, VA, 2012.
- [3] Sackmann, A. Schwachstellengenese an Erddämmen als Resultat sedimentär/diagenetischer Alterungsprozesse: Ursachenforschung und Möglichkeiten der zerstörungsfreien Erkundung. *Dissertation, Julius-Maximilians-Universität, Würzburg*, 2001.
- [4] ICOLD 93. Ageing of Dams and Appurtenant Works. *Bulletin No. 93, International Commission on Large Dams*, 1994.
- [5] USSD. The Aging of Embankment Dams. *United States Society on Dams (USSD)*, Denver, USA, 2007.
- [6] IP Bau. Schutzsysteme im Tief- und Ingenieurbau. Impulsprogramm Bau (IP Bau) – Erhaltung und Erneuerung, *Bundesamt für Konjunkturfragen*, Bern, 1992.
- [7] DIN 19700. Stauanlagen. *Deutsches Institut für Normung (DIN)*, Berlin, 2004.
- [8] DIN 19712. Hochwasserschutzanlagen an Fließgewässern. *Deutsches Institut für Normung (DIN)*, Berlin, 2013.
- [9] Wieland, M. Life-span of storage dams. *International Water Power & Dam Construction (IWP & DC)*, pp. 32-35, 2010.
- [10] Fell, R.; MacGregor, P.; Stapledon, D.; Bell, G. Geotechnical Engineering of Dams. *A. A. Balkema, Taylor & Francis Group*, London, 2005.
- [11] DWA M-507-1. Deiche an Fließgewässern. Merkblatts Nr. 507, Teil 1, *Deutsche Vereinigung für Wasserwirtschaft, Abwasser und Abfall e. V. (DWA)*, Hennef, 2011.
- [12] Haselsteiner, R. Die Alterung von Deichen und Dämmen - Theoretische Grundlagen, Wissenschaft und Praxis. Workshop „Einfluss der Alterung von Erdbauwerken auf die Nachweisführung von Deichen und Dämmen“. 04.07.2017, *Bayrisches Landesamt für Umwelt (LfU)*,

- Länderarbeitsgemeinschaft Wasser (LAWA), Arbeitsgruppe Hydrologie, Hochwasser (AH), Nürnberg, 2017.*
- [13] DWA M-514. Bauwerksüberwachung an Talsperren. Merkblatt Nr. 514, *Deutsche Vereinigung für Wasserwirtschaft, Abwasser und Abfall e. V. (DWA)*, Hennef, 2011.
- [14] DWA M-522. Kleine Talsperren und kleine Hochwasserrückhaltebecken. Merkblatt Nr. 522, *Deutsche Vereinigung für Wasserwirtschaft, Abwasser und Abfall e. V. (DWA)*, Hennef, 2015.
- [15] Haselsteiner, R. Maßnahmen zur Ertüchtigung von Deichen. *Korrespondenz Wasserwirtschaft (KW)*, *Deutsche Vereinigung für Wasserwirtschaft, Abwasser und Abfall e. V. (DWA)*, Hennef, Heft 3/08, S. 139 – 149, 2008.

SUMMARY

An overview of different definitions for ageing is given. Generally ageing depicts a time-dependent alteration and deterioration of material characteristics and/or the complete dam structure.

Internationally accredited life cycle approaches are shortly discussed. In modern dam management life cycle considerations are state of the art starting with the design phase.

The ageing of typical materials, such as clay, geotextiles, concrete, etc. is an important aspect to assess the ageing of complete structures. The long-term behaviour of soils and the underground is more difficult to assess or to predict than the behaviour of artificial materials such as concrete and geosynthetics. For latter materials ageing was investigated in the past precisely.

Recommendations for the design are provided as well as counter measures against the deterioration effect of ageing on the structure. A safety margin should be considered within the design phase in the context with stability analysis and serviceability aspects. The sooner negative ageing effects are detected, the earlier countermeasures can be taken. Early measures are generally cheaper and more efficient than trying to rehabilitate a severely damaged embankment. Measures reach from easy works which can be handled during maintenance routines to a complete demolition and re-construction of the embankment dam.

COMMISSION INTERNATIONALE DES GRANDS BARRAGES

VINGT-SIXIÈME CONGRÈS DES GRANDS BARRAGES
Autriche, juillet 2018

DOI 10.3217/978-3-85125-620-8-103



This work licensed under a Creative Commons Attribution 4.0 International License. <https://creativecommons.org/licenses/by-nc-nd/4.0/>

**HYDRAULIC ANALYSIS OF TEMPORARY FLOOD HAZARD TO SUPPORT
THE PLANNING OF THE CONSTRUCTION PHASES OF HYDROPOWER
PLANTS**

Gašper RAK

FLUID MECHANICS WITH LABORATORY, FACULTY FOR CIVIL AND
GEODETIC ENGINEERING, UNIVERSITY IN LJUBLJANA, SLOVENIA

SLOVENIA

Franci STEINMAN

Chair of FLUID MECHANICS WITH LABORATORY, FACULTY FOR CIVIL AND
GEODETIC ENGINEERING, UNIVERSITY IN LJUBLJANA, SLOVENIA

SLOVENIA

COMMISSION INTERNATIONALE
DES GRANDS BARRAGES

VINGT-SIXIÈME CONGRÈS DES
GRANDS BARRAGES
Autriche, juillet 2018

**HYDRAULIC ANALYSIS OF TEMPORARY FLOOD HAZARD TO SUPPORT
THE PLANNING OF THE CONSTRUCTION PHASES OF HYDROPOWER
PLANTS**

Gašper RAK, Franci STEINMAN

*Chair of Fluid Mechanics with Laboratory, Faculty for Civil and Geodetic
engineering, UNIVERSITY IN LJUBLJANA, SLOVENIA*

SLOVENIA

1. INTRODUCTION

With any major spatial developments (construction projects) it is necessary to analyse both anthropogenic environmental impacts as well as the impact of the environment on the planned structure [1]. One of the technical basis in environmental impact assessment concerning developments in and near rivers and in their impact zone is to analyse the runoff regime, which indicates the difference between the existing and the planned state of water flows, depths, velocities, erosion, etc. Physical and mathematical hydraulic modelling is a commonly established practice to ensure that flood and erosion hazards remain the same, or are even mitigated, and to plan and optimize the expected end situation. In the planning stage of the construction and during the construction itself, neither the analysis of the situation in the individual construction phases nor the impact of temporary facilities and measures (e.g. access roads, bridging structures) must not be neglected or deficient. It can be the case that compared to the completed structure, particularly in major and complex projects, intermediate construction phases can have significantly more adverse impacts on the runoff regime and therefore on flood and erosion hazards of the construction site and other users in space. A hydraulic analysis to determine the extent of flood, velocity or erosion forces flow distribution, and the changes in the entire runoff regime in the area in question is used to determine any potential hazards and adjust or optimise the planned construction phases of the individual structures and accompanying developments, so that risks and costs are reduced.

The hydraulic analysis results of the individual phases allow us to assess the risks under transitional, changing spatial conditions compared to the condition prior to the construction and that after its completion. If excessive deterioration of the

condition in a certain construction stage is identified, mitigation measures can be put in place to prevent hazard and risk increase or other measures are provided for, i.e. different stages of implementing structures and developments.

The planning and implementation of construction phases for the Brežice HPP, which was in the meantime put into regular operation, will be shown based on extensive experience in siting the HPP chain on the Lower Sava, as an example of siting a complex infrastructure facility in an alluvial plain area. Using prescribed spatial planning procedures, site selection and placement of the facilities and accompanying developments necessary for the HPP's operation (river reservoir levees, HPP dam structures, etc.) were carried out along with the many investments planned by other users or developers in the area. Along with this initiative (HPPs), under the National Spatial Plan the siting of developments in public interest was underway, such as updating and upgrading the existing and the construction of new levees and other flood risk reduction developments, developments of sustainable outflow sections of tributaries, improvement of riparian areas, provision of replacement habitats, etc. At the same time many initiatives regarding future land use emerged, including more intensive agricultural land use, various economic activities, and leisure facilities (e.g. a rowing trail).

When balancing the complex system of infrastructure facilities, accompanying developments, and various initiatives in the impact area there was an interplay of many requirements, restrictions, and conditions, which were consistent with each other, conflicting, or indifferent. They reflected the goals of many approving authorities and entities directly included in the spatial development project as well as other participants who take part indirectly but for whom it was assumed that the envisaged developments might, in one way or another, impact their established rights or development goals, and initiators who, upon the HPP chain completion, recognised the opportunity to carry out new or accompanying activities in the area.

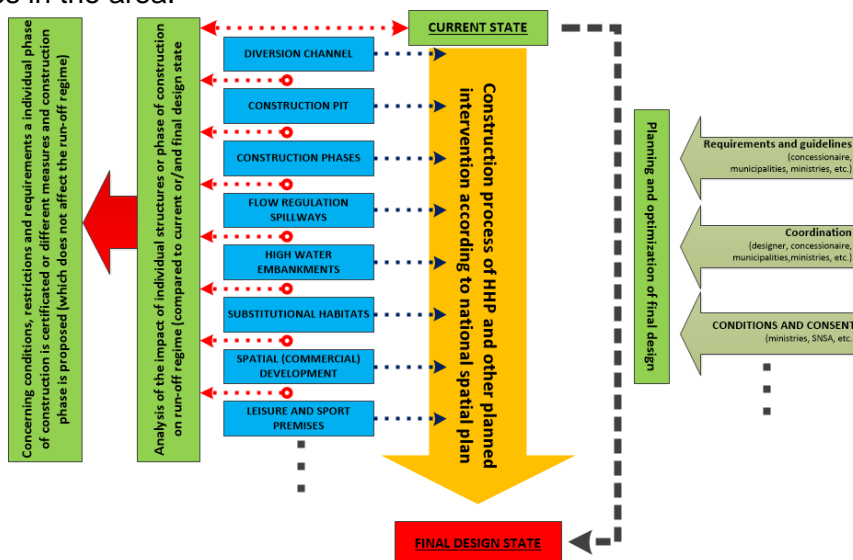


Fig. 1: Conceptual illustration of the activities in stepwise construction planning

For the HPP chain it is also necessary to analyse the morphological, hydrological and hydraulic, and anthropogenic impacts due to the complexity of the

retention area, as they could potentially affect the runoff conditions at the border with the Republic of Croatia. In the downstream country such analyses were conducted in public procedures carried out in Integrated Environmental Impact Assessments. In such demanding interventions, the use of numerical modelling only is not sufficient, therefore the hydraulic analysis of the runoff conditions prior to and upon the construction of the HPP chain (Krško, Brežice, Mokrice) involved the use of hybrid hydraulic models [2-4]. By extensive modelling the locations of reservoir levees, size and locations of flood water overflow structures, HPP spillway structures, and other accompanying developments, including roads and economic structures, were analysed and optimised.



Fig. 2: Locations of HPPs on the Lower Sava River. HPPs Vrholovo, Boštanj, Blanca, Krško, and Brežice are completed, while the Mokrice HPP is in the final design stage.

For the planned situation of the area at the Brežice HPP, where there also is the Krško Nuclear Power Plant (NPP) located at the Sava, it is also necessary to check the fulfilment of all the strict safety requirements regarding the operation of NPP Krško, including the analysis of the conditions during the Probable Maximum Flood (PMF). An overview of the key interventions in the National Spatial Plan area concerning the Brežice HPP is shown in Figure 2.

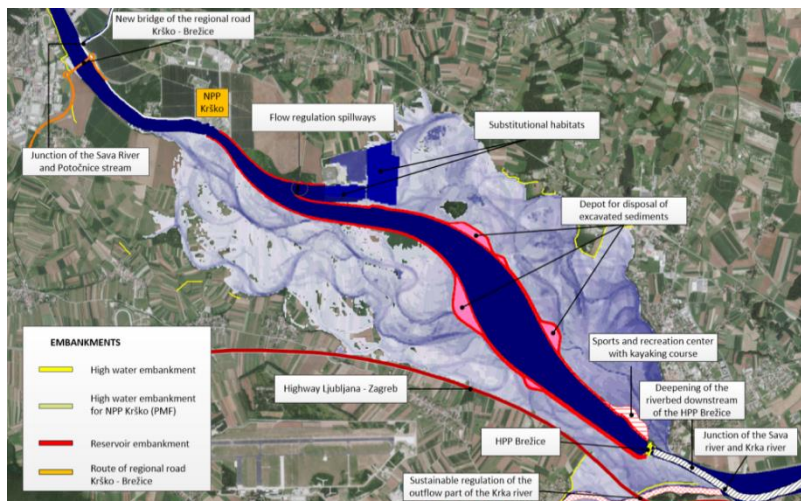


Fig. 3: The run-of-river Brežice HPP facilities with many accompanying measures are shown in terms of the existing flooding situation of the areas along the Sava River between Krško and Brežice at $Q_{100,HW}$.

The preparations for the HPP chain construction took a long time, while over the recent few years intensive analysis concerning the design and implementation of the selected solutions took place. In the individual phases of construction, which took several years, the runoff conditions gradually changed, therefore the previous runoff conditions in the HPP impact area were analysed. Good cooperation with the HPP design engineer and competent authorities was essential to identify relevant or unfavourable scenarios of flood (and other) events to be investigated hydraulically, and to review and evaluate the interim calculation results.

2. HYDRAULIC MODELLING – BREŽICE HPP

The advantage of numerical modelling over physical models is that it is easier to change the geometry and boundary and operational conditions, but unfortunately in the most complex cases it still does not achieve the necessary robustness of results compared with physical models. Therefore, hybrid hydraulic modelling (HHM) was used, which applies the manner of modelling (physical/numerical) that is the most relevant in a particular case. In this case, we applied conventional and distorted physical models for flood areas and various structures, while for the numerical analyses of runoff conditions in the entire area the combined one- and two-dimensional (1D-2D) software MIKE FLOOD was used. The appropriate numerical simulation of the faster 1D flow in the Sava River channel and the slower 2D flow in floodplains was achieved by an extensive calibration in relation to the previous flood events and simulations of conditions in the physical model. The 1D module applied allowed for simulation of the impact of various structures and operational dynamics according to the temporal dynamics of the flow from upstream areas. This enabled a hydraulic analysis of the situation in the wider areas (the entire HPP impact zone) as well as modelling of immediate areas (e.g. the construction pit area) and of individual structures (e.g. spillways).

To analyse the flow conditions in the HPP's immediate areas during the individual construction phases fully-2D modelling was applied, e.g. using the hydraulic software tool CCHE2D [5], which allowed for detailed analyses of velocity fields in critical areas. This tool is well calibrated, too; the same boundary conditions were applied for the HPP's immediate area as well, i.e. the flow conditions from the wider site analysis using HHM. Such case is shown in Figure 3 where left, based on an orthophoto image, the immediate zone of the HPP Brežice construction pit is shown, while on the right the numerical mesh of the same area for 2D analyses is shown.



Fig. 4: Left – an orthophoto image with the developments in the HPP Brežice construction pit site; right – the same site captured using the numerical mesh of the 2D hydraulic model [4]

A physical model in a scale of 1:45 was also built for this case and the conditions in the plant's immediate area were analysed to an extent allowed for by the characteristics of the installations at the Institute for Hydraulic Research. It comprised the area of the entire HPP construction pit with a diversion channel and the Sava River reach 600 m downstream the envisaged dam location. Flow and velocity fields, water levels for dimensioning cut-off barriers at the construction pit and erosive action in riverbanks and the channel during the construction [6].



Fig. 5: Physical model of the HPP Brežice construction pit (Hidroinštitut, 2011). In the diversion channel the remains of the sand left from studying sediment transport capacity are evident

The coupling of physical and numerical modelling is reflected both in determining the boundary conditions for the physical model from investigating the wider area and the additional calibration of the numerical model to analyse the

immediate vicinity of the construction pit and the diversion channel used both for checking the velocity field and/or erosion risk during higher discharges than those enabled by the physical model.

3. ANALYSIS OF SCENARIOS OF GRADUAL INTRODUCTION OF SPATIAL DEVELOPMENTS

During the construction of infrastructure systems many intermediate situations occur, as the individual work phases have different temporal dynamics. Therefore, many situations, i.e. scenarios, emerge, where it is necessary to check whether the individual combinations of (intermediate, temporary) measures do not excessively deteriorate the conditions in space. Such cases are, for example, the study of the impact of the construction pit with the diversion channel in combination with the impact of disposal sites with the material dredged from the construction pit or the determination of the optimal construction of levees along the reservoir. All intermediate conditions were compared in relation to the flow conditions at various discharges to those prior to construction, to remove the responsibility for anthropogenically enhanced flood risk.

For high-discharge conditions the flood risk rate was checked, where the development of the construction pit and the diversion channel shape was taken into consideration, as determined using the physical model, which allows for a discharge capacity of approx. 1800 m³/s. The focus of the physical modelling was the conditions during the construction, e.g. the removal of abrupt changes in the riverbanks, which could lead to vortices that could reduce the throughput of the diversion channel [5]. The choice of locations of temporary disposal sites and the site for disposing of excess material was affected by spatial restrictions, optimisation of construction works, and particularly the requirement to not increase flood and erosion hazard.

When determining the sequence of constructing the individual sections of the embankments along the reservoir, from Krško to Brežice, the main goal was to preserve, as long as possible, the communication between the main channel and floodplains, to preserve the inundation's retention function. Therefore, the embankments were first constructed in the areas where at Q_{100} the communication of the Sava water flow with the inundation was smallest or only local. The calculations showed that the parallel (simultaneous) construction of embankments on the left and right banks preserved the flows on the left and right inundations, while the embankment built in one bank only would cause increased spilling and a rise in water levels in the inundation on the opposite bank. The calculations also confirmed that already the construction of the embankments in the lower part of the reservoir improved the flood safety of the Ljubljana–Zagreb motorway.

These calculations took into account the implementation of other, accompanying interventions (e.g. replacement habitat), therefore the spatial situation changed gradually, while in some cases the impact of the individual spatial interventions was analysed. The calculation results for the individual

scenarios allowed for the design of (temporary) mitigation measures to improve the runoff conditions (lowering of water levels, lower surface erosion, etc.) in the areas where flood risk could increase during the construction.

At the construction pit edges the risk of influx of water into the pit was studied to support the analyses of the design engineer regarding the justification of the degree of protection, i.e. to preserve the construction pit dry. The final decision was reached based on the relevant impacts of the separate interventions as well as on the impact of all the interventions together on the runoff conditions in the following combinations of the Sava and Krka discharges:

Steady flow for simultaneous occurrence of discharges $Q_{20,Sava} = 2900 \text{ m}^3/\text{s}$ and $Q_{Krka} = 80 \text{ m}^3/\text{s}$. and

Steady flow for simultaneous occurrence of discharges $Q_{100,Sava} = 3750 \text{ m}^3/\text{s}$ and $Q_{20,Krka} = 453 \text{ m}^3/\text{s}$.

The Sava River discharges are taken from the hydrological study from 2011 [7] and the 20-year return period discharge of the Krka River after the study from 2004 [8].

4. RESULTS AND DISCUSSION – BREŽICE HPP

Based on the calculations, the impact of the intermediate conditions during the construction was determined by comparing the water levels in the characteristic points, as a difference between the situation during the implementation of the individual phases and the condition prior to the start of construction. According to the various land uses and other boundary conditions, water levels were compared in 43 points in the Brežice impact area (Figure 6).

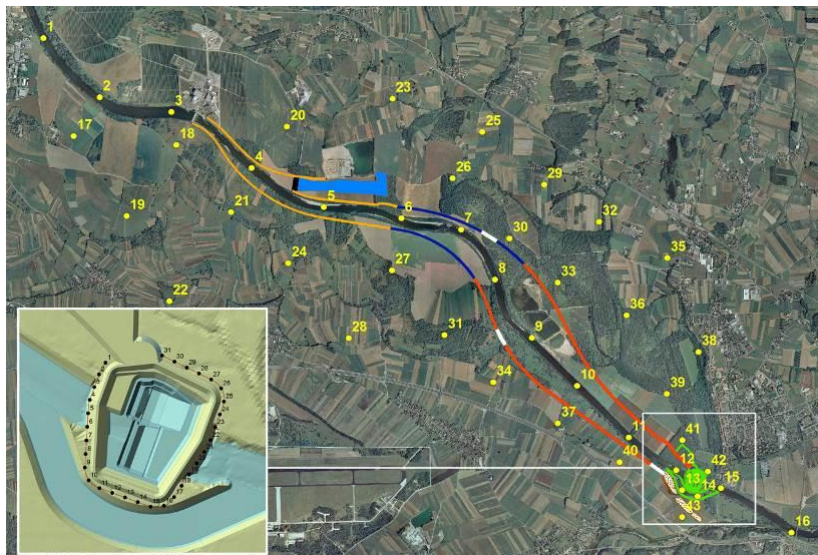


Fig. 6: Locations of points where the water levels were compared to identify the impact of the construction pit and the diversion channel during high-flow conditions

By analysing the differences in the water levels any potential adverse impacts during the construction are determined, so as not to excessively increase flood risk, deteriorate or even disable the functions of infrastructure facilities, or even put the stability of levees at risk, etc. 2D velocity analyses allow for assessing (the changes in) erosion risk in the wider flood area.

4.1. IMPACT OF THE HPP BREŽICE CONSTRUCTION PIT AND THE DIVERSION CHANNEL ON THE RUNOFF REGIME

Prior to HPP construction, the occurrence of a 100-year return period event (3750 m³/s) would result in a quarter of the entire discharge (approx. 900 m³/s) flowing along the right floodplain between the Sava River and the Ljubljana–Zagreb motorway. The location of the construction pit and the diversion channel considerably change the velocity field; as the area of the construction pit is excluded from the flow, throughput is decreased, and the currents are redistributed, causing also a different distribution of depths, velocities, erosion, etc. To minimise the costs of dredging the diversion channel, the best location for the disposal site would be as close as possible to the channel, but the proposed location for the disposal of the material on the right bank would further narrow the already-narrow cross-section. The increase in water levels would increase flood hazard upstream, while, in the narrow cross-section and downstream part, the increased velocities or shear stresses would increase the erosion hazard on agricultural land and the motorway. At the discharges investigated, the mere construction of the construction pit would cause a rise in water levels in the left and right floodplains by up to 45 cm, the effects of which would diminish about 2 km upstream; this would require the construction of dikes near some settlements even in the initial stages of constructing HPP Brežice. The overall impact of the construction pit and the disposal sites would be sufficient to cause flooding of the motorway at a 100-year return period event. The disposal of the material dredged from the diversion channel at the right floodplain would partially obstruct the return of water from the right retention toward the confluence of the Sava and Krka rivers, which would increase the flood hazard vulnerability of the settlements upstream, along the Krka River.

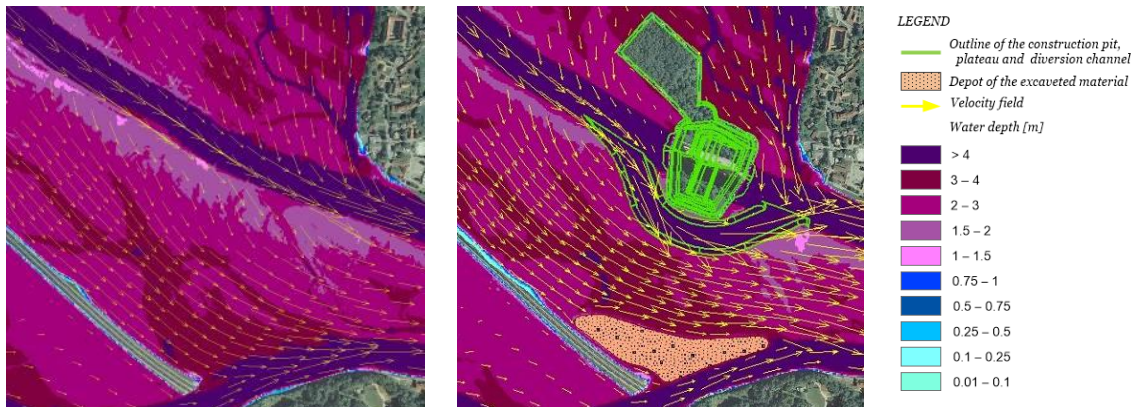


Fig. 7: Comparison of the velocity field and depths for the condition prior to the construction and the final location and shape of the disposal site for the material excavated from the construction pit and the diversion channel at a 100-year return period event.

In terms of costs and flood safety the relocation of the disposal sites upstream from the construction pit would be more suitable, where the cross-section of the right retention (floodplain) is large enough while the impact of the disposal sites would be smaller. Nevertheless this was not possible due to the archaeological site, where the investigations were conducted throughout most of the HPP construction. For other disposal sites on the right bank of the Sava the calculations showed that the critical point in constructing the weir and levees occurs at the narrowing between the construction pit and the Ljubljana–Zagreb motorway, therefore the only option was to remove the disposal sites as far as possible from the Sava River to the left bank of the Krka River. Figure 7 shows the final shape of the disposal site for the total quantity of the material dredged from the diversion channel. The shape is adapted according to the streamlines in the right inundation at the construction pit.

In this way, the disposal site in the corner between the left bank of the Krka River and the motorway embankment would temporarily function as a levee to avert the intrusion of the water from the Sava River into the Krka. This would already in the construction phase decrease the flood hazard of the settlements along the Krka River, as was demonstrated in a previous study [4] about levees along the left bank of the Krka River. In the case of a high-water event during the Brežice HPP construction the water level of the Krka River below the motorway bridge would decrease by up to 50 cm relative to the situation prior to the construction.

Figure 8 shows the conditions in 2014, at the Sava River discharge of approx. 2000 m³/s.



Fig. 8: Photograph of the construction pit site and the diversion channel during high water in September 2014 (discharge approx. 2000 m³/s) (source: 24ur.com).

The surface water formations confirmed the accuracy of the hydraulic analyses. During the event at locations under higher pressure//load//burden due to spiral water current in the diversion channel some erosion damage was caused in the banks of the diversion channel, while the safety of the construction pit was not at risk.

4.2. CHANGES IN RUNOFF CONDITIONS IN THE INDIVIDUAL PHASES OF CONSTRUCTING EMBANKMENTS AT BREŽICE HPP

The calculated conditions for the situation with the construction pit and the diversion channel provided a starting point when trying to find the best sequence of constructing embankments along the reservoir, i.e. such that would minimise any further negative impact on the situation, or even mitigate the situation, particularly along the Ljubljana–Zagreb motorway. The condition prior to the start of works at HPP Brežice provided another basis. The selection of various sections of the dike, various building sequences, etc., provided several scenarios, of which 16 cases were analysed, which addressed the individual developments or temporary conditions in space. Due to their extensiveness, the descriptions of the variants are not provided here. Roughly, they can be divided into four phases as follows: (1) Construction of embankments upstream the weir; (2) construction of embankments from NPP Krško downstream and construction of a flood control relief system; (3) construction of embankments in the middle part, and (4) closing of outflow openings in embankments and the inlet into the diversion channel (Figure 9).

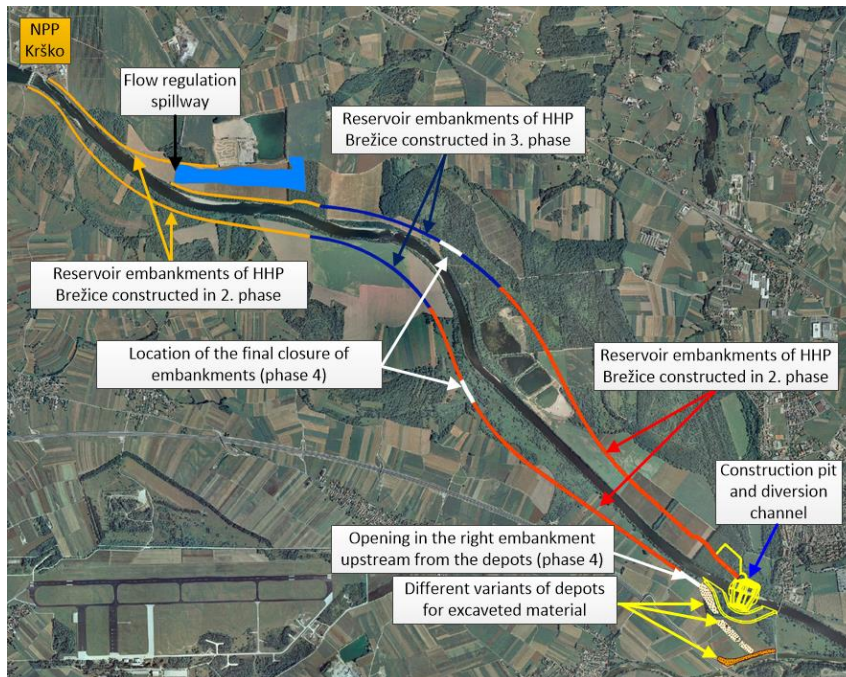


Fig. 9: Basic division of construction phases of building HPP Brežice embankments

In the first phase the embankments at both Sava River banks are built from the HPP weir upstream, with an opening on the right bank at the construction pit due to the inflow into the diversion channel and the upstream outflow opening, which allows for outflow into the right inundation, to preserve the processes as in the existing situation when floods flow from the channel to the retention. The construction of embankments, in fact, obstructs the outflow of water from the channel to floodplains, which would increase the discharge between the already built embankments toward the cross-section at the construction pit. In high-water situations the discharge at the retention, and thus water levels (and flood risk), would decrease, while higher discharge toward the construction pit would require the construction of higher levees along the pit.

Based on these analyses, the second stage involved the building of embankments from NPP Krško dam downstream, including the relief system for retention of peak discharges in the left inundation. After the completion, the latter is fitted with hydromechanical equipment, which is during the construction stage, of course, neither installed nor in operation. In this way, flood water from the channel could flow into the inundation only in the right bank, upstream the NPP Krško dam, and at the section where the embankments are not built yet. Analyses have shown that during high discharges the left retention would partially fill up also through the relief system being constructed as higher discharges would overflow the levee of the construction pit. As the construction of 2nd phase structures additionally reduced the spilling of water from the channel to the retention, at 100-year return period events the water levels of the Sava River in the area between the already built embankments would rise relative to the previous condition (up to 70 cm), while in a major part of the retention areas the water levels would decrease (up to 35 cm). Due to the influence of the construction pit and the disposal site with

the excavated material, in this construction phase the water levels would still remain above the previous state only in the lower part of the right retention.

In stage 3 the middle third of the embankments is built. After the construction of the embankments throughout the length the outflow of water from the channel to floodplains is restricted to the section above the NPP Krško weir, the outflow openings in the built embankments (of a length of approx. 100 m) in the middle part, the inlet into the diversion channel, and the discharge over the relief system. In the latter, the spillway crest elevation of a fully open relief system was considered in the calculations, i.e. in the state where the concrete structure is built, while the hydromechanical installations are still lacking.

In this construction period, retention areas during high waters would be activated to a similar degree than upon the completion of the Brežice HPP, meaning that in the retentions lower discharges than prior to HPP construction would occur, and as a consequence also lower water levels in the most part of the retention areas. To relieve the lower part of the right retention and reduce the water mass spilling across the area at the construction pit, there are still two 100-m long openings in the middle part of the reservoir envisaged (Figure 9). The location of the opening on the left allows for as much outflow as possible (outer part of the curve) to the left retention, while the opening on the right allows for a more favourable flow field in the part between the construction pit and the motorway. The increased mass of the water current from the middle to the lower part in the right retention considerably weakens the transversal water current which is, due to the shape of the construction pit and the diversion channel, directed transversally, towards the motorway. The analysis of the velocity field of the final variant confirmed this effect; at the same time, local velocities (or erosion hazard) and local water levels along the motorway are not increased.

The final construction stage, which was critical mostly because of the potential locally increased velocities and thus erosion hazard, comprised the closing of openings in the embankments in the middle part, the closing of the diversion channel, and the redirection of the flow through the spillways of HPP Brežice. It was also necessary to determine the impact of redirecting the Sava River through HPP spillways on flood safety and the impact on the ongoing works at the reservoir (to estimate the possibility of damage) in the phase when the diversion channel is partially or completely backfilled.

Figure 10 shows the velocity fields in the case of still active 100-m outflow openings in the levees for the case with backfilled diversion channel (left) and the still open diversion channel (right). As evident, the lower part of the right retention between the HPP weir and the Ljubljana–Zagreb motorway was the most affected by erosive action due to maximum flow velocities in retention areas. The calculations have shown that erosion risk can be reduced if backfilling of the diversion channel starts at a later stage, to preserve its discharge capacity as long as possible. In the case of backfilling the diversion channel before completing the embankments the erosion processes would be strongest at downstream ends of the already finished embankments (openings in the middle part and before the inflow into the diversion channel). Water current velocities up to 3 m/s would occur, which can transport gravel and rubble up to a grain size of approx. 100 mm. By preserving the diversion channel open it was possible, due to higher discharge

capacity of the lower part of the basin, to ensure lower water levels and velocities in the most critical sections.

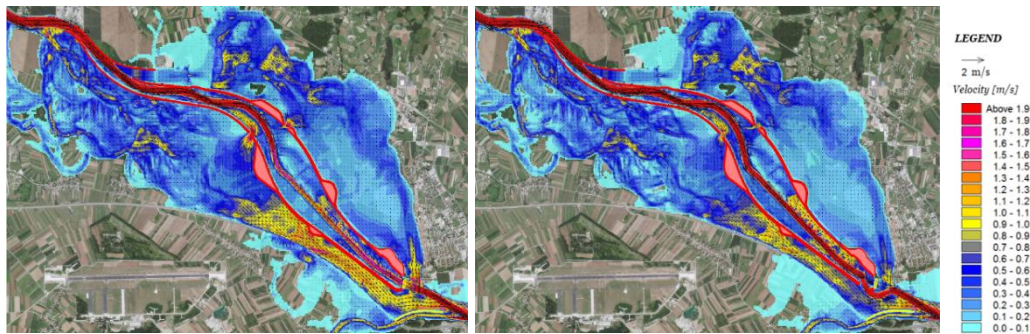


Fig. 10: Velocity field in the case of active 100-m outflow openings in the levees: (a) with backfilled diversion channel (left) or (b) still open diversion channel at the construction pit (right).

Here only some findings from the extensive set of calculations are presented, which show the diversity of the response of the water current to the developments in the floodplains. In the calculations the design engineer could evaluate the different ideas, concepts, scenarios, and thus appropriately designed the excavation of the construction pit and the diversion channel, the sequence of construction phases of embankments and levees and other planned works, and thus tried to minimise the impact on flood and erosion hazard. Despite trying to find the best possible construction sequence, analyses revealed that in the individual construction phases poorer runoff conditions in some areas are to be expected than those prior to the Brežice HPP construction or those upon the completion, as suggested by the calculations. As these areas are populated, and infrastructure facilities of national significance are at stake, the calculation results underlined the need for priority construction of flood levees and additional temporary measures to protect the areas and infrastructure that would be, during the construction, exposed to increased flood and erosion hazards (e.g. of a motorway section).

5. CONCLUSIONS

The appropriate siting of structures and planned developments, which have a significant impact on the runoff regime and can increase flood and erosion hazard for other users in space, needs to take into account both the impact of (stage-wise) construction on the aquatic environment and the impact of action of water on the structures and other works. When determining the acceptability of interventions, the emphasis is usually given to establishing the differences between the existing situation and the planned situation, i.e. the situation after the completion. As shown, during prolonged construction it is necessary to consider the impact of temporary structures, disposal sites, and the individual construction phases, i.e. in a situation when the planned intervention is still not operating as a functional unit.

Therefore, it is necessary to analyse any potential adverse effects of the changing (runoff) conditions on the relevant flood and erosion hazard of users of riparian and downstream space, as temporary conditions can negatively affect the spatial conditions even at high-waters with lower return periods. It was shown that the inclusion of hydraulic analysis into planning the stage-wise implementation is equally important as that in planning and optimising the final solutions of spatial developments. In the case of constructing structures and developments as part of HPP Brežice, the hydraulic calculations provided information about the appropriate planning of construction phases and identifying locations or dimensions of temporary structures and measures, as this provides an important retention area in the section between Krško and the state border and affects the runoff conditions in the border profile with the Republic of Croatia. Notably, NPP Krško is located in the impact area, where any deterioration of runoff and operational conditions is unacceptable, neither during the construction nor afterwards. By comparing intermediate situations and the results of the conditions prior to and upon completion of construction works it was necessary to determine and evaluate the potential deterioration in the individual phases of construction or changes in space, so that the HPP design engineer could predict different construction phases of the individual structures or propose and justify an additional set of (temporary) measures to remedy increased hazard and risk.

This paper also underlines that users of space and activities that take place therein must be made familiar with the processes and impacts of step-wise construction, particularly during prolonged construction. We also recommend that with extensive spatial developments, along longer river section and with larger impact areas, periodic calculations of runoff conditions are carried out. Changes in space have a dispersed character, so it is necessary to check whether any changes or land use affect runoff to a degree when the conditions for siting a structure are no longer met. As in the past the conditions during high-water events have demonstrated, even changes in overgrowth in floodplain areas can significantly affect flows and change the level of flood hazard [9]. Such additional risks should be reduced as much as possible with an appropriate zoning resolution.

6. REFERENCES

- [1] RAK, G., STEINMAN, F. Considering the effects of human activities in flood hazard assessment. *Proceedings of the 15th International Symposium Water Management and Hydraulics Engineering: 2-8*, 2017.
- [2] MLAČNIK, J., RODIČ, P., NOVAK, G., VOŠNJAK, S., STEINMAN, F., RAK, G., ŠANTL, S., MÜLLER, M., CIUHA, D. Izvedba hibridnih hidravličnih modelov za območje spodnje vode HE Krško, območje HE Brežice in območje HE Mokrice, HHM za HE Brežice, Final report, Ljubljana, Inštitut za hidravlične raziskave, 2011.

- [3] RAK, G., MÜLLER, M., STEINMAN, F., ŠANTL, S., NOVAK, G. Hydraulic modeling of future hydro power plants on lower Sava, *ICOLD Symposium*. Austrija, Graz, Verlag der Technischen Universität Graz, 133–138, 2010.
- [4] RAK, G., MÜLLER, M., ŠANTL, S., STEINMAN, F. 2012 The use of hybrid hydraulic models in the process of hydropower plants design on the lower Sava, *Acta hydrotechnica* 25; 42: 59–70, 2012.
- [5] JIA, Y., WANG S.Y. CCHE2D: Two-dimensional Hydrodynamic and Sediment Transport Model For Unsteady Open Channel Flows Over Loose Bed. School of Engineering, University of Mississippi, 2011.
- [6] BOMBAČ, M. Hydraulic research of the construction pit of HPP Brežice on a physical model. *Acta hydrotechnica* 25; 42: 1–17, 2012.
- [7] INŠTITUT ZA VODE RS. Hidrološka študija pritokov Save – na odseku od vtoka Savinje do državne meje, C-1261. Ljubljana, 2004.
- [8] INŠTITUT ZA VODE RS. Verjetnostna analiza spremenjenih vrednosti visokih vod Save za v.p. Radeče, Ljubljana, 2011.
- [9] RAK, G., KOZELJ, D., STEINMAN, F. The impact of floodplain land use on flood wave propagation. *Natural hazards* 83; 1: 425-443, 2016.

SUMMARY

In the planning stage of the interventions in water space and riparian areas hydraulic model research of runoff regime is an established tool in the search of the final solution, which in addition to providing the functionality provides the preservation or mitigation of flood and erosion hazard. To support construction, stepwise planning of temporary structures and measures, etc., is crucial as well. The importance of analysing the runoff regime in a particular intermediate phase of the construction is mainly reflected in siting of an extensive and complex intervention, the construction of which takes place a long time, with changing environmental and hydraulic conditions. One should be aware that during the period of construction the temporary state in the area (particularly in an intermediate phase of construction) could have a significantly more adverse effect on the runoff regime (and consequently on adjacent activities and space users) than a final design state. Temporary flood hazard hydraulic analysis in the planning of construction phases is presented on the case of siting interventions according to the national spatial plan of HPP Brežice, to identify potential intermediate increase of hazard and risk, higher than that predicted for the HPP under full operation. Consequently, the planned construction process was adapted and optimized, which helped to reduce risks as well as costs.

Keywords: Power Plant, Construction Phase, Flood Control, Numerical Model, Physical Model

COMMISSION INTERNATIONALE DES GRANDS BARRAGES

VINGT-SIXIÈME CONGRÈS DES GRANDS BARRAGES
Autriche, juillet 2018

DOI 10.3217/978-3-85125-620-8-104



This work licensed under a Creative Commons Attribution 4.0 International License. <https://creativecommons.org/licenses/by-nc-nd/4.0/>

**THE APPLICATION OF MATURITY MATRIX IN DAMS SAFETY PROGRAM IN
BENGAWAN SOLO RIVER BASIN ORGANIZATION (RBO), INDONESIA**

Agus JATIWIRYONO SOEMARDIJO

Member of Executive Committee of INACOLD

INDONESIA

Antonius SURYONO

Secretary of Dam Management Unit of Bengawan Solo RBO

INDONESIA

THE APPLICATION OF MATURITY MATRIX IN DAMS SAFETY PROGRAM IN BENGAWAN SOLO RIVER BASIN ORGANIZATION (RBO), INDONESIA

Agus JATIWIYONO SOEMARDIJO¹⁾

Member of Executive Committee of INACOLD,

Antonius SURYONO²⁾

Secretary of Dam Management Unit of Bengawan Solo RBO, INDONESIA

1. INTRODUCTION

Safety of dams can be successfully achieved through prudent implementation of solid dam safety program. As stipulated in the Ministerial of Public Works and Housing Regulation number No. 27/PRT/M/2015 concerning Dams (Regulation), the dam management in Indonesia carried out by River Basin Organization (RBO) through the Dam Management Unit (DMU). One of the tasks and functions of DMU is implementation of the dam safety program. To support the DMU in the implementation of the dam safety program, the national government prepared strategy and policy that can be applied by each DMU in the preparation and monitoring of the dam safety program in the basin. With the assistant of the World Bank in cooperation with Damwatch from New Zealand, the Maturity Matrices was introduced as a tool in measuring its performance or level of maturity of the dam safety in their jurisdictions through self-assessment.

Maturity matrix consists of the Master matrix (lists of dam safety program 'Components') on the second column and activity matrices on the third column. Master matrix consists of ten components with each have activities related to dam safety program. Maturity matrix is intended to assess the extent or the level of implementation of activities of dam safety program by the managers of the DMU.

The level of the implementation of dam safety program can be assessed with the maturity matrix is to know how far the program has been conducted by RBO in order to improve the implementation of the program of the dam safety. While the purpose of this assessment is the actualization of reliable dam safety management by RBO.

2. MATURITY MATRIX

2.1. Principle application of Maturity Matrix

The Maturity Matrices^[1] are based on a system used to demonstrate the state of practice in an organization for performing an activity in a qualitative sense. The matrices focus on the operations of the DMU within the RBO and are targeted to the dam safety standards and guidelines in Indonesia. The primary benefit from using dam safety-related maturity matrices is the improved understanding of the effectiveness of the dam safety program across the whole range of dam safety activities. Maturity matrices are intended to reflect the most important components of the dam safety program and its activities as listed in Table 1.

Table 1. Program Components and Activities of Dam Safety Maturity Matrix

No (1)	Components (2)	Activity (3)
1	Governance	A Regulation
		B Delegated Roles and Responsibilities
		C Internal & External Communications
		D Resourcing
2	Information Management	A The standard, Policy, Plan and Procedure
		B Physical Infrastructure
		C Operational
		D Studies, Reviews and Report
3	The Dam safety Training and Education	A Dam Safety
		B Flow Control Equipment
		C Reservoir Operation
		D Incident and Emergency Preparedness
4	Surveillance	A Surveillance Program
		B Inspections
		C Instrumentation and Data Management
		D Dam Safety Assessment
5	Spillway and Outlet Equipment	A Spillway and Outlet Equipment Program
		B Inspections and Maintenance
		C Testing
		D System Performance Assessment
6	Reservoir Operation	A Operation Protocols
		B Relationship with External Stakeholders
		C Debris Management
7	Dams and Spillway Maintenance	A Dam, Reservoir and Access maintenance
		B Spillway and Outlet Structure maintenance
8	Audit and Reviews	A Dam Safety Program Audit
		B Dam Safety Program Reviews
		C Dam Safety Reviews
		D Flow Control Equipment Reviews
9	Managing Dam Safety Problems	A Issue Management System
		B Managing Non-conformances
		C Managing Physical Infrastructure Issues
		D Managing Dam Safety Deficiencies
10	Emergency Preparedness	A Hazard and Consequence Identification
		B Owner Emergency Preparedness Plans
		C Relationship with Community and External Agency
		D Tests and Exercises

^[1] *Dam for Development: Toward Enhancing Water Security in Indonesia, Maturity Matrices p. 21 (draft), The World Bank, 2017*

The matrix shows advancing maturity from a rudimentary or elementary level of practice through stages to advanced, expert or best practice. Maturity matrix has 5 maturity level indicated with different colors. Description and typical characteristic of each proposed maturity level are shown in Table 2.

Table 2. Maturity Level Description and Typical Characteristic

	Maturity Level				
	Level 1 Needing Development	Level 2 Elementary	Level 3 Good Practice	Level 4 Very Good Practice	Level 5 Best Practice
Maturity Level Description	Lacks conformance to applicable guidelines, standards and best practice	Conforms to applicable guidelines, standards and best practice in some areas	Generally conforms to applicable guidelines, standards and best practice	High degree of conformance with applicable guidelines, standards and best practice with good understanding	High degree of understanding and conformance with applicable guidelines, standards and best practice. No significant opportunities for improvement

The 'Master Matrix' lists dam safety program 'Components' on the vertical axis as shown on Figure 1. Components describe the main activities of a dam safety program and align with ICOLD terminology and are common groupings of dam safety activities around the world.

Master Matrix Dam Safety Program Component	Maturity Level				
	Level 1	Level 2	Level 3	Level 4	Level 5
1 Governance					
2 Information Management					
3 Dam Safety Training and Education					
4 Surveillance	→	[summary description]			
5 Spillway and Outlet equipment					
6 Reservoir Operations					
7 Dam and Spillway Maintenance					
8 Audits and Reviews					
9 Managing Dam Safety Problems					
10 Emergency Preparedness					

Fig. 1
Master Matrix Structure

Detailed component matrix and relation between master matrix and component matrices are shown on Fig. 2 and Fig. 3:

Surveillance Component Matrix	Maturity Level				
	Level 1 Needing Development	Level 2 Elementary	Level 3 Good Practice	Level 4 Very Good Practice	Level 5 Best Practice
Activities					
Surveillance Program	[line item descriptions]	[line item descriptions]	[line item descriptions]	[line item descriptions]	[line item descriptions]
Inspections	[line item descriptions]	[line item descriptions]	[line item descriptions]	[line item descriptions]	[line item descriptions]
Instrumentation and Data Management	[line item descriptions]	[line item descriptions]	[line item descriptions]	[line item descriptions]	[line item descriptions]
Dam Safety Assessment	[line item descriptions]	[line item descriptions]	[line item descriptions]	[line item descriptions]	[line item descriptions]

Fig. 2
Surveillance Matrix and its Activities

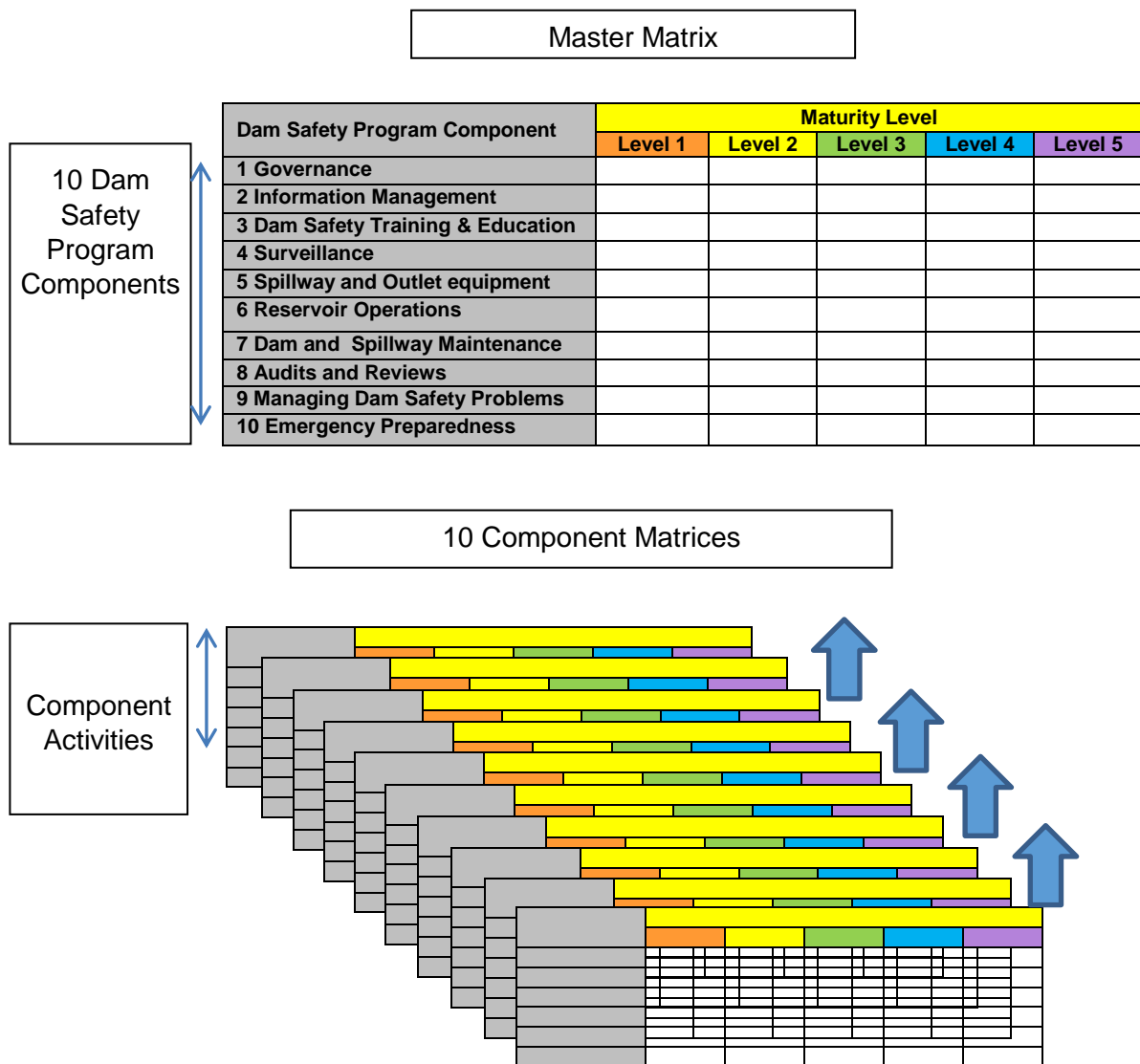


Fig. 3
Relationship between Master Matrix and Component-Matrices

2.2. Limitation of the Matrix

Based on the Regulation, dam construction and management should be implemented based on concepts of dam safety^[2]. The concept of dam safety shall comprise of 3 (three) pillars (Fig. 4), namely: a. structural safety; b. operation, maintenance and monitoring (surveillance); and c. emergency preparedness.

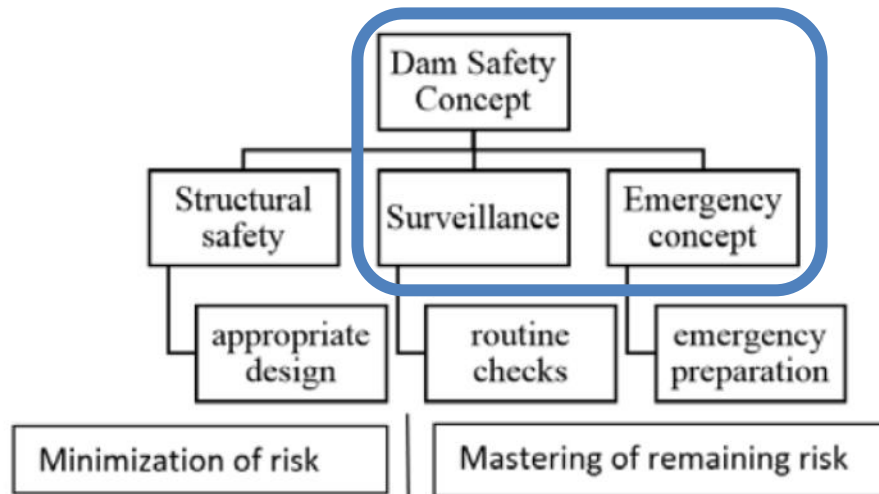


Fig. 4
Dam Safety Concept covered in Maturity Matrices

The maturity matrix primarily concerned with surveillance and emergency preparedness points of the dam safety concept. The discussion will be concentrated on the application of the matrix in Bengawan Solo RBO as the DMU showing the significant progress in the application of the maturity matrices in dam safety program.

3. ASSESSMENT

3.1. Result of self-assessment

Assessment of the performance of the DMU using the maturity matrices have been done with preparing the supporting data in accordance with the activities. The following self-assessment of on the DMU Bengawan Solo RBO which have been carried out, the assessment is using component matrices which

^[2] Article 3, The Ministerial Regulation Number 27/PRT/M/2015 Concerning Dam, Ministry of Public Works and Housing, The Republic of Indonesia, 2015

are summaries into master matrix and plotted in polar graph to show the result of maturity level of dam safety implementation in Bengawan Solo RBO as shown on Fig. 5, then plotted into polar graph (Fig.6).

Components of the Maturity Matrix		Maturity Level				
		Level 1 Needing Development	Level 2 Elementary	Level 3 Good Practice	Level 4 Very Good Practice	Level 5 Best Practices
1	Governance	1	2	3	4	5
2	Information Management	1	2	3	4	5
3	Dam Safety Training and Education	1	2	3	4	5
4	Surveillance	1	2	3	4	5
5	Spilway and Outlet Equipment	1	2	3	4	5
6	Reservoir Operation	1	2	3	4	5
7	Dams and Spilway Maintenance	1	2	3	4	5
8	Audit and Review	1	2	3	4	5
9	Managing Dam Safety Problems	1	2	3	4	5
10	Emergency Preparedness	1	2	3	4	5

Fig. 5
Results of the assessment of the DMU Bengawan Solo RBO

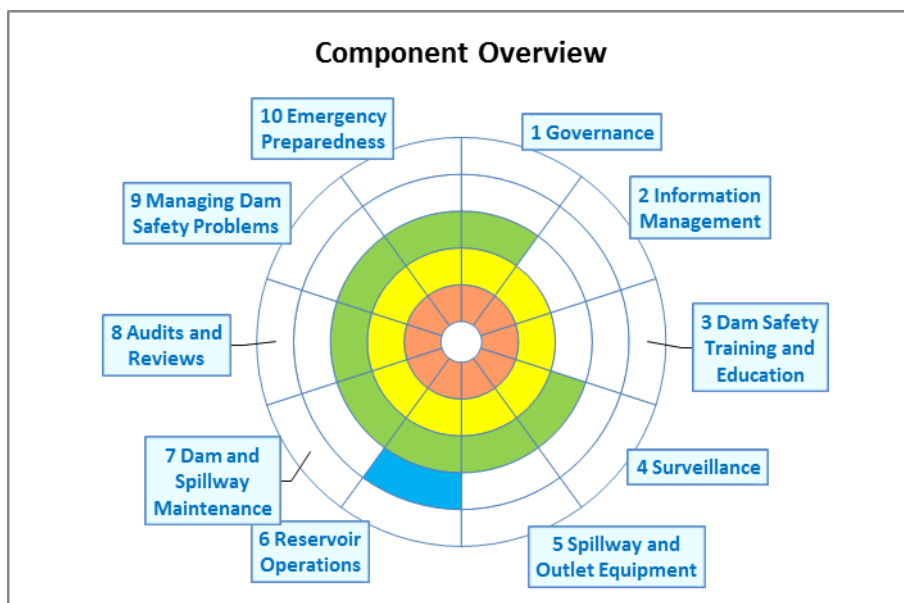


Fig. 6
Polar graph of the assessment result

Evaluation notes that support justification of scoring used in assessment of each components and its activities are as follows:

1. Component 1, Governance with its activities of: Regulation; Delegated Roles and Responsibilities; Internal & External Communications; and Resourcing;
The score is: at good practice (level 3), in general they comply above activities by having Ministerial Regulation and guidelines for managing their dams and already disseminated to all staff concern; the river basin area divided into 3 areas namely: Upper Bengawan Solo sub basin covering 20 dams; Lower Bengawan Solo sub basin covering 3 dams; and Madiun sub basin covering 3 dams respectively. Each sub-basin headed by engineer as sub DMU they also have some competence engineer working at DMU; they have good communication mechanism in the internal DMU, with other unit within the RBOs and other agencies such as local and provincial agencies, ministry of Public Work and Housing; arrangement of resources starting from the personnel, equipment and budget allocation arranged annually.
2. Component 2, Information Management, with its activities of: Standards, Policies, Plans and Procedures; Physical Infrastructure; Operational; Studies, Reviews and Reports
The score is: in the elementary level (level 2) since they have some standards, policies, plans and procedures related to the dam safety in DMU office; inventory of dam physical assets has just started, also existing/ recorded information, operational information and related study but not yet cataloging.
3. Component 3, Dam Safety Training and Education with its activities of: Dam Safety; Flow Control Equipment; Reservoir Operation; Incident and Emergency Preparedness; The score is: at the elementary level (level 2), they prepared just an early of training program which will be held regularly within the DMU with facilitator coming from RBO internally and also from the ministry to improve and refresh knowledge and skill of DMU personnel's. The training subject will include Dam Safety; Flow Control Equipment; Reservoir Operation; Incident and Emergency Preparedness. The training which has been run is mostly practical skill such as training for spillway and outlet operations.
4. Component 4, Surveillance, with its activities of: Surveillance Program; Inspections; Instrumentation and Data Management; Dam Safety Assessment; The score is: at good practice (level 3), DMU prepared standard operating procedures (SOP), annual surveillance program and disseminated to all staff member, including dam inspection program, visual dam inspection and its reservoir, instrumentation data record and management, as well as the dam performance with ultimately safety assessment of the dam. Daily reporting result dam according to SOP and rapid report via WhatsApp reporting.
5. Component 5, Spillway and Outlet equipment, with its activities of: Spillway and Outlet Equipment Program; Inspections and Maintenance; Testing; System Performance Assessment. The score is: at good practice (level 3).

All activities are arranged and in well-organized based on regular SOPs, there is continuous reporting on the observation and maintenance of spillway and outlets equipment. The purpose is to maintain the performance of the spillway and outlets equipment that will contribute to the safety of the dam and its reservoir. The works will include program implementation of the spillway and outlet equipment, examination and maintenance of spillway and outlet equipment to assess the condition and reliability also functional testing of spillway and outlet equipment.

6. Component 6, Reservoir Operation, with its activities of: Operation Protocols; Relationship with External Stakeholders; Debris Management
The score is: at a very good practice (level 4). The DMU of Bengawan Solo RBO has prepared the rule curve for reservoir operation purpose as a protocol and continuously recorded with a structured process as required in the SOP of dam operation. The annual operation plan is prepared based on rule curve and recommendation Basin Coordinating Team for the proposed water requirement from the users. The Debris management is done as part of maintenance works in accordance with SOP which has been made in order to improve the performance of the dam and its reservoir that secure on all the operating conditions.
7. Component 7, Dam and Spillway maintenance, with its activities of: Dam, Reservoir and Access maintenance; Spillway and Outlet Structure maintenance. The score is: at a good practice (level 3). UPB BBWS Bengawan Solo has arranged the operation pattern of reservoir and has been carried out recording with a structured process because it already has SOP of dam operation. Waste management is done in accordance with SOP that has been made the goal is to increase the implementation of maintenance of the structure of the civil society and construction related to the dam and its reservoir. Including structural maintenance or repairs, erosion protection, control vegetation and drainage maintenance (drainage surface and drainage relief internal). Including spillway and electrical outlets that shows the function of the safety of the dam also electrical components and mechanical.
8. Component 8, Review and Audit, with its activities of: Dam Safety Program Audit; Dam Safety Program Reviews; Dam Safety Reviews; Flow Control Equipment Reviews. The score is: at a good practice (level 3). The dam safety program is prepared annually. As a part of the SOP, the implementation and the program are regularly audited and reviewed by DMU manager. While the dam safety review including the flow control equipment being done in semiannual basis by the ministry and 5 years basis for the major inspection by the Dam Safety Commission, not all inspections have been implemented but have been included in the strategic plan related to the implementation of the major dam inspection.

9. Component 9, Managing Dam Safety Problems, with its activities of: Issue Management System; Managing Non-conformances; Managing Physical Infrastructure Issues; Managing Dam Safety Deficiencies
The score is: at a good practice (level 3). Related to the dam safety management issues, periodical and special maintenance have been prepared annually, in addition, related to the problem of dam safety, routine visual inspection and monitoring of the safety parameters of the dam were conducted by DMU staff and implemented well. DMU has set up a reliable safety management of dam through inventory, categorization, priority setting, investigations, and assessment of the dam safety issues.
10. Component 10, Emergency Preparedness, with its activities of: Hazard and Consequence Identification; Owner Emergency Preparedness Plans; Relationship with Community and External Agencies: Tests and Exercises
The score is: at a good practice (level 3), in relation to emergency preparedness, DMU of Bengawan Solo RBO has prepared an Emergency Action Plan though not yet for all dam, so that DMU of Bengawan Solo RBO may increase the awareness in identification of hazard and consequences potential failure of the dam and planning to respond to the incidents that may cause failure of the dam. This includes preparation of the plan for the state of emergency, build external relations and testing and training emergency situations including the simulation for the state of emergency in cooperation with the local government through Regional Disaster Management Authority.

3.2. Review and Discussion

The maturity matrices were launched in early 2017 and followed with two subsequent workshops in Batam (May 11-12, 2017) and in Semarang (July 17-20, 2017). The result of the self-assessment above showed the acceptance of DMU Bengawan Solo RBO to the maturity matrices is promising. The scoring of each activity with its line item descriptions require understanding the nature of the component, activity and also broader context of dam safety management as well as dam safety standards and guidelines. Fortunately the DMU of Bengawan Solo has sufficient competence human resources, so it is helpful in expediting the familiarity to the application of such maturity matrix for evaluating dam safety program.

Yet the objective of such assessment has to be achieved, in order to reach further achievement and to expedite the scoring supporting its assessment result with document as an evidence to facilitate scoring justification may also be necessary. The assessment result and its descriptions is a good start to demonstrate the anticipation of the DMU.

DMU as units that manage dams become vital objects on the application of self-assessment using dam safety program maturity matrix to see their own performance in running the program. Such assessment is conducted in accordance with of the dam safety management based on the applicable rules

and procedures. However associated with workshop of maturity matrices in dam safety program, it is also important to refresh the understanding of participants in the dam safety management based on the applicable rules and procedures.

4. CONCLUSIONS AND RECOMMENDATIONS

4.1. Conclusions

- Dam safety maturity matrices has been understood and possible to be adopted for assessing the dam safety program run by DMU.
- Consistency in self-assessment has yet to be achieved, to expedite the proper assessment its need facilitator which on the other hand will also function in validation of the self-assessment capacity.
- The maturity matrix outcome also can be used as a guide to develop the current level to improve to the desired level depending the available resources within the DMU.
- Variability in DMU capacity may be consider when the tools will be nationally applied. Thus, workshop and training in the subject of maturity matrices in dam safety program and dam safety management should be regularly held.
- Skilled persons in Maturity Matrices application tour of duty has to be anticipate to maintain the capacity of DMU

4.2. Recommendations

- Workshop is very important to anticipate personnel tour of duty and also as a medium to exchange the understanding among DMU.
- The target level of maturity for each DMU shall not be same for all DMU, setting of the target level will be depending on their portfolio of dams.
- The Maturity Matrices could be expanded beyond RBO under the Ministry, such as water supply, hydro power and private dam owner with some modification.
- Dam Safety Maturity Matrices of dam safety program be included as part of annual and comprehensive safety review of all dams in Indonesia

REFERENCES

- [1] *Dam for Development: Toward Enhancing Water Security in Indonesia (draft)*, The World Bank, 2017.
- [2] *The Ministerial Regulation Number 27/PRT/M/2015 Concerning Dam*, Ministry of Public Works and Housing, the Republic of Indonesia, 2015.
- [3] *Guidelines for Dam Safety Studies*, Ministry of Public Works, the Republic of Indonesia, 2015
- [4] *Regulation of Dam Safety – An Overview of Current Practice Worldwide*. The ICOLD Dam Safety Committee, Technical Bulletin, 2015

COMMISSION INTERNATIONALE DES GRANDS BARRAGES

VINGT-SIXIÈME CONGRÈS DES GRANDS BARRAGES
Autriche, juillet 2018

DOI 10.3217/978-3-85125-620-8-105



This work licensed under a Creative Commons Attribution 4.0 International License. <https://creativecommons.org/licenses/by-nc-nd/4.0/>

FULL WAVE BASED DAMAGE IDENTIFICATION IN DAMS

Muyiwa E ALALADE

Institut für Strukturmechanik,
BAUHAUS-UNIVERSITÄT WEIMAR

GERMANY

Frank WUTTKE

Department of Geomechanics & Geoengineering
CHRISTIAN-ALBRECHTS-UNIVERSITY KIEL

GERMANY

Tom LAHMER

Institut für Strukturmechanik,
BAUHAUS-UNIVERSITÄT WEIMAR

GERMANY

COMMISSION INTERNATIONALE
DES GRANDS BARRAGES

VINGT-SIXIÈME CONGRÈS DES
GRANDS BARRAGES
Autriche, juillet 2018

FULL WAVE BASED DAMAGE IDENTIFICATION IN DAMS

Muyiwa E ALALADE^{a)}, Frank WUTTKE^{b)}, Tom LAHMER^{a)}

*^{a)}Institut für Strukturmechanik,
BAUHAUS-UNIVERSITÄT WEIMAR*

*^{b)}Department of Geomechanics & Geoen지니어ing
CHRISTIAN-ALBRECHTS-UNIVERSITY KIEL*

GERMANY

1. INTRODUCTION

A large percentage of dams in operation today are more than 50 years old and as such the true condition of its structural integrity is not fully known. The deterioration of dams may result both from short and from long term effects. In most cases these effects may not be immediately noticed. To prevent sudden dam failure because of accumulated damages overtime, the timely identification of weak heterogeneous zones which may impair the dam's safety and operation is essential. Unfortunately, the conventional methods are tedious, time consuming, expensive and sometimes inefficient. To tackle these challenges, various numerical methods and inverse analysis has been proposed by the authors [1, 2, 3, 4, 5] considering the coupling effects on various phenomena present in the operational life cycle of the dam.

With the recent technological improvements in computational capabilities, waves have increasingly been applied to probe and obtain information on the structural integrity of mainly sub-surface structures. Information from the reflection, refraction and diffraction of these waves gives insight into possible anomalies which may negatively impact the structural stability and performance.

Quite many research projects have been carried out with regards to wave modeling underneath the earths' surface. There exist several code

implementations ranging from simple to complex and using various numerical methods such as Finite Differences, Finite Elements, Ray theory, Integral solution, etc. The finite difference method is a common method used for solving the wave equation in geophysics and oil exploration as can be seen in works by [6, 7] and [8].

Based on the successful application of Full Waveform Inversion (FWI) in geotechnical exploration and non-destructive testing (NDT), especially with subsurface structures [9, 10, 11, 12, 13, 14, 15, 16], our method aims to extend this application to the identification of damaged regions in dams.

2. THEORY

Seismic waves are generally classified into surface waves and body waves. The surface waves as the name implies, generally travel on the while the body waves on the other hand travel through the inner parts of the earth or structure. Seismic inversion can be categorized into seismic reflection and seismic tomography. In seismic reflection the inversion of reflected waves usually gives information on geometry while refracted waves (seismic refraction) give information on elastic parameters. Seismic tomography application on the other hand, employs the inversion of transmitted, reflected and refracted signals from seismic observations to determine the distribution of material properties in a structure. Seismic tomography methods include travel time inversion (kinematic imaging) and Full Waveform Inversion (dynamic imaging).

Full waveform inversion (FWI), initially proposed by [17, 18] and further developed in the last decades, is regarded as the modern seismic imaging technique which utilizes a comprehensive representation of the interaction between wave physics and subsurface properties. It offers unique advantages in terms of generality, fidelity, complexity and robustness and is hence capable of imaging arbitrarily heterogeneous compression and shear-wave velocity profiles of the subsurface constituents [9]. The quality and efficiency of the inversion is sensitive to the initial model, acquisition setup, and the formulation of the inverse procedure (inversion parameters, domain, method, etc.).

To maintain numerical stability and efficiently use computational resources in simulating wave propagation in unbounded media, it is necessary to truncate the numerical domain. Several absorbing boundary conditions (ABC) has been proposed, however most of these ABC become unstable when considering heterogeneous materials in addition to other limitations. The perfectly matching layer (PML) proposed by [19] is used in this paper.

3. MATHEMATICAL MODEL

3.1. FORWARD MODEL

The elastic wave equation is solved numerically for the displacements \mathbf{u} , stresses τ , density and Lamé parameters (λ and μ) using the finite difference method. The wave equation is discretized in time and space with each of the parameters placed on a staggered grid [20, 21]. The 2D elastic wave equation employed for the forward modeling is the stress-displacement formulation (τ - \mathbf{u}) in Eq. [1]. The V_p and V_s velocities can be calculated from Eq. [2].

$$\begin{aligned} \rho (\partial^2 \mathbf{u}_i) / (\partial t^2) - (\partial \tau_{ij}) / (\partial x_j) &= f_i \\ \tau_{ij} - C_{ijkl} \epsilon_{ij} &= T_{ij} \\ \epsilon_{kl} &= (1/2 (\partial \mathbf{u}_i)) / (\partial x_j) + (1/2 (\partial \mathbf{u}_j)) / (\partial x_i) \end{aligned} \quad [1]$$

With

$$\begin{aligned} \mathbf{u}_{t=0} &= \bar{\mathbf{u}}_0 \text{ on } \Omega \\ (\partial \mathbf{u}_i(t=0)) / \partial t &= \bar{\mathbf{v}}_0 \text{ on } \Omega \\ \mathbf{u} &= \mathbf{u}_1 \text{ on } \Gamma_1 \\ (\partial C_{ijkl} \epsilon_{kl}) / \partial x &= \bar{\tau}(t) \text{ on } \Gamma_2 \\ V_p &= \sqrt{((\lambda + 2\mu)) / \rho}; \quad V_s = \sqrt{\mu / \rho} \end{aligned} \quad [2]$$

where:

- u_i is the particle displacement
- $\tau_{ij} = \lambda \theta \delta_{ij} + 2 \mu \epsilon_{ij}$ are stress tensor components
- $C_{ijkl} = \delta_{ij} \delta_{kl} \lambda + (\delta_{ik} \delta_{jl} + \delta_{il} \delta_{jk}) \mu$ is the stiffness tensor
- ϵ_{ij} is the strain tensor
- ρ is the density of the medium
- f_i, T_{ij} are volume and surface source terms
- λ and μ are the Lamé's parameters
- V_p and V_s are the primary and secondary wave velocity

According to [22, 23], the stability of the staggered grid code is guaranteed when λ , μ and ρ are averaged harmonically and arithmetically. The accuracy of the finite difference (FD) operator used to approximate the spatial derivatives is dependent on the order of the FD operator (i.e. truncation error of the Taylor series expansion). Reflection of the wavefield at the boundaries are prevented by using a PML to damp out the wavefield at the boundaries. Furthermore, it is necessary to satisfy spatial and temporal sampling conditions [24] for the wavefield to prevent numerical artifacts and instabilities during the finite difference simulation.

3.2. INVERSE ANALYSIS

The relationship between the experimental/field data and model can initially be expressed as:

$$F(\mathbf{m}) = \mathbf{u}^{exp} \quad [5]$$

Where F is the forward operator, mapping the material properties/damage parameters \mathbf{m} (i.e. λ , μ and ρ) to the measured signals. As the solution of Eq. [5] may not exist as the measured data \mathbf{u}^{exp} are not in the range of F , we follow a least-square solution approach in Eq. [6]. Thus, the main concept behind the inverse analysis is to minimize the data residuals $\delta\mathbf{u}$ or misfit between experimental or field data \mathbf{u}^{exp} and the simulated data from our forward model \mathbf{u}^{mod} . The objective function $C_f(\mathbf{m})$ which is to be minimized is the residual elastic energy in the residuals. That is the L2-norm of the error between the model response and the field or experimental data.

$$C_f(\mathbf{m}) = 0.5 \|\mathbf{u}_m^{mod} - \mathbf{u}^{exp}\|_{L2} \quad [6]$$

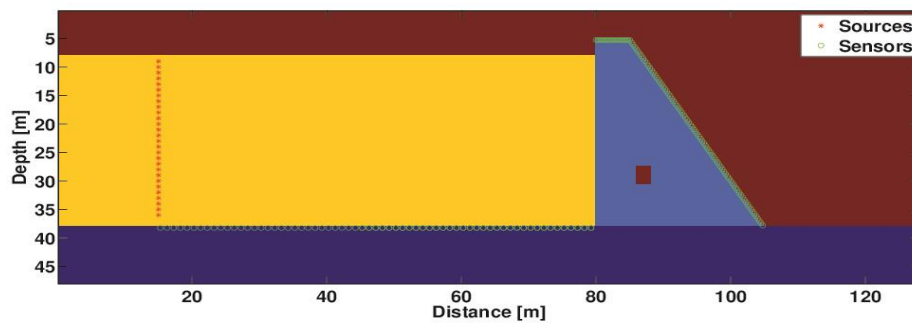
Various strategies are available for inverse analysis, these include both direct and random-search strategies such as Newton methods (Gauss-Newton, Full Newton, etc), Conjugate Gradient, Nelder-Mead simplex methods, Particle Swarm Optimization, Simulated Annealing, Genetic Algorithm and Regularizing Iterative Methods by [25].

4. NUMERICAL SIMULATION AND DISCUSSION

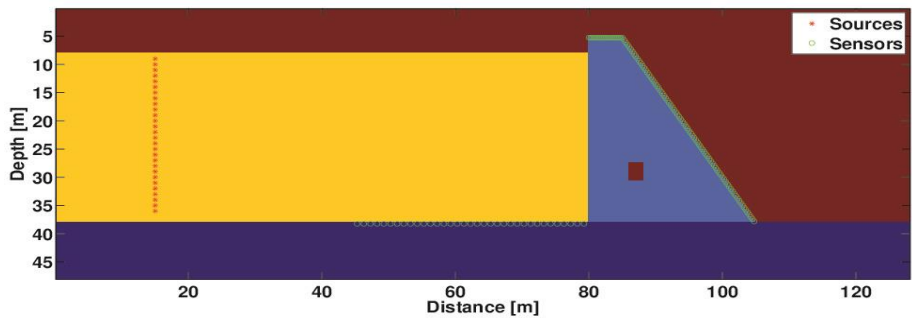
The numerical simulation is carried out for a dam (true model) with material properties defined in terms of seismic velocities summarized in Table 1 and obtainable in Fig. 2. To ascertain the effect of acquisition geometry on quality of results, the sources-sensors setups in Fig. 1 are used to acquire all the waveform data necessary for carrying on the inversion. The dam true model consists of anomalies both in the dam structure and in the foundation. The anomalies represent weaknesses in various regions and of varying magnitudes. In the dam structure, the topmost anomaly represents a 20% reduction in the parameter values (V_p , V_s , ρ), the second 10% and the third (i.e. crack zone) has a 30% reduction. All the anomalies in the foundation have an 70% reduction in the material parameter values.

Table 1
Dam material properties for true model

	V_p	V_s	ρ
Dam body	3500	2200	2000
Dam tunnel	0	0	1.25
Dam foundation	4500	2700	2550
Water	1500	0	1000
Air/Vacuum	0	0	1.25



(a) Setup 1



(b) Setup 2

Fig. 1 Acquisition setup showing distribution of sources and sensors in the domain.

The computational domain has a height of 48m and length of 128m, and it comprises of the dam structure 28m high with a crest and base width of 4.5m and 19m respectively. A 30m by 80m water reservoir, a 10m deep foundation and the surrounding air is also considered. A 2D finite difference scheme on a staggered grid is used to solve the elastic wave equation. The computational domain is truncated using a 2.5m (i.e. 10 grid points) thick Convolutional-PML (C-PML) at both sides and at the bottom of the domain.

Owing to the high number of the systems' global degrees of freedom (i.e. identifying 3 parameters for each node in a domain with $512 \times 192 = 98,304$ nodes), an inverse analysis using methods such as particle swarm optimization (PSO) for anomaly identification, as used in [4, 5] would increase the complexity of the

problem. Gradient and Newton methods involving the computation of the gradient and an approximation of the inverse Hessian operator have been successfully applied by [26, 27, 28]. Thus, motivating the application of the quasi-Newton limited memory Broyden-Fletcher-Goldfarb-Shanno (l-BFGS) method in this paper. The required model parameter gradient calculation is done using the adjoint state method as employed in [29]. Since the FWI is sensitive to the initial model, to enable convergence to the global minima, an initial model which contains the long wavelength part of the model to be resolved is required. Unlike in geophysical exploration, a priori information on the dam material parameters can often be gotten since most of these structures are man-made. Thus, the material properties at construction can be used as an upper bound as done in this case.

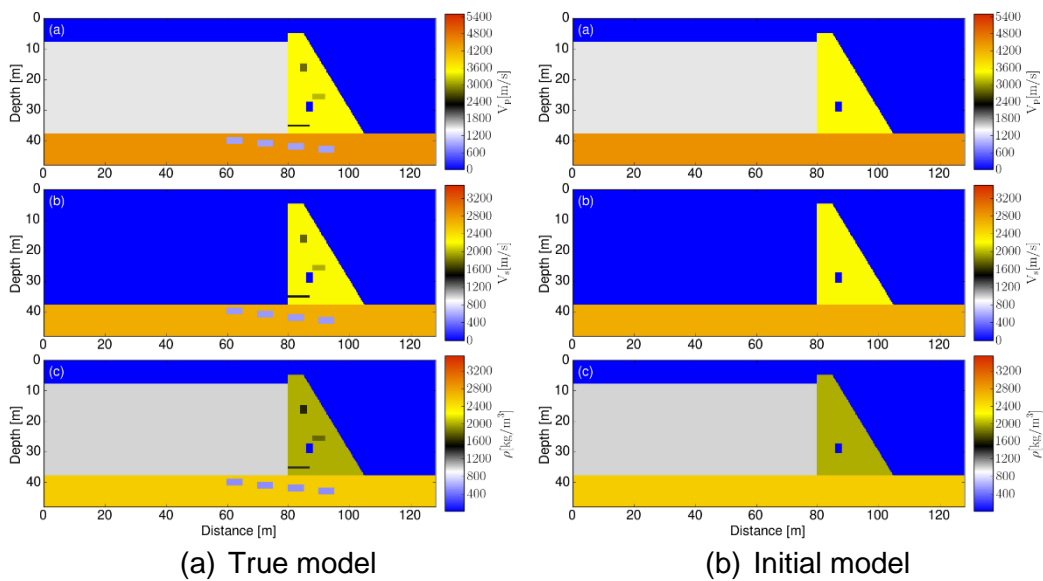


Fig. 2 Distribution of seismic velocities (V_p , V_s) and density in the air, water, foundation and dam structure (true and initial model)

A closer look at Fig. 2 shows that the true model in (a) and the initial model in (b) differ only by the inclusion of regions of degraded material properties in the true model. Therefore, the 'as-built' material properties of the dam are taken as the starting model. To probe the dam material, spike wavelets are sequentially emitted from each of the sources (e.g. air guns). Here, a low-pass filtered spike with upper corner frequency of 1kHz is applied as shown in Fig. 3. For each excitation shot the source wavelet propagates for a duration of 0:1s and the time interval (dt) used for the analysis is 3×10^{-5} s which satisfies the Courant-Friedrichs-Lewy criterion for stability.

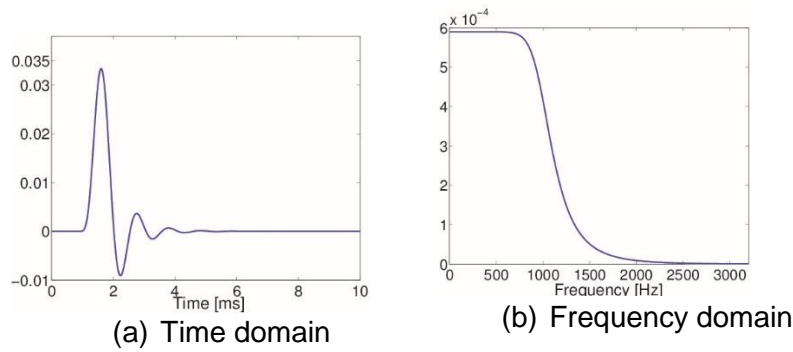


Fig. 3 Source wavelet signal in time domain and frequency domain

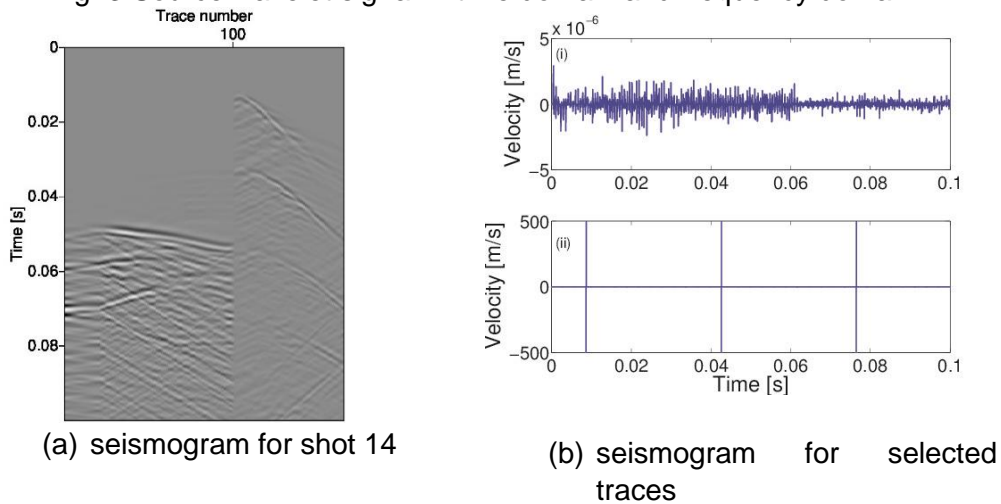


Fig. 4 Sensor response due to propagated waves in medium. (a) Seismogram of all 165 sensor response (b)(i) Response of selected traces.

Dam response recorded by the receivers/sensors due to waves propagating in the medium is obtained in Fig. 4. These synthetically generated seismograms would serve as field data for the inverse analysis (i.e. full waveform inversion). Originally proposed by [30], the FWI is carried out in multiple frequency stages. The inversion is done starting from lower frequencies to higher frequencies (i.e. 0:5-1kHz) to alleviate the non-linearity of the problem. These lower frequencies are less prone to grid dispersion and can identify high velocity regions. The output of low frequency inversion is used as a starting model for higher frequency inversion. Therefore, with each increasing stage of inversion (i.e. increase in frequency), the location/boundaries between different velocity regions becomes more clearly delineated and the quality of the inversion results improves. Inversion results obtained in Fig. 5 shows a good resolution of damages in the dam structure. Anomalies in the dam foundation were not properly resolved, however, from a comparison of the inverted models (i.e. V_p , V_s , ρ) the V_s model can resolve most of the anomalies/damage zones in the dam structure and parts of the foundation. Although less sensors are used in setup 2, better resolution of the damaged regions in addition to more numerical artefacts can be observed.

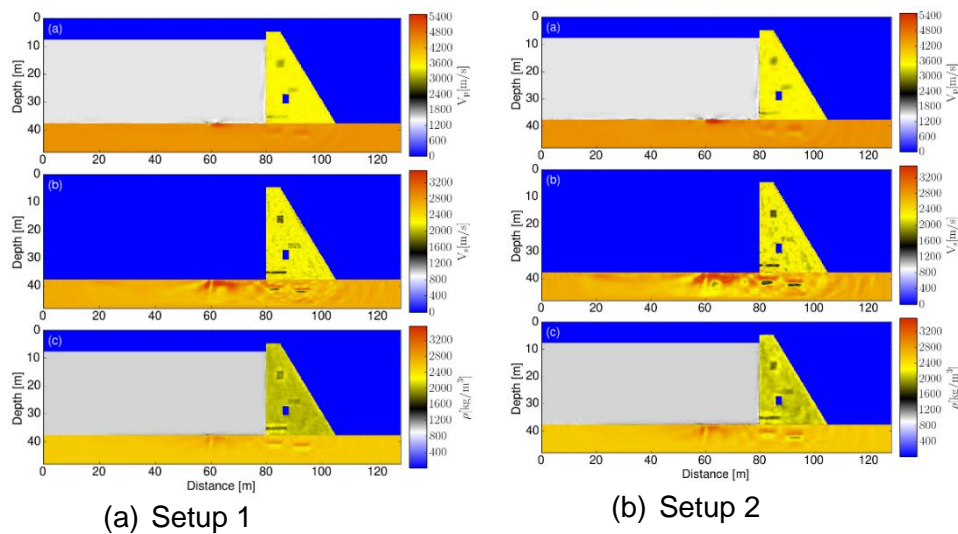


Fig. 5 FWI model comparison for acquisition setup 1 and 2.

5. CONCLUSIONS

Although the Full Waveform Inversion (FWI) has mainly been applied to subsurface exploration of material properties in practice, results obtained in this paper has shown its applicability for non-destructive tests (NDT) of super-structures. The FWI formulation used in our investigation is capable of effectively identifying and quantifying regions of weaknesses (i.e. heterogeneity) in both the dam structure and its foundation. The quality of the inversion is dependent on the initial model, the acquisition geometry and noise level in the measurement data.

5.1. ACKNOWLEDGEMENTS

The authors gratefully acknowledge the financial support of the German Research Foundation (DFG) under the grant LA - 2869/4-1.

REFERENCES

- [1] H. NGUYEN-VINH, I. BAKAR, M.A. MSEKH, J-H SONG, J. MUTHU, G. ZI, P. LE, S. PIERRE A. BORDAS, R. SIMPSON, S. NATARAJAN, et al. Extended finite element method for dynamic fracture of piezo-electric materials. *Engineering Fracture Mechanics*, 92:19–31, 2012.

- [2] T. LAHMER, C. KÖNKE, AND V. BETTZIECHE. Optimal monitoring of gravity dams by multifield considerations. 2011.
- [3] TOM LAHMER. Crack identification in hydro-mechanical systems with applications to gravity water dams. *Inverse Problems in Science and Engineering*, 18(8):1083–1101, 2010.
- [4] M. ALALADE, L. NGUYEN-TUAN, F. WUTTKE, and T. LAHMER. Inverse analysis of coupled hydro-mechanical problem in dynamically excited dams. *In Robert L. Mullen Steffen Freitag, Rafi L. Muhanna, editor, 7th International Workshop on Reliable Engineering Computing: Computing with Polymorphic Uncertainty data*, 2016.
- [5] M. ALALADE, L. NGUYEN-TUAN, F. WUTTKE, and T. LAHMER. Damage identification in gravity dams using dynamic coupled hydro-mechanical XFEM. *International Journal of Mechanics and Materials in Design*. 2017
- [6] D. KÖHN, D. DE NIL, A. KURZMANN, A. PRZEBINDOWSKA, AND T. BOHLEN. On the influence of model parametrization in elastic full waveform tomography. *Geophysical Journal International*, 191(1):325–345, 2012.
- [7] D. KÖHN, DENISE DE NIL, ANDRÉ KURZMANN, and W. RABEL. waveform tomography-part 1 theory. 2015.
- [8] B. E. TREEBY, J. JAROS, A. P. RENDELL, and B.T. COX. Modeling ultrasound propagation in heterogeneous media with power law absorption using a k-space pseudospectral method. *The Journal of the Society of America*, 131(6):4324–4336, 2012.
- [9] A. FICHTNER, B. LN KENNETT, H. IGEL, and H. BUNGE. Full waveform tomography for radially anisotropic structure: new insights into present and past states of the austral asian upper mantle. *Earth and Planetary Science Letters*, 290(3):270–280, 2010.
- [10] R-E PLESSIX and C. PERKINS. Thematic set: Full waveform inversion of a deep water ocean bottom seismometer dataset. *First Break*, 28(4):71–78, 2010.
- [11] L. SIRGUE, O.I. BARKVED, J. DELLINGER, J. ETGEN, U. ALBERTIN, and J.H. KOMMEDAL. Thematic set: Full waveform inversion: The next leap forward in imaging at valhall. *First Break*, 28(4):65–70, 2010.
- [12] C. TAPE, Q. LIU, A. MAGGI, and J. TROMP. Seismic tomography of the southern California crust based on spectral-element and adjoint methods. *Geophysical Journal International*, 180(1):433–462, 2010.
- [13] D. PETER, D. KOMATITSCH, Y. LUO, R. MARTIN, N. LE GOFF, E. CASAROTTI, P. LE LOHER, F. MAGNONI, Q. LIU, C. BLITZ, et al. Forward and adjoint simulations of seismic wave propagation on fully unstructured hexahedral meshes. *Geophysical Journal International*, 186(2):721–739, 2011.
- [14] H. ZHU, E. BOZDÄG, D. PETER, and J. TROMP. Structure of the European upper mantle revealed by adjoint tomography. *Nature Geoscience*, 5(7):493–498, 2012.
- [15] D. VIGH, K. JIAO, D. WATTS, and D. SUN. Elastic full-waveform inversion application using multicomponent measurements of seismic data collection. *Geophysics*, 79(2):R63–R77, 2014.

- [16] S. OPERTO, A. MINIUSI, R. BROSSIER, L. COMBE, L. MÉTIVIER, V. MONTEILLER, A. RIBODETTI, and J. VIRIEUX. Efficient 3D frequency-domain mono parameter full-waveform inversion of ocean-bottom cable data: application to valhall in the visco-acoustic vertical transverse isotropic approximation. *Geophysical Journal International*, 202(2):1362–1391, 2015.
 - [17] P. LAILLY. The seismic inverse problem as a sequence of before stack migrations. 1983.
 - [18] A. TARANTOLA et al. The seismic reflection inverse problem. *Inverse problems of acoustic and elastic waves*, pages 104–181, 1984.
 - [19] J. BERENGER. A perfectly matched layer for the absorption of electromagnetic waves. *Journal of computational physics*, 114(2):185–200, 1994.
 - [20] J. VIRIEUX. P-SV wave propagation in heterogeneous media: Velocity-stress finite-difference method. *Geophysics*, 51(4):889–901, 1986.
 - [21] A. R. LEVANDER. Fourth-order finite-difference P-SV seismograms. *Geophysics*, 53(11):1425–1436, 1988.
 - [22] P. MOCZO, J.F. KRISTEK, and L.V. HALADA. *The finite-difference method for seismologists*. Comenius University, 2004.
 - [23] T. BOHLEN and E. H. SAENGER. Accuracy of heterogeneous staggered grid finite-difference modeling of Rayleigh waves. *Geophysics*, 71(4):T109–T115, 2006.
 - [24] R. COURANT, K. FRIEDRICHS, and H. LEWY. On the partial difference equations of mathematical physics. *IBM journal*, 11(2):215–234, 1967.
 - [25] B. KALTENBACHER, A. NEUBAUER, and O. SCHERZER. Iterative regularization methods for nonlinear ill-posed problems, *volume 6*. Walter de Gruyter, 2008.
 - [26] J. NOCEDAL and S. WRIGHT. Numerical optimization. Springer Science & Business Media, 2006.
 - [27] G. PRATT, C. SHIN, et al. Gauss–newton and full newton methods in frequency–space seismic waveform inversion. *Geophysical Journal International*, 133(2):341–362, 1998.
 - [28] L. MÉTIVIER, R. BROSSIER, J. VIRIEUX, and S. OPERTO. Full waveform inversion and the truncated newton method. *SIAM Journal on Scientific Computing*, 35(2):B401–B437, 2013.
 - [29] D. KÖHN, D. DE NIL, S.A. ALHAGREY, W. RABEL, K. KHALEDI, D. KÖNIG, and T. SCHANZ. Monitoring elastic parameter changes in the vicinity of salt caverns due to cyclic loading by seismic waveform inversion. 2016.
- R. G. PRATT and R.M. SHIPP. Seismic waveform inversion in the frequency domain, part 2: Fault delineation in sediments using crosshole data. *Geophysics*, 64(3):902–914, 1999

COMMISSION INTERNATIONALE DES GRANDS BARRAGES

VINGT-SIXIÈME CONGRÈS DES GRANDS BARRAGES
Autriche, juillet 2018

DOI 10.3217/978-3-85125-620-8-106



This work licensed under a Creative Commons Attribution 4.0 International License. <https://creativecommons.org/licenses/by-nc-nd/4.0/>

SELF-PROTECTED UNDERWATER CONCRETE IN REHABILITATION OF HYDRAULIC STRUCTURES

Feng JIN

Professor in DEPARTMENT OF HYDRAULIC ENGINEERING
TSINGHUA UNIVERSITY, BEIJING

CHINA

Hu ZHOU

Engineer in DEPARTMENT OF HYDRAULIC ENGINEERING
TSINGHUA UNIVERSITY, BEIJING

CHINA

Fengliang LI

Vice President in SINOCONFIX COMPANY, BEIJING

CHINA

Peng WAN

Engineer in SINOCONFIX COMPANY, BEIJING

CHINA

COMMISSION INTERNATIONALE
DES GRANDS BARRAGES

VINGT-SIXIÈME CONGRÈS DES
GRANDS BARRAGES
Autriche, juillet 2018

SELF-PROTECTED UNDERWATER CONCRETE IN REHABILITATION OF HYDRAULIC STRUCTURES

Feng JIN

*Professor in Department of Hydraulic Engineering, Tsinghua
University, Beijing, CHINA*

Hu ZHOU

*Engineer in Department of Hydraulic Engineering, Tsinghua
University, Beijing, CHINA*

Fengliang LI

Vice President in Sinoconfix Company, Beijing, CHINA

Peng WAN

Engineer in Sinoconfix Company, Beijing, CHINA

1. INTRODUCTION

In rehabilitation of hydraulic structures, there are many chances to meet the need of concrete pouring into the water body. The study of underwater concrete technology has been conducted since the early age of concrete development. Some underwater concrete technologies have been developed, i.e. bucket, grouted-intruded aggregate, grouting and tremie^[1]. These construction methods were the efforts the engineers ever made to reduce the serious segregation and loss of cement caused by the scouring of concrete during construction and hardening process, so as to avoid the deterioration of concrete quality and affect the water environment. In the late 1970s, a new type underwater concrete, named

Non-Dispersible Underwater Concrete was first realized by the development of cellulose ethers in Germany. Non-Dispersible Underwater Concrete technology has been employed in other countries in Europe, Japan and USA soon. This technology was adopted in the projects of Access bridge of Kansai International Airport, Akashi strait bridge, Rehabilitation of Copenhagen Port, Breakwater along west coast in Scotland and so on. In 1993, the publish of a Chinese translation of “Design and construction guideline to Non-Dispersible Underwater Concrete” by Research Center of Coastal Developing Technology in Japan, has a positive role in promoting underwater concrete technology in China ^[2]. Now, polymer flocculants with long polymer chain structures are widely used in Non-Dispersible Underwater Concrete. The cement particles absorbed by active functional groups on long carbon chains can be bridged to form stable floc structures. At the same time, the hydrogen bonds between the hydroxyl on the functional group in flocculant and water molecules will form to increase the affinity of water molecules. The long molecular chains of flocculants attract each other and the mesh structures form by these chains. Particles of cement are covered by the meshes and difficult to be dispersed by the washing of external water molecules. However, flocculant will affect the workability of concrete mixture, and also cannot totally avoid the washing effect of water on concrete mixture. The price of non-dispersible underwater concrete is relatively high. In early 2010s , an innovative technology for underwater concrete has been developed and authorized patent in China. It was named Self-Protected Underwater Concrete (SPUC) ^[3] later.

2. WORKING PRINCIPLE AND IMPLEMENTATION OF SPUC

2.1. WORKING PRINCIPLE

The working principle of SPUC is different from that of Non-Dispersible Underwater Concrete. A soluble polymer, called Underwater Protective Agents (UPA) will be poured into the water body prior to the pouring of underwater concrete. Then the water body will be transformed into a solution of UPA, usually the concentration of UPA will be about 100 ppm. The structures of UPA molecules chains will prevent the dispensation of cement particles into the water body, so as to avoid segregation. The employment of self-compacting concrete makes the vibration-free cast of concrete.

2.2. DEMO COMPARISON BETWEEN DIFFERENT TECHNOLOGY

To demonstrate the difference among ordinary concrete, non-dispersible underwater concrete and SPUC , a demo test was conducted, as shown in Fig. 1. In the demo test, three type of fresh self-compacting mortar were poured via a

funnel into the water in the beakers directly. The water-cement ratio and mix are almost identity, while only the flocculant added in non-dispersible mortar. The mortar in case (a) and case (c) are same, but UPA added prior to the pouring of mortar in case (c).

The demo shows that the water in case (c) remain very lucid. Much less cement in the water in case (b) than case (a). It is clear that the performance of SPU mortar is better than that of non-dispersible mortar, and the performance of the later is better than that of ordinary mortar.

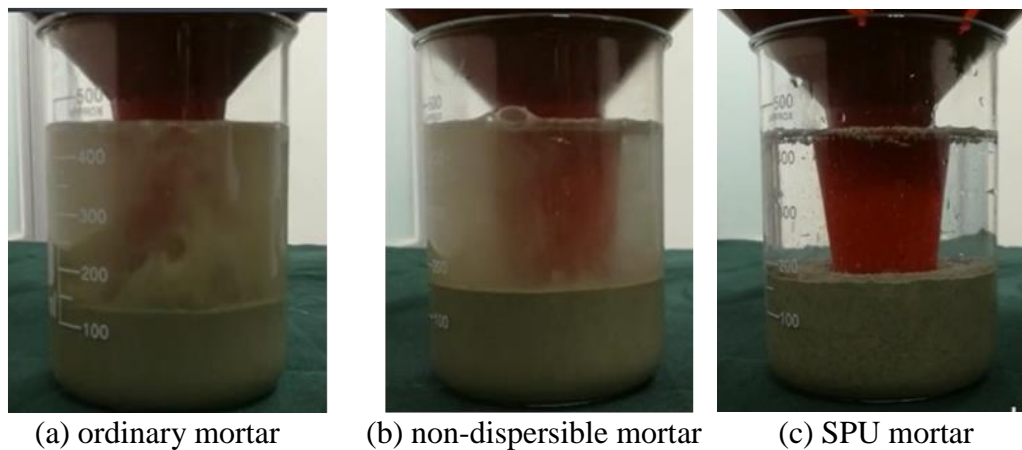


Fig. 1
Demo of three technologies

2.3. IMPLEMENTATION PROCEDURE OF SPUC

The usage of UPA will simplify the construction of underwater concrete. When SPUC employed, the UPA will be poured into the water body where the concrete is poured later. Then SPUC can be vibration-free casted. The construction procedure is shown in Fig. 2.

UPA should be diluted to about 1% before casted into the water to form a 100 ppm UPA solution. After a certain amount of UPA is casted, concrete will be poured at the vicinity of casting point of UPA. At the same time, UPA casting-speed will be control with the speed of concrete pouring. The process will not stop until all workspace filled with SPUC.

3. IN-SITU TEST OF SPUC

3.1 TANJIANG BRIDGE IN-SITU TEST OF SPUC

To validate the SPUC technology, an in-situ test was conducted in Tanjiang bridge, Guangdong Province, China. A pit was dug and paved with plastic sheet with color bands, as shown in Fig. 3. Then water filled and UPA was poured into the water. Concrete had been poured until the pit filled with SPUC.

After concrete harden, the difference of elevation between the cast point and 5 m away is only 60 mm. The average compress strength of drill cores is 36.8 MPa, where design compress strength is only 25 MPa. The bottom concrete of the piers in this huge bridge was decided to pour by using SPUC technology.

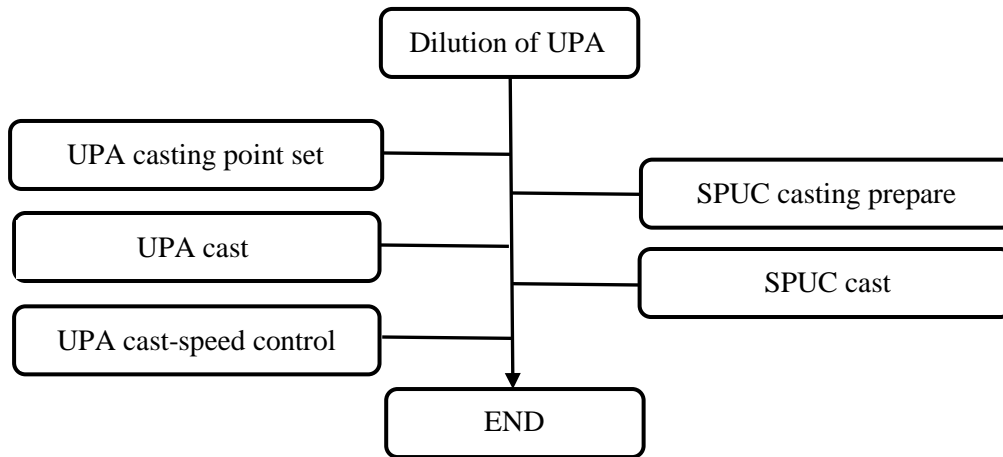


Fig. 2
Flowchart of SPUC casting



(a) commencement of pouring



(b) process of pouring



(c) pouring finished



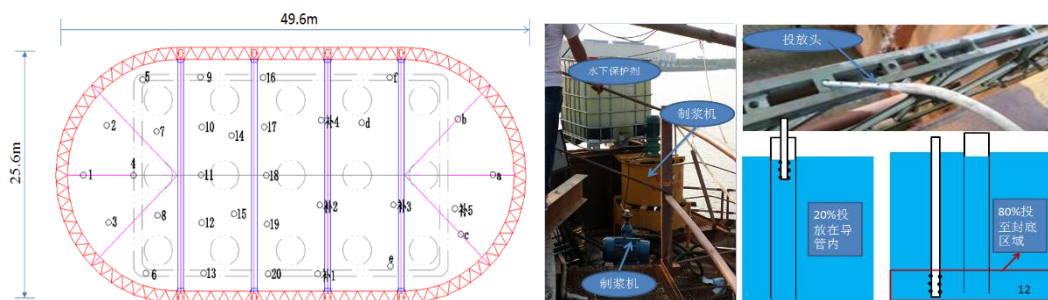
(d) drill cores after harden

Fig. 3
In-situ test of SPUC in Tanjiang bridge

4. ENGINEERING PROJECTS EMPLOYING SPUC

4.1 CONSTRUCTION OF SPUC IN BOTTOM OF PILES IN TANJIANG BRIDGE

The depth of the water is about 10 -15 m. The thickness of bottom concrete is 3.5 m. Area of concrete pouring is about 1000 m², as shown in Fig. 4(a). The small circle with numbers denotes position of 31 designed tremies with a diameter of 300 mm. But only 24 tremies were used since the fluidity of SPUC is better than expected. 80% of consumed UPA was casted into the bottom water in workspace via tremies before concrete pouring started. Then 20% remained UPA was casted into a tremie and an insulate ball with a plug device are installed at the opening of the tremie. Concrete poured into water via the tremie after the insulate ball plugged. The end of the tremie was kept embedded into the concrete about 500 mm depth. The distance between tremies is about 8 m. The slope of concrete surface was about 1:20 – 1:30 during whole pouring process surveyed by measure ropes.



(a) Layout of SPUC construction

(b) Dilution and casting of UPA

Fig. 4

Layout and casting of UPA in SPUC construction in Tanjiang bridge

The whole process of SPUC construction lasted about 36 h smoothly. The total amount of SPUC poured is 2223 m³. The average compress strength of drill cores is about 40 MPa, higher than design value of 25 MPa. The construction of SPUC in Tanjiang bridge was very successful.

4.2 SPUC IN REHABILITATION OF WANYAO DAM

Wanyao reservoir is a Large (Grade II) reservoir with irrigation, water supply, hydropower and flood control functions, which located in Jiangshan city, Zhejiang Province, China [4]. The main dam of Wanyao reservoir is a Roller-Compacted Concrete gravity dam with a height of 79 m. The length of dam crest is 390 m. The whole dam is divided into 11 blocks, where Block 5 is spillway block and others are non-overflow blocks. During the poor construction quality, the dam has to be rehabilitated due to severe seepage problem. An impervious concrete face shall

be installed at the upstream face of the dam. In design phase, the reservoir level is designed to be controlled at the Elevation 158.24. The contractor suggested that the reservoir level shall be lower more 10 m. Then, the layout of rehabilitation is shown in Fig. 5. The shadow part will be poured by SPUC.

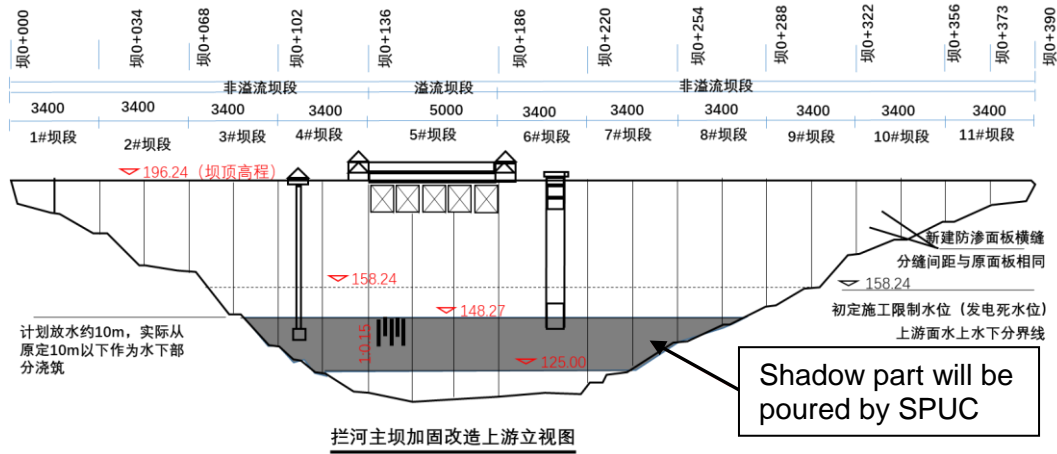


Fig. 5
Layout of rehabilitation by SPUC of Wanyao dam

Two mix of SPUC are suggested, listed in Table 1.

Table 1
Mix suggested

No.	1	2
Requirement	C25W8F100	C25W8F100
Cement, kg/m ³	407	407
Fly Ash, kg/m ³	128	128
Water, kg/m ³	172	172
Sand, kg/m ³	812	812
Coarse Aggregate, kg/m ³	827	827
Superplasticizer, kg/m ³	6.5	9.0
Slump, mm	450	750
Slump Flow, mm	260	280
V-Funnel, s	3.5	1.38
Air Content, %	4.4	4.4

SPUC will be mixed at the mixer plant at the dam crest and casted via a funnel fixed at the crest and a tremie into the workspace underwater. UPA will be diluted and casted into the water prior to the pouring of concrete same as other projects. The photo of the dam and the cast plan is shown in Fig. 6. The width of each block is 34 m and divided into 2 sub-block. 5 casting point will be set for each sub-block since the distance between two casting points is designed as 5 m.

Construction of SPUC will start in the spring of 2018.

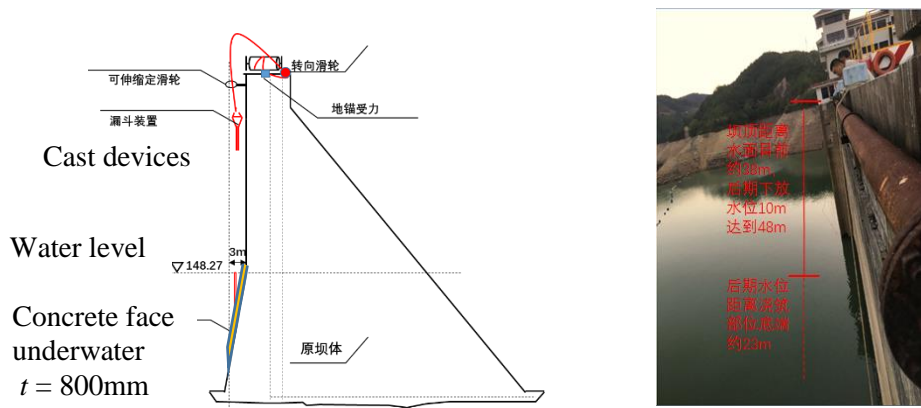


Fig. 6
Casting plan of SPUC and photo of Wanyao dam

SUMMARY

An innovative underwater concrete, named Self-Protected Underwater Concrete technology, is introduced in this paper. SPUC can be used in the case of Non-dispersive underwater concrete employed. SPUC based on the utilization of UPA. Successes of some SPUC engineering projects demonstrates that this technology has a great potential in the underwater concrete field.

ACKNOWLEDGEMENTS

The authors acknowledge the support of the National Science Foundation of China (No. 51239006) and the research funding from the State Key Laboratory of Hydrosience and Engineering, Tsinghua University (No. 2014-KY-01) and China Huaneng Group Co. Ltd. (Contract No. PM2017/D02).

REFERENCES

- [1] C. Gerwick Jr, Ben. UNDERWATER CONCRETE CONSTRUCTION. 94. 29-34, 1972
- [2] Research center on coastal developing technology in Japan, Design and construction guideline for non-dispersible underwater concrete technology (Chinese translation), China Water & Power Press, ISBN 9787120017286, 1993

- [3] Hu ZHOU, Feng JIN, Xuehui AN and Yinpeng LIANG , A construction technology of underwater cement-based self-compacting material, Chinses Patent: CN201310465710.7
- [4] Shanghai Jiaolong Ocean Engineering Co. Ltd., Technical report for underwater concrete construction for Wanyao Reservoir, 2017 (in Chinese)

Keywords: Underwater concrete, Self-Protected, Underwater Protective Agent, Wanyao reservoir

COMMISSION INTERNATIONALE DES GRANDS BARRAGES

VINGT-SIXIÈME CONGRÈS DES GRANDS BARRAGES
Autriche, juillet 2018

DOI 10.3217/978-3-85125-620-8-107



This work licensed under a Creative Commons Attribution 4.0 International License. <https://creativecommons.org/licenses/by-nc-nd/4.0/>

VIBRATIONS IN LARGE DAMS. MONITORING AND MODELLING

Sérgio OLIVEIRA

*Research officer at Concrete Dams Department, NATIONAL LABORATORY
FOR CIVIL ENGINEERING (LNEC), LISBON*

PORTUGAL

André ALEGRE

*PhD research fellow at Concrete Dams Department, NATIONAL LABORATORY
FOR CIVIL ENGINEERING (LNEC), LISBON*

PORTUGAL

COMMISSION INTERNATIONALE
DES GRANDS BARRAGES

VINGT-SIXIÈME CONGRÈS DES
GRANDS BARRAGES
Autriche, juillet 2018

VIBRATIONS IN LARGE DAMS. MONITORING AND MODELLING*

Sérgio OLIVEIRA

*Research officer at Concrete Dams Department, NATIONAL LABORATORY
FOR CIVIL ENGINEERING (LNEC), LISBON*

André ALEGRE

*PhD research fellow at Concrete Dams Department, NATIONAL LABORATORY
FOR CIVIL ENGINEERING (LNEC), LISBON*

PORTUGAL

1. INTRODUCTION

Large dams are civil engineering structures of great importance and present a high potential risk, given their relevant contribution to populations and the costly damage that would result from a collapse situation. Therefore, in the scope of dam safety control, knowledge regarding the dynamic behavior of dams must be continuously updated and improved, relying on the combined use of advanced vibrations monitoring systems and accurate numerical models of dam-reservoir-foundation (DRF) systems (Fig. 1) [1,2,3]. Regarding the monitoring systems, it is important to use quality equipment for measurement, transmission and storage of the recorded data, as well as the appropriate computer software to collect and process said data, and hence analyze/manage the obtained results, with the latter representing a major issue when intending to implement such a system. As for numerical modelling, this is an area that still presents important challenges due to the complexity of DRF systems, namely considering the effects of the water level variations, the dynamic reservoir-dam interaction and the reservoir hydrodynamic behavior, the support conditions, among others.

* *Vibrations dans les grands barrages. Auscultation et modélisation*

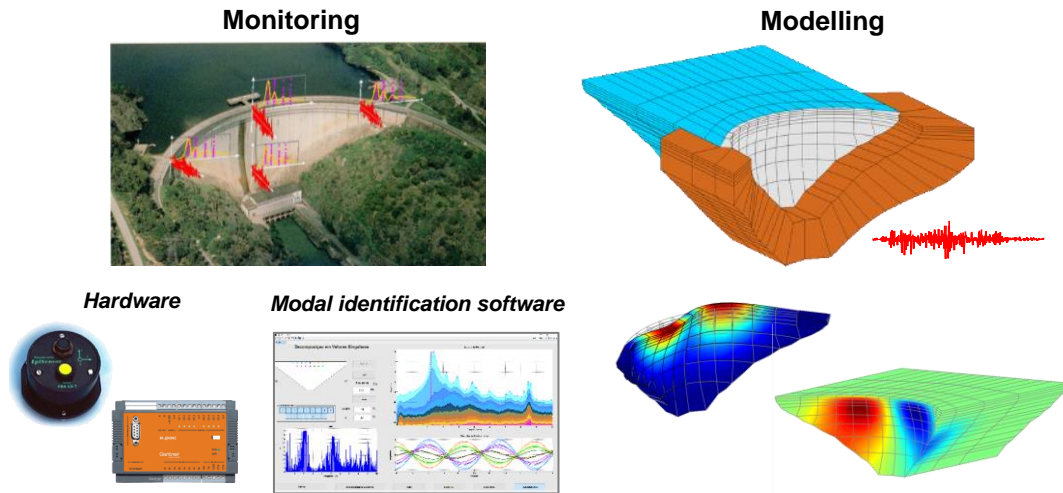


Fig. 1
Monitoring and modelling the dynamic behavior of large arch dams.

2. MONITORING THE DYNAMIC BEHAVIOR OF LARGE DAMS

For large concrete dams, the installation of systems for continuous vibrations monitoring aims to measure and analyze acceleration records in several points in the dam and in the foundation, for different ambient/operational excitation and earthquakes of different magnitudes, based on the latest data acquisition technologies. The data measurements should be performed in as many points as possible, in order to obtain reliable modal identification results. Nonetheless, the efficiency and accuracy of these monitoring systems also depend heavily on the use of sophisticated software for analysis and management of the collected data.

Therefore, it is of the utmost importance to develop and include computational tools, adapted to each dam, for automatic and/or interactive analysis [1,2], aiming to: a) identify the dam's main modal parameters (natural frequencies, mode shapes and modal damping), based on frequency domain and/or time domain modal identification methods [4], and study their evolution over time, considering the water level and seasonal thermal variations, or to detect possible structural changes due to deterioration processes [5]; b) measure the dam dynamic response for different reservoir levels, enabling to evaluate the amplification of the accelerations recorded in the foundation and in the dam [6], as well as to study the influence of the dam-reservoir interaction. Furthermore, the developed software should enable the comparison between the monitored dam dynamic response and its dynamic behavior as predicted with the numerical programs: this is of great value to validate and calibrate the numerical models, which are used to simulate the dynamic behavior of DRF systems and to carry out seismic safety verifications.

3. CABRIL DAM. MONITORING SYSTEM: HARDWARE AND SOFTWARE

Cabril dam was built in 1950's and is the highest Portuguese arch dam (Fig. 2). Located in the Zêzere River, this is a 132 m high double curvature arch dam with crest altitude of 297 m. The arch is 290 m long at the top, and the central cantilever has a maximum width of 19 m at the base and a minimum width of 4.5 m below the crest. In this dam, a significant horizontal cracking phenomena occurred near the crest (at a height of 280-290 m) during the first filling of the reservoir. Also, a concrete swelling process has been detected in recent years.

In the framework of LNEC research activities regarding monitoring and modelling the dynamic behavior of dams, a pioneer project was initiated in 2002 [1] to install a dynamic monitoring system in Cabril dam, which is in operation since 2008 (Fig.2). The outlined configuration for this system was based on experience gathered in LNEC over the years, from both monitoring data and numerical results [2,3,5,6,7]. The goal was to implement a system with a high dynamic range, capable of a continuous accurate measurement of the dam's response for several dynamic excitations: ambient/operation excitations or earthquakes of various magnitudes. This system was designed to measure accelerations in the upper zone of the dam and near the base, at a sampling rate of 1000 Hz and considering time periods of one hour, and it includes 16 uniaxial and 3 triaxial accelerometers.

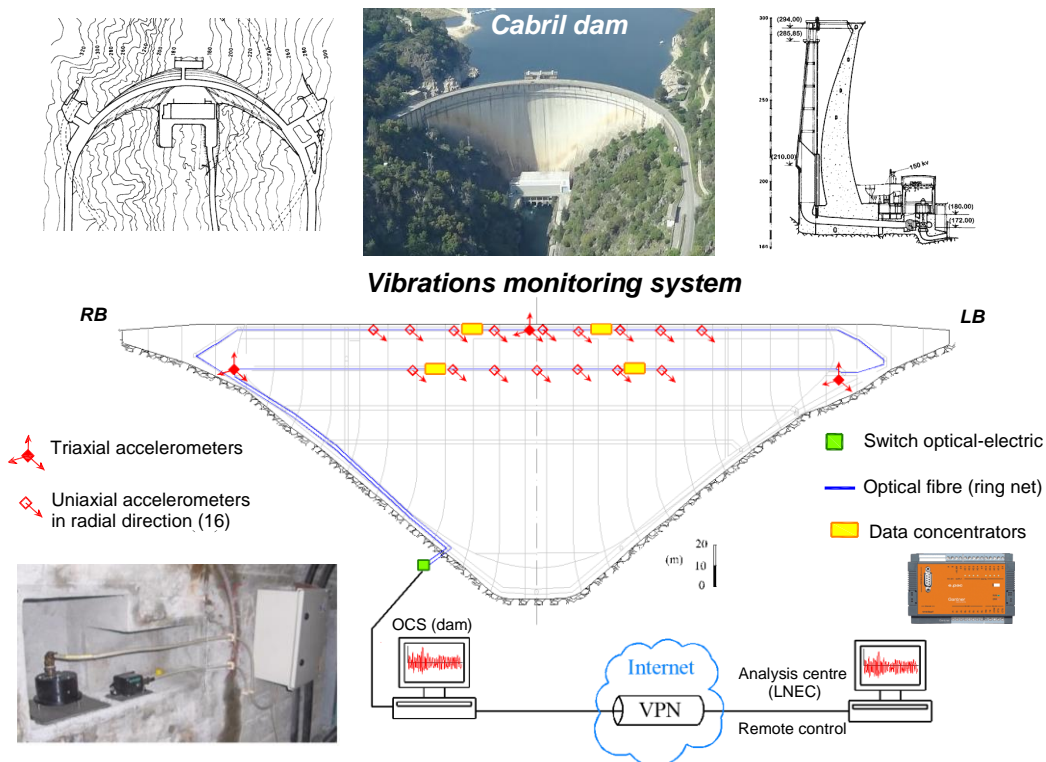


Fig. 3

Cabril dam. Plan and central cantilever (with intake tower) and vibrations monitoring system - schematic representation and main hardware components.

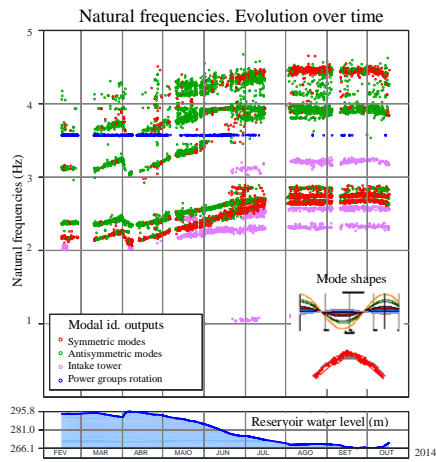
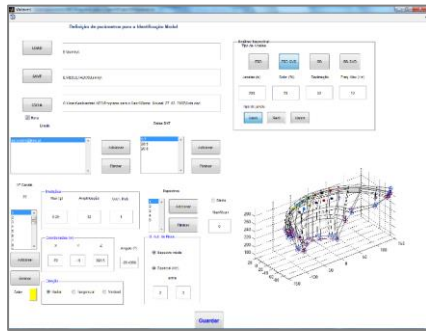
The uniaxial accelerometers (prepared to measure vibrations in a radial direction) are distributed in the upper part of the dam by two galleries, above and below the cracked zone. As for the triaxial accelerometers, one is located in the central cantilever (upper gallery), while the other two are installed near the insertion of the dam base, in both banks. The accelerometers are connected to a modular system composed by acquisition/digitalization units, which in turn are controlled by 4 data concentrators that receive the recorded data. This data is sent through an optical fiber local network (intranet) to a computer in the observation and control station (OCS), located at the dam power station. In total 25 accelerograms are recorded and stored every hour, continuously. The storage and management of the collected data is carried out at the server located in the OCS using appropriate software developed in LNEC. Regarding the remote control of the system, it is important to refer that the server can be accessed via internet from LNEC by computer or even by smartphone, using suitable software, which is of great relevance given that it allows to control and analyze such important data from a distance.

As previously mentioned, the hardware for measuring accelerations and the corresponding data acquisition software must be complemented with suitable software for automatic analysis and management of the collected data, to ensure the efficiency of the dynamic monitoring system and hence accurate results. For the case of Cabril dam, two programs were developed using MATLAB: *Modal_ID_auto2.0* and *Modal_ID2.0* (Fig. 4). Modal identification is performed using a frequency domain method [4], Frequency Domain Decomposition (FDD), including three variants, namely: a) by implementing a Random Decrement technique (FDD(RD)); b) using a Singular Value Decomposition (FDD-SVD); and d) considering the combined use of the previous techniques (FDD(RD)-SV).

As the name indicates, *Modal_ID_auto2.0* is a software that carries out automatic continuous data analysis based on specific outputs defined in advance (e.g. the modal identification technique or the measuring points to analyze). Besides the analysis and management of the data, it automatically generates and sends (via e-mail) files with a synthesis of the obtained results, to be analyzed by the engineers and technicians. Given its continuous analysis of the acceleration records, the results allow to study the evolution of the modal parameters over the year, taking into account water level and thermal variations.

On the other hand, *Modal_ID2.0* is an interactive program that performs the modal identification of the main modal parameters for a certain data file, which is associated to the hour-day-year input chosen by the user. Its interactive feature enables to carefully observe the records and modal identification outputs for a certain water level, and it facilitates the comparison with numerical results. In terms of the results obtained from the collected data, both programs present as outputs: a) the acceleration records for each installed accelerometer and the corresponding amplitude spectrum; b) the medium spectrum, as obtained by applying modal identification techniques; and c) the natural frequencies, which correspond to the main spectral peaks, and the respective vibration modes, including 3D mode shapes and harmonic waves representing the oscillatory movements in each measuring point, all associated to the measured water level.

**Modal_ID_auto2.0:
automatic data analysis**



**Modal_ID2.0:
interactive data analysis**

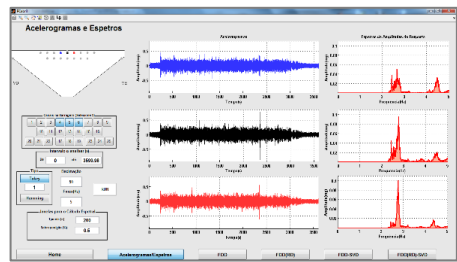
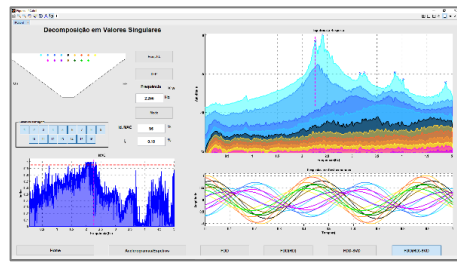
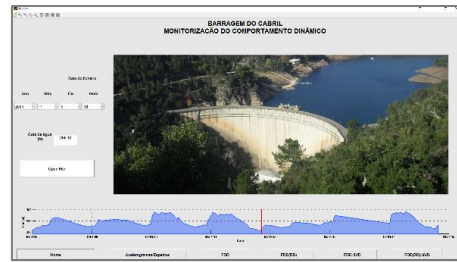


Fig. 4

Modal identification software: *Modal_ID_auto2.0* and *Modal_ID2.0*.

4. NUMERICAL MODELLING OF ARCH DRF SYSTEMS

Considering the utmost importance of the combined use of monitoring systems and numerical models for dam safety control, it is presented the software *DamDySSA2.0*, which has been developed in recent years in LNEC to study the dynamic behavior of dams (Fig. 5). This is a 3D FE program for dynamic state space analysis of arch dam-reservoir-foundation systems, based on a 3DFE coupled model that enables to simulate the dynamic dam-reservoir interaction, considering linear elastic behavior and generalized damping. The outlined Boundary Values Problem for the discrete coupled system is solved through a FE formulation in displacements (solid) and pressures (fluid), considering the solid-fluid motion coupling at the dam-reservoir interface and the hydrodynamic pressure waves propagation throughout the reservoir, which is a semi-infinite domain terminated by a radiation boundary [8]. The dynamic calculations are performed in time domain based on a novel coupled state space approach with two state

matrices using complex modal coordinates [9,10,11]. The implemented coupled approach results in the computation of non-stationary vibration modes, which are usually associated to systems with non-proportional damping, as is the case of arch dams, whose dynamic behavior is highly influenced by dynamic water-structure interaction.

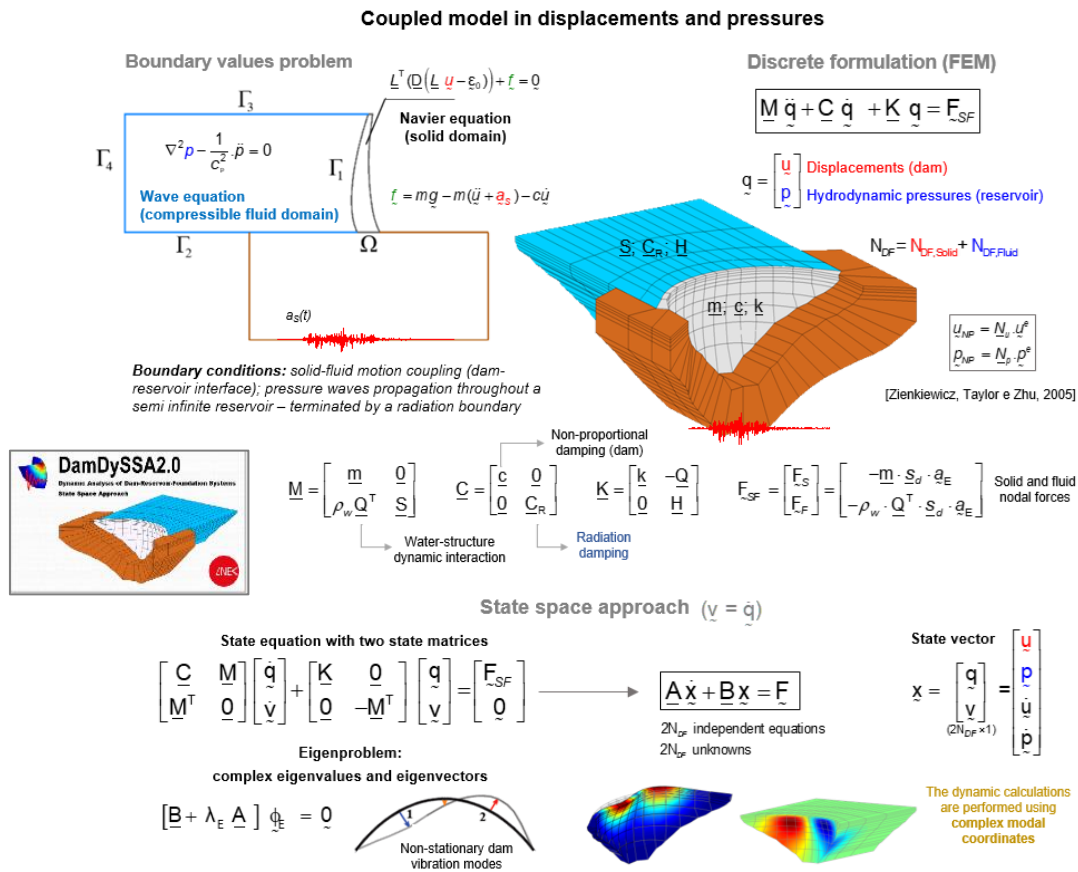


Fig. 5
DamDySSA2.0. Coupled model and state space approach.

5. MODAL IDENTIFICATION RESULTS. COMPARISON WITH NUMERICAL RESULTS

In this chapter the modal identification outputs are compared with numerical results computed using *DamDySSA2.0*, to demonstrate the potential of the combined use of monitoring and modelling to support dam safety control, as well as to validate and calibrate the numerical models and implemented formulations. For the case of Cabril dam, it is necessary to analyze the identified frequencies with great care, in order to distinguish between the dam vibration modes and vibrations related to the intake tower motion or the power groups.

To simulate the dynamic behavior of Cabril dam the coupled model was used, considering a dynamic elasticity modulus (E_{dyn}) of 32.5 GPa and a Poisson coefficient (ν) of 0.2 for the dam. Various water levels are assumed, and a fluid velocity of 1440 m/s is used. Regarding *Modal_ID2.0*, the main modal parameters were obtained based on acceleration records measured on April 1st of 2014, between 10 and 11 a.m., in which the reservoir water level (H_w) was of 291.45 m. As for *Modal_ID_auto2.0*, automatic modal identification was carried out for measured accelerations between February and October of 2014, corresponding to a water level variation between 266 and 296 m. In this work, the modal identification outputs were obtained using the FDD(RD)-SV technique.

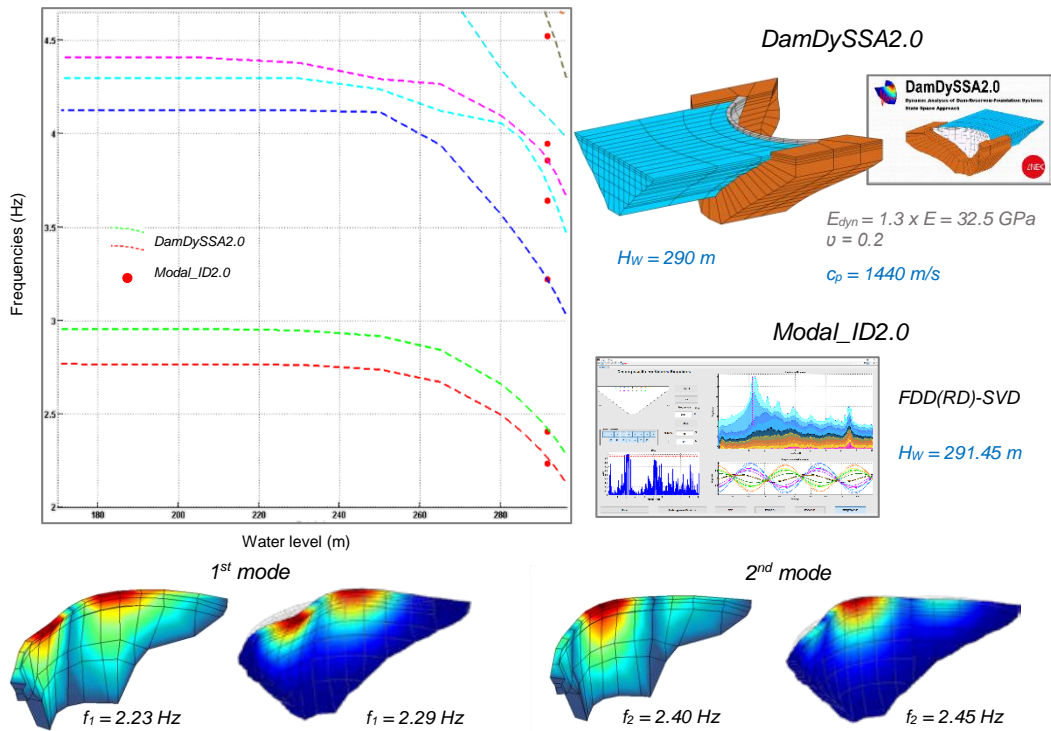
First a comparison between *Modal_ID2.0* and *DamDySSA2.0* is performed (Fig.6a). A graphic representing the evolution of the computed natural frequencies in function of the reservoir water level is shown (colored lines), which also contains the modal identification frequencies for $H_w = 291.45$ m. Second, the outputs obtained from automatic modal identification are presented and compared with *DamDySSa* results (Fig.6b)). A different graphic is presented, containing the natural frequencies obtained from automatic modal identification over time (green and red circles), which are compared with lines representative of numerical natural frequencies, for the referred water level variation (266-296 m). In both cases, identified and computed mode shapes are compared.

By analyzing the presented study, one can note that an excellent agreement was achieved between the results obtained from interactive and automatic modal identification software and the numerical results calculated with a 3D FE program, concerning both natural frequencies and vibration mode shapes. Also, the implemented numerical model enables to compute non-stationary vibration modes, as can be measured in situ. Finally, it is relevant to state that such a close agreement between numerical and experimental results was not possible in previous studies, performed using classic added water mass models [3,4].

6. CONCLUSIONS

A comparative study regarding the dynamic behavior of Cabril dam was presented, namely in terms of the dam's natural frequencies and vibration mode shapes, for different reservoir water levels. The excellent agreement achieved between modal identification outputs and numerical modelling results demonstrates the value of Cabril dam's monitoring system and associated software (*Modal_ID_auto2.0* and *Modal_ID2.0*), and simultaneously proves the reliability of the state space formulation implemented in the 3D FE program *DamDySSa2.0*. Therefore, as intended, this work has proven the importance of vibrations monitoring systems in the scope of dam safety control, which must comprise quality hardware (e.g. accelerometers, data concentrators, etc.) and appropriate software for data analysis and management, as well as the potential of their combined use with numerical models of dam-reservoir-foundation systems.

a) Experimental and numerical results: Modal_ID2.0 & DamDySSA2.0



b) Experimental and numerical results: Modal_ID_Auto2.0 & DamDySSA2.0

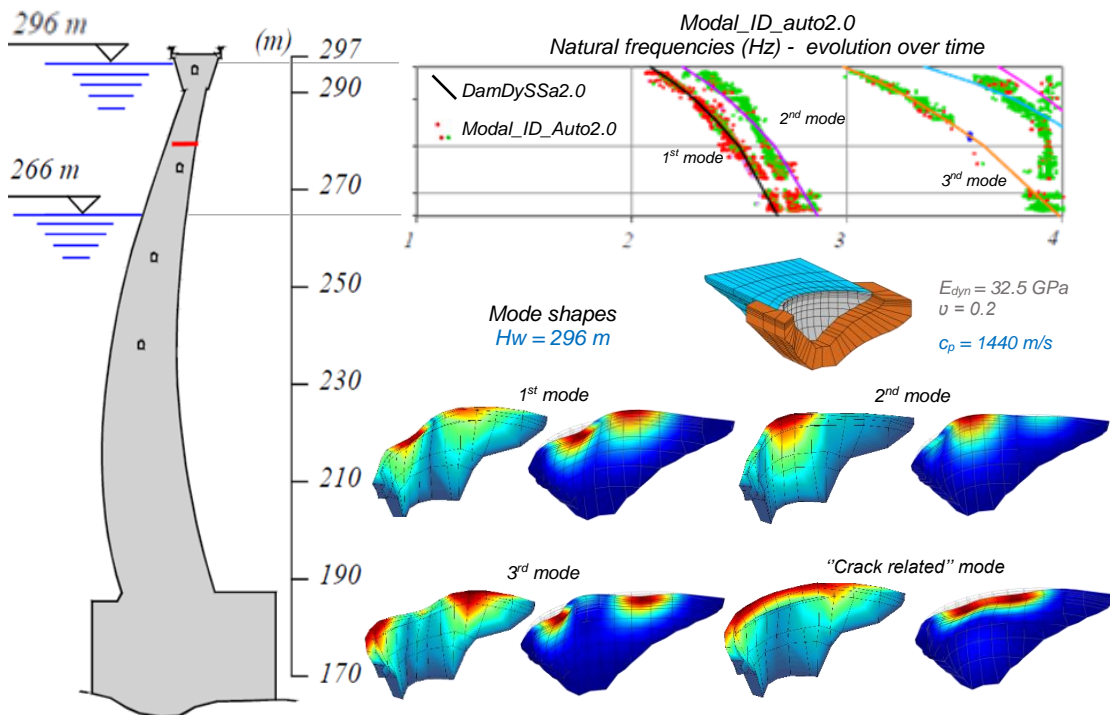


Fig. 6

Comparison between modal identification and numerical results: a) *Modal_ID2.0* (10-11 a.m. April 1st, 2014) vs *DamDySSa2.0* and b) *Modal_ID_Auto2.0* (February to October, 2014) vs *DamDySSa2.0*.

ACKNOWLEDGEMENTS

The authors wish to acknowledge the funding association – FCT, Portugal - for supporting the installation of the monitoring system in Cabril dam (REEQ/815/ECM/2005) and for the PhD grant SFRH/BD/116417/2016.

REFERENCES

- [1] OLIVEIRA S. Continuous monitoring system for the dynamic performance assessment of arch dams. Sub-program D, in Study of evolutive deterioration processes in concrete dams. Safety control over time. *National Program for Scientific Re-equipment, funded by FCT (REEQ/815/ECM/2005)*, 2002.
- [2] OLIVEIRA S., MENDES P. Development of a Cabril dam finite element model for dynamic analysis using ambient vibration test results. *III ECCSM, LNEC, Lisbon*, 2006.
- [3] OLIVEIRA S., ESPADA M., CÂMARA, R. Long-term dynamic monitoring of arch dams. The case of Cabril dam, Portugal. *15th World Conference on Earthquake Engineering, Lisbon*, 2012.
- [4] PEETERS B. System identification and damage detection in civil engineering. *PhD Thesis, KU Leuven Univ., Belgium*, 2000.
- [5] OLIVEIRA S., FERREIRA I., BERBERAN A., MENDES P., BOAVIDA J., BAPTISTA B. Monitoring the structural integrity of large concrete dams. The case of Cabril dam, Portugal. *Hydro2010, Lisbon*, 2010.
- [6] OLIVEIRA S., SILVESTRE A., ESPADA M., CÂMARA R. Modelling the dynamic behavior of dam-reservoir-foundation systems considering generalized damping. Development of a 3DFEM state formulation. *9th Int. Conference on Structural Dynamics EURODYN 2014, Porto, Portugal*. 2014.
- [7] OLIVEIRA S., RODRIGUES J., MENDES P., CAMPOS COSTA A. Monitoring and modelling the dynamic behavior of concrete dams. *VI National Meeting of Computational Mechanics, Évora*, 2003.
- [8] ZIENKIEWICZ O. C., TAYLOR R. L., ZHU J. Z. The Finite Element Method: Its Basis and Fundamentals. *6th ed., Elsevier Butterworth-Heinemann*, 2005.
- [9] OLIVEIRA S. Monitoring of Dynamic Behavior. Part I: Continuous monitoring systems and models for seismic dam behavior simulation. Water structure dynamic interaction. *Dam World Conference, LNEC, Lisboa*, 2015.
- [10] OLIVEIRA S., ALEGRE A., SILVESTRE A., ESPADA M., CÂMARA R. Seismic safety evaluation of Luzzone dam. Use of a 3DFEM state formulation in pressures and displacements. *13th ICOLD Int. Benchmark Workshop on Numerical Analysis of Dams, EPFL, Lausanne*, 2015.
- [11] ALEGRE A., OLIVEIRA S., ESPADA M., CÂMARA, R., LEMOS, V. Hydrodynamic pressures on arch dams. numerical and experimental results. *APAET Journal ISSN 1646-7078, Experimental Mechanics, Vol. 28, pp. 55-62*, 2017.

SUMMARY

This work addresses the subject of monitoring and modelling the dynamic behavior of large arch dams. The continuous vibrations monitoring system installed in Cabril arch dam (132 m high) is described, as well as the associated cutting-edge software for automatic and interactive data analysis and management (*Modal_ID2.0*), based on the frequency domain modal identification techniques. Cabril dam's dynamic behavior is simulated using a recently developed 3DFE program (*DamDySSA2.0*), for dynamic state space analysis of arch dam-reservoir-foundation systems.

A comparative study between modal identification outputs and numerical modelling results is presented, namely in terms of the dam's natural frequencies and vibration mode shapes, for different reservoir water levels. The excellent agreement achieved demonstrates the value of Cabril dam's monitoring system and associated software, and simultaneously proves the reliability of the state space formulation implemented in *DamDySSa2.0*. Therefore, this work showed the importance and potential of the combined use of monitoring systems and numerical models in the scope of dam safety control.

Keywords: Vibrations; Monitoring; Modelling; Cabril arch dam.

RÉSUMÉ

Ce travail porte sur l'auscultation et la modélisation du comportement dynamique des grands barrages. Le système d'auscultation des vibrations installé dans le barrage du Cabril (132 m de haut) est décrit, ainsi que le logiciel de pointe développé pour l'analyse et la gestion automatique et interactive des données (*Modal_ID2.0*), basé sur des techniques d'identification modale au domaine de la fréquence. Le comportement dynamique du barrage du Cabril est simulé à l'aide d'un programme EF3D récemment développé (*DamDySSA2.0*), pour l'analyse dynamique des systèmes barrage-réservoir-fondation en utilisant des formulations d'état.

Une étude comparative entre les sorties d'identification modale et les résultats de la modélisation numérique est présentée, notamment en termes de fréquences naturelles du barrage et des modes de vibration, pour différents niveaux d'eau du réservoir. L'excellent accord obtenu démontre la valeur du système d'auscultation du barrage du Cabril et des logiciels associés, et prouve simultanément la fiabilité de la formulation dans l'espace d'état implémentée dans *DamDySSa2.0*. Par conséquent, ces travaux ont montré l'importance et le potentiel de l'utilisation combinée de systèmes d'auscultation et modèles numériques dans le cadre du contrôle de sécurité des barrages.

Mots-clés: Vibrations; Auscultation; Modélisation; Barrage-voute du Cabril.

COMMISSION INTERNATIONALE DES GRANDS BARRAGES

VINGT-SIXIÈME CONGRÈS DES GRANDS BARRAGES
Autriche, juillet 2018

DOI 10.3217/978-3-85125-620-8-108



This work licensed under a Creative Commons Attribution 4.0 International License. <https://creativecommons.org/licenses/by-nc-nd/4.0/>

COMBINED SEEPAGE AND SLOPE STABILITY ANALYSIS OF EARTH DAMS

Bakenaz. A. ZEIDAN

FACULTY OF ENGINEERING, TANTA UNIVERSITY

EGYPT

Combined Seepage and Slope Stability Analysis of Earth Dams

Bakenaz. A. Zeidan

Faculty of Engineering, Tanta University, Egypt

Email: b.zeidan@f-eng.tanta.edu.eg

ABSTRACT

Earth dams' failure may occur due to different reasons such as structural instability conditions, hydraulic conditions, seepage through the dam body and/or rapid drawdown. The determination of factor of safety for the dam slope stability, under different cases of operations, is vital to ascertain the dam overall safety. In this work, Finite Element modeling is employed for simulating seepage and stress analysis of earth dam problems via GeoStudio software. Thus, phreatic seepage surface, pore water pressure distribution and total hydraulic head variation of an earth dam are analyzed. The model is verified, then it is employed to analyze seepage and stability of Mandali Dam (Iraq). For three different cases of operation, four major analytical methods are used to verify the stability of the dam side slopes. Benchmark safety regulation criteria (USACE and BDS) are obeyed. The results confirm the safety of Mandali dam against combined seepage and slope instability under all cases of operation. The case of rapid drawdown is the most critical operating case; compared to other cases of operation.

Keywords: *Earth dams, Seepage, Stability of slopes, Finite element modeling, Mandali Dam.*

1. Introduction

Dams are built for specific functions such as water supply, irrigation, flood control and hydroelectric power generation. Most of the large dams in the world were built during the middle decades of the twentieth century. There are two types of modern dams, namely: embankment dam and concrete dam. Embankment dams can be classified into two main categories earth-fill dams and rock-fill dams. Embankment dams represent about 85% of dams all over the world. There are several factors to be considered in selecting an earth dam type such as: topography; foundation conditions; environmental impacts, construction facilities and socio-economic studies. A feasible dam should be; built from locally available materials; stable under all operating and loading conditions; watertight enough to control seepage; have appropriate outlet works to crest dam overtopping [1-3].

2. Literature Review

Seepage and slope stability failures are addressed via many authors since *Henry Darcy, 1856* [4], who gave the basic law of flow through porous media. *Darcy's* law was based on series of experiments conducted in a vertical pipe filled with sand. *Fellenius (1936)* [5], developed the Ordinary Method of Slices (OMS) known as Felonious or Swedish method. It is assumed that the forces acting on sides of any slice are neglected. *Zienkiewicz and Chung, 1967* [6], published the first finite element simulation to solve the Laplace equation for steady ground water seepage., *Taylor and Chow, 1976* [7], recorded that the Finite Element Method was used to assess the potential seepage flows and uplift pressure in the foundation rock for Bannett Dam in Canada. *Kratutich, 2004* [8], used thermal mode at ANSYS computer code to simulate numerically the case of no stationary free surface in earth dams. *Karjani, 2009* [9] used Geostudio computer software to analyze Maroon dam, estimate flow net at passing condition and slope stability factor at overall stability for different operating conditions has been calculated. *Zomorodian and Abodollahzadeh, 2010* [10], used Geostudio software to investigate the effect of horizontal drains on upstream slope of earth fill dams during rapid drawdown. *Tatewar and Laxman N. Pawade, 2012* [11], used Geostudio software to investigate the slope stability of the 21m high Bhimdi earth dam, by changing different parameters such as changing berm width and changing position of filter drains. *Hasani et al., 2013* [12], studied the seepage analysis in Ilam earth dam for four mesh size in order to assess the effect of meshing on results accuracy.

3. Seepage flow through Earth Dams

Seepage flow of water through porous media depends on the soil media, type of flow, properties of liquid and hydraulic gradient. Seepage piping account for approximately 40% of all earth dam failures. Different methods have been developed to solve seepage problems, these methods can be classified as analytical, experimental and a numerical methods. Ground water flows in the direction of decreasing potential energy caused by differences in pressure and elevation. A common measure of this potential energy is the total head, ϕ which is simply the sum of pressure head and elevation head. The volume rate of flow per unit area is directly proportional to the rate of change of head as given by the differential form of *Darcy's Law*. The following general governing equation for seepage through earth dams can be considered as [1, 3]:

$$\frac{\partial}{\partial x} \left[\mathbf{K}_x \frac{\partial H}{\partial x} \right] + \frac{\partial}{\partial y} \left[\mathbf{K}_y \frac{\partial H}{\partial y} \right] + \frac{\partial}{\partial z} \left[\mathbf{k}_z \frac{\partial H}{\partial z} \right] = \mathbf{S} \frac{\partial h}{\partial t} \quad \text{In } \Omega \quad \dots\dots\dots (1)$$

where, \mathbf{K}_x , \mathbf{K}_y and \mathbf{K}_z are the coefficient of permeability in x, y, z directions, respectively, \mathbf{S} is specific yield and $\mathbf{H} = p/\gamma_w + z =$ total fluid head, $P =$ pressure, $\gamma_w =$ unit weight of water and $z =$ elevation head. Equation (1) is known as Laplace's equation which is considered as the governing equation for groundwater there dimensions flow through aquifers. For an isotropic, homogeneous aquifer under steady state conditions, Equation (2) can be simplified to the following equation:

$$\frac{\partial^2 H}{\partial x^2} + \frac{\partial^2 H}{\partial z^2} = 0 \quad \text{In } \Omega \quad \dots\dots\dots (2)$$

It is assumed that; the soil media is homogeneous, isotropic, and physically stable; the pressure is atmospheric everywhere on the water table (phreatic surface); the flow of ground water through the flow domain is steady and the hydraulic conductivity through the dam body is constant everywhere.

3.1 Boundary Conditions

Figure (1) shows a schematic representation for the problem statement and boundary conditions for a typical earth dam. These boundary conditions can be briefly summarized as follows:

3.1.1 Entrance Surface (Γ_1)

The upstream boundary surface (Γ_1) is the entrance surface at which the percolation of reservoir water through the media starts. This surface is considered as an equipotential line which is known as *Dirchlet Condition* for a prescribed head as:

$$\mathbf{H}(x, y) = H_1 \quad \dots\dots\dots (3)$$

3.1.2 Phreatic Surface (Γ_2)

The boundary surface (Γ_2) is the phreatic surface of the flow through the dam. This boundary is considered as a stream line. The phreatic surface, although it is considered as a boundary condition, its location and its profile are unknown a priori. For the unknown phreatic surface the boundary condition is:

$$\mathbf{H}(x, y) = y \quad \dots\dots\dots (4. a)$$

$$\frac{\partial H}{\partial n} = 0 \quad \dots\dots\dots (4. b)$$

where n is the normal directions to the boundary (Γ_2).

3.1.3 Exit Surface (Seepage surface) (Γ_3)

The boundary surface (Γ_3) is the exit surface or seepage surface. This boundary is considered as an isobar at which the pressure along it is atmospheric, hence, the boundary condition along such a surface is:

$$\mathbf{H}(x, y) = y \quad \dots\dots\dots (5)$$

The geometry of the seepage surface is known, except its upper limit the exit point, which is laying on the unknown phreatic surface. The location of this point is a part of the required solution.

3.1.4 Dam Foundation Boundary (Γ_4)

The boundary surface (Γ_4) is the dam foundation boundary, which is also known as *Neumann Condition*. In the present study, this boundary is assumed to be impervious i.e. this surface prevents the flow of water across it such that:

$$\frac{\partial H}{\partial n} = 0 \quad \dots\dots\dots (6)$$

where n is the normal directions to the boundary (Γ_4).

4. Stability of Earth Dam Slopes

Every soil mass which has a slope at its end is subjected to shear stresses on internal surfaces or failure plans in the soil mass near the slope. This is due to the gravitational forces that try to pull down parts of the soil mass adjoining the slope. Several models and analytical techniques have been developed to determine the critical slip surface and the associated factor of safety such as method of slices. The factor of safety is:

$$\text{F.S.} = \frac{\tau_f}{\tau} \quad \dots\dots\dots (7)$$

where, F.S. factor of safety, τ_f failure shear strength of the soil, and τ shear stress of the soil. The stability of earth fill dam depends on its geometry, components, materials, properties of each component and the forces to which it is subjected. There are some analytical tools for assessing the stability of a slope by using simple failure models. These techniques are limited to slopes of homogenous material, soils, fractured rocks which are behaving like soils and for plain strain (2-D) problems only. Some of these tools are listed by [13]. For steady state seepage condition the factor of safety using Fellenius method is [5, 14]:

$$F.S. = \frac{\sum_{i=1}^{i=n} (cL_i + (W_i \cos \alpha_i - u_i L_i) \tan \phi)}{\sum_{i=1}^{i=n} W_i \sin \alpha_i} \dots\dots\dots (8)$$

For steady state seepage condition the factor of safety using Bishop Method is:

$$FS = \frac{\sum_{i=1}^{i=n} (cb_i + (W_i - u_i b_i) \tan \phi) \frac{1}{m_{ai}}}{\sum_{i=1}^{i=n} W_i \sin \alpha_i} \dots\dots\dots (9)$$

where, $m_{ai} = \cos \alpha_i + \frac{\tan \phi \sin \alpha_i}{FS}$

c = effective soil cohesion, L = length of the bottom of the slice, b = width of the slice and equal to $(L \cos \alpha)$, u = pore water pressure, W = weight of the slice, α = inclination of the bottom of the slice and ϕ = effective internal friction angle.

5. Finite Element Formulation

The basic concept of the finite element method is to divide the problem region into subdomains (finite elements) connected at their common nodal points and that the unknown function of the field variable is defined approximately within each element. The approximate solution of each element expressed by continuous function is as follows [3]:

$$\mathbf{H} = \sum_{e=1}^{noe} [N_i^e] \{H_i^e\} \dots\dots\dots (11)$$

where, H_i^e = nodal value of (\mathbf{H}) for i^{th} node in element (e) , noe = total number of elements and N_i^e = shape function of element (e) .

There are more different approaches to formulate the approximate solution of the problem. In the present study, the standard weighted residual method with Galerkin's criterion [6] is used to approximate the solution of the unknown variable (\mathbf{H}) . Thus, equation (2) can be written in a matrix form as [3]:

$$[\mathbf{K}]. \{\mathbf{H}\} = \{\mathbf{F}\} \dots\dots\dots (12)$$

in which $\{\mathbf{H}\}$ is the unknown nodal potential head vector, $\{\mathbf{F}\}$ is the nodal external flux vector and $[\mathbf{K}]$ is the conductivity matrix given by:

$$K_{ij} = \int_{V^e} \left(\frac{\partial N_i}{\partial x} K_x \frac{\partial N_j}{\partial x} + \frac{\partial N_i}{\partial y} K_x \frac{\partial N_j}{\partial y} \right) dx dy \dots\dots\dots (13)$$

where, V^e = the domain of element (e) and N_i = interpolation or shape function. Derivations of the above functions are given in detail by [3].

The solution of seepage problem with phreatic surface require a successive adjustment for the location of the phreatic surface and the finite element mesh size till the desired degree of convergence for the head \mathbf{H} is achieved. In all iterative methods, the solution is started by using initial guess for the unknown values and the solution is obtained by repeating the solution of the system of equations successively through recurrence relations to update the old values until the solution converges closely enough to the true values within some prescribed tolerance of error [3].

6. Safety Criteria and Verification of Model

Design and safety evaluation of embankment dams should satisfy the recommended criterion of the experienced agencies in the design of embankment dams. Among the numerous dam safety regulation [13, 15, 16, 17], both USACE (2003) [18] and BDS (1994) [19] criterion are considered as the benchmark for their broad area of validation in the present study. Geostudio computer code [20] is employed in the present study to simulate seepage and stability analysis of atypical earth dam. The model is verified with reference [21] for a solved example with a zoned embankment dam for slope stability analysis. The verification is done for three cases of operation using Bishop's method. Figures (2- 4) and Table (1) show the factor of safety (F.S.) simulation of upstream and downstream slope for all cases of operations. For upstream slope, the absolute mean error (AME) is about 0.16

and the average absolute percentage difference (AAPD) is about 8.8%. For downstream slope, (AME) is about 0.075 and (AAPD) is about 4.1% which are all within the acceptable accuracy.

Table (1): Minimum calculation results of factor of safety

Methods of calculation	F.S upstream slope		F.S downstream slope	
	Rapid drawdown	End of construction	End of construction	Steady state
Present study GeoStudio software (Bishop's)	1.618	2.25	1.911	1.90
Referance [21] Analatical solution (Bishop's)	1.515	2.03	1.86	1.80
Absolute percent difference	6.79%	10.83%	2.47%	5.56%

7. Application of Geostudio on Mandali Dam

Mandali dam is an earth fill dam which is located on Harran Wadi, in the governorate of Diyala which is extends to the northeast of Baghdad, Iraq (Fig.5). The dam has been designed by Directorate General of Dam and Reservoirs, Iraq. The Wadi bed is gravely and permeable to some depths as it is clear from the geological investigations Mandali dam has a central core and the dam total length is about 1316 m. The maximum height of the dam is about 14m [Ministry of water Resources, Iraq] [22]. Figure (6) shows the dam cross-section, while Table (2) gives the material properties of the dam components. The dam geometrical properties can be seen in Table (3).

Table (2): Material properties of Mandali dam, Iraq [22, 23].

Layer (soil type) Physical and mechanical properties	Shell (Sandy soil)	Clay core (Very stiff clay)	Foundation (Stiff clay)	Filter (Sandy gravel soil)
Bulk density (γ) [KPa]	21	19.2	22	21
Angle of internal friction (ϕ) [degree]	40	15	30	37
Cohesion (c) [KPa]	0.0	40	5	0.0
Permeability (k) [m/sec]	1.37×10^{-5}	9.88×10^{-9}	10^{-8}	10^{-2}
Poison's ratio (ν)	0.3	0.36	0.32	0.4
The elastic Modulus (E) [KPa]	35000	19000	100000	30000

7.1 Safety Criteria of Mandali Dam

The Geometric properties of Mandali dam were checked using BDS (1994) [19]. Table (3) gives the results of the comparison. It can be noticed that the geometric design of the dam is acceptable based on the recommendations of The British Dam Society (1994) [19].

Table (3): Comparison between original section of Mandali dam and (BDS) safety limits

Parameter	Mandali Dam	(BDS) Safety limits	Safety of dam status
Crest width	8.0 m	Not less than 2.0 m	Acceptable
Upstream slope	2.7:1	2.5:1	Acceptable
Downstream slope	2.4:1	2:1	Acceptable
Free board	1.50 m	Min. free board = 1.50 m at Max. Fitch = 4 km.	Acceptable (Maximum head over spillway = 2.5 m)
Bed width of core	58 m	Not less than $\frac{H}{3} = (4.67 \text{ m})$	Acceptable
Core slope	1:1.77	1:12	Acceptable

7.2 Seepage Analysis of Mandali Dam

The Finite Element Mesh of the model can be seen in Figure (7). While figures (8) and (9) present the water head variation and pore water pressure through the dam body, respectively. Figure (7) shows that the phreatic line has been lowered down effectively by the central clay core. Figure (8) confirms that the pore water pressure in the internal surface of downstream are far away from downstream which ensures stability of the downstream against seepage failure. Figures (7) and (8) show that the variations of pore water pressure as well as energy lines follow (BDS) safety regulations. Moreover, the flow lines are diverge from the downstream toe of the dam and the drainage filter minimize excess developed pore water pressure, which ensures the stability of the downstream slope.

8. Analysis of Mandali Dam and Results

To investigate the stability of dam slopes, the dam was simulated, using Geostudio software, three different cases of operation are considered, as follows:

Case (1): Just after construction; where reservoir is empty and significant pore pressure development is expected either in the embankment or foundation during construction of the embankment.

Case (2): Steady-state seepage; where reservoir is full and the long-term phreatic surface within the embankment has been established.

Case (3): Rapid drawdown; in the reservoir is drawn down faster than the pore pressures can dissipate within the embankment after the establishment of steady-state seepage conditions.

The considered analytical methods in the present study are Ordinary, Bishop's Simplified, and Janbu's Simplified and Morgenstern-Price methods. The obtained factors of safety (F.S.) are compared to the Limits of USACE (2003) [18] and BDS (1994) [19].

Figures (10 - 14) present F.S. for the dam slopes under different cases of operation using the four analytical tools. Table (4) summarizes the determined upstream and downstream factor of safety (F.S.) for all cases of operation and used analytical tools.

Table (4): Results of Mandali dam stability analysis by Geostudio with Limit of USACE (2003) and BDS (1994).

Critical Stability Condition	End of construction		Steady state		Rapid drawdown	
	Upstream	Downstream	Upstream	Downstream	Upstream	Downstream
USACE (2003)	1.3		1.5		1.2	
BDS (1994)	(1.5-1.3)		(1.5-1.3)		(1.3-1.2)	
Ordinary	1.985	2.394	2.343	2.008	1.958	2.008
Bishop's	2.082	2.427	2.488	2.154	2.061	2.154
Janbu's	1.922	2.357	2.205	1.962	1.895	1.962
Morgenstern-Price	2.12	2.444	2.543	2.187	2.103	2.187
Remark	Stable	Stable	Stable	Stable	Stable	Stable

For steady state condition, the maximum water level was 182.5 m [AMSL], where the dam crest level is 184 m [AMSL] (1.50 m free board). While for rapid drawdown case, the water level was lowered from the estimated maximum flood level of 182.5 m [AMSL] to the minimum operating level of 170 m [AMSL]. As can be seen in the presented figures and table, the factor of safety (F.S.) values ranges from 1.895 to 2.543 which satisfies the minimum limits of factor of safety (F.S.) in USACE (2003) and BDS (1994). The factor of safety (F.S.) values reflects stable slopes of the dam for all operating cases. The least values of factor of safety (F.S.) are given by Janbu method. This is mainly due to the moment equilibrium equations that are not satisfied by Janbu's method. While the largest factor of safety (F.S.) values are given by Morgenstern-price method, as Morgenstern-price method relates the shear and normal force [13].

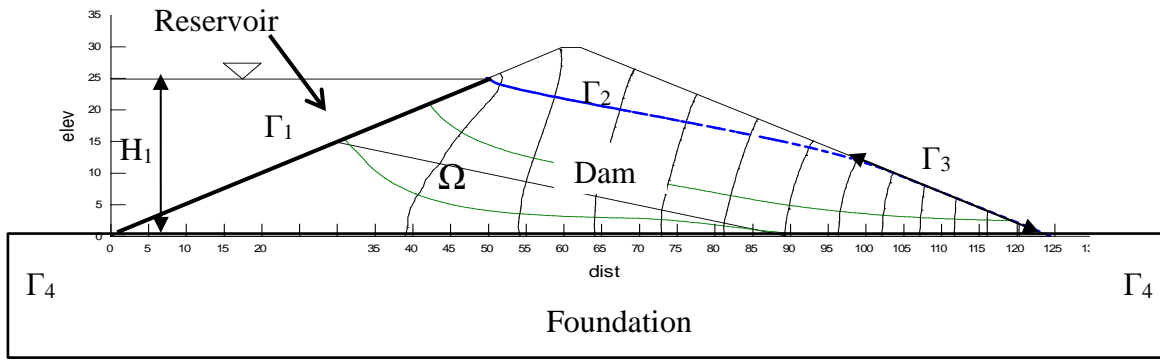
9. Conclusions

Finite element modeling was employed in this study to analyze the combined seepage and slope stability of Mandali earth dam (Iraq). Three different cases of operation were considered, and four different analytical tools were used to analyze the slope stability. The dam safety check was based on the minimum required F.S stated in USACE and BDS. The results showed that the geometric design of the dam is acceptable according to BDS criteria and the seepage through the dam is within the code recommendations. The factor of safety (F.S.) values of upstream and downstream slopes stability satisfy the minimum limits for all cases of operation. Rapid drawdown

case is the most critical case compared to other operating cases. It can be concluded that Mandali dam is safe against seepage failure and slope failure under the different cases of operation. As a conclusion, developing of software for earth dam safety is essential.

REFERENCES

- [1] M. Elshemy, R.I. Nasr, M.M. Bahloul and I.M. Rashwan, *The effect of blockages through earth dams on the Seepage characteristics*, Faculty of engineering, Tanta University, Egypt, (2002).
- [2] M. A. M. Ismail, S. Min Ng and K. Gey, *Stability Analysis of Kelau Earth-Fill Dam Design under Main Critical Conditions*, Malaysia, the Electronic Journal of Geotechnical Engineering (EJGE), (2012).
- [3] Zeidan, B.A., *A Numerical (FEM) Study of the Effect of Anisotropy on Phreatic Seepage Flows*, PhD Thesis, Civil Engineering Department, Indian Institute of Technology IIT, Powai, Bombay, India, (1993).
- [4] M. E. Harr, *Groundwater and Seepage*, McGraw-Hill, New York, (1962).
- [5] Lambe, T. W., and Whitman, R. V., *Soil Mechanics*, John Wiley and Sons, Inc., SI Version, New York, U. S. A, (1979).
- [6] Zienkiewicz, O.C. and Taylor, R.L., *the Finite Element Method*; Volumes I, II", 5th Edition, First Published In (1967) By McGraw-Hill.
- [7] National Water and Climate Center, Watershed Science Institute, EM 1110-2-1901, Sep., (1986).
www.wcc.nrcs.usda.gov/watershed/piedmont/a-a.pdf/
- [8] Kratochvil, J., *Numerical modeling of Non stationary Free Surface Flow in Embankment Dams*, Brno University of Technology CZ, (2004).
- [9] A. Kamanbedast and A. Delvari, *Analysis of Earth Dam: Seepage and Stability Using Ansys and Geo-Studio Software*, Iran, World Applied Sciences Journal 17 (9): 1087- 1094, (2012).
- [10] S.M. Zomorodian and S.M. Abodollahzadeh, *Effect of Horizontal Drains on Upstream Slope Stability During Rapid Drawdown Condition*, Shiraz University, Iran, International Journal of Geology, Issue 4, Volume 4, (2010).
- [11] S.P. Tatewar and Laxman N. Pawade, *Stability Analysis of Earth Dam by Geostudio Software*, India, International Journal of Civil Engineering and Technology (IJCIET), Volume 3, Issue 2, July- December (2012).
- [12] H. Hasani, J. Mamizadeh and H. Karimi, *Stability of Slope and Seepage Analysis in Earth Fills Dams Using Numerical Models (Case Study: Ilam Dam)*, Iran, World Applied Sciences Journal 21 (9): 1398-1402, (2013).
- [13] FERC, (1991), *Chapter IV, Embankment Dams*, Federal Energy Regulatory Commission available at: <http://www.ferc.gov/industries/hydropower/safety/guidelines/eng-guide/chap4.PDF>
- [14] Ismael, KH. S., *Seepage and Stability Evaluation of Duhok Dam*, M. Sc. Thesis, College of Engineering, University of Duhok, Iraq, (2006).
- [15] USBR, United State Department of interior Bureau of Reclamation, *Design Standard DS-13(4), Embankment Dams, Static Stability Analysis*, Chapter (4), October (2011).
- [16] NRCS, *Technical Release No. 60, Earth Dams and Reservoirs*, Natural Resources Conservation Service, (2005); available at www.info.usda.gov/CED/ftp/CED/TR_210_60_Second_Edition.pdf
- [17] ULDC, Urban Levee Design Criteria, *Engineering criteria and guidance for the design*, California Department of Water Resources, May (2012).
- [18] USACE, *Slope Stability*, Engineering Manual 1110-2-1902, Department of the Army, Corps of Engineers, Washington DC, United States of America, (2003); available at www.usace.army.mil/inet/usacoe-docs/eng-manuals/em1110-2-1902/entire.pdf
- [19] BDS, *the British Dam Society at the Institution of Civil engineers*, Great George Street, London, SW1P 3AA, (1994). <http://britishdams.org/conferences>
- [20] GEO-SLOPE INTERNATIONAL. Ltd, Calgary, Alberta, Canada. T2p 2Y5, (2004).
[http:// www. Geo-Slope. com](http://www.Geo-Slope.com)
- [21] MINISTRY OF SCIENCE AND TECHNOLOGY, *Design of Hydraulic Structures*, Earth Dams Design, Chapter (5). www.most.gov.mm/techuni/media/CE_05016_ch5.pdf
- [22] Directorate General of Dams and Reservoirs, *Mandali Dam Project- Geological Report*, Ministry of water Resources, (2004).
- [23] Taylor & Francis / Balkema, *Look, B. G. Handbook of Geotechnical Investigation and Design Tables*, London, UK, pp. 91, (2007).



Γ_4
Fig. (1) Problem statement and boundary conditions accuracy.

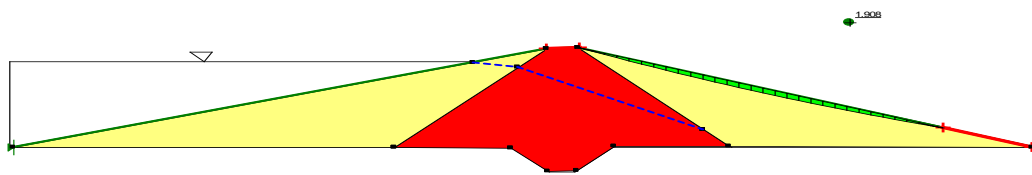


Fig. (2) F.S of downstream slope for steady state case

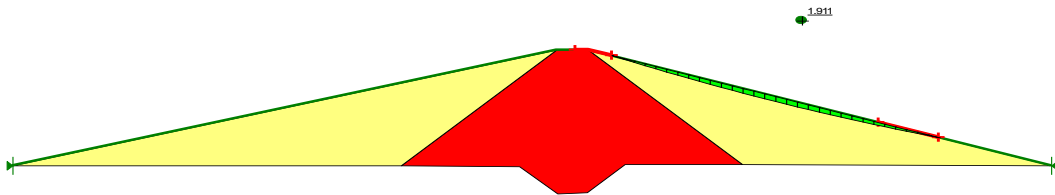


Fig. (3) F.S of downstream slope for End of construction case

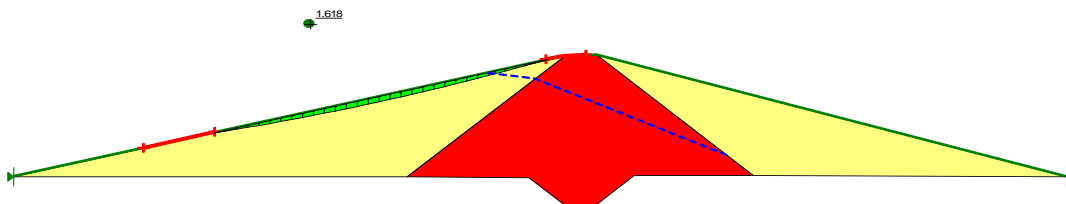


Figure (4) F.S of upstream slope for Rapid drawdown case



Fig. (5) Mandali Dam location [22]

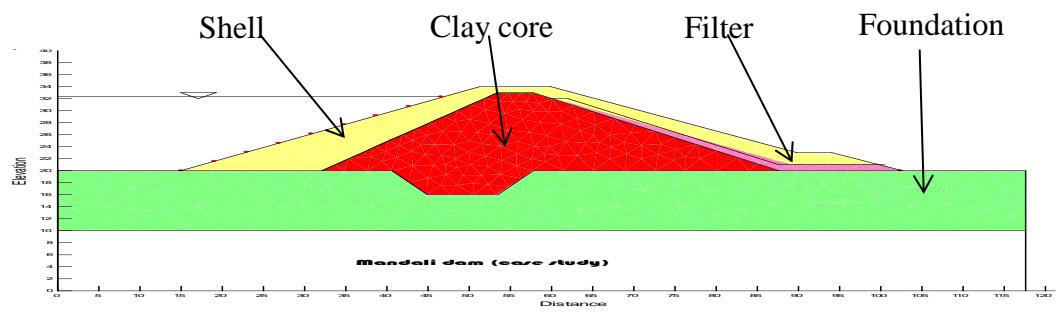


Fig. (6) Cross section of Mandali Dam, Iraq

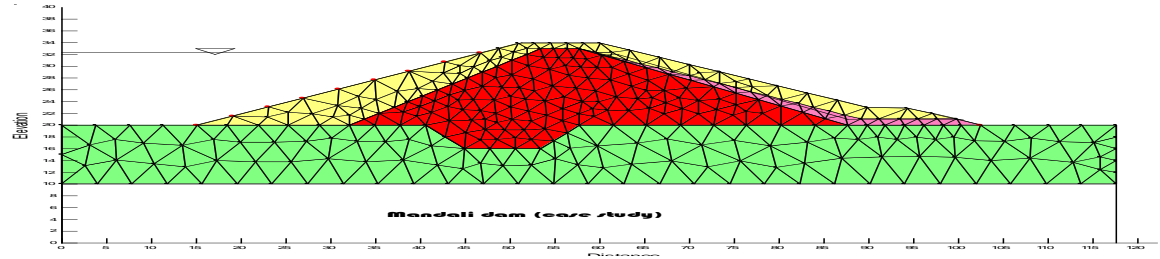


Figure (7) Finite element mesh of Mandali dam

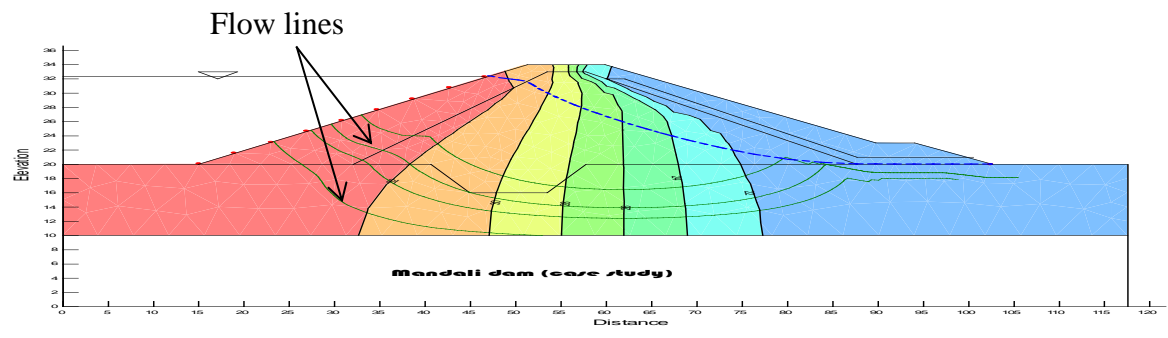


Figure (8) Water head variation and flow line through the dam body

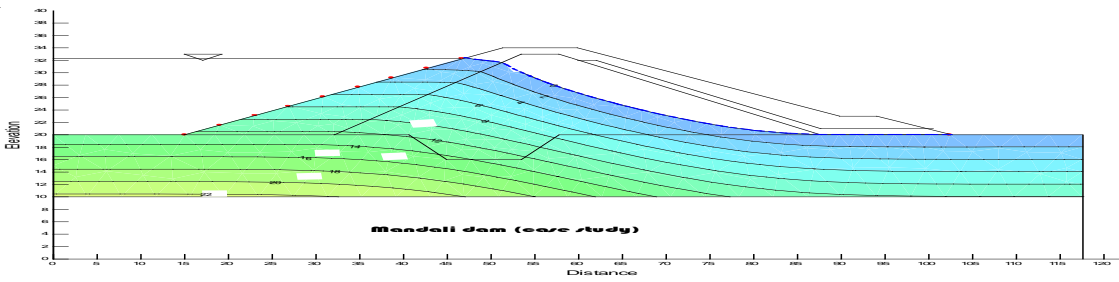


Figure (9) Pore water pressure through the dam body

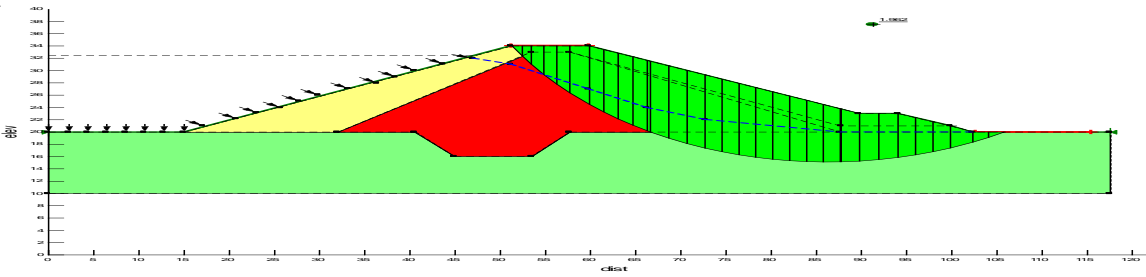


Figure (10) F.S for downstream slope by Janbu's method for case of steady state

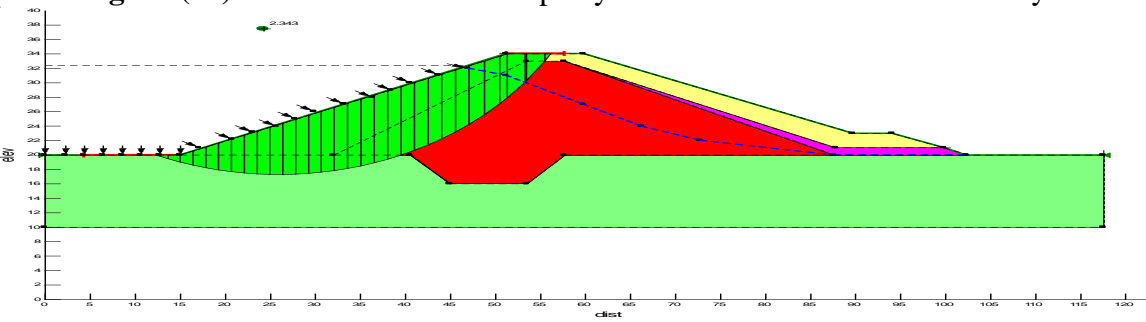


Figure (11) F.S for upstream slope by Ordinary method for case of steady state.

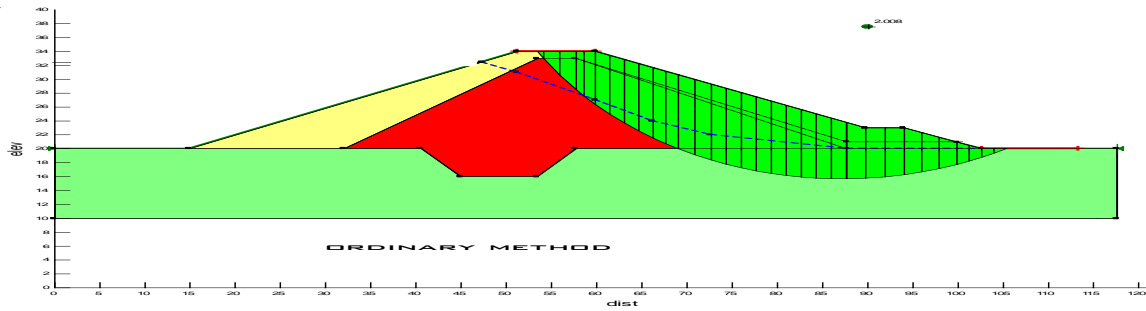


Figure (12) F.S for downstream slope by Ordinary method for case of Rapid drawdown.

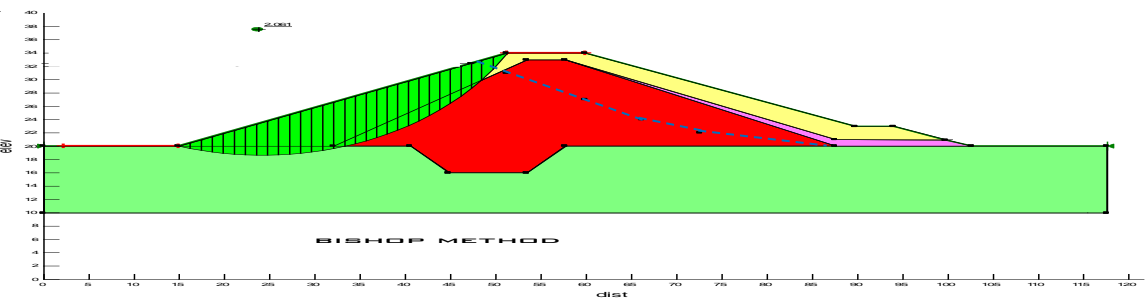


Figure (13) F.S for upstream slope by Bishop's method for case of Rapid drawdown.

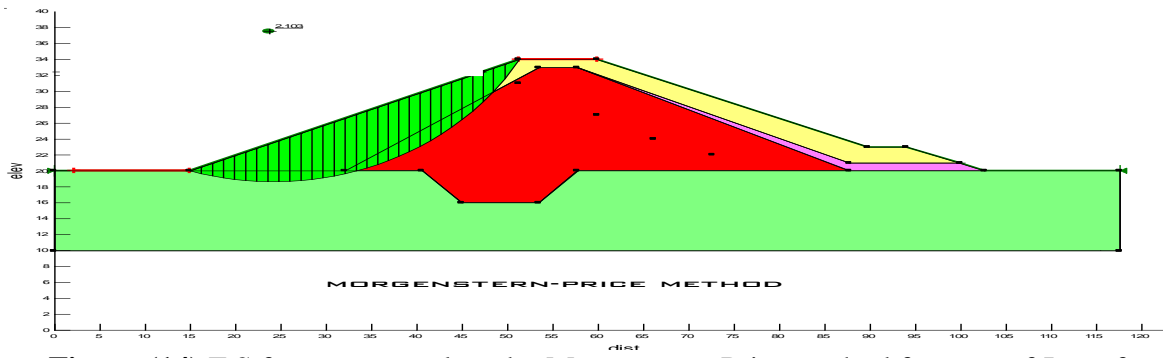


Figure (14) F.S for upstream slope by Morgenstern-Price method for case of Just after construction.

COMMISSION INTERNATIONALE DES GRANDS BARRAGES

VINGT-SIXIÈME CONGRÈS DES GRANDS BARRAGES
Autriche, juillet 2018

DOI 10.3217/978-3-85125-620-8-109



This work licensed under a Creative Commons Attribution 4.0 International License. <https://creativecommons.org/licenses/by-nc-nd/4.0/>

**IMPROVING MODIFIED ICOLD METHOD WITH LOSS OF LIFE INDEX FOR
DAM SAFETY RISK ASSESSMENT IN INDONESIA BY USING RASTER
METHOD**

Anto HENRIANTO

*Dam Engineer, PT. VIRAMA KARYA (PERSERO), Doctor Candidate of Water
Resources Engineering, PARAHYANGAN CATHOLIC UNIVERSITY*

INDONESIA

R.Wahyudi.TRIWEKO

*Professor of Water Resources Engineering, PARAHYANGAN CATHOLIC
UNIVERSITY*

INDONESIA

IMPROVING MODIFIED ICOLD METHOD WITH LOSS OF LIFE INDEX FOR DAM SAFETY RISK ASSESMENT IN INDONESIA BY USING RASTER METHOD

Anto HENRIANTO

Dam Engineer, PT. VIRAMA KARYA (PERSERO), Doctor Candidate of Water Resources Engineering, PARAHYANGAN CATHOLIC UNIVERSITY

R.Wahyudi.TRIWEKO

Professor of Water Resources Engineering, PARAHYANGAN CATHOLIC UNIVERSITY

INDONESIA

1. INTRODUCTION

Indonesia is one of many countries that have the highest number of dams in the world. Related to climate change in the world with so many dams in Indonesia (286 dams) needs to be assessed, the risk assessment action plan is very important to be done. Modified ICOLD Method (MIM), is a risk assessment model that is often used in Indonesia. However, this method has the disadvantage that only provides data on the number of people at risk (PAR) not to the point Loss of Life (LoL). According to the downstream dam area where dominated by densely populated areas and economic centers in Indonesia, which makes the risk level of dam is high or even extreme and considering the effects of climate change that can lead to the destruction of a dam at any time, the aspect of LoL shall be a priority for concerned. Although considered to be a lot of uncertainty, further study of PAR is the prediction of the number of LoL at least a measurable picture for various efforts to reduce the amount of LoL.

2. METHODS

Because this paper only discusses PAR in the inundation area then some conditions, such as PAR who are in the dam and LoL due to traffic accidents due to drift on the highway when disaster does not take into account. Basically, this method involves basic map preparation, parameters affecting the amount of LoL in the inundation area, the development of interaction matrix, coding on the matrix, parameter classification, rasterization, potential risk assessment of LoL, making of risk maps and simulating the reduction of the amount of LoL. Raster method is a method that describes the relationship between risk determinant parameters to a threat in each sub unit of the inundation area. The total number

of LoL predictions of the raster method will be calibrated by the empirical equations of regression results from the number of catastrophic collapse events in Indonesia and the world. If the results are not significantly different, then the prediction of the amount of LoL can be considered close to and can be an additional reference in risk assessment in the Modified ICOLD method.

3. RESULTS

3.1 Basic Map Preparation

The base map is a spatial data that is important in the final decision-making process. The completeness of the base map will have an indirect effect on the final result to be obtained. The basic map used in this paper is the result of running simulated dam and software with ZhongXing HY-21. For example used dam break inundation map at the Cacaban Dam in Central Java, Indonesia.

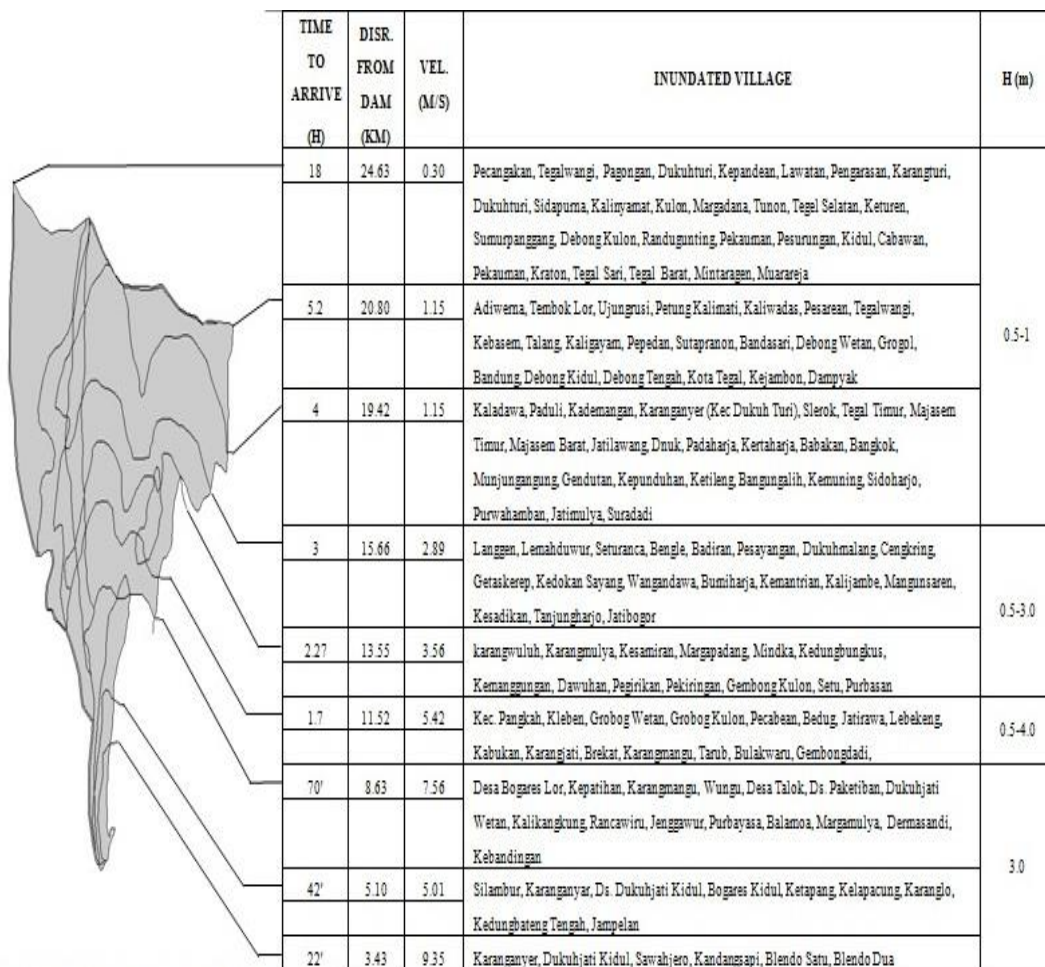


Fig 1. Dam Break Inundation Map of Cacaban Dam

3.2 General Data of Cacaban Dam

Location	: Slawi, Central Java, Indonesia
River	: East Cacaban River
Year Built	: 1952 - 1958
Owner	: Department of Public Works Indonesia
Type	: Homogeneous Earthfill
High	: 38 meter (from deepest foundation) - El. + 80,50 meter
Long of Dam	: 168 meter
Width	: 6 meter
Capacity 2015	: 53,08 million m ³ (Normal) 101,70 million m ³ (Flood) 0,10 million m ³ (Minimum)
Elevation	: + 77,50 meter (Normal) - 790 ha + 78,75 meter (Flood) - 900 ha + 50,00 meter (Minimum) - 100 ha
Catchment Area	: 59 km ²
Q design	: 800 m ³ / s (Free Spillway) T : 125 year
Long of Spillway	: 58 meter
Benefits	: Irrigation
Down Stream	: - Area : 281,71 km ² (Inundation Area) - Tc : 0,5 hour - PAR : 519.518 persons - House : 129.880 unit
Instruments	: Piezometer (30 unit - Standpipe) Inclinometer (2 unit) V Notch (1 unit)

3.3 Developing of Interaction Matrix

In general, the parameters to be used, determined based on the knowledge and experience of experts related to the field to be studied. The more parameters studied, the matrix will have better quality. In this paper, the parameters to be used include the anticipated aspects of flood characteristics that affect the prediction of the amount of LoL. Development and linkages between parameters are labeled as follows:

Table 1. Development of Interaction Matrix

Anticipation of Downstream Dams to Natural Disasters Event	Anticipation Of Disaster That Can Come Every Moment Unexpectedly	Anticipation Of Large Flood That Will Happen	Anticipation Of Disaster Affects Total PAR / PENRIS	Anticipating Disaster Affects Readiness PAR and Related Agency for Evacuation	Quality of Disaster Anticipation Determining Preparedness of Evacuation Sites	Short, Medium and Long Term Anticipation	Main Anticipation is One Vision Reduces Risk Levels to a Safe Level
The Most Extreme Impact of Disasters Affects Anticipation Against Disaster	Disaster Failure of The Dam	Type of Dam Collapse Damming Flood Characteristics	Possible Disaster Affects to Number of PAR / PENRI	The Possibility of an Influential Disaster Against Readiness PAR / PENRIS faces Disaste	The Possibility of an Influential Disaster on the Readiness of Evacuation Site	Incidence of Dam Collapse The Effect of LoL Amount	Disaster Damage Collapse Affects Risk Assessment
Flood Characteristics Affect Anticipation of Disaster	Type of Dam Collapse Damming Flood Characteristics	Flood Characteristic (H, V and WT)	Flood Characteristics affects the number of PAR / PENRIS	Flood Characteristics Affects Readiness PAR and Related Institution	No	Flood Characteristics Affect the Prediction of LoL Amount	Karakteristik Banjir Mempengaruhi Prediksi Jumlah LoL
The number of PAR affects the type of anticipation of disaster	No	No	Amount of People at Risk (PAR)	No	No	The number of PAR affects the Prediction of the LoL Amount	Amount of PAR Affects Prediction of LoL Amount
Quality of Readiness Determining the Value of Anticipatory Efforts	No	No	No	Readiness of PAR and Related Agency Disaster For Evacuation	Depending on the Current Quality of Coordination Between Related Parties Evacuation	Readiness of PAR and Related Agency Affects the Prediction of LoL Amount	PAR Readiness Affects Risk Assessment
Quality of Disaster Anticipation Determining Preparedness of Evacuation Sites	Tidak Ada	No	No	Plotting Lokasi Evakuasi Fix	Readiness from Evacuation Site and Post-Disaster Handling	Readiness of Evacuation Sites Affects the Prediction of LoL Amount	Readiness of Evacuation Sites Affects Risk Assessment
Predicted LoL Amount Affects Anticipation Globally, Especially For Financial Aspects	No	No	Predicted LoL Amount Rated From Amount PAR	Determining the Current of the Program Periodic Activities Improving Quality of Readiness PAR and Related Institution	Effect to Amount and Type of Location Evacuation	Prediction of LoL	Prediction ogf LoL to Risk Assessment
Anticipation for Reduction till safe based on Dam Risk Assessment	Dam Break Disaster give effect to Risk Assessment	Flood Characterists Give Effect to Prediction of LoL	Amount of PAR will effect to Prediction of LoL	Readiness of PAR Related to Risk Assessment	No	Dam Safety Risk Categories for Reduction Prediction of LoL	Risk Assessment LoL for Developing Modified ICOLD Method

3.4 Encoding in Matrix

To know the interaction of all parameters with each other, semi-quantitative method is used with 5 categories with range 0 to 4 with categories: No Interaction (0), Weak Interaction (1), Medium Interaction (2), Strong Interaction (3) and Critical Interaction (4). Encoding In Matrix based on interrelationship between parameters is labeled as follows:

Table 2. Encoding in Matrix and Interrelationship between Parameters

Anticipation of Downstream Dams to Natural Disasters Event	4	4	3	3	3	3	3
3	Disaster Failure of The Dam	3	3	3	3	3	3
3	3	Flood Characteristic (H, V and WT)	4	4	3	3	3
3	0	0	Amount of People at Risk (PAR)	0	0	4	4
3	0	0	0	Readiness of PAR and Related Agency Disaster For Evacuation	3	3	3
3	0	0	0	4	Readiness from Evacuation Site and Post-Disaster Handling	3	3
3	0	0	3	3	3	Prediction of LoL	3
3	3	3	1	2	2	3	Risk Assessment LoL for Developing Modified ICOLD Method

Table 3. The Weighting of the cause and effect relationships for the predicted number parameters of the LoL

Parameter	Cause	Effect	C+E	(C+E) %
Anticipation of Downstream Dams to Natural Disasters Event	23	21	44	32,59
Disaster Failure of The Dam	18	6	24	17,78
Flood Characteristic (H, V and WT)	17	3	20	14,81
Amount of People at Risk (PAR)	8	4	12	8,89
Readiness of PAR and Related Agency Disaster For Evacuation	9	9	18	13,33
Readiness from Evacuation Site and Post-Disaster Handling	6	5	11	8,15
Prediction of LoL	3	3	6	4,44
Total			135	100,00

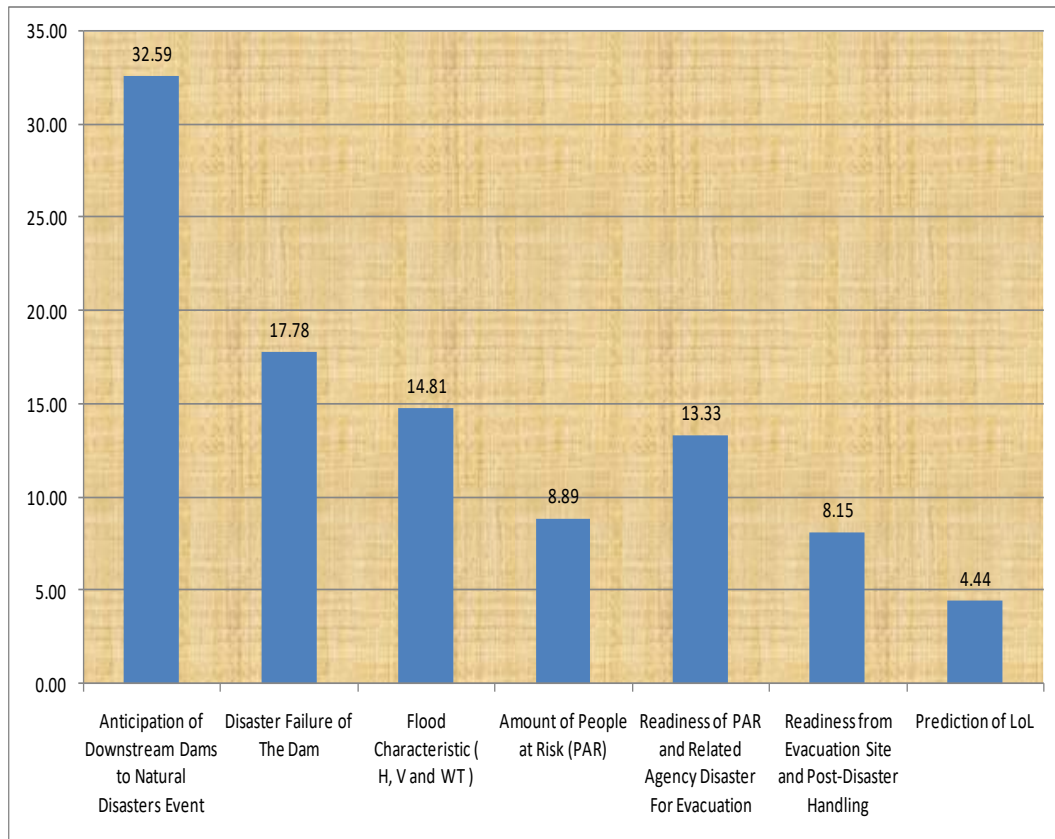


Fig 2. The Weighting Histogram of the Causal Relationship Between Parameters

Based on results with Semi Quantitative Method, it is known that anticipating factors related to natural disasters (32,59 %) , especially the disaster of dam collapse (17,78%), are the dominant parameters that influence the modification effort of dam security risk assessment. The prediction of the amount of LoL itself depends heavily on these two factors. Meanwhile, two other factors that are balanced but interrelated is the information factor predicting the flood flow (14,81%) that will occur with the PAR preparedness factor facing the disaster related evacuation action (13,33%) and evacuation site plus post disaster handling (8,15%). The information (8,89%) and prediction of PAR (4,44%) factor has the lowest weight compared to other parameters.

3.5 Assessment

In accordance with the size of the weighting and classification of predefined parameters, the minimum / lower and upper limit which describes the predicted condition of the LoL amount is as follows :

$$N_{min} = [1 \times (32.59 + 17.78 + 14.81 + 8.89 + 13.30 + 8.15 + 4.4) + (0 \times 14.81)] = 99,92 \quad [1]$$

$$N_{max} = [5 \times (32.59 + 17.78 + 14.81 + 8.89 + 13.30 + 8.15 + 4.4) + (1 \times 14.81)] = 514.41 \quad [2]$$

Thus, the final value classification of the predicted spatial analysis of the LoL amount is labeled as follows:

Table 4. Classification of Results Spatial Analysis to Risk of LoL

No.	Range	Classification	Pixel Color
1	99,92 - 205,92	Very Critical	Red
2	205,93 - 311,93	Critical	Yellow
3	311,94 - 417,94	Fair	Blue
4	417,95 - 514.41	Safe	Green

3.6 Rasterization

The sum of the weights of each parameter per pixel in a flood map area due to the dam break is illustrated as follows:

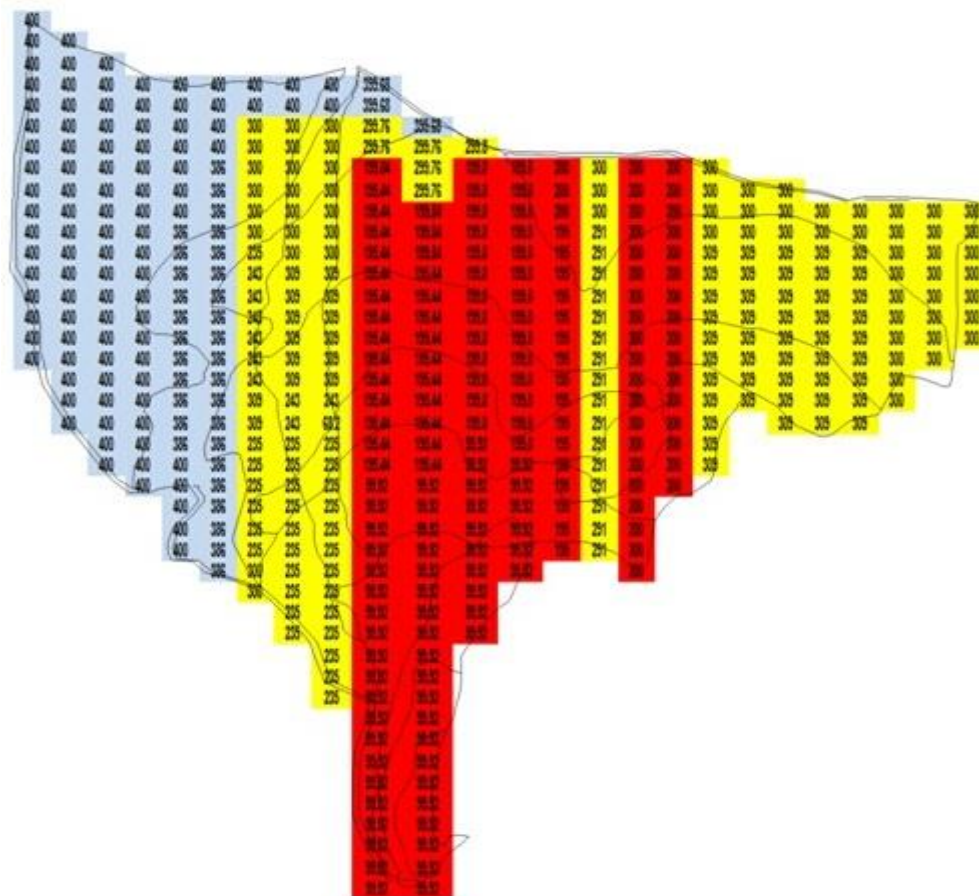


Fig 3. Potential Risk of LoL Map

Based on the potential risk map for the fall of LoL can be seen that the yellow and red areas are still the dominant color. The biggest weight of the parameters is on the anticipation aspect. The ideal step to decrease the risk value is by

removing the PAR in the red and yellow areas but as long as it is difficult, risk reduction efforts can be made by further intensifying the three main points of the parameters: anticipation of dam disasters, preparedness to evacuate and the readiness of the evacuation site and post-disaster handling. If PAR is assisted by the relevant agency is deemed ready for disaster, then the red and yellow color can be changed to blue. Under these conditions, the PAR assessments at the downstream of the dam in MIM can be reduced again with the consideration that PAR together with the anticipated agencies anticipating the disaster has been deemed ready to face the dam disaster that can happen at any time.

3.7 Improving Modified ICOLD Method With LoL Index

In the Modified ICOLD Method, the PAR evacuation requirements at the downstream of the dam have a point 18 (Extreme) where PAR > 250,000 persons, 12 (High) for PAR between 10,000 to 250,000 and 8 (Moderate) for PAR between 1 to 10,000 persons. This condition makes the big dams in Indonesia have high and even extreme categories which gives the impression that it is difficult to reduce the risk level because for the condition of Indonesia, risk assessment with the current condition up to 0 (Low) assessment is difficult to achieve given the increase and mobility of people in Indonesia. so high that it tends to ignore the safety due to future dam breakthroughs. If based on the regression graph that has been created for the condition in Indonesia can be predicted the number of LoL and anticipation can be done to accommodate the amount of LoL it can be said that the result of the assessment that the dam in extreme conditions for example can be proposed down to condition point 6 (Moderate) for PAR between 1 to 10.000 persons. Especially if long and short term action programs are implemented intensively to manage downstream areas of dams at the time of the dam is still standing well, it is not impossible to be reduced to moderate category even though the number of PAR is in the high category and even extreme. The results of this thinking are proposed in order to accompany the action of parallel intensive monitoring of conditions on the dam structure itself. The regression charts that were previously featured in the ICOLD 2017 Symposium in Prague last year are presented as follows:

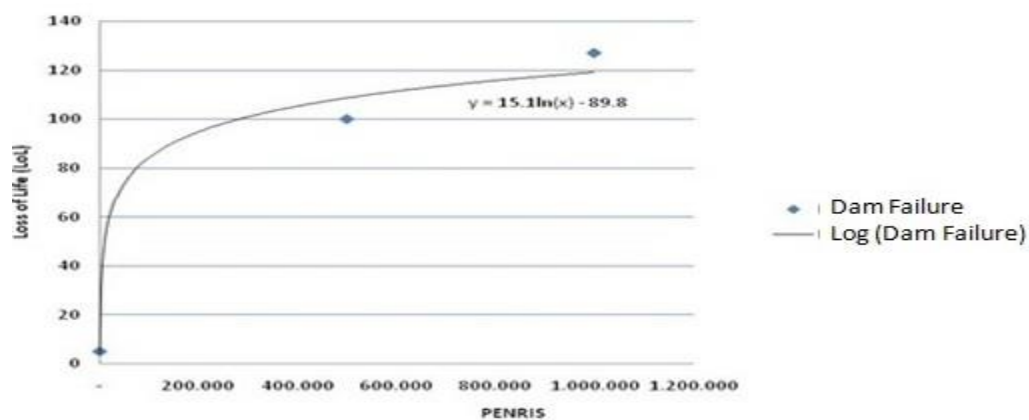


Fig 5 . PENRIS/PAR vs LoL for 3 Dams in Indonesia

The number of LoL predictions of the original Indonesian formula, compared with the calculation formula of De Kay (2003) commonly used in the world, is presented as follows:

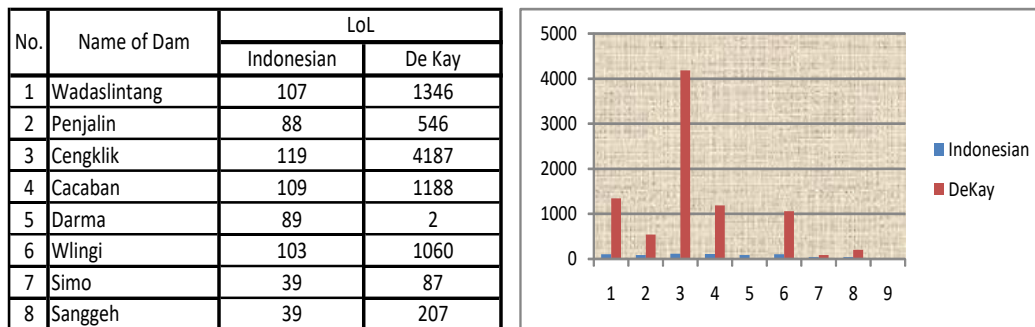


Fig 6 . Comparison of LoL Indonesia vs De Kay - Mc. Clelland for 8 Dams in Indonesia

Indeed there is a considerable difference in the number of LoL from the comparison results from the above table but at least a description of the predicted number of LoL already exists. With such measurable amounts at least if the commitment to take anticipatory action against the dam damage will be more mapped if it will proceed with the amount of costs that must be backed up later by the government and related parties. As an illustration, based on the dam risk assessment at year 2015, Cacaban Dam is categorized as high risk with point 55 and is in the interval 46 to 75. If efforts to reduce the amount of LoL have been well accommodated then no need to worry again to reduce its risk to 43 because it is reduced by 12 points into interval 16 to 45 so it can fit in Moderate category.

4. SUMMARY

Although the prediction of the LoL amount, has the smallest weight but the prediction of the amount of LoL is considered to provide a new argument for efforts to reduce the level of security risks of dams in Indonesia. Dams that with the downstream conditions of densely settled values of extreme or high conditions can be lowered risk level if the downstream preparedness of the disaster is considered good. One of the assessment factors is if it has been able to apply well to the risk reduction effort of LoL with short term anticipation (evacuation preparedness) and long term (preparation of disaster-based spatial design). The calculation of the predicted number of LoL by Raster method should be developed in the form of software program so that it can be applied directly in the field in order to take proper follow-up as well as measured in technical and financial aspects.

5. ACKNOWLEDGMENTS

The author would like to thank PT. Virama Karya (Persero) and KNIBB INACOLD as a sponsor to attend the ICOLD 2018 annual symposium this year. Also to the Parahyangan Catholic University Bandung, for the other support during the preparation of this paper.

6. REFERENCES

1. BOWLES, DAVID.S, 2005, **ICOLD Buletin on Dam Safety Management**, Journal of Dams.
2. BROWN, JACOBS, 2008, **A Step Change in Reservoir Safety Management Quantitative Risk Assessment and It's Strategic Implications**, ICOLD.
3. BROWN, GRAHAM, 1988, **Assessing Threat to Life from Dam Failure**, Published Journal of Dam Safety Office. Pp 5-6
4. GRAHAM, J. WAYNE, 1999, **A Procedure for Estimating Loss of Life Caused by Dam Failure**, USBR. Pp 10-12
5. HONNISVAAG, BJORN, 2007, **Risk Assessment in Dam Safety Management**, Lyse CIGB ICOLD Buletin 130.
6. Mc CLELLAND and DE KAY, 1993, **Predicting Loss of Life in Cases of Dam Failure and Flash Floods**, Journal of Dam Safety Office. Pp 9-12
7. Mc GRATH, SHANE et all, 2013, **Integrated Dam Safety Management Systems**, ICOLD Symposium Seattle 2013.
8. PUSAIR, 1995, **Inventarisasi Bendungan di Indonesia**, Departemen Pekerjaan Umum.
9. REITER, PETER, 2001, **Loss of Life Caused by Dam Failure**, PR Water Consulting. Ltd Helsinki.Pp 12-15
10. SOETJIONO, KARLINA, 2008, **Application of Risk Indexing Tool for Evaluation of Constructed Dam Safety in Java**, Journal of applied Sciences in Environmental Sanitation.
11. TOSUN, HASAN, 2010, **Total Risk Analyses for Large Dams in Kizilmark Basin Turkey**, Journal Natural Hazards and Earth System Sciences.
12. TEEGVARAPU, RAMESH S.V, **Modeling Climate Change Uncertainties in Water Resources Management Models** , Environmental Modelling Software, Elsevier, 2010.
13. YUDIANTO, DODDI, 2004, **Potential Analysis of Raw Water Resources in Cikapundung Hulu Watersheed** , Indonesian Journal of Water Resources.

COMMISSION INTERNATIONALE DES GRANDS BARRAGES

VINGT-SIXIÈME CONGRÈS DES GRANDS BARRAGES
Autriche, juillet 2018

DOI 10.3217/978-3-85125-620-8-110



This work licensed under a Creative Commons Attribution 4.0 International License. <https://creativecommons.org/licenses/by-nc-nd/4.0/>

NEAR-FAULT SEISMIC VULNERABILITY OF GRAVITY DAMS

Y. YAZDANI

TARBIAT MODARES UNIVERSITY

IRAN

M. ALEMBAGHERI

Assistant Professor of Hydraulic Structures, TARBIAT MODARES UNIVERSITY

IRAN

NEAR-FAULT SEISMIC VULNERABILITY OF GRAVITY DAMS

Y. Yazdani, M. Alembagheri*

**Assistant Professor of Hydraulic Structures, TARBIAT MODARES
UNIVERSITY*

I.R.IRAN

1. INTRODUCTION

Near-fault ground motions recorded close to a ruptured fault can be significantly different than those observed further away from the seismic source [1]. The near-fault zone is dependent on the earthquake magnitude. In the near-fault area, depending on the rupture mechanism and slip direction relative to the site, the ground motion may exhibit a unique characteristic known as directivity effects. There is also another property resulted by the permanent ground displacement at the site which is called fling-step. These special aspects of near-fault ground motions should be accounted for in the analysis and design of structures in near-fault areas [2]. The directivity effects, in particular, would lead to high specific pulses in the velocity time-history of the record in the direction perpendicular to the fault rupture. It has been shown that the amplitude and period of the pulse are parameters that control the performance of structures; it cannot be easily predicted by typical measures such as response spectra [1-11]. It has been observed that pulse-like motions have larger elastic spectral acceleration values at moderate to long periods. For the concrete dams, Bayraktar and co-workers [10,11] determined near-fault ground motion effects on the nonlinear response of dams including dam-reservoir-foundation interaction. They selected four different types of dam, which are gravity, arch, concrete faced rockfill and clay core rockfill dams, to investigate the near-fault ground motion effects on dam responses. They showed that near-fault ground motions have different impacts on the dam types. Wang and co-workers [12,13] presented results of a study aimed at evaluating the effects of near-fault and far-fault ground motions on seismic performance of concrete gravity dams. They selected Koyna gravity dam as a numerical application. Four different near-fault ground motion records with an apparent velocity pulse were used in the analyses. The results obtained from the analyses showed the effects of near-fault ground motions on seismic performance of concrete gravity dams and demonstrated the importance of considering the near-fault ground excitations.

2. SEISMIC VULNERABILITY ASSESSMENT

Seismic vulnerability is commonly assessed by estimating the probability distribution of EDP for a given IM, $EDP|IM$. The complementary cumulative distribution function of $EDP|IM$ is used to compute the probability that EDP exceeds a certain level edp , given that $IM = im$. This estimation can be combined with a ground motion hazard $h_{IM}(im)$, to compute the mean annual rate of exceeding the EDP level edp [9]:

$$R_{EDP}(edp) = \int_{IM} P(EDP > edp | IM = im) \cdot dh_{IM}(im) \quad (1)$$

The ground motion hazard $h_{IM}(im)$ is the mean annual rate of exceeding the IM level im , obtained using probabilistic seismic hazard analysis. The conditional probability $P(EDP > edp | IM = im)$ is called as the seismic fragility which is a plot of this probability against various IM levels. $R_{EDP}(edp)$ is a measure of seismic reliability of structure. Relationships between ground motion IM and structural response EDP have been well established for various types of structures in the context of probabilistic seismic demand models. In this approach, probabilistic estimations of the EDP as a function of the IM is computed through statistical analysis of nonlinear dynamic analysis results under a set of earthquake ground motions [9].

3. PULSE-LIKE RECORDS

The near-field earthquakes are recorded close to active faults; they possibly include velocity pulses resulted from the forward-directivity. So they are categorized as “pulse-like” or “non-pulse-like”. The forward-directivity effects may be generated when the site is located at one end of the fault, and rupture initiates at the other end of the fault and travels towards the site, the arrival of the wave front is observed as a pulse with large amplitude that occurs at the beginning of the record. These effects are normally long period and are typically observed in the velocity time-history. However there may be backward- and neutral-directivity depending on the fault orientation and rupture propagation [1]. The velocity pulse may occur in the fault-normal direction; ground motion shaking in the fault-parallel direction is typically less intense. Directivity effects are a major concern for researchers studying velocity pulses, and the effects of these pulses on structures [9]. The period of the velocity pulse T_p , can be determined as the period associated with the peak of the original ground motion’s velocity response spectrum. It is an important parameter such that the ratio of the pulse period to the fundamental

period of the structure can greatly affect the structure's response [9]. In this study, a set of seventy-five pulse-like near-field ground motions collected by Baker [9] is utilized. The pulse in this set has been identified using a wavelet analysis. Sixty non-pulse-like (ordinary) near-field ground motions with no velocity pulse are also used for comparison with the pulse-like record set. Using large number of earthquake records implies an aleatory uncertainty due to record-to-record variability. All ground motions were recorded on firm soil or rock sites. The processed ground motions come from the Next Generation Attenuation project database (<http://peer.berkeley.edu/nga/>), and are oriented in the fault-normal direction. They are from earthquakes with large magnitudes in the range of $5 < Mw < 8$. The acceleration response spectra of the two earthquake sets are shown in Fig. 1. At large periods, the pulse-like ground motions tend to cause larger elastic spectral acceleration than the non-pulse-like ground motions.

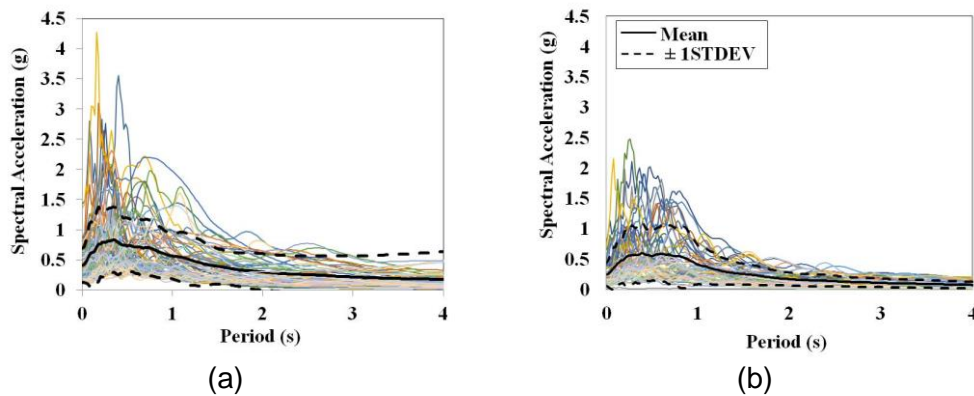


Fig. 1. Acceleration response spectra of the selected earthquakes: (a) pulse-like, (b) non-pulse-like records

4. DAM MODEL

The selected dam model is the tallest non-overflow monolith of Pine Flat gravity dam shown in Fig. 2(a). It is modeled along with its full reservoir using the finite element method; the adopted mesh is illustrated in Fig. 2(b). The water-structure dynamic interaction is taken into account employing Eulerian-Lagrangian formulation. The reservoir length is considered to be five times the dam height and transmitting boundary condition is assigned to its truncated far-end. Zero-pressure condition is assumed for the free surface of the reservoir. The foundation is assumed rigid where the selected earthquakes are uniformly applied.

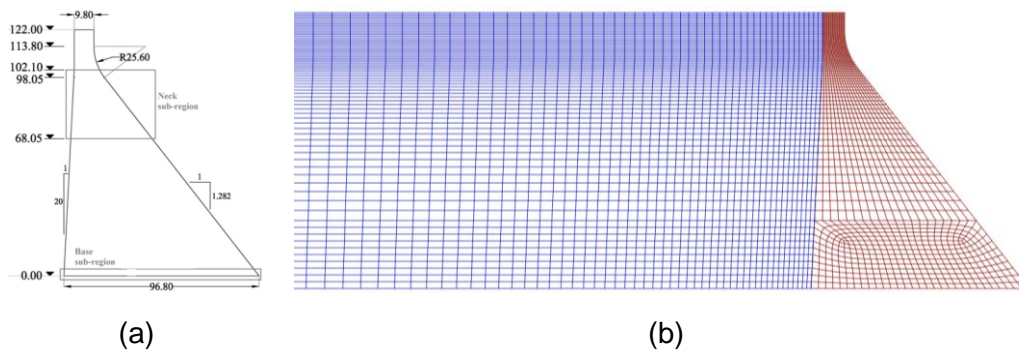


Fig. 2. (a) Non-over-flow monolith of Pine Flat dam used in this study (all dimensions are in meters). (b) finite element mesh of the dam and part of the reservoir.

The nonlinear behavior of dam concrete is modeled using plastic-damage method. In this method, the stiffness of the concrete is degraded beyond its strength using a reduction coefficient of $(1-d_t)$, where d_t is the tensile damage parameter which is assumed to be function of the plastic strains. The damage parameter can take values from zero, representing the undamaged material, to one, which represents total loss of strength. Previous research on this dam showed that only the tensile damage is important in its seismic performance. It is related to concrete tensile cracking which is one of the most important failure modes of gravity dams. The constitutive behavior of the dam concrete is shown in Fig. 3. The finite element mesh of the dam body has been sufficiently refined such that it properly captures its nonlinear response. The concrete properties are: mass density of 2400 kg/m³, initial elastic modulus of 30 GPa, Poisson's ratio of 0.2, and tensile strength of 2.9 MPa. The water has density of 1000 kg/m³ and Bulk modulus of 2.07 GPa.

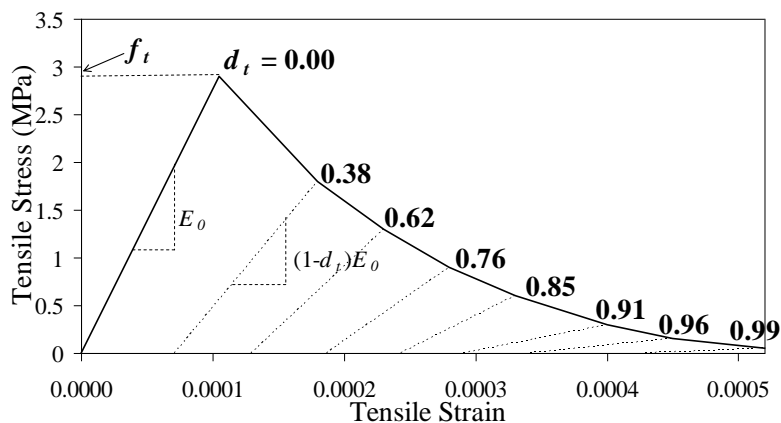


Fig. 3. Constitutive behavior of mass concrete in uniaxial tension

The model is first loaded statically under the self-weight of the dam and the hydrostatic pressure of the full reservoir. Then, it is dynamically analyzed under the selected earthquake ground motions. The Rayleigh damping is employed for structural elements with the coefficients such that produce 5% critical damping in the first and third vibration modes of the intact model. Based on the mentioned properties, the first five natural periods of the dam-reservoir system are: T1=0.38s, T2=0.33s, T3=0.30s, T4=0.26s, T5=0.22s.

The considered EDPs are the crest maximum relative displacement Dc, and the peak hydrodynamic pressure P imposed to the dam heel. Because the dam body has un-symmetric geometry, the crest relative displacements can be separately monitored into the upstream DcU, or the downstream DcD directions. Two local damage indices are defined which are directly related to the cracking response of the dam body. They are computed in the cracking-susceptible sub-regions of the dam body shown in Fig. 2(a) as base and neck sub-regions. These local damage indices, Λ , for both sub-regions are defined as

$$\Lambda_i = \frac{\sum_{e|i} dt|_e A_e}{\sum_{e|i} A_e} \quad i = "b" \text{ or } "n" \quad (2)$$

where $dt|_e$ is the tensile damage of element e with area of A_e . The computation is done on the entire sub-region i . Subscripts b and n show the base and neck sub-regions, respectively. These damage indices are a measure of the amount of damage that the dam may locally experience. Another EDP can be defined as the energy dissipated through cracking process, EC, which can be considered as a global measure of damage imposed to the dam body.

5. RESULTS

The dam-reservoir coupled system is analyzed under the selected pulse-like and non-pulse-like records, and the EDP values are computed. The difference between the pulse-like and non-pulse-like records can be investigated by assessing the cloud of data of, say, $\ln[Dc]-\ln[PGA]$ shown in Fig. 4. Considering all of data as response under the near-field earthquake records (Fig. 4(a)) would result in regression line with slope of 1.022 and goodness of fitting $R^2=0.69$. But, separating the data as response under the pulse-like and the non-pulse-like records (Fig. 4(b)) causes an increase in slope and R^2 value for the non-pulse-like records that shows better correlation for this kind of near-field records. An opposite trend is observed for the pulse-like records. The same trends are observed for other IMs. It is concluded that the pulse nature would lead to more scattered response results. Therefore, it is important to separately investigate the response parameters considering the pulse nature of the earthquake records.

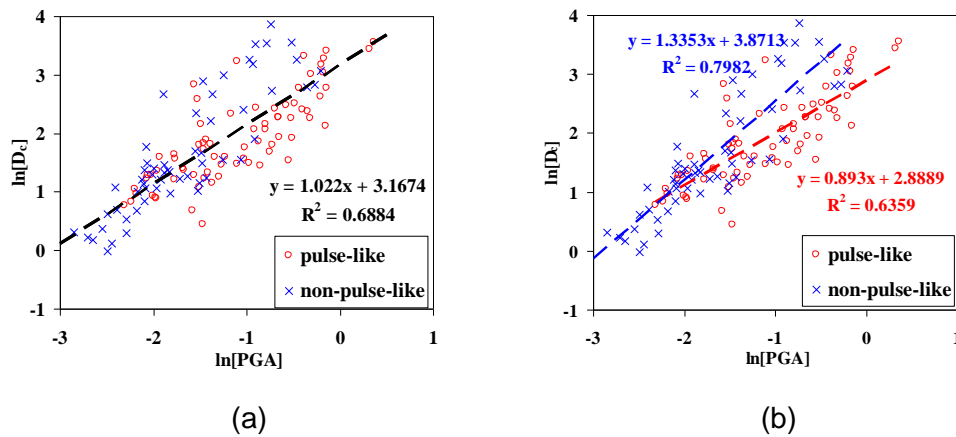


Fig. 4. Cloud of data of Dc-PGA in logarithmic scale: (a) regression line for all of data, (b) separate regression lines for the pulse-like and the non-pulse-like records.

An important parameter of pulse-like motions that affects the structural response is the ratio of the pulse period to the fundamental period of the structure T_p/T_1 . It is particularly important for the first-mode dominated structures such as gravity dams. The response data of the dam-reservoir coupled model under the pulse-like motions are plotted versus the ratio T_p/T_1 in Fig. 5. Because the fundamental period of the model is as low as 0.38s, the ratio of T_p/T_1 is more than 1 for all selected pulse-like motions; this ratio becomes even as high as 34. The local variation of the data is represented using a local average employing the Nadaraya-Watson kernel-weighted average, with a Gaussian weight function. Also shown are the mean and median responses under the non-pulse-like motions; the mean response is totally higher than the median that shows a bias into the higher values. The response of the pulse-like motions may be higher or lower than the average response of the non-pulse-like records. As the ratio of T_p/T_1 increases, approximately, lower response values are observed specifically for the damage dissipated energy which is a global measure of the imposed cracking damage. This trend is somewhat observed for the base local damage index, but it is not so clear for the neck damage index. No all of pulse-like motions would result in Λ_n , i.e. neck cracking; this parameter is observed for motions with $T_p/T_1 < 22$ for only 49 out of 75 records. For the larger period ratios, the pulse period is so much high that it cannot excite the lower main vibration modes of the dam which cause large movements and neck cracking.

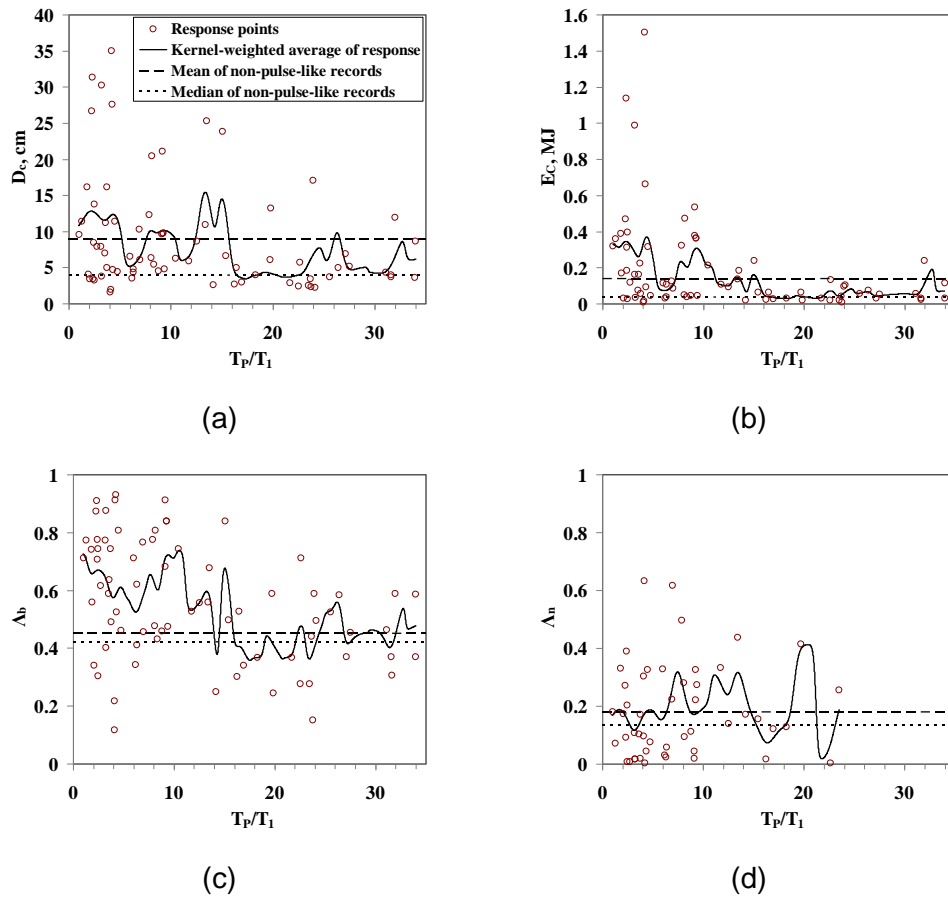


Fig. 5. Response results under the pulse-like records in terms of T_p/T_1 : (a) maximum crest relative displacement, (b) damage dissipated energy, (c) base local damage index, (d) neck local damage index.

Because $S_v(T1,5\%)$ and $S_d(T1,5\%)$ was shown as good predictors of dam's structural response under both pulse-like and non-pulse-like records, the conditional probability of failure is computed using these two parameter as IM. Considering D_c , Λ_b and Λ_n as EDP, the obtained fragility curves are depicted in Fig. 6. The failure threshold of D_c , Λ_b and Λ_n are assumed as 2cm, 30% and 5%, respectively. Although these thresholds are subjective, but they have illustratively used to compare the fragility curves. The probability of failure is higher for the pulse-like records than the non-pulse-like records; however, the fragility curves are very close for D_c and Λ_n . But, the probability of base cracking is much higher under the pulse-like records with respect to non-pulse-like records. The probability of cracking of 30% of the dam's base length under the near-field records with $S_v(T1,5\%) = 20\text{cm/sec}$ is 45% and 85% for the non-pulse-like and the pulse-like records, respectively.

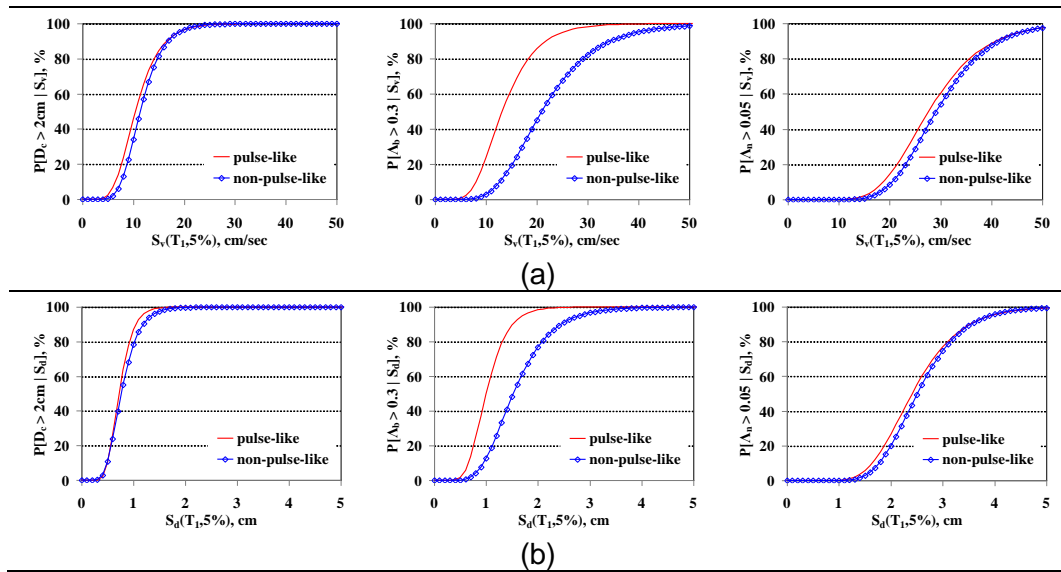


Fig. 6. Fragility curves considering IM as (a) $S_v(T_1, 5\%)$, and (b) $S_d(T_1, 5\%)$. Both pulse-like and non-pulse-like records.

6. CONCLUSIONS

Pine Flat gravity dam was modeled along with its full reservoir as case study. The dam-reservoir coupled system was analyzed under some selected pulse-like and non-pulse-like records, and it was shown that earthquake characteristics other than pulse nature may govern the seismic responses. Also, it was concluded that the pulse nature would lead to more scattered response results. Investigating the seismic EDPs against T_p/T_1 showed that as this ratio increases, approximately, lower response values were observed specifically for the damage dissipated energy which is a global measure of the imposed cracking damage. This trend was somewhat observed for the base local damage, but it was not so clear for the neck damage. Finally, the seismic vulnerability of the dam was assessed by building its seismic fragility curves separately under the pulse-like and the non-pulse-like earthquakes.

REFERENCES

- [1] J.D. BRAY, A. RODRIGUEZ-MAREK. Characterization Of Forward-Directivity Ground Motions In The Near-Fault Region. SOIL DYNAMICS AND EARTHQUAKE ENGINEERING 24 (2004) 815-828.
- [2] M. SASANI, V.V. BERTERO. Importance Of Severe Pulse-Type Ground Motions In Performance-Based Engineering: Historical And Critical Review.

PROCEEDINGS OF THE 12TH WORLD CONFERENCE ON EARTHQUAKE ENGINEERING (12WCEE), AUCKLAND, NEW ZEALAND; 2000.

- [3] J.C. ANDERSON, V.V. BERTERO. Uncertainties In Establishing Design Earthquakes. J STRUCT ENG, ASCE 113 (1987) 1709-1724.
- [4] J.F. HALL, T.H. HEATON, M.W. HALLING, D.J. WALD. Near Source Ground Motion And Its Effects On Flexible Buildings. EARTHQUAKE SPECTRA 11 (1995) 569-606.
- [5] N. MAKRIS. Rigidity–Plasticity–Viscosity: Can Electrorheological Dampers Protect Base-Isolated Structures From Near-Source Ground Motions? EARTHQUAKE ENG STRUCT DYN 26 (1997) 571-591.
- [6] H. KRAWINKLER, B. ALAVI. Development Of Improved Design Procedures For Near-Fault Ground Motions. SMIP 98, SEMINAR ON UTILIZATION OF STRONG MOTION DATA: OAKLAND, CA; 1998.
- [7] G. MYLONAKIS, A.M. REINHORN. Yielding Oscillator Under Triangular Ground Acceleration Pulse. JOURNAL OF EARTHQUAKE ENGINEERING 5 (2001) 225-251.
- [8] Y. ZHANG, W.D. IWAN. Active Interaction Control Of Tall Buildings Subjected To Near-Field Ground Motions. JOURNAL OF STRUCTURAL ENGINEERING, ASCE 128 (2002) 69-79.
- [9] J.W. BAKER. Quantitative Classification Of Near-Fault Ground Motions Using Wavelet Analysis. BULLETIN OF THE SEISMOLOGICAL SOCIETY OF AMERICA 97 (2007) 1486-1501.
- [10] A. BAYRAKTAR, A.C. ALTUNIŞIK, B. SEVİM, M.E. KARTAL, T. TÜRKER. Near-Fault Ground Motion Effects On The Nonlinear Response Of Dam-Reservoir-Foundation Systems. STRUCTURAL ENGINEERING AND MECHANICS 28 (2008) 411-442.
- [11] A. BAYRAKTAR, A.C. ALTUNIŞIK, B. SEVİM, M.E. KARTAL, T. TÜRKER, Y. BİLİCİ. Comparison Of Near And Far Fault Ground Motion Effects On The Nonlinear Response Of Dam-Reservoir-Foundation Systems. NONLINEAR DYNAMICS 58(2009) 655-673.
- [12] WANG G, ZHANG S, WANG C, ET AL. Seismic Performance Evaluation Of Dam-Reservoir-Foundation Systems To Near-Fault Ground Motions. NATURAL HAZARDS, 2014, 72(2): 651-674.
- [13] ZHANG S, WANG G. Effects Of Near-Fault And Far-Fault Ground Motions On Nonlinear Dynamic Response And Seismic Damage Of Concrete Gravity Dams. SOIL DYNAMICS AND EARTHQUAKE ENGINEERING, 2013, 53: 217-229.

COMMISSION INTERNATIONALE
DES GRANDS BARRAGES

VINGT-SIXIÈME CONGRÈS DES
GRANDS BARRAGES
Autriche, juillet 2018

EFFECTS OF FOUNDATION FLEXIBILITY ON THE FAILURE PROBABILITY OF KARUN IV ARCH CONCRETE DAM IN SEISMIC CONDITION

Farid MIARNAEIMI¹, Gholamreza AZIZYAN², Mohsen RASHKI³

¹PhD Candidate, Civil Engineering Department,

²Assistant Professor, Civil Engineering Department,

*³Assistant Professor, Department of Architectural Engineering, UNIVERSITY OF
SISTAN AND BALUCHESTAN*

IRAN

1. INTRODUCTION

Water supply techniques have always been the most important part of the human needs in all of the era. Concrete arch dams are among the main structures in today industrial life. They are built for various purposes such as hydroelectric power generation, water storage for agricultural, industrial, flood control, and preparation of drinking water. It is of particular importance to achieve an adequate safety of dams against earthquakes, because many large dams are constructed in seismic regions.

2. METHOD

In this study, Response Surface Method (RSM) is used for calculate the Limit State Function (LSF) of drift failure mode of KARUN IV arch concrete dam. A three-dimensional model of dam-foundation-reservoir of the dam is created by ABAQUS 6.11 FEM software and the ratio of foundation modulus to dam modulus (E_f/E_d) is considered as the random variable. Material properties of dam and foundation are defined in linear domain and the water is modeled using equations of state (EOS).

Interaction between water and solid areas is considered as frictionless and LAYZMER boundary condition is considered for the free end of the lake. Sliding of the dam heel and abutments is neglected because of being small (2). USBR code is also employed for calculation of the dead, seismic, uplift, hydrostatic and hydrodynamic loads.

3. RESULTS

Five LSFs of drift failure mode for KARUN IV arch concrete dam under earthquakes loading have been extracted by RSM. The functions have been analyzed with six approaches and the \hat{p}_f of dam is presented. RSM is adjusted in polynomial mode. The LSF then obtained by considering the failure drift and the performance of dam (i.e. $g(x = E_f/E_d) = 0.0025 - Drift$). Obtained results by six mentioned approaches are presented.

4. CONCLUSION

It is concluded that CHI-CHI earthquake has the most impact on dam failure and the failure probability is much more than the other earthquakes, considering the foundation flexibility as a random variable. It is also concluded that Subset Simulation method has the best performance in terms of standard deviation of answers and it's results are very close to MCS. Importance Sampling can be also employed for reliability analysis of dam because it is able to find the approximate (near to MCS) failure probability with a few number of function calls.

REFERENCES

- [1] USBR, "Guidelines for preliminary design of arch dams", A water resources technical publication engineering monograph, No. 36, USA, 1977.
- [2] HUAIZHI S., JINYOU L., ZHIPING W., ZHAOQING F., *Dynamic non-probabilistic reliability evaluation and service life prediction of arch dam considering time-varying effect*. Applied mathematical modelling, VOL. 40, p.p. 6908-6923, 2016.
- [3] MAHAB GHODS (MGCE), *Karun IV arch Concrete Dam General Layout and Abutment Stability*, Consulting Engineers.
- [4] RASHKI M., MIRI M., MOGHADDAM M.A., "A new efficient simulation method to approximate the probability of failure and most probable point," Structural Safety, Vol. 39, p.p. 22–29, 2012.
- [5] A. S. NOWAK AND K. R. COLLINS, Reliability of structures. CRC Press, 2012.

COMMISSION INTERNATIONALE DES GRANDS BARRAGES

VINGT-SIXIÈME CONGRÈS DES GRANDS BARRAGES
Autriche, juillet 2018

DOI 10.3217/978-3-85125-620-8-112



This work licensed under a Creative Commons Attribution 4.0 International License. <https://creativecommons.org/licenses/by-nc-nd/4.0/>

**UPGRADING THE PERFORMANCE OF POORLY COMPACTED
EMBANKMENT FOUNDED ON SOFT CLAY USING SECANT AND STABILITY
PILES SYSTEM**

Ashraf A. EL-ASHAAL

Geotechnical Engineering Professor, NATIONAL WATER RESEARCH CENTER

EGYPT

Alaa A. ABDELMOTALEB

Geotechnical Engineering Professor, NATIONAL WATER RESEARCH CENTER

EGYPT

** Amelioration De La Performance D'un Embanchage Mal Comprime Fondu Sur Un
Argile Moyen Au Moyen D'un Systeme De Piles Secondaire Et De Stabilite*

UPGRADING THE PERFORMANCE OF POORLY COMPACTED EMBANKMENT FOUNDED ON SOFT CLAY USING SECANT AND STABILITY PILES SYSTEM*

Ashraf A. El-Ashaal and Alaa A. Abdelmotaleb

Geotechnical Engineering Professor, NATIONAL WATER RESEARCH CENTER

EGYPT

1. INTRODUCTION

The investigation of soil improvement of problematic soils as foundation of soil embankments drew the attention of many researchers. Many techniques have been developed to overcome the negative impact of such problematic soils. In the case under investigation, the presence of deep soft clay layer form an obstacle for adapting the available techniques like soil fracturing and vibro replacemet. Control of seepage water through the soil media was investigated and discussed in many research works. The automated digging apparatus with extensive support facilities required to construct plastic concrete diaphragm wall around Sizewell B. power station at UK was described in [1]. Typical examples of walls to prove the adaptability and advantages of the secant bored pile wall method were summarized in [2]. Field studies have indicated the importance of the monitoring activities in understanding the interaction between the utilized pile and the surrounding soil [3]. Based on the rapid progress in analytical and monitoring techniques, graphs for the design of laterally loaded piles in clay was presented in [4].

In the present work, a stabilizing system of an embankment of one of the major canals north of Egypt was monitored and the collected data are discussed. The soil properties, the embankment cross-section, and the design concept of the proposed upgrading system were pointed out by [5]. The Atlas pile type is used in constructing both seepage control and stability improvement systems. The cast insitu screw piles with very rough shaft (Atlas type) proved to be the most suitable pile type to handle the presence of deep soft clay deposits. A complete review of the developments in Atlas type design and the main factors affecting its performance is in [6]. The monitoring system utilized for evaluating the seepage pattern inside the embankment and the performance of the cutoff secant piles are discussed in the present paper. The main conclusions that prove the effective performance of the tested system are pointed out.

2. MONITORING SYSTEM CONFIGURATION

Figure 1 shows the arrangement the monitoring system. The suggested secant-pile wall consisted of reinforced concrete piles with a diameter of 60 cm spaced at 90 cm from center to center intersected with bentonite piles with a diameter of 60 cm and the over lapping distance is not less than 15 cm. The reinforced concrete pile penetrated the upper fill layer and the soft clay layer and extended in the lower sand layer to about 50 cm with a total length equal to 16.50 m. The bentonite piles extended to 6 m in the soft clay layer with a total length approximately equal to 10 m.

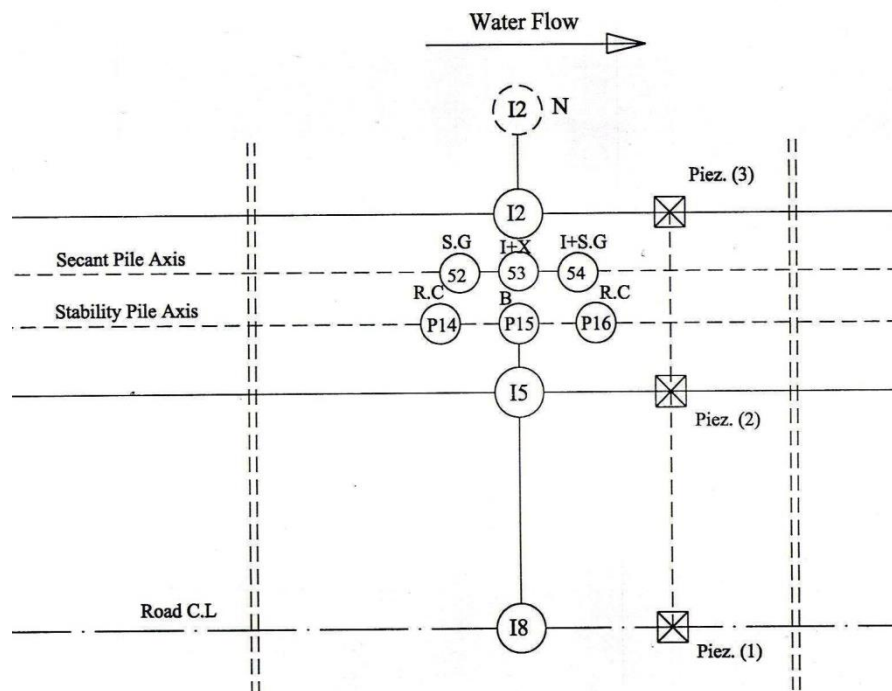


Fig. 1: The arrangements of the monitoring system

The monitored reinforced concrete piles in the wall were named P52 and P54 and the monitored bentonite pile was named P53. Pile P52 was instrumented with vibrating wire strain gages (s.g) on the reinforcing steel bars at levels of -1.80 m, -5.50 m, and -11.00 m relative to the zero sea level. Pile P54 was instrumented with vibrating wire strain gages at levels of -1.80 m, -4.50 m, -7.80 m, -10.80 m, and -13.80 m. In addition to the strain gages, P54 was provided with inclinometer casings and magnetic rings of sondex system at levels of -0.90 m, -3.93 m, -6.94 m, -9.95 m, and -12.96 m. Pile P53 (the bentonite pile) was instrumented with an inclinometer casing and magnetic rings of sondex system at levels of -0.93 m, -2.93 m, and -5.97 m. In addition to the instrumented piles, three piezometers were installed to monitor the variation of water level. Piezometer (1) was installed at the centerline of the road, piezometer (2) was installed adjacent to the secant wall in the roadside, and piezometer (3) was

installed close to the secant wall in the canal side. The overall performance of the embankment mass was monitored through inclinometer I2 in the berm at the canal side, inclinometer I5 in the berm at the road side and inclinometer I8 at the center line of the road.

The monitoring data were collected just after installation of the monitoring equipments, during construction of the secant-pile wall, and during loading of the embankment. The loading process was carried out in three stages. Stage one (I1) covered a distance of 15.00 m to the left of the pile P52, the second stage covered a distance of 15.00 m at the center line of the monitored wall around pile P53, and the third stage covered a distance of 15.00 m to the right of pile P54. In each loading stage an area of 15.00 m × 3.00 m was loaded with a 60-ton lorry load.

3. RESULTS AND DISCUSSION

3.1. EFFECT OF THE SECANT PILE WALL ON THE WATER SEEPAGE IN THE EMBANKMENT MASS

The piezometer readings were collected before the beginning of the secant-pile wall construction, during wall construction, after the end of wall construction, and during the loading stages. Figure 2 shows the variation in the piezometer readings.

The effect of the canal water level on the piezometer readings was the same after the beginning of the wall construction until the construction of the left half of the wall was completed. When completing the construction of the left half of the wall, its left end reached a line passing through the points I8, I5, P53, and I2 in Sept. 17. After Sept. 17, a noticeable difference in the rate of change in the readings between piezometer (3) and both piezometers (1) and (2) was recorded. There are no difference between the readings of piezometer (1) and piezometer (2).

During the different loading stages there was no clear relationship between the readings of piezometer (3) and piezometers (1) and (2). However, the readings of piezometers (1) and (2) still match each other. The difference between the reading of the piezometer in the canal side of the wall and the piezometer in the roadside was increasing with time until eleven days after the end of loading activities where monitoring activities stopped.

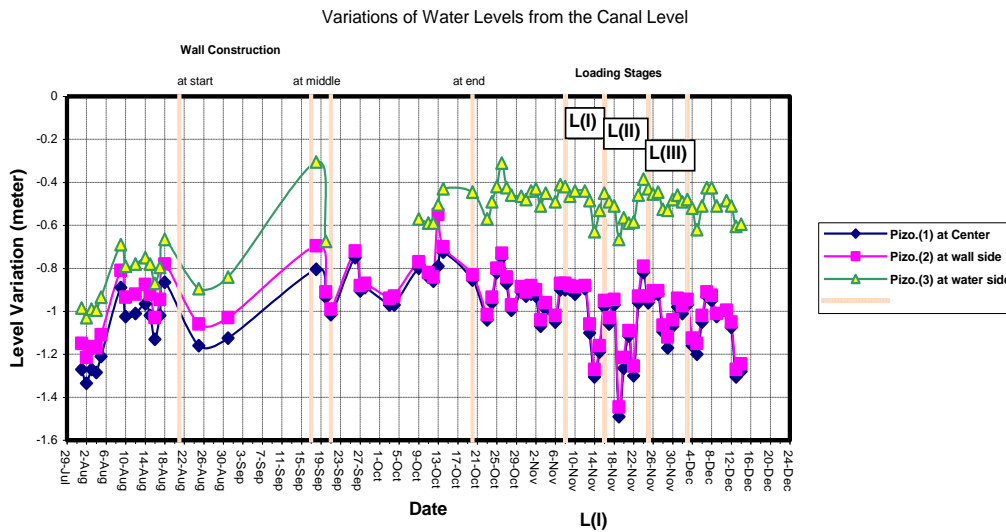


Fig. 2: The variation in the piezometer readings

3.2. EVALUATION OF THE LATERAL DISPLACEMENT OF THE EMBANKMENT AND THE SECANT-PILE WALL

The second monitoring activities were meant to evaluate the lateral displacements of the embankment mass and the monitored piles. The inclinometers I2, I5, and I8 were used to monitor the lateral movement of the embankment mass. Figure 3 shows, as a sample, the readings of inclinometer I2 that is close to the canal section. It can be shown from Fig. 3 that the maximum lateral displacement occurred at the top of the casings in the peat and clay layer with a value of about 17 mm. The maximum lateral displacement occurred during the installation of the inclinometer itself with minor changes due to the installation of the secant-piles wall. It is also clear that while the lateral displacement of the deep sand layer did not exceed 3.5 mm, the soft clay layer suffered from large displacement, which ranged between 12 mm and 16 mm toward the waterside. The previous observation shows the soft nature of the embankment and the high effect of losing the unconfined stress due to canal cut.

Figure 4 shows the collected data of the lateral displacement of the bentonite pile P53. Analysis of the data collected from the inclinometers embedded in the reinforced and the bentonite piles in the wall shows that the 10-m-long bentonite pile P53 suffered from relatively large displacements. Analysis of the collected data reflects the flexibility of the bentonite pile. While the maximum displacement experienced during the different loading and construction activities does not exceed 30 mm, the end toe approximately experienced no lateral displacement. Taking into account that the intersection between the reinforced and bentonite piles is about 150 mm, the maximum lateral

displacement doesn't exceed 20% of such value. It can also be noted that despite such high displacement, the piezometer readings reflect no leakage or escape of water.

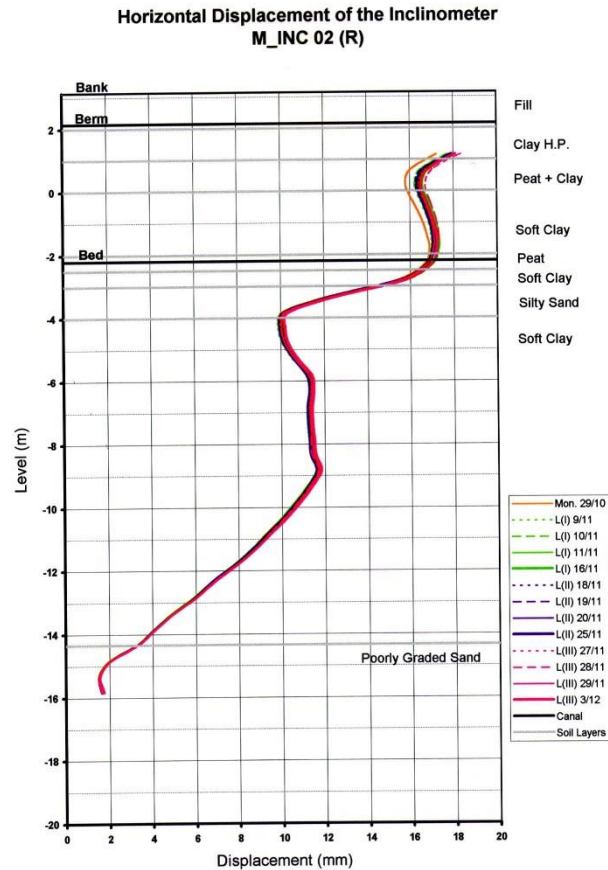


Fig. 3: The readings of inclinometer I_2

Figure 5 shows the lateral displacements of the reinforced concrete pile P54. It is clear from the distribution of the data that the pile experienced lateral displacement smaller than that experienced by P53. The previous observation is true for all the loading and construction stages. The loading stages L(I), L(II), and L(III) resulted in considerable increase in the lateral displacement all over the pile length. The presence of silty sand lenses in the soft clay layers played a vital role in the value of the experienced lateral displacement. It is clear also that the pile experienced high lateral displacement just after loading and then the value of the displacement tends to decrease with time.

It is worth mentioning that the vertical movements of the wall piles were monitored and evaluated but not covered in the present paper. The analysis of the lateral and vertical displacements (movements) of P53 and P54 reflects the ability of the designed monitoring system in tracing the performance of the secant-pile wall. The monitoring system was able to reflect the difference in installation time among its components, and what took place during the construction and the loading stages. The monitoring system was also able to

reflect the effect of the presence of different soil lenses within the soft clay layer on the experienced movements especially during the installation and construction stages.

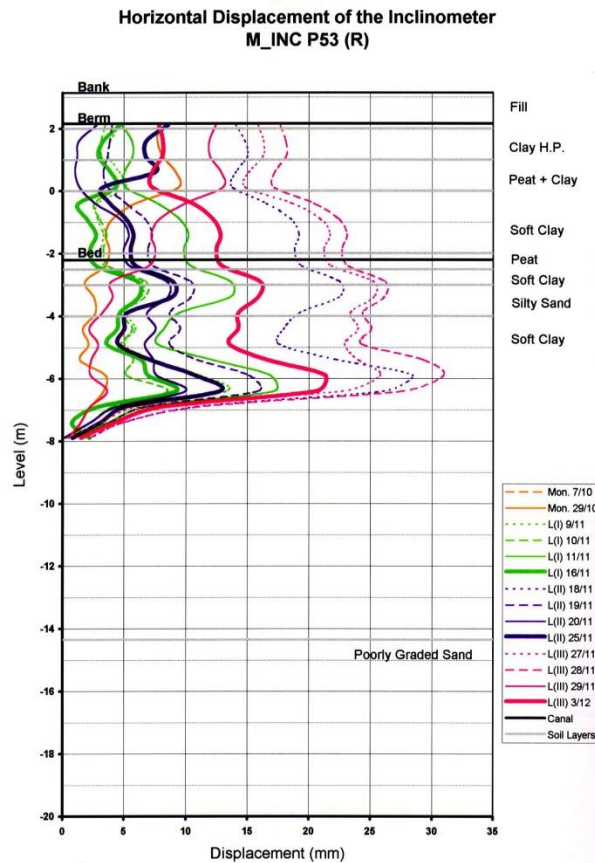


Fig. 4: The lateral displacement of the bentonite pile P₅₃

3.3. EVALUATION OF THE STRAINING ACTIONS OF THE WALL PILES

The strain gages, based on vibrating wire technology, were adapted in measuring the strain in the reinforcement of the reinforced concrete piles in the wall. The vibrating wire was utilized in the monitoring program due to its long-term stability as proved by many investigations such as [7]. In the present monitoring program, both piles P52 and P54 were instrumented with the vibrating wire strain gages.

The strain gages were fixed at the canal side (C) and the roadside (R). Most of the strain gages at the roadside were damaged in the Pile P52. The damage of the strain gages limited the benefit of the collected data for that pile. For the pile P54, the strain gages at both sides C and R were in good condition throughout all activities that took place in the field.

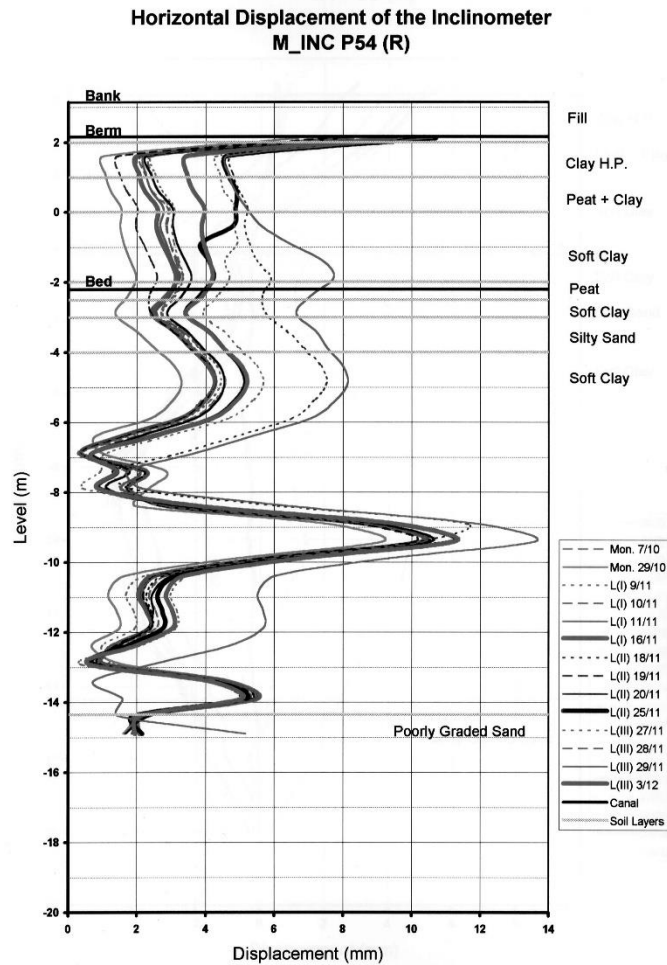


Fig. 5: The lateral displacements of the reinforced concrete pile P₅₄

Fig. 6 shows the readings of the strain gages fixed on the reinforcement bars at side R of the pile P₅₄ shaft. The strain gages were fixed at levels -1.80 m, -4.50 m, -7.80 m, and -10.80 m along the pile shaft. The bending moment, calculated based on the measured strains, reflects high concentration moments at the upper silty sand and the lower very soft clay lenses within the soft clay layer. These sand and clay deposits controlled the pile movements especially during the construction stage, which resulted in concentration of stresses.

4. CONCLUSIONS

The readings of the piezometers embedded in the embankment proved the high efficiency of the secant-pile wall in controlling the seepage through the tested section of the canal embankment. The effect of the secant-pile wall was reflected after finishing the construction of half the wall in the tested section. The readings of piezometer (2), which is adjacent to the wall at the roadside, and

piezometer (1), which lies at the center line of the road, were almost the same from the beginning of the construction of the left half of the wall until the end of the monitoring activities. Hence, it could be concluded that after the construction of the wall, there is no hydraulic gradient through the embankment, which in turn means that there is no erosion due to seepage forces.

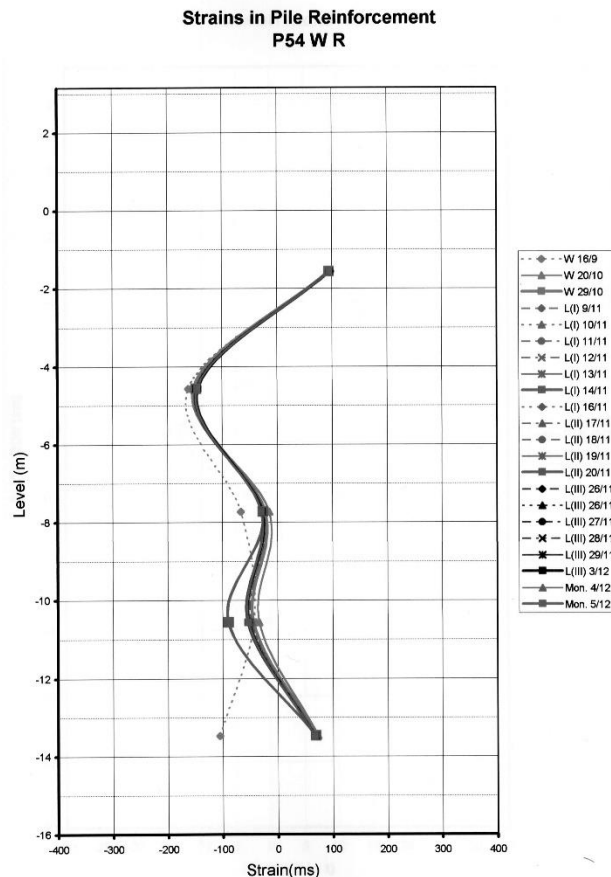


Fig. 6: The readings of the strain gages of direction (r) of pile P₅₄

The readings of the inclinometers embedded in the bentonite piles indicated its high flexibility because of the heave action of the pile after each construction or loading activities. The bentonite piles experienced high lateral displacement compared with the adjacent reinforced concrete pile.

The monitoring system succeeded in reflecting the effect of the presence of hard and/or very soft soil deposit lenses within the soft clay layer on the developed strains and stresses. Monitoring of the reinforced concrete piles showed that they experienced small stresses compared with its ultimate capacity. The shallow embedment of the reinforced concrete pile in the lower poorly graded sand layer did not allow for any fixation or partial fixation of the pile in the sand.

REFERENCES

- [1] COWIE, H. AND CRAWLEY, J. The use of reverse circulation diaphragm walling technique to form a plastic cut-off wall around sizewell b. power station. Proceedings of the international conference on piling and deep foundations, London. 1989, pp. 193-198.
- [2] SHERWOOD, D., HARAN, C., AND BEYER M. Recent development in secant board pile wall construction. Proceedings of the international conference on piling and deep foundations, London. 1989, pp. 211-220.
- [3] PARAKASH, S. AND KUNAR S. Nonlinear lateral pile deflection prediction in sand. ASCE Journal of geotechnical engineering. 1996, Vol. 122, No. 2, pp. 130-138.
- [4] ALEM, A. AND BENAMAR, A. Graphs for the design of laterally loaded pile in clay. Electronic journal of geotechnical engineering. 2002, Vol. 7.
- [5] EL-ASHAAL, A., ABDEL-MOTALEB, A., AND HAGGAG, H. Stabilizing embankments made of and founded over weak soil using piles: a case history. Proceedings of the fourth international engineering conference, cairo university, Cairo, Egypt. 2000, pp. 415-426.
- [6] VAN IMPE, W. Development in pile design. Proceedings of the 4th international conference on piling and deep foundation, Stresa, Italy. 1994, pp. 727-758.
- [7] MCRAE, G. B. AND SIMMONDS, T. Long term stability of vibrating wire instrumented: one manufactures perspective. Proceedings of the 3rd international symposium in field measurements in geo-mechanics, Oslo. 1991, pp 283-293.

SUMMARY

In recent decades great attention was directed toward reclamation of new areas close to the Nile valley in Egypt. North of the Nile delta is one area that has a great potential for developing. Deep deposits of soft clay form an obstacle for such developing process. The embankments of a major canal were made of uncompacted marine deposits and founded over soft clay soil in the north of Egypt. Peat lenses caused slope instability and the sand and Gypsum lenses increased seepage potential and resulted in piping downstream the embankments. The present paper represent the measurements of a monitoring system used to evaluate the performance of an upgrading system of the poorly compacted embankment founded on soft clay. The upgrading is to be achieved through two systems of pile. The first system is meant to handle internal seepage problem while the other is utilized to provide extra stability for the embankment. In the present paper, the monitoring data of the secant-pile wall is presented, discussed, and analyzed. The monitoring system helped to evaluate the performance of the different components of the secant-pile wall. The relative

movement between the reinforced concrete pile and bentonite slurry pile, the lateral and vertical displacement of the bentonite pile and concrete pile, and the strains in the reinforcement of the concrete piles were measured and analyzed. The results show that the seepage control system significantly improved the embankment performance and prevented internal erosion and seepage problems.

RÉSUMÉ

Au cours des dernières décennies, une grande attention a été accordée à la remise en état de nouvelles zones proches de la vallée du Nil en Egypte. Le nord du delta du Nil est un domaine qui a un grand potentiel de développement. Les dépôts profonds d'argile molle constituent un obstacle à ce processus de développement. Les remblais d'un grand canal étaient faits de dépôts marins non compacts et fondés sur un sol d'argile molle dans le nord de l'Égypte. Les lentilles de tourbe ont provoqué une instabilité des pentes et les lentilles de sable et de gypse ont augmenté le potentiel d'infiltration et ont entraîné la formation de tuyaux en aval des remblais. Le présent document représente les mesures d'un système de surveillance utilisé pour évaluer la performance d'un système de valorisation du remblai mal compacté, fondé sur de l'argile molle. L'amélioration doit être réalisée à travers deux systèmes de pile. Le premier système est destiné à gérer les problèmes d'infiltration interne tandis que l'autre est utilisé pour fournir une stabilité supplémentaire pour le remblai. Dans le présent article, les données de surveillance de la paroi de la pile sécante sont présentées, discutées et analysées. Le système de surveillance a aidé à évaluer la performance des différents composants du mur à pieux sécants. Le mouvement relatif entre le pieu de béton armé et le tas de lisier de bentonite, le déplacement latéral et vertical du pieu de bentonite et du pieu de béton, et les déformations dans le renforcement des pieux de béton ont été mesurés et analysés. Les résultats montrent que le système de contrôle des infiltrations a considérablement amélioré les performances du remblai et a empêché l'érosion interne et les problèmes d'infiltration.

COMMISSION INTERNATIONALE DES GRANDS BARRAGES

VINGT-SIXIÈME CONGRÈS DES GRANDS BARRAGES
Autriche, juillet 2018

DOI 10.3217/978-3-85125-620-8-113



This work licensed under a Creative Commons Attribution 4.0 International License. <https://creativecommons.org/licenses/by-nc-nd/4.0/>

PUBLIC SAFETY AROUND DAM: SUTAMI DAM EXPERIENCE

Didik ARDIANTO

Head of R&D Bureau, JASA TIRTA I PUBLIC CORPORATION

Raymond VALIANT

President Director, JASA TIRTA I PUBLIC CORPORATION

Alfan RIAN TO

Director I, JASA TIRTA I PUBLIC CORPORATION

Fahmi HIDAYAT

Deputy of Technical Affairs, JASA TIRTA I PUBLIC CORPORATION

Robert Purba M. SIANIPAR

Commitee Member, INDONESIA COMMISSION ON LARGE DAM (INACOLD)

Kamsiyah WINDIANITA

Chief of Water Resources Infrastructure Unit, JASA TIRTA I PUBLIC CORPORATION

INDONESIA

COMMISSION INTERNATIONALE
DES GRANDS BARRAGES

VINGT-SIXIEME CONGRES DES
GRANDS BARRAGES
Autriche, juillet 2018

PUBLIC SAFETY AROUND DAM: SUTAMI DAM EXPERIENCE

Didik Ardianto¹; Raymond Valiant²; Alfian Rianto³; Fahmi Hidayat⁴; Robert
Purba M. Sianipar⁵, Kamsiyah Windianita⁶

¹*Head of R&D Bureau, JASA TIRTA I PUBLIC CORPORATION*

²*President Director, JASA TIRTA I PUBLIC CORPORATION*

³*Director I, JASA TIRTA I PUBLIC CORPORATION*

⁴*Deputy of Technical Affairs, JASA TIRTA I PUBLIC CORPORATION*

⁵*Committee Member, INDONESIA COMMISSION ON LARGE DAM
(INACOLD)*

⁶*Chief of Water Resources Infrastructure Unit, JASA TIRTA I PUBLIC
CORPORATION*

INDONESIA

1. INTRODUCTION

Dams are critical in terms of population life support and ensuring sustainable economic development. Dams not only for flood control but also provide water for some mutipurpose activities such as hydropower, irrigation water supply, domestic consumption, industrial water use, tourism, aquaculture, navigation, etc. Sutami dam is one of the large dams located in Brantas River Basin. Sutami dam (locally named as Karangates dam) located at Brantas River Basin in Indonesia. The dam is a multifunction dam, which is used for flood control (with the capacity of 1,650 m³/sec), providing irrigation water supply for 34,000 hectares, and also to generate hydro power plant with installed capacity of 3 x 35 mW. Sutami dam has 180 million m³ storage capacity (based on 2016 bathimetry survey) and 1,500 hectares reservoir surface area. The public safety around dam issues surrounding the safety concerns for Sutami dam existed from its beginning of operation because of its critical water storage capacity, structures and massive human activities' surrounding it. This paper addresses some of those public safety requirements throughout the facility and more specifically following the more recent safety risk assessments and mitigation strategies implemented to meet the anticipated safety requirements nowadays.

2. DAM SECURITY

Conceptual approach that used in Dam security is by consider the intersection of the Venn's diagram of dam safety, dam security and public safety around dams comprises intervening activities can be seen in fig.1 below. The activities may be shared, but the objective or narrative of each area may differ.

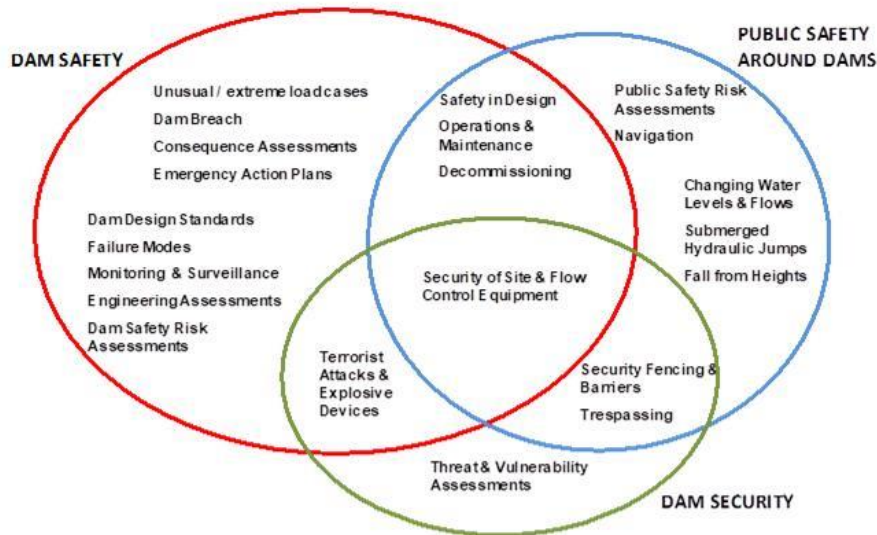


Fig. 1
Venn's diagram of dam safety

To promote the safety of dams, dam operator (PJT I) conducts dam safety management as a part of operation and maintenance activities of water resources infrastructures. As accidents happen at dams all of the time and more people die or are injured in accidents around dams that are not associated with structural failure of dams, Dam operator has a responsibility to safeguard the public and to control hazards that present significant risk of serious harm to the public. Human factor is and remain as an important issue in public safety around dams with the main aim of it was protecting people (visitors and workers) from accidents, drowning, suicide attempts, etc.

Jasa tirta I Public Corporation was implementing ISO as quality management system so Plan-do-actuating-check (PDCA) cycle is an important management approach towards public safety around dams.

- Pre-emptive actions:
 - Installation of proper warning signs
 - Restriction of visitors flow
- Monitoring
 - Close circuit televisions
 - Routine surveillance by reservoir operators
- Restrictions
 - Limitation of traffic flow

- Trashbooms
- Reservoirs zoning

3. IMPLEMENTATION

In implementing the obligation to secure vital objects in in Sutami Dam, Jasa Tirta I Public Corporation as the river basin organization that manage Sutami Dam carries out several activities such as:

- Installation of warning signs
- CCTV Installation
- Vehicles Restricted Area
- Limitation of Vehicle Tonnage
- Security Fences around Main Dams
- Trash boom around hydropower intakes

The example of several activities conducted in order to maintained public safety around dam can be seen in pictures below



Fig. 2
Installation of warning signs



Fig. 3
CCTV Installation



Fig. 4
Vehicles Restricted Area



Fig. 5
Security Fences around Main Dams



Fig. 6
Trash boom around hydropower intakes

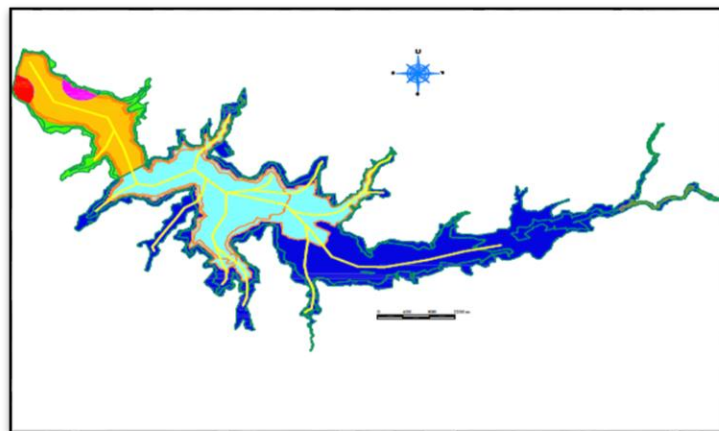


Fig. 7
Reservoir Zoning

4. CONCLUSION

- There are several activities that can be conducted to maintained public safety around dam.
- Dam operator has a responsibility to safeguard the public and to control hazards that present significant risk of serious harm to the public.
- Human factor is and remain as an important issue in public safety around dams with the main aim of it was protecting people (visitors and workers) from accidents, drowning, suicide attempts, etc.

ACKNOWLEDGEMENTS

The study was conducted by Jasa Tirta I Public Corporation, an Indonesian state owned company for river basin organization.

REFERENCES

- [1] Comprehensive Report on the Kali Brantas Overall Project, Nippon Koei Co., Ltd, April 1961.
- [2] Karangates Project Study Report for Operation of Karangates-Lahor Reservoir, Nippon Koei Co., Ltd., Tokyo, Japan, February 1978.

SUMMARY

Dams are critical in terms of population life support and ensuring sustainable economic development. Dams not only for flood control but also provide water for some mutipurpose activities such as hydropower, irrigation water supply, domestic consumption, industrial water use, tourism, aquaculture, navigation, etc. Sutami dam is one of the large dams located in Brantas River Basin. Sutami dam (locally named as Karangates dam) located at Brantas River Basin in Indonesia. The dam is a multifunction dam, which is used for flood control (with the capacity of 1,650 m³/sec), providing irrigation water supply for 34,000 hectares, and also to generate hydro power plant with installed capacity of 3 x 35 mW. Sutami dam has 180 million m³ storage capacity (based on 2016 bathimetry survey) and 1,500 hectares reservoir surface area. The public safety around dam issues surrounding the safety concerns for Sutami dam existed from its beginning of operation because of its critical water storage capacity, structures and massive human activities' surrounding it.

COMMISSION INTERNATIONALE DES GRANDS BARRAGES

VINGT-SIXIÈME CONGRÈS DES GRANDS BARRAGES
Autriche, juillet 2018

DOI 10.3217/978-3-85125-620-8-114



This work licensed under a Creative Commons Attribution 4.0 International License. <https://creativecommons.org/licenses/by-nc-nd/4.0/>

**RISK BASED APPROACH AT THE DAM SAFETY ASSESSMENT DURING ITS
RECONSTRUCTION**

Jaromír ŘÍHA

Water Structures Institute, BRNO UNIVERSITY OF TECHNOLOGY

CZECH REPUBLIC

Miroslav ŠPANO

Water Structures Institute, BRNO UNIVERSITY OF TECHNOLOGY

CZECH REPUBLIC

COMMISSION INTERNATIONALE
DES GRANDS BARRAGES

VINGT-SIXIÈME CONGRÈS DES
GRANDS BARRAGES
Autriche, juillet 2018

RISK BASED APPROACH AT THE DAM SAFETY ASSESSMENT DURING ITS RECONSTRUCTION

Jaromír ŘÍHA, Miroslav ŠPANO

Water Structures Institute, BRNO UNIVERSITY OF TECHNOLOGY

CZECH REPUBLIC

1. INTRODUCTION

The management of floods is of fundamental importance for dam safety. Overviews mentioned in Bulletins [8] and [9] indicate that flood events have been the main reasons for dam failures. According to the recommendations of the International Committee on Large Dams (ICOLD) the dam safety criteria have been significantly stiffened, namely in terms of the design and check flood probabilities related to spillway capacity. In the Czech Republic the criteria were implemented into the decree No. 367/2005 Coll. [6] which was incorporated into the standard CSN 75 2935 [3]. At recent time a wide and systematic reassessment of dams' hydraulic safety have been performed over the whole country. Common result of the assessment is that the dam does not comply with new requirements and should be upgraded as soon as possible.

The experience based on numerous case studies and re-assessments of dam safety in the Czech Republic shows that the crucial problems lie in insufficient spillway capacity, low elevation of clayey core due to imperfections during the construction and also dam settlement and also in lower dam crest than required in terms of prescribed freeboard. One of the reasons of inadequate dam parameters are also less strict requirements on hydraulic safety of dams in the times of their construction.

The reconstruction of the above mentioned dam components practically always calls for provisional disassemble of the dam crest and also significant intervention into the spillway entrance profile and chute line. The crucial question

arises about the degree of dam and construction site safety during remedial works. Relevant dam safety can be usually achieved only through the significant reservoir level drawdown providing sufficient volume to trap potential flood arriving to the reservoir during construction period. The drawdown temporarily harms reservoir purposes like water supply, recreation, hydropower production etc.

This study contains careful examination of aspects and requirements related to the dam safety during its reconstruction. The discussion on the proportion between individual purposes and benefits of the dam is also carried out. The experience with safety analysis during dam reconstruction is mentioned together with the method used. Practical examples demonstrate individual potential conflicts entering into analysis.

2. THE DEGREE OF DAM SAFETY DURING ITS RECONSTRUCTION

The safety issues during the reconstruction of the dam concern two aspects:

- the protection of the construction site during the flood;
- dam safety against its total collapse usually due to water erosion.

2.1. THE PROTECTION OF THE CONSTRUCTION SITE

The construction site protection concerns individual workplaces like spillway, chute, stilling basin, upstream slope lining, dam crest etc. In a view of safety rate these parts should be assessed individually. Some of them like repair of the dam crest or spillway directly relate to overall dam safety (Section 2.2). For other structures not influencing overall safety of the dam some guidance is given by [3]. As a rule cost-benefit analysis has to be performed in case of the threat of significant losses, terms of construction site insurance against floods should be taken into account too. Guidelines in [3] applied in the Czech Republic recommend the following return period N of the flood for preliminary construction site protection:

$$N = T + 1, \quad [1]$$

where T is duration of the construction in years.

2.2. THE SAFETY AGAINST THE DAM FAILURE

The safety of the dam against its collapse during the remedial works should be assessed considering:

- current dam safety;
- potential material losses due to dam break flood;
- potential loss of life.

Usually, it is not advisable to provide higher dam safety during construction than current dam safety.

The material losses contain losses at the dam itself, benefit losses (water supply, power generation, recreation, fish and wildlife), direct losses to the third parties and indirect economic consequences like water shortage, labor reduction, loss of tourism, etc. [5]. The dam break flood extent modelling and hazard mapping is performed by contemporary hydraulic models combined with GIS tools (fig. 1). The census data serve for the assessment of direct losses.

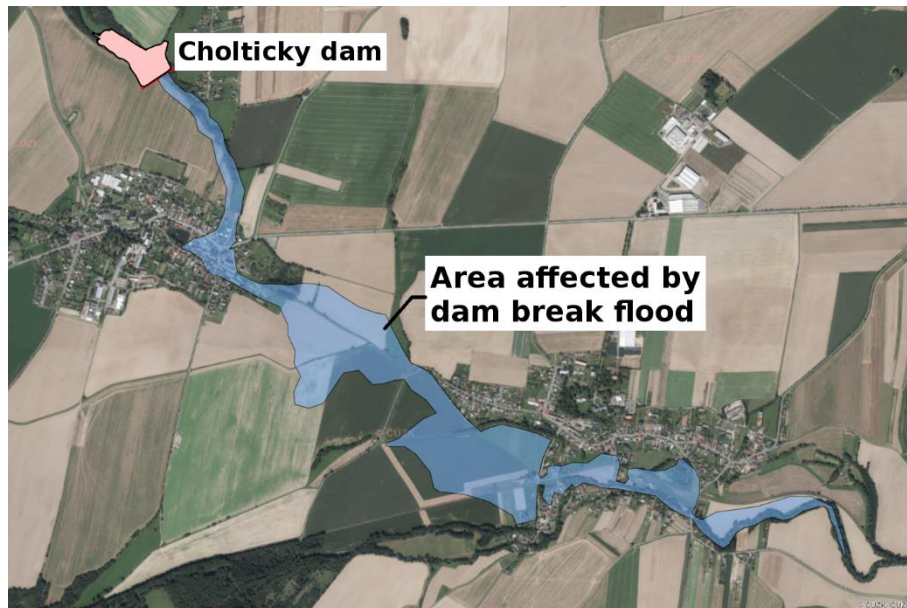


Fig. 1

Area affected by dam break flood cause by breaching of the Cholticky dam [11]

As the principal task is to specify necessary reservoir water level drawdown, losses caused to environment, fish population, recreation and others due to drawdown should be taken into account for selected variants of water levels. The cost benefit analysis should be applied as an appropriate tool for the balancing of material consequences.

The annual probability p_K of the flood for the dam protection during its reconstruction can be determined using the material losses due to dam failure L_K and financial losses L_L due to reservoir level drawdown during the remedial works:

$$p_K \leq \frac{p_L \cdot L_L}{L_K} \quad [2]$$

Probability p_L depends on the duration of necessary drawdown, e.g. in case of one year drawdown $p_L = 1$.

For the potential loss of life estimate numerous guidelines [1; 2; 7] have been published. The experience from the real dam incidents and failures [10] shows extremely strong dependence on warning time, when about 50% of the population at risk can be evacuated in the first hour, 75% within two hours, and that complete evacuation requires more than 10 hours. Expected warning time depends on the level of warning and rescue systems and may significantly differ from country to

country. Definitely the loss of life depends on the density of population in the area in danger. However, certain fatalities cannot be avoided due to randomness in the population migration, behaviour and also day time of dam incident (tab. 1).

Table 1
Numbers of fatalities during the real dam failures [10]

No	Dam	Population at risk	Warning time (hours)	Number of fatalities
1	Allegheny County, PA, 1986	2 200	0	9
2	Austin, TX, 1981	1 180	1	13
3	Baldwin Hills Dam, CA, 1963	16 500	1.5	5
4	Bear Wallow Dam, NC, 1976	8	0	4
5	Big Thompson, CO, 1976	2 500	0.5	144
6	Black Hills, SD, 1972	17 000	0.5	245
7	Buffalo Cr. Waste Dam, WV, 1972	5 000	0.5	125
8	Bushy Hill Pond Dam, CT, 1982	400	2.5	0
9	Centralia, WA, 1991	150	0	0
10	D.M.A.D. Dam, UT, 1983	500	6.5	1
11	Denver, CO, 1965	10 000	3.2	1
12	Kansas City, MO, 1977	2 380	0.5	20
13	*Kansas River, KS, 1951	58 000	3	11
14	Kelley Barnes Dam, GA, 1977	250	0.25	39
15	Laurel Run Dam, PA, 1977	150	0	40
16	Lawn Lake Dam, CO, 1982	5 000	0.75	3
17	Lee Lake Dam, MA, 1968	80	0	2
18	Little Deer Creek Dam, UT, 1963	50	0	1
19	Malpasset Dam, France, 1959	6 000	0	421
20	Mohegan Park Dam, CT, 1963	1 000	0	6
21	Northern NJ, 1984	25 000	3	2
22	Prospect Dam, CO, 1980	100	7.5	0
23	Shadyside, OH, 1990	884	0	24
24	Stava Dams, Italy, 1985	300	0	270
25	Swift and (lower) Two Medicine Dams, MT, 1964	250	0.75	28
26	Teton Dam, ID, 1976	2 000	0.75	7
27	Teton Dam, ID, 1976	23 000	2.25	4
28	Texas Hill Country, 1978	2 070	0.75	25
29	Vega De Tera Dam, Spain, 1959	500	0	150

The dam safety requirements concerning potential fatalities may be assessed using so called F-N curves [4]. The estimated number of fatalities is related to the probability of dam failure which many times directly corresponds with the probability of the arrival of given flood wave during the reconstruction period. Figure 2 shows an example of relevant failure probabilities corresponding to 10 expected fatalities. During the reconstruction special non-structural measures are usually temporarily undertaken like more careful rainfall observations in the catchment, flood forecasting directly linked to actuated flood committee which is ready to initiate prompt evacuation and rescue provisions. This develops sufficient

warning time and efficient activities in case of emergency situation. Therefore, the probability may be assumed within the “tolerable” risk zone in the diagram in fig. 2. It can be seen that failure probability fits the range 10^{-3} to 10^{-5} which corresponds to 1000 to 100 000 years return period.

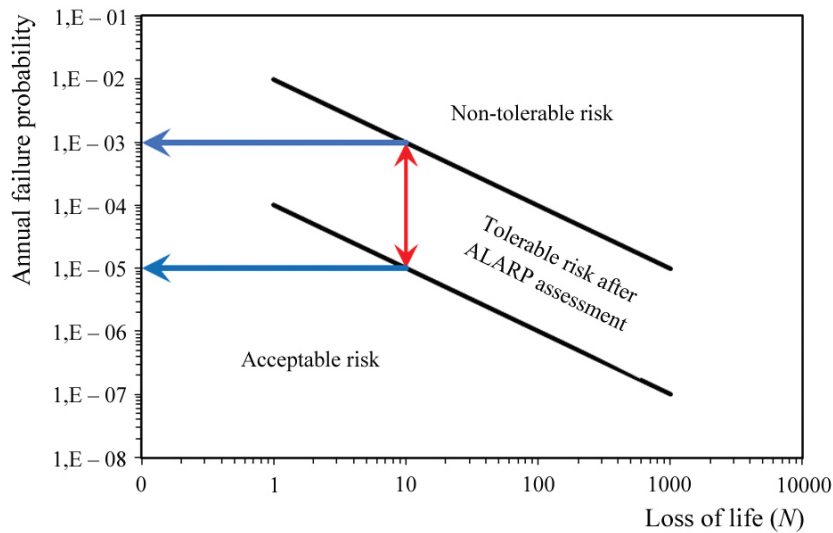


Fig. 2

F-N curves showing situation in case of 10 expected fatalities [4]

For given dam the maximum tolerable failure probability should be specified taking into account previous two aspects – material losses and loss of lives.

The above mentioned procedure gives the guidance for the determination of appropriate probability of the flood for the dam safety assessment during the reconstruction (hereinafter called as “check flood”). The specified probability has to be adapted to the period of the hazard situation, e.g. decreasing of the dam crest level, dismantling the spillway entrance, etc. It reads:

$$P_{adjusted} = 1 - \left(1 - \frac{1}{N}\right)^T \quad [3]$$

where: T is the length of hazardous phase during reconstruction; N is the return period of the flood wave related to one-year occurrence.

It is evident that in case of $T < 1$ year the required return period may be shorter. In tab. 2 the required return periods N are related to the hazardous period T for originally determined return period $N_{1year} = 1\ 000$ years.

Table 2
Approximate required return periods N corresponding to hazardous phase duration T

T (months)	N (years)
12	1000
6	500
2.4	200
1.2	100

3. SAFETY ASSESSMENT DURING THE FLOOD

At the dam safety assessment during floods the maximum water level (MWL) reached while the check flood wave passes the reservoir is compared with the so-called “threshold water level” (TWL) at which the dam is still considered as safe enough (fig. 3).

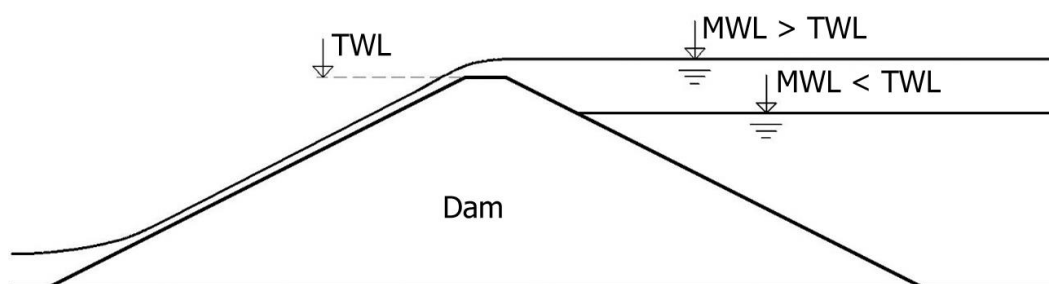


Fig. 3

Scheme depicting the water levels considered in dam safety assessment

During the assessment the reservoir water level drawdown during remedial works is searched to satisfy the condition $MWL \leq TWL$ for given check flood (chapter 2) taking into account the chart flow of the reconstruction works (tab. 2).

4. MAXIMUM WATER LEVEL

The MWL is determined via flood routing procedure for the check flood specified in chapter 2. It is obvious that the construction methods and their duration strongly affect dam safety and its failure probability during refurbishment. The flow chart of the construction steps should be therefore elaborated in variants in advance to enable specification and negotiation of necessary structural and non-structural arrangements and measures in early stage of the preparation of works.

The procedure usually uses trial-and-error method for searching initial reservoir water level (representing the drawdown) during the construction and recommendations on the arrangements on manipulation with water and technical arrangements on appurtenant works.

The flood routing through the reservoir should take into account all appurtenant works available during the reconstruction period. The relevant considerations should contain expected reliability and functionality of bottom outlets and available intakes including possible adaptable measures (e.g. forced opening) in hazardous situation. An example is the opening of the side wall of the emergency spillway at the Mostišť dam (fig. 4) which would attenuate arriving flood more efficiently. Operative measures can be also adapted when the reconstructed dam belongs to the dam cascade to make the flood routing through the system more efficient.



Fig. 4

Opened side spillway during the dam reconstruction

5. THRESHOLD WATER LEVEL

The TWL is determined for each construction phase according to the actual state of the dam and its appurtenant works. The vulnerability of the dam has to be assessed during the construction. Mostly the effect of surface erosion is considered. This is generally represented by the overtopping of the dam body and erosion of subsoil at foundation of the spillway or chute.

The critical phases may be as follows:

- the removal of the breakwater or parapet wall from the dam crest;
- decreasing the dam crest due to increase of clayey core;
- necessary stabilisation of upstream slope/face;
- opening of the spillway chute;
- reconstruction of the chute and stilling basin adjacent to the dam body, etc.

During the construction period, temporarily arrangements improving (heightening) the TWL may be installed.

Theses consist of the following elements:

- cofferdams, fusegates or protecting walls are increasing TWL and protecting the construction site against raising of water level in reservoir (fig. 5);
- wavebreaking arrangements like riprap fill;
- sandbags located along the dam crest to protect it against overtopping (fig. 6).

Some of the above mentioned arrangements are installed for the whole construction period (like cofferdams) some are used as an emergency measure during the flood (like sandbags or fills).



Fig. 5
Concrete cofferdam at the reconstructed dam Šance



Fig. 6
Sandbags located at the crest of the dam Znojmo to reduce risk of overtopping

6. CONCLUSIONS

To assure high dam safety during its reconstruction is essential. In the paper the general guidance is presented to specify the probability of the check flood for dam safety assessment during the remedial works. However, construction activities may, during certain period, call for temporarily both structural and non-structural arrangements which keep dam safety at the prescribed level. These measures concern the attenuation of arriving flood and thus lowering maximum water level during the specified check flood. Here an examples are reservoir water drawdown and/or lowering spillway crest during critical construction phases. Another possibility is to increase threshold water level by cofferdams or also operatively by sandbags. Final safety assessment must prove that the threshold water level is higher than the maximum water level at any construction phase.

7. ACKNOWLEDGEMENTS

This research was supported by the TACR TH03030182 project “Protection of hydraulic structures against action caused by oscillatory wind waves” and FAST-S-17-4066 “The assessment of the filtration instability origin in the soils by the limit state method”.

REFERENCES

- [1] BOWLES D.S., ABOELATA M., 2007, Evacuation and life-loss estimation model for natural and dam break floods, *In Extreme hydrological events: new concepts for security*, O.F. VASILIEV et al. (ed.), NATO Science Series, 78, Springer, Dordrecht, 363-383, DOI: 10.1007/978-1-4020-5741-0_25.
- [2] BROWN C.A., GRAHAM W.J., 1988, Assessing The Threat To Life From Dam Failure, *Journal Of American Water Resources Association*, 24 (6), 1303-1309, DOI: 10.1111/j.1752-1688.1988.tb03051.x.
- [3] CSN 75 2935, 2014, Safety assessment of water structures during floods, Czech standard, (in Czech).
- [4] DAM SAFETY, 2011, Dam safety public protection guidelines. A risk framework to support dam safety decision-making. U.S. Department of the Interior Bureau of Reclamation, Dam Safety Office, Denver, Colorado, USA, 32 p., available online at <https://www.usbr.gov/ssle/damsafety/documents/ppg201108.pdf> (data access 04.07.2017).
- [5] DAMS SECTOR, 2011, Estimating economic consequences for dam failures scenarios, US Department for Homeland Security, USA, 52 p., available

- online at <https://www.yumpu.com/en/document/view/29287776/estimating-economic-consequences-for-dam-failure-scenarios> (access 04.07.2017).
- [6] Decree No. 367/2005 Coll., Regarding technical requirements for water structures, (in Czech).
- [7] GRAHAM W.J., 1999, A procedure for estimating loss of life caused by dam failure, DSO-99-06, Dam Safety Office, U.S. Department of Interior, USBR, Denver, Colorado, USA, 43 p., available online at <https://www.usbr.gov/ssle/damsafety/techdev/dsotechdev/dso-99-06.pdf> (data access 04.07.2017).
- [8] ICOLD, 1995, Dam failures statistical analysis, ICOLD Bulletin, 99, 76 p.
- [9] ICOLD, 2003, Dams and flood. Guidelines and cases histories, ICOLD Bulletin 125, 229 p.
- [10] MCCLELLAND D.M., BOWLES D.S., 2002, Estimating life loss for dam safety risk assessment – a review and new approach, US Army Corps of Engineers, Institute For Water Resources Report 02-R-3, 403 p., available online at <http://www.iwr.usace.army.mil/portals/70/docs/iwrreports/02-r-3.pdf> (access 04.07.2017).
- [11] ŘÍHA J. 2017, Determination of area affected by dam breach flood downstream of the Choltický dam, (in Czech).

SUMMARY

Due to the stricter requirements on the hydraulic safety of the dams in the Czech Republic lot of hydrological and dam safety studies and also extensive remedial works at numerous dams are in progress. The reconstructions concern namely improvement of spillway capacity, adjusting of the dam crest and also clayey core elevation to withstand the check flood according present regulations. As the construction activities often call for provisional reduction of the dam crest elevation and opening of the spillway profile, the dam safety during the civil works has to be carefully analyzed. Usually, considerable drawdown of reservoir water level during the construction period is essential. This however may significantly interfere with main purposes of the dam and may also harm subsidiary effects of the scheme. In the paper the risk based approach is demonstrated at the safety analysis of the dams in the Czech Republic. The results of the analysis may also give some guidance for the optimal sequence of works at the site.

COMMISSION INTERNATIONALE DES GRANDS BARRAGES

VINGT-SIXIÈME CONGRÈS DES GRANDS BARRAGES
Autriche, juillet 2018

DOI 10.3217/978-3-85125-620-8-115



This work licensed under a Creative Commons Attribution 4.0 International License. <https://creativecommons.org/licenses/by-nc-nd/4.0/>

**MASTER PLAN FOR SAFETY OF MAJOR HYDRAULIC STRUCTURES IN
EGYPT**

Khaled M. TOUBAR

*Deputy Head of the Reservoirs and Grand Barrages Sector, MINISTRY OF
WATER RESOURCES AND IRRIGATION*

EGYPT

Pelayo BAZTAN

*Senior Hydraulic Engineer, HYDRAULIC ENGINEERING, GAS NATURAL
FENOSA INGENIERÍA Y DESARROLLO DE GENERACIÓN*

SPAIN

Abeer M. SALAMH

*Civil Engineer, Reservoirs and Grand Barrages Sector, MINISTRY OF WATER
RESOURCES AND IRRIGATION*

EGYPT

MASTER PLAN FOR SAFETY OF MAJOR HYDRAULIC STRUCTURES IN EGYPT*

KHALED M. TOUBAR

*DEPUTY HEAD OF THE RESERVOIRS AND GRAND BARRAGES SECTOR,
MINISTRY OF WATER RESOURCES AND IRRIGATION, k.toubar@mwri.gov.eg*

EGYPT

Pelayo BAZTAN

*SENIOR HYDRAULIC ENGINEER, HYDRAULIC ENGINEERING, GAS
NATURAL FENOSA INGENIERÍA Y DESARROLLO DE GENERACIÓN,
pbaztan@globalpower-generation.com*

SPAIN

Abeer M. SALAMH

*CIVIL ENGINEER, RESERVOIRS AND GRAND BARRAGES SECTOR,
MINISTRY OF WATER RESOURCES AND IRRIGATION, abeer@mwri.gov.eg*

EGYPT

1. INTRODUCTION

The Nile River represents the main source of fresh water in Egypt providing more than 90% Egypt's water resources. To control, regulate and manage Nile water, Egypt has about 1270 different hydraulic control structures on the Nile and the waterways within a network of 33,000 km, to manage water and match between Supply and Demand. These hydraulic structures vary from large dams to small regulators. Their main functions are to provide water for agriculture, domestic potable water, agriculture, industry, navigation and hydropower generation.

Downstream of Aswan high dam and Aswan old dam, seven main large diversion dams/Grand Regulators (known in Egypt as Barrages) are built on the Nile River and its two branches. These Barrages are considered as the most important and sensitive hydraulic structures in Egypt. Their height varies between

* PLAN DIRECTEUR POUR LA SECURITE DES STRUCTURES HYDRAULIQUES MAJEURES EN EGYPTE

rusting. The lifetime of such structures, depend on many variables in design, construction, operation and maintenance procedures.

Some experts estimate the lifetime of these structures in the range of 100 – 200 years. Anyway, these structures must be rehabilitated or replaced after a defined period of time. The oldest functioning regulators in Egypt are Dairout Group of Regulators that were built in 1872.

Table 1
Number of main hydraulic structures according to year of construction and location on the waterway
Nombre de structures hydrauliques principales selon l'année de construction et l'emplacement sur la voie navigable

	Before 1900	1900 - 1920	1920 - 1945	1945 - 1970	After 1970	Sub - total
Nile Barrage	0	2	2	1	3	8
Big Head Regulator (HR)	2	3	4	2	5	16
Big Intermediate Regulator (IR)	5	0	4	6	13	28
Smaller HR/ IR	7	4	27	49	14	101
Sub-total	14	9	37	58	35	153

2. PROBLEM DEFINITION

Having in mind the water scarcity challenges that Egypt face and the vital need to adopt all required measures that improve water allocation and use efficiencies, RGBS initiated a replacement programme to many of these structures several years ago. This programme is in parallel with a continuous maintenance and rehabilitation programme. The rehabilitation programme was generally adopted yearly by reporting urgent defects in certain structures and allocating the required budget for the necessary remedy actions. Longer planning was not possible for more than a 5 year ahead plan.

The (RGBS) authority was in need to have longer ahead plans up to the year 2050. In order to decide action for a certain structure, remedy action or rehabilitation, the optimisation between urgency of remedy action and the importance of the structure was always a debate that could only be settled by own experience of the decision maker.

Capacities and state-of-the-art tools to support informed decisions were not available. Moreover, unavailability of such tools could lead to wrong decisions

that cause misuse of the authority's resources, and even could not achieve the target of the proper management of Nile Water to ensure the reduction of water losses and improve efficiency in water allocation and distribution.

3. CONCEPT FOR SOLUTION

Proper planning should be based on a decision support system that facilitates handling many data about the structures with the planning constraints in order to optimise the best use of the resources with time, achieving the goals in all plans.

A Master Plan (MP) study based on a decision support model for the improvement of structures' functionality and efficiency in water allocation and distribution was adopted. The MP would contribute to the overall River Nile water resource management. The MP study aimed to produce a detailed description of the necessary measures and remedial actions to be undertaken for the selected approximately 150 major existing structures, estimate costs and time schedules for interventions on these structures up to the year 2050, taking into account current and any anticipated future socio-economic and environmental changes.

The study aimed at achieving acceptable efficiency of the Egypt's major control structures with the optimal solution of multi constrained problem. The MP was directed to include all significant criteria that affect the decision of actions in the plan and their proper timing. A multi criteria decision analysis (MCDA) was adopted to obtain the possible plans related to different planning scenarios.

4. METHODOLOGY

First, get a baseline condition. This means to assess current safety, stability and efficiency conditions for all structures.

Second, define all remedy actions required for all structures in order to regain favourable levels of safety and efficiency.

Third, estimate cost for all required actions.

Forth, define criteria that affect prioritising actions in one structure before other actions in another structure.

Fifth, define criteria for different scenario plans.

Sixth, integrate all data and criteria in a multi criteria decision analysis model and obtain the target plan.

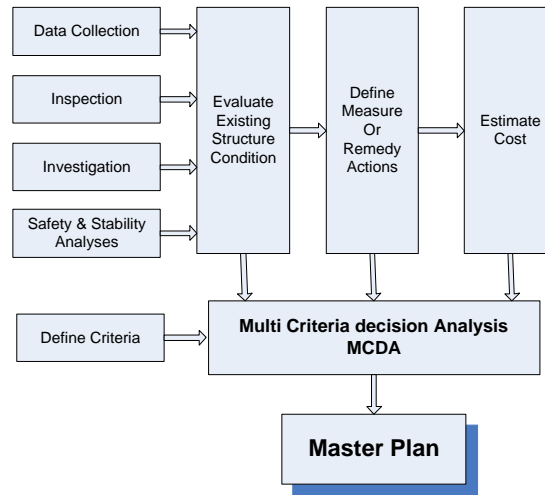


Fig. 2

Flowchart of methodology for preparation of the MP
Organigramme de la méthodologie pour la préparation du PD

5. WORK DONE

5.1. EVALUATE CURRENT STATUS OF EXISTING STRUCTURES

5.1.1. Database

The starting point for evaluation of structures is the collection of basic information about them, then compile in a database. The database was composed of two parts. One part forms the constant or the static data that are almost in need for no regular update, while the other part includes the dynamic data that are in need for periodic update.

The static data portion included:

- Hydraulic structure data (drawings, reports)
- Structure geotechnical investigation (sections, reports, photos)
- Historical events and main rehabilitations (reports, photos)
- Social and environmental data (reports)

The dynamic data portion included:

- Site visual inspection (reports, photos)

- Topographic and bathymetric survey (sections, reports, photos)
- Under water structure inspection (videos, photos, reports)
- Dewatering inspection (videos, photos, reports)
- Structural stability and safety Analysis (reports)

5.1.2. Inspection of current conditions

Inspection of existing structures took place to provide any missing or doubtful data collected and integrated in the Database. Apart from data collection, the main purpose of this activity was to inspect the current situation of the existing structures indicating level of deterioration or inefficiency. The inspection covered the structural and the mechanical elements of the structure.

The inspection programme included different types of inspection as follows:

1. Site visual inspection, collection of missing data for 153 structures.
2. Topographic and bathymetric survey for 150 structures summing a total survey area of 4.264.000 m².
3. Underwater inspections for 192 vents in 48 structures.
4. Dewatering inspections for 19 vents in 15 structures.

5.1.3. Structural and Geotechnical investigations

This is to estimate the current material strength after the age passed since construction in order to perform different technical analyses to check safety and stability of the structures. The decided tool to get this data was to take core samples from the piers and foundations of the existing structure.

Structural and Geotechnical in-site investigations and lab tests for 94 structures have been executed by cores and boreholes summing 4877 m-long.

5.1.4. Analyses for Safety and Stability

Calculations of factors of safety (FOS), for different stability checks, were done to assess the current safety level of the structures. The calculations were based on the material recent properties assessed by the structural and geotechnical investigations.

After fulfillment of parameters requests from the site exploration programme, and the operation data of each regulator, numerical 3D modeling for each structure was carried out to explore the regions of stress concentrations. Implementing the concepts of soil structural interaction (Winckler Assumptions); and the variation of loading within the annual cycle and/or the lock operation was inducted into the model for analysis.

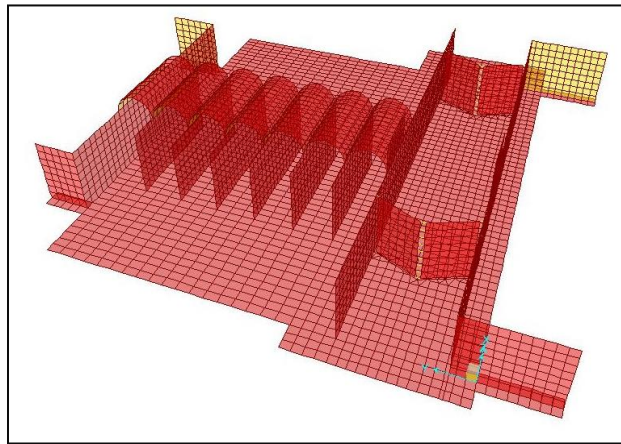


Fig. 3

Example of a 3d model for a control structure (a regulator with a navigation lock)
 Exemple de modèle 3D pour une structure de contrôle (un régulateur avec un verrou de navigation)

5.2. DEFINE CRITERIA FOR DECISION MAKING

The criteria for the decision making are those objectives and constraints that should be considered while looking for the best solution for the problem. There were two types of criteria in this study. The first criteria type included those affecting prioritising of the structure to have the remedy action over other structures. Alternatively, these criteria were named priority factors. They were estimated by the means of an expert system that converted the collected data quantitatively or qualitatively into an arithmetic score. 20 factors were defined expressing the importance of the hydraulic structure (8 factors) and the performance condition of it (12 factors).

Each of these factors has been given a standard scale for scoring. As an example, the first factor is called "Hydraulic structure entity"; and it is related to the classification of the structure accordingly to its location on the waterway and its controlling role. The scale for scoring is as shown in figure 4. The 20 criteria are shown in Figure 5.

Scoring system				
1	2	3	4	5
Intermediate and Spillway (small)	Intermediate Regulator	Head Regulator (small)	Head Regulator (large)	Main Barrage (Nile River)

Fig. 4

Scale for scoring system of the criterion "hydraulic structure entity"
 Échelle du système de notation du critère "entité de structure hydraulique"

MPHS FINAL PRIORITY FACTORS						TOTAL	100%	
#	Description	Data source	Scoring system					Weight
1	Hydraulic structure entity	Site Visits	1	2	3	4	5	5%
			Intermediate and Spillway (small)	Intermediate Regulator	Head Regulator (small)	Head Regulator (large)	Main Barrage (Nile River)	
2	Purposes of the structure	Site Visits	1	2	3	4	5	3%
			Irrigation	Irrigation + Traffic	Irrigation + Traffic + Navigation	Irrig + Traffic + Navig + Water Supply	Irrig + Traffic + Navig + Supply + Power Gen.	
3	Superstructure general condition (Priority Index according to deterioration)	Site Visits	1	2	3	4	5	3%
			Low	Below Average	Average	Above Average	High	
4	Aging and material state	Site Visits	1	2	3	4	5	3%
	Years from commissioning or from fully renovation		<25 or fully renovated<10	25 to 50 or fully renovated 10 to 25	50 to 75	75 to 100	>100	
5	Presence of cracks	Site Visits and Detailed Investigations	1	2	3	4	5	10%
	Detection of visible cracks		Not visible or negligible	Discrete on any part	Continuous on abutment/bridge	Continuous on raft and piers	Critical and continuous on the structure	
6	Presence of holes/abrasion	Site Visits and Detailed Investigations	1	2	3	4	5	10%
	Detection of holes and abrasions		Not visible or negligible	Discrete on <50% vents	Discrete on >50% vents	Critical on <50% vents	Critical on >50% vents	
7	Scouring downstream the structure	Topo and Bathy Reports	1	2	3	4	5	4%
	Depth (m) x 1000 / distance from floor edge DS (m)		<5	6 to 33	34 to 66	67 to 99	>100	
8	Sedimentation upstream the structure	Topo and Bathy Reports	1	2	3	4	5	2%
	Height (m) x 1000 / distance from the floor edge US (m)		<5	6 to 33	34 to 66	67 to 99	>100	
9	Vents mechanical equipment operation	Site Visits and Detailed Investigations	1	2	3	4	5	15%
			Fully operative	Fair operative-basic maintenance required	<50% gates out of order	50-90% gates out of order	All gates out of order	
10	Navigation lock and swinging bridge operation	Site Visits	1	2	3	4	5	5%
			Not implemented/operative	Fair operative-basic maintenance	Bridge inoperative and Lock operative	Bridge operative and lock inoperative	Both Fully Inoperative	
11	Minimum Uplift Factor of Safety	Stability Analysis	1	2	3	4	5	4%
			>3	2 to 3	2 to 1.5	1.5 to 1	<1	
12	Minimum Sliding Factor of Safety	Stability Analysis	1	2	3	4	5	4%
			>3	2 to 3	2 to 1.5	1.5 to 1	<1	
13	Minimum Bearing Factor of Safety	Stability Analysis	1	2	3	4	5	5%
			>3	2 to 3	2 to 1.5	1.5 to 1	<1	
14	Exit Gradient (Piping) Factor of Safety	Stability Analysis	1	2	3	4	5	4%
			>3	2 to 3	2 to 1.5	1.5 to 1	<1	
15	Overall Safety Condition	Stability Analysis	1	2	3	4	5	4%
	Stability analysis conclusion		10	8 to 9	7 to 8	5 to 6	<5	
16	Hazard Potential	Site Visits	1	2	3	4	5	5%
	Distance from inhabited areas DS water way (m)		>2000 m	2000 to 1000 m	1000 to 500 m	500 to 100 m	< 100 m	
17	Seismic Hazard	Site Visits	1	2	3	4	5	6%
			Very low (0 - 0.2 m/s ²)	Low (0.2 - 0.8 m/s ²)	Medium (0.8 - 2.4 m/s ²)	High (2.4 - 4 m/s ²)	Very high (> 4 m/s ²)	
18	Irrigated land served by the water way	Site Visits	1	2	3	4	5	3%
	Number of feddan		< 100.000	100.000 to 500.000	500.000 to 1.000.000	> 1.000.000	Control Structure to feed other intakes	
19	Hydraulic Head (meters)	Site Visits	1	2	3	4	5	3%
			<1 m	1 to 2 m	2 to 4 m	4 to 5 m	>5 m	
20	Nature Park or Historical Archeological site nearby (distance)	Site Visits/SEA	1	2	3	4	5	2%
			>5000 m	5000 to 1000 m	1000 to 500 m	500 to 100 m	< 100 m	

Fig. 5

Criteria used for prioritising actions in the MCDA model
 Critères utilisés pour hiérarchiser les actions dans le modèle MCDA

The second criteria type included those affecting prioritising the actions according to their financial conditions. Different criteria were used to produce different plans till year 2050. Any plan to year 2050 was divided into five year plans. The criteria were:

- Absolute cost of actions
- Different/ equal 5-year-plan budgets
- Benefit/cost-ratio of actions
- Action type
- Structure grouping

5.3. DEFINE THE REHABILITATION ACTIONS NEEDED

After evaluation of current condition of each structure, the required remedy actions were defined. The action in this study varies from maintenance corrective action to rehabilitation or replacement of the structure. Cost of each action was estimated. Expected benefit from that action was assumed as the due enhancement in the scoring system related to the deterioration dealt with by the action.

5.4. MULTI CRITERIA DECISION ANALYSIS (MCDA)

MCDA establishes preferences between options by reference to an explicit set of objectives that the decision-making body has identified, and for which it has established measurable criteria to assess the extent to which the objectives have been achieved.

The scoring and weighting technique was used for the MCDA in this study. Both scoring and weighting rules were set by a series of discussions and meetings by specialised experts in the hydraulic structure work field. Combining the scores and weights of each criterion, shown in figure 6, gave an overall value that reflected the priority of actions.

$$StructureScoring = \sum_{i=1}^n (Priorityfactorscore)_n \times (Priorityfactor\ weight)_n$$

Where n is the total number of factors = 20.

Combining these priority results with the financial criteria led to 6 different scenario plans. The model can handle any number of criteria and lead to many scenarios. But finally, when one set of criteria is selected, only one scenario plan is valid, and that is the best decision.

Table 2
Combination of criteria and corresponding scenario plans
Combinaison de critères et de plans de scénario correspondants

	Plan 1	Plan 2	Plan 3	Plan 4	Plan 5	Plan 6
Absolute cost of actions	•	•	•			
different 5-year-plan budgets	•			•	•	•
Top benefit/cost-ratio actions		•		•		•
Group similar actions in different structures			•		•	•

6. CONCLUSION AND RECOMMENDATIONS

The major hydraulic control structures in Egypt represent the means to manage allocation and distribution of the Nile water with the maximum possible manner. Water scarcity that Egypt is facing adds a pressure on the responsible authority to maintain these structures functioning properly and efficiently to be in-line with other parallel activities the ministry is adopting for better water allocation and use.

The authority prepared a master plan of timely actions for rehabilitation/ replacement of these structures till the year 2050. The master plan is based on a multi criteria decision analysis model that represents an effective tool that allow dynamic planning upon changes of actual efficient conditions of the structures.

It is recommended to follow same methodology in preparation of master plans for other vital infrastructures to provide decision support for decision makers in a way that takes all criteria affecting decision into consideration and have clear rules for decisions.

REFERENCES

- [1] Delivery III.III. Functional Master Plan Model, Master Plan of Hydraulic Structure in EGYPT (MPHS), *ministry of water resources and irrigation, Egypt*, 2017.
- [2] TOUBAR K.M., AL-GOHARY E.A., Rehabilitation of Dams, A Budgetary Point of View, *ICOLD annual meeting, Russia*, 2006.

COMMISSION INTERNATIONALE
DES GRANDS BARRAGES

VINGT-SIXIÈME CONGRÈS DES
GRANDS BARRAGES
Autriche, juillet 2018

FORMAL INVESTIGATION OF LAHOR DAM, INDONESIA

Teguh WINARI¹, Kamsiyah WINDIANITA¹, Didik ARDIANTO¹, Fahmi HIDAYAT²,
Raymond Valiant RURITAN³

¹*Research and Development Bureau*, ²*Deputy Director for Technical Affair*,
³*Director of JASA TIRTA I PUBLIC CORPORATION*

INDONESIA

1. INTRODUCTION

Lahor dam is located in Malang Regency, East Java Province of Indonesia. It is one of the dams in Brantas watershed on the tributary of the Lahor River. Lahor dam was constructed in 1972 for adding capacity of Sutami hydropower. Not only provides great benefits, dam also creates a potential risk to neighboring populations, property, and the natural environment. Therefore, assessment and monitoring of the dam have to be carried out comprehensively and periodically. Formal investigation of Lahor dam aim to evaluate the dam condition during design and construction compare to recent. It is also including visual inspection, instrumentation and slope stability analysis, hydrology and geology condition, and sedimentation analysis. Based on those parameters, the condition of the Lahor dam was ready to be operated.

2. METHOD

Formal investigation of Lahor dam consist of two stages: preliminary stage and advance stage. The former aims to collect all of the information about dam design, construction document, and dam record book (operating and maintenance). While there is an anomaly on the preliminary study, advance study must be carried out that are including re-evaluation of design document, construction method and material type, analysis of operation and maintenance document, and engineering analysis.

3. RESULT AND DISCUSSION

3.1. VISUAL INSPECTION

Visual inspection activities include dam body and complementary building, water quality analysis in laboratory, monitoring of dam instrumentation, hydro mechanical equipment, and concrete structure condition on spillway and access

tunnel. The water quality was monitored on BOD (biochemical oxygen demand), COD (chemical oxygen demand) and DO (dissolved oxygen) parameters from 2013 to 2017. Those BOD, COD, and DO parameters met the standard.

3.2. HYDROLOGY

Spillway design of Lahor dam based on design flood with 1000 years time period and resulted inflow debit 790 m³/second with spillway capacity 399 m³/second. Flood routing with initial elevation of water table +272,70 m obtained maximum flood elevation +274,11 m for 1000 years time period (Q₁₀₀₀) and +277,09 m for Q_{PMF}. The elevation of parapet is +279,00 m.

3.3. INSTRUMENTATION

Some instruments (pore pressure meter, V-Notch, and observation well) was installed in Lahor dam. The pore water pressure at each location is always up and down as the reservoir water level changes. Based on the monitoring results of the seepage discharge shows normal conditions, no significant fluctuations occur, the magnitude is still below the maximum threshold. The amount of seepage discharge depends on reservoir water level and rainfall. The maximum of seepage discharge on toe dam is 1,105.20 liter/minute, the maximum seepage discharge that occurred in toe dam is 896,99 liter / min (April 25, 2017) at water level +273,21 m with seepage water condition looks clear. The amount of spring water discharge at the right bank and left bank (including on the rail way) was fluctuated, because it was influenced by rainfall that occurs. The ground water level conditions also fluctuate along with the water level of the reservoir

3.4. SEDIMENTATION

Based on echo sounding measurement that was carried out in 2016, the dead storage capacity of Lahor reservoir is 3.38 million m³ or 50.45% of the initial dead storage capacity (6.70 million m³). The effective capacity is 28.73 million m³ or 97.72% of the initial effective storage capacity (29.40 million m³) and the total storage capacity is 32.11 million m³ or 88.95% of the initial total storage capacity (36.10 million m³). Sedimentation rates in the Lahor Reservoir from 1977 to 2017 is ± 99,750 m³/year or 0.623 mm/year.

3.5. GEOLOGY

Geological structure (unconformity and fault) around the dam caused several problems during construction. There are agglomeratic tuff as the rock basement, grey clay layer at the middle, and tuffaceous loam as overburden. Those condition lead to land slide around the reservoir. Therefore, in the foundation was carried out rim grouting along the dam axis (433 m). This method could solve the problem effectively.

4. CONCLUSION

Based on formal investigation result in Lahor dam can be concluded that its condition was normal and ready to be operated. There is no anomaly on each inspection parameter.

COMMISSION INTERNATIONALE DES GRANDS BARRAGES

VINGT-SIXIÈME CONGRÈS DES GRANDS BARRAGES
Autriche, juillet 2018

DOI 10.3217/978-3-85125-620-8-117



This work licensed under a Creative Commons Attribution 4.0 International License. <https://creativecommons.org/licenses/by-nc-nd/4.0/>

**FLEXIBLE PROTECTION MEASURES FOR ADAPTATION WITH SEA- LEVEL
RISE ON THE NILE DELTA**

Mohamed HASSAN

*The Project Manager of the Adaptation to Climate Change in the Nile Delta
through ICZM project (ACCNDP)*

EGYPT

Ashraf EL-ASHAAL

*Professor, Geotechnical and Dam Eng., NATIONAL WATER RESEARCH
CENTRE*

EGYPT

Mohamed A MOTALEB

Professor – NATIONAL WATER RESEARCH CENTRE

EGYPT

COMMISSION INTERNATIONALE
DES GRANDS BARRAGES

VINGT-SIXIÈME CONGRÈS DES
GRANDS BARRAGES
Autriche, juillet 2018

FLEXIBLE PROTECTION MEASURES FOR ADAPTATION WITH SEA- LEVEL RISE ON THE NILE DELTA

Dr Mohamed HASSAN¹, Prof. Ashraf EL-ASHAAL², Prof. Mohamed A
MOTALEB³

¹ *The Project Manager of the Adaptation to Climate Change in the Nile Delta
through ICZM project (ACCNDP).*

² *Professor, Geotechnical and Dam Eng., National Water Research Centre*

³ *Professor – National Water Research Centre.*

EGYPT

1. INTRODUCTION

The Nile Delta in Egypt is one the most venerable areas in the world to sea level rise which could cause devastating damages to water resources, agriculture land, people and properties if occurred. Therefore, adaptation measures must be carried out on the ground to protect inhabitants, properties and infrastructure in the Nile Delta. These measures need to be low cost and environmental friendly in order to protect the Delta and preserve the environment in a cost effective way. Therefore, the Government of Egypt (GoE), among its efforts to adapt to Climate Change in different sectors, the Global Environmental Facility (GEF) and the UNDP have jointly funded the Adaptation to Climate Change in the Nile Delta through ICZM project (ACCNDP). The ACCNDP[3] has piloted and assessed the performance of Flexible (soft) techniques to protect the Nile Delta from the anticipated inundation impacts of sea level rise and consequently improve the livelihood of the local population. This paper provides a detailed description of those adaptation options aiming at sharing such experience so they can be up-scaled at local, regional and international scales in similar environments and also present the assessment results of such work.

2. ADAPTATION OPTIONS

Based on the work undertaken by Egyptian researchers at the Coastal Research Institute (CoRI), practitioners at the Shore Protection Authority (SPA) and indigenous people in the Nile Delta, the ACCNDP constructed a number of flexible (soft) dike options. Those options are mainly built from local material to protect the Nile Delta such as sand fences to capture sand blown by wind to accumulate and build sand dunes and dikes with clay and geo-tube cores. These options were constructed at a low laying pilot location between Rasheed (or Rosetta) and El-Burulus. This location was selected based on a survey that was undertaken for the whole area (a length of 60km and a depth of 0.5km) [2].

The construction started in November 2015 and completed in April 2016. The layout of three options is shown in Fig. 1. In the following sections, a description of each option is given.



Fig. 1
Site layout

2.1. SAND FENCES DIKE

This option was selected based on the consultation that was undertaken by the project with the local people in the Nile Delta. They use wooden fences to capture the sand that is blown by the wind to build natural sand dunes around their land and properties to protect them from inundation from the sea (See Fig. 2 Fig. 5). This option was designed by researchers at CoRI and practitioners at SPA according to the Egyptian standards with a length of 250 m and as shown in Fig. 3.



Fig. 2
Local people fences

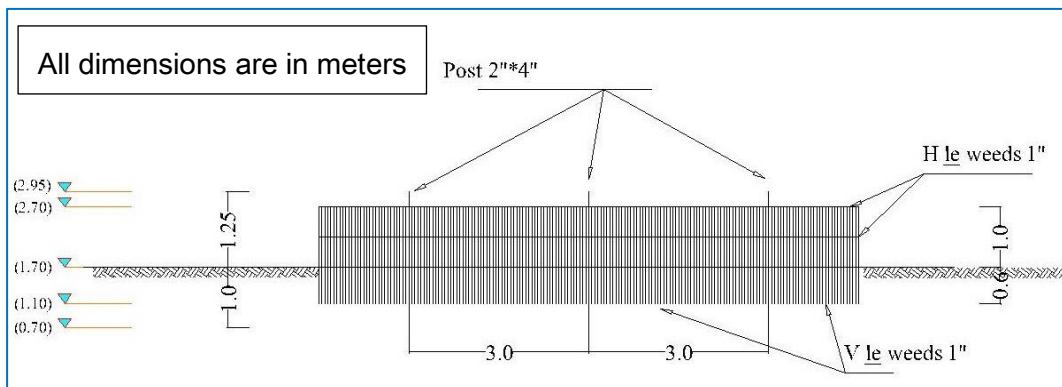


Fig. 3
Sand fences dike design

The sand capturing was monitored since the end of the construction [1] and it was found that the average height of sand accumulation at the fence was increased by approximately over one meter in 8 months, which is considered a good rate of accumulation.

2.2. CLAY CORE DIKE

This option was designed by researchers at CoRI. In this design, the dredged material from El-Burulus Lake was used as a core for the dike. The core is covered with sand up to a level of 3.00 m. Vegetation within sand fence boxes was used to protect the dike faces and crest as shown in Fig. 4. The length of the dike is also 250m. Five monitoring wells were installed within the dike body to monitor the water levels (i.e. seepage) within the dike.

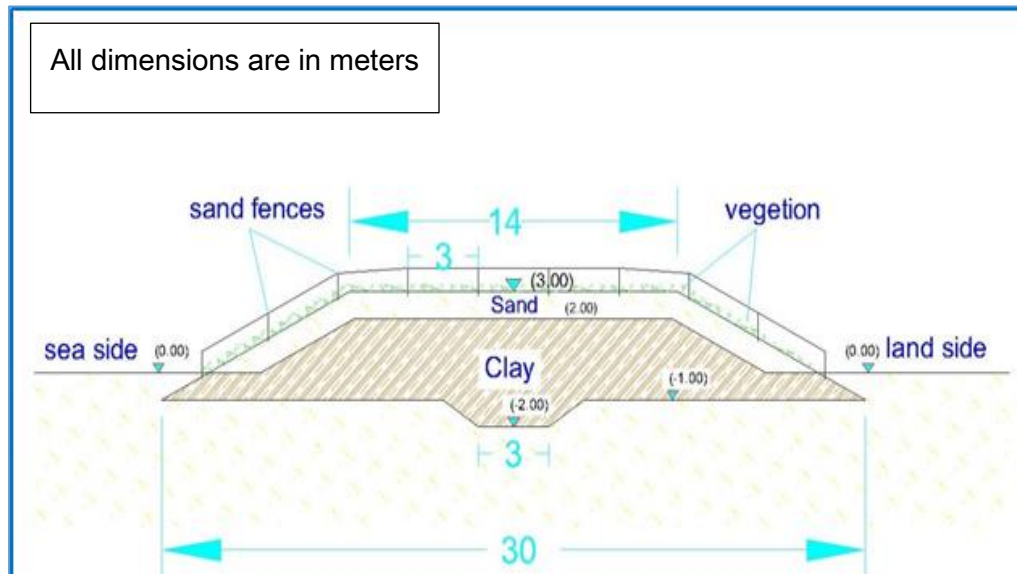


Fig. 4
Clay core dike design

Based on a survey undertaken by the Desert Research Center [DRC] on the natural vegetation in the pilot site location, eight plant species were chosen to protect the sand that cover the dike. These species are:

- *Sarcocornia fruticosa* (L.) A.J. Scot.
- *Juncus rigidus* Desf.
- *Imperata cylindrica* (L.) roeusch
- *Elymus farctus* (viv) Runem
- *Panicratium maritimum* L.
- *Ipomoea stolonifera* (cyr.) J.F. Gmel.
- *Calligonum comosum* (L, Her.) Soskov.
- *Tamarix nilotica* (Ehrenb.) Bunge.

2.3. GEO-TUBE DIKE

This option was designed by practitioners at SPA. In this design, a Geo-tube core was covered with a clay layer from the dredging of El-Burulus Lake up to a

level of 3.00 m. Dolomite stones were used to protect the dike faces and crest as shown in Fig. 5. The length of the dike is also 250m. A monitoring basin was constructed behind the dike body to monitor the overtopping and seepage.

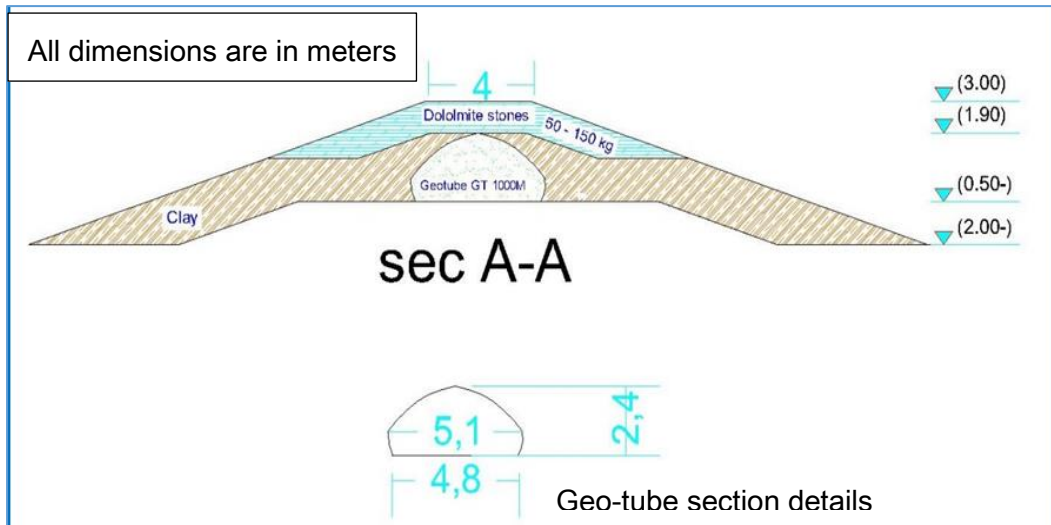


Fig. 5
Geo-tube core dike design

Fig. 6 a, b and c shows a photo of each dike option after the completion of construction in April 2016.

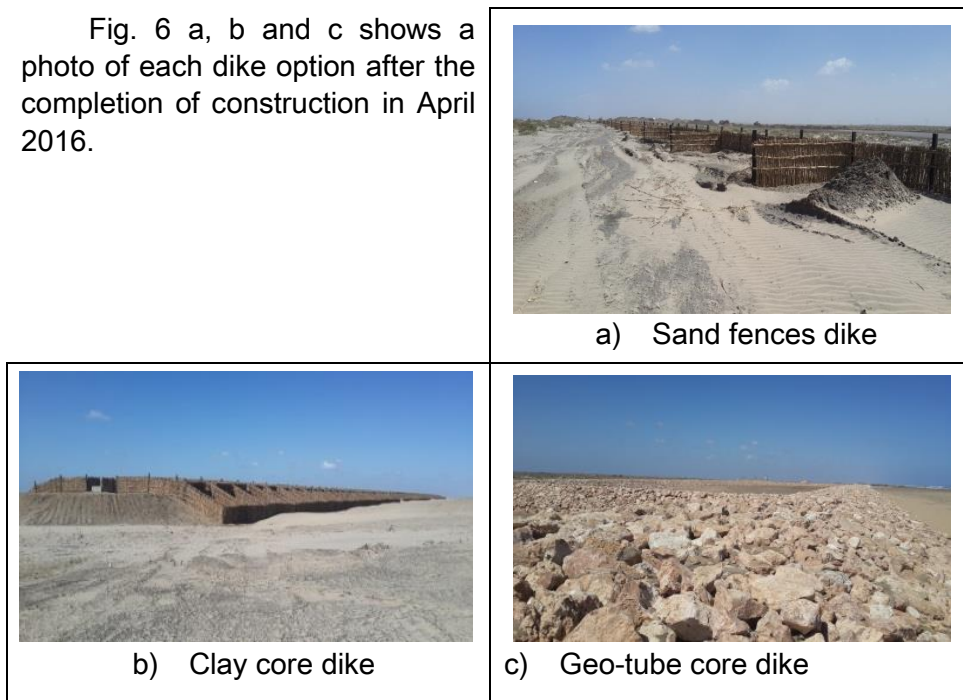


Fig. 6
Dike options after construction

3. ASSESSMENT RESULTS

The performance of the above options was assessed during the winters of 2016, 2017 and early 2018. A number of extreme events occurred during those winters but no damages were observed on the dikes and they remained intact.

The sand fences dike continued to build up and during the events, water did not penetrate through the dike body as no erosion was noted on the whole length of the dike. Water either formed a small pond in front of the dike or flowed within the gaps left between the three dike options.

The clay core dike fences also continued to build up since the end of the construction. Vegetation also grows but at a different rate for each specie [1]. Current results show that *Pancratium maritimum* and *Elymus farctus* are of superior quality at the different locations on the dike (wind and leeward and crest) followed by both *Sarcocorina fruticosa* and *Juncus rigidus*. Monitoring of the five wells revealed that there is no significant increase the water level within each well even after the extreme events which is an indication that seepage is insignificant within the dike body.

The Geo-tube core dike performance was similar to the above two dikes. No wet patches was observed on the back (dry) slope of the dike indicating that seepage is also insignificant within the dike body. The monitoring basin remained dry (apart from small wet batches due to rainfall) indicating that no significant overtopping occurred during the event.

Fig. 7 a, b and c shows a photo of each dike option after a recent extreme event in 2018. Fig 8a shows that a second row of fences was constructed to widen the natural dike (or dune) that was created by capturing the blown sand by wind. Fig. 8b and c show that sea water accumulated in front of the dikes but caused no damage to them.



a) Sand fences dike



b) Clay core dike



c) Geo-tube core dike

Fig. 7

Dike options after a recent storm event

4. CONCLUSION

Low cost and environmental friendly adaptation options have been constructed in Egypt. An assessment of those options against extreme events in 2016, 2017 and early 2018 shows that they provide protection against sea inundation.

Based on the success of this pilot project, The GoE has been able with assistance from the UNDP to secure a grant from the Green Climate Fund. This grant will enable Egypt to almost protect the entire low land in the Nile Delta using flexible techniques covering a length of 69 kms.

REFERENCES

- [1] Desert Research Center, Efficiency of artificial sand barriers for the protection of shoreline at Mastroh area – Kafr El Sheikh Governorate , Progress report, 2017
- [2] Survey Research Institute, survey work between Rasheed (or Rosetta) and El-Burulus, Final report, 2014.
- [3] UNDP, the Adaptation to Climate Change in the Nile Delta through ICZM project, project document, 2009.

ACKNOWLEDGEMENTS

The authors are grateful to GoE, the GEF and the UNDP for their valuable support. The authors are also thankful to the CoRI and SPA staff for their technical support throughout the production of this paper.

KEYWORDS

Embankment, Climate, Cost reduction and Flood control.

SUMMARY

The Nile Delta in Egypt is one the most venerable area in the world to sea level rise, which could cause devastating damages to water resources, agriculture land, people and properties if occurred. Therefore, adaptation measures must be carried out on the ground to protect inhabitants, properties and infrastructure in the Nile Delta. These measures need to be low cost and environmental friendly in order to protect the Delta and preserve the environment in a cost effective way. Therefore, the Government of Egypt (GoE), among its efforts to adapt to Climate Change in different sector, the Global Environmental Facility (GEF) and the UNDP have jointly funded the Adaptation to Climate Change in the Nile Delta through ICZM project (ACCNDP). The ACCNDP has a component to pilot and assess the performance of new innovative techniques to protect the Nile Delta from the anticipated inundation impacts of sea level rise and consequently improve the livelihood of the local population. Based on the work undertaken by Egyptian researchers, practitioners and indigenous people, the ACCNDP constructed a number of flexible dike options that are mainly built from local material to protect the Nile Delta such as sand fences to capture sand blown by wind to accumulate and build sand dunes and dikes with clay and geo-tube cores. In this paper, a detailed description of those options will be given aiming at sharing such experience so it can be up-scaled at local, regional and international scales in similar environments.

Le delta du Nil en Egypte est l'une des régions les plus vénérables au monde à l'élévation du niveau de la mer qui pourrait causer des dommages dévastateurs aux ressources en eau, aux terres agricoles, aux personnes et aux propriétés si elles se produisaient. Des mesures d'adaptation doivent donc être prises sur le terrain pour protéger les habitants, les biens et les infrastructures du delta du Nil. Ces mesures doivent être peu coûteuses et respectueuses de l'environnement afin de protéger le Delta et de préserver l'environnement de manière rentable. Par conséquent, le Gouvernement égyptien, parmi ses efforts d'adaptation au changement climatique dans différents secteurs, le Fonds pour l'environnement mondial (GEF) et l'UNDP ont conjointement financé l'Adaptation au changement climatique dans le delta du Nil à travers le projet GIZC. L'ACCNDP a un volet pour piloter et évaluer les performances des nouvelles techniques innovantes pour protéger le delta du Nil contre les effets d'inondation anticipés de l'élévation du niveau de la mer et améliorer ainsi les moyens de subsistance de la population locale. Basé sur le travail entrepris par les chercheurs égyptiens, les praticiens et les indigènes, l'ACCNDP a construit un certain nombre d'options de digues flexibles principalement construites à partir de matériaux locaux pour protéger le delta du Nil telles que les barrières de sable pour accumuler et construire du sable. Dunes et digues avec des noyaux d'argile et de géotube. Dans ce document, une description détaillée de ces options sera donnée afin de partager cette expérience afin qu'elle puisse être étendue aux échelles locale, régionale et internationale dans des environnements similaires.

COMMISSION INTERNATIONALE DES GRANDS BARRAGES

VINGT-SIXIÈME CONGRÈS DES GRANDS BARRAGES
Autriche, juillet 2018

DOI 10.3217/978-3-85125-620-8-118



This work licensed under a Creative Commons Attribution 4.0 International License. <https://creativecommons.org/licenses/by-nc-nd/4.0/>

**AN INTELLIGENT COOLING CONTROL METHOD AND SYSTEM FOR
XILUODU ARCH DAM CONSTRUCTION**

Peng LIN

*Department of Hydraulic Engineering, TSINGHUA UNIVERSITY, BEIJING
100084*

CHINA

Zeyu NING

*Department of Hydraulic Engineering, TSINGHUA UNIVERSITY, BEIJING
100084*

CHINA

COMMISSION INTERNATIONALE
DES GRANDS BARRAGES

VINGT-SIXIÈME CONGRÈS DES
GRANDS BARRAGES
Autriche, juillet 2018

AN INTELLIGENT COOLING CONTROL METHOD AND SYSTEM FOR XILUODU ARCH DAM CONSTRUCTION

Peng Lin, Zeyu Ning

*Department of Hydraulic Engineering, TSINGHUA UNIVERSITY, BEIJING
100084*

CHINA

1. INTRODUCTION

In hydraulic engineering, heat of hydration develops in fresh concrete, associated with the exothermic chemical reactions of the cement [1]. Due to the poor conductivity of concrete, high temperature gradients may occur between the interior and the surface of the structural elements or between parts of an element with sequential concreting phases [2]. The temperature gradients may lead to tensile stresses and excessive tensile strength will result in the young concrete to crack [3]. Artificial water pipe cooling is an important method used to reduce the interior temperature rise of mass concrete, which can keep the concrete temperature stay near the designed value and to make the construction procedure and property controllable. The first time that water cooling used in hydraulic engineering dated back to the 1930s, when U.S. Bureau of Reclamation tested it in Owyhee concrete arch dam and got a satisfactory result in 1931. Two years later, in the construction of Hoover dam, pre-planted cooling pipes were applied in total concrete pouring blocks and the cooling result was good. Since then, cooling pipes were widely used in concrete dam for its flexibility, reliability and versatility. The method of pre-planted cooling pipes was used in the first concrete arch dam, Xianghongdian dam, for the first time in China and the result of cracking prevention was good. After that, the method was applied in many large hydraulic engineering projects like the Three Gorges Dam, Ertan dam, Xiluodu dam etc. Much engineering practice proved that the method of water cooling has been an

indispensable measure of temperature control and crack prevention in concrete dam [4, 5]. But, the pipe cooling of mass concrete are used in manual mode before Xiluodu (Dam concrete pouring started in March 2009). This pattern of construction and work is very rough, which cannot take full account of the related factors, such as air temperature, pouring temperature, spacing of water pipes, construction process, data collection and control method etc.

In fact, with the rapid development of information and automation control technology, the research and application of intelligent control technology in the civil industry are booming in recent years. There have been many successful cases of applications for some specific areas [6-8]. How to apply information technology and automation control technology to the dam concrete temperature control construction, to solve the drawbacks of the traditional manual pipe-cooling construction mode, and to further improve the quality of concrete in construction and ensure the structural safety? This becomes an urgent problem to be solved in front of water conservancy workers.

A real-time, online and personalized intelligent cooling control method and system for a mass concrete structure (ICCS) is developed in this paper. The proposed method is an important engineering measure to prevent the mass concrete structure from cracking during the construction period. The proposed controlling method and system were successfully used to guide the temperature controlling of Xiluodu arch dam construction. The proposed novel method will be beneficial to the design and construction of the similar projects for controlling thermal stress of mass concrete structure. The following is a detailed introduction to this system.

2. THE METHOD AND PRINCIPLES OF INTELLIGENT COOLING CONTROL

2.1. BASIC PRINCIPLES OF INTELLIGENT TEMPERATURE CONTROL

Temperature is an important index of crack prevention of concrete dam. To achieve the target, the intelligent control method changes the model of setting flow as the control factor into the model of setting temperature as key factor. It follows the three principles below: (1) control the highest temperature during the procedure of cooling down, as well as the highest value in 3-7 days after the pouring of concrete. (2) coordinate the temperature gradient in the whole procedure of cooling down. (3) forecast or warn for anomalous values when the temperature suddenly goes up or goes down. The principles are explained respectively as below.

2.1.1. *control the highest temperature*

Temperature of concrete is related to several factors including the concrete grade, position and duration of the concrete. Controlling the highest temperature is to prevent overlarge difference in temperature of foundation, temperature of adjacent layers or internal and external temperature of concrete, and then to prevent cracking in concrete. The targeted value of highest temperature is determined as following: (1) it should be no higher than the sum of grouting temperature and the allowed difference, for controlling stress caused by temperature difference of the foundation. (2) it should be no higher than the maximum temperature difference between internal and external values. (3) it should be determined differently in confined and unconfined sections. In practice, these different sections include bank sections and riverbed sections. (4) it should vary in different seasons. The previous practice in China generally shows that it is 27°C for confined section and 31 to 33°C for the unconfined. As to large engineering like Xiluodu, the standard is more restricted. The controlled temperature can be determined by local construction practice and the design standard. If the concrete is weak in crack resistance, it should be under 27°C.

2.1.2. *coordinate the temperature change*

Coordinating the temperature change contains three aspects:

(1) keep the temperature curve smooth all along the period of cooling down, as in figure 1(a). In former practice, the temperature curve was manually designed in steps, which added difficulty and labor cost for actual procedure. Assuming that we can automatically adjust the limit of temperature change ratio according to the local highest temperature, then we can keep the temperature curve smooth. Practice in Xiluodu has showed that it is realizable.

(2) make different designed curve in different concrete sections. The stepped time-varying temperature in one concrete section (figure 1(a)) is called time variable curve. It's aimed at limiting the temperature difference between the upper and lower layers from the grouting section to the weighting section of one dam section (figure 1(b)), which is called space variable curve. In a dam, concrete at the bottom is strongly confined while the upper concrete is unconfined. To avoid cracking, it's important to reduce the difference between upper and lower layers. In Xiluodu project, the difference in the range of 1/4 length of old aged concrete (over 28 days) section is limited in 15 to 18°C. In a word, only both time varying and space varying curve controlled can achieve intelligent control. By measures like stage cooling and coordinating temperature change, we can make the temperature gradient in different concrete sections suitable and reduce the concrete stress.

(3) limit the difference in foundation and the difference between interior and exterior. In Xiluodu project, according to the concrete property, using three-dimensional FEM and the design standard method, the difference in confined concrete is 14°C, in base that the cracking-resistance safety factor is no less than 1.8. If the thermal insulation is well conducted, the superficial temperature is 2 °C

to 4 °C higher than the air temperature. In Xiluodu project, according to the stress analysis, the difference should be under 16°C in the most unfavorable condition.

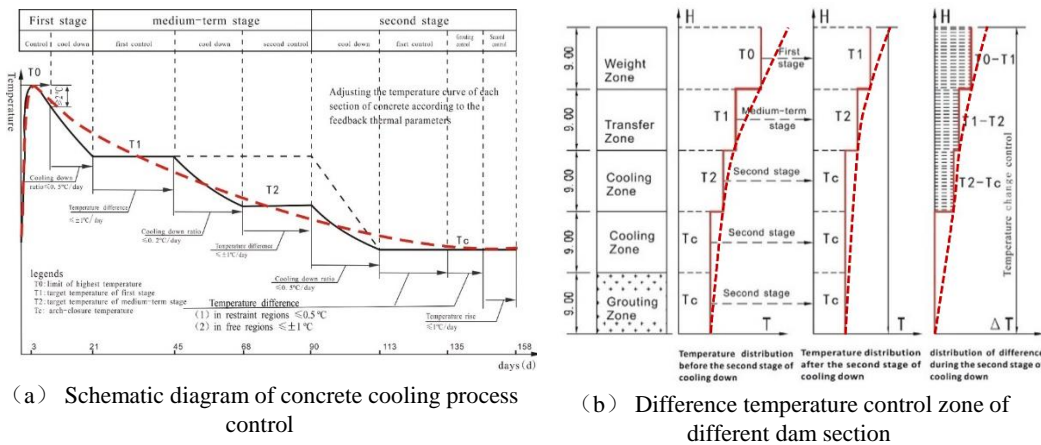


Fig. 1

The time-space control method of the concrete temperature[9]

2.1.3. warn for over transfinite temperature value

Local environment is an important factor affecting the concrete temperature, besides the grouting temperature. Both cold wave in summer and hot wave in winter will cause transfinite temperature. Therefore, the control system has to connect to the system of weather forecasting and timely adjust the limits, considering the principle of coordinating temperature and the problem of cracking in early aged concrete. Like in Xiluodu project, the temperature drop ratio is limited no more than 0.5°C per day in the whole period of cooling down. Particularly, in the middle term of cooling down, the ratio is limited in 0.2°C per day. In practice, continuously and gently reducing the temperature is an important measure for reducing temperature stress. The system must automatically adjust the temperature gradient to the feedback.

2.2. ANALOG PID CONTROL THEORY

In current engineering, the temperature of concrete is affected by many factors. The process is very complex as following: (1) too many unknown factors affect the process. (2) a concrete section is a system of great inertia and delay. (3) the temperature gradient must be limited to as small as 0.2 to 0.5°C per day and the temperature curve must be smooth and steady, neither suddenly going up nor down. (4) temperature in concrete is non-linear distributed. Since these characteristics, classic theory of control cannot meet the requirements. We should combine the modern and classic theory and work out an analogous PID system with property of fuzzy.

First, we get the data such as boundary temperature, temperature difference and change ratio and we can calculate the designed flow and pass the data to the local controller. Then, the controller adjusts the control valve according to PID method thus controlling the temperature of concrete. The system can automatically and timely collect the temperature data and then provide individual method for different concrete sections. It can choose proper thermal parameters for each concrete section thus exactly controlling the flow and temperature. The PID method used by local controller is composited as figure 2. In this system, the output constant $r(t)$, the flow difference, practical integration and differential are combined as a controlled variable to adjust the temperature of concrete.

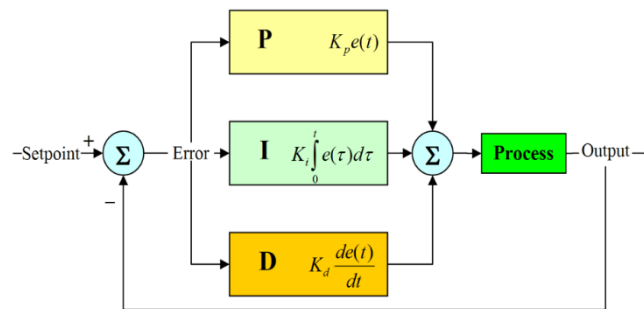


Fig. 2
Control system diagram of analog PID

3. INTELLIGENT COOLING CONTROL SYSTEM

The intelligent cooling control system mainly includes devices for heat exchange, the control device, and the device of monitoring. Here they are introduced respectively.

The device for heat exchange: it is installed inside the concrete or on the surface, for exchanging heat with cooling pipes and achieving individual controlling of temperature of concrete section.

The control device: it mainly includes an integrated control device of temperature and flow, which contains a flow meter, control valve and a thermometer. The integrated device is installed in each closed pipe loop. Under normal circumstances, the system can intelligently calculates the required flow and transmits control commands to the control device. Of course, when an abnormal situation is encountered, manual intervention can also be performed to manually control the integrated device.

The device of monitoring: it includes temperature sensors installed inside the concrete and in the import and export of the cooling pipes. Besides, the system also has a computer server and a software platform for data display data query and control operations. The data acquired by the sensor is transmitted to the computer server through wired or wireless means, and the user can view it on the mobile phone or the computer at any time through the software platform.

In addition, the system also includes an industrial control cabinet, in which many integrated circuit boards, power supply and switches, Plc modules and other electronic components are installed.

4. CASE OF XILUODU ARCH DAM

4.1. THE TEST AND THE FIELD APPLICATION

In order to further explore the evolution law of three-dimensional real temperature field of large-volume concrete through water-cooling, and in the same time improve the system based on the site construction environment, the indoor experiment (at Tsinghua university) and field test (at Xiluodu arch dam) are conducted in the early construction period of Xiluodu.

After the pre-test, the system was initially applied on a large scale at Xiluodu Site. The site installation in Xiluodu project is shown in figure 3. The system control cabinets are set at different elevations of the left and right banks. Each cabinet controls 50 to 100 units of integrated device of temperature and flow. Take the cabinet installed at EL.527m, on the permanent bridge behind the dam and the corresponding integrated devices for example. The pump station is at EL.559m elevation, involving dam sections from number 21 to 29, and its control elevation is from 510m to 630m. The entire local data is transmitted through a wireless bridge to the platform at elevation of 610m at the right bank. And the platform is connected to the server platform in the rear base through the optical fiber.



Fig. 3

The image of intelligence cooling control system in field

4.2. RESULTS AND BENEFITS

This intelligent system can efficiently and accurately collect the real-time data and then transmit it to a unified information platform. The interval of data collecting can be as short as 2 seconds. Using this method can reduce dependence on labor work and avoid data difference caused by personal interference and field cross-operation, thus ensuring the data collected in time and in high accuracy. Take one test section for example, as shown in figure 4.

The cooling intelligent temperature control curves have the following characteristics: (1) compared to the highest temperature value and the point in time of the manually controlled concrete sections, the results of the intelligent controlled sections are basically the same, showing that the intelligent method can effectively control the designed highest temperature; (2) intelligent controlled curves are more smooth and continuous, proving that the data is real-time and the system can coordinate the temperature change; (3) compared to the manually controlled curve, the intelligent controlled one is more fluctuated of flow. This is because the intelligent control platform adjusts the flow size according to the real-time concrete temperature and the entire flow is more saving than that of the traditional method.

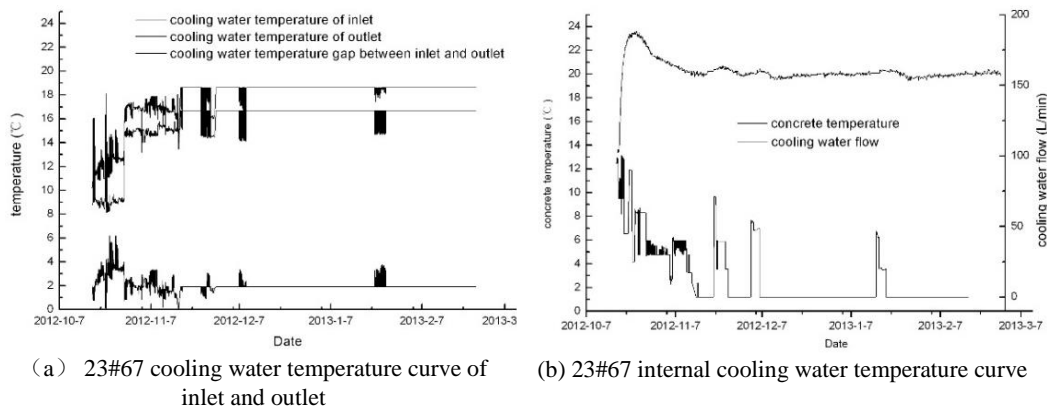


Fig. 4

Cooling intelligent temperature control curves of 23 # 67 of dam[9]

5. CONCLUSIONS

The intelligent cooling control system for mass concrete achieves the online, real-time, intelligent acquisition and control during the operation. It can analyze and control water temperature, flow size and direction as required and provides scientific support for exact, procedural and individual management and control of quality of dam concrete. Through the preliminary application test, the method, which is based on real-time variation of concrete temperature and combined with control of water temperature at the import and export of the cooling pipe, has got

a reasonable result of prediction and control of concrete temperature. It proves that the intelligent cooling control system for mass concrete is feasible.

Based on the current system, more development can be done in directions as following: build an integrated system including monitoring, analysis, control and prediction; synthetically analyze the combination of data like water temperature at the import and export of cooling pipes, temperature of concrete and flow of cooling water; calculate the real-time temperature field and temperature stress of concrete; and at last, control the temperature according to the stress-based indicators and early warning mechanism.

REFERENCES

- [1] Zhu B. Effect of cooling by water flowing in nonmetal pipes embedded in mass concrete[J]. *Journal of Construction Engineering & Management*, 1999, 125(1):61-68.
- [2] Neville, A.M. *Properties of Concrete*. Longman, Essex, England, 1995.
- [3] J. L. Serafim and A. J. Reis, "Thermal stresses in concrete dams during construction," Report CMEST, 1986.
- [4] Zhu Bo-fang, Numerical monitoring of concrete dams, *Water Resources and Hydropower Engineering*. 2008, 39(2):15-18. (in Chinese)
- [5] Wu, Z. R. *Safety Monitoring Theory and Its Application to Hydraulic Structures*. Beijing: Higher Education Press. 2003 (in Chinese)
- [6] Liu Y, Zhong D, Cui B, et al. Study on real-time construction quality monitoring of storehouse surfaces for RCC dams[J]. *Automation in Construction*, 2015, 49(1):100-112.
- [7] Moon S, Yang B, Kim J, et al. Effectiveness of remote control for a concrete surface grinding machine[J]. *Automation in Construction*, 2010, 19(6):734-741.
- [8] Katte N, Konduru N R, Pobbathi B, et al. An integrated expert controller for the oven temperature control system[J]. *Sensors and Transducers*, 2011, 126(3):101-109.
- [9] P. Lin, Q. B. Li, S. W. Zhou, and Y. Hu, "Intelligent cooling control method and system for mass concrete," *Journal of Hydraulic Engineering*, 2013,44(8) :950–957.(in Chinese)

SUMMARY

A real-time, online and personalized intelligent cooling control system for a mass concrete structure (ICCS) is developed in this paper, the proposed method is an important engineering measure to prevent the mass concrete structure from cracking during the construction period. Its main features include: the digital temperature sensors installed in the new pouring mass concrete blocks for real-time measurement of temperature change; one flow, temperature opening measuring and feedback controlling device is installed in the inlet and outlet of cooling pipe, an average reduction of concrete temperature is obtained online through calculating the cooling temperature difference; Thus, according to the Fourier law and conservation of energy the real-time water flow is determined for cooling, then, the intelligent personalized temperature control is carried out by control platform system based on design curve of time with temperature, thereby reducing the concrete tensile stress to achieve purpose of pouring non-cracking concrete dam. The proposed controlling method and system were successfully used to guide the temperature controlling of Xiluodu arch dam construction. The proposed novel method will be beneficial to the design and construction of the similar projects for controlling thermal stress of mass concrete structure.

KEY WORDS

CONTROL METHOD; COOLING; TEMPERATURE; DAM;

COMMISSION INTERNATIONALE
DES GRANDS BARRAGES

VINGT-SIXIÈME CONGRÈS DES
GRANDS BARRAGES
Autriche, juillet 2018

**KEY CONSTRUCTION TECHNOLOGY OF 300M HIGH CORE WALL
ROCK-FILL DAM**

Wu GAOJIAN

Chief engineer, SINOHYDRO BUREAU 5 CO., LTD

Fan PENG

Chief engineer of Branch Company, SINOHYDRO BUREAU 5 CO., LTD

Han XING

*Assistant Chief engineer of Branch Company, SINOHYDRO BUREAU 5 CO.,
LTD*

CHINA

ABSTRACT

As the high rock-fill dam being constructed to 300m, the dam anti-seepage safety attracts much more attention. For the high rock-fill dam constructed at the place where the overburden is deep and the river valley is steep and narrow, the construction quality of foundation treatment, ant-seepage system and dam body filling becomes particularly important. The dam of Changheba Power Station is gravel soil core-wall rock-filling dam, which is construction on the deep overburden, with the dam height of 240m. The height of overburden and dam is 293m in total. The seismic intensity reaches 9 degree. For the above reasons, the control of dam deformation stability and seepage stability is very difficult and it requires high design index and construction quality standard. The deep scientific research was carried out for this project and it made plentiful achievements. This article briefly introduces the engineering characteristics and construction difficulties of

Changheba Power Station dam and describes the key technology adopted during the dam filling works, which has a reference value on the construction of similar projects.

CONCLUSION

The application of the new technologies and new techniques in Chang-he Dam project efficiently guarantees the construction quality. The dam was filled to the crest on 10th September, 2016, which is 4 months ahead of the contract construction period. After 13 times quality inspection carried out by quality monitoring station, it shows that the dam filling is totally under control and the quality is well received by experts. At present the dam seepage controlling and deformation both meet the design requirement and the dam is in good operation condition.

The systematical construction and quality controlling technology developed from the research on Chang-he Dam construction key technology and engineering practices, the engineering problems in 300m high core wall rock fill dam constructed on thick overburden have been solved and the engineering quality and anti-seepage safety have also been guaranteed. 3 industrial standards are formed, more than 50 national patents are obtained and many national and provincial-level construction methods are also formed. The relevant technologies have been applied in some large-scaled hydropower projects, such as the Lianghekou project and the Shuangjiangkou project. It brings remarkable economic and social and environmental benefits and has wide application prospect.

KEY WORDS

Core wall rock-fill dam; construction; key technology; new process

COMMISSION INTERNATIONALE DES GRANDS BARRAGES

VINGT-SIXIÈME CONGRÈS DES GRANDS BARRAGES
Autriche, juillet 2018

DOI 10.3217/978-3-85125-620-8-120



This work licensed under a Creative Commons Attribution 4.0 International License. <https://creativecommons.org/licenses/by-nc-nd/4.0/>

ON-LINE STRUCTURAL HEALTH MONITORING OF REHABILITATED DAMS

Amod GUJRAL

Managing Director, ENCARDIO-RITE ELECTRONICS (P) LTD.

India

Prateek MEHROTRA

Vice President, ENCARDIO-RITE ELECTRONICS (P) LTD.

INDIA



ON-LINE STRUCTURAL HEALTH MONITORING OF REHABILITATED DAMS

Amod GUJRAL, Prateek MEHROTRA

*Managing Director, ENCARDIO-RITE ELECTRONICS (P) LTD., Vice
President, ENCARDIO-RITE ELECTRONICS (P) LTD.*

INDIA

1. INTRODUCTION

Dams are critical components of civil infrastructure of any country. They provide a range of economic, environmental and social benefits like hydroelectric power, irrigation, water supply, flood control and recreation. However, like other assets, dams also age and deteriorate posing a potential threat to life, health, property and environment. The safe functioning of the dam is an important matter of economic benefit and public safety.

Aging dams need to be strengthened and rehabilitated. Improvement of dam instrumentation is an important structural aspect of dam rehabilitation program. This includes replacement of faulty instruments to the extent necessary and practicable. Additional instruments are installed depending on the feasibility and health of the dam.

Continuous monitoring to ensure early detection of failures and to enhance response times to prevent disasters. Changes in the behavioural characteristics of the structure may be indicative of impending dam failure and it is the primary goal of the monitoring system to detect such changes. This calls for online monitoring systems that are capable of near real-time monitoring of the installed instrumentation.

2. DAM INSTRUMENTATION & MONITORING SYSTEM

It is necessary to have a combination of instruments across different sensing technologies to give complete information about potential deformations in a dam. Ease and practicality of installation/replacement of the old instruments for the and communication setup are equally important, apart from proven sensor types and core-technologies to achieve an effective and long-term dam monitoring system. Various building blocks of the system are described in the following paragraphs:

2.1 FIELD INSTRUMENTS

Some surface and subsurface sensors that may be used are mentioned below. Subsurface monitoring gives important information on ground/soil movement which may affect the stability of the structure.

- Tiltmeter and plumb lines to monitor dam tilt/inclination
- Crack meter and joint meter to monitor cracks/joint openings in blocks
- Borehole extensometers to monitor subsurface settlement and deformation
- In-place inclinometers to monitor lateral movement
- Water level & barometric pressure sensors to monitor reservoir level
- Piezometer/uplift pressure sensors to monitor pore and uplift pressure variations
- Seepage/flow meter
- Temperature meter
- Weather station for rainfall, wind velocity, air temperature, humidity and solar radiation

2.2 AUTOMATIC 3-D DEFORMATION MONITORING SYSTEM (ATDMS)

The ATDMS measures movements of targets fixed at critical locations on the dam's structure in three dimensions (x, y & z). It comprises of the following major components:

- 3D prism targets
- Automatic total stations (ATS)
- Control box

- Monitoring database



Fig. 1
Prism target components

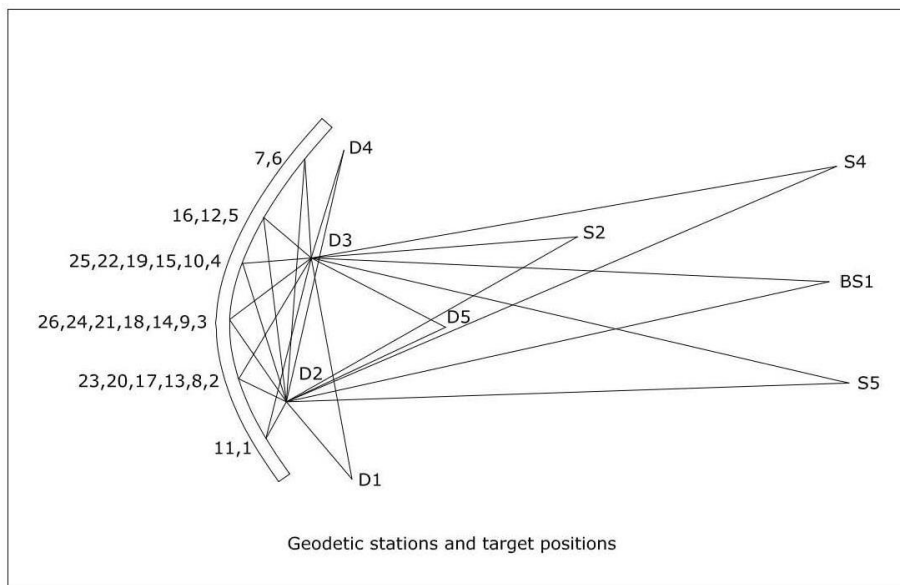
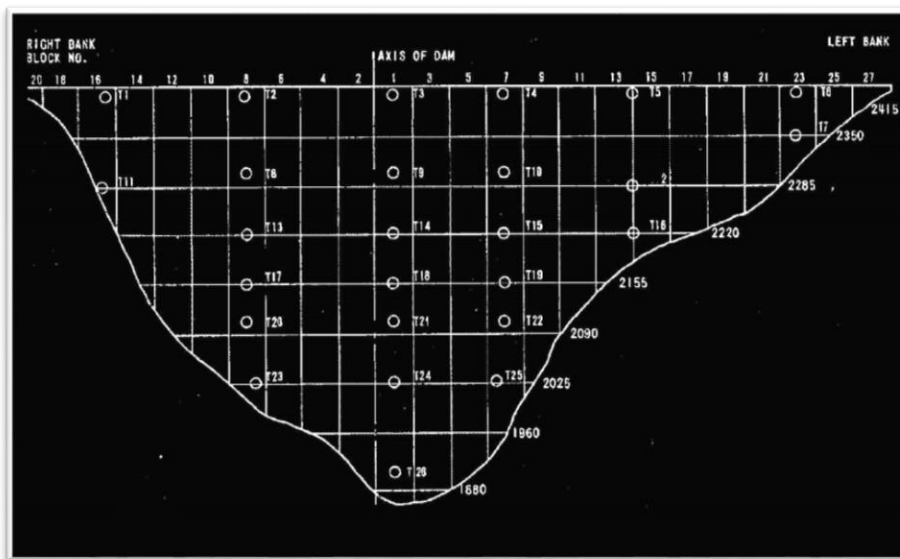


Fig. 2 (Top & Bottom)
Typical locations of targets on the downstream side of an arch dam

3D prism targets (Fig. 1) are installed on the face of the downstream side of the dam in a grid form or at critical locations (Fig. 2)

One or more high precision servo driven, computer controlled ATS is installed at a suitable location on concrete/steel pillar with protective enclosure to automatically sight these points sequentially and record data. Reference prism targets at stable locations make the system complete. Refer to figure 3 for possible mounting arrangements of the ATS.

The ATS is controlled by a control box (Fig. 4) which is essentially rugged field computer. It is powered by 220 V, 50 Hz AC mains and in turn power up the ATS. Solar panels can be used where mains power supply is not available. The control box features GSM/GPRS modem with dual SIM slots for data transmission using the cellular network. Data is collected by the public cloud-based web data monitoring service described in section 3. Alarms can also be programmed in the database resulting in sending SMS/e-mail alerts automatically to the concerned personnel, in case deformation of any point breaches a predetermined trigger value.



Fig. 3
ATS with different mounting arrangements



Fig. 4
ATS control box

2.3 SENSOR COMMUNICATION & DATA TRANSMISSION

2.3.1. Monitoring system with SDI-12 Interface sensors

The SDI-12 system is a bus communication system in which a wide array of dam monitoring sensors can be connected to a single 3-core cable. This is a great advantage and is possible as the electrical interface for the protocol involves three lines: a serial data line, a 12 V power line, and a ground line. The datalogger, featuring GSM/GPRS modem transmits the logged data over the cellular network to the web-based data monitoring service described in section 3. Refer to Fig. 5 for a block diagram of dam monitoring instruments network built on an SDI-12 bus.



Fig. 5
Dam monitoring instruments on an SDI-12 network

The datalogger can be powered either by Lithium or Alkaline cells or by a 12V SMF battery chargeable from AC mains or solar panel.

2.3.2. Wireless monitoring system using radio frequency (RF)



) and features long-range communication on ISM frequency range of permitted in the country of use, of up to 15 km in open field conditions. The low power consumption of the system results in datalogger batteries lasting up to 5 years. Refer to Fig. 7 for a block diagram of a dam monitoring instruments network built on RF data communication technology.

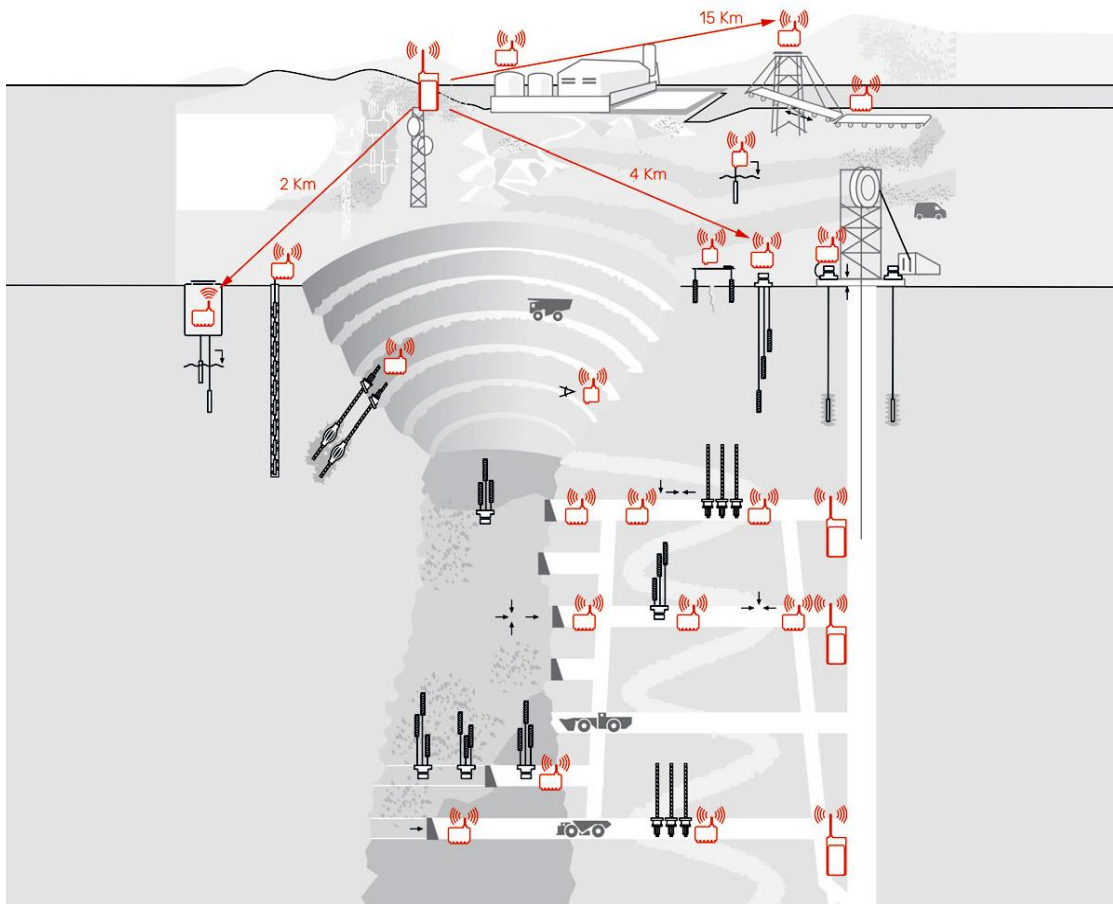


Fig. 6
Typical RF sensor network at field

The RF dataloggers, often called the 'nodes' of the wireless network, can be easily configured in the field using the smartphone Android app provided. These are available in single and multichannel configurations suitable for

receiving the vibrating wire and analogue inputs and automatically collect, store and transmit data from the connected sensors. The RF gateway (

Fig. 8) controls the network and is the aggregator of all data collected by the nodes. It has an integrated 3G modem with antenna supporting HSDPA, EDGE & GPRS, and a high sensitivity GPS-GNSS module. The gateways transmit the data over the cellular network to web data monitoring service described in section 3.

The system offer benefits by means of hassle-free installation- as cable runs-often long and tedious at the dam sites are not involved, cost & time savings, remote monitoring of hard to access locations, easy expansion of the system, if required in future, and easy maintenance.

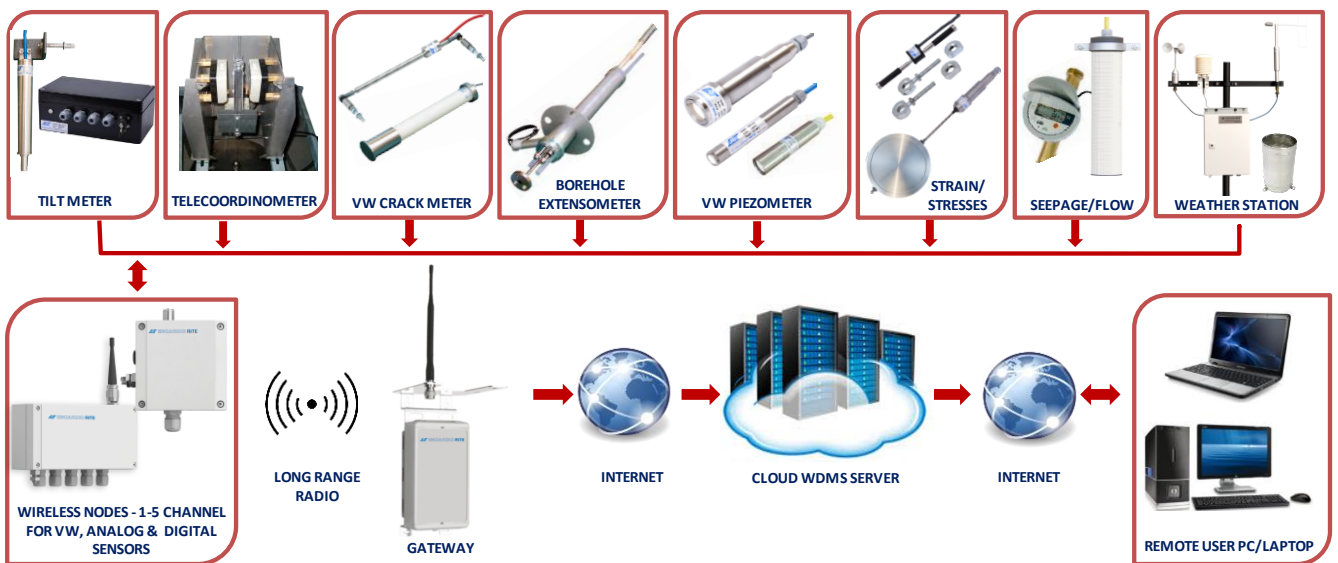


Fig. 7
Dam monitoring sensors connected to an RF network



Fig. 8
RF gateway

3. WEB BASED DATABASE MANAGEMENT SYSTEM

Cloud-based web data monitoring service is available with major geotechnical instrumentation service providers for retrieving data from the dataloggers, archiving retrieved data in a SQL database, processing data and presenting the processed data in tabular and most suitable graphical forms (Fig. 9) for easy interpretation of logged data. This is a highly flexible online monitoring system that can combine data from structural, geodetic and environmental sensors.

Cloud-based WDMS usually work on a rental model. The user has to pay a small setup fee for the first time and then a monthly rental has to be paid for accessing the data over the cloud as long as required.

Web data monitoring service's database management software acts as a data collection agent, a database server and a web server and is hosted on a high-reliability server computer. Choice of the software depends on the measurement technologies deployed.

A master plan of the project is incorporated into the database with locations of each monitoring sensor. From this master plan, the user can get data in the graphical form of any sensor with just a mouse click.

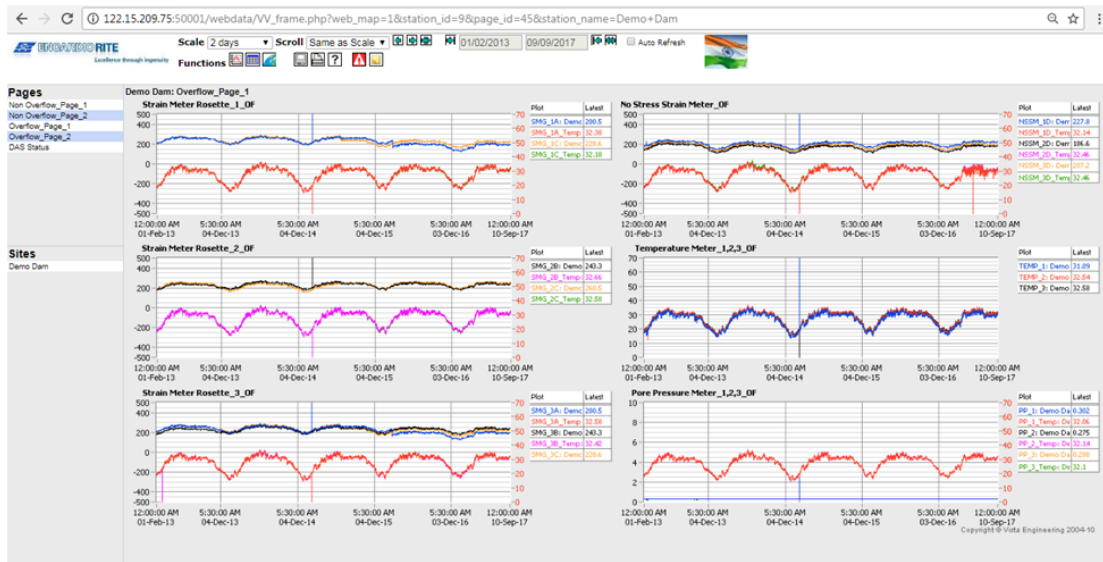


Fig. 9
Graphical data presentation on WDMS

Multiple authorized users at different locations assigned with an individual password are allowed to view any data or report from the structure simultaneously. Graphs & reports can be viewed using popular web browsers like Microsoft Internet Explorer or Mozilla Firefox amongst others.

Details like sensor identification tag, last recorded sensor reading and values of programmed alert levels can generally be viewed on the master plan of the project. If any of the alarm levels of any sensor exceeds, the colour of the marker representing the sensor location changes. Clicking the pop-up table brings up an associated data window where the sensor data can be seen either as a table or as a graph.

Site administrators can set alarm limits, which are generally considered as “alert level” and “evacuate level”. WDMS can also be programmed to send SMS alert messages or e-mail to selected users as soon as any sensor data crosses its predefined alarm levels, either while going above or going below the alarm level.

Features of the data management software can be summarized as follows:

- Data from multiple sensor types are converted into meaningful information in graphical as well as numerical format
- Results available on a wide variety of fixed and mobile devices
- Access to all sensors on one screen
- Instant alerts via SMS or e-mail to authorized personnel
- Combined charts in one report
- Create graphs from any combination of parameters and time period
- Variety of visualization and analysis tools to identify potential failure scenarios
- No special software required for accessing the user sites as information can be viewed using most standard and popular web browsers

4. CONCLUSIONS

While rehabilitation and improvement of dams and its operations and regular maintenance result in restoring their full operational capacity, a balanced and well-executed instrumentation system can provide data for greater understanding triggering mechanisms and deformation behaviour of a dam in great detail. It ensures improved performance on a long-term basis with reduced risk of failure/safety incidents. By monitoring a dam, corrective action may become possible earlier than the occurrence of any failure. The solution for setting up a dam safety instrumentation & on-line monitoring system is not expensive with the advent of new technologies in this field. Considering holistically, the cost of instrumentation and monitoring is a small fraction of what is spent later on in repair and rehabilitation operations.

REFERENCES

- [1] Dunnycliff, John (1988). Geotechnical Instrumentation for monitoring field performance, A Wiley-Interscience publication, USA, pp 199-292; 417-435.
- [2] Website of Dam Rehabilitation and Improvement Project: <https://www.damsafety.in>

SUMMARY

For control and mitigation of disastrous consequences caused by the failure of an ageing dam, it is essential not only to take preemptive corrective action at the site by strengthening and rehabilitating it but also by implementing a good monitoring and forewarning system. The latter is vital for identification of hazardous conditions or developments well before a catastrophic failure takes place and alert personnel with authority to take remedial measures as early as possible. This paper describes advanced instrumentation for dam safety monitoring comprising of field-proven and rugged geotechnical instruments, advanced automatic surveying techniques and public cloud-based web database management system. The field sensors for measuring parameters such as surface and subsurface deformations, porewater pressure, anchor load, rainfall etc. are connected to the field dataloggers either through an SDI-12 bus or through RF signals thus minimizing the cabling costs and increasing system's reliability. Deployment of the robotic total station to automatically monitor 3D prisms at critical locations adds to the comprehensiveness of the data collected and system's integrity. The data collected by the field instruments and sensors, transmitted using GSM/GPRS network, is readily available in real time to the different stakeholders, who may be located in any part of the world. Automatic notification of alarm conditions through e-mail or SMS is realized by the system. The dam safety monitoring network is cost-effective and value-wise is just a small fraction of what is spent later on in repair and rehabilitation.

RÉSUMÉ

Pour maîtriser et atténuer les conséquences désastreuses de la défaillance d'un barrage vieillissant, il est essentiel non seulement de prendre des mesures

préventives préventives sur le site en le renforçant et en le réhabilitant, mais aussi en mettant en place un bon système de surveillance et d'alerte. Ce dernier est vital pour l'identification des conditions ou des développements dangereux bien avant qu'une défaillance catastrophique se produise et alerte le personnel avec l'autorité de prendre des mesures correctives le plus tôt possible. Cet article décrit une instrumentation avancée pour la surveillance de la sécurité des barrages comprenant des instruments géotechniques éprouvés et robustes, des techniques de levés automatiques avancés et un système de gestion de base de données web basé sur le cloud public. Les capteurs de terrain pour mesurer les paramètres tels que les déformations de surface et souterraines, la pression d'eau interstitielle, la charge d'ancrage, les précipitations, etc. sont connectés aux dataloggers sur un bus SDI-12 ou par RF, minimisant ainsi les coûts de câblage. Le déploiement de la station totale robotisée pour surveiller automatiquement les prismes 3D à des emplacements critiques ajoute à l'exhaustivité des données collectées et à l'intégrité du système. Les données collectées par les instruments de terrain et les capteurs, transmises via un réseau GSM / GPRS, sont facilement accessibles en temps réel aux différents acteurs, qui peuvent être situés dans n'importe quelle partie du monde. La notification automatique des conditions d'alarme par e-mail ou par SMS est réalisée par le système. Le réseau de surveillance de la sécurité des barrages est rentable et la valeur n'est qu'une petite fraction de ce qui est dépensé plus tard dans la réparation et la réhabilitation.

KEYWORDS

MONITORING, REHABILITATION, TELEMETERING SYSTEM

COMMISSION INTERNATIONALE DES GRANDS BARRAGES

VINGT-SIXIÈME CONGRÈS DES GRANDS BARRAGES
Autriche, juillet 2018

DOI 10.3217/978-3-85125-620-8-121



This work licensed under a Creative Commons Attribution 4.0 International License. <https://creativecommons.org/licenses/by-nc-nd/4.0/>

**THE OPERATIONAL AND MAINTENANCE OF KEULILING RESERVOIR AS
THE FIRST DAM IN ACEH PROVINCE - INDONESIA**

Ardiana J.

River Basin Organization of Sumatera I,
THE MINISTRY OF PUBLIC WORKS AND HOUSING

INDONESIA

Saputra T. MAKSAL

River Basin Organization of Sumatera I,
THE MINISTRY OF PUBLIC WORKS AND HOUSING

INDONESIA

Mardjono A.

River Basin Organization of Sumatera I,
THE MINISTRY OF PUBLIC WORKS AND HOUSING

INDONESIA

COMMISSION INTERNATIONALE
DES GRANDS BARRAGES

VINGT-SIXIÈME CONGRÈS DES
GRANDS BARRAGES
Autriche, juillet 2018

THE OPERATIONAL AND MAINTENANCE OF KEULILING RESERVOIR AS THE FIRST DAM IN ACEH PROVINCE - INDONESIA

Ardiana J., Saputra T. MAKSAL, Mardjono A.

River Basin Organization of Sumatera I,
THE MINISTRY OF PUBLIC WORKS AND HOUSING - INDONESIA

AUSTRIA

1. INTRODUCTION

Keuliling Reservoir most well known as the first dam in Aceh Province has been serving nearly 10 years. The operation and its maintenance controlled under the surveillance of River Basin Organization Sumatera I - the Ministry of Public Works and Housing of Indonesia. Dam Operation Unit (DOU) is a unit in River Basin Organization Sumatera I which conducting the dam monitoring works in every week, month and year. Three outline duties and responsibilities of DOU; firstly, arranging water reservoir through intake gate in accordance with the needs of water users and operating patterns of Keuliling Reservoir; secondly, supervising the dam instrumentation and hydro-mechanical equipment; and third, maintaining and controlling the dam structure from human activities or animal behavior that may caused a trigger to dam damage.

The Keuliling Reservoir provides as a source of irrigation water supply located in Aceh Province – Indonesia (Fig.1). It is precisely positioned in Bak Sukon Village, Cot Glie Sub-District, Indrapuri, Large Aceh District, Aceh Province. It has 38.2 km² of watershed and an average annual rainfall of 1,791 mm. The flood discharges implied by the Keuliling Reservoir amounted to 203.03 m³/sec for the return period of 20 years and 725.08 m³/sec for the flood discharge of the PMF value. Beside the positive benefits, the dam can cause tremendous flash floods which will result in many casualties, property, public facilities and severe environmental damage due to dam failure state. In preventing such

calamities, the dam must always be monitored and maintained properly. The success of Keuliling Dam monitoring supported by routine, periodic and large inspections. Periodic inspections consist of periodic inspections carried out every 1 (one) year and major inspections undertaken at least once within 5 (five) years.

The River Basin Organization of Sumatera I held the first five years inspection of dam surveillance which evaluated by Dam Safety Committee. The result of the major inspection shows that the dam still able to serve as its main function. The Dam Safety Committee evaluated the dam structure, stability, and its operation system and management. Several recommendation issued for the dam safety and other for dam maintenance. One significant proportion is the human activity surrounding dam area. Hence, the River Basin Organization of Sumatera I interrelated to Dam Safety Committee is implementing and improving dam safety regulation for Keuliling Dam.



Fig. 1. Keuliling Reservoir as the First Dam in Aceh Province, Indonesia

2. BACKGROUND

Considering a dam as multipurpose construction which has a great potential hazard to public salvation, it needs a safety and maintenance guidelines in order to obtain the maximum benefit in long time period. The safeguards and maintenance of the dam need to be followed up with the preparation of operational guidance, maintenance, observation and monitoring of dam. Several government regulations had been established associated with dam construction guidelines in Indonesia that described as follows (Directorate of Water Resources, 2003);

- (1) Law No. 11/1974 on watering;
- (2) Government Regulation No. 22/1982 on the regulation of water;
- (3) Government Regulation No. 35/1991 about river;

- (4) Government Regulation No.25/2000 regarding authority of government and authority of province as autonomous region;
- (5) Presidential Decree No.44/1974 on the principal of departmental organization;
- (6) Presidential Decree No. 102 of 2001 on the status, duties, functions, authority of the organizational structure and working procedures of the department;
- (7) Decree of the Minister of Settlement and Regional Infrastructure No. 01/KPTS/M/2001, on the Organization and Working Procedures of the Department of Settlements and Regional Infrastructure;
- (8) Decree of the Minister of Public Works No. 378/1987, on the Ratification of 33 Indonesian Building Construction Standards;
- (9) Decree of the Minister of Public Works No. 72/PRT/1997, on Dam Safety, Decree of the Minister of Settlement and Regional Infrastructure No. 296/KPTS/M/2001, regarding the amendment;
- (10) Presidential Decree No. 105/M/2002 on the appointment and designation of the Director General of Water Resources, the Ministry of Settlement and Regional Infrastructure;
- (11) Indonesian National Standard Number 1731-1989-F concerning Dam Safety Guidance; and
- (12) Government Regulation of the Republic of Indonesia Number 37 Year 2010 concerning Dams.

Referring to those government regulations mentioned above, the Director General of Water Resources established an operation, maintenance and monitoring dam protocol. There are five subdivisions that include in the operation and maintenance guidance;

Part 1, General :

A guideline on the preparation of the operation, maintenance and dam observation guide, covering general requirements, procedures or operating procedures.

Part 2, Management of Operations dan Maintenance :

Contains detailed description of the implementation of maintenance/operation management and maintenance of dams/reservoirs and their facilities, including a description of their funding needs.

Part 3, Instrumentation and Monitoring :

Describes the basic understanding of the system and the types of instrumentation suitable for the dam and the concrete dam and the procedures for the implementation of the monitoring

Part 4, Dam Inspection for Hydromechanical and Electrical equipment :

Guidance regarding the subjects and targets of inspection and procedures

Part 5, Operational and Hydromechanical and Electrical Maintenance.

3. LARGE INSPECTION DAM

3.1. KEULILING DAM INSPECTION

The regular and large inspection is part of the dam safety evaluation and monitoring process, which purposed to comprehend the condition of a dam related to the security of its structure, hydraulics and operations, identifying the existing problems and establishing suggestions for improving dam security. Large inspection, ie thorough inspection of technical and non-technical aspects supposed to evaluate the dam safety and emergency preparedness. This inspection was led by an expert team who is experienced in the field of dams and at least assisted by Geologists and Hydromechanists. The main work of the large dam inspection executed in five of scope works;

- a. Inventoring and reviewing the existing data
- b. Field inspection work
- c. Instrumentation and interpretation monitoring program
- d. Analysis of inspection result
- e. Report compiling

Three main surveillance conducted in the large inspection of Keuliling Dam were visual inspection, underwater inspection and major inspection. Visual inspection was for ground and water investigating objects, such as dam surfaces, auxiliary buildings, ridges and reservoir cliffs, hydro-mechanical equipment including dam and supplementary buildings. The investigation was for cracks, sub-drainage, crushing, dissolving, leaking, indication of deterioration of quality or chemical reaction, and damage caused by erosion and cavitations. Also, it is aimed to check the contraction joints for water resistance, as well as large signs of expansion or contraction, and the difference in motion of adjacent concrete blocks, the connection of the construction of either vertical or horizontal joints. Elevation of dam crest, cantilever, supporting wall, column, or other wall examined by using previous results as a benchmark to determine the movement of construction. The aeration holes and other openings on the overflow launcher or on the door must be free from mud and other deposits. This action was directed to problems related to scouring and abrasion. Further, the construction also investigated for: cracks, leaks, basins, springs, evaporating holes, incidence of reed erosion, scouring, abrasion, excessive cultivation of plants, crest straightness, bumps and slopes, animal holes, deterioration of riprap quality as well as other slope protective materials and so forth.

Underwater inspection is an investigation of objects under water that executed by beaming or diving method. The objects explored in the upper slope surface of the dam in order to determine the possibility of embankment, avalanches, deterioration of slope protective quality and so on. Upper face of a dam inspected to determine the possibility of cracks, material degradation or openings resulting in increased seepage and leakage.

The main large inspection done through with field investigation and data processing to check the condition of the dam safety in terms of structural, hydraulic, seepage and operational readiness in both normal and extraordinary conditions. Additionally, it is to monitor and evaluate the dam security which consist of the strenghtness of the dam structure, monitoring and operation and maintenances systems and the early warning system of the dam. The main report contains the results of the evaluation and analysis of main dam and its complementary building, hydrology, geology,hydro mechanical and electrical equipments,environmental, dam stability and abundance, sedimentation, operating and maintenance systems, reservoir survey and emergency action plans Keuliling Dam (Multi Karadiguna Jasa Consultant, 2013).

3.2. DAM INSPECTIONS RESUME

The result of major inspection work that was done for 8 (Eight) months start from 23rd March to 19th November 2013 had shown that the main dam of Keuliling Reservoir and its appurtenance in a proper condition. The dam crest has no significant settlement, seepage, crack, joints, sliding and gully erosion but a little deflection and debris. The seepage measurements in downstream area that using a v-notch was found that this gauge had a broken telemetring tool. The spillway of the dam was having no substantial crack, debris, or erosion condition. The intake house of Keuliling Reservoir still in appropriate condition, however it is recommended that there should be an immediat treatment in a structure of the tunnel due to its leaking situation in the joint concrete part. Also, the tunnel should be given a protective paint to maintain the quality of tunnel construction.

The main report for the work of the Large Dam Inspection is the result of the implementation of the inspection work. The main report contains reports of the evaluation and analysis of Keuliling dam and its appurtunance included several evaluations as follow;

- Visual Evaluation of Dam and Complementary Building;
- Hydrological Evaluation and Analysis;
- Evaluation and Analysis of Technical Geology;
- Evaluation and Analysis of Hydro mechanical and Electrical Tools;
- Evaluation and Analysis of Dam Stability and Abundance;
- Evaluation and Analysis of Instrumentation on Body Dam;
- Evaluation and Analysis of Environmental Condition of Reservoir;
- Evaluation and Analysis of Sedimentation Reservoir Survey;
- Evaluation and Analysis of Operating and Maintenance Systems;
- Evaluation and Analysis of Emergency Action Plans;
- Evaluation and Analysis of Dam Security.

It was proposed that the Keuliling Reservoir is provided an emergency control facilities such as gate shaft, controlling system from mechanical and electrical tools and a particular emergency road. Geological condition of Keuliling Reservoir in the main dam, saddle dam, the toehold dam in right and left area, spillway, outlet channel, and its surrounding area had no degradation or

deviation settlement. The dam seismicity investigation resulted in acceptable state where it had no ground tilting, dam cracking, liquefaction processing, and seiches action. In conclusion, the overall assessment of major inspection of Keuliling Reservoir presented that the dam can serve and operate optimally.

4. DAM OPERATION UNIT

The operation and maintenance of a dam must be organized in accordance with standards, operations and its guidelines. The observation works of Keuliling Dam aims in analysing provision data that will result in the state and behavior of the dam whether something is running normally or not. Here, the Dam Operation Unit performing the dam monitoring as one of the main tasks of River Basin Organization of Sumatera – I.

The most recent Keuliling Dam monitoring conducted in November 2017 where it is the third investigation in one year. The unit was monitoring and observing the behavior of dams visually, also reading the instrumentations equipment as a basis and analysis material to evaluate the performance of the dam in order to be followed up if there is a critical situation.

The organizational structure of observation and maintenance of Keuliling Dam is organized under the Dam Operation Unit (DOU) – River Basin Organization of Sumatera I. The organizational structure with number of personnel and the quality of personnel required is a matter of concern in preparing an effective and efficient operation and maintenances organization. The need for personnel required in a dam organization structure is determined by the level and type of complex of a dam construction. Organizational structure of observation and maintenance of Dam Operation Unit in Keuliling Dam is presented in Figure 2.

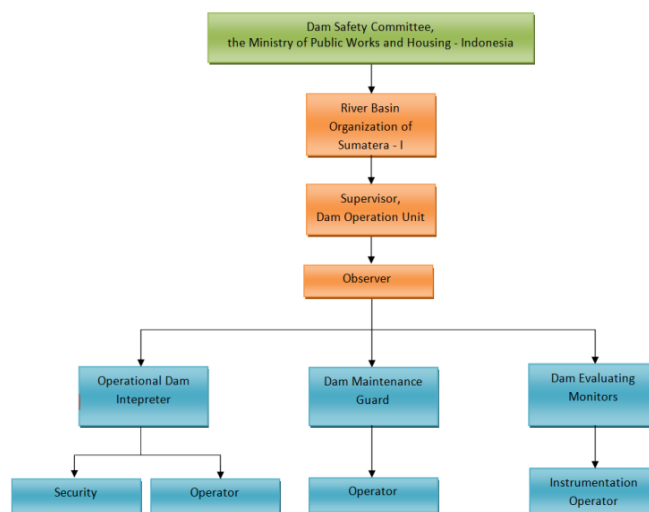


Fig. 2 The Organizational structure of Operation and Maintenance of Keuliling Dam in River Basin Organization of Sumatera – I

4.1. VISUAL EVALUATION

Based on the recent observation works at the end year of 2017, it is desirable that the downstream channel needs to be normalized. It is suggested due to the rainfall in the canal that flowing into the diversion tunnel may affect the stability of the dam. It is also found that there has been no follow-up for sediment removal of a v-notch drainage channel. Thus, may result that the water from v-notch pools cannot be monitored manually.

In investigation of saddle dam 5 and saddle dam 6, it is proposed that there should be re-emphasized to ban illegal connections (water suction) from River Basin Organization Sumatera I, as there have been scouring on the dam body of saddle dam 5 and rock pairs of saddle dam 6 due to the wild connections made by the community (Dam Operation Unit Report, 2017) (see Fig. 3).



Fig. 3. The Water Siphoning Activities by the Community

4.2. MONITORING RESULTS AND RECOMMENDATION

In general, the reading of instrumentation shows a good result without any symptoms of anomaly or deviation. The piezometer at the core zone indicates the filter is working properly and the other located at the foundation illustrates that the wall diaphragm is functioning well. The fluctuation of seepage discharge occurred mostly influenced by the amount of rainfall.

The periodic observation works issued some suggestions. Some buildings and instruments have not been in an optimum maintenance. As a deduction, the Dam Operation Unit (DOU) of River Basin Organization of Sumatera - I submitted

a several recommendation for the urgent maintenance of Keuliling Dam as shown in the the following table 1.

Table 1. The Urgent of Operation and Maintenances Work of Keuliling Dam

No	Building and Instruments	Recent Condition	Recommendation
1.	Data Logger (Instrumentation house)	The automatic instrumentation reading is in a damaged state (data can not be read) caused by lightning that interfere with the program.	Need an immediate reparation.
2.	Vibrating wire piezometer	- Readings were done manually on the house - - Vibrating wire piezometer in the body of the main dam, the data was readable for 5 of 18 points attached to the main dam - Not perfectly accessible digitally on the instrument house	Need a calibration data
3.	Inclinometer	-The box cover is in broken condition -The inclinometer equipment need to be calibrated and the battery should be renewed	The close box need to be repaired immediately to avoid from further destruction which may result in the error reading of inclinometer and the device needs to be re-calibrated
4.	Openstandpipe Piezometer (OP)	The box cover of Openstandpipe is damage	The close box need to be fixed to avoid the clogged pipe holes.
5.	The inundation area	There are fish cages	Control and prohibit the activities of fish cages for water quality and sediment in the reservoir.

5. SUMMARYS

River Basin Organization of Sumatera – I (RBO) as a dam owner has been conducting an operation and maintenance system in Keuliling Reservoir. The monitoring activities operated by Dam Operation Unit. It is found that Keuliling Dam still need an improving of instrumentation monitoring system and it should be controlled 4 (four) times within a year to get an optimum maintenances for a long lifetime of the dam.

Some human activities in Keuliling Reservoir has caused a significant damage. Thus, it is highly recommend that the River Basin Organization of Sumatera I prohibit the illegal activities that may caused a dam destruction. Also, it is suggested that there should be a regional regulation established by the governor about dam preservation including in upstream and downstream area and admissible human activities control surrounds dam area for Keuliling Dam and also the next dam project in Aceh Province.

ACKNOWLEDGEMENT

The great and sincere gratitude is given to Mr. M. Basuki Hadimuljono, the Minister of Public Works and Housing – Indonesia and Mrs. Ni Made Sumiarsih the Head of Dam Project Center from Water Resources Directorate, Ministry of Public Works and Housing Indonesia, for giving all the support to young engineers in participating in the event of international annual meeting ICOLD 2018 and giving the idea of the paper about the operation and maintenance of Keuliling Dam – Aceh, Indonesia.

REFERENCES

- [1] Directorate General of Water Resources. Guidance on Inspection and Evaluation of Dam Safety, *Department of Regional Settlements and Infrastructure*, 2003.
- [2] Directorate General of Water Resources. Operation, Maintenance and Observation Manual – Part 1 & 2 (General, Operation Management and Maintenance), *Department of Regional Settlements and Infrastructure*, 2003.
- [3] Directorate General of Water Resources. Operation, Maintenance and Observation Manual – Part 3 (Instrumentation and Monitoring System), *Department of Regional Settlements and Infrastructure*, 2003.

- [4] Directorate General of Water Resources. Operation, Maintenance and Observation Manual – Part 4 (Safety Inspection for Hydro mechanical and Electrical Equipment), *Department of Regional Settlements and Infrastructure*, 2003.
- [5] Directorate General of Water Resources. Operation, Maintenance and Observation Manual – Part 5 (Operation and Maintenance on Hydro mechanical and Electrical Equipment), *Department of Regional Settlements and Infrastructure*, 2003.
- [6] Government Regulation of the Republic of Indonesia Number 37. Dams. President of the Republic of Indonesia, 2010.
- [7] PT. Multi Karadiguna Jasa Consultant. Large Inspection of Keuliling Reservoir Report. *River Basin Organization of Sumatera I*, 2013.
- [8] Dam Operation Unit. Monitoring Report of Dam Inspection, *River Basin Organization of Sumatera I*, 2017.

COMMISSION INTERNATIONALE DES GRANDS BARRAGES

VINGT-SIXIÈME CONGRÈS DES GRANDS BARRAGES
Autriche, juillet 2018

DOI 10.3217/978-3-85125-620-8-122



This work licensed under a Creative Commons Attribution 4.0 International License. <https://creativecommons.org/licenses/by-nc-nd/4.0/>

**AN ANALYSIS ON THE BEHAVIORS OF A DAM FOR THE EARTHQUAKE
IN SOUTH KOREA**

Taegeun LEE

Department of Inspection for hydraulic structure
KOREA INFRASTRUCTURE SAFETY & TECHNOLOGY CORPORATION

Baegun CHO

Department of Inspection for hydraulic structure
KOREA INFRASTRUCTURE SAFETY & TECHNOLOGY CORPORATION

Gyeongjin KIM

Department of Inspection for hydraulic structure
KOREA INFRASTRUCTURE SAFETY & TECHNOLOGY CORPORATION

Taekang YUN

Department of Inspection for hydraulic structure
KOREA INFRASTRUCTURE SAFETY & TECHNOLOGY CORPORATION

SOUTH KOREA

COMMISSION INTERNATIONALE
DES GRANDS BARRAGES

VINGT-SIXIÈME CONGRÈS DES
GRANDS BARRAGES
Autriche, juillet 2018

AN ANALYSIS ON THE BEHAVIORS OF A DAM FOR THE EARTHQUAKE IN SOUTH KOREA

TAEGEUN LEE, BAEGUN CHO, GYEONGJIN KIM, TAEKANG YUN

Department of Inspection for hydraulic structure
KOREA INFRASTRUCTURE SAFETY & TECHNOLOGY CORPORATION

SOUTH KOREA

1. GENERAL INTRODUCTION

Earthquake was unusual case in South Korea until 2 years ago. However, earthquakes occurring in Gyeongju and Pohang region made people living in South Korea aware that Korea is no longer safe from earthquake.

Especially, Gyeongju Earthquake currently has the largest record since 1978 which seismological observation of South Korea has begun. The fore shock measured to magnitude 5.1 occurred at 9 km point south-south-west in Gyeongju, 7:44 pm on September 12, 2016. After 48 minutes, the main shock measured to magnitude 5.8 occurred at 8 km point south-south-west in Gyeongju.

Table 1. Ranking for magnitude in South Korea

Rank	Magnitude	Date & Time	Epicenter		
			Lat.	Long.	Site
1	5.8	20:32, 12 th Sep. 2016	35.8	129.2	Gyeongju
2	5.4	14:29, 15 th Nov. 2017	36.1	129.4	Pohang
3	5.2	19:14, 29 th May 2004	36.8	130.2	Sea near Uljin
4	5.2	02:07, 16 th Sep. 1978	36.6	127.9	Sangju
5	5.1	19:44, 12 th Sep. 2016	35.8	124.5	Gyeongju



Figure 1. Epicenters and Damage due to earthquake
(Source : www.arirang.com & www.ytn.co.kr)

Gyeongju is one of cities that retain many historical and cultural heritages. Many structures having ancient traditional style are in this region but some of them were damaged by earthquake.

Therefore, KISTEC (Korea Infrastructure Safety & Technology Corporation) thought that main infrastructure near Gyeongju were influenced by earthquake and they performed urgent inspection for a dam which is not far from epicenter.

As a part of dam inspection, the behaviors of a dam were analyzed by comparing with the real-time measured data for before and after earthquake.

In order to perform behavior analysis, displacement and leakage measuring data were selected among entire measuring data. Because these systems are very important for management of type of fill dam and considered to have a relatively high reliability.

Table 2 and Figure 2 show specification of subject dam. Type of Subject dam is C.F.R.D (Concrete Faced Rock fill Dam), operating beginning year is December in 2005 and built purpose of dam is water supply.

This paper shows the results of this analysis and overall conclusions for inspection of a dam after earthquake.

Table 2. Main specification of the subject dam

Dam	Type	Concrete Faced Rock fill Dam	Spillway	Type	Radial Gate (3-Gate)
	Purpose	water supply		Weir crest	EL.117.5 m
	Length	192 m		Length	206.5 m
	Height	52 m		Designed discharge	1,840 m ³ /sec
	Volume	528,000 m ³	Intake facility	Type	Surface intake
	Crest	EL.126.8 m		Scale	D : 4.0 m H : 39.3 m
	Slope	Upstream : 1:1.4 Downstream : 1:1.8			

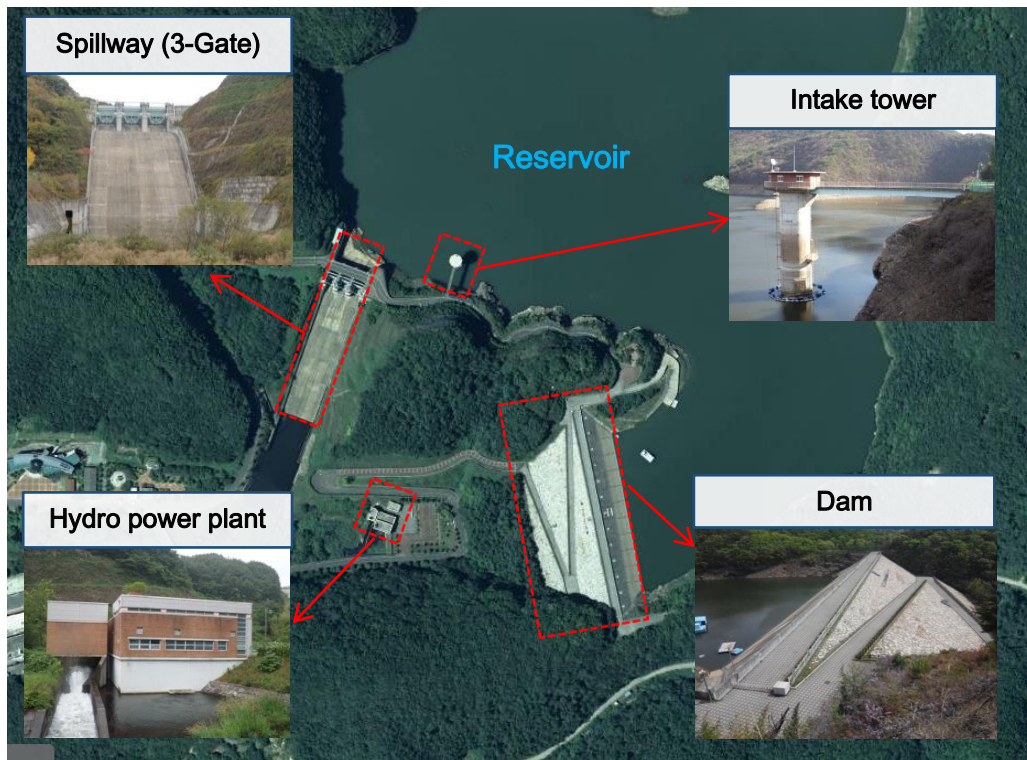


Figure 2. Main specification of The subject dam

2. ANALYSIS RESULTS

2.1. DISPLACEMENT MEASURING

The number of displacement measuring points in subject dam is 14 and these are located at divided section of the subject dam. 5 points are on the dam crest section, 3 points are on the upstream slope section, the others (6 points) are on the downstream slope section. Currently, the displacements of each point are measured automatically every hour.

In order to analyze the influence on earthquake, subject analysis period was decided to 2 months which are Before and after 1 month based on the day (12th, Sep. 2016) of occurring earthquake.

Table 3. Status for displacement measuring points of the subject dam

Classification	Dam crest	Slope		Total
		Upstream	Downstream	
Displacement points (operated)	5	3	6	14

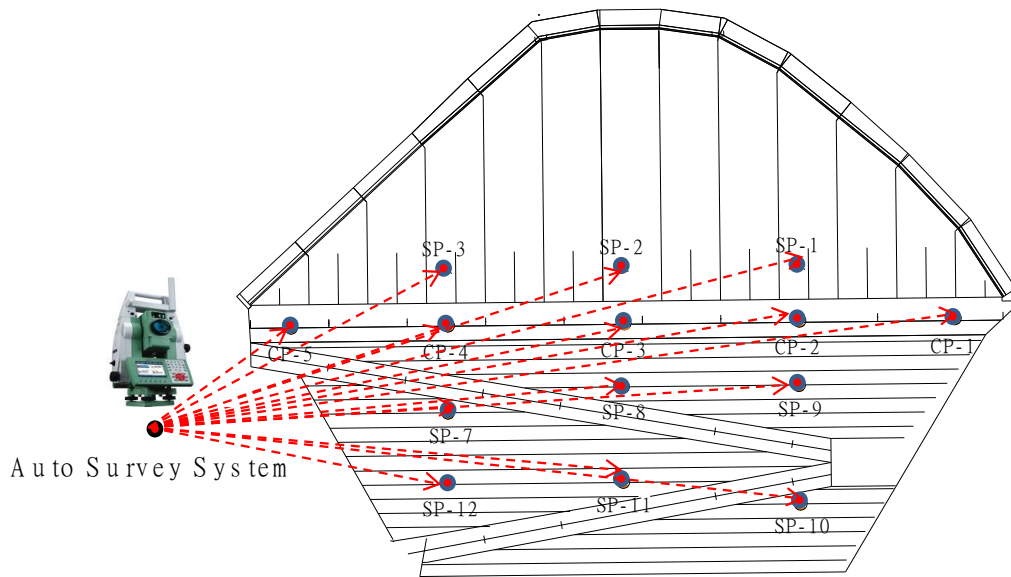


Figure 3. Location of displacement points for the subject dam

Displacement of dam can be measured as 3-Directions (X, Y, Z) and Figure 4 shows displacement direction of the subject dam. X axis is left & right direction and Y axis is upstream & downstream direction. Z axis is up & down direction for the dam crest.

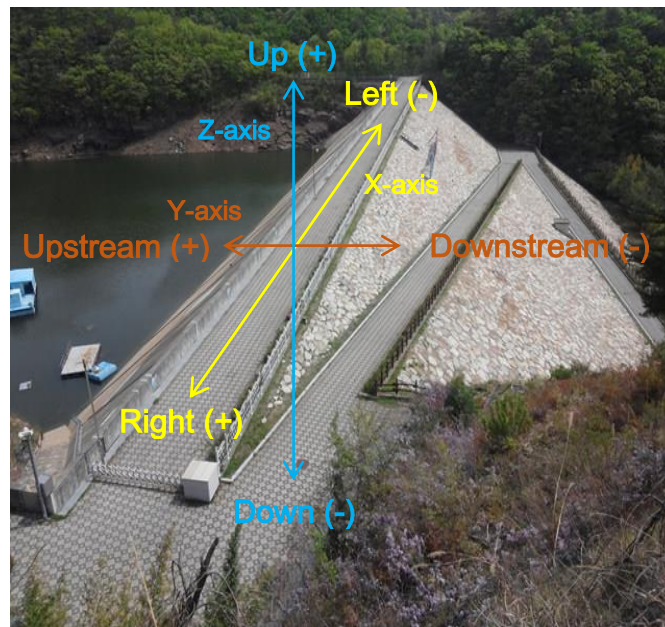


Figure 4. Axis direction of displacement points for the subject dam

Figure 5~6 show status of displacement points for the subject dam. Analysis on SP-12 point excluded because this point needed calibration. In addition, there were unmeasured sections due to the electric errors of measuring instrument.

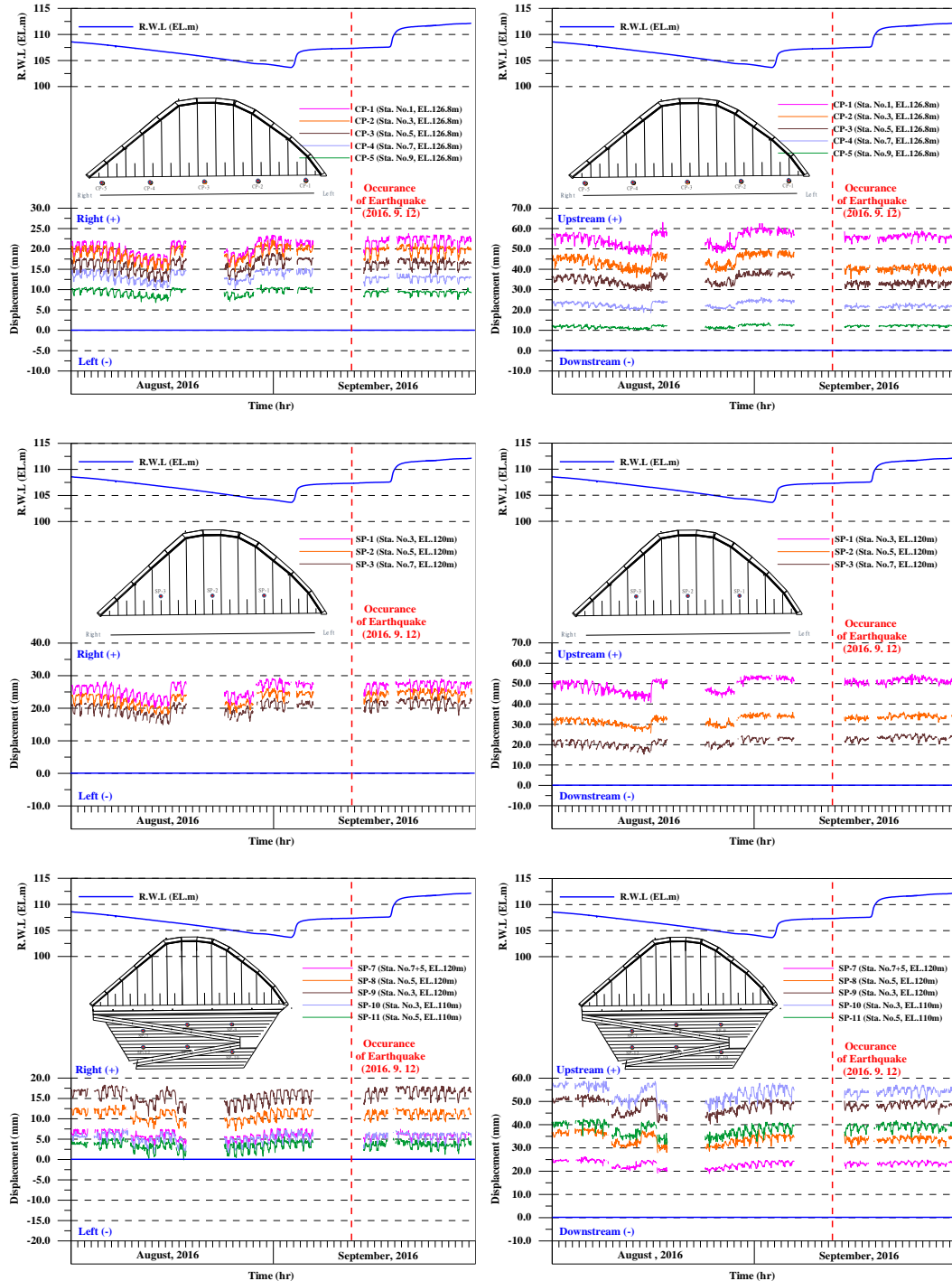


Figure 5. Status of displacement points for the subject dam (X, Y axis)

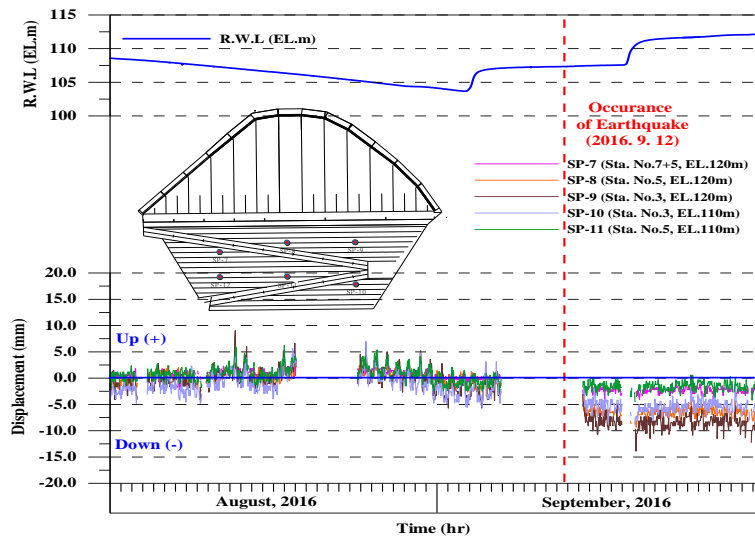
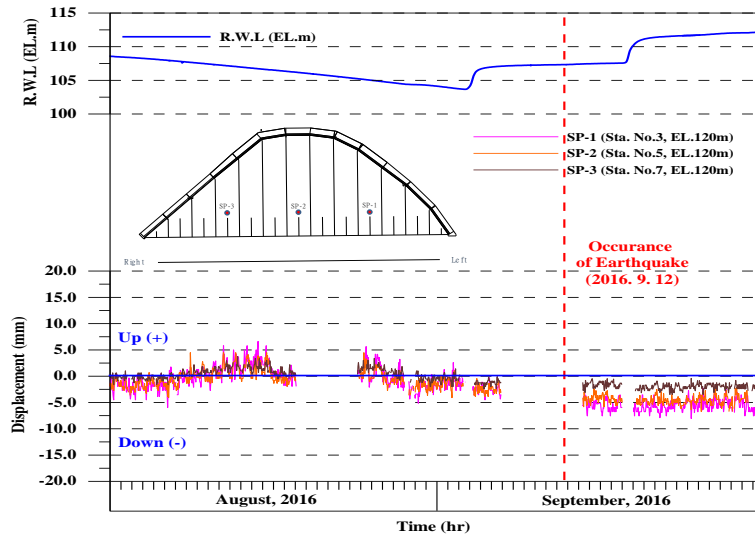
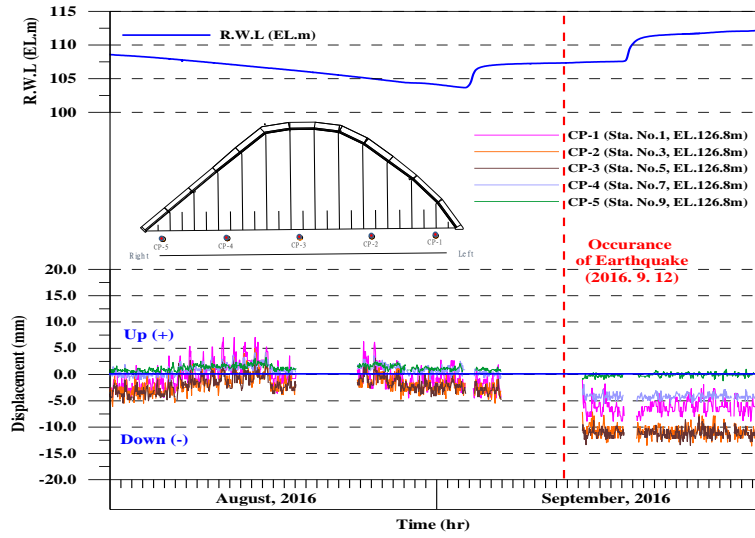


Figure 6. Status of displacement points for the subject dam (Z axis)

Figure 5 shows displacement of x & y directions. As a result, there was little difference between before and after earthquake, but figure 6 shows that displacement of z direction before earthquake was different from after that. This could mean that all points had a change and small displacement occurred on a dam. It was difficult to estimate exactly how much settlement occurred or whether settlement occurred really or not because survey system also had a possibility to be affected by earthquake

Due to a change of only vertical displacements, it was analyzed additionally how much vertical displacement for all points changed.

Figure 7 shows vertical displacement of all points. Lines with rectangular shape are average measured data before earthquake. Period of data is 2 years ago from occurring gyeongju earthquake. Lines with circle shape are average measured data after earthquake. Period of data is 1 month from occurring gyeongju earthquake.

As a result, middle section of dam structure changed larger than other sections. Maximum displacement was about 8.5mm on the middle of dam crest.



Figure 7. Status of vertical displacement before & after gyeongju earthquake

2.2. LEAKAGE MEASURING

Dam structure is always storing amount of water, but perfect blocking of infiltration water is difficult. If infiltration water is increased, dam operators or engineers can think that an Interlocking of rock fill zone or a joint between faced concrete have a problem.

Therefore, in order to properly operate and maintain structures for rock fill dam type, it is very important to check leakage measuring.

The number of leakage measuring points in subject dam is one and this is located at the tip of downstream slope. Currently, quantity of leakage and water quality is measured automatically every hour.

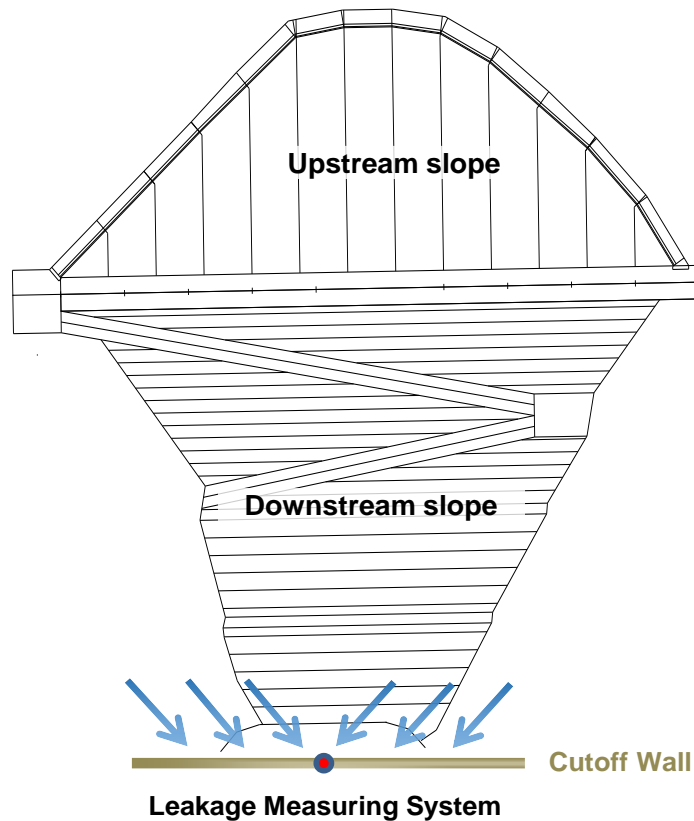


Figure 8. Location of leakage measuring system for the subject dam

In order to analyze the influence on earthquake, subject analysis period is decided to 2 months which are Before and after 1 month based on the day (12th, Sep. 2016) of occurring earthquake in common with displacement measuring.

Analysis for measured leakage data was performed by excluding the data of rainy period because precipitation is negative influence to exact leakage measuring.

Figure 9 shows status of leakage measuring for the subject dam. Simply comparing with quantity of leakage before and after earthquake is not reasonable because precipitation quantity and duration are different every times and analysis period is relatively short term. Important point was that leakage status before and after earthquake was similar, variation was stable. 16th September, Quantity of leakage and turbidity were increased but decreased gradually after that. The reason that leakage increased was precipitation.

Therefore, it seemed that leakage was not affected by earthquake and the leakage measuring system be considered to have no problem to operate.

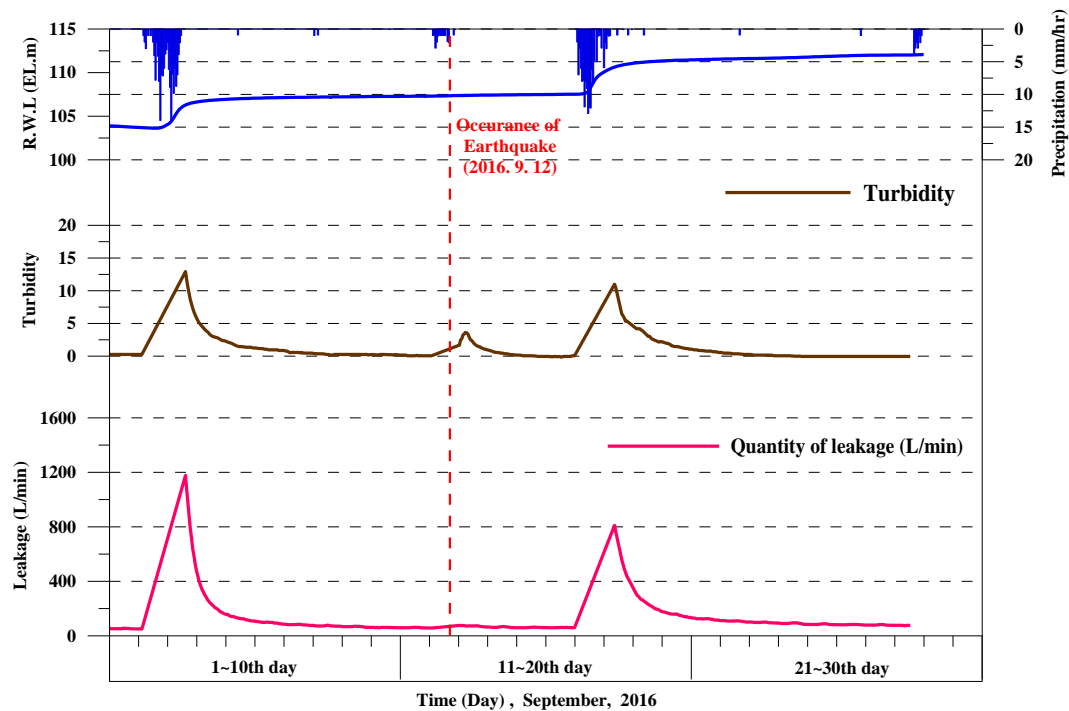


Figure 9. Status of leakage for the subject dam

3. CONCLUSION

In case of displacement behaviors, x & y directions were little difference between before and after earthquake, but z direction after earthquake was different from before that. This could mean that all points had a change and small displacement occurred on a dam. In additional analysis about change of vertical displacement, maximum displacement occurred on the middle of dam crest.

In an urgent field inspection, however, there were no damages by gyeongju earthquake such as crack or breakage of pavement on dam crest, faced slab and change of arrangement for downstream slope.

The leakage status before and after earthquake was similar, variation was stable. It seemed that leakage was not affected by earthquake and the leakage measuring system was considered to have no problem to operate.

As a comprehensive result of inspection and behavior analysis, there are no external damages in the subject dam and leakage measuring was normal and stable. Therefore, it seemed that the subject dam was affected by earthquake but safety and operation of dam structure was evaluated to have no problem.

In spite of no problem about dam safety, dam structure needs in-depth survey using control points because influenced by earthquake.

REFERENCES

- [1] The detailed guideline of the safety inspection and in-depth inspection on dams (In Korean). *KISTEC*, 2010.
- [2] The design standard on dams. *Korea Water Resources Association*, 2011.
- [3] Engineering guidelines. *FERC*, 1991.

COMMISSION INTERNATIONALE DES GRANDS BARRAGES

VINGT-SIXIÈME CONGRÈS DES GRANDS BARRAGES
Autriche, juillet 2018

DOI 10.3217/978-3-85125-620-8-123



This work licensed under a Creative Commons Attribution 4.0 International License. <https://creativecommons.org/licenses/by-nc-nd/4.0/>

**DAM SAFETY REGULATION IN SOUTH AFRICA: 32 YEARS DOWN THE
LINE**

Louis C. HATTINGH

Chief Executive Officer, HATTINGH ANDERSON ASSOCIATES CC, PRETORIA

SOUTH AFRICA

Ivor SEGERS

Principal Engineer: Civil Engineering, EXXARO RESOURCES LTD, PRETORIA

SOUTH AFRICA

COMMISSION INTERNATIONALE
DES GRANDS BARRAGES

VINGT-SIXIÈME CONGRÈS DES
GRANDS BARRAGES
Autriche, juillet 2018

DAM SAFETY REGULATION IN SOUTH AFRICA: 32 YEARS DOWN THE LINE

Louis C. HATTINGH

*Chief Executive Officer, HATTINGH ANDERSON ASSOCIATES CC,
PRETORIA*

Ivor SEGERS

*Principal Engineer: Civil Engineering, EXXARO RESOURCES LTD,
PRETORIA*

SOUTH AFRICA

1. INTRODUCTION

South Africa is the 30th driest country in the world. This is due to low levels of rainfall (relative to the world average) and high variability (60% of river flow arises from only 20% of the land area) as well as high levels of evaporation. Of the total mean annual runoff of 49 000 million m³ per year, only 10 000 million m³ is annually available as assured yield (98% assurance) [1]. As a result, South Africa has been one of the major dam building countries in the world. It is the country with the seventh most large dams (more than 15 m high) on the ICOLD register of dams [2]. It also has a significant number of small dams (less than 15 m high).

Of the total available water resources 67% is currently allocated for irrigation while the rest is made up of domestic and industrial use (22%), mining (5%), afforestation (3%) and power generation (mainly thermal power) and transfers between catchment basins (3%) [1].

This paper not only summarizes the history of Dam Safety implementation in South Africa from its earliest humble beginnings in the 1970s to the implementation of Dam Safety legislation in 1980s [3] and the update of the relevant regulations in

2012 [4] but also provide insight into the required regulatory processes during the lifespan of a dam.

A summary is provided of the lessons learnt in the implementation of the legislation including the positive influence of effective dam safety legislation and the fact that it takes time and significant resources to implement a dam safety regulatory system. It is also important to note that these lessons learnt were used to help some other African countries starting with the implementation of Dam Safety regulatory systems in their countries [5][6].

2. LEGISLATION

2.1. HISTORY

Legislation on the safety of dams was formally introduced in 1984 in South Africa (after earlier attempts dating back to the early 1970s was not successful). It is interesting to note that initially the political decision makers in South Africa considered dams to be inherently safe. This was obviously not correct considering the failure statistics of dams before the 1970s. A visit to the US, UK and several European countries by a team of officials from the Department of Water Affairs in the 1980s lead to the first attempts to introduce dam safety principles in South Africa based on the experiences gained during their visit.

Apart from defining the structures subjected to control, authority has been given to the Minister of Water Affairs (and Forestry) to promulgate dam safety regulations in which conditions and requirements for the design, operation, maintenance, inspection and even decommissioning of dams are prescribed. This was done for the first time in 1986. It is important to note that these regulations initially did not specifically take into account any environmental aspects with regards to dam safety.

Although the Constitution of South Africa of 1996 [7] drawn up after the advent of democracy in 1994, is primarily human centered, it also highlights the protection of the environment. Subsequently a National Water Act was promulgated in 1998 that includes a section on dam safety [8] that also included environmental aspects pertaining to dam safety (impacts). As a result, revised dam safety regulations were promulgated in 2012 [4] which for the first time included the potential impact of a dam on the resource quality downstream of the dam.

2.2. DAM SAFETY LEGISLATION

The National Water Act [8] as well as the Dam Safety Regulations of 2012 [4] aim at "improving the safety of the new and existing dams with a safety risk so as to reduce the potential harm to the public, damage to property or to resource

quality”. It is important to note these only pertain to dams with a safety risk. A “dam with a safety risk” is defined as a dam with a storage capacity of more than 50 000 m³ and a vertical height of equal to or more than 5 m. This definition of height differs from the ICOLD definition – the height is measured from the lowest natural bed level at the downstream toe of the dam wall to the non-overflow crest. Smaller dams that do not satisfy these requirements do not form part of the dam safety legislation. It is of extreme importance to note that these dams, however, still have to comply with water use and environmental legislative requirements.

The authority of dam safety lies with the Minister of Water and Sanitation (DWS). The Minister is assisted with the regulation of the dam safety legislation by the Dam Safety Office (DSO) which forms part of DWS (as designated by the Director-General of DWS) – one could call the DSO the regulator in South Africa. The Minister is also assisted by the Engineering Council of South Africa with the approval of appropriately qualified and experienced professional persons (Approved Professional Persons - APPs) to perform tasks at dams with a safety risk. The mandatory involvement of APPs for all tasks carried out at certain categories of dams is one of the important principles of the dam safety legislation in South Africa.

As in other countries that also had their major dam development in the 20th century, South Africa is experiencing a rapid decrease in the number of available APPs as the majority have either reached and are close to retirement. This is a major area of concern.

One of the founding principles of Dam Safety in South Africa and the rest of the world is that dam owners are responsible for the safety of their dams (the term “dam owners” also includes operators). It is therefore the responsibility of dam owner/s to register their dam with a safety risk with the DSO (including all new or planned dams). Once the registration information is received, the DSO would then classify the dam into one of three categories which determines the required level of control at that particular dam. The classification is based on the size and the hazard potential rating of a dam. The size class is determined by the maximum wall height. The size classification is given in Table 1. It is important to note that in many cases the classification date could be different from the registration date.

Table 1
Size classification (using the South African definition for height)

Size class	Maximum wall height (m) (from the river bed level to the highest point of the dam)
Small	< 12 m
Medium	≥ 12 m but < 30 m
Large	≥ 30 m

The hazard potential is based on an assessment of the potential loss of life (PLL), potential economic loss (PEL) (with respect to downstream development) as well as the potential adverse impact on resource quality (PIRQ) that may result from failure of a dam. In determining the hazard potential rating the PLL, PEL and

PIRQ are considered separately and the highest rating obtained, is accepted. The hazard potential classification is given in Table 2.

Table 2
Hazard potential classification

Hazard potential rating	Potential loss of life	Potential economic loss	Potential adverse impact on resource quality
Low	None	Minimal	Low
Significant	≤ 10	Significant	Significant
High	> 10	Great	Severe

The structural condition of a dam does not influence its category classification (only the size of the dam and its hazard potential are taken into account). There are three categories in the category classification (Category 1, 2 and 3). The relation between the category classification, size class and hazard potential are given in Table 3.

Table 3
Category classification of dams with a safety risk

Size class	Hazard potential rating (*)		
	Low	Significant	High
Small	Category 1	Category 2	Category 2
Medium	Category 2	Category 2	Category 3
Large	Category 3	Category 3	Category 3

(*) Highest level as determined by separate consideration of the potential loss of life, potential economic loss and potential adverse impact on resource quality downstream of the dam

To perform any task at a dam (including construction, enlargement, alteration, repair or decommissioning), the owner needs to obtain a licence for construction from the DSO. This normally includes the completion of an application form accompanied with the required design reports and engineering drawings as well as evaluation of the safety of the existing development. For Category 2 dams all tasks must be carried out under supervision of an APP whereas for Category 3 dams, an APP must be assisted by an approved professional team of experts. For Category 1 dams the involvement of an APP is not required but the dam owner has to fulfil the requirements of the dam safety regulations which includes completing an official application form, submitting design reports and engineering drawings and an evaluation of the safety of the existing development. Most of the small dams in South Africa are classified either as Category 1 or 2. In certain instances dam owners have decided to make use of a panel of experts over and above the APP and the accompanying professional team. This in certain circumstances leads to uncertainty regarding professional responsibilities.

Once construction is completed for Category 2 or 3 dams, the owner needs to obtain a licence to impound water (this is not required for Category 1 dams).

This includes the completion of an application form accompanied by a construction completion report and associated as-built drawings, an operation and maintenance manual, emergency preparedness plan and an affidavit from the owner stating that all residential areas and buildings in the dam basin have been vacated.

With regard to dam safety evaluations, the involvement of an APP and/or supporting professional team are similar to the other tasks (Category 2 dams only require an APP while Category 3 dams require an APP and supporting professional team). Depending on the category and the hazard potential, dam safety evaluations are required at intervals between 5 and 10 years (5 years for Category 3 dams and longer intervals for Category 2 dams).

The dam safety legislation and regulations clearly set out the steps required to satisfy dam safety practice, but within the legislation or regulations there are no specific norms or standards prescribed. The APP has the responsibility to determine appropriate standards for a particular dam and the legislation provides for a review of such standards by the DSO. The appropriate norms are considered to be current acceptable dam engineering practice for site-specific conditions. This is significantly different to a number of other countries in the world where specific norms and standards are applicable. There are, however, a number of guidelines available for use in South Africa including these on Dam Break Floods [9], Safety in Relation to Floods [10] and Freeboard for Dams [11].

Again, it is important to note that the legislation is as such that the owner/s of a dam is at all times responsible for the safety of their dam – South Africa's common law responsibility is applicable in addition to the dam safety responsibility. Included is the responsibility for the implementation of the recommendations of the dam safety evaluations by the owner. The DSO may instruct the owner to implement the recommendations. Failure of the DSO to give such an instruction does however not take the responsibility away from the owner.

2.3. WATER USE AND ENVIRONMENTAL LEGISLATION

In addition to the dam safety requirements of the National Water Act of 1998 [8], a dam owner is also required to satisfy the water use requirements of the act by applying for a water use licence when wanting to construct any new dam or increase the storage capacity of an existing dam (Section 21 of the Act). No construction work may be carried out before a water use licence or written authorization has been obtained from the DWS.

For so called “dirty water” dams (or dams for water containing waste), a dam owner must also comply with the Regulations on the “Use of Water for Mining and related Activities aimed at the protection of Water Resources” promulgated in 1999 [12].

A dam owner must also satisfy the provisions of the National Environmental Management Act and its accompanying regulations [13] with regards to activities which may have a detrimental effect on the environment (construction, enlargement, alteration, repair or decommissioning of a dam or storage of “dirty water” in most cases may be listed as such an activity). This normally requires an

environmental impact assessment (EIA). One of the conditions of the water use licence is the environmental authorization. In other words, no listed activity at a dam may take place before receiving the necessary environmental authorization.

3. LESSONS LEARNT FROM LONG TERM IMPLEMENTATION OF DAM SAFETY LEGISLATION

According to the latest database of the DSO [14] a total number of 5 462 dams with a safety risk according to the Dam Safety Regulations were registered in South Africa at the end of February 2018 (see Table 4). The large majority of these dams (more than 75.3%) can be classified as small (less than 12 m high) while only 3.46% can be classified as high. The rest is classified as medium dams. When comparing the number of dams with the ICOLD definition of a small dam it is evident that there are 458 dams between 12 m high and 15 m high.

Table 4
General dam statistics (using the South African definition for height)

Height of dam (from the river bed level to the highest point of the dam) (m)	Number of dams
Less than 12 m	4 158
12 m to < 15 m	458
15 m to < 30 m	672
30 m and higher	174
Total	5 462

It is important to note that of the 5 462 dams registered, 5 434 dams have been classified by the DSO. Of these 5 434 dams, 57.3% are Category 1 dams that does not require any further regulatory actions other that registration and classification. The remaining classified dams consist of 36.3% Category 2 dams and 5.4% Category 3 dams - both Categories requiring the involvement of an APP and a supporting professional team (for Category 3 dams) and 0.9% dams that does not warrant a classification. In other words, a significant portion of small dams are classified as Category 2 dams due to their adverse hazard ratings.

Fig. 1 provides a graphical presentation of the number of dams registered as well as classified annually since the inception of dam safety regulations in 1986. As expected a large number of dams were registered within the first 5 years (2 632 dams in total). What is however interesting to note is that although the number of dams registered per year has decreased since, the number of annual registrations basically stayed constant since 2000. An increase is evident since 2012 – this could be attributed to the implementation of the revised dam safety regulations in 2012 with an increased focus of the so-called dirty water dams. It has taken another

27 years of dedicated registrations by the DSO to double the amount of registrations to the current 5 462 dams.

However, when considering classification, it is clearly evident from Fig. 1 that all the effort in the beginning was spent on the registration of dams and the classification of dams lagged significantly behind especially the first 2 years after implementation. So, in comparison only 1 692 dams were classified within the first 5 years. This lag was basically eliminated in 2012 with the implementation of the revised dam safety regulations in 2012 with an increased focus on the so-called dirty water dams as the lag was mostly made up of the so-called dirty water dams.

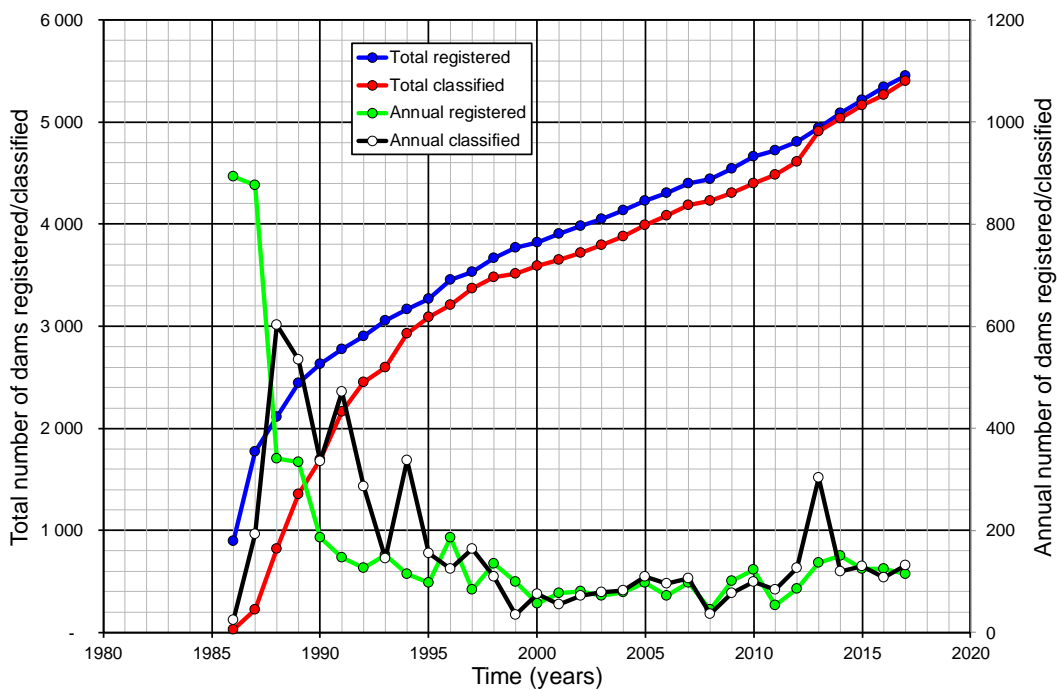


Fig. 1
Number of dams registered and classified since inception of dam safety regulations

Fig. 2 provides more detail on the distribution of completion dates of the dams registered during each year since the first implementation of dam safety legislation. It can therefore be concluded that to effectively implement a Dam Safety regulatory system takes time and effort even for the most basic things like registration and classification of a dam with a safety risk.

The building of dams in South Africa went through a boom period from the 1950's to the 1990's, peaking during the 1980's for both small as well as large dams. Since the 1990's the number of dams constructed has drastically reduced. One of the main reasons can be attributed to a change in the water related legislation in South Africa in 1998 [8]. The old system based on riparian rights changed to a system that recognizes water for the environment and for human consumption as a basic right. Authorization for all other water uses has to be

obtained from the DWS acting as custodian of water resources and responsible for distributing water in an equitable manner.

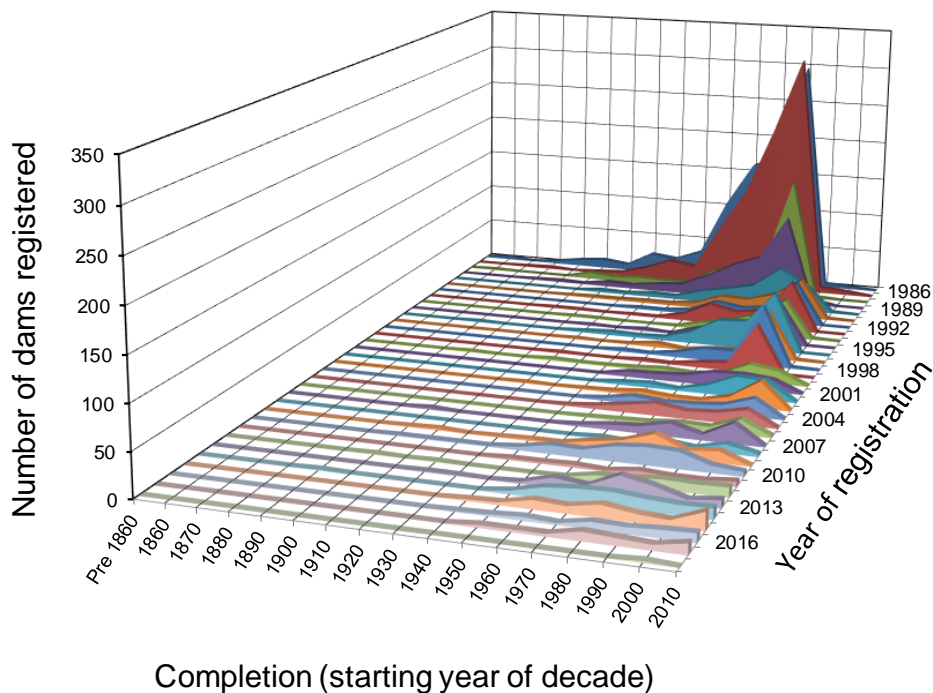


Fig. 2
Timeline of dams registered

So, where a land owner in an uncontrolled area could build a dam on his property up to 250 000m³ without a licence before 1998, presently a licence is required taking into account the water resource situation in the relevant catchment as well as the possible redistribution of water resources. This process together with the scarce nature of the water resources in the majority of South African catchments has subsequently led to fewer dams being built during the last two decades (only 257 small dams were completed in the 2000s and 90 so far in the 2010s compared to a total of 1 303 dams completed during the 1980s). In many catchments the best dam sites have already been utilized and additional storage will not significantly increase the yield of the system.

Prior to the introduction of legislation on the safety of dams in the 1980s not a lot of attention was given to the recording of failures and incidents in South Africa. So much so that in an ICOLD publication on failures and incidents in 1973 [15], only 2 incidents at South African dams were described. Subsequent to the promulgation of the first dam safety regulations in 1986 and the formation of a “DSO” that acts as regulator, failures and/or incidents have been recorded in a “Catalogue of incidents” as part of the information system of the DSO. A number of publications were published with the majority focusing on failures and incidents of large dams. Hattingh and Oosthuizen published a paper in 2017 [16] that

provides a summary of both large as well as small dams. The most important conclusions are as follows:

- With regards to large dams, only earthfill and tailings dams (no large concrete dams) have failed in South Africa. With regards to small dams, the large majority of failures are earthfill dams although some smaller concrete weir structures have also failed.
- Overtopping due to inadequate spillway discharge capacity as well as piping and internal erosion make up the large majority of causes of incidents at and failures of small dams

4. CONCLUDING REMARKS

From the lessons learnt from the implementation of dam safety legislation in South Africa the following is of importance:

- It is of prime importance to convince political decisions makers about the necessity for Dam Safety implementation including the necessary legislative and regulatory environment.
- It takes time and significant resources to successfully implement a dam safety regulatory system – for example after more than 30 years existing dams are still being registered in South Africa. It also takes time and effort to classify the dams as well as establish regulatory compliance;
- Dam Safety legislation, enforced by dedicated and experienced officials (in the DSO), has a positive correlation with the decrease in the number of incidents and failures of dams built since promulgation of dam safety legislation in South Africa. This has also ensured the formal recording of incidents and failures. Not all incidents and failure of especially small dams are however reported to the DSO as required.

ACKNOWLEDGEMENTS

The authors wish to express their gratitude to all other present and past members of the Dam Safety Office as well as Sub-directorate Dam Safety Surveillance of the DWS that contributed in some or other way to the development of the above-mentioned paper.

REFERENCES

- [1] Department of Water Affairs. *National Water Resource Strategy. Second Edition. South Africa.* 2013.
- [2] ICOLD. *Register of dams. ICOLD official website.* 2017
- [3] Republic of South Africa. *Regulations in terms of Section 9c(6) of the Water Act, 1956 relating to Dams with a Safety Risk. Government Notice R 1560 of 25 July 1986.* Department of Water Affairs and Forestry. Republic of South Africa. 1986.
- [4] Republic of South Africa. *Regulations Regarding the Safety of Dams in terms of Section 123(1) of the National Water Act, 1998. Government Notice R 139 of 24 February 2012.* Department of Water Affairs. Republic of South Africa. 2012.
- [5] Eastern Nile Technical Regional Office. *Reference Dam Safety Guidelines for Eastern Nile Countries.* Addis Ababa, Ethiopia. 2014.
- [6] COWI. *Development of Operational Guidelines for Investment in Multi-purpose Small Dams: Module 2B: Guideline 3: Dam Safety.* Ministry of Water Development, Sanitation and Environmental Protection, Lusaka, Zambia. 2017.
- [7] Republic of South Africa. (1996). *The Constitution of the Republic of South Africa.* No 108 of 1996. Statutes of the Republic of South Africa. Government Printer. Republic of South Africa.
- [8] Republic of South Africa. (1998a). *National Water Act.* Act No 36 of 1998. Government Printer. Republic of South Africa.
- [9] SANCOLD. (1990). *Interim Guidelines on Dam Break Floods.* Pretoria, South Africa.
- [10] SANCOLD. (1991). *Guidelines on Safety in Relation to Floods.* Pretoria, South Africa.
- [11] Bosman, DE, Basson, J, Tente, T & Basson GR. (2011). *Review and update of the SANCOLD Guidelines for the design of freeboard of dams.* WRC Report No: 1759/2/11. Pretoria. South Africa.
- [12] Republic of South Africa. (1999). *Regulations on Use of Water for Mining and Related Activities aimed at the Protection of Water Resources.* Government Notice 704 of 4 June 1999. Department of Water Affairs and Forestry. Republic of South Africa.
- [13] Republic of South Africa. (1998b). *National Environmental Management Act.* Act No 107 of 1998. Government Printer. Republic of South Africa.
- [14] Department of Water Affairs. (2018). *Dam Safety Office: Database of registered dams: February 2018.* Department of Water Affairs. Republic of South Africa.
- [15] ICOLD. (1973). *Lessons from Dam Incidents.* Paris, France.
- [16] Hattingh, L. and Oosthuizen, C. (2017). *The History of Dam Safety Implementation in South Africa.* Published as part of proceedings of the International Conference on "Water storage and Hydropower Development for Africa" held in Marrakech, Morocco.

SUMMARY

This paper not only summarize the history of Dam Safety implementation in South Africa from its earliest humble beginnings in the 1970s to the implementation of Dam Safety legislation in 1980s and the update of the relevant regulations in 2012 but also provide insight into the required regulatory processes during the lifespan of a dam.

A summary is provided of the lessons learnt in the implementation of the legislation including the positive influence of effective dam safety legislation and the fact that it takes time and significant resources to implement a dam safety regulatory system. It is also important to note that these lessons learnt were used to help some other African countries starting with the implementation of Dam Safety regulatory systems in their countries.

From the lessons learnt from the implementation of dam safety legislation in South Africa the following is of importance:

- It is of prime importance to convince political decisions makers about the necessity for Dam Safety implementation including the necessary legislative and regulatory environment.
- It takes time and significant resources to successful implement a dam safety regulatory system – for example after more than 30 years existing dams are still being registered in South Africa. It also takes time and effort to classify the dams as well as establish regulatory compliance;
- Dam Safety legislation, enforced by dedicated and experienced officials (in the DSO), has a positive correlation with the decrease in the number of incidents and failures of dams built since promulgation of dam safety legislation in South Africa. This has also ensured the formal recording of incidents and failures. Not all incidents and failure of especially small dams are however reported to the DSO as required.

KEYWORDS

Regulation
Safety of dams
Failure

COMMISSION INTERNATIONALE DES GRANDS BARRAGES

VINGT-SIXIÈME CONGRÈS DES GRANDS BARRAGES
Autriche, juillet 2018

DOI 10.3217/978-3-85125-620-8-124



This work licensed under a Creative Commons Attribution 4.0 International License. <https://creativecommons.org/licenses/by-nc-nd/4.0/>

**BEHAVIOUR OF ASPHALT CONCRETE CORE EMBANKMENT DAMS
(ACED) AND SHEAR ZONE DEVELOPMENT**

Guntram INNERHOFER sen.

*Former Head of Civil Engineering Department, VORARLBERGER ILLWERKE
AG*

AUSTRIA

Peter TSCHERNUTTER

TSCHERNUTTER CONSULTING GMBH, VILLACH

AUSTRIA

Adrian KAINRATH

TSCHERNUTTER CONSULTING GMBH, VILLACH

AUSTRIA

BEHAVIOUR OF ASPHALT CONCRETE CORE EMBANKMENT DAMS (ACED) AND SHEAR ZONE DEVELOPMENT

Guntram Innerhofer sen.¹
Peter Tschernutter² & Adrian Kainrath²

¹*Former Head of Civil Engineering Department, Vorarlberger Illwerke AG*
²*Tschernutter Consulting GmbH, Villach, Austria*

AUSTRIA

1. INTRODUCTION

Asphalt concrete cores as central water barrier provide a cost-effective and highly flexible solution even for small and high embankment dams. The stress and deformation behaviour of such dams is completely different compared to other dam types like surface sealed, homogenous or zoned dams. Worldwide almost 200 asphalt concrete core embankment dams have been built or are under construction in different countries. There are now more than 50 years of successful experience for this dam type. Over the past decades comprehensive material research has been performed and new asphalt concrete placing equipment has been developed.

The comparatively thin asphalt concrete core must withstand the induced deformations of the dam shoulders and the water load without cracking or leaking. Even if an asphalt concrete core tolerates high deformations without structural damage, the understanding of the deformation behaviour of ACE dams is of basic importance. This paper presents fundamental aspects on the stress distribution and the deformation behaviour of ACE dams. Therefore, basic theoretical considerations and monitoring data on existing dams are compared with results of numerical analyses.

2. THEORY OF SHEAR ZONE DEVELOPMENT

Measurements of ACE dams [1][4][5][6] have shown that the deformation behaviour of those types of dams differs from the deformation behaviour of other dam structures. Since the measurements provide only fragmentary information about the overall behaviour of the dam, theoretical considerations are necessary to supplement the data in order to obtain a fundamental understanding about the ongoing effects in the dam. For a long time there have also been presumptions about the existence of shear zones in the dam body, however, general knowledge about the development and the effect on the stability was not theoretically explored in detail. The following chapter provides theoretical considerations about typical stress paths in ACED dams and the formation of shear zones.

When analysing the stress and deformation behaviour of dams, at least two significant load stages have to be considered: end of construction and first impounding. The loads acting on the core and the stress distribution in the dam body completely change when the dam is impounded which means that the dam material undergoes significant stress paths during the impounding as well as during the reservoir operation under fluctuating reservoir levels. Arising stress differences between upstream and downstream are compensated by deformations. The asphalt concrete core acts as a thin impervious and flexible membrane and transfers the horizontal water load to the supporting downstream dam shoulder. Since the core provides limited resistance to the applied horizontal loads, the AC tries to reach an equilibrium state, which can only be achieved by a horizontal deformation in order to mobilize the resistance of the downstream dam shoulders. The magnitude of horizontal deformation depends on the stiffness of the adjacent zones and on the shear strength of the shoulder material. As a result of the horizontal core deformation towards downstream, the horizontal stress in the upstream dam zone adjacent to the core significantly decreases.

For the upstream dam shoulders the stress paths can easily be visualised by a $\sigma - \tau$ diagram as depicted in Figure 1. For the end of construction, the stress state which is depicted by Mohr's circle is far off the Mohr-Coulomb failure line. Due to impounding and the buoyancy of the upstream shoulder material, σ_1 and σ_3 are reduced, whereby Mohr's circle is shifted, but does not reach the Mohr-Coulomb failure line. The horizontal deformation of the asphalt concrete core to the downstream side reduces the minor principal stress σ_3 , $K'_0 = \sigma_3/\sigma_1$ decreases and the diameter of the Mohr circle increases until it reaches the Mohr-Coulomb failure line, activating a sliding wedge. The inclination of the sliding plane ψ and therefore the size of the mobilized wedge depends on the shear strength of the dam shoulder material and can be determined from the $\sigma - \tau$ diagram by Equation 1.

$$\psi = 45 + \varphi/2 \quad [1]$$

The mobilized wedge closes the rising joint between the downstream dam shoulder and the deformed asphalt concrete core. The mobilization of a shear zone reduces the shear stress in the surrounded area and protects those zones against shear deformations.

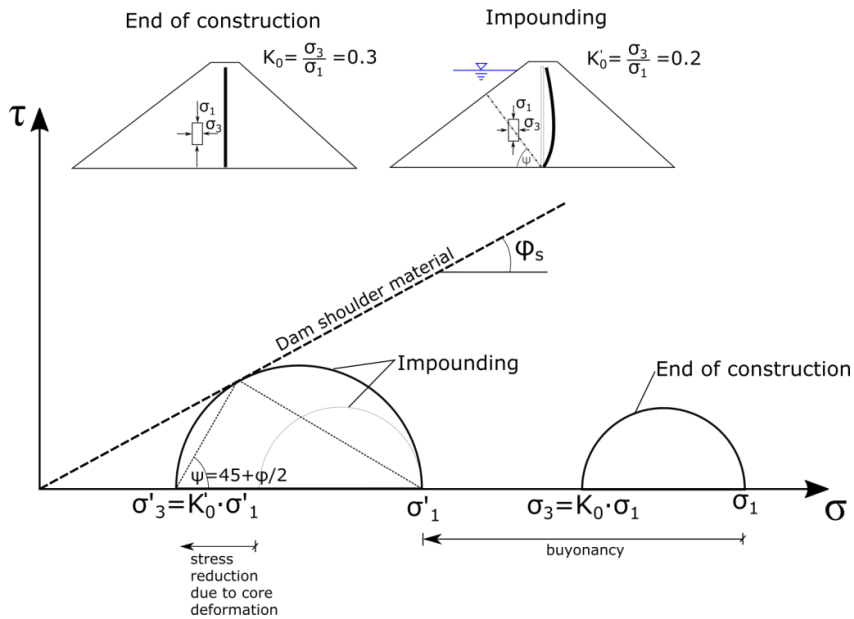


Fig. 1: Stress state in the upstream dam shoulder

At high reservoir levels, the water pressure acts on the core and provides the upstream horizontal support for the core. The horizontal water pressure on the water barrier leads to high horizontal stress in the core and in the adjacent zones downstream of the core. Since the asphalt concrete core material is impermeable, internal water pressures cannot develop and therefore the effective core stress is equivalent to the total stress upstream the core. Due to this high horizontal stresses during impounding, the stress state in the core is almost isotropic ($\sigma_1 \sim \sigma_3$) and the Mohr's circle is reduced and therefore in a stable stress state far off the failure line. The core and the shoulder are shifted downstream. When the reservoir level is lowered, the horizontal support of the core by the water pressure is lost and a sliding wedge which developed during the first impounding provides the necessary horizontal support to stabilize the core and the adjacent upstream "braking" zone. It can be seen from deformation measurements of asphalt concrete cores (see Chapter 3), that the back-deformation due to drawdown is only small compared to the initial deformation during impounding. Figure 2 shows the theoretical model of the mobilized sliding wedge for a vertical core and for an inclined core.

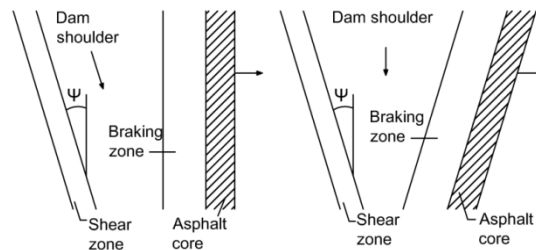


Fig. 2: Mobilization of sliding wedges for vertical (Feistritzbach Dam) and inclined AC core (Finstertal Dam)

During construction, the stress state of the asphalt concrete core depends on the stiffness of the core and the adjacent zones. It is of interest, how the additional

shear stress due to the mobilization of the sliding wedge influences the stability of the core. Figure 3 depicts the situation in the core during impounding, when shear stress τ'' from the mobilization of the wedge superimposes a vertical stress state $\sigma'_1 = \sigma'_v$ and $\sigma'_3 = \sigma'_h$, leading to a rotation of the principal stress with the angle of β . σ''_1 and σ''_3 are the state of the principal stresses after rotation with τ''/z , the mobilization rate of the shear strength. The diagram clearly shows that even if high shear stresses burden the core, the rotation of the principal stresses only have little impact on the mobilization rate of the shear strength τ/z .

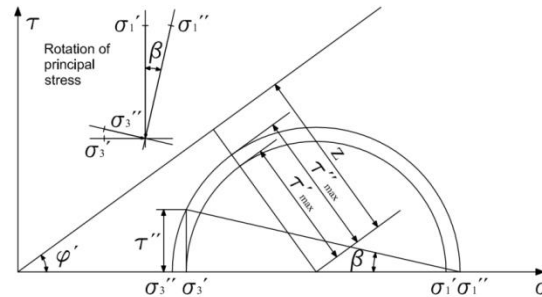


Fig. 3: Stress state in the core (σ'_1, σ'_3), superimposed by shear stress τ'' from the mobilization of an upstream wedge

3. MEASUREMENTS

Different measurements on dams with central sealing membranes [1][4] showed some indications about the existence of shear zones in the upstream dam shoulder. In order to complete the theoretical considerations in Chapter 2, measurements of the 85 m high Feistritzbach Dam and the 155 m high Finstertal Dam (core height 96 m) are presented below.

The Feistritzbach Dam is situated in southern Austria and is designed with a 70 - 50 cm thick vertical asphalt concrete core, slightly inclined in the upper part. Particular tests were performed to examine the physical and mechanical properties of the asphalt concrete core material. In accordance with the design of the dam and the rockfill material properties, a softer bitumen and a less stiff mix were chosen. The tests on the asphalt concrete core material showed a soft behaviour for primary loading and a stiff response for unloading and reloading conditions. If the strain exceeded 5 to 6% (depending on the confining pressure), the material was dilative and the volume increased significantly. The failure criteria of the material was determined with $\phi' = 37^\circ$, $c = 0 \text{ kN/m}^2$, $\nu = 0.25$.

Due to partly severe weathered rockfill materials the settlements of the dam reached about 1.0% of the total dam height after first impounding. Despite large deformations, the dam has been operated for over 28 years and the asphalt concrete core behaves quite well and no leakage through the core was observed. The dam is well instrumented with horizontal and vertical inclinometers, as well as different settlement gauges and earth pressure cells etc. The measurement

data provides a good example for the theoretical considerations discussed in Chapter 2.

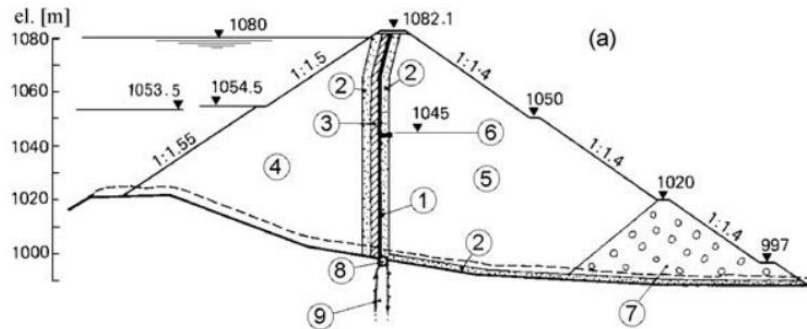
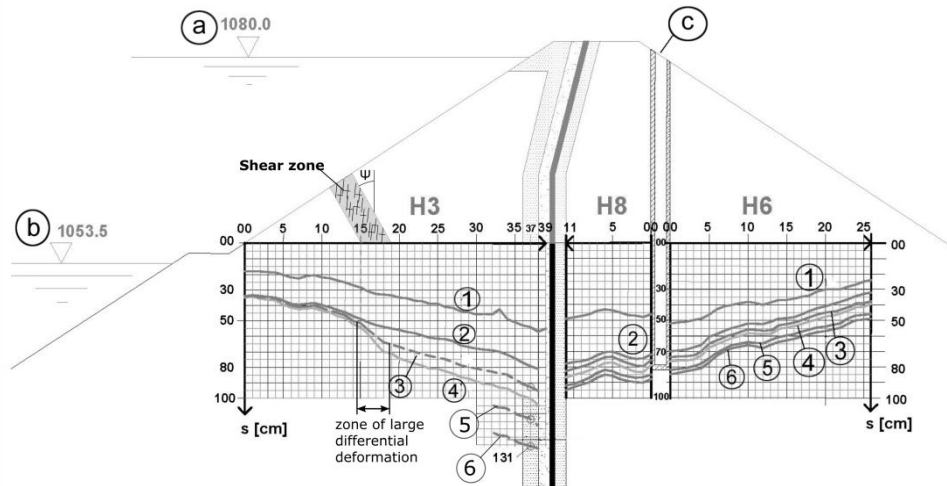


Fig. 4: Cross-section of Feistritzbach Dam [4]

- (1) AC core; (2) filter; (3) fine-graded zone; (4) upstream and (5) downstream shell; (6) horizontal seepage section; (7) drainage toe; (8) grouting gallery; (9) grout curtain

Figure 5 shows the settlements of the dam for different stages. The magnitude of the construction settlements in the core was about 55 cm and increased up to 80 cm before the impounding started. The settlements after construction were distributed equally throughout the entire cross section of the dam. During first impounding, the settlements in the upstream dam shoulder increased up to 95 cm whereas the settlements downstream of the core only increased up to 87 cm. During impounding, almost no significant horizontal core deformations were observed until the reservoir level reached 2/3 of its maximum. Above, the horizontal core deformation amounts up to 10 cm to the downstream leading to a decreasing relative density in the upstream adjacent zone.



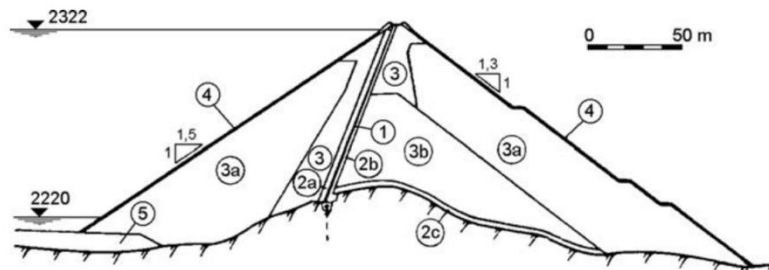
- | | |
|-----------------------------|-----------------------------|
| (a) Normal reservoir level | (3) End of first impounding |
| (b) Minimal operating level | (4) First drawdown |
| (c) Floating shaft | (5) Results 1996 |
| (1) End of construction | (6) Results 2004 |
| (2) Beginning impounding | |

Fig. 5: Settlements of Feistritzbach Dam [5]

The largest rates of differential settlements were observed upstream in a distance of about 20 m to 25 m from the core. The section between this shear zone and the AC core showed only translatory movements and no essential differential settlements were observed, which precludes additional saturation settlements. The results indicate that the shear zone was mobilized together with a sliding wedge deformation, closing the gap between the core and the adjacent upstream zone. After 12 years of reservoir operation the differential settlements between the upstream and downstream side of the core continuously increased up to approx. 36 cm and the maximum horizontal core displacements increased up to 13.5 cm.

The Finstertal Dam is a rockfill dam with an inclined asphalt concrete core and an asymmetric dam body. The plinth for the core is situated on a rock cusp and the foundation of the dam shoulders is inclined on both sides. Figure 6 depicts a typical cross section and the zoning of the dam. The asphalt concrete core with a total height of 96 m is inclined with 1H:4V. The width of the core is 70 cm at the bottom and 50 cm at the top. The core is located at a distance from the dam axis which means it is outside the area with the highest level of strain [7]. A filter and transition zone was designed on the upstream side of the core. Downstream, the core is supported by a drainage zone as well as a stiff zone with moraine (zone 3b) and rockfill (zone 3 and 3a) material.

The dam has a very extensive monitoring equipment with horizontal deformation gauges, vertical inclinometers, earth and pore water pressure cells, piezometers, extensometer, geodetic monitoring devices, perpendiculars, strong motion instruments, seepage collecting systems and three devices to measure a widening of the asphalt core on different elevations (5 m, 21 m and 40 m below storage level) [3].



- | | |
|----------------------------|-----------------------|
| (1) Core | (3b) Moraine |
| (2a) Upstream filter layer | (4) Protective lining |
| (2b,c) Drainage zone | (5) Moraine material |
| (3,3a) Rockfill | |

Fig. 6: Cross-section of Finstertal Dam [3].

In 1981 the AC core thickness devices indicated a widening of the core during the impounding. Figure 7 shows the differential displacements between the upstream filter zone and the downstream core surface at two different elevations (40 m and 5 m below the maximum reservoir level). At the beginning of the first impounding, the dam first behaves as anticipated but when the reservoir level almost reached its maximum, the core was shifted downstream for

12 – 14 cm over the entire height within a short period. The measurement data 5 m below the maximum reservoir level shows a differential horizontal displacement between the upstream filter zone and the downstream core surface of about 3 cm. The first drawdown leads to a back-deformation of the core to the upstream side of about 3 cm. For the reservoir operation until 1999, the measurements show a continuing enlargement of the differential settlements between upstream and downstream while the horizontal deformations remain almost constant. The horizontal deformation of the core between maximum reservoir level and drawdown is elastic with a differential deformation of about 4 cm.

It can be concluded that the deformations as shown in Figure 7 are parallel to the core and a widening of the asphalt concrete core can therefore be excluded. The Finstertal Dam has been successfully operated for 38 years and is consolidated without any problem of the asphalt concrete core.

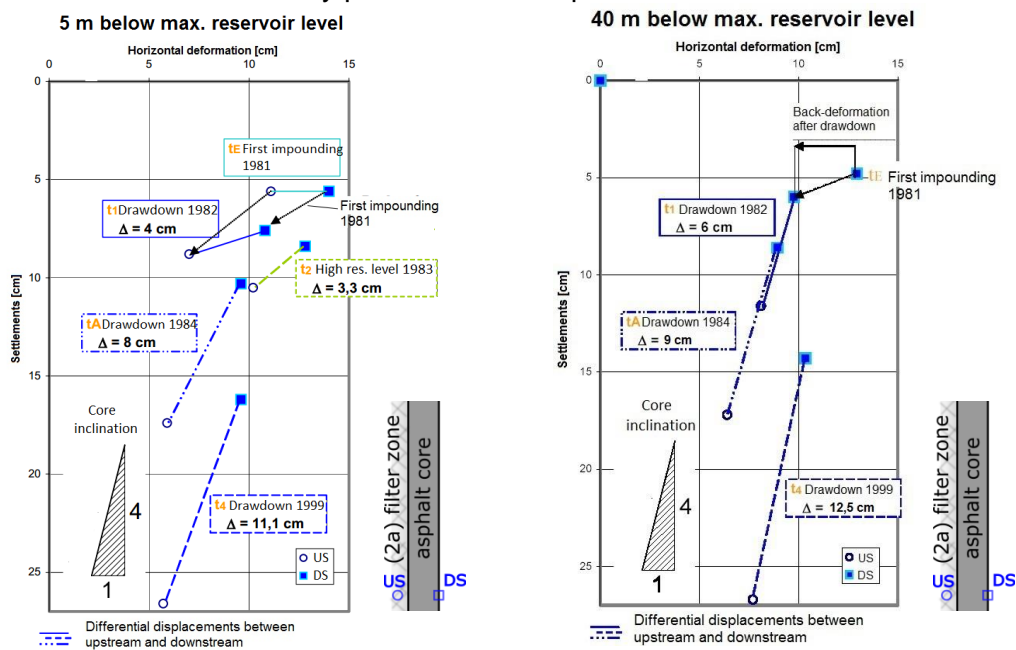


Fig. 7: Finstertal Dam – Absolute and differential displacements between the upstream filter zone and the downstream core surface

4. BEHAVIOUR OF AC DAMS BASED ON THE RESULTS OF NUMERICAL ANALYSES

For the contribution, a numerical simulation of a 128 m high ACRD (asphalt core rockfill dam) was carried out in order to show a typical behaviour of an asphalt concrete core rockfill dam during construction and impounding. Numerical analyses are a useful tool to provide a detailed picture about the stress and

deformation behaviour of dams in order to improve the understanding and to verify theoretical considerations.

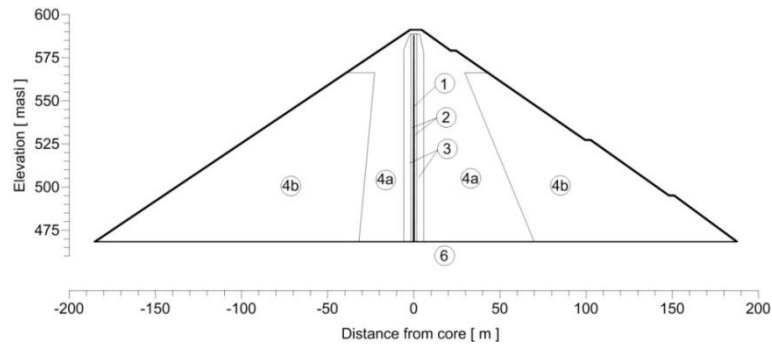


Fig. 8: Model and dam zoning

Figure 8 shows the zoning of the cross section of the dam which was used for the current simulation. The upstream dam slope is inclined with 1:1.5 (V:H) and the downstream slope with 1:1.4. The width of the vertical asphalt core is 95 cm at the bottom decreasing gradually to 50 cm, which is maintained for the top 50 meters. The foundation of the dam is assumed to be on stiff rock. The finite element program Plaxis 2D was used throughout this analysis. The simulations were carried out with a 2D-plane strain model. The non-linear, elastoplastic Hardening Soil Model was used for the numerical analysis. The stress dependency is modeled with three different stiffness moduli: E_{50}^{ref} for primary loading, E_{oed}^{ref} for oedometric loading, E_{ur}^{ref} for unloading and reloading and the parameter m for the amount of the stress dependency. For details on the numerical analysis and material parameters, reference is made to [6]. Table 1 shows the material parameters used in the study.

Table 1: Material parameters

Zone		Asphalt Concrete Core	Transition Zone Gravel	Transition Zone crushed rock	Shoulder rockfill – well compaction	Shoulder rockfill – bad compaction	Bedrock
Zone		1	2	3	4a	4b	6
Model		HS	HS	HS	HS	HS	LE
E	[kN/m ²]	-	-	-	-	-	300000
v	[-]	-	-	-	-	-	0,3
E_{50}^{ref}	[kN/m ²]	15000	76000	95250	76200	50000	-
E_{oed}^{ref}	[kN/m ²]	14.000	60.000	57000	68000	43000	-
E_{ur}^{ref}	[kN/m ²]	30000	210000	300000	210000	120000	-
m	[-]	0,21	0,48	0,25	0,45	0,4	-
ϕ	[°]	45	45	45	45	45	-
c	[kN/m ²]	580	1	1	1	1	-
ψ	[°]	2	7	7	7	7	-
v_{ur}	[-]	0,2	0,2	0,2	0,2	0,2	-

HS...Hardening Soil Model; LE...Linear Elastic Model

Figure 9 depicts the vertical stress distribution of the analysed dam for the end of construction and for the first impounding. It can be seen from the graphs that the stress distribution at the end of construction is depending on the material

stiffness of the dam zones. Arching effects may arise at the end of construction due to the stiffness difference between the core and the adjacent zones, slightly reducing the vertical stress in the core. During impounding, the stress distribution in the dam significantly changes due to the rotation of the principal stresses and the buoyancy of the upstream dam shoulder. Arching effects originating from the dam construction mostly disappear.

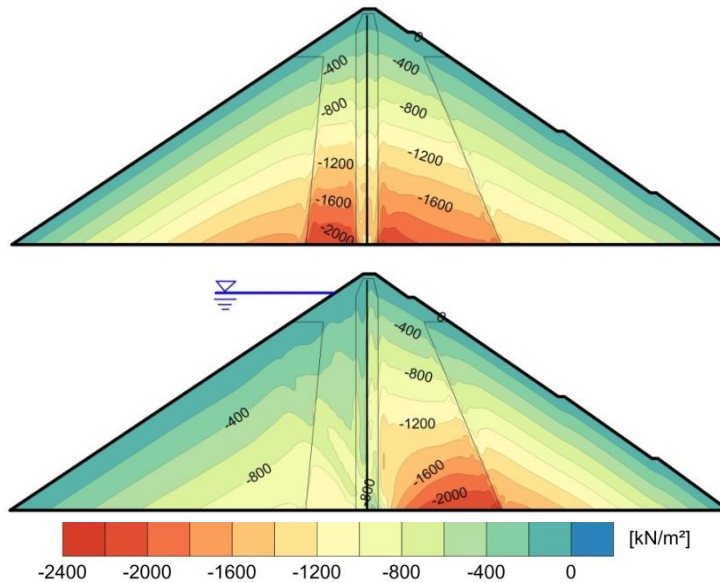


Fig. 9: Effective vertical stress at the end of construction and for impounding

Figure 10 shows the horizontal effective stress distribution during construction and impounding. At the end of construction, the graph shows a homogenous distribution. For the impounded state, the horizontal stress significantly changes in the bottom zones adjacent to the core. While the horizontal stress decreases in the upstream dam shoulder, high horizontal stress arises downstream close to the plinth.

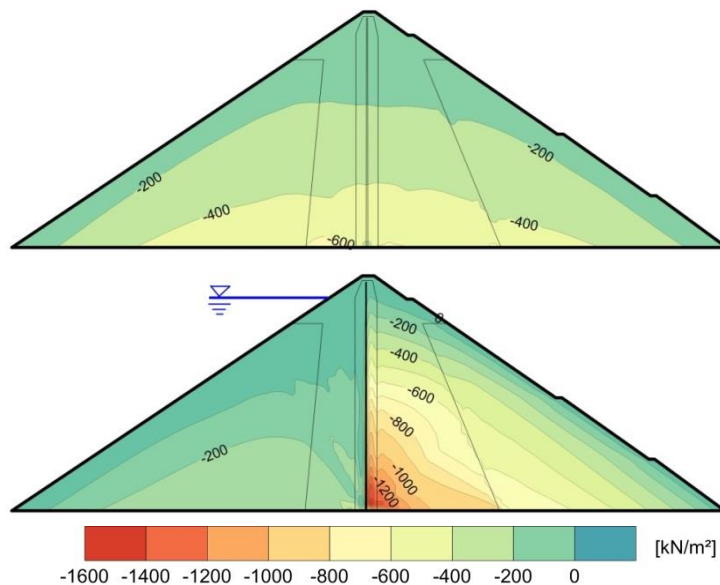


Fig. 10: Effective horizontal stress at the end of construction and for impounding

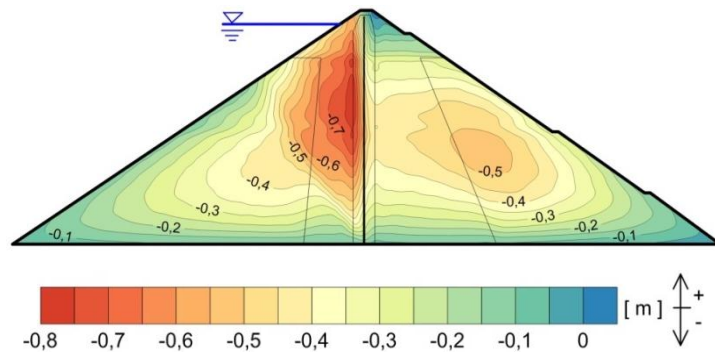


Fig. 11: Settlements after first impounding

The deformation behaviour of dams with a thin impervious central membrane is mainly governed by the dam zoning, material stiffness and shear strength as well as the dam foundation conditions (stiffness, surface inclination). Figure 11 shows the settlements of the analysed dam for the first impounding. Since the stiffness of the asphalt concrete core is generally lower than the stiffness of the adjacent zones, the settlements of the core are governed by adjacent dam zones. The graph shows that the settlements after impounding are concentrated upstream. Figure 12 depicts the horizontal deformations of the analysed dam. Due to impounding, the additional water load, acting on the core leads to a horizontal deformation of the core to the downstream side. The magnitude of those displacements depends on the resistance (stiffness and shear strength) of the downstream shoulder. The largest horizontal deformations occur in the upper part of the dam. The graph clearly shows the mobilization of a wedge in the upstream dam shoulder which is triggered by the downstream deformation of the core due to impounding.

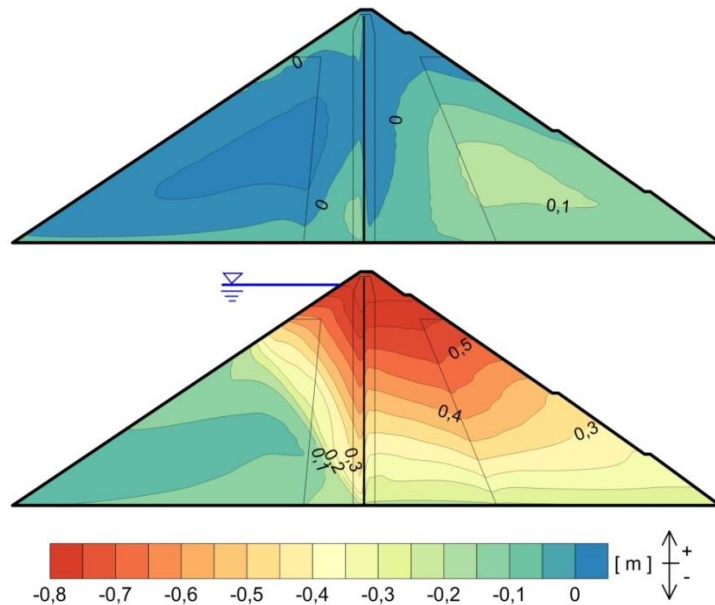


Fig. 12: Horizontal deformations: end of construction and first impounding

The shear strains after impounding are shown in Figure 13, illustrating the deformation characteristics of the dam and indicate the degree of mobilization in the upstream dam shoulder. It can be seen from the graph that the highest shear strains occur in the shear plane on the bottom of the wedge. The inclination ψ of the shear plane is around 60° which is in a good accordance with the theoretical considerations ($\psi = 45 + \varphi/2 = 67,5^\circ$) presented above.

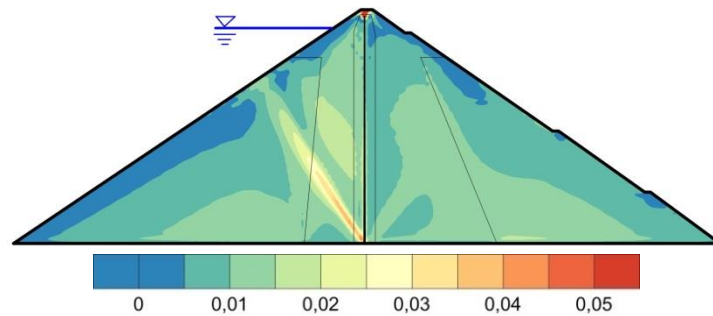


Fig. 13: Shear strains after impounding

SUMMARY

Dams with an asphalt concrete core show a different deformation behaviour compared to homogenous or surface sealed dams. In this contribution, theoretical considerations about the typical behaviour of AC dams during impounding are presented and discussed. It has been demonstrated that the core deformation during the first impounding leads to a mobilization of an upstream wedge. The mobilized wedge closes the joint between the core and the adjacent upstream zone. It also stabilizes the core when the reservoir level decreases and the horizontal support from the water pressure is lost. It has been also demonstrated that the rotation of the principal stresses in the asphalt concrete core, which arise as a result of additional shear stresses along the upstream core, have only little impact on the mobilization rate of the shear strength in the core.

Finally, the measurements of two different Austrian AC dams (Feistritzbach Dam and Finstertal Dam) are discussed in the contribution. The measurements of both dams confirm the theoretical results and showed the development of a shear zone in the upstream shoulder which stabilizes the core.

The results of intense numerical investigations on a typical AC dam are also presented and discussed. The analyses are in a good accordance with the measurements and the theoretical findings. The upstream wedge with the formed shear zone was also clearly evaluated in the numerical analyses.

The presented results and findings contribute to a better understanding of the deformation behaviour of AC dams.

REFERENCES

- [1] INNERHOFER G. (JUN.) Discussion of the long term behaviour of four of the biggest dams in Austria. Master's Thesis, Vienna University of Technology, 2006.
- [2] HÖEG, K. Asphaltic concrete cores for embankment dams. *Stikka Press*, Oslo, Norway, 1993.
- [3] Pircher, W. Schwab H. Design, construction and behaviour of the asphaltic concrete core wall of Finstertal dam, 16th ICOLD Congress, San Francisco, 1988.
- [4] TSCHERNUTTER, P. NACKLER, K. Construction of Feistritzbach Dam with Central Asphaltic Concrete Membrane and the Influence of Poor Quality Rock on Fill Behaviour. *Proceedings of the XVII ICOLD Congress*, Vienna, 1991.
- [5] TSCHERNUTTER, P. Influence of soft rock-fill material as dam embankment with central bituminous concrete membrane. *LTBD09*, Graz, Austria, 2009.
- [6] TSCHERNUTTER, P, KAINRATH, A. A case study on the deformation behaviour of asphalt concrete core dams (ACRD) with different core inclinations. *LTBD17*, Teheran, Iran, 2017.
- [7] Schober, W. Large dams in Austria – Research and development, construction and operation. Volume 34, *ANCOLD*, 2003.
- [8] Wang, W., HÖEG, K., ZHANG, Y., and ZHU, Y., Watertightness, Cracking Resistance and Self Healing of Asphalt Concrete used as Water Barrier in Dams, *Canadian Geotechnical Journal*, 50:3, pp 275 – 287, 2013.

COMMISSION INTERNATIONALE DES GRANDS BARRAGES

VINGT-SIXIÈME CONGRÈS DES GRANDS BARRAGES
Autriche, juillet 2018

DOI 10.3217/978-3-85125-620-8-125



This work licensed under a Creative Commons Attribution 4.0 International License. <https://creativecommons.org/licenses/by-nc-nd/4.0/>

EJECTOR POWER PLANT – VERTICAL KAPLAN

Rudolf FRITSCH

CEO of ZT FRITSCH GMBH / CEO of HYDRO-CONSTRUCT GESMBH

AUSTRIA

COMMISSION INTERNATIONALE
DES GRANDS BARRAGES

VINGT-SIXIÈME CONGRÈS DES
GRANDS BARRAGES
Autriche, juillet 2018

EJECTOR POWER PLANT – VERTICAL KAPLAN

Rudolf FRITSCH

CEO of ZT Fritsch GmbH / CEO of Hydro-Construct GesmbH

AUSTRIA

1. INTRODUCTION

As a contribution to the transition from fossil to renewable energy sources, we need to focus also on power generation from small scale Hydropower plants. The key objective should be to maximize the exploitation of hydro power and one solution in this regard is the utilization of the ejector effect in low head schemes.

A research project was carried out by ZT-Fritsch GmbH / Steyr in collaboration with the Institute HFM (Prof. Dr. Jaberg) - Graz University of Technology in 2013 – 2016.

From this research, and from the appended dissertation on the subject, authored by DI Rudolf Fritsch, scientifically based dimensioning norms for specialized ejector plants in different conditions have been determined.

2. HISTORICAL OVERVIEW

The historical development of ejector power plants goes back to the early 20th century. The first experimental investigations took place in 1905. Mosonyi [1] cites Herschel as having applied special solutions as early as 1909. There were three main types of construction here.

- excess discharge is jetted into the draft tube through the ejector channel
- excess discharge is released through overfall spillways around the draft tube
- excess discharge is released through spillway chute over the draft tube

The heyday for ejector power plants was the 1930s. Especially in the Soviet Union, but also in Europe and the United States, plants of various kinds were planned and built (Hodenpyl power station USA, Kembs power plant on the Rhine, and Alcona power station USA). Hydropower plants utilizing the ejector effect to reduce the loss of drop height in flood conditions by lowering the water level in the tail race were examined in greater detail, for example, in the early 1950s on the basis of built facilities in the then Soviet Union [2].

3. PRINCIPLE OF OPERATION - CURVED DRAFT TUBE

This special concrete hydropower ejector system in a run off river hydropower layout is equipped with a vertical kaplan turbine and a laterally displaced suction tube (Fig. 1), curved in the plan view. This leads to downstream under a special spillway chute, the so-called ejector ramp. In case of excess water, the ejector ramp is activated by opening an ejector gate at the upper side of the ramp. Downside the ramp the energy of the access flow helps to lower the pressure in area of suction tube outlet and so to increase the useable head for the vertical Kaplan Turbine. The annual energy production can be significantly increased by the use of the hydraulic potential.

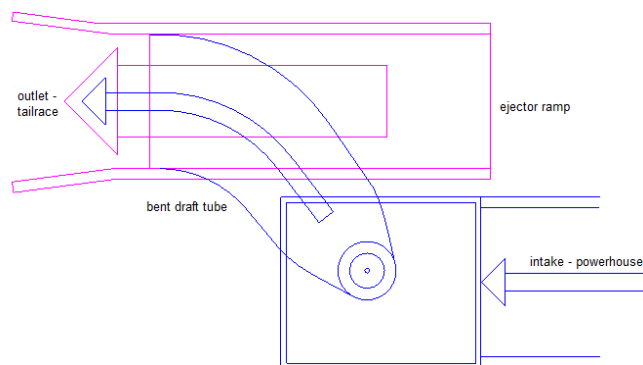


Fig. 1

Situation of the curved draft tube and the ejector ramp in plan view

The goal should therefore be to accelerate the surplus water volume as much as possible in order to achieve a high momentum in the tail race. This increases the suction or creates a lower pressure at the draft tube outlet end and keeps the point of energy conversion as far away as possible from the outlet (Fig. 2), in order to maximize efficient confluence of the two streams.

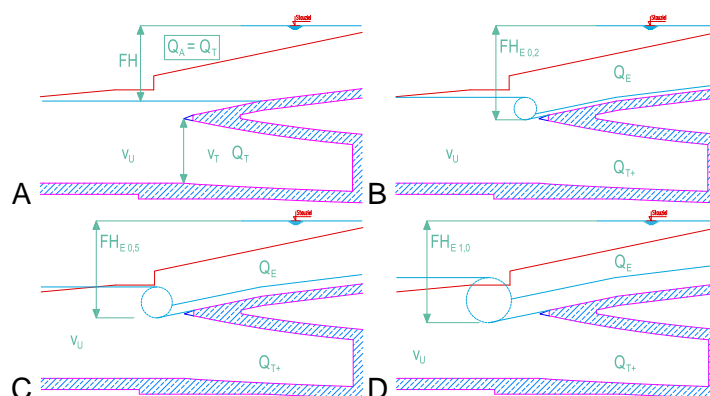


Fig. 2

Principle and effect of the ejector flow

The change in head out of stepwise increased ejector ramp flow is shown in Fig. 2:

- A) Situation without ejector, where Q_T represents the turbine design flow
- B) Flood conditions, ejector operational, increase of the tail race water level
- C), D) Augmented flood condition, showing the shift of hydraulic surge downstream, increasing the useable head

As a result of the momentum, it's clear to see the lowering of the tailrace water level at the draft tube outlet of the turbine, accompanied by an increase in the energy generating head, turbine flow and performance.

A positive side effect of this special draft tube duct under the spillway or ejector ramp, is the elimination of sedimentation problems when flooding occurs. With regard to the operational safety of the plant, safe operation can be ensured even in the event of heavy surplus water or flooding, which nowadays leads to many power plants having to be disconnected from the grid.

As described in Fig. 3 and Fig. 4 the main components of a typical ejector power plant are:

- (1) vertical Kaplan Turbine
- (2) curved suction tube
- (3) intake with horizontal screen
- (4) ejector gate
- (5) ejector ramp
- (6) turbine outlet

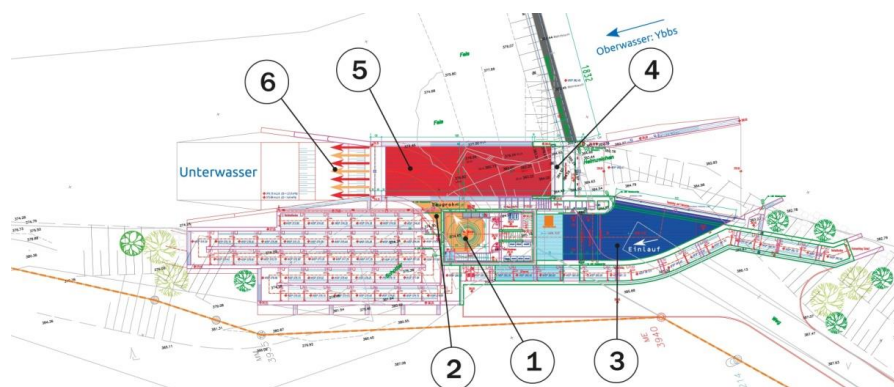


Fig. 3
Plan view of a typical ejector power plant

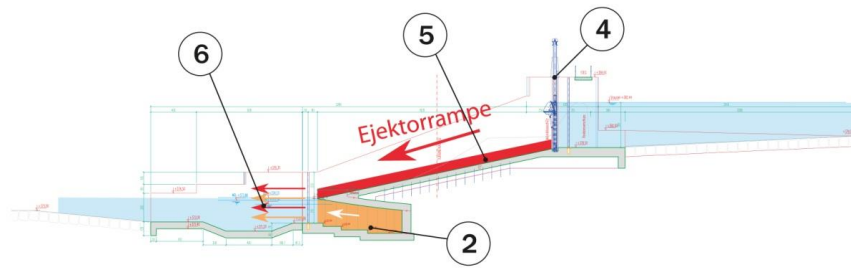


Fig. 4
Section of ejector ramp



Fig. 5
Curved draft tube – example pilotproject KW Stadtwehr Waidhofen / Ybbs

Care must be taken to maintain constant contours throughout the length of the draft tube in order to render negligible any curvature loss.



Fig. 6
Waidhofen Power Station: ejector flow at the end of the
ejector ramp (mixing zone)

A striking drop in water level at the convergence point of the two water streams, where the ramp water mixes with the turbine flow from the draft tube is shown in Fig. 6.



Fig. 7
Ejector ramp flow – Waidhofen Power Station

The ejector flow, regulated at the ejector gate, is accelerated on the ejector ramp and displaces the tail race water body, creating a clearly visible roller wave (Fig. 7).

4. FIELD OF EFFICIENT USE

In low head hydro electric power plants the useable energy height (head) ratios are highly dependent on the runoff conditions within the body of water.

As a rule, the design of the turbine is geared towards the average water flow, in order to ensure optimum operational efficiency of the plant over the longest possible time span.

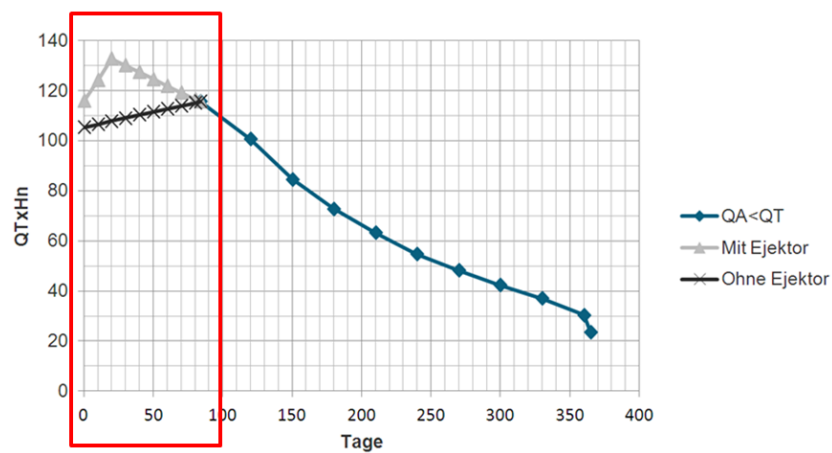


Fig. 8

The hydraulic performance is based on flow duration

The scope of ejector efficiency is limited by full load conditions, where surplus water is present.

5. SCIENTIFIC AND RESEARCH BACKGROUND

In 2013 a scientific research project was started by ZT-Fritsch GmbH in collaboration with TU Graz – Institute HFM (Prof. Dr. Jaberg).

1.1. EXPERIMENTAL INVESTIGATION

In order to achieve an experimental investigation close to reality the substantial parts of the reference power plant Waidhofen were replicated using a scale model ($M = 1:10$).

The three dimensional CAD-model of the designed test rig is shown in Fig. 9. The water delivered by the main pump of the test rig enters the open headwater tank (2) via the inlet pipe (1). With the help of the turbine pipe section (3) a part of the water Q_{Tu} is directed to the draft tube of the turbine (4). The other part of the water flow Q_{Ej} is regulated by an ejector gate (6) and runs in the ejector chute (5) to the mixing zone (7).

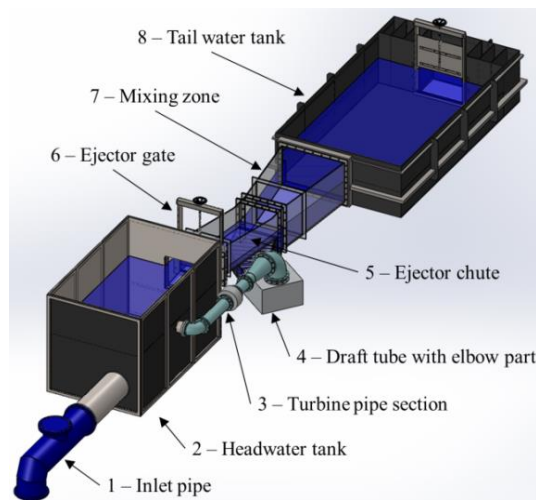


Fig. 9

Three-dimensional view of the CAD-model of the ejector test rig [4]

One of the results of the experimental model is shown in the diagram below (Fig. 10), namely the increase of available hydraulic power due to the ejector effect detected in the course of the measurement program.

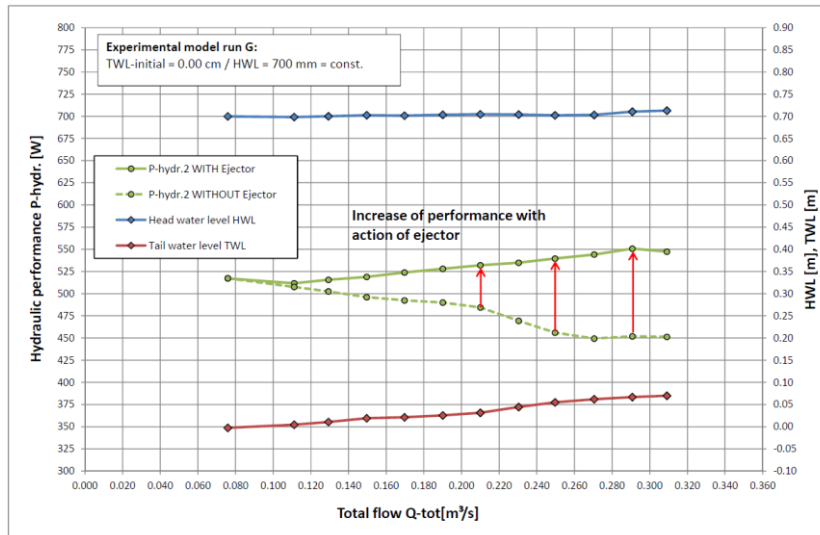


Fig. 10

Experimental model – hydraulic performance with and without ejector [3]

At the operation point with the highest flow rate the hydraulic power available for the turbine is still around 22 % higher than compared to the situation without ejector.

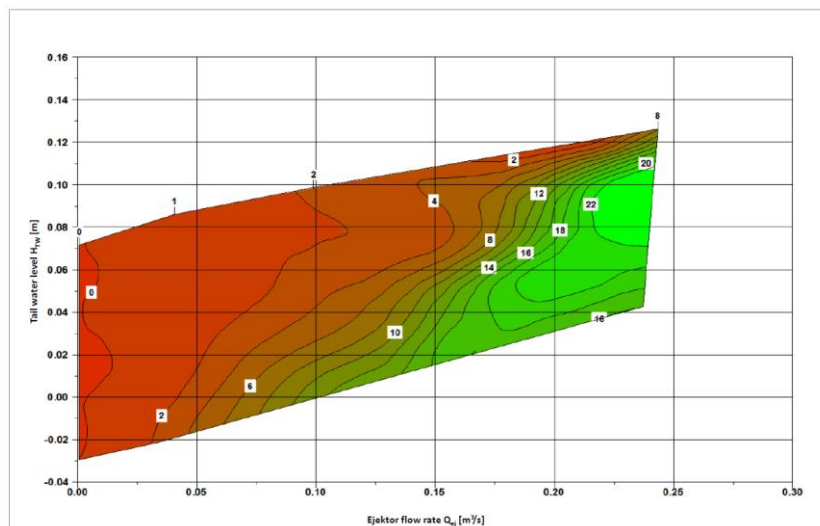


Fig. 11

Contour plot of the percentage of the increased power output due to the ejector effect valid for the experimental model run G

In order to verify whether the increase of the available hydraulic power is reached by an increased turbine head or an increased turbine flow rate the diagram below provides a more detailed analysis of the measurement results. The diagram presents the turbine flow rate Q_{Tu} and the turbine head H_{Tu} plotted against the total flowrate Q for the situation with and without ejector.

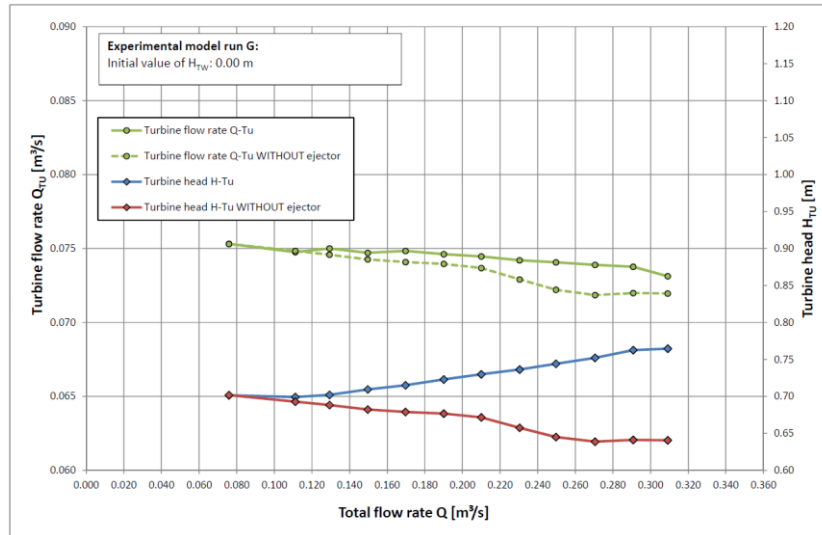


Fig. 12
Turbine flow rate and turbine head measured with and without ejector

It turns out that the ejector effect does not only cause an increase of the turbine head H_{Tu} but also of the turbine flow rate Q_{Tu} which is – though decreasing – higher than the “normal” turbine flow rate. This is due to a suction effect closely connected with the reduction of the tail water level at the draft tube outlet.

1.2. PILOT PROJECTS – MEASUREMENT

At the same time, in our first two ejector pilot projects at hydropower stations KW Mühlthalwehr and KW Stadtwehr Waidhofen, measurement instruments were installed to show the efficiency of ejector technology.

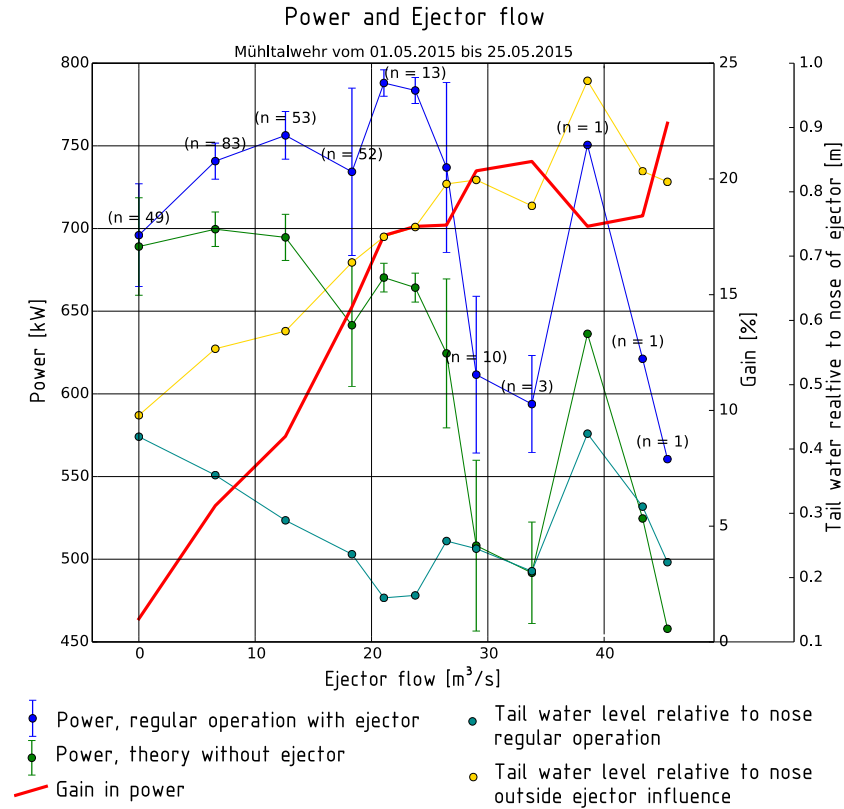


Fig. 13
Documentation main values – May 2015 / KW Mühlthalwehr/Alm [3]

In the diagram above (Fig. 13) the gain in power, the power with ejector, without ejector and also the upstream and downstream level are documented.

1.3. CFD ANALYSIS

Numerical computation was also carried out to verify the experimental model testing with CFD-analysis.

Distinct water waves appear in the tail water especially in the region around the draft tube outlet.

The flow rate dependent change of the wave structure in the tail water is presented by the following Figure.

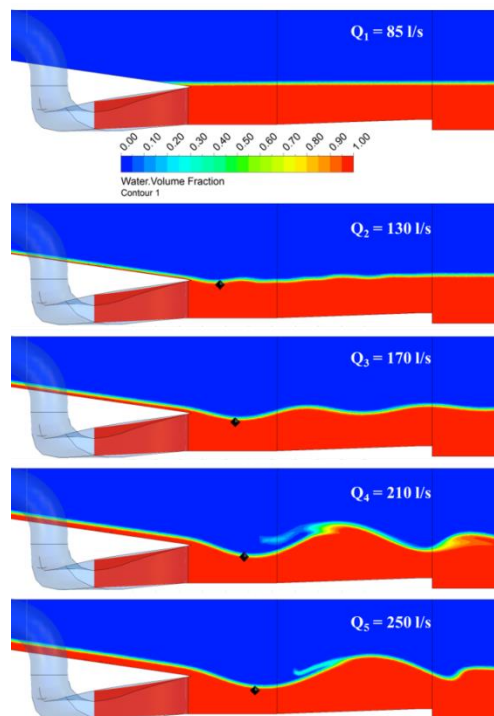


Fig. 14
Water Volume Fraction plotted on a cross sectional area for
 $Q_1 = 87.5$ to $Q_5 = 250 \text{ l/s}$ [4]

On the one hand it turns out that the ejector is capable of increasing the hydraulic power available at the turbine by a maximum of 18 %. On the other hand an analysis of the presented data shows that the positive effect of the ejector does not only depend on the ejector flow rate but also on the tail water level with respect to the level of the ejector nozzle. If the tail water level is too high even a comparably high ejector flow rate does not cause an increase of power output.

In our special design the gate is located immediately below the start of the ramp gradient. This gives the added advantage of increased outflow speed with loss prevention by removing the previously present break at the transition to the ramp and avoiding fill surge.



Fig. 17
Fully opened ejector gate – situation at pilot project KW Mühltalwehr / Alm

Extensive software for the calculation and dimensioning of ejector power plants was produced by DI Rudolf Fritsch [3].

For the retroactive calculation from the model conditions, the following velocity curves of v_1 are shown in Fig. 18, with variable Q_E , directly at the ejector gate before entering the ejector ramp.

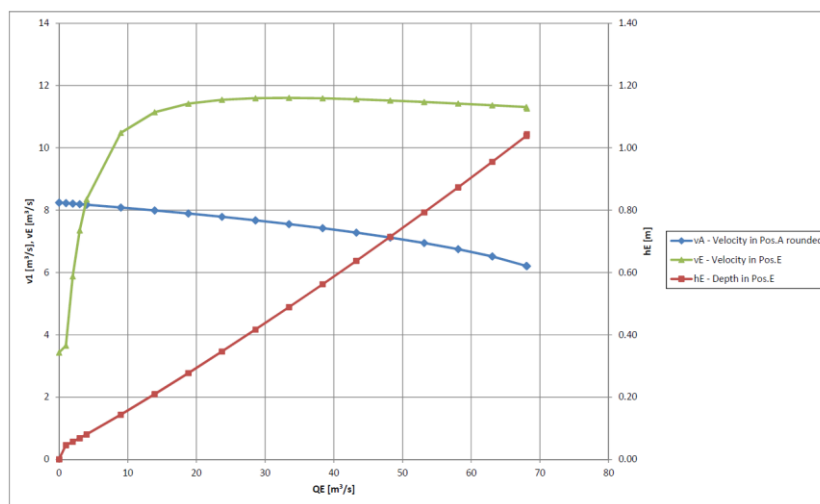


Fig. 18
Example of the typical relation of flow speed (v_E) and height of water on an ejector ramp end to the flow speed (v_A) at the ejector gate [3]

7. GENERATOR OF MOMENTUM – EJECTOR RAMP

A key feature of this installation is the ejector ramp (Fig. 19), whose purpose is to optimize the acceleration of the excess flow.

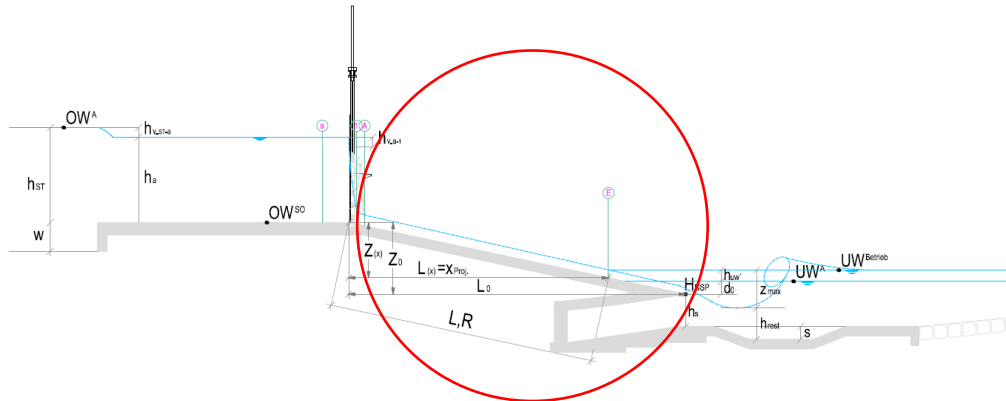


Fig. 19
Section through the ramp with transition to the mixing zone [3]

The spillway and ejector ramp in KW Mühlthalwehr is covered with steel plates to reduce losses to a minimum and to avoid erosion.

Ejector ramps are essentially gravity flow tailraces. For tailraces of this kind, the flow conditions for irregular movement can be calculated using the Strickler method.

$$v = k_{St} \cdot R^{2/3} \cdot J^{1/2} \quad [1]$$



Fig. 20
Ejector ramp – KW Mühlthalwehr/Alm with steel covering

Surface Roughness of the ramp

When constructing the ramp, attention must be paid to minimizing surface roughness along a sufficient length and gradation.

An approach to the calculation of the energy equation for run off on the ramp, taking account of losses due to roughness, is as follows:

$$H_A = H_E \quad [2]$$

$$H_{A,0} + Z(x) = H_{E0} + h_v \quad [3]$$

$$H_{A,0} + Z(x) = h_E + \frac{v_E^2}{2 \cdot g} + \frac{v_m^2 \cdot \Delta X}{K_{ST}^2 \cdot R_h^{4/3}} = \frac{Q}{v_E \cdot b} + \frac{v_E^2}{2 \cdot g} + \frac{v_m^2 \cdot \Delta X}{K_{ST}^2 \cdot R_h^{4/3}} \quad [4]$$

Optimal conditions (for example k_{St} = Strickler values) are to be specified in this development project.

Table 1
List of different materials and roughness values are as follows

Material	Strickler-factor k_{St} in $m^{1/3}/s$
sheet steel	100
skimmed concrete	85
preformed concrete	80
wood	75
rough concrete	50

As can be demonstrated when considering the design of the ramp of an ejector power plant, the main criterion is the reduction of the roughness to a minimum (for example by utilizing sheet steel plate).

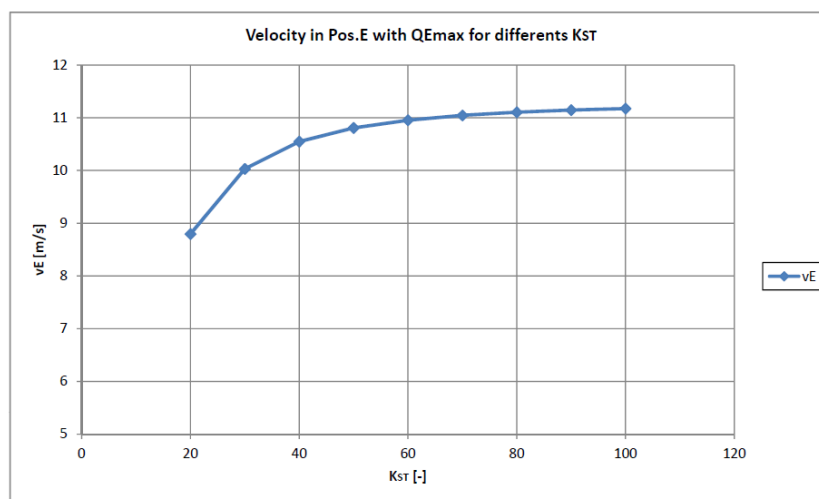


Fig. 21

Water flow speed at the end of the ejector ramp in relation to the roughness [3]

8. ENERGY CONVERSION – MIXING ZONE

Here the core principle of increased head achieved by the ejector comes into play. The analytic approach is based on the equation of energy and the law of momentum

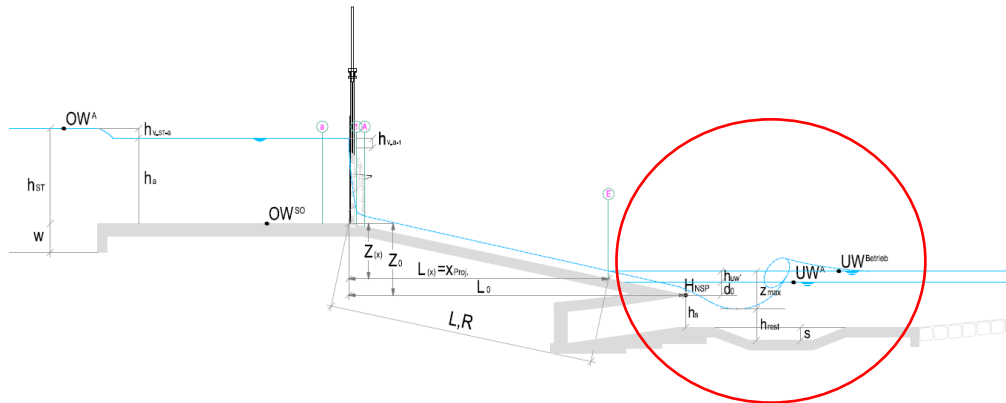


Fig. 22
Section of the ramp with mixing zone [3]

The above scheme (Fig. 22) shows the special configured mixing zone for energy conversion with head increasing effect.

Starting from the energy level, available at the end of the ramp, out of the momentum

$$\text{Pulse current } (I_E) = \text{mass flow } (\rho \cdot Q_E) \cdot \text{velocity vector } (v_E)$$

a power transmission occurs to the existing tailrace water with the water flow from the turbine draft tube.

In this application it is important to utilize the acceleration effect on the ramp, or in other words to further accelerate the volume of water entering the sluice by minimizing surface roughness on the ramp until the water is reunited with the head race water.



Fig. 23
Influence of ramp gradient [3]

The above sketches (Fig. 23) show the speed and momentum components on the end of the ejector ramp, linked to the gradient.

Analytic modelling

At the point of convergence at the end of draft tube the momentum relationships can be written with the equation of momentum, reduced by the pressure component.

$$I_E = \Sigma \left(m \cdot \frac{d\vec{v}}{dt} \right) = \Sigma \rho \cdot Q \cdot \vec{v} = \rho \cdot Q \cdot v_E \quad [5]$$

$$\Sigma \rho \cdot Q \cdot \vec{v} = \Sigma P \Delta t \quad \Sigma P \Delta t = 0 \quad [6]$$

$$\rho \cdot Q_T \cdot v_T + \rho \cdot Q_E \cdot v_{E,H} = \rho \cdot (Q_T + Q_E) \cdot v_{comb} \quad [7]$$

On the basis of the research project, we determined a factor for the effect of the ejector in our calculation approach, which takes into account the difference between the optically visible water level at the decisive confluence point and the actually effective pressure level in the draft tube.

This factor is linked to the momentum component of the ejector flow, as the determining parameter for the gain in head.

The equation of momentum linked to the energy equation can now be written as:

$$\rho \cdot Q_E \cdot v_{E,H} \cdot f_{VE} + \rho \cdot Q \cdot v_T = \rho \cdot (Q_E + Q_T) \cdot v_{eff} \quad [8]$$

The significant result is the useable speed of the mixed flows (v_{eff}) of turbine and ejector:

$$v_{eff} = \frac{Q_E \cdot v_{E,H} \cdot f_{VE} + Q_T \cdot v_T}{Q_E + Q_T} \quad [9]$$

The result for the velocity of the mixed flows (v_{eff}) out of the equation of momentum can be also directly linked to the equation of energy at the confluence point (Fig. 24).

$$h_{UW,B} + \frac{v_{T,B}^2}{2g} = h_{UW,eff} + \frac{v_{eff}^2}{2g} \quad [10]$$

$$z_H = h_{UW,B} - h_{UW,eff} \quad z_H \dots \text{gain in net head} \quad [11]$$

$$z_H = \frac{v_{eff}^2}{2g} - \frac{v_{T,B}^2}{2g} \quad [12]$$

The energy related conditions of the convergence point are projected into the confluence point.

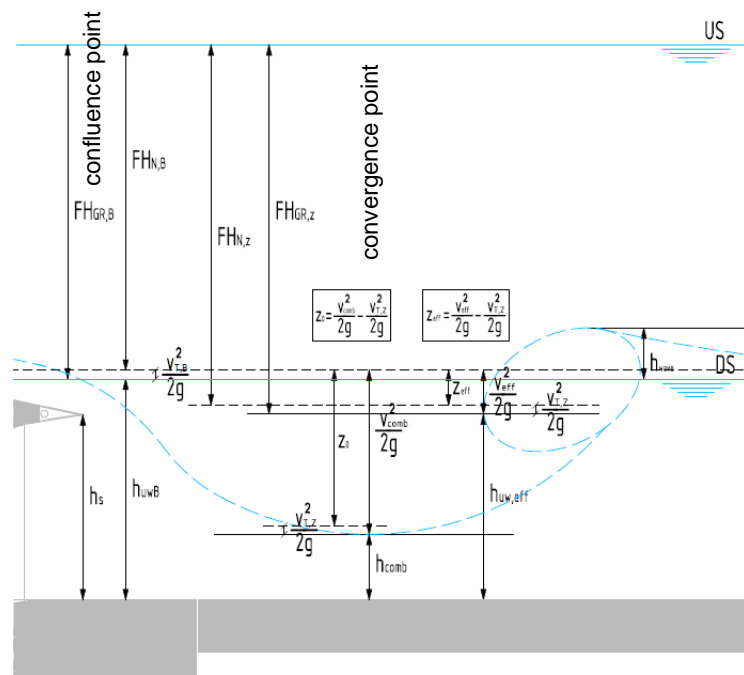


Fig. 24
Energy heights scheme in the mixing zone [3]

A lowering of the water level pressure occurs, together with suction back into the draft tube.

This momentum and consequently the influence on the ejector's effectiveness in increasing drop height can be illustrated in two component parts also, according to influence of the ramp gradient.

$$z = z_H + z_V \tag{13}$$

Conditions at confluence zone

The design of the draft tube discharge or mixing zone is of great significance for the effectiveness of the ejector. The research project results in a special surface design at bed level optimizing the head increasing effect.

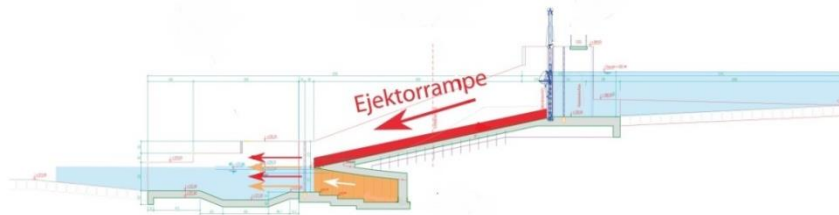


Fig. 25
Section through ejector ramp with the deepened mixing area [3]

The suction effect at the point of confluence, or the point where the ejector exhaust water with higher speed mixes with the slower turbine flow, can of course only take place if the top side of the draft tube is not too severely backed up.

The influence of the draft tube outlet top level is very clearly represented in the results of the model experiment and thus represents a significant boundary condition. The goal should therefore be to determine the underwater conditions very accurately, so that on the one hand during normal to full load operation no risk of air intake to the turbine occurs, but on the other hand water backup remains reduced during ejector operation.

The great importance of the way in which the ejector water and the head race water are brought together is to be seen definitively in the lateral contraction effect we observed in modelling exercise. Increased efficiency from the ejector effect can only be optimized when the water flow from the ejector ramp into the tailrace enables maximum transfer of the energy from the ejector water to the head race water.

The design of the mixing zone which we devised, tested and submitted for patent in this project, ensures an efficient confluence of the two flows and prevents the lateral contraction phenomenon we observed in the test series.

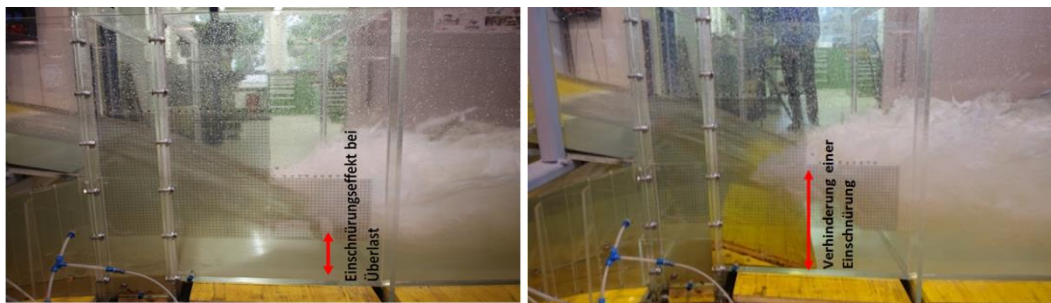


Fig. 26

Pictures with flat bed level in the mixing area in comparison to deepened bed level, show the importance of avoiding a constricting effect, which reduces the positive ejector effect considerably [3].

9. ENERGY PRODUCTION VALUATION

The following chart outlines the results of a comparative study undertaken on the outflows at Gaissulz on Ybbs, taking different heads into account. The key result, in relation to the percentage increase in energy production is, that relative output remains constant.

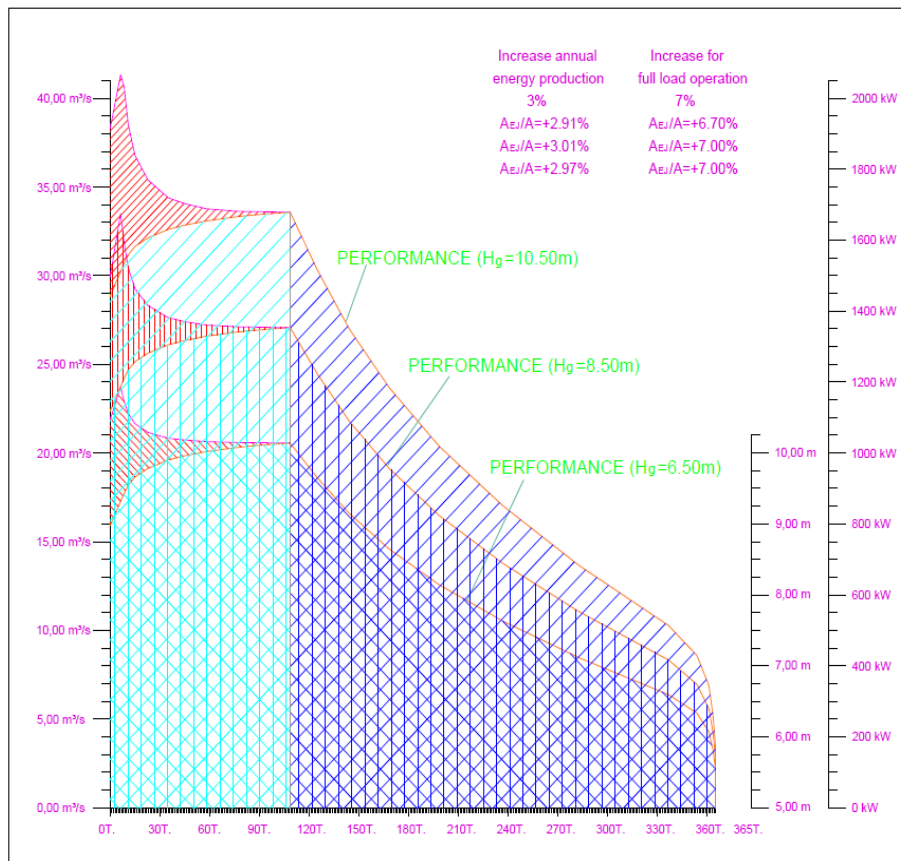


Fig. 27

The duration curve for hydraulic performance is shown in above diagram for different net head with a fixed turbine flow of 20 m³/s [3]

The values for increase of yearly energy production in percentage terms, measured against a fixed full load flow are thus more or less constant and amount to 7% for full load conditions and 3% for the annual average.

10. CONSIDERATIONS – DECISION ON AN EJECTOR PLANT

Assuming a change in the runoff water volume at a constant drop height, and taking into account the annual 3 – 5 % energy increase, you can calculate an equivalent reduction in the full load volume of approximately 7 – 10 %, which compensates for the energy gains, but does not evaluate the further advantages of location and operation, as shown in the below diagram (example KW Gaissulz / Ybbs).

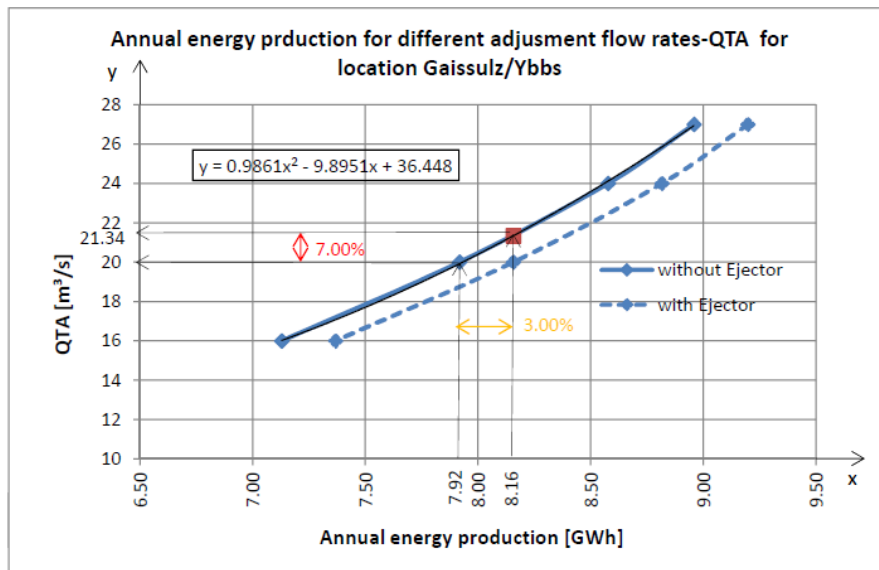


Fig. 28

Annual energy production for different adjustment flow rates Q_{TA} for location Gaissulz/Ybbs [3]

From this comparison and from a desire to reduce the dimensions and costs in general we can conclude the possibility of a smaller design concept using also the further advantages of an ejector power plant.

11. PERFORMANCE PARAMETERS

The performance of ejector is generally considered to be a function of the parameters of hydraulic performance defined in the following:

Internal efficiency parameters

Speed ratio: $\eta_{V,WIRK}^* = \frac{v_{WIRK}}{v_{VER}}$ [14]

Striking drop ratio: $\eta_{Z,WIRK}^* = \frac{z}{z_{BR}}$ [15]

Head increase ratio: $\eta_{FH,N}^* = \frac{z}{FH_{N,Z}}$ [16]

Net head ratio: $\eta^* = \frac{FH_{N,Z}}{FH_{N,B}}$ [17]

Outside total efficiency

Flow ratio: $M = \frac{Q_T}{Q_E}$ [18]

Head ratio: $N = \frac{z}{H_{N,z}}$ [19]

Efficiency – partial: $\eta_{EJ} = M \cdot N = \frac{Q_T \cdot z}{Q_E \cdot H_{N,z}}$ [20]

η_{EJ} gives the ratio of total energy increase of suction flow to the total energy increase of ejector flow.

Efficiency – total: $\eta_{hyd,total} = \eta_T \cdot \eta_G \cdot \eta_{GB} \cdot (1 + \eta_{EJ})$ [21]

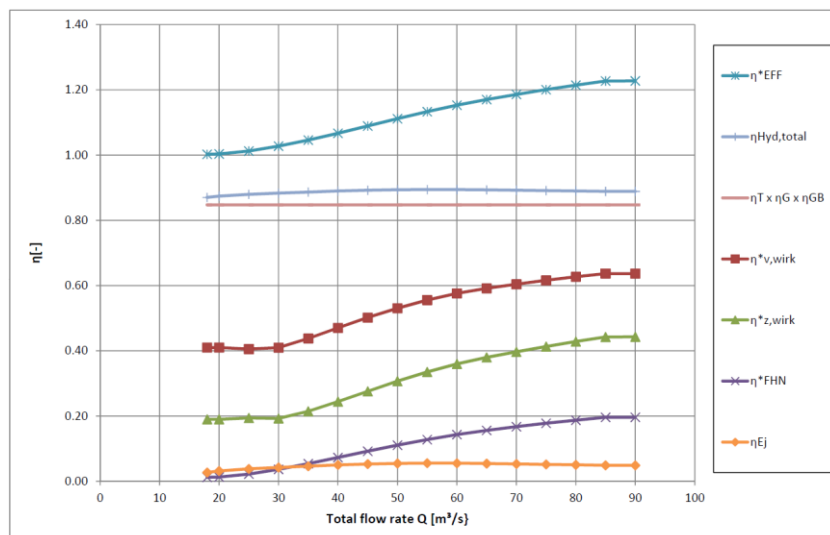


Fig. 29

The diagram shows the different efficiency parameters [3]

REFERENCES

- [1] MOSONYI, E.: Wasserkraftwerke. Band 1 Niederdruckanlagen. Düsseldorf: VDI-Verlag, 1966.
- [2] SLISSKII, S. M.: Ejection into tailraces of hydropower plants. 1. A. Moskau: Gosudarstvennoe Energeticheskoe Izdatel'stvo, 1953.
- [3] FRITSCH, R., J ET AL.: Dissertation – Untersuchung der Ejektorwirkung bei vertikalen Kaplan-turbinen, 2018 [TU Graz – Institute HFM – Prof. Dr. Jaberg]
- [4] SCHIFFER , J ET.AL.: NUMERICAL AND EXPERIMENTAL INVESTIGATION OF THE EJECTOR EFFECT APPLICABLE TO LOW HEAD VERTICAL KAPLAN TURBINES, Conference on Modelling Fluid Flow, At Budapest, Volume: The 16th International Conference on Fluid Flow Technologies
- [5] SCHIFFER, J ET AL.: Experimentelle Untersuchung der Ejektorwirkung bei vertikalen Kaplan-Turbinen; In: WasserWirtschaft, 2015, 05, S33-39.

SUMMARY

In the course of this study we were able to scientifically determine increased outflow performance by utilizing an ejector, as we had indeed observed already in the pilot projects at

Mühltalwehr/Alm and Stadtwehr Waidhofen/Ybbs. Comparative performance increases were also noted in our 1:10 scale model and in CFD simulation. In particular, we were able to demonstrate in the laboratory and in subsequent analyses that the efficiency of the ejector can be significantly increased by specific design measures between the draft tube and the run off, and also by changes in the position of the ejector sluice gate.

The potential of the interaction of the head race water flow out of the draft tube together with the excess water from the ejector ramp represents the sum of the combination of effective drop height and turbine flow rate. First and foremost, the interaction of these two water volumes is accomplished as a result of a pressure drop, dependent on the momentum coming from the ejector, directly at the draft tube exit point. Increased performance of up to 35% is achievable, as compared to theoretical performance without the ejector in flood or excess water conditions. This breaks down to increased energy output of 7% - 10% at full load and 3% - 5% as an annual average. With consistent annual energy yield the development and head race design costs could be reduced by 5% – 10%, a substantial reduction in the construction and investment costs for new installations.

A not insubstantial side effect is that uninhibited operation is possible even in flood conditions, during which previous design models are required to shut down. Additionally, there is no risk of silt build up in the run off zone.

The curved draft tube also results in space saving design outcomes at the construction stage. Surface area reduction of up to 20% can be put to efficient use in the field of environmental considerations, for example the upstream migration of fish. In a typical design configuration as a bay shaped power plant, with a combination of movable weir system, generously dimensioned ejector exhaust and laterally positioned inlet with turbine system, the entire river profile remains free for flood discharge.



Fig. 30
Aerial photography of ejector plant Gaissulz / Ybbs [3]

In addition to the classic measures of increasing energy yield at existing locations, such as increasing the dam height, underwater excavation, more efficient regulation and increasing the amount of full load, the use of ejectors should be considered as a way forward for the redevelopment of hydropower plants.

This special technology, with patented construction details and special software for design calculation, can be offered by ZT-Fritsch GmbH, the company behind the research project and with many years of experience in hydropower design.

About the presenter Rudolf Fritsch:

- after graduating from high school in Steyr, studied civil engineering at University of Vienna
- civil engineer in the construction industry since 1980
- since 1986 CEO of ZT-Fritsch GmbH, engineering office in Enns, specializing in hydro and bridge design, infrastructure and industrial design; certified legal expert
- since 1994, CEO of Hydroconstruct GmbH in addition a company specializing in rubber dam technology
- since 2000 Head Office in Steyr, Austria, currently spending up to 70% of time on hydropower projects

E-Mail contact:

office@zt-fritsch.at

Steyr, June 2018

COMMISSION INTERNATIONALE
DES GRANDS BARRAGES

VINGT-SIXIÈME CONGRÈS DES
GRANDS BARRAGES
Autriche, juillet 2018

FEATURES OF MONITORING TEMPERATURE OF AN RCC DAM DURING CONSTRUCTION BASED ON DATA MINING

Jianwen PAN

*Assistant Professor in Department of Hydraulic Engineering, TSINGHUA
UNIVERSITY*

CHINA

Jinting WANG

Professor in Department of Hydraulic Engineering, TSINGHUA UNIVERSITY

CHINA

1. ABSTRACT

A deep understanding of concrete temperature varying in large concrete dams is of importance for improvement of construction technology. A large number of temperature sensors are installed in the dam blocks as concrete pouring. The temperature of the dam concrete, which increases due to hydration heat in the early stage and decreases when employing water-cooling system, is measured and massive temperature data is stored. The monitoring temperature history varies as time and its changes are affected by many factors, such as the hydration heat temperature rise, the amount and velocity of water flows in the cooling system, environmental temperature, etc. Features of the monitoring temperature may provide insight into possible prevention of temperature-induced cracks in concrete dams.

In this paper, the features of the monitoring temperature data of a roller compacted concrete (RCC) dam (height 203 m), under construction in Yunnan

Province of China, is recognized based on data mining. The raw measured temperature data always contains missing values and outliers. Processing of the missing values and outliers is required before analysis of the data. The density-based spatial clustering of applications with noise method is employed to detect and delete the outliers and the the k-nearest neighbor algorithm is used to estimate and substitute the missing data. The K-means clustering with dynamic time warping algorithm is applied to classified the temperature time series and to find their features.

Four types of temperature series are recognized. Fig. 1 shows the four types of temperature history curves determined by the K-means clustering algorithm. There is a significant difference in the temperature variation between the different types. Type I exhibits a rapid increase due to hydration heat and a decrease as cooling water flows within 20 days after concrete pouring, followed by a gradually increase in the next 3 months. Comparing with Type I, Type II has a stable curve after its drop due to water-cooling. Type III is a approximately horizontal curve, and the hydration heat induced increase and the water-cooling induced drop of temperature are possibly missing. Fluctuation is observed in the later stage of the temperature curve of Type IV, while it is smooth in the other three types, implying that temperature of Type IV is measured near the surface of the dam where the environmental temperature has significant influence and the other three types monitored inside the mass concrete.

This study presents a preliminary analysis of features of monitoring temperature of the RCC dam during construction. Further study based on the big data mining and numerical simulation is needed to understand the cause of the difference between the features and the effect of different features on the concrete dam behavior.

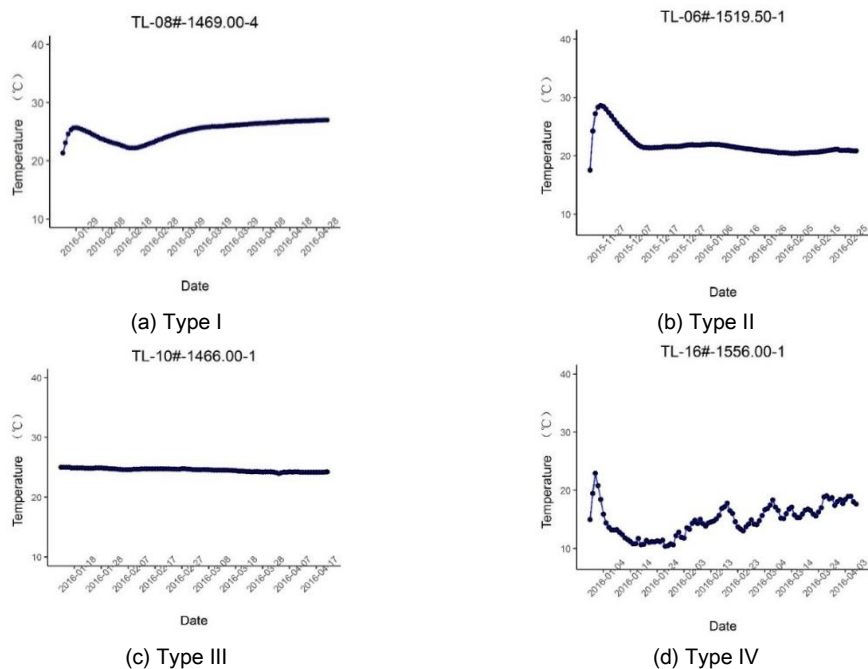


Fig. 1 Types of the monitoring temperatures time series

COMMISSION INTERNATIONALE DES GRANDS BARRAGES

VINGT-SIXIÈME CONGRÈS DES GRANDS BARRAGES
Autriche, juillet 2018

DOI 10.3217/978-3-85125-620-8-127



This work licensed under a Creative Commons Attribution 4.0 International License. <https://creativecommons.org/licenses/by-nc-nd/4.0/>

RUBBER DAM CONSTRUCTION WITH NAVIGATION LOCKS

Paul OBERLEITNER

Partner HYDRO-CONSTRUCT GMBH

AUSTRIA

Rudolf FRITSCH

CEO HYDRO-CONSTRUCT GMBH

AUSTRIA

COMMISSION INTERNATIONALE
DES GRANDS BARRAGES

VINGT-SIXIÈME CONGRÈS DES
GRANDS BARRAGES
Autriche, juillet 2018

RUBBER DAM CONSTRUCTION WITH NAVIGATION LOCKS

Paul OBERLEITNER & Rudolf FRITSCH

*Partner & CEO
Hydro-Construct GmbH*

AUSTRIA

1. INTRODUCTION

Gomti River is a main river in India and is passing the main capital Lucknow in the Indian State Uttar Pradesh. The State Irrigation Department has developed a river rejuvenation program with the following topics:

- Upgrading of the existing Gomti Weir downstream of the Gomti Barrage with a flexible weir structure
- Upgrading comprises also the development of weir cascades
- Improvement of the flood safety by structuring of the river banks
- Creating a water surface with a reservoir with app. 400.000 m³ with a constant water level
- Improvement of water quality in the river stretch by collecting and diverting of the sewage in a new pipe system
- Enabling river boating in the reservoir and passing of boats through the new weir by navigation locks

Alternative Studies carried out came to the solution that a flexible rubber dam with a water filled regulation system meets the requirements as it bests to reach the outlined targets and the economic feasibility. The rubber dam system on the weir is added by navigation locks on both river banks for passing of boats. In the navigation locks there are also moveable rubber dams installed.

2. GENERAL PROJECT DESCRIPTION

2.1. MAIN PROJECT FEATURES

Upgradation of Gomti Weir with water filled rubber dam at Lucknow (at 2.00 km D/S of Gomti Barrage) Uttar Pradesh, India.

The dam system has a length of in total about 256.20 meter and is consisting of 4 sections with inflatable rubber dams and navigation channels on right and left river bank.

The dimensions were chosen by a hydraulic calculation to provide sufficient flood safety.

The system is described with the following data in brief:

- Inflatable main weir sections with rubber dams, 4 main sections (B+C+D+E), each with length 54 m and height 3.00 m
- Navigation channel left side (F), width 16 m and heights 3.30 m at U/S and 3.70 m at D/S, distance between U/s and D/S rubber dam: 17 m
- Navigation channel right side (A), width 16 m and height 3.30 m U/S, provision for a rubber dam on D/S
- Regulation shaft building and water tank
- Connecting pipe system between regulation shafts and rubber dam sections
- Automatic Control & Regulation System (CRS) for all rubber dam sections with SCADA system in control building on top of regulation shaft building
- The Automatic Control & Regulation System (CRS) is maintaining a head water level with up to 3.00 meter over the fixed sill level.
- Manual control of the rubber dams in the navigation locks.

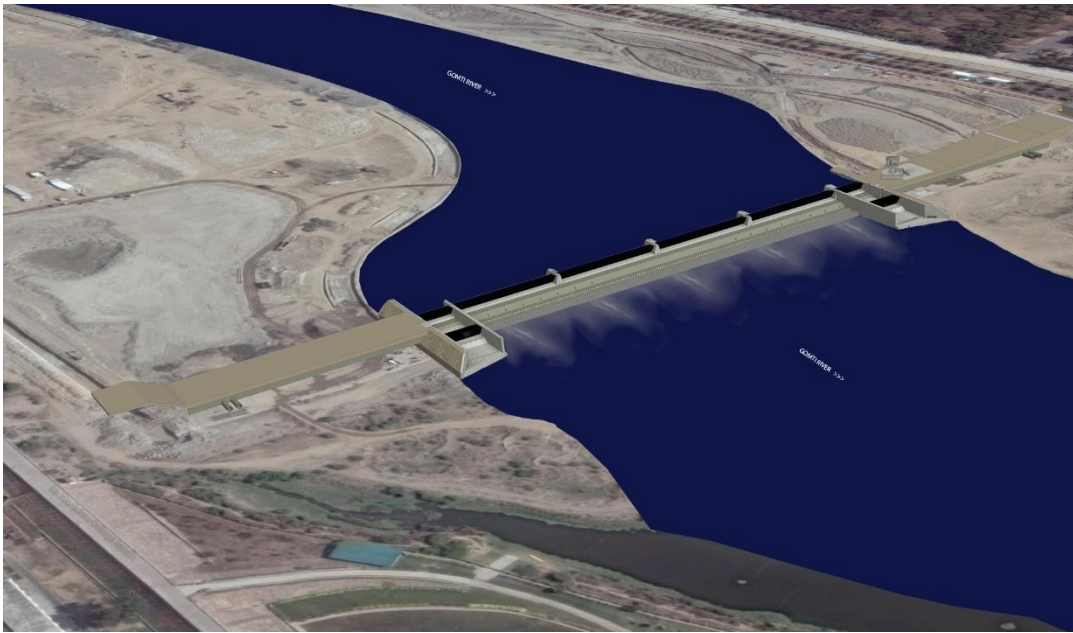


Fig. 1
General view to the new Gomti River Weir

2.2. EXISTING WEIR STRUCTURES BEFORE UPGRADATION

The existing weir was built decades before and serves the river protection measures from erosion and flood control. This old Gomti weir was app. 250 m long and consists of a fixed concrete sill with manually operated flushing channels.



Fig. 2
View to the Gomti Weir in year 2015 before upgradation

The hydraulic behaviour of the old Gomti Weir with a fixed weir sill was resulting in changing water levels depending on river flows. This was resulting in a very small water surface during dry periods.

2.3. DESCRIPTION OF MAIN PARTS

The main sections of the new weir were built on top of the existing concrete structure by removing more than 1 meter of concrete. The new weir slab has a thickness of minimum 1.20 m and is made of reinforced concrete. The crown of the rubber dam lies on EL 106.0 m, the design height of the reservoir at EL 105.50 m.

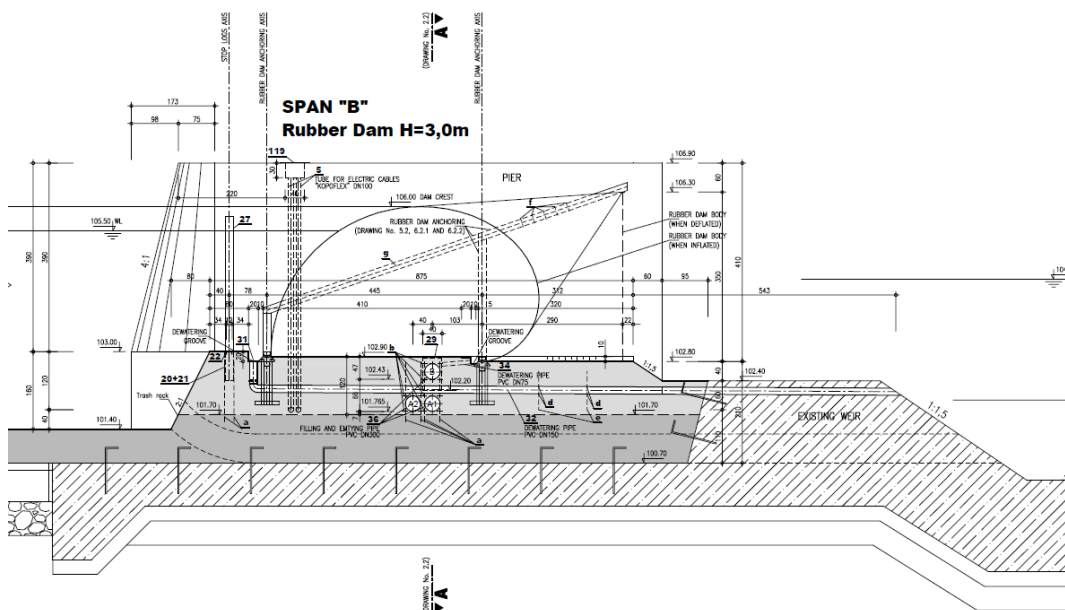


Fig. 3
Cross section through main rubber dam section

For the regulation system water filling is foreseen. This system is providing a more stable and precise regulation range over the whole dam height and is designed for possible tailback up to EL 104.50 m also.

The clamping rail for the 4 weirs sections is fixed in 2 steps with 0.1 m so that the height of rubber dam in downstream side is 3.20 meter.

The rubber membrane is double-clamped and has a minimum wall thickness of 16 millimetres, with three woven fabric reinforcement layers to provide sufficient rupture strength.

In case of flood the rubber dam will be regulated automatically according to the flow until the whole membrane is completely deflated to the fixed weir sill.

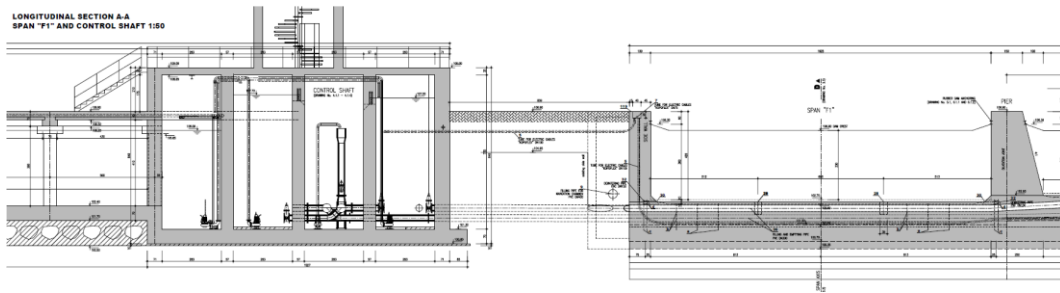


Fig. 4

Longitudinal section through water tank, regulation shaft and weir span "F"

For standard project cases the water for regulation purposes will be taken from the reservoir directly. For the Gomti Project the Irrigation Department has decided to maintain a separate water tank which will be feed by external water from a water pipeline. The volume of the regulation tank was selected with 2,630 m³, which amounts to 60 % of the fill volume (app. 4,000 m³) of all the rubber bodies. This covers the regulation process for almost the whole normal operation of the system.

The general arrangement for the regulation system is consisting of:

- Water Tank with a reservoir volume for 2,630 m³ water
- Regulation Shafts with regulation equipment such as pipes, pumps, valves and safety devices
- Control Building on top of the shaft building at flood safe elevation - with the electric control equipment for the whole rubber dam system including navigation locks.

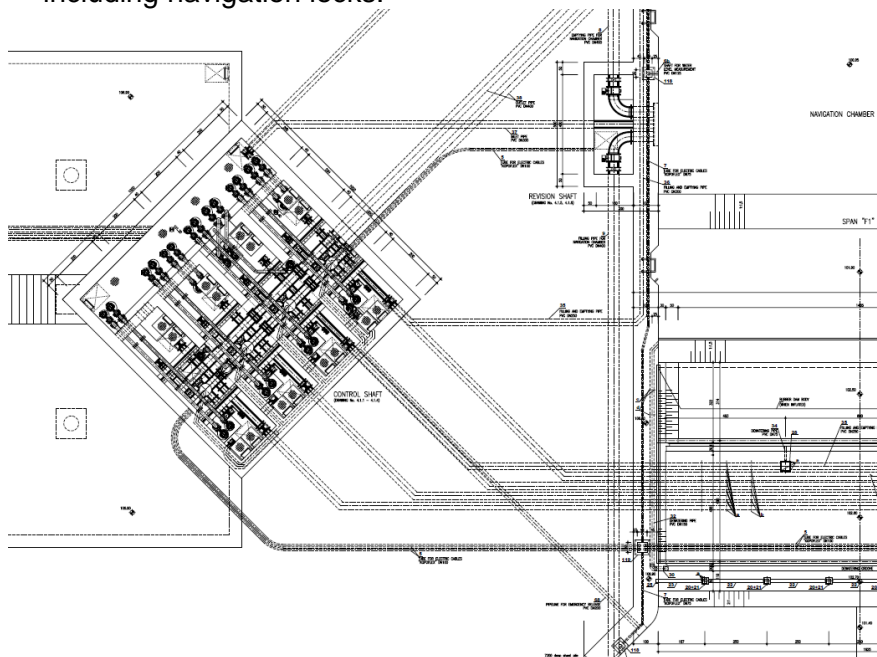


Fig. 5

Layout Control Shafts and Navigation Lock F

Regulation of the upstream level will take place by means of a probe-controlled system. A self-functioning automatic discharge is installed for emergency release. All steel components are hot-dip galvanized; the piping embedded in concrete is made of PE. All screws and bolts are of stainless material.

The control system of the main sections can be operated in manual and automatic mode. Every single section of the rubber dam system can be operated separately. Central control for automatic operation of the rubber dam will be coordinated by means of a PLC and is in a switchboard panel in the control building.

2.4. MAIN DESIGN CONSIDERATIONS

Calculation of the membrane forces assuming firmly inflated water inflated rubber dam shape according to the following figure and equation formula.

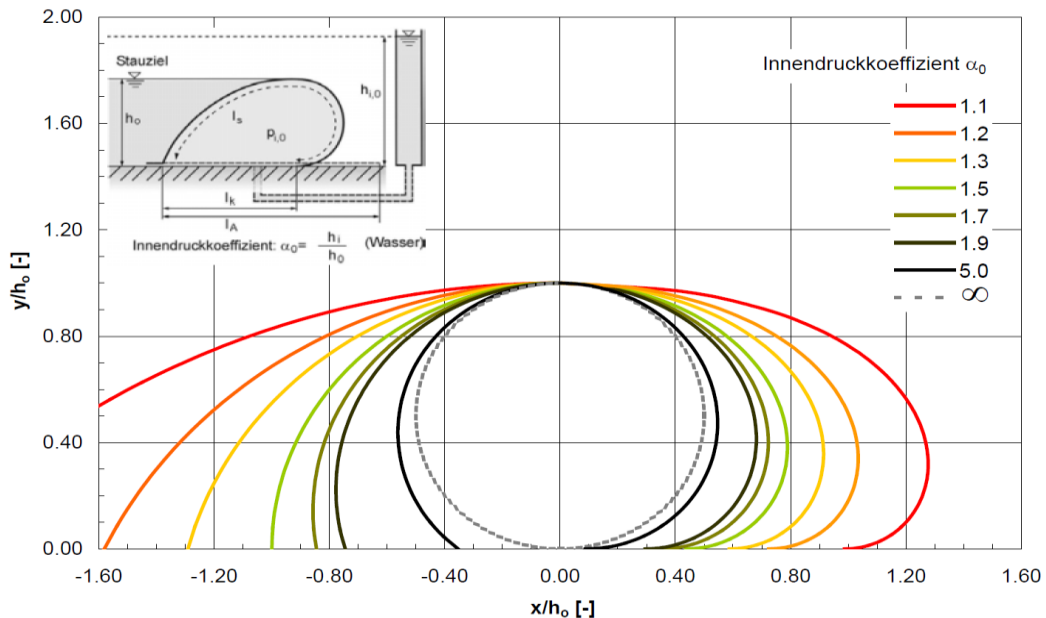


Fig. 6
Inflation pressure coefficient for water filled systems

$$T = \frac{1}{4}(2\alpha - 1)\rho_w g h_s^2 \quad [1]$$

The result of calculation is given in the next following table. The estimated tension force in the membrane has to be held by the membrane and the anchoring system.

hs = ho	[m]	3,2
ρ_w	[kg/m ³]	1000
g	[m/s ²]	9,81
γ_w	[N/m ²]	9810

	[-]	1,1	1,2	1,3	1,5	1,7
hi	[m]	3,52	3,84	4,16	4,80	5,44

T	[kN/m]	30,14	35,16	40,18	50,23	60,27
Tsd = $\gamma_{sd} * T$	[kN/m]	45,20	52,74	60,27	75,34	90,41

$\gamma_{sd} = 1.5$

Fig. 7
Calculation of membrane forces

Membrane properties have to be tested on the supplied material by authorized test institutes. The rupture strength in longitudinal direction of the membrane for this project was tested in laboratory with minimum 670 kN/m which gives a considerable safety margin of factor 9.

3. CONTROL AND REGULATION

3.5. RUBBER DAM MAIN SECTIONS

The regulation shaft system is located on the left bank of the Gomti Weir. It is designed as multiple chamber system enabling independent control of each weir section.

To operate the main rubber dam sections there are two modes available:

- Manual operation mode
- Automatic operation mode.

Water supply for regular operation is provided by the water tank which is linked to the pump shaft. This reservoir with active storage volume of 2,630 m³ is large enough to serve as a buffer for regular operation.

Operation mainly acting with two functions: Raising the rubber dam or lowering the rubber dam. Water filled Hydroconstruct rubber dams are operating at any pressure inside the weir membrane. Thus, the rubber body is stable in any position between full inflated and full deflated position. The state of the rubber dam is continuously monitored. The defining parameters are the head water level, the reservoir level and the pressure inside the related weir section.

Capacity of the installed pumps (app. 60 kW) is designed for app. 2.5 hours filling time for the first filling of the main rubber dam sections B+C+D+E. The reacting times for normal regulation are in the range of 5-10 minutes. After big

flood events, when the rubber dam was completely deflated, the re-inflation time will be with app. 2 days.

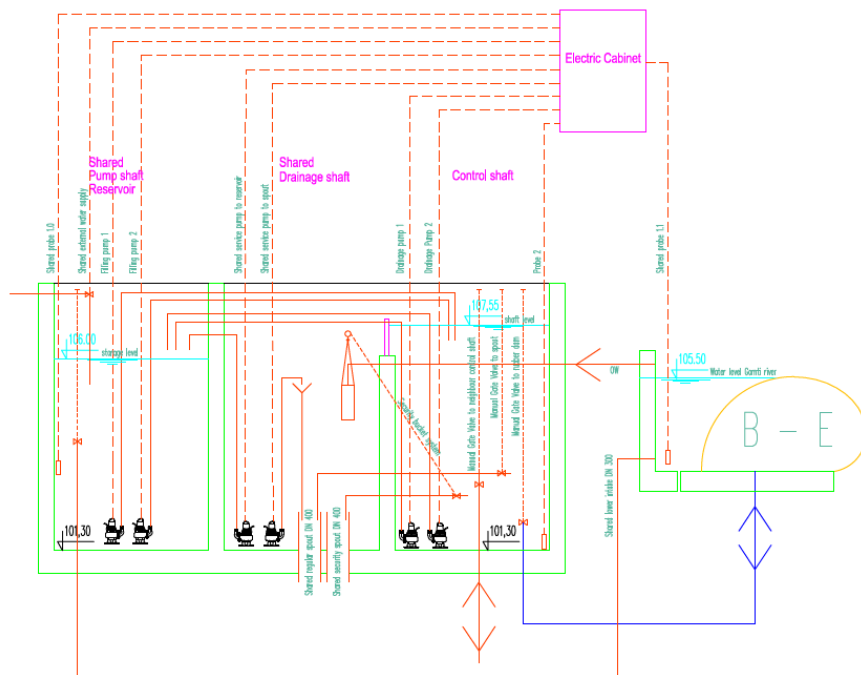


Fig. 8
Control and installation scheme for the 4 main sections B+C+D+E

Automatic operation aims to keep the head water level constant. This is achieved by adjusting the weir crest height according to changes in river flow. In automatic operation the rubber dam will be operated in dependence of the state of the rubber dam and predefined parameters in the control program. An operation priority will be assigned to each of the main weir sections B to E by the operator. It is possible to assign the same priority to two or more sections for parallel operation.

The rubber dam control system for the 4 main weir sections feature a threefold safety system:

- First, there is an overflow section on top of control shaft
- Second, there is a manually operated outlet valve
- Third, the inside pressure in the dam is controlled by an emergency discharge device consisting of a mechanically operating bucket drive for the release valve. This mechanism will be activated if the head water level exceeds a critical elevation.

Water released by the safety system will be drained out to the river through the outlet pipe.

3.6. NAVIGATION LOCKS

The rubber dams of the navigation locks can be used for two purposes. The main purpose of the navigation locks is to give way for boating up and down the Gomti River. Alternatively, they can be used for head water regulation too. The mode of operation can be switched by setting the operational state either to “N”, for navigation lock mode, or to a priority for head water regulation. Since the weir heights of the navigation lock rubber dams differs from the height of the main weir sections, navigation lock rubber dams cannot have similar priorities as any main weir section.

The navigation locks are controlled by the Control & Regulation Shaft System (CRS). Each rubber dam section in the navigation locks can be operated independently. In principle the CRS for the navigation lock systems is the same as for the 4 main weir sections.

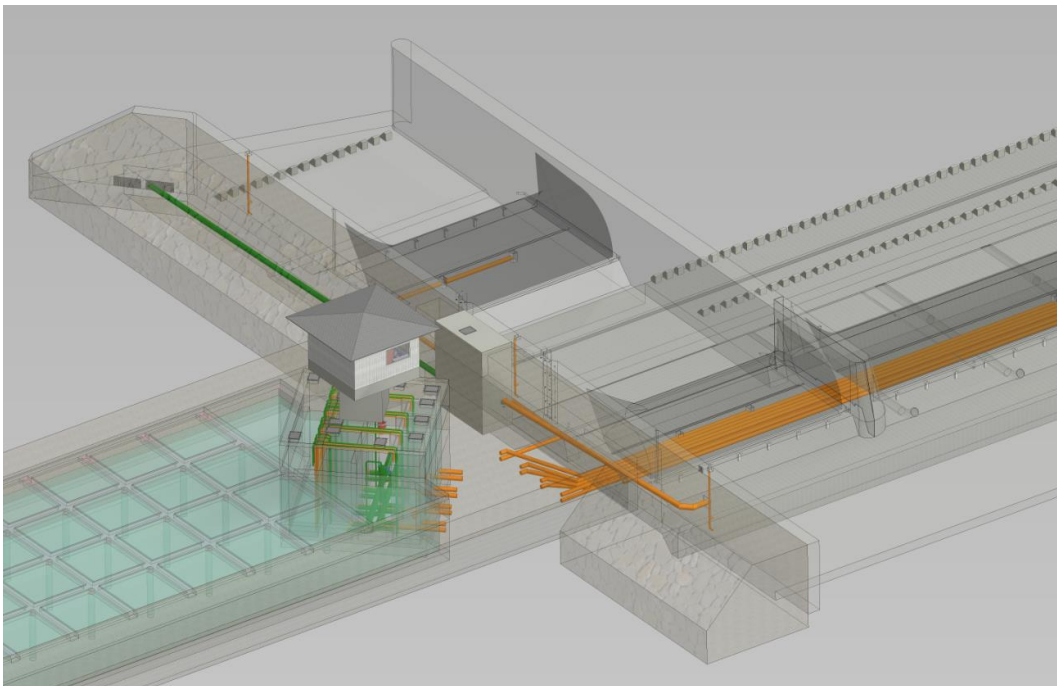


Fig. 9
3D-View to Tank, Control Building and Navigation Lock (left to right)

REFERENCES

- [1] GEBHARDT M. Hydraulic and Statically Calculation for Rubber Dams. Bundesanstalt für Wasserbau (BAW) Proceedings 235, 2006, Publishing Technical University Karlsruhe (TU).

SUMMARY

Rubber Dams are known worldwide for applications creating reservoirs in wide rivers for spans up to 100 m and heights up to 4.5 m. Main advantage is the flexible structure for full automatic reservoir level control allowing discharge of sediments, debris and even ice in Nordic conditions. Numerous applications for reservoir control, spillway gates, irrigation purposes and hydroelectric power generation were realized in the last decade. Several rubber dam projects are under operation in India now.

The said main advantages were the reason why a rubber dam system was selected by the Main Client Government of Uttar Pradesh, Irrigation Department to meet the targets for the Upgrading of the Gomti River weir structure. For the Gomti Project a water filled system with the advantage for regulation of the reservoir level was selected.

In this special project case the rubber dam was added by navigation locks on both sides of the river, allowing passing of boats.

This article highlights the key features of the project and main parts are described in detail. Main design considerations are mentioned to give a picture to the calculation required for such a project. Attention was taken to the special arrangement with an external water tank to provide water for the regulation process.

In a second chapter the control and regulation of the rubber dams and the navigation locks are described.

The project supply parts are already installed on site and the last part for installation of control equipment is expected to be finished before summer 2018. The following commissioning of the rubber dam system will be the last part of project execution phase.

COMMISSION INTERNATIONALE DES GRANDS BARRAGES

VINGT-SIXIÈME CONGRÈS DES GRANDS BARRAGES
Autriche, juillet 2018

DOI 10.3217/978-3-85125-620-8-128



This work licensed under a Creative Commons Attribution 4.0 International License. <https://creativecommons.org/licenses/by-nc-nd/4.0/>

**EVALUATION OF SLOPE STABILITY CONSIDERING EXISTENCE OF THE
SPILLWAY CHANNEL TRENCH AT THE RIGHT AND LEFT ABUTMENTS OF
GELEVAR DAM**

Kayvan RAHIMI

*MSc Student, Geotechnical Engineering Department, ISLAMIC AZAD
UNIVERSITY CENTRAL TEHRAN BRANCH (IAUCTB)*

IRAN

Amir Ali ZAD

*Assistant professor, Geotechnical Engineering Department, ISLAMIC AZAD
UNIVERSITY CENTRAL TEHRAN BRANCH (IAUCTB)*

IRAN

COMMISSION INTERNATIONALE
DES GRANDS BARRAGES

VINGT-SIXIÈME CONGRÈS DES
GRANDS BARRAGES
Autriche, juillet 2018

**EVALUATION OF SLOPE STABILITY CONSIDERING EXISTENCE OF
THE SPILLWAY CHANNEL TRENCH AT THE RIGHT AND LEFT
ABUTMENTS OF GELEVAR DAM ***

Kayvan RAHIMI

*MSc Student, Geotechnical Engineering Department, ISLAMIC AZAD
UNIVERSITY CENTRAL TEHRAN BRANCH (IAUCTB)*

Amir Ali ZAD

*Assistant professor, Geotechnical Engineering Department, ISLAMIC AZAD
UNIVERSITY CENTRAL TEHRAN BRANCH (IAUCTB)*

IRAN

1. INTRODUCTION

Glevar Dam project is located in Mazandaran Province and constructed on Neka Rover, and its middle point situated on the coordination of 36.59 N and 53.61 E. The type of dam is CFRD and maximum height of the dam from riverbed is 103 m and from bedrock is 113 m. Dam crest elevation is 739 m.a.s.l. with the dam crest length of 250 m and width of 10 m as shown in figure 1.

Instead of morning glory spillway, the alternative spillway of the Glevar dam has been considered as a free spillway at the left abutment, with an appropriate safety margin from the fault passing from the abutment site. Figure 2 shows cross section of the geotechnical of the spillway route. The bedrock limestone has been identified through drilling in several boreholes. As already mentioned, spillway crest elevation has been considered as 733 m.a.s.l. and that of the approach canal level as 730 m.a.s.l., which is the normal reservoir water level. Capacity of volume between these two elevations has been considered as 8.65 million m³, which can control 50 and 100-yr floods, with small discharge

* *titre de l'article complet*

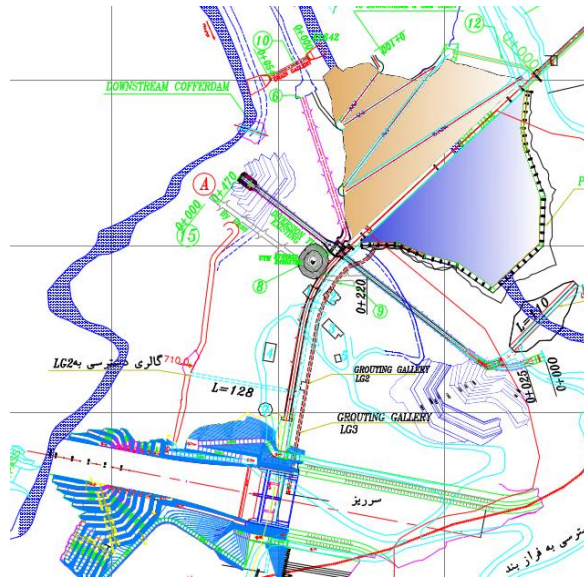


Fig. 1
General Plan of Glevard CFRD

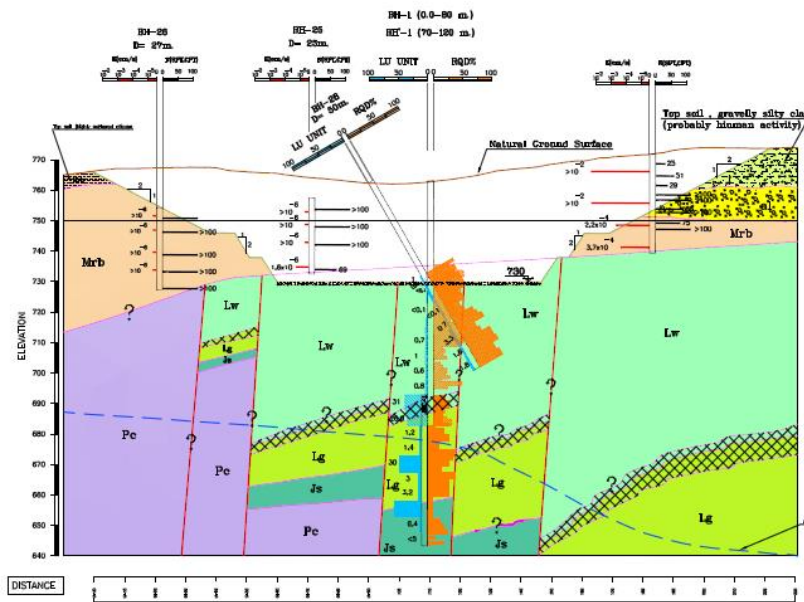


Fig. 2
Geotechnical Cross Section in approach channel of spillway

In accordance with the layout map and geological - geotechnical longitudinal profile as shown in figure 3, after excavation of the top soil, the spillway will be located on an appropriate bedrock. Furthermore, it will be possible to remove the loose soil and rocks and stabilize the trench-excitation slope in approach channel using support Geo-grid as well as cultivation of plants, trees and bushes, in long term surface protection of course after doing slope stability analysis process.

Therefore, trench slope, berms wide and height elaborate and compared base on result of lab tests and “in-situ” test.

The above-mentioned explanations belong to a natural case of cutting with trenches of different heights. To provide slope stability of trenches (with any type of weak materials) the simplest and the major way is to decrease the over burden pressure of the slope, if it is made of soil or eroded, weak rock. Indeed, the lower part will be stable for the required safety factor for all loading cases and various conditions.

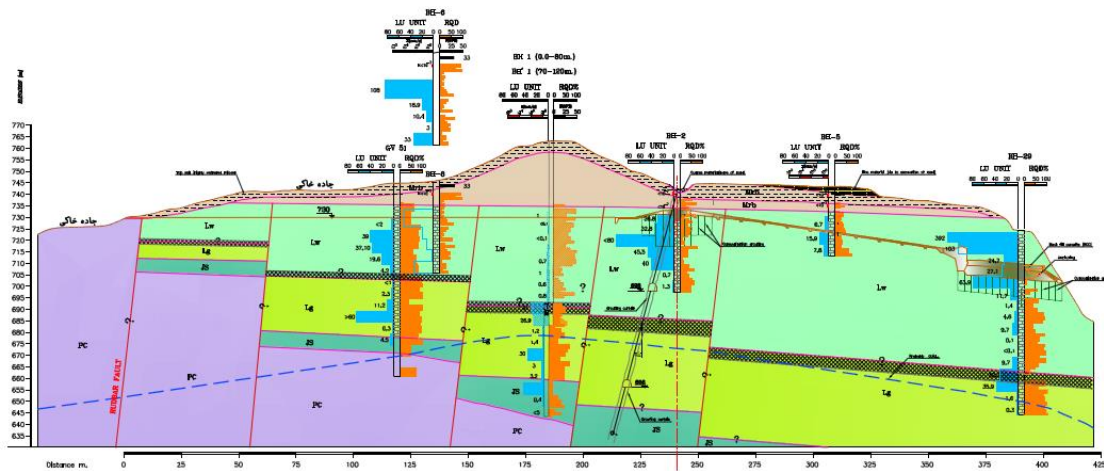


Fig.3. Geotechnical Longitudinal Section along Approach Channel of Spillway

The geometry shape of trench of left and right banks of spillway approach channel was designed considering using appropriate geo-mechanically parameters from lab and “in-situ” tests and engineering judgment on the results, The main point is that to meet the desired width for spillway channel after cutting with trenches (different height) to provide stability of trenches.

2. PROJECT OVERVIEW

In-situ as well as laboratory tests on the fine-grained materials were carried out and sample materials taken from exploration boreholes obtained from test pits for better understanding of Neogene formation materials in free spillway area of the Glevard dam. The Neogen formation consists of an intercalation of siltstone, mudstone, marlstone and sometimes local loose conglomerate and semi-intercalations of loose limestone. SPT test results of different layers had been used for primary estimation of C and ϕ parameters had in stability calculations. For more certainty, some "in-situ tests" were carried out to finalize geotechnical parameters of the soil materials of the approach channel and the spillway location, accordingly.

3. THE DIFFERENT BETWEEN THE "IN-SITU" AND LAB TEST IN NEOGEN FORMATION

With regard to the results of in-situ and laboratory tests, following points should be noted in this regard:

A. Laboratory tests on disturbed samples of any depth are actually face with some cracks due to vibrations and rotation of the drilling bit and due to movements and transportation of samples. Indeed, these samples cannot represent the condition of natural soil on that location where the samples are taken and they show considerably lower strength against the natural state. Cracked soil or normal cracks have considerably lower modulus of elasticity compared to the in-situ soil, and due to natural cementation in the materials.

B. Soil obtained from mudstone, siltstone and marlstone intercalations originally, has higher cohesion among their particles compared to the disturbed or cracked soils, even if the cracks are so tiny, due to their old origin, related to millions of years ago, and to their natural compaction during all these years.

Thus, any kind of disturbance or formation of cracks not only decreases or diminishes cementation among particles, but also causes lower cohesion and modulus of elasticity compare to the ones obtained from in-situ tests. The results obtained from Pressure Meter Test provided in table 1. In a considerable number of tests, even in saturated status of the test place, modulus of elasticity is between 1200 to 2000 kg/cm². Based on the engineering classification of the material strength, as it can be seen, clay, silty clay, grave-sand and clay soils can be classified as hard and very dense soils and their higher modulus of elasticity is an indicative of cementation among the particles. However, triaxial tests (CU or CD) on disturbed soil samples provides a modulus of elasticity of 120 to 230 kg/cm², as the maximum value the saturated compacted clay. This is while in pressure meter test within boreholes, different values were obtained such as higher value than 330 and 410, and even 930, 1200 and 1880 kg/cm², which shows cementation and high cohesion of more than the obtained values in triaxial tests. Meanwhile, it is known that the stress of compressive strength of fine-grained soils has direct relation with modulus of elasticity.

C. Plate loading in-situ test results provided in table 2. As it can be seen, the elasticity modulus of 250, 300 and 500 kg/cm² belong to upper layers (5 to 7 m depth) and it will be increase by depth, unless the layer material is changed. Therefore, this situation was considered in mathematical model of stability analysis.

Table. 1. Pressure Meter Test Results in Exploration Boreholes of Spillway Area

Borehole	Depth (m)	Conditions	γ_s	u	K0	Max. pressure	Max. volume (cm ³)	Em (bar)	Ep (bar)	E (bar)	ϕ °	C kg/cm ²
BH-22	6	N	2.01	0.33	0.47	15	538	62.52	166.3	665.2	32	0.05
BH-22	12	N	2.12	0.33	0.46	18	533	71.14	189.2	756.9	32.5	
BH-22	14	S	2.15	0.33	0.34	24	293	176.9	470.6	1882.6	41	
BH-22	18	N	2.15	-	-	17	54	-				0.05
BH-22	24	S	1.98	0.46	0.86	23	481	92.8	270.9	406.4	36	
BH-22	30	S	1.95	0.37	0.59	24	651	296.8	813.4	1626.9	37	0.05
BH-23	6	N	2.20	0.33	0.48	25	365	266.7	709.6	2838.5	31	
BH-23	12	S	1.9	0.33	0.49	23	739	81.7	217.3	326	30.5	0.2
BH-23	18	S	1.83	0.33	0.5	25	436	455.2	1210		30	
BH-23	25	S	1.83	0.36	0.56	21	798	63	171.4	257	26	0.5
BH-24	6	N	1.95	0.33	0.57	25	437	176	468.2	936.5	25	
BH-22	12	S	1.98	0.35	0.54	18	858	95.2	257.2	358.8	27	0.5
BH-24	3	N	1.88	0.35	.55	25	633	157.5	425.3	850.6	30.5	
BH-25	9	N	1.88	0.36	.57	25	670	101	276.2	552.3	29	0.26
BH-25	15	N	1.88	0	6	0	749				-	
BH-25	21	S	1.88	0.35	0.54	25	2.99	229.4	619.5	1239.1	27	
BH-25	3	S	1.83	0.43	0.74	18	843	38.8	111.1	166.7	-	
BH-26	8	N	1.83	0.39	0.64	25	260	455.1	1265	2530	21	0.3
BH-26	14	N	1.96	0.36	0.57	25	432	320.9	872.9	1745.9	25	0.2
BH-26	21	S	1.89	0.34	0.51	25	390	174	467.7	935.4	29	
BH-26	26	N	1.89	0.36	0.57	20	455	122.6	333.7	500.5	36	
BH-26	14	D	1.96	0.36	0.57	25	432	320.9	872.9	1745.9	25	0.3
BH-26	21	S	1.89	0.34	0.51	25	390	174.5	467.7	935.4	29	0.2

4. LABORATORY TEST RESULTS

In order to determine geotechnical parameters of the sediments and samples taken from exploratory boreholes and test pits, some laboratory tests [4,5,6] were carried out and results have been provided in tables 3 and 4 for the pits (TP-F1 to TP-F5) and exploration boreholes (BH-22) to (BH-24), respectively. Evaluation of laboratory results of these loose and weathered soils which are also sensitive to moisture shows that as their compressive strength has direct relationship with modulus of elasticity, and in in-situ tests these strengths are 3 to 4 times than the strength of the surface soil or the marly layer which is sensitive to water, the laboratory test results generally control field test results and have an appropriate trend, in weakened scale. If due to the cementation of natural undisturbed rocks, their internal friction angle is considered similar to these soils, considering the necessary conservativeness, cohesion values of the natural soil in in-situ case is at least 1.5 to 2 times as the above-mentioned loose, disturbed samples. Certainly,

considering the Mohr — Culomb criteria and the obtained in-situ modulus of elasticity and considering the relationship suggested by Bijrum and other researchers in this regard, the mentioned relationship for fine-grained soils, based on the type of the soil would be as follows:

$$E \cong (250 \text{ to } 500) (\sigma_1 - \sigma_3)_F$$

Hence, it can be seen, due to the high modulus of elasticity obtained in in-situ tests, cohesion of natural soils is higher than the laboratory values of disturbed samples. In table 2, pressure meter tests estimates the minimum cohesion values and considers them for slope stability calculations. However, a conservative approach has been used in selection of the parameters for numerical calculation.

Table.2. Plate loading test results at spillway area in Glevard dam

Borehole	Test cycle	q kg/cm ²	δ mm	u	Es	E
PT-1 Dry	C.1	7.07	2.08	0.35	760	760 Dry
	C.2	14.1	3.35	0.35	8.30	
	C.3	21.2	5.72	0.35	830	
PLT-1 sat	C.1	7.69	4.49	0.35	630	300 sat
	C.2	15.2	18.6	0.35	305	
	C.3	20.8	45.3	0.35	172	
PLT-2 Dry	C.1	7.13	5.2	0.35	511	510 Dry
	C.2	12.7	8.3	0.35	572	
	C.3	-	-	0.35	-	
PLT-2 sat	C.1	7.13	15.8	0.35	168	200 sat
	C.2	15.2	26.7	0.35	213	
	C.3	18	30	0.35	212	
PLT-3 Dry	C.1	7	2.25	0.35	1172	500 Dry
	C.2	19.8	2.1	0.35	599	
	C.3	33.6	42	0.35	310	
PLT-3 sat	C.1	7.2	8.5	0.35	312	250 sat
	C.2	15.3	25.3	0.35	256	
	C.3	17.3	38	0.35	170	
PLT-4 Dry	C.1	7	0.97	0.35	2718	2800 Dry
	C.2	19.8	2.2	0.35	3404	
	C.3	38.2	4.73	0.35	3012	
PLT-4 Dry	C.1	10.3	5.76	0.35	667	500 sat
	C.2	13.5	9.97	0.35	504	
	C.3	21	21.4	0.35	367	
PLT-4 Dry	C.1	7.2	14.8	0.35	180	180 sat
	C.2	14.3	84.3	0.35	63	
	C.3	-	-	0.35	-	

Table.3.Geotechnical parameters results of triaxial lab test of top soil in spillway area

Borehole	Depth (m)	Test	Before test			After test			T		E		E.s		
			Y _d	W %	Y _w	Y _d	W %				Y _d	W %	Y _w	Y _d	W %
TPF-1	4	C.U	1.63	14	1.86	1.88	17.4	2.26	10.37	0.32	21	0.19	70	10	150
TPF-2	3.8	C.U	1.68	12.8	1.89	1.95	16.6	2.27	20.30	0.34	21	0.21	110	14	165
TPF-3	3.8	U.U	1.56	17.2	1.83	1.58	16.8	1.86	9	1.2	-	-	-	-	-
TPF-4	4	C.U	1.77	13.2	2.01	2.15	15.4	2.24	20.27	0.26	-	-	185	23	275
TOP SOIL	-	C.U	1.65	13.4	1.84	1.92	17	2.27	10.38	0.32	24	0.21	90	12	157
TOP SOIL	-	U.U	1.56	17.2	1.83	1.58	16.8	1.86	9	1.2	-	-	-	-	-
TOP SOIL	-	C.D	1.77	13.2	2.01	2.15	15.4	2.24	20.27	0.26	-	-	185	23	275

Table.4.Triaxial Lab Test Results at Spillway Area in Glevard Dam

Borehole	Depth (m)	Tri-axial Test							
		Type	φ°	C kg/cm ²	w%	Y _d kg/cm ³	Elasticity modulus		
							1.5	1.5	1.5
BH-22	9	U.U	3.5	1.1	16	1.7	55	75	115
BH-22	21	C.D	25	0.2	16	1.7	40	70	140
BH-23	4	U.U	3.7	1.1	16	1.7	70	110	155
BH-23	14	C.U	25	0.6	16	1.7	20	25	50
BH-23	23	U.U	2.7	1.5	17	1.7	50	75	105
BH-24	23	CD	26	0.2	16	1.7	30	60	100
BH-26	18	U.U	3.6	1.1	15	1.7	30	45	65

5. DISCUSSION ON “IN-SITU” TESTS RESULT OF GEOTECHNICAL PARAMETERS

As already mentioned, different in-situ tests including pressure meter and plate loading tests (as well as standard penetration tests) have been carried out to determine geotechnical parameters of the bed soil and geo-mechanical parameters of the bedrock mass in the spillway area, to find geotechnical parameter for slope stability analysis; following is a summary result of these tests.

5.1. PROCEDURE IN-SITU TESTS

Plate load test aims to determine the elasticity modulus of the bed with regards to:

$$E_s = qB(1-u_2)lw/\Delta$$

and other geotechnical properties such as the Poisson ratio of the bed, internal friction angle and cohesion values, as a control test and in order to find out anomalies in pressure meter tests.

To attain this objective and perform the test, a number of pits have been tested in different locations and points including the spillway slope, based on the lithological and geological changes of test places in the right and left abutments of the spillway, so that the results are controlled in a number of aspects.

The plate loading test of the soil has been carried out in ASTM-D 1159 method. Steel plates of 30 and 50 cm diameters and a hydraulic jack to implement the load have been used in the tests. At least 3 gauges of 0.01 mm sensitivity have also been used for measurement of plate settlement.

The considered tests have been carried out as cyclic loading, in three consecutive cycles, in accordance with the above-mentioned test method. Table 3 shows the plate loading test results and maximum settlement (S_t), modulus of elasticity and mean Poisson ratio in the concerned layer have been also been provided for the maximum stress implemented in each cycle, at the end of each phase of loading and unloading cycle.

A considerable point in this regard is the fact that the bed reaction modulus is not a fixed number for the soil and varies due to following the plate diameter and stress. It can be considered equal to the above-mentioned values, considering an appropriate safety factor in the foundation and superstructure calculations.

Delineating the stress-strain curve and calculating total settlement and the residual settlement (in zero bar), elastic settlement at each phase of loading has been obtained. Then the maximum stress diagram of each loading cycle against its corresponding elastic settlement has been delineated. Elastic sub grade reaction (C_u) of the soil has been calculated from the delineated diagram. Thus, based on the test, the C_u has been calculated from the following relationship:

$$C_u = q/S_e \text{ (kg/cm}^3\text{)}$$

In this regard, more investigations carried out by Barkan shown that C_u is a function of the load plate area. So that, if C_{u1} and C_{u2} are steady elastic pressure factors for the mats with A_1 and A_2 contact areas, respectively, then the following relationship would be applicable:

$$C_{u2} = C_{u1}\sqrt{(A_1/A_2)}$$

But here, the objective of the test has been controlling the values of the elasticity modulus obtained from the pressure meter tests in the concerned levels.

In the plate loading tests carried out, the values of this parameter in 7 cases out of the 8 tests having been carried out, have been calculated and their first rates have been provided (in test PLT-2 and in the dry state, it has been rejected as the

gauge has been dislocated and in the repeated test, only 2 cycles of the 3 have been performed in the test.

In this regard and as far as possible, the loading is carried out in a way that implementing the loading capacity causes it to enter or get near to the plastic ambience of the rock mass and in other words loading is carried out up to near its loading capacity, so as to distinguish the capacity of the bed affected materials.

The test results are provided as pressure-displacement curves or the soil behavior curve and then analysis of the elasto-plastic ambience and analysis of the behavior curve of the mass is carried out with variations in C , ϕ and γ parameters and finally, the strength parameters can be estimated from the obtained results.

5.2. CONSIDERING TEST RESULTS OF PRESSURE METER TESTING

In the Glevard dam spillway channel area, due to the deep excavation in soil, a total of 21 pressure meter tests have been carried out in the exploration boreholes drilled in the right abutment, including BH-22, BH-23 and BH-24 (totally 12 cases) and in the left abutment, including BH-25 and BH-26 (totally 9 cases), 3-m paces, from 3 to 30 m, in sedimentary materials, fine-grained sub-surface layers (clayey — silty to marly clayey or clayey sandy) and coarse-grained materials (sand, gravel and marlstone) and in dry and saturated states. Mainly, these tests have been carried out in two parts of alluvial surface and silty layer and the middle marlstone layers. These tests have been detailed in table 2.

5.3. CONSIDERING TEST RESULTS OF PLATE LOAD TESTS

Plate loading test has been carried out in totally five locations in the spillway channel slope area and location. They include PLT-1 and PLT-2 locations at the right abutment and PLT-3 and PLT-4 locations at the left abutment and PLT-5 location in the middle of the bed, tending to the right abutment wall. Plate Loading tests have been carried out in saturated state in locations PLT-1, PLT-2 and PLT-3. Test results have been provided in pertaining tables and diagrams in the attachment to the report. In these tables and diagrams, beside determining the tested location, test cycles (1, 2 & 3), maximum load, maximum stress, total settlement (St), elastic settlement (Se), difference between the total and elastic settlements ($St-Se$) and modulus of elasticity and Poisson ratio have been provided in table 3. Summary results of loading tests have been provided in table 3 and actually the modulus of elasticity in dry state is almost 2 to 2.5 times as the saturated state.

Summing up the obtained results indicates relatively reasonable values for the steady pressure coefficient of the soil with regard to the type of materials and sediments of the right abutment, which are mainly coarse grained, and of the left abutment, which are mainly fine grained. In this regard, calculating the values of

modulus of elasticity relating to the tests, the values of these parameters in saturated state for the fine-grained sedimentary materials have been obtained as $E_s=250 - 350 \text{ kg/cm}^2$ and for the coarse grained materials as $E_s= 500-700 \text{ kg/cm}^2$, which are totally correct and reasonable for the loose rock masses of the plate loading location.

5.4. BLOW, STANDARD PENETRATION DENSITY TESTS OF SUB-SURFACE LAYERS

In order to investigate the effect of the blow and standard penetration, the field density tests carried out in the depths of the exploration boreholes and pits drilled in the Glevard dam spillway area. Results obtained in the two states from the exploration boreholes and manual pits were separated and then, with the theoretical description of the samples, the density class of each layer and the fine and coarse grained sediments were determined and finally, with regard to the conclusion and classification of the density in the above-mentioned layers, the expected geometrical parameter values (C , ϕ , q_u and γ) were determined and the results have been provided in table 5. In other words, with regard to the field tests and the blow and standard penetration test results (SPT / CPT) and using the standard codes and relations between the geotechnical parameters obtained from (NAVFAC) and Bowles reference and other national sources, the limits and values of geotechnical parameters of the sub-surface sediments and layers were determined. Table 4 provides summary specifications of geotechnical parameters of the sub-surface sediments and layers obtained in the Glevard dam spillway structure area.

Table.5.The results test of blow, standard penetration test in the spillway area

Borehole	Depth (m)	SPT (N)	Class	Density			q_u	ϕ	C
				γ_d	W	γ_w			
BH-1	3	49	H	-	-	1.9	3	20	1.5
BH-1	5	>100	VH	-	-	2.1	>4	18	>2
BH-1	9	>100	VH	-	-	2.1	>4	18	>2
BH-3	6	>100	VH	-	-	2.1	>4	18	>2
BH-4	4	>100	VH	-	-	1.7	>4	18	>2
BH-5	3	10	S	-	-	2.1	0.7	24	0.4
BH-6	2	33	H	-	-	1.9	3	20	0.5
TPL.1	3	23	VS	1.9	12	1.7	1.5	17	0.7
TPL.1	6	32	H	1.8	16	1.6	3	20	1.5
TPL.2	2	21	VS	1.9	13	1.7	1.5	22	0.7
TPL.2	6	-	VS	1.8	12	1.7	1.5	22	0.7
TPL.3	3	16	VS	1.9	15	1.7	1.5	22	0.7
TPL.3	6	9	S	1.8	18	1.7	.75	24	0.4
TPL.4	2	28	VS	1.9	13	1.7	1.5	22	0.7
TPL.4	4	27	VS	1.9	17	1.9	1.5	22	0.4
TPL.4	3	31	H	1.9	13	1.8	2	19	1
TPL.5	6	>60	VH	2.0	14	2	4	13	2

6. INTERPRETATION OF GEOTECHNICAL PARAMETER OF SPILLWAY TRENCH SLOPE

Previous research has been carried out location of critical slip surface [1,2,3]. Considering the obtained (field and laboratory) results and summation of the geotechnical parameter values in the sub-surface sediments and layers of the slope and spillway structure area in the left and right abutments allows dividing the sub-surface profile into three parts:

1. Upper part, the silty-clayey surface soil in the first 10 m and mainly in the first 4 to 5 m.
2. Middle part, marly-siltstone layer down to the depth of 20 m,
3. Lower part, including the bed rock-mainly of limestone that continues down to lower depths.

Generally, the conclusion from the obtained results indicates that under natural and dry conditions, mean geotechnical parameters of the sub-surface sediments and layers do show stability of the slope and the spillway structure area. This is while under saturation conditions, strength is decreased, where appropriate excavation slope is selected for stability analysis purposes.

7. SLOPE STABILITY ANALYSIS AT THE APPROACH CHANNEL OF SPILLWAY

In the preliminary Slope Stability Analysis at the Approach Channel of spillway Trench at the Right and Left Abutments, based on estimated values for C and ϕ of the soil and soft rock mass of the Neogene era and based on Lab and NSPT tests in the spillway, stability safety factor had been calculated. However, to elaborate design of slope stability and excavation procedure to meet appropriate width to constructing broad spillway, based on the in-situ tests, calculations and selection of design parameters in the slope of the spillway approach channel trench slopes should be separately calculated for the right and left abutments.

This additional analyze refined design parameters selected in calculations of the first alternative, where C and F have been estimated based on the NSPT of the exploration boreholes and test pits (it is pointed out that all SPT tests had shown more than 50 blows in different points for 30 cm penetration). Now, with regard to the drilling of three boreholes BH-22, BH-23 and BH-24 at the right abutment and that of BH-25 and BH-26 at the left abutment and performing pressure meter tests in each meter and in each section, the dry and saturated states have been tested and measured. The results have been provided in table 1 for calculation of the modulus of elasticity, eudiometry, C , ϕ , K_o factor, and the elastic modulus. Meanwhile, table 2 shows the in-situ plate loading tests for identification of the situation of soft rocks and soils resulted from the Neogene formation (in the dry and saturated states, in the locations shown on the spillway plan). For the

limestone, ϕ has been considered as 36° and C' as 115 Kpa, in stability calculations.

8. EXCAVATION GEOMETRY

Invert elevation for the approach channel is 730 m.a.s.l. Excavation of trenches will start, with 1H: 1.5V slope in two 8-m berm and after the first 8 meter, a 4-m berm will be excavated and then, the second 8-m wide berm will be excavated at El. 745 m.a.s.l. After that, the excavation slope will be 2H: 1V for complete excavation to minimize the failure surfaces. In other words, in the first 15 m, there is a 4-m berm at El. 738 m.a.s.l. and then, in a 15-m height, the 8-m berm with 2H: 1V slope will be complied with until excavation in soil is completed. The major excavations to be carried out belong to the approach channel, with a maximum depth of 42 m. However, crossing the approach channel or the access, the concrete flat-edge spillway and its chute will start, whose maximum excavation depth will not exceed 12 to 18 m. Excavation for the spillway with its slope shown in the figures.

9. MECHANICAL AND GEO-MECHANICAL SPECIFICATIONS OF TRENCH MATERIALS FOR STABILITY ANALYSIS

BH-22, BH-23 and BH-24 have been drilled at the right abutment and BH-25 and BH-26 at the left abutment, with following characteristics and pressure meter test has been taken into consideration in its different depths. Meanwhile, the in-situ plate loading test has also been carried out to control the in-situ strength and density of the soil and combination of the results. Mechanical and geo mechanical specifications of the materials have been entered into the calculations based on the pressure meter test results in different boreholes, as provided in table 1, which are totally based on the in-situ pressure meter tests carried out at the site. In depths beyond the values mentioned in table 1, the Lar limestone has been entered in the calculations with $\phi = 36^\circ$ and $C = 115$ Kpa. Most of the concerned soft rocks have had strength more than the foreseen and selected values.

10. ASSUMPTIONS AND CALCULATION PROCEDURE

Calculations have been carried out based on the mechanical and geo-mechanical parameters provided in table 1, limestone properties and drilling

section and also based on the specifications of layers in each borehole and its height conditions, which include three analysis sections at the right abutment and two at the left. In other words, the section belonging to borehole BH-22, which is located at elevation 772 m.a.s.l, due to its more height, is more critical than other sections, and this is the fact shown in calculations, too. Calculations have been performed based on the Geo-Slope V5.16 mathematical model, Mohr-Culomb model of discontinuity and also according to the above-mentioned descriptions and assumptions and for each analytical state, calculations in earthquake conditions with 0.15 factor have also been taken into consideration. Mathematical model of excavation in soil and trench has been provided in figure 1, which has been prepared in Geo-Lope software program.

11. CALCULATION RESULTS

Calculation have been performed in Geo-Slope V5.16 software program based on the Mohr-Culomb model of discontinuity and Modified Bishop linear method [7,8,9].

The first analytical section belong to BH-22, which has been drilled at EI. 722 m.a.s.l. at the right abutment and its pressure meter test results have been provided in table 1. Based on the information mentioned above, drilling section has been analyzed. The maximum Trench height is 42 m. Its slope stability safety factor, based on the pressure meter information and other tests, in this borehole whose different layers have been provided in the analysis has been calculated as 1.585. As safety factor for excavation geometry as shown in figure 4.

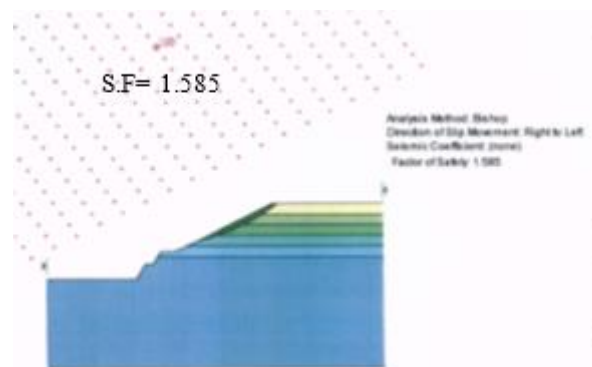


Fig.4.

Numerical model of excavation for slope stability

Allowable values of the safety factor under stability conditions are 1.4 to 1.5 and therefore, the above-mentioned value is acceptable. Figure 2 shows the failure wedge along with the calculated safety factor. Critical failure surface mainly goes beyond the first 8meter.

Section analysis of the borehole BH-22 in the earthquake state with 0.15 factor for pseudo static calculation indicates decrease in the safety factor to 1.153. Under such conditions, the allowable safety factor can also be acceptable for highest slopes in the allowable range. As the obtained factor is higher than the allowable value, the section has no earthquake problems, too. Borehole BH-23 has been drilled at El. 765.2 m.a.s.l. at the right abutment and its drilling depth is 35.2 m.

Based on the above-mentioned conditions, drilling section of the trench different layers has been prepared based on the pressure meter and other tests in Geo- Slope mathematical model and the stability analysis has been carried out under test conditions and with earthquake.

Under conditions without earthquake, the calculations show that the safety factor of the soil or trench excavation at the right abutment in highest slope is 1.798, which is higher than the allowable values of 1.4 to 1.5 and can be acceptable. Calculated safety factor of the analyzed section of borehole 23 under earthquake conditions with 0.15 factor is at least 1.294, which is higher than the allowable value of 1.05 and can be acceptable.

Borehole BH-24 has been drilled at El. 756.28 m.a.s.l. whose maximum excavation is 26.28 m down to the spillway bottom. Analysis of this height under pressure meter test conditions shows the safety factor as 3.351, which is mainly due to the decrease in the excavation height and the safety factor is actually a large one.

Section analysis of borehole BH-24 has been carried out under earthquake conditions with 0.15 factor, whose safety factor has been calculated as 2.4. The minimum safety factor under exceptional load condition is 1.05 but the obtained safety factor is considerably larger and this slope is in the safety margin. Critical failure wedge for excavation based on pressure meter test in borehole 24 plus earthquake with 0.15 factor.

Borehole BH-25 has been drilled at the left abutment, at El. 760.51 m.a.s.l. and its analysis has been carried out for both with and without earthquake conditions, where the calculated safety factors have been estimated as 2.094 and 1.464, respectively, which are totally above the comparing allowable minimums of 1.5 and 1.05 and so, it is actually acceptable.

Borehole BH-26 has been drilled at the left abutment, at El. 754.28 m.a.s.l. and its analysis has been taken into consideration based on the carried out pressure meter tests. For the soil excavation height of almost 25 m, the calculated safety factor has been estimated as 2.003. Allowable safety factor in this state has been 1.5, which is acceptable under such conditions. Based on the information obtained from the pressure meter tests, the critical section crosses the berms in the first 15 m, i.e. due to the material properties; it is in lower elevation layers to the bottom excavation.

Calculation of the safety factor in earthquake conditions for the borehole BH-26 has been carried out with earthquake factor of 0.15, where the safety factor has been shown as 1.468, which is higher than the allowable minimum of 1.05 and it is acceptable.

To put it short, the analyses for the slope stability of trench excavation can be provided as per table 2, appropriate with the carried out analyses. Along with the provided allowable values, they can be compared to ensure acceptability of the excavation slope.

12. CONCLUSION

With regards to pressure meter and other in-situ and laboratory test results in addition to the numerical analysis following design for stable slope was proposed: excavation with 1H: 1.5V slope in the first 15 m height with a 4m berm, at El. 738 m.a.s.l. following by a 8m berm at El. 745 m.a.s.l. and then excavation with a slope of 2H : 1V. For the surface soil, instead of initial design (using geogrid to support top soil) in order to prevent erosion using biological methods such as plantation is recommended. Indeed, the biological methods suggested as the properties of the surface humos soil are instable and can flow down due to rainfall and this support is necessary to prevent erosion and flow of the mud. To support the toe of initial berm gabion is recommended as a facing.

REFERENCES

- [1] Wang, L., Xie, M., Xu, B., & Esaki, T. (2015). A study on locating critical slip surface of slopes. *International Journal of Geotechnical Engineering*, 9(3), 265-278.
- [2] Huang, M., Fan, X., & Wang, H. (2017). Three-dimensional upper bound stability analysis of slopes with weak interlayer based on rotational-translational mechanisms. *Engineering Geology*, 223, 82-91.
- [3] Aas, G., Lacasse, S., Lunne, T., and Hoeg, K. (1986). Use of in situ tests for foundation design on clay, in *Use of In Situ Tests in Geotechnical Engineering*, S. P. Clemence, Ed., GSP 6, American Society of Civil Engineers, New York, pp. 1–30.
- [4] ASTM Standard D2850-07 (2007). Standard Test Method for Unconsolidated-Undrained Triaxial Compression Test on Cohesive Soils, ASTM International, West Conshohocken, PA.
- [5] ASTM Standard D4767-11 (2011). Standard Test Method for Consolidated Undrained Triaxial Compression Test for Cohesive Soils, ASTM International, West Conshohocken, PA.
- [6] Ayres, D. J. (1985). *Stabilization of slips in cohesive soils by grouting, Failures in Earthworks*, Thomas, Telford, London.
- [7] Bishop, A. W., Alpan, I., Blight, G. E., and Donald, I. B. (1960). Factors controlling the shear strength of partly saturated cohesive soils, *Proceedings*

- of the ASCE Research Conference of Shear Strength of Cohesive Soils, Boulder, CO, pp. 503–532.
- [8] Boutrup, E., and Lovell, C. W. (1980). Searching techniques in slope stability analysis, *Engineering Geology*, 16(1), 51–61.
- [9] Bray, J., and Travasarou, T. (2009). Pseudostatic coefficient for use in simplified seismic slope stability evaluation, *Journal of Geotechnical and Geoenvironmental Engineering*, 135(9), 1336–1340.

SUMMARY

This paper presents the results of slope stability analysis at the right and left bank of the spillway in Gelevand dam which is a broad- crested spillway by assuming 739 m.a.s.l. As the dam crest elevation, the width of channel trench will be almost 66 m to discharge the 10,000-yr flood. Based on the design criteria, large spillway channel should be located at the toe of the right and left abutment which will require a special design for the excavation of berms at Neogene era in order to reach a stable slope.

To evaluate the strength parameters of fine-grained materials at spillway area, laboratory test were carried out. According to the strength parameters resulted from lab, the stability of trenches slope of the spillway channel was analyzed. Base on the results, to ensure the stability of spillway trenches, the slopes should be excavated with a gentle slope. Considering the geometry of the current slope and analysis results, a width of 80 meters for approach channel could not be achieved at the level of 730 m.a.s.l. Therefore, to meet the desired width for spillway channel, excavating should be implemented with a steeper slope that this is not possible due to the instability of fine-grained material of the Neogene formation at spillway area, unless by using soil improvement methods for fine grained material. In regards to above mentioned conditions, the cost of the project will be increased. Indeed, considering the nature of the Neogenetic fine, it was decided that "in-situ" tests should be perform to obtain the fine-grained material properties at the spillway area. Based on the strength parameters results obtained from "in-situ" tests again the stability of trenches elaborated.

KEYWORDS

Spillway, In Situ test, Slope stability, Gelevard, CFRD Dam, Approach channel

COMMISSION INTERNATIONALE DES GRANDS BARRAGES

VINGT-SIXIÈME CONGRÈS DES GRANDS BARRAGES
Autriche, juillet 2018

DOI 10.3217/978-3-85125-620-8-129



This work licensed under a Creative Commons Attribution 4.0 International License. <https://creativecommons.org/licenses/by-nc-nd/4.0/>

**ANALYSIS ON THERMAL FIELD EVOLUTION OF WUDONGDE ARCH DAM
CONSTRUCTION SITE BASE OF DISTRIBUTED OPTICAL FIBER
MONITORING**

Haoyang PENG

DEPARTMENT OF HYDRAULIC ENGINEERING, TSINGHUA UNIVERSITY,
BEIJING 100084

CHINA

Peng LIN

Vice president of DEPARTMENT OF HYDRAULIC ENGINEERING, TSINGHUA
UNIVERSITY, BEIJING 100084

CHINA

Zeyu NING

DEPARTMENT OF HYDRAULIC ENGINEERING, TSINGHUA UNIVERSITY,
BEIJING 100084

CHINA

COMMISSION INTERNATIONALE
DES GRANDS BARRAGES

VINGT-SIXIÈME CONGRÈS DES
GRANDS BARRAGES
Autriche, juillet 2018

**ANALYSIS ON THERMAL FIELD EVOLUTION OF WUDONGDE ARCH DAM
CONSTRUCTION SITE BASE OF DISTRIBUTED OPTICAL FIBER
MONITORING**

Haoyang PENG, Peng LIN *, Zeyu NING

*Vice president of Department of Hydraulic Engineering, Tsinghua University,
Beijing 100084*

CHINA

1. INTRODUCTION

In mass concrete temperature monitoring, there are mainly two kinds of methods, i.e., thermometer monitoring (traditional thermocouple or RTD) and optical fiber monitoring based on distributed optical fiber temperature sensing technology. With the rapid development of optical fiber sensing technology, the application of distributed optical fiber temperature measurement technology has been widely used in mass concrete temperature monitoring. Comparing to the conventional thermometer that only is available to the certain spot temperature measurements, the distributed optical fiber temperature measurement techniques can monitor the temperature of concrete along the fibers. With the proper arrangement of optical fiber temperature sensing network, the real-time temperature field information of dam interior could be obtained to actualize the dam temperature control.

In the aspect of foreign development: Barnoski^[1] invented the optical time domain reflectometer (OTDR) in 1976. The University of Southampton originally proposed a distributed optical fiber temperature sensor in 1981. Based on liquid optical fiber laser Raman spectroscopy, Hartog^[2] conducted the principle experiment of distributed optical fiber temperature sensor in 1983. DaMn^[3], Hartog^[4] developed subsequently the experimental device of distributed optical fiber temperature sensor by using argon ion and semiconductor laser light source.

In 1987, Sensa firstly released a distributed optical fiber temperature sensing system (DTS) based on backward Raman scattering. After that, the distributed optical fiber temperature measurement techniques have been commercialized by increasing companies.

In the domestic cases, the earliest optical fiber temperature sensing techniques were actually applied to the project of Shimen Dam by Tsinghua University and Munich University of Technology. Zhang Zaixuan^[5] developed the FGC-W1 laser distributed Raman temperature sensing system in 1995. Afterwards, the FGC-W2 distributed optical fiber temperature sensing system^[6] was further developed and its temperature resolution can reach 0.1 °C. In 2002, Prof. Cai Desuo^[7] introduced a DTS200-8-M2 distributed optical fiber temperature measurement system from Sensa and applied it to the 14th section of the left power house of the Three Gorges Dam. In 2007, Prof. Zhou Yihong^[8] applied the distributed optical fiber temperature measurement techniques to Xiluodu Hydropower Station. In 2011, Prof. Zhang Zixuan successfully reduced the temperature drift of the optical fiber temperature measurement system^[9].

The Wudongde dam located in the dry and hot valley is a concrete double-curvature arch dam with the foundation surface elevation of 718m, crest elevation of 988m and a maximum dam height of 270m. The temperature difference between morning and evening is large, moreover, the ground temperature is high and the evaporation is large. Therefore, it's a big challenge to control the dam temperature. The low-heat cement used in Wudongde dam can improve the crack resistance of mass concrete due to its low heat of hydration and the post-concrete performance close to or over that of medium-heat Portland cement. However, the early strength development of low-heat cement concrete is slow and it is also the first time for the large-scale use of full-dam in China. It is hard to make sure the evolution of the true temperature field inside the low-heat mass concrete. Therefore, using the distributed optical fiber for concrete temperature monitoring is very significant.

2. DISTRIBUTED OPTICAL FIBER INTELLIGENT TEMPERATURE MONITORING SYSTEM

2.1. BASIC PRINCIPLE OF THE SYSTEM

Optical fiber temperature measurement system is composed of the host computer of the DTS (Distributed Temperature System), data network, distributed optical fiber, human-computer interface and cloud platform. The host computer of the DTS is an optical instrument which measures the temperature through the optical fiber. The optical fiber is similar to a sensor that monitor the temperature. The host computer provides the operation interface and it can not only measure the temperature intermittently but also measure continuously in real time. Furthermore, it provides the interface of data file and real-time protocol of data exchange for networking. Data networks can use wired or wireless means.

The basic principle(Fig.1.) of DTS is to make use of the principle of optical time domain reflectometer (OTDR) and the temperature effect of Raman backscattering of fiber. The thermal expansion coefficient of optical fiber can modulate the phase of the laser to reflect the temperature information.

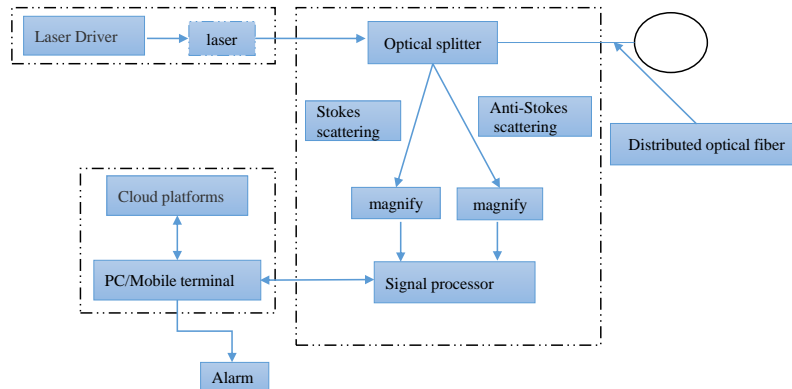


Fig.1

Distributed optical fiber intelligent temperature monitoring system

2.2. FUNCTIONS AND FEATURES OF HARDWARE SYSTEM

In order to obtain the real-time and accurate temperature data of concrete, Tsinghua university has developed the appropriate hardware system in the Wudongde construction site. The hardware system will transmit the temperature data to the cloud platform and the users can read the data from the platform conveniently. The specific functions are as follows:

- (1) the methods of system networking: RS485, 4G and WiFi.
- (2) the alarm function when fiber has been broken.
- (3) visible human-computer interface or mobile terminal interface.
- (4) no blind zone and continuance monitoring.

Compared with the traditional temperature measurement by thermometers, optical fiber temperature measurement has a great deal of advantages: no electromagnetic interference, good temperature stability, long-distance monitoring, large amount of monitoring information, high degree of automation, real-time online monitoring.

2.3. SOFTWARE PLATFORM

The software platform of Wudongde optical fiber temperature measurement system is developed independently by the Tsinghua university. The human-computer interface provides two methods. The first method is the WeChat software platform(Fig.2). The second method is the WEB client on PC. The two interfaces are based on the JavaScript programming language.

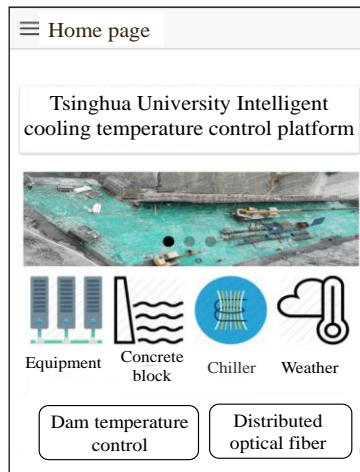


Fig 2

The fiber temperature data display on the WeChat client

3. THE CONSTRUCTION OF DISTRIBUTED OPTICAL FIBER

Wudongde dam is divided into 15 sections. The distributed optical fiber is buried in the 7 # section. The overall layout of the optical fiber is shown in Fig.3.

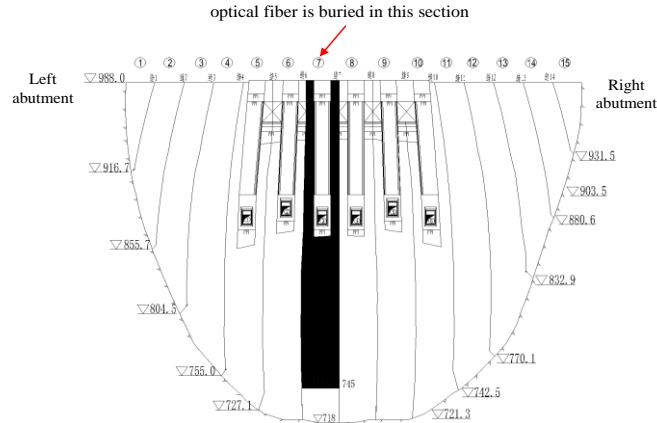


Fig.3

Layout diagram of distributed optical fiber in Wudongde arch dam (unit: m)

In addition to fiber, each dam concrete block is also embedded with three digital thermometers to monitor the temperature. The optical fiber is approximately the same elevation as the buried thermometer during the construction period along the river. The vertical optical fiber at the upstream and downstream surfaces are both 1m away from the upstream and downstream surfaces. The optical fibers below 871m in elevation are laid along the "Z" shape in the 7 # dam section. The optical fibers with an elevation of 871m ~ 988m are laid along the center line of the concrete block.

3.1. THE CONSTRUCTION DESIGN OF VERTICAL OPTICAL FIBER

The optical fibers are alternately in odd and even layers. The odd layers of optical fibers are embedded only in odd-numbered layers and the even layers of optical fibers are embedded in even-numbered layers only (Fig.4).

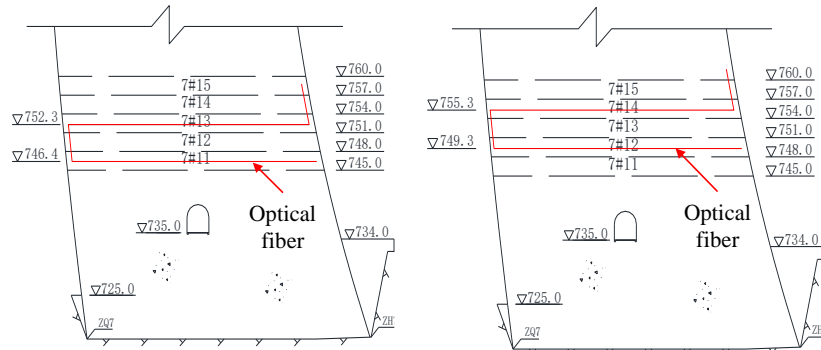


Fig.4

Layout diagram of odd and even layers of optical fiber (unit: m)

3.2. THE CONSTRUCTION DESIGN OF CONCRETE BLOCK OPTICAL FIBER

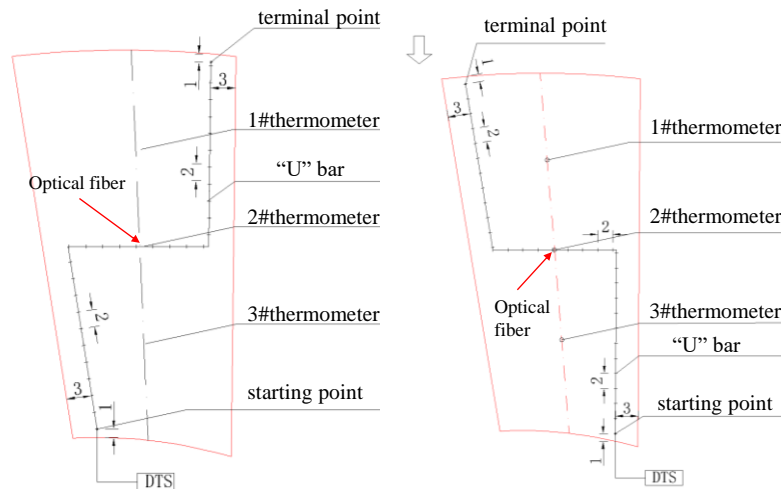


Fig.5

The "Z" shaped alignment of optical fiber in odd and even concrete block

In elevation below 871m, in each concrete block, the optical fibers start from the downstream surface to the upstream surface. The starting point is 1m away from the downstream and 3m away from the transverse joint. when the optical fiber arrives at half of the length of concrete block, it needs to turn to another transverse joint till the distance away from the joint is 3m. Ensuring the turning radius of the fiber is greater than 16cm. The entire fiber is "Z-shaped" (Fig.5).

3.3. THE CONSTRUCTION OF OPTICAL FIBER ON SITE AND COLLECTION OF TEMPERATURE DATA

On-site construction, the workers should embed the optical fiber at the exact location according to design drawings. During the process of the construction of the optical fiber, using the concrete vibrator makes the concrete flaccid. Then pressing the optical fiber vertically into the concrete with a depth of 10-15cm, and fixing it with a U-shaped bar (Fig.6).

After completing the construction of the optical fiber, the workers should test the buried optical fiber with the DTS instrument to ensure that the optical fiber is integrity, has no breakpoint, and is good communication. After confirming that the fiber has survived, the data can be collected and analyzed (Fig.6).

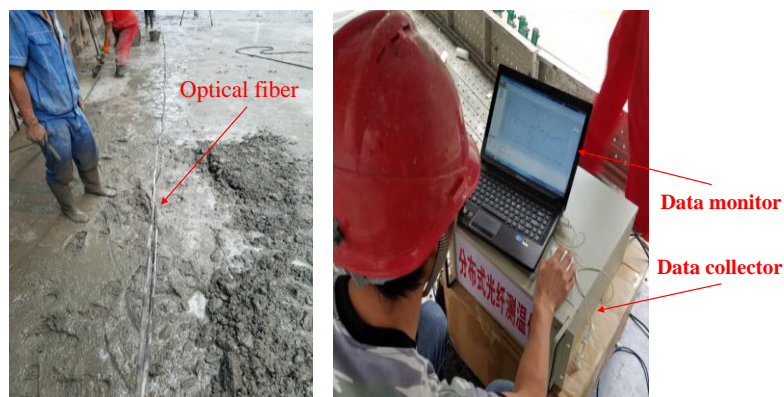


Fig.6

The construction of optical fiber on site and collection of temperature data

4. ANALYSIS OF DISTRIBUTED OPTICAL FIBER TEMPERATURE MEASUREMENT RESULTS

4.1. THE TEMPERATURE DATA CONTRAST BETWEEN OPTICAL FIBER AND CONCRETE THERMOMETER

In order to test the accuracy and reliability of the temperature data by distributed optical fiber, the coincident location of the concrete thermometer and the optical fiber is recorded during the construction process. The temperature at the coincident location is used to compare the data with the two temperature measurement methods later. In 2017/7/25 and 2017/8/4, the temperature data of two different temperature measurement methods are compared (Fig.7 to 8).

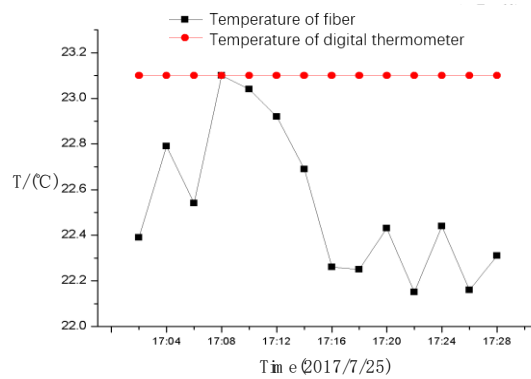


Fig.7

2017/7/25 Temperature data comparison between optical fiber and digital thermometer in 7#11

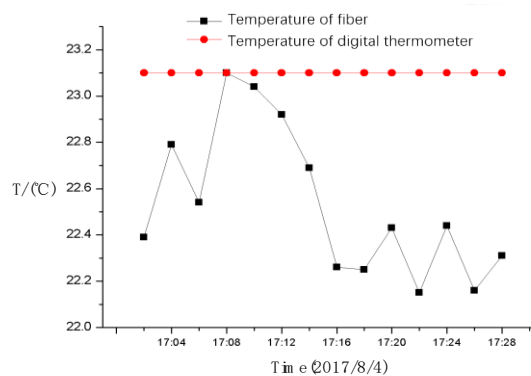


Fig.8

2017/8/4 Temperature data comparison between optical fiber and digital thermometer in 7#11

From Fig.7 and 8, optical fiber temperature measurement data and digital thermometer temperature data are different, but the difference is small. The relative error is within 1 °C between the two methods. Therefore, the optical fiber temperature measurement can meet the engineering requirements.

4.2. VARIATION OF TEMPERATURE INSIDE CONCRETE AT EARLY AGE

Taking the unit 7 # 11 of Wudongde Dam as an example, the temperature Variation is analyzed with age at the starting point at downstream surface and the end point at upstream surface(Fig.9).

During the construction period, the temperature of the dam is controlled by the cooling water. In order to facilitate the expansion of transverse joint, the cooling time is generally 2 to 3 days after the placement. Therefore, the change of concrete temperature is the result of the combined effect of hydration heat and cooling water.

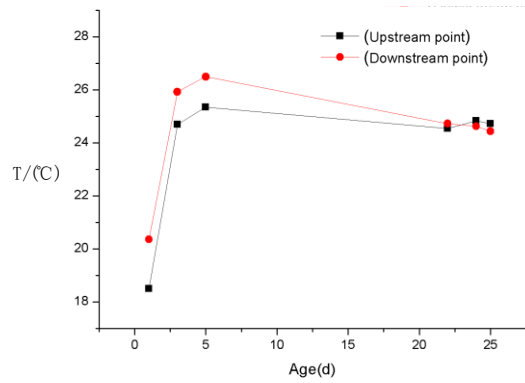


Fig.9

The temperature changes with age at the downstream starting point and upstream end of the optical fiber

From Fig.9, it can be seen that the internal temperature of concrete increases sharply with the increase of the age in the first 2 ~ 3d when there is no effect of the cooling water. Later, under the combined effect of hydration heat and cooling water, the concrete temperature first slowly increases until the maximum temperature (controlled by 27 °C) and then decreases with the increase of the age, and finally becomes stable.

4.3. EVOLUTION LAW OF THE THERMAL FIELD

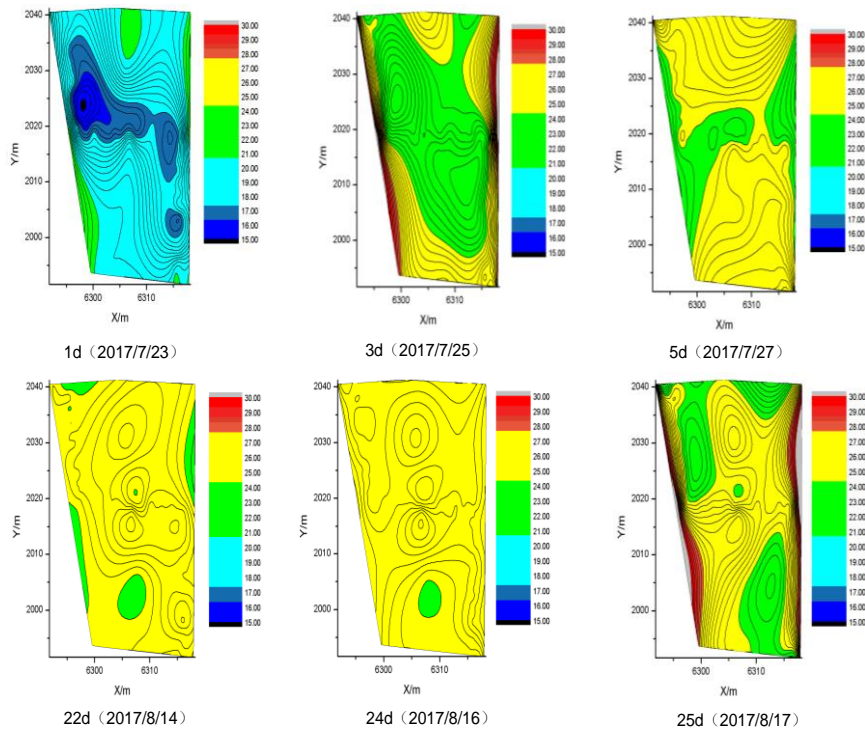


Fig.10

Evolution of the temperature field of unit 11 in 7 # section with age

The thermal field evolution law of unit 11 in 7 # section which bases on distributed optical fiber temperature measurement is displayed as Fig.10.

From Fig.10, when there is no cooling water, the temperature of the upstream and downstream surfaces of the concrete are higher than the temperature at the middle of the concrete block at the age of 1 d. This condition is caused by low pouring temperature and hydration heat, simultaneously, the temperature of the upstream and downstream surfaces is affected by the environment temperature. At the age of 3d, the hydration reaction releases a large amount of heat and causes the temperature inside the concrete to rise sharply. At the age of 5d, under the effect of cooling water, the internal temperature of the concrete continues to rise, but the rate is slowing. When the age reaches 20d and above, the concrete temperature stabilizes at 24 to 26 °C and the temperature field distribution is more uniform.

5. CONCLUSION

The distributed optical fiber temperature measurement system is developed to monitor and analyze the temperature change of low-heat cement concrete in Wudongde arch dam. The conclusions are as follows:

Distributed optical fiber temperature measurement can achieve real-time online monitoring under the complex site condition and the monitoring accuracy can reach $\pm 1^{\circ}\text{C}$.

Distributed optical fiber is alternately buried in the odd-even concrete block along the elevation direction and the "Z" shaped layout of optical fiber is used to enhance the accuracy of the temperature field reconstruction of the entire dam.

At present, the monitoring results show that the internal temperature of low-heat cement concrete increases obviously under hydration action after placement without effect of cooling water. Then the temperature increases with the age at a steady rate under the control of cooling water. After it reaches the highest level (the temperature is controlled at less than 27 °C), the temperature gradually decreases with the age and finally becomes stable under the cooling rate of less than 0.5 °C / d. The temperature distribution of the concrete will tend to be uniform.

6. REFERENCES

- [1] Bamoski M K, Jensen S M. Fiber Waveguides: A Novel Technique for Investigating Attenuation Characteristics[J]. Appl Opt, 1976, 15(9):2112-2115.
- [2] Hartog A H. A distributed temperature sensor based on liquid-core optical fibers[J]. IEEEJ Lightwave Technol, 1983(1):498-509.
- [3] Dakin J P. Distributed anti-stokes ratio thermometry, 3rd International Conference on Optical Fiber Sensor, Postdeadline Session, San Diego, USA,

- 1985.
- [4] Hartog A H, Leach A P, Gold M P. Distributed temperature sensing in solid-core fibres[J]. Electronics Letters, 1985, 21(23): 1061-1062.
 - [5] Zhang Zaixuan, Liu Tianfu. Laser Raman-type Distributed optical fiber Sensor System[J]. ACTA OPTICAL SINICA, 1995(11):1585-1589.
 - [6] Zhang Zaixuan, Feng Haiqi. Distributed optical fiber Raman photonic sensor system[J]. Semiconductor Optoelectronics, 1999(02):83-85.
 - [7] Cai Shunde, Cai Desuo. An Analysis on Monitoring Hydration Heat of the Large Cubage Concrete with the Distributed Fibre [J]. J of China Three Gorges Univ. (Natural Sciences), 2002(06):481-485.
 - [8] TANG Guoqing, ZHOU Yihong. Remote control of distributed temperature sensing for dam temperature monitoring of Xiluodu Hydropower Station [J]. Yangtze River, 2012, 43(23):92-95.
 - [9] Yu Xiangdong, Zhang Zaixuan. An Intelligent Temperature Compensating Circuit for Distributed Optical Fiber Raman Temperature Sensor[J]. ACTA PHOTONICA SINICA, 2011, 40(12):1870-1874.

SUMMARY

Temperature monitoring is the basis for the mass concrete temperature control and is of great significance for the prevention of concrete cracking. According to the requirement of dam concrete temperature control during construction, a set of complete on-site operation technology was put forward based on distributed optical fiber temperature measurement technology and on-line temperature measurement software of optical fiber was also developed. Taking the low-heat concrete of Wudongde arch dam as a case, the temperature data of on-site concrete was collected in real time using the distributed optical fiber temperature measurement system, and the law of temperature evolution of low-heat concrete was analyzed. The results show that the distributed optical fiber temperature measurement system is effective, accurate and reliable, and the real temperature field of concrete can be obtained. The temperature of low thermal concrete in Wudongde is obviously at low level at early age, which helps to reduce cracking risk of dam.

KEY WORDS

Distributed optical fiber, temperature measurement, thermal field evolution, mass concrete, Wudongde arch dam.

COMMISSION INTERNATIONALE DES GRANDS BARRAGES

VINGT-SIXIÈME CONGRÈS DES GRANDS BARRAGES
Autriche, juillet 2018

DOI 10.3217/978-3-85125-620-8-130



This work licensed under a Creative Commons Attribution 4.0 International License. <https://creativecommons.org/licenses/by-nc-nd/4.0/>

OPERATION OF SMALL AGRICULTURAL DAMS IN BULGARIA – STATE-OF-THE-ART

Bogdan R. NIKOLOV

Doctoral student, Department of Hydraulic, Irrigation and Drainage Engineering,
UNIV. OF ARCHITECTURE, CIVIL ENGINEERING AND GEODESY

BULGARIA

Dimitar S. KISLIAKOV

Professor, Department of Hydraulic, Irrigation and Drainage Engineering, UNIV.
OF ARCHITECTURE, CIVIL ENGINEERING AND GEODESY (UACEG)

BULGARIA

COMMISSION INTERNATIONALE
DES GRANDS BARRAGES

VINGT-SIXIÈME CONGRÈS DES
GRANDS BARRAGES
Autriche, juillet 2018

OPERATION OF SMALL AGRICULTURAL DAMS IN BULGARIA – STATE-OF-THE-ART*

Bogdan R. NIKOLOV

*Doctoral student, Department of Hydraulic, Irrigation and Drainage Engineering,
UNIV. OF ARCHITECTURE, CIVIL ENGINEERING AND GEODESY*

Dimitar S. KISLIAKOV

*Professor, Department of Hydraulic, Irrigation and Drainage Engineering, UNIV.
OF ARCHITECTURE, CIVIL ENGINEERING AND GEODESY (UACEG)*

BULGARIA

1. INTRODUCTION

Dams are complex multi-purpose engineering facilities which are always built in connection with a characteristic particular set of local conditions (hydrological, geological, topographical etc.). Their construction is a result of a complicated investment process consisting of several simultaneously running lines of activities such as administrative, financial, technical, economical etc. One activity of special importance in this bunch is the design in all its parts (i.e. special fields) and phases. In the design namely, all parameters, scenarios and modes of the operational life of the dam and its appurtenant facilities incl. the reservoir are formulated with respect to the particular water resources management tasks and to the requirements of the currently active codes and other regulations. It is well known however that the operational life of the dam essentially depends on the maintenance of the facilities, their performance in fulfillment of the operational tasks set with building of the dam is not possible without such proper

* **Exploitation de petits barrages agricoles en Bulgarie - état de l'art**

maintenance. The operation of the dam and its structures ends with conservation or removal of the dam, and such activity also is subject to the development and implementation of special and very particular design solutions.

There are almost 6000 water objects in Bulgaria subject to water right permits. More than 2000 of them are small dams according to the definition of ICOLD [1]. They were built predominantly in the 1960s and 1970s serving most of all agricultural purposes – local irrigation and stock farming. With very few exceptions as parts of some industrial facilities, these are embankment dams. In the decades after the Second World War, large profiled state design and construction enterprises with their local branches were engaged in the design and construction of such dams on the whole territory of Bulgaria for enabling the development of local agriculture besides the large irrigation systems. At the same time, the related national codes and regulations for preliminary surveys, design and maintenance of dams were developed with respect to the obtained experience and the current best practices not only of the Soviet Union and the other socialist countries [2] but also of the world leading countries in the field of Dam Engineering.

After the fundamental political change in 1989 in Bulgaria, all cooperative farms and so-called agricultural-industrial complexes were liquidated. The related administrative procedures were forced in time in connection with the restitution of the land property nationalized after the Second World War. In the frame of this process, many small dams owned previously by cooperative farms and societies were sold, however, without clear definition of the deal conditions as this will be explained in more detail further below. All responsibilities for the further operation of all remaining small dams were administratively transferred to the local municipalities. On the one hand, they still have neither the qualified personnel nor the financial resources to perform proper maintenance of the dams and their facilities. On the other hand, due to the collapse of national agriculture and the steady evacuation of the land population, there is currently in fact almost no need for the water from all these small reservoirs. As a result, the technical maintenance of the small dams as an inherent operation component was disregarded for many years with all related consequences.

The further development up to now is characterized by two other features, too. The municipalities owning small dams have always tried to find mechanisms for financing the technical maintenance of the facilities. Some solutions were found, however, they caused some other problems which will be addressed further below. Simultaneously, there are continuous and intensive attempts for corresponding development of the complicated legislative environment in the field which should enable general solutions of the most important problems related to the dam safety above all.

The present work constitutes an attempt for a short analysis of the current status of the small dams in Bulgaria considering its more recent historical development as well as the wide variety of related problems currently. This is not the first study of these problems, moreover since they become more topical with the time. Here in this connection, the works [3,4] on general and particular issues of the small dams should be mentioned as examples. Of course, a complete study would require large amount of reliable input data, its statistical processing

in the time domain over decades and a comprehensive multi-disciplinary analysis with the boundary conditions of the overall national development in the considered time period. Since such task would go far beyond the frame of this report, further below we'll aim only at the qualitative and structured presentation of the main safety-related groups of problems of the small dams operation, the sources of these problems and some ideas for solutions.

2. CURRENT SITUATION, LEGAL AND REGULATIVE ENVIRONMENT

2.1. STATE OF THE SMALL DAMS IN BULGARIA – GENERAL REMARKS

In the last several years, intensive work is being done by all involved parties for qualitative improvement of the conditions for technical maintenance of the dams in Bulgaria. In fact, there are no problems with the large ones owned either by the National Electricity Company and serving with priority production of electricity from hydropower, or by the state enterprise Irrigation Systems, or by the water supply companies. They all have special operational units with experienced staff and the necessary resources for proper maintenance of the facilities. The main problems with the status – both technical and operational, are connected most of all with the small dams owned by local municipalities. However, a key person in the latter relation is the local district governor who is directly responsible for the safety of every dam in the district and its appurtenant structures. Once a year, he/she must organize an expert commission for analysis of the status of these facilities. Twice yearly, every dam owner must arrange thorough technical review of the facilities. In general, this has become a working mechanism recently, however, the governors hardly have the resources needed for implementation of the results from these analyses.

Since July 2015, the State Agency for Metrological and Technical Surveillance (SAMTS) is officially responsible for all issues of the technical operation of the dams in Bulgaria and their safety. This transition was accompanied by a still running substantial transformation of both administrative structures and regulative documents.

The Main Directorate “Supervision of dams and their appurtenant structures” at SAMTS has only control functions, i.e. it is not engaged itself in performing technical operation and / or maintenance of dams and their facilities. In general, the experts there examine the technical state of the dams periodically, formulate improvement requirements if necessary and control their fulfillment. Currently, a global national information system is being developed with online platform for data management and status monitoring of all dams in Bulgaria.

Although the SAMTS works together with all related parties if necessary, some administrative tension sometimes arises, especially when contradictory interests are present – for example, if an act of violation is drawn up of a dam owner while it is objectively evident that he/she has not had the possibility to

ensure the required activities for the maintenance needed.

All above considerations are related to the technical maintenance of the dams and their facilities as well as to the dam safety, respectively. The other side of the problem is presented by the water resources management of these small dam reservoirs. As already mentioned, after both the collapse of the Bulgarian agriculture and the population migration following the political change in 1989, many of these reservoirs are simply not needed. Hence, the interest for their ownership, operation and maintenance is directly not present. This is a severe problem since on the one hand, these small dams are extremely valuable facilities of the water infrastructure in the conditions of relatively scarce water resources in Bulgaria. Furthermore, although small but numerous, they contribute to the damping of the peaks of flood events in whole catchment areas as this was the case of the flood in August 2014 in Northwestern Bulgaria [5]. On the other hand however, the long-term absence of proper technical maintenance substantially reduces their safety with all dangerous consequences.

2.2. LEGISLATIVE ENVIRONMENT, CODES AND REGULATIONS

Currently, there are almost 40 acts and subordinated legislative documents covering the whole spectrum of hierarchical range which regulate all aspects of the technical operation of the dams, latters' safety and the technical maintenance of the facilities [6]. Discussing them here would go far beyond the frame of the present report. A special feature in this connection is the fact that the property and the operation of the water reservoir is still strictly separated from the operation of the dam and its facilities. In some cases, this causes severe problems in the operation as a whole set of interrelated activities, and attempts at highest administrative level are made currently to overcome this formal separation.

It should also be noted that this regulatory system is a dynamic structure being continuously in development and improvement in terms of more adequate reflection of the reality for decrease of the identified problems – technical, administrative, legislative, operational, environmental etc.

In all cases when a particular problem is not covered by the current national regulations, the most advanced solutions to this problem available worldwide are applied. To serve this purpose, ICOLD Bulletins (for example Nr. 115, 116, 131, 138, 148), EU Directives and related documents, internationally recognized recommendations and guidelines as well as modern best practices are implemented. Other related sources are considered, too – for example [7, 8]. Last but not least, special attention is also paid to the recent research activities in this field, especially to the ones within the European Union. Here, [9, 10, 11] can be mentioned as examples.

The environmental aspects of the small dams are subject to special concern, too. Recently, the legislative component of these aspects is rapidly growing, especially with the implementation of the strategies, policies and directives of the European Union. One important issue related to the operation of

small dams is the water quality in the reservoir. This requires better care not only for the water quality in the dam lake itself but also for the run-off and pollution prevention, respectively in the whole catchment area. Furthermore, the necessity of regular preparation of plans for assessment and management of flood risks (which are regulatory documents) is both formally obligatory and directly related to the dam safety.

3. IDENTIFIED PROBLEMS AND SOME RECOMMENDATIONS

3.1. LEGAL AND ADMINISTRATIVE ISSUES

In this section, the following main issues can be formulated as identified in the operation and maintenance of small dams:

- After having become owners of numerous small dams without having the needed resources for their proper maintenance, many municipalities let the dams for rent. As a result, the renter usually not only restricted the access of any other parties to the reservoir but also to all dam facilities for maintenance. At the same time, the renter had no responsibility for the technical status of the dam and its appurtenant structures. In most cases, the operator used the dam reservoir as a fish farm and installed meshes at the spillway for preventing the fish to escape. Although such installations are indeed extremely dangerous for the dam structural integrity, deficiencies in the actual regulations and in the particular contract formulations made them happen in many cases.
- As mentioned above, the land property was restituted in general in the 1990s. However, during the liquidation of the cooperative farms, many dams were sold by tenders. Later on, it became obvious in many cases that the legal owner of the dam didn't have in fact anything more since the land below the reservoir was returned to its previous owners. The water in the dam lake is public state property, and the dam owner had often even no more access possibility to the facilities. This is indeed a severe issue in many cases still open and directly related to the maintenance and safety of the dam and its structures.
- The previous issue is directly related to the next one as already mentioned above – the rigorous separation between dam with its appurtenant structures and the water in the reservoir. These two items are inherently connected by the purpose of the dam as well as by the Hydraulic and Structural Engineering facilities serving the reservoir water management. Attempts are currently made for overcoming this problem of sharing responsibilities.

- The lack of resources for technical maintenance of the dams and their structures brought some dam owners to the necessity either to keep the corresponding reservoir permanently empty or to cut the dam body and thus to prevent any further impounding. So, they also prevented any flood risks for the downstream residents. Such destruction is usually performed without any technical design and compliance with the related legal requirements. Of course, the result is devastating for the materials of the dam body, too.
- The lack of resources (i.e. finances, qualified personnel, equipment etc.) for technical maintenance of the small dams and their facilities including for carrying out reparatory works sets many municipalities as dam owners between the hammer of the legal requirements and the anvil of resources.
- The emphasis on environmental friendliness has led recently to some curious legal requirements. For example, every new dam must have a fish pass according to the Act for Fishery and Aquacultures. In the process of legislation development, such examples of nonsense should be cleared.

3.2. PERFORMANCE PROBLEMS DUE TO THE LACK OF TECHNICAL MAINTENANCE

The following issues due to the lack or even absence of technical maintenance can be formulated with respect to the performance of the small dams and to the related findings in [3, 4, 5] as well:

- In general, often there has been no technical maintenance of the dams and their facilities. There is no monitoring system, no measurements and analyses of the technical conditions are carried out. Usually, there is no technical documentation including drawings left from the design and construction.
- Settlement of the embankment at the central part of the dam. Thus, the dam crest level has sunk below the maximum water level in the reservoir, and the risk of crest overflow during flood conditions strongly increases with all negative consequences of such event.
- The legal requirement for cleaning the river bed 500 m downstream of the dam is in general not held by the dam owner.
- Many small dams have suffered some damages over the years of operation without proper maintenance. They need a serious and urgent repair for restoring their full operational functionality. Otherwise, subsequent load impacts and floods could lead to heavy damages of the dam body with possibly uncontrolled release of the impounded water. Independantly how small this volume might be, the resulting flood wave could certainly have severe consequences.
- Erosion of the streambed downstream of the spillway. In some cases, the structure of the spillway itself is in a good condition. However, the following spillway race and the stilling basin (if available) have been for

years subjected to erosion without any maintenance and repair. Under some particular geological conditions, this erosion may have become quite intensive.

- Damaged or clogged bottom outlet which leads to the necessity of draining the reservoir only by means of an external temporary siphon.
- With the time and without any maintenance, the spillway inlets of numerous small embankment dams have clogged by floating debris during relatively small flood events. Every time when there was flow in such spillways, additional amounts of debris were added. Thus, without cleaning the spillway inlet, the risk of dam crest overflow increases.
- Non-maintained dam slopes with developed dense plant and tree cover. These slope conditions heavily complicate the access to the dam crest and all appurtenant structures.

3.3. PERFORMANCE PROBLEMS AFTER IMPACTS EXCEEDING NORMAL OPERATING CONDITIONS

At several dams during flood events, the dam crest has been overtopped as well, Fig. 1 [5]. Fortunately, these dams retained their overall structural integrity, and no uncontrolled catastrophic release of the reservoir content occurred. However, the dam body in such cases was damaged, and all necessary repair works had to be carried out as soon as possible, for such dams to be able to further fulfill their basic operational requirements.



Fig. 1

Damaged crest area after overflow

Zone de couronnement endommagée après débordement

It should be noted here that design of such small dams has been performed with relatively high probability of exceedance of the design loads and impacts according to the code requirements. Thus, it is possible that such damages occur during their operational life. This only emphasizes the importance of proper regular maintenance and carrying out of all necessary repair works on time.

3.4. POSSIBLE RECOMMENDATIONS

After the summarizing presentation of the main operation and maintenance problems of the small dams in Bulgaria above, the following recommendations can be formulated:

- The necessary administrative work has to be done for overcoming of the separation in the operational management of the small dams between the dam with its structures and the water reservoir. Careful and justified distribution of the activities and responsibilities, respectively, has to be carried out.
- The performance of the facilities under so-called overload conditions for the particular class of importance has to be regulated.
- The property issues related to the small dams need urgent solution.
- Highest priority has to be assigned to the repair of dams with structural damages of the dam body and to works for restoring the operational ability of the safety-related appurtenant structures.
- The requirements are good but it is a matter of state policy that dam owners have a chance to obtain the resources needed for proper maintenance of the facilities by means of appropriate mechanisms.

4. CONCLUSIONS

From the performed short analysis of the status of the small dams in Bulgaria, the following conclusions can be drawn. First of all, these facilities are essential component of the national water resources management infrastructure at lowest structural level. Hence, their operation and technical maintenance should be subject to strategic national policy in this field.

There is a set of serious problems in several fields related to the operation and maintenance of small dams, as shortly discussed above. The nature of the required solutions is very complex and requires interdisciplinary approach by broader teams of experts. It is quite clear, however, that the process of developing and implementing such solutions is complicated and requires besides expert knowledge high-level skills in the management of sometimes contradictive interests. Moreover, these solutions need considerable resources. One more thing is clear, too. If the state does not set properly its priorities for further development in this field, at least two things will happen. As a result of the

decreasing safety of these dams and their facilities, accidents will occur. We cannot allow this to happen. Further, although possible removal of many such dams (which also requires corresponding design, administrative and construction activities and financing, respectively) seems to be a solution, their subsequent building if needed will be much more difficult and expensive. Hence, similar decisions with long-term effect have to be made very carefully.

We are glad to find that currently, there is the general expert and administrative will in Bulgaria for solving the problems with the status and operation of the small dams.

REFERENCES

- [1] *Small dams: Design, Surveillance, Rehabilitation*, ICOLD Bulletin, 2011
- [2] PETRANOV HR., VALCHANOV L., ANTONOV L., MITEV D., POPOV B. *Small dams – reconnaissance, design, construction* (in Bulgarian), Zemizdat, Sofia, 1955.
- [3] TOSHEV D., CHOLAKOV T., TODOROV O., LISSEV N. State of small dams in Republic of Bulgaria (in Bulgarian), *Vodno delo*, 2012, Nr.5/6
- [4] STANKULOVA D. State and operation control of the small dams (in Bulgarian), Report presented at Water day, April 2017, not published
- [5] KISLIAKOV D. Performance and role of the small dams during the flood in North-Western Bulgaria in August 2014, Proceedings of Conference on topic: The State of the Water Economy Infrastructure, 18th-19th September 2015, Macedonian Committee on Large Dams, Skopje, Republic of Macedonia, 2015
- [6] Bulgarian legislation gateway – www.lex.bg
- [7] *Design of Small Dams*, USDI, Bureau of Reclamation, 3^d Edition, 1987
- [8] DEGOUTTE G. (ENGREF, Coordination), *Small Dams. Guidelines for design, construction and monitoring*, French Committee on Large Dams, 2002
- [9] MEGHELLA M., BUENO I.E., ORTUÑO M.M., LOMBILLO A.S. DAMSE – A European Methodology for the Security Assessment of Dams, Deliverable 3 - v.02, EC funded project, JLS/2006/EPCIP/001 – May, 2008
- [10] PISANIELLO J.D., BURRITT R.L., TINGEY-HOLYOAK J. Dam safety management for sustainable farming businesses and catchments, *Agricultural Water Management*, 2011, 98, 507–516
- [11] MAGILLIGAN F.J., NISLOW K.H., KYNARD B.E., HACKMAN A.M. Immediate changes in stream channel geomorphology, aquatic habitat, and fish assemblages following dam removal in a small upland catchment, *Geomorphology*, 2016, 252, 158–170

SUMMARY

The font size of the Summary should be MS Unicode Arial 11 point, justified, line spacing “exactly” 14 pt; the heading (SUMMARY) should be all capital letters, and centered.

This work is a summary report about the current frame conditions for the operation of more than 2000 small dams in Bulgaria, almost all of them build for agricultural purposes. It is based on both a vast literature survey and specific national experience, and it presents the results from the performed qualitative analysis from the point of view of the following aspects of dam operation:

1) Legislative base, regulatory documents and guidelines: national legislation and administrative procedures, code requirements, international recommendations and good practices.

2) Physical aspects of the operation of small dams aiming at technical and operational reliability in connection with the most commonly used structural solutions for these facilities;

3) Some particular problems of the operation of small agricultural dams.

Finally, based on the presented results from the analysis performed, conclusions are drawn with respect to particular contemporary research and implementation needs.

RESUME

Ce travail représente un rapport de synthèse sur les conditions de base actuelles pour l'exploitation de plus de 2000 petits barrages en Bulgarie, presque tous construits à des fins agricoles. Il est fondé sur une vaste étude bibliographique et sur l'expérience nationale spécifique et présente les résultats de l'analyse qualitative réalisée du point de vue des aspects suivants de l'exploitation des barrages:

1) Base législative, documents réglementaires et directives: législation nationale et procédures administratives, exigences du code, recommandations internationales et bonnes pratiques.

2) Des aspects physiques de l'exploitation des petits barrages visant à la fiabilité technique et opérationnelle en relation avec les solutions structurelles les plus couramment utilisées pour ces ouvrages;

3) Certains problèmes particuliers de l'exploitation des petits barrages agricoles. Finalement, sur la base des résultats présentés de l'analyse réalisée, des conclusions sont tirées en ce qui concerne les besoins contemporains de recherche et de mise en pratique.

COMMISSION INTERNATIONALE DES GRANDS BARRAGES

VINGT-SIXIÈME CONGRÈS DES GRANDS BARRAGES
Autriche, juillet 2018

DOI 10.3217/978-3-85125-620-8-131



This work licensed under a Creative Commons Attribution 4.0 International License. <https://creativecommons.org/licenses/by-nc-nd/4.0/>

COMPARISON OF SELECTED SOFTWARE FOR 3D FLOW MODELING AT THE DAM SPILLWAY

Jan HÖLL

Dam safety engineer in VODNÍ DÍLA - TBD a. s.
CZECH REPUBLIC

Matouš HOLINKA

Ph.D. *student* at BRNO UNIVERSITY OF TECHNOLOGY
CZECH REPUBLIC

Jiří HODÁK

Head of *Department* Brno in VODNÍ DÍLA - TBD a. s., *vice-chairmen* in cluster
CREA Hydro & Energy, z.s.
CZECH REPUBLIC

COMPARISON OF SELECTED SOFTWARE FOR 3D FLOW MODELING AT THE DAM SPILLWAY

Ing. Jan HÖLL

Dam safety engineer in VODNÍ DÍLA - TBD a. s.

Ing. Matouš HOLINKA

Ph.D. student at BRNO UNIVERSITY OF TECHNOLOGY

Ing. Jiří HODÁK, Ph.D.

Head of Department Brno in VODNÍ DÍLA - TBD a. s., vice-chairmen in cluster CREA Hydro & Energy, z.s.

CZECH REPUBLIC

1. PREFACE

Numerical modelling of water flow has been accelerated in recent years by more affordable computer performance and software products for that purpose. Numerical modelling has recently, in some cases, replaced physical models. Sometimes it is worth using their combination, usually with the aim to reduce modelling costs in general. In the case of simple side channel spillways of water works, it is clear that numerical modelling can be used very well for all flow discharges and new possible designs of the spillway geometry as well. Therefore, the objective of this paper was to compare the possibilities of 3D numerical modelling of water flow on the side channel spillway with three software products. The question was not which one is best, but which one is more suitable for special needs of users. The article further describes the difficulty of working with individual software products, especially user interface, setting options, solution speed and accuracy of the results. A common input for all three solvers is an imported STL file, which is individually modified for each program. In the pre-processing section, the differences are mentioned in the settings among the programs themselves. Another objective of the project was to compare these modelling procedures, to show their differences and compare the outputs to each other.

The task outcomes were not primarily focused on the quality (details) of outputs. Also, it was not a priority to compare numerical models with a physical model. The subject of modelling was to create a corresponding virtual model with acceptable simplifications of real geometry. The real structure of the selected spillway was geodetically measured and a 3D spatial model in CAD software was created.

2. PRESUMPTIONS AND SIMPLIFICATIONS OF THE MODEL

These are parameters and facts whose application leads to a partial simplification of the examined phenomenon. In the task, it is not necessary to take into account every detail. Therefore, the task remains with the basic settings of the model, but the examined phenomenon will be sufficiently described. The model should be configured to match the reality or physical model as much as possible.

The following assumptions were implemented to the modelling process:

- *Isothermal system* - is a system where the temperature is constant, throughout the system.
- *Air entrainment* - there are two fluids set in the entire object. It is air and water; however, their mutual mixing is not taken into account, due to pressure changes in the turbulent flow. Requires a very fine computation network.
- *Roughness* - the way to divide this variable into a real object is too complicated. Because the surface is concrete, although partially degraded, there is expected a large flow rate. Therefore, the effect is minimal on the flow rate.
- *Boundary condition* - are for all software products the same (margins = wall, inside = atmosphere, discharge = continuous). Only the inlets are different. It depends on the desired setting of individual software product.
- *Turbulence - option* in all software products is used the same two-equation turbulent model $k - \omega$ [1] for calculation of all parameters.

3. CASE STUDY

The comparison of individual programs took place on the existing water work. Slušovice dam is located near the village of Slušovice in the southeast of the Czech Republic and is managed by state owned enterprise Povodí Moravy. Its primary function is the drinking water supply and flood protection as well.

The side channel spillway is located on the left bank of the reservoir. Spillway and chute are reinforced concrete structures. The shape of the overflow edge in the cross section is circular with a radius of 0.75 m. The length of the spillway edge is 26.8 m and the channel width is 6.0 m. The original (designed) flow capacity of the object is 89.5 m³/s for the maximum level in the reservoir.

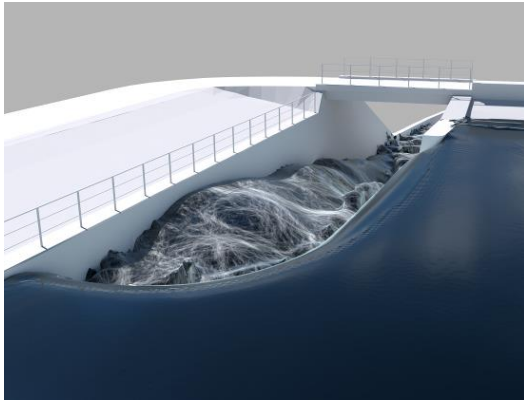


Fig. 1
Virtual model



Fig. 2
Real state (year 2017)

4. OPENFOAM

4.1. INTRODUCTION

OpenFOAM (hereafter referred to as OF) is currently the most widely used CFD (computational fluid dynamics) tool, that is available for download. It is distributed under the GPL (General Public License), which means it can be used free of charge and its source code is freely accessible. GPL licenses give users the freedom to modify and redistribute modified code.

Figures and codes are created with using object-oriented programming and operators. It allows user to create their own solvers relatively easy. Users can create their own objects, boundary conditions or turbulence models that will work with existing solvers without redrawing existing source code.

The OF consists of a large basic library, which contains a number of different types of solvers, tools for creating and manipulating the computing network (mesh networking), monitoring the quality of the computing network, counting variables, parallel calculations on multiple computers and others.

4.2. PROCEDURE

Due to the fact that OF as such is a set of tools for CFD simulation solutions, it does not basically include utility programs for processing object geometry, preparing simulation, selecting boundary conditions, creating a computing network,

etc. (pre-processor). It also does not include a program with a suitable Graphical User Interface (GUI) to perform visualization, verification or manipulation (postprocessor). However, there is a number of available programs for free that can be used for each phase of CFD modelling.

Here is the process of setting numerical model and examples of other implement software products with which the OF works:

- creating STL geometry in Blender or Salome and defining a computational geometry,
- creating a mesh network with snappyHexMesh. This process runs behind the Command-line interface,
- selection of solver for two-phase liquid (interFoam). Again, associated with Command-line,
- definition of physical parameters of liquid,
- definition of initial and boundary conditions,
- the calculation itself, the convergence tests, the residuals assessment, the verification of the existing results,
- post processing in ParaView, verification of results, their graphical interpretation etc.

4.3. SAMPLES OF WORKING INTERFACE

Here are some figures of working in different sub programs for the purpose of creating a valid model, repairing, also setting the fine mesh and setting the variables.

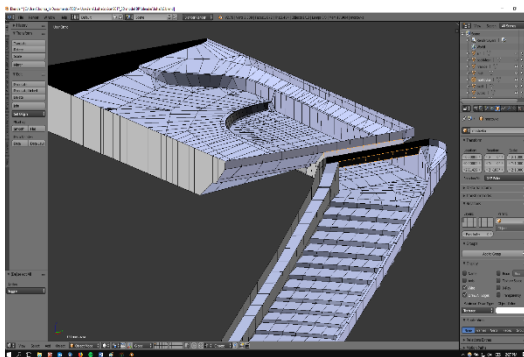


Fig. 3
Blender

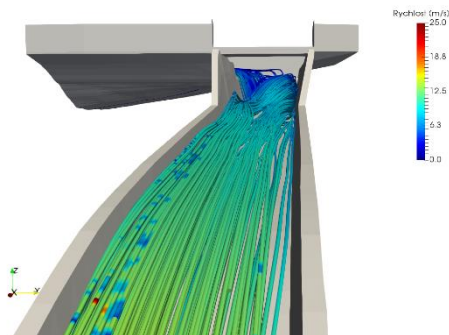


Fig. 4
ParaView

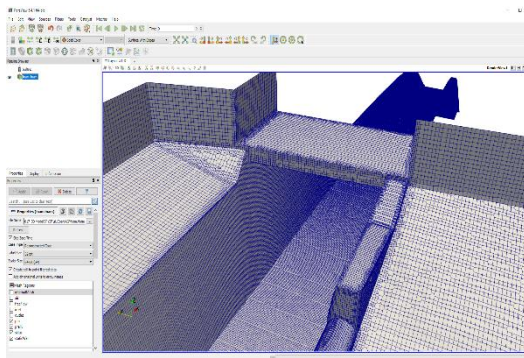


Fig. 5
ParaView

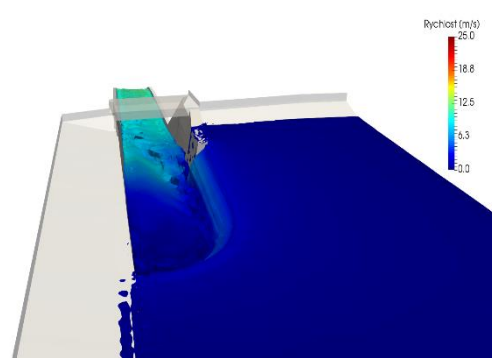


Fig. 6
ParaView

5. ANSYS FLUENT

5.1. INTRODUCTION

Ansys Fluent is today a very common software that deals with CFD issues. It offers a wide range of physical modelling options for flow modelling, turbulence, heat transfer etc. It describes tasks in various branches such as civil engineering, construction, chemistry, etc. There is the choice from a large number of equations for laminar and turbulent flow and their complementary auxiliary elements.

Thanks to step-by-step distribution of the work desktop, which forces the user to continue step-by-step, makes settings very easy to understand and use. The simpler the setting of conditions and model, the more complicated and the less pleasant is the importing of the model and meshing. The software is quite sensitive to various geometry imperfections. Therefore, for more sophisticated models, the body must be properly inspected and handled by the auxiliary functions.

5.2. PROCEDURE

The sequence of individual property settings is determined by the software itself that leads the user through the following points.

- *Analysis systems - fluent* - first step is about the selection of solvers for adequate operation (Fluent),
- *Geometry* - create/import a spatial model, these models are importing through the software SpaceClaim; another step is to check and repair of imported model,

- *Mesh* - a creation and modification of mesh network,
- *Setup* - gradually expanding the sub items to define variables and conditions, only those involved (clearly presented),
- *Solution* - the running of the calculation itself. Writing of the results and comments from the progress. These variables are set in the” Setup “section. The description of the state of the so-called residuals,
- *Results* - post processing, thus visualization of user-selected parameters and variables, in any environment.

5.3. SAMPLES OF WORKING INTERFACE

Here is a group of figures from Ansys workbench.

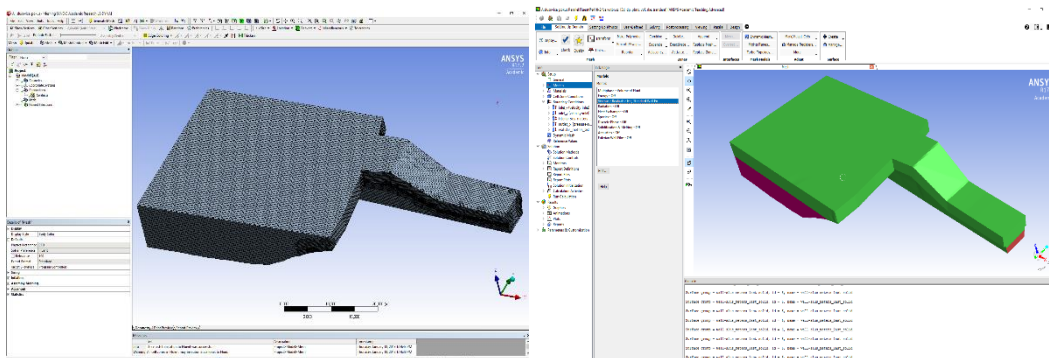


Fig. 7
Mesh networking

Fig. 8
Model setting

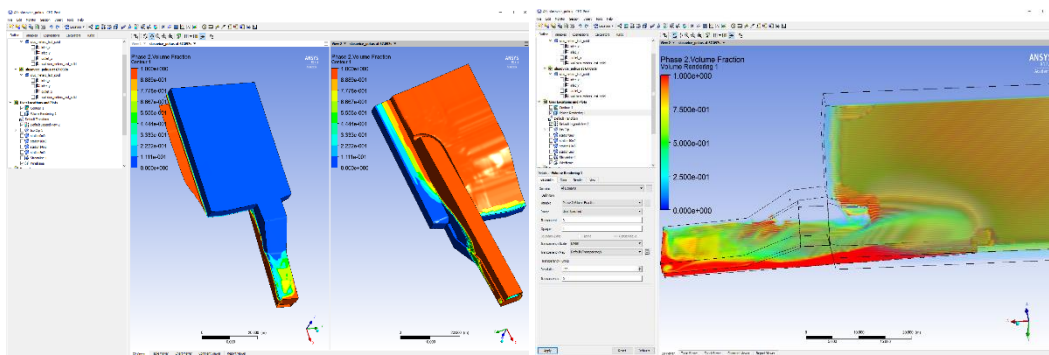


Fig. 9
Post processing

Fig. 10
Volume fraction rendering

6. FLOW-3D

6.1. INTRODUCTION

Flow-3D is software for fluid dynamics in various systems. The user interprets the behaviour of fluids with using numerical methods, the model itself, boundaries and initial conditions, the user interprets the behaviour of fluids. Overall, the survey is performed using the Volume of Fluid mathematical method.

A great advantage is the software's resilience to geometrically complicated and un-repaired models. While other software products require precisely repaired and imported models, Flow-3D also works with very difficult 3D objects without any errors. The software itself includes, among other things, an internal function that corrects the remaining inaccuracies. Its name is Qadmesh. There is lot of tools inside this function, but there is also a risk that the repairing process will change the original model. It will actually fix the imperfections but at the cost of losing real parameters.

6.2. PROCEDURE

After launching the software and looking into the work environment, user can see organized cards. Main cards that have a sub-card group you must expand one after the other and set up the entire process.

Overall, the core part is based on detailed modification of the mesh network. It is simple to create, manipulate and also to import your own shape. Before simulation, it is necessary to know the fact that the smaller cells in the mesh (the smoother the process will be created), the more complicated and longer calculation becomes. Another advantage of the grid is the ability to modify it so that the network is denser at the point where it is needed.

- *New Simulation* - at the beginning user have to choose the type of simulation or physical process (flow over weir),
- *Physics* - another step is to define appropriate condition (gravity, viscous, turbulence etc.),
- *Meshing and geometry* - creating a simple geometry object (or import the complicated) and then create a mesh network,
- *Output and numeric* - in this step user chooses, what he wants to calculate inside the mesh (velocity, pressure, fraction fluid and others),

- *Analyse* - It is used to retrieve the obtained calculations and provide data to plot the process,
- *Display* - It is possible to work separately with the obtained outputs from the previous part of “analyse” (post processing).

6.3. SAMPLE OF WORKING INTERFACE

There are some figures from post processing part of simulation.

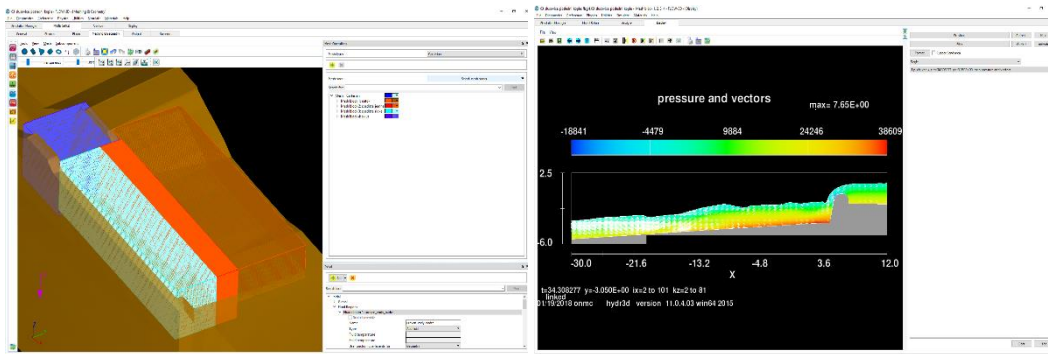


Fig. 11
Dividing mesh blocks

Fig. 12
2D analyse

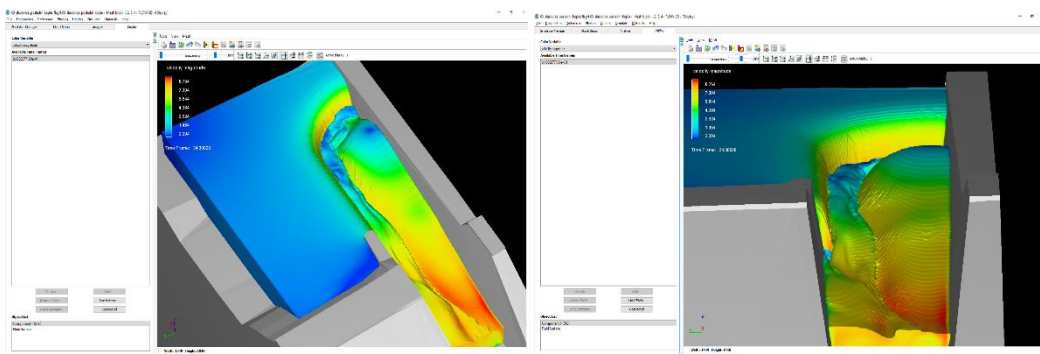


Fig. 13
Complete process edge

Fig. 14
3D view under spillway

7. RESULTS COMPARISON

There is an illustration of flow in spillway cross-section. On the first sight it is evident that Ansys Fluent was set with greater mesh blocks (size = 0,15-0,45 m). The main purpose of this setting was to save the time. Flow-3D and OpenFoam has calculated with size of mesh 0,03-0,15 m.

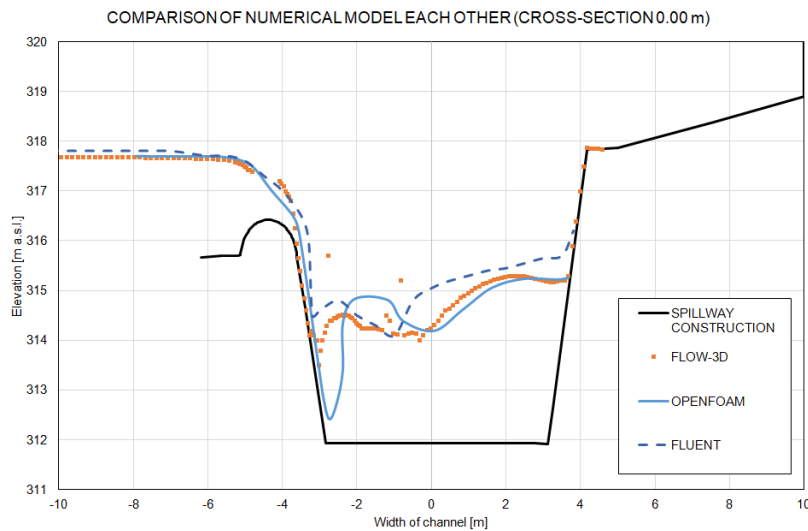


Fig. 15
Cross-section

8. SOFTWARE PRODUCTS COMPARISON

The times given in individual parts in the table below are given approximately. It is only for better understanding, what amount of time the work with software products take. The simulations were handled by single desktop computer (AMD FX 6300 Six-Core, RAM 8.00 GB, NVIDIA GeForce GT 630). That indicates the limited amount of mesh cells, larger amount of time etc. The table below shows the comments to each part of process.

	OpenFoam	Ansys Fluent	Flow-3D
I. Creating of spatial model	in external software (Blender)		
Time for this part	<i>10 hours</i>		
II. Modification and corrections	* it is necessary to do this step in Blender. It contains several tools for geometry repair	* more difficult models need to be edited even more hours	* very simple, program handle also very problematic schemes
III. Meshing	* simple mesh creation, possible refinement of edges, faces and volumes	* the creation of a global mesh is really simple if the spatial model is correctly repaired. Important spots must be described separately	* the possibility of importing, creating of proper interest by dividing into blocks
Time for this part	<i>2 hours</i>	<i>3 hours</i>	<i>1 hour</i>
	OpenFoam	Ansys Fluent	Flow-3D
IV. Settings	* an organized settings, if user knows the basics the solution is way easier and faster	* clear, step-by-step expansion for each step displays all major and minor parameters	* average, at the first sight is everything arranged, but some of the parameters can not be changed or traced without Help-function
V. Boundary conditions	* the selection depends on the tips in help or source files, for user easy manipulation	* there is a simple way how to input, however with simple input might be the simulation sometimes unstable	* with a larger number of blocks grows the amount of BC, but the conditions are not significantly different
Time for this part	<i>2 hours</i>	<i>1 hour</i>	<i>1,5 hour</i>
VI. Simulation	* the check of residues, continuously visualization of results and possibility to change main settings while the calculation is running	* the check of the process depends on residues, it is possible to obtain outputs for verification	* there is possibility continuously evaluate, modify and analyze obtained data
Time for this part	<i>50 hours</i>	<i>62 hours</i>	<i>75 hours</i>
VII. Postprocessing	* the final analysis in postprocessing is available in all dimensions, parameters and output formats. The very clear interpretation and tools help to understand obtained results		
Time for this part	<i>2 hours</i>	<i>4 hours</i>	<i>3 hours</i>

SUMMARY

The main result of numerical simulation is the movement of flowing water in side channel spillway. The level of water surface from all software products is pretty similar, even for the same STL format geometry data. But the STL input must be modified/changed for every solver. Thus, from the beginning are all three

processes completely different. They have all their pros and cons and it is delicate question which is better to use. Same desktop computer, similar settings, similar outputs. Today, the numerical modelling is a perfect way how to perform 3D simulation of water flow on water structures. Of course, the difference makes always the price of the software license. All tested software proven to be worth using for some reasons and some users.

ACKNOWLEDGMENTS

The paper was written thanks to the research project of the cluster CREA Hydro & Energy, z. s. named CREA Hydro & Energy VYZ CZ.01.1.02/0.0/0.0/15_008/0002001.

COMMISSION INTERNATIONALE DES GRANDS BARRAGES

VINGT-SIXIÈME CONGRÈS DES GRANDS BARRAGES
Autriche, juillet 2018

DOI 10.3217/978-3-85125-620-8-132



This work licensed under a Creative Commons Attribution 4.0 International License. <https://creativecommons.org/licenses/by-nc-nd/4.0/>

INVESTIGATION OF THE PROBABILITY OF FAILURE OF A GRAVITY DAM

Roger SCHLEGEL

DYNARDO GMBH

GERMANY

Markus GOLDGRUBER

DYNARDO AUSTRIA GMBH

AUSTRIA

Helmut FLEISCHER

FEDERAL WATERWAYS ENGINEERING AND RESEARCH INSTITUTE (BAW)

GERMANY

COMMISSION INTERNATIONALE
DES GRANDS BARRAGES

VINGT-SIXIÈME CONGRÈS DES
GRANDS BARRAGES
Autriche, juillet 2018

**INVESTIGATION OF THE PROBABILITY OF FAILURE OF A GRAVITY
DAM**

Roger SCHLEGEL

DYNARDO GMBH

GERMANY

Markus GOLDGRUBER

DYNARDO AUSTRIA GMBH

AUSTRIA

Helmut FLEISCHER

*FEDERAL WATERWAYS ENGINEERING AND RESEARCH INSTITUTE
(BAW)*

GERMANY

1. INTRODUCTION

Within the framework of an in-depth review of an old gravity dam in Germany [1], detailed safety assessments are carried out according to the latest state of standardization. Tremendous work has already been done on this topic and especially on this dam. Investigations and results regarding parameter variations and assessment criteria for 3D models of concrete dams have already been published in [11], with the focus on reducing the parameter space and finding

suitable criteria for the reliability analysis. Nevertheless, the following sections in this paper are mostly based on the aforementioned publication [11] for clarification purposes. The main goal of the investigation discussed in this paper is to reduce to amount of needed simulations for the reliability analysis to determine the exceedance probabilities and finding/evaluating suitable assessment criteria.

2. GENERAL INFORMATION

The investigations are based on a three-dimensional finite element model, which takes the loads and resistances into account as realistically as possible. The static and transient thermal analyses are carried out by using nonlinear material laws for the dam (masonry) and brittle rock subsoil, considering the seasonal instationary temperature fields and the load-dependent pore water pressures in the dam body. Additionally, the existing sealing and drainage elements as well as the nature of the rock subsoil are considered.

The investigation of the dam in [11] dealt with the following topics:

- Calibration and verification of the calculation model against measurement results,
- Stability assessment using the EC-compliant safety concept presented in [1] on the basis of partial safety factors,
- Basic studies on the behavior of the dam,
- reliability of the results and main impact factors,
- Stochastic investigations to assess the probability of failure

The gathered knowledge from these topics are the basis of the ongoing investigations.

All simulations are carried out using the finite element program ANSYS®, the elastoplastic material model library multiPlas [10] for ANSYS and the software for stochastic analysis ANSYS optiSLang® [9].

3. NONLINEAR FINITE ELEMENT MODEL

For the nonlinear simulations a 3D model of the dam and the foundation is created. The model has a width of 768 m, a length of 515 m and a height of 218 m. The FE model is shown in Fig. 1.

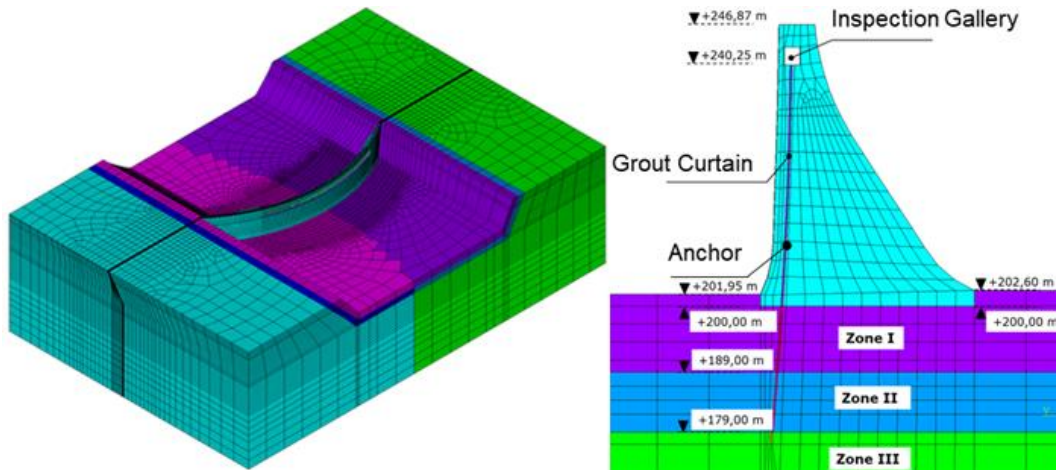


Fig. 1

3D FE-model of the dam and the dam section

The subsoil model is based on the data in [2], [3] and [5]. In total, three zones of different permeability in the vertical direction are considered (see Figure 2). Clay slate is found on the right slope according to [2]. On the left slope, greywacke with clay slate interlinings are found.

A grout curtain is installed and extends to a depth of +177.00 m a.s.l. in the region of the clay ridge and on both sides of the clay ridge to a depth of +191.00 m a.s.l.. 104 anchors stabilize the dam in the middle area. Each anchor contains 34 strands. The cross-sectional area of each strand is 150 mm². The anchor force is 4500 kN/anchor. 52 anchors reach into a depth of +167.0 m and 52 into +172.0 m. The grout length of the anchor for transmitting forces into the rock is 10 m each.

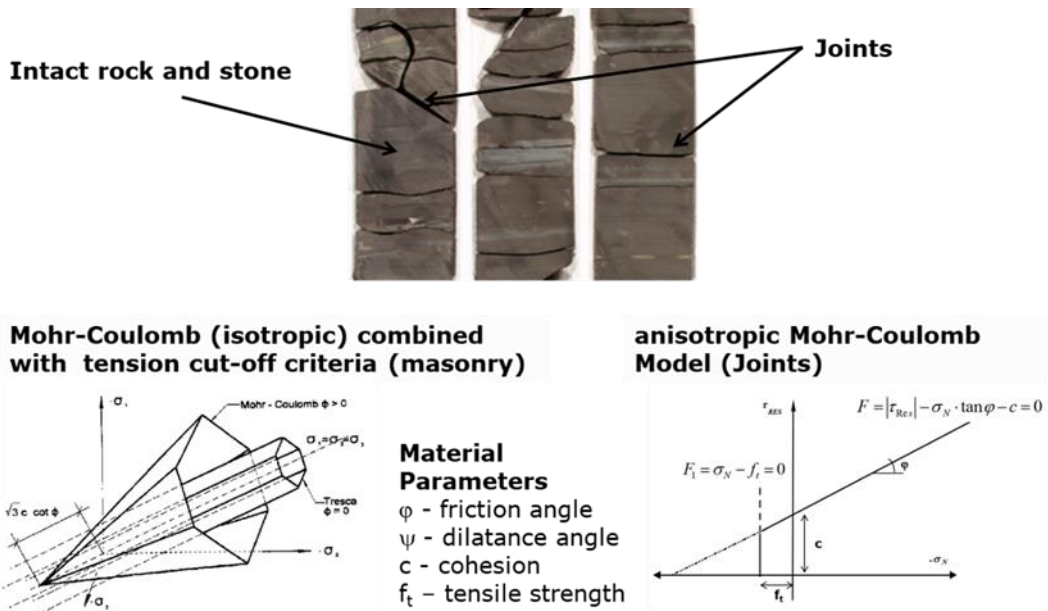


Fig. 2

Constitutive models used for the masonry dam, the intact rock and the joints

The nonlinear behavior of the masonry and the fissured rock subsoil is simulated using isotropic and anisotropic elastoplastic Mohr-Coulomb material models with tensile stress limitation. The position and orientation of the separating surface layers are also considered in the constitutive models. Virtual horizontal separation surfaces are taken in account to allow for stress free openings in vertical direction. Material parameters of the final calibration of the model can be found in Table 2. Fig. 2 illustrates the constitutive models used for the masonry dam, the intact rock and the joints. The final material properties from the calibrations are summarized in Table 2.

The boundary conditions are defined to prohibit the model to move in normal direction to the rock boundaries. The load history is taken into account in all load case combinations (LS) according to the composition in Table 1. The individual loads are multiplied by the corresponding partial safety factors from [1].

Table 1
Load steps of the nonlinear simulation

Loadstep	Action
LS1	Deadweight foundation (Initial Stress State)
LS2	Deadweight dam
LS3	Hydrostatic water pressure for defined water level
LS4	Hydrostatic water pressure at the level of anchor pre-stressing (241,605 m NN)
LS5	Anchor activation
LS6	Anchor pre-stressing
LS7	Hydrostatic water pressure for defined water level
LS8 f.	Additional varying loads according to Eurocode [1]

Non-stationary thermal finite element calculations are carried out for the determination of the temperature stresses in the dam. The external temperatures in the Hessen region are extracted from [7]. The water temperatures are taken into account in the thermal calculations as a function of time and water depth according to temperature data available at BAW (Federal Waterways Engineering and Research Institute). The 3D pore water pressure fields are calculated with a transient thermal analysis using a temperature-flow analogy.

4. MODEL CALIBRATION AND VERIFICATION

In order to increase the realistic proximity of the simulation model and thus to achieve a high quality of the stability tests, the simulation model is calibrated with deformation measurements of the dam. The measured deformation points are shown in Figure 3. Furthermore, pore water pressure and temperature measurements are to verify the hydraulic and thermal analyses.

Parameter identifications and sensitivity analyses are done to determine the dependencies between the model/material parameters and the response variables/measurements to be calibrated.

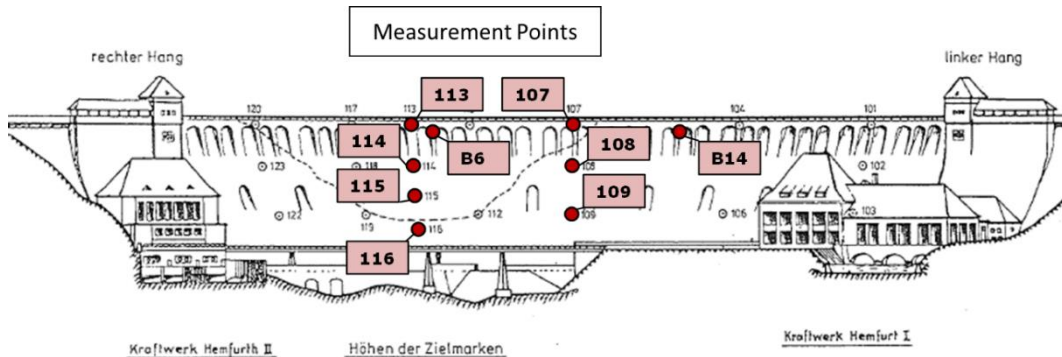


Fig. 3
Displacement measurement points used for calibration

The sensitivity analysis is carried out by means of variations-based correlation analysis in ANSYS optiSLang® [9]. All material parameters are varied as scattering inputs of the sensitivity analysis. The response variables are the radial relative displacements at the measurement points from Figure 3. 200 parameter combinations (designs) are calculated for the sensitivity analysis. Latin Hypercube sampling available in ANSYS optiSLang® [9] is used for sampling the 200 designs. In each design, a nonlinear load history calculation is simulated with the following load steps for calibration (LSC):

- LSC1 Activation of the dead weight in the foundation (Initial stress state)
- LSC2 Activation of the dead weight of the dam
- LSC3 Hydrostatic Water Pressure at 229,02 masl
- LSC4 Hydrostatic water pressure at minimum water level (220,00 masl)
- LSC5 Hydrostatic water pressure at maximum water level (244,95 masl)

The dam is simulated in the sensitivity analysis and model calibration without anchors and restoration measures, because the measured values of the deformation measurements originate from the time before the rehabilitation and the installation of the pre-stressed anchor.

The relevant input parameters (CoP values as a bar histogram) for the maximum water level (244.95 masl) and the minimum water level (220.00 masl) are calculated for each measuring point and the associated dependencies (anthill plots of the relevant input parameters vs. deformation). The CoP values are prognosis parameters and indicate how much the variance of the observed response variable (deformation at the measuring point) can be explained by the variation (or variation) of the respective input variable. Unimportant input parameters (whose scatterings are not correlated with the spread of the response variable) are automatically filtered out by ANSYS optiSLang® [9]. As the sensitivity analysis shows, the stiffnesses of the subsoil and of the masonry of the dam can

be calibrated in particular by means of the deformation measurement values for the observed / measured water levels. It is also plausible that the stiffness of the masonry has a greater influence on the higher measuring points, whereas the deformation on the MP 116 is almost exclusively determined by the foundation stiffness. Fig. 5 shows the calculated and measured deformations. The black line indicates the measured values, gray lines indicate the spread of all designs and red is the best design Nr.186, which is determined by optimization and shows a very good agreement with the measured deformation values. As a result of the model calibration, a simulation model is developed which can easily and reasonably reconstruct the available measurements with regard to the deformations, temperatures and pore water pressures.

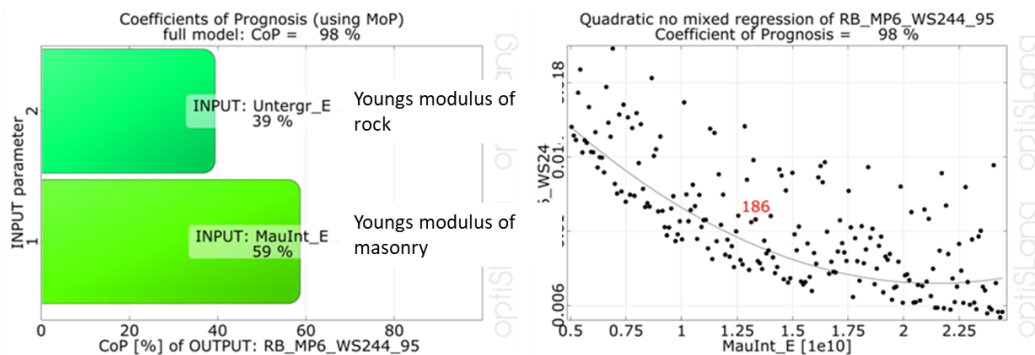


Fig. 4

Results of the sensitivity analysis for measurement point B6; left: Histogram of CoP; right: Anthill-Plot of the E-modulus of the dam (MauInt_E) vs. radial displacement at measurement point B6

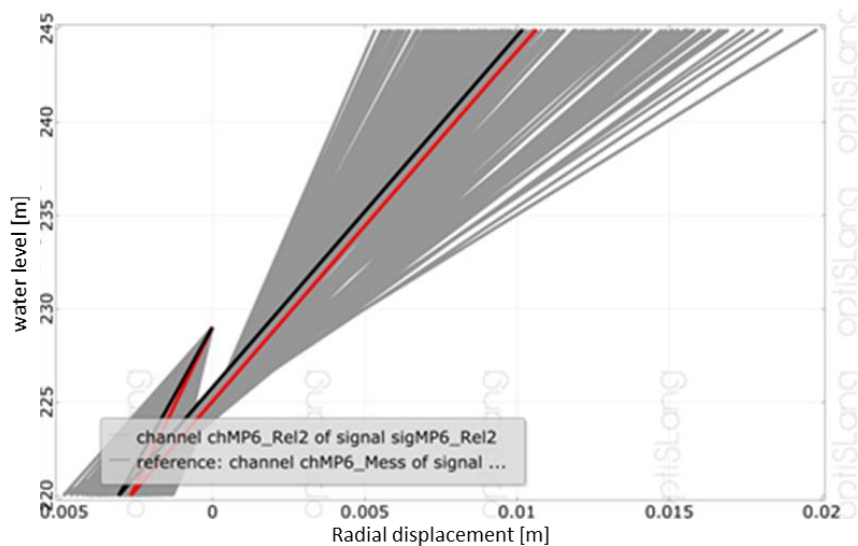


Fig. 5

Radial displacement of measurement point B6, Grey: Band width of all designs; Red: Best design Nr. 186; Black: Measurement

Table 2 summarizes the calibrated material and joint parameters for the dam and the foundation. Zones are depicted in Fig. 2.

Table 2
Calibrated material properties of the masonry and rock

	Dimension	Masonry	Intact Rock
Density	t/m ³	2.2	2.72
E-Modul	N/mm ²	11100	4697
Poisson ratio	-	0.25	0.257
Compressive strength	N/mm ²	5	20
Friction angle	°	45	45
Cohesion	N/mm ²	1.0355	4.14
Tensile strength	N/mm ²	0.5	2
Residual friction angle	°	31.5	31.5
Residual cohesion	N/mm ²	0.1036	0.4142
Residual tensile strength	N/mm ²	0	0
Reference temperature	°C	10	8

5. STOCHASTIC ANALYSIS

Based on the experiences gathered from the stability studies and stochastic analysis from [11] new assessment criteria and more elaborated reliability analyses are carried out using the calibrated FE model.

The motivation for the stochastic analysis results from several questions. For example, a stochastic analysis can be used to circumvent contradictions arising from the use of partial safety factors in nonlinear analyses, where questions arise from whether it should be determined by a load-side increase or by a reduction of the resistance. Both approaches aren't without doubt possible in connection with nonlinear analyzes.

By means of a stochastic analysis, failure probabilities can also be determined in the case of nonlinear analyses when introducing load and resistance-side scatterings. This procedure is included in Eurocode EN 1990:2002 (Annex B and C). In a recent and ongoing cooperation between the BAW (Federal Waterways Engineering and Research Institute) and Dynardo, the example of this dam is worked out, including further fundamental investigations, to develop a procedure for practical projects.

The stochastic analysis consists of the following steps.

- Definition of the scattering of the input parameters.
- Generating the samples in ANSYS optiSLang® [9], various methods (Monte Carlo, Latin Hypercube, Directional Sampling, FORM, ...) are available for this purpose.
- Definition of evaluation criteria, e.g. Displacements in the abutment, Displacement gradients in the abutment, tilt safety - position of the resultant, sliding safety - principal shear strain, pressure failure -

principal normal strain and risk of fracture in the grouting zone - max. plastic vertical strain, etc.

- Performing nonlinear analyses of all necessary designs defined by the sampling method.
- Evaluation and determination of the probability of failure

5.1. RESULTS OF THE STOCHASTIC ANALYSIS

In this investigation two reliability analyses by means of probabilities of failure are carried out. To determine the exceedance probabilities, an adaptive response surface method (ARSM) was used in combination with the First Order Reliability Method (FORM). For each reliability analysis, more than 600 designs were calculated in individual (here three) iteration steps. With each iteration step, new designs are created that are closer to the limit state. The approximation quality of the generated response surfaces is 99%.

The total displacement V (nodal mean value at the abutment) is used as the evaluation criteria. For the derivation of the limit values, limit load analyses were carried out (due to load increase and due to resistance reduction). Two threshold levels were derived for the rating criterion V , which are $V_1 = 0.05$ m (near system failure) and $V_2 = 0.03$ m (transition to non-linear system behavior)

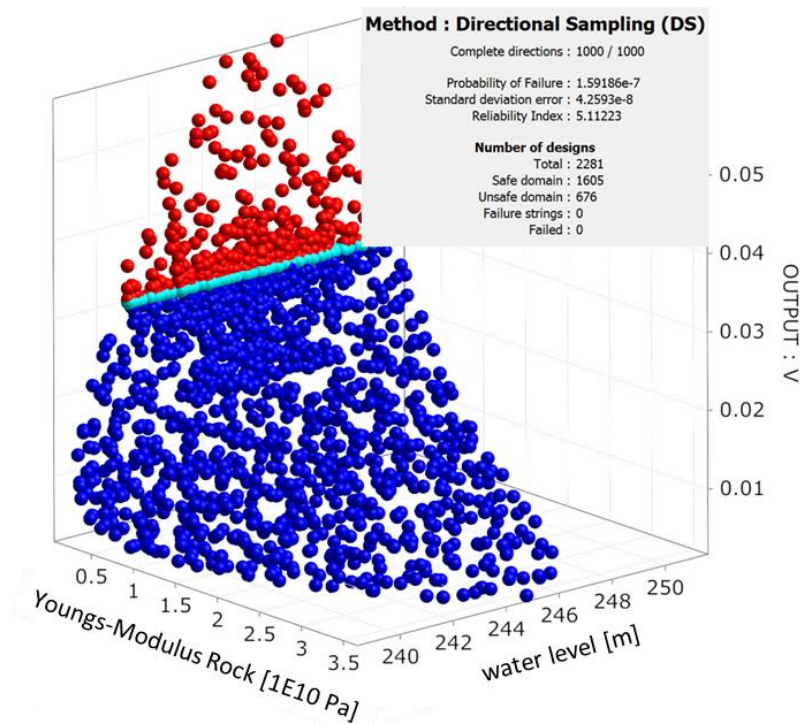


Fig. 7

Reliability analysis V_2 , All Design points in the space of the most important parameters; red dots: $V > 0.03$ m; blue dots: below the limit of 0.03 m

The exceedance probability of the reliability analysis for the limit value of $V_{_1} = 0.05$ m gives a $P_{f(V_{_1})} = 1.59 \cdot 10^{-13}$; which corresponds to a reliability index $\beta_{(V_{_1})} = 7.29$. The result of the reliability analysis for the limit value $V_{_2} = 0.03$ m is shown in Fig. 7. The determined exceedance probability is $P_{f(V_{_2})} = 1.59 \cdot 10^{-7}$; this corresponds to a reliability index $\beta_{(V_{_2})} = 5.11$

As a result of the analyses, it can be stated that both probabilities are below the value of $P_f = 10^{-5}$, corresponding to reliability indexes above $\beta = 4.27$ (Reference period of 100 years). Thus, by using probabilistic analyses and procedures described in the report, a sufficient stability of the Eder dam can be confirmed and the safety margins beyond are quantified.

In addition to the calculation of the probability of failure, the influencing parameters which are decisive for the distribution of the response variable can be output both qualitatively and quantitatively in ANSYS optiSLang® [9]. This allows statements to be made as to which stray input variables (loads, resistances) are relevant for the failure of the dam.

6. ACKNOWLEDGEMENTS

The financial and technical support by BAW (Federal Waterways Engineering and Research Institute) is gratefully acknowledged.

REFERENCES

- [1] FLEISCHER H., FRÖBISCH H.-J. 100 Jahre Edertalsperre – Untersuchungen zur Standsicherheit der Staumauer. *BAW Kolloquium Berechnungen und Analysen für bestehende Wasserbauwerke*, Karlsruhe, 2014.
- [2] HESSISCHES LANDESAMT FÜR BODENFORSCHUNG Ingenieur-geologisches Gutachten. *Hessisches Landesamt für Bodenforschung 345 - 310/85 Hz/Str*, 1985.
- [3] HESSISCHES LANDESAMT FÜR BODENFORSCHUNG Geologisches Ergänzungs-Gutachten. *Hessisches Landesamt für Bodenforschung 345 - 36/92 Hz/Bm*, 1992.
- [4] EDERTALSPERRE Festschrift, Herausgegeben aus Anlaß der Wiederherstellung der Staumauer, Wasser- und Schifffahrtsverwaltung des Bundes, Wasser- und Schifffahrtsdirektion, Mitte Hannover, 1994.
- [5] HOLTZ S. Die geologischen Verhältnisse [4]. 1994, Beitrag 3, S.24-25, Hannover.
- [6] WITTKÉ W. Standsicherheitsberechnungen der Ederstaumauer nach der FE-Methode [4]. 1994, Beitrag 5, S.29-35, Hannover.

- [7] TRY 2011 Aktualisierte und erweiterte Testreferenzjahre von Deutschland für mittlere, extreme und zukünftige Witterungsverhältnisse. 2011, Bundesamt für Bauwesen und Raumordnung (BBR) / Climate & Environment Consulting Potsdam GmbH / Deutscher Wetterdienst, Potsdam.
- [8] WITTKER W. Felsmechanik, Grundlagen für wirtschaftliches Bauen im Fels. 1984, Springer-Verlag, Berlin, Heidelberg, New York, Tokyo.
- [9] OPTISLANG MANUAL The optimizing Structural Language version 6.2.1. 2017, DYNARDO GmbH, Weimar, www.dynardo.de.
- [10] MULTIPLAS MANUAL Elastoplastic Material Models for ANSYS - General Multisurface Plasticity. 2017 DYNARDO GmbH, Weimar, www.dynardo.de.
- [11] SCHLEGEL R., GOLDGRUBER M., MROZEK M., FLEISCHER H. Investigation of the Reliability of Dams with Stochastic Finite Element Methods. *Proceedings of the 14th ICOLD International Benchmark Workshop on Numerical Analysis of Dams, 2018.*

SUMMARY

The analysis of failure probabilities is an important element of risk assessment in dam management. This investigation is illustrating probability of failure calculations of the Eder dam, an old gravity dam in Germany, by means of a parameterized and fully nonlinear 3D-finite element model of the dam and the foundation. The model is calibrated based on measurements (thermal, hydraulic and mechanical) with the software optiSLang®. Therefore, sensitivity analysis with stochastic latin hypercube sampling is performed using a total of 200 designs (parameter combinations) with varying material parameters of the dam and the foundation. For the stochastic analysis of the dam, distribution functions for all relevant effects and resistances, e.g. flood events, are defined. After all, the evaluation of the stochastic analysis is done again with optiSLang®, which is capable to directly yield the failure probability P_f for the specified assessment criteria. Additionally, input parameters influencing the failure probability the most can be indicated quantitatively and qualitatively. Two reliability analyses by means of probabilities of failure are carried out. To determine the exceedance probabilities, an adaptive response surface method (ARSM) was used in combination with the First Order Reliability Method (FORM) with several hundred simulations each. As a result of the analyses, it can be stated that both failure probabilities are below the value of $P_f = 10^{-5}$, corresponding to reliability indexes above $\beta = 4.27$ (Reference period of 100 years). Thus, by using probabilistic analyses and procedures described in the report, a sufficient stability of the Eder dam can be confirmed and the safety margins beyond are quantified.

Keywords: Finite Element Method, Gravity Dam, Safety of Dams, Stochastic Method

COMMISSION INTERNATIONALE
DES GRANDS BARRAGES

VINGT-SIXIÈME CONGRÈS DES
GRANDS BARRAGES
Autriche, juillet 2018

CHALLENGES OF DAMS CONSTRUCTION AND MANAGEMENT IN INDONESIA

Tri HARTANTO

*Geologist of Dam Safety Units, MINISTRY OF PUBLIC WORKS AND HOUSING
REPUBLIC OF INDONESIA*

INDONESIA

Indonesian Archipelago, which is situated in tropical zone, doesn't benefit much its climatic condition from the hydrological point of view. With existence of dry season and rainy season, the rainfall depth is only concentrated in certain months of the year (mostly on November, December, January and February), thereby varying from region to region and from island to island. Such as situation has caused people to look for means of storing up as much as possible water for future use in the dry season when rain is scarce or if it's of not non-existent. One answer to this problem is the construction of dams capable of storing up water in large quantities.

Ministry of Public Works and Housing, who responsible for infrastructure, will construct 65 dams across the region, From 2013 until 2019. It will provide totally 6.5 billion m³ reservoir and irrigated 460,382 Ha and in 2022, it expected that all of 65 dams, will be finished. From 65 dams, 49 are new dams, the other 16 dams still on going. All of them are were owned by the government with 6.5 billion m³ reservoir capacity, not included of those from all other dam stakeholders. So for next 5 years later, Indonesia will have over 270 large dams accros the nation.

This paper will attempt to present some issues and solution regarding to challenges of dams construction and management in Indonesia.

Keywords : land acquitition, human resources, Indonesia

CONCLUSION

As a tropical country and largest archipelago which has abundant water potential, Indonesia plan to build more dam in the future. Building a dam, is the same as we build a dangerous structures. Therefore, Indonesia needs a lot of competent dam engineers to escort this plan to be done. Unfortunately, increasing the number of dams in Indonesia is unbalance with the availability of competent human resources in dam engineering.

Nevertheless, the government realized, they need some breakthrough to solve this issues. Some breakthrough among them is to conduct training and continuously based on the need.

In terms of non-technical issues, land acquisition, handling social impact and budget provision for dam construction must be solve immediately. All those factors should be organized very well, government as a leader, cooperate with other stakeholder and communities with more normative and human approach.

REFERENCES

- [1] BAHAR, UJANG. *Problem of payment of indemnity land procurement for implementation development for general interests*. 38th Law and Development Journal. 2008
- [2] *Dam Operator Training : Analysis of current trend and future outlook*, Department Energy and Water Supply, State of Queensland. 2017
- [3] FIRMAN, A AND RESDIATMOKO, L. A., *Case study on knowledge transfer to the next generation in Indonesia*. *ICOLD International Symposium on Dams For A Changing World*, Kyoto, Japan. 2012.
- [4] HARTANTO, T. AND WAHYUDI, A. P., *Dams engineer in Indonesia*. *Hydropower and Dams Symposium*. Seville. 2017.
- [5] *Material for Strategic Plan on Dams Construction*. Directorate General of Water Resources, Ministry of Public Works and Housing, Center of Dams. Not published. 2017
- [6] MAYANGSARI, A AND BAYU ADJI, T., *Implementation of Dam Safety in Indonesia*. *ICOLD Symposium*. Stavanger. Norway. 2015.
- [7] RIZAL, M AND YUSUF, A., *Challenges of constructing 65 dams for supporting food security, water and energy*. *HATHI Symposium*. Jayapura. 2017.
- [8] SOERJONO, *Dam Engineering in Indonesia*, *Symposium on Problems and Practice of Dam Engineering*. Bangkok. 1980.
- [9] *Strategic Plan of Ministry of Public Works and Housing 2015-2019*, Regional Infrastructure Development Agency, Jakarta. 2015

COMMISSION INTERNATIONALE DES GRANDS BARRAGES

VINGT-SIXIÈME CONGRÈS DES GRANDS BARRAGES
Autriche, juillet 2018

DOI 10.3217/978-3-85125-620-8-134



This work licensed under a Creative Commons Attribution 4.0 International License. <https://creativecommons.org/licenses/by-nc-nd/4.0/>

SEISMIC STABILITY ANALYSIS OF CONCRETE GRAVITY DAMS

Bakenaz. A. ZEIDAN

FACULTY OF ENGINEERING, TANTA UNIVERSITY

EGYPT

Ayman SELEEMAH

FACULTY OF ENGINEERING, TANTA UNIVERSITY

EGYPT

Seismic Stability Analysis of Concrete Gravity Dams

Bakenaz. A. Zeidan, Ayman Seleemah

Faculty of Engineering, Tanta University, Egypt

Email: b.zeidan@f-eng.tanta.edu.eg

Abstract:

The Analysis of dam-reservoir-foundation coupled system is a complicated problem due to mutual interaction between reservoir water, rock foundation and concrete dam. In order to design earthquake resistant dams, it is essential to have accurate and reliable analysis procedures to predict the dam response. In this paper, KOYNA concrete gravity dam subjected to four different normalized ground motion excitations was investigated as a typical case study. A 2-D Finite Element model of the dam was constructed using ANSYS computer code to simulate dam-reservoir-foundation coupled system. The reservoir water domain is represented as incompressible and inviscous fluid continuum having infinite length in the upstream direction. The foundation rock is represented as a viscoelastic half space considering both its mass and flexibility. Both the mass concrete and foundation rock are assumed to have homogenous, isotropic, linearly elastic properties. Seismic dam responses are expressed in terms of dam deformations, dam stresses, spectral displacements and accelerations, hydrodynamic pressure, natural frequency and response time history. Obtained results confirm that El-Centro earthquake caused the minimum displacement and stresses while Aqaba-EW earthquake resulted in maximum displacements and stresses. Spectral results confirm the significant effect of dam natural period on its seismic behavior.

Keywords: *Concrete Gravity Dams, FEM, Seismic Analysis, Dam-Reservoir-Foundation Interaction, Ground motion excitation, Spectral analysis, deformations, Stresses, ANSYS.*

Introduction

Concrete dams are very important structures, regarding to requirements for continuous service during their life time, and catastrophic effects in cases of dam failure. Therefore, the safety of these structures should be investigated quite critically by logical and precise methods. The fluid-structure-foundation interaction is one of the main factors that affect dam behavior during earthquake excitations. The analysis of dam-reservoir-foundation coupled system is much more complicated than that of the structure alone. For a dam-reservoir-foundation system, the earthquake response is significantly influenced by the interaction of the dam with the impounded water and with the underlying foundation region, thus increasing the requirements for the analysis procedure to be used, and complicating what would otherwise have been considered a routine finite element analysis of a concrete cross-section.

State of Art

The seismic behavior of concrete gravity dams under strong ground motion was investigated by numerous researchers. Chopra (1967) conducted a study on the determination of the effects of foundation-structure interaction on the seismic response. Das Gupta and Chopra (1977) presented a procedure to produce a complex valued, frequency dependent stiffness matrix for the surface of a dam base which is supporting the structure. Chopra and Chakrabarti (1981) introduced a general procedure for analysis of the response of concrete gravity dams including the dynamic effects of

impounded water and flexible foundation rock, to the transverse (horizontal) and vertical components of earthquake ground motion. Fenves and Chopra (1984) developed a semi analytical-numerical procedure to analyze the earthquake response of concrete gravity dams. Effect of reservoir-foundation interaction was the subject of a study conducted by Dominguez et al (1990). A boundary integral technique was proposed for the investigation of the response of dam-reservoir-sediment-foundation systems subjected to ground acceleration. Bougacha et al. (1993) introduced a technique based on the Finite Element Method for the analysis of wave generation in a layered, fluid filled poro-elastic media to consider the sediments. Bhattacharjee and Leger (1994) conducted a study on the two dimensional static fracture behavior of dams. Smearred crack models were developed from a nonlinear fracture mechanics point of view that can simulate the tensile and shear softening of the plain concrete. The static fracture behavior of a dam subjected to an incremental increase of the reservoir water level was also investigated by Bhattacharjee et al. (1995). A rotating smearred crack model was considered in the nonlinear finite element analyses. The uplift pressure occurring inside the smearred crack bands was taken into account by effective porosity concept. Ghanaat (2004) introduced an assessment approach that utilized linear time history analyses. The potential failure mechanisms of concrete gravity, buttress and arch dams were discussed and taken into consideration at the performance evaluation approach. Javanmardi et al. (2005) developed a theoretical method to determine the water pressure variations along a tensile crack during dynamic response. The results of the proposed model were compared with experimental test results. Arabshahi and Lotfi (2008) conducted a study on the natural vibration mechanisms due to damage at the dam foundation interface. Zeidan (2013) used ANSYS code to investigate the interaction of reservoir water-dam structure. Yucel (2013) evaluated the hydrodynamic pressures, dam-reservoir-foundation rock interactions and reservoir bottom absorption. Zeidan (2014) analyzed the problem of dam-reservoir-foundation seismic response on concrete gravity dams numerically using ANSYS code. Her results showed that simulation of foundation in dam-reservoir interaction problems significantly affects the seismic response of concrete gravity dams especially in case of mass rock foundation.

Although the dam-reservoir-foundation interaction has been highlighted via many authors, the dam-reservoir-foundation coupled system is a very complicated phenomena and further studies on foundation simulation on seismic response of concrete gravity dams including foundation-structure interaction is required. The objective of the present study is to assess the impact of key parameters which affect the static and dynamic behavior of concrete gravity dams. A 2-D Finite Element model is employed using ANSYS program. KOYNA dam subjected to the S00E component of EL-Centro earthquake is investigated as a typical case of study. The dam is represented as a finite element system, the fluid domain, as a continuum of infinite length in the upstream direction and the foundation rock region as a viscoelastic half-plane. Static, modal and time history analyses are considered in the dynamic simulation. In the static and dynamic analyses, the foundation is simulated considering foundation flexibility. The dam concrete, foundation rock and reservoir water are assumed to have homogeneous, isotropic, linear and elastic properties. Reservoir water is assumed to be incompressible and inviscous fluid. The dam-reservoir-foundation coupled system is idealized as shown in Figure 1.

Governing Equations and Boundary Conditions

Governing equation of wave propagation through fluid is represented in both the Eulerian and Lagrangian methods. The governing fluid-structure system equation is solved using wave propagation through the fluid by assuming linear compressibility and inviscosity. The wave propagation equation through acoustic fluid is as follows (Chopra and Chakrabarti 1981):

$$\nabla p^2 = \frac{1}{c_2} \frac{\partial^2 p}{\partial t^2} = \frac{\rho}{k} \frac{\partial^2 p}{\partial t^2} \dots\dots\dots (1)$$

$$\text{Where } c = (k/\rho)^{1/2} \dots\dots\dots (2)$$

In which p is the pressure function, c is the acoustic wave speed, ρ is the fluid density and k is the fluid compressibility. If the fluid would be incompressible, equation (1) would take the following form:

$$\nabla p^2 = 0 \dots\dots\dots (3)$$

Reservoir upstream boundary (Γ_R)

With the vibration of the dam, volumetric hydrodynamic pressure waves are created in the reservoir and propagate toward the upstream, if the length of the reservoir is assumed to be infinity, then these waves would approach to vanish. It should be noted that the length of reservoir is assumed as a finite length, L, in numerical modeling. Hence, an artificial boundary is applied to simulate effect of infinite reservoir. This boundary is modeled based on the Sommerfeld boundary as

$$\frac{\partial p}{\partial n}(x, y, z) = -\frac{1}{c} \left(\frac{\partial p}{\partial t} \right) (x, y, z) \dots\dots\dots (4)$$

Reservoir bottom (Γ_B)

According to the rigidity of the reservoir bottom, by assuming the horizontal movement of the earth, the pressure gradient is neglected.

$$\frac{\partial p}{\partial n}(x, y, z) = 0 \dots\dots\dots (5)$$

Reservoir free surface (Γ_F)

By neglecting the effects of surface waves, the governing boundary condition is as follow:

$$p(x, y, z) = 0 \dots\dots\dots (6)$$

Fluid-structure interface (Γ_I)

In the common boundary between the reservoir and the dam body, an interaction between these two occurs which the result of inertia force is caused by the movement of the dam body. Hence, the applied pressure on the reservoir face caused by the inertial force is as follow;

$$\frac{\partial p}{\partial n}(x, y, z) = -\rho \cdot \ddot{u}_n(x, y, z) \dots\dots\dots (7)$$

In which ρ is the density of fluid and \ddot{u}_n is the structure's acceleration vector in the direction normal to the common boundary of the fluid and structure.

Foundation region boundary conditions

The nodes on edges A and B at the end of the foundation region are assumed to be constrained in the vertical direction, while it is free in the horizontal direction. The nodes at the horizontal line at the base (edge C) of the foundation region are assumed to be constrained in both vertical and horizontal directions. The nodes at the interface between the dam body and foundation are coupled

in the vertical and horizontal directions. The same coupling is applied at the interface between the reservoir and foundation (Refer to Figure 1).

Coupled Dam-Reservoir-Foundation System FEM Modeling

In the present study, the standard finite element technique is adopted utilizing Galerkin’s method in which the structure displacement vector is discretized as (Zienkiewicz 1991).

$$u = N_u \bar{u} \dots\dots\dots (8)$$

And the fluid is similarly discretized as

$$p = N_p \bar{p} \dots\dots\dots (9)$$

Where u and p are the nodal parameters of each field and N_u and N_p are appropriate shape functions. The standard finite element technique is adopted utilizing Galerkin’s method in which the discrete equation of the concrete dam and the rock foundation dynamic responses reads.

$$M\ddot{u} + C\dot{u} + K\bar{u} - Q\bar{p} + f = 0 \dots\dots\dots (10)$$

$$\int_{\Gamma_1} N_u^T n p d\Gamma = \left(\int_{\Gamma_1} N_u^T n N_p d\Gamma \right) \bar{P} = Q \bar{P} \dots\dots\dots (11)$$

In which [M], [C] and [K] are mass, damping and stiffness matrices of the structure respectively. \bar{u} , \dot{u} and \ddot{u} are displacement, velocity and acceleration vectors respectively. In the above n is the direction vector of the normal to the interface. Standard Galerkin’s discretization applied to the fluid equation and its boundary equations leads to:

$$S\ddot{u} + C\dot{p} + H\bar{p} - Q^T\ddot{p} + q = 0 \dots\dots\dots (12)$$

in which [S], [C], [H] and **q** are pseudo fluid mass matrix, pseudo fluid damping matrix, pseudo fluid stiffness matrix and prescribed flux vector respectively, Q is a transformation matrix which transforms the acceleration of structure to fluid pressure and also transforms the hydrodynamic pressure into applied loads on the structure to simulate fluid structure interaction.

$$S = - \int_{\Omega} N_p^T \frac{1}{c^2} N_p d\Omega + \int_{\Gamma_3} N_p^T \frac{1}{g} N_p d\Omega \dots\dots\dots (13)$$

$$C = \int_{\Gamma_4} N_p^T \frac{1}{c^2} N_p d\Omega \dots\dots\dots (14)$$

$$H = \int_{\Omega} \nabla N^T \nabla N d\Omega \dots\dots\dots (15)$$

The coupled equation of the dam – reservoir - foundation system subjected to earthquake ground motion can be presented as follows (Zeidan 2014):

$$\begin{bmatrix} M & 0 \\ Q^T & S \end{bmatrix} \begin{Bmatrix} \ddot{u} \\ \ddot{p} \end{Bmatrix} + \begin{bmatrix} C & 0 \\ 0 & \tilde{C} \end{bmatrix} \begin{Bmatrix} \dot{u} \\ \dot{p} \end{Bmatrix} + \begin{bmatrix} K & -Q \\ 0 & H \end{bmatrix} \begin{Bmatrix} u \\ p \end{Bmatrix} = \begin{bmatrix} M.I.\ddot{u}_g(t) \\ -\rho Q^T.I.\ddot{u}_g(t) \end{bmatrix} \dots\dots (16)$$

Case of Study KOYNA Dam

The KOYNA Dam, situated in the Maharashtra State, India, is part of the KOYNA Hydroelectric Project, which aims to supply water to western Maharashtra as well as hydropower to

the neighboring areas. It is located on the *KOYNA* River, approximately 120 miles SSE of Bombay. The existing *KOYNA* Dam, completed in 1963, is a rubble concrete gravity dam of 853 length and 103 m height. The reservoir has a capacity of 2780×10^6 m³. Figure 2 shows a schematic model for *KOYNA* dam (Huang 2011), along with its reservoir and foundation.

Results of Seismic Analysis (Case of Full Reservoir)

The effect of foundation stiffness on dam horizontal displacements, vertical displacements and normal stress for case of full reservoir is presented in Figure 3. Obtained results show that dam displacements and stresses are very sensitive to variation in foundation stiffness up to E_F/E_C ratio equals 2.0. For ratios of E_F/E_C greater than 2.0, no significant effect on dam displacements and stresses is noticed. Figure 4 shows hydrodynamic pressure distribution on dam upstream face at various times during El-Centro earthquake. The figure shows that the hydrodynamic pressure distribution is almost linear at the top 25% of reservoir depth. For the lower 75% of reservoir depth it shows nonlinear trend. Moreover, the shape of the nonlinear part of the hydrodynamic pressure distribution at different times has no specific trend. Furthermore, the maximum observed hydrodynamic pressure occurs at $T=0.02$ sec. If it is approximated as linear trend it might be about 6% to 9% of the hydrostatic pressure. From the design point of view, the observed hydrodynamic pressure can be accounted for by increasing the hydrostatic pressure by say 15-25% over the entire height of the dam.

Figures 5 and 6 show time history for dam displacement, stresses and hydrodynamic pressure for ratios of E_F/E_C equal 0.5, 1.5, 5 and fixed base case. Obtained results indicates that the maximum horizontal dam crest displacement decreases as the foundation stiffness increases. The time history for horizontal displacement at different heights on upstream face show that all points move in phase indicating essentially that the first mode dominates the response. Figure shows that in case of full reservoir there are tensile stresses at the heel. This already occurred in 1967 when *KOYNA* dam subjected to *KOYNA* earthquake and a damage was observed in the actual dam due to tensile stresses at *KOYNA* dam heel. This tensile stresses led to a cracks between the dam body at heel and the rock foundation (Hunjie, 2011). **Fehler! Verweisquelle konnte nicht gefunden werden.** shows that the normal stresses at the toe are compression stresses at all times and that the behavior is not affected by foundation stiffness variation. But the compression stresses increase as the foundation stiffness increases. Moreover, the foundation stiffness has no significant effect on hydrodynamic pressure at reservoir base. The time history of displacements and stresses show that when the foundation stiffness is five times that of the dam concrete, the assumption of fixed base is acceptable.

Effect of Ground Motion Excitation

To study the effect of different ground motion excitations on the seismic behavior of dam-reservoir-foundation coupled system, four earthquakes are utilized. These are EL-Centro-S00E components, Taft-N21E component, Aqaba-NS component and Aqaba-EW component. While EL-Centro and Taft earthquakes represent severe and moderate earthquakes, respectively, Aqaba earthquake occurred in the Gulf of Aqaba, Egypt, and represent a minor to moderate earthquake. To have a common base for comparison of the dam behavior under different earthquakes, all ground motions were normalized to have the same peak acceleration of EL-Centro. Table 1. Shows values of peak accelerations and the factor of normalization for each earthquake. Table 2. Shows the effect of four earthquakes; on *KOYNA* dam displacements and stresses. Obtained results show that EL-Centro earthquake-S00E component caused the minimum displacements and stresses, while Aqaba-EW earthquake resulted in maximum displacements and stresses. Figure 7. Shows spectral

displacements and accelerations for the four earthquakes. It is clear that dam natural period has significant effect on dam seismic behavior. Natural period for *KOYNA* dam for first mode of vibration equals 0.38 sec. It is noticed that Aqaba-EW earthquake has the maximum and EL-Centro has the minimum spectral displacement and acceleration.

Conclusions

Based on the results presented in this study, the following conclusions can be drawn:

1. Foundation stiffness affects modal properties and an increase from $E_F/E_C = 0.50$ to 5 leads to significant decrease in natural period. For EL-Centro earthquake-S00E component, when E_F/E_C ratio changed from 0.50 to 5.0 a significant difference in displacement and acceleration occurred. This difference explain the effect of foundation stiffness on seismic behavior of the dam.
2. For static and seismic analysis, foundation stiffness has a pronounced effect on dam displacements and normal stresses up to $E_F/E_C = 2.0$. Up to this value foundation stiffness shouldn't be ignored in dam simulation and analysis especially if foundation stiffness less than two times dam concrete stiffness. When E_F/E_C equals 5.00, it is recommend to assume fixed base to simplify the problem.
3. Ground motion variation affects dam seismic response, although the different ground motions have the same peak acceleration. This difference is dependent on the frequency content of earthquake and the dynamic characteristics of the dam.

References

1. Akkose, M. and E. Simsek (2010) "Non-linear seismic response of concrete gravity dams to near-fault ground motions including dam-water-sediment-foundation interaction." *Applied Mathematical Modeling* 34(11): 3685-3700.
2. Arabshahi, H. and V. Lotfi (2008). "Earthquake response of concrete gravity dams including dam-foundation interface nonlinearities." *Engineering Structures* 30(11): 3065-3073.
3. Bhattacharjee, S. S. and P. Leger (1994). "Application of NLFM models to predict cracking in concrete gravity dams." *Journal of Structural Engineering* 120(4): 1255-1271.
4. Bhattacharjee, S. S. and P. Leger (1995). "Fracture response of gravity dams due to rise of reservoir elevation." *Journal of Structural Engineering* 121(9): 1298-1305.
5. Binnie, A. (1973). "The theory of flexible dams inflated by water pressure." *Journal of Hydraulic Research* 11(1): 61-68.
6. Bougacha, S., J. M. Roesset and L. Tassoulas (1993). "Dynamic stiffness of foundations on fluid-filled poroelastic stratum." *Journal of engineering mechanics* 119(8): 1649-1662.
7. Bougacha, S., J. L. Tassoulas and J. M. Roesset. (1993). "Analysis of foundations on fluid-filled poroelastic stratum." *Journal of engineering mechanics* 119(8): 1632-1648.
8. Chopra, A. K. (1967). "Hydrodynamic pressures on dams during earthquakes." *Journal of the Engineering Mechanics Division* 93(6): 205-224.
9. Chopra, A. K. and P. Chakrabarti (1981). "Earthquake analysis of concrete gravity dams including dam-water-foundation rock interaction" *Earthquake engineering & structural dynamics* 9(4): 363-383.
10. Dasgupta, G. and A. K. Chopra (1977). Dynamic stiffness matrices for homogeneous viscoelastic halfplanes.
11. Domanguez, J., R. Gallego and Bernardo. R (1997). "Effects of porous sediments on seismic response of concrete gravity dams." *Journal of engineering mechanics* 123(4): 302-311.
12. Fenves, G. and A. K. Chopra (1984). EAGD-84: A computer program for earthquake analysis of concrete gravity dams, Report No. UCB/EERC-84/11, Earthquake Engineering Research Center, University of California, Berkeley, 78 pp.
13. Fenves, G. and A. K. Chopra (1984). Earthquake analysis and response of concrete gravity dams, Report No. UCB/EERC-84/10 , Earthquake Engineering Research Center, University of California, Berkeley, 213 pp.
14. Ghanaat, Y. (2004). Failure modes approach to safety evaluation of dams. Proceedings of the 13th World Conference on earthquake engineering.

15. Huang, J. (2011). Seismic Response Evaluation of Concrete Gravity Dams Subjected to Spatially Varying Earthquake Ground Motions, Doctor of Philosophy thesis, Drexel University.
16. Javanmardi, F., P. Leger, and Tinawi. R (2005). "Seismic structural stability of concrete gravity dams considering transient uplift pressures in cracks." *Engineering Structures* 27(4): 616-628.
17. Khosravi, S. and M. Heydari (2013). "Modeling of Concrete Gravity Dam Including Dam-Water-Foundation Rock Interaction." *World Applied Sciences Journal* 22(4): 538-546.
18. Lotfi, V., J. M. Roesset and L. Tassoulas (1987). "A technique for the analysis of the response of dams to earthquakes." *Earthquake engineering & structural dynamics* 15(4): 463-489.
19. Naudi, J. A., E. E. Matheu, Peoppleman. R and Matusевич. A (2005). Foundation flexibility effects on the seismic response of concrete gravity dams. 37th Joint Meeting UJNR Panel on Wind and Seismic Effects, Tsukuba, Japan, May.
20. Novak, P., A. Moffat, Nalluri. C and Narayanan. R (2007). *Hydraulic structures*, CRC Press, Fourth edition.
21. Paul M. Santi, Jason E. Holschen and Richard W. Stephenson "Improving Elastic Modulus Measurements for Rock Based on Geology" *Environmental and Engineering Geosciences*, Vol. No 4 November 2000, pp. 333-346
22. Proulx, J. and P. Paultre (1997). "Experimental and numerical investigation of dam-reservoir-foundation interaction for a large gravity dam." *Canadian Journal of Civil Engineering* 24(1): 90-105.
23. Shariatmadar, H. and Mirhaj, A. (2009). "Modal Response of Dam-Reservoir-Foundation Interaction." 8th International Congress on Civil Engineering, May 11-13, 2009, Shiraz University, Shiraz, Iran.
24. Sun, K. M. and M. R. Bagale (2012). "The study of seismic response and crack dynamic extension rule of the concrete dam under the fluid-solid coupling action." *Mathematical Theory and Modeling* 2(5): 14-26.
25. Westergaard, H. M. (1933). "Water pressures on dams during earthquakes." *Trans. ASCE* 98: 418-432.
26. Yucel, A. R. (2013). "Seismic Analysis of Concrete Gravity Dams Including Dam-Foundation-Reservoir Interaction", Doctor of Philosophy thesis. Middle East Technical University,
27. Zeidan, B. A. (2013). Hydrodynamic Analysis of Concrete Gravity Dams Subjected to Ground Motion. 9th Symposium of ICOLD European club IECS2013, 10-12 April, Italy.
28. Zeidan, B. A. (2013). Seismic Dam-Reservoir Interaction of Concrete Gravity Dams. 9th Symposium of ICOLD European club IECS2013, 10-12 April, Italy.
29. Zeidan, B. A. (2014). Finite Element Modeling for Acoustic Reservoir-Dam-Foundation Coupled System. International Symposium on Dams In A Global Environmental Challenges, ICOLD 2014, Bali, Indonesia, 1-6 June, 2014.
30. Zeidan, B. A. (2014). Seismic Analysis of Dam-Reservoir-Foundation Interaction for Concrete Gravity Dams. International Symposium on Dams In A Global Environmental Challenges, ICOLD 2014, Bali, Indonesia, 1-6 June, 2014.
31. Zeidan, B. A. (2015). Seismic Finite Element Analysis of Dam-Reservoir-Foundation Interaction. International Conference on Advances in Structural and Geotechnical Engineering. Hurghada, Egypt, 6-9 April, 2015
32. Zienkiewicz, O.C. And Taylor, R.L. (1991). *The Finite Element Method; Volume II*. Fourth Edition First Published In 1967 By McGraw-HillPp.407- 419.

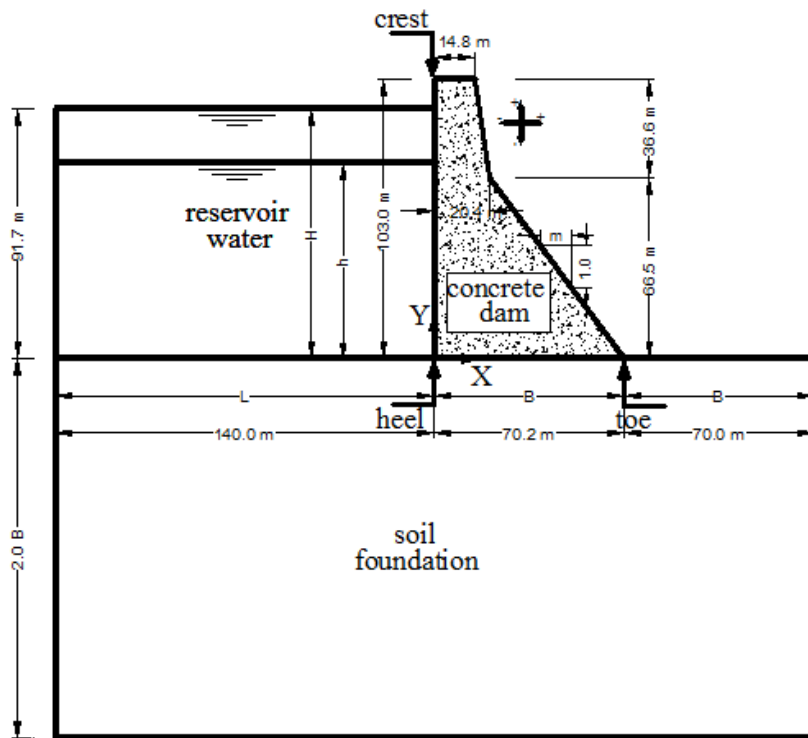


Figure 1. Schematic model for the dam, reservoir and foundation

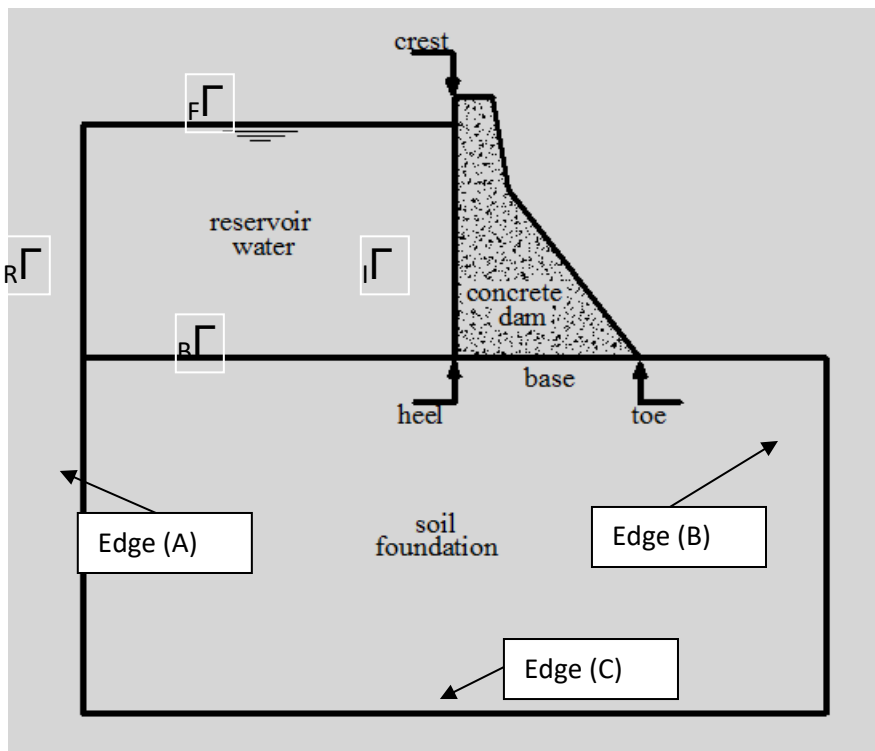
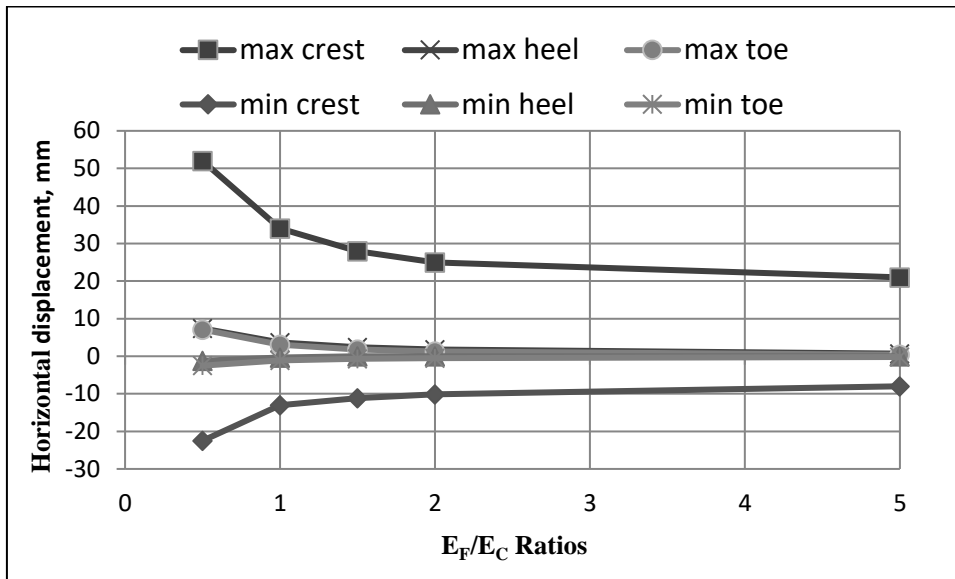
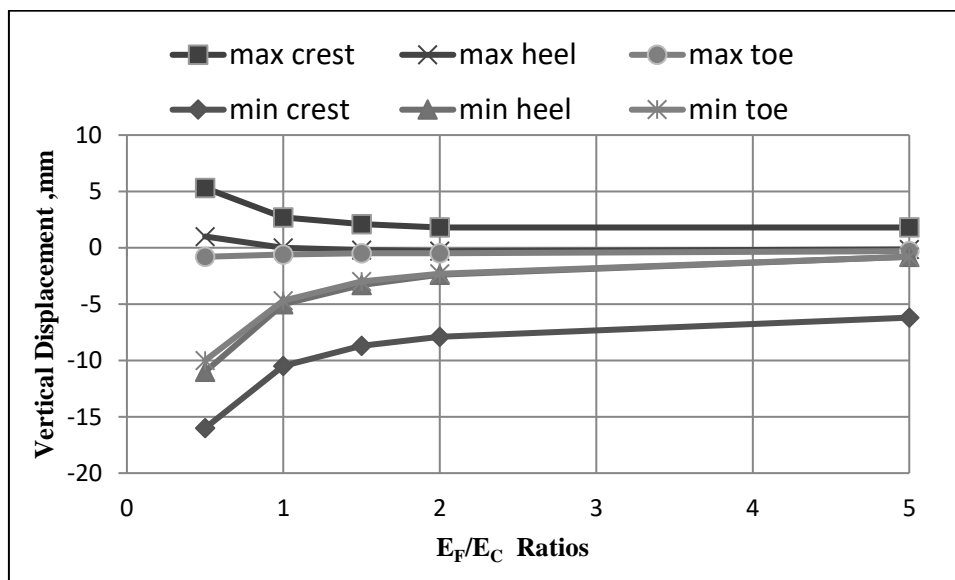


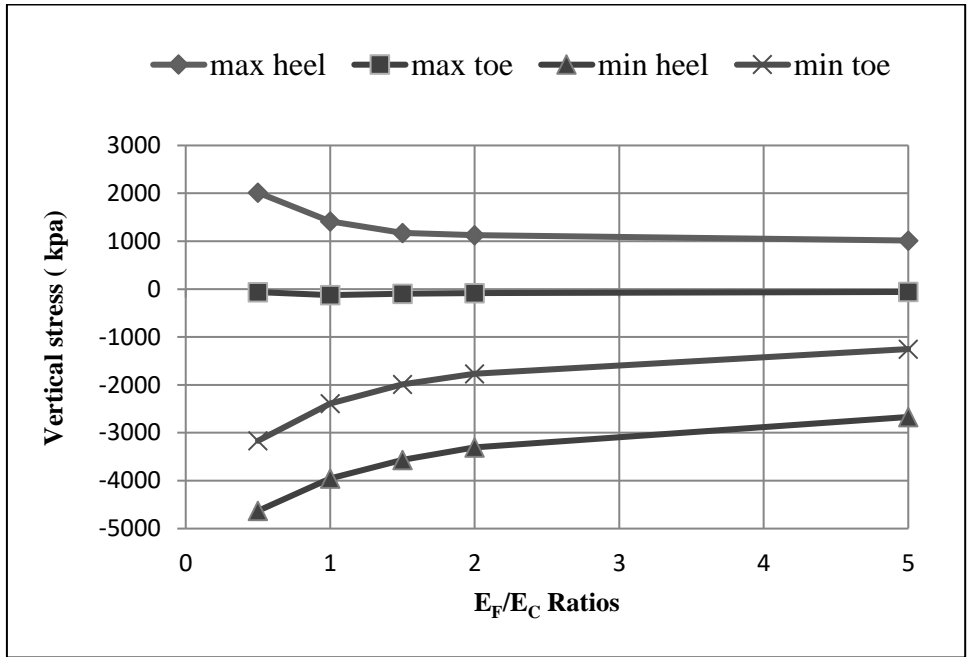
Figure 2. Boundary Conditions of Dam-Reservoir-Foundation System



(a) Horizontal Da displacements

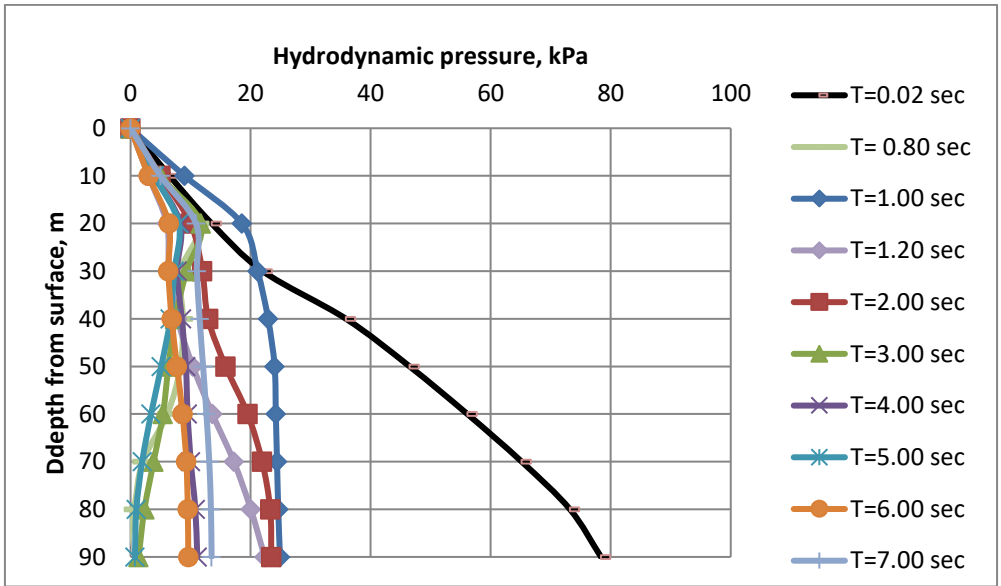


(b) Vertical Dam Displacements



(c) Vertical Stresses

Figure 3. Effect of foundation stiffness on KOYNA dam for case of full reservoir.



Hydrodynamic pressure distribution on upstream face at different times

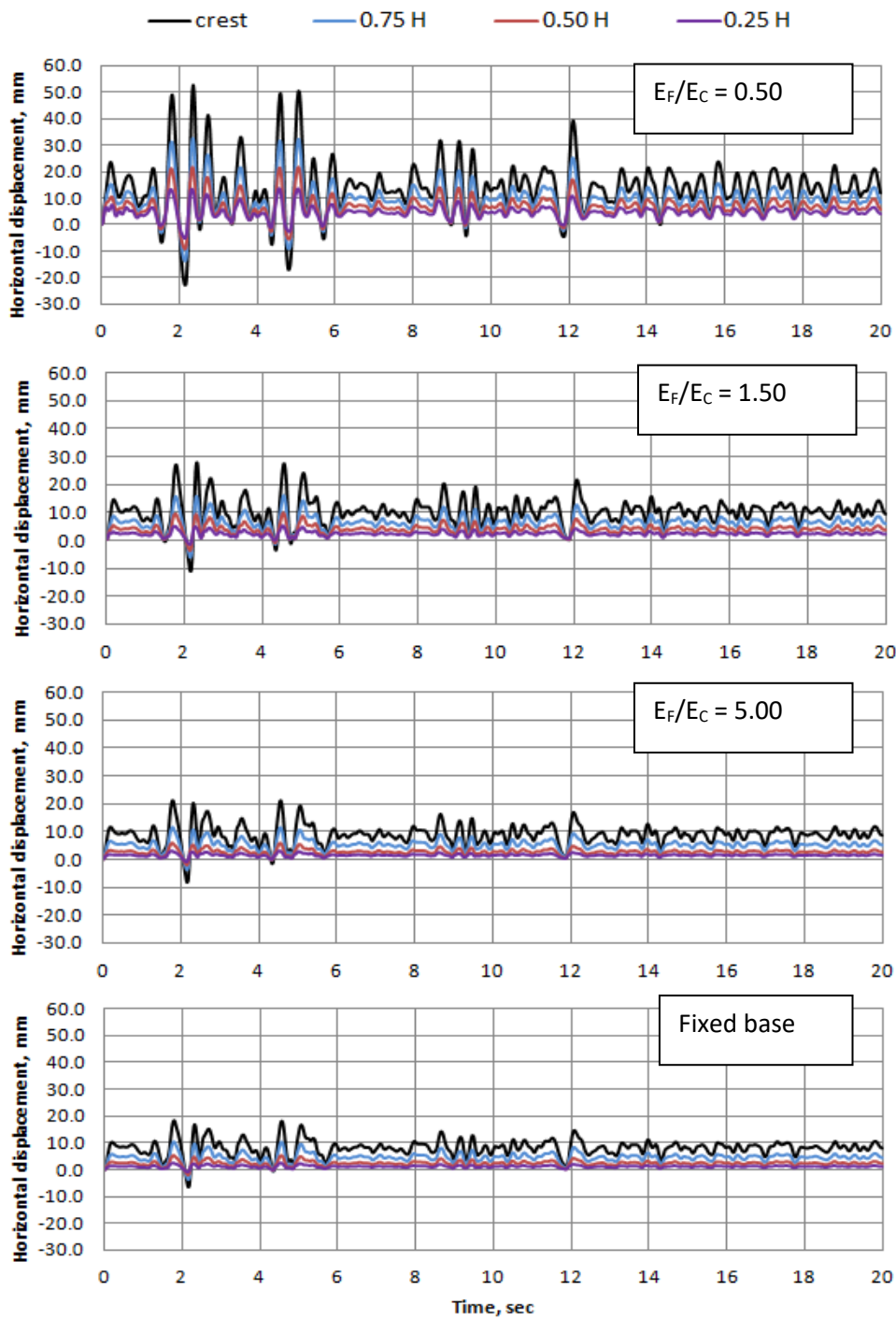


Figure 5a Time history for horizontal displacement at various nodes for case of full reservoir.

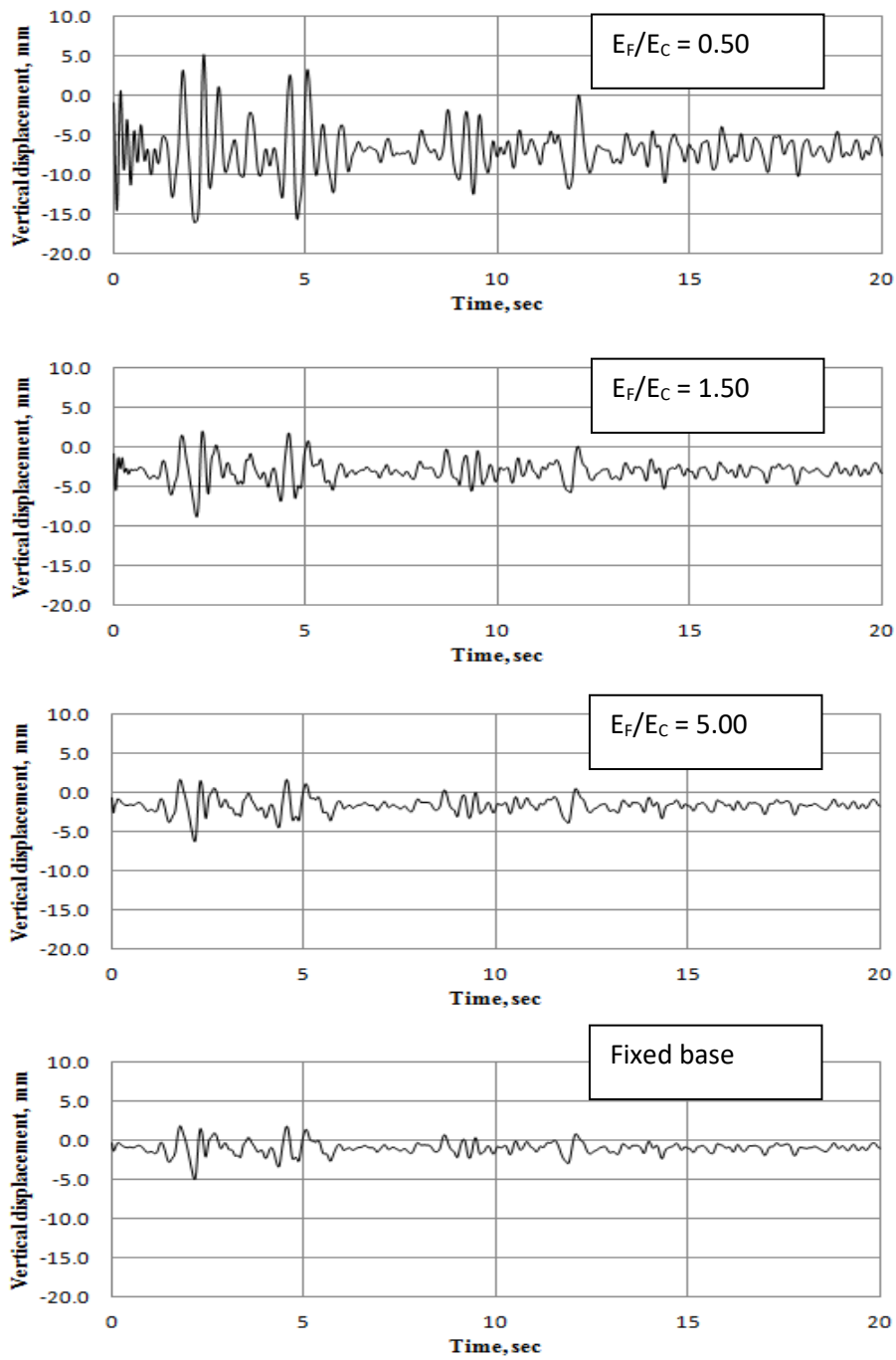


Figure 5b Time history for crest vertical displacement at various nodes for case of full reservoir.

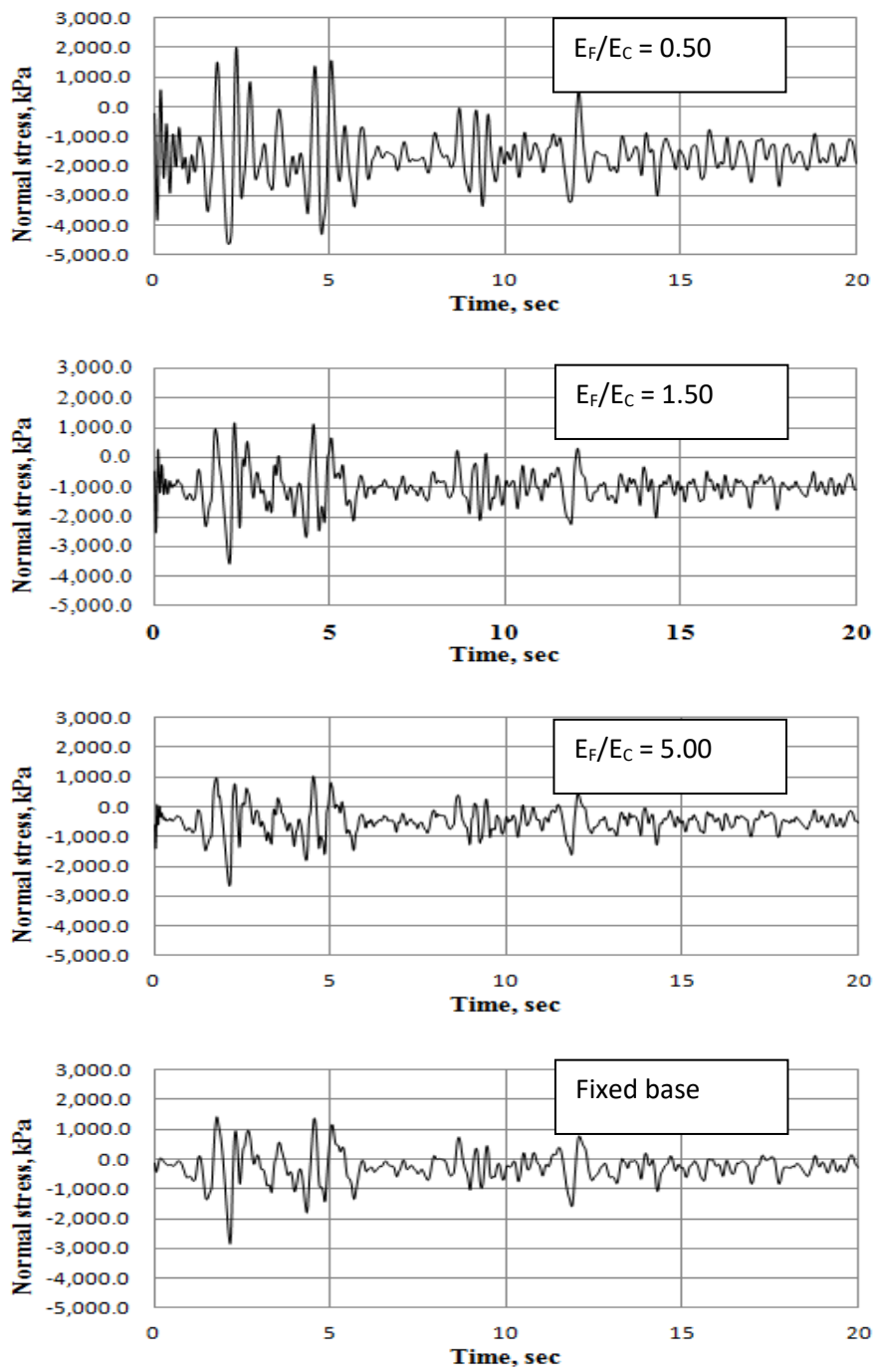


Figure 6a. Time history of normal stress at dam heel

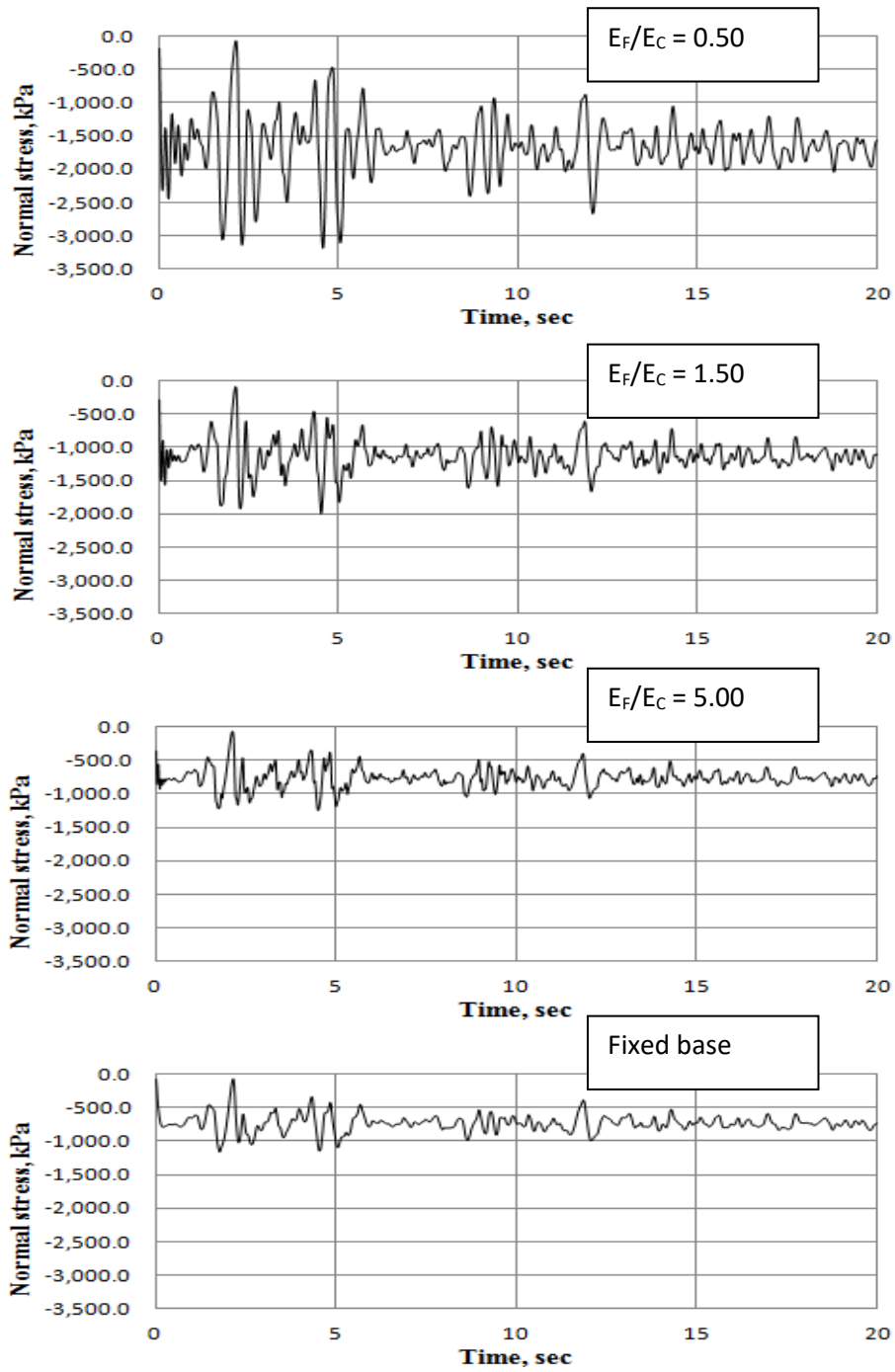


Figure 6b. Time history of normal stress at dam toe

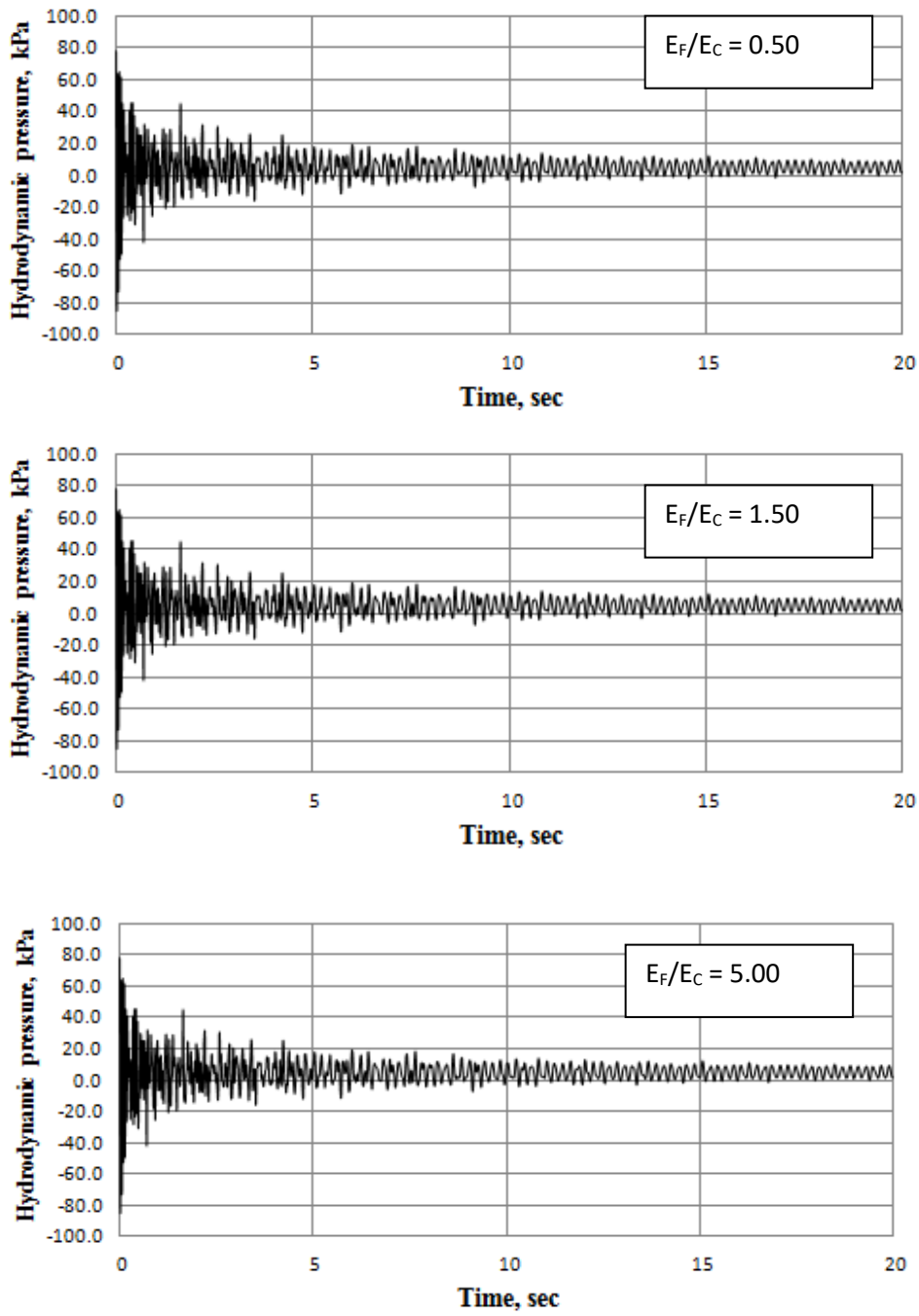


Figure 6c. Time history of hydrodynamic pressure at reservoir base or depth

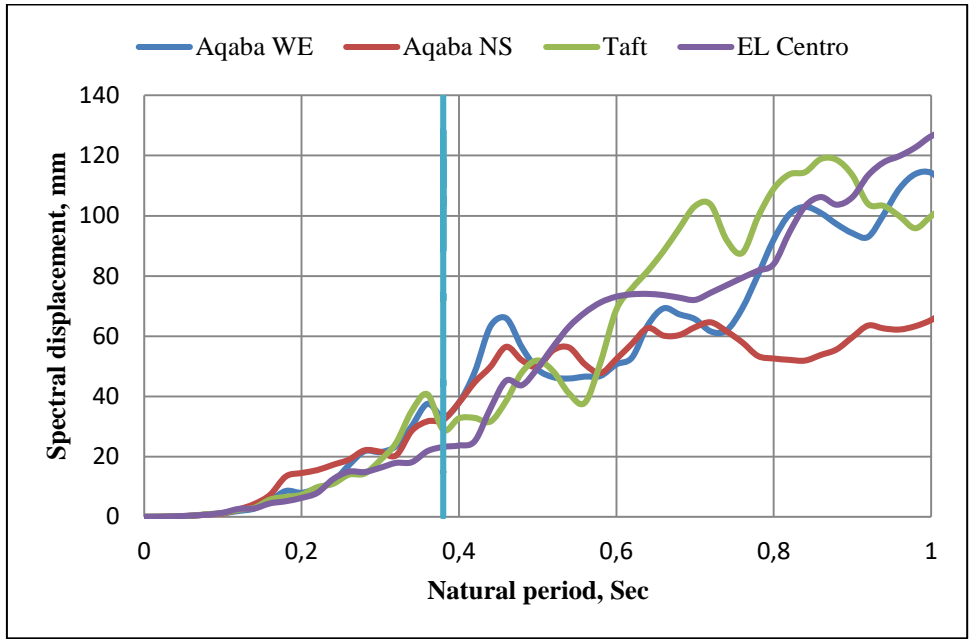


Figure 7a Spectral displacement curves for four normalized earthquake records

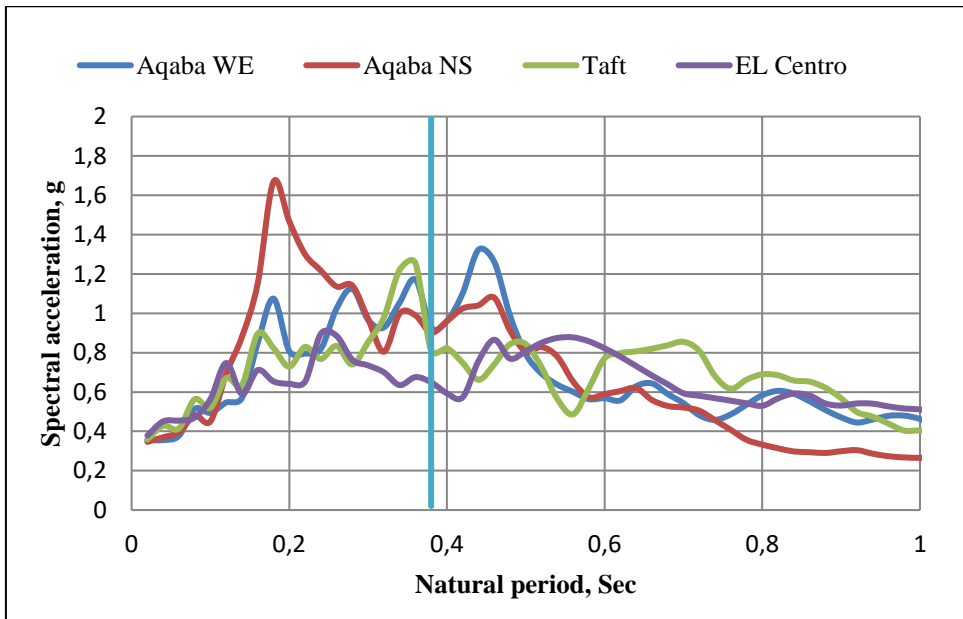


Figure 7b Spectral acceleration curves for four normalized earthquake records

Table 1. Peak accelerations and normalization factors different earthquakes.

Earthquake	Peak acceleration, g	Normalization factor
EL-Centro-S00E component	0.348	1.00
Taft-N21E component	0.156	2.235
Aqaba-NS	0.08	4.35
Aqaba-EW	0.093	3.74

Table 2. Maximum observed response for KOYNA under different earthquakes.

Earthquake		Aqaba-EW	Aqaba-NS	Taft	EL-Centro
Horizontal displacement (mm)	crest	36.1	31.4	32	28
	heel	2.7	2.7	2.6	2.4
	toe	2.2	2.2	2	1.8
Vertical displacement (mm)	crest	-9.8	-9.8	-9.5	-8.7
	heel	-3.5	-3.6	-3.3	-3.3
	toe	-3.1	-3.1	-3	-3
Normal stress (kPa)	heel	-3995	-3975	-3846	-3568
	toe	-2278	-2204	-2120	-1988
Hydrodynamic pressure Reservoir base (kPa)		-100	-100	-85	-85

COMMISSION INTERNATIONALE DES GRANDS BARRAGES

VINGT-SIXIÈME CONGRÈS DES GRANDS BARRAGES
Autriche, juillet 2018

DOI 10.3217/978-3-85125-620-8-135



This work licensed under a Creative Commons Attribution 4.0 International License. <https://creativecommons.org/licenses/by-nc-nd/4.0/>

**3D BLOCK ERODIBILITY: REAL-TIME MONITORING IN AN UNLINED ROCK
SPILLWAY CHANNEL**

Michael F. GEORGE

Senior Geological Engineer, BGC ENGINEERING, INC.

USA

Nicholas SITAR

*Edward G. Cahill and John R. Cahill Professor of Civil Engineering, UNIVERSITY
OF CALIFORNIA - BERKELEY*

USA

COMMISSION INTERNATIONALE
DES GRANDS BARRAGES

VINGT-SIXIÈME CONGRÈS DES
GRANDS BARRAGES
Autriche, juillet 2018

3D BLOCK ERODIBILITY: REAL-TIME MONITORING IN AN UNLINED ROCK SPILLWAY CHANNEL

Michael F. GEORGE

Senior Geological Engineer, BGC ENGINEERING, INC.

USA

Nicholas SITAR

*Edward G. Cahill and John R. Cahill Professor of Civil Engineering, UNIVERSITY
OF CALIFORNIA - BERKELEY.*

USA

1. INTRODUCTION

Scour of rock foundations and spillways pose a significant concern for the safe and reliability operation of dams across the world. The February 2017 events at the Oroville Dam spillways in California, USA are a prime example. Knowledge regarding the mechanics of rock mass break-up resulting from hydraulic loading is still limited and has largely been deduced from scaled laboratory models and testing. This is due, in part, to the challenge of making direct observations of the rock scouring process during spill events from actual dam and spillway sites.

Due to these challenges, nearly all studies on rock erodibility have focused on laboratory testing using simplified rock block geometries (i.e., rectangular/cubic blocks) under idealized flow conditions [1-14]. Extrapolation of the findings of such studies to field conditions can be challenging given the highly irregular 3D geologic structure often encountered at specific sites which, as many rock mechanics practitioners are aware, significantly influences block/rock slope stability.

Accordingly, a research study was undertaken to develop a high-resolution data set from both field and laboratory settings on the erodibility of 3D (non-cubic) rock blocks [15]. This paper presents first-of-a-kind observations made in real-time leading up to the removal of an instrumented rock block in a prototype unlined spillway channel at a dam site in Northern California.

2. SITE DESCRIPTION AND INSTRUMENTATION

Collection of real-time data on 3D rock block erodibility from a prototype setting has several challenges related to selection of a site that is readily accessible, that spills regularly and that has erosion actively occurring. Additionally, instrumentation would need to withstand variable climatic conditions as well as hydraulics loads associated with spill events to allow capture of data.

The basic concept for the prototype set-up was to re-create rock blocks within a spillway channel from locations in the rock mass where blocks once existed but had subsequently been eroded. To do so, two instrumented artificial rock blocks were installed in an unlined rock spillway channel at a dam site in Northern California. The dam is located in the Sierra Mountain Range and founded on hard, blocky granodiorite rock. The spillway consists of a concrete ogee control section that discharges onto rock just downstream (Fig. 1). Ten radial gates are present, three of which are larger and have an invert at a slightly lower elevation. The capacity of the spillway with all gates open is 1,161 m³/s and the maximum flow experienced to date was 968 m³/s in January 1997. Typically, the spillway discharges on an annual basis in the winter and spring months associated with rain on snow events or runoff from snowmelt in the Sierra.

Scour of the granodiorite rock within the spillway has generally been observed throughout the almost 100-year lifespan of the structure, with the first documented instance in the early 1940's. Based on aerial photography, approximately 185,000 m³ (the equivalent of 75 Olympic swimming pools) of material has been eroded from the spillway channel (Fig. 2). Despite several large flows through the spillway, catastrophic erosion has not been witnessed, but rather scour appears to occur more gradually.

Given the propensity for regular spill events and historic erosion of the spillway, the site provided an excellent opportunity to collect real-time scour data from a prototype setting. As mentioned above, two artificial, instrumented blocks were installed within the spillway channel. The blocks were cast into existing block molds, which are locations where a rock block once existed but has subsequently been eroded (Fig. 3). Block 1 was installed below the upper (small) spillway gates, while Block 2 was installed below the lower (large) spillway gates.



Fig. 1

Small discharge (approximately $14 \text{ m}^3/\text{s}$) through gated spillway control section.



Fig. 2.

Aerial photo of unlined spillway channel. Volume of eroded spillway rock material is estimated to be approximately $185,000 \text{ m}^3$.

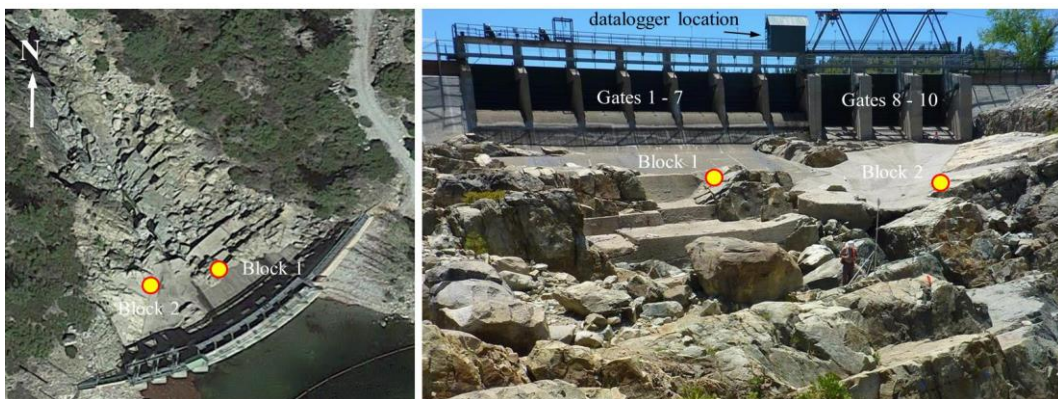


Fig. 3

Location of artificial rock blocks in unlined spillway channel [16].

Both blocks were tetrahedral (4-sided), which is the most basic non-cubic block geometry but also the most likely removable block geometry from a rock mass [17]. The blocks were located close to the spillway gates where flow could still be relatively characterized as 2D channel flow, before becoming more complex further downstream. This was done to facilitate comparison with physical hydraulic model testing done on 3D tetrahedral blocks in a flume channel as another facet of this research study.

The blocks were fabricated out of concrete and instrumented with pressure and displacement sensors on each of the block faces (Fig. 4). This was done to allow measurement of hydrodynamic forces applied to the block during spill events and track block movements precursory to removal. Sensor cables were run through waterproof conduit to a datalogger located above the spillway crest. Measurements were captured at a frequency of 100 Hz to obtain high resolution data sets for hydrodynamic pressure and displacement.



Fig. 4

Artificial rock blocks, as constructed. Note displacement sensors are on block faces within the rock mass and subsequently not shown [16].

3. MARCH 2016 SPILL EVENT

Block 1 was installed in November 2012, while the Block 2 was installed the following year in November 2013. Subsequent drought conditions in California, however, lead to no significant spill events that impacted the blocks. It wasn't until March 2016, when a peak discharge of 126 m³/s resulted in the removal of Block 2 from below the low-level spillway gates. During the afternoon of March 5, 2016 discharge from the spillway began through the low-level outlet gates and at approximately midnight flow through the upper-level gates commenced. The peak discharge occurred around 6 am the following morning. Flow through the upper-level gates terminated on the morning of March 7 around 5 am, while flow

continued to spill from the low-level gates for more than a week after the peak flow occurred. The outflow hydrograph for the event is shown in Fig. 5, while observations of the spill event are shown in Fig. 6.

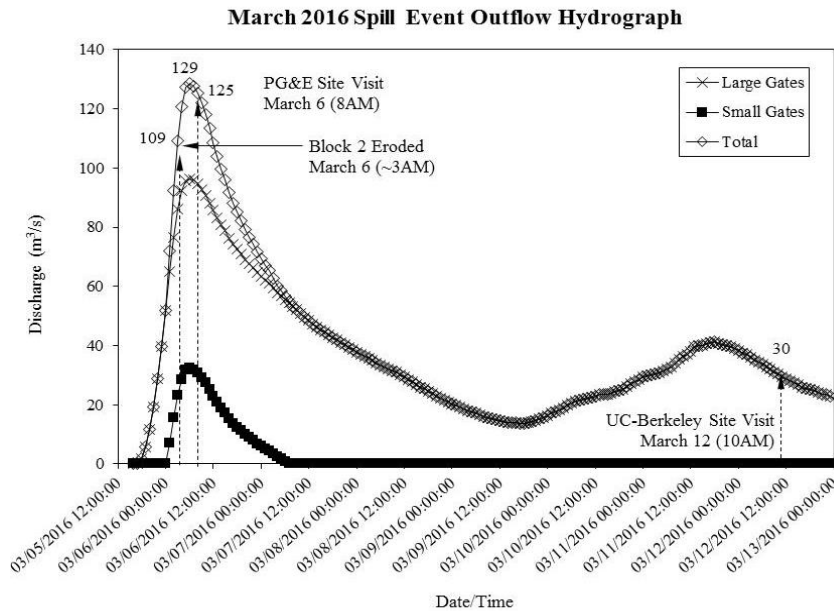


Fig. 5
Outflow hydrograph from March 2016 spill event.



Fig. 6
Discharge on March 6, 8 am (125 m³/s (left), March 12, 10 am (30 m³/s) (right).

Analysis of displacement data recorded for Block 2 indicated the block was eroded from its mold at approximately 3 am on March 6 during the rising limb of the outflow hydrograph at a discharge of 109 m³/s (Fig. 5). After the initial wetting of the block by spillway flows, displacements occurred gradually (at the sub-millimeter scale) until the block was removed (Fig. 7). Prior to removal, the total magnitude of uplift was relatively minor (less than 3 mm) during the approximately 9 hr period when the block was submerged. Some anomalous spikes are observed in the displacement magnitude data, however, review of individual data from each of the displacement sensors suggests that these spikes are erroneous and

potentially related to temporary sensor malfunction (likely due to the turbulent flow environment).

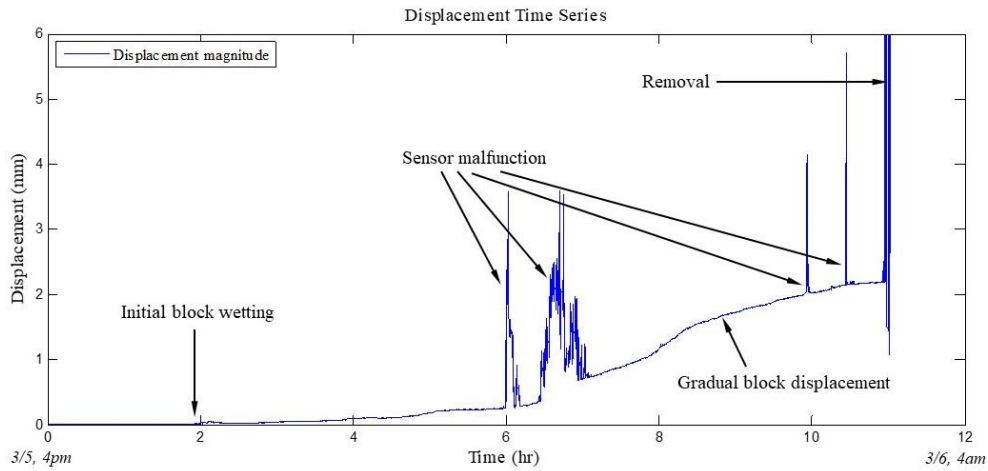


Fig. 7
Displacement magnitude time series leading up to block removal.

Hydrodynamic pressures measured on each of the block faces were used to calculate the active resultant force vector (\mathbf{R}) applied to the block associated with the hydraulic loading from the spillway discharge [16]. Instantaneous measurements were averaged and plotted on a whole sphere, limit equilibrium stereonet in 2 hour increments leading up to removal of the block (Fig. 8). Note that the final resultant vector was calculated at 2:19 am on March 6, corresponding to last measurements obtained prior to failure of the pressure sensors.

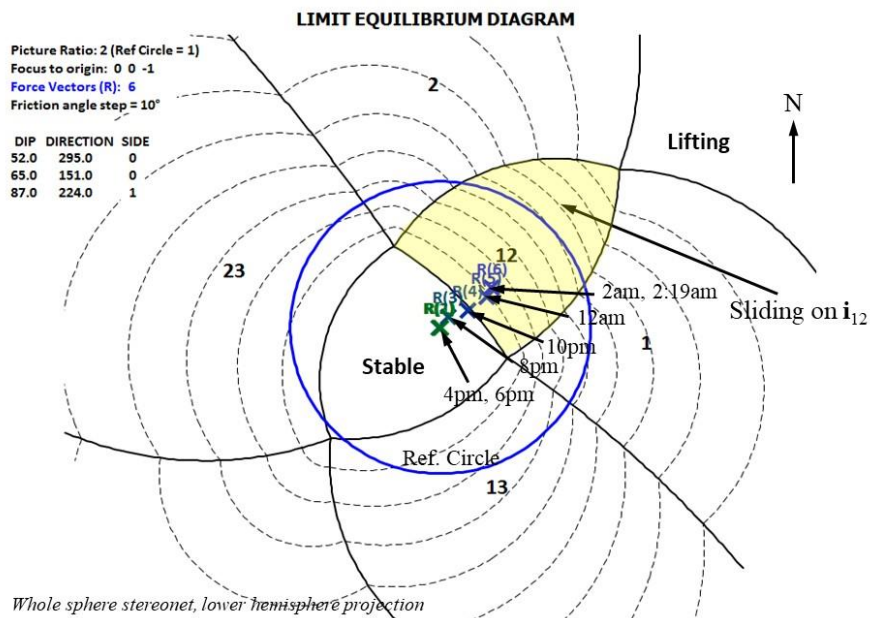


Fig. 8
Limit equilibrium stereonet for 3D stability of Block 2 showing average active resultant force vector (\mathbf{R}) leading up to removal.

The limit equilibrium stereonet presents a graphical solution for 3D stability of the block. The different regions, delineated by the solid black lines, correspond to the different potential kinematic failure modes of the block (e.g., “2” = 1- plane sliding on joint 2, “13” = 2-plane sliding on joints 1 and 3). The dashed lines correspond to contours (10 deg. increments) of the required friction angle on the joint planes to maintain the block at equilibrium. Initially (at 4 pm), the active resultant force vector (**R**) plots within the “stable” region at the center of the stereonet as loading is only due to the self weight of the block. As the block experiences additional loading from hydraulic forces from the spillway flow, **R** rotates outwards away from the “stable” region into region “12” corresponding to the kinematic mode of sliding on joints 1 and 2. Accordingly, the likely failure mode in which the block was eroded was 2-plane sliding on joints 1 and 2.

Flow conditions (velocity and turbulence intensity) in the proximity of Block 2 were assessed using recorded video of the spill event. Particle Image Velocimetry (PIV) software was used to track turbulence structures within the flow field overtime to estimate the instantaneous velocity at the flow surface (Fig. 9). A simplistic free online code, Tracker [18], was used for the analysis. More robust codes are available but are often reserved for more controlled laboratory settings. An existing high-resolution LiDAR point cloud of the spillway was used to spatially scale spillway features in the video used in PIV analysis.

Video for PIV analysis was taken at a discharge of 30 m³/s during a site visit on March 12. From the video a mean flow velocity, $u = 10.3$ m/s and turbulence intensity, $T_u = 19$ % were calculated. Turbulence intensity values compared well with those determined from pressure sensor measurements on the free surface face of the block. Although no video was available during the time the block was removed, the PIV results provided guidance on estimation of flow characteristics at the time of block erosion.

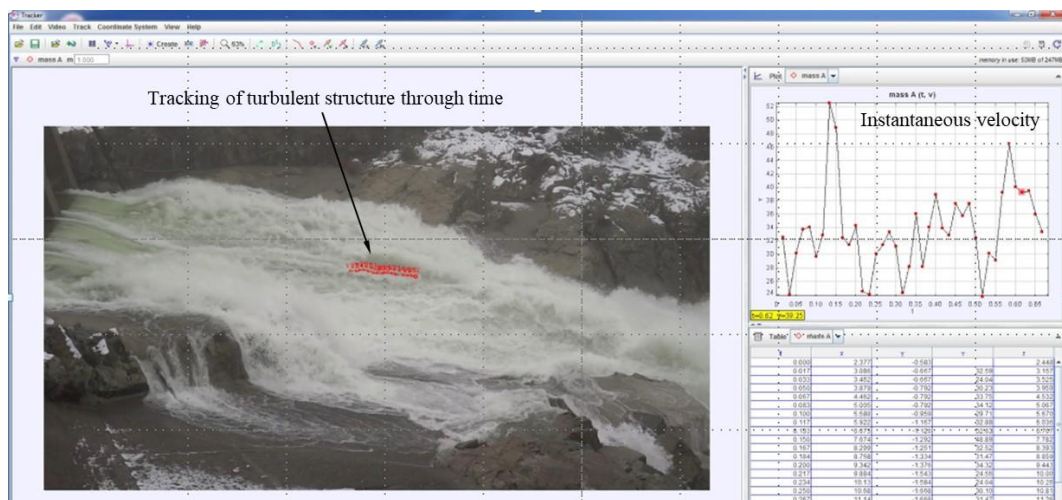


Fig. 9
Screen capture of particle tracking during March 2016 spill event.

4. DISCUSSION AND CONCLUSIONS

The instrumentation of two artificial rock blocks within an unlined spillway channel provided first-of-a-kind, high resolution insight into the rock scour process in a prototype setting. The observations and measurements recorded from the March 2016 spill event that resulted in removal of one of the instrumented blocks allowed assessment of applied hydrodynamic loads and subsequent block response precursory to failure.

The gradual displacement of the block from its mold even under highly turbulent flow conditions agrees with other measurements made on 3D block response from laboratory flume experiments [16]. In these experiments, block kinematics (related to the orientation of the bounding joint planes on the block with respect to the flow direction) played a significant factor in the observed block response. Blocks with limited kinematic resistance to movement exhibited gradual displacement prior to removal whereas blocks with higher kinematic resistance showed a more dynamic response with larger, impulse-type movements. The distinction between low and high kinematic resistance is thought to occur when the active resultant force vector (\mathbf{R}) must be rotated outwards by more than approximately 60 deg. from its initial vertical orientation (due to the self weight of the block). Block geometries requiring rotation of \mathbf{R} less than 60 deg. are considered to have a low kinematic resistance [16]. At the field site, the rotation of \mathbf{R} required for instability of Block 2 (assuming a friction angle on joints 1 and 2 equal to 20 deg.) is 58 deg., suggesting Block 2 has a low kinematic resistance.

Other near-prototype laboratory experiments on 3D block response using a simplified cubic block geometry showed block response was highly dynamic when subject to loading from turbulent jet impact (e.g., [11,12]). In light of the observations from the field study presented herein and the laboratory results presented by [16], this response can be expected given the minimum rotation of \mathbf{R} required for uplift of the cubic block in the above experiments would be approximately 110 deg. (assuming a joint friction angle of 20 deg.). Accordingly extrapolating data obtained from idealized block geometries for analysis of rock scour for sites with highly irregular 3D geologic structure can be challenging.

A framework based on block theory principles [19] has been developed in order to assess 3D rock block erodibility. This has been shown to reasonably predicted block erodibility thresholds obtained from the laboratory flume experiments on 3D tetrahedral blocks [16] as well as in the back calculation of the erodibility threshold of instrumented field block presented herein [20]. Accordingly, this framework can allow practitioners to incorporate site-specific 3D geologic structure into analysis rock erodibility.

5. ACKNOWLEDGEMENTS

Financial support for portions of this work was provided by the National Science Foundation under Grant No. CMMI-1363354, the University of California Cahill Chair, the Hydro Research Foundation, and the United States Society on Dams. All opinions, findings, and conclusions or recommendations expressed in this material are those of the author(s) and do not necessarily reflect the views of the National Science Foundation or any other funding agency. Support for this work is greatly acknowledged.

REFERENCES

- [1] Reinius, E. (1986). Rock erosion. *Water Power and Dam Construction*, (June): 43-48.
- [2] Annandale, G.W. (1995). Erodibility. *Journal of Hydraulic Research*, 33(4): 471-494.
- [3] Annandale, G.W. (2006). *Scour technology: mechanics and engineering practice*, New York, McGraw-Hill.
- [4] Liu, P., Dong, J. and Yu, C. (1998). Fluctuating uplift on rock blocks at the bottom of a scour pool by overfall jets. *Science in China Series E: Technological Sciences*, 41(2): 130-139.
- [5] Robinson, K. and Kadavy, K. (2001). Pressure forces in a fractured matrix. *Proc. of the ASAE Int. Annual Meeting*, Sacramento, CA.
- [6] Bollaert, E.F.R. (2002). *Transient water pressures in joints and formation of rock scour due to high-velocity jet impact*, Communication No. 13. Ph.D. Dissertation. Laboratory of Hydraulic Constructions. Ecole Polytechnique Federale de Lausanne, Switzerland.
- [7] Coleman, S.E., Melville, B.W. and Gore, L. (2003). Fluvial entrainment of protruding fractured rock. *Journal of Hydraulic Engineering*, 129(11): 872-884.
- [8] Dubinski, I.M. (2009). *Physical modeling of jointed bedrock erosion by block quarrying*. Ph.D. Dissertation. Colorado State University, USA.
- [9] Lamb, M.P. and Dietrich, W.E. (2009). The persistence of waterfalls in fractured rock. *Geological Society of America Bulletin*, 121(7-8): 1123-1134.
- [10] Li, A. and Liu, P. (2010). Mechanism of rock-bed scour due to impinging jet. *Journal of Hydraulic Research*, 48(1): 14-22.
- [11] Federspiel, M.P.E.A., Bollaert, E.F.R. and Schleiss, A.J. (2011). Dynamic response of a rock block in a plunge pool due to asymmetrical impact of a high-velocity jet. *Proc. of the 34th IAHR World Congress*, Brisbane, Australia, 2404-2411.
- [12] Duarte, R.X.M. (2014). *Influence of air entrainment on rock scour development and block stability in plunge pools*, Communication No. 59.

- Ph.D. Dissertation. Laboratory of Hydraulic Constructions. Ecole Polytechnique Federale de Lausanne, Switzerland.
- [13] Umumararungu, M.G. (2016). *Physical modeling investigation of rock scour extent due to a plunging jet for typical high head dams*. M.S. Thesis. Stellenbosch University, South Africa.
 - [14] Pells, S. (2016). *Erosion of rock in spillways*. Ph.D. Dissertation. Univ. of New South Wales, Australia.
 - [15] George, M.F. and Sitar, N. (2016). 3D block erodibility: Dynamics of rock-water interaction in rock scour. *Report No. UCB-GT/16/01*, Dept. of Civil and Environmental Engineering, Univ. of California – Berkeley, USA.
 - [16] George, M.F. (2015). *3D block erodibility: Dynamics of rock-water interaction in rock scour*. Ph.D. Dissertation. Univ. of California - Berkeley, USA.
 - [17] Mauldon, M. (1990). Probability aspects of the removability and rotatability of tetrahedral blocks. *International Journal of Rock Mechanics and Mining Sciences & Geomechanics Abstracts*, 27(4): 303-307.
 - [18] Brown, D. (2016). Tracker Video Analysis and Modeling Tool v4.9.5. physlets.org/tracker/.
 - [19] Goodman, R.E. and Shi, G. (1985). *Block theory and its application to rock engineering*, Englewood Cliffs, NJ, Prentice Hall.
 - [20] George, M.F. and Sitar, N. (2017). Real-time capture of rock block erosion: Field measurements of hydrodynamic pressure and block displacement in an unlined rock spillway channel. *In preparation*.

SUMMARY

Scour of rock foundations and spillways during normal and extreme flood events poses an important concern for dam safety. The challenge of making direct observations during a spill event has limited the understanding of the mechanisms driving the break-up of the rock mass when subject to hydrodynamic loading. Historically, methods for scour prediction have been derived from scaled laboratory studies often using simplified rock geometries and flow hydraulics. We present real-time observations of block removal captured using an instrumented block during a flood event in an unlined rock spillway of a dam in northern California. Particle image velocimetry (PIV) from digital video footage provides information on flow characteristics near the time of removal, while pressure and displacement sensors installed on the block faces provide measurements of hydrodynamic loads and block displacement leading up to failure/removal.

COMMISSION INTERNATIONALE DES GRANDS BARRAGES

VINGT-SIXIÈME CONGRÈS DES GRANDS BARRAGES
Autriche, juillet 2018

DOI 10.3217/978-3-85125-620-8-136



This work licensed under a Creative Commons Attribution 4.0 International License. <https://creativecommons.org/licenses/by-nc-nd/4.0/>

**KEY NOTES ON QUALITY CONTROL OF ROLLER COMPACTED
CONCRETE DAMS**

Hamed. MAHDILOUTORKAMANI

Quality Control Engineer, Uma Oya Multipurpose Project Development
FARAB COMPANY

IRAN

COMMISSION INTERNATIONALE
DES GRANDS BARRAGES

VINGT-SIXIÈME CONGRÈS DES
GRANDS BARRAGES
Autriche, juillet 2018

KEY NOTES ON QUALITY CONTROL OF ROLLER COMPACTED CONCRETE DAMS

HAMED. MAHDILOUTORKAMANI

*Quality Control Engineer, Uma Oya Multipurpose Project Development
FARAB COMPANY*

IRAN

1. INTRODUCTION[1, 2]

Roller compacted concrete dam (RCC) construction, including preparation of RCC materials, construction procedures and testing during construction is put into the framework of quality concepts. When put into this framework, the designer and contractor can see the integrated nature of both design and construction processes to achieve project quality objectives that result in safe and cost effective dam construction.

Quality concepts, particularly quality assurance (QA) and quality control (QC) are defined as follows:

Quality assurance (QA) is a program covering activities necessary to provide quality in work, and to ensure that activities that require good quality are being performed effectively. QA specifies actions necessary to provide enough confidence that the project will satisfy the given requirements as established in e.g. design criteria and performance specifications.

Quality control (QC) is the specific implementation of the QA program and includes the monitoring and evaluation of processes and outcome against the requirements and specifications. QC has to facilitate the immediate application of actions to the outcome, thus, allowing the engineer to exert direct influence on the outcome.

The Quality Control system for RCC dams comprised the following main activities:

- Control of production process by inspection of the equipment and material
- Control by testing and inspection of the properties of the RCC constituents
- Control of fresh RCC sampling and testing
- Control of hardened concrete by testing samples and statistical conformity analysis

This paper is concerned with the relationship between the specification of RCC, construction procedures, the properties of RCC and how quality control is used in RCC dams during construction.

2. QUALITY CONTROL OF MATERIALS [1, 2, 3]

The primary objectives of performing RCC mix designs for a dam project are to evaluate the uniformity, compactability, workability, and economic issues of the likely RCC mix components and proportions. These objectives are evaluated relative to the RCC unit weight and strength requirements.

Commonly, RCC mix design is comprised of four main components: aggregate, cementitious materials (pozzolan and cement), water and admixture. The selection, proportioning, and quality of each of these components effect on the RCC quality. Key aspects of each of these components on the quality of the final concrete product are discussed below.

2.1. AGGREGATE

The selection of an appropriate aggregate for RCC production is probably the single most important factor in any RCC project. Aggregate is the one component in RCC that potentially has the greatest variability and impact on quality. Ideally, a suitable RCC aggregate will have the following characteristics:

- Compactable to high density
- High specific gravity
- High Strength
- Suitable gradation to prevent segregation
- Excellent durability/soundness

Aggregate is normally derived from local sources to avoid the considerable cost attached to transport. Some sources will yield aggregate of high quality, which conforms to national or international standards. Specification of processes and RCC mixtures can overcome such defects and produce adequate RCC. Where the aggregate source is known to be of good quality, the specification can be based on published standards such as ACI 221 or ASTM C-33. Table 1 and

figure 1 show QC tests for aggregate in RCC dams and aggregate production in stone crusher.

Table 1
QC tests for aggregate in RCC dams

Quarry or borrow pit		
Petrography	Specific weight	Sulphides
Compressive strength	Absorption	Chloride
Soundness	Alkali-aggregate reactivity	Organic matter
Abrasion resistance	Sulphates	Mica, Clay
Product streams		
Grading	Particle shape	
Before loading into batch plant bins		
Grading	Absorption	
Moisture content	Temperature	

In RCC dam, the physical properties of the source area were measured in the design phase. Tests were carried out to determine rock types, strengths, grading, particle shapes, freeze-thaw resistance, abrasion resistance, specific gravity, water absorption, moisture content and the content of impurities. The chemical soundness of the rock was also investigated and includes tests for alkali-silica reaction (ASR), sulphate resistance and others. Some of these tests are carried out during construction to ensure that the source material and the aggregate produced conform to the design assumptions as embodied in the specifications. Test frequencies will depend on the consistency of the source. Table 3 shows QC chart of aggregate production.



Fig. 1
Aggregate production in stone crusher (Uma Oya project-Sri Lanka)

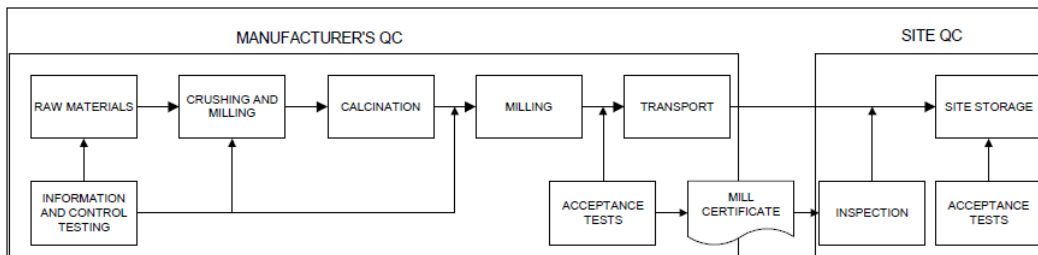
2.2. CEMENTITIOUS MATERIALS

In RCC dams the cement used in concrete determined according to ASTM C150. This determination is based on environmental, materials and structures conditions. For mass concrete, as in the case of RCC Dams, cements with low heat generation -Type 2 or pozzolanic should be used. For cementitious materials, most important is the control of uniformity, which can vary considerably due to heterogeneous sources or caused by the grinding process.

The rate of cement consumption can be very high for RCC dams and the turnover of on-site storage can be rapid. Considerable reliance has to be placed

on the manufacturer's certificates. In the early phases of construction, it may be prudent to arrange for comprehensive testing of the cement at frequent intervals until there is full confidence in the manufacturer's test results. After that, physical tests should be carried out periodically. The tests that can realistically be performed at site are related to setting time and temperature. Table 2 shows QC chart of cementitious material.

Table 2
Quality control chart of cementitious material



2.3. ADMIXTURES

A number of chemical admixtures are available to improve the properties of fresh concrete and RCC. Admixtures commonly used in RCC and concrete are set retarders and water reducing/workability enhancing chemicals and air-entraining agents. Admixtures are available that combine more than one of these properties.

For RCC dams, the effects of admixtures have to be tested with the various RCC mixes. These tests are typical setting times and workability (VeBe test). Poor or undesirable results can arise with particular products because of incompatibility with cement or pozzolan and with some types of aggregates and may arise with seasonal variations in air temperature. These cases require a change of type or brand of admixture. Such tests should be carried out periodically throughout the construction period.

2.4. WATER

Water quality for RCC mixing should satisfy an appropriate standard with respect to the content of contaminants. Potable water is preferred for RCC as it has been filtered for contaminants. When potable water is not available, tests should be made with the precise source of construction water to validate the mix design and RCC properties. Any source of water may be used if the 7 and 28-day strengths of 5-cm cubic mortar specimens be at least 90 percent of the index mortar made using distilled water according to ASTM C109. Besides, the setting

time of the test paste shall not be 60 min shorter or 90 min longer than that of the check paste made using distilled water according to ASTM C191.

3. BATCHING PLANT AND MIXING OPERATION [1, 2]

For RCC dams, the batching plant and mixing operations have an important impact on the in-place properties of the RCC. Table 3 shows quality control activities for batching plant and mixing operations.

When the batching plant is operating, the amount of all constituent materials including cement, and each size group of aggregate, water and admixtures shall be continuously controlled. A daily (24 hour basis) report shall be prepared indicating the type, source, and quantity (actual and SSD basis) of cement, each size group of aggregate, admixture, and water used during each shift of plant operation, based on plant production records. The report shall show the required mix proportions per cubic meter for each mix design, and the average proportions for each mix calculated from the totals used during each shift.

Table 3
Quality Control activities for batching plant and mixing operations

Activity	Frequency
Mixer efficiency tests	At start-up, monthly and changes in material sources
Mixing times	Each batch
Workability	Each batch to hourly (with RCC)
Verification of preventive maintenance	To follow the maintenance schedule
Cleaning and maintenance	Daily

4. QUALITY CONTROL PLAN DURING CONSTRUCTION [1, 4, 5]

4.1. QUALITY CONTROL TESTS DURING CONSTRUCTION

During construction, all of QC tests should be performed according technical specification in specified frequency. Table 4 shows typical quality control tests for RCC dams.

4.2. PLACEMENT

For RCC dams, important factors shall be considered for placement of the RCC include Transportation; RCC placement temperature; Segregation; Timing; Lift joint conditions and Bedding mortar.

Transportation: RCC may be transported from the batching plant to the point of the placement by several means as a function of distance, rate of placement and environmental factors. The method of transport may affect the workability of the RCC and may cause segregation. Transportation and handling equipment should not only have the required capacity but also be capable of being adapted to different mixes and should be designed to minimize segregation. Checks are required to ensure that the method of RCC transport will not adversely affect the fresh RCC properties such as may be induced by drying, wetting or segregation. Maintenance of transport vehicles and conveyor belts has to be carried out and verified. This includes daily maintenance, which entails cleaning off accumulated concrete on the delivery system as well as mechanical maintenance. Figure 2 shows conveyor system for transporting the RCC.

Table 4
Typical Quality Control Tests for RCC dam

Material tested	Test procedure	Test Standard ²	Frequency ³
Cement	Physical and chemical properties	ASTM C150	Manufacturer's certificate or pre-qualification
Pozzolan	Physical and chemical properties	ASTM C618	Manufacturer's certificate or pre-qualification
Admixture		ASTM C494 ASTM C128	Manufacturer's certificate
Aggregates	Relative Density And Absorption	ASTM C127 ASTM C128	One per month or 50 000 m ³
Aggregates	Flat and elongated particles	BS812	One per month or 50 000 m ³
Aggregates	Los Angeles Abrasion	ASTM C131	One per month or 50 000 m ³
Aggregates	Gradation	ASTM C117 ASTM C136	One per shift or One per day
Aggregates	Moisture content	ASTM C566 ASTM C70	Before each shift or as required
RCC	Workability	ASTM C1040	500 m ³ or as required
RCC	Gradation	ASTM C117 ASTM C 136	1000 m ³ or as required
RCC	Fresh density	ASTM C1040	1000 m ³ or as required
RCC	Oven-dry Moisture content	ASTM C566	1000 m ³ or as required
RCC	Temperature	ASTM C1064	100 m ³ or as required
RCC	Variability of Mixing procedures	ASTM C172, C1078, C1079 or special	Two per month or 25 000 m ³
RCC	Compressive Strength	ASTM C1176 or tamper	Two per day or 1000 m ³
RCC	Tensile strength (direct and/or indirect)	Special or ASTM C496	One per day or 2000 m ³
RCC	Elastic modulus	ASTM C469	One per day or 2000 m ³



Fig. 2

Conveyor systems for transporting the RCC (Javeh Dam-Iran)

RCC Placement Temperature: The placement temperature of the RCC is an important consideration relative to the potential for surface and mass gradient cracking in the gravity dam construction. In hot weather, for reducing of RCC temperature, aggregate cooling shall be accomplished by several methods. These methods include mining and processing the aggregate in colder seasons, shading stockpiles from direct sunlight and evaporative cooling of aggregates in the stockpiles. Some reduction in the placement temperature of the RCC can be achieved by cooling the mix water. Under cold weather, heating of mixing water and protection of RCC exposed surface shall be considered. Under the most extreme weather conditions, the RCC placement tasks are stopped.

Segregation: Segregation of RCC during transport and placement shall be controlled by employing means and methods similar to those used in transporting and placing conventional concrete. For this propose the gradation of aggregate, time of mixing in batching plant, transporting system of RCC and concreting equipment should be controlled. Figure 3 shows segregation of RCC.



Fig. 3

Segregation of RCC and effect of segregation on lift surface

Timing: Time limitations are commonly prescribed to keep the RCC from setting before final spreading and compaction. In RCC dams the following time limits for handling, transporting and compacting the RCC:

- Maximum time from plant to spreading on the fill is 45 minutes;
- Compaction starts within 15 minutes of spreading;

- Maximum elapsed time from introduction of water to the mix and final compaction is 60 minutes.

Lift Joint Conditions: The thickness of the layer shall not exceed 300 mm, and shall be aggressively cleaned before applying bedding mortar and placing next layer. Good lift joint conditions are a vital component of good RCC construction. The underlying goal is to place subsequent RCC lifts before the underlying lift has set, allowing the lifts to bond to each other. Cleaning shall include removal of all loose material, cement paste, fine particles, still and current waters, snow, ice, oil and grease and other detrimental materials. In particular, the surfaces of joints shall be kept free of dust at all times. All horizontal joints shall be prepared for the next lift by removing mortar coating, laitance, or other contaminants by water jet or other approved methods. After this initial preparation, the surface shall be kept damp until receiving the bedding mortar application prior to the next RCC placement.

Bedding Mortar: A lift surface is considered a "cold joint" if the surface is damaged by weather or equipment, frozen, Cold joint treatment consists of thorough cleaning of the surface and placement of a layer of bedding mix concrete (bedding mortar) immediately prior to placement of the successive RCC lift. Not more than 15 minutes shall have elapsed after spreading the bedding mortar when RCC is spread on it. Figure 4 shows cleaning of lift Surface and spreading of bedding mortar.

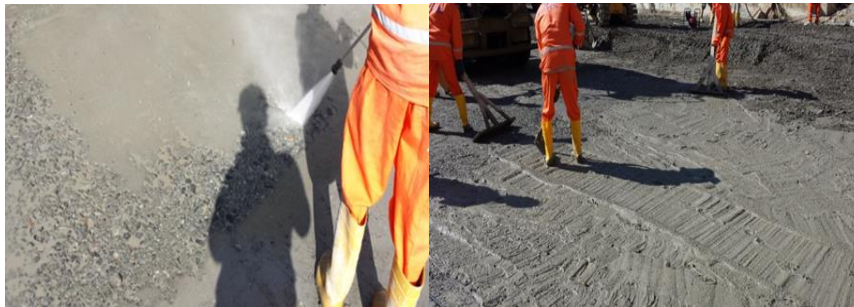


Fig. 4

Cleaning of Surface and spreading of bedding mortar (Uma Oya Project)

4.3. COMPACTION AND VERIFICATION

Compaction is generally viewed as one of the most important elements in RCC Construction. During construction of the RCC, adequate compaction will have one of the most profound impacts on the quality of the finished RCC dam.

In RCC dams, the in-place compaction and water content of the RCC in the lifts are tested using nuclear gauges in accordance with ASTM C1040 and ASTM D1557. The testing shall be performed frequently; Acceptance criteria for in-place density of the RCC require no test less than 98 percent of required compaction. The variation of moisture outside minus 5% and plus 5% of the optimum moisture content shall require aggregate moisture contents testing and control of water contents at the batch plant. Re-compaction of the RCC shall not be allowed

beyond 45 minutes from the batching time of the mix placed at the failing location. Figure 5 shows RCC construction and compaction testing.



Fig. 5
RCC construction and density testing (Javeh Dam-Iran)

5. POST CONSTRUCTION QUALITY CONTROL ACTIVITIES [2, 4, 5]

As with conventional concrete, RCC must be kept continuously moist for the prescribed curing period. Because RCC is dryer than conventional concrete, surfaces tend to dry more rapidly during warm weather. In such conditions, considerable effort will be required to maintain a uniformly moist surface. After compaction of RCC, the curing activates shall be started. Curing activates shall be done according to air condition and weather temperature in summer or winter. Figure 8 shows curing of RCC lift surface.

In RCC Dams, Samples of RCC can be obtained from coring in order to determine the in situ properties. This provides the best evidence of concrete performance by providing samples for strength and density determination, for viewing the density matrix from top to bottom of the lifts, and for identifying lift joint bond or lack of bond. Generally, coring is performed upon completion of the RCC structure. Figure 6 shows Curing of RCC lift surface and Core of RCC.



Fig. 6
Curing of RCC lift surface and Core of RCC- length 3m (Uma Oya Project)

6. CONCLUSION

There are some conclusions in the following:

- RCC mix design is comprised of four main components: aggregate, cementitious materials (pozzolan and cement), water and admixture. The quality of each components effect on the RCC quality
 - For RCC dams, the batching plant and mixing operations have an important impact on the in-place properties of the RCC. When the batching plant is operating, the amount of all constituent materials shall be controlled.
 - During construction, all of QC tests should be performed according technical specification in specified frequency.
 - For RCC dams, important factors shall be considered for placement of the RCC include Transportation; RCC placement temperature; Segregation; Timing; Lift joint conditions and Bedding mortar.
 - During construction of the RCC adequate compaction will have one of the most profound impacts on the quality of the finished RCC dam.
 - After compaction of RCC lift, curing activates shall be done according to air condition and weather temperature in summer or winter.

7. REFERENCES

- [1] International Committee on Large Dams, the Specification and Quality Control of Concrete for Dams," ICOLD Bulletin, Paris, France, 2006.
- [2] Keith A Ferguson, P.E. et al. "Application of Quality concepts to Roller Compacted Concrete Dams and mix designs," National ASDSO Conference, Pittsburg, 1997
- [3] U.S. Army Corps of Engineers, "Roller Compacted Concrete," Engineer Manual EM 1110-2-2006.
- [4] American Concrete Institute, "Roller Compacted Concrete," Report 207.5R-89, Detroit, Michigan, 1988.
- [5] American Society of Civil Engineers, "Quality in the Constructed Project - Manual of Professional Practice (A Guide for Owners, Designers and Constructors)," New York, 1988.

SUMMARY

The purpose of RCC quality control is to maintain uniformity of all constituents and operations entering into the final product. Thus, quality assurance and quality control (QA/QC) systems for RCC dams need to be

established in the preconstruction phase and rigorously continued during the dam construction. In this paper, quality control of RCC dams during construction are discussed along with corresponding quality control (QC) programs, QC tests and acceptance criteria.

Le but du contrôle de qualité RCC est de maintenir l'uniformité de tous les constituants et opérations entrant dans le produit final. Ainsi, des systèmes d'assurance qualité et de contrôle de la qualité (AQ / CQ) pour les barrages des RCC doivent être mis en place dans la phase de pré construction et rigoureusement poursuivis pendant la construction du barrage. Dans cet article, le contrôle de qualité des barrages RCC pendant la construction est discuté avec les programmes de contrôle de qualité (QC), les tests de CQ et les critères d'acceptation correspondants.

COMMISSION INTERNATIONALE
DES GRANDS BARRAGES

VINGT-SIXIÈME CONGRÈS DES
GRANDS BARRAGES
Autriche, juillet 2018

AN EVALUATION SYSTEM OF HYDROPOWER SUSTAINABLE DEVELOPMENT

Chunna LIU

National Research Center for Hydropower Sustainable Development
CHINA INSTITUTE OF WATER RESOURCES AND HYDROPOWER RESEARCH

CHINA

The 13th Five-Year "hydropower development planning (2016-2020)" clearly stated that we must "Make the development of hydropower an important strategic measure of energy supply side structural reforms, so as to ensure energy security and promote the construction of ecological civilization. Sustainable hydropower is an effective way by which to comprehensively understand the social, economic and ecological benefits of hydropower, comprehensively measure the benefits and impacts of hydropower, and coordinate hydropower development and watershed/regional development.

As China's administrative department of energy industry, the State Energy Bureau attaches great importance to the long-term development of hydropower. It has proposed that the concept of sustainable hydropower being established through the innovation of ideas, so as to solve practical problems in the development and management of hydropower industry. The global greenhouse gas emission reduction and China's demand for the prevention and control of smog have given China a new connotation of sustainable hydropower development. China has drawn lessons from international experience, and established a sustainable technology evaluation method for hydropower in China, which is consistent with international standards, in line with the national energy development strategy, and of great significance for promoting sustainable development of the hydropower industry, thereby achieving national emission reduction targets, and promoting the development of green power.

Hydropower development, while generating enormous social benefits, also has an important impact on local immigrants, society and ecological environment. Xie Qingsheng (2013) pointed out that large-scale hydropower development has resulted in the situation of "reservoirs of rivers and rivers, ecological fragmentation,

interest group formation and overall inefficiency" of some of the main tributaries in the upper reaches of the Yangtze River. China's sustainable hydropower is different from the green hydropower of Switzerland and the low-impact hydropower of the United States.

In order to assess and provide guidance on the protection of the ecological environment during the construction of hydropower projects, the Swiss Federal Institute of Water Science and Technology (EAWAG) proposed the certification procedures and standards for green hydropower stations in operation in 2001. The US proposed the implementation of a low-impact hydropower station certification system. German International Cooperation (GIZ) compiled a handbook of watershed ecosystems in hydropower development. In 2000, the World Commission on Dams (WCD), a joint initiative of the World Conservation Union (IUCN) and the World Bank (WB) published a paper entitled Dams and Development - The New Decision Framework and Development: A New Framework for Decision-Making". The International Commission for the Protection of the Danube River (ICPDR) explicitly sets forth the development of sustainable hydropower in the "Sustainable Hydropower Development in the Danube Basin Guiding Principles".

At present, the relevant evaluation of hydropower projects in China mainly focuses on the planning, preparatory stage and implementation stages, while the operational stage is relatively inadequate, especially in terms of environment and immigration. Relevant policies, standards and norms concerning planning, preparation, implementation and operation of hydropower station, are issued to identify stakeholders in China. Sustainable development issues should be addressed, and specific recommendations and supporting policies should be given to promote the sustainable development of hydropower.

China's large and medium-sized hydropower project, has led the local economy, improved the environment, and enrich the social responsibility of immigration. Subsequent research on hydropower development sustainability evaluation has to be combined with other systems, such as negative listing system and ecological compensation system to improve the ecological environmental benefits of hydropower projects. And it's helpful to treat immigration in addition to reservoir anti-poverty policies as well as engineering benefit sharing mechanisms.

The issue of sustainable development of hydropower in China is not only a policy issue, but also a technical issue. Many problems occurred in the process of hydropower development, which affected its positive development and system in the status and in turn. In the future, we must seize the opportunity of power system reform and study-related supporting policies regarding sustainable development of hydropower from the aspects of finance, taxation, electricity price and financial subsidies. We must also establish an incentive mechanism to alleviate the contradictions between local governments and businesses, and achieve a win-win situation.

Keywords: hydropower sustainability, evaluation system, international projects, Belt and Road Initiative

COMMISSION INTERNATIONALE DES GRANDS BARRAGES

VINGT-SIXIÈME CONGRÈS DES GRANDS BARRAGES
Autriche, juillet 2018

DOI 10.3217/978-3-85125-620-8-138



This work licensed under a Creative Commons Attribution 4.0 International License. <https://creativecommons.org/licenses/by-nc-nd/4.0/>

DAM PROTECTION GATES – ARE WE SOFT ON RISK?

Russ DIGBY

Regional Managing Director, KGAL CONSULTING ENGINEERS LTD

UNITED KINGDOM

Ken GRUBB

Consultant Technical Director, KGAL CONSULTING ENGINEERS LTD

UNITED KINGDOM

Paul JONES

Associate Director, KGAL CONSULTING ENGINEERS LTD

UNITED KINGDOM

COMMISSION INTERNATIONALE
DES GRANDS BARRAGES

VINGT-SIXIÈME CONGRÈS DES
GRANDS BARRAGES
Autriche, juillet 2018

DAM PROTECTION GATES – ARE WE SOFT ON RISK?

Russ DIGBY

Regional Managing Director, KGAL CONSULTING ENGINEERS LTD

UK

Ken GRUBB

Consultant Technical Director, KGAL CONSULTING ENGINEERS LTD

UK

Paul JONES

Associate Director, KGAL CONSULTING ENGINEERS LTD

UK

1. INTRODUCTION

At the simplest level, risks associated with dam protection gates can be classified into two headings, namely Hard and Soft. Hard risks are those that have defining factors and a great deal of statistical data. They include machinery failure, power failure and storm events. They are generally quantifiable, analytical and can be stated within statistical limits.

Soft risks are often people-related and include factors which are difficult to analyse. They include, without limit, ethos and culture, leadership and incentives, communications, human psychology, change and complexity. Such risks are often difficult to identify and quantify. As Engineers, do we under-estimate these risks

because we are naturally disposed towards analysis and it is easier to operate where numbers are available?

This paper explores the source of soft risks and attempts to learn lessons by reference to previous studies into fields such as finance, corporate governance and accident investigations. As such, it explores “Human Factors” relating to individuals, groups and organisations. In case there is any doubt as to the need to explore the non-technical issues, we quote below an extract from the Oroville Investigation into the failure of the spillway:

“The fact that this incident happened to the owner of the tallest dam in the United States, under regulation of a federal agency, with repeated evaluation by reputable outside consultants, in a state with a leading dam safety regulatory program, is a wake-up call for everyone involved in dam safety.”

2. HOW PREVALENT ARE SOFT RISKS?

In order to make an immediate case as to the importance of soft risks reference is made to a number of areas, starting with accident investigations. The United Kingdom’s Health and Safety Executive (HSE) in their evidence to a parliamentary science and technology committee previously stated that:

“It has been estimated that 90% of all workplace accidents have a human error as a cause”

Indeed, human error was cited as a significant constituent in many of the notorious industrial accidents, which have led to subsequent independent enquiries. The following examples are quoted as examples of incidents/accidents with a strong human influence:

Accident, Industry and Date	Consequences	Human Contribution
Three Mile Island, Nuclear Industry 1979	Serious damage to core of nuclear reactor	Operators failed to diagnose a stuck open valve due to poor design of control panel, distraction of 100 alarms activating and inadequate operator training. Maintenance failures had occurred before, but no steps had been taken to prevent them recurring.

Kings Cross Fire Transport Sector 1987	A fire at this underground station in London killed 31 people.	A discarded cigarette probably set fire to grease and rubbish underneath one of the escalators. Organisational changes had resulted in poor escalator cleaning. The investigation pointed to poor fire training and a culture that viewed fires as inevitable.
Space Shuttle Challenger Aerospace 1986	An explosion shortly after lift-off killed all seven astronauts on board	An O-Ring seal on one of the solid rocket boosters split after take-off releasing a jet of ignited fuel. Inadequate response to internal warnings about the faulty seal design. Decision to go for launch in very cold conditions. Decision making result of conflicting scheduling/safety goals, mindset and effects of fatigue.
Total IT failure for British Airways 2017	All flights grounded knock-on costs from stranded passengers and planes "in the wrong place".	According to BA, caused by an employee who disconnected a power supply which created a surge when re-connected. Employee was "not authorized to do what he did"
Virgin Galactic crash 2014	Co-pilot unlocked braking system too early	The National Transportation Safety Board determined the cause of the breakup of SpaceShipTwo was Scaled Composite's failure to consider and protect against human error and the co-pilot's premature unlocking of the spaceship's feather system as a result of time pressure and vibration and loads that he had not recently experienced.

<p>Hawaii false missile alert. Hawaii Emergency Management Agency 2018</p>	<p>Panic and fear as the following text alert was issued to residents of Hawaii: "BALLISTIC MISSILE THREAT INBOUND TO HAWAII. SEEK IMMEDIATE SHELTER. THIS IS NOT A DRILL."</p>	<p>The incident occurred when a supervisor gave the arriving day-shift workers a spontaneous drill, according to a Federal Communications Commission report. The supervisor posed as a military official and played a message that warned workers of a fake threat and included the phrase "exercise," three times, as well as "this is not a drill," language that would be used during a real alert.</p> <p>The employee who issued the missile alert claimed he hadn't heard the portion of the message that repeatedly declared it was an "exercise" because a co-worker had placed the call on speakerphone partway into the message.</p>
--	---	--

In the case of commercial corporate crises, several investigations have been made into the reasons behind the failure of large institutions, that were otherwise seen as healthy immediately prior to their problems. In a study of such cases undertaken by the Cass Business School, named "Roads to Ruin", the authors looked at a number of major financial risk events, their origins, impact and implications.

The report investigated "over twenty" corporate crises often involving major international brands (who are named in the report but not important for the purposes of this paper) whose pre-crisis assets were collectively worth about \$6 Trillion. The report noted that:

"The organisations themselves were badly affected by the outcomes. Seven companies collapsed under the strain, in 11 cases the chairman and/or CEO lost their jobs. In 16 cases the company and/or executives suffered financial penalties. Personal reputations were destroyed; Four executives went to prison".

The CASS report noted numerous underlying types of weakness which they distilled into key risk areas including the soft risks of:

- Inadequate ethos, culture and behaviour;
- Poor leadership and inappropriate incentives;
- Poor internal communication, including getting information to the top;
- Change and complexity;
- Reputation

Staying with the financial sector, Anthony Hilton a highly respected City Editor is quoted as saying:

“ Risk systems tend to be numbers-based, and cover potential hazards or current operations. They can cover hard data, technical know-how, systems and strategies. What they don’t do is handle soft issue such as management style, employee motivation, shared values and corporate culture. They are hopeless at behavioural issues. So for that matter are male only boards....

....The trouble with accounting performance measurement and risk control – and indeed the teaching of business schools – is that they treat companies as if they are mechanical. They assume broadly that they are machines which, for a certain level of inputs, will deliver a predictable level of output. But the greater truth, particularly in the modern era where talent is the big differentiator, is that companies are collections of people, and they are as much biological as mechanical”.

Although the above quote was written in the context of financial risk it resonates at the anecdotal level with personal experiences. For “financial accounting performance measurement” could we substitute “engineering reliability studies”?

3. WHAT ARE THE “HUMAN FACTORS”?

Before making further progress, it is worth reviewing what are generally considered to be “human factors” and which are the root cause of many so-called soft risks.

It should also be recognized that cultural differences throughout the World make it difficult to be too universal in our observations. Most of the research drawn upon herein relates to Western civilisations.

3.1. WHY ARE HUMAN FACTORS IMPORTANT?

Estimates suggest that Human Factors are the primary cause of between 60% and 85% of incidents. They emerge because machinery and systems are:

- Designed by humans
- Built by humans
- Programmed by humans
- Tested by humans
- Commissioned by humans
- Operated by humans
- Modified by humans
- Maintained by humans
- Decommissioned by humans
- Disposed of by humans

3.2. HUMANS AS INDIVIDUALS

Human beings are very complex and no two of us are alike. The variability in our capabilities is marked and yet most tasks assume they are being undertaken by a standardised, competent person. In reality each of us is more or less competent from one day to another.

In addition, we tend to over-estimate our own competence usually thinking we are above average. This phenomenon has been given the name “illusory superiority”. In a recent survey, rating how good a car driver they were, most people gave themselves a score of seven out of ten having been told that average was five. In another study 32% of employees in a software company ranked themselves above 19 out of 20 of their colleagues.

It is interesting to note that a common reason given for introducing computers and artificial intelligence into financial processes, is that the computers make better decisions than humans.

In respect of human errors, industrial psychologists sometimes use the terms “slips”, “lapses” and mistakes. The general definition being that:

- A slip is a failure to undertake the task correctly. It could be performing the task too soon or late. Or it could mean omitting to perform a step.
- A lapse is a failure to carry out an action, perhaps one task in a series of tasks. For example the omission of steps in maintenance has been cited as a substantial cause of nuclear power plant incidents.
- A mistake involves doing something wrong that we believe to be right (there is still the problem of a deliberate error or (violation”). These tend to be of two categories knowledge based or rules based.

Such human slips, lapses and mistakes come about for lots of reasons.

3.2.1. Attention

People have a limited attention span which has been estimated to be about twenty minutes before fatigue sets in and errors are more likely to occur.

Regular tasks become habit forming so that when repeated often enough they become automatic responses rather than reasoned decisions. By way of an example, in a historic study of automatic train protection on the UK network the following was observed in respect of train driver behavior:

The automatic warning system installed on passenger trains in the UK is an example of a system that was not designed with the limitations of human attention in mind. It is a device fitted in the train cab, based on the new obsolete mechanical system of signaling that used to signal either STOP or PROCEED. It sounds a bell when a clear (green) signal is passed and a buzzer when caution or danger is signaled. If the buzzer is not acknowledged by a press of the button, then the train begins to automatically

stop. In commuter traffic, most signals will be at “caution” aspect, and given the frequency of signals (spaced 1 km apart), most drivers will face two signals per minute. Given the tendency for the attentional system to automate highly repetitive behavior, many drivers lose focus on the reasons for carrying out this repetitive task, and act in reflex whenever the buzzer sounds. The end result is that drivers often hear the buzzer and press the button reflexively without actively thinking about train speed and location.

3.2.2. *Perception*

Perception relates to how we interpret information from our senses. A particular problem is that people are often required to interpret information rather than receive it directly. The interpretation of the information is a source of error and hence risk.

3.2.3. *Memory*

People’s short-term memory has a limited capacity. Tests have shown that we can typically hold only seven individual items at a time in our memories.

3.2.4. *Logical Reasoning*

Humans are not always good at logical reasoning. During the Three-Mile Island nuclear accident, two valves which should have been open were blocked shut. The operators incorrectly deduced that they were in fact open because of an illogical assumption about the instrument panel.

3.2.5. *Situation Context*

Having identified individual failings in human beings, we should also recognize that our performance in any particular situation is greatly affected by the context we are working in. If we are tired, we will not perform so well and may also work poorly within teams.

We will all have seen people who perform badly when trying to answer a question on a TV quiz show, the answer to which they know but cannot recall under the pressure of the situation.

3.3. HUMANS IN SMALL GROUPS

Over recent decades the principle of building winning teams has become an axiom that few people dispute. The belief that working in teams makes us more creative and successful has become one from which there is little dissent. And yet the Harvard Business Review recently identified a list of problems associated with people working in teams, which included:

- The absence of a team identity such that there is a conflict between team and personal goals. Here individuals are described as being self-centred or half-hearted.
- Difficulty in making decisions because of rigid adherence to individual positions
- Poor communications including silence from some members and constant talking from others. Perhaps personality clashes.
- Inability to resolve conflicts, perhaps because of heightened tensions or perhaps stubbornness
- Lack of creativity prevents seeing problems as opportunities
- “Groupthink” where the team is not open to discussing new alternatives but has a fixed view of a situation into which the members “buy in”
- Ineffective leadership, perhaps by failing to convey a vision or failing to delegate.

3.4. HUMANS IN LARGE ORGANISATIONS

The difference between small teams and large organisations is that the team may have little interaction with their senior management within a large organization. This presents new sets of problems that may lead to risks.

Principal among these risks is the establishment of a culture which may not be appropriate for the organisation as a whole. Frequently this can be driven by inappropriate incentives. For instance, a large oil refining company rewarded their staff if no accidents had been reported over a period. Rather than report minor incidents there was a culture of not reporting them to avoid losing their reward. And so was lost valuable opportunities to identify ways of improving safety. Here is a good example of poor communications and the wrong incentives.

The culture of an organisation is significantly set by its reward systems. Do the compliant get promoted do the dissenters get moved on? Does the Board of Directors want to know?

Much evidence exists that reward systems are a strong indicator of the health of a safety culture. Where employees are rewarded for achieving no accidents, then no accidents are reported. Where they are punished for causing accidents, they will be hidden, or acts will be denied.

What levels of training are available to front-line staff?

4. THE EVIDENCE THAT SOFT RISKS AFFECT DAMS?

In the recent report on the Oroville dam spillway failure, there are a number of references to problems at the human level, including complacency, bureaucracy and an inadequate safety culture. For instance the report notes:

- the California Department of Water Resources, was “significantly overconfident and complacent about the integrity of its State Water Project civil infrastructure, including dams.”
- “insular organization which inhibited accessing industry knowledge and developing needed technical expertise.”
- an “insular organization which inhibited accessing industry knowledge and developing needed technical expertise.” Within the department, the engineering division clashed with the operations and maintenance staff, resulting in a “lack of mutual respect,” it found.

Andrew Brazier reports that upon reviewing the prevalence of Human Error in the US forces:

“Further to this, 20% of defects are missed by inspectors who are specifically looking for them and the U.S. Strategic Air Command claim that 16% of all critical events are made worse by human intervention.

5. APPLYING SOFT RISK LESSONS TO THE PROTECTION OF DAMS

The application of systems and procedures aimed to reduce soft risks, requires commitment from the top. Without an understanding of the issues raised there will be little chance of addressing them. The values inherent in the proposals herein must be communicated from the top and demonstrated by main board actions.

Once the main board is united, they need to get the safety culture right. In general, this needs:

- A single, responsible person at the top for dam safety issues.
- A balanced board, both for skills and gender.
- The avoidance of incentives for the lack of recorded incidents and accidents, since this encourages non-disclosure. Rather the encouragement and celebration of opportunities to learn from experience.
- The non-punishment of mistakes.
- The encouragement of an open, honest and respectful dialogue between work colleagues without dependence on where they are placed in the organization hierarchy. It is important that incidents can be investigated and reported upon without putting a career at risk.
- The regular look for new and better ways of doing things.

- The encouragement of external collaboration, whether with expert consultants or shared experiences with other organisations similar to your own.

Once the culture is right, then:

- Simplify tasks as far as practicable. Design jobs so that the work entailed is less complex. For instance, a shaft containing eight discs has only one way to disassemble them but over 40,000 ways of putting them back together!
- Continually train staff. Make sure they understand the why as well as the what within their jobs. Many human interventions during a crisis only make matters worse
- Try to organize instrumentation so that it presents information and not just data, this reduces the degree of interpretation required of staff.
- Remember that soft risks can be present in the supply chain. Do suppliers share the same safety culture?

6. CONCLUSIONS

The presence of soft risks and the need to control them does not in any way diminish the importance of reliability analysis relating to hard risks. The need is to find ways of addressing and minimizing both.

This paper has explored at a high-level the frailties and quirks of the human condition and shown how these can be embraced in a way that can reduce risk and thereby improve safety.

Finally, in case the reader is still not convinced, here is a direct quote from the official report into the Oroville dam spillway failure:

“The fact that this incident happened to the owner of the tallest dam in the United States, under regulation of a federal agency, with repeated evaluation by reputable outside consultants, in a state with a leading dam safety regulatory program, is a wake-up call for everyone involved in dam safety.”

REFERENCES

- [1] BRAZIER A. Human Error and the Implications for Industry.
- [2] WHITTINGHAM R B. The Blame Machine, Why Human Error Causes Accidents – R B Whittingham published by Elsevier Butterworth Heinemann.
- [3] Reducing Error and Influencing Behaviour – UK Health and Safety Executive

COMMISSION INTERNATIONALE DES GRANDS BARRAGES

VINGT-SIXIÈME CONGRÈS DES GRANDS BARRAGES
Autriche, juillet 2018

DOI 10.3217/978-3-85125-620-8-139



This work licensed under a Creative Commons Attribution 4.0 International License. <https://creativecommons.org/licenses/by-nc-nd/4.0/>

HYDRAULIC ASSESSMENT OF TUNNELS

Balkrishna Shankar CHAVAN

Scientist-D, CENTRAL WATER AND POWER RESEARCH STATION, PUNE

INDIA

COMMISSION INTERNATIONALE
DES GRANDS BARRAGES

VINGT-SIXIÈME CONGRÈS DES
GRANDS BARRAGES

Autriche, juillet 2018

HYDRAULIC ASSESSMENT OF TUNNELS

Balkrishna Shankar CHAVAN,

Scientist-D, Central Water and Power Research Station, Pune

India

1. INTRODUCTION

A river diversion tunnel is used to divert river water during construction of a project. Once construction is over, diversion tunnel is plugged before initiating storage of water consequently tunnel part becomes redundant. No universally accepted standards are available for design of temporary structures like coffer dams and diversion tunnels. Tunnel construction has high costs and usually adopted when other solutions are unfeasible. Length of tunnel is kept minimum as possible. To minimize the project cost, part of diversion tunnel can be reused for depletion of reservoir storage. There are instances where part of river diversion tunnels have been used as depletion tunnel after construction of dam is completed. In India projects such as Yamuna, Doyang, Nagarjunsagar, Salal have successfully used the concept of multipurpose tunnel for diversion of river flow and depletion of reservoir. Hydraulic design associated with such tunnels has to function satisfactorily for high discharge at low head during construction and also high head

low discharge during operation period of project. Present paper describes hydraulic problems associated with design of diversion cum depletion tunnel. Methodology adopted to arrive at solutions for design parameters in selecting flood flow, tunnel flow capacity during diversion as well as depletion, transitions in shape, energy dissipater at tunnel exit and smooth return of flow to river downstream of the structure.

1.1. NEED FOR DIVERSION OF WATER

Urban centers are providing job opportunities, educational facilities and better living, because of which people migrate to cities. The rate of population growth of metropolitan and urban cities of India is unprecedented. Mumbai being the capital city of the state of Maharashtra is also the commercial and financial capital of the country. Actual growth of city and forecast is shown in Figure. 1.

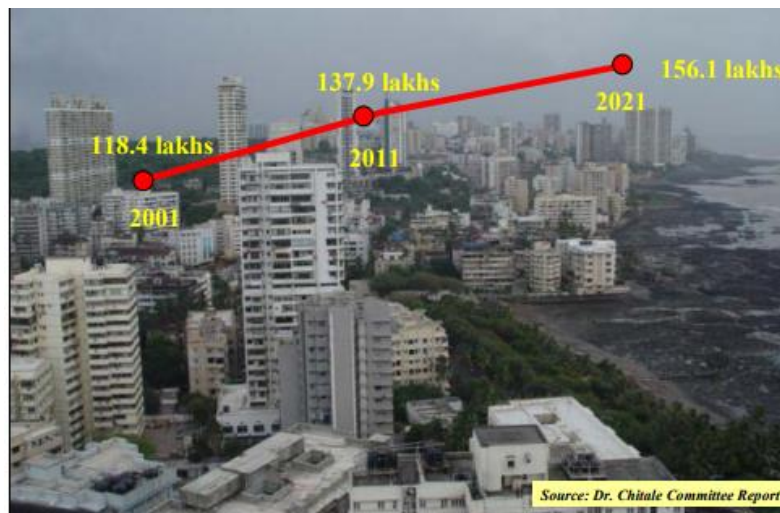


Figure 1: Population Growth of Mumbai City

1.2.

To meet increased demand of water of Mumbai urban agglomerate, a proposal of interlinking Damanganga and Panjal rivers is proposed.

The link envisages transfer of balance available water at the proposed Bhugad reservoir across Damanganga river and at the proposed Khargihill reservoir across Vagh river, a tributary of Damanganga river, in Damanganga basin for augmentation of water supply to Greater Mumbai to meet its domestic and industrial water requirements in the near future. The Bhugad and Khargihill reservoirs (proposed by NWDA) and Pinjal reservoir (proposed by Government of Maharashtra across Pinjal river, a tributary of Vaitarna river) are proposed to be connected through pressure tunnels. The purpose is to make the combined water from Bhugad and Khargihill reservoirs to reach Pinjal reservoir from where further arrangements for transmitting the water to Greater Mumbai will be made by Municipal Corporation of Greater Mumbai (MCGM) and Mumbai Metropolitan Region Development Authority (MMRDA)[6].

The salient details of Damanganga-Pinjal link project are briefly described below:

- A 826.60 m long composite dam is proposed on Damanganga river near village Bhugad in Peint taluka of Nasik district of Maharashtra State and very near to border of Valsad district of Gujarat. The FRL, of the dam fixed on the basis of detailed Surveys & Investigations at 163.87 m. The gross and live storage capacities of the storages are 426.39 Mm³ and 400.00 M m³ respectively. The maximum height of dam is 68.63 metres.
- A 16.85 km long Bhugad-Khargihill link tunnel with 5.0 m diameter connecting Bhugad and Khargihill reservoirs below their minimum draw down levels (MDDLs)is proposed.
- A 572.80 m long composite dam across river Vagh at Khargihill site near village Behadpada in MokhadaTaluka of Thane district of Maharashtra State is proposed. The FRL, of the dam fixed on the basis of detailed Surveys & Investigations at 154.52 m. The gross and live storage capacities have been fixed as 460.79 Mm³ & 420.50 Mm³ respectively. The maximum height of dam shall be 75.62m.
- A 25.70 km long Khargihill-Pinjal link tunnel with 5.25 m diameter connecting Khargihill and Pinjal reservoirs below their MDDLs.
- A 681 m long Pinjal dam on river Pinjal (tributary of Vaitarna river) near village Khidse in Jawhar taluka of Thane district has been proposed by Govt.of Maharashtra. The FRL, have been fixed on the basis of detailed Surveys & Investigations by Government of Maharashtra as 141.00 m. The gross and live

storage capacities have been fixed as 413.57 Mm³ and 401.55 Mm³ respectively.

The divertable water yield to Mumbai city at Pinjal dam site at 75% dependability (as fixed by Government of Maharashtra) is 332 Mm³. Thus, a combined release of 43.84 cumecs of water i.e. 3741MLD will be diverted through Pinjal reservoir. Figure 2 shows typical layout of linking Damanganga and Pinjal rivers.



Figure 2: Linking Damanganga and Pinjal rivers

1.3.

The Beas-Sutlej link is 37.25 km long of which 25.45 km is tunnel through difficult rock formations. The capacity of the tunnel is 254.70 cumec. The main storage on Satluj is at Bhakra, while that on Beas is at Pong. A diversion dam at Pandoh, 140 km upstream of Pong, enables diversion of water from Beas to Bhakra reservoir and generates 165 MW of power. Bhakra system provides irrigation to 26.3 lakh ha. of new area besides stabilization of existing irrigation of 9 lakh ha. The aggregate generation capacity of power on Bhakra Nangal Project is 1,354 MW. Beas-Satluj link in combination with the Indira Gandhi Nahar Project is an example of how the large inter basin transfers brought about all round socio-economic growth with overall enhancement in the ecology and environment of the region.

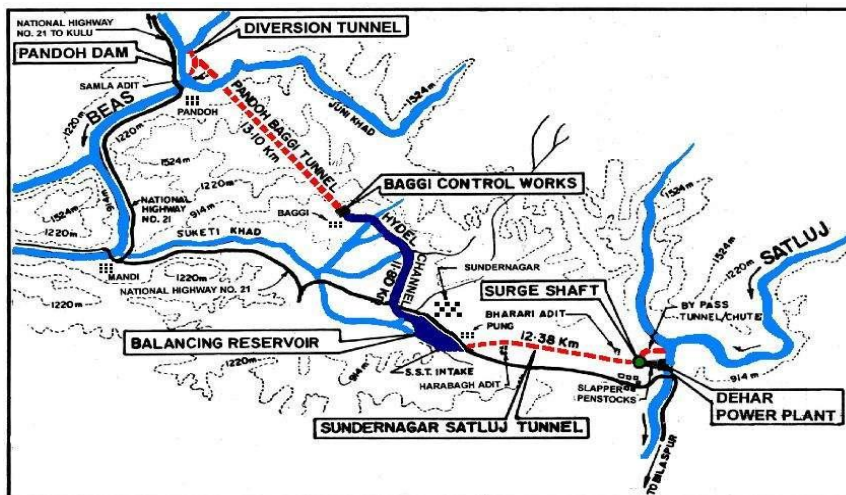


Figure 3: Tunnel for inter linking Beas and Satluj rivers

In addition to transferring water from deficit region, diversion tunnels are used to divert water during construction of dam. The scheme of this type of diversion is characterized by the completion of the diversion tunnel and two coffer dams (upstream and downstream) that will dry the area, in which, it is intend to carry out the dam construction. Tunnels are commonly used to convey water from its source to demand area. Even though costly, compared to surface hydraulic structures, depending upon geological features of the surrounding hills. Complicated geological conditions and extraordinary geological occurrences such as intra-thrust zones, very wide shear zones, geothermal zones of high temperature, cold/hot water springs, water charged rock masses, intrusions, fault planes, etc. should preferably be avoided. Sound, homogeneous isotropic and solid rock formations are the most suitable for tunnelling work. However, in the Himalayan region, such conditions are rather rare compared to the hills of peninsular India. This is because the Himalayan geological formations are mostly sedimentary in nature whereas the peninsular upland of the country is of igneous nature. Hence, geological investigations have to be carried out in detail before a tunnel alignment is finalized. The river diversion tunnel has the function to drain the bypass flow, and may have several sections. However, the sections most frequently used are circular and horseshoe. The choice and design of the type of section employed is related to the final design of the diversion tunnel in relation to its integration or not in the definitive structure. The diversion of the river through tunnels can be held in free surface or pressure flow.

2.

Main components of a water conveyance system for diversion of river water consist of the following components:

1. Intake structure
2. Water conducting system (Tunnel) comprising of control structures.
3. Outflow structure, which joins river flow downstream

2.1. INTAKE STRUCTURE ENTRANCE

An intake is provided at the mouth of a water conveyance system for a diversion of river flow.

It is designed with the following points:

1. There should be smooth entry of water in to the tunnel as water enters from the reservoir behind a dam or the pool behind a barrage into the tunnel.
2. There should not be any formation of vortices that could draw air into the water conducting system.
3. There should be minimum entry of sediment into the water conducting system.
4. Floating material should not enter the water conducting system.

Inlet structure: Inlet transition facilitates the flow acceleration, ensuring the transition from subcritical flow which is established upstream in the reservoir created by the construction of the cofferdam or, in some cases, the channel connecting the bed to the frame, to supercritical flow that occurs in the diversion tunnel. The implementation of this structure aims to promote sufficient air to the flow, so that it develops a pressure equal to atmospheric pressure along the tunnel. This avoids the possibility of reaching pressures near the water vapour pressure, reducing the risk of cavitations phenomena in the diversion tunnel and hence its erosion. Regarding installation of the inlet structure it may be implemented directly on the ground or resort to auxiliary concrete that supports it above the ground level.

For smooth entry of water in to the tunnel, generally following elliptical equation is used

$$\frac{x^2}{D^2} + \frac{y^2}{0.33D^2} = 1 \quad (1)$$

In the inlet structure design it is important to proceed to the analysis of flow velocities that are practiced within and upstream the structure. To this end, the ratio of the velocity flow in the control structure and velocity flow upstream the structure must be in a range of 2 to 5. The inlet separation. In order to drain maximum water sometimes no curve is provided to bottom surface of tunnel which is in touch with invert of approach channel. The flow separation may occur in the transition river section with irregular section for the tunnel section, usually circular or horseshoe sections.

3. GEOMETRIC DESIGN

Sections usually adopted for tunnels are covered in IS 4880 (Part III, Hydraulic design) -2000[1].

The functional requirements are defined in a broad sense. Design requirements include all hydraulic and geometric, ancillary and environmental, logistics, and maintenance requirements and limitations.

3.1. TUNNEL DIMENSIONS

should be decided on the basis of economic studies so as to obtain a most economical section. The following should be taken into account:

Discharge passing through the tunnel flowing partial full is given by:

$$Q = \frac{2}{3} B C_d \sqrt{2g} H^{\frac{2}{3}} \quad (2)$$

Where Q= Discharge passing through the tunnel in m³/s

B= Width of tunnel in m

C_d= Coefficient of discharge

g= Acceleration due to gravity

H= Net head in m

Velocity in tunnel, computed by Manning's equation

$$V = \frac{1}{n} R^{\frac{2}{3}} S^{\frac{1}{2}} \quad (3)$$

Where V= Velocity of water in the tunnel in m/s

n= Coefficient of rugosity for unlined tunnels may range from 0.04 to .06

R= Hydraulic radius in m, for sections other than circular R = 4

S= Longitudinal slope

3.2. HEAD LOSS

- Following losses may be expected for flow in diversion Tunnel:

- Head loss in approach channel, if tunnel is located away from reservoir
- Head loss at intake entrance

$$h_e = k_e \frac{V^2}{2g} \quad (4)$$

Where

h_e , K_e are head loss and loss coefficient s respectively

$K_e = 0.16$ for square bell mouth entrance

= 0.03 for circular bell mouth

= 0.1 for gate wall rounded corners

Head loss due to gradual contraction

$$h_e = K_e \left(\frac{V_2^2}{2g} - \frac{V_1^2}{2g} \right) \quad (5)$$

Here $K_e = 0.10$

Other losses as at bends, transitions, etc.

Head loss due to tunnel friction, calculated with the help of Darcy Weisbach resistance equation:

$$\text{Head loss} = h_f = \frac{fLV^2}{2gD}$$

Where

h_f = Head loss in m

f = Friction factor

L = Length of stretch

3.3. ESTIMATION OF FRICTION FACTOR

Implicit equation for estimation of friction factor was given by Colbrook in 1939

$$\frac{1}{\sqrt{f}} = -2 \log \left[\frac{\frac{e}{D}}{3.7} + \frac{2.51}{Re\sqrt{f}} \right] \quad (6)$$

This equation needs iterative steps for its solution. Many investigators (some of them are listed in Annexure A) proposed approximate solution in form of explicit equation. Two power explicit equation given by the author (2017) Chavan is very convenient :

$$f = \frac{0.0075 \left(\frac{(4000)^{0.05}}{Re} \right)}{0.25 + \left(\frac{4000}{Re} \right)^5} + \frac{20}{Re} \quad (7)$$

Where f = Friction factor

Re = Reynolds Number given by

$$Re = \frac{\rho DV}{\mu} \quad (8)$$

μ = Coefficient of Dynamic viscosity

Exit head loss is

$$h_e = k_e \frac{V^2}{2g} \quad (9)$$

Discharging capacity- Discharge passing through the tunnel flowing full is computed backwardly, using known head loss, known conditions in which tunnel is being operated i.e. Reynolds number, and friction factor curves for operation characteristics of particular tunnel are prepared.

Based on the above losses, the diameter of the tunnel has to be fixed, such that it results in an overall economy. This is because if the diameter of a tunnel is increased, for example, the friction losses reduces

The tunnel diameter determined as a result of economic studies should be examined from practical considerations, such as space requirements for the excavating equipment and the section may be modified if necessary, based on the

above considerations. A minimum height of 2 m is necessary. For mechanized handling of excavated material a minimum section of 2.5m x 2.5 m is required. Approach Channel for diversion tunnel- The dimensions and alignment of the excavated approach channel upstream from the river to the tunnel and of the discharge channel to convey the water back to the river downstream are determined by the hydraulic design requirements and the stable slopes for the material excavated

4. THE TUNNEL SLOPE, LENGTH

The tunnel longitudinal slope, S , has no typical value as it depends on the geometry of the river and the valley but generally is of the order of the riverbed slope at the site. The effect of the slope is to add $L \times S$ to H . Therefore, if the slope increases, the discharge capacity of the tunnel increases and the required cofferdam height decreases. When S is significantly different from the average value assumed, the effect on the cofferdam height estimated from guides in this study should be accounted for. A circular diameter (D) of the tunnel is used to represent and compute the tunnel cross-sectional area available for the flow. In the case of the horseshoe section, the equivalent circular section should be employed. L depends on the extent of the site needed to remain dry and is typically a few tens of meters more than the base width of the dam. It is generally greater for embankment dams than for concrete dams. In any given project, L is fairly fixed and is not subject to optimization here. In the optimization attempt, D and H are inter-related and vary together. Greater H requires smaller D and vice versa. Longer tunnels are generally associated with smaller optimum diameter- D_{optimum} regardless of Q and W and the support type. When the tunnel is very long, an overly large tunnel must be avoided and heightening of the cofferdam should be examined instead. It is prudent that some who follow the tradition of determining D only by Q and W often overlook the simple fact of dependency of D_{optimum} on L . Reservoir depletion tunnel comprises three sub-structures: Inlet Structure, Tunnel body and Outlet Structure. Section of a depletion tunnel studied at Central Water and Power Research Station is shown in Figure 4

5. TUNNELS

Tunnels need to be designed and constructed in an efficient manner for the best performance. The Bureau of Indian Standards code IS: 4880-1976 “Code of practice for design of tunnels conveying water” (Parts 1 to 4)[1] provides guidelines for design of a tunnel under various situations. The following are the salient points.

5.1. TUNNEL LAYOUT

The first aspect that needs to be decided for a tunnel is the alignment, that is, the route layout of the tunnel in plan. Figure 5 shows the possible alignment for the tunnel water conveyance system for a diversion of water through tunnel. The inlet structure geometry must be hydrodynamic, both in plan and in longitudinal profile to avoid flow separation. The flow separation may occur in the transition river section with irregular section for the tunnel section, usually circular or horseshoe sections

The layout is usually governed by the geological features of the surrounding hills. Complicated geological conditions and extraordinary geological occurrences such as intra-thrust zones, very wide shear zones, geothermal zones of high temperature, cold/hot water springs, water charged rock masses, intrusions, fault planes, etc. should preferably be avoided. Sound, homogeneous isotropic and solid rock formations are the most suitable for tunnelling work. However, in the Himalayan region, such conditions are rather rare compared to the hills of peninsular India. This is because the Himalayan geological formations are mostly sedimentary in nature whereas the peninsular upland of the country is of igneous nature. Hence, geological investigations have to be carried out in detail before a tunnel alignment is finalized.

5.2. TUNNEL BODY

The flow in a river diversion tunnel should occur in supercritical scheme to provide quick acceleration required by deploying of upstream structure. In

the river diversion tunnel design it should be noted that in the river diversion through this structure, the flow depth should progress to uniform depth. Thus, it is necessary to define under which conditions the flow is to proceed along the diversion tunnel. Therefore, it is possible to conclude the existence of hydraulic jumps inside the tunnel and determine its location. Studying the flow conditions inside the tunnel consists of analyzing the flow depths along the tunnel by defining the backwater curves. Thus, it is important to trace the backwater curves for diversion tunnel with the goal of establishment the various flow depths along the structure allowing the flow classification.

Flow conditions in tunnel: The occurrence of hydraulic jumps inside the river diversion tunnel can cause structural problems. By establishing the different depths inside the tunnel, it is possible to determine the amount of total movement inside it and the hydraulic jump position. Knowing the flow depths is very important in the study of the river diversion tunnel, so it is imperative to establish backwater curves inside the tunnel. This computation is based on the Bernoulli's theorem.

Free surface flow: In most cases, flow takes place in free surface and should not exceed 70% of the tunnel capacity. When deploying a river diversion with pressure flow, it must be ensured that the structure's altimetry track allow the respective domes to always be situated below the isometric line to avoid depressions that may cause structural and hydraulic inconvenient. The study of flow through the tunnel is hampered by the tunnel geometry. The tunnel cross section assumes generally circular or horseshoe geometry. In case of using a river diversion tunnel is possible to convert it in the bottom discharge of the final structure. This approach has advantages, especially in project costs.

The location of diversion tunnel or tunnels is affected by topography, abutment foundation conditions, hydraulic requirements, and economy of construction. Except for some high-head dams, it usually is economical to place an outlet tunnel near stream elevation and use it for diversion during construction. A tunnel should be located far enough into the abutment to obtain adequate cover for the character of rock encountered, and the tunnel alignment must meet the hydraulic

requirements. The most economical location to pass around or under the dam and meet the foregoing requirements should be selected. An alternate plan used for some deep reservoirs has a high-level intake at the head of an inclined tunnel connecting with a tunnel through the abutment near river level. After serving its purpose of diversion during construction, the low-level tunnel is plugged at the upstream side of the intersection and the inclined tunnel and downstream portion of the low-level tunnel with a connecting curved transition from the permanent outlet. This plan may be economical and satisfactory under special conditions where the reservoir is very deep, the minimum water surface is high, and rock foundation is adequate. Because of the difficult foundation and structural problems involved in this type of construction, thorough foundation investigations and comparative studies should be made and this plan should not be selected without full analysis of its practicability and economy. The advantage of the high-level intakes for a very deep reservoir is the lower intake structure and lower head on intake gates, resulting in a less expensive intake structure. Disadvantages of this type of outlet are: cost of the inclined tunnel, difficulty of obtaining an adequate foundation for the intake structure, and the difficulty of excavation for and the complexity of the transition structure at the junction of the inclined tunnel with the low-level tunnel. Particular care should be taken to obtain high quality concrete, smooth gradual curves, and good alignment at the junction. If the intake structure is located directly over the low-level tunnel, there should be an ample thickness of good, sound rock between the intake base and the tunnel to transmit the foundation loads to the main rock mass. Sometimes conditions may be favourable for locating the intake far enough to one side of the low-level tunnel to simplify the problem of supporting the intake structure. For some high dams, outlet works separate from diversion facilities and located much higher than the river channel may be suitable. In such cases, overall economy may result from use of separate high-level outlets and use of the downstream portion of the diversion tunnel as part of the spillway outlet.

5.3. NUMBER AND SIZE OF TUNNELS

The proper selection of number and size of diversion tunnels depends on hydraulic requirements, the maximum size of tunnel which it is practicable to drive in the rock encountered, operating flexibility, and economy of construction. In some instances it may be necessary to limit the size of tunnel in yielding rock to prevent excessive movement in the surrounding rock. Generally the larger the tunnel within practicable driving limits, the more economical it is per unit flow capacity. Also, the approach and discharge channels and the intake structure usually are more economical for fewer tunnels because the reduced width results in less channel excavation and a narrower intake structure. However, if it is necessary to use two parallel gates in each larger tunnel and only one in the smaller, the intake structure may not be reduced and economy may not be affected by use of larger tunnels. The most economical number of tunnels which will meet the other requirements should be used. A single tunnel is used when, as is frequently the case, the required diameter to handle the entire discharge is not over 20 ft to 25 ft. In order to provide reasonable operating flexibility, a total of not less than two service gates should be provided in the outlet works. In some cases, this requirement may influence the number of tunnels. Detailed design and construction procedures for tunnels are provided in EM 1110-2-2901, A Tunnels and Shafts in Rock[4].

5.4. INFLUENCE OF DOWNSTREAM LEVELS FOR DIVERSION TUNNELS

When dimensioning the river diversion tunnel it is important to study the influence of the downstream level into the flow conditions inside the tunnel, once it may not be guaranteed that the establishment of the uniform system within the diversion tunnel ensures that free surface flow occurs along its entire length. In order to proceed with the study of the downstream level influence, it is necessary to analyze the altimetry placement of diversion tunnel. Submerged flow considerably reduces the discharging capacity of the tunnel. A first stage begins by analyzing the total momentum inside the tunnel, comparing it with the natural bed total momentum. In the case of the natural bed total momentum overcome the values obtained in the tunnel, the hydraulic jump occurs inside the tunnel. Thus it

is possible to determine the existence of hydraulic jump, and if there is, proceeding to its location. The occurrence of a hydraulic jump inside the diversion tunnel involves a correction of the upstream altimetry position. The calculation of the flow depths by defining curves backwater enables the calculation of the total momentum into the river diversion enabling comparison with the total momentum in the natural bed and the location of the hydraulic jump.

5.5. MULTIPLE DIVERSION TUNNELS

For at least two reasons, the designer may choose multiple (mostly twin) tunnels to carry a large design flood: (i) large cross-section needed to divert large flood is associated with specific problems such as higher tunnel stability risks and expensive support measures, need for more complicated excavation or support equipment, and more risks brought about for the abutments specially when the overburden or the rock quality is not sufficient; (ii) the design flood may not happen during construction and the discharge in a great majority of construction days is much below the design flood. Therefore, twin tunnels may be constructed, one to carry the usual low and average discharges another with a higher invert elevation to carry the additional part of the design flood. When the second one is constructed sufficiently higher than the first, it may be mostly used as access road tunnel between upstream and downstream parts of the dam during construction, a double arch 180m high concrete dam under construction in southwest of Iran). The designer may choose to apply support but avoid RC lining in the second tunnel.

6. TUNNEL EXIT

It is also essential to design the entry and exit points of the tunnel very carefully. Where the tunnel emerges out of the hill slope, a structure in the form of an arch is usually provided, which is called the portal. Since at this point the water leaves the tunnel, it is prone to hydraulic head loss and erosion. Proper transition shape has to be provided to keep the loss minimum and to avoid cavitations. The length and slope of the transition depends upon the velocity and flow conditions prevailing in

the tunnel, economics, construction limitations, etc. It is generally preferred that a hydraulic model study is conducted to arrive at an efficient but economic transition. When a circular tunnel flowing partly full empties into a chute, the transition from the tunnel section to one with a flat bottom may be made in the open channel downstream from the tunnel portal or it may be made within the tunnel so that the bottom will be flat at the portal section. Ordinarily, the transition should be made by gradually decreasing the circular quadrants from full radius at the upstream end of the transition to zero at the downstream end. For usual installations the length of the transition can be related to the exit velocity. An empirical rule which may be used to design a satisfactory transition for velocities up to 6 m/s is as follows:

$$\tan \alpha = \frac{1}{F} \quad (10)$$

Where L = length of transition in m, v = exit velocity in m/s, and D = tunnel diameter in m

6.1. OUTLET STRUCTURE

The return diverted flow, through the river diversion, can be made through direct connection to the river or by deploying outlet structure. The deployment of the restitution structure may have two objectives, the dissipation of excess energy or the recovery of part of the kinetic energy. The need to implant a restitution structure is associated with the fact that the flow in the tunnel that is supercritical or if the downstream section of the tunnel is elevated compared to the river bottom, hindering establishment subcritical conditions in the restitution area. The outlet structure can match the deployment of a transition structure or deployment of stilling basin. Diversion tunnel discharge can be led to directly in to river depending upon gradient of river. To avoid bank erosion some form of bank protection is provided. In case of depletion tunnel exits, where high velocity may occur, energy dissipation arrangement has to be provided as shown in fig: 6. It works well as part jet is lifted to 35° splitting and spreading before plunging in to river pool.

7. COST ANALYSIS

Following are the main factors affecting overall cost of the tunnel

- a) Capital investment
- b) Cost of equipments
- c) Interest charges on capital cost of tunnel,
- d) Annual maintenance charges,
- e) Whether lined or unlined and
- f) Cost of gates and their hoists.

8. TUNNEL INSPECTION AND MAINTENANCE

Inspection of tunnel and its maintenance takes an important role in sustainable functioning of the tunnel. Inspection is carried out at lean water levels. Sometime tunnel has to be closed down. As such very little time is available for inspection as compared to other types of tunnels. Another hurdle for inspection of hydraulic tunnels is remoteness.

Cavitations: - Design shall be such that negative pressures are avoided. Cavitation observed at Sardar Sarovar tunnel is shown in Figure 4.



Figure 4. Prototype photograph showing exposed reinforcement inside Tunnel due to cavitations

Closing of river diversion: For diversion tunnels, it is necessary to close the flow through diversion tunnel to start filling the dam or divert the tributary flow through definitive structures that are completed. The temporary diversion closure can be permanent or temporary (Pinheiro, 2002). In temporary closure, it is common to use a gate. For permanent closing it is implanted a concrete plug inside the diversion structure. The planned temporary diversion closure must be programmed according to a study of local flow conditions and the closing of the river coincide with the dry season. The type of diversion structure influences naturally provisional closing. In the case of the structure consist of two diversion tunnels it is possible to make the closing of one of the tunnels continuing the flow to be diverted by other tunnel (ICOLD, 1986)[5].

REFERENCES

- [1] BIS 4880 (Part III, Hydraulic design)-2000, Code of practice for design of tunnels conveying water.
- [2] Balkrishna Shankar Chavan (2017), Unified Equation for Estimation of Friction Factor, Proceedings of 37th IAHR World Congress, Aug13-18, held at Kuala Lumpur, Malaysia Pages 5885-5893
- [3] Bureau of Reclamation (BUREC) 1987, Design of Small Dams, 3rd edition, Bureau of Reclamation, Water Resources Technical Publication, Denver.
- [4] EM 1110-2-2901, A Tunnels and Shafts in Rock Bureau of Reclamation, Water Resources Technical Publication, Denver
- [5] ICOLD. 1986. River Control during Dam Construction, bulletin 48a, Paris. Manzanares, A.A. 1980.
- [6] MMRDA, MCGM, (2006) Development plan for Greater Mumbai.

SUMMARY

Increasing urban population and the pace of industrial and other developments led to increase in water demand. Many of metropolitan and urban cities are facing acute shortage of water for domestic and industrial purposes. To reduce the stress on water supply infrastructure, existing water sources are utilized to fullest and new sources are continuously added to augment the water supply. Major problems in design of tunnel for water flow are flow conditions in approach to tunnels, in tunnel and downstream of tunnel. Even though art of tunneling is very old and well documented, new challenges in design and construction in difficult situations are added over the years. In this paper various hydraulic aspects related to tunnel interlinking rivers are described. Major head loss in tunnel flow is due to friction. Detailed information on investigation by various researchers related to friction factor is attached in Annexure A.

Key Words: Discharge, Diversion Tunnel, Explicit Equation, Friction Factor

ANNEXURE-A

TABLE -1. Application of Friction Factor Formulae for estimation of frictional loss in Tunnel flow

No	Investigator	Year	Formula	Validity Range	R ²
1	Chavan	2017	$f_f = \frac{20}{Re} + \left[\frac{0.0075 \left(\frac{4000}{Re} \right)^{0.05}}{0.25 + \left(\frac{4000}{Re} \right)^5} \right]$	Valid for wide range of Reynolds number	0.9777
2	Morrison	2013	$f = \frac{16}{Re} + \left[\frac{0.0076 \left(\frac{3170}{Re} \right)^{0.165}}{1 + \left(\frac{3170}{Re} \right)^7} \right]$	Inaccuracy crept in for higher values of Reynolds numbers	
3	Barenblatt	2005	$f = \frac{8}{\psi^{2(1+\alpha)}}$	Re < 13 × 10 ⁶	
4	Mckeon	2005	$\frac{1}{\sqrt{f}} = 1.920 \log(Re\sqrt{f} - 0.475 - \frac{7.04}{(Re\sqrt{f})^{0.55}})$		
5	Yen	1991	$f = \frac{1}{4} \left[-\log \left(\frac{e}{12R} \right) + \frac{5.2}{(4R_e)^{0.9}} \right]^{-2}$	30000 < Re , $\frac{e}{D} < 0.05$	
6	Barr	1981	$f = \frac{1}{4} \left[-\log \left(\frac{e}{14.8R} \right) + \frac{5.2}{(4R_e)^{0.89}} \right]^{-2}$		
7	Chen	1979	$\frac{1}{\sqrt{f}} = -2 \log \left[\frac{1}{3.7605} \left[\frac{e}{D} \right] - \frac{5.0452A}{Re} \right]$	4000 < Re < 10 ⁸ 0.000001 < $\frac{e}{D}$	0.9148
8	Churchil	1977	$f = 8 \left[(8/Re)^{12} + \frac{1}{(A+B)^{1.5}} \right]^{\frac{1}{12}}$		0.9066
9	Haaland	1983	$f = \frac{0.308642}{\left[\log \left(\left(\frac{e}{3.7D} \right)^{1.11} + \left \frac{6.9}{Re} \right \right) \right]^2}$		0.85096
10	Colebrook	1938-39	$\frac{1}{\sqrt{f}} = -2 \log \left[\frac{\frac{e}{D}}{3.7} + \frac{2.51}{Re\sqrt{f}} \right]$		0.90416
11	Serghides	1984	$\frac{1}{\sqrt{f}} = \left[A - \frac{(B-A)^2}{C - 2B + A} \right]$	Re > 2100 and any e/D	
12	Swami-Jain	1976	$\frac{1}{\sqrt{f}} = 1.14 - 2 \log \left[\left[\frac{e}{D} \right] + \frac{21.25}{Re^{0.9}} \right]$	5000 < Re < 10 ⁸ 0.000001 < $\frac{e}{D}$ < 0.05	
13	Barr	1972	$f = \frac{1}{4} \left[\log \left(\frac{e}{14.8R} \right) + \frac{5.76}{(4R_e)^{0.9}} \right]^{-2}$		0.9051
14	Zigrang & Sylvester	1982	$\frac{1}{\sqrt{f}} = -2 \log \left[\frac{1}{3.7} \left[\frac{e}{D} \right] - \frac{5.02A}{Re} \right]$	4000 < Re < 10 ⁸ and 0 < $\frac{e}{D}$ < 0.04	0.904104
15	Wood	1966	$f = 0.094 \left(\frac{e}{D} \right)^{0.223} + 0.53 \left(\frac{e}{D} \right) + 88 \left(\frac{e}{D} \right)^{0.44} (Re)^{-\psi}$	4000 < Re < 5 * 10 ⁸ 0.00001 < $\frac{e}{D}$ < 0.04	0.7075
16	Moody	1947	$f = 0.0053 \left[1 + \left(2 * 10^4 \frac{\varepsilon}{D} + \frac{10^6}{Re} \right)^{\frac{1}{3}} \right]$	4000 < Re < 5 * 10 ⁸ 0 < $\frac{\varepsilon}{D}$ < 0.01	

COMMISSION INTERNATIONALE DES GRANDS BARRAGES

VINGT-SIXIÈME CONGRÈS DES GRANDS BARRAGES
Autriche, juillet 2018

DOI 10.3217/978-3-85125-620-8-140



This work licensed under a Creative Commons Attribution 4.0 International License. <https://creativecommons.org/licenses/by-nc-nd/4.0/>

**OPERATIONAL MODES MONITORING FOR PREVENTION OF FAILURE OF
DAMS WITHIN THE DESIGN ENVELOPE**

DND HARTFORD

Dam Safety, BC HYDRO

CANADA

SJ RIGBEY

Dam Safety, BC HYDRO

CANADA

COMMISSION INTERNATIONALE
DES GRANDS BARRAGES

VINGT-SIXIÈME CONGRÈS DES
GRANDS BARRAGES
Autriche, juillet 2018

OPERATIONAL MODES MONITORING FOR PREVENTION OF FAILURE OF DAMS WITHIN THE DESIGN ENVELOPE

DND HARTFORD and SJ RIGBEY.

Dam Safety, BC HYDRO

CANADA

1. INTRODUCTION

For the purpose of promoting debate and discussion this paper introduces two important and difficult questions concerning surveillance and monitoring arise for dam owners that pursue or are interested in pursuing risk-informed dam safety management. The questions, in no particular order because they are related are:

1. To what extent should dam owners rely on risk assessment to guide their surveillance activities? and,
2. Which approach to risk assessment should they use?

Everyone involved in dam safety management is involved in risk management to some degree. This is regardless of whether or not some type of risk assessment is practiced in their country or if they favour risk assessment over established deterministic practices. Further, and again regardless of the approach (deterministic or probabilistic), all dam safety management activities depend to a significant degree on reliable monitoring data and surveillance reports for their integrity. The data and surveillance reports reflect the performance of the dam in its operational mode, where the operational mode refers to any condition of combination of the conditions of containment of the stored volume and passage of flows through and around the dam that the dam has experienced or is intended to experience during its operating life. This definition of operational mode corresponds to that used in the nuclear and other industries [1]. The operational modes of the dam as a whole are derived from the operational modes of its subsystems, components and parts and the activities, or

modus operandi, involved in achieving the overall operational functions. Some form of monitoring and surveillance of the operational modes of the dam and its sub-systems, components and parts provide the starting point for a dam safety analysis, regardless of its form or the level of detail [2], [3]

According to the US Bureau of Reclamation (p.17): *“Many times, weaknesses or deficiencies can be identified from changes in the behavior of the structure, foundation, abutments, or seepage.”*, ..., *“Any unusual behavior, regardless of how seemingly insignificant, should be identified and recorded because any unusual condition may be the forewarning of a newly developing unsafe condition.”*

Monitoring of structural and functional behaviour under normal operating conditions covers the spectrum from visual identification of structural or functional distress (visually observable deformation, overtopping), through visual identification of precursors of physical distress (increased seepage), to detection of actual distress or its precursors via instruments and other technologies. Typically, the monitoring activity is embodied in the broader surveillance process that involves assessing the integrity of the recorded data, interpreting this data and transforming it into meaningful information that then informs safety management actions. Surveillance, which transforms monitoring data into engineering information provides essential analytical and interpretative elements of real-time dam safety assessment.

The notion of basing a surveillance program on monitoring the operational modes of a dam system and its components is not obviously aligned with the notion of focusing the surveillance process on detection of early development of significant failure modes as set out in ICOLD Bulletins 138 and 158 [4], [5]. This is because the latter implies that the effort should be directed at “significant” failure modes that can be identified prior to the establishment of a surveillance program (or prior to re-configuration of an existing program), whereas the former operational modes monitoring approach which is deterministic, does not impose any restrictions or make assumptions about how failures or incidents might develop either physically or temporally.

This paper is underpinned by an unparalleled 25 years of pioneering experience as a dam owner in developing and advancing capability in risk-informed dam safety management while simultaneously maintaining and improving a robust surveillance program as part of a comprehensive dam safety management system. Periodic critical re-assessment of our performance in both of these areas of the dam safety program, which includes independent external audits of the program every 5 years, leads to the question as to whether the dam safety program should revolve around the results of analysis of failure modes in a portfolio risk management process as suggested by some, or maintain and advance the current approach of focusing first on monitoring and surveillance of the operational performance of the dams on an individual basis.

2. THE "AXIS" OF A DAM SAFETY MANAGEMENT PROGRAM

ICOLD Bulletin 154 [6] provides a general process for managing the safety of dams during the operational phase of the life-cycle (Figure 1). This framework and variations of it have a proven track record of effectiveness in managing the risks from dams over many years.

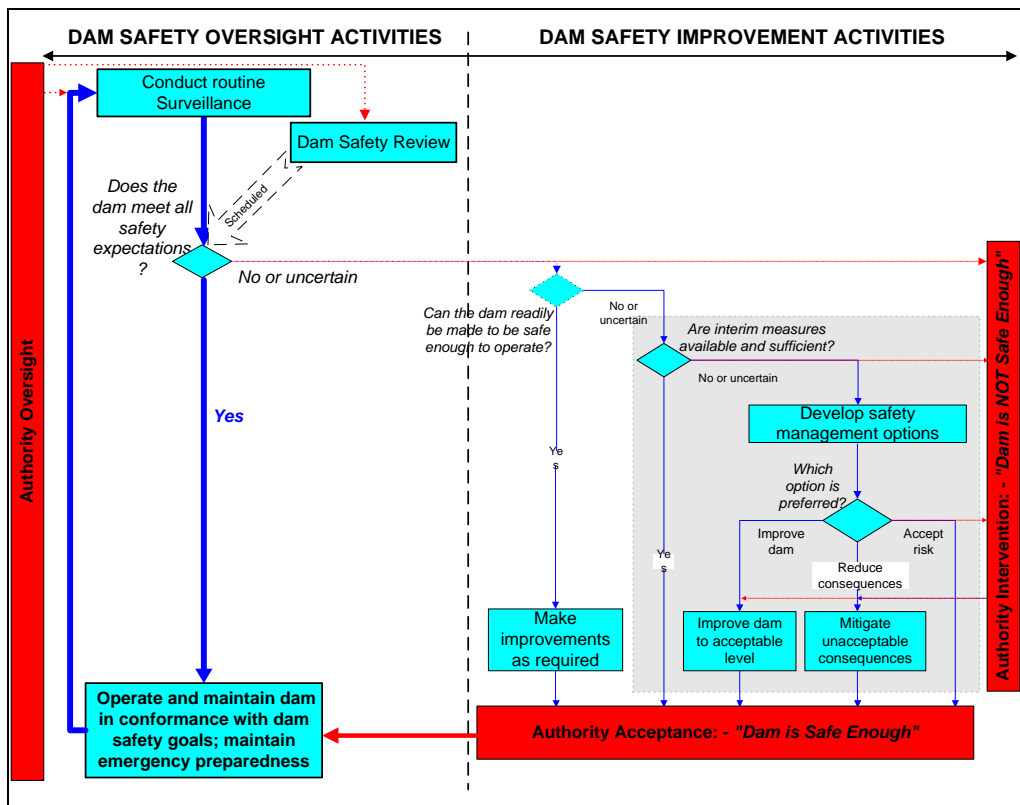


Figure 1. Dam Safety Management Process (ICOLD, 2017)

The effective implementation of the activities shown on the left side of the framework is essential for real-time dam safety management, demanding diligent attention by the dam owner. As such, these ongoing activities under normal operational conditions can be considered to form the axis of a dam safety management program that all other dam safety activities depend on in some way. The importance of diligence and thoroughness in conducting these activities cannot be overstated as investigations into dam failures and incidents invariably point to weakness in implementation of these activities together with other factors such as management and organisational weakness, human error and the likes. For example, the Independent Forensic Report on the Oroville Dam Spillway incident found weakness in the three activities together with significant management and organisational factors and professional practice concerns.

ICOLD Bulletin 154 does not provide detailed treatment of the activities that are carried out in these implementation steps, referring instead to other ICOLD

Bulletins such as Bulletins 118 [8], 138 and 158 on Surveillance. Emergency preparedness typically involves external agencies in the country where the dam is situated and as such is not dealt with in specific detail by ICOLD.

2.1 CONDUCT ROUTINE SURVEILLANCE

A general framework for what is intended by “conduct routine surveillance” is summarised in ICOLD Bulletins 118 and 158 as illustrated in Figure 2 from ICOLD Bulletin 158 [5] which was taken directly from ICOLD Bulletin 118 [8],

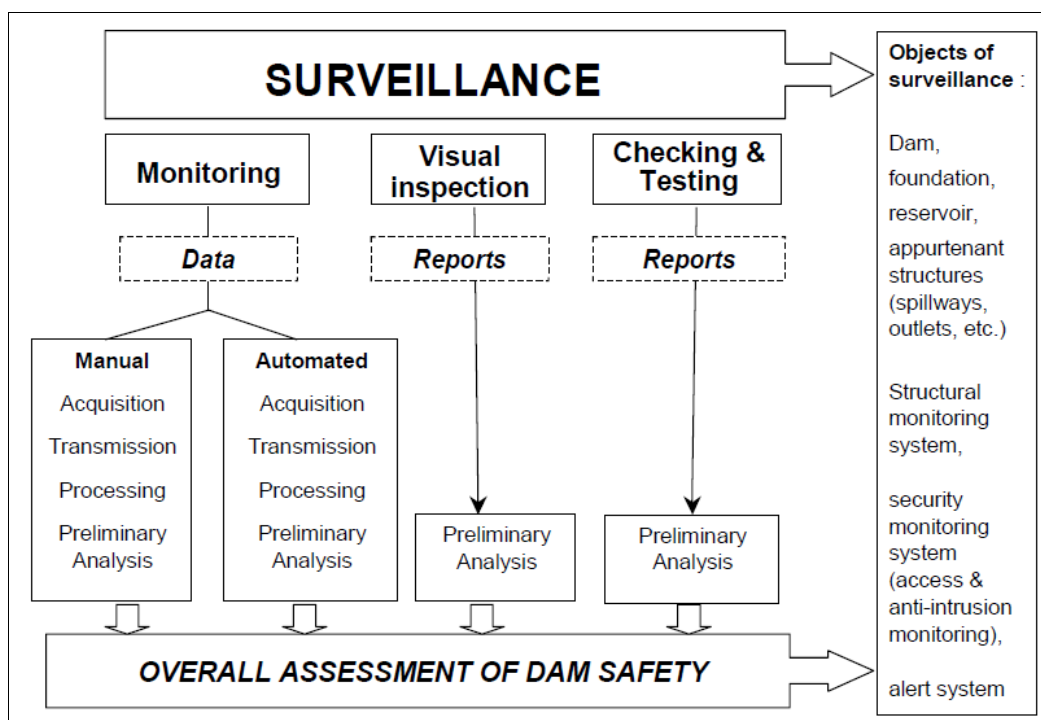


Figure 2. Framework for Surveillance (ICOLD B 118 and B 158)

The definition and intended meanings of the terms failure mode require clarification in Bulletin 158 for instance by referring to ICOLD Bulletin 130 on Risk Assessment [9]. Bulletin 158 refers to the objective of early detection of significant failure modes and some sample potential failure modes of interest provided. These failure modes are clearly defined at a very high level in the dam system similar to the hazards and failure modes framework illustrated in Figure 21 of Bulletin 154. However, the manifestation of such adverse performance characteristics may occur late in the failure process, or be difficult to ascertain such as in the case with seepage, where differentiating between “normal seepage” and “failure inducing seepage” can be exceptionally difficult. Bulletin 158 is unclear with respect to what is meant by a failure mode; what constitutes

significant; and how failure modes can be detected. However, it does provide clear advice on some of the behavioural features of significance to be considered in visual inspections and significant parameters to be monitored by instrumentation.

3. OPERATIONAL MODES AND FAILURE MODES

At the outset, it is important to be clear as to the definition of a “Mode”, be it an operational mode or a failure mode by focusing first on the common use of the term mode:

Mode: A state, condition, way of doing things (modus operandi), manner in which something occurs.

- Common uses include “flight safe” mode; mode of transport (aircraft, car, railway, etc.)

Mode of operation: A mode in which the operational states or objectives of the system manifest themselves.

- In the context of dams, water retention and water conveyance are operational modes; at a more detailed level, the operational modes of a spillway gate system include a) dormant mode (during the dry season); in-service mode (closed to retain water or open to pass flows); and ready mode (just prior to initiation of gate movement).

Failure Mode: The manner in which an element or component fails to achieve its operation (design) objective.

- In the context of spillways, failure modes of a spillway gate include unintended closed state and unintended open state.

Any owner, regardless of degree of sophistication can understand the operational modes of a dam being retention and conveyance when set out in terms of commonly understood terminology.

With reference to well established experience in the nuclear industry, as well as first-hand experience of operational incidents at dams and reflecting on the Oroville Dam Spillway incident where the incident could not be attributed to a specific cause, it is proposed that attempting to define failure modes as sequences of events from initial cause to system end state should be avoided. Referring to the Fault Tree Handbook (Page II-1) [10] (Nuclear Regulatory Commission, 1981): *“For systems that exhibit any degree of complexity (i.e., for most systems), attempts to identify all possible system hazards or all possible component failure modes-both singly and in combination-:-become simply impossible”*. Concerning inductive techniques overall, such as Failure Modes Analysis and Event Tree Analysis, the Fault Tree Handbook points out that *“due to constraints such as time, money and experienced staff, exhaustiveness in the analysis is a luxury that we cannot afford”*. Thus, not only will it be impossible to

capture all possible failure sequences in an inductive analysis, it will typically not be possible to include all identified possible failure sequences in the analysis. Therefore if one defines failure modes as sequences of events from initiation to failure, one should not be surprised if a failure sequence that was not identified in the analysis occurs.

Given that one can reasonably exclude defining failure modes in terms of the sequence of events between initiation and ultimate failure on the grounds that it is impossible for all but trivial systems, one must also accept that failure modes are not uniquely defined, [10], [11]. Rather, failure modes are a matter of the perspective at which the analysis is conducted. System level failure modes are different to parts level failure modes. This has hugely important implications for monitoring and surveillance as these activities are directed at detecting changes in performance of some feature of the dam be it at the system level as is the case with visual inspections of dam (e.g. deformation of the dam body), or tests of functionality of parts (e.g. measuring friction in a trunnion bearing).

The concept of system level and parts level failure modes is illustrated in Figure 3, which also illustrates the relationships between cause-mode-effect for one module of the spillway sub-system, specifically the gate which is further resolved to its component parts.

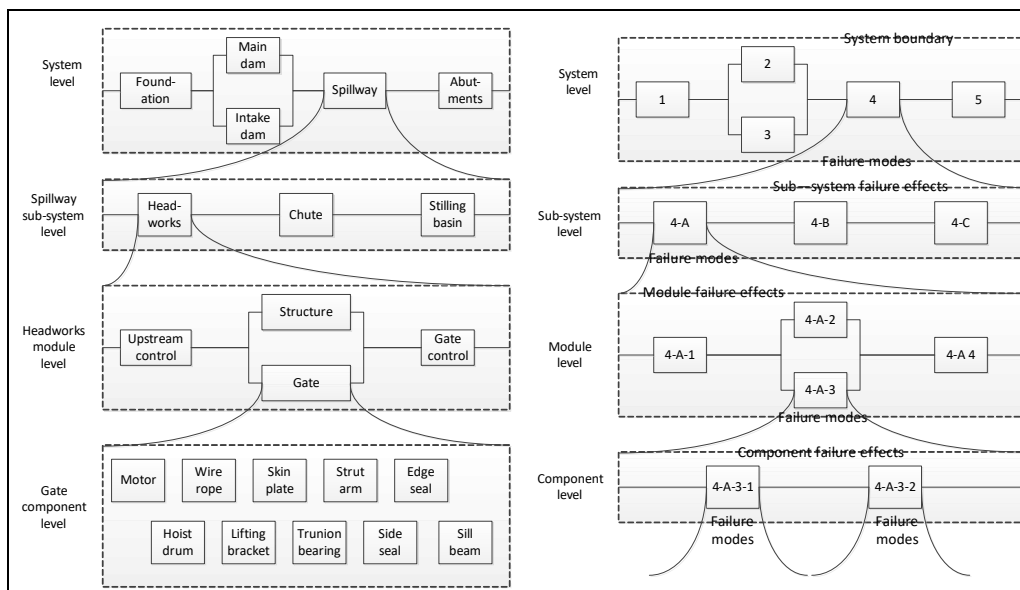


Figure 3. Systems, parts and “cause – mode – effect” relationships

Note, all features at the component level are not shown due to space limitations, and each component can be further resolved into the elements that comprise each component.

At some point, it becomes necessary to ask the question: “To what extent should the system be resolved?” We suggest that the answer is that as a general principle resolution should be to the level at which maintenance and testing can be carried out. This then defines the level in the system at which the monitoring and surveillance effort should be directed because this is the level at which the operational failure risk is managed. Thus, the answers to the questions as to

what should be monitored and tested emerge directly from the practicability of establishing and maintaining the operational integrity of the various features of the dam system be it at the component level (or even further down to the elemental level, such as motor windings), or at the system level, or somewhere in between.

Thus, beginning with the operational modes of water retention and water conveyance, and progressively resolving these system operational modes into their constitutive functional modes, it is possible to determine the overall operational integrity of the dam system and to establish that the dam is functionally safe. This can all be achieved on the basis of operability without consideration of failure modes.

3.1 DERIVATION OF FAILURE MODES

Failure modes can be derived directly from the operational modes of the system and its resolved parts. Figure 4 illustrates a spillway gate at the headworks module level comprising 10 components, and a functional analysis diagram that illustrates the operational modes of the various components in a self-explanatory way.

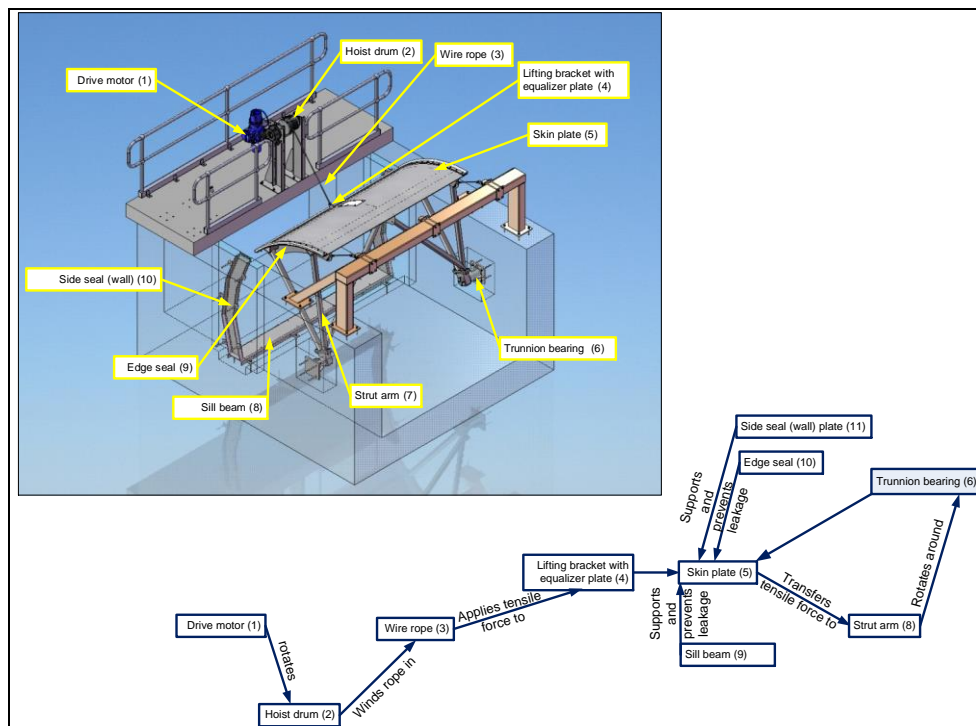


Figure 4. Component level Functional Analysis Diagram of a spillway gate

The function of the motor is to rotate the hoist drum and the failure mode of the motor is loss of rotation, with the effect that the hoist drum does not move. Functionality of the entire gate module is lost as a result and the obvious dam

safety management action in the surveillance process is to verify that the motor does indeed rotate as intended during the inspection and testing process. The failure modes of the various components of the spillway gate module can then be derived by taking the complement of the operational mode of the component. Thus, if the operational modes of the components (or higher levels of the system) are known, then the operational failure modes can be derived directly.

The derivation of failure modes from operational modes is of **crucial** importance, because it contributes greatly to overcoming the problem of a failure modes analysis (of any type) not having the analytical power to reveal the modes. In Failure Modes and Effects Analysis (and its variants), the analysis depends heavily on the ability and expertise of the analyst for finding all necessary modes. [12]

3.2 OPERATIONAL MODES BASED OR FAILURE MODES BASED SURVEILLANCE?

None of the above provides direct answers to the questions that motivated this paper:

1. To what extent should dam owners rely on risk assessment to guide their surveillance activities? And,
2. Which approach to risk assessment should they use and to what extent?

But then, perhaps these are the wrong questions from the perspective of dam safety assurance, where the overriding objective is to demonstrate that the dam and its various subsystems, modules and components are functioning properly and are available to be brought into service as required. Of course, the definitions of what constitutes an “operational mode” and a “failure mode” are vitally important. It is a somewhat straightforward matter if failure modes are derived from operational modes, although it must be recognised that this derivation is not “cut and dried”, as the operational function may not be achieved exactly as intended. Rather than considering failure modes in dam surveillance as forming the basis of real-time dam safety assessment, we suggest that it is more appropriate to consider operational modes as the basis of surveillance for risk management and failure modes as being derived from the loss of the operational modes and from design knowledge. This also means that from a dam surveillance perspective, the effort should be focused on the performance attribute that can be determined in the most efficient and effective way. This said, visual (and now remote via drones etc.) inspections, monitoring and testing all target deviations from the expected performance state of the dam and its various sub-systems, one of which is the failed state (in principle there can be unexpected performance states that are not failed states). Thus, understanding of and focus on the operational modes of a dam, which can be assessed continually in time if necessary, thereby providing the capacity to capture functional and non-functional (failed) states all of which can be validated and verified objectively, provide the foundational basis of a robust dam safety assurance program.

3.3 A ROLE FOR PROBABILITY?

All of the above can and should be achieved in terms of deterministic analysis as there should be no uncertainty in how the designer intended the dam and its constitutive parts to function. This design intent raises the question as to whether or not there is a role for probabilistic assessment of the significance of operational and non-operational (failure) modes, noting that the definition of a failure mode as a sequence of events from initiation to complete failure is unrealistic as explained above.

Given the deterministic nature of the process of setting out the operational functionalities of a dam system and for determining the failure cause – failure mode – failure effect relationships in terms of the intent of the design, any identifiable deviations from the design intent are also determined deterministically; specifically all not intended states are those that do not conform to the design intent. This means that any use of probability pertains to consideration as to whether or not the failure mode is considered to be “significant” or “critical” to safety.

The Fault Tree Handbook [10] provides useful advice as follows: *“In FMEA (and its variants) we can identify, with reasonable certainty, those component failures having “non-critical” effects, but the number of possible component failure modes that can realistically be considered is limited. Conservatism dictates that unspecified failure modes and questionable effects be deemed “critical”.* This observation points to a limited, if any, role if any for screening out failure modes on the basis of probability.

4. CONCLUSIONS

On the basis of the above, we conclude that surveillance of **the operational modes** of a dam in the sense of visual inspections, monitoring, and testing provide the foundation of an effective dam safety management process. These activities can be carried out at various levels of refinement where the most fundamental elements are available to and implementable by all dam owners regardless of their institutional strength and sophistication. We observe that “screening out” of failure sequences on the basis of actual or perceived probability should not be attempted for a complex system such as a dam. This is because the number of possible combinations and interdependencies of functions and functional variances rises exponentially with the size of the system. The number of possible combinations of unfavourable events is correspondingly as large as the probability of any one of them occurring is small. The probability of at least one combination of pernicious events actually happening can be significant.

REFERENCES

- [1] US Nuclear Regulatory Commission. (2017). *Glossary*. Washington DC: US Nuclear Regulatory Commission.
- [2] US Bureau of Reclamation. (1980). *Safety Evaluation of Existing Dams*. Denver: US Department of the Interior.
- [3] ANCOLD. (2003). *Guidelines on Risk Assessment*. Australian National Committee on Large Dams.
- [4] ICOLD Committee on Surveillance. (2009). *Bulletin 138 A General Approach to Dam Surveillance*. Paris: ICOLD.
- [5] ICOLD Committee on Surveillance of Dams. (n.d.). *Buletin 158 Dam Surveillance Guide*. Paris: ICOLD.
- [6] ICOLD Committee on Dam Safety. (2005). *Risk Assessment in Dam Safety Management*. Paris: ICOLD.
- [7] Independent Forensic Team. (2018). *Independent Forensic Team Report, Oroville Dam Spillway Incident*. ASDSO.
- [8] ICOLD Committee on Surveillance of Dams. (2004). *Bulletin 118 Automated Dam Monitoring Systems*. Paris: ICOLD.
- [9] ICOLD Committee on Dam Safety. (2005). *Risk Assessment in Dam Safety Management*. Paris: ICOLD.
- [10] Nuclear Regulatory Commission. (1981). *Fault Tree Handbook*. Washington, DC: US Nuclear Regulatory Commission.
- [11] Hartford, D. N., & Baecher, G. B. (2004). *Risk and Uncertainty in Dam Safety*. London: Thomas Telford.
- [12] Clemens, P., & Simmons, R. (1998). *Systems Safety and Risk Management: A guide for engineering educators*. US Department of Health and Human Services.
- [13] Hand, D. J. (2014). *The Improbability Principle*. Scientific American.
- [14] Hartford, D. N., Baecher, G. B., Zielinski, P. A., Ascila, R., & Rytters, K. (2016). *Operational Safety of Dams and Reservoirs*. London: Thomas Telford.

COMMISSION INTERNATIONALE DES GRANDS BARRAGES

VINGT-SIXIÈME CONGRÈS DES GRANDS BARRAGES
Autriche, juillet 2018

DOI 10.3217/978-3-85125-620-8-141



This work licensed under a Creative Commons Attribution 4.0 International License. <https://creativecommons.org/licenses/by-nc-nd/4.0/>

**STUDY ON THE HARMFUL IMPACT OF SLIT-TYPE ENERGY DISSIPATER
WATER WINGS**

Huang GUOBING

*Director of Hydraulic Department, Changjiang River Scientific RESEARCH
INSTITUTE*

CHINA

Du LAN

*Engineer of Hydraulic Department, CHANGJIANG RIVER SCIENTIFIC
RESEARCH INSTITUTE*

CHINA

Duan WENGANG

*Chief Engineer of Hydraulic Department, CHANGJIANG RIVER SCIENTIFIC
RESEARCH INSTITUTE*

CHINA

STUDY ON THE HARMFUL IMPACT OF SLIT-TYPE ENERGY DISSIPATER WATER WINGS

Huang Guobing¹, Du Lan², Duan Wengang³

1. *Director of Hydraulic Department, CHANGJIANG RIVER SCIENTIFIC RESEARCH INSTITUTE*
2. *Engineer of Hydraulic Department, CHANGJIANG RIVER SCIENTIFIC RESEARCH INSTITUTE*
3. *Chief Engineer of Hydraulic Department, CHANGJIANG RIVER SCIENTIFIC RESEARCH INSTITUTE*

CHINA

1. INTRODUCTION

Slit-type energy dissipaters (STED) change the trajectories of nappes by using specific flip buckets to make the flow contract transversely and extend longitudinally. The energy of flow is greatly dissipated in this progress and then the erosion of downstream channel caused by the nappe can be relieved. Because of its advantage of efficient energy dissipation effect, STED has been widely used in hydraulic projects of high water head, large discharge, and narrow river valley. The energy dissipation problems of many large scale hydraulic projects in China, such as, Longyangxia dam, Ertan dam, Shuibuya dam, and Geheyan dam are successfully solved by the application of STEDs.

From the aspects of energy dissipation effect and structure safety, the water surface in the channel, the characteristics of pressure and cavitation, the shape of the nappe, and the scouring effect of downstream riverbed of STED have been studied theoretically and experimentally. Zhang and Wu (1989), Dai and Yu (1992) observed the movement and extension features of the nappe experimentally, proposed estimated formulas for the water line in contraction section and the distance of the nappe. Wu et al. empirically provided the conversion conditions of

the nappe forms, and experimentally investigated the behavior of the flow choking. The estimated formulas for nappe maximum width and its location of slit-type flip buckets were presented by Liu et al. Huang et al. developed a method to calculate the dynamic water pressure in the contraction section of STED.

Ippen (1943) put forward the ideal shock wave theory based on the mechanical principle, proposed the basic equations of shock wave, then the main theoretical foundation of the contraction type energy dissipaters was laid. Ippen's formulas was then simplified by Hager et al. (1987) and Liu et al. (1999) Ippen's theory following several assumptions: (1) the deflection angle of flow is small; (2) the friction of side wall is negligible; (3) the pressure distribution along the depth of the water conforms to the hydrostatic pressure distribution regularity. However, the flow regime in the STED no longer satisfies the assumptions, for the rather sharp deflection angle, and the narrow width of the surface. So Ippen's formulas would result in large deviation, and need to be modified for the application in STED.

As a special hydraulic phenomenon, the water wing caused by the shock waves in the contraction section of STED may bring about harmfulness to the stability of the bank and the safety of the downstream buildings. However, the harmful effects caused by water wings has been hardly attached enough importance. In hydraulics prototype observation of Geheyan project, it was found that, the water wing caused by the STED diffused transversely, scoured the side bank slope. And the operation of the upper outlet on both side was then limited. The results of model test of Shiubuya project confirmed that, part of the water detached from the main flow from side outlet, and scoured the river bank. Hence it is necessary to carry out special study on the formation mechanism and movement features of the shock waves and the water wings.

In the present study, physical model experiments and theoretical analysis were conducted to reveal the internal relation of the shock wave and the movement characteristics of the water wing. And then the estimation formula for calculating the shockwave - water wings spread area was proposed, based on the experimental data combined with theoretical derivation.

2. EXPERIMENTAL SET-UP AND METHODOLOGY

The experiment model consisted of a water tank, a sloping flume, a STED structure, and a downstream pool, as shown in Figure 1. The high pressure water tank is 10 meters high and provided adequate flow with enough water head. The flow was delivered by a Plexiglas-made sloping flume into the STED structure. The sloping flume is 3.2 m long, 0.2 m wide and 2 m high. A radial gate was set near the downstream end of the flume to adjust the Froude number of the flow in the STED contraction section.

The main geometric parameters of a STED are the length of the contraction section L , the bucket angels α , and the widths before and after the contraction section B and b , as shown in Figure 1. Then, b/B is the contraction ratio.

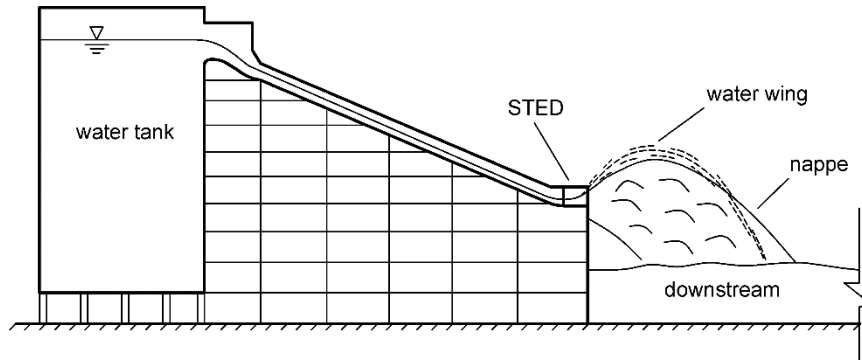


Fig. 1
Experimental set-up

Nine STED models (made of Plexiglas) with various bucket angles ($\alpha = 0^\circ$; 5° ; 10°) and contraction ratios ($b/B = 0.20$; 0.25 ; 0.30) were studied. The length of the STED contraction sections was 0.5m. Table 1 summarized the geometric characteristics of the models. The models were systematically tested for approach flow Fr at the entrance of contraction section ranging from 4.10 to 5.95.

Table 1
Geometric parameters of the STED models

Cases	α ($^\circ$)	b/B	θ ($^\circ$)
M1	0.00	0.20	9.35
M2	0.00	0.25	10.00
M3	0.00	0.30	10.65
M4	5.00	0.20	9.35
M5	5.00	0.25	10.00
M6	5.00	0.30	10.65
M7	10.00	0.20	9.35
M8	10.00	0.25	10.00
M9	10.00	0.30	10.65

The form of the shock wave, the shape and the trajectory of the water wing were observed with high-speed photography. The measuring device for the measurement of the water wing was set in the downstream pool. A rectangular collector was in-house designed to measure the rain strength distribution in the downstream pool and the rainfall caused by the transversely spreading of water wing was analyzed.

3. FLOW REGIME OBSERVATION

3.1. FLOW REGIMES IN CONTRACTION SECTION

As demonstrated in Figure 2, the flow upstream of the STED remained in an open channel condition, with a flat free surface and hydrostatic pressure distribution. Then due to the effects of the side wall contraction, the flow contracted transversely and extended longitudinally when passing through the STED. Figure 3 shows that, the shock waves on both side collided at the center line. The water surface profile no longer remained flat along the contraction section.

The flow in the contraction section was affected by two factors, upstream of the shock wave intersection, i.e. the friction effect caused by the roughness of the side wall and the turbulence inertia effect caused by large vortex. Considering the distance from the inlet of the contraction section to the shock wave intersection point is rather short, the friction effects that caused by the small vortex in the boundary layer of the flow could be ignored. On the other hand, the force acted on the contracted side walls that caused by the inertial impact of the high-speed incoming flow would bring about rapid shock waves (a special form of hydraulic jump). After the shock waves intersected, the turbulence kept growing. As the side walls contracted continuously, the flow depth increased and the velocity decreased, then the inertial effects of the flow reduced accordingly. Large vortexes in the flow constantly split into small vortexes, due to the limitation of the side walls. As a result, large vortexes and small vortexes coexisted in the flow, whereas the turbulence inertia effects caused by large vortexes still played a dominant role in this section.

Upstream of the shock wave intersection, the water-surface curve near the center line of the STED raised slowly, while the water-surface curves near the side wall raised rapidly. The cross section of the flow presented an 'U' shape. Downstream of the shock waves intersection, the water-surface curves near the side wall kept rising, while the water-surface curve near the center line raised sharply, and got above of that near the side wall, due to the collision of the shock wave flow. A 'W' shaped cross section of the flow appeared. Moreover, part of the water detached from the main flow, then ejected out in the form of scattering, with high inclined initial velocity above the main flow. That was how the water wings formed.



Fig. 2
Overall flow regime in STED

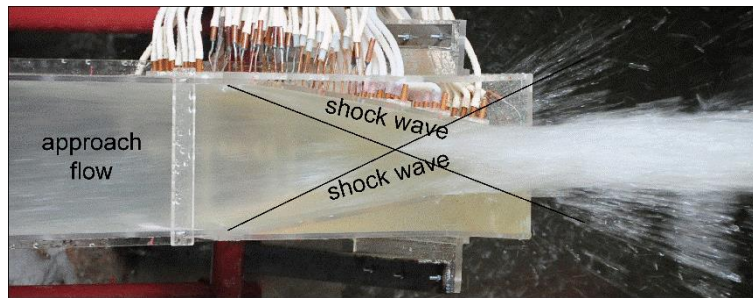


Fig. 3
Flow regime in the contraction section

3.2. NAPPE FORMS

The flow separated into three parts after it left the edge of the STED, i.e. nappe, fin, and water wing. Among these parts, the nappe was formed by the longitudinally extended main flow; the fin was a very thin nappe moved downstream along a straight line trajectory, formed by the flow beneath the main flow under high pressure, which contained negligible quantity of discharge and might hardly cause damage to the buildings; the water wing was caused by the collision of the shock waves, might bring about harmfulness to the stability of the bank and the safety of the buildings downstream.

4. SHOCK WAVES

The shape of the shock wave is the key factor that affects the operation of STED. Ippen proposed the basic formula of shock wave (Eq.1), based on static water pressure assumption.

$$\sin\beta = \frac{1}{Fr} \sqrt{\frac{1}{2} \frac{h_2}{h_1} \left(1 + \frac{h_2}{h_1}\right)} \quad (1)$$

Where, β is the angle of the shock wave, h_1 and h_2 are the depth upstream and downstream of the shock wave respectively; Fr is the Froude number of the incoming flow.

Ippen's formula was then simplified by Hager et al. (1994) and Liu et al. (1999) According to Ippen's theory, there are also two formulas,

$$\frac{h_1}{h_2} = \frac{\text{tg}\varphi}{\text{tg}\beta} \quad (2)$$

Hence,

$$\frac{v_1}{v_2} = \frac{\cos\varphi}{\cos\beta} \quad (3)$$

Where, φ is the angle of the shock wave to the side wall, v_1 and v_2 are the velocity upstream and downstream of the shock wave respectively. According to energy conservation assumption,

$$\sin\varphi = \frac{h_1}{h_2} \frac{v_1}{v_2} \sin\beta \quad (4)$$

Combining Eqs. (1), (4), and (5), the following equation was obtained,

$$h_1 + \frac{v_1^2}{2g} = h_2 + \frac{v_2^2}{2g} = H \quad (5)$$

Eq. (6), could be expanded in Taylor's series, with higher-order small components ignored,

$$\sin\varphi = \frac{1}{Fr} \sqrt{\frac{1}{2} \left(\frac{h_1}{h_2} + 1 \right) \frac{H - h_1}{H - h_2}} \quad (6)$$

Further ignoring one-order small components, a new shock wave simplified formula then derived,

$$\sin\varphi - \frac{1}{Fr} = \frac{1}{2Fr} \left(\frac{\Delta h}{H - h_2} - \frac{\Delta h}{2h_2} \right) \quad (7)$$

Further ignoring one-order small components, a new shock wave simplified formula then derived,

$$\sin\varphi = \frac{1}{Fr} \quad (8)$$

Then, the angle of the shock wave could be simply expressed as

$$\varphi = \arcsin \frac{1}{Fr} \quad (9)$$

However, the flow regime in the STED no longer satisfies the static water pressure assumption, for the rather sharp deflection angle, and the narrow width of the surface. So Eq. (9) would result in large deviation, and need to be modified for the application in STED.

It was assumed that,

$$\gamma = c \cdot \arcsin \frac{1}{Fr} \quad (10)$$

Where, γ is the angle between the shock wave and the side wall; c is a correction coefficient, which depends on the geometric coefficient of the STED, and the incoming flow regime.

Assuming that influencing factors include the bucket angel α , the deflection angle of the side wall θ , and the Froude number of the incoming flow Fr . The results of the orthogonal simulation analysis indicated that, only the deflection angle of the side wall θ , and the Froude number of the incoming flow Fr have significant influences on the coefficient c .

The relationship between the coefficient c and the Froude number of the incoming flow Fr for different deflection angles θ were plotted in Figure 4.

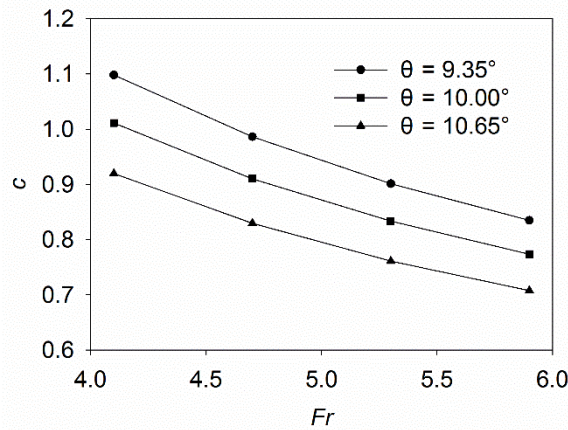


Fig. 4

Relationship between the coefficient c and the Froude number of the incoming flow Fr

According to the results of the least-squares method, c can be calculated as

$$c = \frac{Fr^{0.336} - 0.929}{1.580 - 5.141\theta} \quad (11)$$

As a conclusion, the angle of the shock wave

$$\beta = \theta + \frac{Fr^{0.336} - 0.929}{1.580 - 5.141\theta} \cdot \arcsin \frac{1}{Fr} \quad (12)$$

Eq. (12) is applicable to the STED with the deflection angle $9^\circ \leq \theta \leq 12^\circ$ and the Froude number of the incoming flow $4.45 \leq Fr \leq 5.57$. According to the accuracy test, the calculation results obtained with Eq. (12) are accurate enough to calculate the angle of the shock wave, for the maximum relative error is 0.27% and the average relative error is 0.15%, compared with experimental results.

5. WATER WING IMPACT SCOPE ESTIMATION

Caused by the intersection and collision of the shock waves, part of the water detached from the main flow, and formed the direct source of the water wing. Part of the water wing ejected toward downstream direction or feed into the main flow. This would not cause damage to the bank or the buildings downstream and it was called harmless water wing. Another part of the water wing ejected scattering toward downstream at a certain angle and might lead to continuous rainfall shock to the buildings in a certain area downstream, called harmful water wing. Therefore, estimating the scope of the water wing was of great significance.

Coordinate origin O was set at the bottom of the contraction section inlet. The height of the STED bottom from downstream water surface was denoted as z . The shock waves collided at C point, caused the water wing ejected out with a maximum angle α , then fell to downstream on both sides of the main nappe, with a drop point of D . L_{OC} was defined as the longitudinal distance of the shock waves collision point; L_{CD} was the longitudinal distance between C and D ; L_M was the longitudinal distance between Point D and the origin; T_M was defined as the transversal distance from the center line. Hence, the scope of the water wing could be estimated from the values of L_M and T_M .

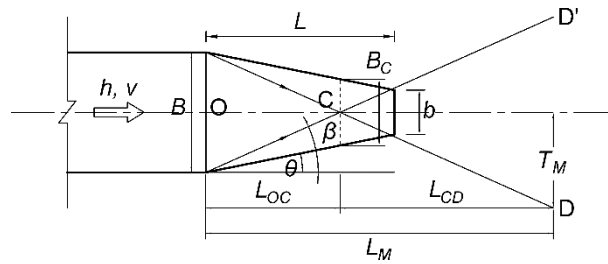


Fig. 5

Sketch of the shock waves and the water wing

According to the geometry relationships,

$$L_{OC} = \frac{B}{2} \cdot \cot\beta \quad (13)$$

$$L_M = L_{OC} + L_{CD} \quad (14)$$

$$T_M = L_{CD} \cdot \tan\beta \quad (15)$$

The shape of the water wing could be regarded as a trajectory of projectile motion. So L_{CD} could be calculated based on the projectile motion theory.

$$L_{CD} = \frac{v_C \cdot \cos\gamma \cos\beta}{g} \left(\sin\gamma + \sqrt{v_C^2 \cdot \sin^2\gamma \cos^2\beta + 2g(z + h_C)} \right) \quad (16)$$

Where, v_c , γ , and h_c are the velocity, the angle of departure, and the depth at the shock waves collision point C respectively; g is the gravitational acceleration. Therefore, the value of v_c , h_c , and γ need to be determined.

The value of v_c could be calculated based on Ippen's theory. The velocity after the shock wave was determined by the angle of the shock wave.

$$v_c = v \frac{\cos\beta}{\cos(\beta - \theta)} \quad (17)$$

Where, v is the velocity of the incoming flow before the shock waves.

The depth at the shock waves collision point could be got from continuity equation,

$$vhB = v_c h_c B_c \quad (18)$$

Where, B_c is the width of the contraction section at the shock waves collision point.

Then,

$$h_c = \frac{vhB}{v_c B_c} = \frac{h \cdot \cos(\beta - \theta)}{\cos\beta (1 - \tan\theta \cdot \cot\beta)} \quad (19)$$

According to the experimental results (as demonstrated in Figure 6), the water surface along the central line could be approximately expressed as the shape of a parabolic function,

$$y = px^2 + h \quad (20)$$

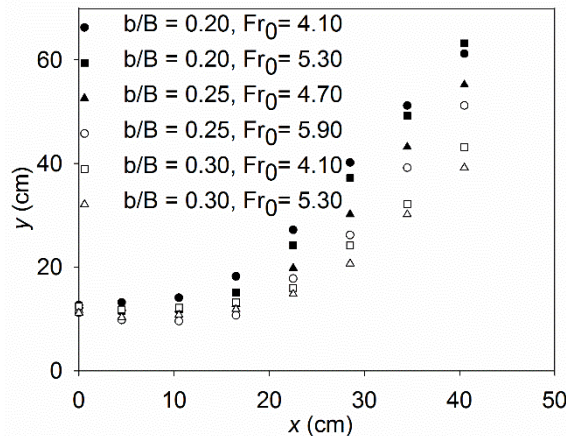


Fig. 6

Water surface along the central line for various conditions

As defined above, the coordinate of the collision point C was (L_{oc}, h_c) . So

$$\rho = \frac{h_c - h}{L_{oc}^2} \quad (21)$$

Substituted into Eq. 20, then the parabolic function turned out to be

$$y = \frac{h_c - h}{L_{oc}^2} x^2 + h \quad (22)$$

From the derivative of Eq. 22 at C (L_{oc} , h_c), the slope at the collision point was obtained,

$$\tan \gamma = \frac{2(h_c - h)}{L_{oc}} \quad (23)$$

Therefore,

$$\gamma = \arctan \frac{2(h_c - h)}{L_{oc}} \quad (24)$$

To validate Eq. (14), and (15), the calculation results L_M and T_M were compared to the experimentally determined area of the rainfall caused by water wing in Figure 7 under different conditions, as listed in Table 2. Furthermore, due to the difficulty of defining the boundary of the water wing, the typical rainfall intensity contour of 500 mm/h was defined for the analysis of the rainfall intensity rainfall area and its distribution characteristics. Table 2 summarized the calculation errors for water wing areas under different conditions.

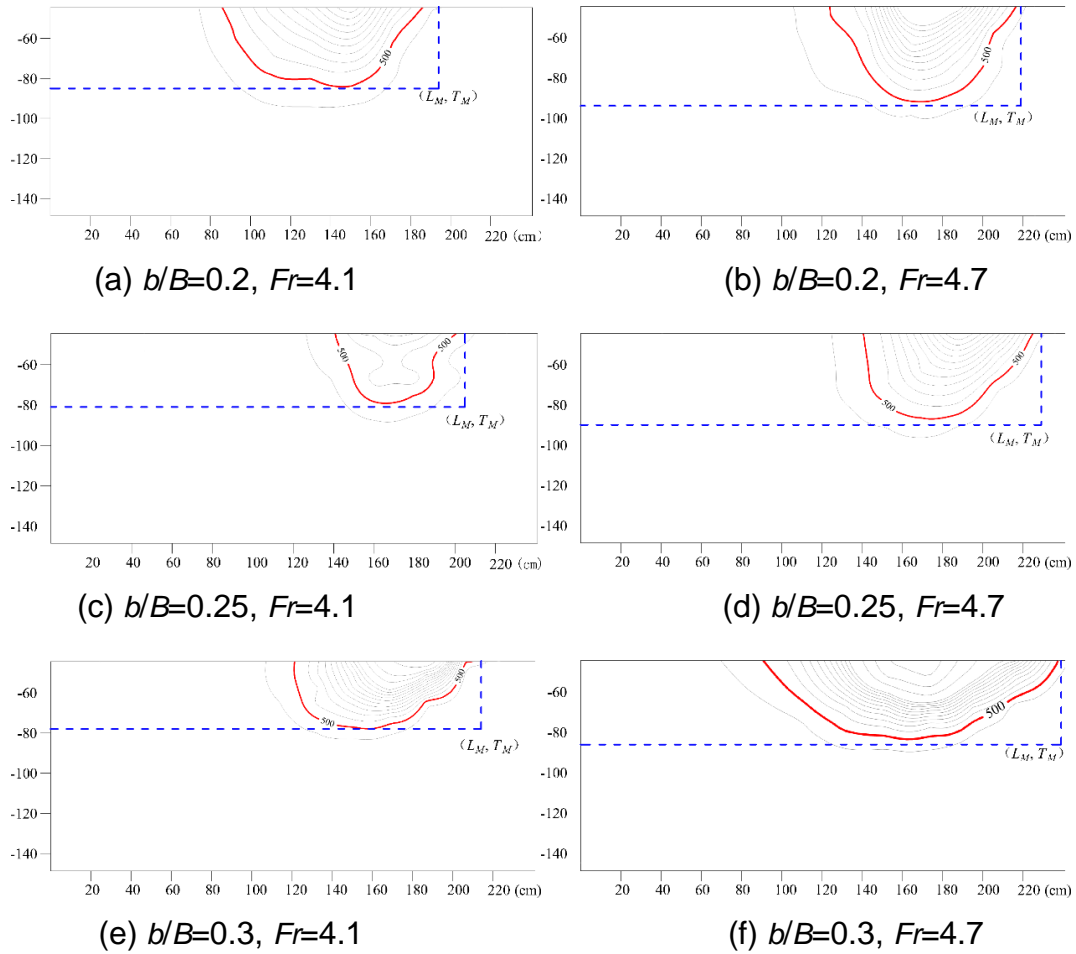


Fig. 7

Comparison of the experimental water wing area and the calculation results for various conditions

According to Figure 7, the typical rainfall intensity contour of 500mm/h were just accurately covered by the calculation results L_M and T_M obtained with Eq. (14), and (15). The maximum relative error of L_M is 4.4% and the average relative error of which is 3.0%; the maximum relative error of T_M is 4.7% and the average relative error of which is 2.6%. So they are accurate enough to estimate the area of the water wings.

6. ACKNOWLEDGEMENTS

The authors gratefully acknowledge the support of the National Nature Science Foundation of China (Grant No. 51709014 & 51609022), and Basal Research Foundation of CRSRI (Grant No. CKSF2016046/SL & Grant No. CKSF2016064/SL).

REFERENCES

- [1] CHEN, Z.R. CHEN, Y.D. AND HUANG, G.B. Research of configuration of narrow opening ski jump spillway and estimation of longitudinally extended width of jet. *Journal of Yangtze River Scientific Research Institute*, 2002, 19 (4), 11-14.
- [2] CHENG, C.T., SHEN, J.J. AND WU, X.Y. ET AL. Operation challenges for fast-growing China's hydropower systems and response to energy saving and emission reduction. *Renewable and Sustainable Energy Reviews*, 2012, 16 (5), 2386-2393.
- [3] DAI, Z.L., YU, Y.Z. A study on jet trajectory length and parameters of water jet deflecting from slit-type flip buckets of deep outlets. *Shanxi Hydropower*, 1992, 8 (1), 7-13.
- [4] HARGER, W. H., BRETZ, N. V. Discussion of "Simplified design of contractions in supercritical flow" by Terry W. Strum. *Journal of Hydraulic Engineering*, 1987, 113 (3), 422-427.
- [5] HARGER, W.H., SCHWALT, M. JIMENEZ, O. Supercritical flow near an abrupt wall deflection. *Journal of Hydraulic Research*, 1994, 32 (1), 103-118.
- [6] HUANG, Z.M., HE, X.H. AND ZHU, H.H. ET AL. Analysis of configuration layout and hydro dynamic pressure characteristics of slit-type bucket. *China Rural Water & Hydropower*, 2006, 5, 69-72.
- [7] IPPEN, A.T. Gas-wave analogies in open channel flow. *Conf. 2nd Hydraulics conf*, 1943, Bulletin 27, studies in Engineering, University of Iowa, Iowa.
- [8] LI, N.W., XU, W.L. AND ZHOU, M.L. ET AL. Experimental study on energy dissipation of flood discharge in high arch dams without impact of jets in air. *Journal of Hydraulic Engineering*, 2008, 39 (8), 927-933.
- [9] LIU, Y., MA, F. AND WU, J.H. Shock waves and jet width of slit-type flip bucket. *Advances in Science and Technology of Water Resources*, 2014, 34 (3), 20-29.
- [10] LIU, H.S., NI, H.G. The simplified formulas for shock wave in open channel. *Journal of Hydraulic Engineering*, 1999, 6, 56-60.
- [11] MA. J.M., ZHANG, Y.J. AND ZHENG, S.L. Experimental study on the characteristics of flow in spillway system with differential slotted flip bucket terminal structures for Shuibuya Hydropower Project. *Journal of Hydraulic Engineering*, 2007, 3, 93-99.
- [12] WU, J.H., MA, F. AND YAO, L. Hydraulic characteristics of slit-type energy dissipaters. *Journal of Hydrodynamics*, 2014, 1 (1), 86-93.
- [13] WU, J.H., WAN, B. AND MA, F. ET AL. Flow choking characteristics of slit-type energy dissipaters. *Journal of Hydrodynamics*, 2015, 27 (1), 159-162.
- [14] XIAO, X.B. Summary of application of slot dissipator for high dam energy dissipation and its development. *Design of Hydroelectric Station*, 2004, 20 (3), 76-81.

SUMMARY

Slit-type energy dissipater (STED) as an efficient device to dissipate energy of flow, is widely used in hydraulic projects of high water head, large discharge, and narrow river valley. However, the water wing caused by the shock waves in the contraction section of STED, may bring about harmful effects, which has been hardly attached enough importance. This paper revealed the internal relation of the shock waves and the water wing in STED through physical model experiments and theoretical analysis. Simplified formulas to calculate the shock wave angle and the water wing area were theoretically derived, which were demonstrated to be accurate enough to estimate the scope of the water wings.

KEYWORDS

Slit-type energy dissipater; Flow shock wave; Water wing; Hydraulic modeling

CLEARANCES AND COPYRIGHT

The author(s) is (are) responsible for obtaining written permission to profile the project or subject matter in their papers from any and all clients, owners or others who commissioned the work. ICOLD assumes proper permission has been obtained by author(s) and accepts no liability for the author(s) failing to do so.

If a figure, table or photograph has been published previously, it will be necessary for the author(s) either to obtain written approval from the original publisher; or refer clearly to the source of previously published material in the caption of the figure, table or photograph.

COMMISSION INTERNATIONALE DES GRANDS BARRAGES

VINGT-SIXIÈME CONGRÈS DES GRANDS BARRAGES
Autriche, juillet 2018

DOI 10.3217/978-3-85125-620-8-142



This work licensed under a Creative Commons Attribution 4.0 International License. <https://creativecommons.org/licenses/by-nc-nd/4.0/>

**SEISMIC ANALYSIS OF MIJARAN EARTH DAM AND OPTIMIZATION
OF ITS PARAMETERS USING PSO**

Seyed razi ANISHEH

Expert on MAZANDARAN REGIONAL WATER COMPANY, SARI

IRAN

Seyed alireza ANISHEH

MAZANDARAN UNIVERSITY, BEHSHAHR

IRAN

COMMISSION INTERNATIONALE
DES GRANDS BARRAGES

VINGT-SIXIÈME CONGRÈS DES
GRANDS BARRAGES
Autriche, juillet 2018

SEISMIC ANALYSIS OF MIJARAN EARTH DAM AND OPTIMIZATION OF ITS PARAMETERS USING PSO

Seyed razi ANISHEH

Expert on Mazandaran Regional Water Company, Sari

Seyed alireza ANISHEH

Mazandaran University ,Behshahr,Iran

1. INTRODUCTION

The Finite Element Method is a good choice for solving wave propagation through bounded and unbounded elastodynamic problems. In the finite element method for unbounded problems such as seismic wave propagation through the soil, a closed boundary must be considered for the foundation so the geometry of the model which has a significant effect on the response changes.

In simplified dynamic analyses of structures, it is normally assumed that the structure is fixed at the ground level and subjected to a base motion [1, 2]. The base motion represents the ground motion anticipated at the proposed site and is influenced by the nature and extent of the soil deposit at the site. In addition, the presence of the structure could also influence this base motion. This mutual influence of the structure and the foundation on their responses is commonly referred to as soil-structure interaction. When the response at the base of the structure is essentially identical to that with no structure present, there is no

interaction between the soil and the structure. On the other hand, when the response at the base is significantly different for the two cases, strong interaction exists between the soil and the structure. For cases where the interaction is strong, the soil and structure systems should be analyzed together using a coupled system. For cases where the interaction is insignificant, the soil and structure systems can be uncoupled and each analyzed separately.

Very little work has been done regarding the seismic response of dams on flexible foundations. Most of the research has been directed toward the analysis of dams on rigid foundations. Finn and Khanas [3] also evaluated the response of an earth dam on a flexible foundation using the finite element method of analysis. Their results indicated strong dependence of the response on the ratio of the fundamental periods of the dam and the foundation layer. Finn and Reimer [4] considered the interaction problem between the dam and the underlying foundation layer. They analyzed both the coupled and the uncoupled dam-foundation systems and showed significant differences in the response depending on the period of the systems compared to the fundamental period of the base input motion.

Chopra et al. [5] by considering dam as an assemblage of two-dimensional finite elements, and the foundation as an elastic half space, determined the dynamic properties of earth dams including foundation interaction effects. Their results indicate that foundation interaction may have significant influence on the frequencies and mode shapes of vibration of earth dams and the influence of foundation interaction depends significantly on the geometry of the earth dam cross-section, being relatively more important for dams with flatter side slopes. Among the geotechnical software, Quad4 and Plaxis can be used to seismic analysis of the dam-foundation model considering foundation-structure interaction. Quad4 is a dynamic, time-domain, equivalent linear two dimensional computer program to evaluate the seismic response of soil structures. Plaxis with dynamic module can be used to model advanced constitutive behaviors for the simulation of the non linear, time dependent and anisotropic behavior of soils and/or rock.

In this study dynamic analysis of Mijaran earth dam (Iran) considering dam-foundation interaction, under Manjil earthquake (after scaling to $a_{max} = 0.28g$), as input motion, carried out by Plaxis. In order to study the effect of the dam height and foundation width in the finite element model, on the calculated earthquake responses, several dam-foundation coupled models have been solved with Plaxis. In addition, dam heights and the foundation width affect on the displacement of the dam. In order to measure displacement of dam, we have used a nonlinear energy operator (NLEO). In this research, NLEO has been defined as a function of both dam heights and the foundation width. We minimize the cost function using PSO algorithm.

Soil-structure interaction (SSI) is an important issue, especially for stiff and massive structures constructed on the relative soft ground, which may alter the dynamic characteristics of the structural response significantly.

Thus, the interaction effects should be accounted for in the dynamic analysis of all soil-structure-system, particularly in severe soil conditions. The SSI system has two characteristic differences from the general structural dynamic system. These are the unbounded nature of the soil and the non-linear characteristics of the soil medium.

The radiation of the energy towards infinity, leading to the so called radiation damping, is the most prominent characteristic in an unbounded soil, which is not relevant in a bounded medium. Various studies and contributions have appeared in the literature regarding the effects of SSI on the dynamic seismic response of buildings (Ben et al.,2000). [6]

This paper is organized as follows: The Mijaran earth dam properties are described in Section 2. Section 3 presents the the numerical modeling for the dynamic analyses. The theoretical foundation of NLEO and PSO have been presented in Section 4. The performanceevaluation of the proposed method are provided in Section 5. Section 6 summarizes our conclusions.

2. METHODS

2.1. DEFINITION OF PROJECT

Mijaran earth dam, which is under construction, is located 20 km north east of Ramsar-Iran. It is constructed on the route of the Nesa River to supply agricultural and drinking water. It's height is 60 m from the foundation and with crest length of 186 m. Fig. 1 shows typical cross section of the dam-foundation coupled model. The dam site is located in Alborz seismic zone where active periods have been observed. One of the most important earthquakes that occurred in this area, was the 1990 Manjil earthquake, with $M_b=7.3$ and $M_s=7.7$.

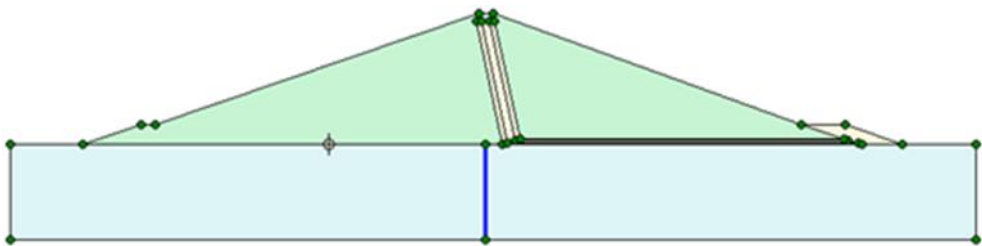


Fig. 1
Typical section of the dam-foundation coupled model

2.2. DYNAMIC ANALYSIS

The numerical modeling for the dynamic analyses has been performed using the Plaxis program, which are based on finite element method. Fig. 2 shows the geometry of the dam-foundation coupled model of the Mijaran earth dam. Dynamic

analyses were performed for the end of construction stage using the elasto-plastic Mohr-Coulomb model for material nonlinear behavior. Material properties of dam body and foundation have been presented in Table 1. In order to absorb the increments of stresses on the boundaries caused by dynamic loading, absorbent boundaries has been used. For accurate representation of wave transmitted in the model, the element sizes should be selected small enough to satisfy the following criteria expressed by Kuhlemeyer & Lysmer [7]:

$$\lambda \leq \frac{\Delta l}{10} \quad [1]$$

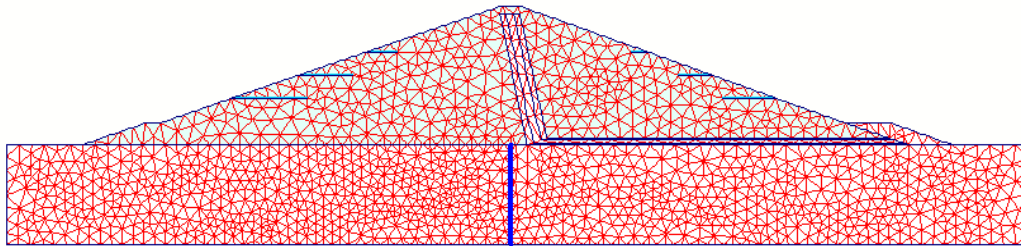


Fig. 2
model of dam-foundation and its elements

where λ is the wave length associated with the highest frequency component that contains appreciable energy and Δl is the length of element. Considering to these criteria, the element size have been selected as fine as possible.

Table 1
Material properties of the Mijaran earth dam

Type of material	γ (KN/m ³)	C (KPa)	ϕ	E (MPa)	ν
Dam body	21.5	27	23	215	0.3
foundation	21.5	1	42	270	0.3
Drain material	20.5	1	42	345	0.25

It should be mentioned that shear modulus, G has been modified according to effective mean stress (σ_0) as

$$G = G_i \sqrt{\frac{\sigma_0}{\sigma_{0i}}}$$

Small viscous damping is added for dam body. This damper was given by Rayleigh damping: the damping factors were assumed 0.005 for the first and second natural periods.

Earthquake response analyses were carried out for Manjil earthquake. The acceleration time histories of the Manjil Earthquake as shown in Fig. 3, were

normalized to a maximum acceleration of 0.28g which has been considered in accordance with Maximum Design Level (MDL).

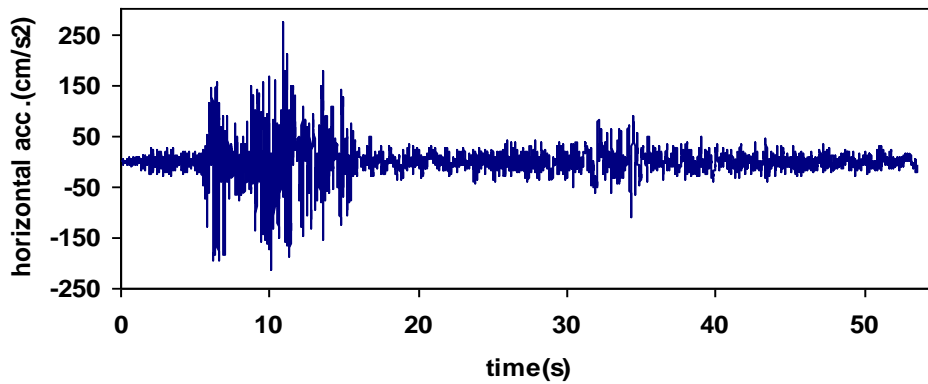


Fig. 3
Normalized horizontal component time history of Manjil earthquake

2.3. NLEO

Teager proposed (as presented in [4]) a simple NonLinear Energy Operator (NLEO) ψ_d given here in its discrete form as

$$\psi_d[x(n)] = x^2(n) - x(n-1)x(n+1)$$

By using simulated signals, Kaiser [4] analyzed this operator and found that it can detect frequency and amplitude of these signals. One of its key properties for a pure tone can be summarized by the rule

$$Q_d(n) = \psi_d[A \cos(\omega_0 n + \theta)] = A^2 \sin^2 \omega_0 \quad [3]$$

The proven can be expressed as:

$$\begin{aligned} Q_d(n) &= \psi_d[A \cos(\omega_0 n + \theta)] = A^2 \cos^2(\omega_0 n + \theta) - A \cos(\omega_0(n-1) + \theta) * \\ &A \cos(\omega_0(n+1) + \theta) = \frac{A^2}{2} [1 + \cos(2\omega_0 n + 2\theta)] - \frac{A^2}{2} \cos(2\omega_0 n + 2\theta) - \quad [4] \\ &\frac{A^2}{2} \cos(2\omega_0) = \frac{A^2}{2} - \frac{A^2}{2} \cos(2\omega_0) = \frac{A^2}{2} [1 - \cos(2\omega_0)], 1 - \cos(2\omega_0) = 2 \sin^2 \omega_0 \quad \omega_0 \\ &\Rightarrow Q_d(n) = \psi_d[A \cos(\omega_0 n + \theta)] = \frac{A^2}{2} * 2 \sin^2 \omega_0 = A^2 \sin^2 \omega_0 \quad \text{much less than the} \end{aligned}$$

sampling frequency, $Q_d(n) = A^2 \omega_0^2 = cte$. Therefore, The output of NLEO is proportional to multiplication of instantaneous amplitude and frequency of the input signal.

With the above motivation, Kaiser [4] used the second order differential equation governing the simple harmonic motion and the energy (sum of the kinetic and

potential energies) required to generate the motion, to introduce a continuous-time counterpart of the NLEO,

$$\psi_c[x(t)] = (x'(t))^2 - x(t)x''(t)$$

The instantaneous energy, E_0 , of an undamped oscillator is constant and is proportional to the output of **(3)** **[4]**.

$$\psi_c[x(t)] = A^2 \omega_0^2 \quad \propto \quad E_0 = \frac{m}{2} A^2 \omega_0^2$$

where $x(t) = A \cos(\omega_0 t + \theta)$ with $\omega_0 = \sqrt{(k/m)}$ is the displacement of the oscillator and k is the spring constant and m is the mass. Kaiser gave an interpretation of **(4)** as the amount of energy required to generate a sinusoid. Unlike the classical mean-square error (*mse*) definition of energy, this definition depends not only on the amplitude but also on the frequency of the sinusoid. To illustrate this difference, consider two sinusoids with frequencies of 1 Hz and 1 kHz but with the same amplitude. It is clear that *mse* energy will be the same for both sinusoids, while **(4)** suggests different amounts of energy requirement to generate these two signals. The latter relates the energy to the physics of generating a sinusoid of a given frequency **[5]**. As such, we will refer to the output of the NLEO **(4)** as the frequency weighted energy (FWE).

2.4. PSO

The basic operational principle of the particle swarm is reminiscent of the behavior of a group of a flock of birds or school of fishes or the social behavior of a group of people [8]. Each individual flies in the search space with a velocity which is dynamically adjusted according to its own flying experience and its companions' flying experience, instead of using evolutionary operators to manipulate the individuals like in other evolutionary computational algorithms. Each individual is considered as a volume-less particle (a point) in the N-dimensional search space. At time step t , the i^{th} particle is represented as $X_i(t) = (x_{i1}(t), x_{i2}(t), \dots, x_{iN}(t))$. The set of positions of m particles in a multidimensional space is identified as $X = \{X_1, \dots, X_j, \dots, X_l, \dots, X_m\}$. The best previous position (the position giving the best fitness value) of the i^{th} particle is recorded and represented as $P_i(t) = (p_{i1}, p_{i2}, \dots, p_{iN})$. The index of the best particle among all the particles in the population (global model) is represented by the symbol g . The index of the best particle among all the particles in a defined topological neighborhood (local model) is represented by the index subscript l . The rate of the position (velocity) for particle i at the time step t is represented as $V_i(t) = (v_{i1}(t), v_{i2}(t), \dots, v_{iN}(t))$. The particle variables are manipulated according to the following equation (global model [9]):

$$v_{in}(t) = w_i * v_{in}(t-1) + c_1 * rand1() * (p_{in} - x_{in}(t-1)) + c_2 * rand2() * (p_{gn} - x_{in}(t-1))$$

where n is the dimension ($1 \leq n \leq N$), c_1 and c_2 are positives constants, $rand1()$ and $rand2()$ are two random functions in the range $[0, 1]$, and w is the inertia weight. For the neighborhood (*lbest*) model, the only change is to substitute p_{ln} for p_{gn} in

equation for velocity. This equation in the global model is used to calculate a particle's new velocity according to its previous velocity and the distance of its current position from its own best experience (*pbest*) and the group's best experience (*gbest*). The local model calculation is identical, except that the neighborhood's best experience is used instead of the group's best experience.

The constants c_1 and c_2 in above equation represent the weighting of the stochastic acceleration terms that pull each particle toward *pbest* and *gbest* positions. Thus, adjustment of these constants changes the amount of 'tension' in the system. Low values allow particles to roam far from target regions before tugged back, while high values result in abrupt movement toward, or past, target regions.

The inertia weight w controls the impact of the previous histories of velocities on the current velocity, thus influencing the trade-off between global (wide-ranging) and local (nearby) exploration abilities of the 'flying points'. By linearly decreasing the inertia weight from a relatively large value to a small value through the course of the PSO run (total number of generations prior termination), the PSO tends to have more global search ability at the beginning of the run while having more local search ability near the end of the run [10].

3. RESULTS

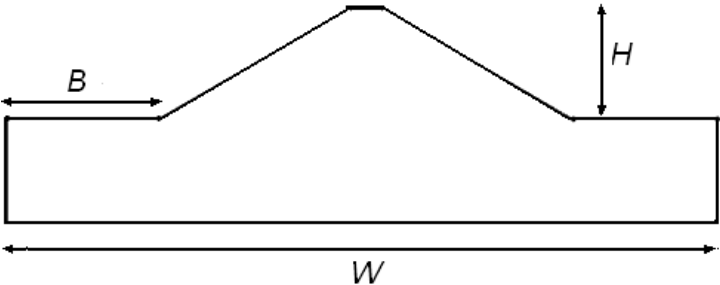
In order to evaluate the effects of dam height (H) and width of the foundation (W) on the finite element solution, some experiments had been carried out in the finite element model [9] (See Table 2). On the basis of experiments, it had been found that lateral extent must be selected less than twice the dam height in the finite element model. In this work an energy fitness function has been defined so that horizontal displacement time history at the dam crest in the finite element model on the earthquake response be minimized. The fitness function has been considered as a function of B/H ratio and we minimize the cost function using PSO algorithm.

In this experiment, the following PSO parameters are used:

Population size: 30; $Weight_{max}=1$; $Weight_{min}=0.4$; $C1 = C2 = 2$; Dimension=2; Iteration: 1000. B and H parameters change between 50-200 and 30-90, respectively. The PSO algorithm were implemented using MATLAB from Math Works. In this experiment, by using the PSO algorithm the B/H ratio should be equal to 1.29.

TABLE 2
Desired Dam Heights Lateral Extents And Foundation Width

Model Number	H (m)	B (m)	W (m)
1	30	50	303
2	30	100	403
3	30	200	603
4	60	50	498
5	60	100	598
6	60	200	798
7	90	50	669
8	90	100	769
9	90	200	969



The diagram illustrates a dam cross-section. It features a trapezoidal dam body with a flat top and sloped sides, resting on a rectangular foundation. The height of the dam is labeled as H . The lateral extent of the dam body is labeled as B . The total width of the foundation is labeled as W .

4. CONCLUSION

In this study, dynamic analysis of Mijaran earth dam (Iran) considering dam-foundation coupled model with various foundation widths and dam heights under horizontal component of Manjil earthquake has been performed using the Plaxis program. In the previous work, B/H ratio has been adjusted experimentally. But, in this research it has been found optimally using PSO algorithm. Several experiments has been carried out and the results shown the efficiency of the proposed idea.

REFERENCES

- [1] BAZIAR M.H., MERRIFIELD C.M., SALEMI Sh., HEIDARI T. Three dimensional dynamic analysis of alborz dam with asphalt and clay cores. *Proc. of 5th International Conference on Case Histories in Geotechnical Engineering*, 2004.
- [2] BAZIAR M.H., NOORZAD. A., SALEMI SH,. GHANNAD Z. Evaluation of

- Earthquake response of 15th Khordad Earth Dam. *Proc. of the 21st ICOLD International Congress, Montreal, 2003.*
- [3] FINN W. D. L., KHANNA J. Dynamic response of earth dams. *Proc. 3rd Symp. Earthquake Engng, University of Roorkee, U.P., India, 1966.*
- [4] FINN W. D. L., REIMER R. B. Effect of soil structures interaction on seismic response, *Proc. Conf. Earthquake, 1970.*
- [5] CHOPRA A. K., PERUMALSWAMI P. R. Dynamics of Earth Dams with Foundation Interaction. *Journal of the Engineering Mechanics Division, Vol. 97, No. 2, 1971,*
- [6] BEN J.S., SHIOJIRI H. A method for three dimensional interaction analysis of pile-soil system in time domain. *Trans Jpn. Soc.Comput. Eng. Sci, 2000.*
- [7] KUHLEMEYER R.L., LYSMER J. Finite Element Accuracy for Wave Propagation Problems. *Journal of Soil Mechanics & Foundation Division, ASCE, 99(5), 1973.*
- [8] EBERHART R. C., KENNEDY J. A new optimizer using particle swarm theory. *Proc. ISMMHS, pp.39-43, 1995.*
- [9] SHI Y., EBERHART R. C. A Modified Particle Swarm Optimizer. *in Proc. IJCNN, , pp. 69-73, 1999.*
- [10] JIRYAEI SHARAH M., ANISHEH S. R. Seismic Analysis of Narmab earth dam (IRAN) considering dam foundation interaction. *ICOLD Conference, Vietnam, 2010.*

Commission internationale Des Grands Barrages

VINGT-SIXIÈME CONGRÈS DES GRANDS BARRAGES
Autriche, juillet 2018

DOI 10.3217/978-3-85125-620-8-143



This work licensed under a Creative Commons Attribution 4.0 International License. <https://creativecommons.org/licenses/by-nc-nd/4.0/>

**REFERENCE PRESSURE CELL, AN EFFECTIVE SOLUTION FOR A
CHALLENGING MATTER OF DAM MONITORING**

Farzin KARIMI

MSc. Geotechnical Eng., Project Manager, GLÖTZL GMBH

GERMANY

Joachim SCHNEIDER GLÖTZL

Dipl. Eng. Geotechnical Eng., Managing Director, GLÖTZL GMBH

GERMANY

COMMISSION INTERNATIONALE
DES GRANDS BARRAGES

VINGT-SIXIÈME CONGRÈS DES
GRANDS BARRAGES
Autriche, juillet 2018

**REFERENCE PRESSURE CELL, AN EFFECTIVE SOLUTION FOR A
CHALLENGING MATTER OF DAM MONITORING**

Farzin Karimi

MSc. Geotechnical Eng., Project Manager, Glöttl GmbH, Germany

Joachim Schneider Glöttl

Dipl. Eng. Geotechnical Eng., Managing Director, Glöttl GmbH, Germany

ABSTRACT

Geotechnical monitoring is an important issue of design, construction and sustainable operation of embankment dams. Two most important categories of geotechnical monitoring by instrumentation are the measurement of pressure and displacement. In many instances of measurement technologies, these two physical parameters help each other to measure a quantity of them. Besides the displacement of soil mass is a source of inconsistent total pressure data. This issue is a challenging matter in geotechnical monitoring of embankment structures, which experience a considerable displacement during construction or consolidation phases.

In case of rotation of a total pressure cell without knowledge of the final inclination, correction of measured values through the theoretical assumptions is either impossible or not completely reliable.

This paper describes an innovative outcome of a project for developing a new measuring instrument, which can solve the above-mentioned problem, increase the reliability of monitoring data and reduce the errors and the costs of instrumentation. The important critical success factor of this measuring system is an optimal mechanical and electrical integration of an inclination sensor and a pressure insert in a tight heavy-duty housing. This type of total pressure cell is capable to measure the inclination in two axes up to 90°.

1. LITERATURE REVIEW

1.1. SOURCE OF ERRORS; HOW CHALLENGING THE MATTER IS?

A total pressure cell installed in the body of an earth-fill, e.g. in the clay core of an embankment dam, must be capable to measure the total stress in a special direction. In many instances, the position of pressure cell changes continuously due to the development of displacements and functionally changes the value of measured pressure. This is the most important reason for the inconsistent total pressure data and uncertainty of monitoring results of embankment structures. This uncertainty can cause some misunderstanding of pressure data and related pressure ratios – such as Arching Ratio - and following mistakes of monitoring.

The rotation of the total pressure cells in the soil material during compaction of an embankment is very likely. Therefore, the analysis of pressure data in an embankment without knowledge of final inclination of the pressure cell is a challenging matter, which sometimes causes resign form installation of total pressure cell.

For reviewing the literature of researches and studies, it would be very helpful starting with the GIN (Geotechnical Instrumentation News) which included an article by Ali Mirghasemi about total pressure cells of Karkheh dam in the 46th episode and subsequently discussions in the next episode. The exchange of ideas mentioned as below about no consistent total pressure data is being still discussed among the manufacturers, geotechnical institutes and consulting companies. The conclusion of Mr. Dunicliff for this very interesting theme is generally accepted for principle of stress monitoring in embankment dams.

" A total of 102 clusters, each of five earth pressure cells, have been installed to determine the total stresses in the embankment – a total of 510 cells. This number is about half of total number of instruments installed in the dam. No consistent data was achieved from the earth pressure cells. " Ali Asghar Mirghasemi, Assistant Professor, University of Tehran; GIN March 2006 [Ref. 1]

" In summary, measurement of total stress in an embankment is extremely difficult and should not be done unless absolutely necessary and, if necessary, particular care must be given to installation details. " Elmo DiBiagio, Norwegian Geotechnical Institute (NGI); GIN June 2006 [Ref. 2]

" My experiences with free field total pressure cells have also been disappointing and the cost of their installation in the clay core of a dam is not justified, in my opinion. The results are rarely reliable. " P. Erik Mikkelsen, Geoengeering & Instrumentation, Geometron Inc.; GIN June 2006 [Ref. 2]

" My experience is, and that of many authors at ICOLD Congresses and other Conferences seems to be, that it is very difficult to interpret and rely on the readings from earth pressure cells installed in embankment dams, especially rockfill dams. Many investigators have spent time and money installing such cells, but have, in general, found the measurements of little value. There are examples of pressure cells giving valuable readings when the cells are installed on a structural interface, but not inside the dam body. " John Dunicliff; GIN June 2006 [Ref. 2]

The conclusion of Mr. Dunicliff, especially mentioning on a solid subsurface, implicates the rotation of total pressure cells as a main source of inconsistent data inside the embankment. Until that time, there were a number of tries to reduce the local initial rotation of total pressure cells, which happens during the earth filling of first layers. However, there are no documented tests attempting to measure the rotation of total pressure cell precise and long-term.

There are wide ranges of studies, which have focused on stress-strain status in embankment projects especially for the verification of monitoring results or numerical back analysis by the instrumentation. These researches have addressed many uncertainties and generally mentioned to the rotation of cells.

As a similar study which has already implicated this inconsistent total pressure data, there is a research on the stress status of Taham dam in Iran. The difference between the numerical modeling and instrumentation data for total normal pressure are shown in figure 1.

Normally if a total pressure cell in an embankment rotates, the measured values are less than vertical stress at the point of measurement. For a better imagination of rotation, two displacement profile of Taham dam, shown in fig. 2, are helpful. In this dam, it is expected to face a rotation of total pressure cells under these large displacement conditions.

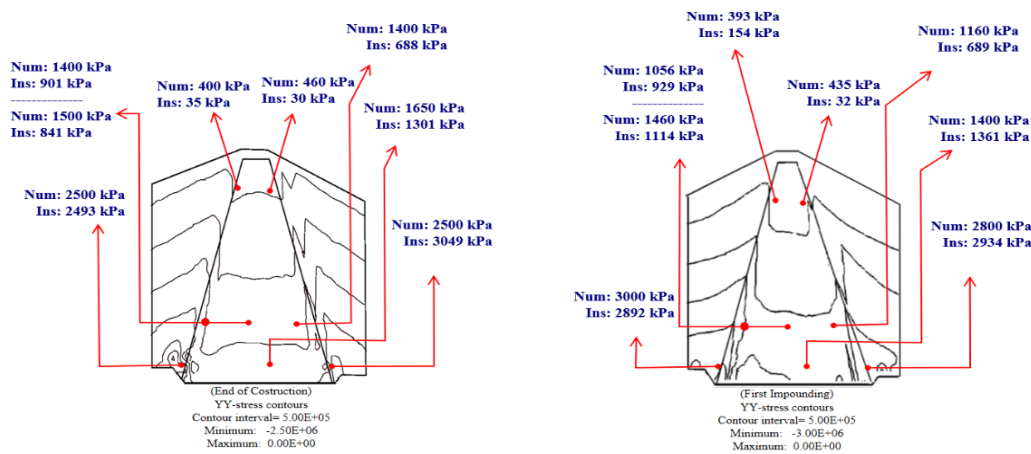


Fig. 1. Total normal pressure before and after impounding of Taham dam reservoir; Numerical analysis: Num. / Total pressure data: Ins. [Ref. 3]

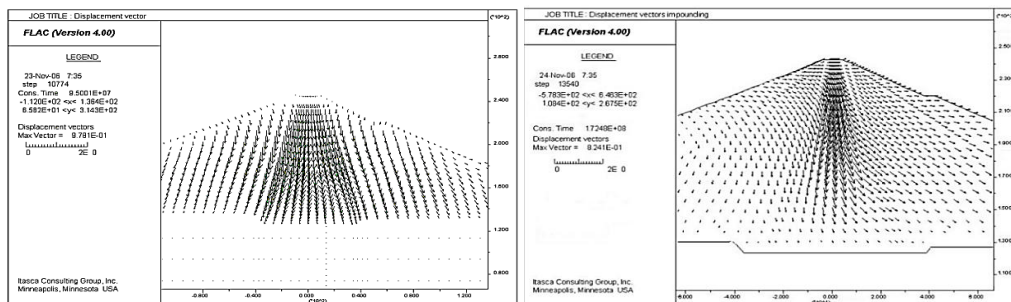


Fig. 2. Numerical Modeling of displacement vectors of Taham dam; [Ref. 3]

As shown in the figure 1, there is a considerable difference between numerical model (Num.) and instrumentation (Ins.). The best compatibility of the pressure data with the calculated values belongs to the lowest level of installation. This level of installation is located in the bottom of the clay core only 30 cm above the roller compacted concrete (Fig. 3). It is very likely that the rotation of total pressure cells in this level is very negligible (remember the conclusion of Mr. Dunicliff: "the structural interface").



Fig. 3. A) Interface of RCC and clay core; Excavated installation banks [Ref. 3]

There are many discussions about some other technical source of errors, in spite of the rotation, which would be mentioned very briefly. For a better understanding of these technical difficulties, a review of the components of a total pressure cell is unavoidable.

The Total Pressure Cell (TPC) consists of one or two active pressure cushion(s), hydraulic oil tube, and housing for diaphragm-type insert as well as hydraulic/pneumatic compensation valve (Fig. 4). The grooved pressure cushions are expressly mentioned as Active Pressure Cushion (or Pad), which cause a quite uniform deformation of pressure cushion (Fig. 5).

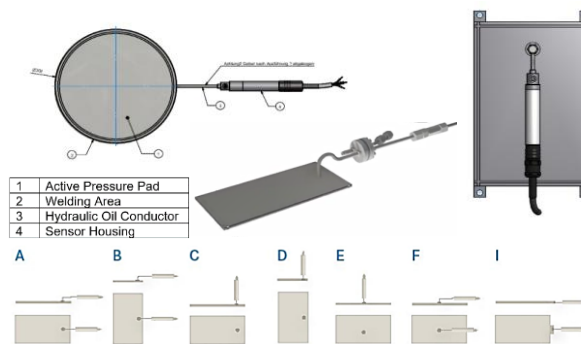


Fig. 4. Total Pressure Cells; Variations of electrical and hydraulic/pneumatic sensor, circular and rectangular, sensor housing connections



Fig. 5. Deformation of welded edge and grooved edge pressure cushions under uniform pressure in fine soil materials

The unqualified mechanical and electrical components are the prior source of errors and inconsistency of data respectively. Each mechanical component of an instrument as well as electrical components is involved in the final precision.

The assembly of cells and the insert in an appropriate housing are all-over important. A thigh housing with one-tenth millimeter tolerance or a slim housing prone to the deformation can reduce the precision tens of percent. In a similar manner the electrical components are enough sensitive to cause the errors.

1.2. SOURCE OF ERRORS; HOW HELPFUL THE CONVENTIONAL SOLUTIONS ARE?

There are some methods, which try to overcome these uncertainties either by some technical considerations during manufacturing, installation or by some recalculating of measured stress values.

First, some special changes in material and configurations of sensors, e.g. reducing drift and creep effects, the heavy-duty housings for inserts, short length hydraulic oil tubes, circular ventilation oil filling, grooving the loading pads, etc. would be listing as important achievements of manufacturers for overcoming the technological sources of errors (Fig. 6). However, they do not definitely warrant an on-site consistent measurement of total pressure.

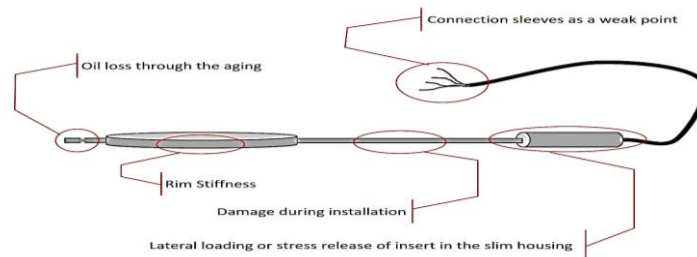


Fig. 6. Total Pressure Cell, Some sources of manufacturing errors

Second, the technical considerations during installation on site for positioning, installation, material filling and compaction don't guarantee in any case a steady fixed direction of installed pressure cells. These methods generally try to make a same compaction conditions around the total pressure cell for preventing local rotation and short-term local arch-action.

On the other hand, the theoretic recalculations are based on many assumptions. There are some methods, which are a combination of both practical and theoretical methods for reducing the negative physical effects and increasing the accuracy of theoretical calculations. These methods have certainly some limitations and disadvantages.

The conventional theoretical solutions, applicable considerations for installation and technological achievements of manufacturers are generally limited to the mechanical aspects of instrument and don't present any solution for overcoming the measuring errors due to the long-term rotation. Consequently, the

theoretical, technological and technical solutions for inconsistent pressure data in an embankment under a large displacement conditions are effective for reducing the sources of short-term errors.

It is to be noticed that there is a considerable quantity of embankment structures, especially embankment dams, in which projects the designer has preferred to resign the stress monitoring by total pressure cells. The current technical and academic literatures implicate that this attitude is becoming rapidly as an accepted design method of instrumentation of embankment structures. In that case the only remaining solution for approximating the pressure ratios is evaluating a pressure value by the average density of overburden materials regardless of unequal layer compaction and arching phenomenon.

2. SOLUTIONS

2.1. CONVENTIONAL SOLUTIONS; CLUSTER CELLS WITHOUT EXCAVATION OF AN INSTALLATION BANK

The non-uniform compaction of installation area causes a short-term local arching and additional rotation on pressure cells. The most known practical method for overcoming this rotation is embedding the cell by spreading soil without excavation an installation bank. The compaction of soil in the bank by using a lightweight roller results lower stiffness at the embedded sections than surrounding fill.

In case of embedding the cell without excavation, using heavy machines for compaction of first soil spreading is possible (Fig. 7). The installation of total pressure cell in the large embankment projects through this method for overcoming the short-term local arching and initial rotation is quite accepted everywhere. However, these phenomena can cause an inconsistent pressure data during the filling of first overburden layers, which is negligible compared to the full-scale pressure and displacement. It would be very careless to account the short-term non-uniform compaction, which would be adjusted during the construction time for long-term source of error.

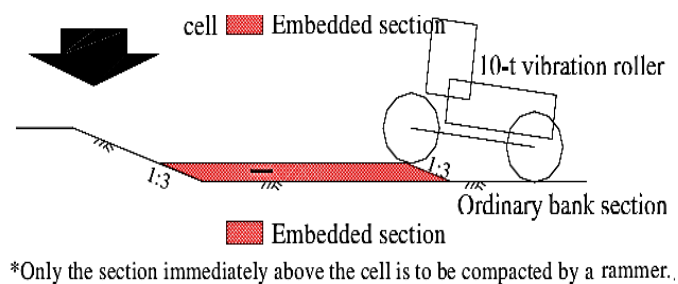


Fig. 7. Embedding cell by spreading soil; Minamiaki dam (Ref. 4)

As a combination of practical and theoretical method, the installation of a cluster of cells makes the recalculation of the rotation possible. In this method, the pressure cells are installed with maximum possible compaction ratio and minimum disturbance of surrounding fill in a cluster form up to five directions. In figure 8, the arrangement of embedded total pressure cells in a cluster of five cells is shown.

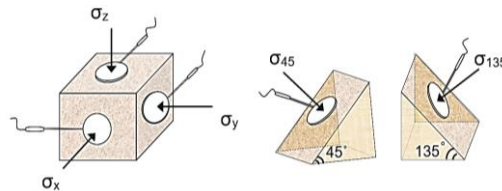


Fig. 8. The angles of embedded total pressure cells in a cluster of five cells.

Since the total pressure cells in one cluster are close enough to each other and adjust equally with the soil mass deformation quite all of them, an equal change of installation angle – the rotation - of whole pressure cells is expectable. Therefore, they can be considered as stresses in different directions for a single point in the embankment. The evaluation of stress ratio (normal stress to lateral stress; σ_{max} and σ_{min}) and the angel of pressure cushions (θ) is possible by theoretic recalculating of pressure data. For this reason, the Plain Strain formulation of strength of materials is used (fig. 9).

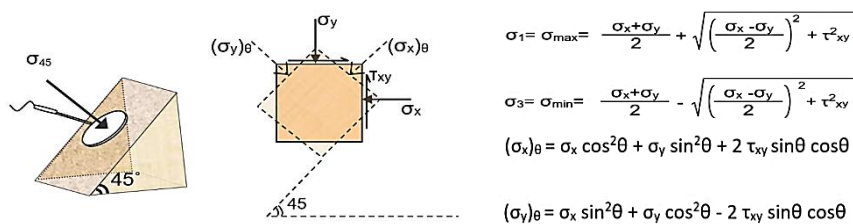


Fig. 9. The normal stresses on the rotated element recorded by the cell embedded 45°

With knowledge of stress ratios from the installed pressure cells and using the pole method of Mohr circle, finding the direction of pressure cushion is possible. Any straight line drawn from the pole will intersect the Mohr circle at a point that represents the state of stress on a plane inclined at the same orientation (parallel) in space as that line (figure 10).

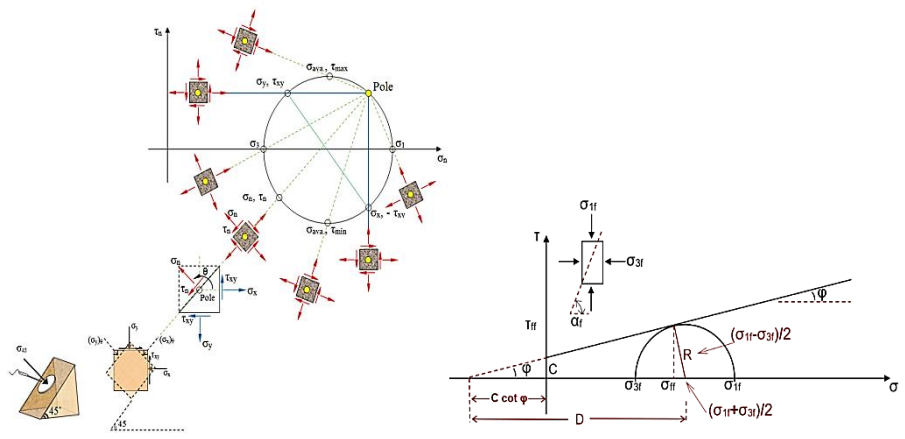


Fig. 10. Mohr circle and Mohr-Coulomb failure envelope for a cohesive soil; Mohr's circle for plane stress and plane strain conditions

2.2. THE EFFECTIVE SOLUTION; MEASURING THE INCLINATION OF PRESSURE PAD

The idea behind the new instrument for measuring the rotation of total pressure cells was very simple. However, there were many limitations to develop this simple idea. One of these limitations, which play a big role in the final product, is the geometry of instrument. The first comment for this idea was to combine a total pressure cell with a building inclinometer (fig. 11). In spite of that the selected inclination sensor for the first idea is very accurate, but the geometry of the product was not appropriate for installation in an embankment.

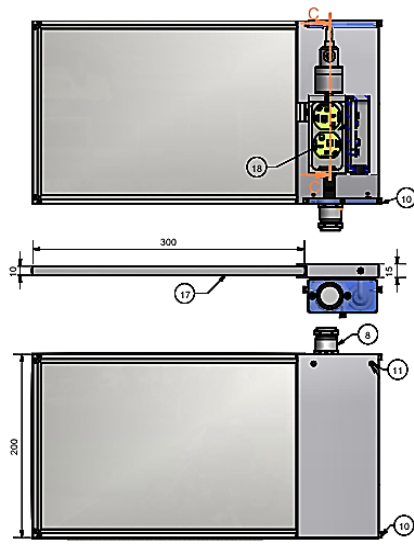


Fig. 11. The first idea for combination of pressure cell with biaxial inclinometer

The final comment on the idea was an integrated on-board sensor in the available standard heavy-duty housing of pressure insert. The standard available Glötzl heavy-duty housing and its mechanical components present an optimum ratio with active pressure pad. Therefore, the maximum dimensions of the electronic board were limited to 44x14 mm (LxW). The sensor which should be printed on the board can only place in a half-round space with maximum 3,5 mm height (fig. 12).

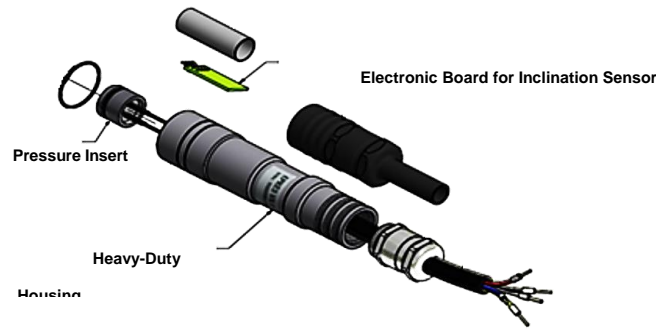


Fig. 12. Integrating an on-board inclination sensor in the standard Glötzl heavy-duty housing

Thank the rapid rise of electronic technologies, there are numerous types of reduced size inclination sensors available on the market. To make a decision for selecting an appropriate precise sensor, which is convenient for a thin electronic board, the significant approaches were dimension of sensor, precision and reproducibility, long-term stability, mechanical shock capacity, temperature sensitivity and price of final product.

The last factor is very decisive. The final price of this product depending on the precision of the sensor should not be expensive and possibly limited to the reasonable value of 30 percent of total pressure cell. On the other hand, the reasonable precision for measuring the rotation of a total pressure cells in an embankment dam are considerably less than a building inclinometer. Therefore, between wide ranges of sensors the MEMS-Sensor appears to be appropriate for the reason. The technical specifications of selected biaxial sensor are as follows.

- Measuring range: $\pm 30^\circ$ and $\pm 90^\circ$
- Measuring accuracy and Resolution: 1 mm / m and 0.06 mm/m
- Mechanical drop shock: 1 m onto a concrete surface
- Temperature operating range / sensitivity: $-40^\circ \dots +125^\circ$ / 0.01 % / $^\circ\text{C}$

The next step for actualizing the idea was data measurement with available hand-held readout units. The output signals of the selected sensor are measured in two axes by Glötzl NMA09 and converted to the sinus values (fig. 13).

Two most important advantages of this development are sealing and dimensions. The dimensions are limited to the above-mentioned size and could be assembled in whole measuring instruments which include the housing. For

example, the settlement gauges, load cells and borehole camera modules. For this reason, it is important to fix the housing with special brackets for preventing any wobble effect.



Fig. 13. Glötzl hand-held readout unit for inclination sensors connected to the MEMS

Since the total pressure cells in a cluster of cells are close to each other, it is enough to equip a total pressure cell with the inclination sensor and making it as reference instrument. For this reason, the total pressure cells equipped with biaxial inclinometer are characterized as Reference Pressure Cell (RPC).

As already mentioned there is no limitation for integrating a biaxial inclination sensor in the housing of whole pressure sensors. Therefore, Glötzl GmbH has developed a new generation of settlement gauges and load cells which are capable to measure the inclination. This possibility helps the engineers to achieve a better understanding of stress status and load distributions in the structures.

SUMMARY

The installation of reference pressure cells in an embankment enables the engineers to recalculate the normal pressure and verified pressure ratios.

Glötzl GmbH has achieved the success by focusing on mechanical and electrical components of a total pressure cell and trying to find an optimal solution for measuring the rotation of total pressure cells. A Reference Pressure-, Load- or Settlement Cell could be used in various type of projects which need to measure the pressure and the displacement.

An accurate measurement of rotation of total pressure cells installed in an embankment is a grate possibility for geotechnical monitoring for overcoming the uncertainties of stress monitoring. The arching (Ar.) and pore water pressure ratio

(Ru) are the critical relationships which are calculated through the knowledge of normal total pressure. It is possible if the rotation of total pressure cell is clear.

KEY WORDS

Earth Pressure, Deformation, Monitoring

REFERENCES

- [1] 46th Geotechnical Instrumentation News (GIN); March 2006
- [2] 47th Geotechnical Instrumentation News (GIN); June 2006
- [3] Farzin Karimi, Numerical Back Analysis of Embankment Dams; Case Study Taham Dam; MSc: Thesis; Amirkabir University of Technology Iran (Teheran Polytechnic)
- [4] Masanori Matsuu, Akira Takahashi, Yoshihisa Uchita, Hideki Ohta; Improvement of Earth Pressure Measuring Method in Rock-Fill Dams; 76th Annual Meeting of ICOLD

COMMISSION INTERNATIONALE DES GRANDS BARRAGES

VINGT-SIXIÈME CONGRÈS DES GRANDS BARRAGES
Autriche, juillet 2018

DOI 10.3217/978-3-85125-620-8-144



This work licensed under a Creative Commons Attribution 4.0 International License. <https://creativecommons.org/licenses/by-nc-nd/4.0/>

**THE APPLICATION OF PERFORMANCE ASSESSMENT OF EMBANKMENT
DAM MODEL BY USING KNOWLEDGE-BASED SYSTEM**

Juliasuti

Lecturer of Civil Engineering Department, BINA NUSANTARA UNIVERSITY

INDONESIA

Widagdo

Commission Member, INACOLD

INDONESIA

Agus Jatiwiryono

Commission Member, INACOLD

INDONESIA

Budy Gunady

*Head of Technical and Business Planning, JASA TIRTA II PUBLIC
CORPORATION*

INDONESIA

COMMISSION INTERNATIONALE
DES GRANDS BARRAGES

VINGT-SIXIÈME CONGRÈS DES
GRANDS BARRAGES
Autriche, juillet 2018

THE APPLICATION OF PERFORMANCE ASSESSMENT OF EMBANKMENT DAM MODEL BY USING KNOWLEDGE-BASED SYSTEM

Juliastuti^{1*}, Widagdo², Agus Jatiwiryono³, Budy Gunady⁴

¹Lecturer of Civil Engineering Department, BINA NUSANTARA UNIVERSITY

^{2,3}Commission Member, INACOLD

*⁴Head of Technical and Business Planning, JASA TIRTA II PUBLIC
CORPORATION*

INDONESIA

1. INTRODUCTION

The performance assessment of embankment dams in respect to main deterioration mechanisms is the major challenge for managers in charge of their security. However, the risk score of dams in Indonesia is moderate until high risk because rarely equipped monitoring instrument and vegetation are often present. To cope with them, the dam owners/managers have first to identify the specific status indicator linked with vegetation and behavior dam based on monitoring instrument.

There was a common belief among communities when damage to embankment dams and dam safety issues associated with tree and woody vegetation penetrations of embankment dams happened, people often immediately assumed that it happened due to lack of maintenance by the dam owners, dam safety regulator and engineers. However, during the Research Needs Workshop on Plant and Animal Impacts on Earthen Dams, a collaboration event between the Federal Emergency Management Agency (FEMA) and the Association of State Dam Safety Officials (ASDSO) in November 1999, they highlighted the realization that damage to earthen dams resulting from plant and animal penetrations was indeed a significant dam safety issue.

Tree and woody vegetation penetrations of earthen dams have been demonstrated to be the causes of serious structural deterioration and distress that can result in failure of earthen dams (FEMA 2005). The workshop itself brought

together technical resources of dam owners, engineers, state and federal regulators, wildlife managers, foresters, and members of academia with expertise in their areas. They agreed that trees and woody vegetation should be removed because they can delay safety inspections also interfere with safe operation, or even leads to dam failure. Until this day, the engineers and dam safety experts were still debating on what kind of method should be used to prevent or control tree growth efficiently. However, they all are agreed that a healthy, dense stand of low-growing grass on earthen dams is a desirable condition and should be encouraged. Therefore removal of trees and other woody vegetation in the embankment area is required.

On the other hand, this removal (of trees and other woody vegetation) action will raise the social issue in communities. Dam safety regulators and inspectors, engineers, and consultants soon will be confronted with the grassroots resistance. This resistance is often associated with sentimental, cultural, ecological, legal, and financial issues. A fundamental understanding, technical knowledge and proper assessment of potential detrimental impacts of trees and woody vegetation growth on the safety of embankment dams are necessary to address these issues.

2. PROBLEM CAUSED BY TREE AND WOODY VEGETATION IN THE EMBANKMENT AREA

Trees and woody vegetation are considered dangerous to grow in the embankment area. The problems caused by tree and woody vegetation growth are: uprooted trees that produce large voids and reduced freeboard; reduced the maintaining stability, the decaying roots create seepage paths and internal erosion problems, interfering the dam safety monitoring, inspection and maintenance for seepage, cracking, sinkholes, slumping, settlement, deflection, and other signs of stress. There is also another problem related to safety dam, they are: hindering desirable vegetative cover and causing embankment erosion, obstructing emergency spillway capacity, clogging embankment underdrain systems, cracking, uplifting or displacing concrete structures and other facilities, inducing local turbulence and scouring around trees in emergency spillways and during overtopping, providing cover for burrowing animals, loosening compacted soil, allowing roots to wedge into open joints and cracks in foundation rock along abutment groins and toe of embankment, which leads increasing piping and leakage potential.

Many misconceptions and common myths regarding trees and woody vegetation spread and have been accepted by many people without any scientific explanation. These myths and misconceptions relative to plant physiology have originated from old, traditional and uneducated interpretations of observations associated with tree growth and tree root development. Not all myths are wrong, however, if we relate with the growth of trees and woody vegetation in embankment area, some of these myths need to be dispelled so that a new level of understanding about the impacts of trees and woody vegetation on earthen dams can be properly developed.

The root systems consist of two primary components that are the root ball and the lateral transport root system. Tree and woody vegetation roots have a primary function of providing oxygen, nutrients, and water to the plant, they also provide stability for the plant. The root ball which is typically directly below the trunk

of the tree provides vertical support while the lateral transport roots provide lateral support for the tree. The root systems that were growing on dam embankment slopes will typically be asymmetrical because of the need for the tree to be stabilized in the sloping embankment soil mass. The lateral transport roots will typically be better developed on the uphill side of the tree than on the downhill side of the tree. Dr Kim D. Coder at the University of Georgia conducted many extensive studies and research on tree growth and tree root development requirements and characteristics. He developed data from these studies and research programs that relate tree trunk size to root ball diameter and lateral transport root system diameter. To relate the research data from Dr Coder, the author compiled a comparative list of soil properties for various soils that have been found in earthen dam embankments. The ranges given in the data presented in Table 1 below are associated with soil in a loose condition and soil in a compacted state that might be required in the construction or remediation of an earthen dam.

Table 1. Summary of typical soil parameter

Soil Type	Specific Gravity	Void Ratio	Porosity (%)	Dry Density, pcf	Permeability, cm/sec
Sand	2.62 to 2.66	0.40 to 0.90	30 to 45	90 to 115	0.01 to 0.0001
Silt	2.60 to 2.68	0.50 to 1.20	35 to 55	75 to 110	0.001 to 0.00001
Clay	2.66 to 2.72	0.60 to 1.40	40 to 60	70 to 105	0.0001 to 0.0000001

Source: FEMA 534, 2005

As shown in the tabulated summary of typical soil parameters, the continual tree root development cannot occur in soils that are well compacted. One of the best methods of controlling tree and woody vegetation growth on new earthen dams and existing earthen dams where remediation requires placement of additional embankment fill soil is to compact the embankment fill soils to a high stage of compaction. Increased compaction of embankment fill soils reduces the air void content and limits the quantity of surface water that can infiltrate into the embankment slope. However, a good ground cover of grasses can be established in well-compacted soils since the depth of grass root penetration is minimal and the surficial soils will typically sustain the shallow grass root penetration.

The initiation of the tree and woody vegetation development on the downstream slope starts soil moisture uptake cycle with the goal that the line of immersion and the leakage line may never totally develop and intercept the downstream slope. In any case, one must comprehend that as the tree and woody vegetation development proceeds compacted soils of the dam embankment are relaxed continuously by the penetration of major tree and woody vegetation roots. Besides, trees that might seem healthy to an untrained inspector might be an unhealthy sample and have a premature death leaving penetrating root frameworks to rot inside the dam embankment. Moreover, soil supplements in the compacted soil embankment of an earthen dam may not be adequate for improvement of growth beyond which the tree can't be properly maintained without premature death. Notwithstanding the reason, trees and woody vegetation do die and stop to take-up soil moisture that they previously used. This change in soil moisture uptake will influence the zone of air circulation, the zone of saturation,

and the area of the leakage line (seepage) near the dead trees and woody vegetation.

When an earthen dam embankment impregnated with many trees and woody vegetation penetrations, routine and even major maintenance activities will likely not be enough to regain the original design lifespan of the dam. At this time in the life of an earthen dam, previously identifiable maintenance problem has become serious dam performance and dam safety issues. Restoration through an engineered dam remediation design and remediation construction is typically required to bring the dam to acceptable standards congener to dam safety requirements. Figure 1 illustrates some of the problems and dam safety issues which can be created by a non-maintained tree and woody vegetation growth in what has been termed by the author as the 'Mid-Life Crisis' of an earthen dam.

Seepage flow might rise out of root ball holes of blowdowns (uprooted trees) since they are no longer using soil moisture and the seepage line has adjusted upward toward the surface of the slope. Expulsion of developing trees by woodcutters decreases the soil moisture take-up of the removed trees along these lines additionally adjusting the area of the seepage line closer to the downstream slope. Root balls and root systems of trees situated at and past the toe of the downstream bank slope end up immersed by the balanced seepage line. Since trees cannot survive through prolonged submergence of their significant root systems, these trees will end up unhealthy and die to leave decaying root balls and root systems as serious penetrations in the earthen dam. Root ball pits staying from blowdowns (uprooted trees), and their relationship to the seepage line create conditions worse to potential slope failure of the embankment dam. Restoring the earthen dam showed in Fig. 1 to a protected condition cannot be brought through periodic maintenance.

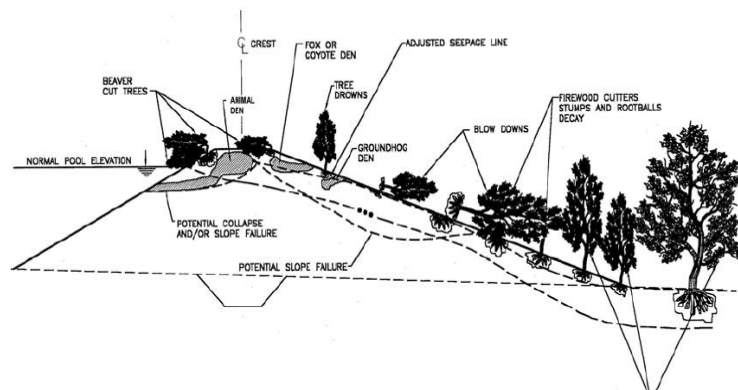


Fig.1 Mid-Life Crisis of a Dam Plant (Tree) and Animal Penetration Problems (Source: FEMA 534, 2005)

3. ASSESSING THE PERFORMANCE OF AN EMBANKMENT DAM

Evaluating the performance of an embankment dam consists in looking for and assessing all the weakness factors which contribute to the damage. It allows

appreciating, at a given moment, the fitness of a hydraulic structure to fulfil the functions for which it was designed and so its level of safety. This assessment will help managers and owners to take the best decisions for carrying out the required maintenance works to secure the safety of their structures. Thus, the managers responsible for the safety of dams' demand methods and tools that they can use to perform detailed diagnostics of their structures then assess their status and performance.

The Authors choose to use knowledge-based systems in this paper due to their interest in performance assessment, especially for complex systems such as dams, as they can reproduce the reasoning of an expert and consider data of various origins and types (visual observations, design-visualisation data, monitoring data, resulting from models). The works cited above focused on the case of dams (i) equipped with monitoring instruments providing the information required to assess their performance with respect to deterioration mechanisms such as internal erosion; (ii) equipped with a drainage system, one of the components ensuring the safety of these structures. However, certain dams such as embankment dams have specific characteristics on which we intend to focus on.

In this paper, the Authors use the models of Curt et al. (2010) and Curt (2013) which are adapted to assess the performance of embankment dams equipped with drainage systems and monitoring instruments for both the “embankment” part and the foundation of the structure, as our basis. This approach analyzes the models to perform until they reached their limits in comparison with the application, then propose modifications and adaptations to take these limits into account. Figure 1 shows the hierarchical model for assessing the performance of an embankment dam with respect to deterioration by internal erosion (Curt et al., 2010), and the limits of this model.

These assessment models have a three-level hierarchical structure: (i) status indicators; these are the input data of the model; (ii) the performance of functions; and (iii) the performance of the component regarding the internal erosion mechanism. The status indicators are formalized data. Different data are used by the engineer to perform an assessment: monitoring data if the dam is equipped with instruments, visual observations, design and construction data and calculation data. It is important to formalize them, to obtain the robust measurement, repeatable and reproducible, however, it is also great to use them in combination. Therefore, a formalization grid is used, based on: the name of the status indicator, its definition, the scale of measurement and the associated references giving the anchoring points on the scale and which allow describing the different possible statuses of the indicator, the spatial characteristics specifying the part of the dam to be analyzed and the temporal characteristics indicating the time step for measuring the indicator and the analysis of the trend presented by this measure (Curt et al., 2010).

The paper proposes using a second assessment scale for all the indicators: an ordinal scale characterized by the ordering of categories as a function of an intensity criterion linked to a scale of intervals that allows working on continuous numerical magnitudes (Fig. 2).



Fig. 2 Scale of the double assessment chosen for assessing the performance of dams

To build our model, we conserve this general structure according to three levels:

- status indicator,
- performance of functions and
- the performance of the component.

The limits of these existing models with respect to the dams dealt with happened because they were developed for embankment dams equipped with drainage systems and monitoring devices. This observation leads us to propose three changes. As shown in Fig. 3, the performance of the embankment of a dam regarding the mechanism of deterioration by internal erosion is evaluated using three function performances: the sealing function, the drainage function and the self-filtration function.

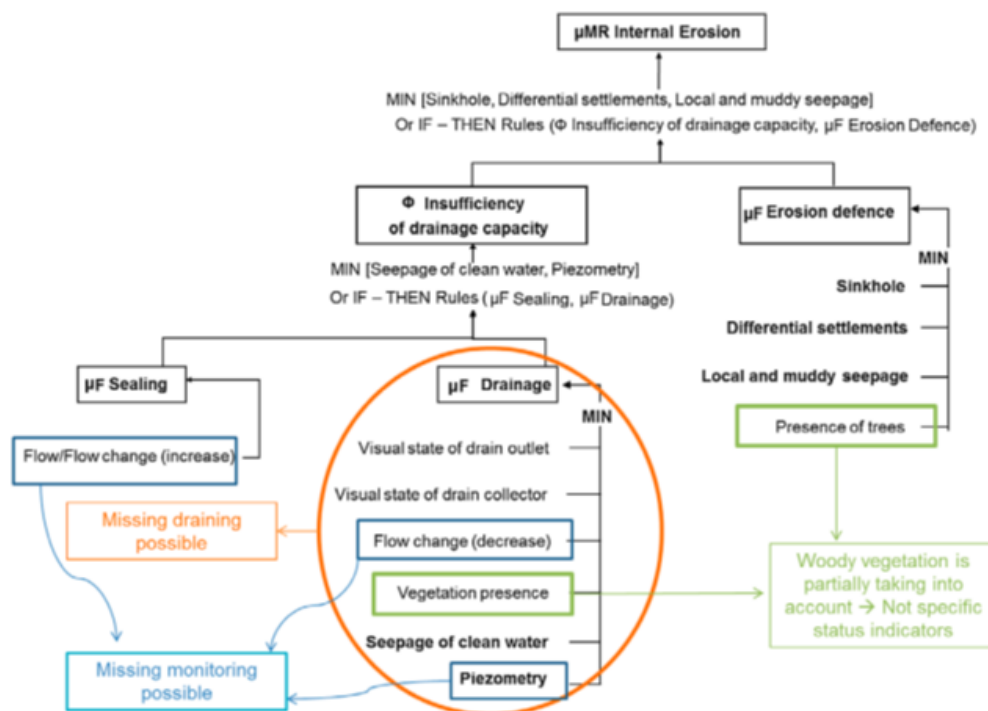


Fig.3 Hierarchical model for assessing an embankment dam built using homogenous fill equipped with a drain and monitoring instruments [μ = performance; Φ = phenomenon] (Bambara et al., 2016)

The performance of the drainage function cannot be evaluated if the structure is not equipped with a drainage system. The structure of the model must be changed to offset this problem. Each of the performances is evaluated based on status indicators stemming in part from monitoring data: “increased flow rate”, “piezometer”, etc. However, this type of information is not readily available for the certain structures we wish to study, thus the aim is to propose other information possibly available to experts, notably design and construction data. In addition, the small embankment dams studied here are often, or have been, subject to a lack of maintenance that has led to abundant woody vegetation on or at the edges of the embankments. The existing models consider woody vegetation only for assessing the performance of the drainage function and the self-filtration function using a single status indicator termed “presence of woody vegetation”. Indeed, they consider only the assessment of the performance of embankment dams regarding the mechanism of deterioration by internal erosion by suffusion. It is important to

characterize this vegetation in greater detail by developing specific status indicators that allow assessing the potential for internal erosion of an earth fill hydraulic structure due to the state of the woody vegetation present on the dam (level of decomposition of root systems of dead trees, etc.). Furthermore, the presence of vegetation leads to another improvement to the models: the components assessed are, as for the existing models, however, the embankment–foundation interface must be considered specifically in the case of a dam that has no drainage system, as this can be a preferential location for the installation of woody roots.

The following steps are aimed at proposing methods to respond to these three main constraints: possible absence of a drainage system, possible absence of monitoring data and presence of woody vegetation.

For specific indicator, we used the safety assessment techniques (Functional Analysis – FA – and Failure Mode and Effects Analysis – FMEA) to identify the indicators specific to woody vegetation by focusing on the external element “woody vegetation”. The FA is carried out in two steps. An external FA makes it possible, initially, to identify the function(s) that the structure must have regarding external constraints, in this case woody vegetation. An internal FA is then performed. It leads to the identification of different functions resulting from the relations between each component of the structure and the external environment.

Following the FA, an FMEA is used to identify the failure modes, their effects and possible causes for each component, and the indicators of the causes and effects of the failures of the different components. This inductive method systematically considers each component of the structure, one after the other. In our case, the failure mode considered is internal erosion linked to the presence of vegetation. The experts use the formalizations on examples of real cases and express their agreement/disagreement regarding the formalizations. The indicators are modified if necessary. The starting point comprises the indicators listed in the FMEA tables. The objective of the sessions is to describe these indicators to ensure their robustness for application. However, it is difficult to assess certain status indicators when there are no known instrumental methods and if visual observation is impossible, since the element to be assessed is inaccessible, as is the case of the status indicator “Degree of decomposition of the woody stump or roots of an individual¹”. Thus, an indirect chemical measure by NIRS (Near Infrared Spectrometry) has been developed (Bambara et al., 2013) and a formalization for this indicator based on the results of the chemical measurement proposed.

4. IDENTIFICATION, FORMALIZATION AND AGGREGATION OF STATUS INDICATORS SPECIFIC TO WOODY VEGETATION

The specific status indicators were identified to assess the performance of embankment dams. These status indicators were identified using an FMEA. Table 2 is the identification of specific indicators for woody vegetation. For the assessment of the sealing function (“Type of root structure of individuals”) and one in the assessment of the drainage function (“Visual condition of the environment of the drainage blanket outlet”). In Table 2, present the formalization grid for assessing the indicator “Diameter of tree trunk from” with the scoring scale of Figure 2. Knowing that diameter of tree trunk is depend of root systems grow as a tree ages, an individual with a stump having a large diameter leads to assuming a tap root system. Thus, the indicator “tree trunk diameter per individual” transposes the measure of the taproot diameter. It is important to know this parameter to

predict the impact in terms of the global increase in dam permeability during root system.

The status indicator “Diameter of tree trunk of individuals” provides a global root characterization next to the profile analyzed. Indeed, the different types of root structure of individuals can act on the internal erosion mechanism to varying degrees during woody root. Thus, individuals with a long horizontal type root structure with the potential for crossing the embankment dam from downstream to upstream would be particularly serious. The taproot would likely form a pipe through the embankment (depends on the material), hence the importance of having an assessment of the status indicator “Degree of decomposition of the taproot or woody roots of an individual”. The status indicator “Visual condition of the environment of the drainage blanket outlet” is appreciated by the “Tree trunk of individuals” present at the outlet of the drainage blanket. Thus, it has the same references as the status indicator “Diameter of individuals”. The status indicators specific to woody vegetation are aggregated according to functional logic. Their successive combinations permit obtaining the propensity to flows within the embankment dam due to the presence of vegetation (Figure 4). This “block” will be used for assessing the performance of the function. The summary of methodology for building embankment dam performance assessment models is shown Fig.5.

		Performance of diameter tree trunk										
		0	1	2	3	4	5	6	7	8	9	10
Performance of internal erosion	0	0	0	0	0	0	1	2	2	8	9	10
	1	0	1	1	2	2	2	3	3	8	9	10
	2	0	1	2	2	2	2	2	3	8	9	10
	3	0	1	1	2	2	4	4	5	8	9	10
	4	0	1	2	2	3	4	4	4	8	9	10
	5	1	1	1	2	3	4	6	6	8	9	10
	6	1	2	2	2	3	5	7	7	8	9	10
	7	8	8	8	8	8	8	8	8	8	9	10
	8	8	8	8	8	8	8	8	8	8	9	10
	9	9	9	9	9	9	9	9	9	8	9	10
	10	10	10	10	10	10	10	10	10	10	10	10

Fig. 4 Truth table for combination of the values of the performances of diameter tree trunk and “to internal erosion” functions

Table 2. Formalization grid for the status indicator “Diameter of tree trunk”

Name	Density of individuals
Definition	Primary look at the diameter of tree trunk for indicator and root typology is taproot. Root typology: vertical taproot, long horizontal root, short root. Never allow any vegetation larger than pasture grass to become established on or near the embankment. Tree roots, especially eucalyptus tree roots can cause the core to crack resulting in the failure of the dam.

Scale	10 (good at very good): Without taproot 5-4 (poor): Diameter tree trunk < 5 cm 1-0 (unacceptable): Diameter taproot > 5 cm
Temporal characteristics	Measure is carried out during a visual examination focused on the characterization of vegetation on dam

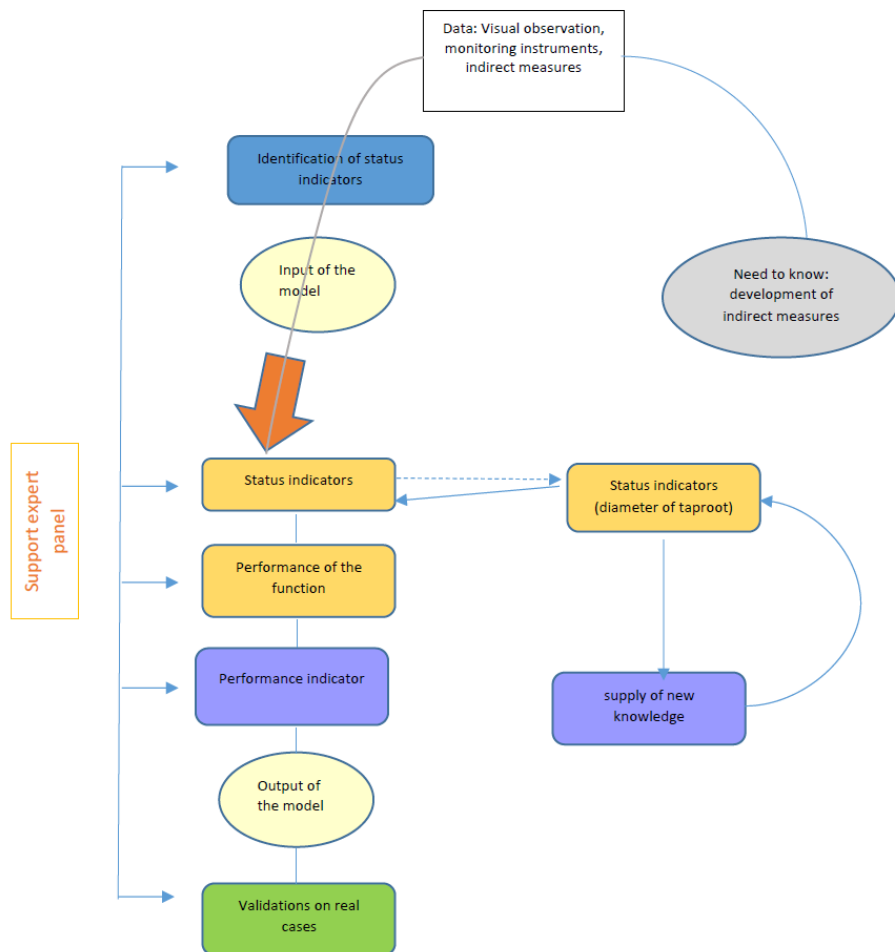


Fig. 5 General methodology for building embankment dam performance assessment models

5. CASE STUDY

The study area is the biggest dam in Indonesia, named Juanda dam at Jatiluhur. The location is 100 kilometers east of the city of Jakarta, Indonesia. The Juanda dam is a multipurpose dam, it is a rockfill-type dam with inclined clay core, and its height is 96 meters. The total storage reservoir capacity is more than 2.5 billion cubic meters and crest length is 1220 meters. It was constructed during the period of 1957 - 1967. The operation of Juanda (Jatiluhur) multipurpose dam was

firstly managed by the Jatiluhur Development Project under the Department of Public Works and Electric Power up to the year of 1970 and since then the dam has been operated under the management of Jasa Tirta II Public Corporation.

Based on the results of the latest visual inspection, on the downstream slope of Juanda Dam is not found any hard trees. The downstream part of the dam body is covered by grass as a protector from rain water splashing, also serves as an indicator when there is a wet area on the downstream slope. In Fig. 6 looks a hard tree, all of which is in the original land, and there is no visible hard tree growing on the dam body (embankment).



a. The downstream of Juanda Dam



b. Upstream toward downstream

Fig 6. Upstream and downstream Juanda Dam
(Source: Jasa Tirta II Public Corporation)

REFERENCE

- [1] BAMBARA, G., CURT, C., MERIAUX, P. (2016). Modular assessment of the performance of Embankment dams
- [2] SCHLEISS, A. (Ed.), BOES, R. (Ed.). (2012). Dams and Reservoirs under Changing Challenges. London: CRC Press.
- [3] FEMA. (2005). Technical Manual for Dam Owners - Impact of Plants on Earthen Dam

COMMISSION INTERNATIONALE DES GRANDS BARRAGES

VINGT-SIXIÈME CONGRÈS DES GRANDS BARRAGES
Autriche, juillet 2018

DOI 10.3217/978-3-85125-620-8-145



This work licensed under a Creative Commons Attribution 4.0 International License. <https://creativecommons.org/licenses/by-nc-nd/4.0/>

**REMEDIAL GROUTING OF EXISTING EMBANKMENT DAM FOUNDATIONS:
LESSONS LEARNED (AND IGNORED)**

Donald A. BRUCE

President, GEOSYSTEMS, L.P.

U.S.A.

Trent DREESE

Vice President, GANNETT FLEMING

U.S.A.

Jim COCKBURN

Independent Consultant

U.S.A.

COMMISSION INTERNATIONALE
DES GRANDS BARRAGES

VINGT-SIXIÈME CONGRÈS DES
GRANDS BARRAGES
Autriche, juillet 2018

REMEDIAL GROUTING OF EXISTING EMBANKMENT DAM *FOUNDATIONS: LESSONS LEARNED (AND IGNORED)

Donald A. Bruce¹, Trent Dreese², Jim Cockburn³

¹ *President, GEOSYSTEMS, L.P.*

² *Vice President, GANNETT FLEMING*

³ *Independent Consultant*

U.S.A.

1. BACKGROUND

Since the late 1990's in the U.S.A. there has been a technological revolution in rock fissure grouting practices, primarily as a result of the technical and dam safety challenges which have typified the dam remediation market. This revolution has been well documented in numerous papers at the New Orleans Grouting Conferences [1] [2], at the Honolulu Grouting Conference [3], in USSD publications and conferences, and in more recent textbooks [4] [5]. Final confirmation is provided in the USACE's new Grouting Manual [6], which is a radical overhaul of the prior version (1984).

An observer of the huge remedial grouting projects at Mississinewa, IN, Clearwater, MO, Center Hill, TN, Boone Dam, TN, East Branch Dam, PA, and Wolf Creek, KY as examples, cannot fail to note the sophistication (and the curious similarities) of the means, methods and materials each contractor has used. It is equally clear that owners and designers are now producing specifications that consistently reflect modern practices, instead of recycling contract documents ("boiler plate") that are inconsistent and awkward amalgam of the old and the new.

The authors are involved in different contractual and oversight roles in a large number of remedial grouting projects for dams. We have noted over the

* INJECTION RÉPARATEUR DES FONDATIONS DE BARRAGES EN REMBLAI EXISTANTES: LEÇONS APPRISSES (ET IGNORÉES)

last few years that certain “lessons learned” during the revolution have not been fully or correctly applied, or have indeed been ignored. If left unchecked, these regressions will have the effect of reducing the quality and reliability of the finished product, and will increase the prospects of contractual disputes.

The following topics focus on practical issues associated with the execution of the works, and so exclude reference to design-related issues such as the number and spacing of grout lines; drill hole spacing and orientation; upstage versus downstage; or grouting control principles.

2. LESSONS LEARNED

2.1. DRILLING TECHNIQUES FOR OVERBURDEN AND ROCK

Most remedial grouting projects will involve drilling and casing through overburden and/or embankment fill so that standpipes can be placed to permit safe access to the rock drilling activities therebelow. In essence, neither compressed air nor water is considered acceptable for fear of compromising the integrity or safety of the embankment [7]. This explains the widespread use of the rotary vibratory method (“sonic drilling”) and dry, double-head duplex, wherein an inner auger is advanced simultaneously with the outer casing. In both cases, minimal amounts of water are introduced to facilitate progress. Every care should be taken to prevent “cleaning water” used on the working platform from escaping down and around the casing (or standpipe once it has been installed).

It is one of the oldest debates in the drilling and grouting industry: percussion versus rotary methods and air flush versus water flush. Past practice has been dictated by the capabilities of the drilling industry: given that air flush is not permissible for rock fissure grouting, or when drilling in karstic limestone formations under existing embankments, much traditional work was done by rotary drilling, either coring or “blind,” using water flush.

Rotary percussion drilling, especially of the Down-the-Hole (DTH) variety, has distinct advantages over rotary drilling in terms of speed and deviation control, but was always synonymous with the use of air flush. The practice of some contractors to “mist” the air with water is totally misguided, as this actually reduces the chances of drilling a clean hole, not improves them. The best of all worlds arrived in 1995 in the form of the water activated (and flushed) DTH (WDTH) [8]. This tool has been the staple of the better resourced grouting contractors since it was first successfully demonstrated at the McCook Quarry Trial (Chicago, IL) in 2001 and consistently provides high quality holes for grouting.

2.2. DESIGN AND TESTING OF GROUT MIXES

One of the major changes in rock grouting technology in recent years has been the increased level of understanding, and almost universal application of multi-component, balanced, stable grouts. Gone, thankfully, are the days of highly unstable, high water content “neat” mixes wherein the only concession to sophistication would be the (unnecessary) addition of superplasticizer and/or a handful of dry bentonite. The dynamic stability of a particulate grout (“pressure filtration coefficient”) is a fundamental control over its ability to penetrate fissures, and is at least equally as important as its grain size and apparent viscosity. Thus, contemporary HMG’s (“High Mobility Grouts”) can be regarded as “high performance” in that they maximize the injection potential value from every grout hole, instead of simply prematurely clogging up the fissures a very short, and uneconomic distance from the borehole wall.

Acceptable grouts should have minimal bleed (< 2%), and low pressure filtration coefficient (a value of 0.06 min^{-1/2} is suitable for most cases). Reflecting current “Apparent Lugeon Theory” practice for controlling injection, dominant now in N. America, these grouts can be manufactured in the field to provide mixes with discrete Marsh Cone ranges, e.g., 35; 45; 60 seconds; and infinite. Bear in mind that Marsh Cone readings over about 60 seconds are imprecise measurements, and other measures such as a Flow Cone or Shear Vane might be required, especially for the “closer” mix. The Baroid Mud Balance, for measuring grout specific gravity, and hence checking water:cement ratio, is a particularly simple, cheap and accurate tool, and stands in sharp contrast to the systematic use of grout cubes as a QC/QA tool: practically useless in rock fissure grouting applications. The true goals of a remedial grouting program should be permeability and seepage reduction, and not production of the highest strength grout cubes possible.

2.3. PLACEMENT AND SEALING OF STANDPIPES AND MPSP’S

This is a process the quality of which is frequently overlooked, even though it is absolutely fundamental to the safe grouting of existing embankment dam foundations.

The USACE Engineering Regulation [7] provides significant discussion on the potential for hydraulic fracturing while backfilling drill holes through embankments. This has led, in some quarters, to the development of specification provisions that require that grouting of standpipes installed through an embankment be performed in stages. A concern over hydraulic fracturing has also led to specifications that require water testing and grouting be performed under very low pressures or under gravity head. The following is a quote from the current version of the Regulation.

“For borings that penetrate zones with low confining stress it is possible to induce hydraulic fracturing from the gravity pressure. When grouting borings in

these locations or if significant grout losses are observed, the grout backfilling should be done in stages allowing the grout to set between stages.”

This statement in the Regulation, together with concerns regarding embankment hydraulic fracturing, have resulted in grouting specifications that limit backfilling of the annular space outside of a standpipe (“casing grout”) to heights of only 10-15 m above the water table. Such requirements are extremely expensive to implement as they require that a drill rig and crew be kept on standby for days for each standpipe installed. Stage grouting of the standpipe annular space also results in the risk of grouting the drill casing into the embankment if the casing is not pulled far enough, or for the embankment to collapse around the standpipe when the casing is pulled above the grout level.

Such staged requirements might be an affordable conservative approach when drilling a limited number of borings for investigation or installing instrumentation. However, in the case where grouting is being performed as a pretreatment for future cutoff wall construction, these requirements are considered to be nonsensical by the authors. The grouting program in these cases is an investigation and treatment program in advance of performing much larger and riskier excavations through the embankment. In the case where a slurry-supported trench is being considered for the cutoff wall construction, this large excavation will be uncased. It seems logical that if a zone of the embankment were prone to hydraulic fracturing under gravity head, the Engineer would want to determine this during the grouting program where only small diameter holes are being drilled, the fluid being used is self-hardening and the fluid quantity is limited and can be easily controlled. If these zones of low confining pressure are not discovered and treated by the grouting program in advance of the cutoff wall construction, the continuous slurry filled panel or trench will most certainly “discover” this zone of weakness. The surface area and volume of non-hardening bentonite slurry in a typical panel excavation is orders of magnitude greater than the surface area and annular space volume around a typical drill hole. Furthermore, if a hydraulic fracturing event does occur during panel wall excavation resulting in slurry loss, the specified procedure is to add slurry to maintain the trench full (i.e. maintain the pressure the caused the fracture to propagate). It seems obvious that the more cautious and prudent approach is to identify any weak zones during the course of the drilling and grouting program and to systematically treat the identified weak zones by compaction grouting or other means prior to excavating uncased higher risk elements through the dam embankment.

Counter to grouting standpipes in stages, some recent grouting programs have elected to limit the amount of annulus standpipe grout used during installation, as a predetermined multiple of theoretical annulus volumes. In these cases, the standpipe annulus was being grouted through the bottom of the standpipe under gravity head. This approach poses several concerns in regards to the effectiveness of grout treatment and more importantly in regards to dam safety. First, the act of prematurely halting the addition of grout into a formation that is readily accepting the grout is counter to the very goals of the grouting program. Second, not continuing to provide grout during the standpipe installation allows for potential incomplete filling of the hole annulus, as the

annulus grout is lost to the formation. This situation lends to defects or incomplete filling of the annulus. These defects can permit direct connection of embankment materials to the foundation and/or connection of grouting fluids up into the embankment during the drilling and grouting operations at lower depths. Both situations are serious dam safety issues.

Arguments for the cessation of annulus grout include avoiding potential hydrofracture of soft embankment or foundation soils above the bedrock. However, it should be noted that most standpipes are drilled and installed into the top of rock immediately below the embankment. This zone of rock is often the most permeable and the zone of rock that most likely led to the need for the remediation being conducted. It is much more likely that any grout take during standpipe installation is flowing into the bedrock or weathered features of the rock (or an alluvium layer remnant immediately above rock) rather than into embankment materials. Bedrock that is being treated during standpipe installation should be viewed as part of the treatment program and should be grouted to refusal just as any other standard grout stage.

In order to adequately backfill and install standpipes, the designer has two options. The first option is to backfill the entire annulus in one complete operation, adding grout as needed and maintaining a continuous head of grout in the annulus at all times until the grout comes to surface and remains at the surface. The second option is recommended for areas of suspected weak embankment soils or zones in which the designer wishes to avoid potential hydrofracture. This option involves the use of Multi-Port Sleeve Pipe (MPSP) with a barrier bag that is inflated with grout at the embankment/foundation interface. The barrier bag hydraulically separates the embankment from the bedrock foundation with the use of a barrier bag. (Figure 1).

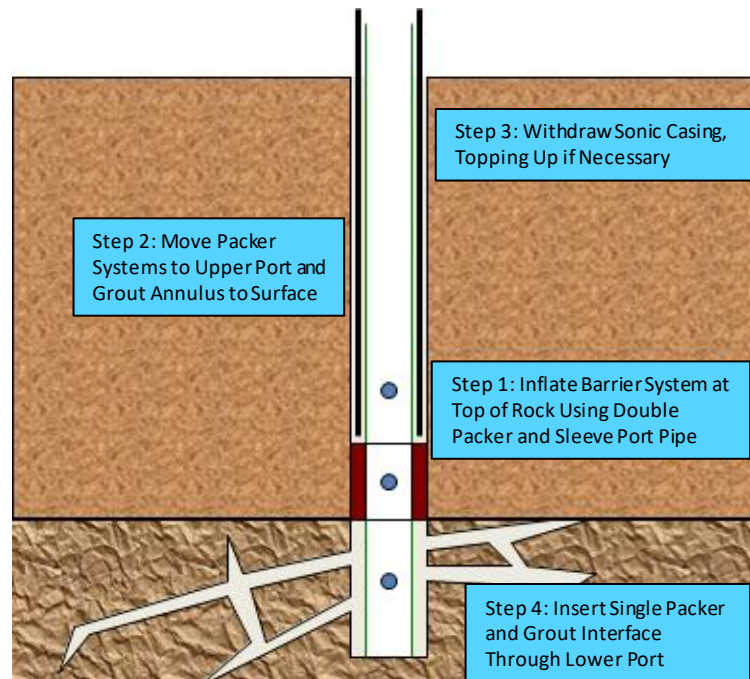


Fig. 1
Separation of embankment and foundation

The annulus can then be filled through a port in the standpipe above the barrier bag, while the critical interface and bedrock immediately below the bag can be treated and evaluated as a separate grouting stage. Either option involves the continuous and uninterrupted backfilling of the hole annulus within the embankment to the top of the hole. Use of the barrier bag to separate and isolate the embankment from the foundation is the only method that verifies that hydrofracturing of the embankment is not occurring. Grout coming to the surface around the outside of a standpipe that was incompletely filled during installation is not evidence of hydrofracturing: it is evidence that the installation method is inappropriate and has created a dam safety concern.

On a similar note, use of very low excess pressures or even gravity head during water testing and grouting due to fears of hydraulic fracturing in advance of cutoff wall construction is misguided. Again, if a zone of the embankment or gouge within rock defects is susceptible to fracture or erosion under low pressures, then one needs to know this prior to excavating the cutoff wall. On one recent project, the allowable water pressures during testing were so low that the headloss through the delivery pipe was not exceeded when flow started and zones with zero water take subsequently consumed very large quantities of grout during pressure grouting. If these zones had not been grouted under pressure due to the low or zero water take and had been backfilled in stages in accordance with the requirements above, then a future large slurry loss during cutoff wall excavation would have been the inevitable result.

2.4. DATA MANAGEMENT SYSTEM (DMS)

It is now common practice for an Owner to insist that the contractor collects, presents and stores all his construction data in real time in some form of an automated DMS (Data Management System). We have found that the contractors are often overwhelmed (initially at least) by the needs, scale and seriousness of such a system. This must not be permitted by the Owner to occur: a fully compliant DMS must be up and running before production work commences. From the technical viewpoint alone, it is integral to controlling and analyzing the treatment in real time, and informing all interested parties on the progress and effectiveness of the work (e.g., via Trend Analyses). It is therefore the only true basis for determining when the work is actually complete or if further work (e.g., higher order holes) is required, and where.

The Contractor's DMS must be controlled by a suitably qualified grouting engineer (not just an IT specialist). There must be a similarly-equipped, dedicated and experienced engineer on the Owner's side. All parties must have simultaneous access to all the information generated during the works.

2.5. REFUSAL AND CLOSURE

Each and every stage of every grout hole must be brought to a true and proper “refusal” in accordance with Apparent Lugeon Theory. This means that the maximum specified pressure has been held over a certain period (say 5 minutes) at a certain maximum flow rate (typically 1-3 liters per minute, depending on the project’s residual permeability goals and the nature of the rock mass). “Closure,” on the other hand, is when a section of the curtain has been judged to have been completed with a degree of certainty that the subsequent verification test holes will indeed confirm that the target residual permeability has been achieved. A proper judgment of closure depends on a holistic analysis of all available and relevant information, such as drilling logs, water tests, optical televiewer logs, grout take analyses and dam instrument response.

Lax refusal criteria will result in incompletely and inefficiently grouted stages. These can also lead to partially grouted fractures resulting in a high residual permeability. Given the limited number of fracture intersections by grout holes and given that the cost of drilling a new hole or holes is likely the most expensive operation in typical foundation grouting programs, each and every hole should be viewed as an opportunity to reduce the bedrock permeability and should be grouted to the fullest extent possible.

Many designers may view the additional time to grout to a low refusal flow criterion as unnecessary and expensive. To the contrary, the last volumes of grout injected during the final refusal of a grout stage can be some of the most important time and effort spent to achieve closure, especially if the time spent reduces the number of additional holes to complete what the prior holes and stages were not able to compete. Designers should consider the costs of drilling additional holes as well as the implications in regards to dam safety (especially for holes that need to be drilled and installed through embankments) when setting refusal flow criteria. Additional time grouting to low refusal criteria will help to reduce the number of additional holes to be added, drilled, water pressure tested, and grouted. All of these operations come with some measured amount of risk involving dam safety, so a reduction in the number of instances that these operations are performed should be viewed as an improvement.

One of the gifts we accept from the use of stable grouts (i.e., those grouts with minimal bleed and pressure filtration) is that they maintain a relatively constant rheology during their period of injection: they do not allow water to be squeezed out of the mix, into fissures, when under pressure. Thus, a grout with constant rheology (i.e., like water has) can thus be regarded as not only a fissure filler, but also a test fluid. This allows us to calculate an Apparent Lugeon Value during the initial grouting of any stage, calculated in the same way as a Water (True) Lugeon Value, but corrected by a factor being Marsh time (grout) / Marsh time (water).

Grout curtains should always be grouted to a target True Lugeon Value (residual permeability). Individual stages should be brought towards refusal by observing and controlling the Apparent Lugeon value, subject to the final “refusal” flow rate. Grout curtains should not be brought to closure based solely on

Apparent Lugeon Values, however, as the authors have observed on a major recent project in the Pacific North West. Water testing of the final hole series and verification holes should always be performed to prove the residual permeability of the treated rock mass.

2.6. ALLOWABLE SAFE INJECTION PRESSURES

A prime rule in any remediation is “First – Do No Harm,” and this is a logical and proper dictum to which the authors fully subscribe. However, the whole issue of safe rock grouting pressures under existing dams has reached levels of hysteria, especially in uninformed and inexperienced circles. Bearing in mind that a) a dam foundation is a 3D structure, b) contemporary computer-aided grouting control and recording systems provide essentially continuous real-time pressure/rate of injection data for each stage, and c) QA/QC programs are generally now quite sophisticated, then the authors believe that the highest safe injection pressures should be used, for both economic and technical reasons. “Rules of Thumb” (e.g., 1 psi/foot) can be discarded provided proper and progressive testing is conducted, and all processes are carefully controlled and monitored during injection.

2.7. JOINT INSTRUMENTATION MONITORING PLANS AND LONG-TERM PERFORMANCE MONITORING

It is normally the case that the dam to be remediated will already have some amount of instrumentation in its body and in its foundation. (It is usually the case that the results of this instrumentation will have highlighted the actual need for remediation, in concert with visual observations.) Further instrumentation should be added just before or during the grouting, to target specific “problem areas,” or simply to ensure a broad coverage without data gaps. The result is a plethora of instruments, typically now configured to provide data in real time.

It is essential for Dam Safety Assurance during construction that the Owner and the Contractor partner to collect, study and act upon these data in real time, regardless of whose contractual responsibility or liability it may be to do so. The most efficient strategy is to create, prior to construction having commenced, a Joint Instrumentation Monitoring Plan (JIMP). This will identify which instruments are to be read, by whom, and at what frequency. The JIMP will also provide Threshold and Action Level guidance for each instrument, and identify courses of action when these levels are reached.

We also note that a JIMP is implemented most effectively when the Owner and the Contractor can view the data while being physically in a joint “Mission Control” facility. In this way, the impact of the Contractor’s work on the dam and its foundation can be seen in real time, and acted upon accordingly when necessary.

We consistently observe that after the curtain or cutoff has been built, little attention is paid to continuing to use the in-situ instrumentation to monitor the long-term efficiency of the cutoff. Even less attention is devoted to publishing such data so that the dam remediation community can have the benefit of a successful (or unsuccessful) case history. Such long-term monitoring is the responsibility of the Owner, and this should be regarded by them as an essential cost outlay – perhaps as part of the routine O&M budget.

3. CLOSURE

It has become very easy to become an “instant” expert, or an “internet” expert, whereupon a great deal of information on any given subject matter can be quickly accessed. However, experience is not so quickly or so easily gained, and its value in a specialty engineering process such as grouting cannot be overstated. The authors’ opinions expressed in this paper reflect their respective experiences, and they have done so in the hope that the opinions will leaven the bread of the internet expert thrown into the midst of a major dam remediation project involving drilling and grouting, both processes previously inexperienced.

REFERENCES

- [1] NEW ORLEANS GROUTING CONFERENCE (2003). Grouting and Ground Treatment, Proceedings of the Third International Conference, Geotechnical Special Publication No. 120. Edited by L.F. Johnsen, D.A. Bruce, and M.J. Byle, American Society of Civil Engineers, New Orleans, LA, February 10-12.
- [2] NEW ORLEANS GROUTING CONFERENCE (2012). Grouting and Deep Mixing, Proceedings of the Fourth Annual International Conference, Geotechnical Special Publication No. 228, Edited by L.F. Johnsen, D.A. Bruce and M.J. Byle, American Society of Civil Engineers,, New Orleans, LA, February 15-18.
- [3] INTERNATIONAL CONFERENCE ORGANIZATION FOR GROUTING (ICO) (2017). 5th International Grouting, Deep Mixing, and Diaphragm Walls Conference, Honolulu, Oahu, Hawaii, July 9-12.
- [4] WEAVER, K.D. AND D.A. BRUCE (2007). “Dam Foundation Grouting, Revised and Expanded Edition,” American Society of Civil Engineers, ASCE Press, New York, 504 p.
- [5] BRUCE, D.A. (2012). “Specialty Construction Techniques for Dam and Levee Remediation,” Spon Press, an imprint of Taylor and Francis, Editor, 304 pp.
- [6] U.S. ARMY CORPS OF ENGINEERS (2014). “Grouting Technology.” Engineering Manual 1110-2-3506, July 3.

- [7] U.S. ARMY CORPS OF ENGINEERS (1997). "Engineering and Design Procedures for Drilling in Earth Embankments," CECW-EG., Report No. 1110-1-1807, September 30.
- [8] BRUCE, D.A., R. LYON, S. SWARTLING (2013). "An Introduction to Water-Powered Down-the-Hole Drilling in Specialty Geotechnical Construction," Deep Foundations Institute 38th Annual Conference, Phoenix, AZ, September 25-28, 7 pp.

SUMMARY

There has been a technological revolution in rock grouting for dam remediation projects in the U.S. stretching back almost 20 years. This has been extensively described in many conferences and publications, and has resulted in a very high level of technical competence and project performance. However, the authors have observed that many "lessons learned" in that period have not been universally applied or, in some cases, have been ignored. This paper reaffirms many of the practical lessons learned in many grouting processes, including:

- Drilling techniques for overburden and rock,
- Design and testing of grout mixes,
- Placement and sealing of standpipes and MPSP's,
- Data management systems,
- Refusal and closure,
- Allowable safe injection pressures,
- Joint instrumentation monitoring plans, and long-term performance monitoring.

Depuis près de 20 ans se déroule une révolution technologique en ce qui concerne l'injection du rocher pour les projets de réhabilitation des barrages aux États-Unis. Ce sujet a été largement traité à plusieurs conférences et dans maintes publications, et en est résulté une amélioration considérable des compétences techniques et de la performance des projets. Cependant, les auteurs considèrent que les « leçons apprises » n'ont pas toutes été considérées, et dans certains cas, ont été ignorées. Cet article réitère plusieurs des meilleurs pratiques dans les processus d'injection, incluant :

- Techniques de forage pour le mort-terrain et le roc,
- Conception et essais de mélanges de coulis,
- Emplacement et étanchéité des conduits,
- Système de gestion des données
- Refus et fermeture
- Pressions d'injection admissibles et sécuritaires
- Programme de suivi de l'injection et suivi à long terme du comportement

KEYWORDS

Automated monitoring, boring, construction, cutoff, embankment dam, foundation treatment, grout curtain, grouting, karst, quality control.

Auscultation automatique, forage, construction, barrage en remblai, traitement des fondations, écran d'injection, injection, karst, control de qualité.

COMMISSION INTERNATIONALE DES GRANDS BARRAGES

VINGT-SIXIÈME CONGRÈS DES GRANDS BARRAGES
Autriche, juillet 2018

DOI 10.3217/978-3-85125-620-8-146



This work licensed under a Creative Commons Attribution 4.0 International License. <https://creativecommons.org/licenses/by-nc-nd/4.0/>

**SEEPAGE CUTOFFS FOR DAMS AND LEVEES: LESSONS LEARNED
FROM 40 YEARS OF REMEDIAL CONSTRUCTION IN NORTH AMERICA**

Donald A. BRUCE

President, GEOSYSTEMS, L.P.

U.S.A.

COMMISSION INTERNATIONALE
DES GRANDS BARRAGES

VINGT-SIXIÈME CONGRÈS DES
GRANDS BARRAGES
Autriche, juillet 2018

SEEPAGE CUTOFFS FOR DAMS AND LEVEES: LESSONS LEARNED FROM 40 YEARS OF REMEDIAL CONSTRUCTION IN NORTH AMERICA *

Donald A. Bruce

President, GEOSYSTEMS, L.P.

U.S.A.

1. INTRODUCTION

The National Inventory of Dams (NID) has listed over 84,000 dams in the United States which meet its criteria for inclusion [1], namely:

1. High hazard classification - loss of one human life is likely if the dam fails.
2. Significant hazard classification - possible loss of human life and likely significant property or environmental destruction.
3. Low hazard classification - no probable loss of human life and low economic and/or environmental losses, but the dam:
 - equals or exceeds 25 feet in height and exceeds 15 acre-feet in storage;
 - equals or exceeds 50 acre-feet storage and exceeds 5 feet in height.

Almost 14,000 dams meet Criterion 1. Only 4% (3,075) are federally owned, and these mainly date from the earlier third of the Twentieth Century. Over 87% of the total are primarily classified as earth embankments, while no other category exceeds 3% of the total. The main primary purposes are recreation (35%), flood control (17%), fire protection in stock/small fish ponds (15%) and irrigation (10%), while less than 3% generate power. Many structures are multipurpose. Figure 1 summarizes their completion dates: about 50% were

* MURS PARAFUILLÉS POUR DES BARRAGES ET DES LEVÉES : LES LEÇONS ONT APPRIS DE 40 ANS DE CONSTRUCTION RÉPARATRICE EN AMÉRIQUE DU NORD

completed between 1950 and 1979, while the median age in the year 2018 is about 67 years.

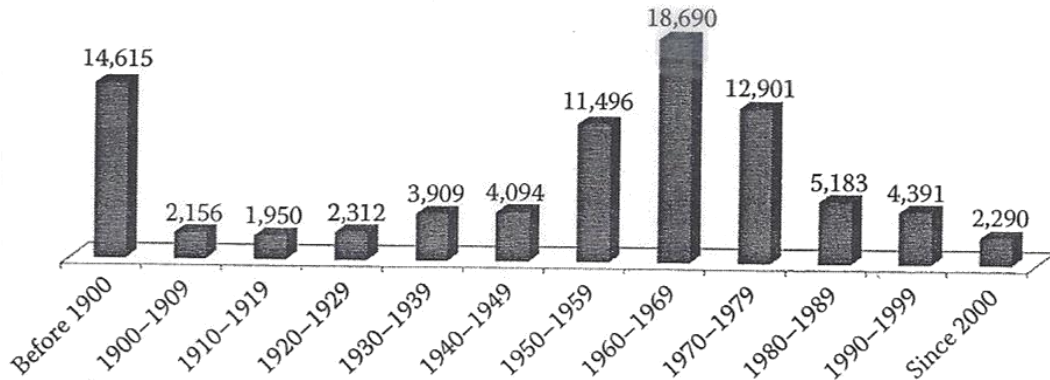


Fig 1

U.S. dams by completion date. (From National Inventory of Dams, CorpsMAP, <http://nid.usace.army.mil>, 2010.)

Whereas it may be calculated from the National Inventory of Dams [2] that the cumulative “end-to-end” length of all the U.S. dams is around 18,000 miles, preliminary estimates put the cumulative length of levees in the U.S. at over 120,000 miles. Only about 14% of this total may be regarded as federal, and considered by Halpin [3] as “robust.” The balance includes municipal, local and agricultural structures often featuring little engineering design, patchwork construction and minimal periodic maintenance, since they were traditionally regarded as “simple” structures.

Certain design assumptions and construction techniques used in the dams and levees built prior to, say, 1960, would not be acceptable today, and have left behind fundamental flaws in some structures. Appropriate filter criteria for embankments and uplift/sliding issues in concrete dams are two obvious design related examples, while old approaches to rock surface preparation and foundation treatment would also fall into the unacceptable category. In addition, there are two overriding geological considerations which directly influence the serviceability, reliability, and performance of the dam and levee system. These considerations are (i) the presence of carbonate and evaporite formations, and (ii) the potential for seismic activity.

Focusing on point (i), there is a huge swath of karstic limestones and dolomites which outcrops from Pennsylvania to Alabama, while it is estimated [4] that evaporites underlie about 40% of the contiguous 48 states. These potentially soluble and erodible foundation conditions underlie many of the major river basins, such as the Mississippi-Missouri basin, and the Tennessee and Ohio River Valley systems – and, of course, the aging dams built thereon.

Beginning with the first Wolf Creek Dam KY remediation in 1975, one can tabulate 27 major cutoff walls which have been built through and under the existing embankment dams, to counteract increasing seepage trends, and the erosional dangers these seepages pose to dam and foundation alike. This paper presents the lessons learned from these projects.

2. SUMMARY OF CASE HISTORIES (1975-2017)

A recent review [5] provides details of 27 major remedial cutoffs using “excavate and replace” methods, as opposed to “mix in place” methods [6]. These projects are listed in Figure 2 which also shows the principal construction method and Specialty Contractor. One project remains in progress (East Branch Dam, PA), while three others are foreseen to commence in 2018, including two in Tennessee and the second phase of Herbert Hoover Dike, FL. Details of construction methods and cutoff material design are provided in older texts (such as [7]), while many of the more recent case histories referred to in Figure 2 are summarized more recently in reference [6]). Several different methods of constructing cutoffs have been successfully and safely utilized on these projects, including the use of clamshells, hydromills and large diameter rotary drills. The choice of method is primarily dictated by the geotechnical conditions, the depth of the cutoff, dam safety considerations, and the traditional preferences of the respective Specialty Contractors.

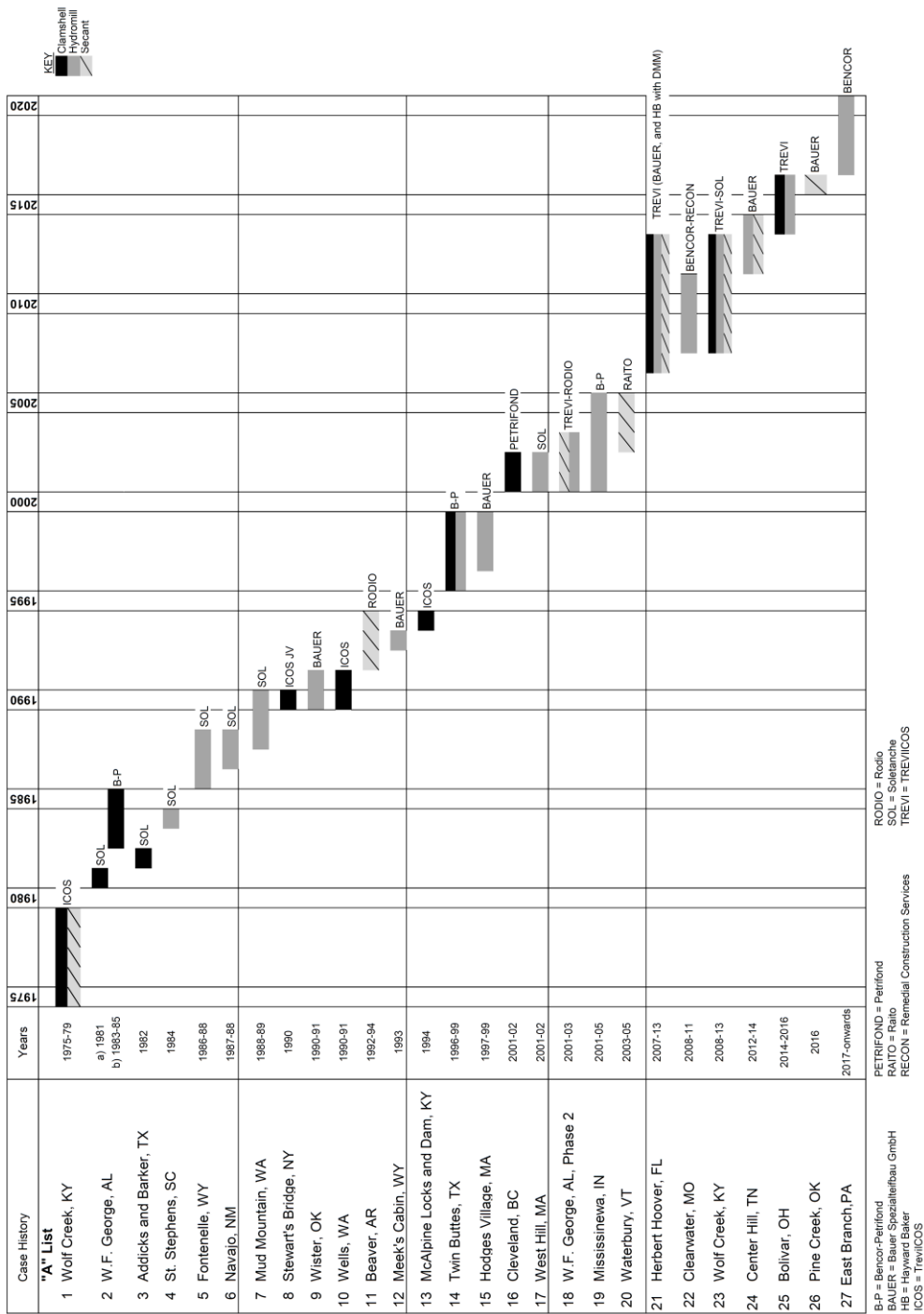
3. LESSONS LEARNED

3.1. DESIGN CONSIDERATIONS

3.1.1 *Geological and Geotechnical Site Characterization*

The following observations are provided, for brevity and clarity, in bullet form. Some readers may find certain lessons to be self-evident and not worthy of consideration. However, each topic has its roots in situations personally observed by the author and, in his opinion, each merits inclusion.

- Before designing a new program of investigation, very carefully reexamine existing, historical information (e.g., grouting programs, original site investigation data, construction photos, as-built drawings), and dam performance data, especially “signs of distress” (sinkholes, seepages, depressions, erratic piezometer readings, etc.). The work product is a basic but robust hydrogeological model.
- The intensity of the new investigation must reflect the variability of the ground conditions as interpreted from the preexisting hydrogeological model (but will be, practically, governed by budget and access, and the project risks).
- Drill holes must extend over the entire length and depth of a foreseen cutoff. Their location should reflect what is suspected to be the main risk areas identified in the preexisting hydrogeological model.



KEY
 Crumshell
 Hydromill
 Secant

B-P = Bencor-Petrifond
 BAUER = Bauer Spezialtiefbau GmbH
 HB = Hayward Baker
 ICOS = Trevicos
 PETRIFOND = Petrifond
 RAITO = Raito
 RECON = Remedial Construction Services
 RODIO = Rodio
 SOL = Soletanche
 TREVI = Trevicos

Fig 2 List of remedial cutoffs for dams showing principal construction method and specialty contractor.

- The investigatory program must inform the design of the cutoff, and produce information essential for bidders to select their construction methods, estimate productivities, and evaluate construction risks.
- All investigations must be conducted in accordance with prevailing standards of care for drilling in dams/levees, and for environmental protection.
- Even the investigatory program may require a certain enhanced level of instrumentation monitoring during its implementation.

3.1.2 *Geotechnical Reports*

- Many different types of Reports can be produced on a project including:
 - Geotechnical Data Report (GDR),
 - Geotechnical Interpretive Report (GIR),
 - Geotechnical Baseline Report (GBR),
 - Geotechnical Design Basis Report (GDBR).
- It is essential that at least the GDR, GIR and GDBR are shared with all bidders, in full. GBR's are relatively uncommon outside the tunneling industry, and have very well-defined contractual and legal significance. The goals of these Reports, considered together, must:
 - allow development and understanding of an accurate hydrogeological model,
 - permit the Engineer-of-Record to design a responsive cutoff,
 - ensure that all bidders are on a “level playing field” when preparing their submittals,
 - clearly identify areas of particular geotechnical construction or performance risk,
 - permit the implementation of an appropriate geotechnical plan to monitor conditions before, during and after construction.

3.1.3 *General Principles of Cutoff Wall Design*

- Plan Location: A cutoff is typically located on the centerline of the embankment (for access reasons), or on upstream slope (to save footage and to ensure tie-in to sloping cores).
- Length: Determined by flow analysis to ensure minimal “end around” seepage. Most cutoffs actually tie-in to existing concrete structures, such as spillways or powerhouses. Their far end typically is determined by the geology and topography of the site (i.e., width of abutment).
- Width: The minimum continuous width (typically 0.3 to 0.6 m) should primarily be determined by the depth of the wall, the variability of the geology, the composition of the wall, and its performance requirements. Note that a cutoff wall does not have to be perfectly vertical to satisfy its design function: it can “ripple” provided the minimum inter-element overlap thickness is satisfied.
- Depth: The terminal elevation of the toe must be chosen to reflect the geological conditions and the design concept of the wall:
 - a “full depth” cutoff into effectively impermeable rock; or

- a “partial depth” (or “floating”) cutoff, to reduce (not eliminate) seepage and/or to prevent internal erosion. Such walls are often constructed through previously installed grout curtains (minimum 2 rows), intended to investigate the ground, pretreat voids to prevent sudden slurry loss; and grout to say < 3 Lu the rock mass under and around the wall in “clean fissure” conditions. This is the concept of the “composite wall” [6].
- Material Properties:
 - In-situ permeability (especially at joints) must be established, and verified. It is typically $\leq 10^{-8}$ m/s for materials, but 1 Lu for joints (i.e., approximately 1×10^{-7} m/s).
 - Strength and deformability must reflect the project conditions (e.g., plastic concrete vs structural concrete). All materials must be non-erodible in service.
 - Homogeneity must be emphasized, e.g., no inclusions of native ground or bentonite slurry, no segregation of the backfill, no contamination of the joints (or the toe) with slurry.
 - Durability/chemical compatibility must be addressed, but is typically not a problem.

3.1.4 Risk and Performance Considerations

- In dam safety considerations, Risk = Probability x Consequence.
- Risk is to be assessed in Potential Failure Mode Analysis sessions (PFMA).
- The individual PFM's, appropriately prioritized, must drive the remedial requirements and the instrumentation requirements.
- The performance of the cutoff and the existing structure must be measured during construction, and after construction. Specific project goals must be set and verified, e.g.:
 - reduction in seepage,
 - acceptable piezometric performance,
 - elimination of other “signs of distress” (e.g., settlements, sinkholes, muddy flows, boils).
- The evaluation of risk may dictate the sequencing and prioritization of the work and the permissible remedial techniques.

3.1.5 Durability of Walls

- The actual backfill materials must be durable. This will be proved by laboratory testing (“pinhole erosion”), quality of construction, and conditions of curing and service.
- There may be some evidence of cracking in old diaphragm walls, but the case is not proven. Newer walls have intense in-situ verification and superior long-term performance monitoring.
- Desiccation cracking may be a concern in embankments where the upper part may be above water level for most of its service life. However, the typical cross-sectional shape of an embankment is favorable (i.e., very broad).

3.2. CONSTRUCTION

- Each Contractor has its own particular mentality and preferences for means and methods, as well as for equipment. Each project's construction details must therefore be evaluated on this basis, with the prime concern being the safety of the dam during construction.
- A proper, stable, working platform (concreted if possible) is essential for a host of reasons, ranging from personnel safety to enhancing productivity.
- Some cutoff walls involve extensive pregrouting such as in the "Composite Wall" concept [6]. Such grouting must be conducted by an experienced and knowledgeable Contractor who may not necessarily be the same business entity as the cutoff wall Contractor. Insufficient or ineffective grouting may create dire problems to subsequent cutoff wall quality and schedule.
- "Technique Demonstration Areas" – thoroughly assessed – are invariably of great value to all the project's stakeholders.
- Time is well spent up front in building high quality, weatherproofed bentonite and concrete storage and batching facilities, and maintenance shops.
- Development of mix designs and their approval by the Owner should not be allowed to negatively impact schedule and should be given high priority during the site mobilization phase.
- All preconstruction permits, etc., must be in place prior to site mobilization.
- Ensure that all equipment is maintained regularly, and that all instrumentation is frequently recalibrated (if necessary).
- Individual cutoff wall elements, be they diaphragm wall panels, or secant piles, should be sized to minimize the number of inter-element joints, consistent, however, with dam safety concerns.

3.3. QA/QC AND VERIFICATION

- Details must be linked directly to the design intent and the project specifications, regulatory requirements, and to the actual construction techniques adopted by the Contractor.
- Key elements promoting success include:
 - Clear and complete contract specifications and drawings;
 - Appropriate organizational structure and qualified personnel;
 - Good communication protocols;
 - Cooperation from all parties (Owner, Engineers and Contractors);
 - Diligent implementation of the Quality Plan.
- A comprehensive, formal Quality Control Implementation Plan is essential, and the effort needed for the drafting and implementation of this Plan should not be underestimated by the Contractor. This project-specific plan must address, as a minimum:
 - Site organization charts showing responsibilities, lines of communication and levels of authority of project personnel from all stakeholders;

- Setting out methods and tolerances;
 - Bentonite slurry properties, production and testing;
 - Wall verticality and panel overlap (by at least 2 independent methods);
 - Wall tolerances;
 - Joint cleanliness criteria;
 - Concrete materials, batching, placement and testing;
 - Coring and in-situ permeability testing (and the use of an Optical Televiewer);
 - Management and communication of data and records (real time, and archived);
 - The development and implementation of a Joint Instrumentation Monitoring Plan (JIMP), between the Owner and Contractor.
- While an essential element of the Quality Plan is timely and accurate transmittal of information, the Plan must be developed and managed by an Engineer or Geologist, and not an IT Specialist in Data Management Systems.

3.4. INSTRUMENTATION AND PERFORMANCE MONITORING

- Prime types are piezometers, settlement gages, inclinometers, seismographs and weirs.
- Data loggers (“trolls”) can detect suspended sediments, change in pH, and temperature in seepages. Real time data transmission is preferable.
- Instrumentation adequacy must be audited, and supplemented if necessary, well in advance of construction (“baselining”).
- Location, intensity, and responsibility during construction must be governed by the JIMP.
- Monitoring must be continued after construction, with clear guidelines for identifying and acting upon Threshold and Action Levels.
- Long-term performance trends should be published in the technical community.

3.5. DEVELOPMENT OF CONTRACT DOCUMENTS AND CONTRACTUAL ARRANGEMENTS

- Performance-based specifications are optimal, and the fundamental performance goals must be clearly and consistently stated.
- Partnering must be implemented rigorously, and with total commitment at all levels in each stakeholder.

- Contractual risks must be allocated fairly, with the Owner being responsible for the site conditions and for the potential impacts and benefits of any previous remediations (e.g., by pregrouting) on the project. Risks to the Owner can be managed in many ways:
 - Ensure all available site-specific data are made available at bid stage;
 - Engage an appropriately qualified, experienced and resourced Design Engineer and Board of Consultants;
 - Clearly define respective roles, responsibilities, and duties, especially for site inspection staff;
 - Select a “Best Value” as opposed to “Low Bid” basis for Contractor selection;
 - Insist on a “Partnering” environment;
 - Select a qualified and experienced Contractor with appropriate human and mechanical resources;
 - Encourage the bidders, via Performance Specifications, to bring their own ideas and expertise to the project;
 - Ensure modifications are issued quickly, and be sympathetic to requests for bid extensions;
 - Allow budget for adequate short- and long-term instrumentation.
- There must be realistic expectations, such as that:
 - The project will satisfy the design intent;
 - The project will be designed and built to the current state of practice and to appropriate referenceable standards of care;
 - Project schedule is actually attainable (especially in “tight” projects with multiple trades);
 - The work will not cause damage or detriment to adjacent preexisting structures;
 - Claims are inevitable, and must be evaluated strictly on merit (often not the case when Construction Managers operating on very small margins are involved).
- The principles of “Early Contractor Involvement” should be applied whenever feasible, and especially on particularly challenging projects, technically or schedule-wise.

REFERENCES

- [1] RAGON, R. (2011). “National Inventory of Dams Provides Interesting Data and Statistics,” *USSD Newsletter*, March, p. 14.
- [2] NATIONAL INVENTORY OF DAMS (NID). (2010). <http://nid.usace.army.mil>.

- [3] HALPIN, E.C. (2010). "Creating a National Levee Safety Program, Recommendations from the National Committee on Levee Safety," *ASDSO Dam Safety Conference*, September 19-23, Seattle, WA, 22 p.
- [4] MARTINEZ, J.D., K.S. JOHNSON AND J.T. NEAL. (1998). "Sinkholes in Evaporite Rocks." *American Scientist*, v. 86, no. 1, pp. 38-51.
- [5] BRUCE, D.A. (2017). "REMEDIAL CUTOFF WALLS FOR DAMS IN THE U.S.: 40 YEARS OF CASE HISTORIES," *5th International Grouting, Deep Mixing, and Diaphragm Walls Conference, International Conference Organization for Grouting (ICOG)*, Honolulu, Oahu, Hawaii, July 9-12, 15 pp.
- [6] BRUCE, D.A. (2012). "SPECIALTY CONSTRUCTION TECHNIQUES FOR DAM AND LEVEE REMEDIATION," Spon Press an imprint of Taylor and Francis, 304 p.
- [7] AMERICAN SOCIETY FOR TESTING AND MATERIALS (1992). "Slurry Walls: Design, Construction, and Quality Control." *ASTM Publication Code Number 04-011290-38*.

SUMMARY

Twenty-seven case histories of major remedial cutoff walls have been reviewed. These cutoffs (excavate and replace methods only) have been installed through existing embankment dams and deep into usually karstic conditions to counteract the dangers to dam safety created by escalating seepage rates and velocities. "Lessons learned" are presented relating to design considerations, construction, QA/QC, instrumentation and development of contract documents.

Vingt-sept études de cas de réhabilitation de grande envergure des parois moulée ont été vérifiées. Ces parois (excavation et méthodes de remplacement seulement) ont été installées à travers des barrages en remblai existants et en profondeur en milieu karstique afin de contrer les risques en lien avec la sécurité des barrages créé par l'augmentation des taux et des vitesses des infiltrations. Les « leçons apprises » présentées concernent la conception, la construction, l'assurance qualité et contrôle de la qualité, l'instrumentation et la rédaction des documents contractuels.

KEYWORDS

Construction method, core wall, cutoff wall, diaphragm wall, embankment dam, foundation, internal erosion, karst, leakage, piping, rehabilitation.

Methode de construction, écran interne, mur parafouille, paroi moulée, barrage en remblai, fondation, erosion interne, karst, fuite, renard, rehiitation.

COMMISSION INTERNATIONALE DES GRANDS BARRAGES

VINGT-SIXIÈME CONGRÈS DES GRANDS BARRAGES
Autriche, juillet 2018

DOI 10.3217/978-3-85125-620-8-147



This work licensed under a Creative Commons Attribution 4.0 International License. <https://creativecommons.org/licenses/by-nc-nd/4.0/>

**THE SEEPAGE ANALYSIS OF THE EMBANKMENT DAMS OF A FLOOD
RETENTION BASIN IN POLAND**

Burcu ERSOY

Hydraulic Engineering Department, BJÖRNSEN CONSULTING ENGINEERS

GERMANY

Ronald HASELSTEINER

Hydraulic Engineering Department, BJÖRNSEN CONSULTING ENGINEERS

GERMANY

*Commission
internationale Des Grands
Barrages*

VINGT-SIXIÈME CONGRÈS DES
GRANDS BARRAGES
Autriche, juillet 2018

**THE SEEPAGE ANALYSIS OF THE EMBANKMENT DAMS OF A FLOOD
RETENTION BASIN IN POLAND**

Burcu ERSOY, Ronald HASELSTEINER

Hydraulic Engineering Department, BJÖRNSEN CONSULTING ENGINEERS

GERMANY

1. INTRODUCTION

All kind of embankment fill dams are faced with seepage body during impoundment and during operation. Therefore, seepage control plays an important role at the design stage to prevent uplift pressures, instability of the downstream slope, piping through the embankment and/or foundation and potential suffusion and erosion processes. In order to guarantee safe seepage conditions for the anticipated load cases, the seepage control design should comprise sealings, dam body specifications, special drainage elements, and their characteristics.

The paper provides the main information and results of the seepage and stability analysis of a case study and aspects considering potential suffusion and erosion processes.

2. PROJECT OVERVIEW – CASE STUDY

A dry/green flood retention reservoir is under construction in Poland since 2013. The project includes embankment dams (head, right and left dam). The lengths of all embankments show approx. 22 km. The reservoir volume is 180 Mio. m³ with a perspective to be enlarged to 300 Mio. m³. The maximum height of the embankment dams is over 11 m in the area of head dam. The maximum water level is specified at a level of 195.2 m a.s.l. and the crest elevation is defined at 197.5 m showing a freeboard of 2.3 m. A selected section of the dam (head dam) is given in Fig. 1. Within specified sections the sand-gravel material was selected as main dam fill material. Gravel material is used as filter material and the seepage control function is provided by a geosynthetic clay liner (GCL). In addition, gravel columns have been placed within the foundation area where weak formations are located beneath the future dam body.

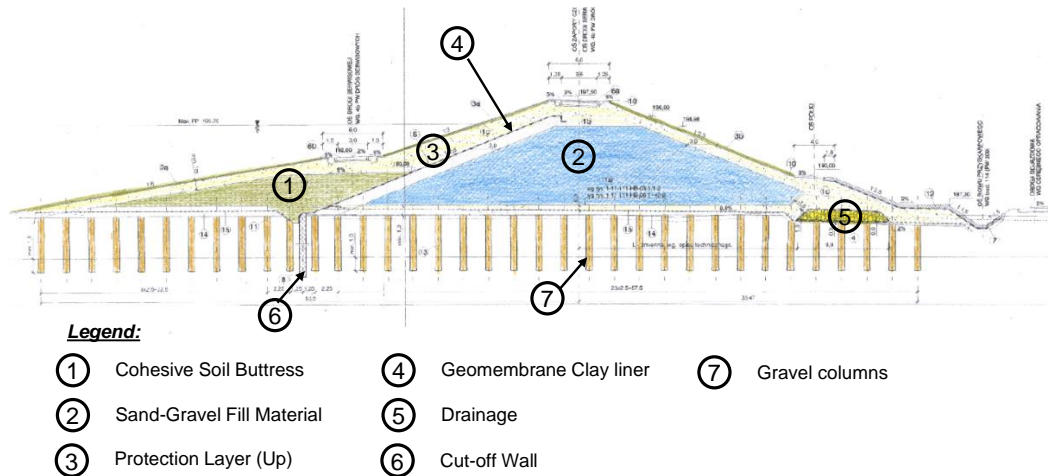


Fig. 1

Main design section of embankment dam (head dam) used for the seepage and stability analysis (sketch)

3. SEEPAGE AND STABILITY ANALYSES

3.1. PREPARATION OF THE FINITE ELEMENT MODEL AND BOUNDARY CONDITIONS

The finite element model (FEM) is defined as a mathematical simulation of a real physical process. For the FEM a typical dam cross section with a height of 11 meters was considered (Fig. 1). The model size (width) was defined in consideration of the dam height. As minimum size two times the dam height to up- and downstream were defined so that the model boundaries are not

influencing the seepage conditions within the dam. This approach results in a model width of 172 m. The modelled underground depth was selected also with a minimum of two times the dam height. The maximum water level is applied at 195.20 m a.s.l. which is 8.7 m above the upstream ground surface level. The geological formation consisting of a clay layer, sand-gravel, and London clay layers are integrated in the model. The thicknesses are established as 6 m, 7 m, and 7 m for clay layer, sand-gravel and London clay, respectively. The thickness and depth of the cut-off wall are applied with 60 cm and up to 13 m respectively. The thickness and depth of gravel columns are assumed as 80 cm and 9 m respectively. The distance between the gravel columns is assumed as 2 m (center to center) so that in total 33 gravel columns are considered in the model section. For a better possibility of evaluation the reference coordinate system used the origin (x, y) = (0, 0) at the upstream dam toe. The final view of the numerical model that used in seepage analysis is given in Fig. 2.

To determine the seepage flow – steady state conditions were considered – through the embankment body, a FEM requires the definition of boundary conditions. Three hydraulic boundary conditions are applied for the numerical model as follows:

- 'Constant head' → Upstream face → at a height of 195.20 masl (water level with 8.7 m above the terrain surface) → dark blue in Fig. 2
- 'Constant head' → Downstream face → the maximum water level that is at a height of -0.44 m → blue downstream line in Fig. 2
- 'Seepage exit', 'Total flux type' → Potential seepage exit areas along the downstream slope → the ground water flow as $0 \text{ m}^3/\text{s}$ → red line in Fig. 2

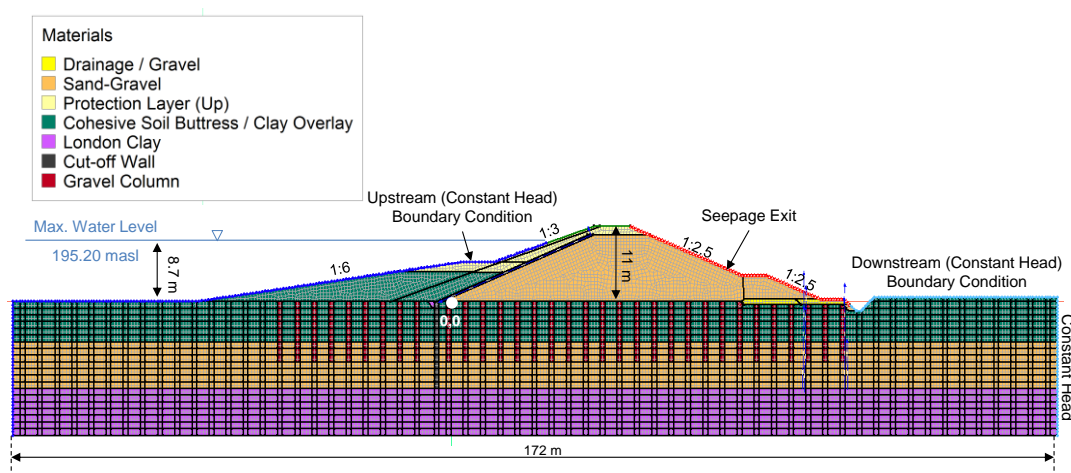


Fig. 2
Finite element model for the seepage analysis

3.2. DEFINITION/DETERMINATION OF THE GEO-HYDRAULIC AND SHEAR STRENGTH PARAMETERS

The next step in developing a numerical model is to assign materials to the regions as defined in the numerical model before. The geo-hydraulic and shear strength parameters are the key parameters for seepage and stability analyses. To assign reliable inputs to the numerical model, geo-hydraulic parameters are implemented that are included in different books and papers, e.g., in Haselsteiner (2007) [8] and the referenced literature sources. In Haselsteiner (2007) [8] the geo-hydraulic parameters are compiled from 17 different literature sources. The compiled geo-hydraulic parameters are categorized in accordance with typical embankment dam zones such as gravel drain, gravel fill used for the dam body and underground, sand material, surface sealing and alluvial clay/loam.

'Saturated only' option was selected for the steady state seepage analysis and for the material shear behavior, the 'Mohr-Coulomb' model was selected. The geo-hydraulic and shear strength parameters that are implemented to the numerical model are given in Table 1.

Table 1
Geo-hydraulic and shear strength parameters for the zones of the embankment dam

No	Type	Name	Color of Zone in Model	geo-hydraulic			shear strength		
				Permeability k_s [m/s]	Anisotropy $A=k_y/k_x$ [-]	Saturated Volumetric Water Content [-]	Unit Weight γ [kN/m ³]	Cohesion c' [kPa]	Friction Angle ϕ' [°]
1	Embankment Zone	Cohesive Soil Buttress		10^{-9}	0.5	0.325	19	4	31.0
2		Sand-Gravel		10^{-3}	0.5	0.225	17	0	37.5
3		Protection Layer (Up)		10^{-3}	0.5	0.200	17	7	31.0
4		Geomembrane Clay liner		10^{-7}	0.5	0.400	20	4	25.0
5		Drainage / Gravel		10^{-2}	1	0.195	18	0	35.0
6		Cut-off Wall		10^{-9}	1	0.500	25	200	40.0
7		Gravel Column		10^{-4}	0.5	0.300	22	3	40.0
8	Soil Layers	Clay Overlay		10^{-9}	0.5	0.325	19	4	31.0
9		Sand-Gravel		10^{-3}	0.5	0.225	17	0	37.5
10		London Clay		10^{-11}	0.5	0.325	20	5	28.0

3.3. DESIGN SITUATIONS AND LOAD CASES

The design, construction and operation of a dam with a reservoir need to be developed in consideration of its long-term performance that is affected by boundary conditions such as reservoir water level, traffic loads, performance of the dam zones, climate impacts, etc. Therefore, corresponding design situations and load cases need to be defined during the design stage especially for the seepage and stability analyses.

Load cases consist of a set of conditions that are taken into consideration in the dam safety analysis. For the analyses, the “Deutsches Institut für Normung e.V.” [1], [2], [3] and DWA [4] codes are considered which regulate dam engineering aspects. The load cases and the revision of guidelines are given in Table 2. Seven load cases are considered within the seepage and stability analyses. The load cases showing unsteady seepage, e.g., for rapid drawdown conditions, and operation earthquake conditions are not taken into consideration for the analyses since they were considered irrelevant.

In addition to the load cases, four design conditions were considered for the numerical model to evaluate the long-term performance of the designed sealing (geo-synthetic clay liner + cut-off wall) and soil treatment systems, e.g., gravel columns as given in

Table 2
Different load cases (design situations) for seepage and stability analyses according to DIN (adapted after DWA, 2015)

No.	Con- sidered		Design Situations according DWA M-522/2015 adapted according EC 7	Load Case according to DIN 19700-10,-11,-12	Loads		Resistance Dam status/situation	
	yes	no						
			DS-P Permanent Design Situations	Normal Load Cases	Temporary/ traffic loads	Water Table	Seepage Conditions	Description
1	1		P.1 Full Flood Water Level Z_v	Load Case 1.1 Full Flood Water Level	$p_1 = 25 \text{ kN/m}^2$	$Z_v = 195.20 \text{ masl}$	steady 2D seepage conditions	All compounds and elements are fully working.
2			P.4 Operational drawdown from Z_v	Not considered within the requirements of DIN 19700.	$p_1 = 25 \text{ kN/m}^2$	Drawdown starting from Z_v .	unsteady conditions analytic approach (not considered)	All compounds and elements are fully working.
			DS-T Temporary Design Situations	Rare Load Cases	Temporary/ traffic loads	Water Table	Seepage Conditions	Description
3	2		T.1 Flood water level at Z_{H1}	Load Case 2.1 Flood level at Z_{H1}	$p_1 = 25 \text{ kN/m}^2$	$Z_{H1} = 196.20 \text{ masl}$	steady 2D seepage conditions	All compounds and elements are fully working.
4			T.2 Rapid drawdown from water level Z_v	Load Case 2.2	$p_1 = 25 \text{ kN/m}^2$	Rapid drawdown with maximum velocity starting from Z_v .	unsteady conditions analytic approach (not considered)	All compounds and elements are fully working.
5	3		T.3 Extraordinary operation situation	Load Case 2.3	$p_2 = 33,3 \text{ kN/m}^2$	Partial impoundment Half of the dam height $Z_{\text{partial}} = 192.00 \text{ masl}$	steady 2D seepage conditions	All compounds and elements are fully working.
6			DS-E Operational earthquake ^{A)}	Load Case 2.4	"For dry basins an analysis considering the load "operational earthquake" can be neglected." (DIN 19700-12) (not considered)			
			DS-A Accidental Design Situations	Extreme Load Cases	Temporary/ traffic loads	Water Table	Seepage Conditions	Description
7	4		A.1 Flood water level at Z_{H2}	Load Case 3.1 Flood level at Z_{H2}	$p_1 = 25 \text{ kN/m}^2$	$Z_{H2} = 196.70 \text{ masl}$	steady 2D seepage conditions	All compounds and elements are fully working.
8	5		A.2a Restricted functionality of sealing/male function	Load Case 3.2	$p_1 = 25 \text{ kN/m}^2$	$Z_v = 195.20 \text{ masl}$	steady 2D seepage conditions	Restricted functionality to complete malfunction of the sealing system.
9	6		A.2b Restricted functionality of to drain	Load Case 3.3	$p_1 = 25 \text{ kN/m}^2$	$Z_v = 195.20 \text{ masl}$	steady 2D seepage conditions	Restricted functionality to complete malfunction of the toe drain.
10	7		A.3 Crest Water Level ^{B)}	Load Case 3.4	$p_1 = 25 \text{ kN/m}^2$	$Z_{\text{crest}} = 197.50 \text{ masl}$	steady 2D seepage conditions	All compounds and elements are fully working.
			DS-E Design Earthquake	Earthquake load case	Temporary/ traffic loads	Water Table	Seepage Conditions	Description
11			Design Earthquake	Load Case 3.3	not considered	not considered	not considered	not considered

Notes:

In DWA M-522/2015 the operational earthquake is not considered within the design situations.

The design situation considering the crest water level is usually not considered within the mentioned load situation but is frequently analysed hand in hand with the

Table 3
Considered design conditions together with considered load cases/design situations (DS)

Design Conditions		Load Cases/Design Situations No.						
Name	Abbreviation	1	2	3	4	5	6	7
Full Sealing with Gravel Column	FS+GC	Load Case P.1 (LCP1)	Load Case T.1 (LCT1)	Load Case T.3 (LCT3)	Load Case A.1 (LCA1)	Load Case A.2a (LCA2a)	Load Case A.2b (LCA2b)	Load Case A.3 (LCA3)
Full Sealing without Gravel Column	FS-GC							
Open Sealing with Gravel Column	OS+GC							
Open Sealing without Gravel Column	OS-GC							

3.4. RESULTS AND INTERPRETATION OF SEEPAGE ANALYSIS

The 2D steady state seepage analysis is performed by using SEEP/W software program that is a part of GeoStudio 2016 software package. As a result of 28 seepage analyses considering the different design situations and load cases, following results are obtained.

Generally, the differences obtained for the different dam/design conditions (FS, OS, with/without GC) regarding total head and pore water pressure are not substantial. Therefore, the application of sand-gravel columns does not worsen the seepage situation critically. But also does not show a benefit in consideration of the performance of the embankment dam.

The comparison of the results for the different design/dam conditions and for selected load cases are given in Fig. 3. The load cases LCT1, LCA1, LCA2a and LCA2b are selected in order to compare the design/dam conditions. In general, the results of the seepage line and pressure head reflect the same trends as theoretically expected.

For the load cases LCA2a “Malfunction of the sealing” and LCA2b “Malfunction of drain”, the drain capacity is not enough to drain the dam body. In addition, an unfiltered exit is the result that may lead to backward erosion.

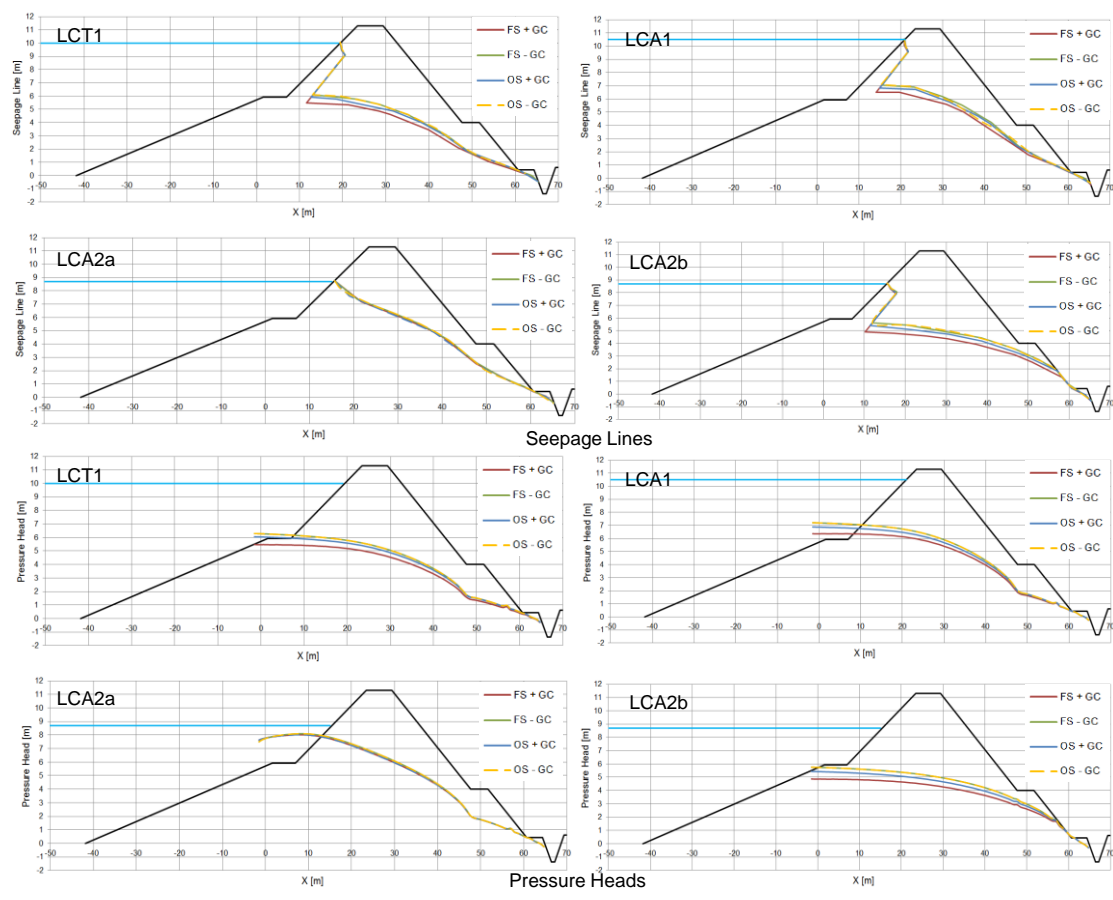


Fig. 3

The comparison of different load cases and design situations in form of on line of seepage and pressure head

The sealing of the actual design does not reach to the crest level. Therefore, a considerable seepage flow may occur within the unsaturated zone, bypassing the sealing in the crest area. Especially, for high water levels this shows an adverse effect.

The gravel columns show a minor effect on the underground seepage conditions. The gravel columns do not show a practical effect when the sealing system is not working, anyway, or the “open sealing situation” is established in the model. The gravel columns increase the seepage flow amount, pressure head and seepage line when the sealing system is working in full sealing (FS) conditions.

3.5. RESULTS AND INTERPRETATION OF THE STABILITY ANALYSIS

The slope stability analysis is performed by applying the limit equilibrium analysis (LEA) method in order to determine the factor of safety (FoS) only for the

downstream embankment slope (using SLOPE/W software, GeoStudio 2016). The FoS values are obtained only for the sliding slope stability considering the downstream slope. Results are presented in Table 4.

The required FoS ([1], [2], [3], [5]) are relatively below the calculated values. In addition, thanks to the conservative dam design and flat slopes in respect to the limited height of the embankment the static stability is not a matter of concern. The FoS range show up to 30 % safety margin.

Table 4
FoS Evaluation of the Downstream Embankment Slope Slip Stability

	Load Cases						
	LCP1	LCT1	LCT3	LCA1	LCA2a	LCA2b	LCA3
Source	Required Factor of Safety						
DIN 19700/2004	BS I	BS II		BS III			
	1.3	1.2		1.1			
Fell et al., 2005	1.5	1.3	-	-	-	-	-
USACE	1.5	1.4	1.3	-	-	-	-
USBR	1.5	1.5	-	-	-	-	-
FERC	1.5	1.4	-	-	-	-	-
Design condition	Calculated Factor of Safety						
FS + GC	1.8	1.8	1.7	1.7	1.7	1.7	1.6
FS - GC	1.8	1.7	1.7	1.7	1.5	1.6	1.5
OS + GC	1.8	1.7	1.7	1.7	1.7	1.7	1.6
OS - GC	1.7	1.6	1.7	1.5	1.5	1.6	1.4

4. HYDRODYNAMIC SOIL DEFORMATION PROCESSES

Fell & Fry [6], [7] developed a process dependent approach for assessing erosion and suffusion processes. The consideration of more assessment steps in order to obtain a full risk assessment approach also in consideration of important aspects such as system identification, detection, measures, etc. [9] supports of a better understanding and more detailed risk assessment.

Beneath the assessment steps (initiation, development, continuation, breaching), which are directly addressing the particle transport, the pre- and post-phases need to be investigated and assessed as well. For the assessment it is also important to localize the transport processes. Within this localization step erosion paths shall be defined which are strongly depending on the dam design and the underground situation. In total three erosion paths are identified as dam body erosion path (DB EP), underground erosion path 1 (UB EP 1) and underground erosion path 2 (UB EP 2). Along the erosion paths different sorts of processes (A to E) are evident which are also checked within the main four phases of the erosion and suffusion assessment (see Fig. 4).

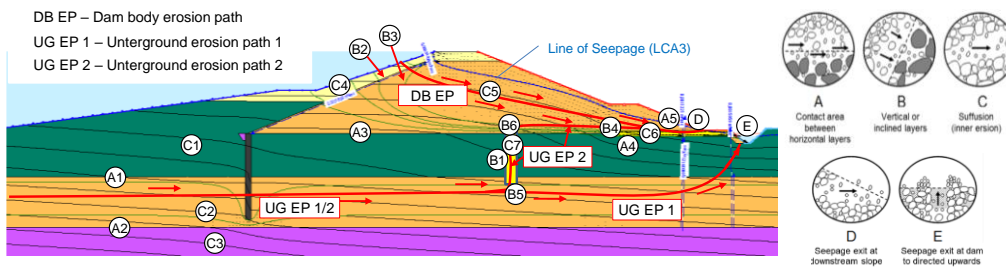


Fig. 4
Defined erosion paths within the embankment dam section

The continuation of erosion shall be assessed by mean hydraulic gradients derived from the seepage analysis. The definitions of the hydraulic head difference and the flow path length are shown in Fig. 5.

The determined hydraulic gradients are given in Table 5. The critical gradient for the present sand-gravels should be approx. $i_c = 0.20$ to 0.40 . For finer sands this can decrease to $i_c = 0.15$ and for silts to $i_c = 0.10$ or even less. For the dam body erosion path the material shows the firstly mentioned gradients. However, the gradients within the dam body (Table 5) are generally small $i < 0.20$, except for load case LCA3 where it reaches a value of $i = 0.30$. Thus, for reaching the crest water level also backward erosion may continue since hydraulic forces are strong enough. For the other load cases the erosion through the dam body should not be a problem due to low gradients.

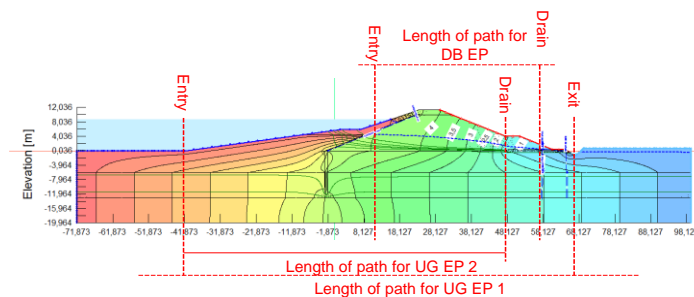


Fig. 5
Determination of the Hydraulic Head difference and Flow Path length using the Total Head results of the Seepage Analysis (here: LCP1, OS - GC)

For the crest water level (LCA3) the hydraulic gradients are strong enough to continue the erosion process through the dam body. This is a result of the seepage control design which does not meet the requirements to European codes and guidelines, especially German design philosophy. Processes within the underground are also considered to be not critical thanks to the protective clay layer and the conservative dam design.

Table 5
Hydraulic and critical gradients for the analyzed load cases and design situations

Erosion path	Load Cases							Design/dam condition
	LCP1	LCT1	LCT3	LCA1	LCA2a	LCA2b	LCA3	
Mean actual hydraulic gradients $i [-]$								
Critical hydraulic gradient for sand-gravels $i_c = 0.20$ to 0.40 (Brandl & Hofmann, 2006)								
Dam body	0.08	0.12	0.02	0.13	0.16	0.09	0.30	OS without GC
Underground 1	0.08	0.09	0.05	0.10	0.08	0.08	0.10	OS without GC
Underground 2	0.09	0.10	0.04	0.12	0.09	0.09	0.12	OS with GC

Suffusion plays a minor role, but as a result of checking selected suffusion criteria some of the applied sand-gravels in the dam fill as well as in the underground might be susceptible to suffusion.

The applied monitoring concept for a 22 km long dam is not able to contribute to an effective detection of potential erosion processes. Intervention measures to stop the erosion through the dam body, once it occurs during accidental load cases, are difficult to realize. Due to the cohesionless fill material in the dam body breaching should proceed relatively fast.

Following recommendations were given. The sealing should be extended to the crest elevation. The drain should be redesigned and extended to be connected to the drainage ditch. The gravel columns do not show a critical negative effect on the design and the dam behavior in respect to erosion and suffusion risks but, therefore, can be spared.

5. CONCLUSION

The dam shows an unsatisfactory seepage behavior resulting in an unfiltered seepage exit which is the first phase to backward erosion. This risk is mainly present for the dam body, which shows a design which does not comply with modern dam design criteria and modern dam safety philosophy. Therefore, the application of an additional sealing or drainage element and redesign of the downstream toe drain are considered to be required. The static stability of the downstream slope is not of concern thanks to the applied flat slope. Erosion risks are mainly related to the embankment dam body. Within the underground erosion risks are tolerable.

REFERENCES

- [1] DIN 19700-10 Stauanlagen, Teil 10: Gemeinsame Festlegungen. *Deutsches Institut für Normung e.V. (DIN), Berlin*, Juli 2004.
- [2] DIN 19700-11 Stauanlagen. Teil 11: Talsperren. *Deutsches Institut für Normung e.V. (DIN), Berlin*, Juli 2004.
- [3] DIN 19700-12 Stauanlagen. Teil 12: Hochwasserrückhaltebecken. *Deutsches Institut für Normung e.V. (DIN), Berlin*, Juli 2004.
- [4] DWA M 522 Kleine Talsperren und kleine Hochwasserrückhaltebecken. *Deutsche Vereinigung für Wasserwirtschaft, Abwasser und Abfall e.V.*, 2015.
- [5] FELL, R. ET AL. Geotechnical engineering of dams. *A. A. Balkema Publishers, Leiden, London New York Philadelphia Singapore*, 2005.
- [6] FELL, R. ET AL. A Framework for Assessing the Likelihood of Internal Erosion and Piping of Embankment Dams and Their Foundations. *Internal Erosion of Dams and their Foundations, Fell & Fry (editors)*, Taylor & Francis Group, London, pp. 65-70, 2007.
- [7] FELL, R., FRY. J. J. The State of the Art of Assessing the Likelihood of Internal Erosion of Embankment Dams. *Water Retaining Structures and their Foundations*, Taylor and Francis, London, pp. 1 - 24, 2007.
- [8] HASELSTEINER, R. Hochwasserschutzdeiche an Fließgewässern und ihre Durchsickerung. *Berichte des Lehrstuhls und der Versuchsanstalt für Wasserbau und Wasserwirtschaft, Technische Universität München*, Nr. 111, 2007.
- [9] HASELSTEINER, R. Die Beurteilung von hydrodynamischen Bodendeformationsvorgängen in Dämmen und Deichen - Ein integraler Ansatz. *3. Symposium Sicherung von Deichen, Dämmen und Stauanlagen, Universität Siegen*, S. 289-338, 2009.

SUMMARY

The seepage control concept that comprises sealing, dam body and drainage elements in order to guarantee safe seepage conditions for the anticipated load cases should be developed where remarkable seepage conditions are expected through the dam body. As long as the seepage conditions are not controlled and hydraulic gradients occur, erosion may occur in form of backward erosion in the underground/subsoil and along all contact borders/interfaces of different materials in the dam body.

The paper presents the seepage and stability analyses of a case study to emphasize the importance of seepage control design and the assessment of hydrodynamic soil deformation process. Based on the analyses' results, recommendations and conclusions are presented to overcome and to improve the specific drawbacks and inherent risks of the present dam design.

COMMISSION INTERNATIONALE DES GRANDS BARRAGES

VINGT-SIXIÈME CONGRÈS DES GRANDS BARRAGES
Autriche, juillet 2018

DOI 10.3217/978-3-85125-620-8-148



This work licensed under a Creative Commons Attribution 4.0 International License. <https://creativecommons.org/licenses/by-nc-nd/4.0/>

**GROUT CURTAIN PERFORMANCE PARTICULARITIES IN THE COMPLEX
GEOLOGICAL CONDITIONS ENCOUNTERED AT GURA APELOR CLAY
CORE ROCKFILL DAM**

Adrian POPOVICI

Professor, TECHNICAL UNIVERSITY OF CIVIL ENGINEERING BUCHARST

ROMANIA

Dan STEMATIU

Professor, TECHNICAL UNIVERSITY OF CIVIL ENGINEERING BUCHARST

ROMANIA

Eugeniu MARCHIDANU

Professor, TECHNICAL UNIVERSITY OF CIVIL ENGINEERING BUCHARST

ROMANIA

GROUT CURTAIN PERFORMANCE PARTICULARITIES IN THE COMPLEX GEOLOGICAL CONDITIONS ENCOUNTERED AT GURA APELOR CLAY CORE ROCKFILL DAM

Adrian POPOVICI, Dan STEMATIU. Eugeniu MARCHIDANU

Professors, TECHNICAL UNIVERSITY OF CIVIL ENGINEERING BUCHARST

ROMANIA

1. INTRODUCTION

Using cement grouting to improve bedrock water tightness is quite common and there are numerous examples of its application to the engineering of dam-foundation improvement. Evaluation methods of the effectiveness and quality of grouting include analysis of drilling data, water pressure testing results, grouting records and monitoring data. Evaluations may be performed on an on-going basis concurrent with grouting, near the end of grouting, or after the completion of grouting [1]. Currently, in-situ water pressure testing over discrete zones in the foundation provides an excellent method for verification of the effectiveness of the grouting program. However, in some particular cases the Lugeon target is hard to achieve in spite of intensive grouting. Areas of abnormally high or low grout takes in comparison to the Lugeon values are identified. For such cases performance evaluations should be based on the general grouting objectives [2]. Post-construction monitoring of seepage from foundation drains and collecting galleries can indicate whether the grouting program has satisfied design seepage requirements. This paper addresses the question by discussing methods one might use to evaluate the adequacy and progress of grouting and items one might choose to consider in evaluating the performance of grouting.

2. GURA APELOR DAM

Gura Apelor dam is a clay core rockfill dam 168 m high, that provides a 230 mil. m³ storage for the 335 MW Retezat power plant. It is the tallest dam in Romania. The crest length is 480 m and total fill volume is 11.2 mil. m³. The core is moderate thick, 64 m at the dam base. The grouting and inspection gallery is located along the clay core – foundation rock contact, in the mid axis of the core. A second gallery is provided downstream of the grouting gallery, inside the downstream filter, in order to collect the water seepage escaped through the clay

core or percolating the grout curtain.

The spillway is located at the right abutment. It is a free flow weir followed by a rapid channel and a 10m diameter tunnel. The end is a flip bucket leading to downstream river bed. The bottom outlet and mid height outlet are also in the right abutment and connected with spillway tunnel.

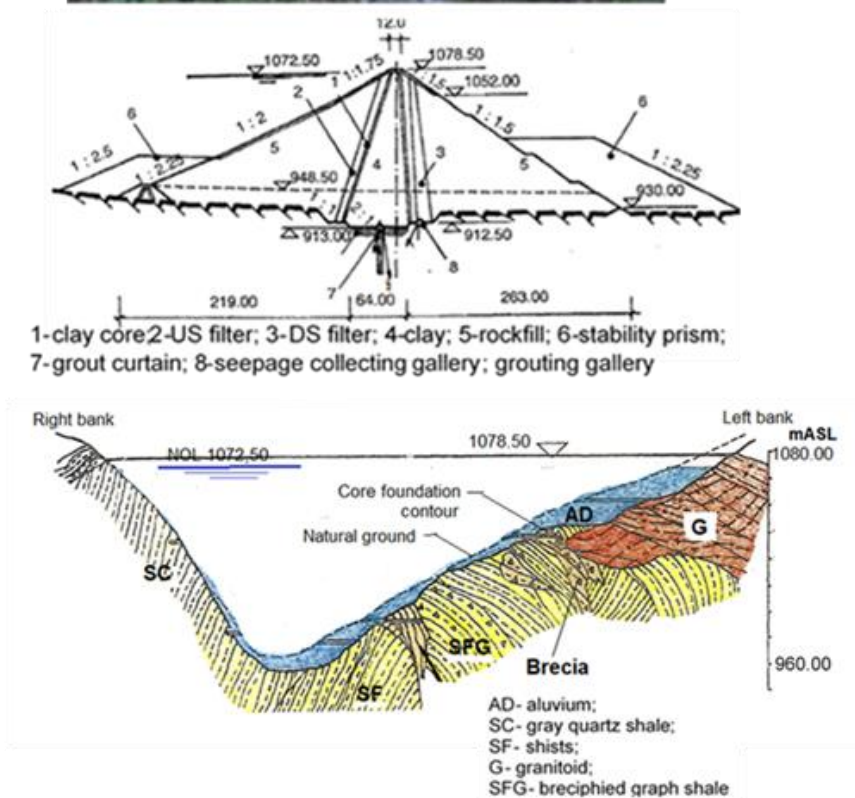


Fig.1

Gura Apelor Dam – cross section, geology and downstream view

The foundation rock is made up of a complex of crystal shale and granite gneiss. The right slope, the river bed and the left slope below 950 mASL consist in gray quartz shale with greenish chlorine-sericitous bands. The left slope above elevation 950 mASL up to elevation 1,030 mASL is made up of tectonised, breciphied graph shale. Above the 1030 mASL the right bank is made of granitoid

rock mass. Water permeability tests performed in investigation drillings pointed out important absorptions on the left slope, particularly in the tectonised area between the granite and the brecciated shale.

3. FOUNDATION WATERTIGHTENING

In order to avoid the seepage along the discontinuities in the upper part of the rock foundation the entire base width of the core was grouted to a depth of 6 to 12 m to form a grout platform, or a grout bulb (fig. 2). The grout curtain was designed based on lugeon values and consists in two rows of grouting holes, with a depth of 60 ... 80 m, performed from the grouting gallery. On the right abutment, on the dam valley and on the lower half of the left abutment the grout curtain achieved the required technical conditions. On the upper part of the left abutment, above the elevation 985 mASL the control drillings have shown very large water absorptions. Areas of abnormally high or low grout takes in comparison to the Lugeon values were identified for further analysis. The grouting records for these abnormal zones were reviewed carefully along with the pressure testing and grouting records from adjacent holes.

The difficulties encountered during the grouting process due to complex geological conditions has imposed the temporary stopping of the grout curtain performance. Consequently, the reservoir water level was severely restricted. The apparent inability of the traditional grouting practices to provide a watertightness barrier of acceptable efficiency and durability led to the idea of replacing the grout curtain with a concrete wall. The attempt was abandoned bearing in mind that the average cost of a concrete wall is many times that of a grouted cut-off, and that there was currently a shortfall in contractor capacity to construct the former,

After 10 years of studies and analyses it was decided to complete the grout curtain. A campaign of high quality drilling, permeability testing and grouting was first conducted. The decision was supported by the fact that grouting equipment, methods and contracting procedures have evolved over the last decade and the engineers can now design, build and verify the performance of permanent grouted seepage barriers for dam structures.

The extension and completion of the grout curtain performed in the first stage was differentiated according to rock mass characteristics (see fig. 2). For the schist zone, between 960 and 1021 mASL elevations, along a length of 146 m, groutings for the bulb underneath the core foundation, 15 m deep were firstly provided. The grout curtain itself, with a depth of 35 m, consists in three rows of grouting drillings disposed at 0.5 m in between and 2m along the curtain. For the breccia zone, with a length of 23.3 m, between elevations 1021 and 1028 mASL, bulb grouting and grout curtain with a depth of 35 m encountered some anomalies. In some places the grout take was quite large in spite of low Lugeon values. For the granitoid zone, with a length of 150 m, between elevations 1028 and 1078.50 mASL, the grout curtain consists in three rows of grouting drillings, with a depth of 55 m for the ones

performed from the grouting gallery and with a depth of 70 m for drillings performed from the platform.

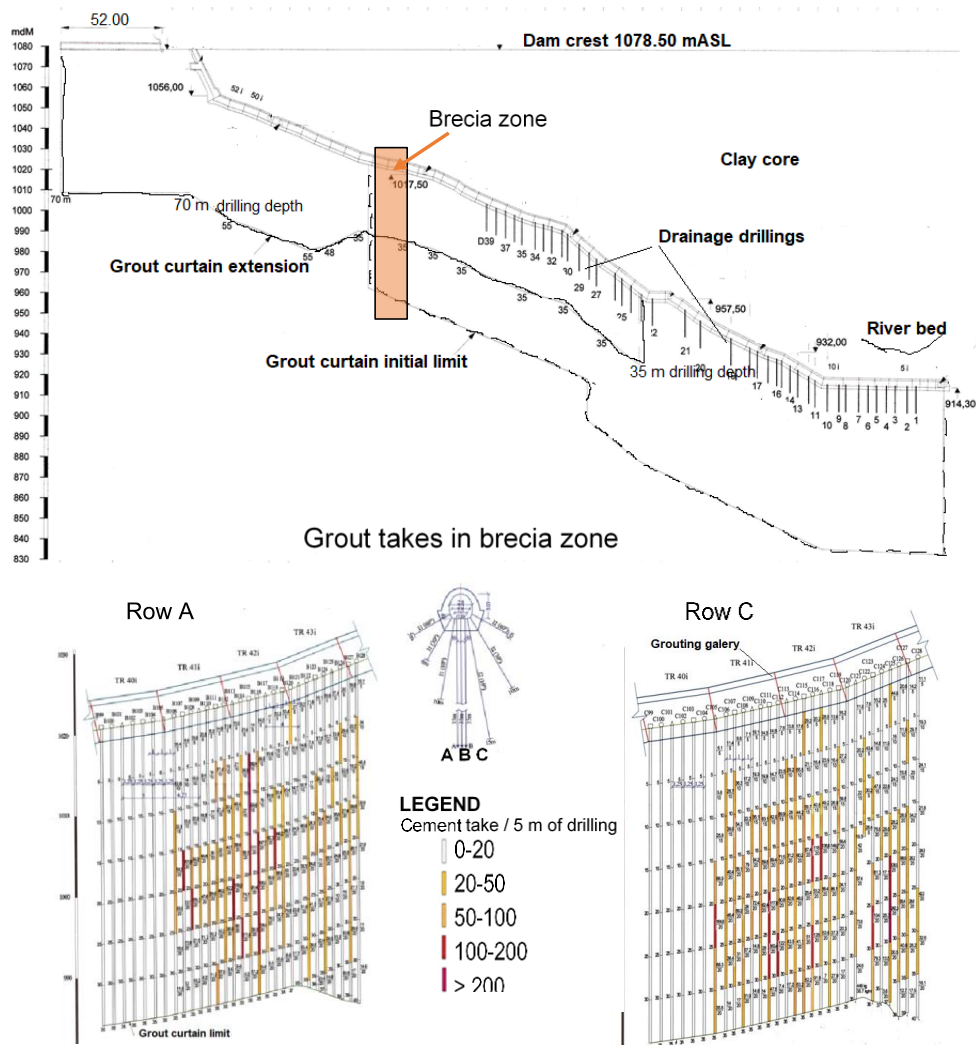


Fig. 2.
The extension and completion of the grout curtain performed in the first stage

3. GROUT CURTAIN EFFICIENCY BASED ON LUGEON VALUES

At the end of the process the criteria based on Lugeon specific absorption [3], [4], [5] were partly fulfilled: some 60% in the case of Romanian standard and ICOLD recommendations and up to 80% in the case of FST criteria.

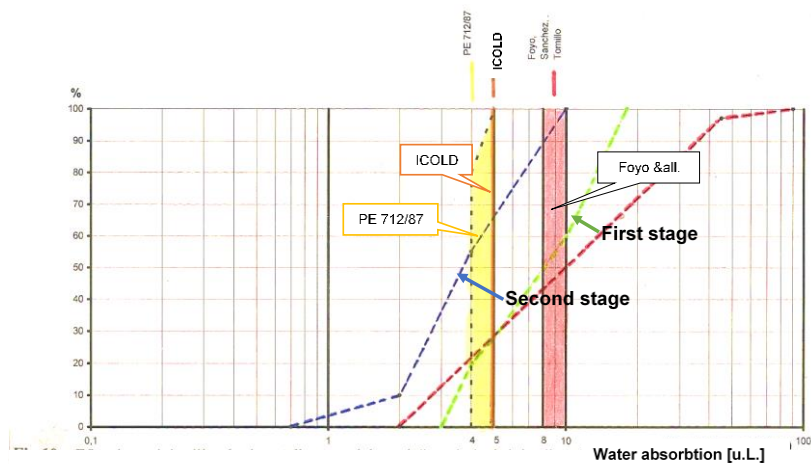


Fig.3
Grout curtain efficiency in terms of water absorption

In spite of intensive grouting the Lugeon target was not achieved. The breccia zone and the brecciated graph shale zone were areas of abnormally high or low grout takes in comparison to the Lugeon values are identified (see fig. 2). Consequently, performance evaluations were based on the general grouting objectives. Monitoring of seepage from foundation drains and collecting galleries was the criterion that indicates whether the grouting program has satisfied design seepage requirements.

4. GROUT CURTAIN EFFICIENCY BASED ON SEEPAGE MONITORING

4.1. MONITORING SYSTEM

Gura Apelor dam is provided with an extensive monitoring system, that allow the record of pore water pressures in the core and inside the rock mass, of the seepage flows, of the strains, of the fill settlements, of the rock displacements, of the joint movement, of the dam body movements. For the grout curtain efficiency, the relevant measurements are the interstitial water pressures in the rock foundation, upstream and downstream of the grout curtain, and the seepage collected in the seepage collecting gallery (fig.4). The interstitial water pressures are measured by manometers that equipped the drainage drillings performed from the grouting gallery. The seepage is collected by provided windows in the collecting gallery and by drainage drillings performed from the same gallery. Concrete diaphragms separate defined zones along the seepage collecting gallery in order to localize the potential large seepage sources.

A drainage gallery was provided in the left abutment, with a length of 100 m, between elevations 996 and 1000 mASL. It is connected to the drainage collecting

gallery. The purpose was to avoid the buildup of large interstitial pressure inside the rock mass thus endangering the slope stability. As it will be seen, the gallery has an adverse effect, increasing the total seepage attributed to lack of imperviousness of the foundation.

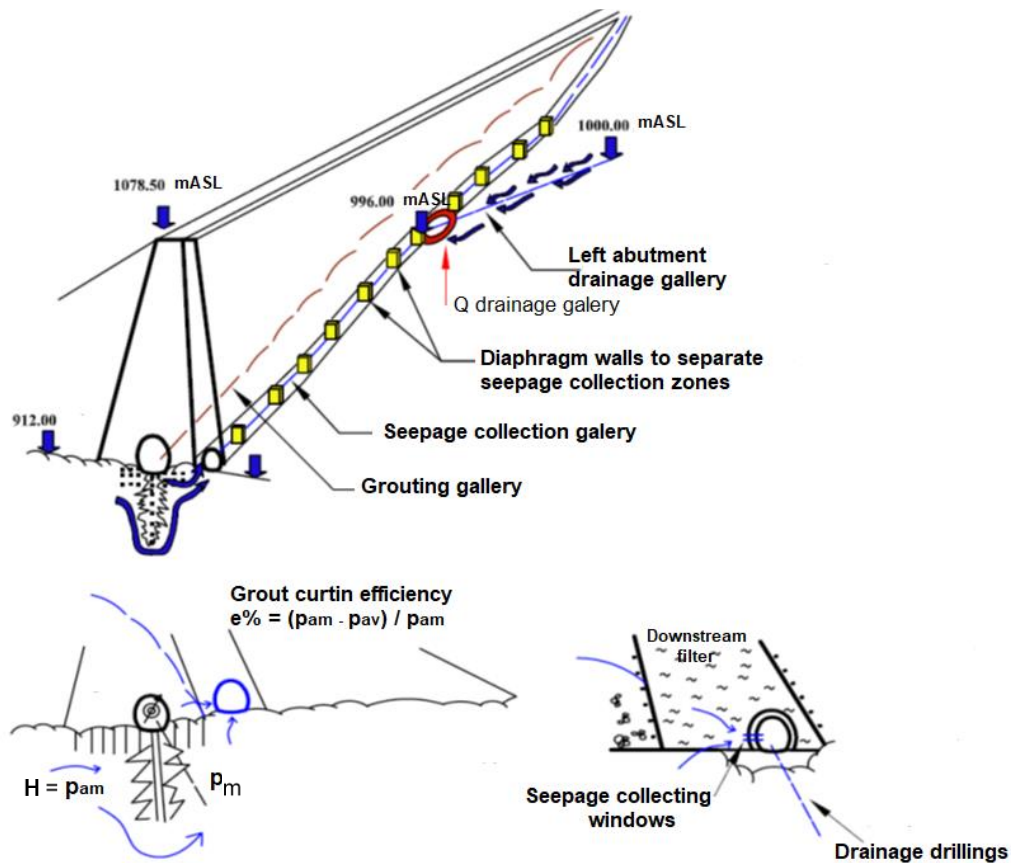


Fig. 4.
Monitoring system for grout curtain efficiency

4.2. MONITORING DATA

Evaluation of the grout curtain efficiency was based on three monitoring values:

- The measured pressures upstream and downstream the grout curtain. The characteristic value was the efficiency defined as $e\% = 100 (H - p_m) / H$, where H is the water column corresponding to water level in the reservoir and p_m is the pressure at the manometer, expressed as meters of water column. At the 1030 mASL reservoir elevation, the efficiency was above 80% on the average, except two local zones where the efficiency was 65 ... 70% (fig.5).
- The seepage flows in the seepage collecting gallery, differentiated into seepage through gallery windows and seepage in drainage drillings.

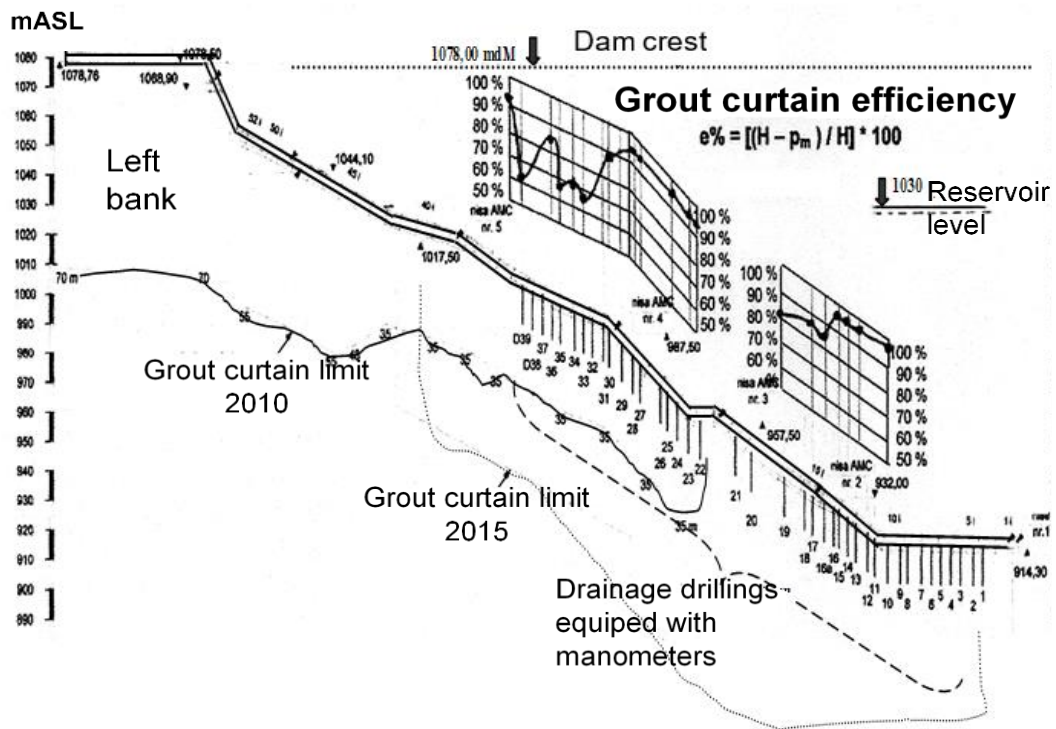


Fig.5.

Grout curtain efficiency in terms of pressure drop

- Total seepage collected at the final weir at the end of the collecting gallery (fig. 6). The total seepage has shown significant decrease i.e. for the same reservoir water level, 1010 mASL, the seepage has decreased from 52 l/s before the grout curtain extension to 23 l/s.

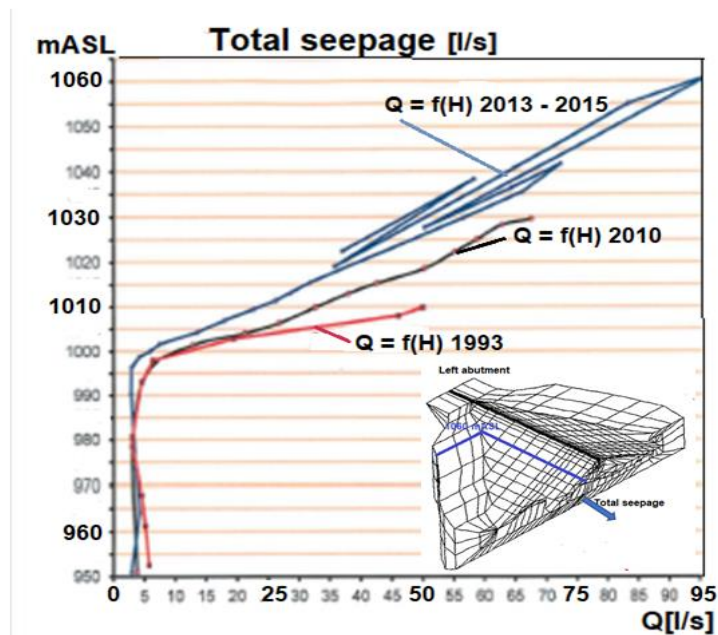


Fig. 6.

Total seepage versus reservoir water level

4.3. EFFECTS OF THE LEFT ABUTMENT DRAINAGE GALLERY

The analysis of the seepage distribution shows that up to 40% of the total seepage is the contribution of the left abutment seepage gallery. The gallery induces a defavorable behavior, increasing the infiltration gradients from the reservoir towards the left bank and consequently the seepage flows. There are gaps and fissured rock zones at the outer surface of the lining and thus the gallery is actually a large diameter drain with a length of 100 m (fig.7). In spite of filling grouting performed from the gallery and decreasing the number of drainage drillings from 32 to 14, the drainage effect is still very active.

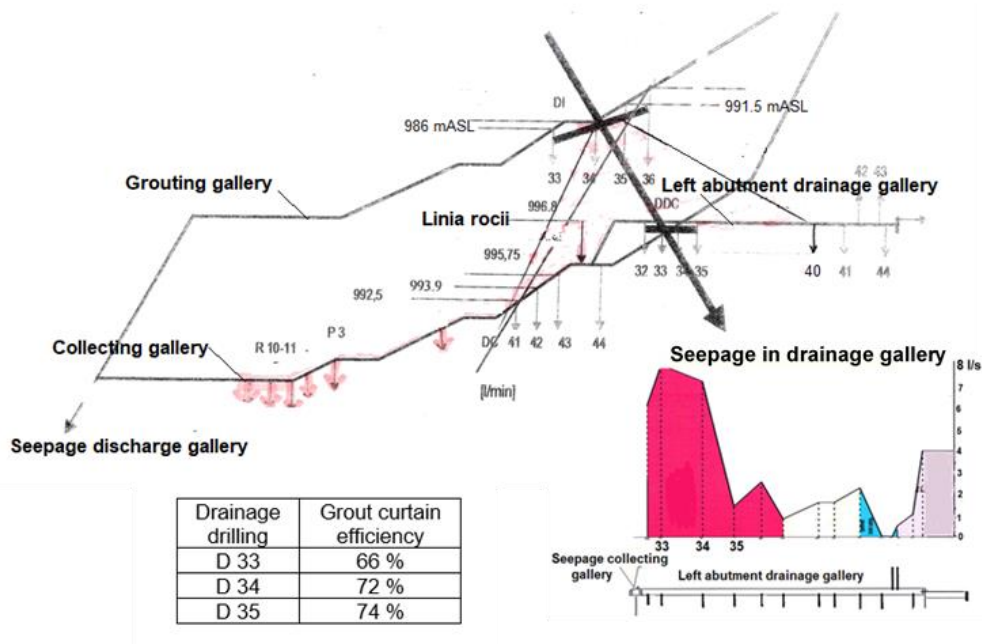


Fig. 7. The seepage contribution of the left abutment drainage gallery

The seepage collected along the left abutment drainage gallery is mainly taken over by the collecting gallery and creates a false image of the seepage pattern corresponding to a more permeable zone in the grout curtain.

The same phenomenon has been revealed by the numerical modeling of the seepage. A 3 D finite element model for dam foundation system was built providing the background for deciding the extent of foundation treatment required to satisfy design and safety criteria and its efficiency (fig. 8). The numerical model was calibrated based on the monitoring data corresponding to a reservoir level of 1030 mASL and was used to predict the dam behavior for reservoir elevation 1050 mASL and normal operation level. The extension of the grout curtain limit from 35 m to 60 m do not improve significantly the seepage control, the reduction being less than 10%. The left bank drainage gallery was included in the model by special boundary conditions. The results underline the need for a retreatment of the drainage gallery.

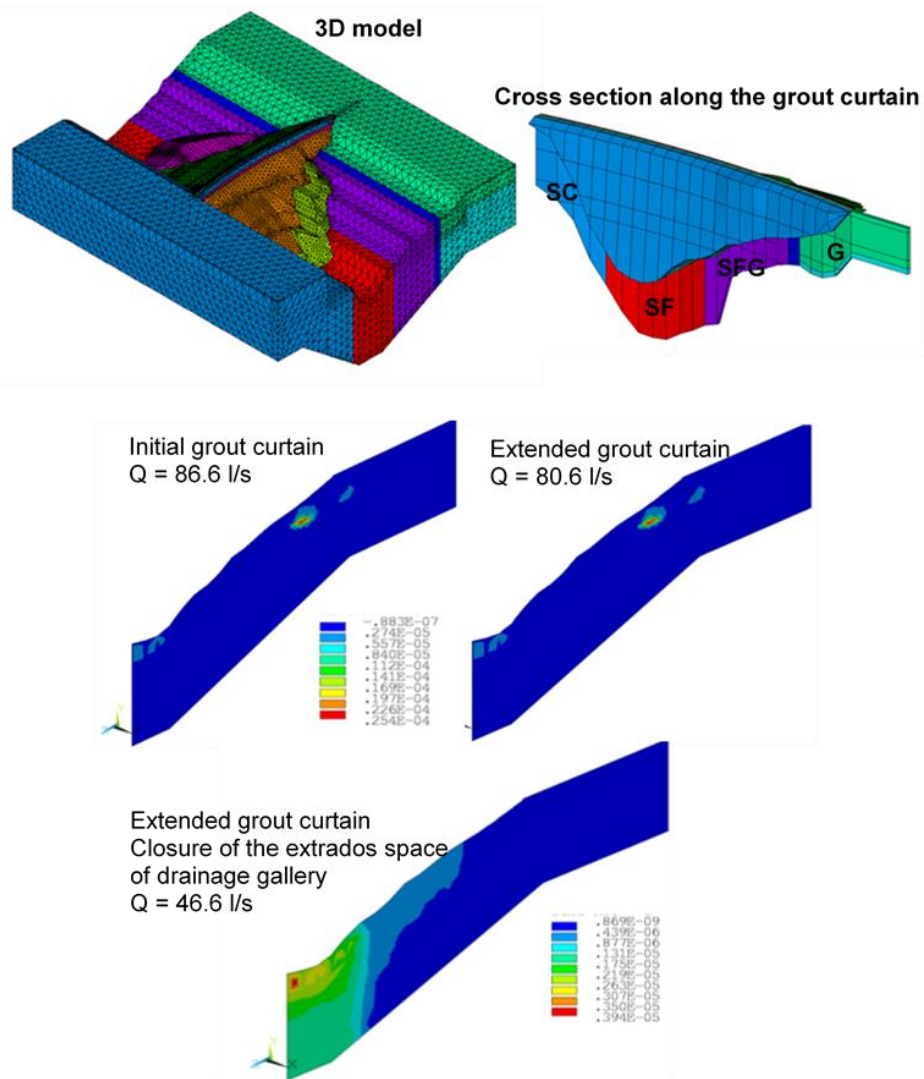


Fig. 8.
Finite element model to predict the grout curtain parameters

5. CONCLUDING REMARKS

The grouting program conducted for Gura Apelor dam has revealed that in some particular cases the Lugeon target is hard to achieve in spite of intensive grouting. For such cases performance evaluations should be based on the general grouting objectives. Monitoring of seepage from foundation drains and collecting galleries can indicate whether the grouting program has satisfied design seepage requirements.

The drainage galleries performed inside the abutment rock of the dam induces a defavorable behavior, increasing the infiltration gradients and consequently the seepage flows. Such galleries are to be avoided unless there is

a real risk to build up large interstitial pressure inside the rock mass of a slender abutment endangering its stability.

REFERENCES

- [1] WEAVER, K. D. AND BRUCE, D. A. Dam Foundation Grouting: *ASCE Press, Reston, VA*, 494 p., 2007.
- [2] DREESE, T., D.B. WILSON, D.M. HEENAN, AND J. COCKBURN. State of the Art in Computer Monitoring and Analysis of Grouting and Ground Treatment, *Proceedings of the Conference sponsored by the Geotechnical Engineering Division of the American Society of Civil Engineers, New Orleans, LA, February 10-12, pp. 1440-1453.*, 2003.
- [3] FOYO, A., SANCHEZ, M., A., TOMILLO, C. Propuesta para obtencion de un indice de calidad del macio mrocoso IPS indice de permeabilidad a partir de los ensayos de carga de agua en cimentaciones de grandes presas. *Proc of Symposium on Dam maintenance and Rehabilitation*, 2003, Lisse
- [4] MEE Romanian Departmental standard 712 /1987. Dam foundation treatment (in Romanian). 1987.
- [5] ICOLD Dam Foundations. Geologic considerations. Investigation Methods. Treatment. Monitoring, *Bulletin 129*, 2005

6. SUMMARY

The difficulties encountered during the grouting process on the left abutment of Gura Apelor dam due to complex geological conditions has imposed the stopping of the grout curtain performance on the last upper quarter of the dam height. Consequently, the reservoir water level was severely restricted. After 10 years of studies and analyses it was decided to complete the grout curtain by the same grouting process but using high performance equipment. Up to now, the reservoir level was raised in stages above the previous restricted level, up to some 12 m below the normal operation level. The closely monitoring seepage phenomena pointed out that the imperviousness of the left abutment was successfully achieved.

KEYWORDS: Embankment dam, Grout curtain, Monitoring, Seepage

COMMISSION INTERNATIONALE DES GRANDS BARRAGES

VINGT-SIXIÈME CONGRÈS DES GRANDS BARRAGES
Autriche, juillet 2018

DOI 10.3217/978-3-85125-620-8-149



This work licensed under a Creative Commons Attribution 4.0 International License. <https://creativecommons.org/licenses/by-nc-nd/4.0/>

**MONITORING AND EVALUATION OF VARIED ANTI-SEEPAGE
MEASURES IN DEEP GRAVEL FOUNDATION FOR AN EMBANKMENT DAM
- A CASE STUDY**

S.J. WANG

NANJING HYDRAULIC RESEARCH INSTITUTE
DAM SAFETY MANAGEMENT CENTER OF THE MINISTRY OF WATER
RESOURCES

Q. PANG

NANJING HYDRAULIC RESEARCH INSTITUTE
DAM SAFETY MANAGEMENT CENTER OF THE MINISTRY OF WATER
RESOURCES

H.B.HUANG

NANJING HYDRAULIC RESEARCH INSTITUTE
DAM SAFETY MANAGEMENT CENTER OF THE MINISTRY OF WATER
RESOURCES

H. WANG

NANJING HYDRAULIC RESEARCH INSTITUTE
DAM SAFETY MANAGEMENT CENTER OF THE MINISTRY OF WATER
RESOURCES

Y.X. WU

NANJING HYDRAULIC RESEARCH INSTITUTE
DAM SAFETY MANAGEMENT CENTER OF THE MINISTRY OF WATER
RESOURCES

CHINA

**MONITORING AND EVALUATION OF VARIED ANTI-SEEPAGE
MEASURES IN DEEP GRAVEL FOUNDATION FOR AN EMBANKMENT DAM
- A CASE STUDY**

S.J. Wang^{1,2}, Q.Pang^{1,2}, H.B.Huang^{1,2}, H. Wang^{1,2}, and Y.X. Wu^{1,2}

1. *Nanjing Hydraulic Research Institute*
2. *Dam Safety Management Center of the Ministry of Water Resources*

CHINA

1. GENERAL SITUATION OF THE DAM

The dam is a homogenous embankment dam with length of 2222m and maximum height of 24m. The elevation of dam crest is 28.72m. The normal water storage level is 21.16m, and the design flood water level is 25.92m. Dam body is filled by four types of compaction, such as heavy roller compaction, light roller compaction, roller compaction in the water and compaction manually. The bedrock is overburdened by Quaternary alluvial and diluvial layer, which includes three permeable layer composed by sand and gravel and two impervious layer composed by clay. Seepage control prevention measures of the dam include cut-off wall in section from 0+700 to 1+250 (extended deeply to the bedrock) and jet grouting in the section from 1+250 to 1+750 (extended to the first imperious layer). The maximum thickness of overburden layer is 42m. The axial geological formation of the dam is shown in Fig. 1.

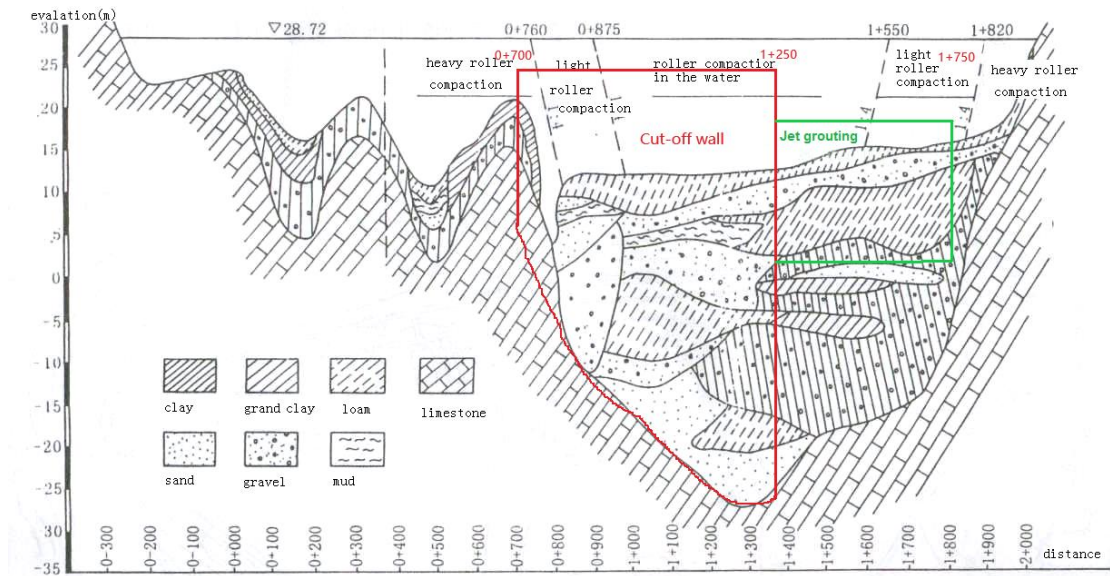


Fig.1
The axial-section geological formation of the dam

2. THE LAYOUT OF SEEPAGE OBSERVATION POINTS

Seepage observation points are distributed in the cross sections of 0+500, 0+850, 1+130, 1+300 and 1+650 (mark B). Observation points of dam body and foundation are distributed in front and back of seepage control measures. Some standpipes are used to monitor the groundwater level also (mark S). There are five seepage discharge observation points in the sections of 1+020 (L1), 1+250 (L2), 1+280 (L3), 1+450 (L4) and 1+650 (L5). The observation layout is shown in Fig. 2 and Fig. 3.

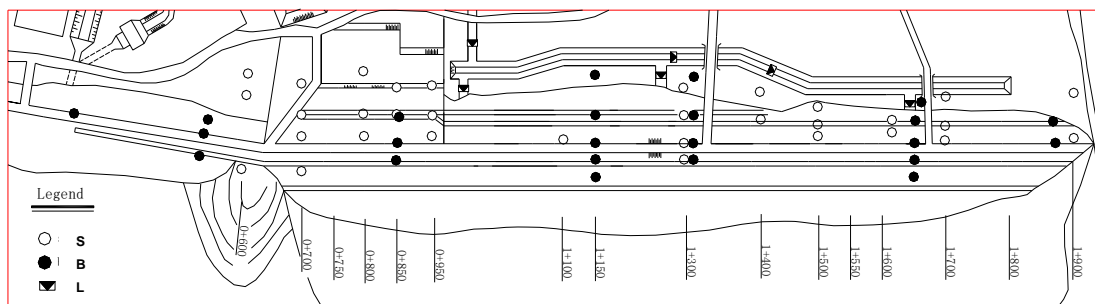


Fig. 2
The plane distribution of seepage observation points

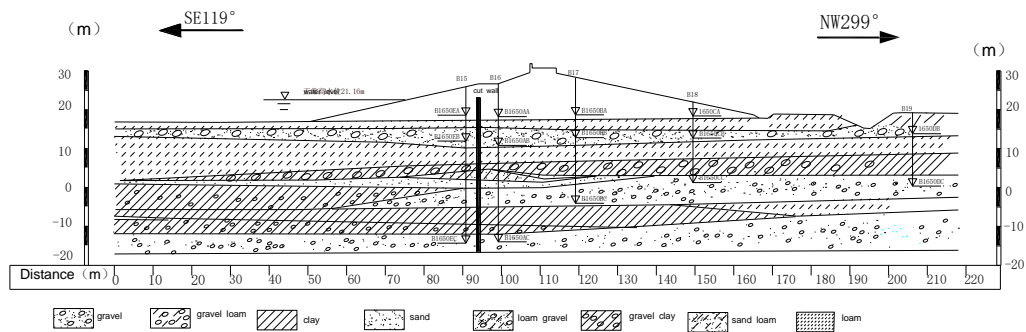


Fig.3
The cross-section distribution (1+650) of seepage observation points

3. EVALUATION OF SEEPAGE CONTROL EFFECT

The seepage pressure hydrograph of dam foundation are shown in Fig.4-Fig7 and the co-efficient between seepage pressures with water level are shown in Table 1. It can be concluded that:

(1) Two dam foundation observation points B0850AB and B0850BB of section 0+850 are located at the back of cut-off wall, and their average potential percent reduce about 75% compared with water level and their seepage pressures have a poor correlation with water level. The measure points B1130AB and B1130AC of section 1+130 are located in the first and third permeable layers at the back of cut-off wall, and their potentials reduce about 72% and 60% respectively compared with water level. These two phenomena mentioned above indicate that the cut-off wall has a significant anti-seepage effect.

(2) B1300AB, B1300BB and B1300CB of section 1+300 located in the same permeable layer, their potentials are almost same, reducing 50% compared with water level and their seepage pressures have a poor correlation with water level. There is small loss of water head and high permeability of dam foundation, which means that the joint area of cut-off wall and jet grouting shows a weaker anti-seepage effect.

(3) B1650AB and B1650AC of section 1+650 located in the first and third permeable layers at the back of cut-off wall, and their potentials reduce about 30% and 40% respectively compared with water level. Besides, the correlation coefficient between their seepage pressures with water level approximate or even exceed 0.9. Section 1+650 shows a more significant correlation with water level compared with other sections on both sides. As a result, jet grouting at this area has a poor anti-seepage effect.

In addition, after cut-off wall set up in 2001, 60% total seepage discharge in the sections of 1+020 (L1) is reduced, whereas seepage discharge of number L3 in the section of 1+280 and number L4 in the section of 1+450 show little

difference. This proves lower efficient of seepage prevention for jet grouting than cut-off wall and leakage happens in the right abutment of dam foundation.

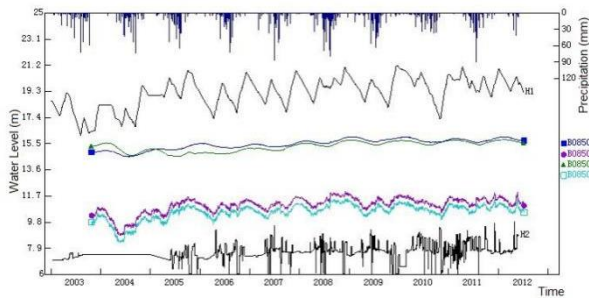


Fig.4

The seepage pressure vs time in cross-section of 0+850

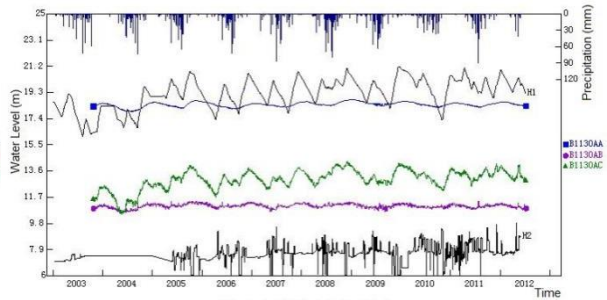


Fig 5

The seepage pressure vs time in cross-section of 1+130

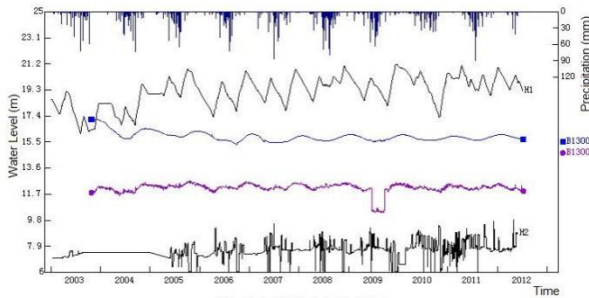


Fig 6

The seepage pressure vs time in cross-section of (1+300)

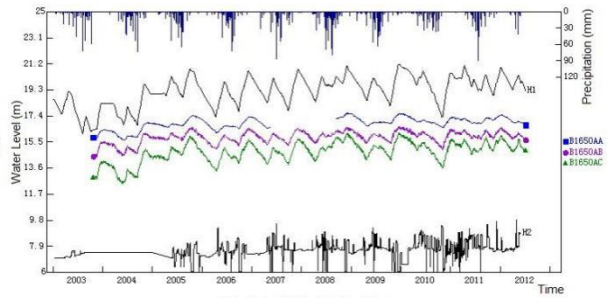


Fig 7

The seepage pressure vs time in cross-section of 1+650

Table 1
Co-efficient between seepage pressures with water level

SECTION	POINT	CO-EFFICIENT	ERROR/m	SECTION	POINT	CO-EFFICIENT	ERROR/m
0+850	B0850AB	0.79	0.3446	1+500	P1500A	0.78	0.2732
	B0850BB	0.79	0.3477		P1500C	0.81	0.1967
1+130	B1130EB	0.98	0.1851	1+600	P1600A	0.36	0.7384
	B1130EC	0.95	0.2609	1+650	B1650EB	0.99	0.1083
	B1130AB	0.55	0.1259		B1650EC	0.96	0.1908
	B1130AC	0.89	0.3126		B1650AB	0.96	0.1085
	B1130BB	0.40	0.1145		B1650AC	0.96	0.2085
	B1130BC	0.81	0.1818		B1650BB	0.96	0.1068
	B1130CB	0.29	0.1599		B1650BC	0.98	0.1162
	B1130CC	0.81	0.1598		B1650CB	0.95	0.1186
	B1130DB	0.24	0.1101		B1650CC	0.96	0.1102
	B1130DC	0.75	0.1573		B1650DB	0.16	0.1171
B1650DC	0.87	0.1131					
1+300	B1300AB	0.47	0.2453	1+700	P1700A	0.75	0.2138
	B1300BB	0.68	0.1203	1+850	B1850CB	0.22	0.1087
	B1300CB	0.54	0.1262				

Grouting is to fill in the pores or holes of the dam body or foundation materials by thin mixture of sand, water, and cement or lime, which aims to make the materials denser and form an impervious barrier in dam. Grouting (include jet grouting) is with advantages as little investment and short construction period. But as its anti-seepage effect is significantly influenced by the condition of the soil layer and the anti-seepage thickness is not uniform, grouting is only suitable for the low water head embankment dam.

Cut-off wall is a technique used to build reinforced concrete walls in dam body or foundation. The technique presents a higher safety and reliability in deep overlying strata. Although the investment of cut-off wall is high, but its integrity is good and anti-seepage effect is remarkable, which makes it more applicable.

Therefore, as shown in the case, for an embankment dam with a deep gravel foundation, cut-off wall is more efficient of seepage prevention than jet grouting.

4. CONCLUSION

Anti-seepage effect of jet grouting is significantly influenced by the condition of the soil layer and it is only suitable for the low water head embankment dam. Cut-off wall presents a higher safety and reliability in aspects of foundations' cutoff in deep overlying strata and it is more applicable. As shown in the case, for an embankment dam with a deep gravel foundation, cut-off wall is more efficient of seepage prevention than jet grouting.

5. ACKNOWLEDGEMENTS

This paper is sponsored by National Key R&D Program of China (grant number 2016YFC0401608) the Nonprofit Industry-Specific Research Project by Chinese Ministry of Water Resources (grant number 201501033) and the International S & T Cooperation Program of China (ISTCP)(grant number 2011DFA72810).

SUMMARY

An embankment is with 30-40m depth of gravel and loams layer. Jet grouting and concrete cut-off wall were implemented in different foundation location for seepage control. Dam seepage observation points were distributed in dam foundation. Seepage-control effect is evaluated by long-term data analysis of dam foundation. Anti-seepage effect of jet grouting is significantly influenced by the condition of the soil layer and it is only suitable for the low water head embankment dam. Cut-off wall presents a higher safety and reliability in aspects of foundations' cutoff in deep overlying strata and it is more applicable. As shown in the case, for an embankment dam with a deep gravel foundation, cut-off wall is more efficient of seepage prevention than jet grouting.

KEYWORDS

EMBANKMENT DAM, FOUNDATION TREATMENT, MONITORING, CUTOFF WALL, GROUTING.

COMMISSION INTERNATIONALE DES GRANDS BARRAGES

VINGT-SIXIÈME CONGRÈS DES GRANDS BARRAGES
Autriche, juillet 2018

DOI 10.3217/978-3-85125-620-8-150



This work licensed under a Creative Commons Attribution 4.0 International License. <https://creativecommons.org/licenses/by-nc-nd/4.0/>

**ASSESSMENT OF HYDRO TASMANIA'S CONCRETE DAMS AND IMPACT
OF UPLIFT**

Richard HERWEYNEN

Principal Consultant - Civil, ENTURA

AUSTRALIA

Tim GRIGGS

Senior Dam Engineer, ENTURA

AUSTRALIA

COMMISSION INTERNATIONALE
DES GRANDS BARRAGES

VINGT-SIXIÈME CONGRÈS DES
GRANDS BARRAGES
Autriche, juillet 2018

ASSESSMENT OF HYDRO TASMANIA'S CONCRETE DAMS AND IMPACT OF UPLIFT

Richard HERWEYNEN
Principal Consultant - Civil, ENTURA

Tim GRIGGS
Senior Dam Engineer, ENTURA

AUSTRALIA

1. INTRODUCTION

Hydro Tasmania is the State-owned generation company for the island of Tasmania, Australia. Hydro Tasmania's power system includes 55 large dams, 30 hydropower stations and two major wind farms and has a total installed capacity of over 2000 MW of hydropower and 300 MW of wind.

Hydro Tasmania's portfolio of dams is ageing, with more than 30 of the dams now more than 50 years old. As a result there has been increased effort to understand the risks associated with this ageing portfolio of dams. Hydro Tasmania has had an active dam safety program since the early 1970s. This program was initially structured around dam surveillance activities; however, in the past two decades risk assessment has become the framework for the program. A full portfolio risk assessment was completed in 2006, which forms the basis for risk-based decision making in relation to dam management.

Hydro Tasmania's dam portfolio consists of a number of different types of dams including a total of 12 concrete gravity dams, ranging in height from 6 m to 49 m.

The portfolio risk assessment, along with an instrumentation monitoring review, resulted in the following findings associated with the concrete dams:

- A key failure mode was overturning or sliding during a flood event, and a key contributing factor to this failure mode was the build-up of uplift pressures under the dam.
- Larger dams were generally designed with a drainage gallery and foundation drain holes to reduce uplift; however, the foundation drain holes were generally of smaller diameter than the industry best practice of 75 mm or more.
- The majority of dams did not include any direct monitoring of uplift and relied on measurement of seepage from drain holes as an indicator of their effectiveness.

A key risk identified was the unknown uplift pressures under the concrete gravity dams, which directly influence stability due to both sliding and overturning. This heightened risk was due to the lack of uplift monitoring, the fact that foundation drains were a smaller diameter than current best practice and the lack of consistent foundation drain cleaning/maintenance since construction.

Based on the outcomes of the portfolio risk assessment and monitoring review, recommendations were made to upgrade both the foundation drainage and the monitoring of uplift at a number of Hydro Tasmania's large concrete gravity dams. The upgrade program of works included:

- Installing piezometers.
- Measuring pressures within the foundation prior to drain cleaning.
- Cleaning of the drains and in some cases increasing the diameter of the drainage holes.
- Ongoing measurement of uplift pressures following drain cleaning.
- Ensure that there was a link between O&M manuals for the dams and the uplift monitoring.

A similar program was also undertaken on Hydro Tasmania's concrete arch dams that range in height from 42 m to 140 m. To demonstrate this program of works, two case studies are provided of the upgrade works undertaken with respect to reduction and monitoring of uplift pressures.

2. TREVALLYN DAM CASE STUDY

2.1. BACKGROUND

Trevallyn Dam is a straight concrete gravity dam that impounds Lake Trevallyn located near the city of Launceston in the north of Tasmania. It is rated as an extreme hazard/consequence category dam. The dam is 33 m high, has a crest length of 178 m and was completed in 1955. It is cast in 15 blocks of up to 15 m in width and it straddles a fault zone which passes diagonally under the dam at its deepest point. Within the dam there is an internal gallery which gives access to the foundation drainage facilities as well as to the control valve for the low level outlets. A two-level free overflow ogee spillway occupies the central 131 m of the crest. Fig. 1 provides a plan and long section of the dam that also shows the location of the drainage gallery and foundation drains.

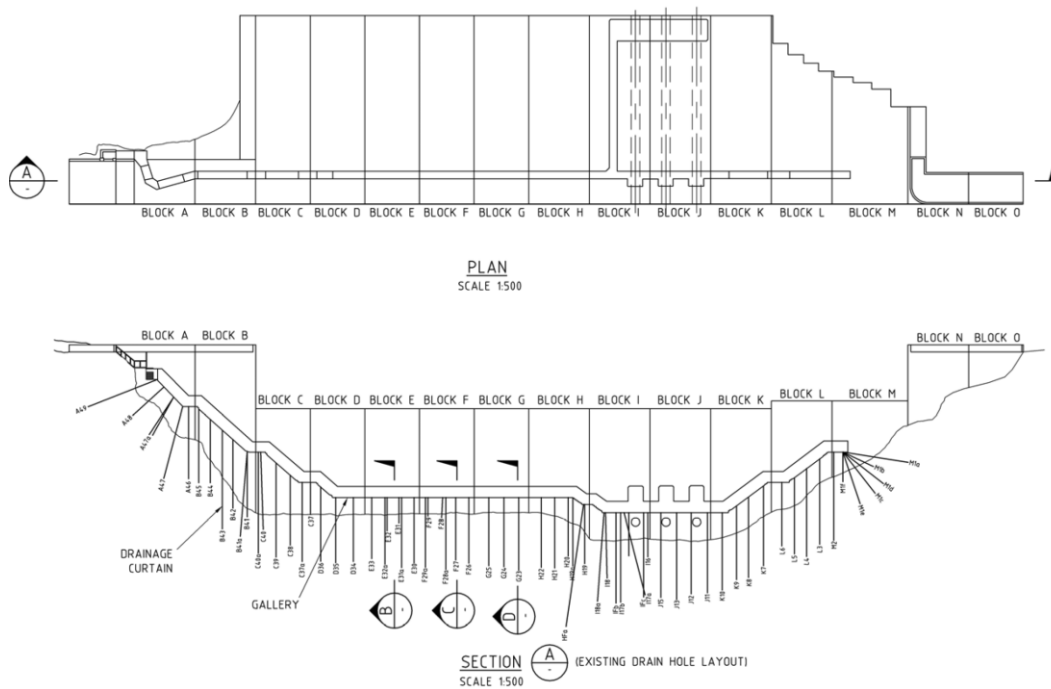


Fig. 1
Trevallyn Dam – Plan and long section

Recommendations were made to upgrade the foundation drainage system by installing new 75 mm diameter drainage holes between each of the existing 50 mm diameter drainage holes. Piezometers were also recommended to be installed at a number of locations across the dam to provide ongoing monitoring of uplift pressures.

The geology of the dam site is dolerite rock with the dominant joint orientation being sub-vertical resulting in columnar sections of rock under the dam. Both the piezometers and the drain holes were therefore orientated in the downstream direction in order to intercept the dominant rock joints.

Piezometer installation was undertaken prior to the foundation drainage upgrade and the uplift pressure monitoring data was reviewed after the works had been completed.

2.2. PIEZOMETER INSTALLATION

Piezometers were installed to monitor the uplift pressure under the dam as shown in Fig. 2. Alternative blocks were selected in order to provide a good coverage of monitoring at an economical price.

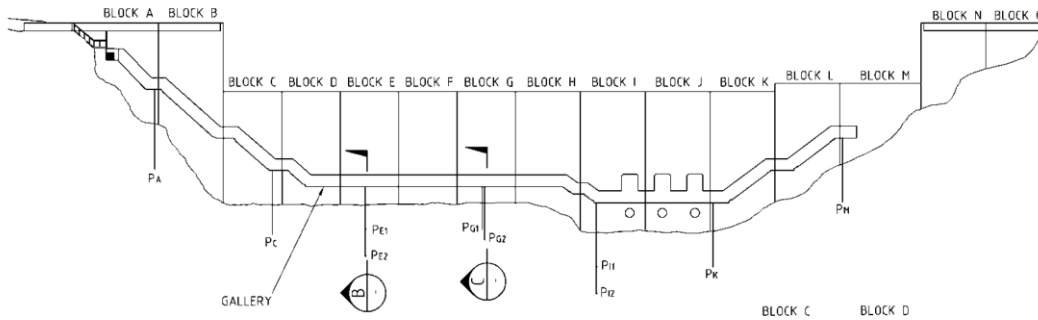


Fig. 2
Trevallyn Dam – Proposed piezometer locations

The following process was followed for the installation of piezometers:

- Holes for piezometers were core drilled and the core was immediately logged by an engineering geologist.
- A dam engineer reviewed the draft core log and provided a mark-up log to indicate the location for the piezometer with the aim of locating the response zone for the piezometer within jointed rock that would be expected to convey seepage and uplift pressures.
- The piezometer was then installed by the instrumentation contractor.

Continuous supervision and logging of the core drilling was a significant portion of the overall cost of the uplift drainage and monitoring upgrade. The supervision and logging was critical to the success of the piezometer installation and this investment was considered necessary in order to have confidence in the monitoring results obtained from the installed piezometers. If this supervision work was not undertaken, there could have been some capital cost savings; however, this would have led to a lack of certainty as to whether the piezometers had been installed in sections of massive rock that would not have exhibited any uplift pressures.

An example of a marked up borehole log that indicated the required position of a piezometer and its response zone is given in Fig. 3. In this example two piezometers were installed in a single hole, with both located in an area that was expected to convey uplift pressures.

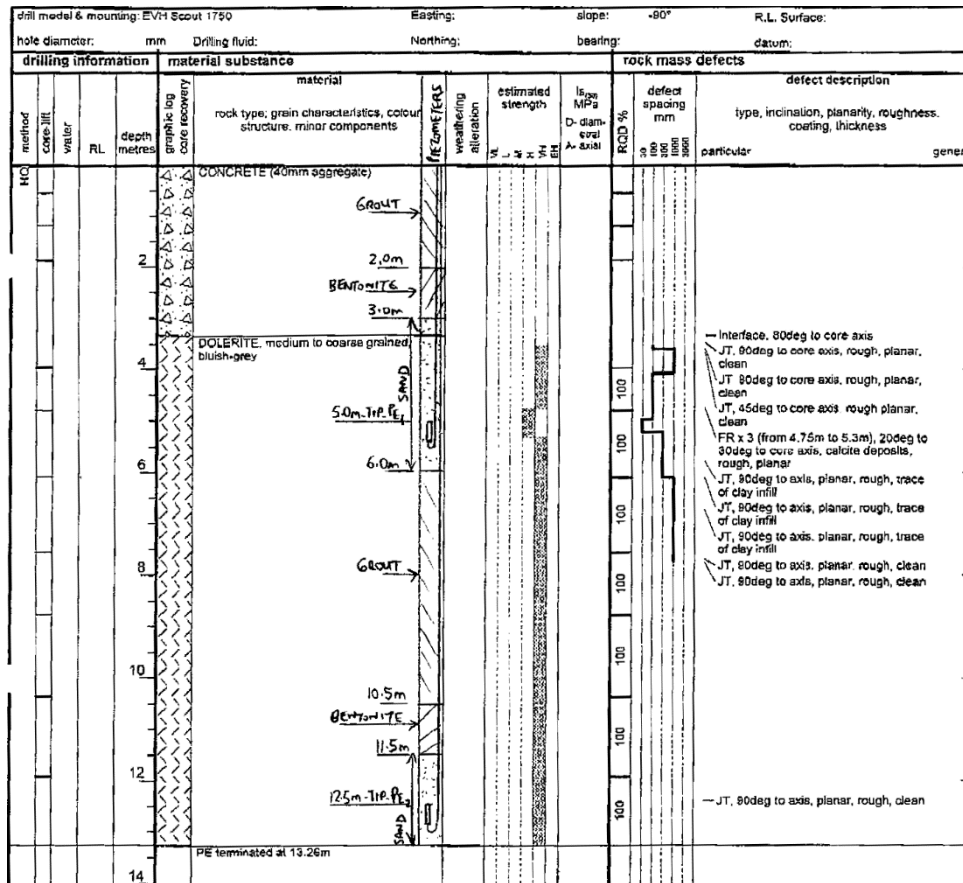


Fig. 3

Trevallyn Dam – Example borehole log showing nominated piezometer location (Pe1 and Pe2)

2.3. REVIEW OF MONITORING DATA

Data collected from the piezometers was reviewed in November 2007 after the piezometer installation and drainage upgrade works had been completed. As background to this review, it should be noted that piezometers were installed and commissioned over the period March–April 2007 and new foundation drainage holes (75 mm diameter) were drilled over the period June/July 2007. The existing foundation drainage holes (50 mm diameter) were flushed with high-pressure water in late July 2007.

An example piezometer plot is provided in Fig. 4. This was for piezometer Pe2 that is the lower piezometer shown in E block in Fig. 2 and Fig. 3. A summary of the findings from this review are given below:

- Prior to drainage hole drilling/flushing, the uplift pressure was measured as near the top of the drainage holes (e.g. at the level of the gallery).

This is below the design assumption of 2/3 reduction of the difference between headwater pressure and tailwater pressure at the line of the drains and therefore indicated that the original foundation drainage was behaving satisfactorily.

- During drainage hole drilling/flushing, the uplift pressures measured by the piezometers reduced by approximately 5 m. This was attributed to the flushing process that resulted in the standing water in the drainage holes being air-lifted out of the holes for a short period. The holes subsequently filled up with water again.
- As a result of the foundation drainage upgrade, it can be observed that the measured uplift pressures have reduced by approximately 0.3 m head from RL 108 to RL 107.7. This could be attributed to the increased drainage efficiency provided by the larger diameter drains.

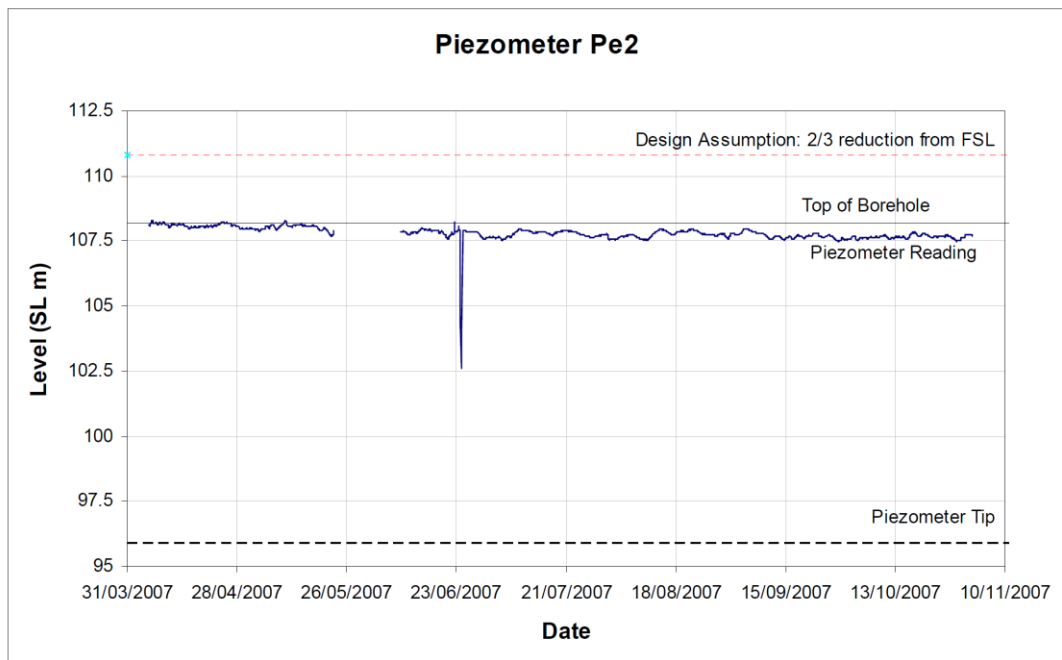


Fig. 4
Trevallyn Dam – Example piezometer plot (Piezometer Pe2)

Other piezometers also generally indicated a similar small reduction in uplift pressures following the installation of new foundation drainage and flushing of the existing foundation drains.

While it could be concluded that the foundation drainage has had minimal effect on uplift pressures, it should be noted that the key failure mode is overturning and sliding during a flood event and it is expected that the larger drainage capacity will be more critical during flood events. As such events are rare, further review and analysis is required to confirm that the upgraded foundation drainage works are adequate to reduce uplift pressures to an

acceptable level. In addition, with the installation of piezometers, there is now greater certainty in relation to the uplift pressures under this dam.

3. CLARK DAM CASE STUDY

3.1. BACKGROUND

Clark Dam is a 67 m high concrete arch gravity dam that impounds Lake King William in the central highlands of Tasmania. Initial construction was completed in 1951 and raising was undertaken in 1964.

As part of the program of works, 12 piezometers were installed from the gallery at locations across the dam in 2011–12. Fig. 5 provides a plan and long section of the dam that also shows the location of the drainage gallery and piezometers.

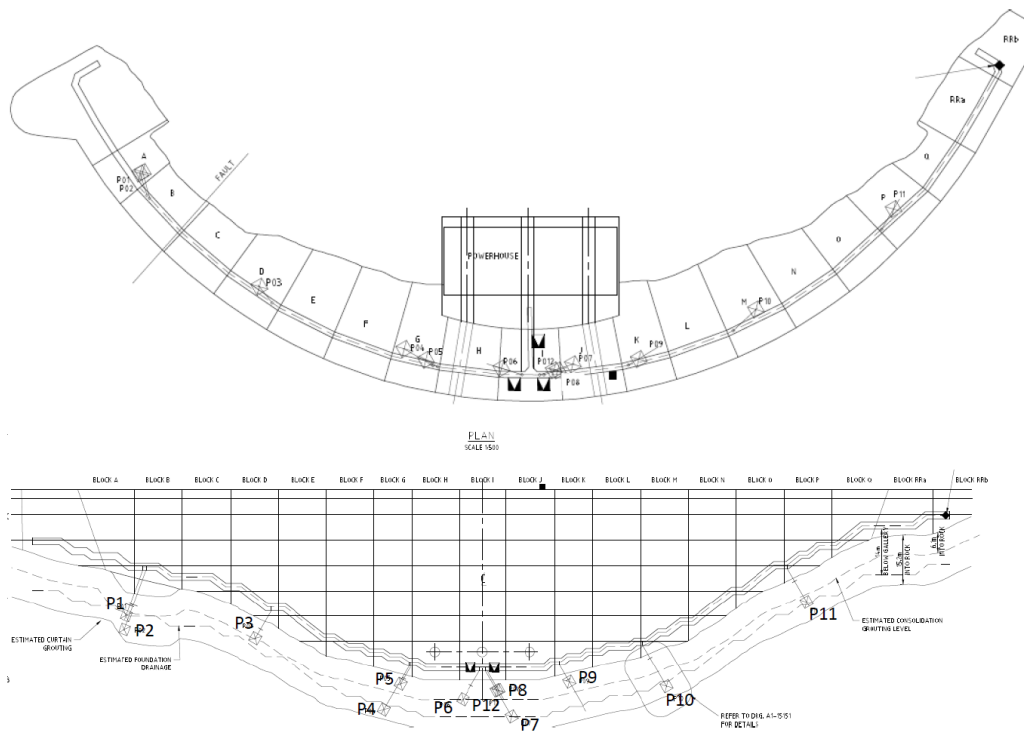


Fig. 5
Clark Dam – Plan and long section

After the piezometers were installed, 95 new drainage holes were drilled from the gallery into the foundation to improve the drainage efficiency. The new drains were 75 mm diameter compared to the existing drain size of 32 mm.

3.2. REVIEW OF MONITORING DATA

A detailed review of the effectiveness of the foundation drainage upgrade was undertaken by monitoring the piezometric pressure before and after the new drainage holes had been drilled. The results of this assessment are provided in Table 1.

Table 1
Clark Dam – Review of foundation drainage effect on piezometric pressure

Piezo	Block	Piezo Level (S.L) (m)	Foundation Level (S.L) (m)	Pressure prior to drain drilling S.L. (m) ^{*2}	Pressure after completion of drain drilling S.L. (m) ^{*2}	Foundation S.L. Pressure Reduction (%)	% of Reservoir Head Before ^{*2}	% of Reservoir Head After ^{*2}
P01	B	676.9	680.9	146.01	140	4.1%	37.7%	35.9%
P02	B	672.7	681	197.9	160.1	19.1%	46.2%	37.2%
P03	D	670.1	673.5	214.1	100.1	53.2%	47.1%	21.9%
P04 ^{*1}	G	648.3	658.3	583.8	617.9	-5.8%	87.1%	88.1%
P05 ^{*1}	G	656.1	658.4	84.6	81.8	3.3%	14.3%	13.1%
P06	I	651.4	656.3	81.8	83.7	-2.3%	12.8%	12.5%
P07	I	646.2	655.7	375.1	330.5	11.9%	54.5%	46.1%
P12	I	654.1	655.7	63.4	64.3	-1.4%	10.4%	10.1%
P08	I	654.2	655.8	77.8	86.2	-10.8%	12.8%	13.5%
P09	K	656.7	657.9	48.5	48.7	-0.4%	8.3%	7.9%
P10	M	655.4	664.6	297.5	170.4	42.7%	49.7%	27.2%
P11	P	681.1	687.5	123.2	110.5	10.3%	35.6%	29.5%

Table 1 indicates that drilling the new drainage holes resulted in an average pressure reduction across the dam of 10%, or 2.5 m of head. The maximum pressure reduction achieved was 53.2%, equating to 11.6 m head relieved from piezometer P03. It is noted that piezometer P04 pressure increased 1% of previous reservoir depth after the works; however, this piezometer had some

installation issues that required removal and subsequent re-insertion which may have increased the pressure slightly.

4. CONCLUSIONS

This paper has outlined the process and reasoning behind upgrade of foundation drainage for Hydro Tasmania's concrete dams.

An important part of the process undertaken was the measurement of foundation pressures before and after foundation drain upgrades/maintenance to quantify the state before and after and the impact of the drainage.

An upgraded drain size of 75 mm was adopted in both case studies with varying results. The foundation drainage upgrade at Clark Dam was noted to be more effective than at Trevallyn Dam. This could be due to the smaller initial drain size at Clark Dam (32 mm diameter) compared to Trevallyn Dam (50 mm diameter) or drain cleaning at Clark Dam being less frequent previously than at Trevallyn Dam.

The data provided in this paper is considered to be of value to the wider dam engineering industry.

REFERENCES

- [1] GRIGGS T. *Hydro Tasmania – Concrete Dams – Review of Monitoring*. Internal report for Hydro Tasmania, 2005.
- [2] JOHNSON L. *Clark Dam Foundation Drain Upgrade – Post-Construction Report and Grout Curtain Defect Investigation*, Internal report for Hydro Tasmania, 2012.

COMMISSION INTERNATIONALE DES GRANDS BARRAGES

VINGT-SIXIÈME CONGRÈS DES GRANDS BARRAGES
Autriche, juillet 2018

DOI 10.3217/978-3-85125-620-8-151



This work licensed under a Creative Commons Attribution 4.0 International License.
<https://creativecommons.org/licenses/by-nc-nd/4.0/>

**RESEARCH AND APPLICATION OF NEW-TYPE MATERIAL IN WUDONGDE
AND BAIHETAN 300M ULTRA-HIGH ARCH DAM - KEY TECH OF
CHARACTERISTICS AND APPLICATION ON LOW-HEAT CEMENT
CONCRETE**

FAN Qixiang

CHINA THREE GORGES CORPORATION, BEIJING

CHINA

LI Wenwei

CHINA THREE GORGES CORPORATION, BEIJING

CHINA

LI Xinyu

POWERCHINA HUADONG ENGINEERING CORPORATION LIMITED,
HANGZHOU

CHINA

COMMISSION INTERNATIONALE
DES GRANDS BARRAGES

VINGT-SIXIÈME CONGRÈS DES
GRANDS BARRAGES

Autriche, juillet 2018

**RESEARCH AND APPLICATION OF NEW-TYPE MATERIAL IN WUDONGDE
AND BAIHETAN 300M ULTRA-HIGH ARCH DAM
----KEY TECH OF CHARACTERISTICS AND APPLICATION ON LOW-HEAT
CEMENT CONCRETE***

FAN Qixiang¹

¹ China Three Gorges Corporation, Beijing

LI Wenwei¹

¹ China Three Gorges Corporation, Beijing

LI Xinyu²

² PowerChina Huadong Engineering Corporation Limited, Hangzhou

Abstract: Ultra high arch dam has higher stress level and requirements in integrity, safety and durability on concrete dam body, it also requires that the dam concrete must have higher strength, impermeability, frost resistance and crack resistance. The low heat Portland cement (P·LH) with high belite content studied for ultra-high arch dam concrete, can effectively reduce the adiabatic temperature rise and improve the crack resistance of the concrete. According to the law of strength and hydration heat influenced by cement compound compositions, suitable content of four major minerals, say, C₂S, C₃S, C₃A, C₄AF and surface area in P·LH cement, was determined, and the relevant standards have been formulated. The concrete applied with P.LH cement standard is characterized as lower water consumption, high strength in late age, lower adiabatic temperature and complicated impermeability. P.LH concrete has been used in Wudongde and Baihetan 300m ultra-high arch dam. The current control results tested have been proven that P.LH concrete quality can meet the technical requirements with Max.temperature within

design limit without temperature crack occurred.

Key words: P·LH cement, dam concrete, temperature control and crack resistance, duration of forms removal, rinsing duration, ultra high arch dam

0. GENERAL

With increase of ultra arch dams constructed or being constructed in China, the dam height is beyond global record, such as Xiaowan(294.5m), Xiluodu(285.5m), the first cascade of Jinping(305m) and Baihetan(289m) together with Wudongde(270m)^[1]. As thin dam body with high stress, compressive strength and durability of concrete, relevantly smaller cementitious ratio and larger unit usage of cementitious material on concrete will cause self-constriction of concrete and temperature shrinkage, and big self-constriction, temperature control and crack resistance are critical. “Moderate heat Portland cement (P·MH) + 35% I fly ash” as cementitious material was generally used in most of 300m high arch dams in China. Although concrete performance can meet the design requirement, the temperature control measures and management have reach current technical limit, and the safe factor can only be greater than 1.8 even in strict accurate management. The temperature crack will occur while careless in the process of implementation, which is harmful to structure safety and impermeability worse to influence the construction duration and investment directly. Therefore, high attention shall be paid to temperature crack resistance of concrete. From the view of the material, it is necessary to research a kind of special low heat Portland cement(P.LH) to own the characteristics of temperature risen slowly, small temperature rise and high performance of complicated crack resistance.

P.LH cement study was started in the regional position in Three Gorges Project, afterwards it has been used in diversion tunnel, flood discharge tunnel and absorption basin in Xiangjiaba, Xiluodu, Wudongde and Baihetan projects. Referring to dam characteristics and tech requirement of Wudongde and Baihetan, further systematic test study and proven consultation^{[2][3]} on P.LH cement have been implemented in the aspects of structure safety, material feature, temperature crack resistance, construction tech and long-term feature. Final decision has been made P.LH concrete will be applied in the two 300m ultra arch dam.

1. SUMMARY OF P.LH CEMENT DEVELOPMENT

C₂S is main component in P.LH cement, which was used in Hoover dam in 30's last century. After Hoover dam completed, concrete strength has increased slowly^{[4][5]}. C₂S content in Hoover dam is 46%^[4] and US national standards ASTM C150 specified the C₂S content should be over 40%^[7]. As lower early strength, difficult production and high cost, P.LH cement was no longer produced and applied in US after 50's and ASTM IV was only remained in US standard list^[8].

C₂S is functioned as lower hydration heat, less water consumption, high step-up strength in late age and well durability, which has incomparable superiority in comparison with C₃S. There are two difficulties existed in traditional calcining process while high C₂S content cement produced, one is how to remain stability of β-C₂S crystal type to prevent transformation to γ-C₂S basically without hydration activation, the other is how to excite C₂S hydration activation to avoid lower early strength in normal ambient temperature, for instance, 7d strength is only 7MPa in accordance with US standard ASTM IV. Breakthrough of high C₂S cement research and production in China were made to realize industrial production and large-scale application with C₂S≥40% as dominant mineral. Chinese standard *Moderate Heat Portland Cement, Low Heat Portland Cement and Low Heat Portland Slag Cement*^[9](GB 200-2003) was published to specify 7d strength of P.LH cement shall be not less than 13MPa.

In the early study and research, consideration has only been taken how to realize higher C₂S content in P.LH. With high C₃A but lower MgO content, P.LH cement was milled finer such that the complicated crack resistance performance would not get obviously different while compared with concrete mixed with P.MH cement^{[16][17]}. It is necessary to optimize P.LH research on the current basis to meet the requirement of ultra arch dam .

2. P.LH CEMENT CHARACTERISTICS APPLIED FOR ULTRA ARCH DAM

The match of clinker's mineral composition, physical performance and overall performance of P.LH cement applied shall be optimized in ultra-high dam .

While C₂S is over 40%, C₃S will be increased properly to ensure that total quantity of silicate mineral is greater than 75% to guarantee a certain early strength. Simultaneously a certain flux mineral(C₃A and C₄AF) shall be existed. In consideration of durability, properly increase C₄AF and decrease C₃A in P.LH cement. Therefore the law of cement strength and hydration influenced by silicate

and flux mineral were researched systematically. Finally it is to ascertain that the available C_3S is 30%~40% and C_2S is 40%~50%. The optimum C_3A is specified under 4% and C_4AF is in the scope of 15%~19%.

A certain chemical shrinkage occurs to cause concrete self-constriction by cement hydration which is seriously critical in low cementitious ratio concrete. The crack risk will easily incur if volume shrinkage and procedure of temperature decrease overlap together. P.MH cement with 3.5%~5.0% MgO was adopted in the Three Gorges Project to improve crack resistance such that the shrinkage can be compensated effectively with well result and concrete was in micro expansion mode while temperature decreased^[18]. In the research of P.LH cement, concrete test in low MgO has ever been conducted and it is resulted that concrete volume constriction became bigger. While other restraints unchanged, concrete volume constriction with P.LH in low MgO obviously became smaller and presented micro expansion. In accordance with relevant research result, concrete volume mixed with P.LH cement in 4.67% MgO is in micro expansion mode^[13], but negative influence to cement strength becomes great while MgO over 5%^[14]. Thus MgO in P.LH cement clinker shall be in the scope of 4.0%~5.0%.

The compressive strength and hydration heat are affected seriously by cement fineness(Fig.1) referring to a great deal of research result. The finer the cement is, the larger the surface area will be, the faster the hydration reacts, the quicker the concrete condenses and hardens to cause high 28d compressive strength and more 3d early hydration heat. Simultaneously not only will the cement cost and water be increased, and more constricted, but also more energy will be needed while milled more finely. The research by the US Bureau of Reclamation indicates concrete frost resistance will become worse while cement was milled finely^[14]. The relationship between cement surface area and RCC frost resistance by Chinese scholars makes clear it is helpful to improve concrete frost resistance while cement surface area reduced^[15]. Surface area of the special P.LH cement applied in ultra arch dam shall be within 340m²/kg in overall consideration of the influence to cement strength and hydration heat, etc.

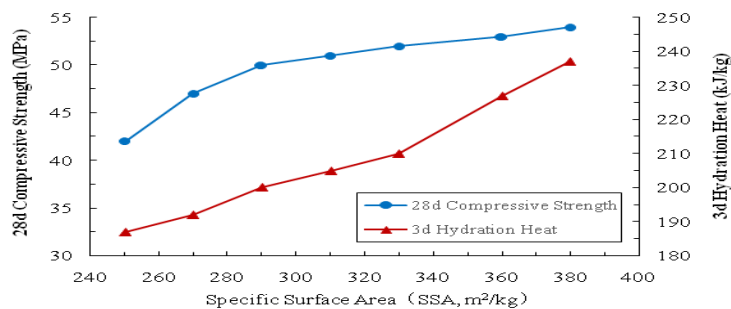


Fig. 1 Effect of specific surface area on compression strength and hydration heat of low heat Portland cement

In accordance with the research above, the mineral composition and chemical components to produce special P.LH cement in ultra arch dam are shown

in Table 1, meanwhile quality acceptance items and index have been put forward in Table 2 to control the quality and stability. For this reason, CTG enterprise standard *Technical Requirement and Test of Low Heat Portland Cement Applied in Arch Dam* (Q/CTG 13—2015) was formulated in Table 2.

Table 1 Composition requirements of specific P.LH used for ultra-high arch dams

Se. No	Mineral composition & chemical component	P·LH requirement in ultra high arch dam(%)	Se. No	Mineral composition & chemical component	P·LH requirement in ultra high arc dam(%)
1	C ₃ S	30~40	4	C ₄ AF	15~19
2	C ₂ S	40~50	5	f-CaO	≤0.8
3	C ₃ A	≤4			

Table 2 Quality requirements of specific P.LH used for ultra-high arch dams

No.	Items	P·LH in Q/CTG13 Index	No.	Items	P·LH in Q/CTG13 Index	
1	SSA5(m ² /kg)	≤340	6	Soundless	qualified	
2	MgO (%)	4.0~5.0	7	Compressive Strength (MPa)	7d	≥13.0
2	Na ₂ O _{eq} (%)	≤0.55			28d	47±3.5
		≤0.50	8	Flexural Strength (MPa)	7d	≥3.5
3	SO ₃ (%)	≤3.5			28d	≥7.0
		≤2.5	9	Hydration Heat (kJ/kg)	3d	≤220
4	Setting time	Initial set(min)			7d	≤250
		Final set(h)			28d	≤300
5	Loss on ignition(%)	≤3.0				

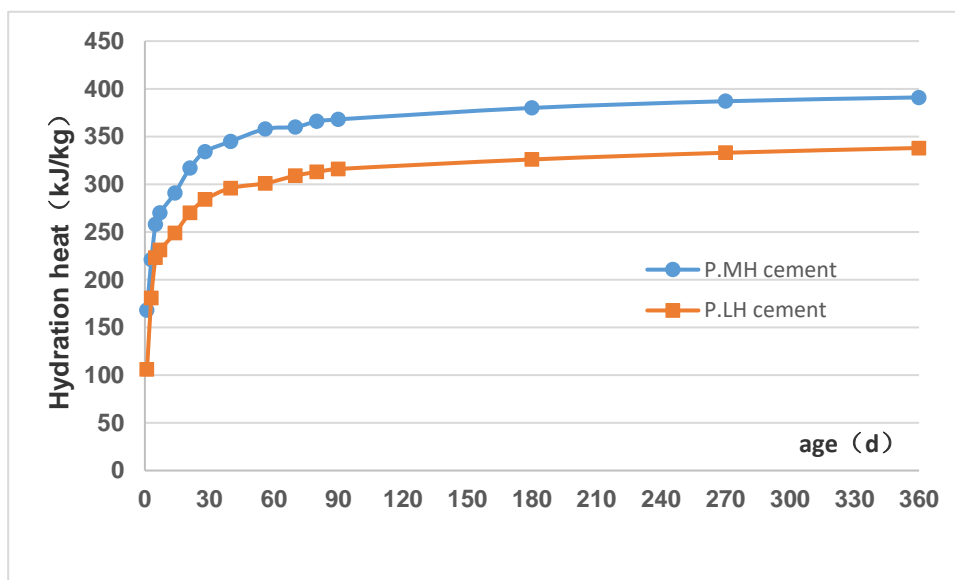


Fig.2 Development of hydration heat of P.LH and P.MH

The comparison of long-term hydration heat has been tested and the result is that P.LH cement has such characteristics of slow hydration release, small peak heat release ratio, low early hydration and lower later-aged hydration than P.MH cement, which the hydration heat of 1d, 3d, 7d, 28d and 360d is only 63%, 82%, 84%, 85% and 86% of the same age. Fig.2 is the developing law of hydration heat between P.MH and P.LH cement.

After many time of industrial production, control point and key parameter were specified during the overall production procedure, and accurate quality management system of P.LH production from quality control and mixture of raw material, calcing and milling of clinker have been established, which mass production have been realized in many cement factories in China.

3. P.LH CONCRETE CHARACTERISTICS OF ULTRA ARCH DAM

In order to ascertain P.LH cement performance, systematical comparison tests have been implemented between P.MH and P.LH cement relying on Wudongde and Baihetan ultra arch dam projects. The research shows that P.LH concrete have such following characteristics of slow early-aged strength and temperature rise developed, high later-aged strength and lower final temperature rise. The concrete mix ratio and performance test of batching mass between P.MH and P.LH are compared in Table 3 while C₁₈₀40 concrete taken from Baihetan ultra arch dam. The test result shows that major parameters are nearly the same, but only early-aged duration has 2h delay and final-aged duration has 7h delay.

The compressive strength and splitting tensile are shown in Table 4 and C₁₈₀40 concrete changing law of the compressive strength are shown in Fig.3.

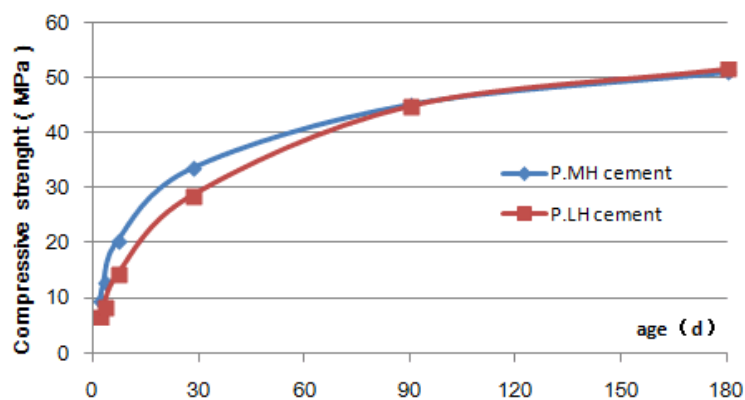


Fig.3 Compressive strength of C₁₈₀40 concrete

Table 3 Mix proportion and fresh properties of C₁₈₀40 concrete

Cement type	Water consumption/(kg/m ³)	cementitious ratio	Fly ash(/%)	Sand(/%)	Admixture(/%)		Slump/mm	Air content(/%)	Consolidation age/(h:min)	
					Water reducer	Air entraining agent			Initial	Final
P.LH	82	0.42	35	23	0.60	0.065	47	4.8	11:07	20:40

Table 4 Compressive strength and splitting tensile strength of C₁₈₀40 concrete

Cement type	Compressive strength(MPa)						Splitting strength(MPa)					
	2d	3d	7d	28d	90d	180d	2d	3d	7d	28d	90d	180d
P.MH	9.4	12.7	20.4	33.5	45.1	50.9	0.73	1.05	1.55	2.17	3.08	3.50
P.LH	6.6	8.3	14.3	28.6	44.9	51.6	0.56	0.75	1.19	2.13	3.01	3.58

Both can meet the design requirement and P.LH compressive strength ahead of 28d is lower than P.MH concrete, the compressive strength is nearly the same at 90d, but 180d compressive strength is greater than P.MH concrete. The increase magnitude of P.LH concrete strength in later age is greater than P.MH.

The ultimate tensile strain and static compressive modulus of elasticity of C₁₈₀40 concrete are shown in Table 5, which are nearly the same as changing law lasted and compressive strength.

Table 5 Ultimate tensile strain and static compressive modulus of elasticity of C₁₈₀40 concrete

Cement type	Ultimate tensile strain $(\times 10^{-6})$				Compressive modulus of elasticity/(GPa)					
	7d	28d	90d	180d	2d	3d	7d	28d	90d	180d
P.MH	72	96	118	121	23.4	26.7	31.4	35.6	39.2	42.5
P.LH	65	93	120	122	21.2	23.1	29.3	35.5	42.7	44.6

The time-lasted difference curve of adiabatic temperature rise are shown in Fig.4. The result is that 28d adiabatic temperature rise as same strength and cementitious ratio level of P.LH concrete is lower than the one of P.MH concrete, and the difference at 2d age is 5.0℃ then to reduce gradually, so is 2.6℃ at 28d age which indicates heat of P.LH concrete in early age release slowly with low adiabatic temperature rise to benefit control concrete Max.temperature effectively.

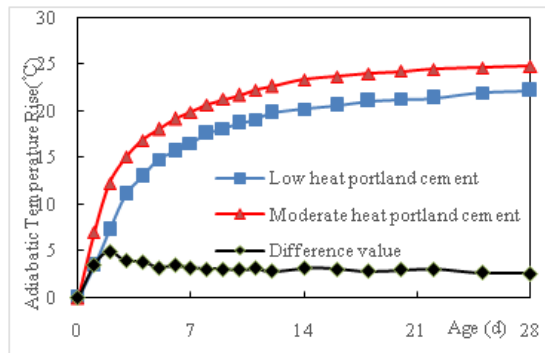


Fig.4 Adiabatic temperature rise of C₁₈₀40 concrete

The frost resistance and impermeability both are nearly the same which can reach F₉₀300 and W₉₀15 respectively with large margin.

P.LH concrete strength, deformation and durability have been tested in Wudongde and Baihetan site sample, the features and developing law mentioned-above in research stage have been witnessed in consistency with test result to meet the design requirements.

4. P.LH CONCRETE CONSTRUCTED IN ULTRA ARCH DAM

Concrete placement in Wudongde and Baihetan arch dam was started on March 16, 2017 and April 12, 2017 respectively, the stable construction process has been formed in these two 300m high arch dam.

4.1 Concrete transportation, pave and vibration

The concrete is transported dumper and poured by chute through cable crane. After concrete poured, concrete will be leveled immediately and vibrated , and manual vibrator will be used in partial corner and reinforcement steel area. In accordance with the site P.LH concrete application, it is well for workability, easy vibration with tiny aggregate segregation and bleed in these two dam, and it is tight from site core sample with high quality.

4.2 Rinse time

The optimum principle is to completely rinse cream in the placement area, tiny expose raw sand and wash cleanly in 32h~36h after pouring. The standard rinsed on transverse joint is in cream rinsed completely, micro exposition of coarse sand and cleanliness generally 10d after cast. The optimum rinse time of P.MH concrete is 16~20h after pouring, the optimum rinse time of P.LH concrete is 14~16h delay while compared with P.MH concrete.

4.3 Time of forms removal

Time of forms removal have been test at 26h, 30h, 38h, 42h and 48h after concrete cast, it is ascertain that the time of forms removal is 42h~48h to guarantee smooth appearance. The time of forms removal for P.MH concrete is 24h after cast, the time of forms removal for P.LH concrete is 18h~48h delay while compared with P.MH concrete.

4.4 Construction time-schedule

Although the rinse time and forms removal are a bit lag 2d after poured, there is no influence to the construction time-schedule even if 1d~2d delay as 7d~10d is required for the next concrete placement preparation which is in the construction time interval. As the rinse to the transverse joint is later, it is witnessed the application of P.LH concrete makes no influence to the construction time-schedule in comparison with the application of P.MH concrete.

5. TEMPERATURE CONTROL EFFECTS OF P.LH DAM CONCRETE

In the procedure of P.LH concrete construction, the intelligent temperature system, such as pre-cooled concrete, intelligent water supply and surface heat preservation are applied.

The secondary air-cooling plus mixing with ice are used in batching system of concrete and the concrete temperature at outlet of the batching system will be adjusted dynamically in accordance with the ambient and concrete temperature poured. Simultaneously, full close heat preservation dumper are adopted for transportation to improve efficiency and accelerate concrete pouring so as to reduce temperature recovery during transportation.

The layer covering time in concrete placement shall be controlled within 4h to decrease temperature recovery, and 2cm thick canvas quilt for heat preservation shall cover to prevent the concrete from temperature flowed backward and air-dry of the surface aggregate. 2h before concrete pouring, mist will sprayed to decrease temperature while temperature in the concrete pouring area in sunshine is over 23℃ (or greater than 28℃ without sunshine). After concrete finished, mist spray shall be continued for curing and it will be changed to spun spray for curing to form flowing water film. In transverse joint and upstream and downstream surface, flower pipe is adopted for curing. 4cm thick urethane foam is coat over the upstream surface and 3cm thick polystyrene extrusion plate is pasted over the downstream surface for annual heat preservation.

In order to guarantee the temperature less than the presettings during water cooling, the Max. temperature will be preset as 2℃ according to Max. Temperature to adjust water temperature and flow, and 0.5℃/d temperature decrease shall be controlled after the temperature reaches peak value. The temperature control principle is small temperature difference and early cooling. The cooling pipe is always full of water after pipeline laid in the concrete placement area, and the cooling water will be changed into intelligent cooling water control system directly after concrete finished.

The result measured shows: it takes 5~10 days to the Max. value in low temperature season. it takes 4~8 days to the Max.value in high temperature season. The average temperature of concrete in the placement area shall be controlled in 24.1℃~26.4℃ which is lower than 27℃ designed as the Max. allowable temperature. There is no temperature crack fund till now.

It is known from the site practice that the Max. temperature of concrete can be more easily controll while adoption of P.LH concrete and the temperature control measures maybe be still optimized.

6. CONCLUSION

From current quality data checked in site, well effect applied of P.LH concrete has been got.

(1) P.LH concrete applied in these two arch dams has meet the requirements specified in CTG enterprise standard with stable quality.

(2) The mixing ratio of 4 grade concrete with unit water consumption is only $79\text{kg}/\text{m}^3\sim 83\text{kg}/\text{m}^3$.

(3) The concrete mix can fulfill the construction specifications, and site core test of concrete strength, ultimate extension and durability is in consistency with design requirements.

(4) The core sample has tight appearance, smooth distribution of aggregate without visible layer joints with construction quality controlled.

(5) The concrete Max. temperature has been controlled in the allowable scope designed without temperature crack and with sufficient safe margin till now to show that P.LH concrete is stronger for crack resistance.

(6) It is still required to grasp the law and mechanism of P.LH concrete, accumulate more experience and adjust temperature control measure if available to make it better for P.LH concrete to apply.

References

- [1] JIA Jinsheng, YUAN Yulan, ZHENG Cuiying, et al. Dam construction in China: Statistics, progresses and concerned issues [J].Water Power, 2010,36(1):6-10. (in Chinese)
- [2] LI Wenwei, FAN Qixiang, LI Xinyu, et al. Development and application of specific low heat portland cement for building ultra-high arch dams [J]. Journal of Hydroelectric Engineering, 2017, 36(3): 113-120
- [3] FAN Qixiang, LI Wenwei, LI Xinyu. Key construction technologies of low heat Portland cement dam concrete [J]. Journal of Hydroelectric Engineering, 2017, 36(4): 11-17
- [4] Bartojay K, Joy W. Long-term properties of hoover dam mass concrete[C]// Wiltshire R L, Gilbert D R, Rogers J R. Hoover Dam 75th Anniversary History

- Symposium, Las Vegas, Nevada, United States, 2010:74-84.
- [5] Dolen T P. Materials properties model of aging concrete[R]. U.S. Department of the Interior, Bureau of Reclamation, 2005.
 - [6] Dolen T P. Advances in mass concrete technology — The Hoover dam studies[C]// Wiltshire R L, Gilbert D R, Rogers J R. Hoover Dam 75th Anniversary History Symposium, Las Vegas, Nevada, United States, 2010:58-73.
 - [7] Standard Specification for Portland cement: ASTM C150/C150M-2016. [S].
 - [8] Concrete manual [M]. 8th ed. Revised Reprint. United States Department of the Interior Bureau of Reclamation, 1981.
 - [9] Moderate heat portland cement, low heat portland cement and low heat portland slag cement:GB200—2003 [S]. Beijing: Standards Press of China, 2003. (in Chinese)
 - [10] LI Jinyu, PENG Xiaoping, CAO Jianguo, et al. Research of high Belite cement dam concrete with low heat and high crack resistance [J]. Journal of the Chinese Ceramic Society, 2004, 32(3):364-371. (in Chinese)
 - [11] LI Jinyu, PENG Xiaoping, SUI Tongbo, LI Wenwei. Study on low-exothermic and high crack-resisting dam concrete with HBC [J]. Water Power, 2003, 29(3):10-14. (in Chinese)
 - [12] CHEN Wenyao, LI Wenwei. Remark on autogenous volume deformation of MgO content cement concrete [J]. Journal of Yangtze River Scientific Research Institute, 2008, 25(4):77-80. (in Chinese)
 - [13] ZHONG Yihui. Study on low heat Portland cement with micro expansion property [J]. Design of Hydroelectric Power Station, 2015(1):88-92. (in Chinese)
 - [14] MA Zhongcheng, YAO Yan, WANG Xianbin, et al. Preparation and performance of high-magnesia moderate heat cement [J]. Journal of Wuhan University of Technology, 2014,36(9):1-6.(in Chinese)
 - [15] Cai YB, Shi Q, Ding JT, et al. Relationship between specific surface area of cement and crack resistance of RCC [J].The Indian Concrete Journal, 2010, 84(1):9-13.

COMMISSION INTERNATIONALE DES GRANDS BARRAGES

VINGT-SIXIÈME CONGRÈS DES GRANDS BARRAGES
Autriche, juillet 2018

DOI 10.3217/978-3-85125-620-8-152



This work licensed under a Creative Commons Attribution 4.0 International License. <https://creativecommons.org/licenses/by-nc-nd/4.0/>

REHABILITATION OF THE CENTER HILL EMBANKMENT DAM

Peter BANZHAF

Head Dam Services, BAUER SPEZIALTIEFBAU GMBH

GERMANY

COMMISSION INTERNATIONALE
DES GRANDS BARRAGES

VINGT-SIXIÈME CONGRÈS DES
GRANDS BARRAGES
Autriche, juillet 2018

REHABILITATION OF THE CENTER HILL EMBANKMENT DAM

Peter Banzhaf

Head Dam Services, BAUER SPEZIALTIEFBAU GMBH

GERMANY

1. INTRODUCTION

The US Army Corps of Engineers (USACE) in the USA is, amongst others, responsible for the surveilling and maintaining of dams. One of these structures is the Center Hill Dam in Tennessee, built in the 1940ies as a combination of a concrete gravity dam and a connected embankment dam. The structure is used for flood control of the Caney Fork River up to the town of Nashville and to generate electricity with a associated power station.

The subsoil mainly consists of karstified limestone. The karstification resulted in water conductivity below the dam soon after the filling. Several grouting measures were not able lastingly sealing these permeabilities. At the beginning of this century, not only damp spots occurred at the embankment dam but also major sinkholes opened up at the left abutment.

Subsequent examinations led to the decision to install a permanent concrete cutoff wall as a sealing-barrier in the until then coreless embankment dam and to permanently tie this cutoff wall to the existing concrete gravity dam. Due to dam safety reasons, an encasement wall for temporary use was specified to prevent uncontrolled trench collapse in case of sudden slurry loss into undetected voids during execution of the cutoff wall. Within this encasement wall, the permanent barrier wall was installed.

Beginning in 2011, BAUER Foundations Corp. (BFC) was tasked by the USACE with the installation of a seepage barrier/cutoff wall at the Center Hill Dam Foundation Remediation project.



Fig. 1 Site overview 2014 – Slurry Plant, BG 50 Drill-rig and MC128 with BC50 Hydrocutter

The executed features of work include the installation of two walls. The first wall, an encasement wall, extends vertically through the clayey embankment and is embedded into the underlying bedrock to provide embankment stability during the construction of the second wall, the barrier wall. The encasement wall is constructed of overlapping panels outstanding 2.25 m wide and up to 64 m deep. The second wall is the seepage barrier and provides a continuous wall, nominally 0.6 m wide, consisting as well of overlapping panels. The barrier wall extends through the concrete encasement wall into the underlying bedrock and is up to 93 m deep. BAUER BC40 and BC50 hydrocutters (Fig. 1) mounted on BAUER MC96 and MC128 foundation cranes were used to perform the majority of the works. Excavations were performed using bentonite slurry (encasement wall) and water (barrier wall) as supporting fluid and concrete was poured with the tremie method. Adding to the challenges, the project had to be executed in an environmentally sensitive area.

2. GEOLOGY AT THE DAM

Based on the Geotechnical Baseline Report (USACE 2011), the right rim of the Caney Fork River is characterized by a steep rock slope, while the left rim rises more gently about 70 m from the riverbed to the crest of the earthen embankment. The earthen embankment section of the dam wraps around the left end of the concrete dam assembled by twenty-nine monoliths and extends about 260 m at the crest to its end at the intersection with the left rim. The

earthen embankment consists of compacted fill made of impervious silty clay and clayey silts.

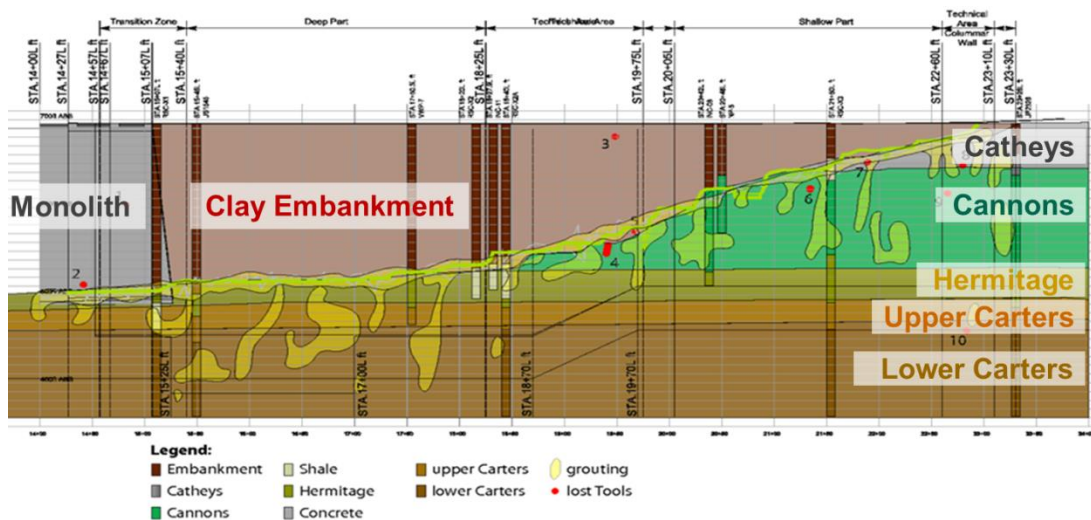


Fig. 2 Geological profile in the wall alignment including areas of high grout takes (upstream view)

The embankment was constructed directly on the existing overburden after topsoil was stripped. The alluvium is underlain by the flat lying Catheys, Cannon and Hermitage formations, with the Hermitage being underlain by the non-daylighting Carters and Lebanon formations (Fig. 2). The Cannon formation is massive bedded, all other formations are thin bedded or medium to thin bedded. The unconfined compressive strength of the rock was up to 220 MPa in the Cannons with formation averages ranging between 50 and 190 MPa.

Physical evidence of karst is visible throughout the site including disappearing streams, sinkholes, caves and extensive solution features. Bedding planes and vertical fractures have the potential to form interconnected systems of open features. These systems are especially threatening if they reach the embankment, creating piping features in the soil rock interface and potentially causing an erosion failure of the embankment.

3. PRIOR REMEDIATIONS

A grout curtain was installed during the original construction of the dam. Later, after several potentially unsafe conditions were detected in the late 1970's, a further grout curtain was installed about 3 m downstream of the embankment centerline through the embankment into the bedrock from 1982-1984. Finally, in order to reduce seepage through the bedrock and in order to allow for a safe

Barrier Wall construction, grout curtains were installed 3.6 m upstream and downstream of the wall alignment from 2009 to 2010.

4. REMEDIATION BY A CONCRETE BARRIER WALL

4.1. ENCASUREMENT WALL FOR DAM SAFETY

Trenches excavated during barrier wall construction had the potential to intersect open solution features and connect the slurry-filled trench with the reservoir or the tail water and in this way cause a sudden and substantial loss of fluid. Apart from the environmental impact, such a fluid loss could destabilize the excavation trench and therefore put the dam embankment at risk. To address such a risk, an encasement wall was built that extends from the crest of the dam down to a minimum of 0.6 m into the foundation bedrock. In this configuration, the encasement wall would support the embankment by bearing earth and water pressure in the event of trench fluid loss, protecting both the embankment and the excavation equipment. The encasement wall was installed using three different approaches ().

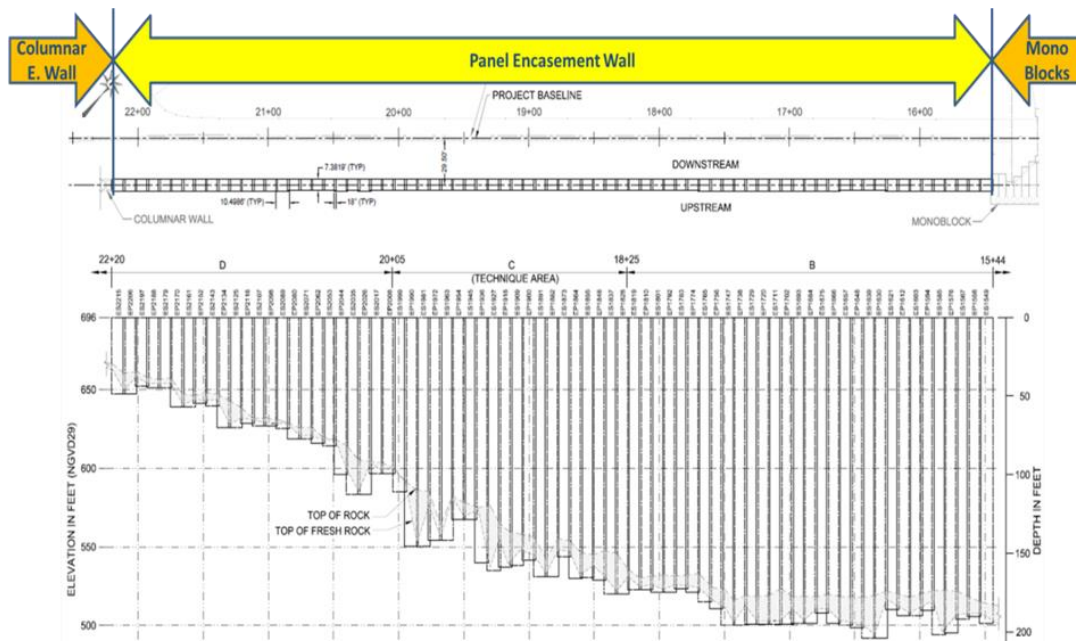


Fig. 3 As build Encasement wall panel layout.

4.2. COLUMNAR ENCASEMENT WALL

In the shallow section at the left rim, about 36 m long, the encasement wall was specified and designed as a columnar wall consisting of 2.3 m diameter and up to 11 m deep unreinforced concrete columns. The columns were excavated under dry conditions using fully cased Kelly drilling by a BAUER BG 50, the most powerful rotary drilling rig made by BAUER at the time, capable of delivering a maximum torque of 468 kNm.

4.3. MONO BLOCKS

In order to tie-into the existing concrete dam monolith at the upstream face, the barrier wall runs parallel to the existing dam for approximately 14 m, which resulted in a section of the encasement wall in close proximity to the sloped upstream side of the concrete dam. This creates a wedge of embankment soil between the barrier wall and the existing dam. BFC decided to fully replace this wedge of soil with a special encasement wall. This was achieved by a series of seven, 2 m wide, 5.5 to 8.2 m long and up to about 60 m deep multi-bite panels called mono blocks, which touch each other along the long side (Fig. 4).

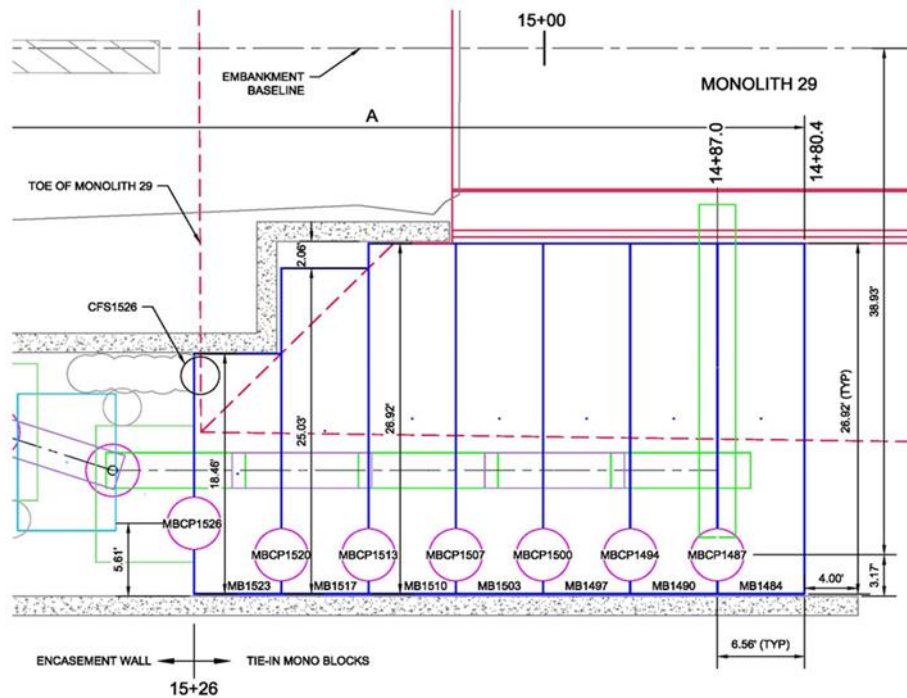


Fig. 4 Layout of Mono blocks

4.4. PANEL ENCASEMENT WALL

The 210 m long main section of the encasement wall was excavated in 3.2 m long panels reaching depths of over 60 m (). Each primary panel was pre-excavated using a hydraulic grab mounted on the MC 96. After pre-excavation of the secondary panels by the onsite available BG50, the element was fully excavated using a BC 50 hydrocutter mounted on a BAUER MC 128 foundation crane. All excavations were performed under bentonite slurry-support. Concrete was placed via two tremie pipes per panel.

The technical specifications (USACE 2011) [2] called for tolerances of 0.25% maximum panel verticality deviation, maximum six degrees panel rotation (twist) and a minimum 0.15 m overlap between primary and secondary panels throughout the full width and depth of the wall. To achieve these goals the cutter needs to be steered, which requires both precise information about the actual position of the tool with respect to design and steering capabilities.

5. BARRIER WALL INSTALLTION

5.1. COLUMNAR BARRIER WALL

BFC's design consisted of twelve 1.22 m diameter primary columns up to 57.3 m deep, and eleven 1.37 m diameter secondary columns up to 56.7 M deep. Downhole water hammers, Wassara W150 and W200, in conjunction with a Klemm KR 806-4 drilling rig were used to drill the pilot holes. All but two pilot holes (maximum verticality 0.35%) achieved the verticality tolerance of 0.25%. Due to the active steering during drilling by means of a bent sub, a piece of drill string with a slight angle to put the hammer at an angle to the borehole axis, the maximum deviations out of plumb were observed above final depth. After final excavation, the pilot holes were tremie-grouted with flowable fill.

BFC used rock augers and drilling buckets, both equipped with stingers (extended pilot bits) to follow the pilot hole, to excavate the columns. Drilling was performed dry at the top and under water at depth with the BG 50. One tremie pipe was used to place the concrete. Geometry surveys were performed using BAUER's proprietary Drilling Inclination System (DIS) and the Koden and SoniCaliper methods with the Koden data being used as as-built data set. Two secondary elements had to be reamed to a diameter of 1.45 m to meet the 0.61 x 0.15 m overlap requirement at all investigated 1.5 m depth intervals.

5.2. PANEL BARRIER WALL

In their proposal, BFC followed the specifications [2] and proposed a hybrid wall configuration (primary columns and secondary diaphragm wall panels). The columns in the USACE plan were designed to provide additional wall thickness at the panel overlaps due to USACE concerns that the required vertical and rotational accuracies would be difficult to achieve at more than 90 m depth. However, based on the ability of the BAUER hydrocutter to excavate the hard rock and maintain excellent verticality as demonstrated at the panel encasement wall, BFC made a value engineering cost proposal (VECP) to eliminate the columns (red circles in Fig. 5) without increasing the nominal overlap between the barrier wall panels. The government accepted the VECP.

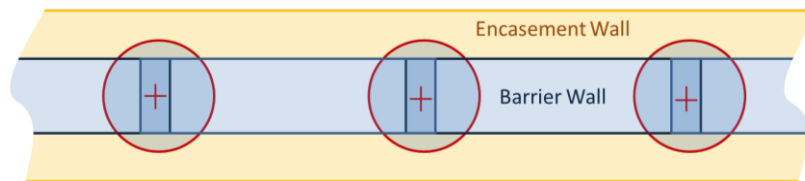


Fig. 5 Hybrid wall as specified

The barrier wall was excavated through the encasement wall concrete into the foundation rock to depths between 44 m and 93 m using two BAUER Hydrocutter. Water was used as trench support and transport fluid. Concrete was again placed using two tremie pipes. Cores and borehole images showed that the use of water as fluid in conjunction with a rigorous joint cleaning procedure allowed for an excellent bond between the primary and secondary panels.

6. TIE-IN CONNECTION TO THE CONCRETE DAM

6.3. TASK TO CONNECT TO THE CONCRETE DAM

Specified was to construct a positive, continuous, full height, water-tight, connection between the encasement/barrier wall and the concrete dam [2]. The tie-in had to accommodate the sloping surface of the concrete monoliths providing a seal along the monolith to prevent floodwaters from circumventing the joint seal with the monolith. A minimum embedment of six (6) inches and a maximum embedment not exceeding four (4) feet had to be met.

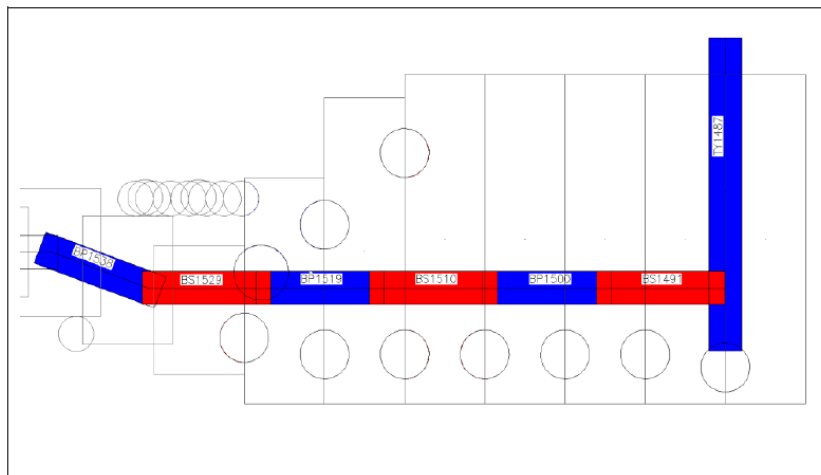


Fig. 6 Layout of barrier wall panels along the monolith 29 with perpendicular tie-in-panel element TY1487.

After installation of the special encasement wall mono blocks adjacent to each other at the upstream side of the existent concrete dam (see chapter 4.3), the joints between individual mono blocks were closed by closing piles to assure the specified function of the encasement wall.

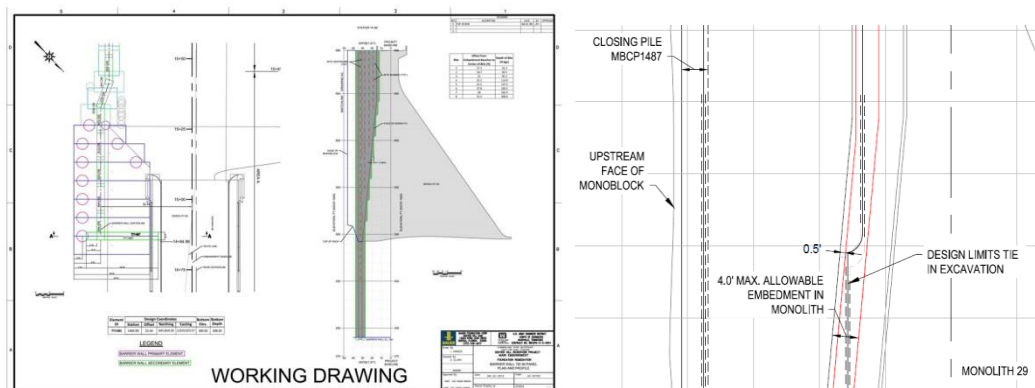


Fig. 7 Tie-in detailed design by BAUER

During the installation of the mono blocks (MB) and mono block closing piles (MBCP) construction data and quality control data had been examined and after acceptance the elements excavated and concreted. Based on these construction and quality control data and the barrier wall construction practices as proven during the installation of other elements in the main barrier wall earlier accepted to be sufficient, permission was granted to install the six typical barrier wall panels (Fig. 6) in the area along the concrete dam for the following reasons:

- All mono blocks and mono block closing piles excavations have held bentonite slurry or water without appreciable fluid loss during their construction.
- Video footage taken in mono block closing pile excavations of the mono block-to-mono block joints, and the rotated cutter panel-to-mono block joints indicate relatively tight joints between adjacent elements.

- Data from verification boring indicate homogeneous concrete from top to bottom, and a clean concrete-to-rock contact.
- Only the tie-in element TY1487 was constructed differently.

The tie-in element TY1487 perpendicular to the concrete dam (Fig. 6) was installed as a primary element with a trench cutter using several bites. The first bite was furthest away from the concrete monolith and was cut to the foundation level of the concrete dam. The cutter was controlled lowered to defined depths cutting into the concrete of the monolith. Guidance was assured by the standard cutter guide frame at the top. After cutting the other bites from top to down into the monolith, finally at the position of the first bite, the cutter was lowered and excavated to the specified final depth. Due to this sequencing, the cleaning of the bottom of the element TY1487 was assured.

SUMMARY

The risks associated with failure of Center Hill Dam were significant and urgent which prompted the USACE to address this risk producing a remediation program of unprecedented scope with stringent specification requirements. Execution of the remediation provided many lessons learned for the USACE and BFC and the project achieved great technical success.

In spite of strict specification requirements, BFC met or exceeded the required plans and specifications with a value engineering approach that also resulted in significant cost savings to the government. BFC was able to achieve this using innovative techniques and equipment for diaphragm wall construction that allows for extremely accurate excavations in very challenging geologic conditions.

It was observed that for the steered hydrocutter excavation the maximum deviations out of plumb – like the maximum panel rotations – typically occur well above final excavation depth since corrections are made during drilling or excavation. The maximum deviation is not a function of depth but the system-inherent result of survey accuracy and steering capabilities. For this reason, the verticality tolerance for deep cut-off walls installed with steerable techniques should be specified as an absolute value similar to rotation and not as a percentage of depth.

The challenging tie-in connection to monolith 29 of the existent concrete dam executed successfully proved, that such connections are feasible. Connecting perpendicular was required due the highway running across the dam. Contractor detailed designed and execution achieved the specified task.

REFERENCES

- [1] ARNOLD M., FAULHABER B.. Cutoff Wall Construction for Center Hill Dam Foundation Remediation, 2017.
- [2] USACE (United States Army Corps of Engineers). Center Hill Foundation Remediation, Solicitation, Amendments, and Technical Specifications, 2011.

KEYWORDS – ENGLISH

CUTOFF WALL, CONCRETE DAM, DIAPHRAGM WALL, EMBANKMENT DAM, TIE-IN

KEYWORDS – FRENCH

MUR PARAFUILLE, BARRAGE EN BETON, PAROI MOULEE, BARRAGE EN REMBLAI, LA VISÉE

COMMISSION INTERNATIONALE DES GRANDS BARRAGES

VINGT-SIXIÈME CONGRÈS DES GRANDS BARRAGES
Autriche, juillet 2018

DOI 10.3217/978-3-85125-620-8-153



This work licensed under a Creative Commons Attribution 4.0 International License. <https://creativecommons.org/licenses/by-nc-nd/4.0/>

REMEDIAL GROUTING FOR EMBANKMENT DAM CORE SEALING – 10 YEARS EXPERIENCES

DongSoon PARK

¹Principal Researcher, K-water Convergence Institute, K-WATER

REPUBLIC OF KOREA

Hee-Dae LIM

Professor, Department of Civil Engineering, CHUNGNAM UNIVERITY

REPUBLIC OF KOREA

COMMISSION INTERNATIONALE
DES GRANDS BARRAGES

VINGT-SIXIÈME CONGRÈS DES
GRANDS BARRAGES
Autriche, juillet 2018

REMEDIAL GROUTING FOR EMBANKMENT DAM CORE SEALING – 10 YEARS EXPERIENCES

DongSoon PARK¹, and Hee-Dae LIM²

¹*Principal Researcher, K-water Convergence Institute, K-WATER*

²*Professor, Department of Civil Engineering, CHUNGNAM UNIVERSITY*

REPUBLIC OF KOREA

1. INTRODUCTION

To address problematic seepage from existing dams, a grouting method can be applied to the deteriorated core layers without reducing the reservoir's water level. Remediation grouting for sealing of aging embankment dam cores has been known as effective, however, no standardization is at present and publication of case histories are rare. Applying remediation grouting directly to the embankment is technically challenging. For remediation grouting of dam core layers, the main purpose should be the improvement of core impermeability. Therefore, it is not desirable to use pressure-type grouting methods such as jet grouting, vibro-type compaction grouting, rock-mass pressure grouting, etc.

For remedial grouting of embankment dam cores, a different design concept is required comparing to typical dam foundation or coffer dam grouting. It should satisfy the opposite conditions, which are the prevention of hydraulic fracturing as well as the maximization of filling of voids and deteriorated areas [1-3].

In this paper, low pressure remediation grouting techniques applied for two large dams over past 10 years are analyzed in detail. More extended case histories can be referred to the reference authored by Park and Oh [4].

Both dams in this study are central core-type fill dams. Technical descriptions of each dam's seepage-related problems are provided. In practice, the deteriorated areas of the clay core layers are not uniformly distributed; rather, the deteriorated areas are randomly distributed, which complicates grouting designs and requires flexibility in the application of the grouting technique. Therefore, the grouting

specifications for each case history vary depending on the characteristics of their respective core materials, voids, and degrees of deterioration.

The study of each dam remediation informs empirical guideline for the recommended permeation grouting methods, including grout mix, injection period per stage, injection rate, and maximum fluid pressure to prevent hydraulic fracturing. This empirical guideline for successful low-pressure permeation grouting constitute the primary contribution of this study, and the guideline can be applied to substantially improve a dam's core layer permeability and efficacy as a water barrier.

2. DAM INCIDENTS

After apparent incidents derived from deteriorated clay cores, carefully designed remediation grouting technique was applied for two earth-cored embankment dams (WM and AG dam) in Korea. Table 1 shows basic dimension, construction period, brief incident description, initial measures, and final remediation by permeation grouting scheme. Fig. 1 shows typical cross-sections of the dams.

Table 1
Case study dam specifications, observed deterioration, and remediation measures

Dam	WM	AG
Construction period	1985.12–1993.06	1968.08–1971.12
Reservoir capacity (million m ³)	135	18
H (m)	55	32.5
L (m)	407	223.5
Hazard type	Exposed event 1998.04–10: Three sinkholes found near crest, excessive leakage	Exposed event 1985.06: Wet zone found on the downstream slope; 2003.07: Downstream slope-sliding after intensive rainfall
Initial remediation	2000.05–08 Partial compaction grouting (L80m)	1986.07–1989.05: General grouting 4 times; 2003.08–10: Emergency slope protection
Ultimate remediation	2003.04–09: Permeation grouting	2004.05–10: Permeation grouting

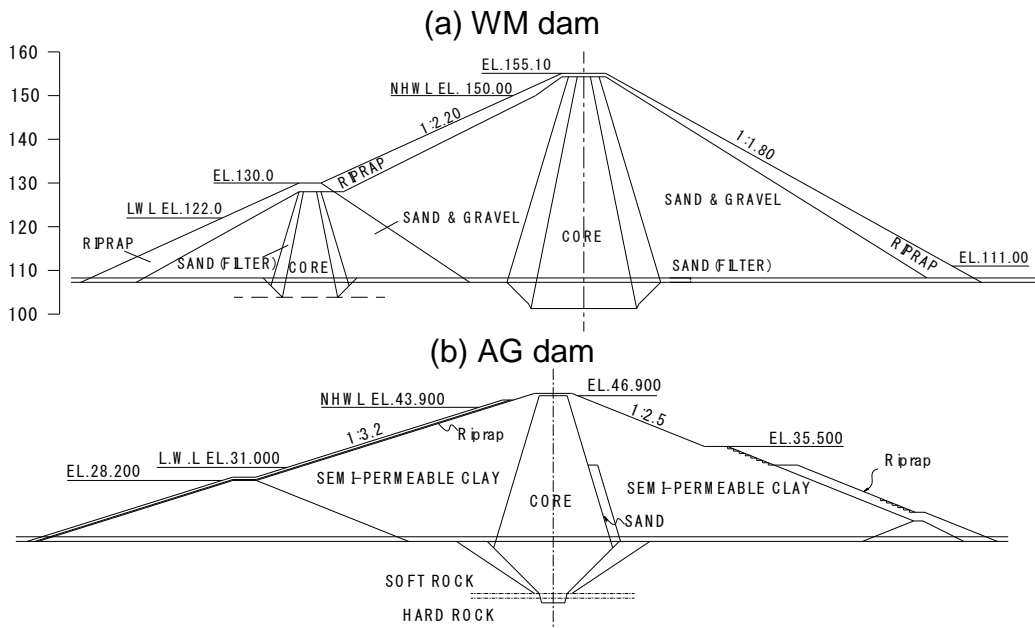


Fig. 1
Typical cross-sections of dams in this study

WM dam is a 55-m-high earth-cored rockfill dam that exhibited distinct deterioration in the form of three sinkholes near the dam crest which were observed over six months during normal dam operation (Fig. 2). Before any remediation, the dam seepage measured at the downstream toe increased up to approximately 2340 m³/day at normal high water level (NHWL) (EL: 150.0 m). After an in-depth diagnosis, an initial remediation measure was applied by compaction grouting on 80 m out of the dam crest's total 407 m [5]. After compaction grouting, the total seepage was reduced to 860 m³/day near NHWL. However, two and a half years later, seepage had increased to up to 1007 m³/day and another in-depth diagnosis revealed diversified flow paths within the embankment, which required remediation to be applied over the whole length of the dam. The final remediation was conducted using low-pressure permeation grouting.



Fig. 2
WM dam sinkhole incidents

AG dam also showed distinct symptoms of core deterioration after first impoundment. The dam embankment's earthfill had very low stiffness and the core material contained a relatively large proportion of sandy soil with fine-grained soils. Various areas of wet zones were found on the downstream surface and general grouting was performed four times. After common grouting applications, heavy rainfall in 2003 induced significant downstream slope-sliding (Fig. 3). After implementing immediate emergency measures to rehabilitate the slope, permanent remediation was undertaken with low-pressure permeation grouting.



Fig. 3
AG dam incident: downstream slope-sliding (2003)

3. REMEDIAL GROUTING

WM and AG dams exhibited distinct incidents such as sinkholes, slope-sliding, excessive seepage, etc. The common feature among all dams was the degraded impermeability of their core layers, and the degrees of deterioration were largely inhomogeneous and anisotropic. Therefore, site-specific remediation grouting designs and applications were essential. Initial remedial grouting design conditions were carefully arranged according to the pilot grouting test results. Additional findings obtained through additional trial tests were applied to correct the initial grouting design conditions. Specific criteria for maximum fluid pressure, grouting duration, and refusal were determined to prevent hydraulic fracturing and grout penetration into filter layers.

Table 2 and Fig. 4 show a typical procedure and a sequence of remedial permeation grouting, respectively. Two rows of grouting holes were spaced 2 m from each other in the dam axis direction and 1 m from each other in the stream direction. The grouting sequence was conducted by interpolation with each incremental grouting spaced at least 8 m from the preceding one. For the remedial grouting of AG dam, three rows of grouting holes were partially drilled, considering a relatively higher degree of core deterioration.

Table 2
Typical permeation grouting procedure for core layer remediation

Sequence	Procedure
Pilot hole drilling	NX-sized no-water boring, accompanied by core sampling, standard penetration test (SPT), and in-situ permeability test
↓	
Pilot hole grouting	Upward grouting (1 stage : 5 m) Grout mix ratio and grout materials follow specified injection pattern
↓	
General hole drilling and grouting	BX-sized rotary washed boring, grouting work based on pilot hole testing results that determined the appropriate maximum amount of grouting, injection duration, and grout mix ratio
↓	
Determination of check holes	Locating equally spaced check holes, adjacent pilot holes, and additional investigation holes
↓	
Check hole drilling and grouting	NX-sized no-water boring, accompanied by core sampling, chemical reaction tests, and in-situ permeability tests; after check hole investigation, final grout injection is made with a cement-to-water mix ration of 1:1
↓	
Determination of additional remediation area	Finding additional remediation areas by additional borehole drilling and grouting, following the same procedure as pilot holes
↓	
Report writing	Reporting on the remediation grouting results

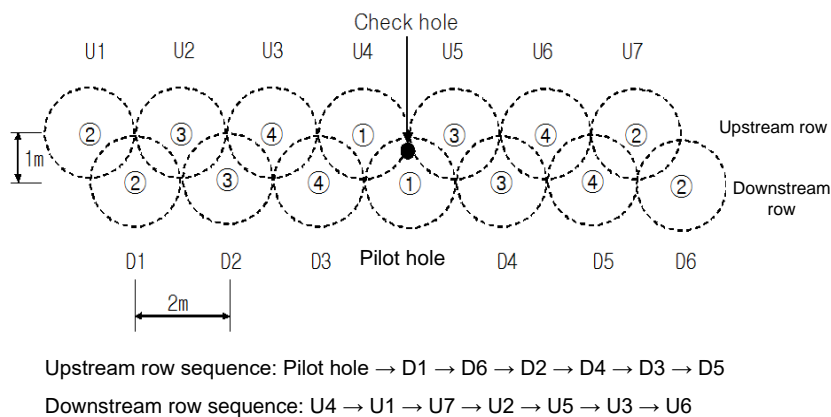


Fig. 4
Remedial grouting sequence applied to WM dam

Table 3 summarizes the specific designs of the low-pressure permeation remedial grouting techniques applied to each of the dam. In Table 3, details of the empirically proven technical specifications are addressed, including maximum grout fluid pressure, grouting duration, initial grout mix ratio, grout mix change condition, refusal criteria for every stage, fluid pressure change condition, and additive ratio. As a main grout material, either ordinary Portland cement (OPC) or micro-cement (MC) was used depending on the groutability, void ratio of the core material, and the degree of core material degradation. For WM dam remediation, two different criteria between those associated with OPC and MC were applied, depending on the type of cement material.

Although different grouting designs were applied, Table 3 reveals a common guideline that should be applied to the maximum grout fluid pressure to avoid hydraulic fracturing in remedial permeation grouting. In these empirical applications, a maximum fluid pressure of $2 \times 10 \text{ kPa/m} \times \text{depth (m)} \times 0.75$ was proposed. The equation can be interpreted as that the maximum fluid pressure is approximately 75% of the hydraulic fracturing pressure at the given depth, with a minimum pressure of 10 kPa per unit depth. Therefore, the maximum fluid pressure increases with depth, limited to 100 to 500 kPa depending on the dam height.

The grouting injection duration per meter in depth varied depending on the depth; in general, the grouting duration was determined to be 8 to 40 minutes for grouting depths of less than 40 m. The commonly applied injection fluid rate was 5 to 20 L/min, and the initial grout mix ratio for core layers was mostly 1:3 or 1:2, as a mass of cement relative to that of water. The grout mix ratio gradually varied up to 1:1 depending on the in-situ condition. The grout mix change criteria during grouting were applied differently depending on the in-situ conditions of the dams; however, in all cases, the flow rate was an important factor in considering changes to the cement-to-water ratio. In some cases, the grout mix ratio was kept constant, and the fluid pressure and grouting duration were adjusted accordingly.

The grouting refusal criteria for every 5-m stage was selected primarily to limit the maximum injection quantity in liters. The fluid pressure change conditions varied a lot for each dam; however, a common approach was to set the pressure value in conjunction with the flow rate (L/min) condition at each depth as shown in Table 3.

More detail information regarding remedial permeation grouting can be referred to Park and Oh [4].

Table 3
Design and application details of permeation grouting for dam core remediation

Dam	WM		AG
	OPC	MC	
Max. fluid pressure (kgf/cm ²)	2~5	2~5	1~4
Grouting duration (min/m) (DS: downstage; US: upstage)	Varied from 8 min for z ≤ 10 m to 40 min for z > 40 m	Varied from 8 min for z ≤ 10 m to 40 min for z > 40 m	Varied from 5 min for z ≤ 10 m to 45 min for z > 45 m
Initial grout mix ratio (C : W)	1:4.5 for z ≤ 20m, 1:3 for z > 20m	1:2 for core embankment 1:1 for rock foundation	1:2 for core embankment 1:1 for rock foundation
Grout mix change condition	(1st) when flow rate > 15 l/min: C:W=1:3 for z ≤ 20m after 5–10 min, C:W=1:2 for z > 20m after 10 min (2nd) when flow rate > 10 l/min: C:W=1:2 for z ≤ 20m after 5 min, C:W=1:1 for z > 20m after 10 min (3rd) when flow rate > 8 l/min: C:W=1:1 for z ≤ 20m after 3–5 min, keep C:W=1:1 for z > 20m	Keep C:W=1:2 constantly	(1st) when flow rate > 55 l/min for 5 min at 1 kgf/cm ² : C:W=1:1 for core embankment, C:W=1:0.8 for rock foundation (2nd) when flow rate ≤ 10 l/min at the max fluid pressure: C:W=1:3 for core embankment, C:W=1:2 for rock foundation
Grouting stop condition for every stage (5m)	After injection, 800–1,000 l maximum	Without duration consideration, 1,000 l maximum for core, 2,000 l maximum for rock foundation	800–1,000 l maximum for core, 1,000–1,200 l maximum for rock foundation
Fluid pressure change condition	Stop injection when there is no flow rate decrease, re-inject after not less than 4 hrs; keep approximately 3 min at least when incremental fluid pressure increase	Keep low pressure when flow rate > 20 l/min at low pressure; stop injection when there is no more flow rate decrease and re-inject after 4 hrs; keep approximately 3 min at least when incremental fluid pressure increase	Increase fluid pressure when flow rate ≤ 10 l/min for 5 min at each pressure stage; maintain the pressure when flow rate is 10–55 l/min for 5 min at each fluid pressure increase; decrease fluid pressure when flow rate > 55 l/min for 5 min at each fluid pressure increase; keep approximately 3 min at least when incremental fluid pressure increase

Note, z = depth from the dam crest, OPC = ordinary Portland cement, MC = micro-cement

Table 4 shows the results of dam core layer remediation by low-pressure permeation grouting for the dams in this study. Both dams that exhibited distinct dam incidents during operation were remediated over the entire crest length of the dams. The grouting depth reached to the bottom of the foundation rock mass.

The majority of the grout material was MC; however, OPC was also used in WM dam, which had sinkholes and granular cores. To stabilize the grout holes and mitigate bleeding during remedial grouting, up to 5% bentonite was added to the mix, and this addition was found to be effective.

The average amount of cement used per meter (kg/m) was 39–40 kg/m for AG and WM dams, which showed distinct incidents. The average grouting quantity was varied from 18–24 l/min for WM and AG dams.

Table 4
Results of dam core remediation by permeation grouting

Dam	WM	AG
Total grout length (m)	16,932	11,131
Total grout quantity (m ³)	1,544	825
Total cement quantity (kg)	690,493 OPC: 94,170 MC: 596,323 Bentonite: 30,718	437,362 MC: 424,139 Bentonite: 13,223
Avg. grout quantity (l/m)	91.2	74.2
Avg. flow quantity (l/min)	23.9	18.2
Avg. cement quantity (kg/m)	40	39
Avg. cement quantity (kg/min)	11	9.7
Mixer RPM (min)	800	1,600
Remarks	Total length of dam remediated; two grouting rows; mainly MC, partially OPC, and bentonite 5% added for core grouting, no bentonite for rock foundation	Total length of dam remediated; two or three grouting rows; MC used, bentonite 5% added for core grouting, no bentonite for rock foundation

4. VALIDATION

Because the remedial grouting state is not visible underground, the remediation work is not easily validated quantitatively. However, a limited validation can be attained by visual inspection of the surface, checkhole drilling and sampling, analysis of the sampled core's reaction to chemical indicator spray, in-situ permeability testing, analyses of grout quantities and total seepage rate change at the dam toe, and electrical resistivity surveys.

Table 5 shows the results of the remedial grouting validation. Visual inspection during checkhole drilling and sampling for WM dam showed a good core sample recovery. For AG dam, which exhibited distinct wet zones on the downstream surfaces, visual inspection after grouting showed the dry state of the previously wet surface soils. Chemical indicator reaction tests were performed on checkhole core samples using Phenolphthalein spray. It was observed that the area penetrated by the grout milk turned red after application of the Phenolphthalein spray, indicating a good filling of soil voids.

Based on in-situ permeability measurements during the checkhole drilling process, all dams showed less core layer permeability after remedial grouting. The maximum permeability coefficient before remediation of approximately 10^{-4} cm/s was reduced down to approximately 10^{-5} cm/s.

The seepage rate measured at the center of the downstream toe after remediation grouting decreased remarkably for WM and AG dams, indicating successful permeation remedial grouting.

Electrical resistivity surveys were conducted. Overall, after remediation, uniformly increasing patterns of resistivity distribution were found as depth increases.

All of the validation findings support the effectiveness of remedial permeation grouting for the dams in this study. Remediation grouting of dam cores is demonstrated using a low-pressure permeation grouting technique that effectively remediates deteriorated core layers. The empirical case studies in this paper are believed to offer an important reference for hazard mitigation technology in a wide range of aging dam rehabilitation projects.

Table 5
Validation of the effect of remediation grouting

Dam	WM	AG
Visual inspection and borehole investigation	Good checkhole core recovery condition	Previously wet zones on the downstream surface become dry
Chemical indicator reaction	Confirmed indicator reaction to grouted core sample using Phenolphthalein spray	Confirmed indicator reaction to grouted core sample using Phenolphthalein spray
Permeability (cm/s)	Before, $k \sim 10^{-4}$ max → After 10^{-5} max	Before, $k \sim 10^{-4}$ max → After 10^{-5} max
Average flow rate (l/min) or grout quantity (kg/m)	24 l/min for general holes → 28 l/min for check holes	18.8 l/min for general holes → 14.5 l/min for check holes
Seepage rate (Q) (m ³ /day)	For reservoir water level = EL:147 m, Q = 640 m ³ /day after 1st remediation by compaction grouting → Q = 4.1 m ³ /day after 2nd remediation by permeation grouting	Leakage decreased remarkably after remediation, as measured by a temporary flowpipe-type device

SUMMARY

As empirical guidelines for the two dams, permeation grouting of two- or three-rows layout was successful with a grout column spacing of 2m in dam axis direction and 1m in stream direction on the crest. Remedial grouting sequence at least 8m spacing in an interpolation method was accompanied. Main grout material was composed of ordinary Portland cement and micro-cement. Bentonite mix with a mixture less than 5% mass quantity was effective as an additive material. Empirically proven recipe of permeation remedial grouting encompasses the maximum fluid pressure (kPa) given as $2 \times 10 \text{ (kPa/m)} \times \text{depth (m)} \times 0.75$.

Seepage rate measured on the center of downstream toe after remediation grouting remarkably decreased for WM and AG dam, which indicated the successful effect of permeation remedial grouting.

Empirical case study in this paper is believed to be an important hazard mitigation technology in the field of aging dam rehabilitation project.

REFERENCES

- [1] USBR. Design Standards No. 13 Embankment Dams - Chapter 10: Embankment construction. U.S. Bureau of Reclamation, U.S. Department of the Interior, 2012.
- [2] U.S. ARMY CORPS OF ENGINEERS. Drilling in earth embankment dams and levees. U.S. Army Corps of Engineers, 2014, Washington DC.
- [3] FELL R., MACGREGOR P., STAPLEDON D., BELL G., FOSTER M. Geotechnical engineering of dams, 2nd edition. CRC Press Taylor & Francis Group, 2015, London, UK.
- [4] PARK D.S., OH J. Permeation grouting for remediation of dam cores. *Engineering Geology*, 2018, 233.
- [5] YEA G.-G., KIM T.-H., KIM J.-H., KIM H.-Y. Rehabilitation of the core zone of an earth-fill dam. *Journal of Performance of Constructed Facilities*, 2012, 27.

KEYWORDS

Seepage – Leakage – Core - Impervious Core Dam – Grouting - Sealing work - Repair

COMMISSION INTERNATIONALE DES GRANDS BARRAGES

VINGT-SIXIÈME CONGRÈS DES GRANDS BARRAGES

Autriche, juillet 2018

DOI 10.3217/978-3-85125-620-8-154



This work licensed under a Creative Commons Attribution 4.0 International License.
<https://creativecommons.org/licenses/by-nc-nd/4.0/>

**THE EFFECT OF THE GROUNDWATER FLOW VELOCITY AND SEDIMENT
DISCHARGE ON INTERNAL EROSION OF RIVERS**

Fereshteh NOORBAKHSH

Ph.D. Candidate, DEPT. OF CIVIL AND ENVIRONMENTAL ENGINEERING,
UNIVERSITY OF LOUISVILLE

KY, UNITED STATES

Mahammad Reza Majdzadeh TABATABAI

Assistant Professor, DEPT. OF WATER AND ENVIRONMENTAL
ENGINEERING, SHAHID BEHESHTI UNIVERSITY OF TECHNOLOGY,
TEHRAN

IRAN

COMMISSION INTERNATIONALE
DES GRANDS BARRAGES

VINGT-SIXIÈME CONGRÈS DES
GRANDS BARRAGES
Autriche, juillet 2018

**THE EFFECT OF THE GROUNDWATER FLOW VELOCITY AND SEDIMENT
DISCHARGE ON INTERNAL EROSION OF RIVERS***

Fereshteh Noorbakhsh

*Ph.D. Candidate, Dept. of Civil and Environmental Engineering, University of
Louisville,
KY, United States*

Mahammad Reza Majdzadeh Tabatabai

*Assistant Professor, Dept. of Water and Environmental Engineering, Shahid
Beheshti University of Technology, Tehran, Iran*

ABSTRACT:

Rivers play an important and life-sustaining role in human societies and provide many critical advantages to human civilizations such as water transport, habitat, economical support, transportation, etc. Degradation of rivers due to the natural occurrences such as flooding or human's interferences like constructions would inevitably lead to undesired environmental and economical situations. Therefore, river engineers have always attempted to monitor the river/coast interactions and control the potential failures which might take place in rivers. Erosion and sedimentation are two key parameters which need to be closely monitored in rivers in order to prevent unfavorable consequences. In this study, internal erosion as one of the main mechanisms for the river degradation and bank erosion has been experimentally investigated and the effect of the groundwater flow velocity and sediment discharge on the internal erosion was evaluated. The results of extensive experimentations showed that the parameters such as the length of internal erosion in sandy layer, hydraulic gradient, sediment transport parameters, and Reynolds number are significantly influenced by river bank slope. Also, an empirical correlation was proposed to predict the length of internal erosion. Results of the present study were found to be in good agreement with the previous measured data and other empirical equations.

Key Words: Internal Erosion, River Bank Slope, Alluvial Layer Slope, Experimental model

1. INTRODUCTION

Rivers are continuously changing. This concept is understood by the people who have settled near rivers for decades or engaged in agricultural activities nearby. Their memories usually involve local motions and gradual or sudden changes in rivers. One of the main sources of sediment is the bank erosion which is significant in the development of floodplain and management of water resources due to its influence on the characteristics of river channels. Bank erosion also induces extensive damages to adjacent lands and buildings [1]. Investigation of channels around the United States of America indicated that bank erosion is an important source of sediment load at most of the rivers [2]. However, channel width is one of the most effective parameters for describing the characteristics of natural channels and rivers as well as their morphology [3]. The larger the river width, the higher the bank erosion rate would become. On the other hand, bank erosion will result in the loss of adjacent fertile agricultural lands; also, it will cause millions of dollars of damages each year [4]. Studies have shown that riverbank sediments constitute about 30 to 80 percent of the total sediment load of the watershed. These sediments are usually a result of the loss of soil pore pressure as well as confining pressure during water surface lowering after a rainfall [5]. Erosion due to seepage flow is one of the causes of river bank erosion. In addition to entering a considerable amount of sediment directly into the river, this type of erosion also causes internal erosion of the river's surrounding layers and mass failure of the upper layers. Important parameters contributing to the formation of this erosion are listed below:

- 1- Flow exchange between the river and aquifers will loosen the surrounding layer materials; hence, sediments are washed to the river by groundwater flows from the aquifer.
- 2- Floods cause fluctuations in surface water level. When the water level rises, some flows enter the surrounding layers, and when the peak flood is passed the back waters from surrounding layers will cause internal erosion.

Many engineers believe seepage force causes the changes in soil particles and decreases particle resistance against the erosive forces. Seepage force is one of the reasons for internal erosion. When seepage flow has been seen in the soil, not only its uplift force decreases the effective stress in the soil, but also seepage force from the hydraulic gradient and consequently, the water velocity in the soil is applied to the particles. Howard et.al. experimented the effect of seepage on sand erosion. They showed that different hydraulic conductivities and the river bank layering has been caused seepage forces and moving soil particles. Internal erosion is a complicated factor of the river morphologic changes [6]. Hagerti did many of studies and field investigations that resulted in the existence of a permeable layer between fine-graded and cohesive layers as being the main reason for the internal erosion. This layer drains water and removes sediments from the river bank and promotes internal erosion. Initiation of the internal erosion depends on the hydraulic gradient. On the other hand, when the rainfall goes into

all soil regions, hydraulic conductivity between soil particles has been decreased, and it causes a reduction in vertical flow velocity and enlargement in lateral flow velocity [7, 8]. Furthermore, buried pipelines or reservoirs can also engender internal erosion in addition to the rainfall infiltration or lateral seepage. Fox et al. accomplished field and experimental investigations to develop a sediment transport model for measuring internal erosion and river bank failure [9]. They continued their studies and experiments to see the effect of lateral subsurface flow on bank slope stability. Experiments were conducted on 26, 36, 45, 60 and 90 degrees' bank slopes. They revealed that they were not able to predict the failure in banks with slope angles less than 45 degrees [10]. Chu-Agor et al. simulated vertical banks in their experimental model and investigated the effect of undermining due to seepage on the elimination of water pore pressure caused by sapping [11]. They did their research for a better understanding of internal erosion in a three-dimensional model, and they limited the number of variables [12]. The researchers investigated the effect of changes in statistical analysis on the bank failure in their three-dimensional model [11,13, 14, 15,16]. Rostami Pour et al. investigated internal erosion as an important parameter in bank erosion and instability in the micro model. Results showed that the particle size of the sand layer and bank height have a significant influence on the critical hydraulic gradient for the initiation of the erosion and erosion rate [17]. Salamat et al. did the experiments and found the probable parameters for erosion near river structures. Results displayed the effectiveness of particle size and changes in gradient on the formation of the internal erosion near the structures [18].

Most researchers have studied the internal erosion in vertical banks with horizontal alluvial layers, and influence of the bank slope and layers have not been considered, simultaneously. Also, in most researches, the relationship between the erosion depth and other parameters were not stated. Therefore, these parameters are experimentally evaluated in this study and attempted to find the relationship between these parameters by getting the ideas from an experimental model which was designed by Fox et al. The aim of this study was to simulate a part of the river bank in a laboratory flume to investigate erosion depth and particles' Reynolds number changes considering the bank slope as well as alluvial layers' slope.

2. EXPERIMENTAL STUDIES

2.1. EXPERIMENTAL EQUIPMENT

The experimental reservoir built in Laboratory was applied to investigate erosion depth and Reynolds number changes of the particles for different bank slopes. In this regard, experimental Plexiglas reservoir with dimensions of 50 cm length, 20 cm width, and 50 cm height was used (Fig.1). The reservoir was divided into two sections for water and materials, and these two sections are connected

with a perforated Plexiglas plate having holes of 1 mm diameter. Length, width, and height of the water reservoir were 10, 20 and 100 cm, respectively. Input and output valves were put on the reservoir to manage the water depth. As shown in Fig.1, the end of the reservoir tried to mimic the channel form and the direction of the water and sediment. Additionally, the discharge from the sandy layer was measured in this section.

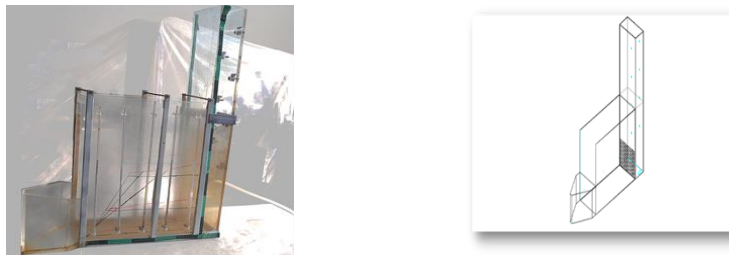


Fig. 1
Schematic view of the laboratory flume

The experiments were conducted in two stages. First, nine experiments with three uniform gradation ranges of 0.4-0.8, 0.8-1.2 and 1.2-2.0 mm and three bank slopes of 1:1, 1.5:1 and 2:1 for horizontal alluvial layers were performed. The second stage was done with the three mentioned gradations and bank slopes with a 5-degree slope for the alluvial layers. In other words, eighteen experiments were designed and carried out in the same situation in this study. For a summary, the results of experiments with gradation range of 1.2-2.0 mm will be presented.

Generally, the sandy river banks with alluvial materials are usually surrounded by non-alluvial materials above and below the sandy layers. So, the model includes three layers of material: clay, sand and mixed soil with a moisture content of 20% as a surface layer with a thickness of 5, 10 and 15 cm respectively. Also, a timber with the same dimensions of the surface layer was used to provide a uniform load distribution for simulating the river bank, and its weight is equal to the weight of a 20 cm soil. All the steps were repeated for three different bank slopes. For the second phase, all of the layers were inclined at 5-degree (Fig. 2).

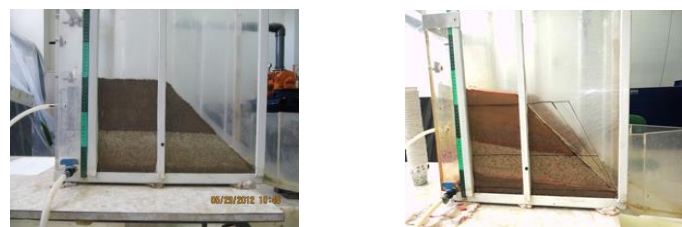


Fig. 2
A view of the laboratory flume, horizontal and steep alluvial layers

Then water enters the reservoir and penetrates into the sample. Based on initial experiments the erosion in the sandy layer has been observed in heights more than 15 cm; therefore, the water level in the reservoir was constant at first (15cm), and it was added every 30 minutes by 2 cm to see and measure the possible changes. When the water level was lower than the sandy layer bed, no significant erosion was seen; while, when the water head was more than 15 cm it caused a critical hydraulic gradient in the sandy layer. However, these values were different for various gradations. The experiment continued until the surface layer was cracked and collapsed.

Measured parameters during the tests included time, water level, output discharge from the sandy layer, the weight of the removed sediments and the depth of erosion. In every step, discharge was measured by using specified volume containers at a specific time; since the maximum compaction was considered in the other two layers and seepage was negligible; so, the measured discharge was for the sandy layer. The sediments were collected and weighted by using specified volume containers during the specific time. Also, erosion depth was measured with a scaled ruler with a precision of mm.

2.2. DIMENSIONAL ANALYSIS AND DETERMINATION OF DIMENSIONLESS PARAMETERS

The purpose of the dimensional analysis is to specify effective parameters on the phenomenon under study and to determine the dimensionless relations. There are a large number of parameters affecting these phenomena; so, it is not possible to develop a specific mathematical relation for the analysis of the problem. Therefore, dimensional analysis is used to present dimensionless parameters. Effective parameters are as follows:

$$f(h, d_{50}, \rho, \rho_s, g, \mu, q_s, L, d, \theta, \alpha, t, t_{max}) = 0 \quad [1]$$

In the Buckingham π theorem, dimensionless groups (π) are selected, and after some calculations, dimensionless relations are established based on the obtained dimensionless groups. Some dimensionless ratios are also established between some parameters.

$$f\left(\frac{\mu}{\rho d \sqrt{gd}}, \frac{q_s}{\sqrt{gd^3}}, \frac{d}{L}, \frac{\rho}{\rho_s}, \frac{t}{t_{max}}, \frac{h}{L}, \theta, \alpha\right) = 0 \quad [2]$$

The first one is Reynolds Number of the porous media. The critical Reynolds Number states that the water flow between the particles changes from laminar flow to turbulent flow has been shown in the range of 1 to 12. However, Reynolds numbers would be considered equal to or less than one as a laminar flow [19]. The second one is sediment transport parameter, and sediment discharge is

considered cumulative. The third one (d^*) is the dimensionless length of internal erosion.

3. RESULTS AND DISCUSSION

As mentioned before, flow discharge, gradient, and internal erosion length were measured for different water levels, and the results are presented in graphs. Hydraulic gradient was calculated by dividing water level by the sample length minus the internal erosion length. The actual velocity was calculated by dividing the average velocity by the porosity coefficient.

3.1. DIFFERENT RIVER BANK AND ALLUVIAL LAYER SLOPES

The dimensionless erosion length (d^*) over dimensionless time (t^*) is shown in Figures 3 and 4 to see the effect of different bank slopes on the erosion length in the alluvial layer.

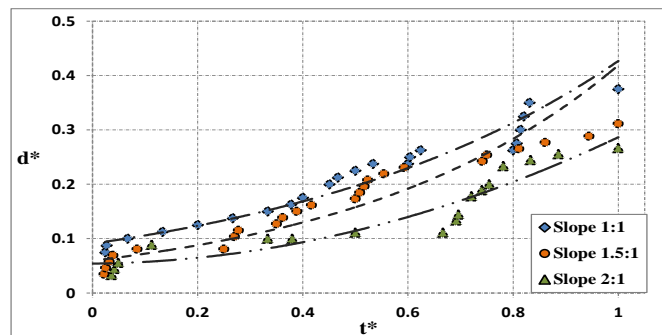


Fig. 3

Changes of d^* and t^* for gradation range of 1.2-2.0 mm for horizontal layers

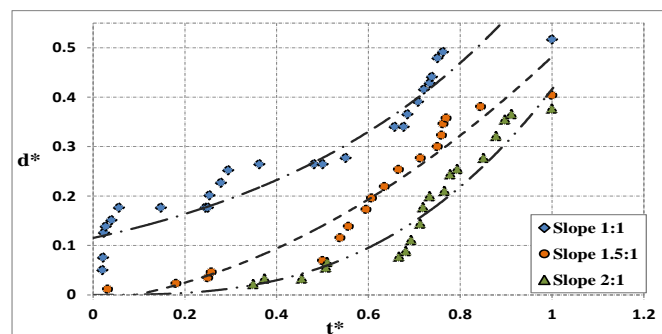


Fig. 4

Changes of d^* and t^* for gradation range of 1.2-2.0 mm for steep layers

It could be seen that by increasing the river bank slope, internal erosion in the horizontal sandy layer has been decreased. The reason might be explained that when the water level in the reservoir rises, the seepage flow through a sample has been increased and it causes growth in discharge and erosion in the layer. Since the sand particles are uniform and don't have any cohesiveness, the sandy layer is washed out through a seepage flow by passing the time. However, when the river bank slope increases, there is more amount of load from the river bank; so, the force doesn't allow to have more undermining. As it can be seen in figure 6, similar trends are observed for steep layers. Figures 5 and 6 show examples of the bank slope effect on the hydraulic gradient over time. Hydraulic gradient calculated by dividing the difference between water levels and the sample length.

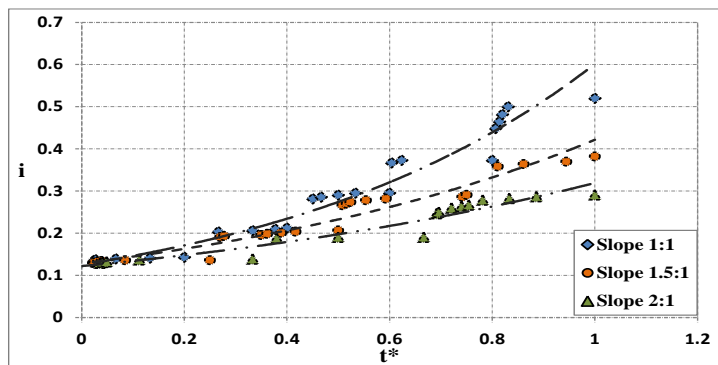


Fig. 5

Changes of the hydraulic gradient and t^* in gradation range of 1.2-2.0 mm for horizontal layers

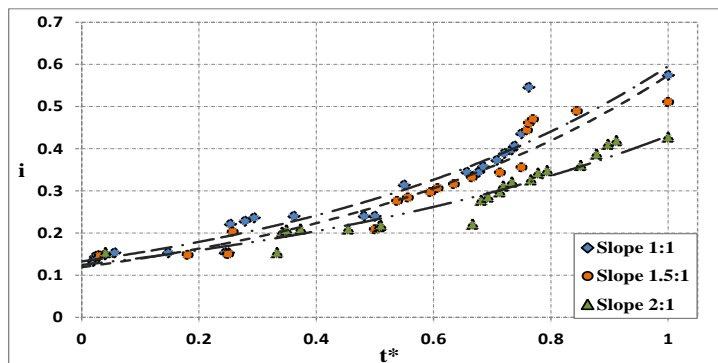


Fig. 6

Changes of the hydraulic gradient and t^* in gradation range of 1.2-2.0 mm for steep layers

Comparison of the hydraulic gradients for different bank slopes, at the same time, shows that by increasing the bank slope, hydraulic gradient is decreased. As mentioned in the previous section, when the bank slope is increased, internal erosion length is decreased; Therefore, according to hydraulic gradient formula, by reducing the internal erosion length, the hydraulic gradient is diminished. The outcomes of the experiments display that the hydraulic gradient for three bank slopes has an increasing trend over time. The reason is attributed to the higher

effect of increased water level in the reservoir than the increased internal erosion length in the sandy layer. To investigate the effect of river bank slope on the particles Reynolds Number, Figures 7 and 8 are presented for various time intervals and considering different layer slopes.

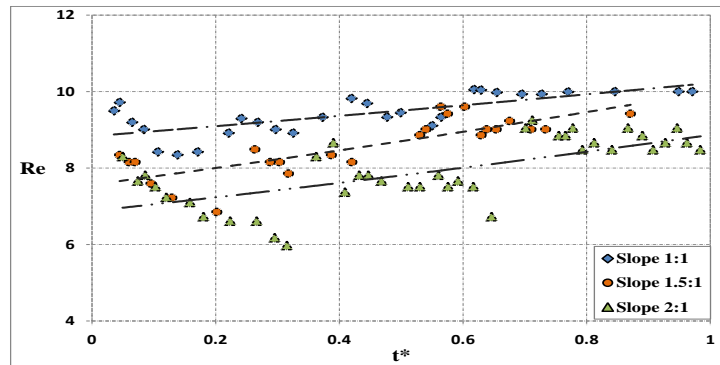


Fig. 7

Changes of Reynolds number and t^* for gradation range of 1.2-2.0 mm for horizontal layers

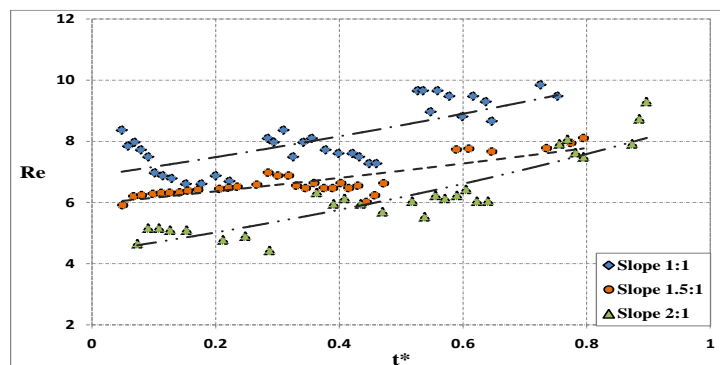


Fig. 8

Changes of Reynolds number and t^* for gradation range of 1.2-2.0 mm for steep layers

The results indicated that in a specific time interval, by reducing the bank slope, the Reynolds Number is increased. This trend is observed for all the slopes. The reason might be explained with Darcy Law; also, based on Darcy's Law when the hydraulic gradient increases, water flow velocity is also increased. On the other hand, there is a direct relation between Reynolds Number and flow velocity, and the fluid density and viscosity coefficient and particle diameter are constant for each gradation; Therefore, Reynolds Number is also increased. The application range of Darcy's Law is extended to Reynolds Numbers ranging from 1 to 10. For higher Reynolds Numbers, the linear state of the seepage law will gradually change [20]. Figures 9 and 10 show cumulative sediment transport parameter curves versus dimensionless time for three different sediment gradations at three different river bank slopes. q_s^* is dependent upon sediment transport rate per unit width (q_s), sediment particle size (d), a relative density of the particles (S) and gravity acceleration. In the results of each gradation,

sediment discharge per unit width was the only variable parameter.

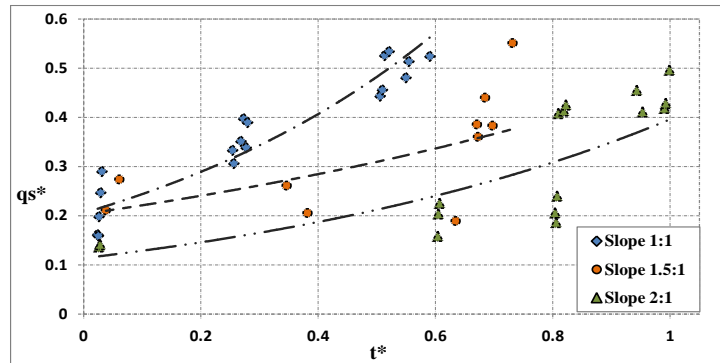


Fig. 9

Changes in q_s^* and t^* in gradation range of 1.2-2.0 mm for horizontal layers

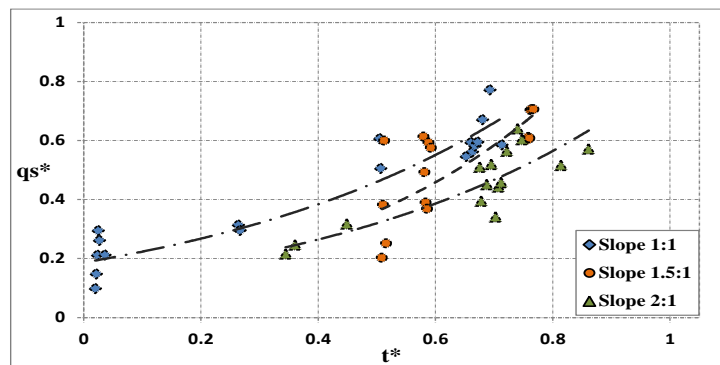


Fig. 10

Changes in q_s^* and t^* in gradation range of 1.2-2.0 mm for steep layers

The figures display that cumulative sediment transport parameter is increased over time for three different bank slopes and three different gradations. The reason is over the natural course of time, Reynolds Number and actual water velocity in the porous media has been raised and it causes the enlargement in cumulative sediments. As mentioned in the previous section, by increasing the river bank slope, internal erosion of the sandy layer is diminished, and thus, the cumulative weight of the sediments is also declined.

3.2. EMPIRICAL RELATIONSHIPS FOR ESTIMATING THE INTERNAL EROSION LENGTH IN THE ALLUVIAL LAYER

According to the dimensional analysis, dimensionless equation of d^* can be written in different experimental conditions by considering the dependent parameter of d^* as a function of the independent parameters of Re_e , i , $\tan \theta$ and $\tan \alpha$. Previous studies were conducted in porous media where flow was surrounded by particles. Fluid viscosity is an effective parameter in porous media, and Reynolds number is the parameter controlling fluid motion in the porous

media. Considering the least error and highest correlation between observed and calculated values, the following equation is presented for estimation of d^* value when Darcy's Law is applied. In this equation, R^2 is calculated 0.94, and its application range is proposed as $Re < 10$.

$$d^* = 0.2 \left(1 + \frac{1}{\tan \theta}\right)^{0.82} \left(1 + \tan\left(\frac{\pi}{4} - \alpha\right)\right)^{1.15} (Re)^{0.47} (i)^{1.62} \quad [3]$$

Figure 11 shows the observed values, d^* versus computed ones when Darcy Law applies, derived from Equation 3. The outcome displays that most of the data lie in the error range of $\pm 25\%$ indicating the appropriate accuracy of the equation.

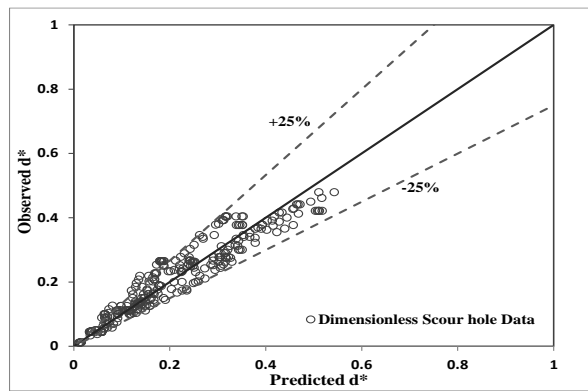


Fig. 11
Comparison of the observed and calculated values

4. CONCLUSIONS

Considering the importance of internal erosion in alluvial rivers, in this project, an experimental study has been carried out to better understand the effect of the bank slope, and alluvial layers slope of the rivers on the internal erosion and output discharge, and experimental results were compared. The results show that, by increasing the bank slope, for both horizontal and steep alluvial layers, the dimensionless internal erosion through the alluvial layer had been decreased. Also, initiation of the internal erosion in the sandy layer with a mild slope occurs more quickly than other slopes, and this issue confirms the role of the load from river bank. It is worth mentioning that by increasing the bank slope, hydraulic gradient, the Reynolds Number and cumulative sediment transport parameters are diminished. The results of this study suggest that the sediment transport parameter is directly related to the slope of the alluvial layer and by increasing the removed sediments from the sandy layer, length of the erosion hole due to undermining is move forward.

REFERENCES

- [1] Samadi, A., 2010, Experimental and analytical investigation of the river bank stability against arc failure, Ph.D. Thesis, Faculty of Engineering and Agricultural Technology, Tehran University.
- [2] Odgaard, A. J., 1987, Stream bank erosion along two rivers in Iowa, *Water Resource Research*, Vol. 23, No. 7, pp. 1225-1236.
- [3] Andrews, E. D., 1982, Bank stability and channel width adjustment, East Fork River, *Wyoming Water Resource Research*, Vol. 18, No. 4, pp. 1184-1192
- [4] Bowie, A. J., 1982, Investigations of vegetation for stabilizing eroding stream banks, *Trans of ASAE*, Vol. 25, No. 6, pp. 1601-1611.
- [5] Simon, A., Curini, A., Darby, S. E. and Langendoen, E. J., 2000, Bank and near bank processes in an incised channel, *Geomorphology*, Vol. 35, No. 3, pp. 193-217.
- [6] Howard, A. D., and McLane, C. F., III, 1988, Erosion of cohesiveness Sediment by groundwater seepage, *Water Resources Research*, 24(10): 1659-1674.
- [7] Hagerty, D. J., 1991a, Piping/Sapping erosion I: Identification and Diagnosis, *Journal of Hydraulic Engineering*, Vol. 117, pp. 991-1008.
- [8] Hagerty, D. J., 1991b, Piping/Sapping erosion II: Basic Consideration, *Journal of Hydraulic Engineering*, Vol. 117, pp. 1009-1025.
- [9] Fox, G. A., Wilson, G. V., and Periketi, R., 2006, The Role of Subsurface water in contributing to Stream bank erosion, US-CHINA Workshop on advanced computational modeling in hydroscience & engineering, Oxford, Mississippi, USA.
- [10] Fox, G. A., Wilson, G. V., Simon, A., Langendoen, E. J., Akay, O. and Fuchs, J. W., 2007a, Measuring Stream bank erosion due to groundwater seepage: correlation to bank pore water pressure, precipitation and Stream Stage, *Wiley Interscience, Earth Surf. Process. Landforms*, Vol. 32, No. 1558-1573.
- [11] Chu-Agor, M. L., Fox, G. A., and Wilson, G. V., 2007, Empirical sediment transport function predicting seepage erosion undercutting for cohesive bank failure prediction, *Journal of Hydrology*, Vol. 377, Issues 1-2, Pages 155-164
- [12] Fox, G. A., Chu-Agor, M. L., Cancienne, R. M. and Wilson, G. V., 2008, Seepage erosion mechanisms of bank collapse: three-dimensional seepage particle mobilization and undercutting, *World Environmental and Water Resources Congress, ASCE*, pp. 1-10.
- [13] Wilson, G. V., 2006, Soil Properties controlling Seepage erosion contributions to Stream bank failure, *Earth Surface Processes, and Landform*, Vol. 10, pp. 1405-1418.
- [14] Fox, G. A., Chu-Agor, M. L. and Wilson, G. V., 2007b, Seepage of noncohesive Sediment by groundwater seepage: Lysimeter experiments and modeling, *American Society of Agricultural and Biological Engineers.*, No. 072235.
- [15] Fox, G. A., Chu-Agor, M. L. and Wilson, G. V., 2007c, Seepage Erosion a Significant Mechanism of Stream bank failure, *World Environmental and Water Resources Congress, ASCE.*, pp. 1-14.

- [16] Fox, G. A., Chu-Agor, M. L. and Wilson, G. V., 2007c, Sediment transport model for seepage erosion of Stream bank sediment, Journal of Hydrologic Engineering, ASCE., Vol. 11, No. 6, pp. 603-611.
- [17] Rostami pour, M., 2007, Experimental model of the river bank erosion considering the erosion due to seepage, M. Sc. Thesis, Department of Water and Environmental Engineering, Water and Power University (Shahid Abbas Pour)
- [18] Salamat, H., 2011, Experimental Study of Internal Bank Erosion in the Vicinity of Cross River Structures, M. Sc. Thesis, Department of Water and Environmental Engineering, Water and Power University (Shahid Abbas Pour)
- [19] Jacques, D., 1999, The Handbook of groundwater engineering, school of civil engineering, Purdue University, West Lafayette, Indiana.
- [20] Behnia, K. V., and Tabatabai, A., 1986-1987, Soil Mechanics, Twelfth Edition, Tehran University Publishing and Printing Institute, Tehran, Iran.

COMMISSION INTERNATIONALE DES GRANDS BARRAGES

VINGT-SIXIÈME CONGRÈS DES GRANDS BARRAGES
Autriche, juillet 2018

DOI 10.3217/978-3-85125-620-8-155



This work licensed under a Creative Commons Attribution 4.0 International License. <https://creativecommons.org/licenses/by-nc-nd/4.0/>

**DESIGN OF DEEP SOIL MIXING WALLS AND THEIR ADVANTAGES OVER
CONVENTIONAL SEALING FOR EMBANKMENT DAMS**

Daniel KERRES

Hydraulic Engineering Department, BJOERNSEN CONSULTING ENGINEERS

GERMANY

Ronald HASELSTEINER

Hydraulic Engineering Department, BJOERNSEN CONSULTING ENGINEERS

GERMANY

COMMISSION INTERNATIONALE
DES GRANDS BARRAGES

VINGT-SIXIÈME CONGRÈS DES
GRANDS BARRAGES
Autriche, juillet 2018

DESIGN OF DEEP SOIL MIXING WALLS AND THEIR ADVANTAGES OVER CONVENTIONAL SEALING FOR EMBANKMENT DAMS

Daniel KERRES; Ronald HASELSTEINER

Hydraulic Engineering Department, BJOERNSEN CONSULTING ENGINEERS

GERMANY

1. INTRODUCTION

1.1. GENERAL

Reconstruction of embankment dams plays a major role in contemporary flood protection projects in Germany. Many old embankment dams are too low and an increase of the height of the dam by earthmoving techniques is difficult in concern of available space. Furthermore, the dam body is often in a poor condition. A lot of embankment dams and dikes/levees show woody vegetation, in some cases this vegetation is nature protected. In order to reconstruct the dam body, static sealing elements are usually the only effective solution.

In general, sheet piles are used as a static sealing element, although they are quite expensive. Unconventional solutions exist like different types of earth concrete walls. Usually earth concrete walls are cost-effective and can be realized even in case of limited space. The selection of a construction method that fits best to the project's boundary conditions can grant a high potential for savings. Therefore, the construction method for implementing static sealing elements should be assessed in detail during the early planning process (preliminary / final design).

1.2. PROJECT AREA

The project area is located on the Neckar River in the southwest of Germany. The length of the river is 362.3 km and the project area is approximately at river kilometer 215 from its mouth. An embankment dam protects the hinterland against flooding. The embankment dam was upgraded and partly rebuilt after a major flood occurred in 1980/81, so the structure of the dam body is partly inhomogeneous. Furthermore, there is no existing floodplain. The embankment dam is directly along the riverbed.

The Neckar River valley is densely populated and intensively agriculturally and industrially utilized (Fig. 1). Hence, the damage potential with the floodplains and hinterland is quite high.

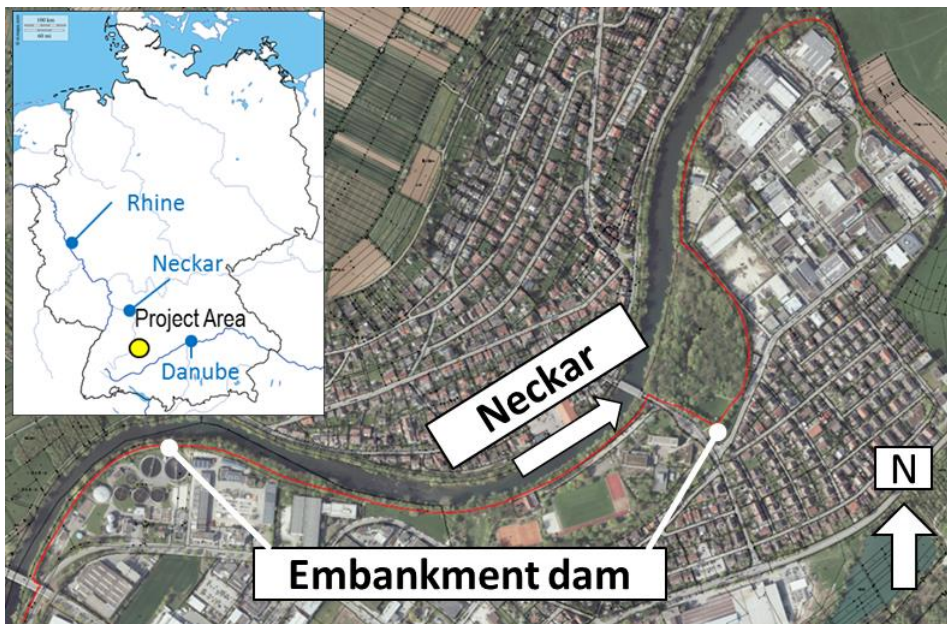


Fig. 1
Project area

Current hydraulic flooding analysis came to the result that the height of the existing embankment dams is partly not sufficient to protect the embankment hinterland from flooding. Furthermore, the existing embankment dam is not stable according to German standards (DIN 19712 [1], DWA M-507 [2], etc.). The standards do not allow woody vegetation on and close to the dam body in general. Nevertheless, many large trees developed on and close to the dam body in the project area (Fig. 2). Nature protection laws dictate that the trees must not to be removed. Thus, the strengthening of the embankment dam can only be realized by the installation of static sealing elements as discussed before.



Fig. 2

View of the crest of the embankment dams along the Neckar River with large trees on both slopes

2. MODELLING

2.3. SOFTWARE TOOLS

In the case study presented in this paper the analyses for the design of static sealing elements were done with a software package developed by GGU (German: Gesellschaft für Grundbau und Umwelttechnik mbH). This software determines the deformation of the construction in consideration of the bedding modulus of the surrounding ground. This bedding modulus is not a real soil parameter. The parameter acts as a spring rate in order to model the interaction between structure and soil. The value of the bedding modulus is depending on the depth of the embedment, etc. The value for the bedding modulus needs to be selected on empirical basis.

The design of sealing elements must comply with several European and German standards as well as technical guidelines (Eurocode 2 [3], EAB [4], EAU [5], etc.). In order to carry out the required analyses, various specifications of the static system need to be defined.

The structure of the system as well as boundary conditions, load cases and material parameters will be discussed within the next sections.

2.4. BOUNDARY CONDITIONS

Load cases were defined corresponding to the specifications of DIN 19712 [1], DWA M-522 [6], Eurocode 1 [7], DIN 19702 [8], etc. They consider different conditions. In addition to standard load conditions such as water level, traffic

load, earth pressure and dead load, the load case "tree failure" is also considered in form of a geometric slope failure criterion. The load case is considered e.g. in the German technical standard for waterways MSD [9].

The mentioned technical standard recommends a reduction of statically required slope inclination. Two different failure modes need to be distinguished. In one case, a tree located on the downstream slope falls, in the other case a tree located on the upstream slope falls. For the tree located on the downstream slope a so-called minimum cross section is defined in MSD [9], which shall be considered for the special load case (Fig. 3). MSD [9] is prepared for embankment dams along waterways with permanent water level, so that trees within the upstream area are not considered, as it is required for levees [13].

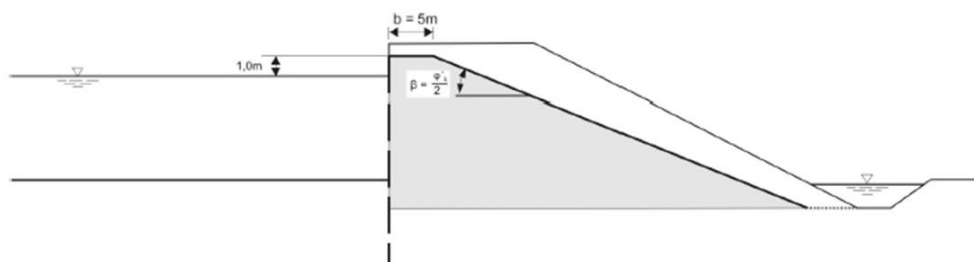


Fig. 3

Minimum statically required cross section according to the load case "tree failure" defined in MSD [9]

Usually trees located at the hinterland or on the downstream slope of an embankment dam are not endangered by flood and a loss of shear strength of the rooted soil area but by strong winds. The coincidence of a flood and storm is quite unlikely to occur. Storm events are preceding flood events. Therefore, the decisive load case for flood embankments and levees is usually the failure of a tree, which is located at or on the upstream slope and which is induced by a loss of shear strength of the rooted area. In consequence, the static sealing element has to be designed as a "free standing" wall which covers a vertical height span. This span can embrace the entire upstream dam shoulder reaching down to the foundation. For the case study, the static function of the sealing element is designed for this total loss of the upstream slope, which is justified by missing foreland, steep slope inclination, and strong flow velocities during flood that might lead to erosion process. The height of the dam crest and the downstream slope was not reduced.

Another boundary condition that has to be set is reflected by the groundwater situation. The software package of GGU allows selecting two different methods. The first method assumes a linear hydrostatic pore water pressure on both sides of the sealing. It is a simplified and conservative approach, since the pore water pressure is usually overestimated. More realistic pore water pressures can be achieved by the second method, which determines the pore water pressure, based utilizing a FEM analysis based on the theory of potentials. For the second approach the geohydraulic parameters for all soils and

materials, such as permeability coefficients, effective pore content, etc. need to be available. Hence, the second approach is likely to produce results that are more realistic. The input parameters were defined by laboratory testing. It was applied for the case study.

In order to guarantee the serviceability of the future dam structure the deformation for the decisive load case was limited to $L/100$ (L = length of the sealing element). The length is defined as the vertical height of the sealing element.

3. DESIGN ASPECTS

3.5. GENERALS

The entire length of the existing embankment dam section in the project area is approximately 2.7 km. 2.05 km of the embankment dam shall be strengthened by placing a static sealing element. A length of 0.8 km shall be fit with an earth concrete wall realized by the so-called mixed-in-place (MIP) wall.

The MIP method destroys the actual the grain structure of the soil in situ and mixes the soil with a cement suspension. The method was developed by the company BAUER. Fig. 4 shows a schematic illustration of the method. This method uses generally three auger drillings which are rotating in opposite directions. The wall itself is established by the pilgrim step method so that each lamella is overlapped by new stitches at least once.

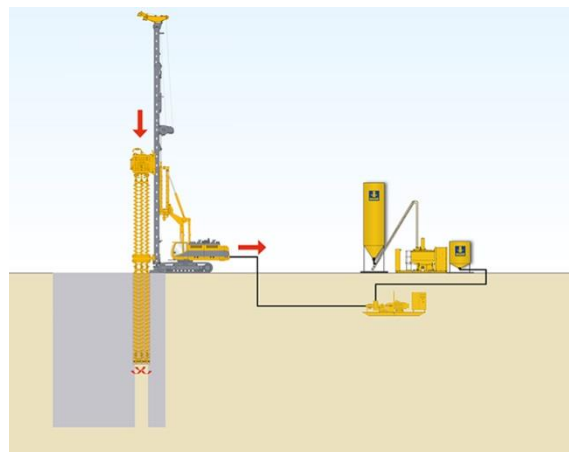


Fig. 4

Schematic illustration of the MIP method (Source: BAUER Spezialtiefbau GmbH)

By placing steel sheet piles into the suspension ditch, the MIP wall can bear loads due to the arching effect utilizing only compressive strength of cement bounded materials.

3.6. DESIGN CROSS-SECTION

The complete embankment dam construction lot was divided into different sections. For each of section a design cross-section was prepared. Fig. 5 shows geotechnical design cross section for the decisive load case “tree failure” which is allocated to the permanent design situation “BS-P” according to DIN 19712 and EC 7.

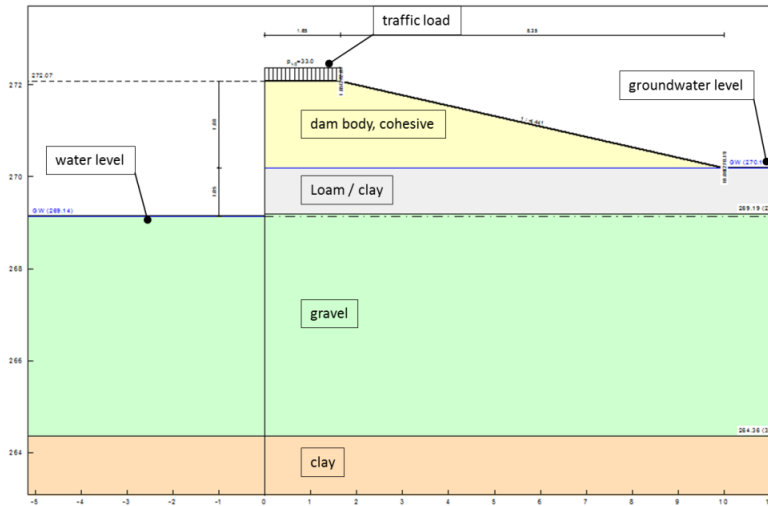


Fig. 5

Geotechnical design cross section for the load case “tree failure” (BS-P)

The height of the considered levee cross section is approximately 2.0 meters. A minimum freeboard of 0.5 m was applied. The embankment slope downstream is not that steep in this design cross-section. It is V:H = 1:4.4. The groundwater level was assumed to reach the ground surface level downstream and a selected rapid drawdown water level upstream.

3.7. CHARACTERISTIC SOIL PARAMETER

In order to carry out the required analyses for design, characteristic soil have to be selected. Table 1 gives an overview of the given characteristic values for the soil layers according to the laboratory tests.

Table 1
Characteristic soil parameters

Soil type	Characteristic soil parameters						
	γ [kn/m ³]	γ' [kn/m ³]	φ [°]	c [kN/m ²]	k [m/s]	δ_a [-]	δ_p [-]
dam fill, cohesive	19	9	25	5	$1 \cdot 10^{-8}$	0.667	-0.667
loam / clay	19	11	30	0	$1 \cdot 10^{-8}$	0.667	-0.667
gravel	18	10	35	0	$1 \cdot 10^{-4}$	0.667	-0.667
clay	18	10	35	0	$1 \cdot 10^{-8}$	0.667	-0.667

Specific weights, friction angles, cohesion and permeability coefficient were determined. The angle of wall friction between sealing and soil can be assumed according to EAB [4] or DIN 4085 [10] (Table 2).

Table 2
Assumptions for the friction angle between sealing and soil

wall texture	according to EAB	according to DIN 4085
teethed wall	$\delta_k = \varphi'_k$	$\delta_k = \varphi'_k$
rough wall	$\varphi'_k \leq 30^\circ: \delta_k \leq \varphi'_k - 2,5^\circ$ $\varphi'_k \geq 30^\circ: \delta_k \leq 27,5^\circ$	$\delta_k \leq 2/3\varphi'_k$
less rough wall	$\delta_k \leq 1/2\varphi'_k$	$\delta_k \leq 1/2\varphi'_k$
smooth	$\delta_k = 0$	$\delta_k = 0$

Due to the construction method of a MIP wall a rough wall characteristic can be assumed, so the friction angle was set to $\delta_k = 2/3\varphi$.

Furthermore, the bedding modulus has to be defined. For this, Weißenbach & Hettler [11] provide reference values depending on the level of mobilization of the earth pressure. Reference values are given for cohesive (Table 3) and non-cohesive soil (Table 4).

Table 3
Reference values for the bedding modulus for cohesive soil according to Weißenbach & Hettler [11]

level of mobilization	bulk density		
	loose	medium	dense
mob $E_{ph,k} : E_{ph,k} = 25 \%$	15.0 MN/m ³	30.0 MN/m ³	60.0 MN/m ³
mob $E_{ph,k} : E_{ph,k} = 37,5 \%$	3.0 MN/m ³	6.0 MN/m ³	12.0 MN/m ³
mob $E_{ph,k} : E_{ph,k} = 50 \%$	1.2 MN/m ³	2.5 MN/m ³	5.0 MN/m ³
mob $E_{ph,k} : E_{ph,k} = 75 \%$	0.5 MN/m ³	1.0 MN/m ³	2.0 MN/m ³

Table 4
Reference values for the bedding modulus for non-cohesive soil according to Weißenbach & Hettler [11]

level of mobilization	bedding modulus
mob $E_{ph,k} : E_{ph,k} = 25 \%$	9.0 MN/m ³
mob $E_{ph,k} : E_{ph,k} = 37,5 \%$	5.0 MN/m ³
mob $E_{ph,k} : E_{ph,k} = 50 \%$	3 MN/m ³
mob $E_{ph,k} : E_{ph,k} = 75 \%$	2 MN/m ³

Bedding modulus and the level of mobilization are interacting so the bedding modulus has to be determined iteratively.

For simplifying the calculation, the bedding modulus can be assumed constant over one soil layer, at least if the embedment depth is small [4]. Furthermore, the MIP wall may only reach down to the gravel layer in order to establish groundwater flow windows (Figure 5).

In addition, the compressive strength of the MIP wall needs to be defined. The compressive strength depends on the soil structure, the content of cement, water, bentonite, etc. According to Witt [12] a characteristic compressive strength of $UCS = 5 \text{ N/mm}^2$ is a reasonable value for earth concrete structures. In DWA (2005) [15] further case studies are mentioned applying less strong mixings with a compressive strength from 0.3 to 1.2 N/mm^2 .

3.8. ANALYSES

The applied software the deformation and moment curve for the indicated system, and it determines the necessary embedment depth. Based on these results a type of steel sheet pile can be selected which meets the requirements for the internal stability and the development of the arching effect.

When selecting the type of the steel sheet pile the dimensions are dictated by the width of the drilling augers, which is, e.g., 370 mm for the smallest rig of BAUER equipment. The steel sheet piles may therefore be maximum 310 mm wide in consideration of at least 30 mm concrete cover. Further, the distance of each sheet pile need to be defined which may vary between 1.0 to 5.0 m in general, mainly depending on the height of the dam (= failure height) and the existing geotechnical conditions.

4. RESULTS

Fig. 6 shows the results of the analysis with the software of GGU, e.g. the moments, shear forces, and the deformation along the MIP wall.

The comparison of different alternatives shows that a wall depth of 7.5 m and a distance between the steel sheet piles of 2.7 m leads to the least amount of steel per meter levees (Table 5). When the embedment depth is reduced or increased, the amount of steel increases. As a result, the MIP wall does not have to be embedded in the impermeable soil layer and the aquifer is sealed so that the groundwater exchange is guaranteed also for normal flow conditions.

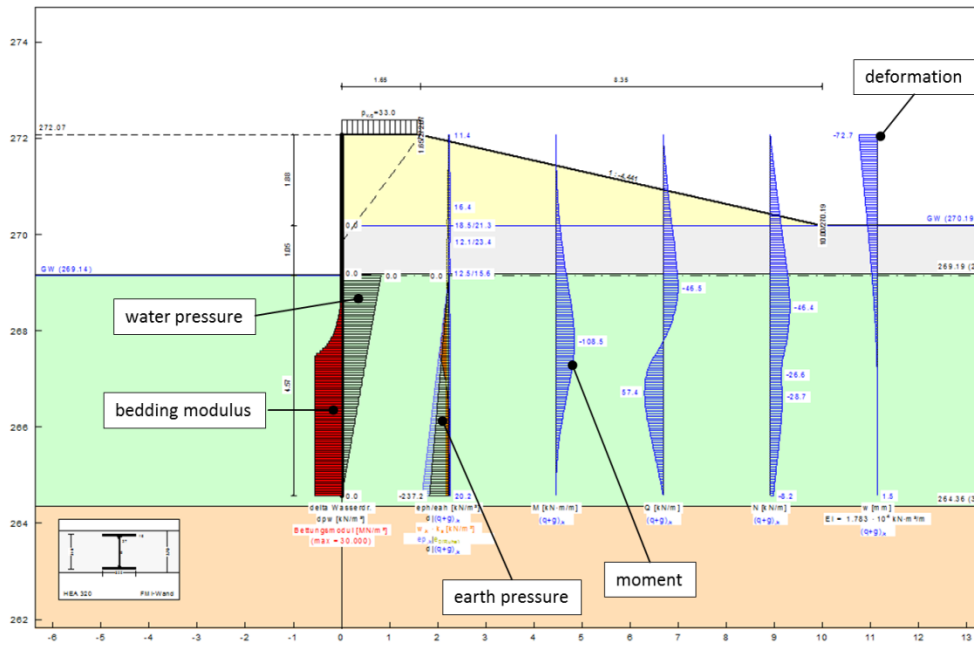


Fig. 6

Results for the design cross-section with an wall depth of 7.5 m and a distance between the steel sheet piles of 2.7 m

Table 5

Required amount of steel for different embedment depths and distances between the steel sheet piles

sheet pile	compressive strength ($f_{c,k}$)	groundwater flow window	depth [m]	distance [m]	amount of steel [t/m]	comment
HEA 320	5	yes	6.5	1.0	not determined	deformation too high, bigger profile or less distance is not possible
HEA 280	5	yes	7.0	1.2	0.45	
HEA 300	5	yes	7.0	1.7	0.37	
HEA 320	5	yes	7.0	2.1	0.32	
HEA 320	5	yes	7.5	2.7	0.27	
HEA 300	5	yes	7.5	2.2	0.3	
HEA 320	5	no	8.0	2.7	0.29	
GU 15N	5	no	8.5	-	1.7	
AZ 12-700	5	no	8	-	1.09	
-		yes	7	-	-	embedment depth too low

5. CONCLUSION

Earth concrete walls, installed by different methods such as MIP method, are an equivalent alternative to sheet pile walls; both are able to bear static

loads. For the described case study groundwater flow windows needed to remain in the underground so that the embedment depth was predefined by this special environmental constraint.

Several design specifications need to be established. The referred German technical standards and guidelines offer practicable hints and suggestions. By using an accredited software program, the MIP walls can be treated like a cut-off wall regarding the design method and the design analysis.

The paper provided an indication of required design alternatives that were considered during the design process. By varying the embedment depth and the distance between the steel sheet piles, an optimum economic solution could be defined which shows the least material consumptions, mainly regarding steel.

REFERENCES

- [1] DIN 19712. Hochwasserschutzanlagen an Fließgewässern. *Deutsches Institut für Normung (DIN)*, 2013.
- [2] DWA-M 507-1. Deiche an Fließgewässern – Teil1: Planung, Bau und Betrieb. *Deutsche Vereinigung für Wasserwirtschaft, Abwasser und Abfall (DWA) e.V.*, 2011.
- [3] EC2. Bemessung und Konstruktion von Stahlbeton- und Spannbetontragwerken. Eurocode 2. *Deutsches Institut für Normung (DIN)*, 2011.
- [4] EAB. Empfehlungen des Arbeitskreises „Baugruben“ – EAB. *Ernst & Sohn Verlag für Architektur und technische Wissenschaften GmbH & Co. KG*, 2006.
- [5] EAU. Empfehlungen des Arbeitsausschusses „Ufereinfassungen“, Häfen und Wasserstraßen – EAU. *Ernst & Sohn Verlag für Architektur und technische Wissenschaften GmbH & Co. KG*, 2004.
- [6] DWA-M 522. Kleine Talsperren und kleine Hochwasserrückhaltebecken. *Deutsche Vereinigung für Wasserwirtschaft, Abwasser und Abfall (DWA) e.V.*, 2015.
- [7] EC 1. Einwirkungen auf Tragwerke. Eurocode 1, *Deutsches Institut für Normung (DIN)*, 2013.
- [8] DIN 19702. Massivbauwerke im Wasserbau – Tragfähigkeit, Gebrauchstauglichkeit und Dauerhaftigkeit. *Deutsches Institut für Normung (DIN)*, 2010.
- [9] BAW. Standsicherheit von Dämmen an Bundeswasserstraßen (MSD). *Bundesanstalt für Wasserbau (BAW)*, 2011.
- [10] DIN 4085. Baugrund – Berechnung des Erddrucks. *Deutsches Institut für Normung (DIN)*, 2017

- [11] WEISSENBACH A., HETTLER A. Baugruben – Berechnungsverfahren. *Ernst & Sohn Verlag für Architektur und technische Wissenschaften GmbH & Co. KG*, 2011.
- [12] WITT K.J. Grundbau-Taschenbuch – Teil 3: Gründungen und geotechnische Bauwerke. *Ernst & Sohn Verlag für Architektur und technische Wissenschaften GmbH & Co. KG*, 2009.
- [13] HASELSTEINER, R.; STROBL, T. Deichertüchtigung unter besonderer Berücksichtigung des Gehölzbewuchses. Sicherung von Dämmen, Deichen und Stauanlagen - Handbuch für Theorie und Praxis. *Hrsg. Prof. Dr.-Ing. Richard A. Hermann und Prof. Dr.-Ing. Jürgen Jensen, Universitätsverlag Siegen – universi*, 2006.
- [14] HASELSTEINER, R. Der Bewuchs an und auf Hochwasserschutzdeichen an Fließgewässern aus technischer und naturschutzfachlicher Sicht. *Dresdner Wasserbaukolloquium, "Wasserbau und Umwelt - Anforderungen, Methoden und Lösungen"*, 17.-18.03.2010 in Dresden, *Institut für Wasserbau und Technische Hydromechanik, Wasserbauliche Mitteilungen, Heft 40*, S. 373-382, 2010.
- [15] DWA. Dichtungen in Deichen. *Deutsche Vereinigung für Wasserwirtschaft, Abwasser und Abfall (DWA) e.V.*, 2005.

COMMISSION INTERNATIONALE DES GRANDS BARRAGES

VINGT-SIXIÈME CONGRÈS DES GRANDS BARRAGES
Autriche, juillet 2018

DOI 10.3217/978-3-85125-620-8-156



This work licensed under a Creative Commons Attribution 4.0 International License. <https://creativecommons.org/licenses/by-nc-nd/4.0/>

FIGHTING CRITICAL UPLIFT AT ATATURK DAM

M. GAVARD

Consultant

LUXEMBOURG

W. RIEMER

Consultant

LUXEMBOURG

FIGHTING CRITICAL UPLIFT AT ATATURK DAM *

M. .GAVARD

Consultant

W. RIEMER

Consultant

LUXEMBOURG

1. INTRODUCTION

With a maximum height above foundation of 179 m and a fill volume of 84 hm³, the Ataturk dam on the Euphrates River in Turkey creates a reservoir with about 49 km³ storage capacity [1], feeds two hydropower plants with a combined capacity of 2.6 GW and offers command over an extensive irrigation area in Southeast Anatolia. A sequence of carbonate sediments – limestone, marl, dolomite – forms the foundation of the Ataturk dam. Exploratory drilling and especially galleries identified important karstification and, in consequence, the design included an extensive grout curtain (1.2 km² area) and provided drainage systems for the spillway and the powerhouse. Nevertheless, with the variation in hydrogeological properties and complexity of the hydrogeological regime in a folded and faulted rock mass, substantial uncertainty in the prediction of the development of seepage and uplift had to be admitted.

To contain the risks potentially associated with this uncertainty, a hydrogeological monitoring system was installed and, concurrent with the progress of construction of the grout curtain and with reservoir filling, the collected data were evaluated for implications related to the performance of the curtain and the building of uplift pressures [2]. Already when river diversion raised the upstream levels, a conspicuous hydrogeological phenomenon materialized: at substantial depth under the dam high artesian pressure developed in karstic rock, potentially affecting the stability of the foundation.

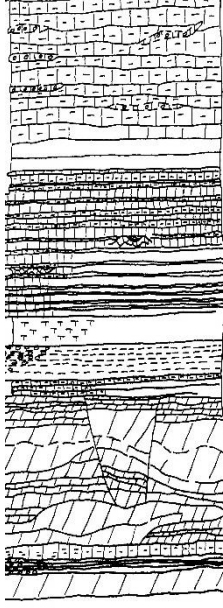
Options for remedial action were studied but their implementation met with technical and economical constraints. Eventually, a balance of grouting and drainage works, which produced an acceptable performance of the foundation, and an observational approach intended to manage the risks associated with conceivable but unpredictable long term effects in the deep underground of the dam was adopted. The contribution explains the concepts applied, summarizes observations obtained and the conclusion resulting for future handling of the hydrogeological problem.

**Lutte contre sous-pressions critiques à Atatürk Barrage*

2. GEOLOGICAL AND HYDROGEOLOGICAL CONDITIONS

The dam rests on a sequence of marls, limestone and dolomite, dating from the Cretaceous, as listed in Table 1.

Table 1
Litho-Stratigraphy
Lithostratigraphie

	Formation	Lithology	Thickness	Karst
	Bozova Formation	Marly Limestone	200-300m	modest or absent
	Sayindere Formation (Plaketli Lst.)	Stratified limestone, marl, chert	100-250m	significant, primarily related with faults
	Karabogaz Fm.	Chert, bituminous limestone	50-100m	locally important
	Karababa Formation	Dolomite, dolomitic limestone	100-150m	caves, cellular and sugary solution
Chert, bitum. lst.		50m	aquitard	
Dolomitic limestone		>100m	significant	

With the loss of calcium carbonate, the limestone of the Sayindere Formation partially became erodible, the dolomites of the Karababa Formation locally had converted into flowable sand or developed a highly porous cellular structure (Figure 1).

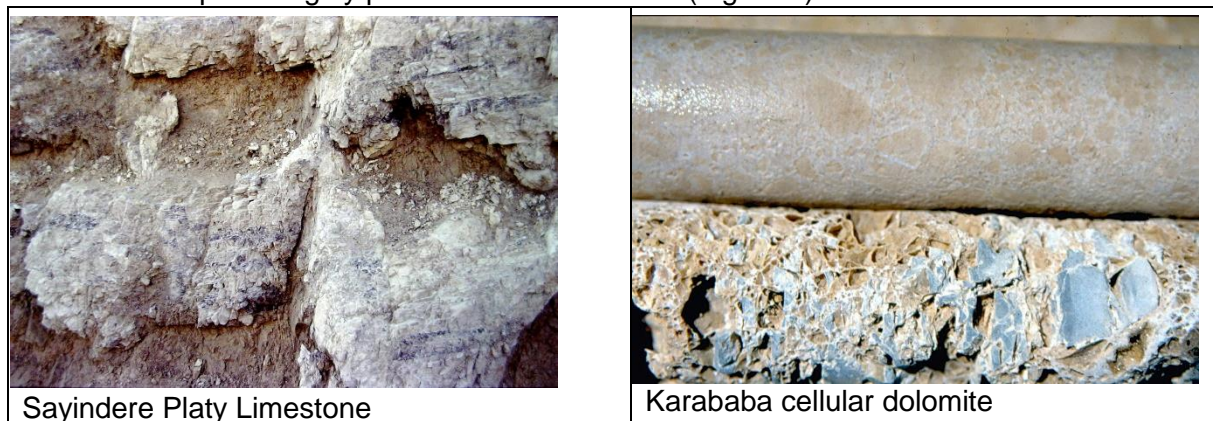


Figure 1

Karstification in Sayindere and Karababa Formations *Karstification des Formations de Sayindere et de Karababa*

A major anticline obliquely crosses the dam axis on the left abutment and raises the upper part of the Karababa Formation to the surface. Downstream of the dam, the Bozova Fault brings the Cretaceous carbonates in contact with clastic sediments of Tertiary age

(Figure 2). A number of minor faults crosses the grout curtain and has promoted the development of karst conduits.

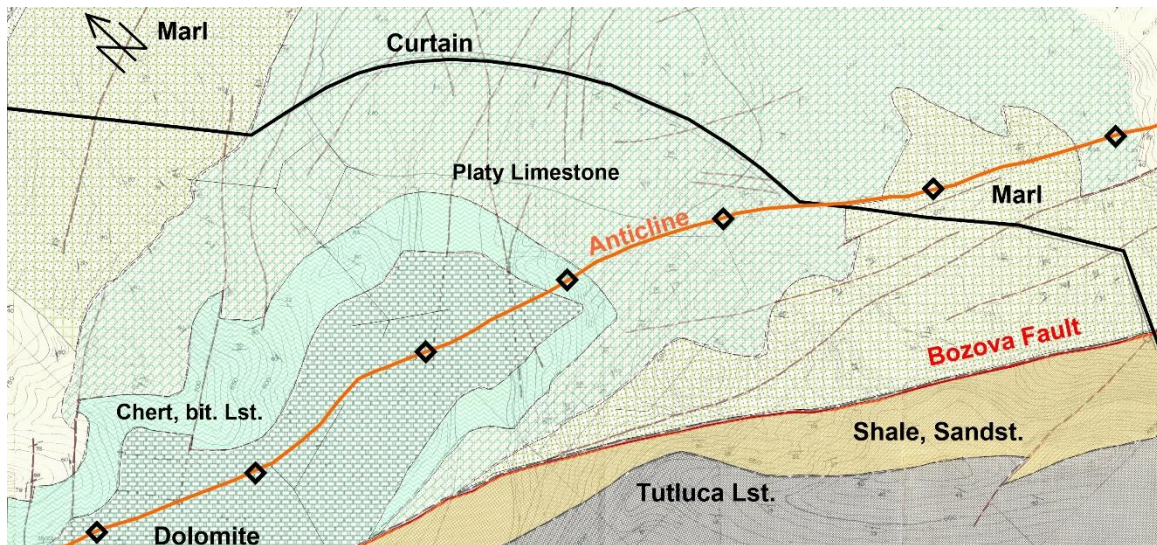


Figure 2
Geological map of dam site
Carte géologique du site du barrage

3. HYDROGEOLOGICAL OBSERVATIONS

After river diversion, springs showed up in the former riverbed, discharging about 1 m³/s. The chemical composition and isotope content of the spring water differed significantly from the Euphrates river water, the elevated temperature suggested deep circulation in a karst system. With rising water levels upstream of the cofferdam, the deep piezometers displayed

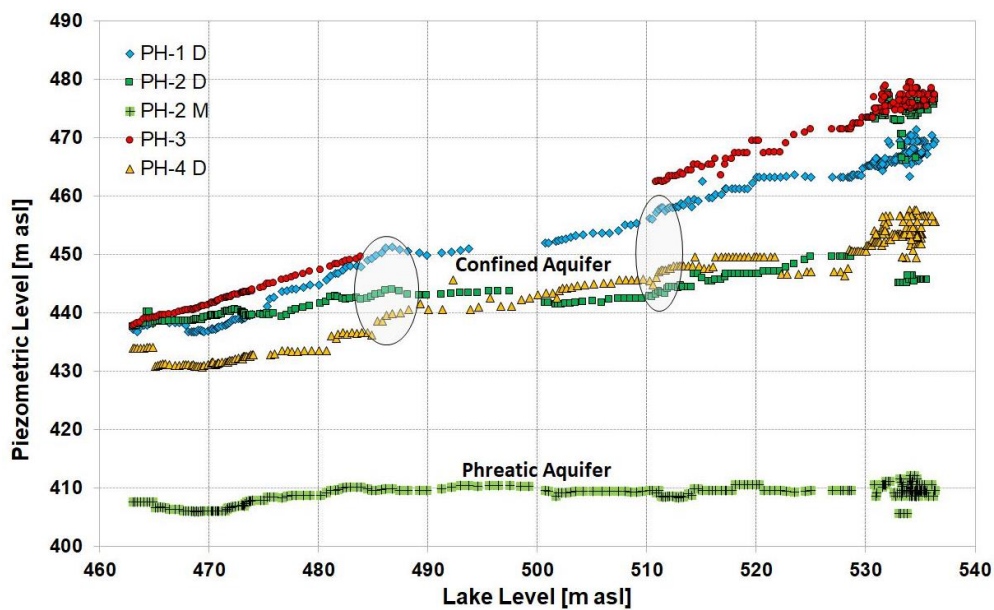


Figure 3
Samples of piezometer response (Location PH 1, 2, 3 see Fig.6)
Exemples des réactions des piézomètres (Location PH 1, 2, 3 voir Fig.6)

a confined response in the lower Karababa Formation, with the intercalated horizon of bituminous limestone acting as aquitard. In response to the upstream water levels, the piezometric head became notably artesian. Already in 1990, river water had replaced the karst water in the deep, confined aquifer. This condition implied recharge from the future reservoir area close to the dam site. Reservoir filling started end of 1989 and Figure 3 illustrates the piezometric response in the deep aquifer. Piezometer PH-2M is completed in the upper Karababa Formation at 120m depth, the other instruments sit below the bituminous layer at around 200 m depth. Although the tectonic faults cut through this layer, the latter continues to act as an efficient aquitard, maintaining a head difference of up to 70 m, reaching an artesian level of about 100 m above the valley floor downstream of the dam. However, the two ellipses in Figure 3 mark events when the response of the deep piezometers changes synchronously, evidencing a change in the hydrogeologic regime, most probably due to the opening of a new drainage path. The observations have the following consequences for the dam: (1) the magnitude of the uplift pressure raises concerns in respect of the hydraulic stability of the valley floor downstream of the dam, (2) the performance of the aquitard is not guaranteed, more important fracturing is conceivable and may raise seepage and concurrent erosion of karst affected domains. Figure 4 illustrates the importance of the piezometric head downstream of the dam.

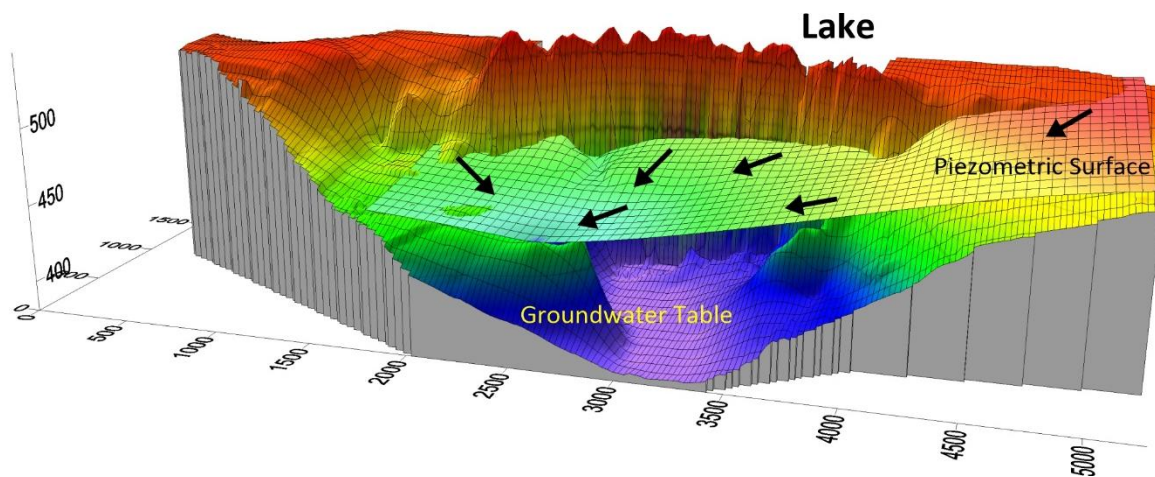
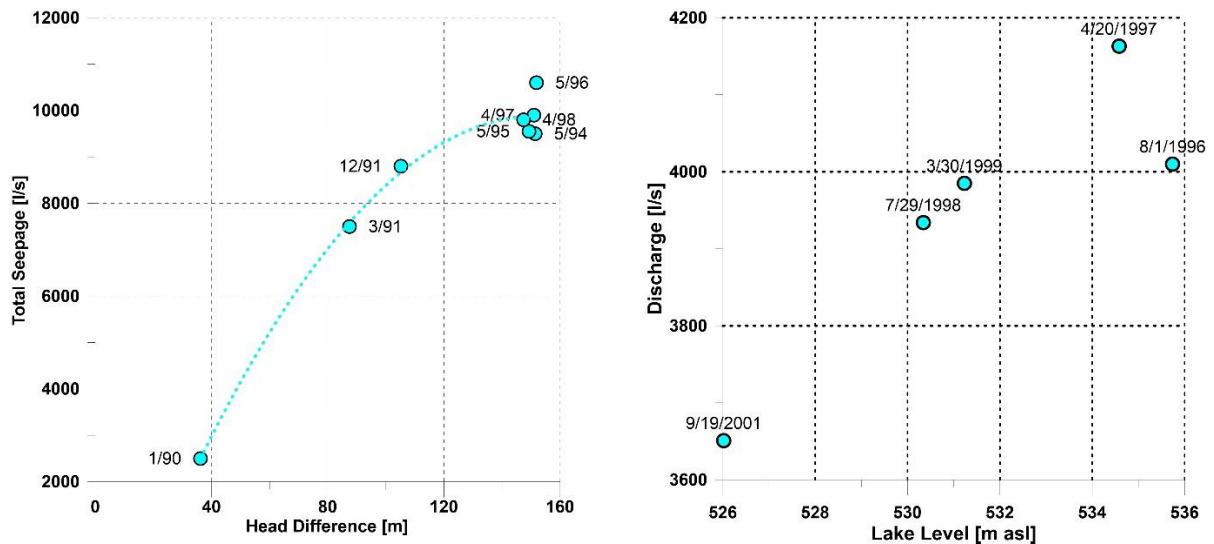


Fig. 4

3D models of groundwater table and piezometric surface downstream of Ataturk grout curtain
Modèles 3D de la nappe phréatique et de la surface piézométrique en aval du voile d'injection

Monitoring of total reservoir seepage is a difficult undertaking. The powerplant has to be shut down for sufficient time to approach steady state and this has trans-border implications. A further complication materialized when the Birecik dam raised the tailwater to the toe of the Ataturk dam. For these reasons, no measurements were taken after 1998. To obtain the value corresponding to reservoir seepage, several other components had to be accounted for, partially poorly defined, and in consequence, a significant error has to be allowed for the data presented in Figure 5. Nevertheless, the data indicate a favorable effect of the complementary grouting works performed after the start of reservoir filling and they also imply a fairly stable performance of the curtain over the period covered by the measurements. Figure 5 also shows the discharge recorded at the drainage galleries driven at the spillway in the left valley flank and in the right valley flank behind the powerhouse and farther downstream. The excavation of these galleries started during the initial stage of reservoir filling in 1990 and was completed at the beginning of 1993. The measurements in these galleries are not very accurate and this circumstance may account for the low value reported for 1996.



Total Seepage in riverbed

Seepage collected by drain galleries

Figure 5

Discharge measurements
Mesures des eaux de drainage

4. ORIGINAL DESIGN AND AMENDMENTS

The design had allocated generous quantities for the grout curtain and these sufficed to handle also the additional geological problems encountered during construction. The design had provided particular precautions for the foundation of the core, with blanket grouting from the surface, a main grouting gallery and an additional control gallery with fan grouting under the core [1, 2, 3]. The design included extensive drainage systems for the powerhouse [4] and for the spillway. A dense network of piezometers allowed monitoring of the efficiency of the grout curtain and the development of uplift in the foundation of the dam and at the appurtenant

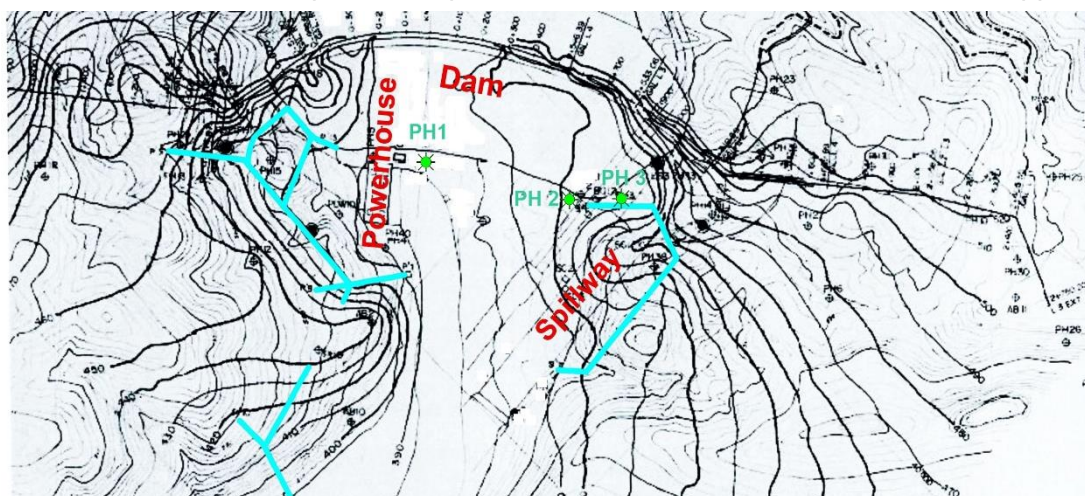


Fig. 6

Dam site, contours for phreatic aquifer, location of drainage galleries in the valley flanks

Site du barrage,

. Contours de la nappe phréatique, emplacement des galeries de drainage dans les appuis

structures. The piezometric records, complemented by tracer tests, guided the works on the grout curtain and also alerted on piezometric hazards rising at the spillway, the powerhouse and in the deep, confined aquifer.

As verified by hydrogeological model simulation, deepening the grout curtain within technical viability promised to reduce reservoir seepage by up to 30%. This effect was not justifiable from an economical point of view. Considering the uncertainty regarding the recharge to the deep aquifer, constraining the seepage at higher levels in the foundation could even risk producing higher loads on the deep aquifer. These considerations led to the decision to implement additional drainage works in both valley flanks and to adopt an observational approach for the deep aquifer. Figure 6 shows the alignments of the drainage galleries, which were constructed in the valley flanks.

After 12 years of safety monitoring, hydrogeological investigations and complementary works on the curtain, the drainage system and the instrumentation, a set of criteria for future action was defined [5], distinguishing three levels of increasing hazard. Level 3, the worst-case scenario, would prompt declaration of an Alarm and immediate start of contingency action under the following conditions:

- If the drainage gallery discharge increases by 20% or if the trend is of the order of 10% per month
- For the curtain and deep aquifer piezometers 20% abrupt change, or 10% persistent monthly trend for an Alarm. For the deep aquifer, these criteria would also apply for a loss of piezometric head because such drop would indicate serious hydrofracturing or erosion of the confining layer.
- An Alarm should be declared if the seepage water in the observation pits, the dam site springs or drainage galleries becomes turbid, indicating erosion of the foundation or the core.
- An Alarm should be given if a sinkhole develops in the vicinity of the dam or the structures
- An Alarm must be declared if the admissible uplift at the powerhouse or the spillway chute is reached or exceeded.

With the data provided by the monitoring system, timely remedial action can be taken and the hazards linked to the karst can confidently be contained.

ACKNOWLEDGEMENTS

Out of the large number of professionals participating in the implementation of the monumental project, a few are mentioned because of their specific support to the installation of the monitoring system and contribution to the geological and hydrogeological investigations: E. Basmaci, A. Öktem, E. Önhon, J. D. Andrey. Credit also has to go to the auxiliary staff who over the years conscientiously collected the wealth of monitoring data.

REFERENCES

- [1] Basmaci, E., 1991: Foundation behaviour of Ataturk dam on first filling. *Proc. 17th Congr. ICOLD, Q. 66, R. 57, pp. 1051-1062*
- [2] Riemer, W., Gavard, M., Soubrier, G., Turfan, M.: The seepage at the Atatürk fill dam. *Proc. 19th Congr. ICOLD, 1997, pp 613-633*

- [3] Riemer, W., Gavard, M., Turfan, M: Atatürk dam - hydrogeological and hydrochemical monitoring of grout curtain in karstic rock. *Verification of Geotechnical Grouting, ASCE Geotechnical Special Publication no. 57, 1995, pp 116-126*
- [4] Riemer, W., Andrey, J. D.: Baugrundbehandlung am Atatürk Damm. *Ber. 8. Nationale Tagung für Ingenieurgeologie, Berlin, 1991, pp 167-174*
- [5] Ataturk Engineers Joint Venture: Hydrogeological Situation at the dam site. Monitoring report. Update October 2001

SUMMARY

The designer of the Ataturk project had provided an extensive treatment for the karstic conditions at the dam site. Nevertheless, with the variation in hydrogeological properties and complexity of the hydrogeological regime in a folded and faulted rock mass, substantial uncertainty in the prediction of the development of seepage and uplift had to be admitted. To contain the risks potentially associated with this uncertainty, a hydrogeological monitoring system was installed and, concurrent with the progress of construction of the grout curtain and with the reservoir filling, the collected data were evaluated for implications related to the performance of the curtain and the building of uplift pressures. The development of high artesian head in a confined aquifer presented a particular problem. Further extension of the grout curtain met with economical and technical constraints and, in consequence, the drainage system had to be strengthened.

In this way, the construction activities for the treatment of the foundation were progressively optimized and the method for managing the risks associated with the complex conditions was developed.

RÉSUMÉ

Les auteurs du projet pour le "Barrage Atatürk" avaient d'emblée prévu un important traitement des fondations karstiques du site. La variété et la complexité du régime hydrogéologique dans un massif plissé discontinu, nécessitaient d'envisager de substantielles incertitudes dans la prédiction et le développement des filtrations et des conditions de sous-pression. Pour y pallier, un vaste système d'observations hydrogéologiques a été mis en place et, durant les travaux pour le voile d'injections ainsi que pendant le remplissage du réservoir, les résultats des mesures d'infiltrations et de sous-pressions ont été évalués et pris en compte. Le développement de forte pressions artésiennes dans un aquifère confiné a représenté un problème particulier car l'extension du rideau d'injections rencontrait des difficultés techniques et financières et il a fallu renforcer le système de drainage.

Cela a permis l'optimisation des dispositions constructives et a grandement contribué à contrôler les risques associés à une fondation complexe.

COMMISSION INTERNATIONALE DES GRANDS BARRAGES

VINGT-SIXIÈME CONGRÈS DES GRANDS BARRAGES
Autriche, juillet 2018

DOI 10.3217/978-3-85125-620-8-157



This work licensed under a Creative Commons Attribution 4.0 International License. <https://creativecommons.org/licenses/by-nc-nd/4.0/>

**WATER TIGHTENING OF RESERVOIR BED AND UPSTREAM FACE OF DAM
IN PERSIAN GULF MARTYRS (CHITGAR) LAKE - A CASE STUDY**

Ali EMAM

Managing Director of ENGINEERING AND DEVELOPMENT ORGANIZATION
OF THE CITY OF TEHRAN (EDOCT), TEHRAN

IRAN

M. ZOLFAGHARIAN

Project Manager of CONSTRUCTION OF PERSIAN GULF MARTYRS
(CHITGAR) LAKE, TEHRAN MUNICIPALITY, TEHRAN

IRAN

Nima RASHIDI

Project Manager, ARMATURE PARDIS CO., TEHRAN

IRAN

Rouzbeh RADMAN

Engineer, ARMATURE PARDIS CO., TEHRAN

IRAN

Water tightening of reservoir bed and upstream face of dam in Persian Gulf Martyrs (Chitgar) Lake - A Case Study

Ali Emam

Managing Director of Engineering and Development Organization of the city of Tehran (EDOCT)
Tehran
Iran

Nima Rashidi

Armature Pardis Co., Project Manager
Tehran
Iran

M. Zolfagharian

Project Manager of Construction of Persian Gulf Martyrs (Chitgar) Lake, Tehran Municipality
Tehran
Iran

Rouzbah Radman

Armature Pardis Co., Engineer
Tehran
Iran

Introduction

Chitgar (Persian Gulf Martyrs) Artificial Lake of Tehran was recently developed for recreational purposes and has significantly changed the landscape of the Iran's Capital. Design and Construction of the lake involved many technical challenges. Shortage of water supply from the nearby river, a four-month impounding constraint and significant surficial evaporation made water tightening at the reservoir bed and the surface of the upstream earth fill dam inevitable. Several solutions were initially considered for the purpose of water tightening among which use of clay blanket, concrete protection layer, injection in alluvium, protective hydraulic asphalt and finally Geomembrane were notable. After carrying out comprehensive technical and economic studies and also considering the time frame of construction, use of Geo-synthetic material was ultimately selected as the best option. In this paper, challenges and lessons learned during construction and installation of Geomembrane for the 130 hectare Chitgar Lake were discussed. Authors hope that information provided herein can be used and applied to many similar projects and help toward improving technical knowledge and successful completion of large scale water tightening projects around the world.

1. Chitgar Lake and City of Tehran

Chitgar Lake was developed with the objectives of improving on recreational, commercial, environmental attractions of the Tehran City. The Lake is located in West side of Tehran near the Chitgar National Park and also in vicinity of the Alborz Mountain Range. These nearby natural features have dramatically improved the scenic beauty and landscape of the area.



Figure 1 Areal View of Chitgar Lake located West of Tehran City

In General, the Lake Project consists of three main components which are illustrated in Figure 2.

A: Diversion Dam

B: Water Conveyance from Kan River to the Lake

C: Rock-fill/Earth-fill Dyke/Dam and Reservoir

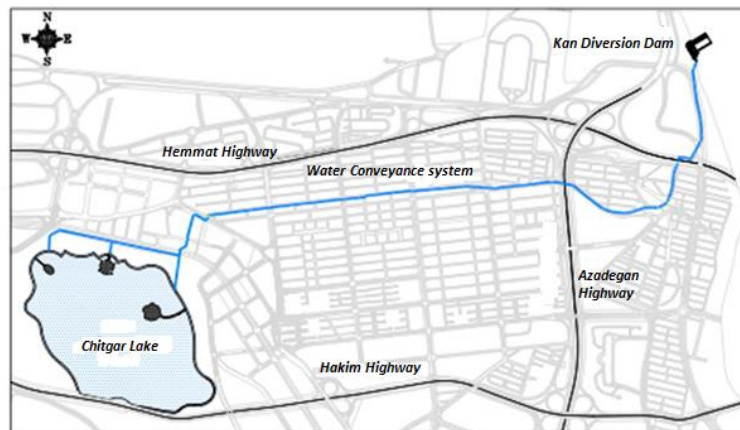


Figure 2. Different components of Chitgar Lake Project (Diversion Dam (Top Right), Water Conveyance and Reservoir)

Kan Diversion Dam is a concrete structure built on the seasonal Kan River at a 7km distance to the Lake in order to increase the level of river water and divert it toward the Lake.

The 7-km Water Conveyance from the Kan River to the Lake is composed of a 3.5km concrete channel (1.5mx1.1m) and 3.5km of GRP Pipes with varying diameters from 600mm to 1200mm. The conveyance was designed to have a maximum discharge capacity of $1.2\text{m}^3/\text{s}$.

The Lake Reservoir spread over a 132 hectare area with a storage capacity of 6.9 million cubic meter was the primary component of the project. The Lake has three artificial islands with a total area of 3 hectares within it. By considering the topography of the area and the required depth and geometry for the Lake, a 10.5 m high and 735 long earth-fill dam plus a perimeter dyke with a total length of 4km were constructed.

2. Necessity of Water tightening for Chitgar Lake

Total allowance for the Lake annual inflow is about 5 million cubic meters while 2.2 million cubic meter is the estimated annual loss through surface evaporation.

In order to identify the soil layer underneath the Lake and estimate the amount of water seepage, investigation bore holes were drilled initially on a 400x400 grid and later on refined to 200x200 and 100x100 grids over the Lake's area. Based on the permeability test results at the depth of 2m, the permeability and seepage potential for the reservoir bed area were listed as given in Table 1. Following assumptions have been used to determine the permeability parameters provided in the table:

- Darcy formula ($Q=k.i.A$) was used for calculation of discharge. (“k” value varies over different areas)
- Depth of reservoir was considered between 4m and 10m with an average depth of 7m.
- Depth of fine-material alluvium layer of reservoir was assumed 4m.
- Hydraulic gradient was considered 1.75. (i.e. $7/4=1.75$)
- Area of the reservoir is roughly equal to 132 hectares

Table 1. Summary of Estimated Seepage Rate for the Reservoir Based on Permeability Test Results

Annual Seepage	Seepage Rate (m ³ /s)	Reservoir Area	Average Permeability	Permeability Range (cm/s)
0.72	0.023	24.4	4.06×10^{-6}	$10^{-6} - 10^{-5}$
1.61	0.051	5.4	4.10×10^{-5}	$10^{-5} - 10^{-4}$
74.35	2.36	32.4	3.15×10^{-4}	$10^{-4} - 10^{-3}$
905.95	28.73	37.8	3.29×10^{-3}	$10^{-3} - 10^{-2}$
983	31.16	100	1.35×10^{-3}	Total

Calculated seepage rate based on the above assumption and parameters was $31.16 \text{ m}^3/\text{s}$. With the assumption of full reservoir, this leads to an annual seepage rate of approximately 1 billion cubic meters. This suggested that water tightening and through insulation for the reservoir was essential for the Chitgar Lake Project.

Due to the significant depth of alluvium (more than 100m), water tightening underneath the dam body and the perimeter dyke was impractical and the only feasible option was continuous interconnection of the water tightening membrane over the entire area of the reservoir and extending to upstream face of the dam. This solution provides many advantages compared to other possible remedies such as elimination of dam foundation water tightening activity, seepage-free dam body resulting in size reduction of the dam's core and finally ease of construction.

3. Lake Water tightening Alternatives

3.1. Water tightening using Clay Blanket

One method for the purpose of reservoir water tightening is to use Clay Blanket. As common practice, in order to have a functional clay blanket with a permeability rate of 1×10^{-7} and less, materials with following specifications should be used: 50% passing rate through No. 200 Filter, a minimum 20% clay material, above 20% Plasticity Index (PI) and above 30% Liquidity Index (LL) Index.

Overall, due to the poor condition of reservoir fine-grain material and unavailability of suitable material in proximity of the project which lead to undesirable seepage, the option of Clay Blanket was rejected. Another disadvantage of the use of Clay Blanket was the possibility of plant growth on the surface which can contribute to pollution of the Lake and have negative environmental impact.

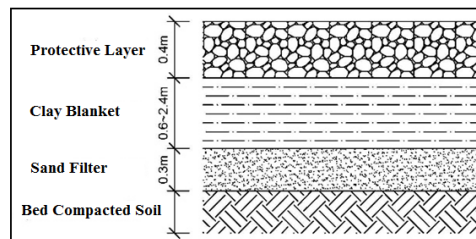


Figure 3. Section Details for Clay Blanket Option

3.2. Water tightening using Impervious Concrete Layer

Use of impervious concrete layer for large reservoirs such as Chitgar Lake's is not common due to the significant size and importance and functional requirements of the Lake. From the geotechnical perspective, impervious concrete layer should be placed on the alluvium with a concrete thickness of about 30cm plus uniform thermal reinforcement and water-tight joints every 12 to 15 meters.

Due to the high cost and relatively lengthy implementation time, the impervious concrete layer was not considered as a suitable option when compared to other feasible options.

3.3. Water tightening using Injection in Alluvium Layer

In principle, injection in alluvium is very rarely used where no other option is available. This method requires heavy research before implementation and is often very costly and time consuming. In addition, injection in fine-grain material would result in rupture and fracture of soil due to hydraulic pressure of injection which is highly undesirable.

For Chitgar Lake, considering the type of soil material, permeability and fine material amount, use of high Belin cement grout injection to achieve allowable permeability (even with injection holes distanced at 75cm) was not feasible. Furthermore, injection using chemicals like Resin and Polyurethane and other stable and unstable materials considering their permeability, even by using 50cm apart injection holes deemed not suitable to achieve the target permeability. Even if this method was somehow technically feasible, due to the large size of the Lake, the projected cost and implementation time makes it impractical within the given time-frame of the project as it required nearly 2.5 million injection holes over the entire Lake area.

3.4. Water tightening using Asphalt Concrete

Another suggested method for water tightening of the Lake was use of Asphalt Concrete with the details shown in Figure 4. In this method, after soil improvements and implementation of the base layer, asphalt concrete with a total thickness of 10cm placed in two 5cm layers is used. Gravel size for this type of concrete is not to exceed 12.6mm according to the ICOLD's Bulletin 114. About 7 to 8 percent bitumen may be used with a porosity of less than 4% to result in a permeability factor of 1×10^{-8} to 1×10^{-9} cm/s. The bitumen has a penetration rate of 80-100 based on ASTM D5-D946 for asphalt concrete. As top finish, a 10mm thick layer of bitumen mastic layer will be placed on top of the asphalt concrete to improve water tightening and provide physical protection.

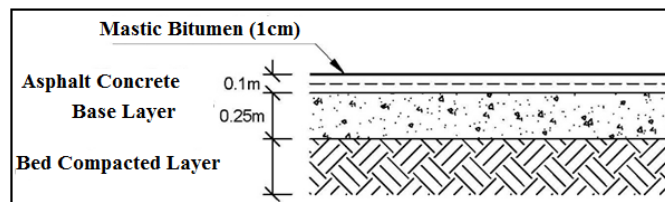


Figure 4. Section Details for Asphalt Concrete Option

With assumption of average reservoir head of 7m and permeability of about 1×10^{-8} cm/s for asphalt concrete, the annual seepage from the reservoir was estimated 300,000 m³ for an intact concrete layer. By considering the possibility of cracking in the asphalt layer the estimated annual loss will be doubled to a total of 600,000 m³/year.

3.5. Water tightening using Geomembrane

Use of Geomembrane was another alternative for water tightening of the Chitgar Lake. The Geomembrane consists of three layers of Geo synthetic material: a Geomembrane layer protected by two layers of Geo textile on top and bottom. Use of Geomembrane has many advantages as follows:

- very low permeability rate to reduce the reservoir seepage
- sufficient flexibility to allow placement on alluvium with minimum base preparation
- a continuous impervious layer extending from the lake to the upstream surface of the earth-fill dam
- ease and high pace of installation process

The main weakness of Geomembrane is its vulnerability to possible physical damage which can be mitigated by soil placement on top of the Geomembrane; however this remedy makes it very difficult to locate and fix the possible damaged area during operation and maintenance.

In this method after soil improvement is complete, the bottom Geotextile layer is placed at the reservoir bed. Then the main Water tightening Geomembrane layer is placed on top of Geotextile

layer and once the top Geotextile layer surface is placed over the Geomembrane, the top surface is covered with a protective soil/rock layer.

The Geotextile layers are provided to protect the Geomembrane against physical damage as well as to provide shear resistance which is critical on the slopes. Due to sensitivity of installation process, extra care and quality control is required for the Geomembrane water tightening procedure.

The top protective layer is made of available alluvium material of higher one inch and with a thickness of 15cm to 20cm with the use of manual non-vibration compactor. Main reason to use the large size material in to avoid a fine-grain layer suitable for growth of plants during the operation period while other benefits are listed below:

- protection against wrinkle effect of Geomembrane due to thermal expansion
- protection against uplift of Geomembrane during extreme wind under empty reservoir condition
- protection against physical damage and act of vandalism

Assuming a 7m reservoir head and a permeability factor of 1×10^{-12} cm/s for the 1.5mm thick Geomembrane, the expected annual seepage from the Lake will be around 2000 m³.

3.6. Finding the Best Solution by Comparison between Water tightening Alternatives

Considering the above figures about the Lake, Water tightening option using the Clay Blanket was eliminated and comparison between Geomembrane and Asphalt Concrete indicated that the Geomembrane option is the most cost-effective solution for the Lake. Another distinctive advantage of Geomembrane is the pace of installation which is much higher for the cold seasons compared to the Asphalt Concrete. Furthermore, reliability of asphalt concrete is of concern as many implemented hydraulic asphalt concrete did not fully meet the expectations for water tightening performance. Ultimately the Geomembrane protection was selected as the preferred water tightening option for the Chitgar Lake.

4. Geomembrane Installation and Quality Control

4.1. Implementation of Water tightening Layer on Chitgar Lake Bed

Water tightening layer for bed of the lake consists of a Geomembrane layer protected by two layers of Geo textile on top and bottom as shown in Figure 5 covered with a protective coarse material layer.



Figure 5. Preparation and Installation Stages for Water tightening of the Chitgar Lake bed

The Specifications for the Geomembrane and Geotextile used in Chitgar Lake bed are provided in the Tables 2.

Table 2. Geomembrane Specifications used in the lake bed

Description	Spec.	Reference
Thickness	1.5 mm	ASTM D5199
Density	0.940 gr/cm ³	ASTM D1505/D792
Tensile strength	:(type IV	ASTM D6693
Yield strength	≥ 22 KN/m	
Break strength	≥ 40 KN/m	
Elongation at Yield	≥ 12%	
Elongation at break	≥ 700% type IV)	ASTM D6693
Tear resistance	≥ 187 N	ASTM D1004
Puncture resistance	≥ 408 N	ASTM D4833
Carbon Content	2-3%	ASTM D4218
Standard Oxidation Induction Time	100 min	ASTM D3895 – 5885
Resistance against crack propagation(SCR)	300h	ASTM D5397
Oven Aging (Hp) After 90 Days	80% of Oxidation Induction Time	ASTM D5885
Resistance against UV radiation After 1600 hours	50% of Oxidation Induction Time	ASTM D5885

Table 3. Geotextile Specifications used in the lake bed

Geotextile Type	400 gr	Reference
Weight per meter square	≥ 400 gr	ASTM D5261
Tensile Strength	≥1.33kN	ASTM D4632
Elongation	≥ 50%	ASTM D4632
Resistance against Rupture	≥ 0.51	ASTM D4533
Resistance against puncture	≥ 0.62	ASTM D4833

4.2. Implementation of Water tightening Layer on Upstream Slope of Chitgar Dam and Perimeter Dykes

The main water tightening member of the dam and perimeter dykes is the Geomembrane protected by Geotextile layers. The recommendations of ICOLD Bulletin 135 were used as reference for installation of Geo-synthetic material and associated details as follows:

- A) Base Layer: To provide a smooth and suitable surface for installation of Geomembrane, first the coarse aggregates and small rocks from the face of the dam were removed and then a 5cm-thick shotcrete was placed on the dam after grading and trimming.
- B) Protective Bottom Geotextile: To ensure the Geomembrane is protected against physical damage and also to provide adequate friction at the base, a 500g/m² Geotextile was used underneath the Geomembrane layer. The GT 12a standards was used for quality control of this protective layer.
- C) Impervious Geomembrane Layer: For the Geomembrane layer on the dam's slope and on top of Geotextile layer, the HDPE type Geomembrane conforming to GM13 standards was used. The specification for the Geomembrane is as follows:
 - Thickness: 2.5 mm (ASTM D5199)
 - Density: 0.94 gr/cm³ (ASTM D792, ASTM D1505)
 - Tensile strength ≥ 37 KN/m (ASTM D6693)
 - Elongation at break ≥ 700 % (ASTM D6693)
 - Tear resistance ≥ 311 N (ASTM D1004)
 - Puncture resistance ≥ 800 N (ASTM D4833)
- D) Top Protective Geo-Textile: The Top Geotextile layer is to protect the Geomembrane during installation and particularly during placement of upper protective soil/rock fill layer. This layer is placed on top of the Geomembrane and is free to move in order to prevent possible stress transfer from the top layer to the Geomembrane.

Table 3. Geotextile Specifications used in the Dam Body and Perimeter Dykes

Parameter	Geotextile Type		Standard
	700 gr	500 gr	
Weight per square meter	$\geq 700\text{gr}$	$\geq 500\text{gr}$	ASTM D5261
Tensile Strength	KN $\geq \geq 2.00$ KN 1.46	KN $\geq \geq 1.64$ KN 1.33	ASTM D4632
Elongation	$\geq 50\%$	$\geq 50\%$	ASTM D4632
Resistance against Rupture	KN $\geq \geq 0.89$ KN 0.46	KN $\geq \geq 0.64$ KN 0.51	ASTM D533
Resistance against puncture	KN $\geq \geq 0.89$ KN 0.46	KN $\geq \geq 0.64$ KN 0.51	ASTM D833

- E) Upper Protective Finish Layer: The upper protective layer on top of the Geotextile layer consists of a 10cm-thick plain concrete layer with a compressive strength of 16 MPa containing Polymer Acrylic additive. This layer was placed from Elevation 1266m to 1268.5m and underneath the riprap and Mallon work. The details of this protective layer are shown in Figure 6. This detail was kept for the entire architectural features and includes a 5cm concrete layer with Polymer additives.
- F) Dam Crest and dyke Details at connection point to the upstream protective layer: At the upstream edge of dam and dyke crest, the impervious Geomembrane is placed and supported in a trench. The crest along dam's width is covered by appropriate finishing layer. In order to protect the accessible surface of the upstream face, a 10cm thick shotcrete layer is placed covered by riprap and crushed rock. This protective layer extends to the crest level and is fixed within the walkway concrete.
- G) Connection Details of the upstream face of dam and dyke to the reservoir impervious layer: The Geomembrane layer is present both at the bed of reservoir and underneath the upstream face of the earth fill dam; however their sub-layer details are different. A concrete bump (hunched concrete zone) was used at the connection point of the Geomembrane as shown in Figure 6. The concrete bump is 1.5m-wide plain concrete with a compressive strength of 16 MPa.

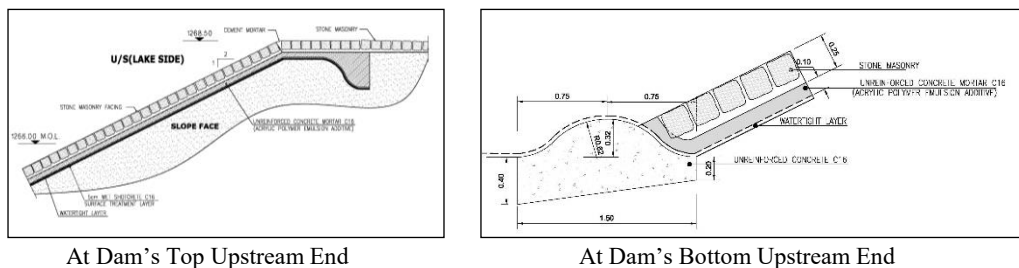


Figure 6. End-Details of the Water Tightening Membrane

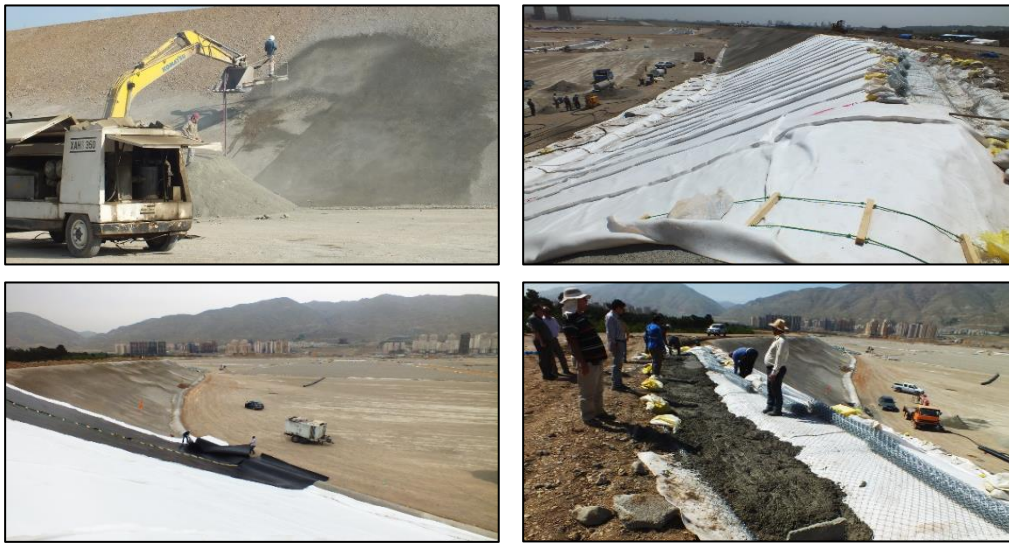


Figure 7. Preparation and Installation Stages for Water tightening of the Chitgar Dam and Dyke

4.3. Quality Control

4.3.1. Short-term Tests

Sampling from the on-site materials was carried out and the measured data was sent to the Laboratory according to GM13 and GT12a for Geomembrane and Geotextile respectively. Prior to installation of each role of Geomembrane and Geo-Textile, laboratory tests were done and results were sent to the Owner's Engineers for approval. One sample every 9 role of Geomembrane and one sample every 7 role of Geotextile were sent to the Labs for testing. After installation, verification on welding process is done. In Table 4 the results for concrete strength placed at the Lake are provided. Table 5 and Table 6 show the results for weld tests and Geotextile strength tests.

Table 4. Geotextile and Geomembrane sampling Specifications used in the Dam Body and Perimeter Dykes

No.	Description	Total samples	Rejected Samples	Accepted samples
1	Geomembrane	206	11	195
2	Geotextile	410	154	256
Total		616	165	451

Table 5. Geomembrane welding tests results

Description	PEEL				SHEAR			
	Elongation		Resistance		Elongation		Resistance	
	%		N		%		N	
	result	allowable	result	allowable	result	allowable	result	allowable
Average	162.47	≥25	525.27	398	993.94	≥50	621.4	525
Number of tests done					10			

Table 6. Geotextile welding tests results

Description	Puncture Strength		Trap Tear Strength			Grab Tensile Elongation			Grab Tensile Strength			Mass Per Unit Area	
	KN		KN			%			KN			g/m ²	
	result	allowable	TD	MD	allowable	TD	MD	allowable	TD	MD	allowable	result	allowable
Average	0.87	0.58	0.66	1.02	0.47	151.6	173.4	50	1.45	2.02	1.27	682.25	373
Number of tests done									453				

MD: Machine Direction, TD: Transverse Direction

4.3.2. Long-term Tests

From every Geomembrane material that was used, two samples were sent to SAGEOS Laboratory in the country of Canada to perform long-term resistance tests against UV radiation and also Oven

Aging. In the process the short-term tests results obtained from Iranian Lab were also verified. Followings test were conducted on the samples:

- Oven Aging for a duration of 90 days
- Resistance Test against UV radiation
- Stress Crack Resistance (SCR)
- Geomembrane Joints Welds

Test results were as follows:

- The Oxidation time reduction amounts from HP-OIT test after over aging were within the acceptable range. The reduction rate was also verified in the 90-Day test.
- The Oxidation time reduction amounts from HP-OIT test after continuous UV radiation were within the acceptable range.
- The procedure for OIT testing for a particular product made by Rowad Company had a direct impact on the obtained results. The difference between the results obtained from in-country and oversea testing Labs (on the over aging results) were mainly due to variation in testing procedures.
- Results obtained from Stress Crack Resistance test from Iranian and Canadian Labs were in complete agreement.

5. Construction Difficulties

Installation of the Water tightening layer for the Lake had its specific challenges and difficulties some of which are listed below:

- Harsh Weather Condition (wind storm and cold weather) during installation of Geomembrane
- Difficulties for Iranian manufactures to supply Geotextile conforming to GT12A standards
- Most Iranian Manufactures failed to provide products certificates
- Foreign Purchase and Import difficulties due to the Sanctions against Iranian Government
- Timeliness for customs clearance and release of products to do standard tests on materials
- Gradual impounding concurrent with the construction to meet the project deadline
- Limited access to different regions of the lake to avoid possible machinery damage to the installed Geomembrane
- Timeliness of quality control process for the membrane
- Fluctuations of exchange rate and associated complications to finalize the price from receipt of Performa to time of approval and budget availability

6. Concluding Remarks

The artificial Chitgar Lake project has significantly contributed to improvement of landscape, environmental and public recreation of Tehran City. Due to limitations on impounding time and also high evaporation rate during summer, the use of Geomembranes was selected as the preferred method among other researched alternatives for Water tightening of the reservoir at the Chitgar Lake. The project faced many challenges in supply and installation of the Geomembrane impervious layer. Since the use of Geomembrane was not common in Iran, finding local manufacturers and test labs specialized in quality control of such products was extremely difficult. In addition, the fluctuations of currency exchange rate during construction made it difficult to order and purchase the products.

Fortunately in spite all the commercial complications and construction difficulties, the project was executed according to plan while fulfilling all the quality control requirements. Considering the time constraint and duration of the project and the direct impact of the Lake Water tightening activity situated on the critical path of the schedule, the client decided to use both Iranian and Foreign Geomembrane products. Therefore the Geomembranes were supplied by four different manufacturers one of which was Iranian. For the quality control, Sageous Test Lab, a Canadian Company along with an Iranian Test Lab was selected.

To this date, according to the monitored operation of the Lake there has been no report or evidence of seepage through the installed Water tightening layer which indicates success of this insulation method for the Chitgar Lake. This project has set records in use and installation of Geo-synthetic materials for an artificial Lake in Iran and also the Middle East Region. Installation of nearly 133 hectares of Geomembrane and 265 hectares of Geotextile while fulfilling latest standards of practice requirements was a great achievement for the Engineering industry and the project has proven to successfully serve the nature, residents and tourists of the Iran's Capital.

References

1. Sadd Tunnel Pars Consulting Engineers (2011): The feasibility study of Chitgar artificial lake, Report on water resource studies, No.: CAL-STP-R-GEN-HY-BD-001A
2. Sadd Tunnel Pars Consulting Engineers (2012): The detail study of Chitgar artificial lake, Studies on water quality of lake, No.: CAL-STP-R-GEN-EN-DD-001A
3. Toos-Ab Company (2013): Studies on promoting the quality of entrance water into the artificial lake
4. Sadd Tunnel Pars Consulting Engineers (2011): The feasibility study of Chitgar artificial lake, Report on reservoir water tightening design, No.: CAL-STP-R-RES-ST-BD-001
5. Sadd Tunnel Pars Consulting Engineers (2014): The feasibility study of Chitgar artificial lake, Report on dam-break studies, No.: CAL-STP-R-DAM-HY-BD-005A
6. Sabir Construction Co. (2011-2013), Monthly Progress Reports.
7. Armature Pardis Co. (2011-2013), Monthly progress report for Management Contractor
8. Danesh Herin Consulting Engineers (2013), Technical Book of Chitgar Lake

Authors

Ali Emam received his B.Sc. degree in civil engineering in 1992 and his M.Sc. degree in hydraulics structures in 1994, both from University of Tehran. He involved in different hydro projects such as earth fill dams, double curvature arch dams and CFRD dams as the head of technical office for more than 15 years. He has been the Managing Director for Engineering and Development Organization of the City of Tehran (EDOCT) (Client of the Chitgar Artificial Lake project) since 2010.

Mehdi Zolfagharian was graduated in civil Engineering from Sharif University (IRAN) in 1998. He received his M.Sc. degree in geotechnical engineering from Sharif University in 2004. He worked in various hydro projects such as earth fill dam, double curvature arch dam and CFRD dam as the head of technical office for 10 years. In the Chitgar Artificial Lake he was the Client's (Tehran Municipality) Project Manager during construction

Nima Rashidi received his Master of Advanced Studies (MAS) in Hydraulic Engineering from EPFL (Ecole polytechnique Fédérale de Lausanne-Switzerland) in 2009. In his previous studies, he received his B.Sc. in Civil Engineering from Amir Kabir University (IRAN) in 2000 and his M.Sc. in Hydraulic Structures from Tehran University in 2003. For more than 14 years he has been engaged in many water resources and hydraulic structure projects. Nima served as the Project Manager of Management Contractor (MC) in Chitgar Artificial Lake Project.

Rouzbeh Radman was graduated from Tehran Polytechnic University (IRAN) in 2001 as a civil engineer and received his M.Sc. degree in water resources management from Tehran's University of Science and Technology (IRAN) in 2003. He has worked for a number of reputable consulting companies as a structural engineer. Also he was involved in various civil projects in different regions of Iran. He joined the Chitgar Artificial Lake as the Technical Manager of the Management Contractor.

COMMISSION INTERNATIONALE DES GRANDS BARRAGES

VINGT-SIXIÈME CONGRÈS DES GRANDS BARRAGES
Autriche, juillet 2018

DOI 10.3217/978-3-85125-620-8-158



This work licensed under a Creative Commons Attribution 4.0 International License. <https://creativecommons.org/licenses/by-nc-nd/4.0/>

**EXPERIENCE ON GROUTING CURTAIN OF EMBANKMENT DAMS WITH
MODERATE HEIGHT IN TURKEY**

Hasan TOSUN

Professor, Engineering Faculty, ESKİSEHİR OSMANGAZI UNIVERSITY

TURKEY

COMMISSION INTERNATIONALE
DES GRANDS BARRAGES

VINGT-SIXIÈME CONGRÈS DES
GRANDS BARRAGES
Autriche, juillet 2018

EXPERIENCE ON GROUTING CURTAIN OF EMBANKMENT DAMS WITH MODERATE HEIGHT IN TURKEY

Hasan TOSUN

Professor, Engineering Faculty, ESKİSEHİR OSMANGAZI UNIVERSITY

TURKEY

1. INTRODUCTION

Grouting in dam foundation is known as a process of injection the fluids by which openings are sealed off so as to minimize seepage and leakage, to strengthen and stabilize rock foundation for the purpose of filling micro and macro features such as joints, fractures, fissures, bedding planes, cavities, or other openings. There are different techniques used to provide impermeability requirement for dam foundation. Control of foundation seepage beneath dam structures can be provided by cutoff trench, sheet piling, slurry trench, diaphragm wall, upstream blanket and grouting curtain [1]. Powell and Morgenstern [2] evaluates the efficiency of seepage control techniques with quantitative data. Fell et al [3] introduce the general requirements to help control seepage, internal erosion and piping mechanics for embankments dams in detail. Some researchers investigated the effectiveness of grout curtain by using in-situ tests and laboratory-scale physical models [4, 5, 6]. World practice indicates that grouting curtain is one of the most effective and widely used techniques to help control foundation seepage beneath dam structures.

In the design standard of USBR for foundation grouting of embankment dams, the dam grouting is categorized into three groups: curtain grouting, blanket grouting and stitch grouting [7]. Curtain grouting is known as the most common method of foundation seepage reduction used beneath dam structures. This standard states that curtain grouting consists of drilling holes into the bedrock at some regular spacing along a line or lines parallel to the dam axis. The curtain is

located at normal position to the seepage flow direction. Blanket or consolidation grouting is commonly used to provide a firm foundation, to reduce seepage within the near-surface foundation bedrock, to reduce seepage from the embankment into the foundation when fractured rock exists at the foundation contact [7]. It helps to reduce the likelihood of internal erosion of the embankment materials into the foundation. Stitch grouting is performed along faults, shear zones or discontinuities exposed on the foundation surface to reduce potential for seepage along these discrete features.

This study introduces design experience on grout curtains of thirty-two embankment dams constructed in Turkey. The depth of grout curtains ranges from 25 to 60 m for the moderate height dams. Table 1 gives the list of dams and their physical properties. Dams considered for this study were selected from different regions of Turkey and their heights from river basin range from 44 to 87 m. Their construction was completed between 1984 and 2013. They were designed for different purposes such as irrigation, energy, flood control, domestic water and industrial use. Their total reservoir capacity changes within a wide range of 12 to 2 120 hm³.

Table 1. Physical properties of dams considered for this study

Dam		River	Aim (*)	Height from river bed (m)	Completed Year	Type (**)	Volume of embankment (hm ³)	Volume of reservoir (hm ³)
No	Name							
1	Aslantas	Ceyhan	I+F+E+D	78	1984	EF	8.49	1 840
2	Bakacak	Kocacay	I	50	1998	RF	2.20	139
3	Batman	Batman	I+E+F	73	2003	RF	7.18	1 244
4	Cat	Abdulvahap	I	76	1996	EF	2.50	288
5	Catalan	Seyhan	I+F+E	70	1996	EF	14.5	2 120
6	Caybogazi	Sancikizik	I	68	2002	EF	9.41	55
7	Demirdoven	Timar	I	58	1988	EF	2.50	37
8	Egrekkaya	Seycayi	I+D	67	1992	RF	3.41	112
9	Erzincan	Gogre	I	75	1997	EF	4.40	12
10	Gazibey	Osgulec	I+F	46	1992	EF	0.90	18
11	Godet	Godet	I+F	64	1988	RF	5.90	158
12	Goksu	Goksu	I	46	1991	RF	1.86	63
13	Guldurcek	Devrez	I	51	1988	EF	1.55	53
14	Havran	Havran	I+E	64	2010	RF	1.05	67
15	Kapulukaya	Kızılırmak	E+D	44	1989	EF	1.49	285
16	Karadere	Karadere	I	70	2007	EF	0.90	44
17	Karaova	Manahozu	I	49	1997	EF	2.30	65
18	Kirklareli	Şeytandere	I+F+D	68	1996	RF	1.64	113
19	Kockopru	Zilan	I+E+F	51	1992	EF	2.03	86
20	Koruluk	Cevizderesi	I	39	2004	EF	4.0	12
21	Madra	Madra	E+I	87	1998	RF	3.17	79
22	Manyas	Kocacay	I+E+F	74	2013	RF	3.30	404
23	Mursal	Nuhcayi	I+E	50	1992	EF	1.57	15
24	Polat	Findıkcayi	I	51	1990	EF	1.83	14
25	Sarımehmet	Karasu	I	47	1991	EF	1.16	133
26	Siddikli	Korpeli	I	51	1999	RF	0.70	29
27	Suat Ugurlu	Yesilirmak	E+I	38	1982	RF	2.15	182
28	Topcam	Madran	I	56	1984	EF	3.27	106
29	Tahtalı	Tahtalı	D	60.5	1999	RF	3.37	307
30	Umurbey	Umurbey	I	61	2002	RF	2.30	53
31	Yaylakavak	Kocacay	I	71	1996	EF	5.27	31
32	Zeyrek	Engil	I+E+F	62	1988	RF	2.1	106

(*) I:Irrigation E: Energy Production F:Flood Control D:Domestic Water

(**) EF:Earthfill dam RF: Rockfill dam RC:Rolled Concrete dam

2. MATERIALS AND METHODS

Grout curtain was firstly used in United States to control seepage in rock masses under and around dam structures in the 1890's [8]. At the beginning, long term behavior of many curtains has not been provided, especially in formations including soluble or erodible materials. However, effective and durable grout curtains have been formed since the mid-1970's using a new design perspective and considering different grout materials. Use of positive cut-offs such as slurry trench and diaphragm wall increased after 1980 [9]. In the past decade, there have significantly been advancements on grout curtain concepts and grouting industry. Especially new developments on real-time monitoring of flow rate and pressure of pumped grout result to more effective and durable grout curtains.

There are generally three separate techniques, which are used for forming grout curtain in engineering sector. These are jet-grouting, high-mobility grouting, and compaction grouting. In jet-grouting technique a cementitious material known as grout is injected into poor rocks or soils with high velocity and high pressure to form soilcrete, which is composed of mixture of soil and grout materials. In high-mobility technique the cementitious grout material is pressurized into the pores and structural features of the underlying soil to form the grout and soil to binding. Its performance is directly related with the size of the pores or void spaces of the underlying soil material. This type of grouting provides an increase on strength properties and a decrease on permeability. Compaction grouting is another technique which use low viscosity grout to displace and densify loose soils. Its use in dam site provides stabilization of large void spaces known as sinkholes. Some scientists have explained these techniques more detail in their research [10]. All three installation techniques mentioned above is commonly used to simply prevent seepage from occurring under water retaining structures, especially for dams.

The depth of grout curtain is a critical issue for performance of dam structures. It is clear that depth for primary holes are based on the geology and permeability of foundation materials and also regional groundwater conditions. In USBR standard, it can extend to a depth below the surface of the rock equal to about 0.5 to 1.0 times the reservoir head, which lies above the surface of the rock [7]. However, an empirical criterion is generally used as guideline which are based on practice ($D = 0.3333xH + C$). In this formula D is depth of grout curtain, H is the height of the dam (the final head of water) and C is a coefficient ranging from 7.5 to 22.5 in m. The Indian Standard [11] introduced guidelines for the design of grout curtain as similar of USBR formula ($D = 0.667xH + 8$). In this empirical formula D and H are the depth of curtain and the head of the reservoir of water given in m, respectively. In Switzerland it is observed that the average of the depth of the curtains grout is stated as 66.7 percent of height of the dam [12] In Sweden, specified deep of grout curtain was depended to the head of the reservoir water at the dam. If height of dam is less than 30 m, the depth of curtain can be selected between 20-30 m. However, its height is greater than 30 m it can be taken between one-third ad two-third of the head of water in reservoir [13]. In Turkey dam engineers consider the simple USBR formula for designing the grout curtains of dams.

3. ANALYSES

In this study thirty-two existing dams are considered and a back analysis was performed for all dams to relieve Turkish experience on the formation of grout curtains of dams. For each dam structural height and water head in the reservoir were determined and more detail geological inspection was performed on the planning report to exactly determine the geological formation, in which grout curtain is installed. Then the depth of curtain was determined from the design sections with inclusion of revised ones. The research on rough data indicates that most of grout curtains was installed by high mobility technique. There are also some examples constructed by other techniques. For example, slurry trench technique was adopted in construction of some parts of curtain for Aslantas dam, which is a 95 m height dams located on Ceyhan River. The diaphragm wall technique was utilized to install the curtain of Tahtali dam, which is a 55 m height dam for providing domestic water of Izmir province in West Turkey.

Table 2 introduces the structural heights and depths of grout curtains with the geological formations, in which curtains were installed, for all dams considered for study. The structural heights of dams, which range from 50 to 100 m, average 72.6 m for all dams. The depths of curtains are between 25 and 60 m and their average is 41.6 m. The type of rock units, in which curtains are emplaced, have different characteristics when considered their strength and permeability. There are limestone, clayey limestone, marl, and their alternation as soluble sedimentary rocks in foundation. Claystone, sandstone, siltstone, ophiolite series, agglomerate and conglomerate can be separated as non-soluble sedimentary rocks. The igneous rocks in foundations of dams considered for this study can be classified as andesite, basalt, brecciated tuff, diorite, granite, granodiorite, meta-granite, monzonite, peridotite, rhyolite, serpentinite, syenite, syenite porphyry and tuff. Chlorite schist, gneiss, quartzite, meta-quartzite, marble, mica-schist and schist are the metamorphic rocks seen in the foundation of dams considered for this study (table 2).

In this study the empirical relationship between the depth of grout curtain and water head in the reservoir was criticized as based on the Turkish practice. For this purpose, a back analysis was performed by means of the simple USBR equation. In this simple equation the depth of curtain is directly related by the height of the dam (the final head of water) additionally with the C-coefficient ranging from 7.5 to 22.5 in m. As based on this equation a C-coefficient was calculated for each dam. Table 3 introduces actual depth of curtain and structural height of dam and the calculated C-coefficient for each dams. This table also includes the exceedance ratio for some cases. It means just the deviation percentage from upper limit for C-Coefficient. There are six dams that their depths exceed the upper limit of C-Coefficient given for the equation. Three of them have too much exceedance ratio. There is no any calculated value which is less than lower limit of C-Coefficient (table 3). If exceedance ratio is represented by (-), it means no exceedance on upper and lower limits.

Table 2. Depth of grouting curtains and rock type in which curtain is emplaced

Dam		Structural Height (m)	Depth of Curtain (m)	Rock units, in which curtain is emplaced
No	Name			
1	Aslantas	95	45	Claystone-sandstone
2	Bakacak	65	40	Brecciated tuff
3	Batman	85	60	Limestone-clayey limestone-marl
4	Cat	78	37	Schist, quartzite
5	Catalan	82	50	Claystone-sandstone
6	Caybogazi	78	40	Claystone-sandstone-siltstone
7	Demirdoven	67	45	Rhyolite, tuff
8	Egrekkaya	100	50	Andesite
9	Erzincan	81	45	ophiolite series
10	Gazibey	58	34	Basalt
11	Godet	93	43	Tuff schist, radiolaritic schist
12	Goksu	53	33	Limestone, clayey limestone, claystone
13	Guldurcek	68	40	Tuff-agglomerate, andesite
14	Havran	80	65	Alternation of limestone, claystone and sandstone
15	Kapulukaya	61	41	Granodiorite
16	Karadere	90	50	Serpentine
17	Karaova	64	35	Conglomerate, schist
18	Kirklareli	72	42	Meta-granite
19	Kockopru	74	33	Agglomerate, basalt, mix of clay, sand and gravel
20	Koruluk	54	35	Tuff, breccia, agglomerate
21	Madra	97	55	Andesite, agglomerate
22	Manyas	91	40	Chlorite schist, meta-quartzite, marble
23	Mursal	58	39	Syenite, syenite porphyry, monzonite, granite
24	Polat	54	38	Diorite, grana-diorite, peridotite
25	Sarimehmet	62	35	Limestone
26	Siddikli	53	28	Limestone, sandstone, conglomerate
27	Suat Ugurlu	51	25	Basalt, agglomerate, tuff, breccia
28	Topcam	62	30	Gneiss
29	Tahtali	55	60	Weathered schist and alluvial soil
30	Umurbey	74	40	Andesite, agglomerate, tuff, siltstone, claystone, sandstone
31	Yaylakavak	89	43	Gneiss, mica-schist
32	Zeyrek	80	35	Limestone, schist, diabase

4. RESULTS AND DISCUSSION

In Turkish design practice, it is a common way to design grout curtain by the simple USBR equation for the dams. For this study thirty-two dams having a height between 50 and 100 m were considered. This study indicates that there are some extreme cases when design engineers consider a curtain, in which soluble rocks are emplaced. The extreme examples can be defined as Tahtali, Batman and Havran dams. The cutoff structure of the Tahtali dam was installed in weathered metamorphic rocks and alluvial soil by diaphragm wall. Therefore, its depth is control by thickness of alluvial soil. However, second and third dams were

constructed on limestone, clayey limestone, marl, sandstone and their alternation. For the grout curtains of Batman and Havran Dams, exceedance ratios are 43.6 and 73.3 percent, respectively. It means that the cost of curtain has high percentage of total structure for these dams. Their expenditures on grout injection could be decreased by means a detail and more sophisticated geotechnical investigation for these dams.

Table 3. Actual depths, calculated c-values and exceedance ratio for the dams considered for this study

No	Dam Name	Structural Height (m)	Depth of Actual Curtain (m)	D = C + 0.3333xH (m)		
				0.333H* (m)	C-value** (m)	Exceedance ratio (%)
1	Aslantas	95	45	30.7	14.3	-
2	Bakacak	65	40	21.0	19.0	-
3	Batman	85	60	27.7	32.3	43.6
4	Cat	78	37	25.3	11.7	-
5	Catalan	82	50	26.7	23.3	3.6
6	Caybogazi	78	40	25.3	14.7	-
7	Demirdoven	67	45	21.7	23.3	3.6
8	Egrekkaya	100	50	32.7	17.3	-
9	Erzincan	81	45	26.3	18.7	-
10	Gazibey	58	34	18.7	15.3	-
11	Godet	93	43	30.3	12.7	-
12	Goksu	53	33	17.0	16.0	-
13	Guldurcek	68	40	22.0	18.0	-
14	Havran	80	65	26.0	39.0	73.3
15	Kapulukaya	61	41	19.7	21.3	-
16	Karadere	90	50	29.3	20.7	-
17	Karaova	64	35	20.7	14.3	-
18	Kirklareli	72	42	23.3	18.7	-
19	Kockopru	74	33	24.0	9.0	-
20	Koruluk	54	35	17.3	17.7	-
21	Madra	97	55	31.7	23.3	3.6
22	Manyas	91	40	29.7	10.3	-
23	Mursal	58	39	18.7	20.3	-
24	Polat	54	38	17.3	20.7	-
25	Sarimehmet	62	35	20.0	15.0	-
26	Siddikli	53	28	17.0	11.0	-
27	Suat Ugurlu	51	25	16.3	8.7	-
28	Topcam	62	30	20.0	10.0	-
29	Tahtalı	55	60	18.3	41.7	85.3
30	Umurbey	74	40	24.0	16.0	-
31	Yaylakavak	89	43	29.0	14.0	-
32	Zeyrek	80	35	26.0	9.0	-

(*) one-third of hydraulic height

(**) C-Values (7.5-22.5 m)

Sarimehmet, Siddikli and Goksu dams are good cases even if their grout curtains were emplaced into limestone and its alternation. Because their C-coefficients range between 11 and 16 m. The curtain of Suat Ugurlu dams, which is emplaced in basalt, agglomerate, tuff and breccia has lowest C-coefficient for

this study. The performance of curtain is currently high, although there are complex geological units in dam foundation and abutments. Therefore, it means that a good engineering service has been spent for designing of this element of Suat Ugurlu Dam.

Fig.1 shows the relationship of curtain depth with water head in reservoir for three separate series. This figure indicates that the relationship between two parameters are very changeable for soluble sedimentary rocks (red color). There is a more acceptable relationship between curtain depth and water head in reservoir for the series including igneous and metamorphic rocks as based on the cases considered for this study (blue color). The series about non soluble sedimentary rocks conforms the relationship belonging to igneous and metamorphic rocks (green color).

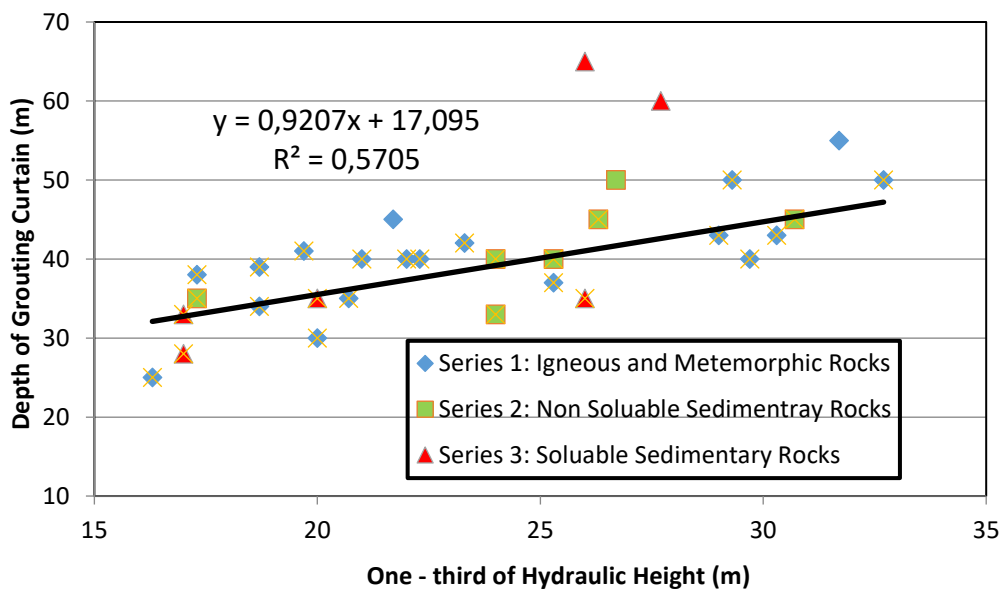


Fig. 1. Direct relationship between gout curtain and hydraulic height for three different series

A simple equation is suggested to relate depth of grout curtain and hydraulic height for non-soluble sedimentary, igneous and metamorphic rocks for the dams having a structural height of 50 and 100 m (eq.1).

$$D = 0.307x H + C_c \quad [1]$$

in which

D= Depth of grout curtain

H= head in reservoir water

Cc = corrected coefficient for grout curtain (averages to 17.01)

Table 4 summarize this study based on thirty-two projects considered for this study. The numbers of projects, range of curtain depths, range and average of C-coefficient are introduced in this table according to rock units, in which curtains are emplaced. This table indicates that range of C-coefficient for soluble sedimentary

rock is too wide when compared with the cases in non-soluble sedimentary, igneous and metamorphic rocks. The percent of projects having the exceeded C-coefficients is also high for soluble sedimentary rocks. Author states that this table can be used as a guideline for designing the grout curtains in all rock units with exception of soluble sedimentary rocks. It should be notified that It can be used for the design of grout curtains of embankment dams having a hydraulic height of 50 m to 100m.

Table 4. Depth of grouting curtains as based on rock types

Number of projects considered for this study	Range of curtain depth (m)	Range of C-value (m)	Average of C-value (m)	Exceeded C-value		Rock units, in which curtain is emplaced
				Number of projects	Percent of projects (%)	
6	28-65	9.0-39.0	20.4	2	33.3	Limestone, clayey limestone, marl, and their alternation
7	33-50	9.0-23.3	16.2	1	14.3	Claystone, sandstone, siltstone, ophiolite series, agglomerate, conglomerate
19	25-67	8.0-23.3	15.4	2	10.5	Tuff, brecciated tuff, schist, quartzite, andesite rhyolite, basalt, granodiorite, serpentinite, meta-granite, chlorite schist, meta-quartzite, marble, syenite, syenite porphyry, monzonite, granite, diorite, grana-diorite, peridotite, gneiss, mica-schist

5. CONCLUSIONS

Turkey has more than 1 250 large dams with different types. The most of them were constructed in embankment type. The thirty-two large dams having a good performance on impermeability of foundation materials were selected for this study. This study indicates that there is a good experience in designing of grout curtains of embankment dams in Turkey and concludes as follows:

- The simple USBR equation is generally used in designing of grout curtain for all foundation materials in Turkey. The equation suggested in this study confirms that one mentioned above for the dams having a height between 50 and 100 m. However, its use for soluble sedimentary rocks is questionable.
- In soluble sedimentary rocks such as limestone, clayey limestone, marl and their alternations the performance of grout curtains depends on nature of material, in which curtain is installed. Detail and more sophisticated geotechnical investigation should be made for this type of dam sites.

Spaces, cavities or holes should be found before designing of curtain and an extended program should be realized for a dam site having soluble sedimentary rocks.

- Table 4 given in this study can be used as a guideline for designing the grout curtains in rock units with exception of soluble sedimentary rocks.
- This study has been realized for only dams having a height of 50 to 100 m. Further study or studies can be performed for the dams having a height less than 50 m and more than 100 m.

ACKNOWLEDGEMENTS

Author would like to thank former and actual authorities of General Directorate of State Hydraulic Works for their sincere supports.

REFERENCES

- [1] TOSUN, H. Geotechnics in Dam Engineering- Pervious Soils and Improvement Techniques. *Civil Engineering Chamber 49/2004-2 No.430*, 2004, 38-47 (in Turkish)
- [2] POWELL, J.J.M and MORGENSTREN, N.R. The Use and Performance of Seepage Prediction Measures in Seepage and Leakage from Dams and Impoundments (edited by R.L. Volpe and W.E. Kelly). ASCE, 1985.
- [3] FELL, R., MACGREGOR, P. AND STAPLAN, D. and BELL, G. Geotechnical Engineering of Embankment Dams. *Taylor and Francis*, ISBN: 978-0415364409, 2005.
- [4] MAGOTO, E.N. and BRYSON, L.S. Evaluation of the Effectiveness of a Grout Curtain using a Physical Model. *Dam Safety 2013*, ASDSO 8-12 September 2013, Providence.
- [5] ANAGNOSTOPOULOS, C and HADJISPYROU, S. Laboratory Study of an Epoxy Resin Grouted Sand. *Grouted Improvement*, 8(1), 2004, 39-45.
- [6] BECKHAUS, K., SCHMITZ, S., and SCHWARZ, W. Deep Cut-Off Walls Constructed Under Dams with Trench Cutters. *Long Term Behavior of Dams. 2008*, 305-310.
- [7] USBR , Design Standards No. 13: Embankment Dams. Bureau of Reclamation, 15-28 DS-13(15), 2014,
- [8] WEAVER, K. D and BRUCE, D. A. Dam Foundation Grouting. Revised and Expanded Edition. American Society of Civil Engineers, ASCE Press. ISBN: 978-0-7844-0764-6, 2007, 504p.
- [9] BRUCE, D.A., A. RESSI DI CERVIA and J. AMOS-VENTI. Seepage Remediation by Positive Cut-Off Walls: A Compendium and Analysis of North American Case Histories, *Canadian Dam Association Conference*, September 30 – October 5, 2006, Québec City, Québec.
- [10] ZOU, Y.J. and ZHOU, X.W. Study and application of key technology to Simultaneous shaft drilling and grouting. *Tunnels & Tunneling International*

- (04): 2012, 130-133.
- [11] INDIAN STANDARD, Guidelines for the Design of Grout Curtain, Part 2, Masonry and Concrete Gravity Dams. IS 11293, 1993.
- [12] SCHLEISS, A. J and POUGATSCH, H. Les Barrages: Du projet à la mise en service; Volume 17. *Presses Polytechniques Universitaires Romandes*. ISBN 978-2-88074-31-9, 2011.
- [13] RIDAS, Gruvindustrins riktlinjer för dammsäkerhet, SweMin, 2007.

SUMMARY

Dam designers believe the fact that grouting curtain is one of most effective techniques used to control seepage and leakage quantity under embankment dams. The efficiency of a grout curtain is directly related with its depth. The empirical equations have been developed to explain the relationships between dam height and curtain depth, and then adapted as design criteria in specifications. In this study a back analysis was performed on grout curtain activities of thirty-two embankment dams, which pose a height of 50 to 100 m in Turkey. The foundation units of these dams are completely igneous and metamorphic rocks and their sedimentary products. The dams having soluble rock units were also considered for this study. The results of this study show that the Turkish design practice for grout curtains of embankment dams generally conform the USBR's approximation for the dams having a height of 50 to 100 m from foundations. A new empirical equation relating depth of grout curtain with hydraulic height of dam and a guideline on depth of grout curtains as based on rock types are suggested for the dam having moderate height as based on the Turkish practice.

KEY WORDS

dam, grout curtain, leakage, permeability, seepage,

COMMISSION INTERNATIONALE
DES GRANDS BARRAGES

VINGT-SIXIÈME CONGRÈS DES
GRANDS BARRAGES
Autriche, juillet 2018

**STUDY ON THE LONG-TERM EFFECT OF INFILTRATION
DEFORMATION ON THE DISTRIBUTION OF UPLIFT PRESSURE IN EARTH-
ROCK JOINT AREA OF EARTH DAM**

Zhiyong MU^{1,3}, Tongchun LI^{1,2}, Zhiwei NIU¹, Xiaoqing LIU¹

¹ COLLEGE OF WATER CONSERVANCY AND HYDROPOWER
ENGINEERING, HOHAI UNIVERSITY

² NATIONAL ENGINEERING RESEARCH CENTER OF WATER
RESOURCE EFFICIENT UTILIZATION AND ENGINEERING SAFETY

³ COLLEGE OF WATER CONSERVANCY AND HYDROPOWER
ENGINEERING, HEBEI UNIVERSITY OF ENGINEERING

CHINA

1. SUMMERY

The earth-rock joint area is generally existed in some earth dams, such as the combination area of dam body with concrete dam, Spillway, dam culvert and other structures. The soil in these areas is susceptible to infiltration failure due to seepage and soil properties, and this kind of damage phenomenon will further affect the distribution of uplift pressure in earth-rock contact surface. In order to study the transformation of the uplift pressure distribution, a contact scouring experiment which is based on the normal stress controlling by the pressure of contact surface is proposed in this paper. The experiment can simulate the seepage failure of soil-rock joint area and reveal the basic law of stress, seepage and soil loss. Based on the experimental results, a mathematical model of contact mechanical state of contact area is established, and the seepage failure in the contact area is simulated using finite element. In conclusions, the evolution

process of the uplift pressure/pore water pressure in the contact area of soil and stone is simulated while taking in to account the aging factors.

COMMISSION INTERNATIONALE DES GRANDS BARRAGES

VINGT-SIXIÈME CONGRÈS DES GRANDS BARRAGES
Autriche, juillet 2018

DOI 10.3217/978-3-85125-620-8-160



This work licensed under a Creative Commons Attribution 4.0 International License. <https://creativecommons.org/licenses/by-nc-nd/4.0/>

**ASSESSMENT OF WATER FLOW MEASUREMENT IN A ZONED DAM USING
ARTIFICIAL NEURAL NETWORK MODELS**

Ricardo C. SANTOS

GEOTECHNICS DEPARTMENT, LABORATÓRIO NACIONAL DE
ENGENHARIA CIVIL

PORTUGAL

Juan T. MATA

CONCRETE DAM DEPARTMENT, LABORATÓRIO NACIONAL DE
ENGENHARIA CIVIL

PORTUGAL

COMMISSION INTERNATIONALE
DES GRANDS BARRAGES

VINGT-SIXIÈME CONGRÈS DES
GRANDS BARRAGES
Autriche, juillet 2018

ASSESSMENT OF WATER FLOW MEASUREMENT IN A ZONED DAM USING ARTIFICIAL NEURAL NETWORK MODELS

Ricardo C. SANTOS

Geotechnics Department, LABORATÓRIO NACIONAL DE ENGENHARIA CIVIL

Juan T. MATA

Concrete Dam Department, LABORATÓRIO NACIONAL DE ENGENHARIA CIVIL

PORTUGAL

1. INTRODUCTION

This paper concerns about the assessment of the hydraulic behavior of a 50 m height zoned dam used for industry water supply, located in Alentejo region, in Portugal. The original draining system of the embankment is composed of a sub-vertical filter, located downstream of the central core, and by a drainage blanket placed over the foundation, in the deeper area of the valley, which, in turn, discharges to a downstream drainage toe. After first filling of the reservoir, resurgences and artesian pressures in the terrain at downstream of the dam body were identified in the left bank. Following that abnormal behavior, the reservoir water level was restricted, and an inverted filter was built over the affected area, to limit occurrence of internal erosion and heave. Additionally, to monitor the hydraulic behavior of the dam and of the inverted filter, several piezometers and a few flowmeters were installed.

Based on the monitoring data (piezometers, flowmeters and reservoir water level) recorded in the last 30 years, a artificial neural network (ANN) model was established for the hydraulic behavior prediction of the zoned dam. The results of this study show that ANN models can be a useful tool for the prediction of the flow rate measured in the flowmeters.

2. SAFETY OF ZONED DAMS

Dams are water-retaining structures that are built to provide water for human consumption, irrigating, generating hydroelectric power and use in industrial processes. They are critical structures for the continuation of life and providing public safety. Statistics from the International Commission on Large Dams (ICOLD) [1,2] reveals that embankment dams represent the most common dam construction type, totalizing about 3/4 of all the existing dams, and, of those, 88% are earthfill dams and 12% are rock-fill dams. Zoned dams account with about 53% of the world population of embankment dams. The most common zoning profiles are zoned earthfill (36%), zoned earth and rock-fill (9%), and central core earth and rock-fill (8%). The main failure modes associated with these type of structures are caused by overtopping (due to inadequate spillway capacity or malfunction of gates), by piping, and by slope instability. Failure modes by piping and overtopping together are responsible, in similar importance, for more than 92% of the total failures [3].

Embankment dam failure and accident statistics [3] show clearly that high average frequencies of failure are associated with dams using profile types without zoning and with inherently poor control of seepage and pressures in the embankment and foundation. On the contrary, embankment dams with downstream rock-fill zones have a particularly low incidence of failure, mainly because they are less likely to progress to breaching if piping erosion initiates compared with dams with earthfill materials in the downstream zones.

In some case studies of zoned dams, leaks appeared at downstream of the embankment, meaning that they bypassed the dam's internal drainage system. Typically, these pathologies appear during first filling or during the first years of exploration of the reservoir. These incidents are usually associated to an inadequate treatment of the foundation, or due to the presence of pervious soil formations or interconnected cracks in a rock formation, not detected during geological prospection of the construction site.

In this paper, we describe the history of a zoned dam, built in the 80s, in which leaks appeared at downstream of the dam during first filling. The remedial actions to overcome the abnormal hydraulic behavior of the foundation are also indicated. Finally, we use a neural network, considering as input parameters the reservoir level and piezometric data, to predict the flowrates measured in a flowmeter located near the leakage area.

3. CASE STUDY

3.1. DAM DESCRIPTION

Figure 1 shows a satellite view of the dam in concern. It is a zoned earthfill dam located in the south center region of Portugal, in particular, in Setúbal district, in Alentejo. The dam crest, following a curve in the longitudinal axis, has an extension close to 2700 m, and a maximum height above foundation of about 52 m (45 m above streambed). The completion of the dam dates the year 1980, and the current dam owner is APA (*Agência Portuguesa do Ambiente*). The dam's reservoir aims mainly the supply of water to industry. The reservoir has an effective storage of 27000 ML.



Fig. 1
Satellite view of the dam (source: Google maps)

Figure 2 shows the typical cross section of the embankment. The crest is defined at level 70 m above sea level and the normal water level (NWL) of the reservoir was initially established from design at 68.3 m. The upstream shell of the embankment has a slope of 1(V):3(H), whereas the downstream shell has a slope of 1(V):2.4(H). The core is made of selected weathered schist materials and has a slope of 2(V):1(H) and 2.5(V):1(H) at the upstream and downstream sides, respectively. The internal drainage system is composed by sub-vertical filter/drains, located at downstream and upstream of the impervious core, a horizontal drainage blanket, located in the downstream shell and above the foundation, and a downstream toe drain, below level 41.5 m.

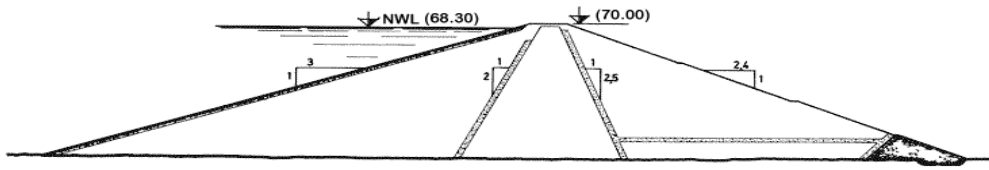


Fig. 2
Cross sectional profile of the embankment of the dam

The dam has a siphon type spillway, located on the left bank, and a bottom outlet, composed by a conduit, under the embankment (in the deepest zone of the valley).

The geological setting for the embankment is characterized by metamorphic rock formations mainly of schist and greywacke. Preparation works involved slush-grouting of the core trench and removal of superficial deposits beneath the shell zones.

3.2. THE MONITORING SYSTEM OF THE DAM

The initial monitoring system of the dam was composed of survey points, to measure vertical displacements of the embankment, inclinometers, to measure the horizontal displacements in the embankment, hydraulic piezometers in the embankment and foundation, to measure pore pressure, and a flowmeter located in the bottom of the valley, to assess the seepage water through the embankment and foundation. Figure 3(a) represents the majority of those monitoring devices.

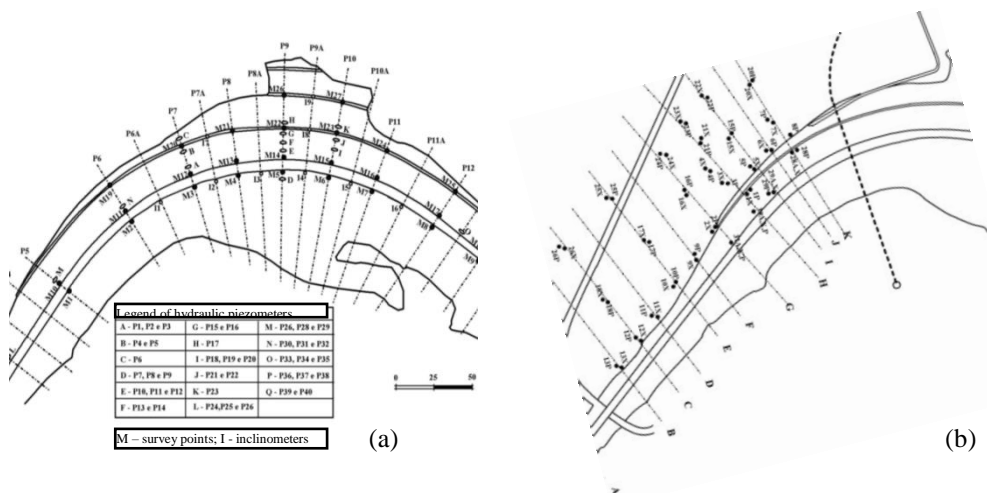


Fig. 3
Partial representation of the monitoring system:
(a) Initial monitoring system; (b) Piezometers installed in the left bank after abnormal hydraulic behaviour of the foundation

Deficient hydraulic behavior of the dam foundation occurred short after first filling of the dam reservoir. In particular, high pore pressures formed in the natural terrain downstream of the embankment, mainly, at the left bank side. Artesian pressures installed in the natural terrain, and, thus, to improve the safety conditions and the monitoring system, an inverted blanket filter and an installation of additional 66 piezometers at downstream of the dam were conducted, respectively. Figure3 (b) shows the location of the majority of these piezometers. In addition, to measure the seepage water collected by the inverted blanket filters a set of flowmeters was installed. In this paper, we evaluate the usefulness of neural network models to predict the hydraulic behavior of such complex dam site. In particular, we correlate the monitoring data from one of the additional piezometers with the data from the closest flowmeter, and confirm that the prediction from the neural network is more accurate than that from a simple linear correlation.

3.3. DATA EVALUATED WITH THE NEURAL NETWORK MODELS

The data used in the model corresponds to a period between March 2003 and August 2017, resulting in more than 120 observations per variable. The time evolution of the reservoir water level, the uplift pressure in the P30, P31 and P17 piezometers (in profile E, shown in Fig 3(b)), and the seepage in the drain MC4 are presented in Fig. 4. The samples were collected every month. Among the different loads acting on dams, it is usual to distinguish, as the most important ones for structures in normal operation, the hydrostatic pressure variation, Fig. 4. Missing data resulted from lack of inspections.

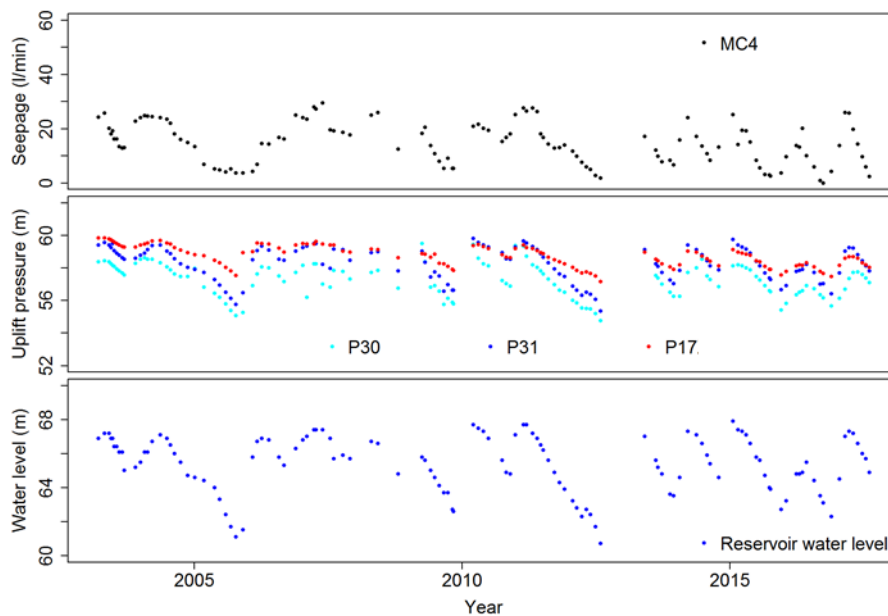


Fig. 4

Seepage, uplift pressure and water level measured between 2003 and 2017

3.4. TRADITIONAL ANALYSIS BASED ON MULTIPLE LINEAR REGRESSION MODELS

The structural response of, for instance, the seepage in any point of the dam, is strongly related to the corresponding variation in the water level in the reservoir. The observations presented in Fig. 3 will be used for the computation of the models presented in this work.

In this case study, the multiple linear regression (MLR) model with the best performance for the seepage of the MC4 drain $y^{MLR,MC4}$ was obtained as the sum of the hydrostatic pressure term $\beta_1 \times h$ (where h is the reservoir water level height), the uplift pressure terms in the upstream zone $\beta_2 \times P31$ and the uplift pressure terms in the downstream zone $\beta_3 \times P17$ e to represent the effect of the head loss variation along the dam and its foundation. The time effect did not seem to have a significant importance in the period examined by this study. The regression coefficients of the quantitative models obtained are $\beta_1 = 1.09$, $\beta_2 = -3.05$ and $\beta_3 = 2.4$, with $k=-257.8$; being the MLR model represented trough the following equation:

$$y^{MLR,MC4} = \beta_1 \times h + \beta_2 \times P31 + \beta_3 \times P17 + k$$

the residuals were obtained through the difference between the observed seepage and the corresponding predicted value obtained through the MLR model.

4. METHODOLOGY FOR SEEPAGE CONTROL

4.5. INTRODUCTION

Seepage measurement devices are installed at the downstream of the dam to measure the amounts of seepage through, around, or under dams. Drain outlets are commonly used as seepage measurement points. The rate of flow is measured either individually in each drain or for a combination of drains grouped by specific zones of the foundation and, in this case, it will also include the infiltrated water through the dam body.

Modelling the hydraulic behaviour of dam foundations is a non-linear problem and a very complex task, mainly because of the discontinuities of the foundation mass and the lack of information concerning the hydraulic properties of foundation mass and the discontinuities characteristics.

As referred before, in order to study the application of the neural network technique in the seepage control of case study, drain MC4 was selected. This measurement point is located at downstream of the embankment (in profile E, Figure 3(b)) and collects the water in the vicinity, from the inverted filter placed

above the natural terrain. The reservoir water level and the pressures measured in the P31 and P17 were considered as inputs for the ANN model.

4.6. THEORETICAL CONCEPTS - ARTIFICIAL NEURAL NETWORK MODEL

Artificial Neural Networks are computational methods inspired on the efficiency of the brain process (Patterson, 1996). The increasing interest for that area derives from the learning ability of these models, which relate the variables without imposing relationships among them. For the creation of these models, it is necessary to define the architecture of the neural networks and to go through a training process with examples (the monitoring data).

Multilayer Perceptron networks have units arranged in layers. The first layer receives the inputs and the last layer produces the outputs. The middle layers have no connection with the external world, and are called hidden layers. A unit is an operator with inputs and outputs, associated with a transfer function, interconnected by synaptic connections.

Each unit in one layer is connected to every unit on the next layer. The information is constantly "feed forward" from one layer to the next.

Multilayer Perceptrons learn by an iterative process, adjusting the weights so as to be able to correctly learn the training data and hence, after the testing phase, to predict unknown data. Fig. 5 illustrates a generic example of a Multilayer Perceptron neural network, with an input layer having input parameters, one hidden layer, l , with Q processing elements and an output layer, L , with M outputs.

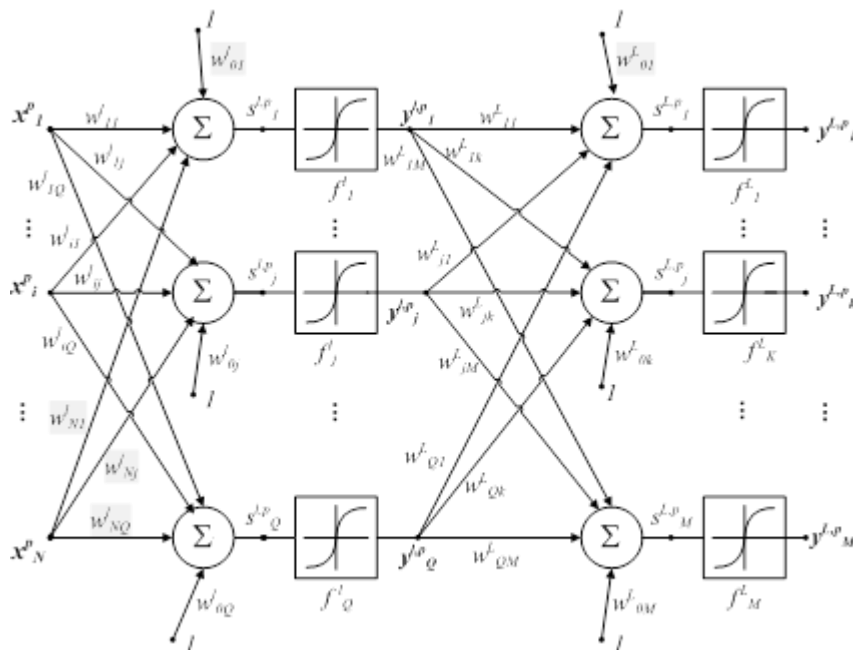


Fig. 5
Multilayer Perceptron neural network designs

The parameters have the following meaning:

- x_i^p - input network i , from pattern p ;
- P - number of patterns;
- L - output layer;
- l - hidden layer;
- N - number of inputs in input layer;
- Q - number of processing elements in the hidden layer;
- M - number of processing elements in the output layer;
- w_{ij}^l - synoptic weight between input network i from layer $l-1$ at processing element j from layer l ;
- $s_j^{l,p}$ - activation value at processing element j from layer l , from pattern p ;
- f_j^l - activation function at processing element j from layer l .
- $y_i^{l,p}$ - output unit i , from layer l , from pattern p ;

First, the neural networks were trained with a small number of processing elements in the hidden layer and the performance over the training set was determined. Then, the procedure was repeated with one more processing unit in the hidden layer and the performance was again calculated. After a sufficient number of architectures were trained, the best architecture was chosen.

4.7. APPLICATION AND RESULTS

The ANN model used in this case study consists of an input layer with 3 input parameters (the reservoir water level and the uplift pressures measures in the piezometer P31 and P17), an output layer (to represent the seepage measured in the MC4) and one hidden layer. Every neuron in the network is fully connected with each neuron of the next layer. A hyperbolic tangent transfer function has been chosen to be the activation function for the hidden layer and the linear function for the output layer. The generalized backpropagation delta learning rule algorithm was used in the training process. The chosen network architecture has shown the best results, considering all the tested networks, from 3 until 30 neurons, at the hidden layer. To find the optimum result, 5 initializations of random weights and a maximum of 5000 iterations were performed on each ANN architecture.

Figure 7 shows the evolution of the seepage at the drain MC4 (black color), and the predicted values from the MLR model (green color) and the ANN model (red color).

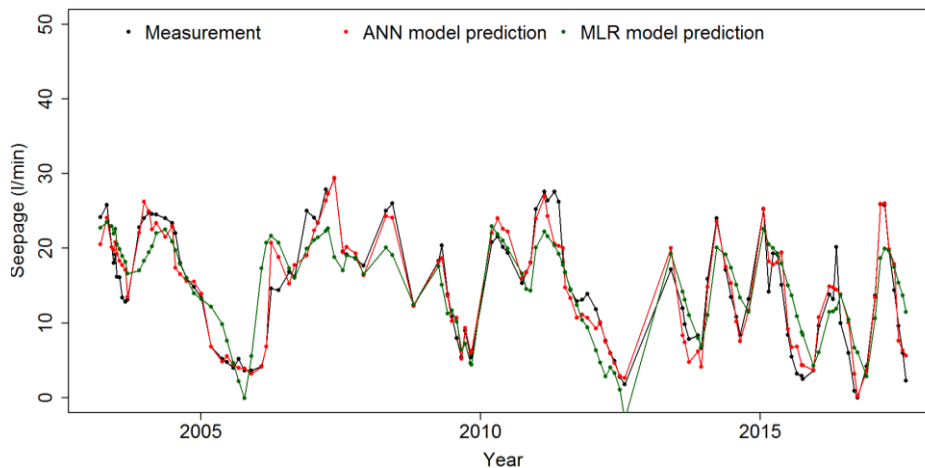


Fig. 6

Measurements, ANN prediction and QI prediction along time

The good fit shown by the models can be seen by comparing observations with the values predicted by the models (Figures 6 and 7) and by the analysis of Table 1, where the values of the maximum residual and the values of the standard deviation of the residuals, σ , for the MLR and the ANN models are presented.

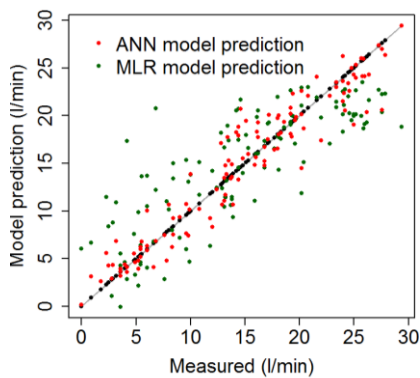


Fig. 7

Model predictions vs measurements

Table 1
Performance parameters for the MLR and the ANN models

Model	Max residual (l/min)	σ of the residual (l/min)
MLR	13.9	4.5
ANN	7.0	2.2

5. FINAL REMARKS

After identification of the main inputs and outputs for the neural network models and after establishing the methodologies for the learning and generalization procedures, the Multilayer Perceptron neural networks may become a new useful tool to support the safety control of seepage in zoned dams.

In this study, the achieved performance of neural network models to predict the flow rate in drain MC4 was very good when compared with traditional multiple

linear regression models. Despite the good results presented for MC4, it is necessary to carry out further studies including the results obtained from other individual drains, and it is not dispensable a global evaluation of the dam safety on the basis of a comprehensive analysis of the various observed parameters. Finally, it is always wise to carry out the safety evaluation simultaneously with various models rather than with just one model.

ACKNOWLEDGEMENTS

We would like to thank APA - Portuguese Environment Agency (dam owner) by given us permission to publish the dam monitoring data results.

REFERENCES

- [1] ICOLD 1995. Dam failures statistical analysis. Bulletin 099-1995, International Commission on Large Dams (ICOLD), Paris.
- [2] ICOLD 2003. World register of dams, International Commission on Large Dams (ICOLD), Paris.
- [3] Foster, M., Fell, R., and Spannagle, M. 2000. The statistics of embankment dam failures and accidents. Canadian Geotechnical Journal, 37: 1000-1024.

SUMMARY

This paper concerns about the assessment of the hydraulic behavior of a 50 m height zoned dam used for industry water supply, located in Alentejo region, in Portugal. The original draining system of the embankment is composed of a sub-vertical filter, located downstream of the central core, and by a drainage blanket placed over the foundation, in the deeper area of the valley, which, in turn, discharges to a downstream drainage toe.

In this study, the achieved performance of neural network models to predict the flow rate in a drain was very good when compared with traditional multiple linear regression models. Despite the good results presented, it is necessary to carry out further studies including the results obtained from other individual drains, and it is not dispensable a global evaluation of the dam safety on the basis of a comprehensive analysis of the various observed parameters. Finally, it is always wise to carry out the safety evaluation simultaneously with various models rather than with just one model.

COMMISSION INTERNATIONALE DES GRANDS BARRAGES

VINGT-SIXIÈME CONGRÈS DES GRANDS BARRAGES
Autriche, juillet 2018

DOI 10.3217/978-3-85125-620-8-161



This work licensed under a Creative Commons Attribution 4.0 International License. <https://creativecommons.org/licenses/by-nc-nd/4.0/>

**APPLICATION OF GEOMEMBRANE AS THE UPSTREAM IMPERVIOUS
LAYER OF KAHIR RCC DAM**

M. SADRI OMSHI

RCC Dam Specialist, WINDAVAR CO.

IRAN

M. JAFARBEGLOO

Technical & Quality Manager, JAHAN KOWSAR CO.

IRAN

H. GHIASSINEZHAD

Project Manager, WINDAVAR CO.

IRAN

A. MOHAMMADIAN

Project Manager, ABFAN CONSULTING ENGINEERING CO.

IRAN

COMMISSION INTERNATIONALE
DES GRANDS BARRAGES

VINGT-SIXIÈME CONGRÈS DES
GRANDS BARRAGES
Autriche, juillet 2018

APPLICATION OF GEOMEMBRANE AS THE UPSTREAM IMPERVIOUS LAYER OF KAHIR RCC DAM

M. SADRI OMSHI¹

M. JAFARBEGLOO²

H. GHIASSINEZHAD³

A. MOHAMMADIAN⁴

1 RCC Dam Specialist, WINDAVAR CO.

2 Technical & Quality Manager, JAHAN KOWSAR CO.

3 Project Manager, WINDAVAR CO.

4 Project Manager, ABFAN CONSULTING ENGINEERING CO.

IRAN

1. INTRODUCTION

Application of geomembrane as the upstream impervious layer of dams, especially of Roller Compacted Concrete Dams, has been increasing worldwide due to its better performance and easier process.

A reinforced concrete slab was in the design phase supposed to be used for waterproofing of dam but within construction phase, it was changed to geomembrane due to some technical and economic reasons.

In this paper, the upstream impervious layer of Kahir dam is described. According to special regional conditions and to prevent any construction stop caused by implementation of waterproofing system, a unique method carried out.

Finally, combination of three methods used in upstream part of the dam including exposed geomembrane in lower levels, geomembrane covered with

precast panels in middle part and geomembrane attached to the precast panels (known as Winchester method) in upper levels.

Kahir dam is the first concrete dam of Iran which uses geomembrane as the waterproofing element and at the moment, the design and construction method have been finalized and the abovementioned system is under construction.

2. PROJECT SALIENT FEATURES

Kahir RCC dam is the first Faced Symmetrical Hardfill Dam (FSHD) of Iran (Fig. 1). The dam is located in southeastern part of Iran, Siatan & Balouchestan province, in a hot climate. The main project information is as below [1]:

Type of dam	Gravity dam, FSHD type
Dam height	54.5 m
Crest width	5 m
Crest length	382 m
Spillway length	120 m
Reservoir volume	314 MCM
RCC volume	485.000 m ³
CVC volume	179.000 m ³
Total concrete volume	664.000 m ³
Diversion system	6 m diam. tunnel with a length of 283 m, upstream and downstream cofferdam

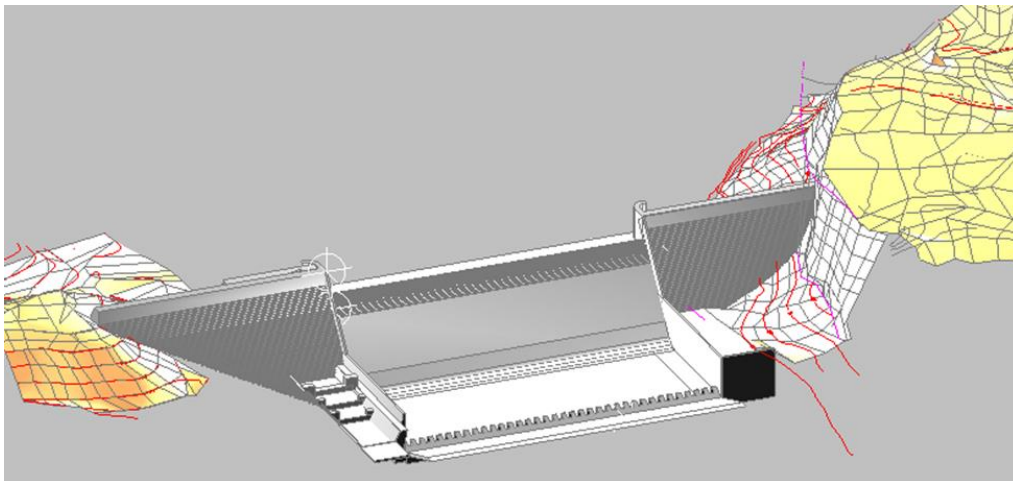


Fig. 1
3-D View of Kahir FSHD

3. MAIN DESIGN OF DAM WATERPROOFING SYSTEM

According to the contract drawings, waterproofing of the dam should be done by a 60 cm-thick reinforced concrete layer. This layer should be implemented after completion of dam body to lessen the tensions on concrete layer induced by settlement. The concrete impervious layer was to start from plinth concrete at the bottom part to the top as shown in Fig. 2:

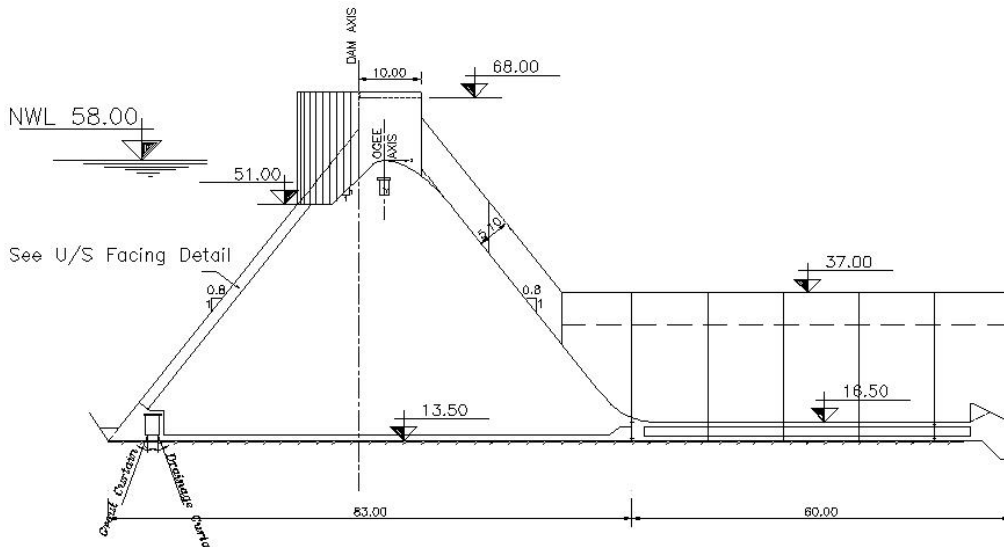


Fig. 2
Dam Section in Spillway

4. GEOMEMBRANE IMPERVIOUS SYSTEM DESCRIPTION

On the one hand, concrete impervious layer of main design should be implemented after the completion of dam body, which increases the time of project and on the other hand, geomembrane is technically more flexible than concrete and eliminates concerns about concrete cracking. For this purpose, a work group named Kahir Dam Waterproofing Design Review Team was formed and after lots of technical meetings, the impervious layer was changed to geomembrane. Eventually, geomembrane waterproofing system was designed as mentioned below (Fig. 3 & 4):

- Expose part from elevation +16 to +42 (bottom outlet level) which is always under water after first impounding. Using geocomposite including a 3 mm PVC geomembrane and 500 gr/m² geotextile attached together. Moreover, a 1000 gr/m² geotextile over it as a protective layer.
- Covered part with precast concrete panels over geocomposite from elevation +45 to +50. Similar to expose part, geocomposite have been

used with 1000 gr/m² geotextile over it to protect from probable damages of precast panels placed later on. However, extra 500 gr/m² geotextile layer used under the geocomposite in order to prevent puncturing.

- Winchester part (geocomposite attached to precast concrete panels) [2]. The impervious element of this part is a 2.5 mm geomembrane and 200 gr/m² geotextile attached to concrete panels.
- At the end, after implementation of all geocomposites, the two berms in elevations +42 and +50 are filled with concrete. These two berms have been designed to support the harness system of cover segments.

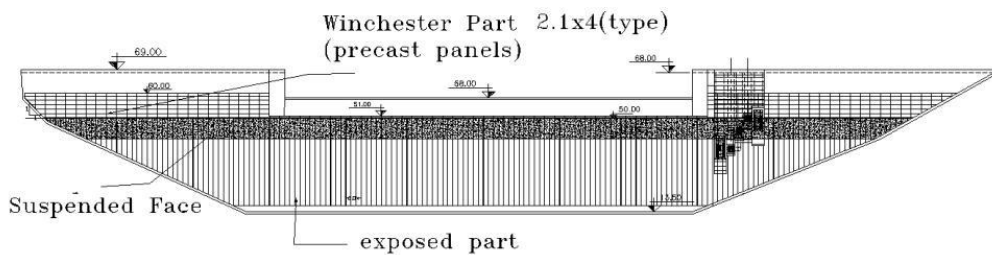


Fig. 3
Geomembrane Impervious System

In items below, the design details and construction method of each part are explained:

4.1. ELEVATION +16 TO +42

After first impounding, up to level +42 is always immersed; therefore, there is no need to have a permanent protection layer over geomembrane. Geomembrane is attached to the plinth concrete in lower parts and vertically to the dam body in every 6 m intervals as well. Plinth concrete is waterproof itself and geomembrane is fastened to plinth concrete by batten strips. There are two drainage pipes in each 12 m of upstream face to collect the probable leakage and lead it to the drainage gallery. The drainage system is designed in a way that the leakage of every 12 m is separately discharged into the gallery.

4.2. ELEVATION +45 TO +50

This part of dam body is above the lower bottom outlet. Since this elevation may sometimes be above water level, the geocomposite needs to be protected. It was supposed to perform Winchester method to seal this part like as upper levels; however due to the time-consuming procurement process, dam body construction reached to this level and the sealing system was inevitably changed to concrete-panel covered geocomposite (CPCG). In this method, without any

significant interruption on construction of upper levels, geocomposite layer is installed and precast concrete panels are thereafter placed on it. It is noteworthy that concrete-panel cover layer's stability and harness system were analyzed.

Being in critical path, geocomposite in elevation of +45 to +50 was implemented first. Lower part can independently be installed; but the upper part should be installed after completion of CPCG in middle part.

4.3. ELEVATION +53 TO +60

Winchester method is used in this part; i.e. precast concrete panels overlaid with geocomposite layer are used as formwork. In this method precast concrete panels stability has been considered as well.



Fig. 4
Berms of Elev.+42 & +50, Dam U/S View

Similar combinational method including Winchester method in upper part and exposed method in lower part (backfilled later on) has been utilized in Rizzanese RCC dam in France [3], [4].

5. IMPERVIOUS SYSTEM DESIGN

As previously mentioned, Kahir dam waterproofing system is specific. Additional to the design of conventional elements -like as stability of exposed geomembrane against uplift induced by wind [5] and stability of Winchester panels and connection anchors- stability analysis of the middle part cover segments, harness system including harness rebars and reinforced concrete berms have been performed. High seismic risk of the region was of great concern. Design loads were considered as below (Fig. 5):

- Weight of concrete cover segments
- Hydrostatic and hydrodynamic loads
- Inertial loads activated by seismic acceleration
- Inertial impact of dam body on concrete cover
- Wind uplift

Although design of different elements has basically been done, the results have been compared to main references; e.g. the number of anchors per unit surface has been calculated less than common construction experiences; therefore the number of steel anchor area has been replaced by the typical quantity mentioned by E. K. Schrader [6].

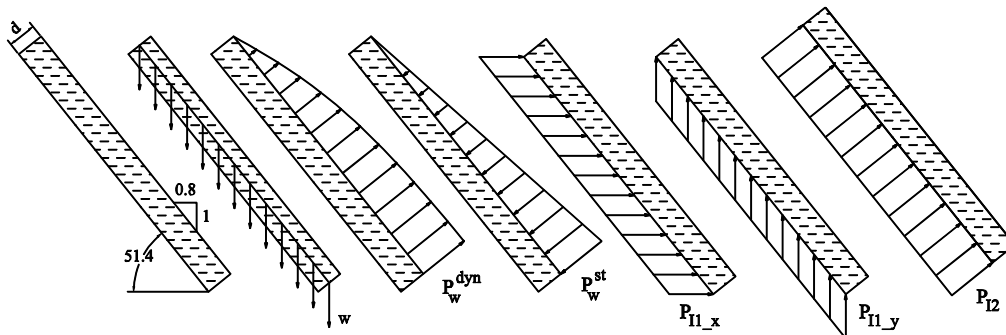


Fig. 5
Schematic Design Loads

Upper and lower harness concrete blocks have been modeled in ANSYS with 4-node plane elements (PLANE42). Some schematic diagrams of this analysis have been shown in Fig. 6.

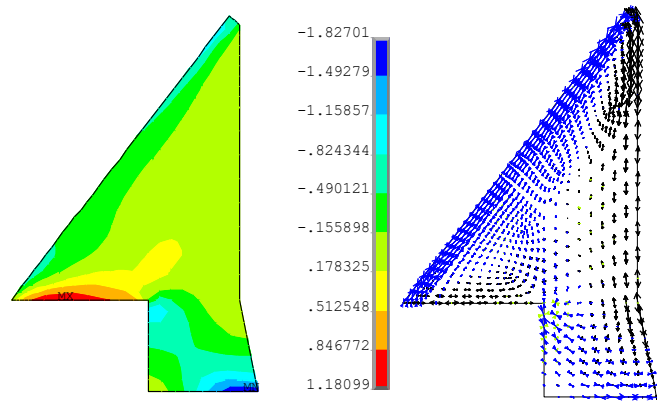


Fig. 6

Horizontal Stress Contour And Normal Stress Direction of Lower Block Also, installation method of concrete panels in Winchester part has been modeled by SAP2000 as demonstrated in Fig. 7.

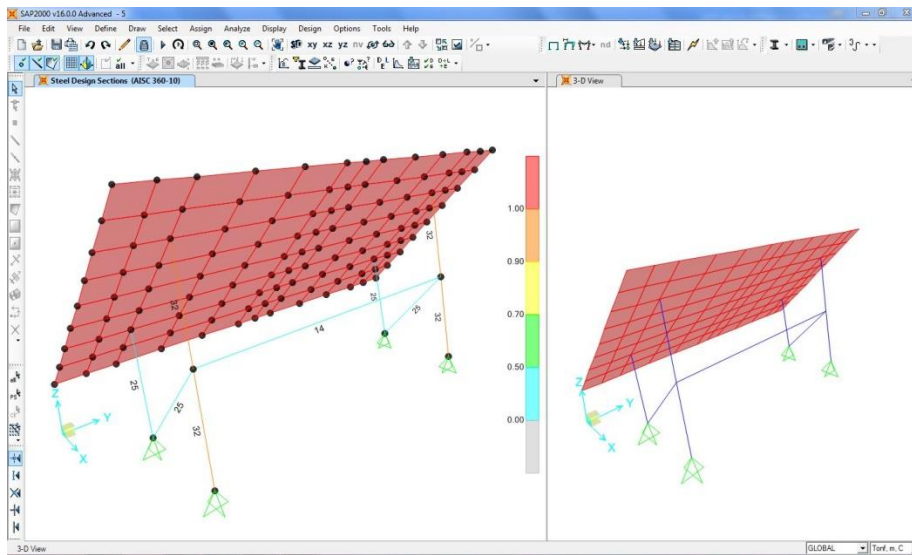


Fig. 7

SAP2000 Model for Installation Method of Winchester Panels

6. CONCLUSION

Based on studies [7], utilizing PVC geomembrane system instead of concrete slab as the impermeable element of Kahir dam has had these advantages:

- From technical aspect; watertightening with geomembrane has better results than upstream concrete slab and brings about higher level of certainty.
- From time aspect; using geomembrane shorten the duration of the project due to simultaneous construction of dam body and impermeable system. However implementing upstream concrete slab should be done after completion of dam body and foundation settlements.
- From cost aspect; both concrete slab and geomembrane system have almost had the same expenditure in this project but as mentioned before, the shorter the time of construction, the less the costs of project.

REFERENCES

- [1] PAZHOUHAB-ABFAN J.V.C.E.; Dam body design report; 2009.
- [2] ACI 207.5R-11; Report on roller-compacted mass concrete; 2001.
- [3] A. SCUERO & G. VASCHETTI; Three recent geomembrane project on new RCC dams; 6th intl. symposium on RCC dams; Spain; 2012.
- [4] A. LOCHU & F. DELORME & P. CARLIOZ; Design and build of Rizzanese RCC dam; 6th intl. symposium on RCC dams; Spain; 2012.
- [5] [J. P. GIROUD, M. H. GLEASON & J. G. ZORNBERG; Design of geomembrane anchorage against wind action, Geosynthetics International; 1999.
- [6] ERNEST K. SCHRADER; Chapter 20 of concrete construction engineering handbook; 2008.
- [7] ICOLD Bulletin No.135; Geomembrane sealing systems for dams; 2010.

COMMISSION INTERNATIONALE DES GRANDS BARRAGES

VINGT-SIXIÈME CONGRÈS DES GRANDS BARRAGES
Autriche, juillet 2018

DOI 10.3217/978-3-85125-620-8-162



This work licensed under a Creative Commons Attribution 4.0 International License. <https://creativecommons.org/licenses/by-nc-nd/4.0/>

**A STUDY ON CAUSE OF PERFORMANCE DEGRADATION OF SEEPAGE
MEASURING FACILITY IN OLD DAM**

Bumlin CHA

*Senior manager of Yecheon Pumped Storage Power Plant, KOREA HYDRO &
NUCLEAR POWER CO., LTD.*

KOREA

Seongho JANG

*Manager of Hangang Hydro Power Site, KOREA HYDRO & NUCLEAR POWER
CO., LTD.*

KOREA

Soowon PARK

*Senior manager of Yecheon Pumped Storage Power Plant, KOREA HYDRO &
NUCLEAR POWER CO., LTD.*

KOREA

COMMISSION INTERNATIONALE
DES GRANDS BARRAGES

VINGT-SIXIÈME CONGRÈS DES
GRANDS BARRAGES
Autriche, juillet 2018

**A STUDY ON CAUSE OF PERFORMANCE DEGRADATION OF SEEPAGE
MEASURING FACILITY IN OLD DAM**

Bumlin CHA

*Senior manager of Yecheon Pumped Storage Power Plant, KOREA HYDRO &
NUCLEAR POWER CO., LTD.*

KOREA

Seongho JANG

*Manager of Hangang Hydro Power Site, KOREA HYDRO & NUCLEAR POWER
CO., LTD.*

KOREA

Soowon PARK

*Senior manager of Yecheon Pumped Storage Power Plant, KOREA HYDRO &
NUCLEAR POWER CO., LTD.*

KOREA

1. INTRODUCTION

The upper dam of Cheongpyeong Pumped Storage Power Plant is an old dam constructed in 1980, which is approximately 35 years ago. A water-collecting wall and a measuring device were installed in the downstream area of the dam structure in order to observe the seepage of water passing through the dam

structure. However, the leakage could not be determined with the measuring device except during the period of localized heavy rain and summer season. It can be assumed that the water passing through the dam structure did not stay in the seepage water-collecting wall but flowed to other places.

Various field surveys were executed in order to determine the path of the water passing through the dam, which found a variety of paths of the seepage passing through the seepage water-collecting wall and the peripheral ground. This study intended to describe the survey and analysis processes designed to determine the cause of performance degradation of the facility for measuring the seepage in old dams.

2. CURRENT STATUS OF SEEPAGE MEASURING FACILITY

2.1. DAM STATUS

The Upper Dam is CCRD (Center core Rockfill Dam) which is a type of fill dam; the impervious core zone is installed in the center of the dam structure, the peripheral area is filled with rocks, and the seepage water-collecting wall is constructed in the downstream area of the dam structure. (Fig.1, Table 1)

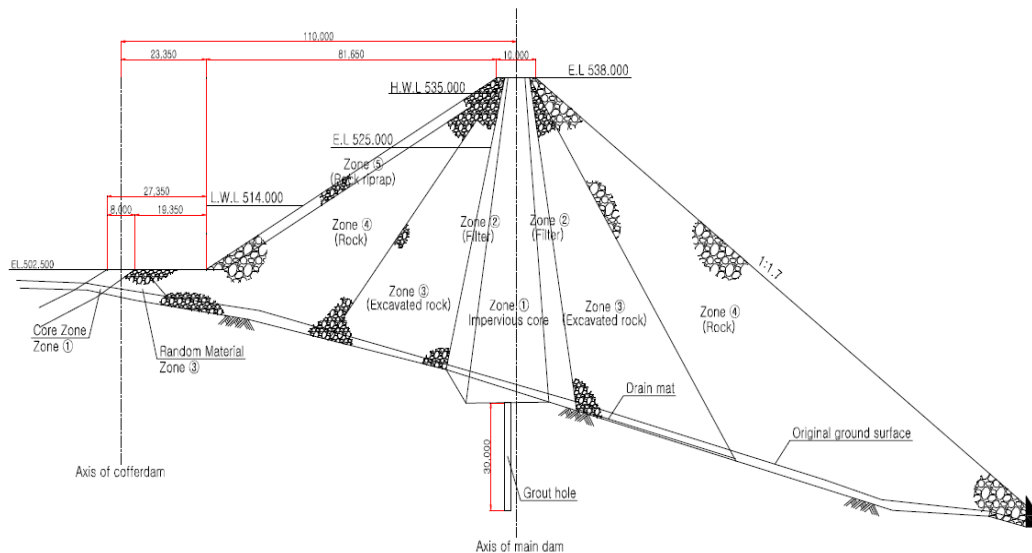


Fig. 1
Sectional Diagram of Upper Dam

Table 1
Specification of Upper Dam

Type	-	Center Core Rockfill Dam (CCRD)
Dam Crest	m	EL. 538.0
Length	m	290.0
Height	m	62.0
Dam Crest Width	m	10.0
Dam Volume	m ³	1,072,600
Inclination of Upstream Slope	-	1:2.3
Inclination of Downstream Slope	-	1:1.7

2.2. CURRENT STATUS OF SEEPAGE MEASURING FACILITY

The seepage measuring facility is composed of a water-collecting wall (Fig. 2) made of a concrete retaining wall (96m in length, 10m in maximum height) and a measuring room for measuring the collected water in the downstream area of the dam. (Fig. 3, Fig. 4)



Fig. 2
Water-collecting Wall



Fig. 3
Appearance of Seepage Measuring
Room



Fig. 4
Inside Seepage Measuring Room

3. FIELD INVESTIGATION

3.1. OVERVIEW

Naked eye investigation, test pit investigation, concrete strength measurement, boring investigation, and Lugeon test were performed to determine the cause of failure of the seepage measurement facility.

3.2. NAKED EYE INVESTIGATION

The concrete of the water-collecting wall has been deteriorated and damages such as local breakage and peeling were found. However, the overall condition was acceptable and did not appear to have functional problems.

The seepage measurement facility using V-notch was constructed by using concrete and stainless steel, and the conditions of all four screen facilities installed inside were acceptable, and it is deemed that the facility has not lost its functionality completely as it maintained consistent water level even after pumping for a long time in the upstream area of the water-collecting wall.

3.3. TEST PIT INVESTIGATION

The test pit investigation was carried out at two points at the corners of both banks where it was expected that the influence of the groundwater level on the excavation would be low and the construction of the water wall would be easy to

check as the height of the locations are relatively high among the sections where water-collecting walls are installed (Fig. 5).

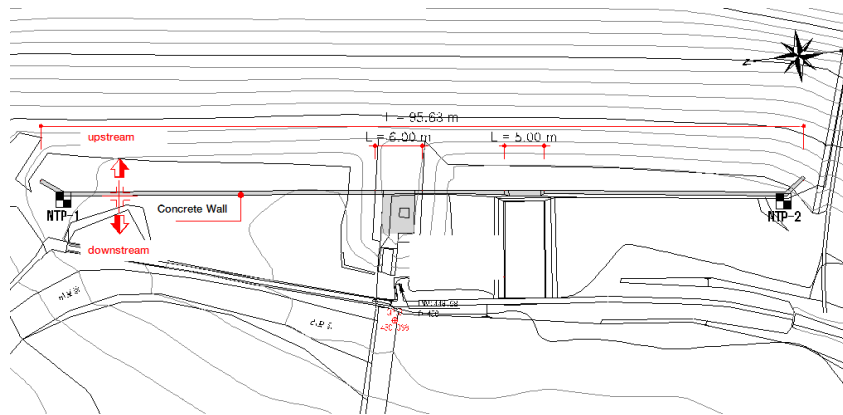


Fig. 5
Position of Test Pit Investigation

The NPT-1 test pit investigation was conducted at the corners of the water-collecting wall in the right bank of the dam. The groundwater was flowing into the excavation surface from 4.5m below the surface and the excavation could continue down to 4.8m below the surface. The mixture of buried layers (silty gravel layer mixed with sand) and boulder stones was distributed down to 1.5m below the surface of the ground. Concrete water-collecting wall (3m high) is installed at the bottom of the buried layer. There was no damage or leakage such as cracks and breakage on the concrete of the collecting wall, indicating the condition of construction is generally acceptable. However, the groundwater leaked from the contact area between the foundation concrete of the collecting wall and the bedrock (Fig. 6)



Fig. 6
Result of NPT-1 Test Pit Excavation

The NPT-2 test pit investigation was conducted at the corners of the water-collecting wall in the left bank of the dam. The groundwater was flowing into the

excavation surface from 3.5 m below the surface and the excavation could continue down to 4 m below the surface. In addition, the bedrock was not found within the excavated depth, and the mixture of buried layer (silty gravel layer mixed with sand) and boulder stones was distributed in the downstream area of the water-collecting wall. There was no damage or leakage such as cracks and breakage on the concrete of the collecting wall, indicating the condition of construction is generally acceptable (Fig. 7)



Fig. 7
Result of NPT-2 Test Pit Excavation

3.4. MEASURING CONCRETE STRENGTH

The concrete strength was measured by using the Schmidt hammer and performed on the collecting wall and the measuring room. As a result of measuring the strength of the collecting wall and the lower spots of the wall in the positions NPT-1 and NPT-2 where the test pit investigation was conducted, the average uniaxial compressive strength was 19.6 ~ 19.7MPa, and the compressive strength compensated based on the age coefficient was estimated at 12.3 ~ 12.4 Mpa.

The concrete strength of the seepage measuring room was measured in one place inside the measuring room. The average uniaxial compressive strength was 23.1MPa and the compressive strength compensated based on the age coefficient was estimated at 18.3 Mpa.

3.5. BORING INVESTIGATION

The boring investigation was carried out at eight positions selected to determine the stratigraphical composition of the lower area of the collecting wall. The depth was determined based on the extent to which the bearing stratum is confirmed and the casing was gradually inserted down to the bottom of the weathering soil and the standard penetration test was performed at the same

time in order to prevent the collapse of the pore wall during boring. As a result of the study, the water-collecting wall is distributed around the depth of 4.4 ~ 10m and is normal or acceptable as TCR was 50 ~ 100% and RQD was 50 ~ 100%.

The foundation the water-collecting wall was in contact with the soft rock layer which had a broad development of cracks and joints being. The soft rock layer was distributed in the lower area of the collecting wall in the depth of 5.4 ~ 9m and was relatively acceptable as TCR was 22 ~ 100% and RQD was 0 ~ 48%

Hard rocks were distributed in the lower side of the soft rock layer and they were relatively acceptable as TCR was 83 ~ 100% and RQD was 25 ~ 100% (Fig. 8).

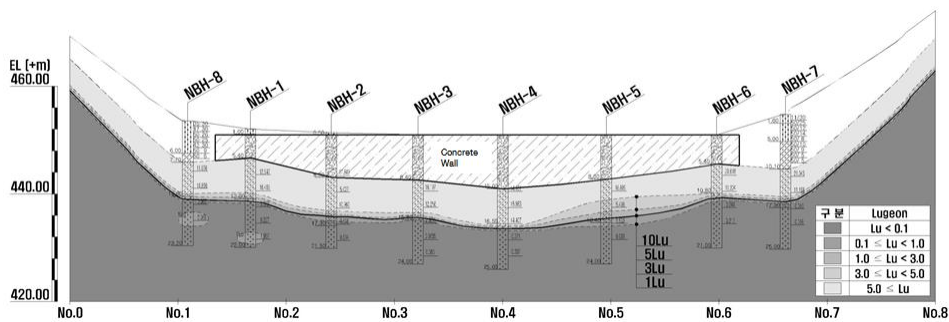


Fig. 8
Boring Investigation & Lugeon Map

3.6. LUGEON TEST

A Lugeon test was conducted within the borehole to determine the permeability of the water-collecting wall and the ground, and some sections of the collecting wall and the soft rock layer showed 3Lu or higher permeability and the hard rock section showed less than 3Lu in all sections (Fig 8). It was assumed then the main seepage pathway of the water-collecting wall is the soft rock layer.

4. ANALYSIS OF SEEPAGE PATH

4.1. LONGITUDINAL SEEPAGE PATH

The major seepage path is the 3Lu or more permeable stratum formed around the water-collecting wall, and this stratum is distributed in the thickness of 6.1 ~ 8.0m in the lower side of the water-collecting wall (a) and in the left side (b) and right side (c) of the water-collecting wall (Fig. 9) in the width of 19.0 ~ 25.2m.

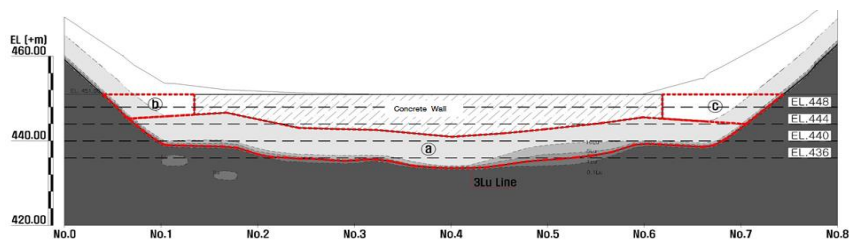


Fig. 9
Longitudinal Map Showing Seepage Path

4.2. PLANAR SEEPAGE PATH

As a result of analyzing planar seepage path at EL. 448m, the seepage pathway greater than 3Lu is distributed in the width of 133.8m, and the area blocked by the water-collecting wall is 95.9m in the center and 16.3m on the left side and 21.6m on the right side of the water-collecting wall. As the water-collecting wall does not completely block the permeable layer, the groundwater can flow in by making a detour around both ends. (Fig. 10)

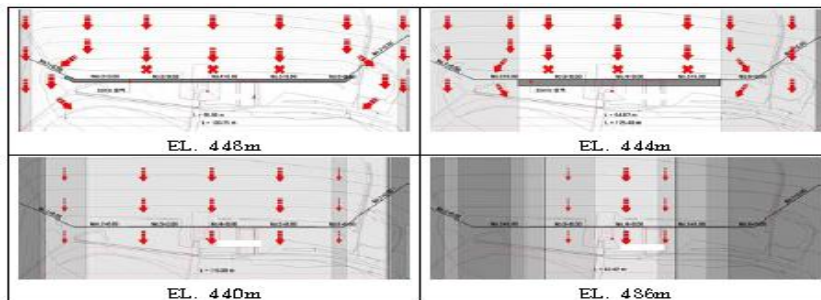


Fig. 10
Floor Plan Showing Seepage Path

At EL. 444m, the seepage pathway greater than 3Lu is distributed in the width of 125.4m, and the area blocked by the water-collecting wall is 64.9m in the center and 29.4m on the left side and 31.1m on the right side of the water-collecting wall. As the water-collecting wall does not completely block the permeable layer, the groundwater can flow in by making a detour around both ends.

At EL. 440m, the seepage pathway greater than 3Lu is distributed in the width of 115.4m. The seepage pathway between 3 ~ 5Lu accounted for 16.2% of the entire seepage pathway and that over 5Lu, 83.8%. It is confirmed that no section at this position is blocked by the water-collecting wall.

At EL. 436m, the seepage pathway greater than 3Lu is distributed in the width of 42.4m. The seepage pathway between 3 ~ 5Lu accounted for 50.8% and

that over 5Lu, 49.2%. It is confirmed that no section at this position is blocked by the water-collecting wall.

5. CONCLUSION

As a result of several investigations which were conducted to identify the cause for functional degradation of seepage measuring facility, the water passing through the dam flew in various paths instead of being collected in the water-collecting wall, and the tracking of seepage path resulted in following conclusions.

First, the foundation of the water-collecting wall is located above the soft rock layer which is the bedrock. The quality of this soft rock layer is poor with the developments of cracks and joints and this layer displays 3Lu or greater permeability in all sections, which identifies the soft rock layer as the major seepage pathway.

Second, the investigation found the leakage of groundwater noticeable by the naked eye in the contact area between the concrete of the foundation of the water-collecting wall and the bedrock and identified the leakage in the contact area as another major cause.

Third, the condition of the concrete of the collecting wall was relatively acceptable. However, the Lugeon test showed that the lugeon value exceeded 3Lu in some sections and it is deemed that the leakage occurs through the wall as well.

We introduced and shared the methods and processes for analyzing the causes of functional degradation of the seepage measurement facility that can occur in dams as above and hope this helps the securing of the stability of the dam in operation.

ACKNOWLEDGEMENTS

The authors would like to express their gratitude for the extensive cooperation provided by Cheongpyeong Pumped Storage Power Plant.

REFERENCES

- [1] DOHWA ENGINEERING CORPORATION. Design report for functional recovery of seepage measuring facility of the upper dam of Cheongpyeong Pumped Storage Power Plant , 2016.
- [2] KOREA WATER RESOURCES ASSOCIATION. Dam design criteria, 2005.

SUMMARY

This study intends to find out the possibility of recovering the original function of the dam by analyzing the cause of functional degradation of the seepage measurement facility that may occur in old dams. The dam concerned is the upper dam of Cheongpyeong Pumped Storage Power Plant constructed in 1980, which is approximately 35 years ago, and it was not possible to measure the leakage except during the period of localized heavy rain as the water was not collected in the seepage measuring facility installed in the downstream area of the dam

Various field investigations were conducted to determine the cause of functional degradation of the seepage measuring facility. According to the result of naked eye investigation, the measuring facility did not have significant problems in carrying out its functions. Two points on both banks of the collecting wall were excavated to confirm the groundwater leakage around the water-collecting wall and it confirmed the leakage of groundwater in the foundation of the collecting wall in the right bank area of the dam. The result of strength measurement to confirm the soundness of the concrete of the collecting wall indicated that the condition of the wall is acceptable. In addition, a boring investigation was carried out to determine the geology of the foundation ground, and the Lugeon test, which was conducted to determine the permeability through the collecting wall and foundation soil, showed the sections with high lugeon values.

The comprehensive analysis of the investigation results showed various paths through which the leaking water flowed instead of being collected in the collecting wall and came to the following conclusions. First, the foundation of the water-collecting wall is located above the soft rock layer which is the bedrock. The quality of this soft rock layer is poor with the developments of cracks and joints and this layer displays 3Lu or greater permeability in all sections, which identifies the soft rock layer as the major seepage pathway. Second, the investigation found the leakage of groundwater noticeable by the naked eye in the contact area between the concrete of the foundation of the water-collecting wall and the bedrock and identified the leakage in the contact area as another major cause. Third, the condition of the concrete of the collecting wall was relatively acceptable. However, the Lugeon test showed that the lugeon value

exceeded 3Lu in some sections and it is deemed that the leakage occurs through the wall as well.

This study could identify various flow paths which deteriorate the function of the seepage measuring facility, and it is necessary to examine a way to recover the intended function of the facility by eliminating such abnormal flows in future studies.

COMMISSION INTERNATIONALE DES GRANDS BARRAGES

VINGT-SIXIÈME CONGRÈS DES GRANDS BARRAGES
Autriche, juillet 2018

DOI 10.3217/978-3-85125-620-8-163



This work licensed under a Creative Commons Attribution 4.0 International License. <https://creativecommons.org/licenses/by-nc-nd/4.0/>

**LONG TERM BEHAVIOR AND PERFORMANCE OF CORE ZONE AGAINST
UPLIFT DISTRIBUTION OF MAE NGAD SOMBOON CHON DAM,
CHIANG MAI, THAILAND**

Chatchai PEDUGSORN

Head of Design Branch, REGIONAL IRRIGATION OFFICE

THAILAND

Kanokwan CHUENUAM

Geologist of Geotechnical Branch, REGIONAL IRRIGATION OFFICE

THAILAND

Pearasynp SRISAWAT

Head of Geotechnical Branch, REGIONAL IRRIGATION OFFICE

THAILAND

Supamitr KRISANAMITR

Head of Dam Safety Management, REGIONAL IRRIGATION OFFICE

THAILAND

**LONG TERM BEHAVIOR AND PERFORMANCE OF CORE ZONE AGAINST
UPLIFT DISTRIBUTION OF MAE NGAD SOMBOON CHON DAM,
CHIANG MAI, THAILAND**

Chatchai PEDUGSORN¹, Kanokwan CHUENUAM², Pearasynp SRISAWAT³,
Supamitr KRISANAMITR⁴

Head of Design Branch, Regional Irrigation office 1¹, Geologist of Geotechnical
Branch, Regional Irrigation office 1², Head of Geotechnical Branch, Regional Irrigation
office 1³, Head of Dam Safety Management, Regional Irrigation office 1⁴

THAILAND

1. INTRODUCTION

Mae Ngad Somboon Chon Dam is located in Mae Tang District Chiang Mai Province in the Northern part of Thailand. The project was initiated under His Majesty King Bhumiphol Adulyadej, originally proposed as multipurpose reservoir for irrigation, Water supply, hydro power and flood control. Construction period was 8 years, started in 1977 and was completed in 1985. Dam details and hydrology condition are as follows. Catchment area 1,281 square-kilometer, Average annual inflow 406 million-cubic meter Maximum reservoir storage 325 million-cubic meter, +398.000 m.-M.S.L. Normal reservoir storage 265 million-cubic meter, +396.500 m.-M.S.L. Dead storage 20 million-cubic meter, +360.500 m.-M.S.L. Dam height 59.00 meter (69.00 meter above bottom of cutoff trench) Dam crest width 9.00 meter (+404.000 m-M.S.L.), Dam length 1,950.00 meter Upstream slope 1:3, Downstream slope 1:2.5, Zone type dam Service spillway, Gate spillway capacity 1,035.00 cubic meter per second Emergency spillway, Earth spillway capacity 535.00 cubic meter per second River outlet 2,500 millimeter (I.D.), Right and Left irrigation outlet 800 millimeter (I.D.)



Fig. 1 Location map of Mae Ngad Somboon Chon Reservoir

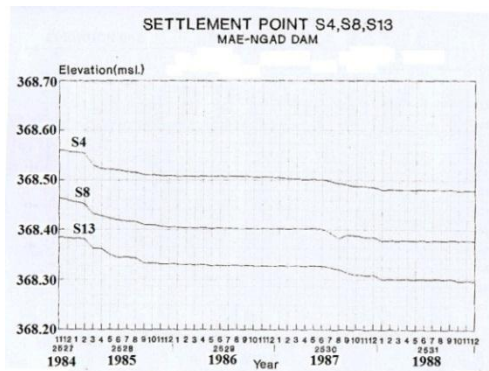
2. DAM INSTRUMENTATION AND DAM INVESTIGATION

During the end of construction, conventional dam instrumentation was installed in 1984 and started to measure manually in November. Dam instrumentation is as shown in Table.1.

Table.1 Dam instrumentation of Mae Ngad Somboon Chon (end of construction)

Dam Instrument			
1. Open end Stand pipe piezometer	18	4. Inclinator	4
2. Surface settlement point	30	5. Observation well	21
3. Foundation settlement point	4	6. Reference Benchmark	6

Measured data from November 1984 to December 1988 is reported by Warathon[5] (1989). Settlement at Sta.0+180, depth section, is in Fig.2. In 2014, Region Irrigation office 1, Royal Irrigation Department (RID), improved dam instrument monitoring system by installation 50 vibration wire electric piezometers (Sta.0+180) (Fig.3), 3 Accelerometers, 2 Seismometers, 1 Seepage flow meter, 5 Observation wells with automatic water leveling sensor. Observation data are input to real-time monitoring system by specific time interval which can adjusted between 10 second to 1 minute. Output of real-time monitoring model display dam cross-section Sta.0+180 by numerical and color gradient display of pore pressure distribution. Dam investigation was done by collecting of large size sample (4 inch diameter) from dam crest to bottom of cutoff trench. Sample is trimmed in laboratory for undisturbed sample for permeability test, triaxial test, and basic soil properties test (Fig. 4).



S.S.P	Degree of Consolidation (1984-1987)/(2014-2017)
S4	65.77%
S8	66.09%
S13	66.36%

Fig. 2 Degree of Consolidation at Sta.0+180 (depth section)

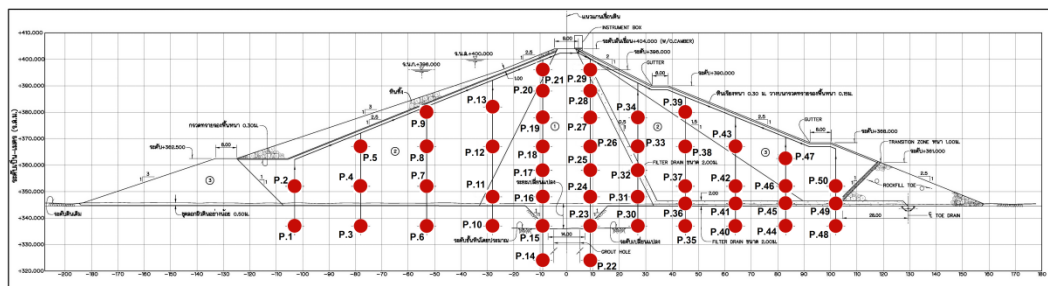


Fig. 3 Vibration wire electric piezometer at sta.0+180



Fig. 4 Dam investigation at Sta.0+180 (depth-section)

3. LONG TERM BEHAVIOR AND PERFORMANCE OF CORE ZONE AGAINST PORE PRESSURE DISTRIBUTION

Measured seepage behavior during period of 1984 to 1987 (before 66 percent degree of consolidation) are compared with recorded pore pressure distribution from 2014 to 2017

(approach 100 percent degree of consolidation) at Sta.0+180, depth section, as example shown in Fig. 5

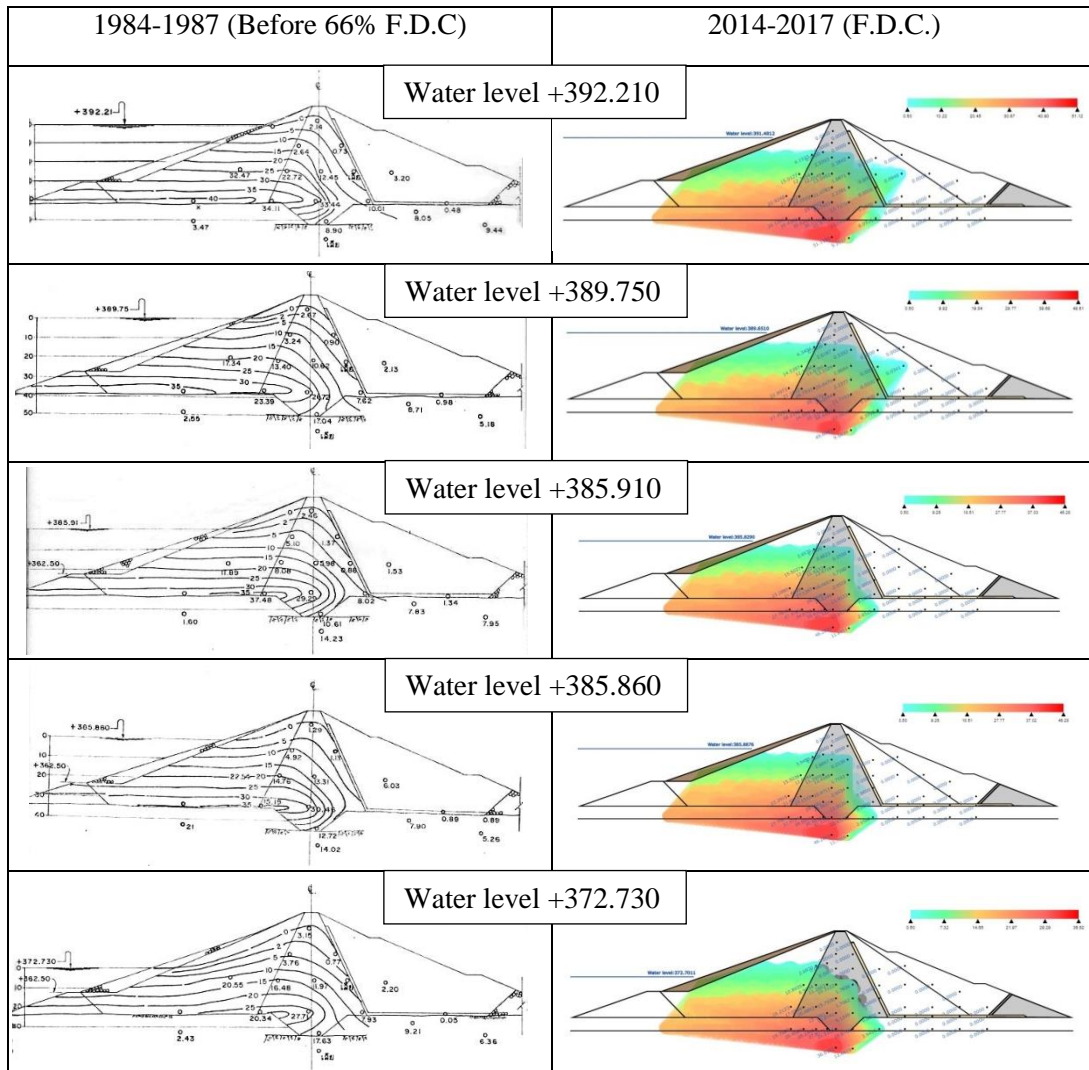


Fig. 5 Comparison between $<2/3$ F.D.C. and F.D.C.

There are 5 seepage indicators proposed to assess core zone subjected to long term seepage pressure distribution as following.

1. Average upstream pore pressure of core zone
2. Average downstream pore pressure of core zone
3. Average seepage gradient of core zone
4. Average seepage velocity of core zone
5. Factor of safety against uplift of core zone

Long term behavior and performance of core zone against uplift distribution is proposed as comparison of indicators between seepage through core zone change from before two-thirds full degree of consolidation and full degree of consolidation under rule curve operation. Core layer seepage distribution a change is shown in Table2.

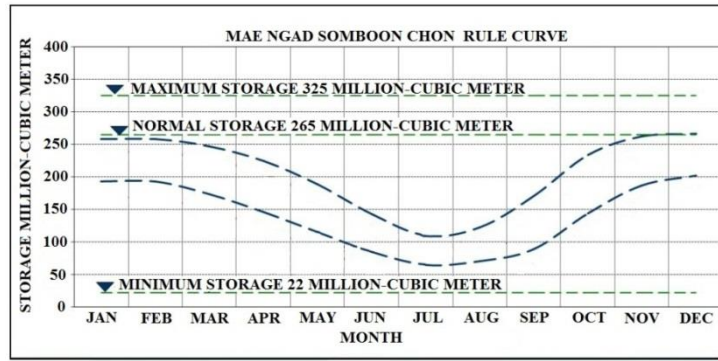


Fig. 6 Rule curve of Mae Ngad Somboon Chon Reservoir

Table2. Core layer comparison between $<2/3$ F.D.C. and F.D.C.

Average	Contact clay $h_i \approx 0$	$h_i=0.1$	$h_i=0.5$	$h_i=0.75$
1.Pore Pressure U/S. core layer	reduce 77.72%	reduce 92.72%	reduce 92.37%	reduce 98.42%
2.Pore Pressure D/S. core layer	reduce 83.42%	reduce 99.05%	reduce 97.66%	reduce 172.26%
3.Seepage Gradient of core layer	reduce 61.40%	reduce 93.53%	reduce 91.60%	reduce 100.94%
4.Seepage Velocity of core layer	reduce 71.80%	reduce 95.63%	reduce 93.84%	reduce 100.50%
5.F.S. against uplift	increase 3.20 times	increase 13.76 times	increase 20.04 times	increase 294.15 times

Core zone investigation was done by dividing core height (H) into layers from bottom of cutoff trench. Core zone layer (i) is identified by height of considered core zone layer from bottom of cutoff trench (h) over core height (H), $h_i=h/H$. Long term seepage performance index (L) of core layers is defined as lump conceptual for seepage indicator changes between first stage and stable stage compared with first stage.

$$L_{h_i} = a_{h_i} \cdot b_{h_i} \cdot c_{h_i} \cdot d_{h_i} \cdot e_{h_i} \quad [1]$$

Where,

- a_{h_i} = average upstream pore pressure of core layer (i) change over first stage
- b_{h_i} = average downstream pore pressure of core layer (i) change over first stage
- c_{h_i} = average seepage gradient of core layer (i) change over first stage
- d_{h_i} = average seepage velocity of core layer (i) change over first stage
- e_{h_i} = factor of safety against uplift of core layer(i) change over first stage
- H = height of core zone (m)
- h = height of considered core zone layer from bottom of cutoff trench (m)

$$h_i = \frac{h}{H_i} \quad [2]$$

$$L_{avg_{h_i}} = -22273.739h_i^6 + 49838.747h_i^5 - 40452.909h_i^4 + 15444.748h_i^3 - 2925.149h_i^2 + 265.718h_i + 0.790, \quad R^2 = 0.9967 \quad [3]$$

$$a_{avg_{h_i}} = -56.605h_i^6 + 156.448h_i^5 - 166.864h_i^4 + 87.455h_i^3 - 23.431h_i^2 + 2.962h_i + 0.793, \quad R^2 = 0.995 \quad [4]$$

$$b_{avg_{h_i}} = 673.074h_i^6 - 1352.221h_i^5 + 990h_i^4 - 309.694h_i^3 + 33.616h_i^2 + 0.679h_i + 0.810, \quad R^2 = 0.954 \quad [5]$$

$$c_{avg_{h_i}} = 305.093h_i^6 - 757.743h_i^5 + 723.474h_i^4 - 333.838h_i^3 + 76.548h_i^2 + 7.990h_i + 0.633, \quad R^2 = 0.982 \quad [6]$$

$$d_{avg_{h_i}} = -233.363h_i^6 + 583.149h_i^5 - 560.129h_i^4 + 259.883h_i^3 - 59.786h_i^2 + 6.276h_i + 0.718, \quad R^2 = 0.977 \quad [7]$$

$$e_{avg_{h_i}} = 37141.727h_i^6 - 57567.110h_i^5 + 30837.041h_i^4 - 5657.709h_i^3 - 277.879h_i^2 + 170.969h_i + 2.558, \quad R^2 = 1.000 \quad [8]$$

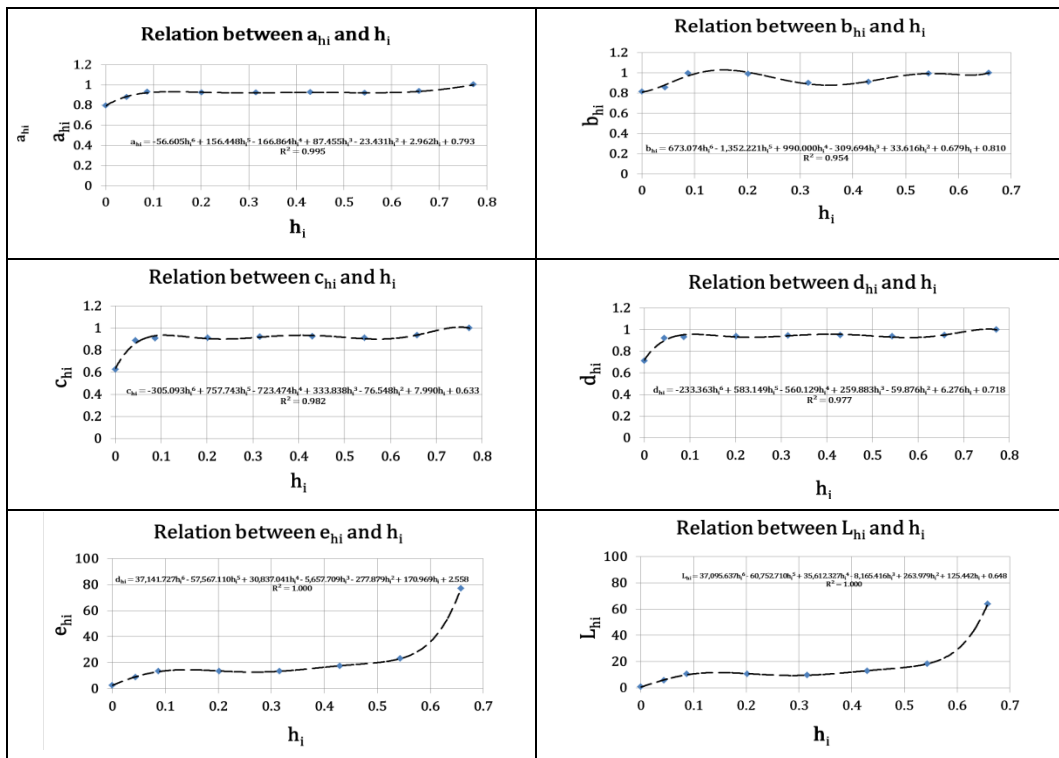


Fig. 7 Relation between a_{h_i} , b_{h_i} , c_{h_i} , d_{h_i} , e_{h_i} , L_{h_i} and h_i

Efficiency of core zone layer (i) can be evaluated as, Efficiency of upstream pore pressure resistance = $a_{h_i} \cdot 100$, Efficiency of downstream pore pressure resistance = $b_{h_i} \cdot 100$, Efficiency of seepage gradient resistance = $c_{h_i} \cdot 100$, Efficiency of seepage velocity

resistance = $d_{h_i} \cdot 100$. Seepage penetration resistance (S.P.R.) for long term is assumed as lump conceptual as resistance of core zone in reducing upstream pore pressure, downstream pore pressure, seepage gradient and seepage velocity.

$$\text{S.P.R.} = a_{h_i} \cdot b_{h_i} \cdot c_{h_i} \cdot d_{h_i} \quad [9]$$

$$\text{S.P.R.} = -381.541h_i^6 + 842.326h_i^5 - 756.158h_i^4 + 354.974h_i^3 - 90.404h_i^2 + 11.201h_i + 0.284, \quad R^2 = 0.999 \quad [10]$$

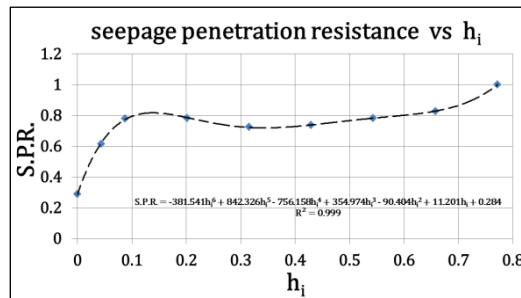


Fig. 8 Relation between S.P.R. and h_i

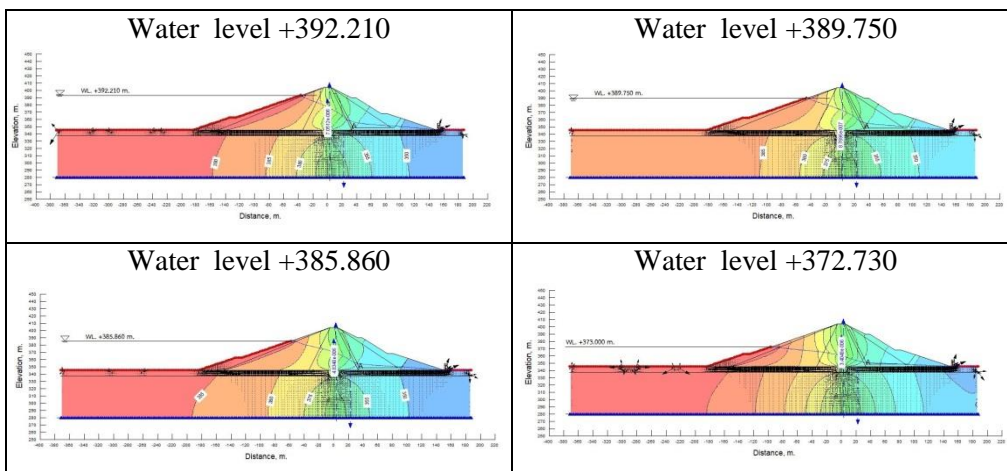


Fig. 9 Finite element seepage analysis

Eq. [3] to Eq. [10] and Fig.7 and Fig.8 show the long term behavior and performance of core layer from bottom of cutoff trench to top of core layer. Upstream core layer pore pressure is minimally decrease at bottom layer $h_i = 0$ and rapidly fall in $0 < h_i \leq 0.1$ from 79.30% ($h_i = 0$) to 92.72% ($h_i = 0.1$) then gradually reduce to 98.42% at $h_i = 0.75$. Downstream core layer pore pressure is minimally decrease at bottom layer $h_i = 0$ and rapidly falls in $0 < h_i \leq 0.1$ from 81.00% ($h_i = 0$) to 99.05 ($h_i = 0.1$) then gradually reduces to 107.23% at $h_i = 0.75$. Core layer seepage gradient is minimally decreased at bottom layer $h_i = 0$ and rapidly reduces in $0 < h_i \leq 0.1$ from 63.30% ($h_i = 0$) to 93.53 ($h_i = 0.1$) then slowly drops to 100.94% at $h_i = 0.75$. Core layer seepage velocity is minimum relaxation at bottom layer $h_i = 0$ and rapidly falls in $0 < h_i \leq 0.1$ from 71.80% ($h_i = 0$) to 95.63 ($h_i = 0.1$) then slowly drops to 100.50% at $h_i = 0.75$. Factor of safety against uplift of core layer is minimally increased at bottom layer $h_i = 0$ and rapidly rises in $0 < h_i \leq 0.1$ from 255.80% ($h_i = 0$) to 1,376.36% ($h_i = 0.1$) then slowly raises to 2,004.10% finally rapidly increases to 68,870.23% at $h_i = 0.65$.

Table4. Seepage distribution from $<\frac{2}{3}$ F.D.C. to F.D.C.

Part	h_i	q (m ³ /sec/m)		Δq (%)
		$<2/3$ F.D.C	F.D.C.	
4 th	$0.5 < h_i \leq 0.75$	5.93×10^{-6}	1.68×10^{-7}	-97.17%
		(2.16%)	(2.94%)	
3 rd	$0.1 < h_i \leq 0.50$	5.12×10^{-5}	2.70×10^{-6}	-94.74%
		(70.42%)	(43.17%)	
2 nd	$0 < h_i \leq 0.10$	1.29×10^{-5}	2.09×10^{-6}	-83.70%
		(17.69%)	(36.61%)	
1 st	$h_i \approx 0$	2.70×10^{-6}	7.62×10^{-7}	-71.80%
		(3.72%)	(13.32%)	
Total		7.27×10^{-5}	5.72×10^{-6}	-92.13%
		(100%)	(100%)	

The measured seepage data from 1984-1987 and 2014-2017 along with finite element seepage analysis result in Table.4 followed 4 parts of seepage penetration resistance. Long term seepage through core zone reduces by 92.13%. Seepage discharge almost penetrates the core zone in range $h_i \leq 0.5$ for short term 97.84% and long term 97.06% of average total seepage discharge. Core zone layers at $h_i > 0.5$ rapidly increased L and S.P.R. but seepage discharge for initial and final stage is 2.16% and 2.94% of average total seepage discharge, respectively. Core zone layers in $0.1 < h_i \leq 0.5$ gradually raise L and S.P.R. however seepage discharge is mostly influence from average total seepage discharge for initial stage ($<2/3$ F.D.C.) and final stage (F.D.C.) about 70.42% and 47.13%, consecutively. Layers in core zone $0 < h_i \leq 0.1$ is rapidly increase L and S.P.R. but seepage discharge for initial and final stage is 17.69% and 36.61% in order. Contact clay layer (0.30meter from bottom of cutoff trench) at bottom of core zone $h_i \approx 0$ is minimum L and S.P.R. and minimum of seepage discharge reduction. Seepage discharge distribution dissipate to bottom layer $0.1 < h_i \leq 0.5$, $0 < h_i \leq 0.1$, $h_i \approx 0$ from initial stage 70.42%, 17.69%, 3.72% to final stage 47.13%, 36.61%, 13.32%, respectively. As part1 $h_i \approx 0$, contact clay layer has minimum reduction of seepage discharge 71.80%, maximum seepage discharge distribution from 3.72% to 13.32% or 3.58 times and minimum increase in factor of safety against uplift 255.80% exhibited boundary condition of core zone weak layer.

4. CONCLUSION

Long term performance index (L), Seepage penetration resistance (S.P.R.) represent an overview and inter-layers seepage through core zone layers changes between initial stage (before $2/3$ full degree of consolidation) and final stage (full degree of consolidation).

Significant seepage discharge penetrated core zone below middle height ($h_i \leq 0.5$) for initial stage 97.84% and final stage 97.06% of total average seepage discharge.

Minimal seepage discharge penetrated the core zone above middle height ($h_i > 0.5$)

for initial stage 2.16% and final stage 2.94% of total average seepage discharge, despite maximum reduction of upstream core layers pore pressure, downstream core layers pore pressure, core layers seepage gradient, core layers seepage velocity, and maximum increase factor of safety against uplift.

Long term seepage through core zone reduce 92.13%

Long term seepage discharge distribution tends to dissipate to bottom layers $0.1 < h_i \leq 0.5$, $0 < h_i \leq 0.1$, $h_i \approx 0$ from initial stage 70.42%, 17.69%, 3.72% to final stage 47.13%, 36.13%, 13.32% respectively.

Contact bottom core layer has boundary condition of weak layer from long term seepage behavior due to minimum reduction of seepage discharge 71.80%, maximum seepage discharge distribution (dissipate from upper core layers) from 3.72% to 13.32% or 3.58 times and minimum increase in factor of safety against uplift 255.80%.

5. RECOMMENDATION

Long term behavior and performance should not be used to design for safety factor but should benefit to additional safety factor.

Future research should extend to boundary condition affecting L, and S.P.R. such as shallow foundation against deep pervious foundation, various dam type, component, and efficiency of internal drainage system, foundation and abutment, reservoir operation, and the like.

Long term seepage performance index, L, and seepage penetration resistance, S.P.R., should benefit long term dam safety management alongside with visual inspection.

REFERENCE

- [1] CASAGRANDE, A., Seepage Through Dams, Contributions to soil mechanics 1925- 40, Boston Society of Civil Engineer, Boston, *Massachusetts*, 1940
- [2] CIVIL ENGINEER DEPARTMENT, Chiang Mai University, The Result of Soil Laboratory of Mae Ngad Somboon Chon Dam, *Chiang Mai, Thailand*, 2016
- [3] GEOTECHNICAL BRANCH, Royal Irrigation Department, Geotechnical Investigations of Mae Ngad Somboon Chon Dam, *Chiang Mai, Thailand*, 2016
- [4] TERZAGHI, KARL, and, RALPH B. PEAK, Soil Mechanics in Engineering, Practice, Second Edition, John Wiley and Sons, Inc., *New York*, 1967
- [5] WARATHORN, A., Dam Behavior Measurement of Mae Ngad Dam from 1984 – 1988, Dam Design Group, Design division, Royal Irrigation Department, *Bangkok, Thailand*, 1989

COMMISSION INTERNATIONALE DES GRANDS BARRAGES

VINGT-SIXIÈME CONGRÈS DES GRANDS BARRAGES
Autriche, juillet 2018

DOI 10.3217/978-3-85125-620-8-164



This work licensed under a Creative Commons Attribution 4.0 International License. <https://creativecommons.org/licenses/by-nc-nd/4.0/>

DAM FOUNDATION SEEPAGE CONTROL IMPROVEMENT BY CEMENT-CHEMICAL GROUTING UNDER STORAGE CODITION OF MAE THI DAM, LUMPHUN, THAILAND

Chatchai PEDUGSORN

Head of Design Branch, REGIONAL IRRIGATION OFFICE

THAILAND

Kanokwan CHUENUAM

Geologist of Geotechnical Branch, REGIONAL IRRIGATION OFFICE

THAILAND

Pearasynp SRISAWAT

Head of Geotechnical Branch, REGIONAL IRRIGATION OFFICE

THAILAND

Supamitr KRISANAMITR

Head of Dam Safety Management, REGIONAL IRRIGATION OFFICE

THAILAND

**DAM FOUNDATION SEEPAGE CONTROL IMPROVEMENT BY
CEMENT-CHEMICAL GROUTING UNDER STORAGE CODITION OF MAE
THI DAM, LUMPHUN, THAILAND**

Chatchai PEDUGSORN¹, Kanokwan CHUENUAM², Pearasynp SRISAWAT³,
Supamitr KRISANAMITR⁴

Head of Design Branch, Regional Irrigation office 1¹, Geologist of Geotechnical
Branch, Regional Irrigation office 1², Head of Geotechnical Branch, Regional Irrigation
office 1³, Head of Dam Safety Management, Regional Irrigation office 1⁴

THAILAND

1. INTRODUCTION

1.1 BACKGROUND

Mea Thi Dam is located in Ban Thi district, Lamphun province in the northern part of Thailand as shown in Fig. 1. The construction of the dam was completed in 1987, for purpose to storing water for irrigation and water supply. The constructed dam is 25.60 m in height , 8 m in width and 437 m in length. The dam is maintained by, the Royal Irrigation Department (RID). Then in 2009, to increase the dam capacity up to 6.0 million cubic meters from 4.5 million cubic meters, 1 m parapet wall was constructed.

Furthermore, in 2012 seepage problem was encountered at the right abutment of the dam including embankment settlement. A hole of size 10 to 20 cm was observed in downstream at the connection zone between abutment and dam body as shown in Fig. 2.

The right side of the dam had water leakage with rate of as much as 60 liter/minute at the downstream along with the soil embankment subsidence. With all these problems encountered which would affect the dam efficiency and safety various solutions were mulled over and the appropriate one chosen as per suitability. To solve these problems without emptying the reservoir and avoiding any excavation works, cement and chemical grouting was proposed by Regional Irrigation Office 1 Chiang Mai province who supervised this project, to improve the foundation, control seepage and maintain stability of the dam. The general working areas to improve the dam condition were at the right abutment, dam embankment and the connection zone between embankment and abutment of the dam.

1.2 CHARACTERISTICS OF DAM

The general information characteristics of the dam is as below [1]

Dam length	437.00	Meter
Dam height	26.50	Meter
Dam crest width	8.00	Meter
Dam crest elevation	+419.00	Meter (M.S.L)
Maximum reservoir elevation	+417.00	Meter (M.S.L)
Retention water elevation	+416.00	Meter (M.S.L)
minimum reservoir elevation	+404.00	Meter (M.S.L)
bed level	+399.00	Meter (M.S.L)
Gross capacity reservoir	5.5	Million-cubic meter



Fig. 1 Location of Mae Thi Dam site, Lumphun province, Thailand
(<https://www.google.co.th/maps/place/Thailand/>)



Fig.2 Area of Water Leakage

2. GEOLOGY

2.1 GENERAL GEOLOGICAL CONDITIONS

Geological mapping of Geological Survey of Thailand, Geological Resources Department (DMR, 2007) identified the rocks in the reservoir area of Lumphun province and neighboring areas. It consists of sediments include gravel, sand, silt, clay and laterite of Quaternary time. Base rocks are Conglomerate, Sandstone, Shale, Slate and Chert of carboniferous period as shown in Fig. 3. [2]

2.2 GEOLOGICAL FOUNDATIONS AND SOIL CONDITION

The soil layer of embankment dam consists of mixture of silt with sand (ML) and sandy silt with gravel (ML). Borehole at the crest of the dam was conducted and stiff to very stiff cohesive soil was observed at depth of 0.00 - 15.00 m. The permeability ranged from medium to high (1.05×10^{-5} to 2.49×10^{-5} cm / sec.) The base of the dam consists of rock foundation extending from ground surface. It is characterized as Grayish-white colored sandstone, moderately weathered hard rock. The average permeability extended from low to moderate (1.09 - 3.46 Lugeon). [3]

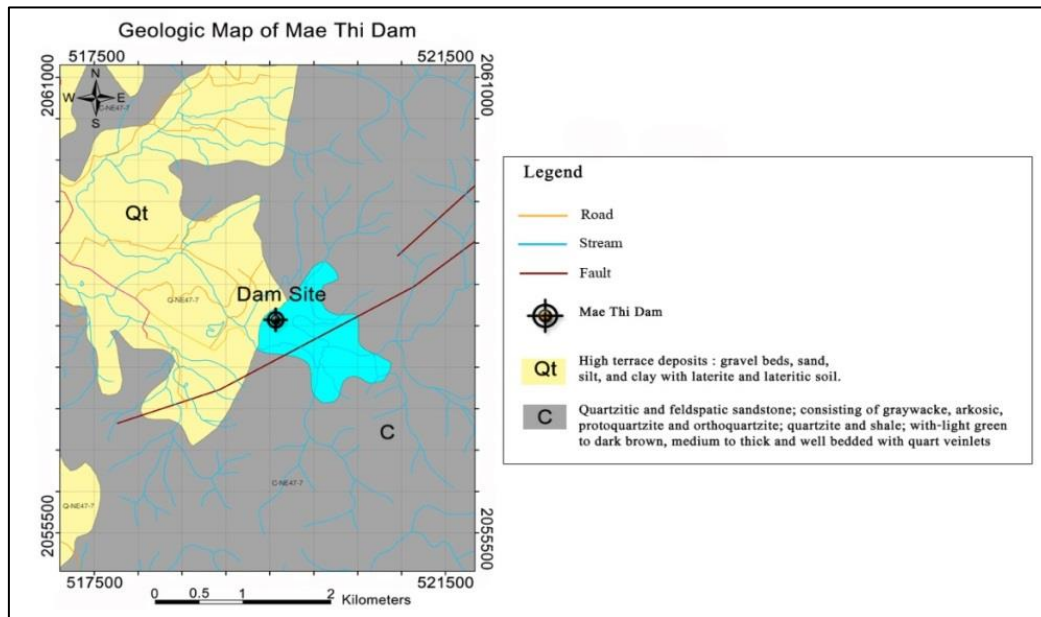


Fig. 3 Geologic Map of Mae Thi Dam Site (DMR, 2007)

3. METHODOLOGY

The main objective of this work was to improve ground condition of dam by carrying out cement and chemical grouting without excavation and emptying reservoir. The profile of grouting works conducted is shown Fig. 4 [3]. Other geotechnical works like the Standard Penetration Test (SPT), permeability tests of the soil, Lugeon Test in rock, drilling holes for cement and chemical grouting were carried out appropriately. Finally, after completion of work requirement quality and limit check was carried regarding the permeability, SPT and Rock Quality Designation (RQD).

3.1 CEMENT GROUTING

For rock foundation, high pressures cement grouting process with quick setting condition was applied. Whereas, for areas with high uplift pressure cement grouting was carried out in discrete steps allowing setting time for grout. Portland Cement Type 1 or Type 3 was used for cement grouting. The compound was used to improve the foundation in stages with varying ratio of cement and water of 1:10, 1:8, 1:6, 1:4, 1:3 and 1:2. Mortar was applied using varying pressure with depth with details given in Fig.5 At first hole was drilled to specified depth then permeability test using water pressure was carried out. Depending upon the permeability the grout mixture was selected as shown below.

Permeability	20	Lugeon	= Cement : Water	= 1:10
Permeability	20-50	Lugeon	= Cement : Water	= 1:8
Permeability	> 50	Lugeon	= Cement : Water	= 1:6

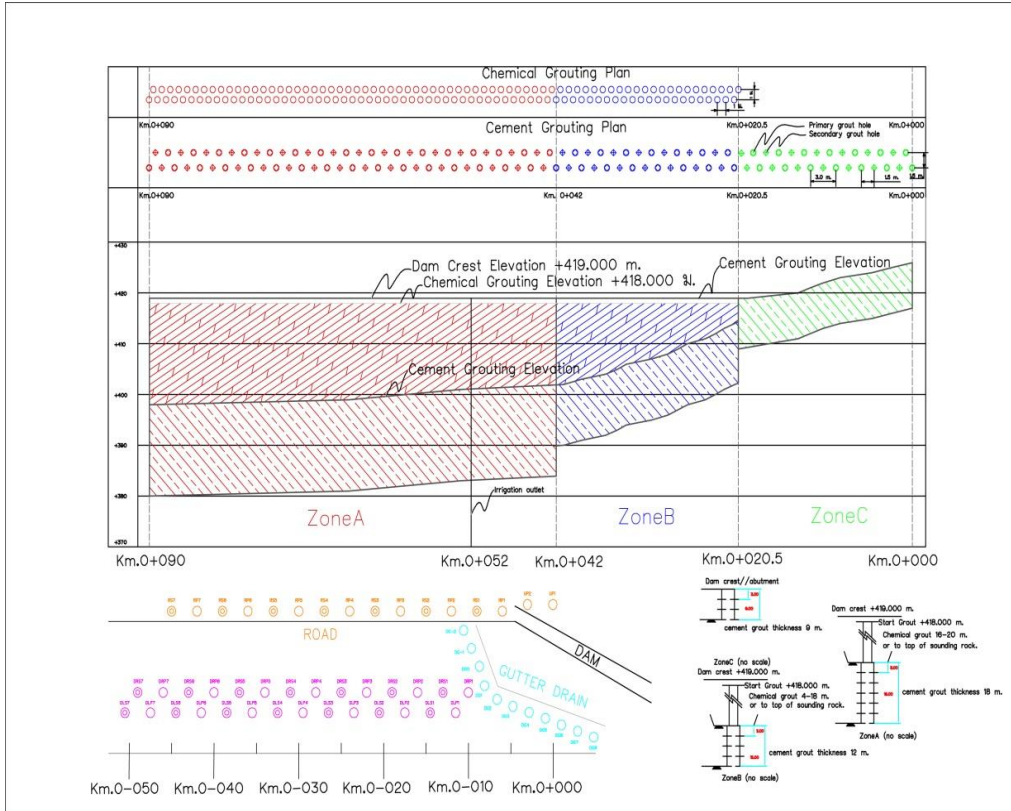


Fig. 4 Profile of Cement and Chemical Grouting Hole Conducted for Mae Thi Dam (Modified from Site plan No. RID1.GEOL. 153/2013)

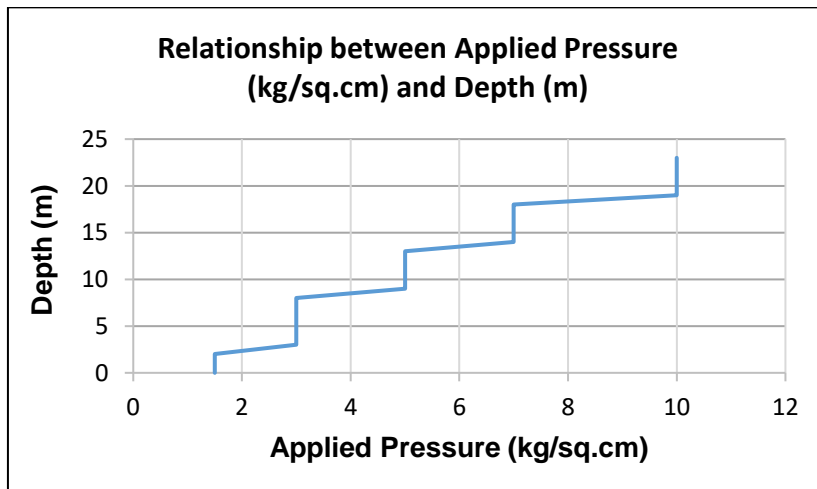


Fig.5 Pressure applied during cement grouting

3.2 CHEMICAL GROUTING

For chemical grouting in clay portion high pressure could not be applied during grouting thus, experiment was carried out to estimate the gel time of water (l), Silicate (l) and Bicarbonate (kg) mix as shown below in the lab. With reference to lab test, field mixture with varying gel time was determined and used accordingly.

The ratio of compound mixture from laboratory is as below

Water	:	Sodium silicate	:	Sodium Bicarbonate	Gel time
173 liters		25 liters		4 kg	2-3 hr.

The actual ratio of compound mixture in the field is as below

Water	:	Sodium silicate	:	Sodium bicarbonate	Gel time
150 liters		10 liters		2 kg	40 min.
115 liters		10 liters		2 kg	20 min.
110 liters		10 liters		2 kg	10 min.

As, due to high uplift pressure on upstream side, chemical grouting was conducted with application of pressure as given in Fig. 6 at the holes spaced at 6 m distance apart.

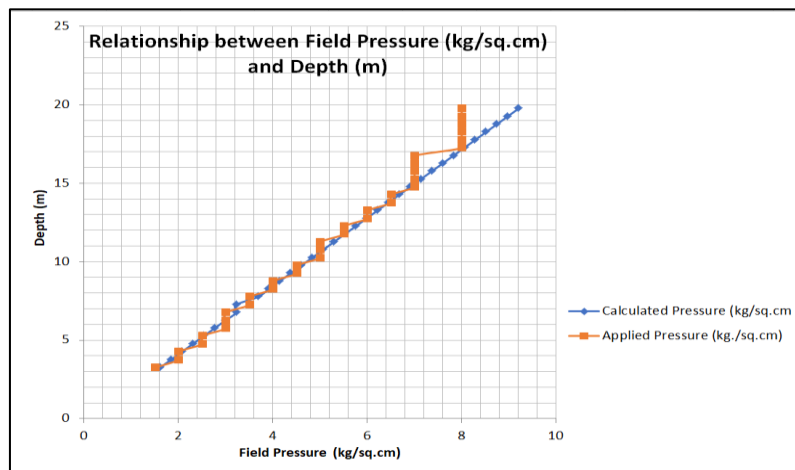


Fig. 6 Pressure applied during chemical grouting

4. WORKING PROCEDURE

The works were separated into Zone A, Zone B and Zone C at connection zone between abutment and dam body, Gutting Drain and right abutment access road [4]. The profile of grouting hole depending upon the requirement conditions cement and chemical grouting were chosen accordingly as shown in Fig. 4. Chemical grouting was carried out in Zone A and Zone B while cement grouting was carried out in Zone B, C, connection

zone between abutment and dam body, Gutting Drain and right abutment access road provided in Fig. 7.



Fig. 7 The working areas as A. Zone C, B. Zone A, B C. Gutting Drain, D. Connection Zone between Abutment and Dam Body, E. Gutting Drain and F. Right Abutment Access Road

5. ANALYSIS

SEEP/W program a finite element analysis of GEO-SLOPE Company [5] was used to calculate factor of safety against uplift of existing Mae Thi dam. The model of SEEP/W analysis of Mae Thi dam is shown in Fig. 8. The factor of safety (FS) calculation have been conducted for core zone separated into 8 layers for existing dam condition Then, it was compared with F.S. that was determined against uplift during chemical grouting for varying pressure from 1.5 to 8.00 kg/cm². The limited recommended factor of safety against uplift from USBR (2014) is 1.5. [6, 7]

Finally, graphical relationship between h_i and F.S. against uplift was plotted as shown in Fig. 9.

Where
$$h_i = \frac{h}{H_i} \quad [1]$$

H_i = height of core zone layer (m)

h = height of considered core zone layer from bottom of cutoff trench (m)

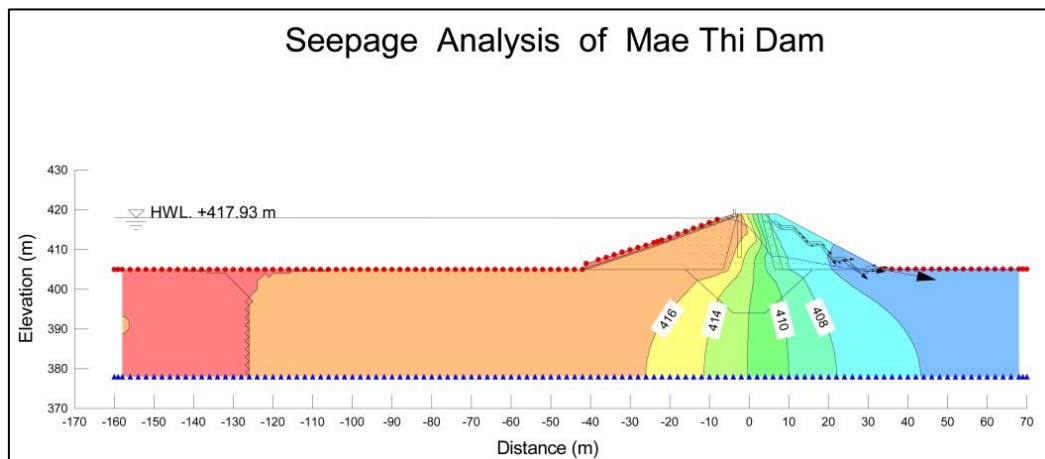


Fig. 8 SEEP/W model of Mae Thi dam, Lumphun province, Thailand

6. RESULTS

At normal reservoir storage condition of +416.00 m, for core layer $0 < h_i \leq 0.5$ computed F.S. against for existing dam varied from 3.5 to 4.5 for $h_i = 0$ and $h_i = 0.5$ and was about 8 for $h_i = 0.75$. Design Chemical grout pressure were in range of 1.5 t/m^2 ($h_i = 0.85$) to 8.0 t/m^2 ($h_i = 0$). The FS calculated for chemical grouting with pressure showed the values extending from 2.0 to 3.0, with was over the limiting value of stability against uplift of FS of 1.5 as show in Fig. 9. During chemical grouting, no embankment heave was measured from the surface settlement markers installed on the crest of dam. To increase the output efficiency of dam after increasing reservoir capacity under full storage condition, dam improvement was carried out to stop water seepage. Outcome cropping yield 10 square kilometers irrigation area are not affected from dam and foundation improvement. Agriculture production value about 2 million US Dollar/crop. The ground improvement works of Mea Thi dam were completed on June 2017. The present condition of still dam reservoir is shown in Fig. 10.

7. CONCLUSIONS

7.1 Ground Improvement of Mae Thi Dam without excavation and emptying reservoir by using chemical grouting showed the F.S. against uplift greater than the limiting value as per USBR standard.

7.2 The apply pressure of chemical grouting varied from 1.50-8.00 kg/cm² in this project.

7.3 The water leakage through the soil embankment and rock foundation with full storage reservoir was within the prescribed limits. (Less than 5 Lugeon, $5.0 \times 10^{-7} \text{ cm}^2$)

7.4 Cement and chemical grouting without excavation and emptying reservoir saved time, cost and utilization excessive manpower or material mobilization without hampering the reservoir operation.

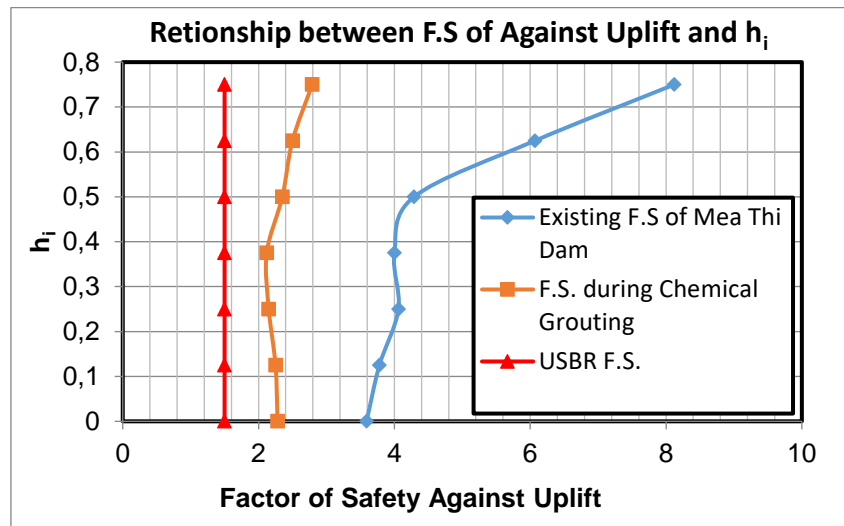


Fig. 9 Graph shown relation between F.S. against uplifts and h_i of Mae Thi dam



Fig. 10 Mae Thi Dam after completion of Ground Improvement

8. RECOMMENDATIONS

8.1 Dam and foundation seepage control improvement by cement-chemical grouting under storage condition should be controlled by F.S against uplift for not less than 2.0 along with measuring surface settlement to ensure the no excessive pressure is applied.

8.2 Grout pressure applied in the field should be gradually increased corresponding with gel setting time and chemical mixture. For Mea Thi core zone compound mixture of water (l), Silicate (l) and Bicarbonate (kg) was used in the ratio of 150:10:2 with the gel-setting time of 40 min., 115:10:2 with the gel-setting time of 20 min and 110: 10:20 mix with gel setting-time of maximum 10 min.

9. ACKNOWLEDGEMENT

Firstly, we would like to express our sincere gratitude and thanks to the Ministry of Agriculture and Cooperatives (MOAC) Thailand and Royal Irrigation Department (RID) for providing us necessary support and information to conduct this project. Also, we would like to appreciate all the colleagues of Chiangmai, RID and other people who are directly and indirectly involved to complete this project.

10. REFERENCES

- [1] PROJECT CONSIDERATION BRANCH, REGIONAL IRRIGATION OFFICE1, Consideration of Mae Thi dam project report, *Chiang Mai, Thailand*, 2009.
- [2] DEPARTMENT OF MINERAL RESOURCES, Geologic Map of Thailand, Scale 1:500,000, *Bangkok, Thailand*, 2007.
- [3] GEOTECHNICAL BRANCH, REGIONAL IRRIGATION OFFICE1, Site Plan of Grouting No. RID1.GEOL.153/2013 of Mae Thi Dam, *Chiang Mai, Thailand*, 2013.
- [4] GEOTECHNICAL BRANCH, REGIONAL IRRIGATION OFFICE1, Ground Improvement of Mae Thi dam, *Chiang Mai, Thailand*, 2017.
- [5] GEO-SLOPE INTERNATIONAL LTD., SEEP/W program, Calgary, *Alberta, Canada*.
- [6] LAMBE, T.W., and R.V. WHITMAN, Soil Mechanics, John Wiley and Sons, Inc, *New York*, 1969.
- [7] U.S. DEPARTMENT of INTERIOR BUREAU of RECLAMATION (USBR), Design Standards Embankment Dams No.13, *United State*, 2014.

COMMISSION INTERNATIONALE DES GRANDS BARRAGES

VINGT-SIXIÈME CONGRÈS DES GRANDS BARRAGES
Autriche, juillet 2018

DOI 10.3217/978-3-85125-620-8-165



This work licensed under a Creative Commons Attribution 4.0 International License. <https://creativecommons.org/licenses/by-nc-nd/4.0/>

FOUNDATION TREATMENT CHALLENGES FOR EARTH AND ROCK FILL DAMS – CASE STUDY OF THE LEFT EMBANKMENT DAM ON ISIMBA (183MW) HYDRO POWER PROJECT, UGANDA

Nicholas Agaba RUGABA

Assistant Project Manager, UGANDA ELECTRICITY GENERATION COMPANY LIMITED (UEGCL)

UGANDA

Chad Silas AKITA

Project Manager, UGANDA ELECTRICITY GENERATION COMPANY LIMITED (UEGCL)

UGANDA

Isaac ARINAITWE

Chief Projects Officer, UGANDA ELECTRICITY GENERATION COMPANY LIMITED (UEGCL)

UGANDA

Harrison MUTIKANGA

Chief Executive Officer, UGANDA ELECTRICITY GENERATION COMPANY LIMITED (UEGCL)

UGANDA

FOUNDATION TREATMENT CHALLENGES FOR EARTH AND ROCK FILL DAMS – CASE STUDY OF THE LEFT EMBANKMENT DAM ON ISIMBA (183MW) HYDRO POWER PROJECT, UGANDA.

Nicholas Agaba Rugaba, Assistant Project Manager, Uganda Electricity
Generation Company Limited (UEGCL)

Co- Authors: Eng. Chad Silas Akita, Project Manager, UEGCL.

Eng. Isaac Arinaitwe, Chief Projects Officer, UEGCL.

Eng.Dr. Harrison Mutikanga, Chief Executive Officer,
UEGCL

Introduction

Uganda will require 8,601MW by 2020, 14,670MW by 2025 and 41,738MW of electricity by 2040 as it works towards middle income status.¹ One of the strategies in the National Development Plans is to construct large hydropower plants and thermal power plants through public and private investments, and Isimba Hydro Power Project is being developed with debt financing to a tune of Five Hundred Million United States Dollars (USD 500m). The EPC Contractor is China International Electric and Water Corporation (CWE). The debt financing is provided by the China Export and Import Banks. For Isimba Hydro Power Project, the reservoir is retained by concrete structures and two earth-rock fill embankment dams on both sides of the concrete structures.

¹ Uganda's National Development Plan 2010-2015

Project Lay-out

The Isimba HPP structures are arranged in a polyline perpendicular to the flow of the river. The structures arranged along the dam axis, from left to right are the Left Embankment Dam section to connect the whole complex to the left bank, the Concrete Gravity Dam section GD1, Powerhouse, Spillways SP1 and SP2, the Concrete Gravity Dam section GD2 and the Right Embankment Dam section to connect the whole dam complex to the right bank . For the connection between the concrete structures and abutments as well as for the closures of the right river channel an earth-rock-fill dam type with central clay core was selected.² The lay-out of the embankment dams for Isimba HPP is shown in Figure 1 below.



Fig 1: Artistic Impression of Isimba Hydro Power Project (Adopted from EPC Contractor's Implementation Proposal, 2014)

² Isimba HPP Feasibility Study Report - Fitchner and Norplan , September 2012

Rationale for Adoption of Earth Rock-Fill Embankment Dams

Embankment dams are a crucial element for different infrastructure projects including hydropower dams for reservoir impounding (to create a “man-made lake”) for water that is used in power generation through the Electro-mechanical and Hydro-mechanical equipment in the plant. For Isimba HPP, the reservoir (retained by concrete structures and two earth-rock fill embankment dams on both sides of the concrete structures) was adopted both at feasibility design, basic design and currently at detailed design and construction stage.

Earth-rock fill embankment dams were preferred to other types of dams e.g. Roller Compacted Concrete dams. This is because of the vast availability of the rock fill and clay core material in the vicinity of the site, compared to the need for very distant transportation of pozzolanic or fly ash material for the Roller Compacted Concrete (RCC) dam. Furthermore, having reviewed test results from the laboratory investigations on the rock samples, it was established that a substantial part of the excavated material (from the foundation of the powerhouse and spillways) could be used for construction of the earth-rock fill dam without as much processing compared to a Roller Compacted Concrete (RCC) dam.

According to the International Committee on Large Dams(ICOLD), a “dam” can be defined as “An artificial barrier, together with appurtenant works, constructed for storage, or control of water, other liquids, or other liquid-borne material (excluding concrete/steel ring tanks reliant on hoop stress for structural stability).” The Left Embankment Dam is part of the appurtenant structures (spillways, power house, concrete gravity dams, right embankment dam etc.) that are used for retaining water and creation of a reservoir or man-made lake, to achieve desired head/ water levels for electricity generation through the electro mechanical and hydro mechanical structures. A rock-fill embankment dam is one composed largely of fragmented rock with an impervious core. The core is separated from the rock shells by a series of transition zones built of properly graded material. The rock-fill

zones are compacted in layers 12 to 24 inches (300 mm to 600 mm) thick by heavy rubber-tired or steel-wheel vibratory rollers. A typical cross-section of an earth rock-fill embankment dam is illustrated in Figure 2 below.

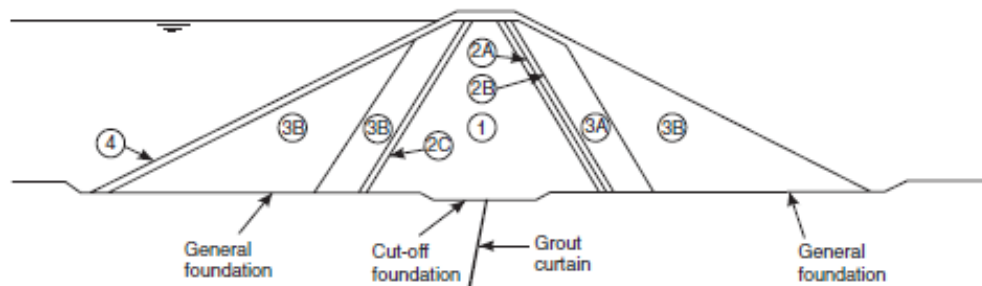


Figure 2: Typical Embankment Dam Section with Central Clay Core. (Key; 1 - Impermeable Clay core, 2 Filters/Transition Zones, 3 - Rock fill 4 - Rip Rap or Concrete face). Adopted from Robin Fell et al, 2005 (Geotechnical Engineering for Dams)

Foundation Treatment and Challenges

Geologic processes cause dam foundations to be much less than perfect for the construction of an embankment dam. Thus, foundation treatment is almost always required to improve a foundation to a suitable condition before a dam is constructed. Recognition of natural processes that damage foundations helps to formulate foundation treatment objectives. Such processes and their effects include; buried river channels, faulting, shearing, slope instability, solution cavities, potholes, benches, overhangs, steps, stress relief joints etc.³ At the Isimba Hydro Power Plant, the right river channel had shear zones in the river bed that needed concreting and treatment. Foundation treatment is the utilization of ground improvement techniques so as to mitigate undesirable foundation concerns of

³ Foundation Surface Treatment, Design Standard 13 USBR Manual

embankment dams namely, excessive seepage and possible piping; collapse of dry, low density abutment soils; and potentially liquefiable soils during earthquake shaking.⁴ Seepage (percolation) is the slow movement of gravitational water through the soil or rock, as illustrated in Figure 3 below.

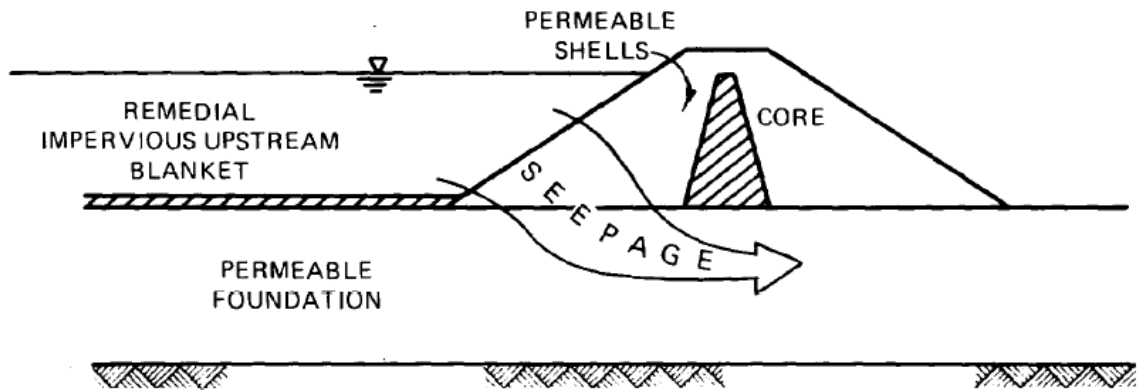


Figure 3: Possible seepage problem in embankment dam. (Adopted from USACE EM – 1110 – 2 – 1901 Seepage Analysis and Control.)

Piping is the washing of fines from soils/ rocks or fractures, dispersive soils. It involves the progressive removal of soil particles from a mass by percolating water, leading to the development of channels. Foundation treatment must therefore be adequate to satisfy the following criteria; minimum leakage, prevention of piping in the foundation, limited settlement and ensuring sufficient friction development between abutments and dam foundations to ensure stability against sliding.

The Left Embankment Dam foundation was also specified to comply with certain permeability parameters and also stability requirements. These include 1 Lugeon value for foundation permeability and dam stability under static and dynamic loading as per USACE EM – 1110 – 2 – 1902 guidelines. This called for robust

⁴ Earth Manual Part 1

foundation treatment to ensure compliance to technical specifications and seepage control measures.

Seepage through a permeable foundation, similar to the weathered rock foundation at the Left Embankment Dam at Isimba HPP, can be reduced by constructing a low permeability cut off through the permeable material. There are various seepage cut-off approaches namely; cut-off trench filled with earth fill, slurry trench, concrete diaphragm wall, contiguous or intersecting bored piles, sheet pile wall, curtain grouting etc. The Left Embankment Dam at Isimba HPP adopted two main ground improvement methodologies as part of foundation treatment, i.e. grouting and construction of concrete cut-off wall, along the longitudinal axis of the dam. Grouting involves the injection under pressure of a liquid or suspension into the voids of a soil or rock mass or into voids between these materials and an existing structure. The injected grout must eventually form either a gel or a solid within the treated voids, or the grouting process must result in the deposition of suspended solids in these voids. The primary purposes of pressure grouting a soil or rock mass are to improve the strength and durability of the mass and/or to reduce the permeability of the mass. Prior to any grouting operation (trial or final), water pressure testing is done. Water pressure test is performed to measure the rate at which water can be forced into a hole under a specific pressure. It is from these water pressure tests, that lugeon values and thus indication of rock mass permeability are established. For the Left Embankment Dam at Isimba HPP, the water pressure testing and trial grouting operations indicated high permeability in the foundation material which was not being significantly reduced by the grouting during the trial phase. Trial grouting was done in the completely weathered and the highly weathered rock foundations. The trial grouting indicated high grout takes and high rock permeability. This thus influenced the decision to adopt utilization of both the concrete – cut off wall and curtain grouting as the seepage control measures for the weathered and sound rock foundations respectively.

CONCRETE CUT-OFF WALL

The concrete cut-off wall together with curtain grouting were thus adopted as the foundation treatment approach for the dam foundation to control under seepage and uplift pressures. The concrete cut-off wall was constructed using conventional concrete of Class C20. Concrete by its nature is too rigid and as the soil mass surrounding the concrete cut-off wall compresses under the weight of the embankment during its construction and the water load as the dam is filled, substantial loads will be shed onto the wall by negative skin friction. This can cause crushing of the wall and penetration of the wall into the dam fill. In this regard, the compressive strength of the concrete used for the cut-off wall should be able to with-stand these stresses associated with skin friction. The test results for the concrete cast for the concrete cut-off wall of the Left Embankment Dam of Isimba HPP range from 23MPa to 28MPa, as reviewed from the EPC Contractor's quality control reports and test results. The concrete cut off wall extends all through the weathered rock foundation and slightly penetrated the sound rock as shown in Figure 4. Whereas the Employer Requirements had not specifically specified the type of concrete to be used for the concrete cut-off wall, the Isimba Panel of Experts and other Dam Engineers recommended use of plastic concrete for the cut-off wall. This was rejected by the EPC Contractor despite numerous demands by the Employer. The site team could not trace literature and or international standards that specified use of plastic concrete for cut-off walls in foundation treatment.

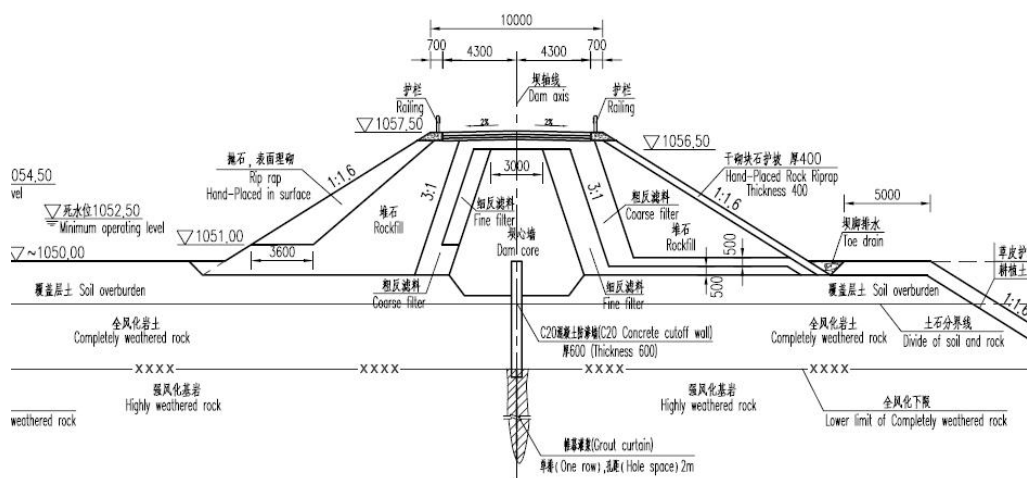


Fig 4: Cross- Section of Left Embankment Dam at Chainage D0+210, showing Concrete Cut-off wall below the central clay core, as part of foundation treatment works. (Adopted from the EPC Contractor's Volume IV of the Basic Design Report)

The concrete cut off wall was excavated in alternating panels with the panel supported by clay slurry. In some other countries or projects depending on availability and economic considerations, bentonite slurry is used to prevent the excavated trench from collapsing. Bentonite is a clay material composed principally of minerals of the montmorillonite group, characterized by high absorption and very large volume change with wetting. For the cut-off wall excavations on the Left Embankment Dam, clay slurry was used for trench support, however for the Right Bank cut-off wall excavations, a mixture of clay and bentonite was used. This was after Employer insisted on better trench support system. From the exposed sections of the cut-off wall on the left bank, it was noted that trench collapse had cause sections of the cut-off wall to have irregular surfaces.

The trench wall thickness was 500 mm, and it extends at least 500 mm into the engineering rock. The cut-off wall trench was excavated by use of percussion tools. Percussion tools and rock chisels are used where boulders, cobbles or other hard materials are encountered. The percussion tools are electricity or compressed air powered tools that operate by striking rapid blows unto the rock, thus break it

up into smaller pieces. The broken pieces are removed by clamshell bucket. Clamshells can also be used to excavate for the cut off wall trenches in soft rocks or foundations with gravely soils. When all the loose and broken up rocks are removed, concrete for the cut off wall is cast. For Isimba HPP, the cut off wall was excavated by use of a percussion hammer. During this excavation and chiseling of the rock and boulders, a lot of rock fragments were generated and these accumulated at the bottom of the slurry trench. To remove these rock fragments, airlift equipment was specified as part of the excavation method statement. However, the EPC Contractor used a bailer to remove the rock cuttings, excavation debris and contaminated slurry but it wasn't suitable to do full cleaning of the bottom of the cut-off trench. As such, a lot of loose rock fragments would stay at the contact between the cut-off wall concrete and the engineering rock. The concrete wall was constructed by tremie pipe placement of concrete. The tremie concrete placement method uses a vertical or near vertical pipe, through which concrete is placed by gravity feed into the bentonite or clay-slurry-filled trench. The lower end of the pipe is kept immersed in the clay slurry/ bentonite slurry so that concrete rising from the bottom displaces the bentonite or clay slurry, thus limiting washing out of the cement content of the fresh concrete to the exposed upper surface. The upper end of the tremie pipe is kept above the trench level during the pour and is provided with a conical hopper for batch loading, or concrete may be pumped into the top of the tremie pipe. Concrete must be poured at a rate which avoids setting in the tremie. Admixtures may be used to control setting time, slump and workability. For the Left Embankment Dam at Isimba Hydro Power Project, admixtures like fly ash were added to improve the workability of the concrete and also minimize the heat generation in the concrete. Since the concrete is poured into the trench through tremie pipes and displaces the bentonite or clay slurry from the bottom of the excavation upward, the concrete must have a consistency such that it will flow under gravity and resist mixing with the bentonite or clay slurry. The steel tubing is inserted (and later removed) as a part of a construction joint to facilitate bonding of the concrete panels.

The concrete cut off wall for the Left Embankment Dam is not a reinforced concrete wall. Reinforced concrete walls may be justifiable for areas susceptible to high and frequent earthquake loading. The concrete for the cut off wall was tested for various parameters including slump, temperature, compressive strength, compressibility and permeability. ICOLD (1985) indicates that the permeability which can be achieved for cut off walls made of normal concrete are in the range of 10^{-9} to 10^{-10} m/ sec. The test results for the concrete cut off wall of the Left Embankment Dam indicate compressive strengths in the range of 23MPa and 28MPa above the design strength of 20MPa (C20). In addition to the compressive strength tests, the EPC Contractor conducted tests on the penetration resistance of the concrete according to ASTM Standard C803, and no water seepage was confirmed for the hardened concrete in the laboratory.

Curtain Grouting

The Left Embankment Dam adopted curtain grouting as a part of the foundation treatment works. Curtain grouting means grouting of rock in one or more lines of holes spaced to form a curtain barrier.⁵ This method consists of drilling bore holes into the foundation bedrock at some regular spacing along a line or lines parallel to the dam axis and normal to the seepage flow direction. A bore hole is a hole of circular cross-section made in soil or rock.

According to Robin Fell et al (2005), since rock substance is generally almost impermeable, the permeability determined in the water pressure test represents an indication of the number, continuity and opening of the rock defects which intersect the wall of the borehole in the test section. Curtain grouting is designed to create

⁵ Employer's Construction Specifications for Civil Works

a narrow barrier (or curtain) through an area of high permeability. It usually consists of a single row of grout holes which are drilled and grouted to the base of the permeable rock, or to such depths that acceptable hydraulic gradients are achieved. For large dams on rock foundations, dams on very permeable rock or where grouting is carried out in soil foundations, 3, 5 or even more lines of grout holes may be adopted. The Left Embankment Dam adopted curtain grouting mainly for dam foundations on sound rock or slightly weathered rock including below the cut off wall. A single line of grout holes was adopted since this was appropriate to achieve the specified permeability parameter/ Lugeon value of 1Lu. The holes were drilled and grouted in sequence to allow testing of the permeability of the foundation (by packer testing) before grouting and to allow a later check on the effectiveness of grouting from the amount of grout accepted by the foundation ("grout take"). Grout take is the measured quantity of grout injected into a unit volume of formation, or a unit length of grout hole. Grout is a mixture of cementitious or non-cementitious material, with or without aggregate, to which sufficient water or other fluid is added to produce a flowing consistency.

The grout holes / borehole were drilled using percussion drilling—a drilling technique that uses solid or hollow rods for cutting and crushing the rock by repeated blows. Percussion drilling methodology that was applied used hollow steel pipes that allow for rock core recovery to be utilized in the logging of the geological profile of the dam foundation along the dam axis. The employer specified drilling of boreholes by use of either percussion drilling method or rotary type diamond drilling. The EPC Contractor utilized the percussion drilling method

since it is more economical. As argued by Fell et al (2005) grout holes should always be oriented and or inclined so as to intercept the major fractures in the rocks and as many discontinues in the rock foundation. The Employer Requirements for Isimba HPP further specified that check holes should be inclined too, to assess the effectiveness of the grouting works.

After the drilling of the boreholes, they are washed to remove any cuttings that may have clogged the rock fractures around the sides of the hole. The borehole is then water pressure tested to establish the rock mass permeability prior to grouting. Pressure testing is a method of testing the permeability of rock mass using water or grout pumped down hole under pressure. The water pressure test is carried out using pressure testing equipment, water and a packer. A packer—*in grouting*, is a device inserted into a hole in which grout or water is to be injected which acts to prevent return of the grout or water around the injection pipe. It is usually an expandable device actuated mechanically, hydraulically, or pneumatically. The results from the water pressure testing are indicated by a lugeon value. Lugeon is a measure of permeability defined by a pump-in test or pressure test, where one Lugeon unit is a water take of 1 L/min per meter of hole at a pressure of 10 bars. This implies that the rock permeability is that in one minute, one litre of water, will flow across a unit (1 metre) section of the rock, under a pressure load of 10 bars. These water pressure test results for the pressure testing prior to grouting are also recorded and submitted as part of the grouting records/ reports. Records of the drilling, grouting and water pressure tests, pressures, flow rates, the quantities

used in the grouting operations and any other general records were kept and submitted to the Employer for review and information.

The curtain grouting was carried out sequentially to achieve a predetermined standard of water tightness in the foundation rock. This required the successive halving of the predetermined spacing of the grout holes. This is called the split spacing method with primary, secondary and tertiary holes. Split-spacing means the system of locating an additional grout hole approximately midway between two grout holes which have previously been drilled and grouted. Primary holes are the first series of holes to be drilled and grouted, usually at the maximum allowable spacing. Secondary holes are the second series of holes to be drilled and grouted, spaced midway between primary holes. The specifications for curtain grouting were also revised by the Employer on the advice of the Owner's Engineer. Whereas initially 1 Lugeon was specified as the limit for permeability, so as to save time and cost, and also optimize the grouting operations, 3-5 Lugeon was later adopted for the curtain grouting works. It was further indicated that industry best practice for grouting works, adopts permeability values in the range of 3-5 lugeon NOT the 1 Lugeon as had been specified by the project owner/ client.

Conclusion

All earth and rock-fill dams are subject to seepage through the embankment, foundation, and abutments. However, it is also evident from geological investigations and tests that compacted earth fill core materials has far less permeability ($< 10^{-8} \text{m/s}$) compared to the permeability of rock foundations. As

argued by Robin et al (2005), nearly all rock foundations have rock mass permeability greater than 1 Lugeon, and most rocks have permeability greater than 5 Lugeon. It is clear that most seepage occurs through the foundation not the embankment itself. However, seepage control is necessary to prevent excessive uplift pressures, sloughing of the downstream slope, piping through the embankment and foundation, and erosion of material by loss into open joints in the foundation and abutments.

The purpose of the project, i.e., long-term storage, flood control, etc., may impose limitations on the allowable quantity of seepage. Although the foundation is not actually designed, certain provisions for treatment are made in designs and specifications to ensure that the essential requirements are met. The foundation treatment for embankment dams requires an array of considerations that range from geological and geotechnical expertise to engineering judgment based on experience. A detailed foundation treatment program that include designs, technical specifications, construction and grouting procedures is critical to sound foundation treatment for dams to ensure dam stability and seepage control.

References;

1. Design of Small Dams
2. USACE EM – 1110- 2 2300 General Design and Construction Considerations for Earth and Rockfill Dams.
3. USACE EM – 1110 – 2- 1901 Seepage Analysis and Control
4. Geotechnical Engineering for Dams, Robin Fell et al (2005)
5. USACE EM – 1110-2 -3506 Grouting Technology
6. ASTM D653 Terminology Relating to Soil, Rock and Contained Fluids
7. USACE EM – 1110- 2 -1902 Slope Stability
8. Earth Manual Part 1
9. Basic Design Report, Isimba HPP
10. Feasibility Design Report, Isimba HPP
11. Engineering Geology Office Manual
12. Design Standard 13, USBR Manuals

COMMISSION INTERNATIONALE DES GRANDS BARRAGES

VINGT-SIXIÈME CONGRÈS DES GRANDS BARRAGES
Autriche, juillet 2018

DOI 10.3217/978-3-85125-620-8-166



This work licensed under a Creative Commons Attribution 4.0 International License. <https://creativecommons.org/licenses/by-nc-nd/4.0/>

**THIRD REMEDIAL GROUTING CAMPAIGN FOR REINFORCEMENT OF
IMPERVIOUS CURTAIN TYPE BATHTUB ON THE CAJON DAM**

R. Flores GUILLÉN

Assessor Senior, GEOCONSULT

HONDURAS, C.A.

M. Flores PEÑALBA

Administrative Manager, GEOCONSULT

HONDURAS, C.A.

J. Andino VALERIANO

Engineer Senior, GEOCONSULT

HONDURAS, C.A.

C. Iglesias ZÚNIGA

Geotechnical Engineer, GEOCONSULT

HONDURAS, C.A.

THIRD REMEDIAL GROUTING CAMPAIGN FOR REINFORCEMENT OF IMPERVIOUS CURTAIN TYPE BATHTUB ON THE CAJON DAM *

R. Flores Guillén

M.Sc. Geology and Geotechnical Engineering, Assessor Senior GeoConsult

M. Flores Peñalba

M.Sc. Engineering, Administrative Manager GeoConsult

J. Andino Valeriano

M.Sc. Geology, Engineer Senior GeoConsult

C. Iglesias Zúniga

*Geotechnical Engineer, GeoConsult
HONDURAS, C.A.*

ABSTRACT

El Cajón Dam is located in a karst limestone geology; during the construction phase (1981-1985) the unusual Bathtub was implemented (no open end curtain in possible deep karst systems, [1]) and also the existence of randomly finding karstic caverns that had to be filled as part of the treatment (empty reservoir), this was presented to the International Community after the construction was finished. Years later (1995) the activities of injection through the Project known as "TRATI" were made known again, these were realized to extend the grout curtain and to remedy the increases in the filtration flows in the proximity of the Power House, on that occasion the project was already in operation and the karstic ducts that were present had water surges, and in some cases suction.

Currently The Third Remedial Grouting Campaign for Reinforcement of Impervious Curtain (2016-2017) is presented, again justified by the rise of filtration flows, this time identified in the left abutment of the dam and on the edge of the Bathtub on

* *Traduction en Français (en attente).*

the right side of the dam (together in the range of 200 L/s). The most important perforated drills presented surge pressure of up to 7 Bars, it is estimated that the anomalies found correspond to mostly vertical Tubular Karts, and permeably connected with the rock stratification planes themselves with dips between 15 ° and 35 ° related to the vertical oriented downstream. The solution implemented could not be equated to the first historical treatment due to the fact that there is a full reservoir and the entrainment of the cementitious mixtures to the exterior (sites downstream of the dam); nor could the unusual methods and materials of the second historic treatment be used because on this occasion there was no suction of the materials and the size of the filtration ducts intercepted by the perforations were less than 2 inches. Finally, as one of the treatments, the injection of concretes with maximum aggregate size of less than 1 inch was arranged, but the injection with the traditional Trailer Pumps was detrimental to the geological environment due to the fact that the "piston effect" [2] increased erosion deposits in the caverns; therefore, for the solution, selected size aggregates were pushed without using a concrete pump and intermittent mortar grout with smaller a size injection pump.

The sealing work on the left abutment had as a relevant factor, improving the contact surface between the concrete masses of the dam and the foundation rock with this treatment.

1. INTRODUCTION

El Cajón hydroelectric Project is located in the central zone of the Republic of Honduras. The dam site is located on the Comayagua river basin about 2 Km downstream from the junction of the Humuya and Sulaco rivers. The structure is a double curvature thin concrete arch dam, of 226 m high.

The foundation of the dam site is located on cretaceous thick limestone rock, the original construction had identified the presence of Karstic Phenomena located in the inside and outside of the bathtub grounding curtain. During the life of the project (around 33 years), the monitoring system has detected periodically changes in the followings parameters: infiltration flow and uplift. These variations have been attributed to process of dissolution and deposit erosion of such Karsts.

Over the past, few years one of the greatest anomalies was the increase in the flow of the "D-1" drain of the drainage system, in the left abutment of the dam, approximately between 106 and 135 m a.s.l. Initially in this drain, there was no infiltration, later between the years 2006 to 2015 an increase of approximate 20 l/s [3] was reported and some sediment drag (erosion). One of the tasks of the third reinforcement campaign was to seal this infiltration.

2. SEAL OF DRAIN "D1"

The initial activities of the project were the execution of grouting drills holes from the upper grouting gallery to the zone drain D1, at level 135 m a.s.l. obviously the execution of these grouting holes would damage the operative of the D1 drain, in case of communication of grouting fluids between both drains.

Due to this, grouting started in drain D1, with the purpose to seal the filtrations. Although later, it would be necessary to perform new drains to repair the drains curtain of the dam.

The first interventions failed, because the drain clogged and grouting mixtures were dragged into the G2 Gallery (located on the outside of the dam body, as shown in Fig. 1). Since then the D1 filtration moved to upper levels and G2 Gallery maintained a permanent filtration in the order of 20 l/s approximately.



Fig. 1
Panoramic View, left abutment

3. GROUTING MIXTURES

3.1. GENERAL

Most of the grouting of the project was done with mixtures that had a relation of between w/c 0.70 - 0.50 (see Table 1). Some cases required the use of mortars (sand/cement). But the grout curtain drill holes which had relation with the source of karsification or empty karst (eroded), it was impossible to seal with these mixtures (each grouting was completed when a volume of grout was reached) and mixtures were dragged to the outside near the G2 Gallery (see filtration number 1 to 7, in Fig. 2).

Table 1
Conventional Mix used in Project

Mix Number	Proportion by Weight			
	Water	Cement	plasticizer	Sand
L-0	0.7	1	1	0
L-1	0.6	1	1	0
L-2	0.6	1	0	0
L-3	0.5	1	0.75	0
M0	0.6	1	1	0.25
M1	0.6	1	1	0.5
M2	0.6	1	1	0.75
M3	0.6	1	1	1
M4	0.6	1	2	1.5

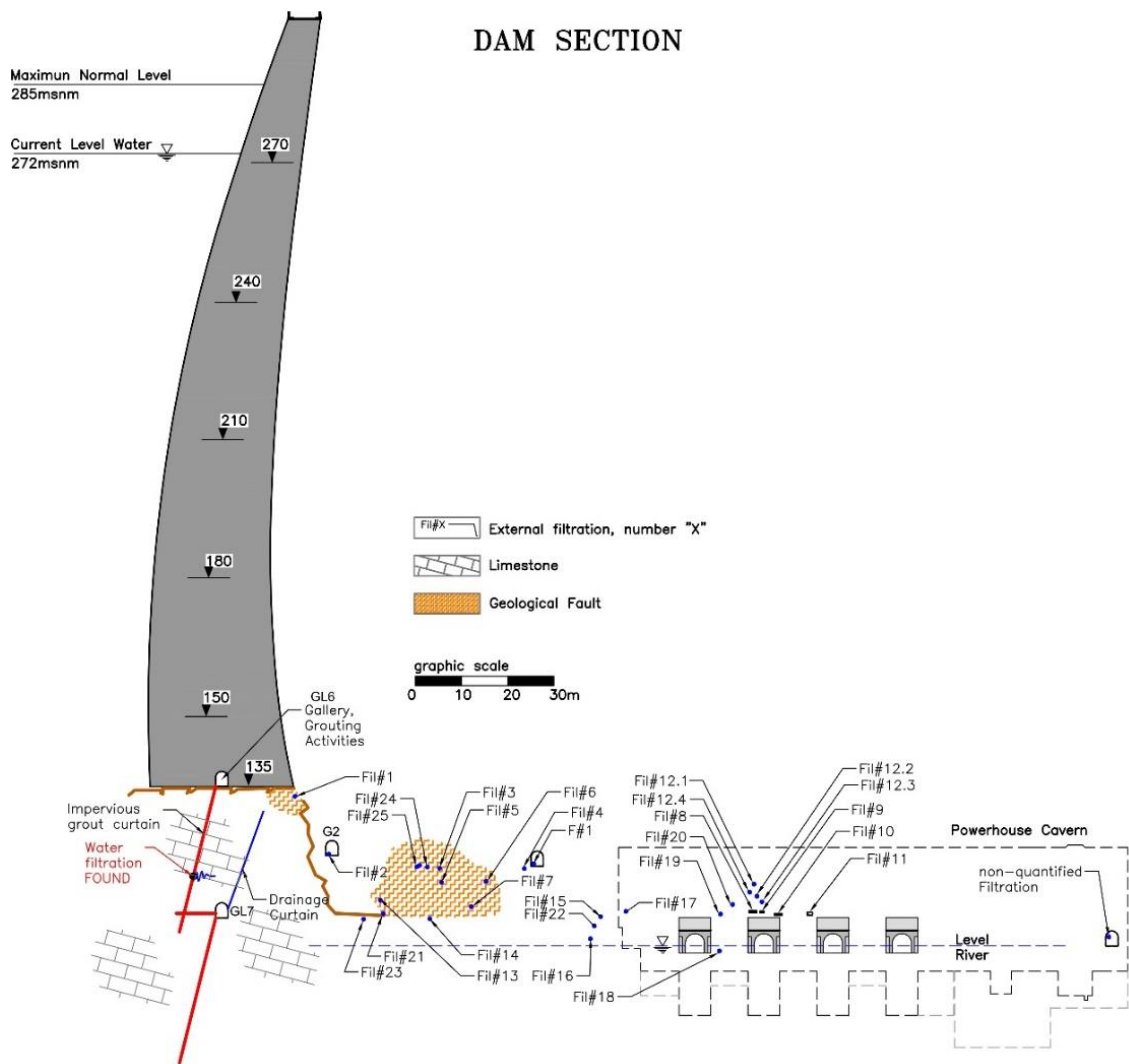


Fig. 2
Dam Section, new filtrations in site

3.2. UNUSUAL MIX

Subsequently, as one of the treatments, the injection of concretes with maximum aggregate size of less than 1 inch were arranged, but the grouting with the traditional Trailer Pumps was detrimental to the geological environment due to the fact that the "piston effect" [2] increased deposits erosion in caverns (see in Fig. 3 left, the erosion process identified in one of the infiltration).

After these activities, the Security Panel of the works (PSO), suggested to avoid the use of concrete pump and only use only traditional grouting pumps. It was recommended to use unusual low-density products for the grouting, such as the sawdust to minimize the drag out of the abutment.

The sawdust was injected to the drill holes in mixtures for water/bentonite (380L / 13.60kg), with a proportion sawdust/bentonite of 400% (by weight). Even in these cases the materials were not deposit in the source of karsification and were dragged to the exterior.

3.3. FINAL SOLUTION

For the final solution, selected size aggregates were pushed without using a concrete pump and intermittent traditional mix with grout or without aggregates was used (nominal size less than 1 inch), for details see Fig. 4.

At the beginning, of the process one part of the aggregate was pushed out to the exterior (see Fig. 3 right) similar to the other occasions but eventually the repetition of this procedure and the variation of the sizes in each grouting allowed to seal the karstic zone and eliminate the infiltration in the zone.



Fig. 3 [4]

Left side: erosion process in filtration (site identifies as “non-quantified Filtration” in Fig. 2); right side: drag de Coarse Aggregates and Rockfill in slope Geological Fault III.

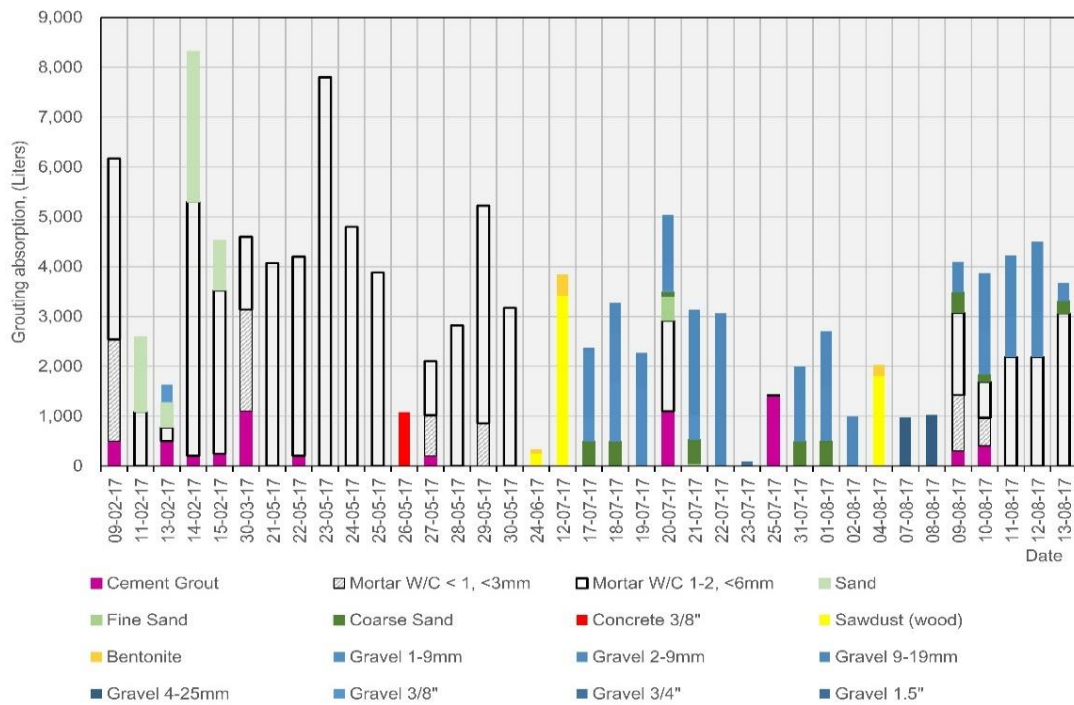


Fig. 4 [5]

Grouting absorption, elapsed time and mixes used. The terms “Gravel” and “Sand”, are utilized to indicate aggregates pushed with water, without cement.

4. CONCLUSIONS

The project experience taught the project participants the dangers of the "piston effect" in the deposits of caverns and joints. This phenomenon is the propagation of hydraulic pressure at large distances [2], in the context of this project the distance can be measured between the site of injection (curtain drillings) and each one of the sites of infiltration which was present in the left abutment of the dam. The hydraulic pressure in the karst tubes was due to: operation (open / closed) of some or all of the infiltration sites (placing grout pipes with valves) and to the pumping cycle of the concrete pump.

The effect was manifested in the short term with the opening of new infiltration sites (the total infiltration flow maintained equal) and in the long term with the erosion process on the unconsolidated deposits in caverns and joints and finally in the increase of in the infiltration flow (see Fig. 5).

At the end of the Project, it was necessary to reactive the drainage curtain of the dam (damaged due to the loss of drain D1), with the drilling of new drain holes between level 106 and 135 m a.s.l.

Currently, the infiltration site originally sealed are inactive, even with the high reservoir level reached this year (2017) (maximum operation level of the powerhouse). Which are above the levels registered during the time of the repairs. (270 vs. 285 m a.s.l.).

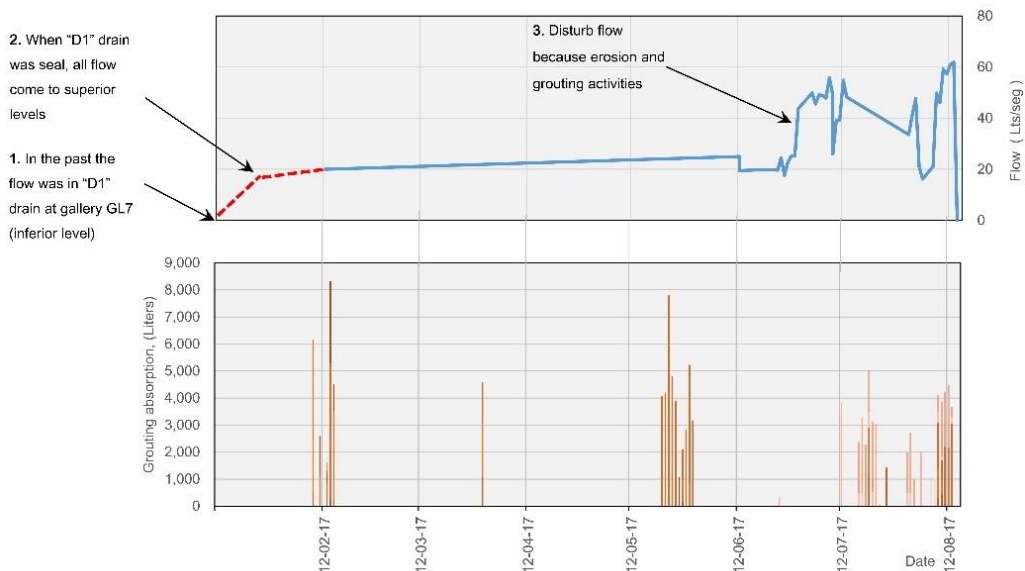


Fig. 5

Above: flow evolution in D1 drain and new filtration. Below: the activities of injection in the same date line (details in Fig. 4).

REFERENCES

- [1] Motor Columbus, Final Construction Report Volume 1, EL CAJON Hydroelectric Power Plant, Chapter 5A and 5B, September 1986.
- [2] Milanović P., Hydraulic Properties of Karst Groundwater and Its Impacts on Large Structures, 2014.
- [3] Panel de Seguridad de Obra (PSO), Reporte No.32, Central Hidroeléctrica “General Francisco Morazán”, Anexo “A”, marzo 2015.
- [4] Consorcio G-A, “Supervisión de los Trabajos Especiales de Mantenimiento de las Obras Subterráneas de la Central Hidroeléctrica General Francisco Morazán” Proyecto MOS. Informe Mensual No. 34, julio 2017.
- [5] Consorcio G-A, “Supervisión de los Trabajos Especiales de Mantenimiento de las Obras Subterráneas de la Central Hidroeléctrica General Francisco Morazán” Proyecto MOS. Informe Mensual No. 35, agosto 2017.

KEYWORDS

Abutment, Aggregate, Arch Dam, Erosion, Flow, Foundation Treatment, Grout Curtain, Karst, Seepage, Cajón Dam.

MOTS-CLES

Appui, Granulat, Barrage-Voute, Erosion, Debit, Traitement Des Fondations, Ecran D´Injection, Karst, Infiltration, Cajón Barrage.

COMMISSION INTERNATIONALE DES GRANDS BARRAGES

VINGT-SIXIÈME CONGRÈS DES GRANDS BARRAGES
Autriche, juillet 2018

DOI 10.3217/978-3-85125-620-8-167



This work licensed under a Creative Commons Attribution 4.0 International License. <https://creativecommons.org/licenses/by-nc-nd/4.0/>

**NECHRANICE DAM – LONG-TERM MONITORING OF SEALING
PERFORMANCE AT THE LONGEST EARTH-FILL DAM IN CENTRAL
EUROPE**

Martin KRUPKA

*Department of Water Management Development, POVODÍ OHŘE, STATE
ENTERPRISE*

CZECH REPUBLIC

Jan SVEJKOVSKÝ

*Head of the Department of Dam Monitoring and Safety, POVODÍ OHŘE, STATE
ENTERPRISE*

CZECH REPUBLIC

COMMISSION INTERNATIONALE
DES GRANDS BARRAGES

VINGT-SIXIÈME CONGRÈS DES
GRANDS BARRAGES
Autriche, juillet 2018

**NECHRANICE DAM – LONG-TERM MONITORING OF SEALING
PERFORMANCE AT THE LONGEST EARTH-FILL DAM IN CENTRAL
EUROPE**

Martin KRUPKA

*Department of Water Management Development, POVODÍ OHŘE, STATE
ENTERPRISE*

CZECH REPUBLIC

Jan SVEJKOVSKÝ

*Head of the Department of Dam Monitoring and Safety, POVODÍ OHŘE, STATE
ENTERPRISE*

CZECH REPUBLIC

1. INTRODUCTION

Nechranice Dam is located on the Ohře River in the North-West of the Czech Republic. The dam is the longest earth-fill dam in the Czech Republic and in Central Europe. The dam was presented to ICOLD Congress 2017 participants as one of the site visit locations.

This paper describes monitoring system and presents long-term data that has been collected since start of the dam operation.

2. DAM DESCRIPTION

Nechranice Dam is situated approximately in the middle of the Ohře River course being the fourth largest reservoir in the Czech Republic. The dam is 3280 metres long and 47,5 metres high. The dam volume is 9.5 million cubic metres [1]. It was constructed between the years 1961 and 1968. Last year the reservoir celebrated its 50 years anniversary since the dam first filling.

The reservoir covers the area of more than 13 km² with the capacity of 287 million m³ – it provides 233 million m³ of active storage and 52 million m³ of flood storage. The main purpose of the dam is enhancing the flow to supply intakes for industry, power generation and maintaining the minimum water flow downstream of the dam.



Fig. 1: Nechranice Dam

The dam is situated in the geologically unfavorable environment of the brown coal mining area at the base of the Ore Mountains. The subsoil is composed of unconsolidated and partly consolidated sediments with the thickness up to 350 m. The overburden layers of clays and claystone are up to several dozen meters thick. The underlying beds consist of coal seams and sand saturated with artesian water.

The dam body is composed of a stabilizing part of local gravel sands and the central earth core of loess loams. The impervious earth core is tied to the subsoil loamy-concrete sealing curtain that extends to the maximum depth

A drain was designed at the downstream toe of the dam to collect water draining from some of the piezometric boreholes.

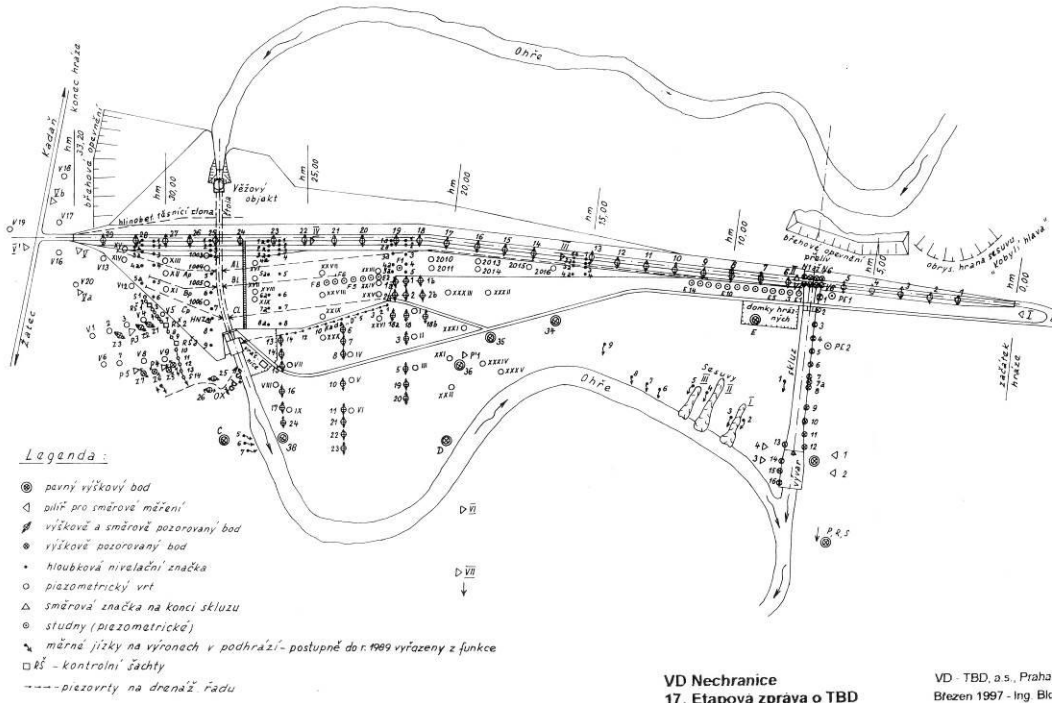


Fig. 3: Plan of the monitoring points

Some of the instrumentation is in operation since the construction of the dam, while other monitored points were added later in order to gather more detailed information at some locations.

The monitoring system comprises of the following:

- Levelling wells (Fig. 4): measure the vertical displacement at the dam foundations level. The wells are also used for the measurement of the water level in the wells providing information about the drawdown curve within the dam body.



Fig. 4: View into the levelling well

- Levelling points (Fig. 5) are used for measurements of vertical displacement.



Fig. 5: Levelling point

- Lateral and vertical movement monitoring points (Fig. 6) are used for measurements of the vertical as well as lateral displacements on the surface of downstream face of the dam.



Fig. 6: Lateral and vertical movement monitoring point

- Piezometric boreholes (Fig. 7) measure the piezometric pressure within the dam body. They are located in five cross-sections across the dam body. At some locations, two piezometric boreholes are present close to each other, reaching to different strata.



Fig. 7: Piezometric boreholes

- Piezometric sensors – are located inside the impervious core of the dam. Sensors are also located below the tower and below the communication tunnel. The measurements of the piezometric pressures are carried out four times per year.

Some of the piezometers at the downstream toe of the dam function also as relief wells. Once the water table reaches certain level it is collected conveyed out by the drain.

The measurements are carried out by the certified company Vodní díla TBD, a.s. Most of the monitoring is done annually fulfilling the Czech legislation requirements for the highest dam hazard classification rank.

4. RESULTS – LONG-TERM MONITORING DATA

4.1. DAM SEALING PERFORMANCE

Ground water table measured in the piezometers and levelling wells has been steady since the construction of the dam [2] allowing for slow changes according to the conditions at the site and water level in the reservoir. The ground water table is present relatively low within the dam body and does not reach the terrain on the downstream toe of the dam. The ground water levels in the dam body downstream of the dam sealing do not move significantly with the reservoir water level changes.

Fig. 8 shows comparison of the piezometric pressure in the four piezometric sensors located in the dam sealing at the dam foundation level over the the 50 years of the dam. The piezometric pressures relate to the water level in the reservoir. While the Sensor 1, located close to the upstream face of the dam sealing, reflects well the water level change, the other sensors react much slower. This applies particularly to Sensors 99 and 113, which are located close to the downstream face of the sealing.

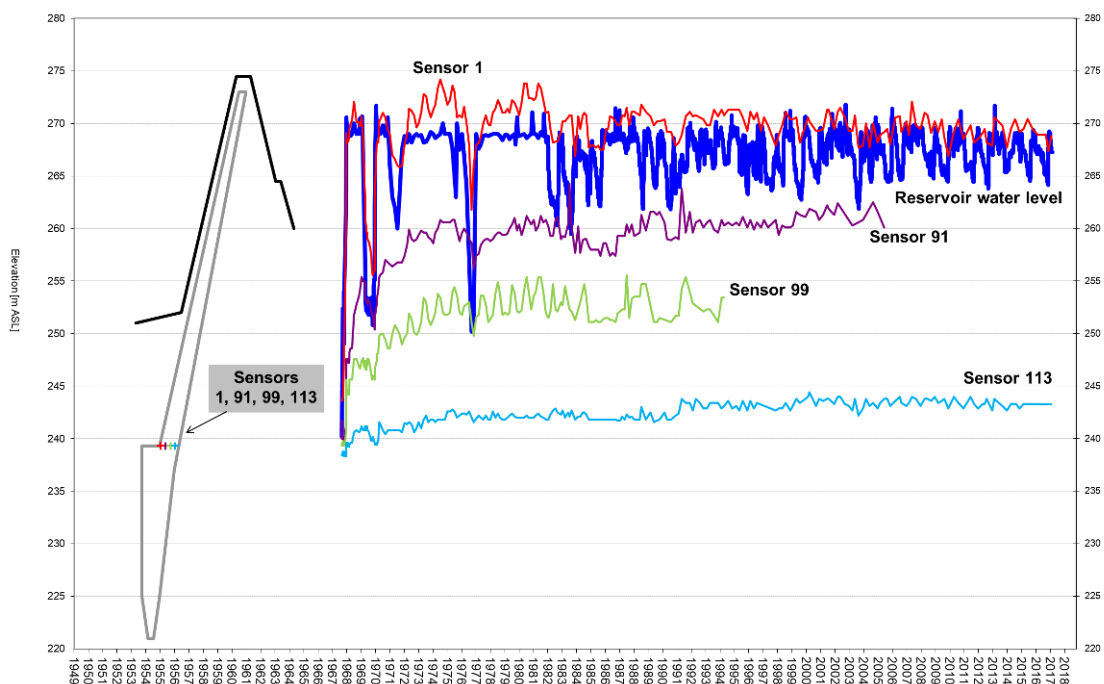


Fig. 8
Dam sealing performance since the dam construction (1967-2017)

The plot also shows that the pressure at sensors located in the dam sealing (91, 99 and 113) increased steadily for the first 7 years of the dam operation until they stabilized at values along which they oscillate since 1974. Sensor 99 and 91 stopped providing data at some point.

The reservoir water level curve shows the update of dam operation rules in 1979. Since then the dam outflow has been optimised and the reservoir storage has been used closer focus on the hydropower production as well as on the maintenance of minimum flow in the Ohře River downstream the dam.

In the period of May 1969 – May 1970, one year after the start of dam operation, the water level was lowered for testing purposes. Fig. 9 shows that the decrease of about 18 m affected the pressure particularly at the sensor 1 located close to the upstream face of the dam sealing. The other 3 sensors reacted to the reservoir water level to much lesser extent and with a delay.

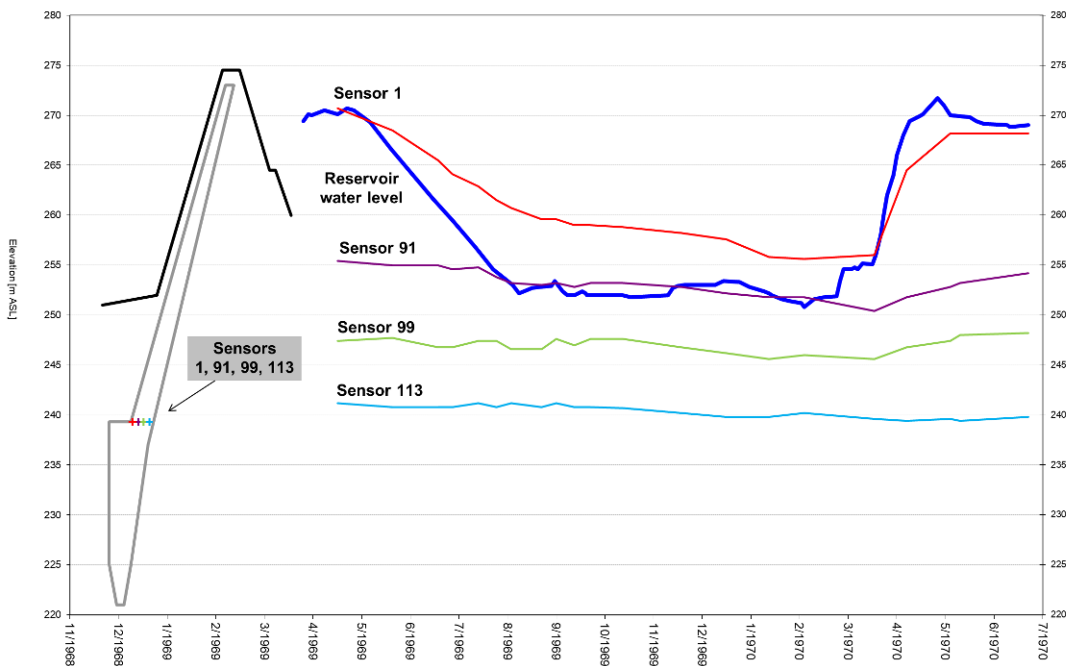


Fig. 9
Piezometric pressures at the dam sealing during the dam testing period (May 1969 – May 1970)

4.2. SETTLEMENT OF THE DAM

The settlement of the dam body has been continuous since the dam construction without any anomalies (Fig. 10). The highest settlement of the dam crest is located near the communication tunnel. At this point the settlement has steadily grown to the value of 550 mm in 2016.

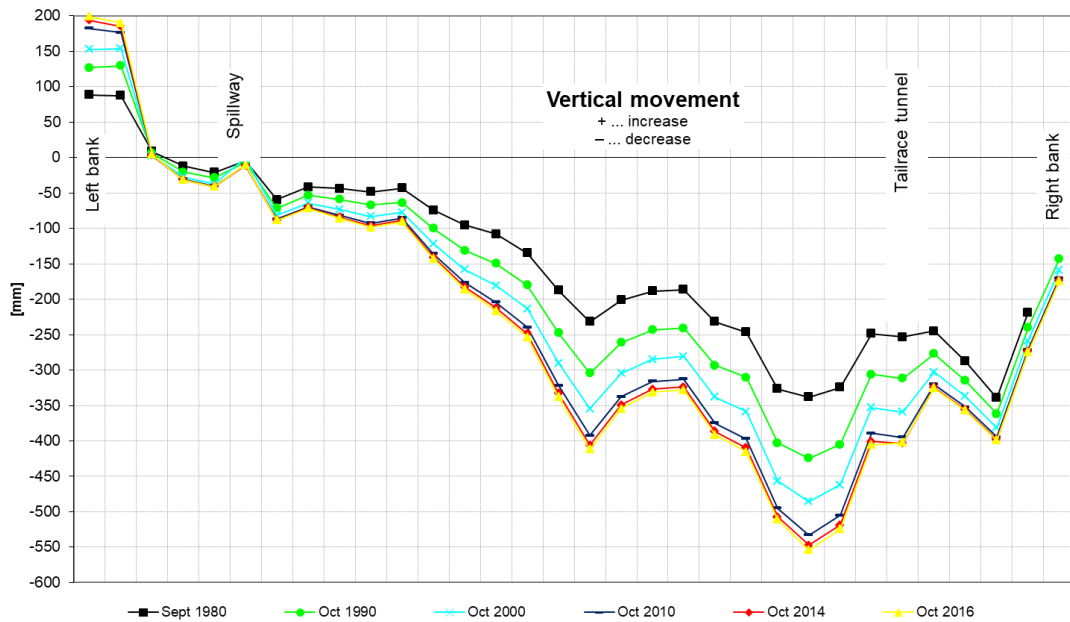


Fig. 10
Vertical movement of the dam crest

The settlement of the dam surface is related to the settlement of the foundation level [3].

The dam settlement was accounted for in the dam design. The dam crest was designed 0,5 m higher than its expected level after the settlement.

Fig. 11 shows the vertical movement of the communication tunnel. It shows that there has been no significant vertical movement since 1982.

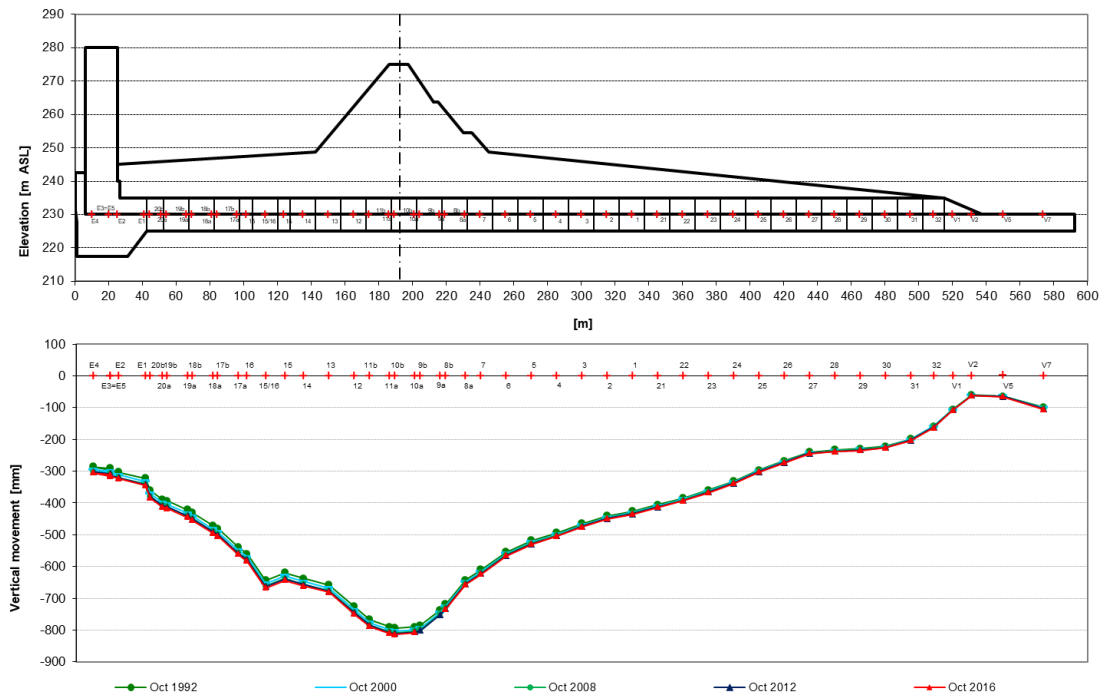


Fig. 11
Vertical movement of the communication tunnel

5. CONCLUSIONS

Presented data show that the water table level is stable and no negative trends have been observed. Short-term movements are result of the specific meteorological conditions.

Settlement of the dam crest is continuous since the dam construction without any anomalies. The highest settlement of the dam crest is located near the communication tunnel. At this point the settlement has steadily grown to the value of 550 mm in 2016. Vertical movements along the communication tunnel show that there has been no significant vertical movement of this structure since 1982. Despite complicated geological conditions at the site, the monitoring has not registered any unexpected behavior.

5.1. ACKNOWLEDGEMENTS

We are grateful to Ing. Ondřej Švarc from Vodní díla TBD a.s. for kindly providing the complete set of the Nechranice Dam monitoring data.

REFERENCES

- [1] POVODÍ OHŘE, STATE ENTERPRISE Nechranice Dam operating manual, 2008.
- [2] VD – TBD, A.S. VD Nechranice, 5. souhrnná etapová zpráva o TBD, 5th Summary report – Nechranice Dam safety monitoring report for the period 05/2008 – 05/2013, issued 06/2013.
- [3] VD – TBD, A.S. VD Nechranice, 29. etapová zpráva o TBD, 29th Nechranice Dam safety monitoring report for the period 06/2015 – 05/2016, issued 06/2016.

SUMMARY

This paper presents Nechranice Dam long-term monitoring data that has been collected since start of dam operation in 1967. Nechranice Dam is located on the River Ohře in the North-West of the Czech Republic. The dam is the longest earth-fill dam in the Czech Republic and in Central Europe. The dam has the highest dam hazard classification rank as defined by the Czech legislation.

The Nechranice Dam monitoring system comprises of geodetic surveying points, wells and piezometers that monitor vertical and horizontal movements at the foundations level as well as on the face of the dam, piezometric pressures, water table elevation and amount of water drained.

The paper presents the piezometric pressures in the dam sealing at the foundation level over the 50-year long period of dam operation. The water table level is stable with no negative trends. Short-term movements are result of the specific meteorological conditions. Attention is then focused particularly on the one-year long period of significant reservoir water level decrease that occurred in 1969 - 1970.

Settlement of the dam crest is discussed. It shows continuous progress since the dam construction without any anomalies. The highest settlement of the dam crest is located near the communication tunnel and has steadily grown to the value of 550 mm in 2016.

Vertical movement along the communication tunnel is presented at the end of the paper. It shows that there has been no significant vertical movement of this structure since 1982.

Despite complicated geological conditions, the Nechranice Dam monitoring has not registered any unexpected behavior.

KEYWORDS

Nechranice Dam, dam, earthfill dam, monitoring

COMMISSION INTERNATIONALE DES GRANDS BARRAGES

VINGT-SIXIÈME CONGRÈS DES GRANDS BARRAGES
Autriche, juillet 2018

DOI 10.3217/978-3-85125-620-8-168



This work licensed under a Creative Commons Attribution 4.0 International License. <https://creativecommons.org/licenses/by-nc-nd/4.0/>

**SEALING OF AND FOUNDATION ON A 70 M ALLUVIUM LAYER OF ARKUN
DAM**

Ronald HASELSTEINER

*Department Manager Hydraulic Engineering, BJOERNSEN CONSULTING
ENGINEERS*

GERMANY

Resul PAMUK

Monitoring Process Leader, ENERJISA ÜRETİM AS

TURKEY

COMMISSION INTERNATIONALE
DES GRANDS BARRAGES

VINGT-SIXIÈME CONGRÈS DES
GRANDS BARRAGES
Autriche, juillet 2018

SEALING OF AND FOUNDATION ON A 70 M ALLUVIUM LAYER OF ARKUN DAM

Ronald HASELSTEINER

*Department Manager Hydraulic Engineering, BJOERNSEN CONSULTING
ENGINEERS*

GERMANY

Resul PAMUK

Monitoring Process Leader, ENERJISA ÜRETİM AS

TURKEY

1. INTRODUCTION

The Arkun Dam and HEPP project is located on the Coruh River in the North East of Turkey. The main purpose is hydroelectric energy generation. Therefore, a main and an environmental powerplant were installed showing a capacity of total 237 MW. The Arkun project is owned by EnerjiSA which was formerly a joint venture of Verbund (Austria) and the Sabanci Group (Turkey) unless E.ON (Germany) took over the shares of Verbund in 2013.

The project was completed and started operation in 2014 after only approximately 5 years of construction. The project construction schedule and the project budget were kept in the range of early project assumptions. The good foundation and suitable dam fill material close to the dam location contributed to the positive project progress and completion.

The project consists of CFSGD, a 14 km long power tunnel, diversion works, a main and an environmental powerhouse as well as a gated spillway. A general layout is shown in Fig. 1. More details concerning the general layout of the project and details had been already published before [1] [2] [3].

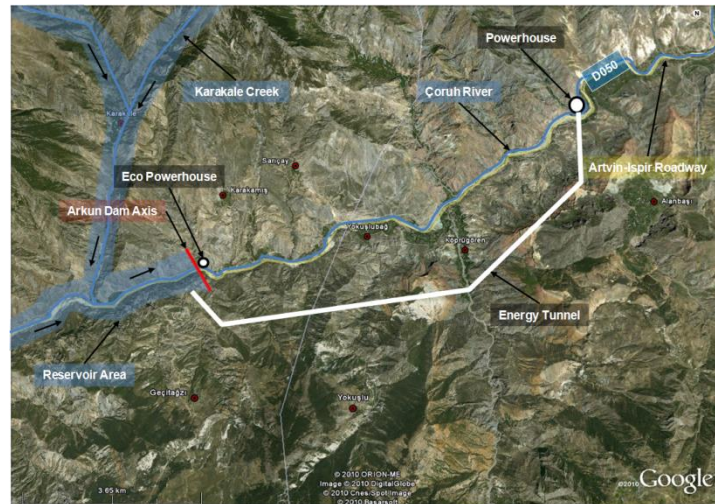


Fig. 1
General layout of the project

2. GENERAL DAM AND FOUNDATION DESIGN

2.1. GENERAL DAM DESIGN

The Arkun dam is of CFSGD type including a rockfill part at the downstream slope. The dam design was prepared according to the corresponding ICOLD bulletin for CFRDs [4] and modern dam design criteria [5]. The design of the main dam was adapted to the special requirements imposed by using not free draining sand-gravel fill at the main dam embankment fill zones as discussed in [9] (see Fig. 2).

A parapet wall was placed at the crest. The upstream surface is covered by a concrete slab sealing which is connected via an articulated plinth to a cut-off wall (COW) which is reaching down to the bedrock which is located underneath a 70 m deep alluvial layer. The slopes are inclined by $H:V = 1.0 : 1.6$.

The spillway is designed for a PMF flood with a discharge of $4,701 \text{ m}^3/\text{s}$. A gated spillway was placed at the right abutment integrating three bays close to the intake of the power tunnel. The power tunnel to the main powerhouse is

approximately 14 km long with a diameter of 6.5 m. The tunnel shows a high pressure grouting pre-stressed concrete lining.

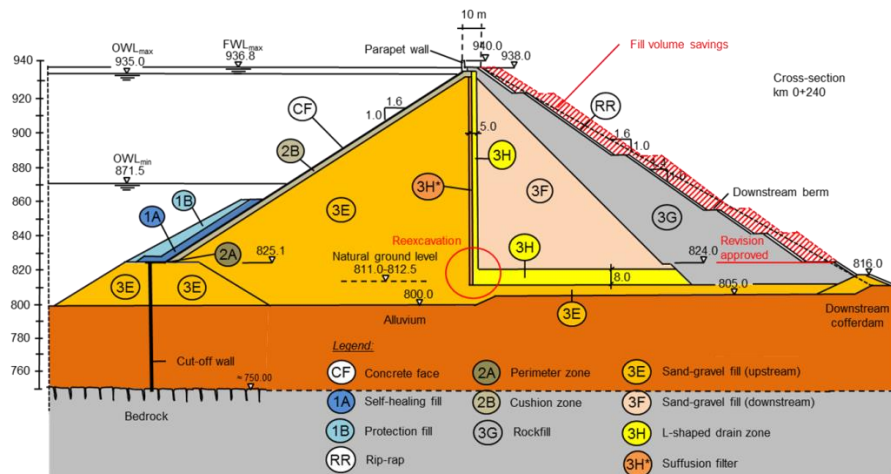


Fig. 2
Typical cross section of the Arkun CFSGD

The diversion tunnel is located on the left side of the dam. The diversion tunnel hosts the pressure tunnel to the environmental powerhouse. The penstock for the environmental powerhouse was constructed after the diversion tunnel was closed and plugged (Fig. 1) when the impoundment of the reservoir started.

2.2. SEALING AND SEEPAGE DESIGN

The Arkun Dam sealing and seepage design consists of an upstream barrier comprising a surface concrete slab sealing, an articulated plinth, and a cut-off wall. An L-shaped drain and a free draining rockfill zone (3G) shall guarantee a high safety level regarding the control of the seepage, also in consideration of critical failure of the upstream sealing barrier.

The drain (zone 3H) itself is protected by a suffusion filter (zone 3H*) in order to hinder small particles which are activated by suffusion processes within zone 3A. The sand-gravel material used for zone 3E was considered to be suffusive. The zoning concept of the dam is shown in Fig. 2.

2.3. FOUNDATION DESIGN

The dam body is placed on a 70 m deep alluvium layer. A stress-strain deformation analysis was performed in order to evaluate the deformation at critical

project milestones such as end of construction and first impoundment **Fehler!
Verweisquelle konnte nicht gefunden werden..**

Particular focus was laid upon the stress-strain behaviour of the cut-off wall in order to assess the cracking potential induced by excessive tensile stresses. The testing results of local laboratories confirmed the design assumptions that intended to create an earth concrete mix with relatively low compressive strength and low stiffness in order to achieve similar deformation behaviour, as the surrounding alluvial material should show. Results of laboratories abroad and of local universities indicated a much stiffer and more brittle material behaviour. Relying on these later results serious cracking could not be excluded anymore, which initiated the Owner to check the impact of this potential cracking of the cut-off by a seepage analysis.

For the determination of the time dependent development of the cut-off wall concrete samples were taken from the ongoing concreting works and were tested after seven and 28 days and further selected periods. Two institutes came to the result that the elasticity modulus reached values exceeding 1,000 MPa after 28 days. One institute persisted to obtain values of approximately maximum 500 MPa also after 70 days after concreting. These contradictory results uncomforted the responsible parties so that further testing and analyses were performed.

Field investigations and the stress strain modelling were the basis for defining the future foundation level in form of the required excavation depth. The field testing results were also contradictory since geophysical investigations indicated a very loose degree of compaction of the alluvium to very large depths which would require extensive excavation works. Finally, an excavation of approximately five to ten meters underneath the dam footprint was realized in order to eliminate the layers showing a high deformation potential and organic particles.

3. APPLIED MODELS, PARAMETER AND ANALYSES

3.1. GENERAL

For the Arkun CFSGD a 2D stress-deformation were prepared using the Geoslope Sigma software package. For the seepage analysis the groundwater module of the Rocscience Slide program was used. The seepage model was further utilized in order to check seepage conditions for extreme load cases neglecting the sealing effect of the upstream barrier consisting of concrete face, articulated plinth and cut-off wall.

A limit equilibrium analysis was performed considering the shear stress behaviour derived from large scale triaxial testing performed in the Karlsruhe Institute of Technology (KIT) in Germany in order to optimize the downstream slope

design and in order to check the stability also for extreme seepage conditions superposed with earthquake loads. For the LEA of the slopes the program Slide/Rocscience was applied.

3.2. FEM MODELS, INPUT PARAMETER AND ANALYSES

The seepage FE model is shown in Fig. 3. The finite element mesh was refined at critical structural objects such as the face slab and the articulated plinth as well as close to the cut-off wall and the L-shaped drain. Steady state conditions were investigated for different water levels and for different sealing and drain conditions which were combined to load cases (LC).

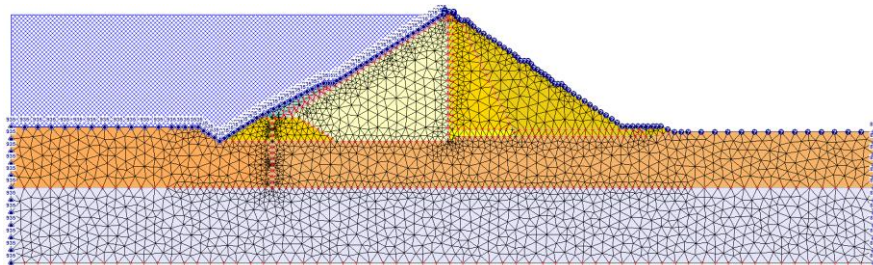


Fig. 3
FE mesh and model for the seepage analysis

For the steady state seepage analysis following parameters, e. g. permeability, were applied (Table 1). Table 1 includes the general Technical Specifications of the dam fill works.

Table 1
Technical specifications of the main dam fill materials **Fehler! Verweisquelle konnte nicht gefunden werden.**

General Technical Specifications for the Fill works ¹⁾⁶⁾										
No.	Name	Description	Passes [-]	Dry density ⁴⁾ σ_d [g/cm ³]	Max. grain size d_{max} [mm]	Layer thickness T [cm]	Elasticity modulus E [MPa]	Permeability k [m/s]	Water [l/m ³]	Model "Set0" k-values [m/s]
1	1A ³⁾	Cohesionless fine grained soil	-	-	63	30	-	-	-	10 ⁻⁵
2	1B ³⁾	Fill, protection material	-	-	400	60	-	-	-	10 ⁻⁴
3	2A	Perimeter filter	8	2.0	40	40	-	-	-	Not modeled.
4	2B	Transition filter I	8	2.0	80	40	-	-	-	10 ⁻⁵
5	3E	Upstream sand-gravel fill	12	2.5	400	60	200	10 ⁻⁴	⁵⁾	10 ⁻⁴
6	3F	Downstream sand-gravel fill	12	2.5	600	80	200	10 ⁻⁴	⁵⁾	10 ⁻⁴
7	3G	Downstream rockfill	12	2.2	600	80	80 ²⁾	10 ⁻¹ to 10 ⁻²	250-500	10 ⁻¹
8	3H	L-shaped drain/filter	8	1.9	150	60	-	10 ⁻²	-	5 10 ⁻²
9	3H*	Suffusion filter	8	2.0	150	60	-	10 ⁻³	-	10 ⁻³
10	RR	Rip-rap	-	-	1,500	150	-	10 ⁻¹	-	Not modeled.

The FE mesh used for the stress-strain analysis (Sigma/W) is given in Fig. 4. The mesh had to be critically refined in the area of stiff objects such as the concrete

slabs and the cut-off wall. In consideration of the laboratory test results particularly the deformation behaviour of the cut-off wall was of major interest. Hence, also observation points were accumulated there and where monitoring instruments were placed.

Thanks to the fact that construction already started when the models were prepared, calibration works could consider the actual construction stages and measurement results derived from inclinometers, settlement gauges and cells. This is a comfortable situation, which contributed to the reliability of the model. The stress-strain model was used mainly to investigate the dam conditions at the end of construction and the first impoundment stage. The deformation at the face slab and the plinth area as well as the stress conditions along the cut-off wall were of major interest.

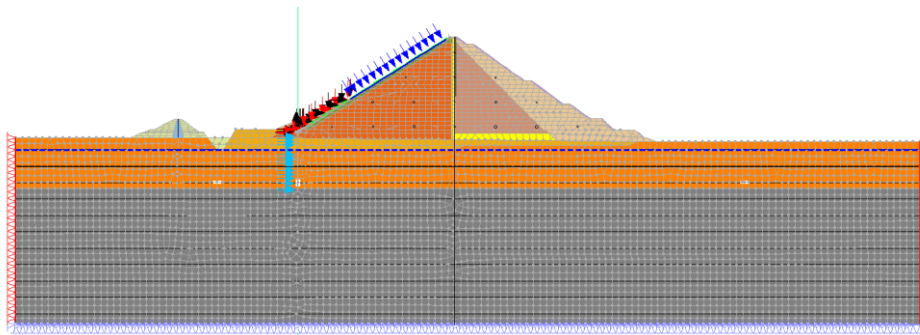


Fig. 4
FE mesh and model for the stress-strain analysis

The model considered 34 construction stages at the main dam before the impoundment was modeled by introducing the corresponding pore water pressures manually. The results of the steady state seepage analysis were considered. Table 2 includes the considered parameters for the stress-strain analysis.

Table 2
Applied parameters for the stress-strain model [2]

Models	Linear-elastic			Linear-elastic			Linear-elastic			Elastic-plastic (MC)				
Source	International consultant			Björnsen Consulting Engineers			Local design engineer			Björnsen Consulting Engineers				
Zone	E [MPa]	v [-]	γ [kN/m ³]	E [MPa]	v [-]	γ [kN/m ³]	E [MPa]	v [-]	γ [kN/m ³]	E [MPa]	v [-]	γ [kN/m ³]	ϕ' [°]	ψ [°]
1A	20	0,35	18	20	0,35	19	20	0,3	17	20	0,35	19	30	0
1B	30	0,3	18	80	0,33	21	200	0,3	21,5	80	0,33	21	35	4
2A	360	0,3	22,5	300	0,3	21	-	-	-	300	0,3	21	38	10
2B	160	0,3	22	250	0,3	21	200	0,3	22	250	0,3	21	40	10
3E	240	0,33	23	220	0,33	24	175	0,38	22	220	0,33	24	38	12
3F	200	0,33	22,5	220	0,33	24	200			220	0,33	24	38	12
3G	120	0,33	20,5	80	0,28	22	200			80	0,28	22	45	15
3H	120	0,33	19	100	0,3	19	150			100	0,3	19	38	4
3H*	-	-	-	100	0,3	19	-	-	-	100	0,3	19	38	4
ALL	200	0,33	22	150	0,33	19	660	-	-	150	0,33	19	35	8
ROCK	5000	0,15	26	20000	0,25	27	15000	0,2	26	20000	0,25	26	-	-
CON	20000	0,25	25	20000	0,2	25	28000	0,2	24	20000	0,20	25	-	-
F-ALL	-	-	-	200	0,33	24	-	-	-	200	0,33	24	38	10
RR	-	-	-	60	0,35	24	-	-	-	60	0,35	24	-	-
COW	-	-	-	800	0,27	23	-	-	-	800/1200/1800	0,26	24	-	-

BCE preferred to apply an elastic-plastic material model rather than the linear-elastic models which were used before. Fundamental considerations concerning the deformation behaviour of rockfill and sand-gravel fill materials were considered as discussed in [4] [6] [7] [8]. Case studies with reference to principle rockfill characteristics are also included in [9] and [10]. Sand-gravel fill materials with a wide, uniform sieve curve tend to show very strong deformation characteristics which is confirmed by several benchmark projects [7].

For the elastic-plastic modeling constant elasticity moduli were considered as well as MC shear strength parameter. This approach is considered especially for the impoundment phase a priori too simplified but, nevertheless, lead to reasonable results, thanks to an accurate calibration of the model by comparison to the actual measurement data to reliable results (see chapter 4).

For the performed slope stability LEA following parameters (Table 3) were applied in order to consider a comprehensive shear-strength behaviour of the different applied materials. For the main fills (zones 3E, 3F, 3G) stress dependent shear curves were implemented which were derived from large scale triaxial tests performed in Germany, as aforementioned.

Table 3
Material parameters used for the LEA of the slope stability

No.	Zone	Name	Dry unit weight	Saturated unit weight	Wet unit weight	Water content	Peak shear strength		Residual shear strength		Shear Type	Saturated permeability
			γ_d [kN/m ³]	γ_s [kN/m ³]	γ_w [kN/m ³]	w [%]	ϕ' [°]	c' [kN/m ²]	ϕ_R [°]	c_R [kN/m ²]	Type	k_s [m/s]
1	1A	Self-healing fill (cohesionless)	17	20	19	10	30	0	30	0	const.	10 ⁻⁵
2	1B	Protection fill	21	22	21	2	35	0	35	0	const.	10 ⁻³
3	2A	Perimeter zone	21	22	21	2	38	0	34	0	const.	10 ⁻⁴
4	2B	Cushion zone	21	22	21	2	40	0	36	0	const.	10 ⁻⁴
5	3E	Sand-gravel fill A	23	25	24	5	53	0	53	0	Curve!	10 ⁻³
6	3F	Sand-gravel-fill B	23	25	24	5	53	0	53	0	Curve!	10 ⁻³
7	3G	Rockfill "Andesite"	22	23	22	2	48	0	43	0	Curve!	10 ⁻¹
8	3H	L-shaped drain	19	20	19	2	38	0	38	0	const.	10 ⁻²
9	ALL	Natural alluvial deposits	18	20	19	5	38	0	38	0	const.	10 ⁻³
10	ROCK	Bedrock	-	26	-	-	40	350	-	-	const.	10 ⁻⁷
11	CON	Concrete face slab / Cutoff wall	25	-	-	-	35	150	-	-	const.	10 ⁻⁹

4. RESULTS

4.1. SEEPAGE ANALYSIS

The seepage analysis showed that also for very unlikely, extreme load cases which consider the situation, that the complete concrete face and the cut-off were not working at all, the seepage is still controlled by the L-shaped drain and the rockfill zone (3G) so that no critical pore water pressures occur within downstream fill. This also emerges a positive effect on the slope stability of the downstream slope. In Fig. 5 the phreatic line of seepage is shown for selected load cases. For comparison also LC2 "Set 0" is included which shows the seepage conditions for complete functional sealing and drain elements.

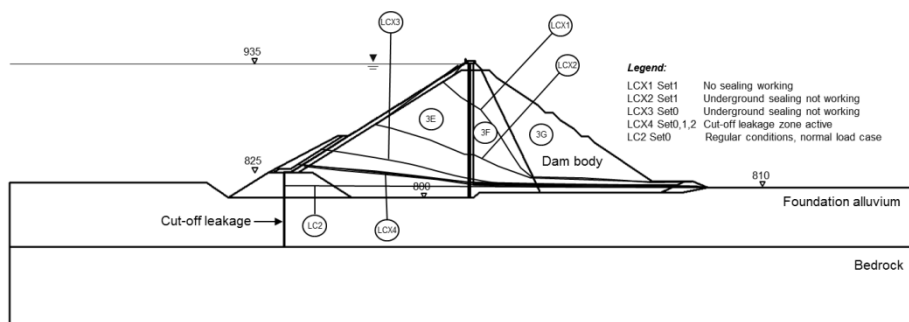


Fig. 5
Phreatic line of seepage of Arkun main dam for selected load cases [1]

Fig. 5 also illustrates that for extreme (unrealistic) load cases, e.g. LCX1 “No sealing working”, the draining zones are able to control the pore water pressure in the dam body and finally the phreativ line of seepage is controlled by the 3G rockfill zone. Thus, the danger of unfavorable pore water pressure conditions at the downstream slope are very unlikely to occur. The sliding stability of the downstream slope shows a sufficient factor of safety, in spite of a complete malfunction of the sealing. This proof was required to comfort all responsible parties due to ongoing discussions concerning the cut-off wall and slab behaviour during first impoundment.

4.2. LIMIT EQUILIBRIUM ANALYSIS

The strong characteristics of the rockfill and the sand-gravel fill material as well as the effective seepage control design resulted in quite confident safety factors considering the LEA for the sliding stability of both slopes (see Fig. 6).

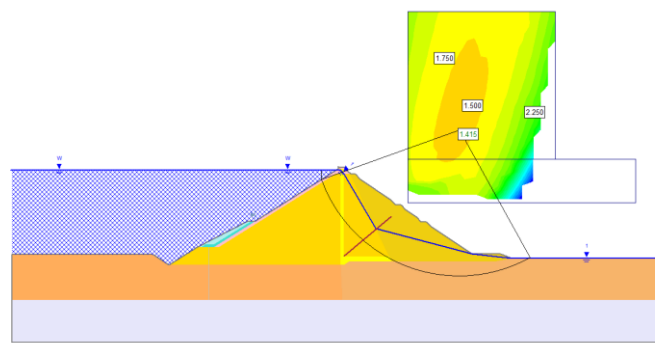


Fig. 6
Decisive sliding circle for the extreme load case 3C, FoS = 1.42

For example, for the extreme load case 3C “Normal operation water level/slab cracking/drain malfunction” (corresponding to LCX1 of the seepage analysis) a factor of safety of FoS = 1.42 is obtained whilst the required safety factor is within the limit between 1.0 to 1.1 according to [5].

4.3. STRESS-STRAIN ANALYSIS

The stress-strain model predicted a total deformation of maximum approximately 75 cm located close to the dam foundation at the EoC stage which conforms to the expectations derived from benchmark projects which were founded on deep alluvium. The results were calibrated using the measurements results from settlement cells and settlement gauges. The obtained 0.5 % total deformation at EoC indicates an realistic value, although it is high in consideration

of the relatively strong elasticity modulus which was achieved mainly for the sand-gravel fill materials.

For the first impoundment a horizontal deformation of the dam crest of 30 cm towards downstream was predicted which fitted quite well to the later measurements of the survey points. The articulated plinth showed total displacements of 45 cm. The alluvial foundation caused a triPLICATION if this value.

The deformation of the cut-off resulted in stresses (> 5 MPa) which indicated a high likelihood of cracking of the cut-off wall during first impoundment. The actual cut-off characteristics are considered to be too stiff.

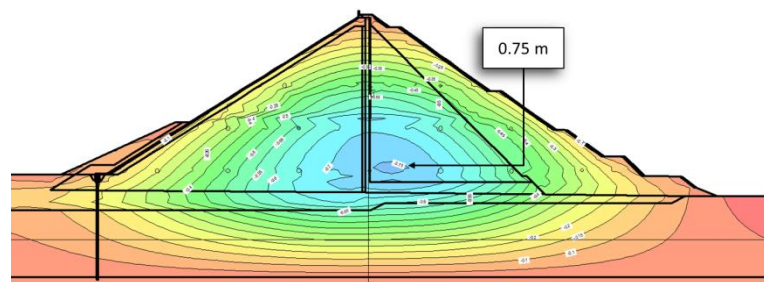


Fig. 7
Total displacements/deformations at the EoC stage

REFERENCES

- [1] HASELSTEINER, R.; KAYTAN, E.; PAMUK, R.; CERI, V. Seepage control design of the Arkun dam in Turkey. *Hydropower and Dams (H&D)*, 1/2012, pp. 90-96.
- [2] HASELSTEINER, R.; PAMUK, R.; KAYTAN, E.; CERI, V. Deformation prediction of a large CFSGD for first impoundment. Conference Proceedings, International Symposium on Dams in a global environmental challenge, *ICOLD 2014*, Bali.
- [3] PAMUK, R.; HASELSTEINER, R., KAYTAN, E.; CERI, V. Design and Construction of the Dam Sealing Structures of Arkun CFSGD. Conference Proceedings, International Symposium on Dams in a global environmental challenge. *ICOLD 2014*, Bali.
- [4] ICOLD 141. Concrete Face Rockfill Dams: Concepts for design and construction. *International Committee on Large Dams (ICOLD)*, Bulletin 141, Paris, 2011.
- [5] FELL, R.; MACGREGOR, P.; STABELDON, D.; BELL, G. Geotechnical Engineering of Dams. A. A. *Balkema Publishers*, Leiden, London/New York/Philadelphia/Singapore, 2005.

- [6] HUNTER, G.; FELL, R. Rockfill Modulus and Settlement of Concrete Face Rockfill Dams. *Journal of Geotechnical and Geoenvironmental Engineering*, Vol. 129, No. 10, pp. 909-917.
- [7] CRUZ, P. T.; MATERON, B.; FREITAS, M. Concrete Face Rockfill Dams. *Dados Internacionais de Catalogacao na Publicacao (CIP)*, Brazil, 2009.
- [8] HASELSTEINER, R.; PAMUK, R.; ERSOY, B. Aspects concerning the shear strength of rockfill material in rockfill dam engineering. *Journal Geotechnik*, Deutsche Gesellschaft für Geotechnik (DGGT), geotechnik 49 (2017), Heft 3, S. 193 - 203
- [9] HASELSTEINER, R.; ERSOY, B. Seepage control of concrete faced dams with respect to the surface slab cracking. *6th International Conference on Dam Engineering*, Lisbon, Portugal, February 15-17, 2011, Proceedings Pina, E. Portela, J. Gomes (ed.), pp. 611-628.
- [10] ICOLD 134. Weak rocks and shales in dams. *International Committee on Large Dams (ICOLD)*, Bulletin 134, Paris, 2008

SUMMARY

The Arkun Dam and HEPP project is located in the North-east of Turkey on the Coruh River. The installed capacity comprises a main powerhouse with 225 MW and an environmental powerhouse with 12 MW. The main dam shows a height of 140 m and is of CFSGD type. The gated spillway is designed for a discharge of 4.701 m³/s. The energy tunnel which is connecting the reservoir with the main powerhouse is 14 km long with a diameter of 6.4 m. The project was commissioned in 2014.

The dam is founded on a deep alluvium layer within the V-shaped valley. The seepage of the concrete face sand-gravel fill dam (CFSGD) is controlled by the concrete face and the articulated plinth which is linked to the maximum 70 m deep two phase cut-off wall. During the construction a seepage analysis, a LEA slope stability analysis and a stress-strain analysis were performed in order to predict the dam's behaviour during construction, first impoundment and for the long-term perspective.

COMMISSION INTERNATIONALE DES GRANDS BARRAGES

VINGT-SIXIÈME CONGRÈS DES GRANDS BARRAGES
Autriche, juillet 2018

DOI 10.3217/978-3-85125-620-8-169



This work licensed under a Creative Commons Attribution 4.0 International License. <https://creativecommons.org/licenses/by-nc-nd/4.0/>

FOUNDATION TREATMENT WITH CUT OFF WALL IN TUGU DAM

Ni Made SUMIARSIH

INDONESIAN DAM CENTRE, INDONESIAN MINISTRY OF PUBLIC WORKS
AND HOUSING

INDONESIA

Airlangga MARDJONO

INDONESIAN DAM CENTRE, INDONESIAN MINISTRY OF PUBLIC WORKS
AND HOUSING

INDONESIA

Nisa Andan RESTUTI

INDONESIAN DAM SAFETY UNIT, INDONESIAN MINISTRY OF PUBLIC
WORKS AND HOUSING

INDONESIA

Ali CAHYADI

INDONESIAN DAM CENTRE, INDONESIAN MINISTRY OF PUBLIC WORKS
AND HOUSING

INDONESIA

COMMISSION INTERNATIONALE
DES GRANDS BARRAGES

VINGT-SIXIÈME CONGRÈS DES
GRANDS BARRAGES

Autriche, juillet 2018

FOUNDATION TREATMENT WITH CUT OFF WALL IN TUGU DAM¹⁾

Ni Made SUMIARSIH

Indonesian Dam Centre, Indonesian Ministry of Public Works and Housing

Airlangga MARDJONO

Indonesian Dam Centre, Indonesian Ministry of Public Works and Housing

Nisa Andan RESTUTI

Indonesian Dam Safety Unit, Indonesian Ministry of Public Works and Housing

Ali CAHYADI

Indonesian Dam Centre, Indonesian Ministry of Public Works and Housing

INDONESIA

ABSTRACT

Tugu Dam is an earth fill dam located in Trenggalek district who has a problem with its foundation which is consists of a relatively thick deposit of pervious alluvium. When the dam foundation consists of a relatively thick deposit of pervious alluvium, the designer must decide whether to make a complete cut off wall (diaphragm wall) or allow a certain amount of under seepage to occur under controlled conditions.

To improve the earth fill dam with pervious foundation by cut off wall can be divided into three types: conventional concrete, slurry trench, and plastic concrete wall. Based on the many reasons, Tugu Dam could be proposed using Plastic Concrete Wall as a cut off wall.

Screen grouting under the cut off wall is considered to make sure the water seepage could be protected.

KEYWORDS

Earth Fill Dam, alluvium deposit, plastic concrete wall, screen grouting.

1. INTRODUCTION

Tugu Dam is a dam which is established to meet the requirements of irrigation water and influent. It was established on Keser River which has a river basin as wide as 43.06 km² with the length of the river is 9.3 km. Administratively, the dam is located in Nglinggis Village, Tugu Sub-district, Trenggalek Regency, East Java Province.

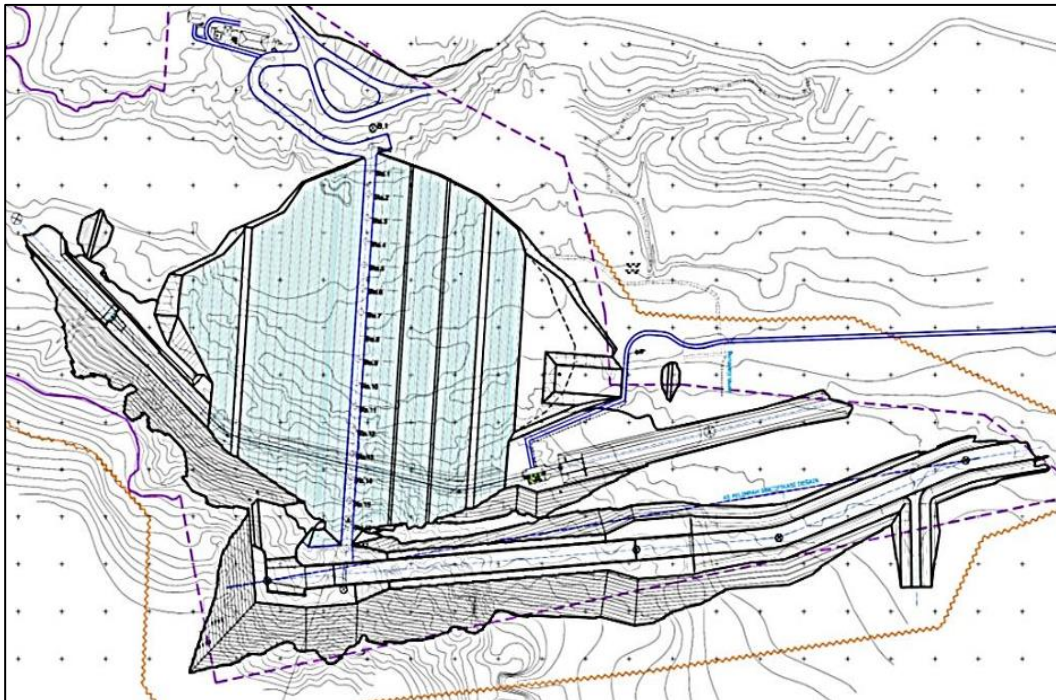


Figure 1. Layout of Tugu Dam

The design of seepage control is one of efforts in obtaining the dam safety and the water storage capacity. The seepage control through many ways is very necessary because there are many factors that have not been exactly known in the construction stage till the life time of the dam, such as:

- a. The geological condition of the dam which is greatly various (not uniform) along the dam axis.
- b. The incident of big earthquake and unpredictable weather.

- c. A decrease in function of one or several efforts of seepage control in line with the age of the dam.

Principally, the efforts of seepage control on the dam foundation are divided into two categories, they are: by restraining the seepage (water barrier) and by controlling the drainage. The design of dam used a combination of the two efforts. The seepage control system on the dam body consists of divisions of embankment zone, blanket drain, and toe drain.

Meanwhile, on the foundation, water barrier, downstream drainage ditch, and relief well are made. Water barrier on the foundation can use a curtain grouting or use a slurry cutoff wall or diaphragm wall.

2. CUT OFF WALL OR DIAPHRAGM WALL

In the area of Tugu Dam, the condition of foundation along the axis is greatly various. The thicknesses of the alluvial deposit and weathering are greatly various starting from 5 meters up to 28 meters. If an excavation of cut off trench is conducted until it reaches the bedrock, this method is not economical. The repair of foundation on the alluvial deposit and the strongly weathered rock using the curtain grouting is also considered as ineffective.

This condition also considered the time function of construction and in line with the age of the dam, with the water head of 80 meters, the water pressure on the foundation will be very high. The effectiveness of material grouting for long term period will not be able to ensure the permeability level is maintained. Considering that the alluvial deposit and the strongly weathered rock are still porous enough, a special repair of foundation is needed using the cut off wall or the diaphragm wall.

The slurry cut off wall is a kind of cut off trench which is very effective in blocking the seepage from passing through the foundation of the dam. It is used if the repair using the methods of either the curtain grouting or the cut off trench which reaches the foundation layer of rock are not economical. The slurry cut off wall is made by digging a vertical narrow trench as wide as 0.8 – 1.6 meter, through the permeable foundation materials (alluvial layer, colluvium layer, or strongly weathered rock layer). The excavation of the hole of slurry cut off trench is conducted until reaching the layer of the bedrock which is relatively impermeable. Then, the trench is filled with the suspension of bentonite slurry in the water during the process of excavation. If necessary, slurry is continuously added during the excavation in order to maintain the slurry stage to keep constant in the surroundings of the top of hole/trench. It is necessary to prevent the collapse of the hole/the slurry trench.

The foundation treatment using the cut off wall aims to reduce the permeability of passing through the layer of porous deposit and to increase the length of equipotential line of the seepage from the reservoir. In the earthfill dam type, the cut off walls which can be used are:

- a. Conventional concrete
- b. Cement- bentonite slurry
- c. Plastic concrete

For Tugu Dam, it is suggested to use the plastic concrete with a width of 80 or 160 cm. The maximum depth is 25-30 m and as long as 150 m (from Sta. 5 until Sta. 11).

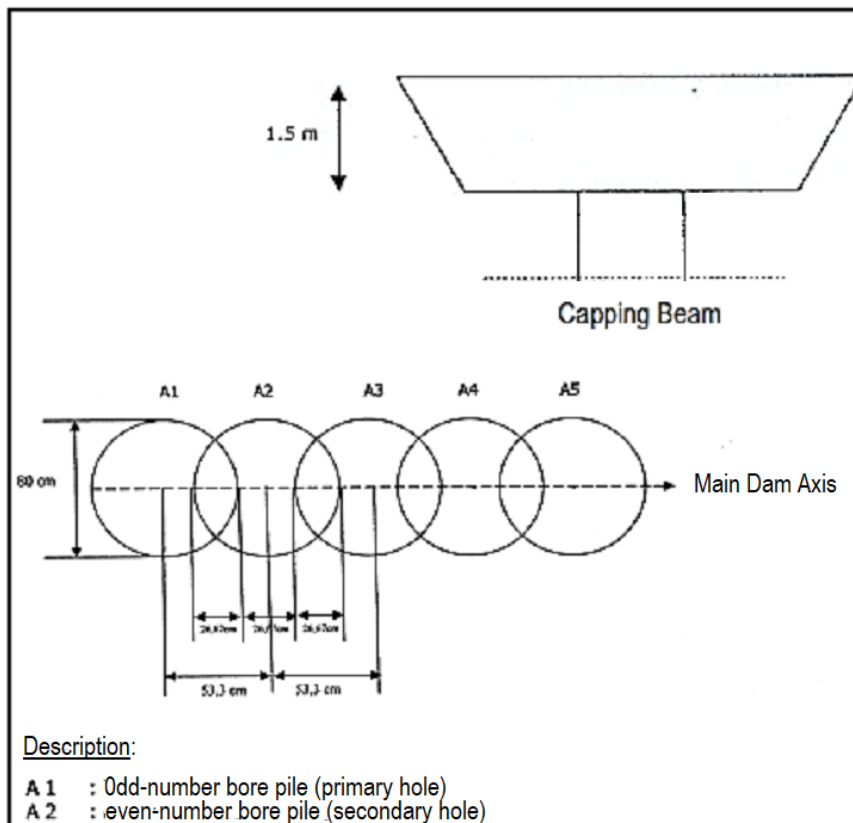


Figure 2. Lay Out of the Cut Off Wall with Bore Pile

3. TRIAL MIX OF PLASTIC CONCRETE

Trial mix of plastic concrete is necessary to be conducted in a laboratory using many varieties of material mix compositions. Several plastic concretes that are suggested are as follows:

Table 1. Trial Mix Composition of Plastic Concrete

Material	Unit	Trial Mix 1	Trial Mix 2	Trial Mix 3	Trial Mix 4	Trial Mix 5	Trial Mix 6
PC Type-1	Kg	185.0	143.6	143.6	185.0	185.0	185.0
Bentonite	Kg	100.0	22.30	36.6	100.0	100.0	100.0
Water	Liter	263.0	300.0	212.5	300.0	378.75	242.86
Coarse aggregate (coral)<2.5 cm	Kg	840.0	707.1	707.1	440.0	440.0	440.0
Fine aggregate (sand)	Kg	700.0	707.1	707.1	1,100.0	1,100.0	1,100.0

Table 2. Characteristics of Material for Diaphragm Wall (ICOLD Buletin 129, 2005)

Kind of Material	Strengt h (Mpa)	Permeabilit y K (m/dt)	Deformabilit y	Characteristi c of Crack	Composition
Tremie concrete	30-50	10^{-12}	Rigid	Fragile	Cement+aggregate slump 20 cm w/c = 0,5-0,7
Plastic Concrete	1,0-3,0	10^{-9}	High	Durable against strain till 10% without any crack	Cement+aggregate +clay+bentonite w/c = 0,5
Slurry cement/bentonite	0,1-1,0	10^{-8}	Very high	212.5	Cement+bentonite w/c = 0,5

Bentonite slurry is made of bentonite slurry mixed with Portland cement type I or type II. The main function of slurry is to maintain the cement still in the suspense form until the initial set up. Cement is added after the bentonite slurry reaches a full hydration. The mixing of bentonite and cement with water is not allowed. The comparison between cement and water will influence the strength, deformability and permeability.

The compositions suggested by ICOLD (1985) for the mix of bentonite slurry-cement per m³ are as follows:

- Cement: 80 up to 350 kg
- Bentonite: 30 up to 50 kg

According to *Xanthakos*, the percentages of the mix are as follows:

- Cement: 15-20%
- Bentonite: 2-4%
- Sand and gravel: 5-10%

The comparison between cement and water:

- For Portland cement, it is around 3.3:1 up to 5:1
- For cement of blast furnish cement (BLF) type, it is around 4:1 up to 10:1.

Cement has a bigger durability against the attack or the reaction of ground water that will dissolve the content of calcium carbonate within the cement. Then, each composition of the mix will be tested for the followings:

1. Compressive strength
2. Slump
3. Elasticity
4. Permeability

4. TRIALS OF CUT OFF WALL

The implementation of trial of the length and width dimensions, the amount of row of the bore pile, and the filed permeability test are necessary to be conducted first. They are necessary in order to know the effectiveness of the cut off wall.

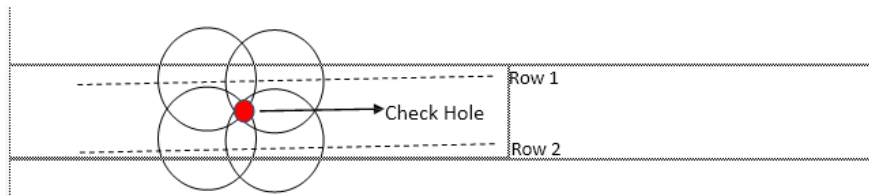
4.1. TRIAL 1

A cut off wall with a width of 80 cm is bored to make point A1 and point A2, then the points are filled with a selected trial mix. After that, the permeability is tested (check Hole) by being bored with rotary core drilling $\varnothing 76$ mm (dry drilling) and Lugeon test. The dry drilling is to prevent the occurrence of construction breakage of the plastic concrete. The coredrill test and Lugeon test are implemented in the overlap between two plastic concrete poles which have reached an age of 28 days. Pressure permeability test (packer test) uses the air packer as the screen. The water pressure is conducted using the pressure pump with a pressure variation of 1 kg/cm^2 up to 6 kg/cm^2 .

If the result of the Trial 1 is not successful in reducing the targeted permeability score of the foundation, Trial 2 is necessary.

4.2. TRIAL 2

A cut off wall with a width of 2 x 80 cm or two rows of upstream and downstream bore piles are filled with the selected trial mix. Then, the permeability test (check hole) is conducted with the above similar pressure.



5. CURTAIN GROUTING UNDER THE CUT OFF WALL

The height of the dam is around 80 meter from the excavation base, meanwhile, the height of the cut off wall is only a maximum of 30 meter. Therefore, an analysis of seepage under the foundation of the dam is necessary to be conducted again. If the result of the analysis shows that the seepage on the foundation under the cut off wall still occurs, the implementation of curtain grouting work is necessary to be considered. Its implementation is by using the rotary machine of $\varnothing 76$ mm in the middle part of the row of the cut off wall, by conducting a non coing drilling until penetrating the bedrock. After that, grouting cement is conducted in the part of the rock foundation, whereas, the hole on the cut off wall is plugged soon using the material of cement.

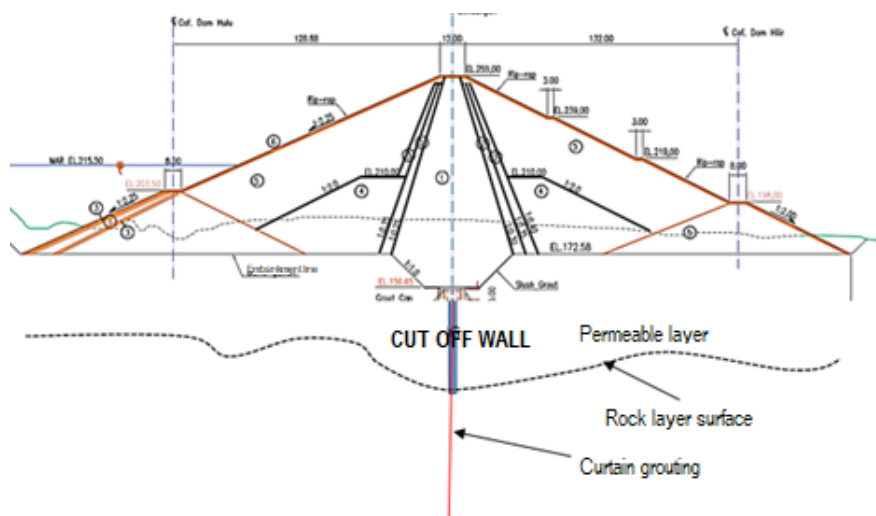


Figure 3. Curtain Grouting under the cut off wall

6. THE RELATION BETWEEN THE CUT OFF WALL AND THE CORE ZONE

For the cement-bentonite slurry cut off wall, a special attention must be paid on the connection between the cut off wall and the core in order that they are really joint. Although the decrease in the cement-bentonite is not too much after being hardened, but the compressibility will be different from the surrounding foundation materials. Therefore, an effort to prevent the occurrence of high-pressure concentration or low-pressure concentration is necessary. It is suggested to install a concrete slab above the rows of plastic concrete as wide as the area of the core zone foundation.

7. THE INSTALLATION OF INSTRUMENTS

The equipment of instrumentation is necessary for monitoring the condition of the foundation permeability. The suggested equipment are as follows:

- a. Inclinator and settlement gauge to monitor the deformation.
- b. Piezometer which is set beside the upstream and the downstream of the cut off wall in order to monitor the efficiency of the cut off wall.

8. THE IMPLEMENTATION OF THE CONSTRUCTION

In the implementation of slurry trenching, commonly, a construction of berm is necessary to be established, as the work surface level as well as for increasing the stability of the work area slope. The placement of berm in a certain elevation is by considering the difference of gap height and utilized as the work berm or the foothold in the implementation of bore pile and casting works.

The cement-bentonite slurry will be hardened in several hours. A retarder can be used to retard the hardening as well as to increase the workability of the slurry. Before giving an agreement on the use of a kind of retarder, a designer should examine first the possibility of the presence of adverse effects on the long-term performance of the wall.

This such type of cut off wall has a round form and is deep, therefore, a tight controlling is necessary on the verticality, besides, the deviation in horizontal direction should be given a maximum limit on the percentage amount from the depth.

The volume of cement-bentonite slurry will be decreased during the early set up due to the loss of water and dewatering. Therefore, it is necessary to implement an extra casting height for the reserve of the volume loss. The top

part of the cut off wall should be cut before implementing the concrete capping work or foundation concrete slab.

The excavation of cut off wall using the method of bore pile (hydraulic rotary drill) can be conducted continuously, by conducting a drilling in rotation with the primary hole series (odd-number bore pile) and then the holes are filled with cement-bentonite slurry and continued with the secondary hole bore pile (even-number bore pile).

REFERENCES

- [1] METTANA. Proposal of Foundation Treatment With Cut Off Wall in Tugu Dam, Indonesia 2016.
- [2] DIRECTORATE OF RIVER LAKE AND RESERVOIR. Guideline For Cut Off Wall In The Earthfill Dam. *Department of Public Works*, Indonesia 2005.

COMMISSION INTERNATIONALE DES GRANDS BARRAGES

VINGT-SIXIÈME CONGRÈS DES GRANDS BARRAGES
Autriche, juillet 2018

DOI 10.3217/978-3-85125-620-8-170



This work licensed under a Creative Commons Attribution 4.0 International License. <https://creativecommons.org/licenses/by-nc-nd/4.0/>

**STRENGTHENING AND SEALING OF GOMAL ZAM RCC ARCH-GRAVITY
DAM FOUNDATION IN PAKISTAN**

Eckhard SCHNÄCKER

LAHMEYER INTERNATIONAL GMBH, TRACTEBEL ENGINEERING

Chongjiang DU

LAHMEYER INTERNATIONAL GMBH, TRACTEBEL ENGINEERING

GERMANY

COMMISSION INTERNATIONALE
DES GRANDS BARRAGES

VINGT-SIXIEME CONGRES DES
GRANDS BARRAGES
Autriche, juillet 2018

STRENGTHENING AND SEALING OF GOMAL ZAM RCC ARCH-GRAVITY DAM FOUNDATION IN PAKISTAN

Eckhard SCHNÄCKER & Chongjiang DU

Lahmeyer International GmbH, TRACTEBEL ENGINEERING

GERMANY

1. INTRODUCTION

Gomal Zam Dam is situated at Khajuri Kach on Gomal River in South Waziristan Agency, Federally Administered Tribal Area, Pakistan. The dam's planned provision is to store water of rivers Gomal, Zhob and Wana Toi ensuring continuous water supply for irrigation and drinking purposes, flood control, and power generation.

The catchment area upstream of the dam site is 29,000 km². Thanks to the favourable topography of the wide-opening of Gomal Valley upstream of the dam, the 13.6-km long reservoir has a total storage capacity of approximately 1,100 mill. m³ and an active storage of 800 mill. m³ to irrigate an area of 66,000 ha of farmland. Moreover, the entire project area is located in an absolutely barren and desolate tribal area where there is no sign of habitation in need of compensation.

The main dam is an RCC arch-gravity structure of 133 m height from its low foundation level at El. 630.0 m and a crest length of 231 m with a crest width of 10 m at El. 763.0 m. The maximum width at base amounts to 78 m. A four-bay spillway of 17.5 m length is integrated in the central part of the dam, and a bottom outlet of 3.0 m in diameter with invert at El. 680.0 m is constructed to release sediment in front of the dam. Both sides of the dam are non-overflow dams. The power intake

is located in the non-overflow dam on right bank to feed power water into the powerhouse, 320 m downstream of the dam on right river bank.

The project was implemented and is owned by WAPDA. The construction work was previously commenced in July 2002 on turnkey basis under an EPC contract, but unfortunately halted in October 2004. In June 2007, the work was resumed and completed in 2012. The initial reservoir impounding started from March 2011.

2. GEOLOGICAL CONDITIONS

The strata in the region are sedimentary rock of neritic to continental facies of Jurassic to Tertiary age. During early Cretaceous, this region was locally uplifted. In Palaeocene or Eocene period, it underwent an overthrusting and inverting movement. Afterwards, in the process of orogenic movement, it suffered further deformation. The formation is strongly folded and fractured due to action of principle compressive stress trending approximately E – W: Consequently folds and major geological discontinuities are striking S - N or SSW – NNE.

The dam foundation consists exclusively of Jurassic limestone with minor intercalation of thinly bedded calcareous marls, marls and fine-sandy claystone/shale. The strata form a wide spanned anticline generally striking perpendicular to the valley dipping with 30° to 70° gently to steeply towards upstream. Obviously, repeated internal folding has caused distinct to heavy tectonization of the thinly to medium bedded limestone.

The limestone is intensely tectonized, fractured and intersected by major faults and shear zones. Traces of faults F2, F3 and F13 are daylighting close to the main dam (Fig. 1), F2 and F3 of which in the right abutment are slightly curved striking approximately parallel to the river stream with a dip of 87° and 80° towards the river. Fault F13, a transpressional fault is striking sub-perpendicular to the river course with an downstream dip of 60° to 80°. Apart from these major faults many other faults and shear zones of minor persistence exist.

The significance of karst is disputed since direct signs of karstification such as open channels or cavities are rare and basically limited to particular faults. However several indirect signs such as increased permeabilities (8 LU to 90 LU) exist. Packer tests in the limestone at the dam site yielded Lugeon values of 50 LU above river level in average with minimum and maximum values of 40 LU and 90 LU, respectively.

Another indication for a high rock mass permeability is the groundwater level. At the dam site the water table is more or less stable at EL. 607 m to 608 m with seasonal variations of 1 m to 3 m. This is 27 m to 28 m below the river level.

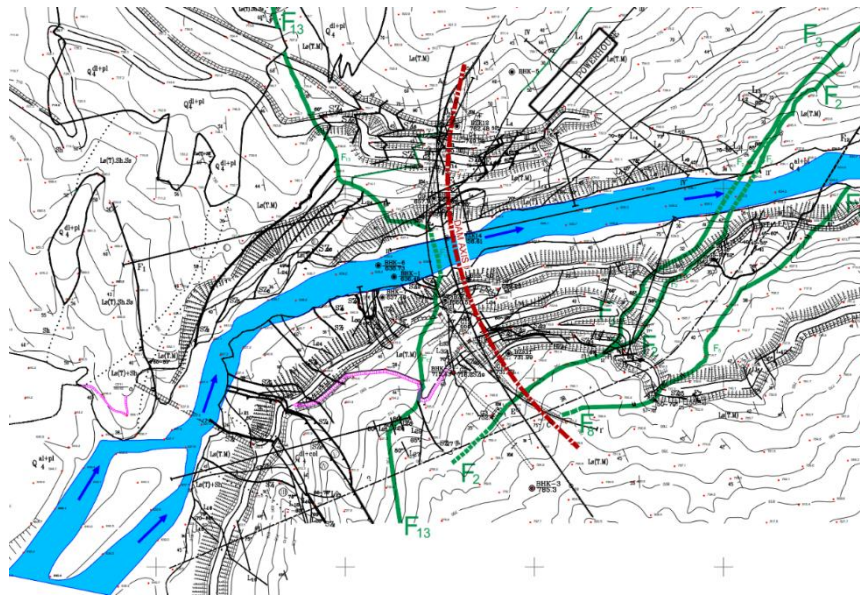


Fig. 1 Excerpt of the geological map at main dam site

3. SELECTION OF DAM AXIS AND TYPE

The river terrace in the confluence area of Khajuri Kach River to Gomal River is a broad unconfined valley with a vast basin. At its immediate downstream, the Gomal River is forced to pass through a narrow ravine named Khajuri gorge of 800 m length. From the topographical viewpoint, it is an ideal terrain to build a dam in the narrow valley which creates a gigantic reservoir for water storage.

At dam site the V-shaped gorge has a bottom width of approximately 25 to 40 m. The narrow canyon is slightly asymmetrical and has very steep flanks with an average slope of 75° and 65° for the left and right flank, respectively, while its upper flanks tend to slightly gentle with an average slope of 40° to 45° . The ratio of width to height of the dam is roughly -1.2:1. This topography is very favourable to an arch dam option. In fact, a double curvature arch dam of conventional concrete was proposed in feasibility studies [1].

Despite very promising conditions at first glance, aforementioned investigations revealed that the geological conditions and rock quality of the foundation leave much to be desired for a double curvature arch dam. The dam site itself lies in a deep gorge which cuts through a thick Jurassic limestone emerging among the shale. Probably through multiphase folding the limestone is intensely tectonized, fractured and intersected by major faults and shear zones, of which the faults F2, F3 and F13 have significant impact on the dam stability. The slightly curved F2 and F3 in the right abutment striking approximately parallel to the river stream with a dip of 87° and 80° towards the river are causing problems

for the dam stability. Fault F13 striking roughly perpendicular to the river course and dipping steeply downstream had to be considered for the selection of dam type and setting up dam axis, since a deep depression on the right bank downstream of the dam, is limiting the possible dam location in downstream direction. Under these conditions, the double curvature arch dam cannot avoid being located across the F13, and its foundation will intersect the fault in each abutment.

Numerical analyses demonstrated that excessive tensile stresses could occur in the double curvature arch dam and thrust act on foundation in an unfavourable direction, so that it would be difficult to obtain an acceptable design satisfying both criterion of stress and criterion of the thrust direction. Preferably, the dam should be completely located downstream of the fault trace. For these reasons, a curved RCC gravity dam with a downstream slope of 1V : 0.7H applying a constant radius over the entire length was proposed for the EPC tendering. This dam can be fully seated downstream of the F13 fault.

During tendering, the dam type was further studied by the EPC Contractor and found that the topography and geology at dam site lends itself to the introduction of two curvatures to the dam axis and reduction of the downstream slope to 1V : 0.6H. Thus, an RCC arch-gravity (also referred to as gravity-arch) dam was developed without crossing the F13 fault, and the stresses in the dam can be adjusted to an acceptable level. This option can combine the advantages of RCC construction with the appreciable reduction in volume of RCC associated with the arch-gravity design concept, which is well suited to the conditions at Gomal Zam site. After weighing the pros and cons of each option, the RCC arch-gravity dam has finally been selected for construction, as shown in Fig. 2.

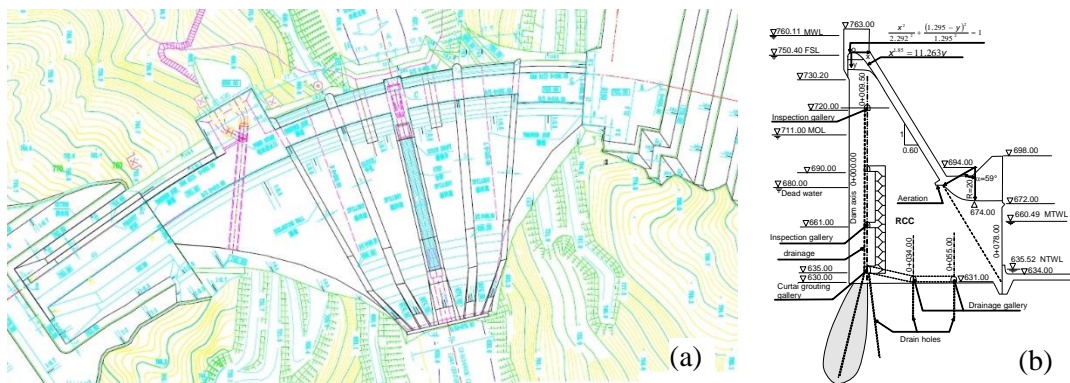


Fig. 2 (a) Layout and (b) cross section of Gomal Zam RCC arch-gravity dam

4. STRENGTHENING RIGHT ABUTMENT WITH CONCRETE SHEAR KEYS

As mentioned above, faults F2 and F3 in the right abutment may affect the stability of the right abutment against sliding. Geological investigation and excavation revealed that fault F2, striking almost parallel to the flow direction and dipping to the river bed at an angle of over 70°, cut through the whole right abutment. The faults have a width of 0.01 to 0.3 m locally up to 0.5 m, and an influence zone of 0.5 m locally 2.0 m thick. The faults have undulated face and are filled with greyish green, pale yellow, greyish black fault gauge, mylonite, breccia and calcite. The fill material is argillaceous cemented and squeezed firmly. The faults F2 and F3 cut the rock mass in the right abutment into prisms and wedges, jeopardizing the stability of the right abutment.

To improve the shear resistance of the faults F2 and F3 in right abutments, several measures were studied and found that the most desirable solution to secure and support the discontinuities is to use concrete shear keys. The shear keys (also named replacement adit) can effectively increase the shear strength of the faults. Furthermore, the seepage paths of groundwater along the faults can be cut off, and consequently, the infilling of the fault gauges is protected from deterioration [2]. Therefore, the stability of the dam and its foundation is ensured.

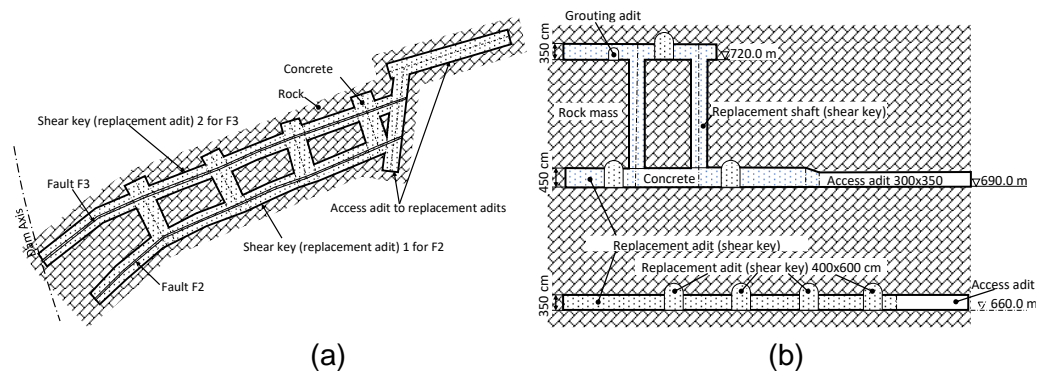


Fig. 3 (a) Layout at El.660.0 m and (b) vertical section at Fault 2 of shear keys

At Gomal Zam dam, the shear keys in form of tunnel and shaft plugs were implemented. In this system the tunnels and shafts were excavated along the faults F2 and F3, and transverse connection tunnels were excavated between F2 and F3, forming the sub-vertical spatial grids. Then the tunnels and shafts were backfilled with concrete of C16 grade. As schematically shown in Fig. 3, the shear keys were accomplished at three levels of El. 660.0, 690.0 and 720.0 m. Between the shear keys at 690.0 and 720.0 m, two vertical shaft shear keys were implemented. In the original design, the vertical shaft shear keys were planned to be extended down to El.660.0 m. After excavation and re-evaluation of the actual conditions of the two faults and re-analysis of the dam stability [3], the two vertical shaft shear keys were cancelled.

5. SEALING THE FOUNDATION

5.1. FOUNDATION GROUTING

The physical characteristics of the natural rock mass are notably insufficient both in regard of the rock mechanical properties of the foundation, as well as with respect to the permeability or water tightness of the sub-surface. Therefore, rock mass treatment with consolidation grouting and curtain grouting was considered necessary, in the early stage already. Contact grouting was performed not only in the lower parts of the dam foundation, but also on the steep abutment slopes to provide a proper bond of the dam concrete to the rock.

The consolidation grouting was generally implemented for the entire dam footprint with extending to the areas 5 m upstream and 10 m downstream beyond the footprint. The holes were drilled vertical in river channel area and inclined on the abutments with a spacing of 3.0 x 3.0 m. High pressure was applied in the consolidation grouting to improve the grouting effectiveness. The purposes were among others (i) to improve the mechanical properties of foundation rock; (ii) to enhance the integrity and reduce deformation and differential settlement of rock mass; and (iii) to strengthen the existing stress-relief rock mass and fill the fissures, cracks and voids/cavities so as to reduce the permeability and seepage of rock mass. After the consolidation grouting of the rock mass, the permeability shall not exceed 5 LU, and the sonic velocity shall be at least 4160 m/s in shallow part and 4250 m/s in deep part, respectively. The deformation modulus shall not be less than 6 GPa for the river channel area, 5 GPa for the lower parts of the abutments and 3 GPa for the upper part.

In the river channel area, the consolidation grouting followed placement of 1 m thick concrete as surcharge. The grout holes were 76 mm diameter in a depth of 20 to 25 m into rock. The method of descending stage grouting with 5 m each was employed. The pressure was limited to 0.8 MPa for the top 5 m at beginning, while it was gradually increased with the depth to 2.5 MPa. The heave monitoring was conducted during grouting of the first stage holes, and soon found that the 0.8 MPa pressure for the top 5 m was too high, causing heave and cracking of the surcharge concrete. Then, the grouting for the top 5 m was divided into two stages of 2 m and 3 m. The pressure was adjusted to 0.2 MPa for the upper 2 m stage and 0.5 MPa for the lower 3 m stage. Additional consolidation grouting was carried out as the surcharge concrete raised to 4.0 m thickness, by which the grouting criteria above were satisfied.

The consolidation grouting for the abutments and placement of RCC dam was alternately carried out. For an RCC lift of 3 m (10 layers), grout holes were firstly drilled into the abutment rock. The grouting was conducted for the stages below the top 5 m and the pressure was gradually increased with the depth to 3.0 MPa. For the top 5 m stage, a PVC pipe was installed at hole entrance and

lead up to the top of next RCC lift. After placement of the 3 m thick RCC lift, the top 5 m stage was grouted. Subsequently, the holes for the next 3 m lift were drilled. Although the consolidation grouting was conducted, the important lesson learnt from this procedure was that the drilling and grouting process of the 3 m high abutments needed at least 5 to 7 days, which forced the RCC placement for the 3m lift in a total 6 to 8 days or more, which considerably hold back the construction progress of the RCC dam. Moreover, grout was found to leak out of the rock surfaces during the grouting due to the high grouting pressure, which required immediately and effectively plugging or caulking.

The dam has a grouting/drainage gallery at El. 634.0 m near the dam heel and two control galleries at El. 675.0 and 720.0 m, respectively. Both sides of the galleries extended into rock in due lengths as grouting/drainage adits. On both sides of dam crest, the grouting/drainage adits were excavated. The galleries are accessible through a vertical stairway shaft in the middle pier of the dam, and from the downstream slopes. Two lines of grout curtains were implemented from the grouting/drainage gallery and adits. The main curtain grout holes are inclined arranged to the upstream with an angle of 5° to vertical in a spacing of 2.0 m, while the auxiliary curtain grout holes (also 2.0 m spacing) downstream of the main curtain are vertical. The hole depth is 74 m down into rock at dam bottom El. 634 m, decreased to 43 m at the crest level at El. 763.0 m. On downstream side of the grout curtains, a line of drainage holes of 110 mm diameter and 3.0 m spacing was drilled from the grouting/drainage gallery and adits inclined to downstream with an angle of 5° to vertical.

5.2. UPSTREAM BLANKET

The upstream cofferdam is a rock fill embankment of 41 m height and 82 m length at crest El. 676 m with an upstream sloping core, located at 85 m to the main dam axis. The cofferdam is 8 m wide at the top with 1V : 2.5H slope on upstream and 1V : 1.75H slope on the downstream surface. The thickness of the sloping clay core is 5 m at top and 17 m at bottom, protected by a layer of 0.4 m thick riprap and 0.6-m thick dry-stone pitching. Beneath the sloping core, a filter layer is placed which is inclined to upstream at an upper and lower slope of 1V : 1.7H and 1V : 1.5H, respectively. The cofferdam is seated on the rock foundation. Because the abutments are steep and the limestone rock mass is well developed in joints, fissures, the clay core is widened in the areas contiguous to the interfaces between the clay core and abutment flanks by 20% of its respective thickness at that level.

In order to additionally enhance the sealing effect of the dam foundation, the upstream cofferdam was utilized. The cofferdam was partially removed to a level below El. 670.0 m. After the space between the main dam and upstream cofferdam was filled and compacted with soil, an impervious blanket was placed on the filled soil from the upstream face of main dam extending to the sloping impervious clay

core of the upstream cofferdam. The impervious blanket is established with clay/weathered shale and compacted layer by layer. The thickness of each layer is limited to 0.3 m as maximum, and the total thickness is not less than 2 m. In the area in front of the dam face, the thickness is increased to 4.0 m or more. The impervious blanket was completed prior to the initial reservoir impounding.

6. SEEPAGE THROUGH FOUNDATION AND FROM RESERVOIR

After completion of the RCC dam construction, the sub-contractor started the initial reservoir impounding on 29th March, 2011. Reservoir filling ran smoothly until 19/20th April, 2011 and the successive days. However, when reaching the reservoir water level El. 689.50 m, a large amount of seepage water flowed out of the existing drainage holes at right abutment into the drainage gallery at El. 634.0 m. The discharge of seepage water exceeded the installed capacity of the 3 pumps of 133.2 l/s, so that the galleries were flooded. The water level in the galleries/vertical shaft reached to their maximum at El. 643.88 m, i.e. 9.88 m above the invert level of the grouting gallery.



Fig. 4: New springs upstream of the Bailey bridge

Some 200 m to 300 m upstream of the Bailey bridge several new springs occurred on the left bank shortly after initial reservoir impounding, others experienced a sudden and drastic increase in discharge (Fig. 4). Four of these springs were perennial with little discharge all over the year [5]. Seepage water is percolating through open joints and fissures of the limestone. The total run-off of these springs in June/July 2011 was estimated to range between 0.05 m³/s and

0.1 m³/s. At least two other leakage points (springs) in the vicinity of the Bailey bridge could be observed. The total discharge of all these springs was estimated to 1.2 m³/s.

Obviously, the quality and/or the dimensions of the grout curtain are responsible for the described seepage. Most likely, the seepage water bypasses the grout curtain vertically or laterally. The curtain might be either not deep, not long or not tight enough to prevent seepage. It could be even possible that seepage water directly passes the grout curtain through portions of increased permeability, using ungrouted open joints. The above statements basically concern the right bank.

At the left bank, the seepage paths may not even touch the actual grout curtain rather than be interrupted and stopped there. Reservoir water may seep into the limestone rock mass outcropping directly upstream of the dam. From there it may flow through joints and fissures, possibly also karst channels inside the rock mass following the general trend of the bedding. In the Bailey bridge area, some 2 km away, it eventually discharges at several springs.

With respect to the events happened during impounding, two potential problems exist. One of which pertains to the amount of seepage losses. The other is related to the forces exerted by the seepage. Loss of water through underground seepage may be of economic concern for the storage dam, but it will not adversely affect the safety of the dam at Gomal Zam. Main concern of the underground seepage is the stability of the dam and the downstream slopes.

The major purpose of the multiannual (carryover) storage reservoir is for irrigation. The average annual flow is 16 m³/s. If the seepage losses exceed 1.2 m³/s, or 7.5% of the natural flow, the losses are considered unacceptable. They may affect the irrigation of 66,000 ha of farmland.

7. ADDITIONAL SEALING MEASURES DURING RESERVOIR IMPOUNDING

In order to improve the existing grout curtain and to further reduce the permeability of the rock mass, additional grouting was carried out as immediate measure, by utilizing existing drainage holes in El. 634 m gallery. Aim of the grouting was to seal big seepage passages and to control the seepage flow into El. 634 m galleries in order to provide normal working conditions in the gallery. In the same time, this measure should enhance the thickness of the grout curtain and to improve its water tightness [6].

Since the permissible uplift pressure on the dam foundation behind the grout curtain is limited, the reactivation of the drainage system after completion of the

additional grouting works had to be done in a timely manner as not to jeopardize the stability of the dam.

In order to reduce the seepage flow through the abutments, the existing grout curtain was extended and/or deepened at both river banks as shown in Fig. 5.

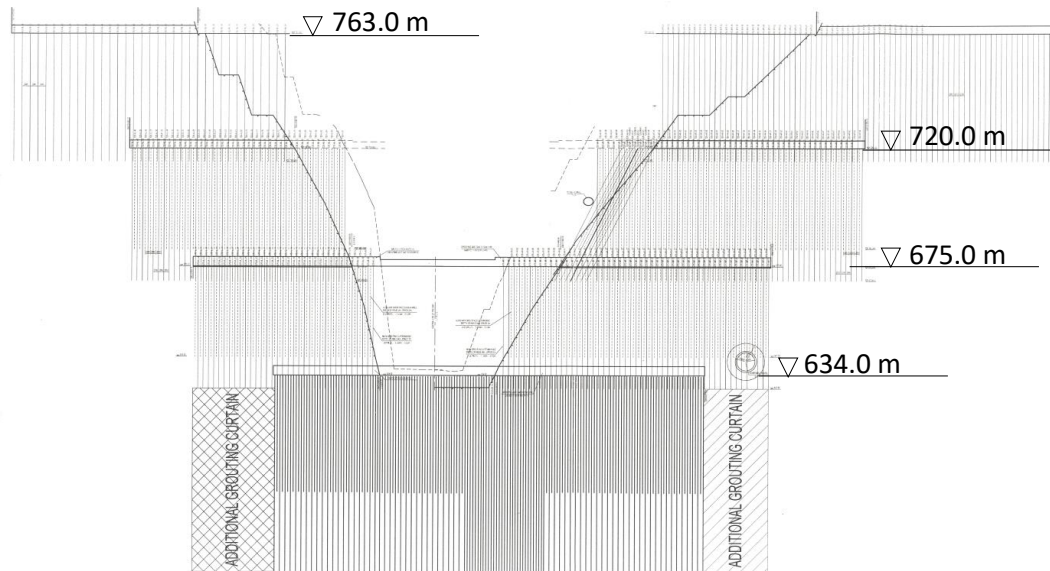


Fig. 5: Grout curtain along the main dam axis after extension

The initial gap between the right end of the EL. 675 m gallery and the right end of the EL. 634 m gallery was closed down to EL. 560 m, similar to the curtain depth below EL. 634 m gallery. Initially the grout curtain drilled from the EL. 675 m gallery ended at EL. 629 m (primary holes) or EL. 641 m (secondary holes), respectively. Accordingly, in order to reduce seepage bypassing the left abutment, additional grouting from EL. 675 m grouting adit down to EL 560 m was carried out in left abutment.

The extension of the grout curtain consisting of a single row of grouting holes was drilled from EL. 675 m gallery. Space-splitting method was applied with a spacing of 8 m for primary holes, 4 m for secondary holes and 2 m for tertiary holes. Quality control criterion for the grout curtain was a Lugeon value of 5 LU [6].

8. REMAINING PROBLEMS AND FURTHER RECOMMENDATIONS

The above described sealing measures did not sufficiently solve the seepage problems inside the gallery on the right bank. Further extension of the grout curtain was carried out after completion of impounding. Details of the additional extension neither laterally nor vertically are known to us.

However, seepage on the left bank being in the order of 0.8 m³/s to 1.0 m³/s did not change considerably. These losses still constitute 5% to 6% of the mean natural discharge of the Gomal River. However, there appears to be a tendency of decreasing seepage discharge on the left bank downstream of the main dam.

Obviously, the measures taken so far are not sufficient to completely reduce the seepage to an acceptable level. Additional measures are required which could be as follows:

On either side of the Gomal River the permeable limestone complex striking sub-parallel to the dam axis is confined by impervious shales cropping out some 200 m upstream of the dam at the left bank. At the right bank the continuation of the shales upstream of the dam exists also. The exact distance between the dam axis and the impervious shales at the right bank is not known, but it could be in the range of 500 m. A detailed geological map of the upstream region showing the outcrops of shale unit up to El. 750 m does not exist.

The main dam together with the grout curtain is built on limestone striking sub-parallel to the dam axis at the footwall of the shales. A possible way to sealing both abutments could be to extend the grout curtain towards the impervious shales on either side:

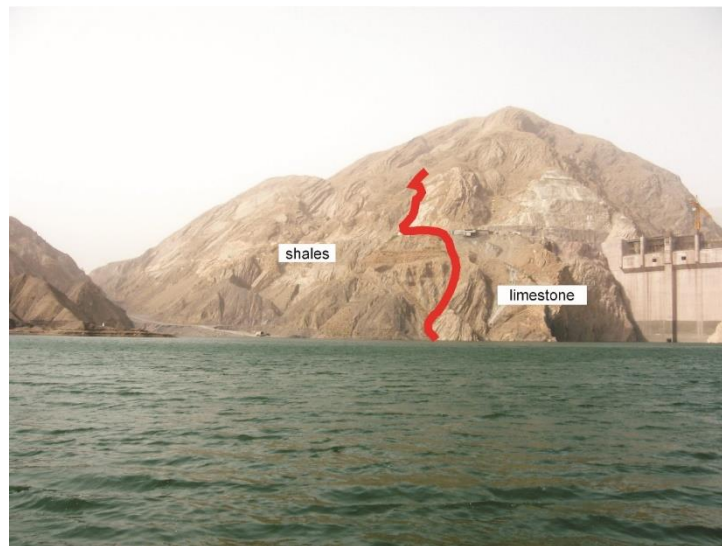


Fig. 6: Exposures of limestone and shales at the left bank of the main dam

Left Bank: The grout curtain of the dam in the left abutment may be extended towards to the impervious shales situated some 200 m upstream of the dam axis (Fig. 6); it has to be studied in details if the thickness of the confining unit is sufficient and if the shales reach up to El. 760 m.

Right Bank: The right bank extension of the deep grout curtain towards the confining shales upstream of the dam axis is unknown. A rough field inspection

indicated the distance between the dam axis and the shale unit to be in an order of 300 m to 500 m.

A more detailed field study and geological map is strongly recommended. The existing geological map is covering the immediate area of the main dam. It has to be extended on both banks to include the distribution of the shales

9. CONCLUDING REMARKS

Already in the early stage of investigations and construction, and later on in the second construction phase when the work was resumed in June 2007, the Consultant has repeatedly expressed his serious concerns regarding the unfavourable engineering geological conditions, and emphasized the need for additional investigation and an appropriate design. This was concerning the possible adverse effect of the faults F2, F3 and F13, as well as potential seepage problems due to the increased rock mass permeability regardless if it were caused by karst or mere tectonization.

The EPC contractor was reluctant to comply with the comments of the consultants. As far as the main dam and the appurtenant structures are concerned necessary measures have been successfully undertaken to ensure the general stability, i.e. concrete shear keys in alignment of fault F2 and F3, consolidation grouting, deep grout curtain and drainage curtain.

The seepage problem visible at the left bank downstream of the main dam involving losses between 5% and 7.5% of the mean natural discharge of the Gomal River has not been solved sufficiently until now. For contractual reasons the EPC contractor could not be persuaded to carry out appropriate sealing measures.

REFERENCES

- [1] DU C.J. Structural features of Gomal Zam RCC arch-gravity dam. *Proceedings of the 6th International Symposium on Roller Compacted Concrete (RCC) Dams*, 23-25 October 2012, Zaragoza, Spain, Paper No. C008
- [2] DU C.J. Concrete shear keys for the foundation treatment of gravity dams. *International Journal on Hydropower and Dams*, 1997, Issue 3, pw.95-99
- [3] PENG X.C. & LIU Z.Y. Abutment stability analysis of Gomal Zam arch-gravity dam in Pakistan (in Chinese). *Design of Water Resources & Hydroelectric Engineering*, 2014, No.3, p.44-45

- [4] LIU Z. Treatments of cracks in surcharge concrete of consolidation grouting for foundation rock of Gomal Zam RCC dam (in Chinese). *Technology Outlook*, 2016, No.10, pp.38
- [5] ZHANG Z. & LUO F. Causes of „Hanging River” at Gomal Zam Dam Project (in Chinese). *Journal of Tianjin City Construction College*, No. 4, 2004
- [6] SINOHYDRO CORPORATION. Technical Measure for Treatment of GZDP Reservoir Seepage. *Unpublished report WAPDA/F.W.C.*, 2011, pp. 8

SUMMARY

Gomal Zam Dam, a multipurpose project in Pakistan, planned for irrigation and drinking water storage, flood control and power generation is an RCC arch-gravity structure of 133 m height, 231 m length, and 10 m top width. The dam foundation consists exclusively of limestone with minor intercalation of various marls. Due to repeated internal folding, the strata underwent distinct to heavy tectonization causing loosening of the rock mass and very high permeability. Major faults in the right abutment striking sub-parallel to the river, as well as the loosening of the highly tectonized limestone belong to the main engineering geological features jeopardizing the dam stability. Furthermore, the high permeability of rock mass with Lugeon values between 8 LU to 90 LU is causing considerable seepage problems through the foundation.

Treatment of the faults in the right abutment comprise the implementation of concrete shear keys with concrete filled shafts and tunnels at several levels. In order to improve and strengthen the jointed rock foundation, deep-extended consolidation grouting with high pressure was carried out over the entire footprint area. To seal the foundation and to prevent considerable seepage beneath the dam, a clay blanket was placed between the upstream face of the main dam towards the clay core of the upstream rock fill cofferdam. Last but not least a deep grout curtain starting from grouting galleries and adits was implemented.

Initial reservoir impounding started in March 2011. Shortly after commencement of impounding significant seepage into the lowest grouting gallery, as well as some 2 km downstream of the dam occurred. Mitigation measures regarding seepage into galleries included immediate grouting of existing drainage holes, reactivation of the drainage system in order not to jeopardize the stability of the dam and lateral extension of the deep grout curtain.

The Gomal Zam RCC arch-gravity dam was completed in 2012. Problems regarding the dam stability appear to be solved. Seepage downstream of the dam in the order of 5% to 7.5% of the natural discharge could not be reduced considerably.

Keywords: geological investigation, foundation treatment, reservoir watertightness, seepage, sealing work, grouting, upstream blanket

RÉSUMÉ

Le barrage de Gomal Zam, un projet polyvalent au Pakistan, prévu pour l'irrigation et le stockage de l'eau potable, le contrôle des inondations et la production d'électricité est un barrage-poids voute incurvé du type béton compacté au rouleau (BCR) de 133 m de hauteur, 231 m de longueur et 10 m de largeur en crête. Le barrage est uniquement fondé sur le calcaire avec intercalation mineure des marnes différentes. En raison du repliement interne répété, les strates ont subi une tectonisation distincte à forte, provoquant un ameublissement considérable du massif rocheux et une perméabilité très élevée. Des failles principales de l'appui rive droite, qui courent sub-parallèlement à la rivière, ainsi que la décompression du calcaire fortement tectonisé appartiennent aux principales éléments géologiques mettant en péril la stabilité du barrage. De plus, la forte perméabilité du massif rocheux avec des valeurs Lugeon comprises entre 8 LU et 90 LU provoque des problèmes d'infiltration considérables à travers la fondation.

Le traitement des failles dans l'appui rive droit comprenait la construction des clavettes de cisaillement en béton à plusieurs niveaux avec des puits et tunnels remplies de béton. Afin d'améliorer et de renforcer la fondation rocheuse, des injections de consolidation profonds à haute pression ont été réalisées sur toute la fondation de l'ouvrage. Pour améliorer l'étanchéité de la fondation et pour prévenir des pertes d'eau considérables sous le barrage, une couverture d'argile a été placée entre le parement amont du barrage vers le noyau d'argile du batardeau en enrochement amont. Enfin, un rideau d'étanchéité profond a été réalisé depuis quatre niveaux de galeries d'injection.

La mise en eau initiale du réservoir a débuté en mars 2011. Peu de temps après le début de la mise en eau dans la galerie de drainage la plus basse, ainsi que quelque 2 km en aval du barrage, de fortes fuites d'eau se sont produites. Les mesures immédiates pour contenir l'infiltration dans les tunnels comprenaient des injections de trous de drainage existants, puis la réactivation du système de drainage pour ne pas compromettre la stabilité du barrage, et enfin, l'extension latérale du rideau d'injections profond.

Le barrage Gomal Zam BCR a été achevé en 2012. Les problèmes d'infiltration concernant la stabilité du barrage ont été résolus. Cependant, les fuites d'eau en aval du barrage de l'ordre de 5% à 7,5% du débit naturel n'ont pas pu être significativement réduites.

COMMISSION INTERNATIONALE DES GRANDS BARRAGES

VINGT-SIXIÈME CONGRÈS DES GRANDS BARRAGES
Autriche, juillet 2018

DOI 10.3217/978-3-85125-620-8-171



This work licensed under a Creative Commons Attribution 4.0 International License. <https://creativecommons.org/licenses/by-nc-nd/4.0/>

**CASE HISTORIES OF TAILINGS DAM WATERPROOFED WITH A
BITUMINOUS GEOMEMBRANE (BGM)**

Bertrand BREUL

Civil Engineering Manager, COMPANY AXTER SAS, PARIS

FRANCE

Jacques MOEGLÉN

*Export Manager for Central, Northern, Eastern Europe, CIS
and Central Asia, COMPANY AXTER SAS, PARIS*

FRANCE

COMMISSION INTERNATIONALE
DES GRANDS BARRAGES

VINGT-SIXIÈME CONGRÈS DES
GRANDS BARRAGES
Autriche, juillet 2018

CASE HISTORIES OF TAILINGS DAM WATERPROOFED WITH A BITUMINOUS GEOMEMBRANE (BGM)

Bertrand Breul, Jacques Moeglen***

**Civil Engineering Manager, company Axter SAS, Paris*

FRANCE

***Export Manager for Central, Northern, Eastern Europe, CIS
and Central Asia, company Axter SAS, Paris*

FRANCE

1. INTRODUCTION

Bitumen emerged as a standard 20th century waterproofing material in civil and water engineering in the form of bituminous concrete, asphalt, and bituminous geomembrane.

For obtaining permission of opening a mine, a very stringent plan is asked by the authorities for containing pollution on site and to be sure that no pollution could impact very remote location in altitude or great North under polar circle.

2. GENERAL PRESENTATION OF BGM

The first applications of BGM were in France in 1975 near Grenoble and for potable water storage reservoirs in altitude around 2000 m in the Alps in Avoriaz.

The structure of BGM is multi-layered including mainly: a polyester geotextile providing the mechanical resistance and especially the high puncture resistance

- Highest mass per unit area giving an important resistance to lifting in windy regions. We can leave the BGM exposed (large economy) and we can install even under bad weather and very windy conditions.
- High puncture resistance. Tire-mounted vehicles and equipment even full loaded can run directly on top of the geomembrane traverse on top of the geomembrane during installation and maintenance. See Fig. 3.



Fig. 3. Tire mounted equipment traffic on top of the BGM

- BGM does not form wrinkles even in case of daily temperature variations. So, installation can take place at any time of the day, without interruption. Also, cover material can be placed on top of the geomembrane at any time of the day.
- The sand surfacing imparts a frictional surface to the geomembrane that reinforces the UV resistance of the bitumen. This face has a friction angle around 34° (values coming from tests "Geosynthetic Friction by the Direct Shear Method ASTM D5321-02" done by Sageos (Qc, Canada) and INSA (Lyon, Fr) and Precision lab (Anaheim, California, USA) daughter company of the US TRI lab and higher, depending of the material placed above it. Based on the above, designers can use slopes steeper than 2H: 1V at the upstream face of a dam or the banks of reservoir.
- BGM can store potable water. Proved by US international certificate NSF 61.
- BGM has a very high resistance to earthquake as demonstrated in the field (Milpo dam having supported an earthquake of a magnitude of 8.1 on the Richter scale and by tests done by TRI. in California for Los Angeles Department Water and Power Interface Friction Testing.
- The density is larger than 1 ton/m^3 , so BGM can be installed under water. The seams under water can be done with a special mastic.
- The manufacturer supplies monitors for training local teams of installers on site.
- The quality of the total length of the seams can be controlled by manual or automatic ultra-sounds apparatus control. Which is recommended for control of the dam watertightness. See Fig. 4.



Fig. 4. Ultrasound equipment to test BGM welds

3. SOME CASE STUDY OF BGM IN HYDRAULIC CONSTRUCTION

In the cases mentioned here-under, all being in altitude (between 1.200 m and 4.800 m), BGM was chosen for one or some of the following reasons:

- High resistance to U.V.
- High resistance to puncturing (geotextile inside geomembrane) so, avoiding protection by geotextile underneath and above. In altitude as you have high speed wind with BGM there are only 1 geosynthetic to install at the place of 3 for thinner geomembrane.
- Highest unit mass means that you can install by wind more than 50 km/hour, with humidity therefore under some rain. Like this you can shorten significantly delays.
- Low cost of installation by local workforces as the manufacturer assumes the training of the installation personnel and you don't need special equipment for welding: only torch and bottles of propane gas.

3.1. In South America

3.1.1. Peru, Milpo tailings dam: a 30-m high earth and rock fill tailings dam in Cerro Lindo (See Fig. 5) to store polluted water.

Milpo is a Peruvian mining company headquartered in Lima. At the Cerro Lindo mine, a 30-m high, earth and rockfill dam was built to store and control process water. The dam was built on a competent substratum reached through shallow excavations in natural soil. It is located at an altitude of approximately 2.000 m. in a region characterized by strong winds. This upstream face of the dam was waterproofed by means of a BGM. The upstream portion of the dam was built with compacted soil consisting of gravelly clay with a 1V/2H face slope. In the middle of the dam, a transition layer of 2 m wide and runs from the bottom to the crest of the dam. At the downstream toe, an infiltration-water collection box and monitoring wells were installed to allow a permanent control of watertightness.



Fig. 5. Cerro Lindo dam:

a) Typical cross section

b) Work completed

c) Dam in use after earthquake

3.1.2. Toromocho Copper Mine (Fig. 6), owned by the Chinese mining company Chinalco), lies at an altitude of around 4.600 m above mean sea level. Water was used throughout the production chain of the mine. The creation of the dam was used to contain water pollution. The water is then recycled.



Fig. 6. Toromocho Copper Mine

The choice of this BGM was done mainly as the installation could be done by local workers able to work at this altitude. They received locally a training by supplier monitor. The work was controlled permanently by the Lima subsidiary of the International consultant firm Amec.

The second reason of the choice was as the installation is possible in extreme weather conditions (rainfall, heavy wind at this altitude (BGM is the heaviest geomembrane per sqm (square meter), quick alternative of temperature during the day).

The third reason was because the membrane will be left exposed. BGM has the best resistance to UV due to the nature of bituminous and the protection by sand of the exposed face see test C.N.A.M – Centre des Arts et Metiers – National Testing Laboratories TEST No: 704-080-DMS/15.107.

3.1.3. In the copper mine Las Bambas, Chuspiri Dam, property of the Chinese company MMG, situated in more than 4.000 m of altitude between the provinces of Cotabambas and Grau, in Apurímac region, to 72 km of Cusco in Peru, Chuspiri Dam was built for the supply of water of the mine. See Fig. 7.

The project was developed by the MWH Engineering of Santiago, Chile. A geomembrane BGM of 4.0 mm of a unit mass of 4,85 kg/m² and of 4,8 mm and of a unit mass of 5,8 kg/m².



Fig. 7. Chuspiri dam:

a) Site overview

b) Start of filling

3.2. In North America

3.2.1 Diavik Diamond Mine (Fig. 8)

The Diavik Diamond Mine is located at 300 kilometres northeast of Yellowknife, Northwest Territories of Canada on an island in the lake of Gras (water the purest in the world). DDMI is the operator of the project. DDMI is a wholly owned subsidiary of Rio Tinto, which is headquartered in London, England.

The choice of BGM was done due the extended period (10 months per year) when it was able to install BGM. January and February were excluded due to very low temperature met (-70°C).

On the same site, they would have been able to install only 4 or maximum 5 months per year.

Installation was completed by a local company based in Yellowknife, NWT, specializing in geomembrane installation in cold weather conditions. A & A retains the flexibility of BGM even when stored and unrolled at -40°C. No special precautions such as inside tunnels were required during welding, which was performed in the open air at -25°C and less till - 35°C.

The manufacturer monitor's presence was required by the international consultant (Golder Associates on their Vancouver and Yellowknife Canadian subsidiaries) to train A & A Technical employees (Native people: Inuit) and ensure that the installation work was done properly.

The second reason of the choice of BGM was the economy induced by the high puncture resistance by BGM comparing with HDPE. Initially, the design specified a 50-mm minus geomembrane bedding and cover material. Tests carried out on site showed that a 150-mm minus material could be used for bedding and cover without damage to the geomembrane. The 150-mm minus bedding material was compacted then the surface was raked by hand to remove the larger particles protruding above the surface. Cover material was dumped along the toe and pushed by a track loader approximately two-thirds up the slope. Cover material was then dumped along the crest and pushed by a track loader, down the slope over the geomembrane.

The use of relatively coarse bedding, cover materials and cushion materials (the cost for producing material on the site was very high) as well as the elimination of the need for a protective geotextile.



Fig. 8. Diavik grain size of the support and the cover

3.2.2 Bloom Lake, Iron Mine (Fig. 9)

Bloom Lake's mine is located approximately 9 miles southwest of Fermont, Quebec, Canada, being part of the southwest corner of the Trough Labrador iron mine.

Operations consist of an open pit mine comprising of a truck and shovel transportation system. A concentrator that utilizes single-stage crushing, an autogenously grinding mill and gravity separator is used to produce an iron concentrate. From the site, concentrate is transported by rail to a ship loading port in Pointe Noire, Quebec, Canada.

This BGM geomembrane was chosen due to:

- Excellent weathering resistance even when exposed.
- Installation in extreme weather conditions (rainfall, wind, cold temperature down -40°C).
- A wider range of materials to be used for the liner bedding and cover zones due to its high resistance to puncture and tearing.
- Installation by local installer after training by manufacturer monitor on site.



Fig. 9. Bloom Lake, anchorage at the toe of the dam

3.3. In Europe, in Finland and in Russia

3.3.1 Kiitilä Gold Mine (Finland) – Fig. 10

Construction is well underway on the Kiitilä mine in northern Finland, approximately 900 kilometres north of Helsinki and 40 kilometres from Kiitilä. The Kiitilä mine will feed 3,000 tons per day surface processing plant.

The Kiitilä Mine site lies within the Arctic Climatic Region (150 km north). Temperatures are cool with an average mean monthly temperature in July of 15°C and in January of -15°C. The mean annual air temperature at the site is approximately 0 °C. Snow falls in every winter month, although rain generally only occurs between May and October.



Fig. 10. Kiitilä site: general view

Dam walls are made from blasted rock with compound structure. This means that the main dam wall is made from maximum 600 mm diameter grain size blasted rock. The “wet” sides of the dam walls are made also from blasted rock (dam max. 300 mm grain size) and gravel (grain size 55 mm).

These layers are also compacted with an excavator equipped with a compacting plate.

BGM was chosen because:

- It can be installed directly over the prepared mineral sealing bottom layer instead of a layer of sand, and then geotextile and finally a polymeric liner. This provided a large cost saving because you don't have to transport materials from outside the site and in the same time, you save many tons of CO₂.
- The low thermal expansion coefficient allows keeping the liner flattened directly on the mineral sealing layer like this, the combination of both moraine and BGM liner is always flat and in permanent contact of the glacial till support so, due to this intimate contact, the watertightness is assumed at 2 levels:
 - At the level of the geomembrane with a permeability of around 10⁻¹⁴ m/sec, that could be considered as an active barrier,

- At the level of the soil around 10^{-5} m/sec that could be considered as a passive barrier.
- It can be installed at very low temperatures such as -30°C for the elastomeric grade of the BGM Liner.

3.3.1 Kupol Gold Mine (Siberia, Russia) – Fig. 11.

The Kupol deposit is in the Chukotka Autonomous Okrug. The total distance between the Kupol and Bilibino the nearest major city, is approximately 200 kilometres.

The climate of the region around the Kupol site is extremely severe, consisting of long and cold winters (8-8.5 months). The average annual temperature is -13°C , ranging from -58°C to 13°C .

BGM in this project has promoted the ease to be installed and welded in extreme weather conditions (rainfall, wind, cold temperatures down to -40°C) permitting to earn more than 1 year in the delay means 1 year of production of gold and the use of wider range of rough materials for the liner bedding and cover zones.



Fig. 11. Kupol Gold Mine (Siberia, Russia)

4. CONCLUSION

The BGM has been used successfully for over 35 years in hydraulics and in protection of Environment. BGM possesses high physical and mechanical properties allowing it to remain exposed and accept a support rougher than with any other type of geomembrane without any external geotextile for protecting it. Subgrade preparation for this liner is reduced to the minimum and the defect rate is low. This leads to wide savings of transport of materials coming from outside the construction site or to reduce the times of crushing thus to a reduction of the environmental impact of construction works.

Its installation is straightforward using propane torch welding and its high unit weight allows it to be installed in rough weather conditions with local installer trained by manufacturer's monitor on site.

These other BGM installations were done at the satisfaction of international consultants (Golder Associates Lima, Vancouver and Yellowknife (NWT, Canada)) and the clients public client, Canadian Government, or private mine companies: Milpo in Peru, Rio Tinto in UK, Agnico-Eagle and Kinross from Canada on time and without any delay due to bad weather or strong winds either in altitude (4800m) or in very cold region, even inside polar circle.

At last, we would highlight that despite the large earthquake at the Cerro Lindo mine, the BGM maintained its core function of waterproofing and there were no defects of seepage because of this. The BGM has maintained the reservoir in the dam at full capacity for the past ten years and there has been no loss of activity at the mine due to seepage.

Furthermore, The City of Los Angeles Department of Water and Power (LADWP) was building two large concrete water reservoirs in Universal City, Los Angeles, California. Each reservoir is designed to hold over 210.000 m³ of fresh water.

LADWP determined that the on-site soils beneath the east reservoir were only medium dense and could if saturated be subject to liquefaction during a strong earthquake and could settle a few inches. An order of magnitude that could lead to structural damage to the concrete reservoir and affect its integrity to remediate the liquefaction potential, LADWP engaged a remediation and mitigation program full seismic phenomenon.

The Precision lab (Anaheim, California, USA) conclusions/ BGM is not affected by the seismic induced shearing and will not be overstressed during a seismic event as the interface friction angle between the soils and the interfaces are in the same value of magnitude, the risk of slippage of the confined BGM is very low.

Installation is much less dependent on weather conditions. Due to the extended construction season of BGM, the completion of the geomembrane portion can be done in half the time of a HDPE solution. The reduced construction period means that the equipment used for the reservoir can be used earlier in mine construction. For investors, this could have the mine operation up and running much sooner, and the financial impact could be huge in mine activity.

5. REFERENCES

GIRARD, H., FISCHER, S., ALONSO, E., 1990, Problems of friction posed using geomembranes on dam slopes – Examples and measurements, *Geotextiles and Geomembranes*, 9, p. 129-143, England, Elsevier.

ICOLD / CIGB, 1991, Watertight geomembranes for dams -State of the art / Etanchéité des barrages par géomembranes - Technique actuelle, *Bulletin technique CIGB*, n° 78, Paris, 140 p. (actualisation en cours).

ROLLIN, A., PIERSON, P., LAMBERT, S., 2002, *Géomembranes, Guide de choix*, Presses Internationales Polytechnique, Montréal, Commercialisation pour la France: Tec & Doc Lavoisier, 312 p.

BLOND, E., *Analysis Report CNN FILE NO.: S549-004-6A*

BREUL, Bt., BREUL, B., 2013, 'Upstream Watertightness of Two Backfill Dams Built in France', ICOLD, *ICOLD 2013 International Symposium*, Seattle (USA)

ASTM D 1557, Standard Test Methods for Laboratory Compaction Characteristics of Soil Using Modified Effort (56,000 ft-lb/ft³ (2,700 kN-m/m³), *American Society for Testing and Materials*, West Conshohocken, Pennsylvania, USA.

CALIFORNIA DEPARTMENT OF TRANSPORTATION (2006), Standard Specifications, State of California, Department of Transportation, Sacramento, California.

BGM (2008), DESIGN AND APPLICATION HANDBOOK FOR BITUMINOUS GEOMEMBRANE.

HUDSON, MARTIN B., CRAIG A. DAVIS, MARSHALL LEW, ALEK HAROUNIAN, AND LIPING YAN (2012), "Seismic Resilient Design of a Concrete Box Reservoir," Proceedings of the 6th China-Japan-United States Symposium on Lifeline Earthquake Engineering, ASCE Technical Council on Lifeline Earthquake Engineering, Chengdu, Sichuan, China.

Koerner, R.M. (1990), *Designing with Geosynthetics*, 2nd ed., Prentice-Hall Inc., Englewood Cliffs, NJ, USA.

LEW, M; PONNABOYINA, H.; DAVIS, C.A.; AND PEREZ, A. (2013). "Interface Friction Testing Between Soil and a Bituminous Geomembrane", Proceedings of Geosynthetics 2013, Long Beach, CA, April 1-4.

COMMISSION INTERNATIONALE DES GRANDS BARRAGES

VINGT-SIXIÈME CONGRÈS DES GRANDS BARRAGES
Autriche, juillet 2018

DOI 10.3217/978-3-85125-620-8-172



This work licensed under a Creative Commons Attribution 4.0 International License. <https://creativecommons.org/licenses/by-nc-nd/4.0/>

**SEALING PERFORMANCE OF SILVEH EMBANKMENT DAM CUTOFF WALL
BASED ON INSTRUMENTATION MEASUREMENTS**

F. JAFARZADEH

Associate Professor, SHARIF UNIVERSITY OF TECHNOLOGY

IRAN

A. AKBARI GARAKANI

Assistant Professor, NIROO RESEARCH INSTITUTE

IRAN

J. MALEKI

Dam Engineer, ABGEER CONSULTING ENGINEERS CO.

IRAN

M. BANIKHEIR

Dam Engineer, ABGEER CONSULTING ENGINEERS CO.

IRAN

R. RAEESI

Dam Engineer, ABGEER CONSULTING ENGINEERS CO.

IRAN

COMMISSION INTERNATIONALE
DES GRANDS BARRAGES

VINGT-SIXIÈME CONGRÈS DES
GRANDS BARRAGES
Autriche, juillet 2018

SEALING PERFORMANCE OF SILVEH EMBANKMENT DAM CUTOFF WALL BASED ON INSTRUMENTATION MEASUREMENTS

F. JAFARZADEH

Associate Professor, SHARIF UNIVERSITY OF TECHNOLOGY

IRAN

A. AKBARI GARAKANI

Assistant Professor, NIROO RESEARCH INSTITUTE

IRAN

J. MALEKI, M. BANIKHEIR AND R. RAEESI

Dam Engineer, ABGEER CONSULTING ENGINEERS CO.

IRAN

1. INTRODUCTION

Controlling, measurement and estimation of the amount of water seepage through the body, foundation and abutments of embankment dams are of great importance [1]. Seepage in earth dams, according to their location, has two parts: seepage through dam body and through dam foundation. Using clay core, filters, and drains are the most common method for controlling the seepage through the earth dam body. To control the seepage through the dam foundation, there are several methods such as using permeation grouting, drainage under some parts of the dam, impervious blanket, and cut-off wall [2, 3, and 4].

Cut-off walls, in general, are constructed beneath the earth's surface to control horizontal flow of groundwater and contaminants. In cut-off wall construction in earth dam foundations, alluvium foundation materials will be removed and the gap will be refilled by good filler material such as drilling mud, rigid concrete or plastic concrete. Most commonly, cut-off walls are vertical and ideally penetrate down to a very low-permeable stratum, a clay or impervious bedrock, which forms a well-sealed base for the controlling the movement of groundwater in dam foundation [5,6]. Because of cut-off walls being influenced by the dam settlement due to its weight, horizontal and vertical displacement influenced during first impounding, and specially, condition such as earthquake, it is necessary to be designed in a way that the deformations due these conditions be the least possible and prevent cracking in the wall. In this regard, using plastic concrete for cut-off walls is one of the best solutions, since it has sufficient strength and flexibility to withstand static and seismic stresses and undergo seismic deformations along the surrounding soil [7].

In this paper, function of the plastic concrete cutoff wall in one of the zoned embankment dams in Iran, namely Silveh Dam, is evaluated by considering instrumentation measurements. In this regard, a performance index, k , has been introduced to evaluate the sealing performance of the water barrier cutoff wall system. For this purpose, related analyses have been performed on the measured pore pressure data obtained from pore pressure gauges located beneath the dam foundation at three different cross sections.

2. SITE AND THE DAM BODY CHARACTERISTICS

Silveh Dam is a recently constructed zoned earth dam located about 12 km Northwest of Piranshahr city in the Western Azerbaijan Province, Iran. Feasibility studies of dam construction on the Lavin-Chai river started in 1975 and Phase-I& II studies and geotechnical site investigations were completed in 2006 with more than 1353 meters of boring, by Abgeer Consulting Engineers. The studied dam body is placed on a wide valley which comprises a coarse-grained alluvial deposits with maximum of 65 m depth in right bank and limestone or schist rock in left bank, underlain by a layer of lightly metamorphosed limestone and shale with lenses of slate, metamorphic sandstones, and powdered layers of schist and mica schist. The dam body encompasses different zones, including a clay core and an impervious upstream blanket, upstream and downstream shells of coarse-grained gravelly sand, drain and filter [8, 9]. The capacity of the dam reservoir, at its normal water level (1573.5 m.a.s.l), is about 84 million cubic meters. With a crest level of 1579 m.a.s.l, the maximum height of the dam is approximately 89 meters from foundation and its crest length is near 720 meters. The maximum height section and the plan of the Silveh dam are shown in Fig. 2 and Fig. 3; respectively. Some Instruments are installed in the dam body and its foundation in order to monitor the behavior of the dam under different loadings, such as the dam body weight, embankment construction stages, dynamic and static pressures from the reservoir,

effects of earthquake loading, and to determine the groundwater levels and the pore water pressure in the body and foundation of the dam. These instruments include electrical pore water pressure meters, inclinometers, earth pressure gauges, Casagrande piezometers, observation wells, earthquake accelerometer, V-notch, and surface settlement benchmarks. Fig. 4 shows the arrangement of the installed instruments in three sections of the dam. In this paper, measurements of pore water pressure have been studied over these three sections, namely 2-2, 5-5, and 7-7 [10]. The cutoff wall on the right abutment is a continuous barrette wall. In the river bed and left abutment, it is installed by the execution of the plastic concrete secant piles with the diameters of 1.2 and 1.0 meters and 45 meters maximum depth (Fig. 5) [11].

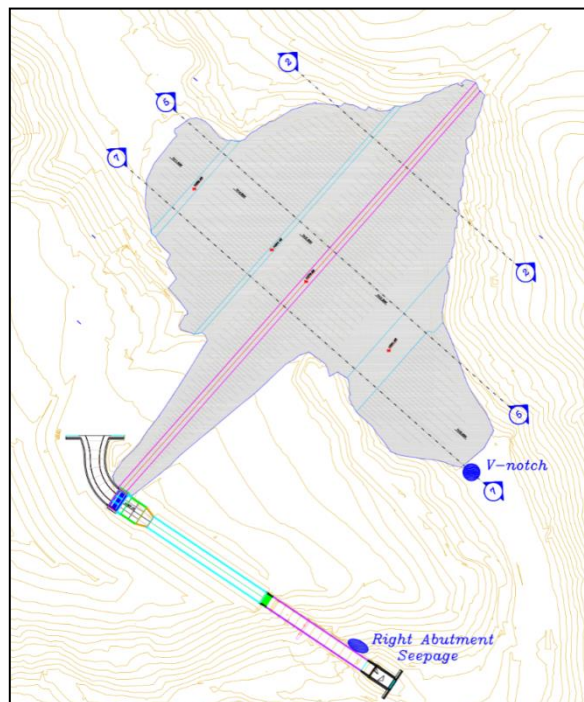


Fig. 2

Plan of Silveh Dam and location of the analyzed cross sections

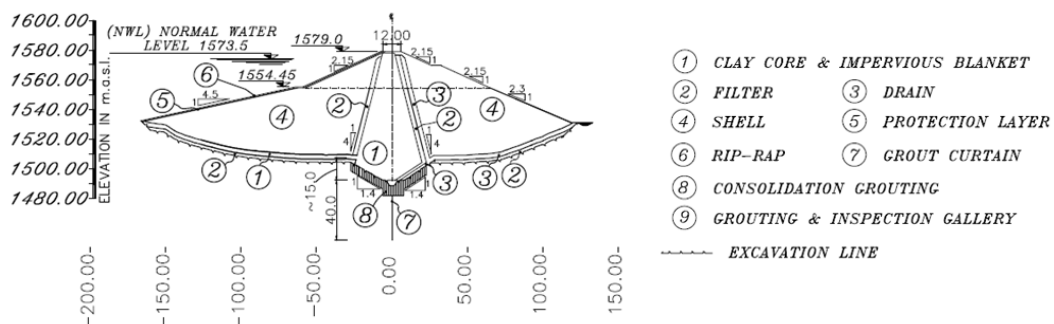


Fig. 3

The maximum height cross section of the Silveh dam

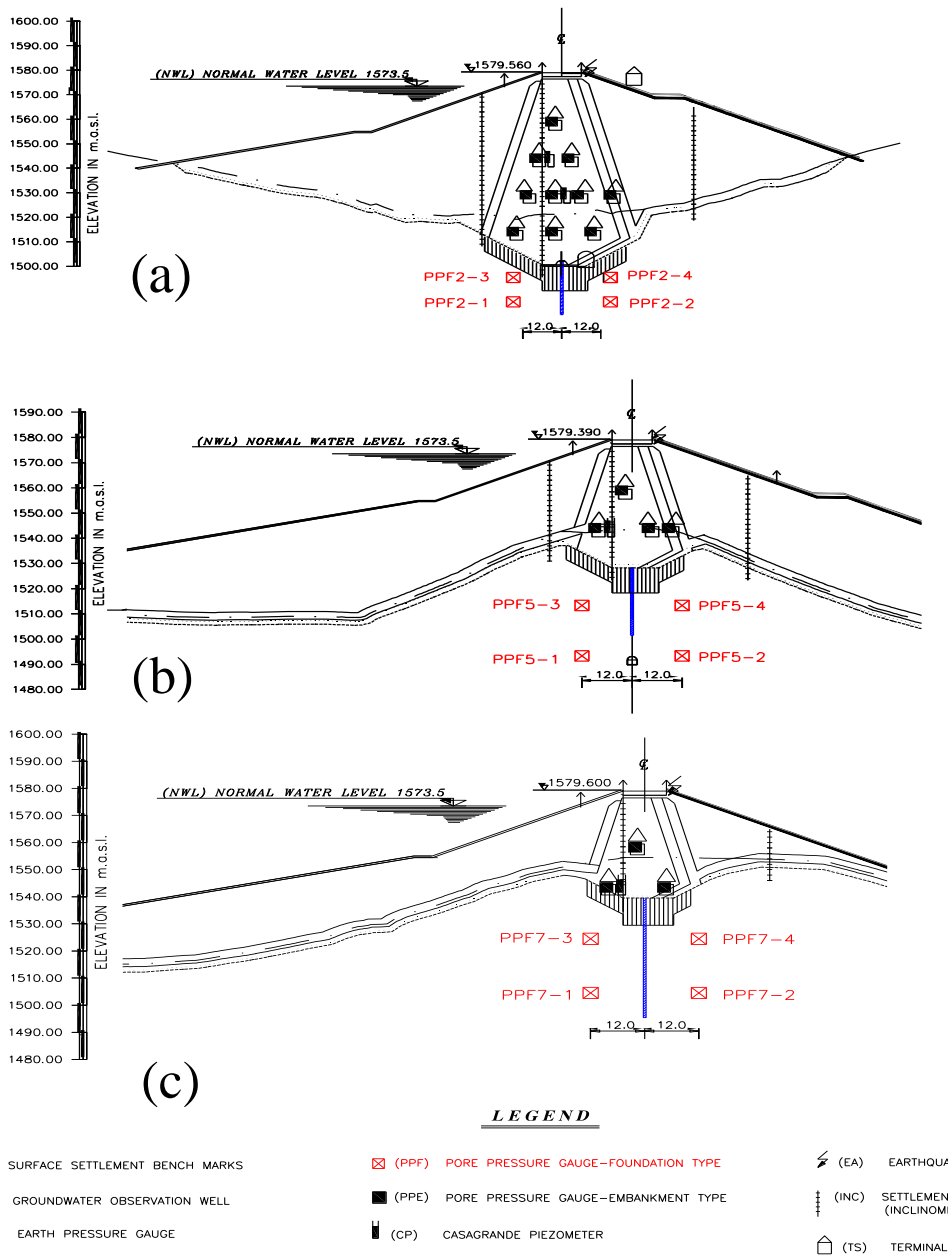


Fig. 4
Details of instrumentation in cross sections a) 2-2, b) 5-5, and c) 7-7

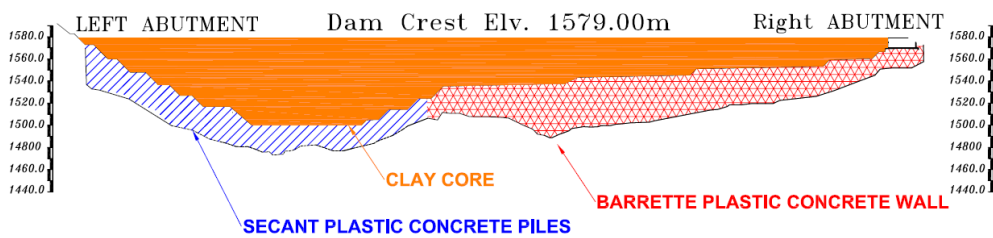


Fig. 5
Longitudinal cross section of the cutoff wall in Silveh Dam

3. RECORDED PORE PRESSURES IN DAM FOUNDATION

As mentioned in part 2 of this paper and depicted in Fig. 4, two pairs of pore pressure measuring gauges are implemented in each cross section of the dam body to study the pore water pressure generations and dissipations through the dam foundation. In Fig. 6, the variation of the measured pore water versus time is depicted for the three studied cross sections of the dam along with the variation of the dam reservoir water elevation and dam body filling level. As illustrated in Fig. 6, in general, pore water pressure in each gauge has been increased by increasing the dam body elevation (during construction) and due to first impounding and then slightly approaches to the constant value. In addition, the recorded pore water pressures at downstream sides of the cross sections are greater than those for the upstream sides, which implies the suitable function of the cutoff wall system.

4. ANALYSIS ON THE CUTOFF WALL PERFORMANCE

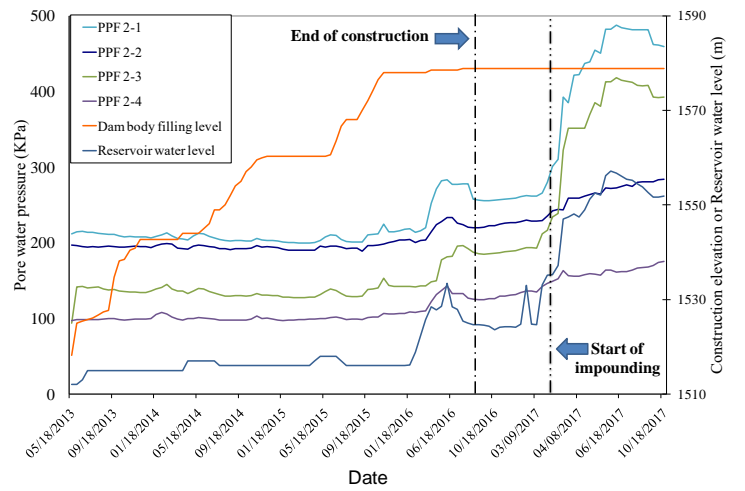
To assess the workability of the cutoff wall, recorded pore water pressures at upstream and downstream sides in dam foundation are considered. In this regard, a performance index, k , has been defined as presented in Eq.[1]:

$$k = (U_{up} - U_{down}) / (W_r - Z_i) \quad [1]$$

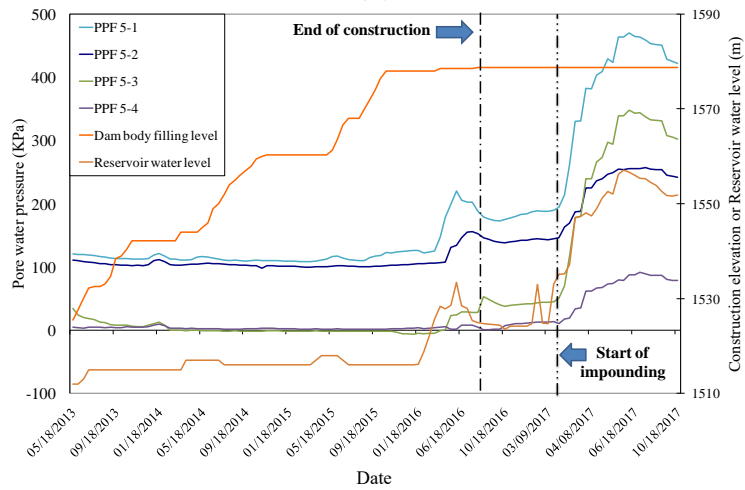
In which, U_{up} and U_{down} are the recorded pore water pressures by two semi-elevated pore pressure gauges placed at the upstream and downstream sides of the cutoff wall, respectively, and W_r and Z_i are the reservoir water and pore pressure gauges elevations, respectively [10, 12].

From Eq.[1], one can postulate that the more value the k gained, the more water head lost occurred due to the better performance of the cutoff wall to elongate the seeping stream lines.

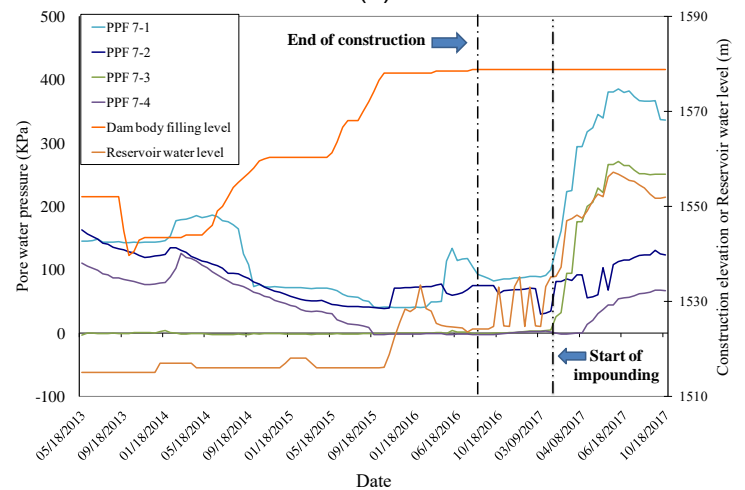
Diagrams of the changes in k v.s time in three studied sections 2-2, 5-5 and 7-7 of the Silveh dam for 2 pairs of pore pressure gauges at each cross section are shown in Fig.7. Data presented in Fig. 7 shows that during dam body construction, k values show oscillations by time increasing which can be related to the simultaneous pore pressure generation and dissipation in dam foundation. The same pattern can be observed during first days of reservoir impounding. Anyhow, after reaching the dam body to its proposed maximum height and stopping the reservoir further impounding, k approaches to an almost constant value, which show the steady and controlled seepage through the dam foundation. Moreover, positive k values in all time ranges shows the pore pressure at upstream sides of the cutoff wall is always greater than the corresponding value at the downstream side (regarding Eq.1) and implies the suitable sealing performance of the cutoff wall.



(a)



(b)



(c)

Fig. 6
Changes of the recorded pore water pressures v.s time in cross sections a) 2-2,
b) 5-5, and c) 7-7

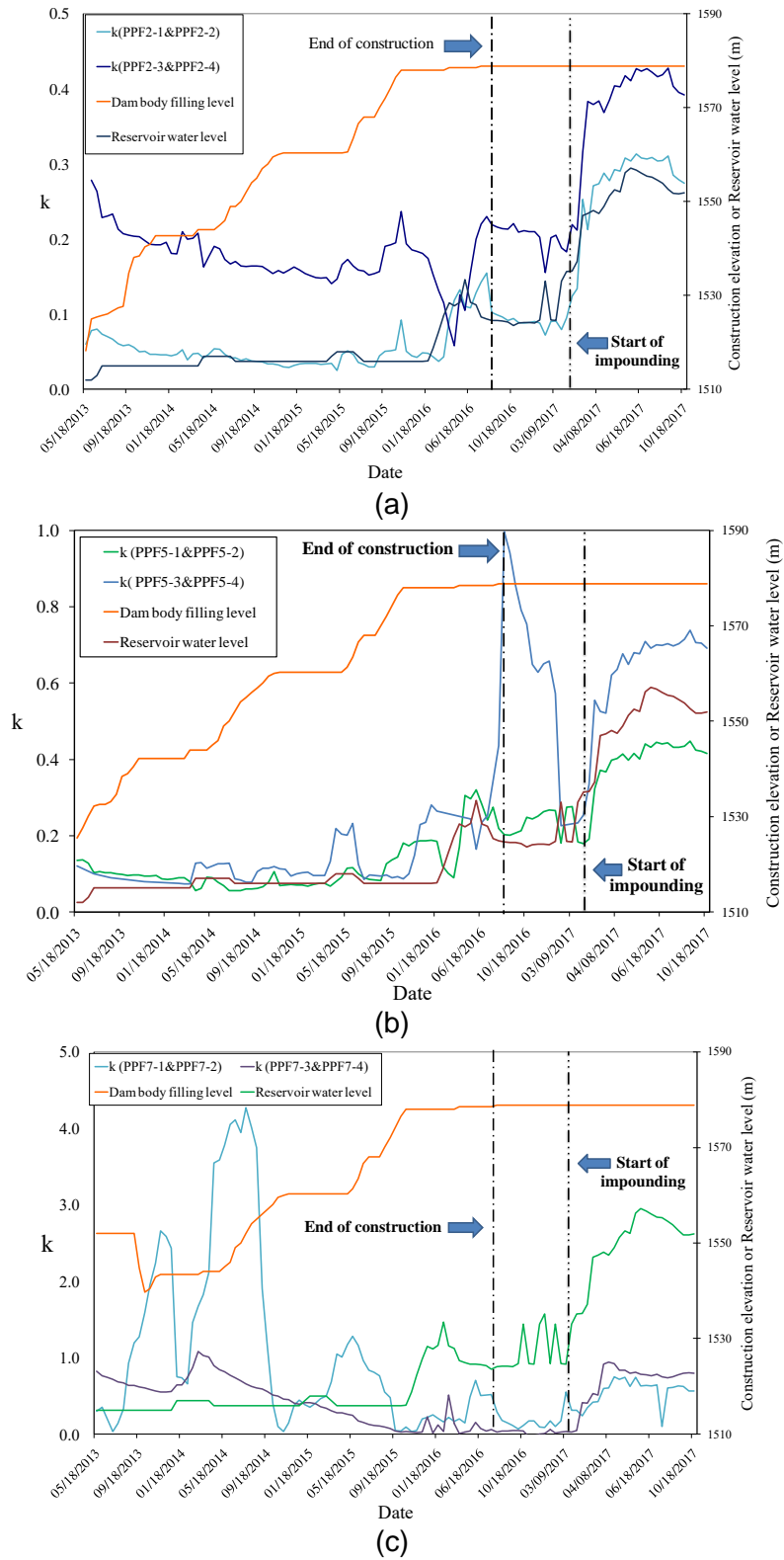


Fig. 7
 Calculated performance index values in cross sections a) 2-2, b) 5-5, and c) 7-7

5. CONCLUSION

In this paper, the sealing function of the executed cutoff wall water barrier system of an embankment dam in IRAN, namely Silveh dam, has been assessed by implementing instrument pore pressure data. For this purpose, at three different cross sections of the dam body and its foundation, recorded pore pressures at both upstream and downstream sides of the cutoff wall have been used to calculate a performance index, k .

The performance function is defined as the ratio of the pore pressure difference at upstream and downstream sides of the cutoff wall to the maximum possible hydrostatic pore pressure at the level of measuring. It actually gains larger values when the pore pressure difference at two sides of the cutoff wall increases, which means the cutoff wall, is working properly. Moreover, the trends of pore water generations and dissipations during dam body construction and first impounding imply the safe condition of the dam and steady seepage occurrence.

Analysis performed on the obtained instrument data from Silveh dam foundation shows that performance index of the dam is rationally great enough which means the suitable function of the constructed cutoff wall.

ACKNOWLEDGEMENTS

This research has been financially supported by “West Azarbayjan Regional Water Authority, Ministry of Energy of Iran” which is greatly acknowledged.

In addition, the second author would like to appreciate the “Niroo Research Institute, Ministry of Energy of Iran” to provide him the opportunity to contribute in this research.

REFERENCES

- [1] ICOLD, International Commission on Large Dams, Neotectonics and Dams. Bulletin 112, 1999.
- [2] GARAKANI, A.A., 2D and 3D Numerical Analysis on the Effects of Sliding Abutment on Stress and Deformation Behavior of Rockfill Dams During Construction, First Filling and Rapid Drawdown - (Case Study: Upper Gotvand Dam), M.Sc. Thesis, Civil Eng. Dept., Sharif University of Technology, 2005.
- [3] SHAFIPOUR NOORAFSHAN, R., Three-Dimensional Seepage Analysis of Inhomogeneous Earth Dam in Narrow Valley and Comparison with Two-Dimensional Analyses, M.Sc. Thesis, Civil Eng. Dept., Sharif University of Technology, 2002.

- [4] JAFARZADEH, F., YOOSEFI, S., BANIKHEIR, M., GHASEMZADEH, H., GARAKANI, A. A., Leakage Evaluation from Foundation of Old Embankment Dam by Instrumentation Data Analysis and Geoelectric Field Tests: A Case Study on Mahabad Dam, International Symposium on Dams in a Global Environment Challenges, Bali, Indonesia, 2014.
- [5] EVANS, J.C., Vertical cutoff walls. In: Daniel D.E. (eds) Geotechnical Practice for Waste Disposal. Springer, Boston, MA, 1993
- [6] YAN, L., TRAPP, D.A., SY, A., Construction of Plastic Concrete Seepage Cutoff Wall for the New Coquitlam Dam, Sixth International Conference on Case Histories in Geotechnical Engineering, 2008.
- [7] Roghani, A., Evaluation of Strength Parameters of Plastic Concrete by Triaxial Tests, M.Sc. Thesis, Civil Eng. Dept., Sharif University of Technology, 2011.
- [8] GARAKANI, A. A., SHAHRABI M.M., JAFARZADEH F., ESKANDARI N., BANIKHEIR M. Determination of critical water level during first impounding in earth dams using unsaturated transient seepage analyses. 19th International Conference on Soil Mechanics and Geotechnical Engineering (19th ICSMGE), Seoul, Korea, 2017.
- [9] ABGEER CONSULTING ENGINEERS CO. Plan view reports of the Silveh dam, 2007.
- [10] ABGEER CONSULTING ENGINEERS CO. Behavioral report of the Silveh dam after construction, 2015.
- [11] ABGEER CONSULTING ENGINEERS CO. Complementary design studies on body and foundation of the Silveh dam, 2012.
- [12] JAFARZADEH, F., GARAKANI, A. A. Foundation Treatment in Rockfill Dams with Consolidation Grouting. Seventh International Conference on Case Histories in Geotechnical Engineering and Symposium in Honor of Clyde Baker. Chicago, USA, 2013.

SUMMARY

In this paper, the sealing function of the executed cutoff wall water barrier system of an embankment dam in IRAN, namely Silveh dam, has been assessed by implementing instrument pore pressure data. For this purpose, at three different cross sections of the dam body and its foundation, recorded pore pressures at both upstream and downstream sides of the cutoff wall have been used to calculate a performance index, k .

The performance function is defined as the ratio of the pore pressure difference at upstream and downstream sides of the cutoff wall to the maximum possible hydrostatic pore pressure at the level of measuring. It actually gains larger values when the pore pressure difference at two sides of the cutoff wall increases, which means the cutoff wall, is working properly.

Analysis performed on the obtained instrument data from Silveh dam foundation shows that performance index of the dam is rationally great enough which means the suitable function of the constructed cutoff wall.

KEYWORDS

Embankment dam, Silveh dam, instrument data, cutoff wall, seepage, performance index.

COMMISSION INTERNATIONALE DES GRANDS BARRAGES

VINGT-SIXIÈME CONGRÈS DES GRANDS BARRAGES
Autriche, juillet 2018

DOI 10.3217/978-3-85125-620-8-173



This work licensed under a Creative Commons Attribution 4.0 International License. <https://creativecommons.org/licenses/by-nc-nd/4.0/>

FOUNDING AND SEALING LARGE DAMS ON VERY WEAK FOUNDATIONS

Wesley. E. SALEIRA

Consulting Engineer, US CONSULTANT

USA

COMMISSION INTERNATIONALE
DES GRANDS BARRAGES

VINGT-SIXIÈME CONGRÈS DES
GRANDS BARRAGES
Autriche, juillet 2018

FOUNDING AND SEALING LARGE DAMS ON VERY WEAK FOUNDATIONS

Wesley. E. SALEIRA

Consulting Engineer, US CONSULTANT

USA

1. INTRODUCTION

Finding appropriate sites to build new storage dams particularly for potable water for drinking, domestic and industrial use, as well as to irrigate land for growing food although on the increase has not kept pace with the population growth across the globe. Engineers are now consistently being called upon to design and build dams at very marginal sites, while on the other hand dam design guidelines and construction quality requirements have been getting more rigorous particularly with regards to seismic and flood hazards.

ICOLD guidelines provide more than adequate basis for designing and building traditional dams be it arch, arch gravity, and gravity dams. Computational methodologies that are currently available do further provide a superior set of tools for the analysis and evaluation to verify the associated performance criteria for any type of conventional dam. The easier access of powerful analysis tools to the modern-day dam design engineer still require appropriate site specific parameters as input which require detailed site investigations specific to the marginal sites. It has also become more than necessary to apply "common sense engineering" to ensure appropriate dam type selection, layout and design.

Crucial lessons being learned on recent dam projects are not being adequately documented. If this is due to preservation of intellectual property rights or propriety design methods, then it is acceptable. But if it is due to liability issues

related to poor engineering design or construction then it would raise integrity questions and should be avoided. The fundamental approach to data collection and interpretation of geological conditions of dam foundation has suffered greatly due to the lack of sufficiently allocated resources and time for site investigations with the pressure to deliver faster but not necessarily the economic and safer solutions. The “Why” question that should continue to persist in planning site investigation logically has been unintentionally taken away. Site investigations which used to be enhanced by local knowledge and experience are routinely being ignored or not attended to, mostly due to budgetary and time constraints imposed by the various stakeholders. A further trend is for stakeholders to persist with original concepts much longer than they should be, even when initial indications are that more economic and technically sound alternative solutions are available.

2. SUITABLE LARGE DAM TYPES FOR WEAK FOUNDATIONS

2.1. DAM TYPES

Traditionally rockfill dams with concrete spillways on one of the banks on competent rock has been preferred in general for weak foundations. Morning glory spillways have been a feasible but less preferred alternative for flood evacuation. Where rockfill is not available in sufficient quantities or quality, earthen embankments have been selected with similar arrangement for spillways and alternatives.

Engineers, in the recent past have begun to consider composite dams for very weak foundations. Composite dams provide a flexible rockfill dam for the geologically weaker parts including over active and inactive faults and fault zones. The relatively more competent part is set aside for providing a spillway section in conventional concrete or RCC after appropriate foundation strengthening treatment are undertaken, if required. Although there are several dams that have been designed and built and in operations currently no guidelines exist for engineering composite dams. This needs to be addressed by ICOLD at the earliest.

2.2. VERY WEAK FOUNDATIONS

Large dams have been built and will continue to be built on very weak foundations that are poor. Engineers who have conducted routine finite element analysis of large gravity dams on such foundations would have observed the following:

1. For embankment dams of similar height, the maximum foundation stresses are similar except for the stress bulb width.
2. A 1:1.5 upstream and downstream sloped rockfill dam imposes less foundation stresses than a flatter 1:2.0 sloped rockfill dam. This observation is very important as widening the width of an embankment dam with flatter slopes does not necessarily provide increased safety nor economy.
3. For the rockfill part of a composite dam the most steeper slopes that provide the required safety margins is adequate and thus must be selected. The foundation improvement will thus be required over a smaller foot-print and the cost savings can be used to provide treatment even deeper that is beneficial.
4. The incremental stresses imposed by even a large dam on the foundation decreases rapidly with depth, with minimal stress increase beyond depths exceeding 15 to 20% of the dam height. The most important zone for consolidation is thus the upper most foundation layers within this impacted depth.
5. RCC dam and/or spillway blocks on weaker foundations are also normally provided an upstream slope partially or for the full height of the dam.

In traditional dam construction, how consolidation grouting is undertaken still remains less effective as it is normally done after exposing the foundation but prior to commencing dam construction. For very weak dam foundations such an approach is not beneficial particularly in zones where a concrete or RCC spillway section needs to be placed. In such areas, it would be more effective if a confining concrete or RCC cap layer, several meters in thickness be placed first and then followed with consolidation grouting. If this confining layer is in mass concrete pipes can be left in place to minimize subsequent drilling for consolidation grouting. Proper consolidation grouting enhances curtain grouting for sealing the foundation for water tightness. This also allows higher grouting pressure such as at the foundation-dam interface where it matters most. Such construction requirements should be put in place at the time of tender.

Irrespective of dam type, proper drainage downstream of the grout curtain is critical for the safety of the dam. Thus the placement of the grouting gallery is also of importance. Usually upstream of the grouting gallery the intent of the consolidation grouting is for both water tightness as well as for strengthening the foundation whereas on the downstream part more emphasis shall be on foundation strengthening. The curtain grout must follow a single axis through the composite dam to be most effective as well as for economic considerations.

2.3. BACKGROUND ON COMPOSITE DAMS

Incidentally most of the early dams, prior to the advent of concrete in early 1900s, were all of composite construction. It is now recognized that the masonry remains of the oldest dams known, the 5000 year old Jawa Dams in Jordan were the spillways. The oldest known continuously operating dam in the world is in South India, built 1800 years ago. It had a main stone masonry structure with earthen embankments on its flanks as its name in the local Tamil language Kallanai also implies. This dam was apparently rehabilitated in 1776 following a major flood by the then English rulers. Strangely one of the earthen spillways ever designed was for the ancient Maduru Oya dam in Sri Lanka. It was placed several kilometres from the main dam on a naturally occurring saddle. The dam was built in the 12th century, but may have never been completed although intact headworks were excavated downstream of the new dam and now saved for posterity.

Of the four RCC dams in Jordan that were built some twenty years ago and have been in operation, two at Wala and Mujib respectively are composite dams. Engineers could obtain additional information from available publications on RCC dam construction in Jordan. Grouting at Mujib dam has also been extensively addressed in several publications and in a text.

Other notable composite dams include the recently completed Neelum Jhelum diversion dam at Nauseri in Pakistan that has recently begun filling up for operation. The main boundary thrust fault crosses this composite dam. Some details of this dam briefly described in a publication by Engineer Khaliq Khan (2012) and other relevant information are available on the internet. After taking into consideration the Chi Chi earthquake damage to the Shih-Kang Dam in 1999, a composite dam was proposed and eventually provided at Nauseri instead of the concrete dam with a Clyde dam type slip joint that was provided in the tender design.

2.4. COMPOSITE DAMS OVER FAULTS AND FAULT ZONES

Fault movements in the footprint of a dam are the most critical seismic hazard for most dam types. If no other site can be selected, then a conservatively designed earth core rockfill dam would be the only solution (Wieland 2012).

Robert C. Lo and Yumei Wang (2012) in their Lessons Learned from Recent Earthquakes - Fault Displacement note Fault displacement caused significant structure damages in the Wenchuan earthquake. Fault displacements reported in the literature range from few metres to tens of metres.

The following is a relevant summary for composite dams from the Lessons Learned from Dam Incidents and Failures as reported by Richards:

- Seepage along penetrations through embankment parts of composite dams should be controlled using a filter diaphragm instead of anti-seep

collars. A concrete encasement or cradle around or under conduit penetrations through earthen/rockfill embankments allow for better compaction of earthfill/rockfill.

- The first filling of a reservoir should be planned, controlled and monitored.
- Treatment of fractured foundation rock for embankment parts of composite dams is important to prevent internal erosion of embankment material that is in contact with the foundation.
- Stability of the dam foundation and other geologic features must be considered during composite dam design.
- The design engineer should be involved in the construction phase of composite dam projects.
- High and significant hazard rockfill parts of composite dams should have internal filter and seepage collection systems.
- External independent peer review of designs and decisions is an effective means of providing quality assurance and reducing the risk associated with design oversights and deficiencies.
- Local experience must be consulted and considered for composite dam solutions for better effectiveness and local compliance.
- PMF magnitude floods do occur. High and significant hazard dams should be designed to pass an appropriate design flood.
- Composite dams need an operable means of drawing down the reservoir.
- Access shall be provided and available at all times for the inspection and routine maintenance of gates and other mechanical systems at composite dams.
- Composite dams and grouting galleries located in areas of potential seismic activity need to be evaluated for liquefaction, cracking, potential fault offsets, deformations, and settlement due to seismic loads.
- Alkali-aggregate reactions (AAR) can cause serious concrete deterioration and other problems at concrete/RCC parts of composite dams.
- Most concrete/RCC parts of composite dam failures are the result of foundation stability problems.
- Concrete/RCC parts of composite dams founded on bedrock require detailed corroborating subsurface investigations and testing of rock properties.
- Outlet works and pressurized conduits in composite dams should be provided with a means for upstream closure.
- Composite dams built from or on loose granular soil can be susceptible to liquefaction of the foundation material.
- Settlement of rockfill parts of a composite dam can reduce freeboard and increase the risk for overtopping. Composite dams should be designed with allowances for settlement.
- For high and significant hazard composite dams, elements that are critical for the safe operation of the dam should all be engineered.
- As for the traditional dams, internal erosion can take decades to progress in composite dams.
- Karstic foundations are difficult to treat and can cause internal erosion issues and require special attention.

- Foundation approval should be documented by designers and geologists.
- Moisture content and compaction of fill material particularly at the interfaces of composite dam parts must be carefully monitored for acceptance during construction.
- Landslides around the rim of a reservoir can cause composite dam overtopping. The stability of the hillsides around the rim of the reservoir as well as the impact of potential slope failures should be addressed.
- The presence of weak zones in natural foundation materials must be evaluated at the time of design and treatment specified at time of tender.
- Brittle materials, such as asphalt and Portland cement concrete, should not be used as reservoir liners without high capacity filtered underdrains.
- Zones of permeable soil, such as old riverbed deposits in dam foundations, should be addressed.
- Grout curtains in a formation where potential seepage paths (joints, fractures, etc.) are filled with either erodible or soluble materials are not permanent and may require periodic maintenance grouting to remain effective.
- Conventional instrumentation may provide early detection of conditions within a composite dam that could lead to failure.
- Construction inspection is critical in assuring proper construction techniques and construction in conformance with approved plans and specifications.
- For concrete and RCC spillway blocks in a composite dam, weak features in rock foundations can be mitigated using concrete shear keys and dental concrete.
- Vertical seismic accelerations can be as high as the horizontal accelerations and this should be considered in the design.
- Reservoir sedimentation can increase destabilizing forces acting on a composite dam and have other detrimental effects that could contribute to a dam failure.
- Rockfill that may become loose following an earthquake should not be placed against a concrete or RCC section in a composite dam.
- Differences in the stiffness of structural materials as well as the foundation can lead to unforeseen stress concentrations particularly concrete/RCC part of a composite dam.

3. DAMS ON VERY WEAK FOUNDATIONS

3.5. SEISMIC CONSIDERATION OF COMPOSITE DAMS ON FAULTS

The rupture of the Chelungpu Fault, led to Shih-Kang dam axis being shortened by about 7 meters with vertical displacement of 9 m.

Activity of a fault was initially taken as “activated” if at least once in the past 10,000 years. An active seismic source is now defined as a fault that has ruptured within the last 35,000 years. However, this or any fault activity criterion is somewhat arbitrary by its very nature. There is no physical reason why a fault that has not moved during the last 35,000 years cannot move again. Case in point is the October 16, 1999 Magnitude 7.1 Hector Mine Earthquake.

Allen and Cluff (2000) note the following:

1. There is no standard definition of what constitutes an "active" fault, which reflects the geologic reality that all degrees of fault activity do, in fact, exist. Any distinction between active and inactive faults is necessarily arbitrary.
2. In worldwide practice, faults in dam foundations that are estimated to have ruptured on the average of once in every few thousand, or every few tens of thousands of years, have typically been considered worthy of engineering consideration.
3. At least some engineers appear to be gaining confidence that, with innovative new techniques, dams of virtually all types can be designed to accommodate moderate foundation fault displacements without major failure.
4. Owing to advances in the ability to obtain absolute ages on geologic materials, mainly through new geochemical techniques, degrees of fault activities can now be estimated far better than only a few years ago. A critical parameter in both probabilistic and deterministic assessments is long-term fault slip rate.
5. Field studies of faults in dam foundations demand the expertise of geologists trained and experienced in neotectonic studies. Classical geological maps, however competently done, often have only limited relevance to earthquake hazard assessments.
6. Seldom are adequate field exposures available in the dam footprint area itself to characterize fully the neotectonic environment of a proposed dam. It is virtually always necessary to carry out such studies, including trenching of suspect faults, throughout a much wider area than that of the dam footprint—typically extending over many tens of kilometers.
7. Seismologic studies of earthquakes in dam areas can play an important role in safety evaluations, particularly in establishing seismic shaking parameters such as maximum ground accelerations and velocities to be expected. But field geologic efforts are nevertheless critical in estimating the likelihood of surface fault rupture through a dam foundation. The abundance or absence of microearthquakes may have little relevance to the probability of large local earthquake associated with surface fault rupture.

S. Gangopadhyay (1993) also noted that many of the dam sites in India had various geological defects creating problems for the construction of the dam. Precise evaluation of these weaknesses of dam foundations at the investigation stage by engineering geological studies had helped cost-effective design and safe construction of the structures after adopting suitable corrective measures.

4. CONCLUSIONS

1. For composite dams, defensive design concepts must be applied until proper ICOLD guidelines become available.
2. Modelling rupture to estimate potential displacement at faults may be useful.
3. Use of elasto-plastic models for analysis of dams for strong earthquake or fault rupture.
4. In the absence of reliable fault displacements for the design earthquakes, flexible joints shall be provided in grouting galleries particularly over faults and fault zones.
5. Simple interface details are only required at the interface between Concrete/RCC and rockfill/clay parts even on a large composite dam.
6. Geological investigations are very crucial for composite dams.
7. Simple aspects of river geomorphology and topology would provide important clues to unexposed faults/fault zones.
8. New Guidelines for Composite dams must include interfaces details and how to handle potential fault displacements.

REFERENCES

- [1] M. WIELAND. Seismic Design and Performance Criteria For Large Storage Dams, 15TH WCEE 2012
- [2] M. WIELAND, R.P. BRENNER AND A. BOZOVIC. Potentially Active Faults in the Foundations of Large Dams Part II: Design Aspects of Dams to Resist Fault Movements, The 14th World Conference on Earthquake Engineering 2008
- [3] CLARENCE R ALLEN AND LLOYD S CLUFF. Active Faults in Dam Foundations: An Update, 12th WCEE 2000
- [4] WILLIAM A. FRASER. California Division of Safety of Dams Fault Activity Guidelines, 2001.
- [5] GREGORY L. RICHARDS. Lessons Learned from Dam Incidents and Failures. 2010.
- [6] ROBERT C. LO AND YUMEI WANG. Lessons Learned from Recent Earthquakes – Geoscience and Geotechnical Perspectives, Advances in Geotechnical Earthquake Engineering - Soil Liquefaction and Seismic Safety of Dams and Monuments, Prof. Abbas Moustafa (Ed.), ISBN: 978-953-51-0025-6, InTech, 2012
Available from: <http://www.intechopen.com/books/advances-in-geotechnical-earthquake-engineering-soil-liquefactionand-seismic-safety-of-dams-and-monuments/lessons-learned-from-recent-earthquakes-a-geoscience-andgeotechnical-perspective>

- [7] KUNG, CHEN-SHAN, NI, WEI-PIN, AND CHIANG, YUN-JEN, Damage and Rehabilitation Work of Shih-Kang Dam, Seismic Fault-induced Failures, 33-48, 2001, January
- [8] N.E. SIMONS AND B.K. MENZIES. A Short Course in Foundation Engineering, 159 Pages, Butterworths, 1977
- [9] PETER AMOS AND MURRAY GILLON. Dams and Earthquakes in New Zealand, Damwatch Vietnam 2009
- [10] ENGR. ABDUL KHALIQ KHAN, Engineering of Headrace Tunnel for Neelum Jhelum Hydropower Project, Centenary Celebration (1912 – 2012), Paper No. 708.
- [11] S. GANGOPADHYAY. Geotechnical Problems of Dam Sites and Their Solution with Reference to the Projects of Eastern India, Third International Conference on Case Histories in Geotechnical Engineering, 1993
- [12] ICOLD Committee on Materials for Fill Dams (2004). Concrete Face Rockfill Dams Concepts for Design and Construction
- [13] FARDIN JAFARZADEH, AMIR AKBARI GARAKANI. Foundation Treatment of Embankment Dams With Combination of Consolidation and Compaction Groutings, Seventh International Conference on Case Histories in Geotechnical Engineering. 2013.
- [14] DONALD A. BRUCE. RCC Dam Foundation Selection and Treatment, RCC 2015 – International RCC Dam Seminar and Duck River Reservoir Study Tour. 2015.
- [15] USBR, Glen Canyon Dam, Foundation Treatment Technical details.
- [16] B.A. FORBES, M. M. LSKANDER, A. I. HUSEIN MALKAWI, High RCC standards achieved at Jordan's Tannur dam, Hydropower & Dams Issue Three, 2001.
- [17] BERNARD BOUYGE, BRIAN A. FORBES, Tannur Dam in Jordan : adapting the project to site conditions and specific construction methods, 2002
- [18] LOPEZ, J & ARIDAH, M & SCHRADER, E. RCC quality control for Mujib dam. Roller Compacted Concrete Dams, Madrid, Spain. 983-994. 2003

SUMMARY

KEY WORDS: Composite Dam, Foundation Treatment, Fault, Grouting Gallery

ICOLD guidelines developed over the past several decades form the basis for current design of large dams of all types. Routinely, such dams have been designed and built on foundations deemed sufficiently competent for the selected dam type, be it concrete, RCC, CFRD, AFRD, Geomembrane faced Rockfill, clay core rockfill, earth embankment, etc., However, over the past few decades dams are being designed and built on foundations that are marginal to poor at best as well as over faults and fault zones due to the increasing need to store water for

various needs. Since dams need flood evacuation capacity, spillway structures and headworks are normally placed on the more competent foundation part of the dam axis, which has given rise to composite dam design and construction. The flexible part of the dam usually comprises of central core rockfill construction. When such composite dams need to span over fault zones, particularly over extensional fault zones, structures such as grouting galleries need to be provided with sufficient flexibility for future likelihood of extension that may occur during an earthquake. However, assessing the allowance for such extensions remain to be more of guesswork. When composite dams are built in developing countries some additional allowance must also be provided as such countries cannot afford the loss of the dam even in the short term. This paper presents how this uncertainty can be adequately addressed. Further, observations on the design and construction of composite dams including interfacing of the flexible segment with the rigid segment are also presented. In addition, a case is presented for this issue to be addressed in greater detail to develop basic guidelines for use by Engineers in the future.

CLEARANCES AND COPYRIGHT

Authors have been identified and also acknowledged. Only publicly available information and publications have been used in preparing the text.

COMMISSION INTERNATIONALE DES GRANDS BARRAGES

VINGT-SIXIÈME CONGRÈS DES GRANDS BARRAGES
Autriche, juillet 2018

DOI 10.3217/978-3-85125-620-8-174



This work licensed under a Creative Commons Attribution 4.0 International License. <https://creativecommons.org/licenses/by-nc-nd/4.0/>

**RELIEF DRAINAGE SYSTEMS AGAINST HYDRAULIC FAILURE DUE TO
UNDERSEEPAGE OF DYKES AND DAMS**

Heinz BRANDL

Emeritus of Institute of Geotechnics, VIENNA UNIVERSITY OF TECHNOLOGY

AUSTRIA

Marek SZABO

Project engineer, 3P GEOTECHNIK ZT GMBH, VIENNA

AUSTRIA

COMMISSION INTERNATIONALE
DES GRANDS BARRAGES

VINGT-SIXIÈME CONGRÈS DES
GRANDS BARRAGES
Autriche, juillet 2018

RELIEF DRAINAGE SYSTEMS AGAINST HYDRAULIC FAILURE DUE TO UNDERSEEPAGE OF DYKES AND DAMS*

Heinz BRANDL

Marek SZABO

*Emeritus of Institute of Geotechnics, VIENNA UNIVERSITY OF TECHNOLOGY
Project engineer, 3P GEOTECHNIK ZT GMBH, VIENNA*

AUSTRIA

1. GENERAL

Many dykes and dams rest on alluvial deposits, which usually grade from fine-grained materials near the ground surface to coarse sediments with high permeability in the lower part of the strata. If dykes or levees do not have a cut-off wall fully penetrating the aquifer, underseepage may occur beneath the earth structure during high river levels. Such seepage may cause an excessive water pressure in the aquifer landside of the embankment dam. Most dangerous situations occur when high hydrostatic pressure acts on the upper low permeable soil layers and ground failure develops in the form of uncontrolled boils or uplift of the blanket.

The risk of dykes or dams failure increases not only with the magnitude of a flood but also with its duration. For instance, the peak period of flood waves along the Austrian section of the river Danube usually lasts one to three days, whereas its tributary, the river March/Morava (Austrian/Slovak border) frequently undergoes flood waves up to three or six weeks (Fig. 1).

After today's practice the hydraulic failure due to underseepage may be prevented mainly by two permanent measures at the landside dyke or dam toe by

* *Systèmes de drainage de la décompression contre les défaillances hydrauliques dues au manque de visibilité des digues et des levées*

installing pressure relief elements or by placing berms. Especially, relief drainages have proved very successful in Austria during the last excessive floods along the rivers Danube and Morava.

However, until now the design of relief drainage systems was based on rather insufficient basic principles, strong simplifications and idealizations. For the quantification of the discharge from relief columns only assumptions based on numerical models are in use. Therefore, various model tests were performed to study the of relief drainage behavior and quantify the water discharge.

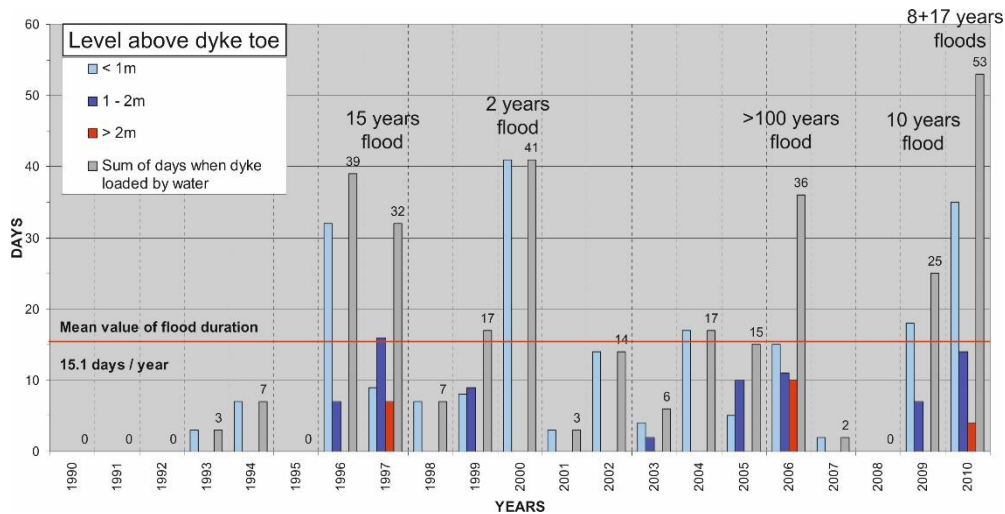


Fig. 1

Duration of floods along the River March dykes (Water level at Dürnkrot – Austria/Slovakia; adapted after via donau). Two floods within three weeks in 2010.

Durée des inondations le long des digues de la rivière March (Niveau d'eau à Dürnkrot – Austria/Slovakia; adapté après via donau). Deux inondations dans les trois semaines en 2010.

2. FAILURE MODES OF DYKES AND LEVEES

Knowledge of possible failure modes due to underseepage is an essential prerequisite, both for a reliable quality assessment of existing dykes and dams and for an optimised design of new ones. The simplified scheme of Fig. 2 illustrates the main failure mechanisms as observed in most cases.

Actually, it is often difficult to precisely determine the causes of a dyke failure. Statistical analyses show that overtopping and internal erosion are the most common failure modes. While many of these failure mechanisms occur relatively fast, the erosion by underseepage develops more inconspicuously. If a groundwater communication below the dyke is possible, the aquifer or the overlaying low permeable layer can be progressively eroded during hydraulic loading. Hydraulic failure is critical because there may not be any external evidence, mostly only soil boiling can be found.

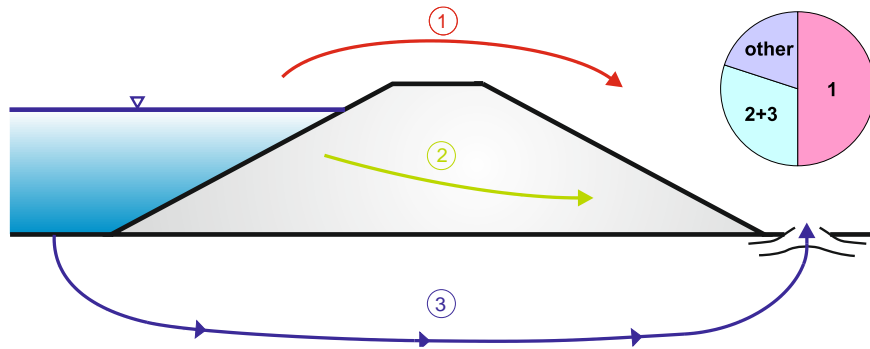


Fig. 2

Main failure modes of dykes: 1 = Overflowing, overtopping → Erosion failure, 2 = Seepage through dyke → Internal erosion, 3 = Underseepage → Internal erosion, Upheave, Ground failure

Principaux modes de défaillance des digues: 1 = Deversement sur le barrage → Erosion, 2 = Infiltration à travers la barrage → Erosion interne, 3 = Infiltration ci-dessous barrage → Erosion interne, Sous-Pression, Rupture ou sol

Due to this unpredictable behaviour hydraulic failure is frequently underestimated in practice and may occur in different forms (e.g. Eurocode 7; CEN 2004):

- By uplift (buoyancy). The pore-water pressure under the low-permeability blanket exceeds the overburden pressure.
- By heave. Upward seepage forces act against the weight of the soil, reducing the vertical effective stress to zero; soil particles are then lifted away by the vertical water flow. This ‘boiling’ dominates in silty-sandy soil, and is combined with internal erosion.
- By internal erosion. Soil particles are transported within a soil stratum or at the interface of soil strata. This may finally result in regressive erosion, leading to ground failure of the dyke, levee or dam.
- By piping. Failure by piping is a particular form of internal erosion, where erosion begins at the surface, and then regresses until a pipe-shaped discharge tunnel is formed. Failure occurs as soon as the water-side end of the eroded tunnel reaches the river bed or bottom of the reservoir. Frequently, several tunnels develop. This process may be induced or significantly promoted by animal activities, as field observations over many years have revealed.

Hydraulic failure may occur despite cut-off walls. If they are “imperfect” (i.e. with underseepage), groundwater communication below the dykes or levees (for environmental reasons) occurs and overpressure can develop beneath the landside blanket and the safety against a failure of the subsoil reduces significantly. The loss of stability is usually initiated by uncontrolled hydraulic rupture (uplift) of the blanket or by concentrated transport of fine particles (erosion, suffusion, piping) from the subgrade.

Hydraulic failure may reach several tens of meters away from dykes or dams, as experience has shown (Fig. 3). This could be observed even for low flood protection embankments with a relatively small hydraulic gradient. Soil boiling may create large volcanos (e.g. Fig. 4) that require urgent flood defense and stabilizing measures.



Fig. 3

Piping far away from the dyke and stabilizing measures to reduce the hydraulic gradient (photo: L. Nagy).

Renard éloignée de la digue et mesures de stabilisation pour réduire le gradient hydraulique (photo: L. Nagy).



Fig. 4.

Boiling "volcanos" after the flood. Retrogressive internal erosion towards the dyke (photo: L. Nagy).

Bouillant "Volcans" après l'inondation. Erosion interne rétrograde vers la barrage (photo: L. Nagy).

3. FLOOD CONTROL MEASURES AGAINST HYDRAULIC FAILURE

Hydraulic failure as an effect of underseepage may be prevented mainly by two permanent measures landside of a dyke or flood protection dam by:

- Filling of berms, thus displacing the possible starting point of internal erosion or piping farther away from the structure, and decreasing the hydraulic gradient at this point. Such berms should be designed and constructed such that they work simultaneously as access ways/roads for quick and easy dam defence in the case of severe floods.
- Installing pressure relief drainage systems in form of trenches, relief stone columns or relief wells.

A filter stable berm compensates through its counterweight the hydrostatic pressure beneath the blanket (Fig. 5a) and prevents hydraulic failure by seepage or uplift, or by internal erosion and piping. When seepage through or beneath the dyke occurs, a free water outflow must be allowed; clogging would be counter-productive. Otherwise an excessive pore-water pressure could cause a failure.

In many cases, berms merely move the hydraulic problem farther away from the dyke, and retrogressive internal erosion may finally reach it in the long term (after several floods). Boiling and internal erosion have been observed up to 20 to 50 m away from dykes and dams (Fig. 3), even though they were only 3 to 6 m high. Moreover, wide berms are often not possible under confined space conditions; therefore relief drainages are preferred under these circumstances.

Pressure relief systems are high permeable linear or punctual drainage elements at the landside embankment toe (Fig. 5b). They connect the terrain surface with the aquifer and allow a controlled pressure relief during floods, while water freely discharges. To prevent the relief elements from clogging due to fine particles transport from subgrade, they must be wrapped into a geotextile.

Filter protection of berms is generally provided by the use of non-cohesive granular material (natural soil) that must fulfil the permeability criterion and the retention criterion. While two criteria are sufficient for granular filters, four criteria are required for geotextile filters (Giroud (2010), Heibaum et al. (2006)): the porosity criterion and the roughness criterion also have to be considered.

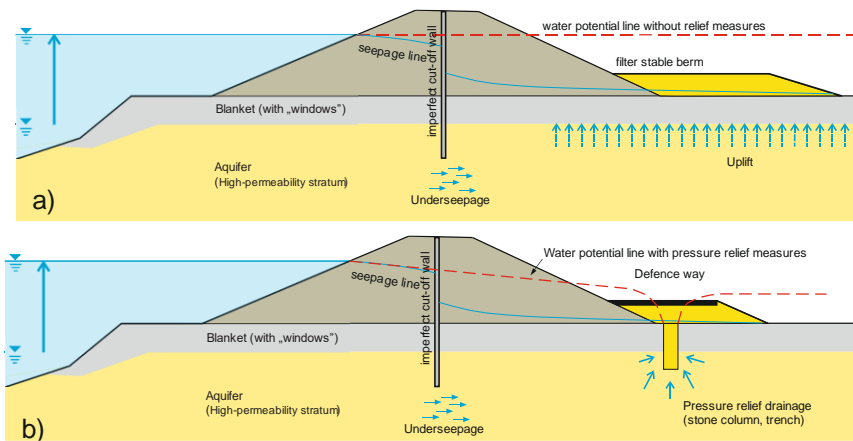


Fig. 5

Permanent measures against hydraulic failure due to underseepage of dykes:
a) Filter stable berm; b) Relief drainage columns or trenches.

Mesures permanentes contre les défaillances hydrauliques dues à la sous-pénétration des dykes: a) berm b) Colonne de la décompression ou tranchées.

3.1. RELIEF TRENCHES

A pressure relief trench is a longitudinal drainage of coarse gravel fill material wrapped in a filter stable geotextile at the landside dyke toe. Wider trenches may consist of granular fill material with horizontally differing grain curves as separating two- or three-stage filters (also in the base). They usually do not penetrate into the permeable aquifer, but rest mostly on top of it. However, a hydraulic connection must always be ensured so that the pressure relief is possible. At the same time, the groundwater must freely discharge the relief drainage and is conducted within the trench or flows into the adjacent hinterland.

3.2. RELIEF STONE COLUMNS (“GRAVEL PILES”)

Jacketed (coated) stone or gravel columns have been installed in Austria since 1992. This method has significant construction advantages over conventional drainage trenches in loose or soft soil.

Pressure relief columns are cylindrical relief elements at the landside dyke or dam toe, which penetrate through the low permeable blanket and embed into the high permeable ground layer (aquifer). They are made of high permeable fill

material (rounded grains, clean: 16/32 mm; permeability factor: $k \geq 1 \times 10^{-2}$ m/s) that is wrapped with a nonwoven geotextile.

The common diameter of these “gravel piles” is about 60 cm to 70 cm, but it can be easily adapted to the required relief effect. The installation is carried out with a designed center-to-center distance by means of vibroflotation or modified auger drilling method (Fig.6).



Fig. 6

Installation methods of relief drainage columns wrapped in nonwoven geotextile. (left: vibroflotation method; right: rotary drilling method with casing).

Les méthodes d'installation des colonnes de la décompression enveloppées dans un géotextile. (à gauche: vibroflotation; à droite: méthode de forage rotatif).

4. EXPERIMENTAL AND NUMERICAL MODELLING OF RELIEF DRAINAGE BEHAVIOUR

The study of pressure relief behaviour and the estimation of discharge from relief drainages were based on a combined modelling by using experimental and numerical techniques. First, a small-scale (1:10) dam model on two-layer strata was used to analyse the influence of main geometric and hydraulic parameters on the relief behaviour of stone columns and trenches. The results of these tests were the basis for calibrating the numerical model and for the large-scale modelling (1:1 scale) as well. Furthermore, this gradual approach allowed parametric studies exceeding the limits of the small-scale model.

4.3. SMALL-SCALE MODELLING

The small-scale dam model represents a vertical cross-section of a dyke including the subgrade in a scale 1:10. The 25 cm high dam model is founded on two-layer strata (Fig. 7). Beneath the silty-clayey blanket ($k = 10^{-9}$ m/s) with a

thickness of about 10 cm follows a homogenous aquifer layer of coarse sand with a thickness of about 18 cm. In addition, the dam has an imperfect cut-off wall (i.e. with underseepage), which slightly embeds into the aquifer.

The pressure beneath the blanket due to underseepage was measured by means of piezometers pipes in the longitudinal and transversal model axis. In addition to these measurements, also the discharge was quantified.

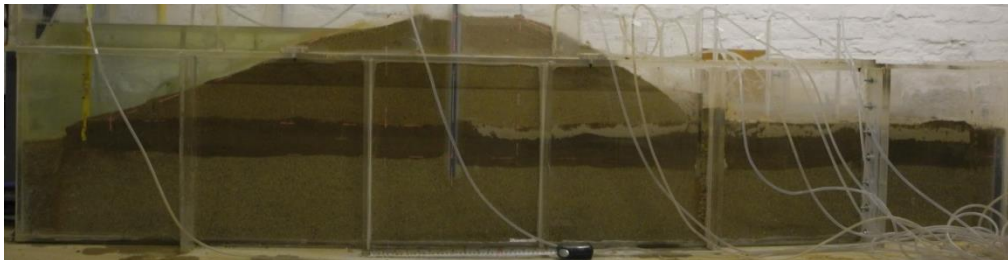


Fig. 7

1:10 small-scale dam model on two-layer strata.

1:10 modèle de barrage à petite échelle sur les strates à deux couches.

Fig. 8 shows the pressure distribution lines beneath the blanket for test series with single relief element depending on its permeability and embedment length into the aquifer. Both – the relief gravel column as well as the relief well – lead to a significant reduction of the hydrostatic pressure. If no relief measures would be installed, due to the blocked outflow boundary the hydrostatic conditions on the landside would become equal to the hydrostatic head on the waterside. It can be also seen that the element permeability significantly influences the pressure reduction. A similar behaviour can also be observed in terms of embedment length. However, the effect of embedment depth on the pressure relief, as supplementary investigations with the calibrated numerical model show, is also strongly influenced by hydraulic parameters of the aquifer.

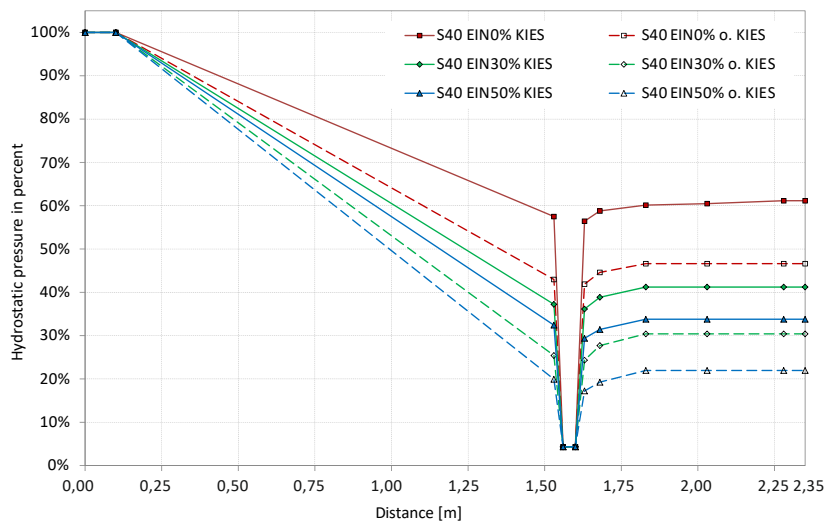


Fig. 8

Pressure along the longitudinal axis of the 1:10 model with a single relief column.

Pression le long de l'axe longitudinal du modèle 1:10 avec une colonne en relief.

4.4. LARGE-SCALE MODELLING

Based on the small-scale modelling, a large scale test facility (1:1) was built to study pressure relief drainages. The ground plan area of the reinforced concrete box was 25 x 4 m with a constant wall height of 5 m.

The 1:1 dam model represents a 4 m wide and 25 m long cross-sectional model of a dyke on two-layer strata (Fig. 9). The homogenous dam had a height of 2.5 m and the slope ratio of 1:2.5. For the dam sealing a silty-clayey core was installed, which penetrated the clayey blanket (thickness of about 0.7 m) and embedded only few centimetres into the 1.3 m thick aquifer layer of sandy gravel.

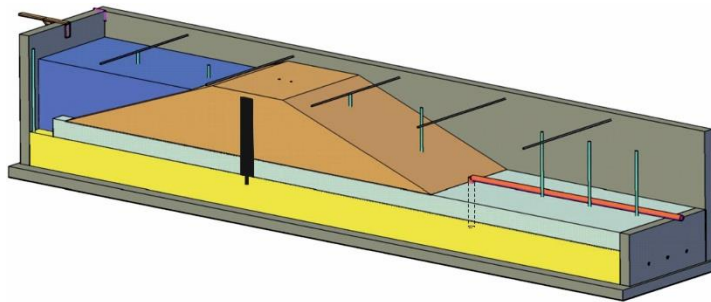


Fig. 9

Schematic drawing of the 1:1 dam model on a two-layer foundation.

Le schéma du modèle de barrage 1:1 sur une fondation à deux couches.

For the pressure relief observation due to the controlled underseepage, a measuring system was used, which allowed a continuous recording of the pressure potentials beneath the blanket as well as a time-synchronous recording of the water discharge from the relief gravel column.

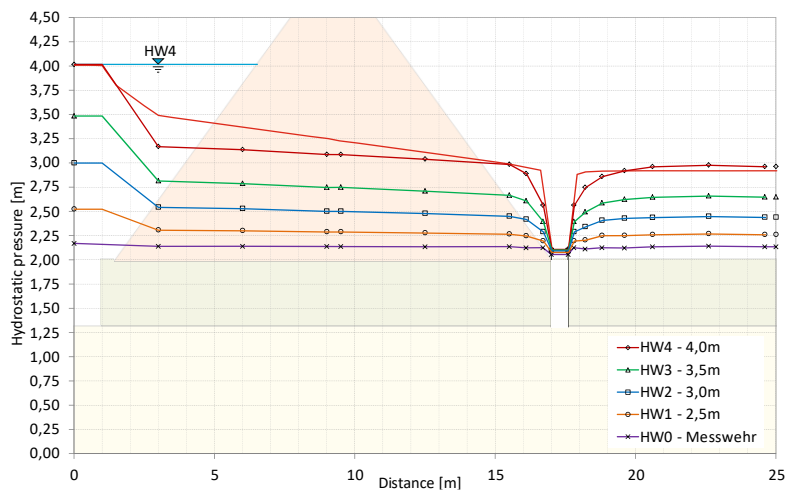


Fig. 10

Pressure distribution due to a single relief drainage column of 600 mm diameter and without embedment into the aquifer in a 1:1 model. (HW = water level)

Répartition de la pression due à une de la colonne de la décompression de 600 mm de diamètre et sans enfoncement dans l'aquifère dans un modèle 1:1.

In numerous series of measurements, a clear relief behavior of drainage columns could be confirmed despite certain anomalies. An example of the pressure relief behaviour due to a single relief column (\varnothing 600 mm) shows Fig. 10. The pressure reduction at the beginning of the measuring profile was partly caused by possible local clogging of the aquifer in combination with the relieving effect by the relief column. This resulted in a reduction of 50% in the hinterland. The maximum discharge for the highest water level was about 0.95 l/s per relief column with 4 m spacing.

4.5. NUMERICAL MODELLING

In order to examine the general application of numerical results, a model calibration with the GGU Software was carried out based on the model tests. For this purpose, the small-scale model test results were used, because the 1:10 model had a higher degree of homogeneity as the 1:1 dam model. The calibration was first carried out for a fully penetrating relief trench by variation of the aquifer permeability and subsequently extended to a three-dimensional model with a single relief column. Based on the model calibration, numerous comparative simulations were performed for both models. They verified the application of the calibrated three-dimensional numerical model for further studies of different geometric and hydraulic parameters (diameter, permeability, embedment length, spacing of a multiple column system) beyond the limits of the physical modelling.

The results from the numerical calibration of the three-dimensional model with a fully penetrating single relief column (with/without gravel) are shown in Fig. 11. The diagrams show the comparison of the measured pressure potential lines and the discharge from the relief column with the results of the numerical calculation.

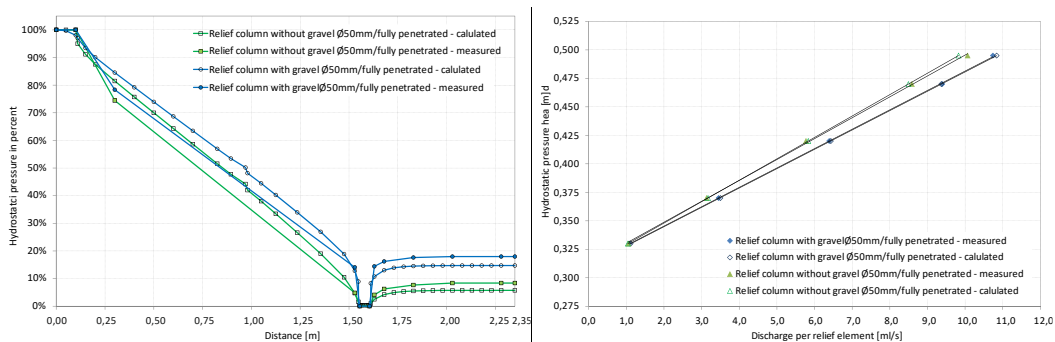


Fig.11

Results of numerical calibration for a model with a single relief column: pressure lines (left) and discharge from the relief column (right)

Résultats de l'étalonnage numérique pour un modèle avec une seule colonne en relief: lignes de pression (à gauche) et décharge de la colonne décompression (à droite)

REFERENCES

- [1] BRANDL H. (2012). Failures and defense of flood protection dykes and levees. *Sicherung von Dämmen, Deichen und Stauanlagen – Handbuch für Theorie und Praxis*, Vol. IV (R. A. Herrmann, J. Jensen), Universität Siegen, 2012, pp. 3-20,.
- [2] BRANDL H., SZABO M. Hydraulic failure of flood protection dykes. *Proceedings of the 18th Int. Conf. on Soil Mech. and Geot. Eng.*, Paris, 2013.
- [3] CEN (2004). EN 1997-1. Eurocode 7: Geotechnical Design – Part 1: General Rules. Comité Européen de Normalisation, Brussels.
- [4] GIROUD, J. P. Development of criteria for geotextiles and granular filters. *Prestigious Lecture 1. Proceedings of the 9th Int. Conf. on Geosynthetics*, Guarujá, Brazil, 2010, pp. 45 – 66.
- [5] NAGY L. *Buzgárok az árvízvédelemben. (ISBN 978-963-12-0319-6) und persönliche Mitteilungen* (TU Budapest), 2014.
- [6] SZABO M. Experimental and numerical analyses of relief drainages by underseepage of dykes and levees, *Doctoral thesis*, Vienna University of Technology, 2017.

SUMMARY

Underseepage of dams, dykes or levees may lead – especially in the long-term – to erosion of the ground due to (subsequent) floods. The pressures that develop landside of the dyke during floods may cause heaving or uncontrolled rupture of the near-surface blanket resulting in a concentration of seepage flow, often accompanied by piping, and potential dyke failure. Such a hydraulic failure develops mostly rather inconspicuously; therefore it is often underestimated in practice. Erosion criteria can be used to describe the critical state for different soil types found during ground investigation. For the control of underseepage pressures in the aquifer and for hydraulic failure prevention stabilizing measures at the embankment toe zone are essential. Filter stable berms, relief drainage columns or trenches, sometimes also relief wells have proven very successful.

If pressure relief measures are required, the selection of a suitable relief system has to consider the geotechnical, hydraulic and local conditions. For the design of the selected relief system (drainage columns, trenches, wells) numerical methods are commonly used in practice. A technically and economically optimized design is only possible, if hydraulic boundaries of the flow field (e.g. long-term data from groundwater observation) and the permeability of the aquifer can be determined as precisely as possible, as could be experienced in experimental and numerical studies. Finally, monitoring of existing projects contributes significantly to continuous calibration and sophistication of numerical modelling and practical design.

KEYWORDS

DAM FAILURE, FLOOD CONTROL, HYDRAULIC MODEL TESTS, INTERNAL
EROSION, RELIEF WELL, SEEPAGE, UPLIFT

COMMISSION INTERNATIONALE DES GRANDS BARRAGES

VINGT-SIXIÈME CONGRÈS DES GRANDS BARRAGES
Autriche, juillet 2018

DOI 10.3217/978-3-85125-620-8-175



This work licensed under a Creative Commons Attribution 4.0 International License. <https://creativecommons.org/licenses/by-nc-nd/4.0/>

SELECTION OF GROUT CURTAIN IN SPATIAL PLANE BASED ON SET JOINTS AND DIRECTION OF GROUTING GALLERY (GLEVARD DAM, IRAN)

Amir Ali ZAD

Assistant professor, Geotechnical Engineering Department, ISLAMIC AZAD UNIVERSITY CENTRAL TEHRAN BRANCH (IAUCTB)

IRAN

Kaivan RAHIMI

MSc Student, Geotechnical Engineering Department, ISLAMIC AZAD UNIVERSITY CENTRAL TEHRAN BRANCH (IAUCTB)

IRAN

Ali NABIZADEH

Assistant professor, Geotechnical Engineering Department, ISLAMIC AZAD UNIVERSITY CENTRAL TEHRAN BRANCH (IAUCTB)

IRAN

SELECTION OF GROUT CURTAIN IN SPATIAL PLANE BASED ON SET JOINTS AND DIRECTION OF GROUTING GALLERY (GLEVARD DAM, IRAN)

Amir Ali ZAD

Assistant professor, Geotechnical Engineering Department, ISLAMIC AZAD UNIVERSITY CENTRAL TEHRAN BRANCH (IAUCTB)

Kaivan RAHIMI

MSc Student, Geotechnical Engineering Department, ISLAMIC AZAD UNIVERSITY CENTRAL TEHRAN BRANCH (IAUCTB)

Ali NABIZADEH

Assistant professor, Geotechnical Engineering Department, ISLAMIC AZAD UNIVERSITY CENTRAL TEHRAN BRANCH (IAUCTB)

IRAN

1. INTRODUCTION

The Glevard Dam project is located in Mazandaran Province and constructed on Neka River, and its middle point situated on the coordination of 36.59 N and 53.61 E. The type of dam is CFRD and the maximum height of the dam from riverbed is 103 m and from bedrock is 113 m. Dam crest elevation is 739 m.a.s.l. with the dam crest length of 250 m and width of 10 m as shown in figure.1.

Based on the geological report of the project, left and right abutments of the dam consist of white limestone (Lw) and grey limestone (Lg). The material of riverbed includes floodplain and alluvium on the top following by gray limestone, Shemshak Formation and Gorgan metamorphic rocks at the bottom, respectively, as shown in figure.2. Selection of the grout curtain and grout boreholes shall be in a way that their direction has the optimum status in relation with the dip and dip direction of discontinuities.

The main criteria for selecting the optimum status of the dip and dip direction of grouting boreholes at Glevard dam site to cover predicted curtain plane appropriately is that pay attention to the direction of grouting galleries especially in bending parts in the left bank. The direction of the galley in the first 130 m is 7°. Afterward, two bends; one is located in 24° direction for 40 m, following 40° for the last bend with 52 m length, towards to the dam axis as shown in figure.3 and 4. Based on the existence of the effective major joint sets in the limestone, selection of inclined boreholes and inclined water tightening grout curtain plane at the left abutment of the Glevard dam proposed according to the following criteria:

- a) The necessity of drilling cross boreholes, b) more appropriate contact with effective major joints and c) more success in sealing the rock mass of foundation.

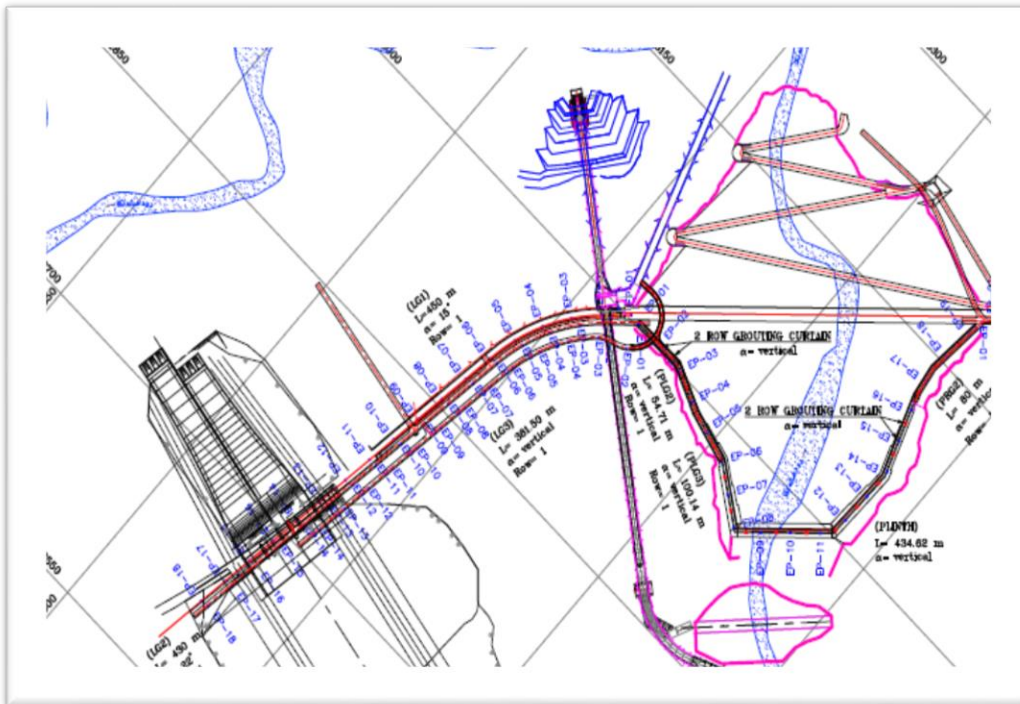


Fig. 1
General Plan of Glevard CFRD Dam

The existing effective joint and fissures crack system in the limestone, mainly with 60 to 90 degrees angle with two dominant directions, using an inclined curtain with drilling inclined borehole, will result in successful sealing of the water-tightening curtain. The inclined grout boreholes should drill in two opposing directions and inside the grout curtain plane with an appropriate angle and direction regarding joint sets at the left abutment with 140/20 and 50/20.

The existing effective joint and fissures crack system in the limestone, mainly with 60 to 90 degrees angle with two dominant directions, using an inclined curtain with drilling inclined borehole, will result in successful sealing of the water-tightening curtain. The inclined grout boreholes should drill in two opposing directions and inside the grout curtain plane with an appropriate angle and direction regarding joint sets at the left abutment with 140/20 and 50/20.

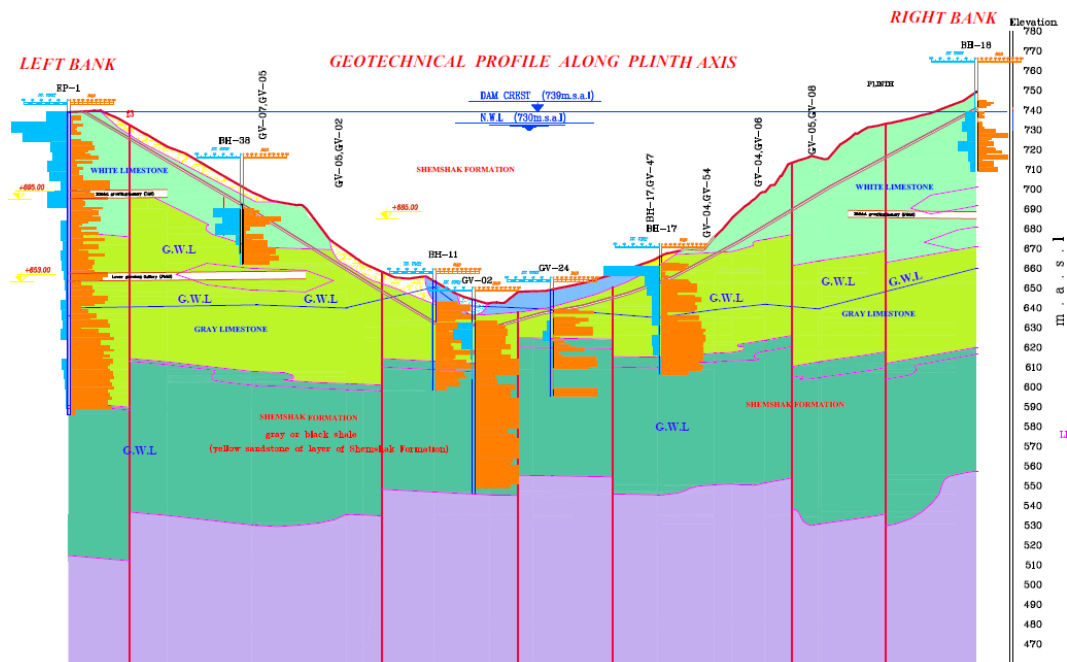


Fig. 2
Geotechnical Profile along Glevard Dam Axis

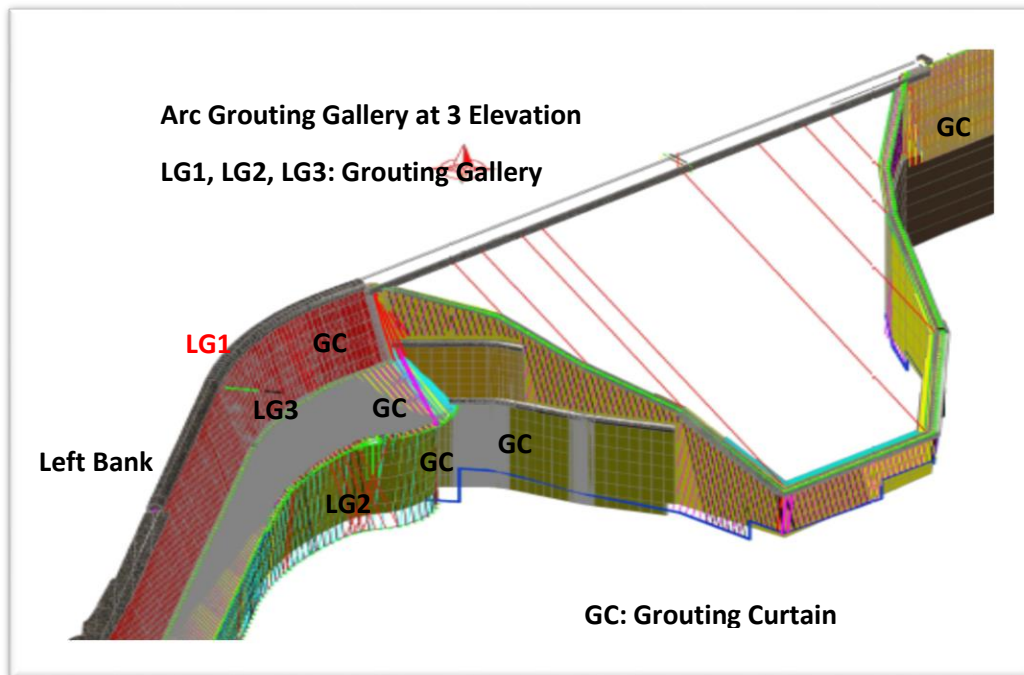


Fig. 3
3D View of curtain grouting along arc direction of grouting galleries at 3 level to guarantee the water tightening system.

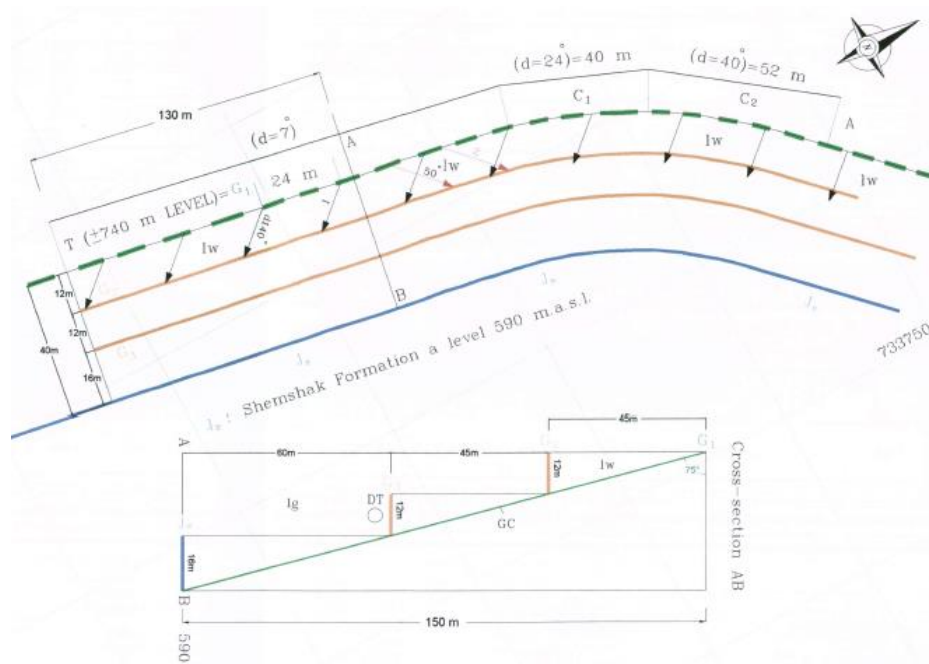


Fig. 4
 Demonstration of three bends in grouting plane (GP) along arc galleries G1, G2 and G3 at Glevard dam site

2. CONCEPT OF DRILLING INCLINED CROSS BOREHOLES FOR THE WATER TIGHTENING

Drilling inclined cross boreholes for the water tightening at the left abutment rock mass in Glevard dam is necessary. However, there are some challenges and uncertainties raised on the rate of success of the inclined curtain compared to the vertical curtain. However, in this project increase the construction costs of the inclined cross boreholes can be justified due to technical and construction reasons, as follows:

1. Based on the Fig. 5, it can be seen that the vertical / inclined combined borehole system produces rhombuses shapes with longer diameters twice as long as the longer diameter of cross boreholes. Therefore, this area is twice as large as the similar rhombus shape obtained from the inclined cross boreholes. It makes the areas among the boreholes twice and with regard to the situation of discontinuities, the limestone rock masses of the area have more uncertainty compared to the cross boreholes. It results in less effective grounding practice.

2. Selection of the inclined cross boreholes system, in terms of the costs and other economical basics, does not increase an additional cost to the project.

3. In this project, inclined boreholes drilled for exploration grouting which shows the grout curtain as almost 15° from vertical, have very good results in terms of crossing the joint and cracks system (discontinuities) and grouting in them will

considerably increase the effect of grouting. The results will be clearer in systematic grouting test panels and drilling of control boreholes. However, with regard to the findings on these boreholes, dominant discontinuities are mainly inclined in different directions in the plane, which indicate more success in contact between the boreholes and joints, as clarified in joint surveys obtained from investigation of surface discontinuities.

3. ASSESSMENT THE JOINTS STUDY OF WHITE LIMESTONE

After measuring discontinuities in the white-colored limestone (Lw) where the LG1 tunnel has been excavated, it was found that the joint sets are a little different from those selected based on the surface mapping. However, the dips are more or less consistent and joints of 104/80 and 113/78 can be considered as one group (50/83 with 63/84). Measurements were done in the 100-m long trench at the LG1 tunnel outlet portal, which is totally 84 joints. Stereographical image of the discontinuities shown in figure 6 and 7 and their engineering geological features have been provided in table 1.

Table 1
Discontinuities in white limestone surrounding gallery LG1. (SP = Spacing, W1 = slightly weathered base on the IAEG suggestion)

Joint sets	spatial	Length (m)	Spacing (m)	opening	weathering
J1	063/84	1-3	20-40	2-10	W 1-3
J2	351/82	0.5-2	15-30	3-4	W 1-3
J3	113/78	3-6	10-40	1-5	W 1-3
J4	284/67	1-4	20-50	3-5	W 1-3

A distinct reality in the white limestone rock masses (Lw) is the formation of slickenside along some joints, which is very crushed and erodible (photos 1 and 2) and the rock mass is highly crushed and full of joints and cracks.

In underground investigations of the boreholes drilled at the left abutment of Glevard dam site [phase I exploratory-grouting boreholes (LG01-EP) and exploratory boreholes (BH02,3,4)] and joints and fissures of 60 to 90 degrees, a large number of joint and fissures have been identified. The summary of the results provided for white and gray limestone in table 2. In upper white limestone which have more joints and fissures, crushing and water seepage, the frequency of joints and fissures in different zones are as follows:

Zone 1: Includes boreholes EP1 to EP4 in the inclined curtain. 272 out of 780 discontinuities (34.8%) have angles of 30 to 60 degrees and most of them have had angles of 80 to 90 degrees. In the inclined plane, these angles identified and assessed as 15°.

Zone 2: Includes boreholes EP-5 to EP-9 in the inclined water-tightening plane. Out of the 743 identified discontinuities, 28% have 60 to 90 degrees angle, showing a slight decrease compared to Zone 1. However, it still includes a large percent. It once more noted that these joints observed in the drilled boreholes in the inclined grout curtain plane.

Zone 3: Includes boreholes EP-10 to EP-12. Out of the 520 identified joints, 37.7% have 60 to 90 degrees angle, most of them have 80 to 90 degrees angles, and all of them are located in the mentioned inclined curtain plane.

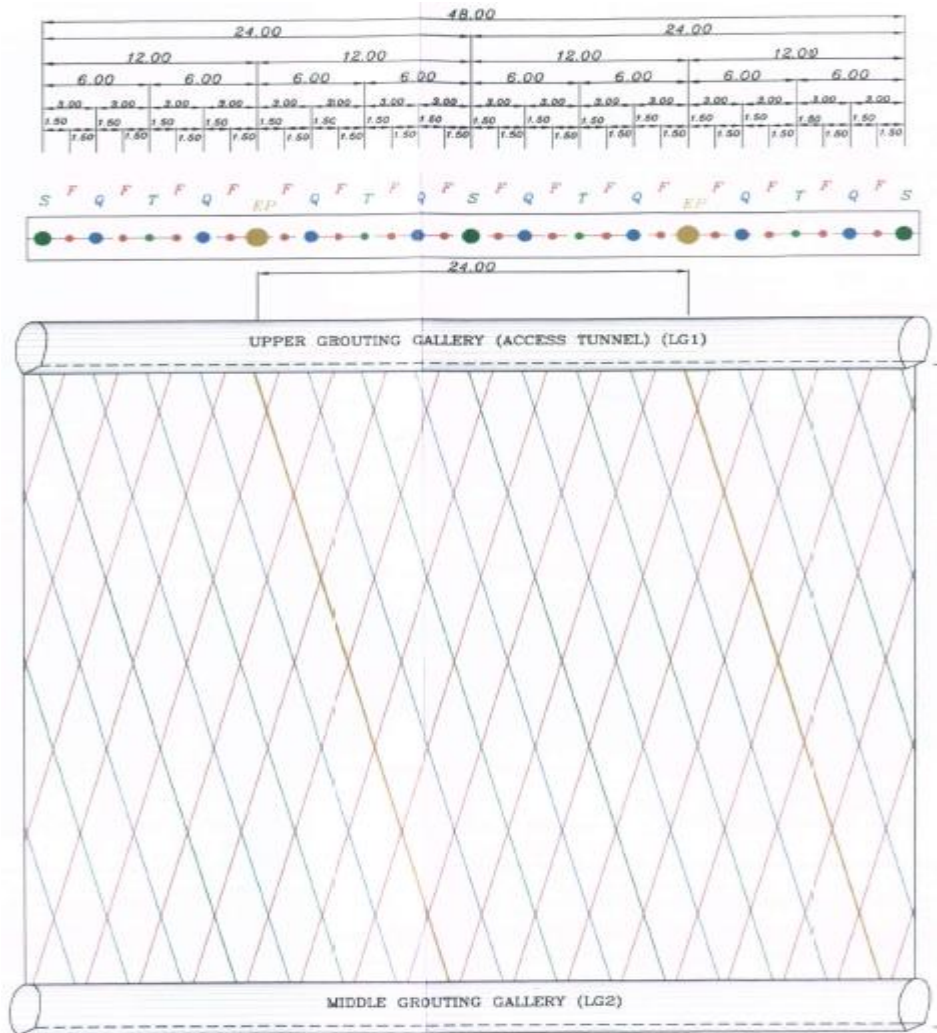


Fig. 5

Schematic Plan and Section of Grouting and Curtain Boreholes at the Left Bank of Gelevar Dam including primary, secondary, tertiary and quaternary boreholes

Zone 4: Includes boreholes BH-2 to EP-13. Out of the 151 identified joints, 69.5% have 60 to 90 degrees angle and most of them have 80 to 90 degrees angles.

Zone 5: Includes boreholes EP-14 to EP-16 and BH-3 to the south of the free spillway. Out of the 385 identified joints, 49.8% have 60 to 90 degrees angles and

most of them have 80 to 90 degrees angles. Drilling of the mentioned boreholes carried out in the 15 degrees inclined plane against the vertical.

The average number of joints with 60 to 90 degrees gradients in these boreholes is 30 to 50, sometimes 70%, which compared to other joints include the maximum number, and most of them have open joints with high seepage and cement consumption. This cause an increase in the grouting radius and thickening of the grout curtain, which is of the main objectives of this work.

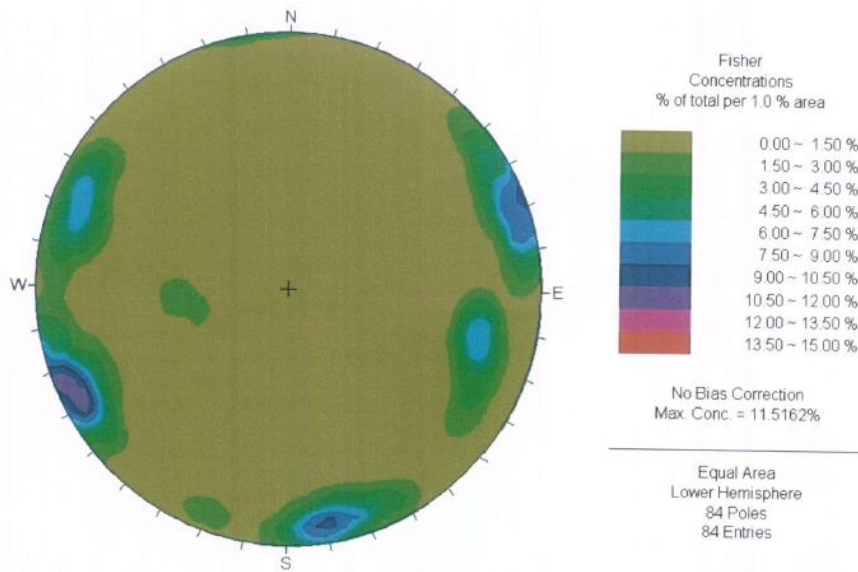


Fig. 6
Cyclographical diagram of the measured joint sets (4 sets) of Lw

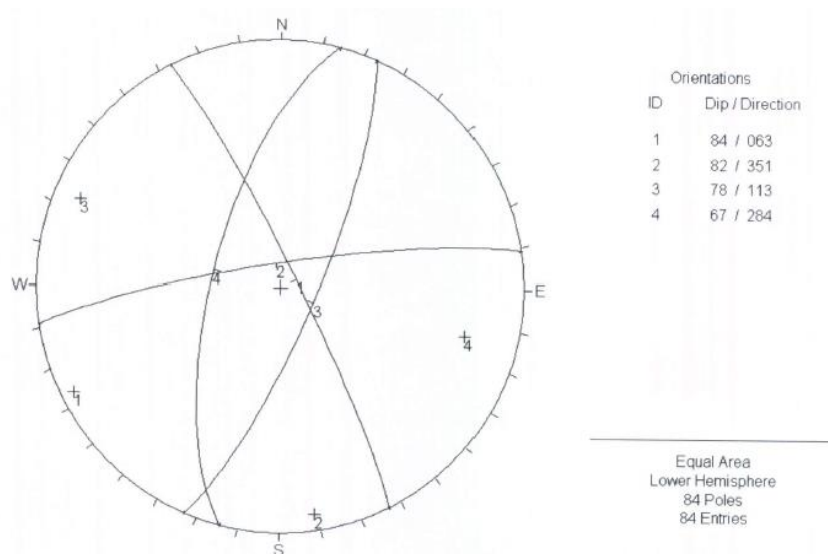


Fig. 7
Stereographical diagram of the measured joint sets in Lw (84 joints).

This investigation only relates to the number of joints, regardless of their effect on seepage). If the effect of joints with high angle compared to the joints with low angle considered on the seepage, their weight effect will be considerably more than the mentioned values.

Table 2
Summary results of classification with the angle of joints and fissures in the limestone

Location	0-30	30-60	60-80	80-90	60-90	No. of Dis.
Z.1	36.3	28.9	11.8	23	34.8	780
Z.2	42.1	29.8	8.9	19.1	28	743
Z.3	41.3	21	9.4	28.3	37.7	520
Z.4	10.6	19.9	19.9	49.6	69.5	151

Joints with high angle have much more length compared to the joints with low angle and length of up to 2.2 m reported in this project. These joints with relatively high width lead to high seepage amount (specifically in zones 1, 2, 3 and 4). As the result, drilling the inclined curtain plane, which will provide the best result in order to cover more joints.

4. SPATIAL LAYOUT OF THE GROUT CURTAIN AND TESTING EXPLORATORY GROUT HOLES

Base on the primary site visit of the outcrop of the limestone (LW) in the trench of the access way to the grouting gallery outlet portal, engineering judgment, and work experiences dip and dip direction of discontinuities are such as 210/74, 104/80, 050/83 and 180/80. This limestone has outcrops in both slopes of the gorge and in the Glevard dam axis; and LW (White Limestone) limestone include milky white, fine-grained, crystallized and dense limestone with average to high compressive strength and high weathered. They are quite different in terms of different tectonic effects, weathering, color, Karstic event, crushing, joints and fissures, filling, etc. However, generally, there have also vertical open joints with medium to high permeability in this area. As the spacing and number of these four joint sets are not available (in the report), it is not possible to use the method suggested by Zhou and Maerz (2003) in finding the spatial layout of the grout curtain [1]. As for a more appropriate evaluation, estimate of the weight of the joint sets is needed, the simplest method which is the homogeneity of the frequency of the joint sets. According to the result of this method, inclined boreholes are more efficient than vertical boreholes (figures 8 & 9).



Fig. 8

View of the crushing and jointed nature of the (Lw) limestone rock mass in trench of outlet portal.

Using the approximate method of bisectors [2], first the appropriate dip of grouting estimated as shown in fig.10. The bisector of the dip of two joints sets 104 and 50 degrees will be in 77-degree direction. The bisector of the dip of two joint sets 180 and 210 degrees is in 195 degrees direction and bisector of 77 and 195 degrees delineated, it will be in 136 degrees direction. homogeneity of the frequency of the joint sets. According to the result of this method, inclined boreholes are more efficient than vertical boreholes (figures 8 & 9).

Table 3
Calculating LSBI θ , (84 joints)

210/74°	104/80°	050/83°	180/80°	Dip	Sum
1.040	1.015	1.008	1.015	0	4.079
1.113	1.064	1.046	1.064	10	4.287
1.236	1.155	1.122	1.155	20	4.668
1.440	1.305	1.252	1.305	30	5.303
1.788	1.556	1.466	1.556	40	6.366
2.459	2.000	1.836	2.000	50	8.295
4.134	2.924	2.559	2.924	60	12.540
14.336	5.759	4.445	5.759	70	30.299
9.567		19.107		80	
3.628	5.759	8.206	5.759	90	23.351
2.281	2.924	3.420	2.924	100	11.549
1.707	2.000	2.203	2.000	110	7.904
1.390	1.556	1.662	1.556	120	6.163
1.206	1.305	1.367	1.305	130	5.184
1.095	1.155	1.192	1.155	140	4.596
1.031	1.064	1.086	1.064	150	4.245
1.002	1.015	1.026	1.015	160	4.060
1.006	1.000	1.001	1.000	170	4.007
1.040	1.015	1.008	1.015	180	4.079

Using this method, the direction between 136 and 142 has been selected for the grouting direction and 140 degrees has been suggested which makes a 47degrees gradient (p) with the tunnel direction. It is clear that a vertical surface in such a direction will cut the four joint sets with 74, 80, 83 and 80 degrees dips, with decreased gradients (apparent dip).

This gradient will be 50, 77.7, 0.0 and 77 degrees. All boreholes are on the mentioned surface. It is clear that each borehole can be located in this vertical surface but a borehole, which is more prominent with the dip of the joint sets, is more appropriate.

This, it is quite clear that inclined boreholes can pass by the highly dipped joints better and more appropriately. Therefore, estimating the average of the

mentioned gradients, which is 63 degrees, 70° accepted as more appropriate than other gradients.

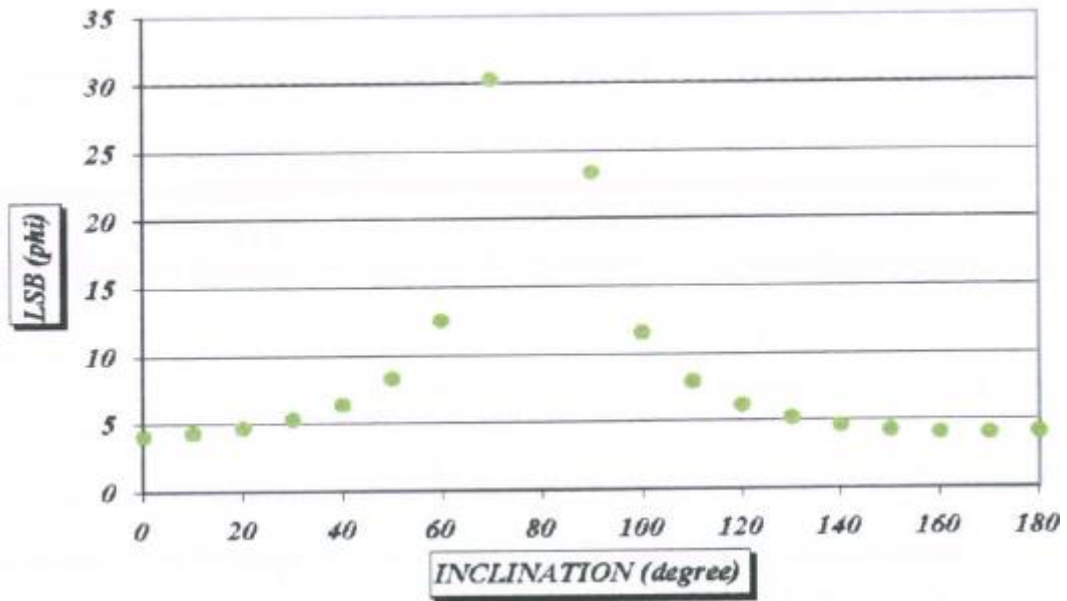


Fig. 9

Diagram Showing Borehole Inclination Direction Relation to Horizontal Line (150° - 180°) Is More Convenient

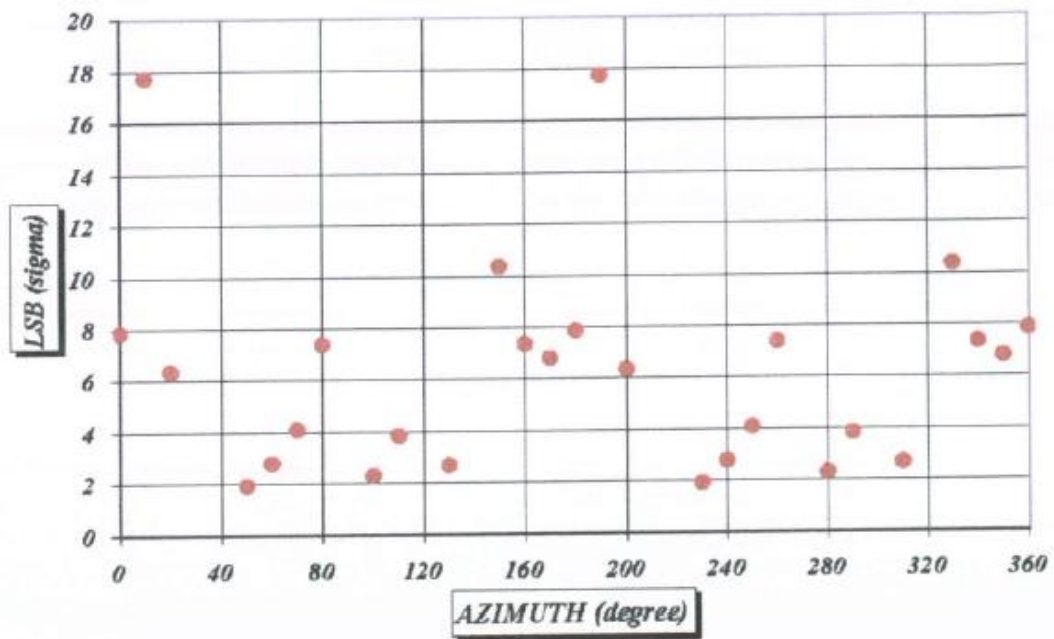


Fig. 10

Borehole Azimuth Angle (100° & 280°)

Table 4
Calculating LSBI β , (84 joints)

$\delta=120^\circ$	$\delta=14^\circ$	$\delta=140$	$\delta=90^\circ$	Azimuth	Sum
1.155	4.134	1.556	1.000	0	7.844
1.064	14.336	1.305	1.015	10	17.721
1.015	9.567	1.155	1.064	20	6.332
1.000	3.628	1.064	1.155	30	0.409
1.025	2.281	1.015	1.305	40	1.055
1.064	1.701	1.000	1.558	50	1.919
1.155	1.390	1.015	2.000	60	2.780
1.305	1.208	1.064	2.924	70	4.087
1.556	1.095	1.155	5.759	80	7.375
2.924	1.002	1.556	5.759	100	2.282
5.759	1.006	2.000	2.924	110	3.829
5.759	1.113	5.759	1.556	130	2.668
2.000	1.440	5.759	1.155	150	10.353
1.556	1.788	2.924	1.064	160	7.332
1.305	2.459	2.000	1.015	170	6.779
1.155	4.134	1.556	1.000	180	7.844
1.084	14.336	1.305	1.015	190	17.721
1.015	9.567	1.115	1.064	200	6.332
1.000	3.628	1.064	1.155	210	0.409
1.015	2.281	1.015	1.305	220	1.055
1.064	1.701	1.000	1.556	230	1.919
1.155	1.390	1.015	2.000	240	2.780
1.305	1.208	1.064	2.924	250	4.087
1.556	1.095	1.155	5.759	260	7.375
2.924	1.002	1.556	5.759	280	2.282
5.759	1.008	2.000	2.924	290	3.829
5.759	1.113	5.759	1.226	310	2.668
2.000	1.440	5.759	1.155	330	10.353
1.226	1.788	2.924	1.064	340	7.332
1.305	2.459	2.000	1.15	350	6.779
1.155	4.134	1.556	1.000	360	7.844

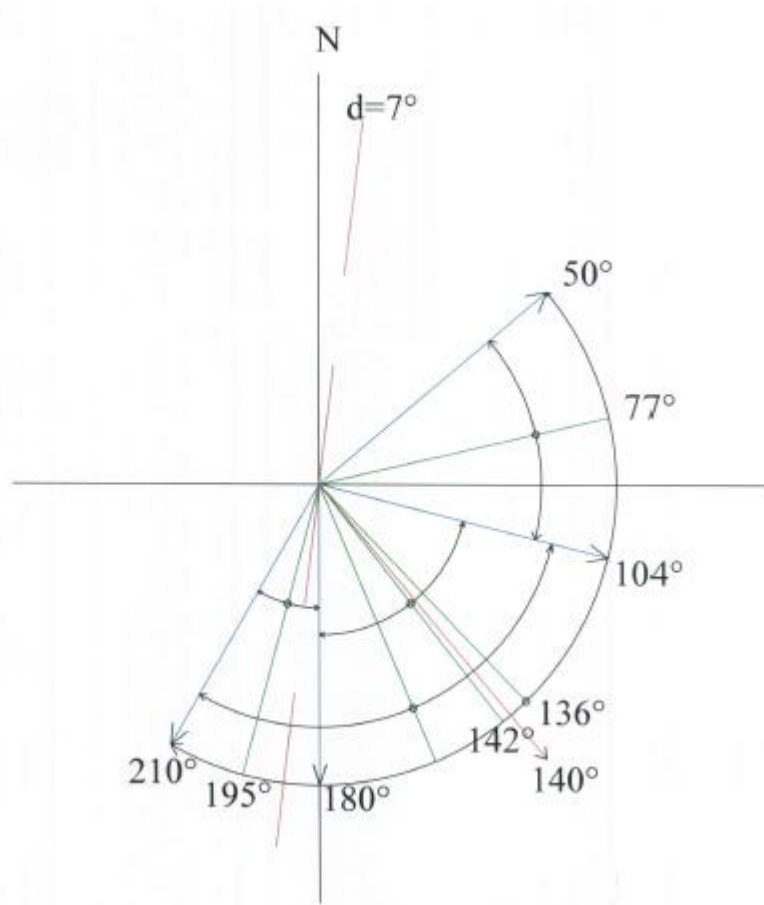


Fig. 11

How to find the more appropriate grouting direction to include all four joint sets. 140° is the direction selected for the azimuth of the exploration grouting borehole (d=7° is the direction of the grouting gallery).

Inclined borehole suggested in the Zhou and Maerz method. Selection of an inclined borehole in 140 degrees direction on a surface with 7 degrees direction (direction of the access tunnel) would be impossible unless with an inclined grouting curtain. Thus, the following method used for finding the gradient of the grout curtain. Boreholes 140/70 will be more applicable in grouting and each of the boreholes drilled in a depth 45 m lower than access tunnel invert in 16 m spacing. For such boreholes to be within the grout curtain, the direction of the grout curtain is the same as the access tunnel (7 degrees), the spatial layout of the grout curtain must be $97/\alpha$. It can be easily found out that if the gallery is lower than the access tunnel in 45 m depth, the spacing between the axis of the access tunnel and the parallel gallery beneath it would be 12 m ($m = m' \sin 13 = 12$ m). This method reveals that the grout curtain should be 45 m deep, with 12 m perpendicular spacing and therefore, the curtain should be inclined, with a dip of $\alpha = (\tan = 45/12)$. Thus, 097°/75° would be its spatial layout as shown in figure.11.

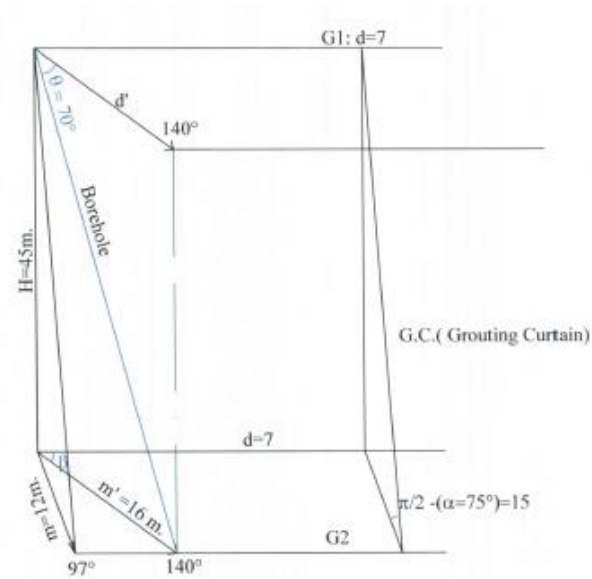


Fig. 12

The layout of the grout curtain and the 140/70 inclined borehole.

Selection of Spatial Layout of the Grout Curtain and Grouting Borehole Based on the white Colored Limestone Joint Sets To estimate the dip and dip direction of the grouting borehole, the following two methods used:

1. Bisector Approximate Method

This is the same method shown in figure 8 & 9. The result of this method provided in the figure.12 where dip direction of the grout borehole obtained as 50 degrees. Thus, the grout borehole will have a 69-degree dip towards 50 degrees.

The bisector of 88 and 318 degrees is in 23 degrees direction, which will be in the grout curtain if the direction of the borehole is 23 to 27 degrees (25°) and its dip is 49° . However, its slope is not so much appropriate. The bisector of 113 and 351 degrees is in 52 degrees direction, which will be in the grout curtain with the slope of 68.7° and will be more appropriate than the borehole with 49° dip and it is so suggested (borehole 0.05/69 or 0.50/70). See figure 5. ($d=70^\circ$: the direction of the access tunnel).

For a borehole of 50° dip to be located in 0.97/75 grout curtain its dip should be 69.9 or 79 degrees. Figure 13 shows how to estimate the gradient and it can also be shown that in case a borehole is drilled towards 50° , the curtain should be inclined, $a = 75$, if it is to be in the 097/a grout curtain. Followings are the marks used in this general figure:

p = gradient between the axis of the access tunnel or galleries and the grout curtain = gallery G1.

d' = direction of the grout borehole which should be in the grout curtain.

m = spacing between the direction of the grout curtain and gallery G2.

m' = spacing between the direction of the grout curtain and the grout borehole (d').

θ = grout curtain gradient

θ' = grout borehole gradient

l = length of the largest dip of the grout curtain to the surface of gallery G2, δ which is H m lower than G1 as shown in figure 14.

With $\theta = 75^\circ$, $m = 12.06$ m, $\theta = 47^\circ$ and $H = 45$, it is easily possible to estimate θ' and m' .

$\theta' = \tan^{-1} (H/m) * (\sin \theta)$, or (conversely, it is possible to obtain θ , having d/δ).

The result would be $\theta = 69.8^\circ$ or 70° and therefore, the grout borehole with the spatial layout of 050/70 will be located in the grout curtain of 097/75.

Conversely, if $\theta' = 70^\circ$, $m = 12$ and $\tan \theta = 45/12$ and so, $\theta = 75^\circ$.

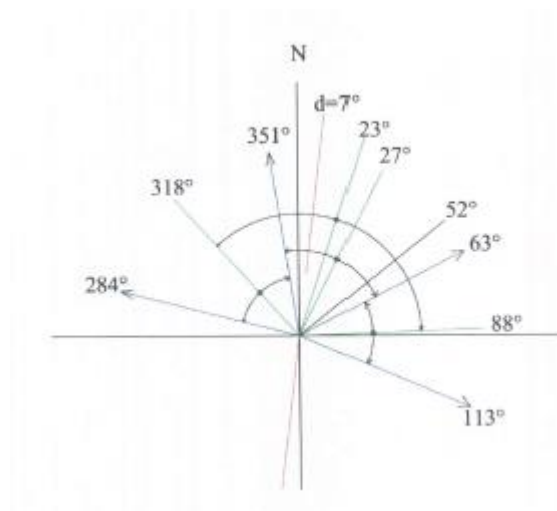


Fig. 13

Selection of grout borehole based on white-colored limestone joints in gallery (bisectors method) is 4 joint sets of 63/84, 351/82, 113/78 and 284/67.

2. Zhou and Maerz Suggested Method (2003)

In this method, based on a bias index of the measured discontinuities (Linear Sampling Bias Index= LSBI), a borehole which will optimally cut all joint sets (optimum borehole of δ/θ). Bias index of the borehole dip slope is:

$$LSBI \theta = \sum_{1}^{n} (1/\sin \alpha_i) * W_i$$

and the bias index of the borehole azimuth is:

$$LSBI \delta = \sum_{1}^{n} (1/\sin \beta_i) * W_i$$

In the above relations, w_i is the weight which is the ratio between the spacing of each joint set and all joint sets. α_i is the dip gradient of the joint set i and β_i is the gradient between δ and direction of the joint.

To estimate optimum θ and δ , their values estimated in the mentioned relationships from 0° to 180° for θ and from 0° to 360° for δ .

In the x and y diagram, where x is θ or δ and y is $LSBI\theta$ or $LSBI\delta$, the least values of these two diagrams provide values of θ and δ .

As shown in figure 15, the value of θ has been selected as equal to 130° in relation to the horizontal surface (0° is another answer which is not used (horizontal borehole)).

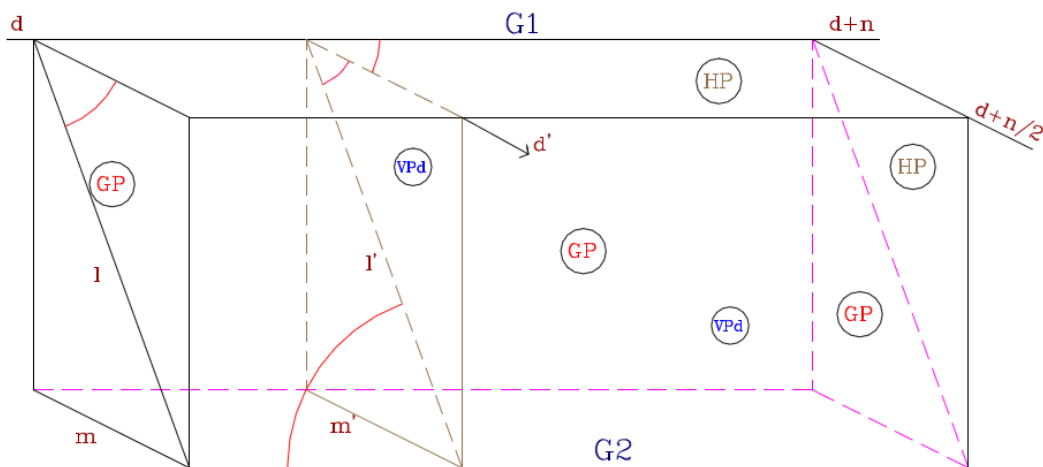


Fig. 14

Demonstration of grouting plane (GP) along galleries LG_1 , LG_2 , Glevard dam site

VP: $d = 7^\circ$, $\theta = 70^\circ$, $H = 45$ m, $l = 47$ m, $m = 12.06$ m
 VPd: $\beta = 47^\circ$, $d' = 140^\circ$, $\theta' = 70^\circ$, $l' = 47.9$ m, $m' = 16.4$
 HP = Horizontal Plane
 VP = Vertical Plane Crossing d'
 VPd = Vertical Plane Crossing d
 G1, G2 = Galleries
 GP = Grouting Plane
 λ = Angle Between l' & axis of G1, G2, on the Gp

Value of δ estimated in figure 16 and the borehole azimuth selected as 125° . According to the mentioned researchers, if the value of θ is more than 90° , δ with a value of less than 180° will be more appropriate. Based on the two values of θ and δ , the spatial layout of the borehole will be $125/160$ and as the dip gradient is against the horizon, the spatial layout obtained as $125/30$.

This spatial layout is for a general statement; however, it cannot be sufficient for a special feature such as grout curtain where grout galleries are within a tunnel or gallery [3]; like grouting in Glevard where the 30° dip never accepted. The mentioned method, which mentioned to clarify that the selection of the requested feature, based on the engineering geological investigation strategies (at least with two methods).

For a borehole which is drilled towards 125° ($D=62^\circ$ and $m'=13.6^\circ$) to be within the grout curtain, it is necessary that its dip is 73°, which is very inconsistent with 30°. As the result, dip of the best borehole, which is 30° with this method, not accepted, as it is not located in the grout curtain.

Therefore, selection method will be the same approximate method that provided the borehole as 50/70, which is quite different from the primary state of 140/70 (perpendicular to it) and these two boreholes, which have crossing state, used to fill out the grout curtain [4].

The least value in this diagram is zero and 130 degree (borehole dip is in the inclined plane). The horizontal borehole is not acceptable and therefore, $\theta = 130^\circ$. The dip of four joint sets is 67, 78, 82 and 84 degrees, with an effective weight of 31, 22, 20, and 27 from 100(w_i).

The least value is 125 and 305 degrees. As the value of θ estimated at 130°, the 125° azimuth selected.

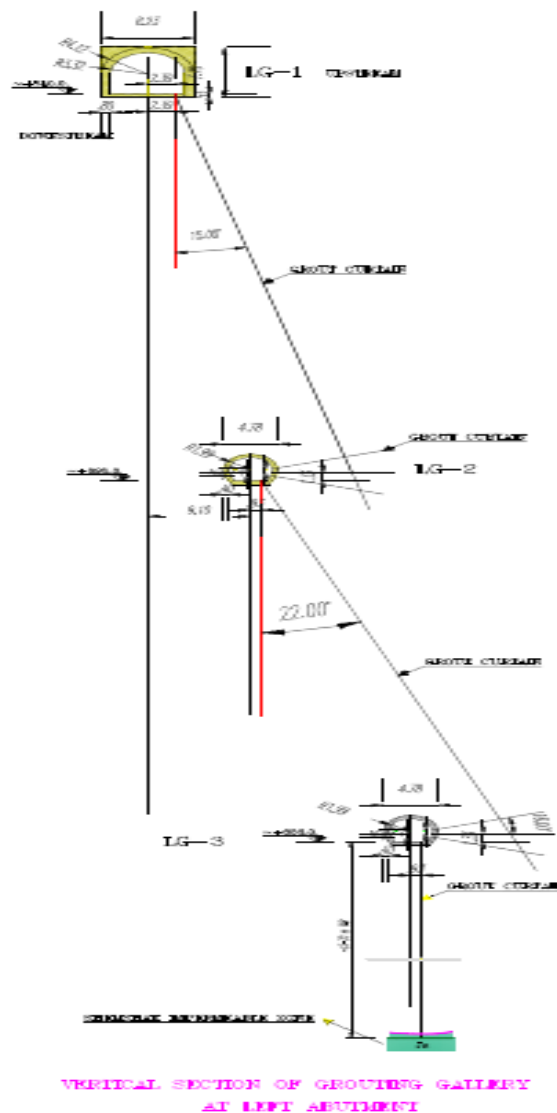


Fig. 15
Vertical section of grouting gallery at left bank of Glevard dam site.

5. MAIN SELECTION OF GROUT GALLERIES IN BENDING PARTS OF THE TUNNEL G1

As already mentioned, the direction of the gallery in its first 120 m is 7 degrees. Afterward, there two bends, one in 24 degrees direction, for 40 m, and then in 40 degrees for 52 m, up to the dam axis. For the grout boreholes to be carried out with the very 140 and 50 degrees directions, they need to have different

dips, which belongs to the values of f_3 and m' . If the dip of these boreholes is not known, there is no way but to change their dip direction.

5.1. FIRST BENDING PART ($D=24^\circ$)

For 140 degrees borehole direction: $13=64$, $m'=13.35$, $O=73.5$ and they are resultant would be a borehole of 140/73/5. For 50 degrees borehole direction: $f=26$, $m'=27.37$, $O=58.7$ and their results would be a borehole of 50/58/7. If the borehole dip direction is selected as 70° , $p=46^\circ$ and $m'=16.68$ and the dip gradient will be 69.6 or 70° , which is more appropriate.

5.2. SECOND BENDING PART ($D=40^\circ$)

For 140 degrees borehole direction: $13=80$, $m'=12.19$, $O=74.8$, with a 140/75 view. For 50 degrees borehole direction: $13=10$, $m'=69.11$, $O=33$, with a 50/33 view, which is not appropriate (the dip is very slight) and if the dip direction is 90° , borehole dip will be 71 degrees ($P=50$, $m'=15.66$).

Zonation of the G1 access tunnel based on the direction of its bending part, has been carried out with the view that the bending parts are replaced with straight parts, so that the ratio of the straight part, (l_i), to its bending part (C_i) is not less than $\{l_i/c_i\} \geq 0.95$. The straight part of the tunnel is 130 m long, which considered as the starting part of the access tunnel. The straight part, with a length of 40 m, has been replaced for the 41.5 m long first bending part (with a ratio of 0.96) and the second bending part which is 52.8 m long and its straight part which is 52 m long will provide a ratio of 0.98 (figure 4).

Access tunnel G1 is located at El. 740 — 743 m.a.s.l. and based on boreholes 01 and 01G, Shemshak Formation with very low permeable to impermeable is located at 150 m below the access tunnel (El. 590 m.a.s.l.). Therefore, at least two galleries parallel with the access tunnel and below is carried out for grouting purpose. Gallery G2 has been foreseen 45 m below the G1 at (El. 695 m.a.s.l.) and dip and gradient of the grout galleries was estimated based on it.

6. FINAL TECHNICAL NOTE

With regard to the explanations provided above, following complementary notes, along with some figures and diagrams seem to be useful for a better understanding of the described technical points. So the following notes provided hereunder:

1. More suitability of inclined boreholes compared to the vertical ones in each vertical surface including the joint sets discussed here. This is a very clear understanding and is certainly known by an expert, however, three directions have been selected here to show it; 7° (access tunnel direction) which will be at the same direction with the grout curtain, too, 140° (azimuth of the grout gallery) and 50° (azimuth of the grout gallery).

2. To do this, joint sets in table 1 (based on the 84 measured joints) have been delineated in 1 m² of the vertical surface, so that the maximum number of joints can be shown. The spacing (SP) of these joints is available which will be as $Sph = SP/\sin a$ on a horizontal line along the dip direction of the joint [5]. Figure 17 shows the vertical boreholes in all the three vertical surfaces with the mentioned directions. It can be clearly seen that at the contact point of the borehole with the joints at 140° direction surface, it is more than the other two directions; 5 against 4.

7° is the direction of the access tunnel and grout curtain. It clearly concluded that there are clear advantages in 50 and 140 degrees directions compared with 7-degree direction, in the vertical curtain. The opening of the joints in three directions have been estimated using the following relationship and β is the gradient between d' and δ [6].

$$Sph \beta = sp. \frac{cotg \alpha'}{cos \alpha}$$

$$\alpha' = tg - 1 (cos \beta. tg \alpha)$$

The number of boreholes to be drilled in this 1 m² with the most contact points, in the 50° direction surface is 3 boreholes and in the other two directions is 2. View of the joints contacts clearly shows more and wider open spaces in the 7° direction. Generally, advantages of the 50 and 140 degrees directions seen from the 7° direction.

This view shown in figure 10 for the inclined boreholes in all the mentioned three vertical surfaces where advantages of inclined boreholes compared to the vertical ones in 50 and 140 degrees direction are quite clear.

3. If we look at the inclined curtain with 097/75 spatial layout, if the same features of the joints existing in vertical surfaces turn by the value of the 0 slope, the difference in the sooner contact of the inclined boreholes with the joints will be clearly recognized. It is impossible to drill a vertical borehole in such an inclined surface. However, the view of the four joints and cross of the boreholes shown with the following relationships

4. All of the observed discontinuities at the ground surface and walls of the river and the excavated trenches, mainly express figures whose geometrical forms and surface forms of the discontinuities shown on figure 18.

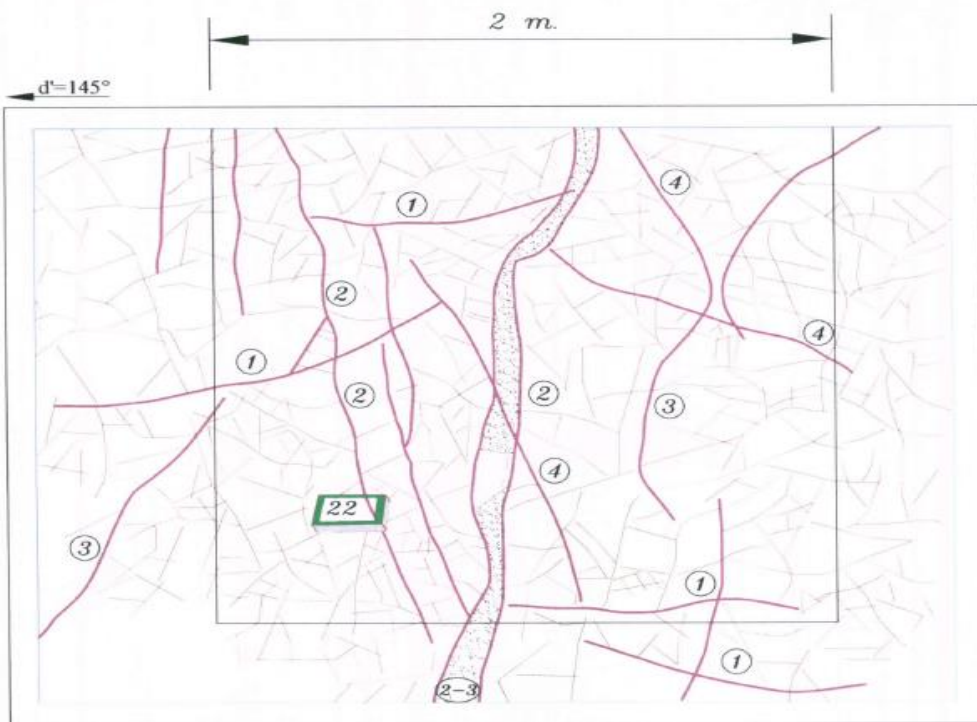


Fig. 16
View based on the spacing of the joints and the decreased angle of the joints at 145° direction, where the difference are very clear.

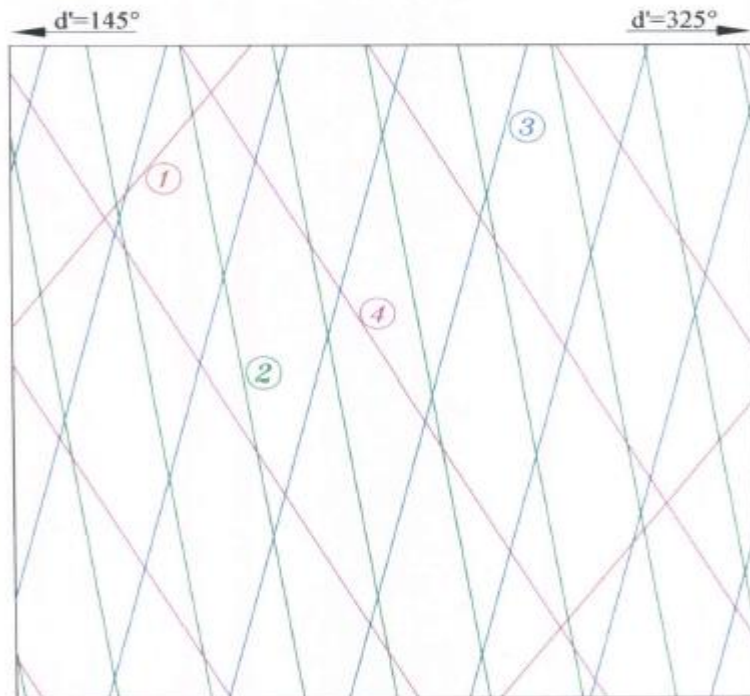


Fig. 17
View of discontinuities in 4 m² of the trench wall

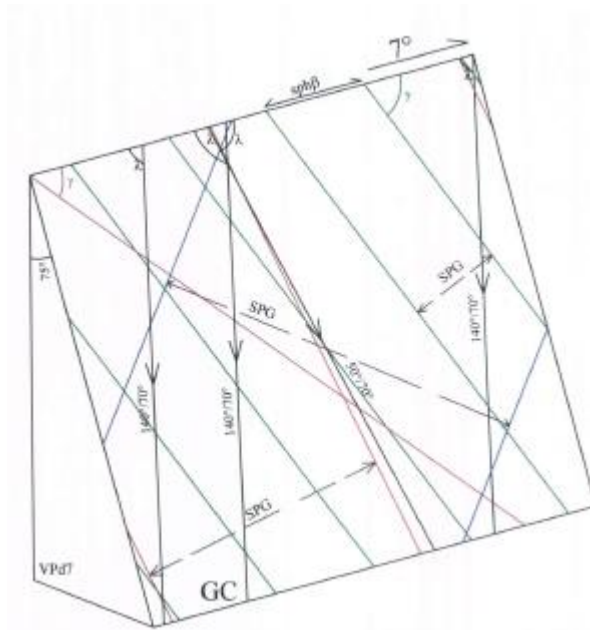


Fig. 18

Number of joint contacts in vertical borehole in vertical surface in the three direction.

5. All of the dominant discontinuities in the white-colored limestone rock mass (1w) at the surface have dips more than 67° and even up to 84° (joint sets J1 and J2 have 84° and 82° degrees dips, respectively). Therefore, the vertical nature of drilled boreholes in terms of cement grout and success is not appropriate, useful, and rejected.

6. Figures 3, 4 and 5 show the delineation status of the planes with 40, 24 and 7 degrees directions. With regard to these values, it can be seen that change in the direction of the planes is highly effective on the contact with the discontinuity planes and the most effective can be seen in the figure below figure 19. As is seen there, what observed on the ground surface has totally complicated and complex conditions and has different bends. This is so that imaging the observed planes on the ground surface on one plane, is not so much compatible and is no help in recognizing their geometrical status with changes from the surface to depth [7]. Thus, the information obtained from the exploration grout galleries in the selected 15° inclined plane for the grout curtain shows a very different situation, in terms of contact with discontinuities through the mentioned boreholes, compared to the surface information.

7. Delineation of the diagram of discontinuities as mentioned here above and referred to in different figures indicate that no important visual feature can be shown in 15° inclined plane. This is because; part of the discontinuities with the provided geometrical relations cannot be in contact with the mentioned inclined plane. However, drilling boreholes in this plane revealed that the effectiveness and usefulness of an inclined grout plane effects on the degree of groutability and success of the work through an increase in the thickness of the grout curtain and

decrease in its hydraulic gradient [8]. This carefully proven after the accomplishment of the work and control of the obtained results.

8. By comparing the above-mentioned, it is seen that the contact of discontinuities in the inclined plane is considerably more than that of the vertical plane. However, some of the discontinuities not shown in the inclined plane.

SUMMARY

1. The grout gallery will so cross that its slope with 70° direction will be equal to λ , $\sin \lambda = \sin \phi' / \sin \theta$. In this equation, $\theta = 75^\circ$ and $\phi' = 70^\circ$ and as the result, for 113/78 joints with $SP = 27$ cm, this angle will be equal to $\lambda = 76.5^\circ$.

2. Decreased angle (α) in the vertical surface ($d=7^\circ$) will be equal to α' and in the vertical surface at the direction of the inclined borehole will be equal to α'' . For the mentioned joints, these two values are: $\alpha' = 52^\circ$ & $\alpha'' = 78^\circ$.

3. Length of the spacing (SP) on each horizontal line, which makes the p angle with the direction of the joint, will be equal to:

$Sph\beta = SP / \cos \alpha (\cos \alpha)$ which will be $Sph13 = 101$ cm for this joint ($SP = 27$ cm), as shown in figure 20.

4. Angle α' which is 52° in the vertical surface ($d = 7^\circ$), will be 62° in the 097/75 inclined surface.

5. $SPG = Sph\beta \sin \gamma$ will be the value of spacing (SP) on the 097/75 grout curtain surface, which will be equal to 89 cm and clearly less than $SPV = Sp / \cos \alpha$, which is almost 130 cm (which shows a more number of joints).

6. Explanations on 113/78 joints are applicable to other joints and therefore, the structural drawing of the inclined grout curtain can be easily delineated having the values of θ , α and SP and angles λ and γ and the value of SPG .

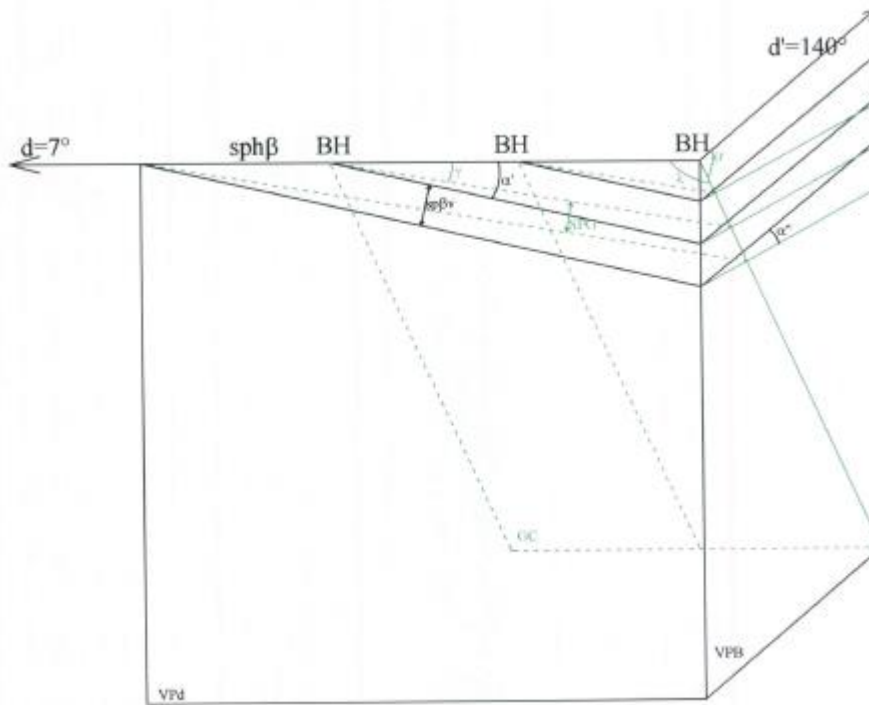


Fig. 19

demonstration of inclined borehole $d'/\theta' = (140/70)$ and joint $\delta/\alpha = (113/78)$ on the inclined grouting curtain $d/\theta = (7/75)$.

VP = vertical plane of $d 7^\circ$.

VPB = Vertical Plane along d' ($d' = 140^\circ$)

GC = inclined grouting curtain.

α' , α'' = reduced dip angle of joint on the vertical plans of $d 7^\circ$ and $d' 140^\circ$.

λ = angle between trace of inclined borehole on the GC.

$$(\lambda = \sin^{-1} (\sin \theta' / \sin \theta))$$

γ = reduced angle of joint on the GC.

$$(\gamma = \cot g - 1 \left(\frac{\sin \theta' + \tan \alpha' \cos k}{\tan \alpha' \sin k} \right), (k = \pi - \lambda))$$

$\text{sph}\beta$ = horizontal spacing of joint set on the line $d 7^\circ$.

$$(d7^\circ) = \left(\frac{sp}{\cos \alpha} \cot g \alpha' \right), \text{ this exhibition undertaken for all joint, beds or fault, ets.}$$

Borehole BH are lying on the GC.

SPG = inclined SP on the GC.

$$(SPG = \text{sph}\beta \sin \gamma)$$

CONCLUSION

1. With regard to the results obtained in the surface and underground investigations in the boreholes, the large number of vertical joints and fissures found with two dominant directions. Indeed, it is necessary to drill cross boreholes to have more appropriate and more numerous contacts with discontinuities and more appropriate grout to attain more success in water tightening.

2. For a better understanding, the conditions of boreholes presented in geometrical view, in both vertical curtains with vertical- inclined and inclined - inclined cross-borehole systems, as shown in Fig. 1. In the inclined cross-borehole system, there is a number of crosses and smaller areas found among the boreholes, which is itself a reason for the necessity of carrying out inclined cross boreholes to obtain more success compared to the vertical — inclined cross boreholes.

3. Regarding the effectiveness of the grouting radius, it again pointed out that the rhombic forms among the inclined cross boreholes have areas equal to one-half of the rhombus forms obtained in vertical-inclined boreholes. Penetration of the vertical-inclined grout obtained with smaller penetration radius but in the inclined-inclined cross borehole system, resulting a better overview of the grouting layout and attain more success. In addition, the construction has no additional cost for the inclined-inclined cross boreholes as well as increasing the grout radius and thickness of the curtain. Based on the results, drilling the inclined curtain plane, which will provide the best result in order to cover more joints.

4. It can be concluded from the above-mentioned descriptions that the grout curtain should drill with the inclined cross boreholes and spatial layout of 97/75, 114/75 and 130/75. These inclined borehole located in the three directions of the access tunnel to the dam crest and middle and lower grout galleries of the limestone rock mass is carried out with a better groutability. With an increase in the grout radius, the thickness of the water-tightening curtain increased and the hydraulic gradient (for a more appropriate longer performance) decreased, which is totally justifiable and necessary for construction purpose.

REFERENCES

- [1] Zhou, W. and Maerz, N. H., Identification the optimum drilling for characterization of discontinuous rock the Geological Society of America.(2003)
- [2] Nabavi, M. H., 2009, Research on defects of RQD estimate and solution in equivalent joint effect on the rock masses – Mining Engineering System Magazine, No. 2, spring 2009, pp 14 – 34.
- [3] Ewert, F.-K.: Rock grouting with emphasis on dam sites, 225 Figures, 428 p. Springer, Berlin(1985)

- [4] Ewert, F.-K.: Rock type related criteria for curtain grouting. In: International Conference Grouting 2003, New Orleans. vol. III, pp. 199–220, 18 Figs. Deep Foundation Institute, Hawthorne (2004)
- [5] Foyo, A., Tomillo, C., Cerda, L.: The low-pressure test. Determination of the permeability and groutability of slate rocks in large dam foundations, XVII ICOLD, Vienna, Q.66, R.5 (1991)
- [6] Foyo, A.: Permeability, groutability and hydraulic monitoring of large dam foundations. Eurock '93, Lisboa, pp. 115–120 (1993)
- [7] Houlsby, A.C.: Construction and design of cement grouting, p. 442. Wiley Inc., New York (1990)
- [8] Lombardi, G., Deere, D.: Grouting design and control using the GIN principle. International Water Power & Dam Construction, June 1993. pp. 15–22, 6 (1993)

SUMMARY AND KEYWORDS

The most important morphological feature of the left abutment at the Gelevard CFRD dam site is the bend and change of direction in the Neka River course at the downstream and its crossing from the downstream of the left abutment at the dam axis. Different factors will provide a place for large seepage from the reservoir water into the tailrace and into the Neka River. Firstly, Existence of steep cliffs on the slopes and a very small distance between the dam reservoir and the Neka River pathway in the downstream. Secondly, the existence of dominant joints sets with 60 to 90 degrees dip and the E-W or SW direction which can connect the dam reservoir to the Neka River at the downstream left abutment, if its length is sufficient and in case of lack of appropriate sealing. These specific conditions make this project an especial case in terms of topography and morphology of the left bank of the Gelevard dam. In this project, drilling of investigation boreholes carried out in phase I and II in the constructed grouting gallery, indicating inclined grout curtain shall be selected with a dip of $\theta = 75^\circ$, according to the estimation of elaborate discontinuities in the rock mass. Therefore, the grout curtains should also be inclined ones.

Based on the proposed design, the locating of the grouting gallery and dip of the joints, spatial layout of the grout curtain for the first 130 m will be 097/75. As the grouting gallery direction towards the dam axis has a double bend, the mentioned spatial layout will be amended after the first 130 m.

In order to elaborate the details of grouting curtain design, a set of discontinuities, specifically, the joints, have been considered. Grout boreholes within the LG1 grouting gallery shall be drilled in the cross inclined direction in the inclined plane of grout curtain.

Key word: Grouting Curtain, Set Discontinuities, spatial layout, Gelevard, CFRD Dam

COMMISSION INTERNATIONALE
DES GRANDS BARRAGES

VINGT-SIXIÈME CONGRÈS DES
GRANDS BARRAGES
Autriche, juillet 2018

**CASE STUDY: ITUANGO HYDROELECTRIC PROJECT-ADDRESSING
GEOLOGICAL AND GEOTECHNICAL ISSUES ON THE ROCKFILL-CLAY
CORE DAM'S FOUNDATION DESIGN***

Maria C. SIERRA

Director of geotechnical department at Integral consultancy company

Juan E. MUNERA

Senior civil engineer Integral consultancy company

COLOMBIA

1. ABSTRACT

The most important hydroelectric project in Colombia's history, located 171 km north of the city of Medellin (Fig. 1), Hydroituango will begin to operate partially in 2018 and with its full capacity in 2026. With 2400 MW of installed capacity distributed in eight Francis turbines, this megaproject icon of the Colombian engineering has presented many challenges before giving its light.



* *Étude de cas: Projet hydroélectrique d'Ituango – Relatif aux affaires géologiques et géotechniques dans la conception de la fondation du barrage en enrochement avec cœur d'argile.*

Fig. 1 Hydro-Ituango dam construction process november 2016
photographic taken downstream

Hydroituango features a rockfill-clay core dam of 235 meters high and 965 meters wide, located in the denominated canyon of the Cauca river. This dam has presented multiple difficulties during its construction process, mainly due to the geological condition of the area, which shows the confluence of two fault systems called Mellizo and Tocayo, along the two sides of the river and that have conditioned sensibly the design of the dam, particularly the left abutment, where, in addition to the faults, has a series of discontinuities with high presence of clay material and fractured rock.

In this paper, a solution to prevent that the clay core of the dam suffers from non-permissible differential settlement is presented, integrating the geology features by means of a 3D numerical model (Fig. 2), to evaluate the shear strains in the core, comparing them with the available results of the big scale triaxial tests, verifying the stability of the dam against construction process, full reservoir and seismic conditions.

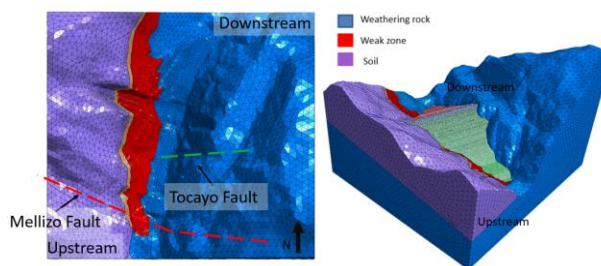


Fig. 2 Finite element numerical model-representation of the dam foundation and rockfill dam.

REFERENCES

- [1] INTEGRAL S.A (2017). "I-2194-122016 *Parámetros de los materiales de la presa*. Doceava Visita Asesores EPM. Febrero de 2017" Technical document.
- [2] FINITE ELEMENT METHOD SOFTWARE MIDAS GTS NX V. 6.1-MIDAS IT-KOREA.
- [3] Y.PARISH, F. NAJAEI ABADI. *Dynamic behavior of earth dams for variation of earth material stiffness*. World academy of science, Engineering and technology international journal of geological and environmental engineering Vol 3, No: 2, 2009.
- [4] US ARMY CORPS OF ENGINEERS (USACE 2003), *Engineering Manual EM-1110-2-1902. Slope Stability engineering and design* 31 Oct. 2003.
- [5] CANADIAN DAM ASSOCIATION (CDA 2007). *Dam Safety Guidelines*. 2007
- [6] ANIL. K. CHOPRA. *Dynamics of structures: theory and applications to earthquake engineering* (1995)

COMMISSION INTERNATIONALE DES GRANDS BARRAGES

VINGT-SIXIÈME CONGRÈS DES GRANDS BARRAGES
Autriche, juillet 2018

DOI 10.3217/978-3-85125-620-8-177



This work licensed under a Creative Commons Attribution 4.0 International License. <https://creativecommons.org/licenses/by-nc-nd/4.0/>

**COMPARATIVE STUDY ON FOUNDATION TREATMENT TECHNICAL
STANDARDS OF HYDROPOWER ENGINEERING BETWEEN CHINA AND
AMERICAN**

Liu Y R

STATE KEY LABORATORY OF HYDROSCIENCE AND HYDRAULIC
ENGINEERING, TSINGHUA UNIVERSITY

CHINA

Zhou H W

STATE KEY LABORATORY OF HYDROSCIENCE AND HYDRAULIC
ENGINEERING, TSINGHUA UNIVERSITY

CHINA

Lv S

STATE KEY LABORATORY OF HYDROSCIENCE AND HYDRAULIC
ENGINEERING, TSINGHUA UNIVERSITY

CHINA

COMPARATIVE STUDY ON FOUNDATION TREATMENT TECHNICAL STANDARDS OF HYDROPOWER ENGINEERING BETWEEN CHINA AND AMERICAN

Liu Y R, Zhou H W, Lv S

State Key Laboratory of Hydrosience and Hydraulic Engineering, TSINGHUA UNIVERSITY

CHINA

1. INTRODUCTION

Engineering technical standards are the basic criterion to guide the construction of engineering project^[1]. However, the inadaptation of the related international engineering technical standards severely restricts the competitiveness of contractors in the international market^[2]. Thus, improving the application level of international engineering technology standards will be great helpful to strengthen project execution ability. Foundation treatments, as the crucial part of hydroelectric project, will be able to keep the stability and improve the bearing capacity of foundation if the treatments are appropriate. But, there still exist some conditions where the engineers are not familiar with the technical standards for foundation treatments in the hydroelectric project. Sometimes, it can cause design errors, unreasonable purchase plans, construction costs increase, delay in time and other situations that relevant technical personnel don't have comprehensive understanding of the difference between Chinese and foreign standards. What's more, there is a lack of systematic and comparative research on the technical standard of foundation treatment for international hydroelectric engineering at present. As a result, the comparative research on international technical standards of foundation treatments have great guiding significance to contractors which will be beneficial for project completion.

2. CONTRASTIVE OBJECTS, CONTENTS AND METHODS

From the whole object, the foundation treatment measures for hydropower projects can be classified into dam foundation treatment and slope treatment, and from the concrete treatment measures, it can be divided into grouting, diaphragm walls, shotcrete, anchorage, deep mixing, etc. China-US standards are selected as the main object of comparison in consideration of Chinese and American hydro-related standards are relatively similar and comprehensive. The scope of comparison includes design and construction of foundation treatment. The standards of dam foundation and slope treatment and kinds of specific foundation

treatment measures between China's electric power industry(DL), water conservancy industry(SL) and United States Army Corps of Engineers(USACE), United States Department of the Interior Bureau Reclamation(USBR) have been comprehensively and systematically compared. The standards contrast framework between China and the United States is shown in Fig. 1.

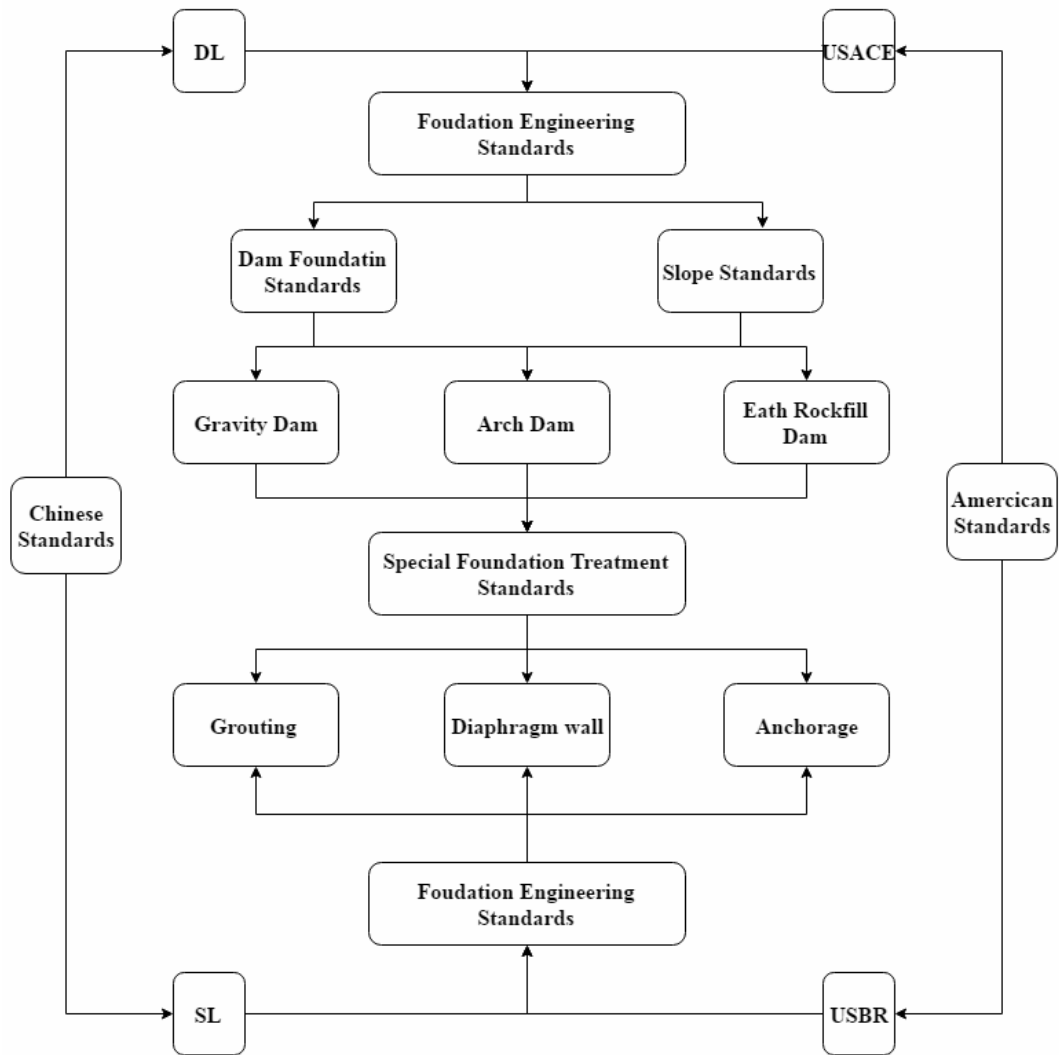


Fig. 1
Standards contrast framework between China and the United States

In order to compare the Chinese and American standards more rationally, hierarchically and systematically, based on Chinese standards as the basic contrast template, the comparison content can be divided into four parts: gravity dam foundation treatment, arch dam foundation treatment, earth-rock dam foundation treatment, slope treatment and specific foundation treatment measures. For the dam foundation treatment, the main contrast points are the treatment of excavation, consolidation grouting, curtain grouting, drainage and weak structural plane treatment. For the slope treatment, the points are excavation, drainage, reinforcement. As for the specific foundation treatment which also includes some the European countries' standards in addition to American standards, the differences in construction materials and technology are compared. Some of the

compared standards have been categorized as shown in Table 1.

Table 1
Category of Compared standards

Object	Chinese Standards	American/ European Standards
Gravity Dam	Design Specification for Concrete Gravity Dams (SL319-2005)	Design of Gravity Dams (USBR)/1976
Arch Dam	Design Specification for Concrete Arch Dams (SL282-2003)	Arch Dam Design (EM 1110-2-2201)/1994
	Design Specification for Concrete Arch Dams (DL/T5346-2006)	Design of Arch Dams (USBR)/1977
Earth-Rockfill Dam	Specifications for Rolled Earth-Rockfill Dam Construction (DL/T5129-2013)	General Design and Construction Considerations for Earth and Rock-Fill Dams (EM 1110-2-2300)/2004
Slope	Design specifications for slope of hydropower and water conservancy project (DL/T 5353-2006)	Slope Stability (EM 1110-2-1902)/2003
	Technical Specifications of Slope Construction for Hydropower and Water Conservancy Project (DL/T 5255-2010)	Rock Foundation (EM 1110-1-2908) /1994
Grouting	Technical Specification for Cement Grouting Construction of Hydraulic Structures (DL/T 5148-2012)	Grouting Technology (EM 1110-2-3506)/2017
Diaphragm Wall	Specification of concrete cut-off wall used for hydropower and water conservancy project (DL/T 5199-2004)	Execution of special geotechnical works —Diaphragm walls (EN 1538:2010)
Anchorage	Design Specification of Prestressed Anchorage for Hydropower Project (DL/T 5176-2003)	Rock Reinforcement (EM 1110-1-2907)/1980
Shotcrete	Construction Specifications for Anchor and Shotcrete Support of Hydropower and Water Conservancy Engineering (DL/T 5181-2003)	Standard Practice for Shotcrete (EM 1110-2-2005) /1993
Deep Mixing	Technical specification for deep mixing method (DL/T 5425-2009)	Execution of special geotechnical works —Deep Mixing (EN14679:2005)

3. COMPARISON OF STANDARD DIFFERENCES

3.1. OVERALL DIFFERENCES

The overall differences are as follows.

(1) The description of Chinese technology standards focuses on the requirements of principle and lack specific guidance on how to operate, leading to the difficulties for designers to understand and apply them. But at the same time, Chinese standards involve more contents and clauses than American standards. On the contrary, the American standards pay more attention to the instruction and explanation of operation methods, which is relatively comfortable to understand. Sometimes, it may adopt a long length to illustrate a concept or method, which Results in less content coverage.

(2) Chinese standards sum up a lot of experience, design parameters and requirements, the design and construction work of architecture can be completed according to the requirements of the code. However, it is easy to ignore the application and analysis of the basic theory. American standards attach great importance to the application of basic theory and for the specific project design, American standards can help engineers carry out a large number of calculation and analysis, giving full play to the initiative of engineers.

(3) The United States standards count the accidents statistics happened in constructed structures from the government level and develop deep analysis into published research findings which have great reference value to similar engineering projects. Chinese standards, by contrast, rarely involve engineering situation which causes many precious experience locked in a very small scope and hinders the exchange and process of technology. So It is suggested that the work of accident analysis and experience exchange should be upgraded to the government level.

(4) The source of many regulations can be found in American standards by the lists of related research references. Chinese standards, however, just give a pure rule which should be strictly implemented causing engineers not to know why they should do like this. For example, about the calculation of the thickness or length of the upstream pavement of the earth rockfill dam constructed on sand and gravel foundation, American standards give the reference of theoretical design method of pavement: "Bennett P.T. The Effect of Blankets on Seepage Through Pervious Foundations. Trans. ASCE, vol. III, 1946.". Chinese standards just give an explanation that the pavement should be gradually thickened from the upstream to the downstream, and the minimum thickness of the front end should be 0.5-1.0m. And any reference can't be found.

(5) On the whole, Chinese standards, in which the requirements on design and construction are incline to keep safe, are stricter than American standards. Chinese standards care about ensuring structures' safety and stability, but simultaneously the cost also increases, which may cause the waste of materials. For example, Chinese standards require the depth of curtain grouting up to the aquifers, but American standards don't have this requirement.

3.2. DIFFERENCES ON MAIN COMPARE POINTS

3.2.1. *Position of the base level for foundation*

Chinese standards determine the base level for foundation by the weathering degree of rock mass(SL) or the the grading of rock mass (DL) The SL's standards stipulate that "when the dam height exceeds 100m, it can be built on fresh, slightly

weathered to weak weathered underlying bedrock. When the dam height is 100m to 50m, it can be built on the bedrock of gently weathered and weak weathered bedrock. When the height of the dam is less than 50m, it can be built on the middle to the upper of the weak weathered underlying bedrock.”^[3] The DL’s standards demand that “high dams should be excavated to class II rock mass and can be excavated locally to class III rock mass. Moderate and low dams can be loosened properly.”^[4] The developing trend of construction base selection in Chinese standards is single weathered estimate to rock mass classification.

The USBR’s standards determine the base level according to the maximum allowable stress in the foundation. The USACE’s standards emphasize the application of the dam’s stress to determine whether the foundation is suitable. The USBR’s standards provide that the maximum allowable stress in the foundation should be less than the compressive strength of the foundation material, divided by the safety factor 4, 2.7 and 1.3^[5], which are respectively for normal, extreme and extreme loading combinations.

The USACE’s standards require that if the deformation modulus value below 500000 pounds per square inch (3.4GPa), the reasonable value of deformation modulus should be adopted to conduct stress analysis fully and if the stress of the dam are within the allowable stress range in a variety of conditions, the design is acceptable^[6].

3.2.2. *The treatment of weak structural plane*

The USBR’s standards introduce the “dental treatment” which means that weak planes and zones require special treatment in case of removing the weak material and backfilling with concrete, and develop general rules for guidance as to how deep transverse seams should be excavated. Based on foundation conditions and stresses at Shasta and Friant Dams, the USBR’s standards have resulted in the development of the following approximate formula for determining the depth of dental treatment^[5]:

$$\begin{aligned} d &= 0.002bH + 5 & H &\geq 150 \text{ feet}(45.72\text{m}) \\ d &= 0.3b + 5 & H &\geq 150 \text{ feet}(45.72\text{m}) \end{aligned} \quad [1]$$

where:

H = height of dam above general foundation level.

b = width of weak zone.

d = depth of excavation of weak zone below surface of adjoining sound rock.

(In clay gouge seams, d should not be less than $0.1 H$)

These rules provide a means of approach to the question of how much should be excavated, but final judgement must be exercised in the field during actual excavation operations.

Chinese standards, however, just suggested that the depth of treatment can approximately equal to 1.0-1.5 times the width of the weak zones or determined by calculation, but didn’t give the specific computational method.

3.2.3. *Cement grouting*

About grouting materials, Chinese standard “Technical specification for cement grouting construction of hydraulic structures” (DL/T 5148-2012) give the requirements of cement sieve: “The sieve residue is not more than 5% through 80 μm hole sieves”. and the demand of specific surface area: “The specific surface area of Portland cement is not less than $300\text{kg}/\text{m}^2$ ”. But the quality requirements of slurry raw materials remain generally high in the foreign projects where the specific surface area of cement must not be less than $350\text{ kg}/\text{m}^2$.and the sieve residue of American standard sieve is 0 through No.200 mesh (0.075mm)^[7].

With regards to grouting pressure, DL/T 5148-2012 tends to make use of high pressure. The definition of “high-pressure cement grouting” can be found – cement grouting whose pressure exceeds 3 MPa. During the domestic grouting construction, the tendency of high-pressure grouting ($\geq 3\text{MPa}$) is more and more obvious, it seems if the pressure must keep high enough to ensure the quality of grouting. However, in international projects, it is not thought to be better to use higher grouting pressure. Merowe Project and the Upper Atbara Project technically require that the maximum grouting pressure does not exceed 1.6 MPa (maximum hole depth exceeds 50m)^[8].

4. CONCLUSION

The differences on foundation treatment technical standards of hydropower engineering between Chinese and American standards have been discussed. The results can be applied in the international hydropower project as a reference for engineers and technicians. Engineering standards are the critical guidelines for the construction of a project. Therefore, the standards need to be used in a specific project item should be clearly studied. The overall and some detailed differences on Chinese and American standards have been compared in this paper, and the differences between China and other countries such as Britain, Germany, France, Australia and so on, whose standards are often applied in international project, remain to be investigated more deeply.

REFERENCES

- [1] TASSCY G. Standardization in technology-based markets. *Research Policy*, 2000.
- [2] ZHANG X.T., YU W.Y., TANG W.Z., et al. Research on the application of international Hydroelectric Engineering related technical standards. Project Management Technology, 2016.(in Chinese)
- [3] Design specification for concrete arch dams. Ministry of Water Resources of the People's Republic of China, 2003. (in Chinese)
- [4] Design specification for concrete arch dams. People's Republic of China national development and Reform Commission, 2006. (in Chinese)

- [5] Design of Arch Dams, United States Department of the Interior Bureau Reclamation, 1977.
- [6] Arch Dam Design, United States Army Corps of Engineers, 1994.
- [7] Standard Test Methods for Fineness of Hydraulic Cement by Air-Permeability Apparatus. American Society for Testing and Materials, 2017.
- [8] OU YANG X, WANG B.F. Research on Sultan Merowe Dam Foundation Grouting Drilling, Water Conservancy Construction and Management, 2010. (in Chinese)

SUMMARY

In recent years, China's international hydroelectric engineering business is growing rapidly, but the inadaptation of the related international engineering technical standards, in which the foundation treatment standards play an important role, has been seriously restricting the competitiveness of Chinese enterprises in the international market. In order to solve this problem, the comparison on foundation treatment standards of hydropower engineering from different countries has been studied. Based on the current understanding of the foundation treatment technology with respect to hydroelectric engineering, taking China-America standards as the primary object, foundation treatment measures as the main content, gravity dam, arch dam, earth-rock dam and slope as the key points, and excavation, consolidation grouting, curtain grouting and drainage as the chief route, the design and technical differences of the standards between China's electric power industry, water conservancy industry and United States Army Corps of Engineers, United States Department of the Interior Bureau Reclamation have been comprehensively and systematically compared. The core differences of gravity dam and arch dam lie in the location determination of dam base and the treatment of weak structural face. About the earth-rock dams, Chinese standards divide them into rolled earth-rockfill dams and concrete face rockfill dams and have the design and construction requirements respectively, but American standards just make unit regulations on earth-rock dam's foundation treatment. As for slope's treatment, specialized standards can't be found in American standard system, where relevant standards only introduce the concept of some treatments. However, Chinese standard system includes many slope specifications and provides corresponding detailed regulations. The comprehensive comparison shows that the overall requirements on foundation treatment of China's hydroelectric industry standards are slightly higher than the American standards, and China's electric power industry a little higher than China's water conservancy industry. This study will be helpful to understand the differences of standard on foundation and slope treatment between China and America, and provides technical support for international projects to strengthen the performance capability of international projects.

Keywords : Specification, Foundation treatment, Dam, Slope protection, Grouting.

COMMISSION INTERNATIONALE DES GRANDS BARRAGES

VINGT-SIXIÈME CONGRÈS DES GRANDS BARRAGES
Autriche, juillet 2018

DOI 10.3217/978-3-85125-620-8-178



This work licensed under a Creative Commons Attribution 4.0 International License. <https://creativecommons.org/licenses/by-nc-nd/4.0/>

**SEALING WORKS WITH MICROFINE CEMENT AND SYNTHETIC RESIN AT
THE CATHALEEN'S FALL DAM, IRELAND - LOW PRESSURE GROUTING
OF POROUS MASS CONCRETE**

Kurt KOGLER

Project Manager, ZÜBLIN SPEZIALTIEFBAU GES.M.B.H.

AUSTRIA

Johann HECHENBICHLER

Senior Site Manager, ZÜBLIN SPEZIALTIEFBAU GES.M.B.H.

AUSTRIA

Patrick GABRIEL

Site Engineer, ZÜBLIN SPEZIALTIEFBAU GES.M.B.H.

AUSTRIA

Harry DOHERTY

Civil Engineering Manager, Donegal Stations, ELECTRICITY SUPPLY BOARD

IRELAND

MISSION INTERNATIONALE DES
GRANDS BARRAGES

VINGT-SIXIÈME CONGRÈS DES
GRANDS BARRAGES
Autriche, juillet 2018

**SEALING WORKS WITH MICROFINE CEMENT AND SYNTHETIC RESIN AT
THE CATHALEEN'S FALL DAM, IRELAND**

-

LOW PRESSURE GROUTING OF POROUS MASS CONCRETE

Ing. Kurt KOGLER

*Project Manager, ZÜBLIN SPEZIALTIEFBAU GES.M.B.H.,
AUSTRIA*

Dipl.-Ing. Johann HECHENBICHLER

*Senior Site Manager, ZÜBLIN SPEZIALTIEFBAU GES.M.B.H.,
AUSTRIA*

Dipl.-Ing. Patrick GABRIEL

*Site Engineer, ZÜBLIN SPEZIALTIEFBAU GES.M.B.H.,
AUSTRIA*

Harry DOHERTY B.Eng. (Hons), CEng., MIEI, MICE

*Civil Engineering Manager, Donegal Stations, ELECTRICITY SUPPLY BOARD,
IRELAND*

1. INTRODUCTION

The Cathaleen's Fall power station is a hydroelectric power plant, located on the river Erne at Ballyshannon in County Donegal, Ireland. It is owned and operated by the ESB (Electricity Supply Board) Group. The construction of the concrete gravity dam started in 1946 and was completed in 1955. The dam is about 256 m long and 10 - 27 m high and has an installed capacity of 45 MW. The associated reservoir has an area of 2 km². The catchment associated with the river is just under 4,350 km². To discharge floods, the dam is equipped with 3 spillway gates, each about 11.0 m long.

The dam was constructed in 11 blocks each with a vertical water bar detail labelled Blocks C to V. The dam was constructed in on average 1.2 m high concrete pours. Over the life span of around 60 years the mass concrete of the gravity dam has begun to leak at some of the horizontal construction joints. The main leaks were within the inspection gallery in blocks S, T, U & V (near the orographic right bank of river Erne) and on the downstream face of these blocks. These were on the north of the spillway gates. To the south of the spillway gates the main leaks were on the downstream face of blocks N, O & P. The inspection gallery and the downstream surface near the orographic left bank of river Erne were in good order.

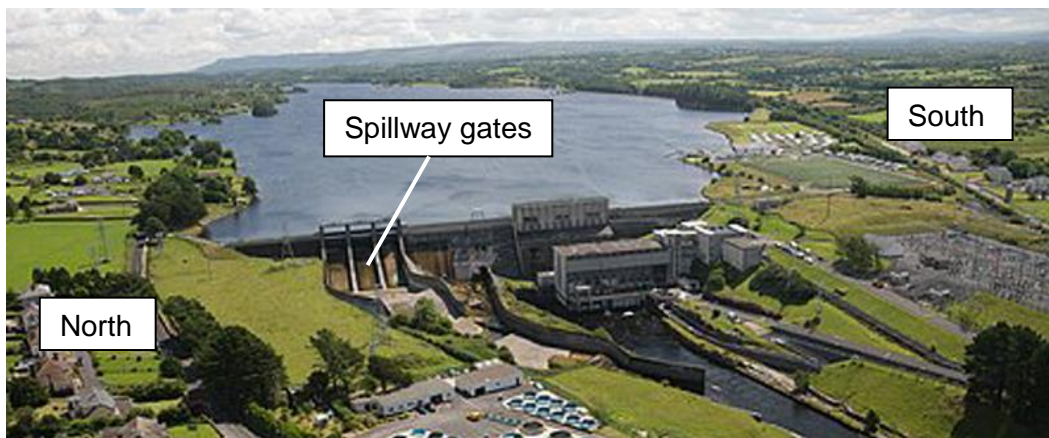


Figure 1: Aerial View of the Cathaleen's Fall Dam

2. DESIGN APPROACH

2.1. HISTORY AND FEASIBILITY STUDY

There had been leakage in the dam for many years since construction. Station Drawings from 1969 detail each leak on the face of the dam. Unsuccessful attempts to seal the leaks had been made in the past. In 1987 grouting was carried out by station staff in Block U from within the inspection gallery. In 2008 divers had tried to seal the upstream face of the joints using an underwater sealing material. None of these attempts had any long-term benefit.

As part of the management of Dam Safety within ESB, an External Dam Safety Committee (EDSC) advise ESB on Dam Safety at each of their installations in Ireland on an annual basis. In their 10 Year Inspection Report of 2010, the EDSC had recommended action to be urgently taken to reduce these seepages in Cathaleen's Fall Dam. ESB considered different sealing options for the dam however the EDSC preferred option was to seal the upstream face of the dam using geomembrane. ESB investigated this option but ruled it out due to the

number of the leaking construction joints being buried in rockfill. To carry out this method would have required underwater excavation works in rock on the upstream side of the dam to expose the joints and create space for sealing works. This would have been a hugely expensive project to undertake. Figure 2 shows the leaking sections of the concrete gravity dam including the section where some of the leaking construction joints were buried.

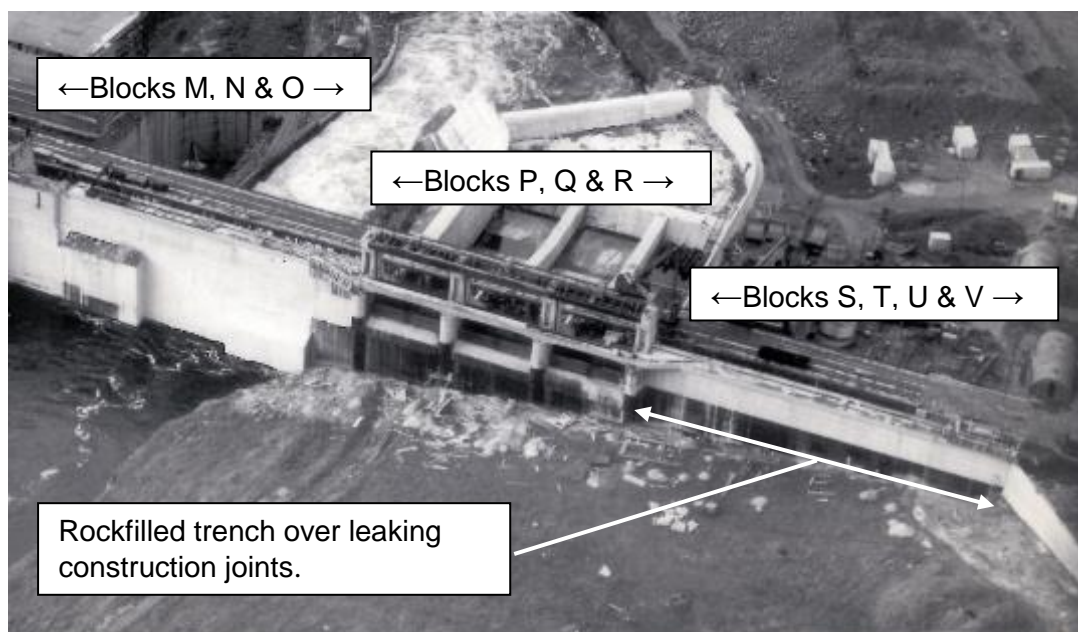


Figure 2: Upstream View of Affected Blocks - Prior to Reservoir Filling

Block O would have been considered the most difficult of blocks to seal due to its history. During construction of Cathaleen's Fall Dam, diversion channels with gates were constructed at Blocks M and O to facilitate completion of the closing Block N. After construction, the gate at Block M was retained as a scour gate and the channel at Block O was blocked up at the upstream end by means of a concrete wall. Over the years the cavities in Block O were filled with concrete on a phased basis. In 1995 the channel cavity was filled and in 1999 the redundant gate shaft was filled with concrete. The integrity of the cavity filling works was questionable and seepages from this block were evident for many years.

ESB consulted with an EDSC recommended Civil Engineer with Dam Sealing experience, Mr. Elmar Netzer from Vorarlberger Illwerke in Austria, who recommended further investigations including drilling boreholes in each block and carrying out water pressure tests. Mr. Netzer recommended drilling and grouting from the inspection gallery and the crest of the dam. ESB accepted this as the only technically feasible option for sealing the leaks.

Following these investigations, with the assistance of Mr. Netzer, ESB International prepared a detailed specification and tender documents for the proposed sealing works.

2.2. TENDER DESIGN

The proposed works involved extensive grouting of the upstream face of ten blocks in Cathaleen's Fall Dam, i.e. Blocks M to V. Grouting had to be carried out in stages, with each of the existing horizontal construction joints, as well as any voids, being treated. Water pressure tests had to be carried out in boreholes during the course of the works to monitor the adequacy of the grouting. Permanent drainage holes had also be provided to reduce the adverse effects of any remaining or future seepage.

2.2.1. Grout Holes

The grout holes in the inspection gallery had to have a minimum diameter of 46 mm and a maximum diameter of 72 mm with depths up to 10 m in downward direction and depths up to 5 m in upward direction. The grout holes on the crest had a depth up to 20 m in downward direction. The grouting sequence of the downward drill holes was bottom-up with ordinary portland cement or microfine cement. The packer had to be raised in a way, so that the packer is always midway between the joints. The primary grout holes were spaced at 2 m, and the secondary grouting holes 2 m between the primary holes, so that there is one hole every meter.

2.2.2. Requirements for Equipment

The drill rigs had to be of a suitable size for use on the crest and particularly in the confined space of the inspection gallery. The inspection gallery was 1.2 m wide and between 1.75 m and 2.1 m high and no widening of or cutting out of recesses in the gallery walls were permitted. The drilling method had to provide accurate results for judgement of the actual conditions in the dam – structural condition of in-situ concrete, cracks, joints, voids, porosity as well as the actual uplift pressure.

2.2.3. Requirements for Grouting Works

Since the dam had to remain in operation during the sealing works, high demands on grouting works were set. The flow rate had to be kept low – under normal circumstances well below 2 ltr/min. The maximum grouting pressures were limited as follows:

- from crest (35.36 m O.D.) to 29.5 m O.D.: 3 bar
- below elevation 22.0 m O.D.: 5 bar for cementitious materials and 4 bar for synthetic resins
- for elevations between 29.5 m O.D. and 22.0 m O.D.: the allowable maximum pressures had to be interpolated

2.3. EXECUTION DESIGN

In the year 2014 Züblin Spezialtiefbau Ges.m.b.H. was commissioned from the ESB (Electricity Supply Board) Group to seal the porous mass concrete with ordinary portland cement, microfine cement and synthetic resin. To meet all requirements for the equipment, the tender design had to be adapted partially in the execution.

2.3.1. Drill Holes from Gallery in Lot 3

The drill holes from the crest in Lot 3 – Spillway Blocks P to S – have been moved to the inside of the inspection gallery as shown in Figure 3. Upward drill holes with a depth of about 7 m simplify the construction progress as there is no need of a platform on the spillway. Furthermore, the discharging of floods over the spillway during the sealing works was guaranteed. The grouting of upward drill holes was only possible using lost single packers.

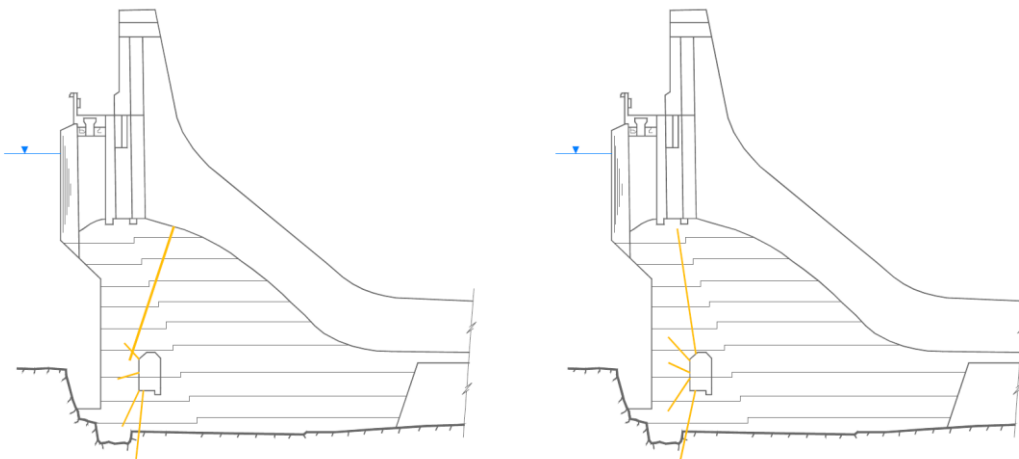


Figure 3: Tender Design (left) with Primary and Secondary Grout Holes (orange) – Drill Holes from Crest; Execution Design (right) with Primary and Secondary Grout Holes (orange) – Drill Holes from Gallery

2.3.2. Drill Holes from Crest in Lot 2

The secondary drill holes from the gallery in Lot 2 - Blocks M to P – have been moved completely to the crest. The use of the adequate drilling method made it possible to drill accurately between the inspection gallery and upstream side of the dam. The length of the secondary downward drill holes was up to 30 m. The primary drill holes have been kept inside the gallery and the crest as shown in Figure 4.

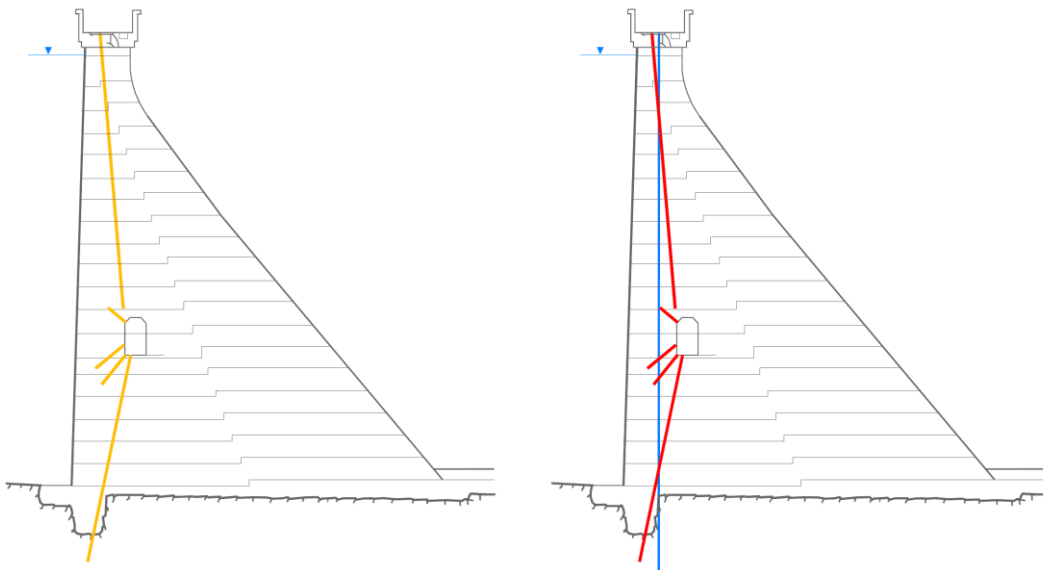


Figure 4: Tender Design (left) with Primary and Secondary Grout Holes (orange); Execution Design (right) with Primary (red) and Secondary Grout Holes (blue)

3. DRILLING WORKS

All drilling operations for the grout holes were performed as rotary core drillings (with diamond core bits) with 46 mm diameter, the drainage holes were performed with 86 mm. For the core extraction (core diameter of 33 mm), a double tube core barrel was used. Narrow space on the crest of the dam required the use of a small, light-weight portable hydraulic core drill. On the crest a Sandvik DE110 drilling equipment was used for the downward grout holes. Confined space inside the inspection gallery and the possibility to drill a grouting fan in 360 degrees required the use of a light rotary drilling rig Hilti DD200.



Figure 5: Drilling Works from Inspection Gallery (Hilti DD200)

4. GROUTING WORKS

Low pressure grouting was used to seal the slightly to highly water-permeable joints. Ordinary Portland Cement (OPC) and microfine cement was generally used to seal thin and slightly water-permeable joints, synthetic resin was used to seal highly water-permeable joints, as the synthetic resin has a high resistance to washout and a short setting time.

The first step of each grouting was the core extraction and judgement of the condition of the in-situ concrete, cracks, joints, voids and porosity. Based on these results, the single packer was brought into the right position within a centimeter to reach all leakages. Furthermore, it was reacted constantly to the actual grouting volumes to define whether tertiary drillings are necessary (split-spacing-method).

The basic grouting sequence was from coarse to fine. Generally, it was started with Ordinary Portland Cement (OPC) such as Dyckerhoff VARIODUR 50 and later grouted with finer materials such as Dyckerhof MIKRODUR R-F/E plus and MIKRODUR R-U/E plus. In exceptional cases (highly water-permeable joints and high flow velocities) synthetic resin such as Sika RODUR 505 / 510 was used.

The stop criteria had to be derived from the Grouting Intensity Number (GIN) and is described as follows:

- Cementitious Grouts: 40 ltr . bar / 1.20 m grouting length with a maximum grout volume of 50 liters / stage
- Synthetic Resin: 30 ltr . bar / 1.20 m grouting length with a maximum grout volume of 40 liters / stage

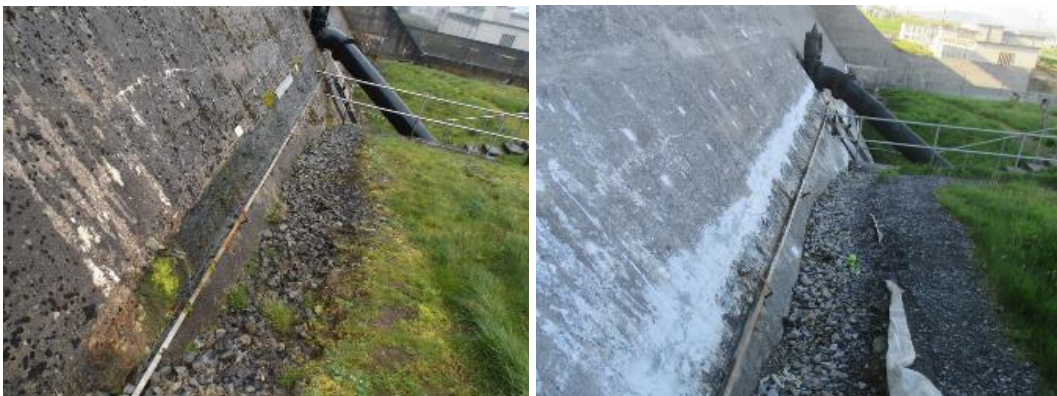


Figure 6: Photo of Downstream Face of Block U showing seepage (left) and results of sealing works (right)

In Figure 7 and Figure 8 the grout volumes per unit grout length are shown for the primary and secondary grout holes. It is clearly visible that the grout volumes have decreased from the primary to the secondary grout holes. The highest grout volumes were recorded in Block O, as there were possibly still remaining cavities in the section of the filled diversion channel.

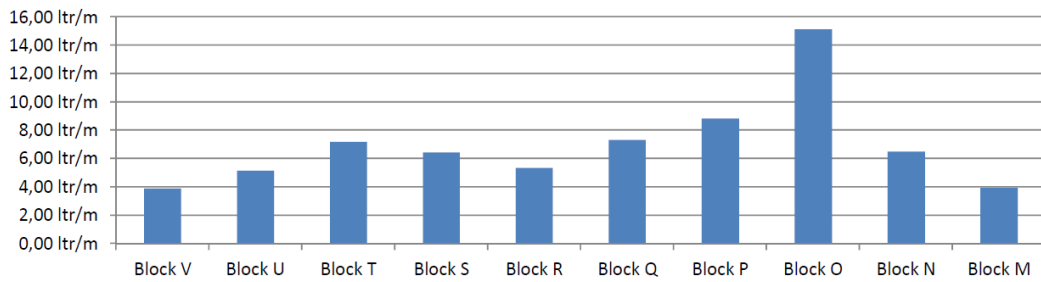


Figure 7: Grout Volume Per Unit Length (Primary Grout Holes)

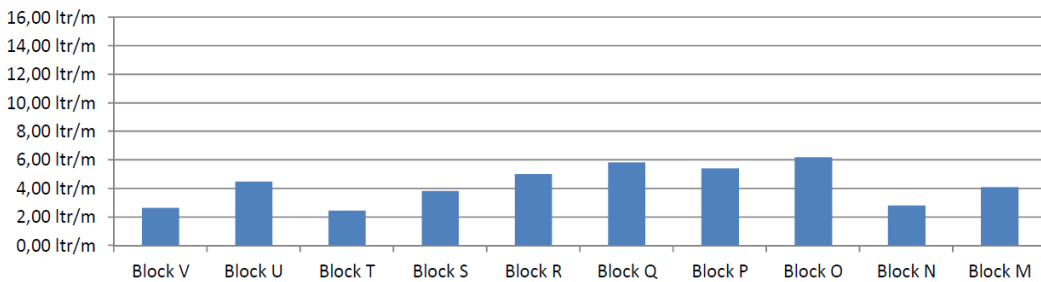


Figure 8: Grout Volume Per Unit Length (Secondary Grout Holes)

5. DATA LOGGING SYSTEM

The grouting module was equipped with a computerized data logging system which provides accurately and continuously monitoring of the grout parameters like flow rate, grout pressures and grout volumes. In Figure 9 (left) a GIN-Graph of a grouting sequence with cementitious material is shown. There the grouting stopped when reaching the GIN-Value of 40 ltr . bar / 1.20 m grout length.

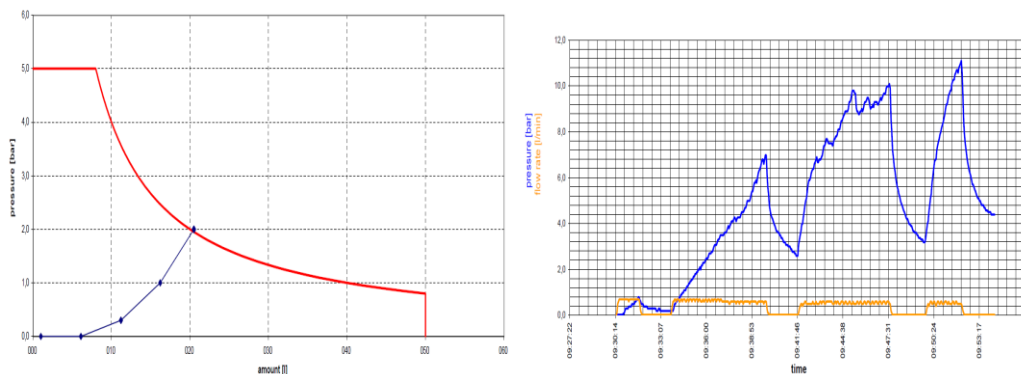


Figure 9: GIN-Graph (left) and Grouting Graph (Pressure / Volume)

In Figure 9 (right) a Grouting Graph of a cementitious grouting (grout pressure in blue, flow rate in orange) is shown. The grout pressure is steadily

increasing until reaching the stop criterion. After every pump stop the pressure decreases and stays steady at the effective pressure (pressure at rest).

6. DRY CRACKS

The last operation was the frictional connection of the so-called “dry cracks”. These cracks were opening more each year and remaining open. Figure 10 shows the seasonal opening and closing of these cracks. The vertical axis shows the deviation from the baseline (mm) and the horizontal axis the date (years).

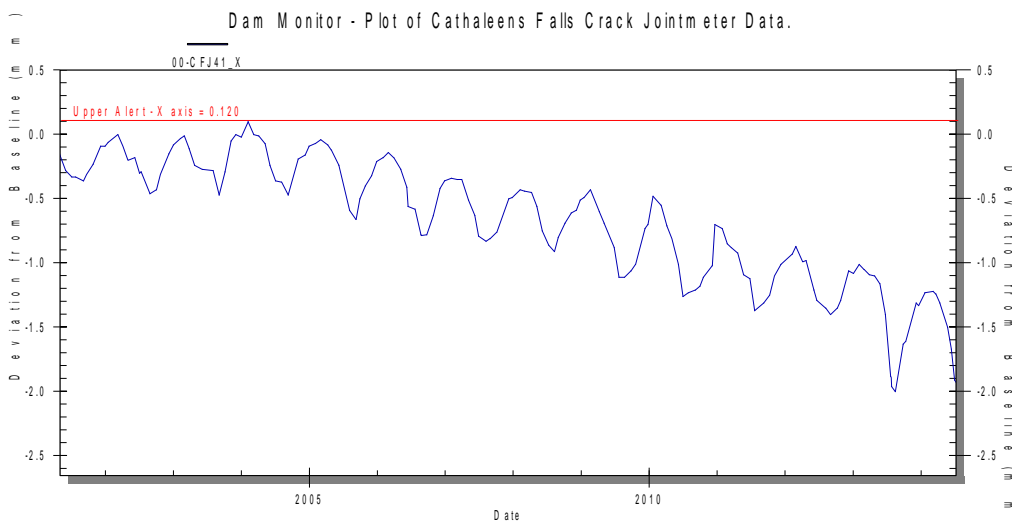


Figure 10: Seasonal Movement of Dry Cracks

These dry cracks were equally sealed and frictionally connected with low pressure grouting using synthetic resin. Figure 11 shows the grouting works of the so called “Dry Cracks” with synthetic resin.



Figure 11: Grouting of the "Dry Cracks"

SUMMARY

Over the life span of around 60 years the mass concrete of the Cathaleen's Fall gravity dam has begun to leak at some of the horizontal construction joints. These joints were sealed with low pressure grouting of microfine cement and synthetic resin. The entire work was finally completed in autumn 2014. The following graphs (Figure 12 and Figure 13) show how the grouting has successfully reduced the seepages in the dam. The vertical axis shows the seepage (ltr/s) and the horizontal axis the date (years).

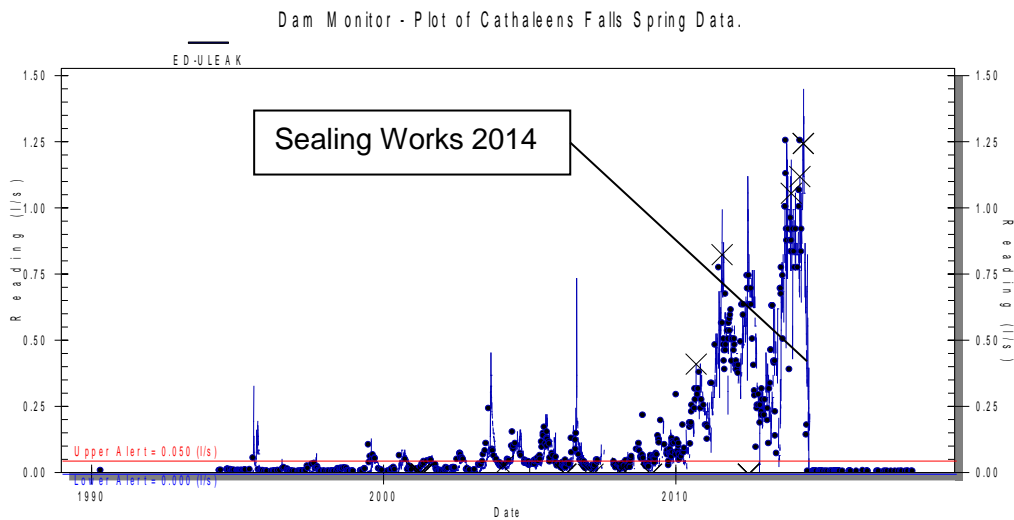


Figure 12: Plot of Seepage 'U Leak' on Downstream Face of Block U (showing results of sealing works)

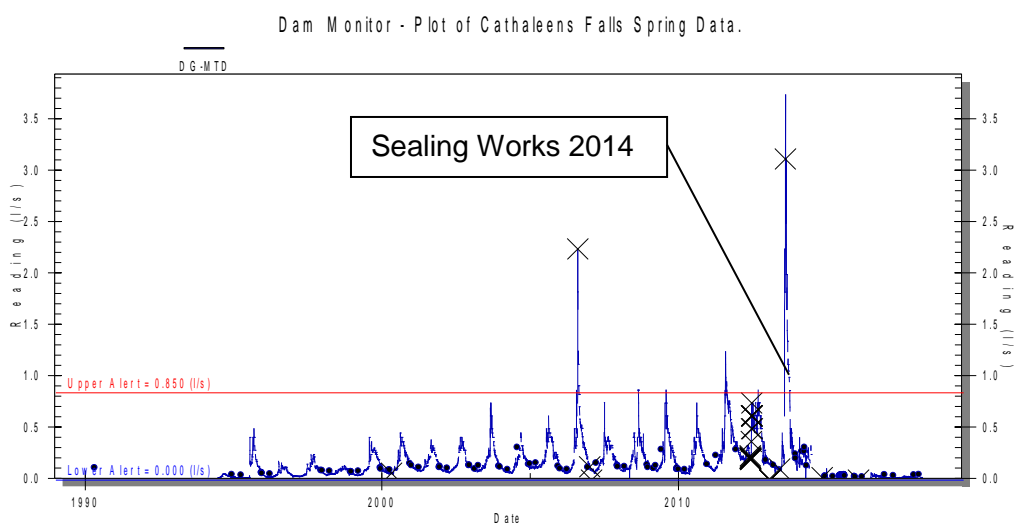


Figure 13: Plot of Seepage 'MTD' within Inspection Gallery from Blocks S & T (showing results of sealing works)

COMMISSION INTERNATIONALE DES GRANDS BARRAGES

VINGT-SIXIÈME CONGRÈS DES GRANDS BARRAGES
Autriche, juillet 2018

DOI 10.3217/978-3-85125-620-8-179



This work licensed under a Creative Commons Attribution 4.0 International License. <https://creativecommons.org/licenses/by-nc-nd/4.0/>

**THE OPERATION AND MAINTENANCE EXPERIENCE OF INDONESIA'S 1ST
UNDERGROUND DAM, CASE OF BRIBIN DAM IN KARST CAVE OF
GUNUNGSEWU GEOPARK; INDONESIAN INSIGHTS ON THE GERMAN-
INDONESIAN IWRM PROJECT (2010-2017)**

Vicky ARIYANTI

Technical Planner, INDONESIA COMMISSION ON LARGE DAMS
PhD Candidate, ERASMUS UNIVERSITY ROTTERDAM

INDONESIA

Ernowo Ary FIBRIYANTORO

Technical Planners, INDONESIA MINISTRY OF PUBLIC WORKS AND
HOUSING, SERAYU OPAK RBO

INDONESIA

Shakti RAHADIANSYAH

Technical Planners, INDONESIA MINISTRY OF PUBLIC WORKS AND
HOUSING, SERAYU OPAK RBO

INDONESIA

COMMISSION INTERNATIONALE
DES GRANDS BARRAGES

VINGT-SIXIÈME CONGRÈS DES
GRANDS BARRAGES
Autriche, juillet 2018

**THE OPERATION AND MAINTENANCE EXPERIENCE OF INDONESIA'S 1ST
UNDERGROUND DAM, CASE OF BRIBIN DAM IN KARST CAVE OF GUNUNGSEWU
GEOPARK; INDONESIAN INSIGHTS ON THE GERMAN-INDONESIAN IWRM
PROJECT (2010-2017)**

Vicky ARIYANTI

*Technical Planner, INDONESIAN COMMISSION ON LARGE DAMS
PhD Candidate, ERASMUS UNIVERSITY ROTTERDAM*

Ernowo Ary FIBRIYANTORO

Shakti RAHADIANSYAH

*Technical Planners, INDONESIAN MINISTRY OF PUBLIC WORKS AND
HOUSING, SERAYU OPAK RBO, INDONESIA*

1. INTRODUCTION

Karst area all over the world always faces water scarcity. However, the water potential runs deep under the ground can be extracted using new technology and high-risk undertaking. The case study presented here is located in a Karst area of the Gunungsewu Geopark (1) Java. The discharge data was the results of MacDonald's & Partners in 1984, which gave a baseline for all potential of groundwater in Yogyakarta(2). This potential is seen as a pilot for the German-Indonesian IWRM project. Since the year 2007, the potential of the cave and its underground streams was under scrutiny. According to the two years feasibility study by KIT, an engineering approach can be used in damming this stream to elevate the height of water to 15m. Thus, the water can be pumped using its kinetic energy (Pump as Turbine) to the surface 100 meters above the cave(3). This study brought hopes of clean water for the severe drought season in the area. As this dam is located in the limestone bedrock 'deep-seated solution channels, the flow of water would not cause rapid erosion or cause instability of the dam' (4).

The catchment area of Bribin in the Gunungsewu Karst Region consists of 1300 km², which originated at Petung (surface) River, Gilap Cave, Luweng

Jomblangan (5). Most of the catchment is still forest, agroforestry or seasonal agricultural land. The Karst type consists of a mixture of labyrinth cone karst type: polygonal karst and residual cone karst with conical shape reached 30 hills/km² (5,6). With the precipitation rate between 2,000-2,500 mm/year, the average humidity is about 60%-90%, and temperatures of 24-28°C (5).

The Bribin Dam project also called Bribin II is supported by the German–Indonesian “IWRM” project, s of scientific, governmental institutions, companies of both countries to develop and implement the management strategies (3,7) of the first underground dam in a natural Karst cavern in Indonesia. The barrage design is of a multi-angular low-reinforced concrete with the dimension of 8.5 x 2.5 meter. This paper would focus on sharing the operation and maintenance experience of the Indonesian operational team of Bribin, from 2010 to 2017.

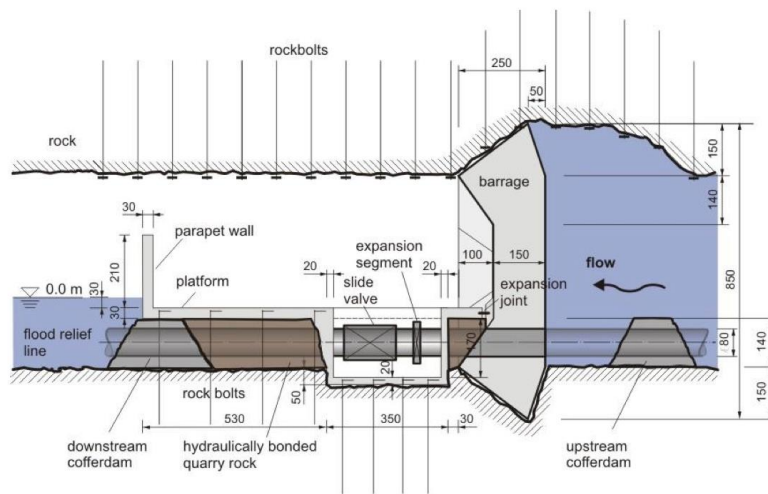


Fig. 1
Longitudinal Section of Bribin Dam (8)

This barrage is used (figure 1) with the pressure head of 15m in the upstream cavern and resulted in the volume of water yield of approximately 400,000 m³. However, this volume is not constant as the water is by-passed through pipes directly linked to Pump as Turbine (PaT) system with five modules, at approximately 400l/s per module. Thus, the hydro-power plant potential water supply discharge at full capacity is supposedly at 62l/s. A dry working platform connected to a vertical shaft housing these modules, where the PaT delivers the water 220 m above it (9). The natural Bribin river discharge is up to 1000 l/s, but due to the limitation of the PaT design and higher safety factors, the yield is only between 30 to 45 l/s (3).

2. CONCEPTS AND METHODS

2.1. CONCEPTS ON DAM OPERATION AND MAINTENANCE IN KARSTS

In general, the Bribin dam operations procedures mainly use the Standard Operating Procedures as the results of lengthy studies within the research cooperation of the German-Indonesian team (3). The lists of core duties:

- Heighten safety standard for a dam in Karst: concrete dam construction
- Dam operation rule curve: water level monitoring
- Hydrological data: upper stream precipitation data

However, as not much literature is found on dams in Karst, let alone an underground one. This condition places the case study in a unique position and a fragile one. The Bribin dam is the first attempt of its kind to be located in Indonesia. Earlier attempts were involving weir and PaT scheme, but not a whole cave structure as in Bribin. The literature review is using the Scopus indexed titles are reviewed on 78 titles, which then eliminated to 14, out of which three were about Bribin. These papers relate directly to underground dams in Karst area construction. Based on these, an overview of what to be expected in dealing with the maintenance of a dam in Karst areas are highlighted as the following check-up activities on:

- Equipment (pump, turbine, etc.)
- The behavior of the underground reservoir (Karstification, flood, etc.)
- Continual watertight structures (suspended grout curtain)
- Instrumentation for geological deformations (piezometer, etc.)

In this research, some of the following concepts are defined for the context of Bribin Dam: (1) normal operation, (2) flood operation, and (3) maintenance. Each of these concepts plays an important role in the daily activities of the Bribin Operation Team as they work 24 hours non-stop. To understand these definitions, the way the PaT system works in Bribin. This system is completed with the ASK and RKV modules as an additional by-pass (added in 2012 after the big flood in the rainy season of 2011/2012).

Firstly, in normal operation pattern in 2011-2016, it includes the condition of water level between 13-15 m. For this pattern, the required data to be calculated would be average discharge and yields annually compared to total annual discharge and yields ranging. Additional data to be compared would be annual rainfall pattern and its correlation to the discharge. This pattern also would highlight normal operation activities by the team. Second, flood operation is when the highest water level will be more than what the modules were designed for. Thus, the PaT will stop operating. The flood happenings set its pattern, which disturbs the normal pattern. This pattern related to the normal should be recorded for future data analysis. Third, the maintenance definition is when downtime is

needed to check the equipment and supporting facilities for the dam to be operationalized.

2.2. METHODS

The methods used here are qualitative research tools. The primary data are acquired using site visits, interviews conducted with main respondents (operation team members), with a historical review of operation reports. The main respondents are the O&M team of Bribin hired by BBWS Serayu Opak, which has been actively involved since the construction phase. These individuals are of high value in the completion of O&M tasks annually and throughout these times. Site visits by the authors' team were done in 2016 and 2017 to make sure the conditions reported in the notes and reports are on point. Meanwhile, the historical reviews of the reports were gathered from 2010 to 2017. They began when the Bribin Dam is operational. The document analysis using Atlas.ti software and coded were based on the activities' types number based on the concepts: (1) normal operation, (2) flood operation and (3) maintenance, which later on being arranged historically. These printed materials were written in Bahasa Indonesia, German or English. All of the field data used are from 2009 to 2016 will be provided by the O&M project office of BBWS SO and the KIT.

3. RESULTS

3.1. DAM MANAGEMENT

This dam management is fully operating under the national government mandate, which is the river basin organization or BBWS Serayu Opak. The operation team at the location in Bribin is fully capable and has been following the development of the dam since its construction phase. The team is highly capable and experienced in managing the dam using the SOP that was put together with the German team. Based on reports and interviews, the following (table 1) are the management units of the Bribin Dam.

Table 1
Management Units of Bribin Dam

Underground dam and reservoir operation	BBWS Serayu Opak (National Government-Ministry of Public Works and Housing, Directorate General of Water Resources)
Pump as Turbine Operation	
On land reservoir (Kaligoro) and water treatment plant	Satker CK SPAM DIY (National Government-Ministry of Public Works and Housing, Directorate General of Cipta Karya/ Human Settlements)
Water Supply Operation	PDAM Tirta Handayani (Local Government Owned Company)
Catchment Management	BPDAS Serayu Opak Progo (National Government-Ministry of Forestry and Environment)

Here these management units performed with the help of the German Team from KIT as the designer and researcher based on the Bribin logger data management (2010-2015), which consist of the water level data and geodetic measurement data. The cooperation continued with the transfer of knowledge in 2014 in managing the measurement data.

3.2. DAM CONDITION

Since the 2011 flood, the modules were submerged during the flood and not running. In 2012, additional modules being installed, the ASK and RKV (figure 3). These modules are by-pass pipes, which are used to evade floodwater. These submerged modules were significant concerns by the BBWS SO as they were not 100% functioning after the flood. Maintenance works were done to the PaT since 2010. Unfortunately, most spare parts for the PaT still need imports from Germany. Ever since then, the maintenance works were done in stages. Also as budgeting standard for the O&M at Bribin by the BBWS SO required one year in advance information, these maintenance works were not done timely. Flexibility for budgeting in this kind of pilot project is also essential for the successfulness of the project in the long run. In 2017, the current condition shows that the PaT and the platform are still functioning. Although, at times there were downtimes due to maintenance work, in principle the Bribin Dam can supply water up to 100l/s to the 369,000 residents of Gunungkidul in the Karst area.

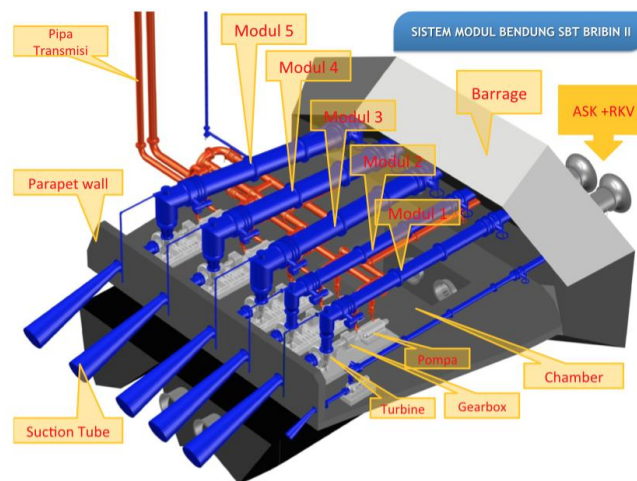


Fig. 2
Elaborated Diagram of Modules of Bribin in 2012 (10)

At other times the events of flooding submerged the platform, which stops the PaT from working and completely hinder the operation. In daily operation, the Bribin team does not have to come down to the platform (110m underground) but monitor through the equipment.

However, based on the interviews with the team members: the team does regular two times daily checkup to the platform (in morning and evening), using the generator run elevator. The main concern of the team; the electricity used for the elevator, the seepage submersible pump, and the instrumental components on the platform is also high, which made the operation of the dam not 100% electricity free as what the KIT suggest. Daily checkups consist of (1) temperature check, when it is over 90°C the module has to be stopped, but when under it, the module works continually, (2) seepage calibration, whether the sensors are working correctly and the submersible pump running, (3) nanometer check, whether it is showing the same number as the panel on the ground. Without the daily checkups the platform could be flooded, and the PaT cannot work effectively.



Fig. 3
The condition of Bribin in 2012-left (10) and 2016-right (BBWS SO documentation)

3.3. HISTORICAL REVIEW

This Bribin Dam review (shown in table 2) at the operational phase starts from 2010 to 2017. Reports, interviews, and notes on the dam operation and maintenance are used came from different sources: the German team and BBWS Serayu Opak team. These reports will be arranged using a timeline to compare and analyze also triangulate using Atlas.ti software to find the patterns of operation and maintenance of Bribin. The following patterns will be sought and numbered as (1) pattern of normal operation, (2) pattern of flood operation, and (3) pattern of maintenance, M for medium scale and L for large scale. The BBWS SO does all the operation, while the maintenance activities were done jointly. From 2010 to 2014, the KIT did the maintenance, while from 2015 and on, the BBWS SO fully maintain the Bribin II. Aside from these activities, the KIT provides annual assessment and monitoring, also consultation. However, the Bribin team at BBWS SO did most of the ground works and since 2014 has been self-reliant to operate and maintain Bribin II.

Table 2
Activities in Bribin Dam O&M (2010-2017)

Year	Condition	Operators	Activities	Type	Information
2010	Normal	KIT & BBWS SO	The first operation of Bribin Dam	1	Water level starts at 13m for the initiation of the operation
		KIT	Modules maintenance	3-M	Spare part change
2011	Normal	BBWS SO	Operation	1	Water level at 13m
	Flood	BBWS SO	Stop operating	2	Water level +15m
	Normal	KIT	Modules maintenance	3-M	Spare part change: all modules
2012	Normal	BBWS SO	Operation	1	Water level added to 14m, as discharge became more reliable
	Normal	KIT	Modules maintenance By-pass installed	3-L	Spare part change: all module Additional ASK and RKV modules
2013	Normal	KIT	Grouting campaign 3 Modules maintenance	3-L	Each grouting campaign has a risk of hydraulic breakthroughs Spare part change: all module
	Flood	BBWS SO	Stop operating	2	Water level +20m
2014	Normal	BBWS SO	Operation	1	Water level at 14m
	Normal	BBWS SO	Modules maintenance	3-M	Spare part change: all modules
2015	Normal	BBWS SO	Operation	1	Water level added to 15m
	Normal	KIT	Installing hanging structure	3-L	To strengthen cave walls and lessening vibration
	Normal	BBWS SO	Modules maintenance coupling change Elevator change	3-L	Rubber coupling and bearing of the PaT modules, spare part change, a safer elevator (with counterweight) and more efficient model (40kW to 15kW)
2016	Normal	BBWS SO	Operation of Bribin Dam	1	Water level at 15m
	Flood	BBWS SO	Stop operating	2	Water level 34m (October)
	Normal	BBWS SO	Modules maintenance	3-M	Spare part change: all modules Ring installations on the bypass
2017	Normal	BBWS SO	Operation of Bribin Dam	1	Water level at 15m
	Normal	BBWS SO	Modules maintenance	3-M	Module 1, 3, 4, module 5 (shaft sleeve, etc.)
	Flood	BBWS SO	Stop operating	2	Water level up to 64m and error occurred

3.4. NORMAL OPERATION

Like any other dam operation pattern, Bribin's is also based on the water level in the reservoir. As the water discharges in underground streams also based on the rainfall, although it needs some time (5 hours) before reaching into Bribin. Thus, there are three basic patterns, wet year, normal year and dry year (PP No.37 on Dams). Indicators of wet, normal and dry are based on rainfall data in Gunung Sewu catchment (2). During normal operation, the current water level is maintained at 13-15m in the reservoir. This condition is due to the supply needs for the drinking water has to be between 40l/s to 60l/s. The PaT is automatic and works 24/7. However, monitoring of the water level also uses human to guard at all times in responding to a sudden change of the upstream condition, especially during rainy seasons. At least twice a day, the O&M team has to check the water level also the PaT condition (temperature, seepage, etc.)

by going down on to the platform using the elevator. This condition shows that the PaT is still in need of human monitoring, even if the modules are automatic.

3.5. FLOOD OPERATION

Flood operation of Bribin II differs as the dam blocks the whole river. Therefore, water level above normal standard operation (more than 15m) would be categorized as a flood. During this condition, all pump modules stop operating:

- Over 15 m: Modules off, ASK+RKV Open 100%
- Over 20 m: Modules off, ASK+RKV+BYpass Open 100%

During the flood, the PaT modules completely stop working and there is only one thing to do, which is to wait until the flood passed. At these times, the O&M team monitors the water level through the panels on the ground. As Bribin river system has input from three locations, it is also possible that sudden flash flood happens. The biggest flood happened on 29 Nov 2017, when the manual log shows these levels in comparison to the panel when the panel shows 64m at 13.40 and the error data of -3.4m at 16.31 (figure 3):

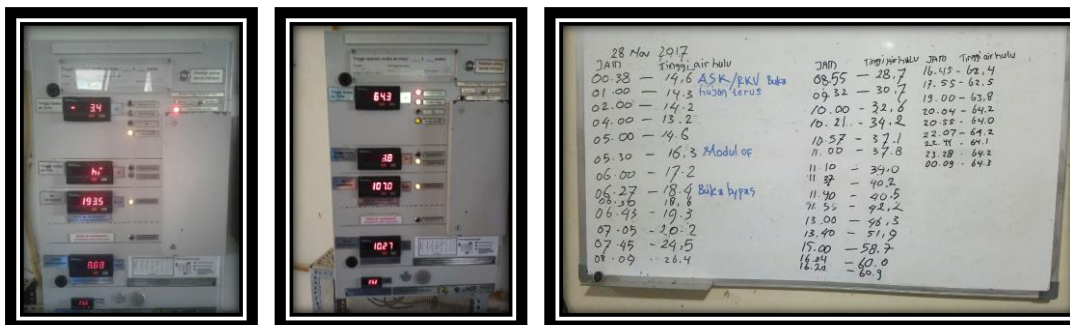


Fig. 4
Flood condition Bribin on 29th November 2017 (BBWS SO documentation)

3.6. MAINTENANCE

Maintenance in Bribin Dam includes all activities in getting the dam to operate normally. Hence, with the specific Karst context, it adds more than regular spare parts and oil change, it also asks for specific timing, especially as the modules work non-stop 24 hours. The following are the maintenance task for the O&M team: (1) Modules check, (2) Platform seepage, (3) Elevator and generator check, (4) Automatic water level and information systems (electrical). The maintenance check is done at least one time per year. However, due to the high humidity of the cave, there are always the possibilities that the equipment

may run down faster than its actual normal lifetime. An excerpt of the annual O&M report is added here to visualize what the activities are consist of. These pictures (figure 4) are taken from 2016 report, where the team works tirelessly in keeping the Bribin Dam up and running. The personnel in this team has been trained to obey the Standard Operating Procedure and updated with new developments as the nature of the pilot project.



Fig. 5
O&M works in 2016 (BBWS SO documentation)

4. CONCLUSION AND RECOMMENDATION

Bribin dam as a pilot project for Indonesia has proven to be a success story, however, as it is the first underground dam in a Tropical Karst, several things that were not calculated at the first phase of construction and first years operation. These things are what made the Bribin, a unique dam, as it is a running project, which supports water supply, but also a research project: cave laboratories. This condition means that there are things not perfected when it was first installed. We have learned from the experience of the O&M team at BBWS SO, the range of activities varies differently and may be interesting to other countries who have similar dam projects in Karst area to make this idea of underground dam works. These activities are divided into normal condition operation, flood condition operation, and maintenance. These categorizations is used by the management unit will be able to note for future reference and transfer this knowledge.

Although there are some things, which were not done ideally as the design, the Bribin Dam is still functioning to supply the drinking water to the much-needed Karst residents of Gunungkidul Regency. Further underground dam development on similar Karst conditions must be as flexible as the current team to facilitate innovations. Other recommendations are: fully automatized operating modules,

waterproof camera systems for monitoring, more intensive use of solar panels for all electrical equipment.

5. ACKNOWLEDGEMENT

The authors would like to express their gratitude to BBWS Serayu Opak and INACOLD for their continuous support in the writing process and also the chance to present this paper at ICOLD 2018.

REFERENCES

- [1] UNESCO. 2017; Available at: <http://www.unesco.org/new/en/natural-sciences/environment/earth-sciences/unesco-global-geoparks/list-of-unesco-global-geoparks/indonesia/gunung-sewu/>, December 2017.
- [2] MACDONALD AND PARTNERS. Greater Yogyakarta ground water resources study. Groundwater. Project report. 1984;Vol.03.
- [3] OBERLE P, IKHWAN M, STOFFEL D, NESTMANN F. Adapted hydropower-driven water supply system: assessment of an underground application in an Indonesian karst area. *Applied Water Science* 2016;6(3):259-278.
- [4] SCAEFER, JA. Risk Evaluation of Dams on Karst Foundations. *Managing Our Water Retention Systems*; 20-24 April 2009; Denver, USA: USSD; 2009.
- [5] ADJI, TN. Upper catchment of Bribin underground river hydrogeochemistry (Gunung Sewu Karst, Gunung Kidul, Java, Indonesia). *Proceeding of Asian Trans-Disciplinary Karst Conference*, Yogyakarta; 2011.
- [6] SEMIADI G, SUYANTO A, SUPRIATNA N. The Diversity of Small Mammals in Gunung Kidul Karst Region. *Proceeding of Asian Trans-Disciplinary Karst Conference*, Yogyakarta; 2011.
- [7] NESTMANN F, OBERLE P, IKHWAN M, KLINGEL P. Adaptive Water Resources Management under Extreme Climatic and Hydrogeological Conditions, *Interdisciplinary Research Activities in Karst Regions of South East Asia. Integrated Water Resources Management Karlsruhe 2010*; 24 - 25 November 2010; Karlsruhe: KIT Scientific Publishing; 2010.
- [8] BREINER R, ET.AL. Grouting of an Underground Concrete Barrage in Karst Limestone. *Asian Trans-Disciplinary Karst Conference 2011*; January 7-10th, 2011; Yogyakarta: Karst Research Group, Faculty of Geography, Gadjah Mada University; 2011.
- [9] NESTMANN F, OBERLE P, IKHWAN M, FRITZ J. IWRM-Indonesia Facts Sheet. *An Innovative Underground Water Supply Plant to Face Water*

Scarcity in Rural Areas of Gunung Kidul, Indonesia. An Indonesia – Germany BMBF Joint R&D Project for Karst Water Management at Gunung Kidul Regency, Province of Yogyakarta Special Region, Indonesia. 2015.

- [10] NESTMANN F. Indonesia: Sustainable development of a poor karst region. The 13th European Forum On Eco-Innovation: Water Sector Eco-Innovation In Practice; 15/01/2013; Lisbon; 2013

SUMMARY

The paper focuses on the operation and maintenance experience of the Indonesian operational team of Bribin, from 2010 up to 2017. The methods used are document analysis of printed materials, reports and site visits and will be dealt through historical review. Lessons learned from this pilot project include normal tasks, curtain grouting injections, spare parts changing, coupling problems, etc., which enriched the Indonesian counterparts to excel on the operational experience on this subject.

Lessons learned from this pilot project's O&M is divided into normal tasks (daily operation tasks, data monitoring, advancing reservoir level, etc.), medium scale maintenance (spare parts changing, coupling fixing, etc.) and big scale maintenance (curtain grouting injections, additional grouting campaigns, lift change, etc.). These experiences enriched the Indonesian counterparts to excel on the operational experience on this subject.

Keywords: CONCRETE DAM, DAM OPERATION, RESERVOIR OPERATION and MAINTENANCE.

CLEARANCES AND COPYRIGHT

The authors have obtained all necessary permissions and clearance to produce this paper.

COMMISSION INTERNATIONALE DES GRANDS BARRAGES

VINGT-SIXIÈME CONGRÈS DES GRANDS BARRAGES
Autriche, juillet 2018

DOI 10.3217/978-3-85125-620-8-180



This work licensed under a Creative Commons Attribution 4.0 International License. <https://creativecommons.org/licenses/by-nc-nd/4.0/>

HYDRAULIC DESIGN OF DIVERSION-CUM-DEPLETION TUNNEL

Balkrishna Shankar CHAVAN

Scientist-D, CENTRAL WATER AND POWER RESEARCH STATION, PUNE

INDIA

COMMISSION INTERNATIONALE
DES GRANDS BARRAGES

VINGT-SIXIÈME CONGRÈS DES
GRANDS BARRAGES
Autriche, juillet 2018

HYDRAULIC DESIGN OF DIVERSION-CUM-DEPLETION TUNNEL

Balkrishna Shankar CHAVAN

*Scientist-D, Central Water and Power Research Station, Pune,
India,*

1.0 INTRODUCTION

A river diversion tunnel is used to divert river water during construction of a project. Once construction is over, diversion tunnel is plugged before initiating storage of water consequently tunnel part becomes redundant. No universally accepted standards are available for design of temporary structures like coffer dams and diversion tunnels. Tunnel construction has high costs and usually adopted when other solutions are unfeasible. To minimize the project cost, part of diversion tunnel can be reused for depletion of storage of reservoir water.

2.0 Components of diversion –cum- depletion tunnel-Main components of a water conveyance system for diversion of river water and depletion of reservoir consist of the following components:

1. Intake structures
2. Water conducting system (Tunnel) comprising of control structures.
3. Transition portion connecting diversion tunnel with depletion tunnel
4. Outflow structure, which joins river flow downstream

2.1 Intake structures Entrance

An intake is provided at the mouth of a water conveyance system for a diversion of river flow. It is designed with the following points:

1. There should be smooth entry of water in to the tunnel as water enters from the reservoir behind a dam or the pool behind a barrage into the tunnel.
2. There should not be any formation of vortices that could draw air into the water conducting system.
3. There should be minimum entry of sediment into the water conducting system.
4. Floating material should not enter the water conducting system.

2.2 Inlet structure: Inlet transition facilitates the flow acceleration, ensuring the transition from subcritical flow which is established upstream in the reservoir created by the construction of the cofferdam or, in some cases, the channel connecting the bed to the frame, to supercritical flow that occurs in the diversion tunnel. The implementation of this structure aims to promote sufficient air to the flow, so that it develops a pressure equal to atmospheric pressure along the tunnel. This avoids the possibility of reaching pressures near the water vapour pressure, reducing the risk of cavitations phenomena in the diversion tunnel and hence its erosion. Regarding installation of the inlet structure it may be implemented directly on the ground or resort to auxiliary concrete that supports it above the ground level.

For smooth entry of water in to the depletion tunnel, generally following elliptical equation is used

$$\frac{x^2}{D^2} + \frac{y^2}{0.33D^2} = 1 \quad (1)$$

In the inlet structure design it is important to proceed to the analysis of flow velocities that are practiced within and upstream the structure. To this end, the ratio of the velocity flow in the control structure and velocity flow upstream the structure must be in a range of 2 to 5. In order to drain maximum water sometimes no curve is provided to bottom surface of tunnel which is in touch with invert of approach channel. The flow separation may occur in the transition river section with irregular section for the tunnel section, usually circular or horseshoe sections are used.

3.0 Geometric design

Sections usually adopted for tunnels are covered in IS 4880 (Part III, Hydraulic design) -2000[1]. Five basic design steps are outlined below:

The functional requirements are defined in a broad sense. They include all hydraulic and geometric requirements, ancillary and environmental requirements and limitations, logistics, and maintenance requirements.

Cross section: Area of cross section of a tunnel shall be of sufficient size 'to carry the maximum required flow on the head available and in addition shall conform to construction requirements.

Tunnel dimensions should be decided on the basis of economic studies so as to obtain a most economical section. The following should be taken into account:

Discharge passing through the tunnel flowing partial full is given by:

$$Q = \frac{2}{3} BC_d \sqrt{2g} H^{\frac{2}{3}} \quad (2)$$

Where Q= Discharge passing through the tunnel in m³/s

B= Width of tunnel in m

C_d= Coefficient of discharge

g= Acceleration due to gravity

H= Net head in m

Velocity in tunnel, computed by Manning's equation

$$V = \frac{1}{n} R^{\frac{2}{3}} S^{\frac{1}{2}} \quad (3)$$

Where V= Velocity of water in the tunnel in m/s

n= Coefficient of rugosity for unlined tunnels may range from 0.04 to .06

R= Hydraulic radius in m, for sections other than circular R = 4

S= Longitudinal slope

3.2 Head loss- Following losses may be expected for flow in diversion Tunnel:

- Head loss in approach channel, if tunnel is located away from reservoir
- Head loss at intake entrance

$$h_e = k_e \frac{V^2}{2g} \quad (4)$$

Where

h_e , K_e are head loss and loss coefficient s respectively

$K_e = 0.16$ for square bell mouth entrance

= 0.03 for circular bell mouth

= 0.1 for gate wall rounded corners

Head loss due to gradual contraction

$$h_e = K_e \left(\frac{V_2^2}{2g} - \frac{V_1^2}{2g} \right) \quad (5)$$

Here $K_e = 0.10$

Other losses as at bends, transitions, etc.

Head loss due to tunnel friction, calculated with the help of Darcy Weisbach resistance equation:

$$\text{Head loss} = h_f = \frac{fLV^2}{2gD}$$

Where

h_f = Head loss in m

f = Friction factor

L = Length of stretch

3.3 Estimation of friction factor

Implicit equation for estimation of friction factor was given by Colbrook in 1939

$$\frac{1}{\sqrt{f}} = -2 \log \left[\frac{\epsilon}{3.7} + \frac{2.51}{Re \sqrt{f}} \right] \quad (6)$$

This equation is implicit in nature and needs time consuming iterative steps for its solution. Many investigators proposed approximate solution of the Colbrook equation in a form of explicit equation (some of them are listed in Annexure A).

Two power explicit equation given by the author Chavan (2017)[3] is very convenient :

$$f = \frac{0.0075 \left(\frac{(4000)^{0.05}}{Re} \right)}{0.25 + \left(\frac{4000}{Re} \right)^5} + \frac{20}{Re} \quad (7)$$

Where f = Friction factor

Re = Reynolds Number given by

$$Re = \frac{\rho DV}{\mu} \quad (8)$$

μ = Coefficient of Dynamic viscosity

Exit head loss is

$$h_e = k_e \frac{v^2}{2g} \quad (9)$$

Discharging capacity- Discharge passing through the tunnel flowing full is computed backwardly, using known head loss, known conditions in which tunnel is being operated i.e. Reynolds number, and friction factor curves for operation characteristics of particular tunnel are prepared.

Based on the above losses, the diameter of the tunnel has to be fixed, such that it results in an overall economy. This is because if the diameter of a tunnel is increased, for example, the friction losses reduces

The tunnel diameter determined as a result of economic studies should be examined from practical considerations, such as space requirements for the excavating equipment and the section may be modified if necessary, based on the above considerations. A minimum height of 2 m is necessary. For mechanized handling of excavated material a minimum section of 2.5m x 2.5 m is required.

4.0 DIVERSION-CUM-DEPLETION TUNNEL – DOYANG PROJECT, NAGALAND

The Doyang H.E. Project envisages generation of 75MW power. It is located on river Doyang in Wokha district of Nagaland State. Project comprises 87.5 m high and 462 m long rock fill dam. During construction of dam river flow is proposed to be diverted through a 12 m dia. Diversion tunnel 633 m long is designed to pass the maximum flow of 2298 Cu.m per second. After construction of dam, it is proposed to make use of major part of diversion tunnel for depletion purpose by connecting it to the reservoir through 6.0 m dia. depletion (Gooseneck) tunnel. During depletion stage of reservoir, gooseneck tunnel is to be operated under maximum head of 37 m and discharge of 568 Cu.m per second.

General lay out plan of the project showing alignment of diversion tunnel, location of control gates, energy dissipation arrangement is shown in figure 1.

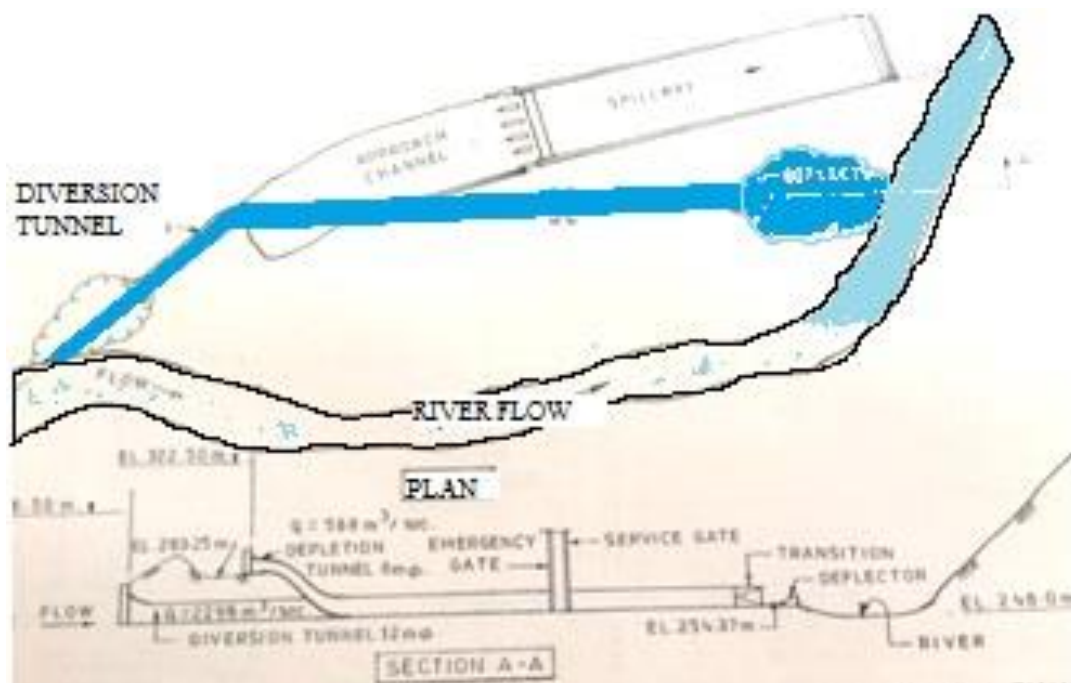


Figure 1. Alignment of diversion tunnel showing location of control gates, energy dissipation arrangement

SALIENT FEATURES OF DIVERSION-CUM-DEPLETION TUNNEL, DOYANG H.E. PROJECT, NAGALAND

(I) DIVERSION TUNNEL

Size of bell mouth entrance	:	9.5 m x 12 m
Length of transition	:	10.4 m
Diameter of tunnel	:	12.0 m
Length of diversion tunnel	:	633.0 m
El. of tunnel entrance	:	255.0 m
El. of tunnel exit	:	254.37 m
Design discharge	:	2298 Cu.m/sec

(II) DEPLETION(GOOSENECK) TUNNEL

Size of bell mouth entrance	:	5.0 m x 9.5 m
Length of transition	:	6.6. M
Size of gooseneck tunnel	:	6.0 m dia.
Elevation of tunnel at entrance	:	El. 287.0 m

(III) SERVICE GATE DETAILS

Size of Gate	:	9.5m x 4.57m
Number of Gates	:	2 Nos
Head on gate at FRL	:	67.5m

Depletion tunnel comprises elliptical entrance, transition from rectangular to circular section, 25m radius vertical bend straight circular section of 6.0m dia. followed by transition to join diversion tunnel.. Energy dissipater for the diversion-cum-depletion tunnel was required to perform for maximum observed flood discharge of 1500 Cumecs in diversion stage and 568 Cumecs under head of 37.0m for depletion stage. Diversion stage was to exist for 3-4 years where as depletion stage is a permanent feature. Keeping in mind site constraints and already constructed end portion of the tunnel, number of alternatives were suggested by NEEPCO, CWC and CWPRS. .Based on model studies and discussions deflector type energy dissipater without splitter blocks was finalized

5.0 THE MODEL

A 1/ 40 scale geometrically similar model of diversion tunnel including bell mouth entrance, circular tunnel, gate well, transitions was reproduced in smooth, transparent acrylic sheets. A high level steel-cum-masonry chamber was constructed to represent the portion of reservoir. Hill contours in the vicinity of entrance to diversion tunnel and depletion (gooseneck) tunnel was reproduced in masonry. A part length of river portion along with hill contours at tunnel exit was reproduced in masonry. For GS model of scale 1/40 various hydraulic parameters for the model are shown in Table i

Table.1 Hydraulic Model Scale for Diversion-cum Depletion Tunnel

Scale type	Length scale	Flow velocity scale	Flow quantity scale	Force Scale	Roughness coefficient scale	Time scale
Actual scale	40	6.325	10120	64000	1.849	6.325

Discharge flowing through the tunnel was measured on a sharp crested Rehbock Weir with an aerated lower nappe. Hydraulic pressures inside the tunnel were observed with piezometric tubes by connecting them to a water manometer. Propeller type current meter was used for measuring velocity of flow. Hydrodynamic forces on service gates were measured with Load Cell fixed on service gate and gate operating mechanism. Load cell readings recorded for gate opening ranging fro 0 % to 30 % with gate opening interval of 10%.



Figure 2 Photograph of the model showing diversion and depletion tunnels

5.1 MODEL STUDIES FOR CONTROL STRUCTURE- SERVICE GATE



Figure-3. Typical Set Up For Estimation of Hydrodynamic Forces on Service Gate

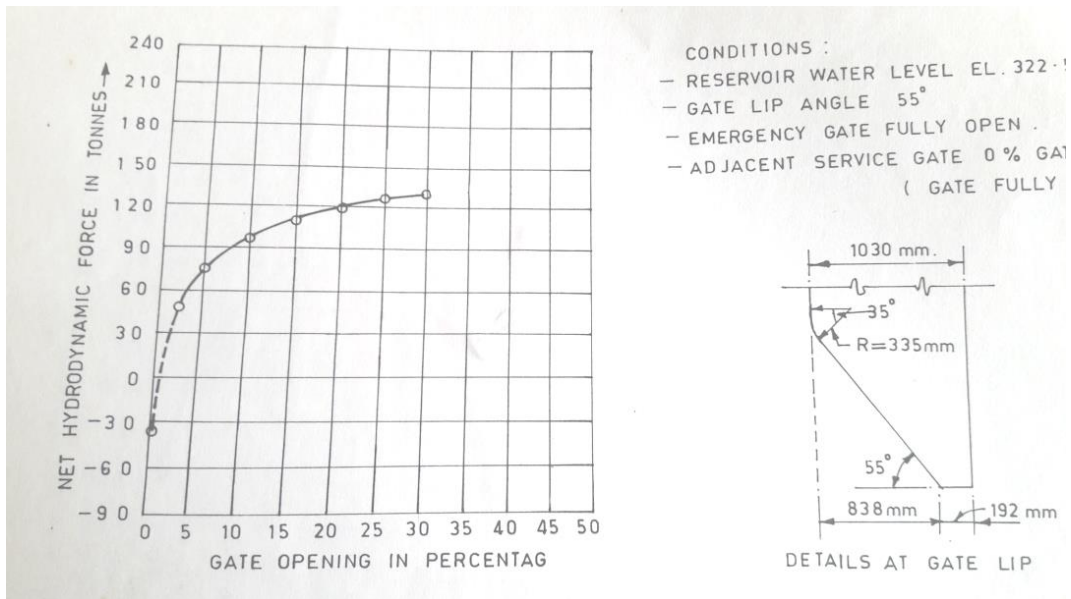


Figure-4. Results of model studies on Service Gate

MODEL STUDIES FOR ENERGY DISSIPATOR DOWNSTREAM OF TUNNEL EXIT

5.2 ALTERNATIVE DESIGN - I

Layout of the energy dissipation arrangement based on the site conditions consisted of a parabolic glacis followed by horizontal stilling basin. It was made curved (35 m radius) in plan to meet the river flow, as shown in the fig 3

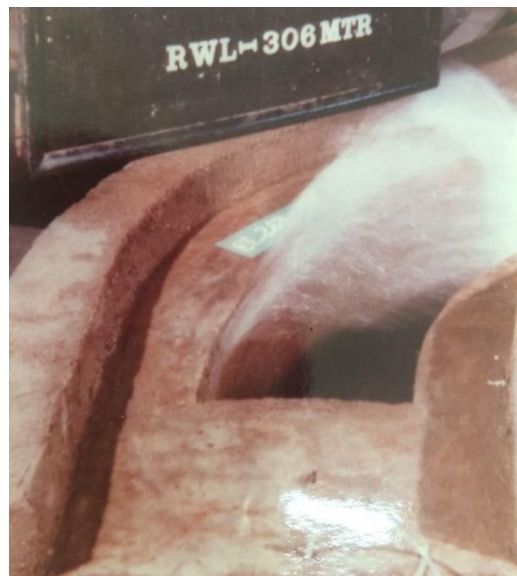


Figure 5. 35m Radial Curve type Energy Dissipator at the exit of depletion tunnel.

Studies for the maximum discharge during depletion stage of about 568 cumecs indicated that due to radial curve in plan, the high velocity jet coming out of the depletion tunnel was hitting and overriding the opposite sidewall as shown in photo-3

ALTERNATIVE DESIGN – II

Layout of the energy dissipation arrangement consisted of a parabolic glacis followed by stilling basin with horizontal apron with flaring sides in plan.

As requirement of sequent depth of 8 m below river bed could not be met with, performance of this dissipater was not satisfactory.

ALTERNATIVE DESIGN - III

Layout of the energy dissipation arrangement consisted of deflector having radius of 70.18 m, exit angle of 13.5 and 15 degree (I) without splitter blocks

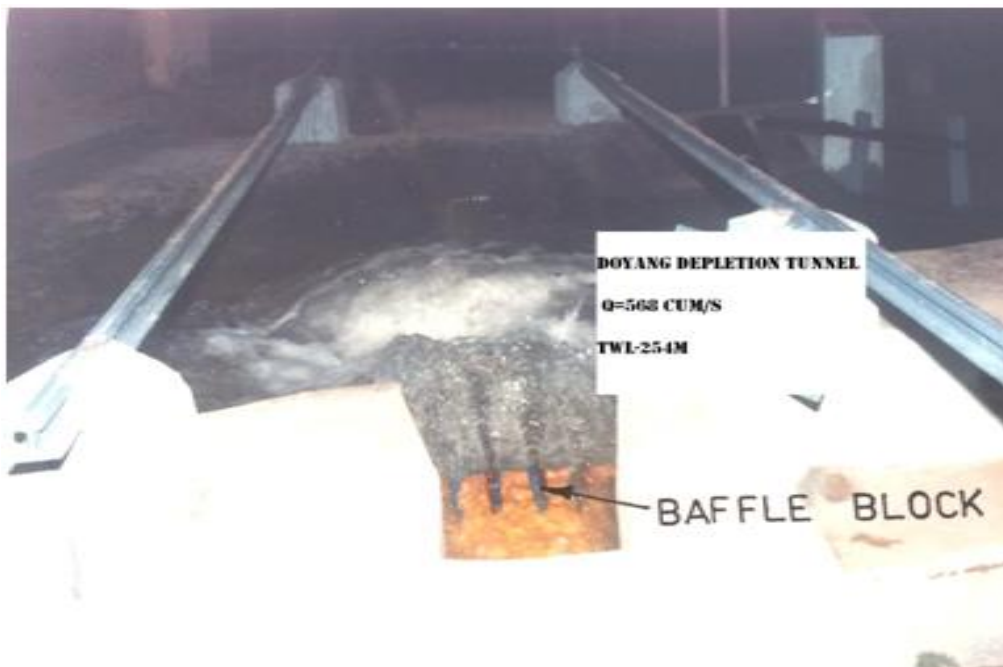


Figure 6. Photo of model showing Energy Dissipator with Baffle Blocks at the exit of depletion tunnel

(ii) with splitter blocks to improve energy dissipation by intermixing jets.

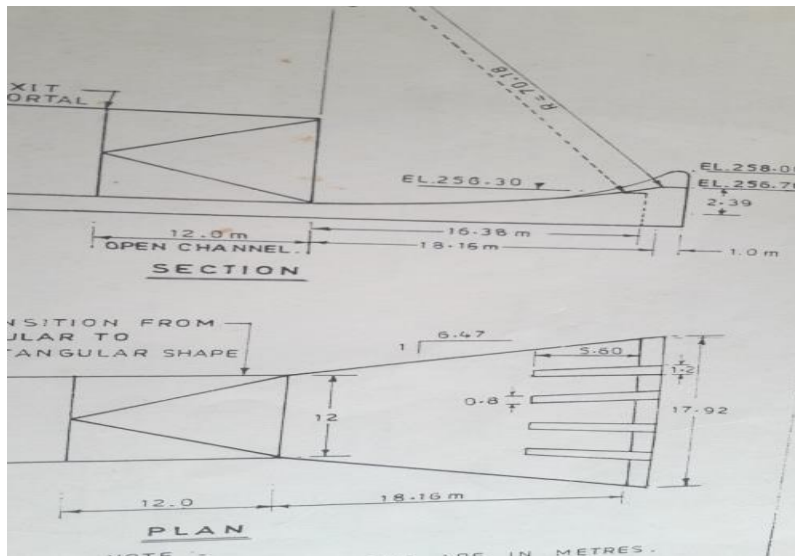


Figure 7. Deflector type Energy Dissipator with Baffle Blocks at the exit of depletion tunnel

DISCUSSION OF RESULTS

Selecting the energy dissipation arrangement for satisfying both conditions of diversion and depletion, model studies were conducted for

- (I) Diversion stage discharge of 2298 Cu.m per second, with RWL 306 m.
- (II) Depletion stage discharge of 568 Cu.m per second with RWL 322.5 m..

Design of the energy dissipater in terms of stilling basin running across the width of river with apron bed at 8 m below river bed were unsuitable due to fear of silting cistern of stilling basin .

The performance of the deflector type energy dissipater for diversion stage –

The performance of the deflector type energy dissipater studied in detail with velocity distribution. It was found to be satisfactory up to 1500 Cu.m. /second discharge. It was observed that high velocity jet after impinging in to river pool rushed along side slopes with rough (boiling) water surface and return flows in both directions. For discharge of 2298 Cu.m/sec, overriding of the jet extended up to el. 261.0 m. Return flow on right bank of river up to 60 to 80 m were observed in both directions. Observed velocities along left banks of river were in the range of 2m/s to 6.1m/s

Performance of deflector type energy dissipater for depletion stage

Deflector with exit angle of 13.5degree without splitter blocks it was observed that equally distributed jet impinged in to the river pool at about 60 m from the exit of the tunnel. Velocity along the right bank of the river varied from 2.5 m/s to 7.6 m/s.

Deflector with exit angle of 15 degree equally distributed jet impinged in to the river pool at about 70 m from the exit of the tunnel. Velocity along the right bank varied from 4.0 m/s to 5.6 m/s and 6.1 m/s to 6.9 m/s. for the conditions of with splitter blocks and without splitter blocks. To avoid the scour at the toe of the

deflector tip before commencement of ski action for small tunnel overflows, suitable protective measures in the form of concrete apron or dumping boulders along full width of deflector was suggested.

For proper aeration of the jet issuing from the deflector a recess of about 5 m on either side of the deflector may be provided .It may effected by cutting the left riverbank and then joining the deflector through suitable curve.

RECOMMENDATIONS:

1. In order to reduce the heavy negative pressures on gooseneck tunnel, its profile is modified to parabolic shape
2. A suitable obstruction in diversion tunnel to reduce area to 25% to prevent negative pressures in gooseneck area .
3. According to model study maximum down-pull force of 180 tonnes and uplift of 36 tonnes is recommended for design of hoist capacity.
4. The transition from 12 m circular to 12 m rectangular in a length of 12 m to be provided between the exit of tunnel and beginning of the deflector (Fig. 5)
5. The deflector type energy dissipater with radius of 70.18 m exit angle of 13.5 degree without splitter blocks recommended for installation.
6. Suitable bank protection measures may be adopted considering maximum velocity along right bank to be without splitter blocks 6.9m/s and 5.6m/s with splitter blocks in energy dissipator .
7. For better aeration of the jet, recess on either sides of the deflector may be provided.
8. Bank protection works may be provided accordingly and toe of the deflector may be founded and keyed to hard rock.

REFERENCES:

- [1] BIS 4880 (Part III, Hydraulic design)-2000, Code of practice for design of tunnels conveying water.
- [2] Bureau of Reclamation (BUREC) 1987, Design of Small Dams, 3rd edition, Bureau of Reclamation, Water Resources Technical Publication, Denver
- [3] Chavan Balkrishna Shankar (2017), Unified Equation for Estimation of Friction Factor, Proceedings of 37th IAHR World Congress, Aug13-18, held at Kuala Lumpur, Malaysia Pages 5885-5893.
- [4] EM 1110-2-2901, A Tunnels and Shafts in Rock Bureau of Reclamation, Water Resources Technical Publication, Denver
- [5] ICOLD. 1986. River Control during Dam Construction, bulletin 48a, Paris. Manzanares, A.A. 1980.
- [6] CWPRS Technical Report Number 3405,1997, Hydraulic Model Studies for Emergency and Service Gates of Depletion Tunnel, Doyang HE Project.
- [7] CWPRS Technical Report Number 3402,1997, Hydraulic Model Studies for Energy Dissipation Arrangement at the exit of Diversion-cum-depletion Tunnel, Doyang HE Project

SUMMARY

There are instances where part of river diversion tunnels have been used as depletion tunnel after construction of dam is completed. In India projects such as Yamuna, Doyang, Nagarjunsagar, Salal have successfully used the concept of multipurpose tunnel for diversion of river flow during construction of project and depletion of reservoir after construction of project is over. Hydraulic design associated with such tunnels has to function satisfactorily for high discharge at low head during construction and also high head low discharge during operation period of project. Present paper describes hydraulic problems associated with design of diversion cum depletion tunnel. Methodology adopted to arrive at solutions for design parameters in estimating frictional head loss, inlet transitions, energy dissipater at tunnel exit and smooth return of flow to river downstream of the structure. Design parameters are illustrated with a case model study of Diversion-cum—Depletion Tunnel, Doyang Hydro Electric Project, Nagaland, conducted at Central Water and Power Research Station (CWPRS).

Paper starts with describing various components of a tunnel. Frictional loss estimation in a tunnel flow by implicit and explicit equations given by various investigators is discussed in detail. Flow control structure such as emergency / service gate needs hoist for operation of gates. Estimation of hydraulic uplift / down pull is essential for finalizing the gate hoist capacity. Energy dissipater downstream of tunnel exit is important to mitigate erosion of river banks. Various alternatives for energy dissipaters studied in the model are described.

ANNEXURE-A

TABLE-2 Application of Friction Factor Formulae

No	Investigator	Year	Formula	Validity Range	R ²
1	Chavan	2017	$f_f = \frac{20}{Re} + \frac{0.0075 \left(\frac{4000}{Re}\right)^{0.05}}{0.25 + \left(\frac{4000}{Re}\right)^5}$	Valid for wide range of Reynolds number	0.9777
2	Morrison	2013	$f = \frac{16}{Re} + \frac{0.0076 \left(\frac{3170}{Re}\right)^{0.165}}{1 + \left(\frac{3170}{Re}\right)^7}$	Inaccuracy crept in for higher values of Reynolds numbers	
3	Barenblatt	2005	$f = \frac{8}{\psi^{2(1+\alpha)}}$	Re < 13×10 ⁶	
4	Mckeon	2005	$\frac{1}{\sqrt{f}} = 1.920 \log(Re\sqrt{f} - 0.475) - \frac{7.04}{(Re\sqrt{f})^{0.55}}$		
5	Yen	1991	$f = \frac{1}{4} \left[-\log\left(\frac{e}{12R}\right) + \frac{5.2}{(4R_e)^{0.9}} \right]^{-2}$	30000 < Re , $\frac{e}{D} < 0.05$	
6	Barr	1981	$f = \frac{1}{4} \left[-\log\left(\frac{e}{14.8R}\right) + \frac{5.2}{(4R_e)^{0.89}} \right]^{-2}$		
7	Chen	1979	$\frac{1}{\sqrt{f}} = -2 \log \left[\frac{1}{3.7605} \left[\frac{e}{D} \right] - \frac{5.0452A}{Re} \right]$	4000 < Re < 10 ⁸ $0.000001 < \frac{e}{D}$	0.9148
8	Churchil	1977	$f = 8 \left[(8/Re)^{12} + \frac{1}{(A+B)^{1.5}} \right]^{\frac{1}{12}}$		0.9066
9	Haaland	1983	$f = \frac{0.308642}{\left[\log \left(\left(\frac{e}{3.7D} \right)^{1.11} + \left \frac{6.9}{Re} \right \right) \right]^2}$		0.8509
10	Colebrook	1938-39	$\frac{1}{\sqrt{f}} = -2 \log \left[\frac{e}{3.7D} + \frac{2.51}{Re\sqrt{f}} \right]$		0.90416
11	Serghides	1984	$\frac{1}{\sqrt{f}} = \left[A - \frac{(B-A)^2}{C - 2B + A} \right]$	Re > 2100 and any e/D	
12	Swami-Jain	1976	$\frac{1}{\sqrt{f}} = 1.14 - 2 \log \left[\left[\frac{e}{D} \right] + \frac{21.25}{Re^{0.9}} \right]$	5000 < Re < 10 ⁸ $0.000001 < \frac{e}{D} < 0.05$	
13	Barr	1972	$f = \frac{1}{4} \left[\log\left(\frac{e}{14.8R}\right) + \frac{5.76}{(4R_e)^{0.9}} \right]^{-2}$		0.9051
14	Zigrang & Sylvester	1982	$\frac{1}{\sqrt{f}} = -2 \log \left[\frac{1}{3.7} \left[\frac{e}{D} \right] - \frac{5.02A}{Re} \right]$	4000 < Re < 10 ⁸ and $0 < \frac{e}{D} < 0.04$	0.9041
15	Wood	1966	$f = 0.094 \left(\frac{e}{D}\right)^{0.223} + 0.53 \left(\frac{e}{D}\right) + 88 \left(\frac{e}{D}\right)^{0.44} (Re)^{-\psi}$	4000 < Re < 5*10 ⁸ $0.00001 < \frac{e}{D} < 0.04$	0.7075
16	Moody	1947	$f = 0.0053 \left[1 + \left(2 * 10^4 \frac{\varepsilon}{D} + \frac{10^6}{Re} \right)^{\frac{1}{3}} \right]$	4000 < Re < 5*10 ⁸ $0 < \frac{\varepsilon}{D} < 0.01$	

COMMISSION INTERNATIONALE DES GRANDS BARRAGES

VINGT-SIXIÈME CONGRÈS DES GRANDS BARRAGES
Autriche, juillet 2018

DOI 10.3217/978-3-85125-620-8-181



This work licensed under a Creative Commons Attribution 4.0 International License. <https://creativecommons.org/licenses/by-nc-nd/4.0/>

**RESEARCH ON CONTROL MEASURES OF LIMNOPERNA FORTUNEI IN
PUMPED STORAGE POWER STATION WATER DELIVERY SYSTEM**

Sheng WAN

HUBEI KEY LABORATORY OF ROAD-BRIDGE AND STRUCTURE
ENGINEERING
QINGYUAN PUMPED STORAGE POWER GENERATION CO., LTD

CHINA

Xueshan LIU

QINGYUAN PUMPED STORAGE POWER GENERATION CO., LTD

CHINA

RESEARCH ON CONTROL MEASURES OF LIMNOPERNA FORTUNEI IN PUMPED STORAGE POWER STATION WATER DELIVERY SYSTEM

Sheng WAN^{1,2} Xueshan LIU²

1. *Hubei Key Laboratory of Road-bridge and Structure Engineering,*
2. *Qingyuan Pumped Storage Power Generation Co., Ltd*

CHINA

1. INTRODUCTION

In the region of southern power grid, there are Guangzhou Pumped Storage Power Station and Huizhou Pumped Storage Power Station, while Qingyuan Pumped Storage Power Station (PSPS) will be soon put into operation. Due to the characteristics of water quality in Guangdong Province, the *Limnoperna fortunei* will breed in the water delivery channels. For this reason, the specialized studies on the prevention and control of *Limnoperna fortunei* or are carried out.

2. CHARACTERISTICS OF LIMNOPERNA FORTUNEI

2.1. BIOLOGICAL CHARACTERISTICS

Limnoperna fortunei is a gregarious mollusks belonging to freshwater mussels, with a thinner shell and developed byssus. They can usually form densely stacked groups, with a growth thickness of up to 3-5 cm, and they live on diatoms, protozoa, organic debris in the water body [1]. For the eutrophication of water body, the water dissolved oxygen content is low and it is not conducive to the growth of *limnoperna fortunei*; a big turbidity of water body is in favor of the formation of mud membrane on the water delivery buildings or facilities, which is conducive to the attachment of *limnoperna fortunei*. Studies have shown that the *limnoperna fortunei* has a stronger reproductive ability and a fast growth when the water temperature is at 16 - 28 °C [2]. The floating stage of the early lifecycle of the *limnoperna fortunei* is key to its distribution and at this stage, the water temperature and dissolved oxygen are the main determinants affecting the larva life [3]. The breeding season of the *limnoperna fortunei* is generally February to September each year, and the best breeding season is March through July. At this stage, it is required to make adequate preparations for the breeding [4]. The survival period of *limnoperna fortunei* is generally two years or so [5].

2.2. HAZARD ON WATER DELIVERY BUILDINGS

In the late 1960s, *limnoperna fortunei* invaded Hong Kong, resulting in a pollution density of 11,000 *limnoperna fortunei* per square meter in the pipelines and pumping stations, and they formed a permanent breeding population since then [6]. The breeding of a large number of *limnoperna fortunei* not only reduces the orifice area of the water delivery pipelines [7], but also increases the pipe wall roughness. The intercepted *limnoperna fortunei* before the grille will not only reduce the discharge capacity of the grille, but also plug or block the pump station pipelines and power station cooling water pipelines. The *limnoperna fortunei* consumes the dissolved oxygen in the water during its respiration and excretes the ammonia nitrogen and nutrients during the metabolism [8], which will result in that the shell attached to the wall is rotten to produce bad smell and deteriorate the water quality so as to indirectly cause the corrosion of water machinery system. In addition, globally, there have also been examples of the destruction of ecosystems caused by the migration and multiplication of *limnoperna fortunei*, resulting in its infringement into the local water delivery pipelines and water conservancy facilities as well as the ecological structure of local water bodies [9].

3. RESEARCH SITUATION OF PREVENTION & CONTROL MEASURES OF LIMNOPERNA FORTUNEI

At present, the prevention & control study of *limnoperna fortunei* is generally aimed at the water delivery pipeline of conventional waterworks, and the study simply on the large cross-section and large flow of hydroelectric power plants has not been carried out yet. In general, the prevention & control measures generally include the following aspects: Biological prevention & control, Surface painting, Manual and mechanical removal and Chemical prevention & control.

4. STUDY ON TREATMENT OF GUANGZHOU PUMPED STORAGE POWER STATION

4.1. GENERATION OF LIMNOPERNA FORTUNEI

Guangzhou Pumped Storage Power Station (hereinafter referred to as “Guangzhou PSPS”) is divided into A/B plants and it is built by two phases and it is put into production in 2000. Guangzhou PSPS found a large amount of *limnoperna fortunei* when it drained the downstream waterway of Plant B on October 11, 2012. The downstream waterway of Plant B was drained up in October

2008 and there was no such a situation at that time. It was thus determined that the large population of *limnoperna fortunei* was bred in the four years from November 2008 to October 2012.

3.2.1. Water quality of the reservoirs: The water quality monitoring report of the Pearl River Basin Water Environmental Monitoring Center shows that the large population of *limnoperna fortunei* in surge shafts and culverts has not yet led to the deterioration of water quality in the reservoir areas. The water quality of Guangzhou PSPS upper reservoir was among poor nutrition and medium nutrition, and the water quality of lower reservoir was in a state of medium nutrition. The abundance of phytoplankton was at the lower middle level and the clear water species predominate. However, the eutrophic cyanobacteria appeared in the lower reservoir and became the dominant species, which indicates that the water quality and nutrient level of lower reservoir was higher than that of the upper reservoir.

3.2.2. Gregarious causes: The bottom material (or sediment) of lower/upper reservoirs in Guangzhou PSPS is sand, only with scattered *limnoperna fortunei* in the sediment. The *limnoperna fortunei* gathered and distributed only on the rough stone walls in the shade of individual banks in lower/upper reservoirs, which indicates that the water quality and sediment condition of the reservoir areas in the reservoir areas were not suitable for the large-scale reproduction of *limnoperna fortunei*. However, they were bred largely in culvert waterways, which indicates that the main factors affecting the distribution of *limnoperna fortunei* in Guangzhou PSPS is not the water quality, but the sunshine and attachment matrix, and other factors.

4.2. TREATMENT MEASURES

4.3.1. Selection of prevention & control materials: According to the selection principle of environmental protection, safety and construction features, 16 sorts of materials were selected for the experiments.

4.3.2. Experiment methods: The erosion effect of *limnoperna fortunei* on the concrete was evaluated by immersing the concrete specimens in flowing water for a certain period of time and then taking them out to test the compressive strength, superficial porosity, depth of carbonization and other indicators; after different protective materials were sprayed or coated on the concrete specimens, the *limnoperna fortunei* were attached naturally or manually to the specimens in the laboratory sinks. After the attachment was stable, the adhesion resistance of protective materials against the *limnoperna fortunei* was quantified and evaluated by regularly observing the adhesion density, biomass, attachment rate, lethality, escape rate, byssus number, adhesion and other indicators. In combination with the safety, construction property, durability and economic benefit of the protective materials, the selected protective materials were comprehensively selected.

4.3.2.1. Natural attachment experiment: The specimens were soaked for

about 9 months. Because only one side of some materials were painted, the black bold numerals in the table represented the blank base without any coating. Facing the downstream direction of the water sink, the base of the left side is defined as the left and the base of the right side is defined as the right. Due to a limited space, only a part of test results are cited here.

Table 1
Results of natural attachment experiment (Part)

Material	Test Result in Month 2		Test Result in Month 4		Test Result in Month 6		Test Result in Month 9	
	Left	Right	Left	Right	Left	Right	Left	Right
Pure polyurea	16	0	1488	2496	1184	1984	2788	5568
Modified silicate	0	0	14848	2096	17152	848	17408	1184
Blank	68	48	3520	15360	1568	5120	2720	11008
Water glass	84	124	29440	824	16640	208	14336	1696
organic-inorganic hybrid material	288	20	1312	164	120	84	2048	592
Modified acrylic resin	16	36	496	388	76	76	2752	560
Modified acrylic resin	12	16	188	4672	28	13312	760	5504
Vinyl resin	36	36	7168	7616	6272	17920	6784	4672
Pasty silane	88	116	11264	784	3776	160	5452	752
Silane impregnation	100	200	592	1200	136	172	320	672
Fluorocarbon resin	276	372	1056	800	204	148	656	448
SK-Polyurea 2	196	200	3296	4352	880	2592	928	1664
SK- Epoxy D50	100	120	6080	3584	720	396	1728	864
SK- epoxy YEC	120	144	1056	32256	560	1616	928	1440
SK-Polyurea 1	0	192	1224	1344	216	348	960	704

Polyurethane	144	184	1280	37888	668	4608	1664	13312
DPS+TS	72	80	6208	1728	3216	3520	8448	2304
Ceramic paint	264	232	2336	3968	3840	116	3360	256

4.3.2.2. Artificial Attachment Experiment: The observation results and calculation results of various materials in artificial attachment experiment (adhesion test) are shown in Table 2.

Table 2
Results of artificial attachment experiment

Material	Escaped mussels, PCS	Attached mussels, PCS	Mussel deaths, PCS	Escape rate, %	Attachment rate, %	Lethality, %	Average of byssus attached, PCS	Average adhesion, N
Blank group	1	37	4	2.48	88.10	9.52	25.47	2.00
Water glass	7	30	5	16.67	71.43	11.90	22.79	1.15
Modified silicate	9	31	2	21.43	73.81	4.76	24.29	1.49
Organic-inorganic hybrid material	5	37	0	11.90	88.10	0.00	21.05	1.29
Modified acrylic resin	9	31	2	21.43	73.81	4.76	23.07	1.18
Modified elastic epoxy resin	0	34	8	0.00	80.95	19.05	20.18	0.96
SK- epoxy D50	9	30	3	21.43	71.43	7.14	21.00	1.54
SK- epoxy YEC	8	30	4	19.05	71.43	9.52	18.82	1.43
SK-polyurea 2	8	25	9	19.05	59.52	21.43	20.77	0.93
SK- polyurea1	9	24	9	21.43	57.14	21.43	17.87	1.01
Pure polyurea	3	33	6	7.14	78.57	13.29	19.43	1.36
Vinyl resin	11	26	5	26.19	61.90	11.90	19.00	0.45
Pasty silane	4	32	6	9.52	76.19	14.29	19.27	0.96
Silane impregnation	5	32	5	11.90	76.19	11.90	16.38	0.69

Fluorocarbon resin	7	32	3	16.67	76.19	7.14	21.00	1.36
Polyurethane	7	33	2	16.67	78.57	4.76	25.92	2.17
DPS+TS	7	35	0	16.67	83.33	0.00	23.56	1.31
Ceramic paint	11	28	3	26.19	66.67	7.14	19.00	1.10

4.3.2.3.Erosion Experiment: The experiments were performed after soaked specimens were taken out and the limnoperna fortunei and attached sediment were scraped from the surface of specimens.

Table 3
Results of erosion experiment

Material/test indicators	Compressive strength, MPa	Porosity, %	Average pore size, nm	Carbonization depth, mm	Bubbling or spalling condition of surface
Saturated calcium hydroxide curing control	39.1	14.16	14.6	7.00	Null
Blank group	30.9	18.31	19.2	9.08	Null
Silane impregnation	33.6	14.47	16.2	9.00	Null
Fluorocarbon resin	32.7	16.82	15.5	7.83	Null
SK-polyurea 1	25.7	15.17	14.0	0.71	Null
SK- epoxy YEC	27.1	14.43	17.1	0.71	Null
Modified silicate	35.1	15.78	16.6	6.17	Null
Organic-inorganic hybrid material	28.9	14.49	18.7	2.54	Null
Pasty silane	26.4	19.29	15.5	4.67	Null
Water glass	27.8	17.28	25.7	3.75	Null
Modified elastic epoxy resin	29.2	15.30	12.8	0.92	Null
Vinyl resin	38.0	17.15	18.5	2.75	Local spalling

Modified acrylic resin	30.0	16.51	18.5	2.75	Local spalling
Polyurethane	30.4	17.32	14.8	0.88	Common bubbling
SK- polyurea 2	29.4	18.06	11.7	0.96	Local bubbling
SK- epoxy D50	30.5	17.33	13.9	0.96	Local bubbling
DPS+TS	34.5	14.12	20.7	3.25	Null

4.3.3. Test Results

4.3.3.1. Adhesion resistance: Centered on the natural attachment density and biomass and supplemented by the remaining test results, SK-polyurea 1, silane impregnation, SK-epoxy YEC and fluorocarbon resin presented a better performance in all indicators, and followed by modified silicate, modified acrylic resin and cementitious permeable crystals.

4.3.3.2. Erosion resistance: From the perspective of erosion resistance, especially carbonization resistance, we can learn that the effect of SK-polyurea 1, SK - epoxy YEC, modified elastic epoxy resin and SK-polyurea 2 are better in all aspects, but SK-polyurea 2 will be blistered after being immersed in water for a period of time, which will affect the durability. Therefore, according to the erosion resistance performance, SK-polyurea 1, SK-epoxy YEC and modified elastic epoxy resin are the best painting materials. However, it shall be noted that, for new concrete, if polyurea and epoxy are selected, the construction time shall not be too early according to their performance of compressive strength and the painting operation cannot be carried out until the concrete is fully hydrated. For the existing concrete, if a better construction effect will be guaranteed, certain construction conditions (for example, surface moisture content shall be within a certain range) shall be satisfied before the construction.

4.3.3.3. Comprehensive result: The attachment experiment results show that SK-polyurea 1, silane impregnation, SK-epoxy YEC, fluorocarbon resin, modified silicate, modified acrylic resin and cementitious permeable crystals have a better adhesion resistance. Considering a poor durability of silane impregnation and fluorocarbon resin and a higher cost of polyurea and other factors, SK-epoxy YEC, modified acrylic resin and cementitious permeable crystals are recommended as the suitable protective materials for concrete in combination with the consideration of adhesion resistance, erosion resistance, environmental protection, construction feature, durability, economic benefit and other factors.

5. STUDY ON TREATMENT OF QINGYUAN PUMPED STORAGE POWER STATION

Qingyuan PSPS is arranged using the “one hole and four machines”, and the longitudinal section of water diversion waterway uses the layout mode of three-stage adit, one-stage shaft and one-stage deviated wells. Other hub structures are the same as Guangzhou PSPS. Qingyuan PSPS takes “beforehand prevention” measures for the treatment of limnoperna fortunei according to the experiences of Guangzhou PSPS and in combination with its own characteristics.

5.1. WATER QUALITY

According to the test result of environmental water erosion in Qingyuan PSPS, the surface water has a medium corrosion of decomposition dissolution type and general acid type; the underwater has the medium acid of decomposition dissolution type, weak-medium corrosion of general acid type and weak corrosion of carbonate type and magnesium sulfate type; the test results show that the environmental water of Qingyuan PSPS has a slightly more serious corrosion.

Table 4

Comparison of corrosively-test results of environmental aqueous

Item	Guangzhou PSPS	Huizhou PSPS	Qingyuan PSPS
pH	6.8 - 7.6	6.0 - 7.6	5.6 - 8.3
Corrosion	5 - 10mg/l	5 - 10mg/l	5 - 10mg/l

5.2. PREVENTION & CONTROL MATERIALS

Based on the experiences of Guangzhou PSPS, it is decided to brush or coat the cementitious permeable crystals onto the concrete of inlet/outlets and brush the epoxy to the concrete of waterways after the comprehensive consideration of the material prices and construction process safety technology and other factors.

5.3. COATING LOCATIONS

Concrete is a building material that absolutely produces cracks [10], so, it is planned to brush or coat all water delivery tunnels of Qingyuan PSPS. However,

since epoxy is a hydrophobic material, it is required to keep the painting surface clean during the coating construction. For the shafts and deviated wells and other special parts, the coating or brushing operation can be carried out only when the grouting facilities are operating. In case of foggy weather, there will be a very serious fogging and condensing phenomenon in the shaft as the main air ventilation channel of diversion tunnel during the brushing or coating construction, so, the brushing test at this site is basically failed. For this reason, Qingyuan PPS only brushes or paints the protective materials of *limnoperna fortunei* at outlet/inlets of lower/upper reservoirs, upper adit, middle adit, deviated wells, lower adit, HP bifurcated pipe, tail water concrete branch pipe, tail water bifurcated pipe and tail water tunnel.

5.4. COATING PROCESS

5.4.1. Coating/brushing procedure: Epoxy coating operation is divided into two stages. Epoxy coating operation of erosion resistance of concrete above 3m at the bottom will firstly be carried out, and then the epoxy coating operations of erosion resistance of concrete at the bottom and below 3m will be performed. During the coating operations, the concrete grouting scaffold is used as the coating work plant. The basal plane is flushed from top to bottom and after it is dried and accepted, it shall be coated or painted also from top to bottom.

5.4.2. Coating Process

(1) Install and check the equipment of work plant to ensure the construction safety.

(2) Before the formal construction, check the construction surface 4 hours in advance to ensure that the concrete surface is dry during the construction.

(3) The coating operation direction is initially determined from top to bottom and it can be adjusted according to the actual situation on the site during the actual construction. The airless high pressure sprayer is used and the body pressure of the sprayer is 12MPa and the outlet pressure is controlled below 1MPa. On the work plant, the spraying nozzles are tied onto the bamboo poles of different length for the coating operations. The long bamboo pole is used to spray the remote ends, and the short bamboo pole is used to spray the near-ends. The length of the bamboo poles is determined experimentally to ensure they can cover all ranges. The nozzle shall be perpendicular to the concrete surface and at 30 -50 cm away from the concrete surface. The prepared paints shall be transported to the storage tank on the work plant through a high pressure hose.

(4) The concrete surface shall be brushed or sprayed twice. For the first spraying operation on the adit wall, the spraying shall be performed along the structural surface from top to bottom. The second spraying operation shall be performed perpendicular to the first spraying direction. The spraying operations shall be performed along certain direction and law to ensure all concrete surfaces

are covered. The paints cover the basal plane and flow slightly when spraying. The operator shall swing the nozzle uniformly and the nozzle pressure shall be controlled not to exceed 1MPa. It is required that the coating thickness shall be even and the surface is level. The first spraying operation cannot be carried out unless the paint of the first spraying operation is not sticky.

(5) During spraying construction, attention shall be paid to the following: First of all, the coating thickness must be under control when the spraying operation is performed, that is, the calculated amount of paint is evenly brushed on the stipulated construction area until the paint is used up. Secondly, if the current working procedure is unqualified, it cannot be transferred to the next working procedure. When any defect is found, it shall be promptly repaired and treated. The surface shall be free from any missing area, sags or bubbles. It shall be solidified completely, with smooth surface and uniform color; thirdly, the construction and curing of coating is completed and the coating meets the requirements of the design specifications. Finally, as for the control range of consumption: the consumption of epoxy resin for spraying two times is about 0.7kg/m².

6. CONCLUSION

As two typical pumped storage power stations, Qingyuan PPS and Guangzhou PPS have done a great deal of in-depth research on the prevention and control of *Limnoperna fortunei* in the operation period and construction period. However, because the implementation time of treating the *Limnoperna fortunei* is not long, the treatment effect cannot be immediately revealed and it shall be announced in the future operation overhaul.

REFERENCES

- [1] FLORENCIA ROJAS MOLINA, MELINA DEVERCELLI. Zooplanktophagy in the natural diet and selectivity of the invasive mollusk *Limnoperna fortunei*. *Biol Invasions*, 2010, 12.
- [2] LI DAIMAO. Probe into Effect of *Limnoperna Fortunei* on Conveyance Capacity of Water Delivery Buildings. *Water & Wastewater Engineering*, 2009, 35.
- [3] DAISUKE NAKANO, TAKUYA KOBAYASHI, ISAMU SAKAGUCHI. Differences in larval dynamics of golden mussel *Limnoperna fortunei* between dam reservoirs with and without an aeration system. *Landscape Ecol Eng*, 2010, 6.

- [4] LUO FENGMING, ZHANG CHONGZHI, HU XIANGPING. Growth law of *Limnoperna fortunei* in raw water pipelines in Shenzhen City. *Science & Technology Economy*, 2011, 1.
- [5] WANG RUI. Research on Oxidative Inactivation and removal technology of *Limnoperna fortunei* in long-distance water pipelines. *Harbin: Dissertation for the Master Degree in Engineering in Harbin Institute of Technology*, 2011.
- [6] DEMETRIO BOLTOVSKOY, ALEXANDER KARATAYEV. Significant ecosystem-wide effects of the swiftly spreading invasive freshwater bivalve *Limnoperna fortunei*. *Hydrobiologia*, 2009, 636.
- [7] GUAN FANG, ZHANG XIHUI, Research on the oxygen consumption and ammonia excretion of invasive mussel *Limnoperna fortunei* in raw water transport pipeline. *Water & Wastewater Engineering*. 2005; 31.
- [8] VALESKA CONTARDO-JARA, LUCAS N. GALANTI. Biotransformation and antioxidant enzymes of *Limnoperna fortunei* detect site impact in water courses of Córdoba, Argentina. *Ecotoxicology and Environmental Safety*, 2009, 72.
- [9] BRUESEWITZ, D.A., J.L. TANK & M.J. BERNOT. Delineating the effects of Zebra Mussels (*Dreissena polymorpha*) on N transformation rates using laboratory mesocosms. *Journal of the North American Benthological Society*, 2008, 27.
- [10] PENG BO. Study on the Mechanism of crack generating of high strength concrete and crack controlling. *Wuhan: Dissertation for master degree in materials in Wuhan University of Technology*, 2002, 33.

COMMISSION INTERNATIONALE DES GRANDS BARRAGES

VINGT-SIXIÈME CONGRÈS DES GRANDS BARRAGES
Autriche, juillet 2018

DOI 10.3217/978-3-85125-620-8-182



This work licensed under a Creative Commons Attribution 4.0 International License. <https://creativecommons.org/licenses/by-nc-nd/4.0/>

**BEHAVIOR ANALYSIS OF THE UNDERGROUND POWERHOUSE BASED
ON PRECISE DISPLACEMENT MEASUREMENT**

Masayuki KASHIWAYANAGI

CHIGASAKI RESEARCH INSTITUTE, ELECTRIC POWER DEVELOPMENT CO.,
LTD.

JAPAN

Keisuke MAEDA

KUZURYUU HYDROPOWER PLANT, ELECTRIC POWER DEVELOPMENT CO.,
LTD.

JAPAN

Norikazu SHIMIZU

YAMAGUCHI UNIVERSITY

JAPAN

COMMISSION INTERNATIONALE
DES GRANDS BARRAGES

VINGT-SIXIÈME CONGRÈS DES
GRANDS BARRAGES
Autriche, juillet 2018

**BEHAVIOR ANALYSIS OF THE UNDERGROUND POWERHOUSE BASED
ON PRECISE DISPLACEMENT MEASUREMENT**

Masayuki KASHIWAYANAGI

*Chigasaki Research Institute,
ELECTRIC POWER DEVELOPMENT CO., LTD.*

Keisuke MAEDA

*Kuzuryuu Hydropower Plant,
ELECTRIC POWER DEVELOPMENT CO., LTD.*

Norikazu SHIMIZU

YAMAGUCHI UNIVERSITY

JAPAN

1. INTRODUCTION

An adequate management of an aging underground powerhouse is recognized to be a mandatory issue through the experience of which significant damages were happened in a few support members of approximately 40-year old cavern for the powerhouse. The studies have been made to verify the soundness of the cavern by arranging two diffused laser range finders at the generator sections for monitoring the convergence, in-situ stress measurements of major concrete structures of the cavern and lift-off tests of pre-stressed (referred to as PS) anchors. Based on these results, the present soundness of the cavern was confirmed with the interpretation by the structural calculation using the simple frame model of the underground powerhouse. The management criterion was

updated by applying the future scenarios of the deterioration of the cavern supports to its present structural condition [1], [2], [3].

Following updated management criteria at the above-mentioned underground powerhouse, seven-year convergence data at two generator sections has been accumulated so far. While one is stable, however another section has been shortened gradually, but does not touch the maintenance criteria. In this paper, the convergence behaviors are examined from the standpoint of the structural response of the cavern.

2. OUTLINE OF AN UNDERGROUND POWERHOUSE STUDIED

The underground powerhouse studied in this paper, is located in the central part of Japan, includes output of 220 MW, two generator units and discharge of 266 m³/s, with completion in 1968. It has the dimension of 23 m wide, 42.25 m high and 70.2 m long. Due to the existence of the reservoir above 100 m of its location, the underground powerhouse was constructed with grouting as the watertight structure. The surrounding weak geological zone caused excessive displacement of the cavern and imposed the additional structures to strengthen the stability of the cavern, such as additional arch structures and thicker side wall and slab during the construction. Its characteristics are shown in Fig. 1.

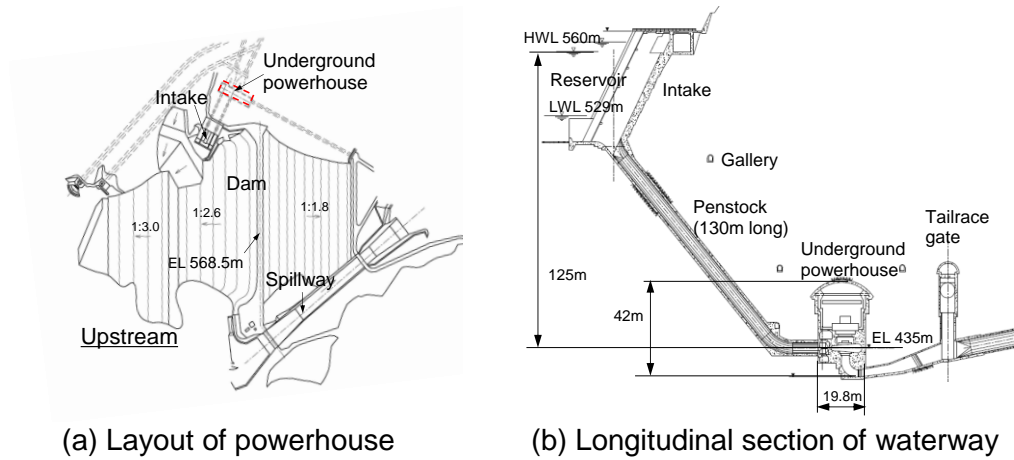
A few damaged PS anchors were identified in 2008, which was 40 years after the completion of the cavern, while no other deterioration in the cavern was found. These are shown in Fig.2. PS anchors arranged in the cavern are a type of un-bond with applying the bituminous coating around the tendon and mortal grouting in the boreholes. It is considered that a few damaged supports did not affect the stability of the cavern. However additional monitoring, which involves measuring the tension stress of existing anchors and monitoring the cavern convergence and major structural beams, was planned to clarify its long-term performance.

The monitored convergence performed in seven years is only examined in this paper from the mechanical view point of the cavern behavior.

3. CONVERGENCE OF THE CAVERN

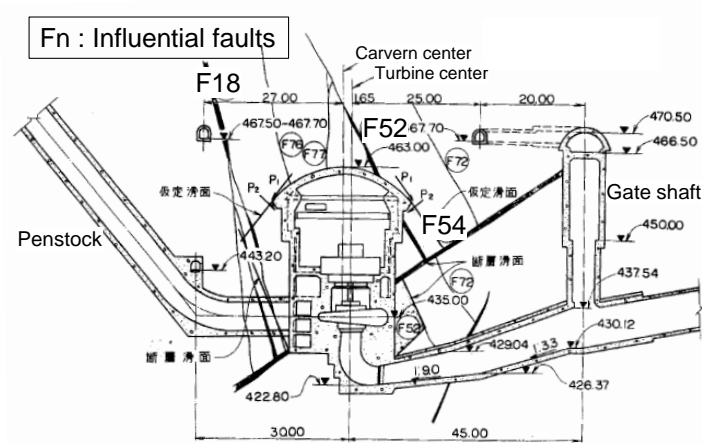
Monitoring plan is shown in Fig. 3. The convergence is monitored at the middle elevation of two generator sections of No. 1 and No. 2 in the machine room using a new device using the diffused laser beam, referred to as the diffused laser range finder (DLRF) [1], which consisting the laser transmitting and receiving unit and the reflecting board. The distance between the unit and the board is continuously measured in a precision of 0.1 mm with any interval. The overview of DLRF is shown in Fig. 4. The circumstance conditions of the

reservoir water depth and the ambient temperature of the cavern are simultaneously measured.



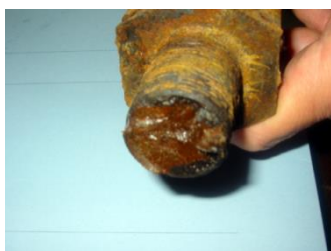
(a) Layout of powerhouse

(b) Longitudinal section of waterway



(c) Geological condition

Fig.1
Situation of underground powerhouse



(a) Broken tendon of PS anchor



(b) Borehole and the broken tendon remained



(c) Broken tendon of PS anchor, which was drawn

Fig.2
Damaged PS anchors

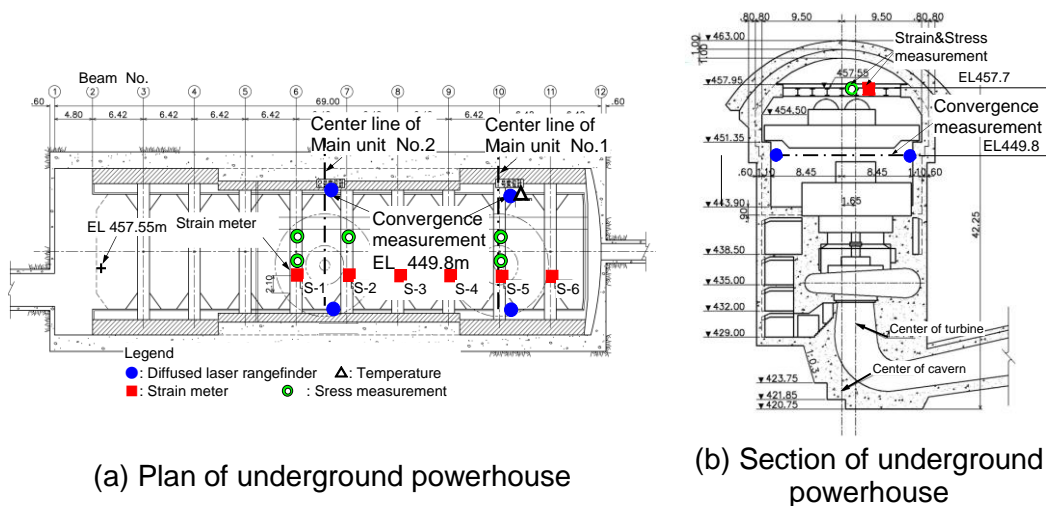


Fig. 3
Underground powerhouse and monitoring arrangement

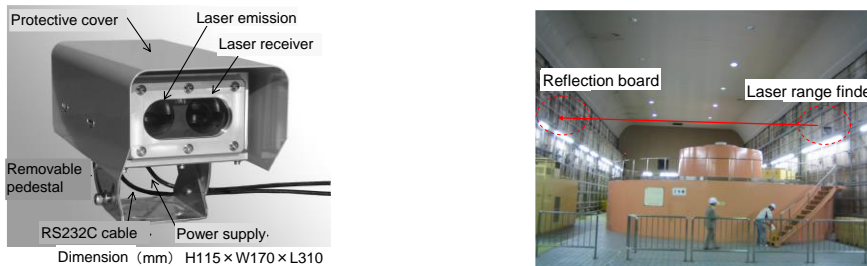


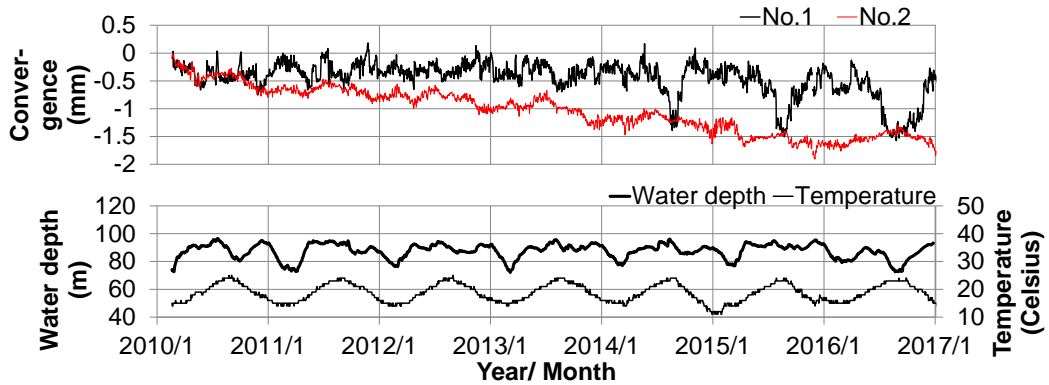
Fig. 4
Diffused laser range finder (DLRF)

The seven-year convergence histories of the cavern are shown in Fig. 5 with the reservoir water depth (referred to as the water depth) and the ambient temperature in the machine room (referred to as the temperature, simply). The data are compiled as daily ones. The water depth is measured from the top of the cavern (EL 463 m) to the reservoir surface. Fourier spectra are shown to identify the frequency characteristics of the data.

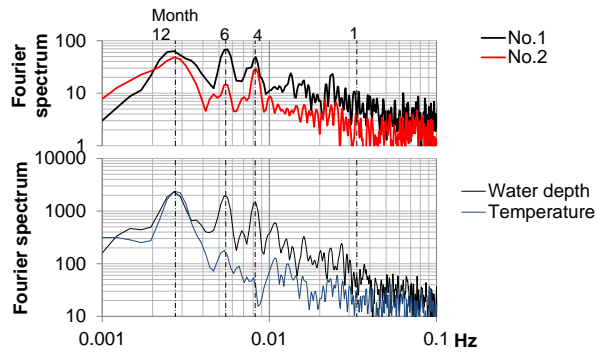
The water depth shows several cyclic fluctuations a year, while the temperature in the powerhouse fluctuates once a year. The convergences of both sections (referred to as No.1 section and No.2 section) show gradual shrinkage with higher frequency fluctuation, which are approximately 1 mm and 1.5 mm for No. 1 and No. 2 sections respectively and still less than the maintenance threshold of 2.5mm [1].

The frequency of the data is characterized with the peak of the Fourier spectrum. The water depth has significant peaks at 12, 6 and 4 months which are considered corresponding to the yearly reservoir operation and seasonal precipitation fluctuation. The temperature spectrum in the cavern shows the peak at 12 months, corresponding to the yearly temperature cycle. The frequencies of both convergences have significant peaks at 12, 6 and 4 months. This figure

implies that the cavern convergence could behave under the influence of the water depth and the temperature in the cavern.

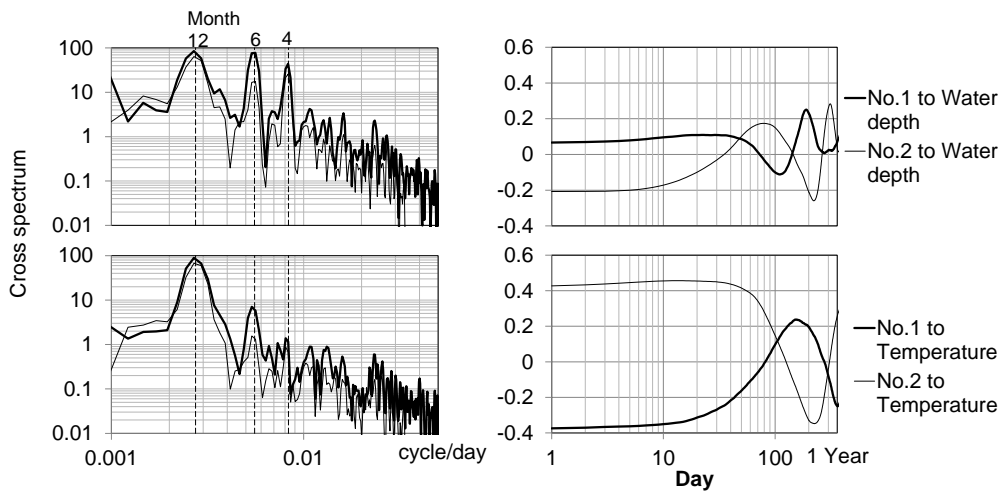


(a) Convergence and related records



(b) Frequency characteristics

Fig. 5
Convergence records of the cavern



(a) Cross spectrum

(b) Cross correlation

Fig. 6
Correlation among convergence, water depth and temperature

The relations among them are examined deeply with cross spectra and cross correlation coefficients (referred to as CCCs) as shown in Fig. 6, the water depth in the above and the temperature in the below. The cross spectra show the similar peaks described above. The convergences of the cavern are affected strongly by the water depth and the temperature in the cavern. The CCCs within one year lag shows low values to the water depth and the temperature. It is considered that the cavern behaves promptly corresponding to the fluctuation of the water depth and the temperature. This paper focuses the relations between the convergences and their circumstances of the reservoir water depth and the ambient temperature of the cavern numerically in the following sections.

4. STUDY OF THE CAVERN BEHAVIOR

4.1. EXAMINATION OF CAVERN BEHAVIOR WITH THE SIMPLIFIED CONVERGENCE

The cavern convergences are processed by eliminating the long term trend and higher fluctuation than ones of the water depth and the temperature. The filtering techniques are applied in the processing using Trifunac method and low-pass-filter of 0.033 cycle/day (ie, once in a month). The processed results are shown in Fig. 7 for the convergences, the water depth and the temperature. The convergences fluctuated in the amplitude of 0.3 mm approximately. One of No.1 section began the wider fluctuation corresponding to the peak of the temperature at most in 0.8 mm from 2014.

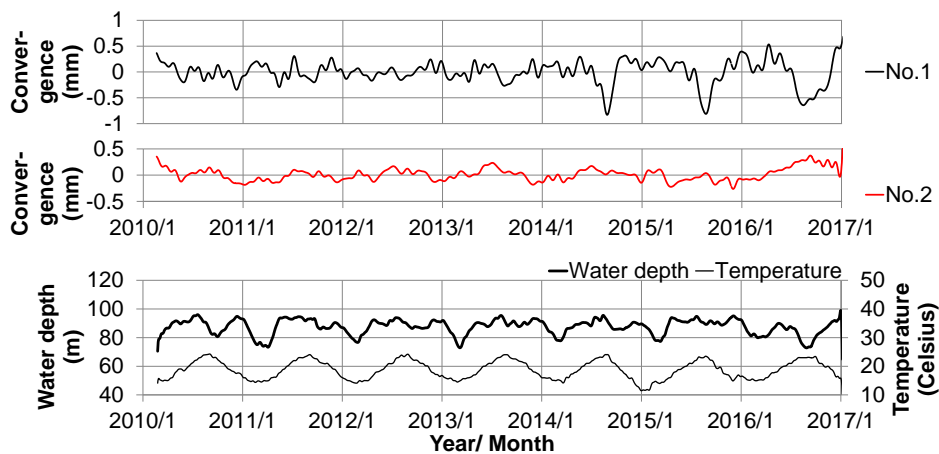


Fig. 7
Processed convergence records

The simple correlations between the convergences and the water depth or the temperature are examined in the durations of (1) 2010 to 2013 and (2) 2014 to 2016 as shown in Fig. 8. The convergence of No. 2 section shows consistent

behavior to the water depth and the temperature in both durations. One of No. 1 section shows relatively complicated manner and has not been consistent in a whole duration. Due to the location of the monitored section of No.1, the three-dimensional behavior may predominate. The further study is necessary to explore the convergence behavior at No. 1 section.

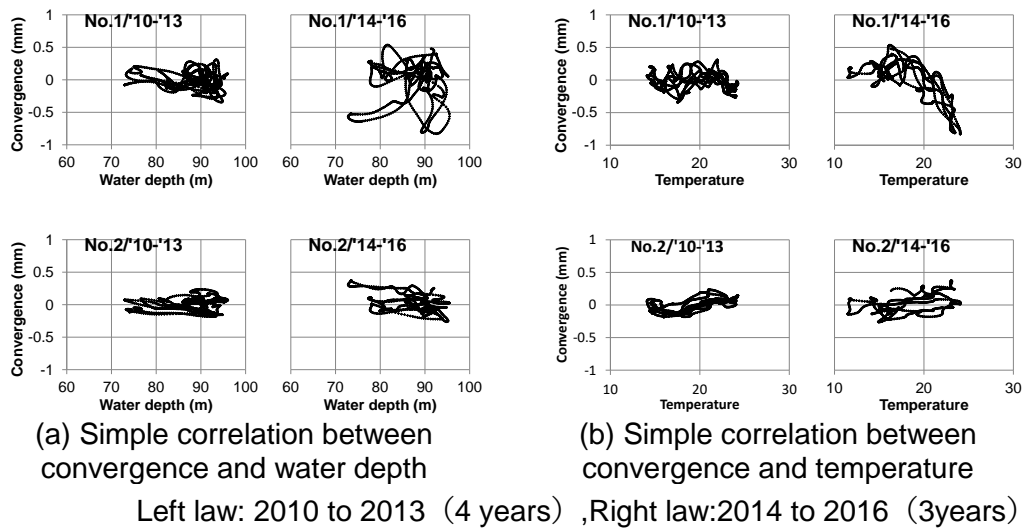


Fig. 8
 Simple correlation among convergence, water depth and temperature

4.2. REGRESSION OF CONVERGENCE

Regression formula is examined for the convergence of the cavern in terms of the water depth and the temperature change in the cavern. A simple physical model of the cavern is introduced as shown in Fig. 9 referred to [1]. The load due to the water depth acts mostly laterally on the model. Considering the physical behavior of the model due to both loads, it will be deformed linearly to the water depth and the temperature changes. The regression formula of Eq. [1] is assumed.

$$u = A + B(p_0 - p) + C(t_0 - t) \quad [1]$$

Where, u: convergence, p: water depth, p_0 : reference water depth, t: temperature, t_0 : reference temperature, A, B, C : constant

The histories of the water depth and the temperature, p and t are examined by ignoring p_0 and t_0 . The constants of A, B, C are estimated by multiple correlation study for the processed data as shown in Fig. 7. The results are illustrated in Fig. 10 and Table 1. The multiple correlation coefficients are 0.54 and 0.59 for the convergence of No.1 and No.2 sections. These indicate a certain degree of the correlation of the convergence to the water depth and the temperature in the cavern. The standard partial regression coefficient indicates

the degree of the correlation among the parameters. The convergence of No.1 section behaves inversely by almost the temperature change. The change of the water depth and the temperature comparably induce the convergence of No. 2 section in an inverse and a proportional manner, respectively. These manners are consistent to the characteristics shown in Fig. 8. The estimated convergences for both sections by Eq. [1] provide reproducible results as a whole, although the wider fluctuation of the No. 1 section since 2014 is not followed. The fluctuations of the convergences are the amplitude of 0.5 mm and 0.2 mm approximately for the yearly changes of the water depth and the temperature, respectively.

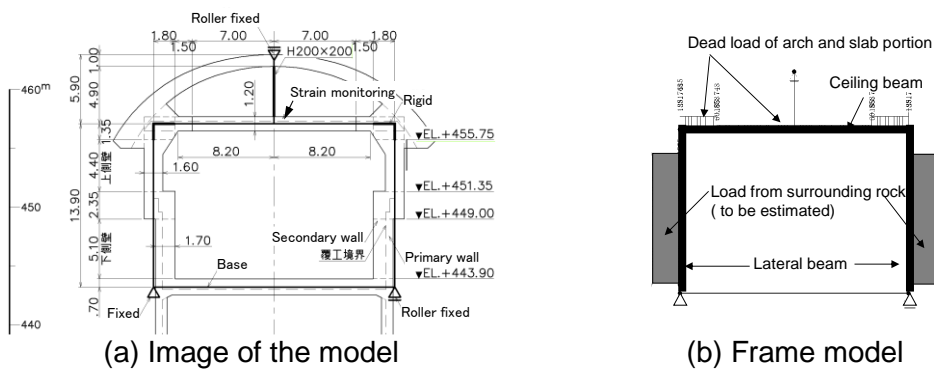
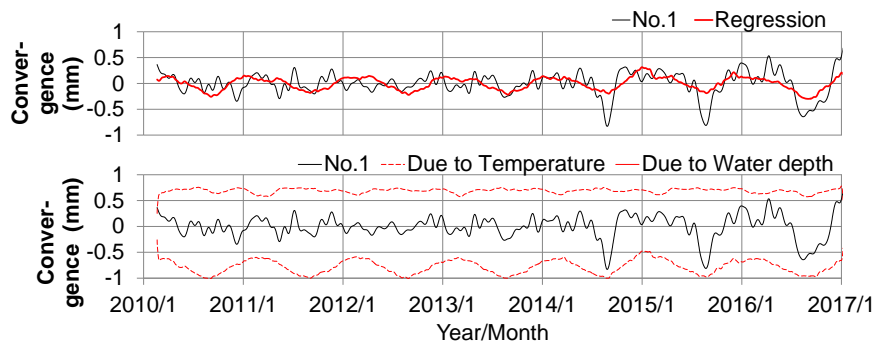
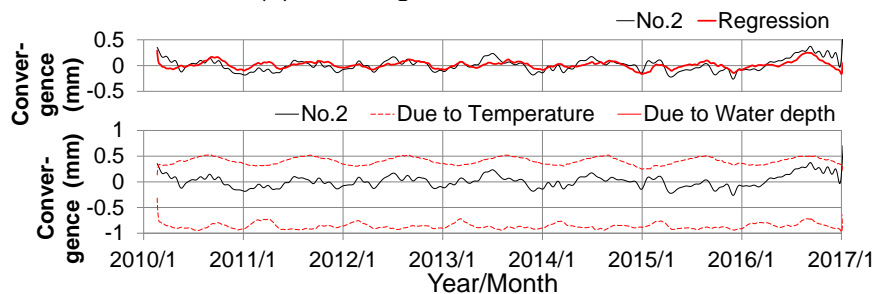


Fig. 9
Representation of the cavern[1]



(a) Convergence of No.1 section



(a) Convergence of No.2 section

Fig. 10
Regression of convergence
Table 1

Regression formula for the cavern convergence

Parameters		For No.1 section	For No. 2 section
Constant	A	0.0862	0.4709
	B	-0.0416	0.0216
	C	0.00787	-0.00986
Cross correlation coefficient		0.54	0.59
Standard partial regression coefficient	B'	-0.590	0.586
	C'	0.195	-0.469

4.3. CONSIDERATIONS

The safety assessment of the cavern has been conducted by the following manner [1], [2]. The current loading condition was assumed by the in-situ stress monitoring of the ceiling beam shown in Fig. 9(a). The convergence of 2.5 mm of the cavern was estimated by incorporating the risk scenario of the loss of the support effect due to the entire deterioration of supports. As the further risk, higher loading which could cause the damage in the main concrete structures was incorporated for the terminal condition of the cavern. These convergences of 2.5 mm and 6 mm were set as the maintenance criteria of the convergence.

The current convergences are less than the criteria and correlate to the water depth and the temperature with repeatability. The fluctuation amplitudes are smaller enough than the criteria. However, the cumulative convergence is clear in the No. 2 section and larger amplitude has been found in the No. 1 section since 2014. The continuous monitoring of the convergence has been essential from the view point of the soundness assessment of the cavern, taking into account the relationship among the convergence, the water depth and the temperature such as Eq.[1]. When the abnormal behavior would be found in the future, the re-evaluation of the cavern behavior will be indispensable.

5. CONCLUSION

The convergence monitoring has been conducted in the cavern of the hydropower plant since 2010 and these data are examined for the soundness assessment of the cavern. The conclusions are listed as follows.

(1) The convergence monitoring using a DLRF provide the useful convergence data with the high precision of 0.1 mm for the soundness assessment of the cavern without any troubles and missing observation in 8 years so far.

(2) The convergence at the representative two sections behaves corresponding to the yearly and/or the seasonal fluctuations of the reservoir water depth and the ambient temperature in the cavern. One of the center section at No. 2 machine develop the cumulative convergence, while one of another section near the end of the cavern shows less cumulative convergence and wider amplitude especially since 2014.

(3) These are less than the unusual convergence which is designated as the maintenance criteria under the assumption of the entire loss of the support effect as the risk scenario. The convergence behavior is stably reproducible to be consistent with the water depth and the temperature fluctuations. No concerns are found in the current situation of the cavern so far.

(4) The DLRF has been renewed in beginning of 2017. It caused certain discontinuities for the convergence monitoring. The cumulative deformation at No. 2 section and the wider amplitude at No. 1 section will be clarified using the data accumulated in the future.

REFERENCES

- [1] Kashiwayanagi M., Matsubayashi S., Shimizu N., Osada N. Re-evaluation techniques of current status of safety for underground caverns of hydropower stations. *24th ICOLD Congress, Kyoto, C.01*, 2012.6
- [2] Kashiwayanagi M., Matsubayashi S., Shimizu N., Osada N. Field measurements aided maintenance for an underground power station under operation, *The 3rd ISRM symposium on rock mechanics, Shanghai, CD*, 2013.6
- [3] Kashiwayanagi M., Shimizu N. Application of Continuous Maintenance Method for Aging Underground Powerhouse, *Vietrock2015 and ISRM specialized conference (Vietrock2015), Hanoi, Vietnam*, 2015.3

SUMMARY

A few damaged pre-stressed anchors were identified in the 40-year aged underground powerhouse, while no other deterioration in the cavern was found. The monitoring of the cavern convergence has been conducted to clarify its long-term performance using a newly developed precise range finder since then. The convergences of two sections during seven years are examined. These have behaved stably reproducible and been consistent with the yearly and/or the seasonal fluctuations of the reservoir water depth and the ambient temperature in the cavern. These are less than the unusual convergence which is designated under the assumption of the entire loss of the support effect as the risk scenario. No concerns are found in the current situation of the cavern so far.

COMMISSION INTERNATIONALE DES GRANDS BARRAGES

VINGT-SIXIÈME CONGRÈS DES GRANDS BARRAGES
Autriche, juillet 2018

DOI 10.3217/978-3-85125-620-8-183



This work licensed under a Creative Commons Attribution 4.0 International License. <https://creativecommons.org/licenses/by-nc-nd/4.0/>

**MODELING TURBULENCE PHENOMENA AND WAVE PROPAGATION IN
AYANUNGA HEPP FOREBAY AND ADDUCTION SYSTEM, THROUGH IBER-
2D AND ANSYS-3D**

Luca MACCHI

*Member of the Center of Excellence in the hydroelectric design unit, involved in
Andeans projects, ENEL GREEN POWER CHILE LTDA, SANTIAGO DE CHILE*

CHILE

Marc Gil FLORES

*Head of the Center of Excellence in the hydroelectric design unit, ENEL GREEN
POWER SPA, ROME*

ITALY

Stefano CAPILLERA

*Head of hydroelectric design unit, Global renewable energies, ENEL GREEN
POWER SPA, ROME*

ITALY

COMMISSION INTERNATIONALE
DES GRANDS BARRAGES

VINGT-SIXIÈME CONGRÈS DES
GRANDS BARRAGES
Autriche, juillet 2018

**MODELING TURBULENCE PHENOMENA AND WAVE PROPAGATION
IN AYANUNGA HEPP FOREBAY AND ADDUCTION SYSTEM, THROUGH
IBER-2D AND ANSYS-3D***

Luca MACCHI¹, Marc Gil FLORES², Stefano CAPILLERA³

*¹Member of the Center of Excellence in the hydroelectric design unit,
involved in Andeans projects,*

ENEL GREEN POWER CHILE LTDA, SANTIAGO DE CHILE

²Head of the Center of Excellence in the hydroelectric design unit
ENEL GREEN POWER SPA, ROME

³Head of hydroelectric design unit, Global renewable energies,
ENEL GREEN POWER SPA, ROME

CHILE, ITALY

INTRODUCTION

Enel Green Power is constructing a RoR hydroelectric power plant in Peru (Monzón district), named Ayanunga. 20 MW installed capacity, 2 small dams of approximately 6m high, equipped with Tyrolean intakes and desanders, 2 free-flow adduction channels in site-cast concrete (total length more than 7km), until the forebay, a penstock made of GRP, and 2 Francis turbines. The plant will have a rated flow of 12.38 m³/s. The gross head is of 190.5 m and the average annual expected production is 141.64 GWh/y. It is currently under construction, first synchronization is foreseen for may-2019, and full production by the end of 2019.

This plant is equipped with a unique forebay, despite of two intakes and two adduction channels: this give advantage as cost savings and increased production.

However, this design generates unexpected problems: vortices in the forebay and problems in the good performance of its emergency spillway. These difficulties usually emerge in the operational phase, but the experience of the group

* Modélisation des phénomènes de turbulence et de la propagation des ondes dans le bief amount et le système d'adduction de la centrale hydroélectrique Ayanunga, à travers IBER-2d et ansys-3d

allowed detecting and optimizing it in the design phase. In order to optimize, two analyses will be performed using IBER-2D and ANSYS-3D:

1) Assess the occurrence of turbulence phenomena in the forebay near the penstock inlet, and evaluate measures to allow good functioning of the system and avoid inlet of air into the penstock, managing to optimize the basic design;

2) Study the propagation of the big wave (surface wave) caused by the turbine load rejection, and model its evolution in time and space from the forebay to its spillway, characterizing discharged water behavior during this case. Furthermore, big wave propagation throughout the plant's adduction system has been modeled, in order to assess the risk that the wave crest touches the upper limit of the adduction conduction.

2. MODELING OF AYANUNGA FOREBAY

2.1. STUDY ZONE DESCRIPTION

The study is on Ayanunga forebay and adduction channel and more specifically in the forebay tank, and outlet, where is located the penstock inlet, according to Figure 1. Ayanunga's forebay receives water from both adduction (north and south) thanks to two inlets that churn in the forebay. At the junction, two sloping floors develop in the pool, and finally the bottom of the tank, which coincides with the lowest point of the penstock inlet.

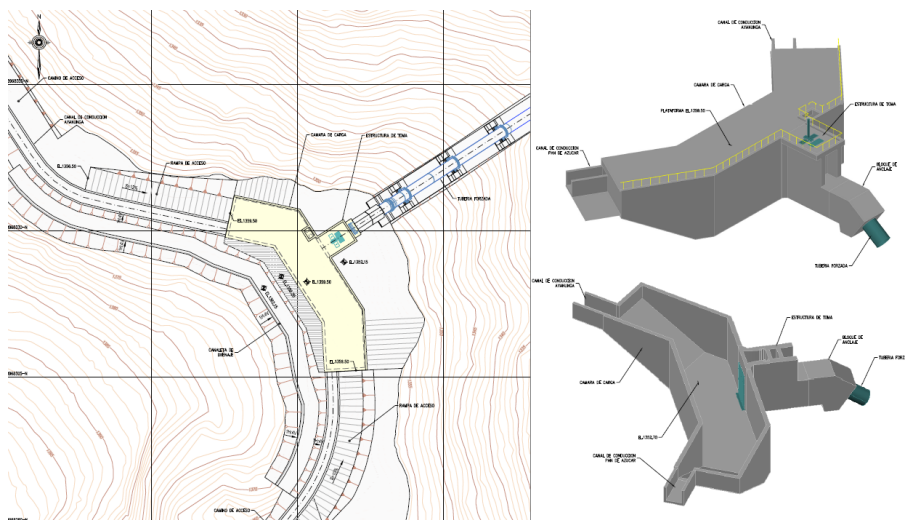


Fig.1
Forebay: Plan view (left) and isometric view with platform (top right) and without platform (bottom right).

2.2. TWO-DIMENSIONAL NUMERICAL MODELING WITH IBER

The 2D numerical modelling approach has been developed with the public domain code IBER [3]. It is a modelling system that uses high resolution schemes (FVM with TVD schemes), with a user friendly interface, compatible with GIS system. IBER solves two-dimensional (2D) depth averaged equation, also known as 2D Shallow Water Equations (2D-SWE) or two-dimensional St. Venant equations. These equations assume a hydrostatic pressure distribution and a uniform vertical velocity distribution. It solves mass and momentum conservation equations in the two horizontal directions:

$$\frac{\partial h}{\partial t} + \frac{\partial(hu)}{\partial x} + \frac{\partial(hv)}{\partial y} = 0 \quad [1]$$

$$\frac{\partial u}{\partial t} + u \frac{\partial u}{\partial x} + v \frac{\partial u}{\partial y} = -g \frac{\partial Z}{\partial x} + \frac{1}{\rho h} \frac{\partial h \tau_{xx}}{\partial x} + \frac{1}{\rho h} \frac{\partial h \tau_{xy}}{\partial x} - \frac{\tau_{bx}}{\rho h} \quad [2]$$

$$\frac{\partial v}{\partial t} + u \frac{\partial v}{\partial x} + v \frac{\partial v}{\partial y} = -g \frac{\partial Z}{\partial y} + \frac{1}{\rho h} \frac{\partial h \tau_{yx}}{\partial x} + \frac{1}{\rho h} \frac{\partial h \tau_{yy}}{\partial x} - \frac{\tau_{by}}{\rho h} \quad [3]$$

Being h depth, u , v the velocity components in the horizontal x and y coordinate directions, g is gravity acceleration, z is water surface elevation, τ_{xx} and τ_{yy} are the normal turbulent stresses in the x and y directions, τ_{xy} and τ_{yx} , are the lateral turbulent shear stresses, τ_{bx} and τ_{by} are the bed shear stresses in the x and y directions and ρ is the water density.

2.3. ORIGINAL FOREBAY DESIGN: INPUTS AND RESULTS THROUGH IBER

In this case of study, the original design of forebay has been modeled in GID by importing a dwf file. The dominium has been discretized with a mesh of rectangle triangle cells, size 100 x 70 x 70 cm. manning roughness has been set equal to 0.014, both the adductions and in the forebay. The penstock is in GRP, Manning= 0.009. On the other hand, the boundary conditions, introduced to the program, that fix the hydraulic behavior, of the system subcritical regime are (for the original case study):

- Upstream (inlet): inflow (Q_i) uniformly distributed, equal to operation condition: 12.38 m³/s divided between 7.49 m³/s for north adduction and 4.89 m³/s for south adduction.
- Initial condition: Forebay and adduction channels without water.
- Downstream (outlet): The condition of pressure inlet into the penstock can be modeled in IBER only using the option "culvert", which allow the program

to calculate flow which go under pressure under a square or circular culvert (the pipe of a penstock for example) in every condition.

The problem has been set with these parameters:

- Initial time = 0 s
- Max simulation time = 3600 s
- Results time interval = each 120 s
- Max increment time = 2 s
- CFL = 0.45
- Wet/dry limit 0.01 m
- Molecular viscosity = 0.000001 m²/s
- Turbulence model = k- ε, limit depth 0.01 m, first order scheme.

Performing this simulation, it can be observed that stabilization time for normal condition (uniform flow at the inlet and at the outlet of the system) is around 2800 s. Finally, in the results are observed two big recirculation areas of turbulence, just near the penstock inlet, affecting the submergence safety conditions.

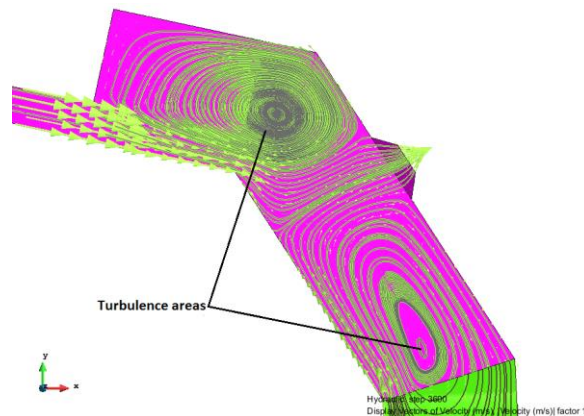


Fig.2

Forebay: Plan view of resulting turbulence areas for the original design

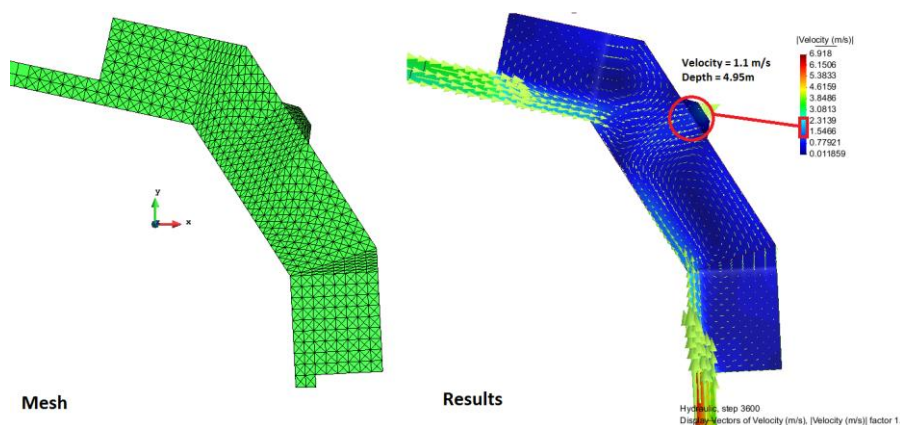


Fig.3

Forebay: Plan view of mesh cells (left) and resulting velocities vectors and contours, with legend.

Furthermore, water velocity in module is around 1.1 m/s in the penstock inlet section, and almost 2.5 m/s just 2 meters upstream the same section, values equals and higher than the maximum recommended in literature (1 m/s).

2.4. THREE-DIMENSIONAL NUMERICAL MODELING WITH ANSYS

Among the different models of turbulence that complements the RANS equations, ANSYS CFX is widely applied in the solution of many flows of engineering interest. This software allows to use two-equation turbulence models based in k - ε and in k - ω . In order to have a better knowledge of the numerical results, the k - ε model has been selected in the two CFD codes, so that results can be compared. This model is implemented in most general purpose CFD codes and is considered the industry standard model. The effective viscosity is calculated as:

$$\mu = C_{\mu} \rho k^2 / \varepsilon \quad (4)$$

where $C_{\mu} = 0.09$ is an empirical coefficient, k the turbulent kinetic energy and ε the dissipation rate of turbulent kinetic energy. The k and ε values can be obtained from the following equations:

$$\frac{\partial(\rho k)}{\partial t} + \frac{\partial}{\partial x_i} (\rho U_j k) = \frac{\partial}{\partial x_i} \left[\left(\mu + \frac{\mu_t}{\sigma_k} \right) \frac{\partial k}{\partial x_j} \right] + P_k - \rho \varepsilon + P_{kb} \quad (5)$$

$$\frac{\partial(\rho \varepsilon)}{\partial t} + \frac{\partial}{\partial x_i} (\rho U_j \varepsilon) = \frac{\partial}{\partial x_i} \left[\left(\mu + \frac{\mu_t}{\sigma_{\varepsilon}} \right) \frac{\partial \varepsilon}{\partial x_j} \right] + \frac{\varepsilon}{k} (C_{1\varepsilon} P_k - C_{2\varepsilon} \rho \varepsilon + C_{1\varepsilon} P_{kb}) \quad (6)$$

$C_{1\varepsilon}$, $C_{2\varepsilon}$, σ_k and σ_{ε} are constants (1.44, 1.92, 1.0 y 1.3, respectively), P_k is the turbulence produced by viscous forces, while P_{kb} and $P_{\varepsilon b}$ represent the influence of the gravity forces. In ANSYS CFX and both phases, air and water, can be solved through an homogeneous model. Actually, in order to compare with IBER model, only the water phase has been solved. Meshes have been compounded with hexahedral elements with a length scale of around 50 cm. Boundary conditions and initial conditions are the same adopted for the 2D analysis in IBER.. Finally, in the results are observed two big recirculation areas of turbulence, just near the penstock inlet, affecting the submergence safety conditions. Furthermore, water velocity in module is around 1.5 m/s in the penstock inlet section, and almost 1.3 m/s just 2 meters upstream the same section, values equals and higher than the maximum recommended in literature (1 m/s) and quite similar to the results of IBER 2D modeling.

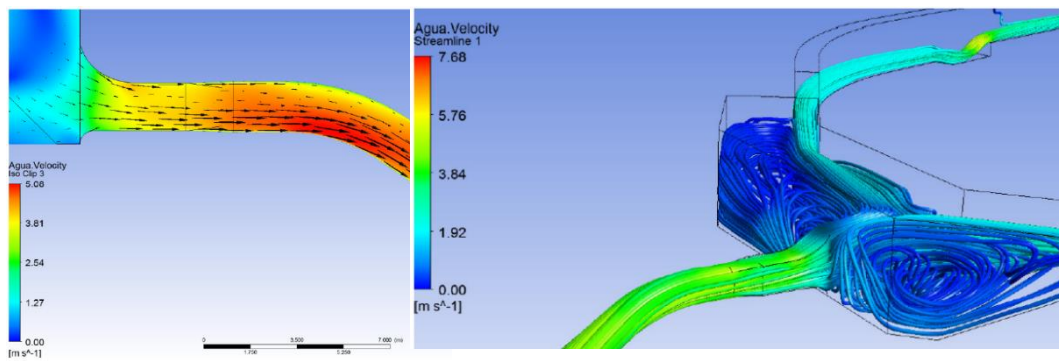


Fig.4
Section view (left) and isometric view (right) of velocities distribution at the penstock inlet in ANSYS

2.5. OPTIMIZATION OF THE EMERGENCY SPILLWAY

Furthermore, through ANSYS has also been studied the propagation of the big wave (surface wave) caused by the turbine closing due to load rejection, and model its evolution in time and space from the forebay to its spillway, characterizing discharged water behavior during this case. The target of this analysis was to assess the safety of the adduction system in case of load rejection, against the

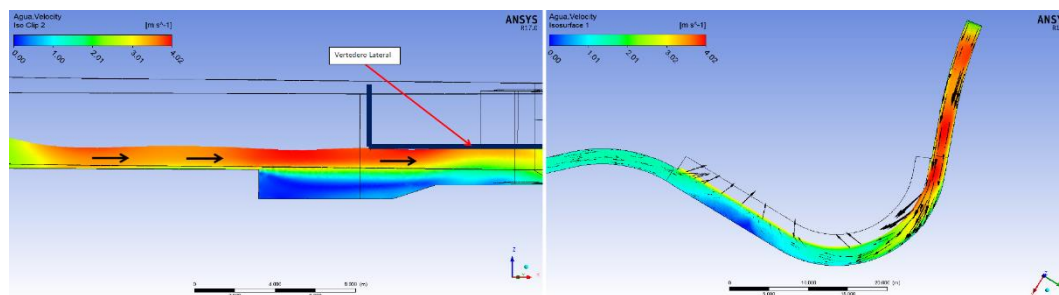


Fig.6
Section view (left) and plan view (right) of diverted flow in case of turbines fast closing due to load rejection in ANSYS.

water local elevations caused by the big propagation wave, in order to avoid that water flow out of the system in not allowed zones. The big wave propagation throughout the whole plant's adduction system has been modeled, in order to assess the risk that the wave crest touches the upper limit of the adduction conduction. It has been observed that wave propagation modeling reduces spillway efficiency. Results helps on proper re-location and optimal design of spillway to improve its discharge capacity.-By optimizing position of the spillway, the wave crest cannot reach the upper threshold of the emergency spillway, due to a proper design of its height. Furthermore, the water along the whole adduction never reaches the top pf the channels walls.

Finally, has been computed and plotted the flow diverted by the optimized emergency spillway, in the same scenery of load rejection and closing of turbine valves. Due to transient condition it's observed that max diverted flow is more than inlet flow, for almost 100 seconds, until stabilization.

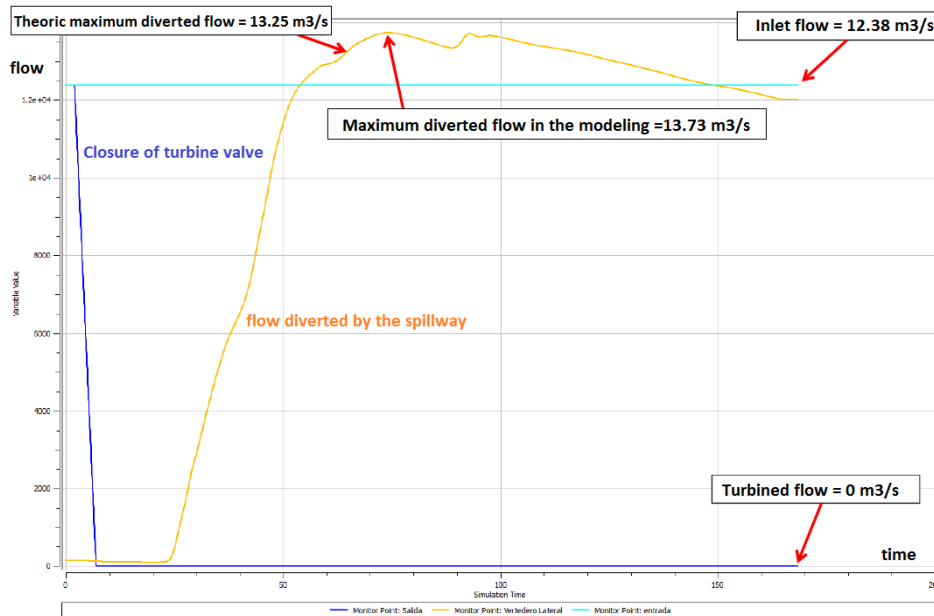


Fig.7

Diagram of diverted flow by the emergency spillway in case of turbines fast closing due to load rejection in ANSYS.

3. DESIGN OF A SYSTEM TO AVOID THE TURBULENT RECIRCULATION ZONES

Due to the big recirculation areas located near the penstock inlet, and to the high velocities affecting submergence stability, original design has been modified, by introducing two internal walls in the forebay. These are located in the slides located just downstream the lateral inlets of the forebay, 6.35 m downstream the channels junction. Inclination of wall is 45° as shown in figure 8, these are 4.5 m long, and its height is equal to internal forebay height. The analysis has been performed both in IBER and in ANSYS and the results obtained are impressively similar. As general outstanding, the vortices are localized upstream of the walls and far from penstock inlet. Maximum velocities of vortices are around 1m/s, and most of the channel energy is lost just some meters downstream their inlet in the forebay, by the formation of a little hydraulic jump, as can be observed in figure 9.

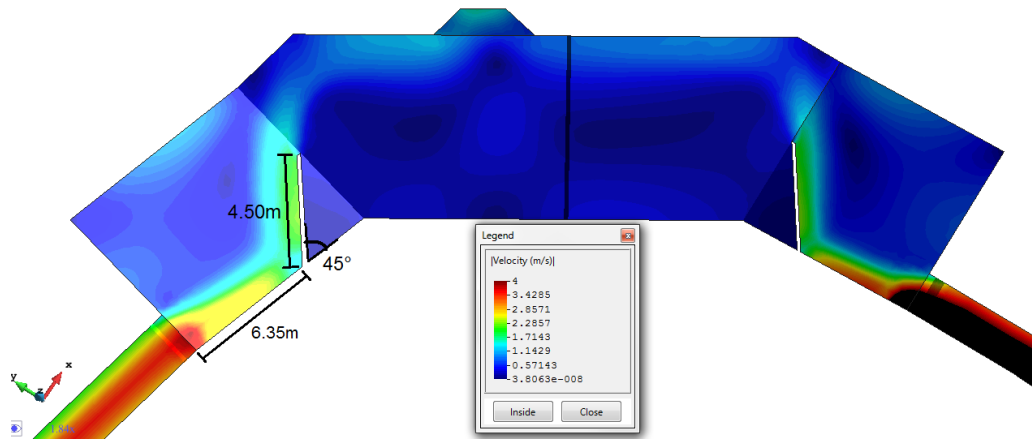


Fig.8

Plant view of velocities contour after installing walls, and dimensions

An unexpected benefit has been obtained: the hydraulic jump is located upstream the walls, in a defined area, increasing only the energy required for the water to flow into the forebay, without increasing the height of water in the forebay more than 5cm. Above all, in the remaining part of the forebay, water velocities are strongly reduced, and near the penstock inlet water velocity in module is less than 0.75 m/s, as shown in figure 9. The walls, so designed, represent a smart solution in terms of cost, because are the simplest and cheapest solution in case you need to make up for a bad basic design.

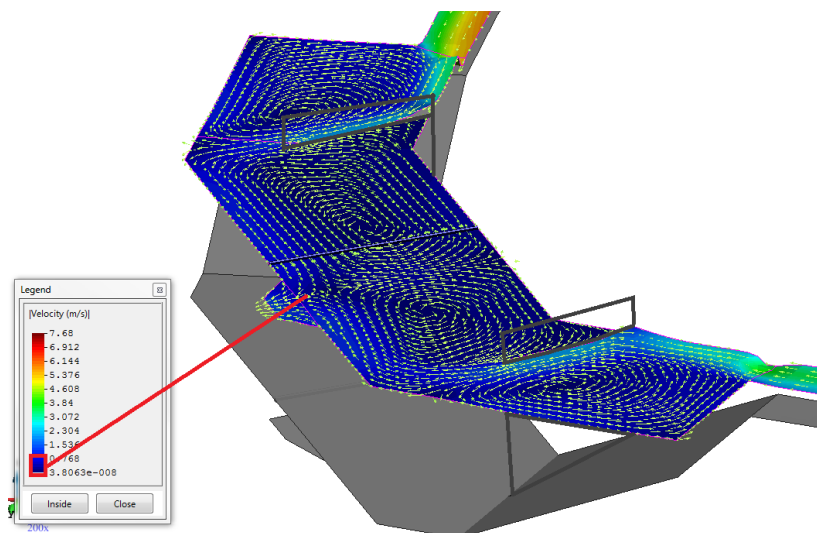


Fig.9

Isometric view of velocities vectors and contours while using walls

4. CONCLUSIONS

In the original design of Ayanunga's forebay, flow velocity near inlet was almost 2 m/s, exceeding submergence safe conditions (1m/s as recommended by good practice). Furthermore, two big vortices were localized near the penstock inlet with noticeable recirculation motion. This was due to high flow speed of water, which enters forebay from adduction channels, and also due to its uncommon shape. Consequently, thanks to the first analysis, original design was modified, by introducing internal walls in the forebay. As result, the vortices are localized upstream of the walls and far from penstock inlet. The second analysis observed that wave propagation modeling reduces spillway efficiency. Results helps on proper re-location and optimal design of spillway to improve its discharge capacity.

In conclusion, a deep knowledge of hydraulics allows savings and efficiencies (forebay optimization): the use of 2D (IBER) and 3D (Ansys) simulations allows to solve complex problems like vortices formation and transients with tools that, until recently, for their cost, were reserved to much larger projects.

REFERENCES

- [1] VEN TE CHOW . Open Channel Hydraulics. 1959.
- [2] HENDERSON, F. M. Open Channel flow. New York, USA. 1996.
- [3] INSTITUTO FLUMEN, UNIVERSIDAD POLITECNICA DE CATALUNYA & CIMNE. IBER ® v.2.4.3. 2017.
- [4] ANSYS INC. Ansys 16.1 ®. 2015.
- [5] ASCE, AMERICAN SOCIETY OF CIVIL ENGINEER. Guidelines for Design of Intakes for Hydroelectric Plants. 1995.
- [6] LEVIN, L. Formulaire des conduits forcées, oléoducs et conduits d'aération, Dunod. 1968.

SUMMARY

This study takes advantage of the power of 2D (IBER) and 3D (ANSYS) calculation codes to analyze and study the flow in a forebay of a hydroelectric plant currently under construction by enel green power, in peru. In the first part, the re-circulation zones in the forebay are modeled and analyzed; in a second part, are studied and modeled the propagation of the wave in the case of load rejection, along the adduction channels, optimizing the position and the threshold height of the emergency spillway. Finally, is provided a very simple and effective solution to the formation of turbulences and recirculation zones, in order to avoid affecting the submergence in the forebay at the penstock inlet. The application of 2 simple ad-

hoc inclined walls, placed in such a way as to locate and limit the recirculation zones, lowering the flow velocities in the area under analysis.

RÉSUMÉ

Cette étude tire parti de la puissance des codes de calcul 2D (IBER) et 3D (ANSYS) pour analyser et étudier le flux dans un bief amont d'une centrale hydroélectrique actuellement en construction par Enel Green Power, au Pérou. Les zones de recirculation dans le bief amont sont modélisées et analysées; dans une seconde partie, on étudie et modélise la propagation de l'onde en cas de rejet de charge, le long des canaux d'adduction, en optimisant la position et la hauteur de seuil du déversoir d'urgence. Enfin, on propose une solution très simple et efficace à la formation de turbulences et de zones de recirculation, afin d'éviter d'affecter la submersion dans le bief amont à l'entrée de la conduite force. L'application de 2 parois inclinées ad hoc simples, placées de manière à localiser et limiter les zones de recirculation, abaissant les vitesses d'écoulement dans la zone analysée.

KEYWORDS

Behaviour, Calculation method, canal, clean energy, computer calculation, conduit, construction, cost reduction, design, discharge, emergency spillway, flow, free surface flow, forebay, hydraulic head, hydraulic model, model, open channel, outlet discharge, penstock, performance, power plant, spillway, water level, wave.

Comportement, methode de calcul, canal, energie propre, calcul par ordinateur, conduite, construction, reduction des couts, calcul, debit, evacuateur de secours, debit, ecoulement a surface libre, bief amont, charge hydraulique, modele hydraulique, modele, canal a ecoulement libre, debit de restitution, conduite forcee, performance, centrale, evacuateur de crue, niveau hydraulique, vague.

COMMISSION INTERNATIONALE DES GRANDS BARRAGES

VINGT-SIXIÈME CONGRÈS DES GRANDS BARRAGES
Autriche, juillet 2018

DOI 10.3217/978-3-85125-620-8-184



This work licensed under a Creative Commons Attribution 4.0 International License. <https://creativecommons.org/licenses/by-nc-nd/4.0/>

**COMPLEX HYDROGEOLOGICAL RESPONSES DEFY CONSERVATIVE
DESIGN OF A PRESSURE TUNNEL – FAILURE OF THE BESAI HEADRACE
TUNNEL**

R. BENSON

Consultant

W. RIEMER

Consultant

GERMANY

M. IIJIMA

Chief Engineer

COMPLEX HYDROGEOLOGICAL RESPONSES DEFY CONSERVATIVE DESIGN OF A PRESSURE TUNNEL – FAILURE OF THE BESAI HEADRACE TUNNEL*

R. BENSON

Consultant

W. RIEMER

Consultant

M. IJIMA

Chief Engineer

1. INTRODUCTION

The performance of pressure conduits has caused costly problems for a significant number of hydropower projects and has prompted studies and investigations with the aim of developing concepts and methods for their safe design. This task has been approached in mainly two different ways: (1) basic physical concepts backed up by empirical data (e.g. [1, 2, 3, 4], with focus on unlined tunnels) and (2) engineered design using rock mechanical parameters (e.g. [5, 6, 7]). The latter approach was further enhanced by incorporation of hydrogeological phenomena (e.g. [8, 9, 10, 11, 12]).

Benson [13] comprehensively discussed the various factors and conditions to be considered in the design of pressure conduits and Swiger [14] cautioned against the use of “rules of thumb” in this context. Nevertheless, in spite of the ample experience accumulated with the performance of pressure conduits and the

* *Les réponses hydrogéologiques complexes défient la conception conservatrice d'un tunnel sous pression – rupture du tunnel d'amenée de Besai*

advances made in the computational analysis since Frey-Baer [5], incidents continue to occur. Some of these incidents are caused by unstable rock and could have happened as well in non-pressurized tunnels (Higuera, Glendow, see [4]) but other incidents resulted from the complex interaction of pressurized water and difficult geological and hydrogeological conditions. This applies to the case history of the Besai headrace tunnel, which, although thoroughly investigated and conservatively designed, developed excessive leakage. The investigations following the incident identified a number of diverse geological details, which in combination caused the failure. In retrospect, the process of the failure that advanced over a sequence of different effects was found to have been virtually unpredictable. It is for this reason that the incident is described in the following, illustrating the particular hazards potentially linked with pressure conduits and the need for particular precautions in their design.

2. THE BESAI HEADRACE TUNNEL

The Besai hydropower plant, with an installed capacity of 90MW, is located in Sumatra, Indonesia. The headrace tunnel, inner diameter 4.30m, descends over a length of 4900m from the intake at el. 708m to the base of the surge tank at el. 636m. The pressure shaft and penstock tunnel connect with the power plant, discharging to the tailwater at el. 472m, giving a net head of 250m with the storage level at el. 722m.

Maximum upsurge: El. 733.37 m, Maximum downsurge: El. 706.28m

Following investigation and design in 1991, construction started 1995.

3. INVESTIGATION AND GEOLOGICAL CONDITIONS

A generous program of subsurface explorations provided geological and geotechnical information for the tunnel, including geophysics, 15 boreholes along the route of the headrace tunnel, totalling 1,540m, drilled with core recovery and, near the level of the tunnel, permeability testing.

Bedrock in the project area consists of a sequence of volcanic and volcanoclastic rocks, dating from the Pleistocene (Fig. 5). The strata with their undulating contacts dip flatly in various directions. Near the level of the tunnel, the boreholes found a cemented, massive volcanic breccia (Tbr), covered by argillaceous tuffs (Tf3 and Tf4). Tuff layer Tf5, encountered at the bottom of the surge tank, was assumed to wedge out intermittently. After the incident, a layer of partially soil-like tuff intercalated in the breccia was encountered. It possibly connects with the Tf5 but differs decisively in geotechnical properties from those observed in the tunnel upstream and downstream of the damaged section. The intercalation has, therefore, been identified as "TfX".

Table 1 compiles geotechnical characteristics for the rock.

Table 1
Rock mass parameters
Paramètres du massif rocheux

Lithologic Unit	Bulk Density	σ_c	ϕ	c	E	Kf
	[g/cm ³]	[kg/cm ²]	[°]	[kg/cm ²]	[kg/cm ²]	[m/s]
Breccia	1.7	30	40	10	7500	2E-6, grouted 5E-7
Tuff	1.6		20- 30	1-5	1000 - 1500	anisotropic 1E-4 - 1E-7

The strength of the TfX detected after the incident reached only half of the values previously found for tuff layers.

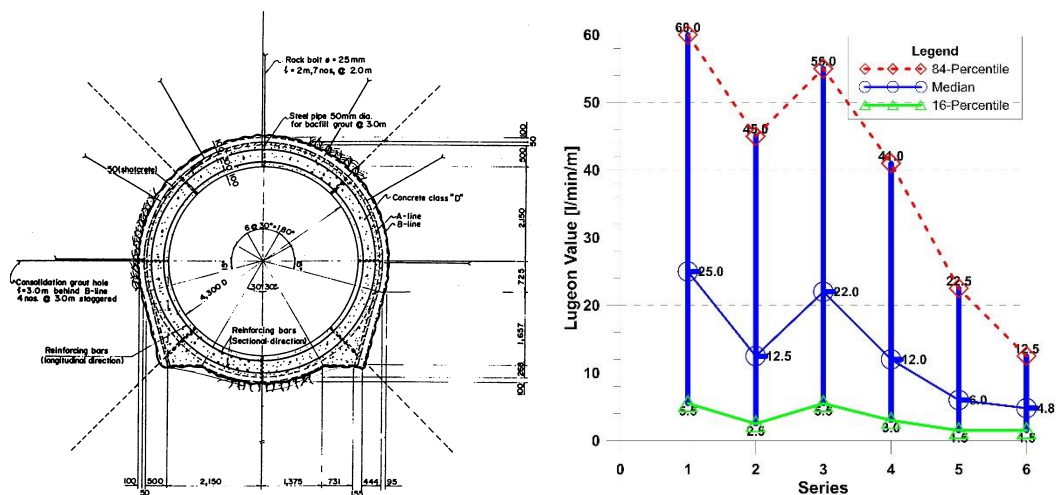
Boreholes in the low-cover stretch found groundwater levels 46 to 48.6m above the tunnel. The design of the lining adopted 30m external head. Jacking pressures estimated from water pressure tests near the failure ranged 4 to 5 bar above the groundwater level.

4. DESIGN AND CONSTRUCTION OF THE TUNNEL

Evaluating several alternatives, the designers, in concurrence with an international Board of Consultants, adopted the following criteria.

- The tunnel should be placed as high as the hydraulic conditions permit to keep the internal pressure low but still maintaining a rock cover of more than 0.7 times the hydraulic static head [2, 15]. Even with these precautions, the design provided a continuous concrete liner, reinforced, with contact and consolidation grouting. As verified by the Frey-Baer method [5], supported by FEM analysis, the width of cracks in the liner would stay below 0.25 mm and the leakage be limited to 20 l/s.
- The Tf4 tuff layer should be avoided, because it was suspected to contain low-modulus horizons, undesirable for the construction and stability of the tunnel.
- The tunnel should run in the tuff breccia, aiming to keep a distance of about 15m from the Tf4 tuff horizon. According to a FEM simulation, the convergence observed in the tunnel would alert on the critical presence of a weak layer in its vicinity.

Excavation and preliminary support followed the concepts of NATM, with geological logging, rock mass classification and convergence monitoring.



a) Preliminary support and final lining, arrangement of consolidation grout holes

b) Reduction of Lugeon Value with successive steps of consolidation grouting

Figure 1:

Support of tunnel in damaged section and results of consolidation grouting
Revêtement du tunnel dans le tronçon endommagé et résultats des injections de consolidation

In the stretch of the failure, RMR averaged 82 – best along the entire tunnel - and only three discontinuities were logged, subvertical and at an acute angle to the tunnel axis. Convergence in the subsequently failed stretch stayed below 1 mm, in agreement with the favorable rock mass classification.

The tunnel was preliminarily supported by 5cm shotcrete and grouted bolts and finally lined with 50cm reinforced concrete (circumferential inner and outer ring $\Phi 22$ at 15cm, longitudinally inner and outer ring $\Phi 19$ at 7,5°, area ratio of steel 1%, see Figure 1). Concrete strength of the liner exceeded 300kg/cm². A 200mm waterstop seals the block joints. After contact grouting in the crown, consolidation grouting followed with rings spaced at 4m, staggered. Grouting pressure reached 6 bar (following [16]). Thus, the rock surrounding the tunnel had been pre-loaded to 6 bar and had built a hydraulic resistance to that pressure.

5. THE LEAKAGE INCIDENT

I. Pinkerton, member Board of Consultants, described the incident: “The Besai power tunnel was pressurized in early December 1999, over a period of about 10 hours with the static pressure head in the downstream section of the tunnel being about 80 metres. Falling water levels in the desanders indicated that water was escaping from the tunnel. Over a period of about 6 hours the tunnel

pressure head fell by around 20 metres but a general inspection the next morning did not reveal where the water was going. The same day the tunnel was again brought up to the operational static pressure over a period of a few hours but again next morning the water level in the tunnel was observed to be falling. After further pressurization the water remained at the static level overnight, but the next morning the water drained rapidly from the tunnel with a calculated loss of the order of 1.5 m³/sec. It was then observed that a failure had occurred on the riverside slope.”

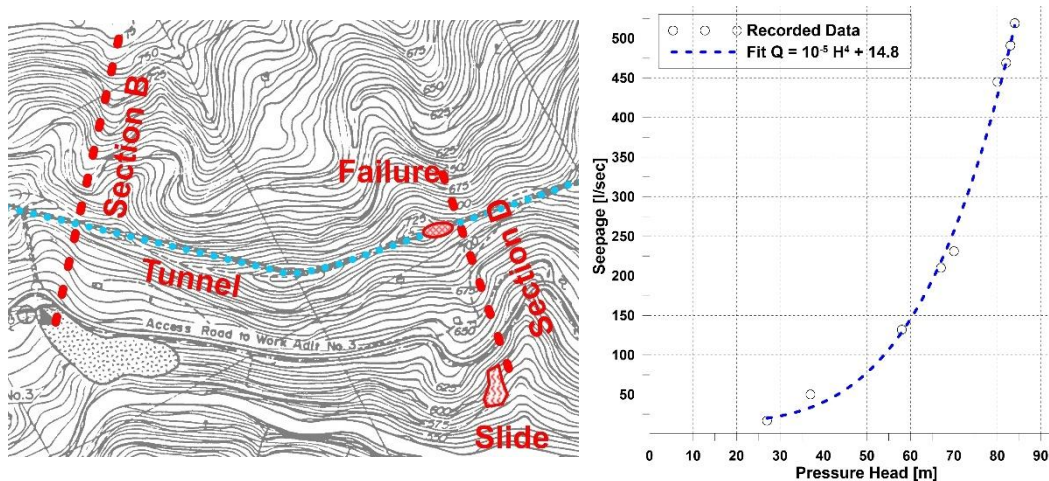


Figure 2:

Location map of low cover stretch and failure of headrace tunnel (grid spacing 500m) and tunnel seepage. Diagram of loss against head.
Endroits du toit minimal et de rupture e tunnel d'amenée (grille 500m) et filtration de tunnel. Diagramme pertes contre pression.

The slope failure affected overburden and decomposed rock, exposing the TfX layer at its back. The water had eroded cm-sized pipes into the tuff.

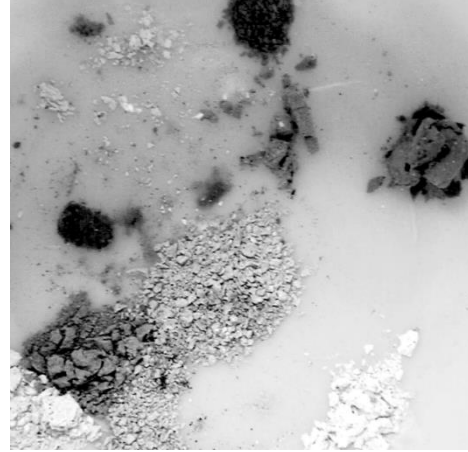
6. POST-FAILURE INVESTIGATION

Mapping and chipping of cracks: Ten blocks displayed longitudinal cracks with more than 0.2mm, finer cracking of liner extended another 100m upstream and downstream. In the most notably affected blocks, mapping was repeated after chipping the concrete. In blocks 337 to 344 isolated cracks continued to 15 cm depth into the concrete, 5 cm beyond the interior reinforcement. Block 342 showed several deep cracks that were opened up to 5 mm. A crack at the downstream end of block 342 could be followed into the rock, where it gaped about 2 cm.

Acoustic probing: notable anomalies from block 338 in half way into block 343. Blocks 340, 341 and particularly block 342 severely affected.

Core drilling: detected a separation between concrete and shotcrete or shotcrete and rock, in some cases with traces of circulation of silt-laden water.

Permeability: notably increased from block 329 to block 353. Water lost from boreholes in some instances issued at the slope failure. Jacking pressures in the most severely damaged stretch 3 and 5 bar, elsewhere >5 bar.



a) eroded crack in TBr above concrete in crown of Block 342

b) crumb test on samples from Tfx above tunnel

Figure 3
Observations after incident
Observations après incident

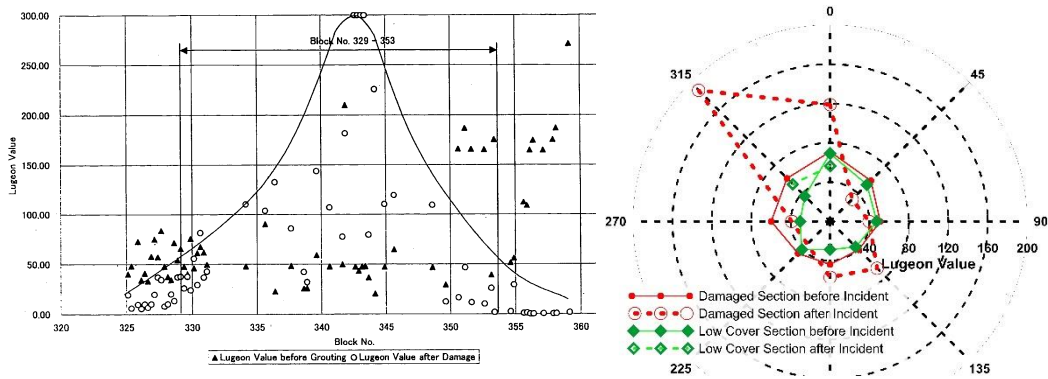


Figure 4
Lugeon values before and after incident in longitudinal distribution and averages in transverse section
Valeurs Lugeon avant et après l'incident, distribution longitudinale et moyennes en coupe transversale

7. INTERPRETATION, ANALYSIS, REPAIR

Seepage discharge quite accurately increased with the fourth power of the internal pressure (Figure 2). Accordingly, hydrojacking did play an important role (crack opening linearly related to pressure and permeability following the “cubic law” with the third power of the opening). Therefore, the adequacy of the burden above the tunnel was checked.

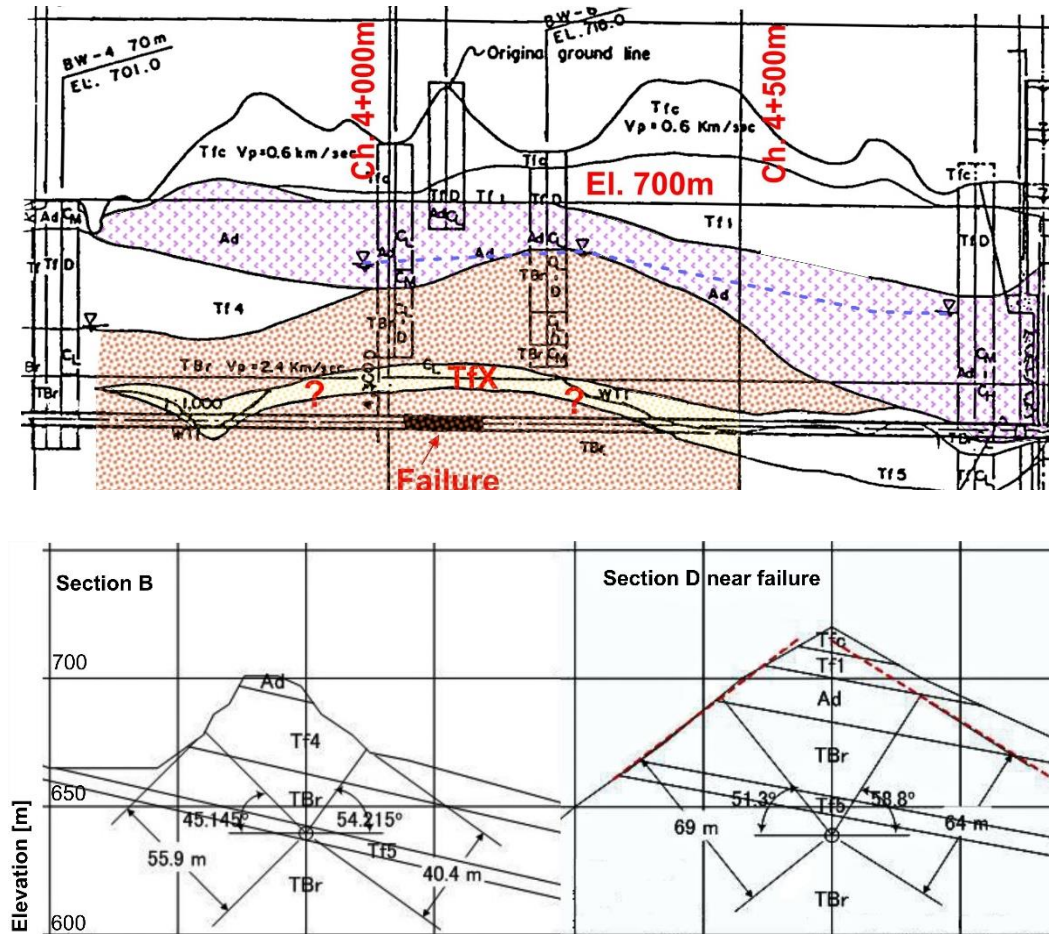


Figure 5

Longitudinal and transverse sections for low cover stretch and failure. Location see Figure 2

*Coupes longitudinale et transversales, toit minimale et site de la rupture.
Emplacement voir Figure 2*

Figure 5 displays a longitudinal and transverse section for the low cover (B) and failed stretch (D) of the tunnel. The sections meet the “Australian Criterion” for lateral cover [1]. For the “Norwegian Criterion” (e. g. [4]), the safety factor arrives at 0.68 for Section B and 1.25 for Section D, the latter with correction for lateral

cover. These safety factors apply to unlined tunnels, disregarding the reinforced liner with consolidation grouting. Therefore, hydrojacking because of low cover cannot constitute the sole cause of the failure. A FEM simulation of the stress distribution in the failed section supports this conclusion. As Figure 6 shows, the TfX layer causes a distortion of the stress field in the ridge, raising σ_3 near the tunnel to arrive at levels similar to that derived from the Lugeon tests (cf. [18] for similar effects).

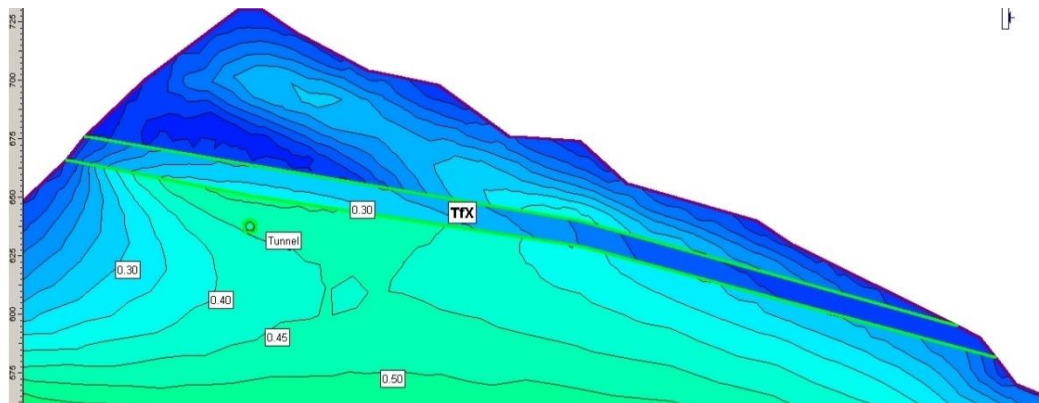


Figure 6
 σ_3 contours for cross section at tunnel failure according to FEM simulation
Simulation MEF des contours σ_3 en coupe transversale près de la rupture

Looking for an explanation for the tunnel failure, the effect of tensile stresses caused by seepage water around the tunnel was also evaluated [according to [11, 12]]. Allowing for an uncertainty in the hydrogeological regime, two alternatives were studied, with 46.5 m external head, as suggested by the piezometer data from the exploratory borehole, and 17 m, as implied by a hydrogeological model introducing a drainage effect due to TfX. For the alternatives, the Fernandez method estimated seepage losses between 0.1 and 0.27 l/s/m (which agreed closely with the results of a hydrogeological simulation) and an average crack width of less than 0.1mm. Estimates following [8, 9] indicated a crack width of up 0.14mm and seepage of 0.38 l/s/m. Thus, also these approaches did not explain the failure of the tunnel. Still other factors and processes must have contributed. In this context, the study of Lugeon and dilatometer tests gives hints: Lugeon values had notably increased (Figure 4) after the incident, but the deformation modulus had not changed, hydrogeological characteristics were more notably affected than mechanical. The crack in the concrete of block 342 was opened 5mm but the continuation into the breccia gaped 2cm. At the slope failure, the water issued from pipes in the TfX layer. Apparently, the clastic dike had collected seepage water and eroded the breccia and dispersivity of TfX had permitted rapid piping. This means, a geological detail – the clastic dike – and a local condition – the pronounced dispersivity – had prominently assisted in the failure process.

Hydrogeologic modelling, assuming high infiltration rates exceeding 600 mm/year, failed to reproduce the groundwater level found in the exploratory boreholes. Therefore, in the original state, the overburden (young tuffs, residual

soil, decomposed rock) had obstructed the drainage of the TfX layer. Initial seepage from the tunnel raised the pore pressure in the slope, triggered the failure and opened the drainage. The hydrogeological regime changed drastically, resembling a scenario, which Benson [13] had presented as Case D, the intercalation of a pervious zone in the rock. The distance of the potentially pervious zone to the failed block measured only 9m, a strong seepage gradient developed (see Figure 7) and the rock eroded. The hydrogeological regime progressively deteriorated and the damages along the tunnel propagated laterally. Figure 8 attempts to interpret and illustrate significant steps in the failure process.

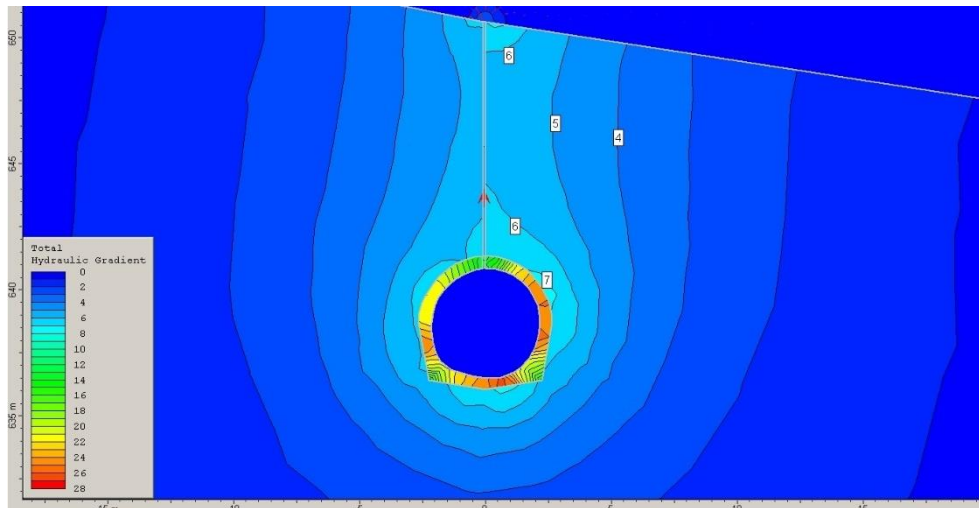


Figure 7

FEM simulation of hydraulic gradient in crown pillar between tunnel and TfX layer
Simulation MEF du gradient hydraulique entre le toit du tunnel et TfX en haute

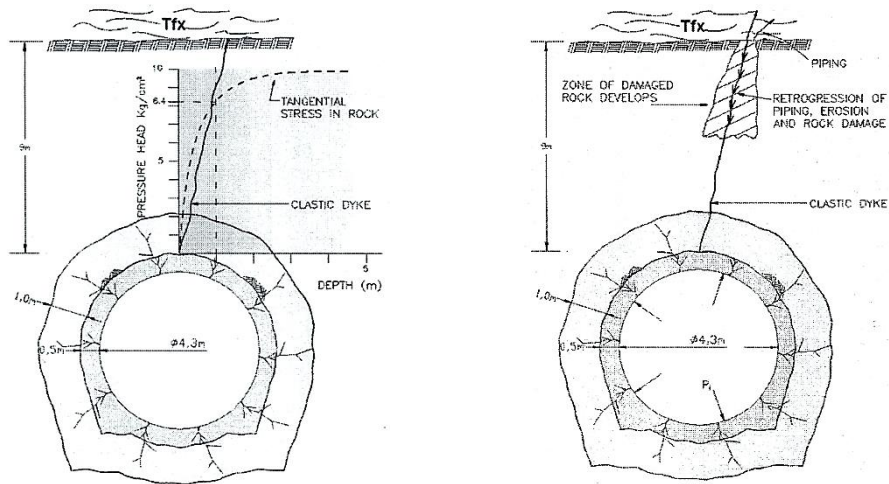
Comparing options for rehabilitation of the tunnel (repair and strengthening of the liner, new concrete liner, geomembrane or steel liners), the steel liner emerged as optimal solution. After installation of 300m steel lining for the damaged stretch, initial leakage amounted to 20 l/s. With time, the losses declined to 6 l/s.

8. CONCLUSIONS

The conservatively designed tunnel failed in a stretch of good rock where the cover according to Norwegian and Australian criteria would have admitted an unlined tunnel. Checking the design against the concepts proposed by Schleiss [8, 9] and Fernandez [11, 12] also predicted an acceptable performance. Analytical methods (e.g. [18]) as well as digital simulation, based on information available at design stage, indicated minor steady state seepage relaxing stresses on the liner.

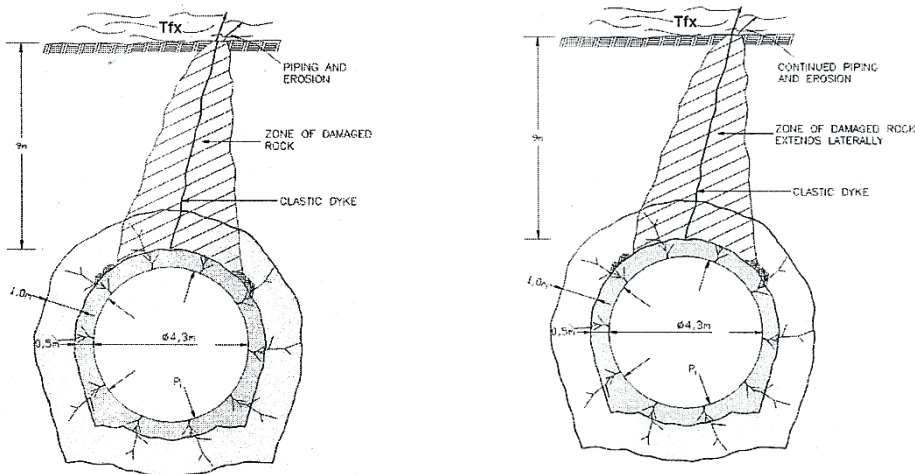
The post-failure investigations traced the causes of the failure to a combination of geological and hydrogeological details. The interaction of these

details in the successive steps in the failure process had defied prediction. The experienced problems essentially derive from an unforeseen instability of the hydrogeological regime, which is attached to several features: the temporarily blocked drainage of the Tfx layer, the dispersivity of the Tfx (not detected previously in the project area), which permitted rapid piping, and the clastic dyke, which promoted hydrojacking and with its erosion paved the way to the failure.



1. Internal Pressure $P=84m$. Hydraulic jacking opens cracks in concrete and starts jacking in rock. Limited leakage

2. Piping and erosions along clastic dyke, full internal pressure builds in clastic dyke, damage to rock pillar and local loss of stress



3. Severe damage to rock pillar. Piping in Tfx opens outlet to ground surface. Vertical offset of tunnel crown, start of collateral damage. Seepage $1.5m^3/s$

4. Propagation of damage along tunnel. Erosion and piping continue. Seepage increases to $1.8m^3/s$

Figure 8

Sketches illustrating significant steps in the development of the failure
Croquis illustrant les étapes importantes dans le développement de la rupture

According to observations in the Besai tunnel, the steel reinforcement does not fully guarantee an even distribution and equal opening of the radial cracks in the concrete liner. The most severe cracking concentrated in the crown, and in these cracks the steel had been strained beyond yield strength. In consequence, the elastic action assisting the balancing of internal and external head was impaired. Perhaps consolidation grouting to notably higher pressures than suggested by EPRI [16] would be helpful in this context.

This case history emphasizes the importance of hydrogeological studies. Such studies are indispensable to assure the geohydraulic steady state assumed for the design methods according to [8 to 12]. Where the geological setting indicates potential for hydrogeological complexities, specific investigations may become necessary, in addition to the geotechnical exploration, and these investigations may have to cover an ample margin beyond the perimeter of the tunnel. Even with such thorough additional studies, it is prudent to monitor the hydrogeological response during construction and filling. Such monitoring will have to be of high quality, e.g. with pore pressure cells and/or multi-port piezometers.

9. ACKNOWLEDGEMENTS

The authors gratefully acknowledge the backing by the owner of the project – Perusahaan Listrik Negara – who supported the investigation and analysis of the incident and granted use of the data and information discussed in this text.

REFERENCES

- [1] Dann, H. E., Hartwig, W. P., Hunter, J. R., 1964: Unlined tunnels of the Snowy Mountains hydro-electric authority, Australia. *ASCE 90, PO3, pp 47ff*
- [2] Deere, D. U., 1983: *Unique geotechnical problems at some hydroelectric projects. Proc. 7th Pan Am. Conf. Soil Mech. Found. Eng., pp 865-888*
- [3] Buen, B., Palmstrøm, A., 1985: Design and supervision of unlined hydro power shafts and tunnels with head up to 590 meters. *Norwegian Soil and Rock Engineering Association, Publication No. 3, pp. 65-73*
- [4] Palmstrøm, A., Broch, E. (2017). The design of unlined hydropower tunnels and shafts: 100 years of Norwegian experience. *Hydropower and Dams, 24, 3, pp 72-79.*
- [5] Frey-Baer, O., 1944: Berechnung der Betonauskleidung von Druckstollen. *Schweiz. Bauzeitg., 124, 14-15*
- [6] Lauffer, H., Seeber, G., 1961: Design and control of linings of pressure tunnels and shafts, based on measurements of the deformability of the rock. *Proc. 7th Congr. ICOLD, Q 26-R91, pp 679-709*
- [7] Seeber, G., 1999: Druckstollen und Druckschächte. *Enke*

- [8] Schleiss, A., 1986a: Bemessung von Druckstollen, Teil I. *Mitt. VAWE, ETH Zürich, # 78*
- [9] Schleiss, A., 1986b: Bemessung von Druckstollen, Teil II. *Mitt. VAWE, ETH Zürich, # 86*
- [10] Hendron, A. J., Fernandez, G., Lenzini, P., Hendron, M. A., 1987 : Design of pressure tunnels. *The art and science of geotechnical engineering at the dawn of the twenty first century. Prentice Hall, pp 161-194*
- [11] Fernandez, G., 1994b: Behavior of pressure tunnels and guidelines for liner design. *ASCE Jour. GE 120, 10, pp 1768-1791*
- [12] Fernandez, G., 1994a: Seepage-induced effective stresses and water pressures around pressure tunnels. *ASCE Jour. GE 120, 1, pp 106-128*
- [13] Benson, R. P., 1989: *Design of unlined and lined pressure tunnels. Tunnelling and Underground Space Technology, 4, 2, pp 155-170*
- [14] Swiger, W. F., 1996: Behavior of pressure tunnels and guidelines for liner design – Discussion. *ASCE GE 122, 3, p. 254*
- [15] Creager, W.P., Justin, J.D., Hind, J., 1944: *Engineering for dams.*
- [16] EPRI, 1987: AP 5273 *Design Guidelines for Pressure Tunnels and Shafts*, University of California (Berkeley) June, 1987
- [17] Niquet, J. J., Brelle, F., 1979 : *Calcul de revêtement des galeries d'adduction d'eau.* *Eau et Aménagement, 21, pp. 24-31*
- [18] Rancourt, A., 2010: Guidelines for the preliminary design of unlined pressure tunnels. Thesis, Mc Gill University

SUMMARY

Upon first filling, the Besai headrace tunnel failed and seepage caused a slope failure. The conservatively designed, reinforced concrete lining had severely cracked along a stretch of good rock where conventional criteria would even have admitted an unlined tunnel. Comprehensive post-failure investigation and analysis identified a complex sequence of processes, which progressively led to the failure. The processes involved hydraulic fracturing/jacking, erosion and in dispersive layers piping. A drastic change in the hydrogeological regime resulted, which in turn promoted damages to the rock in the perimeter of the tunnel as well as of the liner. Steel lining of the failed stretch satisfactorily repaired the tunnel

RÉSUMÉ

La galerie d'amenée de Besai a subi des dégâts lors du premier remplissage et causé un glissement de terrain en surface. Le revêtement du tunnel en béton armé qui semblait à première vue même superflu et d'une conception pourtant très classique, a été sévèrement fissuré le long d'un tronçon en bon rocher. Les

investigations et analyses qui ont suivi les dommages ont identifié une succession de dégradations complexes qui ont abouti à l'incident: fracturation par pression hydraulique et claquage, érosion et renardage à travers des couches dispersives. Il en est résulté un changement fondamental du régime hydrogéologique qui s'est propagé dans le revêtement du tunnel et dans le rocher environnant. La réparation a nécessité la pose d'un blindage métallique le long du tronçon endommagé

COMMISSION INTERNATIONALE DES GRANDS BARRAGES

VINGT-SIXIÈME CONGRÈS DES GRANDS BARRAGES
Autriche, juillet 2018

DOI 10.3217/978-3-85125-620-8-185



This work licensed under a Creative Commons Attribution 4.0 International License. <https://creativecommons.org/licenses/by-nc-nd/4.0/>

**ESTIMATION OF EQUIVALENT PERMEABILITY OF ROCK MASS USING
BACK ANALYSIS AND DFN MODEL- CASE STUDY IN IRAN**

KAMALI

MAHAB GHODSS CONSULTING ENGINEERING, DEPARTMENT OF
ENGINEERING GEOLOGY AND GEOTECHNICS

IRAN

A. ALIANVARI

DEPARTMENT OF MINING ENGINEERING, FACULTY OF ENGINEERING,
UNIVERSITY OF KASHAN, KASHAN

IRAN

M. EI TANI

ROCKGRO, BEIRUT

LEBANON

Kh. NEGINTAJI

MAHAB GHODSS CONSULTING ENGINEERING, DEPARTMENT OF
ENGINEERING GEOLOGY AND GEOTECHNICS

M.A. GHOLAMI

MAHAB GHODSS CONSULTING ENGINEERING, DEPARTMENT OF
ENGINEERING GEOLOGY AND GEOTECHNICS

IRAN

ESTIMATION OF EQUIVALENT PERMEABILITY OF ROCK MASS USING BACK ANALYSIS AND DFN MODEL- CASE STUDY IN IRAN

Kamali¹, A. Aalianvari², M. El Tani³, Kh. Negintaji¹, M.A. Gholami¹

1. *Mahab Ghodss consulting Engineering, Department of engineering geology and geotechnics, Iran, abbas.kamali@aut.ac.ir*
2. *Department of Mining Engineering, Faculty of engineering, University of Kashan, Kashan, Iran*
3. *Rockgro, Beirut, Lebanon*

1. INTRODUCTION

The evaluation of the hydraulic conductivity of a rock mass must take into account the characteristics of the discontinuities. The issue is to define the dimensions of the representative element and deduce its hydraulic behavior from the geometrical and mechanical properties of the discontinuities. The rock mass can then be handled as an equivalent porous medium. The accuracy of the flow estimation in a porous medium depends largely on how well the permeability of the representative element is characterized. It is vital to have a precise estimation of the equivalent permeability for calculating seepage into underground openings such as tunnels and caverns. The uncertainties that characterize the rock mass parameters make the estimation of the equivalent permeability tensor a challenging task.

Many methods are used to obtain the hydraulic conductivity tensor from the geometrical characteristics of the discontinuities. One of these methods is the discrete fracture network (DFN), as a numerical method, that is used to obtain a representation of the rock mass, simulate the flow in the discontinuities and calculate the hydraulic conductivity or HC tensor [1]. There are always some uncertainties in characterizing the entire properties of the discontinuities due to the fact they are buried in the rock mass [2]. DFN models remain advantageous in reproducing 3D realizations of the fracture network in view of determining the overall behavior of a representative element [3, 4].

In this research, the noncommercial discrete fracture network code, 3DFAHAM*, will be used to generate 3D representations of the rock mass at Rudbar-Lorestan pumped storage power plant and predict the HC tensor of a representative element. To this end, the geometrical and mechanical characteristics of 1035 recorded discontinuities at Rudbar-Lorestan powerhouse cavern will serve as input data. The predicted hydraulic conductivity will be compared to the hydraulic conductivities that are obtained by back analysis of the recorded volumetric flow rate. Analytic methods will be used for the back analysis. When the volumetric flow rate in an underground opening is available, the equivalent hydraulic conductivity of the rock mass can be calculated inverting one of the several analytical or empirical equations to calculate discharges into tunnels [5, 6, 7, 8].

2. CASE STUDY

2.1. LOCATION

Rudbar Lorestan Pumped Storage Power Plant with the hydropower generation capacity of 1000 MW is under construction 100 km south of the city of Aligoodar in Lorestan Province of Iran. The main objective of this project is to generate the peak electricity required for the national grid through the storage of the surplus water in a separate reservoir. The powerhouse cavern of the pumped storage plant is located at the right bank of the main dam (earth dam). The distance between the reservoir and the powerhouse cavern is approximately 350 m. The normal water level is 1756 m.a.s.l and the elevation at the powerhouse crown 1700 m.a.s.l. The height, width and length of the powerhouse cavern are 49.5, 26.3 and 129.75 meter respectively. It will be excavated at 400m depth.

2.2. GEOLOGY AND TECTONIC

In accordance with the structural - sedimentary classification of Nabavi (1976), Rudbar Lorestan Pumped Storage Power Plant is located in the structural-sedimentary zone of High Zagros. As per the defined structural characteristics, this zone consists of numerous thrust faults, rough topography and lots of anticlines and synclines. In regional scale, the bedrock of this zone includes the rocks of the Paleozoic to tertiary geological eras. In accordance with the field and laboratory investigations (on local scale basis), the powerhouse cavern area has been constituted by Dalan Formation. The outcrops of Dalan formation with a thickness of about 350 m to 400 m consist of the moderate to thick bedded

*3 Dimension of Fracture Characterization and Hydraulic Analysis using Mapping Methods

limestone and dark gray dolomitic limestone.

Field investigations, discontinuities map inside and around the powerhouse cavern have shown no particular geological feature except for F6, F7 faults and Rudbar fault, Fig. 1. The Geological longitudinal section along the powerhouse cavern is presented in Fig. 1. The Rudbar fault is semi-vertical and has scissors mechanism. According to the field investigations, Rudbar Fault is not completely integrated from downstream of main dam to the powerhouse cavern [9]. The pale blue line is probable underground water level after impounding of the main dam.

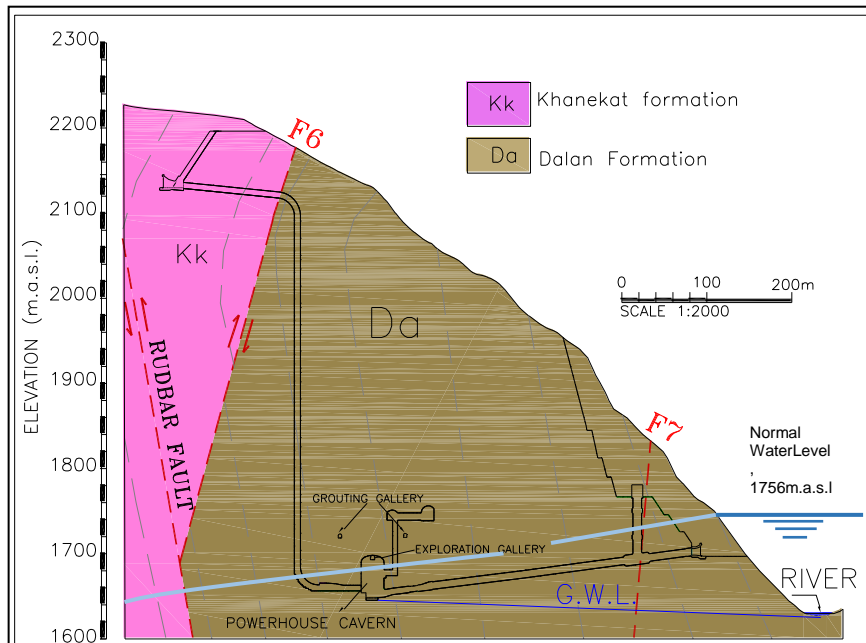


Fig.1

Geological longitudinal section along the powerhouse cavern [9]

2.3. DEFINE THE PROBLEM

Two tunnels have been designed to convey water from the main dam reservoir to the powerhouse cavern and vice versa. More than half of the lengths of these tunnels have been lined keeping the remaining lengths unlined. A 1200m drainage tunnel that starts at the bottom of the powerhouse cavern (1650 m.a.s.l.) and ends downstream of the main dam has been constructed, Fig 2. The main object of this tunnel is discharging of seepage during construction and operational period. A close view of the study area is shown in Fig. 3.

A 120 m exploratory gallery has been excavated in the crown of the power house cavern with a 6mx6m horseshoe-section. Eight exploratory boreholes, with a depth varying between 50 and 100 m have been drilled in the exploratory gallery of the powerhouse cavern Fig. 3. The main dam has been impounded and the powerhouse cavern should be excavated in a distance not longer than 350 m to main dam reservoir. After impounding and increasing the reservoir height (100

m), the water level in the boreholes of the powerhouse cavern raised 30 meter, Fig 4. The location of exploratory boreholes are shown in Fig. 3.

Assessing underground water flow around the powerhouse cavern and estimating the amount of seepage is necessary to understand the observed behavior. Therefore, the hydrogeological modeling of the interaction between the cavern and reservoir is assigned a high priority to understand the problem of the water level raise into the cavern.

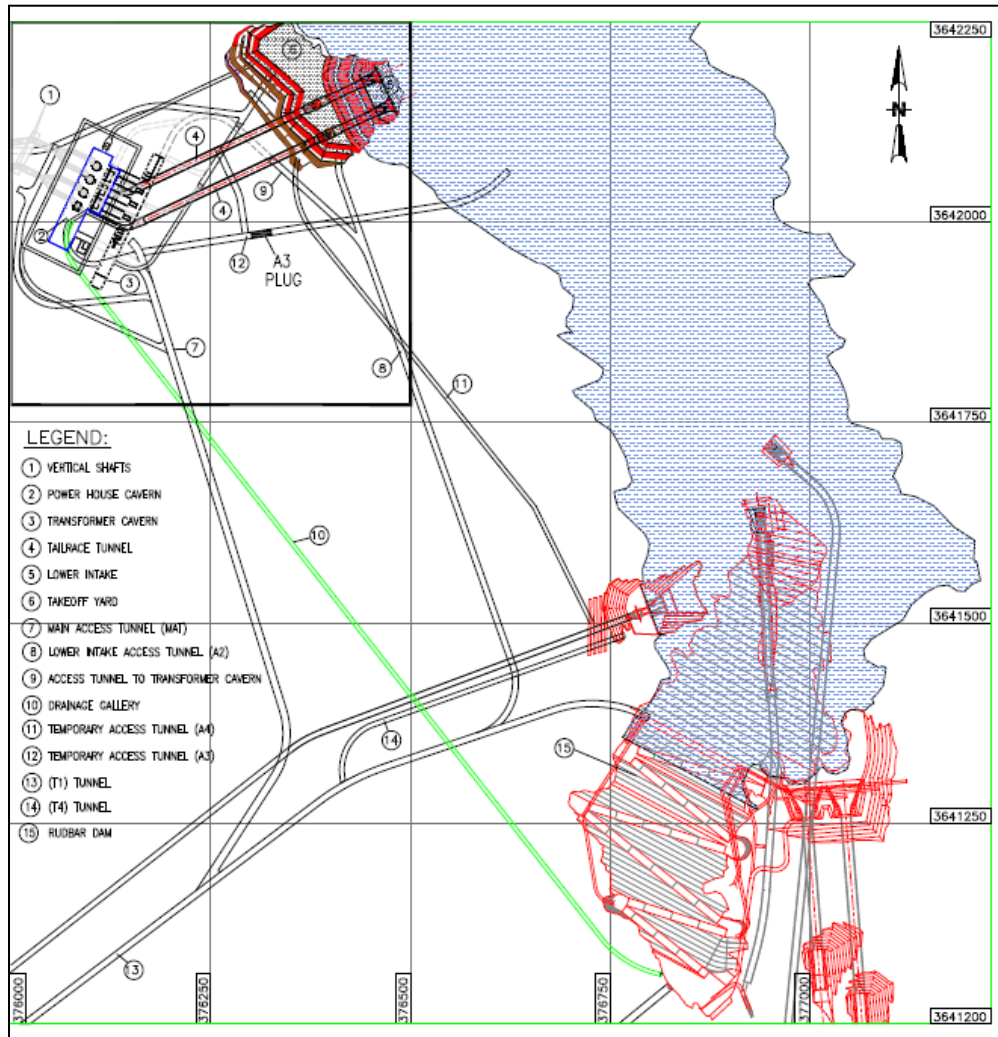


Fig. 2

General Plan of study area

In addition to the mapping of discontinuities in the study area, measuring of seepage in all underground structures and water level in the exploratory boreholes has been done. The water levels in the exploratory boreholes at the beginning and at the ends of the powerhouse cavern are 1665 and 1672 (m.a.sl), respectively, Fig 4. The gradient of the water table along the longitudinal axis of the powerhouse cavern is 7%. And, the gradient perpendicular to the axis of the powerhouse cavern from the main dam reservoir is 27%. In this regards, the measured uplift pressure behind the lining of the drainage gallery varies between 2.2 and 3.2 bar, Fig 5.

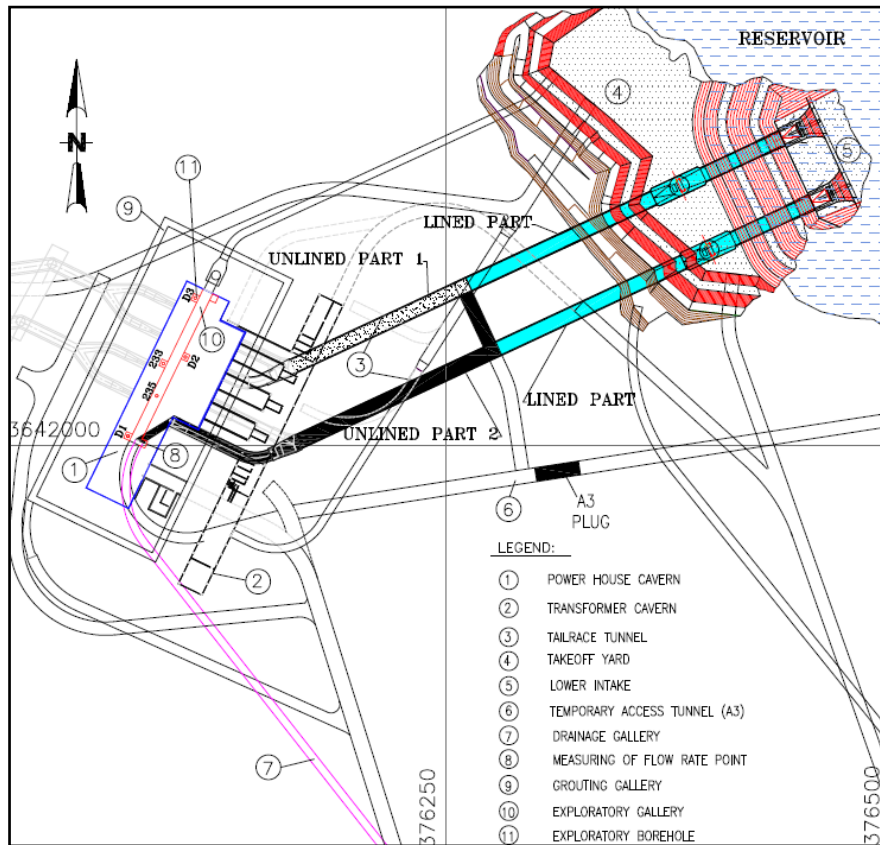


Fig.3

Close view of the powerhouse cavern, unlined part of tailrace tunnel and drainage tunnel

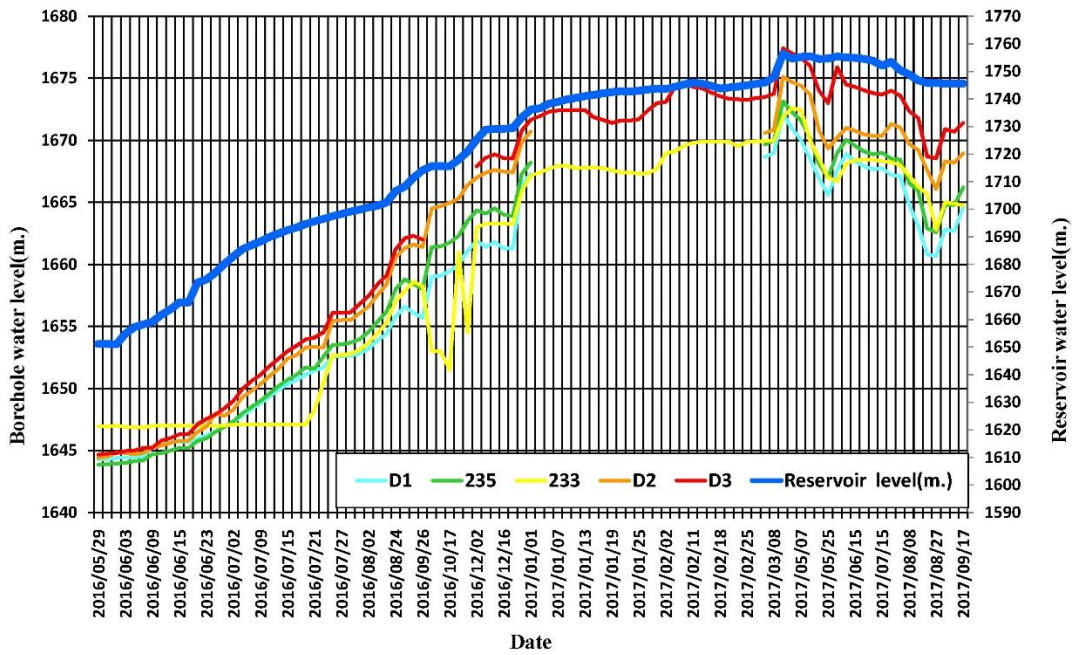


Fig. 4

Variation of the main dam reservoir elevation and water level in the exploratory boreholes



Fig. 5

Measured uplift pressure (P=2.3 bar) behind the lining of the drainage tunnel

3. ESTIMATION OF EQUIVALENT PERMEABILITY

3.4. ANALYTICAL METHODS AND BACK ANALYSIS

There are several analytical and empirical equations to estimate the water inflow into tunnels. The rock mass permeability, water head above tunnel and tunnel radius are the major parameters that enter these equations. In this project, the amount of water ingress into 200 m of unlined tailrace tunnel (part no. 2) has been measured, Fig 3. The groundwater level in the exploratory boreholes, the water level of Rudbar main dam and the radius of the tunnel are known. The equivalent permeability was estimated by back analysis using El Tani's equation [8].

$$Q = 2\pi k \frac{\lambda^2 - 1}{\lambda^2 + 1} \frac{h}{\ln \lambda} \quad \text{where} \quad \lambda = \frac{h}{r} - \sqrt{\frac{h^2}{r^2} - 1} \quad [1]$$

Q is the amount of water inflow into the tunnel per meter, (m³/s/m), k is the equivalent permeability of the rock mass (m/s), h is the water head above tunnel (m) and r is the radius of tunnel (m). The measured amount is 35 lit/s water into the 200 m of unlined part of the tail race tunnel. The device to measure the flow rate is a Moulinet.

The radius of tunnel is constant and the water head is variable around the underground structures. The average of groundwater level measured in these boreholes (22 m from center of tunnel) has been selected for back analysis. The normal water level of main dam reservoir also selected for sensitivity analysis. In order to evaluate the influence of water head variation on the rock mass permeability, the two different cases are considered.

- 1-The tunnel is completely affected by the normal water elevation in the
 - 2-reservoir (1756 m.a.s.l.), about 100 m above the unlined tailrace tunnel
- The head of water in exploratory boreholes, 22 m above the tunnel

The equivalent hydraulic conductivities of the rock mass that are obtained using Eq. [1] are show in Table 1.

Table 1
Estimated rock mass permeability

Tunnel radius(m)	Q(m ³ /s/m)	Water head above tunnel center (m)	Rock mass permeability(m/s)	Permeability (Lu)
3	0.0001753	100	1.15e-6	9
3	0.0001753	22	3.31e-6	26

3.5. FIELD MAPPING

The main input data that are needed to generate a DFN representation of the rock mass and calculate the HC tensor are the geometrical and mechanical characteristics of the discontinuities. Scanline sampling and areal sampling including circular, rectangular and square windows have been resorted to obtain the geometrical and mechanical characteristics of the discontinuities around the powerhouse cavern. Eleven scanline lengths ranging between 10 m and 16 m have been used to survey the discontinuities. Eleven circular windows sampling with radius of 55 cm to 1.5 m and 15 rectangular window sampling with dimensions of maximum 2.2 m*1.9 m have been used as well, Fig 6. The discontinuities were sufficiently mapped in the underground spaces and include 1035 joints, 639 fractures with Scanline and 396 fractures with areal sampling, which are considered well above the required minimum limit that is fixed to 100 for each joint set [10]. The most important parameters to estimate the equivalent permeability of the rock mass and seepage values are the mechanical and hydraulic aperture of discontinuities. With regards to the importance of the mechanical aperture, this characteristic has been measured. Discontinuities aperture have been measured during the detail design period (phase II) and construction period (Phase III). The mechanical aperture values extend on a wide range and have been separated in three classes including low, average and high values (for phase II).

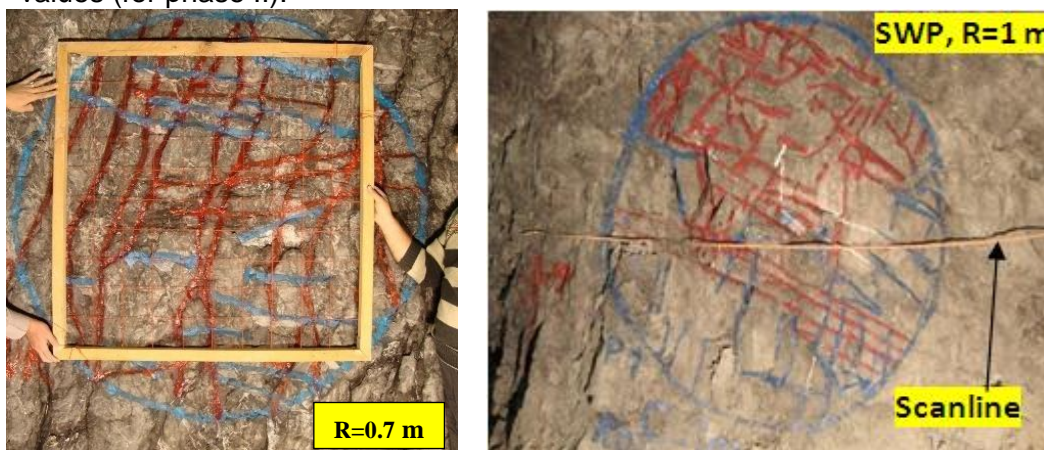


Fig. 6 Scanline and areal samplings in exploratory tunnel in the crown of the powerhouse cavern, (R. is radius of the circle sampling)

According to the discontinuities mapping, four sets of joint sets exist in the

studied area. The geometrical and mechanical characteristics of the joint sets are shown in Table 2.

Table 2
The geometrical and mechanical characteristics of the joint sets

Type of discontinuities	Dip (Deg.)	Dip Direction (Deg.)	K-Fisher	Mean Hydraulic aperture, Phase III (mm)	Persistence (cm)	Spacing (m)
Bedding	76	033	28.6	0.2836	1600	0.52
J1	60	123	13.5	0.0016	56	0.588
J2	46	280	6.6	0.0023	68	0.588
B.P.J.	70	029	11	0.0302	219	0.5

3.6. DISCRETE FRACTURE NETWORK (DFN) METHOD

The geometrical properties of the discontinuities include the number of sets, dip angle, dip direction, length, frequency, intensity, density, Fisher's constant, location and diameter (size). An accurate description of discontinuities network that is based on the geometrical characteristics is an outstanding stage in studying the permeability of the rock mass. The numerical code 3DFAHAM produces a stochastic representation of the rock mass conforming with the statistical nature of the data and the uncertainties in their determination. The fractures center are represented as Baecher's disk and their dip angle are distributed using Fisher's model. The number of fractures has been generated using homogenous and stochastic Poisson's process [3]. The uniform distribution function has been used to simulate the fractures location [11].

In order to study the effective connectivity between the fractures, it is needed to omit the fractures or cluster of fractures which are hydraulically inactive and do not contribute to transferring the flow. This process is called Fractures Regulation. The REV[†] of a fracture network has been estimated on the basis of the network connectivity parameter. The dimensions of an REV have been calculated to determine the size of 3D block and the largest section for calculating the HC tensor (HC window). The REV block is a cube whose edge is 6 m.

The modeling information such as simulation number and dimension of 3D block are presented in Table 3. In each simulation, three sections are considered in each block. Fig.7 illustrates a generated 3D block with its fractures and a regulated 2D section. Due to the uncertainty of hydraulic aperture calculation and high effect of this parameter on the equivalent permeability of the rock mass, four aperture classes have been used in DFN analysis. So, 60 models have been run. The calculated equivalent permeability with DFN code are shown in Table 4 using the hydraulic gradients mentioned in section 2.3 and four aperture classes.

[†] *Representative Elementary Equivalent*

The equivalent permeability according to Table 4 extends over a wide between 7.7 to 157 Lugeon for $i=7\%$ and 5 to 115 Lugeon for $i=27\%$. This is due to the predominance of the aperture on the HC values. On the other hand, according to Tables 1 and 3, the calculated HC by back analysis and those obtained with the DFN code at Phase II with an average aperture are close. The average equivalent permeability that is calculated with the DFN code in the upper aperture range is 136 Lugeon.

Table 3 Specifications of models by 3DFAHAMcode

Simulation number	dimension of 3D block (m)	dimension of HC window (m)	Location of HC window in 3D block (m)	Hydraulic gradient (%)	
				7	27
S1	10*10*10	6*6	3, 6, 8	√	√
S2	10*10*10	6*6	3, 6, 8	√	√
S3	12*12*12	8*8	3.5, 6, 9	√	-

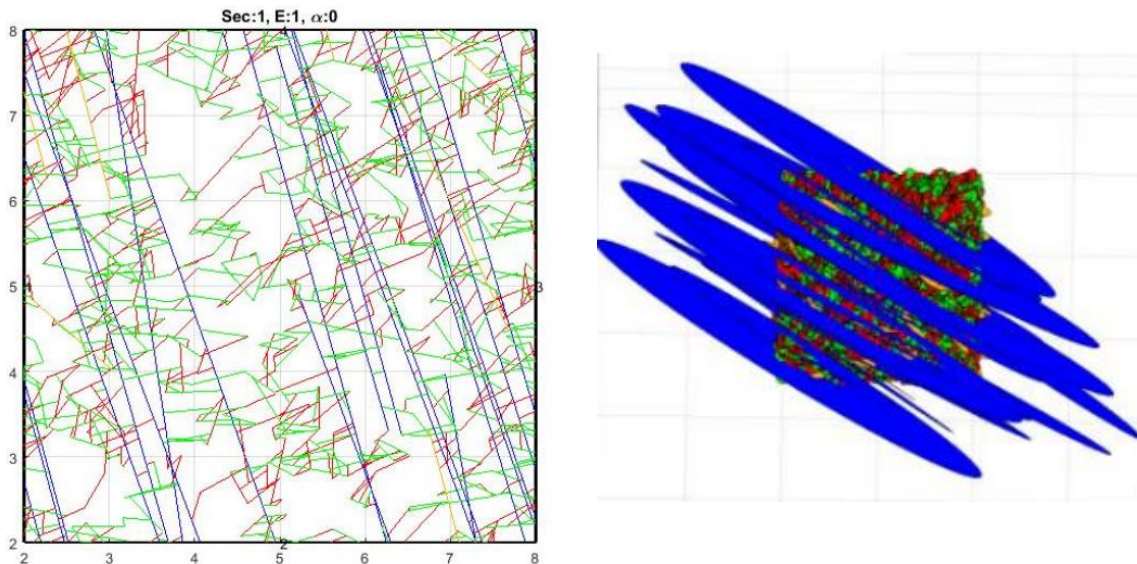


Fig.7
Generated 3D fractures block and regulated 2D section (four joint sets)

Table 4
Calculated equivalent permeability (or HC) with DFNE code (3DFAHAM)

Aperture type	Phase II			Phase III
	Lower	Average	Upper	
Gradient $i=7\%$	0.03	7.7	145	157
Gradient $i=27\%$	0.02	5	104	115
Average of both gradient	0.026	6.4	124	136

4. CONCLUSION

The geological and hydrogeological investigations have been used to calculate the equivalent hydraulic conductivity tensor at the powerhouse cavern in Rudbar-Lorestan hydroelectric project. The estimated values of HC by DFN code are larger than those estimated by analytical method.

Various studies revealed a low level of the water table, a smooth slope of its gradient, water bearing zones with weak and crushed rocks, local openings and various discontinuities and fractures, leak points and local springs. So, the hydraulic conductivity that is obtained by back analysis with the analytic method for a homogeneous aquifer should be considered cautiously. And the calculated value with the DFN code that attained 136 Lugeon should be considered an upper limit or a maximal value for homogenous rock mass.

REFERENCES

- [1] LONG J.C.S., GILMOUR P., WITHERSPOON P. A Model for steady Fluid Flow in Random Three- Dimensional Networks of Disc-Shaped Fractures. *Water Resources research*, Vol.21, No 8, 1105-1115, 1985.
- [2] ZHENG J., DENG J., YANG X., WEI J., ZHENG H., CUI Y. An improved Monte Carlo simulation method for discontinuity orientations based on Fisher distribution and its program implementation. *Computer Geotech*, 61, 266–76, 2014.
- [3] XU C., DOWD P. A new computer code for discrete fracture network modeling. *Int. J. Computer & Geosciences*, 36 (2021) 292-301, 2010.
- [4] REEVES D.W., PARASHAR R., POHLL G., CARROLL R., BADGER T., WILLOUGHBY K. The use of discrete fracture network simulations in the design of horizontal hillslope drainage networks in fractured rock. *Int. J. Engineering Geology*, 163, 132-143, 2013.
- [5] GOODMAN R., MOYE D., SCHALKWYK A., JAVANDEL I. Ground-water inflow during tunnel driving. *Engineering Geology*, vol.1, pp 150-162, 1965.
- [6] LEI S. An analytical solution for steady flow into a tunnel. *Ground Water*, 37, 23–26., 1999.
- [7] Raymer J.H. Predicting groundwater inflow into hard-rock tunnels: Estimating the high- end of the permeability distribution. *RETC*, 201-217, 2003.
- [8] EI TANI M. Circular tunnel in semi-infinite aquifer. *Tunneling and Underground Space Technology*, 18, 49-55, 2003.
- [9] MAHAB GHODSS CONSULTING ENGINEER, Engineering geology report of Rudbar Lorestan pumped storage power plant, Iran, 2014.
- [10] KULATILAKE P.H.S.W, WATHUGALA D.N., STEPHANSON O. Joint Network Modelling With a Validation Exercise in Stripa Mine, Sweden. *Int. J. Rock Mech. Min. Sci. & Geomech. Abstr.* Vol. 30, 503-526, 1993.

- [11] ZHENG J., DENG J., ZHANG G., YANG X. Validation of Mont Carlo simulation for discontinuity locations in space. *Journal of Computers and Geotechnics* 67: 103-109, 2015.

COMMISSION INTERNATIONALE DES GRANDS BARRAGES

VINGT-SIXIÈME CONGRÈS DES GRANDS BARRAGES
Autriche, juillet 2018

DOI 10.3217/978-3-85125-620-8-186



This work licensed under a Creative Commons Attribution 4.0 International License. <https://creativecommons.org/licenses/by-nc-nd/4.0/>

OBERVERMUNTWERK II: NUMERICAL MODELLING AND DESIGN

Christopher DICH

VORARLBERGER ILLWERKE AG, BEREICH PRODUKTION UND TECHNIK,
BAUPROJEKTIERUNG

AUSTRIA

Franz TSCHUCHNIGG

INSTITUTE OF SOIL MECHANICS, FOUNDATION ENGINEERING AND
COMPUTATIONAL GEOTECHNICS, GRAZ UNIVERSITY OF TECHNOLOGY

AUSTRIA

COMMISSION INTERNATIONALE
DES GRANDS BARRAGES

VINGT-SIXIÈME CONGRÈS DES
GRANDS BARRAGES
Autriche, juillet 2018

OBERVERMUNTWERK II: NUMERICAL MODELLING AND DESIGN

CHRISTOPHER DICH¹⁾, FRANZ TSCHUCHNIGG²⁾

*¹⁾Vorarlberger Illwerke AG, Bereich Produktion und Technik,
Bauprojektierung*

*²⁾ Institute of Soil Mechanics, Foundation Engineering and Computational
Geotechnics, Graz University of Technology*

AUSTRIA

1. INTRODUCTION

The pumped storage plant Obervermuntwerk II with an underground powerhouse cavern is located in the western part of Austria. The construction of the approximately 500 million € project began in May 2014 and the power plant is expected to start operating in 2018. In the pre-designing phase 2D-FE analysis for the powerhouse cavern were performed and during the main excavation of the cavern, 3D finite element calculations using Plaxis 3D [1] have been conducted. One objective of the paper is to summarize results from 3D finite element analyses performed in order to assess the performance of the two main caverns of the hydro power plant project. Additionally the headrace system of the power plant and its geotechnical design is presented. Finally, also some experience gained during the construction works is discussed.

2. PROJECT DESCRIPTION

The new pumped storage power plant (PSPP) is located parallel to the existing Obervermuntwerk I. The average construction altitude in the powerhouse

cavern is 1700m above sea level. The Obervermuntwerk II will utilize the existing water capacities of the Vermont and Silvretta reservoir to generate peak and balancing energy. The water from the Silvretta reservoir feeds the underground powerhouse cavern through the 2800m long Silvretta high-pressure tunnel. The maximum overburden is roughly 1100m. Fig.1a shows an overview of the entire project area. The Silvretta high-pressure tunnel is lined with pre-casted segmental linings in the invert and an in-situ concrete shell. The last 600m of the Silvretta tunnel are first lined with a thin steel shell and an interior concrete core ring (length of 255m) followed by a thick-walled steel lining, which is designed to withstand the external pressure.

The Vermont reservoir acts as a storage reservoir for pumping mode and is connected to the cavern with a 380m long tailwater tunnel. The length of the powerhouse cavern is 125m, the width is 25m and the average height is 33m. The powerhouse consists of two ternary machine units with a capacity of 180MW and two pumps of 180MW each. The turbines are designed to have a height between 240m and 310m. Fig. 1b shows a schematic plan view of the two caverns and Fig. 2 shows a detail of a typical cross section through the powerhouse cavern including the anchor design and the different excavation levels. A detailed description of the project and the design procedure can be found in Dich et al. [2].

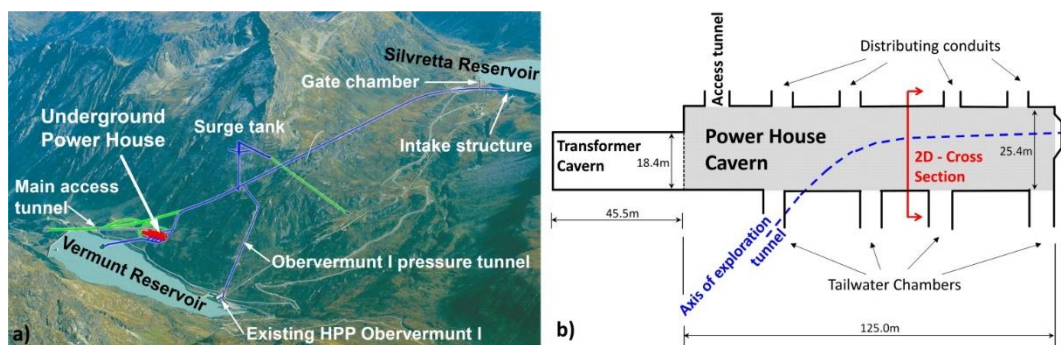


Fig. 1

a) Project overview; b) Plan view of transformer and powerhouse cavern

3. ROCK CONDITIONS

All plant components of the Obervermuntwerk II lie in the Silvretta crystalline. This formation consists mostly of granite gneisses, amphibolites, slate gneisses and mica schist, with the latter being encountered at the intake structure and the gate chamber. The Silvretta tunnel, the pressure tunnel and the tailrace tunnel lie completely in the granite gneiss, as can be seen in Fig. 2. The granite gneisses generally show low to moderate rock mass permeability. A detailed description of the geological conditions is given in Dich et al. [2].

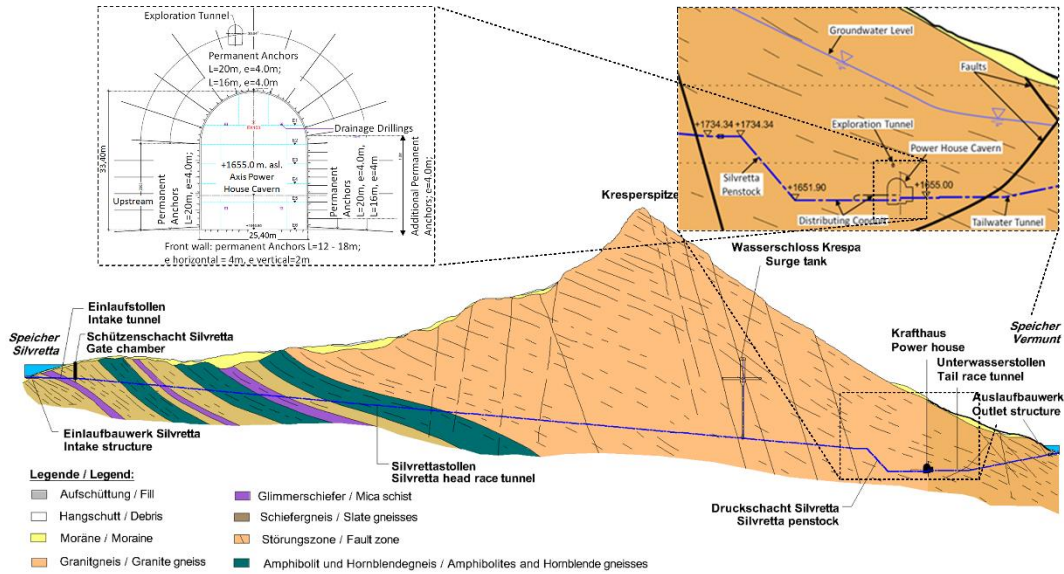


Fig. 2
Longitudinal section and details

In the exploratory tunnel and with investigations from the surface an intense testing program has been performed in 2010 and 2011. Seven drillings with core tests, water pressure tests and joint expansion tests have been conducted. Additionally plate load tests, mineralogical analysis and rock mechanical laboratory testing were executed to obtain uniaxial compressive strength, tensile splitting strength, stress and deformation characteristics. The UCS has a range from 77 to 130N/mm², the tensile splitting strength ranges from 9 to 15N/mm² and the deformation modulus is determined with 15 to 18GPa. For the FE predictions presented in the following only one material set was classified, which is defined with a linear elastic – perfectly plastic constitutive model using a Mohr-Coulomb failure criterion.

4. FINITE ELEMENT ANALYSIS

4.1. PRELIMINARY 2D ANALYSIS

Because of the geological situation (see Fig. 2), it was expected that the principal stresses in the initial state are not horizontal/vertical but rotated. To determine the initial stress situation in the area of the powerhouse and the transformer cavern two dimensional plane strain models were defined in Plaxis 2D (Brinkgreve et al. [3]). A cross section ranging from the sea level of the Vermunt reservoir up to the peak of the Kresper mountain was modelled. The location of the cross section is shown in Fig. 1b.

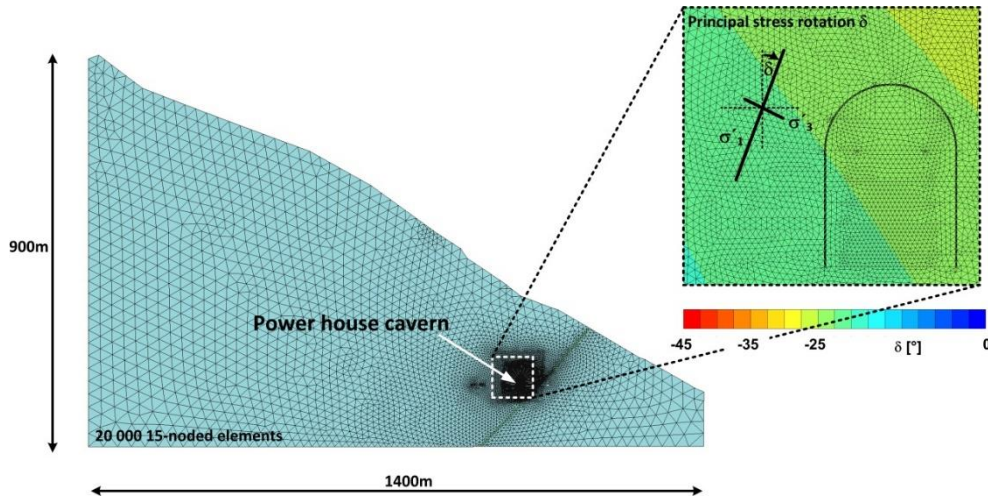


Fig. 3

Preliminary 2D plane strain model and predicted principal stress rotation

The model has a length of 1400m and a height of 900m and consists of about 20000 15-noded elements. The results of this analysis confirmed a significant rotation of principal stresses in the region of the powerhouse cavern. Fig. 3 shows the entire 2D FE model and a zoom of the region next to the powerhouse cavern. The results indicate a rotation of the major principal stress σ_1 to the vertical axis of roughly 25° .

4.2. 3D FINITE ELEMENT ANALYSIS

Since the stress distribution (and redistribution) in the region of the side tunnels and gate chambers during the construction of the caverns is one of the key issues of the 3D FEA, the mesh discretization of the caverns and the surrounding material has to be relatively fine and therefore the finite element models discussed consist of about 500000 10-noded elements with quadratic shape function. The model dimensions L/B/H are 550/165/175m. Fig. 4a shows the geometrical definition and the finite element discretization of the two caverns, the side tunnels and the gate chambers. All calculations were performed under drained conditions. To obtain realistic deformations of the caverns and a reliable stress distribution in the surrounding soil, it is necessary to model a realistic initial stress field and the relevant construction phases. Therefore the "rotated" initial stress field, as defined from the preliminary 2D FE analysis (briefly discussed in chapter 4.1), was imposed (see Tschuchnigg et al. [4]). To include the construction sequence of the caverns, the cross section was subdivided into 6 or 7 main sections respectively (see also Fig. 2 - excavation level E1 to E6). In longitudinal direction, the excavation phases are modelled with excavation lengths between 3.0 to 9.0m. In total, 187 calculation phases are defined in the analysis. Fig. 4b shows exemplary the excavation phase of excavation level E2 in the powerhouse cavern.

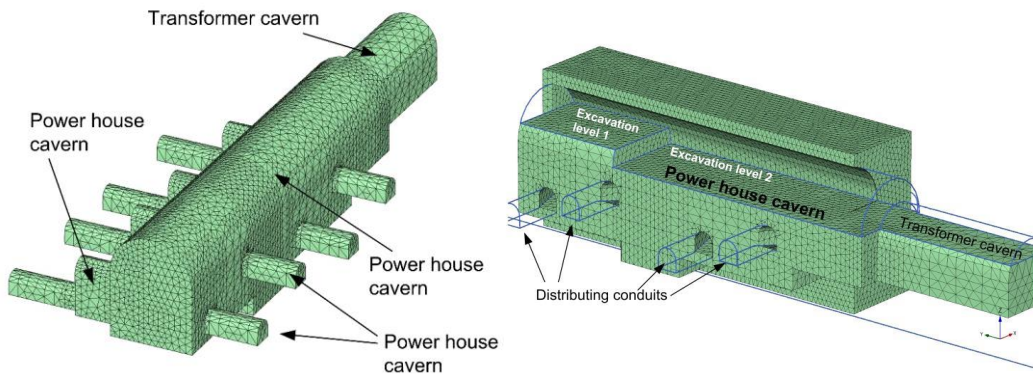


Fig. 4

a) 3D FE model: powerhouse cavern, transformer cavern, side tunnels and gate chambers, b) Calculation phase - excavation level E2 of powerhouse cavern

The maximum vertical displacements in the powerhouse cavern are in the range of 15 to 20mm. Fig. 5a shows the contour lines of vertical displacements after the final construction step. The maximum vertical displacements do not occur at the center of the caverns due to the rotation of principal stresses at the initial stress state. The analysis showed that the maximum deviatoric stresses occur in the powerhouse at and slightly above the gate chambers. In addition, the relative shear stresses (τ_{rel}), which represent the ratio between current shear stress and maximum shear stress, the rock can sustain, indicate sensitive zones at and right above the gate chambers. Fig. 5b represents the contour lines of deviatoric stresses after the final construction phase. However, it has to be mentioned that the anchors and the shotcrete lining are not modelled in this 3D finite element analysis, and the results shown in Fig. 5b indicate that the depth of high shear stresses is relatively small (which corresponds also to the evaluation of relative shear stress). Thus, it can be concluded that this stress concentrations are well covered by the anchors.

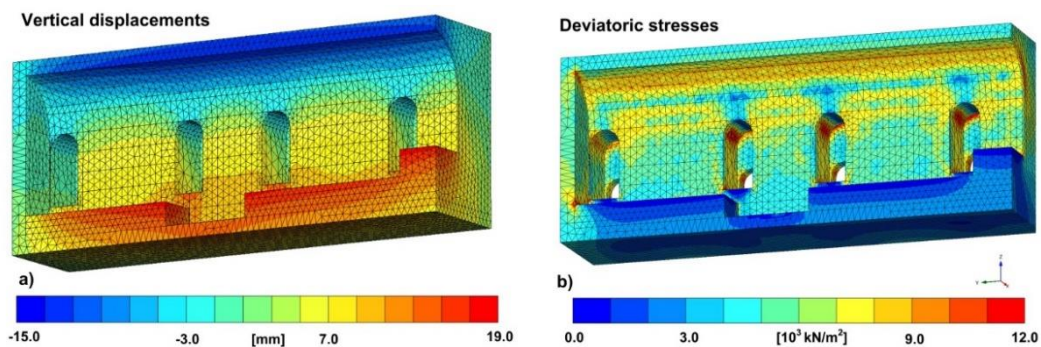


Fig. 5

a) Contour lines of vertical displacements, b) Contour lines of deviatoric stresses

To investigate the behaviour of the shotcrete lining additional 2D finite element analyses have been performed where the three shotcrete layers of the powerhouse cavern were modelled with an advanced constitutive model for shotcrete taking account of tension softening (Schädlich et al. [5]). Details of these FEA can be found in Tschuchnigg et al. [4].

5. HEADRACE SYSTEM OF OBERVERMUNTWERK II

5.1. SILVRETTA TUNNEL, PRESSURE SHAFT, MANIFOLD

The generation water system of the pumped storage works consists of a number of plant components (see Fig. 1 and Fig. 2). In the following the headrace tunnel called “Silvrettastollen”, the pressure shaft and the manifold including tailrace tunnel and outlet structure are presented in detail.

The 2773m long Silvretta headrace tunnel, with a gradient of about 9%, starts downstream of the gate chamber at chainage 184 and ends at the “Kaverne Ausbaurohr” near chainage 2947. At chainage 2490 the headrace tunnel branches off for the Obervermuntwerk I, which is also supplied with headwater from the Silvretta tunnel. The connection tunnel to the Krespa surge tank is located at chainage 2550. Up to chainage 2570 the Silvretta tunnel (with a clear internal diameter of 6.8m) has a 30cm thick unreinforced concrete lining with invert segments. At this chainage is the transition to the 256m long section with thin-walled steel lining (Fig. 6). The thin walled steel lining (with a diameter of about 6m) has a thickness of 10mm. The thin steel lining is protected against external water pressure with a support ring with a wall thickness of 0.55m. In this area, the tunnel has an internal diameter of 4.9m. At chainage 2825 is the transition to the thick-walled armored section (Fig. 6), where the internal diameter reduces to 4.5m. The thickness of the steel lining varies between 44mm at the transition to the thin-walled steel lining and 36mm at the transition to the downstream pressure shaft.

The pressure shaft is designed as an inclined shaft with a slope of 48°; the inclined length is about 110m. The circular flow section has a thick-walled steel lining with wall thicknesses between 32mm at the upper bend and 35mm at the adjoining manifold. The manifold, consisting of the upstream Y-ducting with the two main runs and the subsequent two turbine feed pipes and two pump risers, is designed for hydraulic short circuit operation (simultaneous operation of turbines and pumps). The water from the two machine sets in turbine operation is collected in the tailrace tunnel and flows down to the outlet structure in the Vermunt reservoir. In its vertical alignment, the tailrace tunnel is divided into a horizontal and a sloping section with a constant inclination of 19.5% towards the outlet structure. The internal diameter of the cast concrete ring is 6.4m, with a wall thickness of 0.35m.

5.2. DESIGN OF THE HEADRACE SYSTEM

For the geotechnical design, a difference between the excavation of the cavity in the course of tunneling and the design of the tunnel lining in operation is made. The design of the cavities is done in line with the ÖGG guideline for geotechnical design [6]. The deformation of the excavated cavity have been determined by means of the convergence confinement method (Kolymbas [7]) in each section of 25m and additionally at any important section. Considering the deformations and the depth of the fractured zones, rock mass behaviour types GVT1/2 to GVT 4 can be derived analytically. Rock mass behaviour types GVT 5 to GVT 11, if present, are determined with delineation criteria based on Steiner [8], but modified for the specific project.

Four different lining types were used for the headrace and tailrace tunnels of the Obervermuntwerk II:

- Unreinforced cast concrete
- Reinforced cast concrete
- Thin-walled steel lining
- Thick-walled steel lining

Fig. 6 shows the determination of lining type zones over the whole part of the water system. An unreinforced concrete lining was constructed in the intake tunnel, parts of the Silvretta tunnel and in parts of the tailrace tunnel, where the groundwater table lies securely higher than the internal pressure line of the system.

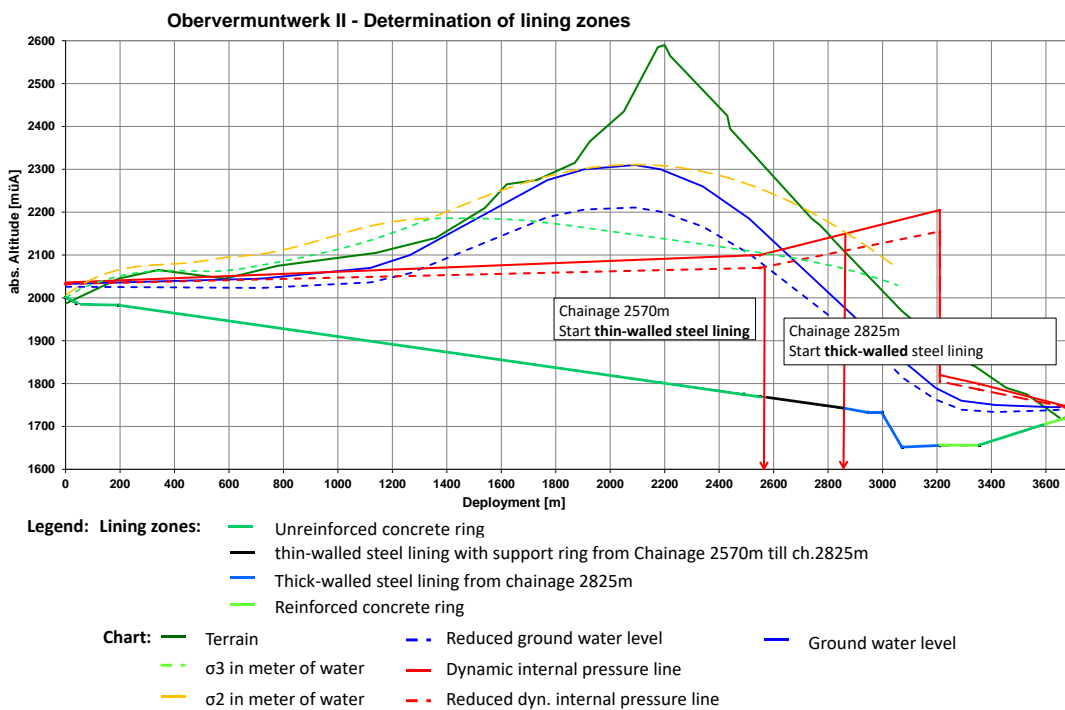


Fig. 6
Determination of lining zones

Cast concrete inner linings with reinforcement (to distribute cracking) were used at the transitions between the rectangular cross section of the gate chamber and the adjoining circular tunnel, as well as at branches. In the tailrace tunnel, further reinforced concrete inner linings were used near the caverns and the outlet structure. In areas where the stresses from internal pressure could indeed be resisted by the rock mass but water losses were possible due to the low groundwater table in relation to the internal pressure, a thin-walled steel lining was used. The thin steel lining is not designed to withstand buckling due to external pressure, therefore it requires a support ring, which was designed to resist the groundwater pressure of up to 39bar in this area. The dimensioning of the thick-walled steel lining was performed in accordance with the work of Seeber [9], including considerations of the collaborative action of the rock mass. Thick-walled steel lining was used in zones where the collaborative action of the rock mass was not able to resist loading from internal pressure alone. Thick-walled steel lining was also used in zones near large cavities with atmospheric pressure conditions, such as the powerhouse or gate chamber. The thick-walled steel lining was designed to resist not only internal pressure but also external water pressure. This design was done in accordance with the calculation models of Amstutz [10]. The transition from the unreinforced cast concrete inner lining of the Silvretta tunnel to the thin-walled steel lining was placed at the intersection of the characteristic dynamic internal pressure curve with the design value of the groundwater table. The transition from thin-walled to thick-walled steel lining was placed at the intersection of the design internal pressure curve with the smallest normal stress in the cross section (estimated from the FE analyses). This procedure includes the consideration of the geological and topographical conditions. The dimensioning of the thick-walled steel lining was based on steel grade S 690. The material parameters for the steel and the rock mass are given in Table 1.

Table 1
Steel and rock parameters

Steel quality S 690	Tensile yield strength $\sigma_{0,2\%} = \sigma_F$	Minimal flexural stress $\sigma_{b,min}$	Young's Modulus	Poisson's ratio
	690N/mm ²	770N/mm ²	210000 N/mm ²	0.3 [-]
Rock parameter	Young's Modulus	Deformation Modulus VF*- Modul	Specific weight	Poisson's ratio
	8GPa	6.3GPa	27kN/m ³	0.27 [-]

5.3. CONSTRUCTION – EXPERIENCE

In summer 2014 conventional tunneling started simultaneously from four starting points. The excavated cross section was horseshoe-shaped for all tunnels. Each face was monitored with instrumentation. The drives generally ran according to the geotechnical calculations made in advance and the geological predictions.

The only surprise was in the Silvretta tunnel, with a significant increased water ingress (peak of about 120l/s) along a length of about 200m. Consequently, the round length was reduced from 3.0m to 1.5m and the instrumentation of the monitoring system was increased.

In the intake tunnel and the Silvretta tunnel, which are lined with cast concrete inner lining, the formwork striking time was ten hours. At the time point of striking, an average early strength of 6MPa was reached, with a specified minimum strength of 2MPa. The concrete was then cured to avoid shrinkage cracking. Concrete repairs were only required to a very small extent. In the sections with thin-walled steel lining, the external ring was backfilled with concrete after installing the 14m long pipe sections. The formwork unit for the concreting of the support ring followed offset at a spacing of 7m. Due to a coordinated sequence, the works proceeded without delays. No concrete repairs were necessary.

The thin-walled steel lining had to be secured against floating in order to ensure its circularity. This provided a binding band and two invert ties in the middle and four invert ties at the ends of each 14m long pipe section. The pipe section lengths for the thick-walled steel lining were generally 10.5m. After attachment and quality controls, each pipe section was concreted. The backfill concreting of the turbine feed and pump riser pipes was carried out in a filled state under pressure in order to achieve a pre-stressing in the longitudinal direction of the manifold.

SUMMARY

3D finite element analyses were performed in order to assess the performance of the two main caverns of the PSHPP Obervermunt II. Of main concern was the stress redistribution within the surrounding rock and the settlement behaviour of the cavern powerhouse during the different excavation phases. The computations predict 15 to 20mm of displacements at the crown of the powerhouse cavern and show that next to the side tunnels stress concentrations have to be expected.

The article provides also a brief overview of construction progress on the major project pumped storage works Obervermuntwerk II. Both the geotechnical design and the experience gained during the construction of selected sections is discussed. The complexity of the project with the technical requirements for the tunnel linings require some special measures, which are presented in detail.

Also described is the headrace system with the 2.4km long Silvretta headrace tunnel, which is first lined with a non-reinforced in-situ concrete lining, then with a thin-walled steel lining (including an inner in-situ concrete core ring) and the last part is lined with a thick-walled steel lining. Both the Silvretta penstock and the distributing conduit are designed with a thick-walled steel lining. The decision where to use which of the four lining parts is based on a number of constraints, namely the rock and steel parameters, the inner and outer pressure and the minor principal stress in the surrounding rock mass.

In the last part of the article an overview of the construction experiences is presented. It can be concluded that almost all parts of the excavation works ran according to the geotechnical calculations and the geological predictions.

REFERENCES

- [1] BRINKGREVE, R.B.J.; ENGIN, E.; SWOLFS, W.M. Plaxis 3D, Finite element code for soil and rock analyses. Users manual. The Netherlands, 2013.
- [2] DICH C., TSCHUCHNIGG F., SCHWEIGER H.F. Hydro Power Plant Obervermuntwerk II – shotcrete phenomena in the power house cavern – decisions and remediation; in EUROCK 2016, Rock Mechanics and Rock Engineering: From the Past to the Future; Taylor&Francis Group London; ISBN 978-1-138-03265-1.
- [3] BRINKGREVE, R.B.J., SWOLFS, W.M. & ENGIN, E. PLAXIS 2D 2011-User Manual. Plaxis bv, Delft, The Netherland, 2011.
- [4] TSCHUCHNIGG F., SCHWEIGER H.F., DICH C. 3D Finite Element analysis of a complex hydropower project. 13th International Conference entitled “Underground Construction Prague 2016”. Prague 2016.
- [5] SCHAEDELICH B., SCHWEIGER H.F. 2014. A new constitutive model for shotcrete. A new constitutive model for shotcrete. Proc. 8th Eur. Conf. Num. Meth. Geot. Eng., 103-108, 2014.
- [6] Österr. Gesellschaft für Geomechanik: RL für die geotechnische Planung von Untertagebauten mit zyklischem Vortrieb; 2. Überarbeitete Auflage 2008, ÖGG, Salzburg 2008.
- [7] KOLYMBAS D. Tunnelmechanik. Institut für Geotechnik und Tunnelbau, Universität Innsbruck, 1995.
- [8] STEINER A. „Criteria for the Determination of Ground behaviour Types“, Diploma Thesis, Graz 2005.
- [9] SEEBER G. Druckstollen und Druckschächte, Bemessung – Konstruktion - Ausführung. Stuttgart: ENKE, 1999. AMSTUTZ E. Das Einbeulen von Schacht- und Stollenpanzerungen. Schweizerische Bauzeitung, 87. Jahrgang, Heft 28, Juli 1969, S. 541-549.
- [10] AMSTUTZ E. Das Einbeulen von Schacht- und Stollenpanzerungen. Schweizer Bauzeitung 68 (1950).

COMMISSION INTERNATIONALE DES GRANDS BARRAGES

VINGT-SIXIÈME CONGRÈS DES GRANDS BARRAGES
Autriche, juillet 2018

DOI 10.3217/978-3-85125-620-8-187



This work licensed under a Creative Commons Attribution 4.0 International License. <https://creativecommons.org/licenses/by-nc-nd/4.0/>

**CONSTRUCTION AND MONITORING OF POWERHOUSE CAVERNS THE
CIRATA HYDRO POWER PLANT**

Pangestu Dwipa AIRLANGGA

PT PEMBANGKITAN JAWA BALI

INDONESIA

COMMISSION INTERNATIONALE
DES GRANDS BARRAGES

VINGT-SIXIÈME CONGRÈS DES
GRANDS BARRAGES
Autriche, juillet 2018

CONSTRUCTION AND MONITORING OF POWERHOUSE CAVERNS THE CIRATA HYDRO POWER PLANT

Pangestu Dwipa Airlangga

PT PEMBANGKITAN JAWA BALI

INDONESIA

1. INTRODUCTION

Powerhouse construction of PLTA Cirata (Hydropower Plant of Cirata) is located underground with 1.008 Mega Watt (MW) of installed capacity and the mean annual generation of electrical energy is 1.428 Giga Watt hour (GWh). To produce 1.428 GWh, eight turbines are operated with the capacity of each turbine is 126.000 KW and 187,5 RPM for *rotative* speed. The effective head through penstock is 112,5 meters and the water discharge is 135 m³ per second. The tunnel (an excavation area) below the rock mountain is one of the largest *Power House Caverns* constructions in the world by regarding to its wide. The construction which is located among the rocks will be affected by enormous pressure from the surrounding rocks; therefore the design of the tunnel is made as it aims to limit the impact of pressure from the rocks as small as possible.

For the construction design of PLTA Cirata, it had been chosen the shape for the tunnel which is rather curved similar to egg shape. The decision was made by considering the simulation result using structural software and the number of stress for reaching the stability of underground structure. Oval tunnel has certain area which is affected by certain stress that is limited to shallow area, so the structural stability becomes better. Since the benefit obtained from the oval shape is very large, thus, the oval shape like egg shape for the tunnel shape is decided for the underground building of PLTA Cirata.

The structure of *Power House Caverns* of PLTA Cirata has 320.000 m³ in volume with longitudinal dimension of 1300 m², 49,5 m of the height and 35 m of

the width of the tunnel. This construction was built by using Geo New Austrian Tunneling Method (NATM) in 1984. The cavern structure reinforcement used rocks around the tunnel as the prior buffer, then it was shotcrete-lined and it was reinforced by rock bolt and pre-stressed concrete. Since NATM was a method for rational construction by using surrounding rocks as the buffer, so it was very important to do monitoring towards the change of the rocks regularly and to keep the safety and the reliability of the underground construction; the monitoring and maintenance activity towards caverns wall were implemented.

The monitoring and maintenance system for the safety of *Power House Caverns* structure of PLTA Cirata, which had been operated for 30 years, are regularly implemented every month. The monitoring activity uses three instruments, i.e. *Rock Displacement Extensometer*, *Crack Displacement Meter*, and *Convergenmeter*. The instruments of Power House Caverns of PLTA Cirata were installed when the cavern construction is being built.

2. MONITORING SYSTEM OF POWER HOUSE CAVERNS

The activity of regular maintenance and monitoring was done to know the structural safety early; it had been mentioned in Ministerial Regulation of PUPR Number 27/PRT/M/2015 as one of the requirements for the management of dam and complementary construction. The Power House Caverns of PLTA Cirata had some monitoring instruments such as Rock Displacement Extensometer, Crack Displacement Meter, and Convergenmeter. The functions of each instrument of PLTA Cirata Power House Caverns could be seen as follows:

Monitoring the instrumentation on the implementation of Power House Caverns of PLTA Cirata has been being done continuously up till now. In geological conditions, the Power House Caverns of PLTA Cirata was located between the rock layers of volcanic breccias which could gradually be decomposed. Based on the phenomenon, the maintenance and monitoring activities was done towards the instruments related to the rocks which become the buffers of Cirata cavern. This is the description about installed instruments and the monitoring result from Power House Caverns of PLTA Cirata:

2.1. ROCK DISPLACEMENT EXTENSOMETER

The monitoring activity of rock mass which was located on the Power House Caverns structure was done by using rock displacement extensometer (Extensometer). This instrument was installed in rock bolt structure to monitor the displacement of rock mass which was located on the roof of Power House Cavern.

The displacement of rock mass at Power House Caverns of PLTA Cirata was measured by using sensor which records the stress and strain happened on the

rocks. Currently, there are seven installed Extensometer lines. Six lines of them were automatic measurements and one line was manual measurement.

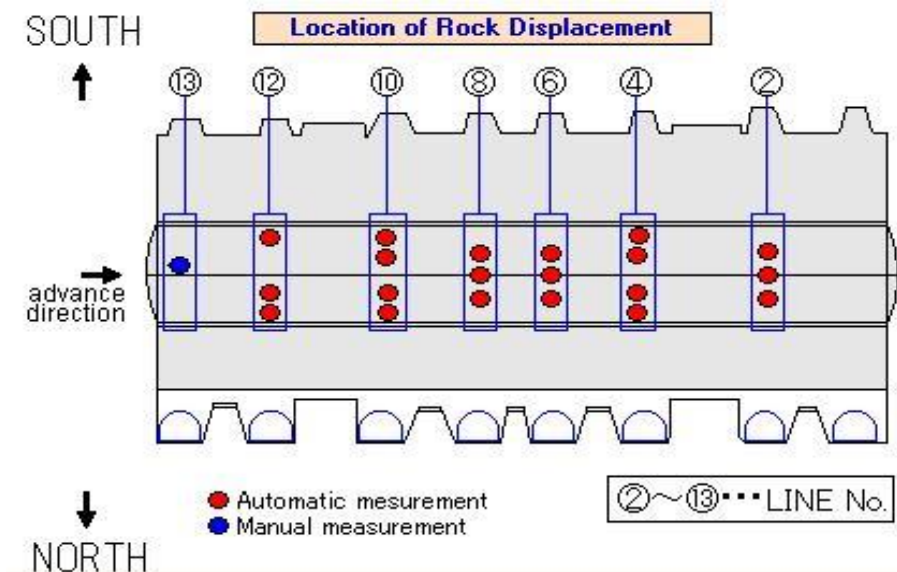
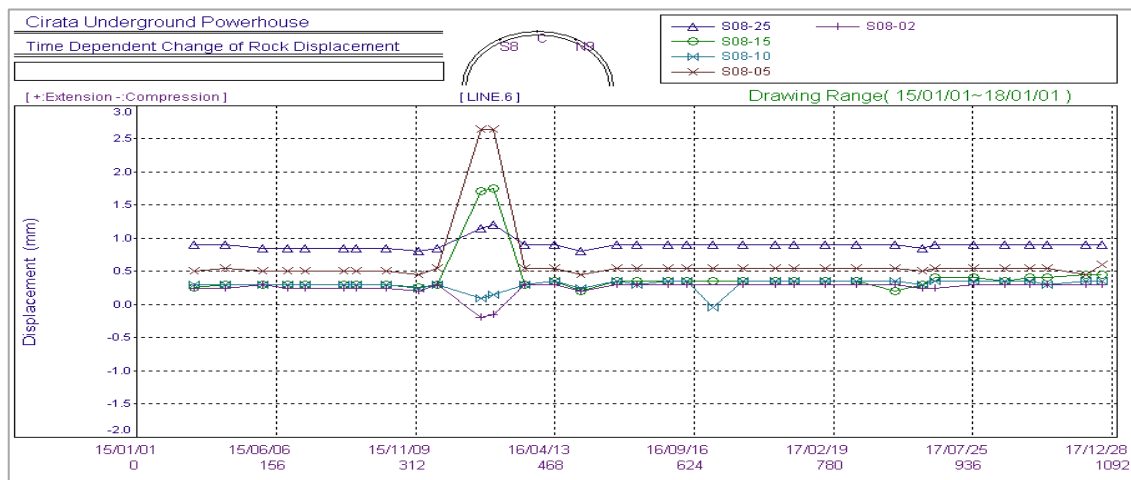


Figure 1. Layout of Location for Monitoring Points of the instrument of Rock Displacement Extensometer

The monitoring result of Rock Displacement Extensometer until December 2017 showed the normal behavior towards the rock displacement of top oval cavern of underground powerhouse. There was no significant fluctuation in every line since the maximum displacement of the design was 2mm.



Graphic 1. The Monitoring of Rock Displacement by using the instrument of Rock Displacement Extensometer

The rock displacement which is monitored until now shows various displacement in every point. The direction from the rock displacement was various. It could be seen in the graphic below. It showed that there were displacement to

the positive area and displacement to the negative area. Thus, the rock structure could be considered as safe.

2.2. CRACK DISPLACEMENT METER

The displacement on the surface of Power House Cavern shotcrete which is indicated by the existence of crack is measured by using Crack Displacement Meter. The installation is located in the existed crack line. It aims for identifying the development of damage of the cracks.

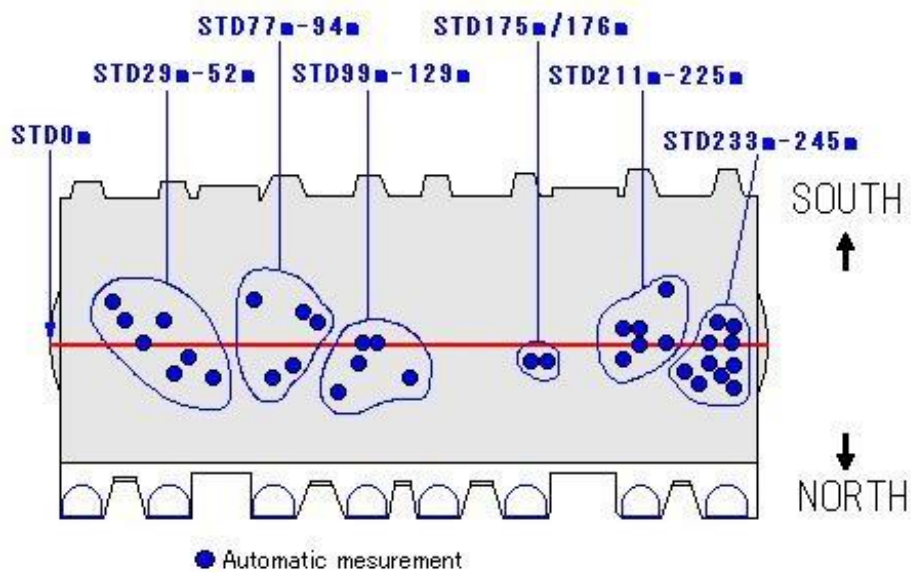
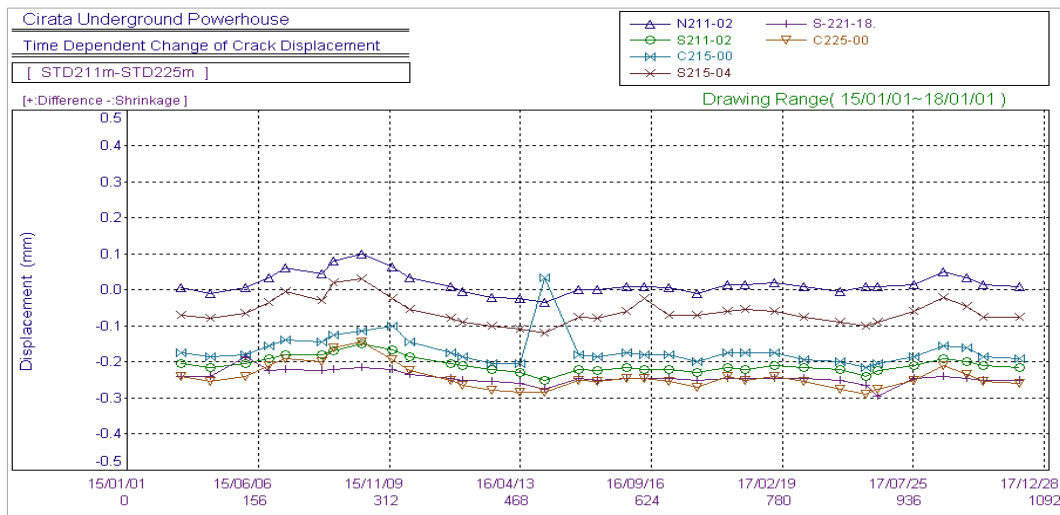


Figure 2. Layout of Location for Monitoring Points of the instrument of Crack Displacement Meter

The instrument of Crack Displacement Meter was installed on six crack lines by using automatic sensor with various numbers. Then, there is manual sensor which is installed on two crack lines. The measurement was done by using Avometer which was located in measurement room.



Graphic 2. The Monitoring of Crack Displacement by using the instrument of Crack Displacement Meter

The monitoring towards crack displacement until year 2017 showed normal digit on the result. It could be seen that the displacement of data trend was still less than the maximum value i.e. between 0,0 mm to 0,3 mm, where the maximum value was 2 mm. The monitoring towards cracks will continuously be done up till now since the bigger number of the age of crack, the bigger cause of crash happens. It happens since the crack caused by the age of building cannot be avoided and the crash signal can be initiated from a crack.

2.3. CONVERGENMETER

Deformation which is happened in Power House Cavern was not only caused by the impact of rock pressure or the characteristic of the rock, but also the moving load inside the cavern such as the generator equipments. Based on the condition, the regular monitoring was applied by using Convergence meter to detect the potential failure and damage early which were happened on cavern wall.

The deformation monitoring towards Cavern wall was done by measuring the displacement of a couple of monuments which were installed along the terrace upstairs by using Convergence meter. The measurement was aiming to know the span between the north wall and the south wall of the Power House. So, the displacement of the wall was known by the difference number between the new and the old measurement.

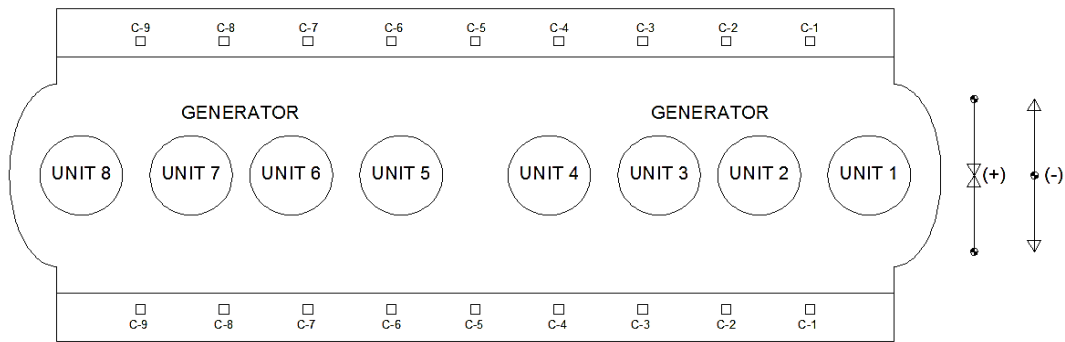
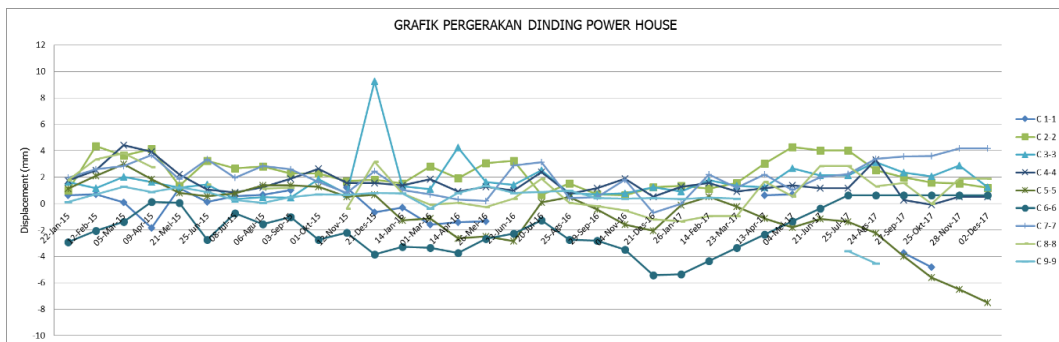


Figure 3. Layout of Location for Monitoring Points of the instrument of Convergometer

In monitoring the wall displacement of Power House, the positive value occurred when the Power House wall was deforming, so both monitoring monuments moved inside or were being closed. Meanwhile, the negative values occurred when the two monitoring monuments moved outside or were being apart. Figure 2. Lay Out of the location of monitoring points on Convergometer instrument

On the measurement for the period 2015-2017, significant trend displacement was happened towards two monitoring points i.e. C 5-5 and C 9-9. The graphic of both monitoring points were deteriorated or it could be said that the condition of PH wall was constricting in both locations. The maximum value of convergence measurement for the period 2015-2017 was about -7.487mm on C 5-5. Meanwhile, the minimum value was about -0.101mm on C4-4.



Graphic 3.The Monitoring of Wall Displacement by using the instrument of Convergometer

From the visual inspection, there was no increasing number of structural damage on the monitoring point. Therefore, the monitoring towards vertical wall of cavern for the period 2015-2017 showed that the displacement was still categorized as normal.

3. CONCLUSION

The monitoring system towards Power House cavern of PLTA Cirata was being done regularly in every month by PT PJB BPWC. Monitoring was done by using three instruments where each of the instruments had different monitoring function. On the cavern age which almost reached 30 years, the monitoring showed that the construction behavior was categorized as normal. These are the conclusion of each monitoring instruments:

3.1. ROCK DISPLACEMENT EXTENSOMETER

The monitoring towards rock mass which was located in the Power House Cavern structure was done by using rock displacement extensometer (Extensometer). The result of monitoring until December 2017 showed that there was no significant displacement. Then, there was no structural damage on the result of visual monitoring.

3.2. CRACK DISPLACEMENT METER

The displacement on the surface of Power House Cavern shotcrete which was indicated by the existence of crack was measured by using Crack Displacement Meter. For the result of monitoring towards the instrument until December 2017, the displacement which was monitored was safe. From visual monitoring, there was no increasing number of cracks or there was no additional number of structural damage.

3.3. CONVERGENMETER

The deformation process happened to Power House Cavern was caused by the impact of rock pressure or the characteristic of rock. Regular monitoring by using Convergence meter aimed at detecting the potential of failure and damage happened early on the wall for crane seats. The monitoring for the period 2015-2017 showed that the displacement was categorized as normal. From the visual inspection, it was found that there was no increasing number of structural damage at the monitoring points.

REFERENCES

- [1] PT PJB CIRATA RESERVOR MANAGEMENT UNIT, Laporan Operasi, Pemeliharaan, dan Pemantauan Waduk, Bendungan dan Power House PLTA Cirata, Bandung Barat, 2017.
- [2] PT PJB CIRATA RESERVOR MANAGEMENT UNIT, report of maintainance, Dam dan Power House Monitoring Cirata Hydro Power Plant, Bandung Barat, 2017.
- [3] STATE MINISTER OF PUBLIC WORKS AND PUBLIC HOUSING, Ministry Regulations Number 27/PRT/M/2015 About The DAM, Jakarta, 2015.
- [4] PT PJB CIRATA HYDRO POWER PLANT UNIT, Large Inspections of Cirata Dam and Complementary Buildings , Bandung, 2010.
- [5] PT PJB CIRATA HYDRO POWER PLANT UNIT, Report of Assesment stability Tailrace Tunnel PLTA Cirata, Bandung, 2013.

SUMMARY

The construction of Power House Caverns of PLTA Cirata has 320.000 m³ in volume with longitudinal dimension of 1300 m², 49,5 m of the height and 35 m of the width of the tunnel. This construction was built by using Geo New Austrian Tunneling Method (NATM) in 1984. The cavern structure reinforcement used rocks around the tunnel as the prior buffer, then it was shotcrete-lined and it was reinforced by rock bolt and pre-stressed concrete. Since NATM was a method for rational construction by using surrounding rocks as the buffer, so it was very important to do monitoring towards the change of the rocks regularly and to keep the safety and the reliability of the underground construction; the monitoring and maintenance activity towards caverns wall were implemented.

The monitoring and maintenance system for the safety of Power House Caverns structure of PLTA Cirata, which had been operated for 30 years, are regularly implemented every month. The monitoring activity uses three instruments, i.e. Rock Displacement Extensometer, Crack Displacement Meter, and Convergenmeter. The instruments of Power House Caverns of PLTA Cirata were installed when the cavern construction is being built.

The monitoring system towards Power House cavern of PLTA Cirata was being done regularly by PT PJB. Monitoring was done by using three instruments where each of the instruments had different monitoring function. On the cavern age which almost reached 30 years, the monitoring showed that the construction behavior was categorized as normal.

Key word: Construction, Monitoring, Power Plant, and Cirata

RÉSUMÉ

La Construction de Power house de Cirata hydro-électricité située à le sous de terre avec une capacité installée de 1 008 méga watts (MW). La production d'énergie électrique par an est à la moyenne de 1 428 Giga watt heures (G Wh). Pour générer les 1 428 G Wh, il fonctionne huit turbines qui chacun a capacité 126 000 kW, et ronde 187,5 tr/mn.

Cette pièce qui a été creusée au sous de la montagne en roche est l'une des plus grandes constructions de Power house tout le monde, en termes de largeur d'envergure. La construction qui est située entre les roches est affectée par l'énorme pression des roches entourages. Ainsi la forme de la pièce est conçue pour baisser la pression de roche devient au peu que possible.

La construction d'hydro-électricité de Cirata est courbe qui semblable au forme d'œuf. La structure de Power House sur les cavernes hydroélectriques Cirata a volume atteint 320 000 m³, avec une superficie de 1300 m², transversale hauteur de section de 49,5 m et la largeur de 35 m Runganan. Cette construction est construite en utilisant la nouvelle méthode de tunneling de GEO (NATM) autrichienne en 1984.

En termes de condition géologique, Power House sur les cavernes hydroélectriques Cirata, situé entre les couches de brèche volcanique, qui peut subir lentement la météorisation. C'est pourquoi on doit faire la maintenance et surveillance de l'instrumentation Rock sur la caverne tampon de Cirata.

Cette hydro-électricité a été opérée depuis 30 ans. La maintenance et surveillance a la sécurité de structure de cavernes Power House sur Cirata hydro-électricité est effectué régulièrement chaque mois. On utilise trois instruments dans cette surveillance, c'est-à-dire extensomètre de déplacement de roches (Rock Displacement Extensometer), compteurs de déplacement de fissures (Crack Displacement Meter) et Convergenmeter. Instrument de Power House Cavernes hydroélectrique est installé quand la construction de caverne était construit.

On utilise le déplacement de roche extensomètre pour surveiller la masse de roche qui est située au-dessus de la structure de caverne Power House. Le résultat de la surveillance jusqu'en décembre 2017 montre qu'il n'y a pas de déformation dépassant à la conception maximale. Tandis que le mouvement a la surface de short crête Power House caverne qui a indiqué la présence de fissures, on la mesure par l'aide de compteur de déplacement (Crack Displacement Meter). La surveillance jusqu'à maintenant donne le résultat avec la bonne et normale condition. Aussi par le résultat de surveillance visuelle il n'y a pas les nouveaux dommages structurels aux cavernes de mur. Donc, les résultats de la surveillance en général des a montré un comportement normal dans la construction.

Mot-clé: Construction, surveillance, centrale électrique et Cirata

COMMISSION INTERNATIONALE DES GRANDS BARRAGES

VINGT-SIXIÈME CONGRÈS DES GRANDS BARRAGES
Autriche, juillet 2018

DOI 10.3217/978-3-85125-620-8-188



This work licensed under a Creative Commons Attribution 4.0 International License. <https://creativecommons.org/licenses/by-nc-nd/4.0/>

**LINING CONCEPT TO CONTROL HYDROFRACTURING OF THE POWER
WATERWAY OF HPP QUITARACSA IN PERU**

Wynfrith RIEMER

Senior Engineering Geologist and Hydrogeology Expert

Michael THIEL

Senior Structural Engineer and Project Manager,
PÖYRY SCHWEIZ AG

Roland SCHMIDT

Senior Hydropower Expert and Project Director,
PÖYRY (PERU) S.A.C.

PERU

COMMISSION INTERNATIONALE
DES GRANDS BARRAGES

VINGT-SIXIÈME CONGRÈS DES
GRANDS BARRAGES
Autriche, juillet 2018

**LINING CONCEPT TO CONTROL HYDROFRACTURING OF THE POWER
WATERWAY OF HPP QUITARACSA IN PERU**

Dr Wynfrith RIEMER

Senior Engineering Geologist and Hydrogeology Expert

Michael THIEL

*Senior Structural Engineer and Project Manager,
PÖYRY SCHWEIZ AG*

Dr Roland SCHMIDT

*Senior Hydropower Expert and Project Director,
PÖYRY (PERU) S.A.C.*

PERU

SUMMARY

Engie's 118 MW Quitaracsa hydropower project is located in the Cordillera Blanca mountain range in Ancash/Peru, on the Quitaracsa River, a main tributary of Río Santa, which is one of Peru's mayor rivers flowing into the Pacific Ocean. HPP Quitaracsa's gross head is 874 m and its design flow 15 m³/s. The plant comprises an hourly regulation reservoir of 270 000 m³ and a 5.5 km long inclined pressure tunnel, with 16% constant slope, connecting the reservoir and intake works with the underground powerhouse.

The entire underground structures of the project are located in granodiorite of the Cordillera Blanca Batholith, and the original design provided for only 160 m of steel lining, followed by 200 m of concrete lining, to protect the powerhouse cavern against seepage inflow. However, the Cordillera Blanca Fault Zone, tectonically active, runs in the immediate vicinity of the power cavern.

In combination with low horizontal and vertical overburden, the presence of this fault affects the stress pattern, and several hydro-fracturing tests, performed during tunnel excavation, determined significantly reduced horizontal stresses, with k_0 -values between 0.2 and 0.3, which is uncommonly low for a young mountain range. Coping with the insufficient in-situ rock stresses, the steel liner had to be extended for 2000 m upstream of the power cavern.

The literature lists ample precedence of unlined pressure tunnels with satisfactory performance and offers empiric and semi-empiric methods and criteria for their design, but the experience with the Quitaracsá pressure tunnel serves as an example of exception from the rules and demonstrates the need for reliable and representative information on rock mechanical and hydrogeological conditions, particularly for projects with medium or high pressure tunnels.

RÉSUMÉ

L'aménagement hydroélectrique Quitaracsá d'Engie, d'une capacité de 118 MW, est situé dans la Cordillère Blanche dans la Province d'Ancash au Pérou, sur la rivière Quitaracsá, affluent principal du Río Santa, l'une des rivières majeures du pays. Sa chute brute est de 874 m et son débit nominal est de 15 m³/s. Il comprend un bassin de régulation horaire de 270 000 m³ et une galerie en charge inclinée à 16% de 5.5 km de long, reliant le bassin à l'usine en caverne.

Les divers ouvrages souterrains étant excavés dans les granodiorites du Batholithe de la Cordillera Blanca, le Projet original ne prévoyait que 160 m de blindage, et 200 m de revêtement en béton, afin de protéger la caverne de l'usine contre les infiltrations, étant donné que celle-ci se trouve à faible distance d'une zone de failles actives de la Cordillera Blanca.

L'influence sur le profil des contraintes de ces failles conjuguée avec des couvertures rocheuses relativement faibles - tant verticales qu'horizontales - a pu être quantifiée par plusieurs tests d'hydrofracturation effectués lors de l'excavation. Ceux-ci ont révélé des contraintes horizontales k_0 comprises entre 0,2 et 0,3, particulièrement faibles donc pour une géologie jeune. Du fait de ces contraintes insuffisantes, le blindage de la galerie en charge a dû être prolongé de 2000 m en amont de la caverne.

Se référant à de nombreuses galeries en charge non revêtues aux performances satisfaisantes, certains auteurs s'aventurent à proposer des méthodes empiriques et semi-empiriques, ainsi que des critères de dimensionnement. L'expérience faite avec la galerie en charge de Quitaracsá illustre bien la validité toute relative de ces méthodes. Elle démontre aussi la nécessité de pouvoir disposer d'informations fiables, représentatives des conditions mécaniques et hydrogéologiques effectives du milieu rocheux, en particulier pour les projets comprenant des galeries en forte et moyenne charge.

INTRODUCTION

Engie's 118 MW Quitaracsa hydropower project is located in the Cordillera Blanca mountain range in Ancash/Peru, on the Quitaracsa River, a main tributary of Río Santa, which is one of Peru's mayor rivers flowing into the Pacific Ocean. HPP Quitaracsa's gross head is 874 m and its design flow 15 m³/s. The plant comprises an hourly regulation reservoir of 270 000 m³ (shown in Fig.1) and a 5.5 km long inclined pressure tunnel, with 16% constant slope, connecting the reservoir and intake works with the underground powerhouse. The scheme does not provide for a surge tank, because of the sufficiently slow closing time of the Pelton turbines, and accepting that pressure fluctuations during turbine start and shutdown cause pressure fluctuations along the inclined pressure tunnel.

The entire underground structures of the project are located within granodiorite of the Cordillera Blanca Batholith, and the original design provided for only 160 m of steel lining, followed by 200 m of concrete lining, to protect the powerhouse cavern against seepage inflow. However, in the immediate vicinity of the power cavern, this bedrock is traversed by a highly fractured zone of the Cordillera Blanca Fault (shown in Fig.2, right), which is an active tectonic fault and considered as an important source of mayor earthquakes.



Fig. 1

HPP Quitaracsa, hourly regulation reservoir with stepped spillway to conduct river Quitaracsa alongside the reservoir slope

Centrale Hydroélectrique Quitaracsa - Réservoir de compensation horaire et torrent confiné le long du pied de sa recharge, avec correction en cascade

GEOLOGICAL SETTING

Granodiorite of the Cordillera Blanca Batholith exclusively forms the bedrock in the project area. The fault zone of the Cordillera Blanca Fault runs at the downstream end of the project area (see Figure 2 left). This is a normal fault, which continues for about 200 km, following the general NNW-SSE direction of the Cordillera. A local fault, the San Mateo Fault, runs in the same direction at the upstream end of the project area.

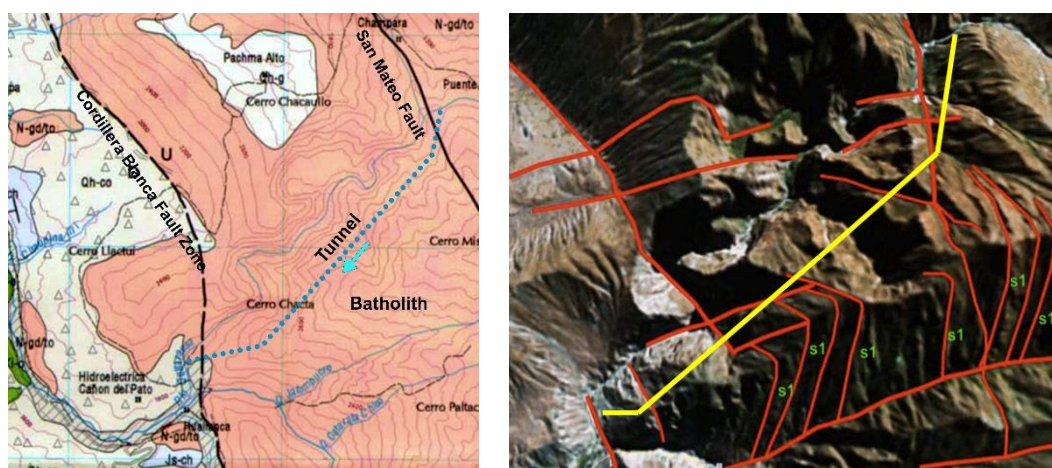


Fig. 2

Geological map of HPP Quitaracsá project area, INGEMMET, 1995 (left);

Carte géologique du site de la C.H. Quitaracsá, INGEMMET, 1995 (à gauche);
Image Google avec linéaments (à droite)

Secondary effects have modified the originally uniform characteristic of the granodiorite: at the Cordillera Blanca fault zone a pronounced schistosity has developed. With increasing distance from this fault this features reduces to a cleavage and eventually to slab-jointing. Concurrent with the grade of schistosity also the mineralogy and the strength of the rock change: the schistose rock in the fault zone becomes friable, along the access tunnel to the power cavern the unconfined compressive strength already reaches 70 MPa, averages 100 MPa near the cavern and increases to 130 MPa farther along the headrace tunnel. The variation in strength is related with the degree of kaolinization of the feldspar.

The rock modulus, determined on core samples, averages 44 GPa.

In the orientation of the schistosity also shear zones have developed, which show up as lineaments in the satellite image. Additionally to the schistosity/slab jointing two more principal sets of discontinuities and another set of shears dominate the fabric of the rock mass (Figure 2 right, Figure 3 left).

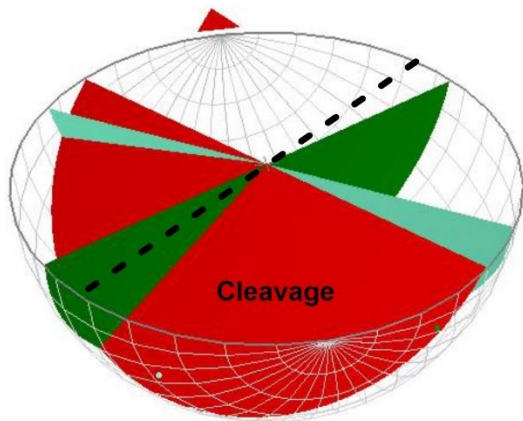


Fig. 3

Stereogram of main discontinuities (left); *Stéréogramme des diaclases principales (à gauche);* rock outcrop in Quitaracsa valley (right) *affleurements rocheux dans la vallée du Quitaracsa (à droite)*

Figure 4 indicates the range of GSI encountered in the headrace tunnel. For most part of the tunnel the GSI exceeded 50, lower values apply to local sheared or faulted zones.

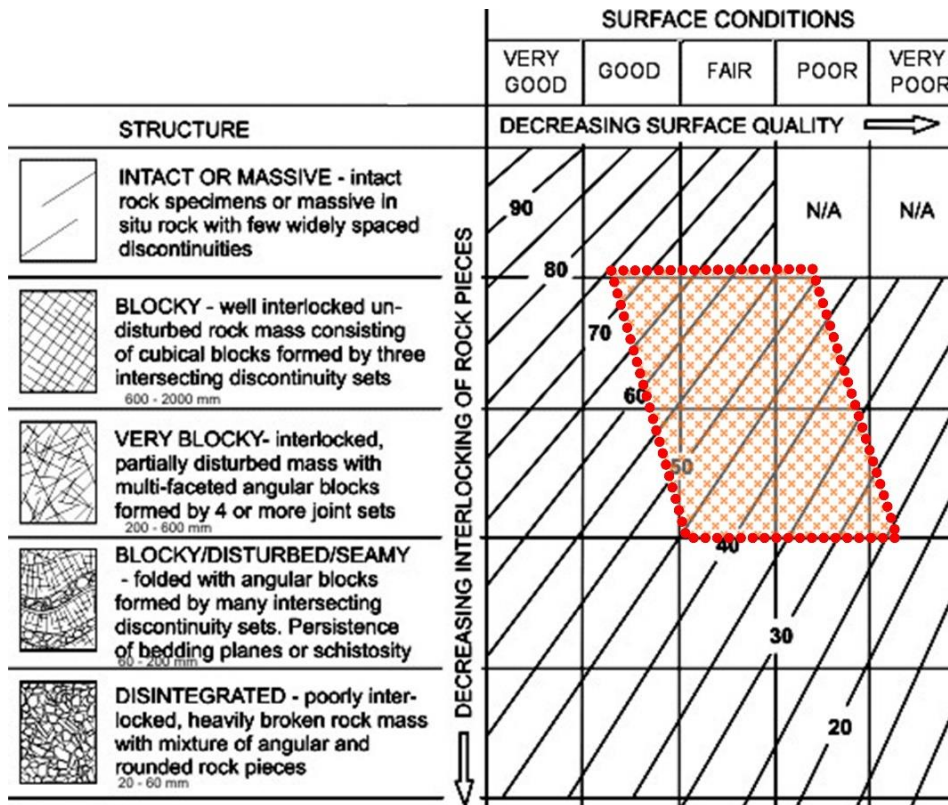


Fig. 4

GSI range recorded in the headrace tunnel *Domaine de variations GSI relevées dans la galerie en charge*

In the exterior zones of the rock mass, the permeability reaches and exceeds 10^{-6} m/s. Along the headrace tunnel in sound rock the permeability stays below 10^{-7} m/s. The tunnel was almost dry with only shear zones notably discharging water.

REVIEW OF DESIGN CONCEPTS

The rock outcrops on the walls of the Quitaracsa canyon are virtually inaccessible, but some information could be derived from the experience with the construction of the Cañon del Pato hydropower plant in the immediate vicinity. On this basis, favorable conditions for the underground works were predicted, with $Q > 40$ for most of the length of the pressure tunnel. Accordingly, an unlined tunnel, only locally supported with shotcrete and bolts, and a 75 m long penstock in the stretch immediately upstream of the power cavern was foreseen. However, a review identified uncertainties in the assumptions with potential impacts for the design and performance of the headrace tunnel. These were primarily:

- Level and pattern of stresses along the tunnel route were unknown. This condition significantly affects the Q-rating and is decisively important in relation to potential hydrojacking of the rock mass due to the high pressure in the tunnel.
- There was no information on hydrogeological characteristics and regime in the rock mass. Discontinuities, specifically shears, traversing the tunnel (Figure 2 right) could convey tunnel seepage towards the canyon and, with the prevailing rock mass structure, locally destabilize the slopes. In several locations, the tunnel alignment did not meet the “Australian Criterion” (Dann et al. [1]) for horizontal lateral cover.

These reservations were debated, alleging that, (a) the route of the headrace tunnel complies with the Norwegian criterion, and (b) the saturation line, calculated according to Bouvard [2] stays safely inside the slope.

However, these arguments are flawed: the respective analyses ignored conditions implicit to the application of the methods. The original Norwegian criterion, as e. g. formulated by Broch [3] assumes $\sigma_h/\sigma_v \approx 1$, a condition, which quite frequently obtains, but is by no means guaranteed. The saturation line, as the title implies, applies to “terrain sec”, with free vertical drainage, which is not the case for the Quitaracsa headrace tunnel.

Figure 5 shows σ_3 contours, the groundwater table and flow lines, simulated by FE-model, with the “saturation line” superimposed. The saturation line rises above the groundwater table, i. e. this method indicates a higher external head than the FE simulation and, in consequence, reduced risk of hydrojacking. In the FE model, the seepage flow from the tunnel drains towards the river, whereas the saturation line would have the seepage disappearing in the depth of the rock mass, which in this case is impossible.

The results of geotechnical and hydrogeological model simulation depend on the input, its completeness and reliability and, therefore, have to be viewed with due reservations. Nevertheless, in this case they clearly demonstrate the

uncertainties inherent to schematic design concepts and emphasize the need for specific investigations and analyses.

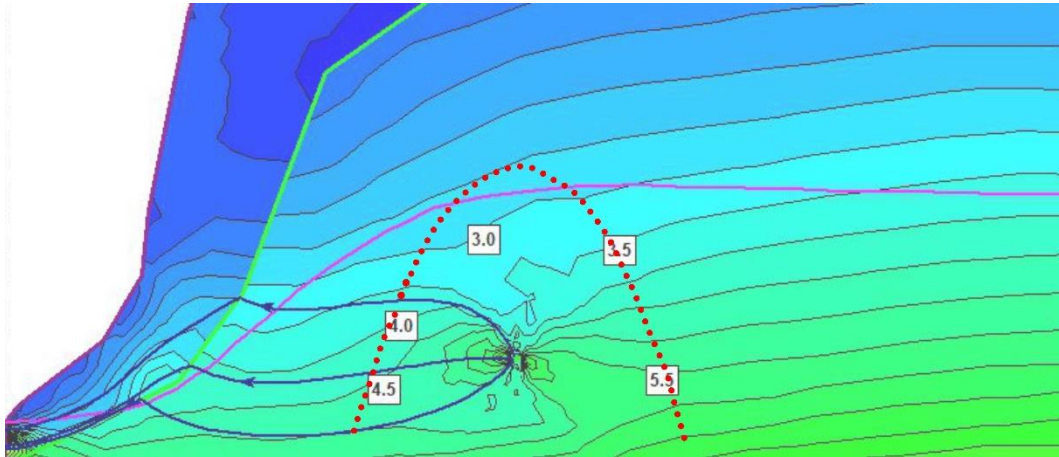


Fig. 5

FE simulation displaying σ_3 contours, groundwater table, flow lines and “saturation line” (dotted line). Labels on contours are σ_3 in MPa

Simulation FE montrant les courbes σ_3 , la nappe phréatique, les lignes de courant et la ligne de saturation. Les contraintes indiquées sur les courbes σ_3 sont en MPa

Table 1
Summary Results of Hydrojacking Tests
Récapitulatif des résultats des essais d'hydrojacking

Chainage	Depth	σ_v	σ_h	σ_H	Azimuth σ_H
[m]	[m]	[MPa]	[MPa]	[MPa]	[°]
3+500	699-734	17.9-18.8	4.5±1.5	4.1	184±2
	780	20.0	2.8		
	788-800	20.1-20.5	5.3±0.7	9.6±0.8	177±11
	805-820	20.6-21.0	9.2±1.7	18.7±3.5	
3+820	712-728	18.2-18.6	5.4±1.3		173±21
	579-585	14.8-15.0	8.9±0.5		169±15
4+100	673-740	17.5-19.1	8.2±1	16.8±1.6	181±1
4+370	955-964	24.4-24.7	5.2±0.7	9.1	179±12
	959-974	24.6-24.9	5.5±0.7	10.6±2.2	
	979-994	25.1-25.4	11.1±0.5	21.4±3.4	183±15
4+750	750-784	20.1-19.2	7.5±1.2		185±1
5+050	589-623	15.6-16.2	2.9-3.2	5.1-5.4	170±10

HYDRO-FRACTURING TESTING AND DESIGN ADJUSTMENTS

Considering the risks linked to the uncertainties in rock mechanical and hydrogeological conditions, the owner of the project decided to conduct investigations concurrent with the construction of the headrace tunnel. From the advancing tunnel, exploratory drilling with core recovery, permeability, dilatometer and hydro-jacking and on core samples laboratory tests was performed. Table 1 summarizes the results of the hydrofracturing tests, and Figure 6 shows the stress ratio σ_h/σ_v at the six test sites.

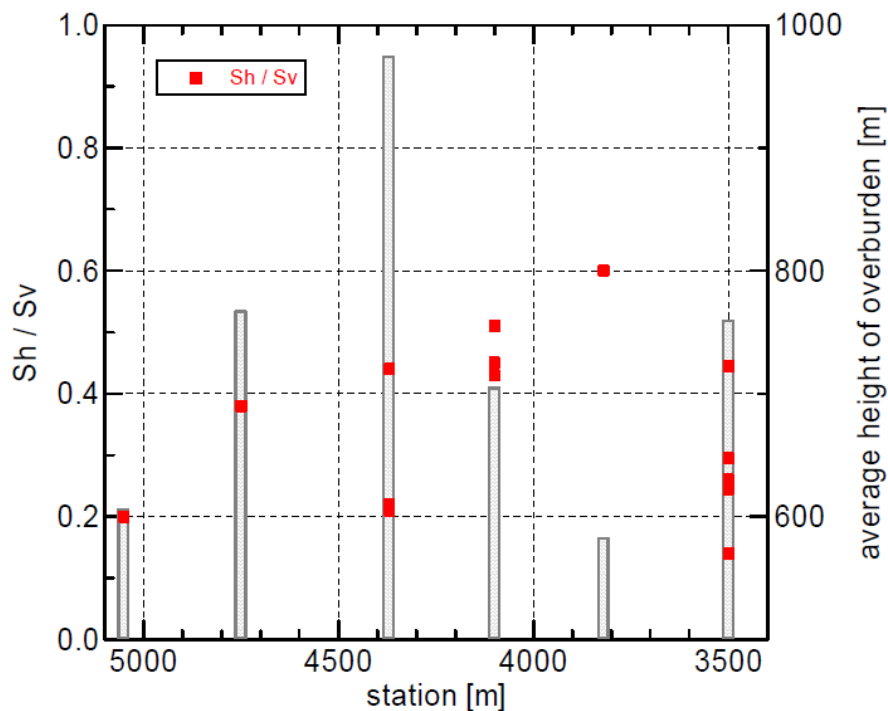


Fig. 6

Cover above tunnel (columns) and stress ratio at the six test sites (upstream on right)

Couverture rocheuse au-dessus de la galerie en charge (colonnes) et rapport de contrainte aux 6 points d'essai (amont à droite)

The minimal in-situ stress in the rock mass, independently of the direction, must be higher than the maximal internal water pressure in the tunnel (confinement criteria above 1.0, cf. Marencé [4]). Under such conditions, leakage water will not be able to open existing joints and discontinuities causing high water losses and possibly instabilities on the surface.

The results of the hydro-fracturing tests performed in the Quitarcaca pressure tunnel indicate unexpectedly low minimal stress levels, basically due to the minor horizontal principal stress σ_h having been found in the order of only 20% to 40% of the corresponding σ_v values. In order to not over-estimate the minimum

stress ratios, a presumed value of 0.25 seemed to be a conservative and thus acceptable assumption for the prediction of the k_0 ratio. In tunnel portions, where existing stresses do not satisfy the confinement criterion, a watertight tunnel lining has to be provided.

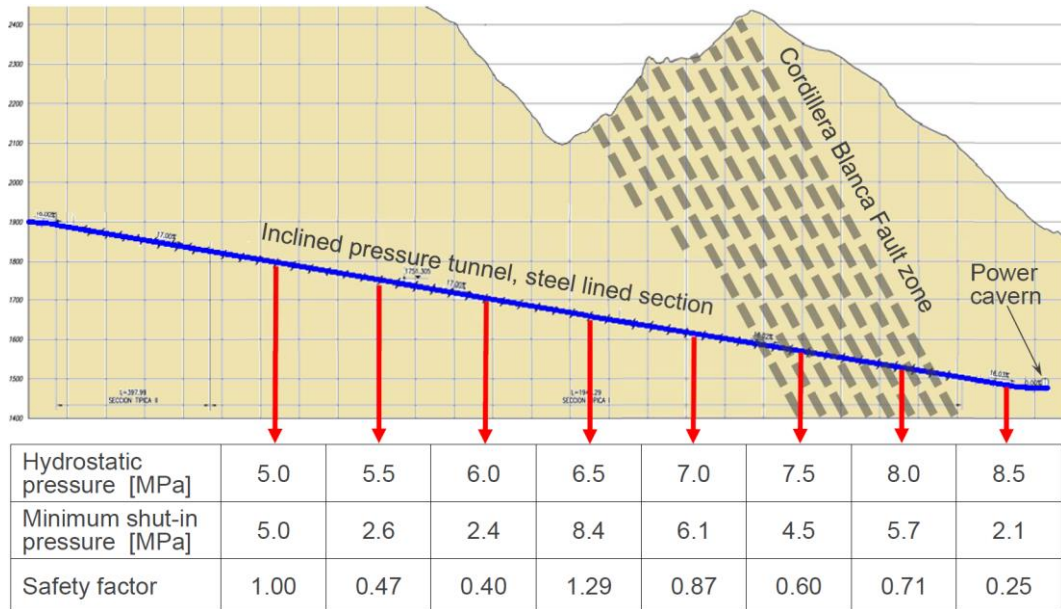


Fig. 7

Comparison of hydrostatic water pressure with the minimum shut-in pressures within the 2000 m of the inclined pressure tunnel close to the power cavern

Comparaison de la pression de l'eau hydrostatique avec les pressions de fermeture minimales dans les 2000 m du tunnel à pression inclinée près de la caverne de puissance.

Figure 7 compiles the minimum shut-in pressures obtained from the hydro-fracturing test campaigns, carried out approximately every 250 metres, starting from the Powerhouse Cavern. By comparison with the hydrostatic water pressures inside the tunnel during operation, the safety factor against hydro-fracturing was determined, resulting in values below 1.0 over large portions of the tunnel length. In order to meet the confinement criteria a watertight element was required along the first 2.0 kilometers from the power cavern, and it had been decided to install a steel lining within this reach, with steel plate thicknesses of up to 34 mm.

In combination with low horizontal and vertical overburden, the presence of the Cordillera Blanca fault zone negatively influences the stress pattern, which was determined during tunnel excavation by several hydro-fracturing tests, showing significantly reduced horizontal stresses, with k_0 -values within 0.2 to 0.3, which is unusually low for a young mountain range.

The diagram Figure 8 indicates the topography (brown line), the elevation of the tunnel axis (blue line), the required level of safety according to EM-1110-2-2901 (yellow line) and shows the achieved safety factors (red and green dots) for a minimum stress ratio of $k_0 = 0.25$ in the tunnel section upstream of the steel lining.

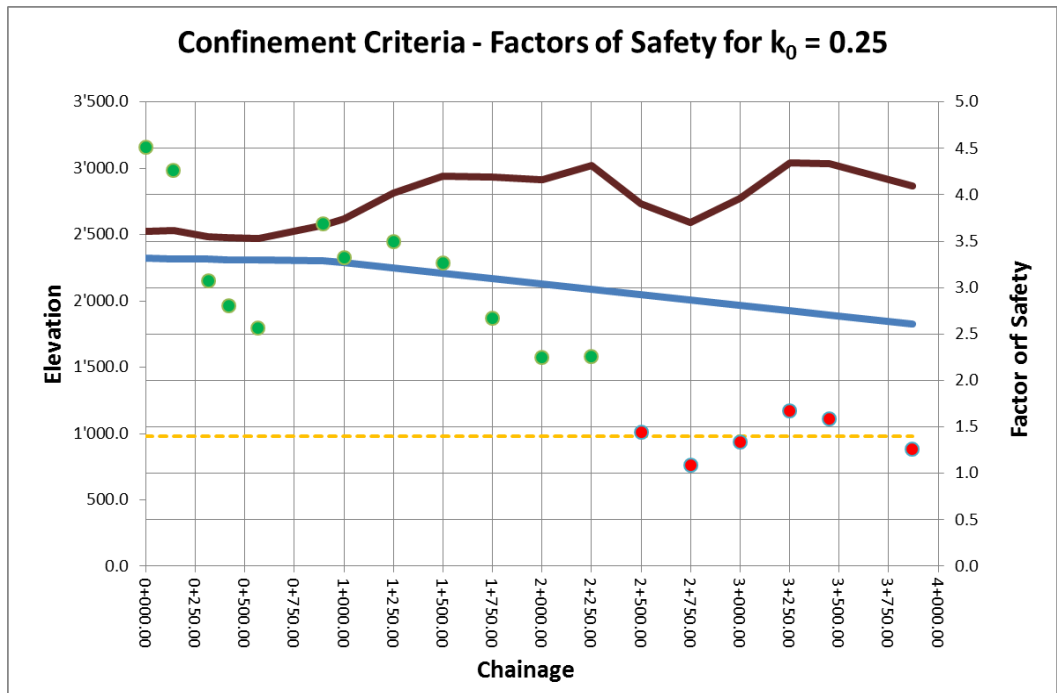


Fig. 8

Surface elevation (brown line), pressure tunnel elevation (blue line) and safety factors according to confinement criteria (red and green dots), along pressure tunnel chainage up to km 4+000

Cote de la surface du terrain (ligne brune), cote de la galerie en charge (ligne bleue) et coefficient de sécurité d'après les critères de confinement (points rouges et verts), le long de la galerie en charge jusqu'au km 4+000

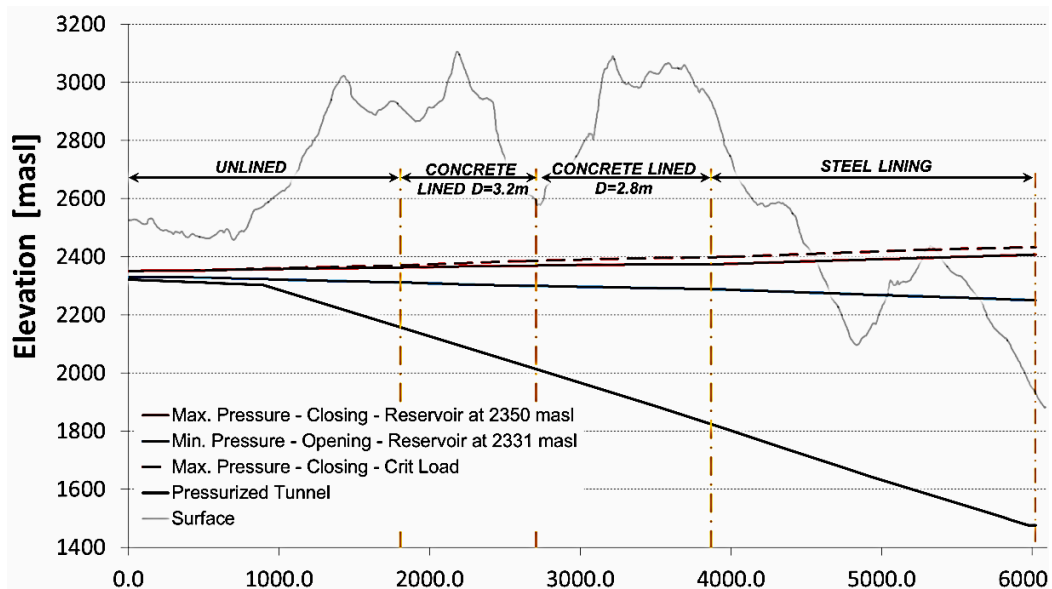


Fig. 9

Distribution of applied lining types, along pressure tunnel chainage up to power cavern

Différents types de revêtement appliqués le long de la galerie en charge depuis le puits amont jusqu'à l'usine en caverne

Even with allowance for accuracy of the test results, they unquestionably establish $\sigma_h/\sigma_v < 1$. This fact was to be taken into account in the design of the headrace tunnel and eventually called for a substantial extension of the steel liner in upstream direction. This had two consequences for the project: (a) added cost for the steel liner and (b) problems with the construction time schedule. The cost for delayed commissioning of the plant was the more serious aspect and remedial measures were taken in this regard, to the best possible extent. A long bypass tunnel allowed opening of additional working fronts and saving of time.

Figure 9 shows the distribution of applied lining types, along pressure tunnel chainage up to power cavern. Thanks to the installation of these linings, performance of the completed tunnel was overall very good, without mayor leakages observed.

CONCLUSION

The literature lists ample precedence of unlined pressure tunnels with satisfactory performance and offers empiric and semi-empiric methods and criteria for their design, e. g. Blind et al. [5], Broch [3], Buen et al. [6], Deere [7], Palmström et al., [8]. However, Benson [9] described the complexity of the subject and Swiger [10] questioned the use of rules of thumb. Schleiss ([11], [12]), Hendron et al. [13] and Fernandez ([14], [15]) analyzed the hydrogeological effects on the performance of pressure tunnels.

The uncertainties, critical for the design of the Quitaracsa headrace tunnel, were identified in time for the required investigations and adjustments. Without these adjustments, the Quitaracsa tunnel would have failed and required extensive repair works, resulting in a long interruption of plant operation with high consequential loss of production.

Under conditions similar to those present at Quitaracsa, empirical methods for the design of pressure tunnels can offer a reasonable approach in early stages of a project, but for final design it must be carefully checked if the assumptions inherent to such methods do apply. This was not the case for the Quitaracsa tunnel and similar experience was also made on other projects. The uncertainties, critical for the design of the Quitaracsa pressure tunnel, were identified in time for the required investigations and adjustments. Without these, extensive repair works would have resulted in long interruptions of plant operation and loss of production.

In this context, the experience with the Quitaracsa pressure tunnel serves as an example of exception from the rules and demonstrates the need for reliable and representative information on rock mechanical and hydrogeological conditions, particularly for projects with medium or high pressure tunnels.

REFERENCES

- [1] DANN, H. E., HARTWIG, W. P., HUNTER, J. R. Unlined tunnels of the Snowy Mountains hydro-electric authority, Australia. *ASCE* 90, PO3, 1964, pp 47-79.
- [2] BOUVARD, M. Les fuites de galeries en charge en terrain sec. *La Houille Blanche*, 1975, 4, pp 255-265.
- [3] BROCH, E. Development of unlined pressure shafts and tunnels in Norway. *Norwegian Soil and Rock Engineering Association*, Publication No. 3, Norwegian Hydropower Tunelling, 1985, pp 23-30.
- [4] MARENČE, M. Geotechnical input essential for power waterway design, Rock Engineering in Difficult Ground Conditions – Soft Rocks and Karst – Vrkljan (ed), *Taylor & Francis Group*, 2010.
- [5] BLIND, H., SCHWARZ, J. Limits for pressure tunnels without steel linings. *Water Power*, 1987, 7, pp 51-54.
- [6] BUEN, B., PALMSTRÖM, A. Design and supervision of unlined hydropower shafts and tunnels with head up to 590 meters. *Norwegian Soil and Rock Engineering Association*, Publication No. 3, Norwegian Hydropower Tunelling, 1985, pp. 65-73.
- [7] DEERE, D. U. Unique geotechnical problems at some hydroelectric projects. *Proceedings 7th Pan-American Conference on Soil Mechanics and Foundation Engineering*, 1983, pp 865-888.
- [8] PALMSTRÖM, A., BROCH, E. The design of unlined hydropower tunnels and shafts: 100 years of Norwegian experience. *Hydropower and Dams* 24, 2017, 3, pp 72-79.
- [9] BENSON, R. P. Design of unlined and lined pressure tunnels. *Tunnelling and Underground Space Technology*, 1989, Nr. 4/2, pp 155-170.
- [10] SWIGER, W. F.: Behavior of pressure tunnels and guidelines for liner design – Discussion. *ASCE GE* 122, 1996, 3, p. 254.
- [11] SCHLEISS, A. Bemessung von Druckstollen, Teil I. *Mitteilungen VAWE, ETH Zürich*, #78, 1986a.
- [12] SCHLEISS, A. Bemessung von Druckstollen, Teil II. *Mitteilungen VAWE, ETH Zürich*, #86, 1986b.
- [13] HENDRON, A. J., FERNANDEZ, G., LENZINI, P. HENDRON, M. A. Design of pressure tunnels. The art and science of geotechnical engineering at the dawn of the twenty first century. *Prentice Hall*, 1987, pp 161-194.
- [14] FERNANDEZ, G. Seepage-induced effective stresses and water pressures around pressure tunnels. *ASCE Journal GE* 120, 1994a, 1, pp 106-128.
- [15] FERNANDEZ, G. Behavior of pressure tunnels and guidelines for liner design. *ASCE Journal GE* 120, 1994b, 10, pp 1768-1791.
- [16] RIEMER, W. Fels-Klassifikationen – Einige kritische Anmerkungen. 18. *Tagung Ingenieurgeologie*, 2011, pp 53-60.

KEYWORDS

Failure, Fault, Geology, Geotechnical Investigation, Hydraulic Fracturing, Penstock, Safety Factor

COMMISSION INTERNATIONALE DES GRANDS BARRAGES

VINGT-SIXIÈME CONGRÈS DES GRANDS BARRAGES
Autriche, juillet 2018

DOI 10.3217/978-3-85125-620-8-189



This work licensed under a Creative Commons Attribution 4.0 International License. <https://creativecommons.org/licenses/by-nc-nd/4.0/>

**IN-SITU TESTING AND MONITORING OF TUNNELS AND CAVERNS AT A
PUMPED-STORAGE POWER PLANT IN THE SWISS ALPS**

Marcel HUBRIG

Deputy Head of Geotechnical Department, SOLEXPERTS AG

SWITZERLAND

Andreas KERN

Project Leader Hydrogeological Department, SOLEXPERTS AG

SWITZERLAND

Ursula RÖSLI

Project Leader Hydrogeological Department, SOLEXPERTS AG

SWITZERLAND

Holger WÖRSCHING

Head of Geotechnical Department, SOLEXPERTS AG

SWITZERLAND

COMMISSION INTERNATIONALE
DES GRANDS BARRAGES

VINGT-SIXIÈME CONGRÈS DES
GRANDS BARRAGES
Autriche, juillet 2018

IN-SITU TESTING AND MONITORING OF TUNNELS AND CAVERNS AT A PUMPED-STORAGE POWER PLANT IN THE SWISS ALPS

Marcel HUBRIG

Deputy Head of Geotechnical Department, SOLEXPERTS AG

Dr. Andreas KERN

Project Leader Hydrogeological Department, SOLEXPERTS AG

Dr. Ursula RÖSLI

Project Leader Hydrogeological Department, SOLEXPERTS AG

Holger WÖRSCHING

Head of Geotechnical Department, SOLEXPERTS AG

SWITZERLAND

1. INTRODUCTION

Since 1968, the original Linth-Limmern power station with the Limmern dam, located in the Swiss Alps in the Canton of Glarus, was fully operational. To increase the peak-shaving capacity in meeting fluctuating electricity demands, the project "Linthal 2015" for the underground pumped-storage power plant Limmern was one of the most important expansion projects of Axpo, a Swiss energy utility. Water is pumped from the storage reservoir Limmern to the upper lake Mutt, situated 630 m higher up. The pumping and turbine capacities of the new pumped-storage power plant reach 1,000 megawatts (MW), increasing the output of the Linth-Limmern power plants up to 1,420 MW. The project realization took one decade between the decision of the local government and the start of full operation in 2017. Pressure, head race and access tunnels as well as three large cavern (max. length 150 m, max. width 29 m and max. height 51 m) for the turbines, power house and valve chamber were excavated and a large gravity

dam built to increase the storage volume of the lake Mutt. A comprehensive hydrogeological and geotechnical in-situ testing and monitoring program was implemented [1]. An overview is given in Fig. 1.

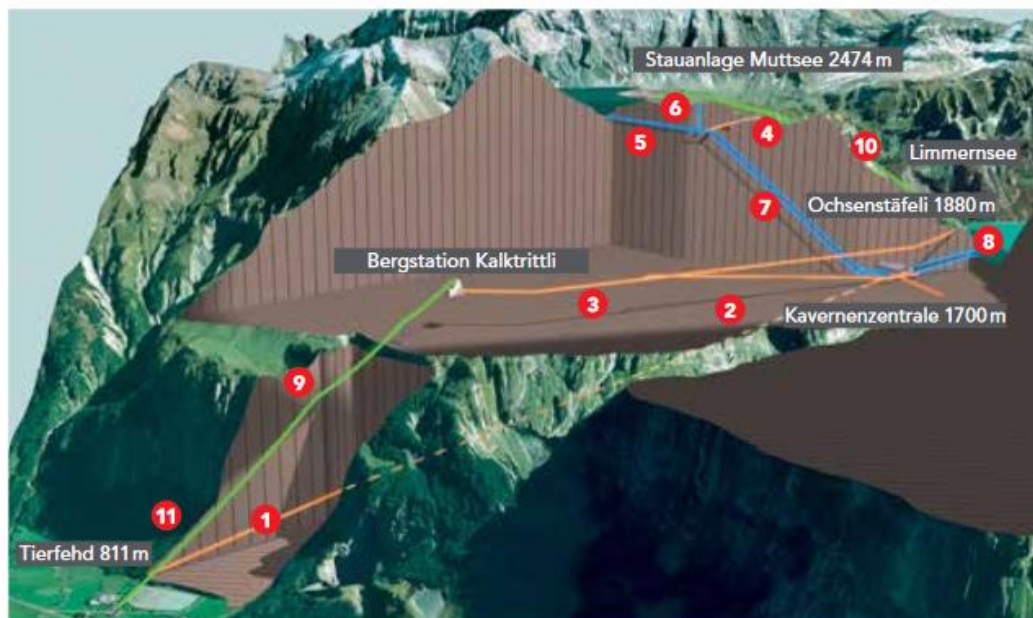


Fig. 1
Overview of the pumped-storage power plant Limmern

2. PRELIMINARY IN-SITU TESTS

The central cavern is partly located in the Quintner limestone of Malm and Cretaceous origin with locally developed schistosity and karst formation. Because of the extension of the caverns, the hydraulic and rock mechanic properties were estimated during a preliminary investigation phase. Therefore, in-situ tests were performed in ten boreholes between horizontal and upwards vertical direction with a diameter of 96 mm (HQ) and a length of maximum 130 m. The locations of the boreholes are shown in Fig. 2. The main goal of these in-situ tests was:

- Information on rock structure, schistosity, fractures, faults, karst
- Determination of the mechanical rock properties, elasticity and deformation moduli through dilatometer tests
- Determination of the minimal principal stresses through hydraulic fracturing tests
- Identification of water-bearing features and determination of static formation pressures and rock permeabilities through hydraulic tests.

The task was particularly demanding, as all the tests had to be performed in boreholes drilled from small exploration tunnels without the help of the drilling crew (Fig. 3). The particular boundary conditions of the test sites and the relatively short time window for the performance of these extended test series in combination with the logistic challenges required a careful planning and a novel testing approach for the more time-consuming implementation of the hydraulic tests.

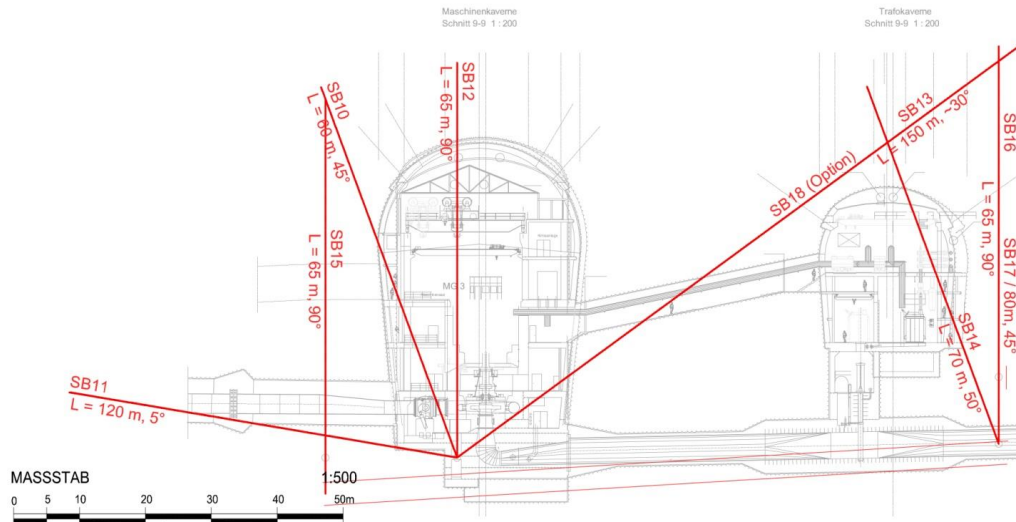


Fig. 2
Overview of boreholes drilled in the area of the future central cavern



Fig. 3
Installation of dilatometer system in small exploration gallery

The main challenge was the performance of the hydraulic tests. To avoid the slow natural saturation of the de-saturated formation due to the drilling of the upwards inclined boreholes and the trapping of air in the intervals, a customized 4-fold packer system was developed (Fig. 4). In total, three similar systems were simultaneously used to cope with the time limitations. The advantages of the systems can be summarized as follows:

- Saturation of the entire borehole after inflation of the packer nearest to the well head
- Simultaneous de-airing of the boreholes through the line situated at the bottom of the system
- Simultaneous monitoring and performance of parallel hydraulic tests in different intervals because of two individual lines within each test/observation interval (Fig. 4)
- Long-term monitoring of the pressure recovery
- Optional cross-hole tests.

A total of 40 hydraulic tests were performed. In addition, 55 dilatometer tests, 23 hydraulic fracturing tests and 18 impression packer tests were conducted without problems. Dilatometer tests supplied reliable ranges of in-situ rock E- and D-moduli. Hydraulic fracturing tests defined principal stress magnitude and orientation [2]. The results considerably contributed to the proper design of the caverns and the optimization of the layout and the construction work [3] [4].

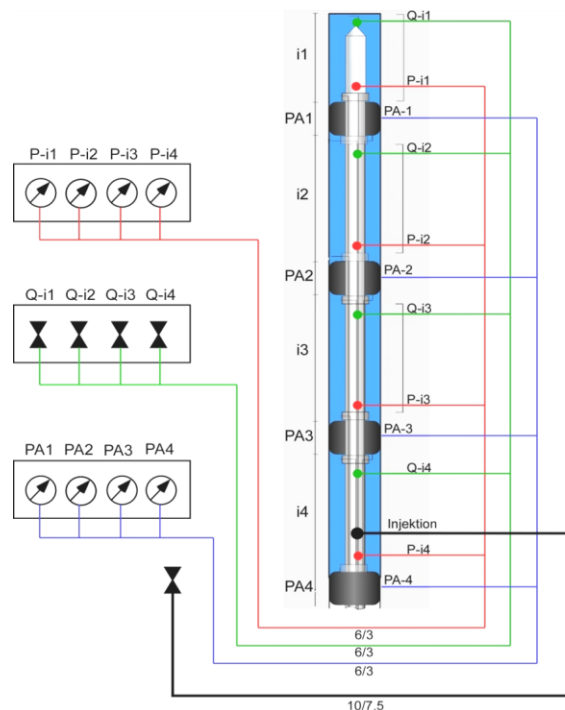


Fig. 4
4-fold packer system used for hydraulic testing

In addition, the hydraulic properties of the debris cones around the lake Mutt were investigated. Hydraulic tests were performed in three boreholes up to a depth of 38 m using a standard double packer system. These tests provided essential information, which was used to estimate the debris behaviour under the expected lake level increase from 2446 m asl to 2474 m asl and the water level changes during the operation of the power plant and to prevent slope instabilities along the lake Mutt.

3. MONITORING OF CAVERN EXCAVATION

The excavation of the central machinery caverns, consisting of machine and transformer caverns and the valve chamber (machine cavern see Fig. 6, left) was performed from top to bottom. This required a continuous monitoring of the rock deformations and the anchoring forces during the excavation process. The convergences were recorded with 30 m long 4-point extensometers, installed in cross-sections (Fig. 5). As the extensometers were immediately installed close to the working surface to obtain a complete data set of the convergences, their heads had to be protected from the potential damage by blasting. Initially the extensometers were equipped with data loggers and were wirelessly readout. In a later stage, the extensometers and the anchor load cells were connected via a bus cable (Fig. 6, right) to a central data acquisition system and subsequently uploaded to a Web database with close-to-real-time data plots, which were available to the responsible engineers at their workstation for permanent control.

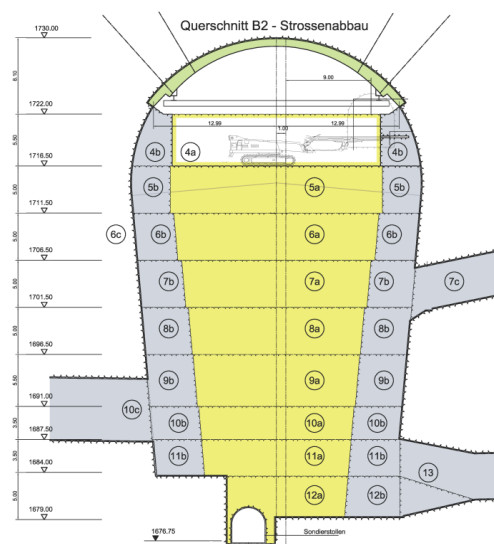


Fig. 5
Cross section of the machine cavern with excavation stages and uppermost extensometers

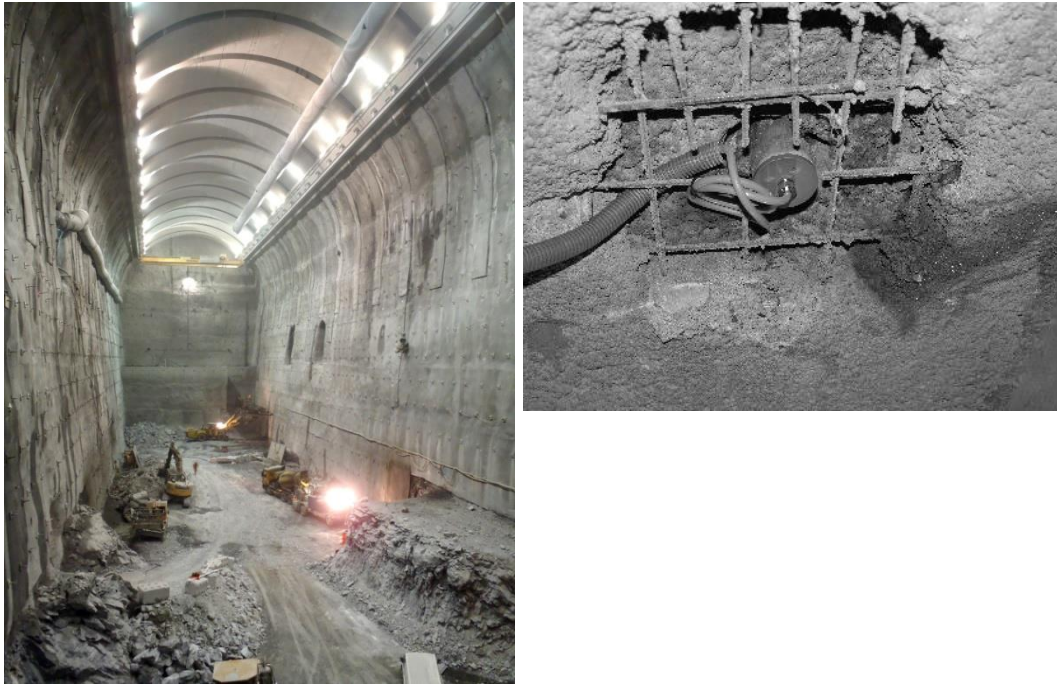


Fig. 6

Machine cavern during 2012 (left), extensometer head with bus cable (right)

4. INSTRUMENTATION OF LAKE MUTT DAM

The new dam of the lake Mutt has a length of 1050 m and a height of 35 m and is Europe's longest gravity dam. The total volume of the lake is thus increased from 9 to 25 million cubic meters. The installation of the dam safety monitoring started in 2015 and included:

- 76 pressure sensors for flotation measurements
- 74 concrete temperature
- 7 seepage surveillance points
- 8 pendulums
- 1 lake water table measurement station.

Solexperts obtained the task to install the flotation measurement points. Eleven cross-sections were instrumented. The flotation, which normally depends on the lake water level, is measured at different depths in the underground and at the contact between concrete and rock. The boreholes were drilled from the control gallery over the entire foundation width to monitor the pressure potential decrease from the upstream to the downstream side of the dam (Fig. 7, left). One to three vibrating wire pressure sensors were installed at different levels in each borehole. One measuring position in each cross-section was equipped with a

retrievable pressure sensor using a Solexperts Piezopress system consisting of a plastic casing with a filter element and the sensor seat at the bottom (Fig. 7, right). After the installation of the casing, the borehole was filled with sand along the filter section and with a cement injection as sealing section. The sensor was installed after the backfilling at the sensor seat in the filter section and sealed to the casing by O-rings. The other sensors were directly installed as lost sensors at the required depth in a sandy filter section, which was isolated by cement injection to avoid a hydraulic short circuit between different aquifers.

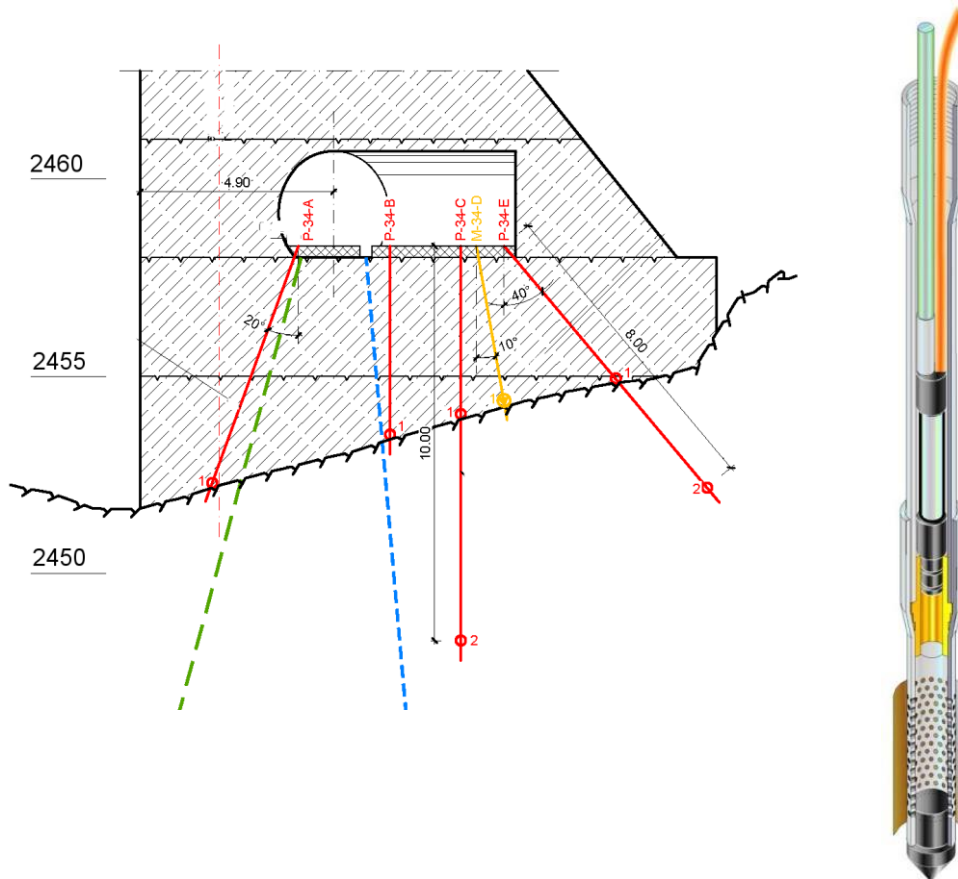


Fig. 7

Measuring section in the lake Mutt dam, in red the boreholes for the flotation measurements (left), schematic cross-section of a Piezopress (right)

All sensors installed in one measuring section are connected with a measuring box with the possibility to manually readout all sensors. Furthermore, the sensors are connected to the automatic data acquisition system and the current calculated heads are automatically displayed at the front of the measuring box (Fig. 8).

Besides the flotation, further parameters are monitored. The concrete temperature sensors are installed in several cross-sections and primarily serve for the quality control of the concrete. The seepage water is collected in a canal

along the downstream side of the dam and the water amount is measured at seven V-weirs with ultrasonic sensors. Furthermore, the position of the dam is recorded to estimate its stability. Therefore, four measuring sections are equipped with a pendulum and an inverted pendulum. The pendulum measures the inclination from the dam crest to the measuring location in the control gallery. The inverted pendulum is anchored in the rock and provides information on the relative movement of the dam with regard to the foundation. In addition, the water level in the lake Mutt is recorded.



Fig. 8

Measuring box for the flotation measurements with digital displays of the current heads

5. DATA ACQUISITION SYSTEM

An automatic data acquisition system was installed in the dam guard cabin directly besides the lake Mutt dam. The power supply includes a UPS (uninterruptable power supply). All described instruments are readout via a data bus system. The communication of the DAS with the sensors is ensured by a backbone system and multiple sub-bus systems. Therefore, most parts of the measuring points would still be monitored also in the case when main components of the system might be subject to failure. A total of about 250 sensor channels is recorded which, in addition, are partly calculated into target units. All data is integrated in the higher-level analysis system of the dam operator.

REFERENCES

- [1] BECKER H.J., HUBRIG M. STOLZ M., THUT A., WÖRSCHING H. Instrumentierung und Monitoring in der Geotechnik. *Grundbau-Taschenbuch, Teil 1: Geotechnische Grundlagen*, Witt, K.J. (ed.). 8. Auflage - April 2017, pp 867-967. Ernst & Sohn Verlag, 2017.
- [2] KECH M., NATEROP D., SENTI R. Hydrogeological and geotechnical in-situ testing for large caverns. *Rock Engineering in Difficult Ground Conditions- Soft Rocks and Karst (Vrkljan I., ed.)*, London 2010.
- [3] MÜLLER U., MARCLAY R., DUNN J., HOHBERG J.-M., HASE M. The Linth-Limmern hydro-power plant – Design and construction of a large pumped storage scheme. *Underground – the way to the future! (G. Anagnostou G, & H. Ehrbar H., eds.)*, World Tunnel Congress 2013, Geneva 2013.
- [4] MARCLAY R., HOHBERG J.-M., JOHN M., MARCHER T., FELLNER D. The new Linth-Limmern hydro-power plant – design of caverns und 500 m overburden *Rock Mechanics in Civil and Environmental Engineering (J. Zhao et al. eds.)*, Proc. EUROCK 2010, pp. 467-470. CRC Press/Balkema 2010.

SUMMARY

The pumped storage power plant Limmern in the Swiss Alps was an important hydropower project during the last years. To pump water from the lake Limmern in the about 600 m higher lake Mutt and to increase the power production up to 1,420 MW, a new underground machinery centre and a new gravity dam for the lake Mutt were constructed. The design required comprehensive investigations of rock parameters. Hydraulic tests were performed to obtain information on the hydraulic conductivities and the static formation pressures in the partly schistose and karstic Quinter limestone. The E- and D-moduli of the rock were determined with dilatometer tests. Finally, hydraulic fracturing tests were conducted to estimate the minimum primary stresses in the rock. These investigations considerably helped to improve the models of the underground and to adjust the design of the three caverns.

During the construction of the central machinery cavern, a complete data set of the convergence behaviour was obtained from the anchor forces and the extensometers, which were installed in cross-sections close to the advancing excavation.

A further task was the long-term monitoring of the lake Mutt dam. 166 sensors were installed, including pressure sensors for flotation measurements and lake level monitoring, sensors for temperature and seepage measurements and pendulums. All sensors were connected with a redundant bus system to a

data acquisition system installed in the dam guard cabin. The database is transferred to the dam operator's main analysis system.

The combination of in-situ measurements and monitoring of critical geotechnical parameters for the design and during the construction of the pumped-storage power plant has significantly contributed to optimize the construction process by reducing uncertainties regarding the subsurface properties and their associated risks. The final geotechnical monitoring of the lake Mutt dam is still ongoing and represents an essential part of the safety assessment of the dam.

La centrale de pompage-turbinage de Limmern dans les Alpes suisses a été un important projet hydroélectrique au cours des dernières années. Pour pomper l'eau du lac de Limmern vers le lac de Mutt situé 600m en amont, une nouvelle caverne souterraine pour la salle des machines et un nouveau barrage-poids au niveau du lac Mutt ont été construits dans l'objectif d'augmenter la capacité de production de la centrale à 1,420 MW.

Des études approfondies des paramètres du massif rocheux ont été nécessaires pour la conception du projet. Des tests hydrauliques ont été effectués afin d'obtenir des informations sur les conductivités hydrauliques et les pressions hydrostatiques dans la formation calcaire de Quinten partiellement schisteuse et karstique. Les modules d'élasticité des roches ont été déterminés à l'aide de tests au dilatomètre. Enfin, des essais de fracturation hydraulique ont été menés pour estimer les contraintes primaires minimales dans le massif rocheux. Ces études ont considérablement aidé à améliorer les modèles du sous-sol et à adapter la conception des trois cavernes de la centrale.

Durant la construction de la caverne pour la salle des machines, une multitude de données sur les caractéristiques de convergence du massif rocheux ont été récoltées par le biais des mesures des cellules de chargement sur les ancrages, ainsi que des extensomètres installés au niveau des sections transversales proche du front d'excavation.

Une autre tâche a consisté en la surveillance à long terme du barrage du lac de Mutt. 166 capteurs ont été installés, comprenant des capteurs de pression pour les mesures de flottabilité et la surveillance du niveau du lac, des capteurs de température, des capteurs pour les mesures d'infiltration et des niveaux à pendule. Tous les capteurs ont été connectés de façon redondante à un système BUS contrôlé par une centrale d'acquisition des données installée dans la station de surveillance du barrage. Les données sont ensuite envoyées vers le système général de l'opérateur du barrage.

Le couplage des mesures in-situ avec la surveillance du comportement hydro-mécanique du terrain avant et pendant la construction de la centrale de pompage a contribué significativement à optimiser le processus de construction de la centrale en réduisant les incertitudes sur les propriétés du sous-sol et les risques associés. La surveillance géotechnique du barrage du lac de Mutt est toujours en cours et représente une composante importante dans l'évaluation de la sécurité du barrage.

KEYWORDS

Lake Mutt dam, power plant, gravity dam, deformation measurements, extensometer, hydraulic fracturing, hydraulic head, hydrogeology, permeability, piezometer, sounding, stress, tunnel

Barrage du lac de Mutt, centrale, barrage-poids, mesure de déformation, extensomètre, fracturation hydraulique, hydrogéologie, perméabilité, piézomètre, sondage, contrainte, galerie

COMMISSION INTERNATIONALE DES GRANDS BARRAGES

VINGT-SIXIÈME CONGRÈS DES GRANDS BARRAGES
Autriche, juillet 2018

DOI 10.3217/978-3-85125-620-8-190



This work licensed under a Creative Commons Attribution 4.0 International License. <https://creativecommons.org/licenses/by-nc-nd/4.0/>

**SIPHON INTAKE AS SHPP INTAKE & WATER WAY, A SOLUTION DESIGN
FOR SECURING THE LEFT BANK OF WLINGI DAM IN BLITAR, INDONESIA**

Ulle Mospar DEWANTO

Deputy of Operational II, JASA TIRTA I PUBLIC CORPORATION

INDONESIA

Gede Nugroho ARIEFianto

*Chief of Water Supply and Hydropower Division, JASA TIRTA I PUBLIC
CORPORATION*

INDONESIA

Bayu Pramadya Kurniawan SAKTI

*Civil Engineer of Water Supply and Hydropower Division, JASA TIRTA I PUBLIC
CORPORATION*

INDONESIA

SIPHON INTAKE AS SHPP INTAKE & WATER WAY, A SOLUTION DESIGN FOR SECURING THE LEFT BANK OF WLINGI DAM IN BLITAR, INDONESIA

Ulle Mospar Dewanto

Deputy of Operational II, JASA TIRTA I Public Corporation

Gede Nugroho Ariefianto

Chief of Water Supply and Hydropower Division, JASA TIRTA I Public Corporation

Bayu Pramadya Kurniawan Sakti

Civil Engineer of Water Supply and Hydropower Division, JASA TIRTA I Public Corporation

INDONESIA

Wlingi Dam in Blitar, East Java Province, Republic of Indonesia is a multipurpose dam which one of the purposes is to supply Lodoyo Irrigation Area in Blitar and Tulungagung District of 12,687 Ha, through Lodagung Irrigation Canal. According to the importance of this food security infrastructure, the guarantee of discharge dependability becomes an absolute necessity. The outflow for irrigation is 8.89 m³/s to 13.78 m³/s that is available throughout the year. There is also a gross head of 12.50 m between the water level on Wlingi Reservoir and after canal escape. Thus, the availability of head and discharge make the potential of additional small hydroelectric power plant (SHPP) in Lodagung Irrigation Canal sounds very promising.

Jasa Tirta I Public Corporation, a State-Owned Corporation on Water Resources Management in the Republic of Indonesia has been constructing SHPP Lodagung 2x850 kVA since August 2016 and scheduled to be completed on December 2017. This project is expected can meet the lack of electricity supply that has been relied only on two local hydropower plants, HEPP Wlingi and HEPP Lodoyo with total installed capacity of 75.38 MVA. These supplies have not increased since 1983, whereas in 2010 the peak load exceeded 75 MVA and in 2017 is projected to be at 92 MVA.

The Wlingi Dam itself encountered geological problems during impounding in 1977. At that time, there was an excessive leak in the formation of lime soil, in form of seepage in left abutment of the dam. The seepage appeared also in the raising of well water level in the village around downstream of the dam and reached parallel to the yard. The investigation was conducted on 12 February – 14 March 1978 using radio isotope tracer with “multi well technique” method. Radioisotope Cr⁵¹ and Br⁸² injected into a borehole and then observed on the other holes. The investigation concluded that seepage raised on the left bank of the dam, mainly through the upper part of the limestone rock and centered near the irrigation outlet. Then the problem was dealt with the three curtain grout lines on the left bank area, and until now is an effective treatment.

Crossing curtain grout lines that intersect with the irrigation canal, so far become the most economical path for intake pipes and penstock. However excessive digging will surely disturb curtain and have bad impact on overall dam safety. Therefore, the design of the intake and water way are planned to be placed on top of crest dam. Siphon intake that made from steel pipe was chosen as a best solution for the design, even though need precise hydraulic calculation to ensure that it will work properly. The challenge is that it will be also the first application for hydropower intake and water way in Indonesia.

Siphon intake was designed by steel material SS 400 with specification technical data: 2 units each diameter 1.5 m, thickness 10 mm, length 60 m. The specification technical data of penstock i.e.: Inner Diameter 2.5 m, thickness section-I 10 mm with length section-I 315 m, thickness section-II 12 mm with length section-II 30 m, total length 345 m. After the installation and construction works has completed in January 2018 since construction works started in August 2016 (18 months), the system performed well. The turbines and generators worked with the pressure in penstock similar with turbines in range 0.83 – 1.03 bar with output capacity of each turbine 407 – 643 kW.

(Keywords: SEEPAGE, SIPHON, POWER PLANT)

1. Introduction

1.1 Background

The deficit of electricity supply in Blitar Regency, East Java Province, Republic of Indonesia was strived to be fulfilled by the development of hydro electricity. The supply of electricity by HEPP Wlingi and HEPP Lodoyo of 75.38 MVA through the Wlingi Substation has not increased since 1983, while the peak load of the surrounding areas of Blitar and beyond has exceeded 75 MVA after 2010. In 2017, the peak load is projected at 92 MVA. In accordance with Government of Indonesia policy set forth in Power Supply Business Plan (RUPTL) 2015-2024 (PT PLN (Persero), Electricity Supply Business Plan (RUPTL) PT PLN (Persero) 2015-2024 Jakarta, 13 and 25.) that every new primary source of local electrical energy derived from renewable energy, i.e geothermal and water power, can be fed in directly to the power network system whenever it is available. This is one of a government policy for climate change mitigation.

There was a potential of hydroelectricity that can be generated in Lodagung Irrigation Channel, one of the Multipurpose Dam “Wlingi” facilities in Blitar. One of the development goals of Wlingi Dam was to supply irrigation demands for agricultural land in Blitar and Tulungagung regencies and operated since 1978. Water from the Wlingi Dam is flowed through Lodagung Irrigation Channel to irrigation area of 12,687 Ha. Considering the important role of the irrigation infrastructure, the guarantee of water availability throughout the year becomes an absolute demand for farmers. Maximum outflow for irrigation water is 13.78 m³/s with probability 2.70%, while minimum is 8,89 m³/s with probability 97,30%. The Wlingi Reservoir has a high water level at El + 163.50 m, normal at El + 162.00 m, and average at El + 162.75 m. The water level ini irrigation channel in the lowest segment after the plunge escape regulator is at El + 150.25 m. From the data there is a gross head of 12.50 m. The availability of heads and constant discharge makes the potential of electricity in Lodagung Irrigation Channel was feasible to be realized.

But, there is an important issue that must be considered if the hydropower potency in Wlingi Dam will be generated. That is “How to flow the water from reservoir to power house without build an intake and water way with excessive digging?” There are two reasons why it should be built on that condition. First, Wlingi Dam itself encountered geological problems during impounding in 1977, then the problem was dealt with the three curtain grout lines on the left bank area, and until now is an effective treatment. Excessive digging will surely disturb curtain and have bad impact on overall dam safety. The second, the strength of the existing irrigation conduit channel initially designed for free flow, so when connected to the penstock it becomes a pressurized conduit. It will result significant construction works on left bank of the dam if the existing conduit is connected to the penstock. The strength of the conduit channel strengthens the motivation to design the intake and water way at Lodagung Hydropower does not connect to existing irrigation conduit outlet.

1.2 The Problem

The problem examined in this paper is: what is appropriate type of water intake of hydropower plants which crossing the dam body, without disturbing the dam structures and keeping the reservoir performance in supplying water requirements for irrigation at best level?

2. Library Review

2.1 Formula for Annual Energy Generating and Production Capacity

To calculate the capacity (P) and annual energy production (E), the equation formula (Damanik, A.K. et.al) Main Book of Feasibility Study of MHP PLATMH Directorate General of Electricity and Energy Utilization of Department of ESDM Jakarta, 9.), namely:

$$P = g \times Q \times H \times (E_f \text{ system}) \quad [1]$$

information :

P : Estimated power generated (kW)

G : Gravity (9.81 m / s²)

Q : The water discharge (m / sec)

H : High effective fall (m)

E_f system is the mean value of the efficiency of the turbine: $\eta_T = 0,925$, efficiency of generator: $\eta_G = 0,97$, transformer efficiency: $\eta_{TR} = 0,98$. If the generation discharge decreases to 40%, the turbine efficiency is estimated to decrease by 70% (Perum Jasa Tirta I, 2014, Final Report of Capacity Design and Layout of Lodagung MHP Project (2 x 0.65 MW) .Wiratman Power Jakarta, 2 .).

To calculate the annual energy production used the formula:

$$E = \xi \times P \times 8.760 \text{ hours} \quad [2]$$

E : annual energy (KWh)

ξ : Capacity Factor

2.2 FAO method (Food Agriculture Of Organization) for Siphon Intake

$$Q = CA \sqrt{2gH} \quad [3]$$

C = discharge coefficient

A = cross-sectional area (m²)

H = gross head (m)

Discharge coefficient can be calculated by this formula:

$$C = \frac{1}{1 + \lambda \frac{L}{d} + \sum k} = \frac{1}{1 + \frac{\text{TotalHeadloss}}{\frac{V_{siphon}^2}{2g}}} \quad [4]$$

λ = roughness coefficient of pipe = 0.02 (Steel pipe)

L = length of conduit

d = siphon diameter

$\sum k$ = loss coefficient in pipe

3. Discussion

The power plant utilizing the Lodagung Irrigation Channel is a small-scale hydro power plant, hereinafter called Lodagung Small Hydro Power Plant (SHPP Lodagung), located in Jegu Village, Sutojayan District, Blitar Regency, East Java Province. Discussions on the power plant plan are as follows:

3.1 Capacity of Power Generation and Annual Energy Production

The installed capacity (P) and annual electric energy (E) capacity are calculated as follows equation [1] and [2]:

$$\begin{aligned} P &= g \times Q \times H \times \eta_T \times \eta_G \\ &= 9,81 \text{ m/s}^2 \times 14 \text{ m}^3/\text{s} \times 10,30 \text{ m} \times 0,925 \times 0,97 \\ &= 1.276 \text{ kW} \rightarrow \text{installed capacity} = 1.300 \text{ kW (common value)} \end{aligned}$$

$$\begin{aligned} E &= \xi \times P \times 8.760 \text{ hours} \\ &= 83,43 \% \times 1.276 \text{ kW} \times 8.760 \text{ hours} \\ &= 9,325 \text{ GWh} \end{aligned}$$

3.2 Main Building Arrangement

The optimization of SHPP Lodagung layout is based on survey measurement and field condition identification to determine the location of penstock and powerhouse, with the following development criteria:

- a. Determination of the location of the penstock to the powerhouse refers to the longitudinal section of Lodagung Irrigation Channel.
- b. Determination of the penstock line is made by avoiding turns with sharp angles, with the shortest length to minimize losses, and is in a good soil structure and stable.
- c. Determination of powerhouse locations in areas with good accessibility and location stability, located not far from the tailrace outlet.
- d. The location of SHPP Lodagung building placement (penstock and powerhouse) also consider the topography, geology, access roads, the nearest 20 kV transmission line.

Conditions that must be considered is the geological history when impounding Wlingi Reservoir in year of 1977 in the form of excessive seepage on the left back of the dam (left abutment). The investigation was conducted on 12 February to 14 March 1978 with tracer technique. Tracers use the radioisotope Cr51 and Br82 with multi well technique, ie the tracer is injected into a borehole and the observations are performed on other holes. The investigation concluded that the seepage encountered on the left back of the dam came from the eastern direction veering northwest to tailrace hydropower. Details of the conclusions on the seepage description are described as follows:

- a. Right abutment area there is no seepage from the reservoir on the right side downstream.
- b. Seepage occurs in the left back area mainly through the upper part of the limestone rock.

- c. Direction of seepage in the left back area is concentrated to the left open channel area near the irrigation outlet, then flows to the tail race area through fractures in the rock chalk.
- d. There is direct seepage from the left side reservoir area (see attachments 1 and 2: C-11 and C-20) to the power house (PH) hydropower and spillway (SPL).

Impounding of Wlingi Dam in 1977 had a problem of water leakage in the formation of lime soil that resulted in raising of the land water table. The elevation caused the well water to reach parallel to the land in the settlement of residents around the downstream of the dam or powerhouse of hydropower. To overcome it then the protection with 3 (three) curtain grout path in the left bank area / left bank body dam were built. The "Additional Curtain Grout Line Section I, II and III" show the location of the intersection of the three curtain grout lines located near the conduit channel outlet of Lodagung Irrigation Channel. One path of curtain grout consists of two types, namely:

- a. The inner side adjacent to the reservoir is 2 (two) cement grouting lines;
- b. The outside as a curtain is 1 (one) line of chemical grout.

The initial phase of the study was to establish the main structures of SHPP Lodagung and its layout taking into account the geological history during the implanting of the Wlingi Reservoir in 1977, thus setting the following structure:

- a. The generator discharge is taken directly from the reservoir using the siphon pipeline intake. The siphon pipeline intake is the most likely design to be realized because it does not modify the irrigation conduit channel based on the dam safety considerations.
- b. After being sucked by the siphon pipes, water flows to the pipe (penstock) on the left and parallels the open irrigation canal.
- c. Consideration for optimum head and dam safety, which is the minimum of vibrations occurring to the dam body during construction, the power house is placed more than 400 meters from the dam near the escape gate.
- d. The flow of water coming out of the turbine (draft tube) is redirected back to the tailgate and returns to Lodagung Irrigation Channel. This design will keep water allocation for irrigation is still full filled

3.2.1 Intake

The design of the selected intake building is siphon pipes and it is decided that irrigation conduit outlet lines are not disturbed. The siphon intake design and water way are planned to be placed on top of crest dam, and sucked water from Wlingi reservoir without pump or other mechanism except first pumping to make pre-condition of water pressure along the pipe. Then, waterflow goes down to penstock and finally run the turbine. The system, therefore needs

precise hydraulic calculation to ensure it will work properly. Consideration of choosing the intake design are:

- a. A similar risk during impounding in 1977 is worried to recur when the existing curtain grout layer is disrupted or broken by heavy engine vibration or deep excavation in the area around the irrigation outlet located on the third intersection of the grout path.
- b. The strength of the existing irrigation conduit channel originally designed for free flow. When connected to a penstock, it will become a pressurized channel then, and the strength of conduit will not be adequate. So, new intake was designed and use siphon intake system. Data planning intake siphon as follows:

Design discharge	= 14 m ³ / s @ 7 m ³ / s
Number of siphon pipe	= 2 units
Siphon pipeline length	= 60 m
Elevation of the dam peak	= +167.00 m
Upper elevation siphon pipe	= +168.50 m
Low water level	= +162.00 m
Suction head siphon on low water level	= 6.5 m (ΔH critical)
Suction head maximum	= 7.11 m
Total Gross Head	= 2,20191 m

The calculation of siphon intake based on equation [3] and [4]:

$$C = \frac{1}{1 + \lambda \frac{L}{d} + \sum k} = \frac{1}{1 + \frac{\text{TotalHead}bss}{\frac{V_{siphon}^2}{2g}}} = \frac{1}{1 + \frac{2,20191}{3,96^2 / (2 \times 9.81)}}$$

$$= 0,556$$

$$Q = CA \sqrt{2gH} = 0,556 \times (\pi \times 1,5^2 / 4) \times \sqrt{2 \times 9.81 \times 12,50}$$

$$= 15,38 \text{ m}^3/\text{det}$$

Based on the calculation obtained the maximum discharge (without regulation) on the channel of 15.38 m³/s. With the help of pipe regulation, the design discharge 2 x 7 m³/s using 2 pcs of 1.5 m diameter then the water velocity in siphon pipes is 3.96 m/s. Suction head siphon on low water level (6.5 m) is lower than Suction head maximum (7.11 m).

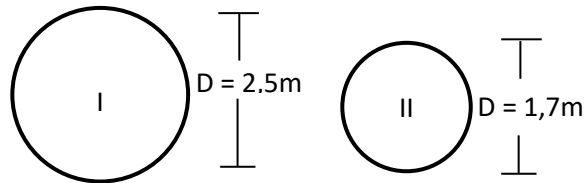
The siphon method of operation is a filling method that utilizes pressure differences due to the high difference between upstream water level (reservoirs) and turbine inlet valves. The way it works are described consecutively, firstly, the turbine inlet valves at the end of the penstock are closed, fulfill the pipe with water, using small pump to make desire vacuum condition at beginning of siphon until penstock so that due to the difference water pressure, water from the reservoir will be constantly inhaled and rotating the turbine. The tip of the siphon pipe is fitted with a litter filter and a rough material (trash rack) that protects the area around the end of the pipe. Its function is to select the material

that goes into the penstock and turbine with water to fit the allowed size.

3.2.2 Penstock

The penstock path to the powerhouse location is located on the left and parallel to the existing open irrigation channel of 367.59 m. The minimum distance from the irrigation channel to the penstock is 15.00 m. The technical data for hydrolysis calculations on penstock are:

- a. Debit = 14 m³ / s
- b. Manning Roughness = 0.014
- c. Total penstock length (I and II) = 367.59 m
- d. Types of tunnels = Circles



Types of tunnels = Circles

The press flow occurs when the ratio of water level to the penstock (h / D) diameter is more than 1.5 with the following checks:

Water level, H = 12,50 m

Diameter penstock, D = 2,50 m

$$\frac{h}{D} = 5 > 1,5 \text{ (OK)}$$

From the penstock calculation, primary penstock diameter was set at 2.50 m by the cross-sectional area of the penstock pipe was 4.91 m². With the generation discharge Q = 14.00 m³ / sec, the flow velocity in the penstock pipe is (14.00 m³ / s) / (4.91m²) = 2.85 m / s. From the calculation results, a 2.50 m diameter penstock was selected based on several considerations, among others:

- a. Ease of pipeline treatment process,
- b. Minimal energy loss levels
- c. The economic value of the penstock pipe,
- d. Pipes that have larger diameters have a lower level of energy loss because the water flow rate is smaller, but the size is bigger, heavier and the price is higher. While the pipe that has a smaller diameter the price is cheaper, but has a greater energy loss rate.

3.2.3 Turbine and Generator

Data design of turbine i.e.:

Net Head	10,3 m
Flow	14 m ³ / s
Turbine Type	S-Type Horizontal Kaplan
Turbine Capacity	2 x 675 kW
Flow/unit	7 m ³ / s
Speed	400 rpm

runway speed	800 rpm
Specific Speed	555,21
Diameter Runner	1,13 m
Suction Head	2 m
Turbine efficiency at 100% load	93 %
Runner Material	X3CrNiMo 13-4 or equivalent
Draft tube, elbow and cone material	S355J2G3 or equivalent, after welding galvanized

Data design of generator i.e.:

Generator efficiency	97 at pf-0.8 %
Generator Output	2 x 650 kW
Voltage Output	6,3 kV
Excitation System	Brushless
Frequency	50 hz
Speed	1000 rpm
Runaway speed	2000 rpm
Automatic Voltage Regulator	+5 to -10 %

3.2.4 Power House

Turbines and generators with other equipment are placed in a power house. The structure of the building is designed to be stable against the load of hydro mechanical engines and earthquake, and meet the limits of the voltage permit according to the design criteria.

3.2.5 Tailrace

Tailrace is planned to boil down the existing irrigation channel in the form of a natural channel located after the irrigation measurement or bridge building for access to Wlingi hydropower. The natural channel base elevation as tailgate channel outlet location is +149.00 m, tailrace water level is +150.25 m with a threshold width of 6 m).

3.2.6 Spesification Technical of Siphon pipe and Penstock Intake Siphon by Material SS 400

Diameter	1,5 m
Thickness	10 mm
Units	2
Lenght	60 m
Connection Box (Expansion and Reducer)	1 unit

Penstock by Material SS 400

Inner Diameter	2,5 m
Thickness Section-I	10 mm
Length Section-I	315 m
Thickness Section-II	12 mm
Length Section-II	30 m
Total Lenght	345 m

3.2.7 The Performance of Lodagung SHPP

After the installation and construction works has completed in January 2018 since construction works started in August 2016 (18 months), the system of Lodagung SHPP performed well. The turbines and generators worked with the pressure in penstock similar with turbines in range 0,83 – 1,03 bar with output capacity of each turbine 407 – 643 kW.

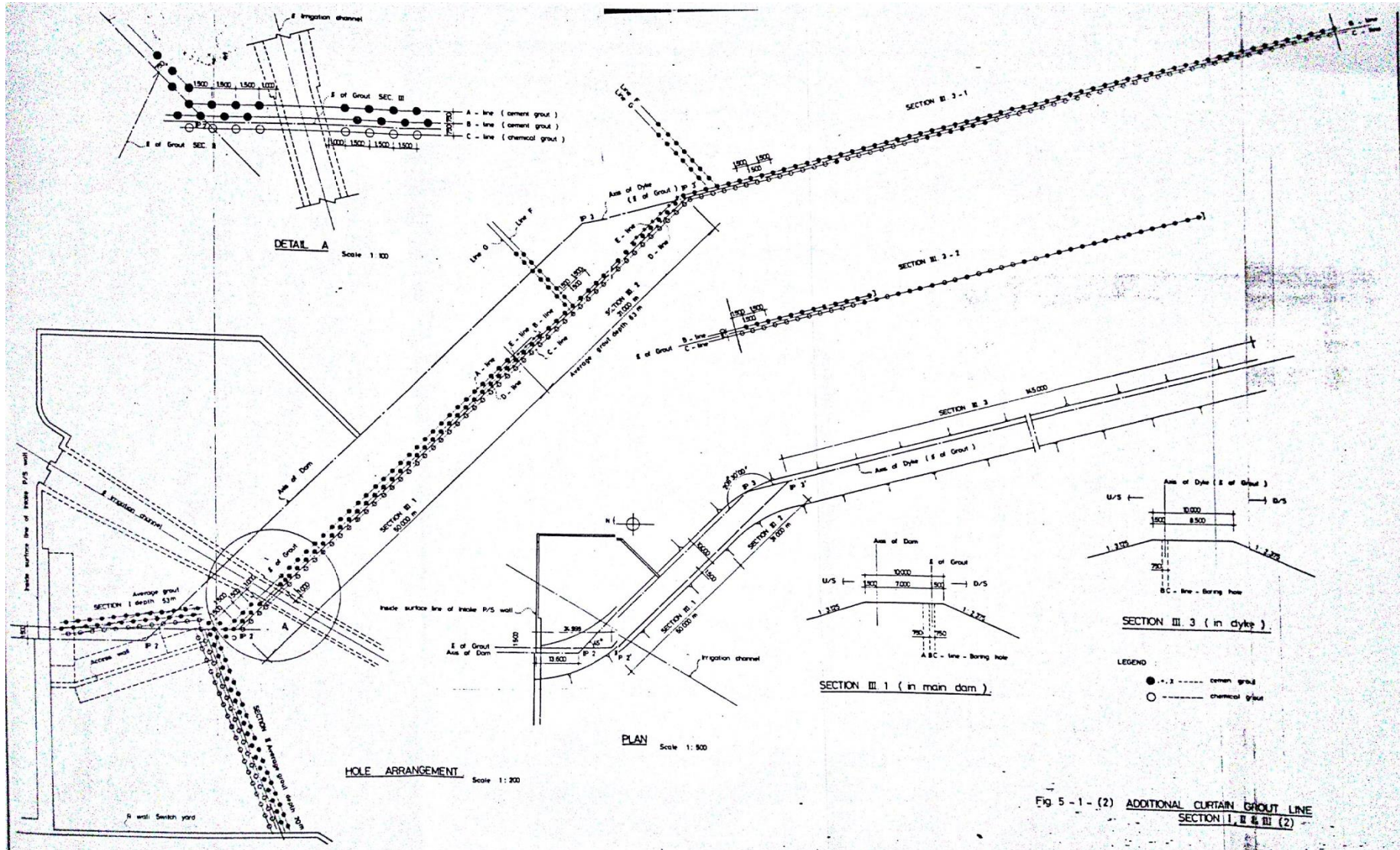
4. Conclusion

- a. The small scale hydropower is potential and promising to be built because there is continuity of flow which using irrigation water allocation and effective head is adequate
- b. There is a need of additional electricity supply in the adjacent and surrounding area
- c. The construction of hydropower particularly water intake should not disturb dam embankment and also keep reservoir performance for irrigation supply.
- d. Development of siphon intake model then become best solution, even though needs precise hydraulic calculations.
- e. Small scale hydroelectric power with siphon intake technology which may be first been built in Indonesia finally come through in early of year 2018.
- f. It becomes a challenge that siphon intake as hydro power water way or water way for other purposes, could be implemented to other small dams without disturbing existing dam embankment, in consideration with dam safety.

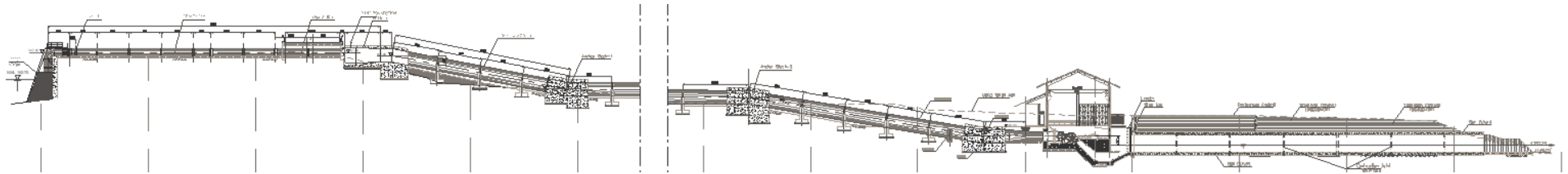
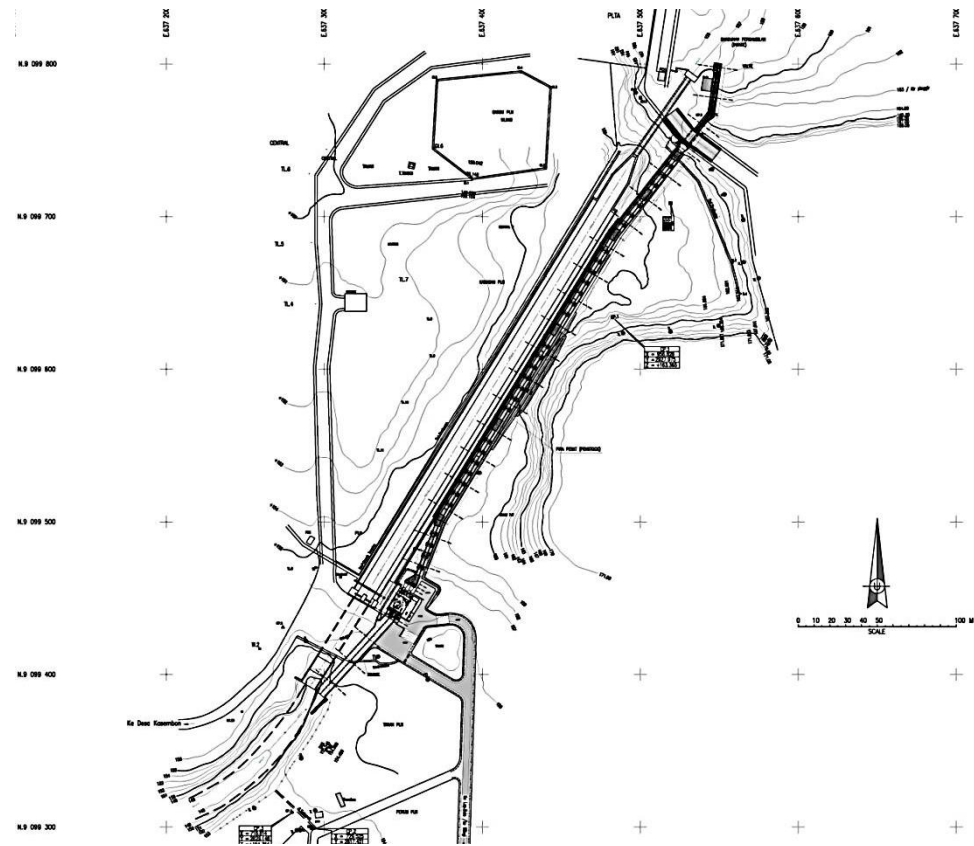
5. References

- [1] ATOMIC ENERGY RESEARCH CENTER - BATAN, Report of Seepage Investigation at Wlingi Dam with Radioisotope Bapel of Kali Brantas Versatile Master Project, 1 and 19, 1978.
- [2] TECHNICAL CONSULTANT OF NIPPON KOEI Co., Ltd., Wlingi Multipurpose Project Report on Ground Water In Limestone Foundation and Dam Safety, Jakarta, 1980.
- [3] JASA TIRTA I, Final Report of Capacity Design Review and Layout of Lodagung MHP Project (2 x 0.65 MW) PT Wiratman Power Jakarta, 2015.
- [4] VONNY CS, BAYU PKS, Lodagung SHPP Development In Using Hidro Power Potential In The Wlingi Dam In Blitar, East Java Province, *INACOLD Jakarta*, 2015.

Attachment 1. Curtain Grout Lining I, II, and III in Wlingi Multipurpose Dam



Attachment 2. Main Building Scheme of Lodagung SHPP 2 x 0,65 MW



COMMISSION INTERNATIONALE DES GRANDS BARRAGES

VINGT-SIXIÈME CONGRÈS DES GRANDS BARRAGES
Autriche, juillet 2018

DOI 10.3217/978-3-85125-620-8-191



This work licensed under a Creative Commons Attribution 4.0 International License. <https://creativecommons.org/licenses/by-nc-nd/4.0/>

**MODIFYING METHOD FOR VORTEX FLOW IN TRIFURCATION IN
HYDROPOWER PLANT**

Yeonju LEE

Senior Manager, K-WATER

PAKISTAN

Waqar Ahmad KHAN

CEO, STAR HYDRO POWER LIMITED

PAKISTAN

Junaid KHAN

Manager, STAR HYDRO POWER LIMITED

PAKISTAN

COMMISSION INTERNATIONALE
DES GRANDS BARRAGES

VINGT-SIXIÈME CONGRÈS DES
GRANDS BARRAGES
Autriche, juillet 2018

MODIFYING METHOD FOR VORTEX FLOW IN TRIFURCATION IN HYDROPOWER PLANT

Yeonju Lee

Senior Manager, K-water

Waqar Ahmad Khan, Junaid Khan

CEO, Manager Star Hydro Power Limited

1. INTRODUCTION

The Patrind hydropower project developed by SHPL (being a special purpose company established for the project) and owned by K-water (being the main sponsor for the project) is a run of river type hydropower project on the Jhelum River, approximately 200km northeastward of Islamabad and at the west bank to the township of Muzaffarabad in the Azad Jammu & Kashmir, Pakistan.

According to the project overall layout conditions, water diversion and power plant using a three-hole machine layout. The inner diameter of the straight penstock is 5.5m and the branched penstock is 3.2m. The maximum water level for the dam is 767.5masl. The installation elevation of turbine that is the elevation of steel liner center in the lower part is 645.0masl. The discharge of single unit is 51.22 m³/sec, that is, when in full load, the discharge of the straight penstock is 153.66m³/sec.

In order to minimize the head loss, the hydraulics conditions of two trifurcation types (spherical type and shell type) are compared. Because of the significant head losses are suspected to be increased in the water flows through trifurcation.

In general, due to the sudden change at the joint point of straight penstock, branched penstock and the spherical trifurcation, the flow condition is bad and the head loss is large. The water flow is expected to be smooth and head loss will be relatively small through the shell type trifurcation employing gradual taper penstock. From the hydraulic conditions aspect, the shell type trifurcation with deflecting plates is chosen as shown in Fig. 1 and Fig. 7.

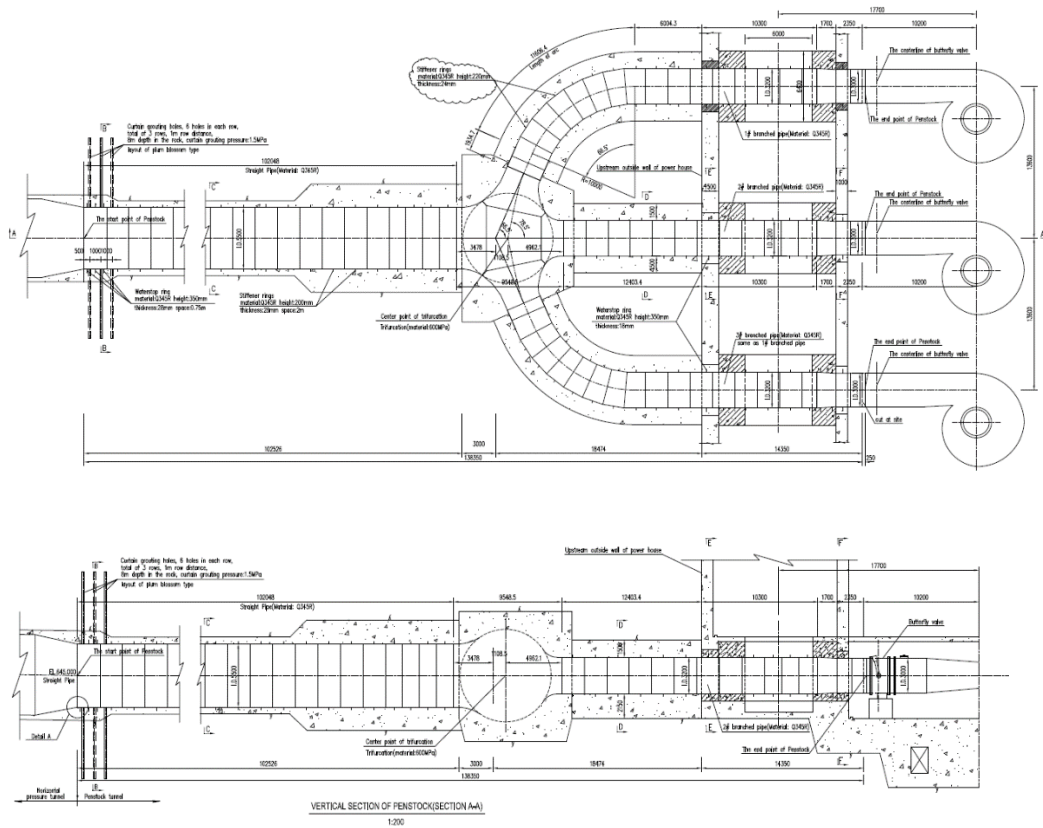


Fig. 1
Installation Condition of Penstock and Trifurcation

2. OCCURRENCE OF POWER SWING

2.1. OCCURRENCE OF POWER SWING

The active power is shown in Fig. 2 below. It can be seen that with increasing power output, severe power oscillations occur especially at the conditions of three units' simultaneous full load operation.

The size of oscillation did not meet the IEC 60308 standard, and for this reason, the power output test failed during the commissioning test and substantial completion of the project was not achieved on time and got delayed several times under this situation.

According to the IEC standard, the acceptable power swings on a hydro generation unit should not be more than 5%(peak to peak) of the rated power, but, the measured power swings on two of the three units in the Patrind plant were approximately around 20%.

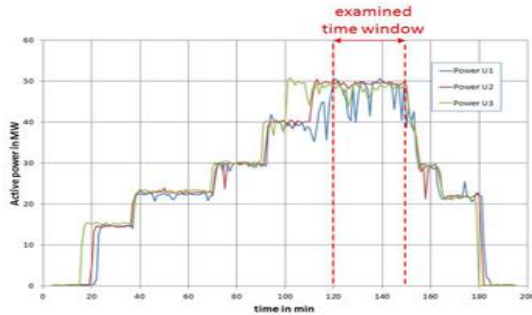


Fig. 2
Active power output

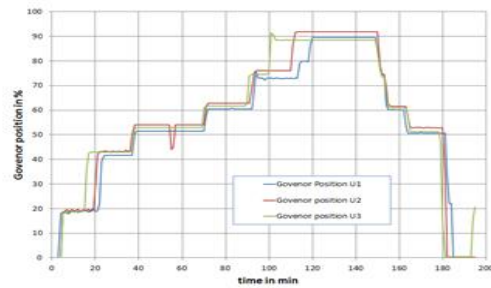


Fig. 3
Governor position

2.2. CAUSE ANALYSIS OF POWER SWING

In Fig.3 above, the corresponding governor position is shown. It can be clearly seen that the governor position shows no oscillation. Consequently, the power oscillations are not expected to be caused by an insufficient control algorithm or by the governor's instabilities.

Since the severe power oscillations occur at high loads, we concentrate our examination on the time region between 120 minutes and 150 minutes of the measured data. In Fig.4 below, the governor position is plotted again but only in the examined time region. Here again, it can be observed that the governor position is nearly constant and cannot be the reason for the oscillations.

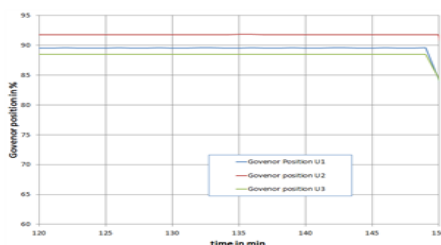


Fig. 4: Governor position in the examined time region

Fig. 4
Governor position

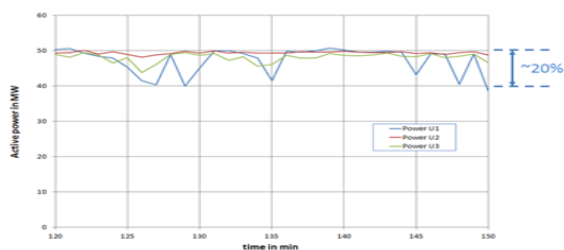


Fig. 5: Active power output of the three units in the examined time region

Fig. 5
Active power output of three units in the examined time region

In Fig.5 above, the active power is shown for the examined time region. It can be seen that the power fluctuations of unit 1 are higher than those of unit 3. Unit 2 shows nearly constant power output. The maximum power changes are approximately 10 MW, which is approximately 20% of the output.

Assuming that by relations of output variation with head variation according to hydraulic similarity;

$$N \propto H \cdot Q = H^{3/2} \quad [1]$$

{N : Active power(MW), H : Head(m), Q : Discharge(CM/s)}

According to the above formula, 12% of pressure variation makes 17.4% of power variation. Referring to Fig. 6 below, there are some gaps between measured power variation (20%) and calculated power variation (17.4%).

The reason for the gap is the inaccuracy of the pressure data, which was measured at a certain cross section having unsteady water flows due to the vortices, so that the measured pressure is not representing the real pressure at the certain cross section. Anyway, we can verify, there is a strong relation between power variation and head variation.

It can be found that the power oscillations are caused by the pressure drop. This pressure drop is caused by the unsteady vortices in the trifurcations. When a vortex from the trifurcation enters one of the penstocks (left or right), the head losses at the penstock inlet significantly increase because of the swirl component. It could be observed from the measurement data that the dominant reason for the power oscillations is the pressure drop in penstock and consequently the reduction of pressure in the spiral case and turbine leading to critical velocity of 4 m/sec (approx.). Therefore, it seems obvious that the unsteady water flow, vortices in the trifurcation and the critical velocity of around 4 m/sec are causing the power oscillations and not the other factors such as the governor or unsteady water flow through the draft tube and tailrace.

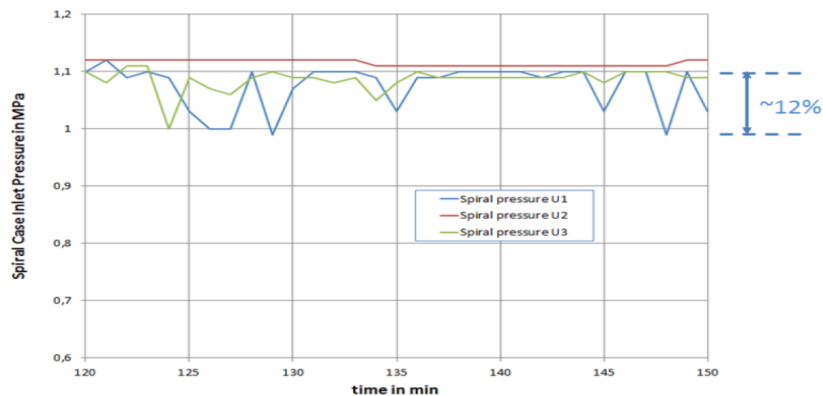


Fig. 6
Pressure at the spiral case inlet in the examined time region

To minimize the head losses and vortices through the trifurcation, the shell type trifurcation with deflection plates is chosen as shown in Fig. 7 below. Despite of this consideration, there is still a possibility of occurring unsteady water flow because of the sudden change at the joint point of straight penstock, branched penstocks and the trifurcation.

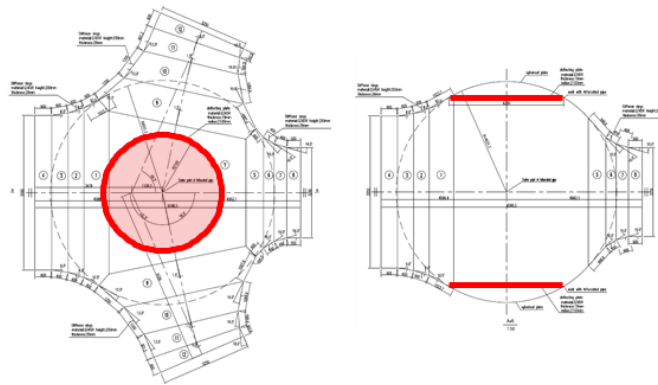


Fig. 7
Shape of previous trifurcation

After examining the data in detail, the power oscillations having a certain regular period were detected in unit 1 and unit 3 in the Patrind plant. We can estimate that the period of power oscillations is determined by the velocity of water passing the penstock and the length from the trifurcation to the spiral case.

The discharge through the branched penstock is reduced with growing vortices and the velocity passing through the trifurcation is also decreased. When the growth of vortices is culminated, the power output drops most. The next moment the size of vortices is gradually reduced in proportion to the decreasing rate of velocity.

When the vortices are almost disappeared, the velocity and power output get back to the normal status and the next moment creation of vortices kicks and grow to maximum. This process is repeated and continuous. To the contrary, the other sides of the branched penstock faced the reverse process at the same time means if vortices are created in one side branch penstock the other side branch behaves normal.

It is obvious that the discharge varies alternatively between branched penstocks of unit 1 and unit 3. Low discharge corresponds with the location of the branched penstock having large vortices. If the vortices are located in the other side of the branched penstock, the discharge is higher. The discharge in the middle branched penstock only shows much smaller oscillations.

3. METHOD OF MODIFYING

It is not possible to replace readily the trifurcation with modified trifurcation because the trifurcation is embedded in the deep underground and covered with thick steel-concrete.

The only one solution is to modify the inner side shape of the trifurcation and improve the water flow conditions as shown in Fig. 8. For more stable water flow distribution, it is planned to install the enlarged deflection plates linearly connecting and covering the inner space of trifurcation between the main penstock and the branched penstocks.

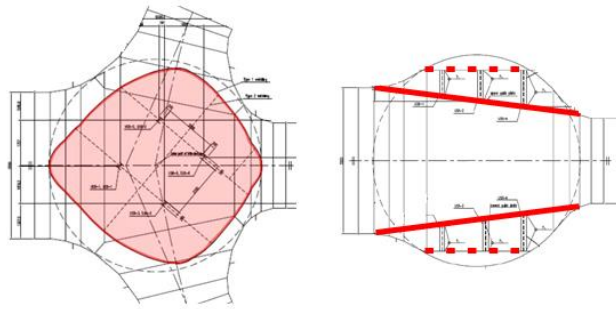


Fig. 8
Shape of modified trifurcation

4. COMPARING THE BEFORE AND AFTER MODIFYING THROUGH THE SIMULATION

4.1. SIMULATION CONDITIONS

For the simulation, a computational grid of approximately four million grid nodes was applied for a numerical model. The grid was refined towards the wall in order to satisfy that the relative wall distance y^+ of the nearest cell is in the range between 10 and 300, which has to be satisfied for an accurate prediction. The distribution of the y^+ -value is shown in Fig. 9 below.

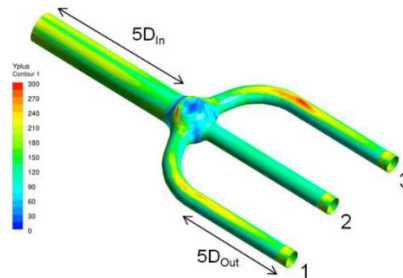


Fig. 9
Distribution of the y^+ -value on the geometry

The investigated load cases are shown in Table 1 below. Since the geometry is completely symmetric, it was not necessary to simulate all combinations, so we concentrated on the operation of unit 1.

Table 1
Investigated load cases

OP	Penstock 1(Side)	Penstock 2(Middle)	Penstock 3(Side)
1	100%	100%	100%
2	100%	-	-
3	100%	100%	-
4	100%	-	100%

Because in the previous investigation of the measurements it was found that the reason for the oscillations is the pressure drop, the variation of the total pressure between inlet and outlet is examined. This is done for different load cases.

4.2. LOAD CASE 1

This load case corresponds to the measurement data. In Fig. 10 below, the total pressure differences are shown.

For the reference geometry in the left and right penstock, oscillations of pressure differences of approximately 70 kPa can be observed. This corresponds quite well to the value of measurements even when the amplitude in the simulation is smaller. This can be explained because in strong swirling water flows, the simulation usually under-predicts the swirl intensity.

As a consequence, the losses caused by the swirl component are under-predicted as well. However, it is obvious that the original geometry pressure vibrations exist, which would lead to power oscillations.

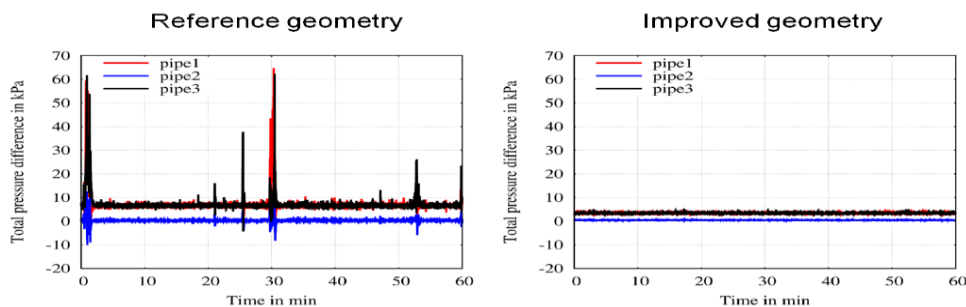


Fig. 10
Total pressure difference between inlet and outlet cross-sections, load case 1

In Fig. 11 below, the vortex behavior in the trifurcation for different time steps can be plotted. It can be seen that the vortex structures and intensities are unsteady and lead to the oscillations. Also, it can be observed that in the middle penstock, there is little vortex. Therefore, unit 2 in the middle shows no power oscillations.

Looking at the right hand side of Fig. 11 below (the improved geometry), it can be observed that pressure oscillations no longer occur. The pressure shows a smooth behavior and no power oscillations would be expected.

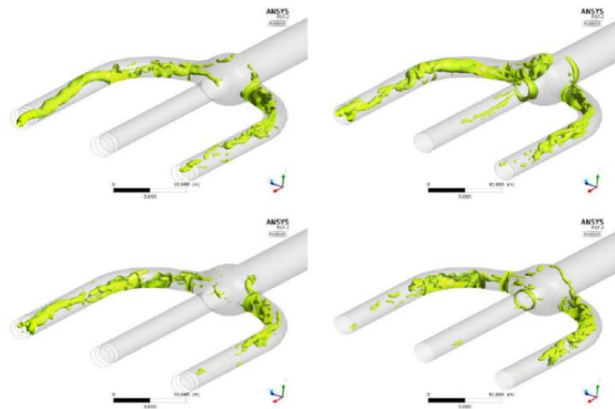


Fig. 11
Vortex structures for different time steps, load case 1

4.3. LOAD CASE 2

When operating only unit 1 there are also pressure oscillations with the original geometry as shown in Fig. 12 below. However, the amplitudes are significantly smaller (less than 20% of the oscillations in load case 1). The installation of deflection plates significantly reduces these pressure oscillations and are assessed to be tolerable.

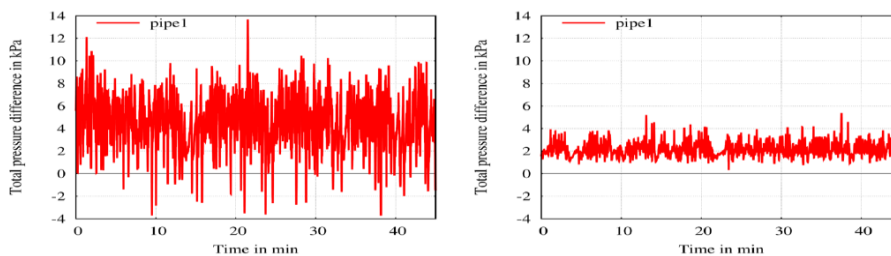


Fig. 12
Total pressure difference between inlet and outlet cross-sections, load case 2

4.4. LOAD CASE 3

The same applies for the operation of the middle unit and a side unit. Here also pressure oscillations occur for the existing geometry as shown in Fig. 13 below. When installing the deflection plates, pressure oscillations no longer occur.

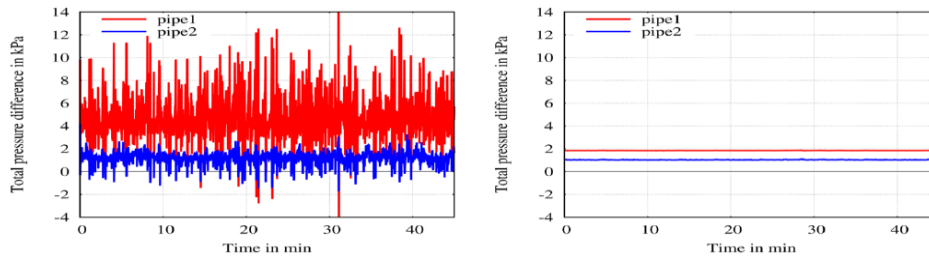


Fig. 13
Total pressure difference between inlet and outlet cross-sections, load case 3

4.5. LOAD CASE 4

When both side units are in operation, severe oscillations reoccur. The amplitudes are approximately half of those in load case 1 as shown in Fig. 14 below. However, the installation of deflection plates cures the problem and no further oscillations occur.

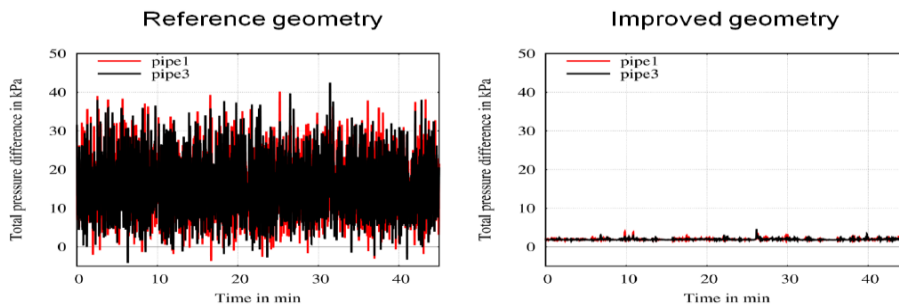


Fig. 14
Total pressure difference between inlet and outlet cross-sections, load case 4

4.6. THE RESULTS OF NUMERICAL ANALYSIS

The analyses of the measurement data and the numerical simulation of the existing geometry clearly show that the power oscillations are caused by the

trifurcation. The installation of enlarged deflection plates leads to a significant reduction of the oscillations for the investigated operation conditions.

With the modified design of the trifurcation, the power plant is expected to operate without oscillation problems that may be caused by the trifurcation without modification.

5. CONDUCTING MODIFYING WORKS

For more stable water flow distribution, enlarged deflection plates are installed at the top and bottom of trifurcation. ASTM A537 steel plate (22mm in thickness) is selected for the deflection plate and it is installed from the main penstock to each branched penstocks at the top and bottom areas.

To keep the structural reliability, each deflection plate has four supports which are selected with H-beam (200mm x 200mm). The deflection plate, except for 300mm edge, has holes for the water path, it is drilled each 200mm in length.

To improve water flow distribution at the trifurcation, it is planned to restrict the water path through deflection plates at the top and bottom of trifurcation. However, to avoid the reduction of trifurcation air volume, the deflection plate has enough holes to fill with water.

For the sake of material transportation works to the inside of trifurcation, the deflection plate is divided into suitable size of 7 pieces, considering the diameter of branched penstocks and the narrow gap of extension-joint of main inlet valve as shown in Fig. 16 and Fig. 17 below.

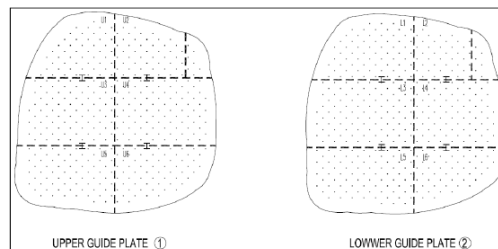


Fig. 16
Drawings of deflection plate



Fig. 17
Photographs of installing deflection plate

6. POWER OSCILLATION AFTER MODIFYING THE TRIFURCATION

The size of power oscillations is smaller than the older and meet the IEC standard such as shown in Fig. 18 below after completing remedial works.

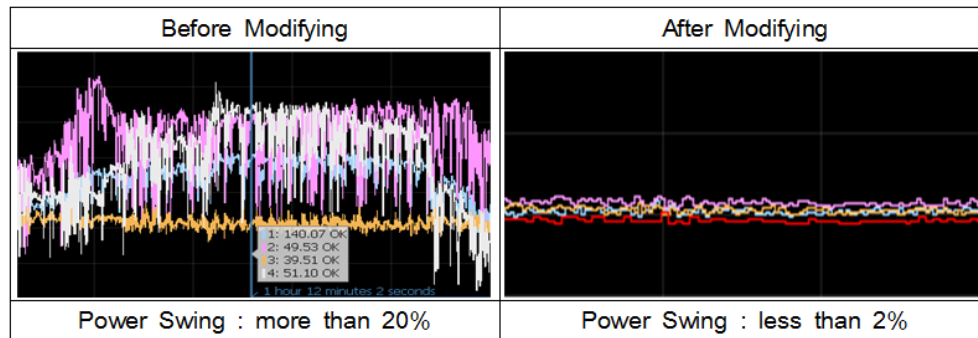


Fig. 18
Comparison of power oscillation after modifying

7. CONCLUSION

Except for the case of very slow velocity of water flow, sudden expansion and reduction through the water way should be removed, especially in the trifurcation.

Where there are some uncertainties about water flow conditions, the hydraulic model test should be conducted in order to get an optimized design and mitigate the risks from uncertain hydraulic conditions.

REFERENCES

- [1] IEC 60308, Hydraulic Turbines –Testing of Control System, 2005.
- [2] MIROSLAV NECHLEBA, Hydraulic Turbines, 1957.
- [3] ALBERT RUPRECHT, Very Large Eddy Simulation for the Prediction of Unsteady Vortex Motion, January 2004.

COMMISSION INTERNATIONALE DES GRANDS BARRAGES

VINGT-SIXIÈME CONGRÈS DES GRANDS BARRAGES
Autriche, juillet 2018

DOI 10.3217/978-3-85125-620-8-192



This work licensed under a Creative Commons Attribution 4.0 International License. <https://creativecommons.org/licenses/by-nc-nd/4.0/>

**HOLLOW CONE VALVE (HCV) IR. H. DJUANDA DAM AND MURI INDONESIA
RECORD**

Yudha MEDIAWAN

KEPALA BALAI BESAR WILAYAH SUNGAI CITARUM

INDONESIA

Angga PRAWIRAKUSUMA, ST. MT

PPK OP III SDA BBWS CITARUM

INDONESIA

Ir. Joko MULYONO, ME

JAFUNG TEKNIK PENGAIRAN AHLI MADYA, AHLI TEKNIK BENDUNGAN
BESAR – UTAMA

INDONESIA

Dwi Aryani SEMADI, ST. SP1

KABID PJSA BBWS CIMANUK CISANGGARUNG, AHLI TEKNIK BENDUNGAN
BESAR – MADYA

INDONESIA

HOLLOW CONE VALVE (HCV) IR. H. DJUANDA DAM AND MURI INDONESIA RECORD

Yudha Mediawan¹⁾, Angga Prawirakusuma, ST. MT²⁾, Ir. Joko Mulyono, ME³⁾,
Dwi Aryani Semadi, ST. SP1⁴⁾

¹⁾ Kepala Balai Besar Wilayah Sungai Citarum

²⁾ PPK OP III SDA BBWS Citarum

³⁾ Jafung Teknik Pengairan Ahli Madya, Ahli Teknik Bendungan Besar – Utama

⁴⁾ Kabid PJSA BBWS Cimanuk Cisanggarung, Ahli Teknik Bendungan Besar –
Madya

ABSTRACT

Construction of Ir. H. Djuanda Dam or better known as Jatiluhur dam which was implemented from 1957 until 1967, this construction project called "Jatiluhur Multipurpose Project" and after its completion was named as Juanda Dam and Power Plant, after finished the name was changed to Juanda Dam and Power Plant because remembering the role of Prime Indonesia's last minister that is Ir. H. Djuanda. Basically Jatiluhur / Juanda Dam construction project is designed to irrigate tens of thousands hectares farmland and fisheries, electricity for Java - Bali lighting, main supplier of water for industry, raw water supply for capital city and tourism. Currently Jatiluhur Dam/Juanda age have reach 50 years, pollution and sedimentation become a worrying problem so that in 2012 there is great inspection by ACE Pakistan JV consultant through Dam Operation Improvement Safety Project (DOISP) obtained description of dam condition and facility building has decreased function as in mechanical equipment that is hollow cone valve. Referring to Decree of Public Works Minister Number 315/KPTS/M/2011 about Authority Delegation to General Director of Water Resources to regulate operation of Saguling Dam, Cirata Dam and Jatiluhur Dam which main task is monitoring and evaluation cascade dam by Balai Besar Wilayah Sungai Citarum through Operation and Maintenance of Citarum Water Resources for doing repair/replacement the mechanical equipment above.

Replacement of two hollow cone valve diameters of 3.85 m with material (stainless steel) meets the same standard as Z5 CN 17-04 M in accordance with asbuilt drawing on previous data. The making of this HCV has been awarded the Indonesian Record Museum (MURI) which is work of nation's children, as well as manufacture and installation of replacements process has been written simply.

There are several problems in the implementation that can be solved there are:

1. HCV manufacturing and auxiliary equipment (cantilever) are new in Indonesia both from size and mounting method with mathematical models only for model test.

2. HCV mobilization from Gresik factory to location is doing by a special trailer that refers the rules of freight traffic to reservoir, from that location using phonton for morning glory and cantilever tool must be installed.
3. When disassembling and installation operations with condition of water surface elevation should be maintained for reservoir operations.

KEYWORDS

HCV, Manufacturing, MURI Record

1. INTRODUCTION

1.1. BACKGROUND

The construction of Jatiluhur Dam (Ir H. Djuanda) was built from 1957 to 1967 by Compagnie française d'entreprise, French contractor. This construction project named "Jatiluhur Multipurpose Project", after finished the name was changed to Juanda Dam and Power Plant because remembering the role of Prime Indonesia's last minister that is Ir. H. Djuanda. Basically Jatiluhur / Juanda Dam construction project is designed to irrigate tens of thousands hectares farmland and fisheries, electricity for Java - Bali lighting, main supplier of water for industry, raw water supply for capital city, tourism, and equally important as flood control for downstream Citarum area.

Currently Jatiluhur Dam/Juanda age have reach 50 years, pollution and sedimentation become a worrying problem so that in 2012 there is great inspection by ACE Pakistan JV consultant through Dam Operation Improvement Safety Project (DOISP) obtained description of dam condition and facility building has decreased function as in mechanical equipment that is hollow cone valve. Referring to Decree of Public Works Minister Number 315/KPTS/M/2011 about Authority Delegation to General Director of Water Resources to regulate operation of Saguling Dam, Cirata Dam and Jatiluhur Dam which main task is monitoring and evaluation cascade dam by Balai Besar Wilayah Sungai Citarum through Operation and Maintenance of Citarum Water Resources for doing repair/replacement the mechanical equipment above.

1.2. PURPOSE AND OBJECTIVES

This HCV replacement is one of main tasks of BBWS Citarum, and with this paper as material information in maintenance implementation of mechanical replacement and electrical equipment hollow cone valve on Jatiluhur/Juanda Dam. The purpose of this paper as one example reference for other dams in replacement maintenance of mechanical and electrical equipment hollow cone valve.

1.3. GENERAL DESCRIPTION

Jatiluhur Dam (Ir. H. Juanda) is located approximately 100 km southeast of Jakarta, which can be reached through Jakarta-Cikampek toll road and Cipularang toll road (Cikampek-Jatiluhur), and 60 km northwest of Bandung, which can be reached by road toll Cipularang (Bandung-Jatiluhur). From Purwakarta City about 9 km west. Based on geographical coordinates, main position of Jatiluhur Dam is 6° 31' South Latitude and 107° 23' East Longitude. This dam began built in 1957 marked with laying the first stone of development by first Indonesia President that is Ir. Soekarno.

Jatiluhur Dam is the largest dam in Indonesia, damming Citarum River flow in Jatiluhur District - Purwakarta District - West Java Province, forming a reservoir with an area of ±8300 ha and around 150 km of reservoir at normal water surface elevation ±107 m above sea level (mdpl). Total area of Jatiluhur Dam catch is 4,500 km². While catch area large that direct to dam after built Saguling and Cirata Dam in upstream reaches 380 km² which is 8% from catch area total. The catch area (upper Citarum) covers Bandung district, West Bandung district, Bandung city, Cimahi city, Cianjur district and Purwakarta district. Originally designed to have a capacity of 3 billion m³, but currently only 2,685 billion m³ (bathymetry in 2013) this reduction is due to sedimentation. However after built Saguling and Cirata Dam in Jatiluhur upstream area, sedimentation rate is decreasing. Jatiluhur Dam is a multipurpose dam, with 6 turbines with capacity 248 m³/s and power plant with capacity 187 MW, irrigation water supply for ±240.000 ha rice field, capital city raw water, fishery cultivation and flood control at downstream of Citarum river which managed by Perum Jasa Tirta II.

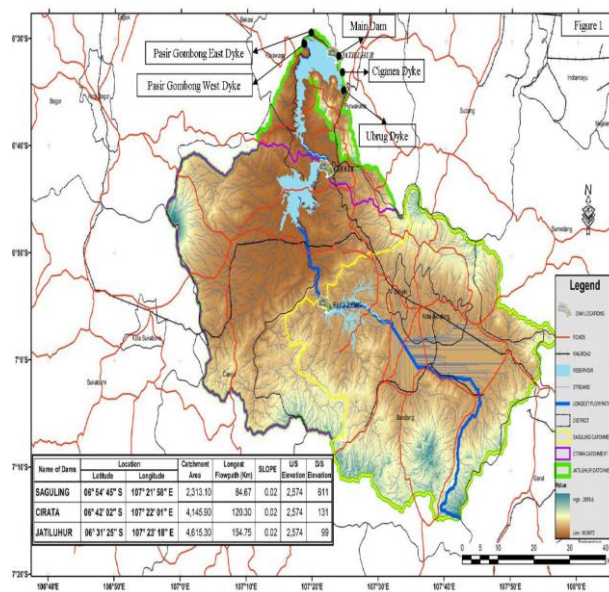


Figure 1.1 Cascade Dam of Saguling, Cirata, and Jatiluhur

1.4. ACTIVITIES

Activities that implemented in this writing papers by:

- Primary and secondary data collecting
Primary data collecting is doing by field survey to get accurate data while secondary data by collecting existing and related literature.
- Doing discussion and problem solving
The discussion is doing by reviewing existing data of existing condition that get from survey and literature then expected conditions. While problem solving is doing by adjusting implementation plan above.
- Conclusion and recommendation
Make conclusion from paper that have been made and recommend which related or needed.

2. EXISTING CONDITIONS AND PROBLEMS

2.1. EXISTING CONDITIONS

Mechanical equipment existing condition in Jatiluhur Dam at this time has decreased function, hollowcone valve only optimal at opening position 20%.

Hollowcone equipment is under the morning glory tower which is a tower structure made from concrete that has an outside diameter of 90 m and height 110 m. This tower function as main valve (spillway threshold elevation ± 107.00 m) and hollow cone valve is located on el. 49.00 m. Morning Glory has 14 windows without a door (ungated spillway) with an overall length of 151.1 m. Abundant capacity is $3,000 \text{ m}^3 / \text{s}$ at water surface elevation of 111.6 m.

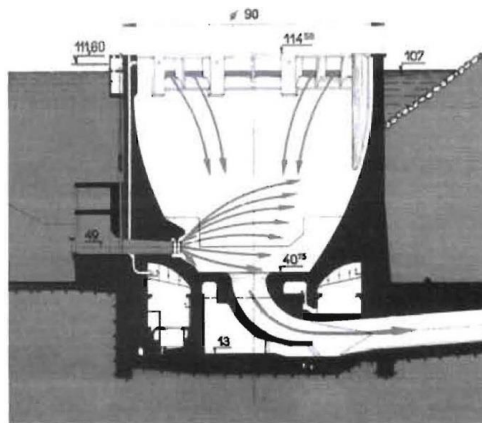


Figure 2.1 Cutting of Morning Glory Tower and Hollow Cone Valve

2.2. CURRENT PROBLEMS

Based on results from a large inspection in 2014, hollow cone valve left there is a leak due to stoplog is not able to close perfectly. As well as the unbalanced of openings up to 100%. The following photos show the current hollow cone valve and rail condition.

3. THE PROBLEM ISSUES

3.1. PROBLEM SOLVING

3.1.1. *Technically*

With the mechanical equipment condition of Jatiluhur dam which has decreased function on two hollowcone and two stoplog so it needs to replace and repair. For hollowcone valve will be total replacement while stoplog only on rubber seal. In the implementation of hollowcone valve replacement, problems

will arise because in Indonesia never implemented Hollowcone manufacture and replacement with a large enough size (3850 mm) with technical specification material in accordance with the original so that most of materials imported from abroad (manufacture time 7 months).

HCV delivery requires a review of traffic and possible road conditions by using trailers to climbs then derivatives and bridges to location of dam puddles. Hollowcone installation implementation requires special tool such as cantilever which doing by own fabrication (manufacture 3 months) mounted on top of morning glory, so it requires special calculation and skill at dam water surface in operating condition as needed. Disassembly and installation Hollowcone valve takes four months. Before the replacement of hollowcone must repairs stoplog so that hollowcone replacement implementation is not disturbed by stoplog rubberseal leak. Replacement rubber seal takes three months.

Rules of works this activity are limited by reservoir water surface elevation, which the unloading implementation is optimized at elevations below ± 105.50 mdpl.

3.1.2. Administration

Funding for replacement of Hollowcone valve and stoplog is funded by loan from World Bank and APBN companion with activity value 43.230.000.000 rupiah. The implementation of the activity is required to be completed before June 30th, 2017.

4. UNLOADING AND INSTALLATION HCV PROCESS AT IR. H DJUANDA DAM

4.1. MANUFACTURING PROCESS

In November 2016, HCV metal structures construction and installation support tools such as balanced cantilever, custom pontoon HCV, and others are ready delivered to Jatiluhur Dam, where the manufacturing and testing process is doing at PT. Barata Tegal. Workshop distance from Tegal to Jatiluhur Reservoir, Purwakarta District is ± 250 km by road, or approximately 2 days by truck, due to steering effective time at night. The technical data of hollow cone valve diameter is 3850 mm, with material ASTM A240 Gr. 2205, is planned to burdened with pressure of 15 Bar. In mobilizing HCV to site using low bad trailer with packing size of 5070 mm long and 5020 mm wide and 4120 mm height, if height of

packing is added with tub height of transport vehicle to road 600 mm it becomes 4720 mm so it is still safe against high net between road and bridges girder concrete along toll roads having an average of 4900 mm.

4.2. UNLOADING AND INSTALLATION

4.2.1. *Supporting Equipment*

In November 2016 until beginning of February 2017 water surface elevation above 105.50 and even runoff, which means that contractor/implementer does not get discharge recommendation permit due to work safety support at bottom. As a result of limpas water in morning glory there are some workbench components process of disassembly and installation hollow cone valve lost carrying water flow. Some missing components are immediately followed up by creating a replacement. The material is unloaded from the freight at logistics warehouse location and gradually shipped to morning glory gradually due to load for passing main dam should not exceed 3 tons.

In February 11th, 2011 Jatiluhur water surface elevation is still above the elevation 105.5 but if see the trend of reservoir water surface elevation is decreasing plus reference from Prakirawan BMKG West Java through portal <http://www.bmkg.go.id> weather for upstream area which precipitate reservoir tends to narrow with frequency decreasing so that decided as beginning of discharge old HCV followed by installation new HCV. Beginning installation of work aids discharge and installation HCV begins with installation of safety net that functioned as last safeguard in case of work accidents and material tools that fall not directly into drainage hole.

The next installation work tool is installation of lifting table components which lost due to washed away by water runoff. The next work process is checking the wheels of trolley wheels and coloumn wheels lifting whether the bearings on the wheels are still functioning properly.

Another work tool is lifting column which function to lifting and lowering old and new HCV from moving table to lifting table then vice versa.



Figure 4.6 Installation Lifting Table Component

Working tools for HCV lift overhaul using balanced cantilever. The tool was designed by LAPI ITB then tested on September 8th, 2015 at PT. Barata Tegal and test site on February 20th, 2017 with conclusion that this tool can lifting and lowering HCV.

The next step is preparation path road for vehicles and destruction heavy equipment at dock/port. Preparation that has been done by adding *sirtu* (sand stone) on the entrance to dock (entrance portal) and dredging of pontoon area for pulled over and stone pile addition in heavy equipment position (car crane) which lifting HCV.

4.2.2. Unloading

Process of diasassemble old HCV begins with release 84 pieces flange bolt then right and left arm drive bolts, then the trolley is positioned just below the HCV and tied with the trolley by using the sling.

The detached HCV and above trolley move out just below the lifting table and lifting column.

Lifting process the old HCV from trolley upwards using a 20 ton chain block of 2 pieces which located at lifting column, was manually lifted with human power.

Balanced cantilever is prepared for lifting old HCV by lowering binding hook on hoist and tied to old HCV. Lifting process approximately 2 hours get to morning glory side because lifting equipment speed is made at low speed to HCV that weighs nearly 35 tons in process of lifting is not rocking.

After old HCV on morning glory side and shifts to outside then the pontoon that has been prepared with holder/saddle near to morning glory just

beneath balanced cantilever arm and continued lowering process of old HCV which placed on pontoon saddle.

Old HCV on the pontoon are tied with steel string sling and chain block to avoid rocking then immediately sent to blue dock/harbor with assistance of 2 tug boats.

Heavy equipment (capacity of crane car is 100 ton) is prepared to disassemble/lift old HCV from pontoon and lift new HCV. Furthermore, new HCV is delivered to morning glory.

4.2.3. Installation

New HCV removal process from pontoon and drop to baseline morning glory, the sequence is almost same as old HCV lifting process but reversed sequence. It starts from new HCV lifting from outside of morning glory and lowered down using balanced cantilever.

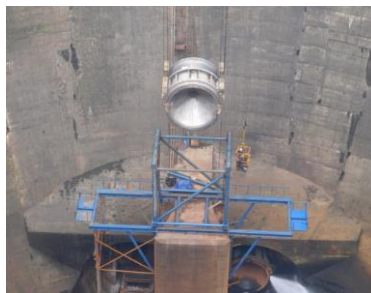


Figure 4.15 New HCG Lifting and Lowering Process

Before new HCV installation, first doing the rail replacement and brushing flange existing.



Figure 4.16 Replacing Process of Rail and Brushing Flange Existing

After the work of rail replacement and brushing flange then continued by lowering new HCV using chain block and shifted trolley into approaching flange. Flange bolts installation is doing with a firming load of ± 610 kg for each bolt by looking at digital scales.



Figure 4.17 Bolt Installation Process with Specified Load

5. COMMISSIONING

5.1. COMMISSIONING TEST

After Hollow Cone Valve is mounted, continuously with disassembly of work desk tool, safety net and doing the Commissioning Test on June 12th, 2017.

Commissioning test is a part of final stage to try hydromechanical and mechanical reliability of Hollow cone valve, in implementation of this test is divided into two parts. Dry test is a test of HCV motion function without any load with stop log concrete (check name to pjt) in closed position. This test only checks the HCV motion when open and close 5% increments start from 0 until 100% and 100% to 0 position. Load Test is a test such as dry test but with hydrostatic load which stop log concrete in opened position so that causing burden to mounted HCV.



Figure 5.1 Commissioning Test

Testing of HCV load test reliability that has been installed is implemented until 100% aperture, because in order to anticipate the cessation of 6 turbines simultaneously which water drainage for industry and raw water to DKI Jakarta can be disbursed through two HCV each has opening discharge 197 m³/s on reservoir water surface elevation $\pm 105,00$ mdpl.

5.2. COMMISSIONING RESULT

For this test, HCV reliability is tested with the parameters seen from testing time, bolt ampere read, rail condition, etc. which presented in the table:

Table 5.1 Ampere Load Test Measurement Data HCV-1 (Right) and HCV-2 (Left)

<u>Load Test Open 20 %</u>					
No.	HCV	Open	Ampere	Time (Minute)	Information
1.	HCV-1 Right	0 % - 20 %	12,5 A	01. 28. 40	Bolts, rail and wheels are all still safe
2.	HCV-2 Left	0 % - 20 %	12,2 A	01. 30. 40	Bolts, rail and wheels are all still safe
<u>Load Test Open 40 %</u>					
No.	HCV	Open	Ampere	Time (Minute)	Information
1.	HCV-1 Right	0 % - 20 %	11,9 A	01. 29. 96	Bolts, rail and wheels are all still safe
		20 % - 40 %	12,1 A	01. 27. 92	Bolts, rail and wheels are all still safe
2.	HCV-2 Left	0 % - 20 %	12,0 A	01. 27. 96	Bolts, rail and wheels are all still safe
		20 % - 40 %	12,2 A	01. 27. 92	Bolts, rail and wheels are all still safe
<u>Load Test Open 100 %</u>					
No.	HCV	Open	Ampere	Time (Minute)	Information
1.	HCV-1 Right	40 % - 70 %	13,1 A	02. 12. 40	Bolts, rail and wheels are all still safe
		70 % - 100 %	15,1 A	02. 15. 80	Bolts, rail and wheels are all still safe
2.	HCV-2 Left	40 % - 70 %	12,6 A	02. 12. 30	Bolts, rail and wheels are all still safe
		70 % - 100 %	14,4 A	02. 13. 70	Bolts, rail and wheels are all still safe
<u>Load Test Close 100 % - 0 %</u>					
No.	HCV	Open	Ampere	Time (Minute)	Information
1.	HCV-1 Right	100 % - 70 %	14,5 A	02. 14. 60	Bolts, rail and wheels are all still safe
		70 % - 40 %	12,7 A	02. 13. 10	Bolts, rail and wheels are all still safe
		40 % - 0 %	12,8 A	01. 56. 20	Bolts, rail and wheels are all still safe
2.	HCV-2 Left	100 % - 70 %	12,9 A	02. 13. 90	Bolts, rail and wheels are all still safe
		70 % - 40 %	12,3 A	02. 12. 30	Bolts, rail and wheels are all still safe
		40 % - 0 %	12,6 A	02. 57. 80	Bolts, rail and wheels are all still safe

5.3. OLD HOLLOW CONE VALVE MONUMENT

Old HCV are moved and placed at designated place near PJT II archives warehouse area. This HCV is temporarily stored near the building of hydropower plant in Jatiluhur, HCV is planned to be a monument in Jatiluhur dam main area. For this HCV get MURI record from Museum Muri Records, category largest HCV with diameter 3850 mm.



Figure 5.2 Old HCV

6. CONCLUSION AND RECOMMENDATION

6.1. CONCLUSION

- Hollowcone valve (HCV) mechanical replacement at Jatiluhur / Juanda Dam requires special skills to be initiated during HCV manufacture at the plant up to the installation in the field (Jatiluhur Dam / Juanda). Hollowcone valve Jatiluhur / Juanda Dam is the largest HCV in Indonesia even in the World, so MURI Indonesia record museum awarded the certificate with the largest valve category (diameter 3850 mm)
- All activities ranging from manufacturing process, transportation, demolition, HCV installation, and Dam history Ir. H. Djuanda, fully documented recorded and popularized into the book "SETENGAH ABAD HCV BENDUNGAN IR. H. DJUANDA" compiled and written by Joko Mulyono and Chainur Fauzi
- The success of this HCV replacement is inseparable due to good coordination between Balai Besar Wilayah Sungai Citarum (BBWS CITARUM), Pembangkit Jawa Bali (PJB) Saguling Dam, Indonesia Power (IP) Cirata

Dam, PJT II Juanda Dam and BMKG. This HCV installation activity is limited when the water elevation of reservoir is below 105.5 mdpl according to the agreement in Tim Koordinasi Pengelola Bendungan Kaskade Citarum (TKPBKC).

6.2. RECOMMENDATION

Implementation of Operation and Maintenance must be as much as possible with the implementation of development, since continuous of Operation and Maintenance can make development outcomes more guaranteed useful life and function. Therefore continuity according to Operation and Maintenance manual should be implemented.

REFERENCES

1. Pekerjaan Replacement Hydromechanical HCV CT-CW 02, 2014
2. Inspeksi Besar Special Study Ir. H. Djuanda, 2012
3. Bendungan Besar Upaya Mensejahterakan Rakyat, Direktorat Jenderal Sumber Daya Air
4. Departemen Permukiman and Prasarana Wilayah, Agustus 2004
5. Dams of Indonesia, A Journey toward National Water Security, Directorate General of Water Resouces Ministry of Public Works, June 2014
6. Setengah Abad HCV Bendungan Ir. H. Djuanda, Joko Mulyono, Chainur Fauzi, 2017

COMMISSION INTERNATIONALE DES GRANDS BARRAGES

VINGT-SIXIÈME CONGRÈS DES GRANDS BARRAGES
Autriche, juillet 2018

DOI 10.3217/978-3-85125-620-8-193



This work licensed under a Creative Commons Attribution 4.0 International License. <https://creativecommons.org/licenses/by-nc-nd/4.0/>

**THE GROUTABILITY INVESTIGATION OF PUMICE PACKED BEHIND
TUNNEL LINING SYSTEM**

Ghasem DERA VI

*Head of site supervision of drilling and grouting department on dam and tunnel
design/inspection, MAHABGHOODS CONSULTING ENGINEERING COMPANY*

IRAN

Ali Akbar VAHEDI

*Project manager, designing department on main office,
MAHABGHOODS CONSULTING ENGINEERING COMPANY*

IRAN

Amir HAFEZQURAN

*Engineer site supervision of drilling and grouting department on dam and tunnel
inspection, MAHABGHOODS CONSULTING ENGINEERING COMPANY*

IRAN

COMMISSION INTERNATIONALE
DES GRANDS BARRAGES

VINGT-SIXIÈME CONGRÈS DES
GRANDS BARRAGES
Autriche, juillet 2018

THE GROUTABILITY INVESTIGATION OF PUMICE PACKED BEHIND TUNNEL LINING SYSTEM

GHASEM DERA VI

*Head of site supervision of drilling and grouting department on dam and tunnel
design/inspection, MAHABGHOODS CONSULTING ENGINEERING COMPANY*

ALI AKBAR VAHEDI

*Project manager, designing department on main office,
MAHABGHOODS CONSULTING ENGINEERING COMPANY*

AMIR HAFEZQURAN

*Engineer site supervision of drilling and grouting department on dam and tunnel
inspection, MAHABGHOODS CONSULTING ENGINEERING COMPANY*

IRAN

1. INTRODUCTION

Today's, construction of dam and power plant projects with the aim of electricity generation, flood control and water storage for use in industry, agriculture and drinking is a part of the government's development plans, and in Iran, these plants are being pursued. For instance, one of the projects is a 4 km pressure tunnel under construction in West Azerbaijan province, northwest of IRAN.

The construction of each tunnel always has unique technical geological/engineering problems. On-time solution of such problems is very effective in achieving the schedule of project planning, and it can provide the satisfaction of the client.

Rock mass classification systems developed by international society of rock mechanics to achieve uniformity of rock mass description all around the world. Rock mass classification is a basic communication between the geologists and engineers [1]. The RMR and Q systems are two rock mass classifications most commonly used in rock engineering, which values of each rock mass class relating it to specific engineering problems [2]. These systems provide guidelines for the selection of rock reinforcement for exposed area. The guidelines present shotcrete and lattice girded/Steel Ribs for weak unstable rocks during tunnel excavation [3].

In traditional tunneling methods, over-excavation due to geological conditions and collapse of weak rock area is almost inevitable [4]. In these situations, reinforcing methods should be used, in according to rock mass classification systems, to prevent occurring and/or development of rock collapse [5]. However, empty spaces remain behind the rock reinforcing systems.

Any gaps between tunnel ceiling and reinforcement system can cause unpredictable deformations (such as collapse etc.) of the surrounding rock [6]. Therefore, such gaps should be filled with stiff and solid materials. Contact grouting is a most common practice for backfilling of the gaps [7], [8]. In case of collapsed area, empty spaces behind the reinforcing systems mainly could be filled by desirable material for instance packed pumice pieces in, and then injected by cement grout to get a solid portion between rock and lining [9].

2. DEFINATION OF THE PROBLEMS

The project is a hydroelectric power plant, including of about 4 Km water transfer tunnel. The tunnel is excavated by the traditional method, using excavation machines such as Jack Hammer, Rodheader and sometimes with explosives. Type of the rock along this tunnel is a poorly-grade of metamorphic rocks, often containing meta-sandstone, slate and phyllite, and in some cases schist. During the tunnel excavation, problems such as rock collapse and over-excavation due to the intersection of faults, major joints, crushed zones and particularly wet areas are encountered; several times. If necessary, initial tunnel-supporting systems consist of lattice girded/steel ribs; wire mesh and shotcrete were installed at collapse and over-excavated areas during the excavation phase. Two type of plastic sacks was used for placing of pumice pieces in gaps behind reinforcing systems, as shown in figure 1, type A: flour sacks and type B: onion sacks. After the completion of the tunnel excavation, the final concrete lining was installed.

Now, there are three main questions?

First: is it possible to filling the porosity between sacks and inside pumice pieces? On the other hand, which type of sacks is better to use that has cement grout penetrability?



Type " A "

Type " B "

Figure1
Types of Sacks for Pumice Packing

Second: when is the appropriate moment for contact grouting? Before or after concrete lining was completed?

Third: Is it necessary to revise the contact grout holes' arrangement? which has already designed.

To find the answer of the first question, a simulation phase has been done on the workshop. Answering the second question by selecting of two situations in tunnel. One situation was shotcrete face finished and the other was finished face of lining. The last question was find out after implementation of grouting and according to the check-holes result.

3. SIMULATION OF CONTACT GROUTING

The purpose of this simulation is to investigate the grout penetration in the empty space between the pumice pieces as well as the gap between the sacks. Metal barrels were used to simulate contact grouting. One side of the barrels were cut and two type of pumice sacks placed in and packed by welding. Two valves were installed at the other side of barrels in order to grout injection and air evacuation. Barrels abide for injection was maximum pressure of 1.5 bar. Water Cement ratio of contact grout is 0.8.

Seven days later, grouted portion was hardened, then in laboratory the barrels were rifted carefully and solid portion were taken out to prepare for core drilling. Samples were used to determine the uniaxial compressive strength and control the quality of the grouted solid portion.

The quality of core samples can be seen in figure 3. It shows two different pumice packed types. As it shows the grout has penetrated in both types of packed pumices and the voids between pumice pieces and gaps around the sacks filled by injected cement properly. On the other hand, type of sacks has not affected the grout penetration.

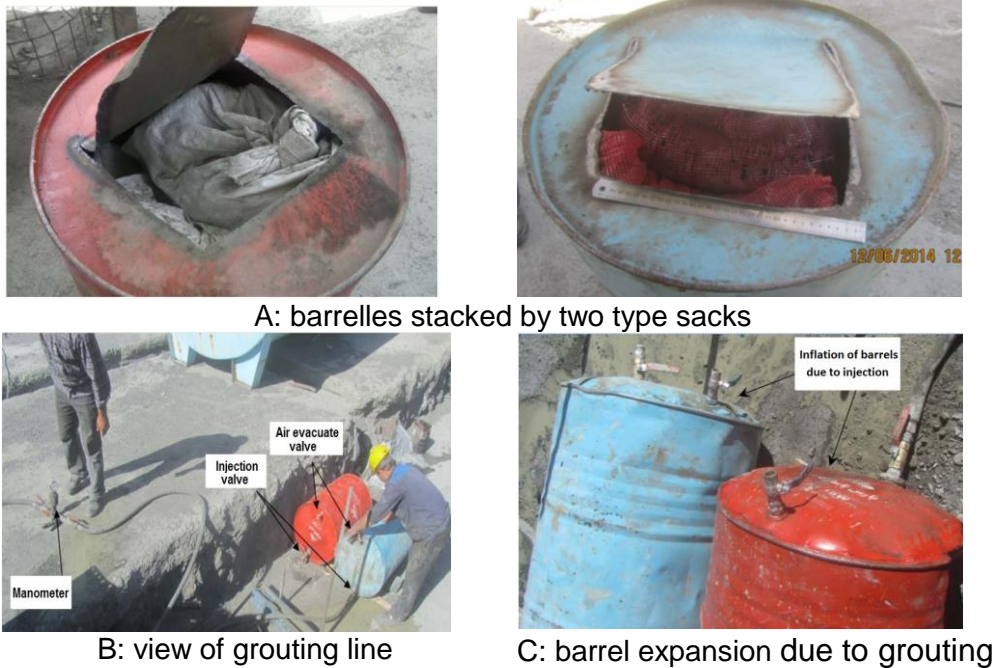


Fig. 2
Sequence of Simulation in Metal Barrels

Cores of both types of packed pumice indicate that solid specimens with no voids or un-cemented pumice pieces. Average of compressive strength 28 days' age were 165 and 151 kg/cm² for onion sacks and flour sacks respectively. As a result, the both pack of sacks get acceptable groutability.



Fig. 3
Left: Core of Onion Sacks, Right: Core of Flour Sacks

4. COMPARE OF CONTACT GROUTING IN PHASE

In order to grouting gaps during tunnel construction, two opinions have proposed. When is the appropriate time for grouting? After initial supporting (lattice grade, shotcrete and wire-mesh) or after final concrete lining?

To answer the above questions, two test panels have selected in tunnel. One panel was located in initial support area (ISA). Second panel was in final lining area (FLA).

4.1 CONTACT GROUTING IN INITIAL SUPPORT AREA

Sequence of initial support system execution in ISA panel including first shotcreting on collapse area rock face, installation of lattice/steel ribs, wire-mesh installation, stacking of pumice sacks and final shotcreting on wire-mesh to cover the area (see figure 4).

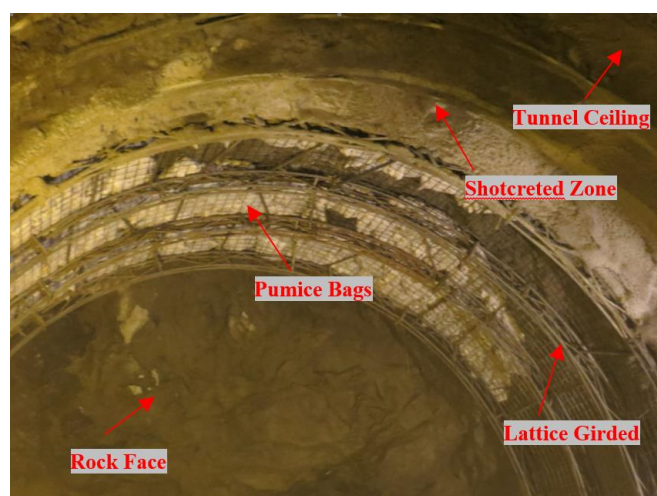


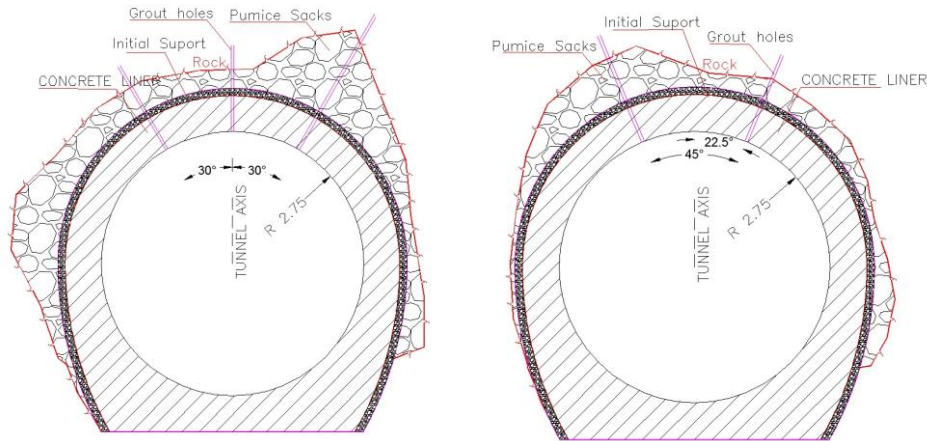
Fig. 4
Inside Tunnel, View of Initial Support System

When the initial support was completed, drilling and grouting activities were carried out. Because of the inadequate strength of the initial support, it was not possible to apply injection pressure greater than two bars. Therefore, it was decided that the grouting activities would be tested in a panel where the final concrete lining was performed in that area.

4.2 CONTACT GROUTING IN FINAL LINING AREA

Based on technical office protocol, it was decided that drilling and grouting activities would be done within the concrete lining area as a comparing panel. The process and consequences of this panel (FLA) will be compare with ISA panel. According to the technical specification, drilling and grouting in FLA panel will be done after final lining installation. Concrete lining were placed whole the tunnel, so it cover the initial supporting system. The grout holes arrangement was carried out according to the design drawings in initial "A" and secondary "B"

series separately (see figure 4). Spacing of A and B series were 3 meters. Pressure for contact grouting in FLA panel increased up to 7 bars due to concrete lining bearing. Water cement ratio of grout is 0.8 by weight.



A: pattern of initial holes B: pattern of secondary holes

Fig. 4
Contact Grout Holes Arrangement

4.3 COMPARING OF ISA AND FLA PANELS GROUTING PROCESS

Although drilling of borehole in ISA panel could be done faster and lower cost also does not delay the project schedule, but due to technical limitations in applying the injection pressure, satisfied results of grout penetration inside the gaps and sacks h not achieved. Inspection of core samples indicate that the grout penetration in the voids is not desirable and the pumice pieces were not consolidated predominantly (see figure 5-a).

In FLA panel, injection pressure up to 7 bars were possible, so the penetration of grout in the voids were acceptable. As a result, injection in the FLA panel were get the pumice pieces and cement parts integrated, and solidified in the cores mostly (figure 5-b).



A: Core sample of ISA panel B: Core sample of FLA panel

Fig. 5
Core Samples from ISA and FLA Panels

Figure 6 shows the results of grouted cement of A and B series for FLA panel. In general, the amount of injected cement in the B series has been significantly reduced compared to the A series, but the B series still shows a peak absorbed cement locally.

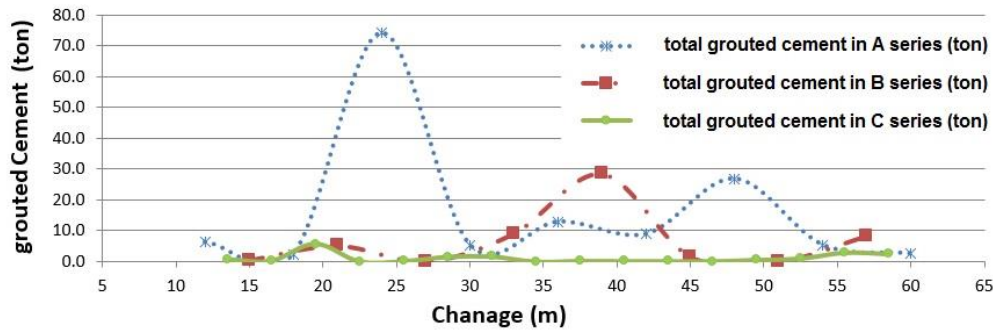


Fig. 6
Grouted Cement in Contact Holes Series

The necessity of implementation the third series “C” was established. C series were placed between A and B series (see figure 6). Cement absorption in C series could be seen in figure 7. Cement grouted in the C series has been extremely reduced compared with A and B series and cement absorbed peak is not seen in this chart.

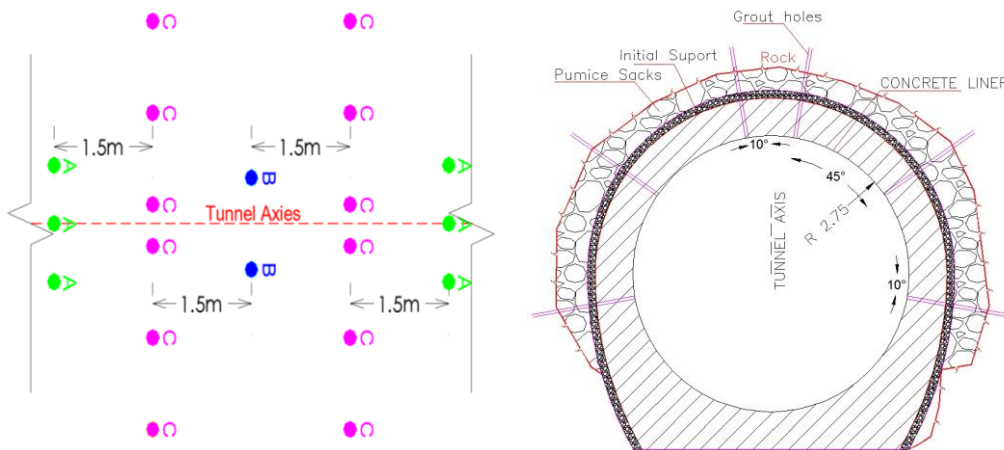


Fig. 5
Left: Plan View of Grout Holes Right: Typical Section of C Series

When the grouting of all three series completed as mentioned above, check-holes were drilled to evaluate the effectiveness of grouting. Therefore, the check-holes indicated the gaps behind final concrete lining, have filled and consolidated with cement firmly (see figure 8).



Fig. 8
Consolidated of Core Sample – Checkhole, FLA Panel

5. REFERENCES

- [1] Singh B, Goel RK. Engineering rock mass classification. Butterworth-Heinemann; 2011.
- [2] Sivakugan N, Shukla SK, Das BM. Rock mechanics: an introduction. Crc Press; 2013.
- [3] Hoek E, Kaiser PK, Bawden WF. Support of underground excavations in hard rock. CRC Press; 2000.
- [4] MAERZ, N. H.; IBARRA, J. A.; FRANKLIN, John Allan. Overbreak and underbreak in underground openings Part 1: measurement using the light sectioning method and digital image processing. Geotechnical & Geological Engineering, 1996, 14.4: 307-323.
- [5] Hoek E, Brown ET. Underground excavations in rock. 1980.
- [6] Karlovšek, J, Voids and cavities in tunneling: why do they occur and how to detect them using non-destructive methods?
- [7] HENN, RAYMOND W. Practical guide to grouting of underground structures. Thomas Telford, 1996.
- [8] HOULSBY, A. Clive. Construction and design of cement grouting: a guide to grouting in rock foundations. John Wiley & Sons, 1990.
- [9] Warner J. Practical handbook of grouting: soil, rock, and structures. John Wiley & Sons; 2004 Apr 5.

SUMMARY

Both types of sacks (onion and flour sacks) used to placing pumice pieces in the empty space behind the lining have acceptable groutability.

The results of contact grouting taken after the initial supporting is not satisfactory, therefore the implementation of contact grouting was postponed after the installation of the final lining.

The grouted cement in secondary grout holes still shows a peak absorbed cement locally, therefore the third grout holes grouted between initial and secondary holes.

Check-holes drilled after grouting of third series shows that the voids inside the pumice sacks and the gaps between sacks completely filled with cement grout.

RÉSUMÉ

Les deux types de sacs (sacs d'oignon et de farine) utilisés pour placer des morceaux de pierre ponce dans un espace vide derrière la doublure ont une aptitude au coulage acceptable.

Les résultats du jointoiment de contact pris après le support initial ne sont pas satisfaisants, par conséquent la mise en place du joint de contact a été reportée après l'installation du revêtement final.

Le ciment injecté dans les trous de coulis secondaires montre encore un pic de ciment localement absorbé, donc les trous de coulis troisième joint entre les trous primaires et secondaires.

Les trous de contrôle forés après le jointoiment de la troisième série montrent que les vides à l'intérieur des sacs de ponces et les espaces entre les sacs sont complètement remplis de coulis de ciment.

6. CLEARANCES AND COPYRIGHT

The authors are responsible for obtaining written permission to profile the project or subject matter in their papers from any and all clients, owners or others who commissioned the work. ICOLD assumes proper permission has been obtained by author(s) and accepts no liability for the author(s) failing to do so.

If a figure, table or photograph has been published previously, it will be necessary for the authors either to obtain written approval from the original publisher; or refer clearly to the source of previously published material in the caption of the figure, table or photograph.

KEYWORDS:

Pumice, Sack, Contact Grouting, Tunnel, Lining, Voids, Gap

COMMISSION INTERNATIONALE DES GRANDS BARRAGES

VINGT-SIXIÈME CONGRÈS DES GRANDS BARRAGES
Autriche, juillet 2018

DOI 10.3217/978-3-85125-620-8-194



This work licensed under a Creative Commons Attribution 4.0 International License. <https://creativecommons.org/licenses/by-nc-nd/4.0/>

**STATUS AND FUTURE PROSPECTS OF RENEWABLE ENERGY IN
SUBSAHARAN AFRICA**

Daniel ADU

NATIONAL RESEARCH CENTER OF PUMPS, JIANGSU UNIVERSITY,
ZHENJIANG 212013

CHINA

Jinfeng ZHANG

NATIONAL RESEARCH CENTER OF PUMPS, JIANGSU UNIVERSITY,
ZHENJIANG 212013

CHINA

Stephen ASOMANI

NATIONAL RESEARCH CENTER OF PUMPS, JIANGSU UNIVERSITY,
ZHENJIANG 212013
JIUQUAN SATELLITE LAUNCH CENTER, JIUQUAN CITY, GANSU PROVINCE

CHINA

Lv SUOMING

JIUQUAN SATELLITE LAUNCH CENTER, JIUQUAN CITY, GANSU PROVINCE

CHINA

COMMISSION INTERNATIONALE
DES GRANDS BARRAGES

VINGT-SIXIÈME CONGRÈS DES
GRANDS BARRAGES
Autriche, juillet 2018

- **STATUS AND FUTURE PROSPECTS OF RENEWABLE ENERGY
IN SUBSAHARAN AFRICA**

Daniel Adu¹, Jinfeng Zhang¹, Stephen Asomani^{2,1} Lv SUOMING²

1. *national Research Center of Pumps, Jiangsu University, Zhenjiang
212013 China.*
2. *Jiuquan Satellite Launch Center, Jiuquan City, Gansu Province*

1. INTRODUCTION

Worldwide use of hydropower grew over 5% between 2009 and 2010, according to new research published by the (World watch Institute for its Vital Signs Online publication). Hydropower use reached a record 3,427 TWh, or about 16.1% of global electricity consumption, by the end of 2010, continuing the rapid rate of increase experienced between 2003 and 2009. And continued to increase in 2011, reaching 3,498 (TWh) and 970 GW respectively. Total consumption got increased each year between 2003 and 2011. But in 2011 the growth rate slowed, recording only 1.6% increase from the previous year. China was the largest hydropower producer and is expected to continue to lead global hydro use in the coming years. The country produced 721TWh in 2010, representing about 17% of national electricity use. China also had the highest installed hydropower capacity, with 213GW at the end of 2010. It added more hydro capacity than any other country, 16 GW in 2010, and plans to add 140 GW by 2015. Hydropower is produced in at least 150 countries but is concentrated in just a few countries and regions. The Asia-Pacific region produced about 32% of world hydropower in 2010. Africa produces the least hydropower, accounting for 3% of the world total, but considered the region with the greatest potential for increased production. According to China's first national water census data released in 2013, the number of hydropower stations and the installed capacity of the distribution in China [1], as shown in Figure 8, the size of the following (i.e., power plant installed capacity of less than 500 kW) 658, accounting for 52.5% of the total number of 46 758 units, the corresponding installed capacity of 5.5914×10^6 kW, the total installed capacity of 3.3×10^8 kW of 1.7%. These data show that small and micro hydroelectric power generation benefits are small.

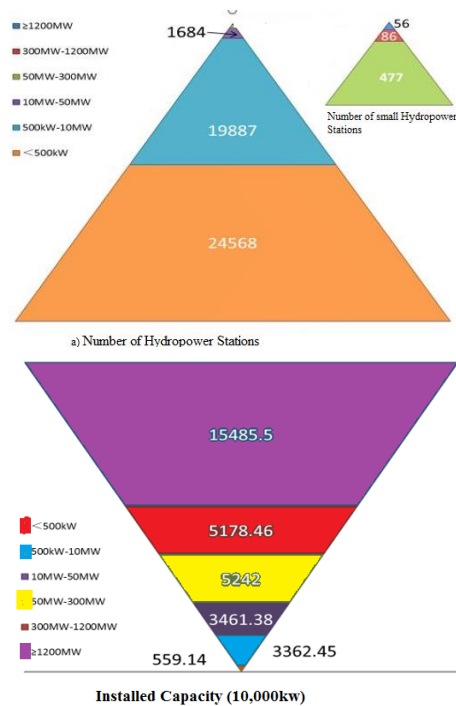


Fig.1 Statistics of hydropower plants of first national census for water

2. CURRENT SITUATION AND STRATEGIC PLANNING OF SMALL HYDROPOWER IN EU 27 COUNTRIES

INTRODUCTION

In 1989, when the European Commission initiated the establishment of the European Association of Small Hydropower Stations to stimulate the growth of small and micro hydroelectric power generation, the importance of developing small hydropower was recognized: in the energy plan of 2050, the energy plan of the year stressed that the proportion of renewable energy must be increased with the proportion of demand for energy growth in the future, in order to achieve the following objectives [2]:

- Maintain the sustainability of energy production;
- Independence of energy production;
- Adopt positive measures to address climate change.

Over the past 20 years, the development of small hydropower in the EU-27 has achieved very positive results, appreciations to the EU's Water Framework Directive, 2020 targets for renewable energy and greenhouse gas emissions reductions, and the active promotion of the European Association of Small Hydropower Stations. Fig.2 shows the Statistics and prediction of SHP installed capacity in the EU countries from 2005 to 2020. In 2010, nearly 21,800 small hydropower stations were in operational, that is in Germany (more than 7,500), Austria (2,590), Italy (2,303), France (1,900), Sweden 1 900), the Czech Republic (1 450). The total number of small hydropower stations is expected to reach 24,000 by 2020 [1]. From 2010 to 2020, the installed capacity of the power station is expected to increase from 13.7 GW to 17.3 GW, with the annual power generation capacity also increase from 49.3 TWh to 59.7 TWh, the annual growth rate of small hydropower generation should also reach Total of 21%., the strategic plan for small hydropower in EU-27 from 2010 to 2020 is to increase the installed capacity of small hydropower by adding 2,100 small hydropower stations (with an average annual increase of 210 power stations) 3.62×10^6 kW (an average annual increase of 3.62×10^5 kW) and an increase of about 10.37 GWh (an average annual increase of 1.037 GWh) in the annual production of small hydropower.

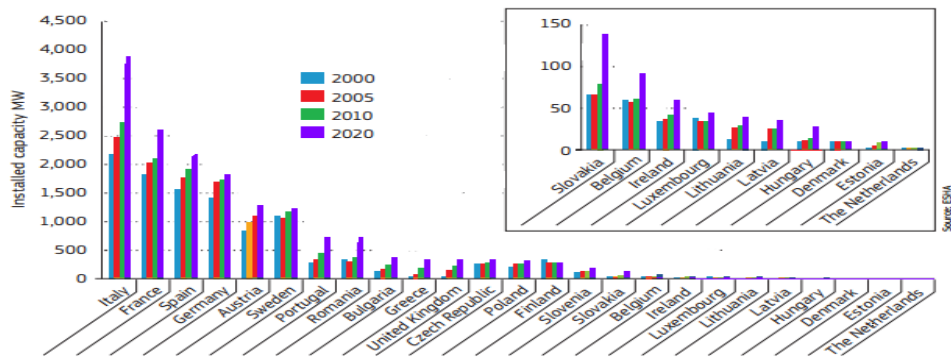


Fig.2 Statistics and prediction of SHP installed capacity in the EU countries from 2005 to 2020

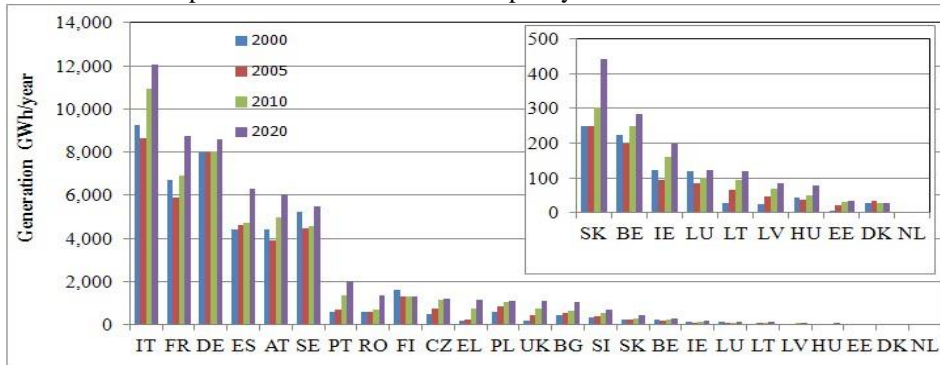


Fig.3 SHP electricity generation in the EU countries

Figure 2 and Figure 3 for the EU countries from 2000 to 2020, showing hydropower installed capacity and small hydropower generation statistics and forecasts [2]. Italy is far ahead in the EU countries, in the installing capacity of small hydropower and annual electricity generation. Italy in 2010 had an installed capacity of 2735MW small hydropower with an annual Energy generation reaching 10958GWh; and still expecting the installed capacity of small hydropower to reach the scale of 3,900 MW by 2020, compared to 2010 growth of 42%. Ranked 2nd to 4th countries are France, Spain and Germany respectively. Countries with low installed capacity and annual electricity generation are countries or regions with relatively low terrain, for example, the Eastern Baltic Sea region, Hungary, Denmark and Ireland. (Note: Figures for Malta, Cyprus and Greece are not included in the charts). From the structure of the whole renewable energy and distributed energy, the current situation of the EU and the forecast for 2015 and 2020 are shown in Table 1. The data in the table are from the report of the European Small Hydropower Association [2]. Data may be available 0.1% of the error.

	CLASSIFICATION	PARTICULAR			
		2005	2010	2015	2020
Hydropower generation	Hydropower generation	71.3	53.7	39.4	30.9
	Small hydropower	8.9	7.8	6.1	4.9
	Large hydropower	62.2	45.7	33.2	25.4
	Tidal energy wave energy ocean energy	0.2	0.2	0.1	0.6
Solar energy		0.2	3.3	6.8	8.5
Biomass energy		12.7	16.3	18.8	19.1
Wind power		14.8	25.8	34.3	40.7
geothermal energy		1.1	0.9	0.8	0.9

Table 1 Structure of renewable energy and distributed power generation%

According to China's first national water census data released in 2013, the number of hydropower stations and the installed capacity of the distribution in China [1], as shown in Figure 8, the size of the following (i.e., power plant installed capacity of less than 500 kW) 658, accounting for 52.5% of the total number of 46 758 units, the corresponding installed capacity of 5.5914×10^6 kW, the

total installed capacity of 3.3×10^8 kW of 1.7%. These data show that small and micro hydroelectric power generation benefits are small.

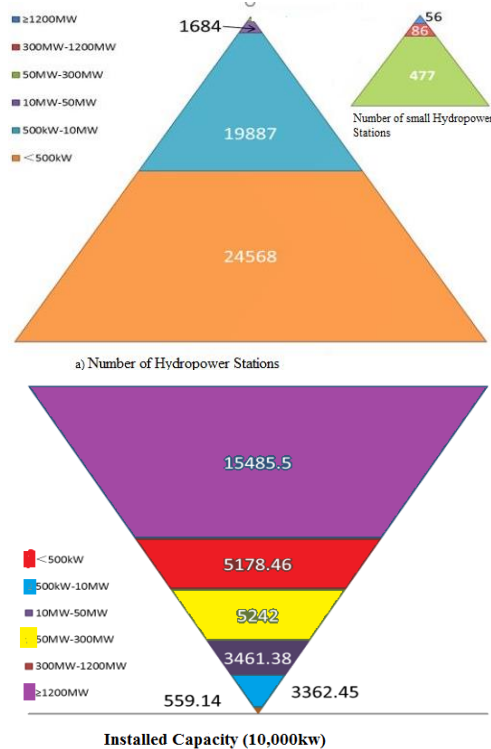


Fig.4 Statistics of hydropower plants of first national census for water

2.1. OVERVIEW OF AFRICA'S ENERGY

Africa's hydropower investment channel highlights the potential for renewable energy expansion across the continent. Hydroelectric power is a very attractive investment in Africa due to its huge potential for hydro power generation. access to modern energy, is minimal in the Region, over 645 million people live in the region without access to modern Energy especially those in the rural areas. The Democratic Republic of the Congo has a large part of Africa's stated potential It currently carries 40 projects for hydropower of which nine of them are located in Democratic Republic of the Congo in addition to the two largest Inga I (354 MW) and Inga II (1,424 MW). The Zambezi River is the most important resource of hydropower and the terrain of Zambia dwell in a larger portion of the river basin i.e. 41%, compared to the other seven riparian countries. Zambia has reached hydropower installed capacity of 2,257 MW, based on the accomplishment of the upgraded Lunzua station (14.8 MW) in 2014, Representing 94% of the total energy mix of the nation [3]. The total highest SHP potential in the African continent is located in The Eastern Africa region with a total potential of 6,759 MW. With only 216 MW installed capacity. Western Africa has the second-highest SHP potential in the continent with 3,113 MW yet the second lowest in installed capacity with only 86.1 MW representing only 3% of the total potential. the Middle African region on the other hand has the largest amount of undeveloped SHP potential. Northern Africa has insufficient potential of 225 MW, being one of the lowest in the world, with 112 MW already developed. Africa's Small Hydro Power can be considered as having a comparatively low level of installed capacity but with huge potential for development. The total SHP potential is estimated at 12,197 MW with an installed capacity of 580 MW. This indicate that only about 5% of the potential have been developed. Figure5 shows the Share of Small Hydro Power installed capacity in Africa (%) [4]

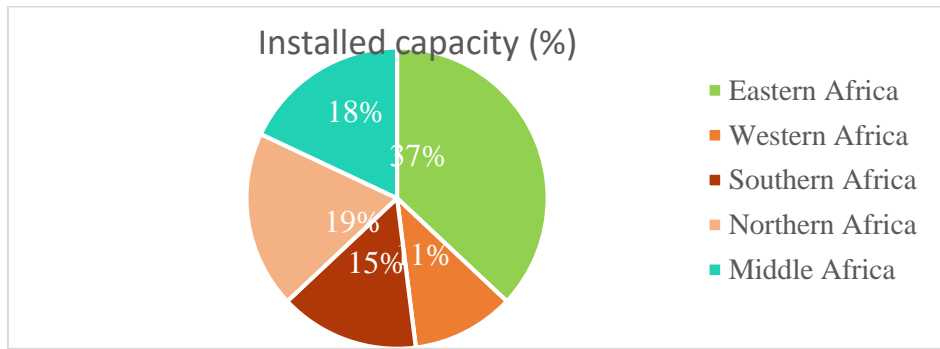


Fig. 5 Share of installed SHP capacity in Africa (%)

Countless of the world's fastest-growing economies are located in the resource rich African continent. Accelerated economic growth in the region is determined by rising in commodity prices. Nevertheless, growth in sub-Saharan Africa is not always comprehensive, and there is a low level of access to modern energy, water and other basic services throughout the region. Access to energy will continue to achieve a high level on the policy agenda, Particularly the work of the new United Nations sustainable development goals agenda which includes a devoted goal to deliver universal access to modern energy services, relying on Millennium Development Goals which they supplanted in 2016[5]. Reasonable price along with Consistent power supply is an important requirement for economic growth. Electricity from renewable sources can play an important role in the improvement of electricity supply in Africa [6]. Access to electricity in Africa is a very big canker to the continent. In adequate electricity supply in many African countries has been noticed as the most pressing obstacles to economic growth. roughly 10% of the worldwide small hydropower potential is located on the African continent, specifically in the sub-Saharan African region but only few of these potentials have been developed. [7,8]. It is therefore necessary to adopt the pumping method for power generation by using Pump As Turbine for small hydropower power generation. fig.6, Electricity generation by fuel in sub-Saharan Africa under the new policies scenario, 2012 and 2040.

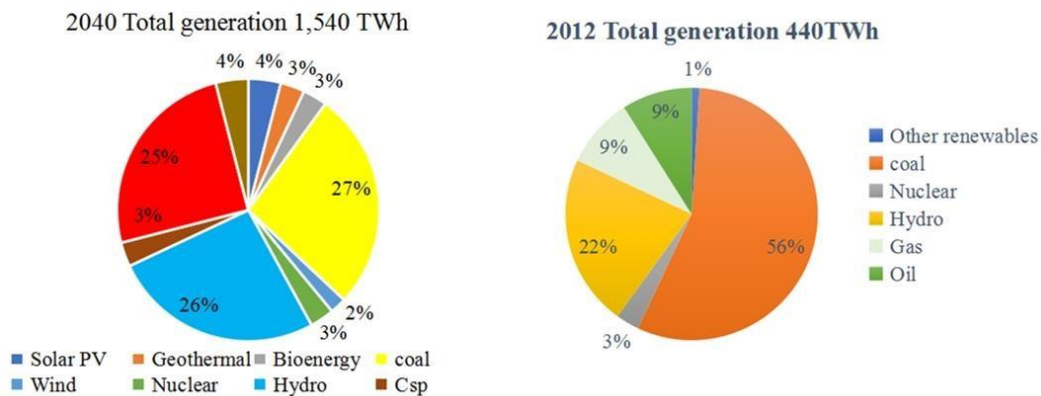


Fig. 6 Electricity generation by fuel in sub-Saharan Africa under the new policies scenario, 2012 and 2040

CURRENT SITUATION OF SUB-SAHARAN AFRICAN RENEWABLE ENERGY

The potential for renewable energy development in sub-Saharan Africa is experiencing an increase attention recently as investors and world leaders seek a new clean energy boundary. The continent could become a gold mine for renewable energy because of its abundant solar and wind resources for instance According to Statistics Botswana figures, there was a decrease of 63.9% in power generation imports during the first quarter of 2017. Comparing figures from the first quarter of 2016, there is an indication that decreased in electricity imports from 523,736MWh to 189,052MWh accounting for 63.9% decrease. This is as a result of the enhancement in local power generation at Morupule B, as the plant is now said to be producing more than half of its capacity. It can further be

explained that the physical volume of electricity generation in the first quarter of 2017 was 698,451MWh, causing an increase of 57.4% compared to the first quarter of 2016 generation of 443,628MWh [9]. But barriers to clean energy worldwide are augmented all over the concerned countries of sub-Saharan Africa, also financial resources are minimal as well as unreliability of infrastructure. In sub-Saharan Africa, there is a lack of electricity infrastructure for large-scale renewable energy industries. For example, in Kenya, there are at least 50 power outages per year. Increasingly, countries in sub-Saharan Africa are implementing energy through renewable energy resources and efficacy. Kenya, as one of the most dynamic countries, increased its geothermal energy capacity to 740MW in 2015, and plans to launch a \$ 150 billion project to invest solar energy in areas where Electricity is not accessible and are not connected to the grid. Ethiopia on the other hand is also principally active in wind power (150MW), and also stepping up its efforts in solar energy with the construction of a 5.200MW plant which is the largest in the region. In addition, several projects in Addis Ababa are underway, including geothermal and solar projects, and are intended to be open to the private sector. The figures below show renewable status in the region between 2010 to 2016[10]

2.2. CONCEPT OF PUMP RUNNING IN REVERSE MODE AS TURBINE

The velocity diagram for the flow at the inlet and discharge of a pump runner are basically matching when the unit operates as a turbine, except for the reversing of each vector as can be seen Fig. 9.5 and Fig. 9.6. Fig. 10 provides better understanding to the concept of pump operating in pump mode and in reverse mode as turbine

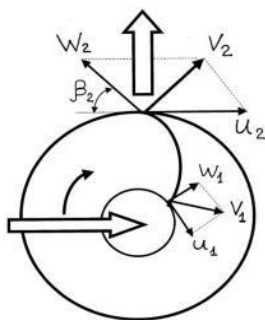


Fig. 7.5: Velocity Diagrams at the Inlet and Outlet of Centrifugal Pump [11]

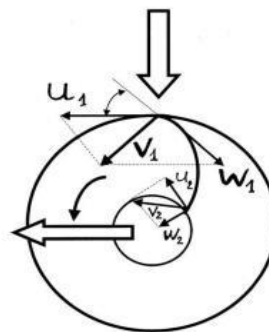


Fig.7.6: Velocity Diagrams at the Inlet and Outlet of Impeller Under Reverse Flow [11]

PAT CHARACTERISTICS

It is well known that efficiency of a centrifugal pump decreases rapidly with a drop of specific speed, and the impeller outlet diameter should be reduced considerably to increase its efficiency. With a reduced outlet diameter, it is necessary to select a larger blade discharge angle and more blades to produce the rated head. However, too many blades result in a decrease in efficiency due to the increasing blockage and skin friction in the impeller passage. Yuan [13] revealed that the splitter blade technique is one of the techniques to solve three hydraulic problems of low specific speed centrifugal pumps (lower efficiency, drooping head-flow curve and easily overloaded brake horsepower characteristics). It was observed from the studies that low or high blade numbers had increased the instability risk of head-flow curves [14], and the optimum efficiency was obtained when the blade number was between 4 and 6 [15]. M Asuaje et al. [16] studied the splitter blades effect on the performance of a centrifugal pump through both numerical simulation and experimental results. Adding splitters has negative and positive effects on the pump behavior. It increases the head rise compared to the original impeller, it has positive effect on decreasing the vibrating and radiated noise; but the efficiency is not improved since the hydraulic losses are greater. J. Zhang et al. conducted a study using the A BP artificial neural network (BPANN) model of a three-layer with 5

inputs, 20 hidden neurons and 2 outputs for predicting the efficiency and head of centrifugal pumps with splitters were built. The average relative deviation for the predicted efficiency and head were 5.97% and 4.78% respectively. And by comparing with test data, the predicted data has the similar trend, and the value of R for the predicted efficiency and head are 0.978 and 0.989 respectively, which prove that the correlation between the predicted and test value and the generalization capability are very good, and the trained network model can meet the requirement for the performance prediction of centrifugal pumps with splitters [17].

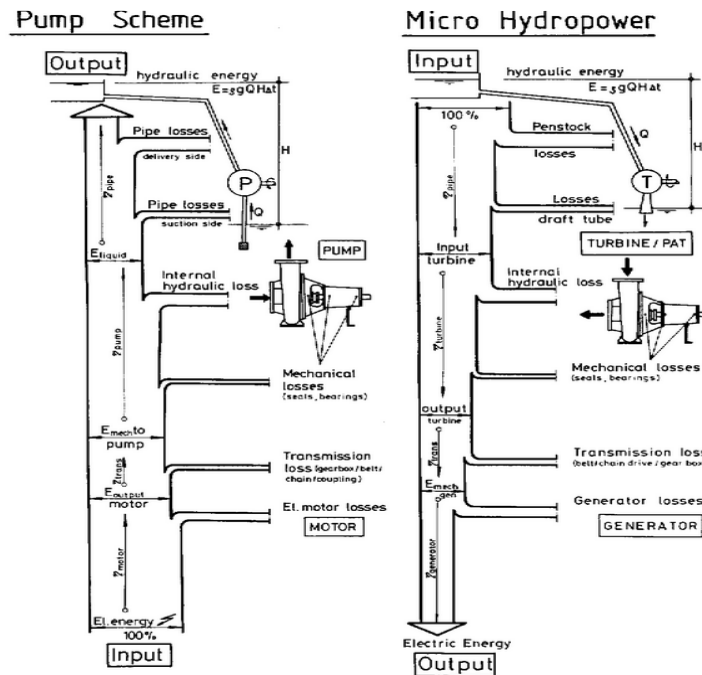


Fig.8 Working of Pump in Pump Mode and Pump in Turbine Mode and Losses

RENEWABLE ENERGY PROSPECTS AND FUTURE PREDICTIONS IN SUB-SAHARAN AFRICA

sub-Saharan Africa has a vast renewable energy potential, some of which are the world's largest alternative energy sources in the form of solar, wind, hydro and biomass. A total of 17 sub-Saharan African countries are among the world's top 33 countries with joint solar, wind, hydro and geothermal energy reserves far more than the annual consumption. The majority of sub-Saharan countries have a solar radiation range of 6-8 kWh / m² / day, which counts among the world's largest solar radiation. So far, only a small part of sub-Saharan Africa's huge potential for renewable energy has been tapped out. Renewable energy has the potential to meet the energy needs of the entire continent. Several African countries, such as South Africa, Egypt, Morocco, Kenya, Senegal, Madagascar, Rwanda and Mali, have adopted national targets for renewable energy and have proposed feed-in tariffs on renewable energy. In South Africa and Kenya. Countries such as South Africa, Morocco, Egypt, Cape Verde, Ethiopia, Kenya and Tanzania are developing wind farms. sub-Saharan Africa's investment lines in hydropower, wind farms, solar PV, solar thermal, geothermal and biomass technologies underscore the potential for future expansion of renewable energy in the continent. Sub-Saharan Africa has abundant renewable energy resources that have yet to be developed to meet its electricity demand. Its technical generation capacity potential largely from renewables is estimated to be 11,000GW. Almost all the countries in the region have a solar potential of up to about 10,000 GW, and the PV potential is estimated at 6,500 TWh per year [18]. Majority of its coastal countries have huge potential for wind power, with a total of about 109 GW. the main power source in many sub-Saharan Africa countries is hydropower, with an Estimated power generation of about 350 GW, largely in Ethiopia, South Africa, Egypt, the Democratic Republic of the Congo, Zambia and Mozambique this is as a result of the Congo and the Nile Rivers

which are among the world's longest rivers are located in the region. For example, Mozambique has twice as much hydropower generation capacity as the UK and it accounts for 99.9% of all electricity generated. Coal resources are estimated at 300 GW, mainly in Botswana, Mozambique and South Africa [19]. Over the past decade, the average annual growth rate of sub-Saharan African financial prudence is 5.3%. Energy demand has increased dramatically even though the region has the lowest per capita power consumption Estimated at 157kWh, despite the fact that there is a rapid population growth and is expected to double by 2050[20]. on the word of IEA Renewable energy will virtually constitute half of sub-Saharan Africa's energy generation growth by 2040. There has been a rapid growth in Sub-Saharan Africa's economy since 2000, nevertheless there is a confusing in the growth.as two-thirds of the population in the regions have no access to electricity. at present only about 10% of sub-Saharan's hydropower potential has being developed. it is expected that sub-Saharan Africa will start developing these huge untapped renewable energy potentials resources. [21] The report predicts that, over the next 26 years, sub-Saharan Africa will start to unlock its "vast renewable energy resources" and that solar energy will lead the growth in renewables in the region. According to the report, just 10 percent of sub Saharan's hydropower potential is currently being exploited.

SOLAR POTENTIAL IN SUB-SAHARAN AFRICA

Sub-Saharan Africa has abundant renewable energy resources which are yet to be developed to meet their electricity call. Its technical generation capacity potential largely from renewables is estimated to be 11,000GW. Almost all the countries in the region have a solar potential of up to about 10,000 GW, and the PV potential is estimated at 6,500 TWh per year [18]. The entire continent has a long day of sunshine with an annual period of about 4300 hours [22], which equates to 97% of the total possible. [23] The continent has the highest average annual solar radiation values [24] (up to over 220 kcal/cm² [18]). The low latitude of the landmass is another source: most parts of the continent are in the equatorial regions where the intensity and strength of the sun's rays are always high. There are arid and semi-arid forests in the northern part of the region, with fewer in the south and east. The combination of all these geographical and climatic factors is the reason for a huge potential of solar energy in sub-Sahara Africa. This enables solar to be powered in almost all of Africa devoid of the costly, large-scale grid level infrastructural developments. solar equipment costs reductions are anticipated to promote solar installations in sub-Saharan Africa with an industry projection estimating that there will be an annual PV market expansion of 2.2 GW in the region by 2018. [25]

-Saharan African continent is leading solar power in Africa with an installed capacity of 1329 MW in 2016. [26] South Africa Solar power is rising faster. Quite a lot of 75 MW PV plants and 2 CSP plants at 100 MW each were the largest in the country and among the largest in Africa. South Africa is currently leading in both solar thermal and PV solar energy in Africa. And has developed a lot of solar thermal plants, both parabolic trough and power tower types. A 50 MW photovoltaic power plant is planned for Garissa in Kenya which is projected to produce about 76,473 MWh/year. [27] Ghana has also planned for a 155 MW Pv plant with the government planning to increase solar power in the country from 22.5MW in 2017 to 300MW by 2020. [28] [29] There are also many small-scale modular solar power installations being implemented across the continent at villages and household levels. [29] Sub-Saharan Africa was on top for purchases of off-grid solar products in 2015, [30] Morocco's solar plan, which is one of the world's largest solar energy projects aim to produce 2,000 MW of solar power by 2020. with the 500MW phase one solar power complex at OuarZarate being the first to be developed. [31] The first part of the 500MW project. Morocco happens to be the only African country having a power cable link to Europe. Morocco's solar plan, which is one of the world's largest solar energy projects aim to produce 2,000 MW of solar power by 2020. with the 500MW phase one solar power complex at Ouarzazate being the first to be developed. The first part of the 500MW project. Morocco happens to be the only African country having a power cable link to Europe, South Africa is currently leading in both solar thermal and PV solar energy in Africa. And has developed a lot of solar thermal plants, both parabolic trough and power tower types [31] [32]

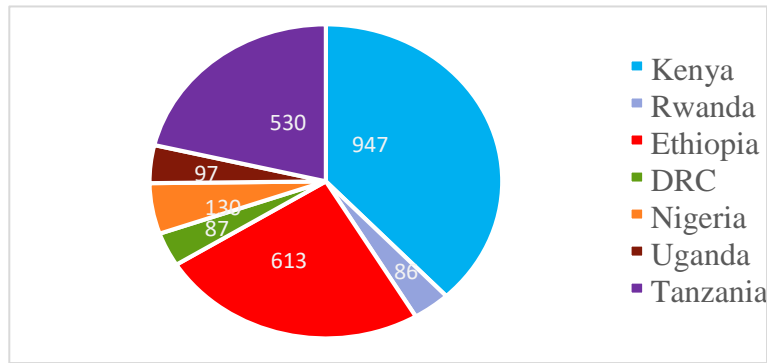


Fig. 10 Sales of Pico-solar production in sub-Saharan Africa 2014-2015 (thousands of units)

Challenges to The Renewable Energy Development

Absence of system capacity. Continued electricity shortages in the region have led to a slowdown in economic growth, obstructing the implementation of various health and educational development goals [14]. This is due to insufficient power generation capacity in the network area, inadequate power grid infrastructure, poor power generation maintenance, new generation capacity investment, and decentralization in remote areas. The lack of systematic planning of renewable energy sector led to a transmission and distribution of larger losses in the region.

Policy and regulatory framework: undefined or non-appearance of policies and regulations that sees renewable energy development in most of the Countries in sub-Saharan Africa is one of the major challenges. The region wastes billions of dollars in lost public services and oil subsidies, that are not beneficial for the energy sector development. Assuming that most utilities cannot recover their costs without these subsidies, the development of energy systems is perceived as a high risk and therefore not attractive to private investors [33].

Lack of Finance: One of the biggest challenges facing sub-Saharan Africa on solar power development is financing. Funds are not available for the feasibility studies on these potential site as well as construction and maintenance. Almost all the new developments on the continent are relying in one Way or the other on donor financing.

SUMMARY

Renewable energy technologies can play an important role in the energy sector of sub-Saharan African continent. sub-Saharan Africa's renewable energy industry can become a major player in the energy sector to meet the energy needs of a large part of the population through the use of centrifugal carefully chosen as turbine for small hydropower generation. since pump As turbines are a leading solution for small hydropower generation, especially in rural areas. The initial project cost has dropped significantly, making it more viable. The specific location of the pump can be further limited by selecting the appropriate pump turbine. The characteristics of the best efficacy point can also be improved by applying the various modifications proposed by the earlier researchers. There is a need to actively lobby for renewable energy at the national, regional and sub-regional levels. Development and promotion of new business models for the maintenance of renewable energy development for rural electrification should also be mainstreamed in the continent. Supportive inducements at the local level, when combined with energy sector reform, can become a powerful lever for private

investment, but they must be specific, beyond the political correctness of high-level statements. This solution will make the region economically and environmentally sound and promote development of the people. Achieving 100% power access Throughout the area needs mix of pathways and scales

REFERENCES

- [1] EUROPEAN SMALL HYDROPOWER ASSOCIATION. Small Hydropower Roadmap-Condensed Research Data for Eu-27 [R / OI]. Brussels: ESHA, 2013: 6-11 [2013-12-17] [Http://Streammap.Esha. Be / Fileadmin / Documents / Press_Corner_Publications / Shproadmap_Final_Public.Pdf](http://Streammap.Esha.Be/Fileadmin/Documents/Press_Corner_Publications/Shproadmap_Final_Public.Pdf)
- [2] KARL SCHWAIGER, MARTIN PFAUNDLER. Situation report on hydropower generation in the alpine region focusing on small hydropower[r/ol]. evian: the alpine convention, 2011:26. [2014-06-16]. http://www.alpconv.org/en/organization/conference/documents/ac11_b8_1_situation_report_fin_annex024_1.pdf?aspxautodetectcookiesupport=1
- [3] IEA (2015A), World energy outlook, OECD/IEA, Paris.
- [4] (ICSHP) World Small Hydropower Development Report, Zhejiang Prov. International Center On Small Hydro Power 136 Hangzhou, China 2016.
- [5] HOLM, D. Renewable Energy future for the developing world. ISES White Paper, 2010.
- [6] ESHA, It Power, Small Hydropower for Developing Countries, (2006).
- [7] MIN CONF WATER FOR AGRICULTURE AND ENERGY IN AFRICA, Hydropower Resource Assessment of Africa, (2008).
- [8] STATISTICS BOTSWANA REPORTS A 63.9% decrease in power imports<https://www.esi-africa.com/news/statisticsbotswana-generation-capacity/> accessed July 14 2017
- [9] SUB-SAHARAN AFRICA'S Hunger for Renewable Energy, Bonelli Erede Pappalardo Studio Legale 2015 [Https://Www.Belex.Com/En/News/Sub-Saharan-Africas-Hunger-For-Renewable-Energy](https://Www.Belex.Com/En/News/Sub-Saharan-Africas-Hunger-For-Renewable-Energy)
- [10] WILLIAMS, A. A., 1994. The Turbine Performance of Centrifugal Pumps: A Comparison of Prediction Methods. Proc. Ants. Mech. Engrs, Vol. 208, Pt A, Pp. 59-66
- [11] MANKBADI R.R., and MIKHAILS.A., A Pump As Turbine", Energy Conversion, Mgmt. Vol.25, No. 3. Pp. 339-344, 1983 Accessed On 15/8/2017
- [12] YUAN SHOUQI: advances in hydraulic design of centrifugal pumps. in: ASME, fluid engineering division summer meeting, Vancouver, Bc, Canada; p. 1–15 (1997)
- [13] YUAN SHOUQI: The Theory and Design of Low Specific-Speed Centrifugal Pumps. Beijing: Mechanical Industry Press (1997) (In Chinese)
- [14] IEA (2014). Africa Energy Outlook: A Focus on Energy Prospects in Sub-Saharan Africa. Paris.

- [15] YUAN SHOUQI, CHEN C. Q., CAO WULING: Design Method of Obtaining Stable Head-Flow Curves of Centrifugal Pumps. ASME. Pumping Machinery Meeting, Fed, Vol. 154, Pp.171--175. (1993)
- [16] ASUAJE M., BAKIR F., NOGUERA R. ET AL.: 3-D Quasi-Unsteady Flow Simulation in A Centrifugal Pump. Influence of Splitter Blades in velocity and pressure field. ASME Fluids Engineering Forum - Ht-Fed2004-56600 (2004)
- [17] J. ZHANG ET AL. Numerical characterization of pressure instabilities in a vaned centrifugal pump under part load condition, IOP conf. ser.: mater. sci. Eng. 52 022044,2013.
- [18] CARTWRIGHT, A. (2015). Better Growth, Better Cities: Rethinking and Redirecting Urbanization in Africa. Working Paper. London and Washington, Dc: New Climate Economy.
- [19] ESI AFRICA, RWANDA: PPP Launches Musanze Hydropower Plant [https://www.Esi-Africa.Com/News/Rwandalaunches-Musanze-Hydropower-Plant/26 June 2017](https://www.Esi-Africa.Com/News/Rwandalaunches-Musanze-Hydropower-Plant/26%20June%202017) Access 14 July 2017.
- [20] ESI AFRICA, NAMIBIA: 5MW wind project near to completion [s://www.ESi-africa.com/news/namibiawind-project-near-completion/2017/07/13](https://www.Esi-africa.com/news/namibiawind-project-near-completion/2017/07/13) Accessed 13 July 2017
- [21] AFRICA PROGRESS PANEL. (2015). Power, People, Planet: Seizing Africa's Energy and Climate Opportunities: Africa Progress Report 2015. Geneva.
- [22] DUNLOP, S. (2008). A dictionary of weather. oup oxford. isbn 9780191580055. retrieved 2017-01-29.
- [23] [HTTPS://BOOKS.google.fr/books?hl=fr&id=n_gohp1ws3cc&dq=eastern+sa hara+bright+sunshine &focus=searchwithinvolume&q=4300](https://books.google.fr/books?hl=fr&id=n_gohp1ws3cc&dq=eastern+sa+hara+bright+sunshine&focus=searchwithinvolume&q=4300)
- [24] RIORDAN, P.; PAUL G. BOURGET; U.S. Army engineer topographic laboratories (1985). world weather extremes. the laboratories. p. 66.
- [25] CLIMATE and life. Elsevier science. 1974. p. 151. ISBN 9780080954530. retrieved 2017-01-29.
- [26] WADSWORTH, F.H.; United States. Forest Service (1997). forest production for tropical America. U.S. department of agriculture, forest service. retrieved 2017-01-29.
- [27] "MIDDLE EAST and Africa solar PV demand to grow by 50 % in 2014, according to NPD solar buzz". 2014-04-24. retrieved 2014-08-19.
- [28] "Monitoring of renewable energy performance 2016". www.nersa.org.za. retrieved 2017-06-03.
- [29] "Ghana solar energy plant set to be Africa's largest - BBC news". bbc.co.uk. retrieved 2017-01-29
- [30] Government Targets 300mw of Solar by 2020, Ghana Web, 25/09/ 2017
- [31] KEMENY, P; MUNRO, P G; SCHIAVONE, N; VAN DER HORST, G; WILLANS, S (2014). "Community charging stations in rural sub-Saharan Africa: commercial success, positive externalities, and growing supply chains". energy for sustainable development. 23: 228–236.
- [32] RENEWABLES 2016 GLOBAL STATUS REPORT, REN 21, P. 91
- [33] REUTERS EDITORIAL. "Morocco says investors lining up for \$9 bln solar project | Reuters". uk.reuters.com. retrieved 2017-01-29.

COMMISSION INTERNATIONALE DES GRANDS BARRAGES

VINGT-SIXIÈME CONGRÈS DES GRANDS BARRAGES
Autriche, juillet 2018

DOI 10.3217/978-3-85125-620-8-195



This work licensed under a Creative Commons Attribution 4.0 International License. <https://creativecommons.org/licenses/by-nc-nd/4.0/>

**"THEORY OF EVERYBIM" – WORKFLOW OPTIMIZATION HYDROPOWER
NORWAY**

Kristoffer S. BUGGE

Hydropower Engineer and Head of BIM Coordination - Energy Division,
NORCONSULT AS

NORWAY

COMMISSION INTERNATIONALE
DES GRANDS BARRAGES

VINGT-SIXIÈME CONGRÈS DES
GRANDS BARRAGES
Autriche, juillet 2018

**"THEORY OF EVERYBIM" – WORKFLOW OPTIMIZATION
HYDROPOWER NORWAY**

Kristoffer S. BUGGE

*Hydropower Engineer and Head of BIM Coordination - Energy Division,
NORCONSULT AS*

NORWAY

1. INTRODUCTION

Traditionally, construction and hydropower projects have been designed and built based on multiple 2D drawings. Drawings have been used since ancient times, when they were cut into stone. Our experience with drawings is that a lot of time is spent on unnecessary perfection of the appearance of the drawings, such as line thickness, textures, company standards, etc. Much of this is not relevant for building the desired construction and can be considered poor use of valuable time. Technology is at the same time changing rapidly around us, and its growth is almost comparable to an exponential curve (Fig.1).

This growth/development is particularly relevant in our industry, as it represents an enormous potential that is accessible to all. We wanted to take advantage of this potential and we had to make a major change in the way we worked. Major changes are not easily implemented in a company or in a project since humans by nature are reluctant to change and tend to favor established routines. We had to challenge the established routines and get started. Our main goal was to be the first to complete an entire project without traditional 2D drawings at all. We wanted to deliver a fully integrated "Building Information Model" (BIM) that was available to everyone at any time throughout the project, consisting of all necessary geometry and information for both design and construction phase. This leads to more constructive use of time since changes will be made on dynamic objects rendered in an interdisciplinary model and not on many drawings with countless references. The concept was "Paperless Design, Paperless Construction". No one had done this before. The whole Industry said it was too early, even the software developers said we had to wait a couple of years before this could be done in full scale. Someone had to take the first step.

The 125 MW Run Of the River hydro power plant “Vamma 12” was our “chosen one”. The interdisciplinary complexity, size and location made it the perfect choice. Today, in line with our goal, the project is close to being finished and represents a milestone for us and the construction industry in relation to how projects are being implemented. The work has been innovative and inclusive where the team was put before individuals and the project itself was delivered by close collaboration of the involved firms. It has turned a lot of skepticism into motivation. Following the successful delivery of the Vamma project, a new generation of many fully integrated BIM projects of all sizes and complexity are being undertaken. All project teams work on a continuation of the same theory / workflow, so that we can shift resources between projects in case of sickness and produce the same quality on a wider range of deliverables. At the same time no project teams can work without asking critical questions or looking for places where the theory can be improved. It is accessible to all and is regularly updated in line with smarter processes and technological development. This paper gives an insight into how we have worked as a team to establish our current workflow for fully integrated BIM projects. BIM is so much more than just the 3D-model. It is a process enhanced by technology, combining everything that has to do with delivery and construction of a project. This is the reason why we have called it – “The Theory of EveryBIM”.

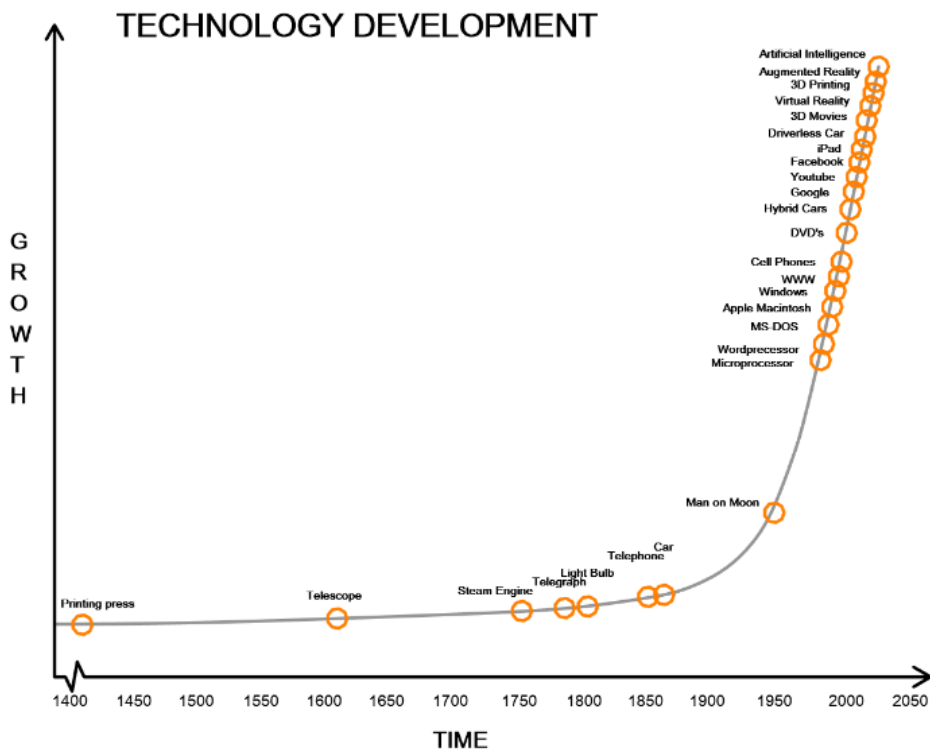


Fig. 1
Technology growth illustrated by an exponential curve

2. THE THEORY OF EVERYBIM

The first we did was to carry out a creative process to look at the big picture. Here we decided to make a solid overall plan, not to plan everything in detail. Many of the necessary details evolve through cooperation in the project and uncovering of relevant issues. We identified that our goal required much more than just better utilization of technology. It is more about man than machine (the things that cannot be measured). We ended up with four main categories for our theory; Strategy, Mindset, Technology and Collaboration.

(Strategy + Mindset³ + Technology) x Collaboration ~ Theory of EveryBIM

2.1. STRATEGY

2.1.1. *Gears of change*

“It is not the strongest of the species that survive, but the one most responsive to change” – Charles Darwin.

The constant pressure to achieve sufficient billable hours and to deliver to agreed deadlines, might be reasons why many leaders and employees avoid risk and keep on doing what is already known. Companies or projects solely consisting of this kind of employee provide a poor environment for innovation and change and will most likely fall behind competition in the long run. They need those who believe the impossible is possible, who never give up and are willing to fight for a change regardless of potential internal and external skepticism. If you manage to place a few of them together in a team and trust them to work towards a goal, you have what we in Norconsult like to call a “Gear of Change” (Fig.2). Work with establishing new workflows usually needs to withstand some initial disappointment and anxiety from leaders and clients regarding time and progress since you don’t know all the answers to begin with. Perseverance is the key to success. When new solutions emerge, and useful experiences prove to be better than existing ones, the small “gear” moves a “click” and starts off a reaction that inspires and moves adjoining “gears” that want to be part of the new process. This movement goes on to the next “gear” until the change (if relevant) has been established in the entire company or project. This chain-reaction is incredible to experience. It is happening from the inside and out, usually ignited by motivation, curiosity and ambition. Trying to make a change for an entire company or project at once (make all gears rotate at the same time) is probably not beneficial but quite common. Such initiatives are often stopped by bureaucracy or by fear of failure when the amount of information and digital tools provide so many alternatives that it seems overwhelming.



Fig. 2

One “Gear of Change” can inspire and affect an entire company or project

2.1.2. Linear or exponential workflow

We looked at the curve that illustrates technology development and discussed the potential of exponential growth further. We saw that we could use a similar representation to illustrate the expected results over time by working with either known (2D drawing production) or unknown (full BIM) workflows and routines (Fig.3). We like to think that if you are skeptical to changes, don't take any risks and only work by established routines that are already known; you work linearly. You know where to start, how long it takes, what tools to use and what results to expect. On the other hand, if you challenge existing workflows and search for efficient processes, investigate the latest technology, help to establish and share new experiences and dare to fail without giving up; you work exponentially. When working exponentially, you must make it through “the disappointment” phase to reach the “turning point” where you cross the linear workflow. From this point on, both foreseen and unforeseen results take place. This is where the hard work pays off. Do not let others take away your inherent initiative before you reach it.

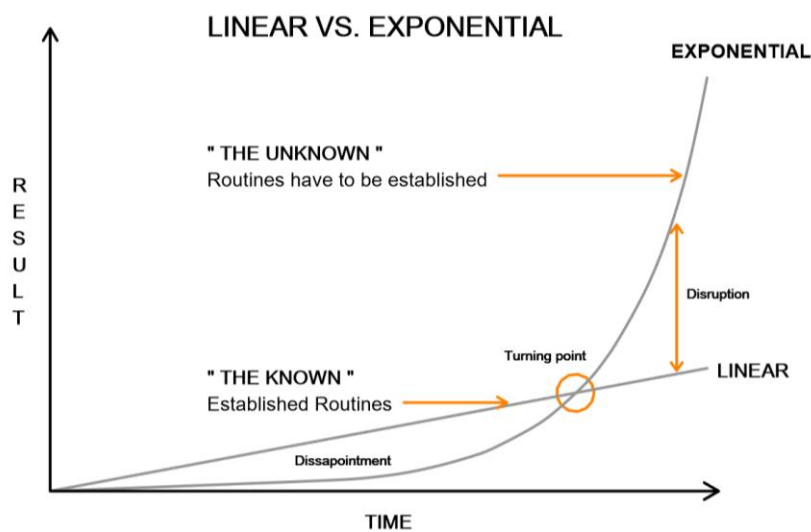


Fig. 3

Linear and Exponential workflow

2.1.3. The Trinity

A project is an interaction between several parties, and it is insufficient if everyone focuses on their own needs instead of the project and the team. Too many projects have been undertaken in separate "trenches" where the different parties try to point out where the others are doing wrong, instead of communicating and helping one another. Although this conservative behavior is probably motivated by financial reasons it leads to poor cooperation and progress which is very expensive. Major disagreements are often pushed to the end of the project when much is forgotten, and everyone ends up losing money in a time-consuming final settlement. The project itself can then be considered as unsuccessful (Fig.4).

This time we wanted to do it differently. We wanted to work more closely with the other parties in an a more humble and inclusive manner, listening to and respecting their expertise, as well as realizing that we may not always be right. It was important to prepare a new contract adapted to the workflow we planned to implement together. We had to make a clear delineation off who was responsible for what. We solved this by first inviting the major contractors in Norway to hear from them what they need in the coordination model (BIM) to be able to build from it. Then we invited the major owners in Norway to clarify their needs and wishes. Overall, this enabled us to create the contract in a constructive way.

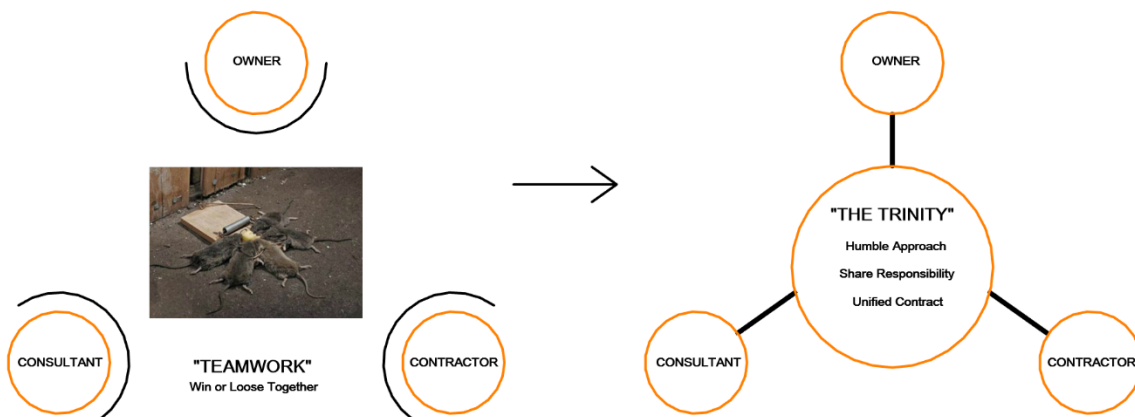


Fig. 4
What happens if the team and project come first or last

2.2. MINDSET

"Not everything that counts can be counted, and not everything that can be counted counts" – Albert Einstein

Good attitudes and mindset throughout the project are the single most important factor in our theory and the reason why we have highlighted this as a cubic function in our Theory of EveryBIM. Negative attitudes are far more infectious

than positive, so providing this got highest priority. The team motivated itself by establishing and following some simple principles.

2.2.1. “Don’t ever give up”

Giving up is never an option. It's about endurance every time a problem occurs and there are no projects without problems. When they occur find a solution. It is most likely not the perfect solution to begin with, but it can be evaluated by others, improved and optimized over time until it's final. Difficult technology, poor time, external pressures, and anxiety can feel overwhelming. Adopt and overcome to turn the problem into improved technology, good timing, inner calm and excitement.

2.2.2. Don’t sit on your egg

It is common practice for individuals or companies to keep smart solutions and innovations for themselves. We call this to “sit on an egg”. This is probably done to acquire an advantage over the others and to feel irreplaceable. We wanted to avoid this and made a rule about mandatory sharing of good ideas (hatching of eggs). This increases the ideas value by getting different considerations from others, and in most cases the origin is known anyway.

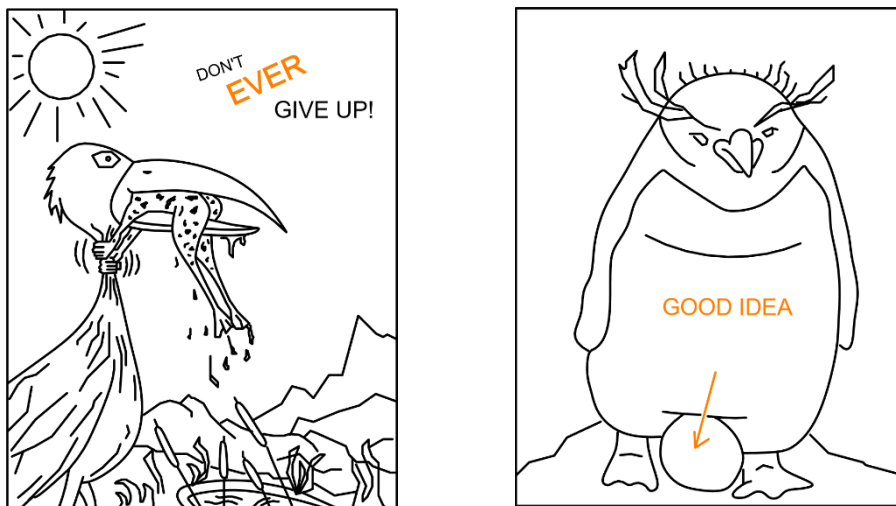


Fig. 5
Don't ever give up – don't sit on your egg

2.3. TECHNOLOGY “ATTACK ALL FRONTS”

When attitudes and mindset were in place, the project team could begin to look at how to utilize today's available technology. We agreed to consistently evaluate whether we were working with the right digital tools. "Attack all digital fronts" is our motto. We focused on digital interaction with those who would receive the models, not just what gets the job done at our end of the process. If the Contractor would be unable to build from the model, then it would have no value. Our initial plan had basic guidelines for technology as well.

2.3.1. *Utilization of existing software.*

We investigated how far we could push the software we already possessed. This was fun and gave us a lot of new and useful methods valuable for our design. Our biggest discovery was Parametric Design. We utilized our existing software in a new and better way to create formulas which were able to solve problems we were not able to do before. This was especially relevant for our rebar design. We believe that in a matter of years we will be able to model entire projects based on formulas that can be reused with minor changes in required input.

2.3.2. *Cooperation with external developers*

Even though we pushed our existing software to the extreme, we discovered that some of them were not suitable. We still had processes to improve. We started searching for alternative software elsewhere. This gained huge benefits as we found several small external partners that could deliver niche tools to solve issues for us and even adjust and upgrade their functionality to meet our specific needs. It required some hard work to learn the new platforms but it payed off.

2.3.3. *In-House Development.*

Where neither existing or new software could solve our problems, we had to develop our own functionality. We are lucky in Norconsult to have our own sister company, Norconsult Information Systems (NOIS), who work with programming and software development. They were able to develop indispensable tools that have revolutionized the way we work. The best application they developed was to integrate functionality for a dynamic link between the project's bill of quantity and the BIM Model. This made us feel innovative and not restrained by old methods and rules.

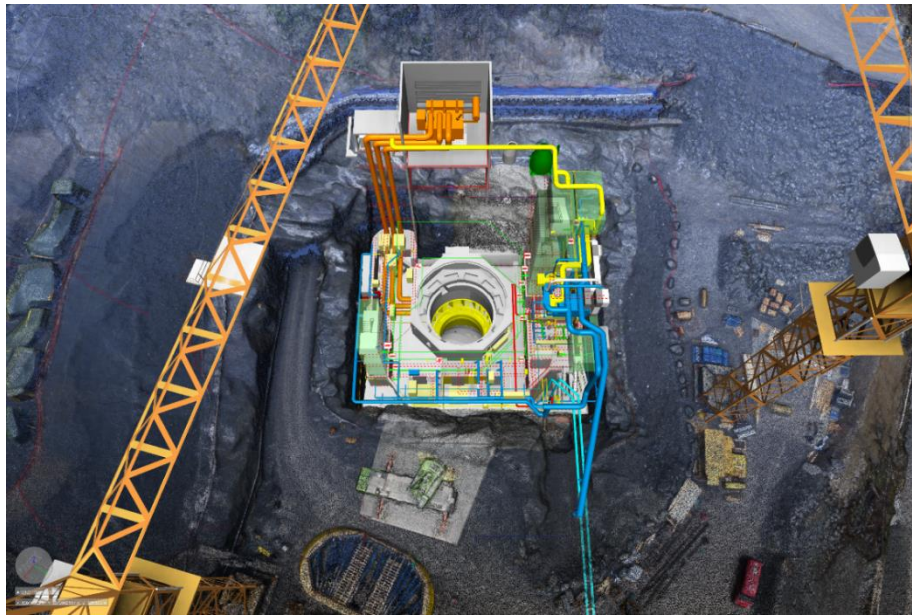


Fig. 6
The Digital Coordination Model – Vamma 12

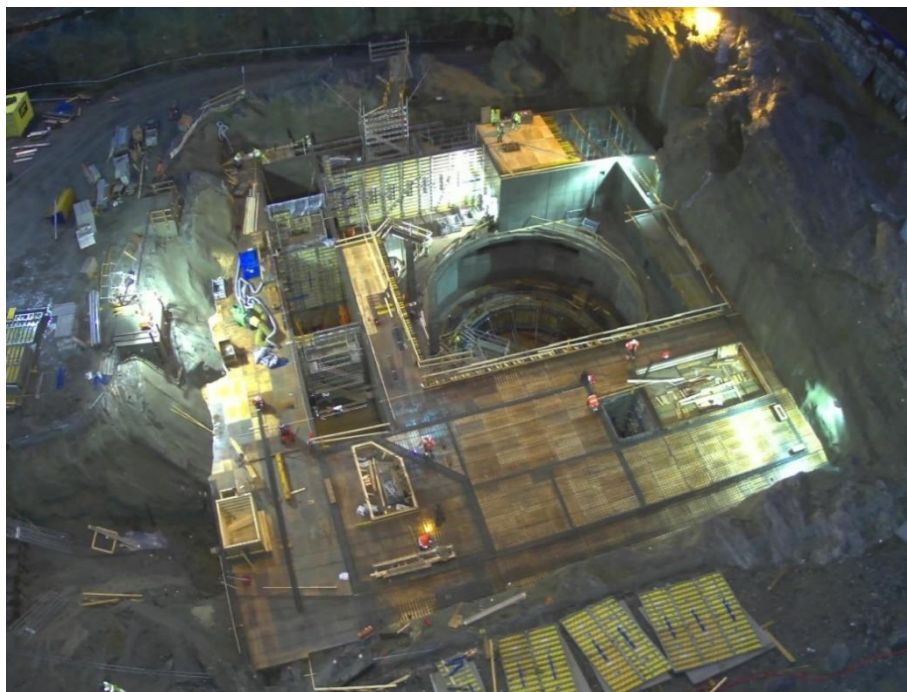


Fig. 7
The construction site – Vamma 12

2.4. COLLABORATION

Collaboration with the chosen contractor is perhaps the area that has changed the most. We compared the necessity of our cooperation with two people on a tandem bike, one missing both arms and the other missing both feet. The entrepreneur's contribution to the workflow, endurance in the field and the ability to find new solutions has been inspiring and crucial to our success in meeting our common goal. We met regularly and had good discussions on how we could improve the model and procedures for the best possible performance. We called ourselves "The Fellowship of the BIM". It has been practical to have a contractual agreement which defined responsibilities at all times, coupled with a mindset which allowed all parties to contribute across responsibilities for the project's best. Our meetings led to "tailored" digital communication. The Contractor had a proprietary tool which is used by all their personnel and machines in the field. They recommended that we also used this tool in design, so they could receive models directly without the need for further processing. Furthermore, we identified what information was necessary in the elements of the model and used this to structure the model to be readable and useful for construction. The experiences we have shared together have been written down and put into system. In addition to the overall theory, we have many detailed recipes of a technological nature that can be used and updated further.

3. CONCLUSION

We discovered that we worked with outdated methods and digital tools. Why do we still design and build from 2D drawings when technology has so much more to offer? This was the starting point for our bold goal of being the first to design and build from one collaborative model. We worked patiently and discovered early in the planning phase that it was about much more than technology alone. It was just as much about attitudes, mindset and teamwork. Our workflow and routines have been completely revised. All work is based on a unified, but not limiting, plan. Many solutions have emerged along the way in collaboration with all parties in the project. We have succeeded in reaching our common goal.

The results from the Vamma project are beyond expectations. The model ("the digital twin") is a realistic duplicate and has a lot of potential for further operation and maintenance of the plant. Never before has the owner had the same opportunity to use the product as a tool throughout the life of the construction. They must use the same curiosity and innovation that they have had in the design and construction phases to make the most of this phase. The whole process has been a team and project victory. We have experienced a reduced number of misunderstandings and better communication. There has been a massive reduction in change orders and discussions around quantities are almost non-existent. The management of health and safety has been better because we have

been able to see all the different disciplinary designs together and dynamically changed designs accordingly as the project has developed.

The project has gained national and international attention and was awarded 1st place (Autodesk AEC Excellence Awards) at the world's largest BIM conference in 2016 for its innovative use of BIM. It all started with a gear of change.

Today we see a number of new tools and opportunities that should be explored; Virtual reality, artificial reality, artificial intelligence, 3D printing etc. Where will we be within the next year, in 5 years or 10 years? Nobody knows the answer, but it is likely that we will do everything in a whole new way. We will never stop exploring new opportunities or conclude that what we do today is good enough for tomorrow. The theory will never be completed but is as good as it gets today.

*“People who say it cannot be done should not interrupt those who are doing it” –
George Bernard Shaw*

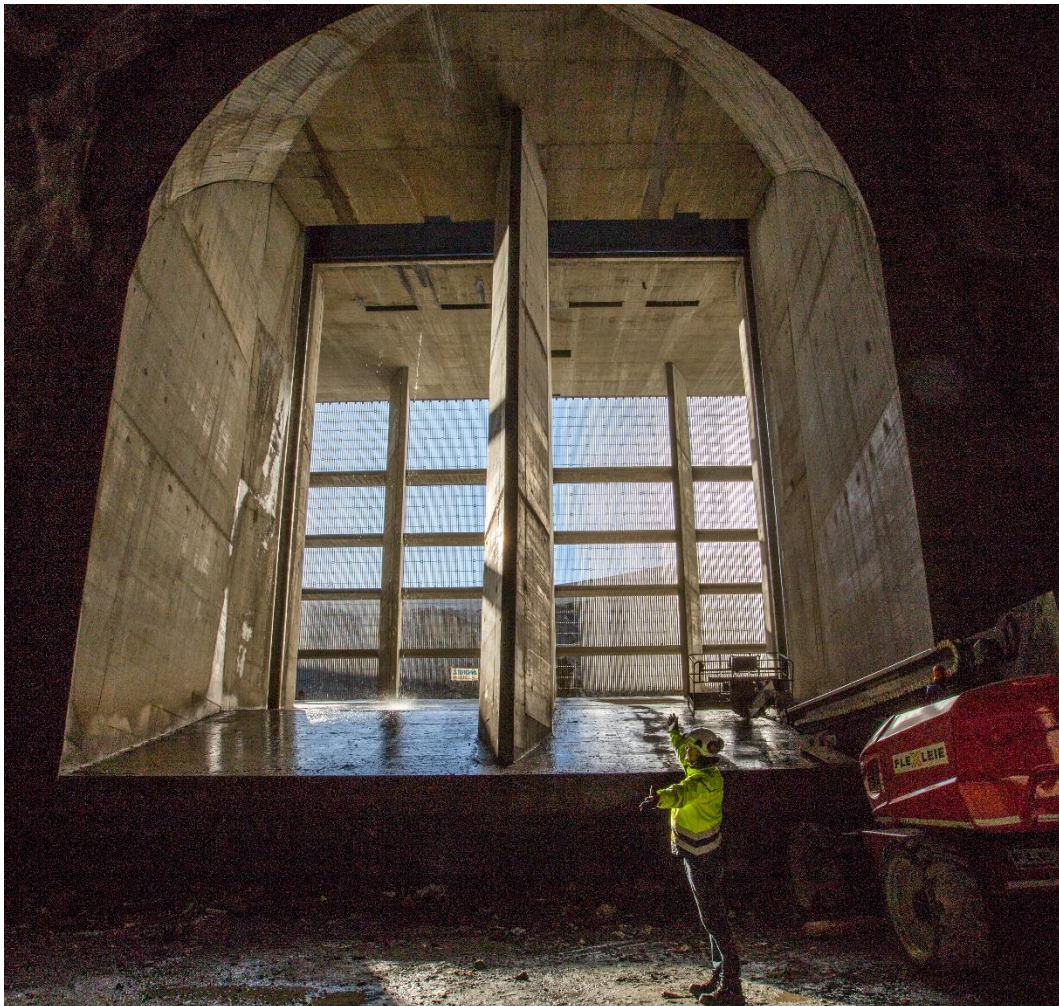


Fig. 8
The Inlet Gate (500m²) – Vamma 12

COMMISSION INTERNATIONALE DES GRANDS BARRAGES

VINGT-SIXIÈME CONGRÈS DES GRANDS BARRAGES
Autriche, juillet 2018

DOI 10.3217/978-3-85125-620-8-196



This work licensed under a Creative Commons Attribution 4.0 International License. <https://creativecommons.org/licenses/by-nc-nd/4.0/>

HIGH PERFORMANCE PRESSURE TUNNEL EXCAVATION AND LINING

A. VIGL

CEO of viglconsult ZT, VIGLCONSULT ZT, SCHRUNS

AUSTRIA

C. BARWART

Chief project engineer of viglconsult ZT, VIGLCONSULT ZT, SCHRUNS

AUSTRIA

HIGH PERFORMANCE PRESSURE TUNNEL EXCAVATION AND LINING

A. Vigl¹⁾, C. Barwart²⁾

1) *CEO of viglconsult ZT*, 2) *chief project engineer of viglconsult ZT*,
VIGLCONSULT ZT, SCHRUNS

AUSTRIA

1. INTRODUCTION AND SUMMARY

Pressure tunnels of either, the headrace- and/or the tailrace system of high head (gross head >500m) hydroelectric power plants commonly are those parts of the plant that are bearing the maximum costs and the maximal potential of cost saving as well. For that reasons the optimization of the technologies applied has performed steadily within the last 20 years.

The performance has rather developed within the following topics:

- Optimized layout selection allowing a maximal benefit from the geological and hydrogeological surroundings.
- TBM- excavation predominantly based upon hard rock double shield technology.
- Precast segmental linings optimized towards the fundamental requirements of pressure tunnels.
- Grouting technologies in order to involve the rock mass into the lining concept as much as possible.
- Construction concepts that allow the performance of construction with a high percentage of semiskilled local workers supported by a small, specific skilled key staff.

The paper at hand is dealing with the key tasks lined out above. It mainly is focusing upon pressurized headrace tunnels. Regarding pressure shafts, references are given [14], [15].

2. CLASSICAL ALPINE HHP PROJECT SCHEMES

Figure 1 is showing a classical Alpine high head power plant (HHP) project scheme with a gross head above 500m.

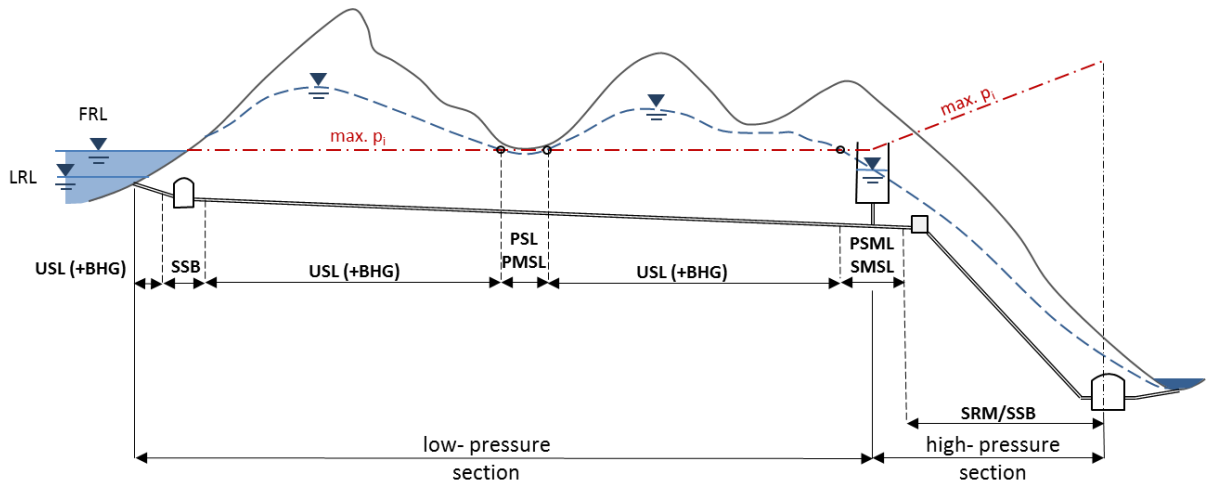


Figure 1: Longitudinal section of a typical Alpine high head power plant

The key task of the headrace system is to transfer the turbine water from intake to the power station with reasonable head losses and to bear the maximal internal pressure. The goal is to gain as much support as possible from the surrounding rock mass. Economically sealing and grouting of the pressure tunnel will require sufficient overburden. This can be achieved by an optimized layout design. A special benefit can be gained, if the ground water table is located above the internal pressure of the tunnel. For those reasons, a typical Alpine high head power plant tries to meet the following goals [1]:

- To subdivide the headrace system in a long low- pressure section and a short high- pressure section.
- To gain the benefit from a ground water pressure above the maximal internal pressure and to remain beyond the “Walch’ border” [1] as far as possible.
- To place the surge system completely below the surface

This can be achieved if the layout (Fig. 2) is designed in a way that most of the cross sections fulfill the conditions shown in Fig. 3.

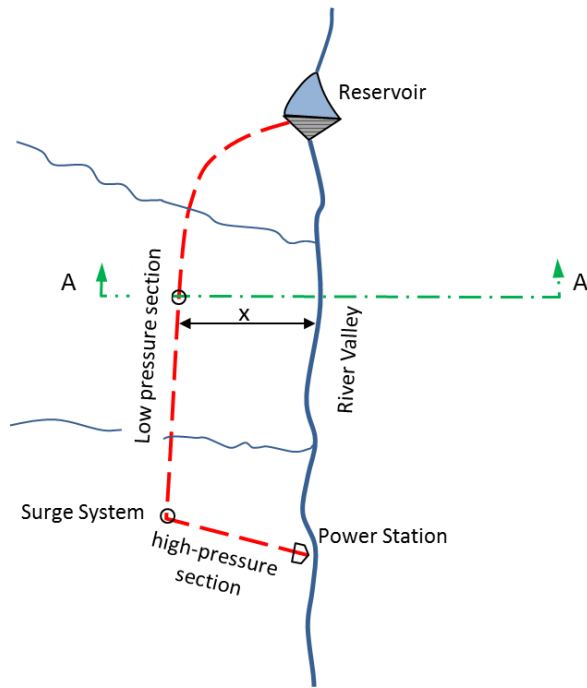


Figure 2: Layout of a typical Alpine high head power plant

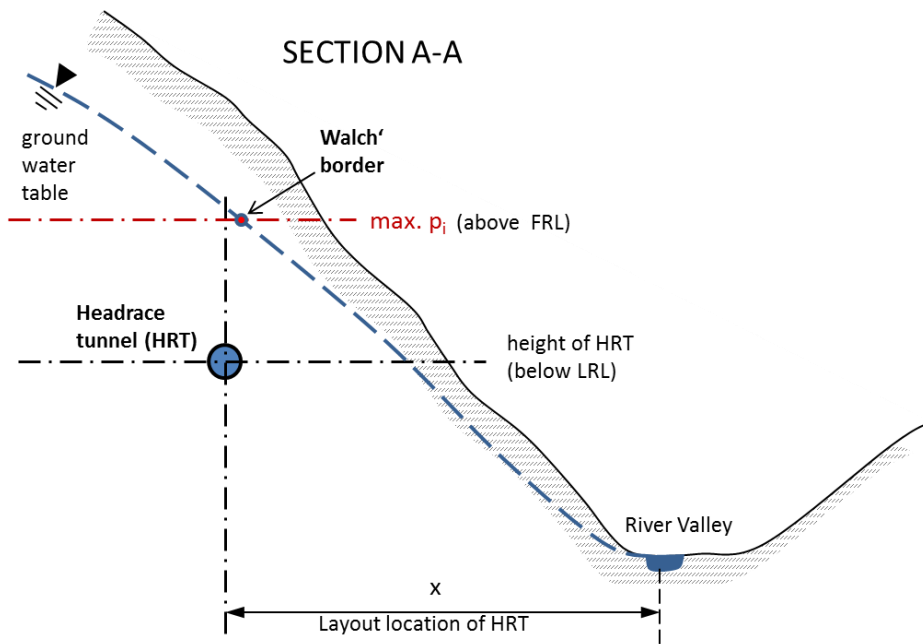


Figure 3: Cross section to place the headrace tunnel behind the Walch' border [1]

3. GEOTECHNICAL APPROACH & HYDRAULIC DIMENSIONING

The focus of the geotechnical approach predominantly has to be laid upon the feasibility of the excavation method and not upon the lining. Since mechanical excavation in most cases is a preferable method to excavate headrace systems, the focus will lay upon the feasibility of TBM excavation for the headrace tunnel of the low-pressure section. The same is due for an inclined shaft of the high-pressure section or for raise boring, in case of a vertical shaft.

Regarding the geotechnical approach, it has proved to follow the guideline for the Geotechnical Design of Underground Structures of the Austrian Society for Geomechanics [2] and to determine the “ground behavior types” (BT) systematically along the longitudinal section and especially in disturbed zones. If the ground behavior predominantly works out “stable” (BT1) to “disintegrated” (BT2) behavior types, excavation with an open Gripper TBM might be a proper solution. If the ground behavior predominantly offers disintegrated rock, as well as shallow and deep reaching rock-mass failure or rock burst (BT2 and above), an open Gripper TBM especially equipped for such behavior or a shielded TBM may be the best choice [3], [7].

For hydraulic dimensioning, the “Strickler- Formula” is serving properly and with sufficient accuracy. For cast in situ concrete, the Strickler roughness coefficient k_{STR} might be chosen with 80-90 [$m^{1/3}s^{-1}$]. For a segmental lining with mortar joint fill, the Strickler roughness coefficient k_{STR} might be chosen with 75-80 [$m^{1/3}s^{-1}$]. The roughness coefficient for segmental linings is considering smooth surfaces without pockets, which may exist in bolted linings.

4. HIGH PERFORMANCE EXCAVATION AND ROCK SUPPORT

The internal diameter of pressure tunnels most frequently is ranging from 4 to 7 meters with a tendency towards bigger diameters. This range of diameters is a range, where TBM-tunnelling in most cases is the most preferable and economical construction method.

Fig. 4 is showing the results of a comparison of achievable net advance rates between TBM and D&B excavation with a single heading either (1 D&B heading) and a D&B counter heading in addition (2 D&B headings). For the TBM heading, the net advance rate [m/wd] can be derived as follows:

$$net\ advance\ rate = \frac{p \cdot n \cdot 60 \cdot 24}{1000} \eta_{TBM,24h} \cdot \eta_{(p \cdot n)} \quad [1]$$

- p... penetration with, p=7mm/rev
- n... cutter head speed [rev/min], derived with
- $n = 50/D_{exc}$ [2]
- D_{exc} ... Excavation diameter [m]
- $\eta_{TBM,24h}$... TBM net boring time utilization, with $\eta_{TBM,24h} = 35\%$

- $\eta_{(p \cdot n)} \dots$ Utilization of penetration & cutter head speed : $\eta_{(p \cdot n)}=65\%$.

For D&B it has been anticipated, that the length of one round is 3m and 3 rounds can be achieved per working day, independent from the excavation diameter $D_{exc.}$. Fig. 4 clearly shows that for the common diameter range for headrace tunnels, the TBM is the preferable method regarding net-advance rates. This of course only is due if TBM has worked out as a feasible excavation method.

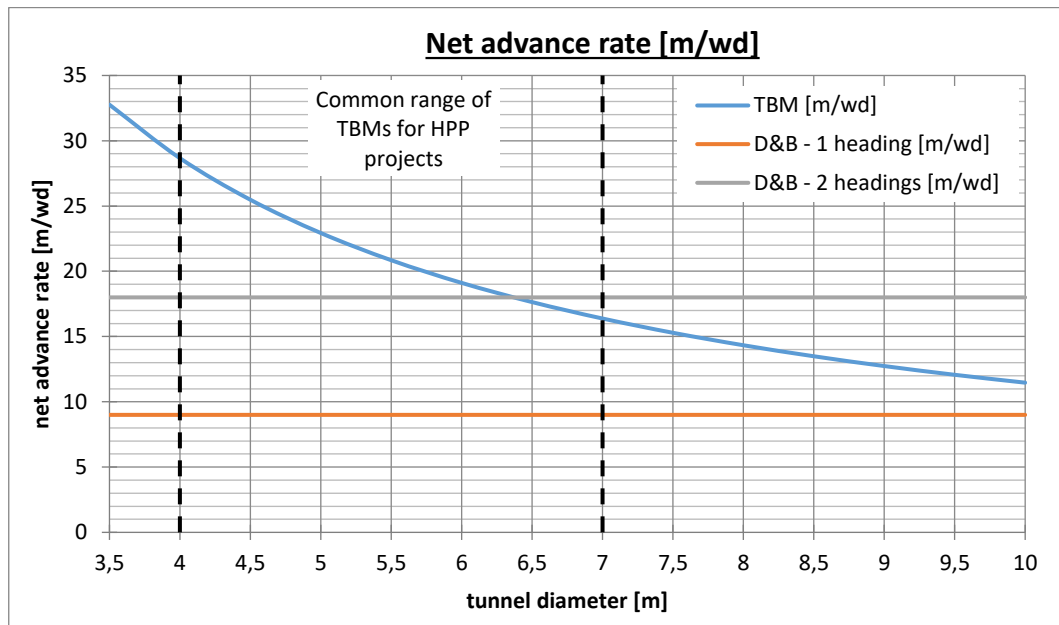


Figure 4: comparison of TBM and D&B regarding achievable net advance rates

Considering the TBM preferable for high performance excavation and a shielded TBM most appropriate for a wide range of rock mass behavior (BT), the maximal benefit can be gained from a double shield TBM (TBM-DS) together with a simple segmental lining. The TBM-DS is offering a Gripper mode for high performance under preferable geological conditions and a single shield mode, probably together with special pretreatment measures, for special zones.

Tunnel support according NATM and in situ concrete lining of course can be the best choice on a Gripper TBM [4] for special projects with a short length and / or small diameters. However, most probably it requires especially skilled workers and is bearing a high risk regarding construction time and costs. The qualification in skills and the risks regarding construction time and costs can rather be reduced by applying the technology of mono shell precast tunnel linings. Such precast segmental linings are linked to high performance excavation, predominantly with double shield hard rock TBM's.

For worldwide application of economically high performance pressure tunneling and lining, it is a postulate, that construction can be performed with a high percentage of semiskilled local workers supported by a small specific skilled

key staff. This postulate is fulfilled with the technologies lined out. Segmental lining is offering the advantage of high quality segment prefabrication outside the tunnel and quick and accurate installation within one working cycle inside the tunnel. Remaining in full compatibility with high performance TBM-DS excavation, simple precast lining systems, meeting all requirements of common headrace tunnels, have been developed and optimized during the recent 20 years [5], [6], [8], [9] [10], [12], [13].

Such lining systems commonly are composed of a parallel ring system with rhomboidal or hexagonal precast segments. The annular gap fill most frequently is mortar in the invert and pea-gravel in the circumference, which is systematically contact grouted within a separate step, followed up by borehole grouting where required. Such a lining system is able and suitable to fulfill most requirements of a final lining of a headrace tunnel.

5. BEST FITTING LINING SYSTEMS

As already lined out above, the key task of designing a headrace tunnel, is to gain as much benefit and cost saving potential from the surrounding rock mass. In terms of the sealing and bearing requirements, the most common lining types for headrace tunnels can be defined as follows (Tab. 1):

NOL	no lining(invert only)
USL	unsealed concrete lining
USL+BHG	unsealed concrete lining + borehole grouting
PSL	pre stressed lining
PMSL	plastic membrane sealed lining
SMSL	steel membrane sealed lining
SRM	rock mass supported steel liner
SSB	self bearing steel liner

Table 1: Legend for different lining systems

Tab.2 comprises the main tasks and requirements for the applicability of the common lining types.

Requirements	no lining (invert only)	unsealed lining (USL)	unsealed lining + borehole grouting (USL + BHG)	pre-stressed lining (PSL)	plastic membrane sealed lining (PMSL)	steel membrane sealed lining (SMSL)	rock mass supported steel liner (SRM)	self bearing steel liner (SSB)
rockmechanical requirements	stable rock-mass under internal pressure fluctuation too; non erodable rock mass	massive to disintegrated, non erodable rock mass	highly jointed to disintegrated rock mass	every kind of rock mass; minimal principle stress above grouting pressure			every kind of rock mass; minimal principle stress must be known	no relevant requirements
hydrogeological requirements	external watertable above inner pressure; or watertight rock mass	external watertable above inner pressure; or watertight rock mass ($k_f < 10^{-7}$ m/s)	external watertable preferable above inner pressure; groutability with cement grout ($k_f > 10^{-5}$ m/s)	no relevant requirements; groutability with cement grout ($k_f > 10^{-5}$ m/s) in case of consolidation grouting			external water pressure must be known; groutability with cement grout ($k_f > 10^{-5}$ m/s) in case of consolidation grouting	external water pressure must be known
int. pressure conditions	slow dynamic pressure fluctuation (up- and downsurge only)			minimal principle stress emply above dynamically internal pressure			no relevant requirements	
environmental restrictions	expected water inflow in line with restrictions			no relevant impact				

Table 2: Basic requirements for different lining systems

Fig. 5 is showing a comparison of those lining types regarding construction cost. As a basis, a design discharge has been chosen with 30m³/s. Considering tunnel diameter optimizations, for the concrete or segmental lined types, a flow velocity was anticipated with about v=3m/s; for the steel lined types the flow velocity was anticipated with about v=6m/s.

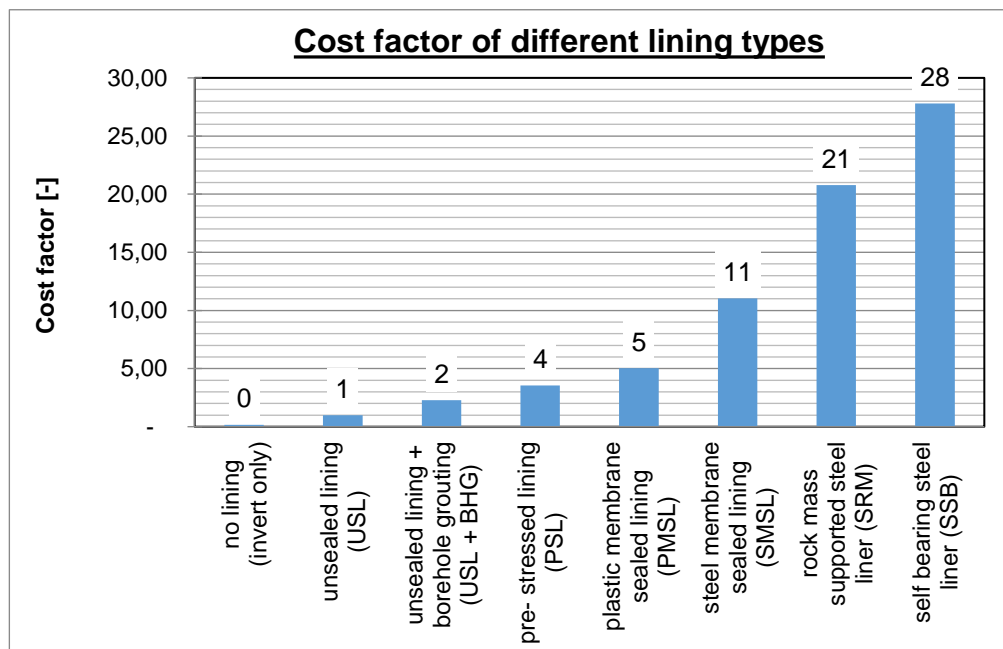


Figure 5: Cost factor for different lining types considering lining costs

The “cost factor” shown in Fig. 5 comprises the relation of the construction costs of the lining calculated for the different lining types. The costs per meter for an unsealed concrete lined tunnel was taken as a reference value with “1”. From Fig. 5 the benefit can be derived, to remain with an unsealed lining as far as possible. Unlined tunnels, which would comprise the lowest construction costs nowadays, became more and more out of fashion due to risk in terms of falling rock into turbine water.

6. GROUTING AS A KEY TASK

The principle to gain most benefit from the surrounding rock mass in order to achieve the most economical lining type is determined by the following tasks:

- To activate a sound rock mass load bearing ring in order to reduce the bearing capacity required from the lining.
- To hide below the ground water table in order to reduce sealing tasks to a minimum.
- To improve the surrounding rock mass by grouting in order to achieve most uniform and consolidated rock mass conditions, to reduce the rock mass permeability in order to control water communication between inside and outside the tunnel and pre-stress the lining system in order to improve with regard to internal pressure fluctuation.

The first task can be met by applying the construction principles of NATM. The second can be met by a sound layout design of the headrace system [1]. The last can be met by grouting. Grouting in any case should comprise systematically contact grouting as a basis and consolidation- and/or sealing grouting, in terms of borehole grouting, systematically or where required [11].

7. HOW THE CIRCLE GETS CLOSED

At high head hydropower plants with gross height greater than 500m of the conventional “Alpine type”, in most cases the headrace system comprises the mayor part of the plant costs. At the other hand, especially this part comprises the mayor chance to gain as much benefit from the surrounding rock mass, to keep the overall projects costs low, and to turn a project towards economic feasibility.

The first step starts with a layout design keeping the cost-factor of the lining type in focus. The next step is to achieve a high performance excavation method and economic support method comprising already a final lining, meeting the

requirements of a headrace tunnel. Both steps are linked to each other and must be considered as a decision loop (Fig. 6).

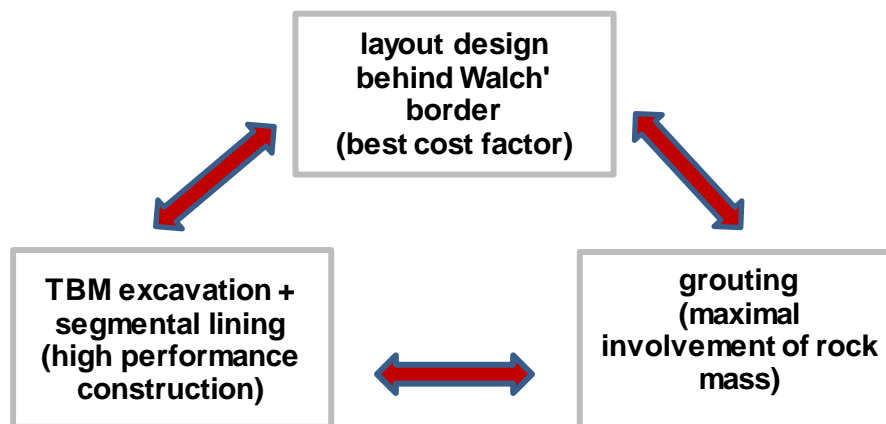


Figure 6: Link between layout, excavation, lining and grouting

REFERENCES

- [1] G. SEEBER; „Druckstollen und Druckschächte“; *ENKE im Georg Thieme Verlag; Stuttgart/Germany; ISBN 3-13-117511-7; (1999)*
- [2] ÖGG „Guideline for the Geotechnical Design of Underground Structures“; *Austrian Society for Geomechanics Salzburg/Austria; (2010)*
- [3] W. GÜTTER, W. WEBER, “Two tunnels in totally different geologic formations excavated by the same Double- Shield TBM” – *Felsbau 19 (2001) Nr. 3*
- [4] G.SEEBER, A. VIGL, "Die Neue Österreichische Tunnelbaumethode und der mechanische Vortrieb mit Tunnelbohrmaschinen" (New Austrian Tunnelling Method and excavation with TBM's) – *Felsbau 6 (1988) Nr. 2*
- [5] A. VIGL, "Planung Evinos-Tunnel" (Design of the Evinos-Tunnel) – *Felsbau 12 (1994) Nr. 6*
- [6] R.GRANDORI, M.JÄGER, F.ANTONINI, A.VIGL "Evinios-Mornos Tunnel - Greece" – *Proceedings of the Rapid Excavation & Tunneling Conference – RETC(1995)*
- [7] A.VIGL, M.JÄGER, "Double shield TBM and open TBM in squeezing rock - a comparison" – *Proceedings of the world tunnel congress '97 - Vienna/Austria 1997 - ISBN 90 4510868 1 Balkema, Rotterdam)*

- [8] A.VIGL, E.PÜRER, "Mono-shell segmental lining for pressure tunnels" – *Proceedings of the world tunnel congress '97 - Vienna/Austria 1997 - ISBN 90 4510868 1 Balkema, Rotterdam*)
- [9] G.INNERHOFER, A.VIGL, "Tunnel lining without reinforcement" - *Proceedings of the world tunnel congress '97 - Vienna/Austria 1997 - ISBN 90 4510868 1 Balkema, Rotterdam*)
- [10] A.VIGL "Design method for TBM-driven water-and pressure tunnels" – *Proceedings of 2nd Mexican Congress of Tunnelling Engineering and Underground Works - by AMITOS- Mexico City, Mexico(14.-17.May 1997)*
- [11] VIGL A., R. GERSTNER; "Grouting in pressure tunnel construction – Injektionen im Druckstollenbau" – *Journal of Geomechanics & Tunnelling 2 (2009), No.5*
- [12] VIGL A., C. BARWART; "Kopswerk II headrace tunnel – geomechanical and construction design – Triebwasserstollen Kopswerk II – geomechanische und bautechnische Planung" – *Journal of Geomechanics & Tunnelling 4 (2011), No.2*
- [13] VIGL, A.; R.GERSTNER, F.BARTIMOCCIA, M.CRUCIANI; „Headrace tunnel and tailrace tunnel of the Beles MPP in Ethiopia“;– *Journal of Geomechanics & Tunnelling 6 (2013), No.5*
- [14] VIGL, A., "Conventional design of HPP pressure shafts according to G.Seeber, considering the surrounding rock mass" *Proceedings of the 3rd. international HSS conference (ISBN 978-3-85125-292-7) TU Graz (2013)*
- [15] VIGL, A., „System solutions for headraces in high head hydropower plants“;– *Journal of Geomechanics & Tunnelling 8 (2015), No.1*

COMMISSION INTERNATIONALE DES GRANDS BARRAGES

VINGT-SIXIÈME CONGRÈS DES GRANDS BARRAGES
Autriche, juillet 2018

DOI 10.3217/978-3-85125-620-8-197



This work licensed under a Creative Commons Attribution 4.0 International License. <https://creativecommons.org/licenses/by-nc-nd/4.0/>

GEOMEMBRANES IN HIGH-PRESSURE TUNNELS AND SHAFTS

David A. DEL RIO

Project Controller – Construction and Engineering, AES CHIVOR

COLOMBIA

Marco SCARELLA

Design Manager, CARPI TECH

SWITZERLAND

Gabriella L. VASCHETTI

Vice President - Technical & Marketing Manager, CARPI TECH

SWITZERLAND

COMMISSION INTERNATIONALE
DES GRANDS BARRAGES

VINGT-SIXIEME CONGRES DES
GRANDS BARRAGES
Autriche, juillet 2018

GEOMEMBRANES IN HIGH-PRESSURE TUNNELS AND SHAFTS

David A. DEL RIO

Project Controller – Construction and Engineering, AES CHIVOR

COLOMBIA

Marco SCARELLA

Design Manager, CARPI TECH

SWITZERLAND

Gabriella L. VASCHETTI

Vice President - Technical & Marketing Manager, CARPI TECH

SWITZERLAND

1. INTRODUCTION

Hydraulic tunnels and shafts are underground water ways that, with the exception of old tunnels excavated in rocks, are usually lined. The lining provides stability and watertightness to the excavation line, avoiding that excessive water infiltration may undermine the stability of the slopes and of the structure itself, and minimises head losses, due to the low friction of the lining in contact with water.

Traditional lining systems have been steel, and reinforced or un-reinforced concrete. The construction of steel and concrete linings is expensive and time

consuming, can be further complicated in locations with difficult access, and may require expensive maintenance: over time, or in presence of particularly difficult geological conditions, concrete linings deteriorate, water infiltrates into the soil through fissures, and/or failing joints and increased permeability, increased roughness results in reduced hydraulic efficiency. Similarly, steel liners may be stressed above their yielding point.

Deterioration of the lining and subsequent loss of watertightness can have serious consequences: continuous water seepage into the surrounding soil may in the long term affect the stability of steep natural slopes, eventually triggering landslides that can ultimately cause the partial or total collapse of the structure. Deterioration of a concrete liner means not only in loss of water but also increased roughness. The Owners therefore face risk of instability, power loss, and head loss.

Rehabilitation must restore watertightness and bring the pressure tunnel/shaft back to its design conditions. Local repairs with mortars and resins have shown drawbacks in respect to efficiency and durability. Overall repair with a new liner must be designed to optimise several parameters: hydraulic efficiency, lifetime, outage time for installation, costs, future maintenance. Geomembrane lining systems have proved to be a permanent repair solution, and in case of new construction a solution increasing the project's safety. This paper focuses on exposed geomembrane systems, which are applied to rehabilitation and new construction.

2. THE GEOMEMBRANE SYSTEM

2.1. RATIONALE

The rationale of the system is to provide a practically watertight liner capable to maintain imperviousness under the acting loads, and with elongation characteristics allowing bridging those discontinuities that may arise in the subgrade (e.g. cracks forming in the concrete liner on which the geomembrane is applied). A geomembrane liner stops leakage: it prevents water entering the deteriorated concrete lining through cracks and joints, and affecting the durability of the reinforcement, and avoids that water inside the tunnel can escape into the surrounding ground with potentially dangerous effects on the stability of the slopes and consequently of the structure. Additional assets are that an exposed geomembrane system does not significantly reduce the tunnel envelope, improves hydraulic efficiency through low friction, and by deleting future maintenance provides savings on costs due to outage.

Design parameters for the choice of the liner, of its anchorage system, of drainage and support layers if any, are water head, static and dynamic pressure,

water velocity, negative pressure outside the structure when it is empty, way of operating the structure, roughness of the subgrade, etc. The geomembrane liner is anchored by mechanical fastening lines whose type, number and position is designed based on the mentioned designed loads at full and empty tunnel, and taking into account also the dynamic action of water that would result from a tear in the geomembrane liner. Water velocities of several meters/second and pressures of several MPa can be accommodated.

A drainage system is provided behind the geomembrane to collect and discharge water that should be present behind the geomembrane liner, be it water migrating from the slopes towards the structure, or already impregnating a deteriorated concrete liner. The drainage system avoids that if the tunnel is dewatered backpressure can build up and ultimately exceed the resistance to burst of the geomembrane.

2.2. COMPONENTS

The liner adopted in all state-of-the-art projects is SIBELON® CNT, a geocomposite consisting of a flexible polyvinylchloride geomembrane, heat-bonded to an anti-puncture geotextile. The geomembrane, with hydraulic conductivity $k = 6.25 \cdot 10^{-14}$ cm/s, provides the water barrier, the geotextile protects the geomembrane against puncturing from the substrate. The geocomposite shows the tensile stiffness of the geotextile up to a strain > 60%, for larger stresses the material presents the characteristic elastic behaviour of the geomembrane up to a strain > 250%. The design strength of the geocomposite liner is assumed to be the geotextile break tension, in the range of 50-60 kN/m, while the geomembrane elasticity is activated only in case excessive stresses would produce delamination of the backing geotextile. For design purpose, the strength parameters of the geocomposite, are corrected to account for potential defects not detected by the QC process, for incorrect installation, and for ageing of the polymeric material.

The anchorage system consists of continuous stainless-steel anchorage lines parallel to the water flow. These longitudinal fastening lines can be tensioning profiles, or batten strips, designed/installed to avoid slack areas and folds in the liner. The design of the anchorage lines is based on exceptional scenarios, aiming at avoiding that extreme loads may cause the failure of the anchorage system with the risk of detachment of metal elements and geocomposite fragments. The calculations are based assuming that, in case of accidental damage resulting in the perforation and/or cutting of the geocomposite liner, the water infiltrating through the damage can generate a negative pressure behind the liner equal to the internal pressure in the tunnel/ shaft. In this condition, remote but crucial for a correct design, the kinetic head of the water flow can generate uplift and deformation of the geocomposite liner. The tension in the geocomposite is obtained by an equation based on the kinetic head (function of the water velocity

and density) and on the geometry of the deformation, and using the stress-strain curve of the selected geocomposite. The tension in the geocomposite liner thus obtained must be at least equal to what imposed by the established Factor of Safety (FS). The tension transmitted to the anchorage lines results in a pull-out component and a shear component: the design condition for the calculation of the pull-out force on the anchors corresponds to the case in which two adjacent sheets of geocomposite liner are simultaneously damaged and uplifted, resulting in the combination of the pull-out components (one for each sheet), while the design condition for the calculation of the shear force on the anchor corresponds to the case in which only a single sheet of geocomposite liner is uplifted, resulting in an asymmetric shear component. The data obtained by calculations of the tension in the geocomposite, of FS on the geocomposite, of pull-out and shear forces on the anchors, and of FS for pull-out and shear, verify the soundness of the anchorage system.

A transverse stainless-steel watertight seal is placed at the beginning and end of the lined area to avoid water infiltrating behind the liner.

The drainage system is designed based on an analysis of the estimated amount of water that can accumulate behind the liner, leaking through the ground/cracked concrete lining when the tunnel/shaft is empty. The inflow is essentially due to a) the intrinsic permeability of the outer ring/concrete lining and b) the leakage through the concrete cracks. Given the low permeability of the concrete, leakage through cracks can be considered as the primary source of inflow, while other sources can usually be neglected. A continuous drainage layer consisting of a geosynthetic having high in-plane transmissivity is often applied to enhance efficiency of drainage transmission to the custom-designed drainage discharge components. In case of subgrade with large cracks/discontinuities/irregularities, additional geosynthetic layers are used to provide support/anti-puncturing.

2.3. PAST EXPERIENCE AND PERFORMANCE DATA

To the knowledge of the authors, experience of watertight geomembranes in high-pressure conduits dates back to the late 1970ies- early 1980ies, when Austria saw several applications with water heads in the range of 0.2 to 0.7 MPa, where the geomembrane was sandwiched between the outer regularization ring and the inner concrete ring. Carpi started installing totally or partially exposed geomembranes in pressure tunnels in 1984 (Gorghiglio pressure tunnel, Italy). The feedback of several installations proves the effectiveness of the system and its capability to resist high pressures and water velocity. Outstanding examples summarized below and detailed in international literature are Thissavros [1] and Belden [2].

Thissavros is a 11 meters diameter pressure tunnel in Greece. The inside water pressure is 1.5 MPa, maximum water velocity exceeds 4 m/s. Water infiltrating from the reservoir generates a negative uplift pressure of about 0.5 MPa. The tunnel was originally lined with concrete, which started to crack. At first reservoir filling, because of some changes in the location of the dam grout curtain and of the cracks in the concrete of the tunnel, the dam galleries were flooded. It was decided to extend upstream the concrete plug for a length of 60 m. Time constraints and a much more attractive price suggested to split the required extra works in two sections: one section by extending the conventional concrete plug and its steel lining, the second section by using only an exposed geomembrane against the fractured concrete liner. Installation of a watertight SIBELON® CNT geocomposite, anchored with tensioning profiles and watertight sealed at peripheries, upstream on concrete and downstream on steel, required 3 weeks and cost was approximately 25 % of the cost of an equivalent steel liner, which would have required more than 3 months' time for installation. The geomembrane system was installed in 1997. A few weeks after it had been installed and the tunnel had started operating, the tunnel had to be emptied to execute some extra grouting works in correspondence of the concrete plug. That situation allowed testing the fully satisfactory behaviour of the geocomposite and of its drainage system, which worked as designed. After grouting works were completed, the tunnel was filled again and it will be always full of water, with no plan to dewater it again. The geomembrane liner is working effectively since 1997.

Belden hydropower plant, built in 1958 and owned by Pacific Gas and Electric Co. (PG&E), includes a 2941.41 m long concrete lined tunnel (Tunnel 2). In 1970, during an outage, two large circumferential cracks and additional cracks were identified in the lining of Tunnel 2. The cracks were repaired on several occasions; instrumentation showed that the ground was continuously moving and slowly accelerating. PG&E undertook studies to determine the best method to rehabilitate the tunnel whose leakage was the main cause for the sliding of the ground. A geomembrane liner was selected because of speed of installation, lower cost, and potential ability to accommodate future ground movements. The geomembrane design was challenging due to the changing shape of tunnel, the water velocity (4.27 m/s), the hydraulic head (0.54 MPa), the groundwater pressure (0.24 MPa), and the drainage requirements due to the high water table in the mountain and the need to drain upstream. A complete survey of the tunnel showed that in one section the cracks could reach width > 22 mm over the design life of the project. Such opening, together with the pressure applied to the surface, could induce large strains in the selected watertight SIBELON® CNT geocomposite. A support system able to withstand the load transmitted by the water pressure on the span created by the big cracks was designed, consisting of a support geogrid placed on the concrete. A drainage geonet was installed on the geogrid. Both under-layers were placed in the full area to be lined, and anchored with mechanical anchors. The geocomposite was anchored with tensioning profiles and watertight sealed at peripheries with a mechanical seal consisting of 80 x 8 mm batten strips with regularising resin, gaskets and splice plates to evenly distribute compression. Installation was made in 2008, the tunnel was immediately put back to operation

for a couple of days, then dewatered and inspected, and put back in service. In 2014, 6 years after installation, the tunnel was again dewatered and inspected by PG&E. The detailed inspection did not find one single damage, no repairs were needed, and the tunnel was put back in service. Data readings have shown that the geomembrane system is successfully dewatering the mountain and preventing seepage that could aggravate ground movement.

3. RECENT CASE HISTORIES

3.1. HELMS HIGH-PRESSURE TUNNEL

The Helms Pumped Storage Project conduit and penstock system, owned by PG&E, connects Courtright and Wishon reservoirs in the Sierra Nevada Mountains of central California. The powerhouse complex is located more than 330 meters underground in granitic rock. The Helms Penstock Access Tunnel, approximately 76 m long and > 8 m in diameter, terminating into a 10.6 m thick concrete plug with maximum static hydrostatic pressure exceeding 5.1 MPa, has been in operation for more than 30 years and there was a desire to reduce seepage of high pressure water from the tunnel into the mountain. PG&E had installed a geocomposite liner into Belden hydraulic tunnel in 2008. Helms represented an approximately tenfold increase in pressure in respect to Belden, and more than threefold in respect to the Thissavros tunnel cited above.

Full scale testing was undertaken to validate a preliminary design based on anchorage with special tensioning profiles and perimeter seals conceived to resist the high pressure. The Deep Ocean Test Facility in Maryland, where the US Navy deep submergence vehicles were tested, was the only facility found with adequate equipment to allow testing under the required maximum pressure of 8.52 MPa. All components and design details of the geocomposite system ("Fig. 1") were tested to full dynamic pressure. The results proved a SIBELON® CNT 5050 geocomposite, a 3.5 mm geomembrane with a geotextile layer heat-bonded onto bottom sides of the liner, and its all-stainless-steel anchorage components, would withstand the pressures.

In the final design, the SIBELON® CNT 5050 geocomposite is anchored to the concrete subgrade by sixteen longitudinal fastening lines consisting of tensioning assemblies placed at appropriate spacing, and of one fastening line consisting of flat profiles, centred at the crown of the vault. The tensioning assemblies consists of two profiles: a first solid trapezoidal profile is fastened to the concrete ("Fig. 2" at left), the geocomposite is laid and punctured on the anchors fixing the first profile, and then permanently anchored by installing over it a second profile, whose shape is such that when the two profiles are tightly connected they achieve tensioning of the geocomposite ("Fig. 2" at right).

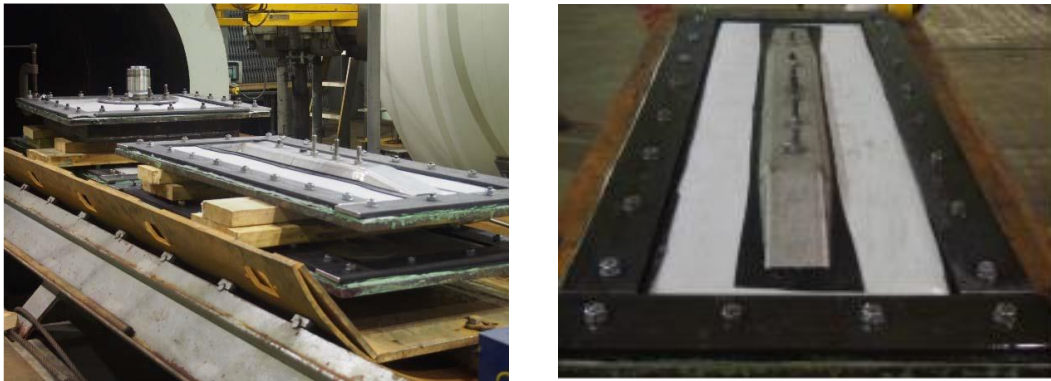


Fig. 1

Testing under 85.2 bar pressure for Helms. At left the tested components (drainage discharge valve, tensioning profiles and perimeter seals) ready for testing on wood blocks. In each test, the tank is filled with water through the instrument port. Water and air are pushed out of the system while the tank is pressurizing. At right, detail of the tensioning profiles and of the perimeter seal after a test

The anchors penetrating the geocomposite are equipped with suitable outfits and gaskets to make the penetrations watertight.



Fig. 2

Helms high-pressure tunnel. At left the solid trapezoidal tensioning profiles and flat profile anchored at the vault. At right a view of the completed anchorage lines

The upstream and downstream transverse perimeter seals consist of flat profiles, section 80 x 8 mm. Seven one-way mechanical pressure relief valves, distributed along the lined area, act as drainage discharge when the tunnel is emptied ("Fig. 3"). Construction of the waterproofing geocomposite began in September 2017 and was completed in October 2017, with the reservoir being placed back into operation in early November 2017.



Fig. 3

Testing drainage discharge capacity at Helms high-pressure tunnel. At left, after sealing of the geomembrane system, water present behind the liner exerts backpressure deforming the geocomposite. At right, the pressure relief valves have discharged the water inside the tunnel, the geocomposite is recovering the deformation

3.2. TUNJITA SURGE CHAMBER AND SHAFT

The Tunjita scheme in Colombia includes a surge shaft, an access gallery at the bottom of the shaft and a headrace tunnel (“Fig. 4”). All these structures are lined with three 0.05 m thick layers of shotcrete reinforced with a steel mesh, and with a 0.25 to 0.40 m thick layer of reinforced concrete. In 2017, an exposed SIBELON® CNT geocomposite system has been installed as safety water barrier on the surge chamber and shaft, and on the tunnels.

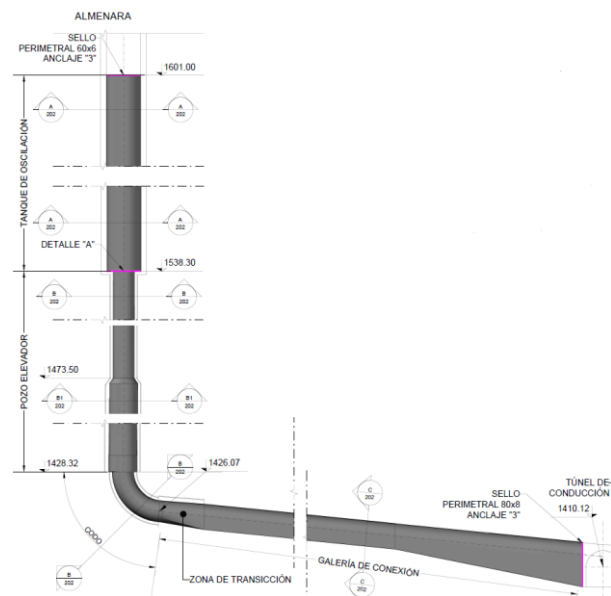


Fig. 4
The Tunjita scheme

The upper shaft is about 71.5 m high and with internal diameter 4.1 m, the surge shaft about 108.9 m high with an internal diameter of 2.5 m. The maximum hydrostatic pressure in the surge chamber is about 0.6 MPa, in the surge shaft about 1.74 MPa. The elevation of the water table is such that the bottom part of the upper shaft and the rest of the structure are permanently below the water table, with consequent presence of water in the rocky mass during the period of emptying.

The selected waterproofing liner is the geocomposite SIBELON® CNT 4400 (3.0 mm thick geomembrane heat-bonded to a 500 g/m² geotextile). Due to the water pressure, a support geocomposite layer, consisting of a geogrid backed by a nonwoven polypropylene geotextile, is placed under the SIBELON® geocomposite ("Fig. 5" at left). The geocomposite is fastened longitudinally by stainless-steel batten strips, section 60 x 6 mm, anchored by mechanical anchors selected in function of the strength of the concrete. The surge chamber has 10 fastening lines, the surge shaft has 8 fastening lines. Tensioning of the geocomposite is achieved by an installation sequence of progressive closure, placing the "First phase" anchorage lines and subsequently the "Second phase" anchorage lines, which produces a tensioning effect on the geocomposite liner in between two adjacent first phase anchorage lines. This method avoids formation of slack areas and wrinkles in the geocomposite. Perimeter seals are the same as for Belden.



Fig. 5

Tunjita surge shaft. Vertical view from bottom to top of the support geocomposite, and of the waterproofing geocomposite fastened and tensioned

3.3. TUNJITA TUNNELS

The connection and pressure tunnels, have a length of about 142 meters and a horseshoe section 3.60 m wide and with height varying up to 5.85 m. The maximum hydrostatic pressure in the connection tunnel is about 1.90 MPa, and in the pressure tunnel about 1.91 MPa, and 2.2 MPa at closing of the gates. The maximum water velocity is 2.4 m/s.

The waterproofing system is the same adopted in the surge chamber and shaft. The tunnels have 8 fastening lines, except than in correspondence of the sand trap, where the bottom is not lined and there are 7 fastening lines.



Fig. 6

Tunjita tunnels. At left the support geocomposite, at right the waterproofing geocomposite fastened and tensioned

4. FUTURE PROJECTS

The same geocomposite, and the same approach for the fastening system, has been adopted for the high-pressure shaft that is part of the Gilboa Pumped Storage Power Plant under construction in Israel. The PSPP comprises a nearly 480 m high vertical shaft with 4.5 m constant internal diameter. The rock excavation has been stabilised by a nearly 0.1 m thick shotcrete layer. The shaft lining consists of a 0.5 m thick heavily reinforced concrete (external diameter 5.5 m), increased to 1.5 m (external diameter 7.5 m) in the bottom section. Maximum internal pressure at the bottom bend is about 5.94 MPa; maximum external (negative) pressure is potentially equal to internal static pressure due to leakage through concrete lining; steel reinforcement concrete cover is 50 with tolerance ± 10 mm, which will require using special anchors for short embedment. The design water velocity is 6 m/s, resulting in 14 fastening lines placed at regular spacing.

REFERENCES

- [1] SCUERO A., VASCHETTI G. Stopping water and power losses in hydraulic tunnels. Proceedings, *Conference on Techniques of Reinforced Concrete for Hydraulic Engineering*, 2005.
- [2] WILKES J., YU A., MCMANUS R., JARAMILLO C., VERANI C. Lining Belden Hydraulic Tunnel with a Geomembrane. *WTC11 Congress*, 2011.

COMMISSION INTERNATIONALE DES GRANDS BARRAGES

VINGT-SIXIÈME CONGRÈS DES GRANDS BARRAGES
Autriche, juillet 2018

DOI 10.3217/978-3-85125-620-8-198



This work licensed under a Creative Commons Attribution 4.0 International License. <https://creativecommons.org/licenses/by-nc-nd/4.0/>

**INCREASING POWER OUTPUT AND FLEXIBILITY OF EXISTING HIGH HEAD
POWER PLANTS WITH THE HELP OF WATERHAMMER SIMULATIONS**

Stefan HÖLLER

INSTITUTE OF HYDRAULIC FLUID MACHINERY, GRAZ UNIVERSITY OF
TECHNOLOGY

AUSTRIA

Helmut JABERG

INSTITUTE OF HYDRAULIC FLUID MACHINERY, GRAZ UNIVERSITY OF
TECHNOLOGY

AUSTRIA

COMMISSION INTERNATIONALE
DES GRANDS BARRAGES

VINGT-SIXIÈME CONGRÈS DES
GRANDS BARRAGES
Autriche, juillet 2018

INCREASING POWER OUTPUT AND FLEXIBILITY OF EXISTING HIGH HEAD POWER PLANTS WITH THE HELP OF WATERHAMMER SIMULATIONS

Stefan HÖLLER, Helmut JABERG

*Institute of Hydraulic Fluid Machinery,
GRAZ UNIVERSITY OF TECHNOLOGY*

AUSTRIA

1. INTRODUCTION

In a changing energy market with decreasing energy prices, energy suppliers try to sustain their financial return with their existing hydro power plants. One possibility to increase the annual turnover is not only to increase the power output but also the availability and flexibility of an existing power plant. Most of the older power plants – in particular storage power plants – are not designed for such operating modes – especially not for rapidly changing and fluctuating loads.

As many plants operated today were constructed decades ago, the original plant design was based on operating conditions that were completely different to the ones actually required. To prove the ability for higher flexibility in power generation, detailed investigations of the power water way, especially the surge tank limitations, are necessary. Since the main constructive infrastructure cannot be changed or just in a restricted way, usually only limited additional power generation is possible. The higher the demand for an increasing power output, the higher are the limitations in operational flexibility. An overflow of the surge tank must be prevented in any potential operational or exceptional scenario of the power plant. On the other hand, a ventilation of the headrace system by means of an inelible empty surge tank must not occur during operation.

Flexible operation induces a highly transient fluid flow in the hydraulic system and especially the surge tanks of high head hydro power plants. In the planning phase of activities to increase the power output and/or the flexibility, a

reliable prediction of the transient plant behaviour and especially the surge tank performance in unsteady load cases – such as periodic machine starts and stops or switching load cases – is necessary.

Modern techniques in numerical simulation methods provide the only feasible possibility to accurately calculate the occurring mass oscillations and pressure pulsations. Thus providing a for the optimization of the transient behaviour. Commercial software-packages for water hammer simulations usually do not provide numerical models for a realistic calculation of complex components like surge tanks, hydraulic turbines or emergency closing valves in a high head hydro power plant. But especially these components need to be modelled correctly in order to get a significant and reliable solution [1], [2].

2. OVERVIEW OF THE INVESTIGATED POWER PLANT

The Kops I hydro power plant was set into operation in 1970 with a maximum power output of 245 MW. The hydraulic system consists of a headrace tunnel with a length of 4.500 m which connects the Kops lake (upper reservoir) with the surge tank of the power plant from where the penstock feeds three Pelton units with four nozzles for each turbine.

The throttled chamber surge tank (see Fig. 2) is constructed with an upper and a lower chamber, which is quite common for alpine high head power plants [3]. At the base point of the surge tank, at the connection with the headrace tunnel, one of two throttles is located. Since there is a second vortex throttle at the intersection of the surge tank main shaft and the upper chamber, a differential effect is created that supports damping of the mass oscillations. The fluid flow in the lower chamber of this surge tank design will have two different states:

- open channel flow if the lower chamber is aerated
- pressurized flow in case of a full lower chamber combined with a charging or discharging procedure of the surge tank

Fig. 1. shows a general hydraulic layout of the power plant, for the main data of the original power plant setup see Table 1.

In the course of a rehabilitation of the generator sets of the power plant, there was an attractive possibility of a power increase of the machinery sets.

Table 1
Power Plant data of HPP Kops I

set into operation	1969-1970	maximum gross head	780	m	
number of units	3	#	minimum gross head	700	m
nozzels per unit	4	#	maximum power	245	MW

3. NUMERICAL MODEL

A large number of simulations was performed to examine the maximum power increase where a secure plant operation is guaranteed in a wide operation range and under all circumstances. It would be far out of the scope of a conference paper to show even a larger portion of the results found.

The focus of the presented results is on the water level in the surge tank and its chambers as this is one of most crucial components of the plant. Additionally, some of the most challenging operational modes will be presented.

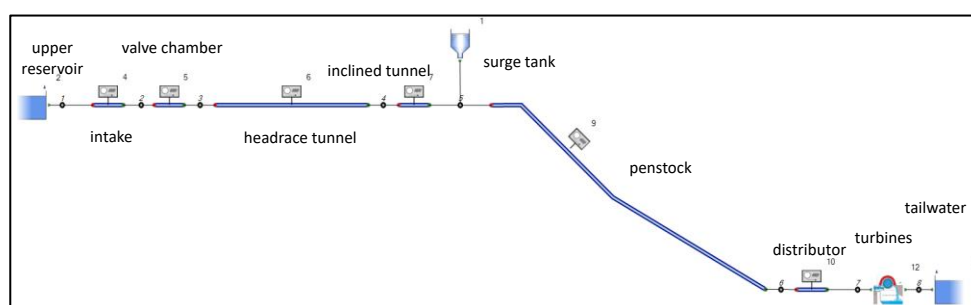


Fig. 1
Numerical model of HPP Kops I

The 1-dimensional water hammer analyses, which are shown in this paper, were performed using the commercial software package Flowmaster [4]. In addition to the standard components further improved hydro power components were especially developed for this purpose [1], [2]. In fact, Flowmaster is designed to enable the implementation of these customized components in form of user built Component Analytical Models (CAM). Their purpose is to model their hydrodynamic behavior by a linear function for the mass or volume flow rate, respectively of the pressure of the connected pipe work and a constant that hydrodynamically would be a source or sink. In case of the simulation network for Kops I the custom designed numerical models are the surge tank and the Pelton turbine. Sophisticated mathematical models were required in order to find detailed results on different positions in the surge tank chambers such as water levels, throttle flow rates and pressures. It also allowed the estimation of the probability of air being sucked into the headrace system when the lower chamber of the main surge tank is being emptied.

3.1. SURGE TANK MODEL

Since the surge tank is the most critical component for the given task, the numerical model for this component must be able to represent the real behavior in a detailed way. The invented simulation model is therefore able to represent the above-mentioned states of the lower chamber. It can act as pressurized pipe

or as a partially filled pipe with open channel behavior. If the lower chamber is full, liquid inertia of both, the chamber and the rising shaft, is considered. A local rise or fall of the liquid level at the base point throttle is also numerically possible as well as different liquid levels in the rising shaft and the upper chamber mainly resulting from the differential effect caused by the vortex throttle. Horizontal liquid levels in the aerated chambers are assumed since there were no significant effects of surface waves expected. This assumption is confirmed by the comparison with measurements shown below. The charging and discharging of the upper chamber is possible in two different ways depending on the liquid level:

- By means of the vortex throttle if the liquid level is below the weir crone of the rise shaft (1)
- And additionally by means of weir overflow if the liquid level is above the weir crone (2)

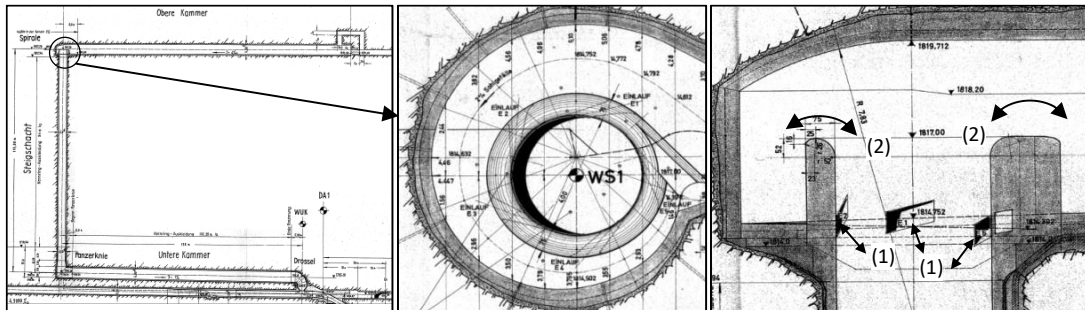


Fig. 2

Surge Tank of HPP Kops I: left: general view, middle: top view of vortex throttle, right: cross section of vortex throttle

For a correct modelling of the surge tank behavior in such detail, additional information and boundary conditions are necessary. To get appropriate data of the hydraulic losses of the throttles and the hydraulic behavior of the chambers and weirs, analytical models based on technical literature [5], [6], [7], [8] or 3D numerical simulations have to be developed. A successful application of 3D numerical simulations to get the necessary information of hydraulic data to model the surge tank behavior correctly in the course of 1D numerical waterhammer simulations has been shown by Meusburger [9] and Veide et al. [3].

4. NUMERICAL RESULTS AND COMPARISON WITH MEASUREMENTS

4.1. VALIDATION OF THE NUMERICAL RESULTS

A comparison of the numerical result for the original power plant configuration with on-site measurements was carried out at the beginning of the numerical simulations. In that course a validation of the numerical model, especially for the surge tank behavior, as well as the losses in the power water way, was possible. Measurement data of the pressure at the base point of the surge tank, at the downstream end of the penstock and at the inlet of the pelton turbines, as well as the position of the pelton needles were available. In the bottom diagram of Fig. 3 the liquid levels in the surge tank are shown for both simulation and measurement results for a serial starting of the units followed by a synchronous stopping off all units in parallel. The corresponding measured nozzle positions supplied the boundary conditions for the numerical simulations and are drawn in the top diagram in Fig. 3.

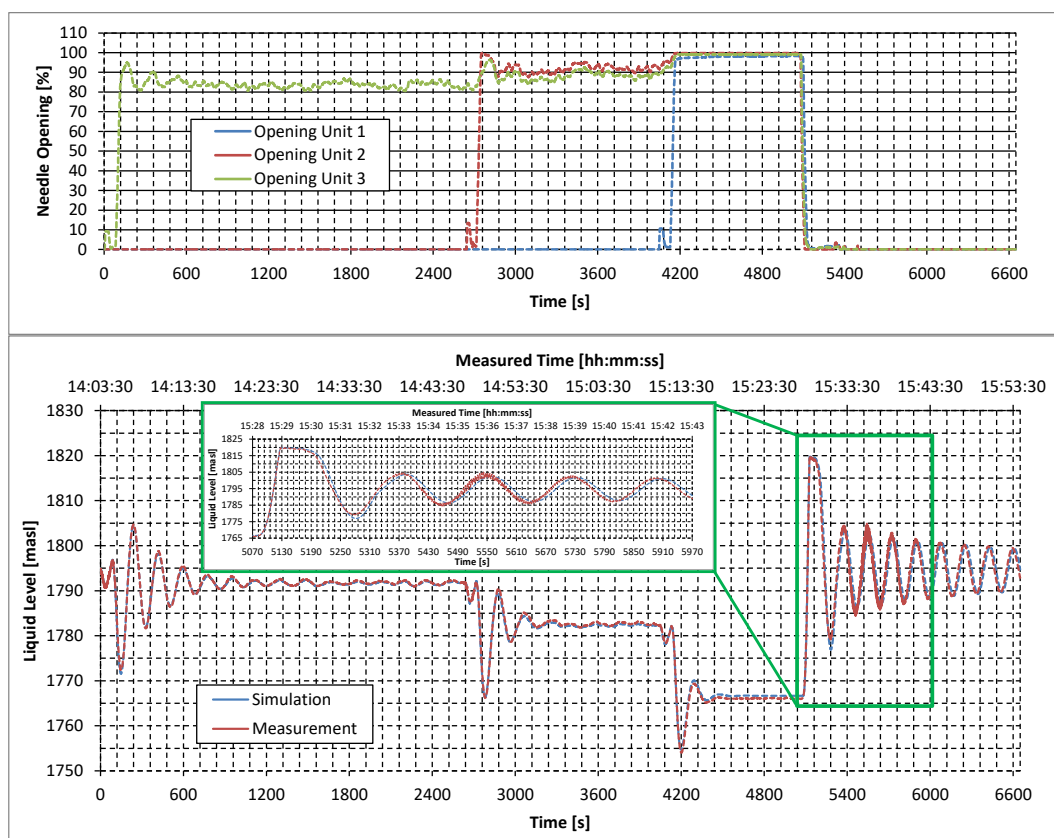


Fig. 3
Comparison of simulation results and field measurements

The comparison shows very good correlation for the measured and simulated liquid levels in the surge tank. A detail view of the time when the units are stopped (after around $t = 5100$ s) is presented in the small diagram in Fig. 3. After approximately $t = 5130$ s the upper chamber is activated, indicated by a nearly horizontal water level. Again, a very good correlation of the simulation and the measurement is shown for both, filling (rising liquid level) and emptying (falling liquid level) of the upper chamber as well as the surge tank in general.

Therefore the accuracy of the numerical model is confirmed and yields additional confidence for the simulation results.

4.2. MAXIMUM SURGE TANK OSCILLATION

In order to achieve the allowable operating limits for the power plant with increased power output, the maximum occurring surge tank oscillation must not exceed the allowable limits in any possible operating mode. Therefore the maximum and minimum liquid levels in the surge tank for a given gross head and power output have to be identified.

The criterion for determining the **maximum water level** in the upper reservoir (i.e. gross head) for a given power output is the maximum surge tank oscillation (i.e. the maximum filling of the upper chamber). The maximum allowable gross head is determined by following worst case scenario:

If all three turbines are put into operation from a standstill, the increasing turbine flow rate will lead to a rapid decrease of the water level in the surge tank. The nozzles are opened as far as possible for the given gross head, but the maximum opening is limited with the maximum power output of the generator. The system inertia of the headrace tunnel leads to an oscillation of the liquid level in the surge tank. When the turbines are stopped in parallel at the same time when the liquid level rises again, the surge tank oscillation can be forced to its maximum amplitude.

The resulting maximum water level in the surge tank increases with increasing gross head and turbine flow rate.

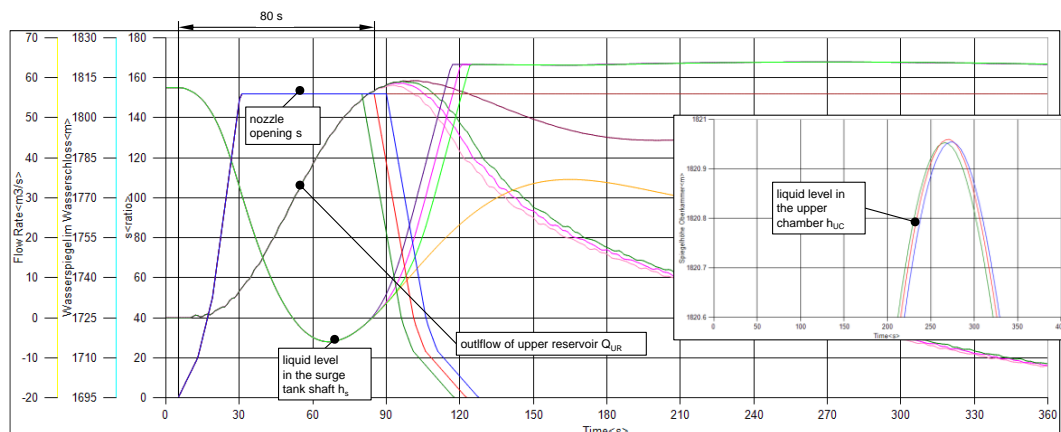


Fig. 4
Determination of maximum liquid level in the surge tank

The most critical time for stopping the turbines was found iteratively at 80 seconds after the start of the previous nozzle opening, by varying the closing time. An example procedure is shown in Fig. 4 where the nozzle opening (s), the

liquid level in the surge tank (h_s) and in the upper chamber (h_{UK}), as well as the outflow of the upper reservoir (Q_{UR}) are shown for four different load cases:

- start-up of 3 units in parallel
- start-up of 3 units in parallel followed by synchronous stopping at 3 different times.

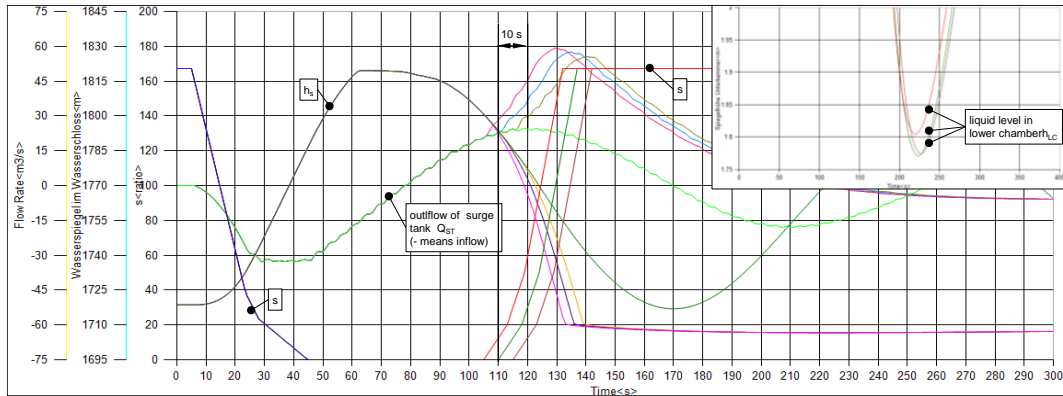


Fig. 5

Investigation of minimum water level in the surge tank

The **minimum water level** in the surge tank is determined when the units are started in parallel in resonance after a previous synchronous shut-down of the power plant. The procedure for the iterative investigation process is shown in Fig. 5. It shows the nozzle opening as well as the transients for h_s , the flowrate in the surge tank (Q_{ST}) and the liquid level in the lower chamber (h_{LC}) for four different loadcases.

The synchronous closing of the nozzels leads to a water level oscillation with corresponding flowrate in (- sign) and out of (+ sign) the surge tank. It turned out that the lowest liquid level in the lower chamber results when the opening of the nozzels is started 10 seconds before Q_{ST} would reach its maximum value of the preceding turbine stop.

If the above described maximum or minimum liquid level exceeds the surge tank limitations the power output will be decreased until the resulting surge tank oscillation is below the limitations. This procedure is then repeated for different gross heads to receive the maximum allowed power output.

4.3. CYCLICAL OPERATION

As already described above forced, water level oscillations caused by synchronous start and stop in resonance to the natural frequency of the hydraulic system must be given extra attention. With completely free power plant operation, it might be possible that such cyclic resonance manouvers are necessary several times in succession for grid service reasons (e.g. power control or frequency

control). Therefore also multiple surge tank excitation has to be examined in order to investigate whether possibly even higher water level amplitudes can result. Again several iterations are necessary to identify the worst time for each closing or opening cycle to gain highest or lowest liquid levels in the surge tank of the power plant.

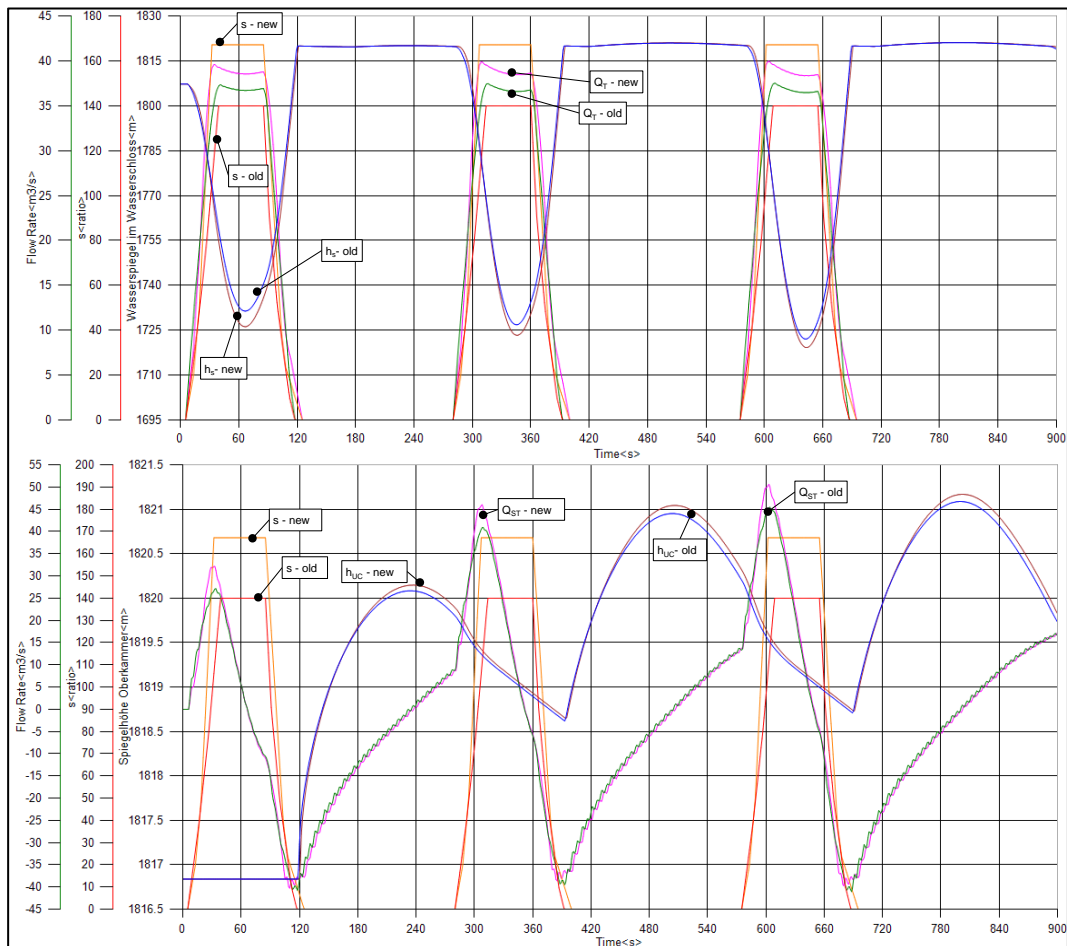


Fig. 6
Cyclical forced surge tank oscillation before and after power increase

An exemplaric multiple resonance cycle for both, the existing power plant configuration (old) as well as with increased power output (new), is shown in Fig. 6. In the upper diagram the transients for the nozzle opening (s), the liquid level in the surge tank shaft (h_s) and the turbine flowrate (Q_T) for both configurations are shown, whereas in the lower diagram the history for Q_{ST} and h_{UC} are drawn. It turns out very clearly that the maximum liquid level in the surge tank is increased if multiple resonance cycles are applied.

Investigations have shown that after 3 starts and stops the maximum water level amplitude is resulting. More cycles will not increase the liquid level oscillations for both load cases maximum and minimum liquid levels.

The new configuration with increased Q_T and thus increased power output has also increased operational flexibility since the maximum nozzle opening is reached in a shorter duration compared to the old configuration. In both scenarios the liquid level in the upper reservoir is at the same level near its maximum. It is clearly visible, that due to increased turbine flowrate, Q_{ST} is also increased and thus higher maximum amplitudes of the surge tank oscillations are resulting.

Like described above, the admissible water level in the upper reservoir for a certain maximum power output was found by stepwise reducing the gross head if the maximum surge tank limit was exceeded. Thus operational limits for a totally free power plant operations are necessary. For each gross head again several iterations were needed to determine the maximum amplitudes of the surge tank oscillations.

An overview of the resulting permissible operating range between minimum and maximum liquid level in the upper reservoir is given in Fig. 7 where the power limits for fully flexible operation are drawn. Due to massive numerical simulations linear operating limits within the range of minimum and maximum gross head could be found. Compared to stepwise limits additional operating range and therefore increased gross annual earnings were gained (orange areas in Fig.7).

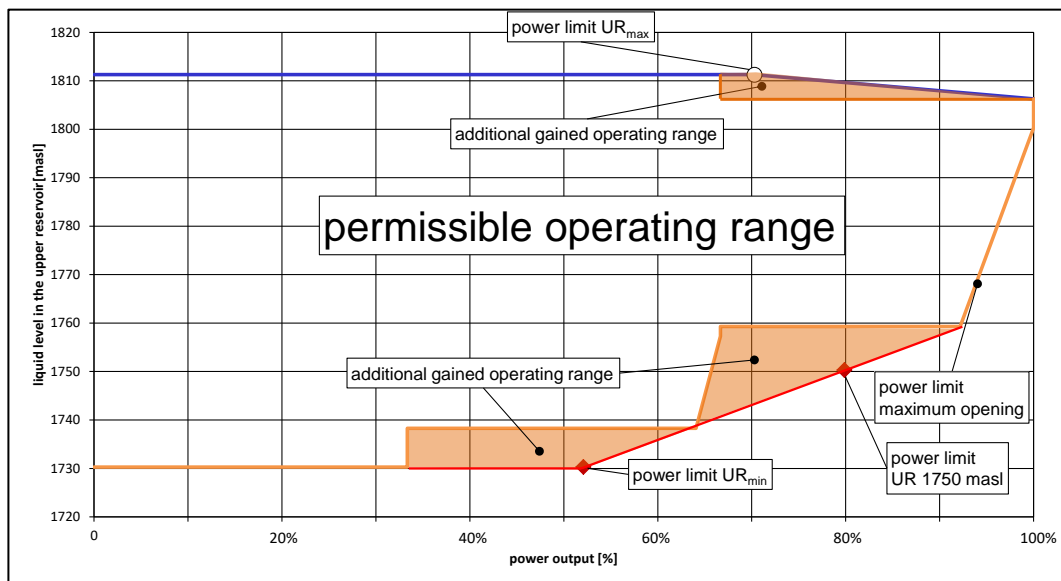


Fig. 7
Permissible and additional gained operating range

5. CONCLUSION

This paper presents a way to identify the possibility of an increase of power output and power plant flexibility at the same time for high head hydro power plants. With the help of transient 1-D numerical simulations and a validation with measurements on the existing power plant, the surge tank oscillations with increased power output can be calculated precisely. It could be shown that the given hydraulic infrastructure is able to allow for greater flexibility and higher power with only minor additional limits in the permissible operating range.

The focus in the present paper was on mass oscillation and the surge tank limitations. Additional investigations like the maximum pressure in the penstock due to increased waterhammer have also been carried out but exceed the scope of the present paper.

REFERENCES

- [1] MEUSBURGER P. Die 1D transiente, numerische Simulation von modernen Hochdruckwasserkraftanlagen. Dissertation, TU Graz, 2009.
- [2] HÖLLER S., JABERG H. Ein Beitrag zur Druckstoßberechnung von Pumpspeichieranlagen. Wasserwirtschaft, 2013, Nr. 1.
- [3] VEIDE K., RICHTER W., ZENZ G., LEIF L. Surge Tank Research in Austria and Norway. Wasserwirtschaft Extra, 2015 Nr. 13.
- [4] Flowmaster Ltd. Flowmaster Reference Help. Towcester, Northants, United Kingdom, 2009.
- [5] Bollrich G. Technische Hydromechanik. 5. Auflage, Berlin, Verlag Bauwesen, 2000.
- [6] Idelchik I.E. Handbook of Hydraulic Resistance. 2nd Edition, Berlin, Springer, 1986.
- [7] Naudascher E. Hydraulik der Gerinne und Gerinnebauwerke. 2. Auflage, Wien, Springer, 1992.
- [8] Knapp, F.H. Ausfluss, Überfall und Durchfluss im Wasserbau. Verlag Braun, Karlsruhe, 1960.
- [9] MEUSBURGER P. Pumped Storage Power Plant Obervermuntwerk II – Plant Layout and Study of different surge tank design. 18th Intern. Seminar on Hydropower Plants, Vienna, 2014.

COMMISSION INTERNATIONALE DES GRANDS BARRAGES

VINGT-SIXIÈME CONGRÈS DES GRANDS BARRAGES
Autriche, juillet 2018

DOI 10.3217/978-3-85125-620-8-199



This work licensed under a Creative Commons Attribution 4.0 International License. <https://creativecommons.org/licenses/by-nc-nd/4.0/>

IMPROVEMENT OF INTAKE STRUCTURES WITH NUMERICAL SIMULATION

Helmut BENIGNI

INSTITUTE OF HYDRAULIC FLUIDMACHINERY, GRAZ UNIVERSITY OF
TECHNOLOGY

AUSTRIA

Jürgen SCHIFFER

INSTITUTE OF HYDRAULIC FLUIDMACHINERY, GRAZ UNIVERSITY OF
TECHNOLOGY

AUSTRIA

Stefan HÖLLER

INSTITUTE OF HYDRAULIC FLUIDMACHINERY, GRAZ UNIVERSITY OF
TECHNOLOGY

AUSTRIA

Helmut JABERG

INSTITUTE OF HYDRAULIC FLUIDMACHINERY, GRAZ UNIVERSITY OF
TECHNOLOGY

AUSTRIA

COMMISSION INTERNATIONALE
DES GRANDS BARRAGES

VINGT-SIXIEME CONGRES DES
GRANDS BARRAGES
Autriche, juillet 2018

IMPROVEMENT OF INTAKE STRUCTURES WITH NUMERICAL SIMULATION

Helmut BENIGNI, Jürgen SCHIFFER, Stefan HÖLLER, Helmut JABERG

*Institute of Hydraulic Fluidmachinery,
GRAZ UNIVERSITY OF TECHNOLOGY*

AUSTRIA

1. INTRODUCTION

The design of inlet and outlet areas of hydro power plants significantly influences the overall cost of a plant not only in the design and construction phases but also during operation. Due to an incorrectly shaped inlet geometry, vortices and flow separation occurred at several river power plants. These phenomena can cause flow problems and losses at the turbines and must not be neglected, especially for low head turbines with relatively high specific speed turbines. Sources of such inhomogeneous inlet flow distribution could be a wrong design of dividing piers, gravel steps and other points of discontinuity in the flow guiding walls and river bed. In this paper, samples of water way designs and their optimisations, whose target is to avoid wrong inflow and outflow designs, are presented together with cost-optimised design.

During the last decades, turbine intake structures have been investigated in more detail. Based on the systematic analysis of vortex types, design rules for the design of intakes to avoid free surface vortices as well as other publications referring to swirling flow problems at intakes have been published [1]. Problems of intake vortices have long been known [2, 3] and tests at laboratory scale were realised in a systematic way including categorisation of vortices and empirical correlations ([1], [4] newer ones [5], [6]). Since numerical simulations are getting more and more reliable, investigations of these flow phenomena increased – but also the effort connected to them. During the last few years LES and SAS simulations [7, 8] captured the flow field with acceptable accuracy.

2. HPP GÖSSENDORF

2.1. PLANT OVERVIEW AND CFD MODEL

The plant consists of two units with a maximum discharge of $Q = 100 \text{ m}^3/\text{s}$ per turbine and a total nominal power of $P = 18.75 \text{ MW}$. Its yearly production amounts to 89 GWh, and the units were brought into operation in 2012. Each unit consists of a bulb turbine with 16 guide vanes, a 4-blade runner and a nominal diameter of $D_{\text{Nominal}} = 3.6 \text{ m}$ as well as a straight conical draft tube (Table 1).

Table 1: Turbine main data of HPP Gössendorf

Year of construction	2010-2012		Rotational speed	150	rpm
Number of units	2	#	Runner diameter	3.6	m
Max. flowrate per unit	100	m^3/s	Number of blades	4	#
Net head	11.2	m	Level machine axis	314	masl
Maximum power	18.75	MW	Head water level	330.8	masl

A lack of efficiency could be identified for turbine no. 2 (closer to the pier, see Fig. 1) at only a short time of operation after the start-up of the turbines in 2012. At identical runner blade and guide vane positions of both units the power output of the two identical turbines was different (see measurement curves later in Fig. 3). With the help of index tests, a failure at the turbines could be excluded and the efficiency level in general was tested in a model test as well. During the hydraulic development phase also a comprehensive numerical investigation of the turbine with the help of CFD was carried out. An idea regarding the reason for the lack of power was, that the flow distribution to the turbine must be disturbed and thus vortices are generated.

During the planning phase of the power plant a model test was carried out in the course of the hydraulic engineering [9]. During this model test (scale 1:40) vortex generation could be found in the intake and a new design of the pier was realised. This new pier works well for flood water, but influences the inflow situation negatively. The finally designed pier ends 3.5 m below the head water level and is shown in Fig. 1b. To avoid vortex generation in the intake bed, a smooth crossover with a ramp (Fig. 1c) and a gravel step (Fig. 1d) with a height of 2 m (due to rubble in the river bed) were realised.

The model starts 240 m upstream the machine runner. Based on 2D drawings and profiles for different sections of the river bed, a smoothed simplified section of the river was generated and is shown in blue in Fig. 1e. Then, the exact remodelling of the intake situation of the two units, including the three weirs, started. First, the turbine itself was calculated with a complex model which is shown in Fig. 1f. It consists of the intake, the bulb and a 360° section of the guide vanes, a whole runner and the straight draft tube with an enlarged section downstream. Finally, the entire power plant was investigated. This means, that the two units were installed in parallel (including turbine, guide vane, draft tube

and inflow structure as well as the intake structure and the two installed screeners visualised in red in Fig. 1g with a useable clearance of 88 mm). Downstream of the draft tube an additional component, the so-called outblock, was connected directly to the draft tube. The function of this component is not exactly a representation of the tail water, but helps to avoid the setting of boundary conditions directly at the draft tube outlet, which would influence the draft tube simulation and prescribe the flow situation. Pressure type boundary conditions were set for inlet and outlet, and thus the flow rate resulted. Menter's SST turbulence model with automatic wall functions was applied for the stationary calculations, and in order to achieve a satisfying convergence level all sensitive variables and imbalances were monitored.

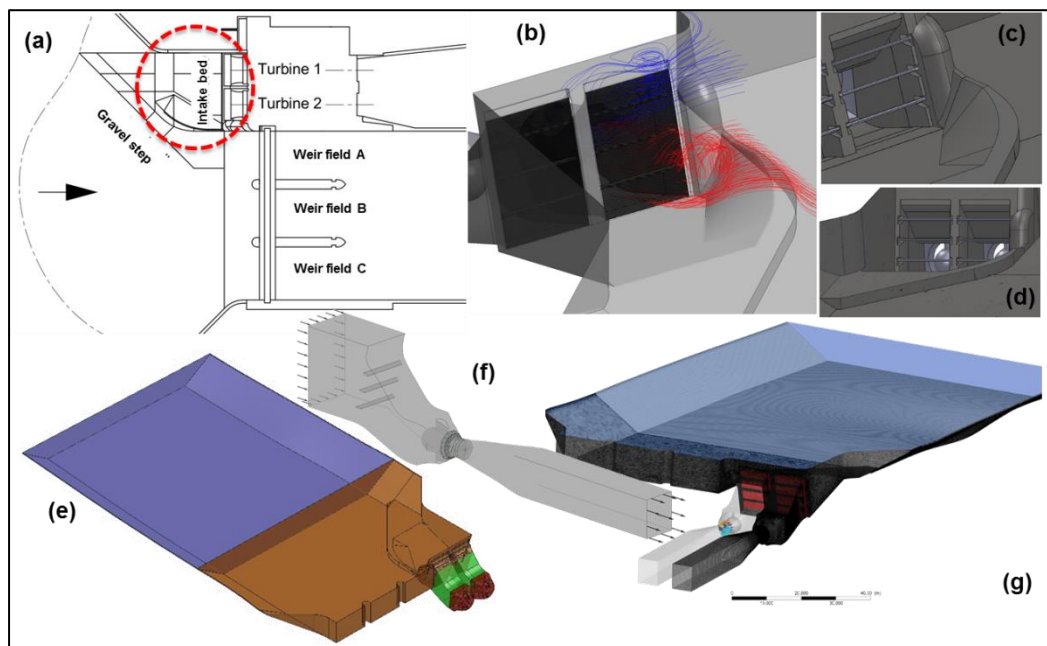


Fig. 1: Inflow situation

2.2. FULL MODEL, INTAKE FLOW SITUATION, PERFORMANCE DIFFERENCE

When analysing the numerical simulations results for the intake only and for a full model calculation, an influence on the flow distribution to the bulb could be detected. The plane shown in Fig. 2 is located just in front of the bulb. It is clearly visible that the flow distribution is strongly inhomogeneous for turbine 2 (left) in comparison to turbine 1 (right). Anyway, both are outside of the Fisher-Franke criteria [10]. For the evaluation of the flow situation the velocity was evaluated, normalised and sorted from the largest deviation to the mean value and to the lowest.

For the simulation including the turbines the situation was slightly better, as the distance to the allowed values (marked in grey) is smaller, however unit 2 was definitely outside of these criteria. Also, during the model test in the lab a

similar situation happened and optimisation was provided, but due to a lack of time and higher costs not all modifications could be integrated into the final intake design. Yet, according to [11], more deviation is allowed for the velocity in the intake and a summary of additional criteria is given by [12].

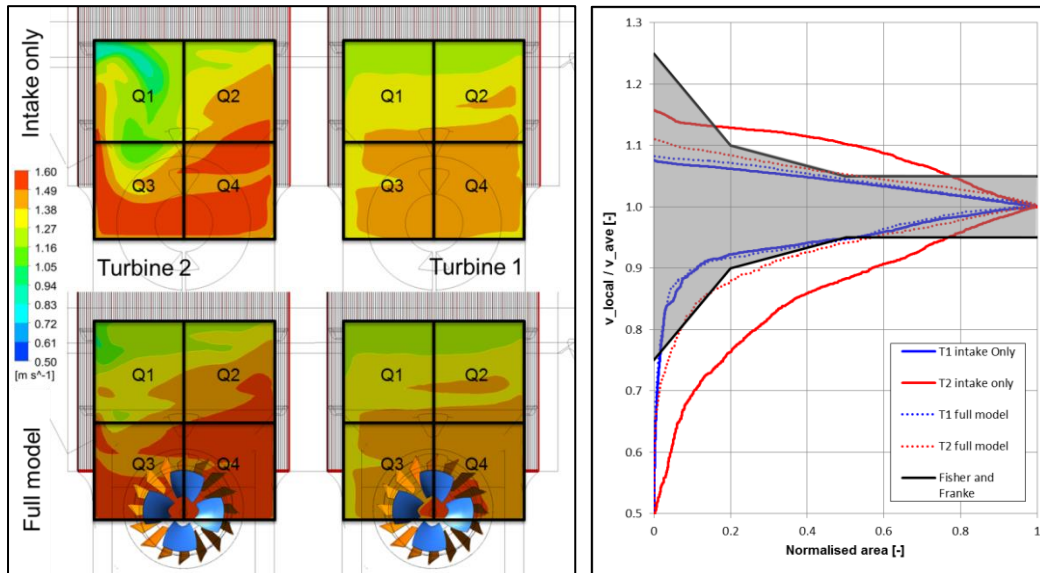


Fig. 2: Left: Velocity distribution at intake, full model and intake only simulation, Right: Fisher Franke analysis for full model and intake only simulation

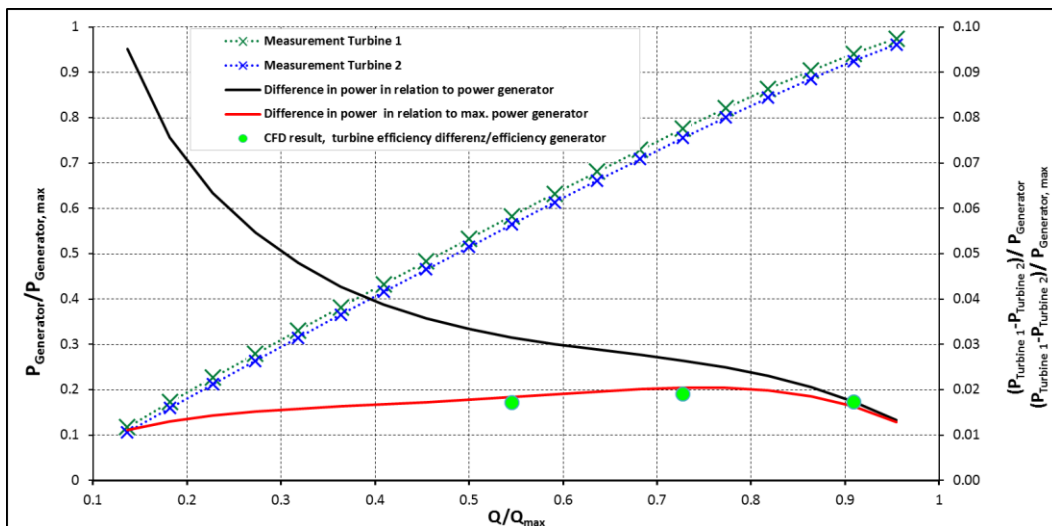


Fig. 3: Numerical simulation versus prototype test

The turbines were model-tested and during the development phase also numerically analysed. After the start-up of the turbines a comprehensive test of the two units was realised, including efficiency and vibration tests. In Fig. 6 the measurement data for the electrical power is shown versus the flowrate for the two units normalised with a maximum flowrate of $Q_{Max} = 115 \text{ m}^3/\text{s}$ and the maximum generator power of $P_{Generator,max} = 11 \text{ MW}$. The differences between the two units are visualised in red for the relative difference and in black for the

absolute difference. Three operation points were calculated for the full model with the intake and the operation of the two units in parallel.

The difference in efficiency is shown by means of green dots. For the generator efficiency and other losses a constant value of η_{Geno} and other losses = 98% was used to calculate the electrical power output based on the CFD data. The CFD analysis correlates with the on-site measurement data and confirms the findings established during the hydraulic structure model test [9]. Over the whole operation range the measurement of turbine 1 shows a higher performance as turbine 2. In relation to the generator output the relative losses are in the range of 7% at 20% flowrate and approx. 1.5% at 95% of the maximum flowrate (black line). In terms of losses in relation to the maximum generator output the range is between 1 and 2% (red line).

2.3. OPTIMISATION

Multiphase calculations were realised to verify the air sucking turbulences and swirls. Based on the results of these simulations, different kinds of structural measures were developed. The various types of measures were simple accessory elements as well as large-scale structural interventions at the inlet area of the power plant. The effects of all these different structural adjustments on the inflow were further investigated by means of computational fluid dynamics. The inferior inflow situation is a fact, optimisation with additional guide walls and other modification was analysed. 34 different variants were investigated, but with simple elementary structures no substantial improvement could be realised. With more complex and extensive guide walls also at the bottom of the intake a flow distribution approximately comparable to turbine 1 could be realised. However, with no option the Fisher-Franke [10] criteria are satisfied.

Fig. 4 shows the initial situation and 2 modifications. With the modification of 3 guide walls a more homogeneous flow distribution could be realised (see velocity distribution), and with the second modification presented even the swirl at the bottom could be avoided (red streamlines). The velocity distribution presented in absolute values at the right side of Fig. 4 also shows a flat gradient for version (c), which indicates a smoother velocity distribution. Still, all these variants could not satisfy the Fisher-Franke criteria or a comparable velocity distribution of turbine 1. The operator of the power plant defined the possible frame conditions with a few mandatory criteria. This includes the project costs, the operational capability of the track rack cleaner, secure operation and massive construction of the structures (e.g. guide wall made of steel) especially for flood water. A solution without modifications of the pier made of concrete and other structures has to be found in order to avoid the necessity of emptying the head water reservoir. The best solution would be a massive guide wall made of steel (Fig. 4), which is a modified and enhanced version of the principle idea presented in [9]) and a modification of the pier made of concrete. These measures would incur expenses more than 3 times higher as the given budget (calculated by the operator including operation interruption).

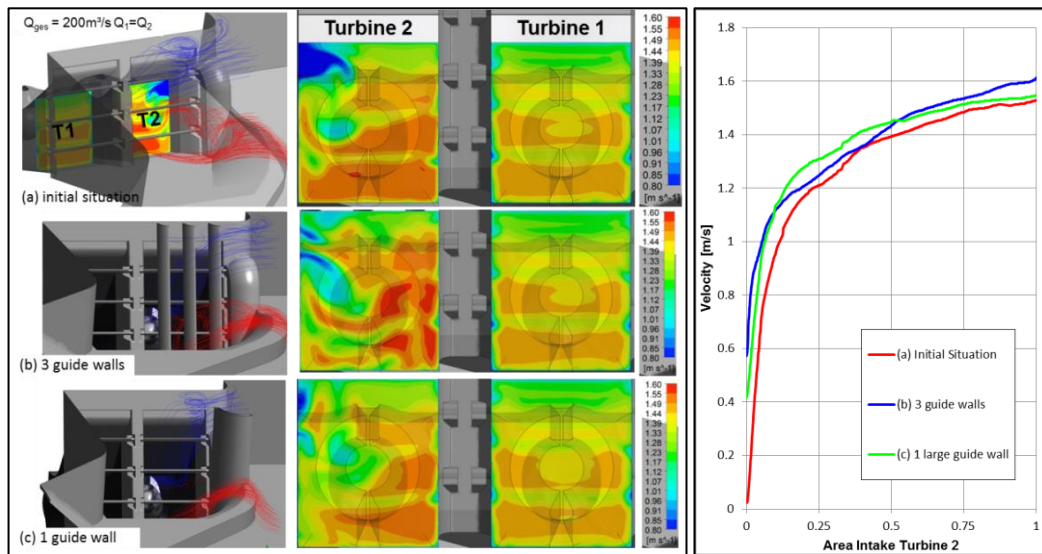


Fig. 4: Numerical simulation versus prototype test

3. GRENZKRAFTWERKE INN HPP GKI

A new diversion power plant located at the Swiss-Austrian border at the river Oberer Inn is currently under construction. In Ovella the intake structure consist of a 15m high weir canal to collect water for the GKI power plant. The weir was planned as a multi-functional structure and includes the weir valves for the barrage, the inlet channel for the approximately 23 km long gallery to the main stage (powerhouse Prutz / Ried), a small turbine for residual water delivery and a device for barrier-free fish migration. The plant data of the power plant project are summarised in Table 2.

Table 2: Turbine main data of HPP GKI

	Main turbine	Residual water turbine
Planned start-up	2018	
Type of turbines	2 x verticale Francis	1 x Kaplan-S
Net head rated	160.7 m	15 m
Flow rate rated	75 m ³ /s	20 m ³ /s

Fig. 5 (left) shows a visualisation of the planned reservoir with the intake structure on the orographic side (right), which was examined in the course of a comprehensive CFD study. The flow rate at the intake structure is max. 95 m³/s. Then 75 m³/s feed the headrace channel to the inclined shaft where the powerhouse Prutz / Ried is connected. The remaining amount of water is processed at the small turbine and discharged as residual water in the original river. It should be mentioned, that – as an additional special feature – the use of a fine screener with a clear width of only 20 mm was prescribed at the transition

from the reservoir to the intake structure. In order to obtain a flow velocity of max 0.75 m/s in front of the trash rack and a mean velocity of 1 m/s in the trash rack itself, the dimension of the screener was determined to be: width = 19 m and height = 6.5 m (steel bar width 8 mm).

The focus of the investigations carried out based on CFD calculations lay on the optimisation of the flow guidance in the inlet structure in order to obtain an ideal flow of the calculation field and to improve the geometric connection of the small residual water unit and thus to ensure a swirl free homogenous flow situation at the inflow there. Fig. 5 shows the two-axis 3D CFD model used as well as an example result of the calculated phase boundary (= water surface).

The CFD calculations were all carried out for the maximum intake at the intake structure ($Q = 95 \text{ m}^3/\text{s}$) at the design water level ($H_{\text{max}} = 1029.5 \text{ m}$) and the minimum water storage elevation ($H_{\text{min}} = 1025.5 \text{ m}$). The implementation of the fine screener was a specific challenge in the CFD calculation, as it resulted in a particularly complex two-phase CFD model. While a mesh with approximately 5 million nodes was created for the course of the river and the inlet channel, approximately 25 million hexahedral elements had to be used in the area of the fine screening. The CFD model used for the calculation from the storage reservoir to the intake structure is shown in Fig. 6. Velocity vectors were plotted on an evaluation plane placed in the middle of the arithmetic field. The left diagram shows the flow situation in the case of the originally planned geometry variant. While the screener field in the middle (pos. 2) is expected to flow well, a false flow appears to occur at the edges (pos. 1 and pos. 3). This leads to pronounced flow separations between the screen bars in these areas (see Fig. 6 – left) and thus the flow is not divided equally across the screener field. Furthermore, the inclined computing field of the inflow can cause vibrations on the bars. The justified alignment of inlet structure and screener field therefore appears to be inappropriate.

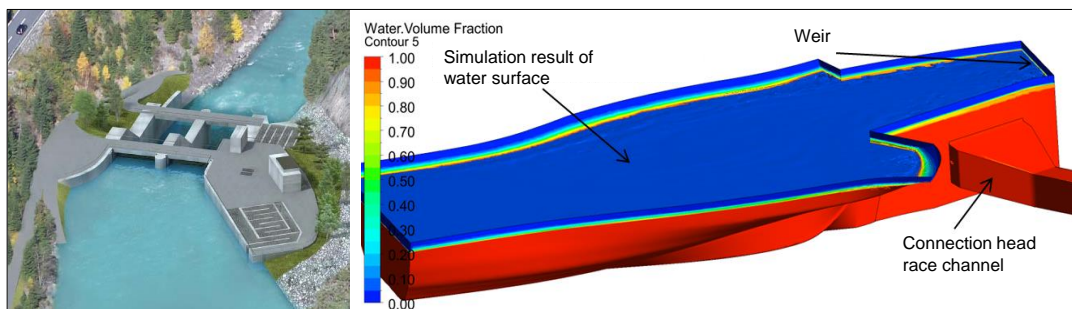


Fig. 5: Planned hydro power plant intake structure and CFD model

The flow situation at the inflow is more homogeneous and looks much better in the case of the improved geometry (see Fig. 6 – right). Due to the offset of the plane, where the screener is located in a distance of about 2 m to the rear and the attachment of an elliptical fillet before the area 1 and a the circular contour in front of the area 3, a false flow can be prevented (see also Fig. 6 – right) and a homogeneous velocity distribution over the entire calculation field is ensured.

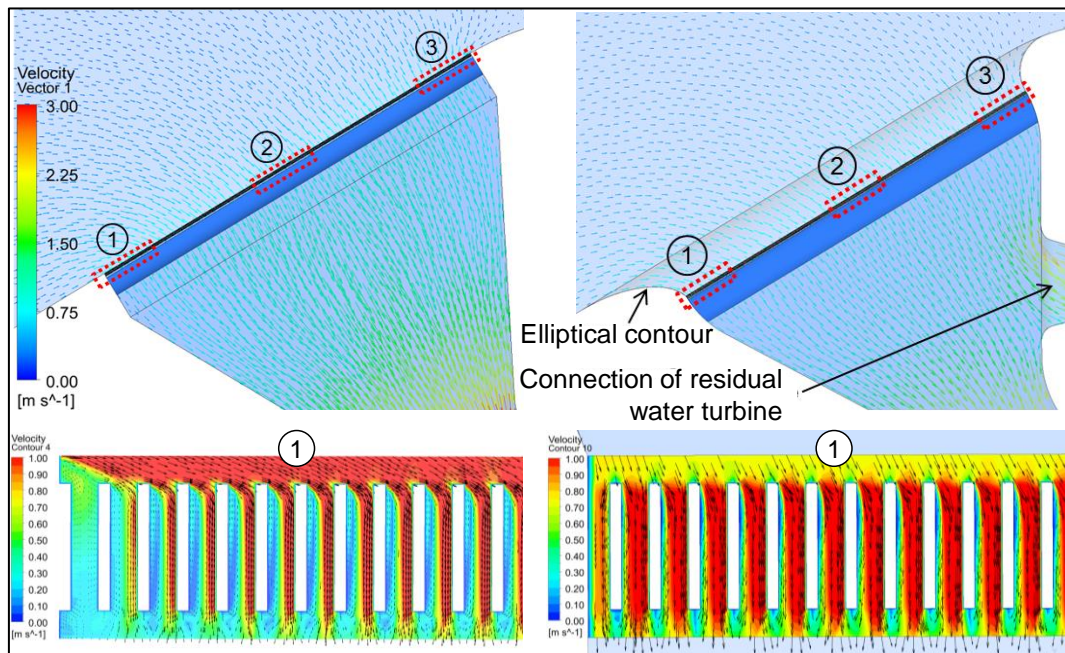


Fig. 6: Velocity distribution at different locations

Further improvement of the originally planned design of the intake structure becomes apparent when analysing the flow situation in a side view. Figure 8 shows a visualisation of streamlines in a vertical central section through the inlet structure. The left-hand illustration shows, that in the original design along the sharp edge at the transition from the flow to the inlet channel (marked red) pronounced detachment zones occur, which on the one hand cause flow losses, on the other hand these zones can lead to oscillation problems in the screener area. Furthermore, the shape of the screener's beam also does not seem ideal. A fillet around the intake structure and the use of two beams turned into the flow direction significantly improve the flow situation.

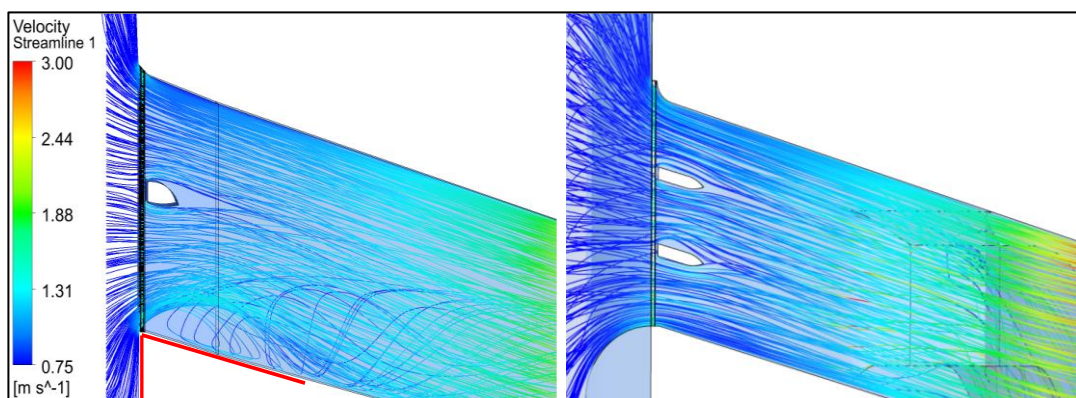


Fig. 7: Streamlines, connection of headrace channel

4. MUR POWER PLANT FRANZ, HPP MKF

The new MKF hydro power plant, designed as weir turbine, is located at the intake structure of an existing headrace channel for a diversion power plant with a maximum flow rate of $Q_{\max, \text{Diversion}} = 100 \text{ m}^3/\text{s}$ at the river Mur. The design flow rate for the new power plant is $Q_{\max, \text{MKF}} = 40 \text{ m}^3/\text{s}$ whereas the minimum residual water through the turbine is $Q_{\min, \text{MKF}} = 11 \text{ m}^3/\text{s}$. The power plant is located on the inner curvature of the river bend opposite the headrace channel for the existing power plant (Fig. 8). The turbine's direction of rotation must be investigated as it has an enormous influence on the civil engineering construction cost due to power transmission lines located in the air space above the excavation zone. The investigation was based on qualitative flow evaluations at different planes. The evaluation levels 1, 2 and 3 each represent horizontal sections through the flow field at different height levels (Fig. 8c). Additional evaluation criteria represent the ratios of maximum and minimum occurring flow velocity to average flow velocity for the evaluation of a uniform flow towards the turbine. The comparison for the left- and right-hand turbine configuration is shown for load case 1 (see Table 3 for load case details) with Fig. 9. It clearly shows that the right-hand variant for evaluation levels 1, 2 and 3 has a more inhomogeneous flow distribution in the MKF bay compared to the left-hand turbine. This statement is also confirmed by the evaluation of the maximum and minimum relative flow velocity at the spiral inlet – there are increased secondary flows at the spiral inlet when using a right-hand machine. Other load cases are presented in Table 3. Based on these test results, the installation of left-hand machines is recommended, the construction of which is also cheaper.

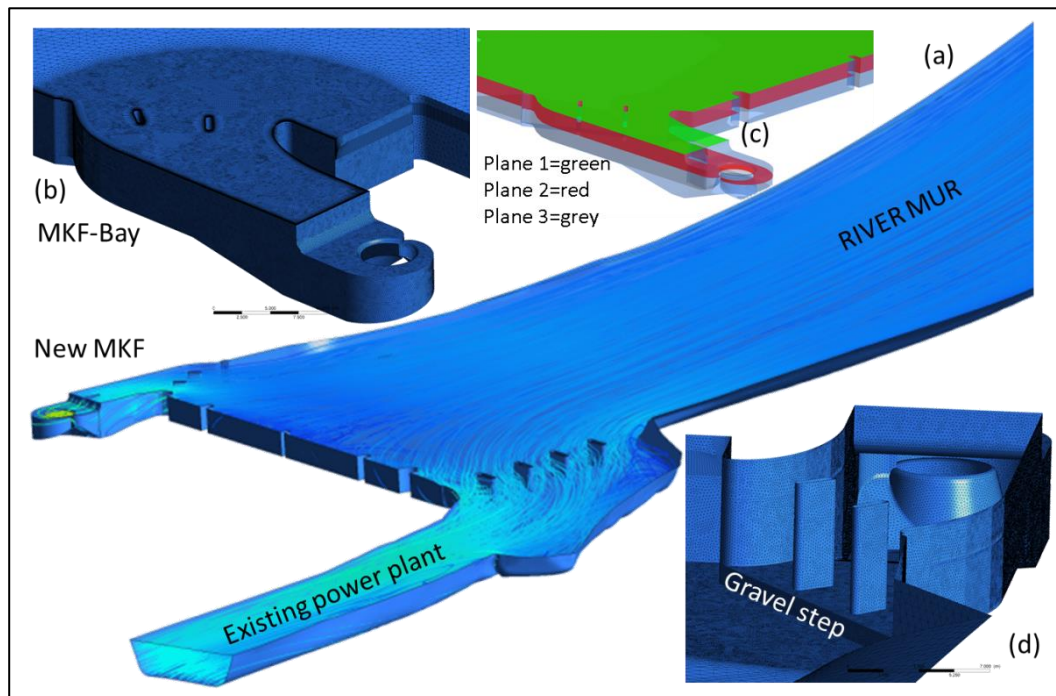


Fig. 8: Velocity distribution at different locations

Table 3: Load cases HPP MKF

Load case	Q _{Mur}	Q _{MKF}	Q _{Existing}	C _{ratio,min}		C _{ratio,min}	
				left	right	left	right
	m ³ /s	m ³ /s	m ³ /s	m ³ /s	m ³ /s	m ³ /s	m ³ /s
1	140	40	100	1.827	2.073	0.054	0.031
2	111	11	100	1.810	1.961	0.005	0.046
3	61	11	50	1.820	2.071	0.059	0.013
4	40	40	0	1.944	2.033	0.028	0.054

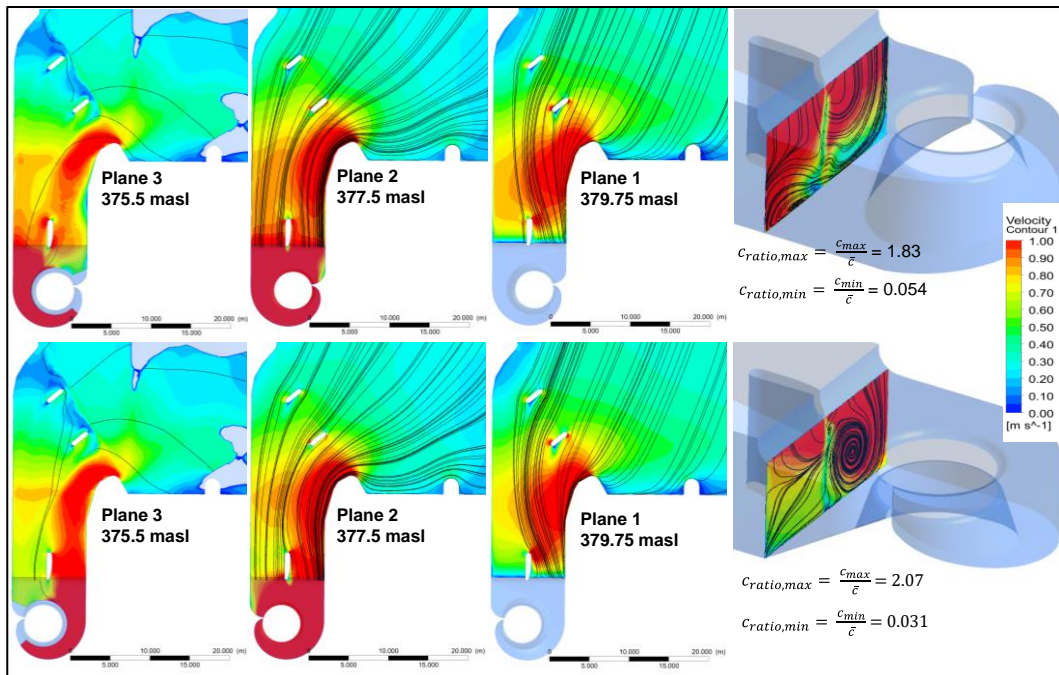


Fig. 9: Streamlines for left-hand (top) and right-hand (bottom) turbine configuration

4.1. OPTIMIZED GEOMETRY

The single-phase calculation shows a non-optimal orientation of the supporting pillars in the inflow region of the power plant inlet for the left-hand rotating turbine. In all tested load cases it shows, that the pillars should be rotated by up to 15° counter clockwise. In addition, the analysis of the flow field in the horizontal evaluation levels shows optimisation potential in the hydraulic design of the existing wall between the MKF bay and the right bottom outlet.

The flow situation at the water surface shows that a dead water zone is to be expected in the inlet area in the bay power plant on the orographic side (right). A hydraulic optimisation (enlargement of the radius) of the right orographic boundary in the inlet area of the MKF bay has been proposed in order to avoid

this unfavourable flow situation together with a gravel step (see Fig 8d). A stationary approach is used with the SST turbulence model, with the flow rate as boundary condition at the MKF and the existing power plant, and furthermore a pressure boundary condition was set at the inlet. The investigations now were all carried out by means of two-phase CFD simulation. For the numerical modelling of the flow with free water level for the project in question the "homogeneous multiphase model" in Ansys CFX, the one based on a Volume of Fluid approach (VOF), is used. For the multiphase studies the calculation area was extended upwards (airspace) and very finely resolved with prismatic layers in the area of the expected water level. This ensures, that the water level can be precisely calculated during the CFD simulation. An optimised geometry proposal of the hydraulic contour of the MKF bay was developed. Turning back the pillars and the removal of the right bank embankment detected and included in the new geometry model with 4.87 million nodes, respective 15.44 million elements. The hydraulic contour of the existing wall between MKF bay and right to bottom outlet was modified to achieve the desired effect of no detectable level reduction. The water level is now constant along this wall as visualised in Fig. 10, whereby the optimised contour is shown at the bottom left.

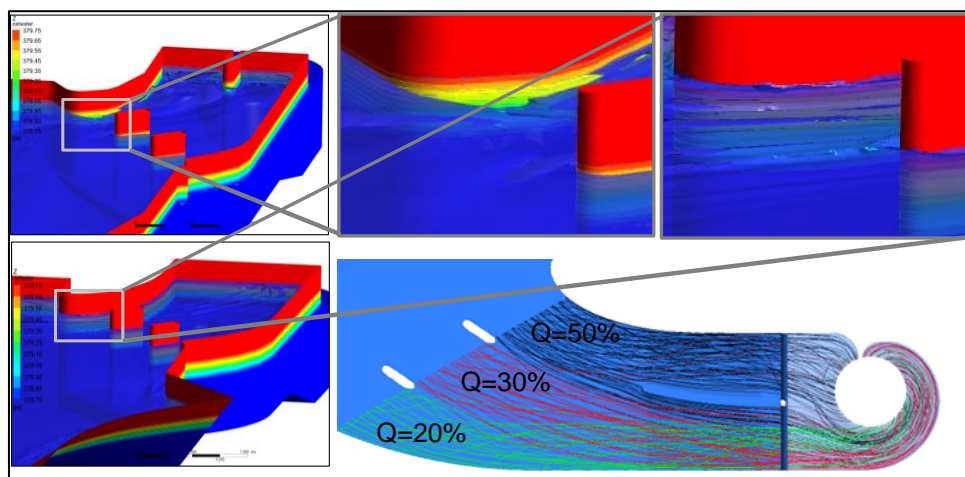


Fig. 10: Water level at wall, distribution of intake water

The last optimisation step deals with the installation of a baffle before the spiral entry. This should attenuate the formation of the vortex structures on the water surface or, in an ideal case, suppress it completely and lead to a further homogenisation of the velocity distribution in front of the turbines. At the same time, an extended partition before the spiral entry can be used as a support structure for a pedestrian walkway in this area of the power plant.

However, Kaplan turbines with a concrete semi-spiral have an asymmetrical quantity distribution due to the geometric conditions at the entrance to the spiral. The water masses entering MKF bay through field 1 are shown in green, those in field 2 in red and those in field 3 in black (Fig. 10 right bottom). An approximate distribution of volumes between the fields at the entrance to the bay shows the previously mentioned circumstance of an unequal collection of quantities in a concrete semi-spiral ($Q_{\text{Field1}} = 20\%$, $Q_{\text{Field2}} = 30\%$, $Q_{\text{Field3}} = 50\%$).

REFERENCES

- [1] KNAUSS, J., Coordinate Editor, "Swirling flow problems at intakes", Hydraulic Structures Design Manual, ISBN 9061916437, 1987.
- [2] ROUVE, G., „Anströmungsverhältnisse bei Niederdruckanlagen“, Escher Wyss Mitteilungen, Issue 2/3, pp 25-40, 1961.
- [3] QUICK, M.C., "Efficiency of air-entraining vortex formation at water intake", J. Hydraulics Div. ASCE 96(HY7), pp. 1403–1416, 1970.
- [4] DENNY, D.F., "An experimental study of air-entraining vortices in pump sumps". In: Proc. of the Institution of Mechanical Engineers, Volume 170 / 1956, 106-125, London, UK, 1956.
- [5] SUERICH-GULICK, F., GASKIN, S.J., VILLENEUVE, M., PARKINSON, E., "Characteristics of Free Surface Vortices at Low-Head Hydropower Intakes", Journal of Hydr. Engineering, Volume 140, Issue 3, March 2014.
- [6] GULLIVER, J.S., RINDELS, A.J., LINDBLOM, K.C., "Designing intakes to avoid free-surface vortices", Int. Water Power Dam Constr. 38(9), 1986.
- [7] NAKAYAMA A., HISASUE N., "Large eddy simulation of vortex flow in intake channel of hydropower facility", Journal of Hydraulic Research", 48:4, 415-427, 2010.
- [8] MENTER, F.R., EGOROV, Y., „A Scale-Adaptive Simulation Model using Two-Equation Models“, AIAA, Paper 2005-1095, 2005.
- [9] TSCHERNUTTER, P., PUCHER, M., SCHÜLL, M., MAYR, T., „Modelldurchführung für das Kraftwerk Gössendorf“, 2008.
- [10] FISHER, R.K., FRANKE, G.F., "The Impact of Inlet Flow Characteristics on Low Head Hydro Projects", Proc. Int. Conf. on Hydropower, Portland, 1987.
- [11] NICHTAWITZ, A., ABFALTERER, J., "Discussion on inflow and outflow conditions of a hydro turbine", Waterpower – Proceedings of the International Conference on Hydropower San Francisco, CA, USA, 25 July 1995 through 28 July 1995, Volume 2, 1995
- [12] GODDE, D., „Experimentelle Untersuchungen zur Anströmung von Rohrturbinen“, Mitteilungen des Institutes für Wasserbau der TU München, Band Nr. 75, 1994.

SUMMARY

Based on three case studies the Institute of Hydraulic Turbomachinery at the Graz University of Technology has worked on in recent years, it can be shown that the numerical flow simulation is very well suited for the detailed analysis of the inflow of power plants as well as for the development of geometric improvements. Especially in the area of low head power plants, where axial turbines are often used (such as Kaplan tube or S-turbines), such studies should be carried out in the planning phase already in order to avoid potential problems in advance.

COMMISSION INTERNATIONALE DES GRANDS BARRAGES

VINGT-SIXIÈME CONGRÈS DES GRANDS BARRAGES
Autriche, juillet 2018

DOI 10.3217/978-3-85125-620-8-200



This work licensed under a Creative Commons Attribution 4.0 International License. <https://creativecommons.org/licenses/by-nc-nd/4.0/>

**THE IMPACTS OF THE DIFFERENCES BETWEEN CHINESE AND
FOREIGN TECHNICAL STANDARDS ON DEVELOPING INTERNATIONAL
HYDROPOWER PROJECTS**

Richun YOU

DEPARTMENT OF HYDRAULIC ENGINEERING, TSINGHUA
UNIVERSITY
STATE KEY LABORATORY OF HYDROSCIENCE AND ENGINEERING,
TSINGHUA UNIVERSITY

CHINA

Wenzhe TANG

DEPARTMENT OF HYDRAULIC ENGINEERING, TSINGHUA
UNIVERSITY
STATE KEY LABORATORY OF HYDROSCIENCE AND ENGINEERING,
TSINGHUA UNIVERSITY

CHINA

Qingzhen ZHANG

DEPARTMENT OF HYDRAULIC ENGINEERING, TSINGHUA
UNIVERSITY
STATE KEY LABORATORY OF HYDROSCIENCE AND ENGINEERING,
TSINGHUA UNIVERSITY

CHINA

COMMISSION INTERNATIONALE
DES GRANDS BARRAGES

VINGT-SIXIÈME CONGRÈS DES
GRANDS BARRAGES
Autriche, juillet 2018

**THE IMPACTS OF THE DIFFERENCES BETWEEN CHINESE AND FOREIGN
TECHNICAL STANDARDS ON DEVELOPING INTERNATIONAL
HYDROPOWER PROJECTS**

Richun You^{a,b}, Wenzhe Tang^{a,b,*}, Qingzhen Zhang^{a,b}

^a *Department of Hydraulic Engineering, Tsinghua University*

^b *State Key Laboratory of Hydrosience and Engineering, Tsinghua University*

CHINA

1. ABSTRACT

Chinese contractors play a more and more important role in the hydropower industry worldwide due to the experience and technological strength accumulated from delivering many significant hydropower projects such as the Three Gorges Dam. However, the Chinese contractors encounter ongoing difficulties in achieving the objectives of developing international hydropower projects, which arise from unfamiliarity with the differences between Chinese and foreign technical standards. This research collected the data from international hydropower projects, which are scattered in Asia, Africa, Oceania and Latin America. With support of the case studies, this research reveals the impacts of the technical standards' differences on hydropower project development processes, including bidding, design, procurement, construction, occupational health and safety management, and environment protection. It is suggested that Chinese contractors should more

* Corresponding author at: Department of Hydraulic Engineering, State Key Laboratory of Hydrosience and Engineering, Tsinghua University, China, New Hydraulic Building, Tsinghua University, Beijing 100084, China.
E -mail addresses: twz@mail.tsinghua.edu.cn

clearly understand the differences between Chinese technical standards and foreign technical standards in project delivery for providing more cost-effective and environment-friendly hydropower projects worldwide.

2. INTRODUCTION

Over the past 15 years, Chinese contractors play a more and more important role in the international construction industry with more than 20% annual growth rate of contract amount (Zhao et al., 2017). Nevertheless, when delivering a global project, participants from different countries with differing institutionalized practices may come into conflict (Mahalingam, 2006). Although there exist opportunities, international hydropower projects also face more uncertainties than domestic projects since foreign contractors have to work in unfamiliar environments, including different regulations, norms, and cultural beliefs (Javernick-Will et al., 2010). In these situations, the unfamiliarity with different environments can increase misunderstandings and risks, thus result in project delays and cost overruns (Javernick-Will et al., 2009). Many researchers have studied the impact of unfamiliar environments on international project delivery. For example, Orr et al. (2008) built a conceptual framework to analyse unforeseen costs of a project in an unfamiliar host societal context base on an examination of 23 cases; Han et al. (2007) indicated that unfamiliarity with different regulations and norms was one of the significant distinctions between successful and failed international projects from a comparative case study; Chua et al. (2003) identified five risk factors, namely business environment discontinuity, contractual issues, differences in standards, regulation obstacles, and cultural differences, that can lead to cost overrun in the East Asian construction industry. Among the unfamiliar environments, such as different regulations, norms and cultural beliefs, technical standards particularly remain a great challenge for Chinese contractors (Lu et al., 2009), since technical standards of Chinese and other countries in hydropower industry can vary significantly. Lei et al. (2017) confirmed that Chinese contractors perceived significant difference between foreign standards and Chinese standards, which resulted in greater challenges in implementing foreign standards in international projects. In order to provide more cost-effective and environment-friendly projects worldwide, Chinese contractors should more clearly understand the differences between Chinese technical standards and foreign technical standards in project delivery.

Although many researchers have pointed out the importance of understanding the differences of technical standards (Orr et al., 2008; Javernick-Will et al., 2009; Kwon and Kareem, 2013; Lee et al., 2016; Lei et al. 2017), there is still a lack of solid and practical investigation to reveal the impacts of the differences in technical standards on developing international hydropower projects. Thus, this research aims to demonstrate such impacts on international hydropower project development processes together with the outcomes.

3. RESEARCH METHODOLOGY

3.1. DATA COLLECTION

Data was collected through questionnaire survey. The questionnaire aims to investigate Chinese contractors' perceptions on how technical standards affect the delivery of an international project according to their practical experience in a specific project. The questionnaire is divided into 5 sections: 1) Background of the respondent under investigation and the project that he/she participated in; 2) Frequency of using different technical standards; 3) The differences between Chinese and foreign technical standards; 4) Technical standard differences related problems in project implementation; 5) Project performance. The respondents were requested to answer the questions according to their experience learned from international hydropower projects that they were engaged. They were asked to answer the questions using a 5-point Likert scale, except the question on the frequency of using technical standards.

Questionnaires were sent to 17 Chinese construction companies, which all have rich experience in international hydropower projects with over \$30 million contract value in international market annually, through fieldtrips as well as e-mail. The selected respondents have 8.82 years (on average) of experience in overseas projects. All sent 362 questionnaires were collected and 294 of them were used for analysis, excluding 68 invalid ones with incomplete information.

3.2. DATA ANALYSIS

With the help of the software Statistical Package for Social Science (SPSS), ranking analysis and Pearson correlation analysis were applied in this research. Rank analysis was used to reveal current application status of different technical standards applied in international hydropower projects and to identify the most significant factors that affect the technical standard selection; Pearson correlation analysis was performed to exhibit the relationships among the differences between technical standard differences related problems in project implementation and project performance.

4. RESULTS AND DISCUSSION

4.1. FREQUENCY OF USING DIFFERENT TECHNICAL STANDARDS

18 kinds of technical standards were selected, because they have important influence worldwide. Respondents were requested to identify whether or not these selected technical standards were used in the projects that they were engaged. The using frequency of each technical standard was then calculated and is shown in Table 1.

Table 1
Frequency of using technical standards in international hydropower projects

Technical standards	Using frequency (represented by percentage)	Rank
American Society for Testing and Materials (ASTM)	52%	1
International Organization for Standardization (ISO)	47%	2
Chinese Standards (including GB, DL, SL, NB, etc.)	46%	3
American Concrete Institute (ACI)	32%	4
European Norm (EN)	31%	5
British Standard (BS)	29%	6
International Electrotechnical Commission (IEC)	20%	7
The American Society of Mechanical Engineers (ASME)	19%	8
Institute of Electrical and Electronics Engineers (IEEE)	17%	9
German Institute for Standardization (DIN)	15%	10
The American Society of Civil Engineers (ASCE)	14%	11
French Standards Association (NF)	13%	12
American Association of State Highway and Transportation Officials (AASHTO)	13%	13
United States Army Corps of Engineers (USACE)	12%	14
United States Bureau of Reclamation (USBR)	8%	15
International Telecommunication Union (ITU)	6%	16
Australian Standards/New Zealand Standards (AS/NZS)	4%	17
Indian technical standards	2%	18

Since the data was collected through survey of 17 representative Chinese construction companies, the result can well reflect the frequency of using different kinds of technical standards in international hydropower projects delivered by

Chinese contractors. As shown in Table 1, ASTM, ISO and Chinese technical standards are most frequently used in international hydropower projects delivered by Chinese contractors, with a frequency of 52%, 47% and 46% respectively. Other frequently used technical standards are ACI, EN, BS and IEC, with frequency larger than 20%. In general, USA, ISO, Chinese and European technical standards have significant influence on international hydropower projects conducted by Chinese contractors.

4.2. THE DIFFERENCES BETWEEN CHINESE AND FOREIGN TECHNICAL STANDARDS

Eight aspects were selected to evaluate the differences between Chinese and foreign technical standards, including *philosophy of the standard*, *completeness of the standard*, *application conditions of the standard*, *logical structure of the standard*, *material*, *theory for calculation*, *construction method* and *test method*. The respondents were asked to rate the differences on these aspects using a 5-point Likert scale, with 1= no difference and 5= huge differences. Results are shown in Table 2.

Table 2
The differences between Chinese and foreign technical standards

Aspects	Score	Std.	Rank
Philosophy of the standard	3.36	0.98	1
Material	3.30	0.89	2
Completeness of the standard	3.27	0.85	3
Construction method	3.21	0.87	4
Application conditions of the standard	3.16	0.86	5
Logical structure of the standard	3.16	0.84	6
Test method	3.13	0.88	7
Theory for calculation	3.10	0.94	8

The results in Table 2 show that the scores of all the aspects are above 3.0, indicating that there are significant differences between Chinese and foreign technical standards from all angles. Among them, *philosophy of the standard* is ranked first with a score of 3.36, and other aspects with relatively larger scores are *material*, *completeness of the standard* and *construction method*. Nonetheless, although *theory for calculation* ranks last among these 8 aspects, it still gets a score of 3.10, which must not be neglect.

4.3. TECHNICAL STANDARD DIFFERENCES RELATED PROBLEMS IN PROJECT IMPLEMENTATION

During the implementation of an international hydropower project constructed by Chinese contractors, different kinds of problems may occur due to the unfamiliarity with the differences between Chinese and foreign standards. 19 problems were selected and displayed for the respondents to rate on their occurrence frequency using Likert scale with 1= never happened and 5=usually happened. These problems were then classified into 5 kinds, shown as Table 3. The results are presented as below.

Table 3
Technical standard differences related problems in project implementation

Problems	Score	Rank	Cronbach'α
Standard management problems	3.11		0.892
Lacking well-rounded talents	3.46	1	
Incompletely understanding foreign standards	3.14	7	
Inadequate collection of foreign standards	3.02	10	
Barriers to learning foreign standards	3.01	11	
Poor translation of foreign standards	2.94	14	
Engineering-Procurement-Construction integrated management problems	3.10		0.858
Low coordination efficiency between design, procurement and construction	3.17	4	
Lacking incentives for design optimization	3.16	6	
Poor constructability of designs	2.96	13	
Design problems	3.06		0.894
Design's low approval rate from engineers	3.19	3	
Poor communication with engineers	3.17	5	
Design delay	3.12	8	
Uncompetitive design for bidding	2.99	12	
Design error or defect	2.83	18	
Procurement problems	2.92		0.887
Procurement scheme not cost-effective	3.03	9	
Unreasonable procurement scheme	2.87	16	
Improper selection of suppliers	2.86	17	
Construction problems	2.89		0.933
Construction cost increasing	3.30	2	
Construction delay	2.93	15	
Improper construction method	2.70	19	
Poor construction quality	2.64	20	

The reliability test shows that the value of Cronbach's α for all the 5 sorts of problems are larger than 0.85, indicating a good consistency for all the 5 sorts, hence the classification is reliable. The results shown in Table 3 reveals the following findings:

1. In general, *standard management problems* gets the highest score, reaching 3.11. It shows that integrated management in standard issues is a key to promote the ability of Chinese contractors;

2. *Engineering-Procurement-Construction integrated management problems* gets a high score of 3.10. Specifically, *low coordination efficiency between design, procurement and construction* gets 3.17, indicating the significance of interface management between design, procurement and construction.

3. *Design problems* scored 3.06, ranked third. Moreover, we can find that *low approval rate for design* and *poor communication with engineers* scored 3.19 and 3.17. These reveal that there is an urgent need to improve the design capability of Chinese contractors using foreign standards.

4. *Construction problems* scored 2.89 with the rank of 5, showing a good construction ability of Chinese contractors. Nevertheless, *construction costs increasing* got a 3.30 score, ranking second among all. This demonstrates that cost increasing due to unfamiliarity with the differences between Chinese and foreign standards is a critical issue that Chinese contractors need to deal with.

4.4. PROJECT PERFORMANCE

In order to understand the performance of an international hydropower project conducted by Chinese contractors, respondents were asked to rate the status of 11 indexes (see Table 4).

Table 4
Performance of international hydropower projects

Performance	Score	Std.	Rank
Safety	4.16	0.68	1
Client's satisfaction of the contractor's service	4.16	0.75	2
Corporate-Social-Responsibility (CSR)	4.15	0.72	3
Environment protection	4.14	0.72	4
Client's satisfaction of the product	4.11	0.72	5
Quality	4.07	0.76	6
Enhancing the brand effect	3.99	0.84	7
Occupational health	3.98	0.72	8
Time	3.82	0.88	9
Cost	3.66	0.78	10
Profitability	3.51	1.05	11

As shown in Table 4, Chinese contractors performed well in international hydropower projects, with all scores higher than 3.50, among which *safety* ranked

first with a score of 4.16. In addition, the project's quality, time and cost performance ranked 6, 9 and 10 with scores of 4.07, 3.82 and 3.66 respectively, indicating that Chinese contractors' time and cost control abilities have more room for improvement. Profitability got the lowest score of 3.51, which needs to be enhanced urgently.

4.5. IMPACT OF TECHNICAL STANDARD DIFFERENCES RELATED PROBLEMS ON PROJECT PERFORMANCE

Pearson correlation analysis was performed to reveal the relationships among the differences between technical standard differences related problems in project implementation and project performance, with the results shown in Table 5.

Table 5
Impact of technical standard differences related problems on project performance

	I	II	III	IV	V
Quality	-0.207*				
Cost	-0.296**	-0.292**	-0.214**	-0.167*	-0.229**
Time	-0.246**	-0.232**	-0.272**		
Client's satisfaction of the contractor's service	-0.189*				
Profitability			-0.207*		-0.240**
Enhancing the brand effect					-0.212**

Note : I =Standard management problems; II =Engineering-Procurement-Construction integrated management problems; III=Design problems; IV=Procurement problems; V=Construction problems.

*=correlation is significant at the 0.05 level (two-tailed); **=correlation is significant at the 0.01 level.

As shown in Table 5, *quality*, *cost*, *time*, *client's satisfaction of the contractor's service*, *profitability* and *enhancing the brand effect* have significant negative correlations with technical standard differences related problems. Specifically, cost performance is negatively correlated with *Standard management problems*, *Engineering-procurement-construction integrated management problems*, *design problems* and *construction problems* at 0.01 significance level, and negatively related to *procurement problems* at 0.05 significance level, indicating that technical standard differences related problems due to unfamiliarity with the differences between Chinese and foreign standards have a significant impact on the project cost performance.

Time performance is significantly correlated with *Standard management problems*, *engineering-procurement-construction integrated management problems* and *design problems*, which indicates that the key to improve time performance is to focus on these technical standard differences related problems. *Profitability* performance has a significant negative correlation with *design problems* and *construction problems*, showing that the impact of design and construction problems on the profitability of the project is of the utmost importance.

5. CONCLUSIONS

This study investigates the current status of applications of different standards in international hydropower project conducted by Chinese contractors and further reveals the impact of the differences between Chinese and foreign standards on developing international hydropower projects with the findings as follows:

- USA, ISO, Chinese and European technical standards have significance influence on international hydropower projects conducted by Chinese contractors, with ASTM most frequently used in international hydropower projects;
- *Philosophy of the standard* ranks first among 8 aspects of differences between Chinese and foreign standards. Other aspects with relatively larger scores are *material*, *completeness of the standard* and *construction method*;
- *Standard management problems* are most frequently occurred in implementation of an international hydropower project, indicating that integrated management in standard issues is a key to promote the ability of Chinese contractors;
- *Engineering-Procurement-Construction integrated management problems* also happen constantly, which reminds Chinese contractors to concentrate on interface management between design, procurement and construction;
- *Design problems* usually occur, showing that there is an urgent need to improve the design capability of Chinese contractors using foreign standards ;
- *Construction cost increasing* has a significant impact during project implementation, revealing that cost increasing due to unfamiliarity with the differences between Chinese and foreign standards is a critical issue in international hydropower project delivery;
- Technical standard differences related problems have a significant impact on project performance, especially on project cost and time performances. It is necessary for Chinese contractors to figure out the differences between Chinese and foreign standards in order to perform better and provide more cost-effective and environment-friendly hydropower projects worldwide.

6. ACKNOWLEDGEMENTS

Sincere thanks are given to the National Natural Science Foundation of China (Grant Nos. 51379104, 51579135 , 51079070), the State Key Laboratory of Hydroscience and Engineering (Grant Nos. 2015-KY-5 , 2013-KY-5) and Major Science and Technology Research Project of Power China (Grant Nos. DJ-ZDZX-2015-01-02, DJ-ZDZX-2015-01-07). Special thanks are also given to the respondents for their contributions during the survey.

REFERENCES

- [1] ZHAO, Z., YAO, J., & TANG, C. Chinese Contractors in the International Market: Business Distribution and Competitive Situation. *In Proceedings of the 20th International Symposium on Advancement of Construction Management and Real Estate*, 2017, (pp. 1261-1277). Springer, Singapore.
- [2] MAHALINGAM, A. Understanding and mitigating institutional costs on global projects, *Doctoral dissertation, Stanford University*, 2006.
- [3] JAVERNICK-WILL, A. N., & SCOTT, W. R. Who needs to know what? Institutional knowledge and global projects. *Journal of Construction Engineering and Management*, 2010, 136(5), 546-557.
- [4] JAVERNICK-WILL, A. N., & LEVITT, R. E. Mobilizing institutional knowledge for international projects. *Journal of Construction Engineering and Management*, 2009, 136(4), 430-441.
- [5] HAN, S. H., PARK, S. H., KIM, D. Y., KIM, H., & KANG, Y. W. Causes of bad profit in overseas construction projects. *Journal of construction engineering and management*, 2007, 133(12), 932-943.
- [6] CHUA, D. K. H., WANG, Y., & TAN, W. T. Impacts of obstacles in East Asian cross-border construction. *Journal of construction engineering and management*, 2003, 129(2), 131-141.
- [7] LU, W., LI, H., SHEN, L., & HUANG, T. Strengths, weaknesses, opportunities, and threats analysis of Chinese construction companies in the global market. *Journal of Management in Engineering*, 2009, 25(4), 166-176.
- [8] LEI, Z., TANG, W., DUFFIELD, C., ZHANG, L., & HUI, F. K. P. The impact of technical standards on international project performance: Chinese contractors' experience. *International Journal of Project Management*, 2017, 35(8), 1597-1607.
- [9] LEE, J.H., HUH, J., LEE, J.J. A comparative study on wind loads between design standards for the design of pipe-rack structures. *KSCE J. Civ. Eng.*, 2016, 20 (1), 293–300.
- [10] KWON, D.K., KAREEM, A. Comparative study of major international wind codes and standards for wind effects on tall buildings. *Eng. Struct.*, 2013, 51, 23–35.

COMMISSION INTERNATIONALE DES GRANDS BARRAGES

VINGT-SIXIÈME CONGRÈS DES GRANDS BARRAGES
Autriche, juillet 2018

DOI 10.3217/978-3-85125-620-8-201



This work licensed under a Creative Commons Attribution 4.0 International License. <https://creativecommons.org/licenses/by-nc-nd/4.0/>

TWO YEAR OF PERFORMANCE OF A PENSTOCK ANCHORED BY PU-FOAM

Leif LIA

*Professor, Department of civil and environmental engineering, NORWEGIAN
UNIVERSITY OF SCIENCE AND TECHNOLOGY - NTNU*

NORWAY

Tor OXHVD SVALESEN

Project manager, STAKRAFT ENERGI AS, NARVIK

NORWAY

Stian L. AAKER

Project engineer, NGK UTBYGGING AS, OSLO

NORWAY

Guy HARRIS

Mechanical engineer, VELOCIFOAM LTD, SAINT JULIAN

MALTA

Mattias KULLBERG

Mechanical engineer, MULTICONSULT ASA, OSLO

NORWAY

COMMISSION INTERNATIONALE
DES GRANDS BARRAGES

VINGT-SIXIÈME CONGRÈS DES
GRANDS BARRAGES
Autriche, juillet 2018

**TWO YEAR OF PERFORMANCE OF A PENSTOCK ANCHORED BY PU-
FOAM**

Leif Lia

*Professor, Department of civil and environmental engineering
NORWEGIAN UNIVERSITY OF SCIENCE AND TECHNOLOGY - NTNU*

NORWAY

Tor Oxhøvd Svalesen

Project manager, Stakraft Energi AS, Narvik

NORWAY

Stian L. Aaker

Project engineer, NGK Utbygging AS, Oslo

NORWAY

Guy Harris

Mechanical engineer, VelociFoam Ltd, Saint Julian

MALTA

Mattias Kullberg

Mechanical engineer, Multiconsult ASA, Oslo

NORWAY

1. INTRODUCTION

Due to a high number of new small hydro projects (SHP) in the last decade many cost-reducing innovations have been developed [1]. Still, the conduit system remains the most costly item in the SHP, representing 40 – 60% of the total investment cost. In the same period, electricity prices in Europe have dropped and further cost-saving innovations must be made to maintain SHP as one of the alternatives for feasible new renewable energy.

Today, the construction of buried penstocks is based on the principle of gravel/crushed rock as backfill, and anchoring of bends with concrete thrust blocks. With SHPs often located in remote areas without pre-existing connection to the main road network, the transportation of materials for penstock construction has to be carried out by constructing new access roads or by helicopter, which is both time consuming and costly.

Penstock BV (now VelociFoam Ltd) invented a method using polyurethane foam (PU-foam) as a replacement for gravel and rockfill. The PU-foam concept was presented internationally in 2017 in [2] after the commissioning of the first full scale penstock constructed using this concept. The project at Lille Måsevann was a development project; a brief program to study and follow up the quality and performance of the penstock was implemented. This paper describes the performance of the penstock in two full seasons of pumping. Since completion in November 2016 the penstock has performed perfectly well without any indication of unexpected behaviour.

2. THE PU-FOAM CONCEPT

The main motivation of the concept is to lower cost of buried penstocks with the same safety or better. Applied at straight sections of the penstock, the main purposes of the foam are:

- To provide mechanical protection of the pipe, against sharp edged gravel and stones
- To allow more native soil material to be used as backfill, reducing the amount of transported or locally-crushed gravel/aggregate and reducing the need to dispose of unused excavated material
- To increase the periphery towards the native soil material (normally not a critical condition)

In bend application, the function is different; the PU-foam act as a structure exposed to tensile stress and absorbs the hydraulic forces from the bend. In addition, the effects of adjacent 'straights sections' are still taken into consideration as part of the bend system. This lower the costs of bends by eliminating the demand for expensive on site constructed concrete blocks.



Fig. 1
PU-foam used as backfill

3. PU-FOAM

The quality and the performance of rigid closed-cell PU-foam for outdoor use is briefly described in [2]. The foam typically expands up to 30 times, and is 70 % cured 10 minutes after the initial reaction, although the reaction profile can be controlled by manipulation of pressure and heat. In order for the foam to expand, a blowing-agent is needed. The most commonly used blowing-agent is water – an eco-friendly blowing-agent where no harmful gasses are released into the atmosphere.

Rigid closed-cell PU-foam is normally divided into two categories; ‘pour foam’ and ‘spray foam’. The main difference between the types is the proportion of mixing between the components and the way they are applied to the object. For experimental purposes and to optimize the total concept of anchoring of penstocks by PU-foam both methods have been fully tested in lab and in the field. Both the behavior of the foam and the procedure for application is very different and requires two very different set of equipment and set-up of the working teams. The experience from both quality and speed of construction will be discussed in later parts of the article.

No prior findings indicate that the foam, after curing, has a negative effect on the environment [4]. Cured foam is considered ‘inert’ and does not react easily with other substances in any natural environment. During application of the foam, health and safety measures need to be met. This certificate information has not been possible to verify during the rather short available lifetime of this specific penstock.

4. THE PENSTOCK AT LILLE MÅSEVANN

The penstock at Lille Måsevann is the first of its kind that uses PU-foam as backfill at parts of the penstock. Lille Måsevann is a pumping station for lifting water with maximum discharge 1,4 m³/s from Lille Måsevann reservoir up to Store Måsevann reservoir. The water is further used in the 50 MW Adamselv hydropower project and increases the annual energy output with 7 GWh. Construction took place during the summer and fall of 2016 and were commissioned by a start-up and sudden shut down at the 24. November 2016, see Figure 6. The pumping station conduit consists of an 1130 m long, buried DN800 and 900 GRP pipe. Approximately 1/3 of the total length, including two bends, was covered by foam. A map showing the penstock alignment can be seen in Figure 2a. On the same Figure 2b, the penstock both with and without PU-foam is shown, before application with gravel.



Fig. 2

a) Map of the penstock alignment b) The penstock at Lille Måsevann (from west)

Three different methods were used to apply the foam to the penstock; 'Open formwork' (Figure 3a), 'Closed formwork' (Figure 3b) and 'Spray application' (Figure 3c).

Both methods using formwork is developed for 'pour foam' material. The open formwork application gave dry conditions in the formwork and controllable curing conditions see Figure 3. The closed formwork application is a better concept on the way to automatize the construction process but there is still large challenges to overcome about the quality, see Figure 3. The direct spray application is a manual based process with limited speed of construction but with very good conditions to control the curing and the quality of the foam.



a)



b)



c)

Fig. 3

Different methods for foam application a) Open formwork with roof to protect against rain b) Closed formwork to be placed around the penstock c) Spray-foam is applied to the pipe, two persons are required as work force

As in many development projects the progress and quality were not uniform. The foam produced at the start of the project showed greater property deviation compared to the final product. The method with direct application to the pipe provides for the best progress and predictability in the project. Besides, research by [3] indicate that spray-foam end up with better mechanical properties and density than pour-foam.

5. ANCHORING OF BENDS

The penstock at Lille Måsevann includes two 15° bends which were constructed without any concrete or rock bolt measures. Static head acting on the bends are 44 mWC. Both bends were anchored using 300 mm of spray-foam with spray application. The bends were anchored to the gravel bed by a combination of

the gravity of the penstock system and the resulting "locking" interaction between the foam and the gravel.



Fig. 4

a) Application of foam at the bend b) The bend after removal of the tent

To monitor displacement over time, four displacement transducers were installed at one of the bends, described in [5]. The type of equipment used was WA Inductive displacement transducers with a measuring range of 20 mm. The measuring is based on the differential inductor principle with an inductive quarter bridge. The system is highly accurate to 0,2% of the measuring length, in this case 0,04 mm. The deformations can be monitored in real-time inside the pumping station. Figure 5 shows which direction the plunger is extended. The axial deformations in the direction is given as decreasing values in the graph Figure 6.

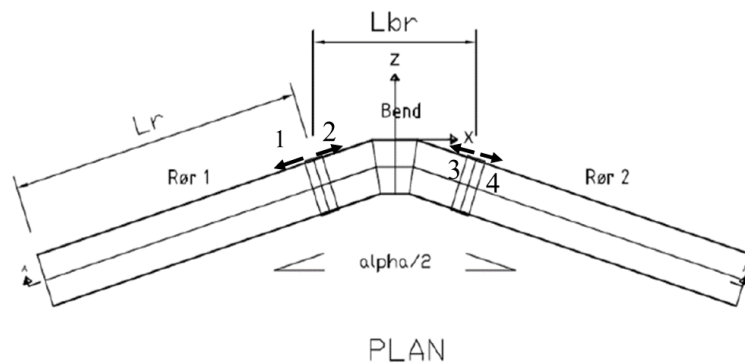


Fig. 5

Placement and measured direction of the displacement transducers

Two full seasons with pumping have been experienced at the time of this presentation. Figure 6 shows measurements conducted 28.04.17, during first filling of the penstock. The displacement transducer's position is given on the left axis, and water pressure (black line) is given on the right axis.

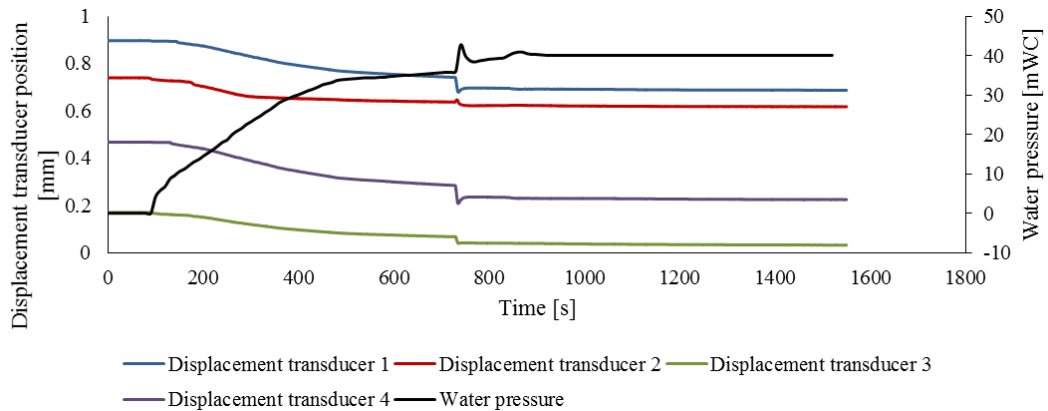


Fig. 6
Deformation measurements at Lille Måsevann, 28.04.17

The results shows that the bend has very small deformation in the pipes axial direction (~ 0.2 mm). The small deformation can indicate that the forces are distributed as a combination of compression and tension in the foam. The measurements confirm that the foam distributes a fraction of the hydraulic forces as tensile stress in the pipe axial direction. No measurement of foam compression deformation in force resultant direction was carried out.

In addition, deformation and angle deflection in the pipe joints had to be verified within the engineering requirements set by the regulator. Deformation calculation was carried out, stiffness of foam, backfill and in situ soil was taken into account. As a conservative approach for first time use in penstock, tensile restraining capacity was not included. Further, a scale test rig was set up at NTNU the spring of 2016, to investigate the capacity of bends anchored with PU foam. The scale test rig is shown in Figure 7a.



a) Setup of the bend test rig b) Bend in full scale

The test rig was set up without a bend coupling to ensure that all forces acting on the bend was distributed in the foam. A concentrated load was set up directly in the bend with a metal hook inserted in the pipes to simulate forces from internal pressure in the pipe. Test results indicate that the capacity of the foam increases with larger cross-sections and increased bend angle. For instance, the test with foam thickness of 40 mm at 30° bend had an ultimate bend load of 1 kN corresponding to 19 mWC internal pressure. The idealised distribution of the forces in the foam in the test is not possible to verify exactly by the full-scale monitoring program. In the field distribution of forces in the bend will not only occur in the foam; the surrounding masses, bend coupling and interface layer between the foam and drainage layer will also absorb the forces. This is the main explanation of the large difference in displacement between laboratory and field results; the field displacements are much lower than predicted, according to the conservative calculation model, which is a result of not taking the full set of stabilizing factors into account.

6. VIBRATIONS IN THE PENSTOCK

Vibrations from the rotating runner propagate along the penstock. This was recognized even the first hour of operation in November 2016 for a long distance upstream of the pumping station. Both sound and remarkable vibrations on the frozen ground were recognized. The frequency in the vibration corresponded with the rotational speed of the runner. This could easily be proved, because the unit was operated by the frequency controller on several different rpm's. The runner is an asymmetric 'pump wheel' which introduce significant but predicted vibrations in the unit. The test program in the lab in 2015, 2016 and 2017 didn't include yield tests for the foam and it's not clear how this may will influence the long-term quality of the anchoring. The effect of the foam layer on the pipe is to attenuate the energy propagating from the runner through the water mass, by reducing amplitude and dissipating the energy as heat. The energy absorbed in this dampening effect would otherwise be transmitted from pipe surface to granular backfill in a classic system, with the attendant risk of damage of the pipe surface from sharp stones edges. Absorption of acoustic wave energy in foam is a well-understood phenomenon. The full set of mechanical interactions between pipe, pipe bend and surrounding PU-foam and soil masses are not yet fully understood or modelled, but this is an objective of further research, both in academic and operational settings.

The long term behavior of the foam in frozen soil is still based on the results from the lab tests. Samples may subsequently be extracted from the foam in the field and tested. This will verify the extent to which foam in the field is sensitive to the freeze-thaw processes. How any variations in mechanical properties due to freeze-thaw cycle affect system performance can only be established by pushing comparative samples to failure, which is not possible in the field.

7. CONCLUSIONS FROM OPERATION

At Lille Måsevang 300 m of buried penstock was enveloped in foam, including two bends. The commissioning of Lille Måsevang penstock proves that the method with PU-foam as backfill works on a full-scale project, both for construction and operation.

The PU-foam absorbs water at varying rates, but tests in the frost laboratory indicate very little influence on the strength. Long term deformations in the bends shows no development, while displacements are followed closely by the monitoring program.

PU-foam as backfill and for anchoring of bends is a promising alternative to the traditional method. However, to obtain desired quality and safety, precautions on-site needs to be met. As such a strict quality test program must be followed to verify the statement in a longer term perspective.

ACKNOWLEDGEMENTS

The authors like to acknowledge Nina Johnsen for contribution to this article and ENOVA for financial support to make this project possible.

REFERENCES

- [1] LIA, L, JENSEN, T., STENSBY K.E., MIDTTØMME, G.H., RUUD, A.M. The current status of hydropower and dam construction in Norway. *Hydropower & Dams, Issue 3*, 2015.
- [2] JOHNSEN, N., AAKER, S.L., KULLBERG, M., HARRIS, G., SVALESEN, T.O., LIA, L. PU-foam in buried penstocks. *Hydro2017*, Seville, Spain, 2017.
- [3] JOHNSEN, N. Legging av rørgater med PU-skum som omfylling. *NTNU Trondheim*, 2017.
- [4] PU Nordic, n.d. Heat insulation in materials made from rigid closed-cell PU-foam. s.l.:s.n. 2016.
- [5] AAKER, S.L. Forankring av bend på rørgater med PU-skum. *NTNU, Trondheim*, 2017.

SUMMARY

Today the most commonly used backfill for penstocks for small hydro are gravel and rockfill, which is time consuming and costly due to transportation. Penstock BV with Guy Harris developed a method with polyurethane foam as a replacement for gravel and rockfill which may lead to lower investment costs and reduced construction time. NTNU made the required initial laboratory tests in 2015 and Statkraft AS initiated a research project to verify the method in 2016. The project involves the construction of Lille Måsevang Pump with a buried penstock connecting Lille Måsevang to Store Måsevang – the intake reservoir for Adamselv hydropower plant. Lille Måsevang Pump is the first of its kind where sections of the penstock, including two bends, are enveloped in polyurethane foam (PU foam). Previously only scale tests have been carried out. The full-scale project is located in Finnmark County, Norway, and the construction work was done the summer of 2016. By the summer 2018 this DN800/900 mm penstock have experienced two years of operation. Monitoring of elastic and non-elastic displacement of the bends proves the behavior during start/stops and other dynamic load situations. Out of the total length (1130 m) approximately 300 m were anchored by in foam.

The experiences made from both construction and two years of operation at Lille Måsevang Pump has acquired new knowledge to the subject. The behavior of the penstock is without any kind of unexpected observations and the penstock performance is as for other penstocks constructed in traditional ways.

COMMISSION INTERNATIONALE DES GRANDS BARRAGES

VINGT-SIXIÈME CONGRÈS DES GRANDS BARRAGES
Autriche, juillet 2018

DOI 10.3217/978-3-85125-620-8-202



This work licensed under a Creative Commons Attribution 4.0 International License. <https://creativecommons.org/licenses/by-nc-nd/4.0/>

DESIGN OF AERATOR FOR ORIFICE SPILLWAY

Balkrishna Shankar CHAVAN

Scientist-D, CENTRAL WATER AND POWER RESEARCH STATION, PUNE

INDIA

COMMISSION INTERNATIONALE
DES GRANDS BARRAGES

VINGT-SIXIÈME CONGRÈS DES
GRANDS BARRAGES

Autriche, juillet 2018

DESIGN OF AERATOR FOR ORIFICE SPILLWAY

Balkrishna Shankar CHAVAN.

*Scientist-D, Central Water and Power Research Station, Pune
India.*

1 INTRODUCTION

Orifice spillways combine the advantages of greater depth of flow over the crest and moderately sized gates – an arrangement made possible by inclusion of a breast wall. An orifice spillway would allow the setting of its crest at significantly lower elevation, yet retaining the choice of a high dam for creating head for power generation. The main advantages of orifice spillway are: Reduction in height of the spillway gates, reduction in number of spillway spans, ease in regulating flood discharge and storage, reduction in the cost of gates and operating mechanism.

ORIFICE SPILLWAY BREAST WALL Breastwall / sluice spillways have been widely recognized as the most appropriate especially for run-off river projects for handling both flood releases and flushing of sediment. Generally, two configurations of the breast walls are provided on a high head spillway. In one of the alternatives, bottom profile of the breast wall starts from the upstream face of the over flow spillway crest. In other alternative the bottom profile of the breast wall starts at an intermediate location on the spillway pier. In the latter, the breast wall facilitates provision of stoplog gate groove upstream of crest axis, whereas in the former arrangement, the stop log groove has to be provided through the body of the breast wall and is not desirable because of the high velocity flow or the stoplog gate groove has to be provided upstream of the spillway face by providing cantilever structure.

The bottom profile of the breast wall starts at an intermediate location on the spillway pier, the breast wall facilitates provision of stoplog gate groove upstream of crest axis, whereas in the former arrangement, the stop log groove has to be provided through the body of the breast wall and is not desirable because of the high velocity flow or the stoplog gate groove has to be provided upstream of the spillway face by providing cantilever structure.

Sluices are essentially large capacity outlets placed in the body of the dam and controlled by gates.

The following parameters are required to be determined for the orifice spillway :

- a) Bottom profile of the spillway crest including the upstream and downstream quadrants
- b) Roof profile of the breastwall or sluice barrel
- c) Estimation of discharge characteristics of the spillway
- d) Size and dimensions of the orifice spillway and its disposition with respect to power intakes
- e) Structural design considerations and Protection of the spillway surface to resist abrasion
- f) Special considerations for energy dissipater.

2.DESIGN OF SPILLWAY CREST PROFILE

The hydraulics of orifice spillway changes with the varying reservoir levels. The flow is free flow for reservoir water levels below the top of the roof of the sluice. For higher water levels the flow is orifice flow. The crest profile is required to be designed for orifice (pressurized) flow. The spillway crest profile is flat as compared to the standard WES crest profile to avoid separation and negative pressures on the crest for small partial gate openings. The crest profile follows the equation $x^2 = 4 H y$, where H is the head over the centreline of the orifice. Design of Roof Profile of Breastwall / Sluice Spillway

Hydraulic design of roof profile of breast wall is very important, because the bottom profile of the breast wall guides the flow smoothly. This governs the coefficient of discharge of the spillway. This profile should be simple to construct and the pressures on the profile should not be excessively negative. Usually, a profile in the form of quarter of an ellipse is provided bearing the equation

$$\frac{x^2}{a^2} + \frac{y^2}{b^2} = 1$$

where

- a = width of semi-major axis i.e. the width of breast wall,
- b = width of semi-minor axis which governs the steepness of the profile.

Figure 1 shows the setup constructed for testing of spillway profile and aerator.



Figure1. Model set up for measurement of air concentration in an orifice spillway overflow

Usually steep profiles yield increased coefficient of discharge, whereas flat profiles tend to reduce the discharging capacity. However, negative pressures increase as the profile becomes steep. High negative pressures with cavitation index below 0.2 are undesirable. The bottom profiles of breast wall are usually steel lined to avoid cavitation damage.

Discharge Characteristics of the Orifice Spillway

The spillway operates as free overflow spillway for lower discharges whereas for higher discharges effect of breast wall comes into play and flow through the spillway is governed by the orifice flow. Generally, the orifice flow condition sets in for heads over crest in excess of about 1.5 to 1.7 D, where D is the height of the orifice opening.

For free flow conditions the discharge is given by

$$Q = \frac{2}{3} \sqrt{2g} \, cd. \, LH^{3/2}$$

when Q = discharge in cumec

Cd = coefficient of discharge

L = length of spillway in m

H = head over the crest in m

For orifice flow,

$$Q = C_d \cdot n \cdot A \cdot \sqrt{2g(H - H_m)}$$

Q = discharge in cumec

C_d = coefficient of discharge

n = number of span

A = area of orifice in m² = L x D

H - H_m = head over the center line of orifice

The coefficient of discharge is influenced by the entrance profile – composed by root profile or the bottom profile of the breast wall, spillway crest profile, side wall profiles if provided, inclination of the orifice barrel with reference to horizontal. The coefficient of discharge for the orifice flow is in the range of 0.75 to 0.95. Figure 2 shows a typical discharging capacity curve. Unlike ogee spillways, the design of breast wall spillways has not been standardized. Therefore, a recourse is taken to study the existing structures, while designing a new project.

3. Size and Dimensions of the Orifice Spillway and its Disposition with respect to Power Intakes

In the past, flushing used to be carried out by providing small sluices (of the size of 3 m x 4 m or so) at very low level. However, it was realized that these sluices were effective only locally. Also, there was a tendency of choking of sluices within a short period. Large openings of the size of [6-10 m (w) x 10 m x 15 (H)] are required to be located 30-40 m (w) below the full reservoir water level for flushing of the reservoir. This results in high velocities of the order of 20-25 m/s over the spillway crest corresponding to discharge intensity of the order of 200-250 cumec /m.

Structural design Considerations and Protection of Spillway Surface to resist Abrasion

3.1 Breastwall spillways necessitate some special design considerations. Breastwalls have to bear the upstream water head with beams or slabs spanning between and fixed with two piers. As such, the breastwall and both the piers have to be constructed as a single structural unit. The construction joint is, therefore, provided at the center of each pier, except the end piers. Thus, a single pier is virtually a combination of two full piers separated by a construction joint, and a typical spillway monolith is composed of two piers and breast wall. In a standard overflow spillway without breast wall, construction joints are provided at the center of the monolith. Special care is also required in respect to the top seal of the radial gate in ensuring water tightness.

3.2 The larger velocities associated with the high heads may increase the potential for cavitation and erosion damage to the structure. Adequate protection measures should be taken during the construction of the sluice barrel and breastwall spillway, to withstand the erosive power of the silt laden water while flushing the reservoir

and flood routing, by way of special type of concreting (poly impregnated concrete) or providing steel lining along the discharge channel of the spillway.

4 Special Considerations for Energy Dissipator

Special considerations are required for design of suitable energy dissipator, since the spillway has to surpass both the flood and the sediment. Ski-jump bucket is found to be the most suitable form of energy dissipator because of its obvious advantage during flushing operation. The sediment passes down the spillway with supercritical flow without deposition and churning in the bucket. Fortunately, steep bed slopes of the rivers result in low tail water depth permitting this type of energy dissipator. If the geological conditions are not favourable, a hydraulic jump stilling basin may have to be adopted. Because of the requirement of passing silt-laden flows, use of energy dissipating appurtenances like chute and baffle blocks is not advisable. The resulting basin is excessively long and often deep-seated below the general river bed, making it vulnerable to deposition by silt during flushing operation. A trade-off is desirable between the hydraulic efficiency of energy dissipation and the self-cleansing potential of the stilling basin during flushing operation. Cylindrical end - sills are generally preferred for easy movement of sediment out of the basin. A concrete apron downstream of the end sill is required to protect the spillway against undermining due to scour during transition action from hydraulic jump to flip action and vice versa. Provision of roller bucket is generally avoided as an energy dissipator due to likelihood of abrasion damage of the bucket due to churning of sediment. The flow surfaces of spillway and energy dissipator suffer abrasion damage due to passing of sediment laden flow. Adequate care should be taken in the structural design.

5.0 Data Acquisition System-Industrial PC based multifunction Data Acquisition System consists of Kulite make pressure transducers 20 Nos. of +/- 2 & +/- 5 psi range. A lab make linear power supply for pressure transducer excitation. PCI-6143 DAQ -2 Nos. . BNC-2110 analog input board - 2 Nos. air vent tube. 4-core shielded cable. Data Cables-2 Nos. Industrial PC having 2 GB RAM, 200 GB Hard Disc Drive. Core 2 Duo processor with LG make 17" LCD display. Application software is based on Labview 8X platform for data acquisition, monitoring & reporting. Data Acquisition System (DAS) can collect data samples at a rate of 10,000 samples per second per channel for 10 channels continuously for 30 minutes. Pressure transducer works on the principle of piezoresistive technology. It converts applied hydraulic pressure into an electrical signal using diaphragm as a pressure sensing element. Miniature ruggedized pressure transducers of size 4mm diameter having 0.15mm diameter holes positioned on a circle are used. Resonance frequency of the sensor is 160KHz. Analog to Digital Converter has a resolution of 1 part in 65536. The accuracy of the ADC is 0.01%, taking care of A/D nonlinearity, amplifier non linearity, gain, offset errors, drift and noise. Facility of simultaneously viewing and analyzing experimental data in digital and analog form

6. MODEL STUDIES FOR AERATOR OF ORIFICE SPILLWAY- DESIGN TESTING. Preventive measures such as control by geometry, smoothness of surface, use of cavitation resistant materials etc. are expensive and labour

intensive. Aeration on the spillway surface is one of the most reliable and economic measures used at present for mitigating cavitation damage. An aerator is a device that deliberately causes a large cavity to be formed underside of a high velocity jet.

The void created is a negative pressure region relative to atmospheric pressure.

Air is drawn into the void when a vent is connected

Performance of aerator on orifice spillway was assessed based on following aspects:

- General flow conditions
- Length of trajectory
- Pressure field around aerator and in cavity below jet
- Air entrained by aerator
- Air concentration downstream of aerator

Jet Length $\lambda = L / d_n$

λ = non dimensional jet length

L = length of the jet in m

d_n = incoming depth of water at aerator in m

- Cavity Pressure $P_n = \Delta p / \rho a d_0$

P_n = non dimensional cavity pressure

Δp = cavity pressure in Pascal

ρ = density of water in kg/m³

d_0 = incoming depth of water at aerator in m

- Air Entrainment Coefficient $\beta = Q_a / Q_w$

β = air entrainment coefficient

Q_a = air discharge m³/sec

Q_w = water discharge m³/sec

- Three alternatives of spillway profiles

- Profile conforming to $x^2 = 220y$ (Subansiri spillway)

(slope varying between 100 and 200)

- Slope 150

- Slope 200

- Two alternatives of aerator

- No ramp and;

- 3° ramp

- Precise mechanism by which small air concentration protects concrete surface is unclear, however it decreases the velocity of compression wave and hence any shock pressure.
- For zero air concentration this velocity is 1470 m/s, but for C=10% this velocity is approximately 50 m/s.

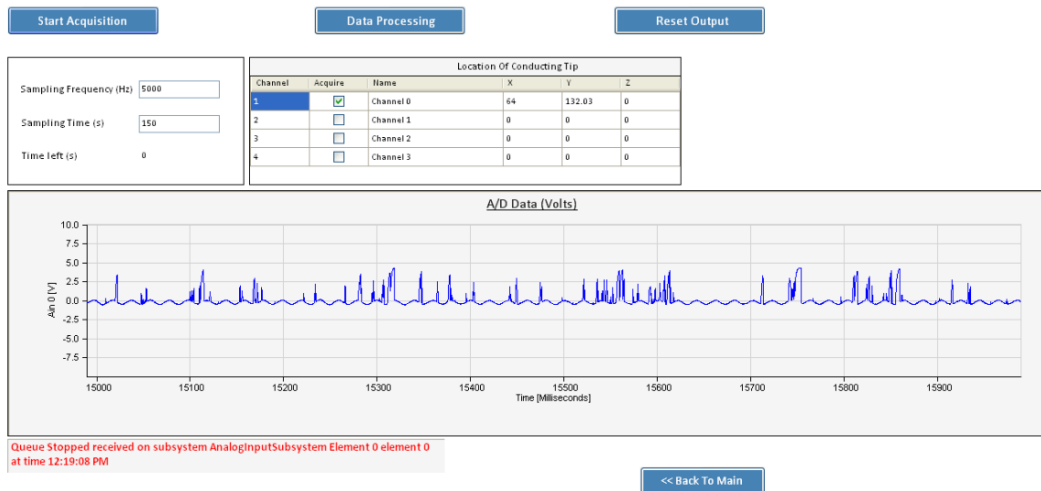


Figure2. Typical air concentration measurement output.

is available. During the data acquisition elapsed time, channel details, its configuration and hydraulic parameters with respect to time can be viewed. For system calibration special water column of height 3.75m was fabricated. This system was calibrated & tested on hydraulic model for obtaining experimental data.. Analysis of experimental data collected from model was done to obtain values of maximum, minimum, mean, standard deviation, turbulence intensity, no. of zero crossings, skewness, kurtosis, and stationarity test. In addition FFT analysis, Probability Density Function, Cumulative Distribution Function, Auto correlation, Cross correlation can be performed.

- Advanced DIAdem computing software is installed in the system to overcome the limitation of the excel file format which can store only 60,053 data points. DIAdem is an interactive tool for mathematics and visual data analysis and report generation. It is used to abstract necessary information from experimental data in order to make technical decisions.

7. SALIENT FEATURES OF ORIFICE SPILLWAY OF SUBANSIRI PROJECT

- Maximum design discharge 35000 m³/s , q = 338 m³/s/m
- Head over orifice spillway crest = 60 m
- Velocity =25 to 30 m/s
- Spillway profile equation $x^2 = 220 y$, Spillway length 88 m
- Energy dissipator ski jump bucket
- Positive pressures on the surface of spillway for ungated operation
- Negative pressures of - 1.0 m to - 3.0 m with partial gate operation
- Cavitation index for negative pressures between 0.16 and 0.13 which was lower than critical cavitation index of 0.2

PRESSURE PROFILES FOR ALL ALTERNATIVES OF SPILLWAY PROFILES WITH RAMP

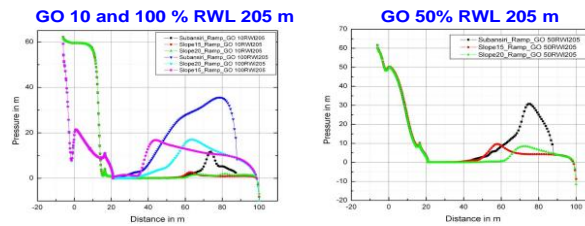


Figure 3. Typical pressure measurement on orifice spillway

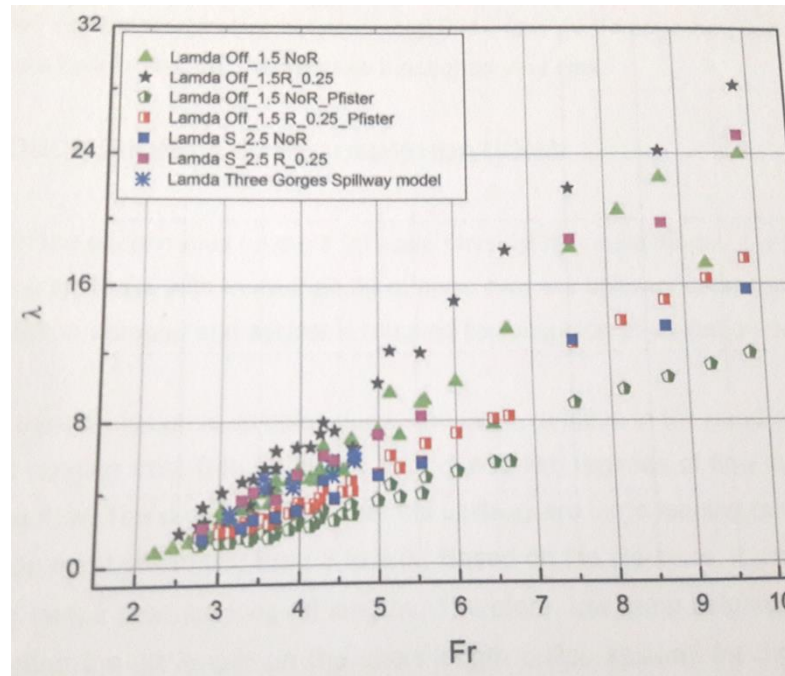


Figure 4. Plot of Froude Number and Jet length

Following ideas were gathered and research gaps identified:

- Various design approaches proposed by IAHR, ICOLD and USBR are for overflow spillways with steep slopes
 - Scantv data is available for spillway slopes < 300
 - Large ramp angles 7-110 are not studied
- Recently, Pfister and Haer (2010a and b) published the research work on flat slope overflow spillway with steep ramps
- No systematic research work is reported for aerator on orifice spillway
Orifice spillways with more than 50 m head over crest are susceptible to cavitation damage and aerator is required for mitigation of cavitation damage

- Aerator design is complex due to large variation in the head over spillway crest and also due to two regimes of flow viz. free flow and orifice flow
- Low ramp heights are preferred for restricting jet length on short length orifice spillway
- Jet action does not start up to a head of 17 m above the orifice spillway crest. Cavitation index is much above the critical cavitation index of 0.2. Therefore, there is no danger of the aerator inducing cavitation
- Jet reattachment point is farthest for lowest gate opening and decreases for increasing gate openings for a given reservoir water level
- Jet length and air entrainment increase with increase in air vent size till the cavity pressure reaches near atmospheric
- Non dimensional pressure in the cavity below jet decreases with increase in Froude number
- Air entrainment coefficient β decreases with increase in gate opening
- Addition of ramp enhances performance of aerator
- Flow is fully aerated across the depth and air concentration is found in the range of 30 to 50% for low gate openings.
- Clear water core appears in the central portion of the jet between upper and lower nappe aeration with increase in gate opening and the air concentration along the spillway surface decreases
- Physical model studies provided a good first hand information and insight in the hydrodynamic characteristics of aerator on orifice spillway
- Comparison of present study with aerator on flat slope overflow spillway revealed that characteristics of aerator on flat slope orifice spillway are totally different
- Philosophy of the functioning of aerator on orifice spillway is different than the aerator on flat slope overflow spillway
- Jet is lifted from the spillway floor in the area susceptible for cavitation damage. Smaller quantity of air induced by flat ramp remains in the flow till the end of short spillway length and is sufficient to mitigate cavitation damage

Reference

- [1] Chanson H (1997) Air Bubble Entrainment in free surface turbulent shear flow, Academic Press London
- [2] ICOLD Bulletin 81 (1992) Spillway Shockwaves and air entrainment, Cassidy J J (editor)
- [3] IAHR hydraulic Structures design Manual No 4 (1991) Air Entrainment in free Surface Flows, A A Balkema Publications
- [4] CWPRS Technical Report No 5004(2012), Hydraulic Model Studies for Aerator for Orifice Spillway, Subansiri Lower Dam Arunachal Pradesh/Assam 1/25 Scale GS model

SUMMARY

Recent trends in run of the river projects involves high intensity discharge and high heads. Such situation leads to pressures on the surface of spillway to drop below atmospheric leading to cavitation damages. To mitigate cavitations damage, measures such as control of geometry, smoothness of the spillway surface, use of cavitation resistant materials are adopted. There are limitations for adopting preventive measures. Provision of aerator only alternative to mitigate cavitations damage. There are various methods to measure air concentration in a spillway overflow flow. Most reliable being intrusive phase detection probes, like optical probe and resistivity probes. Present study employs use of resistivity probes along with PC based Data Acquisition System (DAS) to measure air concentration in a spillway over flow downstream of aerators. Two locations were selected to measure the air concentration. Two alternatives with offset of 1.5m and 2.5m namely without ramp and with ramp upstream of aerator were studied in the model. Comparison of various alternatives are presented in a table using non dimensional parameters jet length λ , air entrainment coefficient β , cavity pressure. Model study indicated that provision of ramp increases the air entrainment. Air concentration along the bed is more for small gate openings and decreases drastically in the vicinity of 2-3% for decreasing Froude number. Flow depth is fully aerated for small gate openings. β decreases with increase in gate openings. Addition of ramp improved pressures in aerator, jet length increases with addition of ramp. Study also proved that functioning of an aerator on the orifice spillway is different from the flat slope chute spillway. Spillway surfaces of high dams are susceptible to cavitation damage due to high velocities, surface roughness and geometrical deformities.

COMMISSION INTERNATIONALE DES GRANDS BARRAGES

VINGT-SIXIÈME CONGRÈS DES GRANDS BARRAGES
Autriche, juillet 2018

DOI 10.3217/978-3-85125-620-8-203



This work licensed under a Creative Commons Attribution 4.0 International License. <https://creativecommons.org/licenses/by-nc-nd/4.0/>

**STRAIN MEASUREMENTS AND AXIAL FORCE PREDICTIONS AT THE END
OF A STEEL LINED PRESSURE TUNNEL**

HAMMER A.

TIWAG – TIROLER WASSERKRAFT AG

AUSTRIA

BONAPACE P.

TIWAG – TIROLER WASSERKRAFT AG

AUSTRIA

UNTERWEGER H.

INSTITUTE OF STEEL STRUCTURES, GRAZ UNIVERSITY OF TECHNOLOGY

AUSTRIA

ECKER A.

INSTITUTE OF STEEL STRUCTURES, GRAZ UNIVERSITY OF TECHNOLOGY

AUSTRIA

COMMISSION INTERNATIONALE
DES GRANDS BARRAGES

VINGT-SIXIEME CONGRES DES
GRANDS BARRAGES
Autriche, juillet 2018

STRAIN MEASUREMENTS AND AXIAL FORCE PREDICTIONS AT THE END OF A STEEL LINED PRESSURE TUNNEL

Hammer A.¹, Bonapace P.¹, Unterweger H.², Ecker A.²

¹ *TIWAG – Tiroler Wasserkraft AG*

² *Institute of Steel Structures, GRAZ UNIVERSITY OF TECHNOLOGY*

AUSTRIA

1. INTRODUCTION

A new steel lined pressure shaft was constructed for the existing Kaunertal high head hydro-power plant in the years 2012 to 2015. The project included the construction of a 1430 m long 4.3 m diameter inclined pressure shaft, a 325 m long penstock tunnel section, a new surge tank consisting of two chambers connected by a 150 m deep vertical surge shaft [1].

Before starting operation, initial filling tests were carried out in particular to investigate the stress and strain distribution of the steel penstock. Each test consisted of two loading and unloading cycles of the new facilities. The first fill-test was carried out before the interface between steel lining and backfill concrete was grouted. The second fill-test started after interface grouting was completed. This rather lengthy testing procedure should primarily facilitate the grouting. The rock mass / steel lining response to loading and unloading of the shaft and eventual benefits gained from interface grouting were recorded with optical strain gauges spot-welded to the steel lining.

The axial force in the pipe due to internal pressure acting on the end cover of the pipe is necessarily transferred via friction into the rock mass embedding the penstock. Based on strain measurements at several pipe sections the distribution of the axial forces was studied in detail.

In particular the following scope was investigated

- Adequacy of assumptions in the structural analysis
- Back-analysis of rock modulus " V_F " and thermal gap " u_0 "
(Reduction of pipe stresses in circumferential direction)
- Behavior of the shaft lining in case of several loading and unloading cycles
- Isotropic / anisotropic rock mass reaction
- Distribution of strains at transitions of embedded to the exposed penstock
- Redistribution of internal (cover-) pressure into the rock mass

2. STRAIN MEASUREMENT

2.1. MONITORING ARRANGEMENT

Monitoring sections were situated at various locations along the alignment. Eight sections "A" aiming to monitor a standard shaft section in varying geologic conditions and three locations "B" aiming to monitor the lining behavior at transitions into the rock mass were installed (Fig. 1).

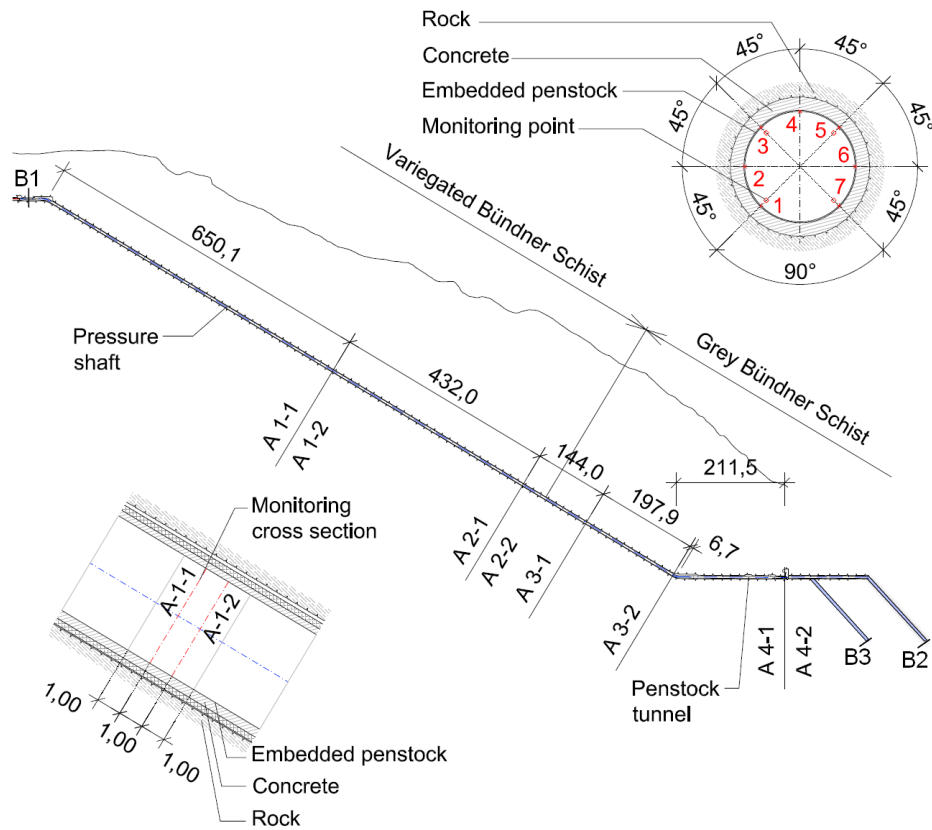


Fig. 1
Monitoring cross sections "A" and locations "B"

Monitoring cross section “A” arrangements (Fig. 1) consisted of two identical monitoring cross sections at a distance of 1.0 m to cover redundancy (e.g. A1-1 and A1-2). Each monitoring cross section included seven monitoring points around the circumference to measure circumferential strains at 45° angles. Every second monitoring point was also fitted with a longitudinal strain gauge to measure in addition the longitudinal stress behavior of the steel lining. For practical reasons no strain gauges were installed in the invert of the lining (see Fig. 1, danger of damage).

Each monitoring location “B” arrangement was fitted with strain gauges inside the pipe at an angle of 45° left and right of the center line in the invert of the steel lining. Six monitoring cross sections were placed near each transition of embedded to exposed penstock. Spacing of monitoring cross sections was selected to take measurements approx. 10 m deep into the rock mass along the penstock axis. At one monitoring location “B3” (Fig. 2) additional strain gauges were mounted on the outside of the pipe before it was embedded in concrete. For monitoring the outside of the steel pipe electrical strain gauges were used.

Due to long distances (up to 700 meters) between monitoring cross sections, the feedthrough traversing the penstock lining and the long monitoring period, standard electrical strain gauges could not be used inside the penstock. Optical strain gauges were applied instead. The optical sensors were mounted on thin metal strips which were spot welded onto the lining. The spot weld points were grinded and tested after removal of the strain gauges to exclude damages to the pipe surface.

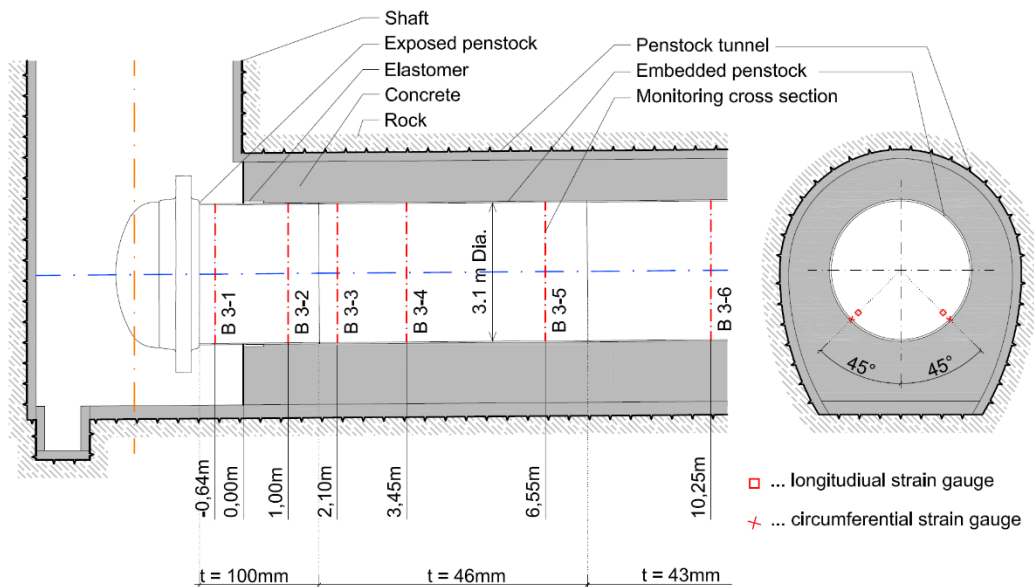


Fig. 2
Monitoring cross section “B” at pipe transition into the rock mass [2]

2.2. MEASURING PRINCIPLE OF OPTICAL SENSORS

Optical strain sensors use light with the initial Bragg-wavelength (λ_0), which is reflected by a grating. The wavelength is measured by an interrogator. Strains applied to a Fibre Bragg Grating (FBG) increases/decreases the distance between the “mirrors” of the grating. This shifts the Bragg-wavelength of reflected light, dependent on the compression or tension and length. The Bragg-wavelength shift ($\Delta\lambda$) on a FBG subjected to strain is dependent in a linear way on the applied strain [3].

$\Delta\varepsilon = \frac{\Delta\lambda}{k \cdot \lambda_0} = \Delta\lambda \cdot S$	$\Delta\varepsilon$... measured strain [$\mu\text{m}/\text{m}$]
	k ... gauge factor [-]
	S ... strain sensitivity [$\mu\text{m}/\text{m}/\text{nm}$]

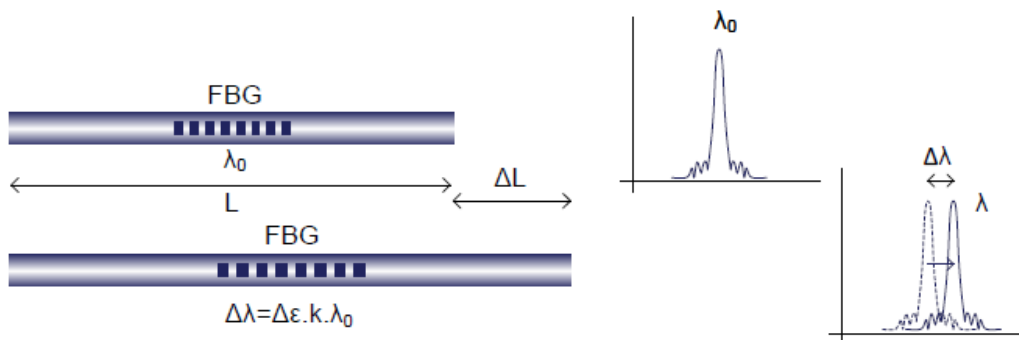


Fig. 3
Measuring principle of optical sensors using FBG [3]

The FBG is “written” into a single-mode optical fiber by activation of Germanium dopings or by inscription of morphological defects into the fiber core with high level energy lasers [4]. The advantages of the FBG technology as compared to standard electrical strain gauges are:

- Application of up to 20 sensors in one measurement chain
- Possible length of measurement chains up to several kilometers
- Redundancy when providing a measurement loop
- No destruction of FBGs due to high water pressure
- Small number and diameter of cables permit small feed-through
- Linear correlation between applied strain and measurement unit
- No danger from humidity (no short circuit, no electrical issues)

As shown in Figure 4 a typical measurement chain consists of a connection fiber which may be as long as required. At the end it is spliced with the sensor fiber which is up to 200 meters long. Up to 20 FBGs with different nominal wavelengths are provided in one measurement chain. The total amount of damping loss in the measurement chain has to be smaller than the value allowed by the interrogator. Finally the emitted light reflects at each FBG and the wavelength of the reflection is measured by the interrogator $\Delta\lambda_1$.

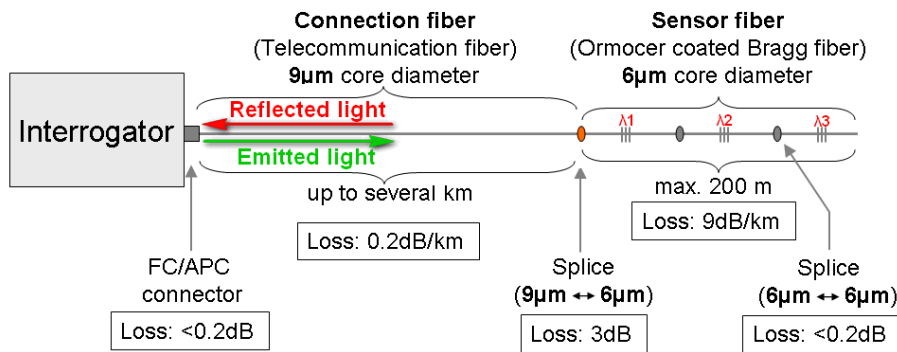


Fig. 4
Typical measurement chain with several FBGs

3. INITIAL FILL-TESTS AND RESULTS

3.1. PENSTOCK BEHAVIOR

In June 2015 the new shaft was filled for the first time and measurement results recorded for this Fill test 1 (FT 1). A pressure of 88 bar was reached at the shaft bottom after three days of filling and held for another three days until the facility was emptied again (Fig. 5).

After a waiting time of approx. one day the shaft was filled again and emptied. At first loading the measured strains at sections “A” were already close to values predicted in the analysis (Fig. 6). Compared to the calculated strains without any rock support, substantial interaction between rock mass and steel lining could be registered even not any interface grouting had taken place. On average the internal pressure was shared half and half between the steel lining and the rock mass. When emptying the facility for the first time the reduction of the shaft diameter due to pressure decrease and temperature effects resulted in a “thermal gap” between steel pipe and backfill concrete. A sudden release of pipe friction along a substantial length of the shaft was the consequence and longitudinal movements associated with substantial negative strains could be measured (e.g. Fig. 7, First Fill-Test (FT 1) at 25-20 bar).

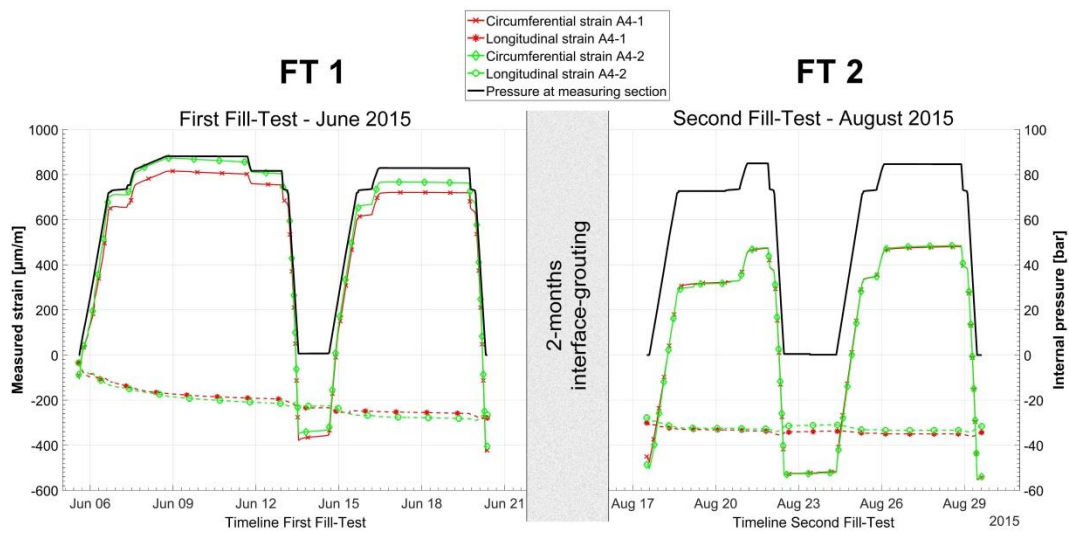


Fig. 5

Measured strains at sections A4-1 und A4-2 for both Fill-Tests (FT1 and FT2) [2]

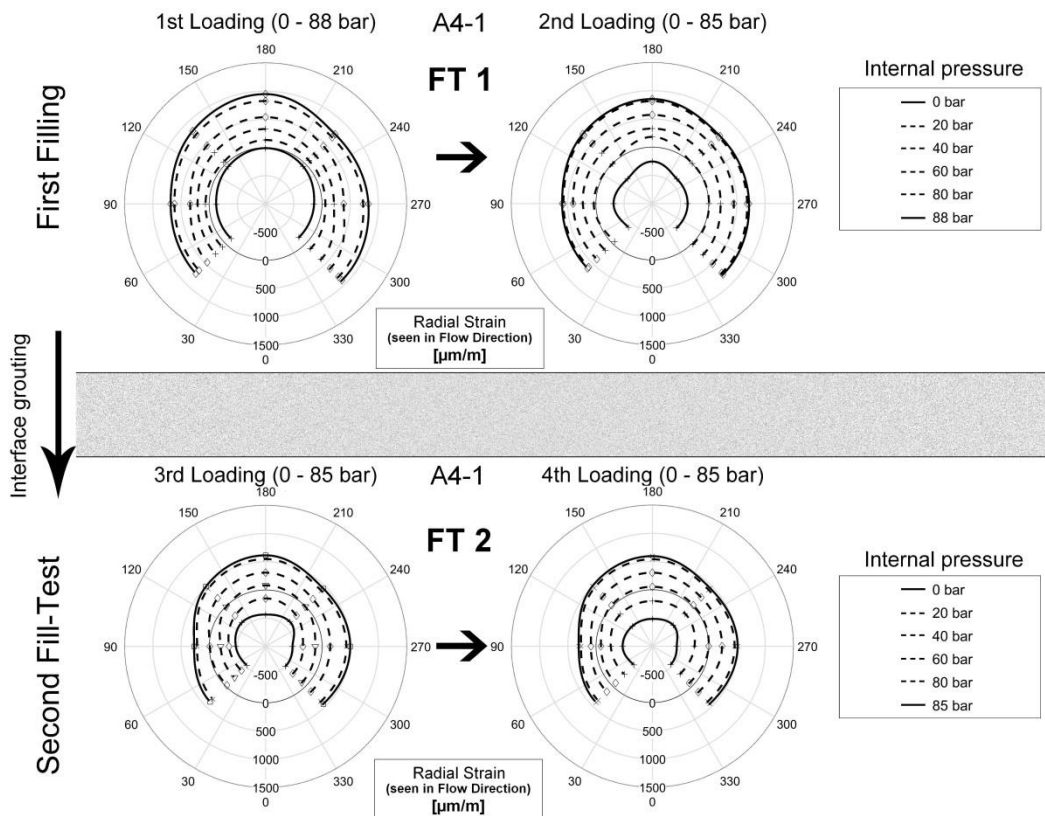


Fig. 6

Typical measurement cycle before (FT1) and after interface grouting (FT2) at section 4-1 [2]

The “thermal gap” provided space for free deformation of the steel lining at the second loading and unloading cycle of FT 1, which was still before interface grouting took place. This gap closed at moderate internal pressure causing circumferential strains ϵ_y of 200 to 400 $\mu\text{m}/\text{m}$ (equals 0.02 - 0.04%, Fig. 7: FT 1). Subsequently the steel lining was bedded in the rock mass again. The reason for this behavior may be associated with an initial settling of the strain gauges, temperature difference, shrinkage of concrete and creep, which was, however, not predicted to such an extent. The gap had to be filled with grout to improve uniform radial bedding of the penstock in the rock mass. At the second Fill-Test after interface grouting (FT2, loadings 3 and 4) longitudinal strains ϵ_x were zero. Circumferential strains ϵ_y responded purely elastically and returned to the starting point at the pressure-strain diagram after emptying the pipe (Fig. 7: FT 2).

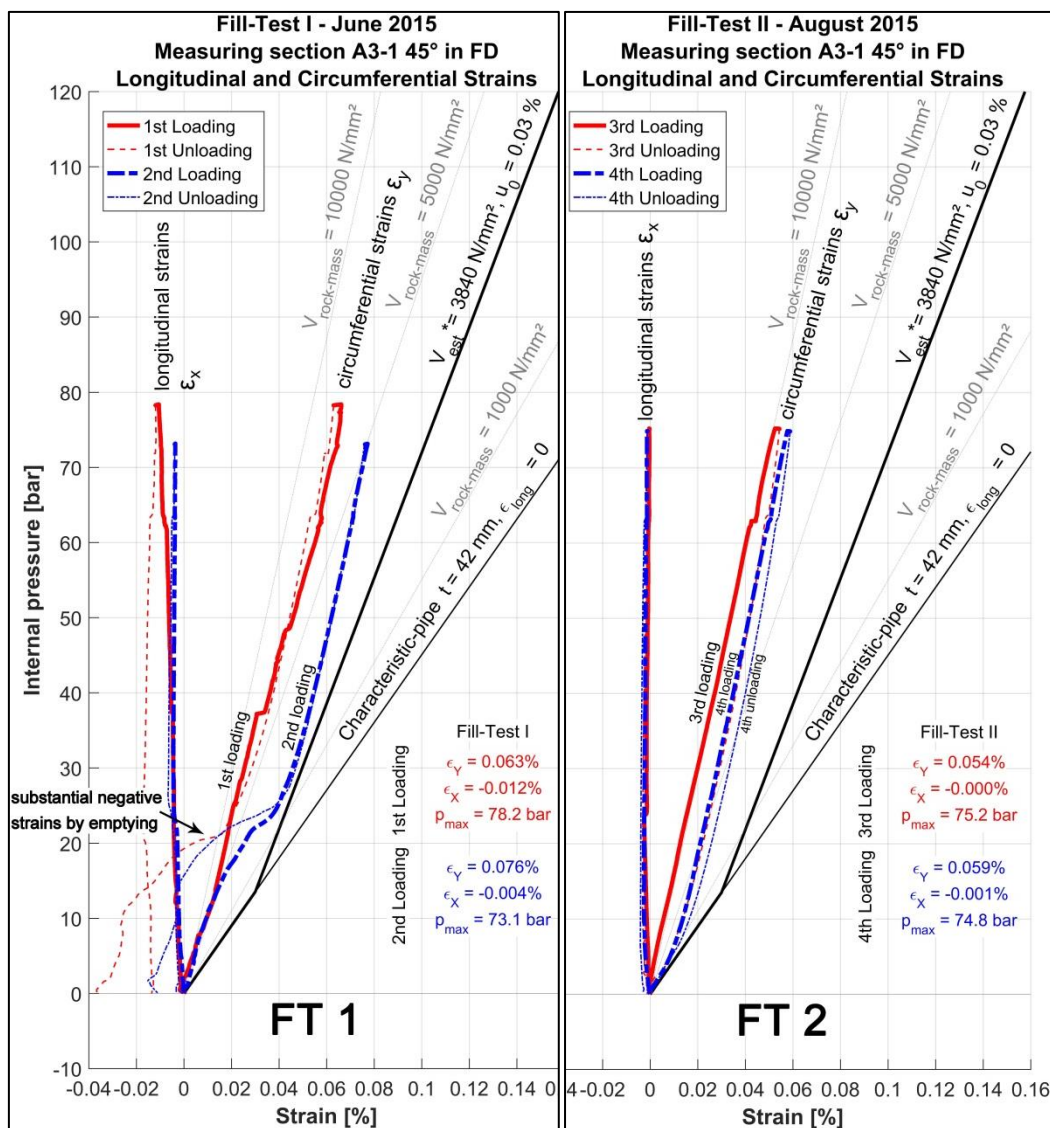


Fig. 7: Typical steel lining response before (FT1) and after (FT2) interface grouting

At locations “B” (Fig. 2) it was discovered that even without any shear rings a high portion of the full cover pressure of up to $D = 60$ MN, acting as an axial force at the pipe end was redistributed near the transition after only 3 m to 4 m (1.5 diameters) of embedded pipe length. At short distance from the transition a remarkable reduction of axial stress was registered in pipes with moderate wall thickness as compared to thick walled pipes [5], [6]. A considerable improvement for stress redistribution from the steel pipe into the rock mass was noticed in Fill-Test 2 after the interface grouting had taken place. After having redistributed a high portion of the cover pressure into the backfill concrete and rock mass close to the transition, the pipe was locked in with restricted constant longitudinal strain equivalent to a rather constant longitudinal pipe force (e.g. Fig. 8, at 4.0 m to 10.0 m distance to the transition). This remaining portion of the cover pressure results from axial stresses σ_x in the pipe due to internal pressure and full restraint of lateral contraction (see [6]).

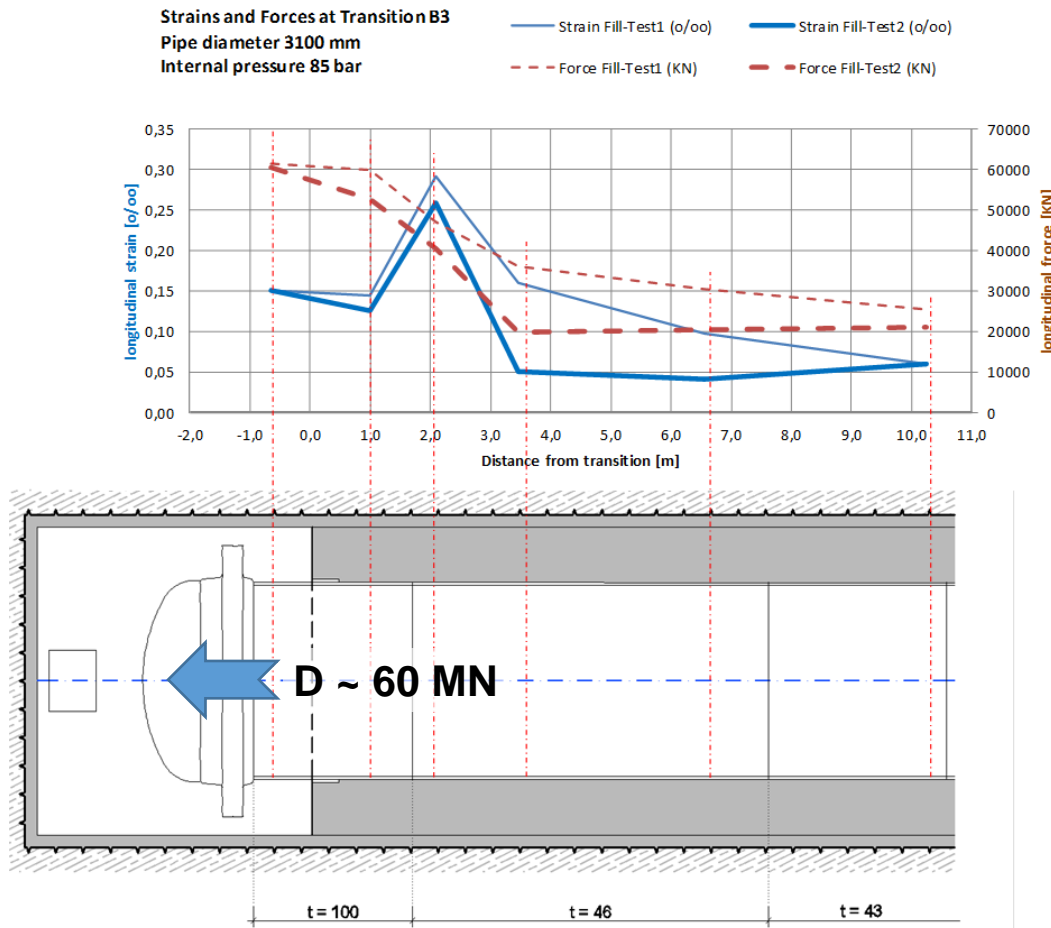


Fig. 8: Typical longitudinal strain and longitudinal force in the pipe at the transition into the rock [2]

SUMMARY

A new steel lined pressure shaft was constructed for the existing Kaunertal high head hydro-power plant. Before starting operation, initial filling tests were carried out in particular to investigate the behavior of the steel penstock. Various monitoring arrangements were used to monitor the rock mass / steel lining interaction and the axial force distribution at the end of the embedded penstock. To verify the effects of grouting the tests were carried out before and after interface grouting took place. The most important findings regarding the results of strain measurements in the steel pipe are listed below:

- Strain measurements can be realized with optical strain sensors at high accuracy, bridging distant locations and sustaining high water pressure.
- At the second loading and unloading cycle of the first fill test (still before interface grouting took place), a “thermal gap” between steel pipe and backfill concrete, which could be detected, provided space for free deformation of the steel lining.
- A considerable improvement of stress redistribution from the steel pipe into the rock mass was noticed in Fill-Test 2 after the interface grouting took place.
- After interface grouting took place circumferential strains responded purely elastically and returned to the starting point of the pressure-strain diagram
- After only 3 m to 4 m (1.5 diameters) of the embedded pipe length a substantial portion of the full cover pressure acting as an axial force in the steel pipe was transferred to the rock mass even without any shear rings.

REFERENCES

- [1] BONAPACE P., The renewal of the pressure shaft for the high head hydropower plant Kaunertal in Austria: Civil engineering and civil works, Vienna Hydro, 2012
- [2] HAMMER A., Strain monitoring with optical sensors in the Kaunertal penstock, Vienna Hydro, 2016
- [3] GRAHAM-ROWE D., Sensors take the strain, Nat. Photon.1, (2007), 307ff.
- [4] BRINKMEYER E., “Faseroptische Gitter”, Optische Kommunikationstechnik, Eds. E. Voges and K. Petermann, Springer, 2002
- [5] UNTERWEGER H., ECKER A., Abklingverhalten von Rohrlängskräften in Druckschachtpanzerungen bei Berücksichtigung der Reibung zwischen Rohrwand und Hinterfüllbeton – Parameterstudie mit und ohne Schubringe, Institut für Stahlbau, TU Graz, 2016
- [6] UNTERWEGER H., ECKER A., Load transfer of longitudinal pipe forces in penstocks through friction, Journal on Hydropower and Dams, Vol. 24, No. 5, pp. 92-96, 2017

COMMISSION INTERNATIONALE DES GRANDS BARRAGES

VINGT-SIXIÈME CONGRÈS DES GRANDS BARRAGES
Autriche, juillet 2018

DOI 10.3217/978-3-85125-620-8-204



This work licensed under a Creative Commons Attribution 4.0 International License. <https://creativecommons.org/licenses/by-nc-nd/4.0/>

**END OF STEEL LINED PRESSURE TUNNELS - LOAD TRANSFER OF
LONGITUDINAL PIPE FORCES**

UNTERWEGER H.

INSTITUTE OF STEEL STRUCTURES, GRAZ UNIVERSITY OF TECHNOLOGY

AUSTRIA

ECKER A.

INSTITUTE OF STEEL STRUCTURES, GRAZ UNIVERSITY OF TECHNOLOGY

AUSTRIA

HAMMER A.

TIWAG – TIROLER WASSERKRAFT AG

AUSTRIA

BONAPACE P.

TIWAG – TIROLER WASSERKRAFT AG

AUSTRIA

COMMISSION INTERNATIONALE
DES GRANDS BARRAGES

VINGT-SIXIÈME CONGRÈS DES
GRANDS BARRAGES
Autriche, juillet 2018

END OF STEEL LINED PRESSURE TUNNELS - LOAD TRANSFER OF LONGITUDINAL PIPE FORCES

Unterweger H.¹, Ecker A.¹, Hammer A.², Bonapace P.²

¹ *Institute of Steel Structures, GRAZ UNIVERSITY OF TECHNOLOGY*

² *TIWAG – Tiroler Wasserkraft AG*

AUSTRIA

1. INTRODUCTION

Within a recently finished research-project the load transfer of axial loads in penstocks only due to friction between the filled steel pipe and the surrounding concrete and rock, without thrust rings, was studied. Axial loads arise due to water pressure on caps or valves and temperature differences between steel pipe and surrounding concrete. Thrust rings are traditionally used to transfer the axial loads in the steel pipe into the surrounding concrete and further into the rock. The load carrying and stiffness behavior of thrust rings was recently studied in detail by the authors ([1], [2]), because it was not regulated in common design codes for penstocks ([3] - [5]).

This paper deals with a summary of the measurements on a part of a penstock to evaluate appropriate coefficients of friction μ between steel pipe and the backfill concrete. Then parametric studies are presented to show the principal behavior of load transfer along the pipe, with and without thrust rings.

Based on that, a simplified analytic model was developed for practical design including regions without friction. In addition, the effects of the important boundary conditions – longitudinally free or fixed – of the steel pipe within the rock are presented.

This paper also sums up the results of [6].

2. MEASUREMENTS FOR EVALUATION OF COEFFICIENTS OF FRICTION

During renewal of the penstock of the high head hydropower plant called “Kaunertal” (owner TIWAG Innsbruck/Austria) very comprehensive strain measurements at parts of the penstock after water filling – before and after injection of the interface between steel pipe and concrete – were carried out. Here only the results at a part of the penstock are presented, where in this erection phase a transfer of longitudinal forces via friction only occurs. Fig. 1 shows this part, with an internal diameter $d_i = 3100$ mm. The six test sections (TS 1 to TS 6) are shown, with two measure points along the circumference. In each point both the longitudinal strains (ε_x) and the strains in circumference direction (ε_θ) were measured, at the inner and outer wall surface, leading to four individual results ($\varepsilon_{i,x}$, $\varepsilon_{i,\theta}$ and $\varepsilon_{o,x}$, $\varepsilon_{o,\theta}$). At the left side of Fig. 1 the steel pipe is longitudinal free and has no concrete surrounding. The pipe has temporarily a bolted steel end cover. In total four measurements for filling situations were carried out.

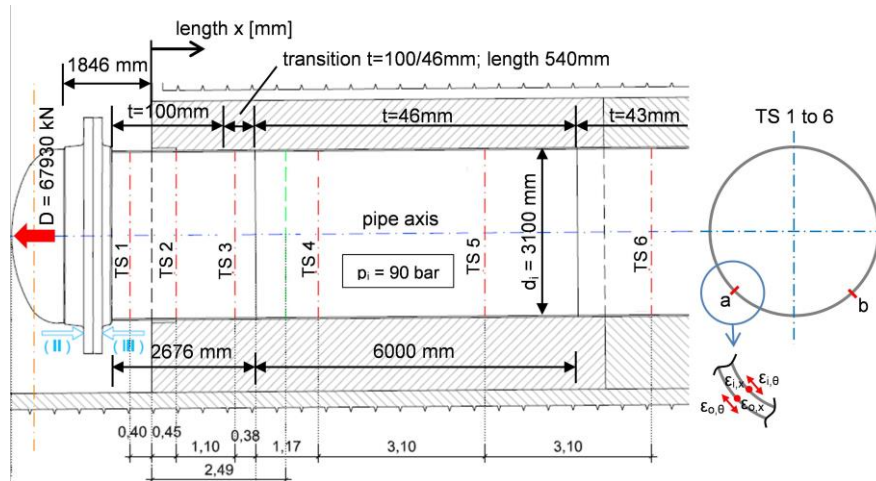


Fig. 1

Penstock at Kaunertal in the erection phase. Transfer of longitudinal force due to internal pressure without thrust ring and measuring points in the individual test sections (TS1 to TS6)

Fig. 2 shows only the results for the 2nd filling after injection of the interface between steel pipe and concrete. Fig. 2a shows the strains in longitudinal, Fig. 2b in circumferential direction. The dots are the measured strains due to internal pressure $p_i = 9.0$ N/mm² (90 bar), also leading to the total force D (Eq. [1]) in longitudinal direction of the pipe (r_i is equal to the inner radius of the pipe). Some measure points were not directly situated at the test sections, leading to the shown shift of $\Delta x = 0.25$ m.

$$D = p_i \cdot r_i^2 \cdot \pi = 9 \cdot 1550^2 \cdot \pi \cdot 10^{-3} = 67930 \text{ kN} \quad [1]$$

Some strain measurements failed. Therefore not in each test section four values are visible in Fig. 2. The measured strains in the individual points of each

test section show a considerable scattering, probably due to different radial stiffness of the surrounding concrete and rock. Within a parametric numerical study, calculations for constant radial stiffness C_F and coefficient of friction μ were done. The radial stiffness C_F in N/mm^3 depends on the modulus of subgrade reaction V_F in N/mm^2 of the surrounding rock, as shown in Eq. [2].

$$C_F = V_F/r_i \quad [2]$$

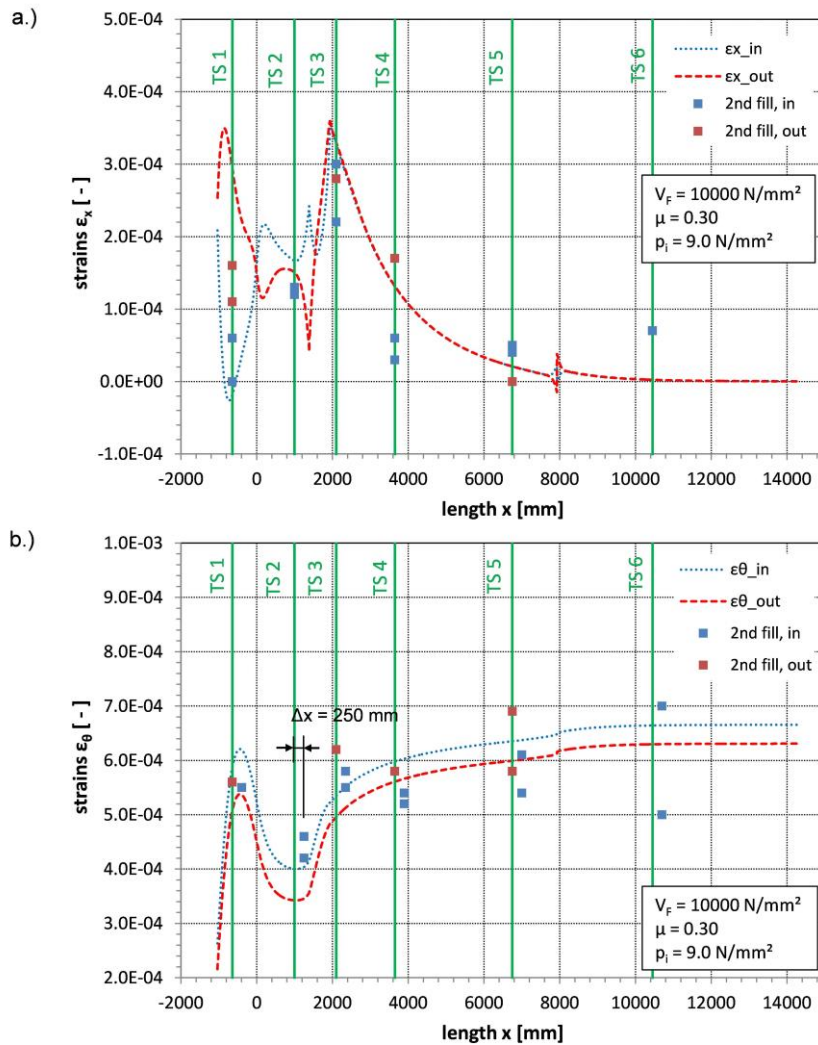


Fig. 2

Strain measurements in the penstock at Kaunertal due to infill ($p = 9.0$ bar). Comparison with results of the numerical study, a) strains ϵ_x in longitudinal and, b) strains ϵ_θ in circumferential direction

Based on the strains in circumferential direction ϵ_θ the accurate radial stiffness C_F can be estimated, because for a pipe with internal pressure according to the simplified Eq. [3] the strains ϵ_θ decrease with increased radial stiffness (u_0 corresponds to the radial gap between steel and concrete).

$$\varepsilon_{\theta} = \left(p_i - \frac{u_0 \cdot E^* \cdot t}{r^2} \right) \cdot \frac{r}{E^* \cdot t + C_F \cdot r^2} \quad [3]$$

with: $E^* = \frac{E}{1-\nu^2} = \frac{210000}{1-0.3^2} = 230770 \text{ N/mm}^2$...modulus of elasticity for plane strain

On the other hand the distribution of the strains ε_x in longitudinal direction and the longitudinal deformation u_x at the free end have a direct relationship to the coefficient of friction μ . Reasonable values within the numerical study for best fit with the measured test data are $\mu = 0.25$ and $V_F = 10000 \text{ N/mm}^2$. In Fig. 2 the strains for $\mu = 0.30$ are shown, because the exact friction coefficient was determined with the longitudinal displacements at the cover and for the calculation with $\mu = 0.25$ only the displacements were plotted (see Fig. 6). In contrast the specific value $V_F = 3800 \text{ N/mm}^2$ was also used in the numerical studies, because in the past during tunneling of the penstock additional tests with a radial jack gave this value.

3. NUMERICAL STUDY FOR VERIFICATION OF THE TYPICAL BEHAVIOR

3.1. OVERVIEW

The results of the measurements are hard to interpret, on the one hand due to the different thicknesses of the pipe and on the other hand due to the large scattering. To get a better understanding of the transfer of longitudinal pipe forces to the surrounded part of the steel pipe (for $x > 0$ in Fig. 1, 2) an additional numerical study was done with constant thickness ($t_1 = 50 \text{ mm}$ at the free pipe, for $x < 0$, thickness t_2 in the region with concrete surrounding). Different radial stiffness C_F were assumed, leading to different thickness t_2 , based on the assumption that the stresses in circumference direction due to internal pressure are equal to 60% of the yield strength (calculations were done with $f_y = 460 \text{ N/mm}^2$ leading to thicknesses t_2 shown in Table 1). For the simplified systems with constant pipe thicknesses a FE-model and also a simplified analytical model were developed. Pipe transitions with and without thrust rings were analyzed.

3.2. FE-MODEL

Due to the assumed axial symmetric behavior, also axial symmetric elements were used within the software-code ABAQUS. The steel pipe and thrust ring was assumed with linear elastic behavior ($E = 210000 \text{ N/mm}^2$; $\nu = 0.30$). For the thickness transition an inclination of 1:10 was adopted only at the outer surface. For the calculations without a thrust ring linear shell elements (SAX2), otherwise volume elements (CAX4R), were used. For the concrete a nonlinear behavior was assumed (concrete damage plasticity [7], [8]), based on the studies with thrust

rings ([1], [2]). In the FE-model only the steel pipe, the thrust ring, the concrete surrounding and the radial stiffness of the rock were considered. The end cover was not part of the model, therefore instead of the total force D the membrane force n_D (Eq. [4]) along the circumference was used (similar FE-model as in Fig.7) in longitudinal direction.

$$n_D = p_i \cdot \frac{d_i}{4} = 9.0 \cdot \frac{3100}{4} = 6975 \text{ N/mm} \quad [4]$$

3.3. RESULTS OF LONGITUDINAL FORCE DISTRIBUTION – WITHOUT THRUST RING

In Fig. 3 the typical distributions for the longitudinal membrane stresses $\sigma_{x,m}$ are shown for a varying coefficient of friction and with a very low radial stiffness $V_F = 1000 \text{ N/mm}^2$. In addition also the radial stresses σ_r between steel and concrete are shown. The shown characteristic of the longitudinal membrane stresses $\sigma_{x,m}$ is equal to the longitudinal membrane forces n_x .

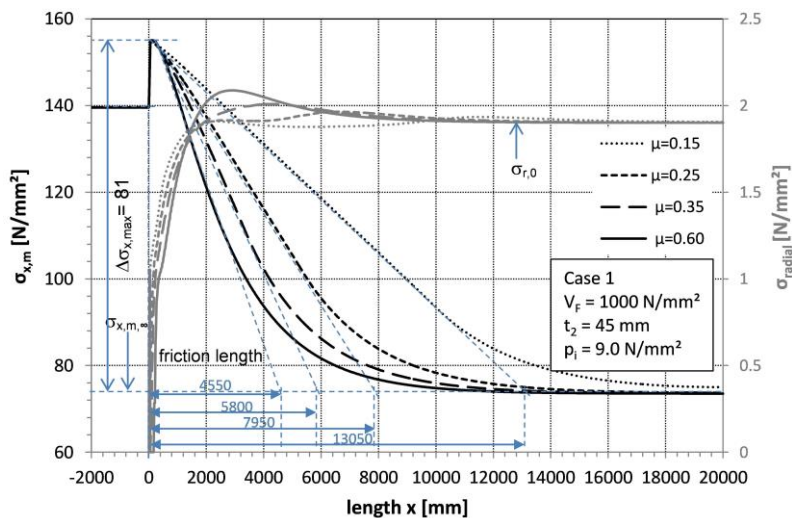


Fig.3

Transfer of the longitudinal force along the length of the steel pipe for $V_F = 1000 \text{ N/mm}^2$. Stresses $\sigma_{x,m}$ in longitudinal and stresses σ_r in radial direction at the steel pipe.

Worth mentioning is that not the entire longitudinal force D is transferred via friction. After a so called friction length l_{fr} (shown with a simplified linear extrapolation for the $\sigma_{x,m}$ curves in Fig. 3) the stresses $\sigma_{x,m}$ doesn't change any more. The background of the limit value $\sigma_{x,m,\infty}$ in Fig. 3 is, that no axial strains in the steel pipe in this region occur. The tension strains due to $\sigma_{x,m,\infty}$ are equal to the compression strains due to the lateral contraction of the tension stresses σ_θ in circumferential direction, due to water infl. This leads to Eq. [5]:

$$\sigma_{x,m,\infty} = \nu \cdot \sigma_{\theta,m,\infty} = 0.3 \cdot \sigma_{\theta,m,\infty} \quad [5]$$

For the tension stresses $\sigma_{\theta,m,\infty}$ in the circumferential direction also an analytic formulation based on Eq. [6] can be used.

$$\sigma_{\theta,m,\infty} = \frac{E^* \cdot u_0}{r_i} + \frac{E^* \cdot \left(p_i - \frac{E^* \cdot u_0 \cdot t_2}{r_i^2} \right)}{r_i \cdot \left(C_F + \frac{E^* \cdot t_2}{r_i^2} \right)} \quad [6]$$

If a radial gap u_0 can be ignored Eq. [6] leads to Eq. [7]:

$$\sigma_{\theta,m,\infty} = \frac{E^* \cdot p_i}{r_i \cdot \left(C_F + \frac{E^* \cdot t_2}{r_i^2} \right)} \quad [7]$$

Eq. [7] and [5] lead to $\sigma_{x,m,\infty} = 74 \text{ N/mm}^2$ for $V_F = 1000 \text{ N/mm}^2$. This stress value is identical to the numerical result given in Fig. 3. Based on the longitudinal stress $\sigma_{x,m,\infty}$ the reaction force at the anchor point of the steel pipe is determined (n_{AP} in N/mm and N_{AP} in N; with D_m as diameter of the pipe; mean value of inner and outer diameter).

$$n_{AP} = \sigma_{x,m,\infty} \cdot t_2 = \nu \cdot \sigma_{\theta,m,\infty} \cdot t_2 = 0.3 \cdot \sigma_{\theta,m,\infty} \cdot t_2 \quad [8]$$

$$N_{AP} = n_{AP} \cdot D_m \cdot \pi \quad [9]$$

The part of the overall longitudinal force transferred by friction n_{fr} at the beginning of the concrete surrounding ($x > 0$) is based on Eq. [10], considering also additional longitudinal forces n_{Temp} due to temperature differences ΔT , calculated with Eq. [11] (α_T = coefficient of thermal expansion).

$$n_{fr} = n_D - n_{AP} \pm n_{Temp} \quad [10]$$

$$n_{Temp} = \Delta T \cdot \alpha_T \cdot E^* \cdot t \quad [11]$$

In Table 1 the longitudinal forces transferred by friction n_{fr} for different assumptions of the radial stiffness V_F are shown. With higher radial stiffness the transferred longitudinal force by friction increases and the support force at the anchor point decreases. If no anchor point for the steel pipe is performed, the longitudinal forces will be transferred at the free end inside the mountain also by friction (see section 4).

Table 1
Part of the overall longitudinal force n_D which is transferred by friction (n_{fr}) and support reaction n_{AP} at the anchor point inside the mountain

V_F [N/mm ²]	t_2 [mm]	n_{fr} [N/mm]	n_{fr} / n_D	n_{AP} / n_D
1000	45	3645	52 %	48 %
3840	30	4785	69 %	31 %
10000	10	6345	91 %	9 %

In Fig. 3 also the radial compression stresses between steel pipe and

concrete are shown. They are nearly constant after a short length x . For the reference value $\sigma_{r,0}$ only a 2D ring model with plane strain conditions is necessary. Alternatively based on an analytical model Eq. [12] is available, leading to the same values as in the numerical study, if the stiffness of the concrete is neglected (for $V_F \geq 3800 \text{ N/mm}^2$ the influence of the concrete ring is very small).

$$\sigma_{r,0} = \left(p_i - \frac{u_0 \cdot E^* \cdot t}{r^2} \right) \cdot \frac{V_F \cdot r}{E^* \cdot t + V_F \cdot r} \quad [12]$$

Based on this constant radial compression stresses $\sigma_{r,0}$ a simplified solution for the friction length l_{fr} is available:

$$l_{fr} = \frac{n_{fr}}{\mu \cdot \sigma_{r,0}} \quad [13]$$

This simplified solution leads to a small underestimation of the friction length l_{fr} in the numerical studies, which is shown in Fig. 3 ($< 5 \%$). An overview of the friction length l_{fr} for all studied cases is given in Fig. 4. Based on the determined coefficient of friction $\mu = 0.25$ (see section 2) and a common radial stiffness $V_F > 3000 \text{ N/mm}^2$, it is worth mentioning that only very short friction lengths l_{fr} , smaller than two times the diameter of the pipe ($l_{fr} < 2 \cdot d_i$), occur.

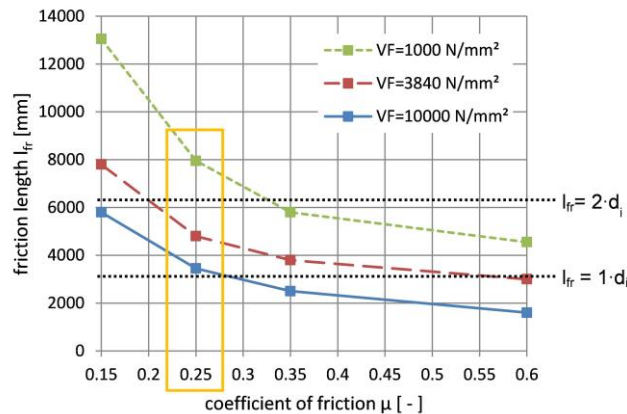


Fig. 4

Summary of the calculated friction lengths l_{fr} for different coefficient of friction μ and stiffness of rock V_F

3.4. RESULTS OF LONGITUDINAL FORCE DISTRIBUTION – WITH ADDITIONAL THRUST RING

In Fig. 5 the results for the solution with and without thrust rings for a small radial stiffness $V_F = 1000 \text{ N/mm}^2$ are compared. The position of the thrust ring was assumed at a distance of $x = 6 \text{ m}$ (equal to two times the diameter of the pipe) inside the mountain. The results in Fig. 5 show that for higher coefficients of friction ($\mu = 0.25$ and 0.35) nearly no longitudinal forces are transferred by the thrust rings.

Only for a very low value $\mu = 0.15$ approximately 20 % of the overall force is transferred by the thrust ring ($n_{TR} / n_{fr} \approx 0.20$). In case of higher radial stiffness V_F also for this low value of the coefficient of friction $\mu = 0.15$ nearly no part of the longitudinal force is transferred by the thrust ring.

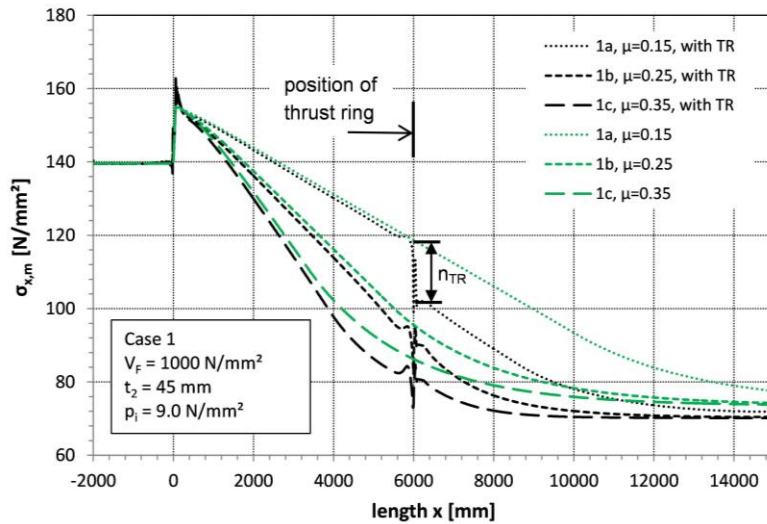


Fig. 5

Transfer of the longitudinal forces along the steel pipe with and without thrust ring (TR). Stresses $\sigma_{x,m}$ at the steel pipe in longitudinal direction.

3.5. PIPE DISPLACEMENTS AT THE PIPE END – WITH AND WITHOUT THRUST RINGS

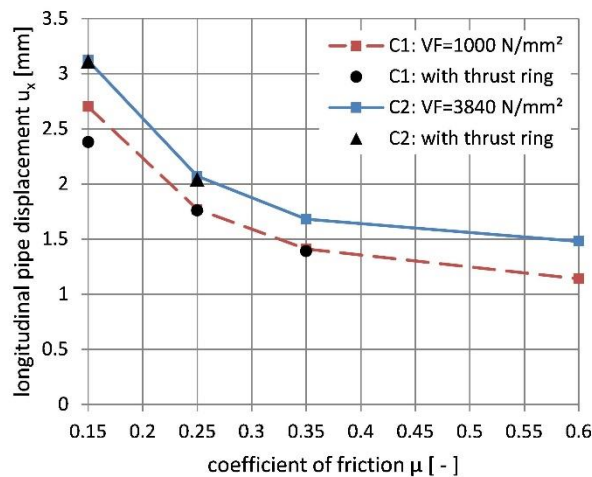


Fig. 6

Longitudinal pipe displacements u_x at the free end of the steel pipe, depending on the coefficient of friction μ and stiffness of the rock V_F – with and without thrust ring at $x = 6000$ mm

An important issue for the erection of thrust rings is the limited values allowed

for longitudinal displacements of the steel pipe near the power houses. In Fig. 6 a summary of the calculated values u_x of the longitudinal pipe displacements at the free end are plotted, depending on the coefficient of friction μ . Due to the assumed position of the thrust ring ($x = 6.0$ m) nearly no difference in the displacements occurs in the calculation with and without thrust ring.

4. NUMERICAL STUDY FOR DIFFERENT BOUNDARY CONDITIONS AND REGIONS WITHOUT FRICTION

4.1. TYPICAL BEHAVIOR BASED ON FEM-STUDIES

In section 3 the typical behavior for the transfer of longitudinal pipe forces was shown, with constant coefficient of friction between the steel pipe and the surrounding concrete (for $x > 0$). The steel pipe had a longitudinally fixed boundary condition inside the mountain (boundary condition BC1 in Fig. 7).

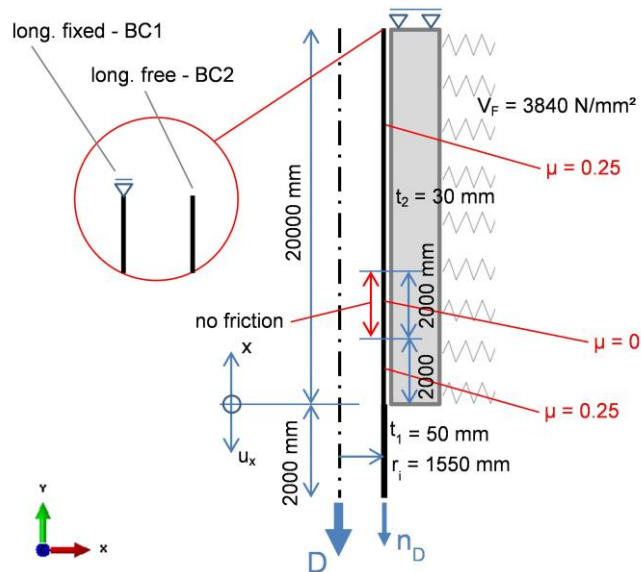


Fig.7

Numerical FE-model to study regions of the steel pipe without friction and different boundary conditions at the pipe end within the mountain.

In Fig. 8 the typical behavior is shown, when along a short region no friction is available ($2.0 \text{ m} < x < 4.0 \text{ m}$). In this region no longitudinal forces are transferred, leading to constant stresses $\sigma_{x,m}$ along this distance. This means that the friction length l_{fr} must be extended by the length without friction ($l_{fr}^* = l_{fr} + l_{\mu=0}$). In Fig. 8 also the results for the steel pipe with a longitudinal free boundary condition inside the mountain are shown (BC2 in Fig. 7). Now at this end the longitudinal stresses $\sigma_{x,m}$ must disappear ($\sigma_{x,m} = 0$). As Fig. 8 shows, there is a similar behavior

of the transfer of the remaining part n_{AP} of the total longitudinal force (see Table 1) at $x=14000$ mm to $x=20000$ mm. Therefore again for the simplified approach Eq. [13] is applicable, based on the force n_{AP} .

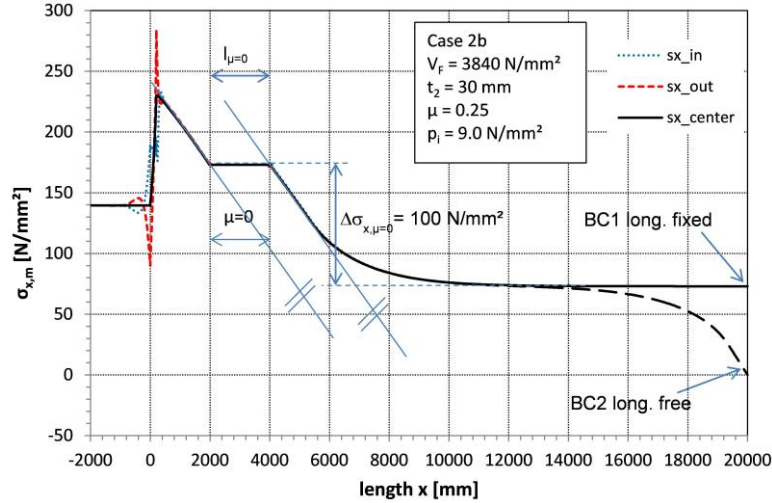


Fig. 8

Transfer of the longitudinal forces along the steel pipe for different boundary conditions of the steel pipe and a region without friction (length $l_{\mu=0}$) within the length l_{fr} .

4.2. SIMPLIFIED ANALYTICAL MODEL FOR END DISPLACEMENT U_x

The occurrence of regions without friction within the friction length l_{fr} significantly increases the longitudinal displacement u_x at the free end (see Fig. 7). Based on the results of the numerical study, for the calculation of the displacement u_x Eq. [14] can be used, leading to underestimations of the correct values of approximately 10 % (for $\mu = 0,25$). This Eq. [14] is applicable for both boundary conditions in Fig. 7, because the boundary condition has no influence on the displacements at the free end.

$$u_x = \frac{\Delta\sigma_{x,max}}{2 \cdot E} \cdot l_{fr} \quad [14]$$

If within the friction length l_{fr} also regions without friction ($l_{\mu=0}$) are expected the increased deformation u_x can be estimated based on Eq. [15], with $\Delta\sigma_{x,\mu=0}$ given in Fig. 8.

$$\frac{\Delta\sigma_{x,max}}{2 \cdot E} \cdot l_{fr} + \frac{\Delta\sigma_{x,\mu=0}}{E} \cdot l_{\mu=0} \quad [15]$$

5. SUMMARY

Within this research project, based on measurements on a penstock during erection and a comprehensive numerical study the following results are worth mentioning:

- High local longitudinal forces acting on the steel pipe in penstocks, due to closed valves for example, may also be transferred to the surrounding concrete and rock due to friction only – without thrust rings.
- This requires internal pressure in the steel pipe. Then the length for transferring the longitudinal forces l_{fr} is very short ($l_{fr} < 2 \cdot d_i$, for $\mu = 0.25$ and $V_F > 2500 \text{ N/mm}^2$).
- Only a part of the longitudinal force n_D is transferred locally over the length l_{fr} . This proportion n_{fr} / n_D increases with higher radial stiffness of the rock.
- Additional thrust rings, when they are not directly situated at the beginning of the rock and concrete surrounding, get only small amounts of the longitudinal forces.
- If the transfer of longitudinal forces within the friction length l_{fr} is possible (guaranteed coefficient of friction μ) also the longitudinal displacements u_x of the steel pipe on the free end will be small.
- If the steel pipe has also a free end inside the mountain also the remaining part of the longitudinal force $n_{AP} = n_D - n_{fr}$ will be transferred over a very short length l_{fr} . For the estimation of this length the same behavior is given as at the free end of the steel pipe. It is highly recommended to set up an anchorage point inside the mountain due to safety reasons. If this is not possible, the friction length should be long enough, because the whole longitudinal force is transferred by friction.
- A simple analytical model was developed to calculate the transferred load n_{fr} , the friction length l_{fr} and the displacements u_x at the free end of the steel pipe.

REFERENCES

- [1] H. UNTERWEGER, A. ECKER, Load carrying behaviour of thrust rings for transferring longitudinal pipe forces. *Journal of constructional steel research*, Band 114, pp. 178-187, 2015
- [2] H. UNTERWEGER, A. ECKER; Design Model for Transferring Longitudinal Pipe Forces Using Thrust Rings. *Structural Engineering International, IABSE*, Volume 26, Nr. 2, pp. 139-149, 2016
- [3] Engineer Manual 1110-2-2901: *Engineering and Design – Tunnels and Shafts in Rock*. U.S. Army Corps of Engineers, Washington, 1997
- [4] C.E.C.T: Recommendations for the Design, Manufacture and Erection of Steel Penstocks of Welded Construction for Hydro Electric Installations. European Committee for Boilermaking and Kindred Steel Structures, 1984

- [5] ASCE 1993: Steel Penstocks, *Manual on Engineering Practice No. 79*, America Society of Civil Engineers, New York, 1993
- [6] H. UNTERWEGER, A. ECKER, Load transfer of longitudinal pipe forces in penstocks through friction. *Journal on Hydropower and Dams*, Vol.24, No. 5, pp. 92-96, 2017
- [7] J. LUBLINER, J. OLIVER, S. OLLER, E. ONATE, A Plastic-Damage Model for Concrete. *International Journal of Solids and Structures* Vol. 25, No. 3, pp. 299-326, 1989
- [8] J. LEE, G. L. FENVES: Plastic-Damage Model for Cyclic Loading of Concrete Structures. *Journal of Engineering Mechanics*, Vol. 124, pp. 892-900, 1998

COMMISSION INTERNATIONALE DES GRANDS BARRAGES

VINGT-SIXIÈME CONGRÈS DES GRANDS BARRAGES
Autriche, juillet 2018

DOI 10.3217/978-3-85125-620-8-205



This work licensed under a Creative Commons Attribution 4.0 International License. <https://creativecommons.org/licenses/by-nc-nd/4.0/>

**THRUST RINGS FOR TRANSFERRING LONGITUDINAL PIPE FORCES –
DEVELOPMENT OF A DESIGN MODEL**

ECKER A.

INSTITUTE OF STEEL STRUCTURES, GRAZ UNIVERSITY OF TECHNOLOGY

AUSTRIA

UNTERWEGER H.

INSTITUTE OF STEEL STRUCTURES, GRAZ UNIVERSITY OF TECHNOLOGY

AUSTRIA

THRUST RINGS FOR TRANSFERRING LONGITUDINAL PIPE FORCES – DEVELOPMENT OF A DESIGN MODEL

Ecker A., Unterweger H.

Institute of Steel Structures, GRAZ UNIVERSITY OF TECHNOLOGY

AUSTRIA

1. INTRODUCTION

Thrust rings with rectangular cross-sections are mainly used in penstocks to transfer the longitudinal pipe forces via the exterior concrete to the surrounding bed rock (Fig. 1). The design model is limited to usual applications with continuous full penetration welds at the thrust rings over the whole circumference.

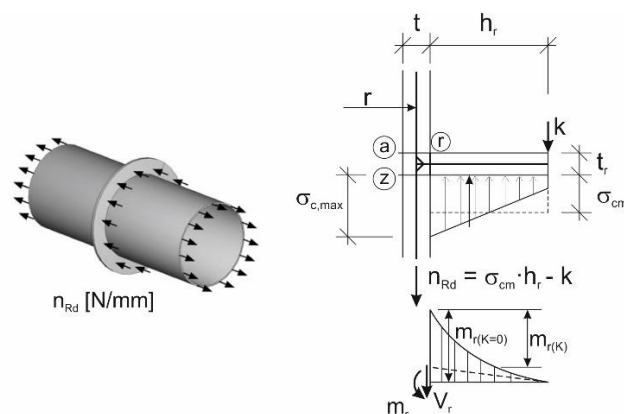


Fig. 1

Overview of pipe and thrust ring and simplified cantilever model used in practice

Thrust rings can be seen as a composite component, which transfers very high pipe forces – up to 50.000 kN, because of increasing diameter and pressure in recently erected penstocks.

Longitudinal forces in penstocks can have various reasons. For example they act due to the internal pressure on a closed valve, throttle, or temperature changes. Surprisingly in relevant design codes for penstocks (e.g. [1], [2], [3]) no detailed information is given for the design of thrust rings. In practice simplified models are used, considering the thrust ring as a cantilever (Fig. 1). The maximum force n_{Rd} and also the maximum moment m_r at the thrust ring are depending on the distribution of the concrete pressure σ_c and the maximum concrete stress $\sigma_{c,max}$ at the thrust ring. In practice different assumptions with no physical background based on test results are used. In some cases an additional prying force k at the non-loaded side of the thrust ring is assumed, which reduces the maximum moment m_r (e.g. [4]). Based on the internal forces m_r and V_r transferred from the thrust ring to the pipe the stresses in the relevant sections (r , a and z in Fig.1) of the thrust ring and the pipe can be calculated, based on shell theory.

For usual large penstock diameters ($d = 3\text{-}5$ m) the cantilever model for the thrust ring is quite accurate, because the effect of the circular ring plate is negligible. These results are based on 3D-FEM-analyses by the authors for cases in practice. That means, if the pressure distribution σ_c and the acting contact force k are known for the simple model in Fig. 1 the design of the thrust ring and the pipe are based on the well-known codes for steel design. Therefore a research project was executed by the authors which includes also laboratory tests to calibrate FEM-models for the prediction of these pressure distributions σ_c at the thrust ring (see [5], [6]).

At the beginning of this paper the load carrying behaviour of thrust rings will be shown based on a practical example with a pipe of an inner diameter $d_i = 3800$ mm, a thickness $t = 74$ mm and a thrust ring $h_r/t_r = 370/62$ mm. In the second part of this paper a design model for thrust rings is presented. In this brief paper only the basic model, considering the elastic behaviour of thrust rings is shown in detail. For thrust rings also a higher plastic ultimate load carrying capacity can be utilized, if a continuous radial elastic support is given by the surrounding bedrock (details are given in [6]). In [5] and [6] the background of the simple design model is presented in detail, based on many FEM-calculations for individual examples within the accurate parameters range of practical application.

2. LOAD CARRYING BEHAVIOUR OF THRUST RINGS – MAIN FINDINGS BASED ON A PRACTICAL EXAMPLE

Varying the main parameters (pipe diameter d ; pipe thickness t , thrust ring dimensions h_r/t_r , material parameter for steel and concrete) it can be seen (based on [6]) that the typical load carrying behaviour for transferring longitudinal forces is similar. Therefore in the following only one example is presented in detail. The results are based on a numerical 3D-FEM-calculation with axisymmetric elements, with the assumptions given in Fig. 2. This FEM-model was also calibrated with tests. A pipe with an inner diameter $d_i = 3800$ ($r_i = 1900$) mm, a wall thickness $t = 74$ mm and a thrust ring $h_r/t_r = 370/62$ mm is assumed. The surrounding concrete

cylinder is supported at the bottom. The longitudinal force N_{sr} and the displacement u_2 respectively are also applied at the bottom of the steel pipe. This force will be transferred to the surrounding concrete by the thrust ring, located in the middle of the pipe (at $x = 2500$ mm from the pipe top). Here an intact rock mass is assumed, leading to a minimum bedding modulus $V_F = 2000$ N/mm², which gives the additional elastic support in radial direction. In the FEM-calculation an equivalent radial spring stiffness is used: $C_f = V_F / ((1+\nu_F) \cdot r)$. In this equation r is the outer radius of the concrete cylinder and ν_F is the Poisson's ratio of the rock mass. Without that radial elastic support the results in the elastic range are very similar, but the elastic limit $N_{R,el}$ is smaller (see [5]).

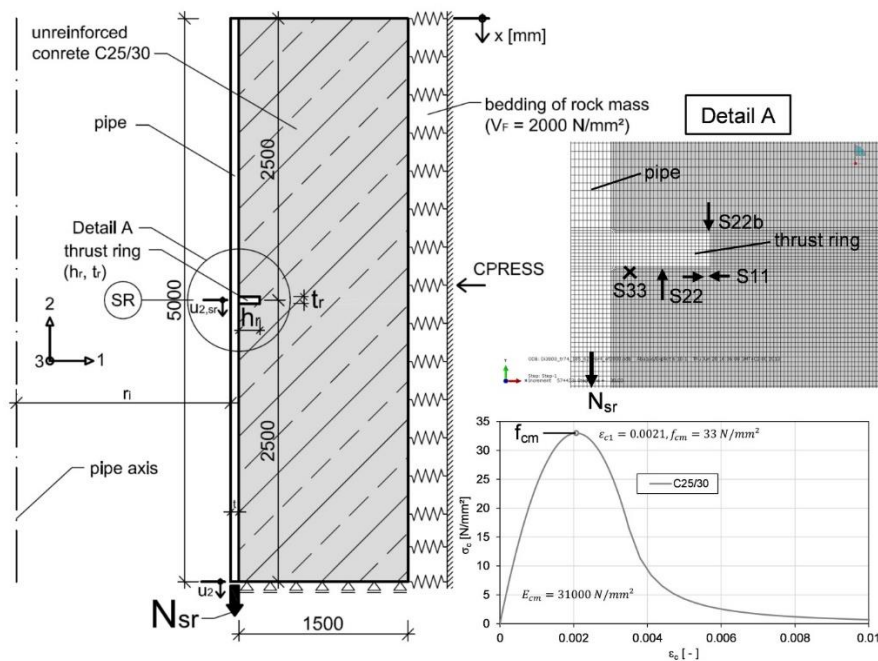


Fig. 2

FEM model for the representative example of a thrust ring, surrounded by a concrete block and the intact rock mass

In Fig. 2 also the fine mesh of the elements in the region of the thrust ring is shown. Conservatively no friction between steel part and surrounding concrete is taken into account. To simulate the ductile behaviour of the thrust ring after exceeding the elastic limit, it is necessary to define the post critical stress – stain curve for concrete in compression (in general concrete C25/30 is used in the FEM-calculations) – in Fig. 2 the assumed realistic assumptions for uniaxial behaviour in the numerical calculation are shown. The concrete has a tensile strength of 2.6 N/mm² in the calculations. The steel has got a yield-strength of 650 N/mm² with an ideal elastic-plastic material law. No gap between steel pipe and concrete is assumed, due to injection grouting used in practice.

The load carrying behaviour of the thrust ring is summed up in Fig. 3. Fig. 3a shows the overall load-deformation behaviour. With increasing overall force N_{sr} transferred at the thrust ring, the maximum displacement u_2 at the pipe increases.

In the following the stresses are presented at the end of the elastic range – $N_{R,el}$ and at ultimate limit load – $N_{R,u}$ as shown in Fig. 3a.

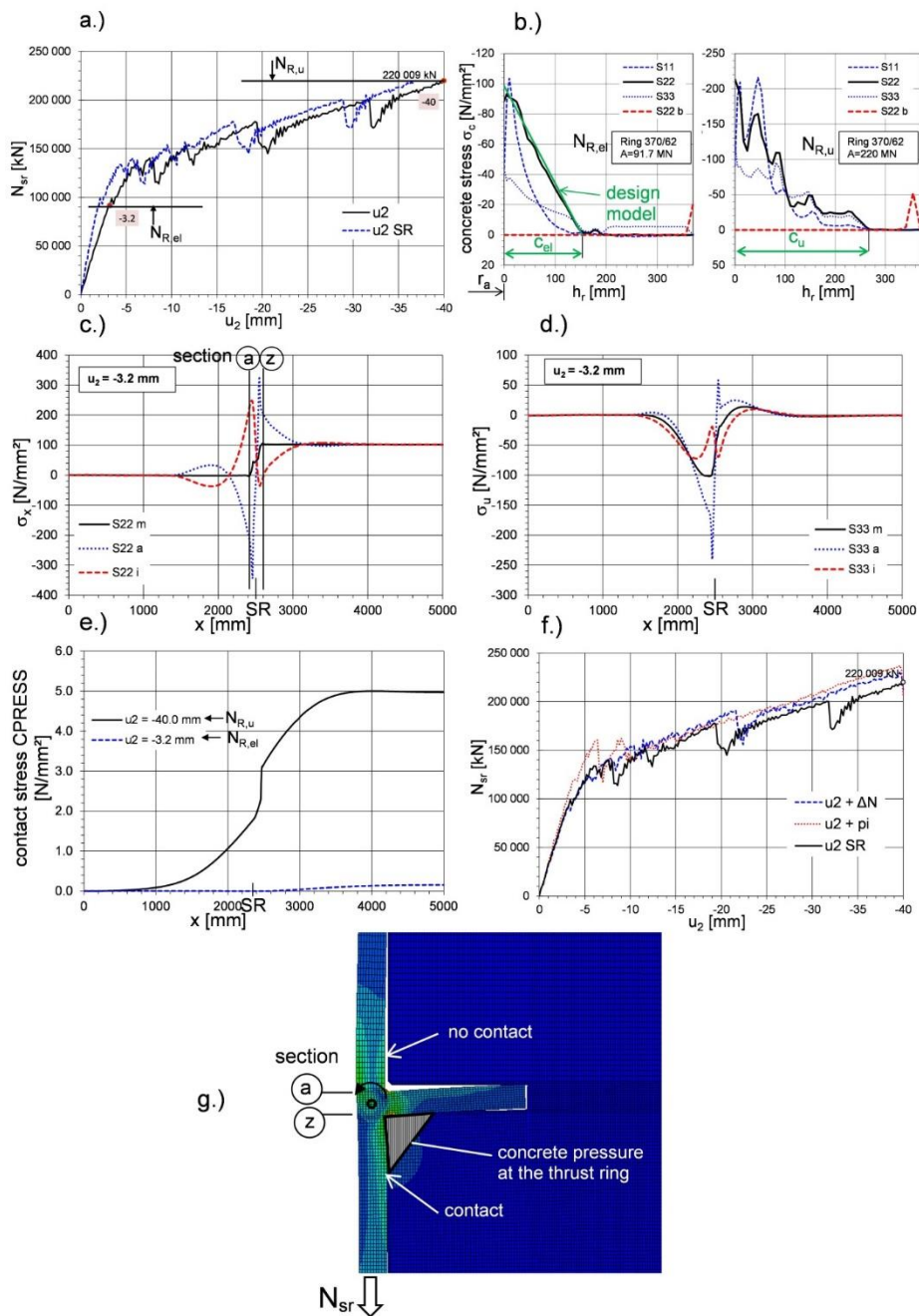


Fig. 3

Load carrying behaviour at the thrust ring – based on an example ($d_i = 3800$, $t = 74$, $h_r = 370$, $t_r = 62$ mm, material S690 – steel, C25/30 – concrete)

Fig. 3b shows for that two load levels the concrete pressure at the thrust ring along the height h_r (the steel pipe is at the left end of both diagrams). The concrete stress is presented in all three directions (notation S11, S22, S33 see Fig. 2) at the

“loaded” side of the thrust ring. At the back of the thrust ring only the pressure parallel to the pipe (S22 - b) is plotted. It can be seen that up to the elastic range (force $N_{R,el}$ is explained in Fig. 3a and based on Eq.[2]) there is only a very small negligible contact force at the outer end of the thrust ring. In the elastic range a nearly triangular pressure distribution at the thrust ring (acting parallel to the pipe axis and force direction) will be activated, which is well predictable in the design model (length c_{el}). Due to the compression stresses in all three directions in the concrete directly at the steel pipe, the maximum concrete stress – also at the end of the elastic range $N_{R,el}$ – is highly above the uniaxial concrete strength ($S11_{max} = 90 \gg f_{cm} = 33 \text{ N/mm}^2$). If the elastic range is exceeded, a pressure re-distribution starts, leading to an increased length c_u . This behaviour leads also to a significantly increased bending effect in the pipe, which must be considered in design if the higher plastic load carrying capacity $N_{R,u}$ should be utilized.

In Fig. 3c the longitudinal stresses (S22; m...middle surface; a...outside; i...inside) in the pipe are shown at the load level $N_{R,el}$. On the one hand the membrane stresses with the discontinuity at the thrust ring are shown and on the other hand the stresses at inner and outer side of the pipe are presented. The latter ones show the significant bending effect in the pipe. The sections a and z are directly at the thrust ring with the highest bending effect. These sections are decisive for the design model.

The Fig. 3d shows the circumferential stresses (S33; m...middle surface; a...outside; i...inside) in the steel pipe. There are compression membrane stresses near the thrust ring, due to the radial component of the support reaction at the thrust ring, based on the radial eccentricity of N_{sr} (resulting vertical reaction force at the bottom of the concrete block acts outside the pipe wall). Also limited bending effects near the thrust ring in circumferential direction are acting due to the Poisson effect. They can be neglected in the design model.

The Fig. 3e shows the radial pressure CPRESS between concrete and bed-rock. Up to the end of the elastic range the compression stresses are negligible small, but they significantly increase in the plastic range. Therefore if the significantly higher ultimate load $N_{R,u}$ should be utilized, a verification of the rock to resist these radial stresses is necessary.

In Fig. 3f again the overall load-deformation behaviour as in Fig. 3a is shown, but now in comparison with cases where additional load cases of very high magnitude are considered. On the one hand an additional longitudinal force ΔN (ΔN results in longitudinal stresses σ_x in the pipe of half of the yield stress) and on the other hand an additional internal pressure $p_i = 12.7 \text{ N/mm}^2$ (p_i results in circumferential stresses σ_u in the isolated pipe equal to the half of the yield stress). It can be seen that the overall behaviour is nearly the same – therefore in the design model for the elastic limit $N_{R,el}$ additional load cases can be ignored, but they must be taken into account for the verification of the section capacity (section a, z). In Fig. 3g finally the deformations of the pipe and the thrust ring are represented. It is visible that only on the loaded side of the thrust ring the pipe is radially supported by the concrete, at the opposite side there is a gap between pipe and concrete. This behaviour also leads to the result, that the bending effect in the pipe is significantly higher in section a, which must be considered in the design model.

3. ELASTIC DESIGN MODEL FOR THRUST RINGS

The developed design model is summed up in Fig. 4. Here only the elastic limit $N_{R,el}$ is presented and the associated verifications in the thrust ring and pipe. Nevertheless the given design procedure guarantees ductile behaviour, as shown in Fig. 4a. The parts of the design model of a cantilever-beam with unit width are (see Fig. 4):

- Elastic limit load $N_{R,el}$ for the thrust ring
- Overall stiffness C_{ges} in longitudinal direction of the pipe in the elastic range
- Simplified cantilever mechanical model with idealised pressure distribution for verification in the thrust ring (section A) and the pipe (section a and z).

The following paragraphs explain the procedure for the elastic design for thrust rings in detail.

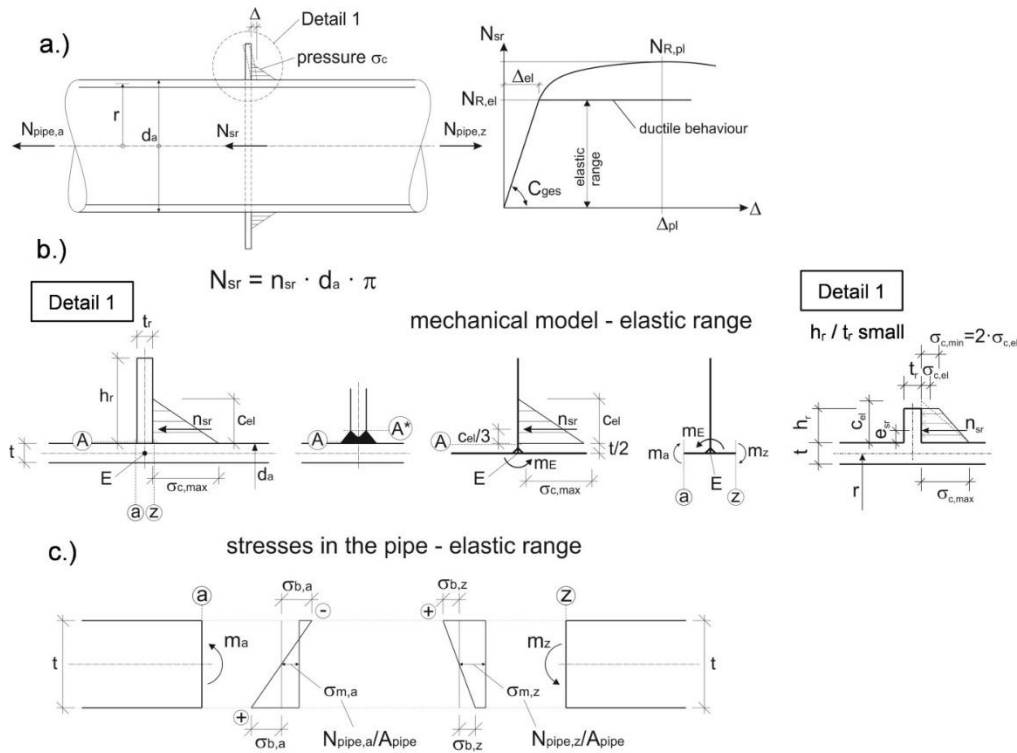


Fig. 4
Basics of the new design model for thrust rings

Limitations of the Design model

Based on the parametric study of the accurate FEM-calculations for verification of the developed design model the following limitations are important:

- Geometry of the thrust ring: $2 \leq h_r/t_r \leq 10$; $t_r \geq 20$ mm
- Thickness relationship: $t_r/t \leq 1,5$
- Constant pipe thickness t on both sides of the thrust ring over a length

- of at least $r_i/2$
- Rectangular thrust rings – fully welded (butt welded) along the circumference of the pipe

Idealized pressure distribution at the thrust ring

In general a simple triangular stress pattern (see Fig. 4b) – without any contact force at the backside – is applied. The pressured length c_{el} is calculated using Eq. [1]. This equation is empirically determined with the numerical calculations. The accuracy of Eq. [1] is shown in [5].

$$c_{el} = 0.85 \cdot t + t_r \cdot \left[1 + 0.1 \left(\frac{h_r}{t_r} - 2 \right) \right] \leq 0.85 \cdot t + 1,5 \cdot t_r \quad [1]$$

For stocky thrust rings in case of thicker pipes, with $c_{el} > h_r$, a modified trapezoidal stress pattern with an increased stress at the outer edge ($\sigma_{c,min} = 2 \cdot \sigma_{c,el}$) is assumed (see Fig. 4b).

Elastic load capacity $N_{R,el}$

Based on the simplified concrete pressure at the thrust ring (Fig. 4b) and an increased maximum concrete strength of $\sigma_{c,max}$ (with f_{cd} uniaxial concrete strength, design value) is available:

$$\sigma_{c,max} = 2 \cdot f_{cd} \text{ (in general)}$$

$\sigma_{c,max} = 3 \cdot f_{cd}$ (special case with radial elastic support of the rock mass and $V_F \geq 2000 \text{ N/mm}^2$); limited value $2,5 \cdot f_{cd}$ (if also $h_r / t_r > 7$)

Note: if an increased strength of $\sigma_{c,max} > 2 \cdot f_{cd}$ is used, the rock mass must be able to resist a radial pressure of 0.15 N/mm^2 and the concrete thickness should be at least $d_c > 10 \cdot c_{el}$. The extraordinary high increase of concrete strength is based on the beneficial local 3D-stress state with significant compression in all directions. The elastic load capacity $N_{Rd,el}$ (Note: notation $N_{Rd,el}$ instead of $N_{R,el}$, because design value f_{cd} is used) is based on Eq. [2]

$$N_{Rd,el} = n_{Rd,el} \cdot d_a \cdot \pi = \frac{\sigma_{c,max} \cdot c_{el}}{2} \cdot d_a \cdot \pi \quad [2]$$

For a trapezoidal pressure distribution Eq. [3] must be used

$$N_{Rd,el} = n_{Rd,el} \cdot d_a \cdot \pi = \left(\frac{c_{el} - h_r}{c_{el}} + 0,5 \right) \cdot \sigma_{c,max} \cdot h_r \cdot d_a \cdot \pi \quad [3]$$

The elastic load capacity $N_{R,el}$ is limited by the increased shear capacity of the thrust ring, based on Eq. [4]

$$N_{Rd,el} \leq N_{Rd,V} = d_a \cdot \pi \cdot t_r \cdot (f_{yd,sr} / \sqrt{3}) \quad [4]$$

with: $f_{yd,sr}$ design value of the yield strength at the thrust ring.

Verification of the section capacity of the thrust ring (section A)

Note: The 2D-beam model, shown in Fig. 4b, leads to unit width for the thrust ring and the pipe. Based on the acting overall force $N_{sr} < N_{Rd,el}$ at the thrust ring the

bending moment m_A is based on Eq. [5]

$$m_A = n_{sr} \cdot \frac{c_{el}}{3} = \frac{N_{sr} \cdot c_{el}}{3 \cdot \pi \cdot d_a} \quad [5]$$

If a trapezoidal pressure distribution is relevant ($c_{el} > h_r$), then:

$$m_A = n_{sr} \cdot e_{sr} = \frac{N_{sr}}{\pi \cdot d_a} \cdot e_{sr} \quad [6]$$

Stress verification in section A

$$\sigma_A = m_A / (t_r^2 / 6) \leq f_{yd, sr} \cdot f_V \quad [7]$$

$$f_V = 1 - \left(\frac{2 \cdot N_{sr}}{N_{Rd, V}} - 1 \right)^2 \leq 1.0 \quad [8]$$

with: $f_{yd, sr}$... design value of the yield strength at the thrust ring

f_V ... reduction factor, considering additional high shear stresses due to N_{sr} ;
only relevant if $N_{sr} / N_{Rd, V} \geq 0.50$

$N_{Rd, V}$... shear capacity of the thrust ring, based on Eq. [4]

Eq. [8] is identical with the formulation in Eurocode EN 1993-1-1, for interaction of bending and shear.

Verification of the section capacity at the pipe (section a and z)

The bending moment m_E , related to the pipe axis is given by Eq. [9]

$$m_E = n_{sr} \cdot \left(\frac{c_{el}}{3} + \frac{t}{2} \right) = \frac{N_{sr}}{\pi \cdot d_a} \cdot \left(\frac{c_{el}}{3} + \frac{t}{2} \right) \quad [9]$$

In case of a trapezoidal pressure distribution ($c_{el} > h_r$) Eq. [10] must be used

$$m_E = \frac{N_{sr}}{\pi \cdot d_a} \cdot \left(e_{sr} + \frac{t}{2} \right) \quad [10]$$

Stress verification in section a: The bending moment in section a is calculated based on Eq. [11]. The factor 0.50 in this equation is empirically determined with the numerical calculations.

$$m_a = 0.50 \cdot m_E \quad [11]$$

$$\sigma_a = \sigma_{m, a} \pm \sigma_{b, a} = \frac{N_{pipe, a}}{A_{pipe}} \pm m_a / \left(\frac{t^2}{6} \right) \leq f_{yd} \quad [12]$$

Stress verification in section z: The bending moment in section z is only half the value of section a, therefore the stress verification is only relevant for high axial forces $N_{pipe, z}$. The factor 0.25 in Eq. [13] is empirically determined with the numerical calculations.

$$m_z = 0.25 \cdot m_E \quad [13]$$

$$\sigma_z = \sigma_{m, z} \pm \sigma_{b, z} = \frac{N_{pipe, z}}{A_{pipe}} \pm m_z / \left(\frac{t^2}{6} \right) \leq f_{yd} \quad [14]$$

Worth mentioning is that the sum of the bending moments in section a and z is smaller than the overall moment m_E , due to the beneficial bending moment distribution in the pipe (see explanation in [5]).

Additional requirements for anchor points are also given in [5].

Elastic stiffness of the thrust ring in longitudinal direction

Worth mentioning is, that the elastic stiffness C_{ges} , given in Eq. [15], is based on a length of 1 mm in circumferential direction. If for the global analysis a beam model for the pipe is used, the resulting spring stiffness C_{sr} using Eq. [16] is necessary.

$$C_{ges} = 0.28 \cdot C_{ring} + 2.9 \quad [kN/mm^2] \quad [15]$$

$$C_{sr} = C_{ges} \cdot d_a \cdot \pi \quad [kN/mm] \quad [16]$$

$$\text{With: } C_{ring} = E \cdot A_{ring} / r_a^2 \quad [17]$$

$$A_{ring} = h_r \cdot t_r + b_{eff} \cdot t \quad [18]$$

The parameter C_{ring} is equal to the radial stiffness of the ring with an effective width of the pipe for the internal pressure. Instead of the radius of the centroid of the ring, the outer radius of the pipe r_a can be used to simplify the calculation (see Fig. 5).

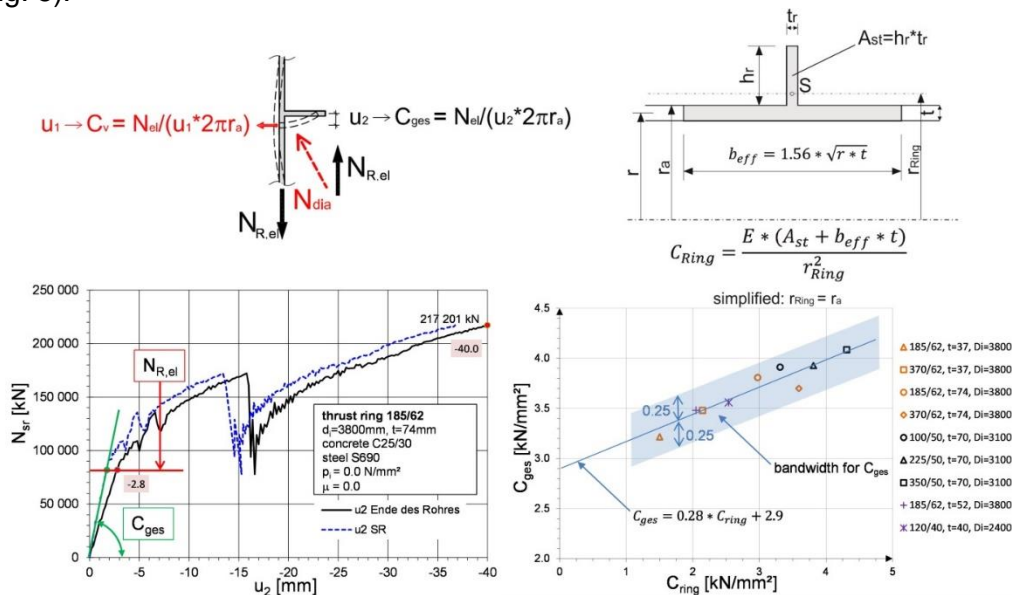


Fig. 5

Elastic stiffness C_{ges} of the thrust ring; real behaviour and background of the design model with most important parameter C_{Ring}

For smaller thrust rings with $20 \leq t_r < 40$ mm, a reduced stiffness, based on Eq. [19], must be used.

$$C_{ges} = 0.28 \cdot C_{ring} + 2.1 + \frac{0.8}{20} \cdot (t_r - 20) \quad [19]$$

Eq. [15] and [19] are based on curve fitting of the FEM-results for a lot of

practical examples, shown in Fig. 5. In this Figure the accuracy of Eq. [15] can be seen (for all given cases $t_r > 40$ mm). To capture the variation of the elastic stiffness, based on the FEM-calculations, it is recommended to use a maximum/minimum value of C_{ges} by increasing/reducing of the second term in Eq. [15] and [19] with a factor of 1.10/0.90.

The accuracy and background of the design model is shown in [5].

4. CONCLUSION

Based on tests and numerical results of a research project operated by the authors [5] a comprehensive design model for thrust rings was developed. It includes the elastic load carrying capacity of the thrust ring and the verification of the stresses in the steel pipe and the ring. Now it's also possible to calculate the stiffness of a thrust ring. Also the interaction behaviour of several thrust rings was investigated, leading to a very simple design rule (see [5]). As a result a significantly higher load carrying capacity $N_{R,el}$ of the thrust ring can be achieved, in contrast to the current design concepts (e.g. [4]). Also higher load carrying capacities than $N_{R,el}$ can be utilized in case of an additional radial elastic support of the rock mass, but they are not described in this brief paper.

REFERENCES

- [1] Engineer Manual 1110-2-2901: *Engineering and Design – Tunnels and Shafts in Rock*, U.S. Army Corps of Engineers, Washington, 1997
- [2] C.E.C.T: Recommendations for the Design, Manufacture and Erection of Steel Penstocks of Welded Construction for Hydro Electric Installations, European Committee for Boilermaking and Kindred Steel Structures. 1984
- [3] ASCE 1993: Steel Penstocks, *Manual on Engineering Practice No. 79*, American Society of Civil Engineers, New York, 1993
- [4] R. OFNER, R. GREINER, Beanspruchungen von Schubringen für Druckrohrleitungen, *Stahlbau* 76, Heft 10, p. 739-746, 2007
- [5] H. UNTERWEGER, A. ECKER, Design model for transferring longitudinal pipe forces using thrust rings. *Structural engineering international*, Vol. 26, Nr. 2, 2016
- [6] H. UNTERWEGER, A. ECKER, Load carrying behaviour of thrust rings for transferring longitudinal pipe forces. *Journal of constructional steel research*, Vol. 114, p. 178-187, 2015

COMMISSION INTERNATIONALE DES GRANDS BARRAGES

VINGT-SIXIÈME CONGRÈS DES GRANDS BARRAGES
Autriche, juillet 2018

DOI 10.3217/978-3-85125-620-8-206



This work licensed under a Creative Commons Attribution 4.0 International License. <https://creativecommons.org/licenses/by-nc-nd/4.0/>

**A CASE STUDY OF A HIGH STRENGTH STEEL DESIGN: APPLICATION OF
DIFFERENT SAFETY CONCEPTS AND THE RESULTING IMPACTS ON A
BIFURCATION**

Claudia POLLAK-REIBENWEIN

*Lead Engineer Structural Analysis, Penstock and Gates, ANDRITZ HYDRO
GMBH, LINZ*

AUSTRIA

Bettina NEUGSCHWANDTNER

*Head of Structural Analysis, Penstock and Gates, ANDRITZ HYDRO GMBH,
LINZ*

AUSTRIA

COMMISSION INTERNATIONALE
DES GRANDS BARRAGES

VINGT-SIXIEME CONGRES DES
GRANDS BARRAGES
Autriche, juillet 2018

**A CASE STUDY OF A HIGH STRENGTH STEEL DESIGN:
APPLICATION OF DIFFERENT SAFETY CONCEPTS AND THE RESULTING
IMPACTS ON A BIFURCATION**

Claudia POLLAK-REIBENWEIN¹, Bettina NEUGSCHWANDTNER²

¹*Lead Engineer Structural Analysis, Penstock and Gates, ANDRITZ
HYDRO GMBH, LINZ*

²*Head of Structural Analysis, Penstock and Gates, ANDRITZ HYDRO
GMBH, LINZ*

AUSTRIA

1. INTRODUCTION

The application of high strength steels for modern, highly pressurized penstocks allows for reduced wall thicknesses. Hence, this should result in lighter components and easier fabrication, transport and handling conditions. This paper presents a case study of a complex geometric steel liner component – a bifurcation for access to a vertical tunnel – made of steel grade S620QL.

Besides geometrically optimizing the design of a bifurcation with respect to the reduction of hydraulic losses, the choice of an appropriate safety concept influences the layout strongly. Usually, the owner or the owner's engineer specifies a safety concept, which is stipulated by a standard or a guideline. As for steel penstock design, several international standards and guidelines with their own integral safety concepts are available throughout the world. The most common European standard for steel penstocks is still C.E.C.T. [1]. English speaking countries prefer for example ASCE manual no.79 "Steel Penstocks" [2].

The problem now is that the safety concept of C.E.C.T. is historically based on nominal design stress, which means that stresses or minimum required plate thicknesses are calculated by analytical formulae. This approach does not match

with the application of finite element analysis, which is the state-of-the-art approach for complex structures (and often required by owner's engineers) and where dimensioning by means of formulae is not possible any more. Moreover, finite element analysis usually shows regions with locally increased stresses due to structural discontinuities. Compared with allowable stresses derived by nominal stress concepts this would unnecessarily lead to increased plate thicknesses and thus a higher dead weight of the component.

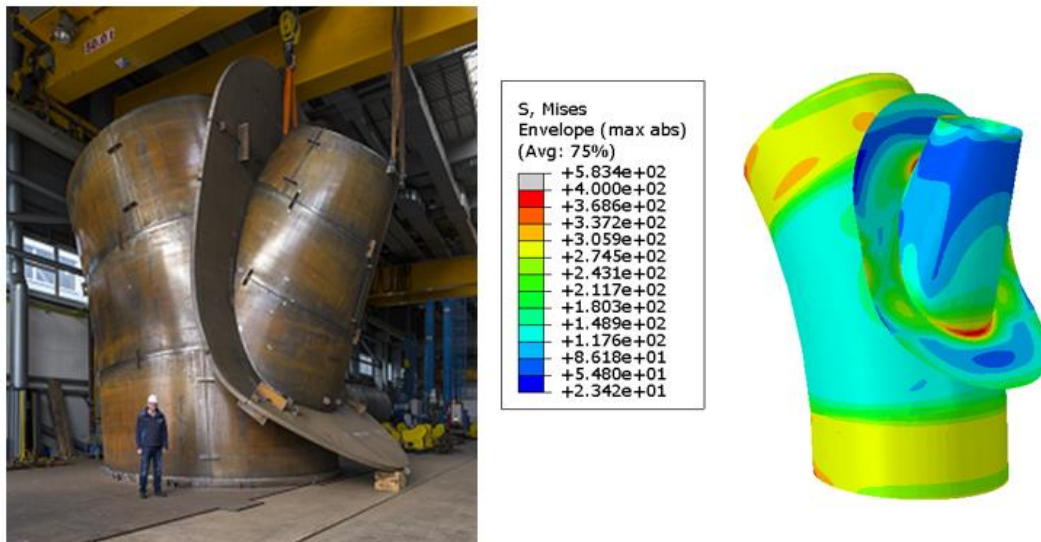


Fig. 1

Left: Shop assembly of a bifurcation; right: Stress plot of numerical simulation model

ASCE manual no. 79 clearly denotes allowable stress intensities for finite element models, which can be increased depending on the respective stress category. It is distinguished between different primary and secondary stresses (e.g. allowable local primary membrane stress for a reinforcing girder of a bifurcation is 1,5-times of the allowable stress intensity). Peak stress assessment, which becomes relevant for fatigue analysis, is also dealt within this guideline. The case study of a bifurcation presented in this paper opposes the traditional C.E.C.T. safety concept to the ASCE safety concept and points out the problems transferred to successive processes, e.g. fabrication and welding procedure, assembling and erection problems, which originate from an inadequate safety concept application and makes the economic benefits from high strength steel irrelevant.

2. EVALUATED SAFETY CONCEPTS

Penstocks and their appurtenances must be designed in accordance with the requirements of certified design criteria which must be prepared by experienced professional engineers. These requirements also comprise a safety concept to be applied.

Two major safety concepts and their further consequences and impacts on the design of special components are analysed in detail in this paper: C.E.C.T. recommendations for the design, manufacture and erection of steel penstocks from 1979 (exceptionally based on the application of analytical formulae for nominal stress assessment and still widely specified in certified design criteria) and ASCE steel penstock manual no.79 from 2012 (including recommendations for finite element analysis of wye branches).

State of the art requires finite element analysis for special and complex parts, such as bifurcations. This method is commonly specified by owner's engineers, regardless of the stipulated safety concept being suitable or not.

ASCE manual clearly distinguishes different stress categories which are based on the stress intensity limit S . These classifications are either of general or of local nature (see Table 1). The stress intensity S follows closely that of ASME Boiler and Pressure Vessel Code. ASCE manual recommends the use of the maximum shear stress theory and also recognizes as acceptable the Huber-Hencky-von Mises or distortion energy theory. ASCE manual denotes allowable stress intensities for steel penstock components for general application (denoted in chapter 3.4.10) and especially in chapter 7.3.3 for wyes in combination with the application of finite element method.

C.E.C.T. recommends minimum dimensioning factors C' which depend on the loading case and apply to the equivalent stress (Huber-Hencky-von Mises theory) calculated with primary stresses. Unfortunately stress categories are not distinguished. Solely two hints regarding secondary stresses are given: *"...the permissible stress will be higher (...) when the secondary stresses are taken into account."* and *"Under the effect of secondary stresses, a certain elongation beyond the elastic limit may be permitted in so far as it is consistent with the conditions under which the part is used and taking into account possible changes that it could cause in the properties of the materials."* A value for this dimensioning factor remains open and is often even not specified.

The stress concepts with their allowable stress limits are summarized in Table 1.

Table 1
Comparison of Stress Concepts

BIFURCATION STRESS ASSESSMENT	STRESS CONCEPTS (for normal conditions)		
	ASCE manual no.79 (chapt. 3.4.10)	ASCE manual no.79 (chapt. 7.3.3)	C.E.C.T.
SHELL PLATES			
$P_m^{3)}$ (primary, evaluated in middle fiber)	$\leq S = \text{MIN}\left(\frac{R_{eH}}{1.5}; \frac{R_m}{2.4}\right)$	$\leq S = \text{MIN}\left(\frac{R_{eH}}{1.5}; \frac{R_m}{3}\right)$	$\leq \sigma_{SFI} = \frac{R_{eH}}{C'}^{1)}$
$P_l^{4)}$ or $(P_l + P_b)^{6)}$ (primary, evaluated in middle and surface fiber)	$\leq 1.5 \cdot S$	$\leq 1.5 \cdot S$	$\leq \sigma_{SFI} = \frac{R_{eH}}{C'}$
$(P_l + P_b^{5)}) + Q^{7)})^{8)}$ (secondary, evaluated in decisive surface fiber)	$\leq \text{MIN}(3 \cdot S; R_m)$	$\leq \text{MIN}(3 \cdot S; R_m)$	$\leq \sigma_{SFI} = \frac{R_{eH}}{C'} \cdot f^{2)}$
REINFORCING GIRDER PLATES (SICKLE)			
$P_l + P_b$ (primary, evaluated in middle and surface fibers)	$\leq 1.5 \cdot S$	$\leq 1.5 \cdot S$	$\leq \sigma_{SFI} = \frac{R_{eH}}{C'}$

1) For distributors and special parts C.E.C.T. recommends a factor of $C' = 1.8$ if the structure is embedded in concrete/rock.

2) The allowable primary stresses are increased by a factor f , which allows higher permissible stresses when accounting for secondary stresses. The value $f = 1,35$ is a value supposed by Andritz Hydro and other professionals to define analytically calculated secondary stress limits which are not clearly defined by standards or specifications.

3) P_m : General Primary Membrane: Membrane stress intensity away from reinforcing girders, from changes in direction and from discontinuities. Stress averaged across the thickness necessary to satisfy the law of equilibrium, e.g. hoop stress from internal pressure.

4) P_l : Local Primary Membrane: Membrane stress intensity adjacent to reinforcing girders and changes in direction, e.g. stress in the immediate vicinity of miters. A stress region may be considered as local if the distance over which the stress intensity exceeds $1.1S$

does not extend in the meridional direction more than $\sqrt{R \cdot t}$, where R is the midsurface radius of curvature measured normal to the surface from the axis of rotation and t is the minimum thickness in the region considered.

5) P_b : Primary Bending: Bending stress across the thickness of the plate/shell with no redistribution of the load due to yielding.

6) $P_l + P_b$: Local Primary Membrane plus Primary Bending.

7) Q: Secondary Stress: Normal stress, either bending or axial, or a shear stress developed by constraint of adjacent parts or by self-constraint of a structure. The basic characteristic of a secondary stress is, that it is self-limiting, e.g. stress due to thermal constraints, bending stress intensities across the thickness of a shell or plate at a gross structural discontinuity. The combination of Q with primary stress intensities should be limited to the lesser of minimum tensile strength (R_m) or $3S$.

8) PI + Pb + Q: Secondary: Combination of secondary stress with local primary membrane and local bending stress.

3. CASE STUDY BIFURCATION – MATERIAL AND BOUNDARY CONDITIONS

This report's case study is a vertical 90°-bend which is part of a high head power plant penstock. The bend with an internal diameter of 3800mm is intersected by a vertical access pipe with an internal diameter of 1500mm. The intersection of these bodies (which means huge opening interrupting the hoop stress) is reinforced by an exterior, multiple curved and massive reinforcement or sickle plate.

The internal design pressure at this location is assumed to be approximately 700mWC or 7N/mm².

The purpose of the access pipe is to enable the lowering of inspection platforms and additional maintenance equipment.

The material of the bifurcation is S620QL with the following guaranteed material properties (deviating from EN 10025-6 but in this case study specified by owner's engineer, a trend being observed in recent projects):

Table 2
Material properties S620QL (special requirements, values from inspection and test plan)

Material	Thickness [mm]	R_{eH} [N/mm ²]	R_m [N/mm ²]
S620QL	$50 < t \leq 150$	620	770

with:

R_{eH} : Minimum specified yield strength of the material

R_m : Minimum specified tensile strength of the material

The stress assessment of the bifurcation is done by means of finite element analysis (FEA). The FEA model has to account for the static system of the conveyance system by applying adequate boundary conditions at the up- and

downstream ends of the model. The pre- and post-processing of this case study is done by Abaqus/CAE 2017.

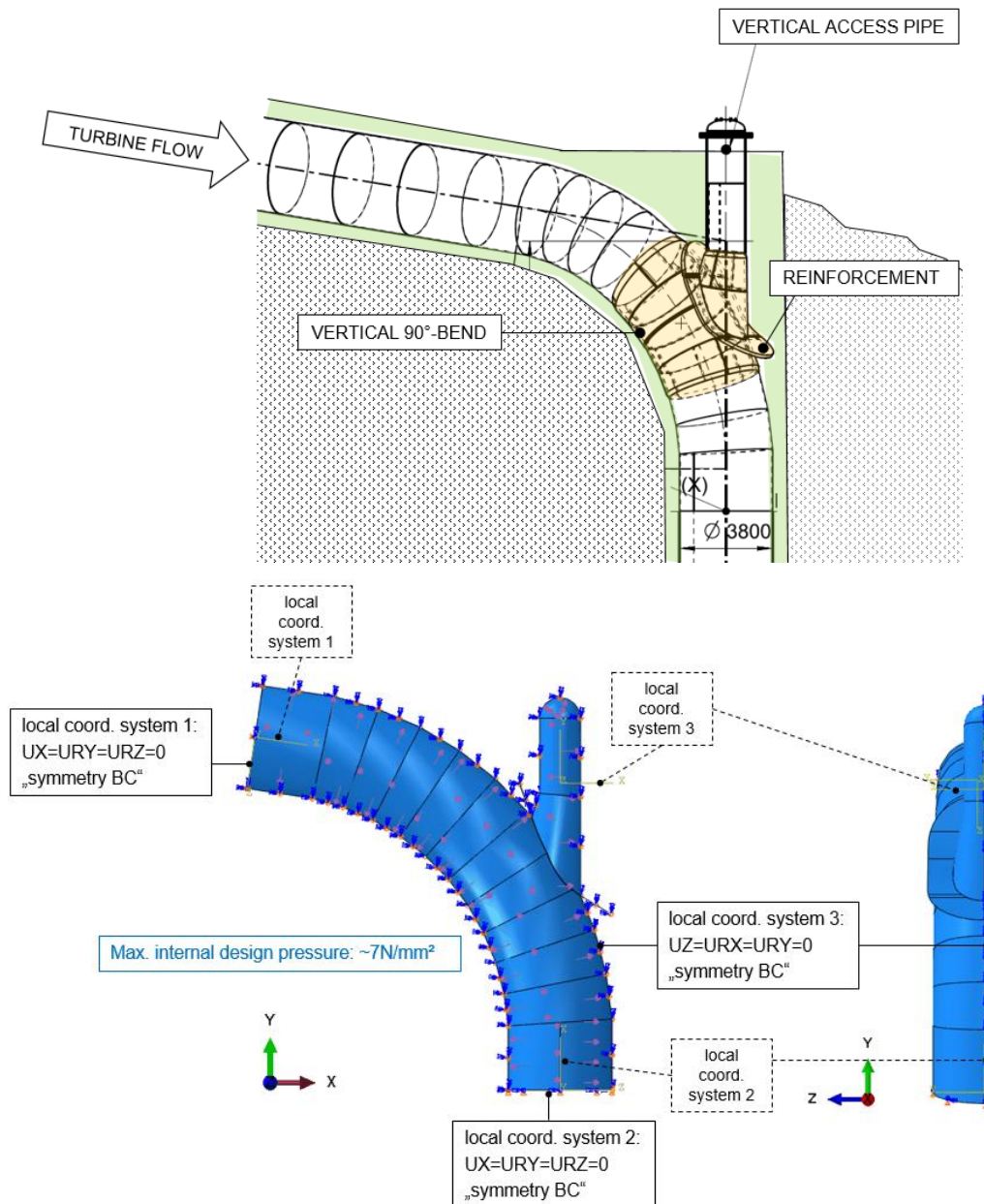


Fig. 2

Case study: Above - vertical 90°-bend with vertical access; below - FEA- model of the bifurcation with boundary conditions

Bifurcations or wye branches are huge, slender structures which justify simulating them on basis of shell models. The stresses across the plate thickness of shell models are evaluated in the middle and in the surface fibers of those elements.

The finite element model is meshed with quadratic shell elements having a maximum element size of 50mm.

Usually such structures are embedded in concrete and surrounded by stable rock. But special components are commonly specified as self-supporting systems without considering the surrounding material in a numerical analysis, as it is assumed for this case study.

3.1. ALLOWABLE STRESS AND RESULTING PLATE THICKNESS

The allowable stresses for the applied high strength steel are summarized in Table 3. Hence it appears that the permissible general primary membrane stress (P_m , hoop stress, undisturbed region) is most strictly restricted by ASCE approach for finite element models (chapter 7.3.3). But for locally increased stress regions (e.g. miters, attachment regions) or for reinforcing girders under mainly bending stress (sickle plate) ASCE concepts allow for higher local stress limits than C.E.C.T. Unfortunately these local stress concentrations often become decisive for plate dimensions. The evaluation of the reinforcement is especially affected since C.E.C.T. makes no difference between certain stress categories (general membrane vs. local membrane/bending). The bending stress of the sickle plate is of general primary nature and is often specified to be evaluated by applying the dimensioning factor for primary stresses (C') acc. to C.E.C.T.

Table 3
Allowable stresses

BIFURCATION STRESS ASSESSMENT	STRESS CONCEPTS (for normal conditions)		
	ASCE manual no.79 (chapt. 3.4.10)	ASCE manual no.79 (chapt. 7.3.3)	C.E.C.T.
SHELL PLATES – Material S620QL			
P_m <i>(primary, evaluated in middle fiber)</i>	$\leq 321\text{N/mm}^2$	$\leq 257\text{N/mm}^2$	$\leq 344\text{N/mm}^2$
P_1 or $(P_1 + P_b)$ <i>(primary, evaluated in middle and surface fiber)</i>	$\leq 482\text{N/mm}^2$	$\leq 386\text{N/mm}^2$	$\leq 344\text{N/mm}^2$
$P_1 + P_b + Q$ <i>(secondary, evaluated in decisive surface fiber)</i>	$\leq 770\text{N/mm}^2$	$\leq 770\text{N/mm}^2$	$\leq 465\text{N/mm}^2$
REINFORCING GIRDER PLATES (SICKLE) – Material S620QL			
$P_b + P_1$ <i>(primary, evaluated in middle and surface fibers)</i>	$\leq 482\text{N/mm}^2$	$\leq 386\text{N/mm}^2$	$\leq 344\text{N/mm}^2$

Problematic evaluation areas become visible by numerical simulation and are e.g. intersections with locally increased stress concentrations or sickle plate attachments at sharp miters, as illustrated in Fig. 3.

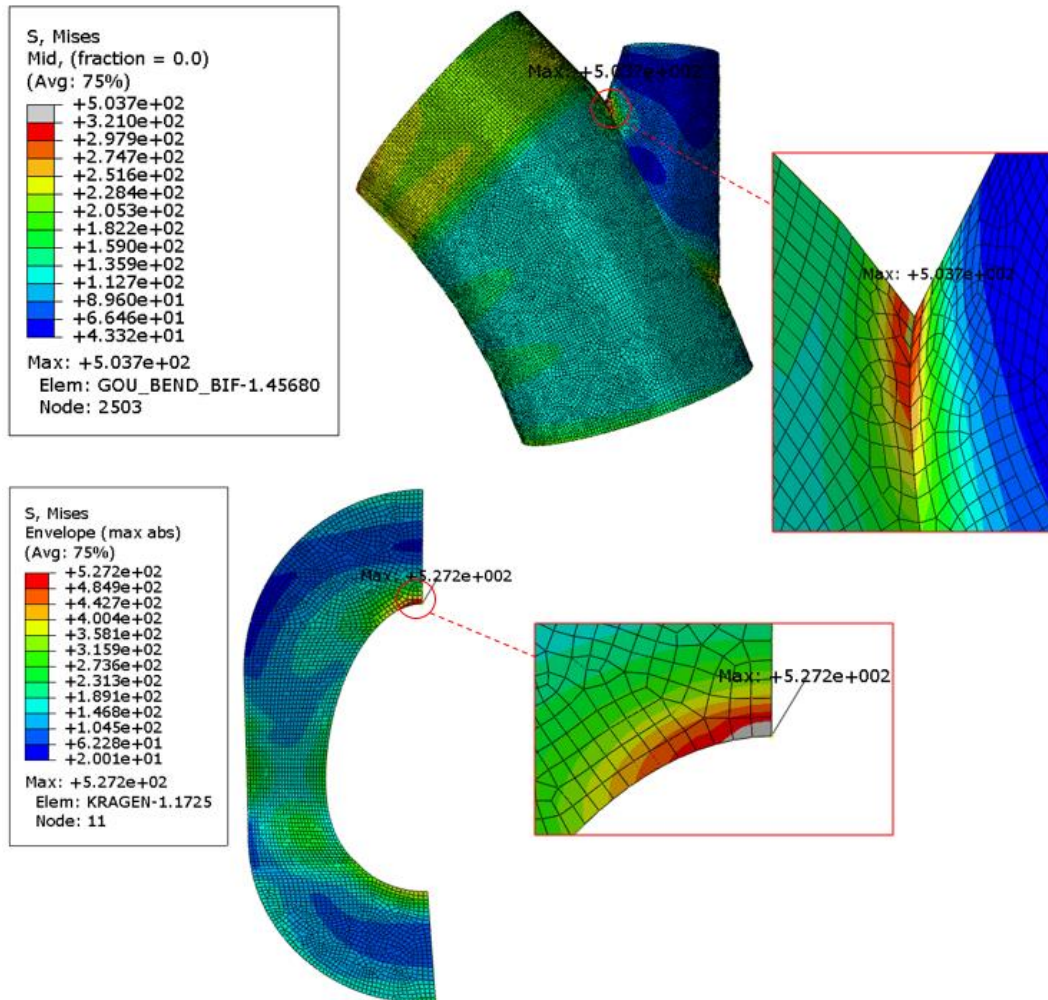


Fig. 3

Local stress concentrations of a bifurcation and a reinforcement; stresses in [N/mm²]

The ASCE approach (regardless of applying chapter 3.4.10. or chapter 7.3.3.) accounts for locally increased stresses and allows a more appropriate stress evaluation with regard to FEA application from authors' point of view.

A comparison of the required plate thicknesses as a consequence of applying above mentioned safety concepts clearly points out the difference in terms of total dead weight, as depicted in Fig. 4: It becomes apparent that the evaluation according to ASCE manual No.79 leads to 20 tons less weight.

It is worth highlighting two more points: Firstly, special parts are usually calculated as self-supporting components without consideration of surrounding

concrete/rock. Secondly, advanced quality tests and supervision have evolved in the course of time, which could not be considered in C.E.C.T.

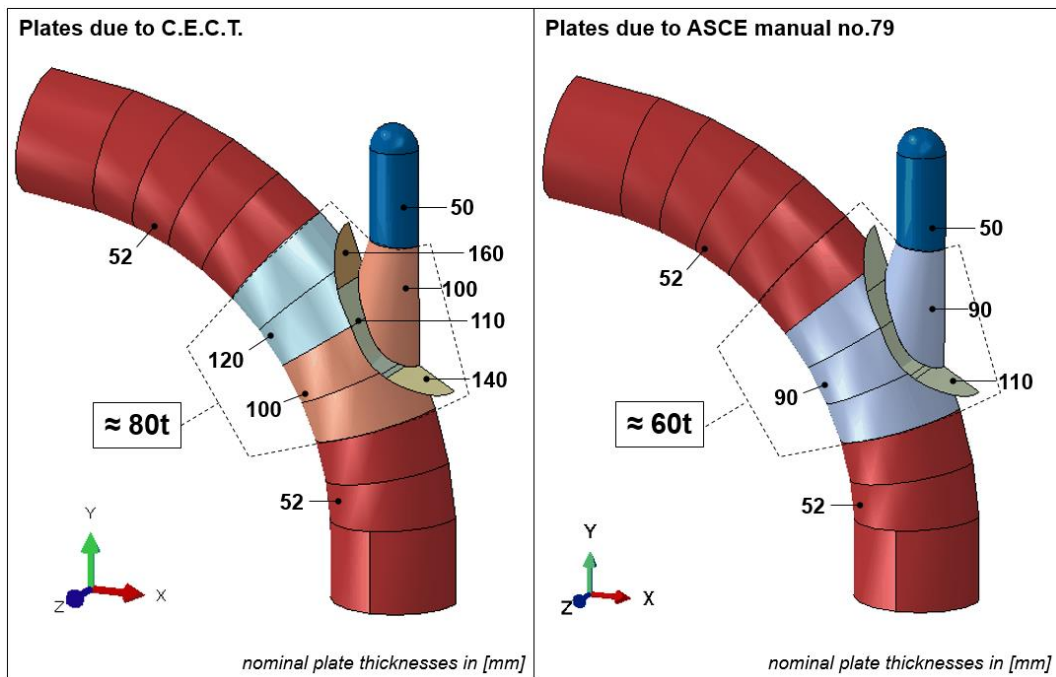


Fig. 4
Comparison of plate thicknesses and total weight

4. IMPACTS ON FURTHER PROCESSES

The choice of an appropriate material quality and its resulting plate thickness is very important. The designed weight due to specified safety concepts strongly impacts further processes. Unnecessarily material, fabrication and installation time and costs will be increased. The whole fabrication and installation method has to be reconsidered. Plate bending machines are limited to certain plate thicknesses. Besides affecting welding preparation requirements (pre-heat, edge prefabrication), also higher welding volume under difficult welding conditions and non-destructive testing needs have to be re-evaluated for example.

Highly pressurized special components are usually made of high strength steel in order to minimize these costs and efforts. As it was pointed out in the previous chapter, safety concepts strongly influence the dead weight of a structural component: The thicker or more robust a structural component is designed with respect to safety against yield, the more complicated it might become for fabrication and welding. Fig. 5 illustrates the high demands on the execution carried out by mounting and welding personnel using the example of full penetration welds between sickle and bifurcation plates. One has to be aware that

such huge and heavy components are usually assembled and welded in situ under limited space conditions, where every ton counts. When processes become more complex or complicated, the susceptibility to errors tend to increase and safety margins might be reduced. The application of high strength steel and the determination of plate thicknesses derived by FEA stress results should make such special components both robust and economically justifiable and not lead to the opposite.

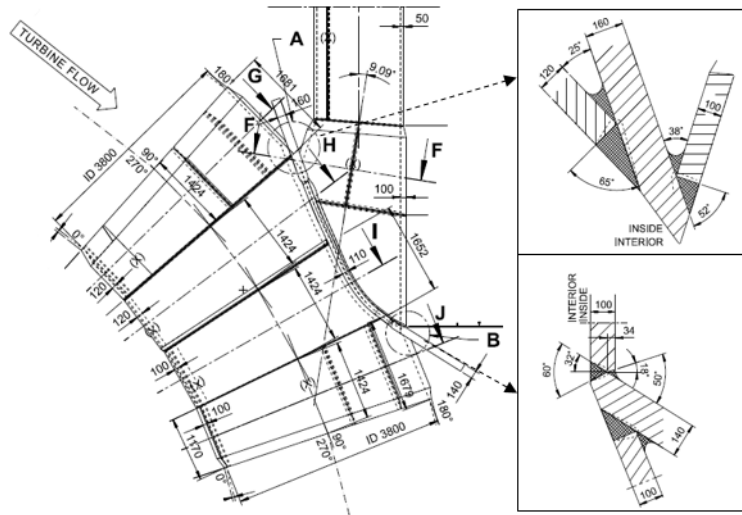


Fig. 5
Weld details of a bifurcation

SUMMARY

Based on a bifurcation design made of high strength steel a comparison between traditional C.E.C.T. safety concept and ASCE manual no.79 approach leads to following conclusion: ASCE manual on steel penstocks which is intended for the design of higher pressure, larger diameter and/or more critical conveyance systems used for power generation appears to be a more accurate standard to numerically evaluate special and geometrically complex parts. Its safety concept accounts for local stress concentrations which become visible by finite element analysis and therefore helps to profit by the benefits of high strength steel applications such as reducing the total weight.

REFERENCES

- [1] C.E.C.T. Recommendations for the design, manufacture and erection of steel penstocks of welded construction for hydro electric installations, Comité Européen de la Chaudronnerie et de la Tolerie, edition 1979, including modifications 1984, SNCT Publications, Paris.
- [2] ASCE Manuals and Reports on Engineering Practice No.79 (2012), Steel Penstocks, 2nd Edition, American Society of Civil Engineers, Reston, VA.

KEYWORDS

Analysis, Finite Elements Method, Penstock, Safety Factor, Stress, Weight

COMMISSION INTERNATIONALE DES GRANDS BARRAGES

VINGT-SIXIÈME CONGRÈS DES GRANDS BARRAGES
Autriche, juillet 2018

DOI 10.3217/978-3-85125-620-8-207



This work licensed under a Creative Commons Attribution 4.0 International License. <https://creativecommons.org/licenses/by-nc-nd/4.0/>

**DESIGN OF STEEL LININGS OF PRESSURE SHAFTS MADE OF HIGH
STRENGTH STEEL – ULTIMATE LIMIT STATE AND CYCLIC LOAD
CONDITIONS**

Richard GREINER

*Em. Professor, Institute of Steel Structures, GRAZ UNIVERSITY OF
TECHNOLOGY*

AUSTRIA

Guntram INNERHOFER sen.

VORARLBERGER ILLWERKE AG, VANDANS

AUSTRIA

Guntram INNERHOFER jun.

VORARLBERGER ILLWERKE AG, VANDANS

AUSTRIA

COMMISSION INTERNATIONALE
DES GRANDS BARRAGES

VINGT-SIXIÈME CONGRÈS DES
GRANDS BARRAGES
Autriche, juillet 2018

**DESIGN OF STEEL LININGS OF PRESSURE SHAFTS MADE OF HIGH
STRENGTH STEEL – ULTIMATE LIMIT STATE AND CYCLIC LOAD
CONDITIONS**

Richard GREINER.

*Em. Professor, Institute of Steel Structures, GRAZ UNIVERSITY OF
TECHNOLOGY*

Guntram INNERHOFER sen., Guntram INNERHOFER jun.

Vorarlberger Illwerke AG, VANDANS

AUSTRIA

1. INTRODUCTION

Developments of the design of steel linings for pressure shafts are an ongoing process, stimulated by the erection of new plants and the increased dynamic loading due to pumping and intensified operation. At the 3. International Conference “HSS for Hydropower Plants” in 2013 [1] the state of developments of that time was reported, - this paper is to present the progress achieved since then in Austria.

One topic deals with the composite behaviour of the HSS-liner with the rock mass. It gives an overview on a consolidated design concept based on the ultimate limit state of the combined system of steel liner plus rock mass, which accounts for the post-failure capacity of the rock in the cracked state. The new concept results in a mechanical consistent approach and leads to a significant increase of rock participation and saving of steel.

The second topic deals with the effects of cyclic loadings, which arise in the steel liner due to operational pressure variations and to pressure oscillations resulting from emptying the penstock. The first may cause fatigue, the second cyclic plasticity. Both may significantly determine the design of the steel liner and affect

the detailing and fabrication of welds and local structural parts. As result of the intensified operation of hydropower plants and of pumping these effects become more important nowadays.

2. ULTIMATE LOAD DESIGN

The design of the composite system of a steel-liner with the rock mass is traditionally based on elastic rock behaviour expressed by the modulus V_R^* and on the elastic behaviour of steel expressed by the allowable stress $kx f_y$ (f_y denotes the yield stress). The design criteria currently used in Austria were discussed in [1] and Fig.1 illustrates them here again for better understanding (thereby the terms V_F, p_F, p_s, σ_s correspond to $V_R, p_R, p_{ST}, \sigma_{ST}$ of the present paper).

Criterion 1 describes the uniform state of elastic rock behaviour around the liner and the splitting of the internal pressure into p_{ST} of the steel lining and p_R of the rock. The interaction is both elastic and axially uniform.

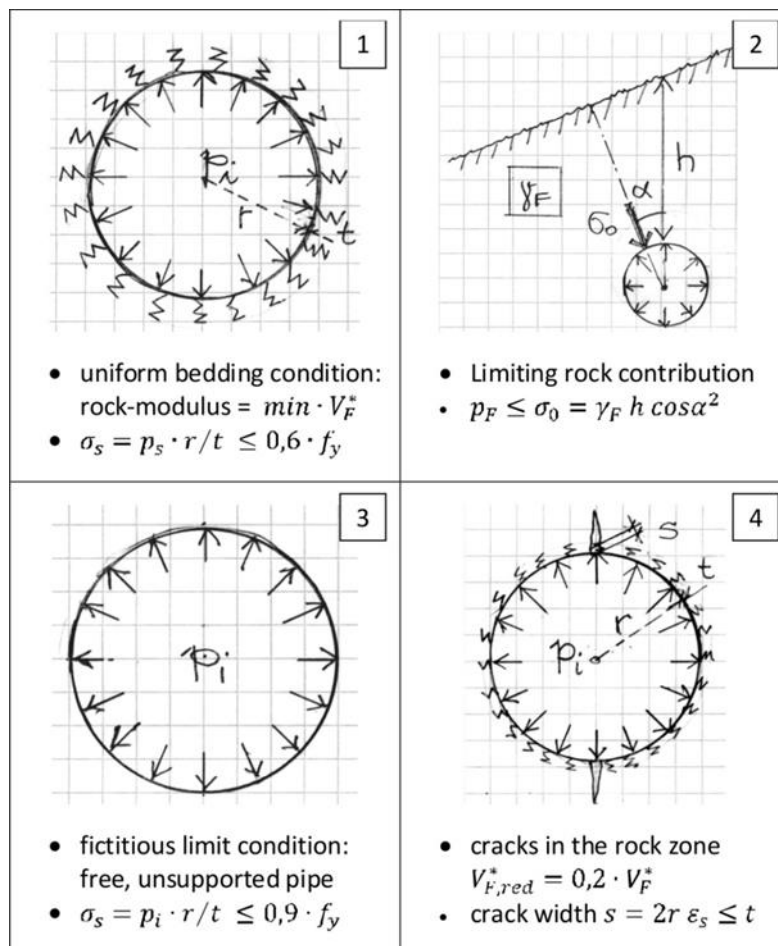


Fig. 1: Current design criteria of steel liners for internal pressure

Criterion 2 defines the limit condition for the rock participation p_R by the overburden of the rock mass.

Criterion 3 represents a fictitious ultimate limit-condition of the steel liner by ignoring any support by the rock and using $0,9x_{fy}$ as limit stress.

Criterion 4 deals with the bridging of a potential crack in the rock soffit by the ductility of the steel lining. The reduction of V_R^* to 20% of the elastic one may be considered as conservatism, but nonetheless it cannot describe the mechanical behaviour in realistic way.

Considering the four criteria in practical design conditions offers that the stress state at the service load level is mechanically reliable and has often been verified in real structures, but that a sound prediction of the capacity of the liner-rock system at the ultimate load level cannot be made. As result - especially in cases of firm rock stiffness - the design is dominated by the criterion 3 leading to unfavourable liner thicknesses.

To this purpose the new concept developed by G. Innerhofer sen. closes the existing gap by providing design rules for the ultimate load resistance of steel liners considering the post-failure capacity of the rock mass in the cracked state. This means that the rock participation is not only the result of the elastic rock behaviour, but is extended to its cracked ultimate state. Further, the steel liner in this interaction may also be considered with its plastic limit capacity. The concept has been mechanically derived for axial uniformity of the rock parameters and conservative preconditions as neglect of tension resistance of the rock and the formation of just one concentrated through-crack (see Fig 1 - 4) have been made.

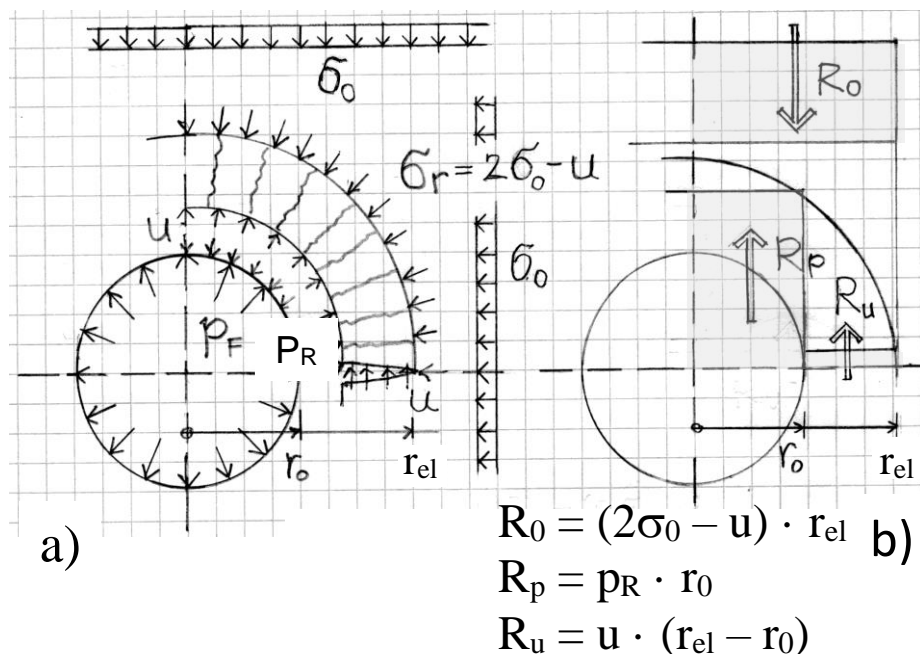


Fig. 2: Ultimate limit state of rock with cracked zone: (a) stress state, (b) stress resultants.

The background of the concept and its derivation is given in [2] but the basic steps are again illustrated here to establish a better context. Fig.2 shows the equilibrium state of the rock mass in the cracked state. Under increasing pressure p_R on the rock surface the radial crack opens and grows to a certain depth r_{el} . Thereby, the crack water pressure u starts acting along the length $(r_{el}-r_0)$ of the crack. The cracked zone propagates as long as equilibrium is found with the primary stress state σ_0 and the crack-water pressure u . Outside of the boundary r_{el} the rock is in the elastic range.

Crack formation at the soffit r_0 starts when p_R reaches the limit $(2\sigma_0-u)$; - the same is found at r_{el} for $(\sigma_r=2\sigma_0-u)$. This limit $(2\sigma_0-u)$ considers small initial fissures along the soffit after excavation so that $2\sigma_0$ is reduced there by the effect of u before the real cracks start forming.

In form of resultants the equilibrium condition can be set up by the components R_0 , R_p and R_u . As result one may find expressions for the crack depth under a given pressure p_R or for p_R under a given crack ratio r_{el}/r_0 :

$$\frac{r_{el}}{r_0} = \frac{p_R - u}{2(\sigma_0 - u)} \quad \text{or} \quad p_R = 2(\sigma_0 - u) \frac{r_{el}}{r_0} + u \quad (1)$$

The approach leads to increased radial deformations in the cracked state compared to the current elastic design and therefore the ductility demands on the steel liner for bridging the crack width at the rock soffit play an important role. The crack width must be covered by the critical width of the steel. This condition limits the allowable crack propagation of the rock in the ultimate limit state. Since the plastic elongation of the steel liner –in the local area bridging the crack- is restricted by the friction effect between the outer liner surface and inner surface of the filling concrete this condition may pose a challenge for HSS-liners due to their reduced ductility parameters, particularly in the welds.

The radial deflection Δr_0 of the rock soffit at r_0 consists of 2 parts, i.e. Δr_{cz} of the cracked zone in radial compression plus Δr_{el} of the sound elastic zone outside of r_{el} , see [2]. Thereby ν denotes the Poisson-factor of the rock material:

$$\begin{aligned} \Delta r_{cz} &= (p_R - u) \cdot r_0 \cdot \ln\left(\frac{r_{el}}{r_0}\right) + \nu \cdot \sigma_0 \cdot r_0 - (1 - \nu) \cdot (\sigma_0 - u) \cdot (r_{el} - r_0) / V_R \\ \Delta r_{el} &= (\sigma_0 \cdot r_0 + (\sigma_0 - u) \cdot r_{el}) / V_R^* \quad \text{with } V_R^* = V_R / (1 + \nu) \end{aligned} \quad (2a), (2b)$$

The crack width for the assumed through-crack is taken equal $S_w = 2 \cdot (\Delta r_0 - \Delta r_A)$ where $\Delta r_A = (2\sigma_0 - u) \cdot r_0 / V_R^*$ denotes the radial deformation at the point when crack initiation starts at the soffit r_0 .

The critical crack width S_{cr} - assuming linearized stress-strain behavior for the rather small stretched length L_S - can be determined from (3a, 3b). Thereby, the notations apply as follows: $\Delta \varepsilon_{pl} = \varepsilon_u - \varepsilon_y$, $\Delta \sigma_{pl} = f_u - f_y$ and $\mu_F =$ friction factor. As mentioned above the ductility parameters of HSS may be rather low for thermo-mechanically produced grades, in particular in welded plates where $\Delta \varepsilon_{pl}$ –values may sag to about 2,5% [for more information see [1]].

$$L_S = 2 \cdot \Delta \sigma_{pl} \cdot t / \mu_F \cdot p_R \quad S_{cr} = (\Delta \sigma_{pl} \cdot \Delta \varepsilon_{pl}) \cdot t / (\mu_F \cdot p_R) \quad (3a), (3b)$$

Concerning the safety requirements specific elements for the rock and the steel behaviour underlie the concept. The hydrodynamic pressure line is usually defined in a conservative way covering also exceptional effects and does not need a further safety factor. The safety factor of the rock parameters is to cover the radial deformations and the crack width and follows from experience and measurements. A factor of 2,0 on the rock modulus V_R^* for design calculations can be considered as recommended value. Further, a limitation of the crack-depth would be reasonable. The safety factor of the steel is recommended to 1,75 on f_y . Both factors should be adapted to the risk potential and the state of knowledge of the geotechnical conditions.

Fig.3 presents an example showing the basic design aspects under internal pressure loading for a liner of the steel grade S690 and the rock with the modulus V_R^* of 6GPa. The parameters describe a very shallow shaft where the effect of cracked rock is most significant. The outcome may be summarized as follows:

- On the ultimate load level (ULS) based on the reduced $V_R^* = 3\text{GPa}$ radial cracking starts at the strain $\Delta r/r_0$ of 0,53‰ and the design pressure of 10MPa is reached at 3,25‰, just in the plastic range of the steel with the yield strain of 3‰. The internal pressure is split there to about 60% for the rock mass and to 40% for the liner. The allowable strain of the steel in the ULS is limited by $\Delta r/r_0 = 3,3$ ‰ where the crack width 5,5mm reaches the critical value. Thus, the limiting condition of crack bridging has just been achieved.

- On the service load level (SLS) -based on $V_R^* = 6\text{GPa}$ - the design pressure is reached at 1,7 ‰ of strain where the rock is in the cracked state. However the steel liner is elastic, except in the local points where crack bridging occurs. Since crack bridging is an action of imposed local deformation, the stress state may be considered as secondary stress.

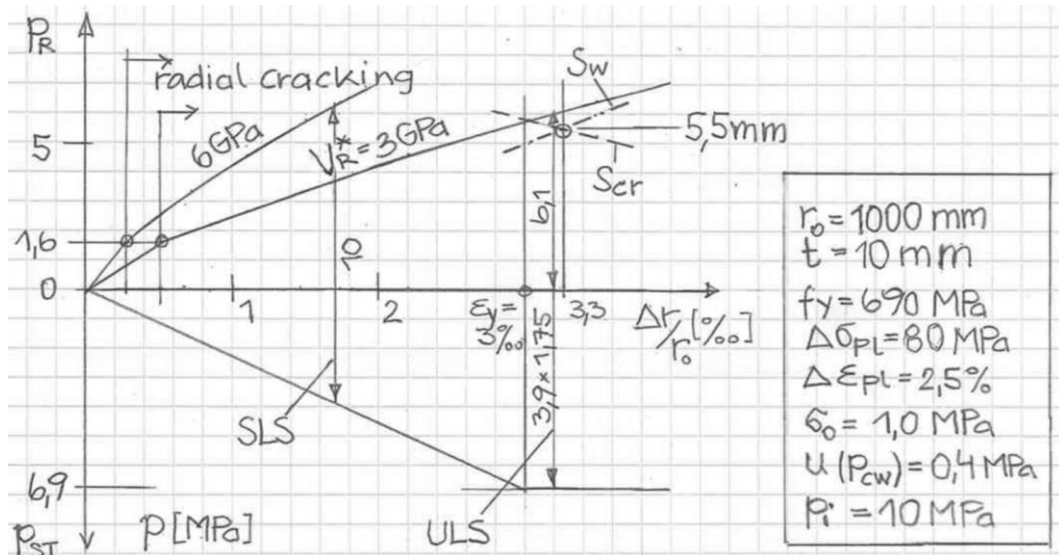


Fig.3: Design example of HSS-lining based on interaction with cracked rock mass in a shallow shaft (friction factor $\mu_F = 0,6$)

Three main results of liner-design follow from the new concept:

Firstly, the traditional rock participation is no longer limited by the elastic resistance of the rock in the uncracked state which would amount in the given example to just 1MPa due to the current design philosophy.

Secondly, the traditionally used ULS-check under internal pressure based on the fictitiously free, unsupported liner with the allowable limit stress of $0,9x\sigma_y$ is now overcome. In the given example, this leads to a reduction of wall thickness by about 33% in case of ultimate design under internal pressure.

Thirdly, liners in shallow shafts may exhibit the phenomenon of crack bridging even on service load level – and if, this occurs also in case of the current design conditions. Although any damage due to this effect has not yet been discovered, for such cases further studies are needed to evaluate this influence also under cyclic load conditions. Accordingly, this topic is not included in the next chapter.

3. CYCLIC LOADING OF HS-STEEL LINERS

The second topic deals with the effects of cyclic loading on the steel liner. There are two kinds of cycles; - those with high frequency leading to failure by fatigue and those with low frequency, which may lead to cyclic plasticity. The first ones are summarized by load spectra ($\Delta p_i, N=2 \cdot 10^6$) resulting from pumping and turbine-operation, the second ones are pressure oscillations due to emptying the penstock, which arise between the maximum hydrodynamic level p_{imax} and the level of crack-water pressure p_{cw} in the empty state ($\Delta[p_{imax} - p_{cw}], N=50$). Thereby, both states also include their specific temperature variations.

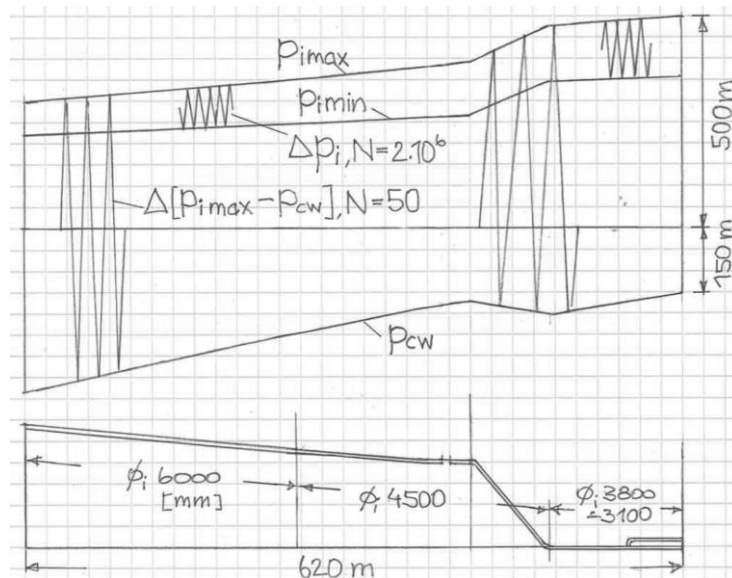


Fig.4: Example of cyclic loading conditions of a steel lining

These effects - mainly resulting from intensified operation- nowadays may lead to limiting design conditions for the linings and cause great demands on the detailing and fabrication of welds and structural parts like injection-nipples, openings, thrust-rings etc.

Fig. 4 illustrates the load conditions of a penstock recently under construction with linings in HSS 690. The load spectrum Δp_i has been based on an operating time of 100 years including pumping and the pressure variation Δp_i results in about 28% of the maximum hydrodynamic pressure. The variation $\Delta[p_{i\max} - p_{cw}]$ is rather large too, due to the high crack-water level.

The specification of the load spectrum is usually provided by the hydro-power company of the plant since it is in close context with the planned service life of the penstock. In the given case it was composed of a mixture of expected operating sequences over 100 years and then increased with a factor of 1,2 on Δp_i and 5 on the number of cycles; - just for understanding, the latter means that the spectrum-length is increased by $5^{1/3}$. This approach is not a standard in Austria but it seems reasonable in view of a longstanding use of penstocks.

The design of these linings illustrated that a large part of them is dominated by the buckling phenomenon so that the general stress level under internal pressure is rather moderate there (see Fig.5). Nonetheless, the cyclic loads result in a high utilisation level at points of stress raisers like welds and local structural parts mainly resulting from grouting. The utilisation factors - both of fatigue and cyclic plasticity- may increase there up to 95%, which leads to the conclusion that the cyclic stress states surpass the static ones. This means that - in view of linings with higher utilisation under internal pressure - high attention must be paid to the cyclic material behaviour of HS-steels.

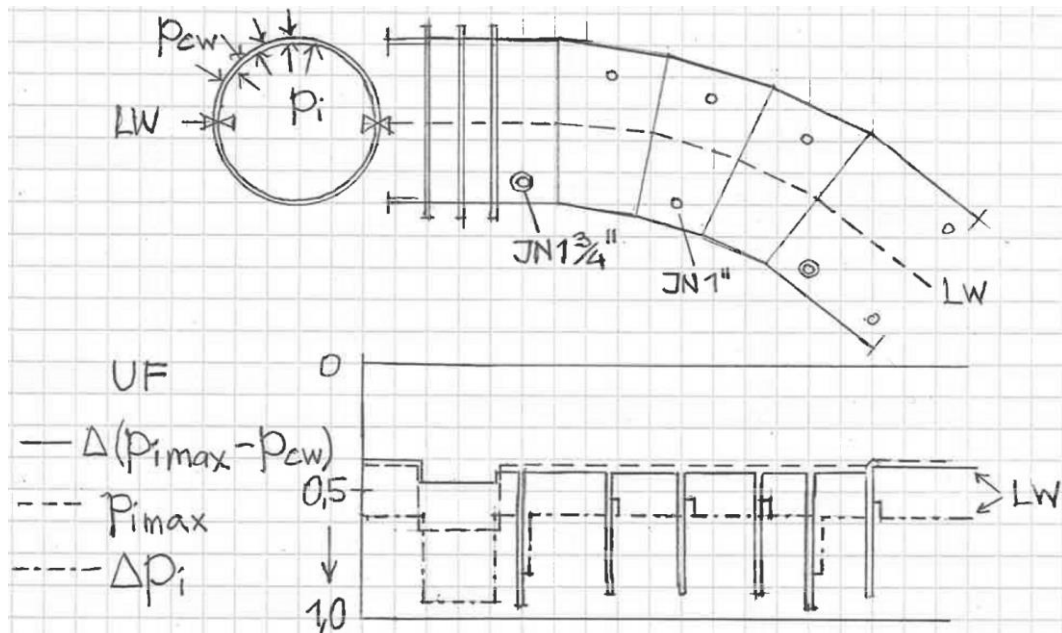


Fig.5: Example of a liner section under cyclic load, - utilisation factors UF

The above findings –as already mentioned above- are the result of the stress concentrations arising at local parts in the liner. Fig.6 demonstrates just some examples of stress concentration factors SCF, which may appear in such details in a large range of magnitude. These SCF mainly affect both the phenomena of fatigue and cyclic plasticity while ultimate stress design usually based on the area replacement method is not decisive in ordinary cases.

Cyclic plasticity is the limit state, which assures that incremental strain accumulation is avoided, and it is understood by the term “Shakedown”. It is the condition that after the first cycle of load, where some plastic strain occurs, the component behaviour is purely elastic in all following cycles. The target of it is avoiding any kind of plastic strain accumulation, which can lead to incremental collapse. For elastic-perfectly plastic material in a uniaxial stress state the maximum allowable elastic stress range is $2\sigma_y$, which is called shakedown-factor of 2,0 (Fig.7a). The actual shakedown factor for a general component is below this limit and depends on both the geometry and the type of loading [3]. Fig.7b illustrates the condition for a biaxial stress state of a cylindrical vessel under radial line-load [4] leading to the shakedown factor of 1,75.

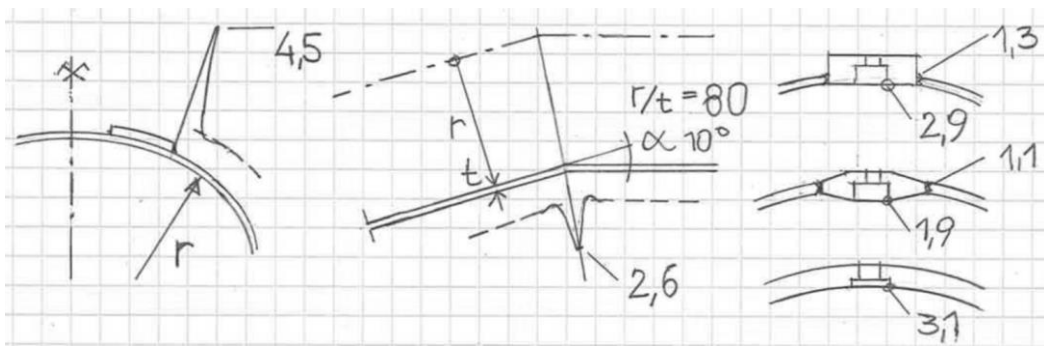


Fig.6: Stress concentration factors SCF for local structural parts

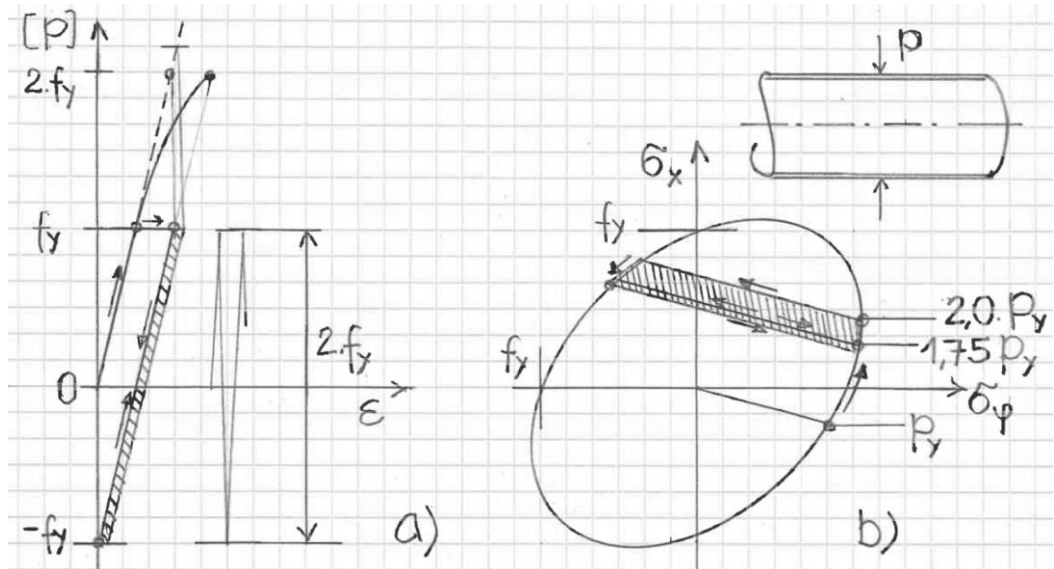


Fig.7: Shakedown for uniaxial (a) and biaxial (b) stress states

An example of nozzles in cylindrical vessels under cyclic internal pressure shows the progress of plastic strains in form of test results (Fig.8). When a cyclic pressure of $1,7x_{fy}$ is applied, the incremental strain reduces to zero after 20 cycles. If the pressure is increased to $1,82x_{fy}$, small values of (constant) plastic strain still occur after 45 test cycles, which creates the case when progressive plastification occurs [3].

Some standards like the BS5500 for pressure vessels use a method for the shakedown factor, which is linked with the SCF of the component and leads to lower factors than 2,0, e.g. to 1,67 for the SCF=2. The Eurocode 3-1-6 for shell structures defines the shakedown by the factor of 2,0, which in light of the above results does not well fit to the to shell-type components of liners. For design purposes of HSS-liners a shakedown limit of $1,2x_{fy}$ has presently been fixed, which is conservatively derived from $1,6x_{fy}$ divided by a safety factor of 1,35, - the latter, to cover unknown effects of high steel grades, since relevant shakedown tests for HSS are not available so far. This limitation may later be raised when deeper insight into the behaviour of HSS is available. Experimental investigations would therefore be required.

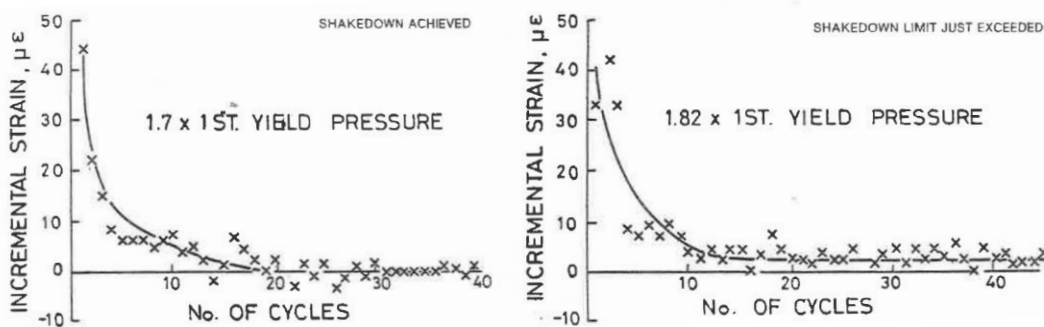


Fig.8: Incremental strains at crotch of a nozzle during shakedown tests [3]

The design limits for fatigue may be taken from the Eurocode 3-1-9 or from the IIW-Recommendations [5], which are identical for nominal stress design. For structural hot spot design however, the rules in [5] are more advanced and should therefore be applied where required. For certain structural details of liners specific solutions are missing in the above codes, like for welds at transitions of different wall thickness or intersections of longitudinal and circumferential welds at rings (see detail A in Fig.9). For the fatigue design of nipples or openings for grouting, which are the main stress raisers in liners, recommendations have already been elaborated [6].

Another structural part creating high utility are thrust rings, as shown in the example of Fig. 5. Some remarks are given in the following, since just few specific investigations of thrust rings are available so far. The design problem splits firstly into the load introduction of the thrust-force into the concrete and into the rock mass respectively and secondly into the fatigue design of the steel structure itself. The former has been elaborated recently [7] including rules for the elastic spring constants of the rings in axial direction. The latter comprises the

calculation of the thrust forces subdivided into the individual rings and then the diverse fatigue checks at the different weld details shown in Fig 9. The individual thrust forces may be determined on basis of a bar with axial springs, however the shell-behaviour in form of the Poisson-effect due to internal pressure variation must be included because of its significant influence. It is interesting to see that – contrary to expectations - not the first ring but the last one –depending on the Poisson-effect - may take the highest percentage of the force as given in case of the example in Fig.9a. The diverse fatigue checks at the welds are indicated in Fig.9b – in particular the check at position A, where the longitudinal weld LW crosses the transverse circumferential weld of the ring. Although longitudinal welds are usually ground flush it should be investigated if the detail may be assumed comparable with that of the transverse-welded attachment on a plane plate.

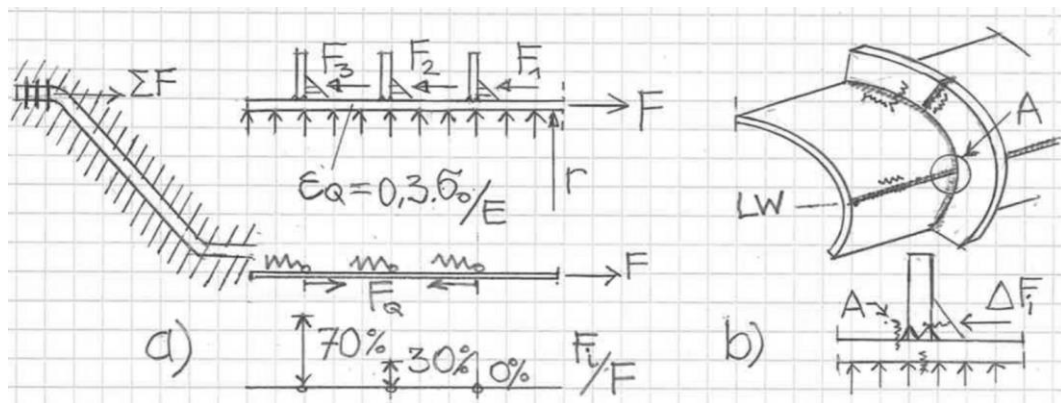


Fig.9: Thrust rings: calculation of force distribution (a) and points of relevant fatigue checks (b)

REFERENCES

- [1] Greiner R., Innerhofer G. and Stering W.: New design aspects for steel linings of pressure shafts made of high strength steel, Proc. of the 3rd International Conference, High Strength Steels for Hydropower Plants, 16.-20. Sept.2013, TU Graz, Austria
- [2] Innerhofer sen. G, Greiner R, Innerhofer jun. G.: Bemessungskonzept für Druckschächte bei Nutzung des passiven Gebirgswiderstandes. Geomechanik und Tunnelbau, 2018, Heft 2
- [3] Spence J. and Tooth A.S.: Pressure Vessel Design-Concepts and Principles, E & FN SPON, 1994, London, UK
- [4] Ofner R.: Zum Tragverhalten des ringversteiften Zylinder-Konus-Überganges von Behältern aus Stahl, Diploma-Work, TU Graz, 1988
- [5] Hobbacher A.: Recommendations for Fatigue design of welded joints and components, International Institute of Welding, 2014

- [6] Greiner R. and Lechner A.: Fatigue strength of high strength steel-linings with different types of grouting openings, Proc. of the 3rd International Conference, High Strength Steels for Hydropower Plants, 16.-20. Sept.2013, TU Graz, Austria
- [7] Unterweger H. und Ecker A.: Bemessungsmodell für Schubringe von Druckrohrleitungen und Druckschächten mit Rechteckquerschnitt-Beanspruchungen, Steifigkeiten und Tragfähigkeiten infolge von Rohrlängskräften N_{sr} , April 2015, TU Graz, Austria

SUMMARY

The new developments presented in the paper comprise two aspects of design of Pressure shafts with high strength steel liners in context with the planning of new shafts or the experience from recently erected ones.

The first one is a consolidated design concept aimed at the ultimate load resistance of steel liners of pressure shafts, which includes an enhanced rock participation in the cracked state of the rock mass. Thereby, the limiting condition is the radial deformation of the soffit, which is restricted by the phenomenon of crack bridging of the steel; - whereby the latter may make high demands on the ductility parameters of HSS. Further, an amended safety concept has been proposed with individual factors for the rock and the steel liner. It on the one hand presents a mechanically consistent approach and on the other may also help to reduce the amount of steel.

The second part deals with the effects of cyclic loading on the design and detailing of the steel liner. It illustrates the design for the limit state of cyclic plasticity (shakedown) and its influence on the utilization of the steel liner. It further indicates that experimental investigation of the cyclic behavior of HSS is needed in order to define a sound shakedown limit for HSS.

Similarly, the effects of fatigue on the utilization at points of local structural parts have been addressed here illustrating their strong impact on the service life of the plant. Also shown is the need to investigate shell-specific details of steel liners, which are not covered by the standardized details of steel structures or pressure vessels so far.

KEY WORDS

pressure shafts, internal pressure, rock-participation, steel liners, ultimate resistance, crack bridging,

cyclic loading, high strength steel, shakedown design, cyclic plasticity, fatigue design

COMMISSION INTERNATIONALE DES GRANDS BARRAGES

VINGT-SIXIÈME CONGRÈS DES GRANDS BARRAGES
Autriche, juillet 2018

DOI 10.3217/978-3-85125-620-8-208



This work licensed under a Creative Commons Attribution 4.0 International License. <https://creativecommons.org/licenses/by-nc-nd/4.0/>

**ADVANCED DESIGN OF HIGH STRENGTH STEEL-LINED PRESSURE
SHAFTS ACCOUNTING FOR FATIGUE CRACK GROWTH**

Alexandre J. PACHOUD

Project Engineer, STUCKY SA
Formerly PhD Candidate at the LABORATORY FOR HYDRAULIC
CONSTRUCTIONS (LCH), ECOLE POLYTECHNIQUE FEDERALE DE
LAUSANNE (EPFL)

SWITZERLAND

Pedro A. MANSO

Senior Research Associate at the LABORATORY FOR HYDRAULIC
CONSTRUCTIONS (LCH), ECOLE POLYTECHNIQUE FEDERALE DE
LAUSANNE (EPFL)

SWITZERLAND

Anton J. SCHLEISS

Full Professor and head of the LABORATORY FOR HYDRAULIC
CONSTRUCTIONS (LCH), ECOLE POLYTECHNIQUE FEDERALE DE
LAUSANNE (EPFL)

SWITZERLAND

COMMISSION INTERNATIONALE
DES GRANDS BARRAGES

VINGT-SIXIÈME CONGRÈS DES
GRANDS BARRAGES
Autriche, juillet 2018

**ADVANCED DESIGN OF HIGH STRENGTH STEEL-LINED PRESSURE
SHAFTS ACCOUNTING FOR FATIGUE CRACK GROWTH**

Alexandre J. PACHOUD

Project Engineer, STUCKY SA

*Formerly PhD Candidate at the LABORATORY FOR HYDRAULIC
CONSTRUCTIONS (LCH), ECOLE POLYTECHNIQUE FEDERALE DE
LAUSANNE (EPFL)*

Pedro A. MANSO

*Senior Research Associate at the LABORATORY FOR HYDRAULIC
CONSTRUCTIONS (LCH), ECOLE POLYTECHNIQUE FEDERALE DE
LAUSANNE (EPFL)*

Anton J. SCHLEISS

*Full Professor and head of the LABORATORY FOR HYDRAULIC
CONSTRUCTIONS (LCH), ECOLE POLYTECHNIQUE FEDERALE DE
LAUSANNE (EPFL)*

SWITZERLAND

1. INTRODUCTION

The recent development of high strength weldable steels has enlarged the range of design alternatives for the optimization of high-head steel-lined pressure tunnels and shafts in the hydropower industry. With the liberalization of the European energy market and increasing contribution of new renewable volatile energies in the electricity grid, storage hydropower and pumped-storage plants are subject to more severe operation conditions than before, resulting in frequent

transients. Whilst the use of high strength steel allows the design of thinner steel liners, welded high strength steel do not provide higher fatigue resistance than lower steel grades, and may be subject to the risk of cold cracking [1]. Fatigue behavior may become the leading limit state criterion [2].

The research project presented hereafter aimed at: (i) improving the comprehension of the mechanical behavior of steel-lined pressure tunnels and shafts (presented in the Section 2 herein); and (ii) developing a framework for probabilistic fatigue crack growth and fracture assessment of cracks in the weld material of longitudinal butt welded joints, considering all possible steel grades for high-head hydropower schemes (presented in Section 3 of this paper).

The influence of anisotropic rock behavior and geometrical imperfections at the longitudinal joints on the structural stresses was studied by means of the finite element method (FEM) accounting for the interaction with the backfill concrete-rock multilayer system [3-4]. Parametric correction factors were derived to estimate structural stresses in steel liners with ease in practice. Stress intensity factors (SIF) for axial cracks in the weld material of the longitudinal joints were also obtained by means of computational Linear Elastic Fracture Mechanics (LEFM). The use of the previously developed parametric equations in the classical formulas for SIF in cracked plated structures was validated [5].

Finally, a probabilistic model (the Monte Carlo simulation procedure) for fatigue crack growth assessment was developed in the framework of LEFM and the Paris-Erdogan law. A week-long normalized loading spectrum derived from prototype measurements on an alpine pumped-storage hydropower plant in Switzerland was used [6]. This approach provides relative and quantitative results through parametric studies, giving new insights on the fatigue behavior of steel liners containing cracks in the weld material of the longitudinal joints.

2. STRESS INTENSITY FOR CRACKS IN THE WELD MATERIAL

2.1. GENERAL FORMULATION OF STRESS INTENSITY FACTOR IN PLATED STRUCTURES

Parametric equations for axial semi-axial surface cracks in cylinders are available in literature (vide [7]). However these solutions either cannot account for geometrical imperfections, or require the stress distribution on the crack face. Given the slenderness of the steel liners of pressure shafts, solutions for semi-elliptical surface cracks in plated structures can be considered as follows, according to Newman [8]:

$$K_I = M_w [M_m (\sigma_m + p_{cr}) + M_b \sigma_b] \sqrt{\pi a / Q} \quad [1]$$

where: σ_m and σ_b are the membrane and bending stresses, respectively; p_{cr} is the pressure applied on the crack face (for a surface crack at the internal surface

of a steel liner, the internal water pressure); M_m and M_b are the shape correction factors applied to the membrane and bending stresses, respectively; M_w is the weld shape correction factor; a is the minor semi-axis for an elliptical crack (e.g., crack depth for a semi-elliptical surface crack); and Q is the flaw shape parameter.

In the case of steel-lined pressure shafts, the complex interaction between all geometrical imperfections and the contact between the steel liner and the concrete-rock system have never been studied, particularly in anisotropic rock. Those specific features of these complex structures may greatly influence the input of Eq. [1], such as the membrane and bending stresses σ_m and σ_b .

2.2. INFLUENCE OF ANISOTROPIC ROCK BEHAVIOR ON THE NOMINAL STRESS

2.2.1. Conceptual model

The conceptual model for the calculation of stresses in steel line pressure shafts is presented in Fig. 1.

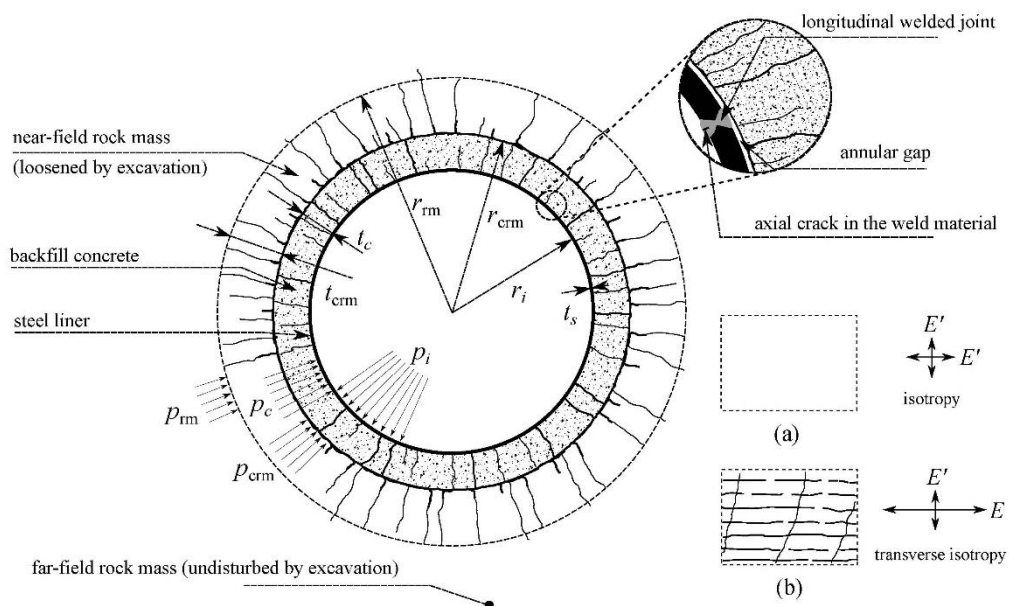
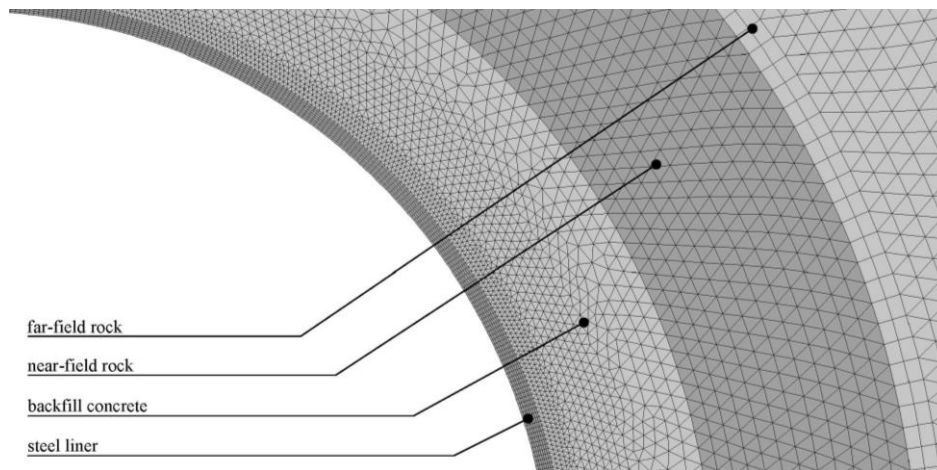


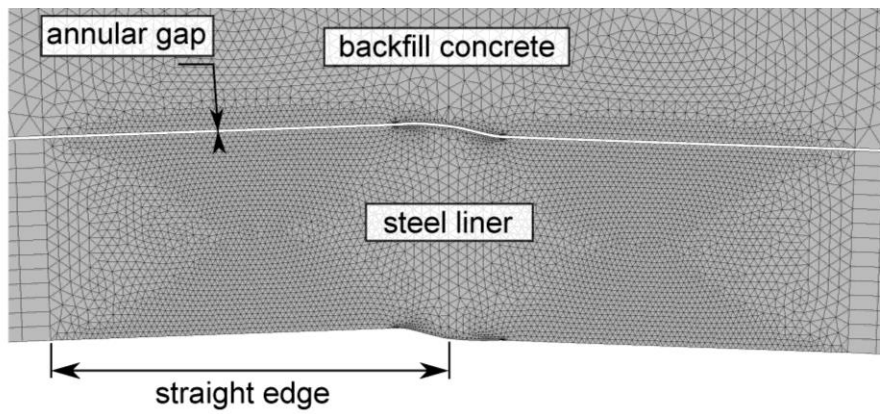
Fig. 1

Conceptual model (cross-section) of a steel-lined pressure shaft in different rock masses, with an emphasis on a longitudinal surface crack at the longitudinal weld (modified after [2])

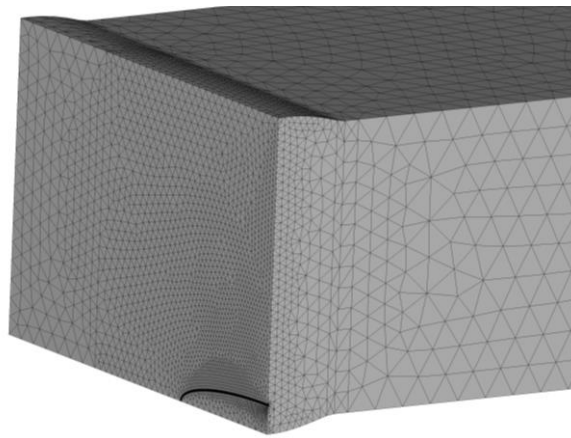
Modèle conceptuel (section transversale) d'un puits blindé en charge dans différents rochers, avec emphase sur une fissure longitudinale de surface à la soudure longitudinale (modifiée d'après [2])



(a) Finite element model to study the influence of anisotropic rock



(b) Finite element model to study the influence of geometrical imperfections



(c) Finite element model to study stress intensity factors

Fig. 2

Finite element models developed to investigate the mechanical behavior of steel-lined pressure shafts

Modèles éléments finis développés dans le but d'étudier le comportement mécanique des puits blindé en charge

In this multilayer system, five layers are generally distinguished as presented in Fig. 1. A detailed description of these layers can be found, e.g., in [3]. In isotropic rock (vide (a) in Fig. 1), the system is axisymmetric, and stresses and displacements can be computed via an analytical solution [3].

2.2.2. *Correction of the isotropic formulation*

Pachoud and Schleiss [3] have studied systematically the influence of anisotropic rock behavior on the maximum stresses in the steel liner by means of the FEM (vide Fig. 2(a)). The particular case of transverse isotropy (e.g., foliated rock with a plane of isotropy parallel to the main foliation, see Fig. 1) was considered within ranges found in situ. It was found that such anisotropy mainly influences the nominal stress in the steel liner. The authors developed correction factors to be included in the analytical solution in isotropic rock allowing to determine the maximum stress in the steel liner considering the anisotropy [2,3,9].

2.3. INFLUENCE OF GEOMETRICAL IMPERFECTIONS ON THE STRESS CONCENTRATION FACTOR AT THE LONGITUDINAL WELDS

Geometrical imperfections are expected to produce bending stresses σ_b at the longitudinal butt welded joints. The effects of the geometrical imperfections presented in Fig. 3 have been studied by Pachoud [9] by means of the FEM (vide Fig. 1(b)), partly based in the descriptions provided in the C.E.C.T. recommendations [10].

Pachoud [9] has shown that the embedment removed the effect of out-of-roundness, whilst the roof-topping (“peaking”) and the misalignment effects remain, barely influenced by the contact with the concrete-rock system. It was also shown that the stress concentration factors (SCF) at the longitudinal welds can be computed using SCF formulas for plated structures and shells [9,11].

2.4. ESTIMATION OF THE STRESS INTENSITY FACTOR FOR CRACKS IN THE LONGITUDINAL WELDS

The SIF for semi-elliptical surface at the longitudinal welds of steel liners (vide Fig. 4) was studied by means of the FEM (vide Fig. 2(c)) and the LEFM by Pachoud et al. [5]. It was shown that the previously published analytical/empirical solutions for cracks in plated structures can be used in the case of steel liners of pressure shafts, using the SCF studied by the authors [2,3,9]. The influence of the weld shape was also studied, and an empirical solution for M_w was proposed [5].

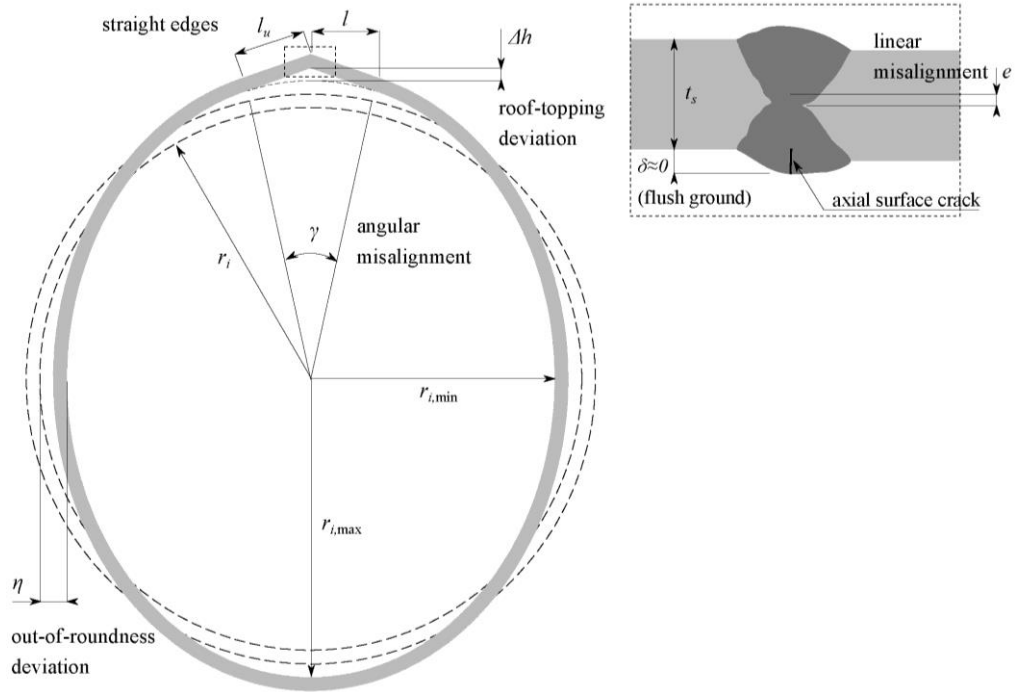


Fig. 3

Schematic representation of the geometrical imperfections at a longitudinally butt welded steel lining (modified after [2])

Schéma représentant les imperfections géométriques dans un blindage avec soudure longitudinale (modifié d'après [2])

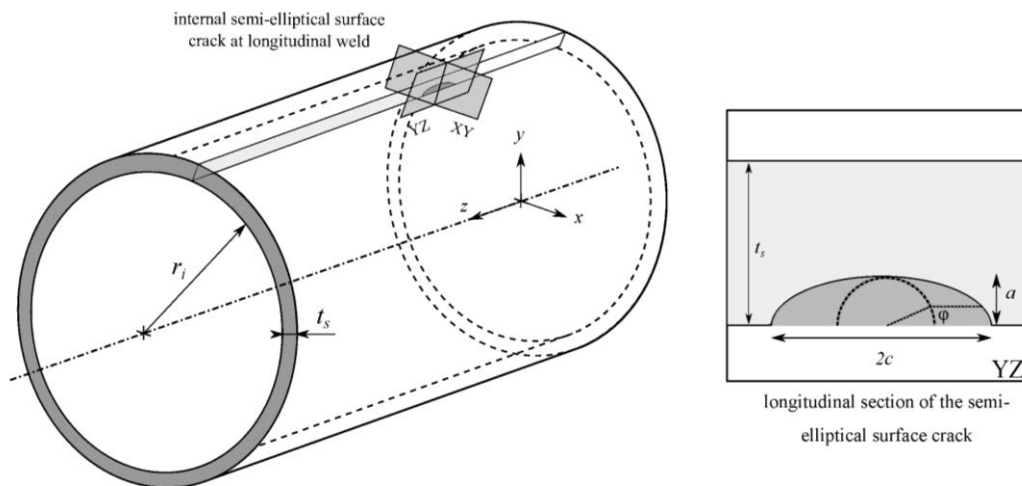


Fig. 4

Schematic representation of a semi-elliptical surface crack (flush ground weld) at the longitudinal weld of a steel liner (modified after [5])

Schéma représentant une fissure semi-elliptique de surface (meulée) à la soudure longitudinale d'un blindage (modifiée d'après [5])

3. FATIGUE CRACK PROPAGATION

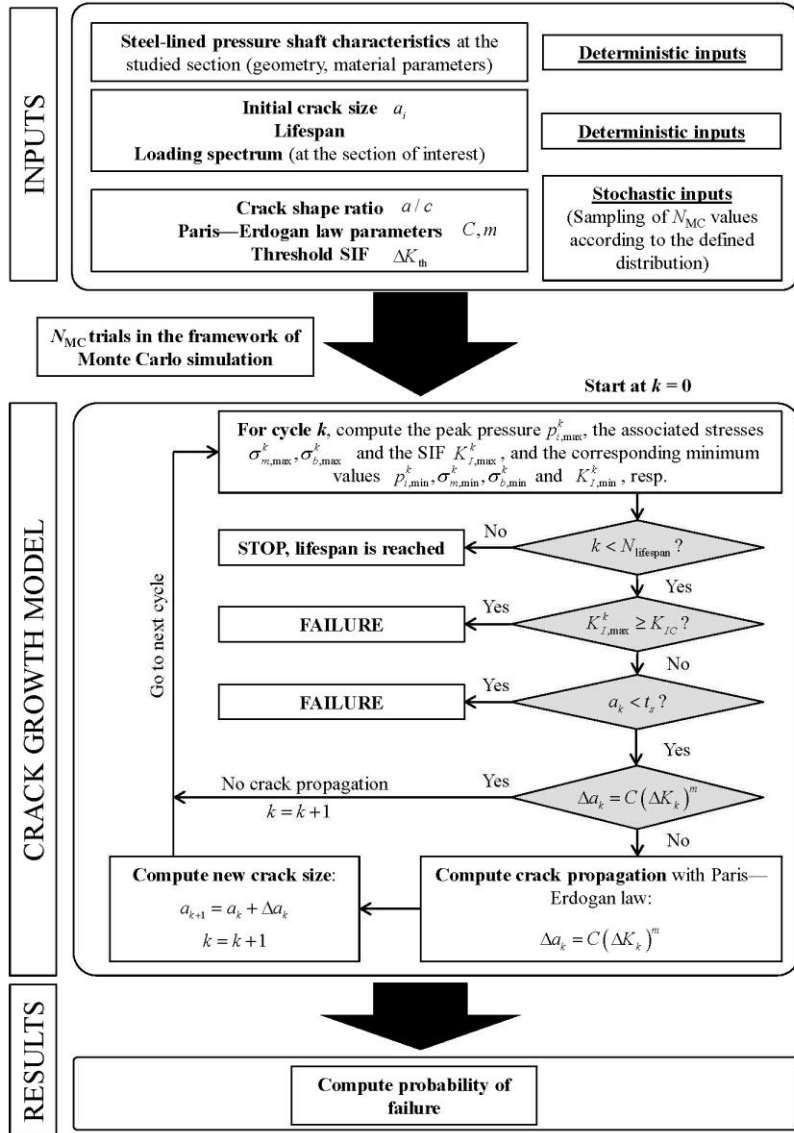


Fig. 5

Flowchart of the proposed Monte Carlo simulation procedure (modified after [2])
Fluxogramme de la procédure de Monte Carlo proposée (modifiée et étendue d'après [2])

3.5. LOADING SPECTRUM

Hachem and Schleiss [12] have measured transients generated within the course of one week of normal operation of an alpine pumped-storage scheme in

Switzerland, equipped with horizontal axis ternary groups with single-stage pumps and Francis turbines. These data were filtered and assembled by Hachem and Giovanola [6]. Pachoud [9] analyzed these data using the Rainflow Counting technique and derived a loading spectrum, which was then normalized with respect to the mean pressure $p_{i,mean}$. The normalized spectrum was used and scaled up for fatigue crack propagation in steel-lined pressure shafts cases.

3.6. PROBABILISTIC MODEL FOR FATIGUE CRACK GROWTH AND FRACTURE

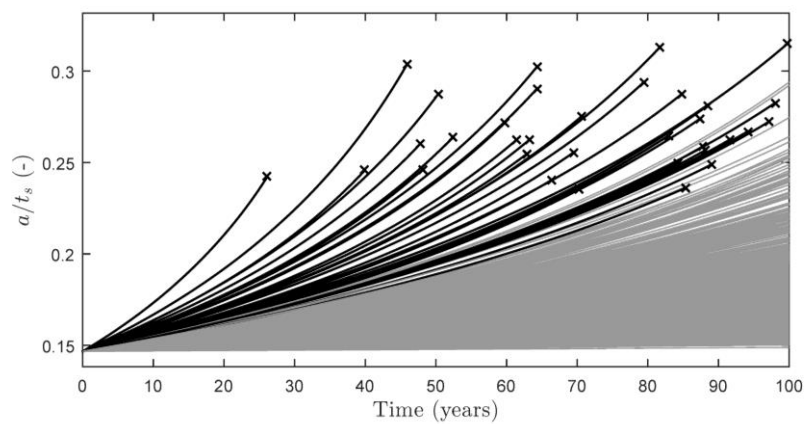


Fig. 6

Semi-elliptical surface crack growth as a function of time ($x = \text{failure}$) from the probabilistic model (1000 trials, in aggressive environment)
Propagation de fissures semi-elliptiques en fonction du temps ($x = \text{rupture}$), issue du modèle probabiliste (échantillon de 1000 valeurs, environnement agressif)

Pachoud [9] developed a probabilistic model for fatigue crack growth and fracture of initial axial cracks in the weld material of longitudinal butt welded joints of steel liners of pressure shafts. This model was implemented in the scope of the Monte Carlo simulation procedure, considering the well-known Paris-Erdogan law. The flowchart of the procedure is presented in Fig. 5. The complete and detailed methodology to compute pressures, stresses and SIF at each loading cycle is presented in [2] in the scope of a deterministic approach. More details on the probabilistic approach are presented in [9].

An example of result that can be obtained with the proposed approach is shown in Fig. 6, for only 1000 trials for the sake of presentation herein (mean static pressure of the load spectrum $p_{i,mean}=15$ MPa; steel liner thickness $t_s=27.3$ mm; initial crack depth $a_i=4$ mm; steel yield strength $f_y=960$ MPa, safety factor $SF=1.8$ on the yield strength for the design; elastic modulus of the isotropic rock $E=5.0$ GPa). The same procedure can be used to obtain the probability of failure of the steel lining within a given timespan and to determine the acceptable undetected initial crack sizes in the steel liner, for different steel grades options.

4. ACKNOWLEDGEMENTS

This study is part of *HydroNet 2: Modern methodologies for design, manufacturing and operation of hydropower plants*, a research project funded by the Swiss Competence Center Energy and Mobility (CCEM-CH). Additional support was obtained from the Swiss Committee on Dams (SwissCOD) and the Swiss Competence Center for Energy Research—Supply of Electricity (SCCER-SoE).

REFERENCES

- [1] CERJAK H., ENZINGER N., PUDAR M. Development, experience and qualification of steel grades for hydro power conduits. In *Proceedings of the Conference of High Strength Steels for Hydropower Plants, Graz, Austria, Graz University of Technology*, 2013.
- [2] PACHOUD A.J., MANSO P.A., SCHLEISS A.J. New methodology for safety assessment of steel-lined pressure shafts using high-strength steel. *International Journal on Hydropower & Dams*, 2017; Issue 3:80-88.
- [3] PACHOUD A.J., SCHLEISS A.J. Stresses and displacements in steel-lined pressure tunnels and shafts in anisotropic rock under quasi-static internal water pressure. *Rock Mechanics and Rock Engineering*, 2016;49(3):1263-87.
- [4] PACHOUD A.J., MANSO P.A., SCHLEISS A.J. Contraintes aux soudures longitudinales des blindages sous l'effet de l'anisotropie du rocher et des imperfections géométriques. *Wasser Energie Luft*, 2017;109(2):91-95.
- [5] PACHOUD A.J., MANSO P.A., SCHLEISS A.J. Stress intensity factors for axial semi-elliptical surface cracks and embedded elliptical cracks at longitudinal butt welded joints of steel-lined pressure tunnels and shafts considering weld shape. *Engineering Fracture Mechanics*, 2017;179(June):93-119.
- [6] HACHEM F., GIOVANOLA F. Fatigue cracks propagation in steel-lined pressure shaft of pumped-storage power plants under normal operation conditions. In *Proceedings of the Conference of High Strength Steels for Hydropower Plants, Graz, Austria, Graz University of Technology*, 2013.
- [7] NEWMAN JR J.C., RAJU I.S. Stress-intensity factors for internal surface cracks in cylindrical pressure vessels. *International Journal of Pressure Vessel Technology*, 1980;102(4):342-346.
- [8] NEWMAN JR J.C., RAJU I.S. An empirical stress-intensity factor equation for the surface crack. *Engineering Fracture Mechanics*, 1981;15(1-2):185-192.
- [9] PACHOUD A.J. *Influence of geometrical imperfections and flaws at welds of steel liners on fatigue behavior of pressure tunnels and shafts in anisotropic rock*, Ph.D. Thesis No. 7305 and LCH Communication 69, Ed.

- A. Schleiss, Ecole Polytechnique Fédérale de Lausanne, Switzerland, 2017.
- [10] C.E.C.T. *Recommendations for the design, manufacture and erection of steel penstocks of welded construction for hydroelectric installations*. European Committee of Boiler, Vessel and Pipe Work Manufacturers, 1980.
- [11] HOBACHER A.F. *Recommendations for fatigue design of welded joints and components*. IIW Collection, Springer International Publishing, 2016.
- [12] HACHEM F.E., SCHLEISS A.J. Online monitoring of steel-lined pressure shafts by using pressure transient signals under normal operation conditions. *Journal of Hydraulic Engineering*, 2012;138(12):1110-1118.

SUMMARY

This paper presents a novel contribution for the design of steel lined pressure tunnels and shafts considering (i) the influence of anisotropic behavior of rock as well as (ii) the geometrical imperfections and flaws at welds on the fatigue resistance of the steel liners. This issue is of utmost interest for high-head hydropower plants, in particular when considering the use of high-strength steels and low overburden. For fatigue assessment, a probabilistic model for steel liner crack growth and fracture in the steel liner was developed by using a set of new parametric equations for stress concentration at welds and stress intensity factors for cracks. The application of this model is illustrated in the paper for a case study subjected to dynamic loading. The probabilistic model allows to determine the acceptable undetected initial crack sizes in the steel liner depending on the choice of the steel grade, which is crucial for engineering practice using high-strength steels for pressure tunnels and shafts.

L'article présente une nouvelle contribution à la conception et au dimensionnement de galeries et de puits blindés, en tenant compte de l'influence (i) de l'anisotropie du massif rocheux et (ii) des imperfections géométriques du blindage et des défauts aux soudures, dans la résistance des blindages à la fatigue. Ce sujet est important pour les aménagements hydroélectriques à haute chute, en particulier ceux avec des structures blindées avec des aciers à haute limite de résistance ou avec un faible recouvrement rocheux. Pour l'analyse de la résistance à la fatigue l'article propose un modèle probabiliste basé sur un nouveau jeu d'équations paramétriques pour les concentrations de contraintes dans les blindages et pour l'intensité des contraintes aux fissures. L'application du modèle est illustrée pour un cas d'étude soumis à un chargement dynamique. Le modèle probabiliste permet d'obtenir les dimensions initiales maximales des fissures non-détectées selon le type d'acier, ce qui est primordial pour le choix en pratique du type d'acier à haute résistance pour les galeries et puits blindés.

COMMISSION INTERNATIONALE
DES GRANDS BARRAGES

VINGT-SIXIÈME CONGRÈS DES
GRANDS BARRAGES
Autriche, juillet 2018

EFFECT OF RTE TREATMENT ON TOUGHNESS OF HSS WELD METAL

Horst-Hannes CERJAK¹, Ozan CALISKANOGLU², Norbert ENZINGER¹,
Gunter FIGNER², Milan PUDAR³

¹ *Institute of Materials Science, Joining and Forming, GRAZ UNIVERSITY OF
TECHNOLOGY*

²STIRTEC GMBH

³MAGNA STEYR FAHRZEUGTECHNIK GMBH

AUSTRIA

During pressure test of a manifold of a brand new huge hydro power penstock fabricated from advanced high strength steel a catastrophic fracture appeared by breaking the circumferential weld of the closure head before reaching the design pressure. By analysis of the reasons of this event severe embrittlement of weld metal has been detected by observing intergranular fracture surface and toughness testing of the weld metal. Further investigations revealed that the embrittlement was caused by unqualified post weld heat treatment (PWHT) during fabrication, characterized by extremely low cooling rate of 15°C/h from holding temperature at 570°C. Temper embrittlement has been found as root cause for the embrittlement. For assuring safe service conditions all PWHT treated welds has completely been removed and re-welded. This was possible because of full access to the manifold welds in the tunnel. Further investigations revealed that many welds present in the inclined shaft has also been PWHT treated by application of the slow cooling rate. In these welds also severe embrittlement has been observed. The welded shells present in the inclined shaft has already been fixed in the mountain by concrete. That fore re-welding could not be applied because of water intake after removal of the existing welds. Therefore, consequently the fabrication of a new penstock in a newly drilled tunnel had to be considered, taking into account costs and schedule consequences.

Various possibilities has been studied to solve that severe problem. Reversible temper embrittlement treatment (RTE), a short time heat treatment at a

peak temperature around 600°C, was found as method to recover the toughness of the embrittled welds. Intensive investigations has been performed to realize this idea in the project. Electrical mat heating was selected and carefully qualified to be applied in the shaft.

The procedure of application of electrical mat heating on brittle welds in the penstock is discussed in this contribution. By qualified controlled application of electrical mat heating in the shaft, rehabilitation of the brittleness in the existing welds could successfully be achieved. The penstock after finishing this procedure has successfully been commissioned and could start service operation. (1)

The results of the industrial application of RTE treatment performed are doubtless very successful and reproducible. Basic scientific investigations to explain the surprising positive effect of RTE treatment on the recovery of the toughness of temper embrittled weld deposit have been performed. By application of Atom Probe investigations, the effect of embrittlement observed as well the surprising effect of de-embrittlement by RTE application could be explained. (2) (3)

REFERENCES

- [1] H. CERJAK, O. CALISKANOGLU, N. ENZINGER, G. FIGNER, M. PUDAR: *Increasing of toughness of brittle type S690 HSS weld metal by application of reversible temper embrittlement (RTE)*, Welding in the World, 2017, Vol.61.
- [2] H. CERJAK, F. MENDEZ-MARTIN, M. DOMAKOVA: *Atom probe investigations on temper embrittlement and reversible temper embrittlement in S 690 steel weld metal*, Science and Technology of Welding and Joining, 2 -2017.
- [3] H. CERJAK, F. MENDEZ-MARTIN: *Atom probe investigations on temper embrittlement and reversible temper embrittlement in S 690 steel weld metal*, to explain successful Rehabilitation of Brittle Penstock welds ICOLD AUSTIA 2018

COMMISSION INTERNATIONALE DES GRANDS BARRAGES

VINGT-SIXIÈME CONGRÈS DES GRANDS BARRAGES
Autriche, juillet 2018

DOI 10.3217/978-3-85125-620-8-210



This work licensed under a Creative Commons Attribution 4.0 International License. <https://creativecommons.org/licenses/by-nc-nd/4.0/>

**INFLUENCE OF PIPE FABRICATION QUALITY ON LIFETIME OF
PENSTOCKS OF PUMPING STORAGE POWER PLANTS**

Christian BUZZI

*External Lecturer, Institute of Machine Components and Methods of
Development, Division for Structural Durability and Railway Technology,
GRAZ UNIVERSITY OF TECHNOLOGY*

AUSTRIA

Horst CERJAK

*Emeritus Professor, Institute for Materials Science, Joining and Forming, GRAZ
UNIVERSITY OF TECHNOLOGY*

AUSTRIA

Christian MOSER

*First Deputy Head, Institute of Machine Components and Methods of
Development, Division for Structural Durability and Railway Technology,
GRAZ UNIVERSITY OF TECHNOLOGY*

Manel AKROUT

Expert Hydromécanique, TRACTEBEL ENGINEERING S.A.

Bertrand CHANZY

Expert Hydromécanique, TRACTEBEL ENGINEERING S.A.

FRANCE

COMMISSION INTERNATIONALE
DES GRANDS BARRAGES

VINGT-SIXIÈME CONGRÈS DES
GRANDS BARRAGES
Autriche, juillet 2018

**INFLUENCE OF PIPE FABRICATION QUALITY ON LIFETIME OF
PENSTOCKS OF PUMPING STORAGE POWER PLANTS ***

Christian BUZZI

External Lecturer

*Institute of Machine Components and Methods of Development
Division for Structural Durability and Railway Technology, GRAZ UNIVERSITY
OF TECHNOLOGY*

AUSTRIA

Horst CERJAK

Emeritus Professor

*Institute for Materials Science, Joining and Forming, GRAZ UNIVERSITY
OF TECHNOLOGY*

AUSTRIA

Christian MOSER

First Deputy Head

*Institute of Machine Components and Methods of Development
Division for Structural Durability and Railway Technology, GRAZ UNIVERSITY
OF TECHNOLOGY*

AUSTRIA

MANEL AKROUT

Expert Hydromécanique

* INFLUENCE DE LA QUALITÉ DE FABRICATION DES CONDUITES SUR LA DURÉE
DE VIE DES CONDUITES FORCÉES DES STATIONS DE TRANSFERT D'ÉNERGIE
PAR POMPAGE (STEP)

TRACTEBEL ENGINEERING S.A.

FRANCE

BERTRAND CHANZY

Expert Hydromécanique

TRACTEBEL ENGINEERING S.A.

FRANCE

1. INTRODUCTION

With the increasing demand for energy and dynamic distribution of electric power the requirements on power plants are rising. This means for penstocks of pumped storage hydro power stations an increasing amount of load cycles per year. For penstocks of welded pipes the welding seams demand attention because of possible deviation of the idealized geometry and microstructure. This paper deals with the influence of fabrication on the stress situation and its influence on penstock life time.

2. MOTIVATION

The penstock of the hydro power station described in this paper covers a water head of 600 m. The inner diameter of the penstock has a constant value of 3700 mm, the wall thickness starts at 12 mm near the basin and ends with 36 mm at the foot of the mountain. The materials used for the penstock are steels grades S355J2, S500QL and S690QL according to the increasing hydrostatic pressure. The projected term is 80 years, the combination of high stress fluctuations and existing cold cracks leads to high cycle fatigue damage, which caused leakage after 5 years of service. To investigate this case, studies initiated between the operator of the hydro power station, a consultancy and engineering company and several institutes of the Graz University of Technology.

3. PRELIMINARY WORK FOR A FATIGUE CALCULATION

The aim of a fatigue calculation is the estimation of the achieved damage respectively remaining lifetime or a forecast of lifetime respectively expectation of loadcycles of a mechanical part.

The resources needed to achieve this aim are the “as-built” geometry of the part, the resulting stresses in combination with the loads and load cases and the material parameters.

3.1. GEOMETRY

The quality of a welding seam depends on the mechanical preparation of the plate (chamfer, rolling ...) the welding process applied, and in addition, the remaining geometry (Fig. 1) of the welding seam, defined by misalignment d_1 , roof topping d_2 and notch radius. These items have high influence on the resulting stress under service conditions. The notch factor depends on the notch radius and is the quotient of notch stress to nominal stress. Fig. 2 depicts as an example the influence of misalignment, peaking (outward known as roof topping and inward) and notch radius on the local stress situation of a weld seam. With a standard geometry of a welding seam, the nominal stress is about 2.2-times magnified (Fig. 2, a). A moderate roof topping raises the notch factor up to nearly 2.4 (Fig. 2, b). A combination of misalignment and roof topping increases the notch factor up to 3.1 (Fig. 2, c). Fig. 2, d shows the measured geometry of a sample with a quite smooth notch radius and thus a low notch factor of about 1.8.

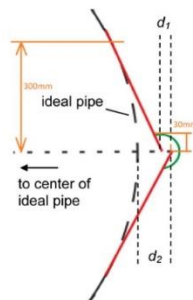


Fig. 1
Geometry of welding seam

To gain all the information needed, the process to generate the geometry for the penstock is split up into two parts. The first part is the overall geometry used in the global fe (finite element) model, the second part is the detailed geometry used for selected local fe models of the longitudinal welding seams. The local models are based on data gained during the laser measurement performed by the Institute of Engineering Geodesy and Measurement Systems (IGMS) of TU Graz [1].

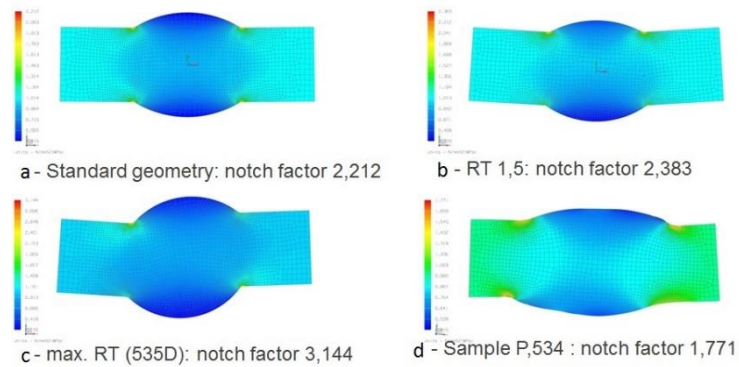


Fig. 2
Influence of the geometry on the local stress

3.1.1. Global Model

The global model developed covers the total penstock length of roughly 1000 meters (300 shells), considering its geometry of length, altitude, angle, plate thickness, supports and basements. The result of the global model is the stress caused by the hydrostatic pressure acting along the penstock with idealized plate thickness and without welding seams. The global model of the penstock is built as a 3D CAD model consisting of the penstock and the supports. All parts are meshed with linear 2D quad elements. The wall thickness changes according to the build penstock and the material is steel with a linear elastic behaviour.

3.1.2. Misalignment and roof topping

The actual measured geometries of the longitudinal welding seams are compared to the CECT values, which represent the specified allowable geometric deviation at this installation. As an example, Fig. 3 shows the measured misalignment and roof topping of the penstock.

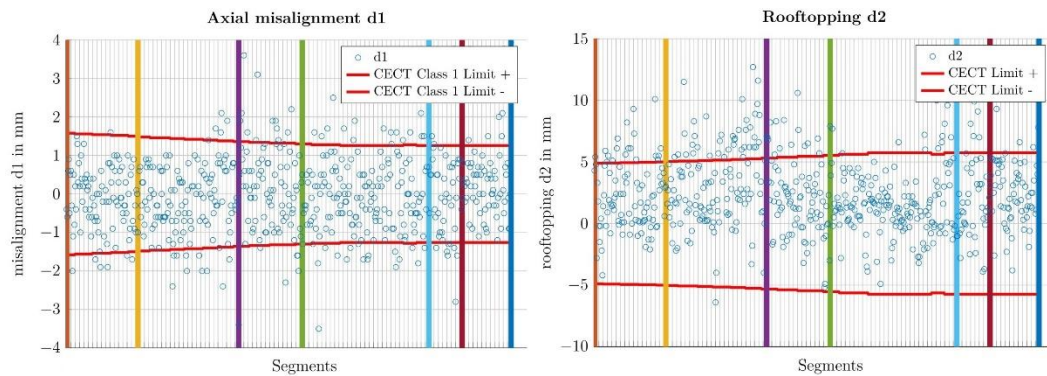


Fig. 3
Measured data of misalignment d1 and roof topping d2 of the penstock segments

3.1.3. *K_m factor*

At the beginning of the project, the question arised how to select the locations for the selection of local models. It was a common consent, that high values of misalignment and roof topping at the longitudinal welding seams results in high stresses The influence of misalignment and roof topping and their combination was calculated by application of the K_m factor [2] which describes the influence of the macro geometry of a welding seam on the stresses.

The measured and prepared data from IGMS (Fig. 3) have been evaluated and used in Eq. [1] to [4]. This allows on generating an overview of the influence of geometry along the entire penstock. The next step was a combination of K_m with the circumferential stress from the global model, which will give a first idea of the “structural stress” along the penstock.

$$K_{m,ax,mis} = 1 + \frac{6 \cdot d1}{t_1(1-\nu^2)} \cdot \frac{t_1^n}{t_1^n - t_2^n} \quad K_m \text{ for axial misalignment} \quad [1]$$

$$K_{m,ang,mis} = 1 + \frac{3 \cdot d2}{t(1-\nu^2)} \frac{\tanh\left(\frac{\beta}{2}\right)}{\frac{\beta}{2}} \quad K_m \text{ for roof topping} \quad [2]$$

$$\beta = \frac{2 \cdot l}{t} \sqrt{3(1-\nu^2) \frac{\sigma}{E}} \quad [3]$$

$$K_m = 1 + (K_{m,ax,mis} - 1) + (K_{m,ang,mis} - 1) \quad [4]$$

d1	...	misalignment	d2	...	roof topping
β	...	geometry parameter	t1	...	thickness of plate 1
t2	...	thickness of plate 2	ν	...	poisson's ratio (0.3)
E	...	Young's modulus	n	...	factor for longitudinal joints (0.6)

3.1.4. *Local Models*

The local models are necessary for the fatigue calculation and therefore to obtain a forecast of the residual lifetime. The combination of stress from the global model and the calculated K_m from the measurement results in a “structural stress” at the welding seam. The notch stress is in addition to the misalignment, roof topping and plate thickness an important factor for local stress value and therefore for the fatigue calculation.

Based on the imported local models to CAD the geometry of the notch is defined and the notch radius could be derived. For the simulation it is necessary to use a half cross section of the penstock. A part of this cross section is covered by the measurement, the other parts of the geometry are build up by assumptions.

1. The absent part of the diameter of the penstock has an idealized geometry and corresponds with the delivered drafts.
2. The wall thickness is idealized and corresponds with the delivered information.

3. During the measurement campaign, only the outside surface of the penstock has been measured. There is no information about the geometry inside. That's why the geometry of the welding seam inside the penstock, used in the local models, can't be the exact geometry.

4. The grinded welding seams are idealized with a smooth transition from the wall to the grinded part without edges, scratches or cracks.

3.1.5. Influence of weld notch radius

The actual existing weld geometry of the penstock investigated can be rated, by the used actual welding procedure, as relatively smooth. For quantification of the influence of notch radius, the stress rising factor K_t is introduced. The maximum stress $\sigma_{max,static}$ (Eq. [5]) in the notch radius for hydrostatic pressure in the penstock is a combination of

- circumferential stress caused by hydrostatic pressure
- misalignment and roof topping and their influence factor K_m
- notch radius at the welding seam and the influence factor K_t

$$\sigma_{max,static} = K_m \cdot K_t \cdot \sigma_{hydrostatic} \quad [5]$$

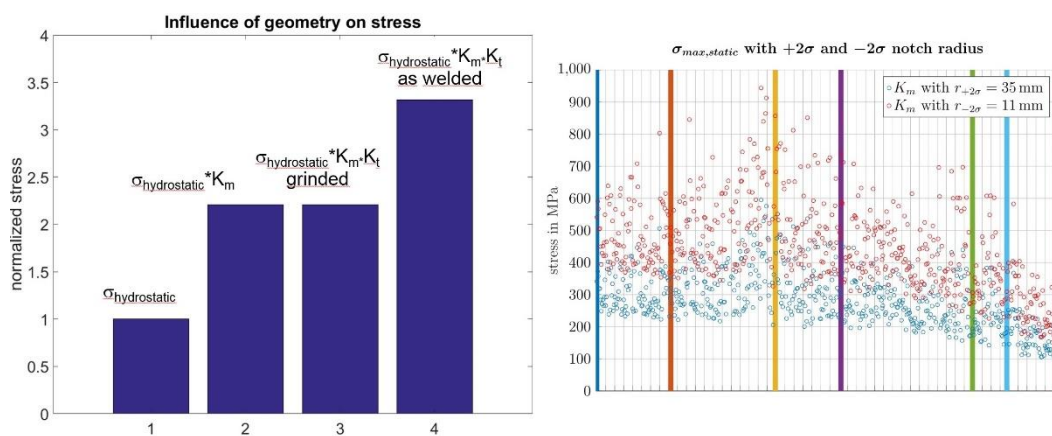


Fig. 4

a.) Comparison of the influence of geometry on stress and the calculated b) frequency bandwidth of stresses along the penstock segments

The notch radii used for calculation of the selected local models have been derived from the geometric data. For this selected positions a statistical analysis has been made. The standard deviation ($\pm 1\sigma$ and $\pm 2\sigma$) of the notch radius from the local models is made by statistical analysis. The factor K_t is used to describe the additional effect of notch radius on the acting stresses in the weld region (Fig. 4, a). It was tried to perform a combination of K_m and K_t for r_{μ} , $r_{\pm 1\sigma}$ and $r_{\pm 2\sigma}$ which results in an overview of possible stresses $\sigma_{max,static}$ for all measured locations (Fig.

4, b). The estimated minimum stress along the penstock segments is about 100 MPa, the maximum stress about 950MPa.

3.2. MATERIAL

High strength steels promise higher fatigue strengths and gently inclined gradients compared to the standard steel SN-curves. On the other hand, high strength steels are more sensitive on notches, cracks and residual stresses. The penstock is fabricated with three different steel grades: S355J2, S500QL and S690QT. The steel S355J2 steel is well known and the static and dynamic data are based on the data from FKM [4] and IIW [3]. At the beginning of the project, it was decided to use for the S500QL the same material data as for the S355J2. For S690QT less valuable data are available in the literature, so own SN-curves have been established. Because of the expected high stresses and strains in the welding seam notches an elastic-plastic material law have been used for the simulations. For the S355J2 the elastic-plastic material law is used which is delivered by the simulation software, for grade S690QL the data have been used from a former project.

4. RESULTS FE SIMULATION

4.1. RESULTS GLOBAL MODEL

The results from the global model are necessary for developing the local models. These stresses are similar to the results at the same location of a former project. The circumferential stress along the penstock is used for the local model calculations. With this stress distribution, the “structural stress” in combination with K_m has been calculated. It is also an indicator for the mean stress in the penstock wall for local models.

4.2. RESULTS LOCAL MODEL

The result of simulation are stresses and deformations of the penstock at the positions in the selected shells of the penstock. Fig. 5 presents an example of the influence of notch radius, roof topping and misalignment on the stress distribution represented by equivalent von Mises stress Fig. 5, a and examples of the influence of different extensive shapes of geometric discontinuities on the deformation of the pipe in an oversubscribed presentation Fig. 5, b. When evaluating these results it can be concluded, that across the local models calculated no commonly valid

representative behaviour of the welds can be derived. The local deformation, and as a conclusion the stress distribution varies as a function of misalignment, roof topping, and notch radii in the measured position. In addition, it has to be considered because of the fact that the real geometry of the weld inside the pipe could not be measured. So, for the calculation the outside was “mirrored” to the inside and is therefore not quantitatively represented.

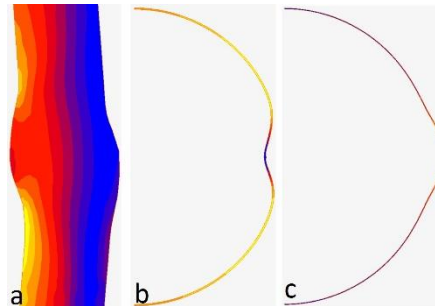


Fig. 5

- a.) notch stress at local model with a maximum of 590 MPa at the welding notch
 Examples of deformation (oversubscribed) of the penstock with hydrostatic pressure and positive b) and negative c) roof topping

5. FATIGUE CALCULATION

The fatigue calculation is based on fluctuation data, SN-curves, geometric measurement of the penstock and the FE simulation of local models. The whole fatigue calculation was performed by using MATLAB R2015b and the WAFO toolbox [5]. For the fatigue calculation the knowledge of the resulting stresses, allowable stresses and the load cases are essential. The resulting stresses are derived from the local models. The allowable stresses applied, are taken from the own test results and from [3]. The load cases and load cycles (fluctuation data) are provided by the operator of the power station (history of operations of the pump-turbine).

5.1 FLUCTUATION DATA

The fluctuation data consists of the loadcases and the amount of the loadcycles. The loadcases are separated in turbine and pump operations and the loadcycles are separated in different time periods. Each loadcycle consists of sinusoidal pressure fluctuations. The four main loadcases are separated into stop and shut down (trip) for each turbine and pump mode. For the loadcases fluctuation measurements exists from the pressure and strain fluctuations of the penstock.

The measured strain fluctuation has been converted to stress which have been combined with stress caused by hydrostatic pressure.

5.2 CALCULATION OF DAMAGE AND RESIDUAL LIFETIME

In a first step, the damage is calculated for one load cycle per load case. In the next step the damage for one load cycle is multiplied by the number of load cycles per time period. This was performed for all load cases and time periods. The sum of this damage per load cycles and different time periods represents the whole damage at the selected locations. Fig. 6 shows the wide scatter band of the remaining lifetime at selected positions along the penstock. The result covers a remaining lifetime starting with about 3 years up to several hundred years. As it can be revealed from measuring of misalignment and roof topping a wide scatter band of K_m factor in the shells is present. It can be concluded that the wide scatter of $\sigma_{max,static}$ acting in the shells (Fig. 4) including the strong influence of notch radius might confirm that a wide range of scatter of residual lifetime of the single shells have to be expected. To show the improvement of grinding a second fatigue calculation was made for 3 positions. Removing the notch radius increases the remaining lifetime clearly (Fig. 6).

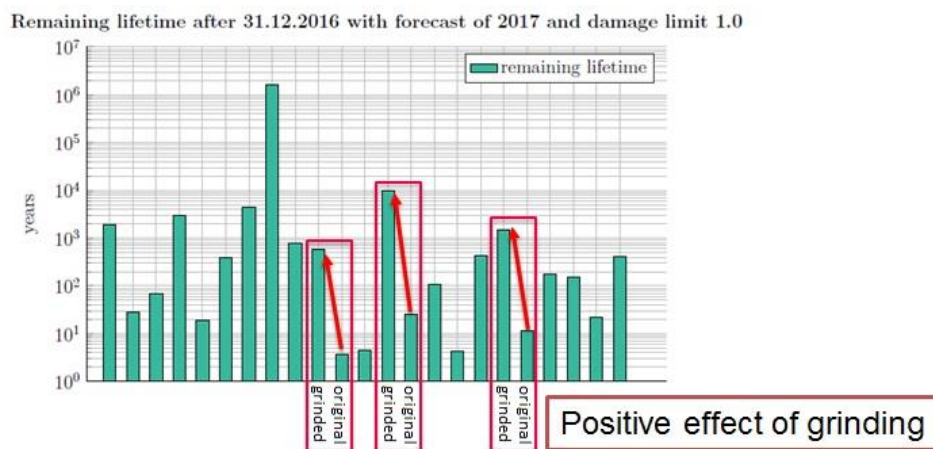


Fig. 6
Calculated remaining lifetime for selected local models

6 IMPROVING THE LIFE TIME BY MECHANICAL TREATMENT (GRINDING)

The question was if it is possible to determine those locations of the more than 600 measured positions which exceed the damage sum of $D = 1.0$ in 70 years if they are grinded during year 2017. The local models show detailed points of the

fatigue calculation (Fig. 6) but it is not legitimate to conclude from the results of the local models from 23 positions to the complete longitudinal welding seam of the penstock. For this fatigue calculation, the damage sum consists of the damage accumulated until year 2016 and the approach for 70 years of the damage if all locations are grinded during year 2017. The calculations had shown that the number of shells which exceeds damage $D \geq 1$ is increasing when the notch radius became smaller than $r_{-1\sigma} = 17$ mm (Table 1). Grinding and polishing of surfaces principally reduce the probability of fatigue crack initiation because of eliminating of local stress risers caused by microscopic roughness or notches. From this results the dominating influence of notch radius in addition on the existing geometric situation, represented by K_m factor is confirmed. Having the same K_m factor, the damage is dramatically in- respectively the residual lifetime is decreasing by smaller notch radii. Furthermore, it cannot be excluded, that within the entire length of welds outside and unknown weld length inside the pipe, positions exists with even smaller notch radii, which can increase the damage substantially. This observation explain clearly that the negative influence of notches will be eliminated by grinding of all welds.

Table 1
Number of shells, which probably exceed the damage limit in 70 years

notch radius	$D \geq 1$	$0.5 \leq D < 1$
$r_{+2\sigma} = 35\text{mm}$	1	8
$r_{+1\sigma} = 29\text{mm}$	1	8
$r_{\mu} = 23\text{mm}$	1	8
$r_{-1\sigma} = 17\text{mm}$	9	17
$r_{-2\sigma} = 11\text{mm}$	44	47

SUMMARY

The result of this study clearly confirms that geometric deviations of welded pipes like roof topping, misalignment cause serious increasing of acting stresses in penstocks of pumping storage power plants, which can cause serious reduction of expected lifetime of the installation. In addition remaining notches caused by the welding procedure increase dramatically the local stress situation which additionally to roof topping and misalignment increase fatigue caused damage. For existing plants the removal of local notches by grinding can effectively reduce the sensitivity to fatigue damaging. In any case safe service behaviour can only be achieved by controlled fabrication processes considering prevention of geometric deviations roof topping and misalignment and providing of notch free surfaces on the pipes by application of grinding or polishing.

Les résultats de cette étude confirment clairement que les déviations géométriques des tubes soudés en acier comme l'effet de toit, le désalignement engendrent une augmentation importante des contraintes agissant sur les conduites forcées des stations de pompage-turbinage, ce qui peut entraîner une réduction importante de la durée de vie prévue de l'installation. En outre, les entailles existantes dues au procédé de soudage amplifient considérablement le niveau de la contrainte locale qui, en plus de l'effet de et du désalignement, augmente le dommage causé par la fatigue. Pour les sites existants, l'élimination des entailles locales par arasage peut réduire efficacement la sensibilité au dommage par fatigue. Dans tous les cas, une exploitation fiable et sûr ne peut être obtenu que par des procédés de fabrication contrôlés, en tenant compte de la prévention des déviations géométriques, d'effet de toit et des désalignements et de l'obtention de surfaces exemptes d'entailles ou autres discontinuités géométriques par meulage ou polissage.

REFERENCES

- [1] MATTHIAS EHRHART, ed. 20151203-Rooftopping Misalignment d1 d2 all DRAFT.xls. Dec. 3, 2015
- [2] ADOLF HOBACHER ET AL. RECOMMENDATIONS FOR FATIGUE DESIGN OF WELDED JOINTS AND COMPONENTS . Tech. rep. International Institute of Welding, 2008.
- [3] MANFRED KASSNER ET AL. "FATIGUE DESIGN OF WELDED COMPONENTS OF RAILWAY VEHICLES – INFLUENCE OF MANUFACTURING CONDITIONS AND WELD QUALITY". In: *Welding in the World (2010)*.
- [4] ROLAND RENNERT ET AL. RECHNERISCHER FESTIGKEITSNACHWEIS FÜR MASCHINENBAUTEILE. aus Stahl, Eisenguss- und Aluminiumwerkstoffen . Tech. rep. Forschungskuratoriums Maschinenbau e.V. (FKM), 2012.
- [5] WAFO-group. WAFO - A Matlab Toolbox for Analysis of Random Waves and Loads - A Tutorial . ISBN XXXX. Math. Stat., Center for Math. Sci., Lund Univ. Lund, Sweden, 2011. url : <http://www.maths.lth.se/matstat/wafo> .

ATOM PROBE INVESTIGATIONS ON TEMPER EMBRITTLEMENT AND REVERSIBLE TEMPER EMBRITTLEMENT IN S 690 STEEL WELD METAL, TO EXPLAIN SUCCESSFUL REHABILITATION OF BRITTLE PENSTOCK WELDS

Em.Univ.-Prof. Dipl.-Ing. Dr.mont. Horst CERJAK

Emeritus Professor at Institute of Materials Science, Joining and Forming,
GRAZ UNIVERSITY OF TECHNOLOGY

AUSTRIA

Dr. techn. Francisca MENDEZ MARTIN

Senior Scientist of the Department Physical Metallurgy and Materials Testing, MONTANUNIVERSITÄT LEOBEN

AUSTRIA

During the hydrostatic pressure test of a penstock, in a brand new large pumped-storage hydropower plant, a spectacular brittle fracture of a closure head occurred. The embrittlement was located in the manifold weld seams as well as in the post weld heat treated welds of the completed penstock.

The reason for the failure was temper embrittlement (TE), produced by a low cooling rate during the post weld heat treatment, having a strong influence on the toughness of the weld material. Our investigations were focused on one side in the clarification of the failure cause and on the other side to clarify why by application of a short time heat treatment (starting at 10 seconds at 600° C) the toughness of the embrittled weld material significantly recovered - effect of reversible temper embrittlement (RTE).

In order to understand the mechanism of RTE, high resolution analytics as Atom Probe Tomography (APT) were applied. The investigations reveal phosphorus segregation in the high angle grain boundaries of the temper embrittlement material, see Fig. 1. When RTE treatment for few seconds was applied, phosphorus segregation in the grain boundaries disappears keeping the concentration of the other alloying elements unchanged.

The mechanism of this behavior could be explained by referring the Mc Lean [1] based grain boundary equilibrium segregation of phosphorous. Grain boundary impurities, as can be phosphorus, can produce embrittlement in steels which can be explained by electronic models based on quantum mechanical cluster

calculations. The impurity is electronegative with respect to the metal and draw charge from the metal onto themselves. As result, less charge is available to participate in the metal–metal bonds and they are weakened. By the application of a RTE treatment around 600°C, diffusion of the impurities elements occurs faster because segregation starts at lower temperatures (around 550°C) [2]. During RTE treatment, the diffusion is much faster, producing the fast recovery of toughness.

The brittleness occurred in the post weld heat treated penstock welding's could be recovered by site by application of qualified local electrical mat heating [3].

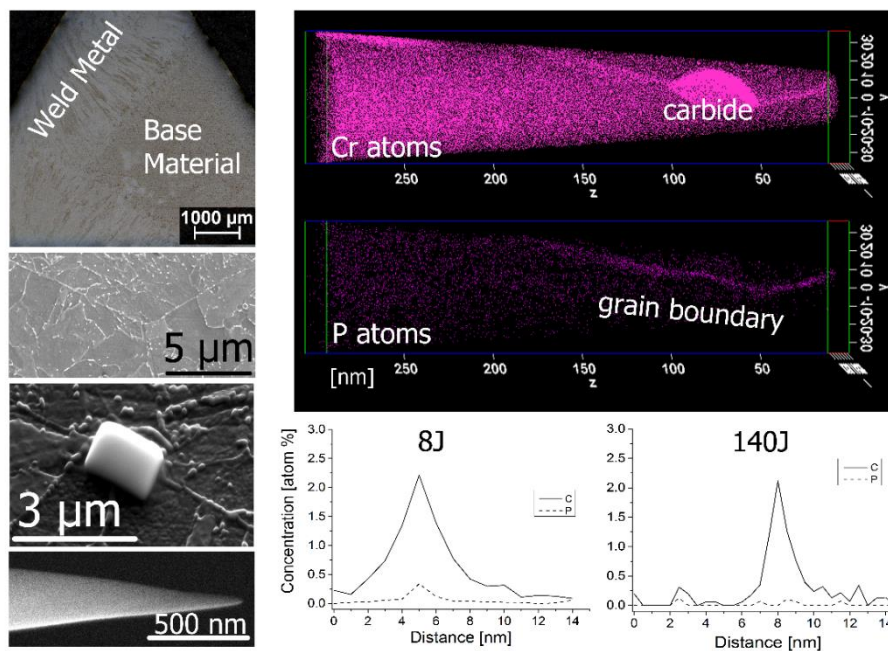


Fig. 1 shows the specimen preparation of a high angle grain boundary tip for atom probe tomography analysis. The results reveal segregation of phosphor at the high angle grain boundaries in the temper embrittled specimens (8J). The RTE specimens (140J) show phosphor free grains.

REFERENCES

- [1] McLEAN D. Grain boundaries in metals. *Oxford: Clarendon Press*, 1957.
- [2] CERJAK H., MENDEZ-MARTIN F. and DOMAKOVA M. Atom probe investigations on temper embrittlement and reversible temper embrittlement in S 690 steel weld metal, *Science and Technology of Welding and Joining*, 2017, Vol.23, 2.
- [3] CERJAK H., CALISKANOGLU O., ENZINGER N., FIGNER G., PUDAR M. Increasing of toughness of brittle type S690 HSS weld metal by application of reversible temper embrittlement (RTE), *Welding in the World*, 2017, Vol.61.

COMMISSION INTERNATIONALE DES GRANDS BARRAGES

VINGT-SIXIÈME CONGRÈS DES GRANDS BARRAGES
Autriche, juillet 2018

DOI 10.3217/978-3-85125-620-8-212



This work licensed under a Creative Commons Attribution 4.0 International License. <https://creativecommons.org/licenses/by-nc-nd/4.0/>

**SEISMOTECTONIC FEATURES AT RUDBAR LORESTAN DAM IN IRAN AND
RESERVOIR SLOPE STABILITY DURING FIRST IMPOUNDMENT**

Martin WIELAND

*Chairman, ICOLD Committee on Seismic Aspects of Dam Design, POYRY
SWITZERLAND LTD., Zurich*

SWITZERLAND

Mohammad HAJILARI

Senior Engineering Geologist, POYRY SWITZERLAND LTD., Tehran

IRAN

COMMISSION INTERNATIONALE
DES GRANDS BARRAGES

VINGT-SIXIÈME CONGRÈS DES
GRANDS BARRAGES
Autriche, juillet 2018

SEISMOTECTONIC FEATURES AT RUDBAR LORESTAN DAM IN IRAN AND RESERVOIR SLOPE STABILITY DURING FIRST IMPOUNDMENT

Martin WIELAND

*Chairman, ICOLD Committee on Seismic Aspects of Dam Design, POYRY
SWITZERLAND LTD., Zurich*

SWITZERLAND

MOHAMMAD HAJILARI

Senior Engineering Geologist, POYRY SWITZERLAND LTD., Tehran

IRAN

1. MAIN FEATURES OF RUDBAR LORESTAN DAM PROJECT

1.1 THE RUDBAR LORESTAN DAM PROJECT

The Rudbar Lorestan dam project shown in Fig. 1, located in a narrow canyon, comprises (i) a 156 m high earth core rockfill dam with a crest length of 185 m, (ii) two ungated tunnel spillways, with a length of 631 m and a total discharge capacity of 3342 m³/s, and (iii) two bottom outlets. The dam body has a volume of 4.36 Mm³ and was completed in 2016. The reservoir volume and surface area are 228 Mm³ and 4.1 km², respectively. The power intake structure is at the right abutment near the dam. Twin penstocks, each about 2.2 km long, cross a long bend of the Rudbar River to serve a surface powerhouse. The head of the project is 430 m and the installed capacity of the two Francis turbines is 460 MW.

The main challenging features of this project are the location of the dam in a very narrow gorge, the high seismicity of the dam site and the presence of discontinuities and faults in the footprint of the dam.



Fig. 1

View of downstream face of Rudbar Lorestan rockfill dam with two spillway tunnels on left bank and two bottom outlets

1.2 MULTIPLE SEISMIC HAZARDS AT DAM SITE

The main seismic hazards of the Rudbar Lorestan dam site are:

- (1) Ground shaking causing inelastic deformations in dam body;
- (2) Movements at discontinuities in footprint of the dam that can cause distortions in the dam body and offsets in the filters;
- (3) Mass movements (rockfalls, landslides) causing damage to dam crest, power intake structure and bottom outlet, block intake of bottom outlet, or causing impulse waves in the reservoir and overtopping of the dam crest; and
- (4) Reservoir-triggered seismicity (RTS) [3] and [7].

There are other seismic hazards, which can affect large dam projects as discussed in [5] and [6].

Ground shaking: Ground shaking is the main seismic hazard addressed in all design guidelines. The other hazards listed above may not be relevant for most dam sites, therefore, they are rarely included in seismic design guidelines and thus may be ignored or forgotten. The peak ground acceleration of the worst-case earthquake scenario at Rudbar Lorestan dam site, i.e. a magnitude 7.5

earthquake along a major fault at a distance of about 1.5 km from the dam site, was estimated as 0.74 g (horizontal component on outcropping rock).

Fault movements: Seismotectonic studies at the dam site revealed different faults and discontinuities in the footprint of the dam. The faults are not seismogenic but rather secondary or splay faults, where movements may occur during strong nearby earthquakes. The maximum observed single event fault movement was 1.2 m along a relatively short fault, which has created a cumulative dislocation of about 8 m. Some of the faults are sub-parallel with almost identical features as found during excavation of the dam foundation. There are other discontinuities in different directions, i.e. fissures, joints, bedding planes, shear zones, and faults, which could experience different degrees of block-type movements as the limestone rock is of brittle nature. As there was no suitable material in the faults, dating of the last fault movements was not possible. Because of the complexity of the seismotectonics at the dam site and the difficulties in estimating possible movements along the different discontinuities, maximum horizontal and vertical movements were assigned to the main faults and discontinuities. For the main faults the horizontal and vertical design displacements were specified as 2 m and 1 m, respectively. Smaller displacement values were assigned to the other discontinuities. However, the dam design was governed by the larger displacements. The unique feature is that there are several faults and discontinuities in the footprint of the dam with different orientation, which could experience movements during a strong earthquake. In the selection of the dam type and dam design, these movements played an important role. At the time of the design, it was not possible to exclude such displacements, therefore they had to be considered in the design.

Mass movements: At dam sites, mass movements (landslides and rockfalls) are the seismic hazards that are often underestimated. Depending on their consequences, the stability of the dam abutments and reservoir banks has to be checked for different types of design earthquakes. For example, if the intake of the bottom outlet will be blocked by debris, then the slope must be stable for the ground motion of the safety evaluation earthquake (SEE), which in the case of a deterministic worst-case earthquake scenario is equal to the ground motion of the maximum credible earthquake (MCE). For other slopes with no dam safety consequences, the slopes must be stable for smaller earthquakes, as for example, those specified in building codes.

Reservoir-triggered seismicity: If a large dam has been designed according to the current state-of-practice, which requires that the dam can safely withstand the ground motions caused by the SEE, it can also withstand the effects of the largest reservoir-triggered earthquake, as the maximum reservoir-triggered earthquake cannot be stronger than the SEE. Thus, RTS is not a safety problem for a well-designed dam or the people who could be at risk in the case of a dam failure. However, RTS may still be a problem for the buildings and structures in the dam and reservoir area, because in seismic building codes the ground motion parameters are given for return periods of 475 years, whereas for large storage dams the corresponding value is 10,000 years. In the great majority of RTS, the magnitudes are small and of no structural concern. Up to now, the maximum magnitude of reservoir-triggered earthquakes is 6.3. As the correlation between

the filling of the reservoir and the occurrence of a damaging earthquake in the reservoir region is extremely weak, severe doubts remain if some of the largest observed earthquakes are actually RTS events. Therefore, dam owners would object to the classification of strong earthquakes in the reservoir region of large storage dams as being triggered by the reservoir [3] and [7].

2. SEISMIC DESIGN ASPECTS OF RUDBAR LORESTAN DAM

2.1 CONCEPTUAL SEISMIC DESIGN GUIDELINES FOR EMBANKMENT DAMS

The seismic design of embankment dams is based on (i) conceptual criteria, which are mainly based on the observation of the behaviour of embankment dams during strong earthquakes and the behaviour of soils and rockfill under dynamic loadings, and (ii) the results of seismic analysis of dams subjected to different types of design earthquakes. Usually several earthquakes must be analyzed – at least three. As a basis for the dynamic analysis a static analysis that simulates the incremental construction of the dam body and the filling of the reservoir and if applicable a seepage analysis must be performed first before the earthquake ground motion can be applied. The basic conceptual criteria are as follows [1].

- 1) Foundations must be excavated to very dense materials or rock; alternatively, the loose foundation materials must be densified, or removed and replaced with highly compacted materials, to guard against liquefaction or strength loss.
- 2) Fill materials, which tend to build up significant pore water pressures during strong shaking must not be used.
- 3) All zones of the embankment must be thoroughly compacted to prevent excessive settlements during an earthquake.
- 4) All embankment dams, and especially homogeneous dams, must have high capacity internal drainage zones to intercept seepage from any transverse cracking caused by earthquakes, and to assure that embankment zones designed to be unsaturated remain so after any event that may have led to cracking.
- 5) Filters must be provided on fractured foundation rock to preclude piping of embankment material into the foundation.
- 6) Wide filter and drain zones must be used.
- 7) The upstream and/or downstream transition zones should be self-healing, and of such gradation as to also heal cracking within the core.
- 8) Sufficient freeboard should be provided in order to cover the settlement likely to occur during the earthquake and possible water waves in the reservoir due to mass movements etc.

- 9) Since cracking of the crest is possible, the crest width should be wider than normal to produce longer seepage paths through any transverse cracks that may develop during earthquakes.
- 10) One of the most dangerous consequences of the dynamic loading of an embankment dam is the liquefaction of foundations or embankment zones that contain saturated fine-grained cohesionless and/or uncompacted materials.

2.2 DAMS ON ACTIVE OR POTENTIALLY ACTIVE FAULTS OR DISCONTINUITIES

In designing dams for fault movements, the following situations have to be considered:

- active or potentially active fault passing through the dam foundation (footprint of dam),
- multiple faults passing through the dam foundation or fault with wide fractured zone, and
- dam located in the near-field of a major fault, which is capable of producing large magnitude earthquakes: if fault displacements spread as far as the dam site, they can cause movements along fractures or secondary faults in the dam foundation.

In [2] the following recommendations are given:

- 1) When a major active fault is crossing the dam foundation the site should be abandoned and a more appropriate site should be looked for.
- 2) In highly seismic areas it may not be possible to find any site without fault slip hazard: In such a case, concrete dams should be avoided and preference be given to a conservatively designed embankment dam, designed with ample filter and transition zones, on both sides of a rather wide core, displaying ductile properties. There is a considerable confidence that such a structure can withstand, without failure, significant fault offsets.
- 3) If the seismotectonic conditions at a dam site are not clear, then the engineer should avoid concrete dams and select a conservatively designed embankment dam.

In highly seismically active regions, such as the Zagros Mountain Range in Iran, most of the faults could be potentially active or could undergo some movements by nearby strong earthquakes. Therefore, conservatively designed rockfill dams with earth core might be the safest seismic solution.

2.3 GENERAL GUIDELINES FOR THE DESIGN OF DAMS ON FAULTS

The basic ingredients of an embankment dam, which can resist both differential ground movements and strong earthquake ground shaking, are the following [1] and [2]:

- 1) Impervious core made of ductile material with a high failure strain to minimize the propagation of the rupture zone; prevention of internal erosion if core is cracked;
- 2) Thick filter and transition zones: about 50% shall still be available after faulting and slip movements;
- 3) Wide dam crest;
- 4) Flat slopes;
- 5) Generous freeboard: to prevent overtopping due to possible impulse waves in reservoir and settlement of the dam crest; and
- 6) Material selection and compaction of rockfill.



Fig. 2

View of core, filter and transition zones near the left abutment (top left), 5 m wide contact clay zone and treatment of rock surface in the core zone by shotcrete (top right) and detail of widened fine sand filter at the right abutment (bottom)

The main concern of any embankment dam with impervious core is the erosion resistance of the core material. The filter and transition zones provide the first line of defense against cracks in the core, adequately graded, cohesionless transitions are provided. A leak can only get out of control if embankment distortions exceed the width of the thin sand filter.

In view of the high seismic hazard from ground shaking and fault movements in the footprint of the dam and in order to account for the possible arching due to the location of the dam the following design features of the dam were provided as shown in Fig. 2:

- 1) Large freeboard,
- 2) Thick filter zone consisting of fine sand filter, coarse sand filter and transition zone, each 5 m thick, located at upstream and downstream faces of the core, to control internal erosion from seepage through any cracked portions of the core
- 3) Widening of the fine sand filter from 5 m to 10 m at the downstream faces of the core near the abutments to prevent contact erosion due to seepage along the abutment, and
- 4) Provision of a 5 m wide plastic clay zone at the interface with the rock abutment, in order to minimize any arching effects in the core and to increase compressive stresses in all zones of the core.

Ultimately, the seismic safety depends on the quality of the work done by the contractor. Moreover, in the core high pore pressure were induced in the core during construction, which do not deviate much from the pore pressure due to the long-term seepage process. This will minimize any seepage movements in the core and can be considered as a special type of “pre-stressing”.

2.4 SEISMIC DESIGN AND PERFORMANCE CRITERIA OF DAM BODY

The following design earthquakes are specified for large dam projects according to ICOLD [4]:

- (1) Safety Evaluation Earthquake (SEE): The SEE is the earthquake ground motion a dam must be able to resist without uncontrolled release of the reservoir. The SEE is the governing earthquake ground motion for the safety assessment and seismic design of the dam and safety-relevant components (spillway and low level outlets), which have to be functioning after the SEE.
- (2) Operating Basis Earthquake (OBE): The OBE may be expected to occur during the lifetime of the dam. No damage or loss of service must happen. It has a probability of occurrence of about 50% during the service life of 100 years. The return period is taken as 145 years [4]. The OBE ground motion parameters are estimated based on a PSHA. The mean values of the ground motion parameters of the OBE can be taken.

The SEE ground motion parameters can be obtained from a probabilistic and/or a deterministic seismic hazard analysis, i.e.

- Maximum Credible Earthquake (MCE): The MCE is the event, which produces the largest ground motion expected at the dam site on the basis of the seismic history and the seismotectonic setup in the region. It is estimated based on deterministic earthquake scenarios. According to [4] the ground motion parameters of the MCE shall be taken as the 84 percentiles (mean plus one standard deviation).

- Maximum Design Earthquake (MDE): For large storage dams the return period of the MDE is taken as 10,000 years. The MDE ground motion parameters are determined based on a probabilistic seismic hazard analysis (PSHA). According to [4] the mean values of the ground motion parameters of the MDE shall be taken.

The general performance criteria for large storage projects are as follows:

- (1) The dam must be able to safely retain the water in the reservoir during and after the SEE. No uncontrolled release of large quantities of water that may flood the downstream area is accepted, however inelastic deformations are accepted. The stability of the dam must be ensured.
- (2) It must be possible to control the reservoir level after the SEE.
- (3) It should be possible to lower the reservoir level after the SEE to carry out any repair works on the upstream face of the dam or to increase the safety of the dam in case of doubts about its seismic safety.

3. STABILITY OF RESERVOIR BANKS DURING FIRST IMPOUNDMENT

The slow sliding of a rock mass into the reservoir may rise the lake level. But in the case of a fast slip into the reservoir an impulse wave will be generated, which, depending on the geometry of the reservoir and the direction of the impulse direction of the sliding mass may cause damage along the shoreline and the dam. The most severe event would be an overtopping of the dam. Calculation methods to estimate the height of such waves are available. Landslides also reduce the active storage volume of the reservoir.

From a dam safety point of view, the slope stability in the narrow reservoir of the Rudbar Lorestan project is of great importance particularly in the area near the dam (up to about 2 km). Any instability of the slopes (rock, overburden or spoil materials) may create impulse waves in the reservoir.

Among several potential unstable zones in the area close to the dam, five potential sliding zones including two spoil areas plus three zones composed of overburden materials were identified prior to reservoir impounding. Another three Areas at greater distance from the dam were also considered, but due to the geometry of the reservoir, these slides could not generate waves that could overtop the dam.

For each unstable zone a simplified impulse wave analysis was carried out. The results showed that at the dam, the maximum wave run-up could reach up to 8.8 m above the reservoir normal water level. The freeboard provided for the dam is 9 m, which is higher than the maximum estimated wave run-up.

The total volume of the sliding mass of all identified zones located above the normal water level is about 4.5 Mm³. A simultaneous failure of these slopes and the sliding into the reservoir would induce a change in the reservoir elevation of 0.85 m, which is negligible compared to the maximum height of impulse waves and the available freeboard of 9 m.

During the first filling of the reservoir, several sliding movements were observed. The largest slope movement occurred at the right reservoir bank at a distance of 7.1 km from the dam. The first signs of slope movements were detected on October 7, 2016. Two months later, a vertical escarpment with a height of up to 15 m was formed as shown in Fig. 3, when the reservoir reached the sill level of the free-flow spillway. In the following months, the reservoir level has decreased due to the start of operation of the first unit in the powerhouse. Since then, no further movements have occurred, although this slope remains unstable and further movements may develop if the reservoir level is increased or lowered. Heavy rainfall in winter and spring and strong earthquake are additional triggers of natural slopes or slopes partially submerged by the reservoir. The consequences of failure of this slope will be relatively small on the dam, due to the great distance to the dam and due to the geometry of the reservoir.



Fig. 3

Unstable mass with vertical scarp of up to 15 m triggered during reservoir impounding (distance to dam: approx. 7.1 km; volume: 1.5-2.5 Mm³) (photo taken May 5, 2017)

Several other rock slope failures were observed on the right bank of the reservoir as shown in Fig. 4. These failures occurred relatively slowly and did not cause any impulse waves in the reservoir. Nevertheless, due to the steep slopes and the possibility of mass movements, the number of people staying at the upstream face of the dam, were requested to stay away from the reservoir.

Furthermore, due to water wave action several small slides developed in zones with loose material on both reservoir banks as shown in Fig. 5. Although

there are several mass movements observed during impounding of the reservoir, none of them has created any impulse wave yet.



Fig. 4

Local failure of rock slopes during reservoir impounding (distance to dam: approx. 4.3 km; volume: 0.4 Mm³)



Fig. 5

Local slides in loose material on left bank, caused by surface waves in reservoir

Besides mass movements into the reservoir, mass movements could be triggered by the operation of the spillway due to the wetting of loose overburden materials above the plunge pool or erosion of the relatively weak rock. Tests of the bottom outlets were carried out, while construction of the plunge pool was not yet completed. Such tests have caused substantial river bank erosion. But these phenomena are not related to the impounding of the reservoir.

Finally, due to the almost vertical rock abutments and the presence of loose rocks at high elevations, it is expected that extensive rockfalls could be triggered by strong earthquakes. These rockfalls are not considered as a threat to the dam body, but may prevent access to the dam, damage the road surface near the abutments and may damage the power intake structure, spillway chute and others. For that reason, rockfall protections have been provided in the portal areas of the surface penstocks and the two surge tanks. Stabilization of the loose rocks above the dam is very difficult.

Due to the high seismicity of the dam site, a microseismic monitoring system was installed, to monitor any signs of reservoir-triggered seismicity. The network consists of 7 stations at distances from 8-25 km of the dam site and cover the reservoir and the most important faults around the project. Up to now,

the largest recorded magnitudes were less than 3 and no changes in seismicity patterns were observed.

4. CONCLUSIONS

In the seismic design of the Rudbar Lorestan rockfill dam the following items are of main concern:

- (1) The seismic hazard is a multi-hazard for most dam projects. Ground shaking is the main hazard considered in all earthquake guidelines for dams and other structures.
- (2) Movements of active faults in the footprint of a dam or movements at discontinuities (faults, joints, bedding planes), which can be activated during strong nearby earthquakes, are the most critical seismic hazards for most dams. A conservatively designed earth core rockfill dam with wide filter and transition zones is the only feasible solution for such sites.
- (3) Due to the topography, geology and the rock properties, mass movements affect the reservoir, the dam body and all appurtenant structures as well as access roads. Slope stability problems have been observed during impounding of the Rudbar Lorestan reservoir. Many more mass movements will occur during strong earthquakes.
- (4) Impounding of the reservoir has not caused any changes in the seismicity of the dam and reservoir region. Reservoir-triggered seismicity is monitored by a dedicated microseismic network.
- (5) The Rudbar Lorestan earth core rockfill dam includes several advanced features such as (i) wide filter zones, which are widened towards the abutments (doubling of width of fine sand filter at the downstream side of the dam), (ii) a wide impermeable core with a plastic clay zone at the core-abutment contact, in order to minimize any tensile cracks in the core, and (iii) a generous freeboard to account for large seismic deformations of the dam and the run-up of impulse waves due to mass movements into the reservoir.

Up to now, the dam behavior has been as expected. Despite all the antiseismic design features provided by the consultant, we shall not forget that it is equally important that the dam contractor is doing a perfect job.

ACKNOWLEDGEMENTS

This article is published with the permission of Iran Water and Power Resources Development Company as owner of the Rudbar Lorestan Dam and Hydropower Project.

REFERENCES

- [1] ICOLD. Design Features of Dams to Effectively Resist Seismic Ground Motion, Bulletin 120, Committee on Seismic Aspects of Dam Design, ICOLD, Paris, 2001.
- [2] ICOLD. Neotectonics and Dams, Bulletin 112, Committee on Seismic Aspects of Dam Design, ICOLD, Paris, 1998.
- [3] ICOLD. Reservoirs and Seismicity - State of Knowledge, Bulletin 137, Committee on Seismic Aspects of Dam Design, ICOLD, Paris, 2011.
- [4] ICOLD. Selecting Seismic Parameters for Large Dams, Guidelines, Bulletin 148, Committee on Seismic Aspects of Dam Design, ICOLD, Paris, 2016.
- [5] WIELAND M. Seismic Aspects of Dams, General Report, Q.83 Seismic Aspects of Dams. Proc. 21st Int. Congress on Large Dams, Montreal, 2003.
- [6] Wieland M. Features of Seismic Hazard In Large Dam Projects and Strong Motion Monitoring of Large Dams, Int. Journal Front. Archit. Civ. Eng. China, December 2009.
- [7] Wieland M. Reservoir-Triggered Seismicity and Effect on Seismic Design Criteria for Large Storage Dams, Proc. 16th World Conf. on Earthquake Engineering, 16WCEE, Santiago de Chile, Chile, Jan. 9-13, 2017.

SUMMARY

The 156 m high Rudbar Lorestan earth core rockfill dam, located in a narrow canyon in the seismically very active Zagros Mountain Range in Iran, had to be designed against multiple seismic hazards including ground shaking, movements along discontinuities in the footprint of the dam caused by nearby strong earthquakes, and rockfalls. Furthermore, in view of the proximity of a large fault, reservoir-triggered seismicity may occur during impounding and the first years of operation of the reservoir. The main concerns in the dam design were the discontinuities formed by joints, bedding planes, fissures and faults although there exist no active faults in the dam foundation, which could produce large earthquakes. The special design features of the dam, to cope with movements along multi-directional discontinuities in the footprint of the dam and the deformations in the dam body due to ground shaking are discussed. Construction of the dam body was completed in 2016 and first reservoir impounding was done in early 2017. The possible hazards from the failure of steep slopes in the reservoir are presented. The different types of slope failures and wave erosion of the slopes, observed during the first impounding of the reservoir, are described. The volume of the largest activated slope is about 1.0-1.5 Mm³. Further mass movements could be triggered in the future by earthquakes or heavy rainfalls.

KEYWORDS

Rudbar Lorestan dam, rockfill dam, seismic hazard, seismic design, active faults, slope stability, reservoir impoundment

COMMISSION INTERNATIONALE DES GRANDS BARRAGES

VINGT-SIXIÈME CONGRÈS DES GRANDS BARRAGES
Autriche, juillet 2018

DOI 10.3217/978-3-85125-620-8-213



This work licensed under a Creative Commons Attribution 4.0 International License. <https://creativecommons.org/licenses/by-nc-nd/4.0/>

**EVOLUTION OF STABILITY OF THE VERNAGO RESERVOIR SLOPE UNDER
WATER LEVEL VARIATION, DURING SIXTY YEARS OPERATIONS**

Francesco FEDERICO

DEPARTMENT OF CIVIL ENGINEERING AND INFORMATION ENGINEERING,
UNIVERSITY OF ROME 'TOR VERGATA', ROME

ITALY

Marina MAESTRI

ALPERIA S.p.a., BOZEN

ITALY

Chiara CESALI

DEPARTMENT OF CIVIL ENGINEERING AND INFORMATION ENGINEERING,
UNIVERSITY OF ROME 'TOR VERGATA', ROME

ITALY

Martina CACCIOTTI

Civil Engineer, ROME

ITALY

COMMISSION INTERNATIONALE
DES GRANDS BARRAGES

VINGT-SIXIÈME CONGRÈS DES
GRANDS BARRAGES
Autriche, juillet 2018

EVOLUTION OF STABILITY OF THE VERNAGO RESERVOIR SLOPE UNDER WATER LEVEL VARIATION, DURING SIXTY YEARS OPERATIONS

Francesco FEDERICO^(*); Marina MAESTRI^(**); Chiara CESALI^(*);
Martina CACCIOTTI^(***)

() Department of Civil Engineering and Information Engineering,
UNIVERSITY OF ROME 'TOR VERGATA', ROME
(**) ALPERIA S.p.a., BOZEN; (***) Civil Engineer, ROME*

ITALY

1. INTRODUCTION

The earthfill dam of Vernago is located in the east portion of the Alps, in northern Italy, and intercepts the Senales River (tributary on the left of the Adige River), giving rise to an artificial reservoir which feeds the Naturno hydroelectric power plant, managed by Alperia Spa. The dam has about 55 m maximum height and its length at the top is about 480 m. In standard operation, a single drawdown and filling cycle of the reservoir takes place each year [1]. Consequently, the water level ranges from 8 to 48 m from the bottom of the dam.

The slope bounding on the rightside the reservoir of Vernago (Fig. 1a) showed slow and small movements associated with each drawdown-filling cycle, mainly occurring in the glacial deposit that hosts the experimentally observed sliding surface [1]. These monitored movements, first recorded during the early '70s, suggested the need of geophysical and geotechnical investigations.

Inclinometer measurements showed that the displacements generally increase during the slow reservoir drawdown [2],[3]. To reduce its strain rate and increase its safety, a stabilizing berm at the bottom of the slope was built (Fig. 1b). *Piezometer readings* revealed differences between the reservoir water level (r.w.l.) and the piezometric head (p.h.) within the upper portion of the slope, during operation; therefore, a transient seepage flow regime occurs [4],[5],[6],[7].

Regression analyses preliminarily allowed to identify the correlation between the cumulated measured displacements and the variation of the r.w.l.. The effectiveness of the stabilizing berm is confirmed by the reduction of the rate of displacement accumulation (Fig. 3) [1],[7].

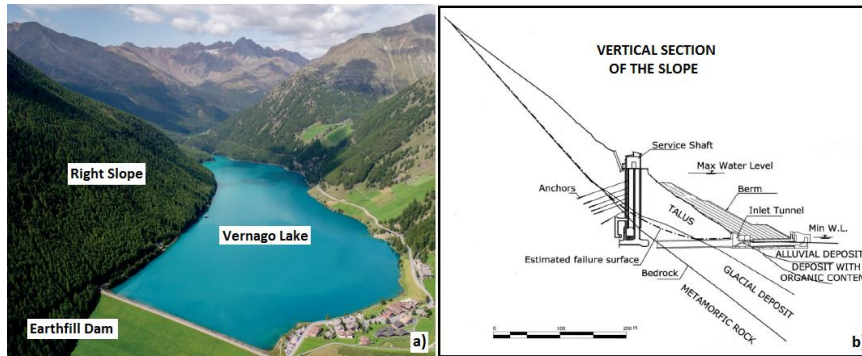


Fig. 1. a) Aerial view of the Vernago reservoir; b) Vertical section of the slope

2. REGRESSION ANALYSES OF INCLINOMETERS MEASURES

Slope displacements are monitored through several inclinometers [8],[9]; particularly, horizontal slope displacements refer to the T3, TM, TB, T4 inclinometers, located in front of the service shaft [9], at the elevation 1692 m a.s.l., and to the T5 and T6 inclinometers behind the shaft, at the elevation 1720 m a.s.l. (Fig. 2). In the period 1983-1999 the measures were not regularly recorded; few measures are thus available for the years 1987, 1990, 1991, 1993, 1995, 1996 and 1999. From 1999 until August 2015, the measurements were carried out every six-month, approximately; in the period of construction of the stabilizing berm (2000-2001), a greater frequency of measures was observed. From August 2015 until February 2016, due to a particular operation, the slope displacements were measured every 15 - 20 days.

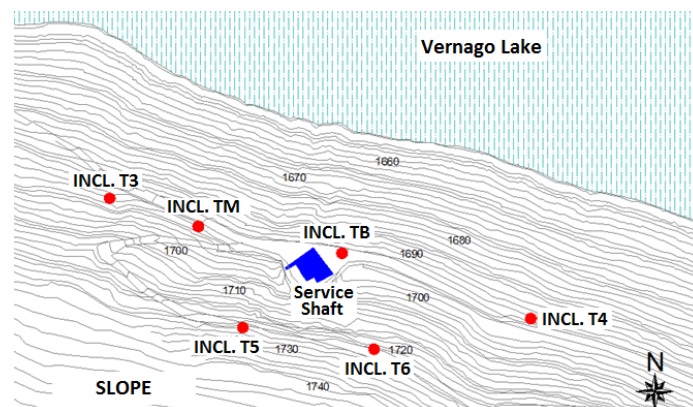


Fig. 2. Location of inclinometers

The measured slope displacements exhibit both reversible and non-reversible components [1],[7],[8],[9], the later generally increasing during the slow reservoir drawdown (Fig. 3); these movements are not uniformly distributed along the cross (towards the reservoir) and longitudinal directions.

To analytically describe the dependence of the slope movements on the variation in the reservoir water level (r.w.l.), regression analyses of the inclinometric measures have been carried out [7]. These analyses take into account the construction of the stabilizing berm, as well as the operation conditions (law of variation of r.w.l.). Therefore, the displacements (at the ground level) measured through the T3, T4, T5, T6 inclinometers have been distinguished during the following periods: *i*) 1982-1999 (before the construction of the berm); *ii*) 2009-2013 (after). The filling/drawdown cycles in these periods have been schematized to identify the governing hydraulic variables (e.g. H_{max} and H_{min} , that are the max and minimum reservoir water levels [m a.s.l.]; $\Delta T_{max,fill}$, the persistence period of H_{max} [days]; $\Delta t_{filling/drawdown}$, the duration of the filling/drawdown phase [days]; $v_{fill/dd}$, the rate of change in water level during the filling/drawdown phase [m/day]) on which the slope displacements could depend (Fig. 4). The following general relationship has been thus developed [7]:

$$s = C_0 + C_1 \cdot H_{max} + C_2 \cdot H_{min} + C_3 \cdot v_{fill/dd} + C_4 \cdot \Delta T_{max,fill} \quad [1]$$

s [cm] being the horizontal displacement (h.d.) of the slope occurred from the initial time instant of the considered period (relative h.d.); C_0, C_1, C_2, C_3, C_4 , the multiplier constants, derived from the regression analysis, related to the considered inclinometers (Table 1). The best agreement between the theoretical and measured displacements, for both periods (before and after the construction of the berm), is observed for the T4 and T6 inclinometers (Fig. 5).

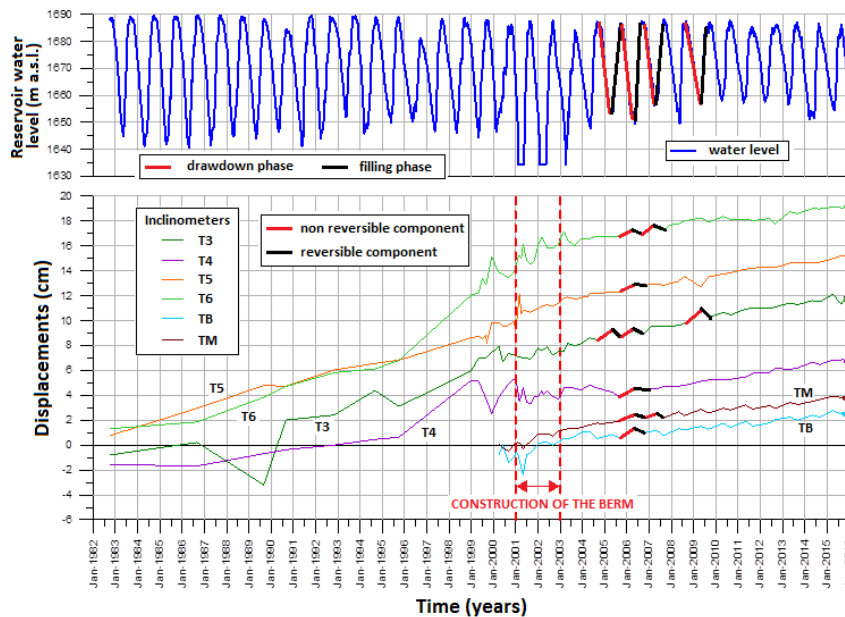


Fig. 3. Cumulated displacements measured through inclinometers

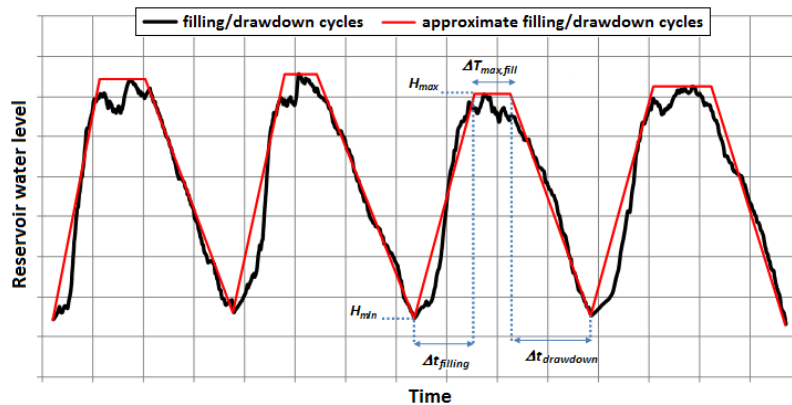


Fig. 4. Definition of the variables on which slope displacements depend.

The comparison between the relationships referred to the two considered periods show the effectiveness of the variation in the reservoir water level excursion (increase of H_{min} and decrease of H_{max}) and the construction of the berm (increase of effective normal stresses at the slope toe) in the reduction of the rate of the slope cumulated displacements (Fig. 6). Furthermore, the relationships obtained from the regression analyses (Table 1) of the slope displacements measured after the construction of the berm (2009-2013) have been applied to back analyze the displacements measured during filling/drawdown cycles (2006-2008), different from which previously considered [7].

Table1. Relationships from regression analyses for the T3, T4, T5, T6 inclinometers (R^2 = regression coefficient).

Period: 1982 - 1999 (before the construction of the berm)		
Incl.	Relationship	R^2
T3	$s = 479.8 - 0.75 \cdot H_{max} + 0.47 \cdot H_{min} + 14.0 \cdot v_{fill/dd} + 0.14 \cdot \Delta T_{max,fill}$	0.70
T4	$s = 783.4 - 0.46 \cdot H_{max} - 0.0003 \cdot H_{min} + 1.29 \cdot v_{fill/dd} - 0.013 \cdot \Delta T_{max,fill}$	0.96
T5	$s = 343.9 - 0.16 \cdot H_{max} - 0.044 \cdot H_{min} + 1.67 \cdot v_{fill/dd} - 0.010 \cdot \Delta T_{max,fill}$	0.97
T6	$s = 948.7 - 0.55 \cdot H_{max} - 0.01 \cdot H_{min} + 0.25 \cdot v_{fill/dd} - 0.013 \cdot \Delta T_{max,fill}$	0.90
Period: 2009 - 2013 (after the construction of the berm)		
Incl.	Relationship	R^2
T3	$s = -3.56 + 0.025 \cdot H_{max} - 0.023 \cdot H_{min} - 1.34 \cdot v_{fill/dd} + 0.0001 \cdot \Delta T_{max,fill}$	0.53
T4	$s = 94 - 0.037 \cdot H_{max} - 0.0187 \cdot H_{min} + 0.63 \cdot v_{fill/dd} + 0.002 \cdot \Delta T_{max,fill}$	0.86
T5	$s = 322 + 0.135 \cdot H_{max} - 0.332 \cdot H_{min} + 0.17 \cdot v_{fill/dd} + 0.00003 \cdot \Delta T_{max,fill}$	0.49
T6	$s = 265.2 + 0.008 \cdot H_{max} - 0.17 \cdot H_{min} - 1.62 \cdot v_{fill/dd} + 0.004 \cdot \Delta T_{max,fill}$	0.81

The appreciable agreement of the theoretical results with the in situ measures (Fig. 7) demonstrates the time cyclicity of the slope displacements.

Thus, the same relationships can be also applied to approximately estimate slope displacements evolutions following new operation procedures [7].

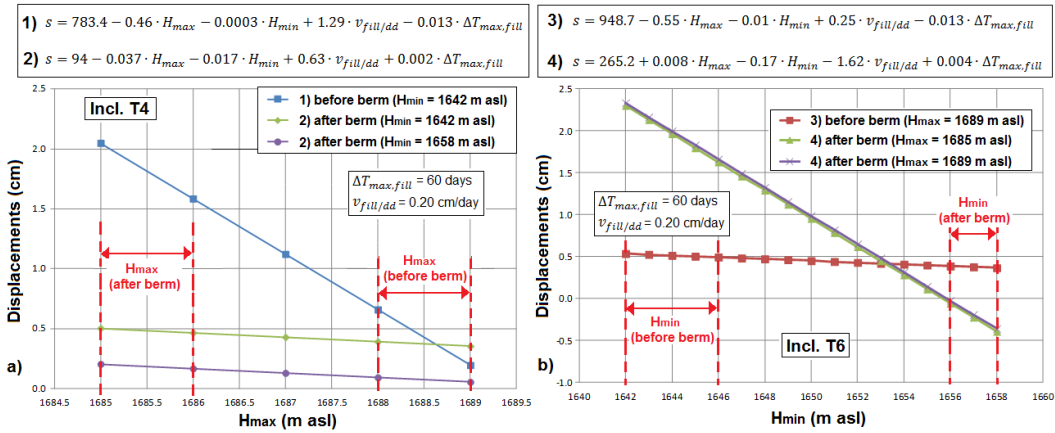


Fig. 5. Measured vs theoretical displacements, before and after the construction of the berm, for the a) T4 and b) T6 inclinometers, respectively

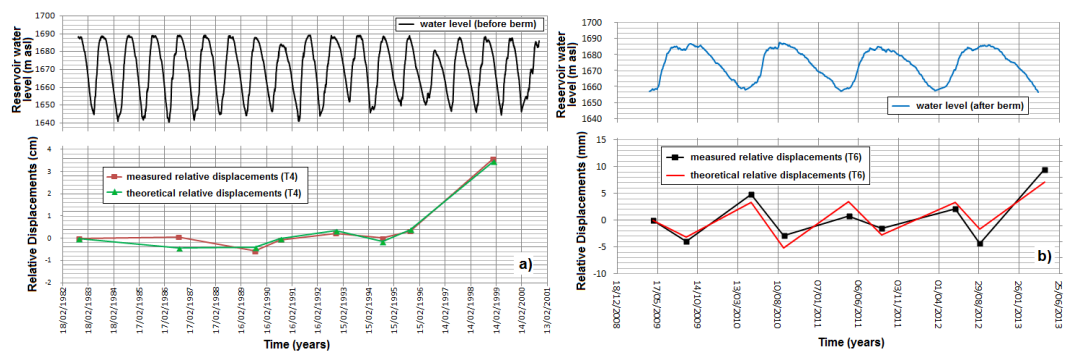


Fig. 6. Theoretical displacements for a) T4 and b) T6 inclinometers

3. COUPLED SEEPAGE AND STABILITY NUMERICAL ANALYSES

To measure the piezometric heads (p.h.) within the slope of the Vernago reservoir, 3 open standpipe piezometers and 8 Casagrande piezometers were installed [7],[8],[9].

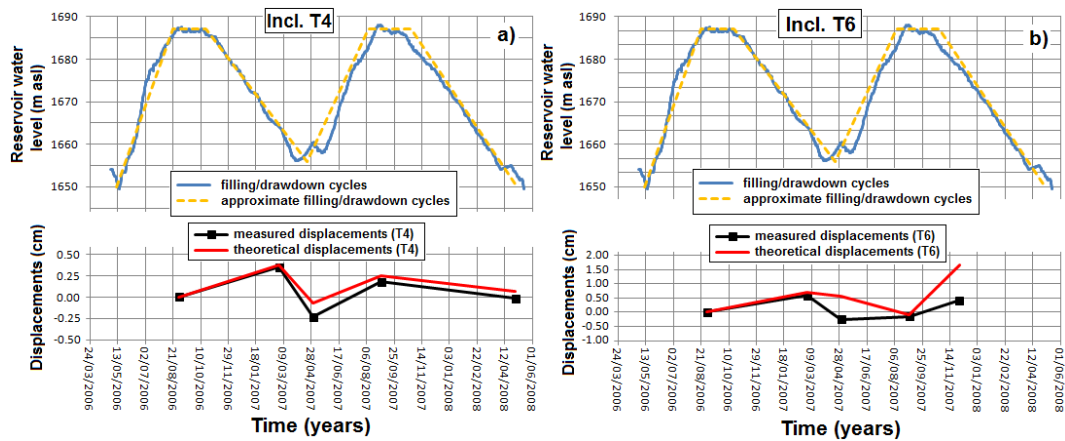


Fig. 7. Theoretical vs measured displacements for the period 2006-2008

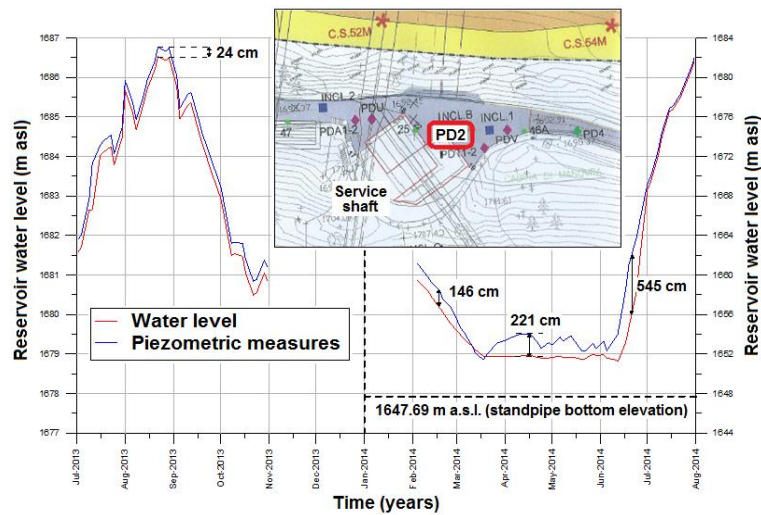


Fig. 8. Piezometric head measurements vs reservoir water level

P.h. measurements through the PD2 open standpipe piezometer (located near the service shaft [9]) revealed differences (Δh) between the reservoir water level and the piezometric head within the upper portion of the slope subjected to movements during operations (Fig. 8). Particularly, the progressive saturation of the slope during the filling phase is slower than its desaturation during the drawdown phase: in particular, Δh is about 146 cm and 545 cm during the drawdown and filling phases, respectively (Fig. 8). This phenomenon influences the progressive change of the bulk unit weight of the soil during the unsteady seepage flow associated with the operation [2],[3],[7]. The coupled analyses of slope displacements and piezometric heads (p.h.) measures highlight *i*) the cyclicity of the slope movements, following the variation of the reservoir water levels; *ii*) the occurrence of unsteady state seepage flows; *iii*) the effectiveness of the berm in the reduction of movements by increasing the effective stresses.

The hydro-mechanical response of the slope has been thus investigated through coupled seepage (FE) and stability (LEM) analyses, carried by SEEP/W

and SLOPE/W codes [1],[7]. The (initial) values of the permeability coefficients (deduced by previous geotechnical analyses [7],[8],[9]) has been progressively refined (through parametric simulations referred to the scheme in Fig. 9) to obtain the best fitting between the p.h. measurements and the computed (final) values of the piezometric heads. The agreement between the computed and measured (through PD1 piezometer) values of piezometric head (p.h.) can be observed in Fig. 10. The importance of the unsteady 2D seepage flow, affected by both horizontal and vertical components of the flow velocity vectors, inlet and outlet from the slope, is confirmed [7]. The inclinometric measures have also allowed to identify, for the reference slope cross-section (Fig. 9), the potential sliding surfaces (Fig. 11): the evolution of the slope safety factor, in dependence on the r.w.l. along time, has been determined (Fig. 12) [7]. Particularly, the safety factor generally reduces during the filling phase, reaching the unit value at the maximum water level (Fig. 12 a); its values *just below the unit value*, thus allowing slope movements, occur and persist during the most of the drawdown phase (Fig. 12b), according to the previously analyzed measures (Fig. 3).

For a careful comprehension of the hydro-mechanical behaviour of the slope, numerical models to simulate the recorded displacements have been previously developed [1],[7].

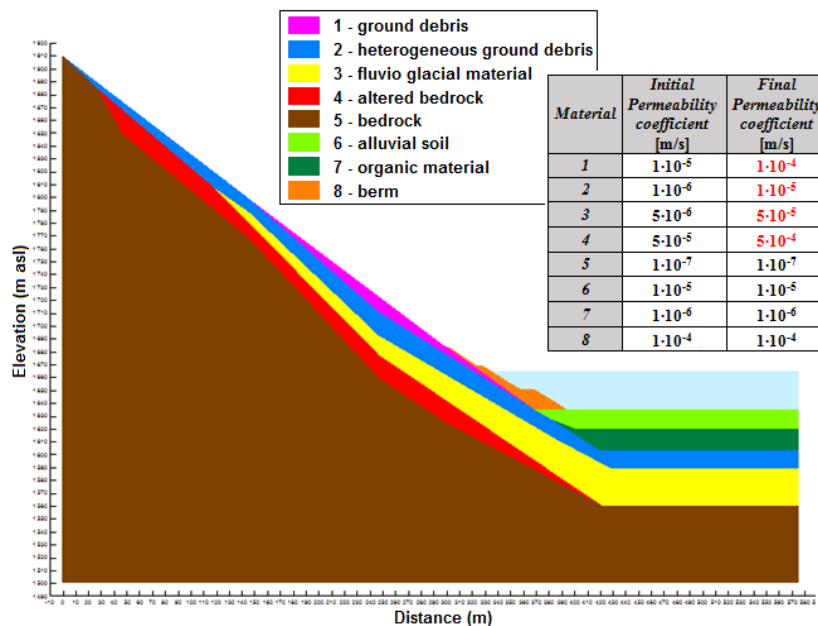


Fig. 9. Schematization of the slope of Vernago reservoir

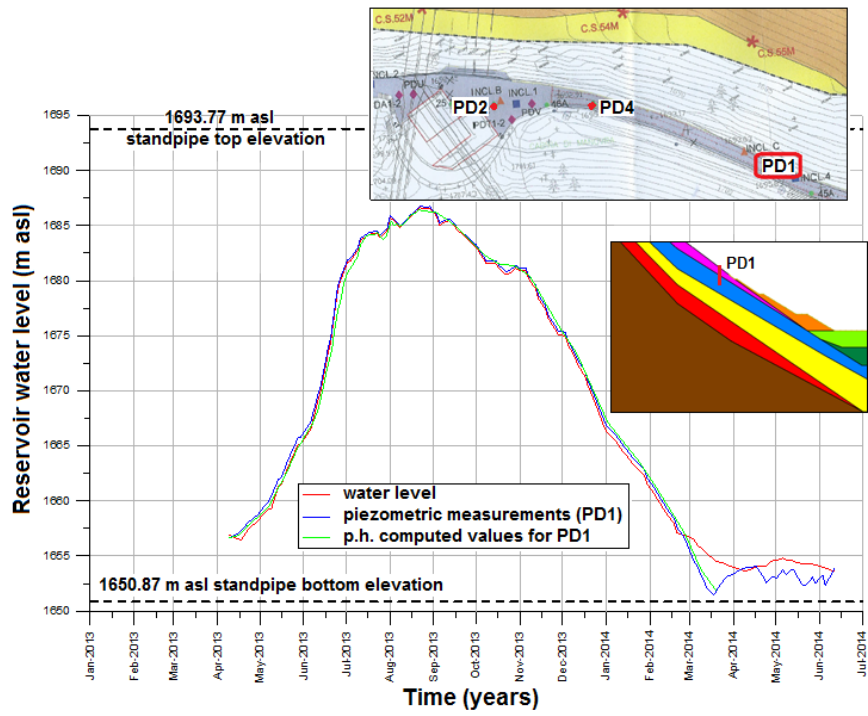


Fig. 10. Computed vs measured values of p.h. (PD1 open standpipe piezometer)

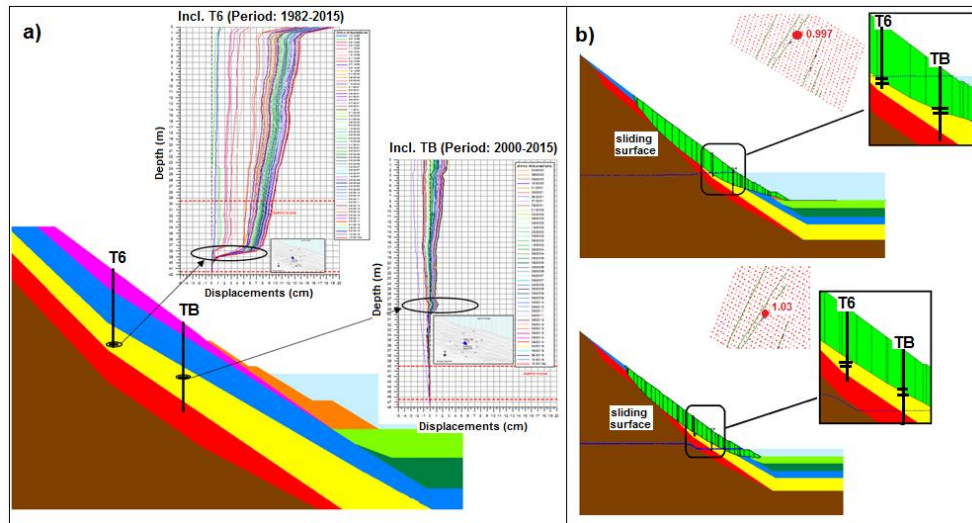


Fig. 11. a) Determination of sliding surface through inclinometric measurements;
b) possible sliding surfaces from LEM analyses

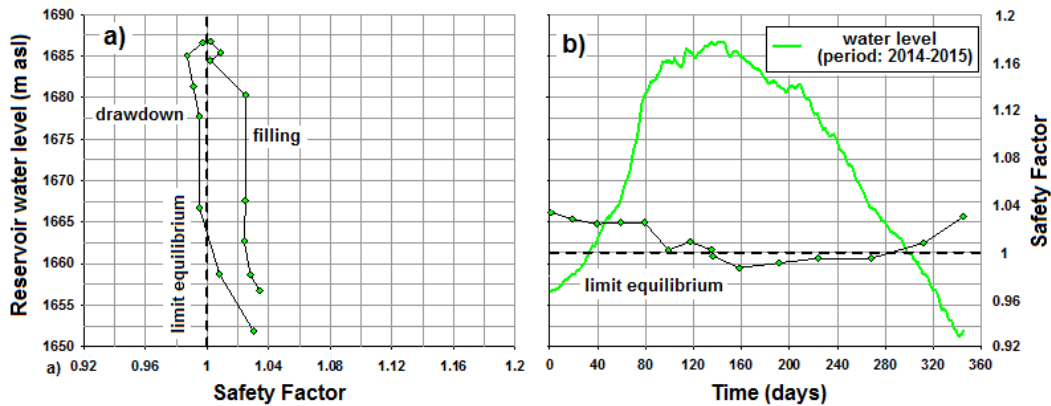


Fig. 12. a) Safety factor vs reservoir water level; b) safety factor vs time

Particular attention should be given to the mechanical characterization of the slope materials, specifically along the sliding surface [7]: due to the lack of specific experimental evidences on the validity of the rheological laws available in literature for the involved materials, specific calibration analyses, based on the interpretation of the available measured displacements, are needed [7]. To this purpose, advanced numerical simulations of the slope displacements are still in progress.

4. CONCLUDING REMARKS

The hydro-mechanical response of the slope of the Vernago reservoir has been firstly investigated through regression analyses of the displacements measured before and after the construction of the stabilizing berm. The obtained results highlighted the cyclicity of the slope displacements and the effectiveness of the berm in the reduction of movements. The obtained regression relationships may be applied to estimate slope displacements following new operation rules, according to the hydraulic variables H_{max} , H_{min} (max and minimum reservoir water levels), $\Delta T_{max,fill}$ (persistence of H_{max}), $v_{fill/dd}$ (rate of change in water level during the filling/drawdown phase). To better understand the hydro-mechanical response of the slope, according to the variation in the reservoir water level, coupled numerical unsteady seepage flow within (FE) and stability (LEM) simulations of the slope have been run. After a better characterization of the permeability coefficients (k) of the slope materials, through the best correspondence between those computed and measured piezometric heads, it has been clearly demonstrated that the hydraulic conditions within the slope don't correspond to hydrostatic conditions.

FE and LEM results coherently interpret the pore pressure and stress state evolution within the slope during the imposed operation conditions, both before and after the construction of the stabilizing berm. The hydromechanical response of the slope always depends on the operation conditions that, in turn, induce unsteady state seepage flows within the slope according to the filling and drawdown phases. Thus, the global stability of the slope strongly depends on the specific drawdown

phase. In particular, its safety factor mainly reduces just below the unit value during the drawdown, confirming the observed displacements of the slope in the same phase.

REFERENCES

- [1] GIODA G., BORGONOVO G. Finite element modeling of the time-dependent deformation of a slope bounding a hydroelectric reservoir. *International Journal of Geomechanics*, ASCE, 2004, 4(4).
- [2] DESAI C.S. Drawdown analysis of slopes by numerical methods. *J. Geotech. Eng. Proc.* ASCE, 1977, 109(7), pp. 946-960.
- [3] CHEN X., HUANG J. Stability analysis of bank slope under conditions of reservoir impounding and rapid drawdown. *Journal of Rock Mechanics and Geotechnical Engineering*, 2011.
- [4] WANG J., XIANG W., LU N. Landsliding triggered by reservoir operation: a general conceptual model with a case study at Three Gorges Reservoir. *Acta Geotechnica*, 2014, Springer, DOI 10.1007/s11440-014-0315-2.
- [5] XIA M., REN G.M., ZHU S.S., MA X.L. Relationship between landslide stability and reservoir water level variation. *Bull. Eng. Geol. Environ.*, 2014, Springer, DOI 10.1007/s10064-014-0654-0.
- [6] ZHOU Q., YAN S., DENG W., FU X. Analysis of the influence of reservoir water level fluctuation on bank slope stability. *J. of Highway and Transportation Research and Development*, vol. 6, n. 2, 2012.
- [7] FEDERICO F. Slope displacements of the Vernago reservoir: measures, interpretation and evolution of the slope safety. *Alperia Spa, Internal Report*, 2016 (*in Italian*).
- [8] BALDOVIN E., MARTINI G., MORELLI. Vernago Reservoir southern slope stabilization and operation shaft reinforcement. *76th Annual Meeting ICOLD, Sofia*, 2008.
- [9] BALDOVIN E., MAESTRI M., MARTINI G. Realizzazione di tiranti all'interno del pozzo di manovra del Serbatoio di Vernago. *AGI Conference Naples, Italy*, 2011.

SUMMARY

The slope bounding the reservoir of Vernago, in northern Italy, showed slow and small movements associated with the drawdown/filling cycles of the reservoir. Preliminary regression analyses of the measured displacements highlighted their cyclicity in time. Coupled transient seepage flow (FE) and stability (LEM) analyses have been also carried out. Numerical results coherently interpret the pore pressure and stress state evolution within the slope during the imposed operation

conditions that induce unsteady state seepage flows on which in turn the hydromechanical response of the slope depends, according to the filling and drawdown phases.

KEYWORDS: Reservoir Slope, Stability, Water Level, Drawdown

ÉVOLUTION DE LA STABILITÉ DE LA PENTE DU RÉSERVOIR DE VERNAGO SOUS UNE VARIATION AU NIVEAU DE L'EAU, PENDANT LES OPÉRATIONS DE SOIXANTE ANS

RESUME

La pente qui borde le réservoir de Vernago, dans le nord de l'Italie, a montré des mouvements lents et faibles associés aux cycles de rabattement / remplissage du réservoir. Les analyses de régression préliminaire des déplacements mesurés ont mis en évidence leur cyclicité dans le temps. Des analyses de flux d'infiltration transitoire couplé (FE) et de stabilité (LEM) ont également été effectuées. Les résultats numériques interprètent de façon cohérente la pression interstitielle et l'évolution des contraintes dans la pente pendant les conditions de fonctionnement imposées qui induisent des flux d'infiltration instationnaires dont dépend la réponse hydromécanique de la pente, en fonction des phases de remplissage et de rabattement.

MOTS-CLÉS: Versant de retenue, stabilité, niveau hydraulique, vidange

COMMISSION INTERNATIONALE DES GRANDS BARRAGES

VINGT-SIXIÈME CONGRÈS DES GRANDS BARRAGES
Autriche, juillet 2018

DOI 10.3217/978-3-85125-620-8-214



This work licensed under a Creative Commons Attribution 4.0 International License. <https://creativecommons.org/licenses/by-nc-nd/4.0/>

**RESEARCH ON STABILITY OF RESERVOIR ACCUMULATIVE BODY SLOPE
AND THE IMPACT OF WATER STORAGE**

Ji LU

*Head of Engineering Safety Research and Development Department, Science
and Technology R & D Center, HUANENG LANCANG RIVER HYDROPOWER
INC.*

CHINA

Zheng-gang ZHAN

*Deputy Chief Engineer of POWERCHINA GUIYANG ENGINEERING
CORPORATION LIMITED*

CHINA

Meng-Xi WU

INSTITUTE OF MECHANICS, CHINESE ACADEMY OF SCIENCES,
UNIVERSITY OF CHINESE ACADEMY OF SCIENCES

CHINA

Hong-Jie CHEN

*Engineer of Engineering Safety Research and Development Department,
Science and Technology R & D Center, HUANENG LANCANG RIVER
HYDROPOWER INC.*

CHINA

**RESEARCH ON STABILITY OF RESERVOIR ACCUMULATIVE BODY
SLOPE AND THE IMPACT OF WATER STORAGE ***

DR. Ji Lu

*Head of Engineering Safety Research and Development Department,
Science and Technology R & D Center, HUANENG LANCANG RIVER
HYDROPOWER INC.*

CHINA

Mr. Zheng-gang Zhan

*Deputy Chief Engineer of POWERCHINA GUIYANG ENGINEERING
CORPORATION LIMITED*

CHINA

Prof. Dr. Meng-Xi Wu*

*INSTITUTE OF MECHANICS, CHINESE ACADEMY OF SCIENCES,
UNIVERSITY OF CHINESE ACADEMY OF SCIENCES*

CHINA

DR. Hong-Jie Chen

*Engineer of Engineering Safety Research and Development Department,
Science and Technology R & D Center, HUANENG LANCANG RIVER
HYDROPOWER INC.*

CHINA

1. INTRODUCTION

* *titre de l'article complet*

The landslides of reservoir slopes may cause heavy casualties and loss of property. A large-scale high-speed landslide may cause high wave surge which may even endanger the safety of a waterpower project. Therefore, the stability of those slopes is an important subject in the design of a hydropower station. Landslides of reservoir slopes can occur during the operation of a reservoir (Jones et al., 1961 ; Schuster, 1979; Gutiérrez et al., 2010; Jiao et al., 2014; Da Huang et al., 2017). Statistics show that in general, approximately 50% of reservoir landslides occur during the first impoundment, with the others occurring during the first 3–5 years after the construction of the dam (Jones et al., 1961 ; Cojean and Cai, 2011). The raise in the water level during reservoir filling causes saturation of slope materials, reducing mechanical strength of soil and rock (Záruba and Mencl, 1982; Wang et al., 2007), and decreasing slope stability. The impact of water impoundment of a reservoir to the stability of a large scale accumulative body (ACC for short) slope is analyzed with an enhanced limit strength method based on a linear finite element stress analysis.

2. BRIEF INTRODUCTION OF THE RONG-SONG ACCUMULATIVE BODY

Rong-song ACC is located at the left bank of the Lan-cang River 5.5km away from a 315m high rockfill dam of the hydropower station in the south-west china. The photo of the ACC is shown in Figure 1. The elevation of the front of the ACC is 2654m and the height of the trailing edge is 3200m. It extends up to 3400m locally along a small gully. The length of it along the river is about 1.4km, the width vertical to the river is about 700m, and the natural slope is between 32 ° and 37 °. It is slightly steep near the riverbed which is at about 40 °. The total height of the ACC is up to about 750m. The slope is currently in a stable state and there is no signs of sliding. Groundwater can be divided into soil pore water which is stored at the Quaternary overburden soils and bedrock fissure water according to their presence conditions. Soil water is recharged mainly by atmospheric precipitation and the water content is dynamically unstable and changes with seasons. There is very few vegetation on the slope surface. The annual rainfall is much smaller than the evaporation. The bedrock fissure water is found in the fractures of the dacite, mainly receives the infiltration and precipitation recharge of the upper soil pore water. The depth of the groundwater at a surface level below 2800m exposed by drilling is 40m ~ 60m below the level. The groundwater in the middle and rear elevation above 2800m is not exposed in the ACC. After the reservoir is impounded, most of the accumulation is below the normal high water level of 2895m. The deposit below 2895m will be submerged during the impoundment of the reservoir, the stability of the accumulation will decrease. It may lose stability during the process of reservoir filling or operation, and the landslide wave surge is dangerous to the safety of the rockfill dam. Therefore, the analysis of the stability of the accumulation and its sliding mode is important to the design.



Fig.1 Photo of Rongsong accumulative body (oblique view from top to bottom)

2.1. TERRAIN GEOLOGY

The geological plane with 8 profile lines is shown in Figure 2. A typical profile R2-R2' is shown in Figure 3. The main body of the deposit was explored by drilling, adit and geophysical work. The ACC is composed of a gravel with fine soil layer with multi-layers gravel sandwiches and a gravel soil. Photo of materials at the surface and exposed by adit is shown in Figure 4. The deposit above 2800m is mainly gravel soils, forming oblique stratification of alternative distributed slope gravelly soil and crushed gravel as shown in Figure 4 (a). The cementation of slope gravel soil is good, and that of crushed gravel is slightly worse. It can be divided into two soil layers, including fine grained gravel soil $Q^{col+dl-2}$ and crushed gravel layer $Q^{col+dl-1}$. The thickness of a gravel soil layer ($Q^{col+dl-2}$) is 5 to 10m. The gravel grain content is about 50 ~ 60% with the size generally between 3 and 6 cm. With sandy soil packed between gravel grains, it is relatively dense and have some cementation. It is slightly loose at the slope surface. The soil can keep stable temporarily in a short time during tunnel excavation. The thickness of a crushed gravel layer ($Q^{col+dl-1}$) is 0.3 to 1.0m. The contact angle between layers is 27° to 32° . Gravel diameter is generally 5 to 20cm, with a small amount of gravel grains which is 20 to 50cm in diameter locally. It is loose and poor cemented. When the adit is excavated to this layer, it is muddied. Deposit about 2800m below is early diluvial gravel soil, collapsing fragment stone terrace accumulation and accumulation of colluvial deposit fragment stone with small amount of alluvial sand gravel $Q^{col+dl+al}$. As shown in

Figure 4(b), particle size is mostly 5 to 20cm, there is about 1m diameter boulder locally. Several profiles shows that there is a small amount of sand and gravel Q^{dl+al} at the lower part of $Q^{col+dl+al}$ (Q^{dl+al} is not appear at R2-R2' as shown in Figure 3). The alluvial sand and gravel Q^{al} is located on the part of the riverbed and on the part of the old river bed on the slope in several profiles. There is gravel filled with gravel soil at the interface of bedrock and overburden as shown in Figure 4(c). Dacite rock is exposed at the front of the ACC along the river as shown in Figure 4(d).

At the bottom of the ACC, there is no obvious weakness in the contact interface between the bedrock and the overburden layer, the soil there is basically the same as that inside the ACC. The internal weakness of the ACC is mainly gravel layer $Q^{col+dl-1}$. Through field investigation, there are two possible types of failure mode in the ACC: (1) an circular sliding arc inside the ACC; (2) non-circular sliding mode including the overall stability failure sliding along the contact interface of the ACC and the bedrock, or a local non-circular sliding surface along the gravel layer within the ACC.

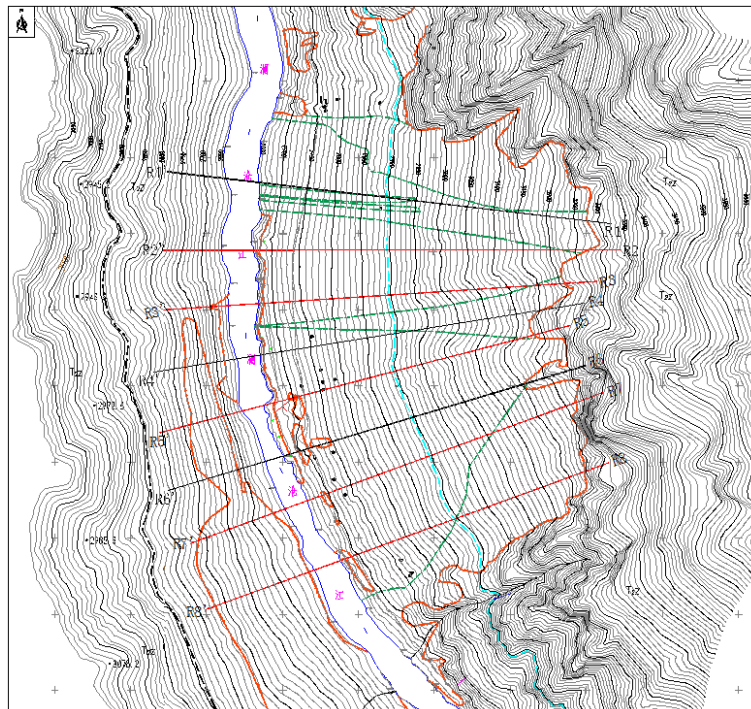


Fig.2 A schematic of the geological plane of the accumulation body

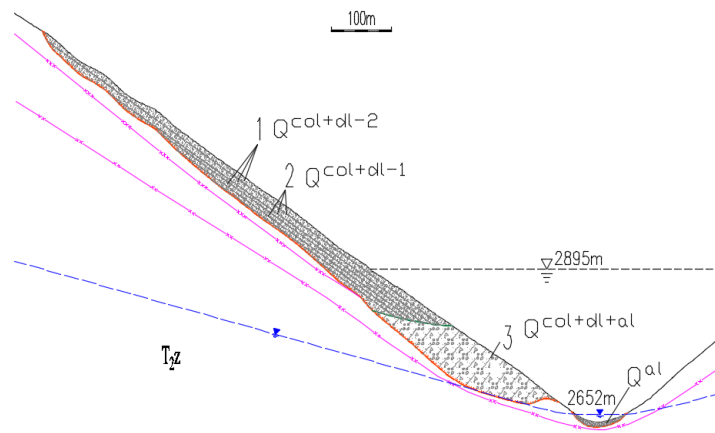


Fig.3 The typical geological section of the reservoir slope R2-R2'
 1 Gravel soil $Q^{col+dl-2}$; 2 Gravel $Q^{col+dl-1}$ 3 Sand gravel $Q^{col+dl+al}$



(a) Oblique stratification of $Q^{col+dl-1}$ and $Q^{col+dl-2}$ (b) Sand gravel layer $Q^{col+dl+al}$



(c) Bedrock and overburden contact interface (d) Bedrock exposed at the slope surface leading age

Fig.4 Photo of materials at the surface and exposed by adit

2.2. PHYSICAL AND MECHANIC PARAMETERS

Based on exploration and experiment, the bulk density and the Mohr-Coulomb strength parameters of soils are obtained as shown in table 1. In the stress calculation of the ACC, the adopted values of the elastic modulus and Poisson's ratio of all the deposit soils were 0.35GPa and 0.35 respectively. The bedrock is divided into three layers: strong weathering, weak weathering, and fresh rock mass. Their elastic modulus are 3, 7 and 15GPa respectively, and their Poisson's ratio are 0.3, 0.28 and 0.22 respectively.

Table 1 Bulk density and the Mohr-Coulomb strength parameters of soils

Soil name	Unit weight (kN/m ³)		Shear strength above water level		Submerged shear strength	
	Nature	Saturated	Cohesion (kPa)	Friction angle (°)	Cohesion (kPa)	friction angle (°)
Bedrock	26.5	27.0	900	45	900	45
Q ^{col+dl-1}	22.0	23.0	5	34.2	0	28.8
Q ^{col+dl-2}	21.0	22.5	50	33	25	28
Q ^{col+dl+al}	21.5	22.5	20	35.7	10	30.5

3. STABILITY ANALYSIS

The enhanced limit equilibrium method based on finite element stress is adopted. The combination of a finite element stress analysis with a limit equilibrium analysis provides greater certainty and flexibility regarding the internal distribution of stresses within the soil mass (Fredlund & Scoular, 1999). The normal force along any selected slip surface can be calculated from the stress distribution that has been calculated using a linear and non-linear stress analysis. The overall factor of safety for a slope, when the finite element method is used, can be defined as the available shear strength of the soil divided by the shear stress. The overall factor of safety is a combination of the local factors of safety within the slope. The resulting factor of safety retains the basic assumptions inherent to the limit equilibrium definition of the factor of safety. Optimization techniques should be used to find the critical slip surface of the slope.

3.1. STRESS INSIDE THE SLOPE

The finite element grid of profile R2-R2' is shown in Figure 5. The meshes in the overburden area are denser than that in the bedrock areas. The control

length of a mesh side in the overburden areas is 3m. The elevation of the accumulation in the profile is 2689.5m to 3269.1m, with a height of 579.6m.

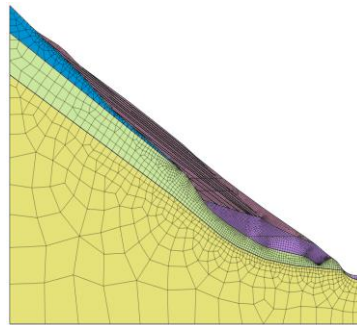


Fig.5 Finite element grid of profile R2-R2'

The steady seepage field with natural or varied water level during reservoir impoundment is calculated followed with the stress field calculation by the effective stress method. Due to the small amount of water influxion in the mountain side and the permeability coefficient of the accumulation material is large, so the phreatic line in the ACC is almost horizontal and flush with the reservoir water level during the reservoir impoundment.

Effective stresses of the slope were obtained by a linear stress analysis. The normal stresses at natural water level(2654m) and at the normal storage water level (2895m) are shown in Figure 6 and 7 respectively. The horizontal normal stress is tensile in the middle and upper part of the ACC (above elevation 2950m), while the actual stress in the ACC should not be tensile because it will crack when tensile stress occurs. The vertical normal stress is directly proportional to the depth of the deposit, which is agree with the actual situation. There is of course a certain difference between the obtained stress and the actual situation of the ACC with a linear stress analysis.

Compared with the natural state, the vertical normal stress in the ACC below elevation 2895m in the normal water level condition is basically reduced by the ratio of the buoyancy and the natural density.

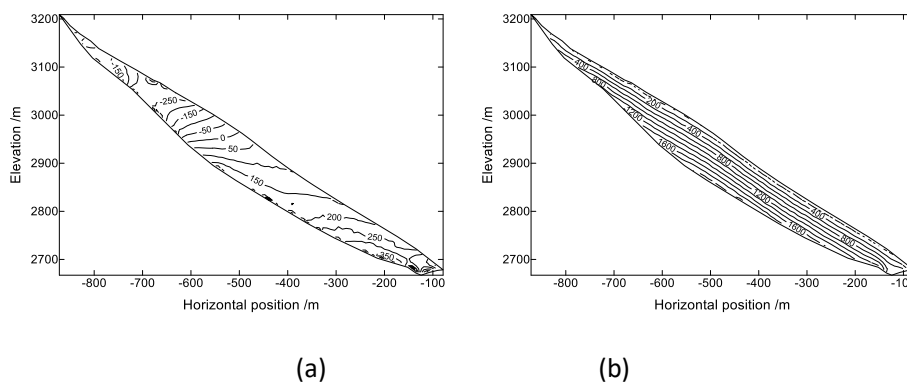


Fig.6 Effective stresses of profile R2-R2' at water level 2654m (a) horizontal normal stress and (b) vertical normal stress (kPa)

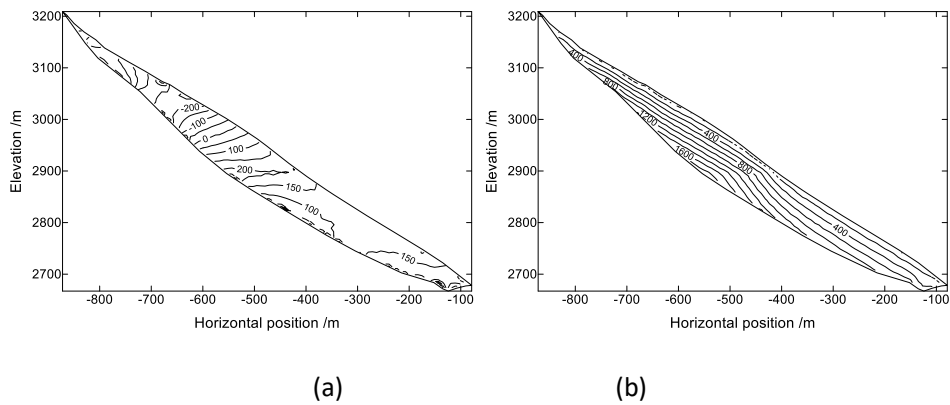


Fig.7 Effective stresses of profile R2-R2' at water level 2895m (a) horizontal normal stress and (b) vertical normal stress (kPa)

3.2. CIRCULAR SLIDING MODE

Firstly, the factor of safety (FOS) of an arc sliding mode is studied. The position of an slip arc is defined by the position of the two intersection of the arc and the slope surface lines, a sliding into point and a sliding out point, and the arch height. 201 points were evenly arranged on the slope surface according to the distance as sliding into or out points. The FOS of each slip curve inside the overburden deposits with a chord not less than 20m and a arch not less than 5m is calculated. Firstly, the variable arch height is optimized. For a given pair of sliding into and out points, the search of the critical slip arc is a single variable optimization problem for arch height and the golden section method was adopted. Thus, the FOS of the critical slip arc of all pairs of sliding into and out points can be obtained. With the elevations of the sliding into and out points as the vertical and horizontal coordinates respectively, a contour map of the FOS of circular arc sliding mode can be plotted.

FOS contour map of profile R2 - R2' at the natural water level (2654m) is shown in Figure 8. The minimum FOS of arcs sliding from the upper part of the ACC and sliding out from the lower middle part is within 1.08, and the FOS increases with the distance deviation of the pair of sliding into and out points from this area.

As shown in Figure 9, when the water level rises to a higher level, the FOS of sliding arc with a sliding out point below that level decreases. At water level 2744.8m, the range of sliding out point with FOS lower than 1.08 extends to the bottom of the slope. At water level 2815 m, there is area with FOS less than 1.0, the sliding into point position is between 2950m and 3180m, and the sliding out point is located at the bottom of the slope. At water level 2863.8m, the FOS decreases further. At water level 2895m, the range with FOS less than 0.9 appears. Water level rising reduces the FOS of sliding arc with a sliding out point below the water level, but almost have no effect on the FOS of sliding arc above the water level.

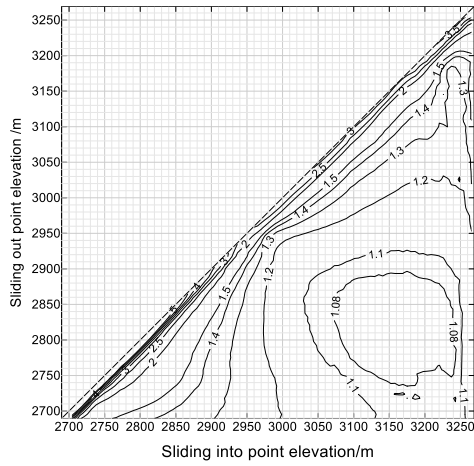


Fig.8 FOS contour map of circular sliding mode at the nature water level

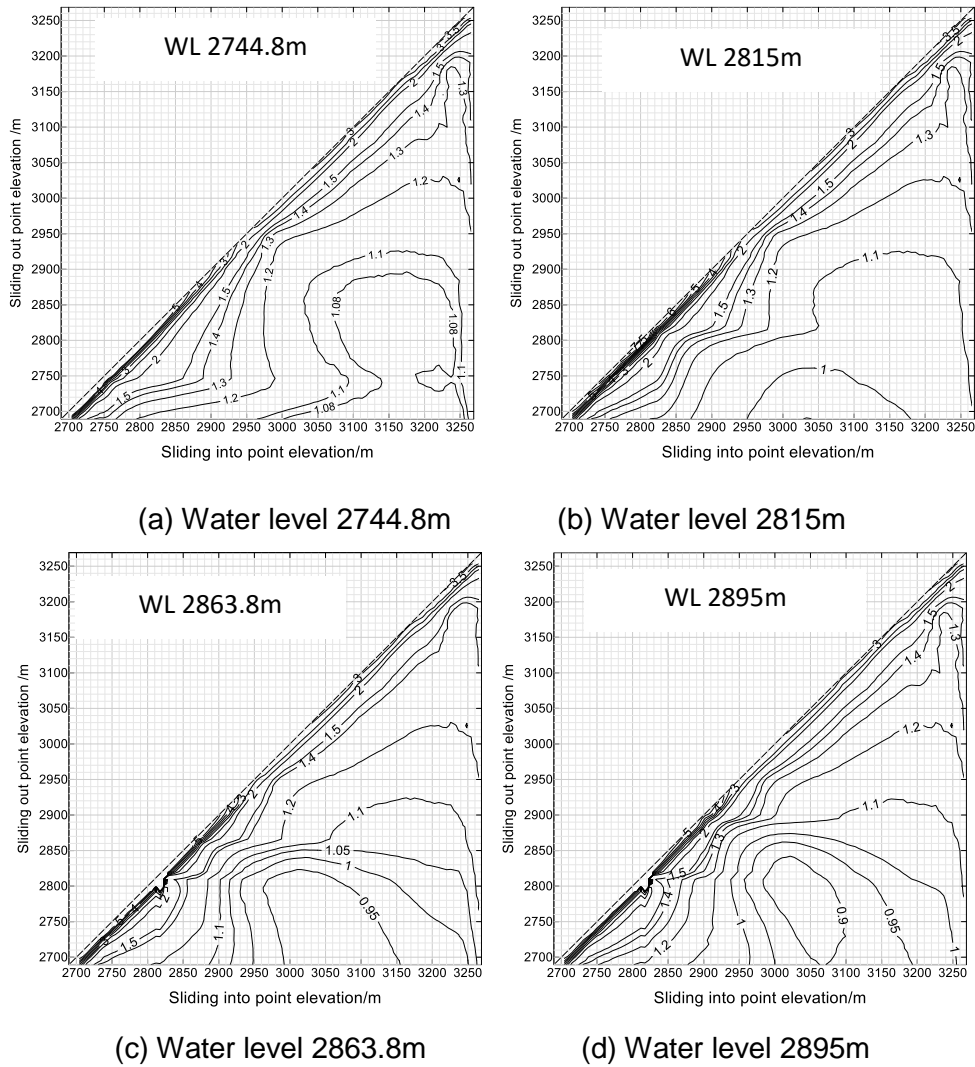


Fig.9 FOS contour map of circular sliding mode during impoundment

Figure 10 shows the critical circular slip arcs and their FOS at each water level. The FOS decreases with the water level, and the FOS decreases by 0.205, from 1.065 in the natural state to 0.860 at the normal storage water level 2895m. Because the FOS is decreased to less than 1.0, the slope may sliding during the impoundment of the reservoir.

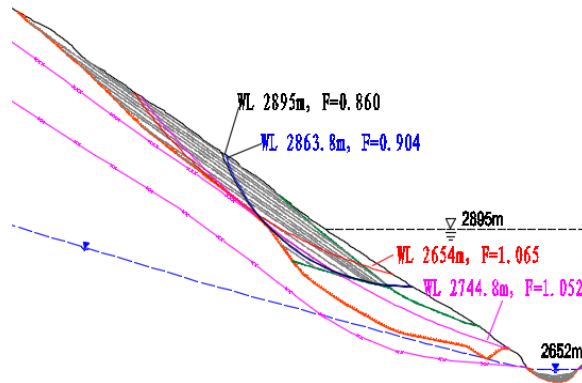


Fig.10 The critical slip circular arc and FOS at each water level

3.3. NON CIRCULAR SLIDING MODE

The non-circular sliding mode along one of the gravel layer in the upper part of the ACC is a typical sliding mode. The FOS of the critical sliding curve in the natural condition (WL 2654m) is 1.033. The position of the critical sliding curve along a gravel layer and the FOS doesn't change during the impoundment.

The FOS of the ACC as a whole sliding along the interface of bedrock and overburden is 1.12 in the natural condition. It decreases with the water level. The FOS at the normal storage water level 2895m decreases to 0.996 which is 0.12 less than that in the natural condition. The FOS of the ACC as a whole at a high water level during the impoundment is less than that of a circular arc sliding mode.

The stability situation of the other seven profiles are similar to profile R2-R2'. On the whole, the present situation of Rong-song ACC is stable. The possible sliding modes are circular slip mode and non-circular mode. The sliding probability along a circular arc and along a gravel layer are quite equal in natural condition. As the water level rises, the probability of circular sliding mode becomes higher than that of a non-circular sliding mode along a gravel sandwich layer or along the interface of the bedrock and overburden.

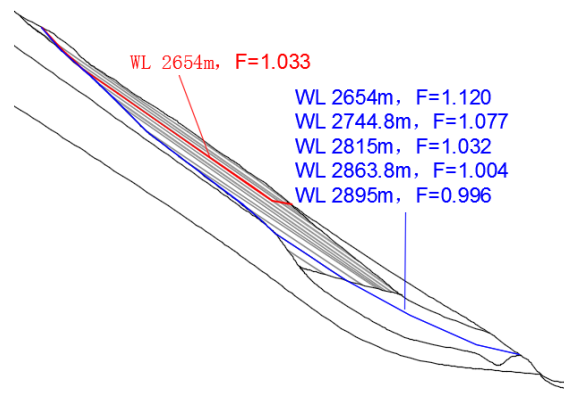


Fig.11 FOS of non circular slip arc at each water level

4. SUMMARY AND CONCLUSION

Based on the finite element stress, the stability of the Rong-song accumulative body in the natural state and during the reservoir impoundment is analyzed. There are two possible sliding modes for the instability accumulative body: the first is the circular arc sliding mode; The other is a non-circular sliding mode along the bedrock and overburden interface or along a sandwich gravel layer in the upper part of the ACC (accumulation body).

The ACC is stable in the natural state. As the water level rises during the reservoir impoundment, the lower part of the ACC will be submerged in the reservoir water. Due to the changes of the effective stresses and the reduction of the strength parameters of soils while it is submerged, the FOS of the ACC decreases with the reservoir water level.

The FOS of both the slip along the interface of the bedrock and overburden and along a critical circular arc decreases to less than 1.0 during the reservoir impoundment. The FOS of a critical circular arc is falling faster than that of the non-circular sliding mode. In the process of water storage, the accumulative body is most likely to lose stability in a circular sliding mode.

AKNOWLEDGEMENT

This work was supported by the The National Key R & D Program of China, Grant No. 2017YFC1501100, by The National Key R & D Program of China, Grant No. 2017YFC1501106, and by Huaneng Lancang River Science and Technology Project HNKJ15-H13.

REFERENCES

- [1] Jones, F.O., Embody, D.R., Peterson, W.L., 1961. Landslides along the Columbia River Valley, Northeastern Washington. In: U.S. Geological Survey Professional Paper. 367. Government Printing Office, Washington, DC, U.S., pp. 98.
- [2] Schuster, R.L., 1979. Reservoir-induced landslides. *Bull. Int. Assoc. Eng. Geol.* 20, 8–15
- [3] Gutiérrez, F., Lucha, P., Galve, J.P., 2010. Reconstructing the geochronological evolution of large landslides by means of the trenching technique in the Yesa reservoir (Spanish Pyrenees). *Geomorphology* 124 (3), 124–136.
- [4] Jiao, Y.Y., Zhang, H.Q., Tang, H.M., Zhang, X.L., Adoko, A.C., Tian, H.N., 2014. Simulating the process of reservoir-impoundment-induced landslide using the extended DDA method. *Eng. Geol.* 182, 37–48.
- [5] Záruba, Q., Mencl, V., 1982. *Landslides and Their Control*. Elsevier, Amsterdam.
- [6] Wang, H.B., Xu, W.Y., Xu, R.C., Jiang, Q.H., Liu, J.H., 2007. Hazard assessment by 3D stability analysis of landslides due to reservoir impounding. *Landslides* 4 (4), 381–388.
- [7] Da Huang, , Dong Ming Gu, 2017. Influence of filling-drawdown cycles of the Three Gorges reservoir on deformation and failure behaviors of anacinal rock slopes in the Wu Gorge. *Geomorphology* 295 (2017) 489–506.
- [8] D.G.Fredlund, R. E. G. Scoular. Using limit equilibrium concepts in finite element slope stability analysis. *Proceedings of the International Symposium on Slope stability Engineering-IS-Shikoku'99*, Invited Key note paper, Matsuyama Shikoku, Japan. November 8-11, 1999, 31-47

COMMISSION INTERNATIONALE DES GRANDS BARRAGES

VINGT-SIXIÈME CONGRÈS DES GRANDS BARRAGES
Autriche, juillet 2018

DOI 10.3217/978-3-85125-620-8-215



This work licensed under a Creative Commons Attribution 4.0 International License. <https://creativecommons.org/licenses/by-nc-nd/4.0/>

DAM UPGRADES USING MECHANICALLY STABILIZED EARTH

John E. SANKEY, P.E.

International Engineering Manager, TERRE ARMEE

USA

Gary POWER

Manager Asia Pacific Zone, THE REINFORCED EARTH COMPANY

AUSTRALIA

COMMISSION INTERNATIONALE
DES GRANDS BARRAGES

VINGT-SIXIÈME CONGRÈS DES
GRANDS BARRAGES
Autriche, juillet 2018

DAM UPGRADES USING MECHANICALLY STABILIZED EARTH

John E. SANKEY, P.E.

International Engineering Manager, TERRE ARMEE (USA)

Gary POWER

*Manager Asia Pacific Zone, THE REINFORCED EARTH COMPANY
(AUSTRALIA)*

1. INTRODUCTION

The current limitations to space and access to permitting approvals has reduced construction of new dams in several parts of the world, particularly those located in or near densely populated areas. Upgrades to capacity and supplemental structures, including spillways and outlet structures, have resulted in turning toward technologies such as Mechanically Stabilized Earth (MSE) to maintain existing plan areas, while allowing vertical construction means to achieve increased water holding volumes and continued stability. This paper will provide an overview of MSE technology used in the raising of earth dams and dam restoration. In addition to its cost efficiency, MSE wall systems such as Reinforced Earth® provide uniform distribution of loads throughout its mass and increases the overall stability of the resulting composite earth dam. Two separate general types of reinforcement materials, steel and polymeric, will be addressed as to design considerations for safe and expanded performance of earth dam structures. This paper will in turn be supplemented by two case studies representing each of the general reinforcement types to show the viability of each system for dam upgrades.

2. MSE STRUCTURES FOR DAM UPGRADE APPLICATIONS

2.1 BACKGROUND ON TECHNOLOGY

MSE technology as now used in civil engineering in the modern era was first developed by Henri Vidal, a French architect, in the early 1960s. It is more widely associated with road transportation construction on such applications as retaining and bridge abutment walls, but the breadth of MSE technology encompasses industrial, mining, waterway, military and railway support just to name a few of the applications where the technology has spread.

MSE structures are typically composed of precast concrete facing panels joined by reinforcing strips or grids (either steel or geosynthetic) within a granular select fill matrix (Fig. 1). The frictional bond between the backfill and the reinforcements is permanent and predictable and there is a reliable mechanical connection between reinforcements and facing panels. As a retaining structure, MSE represents a unique, composite construction having great strength and stability, a limited footprint and the ability to distribute loads uniformly, even on poor or sensitive foundation soils.

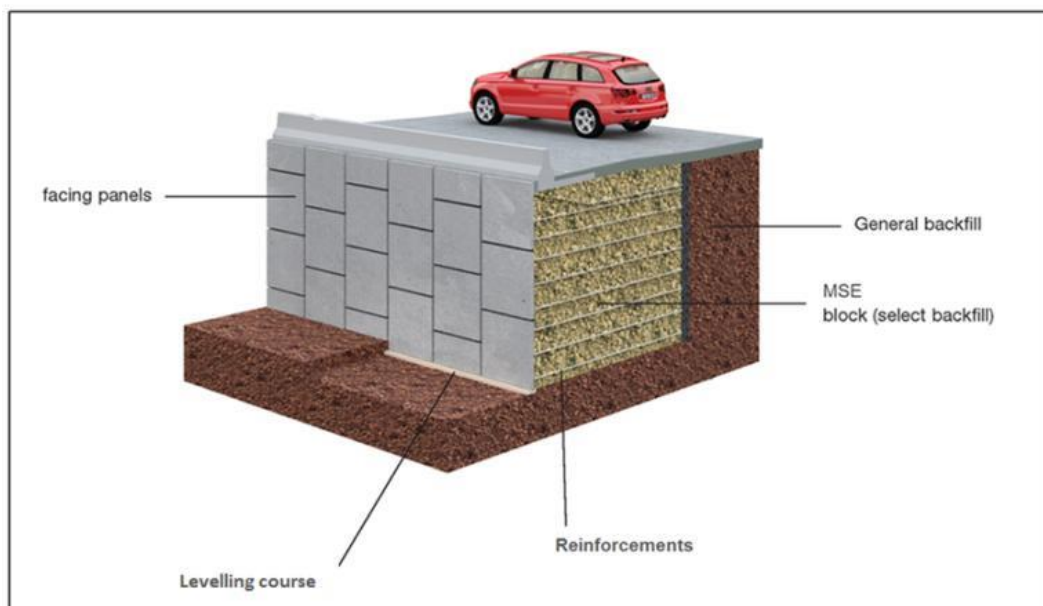


Fig. 1
Typical MSE Wall Components

The advent of MSE technology for use in waterway structures eventually resulted in its development for dam applications. In the mid-1980s, MSE walls were first used to construct new earth dams. One of the earliest dams that was constructed using the technology was Taylor Dam completed in 1984 (Fig. 2). The dam built across the White River in Rangeley, Colorado (USA) was approximately

22.6 m tall and was essentially developed as a core to save on the plan area, thus reducing project costs by approximately US \$1 million dollars. Phreatic and drawdown considerations were incorporated, along with special toe stabilization support and incorporation of spillway and piping inclusions. Galvanized steel reinforcing strips were used within the MSE volume.

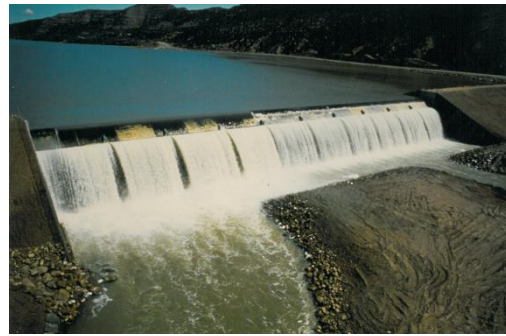
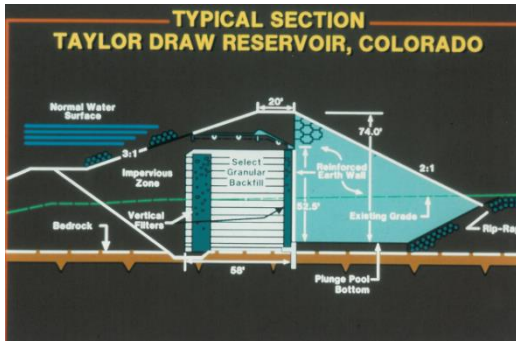


Fig. 2
Taylor Dam

Soon after completion of initial full scale dam projects, use of MSE technology turned to upgrades in existing earth dams to increase reservoir volume and improve embankment stability. One such example was the 60-year-old earth dam at Lake Sherbourne in Montana (USA). The 26m tall earth dam was topped by a 6m tall back-to-back MSE wall that increased the reservoir capacity by 200 m³ at a cost savings of 35%. The use of MSE technology also had the additional benefit of preventing overloading of the foundation soils.

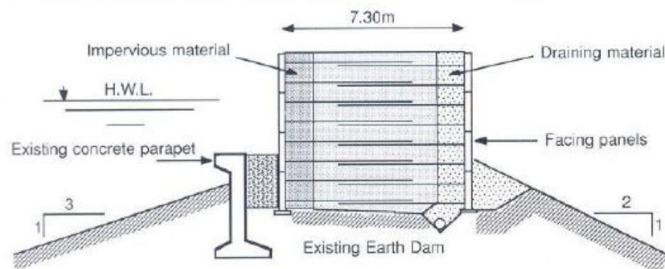


Fig. 3
Lake Sherbourne



Use of MSE technology in dam improvements continues today with less focus on newly established earthen dams (though still a most viable technology consideration). The earliest versions of MSE technology relied on galvanized steel reinforcements; however, geosynthetic strips have become recent reinforcement alternatives where elevated salts in the backfill and/or retained water make considerations for long term metal losses a factor in design and performance. Design and construction differences do exist in selection of reinforcement types, so an early assessment of project physical features needs to be confirmed during development and planning at the outset.

2.2 DESIGN CONSIDERATIONS

Earth dams using MSE technology, whether as new or upgraded structures, have a number of design considerations to be evaluated. These include internal reinforcement pullout and tension considerations typical of MSE walls along with impermeable barriers, drainage and filter features. External stability with respect to prevention of sliding and global stability that is also typical of MSE design, must more closely evaluate erosion and external protection along with through-spillway features.

2.2.1 REINFORCEMENT AND FACING

The use of discrete galvanized steel or geosynthetic strips are the dominant reinforcement types used internationally for MSE walls in water-related applications. A predictable metal loss rate for the metallic strips is possible thanks to the interaction between the hot dip galvanization and the underlying carbon steel during the life of the structure. Geosynthetic strips on the other hand depend on the durability and long term plastic deformation of the polymer type used in the reinforcement. In most cases the design life for critical MSE structures is assessed within a range of 75 to 120 years depending on the criticality of the structure involved.

The facing for permanent MSE walls in dam applications is usually precast panels in the range of 1.5 to 3m length and 1 to 2m height, though wire faced walls are sometimes used or panels tailored to resist unique conditions such as shipping or unusual impact loads. In relationship to the face dimensions of the panels, the thickness of the precast units is relatively thin (panel thicknesses as small as 140mm are not unusual with or without concrete reinforcement). Galvanized steel connectors are embedded or polymer recesses are cast into the precast concrete facings to offer mechanical anchoring of galvanized steel or geosynthetic strip reinforcements, respectively.

2.2.2 *BACKFILL*

The largest material component of a MSE structure is the select backfill used to construct it. Good design practice requires the use of materials that ensure adequate frictional interaction with the reinforcements within the resistant zone of the MSE structure (approximately 0.3H behind the wall face, where H is the wall height). Codes for MSE structures usually allow default friction values of 34° to 36° for backfill when less than 15% low plasticity fines are considered.

At the same time, the backfill near the face(s) of the MSE structure must incorporate zones of impermeable backfill backed by adequate drainage means to address rapid drawdown and other variations in internal water level (a central impermeable core may be considered in back-to-back walls where there is horizontal space between reinforced sections). Drainage can be achieved with backfill materials containing less than 5% fines (< 74µm), which is consistent with a permeability coefficient that should exceed 10⁻³cm/sec. Higher fines in the impermeable zone or backfills treated with soil cement may be considered in dam-related structures. Grain size compatibility is needed to prevent piping and loss of fines between zones. Maintaining vertical impermeable and drainage zones poses potential construction difficulties, which is why use of geomembranes to accommodate water retention and permeable geosynthetics to promote drainage have been incorporated into MSE water retention structures.

The durability of galvanized steel in MSE applications is dictated by the backfill where it is embedded during its intended design life. Electrochemical conditions for the select fill in galvanized steel reinforcements follow guidelines in local codes for resistivity, pH and salts (typically chlorides and sulfates). Geosynthetic strips have separate durability conditions to be met including pH, temperature/creep resistance, construction survivability and chemical/biological degradation. Polymers commonly used in geosynthetic strips for MSE applications are coated high tenacity and molecular weight - polyester (PET) or polyvinyl alcohol (PVA). Though either galvanized steel or geosynthetic strips may be used in submerged freshwater MSE applications, only geosynthetic reinforcements are commonly used in saltwater exposure conditions.

2.2.3 *DRAINAGE, FILTERS AND EXTERNAL STABILITY*

As has been addressed briefly in the foregoing sections, the basic elements typical of all MSE walls must be further modified to address functional components that verify internal and external stability of the dams using the technology. Since the basis and analysis of the functions are specific to the dam upgrade being considered, Table 1 has been provided as an overview and further details are left to two case examples provided hereafter.

Components	Function
Foundation load-bearing soil	<p>Support the dam embankment; distribute MSE bearing pressure per Meyerhof Method</p> <p>Resist geotechnical destabilization phenomena (sliding, settlement, bearing pressure, overturning and deep circular rupture),</p> <p>Resist water flow and internal erosion, prevent particle migration</p>
Dam embankment or mass core	<p>Ensure stability</p> <p>Limit the flow towards the other embankment components</p> <p>Prevent particle migration</p>
Central core between MSE zones or immediate backface impermeable zone	<p>Ensure the structure's watertightness</p> <p>Composed by low permeability materials (such as clays or compacted silts)</p> <p><i>This function can be ensured by the MSE mass block in some cases (e.g., cement treated soils) or use of geomembranes</i></p>
Filters	<p>Prevent leakage of materials in order to maintain the watertightness and structural integrity by resisting to internal erosion</p> <p>Prevent particle migration at the interface of granular elements. The main use is geotextiles</p>
Drains	<p>Monitor the occurrence of overpressure phenomena, swelling/shrinking events and destabilization</p> <p>Positive discharge of water seepage</p> <p>Additional design for internal or deep drainage</p>
Berms	<p><u>Watercourse side</u>: used as protection system or as an element to add stability and watertightness (by decreasing the hydraulic gradient)</p> <p><u>Protected Zone side</u>: used in order to provide stability and/or filtration, to control internal erosion and/or under pressure of the foundation ("sand boil", which can lead to liquefaction)</p>
External protections	<p>Protection by grass vegetation or hard shell</p> <p>Riprap, concrete artificial blocks (tetrapod) or dressed stones' riprap or masonry.</p>

Table 1 MSE Dam Functional Components

3. PROJECT CASE STUDIES

3.1 CHAFFEY DAM, TAMWORTH, NSW, AUSTRALIA

Chaffey Dam is a 54m high and 430m long clay cored, rockfill embankment with a combined Morning Glory (MG) Spillway and outlet works. Construction began in 1976 and the dam was commissioned in 1979 with storage capacity of 62 gigalitres at full supply level (FSL). The dam is located 43 km south-east of Tamworth on the Peel River in New south Wales and provides town, industrial and irrigation water supplies, flood mitigation and drought security to the Tamworth Region. The dam, as it was originally constructed, had an inadequate flood capacity of 1:50,000 AEP and the crest was raised in 2004/5 by 1.8m using a precast concrete wall on the upstream edge improving the capacity to 1:98,000 AEP. However, Chaffey Dam is classified by the NSW Dam Safety committee as an Extreme Consequence Category dam and consequently the State Water Corporation decided to improve the flood capacity to the full Probable Maximum Flood and to augment its storage to 100 gigalitres. A detailed study in 2006-7 recommended the combined measures of forming an auxiliary spillway through the left abutment, raising the dam crest by 8.4m and raising the bellmouth of the MG spillway by 6.5m.

The raising of the crest to RL 541.6m and the increase in the FSL to 525.1m was predicted to induce settlement in the crest in the order of 100mm, and downstream deflection in the order of 20mm to 50mm so a camber allowance of 100mm was introduced. The PMF loading was predicted to induce crest deflection at the top of the structure in the order of 300mm to 350mm. The raising of the dam crest was detailed as two Mechanically Stabilized Earth (MSE) retaining walls, constructed 7.35 meters high, back to back, to RL 539.75 and topped with a precast concrete parapet 1.8 meters high to RL 541.8. The bearing pressure below the MSE block was estimated to be a maximum 270 kPa at the downstream toe for the PMF load condition, which controlled the design.

The MSE walls were designed by The Reinforced Earth Company (RECO) in accordance with NSW Roads and Maritime Services QA Specification R57 "Design of Reinforced Soil walls" with modular precast concrete facing panels and galvanized steel reinforcing strips for a design life of 100 years. Whilst both steel and polyester reinforcing strips were considered, steel was ultimately preferred due to concerns about possible damage to the polyester strips from the compacted gravel backfill.

Design load cases considered both dry and saturated MSE blocks for the PMF event using factored ultimate limit state (ULS) design loads that are calculated by moment equilibrium equations and assuming a Meyerhof vertical stress distribution. To satisfy R57 design requirements, an overdesign factor of 1.0 must be achieved. Earthquake load cases considered included the Operating Basis Earthquake (0.21g horizontal and 0.15g vertical accelerations) and Maximum Design Earthquake (0.99g horizontal and 0.73g vertical accelerations). Following pseudo-static analysis to determine the likely failure mode, an elastic finite element analysis using backfill stiffness varying from 50MPa to 200MPa predicted that the maximum likely movement of the MSE block could be in the order of 80-100mm under an MDE event.

The upstream facing panel joints were sealed with an impermeable membrane and the MSE block was constructed in zones which varied from a silty, sandy gravel (Zone 4) at the upstream face and above the existing dam's clay core, to a well graded gravel (Zone 4A) above the existing fine filter, to coarse gravel (Zone 4B) above the existing coarse filter (Fig. 4). Construction of the project was completed in December 2015.

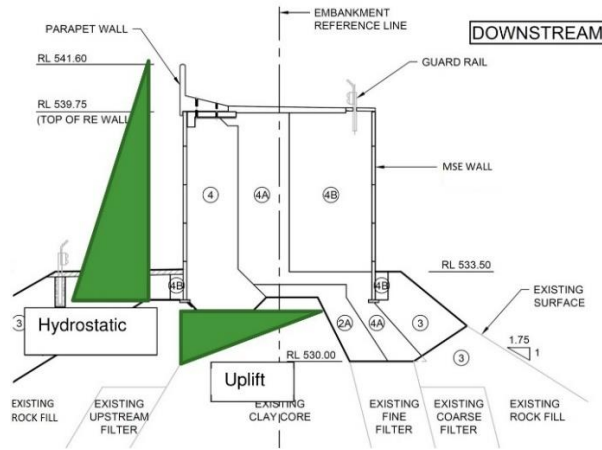


Fig. 4
Water Pressure Diagram for PMF Loading Case (Consultant Design Report)

3.2 LOS VAQUEROS DAM, CALIFORNIA (USA)

Los Vaqueros Dam was originally built in 1998 to create the Los Vaqueros Reservoir to improve the quality and amount of water available to the Contra Costa Water District (CCWD). In 2011, CCWD expanded the reservoir from 123,000 million liter (ML) (100,000 acre-ft) to 197,000 ML (160,000 acre-ft) in capacity by raising the dam height by 10.4m (34 ft).

The principal elements of the project were to excavate the crest of the existing dam by 14.3m (47 ft) and then to add 24.7m (81 ft) to the dam height, making a total dam height increase of 10.4m (34 ft), as shown in Figure 5. Approximately one million cubic meters of additional engineered embankment fill was placed; coming from borrow areas located near the dam.

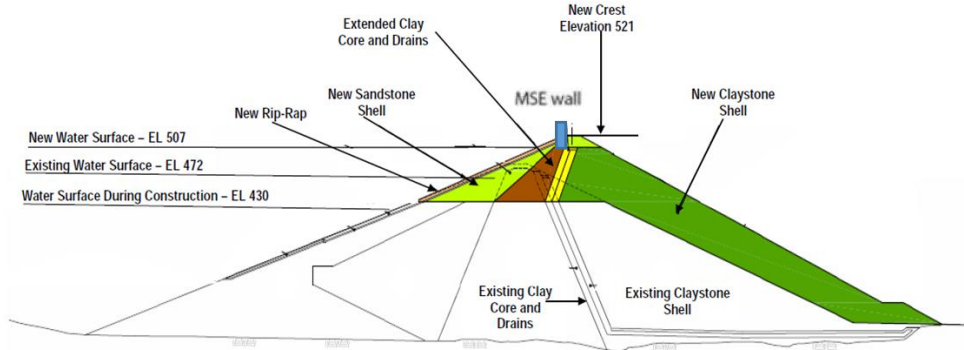


Fig. 5
Section of Dam Expansion

The project site was within a relatively high seismicity zone with a specified ground acceleration coefficient of 0.50g. Two MSE structures with a maximum height of 15m (49 ft) were utilized to widen the roadway at the crest of the dam on the upstream side. The other two structures were used on the downstream side. The upstream walls were located within the phreatic zone and subjected to submerged design conditions with one meter (3 ft) of rapid drawdown.

Design was performed on the basis of AASHTO codes modified to address special criteria related to PET geosynthetic strips and dam functionality. The MSE walls were founded on competent compacted shell-sandstone material that was also a part of the dam embankment. The bearing capacity was adequate to support the MSE wall with narrower base width at some sections of upstream walls. The final vertical plumbness of the walls was measured to be within 38mm (1.5 inches) in 3m (10 ft) of vertical distance. No movements were detected after the construction of the walls (Figure 6).



Fig. 6
Completed Los Vaqueros Dam Expansion

CONCLUSIONS

The use of MSE walls in upgrades to existing dams allows expansion to capacity while combining a more limited plan area and loading scheme with relative economy. Selection of reinforcements for the MSE walls depends upon the salts content of the retained backfill and water, but on the whole, either galvanized steel or geosynthetic reinforcements can perform equally well with the material considerations taken into account during design and construction. MSE walls are a well understood and mature technology that should be considered for their reliability, stability and flexibility, particularly in the face of seismic conditions.

REFERENCES

- [1] Association of American State Highway and Transportation Officials (2004, 2007, 2012), "AASHTO LRFD Bridge Design Specifications."
- [2] Beukes. J., "The Use of Mechanically Stabilized Earthfill in Raising of Earth Dam", Dept. of Water Affairs, Directorate:Strategic Asset Management, South Africa.
- [3] Hardianto, F., Lozano, R., Sankey J., Hughes, D., "The Use of Mechanically Stabilized Earthfill in Raising of Earth Dam", 2013 GeoCongress, Oakland, California (USA).
- [4] Ministère Des Transports (1979). "Les Ouvrages en Terre Armée, Recommendations et Regles De l'Art", Direction Desroutes et De La Circulation Routiere, Paris, France 1-189.
- [5] NSW Roads and Maritime Services QA Specification R57, "Design of Reinforced Soil Walls" Guide Note, Ed.2/Rev6 (2012), Australia.
- [6] Reinforced Earth Marine and Dam Structures Brochure, USA, 2018.
Taylor Draw Dam Case Study, The Reinforced Earth Company, USA, 2018.

SUMMARY

The first Mechanically Stabilized Earth (MSE) walls for dam applications were constructed using Reinforced Earth® in 1973, soon after development of the MSE technology by Henri Vidal in the late 1960s. Since these first structures, MSE walls have been used around the world to meet the challenges represented by a variety of waterway structures that include dams and dam upgrades. With time, the technology has evolved primarily in the type of reinforcements used to meet the site conditions imposed by geotechnical and hydraulic conditions. Case studies are provided to represent the primary applications of galvanized steel and geosynthetic reinforcements used in MSE walls for dam upgrades.

Les premières parois mécaniquement stabilisées (MSE) pour les barrages ont été construites en utilisant Reinforced Earth® en 1973, peu après le développement de la technologie MSE par Henri Vidal à la fin des années 1960. Depuis ces premières structures, les murs MSE ont été utilisés dans le monde entier pour relever les défis représentés par une variété de structures de voies navigables qui incluent des barrages et des améliorations de barrage. Avec le temps, la technologie a principalement évolué dans le type de renforcement utilisé pour répondre aux conditions du site imposées par les conditions géotechniques et hydrauliques. Des études de cas sont fournies pour représenter les principales applications de l'acier galvanisé et des renforts géosynthétiques utilisés dans les murs MSE pour la modernisation des barrages.

KEYWORDS

Earthfill Dam, Internal Friction, Reinforcement, Reinforced Earth

COMMISSION INTERNATIONALE
DES GRANDS BARRAGES

VINGT-SIXIÈME CONGRÈS DES
GRANDS BARRAGES
Autriche, juillet 2018

STUDY OF RESERVOIR RIM SLOPE STABILITY DUE TO OPERATION OF SUSU DAM

Ahmad FADHLI MAMAT

Project Leader, TNB RESEARCH SDN BHD

MALAYSIA

1. INTRODUCTION

Susu Dam is part of the Ulu Jelai Hydroelectric Project undertaken by the national power company (TNB) which could generate 372MW. Its main dam, with a height of 88m, is located in Cameron Highlands, about 200km north of Kuala Lumpur. This reservoir is one of the dams in Malaysia with major fluctuation during its operation. Leryar Village, which is a settlement for about 400 aborigines, is located on the bank and a rim slope failure could be catastrophic to the community. As such, this study investigates the landslide hazards due to the fluctuation of Susu reservoir and rainfall infiltration, by conducting soil investigation, hazard mapping and advanced laboratory tests.

2. METHODS

Rainfall data for the past 30 years were analyzed so that the intensity and duration of a rainfall event with a return period of 1:10 years could be estimated. Field assessments and GIS analyses were conducted so that hazard maps could be produced using methods proposed by Anbalagan (1992). Advanced lab tests, i.e. permeability, CU, CD and SWRC, were carried out to obtain the hydraulic and mechanical properties of the top soil layer, in the saturated and unsaturated

states. The hydraulic conductivity relationship and the shear strength contribution with increase in suction were then deduced using methods proposed by Van Genuthen (1980), Freudland & Morgenstern (1977) and Ho & Freudland (1982).

3. RESULTS

Results of Factor of Safety (FOS) from slope stability analyses using this method differs greatly from the methods normally used by practitioners. Conventional methods would conclude that the slopes are sufficiently stable with FOS values of at least 1.47, while this method, which involved rigorous testing and numerical modeling, resulted in FOS as low as 0.37. It is also noted that hazard maps produced using a qualitative and probabilistic approach agrees well with the FOS of the specific slopes, which is quantitative and deterministic.

4. CONCLUSION

This study exhibits the need to conduct extensive soil tests and apply the latest theories in soil mechanics to obtain reliable FOS for shallow failures involving transient flow conditions, such as rapid drawdown and rainfall infiltration. It also suggests that qualitative hazard assessment could be used as a precursor to advanced soil tests and numerical modeling, which are costly.

REFERENCES

- [1] ANBALAGAN R. Landslide hazard valuation and zonation mapping in mountainous terrain. *Engineering Geology*, 32, 269-277, 1992.
- [2] VAN GENUCHTEN, M. T. A closed-form equation for predicting the hydraulic conductivity of unsaturated soil. *Soil Science Society of America*, 44, 892-898, 1980.
- [3] FREDLUND, D. G. & MORGENSTERN, N. R. Stress state variables for unsaturated soils. *Journal of Geotechnical Engineering Division, ASCE*, 103, 447-466, 1977.
- [4] HO, D. Y. F. & FREDLUND, D. G. Increase in strength due to suction for two Hong Kong soils. *Proceeding ASCE Specialty Conference Engineering and Construction in Tropical and Residual Soils*, 263-295, 1982.

Keywords: Landslide, Stability, Safety Factor, Finite Elements Method, Soil Mechanics, Soil Investigation, Shear Stress, Susu Dam.

COMMISSION INTERNATIONALE
DES GRANDS BARRAGES

VINGT-SIXIÈME CONGRÈS DES
GRANDS BARRAGES
Autriche, juillet 2018

**MONITORING OF THE SLOPE STABILITY OF RESERVOIRS: AN UPDATE
ON THE OBSERVATIONAL METHOD. THE CASE OF A DAM IN PORTUGAL**

Josep RAVENTÓS FORNÓS, Carles COUSO, Maite GARCIA

TRE ALTAMIRA

SPAIN

Nadir PLASENCIA, Elisa ALMEIDA

EDP PRODUÇÃO

PORTUGAL

1. INTRODUCTION

The observational method applied to monitoring slope stability in dams and reservoirs aims to provide substantial information for a proper risk management, during the construction and operation of these critical infrastructures.

This paper proposes to describe, explore and discuss the advantages and limitations of the data obtained by geological in situ inspections, classical geotechnical monitoring techniques (such as inclinometers, piezometers, etc.) and geodetic surveying techniques applied in large areas, together with the use of remote sensing techniques, like InSAR. This combination allows the information to be maximized in terms of areal coverage, accuracy and data integration.

In the case study presented, this analysis proved to be a great help to decision making in the context of a hydropower reservoir in Portugal owned by EDP, with a capacity of 106 hm³ and an area of 421 ha, created by a dam 110 meters high and 275 meters long at the crest, which has associated a powerhouse with a generation capacity of 263 MW.

2. MONITORING PROGRAMME FOR SURVEYING SLOPE STABILITY

The program for monitoring the slope stability of the reservoir included, locally, the installation and reading of several inclinometers and also the observation of several particular slopes whose safety can be compromised for geotechnical reasons and/or for their specific characteristics.

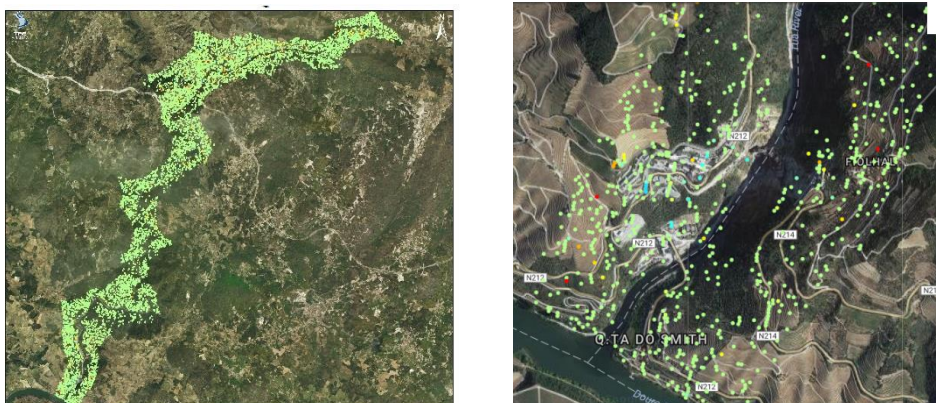
Dam monitoring includes the installation of topographical prisms over the dam body and also several topographic references that help the stability of the system in terms of precision and accuracy. Those reference prisms are also installed in the slopes, so in areas of potential movement. The use of other systems that can help to monitor these references and correct the final real displacement is also of interest.

InSAR remote sensing monitoring was analyzed in order to verify if this technique could be applied to:

- obtain displacement information over the remote slopes where there is no option to install in-situ devices,
- check if the reference prisms are in moving areas,
- obtain a general overview of the stability of the slopes and also helps to optimize the installation and readings of other geotechnical instruments.

Figure 1

Results obtained for slope monitoring with InSAR technology. Displacement map with general overview on the area (left) and results showing motion on the slopes close to the dam body (right).



COMMISSION INTERNATIONALE DES GRANDS BARRAGES

VINGT-SIXIÈME CONGRÈS DES GRANDS BARRAGES
Autriche, juillet 2018

DOI 10.3217/978-3-85125-620-8-218



This work licensed under a Creative Commons Attribution 4.0 International License. <https://creativecommons.org/licenses/by-nc-nd/4.0/>

**COUNTERWEIGHT AS JATIGEDE DAM LANDSLIDE STABILITY
COUNTERMEASURE**

Cristina D. YULININGTYAS

*Dam Engineer, Dam Safety Unit, MINISTRY OF PUBLIC WORKS AND
HOUSING*

INDONESIA

Dwi A.S.KUBONTUBUH

*Head of Water Resouces Network Development, Cimanuk Cisanggarung River
Basin Unit, MINISTRY OF PUBLIC WORKS AND HOUSING*

INDONESIA

H. MULDIANTO

*Head of Dam Project, Cimanuk Cisanggarung River Basin Unit, MINISTRY OF
PUBLIC WORKS AND HOUSING*

INDONESIA

P. RADITYO

*Head of River and Coastal, Cimanuk Cisanggarung River Basin Unit, MINISTRY
OF PUBLIC WORKS AND HOUSING*

INDONESIA

COMMISSION INTERNATIONALE
DES GRANDS BARRAGES

VINGT-SIXIÈME CONGRÈS DES
GRANDS BARRAGES

Autriche, juillet 2018

**COUNTERWEIGHT AS JATIGEDE DAM LANDSLIDE STABILITY
COUNTERMEASURE**

Cristina D. YULININGTYAS

*Dam Engineer, Dam Safety Unit, MINISTRY OF PUBLIC WORKS AND
HOUSING*

Dwi A.S.KUBONTUBUH

*Head of Water Resources Network Development, Cimanuk Cisanggarung River
Basin Unit, MINISTRY OF PUBLIC WORKS AND HOUSING*

H. MULDIANTO

*Head of Dam Project, Cimanuk Cisanggarung River Basin Unit, MINISTRY OF
PUBLIC WORKS AND HOUSING*

P. RADITYO

*Head of River and Coastal, Cimanuk Cisanggarung River Basin Unit, MINISTRY
OF PUBLIC WORKS AND HOUSING*

INDONESIA

1. INTRODUCTION

Jatigede Dam is the second largest storage dam in Indonesia that reaches almost 1 billion m³. Completed in 2016, this dam is located in Cimanuk River, Jatigede Subdistrict, Sumedang District of West Java Province, Jatigede Dam is a center core rockfill dam with 114 m height and 1,715 m length. The main purposes of Jatigede Dam are to fulfill 90,000 ha irrigation area, 3,500 l/s of

Cirebon and Indramayu water supply, 2 x 55 MW of hydropower, and flood control of 14,000 Ha area around Cimanuk River.

The dam site area generally has an intensive and complex tectonic geological structure. The existence of this complex structure causes the dam site area be vulnerable of landslide. Downstream of the left and right slope of the dam and the upper left bank of main cofferdam are the landslide locations. Geological structure and high rainfall intensity are the main factors that cause the landslide.

During the construction phase of Jatigede Dam, it was discovered that some landslides were in motion around the main dam area particularly at the downstream left bank in Cipinang and at the right bank in Eretan. These landslides disrupted the work progress thus leading to initiation of several countermeasures. While the landslide at the right bank had been taken care of successfully, the one occurs at the downstream left bank is still in progress of stabilization up to date.

2. GEOLOGICAL REVIEW

2.1. LOCAL GEOLOGY

The left saddle bedrock is formed by a mixture of sand-stone and clay-stone with thickness ranging between 10 to 40 centimetres, grey to yellowish grey in color, friable, slaking, and moderately weathered. This bedrock formation is classified as folded breccia. The upper part has weathered and mixes up with yellow to reddish brown soft soil.

The river bedrock consists of sedimentary rocks and rigid breccia formation utilized as the main dam's footing. There is also an evidence of fault in the riverbed as indicated in geological maps. In general, the bedrock on both left and right banks is formed by volcanic breccia of Lower Halang formation.

Within the bedrock of the right bank, the Lower Halang volcanic breccia starts to shift to the Upper Halang clay-stone. This transition manifests in the form of fault with angle of strike/dip $N242^{\circ}E/82^{\circ}$, inclined to the west with angle of $N124^{\circ}E/64^{\circ}$. This bedrock formation is more than five hundred metres spanning to the upstream and downstream of the main dam.

2.2. LANDSLIDES ZONE

Landslides area on the left bank is estimated about twenty hectares. The sliding crown is situated close by the sand sieving plant, spans toward the edge of river body in the east. The sliding border is easily recognized due to trapped topographical surface and highly steep slope (approximately $60^{\circ} - 70^{\circ}$).

Its bedrock formation is the lowest layer of Lower Halang breccia. The upper layers consist of Upper Halang flakish clay-stone and folded breccia, with the latter being white to brownish yellow in color, relatively permeable (permeability coefficient of 10^{-4} cm/s).

A layer of old unconsolidated volcanic sediment is situated above the aforementioned folded breccia. The sequential upper layer is filled by a mixture of solid aggregates and residual soil with 10^{-4} cm/s permeability coefficient. The debris is a mixture of weathered soil layer and old volcanic breccia layer, permeable and unconsolidated.

The landslide at the right bank consists of rock and soil fragments, permeable and consolidated, which is a suitable indication for instability during or even after construction phase. Result of geology investigation gives a clear picture of quarter volcanic layer slides over the claystone layer, on which the claystone is indicated as heavily weathered and extremely soft, black in color. Geologic characteristic shows the volcanic quarter debris is a mixture of rock fragments and silty clay, with thickness between 8 up to 14 meter from top soil.

Ground water level is at the depth of 15 meter, adjacent to the landslide's crown, 5 meter downstream

3. FACTORS OF LANDSLIDES

According to the national standard issued by Ministry of Public Works and Housing namely SNI 03-1962-1990 regarding the Planning on Landslides Countermeasures, the general driving forces for any landslides are identified from the source of disturbance, whether internal or external.

3.1. EXTERNAL DISTURBANCE

- (1) Overburden due to human activities, such as buildings or soil dumping on top of banks.
- (2) Loss of lateral support, might be induced by bank erosion (natural cause or sand mining).
- (3) Lack of vegetation cover leading to gully erosion.

3.2. INTERNAL DISTURBANCE

- (1) Increase of soil mass due to over-saturation.
- (2) Groundwater table raises up causing a higher pore pressure, which in turn lowers the friction among soil particles.
- (3) Swelling on some certain clay soil.

In the case of Jatigede Dam, a heavy rainfall was accounted as external factor causing oversaturation in the soil, then the soil become an overburden toward itself with a higher pore pressure.

A similar phenomenon is expected to reoccur with a higher severity during the initial impounding. Thus, it is necessary for an intensive monitoring to be carried out during this phase.

3.3. LANDSLIDE SURVAILLANCE

3.3.1. *Left Bank Landslide*

A. Inclinometer Reading

After the completion of bored piles line A, B, and C, inclinometer IKI-1 was installed at the center of landslide direction which was giving a reading with no signs of movement. In contrast, the inclinometer IKI-2 which was installed at the edge of the upper part landslide showed an eight millimeter movement at the depth of 16 meter. According to technical discussion on this matter, held in Bandung in June 2014, it had been then decided to install additional bored piles and inclinometers namely bored piles line D and IKI-3 and IKI-4, which were completed in August 2014. From these additional installations, another movements were detected (IKI-3 at the depth of 43 m; IKI-4 at the depth of 16 m and 24 m), thus leading to three more bored piles installation at the base of landslide (line E, F, G) which is still in progress.

Sliding movement showed by IKI-4 is situated on an exposed clay-stone with steep slope, with a creep movement and is calssified as translation sliding.

Reading of IKI-3 shows a deep slide at the depth of 43 m on the transition between breccia tuffs (semi-impermeable with coefficient 10^{-4} cm/s) and clay-stone (coefficient 10^{-6} cm/s) layers, therefore it is estimated that this transition layer is responsible as the sliding plane. This plane's slope, indicated as translation sliding, is in alignment with the top soil surface layer with slope of $5^0 - 10^0$.

Inclinometers and Piezometers placement layout on the left bank is shown in figures below. Visual results of inclinometers display the rate of movement from IKI-3 (1.4 mm/day) and IKI-4 (1.5 mm/day), which are according to SNI 03-1962-1990 classified as creep movements (less than 4 mm/day).

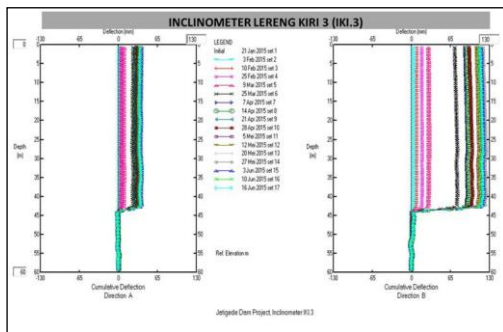


Figure 1.
Inclinometer Reading IKI-3 at Left Bank

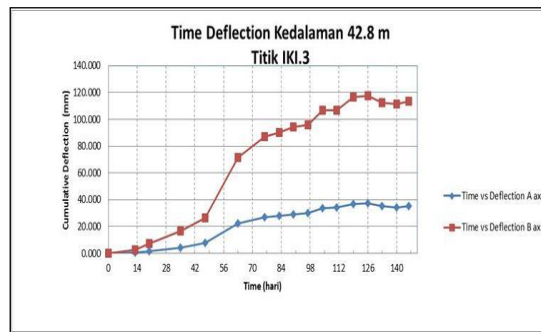


Figure 2.
Inclinometer IKI-3 at Left Bank,
Landslide Motions in Time

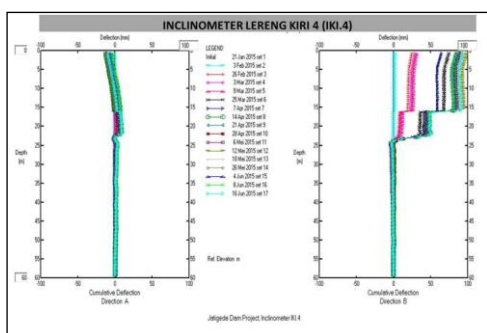


Figure 3.
Inclinometer IKI-4 at Left Bank

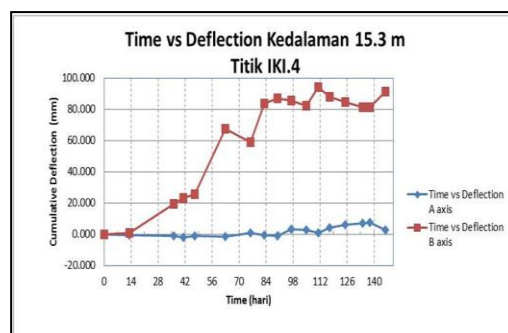


Figure 4.
Inclinometer IKI-4 at Left Bank,
Landslide Motions in Time

B. Robotic Monitoring System Reading

At the left landslide zone, the result of robotic monitoring system shows that all observatory prisms tend to move toward the old river body (right side) by 18 mm in 2 months. This magnitude is considered to be relatively small in accordance with the inclinometer reading during period of March – May 2015 (Figure 7).

3.3.2. Right Bank Landslide

At the right landslide zone, the reading from observatory prisms shows tendency of movement toward the left direction with a relatively low magnitude (0 – 4 mm) (Figure 8).



Figure 5.
Situation of landslides around
Jatigede Dam

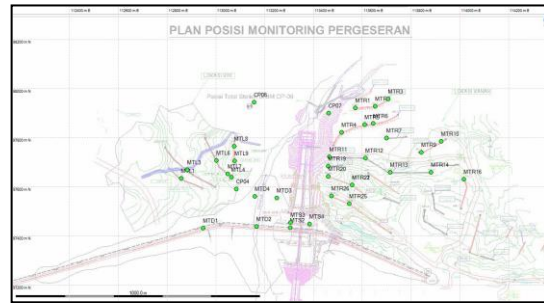


Figure 6.
Observatory Prisms on landslides around
Jatigede Dam

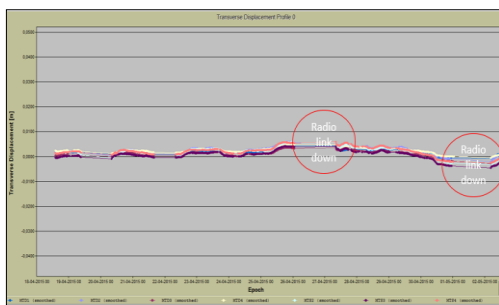


Figure 7.
Transversal Displacement of Left
MTL (March-May 2015)

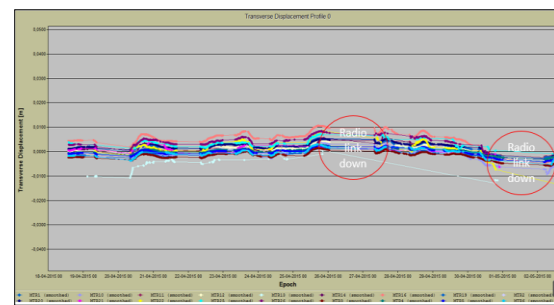


Figure 8.
Transversal Displacement of Right MTR
(March-May 2015)

4. PROPOSED OF COUNTERMEASURES

Some countermeasures to prevent potential landslides has been prepared and constructed, they are:

1) Reduce the driving force

- (a) Reduce static force:
 - Reduce slope steepness (accomplished)
 - Terraces construction at the upstream of bored piles line (accomplished)
- (b) Minimize contact with surface run-off and groundwater:
 - Rearrange drainage network (on progress)

2) Anchor Placement and Improvement of Sustaining Force

- (a) Arrange bored piles lines along the bank (on progress, with some part has already accomplished).
- (b) Construct a counterweight at the toe of the left bank (dependant on short-term monitoring result).

3) Various Improvement Activities

- (a) Subsurface drainage system (horizontal-pipe drain).
- (b) Robotic surface-coordinate monitoring (accomplished).

- (c) Inclinator installation (on progress).
- (d) Installation of additional piezometers (on progress).
- (e) Observation wells probing at the landslides site.
- (f) Periodic observation and evaluation to determine the necessity of long-term countermeasures.
- (g) Calculation of a three-dimensional mathematic model on the correlation of landslides and main dam.

5. CONCLUSION

Constructed countermeasures has showed that:

- Right Bank landslide had been taken care of successfully, and recent visual inspection and instrumental observation show no evidence of any significant displacements.
- Left bank landslide has undergone a similar treatment method assuming 12 to 14 meter depth of sliding plane. However, inclinometers reading shows indication of another movements at the depth of 43 m (IKI-3) and 16 – 24 m (IKI-4) with the rate of 1.4 mm/day, thus classified as a creep movement.
- These sliding movements are highly correlated to rainfall intensity.

However some recommendation countermeasures are still needed to make sure the stability due to landslide potential areas, such as:

- 1) Complementary constructions in order to mitigate the additions of impending loads due to external disturbance as follows :
 - (a) Deeper additional bored piles (in progress) or soil nailing at the toe of left bank.
 - (b) Construction of counterweight at the toe of left bank which supports the right bank.
 - (c) Continuation of subsurface drainage with horizontal pipes to lower groundwater level.
 - (d) Continuation of surface drainage with Y-drains (bee hives construction) to reduce the rainfall effect.
- 2) Intensive monitoring and evaluation on both visual inspections and instrumental readings.
- 3) Reservoir impounding to be carried out thoroughly and gradually. Construction of point 1) could be implemented during or after the initial impounding.
- 4) Establish a discrete monitoring and evaluation task force, solely responsible during initial impounding phase.

6. ACKNOWLEDGEMENT

The authors would like to thank to Cimanuk Cisanggarung River Basin Unit for the authorization to publish the main result of the present study.

KEYWORD

Counterweight, Jatigede Dam, Landslide

REFERENCES

- [1] Dam Safety Unit. *Jatigede Dam Safety Review Report*, 2014.
- [2] Departement of Public Works. *Landslide Countermeasure Design*, 1987.
- [3] Cimanuk Cisanggarung River Basin Unit. *Design Report, Landslide Countermeasure at Downstream of Jatigede Dam*, 2011.

COMMISSION INTERNATIONALE DES GRANDS BARRAGES

VINGT-SIXIÈME CONGRÈS DES GRANDS BARRAGES
Autriche, juillet 2018

DOI 10.3217/978-3-85125-620-8-219



This work licensed under a Creative Commons Attribution 4.0 International License. <https://creativecommons.org/licenses/by-nc-nd/4.0/>

**EVALUATION OF SEISMIC PERFORMANCE OF EARTH DAMS DUE TO THE
LEVEL OF ITS RESERVOIR USING FINITE ELEMENT METHOD**

Amin DIDARI

DEPARTMENT OF CIVIL ENGINEERING, ESTAHBAN BRANCH, ISLAMIC
AZAD UNIVERSITY, ESTAHBAN

IRAN

Mohammad Hassan SADDAGH

DEPARTMENT OF CIVIL ENGINEERING, ESTAHBAN BRANCH, ISLAMIC
AZAD UNIVERSITY, ESTAHBAN

IRAN

Zahra GHADAMPOUR

DEPARTMENT OF CIVIL ENGINEERING, ESTAHBAN BRANCH, ISLAMIC
AZAD UNIVERSITY, ESTAHBAN

IRAN

EVALUATION OF SEISMIC PERFORMANCE OF EARTH DAMS DUE TO THE LEVEL OF ITS RESERVOIR USING FINITE ELEMENT METHOD

Amin DIDARI

DEPARTMENT OF CIVIL ENGINEERING, ESTAHBAN BRANCH, ISLAMIC
AZAD UNIVERSITY, ESTAHBAN

IRAN

Mohammad Hassan SADDAGH

DEPARTMENT OF CIVIL ENGINEERING, ESTAHBAN BRANCH, ISLAMIC
AZAD UNIVERSITY, ESTAHBAN

IRAN

Zahra GHADAMPOUR

DEPARTMENT OF CIVIL ENGINEERING, ESTAHBAN BRANCH, ISLAMIC
AZAD UNIVERSITY, ESTAHBAN

IRAN

ABSTRACT

One of the challenges in engineering world is investigation on seismic behavior of earthdams during an earthquake. The complexity of this issue is lack of adequate information about the impact of the earthquake on earthdams behavior. Many scientists presented an important research in this area. Dam stability during the earthquake is one of considerable factors which can be estimated by various parameters. In this paper, as a reliable parameter, safety factor is estimated using finite element method in PLAXIS 2D software. In this paper, reservoir water level is considered as a noticeable parameter which affects on stability of earthdam and safety factor during an earthquake. For this purpose, two different water levels, %30 and %70 of earthdam height, is assumed for reservoir. Also, in order to consider effects of earthquake, a magnitude MW 6.8 earthquake is applied to model. Angle of internal friction of earthdam materials is 30 to 35 Degree and the side slopes are 1:2.7. Additionally,

as isotropy has no enormous impact on results, isotropic materials are assumed for earthdam. Analysis results indicate reservoir water level increasing from %30 to %70 of earthdam height has direct impact on safety factor reduction up to %8.

KEYWORDS

Earthdam, reservoir level, finite element method, seismic performance, safety factor

1. 1.INTRODUCTIONS

It has been a long time since the construction of earth dams was used to control and store water. One of the issues that is important in earth dams is the seismic behavior of earth dams due to landslide of neighboring areas or earthquakes. Mostly failure due to an earthquake was not in areas where the dams are concentrated; however, to investigate this comment a few practical experiences are available. Earthquake-related failures can be sub-categorized and for each group the stability prediction can be considered:

- The earthquake shake causes cracks in the upper parts of the dam and these cracks may happen exclusively in the core and water can flow from cracks and if there are no precautionary measures, the piping will eventually lead to the destruction of the dam.
- The earthquake shake causes the body or foundation to subsidence, therefore the dam's crest moves. As a result of the free height reduction, the water flows above the dam and the dam will destroy.
- The reservoir shake causes the formation of oscillary waves which are large and slow at the surface of the water. If there is not enough free height, the water inside reservoir passes the crest of dam toward downstream and possibly destroys the dam.
- Slopes of dam in the both sides might reach to failure due to earthquake and the dam can be destroyed from the both sides. One of the attractive factors is the stability of dams. To measure the stability of dams, various parameters can be used which one of the most accurate and reliable is the Safety factor.

Shong-Loong Chen et al. [4] entitled the effect of upward water level on dynamic response of embankment dams conducted a dynamic survey on embankment dams according to seismic conditions of Taiwan in DIANA-SWANDYNEII with different water levels and numerical simulations. In this paper, the penetration and dynamic stability of embankment dams making by three

different types of soil such as clay, silt and silty sand have been examined. Results obtained from dynamic survey on five different water levels indicate that areas above foundation line and membrane part of upstream silty link to dam height have seep ability; moreover, pore water pressure makes rapidly and increase in medium of upstream silty part. Also, results indicate that pore water pressure in more than one third of upward out membrane mostly be negative until water height reaches to 0.75% of the dam height which is indicative of area stability and any seepage is impossible in this passive time.

Yu-xin Jie et al. [5] in a study examined penetration, seepage and also stress and strain on different water levels in embankment dams. In this research, in order to perform numerical simulation for filling water in a rock embankment dam, a simple approach has been used for analysis of unsaturated soil stabilization. In addition to stress and movement in dam, pore water pressure and phreatic line have simultaneously obtained. Results indicate that according to simultaneous effect between deformation and pore water pressure, progress of phreatic line in body and core of dam is faster than analysis of unsaturated penetration and seepage without simultaneous effect of deformation. Changes of pore water pressure is not only related to unsaturated penetration due to water surface changes, but also related to cavity due to deformation.

2. MATERIAL AND METHODS

In order to examine the dynamic behavior of embankment dams, a model was designed and safety factor for two cases of friction internal angles of 30 and 35 degrees in top and bottom levels of reservoir was investigated. For this purpose, a dam with 70 meters height, sides slope 1:2.5 and 9 meters length of crest was assumed. Clay soil was used for a core and a sand for drainage and also a foundation consist of clayey-sand. The dam has also a cutoff consist of grout (Figure 1), and then was meshed by the program (see Figure 2).

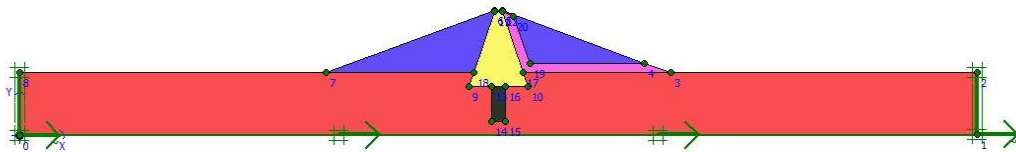


Fig. 1. soils cluster

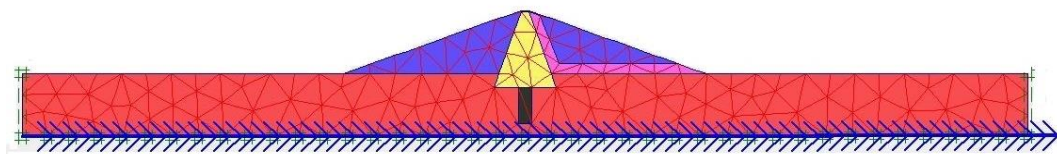


Fig. 2. mesh formation

2.1. SOIL DATA

In this model, five soil specimens (grouted ground to seal the foundation by, clay soil for core, sand and gravel for soil draining, clayey sand for soil of and at last, silty sand for dam surface) were used which properties of each of them separately shown in Table 1.

Table 1. soils specifications

Soil	E(KN/m ²)	C(KN/m ²)	Φ	K(m/day)
Silty Sand	5500	30	35	0.2
Clay	2500	60	30	0.001
Clayey sand	3500	1	33	0.4
sand	30000	1	35	10
Grout	4000	1	33	0.05

the information above and also initial values of computations can be extracted by Allpile [1] program, Advance Soil Mechanic written by Das[6] and Foundation Analysis and Design written by Bowles[2] and other parameters can be computed. The table in this guideline and books has been taken for helping in selection of soils property.

Penetration of some soils has been mentioned in book of Advance Soil Mechanic from which can be used for selecting the most appropriate soil. Test standard method for standard penetration test [3] and sampling soils by split rib tube (two scales sampling). This test method describes way of going forward two scales tubular sampling for obtaining definite soil specimen and measuring soil strength against sampling penetration, and generally it has been known as Standard Penetration Test (SPT). This standard does not express all safety cases related to its application, consumer of this standard account to provide appropriate health and safe instructions and define applicability of equality limitations before using. Values which is expressed in inches-pounds units as standard. This test provides both a sample in order to detection and appropriate experimental tests related to the soil, and another sample that it may lead to much touched shear deformations. This test has been widely used in exploratory geotechnical projects. There are any local and widely propagated relationships which number of SPT impact or N related to engineering behavior of earth works and foundations. Also, elasticity modulus of some soils can be determined by Foundation Design and Analysis book which is taken in the following using SPT.

Table 2. modulus of elasticity specifications

Soil	Es(kN/m ²)
Sand	Es=500(N+15) Es=18000+750N Es=(15200 to 22000)ln N
Clayey sand	Es=320(N+15)
Silty sand	Es=300(N+6)
Gravelly sand	Es=1200(N+6)

2.2. EARTHQUAKE DATA

Magnitude (Richter) and amplitude logarithmic measuring of earthquake is in conjunction with released energy as earthquake waves in earthquake center. Earthquake magnitude do not have top and bottom limits; however, the most and least earthquake magnitude are 9.5 and -3.5. In this logarithmic scale, shallow earthquakes have been shown that elastic wave of earthquake with magnitude 6 Richter, has an energy about 30 times energy of an earthquakes with magnitude 5 Richter, and also more than 900 times one with magnitude 4 Richter and so on. Different factors are effective on determination of earthquake power including focus depth, distance of earthquake center to measure station, frequency of sampled energy and pattern of earthquake propagation (angle variety in vibration amplitude).

According to the statistics of earthquakes occurred in California[7], America between 1898 to 1989, at least 23 earthquakes with magnitudes between 6.5 to 7.2 are reported and also, so other earthquakes observed in less or more magnitudes. Measurement is done by the shaking caused by earthquake in any time. In whole, in three past decades in California, the scales which have had more strong shaking and acceleration during earthquake, have been measured by organization of coastal and geodetic of America. On the base of statistics, earthquakes are differed on different cases. Thus herein, an earthquake with the following characteristics has been considered which these cases can be accounted in possibility occurrence in an acceptable range among earthquakes which may cause damage. Earthquake characteristics used in this analysis, have been taken in Table 3 and also, acceleration in cm/s², velocity in cm/s and displacement in cm versus time observed in the following Figures.

Table 3. Earthquake specifications

Earthquake magnitude	6.8	Mw
The distance from the epicenter	77.7	Km
Peak value	-2.4	Cm
Sample rate	200	Hz
Acceleration	52.5	cm/s ²
Velocity	3.12	cm/s

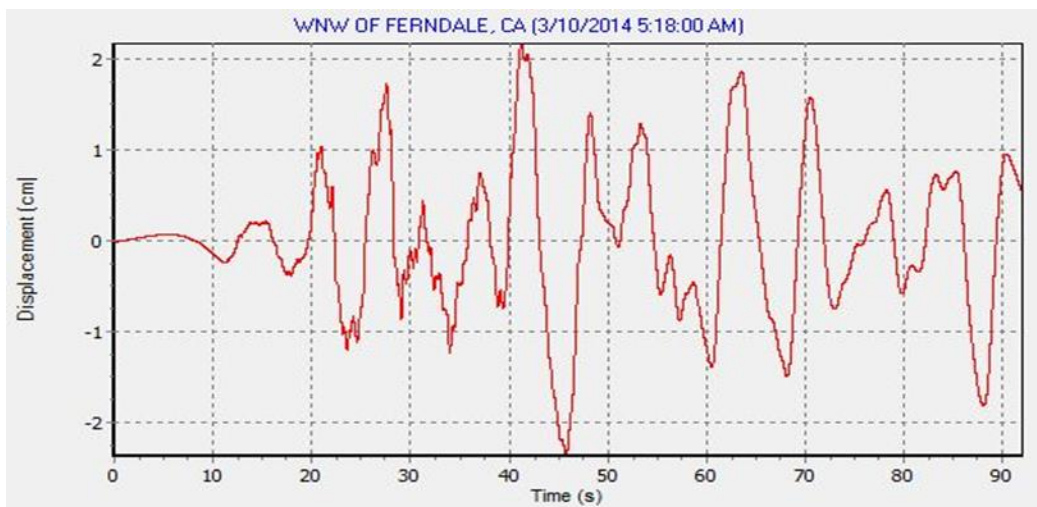


Fig. 3. Earthquake Displacement-Time diagram

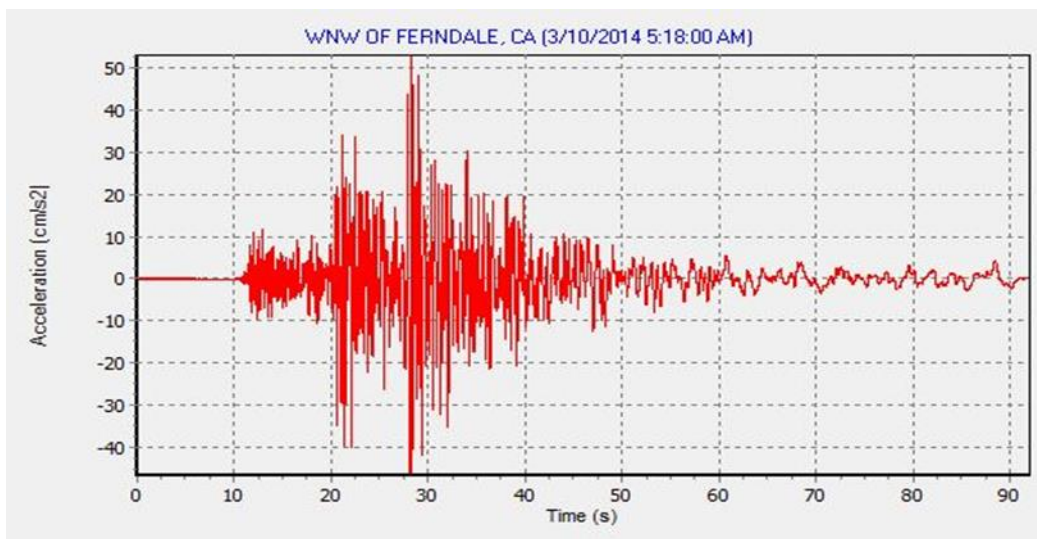


Fig. 4. Earthquake Acceleration-Time diagram

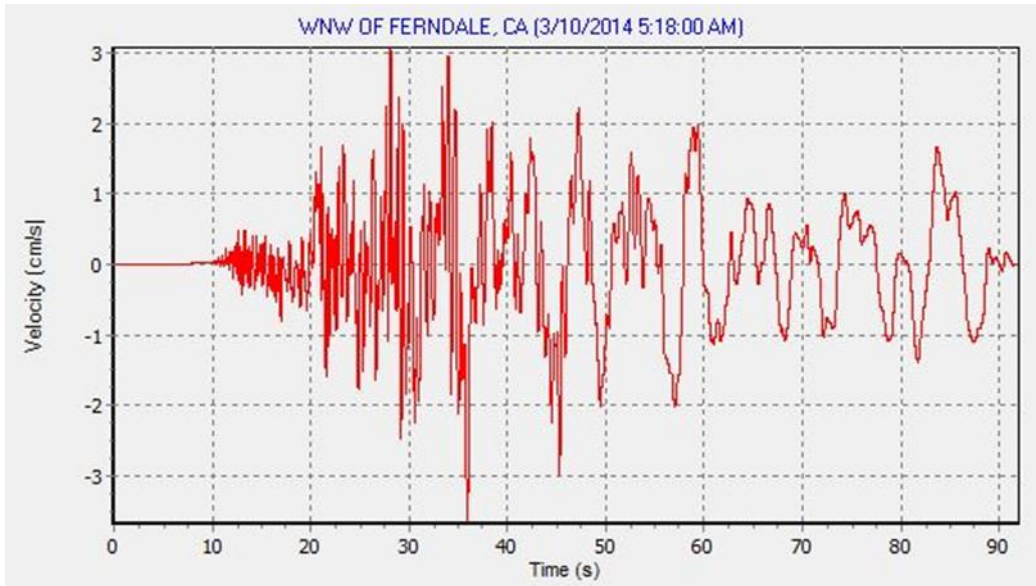


Fig. 5. Earthquake Velocity-Time diagram

3. RESULTS AND DISCUSSION

After modeling and applying initial conditions, seismic conditions of dam were considered according to two levels of water reservoir (30% and 70% of reservoir volume). These investigations were conducted in two different levels of water reservoir and each level by 3 times repetition. In the following, computation charts of safety factor were taken for different water levels with separation of reservoir water height that would be analyzed.

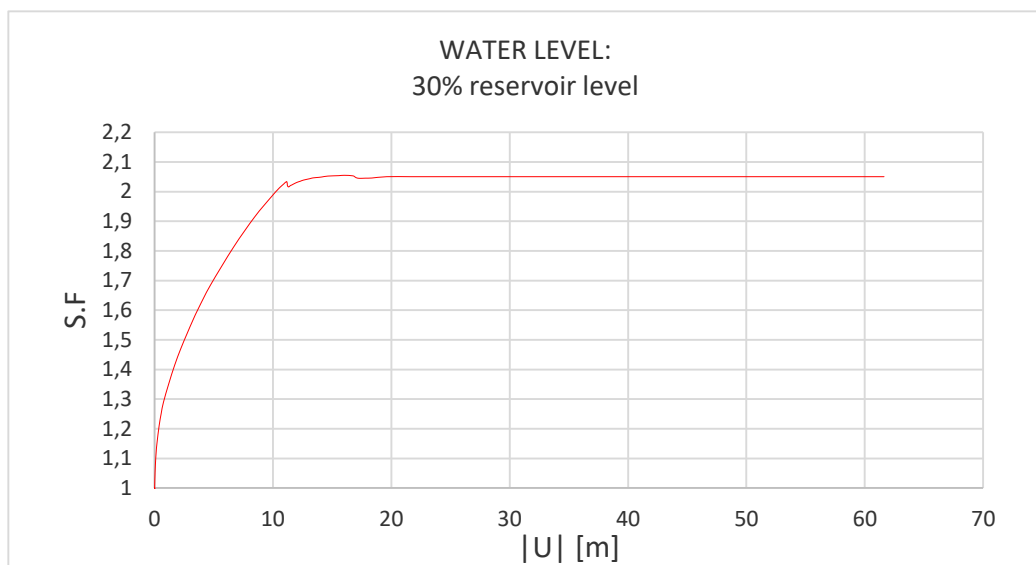


Fig. 6. Safety factor diagram-30% reservoir level

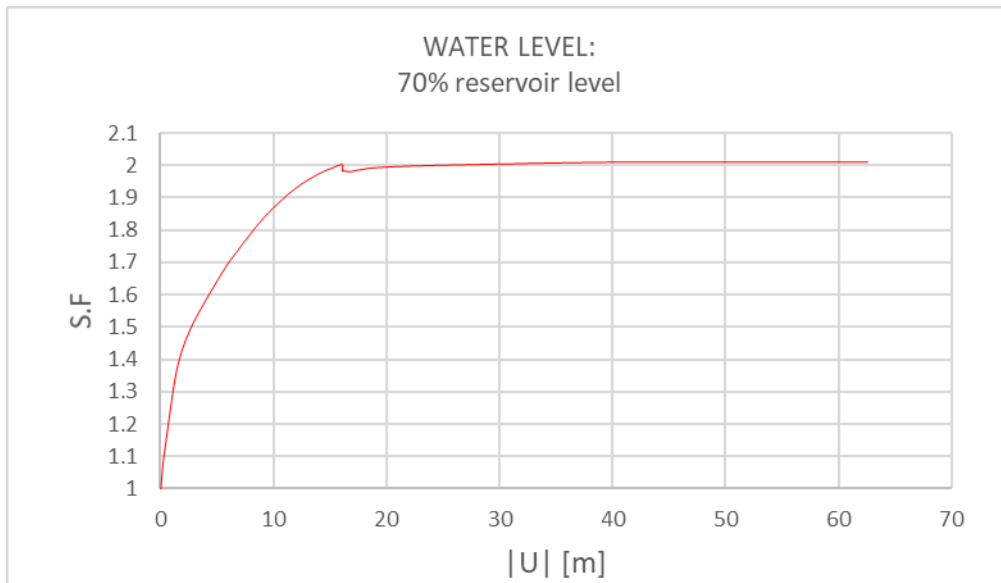


Fig. 7. Safety factor diagram-70% reservoir level

As it is observed in above charts, increasing water surface from 10% to 90% of reservoir height cause decreasing factor of safety.

4. CONCLUSION

Figures 6 and 7 indicates FS for two water levels. As it is obvious in these charts, curves slope reduced from level 30% to 70%. By drawing a tangent line between them to find safety factor, it's value becomes smaller. This means that, seismic stability of embankment dam is reduced by increasing water level of reservoir.

the Results indicate that FS is reduced by increasing upward water level of dam; if water level is increased from 30% to 70% of upward water level, this reduction would be about 8%.

REFERENCES

- [1] AllPile (Version 7)- User's Manual (Volume 1 and 2)(2015)
- [2] Bowles , 1979 , physical and geotechnical properties of soils, Mc Graw – Hill , Inc.
- [3] Introduction of standard penetration test, Department of Engineering Dari, (www.daryan.co)

- [4] Chen S.-L., Lin C.-F., Ni J. C., and Gui M.-W., Effects of Upstream Water Level on Dynamic Response of Earth Dam, Hindawi Publishing Corporation Mathematical Problems in Engineering. (2015)
- [5] Jie Y.-x., Wen Y.-f., Deng G., Chen R. and Xu Z.-p., Impact of soil deformation on phreatic line in earth-fill dams, Computers & Geosciences. (2012)
- [6] Das B.M. (1983). Advanced soil mechanics, 270 Madison Ave, New York, NY 10016, USA.
- [7] STOVER C. W. and COFFMAN J. L.. Seismicity of the United States. (1568-1989)

COMMISSION INTERNATIONALE DES GRANDS BARRAGES

VINGT-SIXIÈME CONGRÈS DES GRANDS BARRAGES
Autriche, juillet 2018

DOI 10.3217/978-3-85125-620-8-220



This work licensed under a Creative Commons Attribution 4.0 International License. <https://creativecommons.org/licenses/by-nc-nd/4.0/>

**THREE LARGE RESERVOIRS OPERATION IN THE CASCADE SYSTEM
CITARUM RIVER – INDONESIA**

Hari SUPRAYOGI

Director of River and Coastal, MINISTRY OF PUBLIC WORK AND HOUSING

INDONESIA

Harry M. SUNGGUH

Director II, JASA TIRTA II PUBLIC CORPORATION

INDONESIA

Reni MAYASARI

*Special Expertise Level I of Water Resources Management, JASA TIRTA II
PUBLIC CORPORATION*

INDONESIA

**THREE LARGE RESERVOIRS OPERATION IN THE CASCADE SYSTEM
CITARUM RIVER – INDONESIA**

Hari SUPRAYOGI

Director of River and Coastal, MINISTRY OF PUBLIC WORK AND HOUSING

INDONESIA

Harry M. SUNGGUH

Director II, JASA TIRTA II PUBLIC CORPORATION

INDONESIA

Reni MAYASARI

Special Expertise Level I of Water Resources Management, JASA TIRTA II
PUBLIC CORPORATION

INDONESIA

1. INTRODUCTION

The three reservoirs are all situated on the Citarum, West Java. The Ir. H. Djuanda reservoir, which already exists since 1967 is the most downstream one. The next upstream reservoir is Cirata which is expected to become operational by 1987. The Saguling reservoir is the most upstream one and will start its operation in the most upstream one and will start its operation in the course of 1985. Downstream of Ir. H. Djuanda reservoir two weirs across the Citarum divert water into three main canals; the west tarum canal, the East tarum canal and the north tarum canal.

More than 20 million people are depend on Citarum with three reservoirs for irrigation (240,000 ha), water supply for domestic, municipal and industry (800 million m³/year), Electricity (3,200 MW), flood control and environment water, therefore optimize operation three reservoirs is necessary for maximizes dependable water to meet several needs with existing limitation. Reservoirs can be operated by means of rule curves. These curves relate storage and time, several curves can be applied at the same time. Depending on the position of the release for the next periods are taken. The linier or dynamic programming method is a famous and classic method to optimize a reservoir system, and it was therefore chosen for application here. With this method it is possible to decide under uncertainly with in the most optimal "path" of reservoir level.

For the integrated hydro-power optimization from the three reservoirs cannot be special for the power production, caused by the multipurpose dam in downstream which fulfill water requirements and the system as a whole has to be operated such that flood control is maximal. Ad hoc adjustments are made during emergency situations on daily or even shorter basis. The rule curves produced had been optimized with respect to power production in the system. At the same time monthly target storage was derived with respect to flood protection and water supply for all purposes. Different purposes and various operators on managing reservoir operation induce conflict of interests. Optimization method cannot always be applied considering the complexity of constraints that must be adopted. To overcome the limitation of the method, the policies are brought about in the form of coordination forum. Optimization is conducted by simulation and sometimes without optimizing the hydropower production.

2. EXISTING INFRASTRUCTURE DAM IN CITARUM

The Jatiluhur project conceived in 1957 to supplement the run-of-river technical irrigation systems on the basin was completed in 1981. It is the largest contiguous irrigation system in Indonesia and is major rice production area. It comprises of the main Ir. H. Djuanda reservoir (estimated net capacity 1,860 M m³ in 1997), the associated Jatiluhur dam, hydro-electric power station (150 MW) and a conveyance system that provides irrigation to about 240,000 ha in West Java through the West Tarum Canal (WTC) system, East Tarum Canal (ETC) system and the North Tarum Canal (NTC) system. In addition, the project provides domestic, municipal and industrial (DMI) raw water supply to DKI Jakarta metropolitan area, to a number of urban center such as Bekasi, Karawang etc., and to industries along the corridor from Jakarta to Cirebon, including the region around Purwakarta. The Project also provides flushing water to Cirebon, including the region around Purwakarta. The project also provides flushing water flush rivers in DKI Jakarta metropolitan area during the dry season.

During the 1980's the State electric Corporation (PLN) constructed two hydro-power projects upstream of the Ir. H. Djuanda reservoir. These are the Saguling Dam (750 MW) completed in 1985 and the Cirata Dam (500 MW) completed in 1988. The capacity of the Ciarata hydro-power station is currently being increased by 500 MW. The Saguling (estimated net capacity 620 M m³) and Cirata (estimated net capacity 800 M m³) reservoirs further regulate the flow in the Citarum and thus enable an increase in the utilization of the water resources of the basin. These reservoirs are operated by the State Electricity Company (PLN) instead of the Jasa Tirta II Public Corporation (PJT-II) with the generation of firm peak power as their main objective. The salient data of the Citarum cascade dams and hydropower plants is shown as "Table 1, 2 and 3".

Table 1.
Data of Citarum Cascade Reservoirs

	Saguling	Cirata	Ir. H. Djuanda
Operational	1985	1988	1967
Dam Data			
Type	Rock fill dam with clay core	Rock fill dam with concrete face	Rock fill dam with inclined clay core
Height	99 m	125 m	105
Crest length	301 m	453.5 m	1220 m
Crest elevation	650.20 m	225.0 m	114.5 m

Table 2.
Data of Citarum Hydropower Plants

	Saguling	Cirata	Ir. H. Djuanda
Tail level (m)	252	103	27.0
Head loss (m)	28.4	4.0	1.0
Spillway characteristics	Gated spillway	Gated spillway	Ungated (ogee) spillway
Installed capacity (max. power, MW)	750	1000	187.5
Number of turbines	4 units	8 units	6 units
Type of turbines	Francis	Francis	Francis

Table 3.
Data of Specific Citarum Reservoir

	Saguling	Cirata	Jatiluhur
Full supply level	643 m	220 m	107 m
Dead storage level	623 m	205 m	56 m [*])
Minimum power level	-	-	75 m
Maximum storage	880 x 10 ⁶ m ³	1,973 x 10 ⁶ m ³	2,970 x 10 ⁶ m ³
Minimum storage	271 x 10 ⁶ m ³	1,177 x 10 ⁶ m ³	599 x 10 ⁶ m ³ **)
Surface area at max operating level	49 km ²	62 km ²	83 km ² ***)

In order to operate the whole cascade reservoir consistently, a special working group committee consisting of representatives from Jasa Tirta II Public Corporation, Electrical State Company, Research Institute of Water Resources keeps monthly meetings.

3. CITARUM WATER AVAILABILITY AND DEMAND

The Citarum river originates from mountainous area of Bandung region and flows northward to Java Sea through central portion of West Java Province. Bandung City, the capital of the West Java Province with inhabitants of 6,578,829 is located in the mouth of Saguling Reservoir. Topographically, the Citarum catchment upstream of Jatiluhur is characterized by a ring of high mountain ridges around a slightly undulating plain. Saguling dam is located in the upstream ridge while Cirata and Jatiluhur are in the downstream ridge. The seasonal variation in river runoff closely follows the rainfall distribution, marked by a distinct dry and wet season. The dry season fall in April – September and rainy season fall in October – March. The season not always like this, but depended from condition of season every year. Rainfall in the basin varies from about 4,000 mm/year in the mountainous areas in the upper catchment to about 1,500 mm/year along the coast.

Citarum River basin is covering an area of about 12,000 km² with the average annual flow of 12.95 billion m³, out of which 6.0 billion m³ flows in Citarum River and 6.95 billion m³ flows in the other rivers in the basin. By employing water resources infrastructures in basin the water that could be regulated is about 7.65 billion m³ per annum and the rest is wasted flows to the sea. The utilization of water by far is goes to irrigation of 6.0 billion m³ equal to 88%, and to domestics, municipalities, and industries of 800 million m³ equal to 12%.

At the present time the water demands on the Citarum cascade are mainly on Djuanda reservoirs as far DMI and irrigation water are concerned, of which irrigation water is by far the biggest (80%). This means that the actual demand has to be met in Djuanda. Of course, some demands are on Saguling and Cirata as well, but they are not consumptive. Water used for the generation of hydro-power and up in Djuanda reservoir, where it can be used for all other demands.

In the as “Table 4”, total water demands are shown for 2017 in as far they have been used by the preparation of the annual operational plan for the Citarum reservoir cascade, compared with irrigation water demands for a dry, normal and wet year, from Djuanda only, i.e, unregulated flows of the rivers intercepted by the West Tarum Canal, North Tarum Canal, East Tarum Canal system have already been taken into account. Although the demands are to be met by the reservoir system as whole, the location of the demands is from Djuanda Reservoir.

Table 4.
Water demands (m³/sec) from Ir. H. Djuanda Djuanda Reservoir in 2017 according the Annual Operational Plan for the Citarum Reservoir Cascade.

Condition	Dry year	Wet Year	Normal Year
Month			
Jan	116,8	82,4	83,7
Feb	88,3	79,1	79,1
Mar	109,6	90,3	90,3
April	137,3	103,8	105,5
May	183,4	119,1	143,2
June	247,0	167,9	220,9
July	255,5	203,5	242,5
Aug	154,5	133,3	149,7
Sept	72,7	54,6	68,6
Oct	165,8	126,9	156,0
Nov	189,0	107,5	152,7
Dec	162,1	94,2	115,8
Average	156,8	113,5	134,0

The demand of the system can be generalized into three parts: (i) irrigation water supply to the North, East, and West Tarum areas, (ii) raw water supply to drinking water treatment plants for the districts and municipalities in the corridor of the canals including Jakarta, and (iii) to industrial zone along the corridor from Capital District of Jakarta to Indramayu, including the region around Bekasi, Karawang, Purwakarta, Subang district. These demands can partially be satisfied by rivers which are intersecting the main canals. The balance has to come from the Citarum, which are the greatest part of the intake requirements at the diversion weirs has to come from the Jatiluhur reservoir. As the biggest consumer and the largest contiguous irrigation area, irrigation water supply should be arranged into several crop plantation schedule. To cope with the available water resources, the irrigation plan is prepared as major input for Citarum cascade reservoirs operation.

The methodology to develop normal system operations in a multipurpose reservoir, include development of optimal end-of-month storage which maximize the expected value of selected primary objective function for the system, subject to satisfying other system objectives based on the specification of target performance levels. The domestic, municipal, and industry water demands (DMI) and irrigation water requirement as calculated from the previous procedure become an input to the reservoir operation model and synchronized with hydro-power to evaluate reservoir rule curves. Based on this model, an annual operational plan for Citarum cascade reservoirs is made using expected demands, statistical inflows based on dry, wet, normal years (each month). In this plan, the total energy of the system is maximised subject to a number of conditions:

- The demands at Jatiluhur reservoir should at least be met.
- The upper and lower rule curves for the reservoirs should be observed as much as possible.
- At the end of the year (or planning period) certain reservoir levels should be met.
- The maximum water level at the end of rainy season.
- To provide two times of yearly flood intercept and retain falling water and to control the flood periodically which released from Cirata reservoir (peak load).
- In order to prevent individual reservoir levels from changing too much from month to month, the relative net. storage of each reservoir with respect to the total net storage in the system should be kept constant.

For the preparation of the annual operation plan by working group for the monthly meeting, historical inflows since 1988 when the complete cascade was in operation are used by analyses Log Normal type 3 (LN-3). For Saguling, the inflows are derived from observations at Nanjung and intermediate inflows from reservoir balance calculations at Saguling. For Cirata and Djuanda historical inflows are calculated from reservoir balance calculations only. A problem with these calculations is that they notoriously inaccurate and difficult to check. Improvement by installing good automatic hydrometric stations just of each reservoir is therefore highly recommended.

Definition of wet and dry, and the way to calculate this is not universal. For instance NEDECO, 1985 uses a definition based on annual totals, but adjusted over the months by 2 two methods:

- Dry or wet year is defined according to the total annual flows. Monthly flows are distributed proportionally to the total annual flows.
- Dry or wet year is defined according to the total annual flow. Wet period monthly flows are distributed proportionally to the total wet period flow, while the remainder is distributed over the dry months.

Dry is defined as annual total 80% of the observation exceeded, wet as 20% exceeded (statistically known as the 80- and 20- percentile respectively). No underlying spastically distribution is used. If long historical records are used, additional years of data do not influence the picture very much. Based on any of the two approaches mentioned, additional very dry and very wet years can be defined. The biggest problem is, of course, to determine whether the present month belongs to a dry, normal or wet year.

4. RESERVOIR CASCADE OPERATION

4.1. RESERVOIR OPERATION CONCEPT

The Citarum cascade reservoirs have a combined effective volume of $3,276 \times 10^6 \text{ m}^3$ which is approximately 57% of annual mean run off of Citarum, indicating that the system was not designed to provide carry-over storage during year-long periods. Using non-shared optimised reservoir operation, the total water released of the Citarum cascade reservoirs can reach $5,531 \times 10^6 \text{ m}^3$, which is nearly 100% of water resources potential has been controlled. The water resources potential in the Citarum river is around $6 \times 10^9 \text{ m}^3$ annually. The biggest consumer so far is irrigation which uses up about 87% of total regulated water from Ir. H. Djuanda reservoir and other rivers in the system.

The present cascade operation is based on the guidelines produced by PLN-P2B in 1991. First an annual operational plan is made using expected demands, statistical inflows based on dry, wet and normal years (by each month). This plan forms the basis of the reservoir operation. It result in a recommended rule curve for the year under consideration actual operation is adjusted during monthly consultative meetings group Citarum Basin. Ad hoc adjustments are made during emergency situations on a daily or even shorter basis. In this plan the upper two reservoirs are operated for power production, while the bottom reservoir, Ir. H. Djuanda, has to meet the water supply requirements. The systems as a whole has to be operated such that flood control is maximal

Main difficult with this way of operations are ; (1) the established of upper and lower rule curves, (2) how to adjust in an optimum manner if the actual situation differs from the planned one, (3) how to decide on the actual situation with the respect to very dry, dry, normal, wet or very wet situation, and (4) how to forecast inflows into the reservoir.

Apart from these major issues, other difficulties arise from:

- Maintenance (e.g. power plant units cannot be used, water levels are restricted due to maintenance of the dams, intake gates, etc)
- Water quality aspects (e.g. extra water for dilution is required to offset over-feeding of fish farms)
- Certain high water level are desired for recreational purposes.

In the following, a procedure will be shown, to derive an annual plan in a relatively simple and very flexible manner using a spreadsheet and its standards (non) linear optimization solver add-in.

The reservoir cascade has a combined net storage capacity of 2800 Mm³, where net storage is defined as the storage between the spillway crest level and minimum storage level. The later level is the minimum operating level for hydro-power generation. For Saguling, Cirata and Ir. H. Djuanda these level and storages have been taken as "Table 5".

Table 5.
Data of Water Level Citarum Cascade Dams

	Saguling		Cirata		Ir. H. Djuanda		Total Cascade
	(m +MSL)	(Mm3)	(m +MSL)	(Mm3)	(m +MSL)	(Mm3)	
Maximum Level	643	889	220	1,977	107	2,458	5,324
Min. Storage	623	272	205	1,177	75	599	2,048
Net Storage (Mm3)	617		800		1,859		3,276
Net storage (%)	18.8 %		24.4 %		56.8 %		100.0 %

The Citarum basin at Jatiluhur os about 5,750 Mm3. Thus the combined net storage capacity is about 49% of the MAR, indicating that the system was not designed to provide carry-over storage during year long drought periods. This typical for a reservoir in Java where there are very pronounced dry and wet season.

Before the construction of Saguling and Cirata, the multipurpose Ir. H. Djuanda reservoir, operated by PJT II, had to meet the following water supply objectives, ordered by priority based on the Water Resources Law No. 7/2004 as follow:

- Requirement of human life (drinking water, sanitation etc)
- Domestic, Municipal and Industry
- Irrigation
- Generation of (peak) hydro-power

Apart from these objectives, there is a standing operational obligation with respect to flood control. The following remarks can be made on the list.

4.2. CONCEPT THE RULE CURVES

Reservoirs can be operated by means of rule curves. These curves relate storage and time (month). Several curves can be applied at the same time. Depending on the position of the actual storage at a certain moment, decision on the release for the next period are taken. Quite often two rule curves are in uses; an upper rule curve and a lower rule curve. If the reservoir storage at the start of a month is greater than the storage indicated by the upper rule curve an above target amount of water is released from the reservoir in order to come back of the curve. In this way one can be observe the required storage capacity for floods, or spill can be prevented later on by routing an additional amount of water through the turbines. If the reservoir level drops below the lower curve water conservation measures have to take, which can be: (1) reduce the power target, (2) reduce the release target. Because above target releases for water supply do not yield any extra benefits, one can only prevent spill by producing more electricity.

If the upper rule curves is not meant to prevent spill or to provide storage for floods, a different decision may be assigned to it. This could be the case if the curve is used to maximize the average power output. In that case one may decide to release the expected average inflow plus the difference in storage which is indicated by the (gradient) rule curves. The function of the lower curve is mainly to prevent a great failures, either in irrigation or in power and to replace it by a controlled reduction in output. The number of organized failures through is greater that if nothing is done at all.

4.3. OPTIMAL INTEGRATED OPERATION

This method derived for a truly integral operation of the three reservoir together. For this purpose an optimization model has been developed which is based on the dynamic programming method. Three features of the model however have to be mentioned here.

- The dynamic programming model can only solve the problem for a set of discrete storages into which the reservoirs are schematized. The answer produced by the model is expressed as required storages at every time step, which always are one of the set of discrete stages. It is clear that by increasing the number of discretization a more precise answer is obtained. It must however be stressed here that the computational effort involved, is a quadratic function of the number of stages. In the present model, the number of stages is limited to 10. In some cases this even proved to be unpractical. The calculations were then first executed roughly with smaller number of stages. Then the 10 stages were introduced, but allowing only a limited range around the first solution.
- Secondly the optimization is only possible when a set of values, which are attributed to outflows and power productions are available. The problems are solved by using factious values. They do not represent real values in rupiahs but express more the priorities of several goals. The object is to find an operation which protects irrigation and urban water supply, and taking that into account maximizes the energy and power output. Producing power does yield a higher income at increase levels. In general 1,000 points per MW continuous production are allocated. The gain in power is of a much lower order of magnitude than the loss which is involved in not giving the release target. In this way, a solution which does not match the release target is highly improbable.
- The model is able to solve the operational problem for a dry, average wet year of for a combination of all three. The last method computes at every moment the benefits in a wet, average and dry case and combines the benefits according to the ration 3:4:3. This, because its is assumed that a 90% dry year and a 90% wet year each represent 30% of all possibilities and the average 40%. This is very roughly what is called "stochastic" dynamic programming. It would be better even to use all historical inflow data and to

compute the value in each case. The final value attributed to a certain decision is then just the average benefit. In the practical situation, such a model would be useless due to the core capacities of the minicomputer and because computer times were already very extensive (12 hours for a full calculation).

The optimal operational patches found in this way were tested with the simulation model. This verification was necessary to see whether violations of the criteria do occur. In that case adaption's of the optimal lines have to be made. This difference may occur due to the different set of flow data which are used in both models.

4.4. PRESENT ANNUAL OPERATIONAL PLAN PREPARATION

Each year, the representative of State electricity Company (PLN), Research Institute of Water Resources and PJT II prepare an operational plan for monthly meeting. It is based on the predicted Domestic, Municipal, Industry and irrigation demands, existing reservoir levels and expected inflows, and evaporation and tries to optimize the total power output of the system by varying the monthly outflows of the individual reservoirs. This is done on a monthly basis by hand.

A few other principles (constrains) are adhered to as well; (1) spilling is not allowed, (2) the ending reservoir water level is the same, or higher than the starting water level, (3) the principle of shared in each month is kept constant, at 21,12 %, 28,94 % and 49,94 % for Saguling, Cirata and Djuanda respectively.

In regular (at least monthly) consultative meeting of during the year this plan then is revised according to the real situation.

5. CONCLUSION

The three reservoirs are all situated on the Citarum River, West java, The Ir. H. Djuanda reservoir is the most downstream one, the next upstream reservoir is Cirata and the Saguling reservoir is the most upstream one. Downstream of Ir. H. Djuanda reservoir two weirs across the Citarum divert water into the three main canal.

Reservoirs can be operated by means of rule curves. These curves relate storage and time, several curves can be applied at the same time. Depending on the position of the release for the next periods are taken. The linear programming method is a famous and classic method to optimize a reservoir system, and it was therefore chosen for application here. With this method it is possible to decide under uncertainty with in the most optimal "path" of reservoir level.

Analysis and optimization of the annual operation plan by spreadsheet is both very flexible and easy to do with the built in solver. From the annual operation plan analysis by spreadsheet, it has been shown that operational principles have a large influence on the generation of (firm) power. In particular, a marked difference in result exists between so-called shared and non shared operation. Existing rule curves have not been updated in accordance with the latest flow figures. Similarly, elevation area capacity data for the three reservoirs are not recent. At least not for Ir. H. Djuanda. Local flow are determined by indirect reservoir balance calculations. Flow forecasting is not used for reservoir operation.

REFERENCES

- [1] ASSOCIATED CONSULTING ENGINEERS ACE (PYT) LTD, "Additional safety related to Jatiluhur dam" Brief on Main Dam, 1992.
- [2] ASSOCIATED CONSULTING ENGINEERS ACE (PYT) LTD, "Additional safety related to Jatiluhur dam" Design Note Volume 2, 1992.
- [3] IDRUS HERMAN, "Water Utilization for Industry and Public Purposes in Citarum River Basin", Juli 2005.
- [4] NETHERLAND ENGINEERING CONSULTANTS BV (NEDECO), "Jatiluhur Water Resources Management Project Preparation Study" Feasibility Report, 1998.
- [5] NETHERLAND ENGINEERING CONSULTANTS BV (NEDECO), "West Tarum Canal Improvement Project Report on Integrated Reservoir Operation Ir. H. Djuanda, Cirata, Saguling" Main Report, 1985.

COMMISSION INTERNATIONALE DES GRANDS BARRAGES

VINGT-SIXIÈME CONGRÈS DES GRANDS BARRAGES
Autriche, juillet 2018

DOI 10.3217/978-3-85125-620-8-221



This work licensed under a Creative Commons Attribution 4.0 International License. <https://creativecommons.org/licenses/by-nc-nd/4.0/>

ANALYSIS THE EFFECT OF SOIL PERMEABILITY OF THE UPSTREAM SHELL ON THE DAM STABILITY UNDER RAPID DRAWDOWN (BRADON DAM)

Fatima S. FOUITI

FACULTY OF CIVIL ENGINEERING - WATER ENGINEERING AND IRRIGATION DEPARTMENT TISHREEN UNIVERSITY

SYRIA

COMMISSION INTERNATIONALE
DES GRANDS BARRAGES

VINGT-SIXIÈME CONGRÈS DES
GRANDS BARRAGES

Autriche, juillet 2018

**ANALYSIS THE EFFECT OF SOIL PERMEABILITY OF THE UPSTREAM
SHELL ON THE DAM STABILITY UNDER RAPID DRAWDOWN
(BRADON DAM)***

Prof. Dr. Fatima S. Fouiti

*Faculty of Civil Engineering - Water Engineering and
Irrigation Department Tishreen University*

SYRIA

1. INTRODUCTION

The drawdown is one of the most dangerous conditions for the upstream slope. During the investment of the dams, rapid reduction of the water level is necessary when a defect threatens its stability, or when needed absorbing the flood wave or in case of dam rehabilitation in a short period.

The stability analysis of the upstream shell of the dam during rapid reduction has a significant impact. The reduction rate of 0.1 m / day is common, 0.5 m / day is large and the reduction of 1 m / day and above is a special rate [1]. The porous water pressure in the upstream shell remains for a period of time with high values [2] [3]. Dissipation of the porous water pressure is related to soil characteristics of the up-stream side (Permeability, mechanical and physical properties) [4] [5] [6]. It has been shown that high permeability soils respond hydraulically quickly where water is released from pores (consolidation process), while the low permeability soils need a long period of time to get the water out [7] [8]. In this paper, the rapid reduction of the Bradon dam reservoir was studied taking into account the slope properties for several types of soil (14 types), which could formed the upper shell with different properties, the amount and the time of reduction using Geo-Studio

package [9] [10] [11]. Computed safety factors for each type of soil have been compared with the permissible safety factor values shown in "Table 1".

Table 1
Minimum safety of factors for slope stability [12]

Upstream slope	First full state (steady state)	1.3-1.5
	Rapid discharge (transient state)	1.2-1.3
Downstream slope	First full state (steady state)	1.5
	Earthquake and full reservoir	1.2

2. RESEARCH METHODS

2.1. COMPUTATION THEORY

To study the leakage in saturated and unsaturated media, a Darcy law is adopted [11] which is given according to the following equation "Eq. [1]" :

$$q = k * I \quad [1]$$

Where: q - specific discharge, k- hydraulic conductivity, I – hydraulic gradient. Where the hydraulic conductivity takes a constant value of saturated soil. The only difference is that under conditions of unsaturated flow the hydraulic conductivity is no longer constant but varies with changes in water content and indirectly varies with changes in pore water pressure.

The governing differential equation used in the formulation of seep/w is:

$$\frac{\partial}{\partial x} \left(k_x \frac{\partial H}{\partial x} \right) + \frac{\partial}{\partial y} \left(k_y \frac{\partial H}{\partial y} \right) + Q = \frac{\partial \theta}{\partial t} \quad [2]$$

Where: H - total head, k_x - hydraulic conductivity in the x-direction, k_y - hydraulic conductivity in the y-direction, Q - applied boundary flow, θ - volumetric water content, t – time.

Under steady-state conditions, the flux entering and leaving an elemental volume is the same at all times, the right side of the equation consequently vanishes and the equation reduces to the form:

$$\frac{\partial}{\partial x} \left(k_x \frac{\partial H}{\partial x} \right) + \frac{\partial}{\partial y} \left(k_y \frac{\partial H}{\partial y} \right) + Q = 0 \quad [3]$$

Changes in volumetric water content are dependent on changes in the stress state and the properties of the soil. Seep/w program is formulated for conditions of constant total stress that, there is no loading or unloading of the soil mass. The

second assumption is that the pore-air pressure remains constant at atmospheric pressure during transient processes.

A change in volumetric water content can be related to a change in pore-water pressure by the equation:

$$\partial\theta = m_w \partial u_w \quad [4]$$

Where: m_w - the slope of the water content function. The total hydraulic head is defined as:

$$H = \frac{u_w}{\gamma_w} + y \quad [5]$$

Where: u_w - Pore-water pressure, γ_w - Unit weight of water, y - Elevation,

"Eq. [5]" can be rearranged as: $u_w = (H - y)$ [6]

Substituting "Eq. [6]" into "Eq. [4]" then the result in equation 3 leading to the following expression:

$$\frac{\partial}{\partial x} \left(k_x \frac{\partial H}{\partial x} \right) + \frac{\partial}{\partial y} \left(k_y \frac{\partial H}{\partial y} \right) + Q = m_w \gamma_w \frac{\partial (H - y)}{\partial t} \quad [7]$$

Since the elevation is constant, the derivative of y with respect to time disappears, leaving the following governing differential equation:

$$\frac{\partial}{\partial x} \left(k_x \frac{\partial H}{\partial x} \right) + \frac{\partial}{\partial y} \left(k_y \frac{\partial H}{\partial y} \right) + Q = m_w \gamma_w \frac{\partial H}{\partial t} \quad [8]$$

The finite element equation that follows from applying the Galerkin method of weighed residual to the governing differential [11] equation is:

$$\int_v [B]^T [C] \cdot [B] \cdot \partial v \cdot (H) + \int_v \lambda \langle N \rangle^T \langle N \rangle \cdot \partial (v) \cdot (H), t = q \int_A \langle N \rangle^T \partial A \quad [9]$$

Where: [B] = gradient matrix, [C] = element hydraulic conductivity matrix

{H} = vector of nodal heads, $\langle N \rangle^T \langle N \rangle = [M]$ = mass matrix

(H),t = change in head with time, q = unit flux across the side of an element

Slope/w uses the theory of limit equilibrium of forces and moments to compute the factor of safety. A factor of safety is defined as that factor by which the shear strength of the soil must be reduced in order to bring the mass of soil into a state of limiting equilibrium along a selected slip surface. For an effective stress analysis, the shear strength is defined as:

$$S = C' + (\sigma_n - u) \gamma g \phi' \quad [10]$$

Where: S - Shear strength, C'- Effective cohesion, ϕ' - Effective angle of internal friction, σ_n - Total normal stress, u - Pore-water pressure.

2.2. COMPUTATION MODEL:

The Bradon dam is located in the northwestern part of the Syrian Arab Republic, at the top of the northern Great River, 64 km from Latakia city. The dam is an earth-rock fill dam with a central clay core, tow filter zones and rock fill shoulders. The normal water level behind the dam is 193.8 m, the high is 62.5 m, the length is 806 m, and the width is 366 m at the base and 12 m at the top. The surface area of the reservoir is 5.3 km², the maximum storage level of 193.8 m, and a maximum storage volume of 164.5 Mm³. "Figure 1" shows the cross-section at the maximum height.

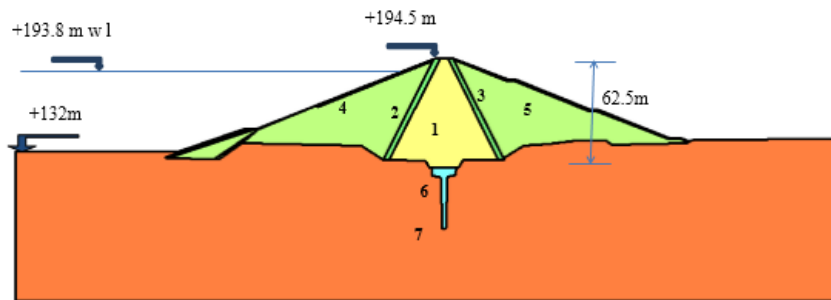


Fig. 1

Cross-section of the dam, 1 - central core, 2-3 filters, 4 - downstream shell, 5 - upstream shell, 6 - injection Curtain, 7 – foundation.

The Material properties of the dam, core and foundation are shown in "Table 2".

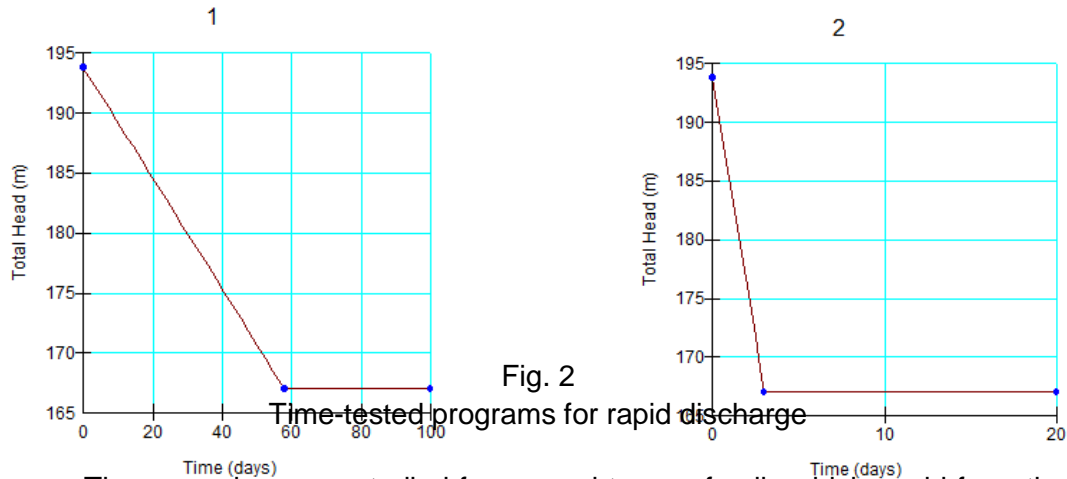
Table 2
The Material Properties of dam, core and foundation materials

Soil number	Soil location	γ_d (t/m ³)	porosity n	Cohesion coefficient C (Kpa)	Angle of friction ϕ	Permeability coefficient (m/day)
1	Central core (clay)	1.76	0.562	64	30	Kc=0.00059
2-3	Filters	1.8	0.38	0	25	-
4-5	Downstream and upstream shell	2.1	0.33	30	38.5	10
6	Injection Curtain					
7	Foundation	2.68	-	120	31	0.3

3. RESULTS AND DISCUSSION

3.1. SEEPAGE ANALYSIS:

The seep/w program was used to analyze seepage in complex and simple models according to the finite element method with two-dimensional flow. The leakage line within the body of the dam calculated first as steady state in case of maximum level of storage for each type of studied soils shown in "Table 3". The leakage line was used as a boundary condition for rapid drawdown (transient seepage). The scenarios of rapid discharge were studied to determine the effect of water drop from 193.8 m to 167 m in linear form, for two cases of discharge programs as shown in "Figure 2". The first case through the irrigation outlet of 25 m³/s, it will take 58 days. And the second case through the transforming tunnel of 500 m³/s, it will take 3 days.



The scenarios were studied for several types of soils which could form the slopes according to "Table 3", K_s - is the hydraulic conductivity factor of the soil, and K_c - The hydraulic conductivity factor of the core.

Table 3
Studied soil samples

Soil type	Permeability Coefficient K_s (m/day)
gravel-pebble(Bradon state)	10
Gravel	8.64
Sand	4.66
Uniform Fine Sand #1	1.8576
Embankment (Silty clay)	0.1
Uniform Fine Sand #2	0.0976
Silt #2	0.0864
Silt Loam	0.0605
Sandy Loam	0.0506
Silty Sand	0.0432

Sandy Silty Clay	0.0121
Silty Clay	0.0026
Very Fine Sand	0.0017
Clay (Core soil)	Kc=0.00059

The leakage curves change during rapid drawdown were calculated using seep/w program for all types of soil mentioned above "Figures 3 and 4" show some of them for two cases of discharging.

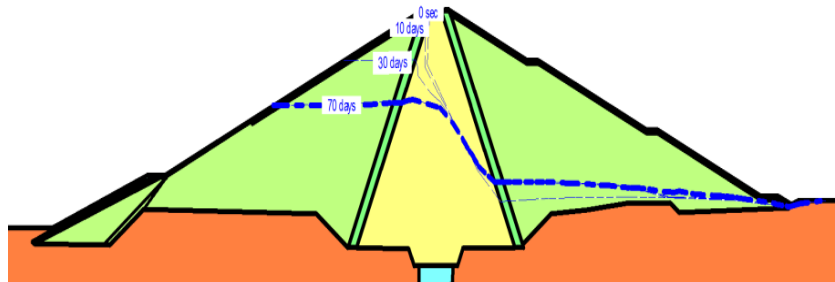


Fig. 3

Curves of leakage in case of discharge through Irrigation outlet. Soil type (gravel-pebble)

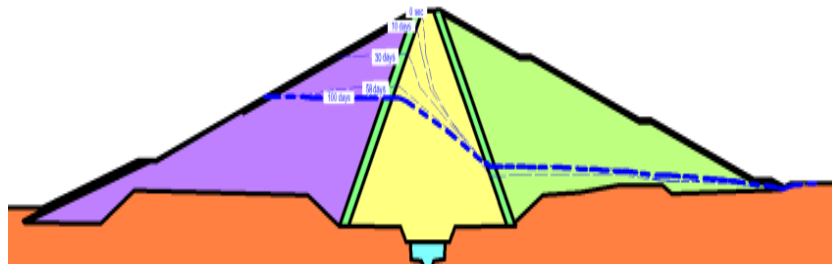


Fig. 4

Curves of leakage in case of discharge through transforming tunnel. Soil type (Uniform Fine Sand #1)

3.2. STABILITY ANALYSIS:

The stability of the upstream shell was studied using the slope/w program, which uses several methods for analyzing and calculating the safety factor. These methods are Bishop, Phellinus, Janbu, Ordinary-Morgenstern-Price and others. The safety factors were obtained from the Morgenstern-Price method, which takes into account the balance of forces and moments [13].

The safety factor of the upstream slope and the critical slip surface for all types of soil have been calculated, under influence of the applied boundary conditions, "Figures 5 and 6" show some results in two cases of discharge. And "Table 4" and "Table 5" show the values of the minimum safety factors.

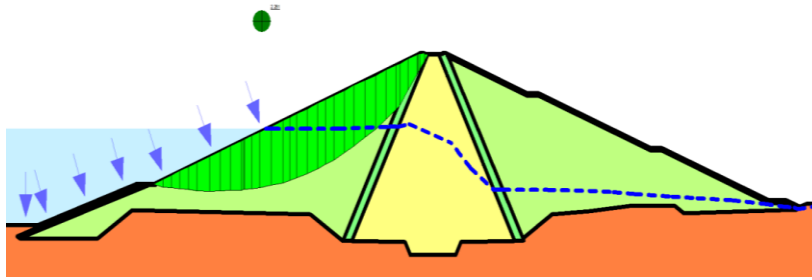


Fig. 5
Upstream slope safety factor in case of discharge through
Irrigation outlet. Soil type (gravel-pebble)

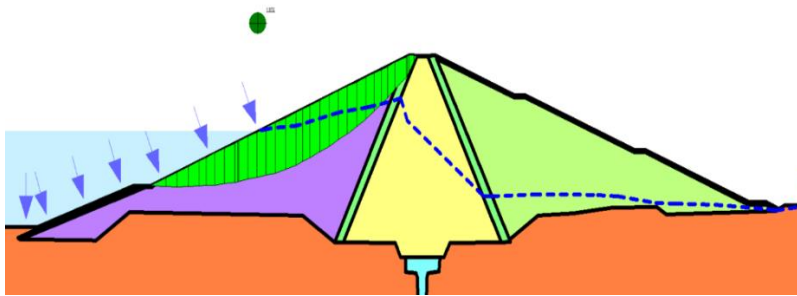


Fig. 6
Upstream slope safety factor in case of discharge through
transforming tunnel. Soil type (gravel)

3.3. ANALYSIS THE EFFECT OF THE RATIO (k_s/k_c) CHANGES

The ratio between the permeability of the upstream shell (k_s) and the permeability of soil core (k_c) within the dam body has effected on the stability of the upstream shell. The variation was studied according to soil types and the ratio (k_s/k_c) were calculated. The obtained results shown in "Table 4" for the first case of discharge through the irrigation outlet, the discharge rate is 0.5 m/day, and in "Table 5" for the second case of discharge through the transforming tunnel, the discharge rate is 8.93 m/day.

Table 4
Minimum safety factor in the case of the first discharge program

Soil type	Safety factor	the ratio k_s/k_c	The range
gravel-pebble (Bradon dam state)	2.25	16949.15	>10000
gravel	1.729	14644.07	
Sand	1.595	7898.305	>1000
Uniform Fine Sand #1	1.359	3148.475	

Embankment (silty clay)	1.279	169.4915	>100
Uniform Fine Sand #2	1.198	165.4237	
Silt #2	0.981	146.4407	
Silt Loam	0.968	102.5424	
Sandy Loam	1.169	85.76271	>10
Silty Sand	0.984	73.22034	
Sandy Silty Clay	1.166	20.50847	
Silty Clay	0.936	4.40678	<10
Very Fine Sand	1.046	2.881356	
Clay (Core soil)	2.01	1	1

Table 5
Minimum safety factor in the case of the second discharge program

Soil type	Safety factor	the ratio ks/kc	The range
gravel-pebble (Bradon dam state)	2.063	16949.15	>10000
gravel	1.576	14644.07	
Sand	1.429	7898.305	>1000
Uniform Fine Sand #1	1.095	3148.475	
Embankment (silty clay)	0.598	169.4915	>100
Uniform Fine Sand #2	0.359	165.4237	
Silt #2	0.44	146.4407	
Silt Loam	0.677	102.5424	
Sandy Loam	0.947	85.76271	>10
Silty Sand	0.668	73.22034	
Sandy Silty Clay	0.821	20.50847	
Silty Clay	0.679	4.40678	<10
Very Fine Sand	0.235	2.881356	
Clay (Core soil)	1.782	1	1

3.4. CONCLUSIONS

- 1- Using some types of soil causes a collapse of the upstream slope according to the dimensions and slope of the cross-section of the Bradon dam, i.e. the suitable soil type can be chosen from the design stage, which does not cause danger in the conditions of rapid drawdown.
- 2- The safety factor values in the second discharge program are lower than the safety factors in the first discharge program, i.e. that the greater of water reduction, the lower safety factors.

- 3- For the studied soils, the ratio $K_s/K_c = 165$ is the interval value between stable and unstable soils in the first case of discharge, and for the second case of discharge, the ratio is $K_s/K_c = 7898$.

REFERENCES

- [1] ALONSO E., PINYOL N. Slope stability under rapid drawdown conditions, *University Polytechnic de Catalonia, Barcelona, Canada 2003*, 367
- [2] FREDLUND M. Combined seepage and slope stability analysis of rapid drawdown scenarios for levee design. *Geo-Frontiers 2011© ASCE 2011*, 1595-1604.
- [3] TRAN T. Stability problems of an earth fill dam in rapid drawdown condition. *Slovak Republic Grant Project No. 1/9066/02, 2004*.
- [4] NIAN T. JIANG J. WAN S. LUNA M. Strength reduction FE analysis of the stability of bank slopes subjected to transient unsaturated seepage. *China EJGE Vol. 16Bund A, 2011*, 165-177. KINI R.L., RAIFA X.
- [5] KUNITOMO N. Design and construction of embankment dams, *Dept. Aichi Institute of Technology, 2000*.
- [6] Fouiti F. Study of the effect of porous water pressure on earth dams stabilization (al-hawiz dam case). *Tishreen University Journal of Research and Scientific Studies, Engineering Sciences Series, 2013*.
- [7] XINTING L. ZEHNHUA Z. Stability of bank slope under reservoir water drawdown, *China Three Gorges University under grant No. 2008KDZ07, 2008*, 533-537.
- [8] US Army Corps of Engineers. Engineering and design slope stability. *EM 1110-2-1902, 2003*.
- [9] Stability Modeling with SLOPE/W 2007 Version. *Engineering Methodology Third Edition, March 2008, GEO-SLOPE International Ltd*.
- [10] Seepage Modeling with SEEP/W 2007 Version, *Engineering Methodology, Third Edition, University Polytechnic de Catalonia, March 2008*.
- [11] MURRAY F., TIEQUN F. Slope stability modeling software. *Verification Manual, Soil Vision Systems Ltd, Canada, 2012*.
- [12] State of Colorado department of natural resources. Rules and regulations for dam safety and dam construction. *Colorado, 2007*, 76.
- [13] The website of the Hydraulics Engineering Forum. Slope stability Morgenstern - price Method, *www.water-eng.com, Date: 17/9/2009*.

SUMMARY

The aim of this study is to determine the effect of the rapid drawdown of the Bradon dam reservoir on the upstream shell stability for two different discharge scenarios and different types of available soils in situ.

The dam to be considered is 62.5 m high and the width is 366 m at the base and 12 m at the top. The dam consists of a central clay core, tow filter zones and rock fill shoulders. The normal water level behind the dam is 193.8 m high.

Various scenarios for rapid discharge cases were studied to determine the safety factor of water drop from 193.8 m to 167 m in linear form for two discharge cases. The first case is through the irrigation outlet 25 m³/s and the second is through a tunnel transforming 500 m³/s.

The obtained results show that the stability of the upper slope change under considered boundary conditions according to the soil type. And the appropriate type of soil can be chosen from the design stage. Also, the effect of the ratio between the permeability of the upper slope and the permeability of the clay core (k_s/k_c) was calculated, the results show for the studied soils in the first case of discharge that the ratio (k_s/k_c)=165 is interval value between stable and unstable soils. While for the second case of discharge, the ratio is (k_s/k_c) =7898.

KEY WORDS: Rock fill dam, safety factor, stability, transient seepage, Bradon dam.

SOMMAIRE

Le but de cette étude est de déterminer l'effet du rabattement rapide du réservoir du barrage de Bradon sur la stabilité de la coquille en amont pour deux scénarios de décharge différents et différents types de sols disponibles in situ.

Le barrage à considérer a une hauteur de 62,5 m, et une largeur de 366 m à la base et de 12 m au sommet. Le barrage se compose d'un noyau d'argile central, de zones de filtre de remorquage et d'épaulements de remplissage rocheux. Le niveau d'eau normal derrière le barrage est de 193.8 m de hauteur.

Différents scénarios de décharges rapides ont été étudiés pour déterminer le facteur de sécurité de la chute d'eau de 193.8 m à 167 m sous forme linéaire pour deux cas de décharge. Le premier cas est à travers la sortie de l'irrigation 25 m³/s et le second est à travers un tunnel transformant 500 m³/s.

Les résultats obtenus montrent que la stabilité de la pente supérieure change dans des conditions aux limites déterminées en fonction du type de sol. Et le type de sol approprié peut être choisi dès la conception. Aussi, l'effet du rapport entre la perméabilité de la pente supérieure et la perméabilité du noyau argileux (k_s/k_c) a été calculé, les résultats montrent pour les sols étudiés dans le premier cas de décharge que le rapport (k_s/k_c) =165 est la valeur d'intervalle entre les sols stables et instables. Alors que pour le second cas de décharge, le rapport est (k_s/k_c) = 7898.

MOTS CLÉS: Barrage de remplissage rocheux, facteur de sécurité, stabilité, infiltration transitoire, barrage de Bradon.

COMMISSION INTERNATIONALE DES GRANDS BARRAGES

VINGT-SIXIÈME CONGRÈS DES GRANDS BARRAGES
Autriche, juillet 2018

DOI 10.3217/978-3-85125-620-8-222



This work licensed under a Creative Commons Attribution 4.0 International License. <https://creativecommons.org/licenses/by-nc-nd/4.0/>

**EARTH DAMS SAFETY UNDER SEISMIC MOTION USING LIMIT
EQUILIBRIUM METHOD AND PHYSICAL MODELING**

Behrouz GORDAN

ENGINEERING SEISMOLOGY AND EARTHQUAKE ENGINEERING
RESEARCH GROUP (E-SEER), UNIVERSITI TEKNOLOGI MALAYSIA 81310
SKUDAI, JOHOR

MALAYSIA

Azlan ADNAN

ENGINEERING SEISMOLOGY AND EARTHQUAKE ENGINEERING
RESEARCH GROUP (E-SEER), UNIVERSITI TEKNOLOGI MALAYSIA 81310
SKUDAI, JOHOR

MALAYSIA

Earth dams safety under seismic motion using limit equilibrium method and physical modeling

Behrouz Gordan, Azlan Adnan

Engineering Seismology and Earthquake Engineering Research Group (e-seer), Universiti Teknologi Malaysia 81310 Skudai, Johor, Malaysia

**Corresponding Author: bh.gordan@yahoo.com*

Abstract

The aim of the present research is the evaluating of Limit Equilibrium method to assess factor of safety under seismic load in earth dam using physical small-scale modeling. For this purpose, numerical analysis to evaluate slope stability under vertical peak ground acceleration (PGA) was carried out using Geostudio program. In parallel, small-scale physical modeling (1/100) was tested using vibrator table device in order to observe slope stability in induced dam by seismic motion. As result, the weak performance was obtained for assessing factor of safety under seismic load using Limit equilibrium method (LEM). Based on Physical modeling, damage with respect to longitudinal cracks was dramatically observed at upstream and crest during seismic motion while the simulated models were safe under same acceleration. Consequently, the good agreement was found between modeling tests and lesson learned from literature. Finally, due to predict dam safety along seismic motion using LEM, design acceleration of the dam site should be increasingly applied using (PGA+ 0.2g) for simulation.

Keywords: Factor of safety, Vibrator table, Acceleration, Physical modeling, Limit Equilibrium

1. Introduction

Due to slope stability in the field of geotechnical engineering, determination of the critical slip surface to compute factor of safety is one of the main concerns in the earthquake engineering. In this case, slope stabilization methods are based on specific skills that must be exactly understood and realistically simulated. This analyze significantly depends on many main factors such applied loads, foundation properties and soil behavior. However, factor of safety is the essential function to establish a safe and economical design. In this context, the limit equilibrium method (LEM) was presented using circular slip line (Fellenius 1936, Bishop 1955 and Spencer, 1967), which can be appreciated. After that, several attempts were also recommended based on general slide line (Janbu, 1973; Morgenstern and Price, 1965). After that, an additional equation of vertical force equilibrium was individually taken into account for each slice (Sarma, 1973 and 1979). In recent decades, Finite-Element Method (FEM) has been developed based on displacement, in particular used to evaluate safety regarding the shear strength reduction" SSR or "phi-c reduction" techniques (Huang et al, 2009; Baker, 2006). Some combined methods based on probabilistic approaches of slope analysis and design with an aid of LEM and FEM (El-Ramly et al, 2002; Li et al, 1987 and Griffiths et al, 2004) were also presented. Furthermore, an artificial neural network (ANN) was carried out using optimization techniques to compute factor of safety (Cho, 2009). Moreover, Two-stepped self-optimizing method was performed using genetic algorithm (GA) with structure evolution and parameter optimization (Yang et al, 2004). According to report from case studies, the underwater slide during the San Fernando earthquake (1971) was observed in Lower San Fernando dam. Fortunately, the dam barely avoided collapse, thereby preventing a potential disaster of flooding of the heavily populated areas below the dam. Two decades later in 1994, the Los Angeles Dam concrete face rock-fill dam (CFRD) was confronted by Northridge earthquake. The Northridge earthquake was almost equal in magnitude to the previous San Fernando earthquake. Ground shaking was very strong, with amplitudes among the highest ever recorded but consistent with the USGS estimates. Yet the dam showed only minor deformation and superficial cracking. Despite the intense shaking, the crest of the dam moved only 1 inch sideways and settled only 3.5 inches. In 2008 by earthquake 7.9 magnitude, the longitudinal crack was found in Fengshou reservoir dam. However, numerical analysis to evaluate dam

behavior during seismic motion was commonly used (Parish et al, 2009; Berhe et al, 2010; Xia et al, 2010; Kong et al, 2010; Bayraktar et al, 2011; Risheng et al, 2006; Gordan et al, 2013). There are two reasons for using numerical method in this context such the lack of monitoring data and technology development. In the last decade, shaking table and centrifuge based on small-scale physical modeling were commonly used to evaluate dam behavior during the seismic motion (Matsumaru et al, 2008; Namdar et al, 2010; Wang et al, 2011). In the present paper, the performance of slope stability under severe seismic motion for homogenized earth dam is the main purpose of study. For this purpose, two physical small-scale models with different slope constructed for vibrating on top of the vibrator table. In parallel, factor of safety was computed using numerical analysis based on limit equilibrium method. Based on comparing result in both cases as mentioned earlier, the performance of Limit Equilibrium method under seismic load will be discussed.

2.0 Background of limit equilibrium method (LEM-slices)

Based on limit equilibrium method (LEM) with respect to slices from potential slip surface, Fellenius and Bishop's methods are the simplest and most applicable in the geotechnical engineering. As shown in Figure 1, the soil mass above a failure surface divided into slices with vertical sections. Each portion was taken as having a straight-line base, denoting mutual support between the slices. Based on Fellenius approach, the forces acting between each pair of slices (E, X) are neglected, so only the forces acting on the base of each slice (W, N and S) are left for consideration (Yu, 1998). Factor of safety (FOS) is the suitable relation between opposing and toppling moments. It can be computed according to the center point of an assumed slip circle. The final formulation of the safety factor has comprised only resisting and sliding forces (S, T).

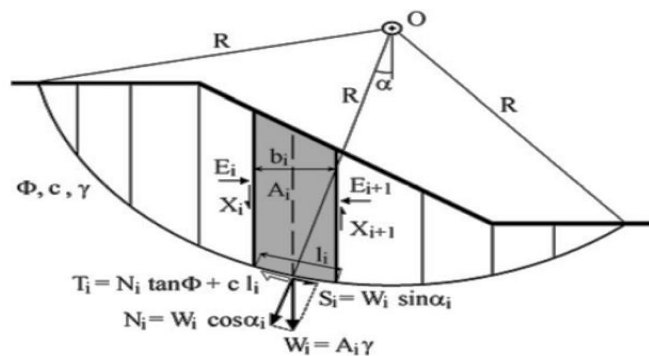


Figure 1: The idea of slice method and definition factor of safety (See Eq.2)

In Bishop's method, apart from the total moments' equilibrium conditions, an additional equation of vertical force equilibrium was taken into account individually for each slice. Such consideration leads to an implicit formulation of the safety factor that needs an iterative procedure (Zhu et al, 2003).

$$\Sigma H = 0, \Sigma V = 0 \text{ and } \Sigma M = 0 \quad (1)$$

$$F_S = \frac{\Sigma_i [c b_{i+} + (w_i + x_i - x_{i+1}) \tan \phi] \frac{\sec \alpha_i}{1 + (\tan \alpha_i \tan \phi) / F_S}}{\Sigma_i S_i} \quad (2)$$

However, the general equilibrium equations as mentioned below should be persuaded (See Eq.1). Finally, the Bishop's method explained in Eq.2.

3.0 Method of research

Two types of tests such as soil mechanic and physical modeling test were carried out in this study. Soil properties were collected based on British standard test (BS). The physical small-scale modeling was performed using vibrator table. For this purpose, two models with sinusoidal motion were vibrated. For numerical analysis, Geostodio 2007 (Slope /W) was utilized for evaluations factor of safety based on limit equilibrium method. Figure 2 shows the research flowchart.

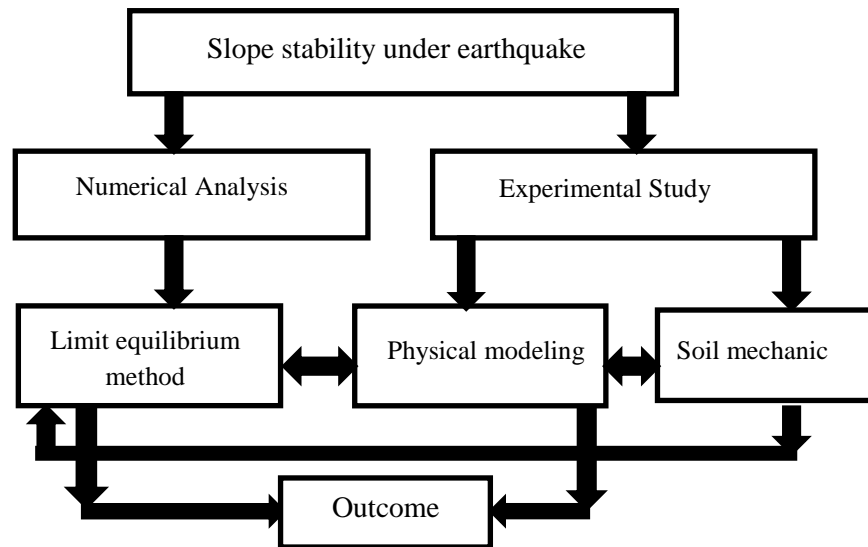


Figure 2: Flowchart

3.1 Soil mechanics laboratory tests

Due to collect soil physical properties, soil mechanics tests were completely carried out using British Standard (BS). Table 1 presents the physical properties for river sand with 75% relative density (dense sand). Physical characteristics of the tropical laterite soil were presented in Table 2. It is important noting that river sand and tropical laterite soil were respectively utilized in the foundation and dam body for small-scale models.

Table 1: Characteristics of sands

Engineering and physical properties	Content
Specific gravity	2.574
Maximum dry density (gr/cm^3)	1.721
Minimum dry density (gr/cm^3)	1.366
Maximum size (mm)	2.00
Minimum size (mm)	0.075
Uniformity Coefficient (C_u)	4.375
Coefficient of curvature (C_c)	2.725
Relative density %	75

Table 2: Characteristics of the laterite soil

Characteristics of the laterite soil	Content
Specific gravity	2.40
Liquid limit, LL (%)	75
Plastic limit, PL (%)	41
Plasticity index, PI (%)	34
BS classification	MH
Maximum dry density (g cm^{-3})	1.33

Optimum moisture content (%)	35
Unconfined compressive strength (KPa)	306.26
Cohesion (KPa)	25.18
Angle of internal friction (Degree)	30.00
Secant modulus elasticity (KPa)	15283.72
Coefficient of Volume Compressibility (m _v , m ² /MN)	0.1055
Coefficient of Consolidation (c _v , m ² /yr)	44.16
Permeability (cm/seconds)	1.29E-5

Figure 3 and 4 show the distribution of the particle size for both type of soil as mentioned earlier. The determination of particle size distribution was tested based on BS 1377-2 1990. As seen, maximum size was 2.00 mm and minimum size was 0.75mm.

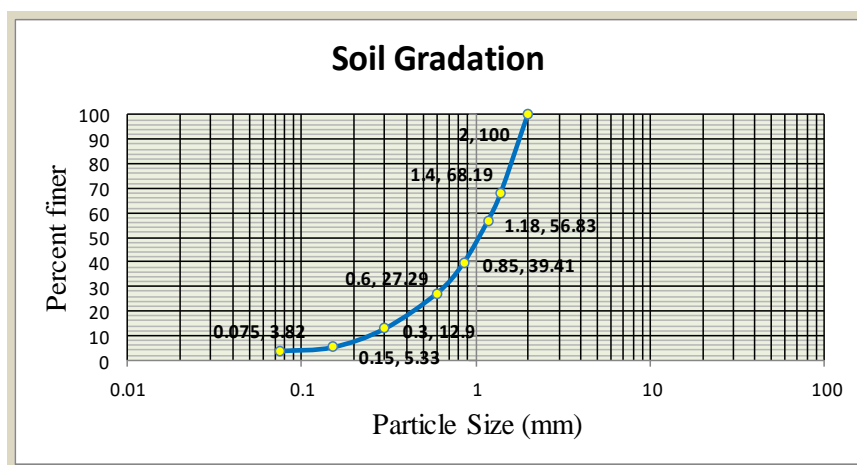


Figure 3: Laterite soil gradation

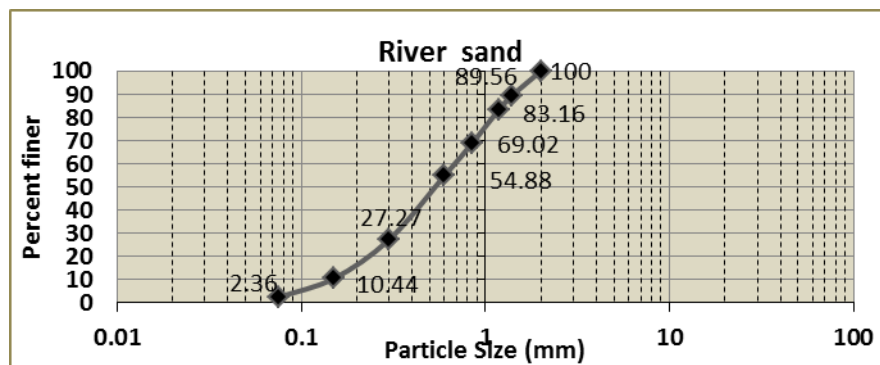


Figure 4: River sand gradation

3.2 Small-Scale physical modeling

Small-scale model is explained in the present section. In terms of utilizing apparatus for this study, some devices were applied such as vibrator table, displacement transducer, and data logger. In terms of dynamic loading, sinusoidal motion was used for evaluating slope stability for small-scale modeling (1/100).

3.2.1 Vibrator table

Vibrating table 24-9112 (CN-166) was used in this study, as shown in Figure 3. The vibrating desk was cushioned steel and semi noiseless electromagnetic vibrator with 3600 vpm operating frequency. In addition, it was a separate controller to vary vibrator amplitude in case of frequency capacity limit to 100 Hz. Table capacities was equal to 750 lbs (340 kg). Double amplitude range was located at 0.002 inch (0.05 mm) to 0.015 inch (0.38mm). Actuator was an electromagnetic vibrator over 100 lbs (45.30kg). The table was square shape 30 inch (762 mm). The table thickness was 33.3mm of steel. In terms of weight, it was net 555 lbs (252 kg) and shipping 605 lbs (274 kg). Figure 5 illustrates the vibrator table that used in this study, as shown actuator is in the vertical direction.



Figure 5: Vibrator Table

3.2.2 Displacement transducer and data logger

Displacement transducer CDP-D was applied with dual isolated ports (I/O). By using transducer, one set of cables for input and output were connected to the analog measuring instrument and other set to the digital measuring instrument. With two different types of measuring equipment connected to this transducer, simultaneous measurements can be made without interference. Figure 6-a shows the displacement transducer which was used in this study. Besides, Figure 6-b shows the dimension detail for CDP-100 to measure displacement at both edges of the crest in small-scale modeling.

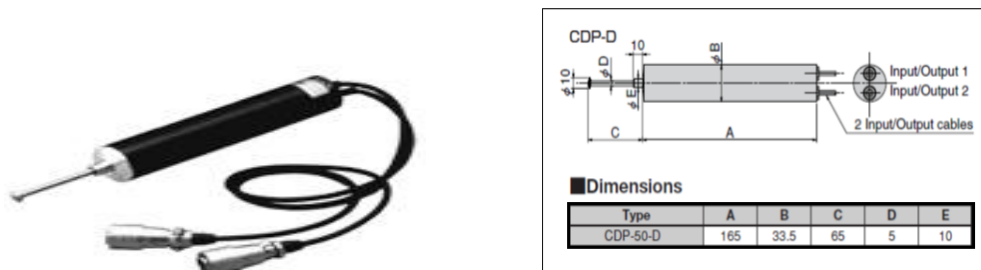


Figure 6: a) Displacement transducer, CDP-100 b) Dimension of displacement transducer

In terms of data record, data logger or data recorder is the electronic device. It can record data over time or in relation to location either with a built in instrument or sensor or via external instruments and sensors. Figure 7 illustrates the data logger that used in this study.



Figure 7: Data logger, UCAM-70A

Based on device ability, results were printed during the duration of vibration. After that, results were classified by using Excel program. It should be noting that, both transducers as mentioned previously were connected to this data logger (UCAM-70A) in order to record vertical displacement during the vibration. In addition, the sub step of vibration period was equal two seconds based on device ability with respect to print.

3.2.3 Sinusoidal vibrate loading

There is a mathematical relationship between frequency, displacement, velocity, and acceleration for sinusoidal motion in order to consider the peak value. This relationship is such that if any two of the four variables are known, the other two can be calculated. all equations with respect to required combination are presented in Table 3. In addition, Table 4 illustrates distribution of displacement and acceleration based on different frequency. As seen, the amplitude of frequency is between 5 to 30 hertz. Also in this Table, it is obvious that, displacement and acceleration were increased while frequency was increased. It is important to note that, G in these formulas is not the acceleration of gravity. It is a constant for calculation within different systems. Respectively, for metric, imperial and Si G is 9.80665m/s², 386.0885827 in/s² and is 1.00 m/s².

Table 3: Equations for sinusoidal motion, Displacement (D), Velocity (V), Acceleration (A), and Frequency (F)

Displacement (D)	Velocity (V)	Acceleration (A)	Frequency (F)
$\frac{V}{\pi F}$	$\pi F D$	$\frac{2\pi^2 F^2 D}{G}$	$\sqrt{\frac{GA}{2\pi^2 D}}$
$\frac{GA}{2\pi^2 F^2}$	$\frac{GA}{2\pi F}$	$\frac{2\pi F V}{G}$	$\frac{V}{\pi D}$
$\frac{2V^2}{GA}$	$\sqrt{\frac{GAD}{2}}$	$\frac{2V^2}{GD}$	$\frac{GA}{2\pi V}$

Table 4: Distribution of acceleration using different frequency in vibrator table

Frequency (Hz)	5	10	15	20	25	30
Displacement (mm)	0.06875	0.083	0.0995	0.116	0.1325	0.149
Acceleration (Gn)	0.003341	0.01668	0.045	0.0933	0.166	0.269
Acceleration	0.034g	0.17g	0.46g	0.95g	1.69g	2.74g

Since the motion is sinusoidal, the displacement, velocity, and acceleration are changing sinusoidal. However, they are not in the same phase. The phase relationship between displacement, velocity, and acceleration is that such that velocity is 90° out of phase with acceleration and displacement is 180° out of phase with acceleration. In other words, when displacement is at a maximum, velocity is at a minimum, and acceleration is at a maximum. It should be noting that, $1 g_n = 9.80665 \text{ m/s}^2 = 32.174 \text{ ft/s}^2 = 386.0886 \text{ in/s}^2$.

3.2.4 Scaling laws

In case of using scale parameter, the scale factor according to Eq.2 was used in this study.

$$x^* = \frac{x_m}{x_p} \quad (3)$$

The subscript m represents "model" and the subscript p represents "prototype" and x^* represents the scale factor for the quantity x (Garnier et al, 2007).

The reason for spinning a model on a centrifuge is to enable small-scale models to feel the same effective stresses as a full-scale prototype. This goal can be stated mathematically as

$$\sigma^* x = \frac{\sigma'_m}{\sigma'_p} = 1 \quad (4)$$

Where the asterisk represents the scaling factor for the quantity, σ'_m is the effective stress in the model and σ'_p is the effective stress in the prototype.

In soil mechanics the vertical effective stress, σ' for example, is typically calculated by

$$\sigma' = \sigma^t - u \quad (5)$$

Where σ^t and u are total stress and pore pressure, respectively. For a uniform layer with no pore pressure, the total vertical stress at a depth H may be calculated by:

$$\sigma^t = \rho g H \quad (6)$$

Where ρ represents the density of the layer and g represents gravity. In the conventional form of centrifuge modeling (Garnier et al, 2007), it is typical that the same materials are used in the model and prototype; therefore the densities are the same in model and prototype, i.e.

$$\rho^* = 1 \quad (7)$$

Furthermore, in conventional centrifuge modeling all lengths are scaled by the same factor L^* . To produce the same stress in the model as in the prototype, we thus require

$$\rho^* g^* H^* = 1 g^* L^* = 1 \quad (8)$$

This may be rewritten as

$$g^* = \frac{1}{L^*} \quad (9)$$

The above scaling law states that if lengths in the model are reduced by some factor, n, then gravitational accelerations must be increased by the same factor, n in order to preserve equal stresses in model and prototype.

3.2.5 Dynamic problems

For dynamic problems where gravity and accelerations are important, all accelerations must scale as gravity is scaled, i.e.

$$a^* = g^* = \frac{1}{L^*} \quad (10)$$

Since acceleration has units of $\frac{L}{T^2}$, it is required that

$$a^* = \frac{L^*}{T^{*2}} \quad (11)$$

Hence it is required that: $\frac{1}{L^*} = \frac{L^*}{T^{*2}}$, or

$$T^* = L^* \quad (12)$$

Frequency has units of inverse of time, velocity has units of length per time, so for dynamic problems we also obtain

$$f^* = \frac{1}{L^*} \quad (13)$$

$$v^* = \frac{L^*}{T^*} = 1 \quad (14)$$

For model tests involving dynamics, the conflict in time scale factors may be resolved by scaling the permeability of the soil (Garnier et al, 2007).

3.2.6 Model introducing

In this study, two small-scale models vibrated in the vertical direction, as shown in Figure 8 and 9. In Figure 8, slope covers 0.785 vertical and 1.00 horizontal. The width of the crest is 10.00 meter. Both slopes and crest width were changed in Figure 9, as seen in the second model.

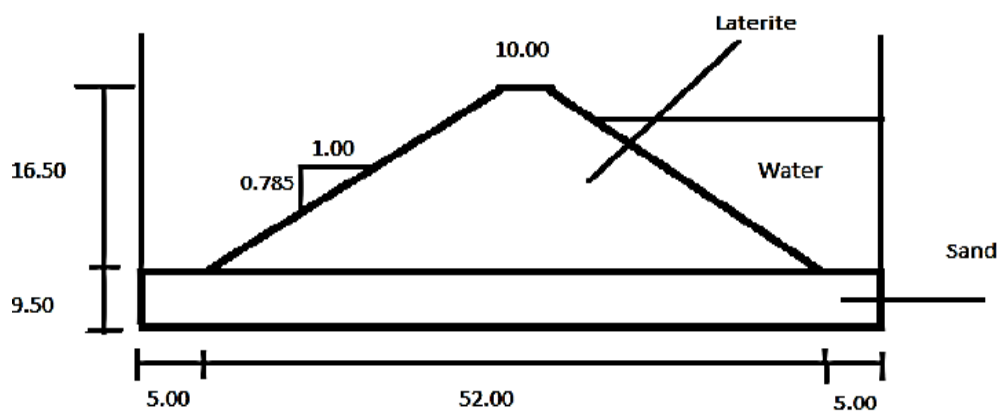


Figure 8: First physical small modeling; (S=1/100)

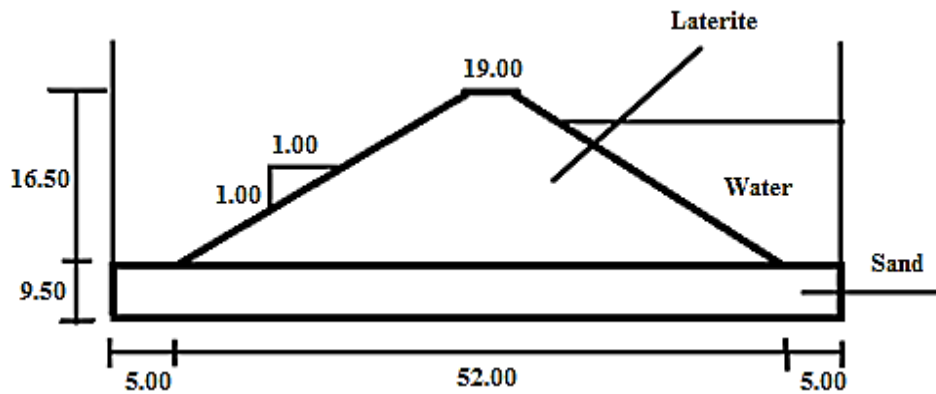


Figure 9: Second physical small-scale modeling; (S=1/100)

In models, both slope for upstream and downstream are same. In the second model, the crest width is 19.00 meter in order to make sharp slope. For both models, river sand (75%RD) was used in the foundation.

4. Results and analysis

Figure 10 show that, both points are at uplift position. In order to hydrodynamic pressure during the vibration, vertical displacement at upstream is larger than downstream. It can be

respectively seen that, maximum displacement for downstream and upstream are 0.29 mm and 0.48 mm. However, the displacement peak is respectively occurred after 62 and 90 second. In addition, the fixed trend after peak was shown by both distributions.

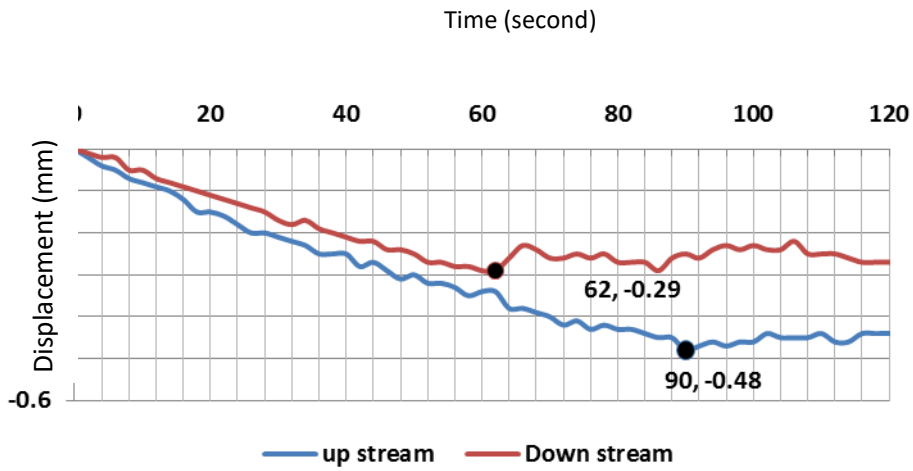


Figure 10: Vertical displacement distribution at the middle of crest length, first model

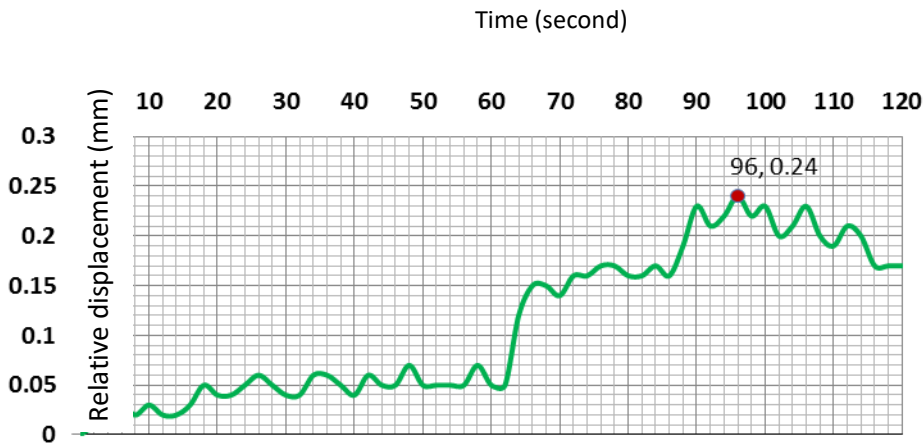


Figure 11: Relative displacement at the middle of crest length, first model

Moreover, in terms of relative displacement at the crest, Figure 11 shows that, maximum value is 0.24 mm at 96 seconds. It worth noting that, relative displacement was increased before than 60 seconds by 0.07 mm. In fact, dam performance is reliable for half time of vibration, because the maximum value is observed after three-fourth of duration. Furthermore, Figure 12 shows small-scale model before than vibration in the first situation. It can be seen that, two LVDT are installed at the middle of dam crest.



Figure 12: First small scale model on vibrator table



Figure 13: Upstream damage after reservoir with vibration at resonance condition

In terms of damage observation, Figure 13 shows model at the end of vibration, after reservoir drainage. It can be observed that, there is some longitudinal crack in the upstream. In particular, most of them are located at one-fourth of dam height near to the crest, as shown with some lines such as A, B, C and D. Moreover, line-E shows longitudinal crack at the middle of upstream surface. It is also worth noting that, the maximum length of crack is exhibited by Line-c, as can be seen in Figure 14. Significantly, it was near to the middle of length crest.



Figure 14: Longitudinal crack at line-c

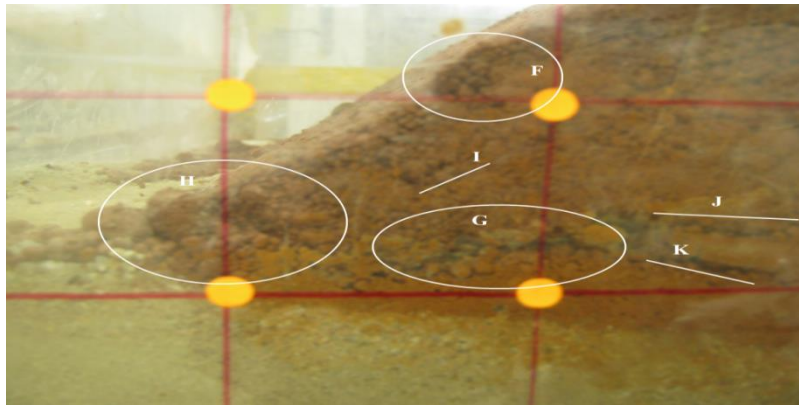


Figure 15: Transverse crack at downstream-toe

Furthermore, Figure 15 shows transverse crack in the downstream-toe. However, cracks are dramatically developed in this location. This area is restricted by four yellow circles with respect to network index for this photo, as shown by one-fourth of dam height near to foundation.

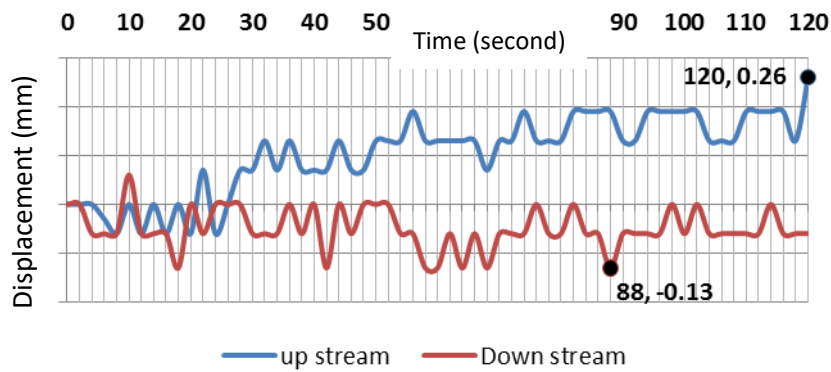


Figure 16: Vertical displacement distribution at the middle of crest length, third model

In terms of slope stability, the crest width in third small scale model is enhanced. Based on results, Figure 16 shows displacement distribution at the middle length of crest. Displacements at upstream and downstream are shown by different behavior, as can be seen that, the maximum values are respectively located at the end of vibration and 88 seconds. It means that, the edge of crest at upstream was in settlement while it was uplift at downstream, reversely. Also, in compare of maximum displacement at both edges of crest, the double ratio in upstream is observed. Furthermore, Figure 17 shows distribution of relative displacement at the middle length of crest in third physical modeling. It can be seen that, maximum value is occurred at the end of vibration with 0.32 mm, but this value also at the 88 seconds has been repeated.

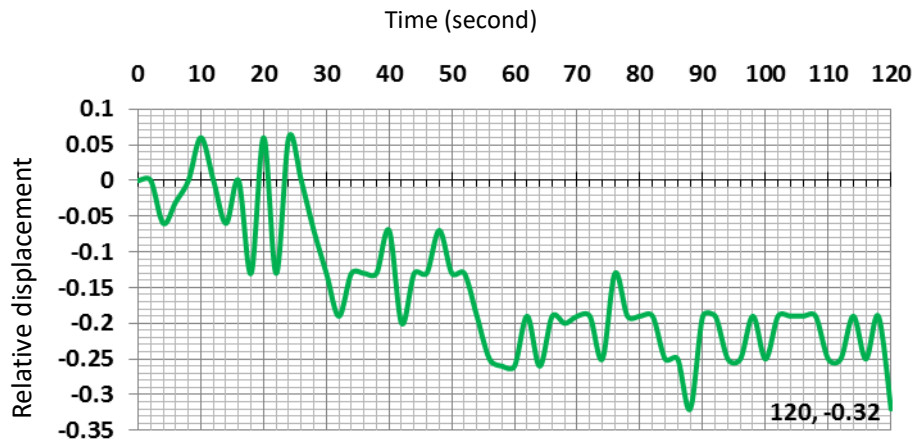


Figure 17: Relative displacement at the middle of crest length, third model

Figure 18 shows third model physical small scale. It can be observed that, dam is constructed on the river sand before reservoir. However, the upstream is located at right side. Also, some stud with different color at upstream (red color) and downstream (green color) in order to better identification of damage location are installed.

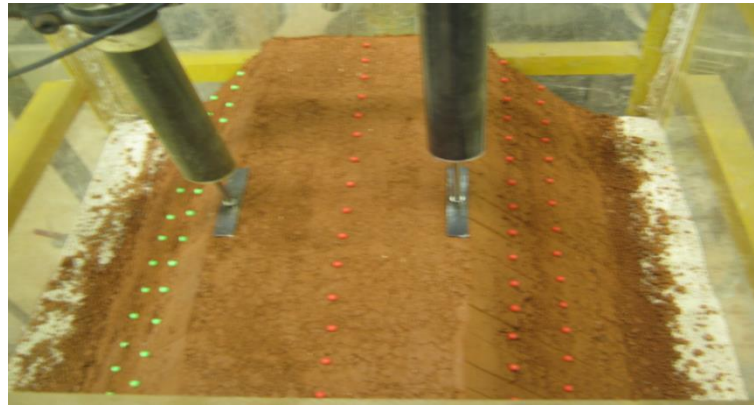


Figure 18: Second model view, upstream at right side



Figure 19: Third model view with reservoir

Also, Figure 19 shows model during tank process. It should be noted that, the rate of filling was very slowly. After vibration, damage location in this model shown by Figures 20 and 21.



Figure 20: Damage at upstream, middle to left side, near to abutment

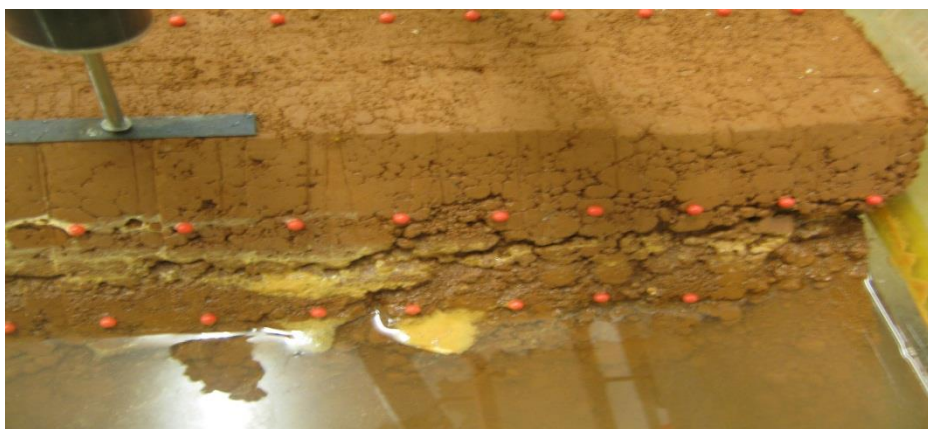


Figure 21: Damage at upstream, middle to right side, near to abutment

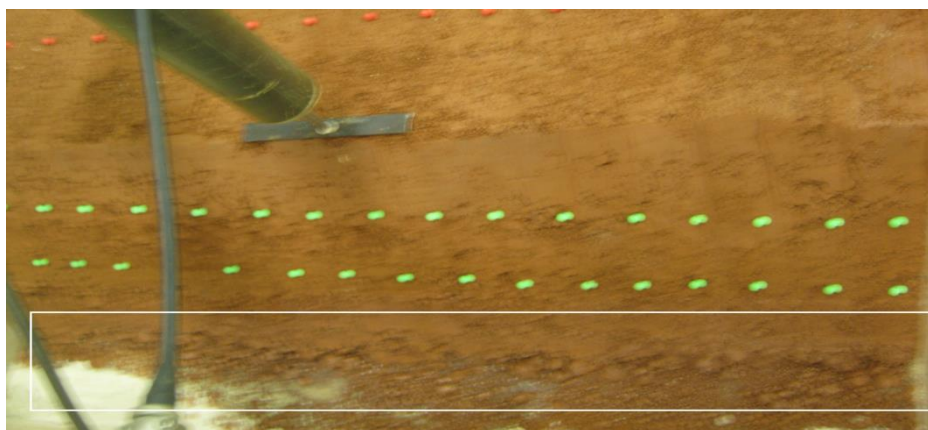


Figure 22: Damage at downstream, total length of the toe

The significant damage at upstream are occurred at hydrodynamic pressure level between half of upstream surface and freeboard. In particular, the huge damage with respect to intensity at area near to both abutments was observed. In parallel, Figure 22 shows damage at downstream of dam, as can be observed by white rectangular. The damage location at downstream was at toe area in total length.

Factor of safety for models

To evaluate factor of safety based on vibration, models have been simulated using Geostudio 2007 in the present study. In this case, seismic load in ranges of 0.05g to 0.4g was used. Table 5

compares the factor of safety based on different peak ground acceleration in both models. Static safety presented using acceleration equal zero. As seen, factor of safety are respectively 1.199 and 1.31 for both models in the static position.

Table 5: Factor of safety for different seismic load in models

Model	FOS								
	0	0.05g	0.1g	0.15g	0.2g	0.25g	0.3g	0.35g	0.4g
First	1.199	1.141	1.109	1.08	1.037	0.996	0.958	0.922	0.889
Second	1.31	1.247	1.191	1.139	1.092	1.048	1.008	0.97	0.936

Figure 23 shows the safety map for both models as mentioned earlier. However, factor of safety is bigger in the second model. As seen in this Figure, critical slip was occurred at slope for second model while it was expanded towards foundation, as observed in the first model. It can be concluded that increasing of the crest width can be led to increase factor of safety in static situation. In order to effect of peak ground acceleration on the factor of safety, this value was less than one for 0.25g in the first model while it is unsafe for 0.35g in the second model. It should be noting that, both physical models have been vibrated using 10 Hz (0.17g), and should safe without any damage with respect to Table 5. In reality, models are safe under simulations using Limit equilibrium method but unsafe under sinusoidal motion using vibrator table. It means that, dam performance is very complex during vibration. In fact, Finite-element method should be applied to assess the accurate results. Therefore, more peak ground acceleration (PGA+0.2) is the best suggestion for using limit equilibrium method. For example, factor of safety for one case study using limit equilibrium method is the main purpose when site background is 0.15g; therefore, we suggest using 0.35g instead of 0.20g.

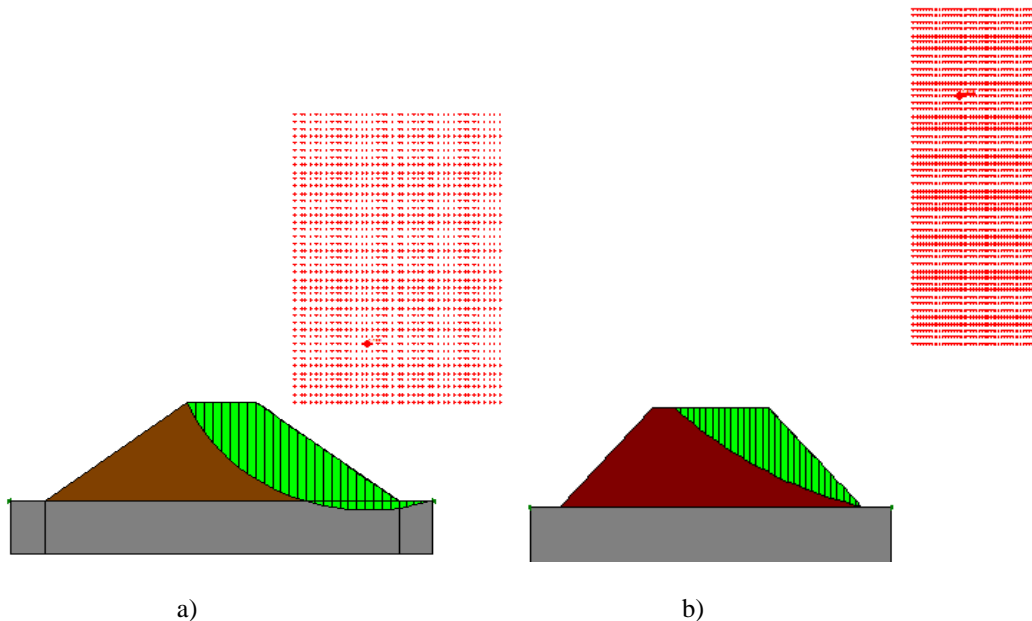


Figure 23: Factor of safety in static situation, a) First model b) Second model

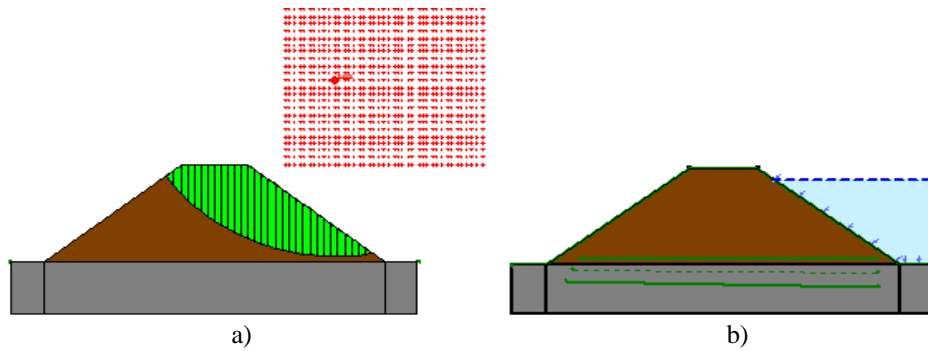


Figure 24: Factor of safety in dynamic condition, a) Safety map b) model with tank

As a mentioned, critical slip surface was expanded in the static situation for first model. Figure 24 shows that, this condition was changed for seismic loading. Also in Figure 25, this position was similar to static state as explained earlier for second model. Finally, Limit equilibrium method was the weak prediction of safety in dam under dynamic loading. The location of damage was at upstream under seismic motion in physical small-scale modeling, when it was safe according to results from numerical analysis.

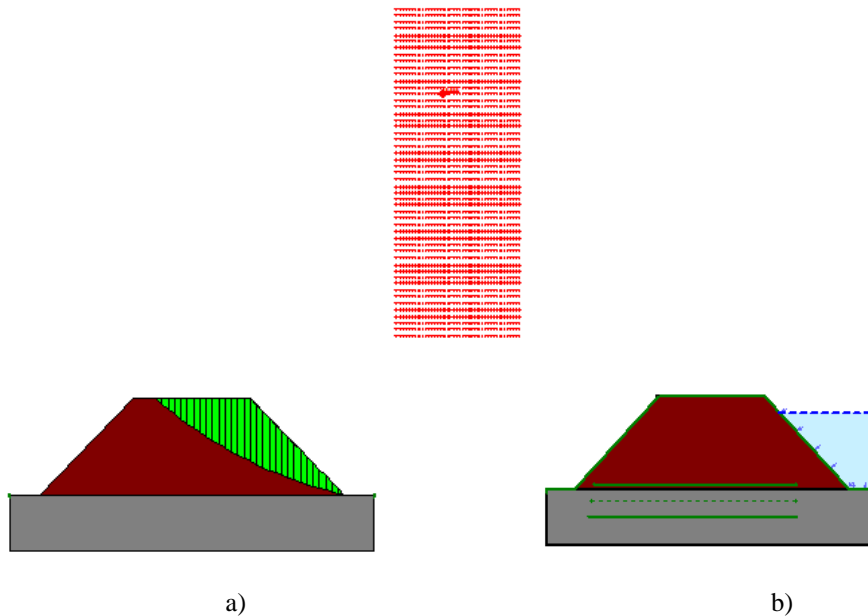


Figure 25: Factor of safety in dynamic condition, a) Safety map b) Second model with tank

5.0 Conclusion

In this study, earth dam safety using physical small-scale modeling and numerical analysis was carried out. As concluded, Limit equilibrium method was the weak assessment for factor of safety under seismic load. Damage during seismic vibration observed using Physical modeling while models as simulated were safe under same acceleration. It is the best recommendation to compute factor of safety using limit equilibrium method that acceleration of the dam site should be increased (PGA+0.2).

6.0 Acknowledgment

This study is made possible by the support of the International Doctorate Fellowship of Universiti Teknologi Malaysia, and it is very much appreciated.

References

- Baker, R. (2006). A relation between safety factors with respect to strength and height of slopes. *Computers and Geotechnics*, 33(4), 275-277.
- Bayraktar, A., Kartal, M. E., & Adanur, S. (2011). The effect of concrete slab–rockfill interface behavior on the earthquake performance of a CFR dam. *International Journal of Non-Linear Mechanics*, 46(1), 35-46.
- Berhe, T. G., Wang, X. T., & Wu, W. (2010). Numerical Investigation into the Arrangement of Clay Core on the Seismic Performance of Earth Dams. In *Soil Dynamics and Earthquake Engineering* (pp. 131-138). ASCE.
- Bishop, A. W. (1955). The use of the slip circle in the stability analysis of slopes. *Geotechnique*, 5(1), 7-17.
- Cho, S. E. (2009). Probabilistic stability analyses of slopes using the ANN-based response surface. *Computers and Geotechnics*, 36(5), 787-797.
- El-Ramly, H., Morgenstern, N. R., & Cruden, D. M. (2002). Probabilistic slope stability analysis for practice. *Canadian Geotechnical Journal*, 39(3), 665-683.
- Fellenius, W. (1936). Calculation of the stability of earth dams. In *Transactions of the 2nd congress on large dams*, Washington, DC (Vol. 4, pp. 445-463).
- Geostudio2007 manuel. [www. Geo-slope.com](http://www.Geo-slope.com).
- Griffiths, D. V., & Fenton, G. A. (2004). Probabilistic slope stability analysis by finite elements. *Journal of Geotechnical and Geoenvironmental Engineering*, 130(5), 507-518.
- Garnier, J., Gaudin, C., Springman, S. M., Culligan, P. J., Goodings, D. J., Konig, D., ... & Thorel, L. (2007). Catalogue of scaling laws and similitude questions in geotechnical centrifuge modelling. *International Journal of Physical Modelling in Geotechnics*, 7(3), 1-23.
- Gordan, B. & Azlan, B. A. (2013). Effect of material properties in CFRD tailing-embankment bridge during a strong earthquake. *Caspian Journal of Applied Sciences Research*, 2(11), pp. 61-72.
- Huang, M., & Jia, C. Q. (2009). Strength reduction FEM in stability analysis of soil slopes subjected to transient unsaturated seepage. *Computers and Geotechnics*, 36(1), 93-101.
- Janbu, N. (1975, April). Slope stability computations: In *Embankment-dam Engineering*. Textbook. Eds. RC Hirschfeld and SJ Poulos. JOHN WILEY AND SONS INC., PUB., NY, 1973, 40P. In *International Journal of Rock Mechanics and Mining Sciences & Geomechanics Abstracts* (Vol. 12, No. 4, p. 67). Pergamon.
- Kong, X. J., Zhou, Y., Xu, B., & Zou, D. G. (2010). Analysis on seismic failure mechanism of zipingpu dam and several reflections of aseismic design for high Rock-fill dam. *Earth and Space*, 3177-3189.
- Li, K. S., & Lumb, P. (1987). Probabilistic design of slopes. *Canadian Geotechnical Journal*, 24(4), 520-535.

- Matsumaru, T., Watanabe, K., Isono, J., Tateyama, M. and Uchimura, T. (2008). Application of cement-mixed gravel reinforced by ground for soft ground improvement. Proceedings of the 4th Asian Regional Conference on Geosynthetics June 17 - 20, 2008 .Shanghai, China.
- Morgenstern, N. R., & Price, V. E. (1965). The analysis of the stability of general slip surfaces. *Geotechnique*, 15(1), 79-93.
- Namdar, A. and Pelko, A. K. (2010). Seismic Evaluation of Embankment Shaking Table Test and Finite Element Method. *The Pacific Journal of Science and Technology - volume11, Number2, November*.
- Parish, Y., & Abadi, F. N. (2009). Dynamic Behaviour of Earth Dams for Variation of Earth Material Stiffness. Proceedings of World Academy of Science: Engineering & Technology, 50.
- Risheng Park Piao, P. E., Rippe, A. H., Barry Myers, P. E., & Lane, K. W. (2006). Earth dam liquefaction and deformation analysis using numerical modeling.
- Sarma, S. K. (1973). Stability analysis of embankments and slopes. *Geotechnique*, 23(3), 423-433.
- Sarma, S. K. (1979). Stability analysis of embankments and slopes. *Journal of the Geotechnical Engineering Division*, 105(12), 1511-1524.
- Spencer, E. (1967). A method of analysis of the stability of embankments assuming parallel inter-slice forces. *Geotechnique*, 17(1), 11-26.
- Wang, L., Zhang, G., & Zhang, J. M. (2011). Centrifuge model tests of geotextile-reinforced soil embankments during an earthquake. *Geotextiles and Geomembranes*, 29(3), 222-232.
- Xia, Z. F., Ye, G. L., Wang, J. H., Ye, B., & Zhang, F. (2010). Fully coupled numerical analysis of repeated shake-consolidation process of earth embankment on liquefiable foundation. *Soil Dynamics and Earthquake Engineering*, 30(11), 1309-1318.
- Yang, C. X., Tham, L. G., Feng, X. T., Wang, Y. J., & Lee, P. K. K. (2004). Two-stepped evolutionary algorithm and its application to stability analysis of slopes. *Journal of computing in civil engineering*, 18(2), 145-153.
- Yu, H. S., Salgado, R., Sloan, S. W., & Kim, J. M. (1998). Limit analysis versus limit equilibrium for slope stability. *Journal of Geotechnical and Geoenvironmental Engineering*, 124(1), 1-11.
- Zhu, D. Y., Lee, C. F., & Jiang, H. D. (2003). Generalised framework of limit equilibrium methods for slope stability analysis. *Geotechnique*, 53(4), 377-395.

COMMISSION INTERNATIONALE DES GRANDS BARRAGES

VINGT-SIXIÈME CONGRÈS DES GRANDS BARRAGES
Autriche, juillet 2018

DOI 10.3217/978-3-85125-620-8-223



This work licensed under a Creative Commons Attribution 4.0 International License. <https://creativecommons.org/licenses/by-nc-nd/4.0/>

FLOOD WAVE ANALYSIS OF EMBANKMENT DAM FAILURE BY USING 2D MODELS

Michael BERGER

Institute of Hydraulic Engineering and Water Resources Management, Research Center of Hydraulic Engineering, VIENNA UNIVERSITY OF TECHNOLOGY

AUSTRIA

René DÜNKNER

Institute of Hydraulic Engineering and Water Resources Management, Research Center of Hydraulic Engineering, VIENNA UNIVERSITY OF TECHNOLOGY

AUSTRIA

COMMISSION INTERNATIONALE
DES GRANDS BARRAGES

VINGT-SIXIÈME CONGRÈS DES
GRANDS BARRAGES
Autriche, juillet 2018

FLOOD WAVE ANALYSIS OF EMBANKMENT DAM FAILURE BY USING 2D MODELS

Michael BERGER, René DÜNKNER

*Institute of Hydraulic Engineering and Water Resources Management, Research
Center of Hydraulic Engineering, VIENNA UNIVERSITY OF TECHNOLOGY*

AUSTRIA

1. INTRODUCTION

Despite a very careful planning and construction as well as a meticulous surveillance, the risk of a dam failure cannot be neglected completely. According to [1], the two most common modes of failure for embankment dams are overtopping and piping. In order to estimate the consequences for a dam break scenario (loss of life, economic consequences), a flood wave analysis is mandatory. The present paper deals with the topic of flood wave analysis due to embankment dam failure by using 2D models. Key parts of this work are the estimation of the failure hydrographs on the one hand and the flood routing for different failure scenarios on the other hand.

2. INVESTIGATED CASE STUDIES

The following chapter summarizes the characteristic features of the two investigated case studies. Beside the specification of the embankment dams, a general description of the investigated downstream area is presented. Based on airborne LIDAR data, a 3D point cloud is used to generate a geometrical model of the area studied, in order to build the basis for hydraulic model.

2.1. CASE STUDY 1 – FLOOD RETENTION BASIN IN LOWLAND AREA

The embankment of the flood retention basin is a homogeneous earth-fill dam with a maximum height of 12,0 m, a crest length of about 115 m and slopes of 1:3 for both upstream and downstream face. According to the design criteria of retaining a 100-year flood, a retention volume of $V_{ret,100} \approx 2,5 \cdot 10^5 m^3$ can be determined. During this flood event, a maximum discharge of the bottom outlet of $Q_{ret,100} = 8,2 m^3/s$ will run off to the downstream area. For a 5000-year safety flood, the maximum reservoir volume of the basin can be calculated to $V_{ret,5000} \approx 3,3 \cdot 10^5 m^3$. For this extreme scenario, a maximum discharge of $Q_{5000} = 61,1 m^3/s$ can be stated for both the bottom outlet and the emergency spillway. The investigated downstream area of the basin is located in a lowland region. The total length of the hydraulic model is about 23,57 km, with an average bottom slope of 0,7 % (see Fig. 1). The meandering main channel often leads through woodlands and is surrounded by hedgerows over long distances. Furthermore, the channel runs through several culverts in order to cross some main streets of the region.

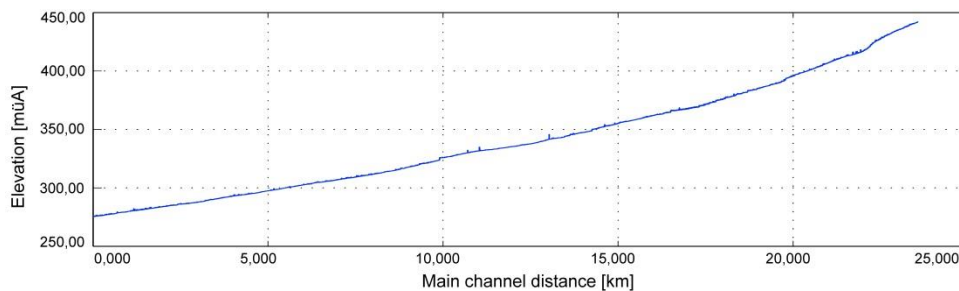


Fig. 1
Longitudinal section of the main channel – case study 1

2.2. CASE STUDY 2 – RESERVOIR IN ALPINE AREA

The second case study deals with the failure of a permanently impounded reservoir in an alpine region. With a maximum height of 92 m, a crest length of 275 m and slopes of 1:1,4 for the upstream, respectively 1:1,5 for the downstream face, the dam retains a volume of $V_{MOL} \approx 8,2 \cdot 10^6 m^3$ for maximum operation level. For a 5000-year safety flood, the reservoir volume results to $V_{SHQ} \approx 9,0 \cdot 10^6 m^3$. The corresponding water level in the reservoir for this scenario is about 1,5 m above the maximum operation level. The additional freeboard to the dam crest are another 1,5 m. The investigated downstream area of the dam is generally located in the Austrian Central Alps and can be subdivided into two main parts. The first upper part reaches over 5,5 km from the dam site, through a steep and narrow side valley to the 17,0 km long main valley (see Fig. 2).

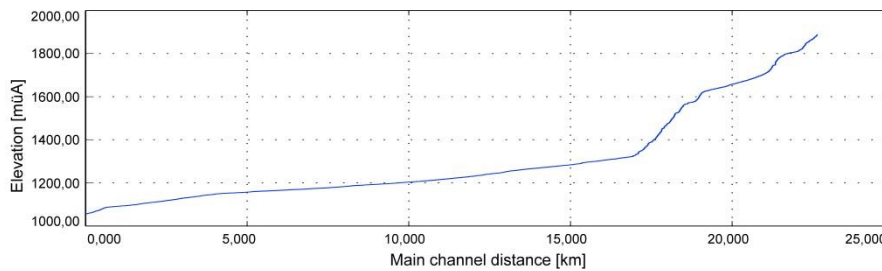


Fig. 2
Longitudinal section of the main channel – case study 2

3. THEORETICAL BACKGROUND AND GOVERNING EQUATIONS

The following chapter deals with the governing equations both of the breach outflow hydrographs and the 2D hydraulic model of the downstream area of the dam.

3.1. BREACH OUTFLOW

As a basis for the flood wave analysis, the discharge curve of the failure event has to be determined. The widespread approaches like those of Pierce [2] or Froehlich [3] provide only a peak outflow and are not immediately applicable for a transient flood wave analysis.

The DEICH parameter program developed by Broich [4] provides a transient failure hydrograph for both overtopping and piping failure of the embankment dam. The program assumes a trapezoidal initial breach cross section with a horizontal breach bed and a constant lateral inclination of the breach slopes (see Fig. 3). In order to calculate the enlargement of the breach, DEICH draws on standard empirical sediment transport formulae like those of Meyer-Peter and Müller [5] or Smart and Jaeggi [6]. Furthermore, the program uses an explicit algorithm for the calculation of water level, breach outflow and breach widening. The water level in the reservoir is either determined by the water level line or calculated using the volume balance. The outflow is calculated using the weir formula of Poleni-Weissbach.

In both case studies, DEICH is used to generate different outflow hydrographs. In addition, the empirical approaches of Rüdissler and Pierce are also used, in order to get an extended range of possible failure hydrographs. The peak discharge of both Ruedissler [7] and Pierce [2] follows Eq. 1.

$$Q_{\text{Pierce}} = 0,0176(VH)^{0,606} \quad Q_{\text{Rüdissler}} = 0,0328(VH)^{0,625} \quad [1]$$

where V describes the stored water volume and H the height of the dam.

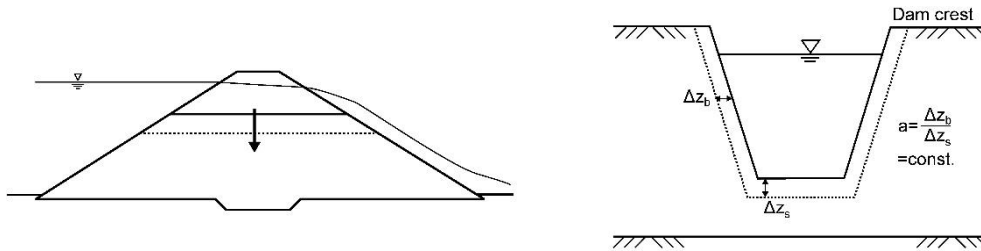


Fig. 3

Longitudinal and transversal development of a dam breach

3.2. FLOOD WAVE ANALYSIS

The 2D hydraulic calculations of the dam break scenario performed with HEC-RAS are based on a relationship of two basic equations. These are the Navier-Stokes and the Saint-Venant equations. As a simplification, an incompressible fluid, a consistent density of the fluid as well as a hydrostatic pressure and an averaged Reynolds number are assumed. Furthermore it is assumed, that the surface propagation of the water is much larger than its vertical spread. This assumption leads to low vertical velocities as well as a hydrostatic pressure in the fluid. Subsequently, the differential form of the Saint-Venant equations can be derived. In shallow water, the terms of the barotropic pressure gradient and soil friction are the dominant factors in the momentum equations. The terms of discontinuity, advection and viscosity can be neglected. The momentum equation is needed for the approximation of the two-dimensional form of the diffusive wave equation. Combining the momentum equation with mass conservation, the Diffusive Wave equation represents an equation system of the Saint-Venant equations that is easy to solve.

In order to reduce computation time, a sub-grid bathymetry method is used [8]. The basic idea here is, that a coarser calculation mesh is used for the hydraulic calculations. In post-processing, the results of the gross discretization with the information (exact altitude, storage area of the area element) of the finer discretization are revised. Assuming an incompressible fluid, the unsteady differential form of the mass conservation (continuity) equation takes the following form:

$$\frac{\delta H}{\delta t} + \frac{\delta(hu)}{\delta x} + \frac{\delta(hv)}{\delta y} + q = 0 \quad [2]$$

In vector form, the mass conservation equation takes the following form:

$$\frac{\delta H}{\delta t} + \nabla \cdot hV + q = 0 \quad [3]$$

Due to the significantly larger horizontal spread, compared to vertical water depth, the vertical velocity in the fluid is very low. In the Navier-Stokes momentum equation, the pressure in the fluid is assumed to be hydrostatic. As a result of the absence of baroclinic pressure gradients, atmospheric pressure, strong wind forces and pressure changes resulting from the vertical velocity component can be safely neglected in both mass and momentum equations. The 2-dimensional Saint-Venant equations take the following form:

$$\frac{\delta u}{\delta t} + u \frac{\delta u}{\delta x} + v \frac{\delta u}{\delta y} = -g \frac{\delta H}{\delta x} + v_t \left(\frac{\delta^2 u}{\delta x^2} + \frac{\delta^2 u}{\delta y^2} \right) - c_{fu} + f_v \quad [4]$$

and

$$\frac{\delta v}{\delta t} + u \frac{\delta v}{\delta x} + v \frac{\delta v}{\delta y} = -g \frac{\delta H}{\delta y} + v_t \left(\frac{\delta^2 v}{\delta x^2} + \frac{\delta^2 v}{\delta y^2} \right) - c_{fv} + f_u \quad [5]$$

In order to get a more compact and easily readable equation, the momentum equations can also be written in vector form:

$$\frac{\delta V}{\delta t} + V \cdot \nabla V = -g \nabla H + v_t \nabla^2 V - c_f V + f_k \times V \quad [6]$$

Starting from left to right, the following terms are shown: unsteady acceleration, convective acceleration, pressure term, turbulent diffusion, bottom friction term and Coriolis term. On closer inspection, it can be seen that at low water depth, the bottom friction term becomes decisive. For this reason, Eq. [6] for dry cells is limited to $V=0$ and thus represents a special case.

The diffusive wave equation can be used under the previous conditions instead of the momentum conservation equations. The sub-grid bathymetry method also serves as a simplification of the numerical solution. The calculation is simplified insofar as the determination of the hydraulic radius $R=R(H)$ and the wetted surface $A=A(H)$ are outsourced as cell functions of the water level H . The simplifications and neglects for shallow waters also apply here. The simplified form of the momentum equation takes the following form:

$$\frac{n^2 |V| V}{(R(H))^{4/3}} = -\nabla H \quad [7]$$

Dividing both sides of the equation by the square root of their norm, the equation can be rearranged into the more classical form:

$$V = \frac{-(R(H))^{2/3}}{n} \frac{\nabla H}{|\nabla H|^{1/2}} \quad [8]$$

By inserting the diffusive wave equation from Eq. [8] into the mass conservation equation Eq. [3], the classical differential form of the diffusive wave approximation of the Saint-Venant Equations can be obtained.

$$\frac{\delta H}{\delta t} - \nabla \cdot \beta \nabla H + q = 0 \quad [10]$$

with

$$\beta = \frac{(R(H))^{5/3}}{n|\nabla H|^{1/2}} \quad [11]$$

4. ESTIMATION OF THE FAILURE HYDROGRAPHS

With reference to the introduced approaches for estimating the breach outflow in case of a dam break (see chapter 3.1), a range of failure hydrographs for each of the case studies is generated.

4.1. CASE STUDY 1 – FLOOD RETENTION BASIN IN LOWLAND AREA

Different flood waves are used, in order to investigate the influence of peak discharge and wave run time on the flooded downstream area (see Fig. 4). With a peak discharge of about $Q_{HQ5000 \text{ Rüdissler}} = 574 \text{ m}^3/\text{s}$, the flood wave estimated with the approach of Rüdissler superposed with a 5000 years flood reaches this point 5 minutes after the break. In comparison to that, the wave following the approach Broich Smart shows a peak discharge of $Q_{Broich \text{ Smart}} = 138 \text{ m}^3/\text{s}$ by reaching this value 27 minutes after the initial breaching.

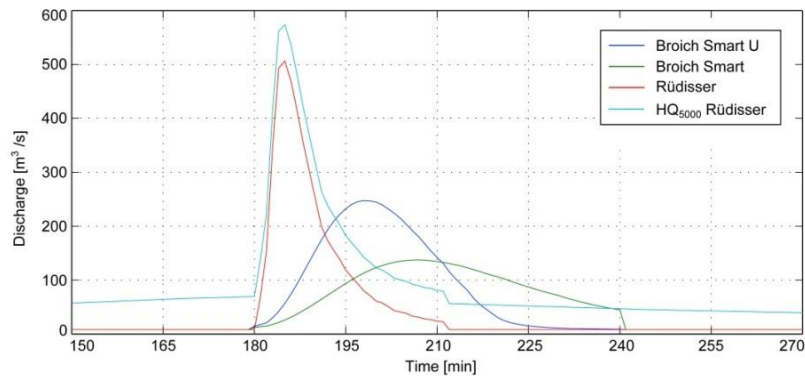


Fig. 4
Investigated failure hydrographs of case study 1

4.2. CASE STUDY 2 – RESERVOIR IN ALPINE AREA

The investigated failure hydrographs of case study 2 are based on different storage levels in the reservoir. The peak values of the discharge differ between $Q_{Broich\ Smart} = 1265\ m^3/s$ and $Q_{Pierce} = 3010\ m^3/s$. The timespans between the initial breaching and the peak discharge range between 25 and 45 minutes (see Fig. 5).

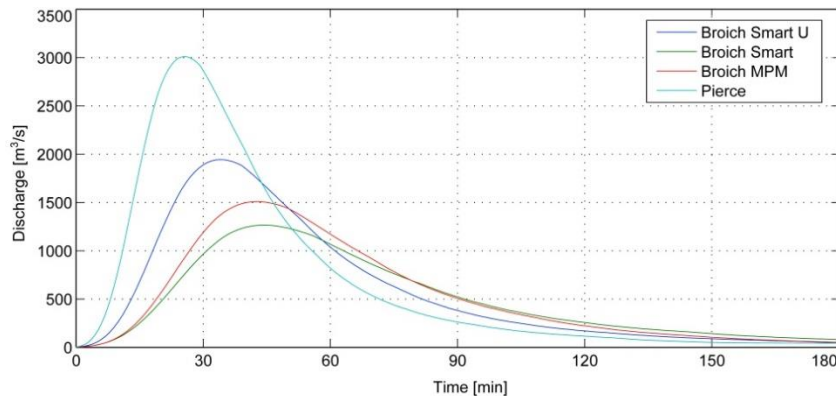


Fig. 5
Investigated failure hydrographs of case study 2

5. RESULTS OF THE FLOOD WAVE ANALYSIS

In the following chapter, an overview of the gained results of the flood wave analysis is presented. More detailed results and information can be found in [9] or [10].

5.1. CASE STUDY 1 – FLOOD RETENTION BASIN IN LOWLAND AREA

Due to the mainly flat investigation area as well as the several culverts, situated along the main channel, a strong retention character of the downstream region can be observed. Evaluating the first flood marker PP1, situated about 1,5 km downstream of the retention basin, a significant accordance to the input data of the failure hydrographs can be observed (see Fig. 6 – left). Along the section between the flood markers PP1 and PP2, two bridges cross the main channel and generate smaller flood retention area before the culverts. By studying Fig. 6 – right, a significant damping of the hydrographs can be noticed. Evaluating the further flood markers in the area studied, a continuing and reinforcing effect of flood retention can be observed.

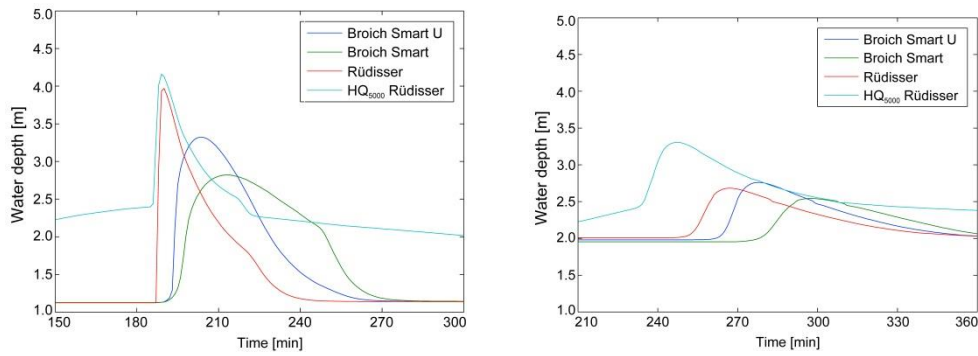


Fig. 6

Flood markers PP1 (km 22,000) and PP2 (km 16,800) in the investigation area of case study 1

The water depths of the flooded area strongly vary as a function of the respective failure hydrograph. Those failure scenarios with a higher peak discharge show higher flood levels as well as higher flow velocities in the area studied. Fig. 6 show water depths (left) and velocities (right) of the surrounding area of PP2. Due to the bridge crossing the main channel, a natural retention basin is build, which leads to higher water levels in the upstream and higher velocities in the downstream region.

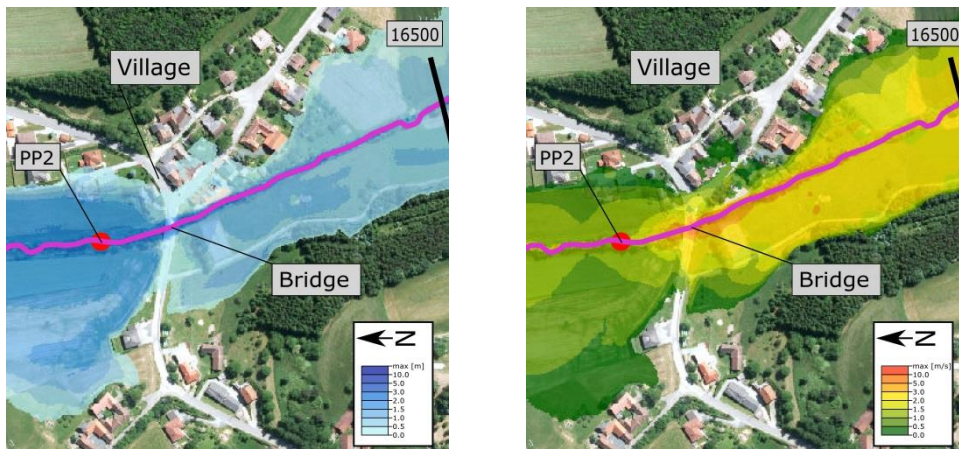


Fig. 6

Water depths and flow velocities around PP2 (16,800) in the investigation area of case study 1

5.2. CASE STUDY 2 – RESERVOIR IN ALPINE AREA

Along the first about 5,7 km long (km 22,650 – km 17,000), mostly steep and narrow part of the area studied, nearly no considerable flooding can be observed. The subsequent and more flat main valley (see also Fig. 2) allows an

extensive propagation by effecting larger settlement areas. A significant retention of the flood waves can be observed. Furthermore, a correlation between the peak value of the failure hydrograph and the arrival time of the flood wave as well as the resulting flood levels can be noticed. By studying the flood markers along the area studied (see Fig. 7), a most sudden impact of the flood wave can be observed.

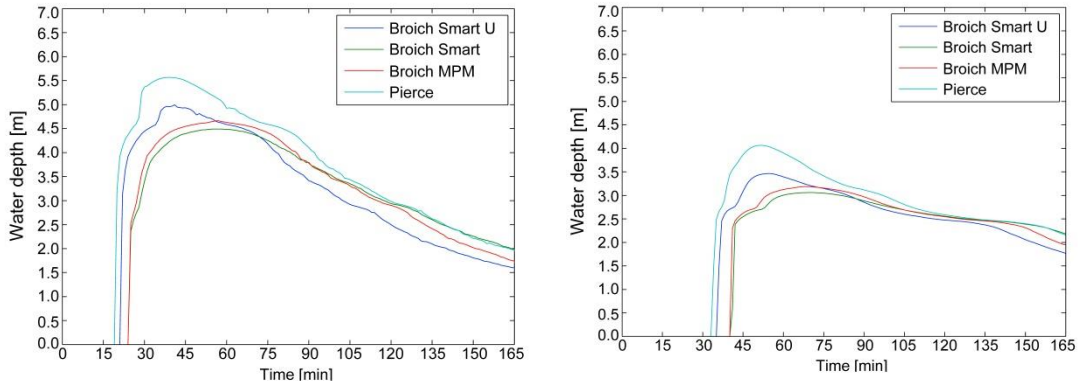


Fig. 7

Flood markers PP2 (km 15,000) and PP4 (km 9,000) in the investigation area of case study 2

The flood regime along the main valley is characterized by a rail embankment following the main channel and several underpasses. These underpasses mainly influence the flooding of certain villages. In some cases, an overtopping of the rail embankment can be observed as well (see Fig 8).

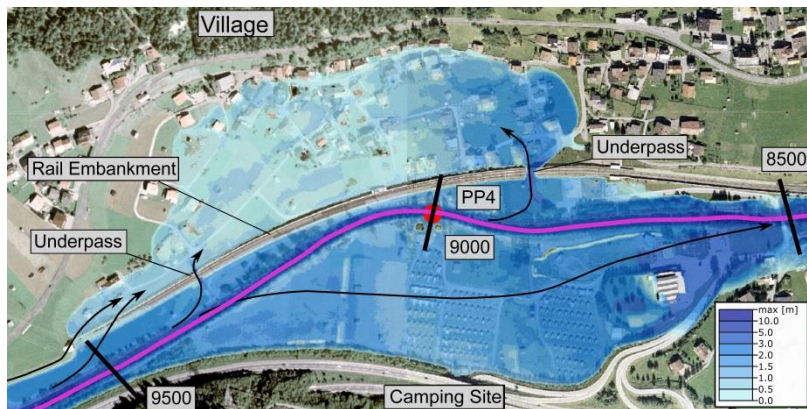


Fig. 8

Water depths around PP4 (km 9,000) in the investigation area of case study 2

Flow velocities around 15 m/s in the main channel and 5-10 m/s in the surrounding area can be noticed (see Fig. 9).

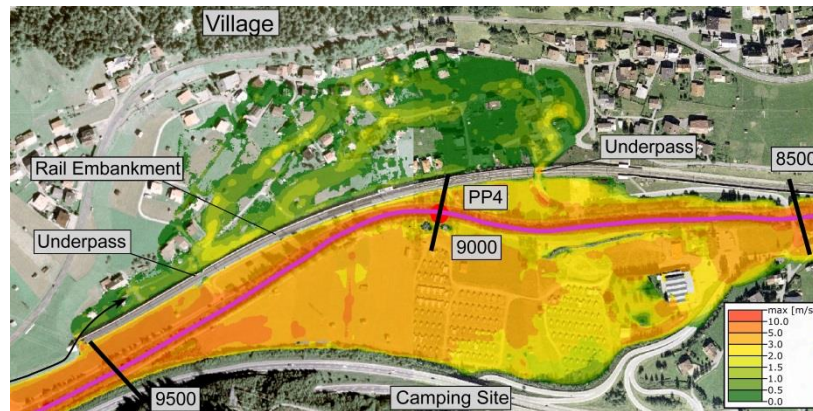


Fig. 9

Flow velocities around PP4 (km 9,000) in the investigation area of case study 2

REFERENCES

- [1] FOSTER, M.A., FELL, R., SPANNAGLE, M. The statistics of embankment dam failures and accidents. *Canadian Geotechnical Journal*, 2000, Nr. 37: 1000-1024.
- [2] PIERCE, M.W., THORNTON, C.I., ABT, S.R. Predicting Peak Outflow from Breached Embankment Dams. Colorado State University, Fort Collins, CO, USA, 2010.
- [3] FROELICH, D.C. Peak Outflow from Breached Embankment Dams. *Journal of Water Resources Planning and Management*, 1995, Nr. 121(1):90-97.
- [4] BROICH, K. Computergestützte Analyse des Dammerosionsbruchs. *Universität der Bundeswehr München*, 1996.
- [5] MEYER-PETER, E., MÜLLER, R. Formulas for bed-load transport. *Proceedings of the 2nd Meeting of the International Association for Hydraulic Structures Research*, 1948, 39-64.
- [6] SMART, G.M., JAEGGI, M.N.R. Sedimenttransport in steilen Gerinnen. *Mitteilungen der Versuchsanstalt für Wasserbau, Hydrologie und Glaziologie*, ETH Zürich, SUI, 1983.
- [7] RÜDISSER, B. Einfluss der Kornverteilung des Schüttmaterials und einer Oberflächendichtung auf die Breschenentwicklung und die Abflusskurve beim Versagen eines Schüttdammes durch Überströmen. Vienna University of Technology, 2017.
- [8] USACE. HEC-RAS River Analysis System - Hydraulic Reference Manual, CDP-69, Davis, CA, USA, 2016
- [9] BERGER, M. Sicherheit von Staudämmen – Probabilistische und deterministische Sicherheitskonzepte für Dammbauwerke. Vienna University of Technology, 2018.

- [10] DÜNKNER, R. Flutwellenanalyse beim Versagen von Schüttdämmen. Vienna University of Technology, 2018.

SUMMARY

In order to estimate the possible consequences for a dam break scenario, a flood wave analysis is wisely required. Especially for embankment dams, the investigations should contain a study of potential failure hydrographs. By using different approaches for calculating the breach outflow on the basis of variable storage levels in the reservoir, it is possible to obtain a range of outflow hydrographs as a mandatory input data for the flood wave analysis.

Using 2D hydraulic models for this analysis allow to investigate the flood regime in detailed way. On the basis of airborne LIDAR data, geometric boundary conditions, such as culverts or underpasses in the area studied, can be implemented into the model in an easy way. Due to the influence of these geometric boundaries on the flooding, a special focus has to be set on the accurate modelling of the investigation area.

KEYWORDS

DAM FAILURE, EMBANKMENT DAM, FAILURE, FLOOD, NUMERICAL MODEL, RISK ANALYSIS,

COMMISSION INTERNATIONALE DES GRANDS BARRAGES

VINGT-SIXIÈME CONGRÈS DES GRANDS BARRAGES
Autriche, juillet 2018

DOI 10.3217/978-3-85125-620-8-224



This work licensed under a Creative Commons Attribution 4.0 International License. <https://creativecommons.org/licenses/by-nc-nd/4.0/>

**RISK MANAGEMENT FOR THE LAGO BIANCO RESERVOIR IN CASE THE
CAMBRENA GLACIER RUPTURES**

Johannes MAIER

SUPERVISION OF DAMS, SWISS FEDERAL OFFICE OF ENERGY, BERNE

SWITZERLAND

Alexandra BECKSTEIN

SUPERVISION OF DAMS, SWISS FEDERAL OFFICE OF ENERGY, BERNE

SWITZERLAND

Georges R. DARBRE

SUPERVISION OF DAMS, SWISS FEDERAL OFFICE OF ENERGY, BERNE

SWITZERLAND

RISK MANAGEMENT FOR THE LAGO BIANCO RESERVOIR IN CASE THE CAMBRENA GLACIER RUPTURES*

Johannes MAIER

Alexandra BECKSTEIN

Georges R. DARBRE

Supervision of Dams, SWISS FEDERAL OFFICE OF ENERGY, BERNE

SWITZERLAND

1. INTRODUCTION

The average annual temperature in Switzerland has increased by 2°C since the start of measurements in 1864. This increase is almost twice as high as for other land areas in the northern hemisphere. Today, the zero degree line in Switzerland is about 350 m higher than 60 years ago. Mainly because of these rising temperatures the alpine glaciers are melting.

In 2015, it was discovered that the retreating Cambrena glacier in southwestern Switzerland had introduced a new risk to the Lago Bianco reservoir: A melting glacier tongue is slowly retreating into a steep rock step and therefore losing its support at the front end and on both sides. According to the glacier specialists, there is a danger for a rupture of up to 1.5×10^6 m³ of ice. The ice rupture could generate a flood wave in the reservoir and cause a sudden dam breach. Therefore, the owner of the Lago Bianco reservoir Repower AG had to add this new danger into his risk management.

2. LAGO BIANCO RESERVOIR

The Lago Bianco reservoir (see fig. 1) is located just west of the Bernina pass in southwestern Switzerland, only a few kilometers from the border to Italy. The reservoir is part of the water divide between the Mediterranean Sea and the Black Sea. The highest peaks of the eastern Alps (with altitudes around 4'000 m a.s.l.) flank the western side of the reservoir. The narrow gauge Bernina railway follows the eastern reservoir shore; the northeastern corner of the reservoir is close to the Bernina highway. Both traffic lines are all-the-year open, except winter days with

* *Gestion du risque au réservoir de Lago Bianco en cas de rupture du glacier de Cambrena*

high avalanche risk. The water stored in the reservoir is used in several power stations to produce electricity.

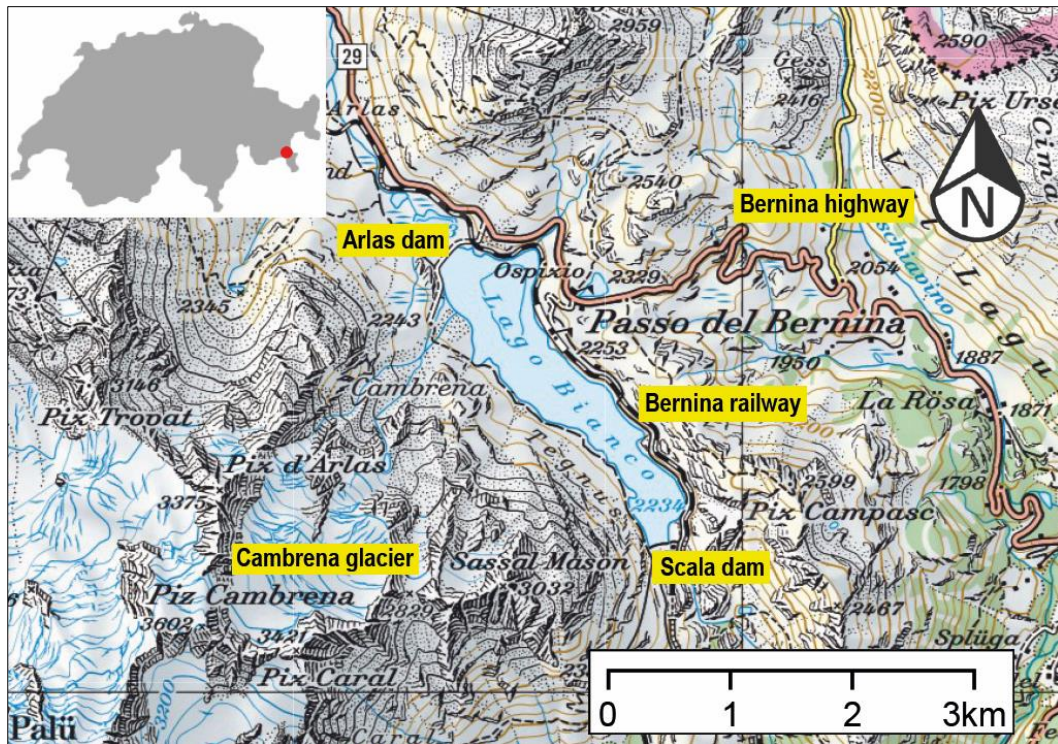


Fig. 1: Location of the Lago Bianco reservoir in southwestern Switzerland.
Img. 1 : Situation du réservoir de Lago Bianco au sud-est de la Suisse.

The two dams of the Lago Bianco reservoir, the Arlas gravity dam in the north and the Scala arch-gravity dam in the south, were originally built in 1910–12 with cyclopean concrete. The impounding of the reservoir connected two natural lakes. In 1941/42 the height of the two dams was increased by adding at the crest 4 m of concrete and so enlarging the reservoir capacity. Later on this additional concrete started to show signs of alkali aggregate reaction; furthermore, only an incomplete connection between the original and the additional concrete was discovered at the Scala dam. To solve these problems an extensive renovation of the two dams took place in 2000/01. The eastern two-thirds of the Arlas gravity dam were totally demolished and rebuilt with regular concrete above the old foundation. The demolition waste together with fresh rock material was used to cover the western third of the dam. The Scala arch-gravity dam got a shotcrete cover and PP-Dam sealing on the upstream face, a drainage and inspection gallery at the upstream foot, a new concrete crest and a systematic anchoring on the downstream face. Fig. 2 shows the actual cross sections of the Arlas and Scala dams.

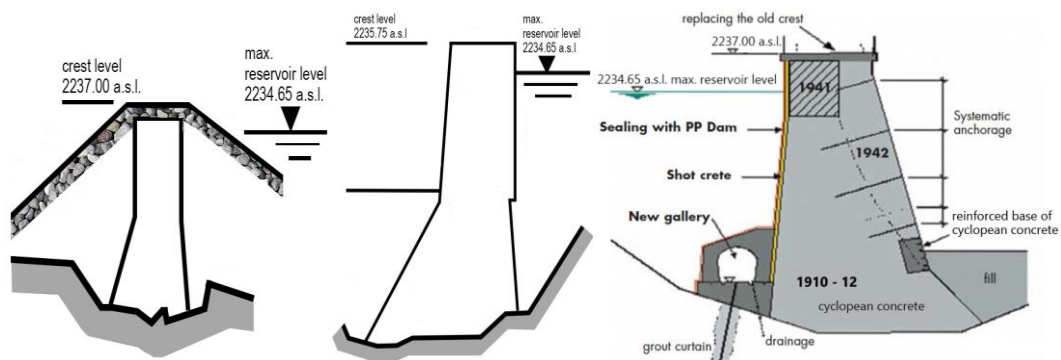


Fig. 2: Cross sections of the western part of the Arlas dam (left), the eastern part of the Arlas dam (middle) and the Scala dam (right).

Img. 2 : Coupe transversale de la partie ouest du barrage d'Arlas (à gauche), de la partie est du barrage d'Arlas (au centre) et du barrage de Scala (à droite).

The following list summarizes the characteristics of the Lago Bianco reservoir:

- Catchment area 10.85 km² (currently 15 % covered by glaciers)
- Reservoir area 1.43 km²
- Reservoir volume 18.6×10⁶ m³
- Maximum reservoir level 2'234.65 m a.s.l.
- Length of Arlas dam 290 m
- Height of Arlas dam 15 m
- Crest level of Arlas dam 2'235.75 m a.s.l. (western part 2'237.00 m a.s.l.)
- Length of Scala dam 190 m
- Height of Scala dam 26 m
- Crest level of Scala dam 2'237.00 m a.s.l.

All dam outlets are located in the Scala dam. The bottom outlet has a maximum capacity of 6.0 m³/s; the intermediate outlet with a base level of 2'231.40 m a.s.l. allows a maximum discharge of 24.0 m³/s. Flood waters are controlled with a 37 m long overflow section, its crest is at the maximum reservoir level 2'234.65 m a.s.l. The turbination capacity amounts to 4.4 m³/s and 0.75 m³/s can be pumped from the reservoir below. Today, the Lago Bianco reservoir is used as a seasonal water storage with maximum level in autumn and minimum level in spring.

The regular surveillance of the Lago Bianco reservoir consists of visual inspections and measurements carried out by personnel of the reservoir owner. They are also responsible for the annual tests of the outlets with mechanical gates. Once a year a dam engineer carries out his inspection. He is also the author of the annual report about the condition and behavior of the reservoir and its two dams. Every fifth year a geodetic measurement and an in-depth safety review by a dam expert and a geology expert take place. All reports are submitted to the Supervision of Dams Section of the Swiss Federal Office of Energy. The responsible supervisor reviews these reports and carries out his own inspections at least every third year. The Supervision of Dams Section is also present at the site inspections of the experts.

3. RETREAT OF CAMBRENA GLACIER

During project work for the development of the current seasonal reservoir into a high capacity pumped storage facility it was detected that there is a risk of a rupture of the southern tongue of the Cambrena glacier. The reservoir owner asked glacier specialists from the ETH Zurich to study the situation and give their advice. Their findings [1] can be summarized as follows:

- **Actual situation:** The Cambrena glacier covers a surface of about 1.37 km² and has a volume of 50×10⁶ m³. The current lower end of the southern glacier tongue is at an altitude of 2'520 m a.s.l. Due to the strong glacier retreat a lake has developed in front of it. The terrain behind the end of the glacier gets steeper and steeper over a distance of 550 m until a flattening starts at an altitude of 2'820 m a.s.l. The inclination below the steep part is at 24°, in the steep part it is at 35°.
- **Prognosis of glacier melting:** Fig. 3 shows the result of model calculations for the ice volume of the Cambrena glacier from 1900 until 2100. Between 1985 and 2008 the volume loss amounts to 40×10⁶ m³ of ice. Furthermore, the diagram shows that the Cambrena glacier is expected to disappear totally between 2050 and 2080. Fig. 4 presents the prognosis of the surface covered by the glacier between 2010 and 2050. Around 2025 the glacier will have retreated above the steep part.

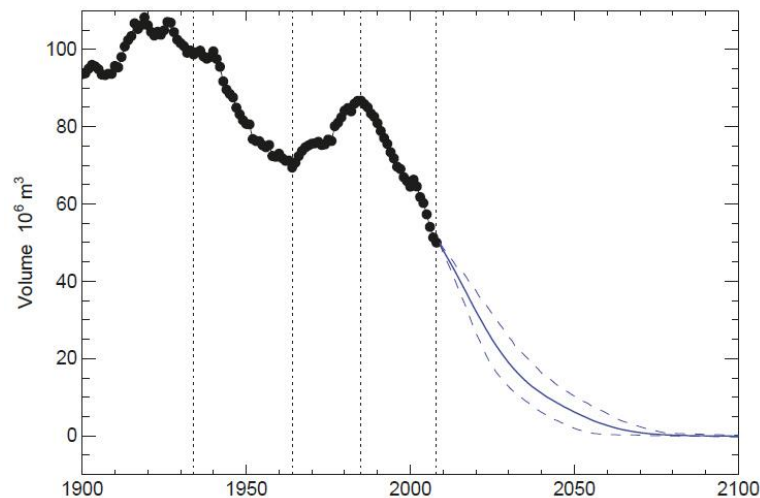


Fig. 3: Changes in the ice volume of the Cambrena glacier between 1900 and 2100 (the potential future changes are given by an average value and a band width from 10 scenarios; the vertical dotted lines indicate dates with known extent of the glacier surface) [1].

Img. 3 : Changements de volume de la glace du glacier de Cambrena entre 1900 et 2100 (les potentiels changements futurs sont obtenus avec une valeur moyenne ainsi qu'une variation de volume tirée de 10 scénarios ; les lignes pointillées verticales indiquent les dates avec la mesure connue de la surface du glacier) [1].

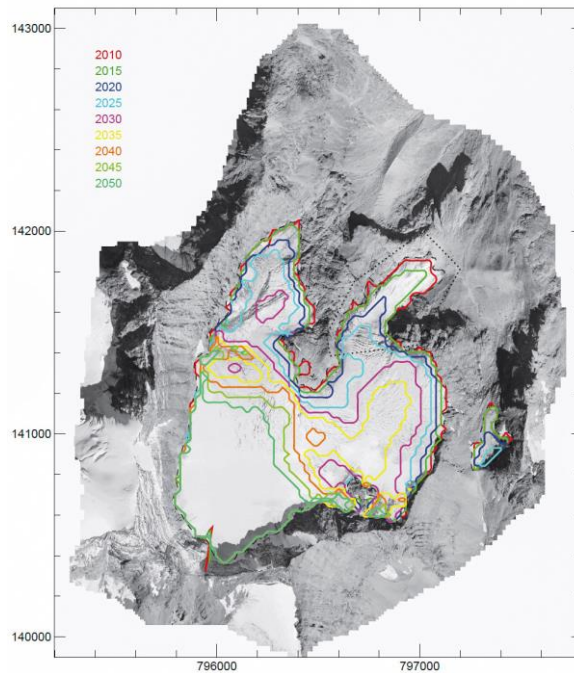


Fig. 4: Prognosis of the surface of the Cambrena glacier until 2050 (the base photo shows the situation in 2008) [1].

Img. 4 : Pronostic de la surface du glacier de Cambrena jusqu'en 2050 (la photo de base montre la situation en 2008) [1].

- Threat of glacier tongue rupture:** Currently the glacier tongue is stabilized by its lowest part with the inclination 24° and the contact at its bottom and the two sides. As soon as the glacier tongue retreats into the steeper part with the inclination 35° and gets thinner on both sides, the ice is only stabilized by the contact to the terrain at its bottom (see fig. 5) and a risk of sudden ice rupture emerges. According to studies at other glaciers, a rupture requires a water flow between the glacier and the terrain surface. Therefore, such events usually occur with alpine glaciers in the months of July to October.

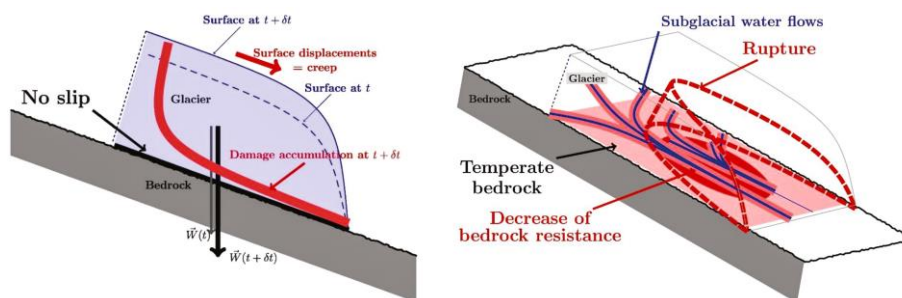


Fig. 5: Displacement of a glacier frozen to the bedrock (left); rupture of a glacier due to subglacial water flow on the temperate bedrock (right) [2].

Img. 5 : Déplacement d'un glacier gelé sur un socle rocheux (à gauche); décrochement d'un glacier en raison de flux d'eau sous-glaciaire sur le socle rocheux tempéré (à droite) [2].

4. RUPTURE OF CAMBRENA GLACIER TONGUE, ICE AVALANCHE AND IMPULSE FLOOD WAVE IN THE LAGO BIANCO RESERVOIR

The report of the glacier specialists [1] gives a forecast on the decrease of the ice volume in the steep part with time (see fig. 6): In 2015 the potential rupture volume equals to $1.5 \times 10^6 \text{ m}^3$, this corresponds to the worst-case scenario to be taken into account in the risk management of the Lago Bianco reservoir. By 2020, the potential rupture volume will diminish below $0.5 \times 10^6 \text{ m}^3$ of ice.

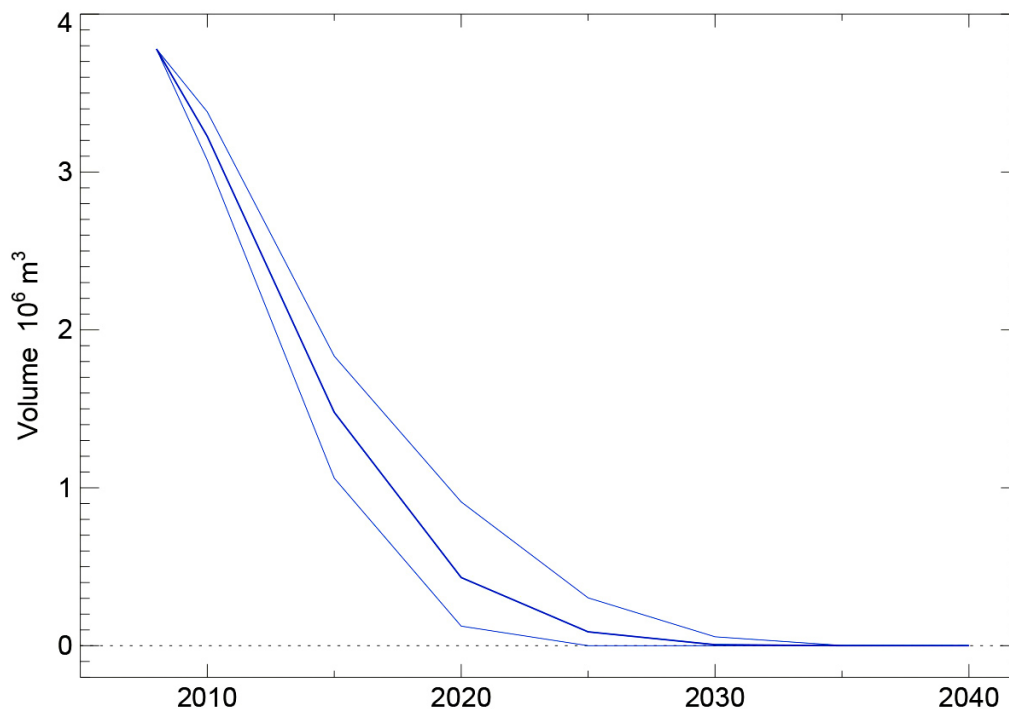


Fig. 6: Prognosis of the decrease of the ice volume in the steep part of the southern tongue of the Cambrena glacier (an average value and a band width from 10 scenarios are shown) [1].

Img. 6 : Pronostic de la diminution du volume de glace dans la partie raide de la langue glaciaire sud du glacier de Cambrena (une valeur moyenne ainsi qu'une variation de volume tirée de 10 scénarios sont représentées) [1].

The ruptured ice would move as an avalanche towards the Lago Bianco reservoir. The report [3] presents the calculations carried out by avalanche specialists with the computer program RAMMS [4]. The calculation results show that the ice rupture volume in the worst-case scenario of $1.5 \times 10^6 \text{ m}^3$ gives an avalanche with a volume of $1.8 \times 10^6 \text{ m}^3$, which reaches the reservoir with a speed of 10–20 m/s, a flow height of 5–10 m and a volume of approximately $0.25 \times 10^6 \text{ m}^3$ (see fig. 7). The avalanche produced by an ice rupture volume of $0.5 \times 10^6 \text{ m}^3$ reaches the reservoir with a volume of a few thousand m^3 and can be neglected.

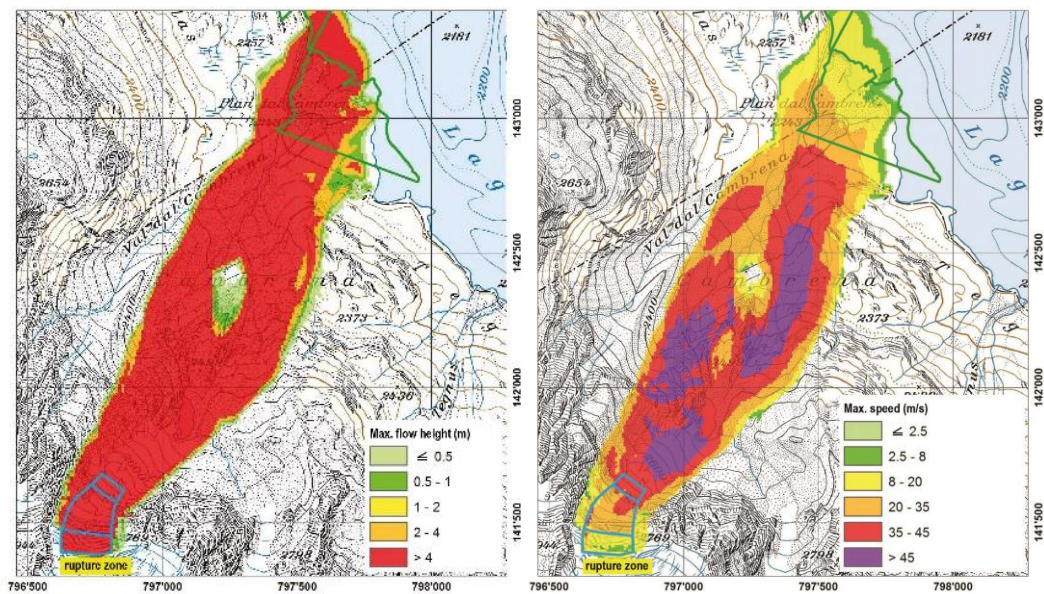


Fig. 7: Maximum flow height (left) and speed (right) according to the RAMMS calculations for the ice avalanche produced by the worst-case glacier rupture of $1.5 \times 10^6 \text{ m}^3$ [3].

Img. 7 : Hauteur (à gauche) et vitesse (à droite) maximum de l'avalanche calculées selon la méthode RAMMS lors de la rupture du glacier pour le cas extrême de $1.5 \times 10^6 \text{ m}^3$ [3].

Based on the results of the avalanche calculations the dam expert responsible for the Lago Bianco reservoir conducted impulse flood wave calculations [5] with a spreadsheet program developed at the demand of the Swiss Federal Office of Energy at the ETH Zurich [6]. For the worst-case ice rupture and the maximum reservoir level of 2'234.65 m a.s.l. the calculations for the Arlas dam give the following results:

- Wave height 1.5–4.5 m
- Overtopping volume 200–4'000 m^3 (minimum freeboard of 1.1 m taken into account)

The overtopping volume is rather small. It would only cause minor damages downstream of the Arlas dam. On the other hand, the flood wave reaches well above the danger level (= crest level of the eastern part of the dam at 2'235.75 m a.s.l.) and therefore puts the stability of the dam at risk.

The impulse flood wave can only reach the substantially more distant Scala dam after reflection. Thus, the wave height will be much smaller and pass the dam by the overflow section. The substantial freeboard of 2.35 m from the maximum reservoir level up to the crest level at 2'237.00 m a.s.l. (= danger level) is expected to guarantee the integrity of the Scala dam.

5. ICE FLOW SPEED AS EARLY INDICATOR OF GLACIER RUPTURE

Experiences with several glacier ruptures have demonstrated, that the ice flow speed is a good early indicator for a situation becoming dangerous [1, 2]. Fig. 8 presents the flow speed of the tongue of the Allalin glacier in the Saas valley in the southern Swiss Alps for the years 1965 to 1967. The two decreasing curves from 1965 were measured after the rupture of more than 2×10^6 m³ ice on August 30th 1965, which killed 88 people on the construction site of the Mattmark dam. The curves from 1966 and 1967 show speed increases by a factor of 10 or more from a few decimeters/day to several meters/day. Important is also the fact that the increase periods lasted many days or weeks.

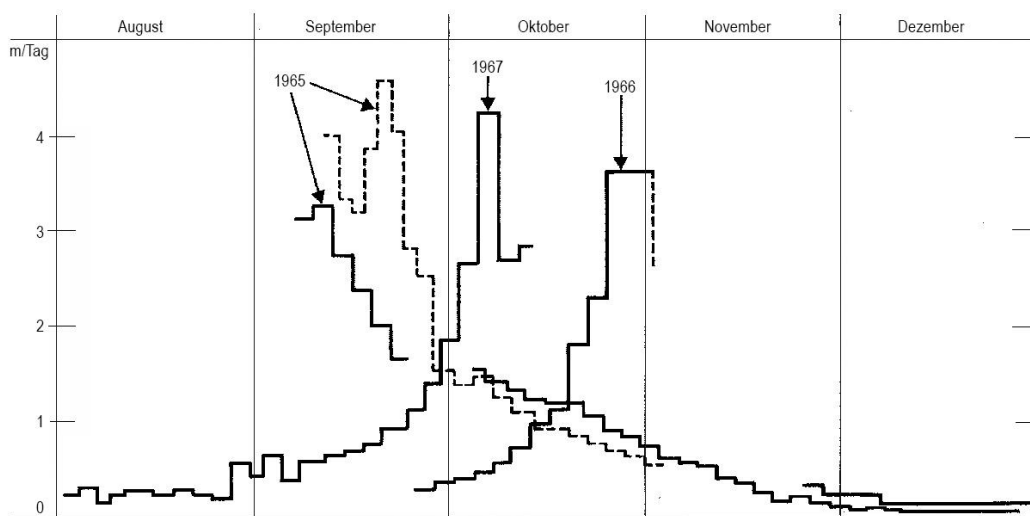


Fig. 8: Flow speed of the Allalin glacier in the southern Swiss Alps for the years 1965 to 1967 [1].

Img. 8 : Vitesse de déplacement du glacier d'Allalin dans le sud des Alpes suisses durant les années 1965 à 1967 [1].

Based on the findings given above, the ETH Zurich glacier specialists recommended in the case of the Cambrena glacier the installation of an automatic photographic camera with energy supply from a photovoltaic panel and mobile phone data transmission to follow the ice flow speed on a daily basis. The camera (see fig. 9) was installed in July 2015 at a cost of about 30'000 CHF (\approx 25'000 EUR) [7]. The annual costs amount to 12'500 CHF (\approx 10'500 EUR) and include the analysis of the daily pictures by the glacier specialists. Fig. 10 shows as an example the ice flow speed calculated from the camera pictures for two different periods of the year 2016.

Ice flow speeds between 0.04 and 0.12 m/d, averaged over periods of several days, were measured for the steep part of the southern tongue of the Cambrena glacier during the year 2016.

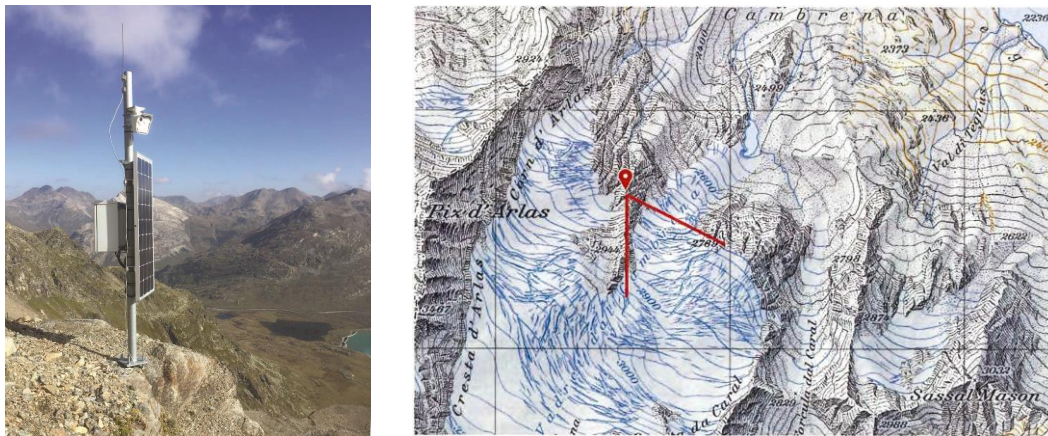


Fig. 9: Automatic camera with photovoltaic energy supply and mobile phone data transmission for the surveillance of the Cambrena glacier (left) [2]; camera position and view angle over southern glacier tongue (right) [7].

Img. 9 : Appareil photo automatique avec approvisionnement en énergie photovoltaïque et une transmission des données par le réseau de téléphonie mobile pour la surveillance du glacier de Cambrena (à gauche) [2] ; position de l'appareil photo et angle de vue sur la langue glaciaire sud (à droite) [7].

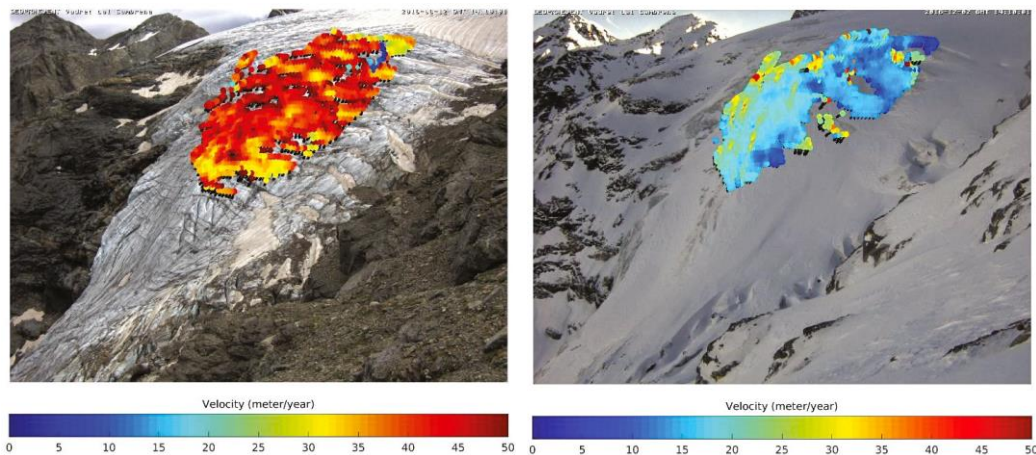


Fig. 10: Ice flow of the southern tongue of the Cambrena glacier based on the analysis of camera pictures (left: high flow speed in August 2016; right: low flow speed in December 2016) [2].

Img. 10 : Déplacement de la glace de la langue sud du glacier de Cambrena basé sur l'analyse d'images photographiques (à gauche : vitesse maximum en août 2016 ; à droite : vitesse minimum en décembre 2016) [2].

6. EMERGENCY PREPAREDNESS PLAN

Emergency preparedness plans for reservoirs and their dams use five danger levels [8, 9], as it is common for different risks in Switzerland:

- Danger level 1 = normal situation → regular surveillance and maintenance
- Danger level 2 = moderate danger → preparation of emergency organization
- Danger level 3 = serious danger → emergency organization in action
- Danger level 4 = high danger → preparation of alarm of population
- Danger level 5 = very high danger → alarm and evacuation of population

At a meeting with the owner of the Lago Bianco reservoir, the ETH Zurich glacier specialists, the dam engineer, the dam expert and the geology expert the supervision of dams authority assigned danger level 2 for the Lago Bianco reservoir. Thereafter, the reservoir owner developed a special emergency preparedness plan for a rupture of the Cambrena glacier tongue [10]. This plan uses two basic elements:

- Continuous surveillance of the Cambrena glacier to measure the ice flow speed.
- Lowering of the Lago Bianco reservoir in case of a high ice flow speed to a level, which still guarantees the stability of the Arlas dam.

Based on the calculations presented in the preceding chapter 4 the safe reservoir level was determined by the dam expert for the worst-case glacier rupture of 1.5×10^6 m³ of ice to be 2'232.15 m a.s.l., i. e. 2.50 m below the maximum reservoir level. The time needed for this lowering plays a key role in the emergency preparedness plan. With an inflow of 1.0 m³/s to the reservoir, the available outlets (see chapter 2) give the following times for reaching the safe level:

- Turbination only: 10.9 days
- Bottom outlet only: 7.4 days
- Intermediate outlet only: 2.6 days

The use of the intermediate outlet at maximum capacity would cause substantial damage downstream of the Scala dam. To reduce this, the reservoir owner has decided to open the intermediate outlet stepwise as long as the danger does not reach level 4. Therefore, the lowering of the reservoir level including a preparation period of 24 hours is prolonged to 100 hours \approx 4 days. This agrees with the statement of the glacier specialists, that the increase period of the ice flow speed lasts many days or weeks before it comes to a glacier rupture. In case of danger levels 4 and 5, an immediate full opening of all outlets down to the safe level is intended.

Based on the previous statements the following conditions and procedures were established for the danger levels 2 to 5 (see fig. 11):

- **Danger level 2:** The reservoir may be operated over its full range. The glacier specialists of the ETH Zurich check the ice flow speed, during the critical time of the year on a daily basis. The operation center of the reservoir owner is active on a 24 hours and 7 days basis.
- **Danger level 3:** A reported glacier flow speed ≥ 2.5 pixel/day (≈ 0.5 m/d) and a reservoir level $> 2'232.15$ m a.s.l. (= safe level) triggers danger level 3. Between June 1st and November 30th, a camera blackout of 5 days and a reservoir level $> 2'232.15$ m a.s.l. would also lead to danger level 3. Immediately, the reservoir owner informs the emergency center of the police about the new danger level and sends personnel to the reservoir. After a 24 hours preparation period, the lowering of the reservoir with a stepwise opening of the intermediate outlet starts.
- **Danger level 4:** A reported glacier flow speed ≥ 5 pixel/day (≈ 1.0 m/d) and a reservoir level $> 2'232.15$ m a.s.l. (= safe level) triggers danger level 4. Immediately, the reservoir owner informs the emergency center of the police about the new danger level and the intermediate outlet is totally opened; if possible, the bottom outlet and the turbines are additionally used with maximum capacity. The water alarm center at the Lago Bianco reservoir is now permanently manned. The police closes down both railway and highway over the Bernina pass.
- **Danger level 5:** A glacier flow speed ≥ 5 pixel/day (≈ 1.0 m/d) continuously reported over 5 days and a reservoir level $> 2'232.15$ m a.s.l. (= safe level) triggers danger level 5. Immediately, the water alarm is activated and the Swiss civil protection sirens alarm the population to evacuate the possible flooding area of an Arlas dam breach. The reservoir owner informs the emergency center of the police about the new danger level and the activation of the water alarm. The lowering of the reservoir continues with the totally opened intermediate outlet and if possible with the full capacity of the bottom outlet and the turbines.

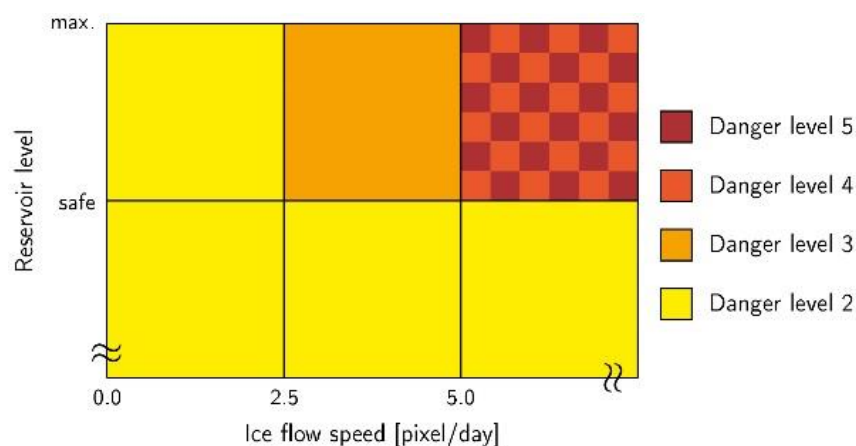


Fig. 11: Emergency levels 2 to 5 as a function of the ice flow speed of the Cambrena glacier and the water level in the Lago Bianco reservoir.

Img. 11 : Niveaux d'urgence 2 à 5 en fonction de la vitesse de déplacement de la glace du glacier de Cambrena et du niveau d'eau dans le réservoir de Lago Bianco.

7. ADJUSTMENTS TO THE EMERGENCY PREPAREDNESS PLAN

The measuring of the actual ice thickness allows a more precise estimate of the possible ice rupture volume. In May 2017, a first such measurement was carried out [2]. Fig. 12 presents the glacier profiles measured with a helicopter-based radar system. The measurements showed ice thicknesses between 40 and 60 m. Repetitions of these measurements are planned in the coming years until the Cambrena glacier has retreated out of the steep zone.

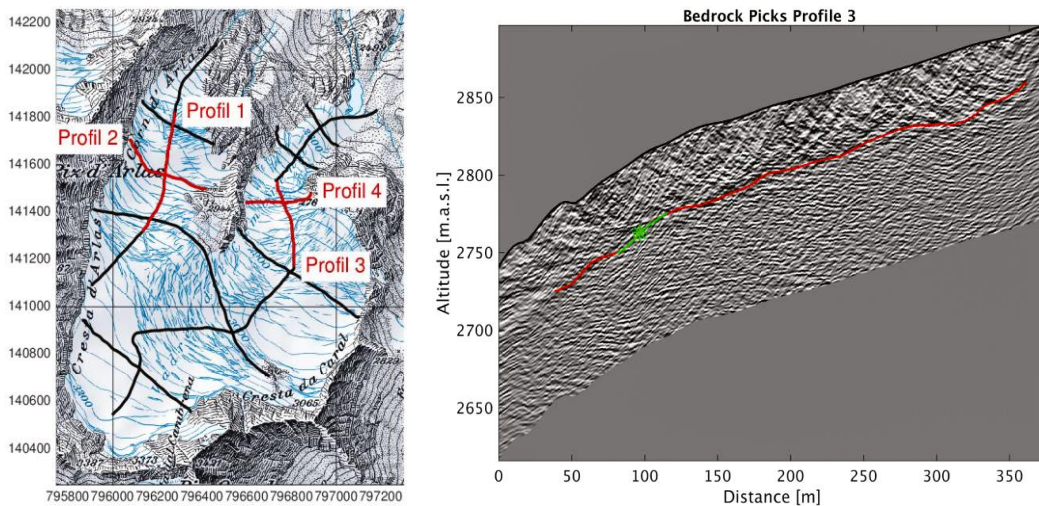


Fig. 12: Profiles for the thickness measurements on the Cambrena glacier carried out in May 2017 (left); results for profile 3 with red line showing the bedrock altitude (right) [2].

Img. 12 : Profils des mesures d'épaisseur sur le glacier de Cambrena en mai 2017 (à gauche) ; résultats du profil 3 au moyen d'une ligne rouge indiquant l'altitude du socle rocheux (à droite) [2].

As soon as a new estimate of the possible rupture volume becomes available, the calculations of the ice avalanche and the impulse flood wave can be repeated. Eventually the results will allow for an adjustment of the safe level of the Lago Bianco reservoir. This would permit a slower reservoir lowering process with less damage downstream of the Scala dam.

ACKNOWLEDGEMENTS

The authors want to express their thankfulness for the support given by R. Vassella and C. Pelazzi from Repower AG, R. Baumann from Rebau Engineering AG, K. Steiger and W. Schmutz.

REFERENCES

- [1] M. Funk and A. Bauder: *Vadret dal Cambrena — Untersuchungen zur Gefahr von Eislawinen im Zusammenhang mit dem Projekt Lago Bianco*, Report 70.03.2013, VAW ETH Zurich, February 2013.
- [2] A. Bauder: *Überwachung des Cambrena Gletschers*, VAW ETH Zurich, presented at the conference *ATCOLD-STK Fachtagung 2017*, Dornbirn, July 28th 2017.
- [3] N. Pitsch: *Vadret dal Cambrena — Gefahrenanalyse betreffend Eislawinen*, pitsch-ing.ch, July 2014.
- [4] Program RAMMS (Rapid Mass Movement Simulation): *Two-dimensional dynamics modeling of rapid mass movements in 3D alpine terrain*, SLF WSL, program homepage <http://ramms.slf.ch/ramms/>
- [5] K. M. Steiger: *Stauanlage Bernina — Expertenbericht über die 9. Fünfjahreskontrolle 2014*, AF-Consult Switzerland AG, June 2015.
- [6] V. Heller, Willi. H. Hager and H.-E. Minor: *Rutscherzeugte Impulswellen in Stauseen*, VAW ETH Zurich, July 2008.
- [7] M. Blum: *Überwachung Vadret dal Cambrena — Vorprojekt Überwachung 2015–2019*, Amt für Wald und Naturgefahren Graubünden, January 2015.
- [8] Swiss Federal Office of Energy: *Directive on the Safety of Water Retaining Facilities — Part E: Emergency plan*, version 2.0, May 2015.
- [9] Swiss Federal Office of Energy: *Beispiel Notfallreglement Stauanlage mit Wasseralarmsystem*, version 2.0, May 2015.
- [10] Repower AG: *Stauanlage Lago Bianco — Notfallreglement Cambrenagletscher*, Poschiavo, April 2017.

The reports referenced by the numbers 1, 3, 5, 7 and 10 have not been published. Eventually they are available from the owner of the Lago Bianco reservoir Repower AG, via da Clalt 307, CH-7742 Poschiavo, Switzerland or from the Amt für Wald und Naturgefahren, Kantonale Gefahrenkommission 3, Islas 244, CH-7524 Zuoz, Switzerland.

SUMMARY

In 2015 it was discovered that the retreating Cambrena glacier had introduced a new risk to the Lago Bianco reservoir in southwestern Switzerland. The melting southern glacier tongue could eventually lose its support, rupture off, move as an ice avalanche down to the reservoir and initiate an impulse flood wave with danger of a breach of one of the reservoirs two dams. Therefore, the owner of

the Lago Bianco reservoir Repower AG established a special emergency preparedness plan. It is based on two elements:

- Continuous surveillance of the Cambrena glacier by an automatic photographic camera to measure the ice flow speed.
- Lowering of the Lago Bianco reservoir in case of a high ice flow speed to a level, which still guarantees the stability of the dam.

If the ice flow speed increases faster than predicted before the safe reservoir level is reached, the emergency service of the Swiss civil protection will alarm the population in the danger zone to evacuate and close down both railway and highway passing by the reservoir.

KEYWORDS

- LAGO BIANCO RESERVOIR
- RESERVOIR OPERATION
- AVALANCHES
- IMPULSE WAVES
- DAM BREACH

COMMISSION INTERNATIONALE DES GRANDS BARRAGES

VINGT-SIXIÈME CONGRÈS DES GRANDS BARRAGES
Autriche, juillet 2018

DOI 10.3217/978-3-85125-620-8-225



This work licensed under a Creative Commons Attribution 4.0 International License. <https://creativecommons.org/licenses/by-nc-nd/4.0/>

SERVER DESIGN STANDARDS OF RESERVOIR FAILURE ALERT SYSTEM

Baeg LEE

*Researcher of Region & Infrastructure Research Group, RURAL RESEARCH
INSTITUTE, KRC*

KOREA

Byoung-Han CHOI

*Researcher of Region & Infrastructure Research Group, RURAL RESEARCH
INSTITUTE, KRC*

KOREA

SERVER DESIGN STANDARDS OF RESERVOIR FAILURE ALERT SYSTEM

Baeg LEE, Byoung-Han CHOI

*Researcher of Region & Infrastructure Research Group, RURAL
RESEARCH INSTITUTE, KRC*

KOREA

1. INTRODUCTION

In recent years, a great number of reservoir failures have been reported in many countries including Korea. Especially, the large increase in hydrologic variables due to meteorological variability & climate change and the rapid progress of facility aging are factors that threaten the stability of reservoirs. The lack of flood control capacity due to the hydrologic variables which have increased from the stage of design and the loss of function due to aging are directly linked to reservoir overflows and structure failures & damage. In addition, the increased number of residents due to the development of downstream areas is directly related to massive casualties and property damages. Therefore, along with the existing safety evaluation, a failure alert system that detects and controls early signs of failure and damage in real time, considering various risk factors and uncertainties, is desperately needed.

In order to propose server design standards for the Reservoir Failure Alert System, similar cases in Korea were analyzed and pros and cons were examined. Design standards have been established after considering them. The server design standards set goals in each of the four aspects: database (DB) design, hardware (H/W) configuration, software (S/W) configuration, and framework (F/W) configuration. Server design standards are proposed to achieve each goal.

2. SERVER DESIGN STANDARD ESTABLISHMENT METHODS

2.1. RESERVOIR STATUS AND TARGETS

Over the past 100 years, rainfall intensity has decreased by 18%, while precipitation has increased by 17% (KMA, 2004). The increase in hydrologic variables due to climate change along with the aging of reservoirs are factors that threaten the stability of reservoirs. According to the "Statistical Yearbook of Land and Water Development for Agriculture (2014)", there are 17,427 reservoirs

designated as agricultural irrigation facilities, and about 51% of them are over 70 years old.

According to the Rearrangement of Agricultural and Fishing Villages Act (MAFRA, 2016), domestic reservoirs are classified into Level 1 of 1,197 and Level 2 of 16,203, and subject to safety management according to the safety grade (Table 1) (Choi and Lee, 2015). In the case of Level 1 reservoirs (reservoirs with a capacity of 300,000 tons or more), they are checked for safety inspection and precision safety diagnosis according to the system. However, Level 2 reservoirs (reservoirs with a capacity of 300,000 tons or less) can receive safety inspections only on a quarterly basis, and if there is a sign of abnormality, precision safety diagnosis can be requested.

Table 1 Classification of state evaluation of structures

Safety grade	Condition of Structures
A	Excellent condition of structure
B	Mostly excellent condition of structure
C	Normal condition without difficulties in the safety management
D	Condition requiring partial repair and reinforcement
E	Condition requiring urgent repair and reinforcement

Among domestic reservoirs, the reservoirs which are actually subject to failure, are small and medium reservoirs with reservoir capacity between 200,000 and 300,000 tons. There are 884 such reservoirs scattered throughout the country. It also shows that the safety grade does not guarantee the actual safety of reservoir. In this reality, the configuration of the failure alert system should be constructed and operated for small and medium reservoirs, which are vulnerable due to poor management, by counteracting the aging of facilities, the rapid increase in hydrologic variables due to climate change, and the increased number of residents due to the development of reservoir downstream areas, in order to minimize damage on humans and properties.

2.2. STRUCTURAL HEALTH MONITORING

Structural health monitoring is a technique to diagnose the exact state of a structure by collecting and analyzing the responses of the structure from the sensors installed in the structure. It began in the aerospace industry and has expanded into many areas.

Real-time integrated disaster management is possible if the structural (or facility) health monitoring methodology is applied to social infrastructures such as reservoirs (dams). This benefit should be introduced into the Reservoir Safety Management System; such a system enables to minimize damages by identifying and remediating risks before a disaster occurs, and minimize damages on humans and properties by forecasting to the public in case of failure (Choi et al., 2014).

2.3. RESERVOIR MONITORING REGULATIONS

According to Article 3 Paragraph 3 of the 'Reservoir and Dam Safety Control and Disaster Prevention Act' (MPSS, 2014), reservoirs and dam caretakers shall install various monitoring facilities or observation facilities for reservoirs and dams designated as dangerous, and keep & manage records through monitoring and observation. According to Article 15 of the 'National Disaster Management Standards' (2010), in the case of reservoirs which are under control of local governments, the competent disaster management authority shall collect and analyze risk factors present in the area and detect the likelihood of disaster in advance, according to the content of the disaster health monitoring. The authority shall then establish a disaster health monitoring plan in order to support decision making by making reviews on installing a sensor system, collecting and analysing data, issuing a forecast or warning in accordance with monitoring, and establishing measures to minimize damage.

2.4. ALERT SYSTEM CONFIGURATION DESIGN GOALS

The C/S (Client-Server system) has the advantages of relatively short development period due to simple design application in handling calls to business logic and operating data service results, but it also has the disadvantages that client processing performance becomes degraded when dealing a rapid change of work and a large amount of data, the software is difficult to manage, and the scalability and flexibility of the system are difficult to achieve. Therefore, this alert system is aimed to be developed as a web system to respond actively to various sensors, business logic and changes of user's work, and to improve system utilization by reducing logic changes and client maintenance with minimal interface change.

3. CASE STUDY AND ANALYSIS

Similar cases related to domestic failure alert include the "Ubiquitous Sensor Network (USN) Reservoir Failure Forecasting and Warning System", an information pilot project of Korea Rural Community Corporation, the "Disaster Prevention Monitoring System", the "USN Steep Slope Failure Forecasting and Warning System " of the Ministry of Public Safety and Security, and the "Waterfront Structure Integrated Safety Management System" of Korea Water Resources Corporation (K-water).

3.1. USN RESERVOIR FAILURE FORECASTING AND WARNING SYSTEM

In the case of the USN Reservoir Failure Forecasting and Warning System, the monitored values collected from the sensors are managed by single tables, and the monitored data manages the correction values of the monitored data with meta information of monitored items, length, conversion formulas, etc. in the "Sensor Information" table. It also manages reference values for real-time forecasting and warning by managing the per-sensor-related risk criteria in separate tables (Fig. 1). The DB is a meta information management, which has a design structure in which a table change can be applied even if other kinds of sensors are added in the future.

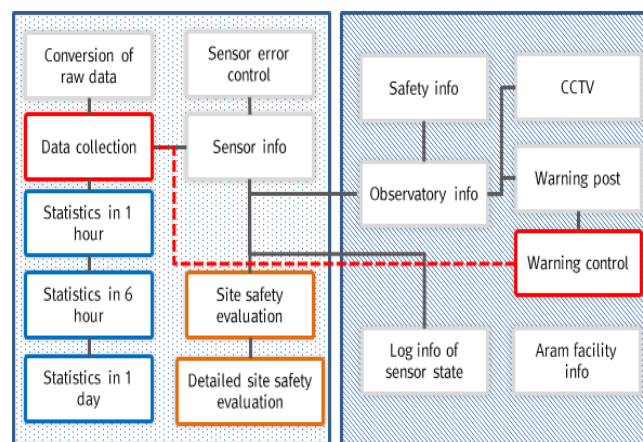


Fig. 1 DB Structure of Forecasting and Warning System for Reservoir

The configuration of H/W, S/W and F/W of the USN Reservoir Failure Forecasting and Warning System is in pilot operation constructed as follows. Sensors installed in reservoirs are connected to the data loggers by wire, and data collected by the sensors are delivered to the branch offices through the internet network. Monitored information gathered at the branch offices is used to search for forecasting and warning status and monitored values in real time through the monitoring system of the branch offices. The monitored data is sent through an external commercial network to the integrated monitoring system of the Rural Research Institute (Fig. 2). Due to this system configuration, the types of services between the branch offices and the Rural Research Institute Headquarters are different, requiring double management in maintenance and operation. In addition, there is a possibility of error in ensuring the consistency of data, and the data loggers may be dependent on a specific company and may be impossible to be upgraded in the future.

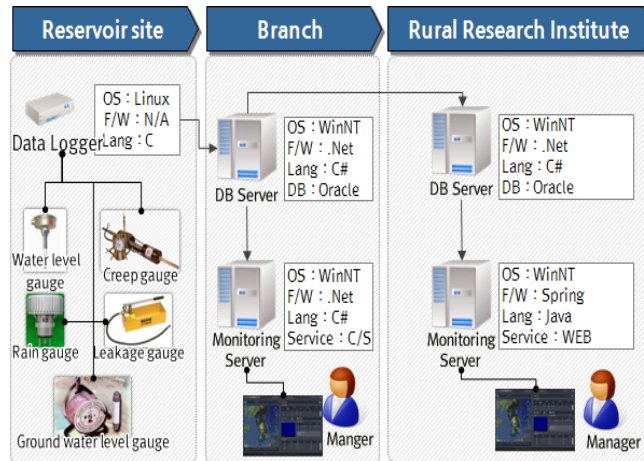


Fig. 2 System Structure of Reservoir Forecasting and Warning System

3.2. DISASTER PREVENTION MONITORING SYSTEM

The disaster prevention monitoring system is constructed for the reservoirs, which are more than 15m high and with a storage capacity of more than one million tons of water, among Level 1 reservoirs. It is a system which automatically collects and manages data from the installed sensors and manages the monitored values collected from the sensors by making separate tables for each gauge. It also provides scalability by generating up to 150 data table columns in case a sensor type is changed. The threshold value for each sensor is also managed as a separate table, and the reference values for real-time warning are stored and used for warning management (Fig. 3). The implications are as follows: "When a new sensor is added, a table for storing data of a new sensor must be newly created, and a screen for displaying the stored data must be newly developed. This limits the scalability."

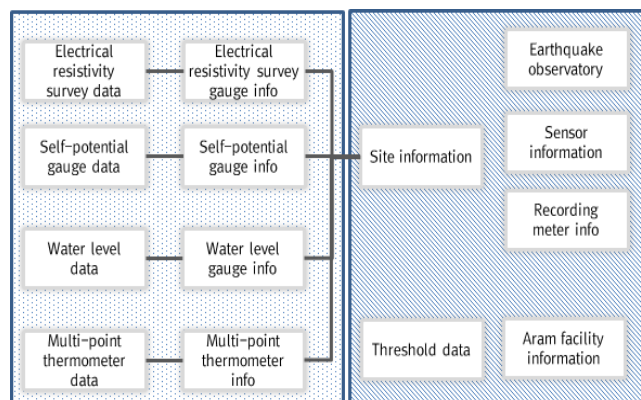


Fig. 3 DB Structure of Disaster Prevention Monitoring System

The configuration of H/W, S/W, and F/W of the disaster prevention monitoring system is as follows. The Rural Research Institute collects and manages the data of reservoirs directly, and the sensors installed in the reservoirs are communicated and monitored in a manner provided by the manufacturer. The central monitoring system is composed of the collection server, the DB server, and the monitoring server. The monitoring server uses the WEB server (server for static data processing) and the WAS (Web Application Server) server (server for dynamic data processing) without distinguishing them. In addition, the reservoirs equipped with an electrical resistivity sensor and a seismic accelerometer have installed and is currently operating a virtual private network (VPN) solution in order to achieve data security (Fig. 4).

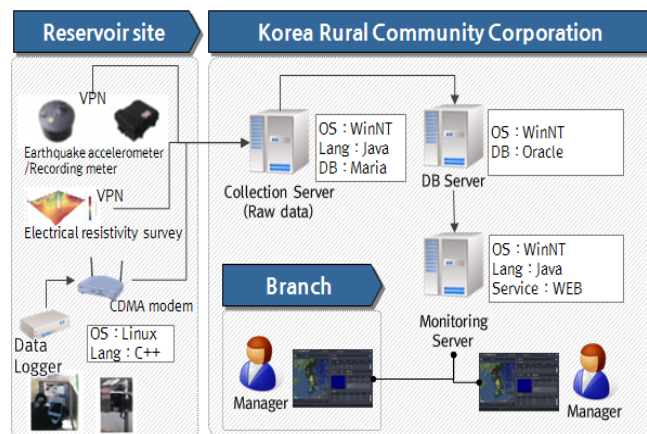


Fig. 4 System Structure of Disaster Prevention Monitoring System

3.3. USN STEEP SLOPE FAILURE FORECASTING AND WARING SYSTM

The USN Steep Slope Failure Forecasting and Warning System of the Ministry of Public Safety and Security is a pilot system constructed and operated in six districts up to the 3rd project from 2013, targeting the steep slope danger zones managed by local governments. It is a system which identifies risk of steep slopes with monitored data and makes a forecast and warning at the site. However, as of 2016, it has been merged with the National Disaster Management System (NDMS), and its programs have been revised mainly to focus on steep slope status management and monitored data retrieval rather than the forecasting and warning function. Accordingly, it is being operated with the tables for managing the established values for forecasting and warning removed, so that the function of the forecasting and warning system is lost (Fig. 5).

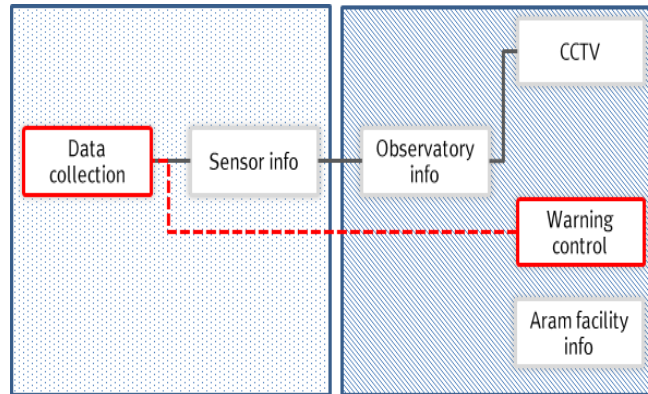


Fig. 5 DB Structure of Forecasting and Warning System for steep slope

The system configuration of H/W, S/W, and F/W of the USN Steep Slope Forecasting and Warning System is constructed as follows. The sensors installed in steep slopes are connected to the data loggers by wire. Collected data of the sensors are compiled into Si/Gun/Gu through internet. The monitored information collected in Si/Gun/Gu is transmitted to the NDMS system of the Ministry of Public Safety and Security via the administrative network. The monitored values are then monitored through the steep slope monitoring system of the NDMS (Fig. 6).

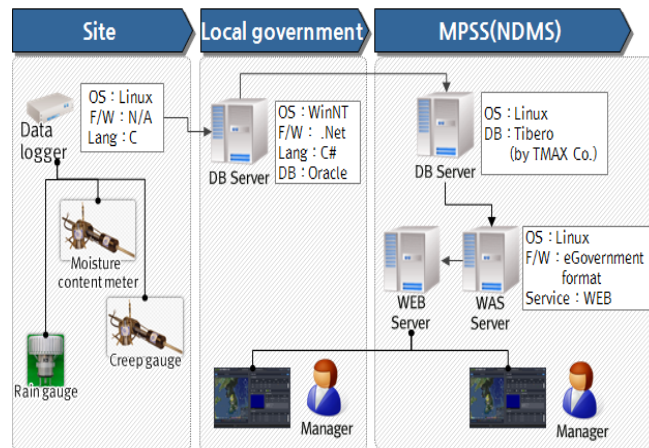


Fig. 6 System Structure of Forecasting and Warning System for steep slope

The H/W, S/W, and F/W that make up the system are installed in the G-Cloud environment of the National Computing and Information Service located in Daejeon. For this reason, they are being developed and operated as the Linux- and Java-based e-government framework that is established as the standard in e-government. All systems are made redundant, which are composed of a non-disruptive system in case of failure.

3.4. INTEGRATED WATERFRONT INFRASTRUCTURE SAFETY MANAGEMENT SYSTEM

The integrated safety management platform based on the disaster scenario of Korea Water Resources Corporation is designed to standardize and store the monitored values of five items per sensor in single measurement tables, and issue a warning after comparing the stored data values with the values of the safety evaluation table of river water level and earthquake monitoring (Fig. 7). A system for the pilot service is currently under construction and will be launched in 2017. The safety evaluation values are managed based on river water level and earthquake monitoring values. A notable point is that it manages the SOP (Standard Operating Procedure) response status in the system by managing the SOP DB in case of a disaster.

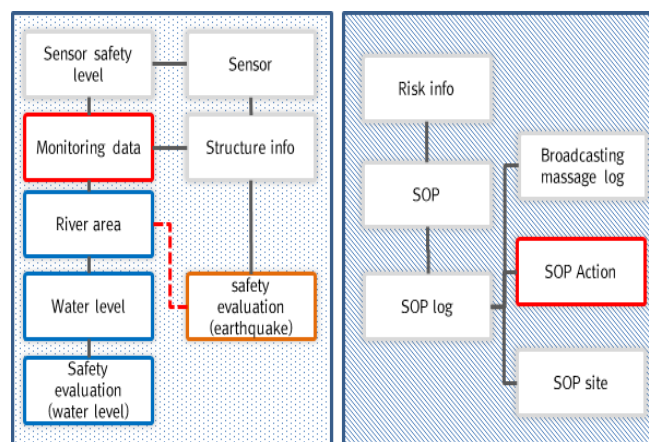


Fig. 7 DB Structure of Integrated Waterfront Infrastructure Safety Management System

The structure of H/W, S/W, and F/W of the integrated safety management platform based on the disaster scenario of Korea Water Resources Corporation (K-water) is composed of the following structure. Sensors installed in the Test Bed are connected with the data loggers. Monitored data is collected in the collection server of Korea Water Resources Corporation (K-water) through the CDMA wireless internet network. The monitoring system then monitors monitored values and safety assessment.

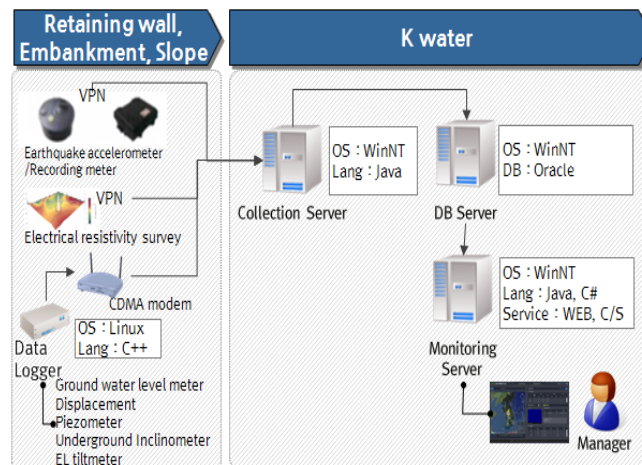


Fig. 8 System Structure of Integrated Water Infrastructure Safety Management System

The structure of H/W, S/W, and F/W of the integrated safety management platform based on the disaster scenario of Korea Water Resources Corporation (K-water) is composed of the following structure. Sensors installed in the Test Bed are connected with the data loggers. Monitored data is collected in the collection server of Korea Water Resources Corporation (K-water) through the CDMA wireless internet network. The monitoring system then monitors monitored values and safety assessment.

The H/W, S/W, and F/W that make up the system configuration are installed in Korea Water Resources Corporation (K-water). As the system is configured for a trial service, it is not redundant. It is based on the WinNT server, and the programs in use are mixed with C# and JAVA (Fig. 8). For S/W, the DB is configured with Oracle and the WAS with Tmax's JEUS product. In case of expansion of the system in the future, it is expected that the cost of introducing S/W will be increased. In addition, the transmission programs for each sensor use the program of the supplier, and the program for each function is not standardized and developed as WEB, C/S, single application or other ways. Therefore, it is considered that standardization work of the frameworks and programs should be carried out in various parts in case of dissemination after the test operation.

3.5. CASE ANALYSIS RESULTS

From a result of the analysis of similar cases, four programming languages such as C, C#, C++, and JAVA are being used as the development languages. When the development languages used in the data logger, the collection server, and the monitoring server are different, the maintenance cost for each program increases. In addition, as there are not enough people who can use four languages at the same time, there is a difficulty that programmers who can use each programming language must be secured separately.

The IoT framework is widely used for data analysis and communication. This framework is mainly based on Open Source. In the Reservoir Failure Alert System, the IoT framework can be used for the data logger that transmits the data collected by sensors to the collection server. If the data logger is constructed of a proprietary program of the development company, there will be problems due to dependency on the specific company in the future maintenance and expansion.

Oracle, Maria, and Tiberio are used for the DB server management programs, and many commercial products and open source solutions exist today. The use of commercial products implies additional costs of program purchase, installation and operation.

The table configuration of the DB server is configured in various ways according to the structure of the system. Two representative methods are used: the method which is intuitive but lacks scalability by organizing tables by sensor type; and the method of considering scalability by managing single table configurations and alert reference values in separate tables.

The WAS server is a software to save the program and compute dynamic data during the time of the WEB service. It is not applied in most cases, but it is a necessary solution to distribute the system load for ensuring efficiency and performance when the number of users increases.

The processed sensor data is displayed to the C/S or the WEB system via the WEB server to be delivered to users. The C/S has the disadvantages of software management difficulties and difficulty in securing system scalability and flexibility.

Table 2 Purpose of H/W structure

Item	Purpose
Data Logger	To collect data from installed sensors in site
Collection Server	To collect data from Data Logger and send to DB Server
DB Server	To save observed data in the format of raw, statistic, backup, and processed
WAS Server	To access sensor data and to drive alert program
WEB Server	To save/service HTM and, image file

Table 2 shows the H/W and configuration purposes to be achieved in the failure alert system. The collection server, the DB server, the WAS server, and the WEB server must be configured independently to ensure efficiency and performance when the number of users increases. When constructing S/W, it is necessary to consider that the maintenance cost increases when a commercial S/W is introduced, and the program redevelopment cost occurs when the DB management system is changed. Since the monitored data volume is not vast, Open S/W must be configured as a basis. When configuring F/W, it must be configured in such a way that the transmission method for each sensor be unified, and could be integrated into the e-government framework, so as not to be dependent on the sensor and data logger vendor's program.

4. SERVER DESIGN STANDARD SUGGESTIONS

The analysis of the designs and operation status of similar cases and pre-installed systems led to the drafting of standards from the following three perspectives.

1. To integrate the Reservoir Forecasting and Warning System composed of two sides – sites and users & managers – into a single system
2. To introduce and operate a framework for monitored data collection and transmission, suitable for the failure alert system to remove the dependency to the sensor and data logger vendor.
3. To select the DB design considering convenience and extensibility in similar cases and pre-built system

In order to implement the above design standards, optimal solutions should be selected by examining the status of H/W in each programming language, in the DB server, in the WAS server and in the WEB server, and comparing with the existing frameworks and solutions used as the standards of electronic government businesses. The functional comparison between solutions is pointless in nature as there is currently a small variation in performances and functions for each solution. Therefore, the solutions are chosen considering both popularity and cost savings.

4.1. DEVELOPMENT LANGUAGE SELECTION

Currently, JAVA has been designated as the standard programming language for e-government projects. Looking at the global programming language share of August 2016, the most popular programming language used is JavaScript followed by Python, Java, and C (Nunns, 2016). Because the languages defined as the standards by the e-government among the four languages are Java and JavaScript, they have been selected as the standards in the reservoir alert system.

4.2. DATA LOGGER FRAMEWORK SELECTION

If the framework of data logger is built on the development company's own program, there will be problems caused by the dependency on the specific company in maintenance and expansion. In order to prevent these problems, basically public frameworks that are widely used around the world are applied and functions specialized for the reservoir alert system are built together. Docker and Apache Spark rank first and second in the global framework interest of 2016 (Nunns, 2016). In the case of Docker, there is a lot of interest but the cases of actually being applied to the field is still lacking. Therefore, Apache Spark, which is widely used as a core framework for other commercial solutions, is chosen to be used in the data logger framework of the reservoir alert system.

4.3. DB SERVER SOLUTION SELECTION

The DB server is used to store and manage data. It stores monitored information of sensors for the Reservoir Failure Alert System. Although many commercial products and open source solutions exist, open source solutions are chosen in terms of cost saving because there is a small variation in performance and function. Currently, CUBRID, MariaDB, MongoDB, and MySQL are used. CUBRID is a free open source option specifically optimized for web applications, and has the advantage that its complex web services can handle large amounts of data and generate simultaneous requests of large amounts of data (Champagne, 2016). Thanks to these advantages, the standards of the domestic e-government system recommends CUBRID, a domestic open source DB solution. Therefore, it is selected as the standard in the Reservoir Failure Alert System as well.

4.4. DB TABLE DESIGN SELECTION

DB table is composed of a single table with the monitored values collected from the sensors. It enables the management of reference values for the real-time alert by managing risk criteria per sensor in a separate table (Fig 9).

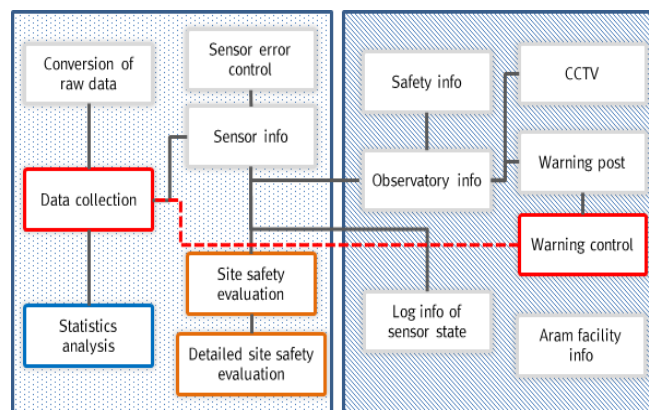


Fig. 9 Proposal of DB Table Design

Since extensibility needs to be considered for the DB table, the DB table is structured as follows. The transmission format of the monitored data of each sensor is standardized to organize the data into 4 kinds and the measurement value columns of the monitored data storage table are limited to four (Fig. 10 (a)). It is reflected in the design in order to operate the system regardless of the sensor manufacturer, by conforming to the standard data format even if a sensor is added in the future. The DB is a meta information management which has a design structure adjustable to a table change, even if other kinds of sensors are added in the future.

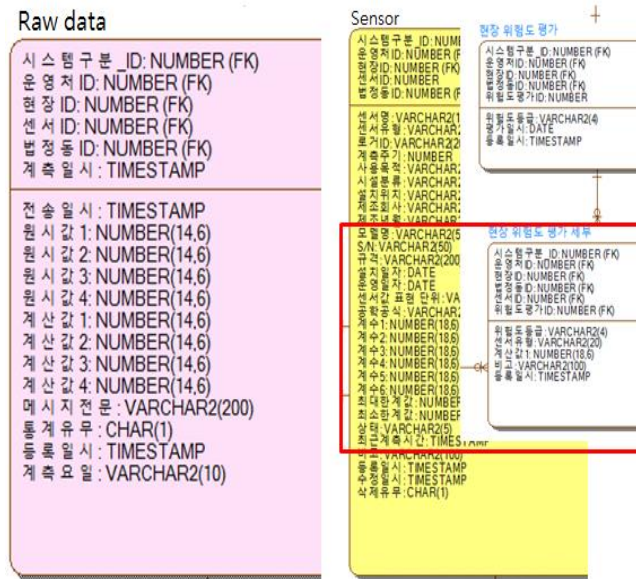


Fig. 10 Proposal of DB Table Design; (a) Raw Data table structure (left), (b) Basic and correction data table structure (right)

The table columns of the DB are constructed considering the inclusion of the following: the general information of sensors, such as sensor type, model name, manufacturer, warranty period, and image storing column, as well as engineering formulas and coefficient values for correcting the monitored values of sensors, such as engineering formulas, coefficients, minimum limit value, and maximum limit value (Fig 10(b)). Even if sensors of the same nature are used, the methods of correcting deviation of measurement values are different according to the sensor manufacturer. Therefore, columns are used to reflect the measures for securing future scalability in the DB design. Furthermore, it is necessary to construct a table that can set the threshold separately for each sensor installed, and to use it as a reference value.

4.5. WAS SERVER SOLUTION SELECTION

The WAS server is a software that processes business logic like calculating and storing data by storing the program during the time of the WEB service, and is a solution located between the WEB server and the DB server. Currently, commercial products and open source solutions are being used as the WAS server. Typical WAS platforms used in 2016 include IBM WebSphere, Oracle WebLogic, RedHat JBoss, and open source Tomcat. The domestic product is Tmax's JEUS product (Kharkovsk, 2016). IBM's WebSphere product offers many features, but not all of these features are necessary. The reservoir alert system intended to be built is fully operational with RedHat's Jboss solution, which is based on open source. It is also a recommended standard for the e-government system. Therefore, Jboss solution is selected for the above reasons.

4.6. WEB SERVER SOLUTION SELECTION

The WEB server is a software that is used to store and serve HTML documents, images and files during the time of the WEB service, and is located at the front of WEB service. Currently, commercial products and open source solutions are being used as the WEB server. In terms of worldwide share of Web servers in 2016, the open source Apache solution accounts for 45%, followed by Microsoft's IIS, a commercial solution (Netcraft, 2016). The open-source Apache is currently being recommended as the e-government standard. Therefore, the Apache solution is chosen as the standard of the reservoir alert system as well.

4.7. DRAFT OF RESERVOIR FAILURE ALERT SYSTEM DESIGN STANDARDS

Table 3 Selected S/W for alert system

Item	S/W	Reason
Development language	JAVA	- WEB program standard - e-Government standard framework
Operating system	Linux	- Open source so low application cost - To work in low H/W spec
Communication F/W	Apache spark	- Open source so no application cost - IoT real time data collection and analysis
DB	Cubrid	- Open source so no application cost - DB of eGovernment standard
WAS Server	JBOSS	- Open source so low application cost - WAS S/W of e-Government standard
WEB Server	Apache	- Open source so low application cost - WEB S/W of e-Government standard

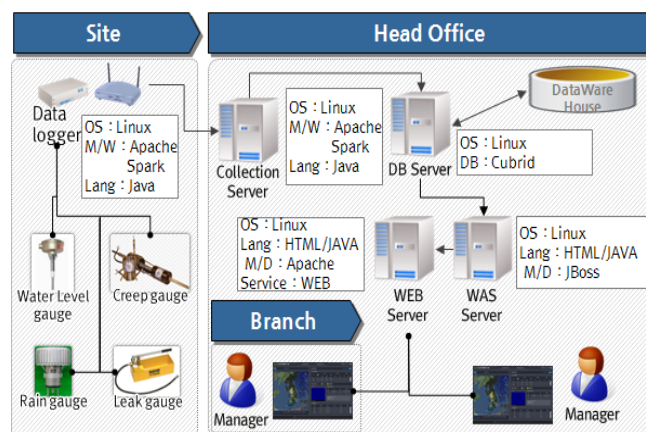


Fig. 11 Proposal of Server H/W, S/W, and F/W design

The H/W and S/W introduced to establish the system design standards are structured using the G-Cloud construction and operation environment of the National Computing and Information Service located in Daejeon as a reference, which is currently being used as the standard of the e-government system. The H/W configuration of the introduced WEB, WAS, and DB server use the introduced H/W that supports the open O/S Linux as the standard, and the basic O/S is based on the Open S/W Linux. Table 3 shows the results and the server design is constructed as shown in Fig 11. DB table is structured as a single table, and since extensibility has to be considered, measurement value columns of the monitored data storage table are limited to four. In addition, for a stable service, all the system configurations are made redundant from collection to display for non-disruptive service as a principle.

5. CONCLUSION

In order to present the server design standards (draft) in this study, the analysis of similar cases and the e-government standard frame were comprehensively considered to derive the directions of the system as follows:

First, Java and JavaScript are chosen as the standard languages, taking into consideration the unification of development language, program share, and the e-government standard framework.

Second, Apache Spark is chosen as the data logger solution in order to avoid problems caused by dependency on specific companies, and to fit the e-government standard frame.

Third, CUBRID is selected as the DB solution because it is an open source program good for cost saving and fits the e-government standard framework.

Fourth, The DB table consists of single tables of collected measurement values, the risk standards for each sensor is managed in a separate table, and the DB adopts the table methods that can manage with the meta information.

Fifth, RedHat's JBoss solution based on open source is selected as the WAS server to handle business logic.

Sixth, the Apache solution is chosen as the standard of the WEB server solution to be strong in security and minimize maintenance cost according to the e-government standard framework.

ACKNOWLEDGEMENTS

This research was supported by a grant(2017-MOIS31-002) from Fundamental Technology Development Program for Extreme Disaster Response funded by Korean Ministry of Interior and Safety(MOIS).

REFERENCES

- [1] Champagne, J., 2016, The Top 7 Free and Open Source Database Software Solutions, IT Management.
- [2] Choi, B. H., Jung, M. C., Heo, J. and Lee, B. (2014), Toward advancing risk management on irrigation facilities-Non structural risk management, Korea Rural community Corporation, 149-164.
- [3] Choi, B. H. and Lee, B. (2015), Investment Priorities for the Decision-making Support Based on the Evaluation of Downstream Areas and Surrounding of Dam, *Journal of Korean Society of Hazard Mitigation*, Korean Society of Hazard Mitigation, 15(1), 305-313.
- [4] KMA (Korea Meteorological Administration) (2004), 100-Year Climate Change and Future Prospects on the Korean Peninsula.
- [5] MAFRA (Ministry of Agriculture, Food and Rural Affairs) (2106) Rearrangement of agricultural and fishing villages act.
- [6] MPSS (Ministry of Public Safety and Security) (2014) Reservoir and dam safety control and disaster prevention act.
- [7] National Disaster Management Standards (2010).
- [8] Netcraft, 2016, December 2016 Web Server Survey, (<https://news.netcraft.com/>)
- [9] Nunns, J. (2016), What are the 5 most popular programming languages and which pays the best salary?, Computer Business Review, (<http://www.cbronline.com>).

COMMISSION INTERNATIONALE DES GRANDS BARRAGES

VINGT-SIXIÈME CONGRÈS DES GRANDS BARRAGES
Autriche, juillet 2018

DOI 10.3217/978-3-85125-620-8-226



This work licensed under a Creative Commons Attribution 4.0 International License. <https://creativecommons.org/licenses/by-nc-nd/4.0/>

**SLOPE MONITORING BY DISTRIBUTED FIBER-OPTIC SENSING: PROJECT
EXAMPLES, RESULTS AND LIMITATIONS**

Michael ITEN

MARMOTA ENGINEERING AG, ZURICH

SWITZERLAND

Frank FISCHLI

MARMOTA ENGINEERING AG, ZURICH

SWITZERLAND

COMMISSION INTERNATIONALE
DES GRANDS BARRAGES

VINGT-SIXIÈME CONGRÈS DES
GRANDS BARRAGES
Autriche, juillet 2018

SLOPE MONITORING BY DISTRIBUTED FIBER-OPTIC SENSING: PROJECT EXAMPLES, RESULTS AND LIMITATIONS

Michael ITEN & Frank FISCHLI

Marmota Engineering AG, ZURICH

SWITZERLAND

1. INTRODUCTION

Reservoir slopes, dams and hydropower infrastructure, such as water pipelines or transportation ways, often lay within areas of potential soil movements. These areas, affected by unstable slopes and differential settlements, mostly have a large aerial extension, which makes it particularly difficult to identify the critical zones. Distributed fiber-optic sensors, that are capable of providing monitoring data for thousands of individual sections along a sensor of up to several kilometers of length, can reveal possible threats over a large area.

The authors have wide experience with soil- and rock-embedded fiber-optic sensing solutions for landslide and infrastructure monitoring, particularly:

- Pipeline monitoring in creeping landslides;
- Dam stability monitoring by borehole-embedded sensors;
- Landslide site investigation by horizontal and vertical sensors;
- Possible substitution of inclinometers by fiber-optic sensors.

Besides detailed project examples and monitoring data of these projects, the challenges and limitations of the fiber-optic methods are discussed. In addition, a short introduction into the most prominent distributed fiber-optic strain sensing technologies is provided.

2. METHODOLOGY

2.1. DISTRIBUTED FIBER-OPTIC SENSING TECHNOLOGIES

A distributed sensing system means that sensor data is continuously (distributed) obtained over the full length of a sensor cable. This can be idealized as a gapless array of numerous point sensors aligned one after another. Continuous strain along optical fibers can be measured by several techniques based on the Brillouin scattering effect: spontaneous Brillouin scattering occurs when a light pulse guided through a silica fiber is backscattered by a nonlinear interaction with thermally excited acoustic waves. The scattered light undergoes a frequency shift, which is directly related to the strain and temperature in the medium. Thus, in addition to the strain sensor cable, a loose fiber must be placed for temperature compensation. The backscatter is recorded in the time domain to obtain information of the scattering location along the fiber. The frequency shift of the signal is analyzed and converted into strain and temperature data.

When using spontaneous Brillouin scattering (Brillouin Optical Time Domain Reflectometry - BOTDR), the signal is weak and thus, frequency shift information not very accurate as well as possible distance of signal transfer is limited. In the more refined stimulated Brillouin setup (e.g. Brillouin Optical Time Domain Analysis - BOTDA), two counter-propagating light waves at different frequencies interact via stimulated acoustic waves [1]. The interaction results in an energy transfer and thus, amplifies the signal, which leads to higher accuracy of the measured strain as well as longer sensor lengths. With BOTDA technology, the strain measured is an average value over the spatial resolution (typically 1 m), which corresponds directly to the wavelength of the light pulse sent down the fiber. The readout resolution is about $2 \mu\epsilon$ and the maximum sensing distance is > 30 km.

Distributed strain measurement technologies can also be based on Rayleigh scattering. Commercially available Rayleigh technology is currently limited to 70 m sensing length and due to this limitation, it has not been used in the monitoring projects below.

2.2. MONITORING CONCEPTS

The different sensing concepts can mainly be divided in terms of the angle between movement and sensor direction and type of movement which is to be detected (see Figure 1). A distributed fiber-optic sensor measures strain and or temperature changes along its longitudinal direction. Therefore, the most obvious application is a situation in which the main movement acts in the direction of the installed sensor (e.g. in vertically installed sensors in boreholes or piles for load monitoring). In many cases however, the direction of movement is not parallel to the installed sensor, since such installation is not possible, or the exact location of the movement is not known and needs to be detected. Applications where the

sensor is subjected to angled movements can be used for qualitative assessments of movements and for quantitative analysis by adopting a suitable model for the data interpretation.

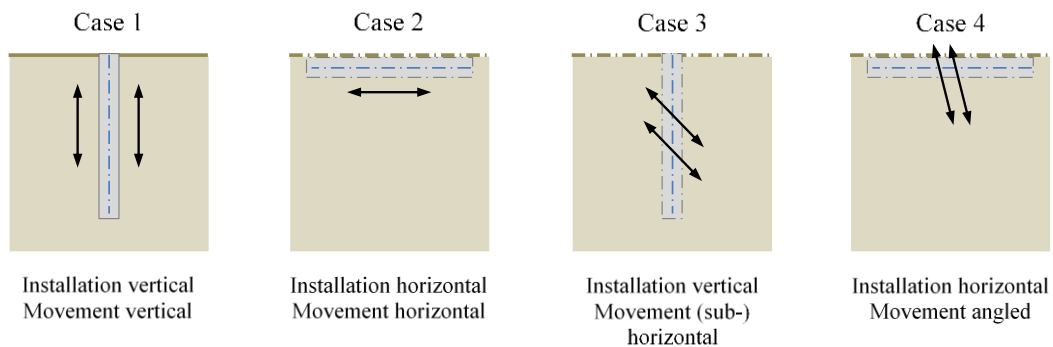


Fig. 1

Schematic layout of the different sensing cases (blue dotted line shows sensor).

2.3. DATA INTERPRETATION FOR ONE LONGITUDINAL SENSOR

In Figure 2a, a movement of point B induces strain in the sensor section AB (of length equal to the spatial resolution of the applied measurement technology). Thus, for a measured strain ϵ in the fiber sensor, L_0 changes to L_n . This means, that the new location of B is anywhere on the circle with center A and radius L_n . In the case where the movement angle can be sufficiently well estimated, a good quantitative assessment is possible. This is especially true for movements at angles β below 85° and above 95° to the sensor axis. Figure 2b shows the movement that can be detected over the typical spatial resolution of 1 m with a typical measurement resolution of $2 \mu\epsilon$.

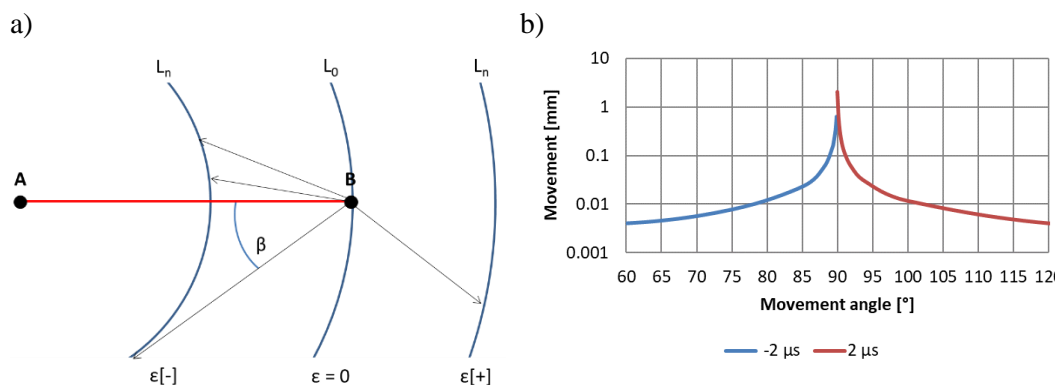


Fig. 2

(a) Possible movements of point B for a given measured strain with unknown movement angle β ; (b) influence of movement angle for the data interpretation.

2.4. DATA INTERPRETATION FOR THREE OR MORE LONGITUDINAL SENSORS OVER THE CROSS SECTION

As shown in Figure 3 below, it is possible to arrange several longitudinal sensors over the cross section of a circular structure. A movement of point F then induces strains in the sensor sections AB and CD. Assuming the cross section stays planar and the geometry does not change, the movement of point F can be calculated as well as its movement angle. An advantage is also that this model does not need a temperature compensation but is self-compensating.

It must be noted that for both concepts shown above (one or three and more longitudinal sensors), it is necessary to know at least one point along the structure in its absolute coordinates. Preferably, this is obtained geodetically.

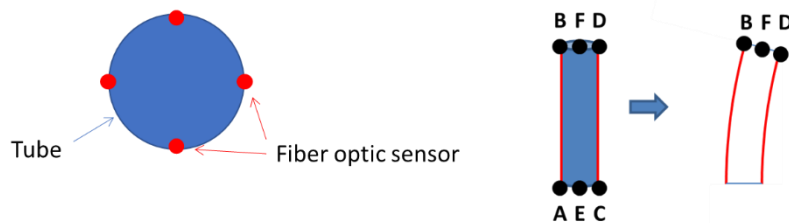


Fig. 3

Arrangement of four longitudinal sensors over the cross section of a tube.

3. PROJECT EXAMPLES

3.1. SUCCESSFUL APPLICATIONS

Possible applications for geotechnical monitoring using fiber-optic sensors are numerous and soil-embedment of sensors has been studied by the authors for years (e.g. [2]). In order to bring it to a successful practical implementation, the concepts have to satisfy certain requirements: sufficient reliability for a given task, practical applicability, acceptance by infrastructure experts/decision makers and commercial effectiveness. In the next paragraphs selected successful applications that have been awarded as commercial projects (i.e. the authors have been contracted by private or public entities to carry out the job) are shown.

3.2. LANDSLIDE SITE INVESTIGATION

Unstable reservoir slopes can endanger the reservoir itself as well as constructions on them. However, the extent of the landslides and its boundaries

may not be sufficiently known from surface observation only. Distributed fiber-optic sensors can help to localize the shear zones and quantify their extent, as well as specify the moving areas. To localize shear zones, sensors can be placed vertically into boreholes (c.f. Figure 1 Case 1) or horizontally, directly into the soil or into roads (c.f. Figure 1 Case 2). Several landslide site investigation projects have been carried out in the Swiss Alps from 2006 to 2016:

In the mountain resort of St. Moritz, which is partly built on a creeping landslide, selected roads and boreholes have been instrumented with the goal of identifying if constructions will be on stable or moving ground. For example, a horizontal sensor was embedded in a road (Figure 4a) ahead of the construction of a new water reservoir. Another sensor was installed vertically in a borehole (Figure 4b) to detect possible sliding surfaces and its depths. A fiber-optic sensor was chosen over an inclinometer since it was more economical and faster to detect, and the main interest was the sliding surfaces depth. Only of secondary interest was the magnitude and the direction of the movement. The depth of the borehole was 42 m which coincides with the stable rock surface. Thus, a deeper sliding surface could be excluded. After a measurement period of only 3 months, one sliding surface could already be detected at 35 m depth within the overlaying soil layer (Figure 4c). The magnitude of displacement (approx. 4 mm) was estimated assuming a movement in direction of the dip at 80° to the sensor axis. The identification of this sliding layer was significant for the new building construction measures that were applicable according to the construction regulations.

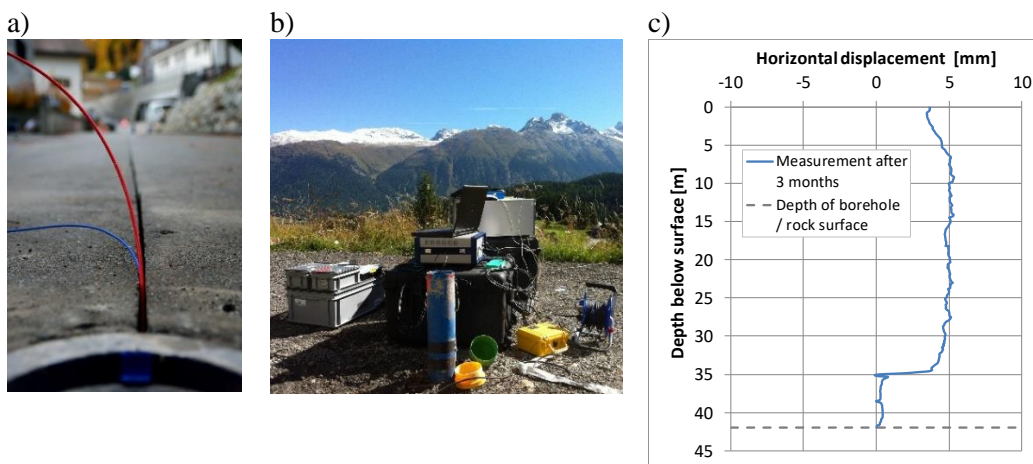


Fig. 4

Strain sensors for the detection of landslide boundaries: (a) embedded into a road; (b) vertical sensor embedded into a borehole; (c) results of borehole measurements.

Below the small town of Brienzau, which apparently lies on a rather fast creeping landslide, a 125 m deep borehole was instrumented (Figure 5a). The objectives of the installation were to detect the presumably several sliding layers and quantify the magnitude of displacements. The usage of distributed fiber-optic sensors was ideal for this application as the depth and numbers of the sliding

surface was unknown. In addition, the sensors could be assembled with high flexibility to adjust for the reached borehole depth. The results of the horizontal movements calculated from strain measurements and combined with the geodetic measurements at the borehole head are shown in Figure 5b. Different sliding surfaces could be detected. Further, it can be observed that the geodetically measured displacements do not only accumulate over the depth of the borehole but also below. It is assumed that more sliding layers exist in greater depths. This first installation provides a deeper insight in the behavior of the unstable slope and now serves as a basis to more extensive instrumentation and deeper boreholes.

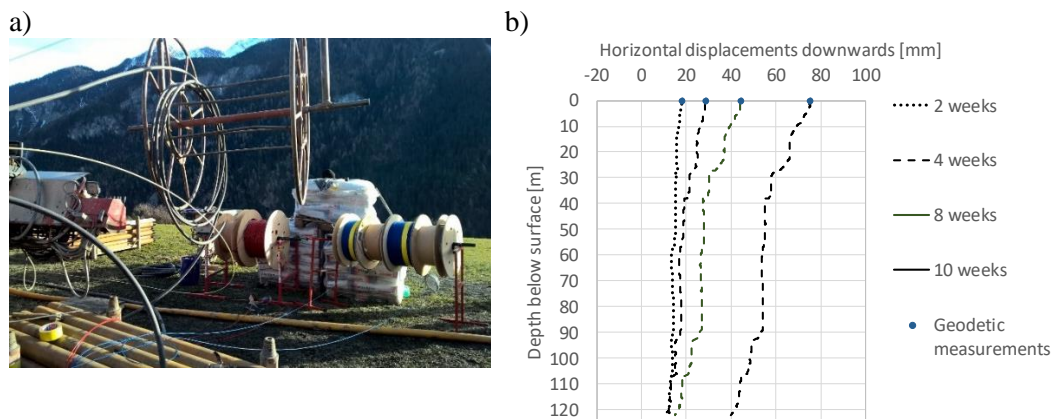


Fig. 5

(a) Installation of strained temperature sensors in the borehole; (b) horizontal displacements over the depth of the borehole.

3.3. PIPELINE MONITORING IN CREEPING LANDSLIDES

The headrace pipe of a newly built hydropower plant crosses steep slopes in a mountain area close to the small village of Tschierschen, Switzerland (Figure 6a). The slopes within the first pipeline kilometer are known to be unstable, however the exact locations and the extent of the movements were not known. The use of conventional monitoring techniques (e.g. geodetic measurement or radar) was not optimal due to the changing vegetation (forest and fields) and the large extension of the endangered area. Therefore, it was decided to install a distributed fiber-optic measurement system running parallel to the pipe (Figure 6b) allowing for gapless monitoring. The cables were embedded into soil, starting from a service building at the water intake from where also the measurements are carried out.

The measurements are reported as strain along the sensor and thus in the direction of the pipeline. For example, Figure 7a shows the strain data for a two year period. Qualitatively, stable ground can be read out from the smooth strain sections (i.e. 150 m to 280 m, 470 m to 650 m, 730 m to 830 m). Strain peaks indicate shear zones (i.e. around 720 m and 950 m) and a large creeping zone can be evaluated from 850 to 1000 m (unstable strain profile). Further details are

highlighted in Figures 7b and 7c. The most probable interpretation of the compression in Figure 7b is a shearing movement angled to the pipeline. The magnitude of the movement can be calculated by assuming a movement parallel to the surface with a direction of the dip at an angle of 75 to 82 ° to the pipeline. Having a maximum strain of roughly 0.35%, this results in a movement of 4 mm to 40 mm. In Figure 7c, two elongation peaks are combined with a compression in between. The section lies in a concave part of the slope and can be interpreted as a sliding within the concave part. This results in compression in the center and extension at the outer ends.

Similar monitoring systems were successfully installed in further projects during 2015 and 2016 for hydropower and gas pipelines. Monitoring is ongoing.

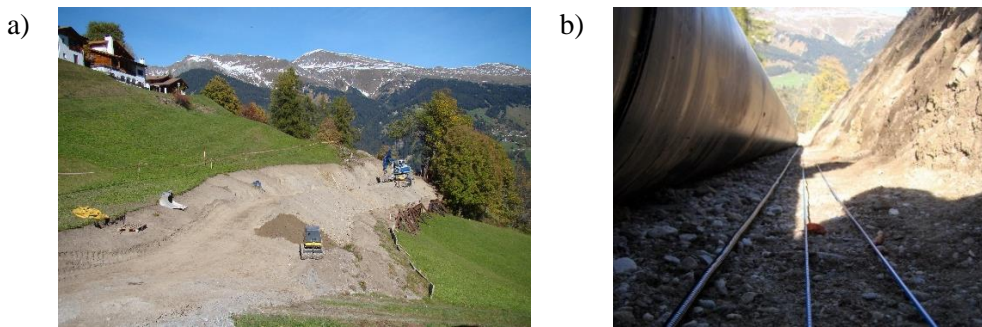


Fig. 6

(a) Water pipeline running through steep slopes below a small village; (b) installation of sensor cables parallel to the pipeline.

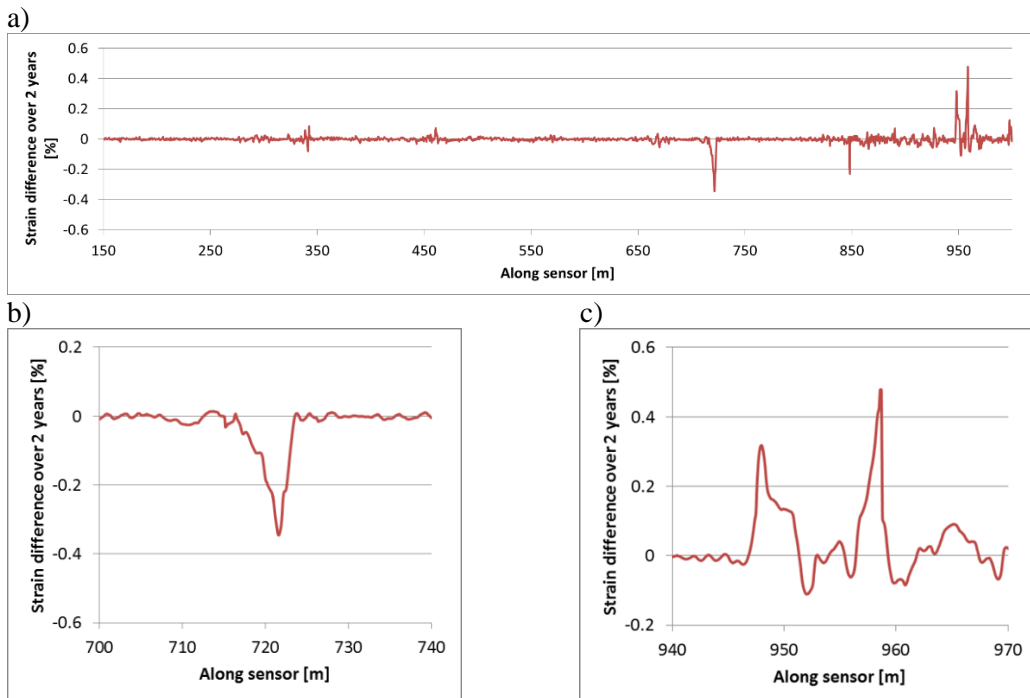


Fig. 7

Field data for pipeline monitoring over a roughly two year period: (a) over the first kilometer; (b) around 720 m; (c) around 950 m.

3.4. DAM STABILITY MONITORING

For mining repositories, the material is often disposed of in tailings. Such tailings dams can grow up to a height of 100 m and more, thus loading the ground below significantly up to its limit. Settlement as well as sub-surface monitoring by inclinometers are the main methods to detect a sliding surface development. Since borehole-embedded distributed fiber-optic sensors may offer a more efficient alternative, a trial was performed in two 150 m deep boreholes between 2014 and 2017 in a mine in Poland. In Figure 8, the results of one installation, which consists of four longitudinal sensors fixed to the outside of an inclinometer tube (c.f. 2.4) are displayed. This installation allowed to measure and compare the fiber-optic setup and the inclinometer simultaneously. The main shear surface at 80 m elevation is well recognized by both methods as well as the general amplitude of the movements. Below the main shear surface, the absolute data varies significantly.

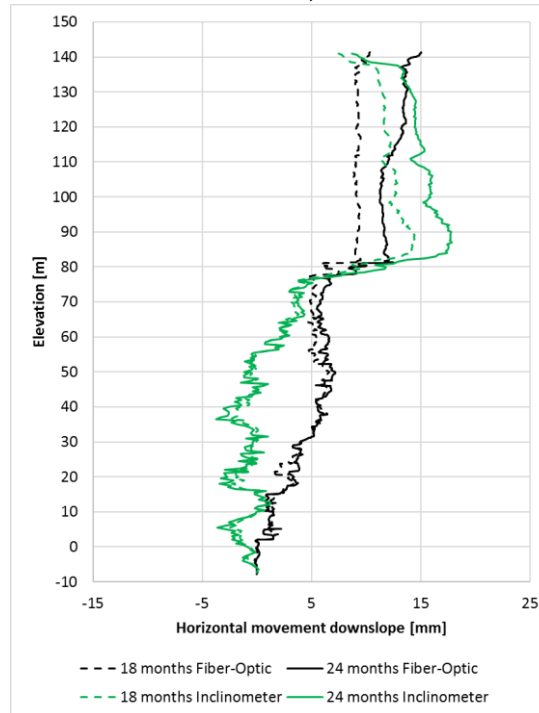


Fig. 8

Comparison of the movements measured by inclinometer and fiber-optic sensors.

4. DISCUSSION AND CONCLUSIONS

4.1. MONITORING RESULTS AND LIMITATIONS

For one-dimensional problems, where the main strain vector is in the direction of the sensor axis, accurate results of good quality can be obtained

straightforward. When the movement is not in the direction of the sensor axis, which is the case for most projects, the interpretation is more challenging. The angle of movement direction (in relation to the sensor axis) plays a major role for the accurate interpretation of the measured strain. The strong dependency of a fixed measured strain value (e.g. $2 \mu\epsilon$) interpreted into movement is shown in Figure 2b. Particularly at angles between 85° and 95° , quantitative interpretation is prone to large uncertainties. Additional difficulties for quantitative interpretation arise for cases where changing angles are expected, either over time or over distance or even both. Despite the difficulties in movement quantification, especially in the following situations good results are possible:

a) Only qualitative interpretation expected: detection and localization of shear zones (strain peaks), moving grounds (unstable strain profile) and stable ground (smooth strain profile). This can be seen for example in Figure 7a.

b) Strain profiles in boreholes: qualitative information about shear zones, moving and stable ground. By measuring the borehole head and or estimating the movement angle, the horizontal movement over depth can be estimated and a good idea of quantitative behavior is obtained. Yet, it is important to distinct between this kind of instrumentation and inclinometers: not the same results are produced, and this shall not be expected or promised for such instrumentation.

c) Pipeline monitoring: since the sensor axis is in the direction of the pipeline axis, the actual impact of a movement on the pipeline can be measured. The amount of the movement is not the major interest, but more the effect of the movement on the pipeline strain.

4.2. CONCLUSIONS

From the theory outlined and the projects shown in this paper, the following main conclusions can be drawn:

- 1) Well-funded monitoring results were obtained and compared with data obtained by third parties (e.g. geodetic measurements). Due to the high sensitivity of the fiber-optic sensors (resolution of $2 \mu\epsilon$) as well as the possibility to place the sensors as close to the location where measurements are desired (e.g. inside the soil, not only on the surface), movements are often much quicker detected as compared to other methods. Thus, additional time for decision making and reaction is gained.
- 2) The equipping of soil (horizontal and vertical) with only one longitudinal sensor is a simple and efficient method. Especially when it comes to assessing the effect of a movement for a one-dimensional structure (pipeline), the detection and quantification of the extent of shear zones, as well as the order of magnitude of the movement of individual ground layers. The installation is straightforward and cost-efficient, even for large size projects.
- 3) For boreholes, one must be aware, however, that this is not a one to one substitution of an inclinometer. Nevertheless, depending on the project,

it may as well provide more than sufficient information about the ground behavior. And in contrary to the inclinometer this information can be obtained by a moderate installation and readout effort. In general, the authors see a large potential for the instrumentation of boreholes. The main challenge is not on the technical side, but rather in convincing the engineers that often, full inclinometer information is not required.

- 4) For most cases, the main priority should be the qualitative assessment since it is rather difficult to obtain quantitative results.

REFERENCES

- [1] Horiguchi T., Tateda M. Optical-fiber-attenuation investigation using stimulated Brillouin scattering between a pulse and a continuous wave: *Optics Letters*, Vol. 14, n° 8, Optical Society of America, pp. 408-410, 1989.
- [2] Hauswirth D., Iten M., Richli R., Puzrin A.M. Fibre optic cable and micro-anchor pullout tests in sand: *Physical Modelling in Geotechnics, Proceedings of the 7th International Conference on Physical Modelling in Geotechnics*, 2010.

SUMMARY

Reservoir slopes, dams and hydropower infrastructure, such as water pipelines or transportation ways, lay often within areas of potential soil movements. These areas affected by unstable slopes and differential settlements mostly have a large extension, which makes it particularly difficult to identify the critical zones. Distributed fiber-optic sensors that are capable of providing monitoring data for thousands of individual sections along a sensor of up to several kilometers of length can reveal the possible threats over a large area. The authors have wide experience with soil- and rock-embedded distributed fiber-optic sensing solutions for landslide and infrastructure monitoring and share their particular experience in this paper. Besides detailed project examples and monitoring data, the challenges and limitations of the fiber-optic methods are discussed.

Les pentes du réservoir, les barrages ainsi que les infrastructures hydroélectriques, se trouvent souvent dans des zones de mouvements potentiels du sol. Ces zones ont pour la plupart une extension importante, ce qui rend particulièrement difficile l'identification des zones critiques. Des capteurs à fibre optique distribués pouvant atteindre plusieurs kilomètres de longueur peuvent révéler les menaces possibles sur une grande surface. Les auteurs aimeraient partager leur expérience avec des solutions de détection à fibres optiques distribuées enrobées de terre pour la surveillance des glissements de terrain.

COMMISSION INTERNATIONALE DES GRANDS BARRAGES

VINGT-SIXIÈME CONGRÈS DES GRANDS BARRAGES
Autriche, juillet 2018

DOI 10.3217/978-3-85125-620-8-227



This work licensed under a Creative Commons Attribution 4.0 International License. <https://creativecommons.org/licenses/by-nc-nd/4.0/>

**INSAR & PHOTOMONITORING™ FOR DAMS AND RESERVOIR SLOPES
HEALTH & SAFETY MONITORING**

Benedetta ANTONIELLI

NHAZCA S.R.L., SPIN-OFF OF “SAPIENZA” UNIVERSITY OF ROME

ITALY

Paolo CAPOROSSI

“SAPIENZA” UNIVERSITY OF ROME, DEPARTMENT OF EARTH SCIENCES

ITALY

Paolo MAZZANTI

NHAZCA S.R.L., SPIN-OFF OF “SAPIENZA” UNIVERSITY OF ROME
“SAPIENZA” UNIVERSITY OF ROME, DEPARTMENT OF EARTH SCIENCES

ITALY

Serena MORETTO

NHAZCA S.R.L., SPIN-OFF OF “SAPIENZA” UNIVERSITY OF ROME

ITALY

Alfredo ROCCA

NHAZCA S.R.L., SPIN-OFF OF “SAPIENZA” UNIVERSITY OF ROME

ITALY

COMMISSION INTERNATIONALE
DES GRANDS BARRAGES

VINGT-SIXIEME CONGRES DES
GRANDS BARRAGES
Autriche, juillet 2018

**INSAR & PHOTOMONITORING™ FOR DAMS AND RESERVOIR SLOPES
HEALTH & SAFETY MONITORING**

*Benedetta Antonielli ^a, Paolo Caporossi ^b, Paolo Mazzanti ^{a,b}, Serena Moretto ^a,
Alfredo Rocca ^a*

*(a) NHAZCA S.r.l., spin-off of “Sapienza” University of Rome, Via Vittorio Bachelet
12, Rome, 00185, Italy*

*(b) “Sapienza” University of Rome, Department of Earth Sciences, P.le Aldo Moro
5, Rome, 00185, Italy*

AUSTRIA

ABSTRACT

This paper is focused on the use of InSAR (Synthetic Aperture Radar Interferometry) and PhotoMonitoring™ techniques for dams and reservoir slopes monitoring.

The technological and scientific advances in the field of remote sensing have allowed the spread of different technologies that currently represent powerful tools for the surficial monitoring of ground and infrastructures. This paper allows to circulate and to make known the capabilities of these technologies for dams monitoring applications. In particular, Terrestrial and Satellite SAR interferometric techniques and the innovative remote sensing approach called PhotoMonitoring™, are introduced highlighting their potential and the possible applications for dams and reservoir slopes monitoring. Furthermore, two example of applications based on Terrestrial and Satellite SAR interferometric techniques have been described.

1. INTRODUCTION

Remote sensing techniques can be a powerful tool for structural health assessment of dams and for reservoir slopes monitoring. The evolution of traditional technologies and the development of emerging technologies (e.g., satellite and terrestrial radar technologies and PhotoMonitoring™) offer a wide spectrum of monitoring solutions. These technologies find application during different stages of the life cycle of a dam (e.g., design, construction, operation and maintenance) and can be applied effectively in several crucial operations, such as (i) dam reservoir site selection, (ii) reservoir catchment management, (iii) detection and control of geohazard-prone areas, (iv) structural health monitoring (SHM) of dams, (v) risk management and risk-informed decision-making.

Over the last decades, several monitoring approaches have been adopted, ranging from visual inspection to instrumental continuous monitoring [1-4]. At this regard, Satellite and Terrestrial SAR Interferometry can be an effective tools for the engineers in charge of SHM [5,6], representing a unique solution in the monitoring of structures, such as the capability to provide information about the ongoing and past deformations with millimeter accuracy.

As regards the radar-based technologies, satellite and terrestrial SAR (Synthetic Aperture Radar) interferometry represents one of the most advanced and effective techniques for monitoring deformation of both ground and man-made structures.

The main strengths of satellite SAR interferometry are the capability of monitoring large areas with high accuracy and the ability to perform historical analyses (thanks to archive satellite SAR images available from 1992). These characteristics allow to observe and measure reservoir slopes and to detect potentially unstable slopes at reservoir scale, in order to undertake the appropriate risk management strategies.

Terrestrial SAR interferometry, on the other hand, thanks to its high sampling frequency of data collection (in the order of few minutes or even seconds) and its high accuracy of displacement measurement (up to decimal millimeter order), has proven to be effective for local-scale, real-time slopes and structures monitoring, currently considered a proper technology for early warning purposes.

In addition to radar-based technologies, cutting-edge solutions like the PhotoMonitoring™ are now available for dams and reservoir slopes monitoring. The concept PhotoMonitoring™ refers to different image processing techniques, used for geotechnical and structural monitoring purposes. Among these techniques are included the digital image correlation (DIC), the change detection and the 3D photogrammetry.

In the following paragraphs, the description of the techniques and an overview of some projects carried out by NHAZCA S.r.l. using terrestrial and satellite SAR interferometry and PhotoMonitoring™ techniques are presented.

2. TERRESTRIAL SAR INTERFEROMETRY

2.1. BASIC PRINCIPLES AND APPLICATIONS

Terrestrial SAR Interferometry (TInSAR) is an all-time (night and day), all-weather, non-contact, high-accuracy and fully remote sensing technique based on an active radar sensor that emits microwaves and receives the return of scattering objects. The final output is a 2D displacement map of the investigated scenario along the instrumental Line of sight (LOS), i.e., the path between the sensor and the target. In addition, for every measurement point characterized by high backscattering features, it is possible to obtain the time series of displacement.

The SAR principle is achieved by moving the sensors along a rail and by combining the backscattered signals using focusing algorithms, that allow to obtain high resolution 2D images in range (sensor-target direction) and cross-range (orthogonal to the range; [7]) directions. The length of the rail determines the cross-range resolution of the acquired images (i.e., the longer the rail, the higher the cross-range resolution), while the distance between the instrument and the observed scenario determines the range resolution [8].

By the comparison of the phase value of SAR images collected at different times, sub-millimeter accuracy measurements can be obtained (interferometric principle). According to the site-specific conditions, the system's accuracy can range between some tenths of a millimeter, in the optimal monitoring conditions (very high signal to noise ratio values), to some millimeters (Figure 1).

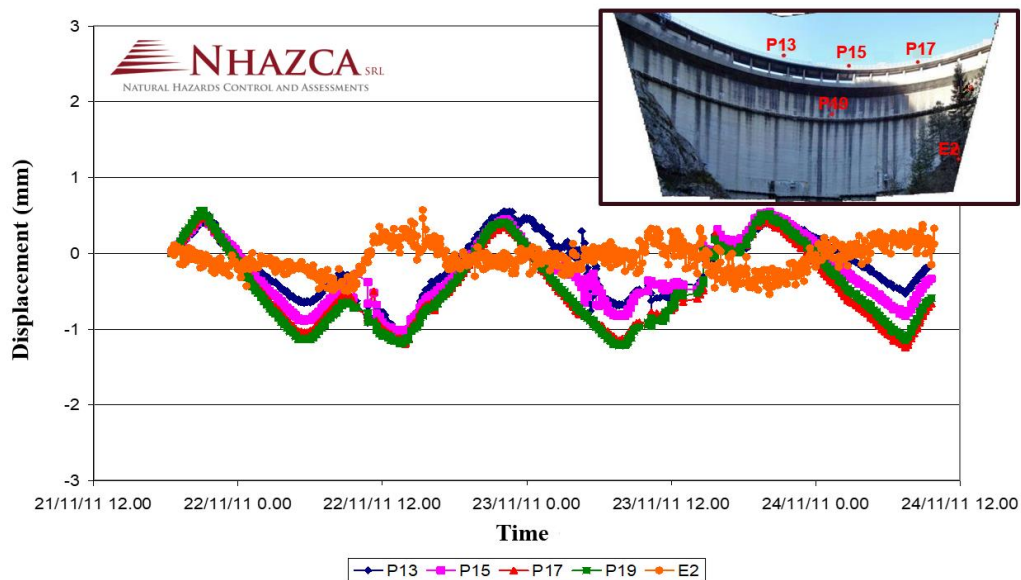


Figure 1. Example of time series of displacement (in millimeters) obtained with TInSAR in correspondence of a concrete arch dam in Northern Italy. The high accuracy of the collected displacements (up to a few hundredths of a millimeter) allowed to capture the thermal deformation behavior of the concrete dam.

Thanks to the active nature of the sensor, the TInSAR instrument does not need artificial reflectors, allowing to monitor the deformational behavior of ground

and structure/infrastructure from a completely remote point of view. However, in particular conditions, artificial reflectors on the ground (i.e., the so-called corner reflectors) would allow to improve the data accuracy and the density of measurement points.

The high data sampling frequency (up to 30 seconds), the high spatial resolution, the continuous monitoring capabilities (both in time and in space) and the high accuracy in terms of displacement monitoring, make TInSAR a suitable instrument for different applications and purposes such as [9]:

- knowledge monitoring, to characterize and assess the processes under investigation in ordinary operational conditions;
- control monitoring, to quantitatively check the evolution of known issues;
- emergency monitoring, in order to provide alert in case the risk become unacceptable.

An example of application of the TInSAR technique for the monitoring of the right flank of an earth dam is reported in paragraph 2.2.

2.2. TINSAR MONITORING OF AN EARTH DAM

In the frame of the engineering works for the stabilization of the right flank of an earth dam in Central Italy, a continuous 24/7 TInSAR monitoring has been setup. The activity has been performed for the following purposes: i) early warning for the safety of workers and ii) improvement of knowledge about the deformational behavior of the slope, also thanks to the correlation of TInSAR data with weather data and information from other monitoring instruments.

The measurements have been acquired in continuous, with a sampling period of few minutes. The data have been pre-processed on site through suitable algorithms and then transferred to the NHAZCA monitoring center, where they have been processed using a semi-automatic software. A phase of automatic image processing and internal alarms notification was performed to guarantee the early warning purposes. In case defined thresholds were exceeded, after the data validation performed by an expert user, the alarm procedure is activated.

During the 2 years of monitoring, localized surface displacements have been observed in the central part of the slope (Figure 2). In particular, more than 300 mm of displacements have been detected on the right flank of the earth dam. However, the deformations were ascribed to anthropic work activities and shallow debris movements correlated with rainfalls that did not cause concerns among the decision makers.

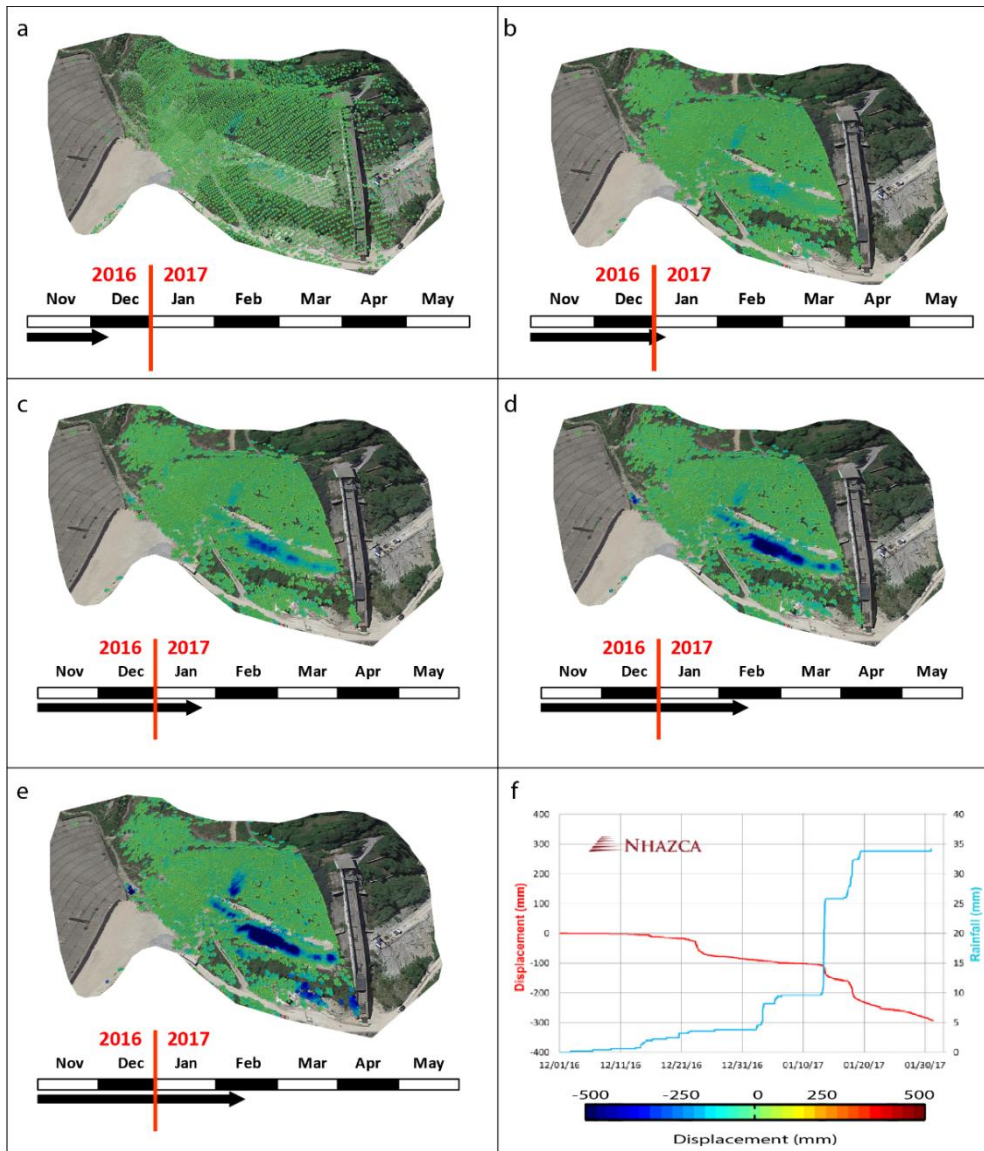


Figure 2. a - e) TInSAR multi-temporal deformation maps in tridimensional view; f) time series of displacement of one of the measured point inside the moving area and the relation between rainfall and displacements can be observed. The color of the points indicates the intensity and the direction of displacements. Specifically, negative values (light blue to dark blue) are points with deformation direction towards the sensor, while positive values (yellow to red) refer to points moving away to the sensor. Green points are considered stable.

3. SATELLITE SAR INTERFEROMETRY

3.1. REPEAT PASS SATELLITE SAR INTERFEROMETRY

Satellite Synthetic Aperture Radar (SAR) Interferometry has proved its capability in monitoring the ground and structures deformation with high accuracy

[10-14]. With respect to other traditional methods, this technology can work at all-time, with all-weather conditions and it is suitable for both wide areas and site-specific applications. A further relevant characteristic of Satellite SAR Interferometry is the possibility to retrieve information on the deformation history of the area of interest, looking back in time using the SAR data archives of the Spatial Agencies. In fact, the first global systematic acquisition of SAR imagery started in the early 1990s, with ERS-1 and -2 satellites (European Space Agency). Since then, images have been collected in several parts of the world with revisit times of the order of some days (for examples the Envisat-ASAR sensor had a revisit time of 35 days, while the recent Sentinel-1 constellation has a revisit time of only 6 days).

A SAR image consists of a matrix of resolution cells (i.e., pixels) that contain the information about the satellite-target distance. Surface deformations can be investigated through the Differential InSAR (DInSAR) methodology, that is based on the phase difference between two SAR images collected in different times (computing in the so-called interferogram), allowing to estimate the displacement occurred between the two acquisitions. In order to overcome the major limitations of the DInSAR technique, like the influence of the atmospheric phase screen (APS), long time series of SAR images are used in the Advanced Differential InSAR (A-DInSAR) technique. This latter takes advantage of several SAR images collected in the same area over time to perform deformation measurements [10, 11]. A-DInSAR methodology allows to obtain the displacement-time information of natural targets on the ground, which are measured along the satellite Line of Sight (LOS).

The Persistent Scatterers Interferometry (PSI) is one of the most effective A-DInSAR techniques, based on the analysis of specific targets on the Earth's surface (called Persistent Scatterers, PSs) characterized by long time-coherent behavior [10, 12].

The main outputs of a PSI analysis are: i) the trend of deformation during the investigated time period; ii) the time series of displacement, with an accuracy up to few millimeters; iii) the height of the target on the ground; iv) cyclic (non-linear) deformation due to several factors (e.g., temperature variations).

3.2. A-DINSAR HISTORICAL ANALYSIS OF 2 ROCK-FILL DAMS

A preliminary site-specific PSI analysis has been carried out for two rock-fill dams in USA (Figure 3a, b). The two reservoirs serve as terminal basins for the water supply of Colorado Springs and surrounding municipalities.

The A-DInSAR historical analysis has been performed using a stack of 114 high-resolution COSMO-SkyMed (from Italian Space Agency, ASI) scenes collected in the time span ranges between 2011 and 2016, in the ascending geometry of acquisition.

The multi-image processing technique allowed the analysis of the past deformational behavior of the dam bodies. The velocity measurements have been obtained with millimeter accuracy in the LOS direction (the average velocity map

is showed in Figure 3c). The measurement points in correspondence of the dam flanks show a general stability, while constrained ground deformations have been observed in the lower portion of the dam 'b' in Figure 3c, where linear deformation behavior has been observed during the 5 years monitoring period, with an average velocity trend ranging between 3 and 7 mm/year.

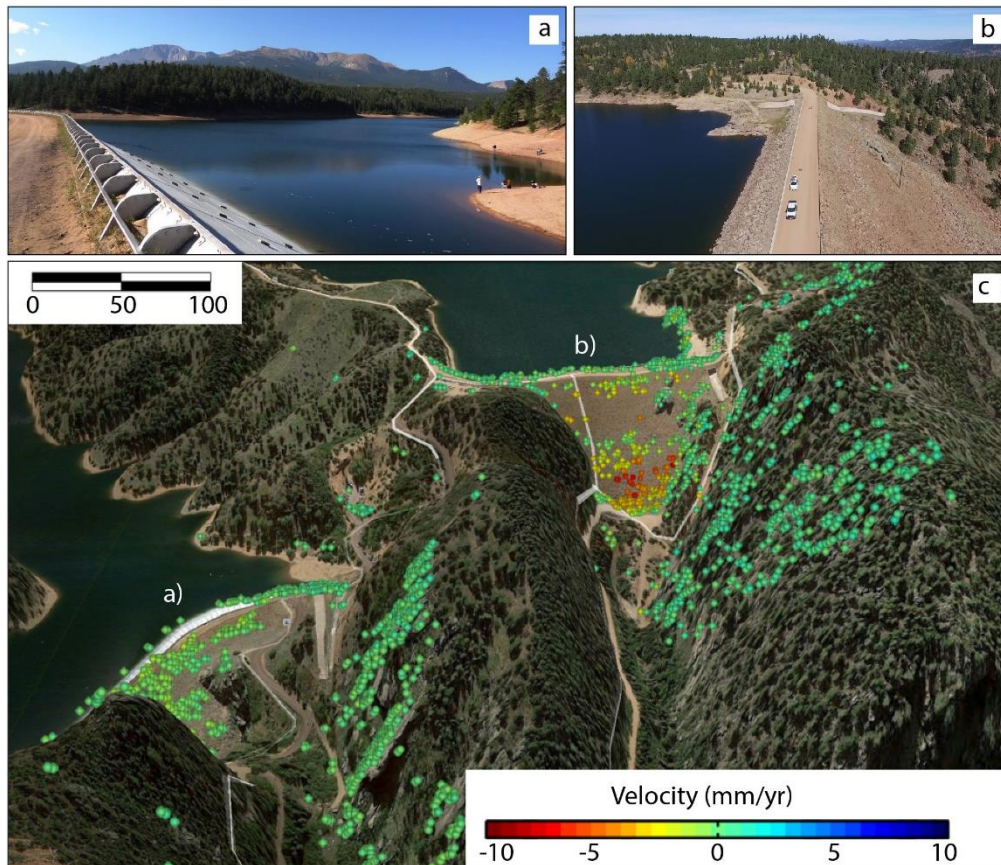


Figure 3. The two dams under investigation (a, b) and A-DInSAR results (c). For every measurement point, it is possible to observe the displacement rate in mm/year. Negative values (yellow to red) are points with deformation rate away from the satellite, while positive values (light blue to dark blue) are points that move towards the sensor. Green points are stable. (COSMO-SkyMed Product - ©ASI - Agenzia Spaziale Italiana – (2017). All rights reserved).

4. PHOTOMONITORING™: AN INNOVATIVE MONITORING SOLUTION

In addition to radar-based technologies, cutting-edge solutions are now available for dams and reservoir slopes deformation analyses. PhotoMonitoring™ is one of the most innovative remote sensing solutions, useful for geotechnical and structural monitoring.

The increasing number of satellite-based, airborne and ground-based optical and radar sensors, have greatly increased the potential of PhotoMonitoring™ for engineering applications. Ranging from very high resolution (VHR) optical and/or multispectral cameras to low-cost and low resolution sensors, today an incredible

amount of source of information can be exploited using the PhotoMonitoring™ approaches.

The approach of PhotoMonitoring™ is based on the integration of different remote sensing measurement techniques that allow to identify, analyze and quantify the surface changes/variations over time by processing two or several optical or multispectral images (e.g., satellite, aerial imagery or simple photos), collected at different times over the same area (www.photomonitoring.com).

Specifically, Change Detection (CD), Digital Image Correlation (DIC) and 3D Photogrammetry techniques can be combined, also with other remote or contact instruments for dams and reservoir slopes monitoring. In fact, it is possible to retrieve quantitative and qualitative measurement of surface changes on the investigated object (e.g., the surface of a concrete or earth dam, unstable reservoir slopes) with both Change Detection and Digital Image Correlation techniques. If Change Detection technique allows to identify, describe and quantify any changes of the area of interest, Digital Image Correlation technique allows the measurement of "full-field" deformation on the surface of investigated area. This is possible through the correlation of co-registered images, collected at different time intervals [15-19] (Figure 4).

The great adaptability of the technique makes PhotoMonitoring™ appropriate for several kinds of dam related applications. PhotoMonitoring™ can be an effective solution at different scales of investigation, from the single crack measurement to the reservoir scale.

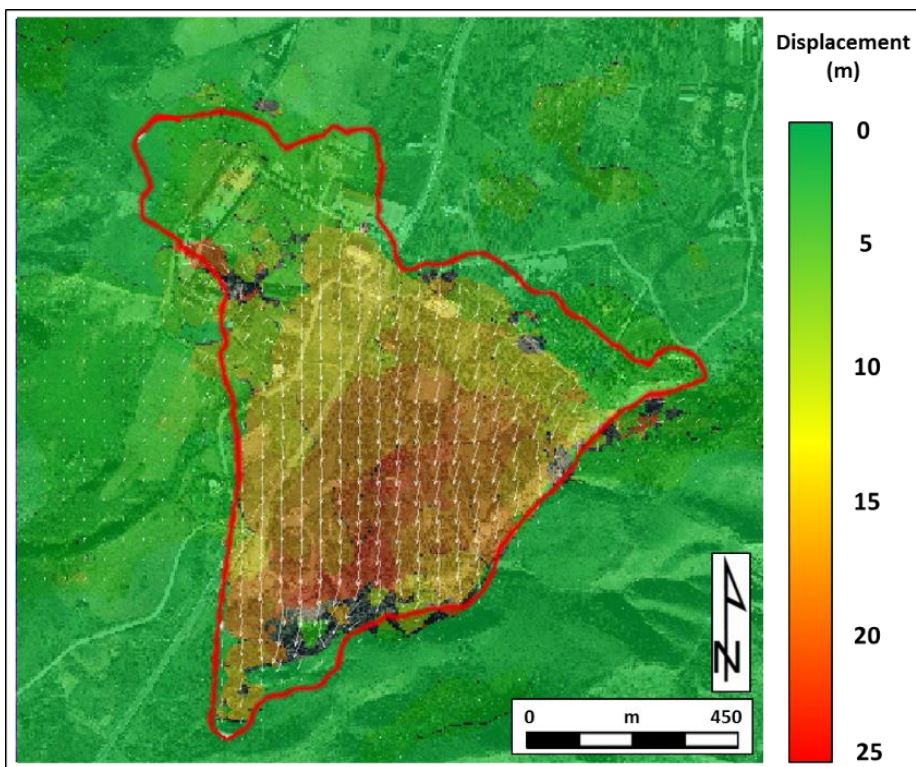


Figure 4. Example of 2D displacement map retrieved by DIC analysis performed on very high-resolution optical imagery. Here it is reported the displacement related to a large earth-slide, occurred in Italy. The landslide boundary is highlighted in red, while the displacement field is highlighted with white arrows.

In fact, satellite multispectral and/or radar images can be exploited with PhotoMonitoring™ approach for big scale application in order to investigate the stability of reservoir slopes and identifying insights of slope instability processes, thanks to the application of semi-automatic digital image analysis techniques. At the same time, terrestrial instrument based on the acquisition and processing with CD and DIC techniques of high-resolution photos can be installed for local-scale analysis, in order to monitor the 2D displacement field of the dam body or of a slope of interest. The accuracy in displacement measurement strictly depends on the kind of sensor used, the distance between the target and the collecting instrumentation and the environmental features, reaching a theoretical accuracy of 1/10 of pixel [20-24]. The terrestrial instrument, known as Virtual Digital Extensometer (VDE), can be completely managed from a remote location, allowing considerable advantages during emergency scenarios, where a quickly monitoring service is required and when traditional geological, geotechnical and structural monitoring techniques (such as inclinometers, strain gauges, crack-meter, etc.) cannot be applied avoiding risks and logistical problems.

3D Photogrammetry technique allows the reconstruction of 3D digital models, by using optical images with a high percentage of overlapping and through the implementation of Structure from Motion (SfM) algorithms. This latter can be the most suitable solution to have a comprehensive three-dimensional overview of the dam of interest [25-28]. As reported also in Buffi et al. (2017) [25], the 3D Photogrammetry technique, integrated with an UAV-based platform (Unmanned Aerial Vehicle) and traditional topographic techniques, can be the most suitable solution for the reconstruction of a 3D model of a dam. In addition, through the digital analysis of the three-dimensional model, it is possible to perform an accurate virtual inspection of the dam, even in correspondence of inaccessible or dangerous dam sectors.

5. CONCLUSIONS

This paper showed the potential of three different remote sensing monitoring solution for dams surveillance: Terrestrial SAR Interferometry (TInSAR), Satellite SAR Interferometry and PhotoMonitoring™.

The main capabilities of TInSAR (i.e., the high sampling frequency and the high accuracy of measurements) make it possible to use the technique to improve the knowledge about a deformation process, to control it over time and for emergency applications.

Satellite SAR Interferometry, and in particular, A-DInSAR technique, allows to perform both wide areas investigation and local scale analysis with high accuracy in terms of displacement measurements. The large-scale analysis can be very useful in order to investigate the state of activity of reservoir slopes, possibly detecting deformation anomalies where to focus the attention, allowing decision makers to plan further investigations. On the other hand, site-specific investigations can be carried out on localized area or structure, allowing to

characterize and monitor the possible occurrence of deformations. The peculiarity of satellite InSAR is the possibility to perform historical analyses, exploring the deformation processes occurred in the past in order to improve the know-how about the investigated phenomena.

The PhotoMonitoring™ is an emerging group of technologies, which can be effectively used for long term monitoring surveys but also for quick analyses, taking advantage of the relatively low-cost of the technology.

In conclusion, the aforementioned remote sensing technologies represent powerful tools for several applications at different stages of the life cycle of a dam (design, construction and operation), such as: the reservoir catchment management, the structural and health monitoring of dams, geo-hazard monitoring and risk management.

REFERENCES

- [1] FUHR P.L., & HUSTON D.R. (1993). Multiplexed fiber optic pressure and vibration sensors for hydroelectric dam monitoring. *Smart Materials And Structures*, 2(4), 260.
- [2] KRONENBERG P., CASANOVA N., INAUDI D., & VURPILLOT S. (1997). Dam monitoring with fiber optics deformation sensors. In *Smart Structures And Materials' 97* (Pp. 2-11). International Society For Optics And Photonics.
- [3] ALONSO PEREZ DE AGREDA, E., & GENS SOLE, A. (2006). Aznalcollar Dam Failure. Part 1: Field Observations and Material Properties.
- [4] ALBA M., FREGONESE L., PRANDI F., SCAIONI M. & VALGOI P. (2006). Structural Monitoring Of A Large Dam By Terrestrial Laser Scanning. *International Archives Of Photogrammetry, Remote Sensing And Spatial Information Sciences*, 36(5), 6.
- [5] WANG T., PERISSIN D., ROCCA F., & LIAO M. S. (2011). Three Gorges Dam stability monitoring with time series insar image analysis. *Science China Earth Sciences*, 54(5), 720-732.
- [6] TOMAS R., CANO M., GARCIA-BARBA J., VICENTE F., HERRERA G., LOPEZ-SANCHEZ J. M., & MALLORQUI J. J. (2013). Monitoring an earth fill dam using differential SAR interferometry: la Pedrera dam, Alicante, Spain. *Engineering Geology*, 157, 21-32.
- [7] MAZZANTI P., ROCCA A., BOZZANO F., COSSU R. & FLORIS M. Landslides forecasting analysis by time series 413 displacement derived from satellite InSAR data: preliminary results. In: *ESA-ESRIN, Frascati (RM), 2012; 414 Italy, September 2011, Noordwijk:L. Ouweland, ISBN: 9789290922612.*
- [8] MONSERRAT O., CROSETTO M., LUZI G. 2014. A review of ground-based SAR interferometry for deformation measurement. *ISPRS Journal of Photogrammetry and Remote Sensing* Volume 93, July 2014, Pages 40-48

- [9] MAZZANTI P. 2017. Toward transportation asset management: what is the role of geotechnical monitoring? *J Civil Struct Health Monit.* <https://doi.org/10.1007/s13349-017-0249-0>
- [10] FERRETTI, A., PRATI, C. & ROCCA, F. Permanent scatterers in SAR interferometry. *IEEE Trans. Geosc. and Remote Sens.*; 2001; 39(1), 8-20
- [11] BERARDINO, P.; FORNARO, G.; LANARI, R.; SANSOSTI, E. A new algorithm for surface deformation monitoring based on small baseline differential SAR interferograms. *IEEE Trans. Geosc. Remote Sens.* 2002, 40, 2375–2383.
- [12] KAMPES B. M. 2006. *Radar Interferometry Persistent Scatterers Technique.* Springer, Ed.. DORDRECHT, THE NETHERLANDS.
- [13] HANSSEN R.F., 2005. Satellite radar interferometry for deformation monitoring: a priori assessment of feasibility and accuracy. *International Journal of Applied Earth Observation and Geoinformation*, 6(3), 253-260.
- [14] STROZZI T., FARINA P., CORSINI A., AMBROSI C., THÜRING M., ZILGER J., WIESMANN A., WEGMULLER U., WERNER C. (2005). Survey and monitoring of landslide displacements by means of L-band satellite SAR interferometry. *Landslides*, 2(3), 193–201, doi:10.1007/s10346-005-0003-201.
- [15] PAN B., XIE H., WANG Z., QIAN K., WANG Z., 2008. Study on subset size selection in digital image correlation for speckle patterns. 12 May 2008/Vol. 16, No. 10 / *OPTICS EXPRESS* 7037. Optical Society of America.
- [16] SUTTON M. A., ORTEU J. J., SCHREIER H. W., 2009. Shape, motion and deformation measurements. Basic concepts, theory and applications. Springer Science, chap. V.
- [17] LAVA P., COOREMAN S., COPPIETERS S., DE STRYCKER M., DEBRUYNE D., 2009. Assessment of measuring errors in DIC using deformation fields generated by plastic FEA. *Opt. Las. Eng.* 47 (2009): 747-753.
- [18] LAVA P., COOREMAN S., DEBRUYNE D., 2010_a. Study of systematic errors in strain fields obtained via DIC using heterogeneous deformation generated by plastic FEA. *Opt. Las. Eng.* 48 (2010):457-468.
- [19] LAVA P., COPPIETERS S., WANG Y., VAN HOUTTE P., DEBRUYNE D., 2010_b. Error estimation in measuring strain fields with DIC on planar sheet metal specimens with a non-perpendicular camera alignment. *Opt. Las. Eng.* 49 (2011): 57-65.
- [20] DELACOURT C., ALLEMAND P., BERTHIER E., RAUCOULES D., CASSON B., GRANDJEAN P., PAMBRUN C., VAREL E., 2007. Remote-sensing techniques for analysing landslide kinematics: a review. *Bull. Soc. géol. Fr.*, 2007, t. 178, no 2, pp. 89-100.
- [21] LEPRINCE S., BARBOT S., AYOUB F., AYOUCAC J.P., 2007. Automatic and precise orthorectification, co-registration, and sub-pixel correlation of satellite images, application to ground deformation measurements. *IEEE Trans. Geosci. Remote Sens.*, vol. 45, no. 6, pp 1529–1558.
- [22] LEPRINCE S., MUSE P., AVOUAC J. P., 2008. In-Flight CCD Distortion Calibration for Pushbroom Satellites Based on Subpixel Correlation. *IEEE*

TRANSACTIONS ON GEOSCIENCE AND REMOTE SENSING, VOL. 46, NO. 9, SEPTEMBER 2008.

- [23] AYOUB F., LEPRINCE S., AVOUAC J. P., 2009. Co-registration and Correlation of Aerial Photographs for Ground Deformation Measurements. *ISPRS Journal of Photogrammetry and Remote Sensing*, vol. 64, no. 6, pp 551-560, November 2009.
- [24] TRAVELLETTI J., DELACOURT C., ALLEMAND P., MALET J. P., SCHMITTBHUL J., TOUSSAINT R., BASTARD M., 2012. Correlation of multi-temporal ground-based optical images for landslide monitoring: Application, potential and limitations. *ISPRS Journal of Photogrammetry and Remote Sensing* 70 (2012) 39–55.
- [25] WESTOBY M. J., BRASINGTON J., GLASSER N. F., HAMBREY M. J., REYNOLDS J. M., 2012. 'Structure-from-Motion' photogrammetry: A low-cost, effective tool for geoscience applications. *Geomorphology* 179 (2012) 300–314.
- [26] JOHNSON K., NISSEN E., SARIPALLI S., ARROWSMITH J. R., MCGAREY P., SCHARER K., WILLIAMS P., BLISNIUK K., 2014. *Geosphere*; October 2014; v. 10; no. 5; p. 1–18; doi:10.1130/GES01017.1.
- [27] NOUWAKPO S. K., JAMES M. R., WELTZ M., A., HUANG C. H., CHAGAS I., LIMA L., 2014. Evaluation of structure from motion for soil microtopography measurement. *The Photogrammetric Record* 29(147): 297–316 (September 2014) DOI: 10.1111/phor.12072.
- [28] BUFFI G., MANCIOLA P., GRASSI S., BARBERINI M. & GAMBI A. 2017. Survey of the Ridracoli Dam: UAV-based photogrammetry and traditional topographic techniques in the inspection of vertical structures. *Geomatics, Natural Hazards and Risk*, Volume 8, 2017 - Issue 2. <https://doi.org/10.1080/19475705.2017.1362039>

KEYWORDS

Monitoring, Control, Landslide.

COMMISSION INTERNATIONALE DES GRANDS BARRAGES

VINGT-SIXIÈME CONGRÈS DES GRANDS BARRAGES
Autriche, juillet 2018

DOI 10.3217/978-3-85125-620-8-228



This work licensed under a Creative Commons Attribution 4.0 International License. <https://creativecommons.org/licenses/by-nc-nd/4.0/>

SLOPE STABILITY ANALYSIS IN GAMBIRI DIVERSION DAM USING NUMERICAL MODELS

S. SOLEYMANI

*Expert of Engineering Seismology, TOOSSAB CONSULTATNT ENGINEERING
COMPANY*

IRAN

A. HEMMATI

*Expert of Geotechnical Engineering, TOOSSAB CONSULTATNT ENGINEERING
COMPANY*

IRAN

H. BAHRAMI

*PhD candidate in Engineering Geology, FERDOWSI UNIVERSITY OF
MASHHAD*

IRAN

SLOPE STABILITY ANALYSIS IN GAMBIRI DIVERSION DAM USING NUMERICAL MODELS

S.SOLEYMANI¹, A.HEMMATI², H.BAHRAMI³

¹*Expert of Engineering Seismology, TOOSSAB CONSULTATNT ENGINEERING COMPANY*

IRAN

²*Expert of Geotechnical Engineering, TOOSSAB CONSULTATNT ENGINEERING COMPANY*

IRAN

³*PhD candidate in Engineering Geology, FERDOWSI UNIVERSITY OF MASHHAD*

IRAN

1-INTRODUCTION

Among various engineering projects, dams construction and their industry involves major challenges. Since 1980 construction of earth and rock fill dams are more common than other type of dams. The reasons for this common usage are: the method of construction is based on ordinary technology with utilization of cheap raw soil materials, subsurface materials and does not depend on particular valley shape. Also, geometric design of embankment dams depends on barrowed soil materials, subsurface conditions and type of construction. Consequently feasible design can cause significant reduction on construction time, materials and costs. One of the main important factors for the failure of earth dams is the slope stability analysis in their body and abutments. In order to prevent the dam failure, it is essential to control the stability in the earth dam.

In this paper, software analysis results consisting of slope stability analysis at different loading conditions of dam performance within its effective life, analysis of seepage from Gambiri diversion dam earth dyke body and foundation, are presented, based on which, geometric design of Gambiri diversion dam parts is performed.

The Gambiri diversion dam site is located in Kunar province, eastern Afghanistan, near Asadabad city as shown in "Fig. 1". The site location in the global coordinates system is defined with X =680248 and Y =3842647. The Gambiri diversion dam is an earth dam with a clay core and elevation from river bed is 10.5 meters.



Fig. 1

Location of the Gambiri diversion dam site in the eastern Afghanistan.

In order to identify and develop geological units within the project, geological map has been prepared based on field studies “Fig. 2”. According to the map, four sedimentary units with one hard formation of metamorphic rocks are observed within the project area. The sedimentary units include Quaternary sediments within the project area, deposited in the river-bed. Based on field surveys and the results of geotechnical studies, the Kunar River-bed sediments are mostly of rounded coarse aggregates in sizes of cobble, gravel, sand and small percentage of fines. From lithological point of view, some pieces of granite and gneiss stone are observed in these deposits. The Quaternary units overly the metamorphic unit in the diversion dam area. Metamorphic rocks are related to an early Proterozoic metamorphism (marked with X1gm sign).

No outcrops of this unit are observed around diversion dam site. The results of geophysical studies indicate that the depth to bedrock below earth surface at the diversion dam site is about 120 meters.

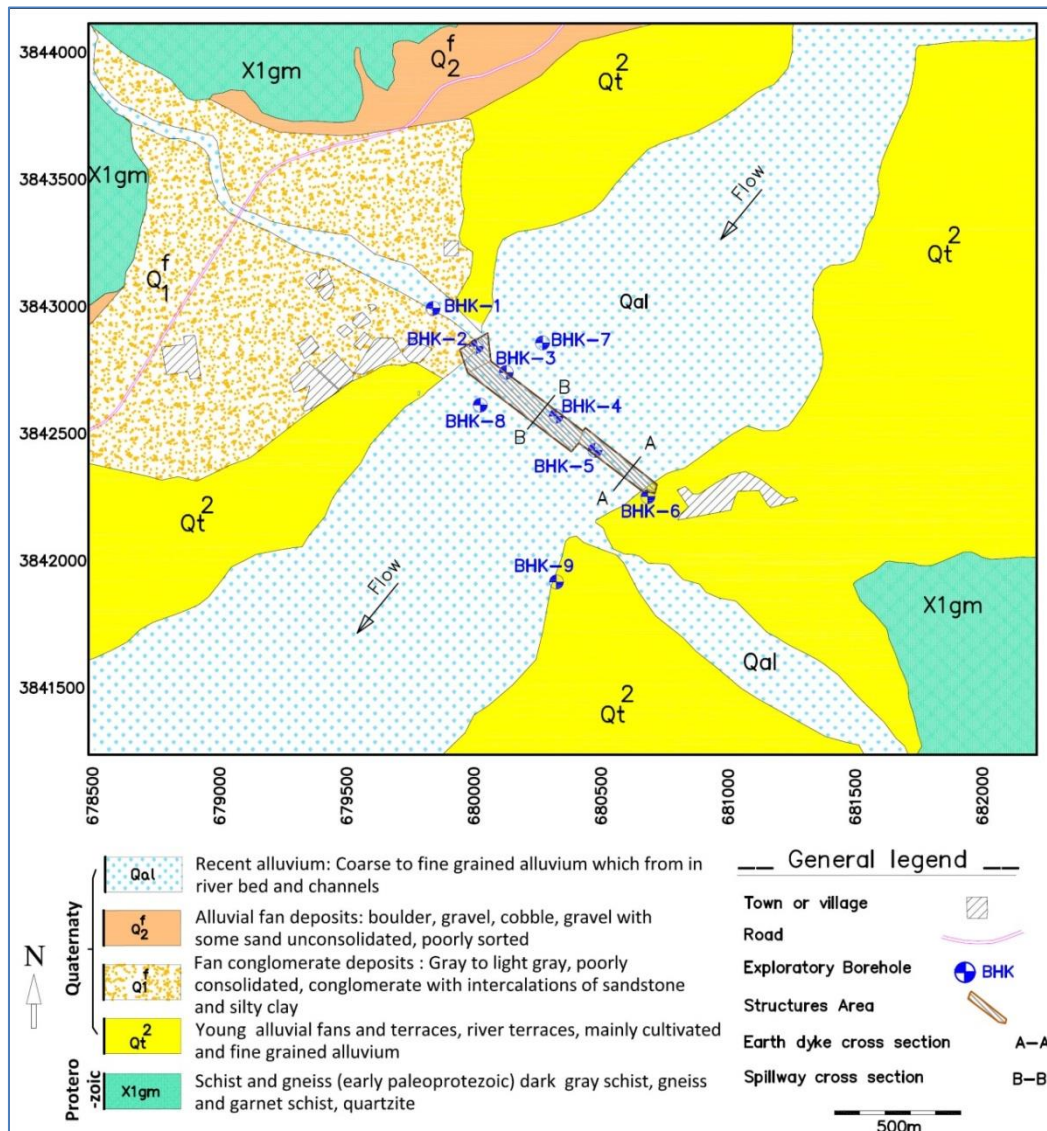


Fig. 2
Dam site geological map

2- ANALYSIS METHOD

In order to achieve the objectives of this study, Slope/W software [1] is used. This program can calculate the safety factor (FOS) using Bishop [2], Janbu [3], Morgenstern-Price [4] and Spencer [5] methods. SLOPE/W is one component in a complete suite of geotechnical products called Geo-Slope, one of whose powerful features of the integrated approach is that it opens the door to types of analyses of a much wider and more complex spectrum of problems, including the use of finite element computed pore-water pressures and stresses in a stability analysis [6]. Slope/W can effectively analyze both simple and complex problems for a

variety of slip surface shapes, pore-water pressure conditions, soil properties, analysis methods and loading conditions. In the present study, Morgenstern-Price method for slope stability analysis is used, which has more accuracy than modified Bishop Method while its difference with this method is negligible.

Minimum safety factor recommended for stability analysis in different loading conditions are given in “Table 1”. This table is prepared according to U.S. Army Corps of Engineers [7]. In slope stability analysis, failure safety factors calculated by limit equilibrium methods in different conditions of construction and operation are compared with allowable amounts recommended by references for downstream and upstream slopes [8].

Table 1.
Recommended safety factors for stability analysis at different conditions of diversion dam earth dyke

State	Situations	Minimum Safety Factor allowed	Explanations
1	End of Construction	1.3	Upstream & Downstream Slope
2	Seepage from partially full Reservoir	1.5	Upstream Slope
3	Water Rapid drawdown from Normal Level	1.2	Upstream Slope
4	Steady seepage from Normal Level	1.5	Downstream Slope
5	States 1.2 and 4 with Earthquake	1.0	Earthquake Coefficient

In the slope stability of upstream and downstream slopes of an earth-fill dam, stability analysis is generally performed in the following states:

- During or at the end of construction
- Operation state (steady seepage) and full reservoir (maximum water level)
- Each of above states in earthquake conditions
- Reservoir rapid drawdown

Considering each of these states, depends on the conditions of construction and operation stages. Important forces in slope stability analyses include water load and earthquake. In SLOPE/W software, excess pore pressure for different parts of materials can be defined. Pore pressure in soil resulted from construction can be defined as a percentage of vertical stress. In the current methods, pore pressure ratio (ru) is used instead of pore pressure (U_w). Usually according to experiences, ru is considered as 0.1 to 0.5. Pore pressure ratio (ru) is defined by [Eq. 1].

$$r_U = \frac{U_w}{\gamma z} \quad [1]$$

In which U_w is pore pressure, γ is soil specific gravity and z is the depth of study point. Earthquake effects can be simulated by pseudo-static method. Pseudo-static slope stability analysis is done by introduction of a horizontal earthquake coefficient (static acceleration as in seismic studies). Earthquake force is considered as a percentage of weight of each segment in this method.

In order to select pseudo-static acceleration, references suggest a ratio of 0.27 - 0.5 of peak seismic acceleration [9].

So for selection of final seismic acceleration, "Eq. [2]" is used:

$$K_h = 0.5 \frac{PGA_H}{g} \quad [2]$$

In this relation, PGA_H is the horizontal peak seismic acceleration. On this basis, seismic coefficients 0.14g and 0.18g are used for DBE seismic level (for end of construction and seepage from half full reservoir) and MDE seismic level (for other loading cases), respectively.

3- STABILITY ANALYSIS OF EARTH DYKE BODY SLOPES

All of the cross sections of an earth dam must be sufficiently stable in different loading conditions, to consider it safe and stable. Stability analysis of the critical cross section is done by investigation of foundation and abutments conditions. On this basis, body height and crest width of the maximum cross section are considered as 10.5 and 5 meters respectively.

3.1 ENGINEERING CHARACTERISTICS OF EARTH DYKE FOUNDATION AND BODY MATERIALS

In this analysis, dyke foundation is assumed to consist of two major layers:

- Upper alluvial layer consisting of sand and gravel with average density and a thickness of about 10 m
- Lower dense layer of sandy gravel with thickness about 60 m

Shear strength parameters used in the stability analyses for different parts of body and foundation are presented in "Table 2".

Table 2
Strength parameters of the different parts of body and foundation of earth dyke
of Gambiri diversion dam

Materials	γ_{wet} (KN/m ³)	γ_{sat} (KN/m ³)	Internal Friction Angle (Degree)	Cohesion (KN/m ²)
Upper Foundation (0-10m)	-	20	33	0
Lower dense Foundation (10-70m)	-	22	40	0
Rip Rap	22	22.5	40	0
Mixed Materials of Dyke Body (UU Parameters)	20.5	20	33	5
Mixed Materials of Dyke Body (Total Parameters)			25.4	10
Mixed Materials of Dyke Body (Effective Parameters)			29.2	6
Filter	19.5	20.5	30	0
Drain	20	20.5	31	0

3.2 ANALYSIS CONDITIONS

With attention to prior comments and according to construction and operation conditions, stability analyses of earth dyke were performed as below.

3.3 END OF EMBANKMENT CONSTRUCTION (EARTH DYKE)

In this state, embankment (earth dyke) construction is assumed to have been terminated but pore pressures due to dam construction still exist. Both upstream and downstream slopes are subject to instability. Critical condition is when the pore pressure in low permeable parts of embankment (earth dyke) is in maximum. To take pore pressures into account, stability analyses are performed by use of total stress parameters from UU triaxial test.

For relevant pseudo-static analysis, because of rather short duration of this state compared to dam life, using MDE seismic level is conservative. So DBE seismic level and acceleration of 0.14g is selected.

3.4 SEEPAGE FROM PARTIALLY FULL RESERVOIR

Here, half of the reservoir is assumed to be full and upstream slope is prone to instability. In this state, parameters of materials are selected from CD (drained) triaxial tests. Subjects mentioned about pseudo-static analysis at the end of construction, are universal in this condition too. So by DBE seismic level and prior comments acceleration 0.14 g is selected.

3.5 RAPID DRAWDOWN

Rapid drawdown happens when it is required to discharge reservoir water in a short time. It can cause upstream slope instability. Upstream slope stability in this condition is usually related to permeability of shell. Occurrence probability of this state in the diversion dams is too low.

In this state, parameters of low permeable materials are selected from CU triaxial test. This state is analyzed by assuming water in the maximum and normal levels.

3.6 STEADY SEEPAGE

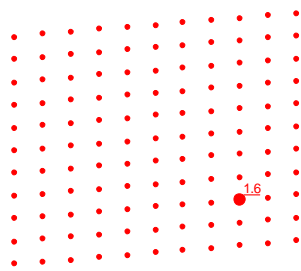
In this state, downstream slope is subject to instability due to seepage forces. In this state parameters of materials are selected from CD triaxial test (like "seepage from partially full reservoir" condition). In this report steady seepage state is analyzed considering reservoir water in the maximum and normal levels. In the pseudo-static analysis using MDE seismic level and prior comments acceleration 0.18 g is selected.

Summary of results has been presented in "Fig. 3 to 6".

4- CONCLUSION

In the present study Slope/W software is used under different conditions to evaluate slope stability. Analyzes for each state and each slope with Morgenstern-Price methods is calculated that the minimum safety factor in each of this method, be considered as a safety factor (FOS) of slope stability. Stability analyses has done based on common finite element method at different loading conditions, and the results showed that dam body has no specific problem in terms of stability.

Based on the results from all slope stability analyses performed on critical section of Gambiri earth dyke in different loading conditions (static and pseudo-static analysis), it is observed that dyke body with upstream slope of 1:3 (vertical: horizontal) and downstream slope of 1: 2.5 (vertical: horizontal) is always stable.



Gambiri Dam:
 Analysis Method: Morgenstern-Price
 Direction of Slip Movement: Right to Left
 Slip Surface Option: Grid and Radius
 P.W.P. Option: Piezometric lines with Ru
 Tension Crack Option: (none)
 Seismic Coefficient: (none)

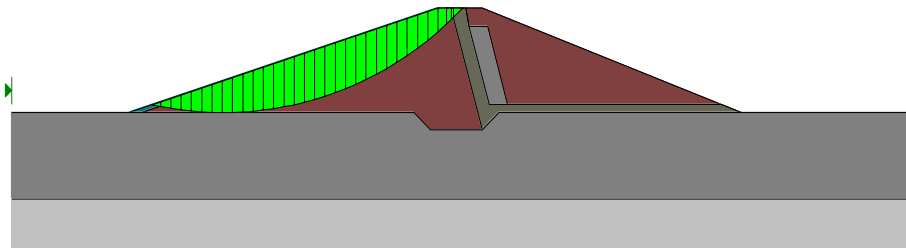
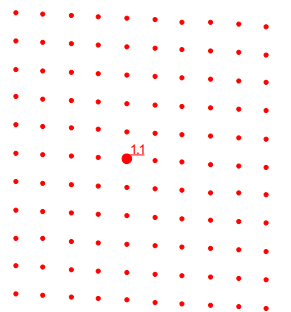


Fig. 3
 Failure plane of upstream slope of Gambiri earth dyke at the “end of construction”
 - static analysis



Gambiri Dam:
 Analysis Method: Morgenstern-Price
 Direction of Slip Movement: Left to Right
 Slip Surface Option: Grid and Radius
 P.W.P. Option: Piezometric lines with Ru
 Tension Crack Option: (none)
 Seismic Coefficient: Horizontal

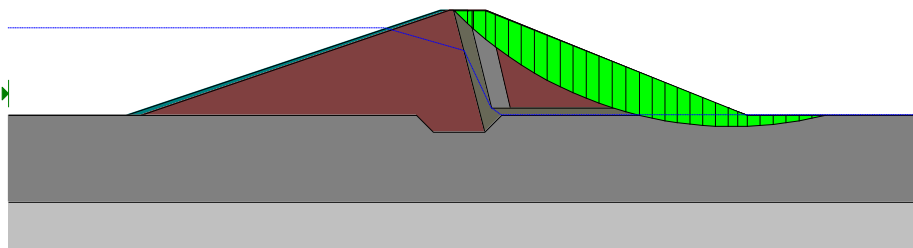
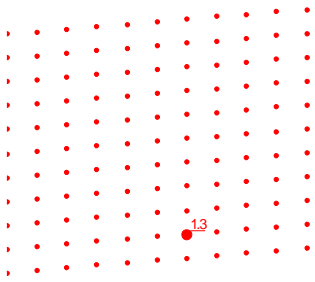


Fig. 4
 Failure plane of downstream slope of Gambiri earth dyke in “steady seepage”
 conditions - pseudo-static analysis (0.18 g)



Gambiri Dam:
 Analysis Method: Morgenstern-Price
 Direction of Slip Movement: Right to Left
 Slip Surface Option: Grid and Radius
 P.W.P. Option: Piezometric lines with Ru
 Tension Crack Option: (none)
 Seismic Coefficient: Horizontal

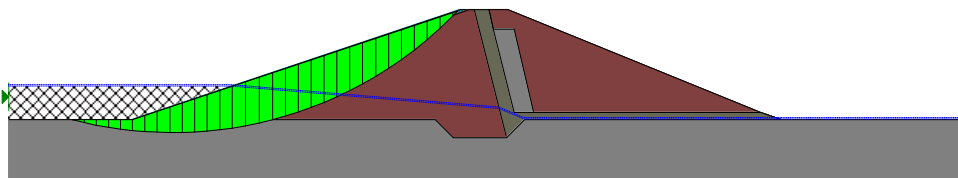
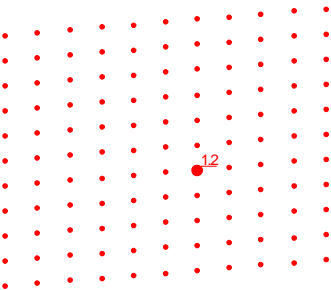


Fig. 5
 Failure plane of upstream slope of Gambiri earth dyke in “partially full reservoir conditions”- pseudo-static analysis (0.14 g)



Gambiri Dam:
 Analysis Method: Morgenstern-Price
 Direction of Slip Movement: Right to Left
 Slip Surface Option: Grid and Radius
 P.W.P. Option: Piezometric lines with Ru
 Tension Crack Option: (none)
 Seismic Coefficient: (none)

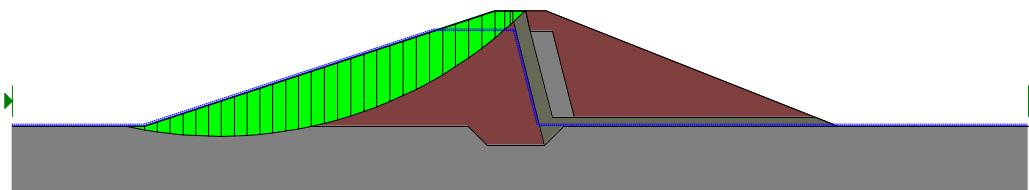


Fig. 6
 Failure plane of upstream slope of Gambiri earth dyke in “rapid draw-down from maximum water level” conditions-static analysis

REFERENCES

- [1] GEO-SLOPE, Slop/W. software user guide, *Geoslope International Ltd., Calgary, 2004, Canada.*
- [2] BISHOP, A.W. The use of the slip circle in the stability analysis of slopes, *Geotechnique*, 1955, 5 (1), 7–17.
- [3] JANBU, N. Applications of Composite Slip Surfaces for Stability Analysis. *In Proceedings of the European Conference on the Stability of Earth Slopes, Stockholm, 1954, Vol. 3, p. 39-43.*
- [4] MORGENSTERN, N.R., AND PRICE, V.E. The Analysis of the Stability of General Slip Surfaces. *Geotechnique*, 1965, Vol. 15, pp. 79-93.
- [5] SPENCER, E. A Method of Analysis of Embankments assuming Parallel Interslice Forces. *Geotechnique*, 1967, Vol 17 (1), pp. 11-26.
- [6] KRAHN, J. Stability Modelling with Slope/W, an engineering methodology, *Geo-slope/W International, Ltd, 2004.*
- [7] U.S. ARMY CORPS OF ENGINEERS, Stability of Earth and Rock-Fill Dams ,*U. S. Department of Army, Corps of Engs., 1970, EM110-2-1902 .*
- [8] SHARMA, H. D., Embankment Dams, *Oxford & IBH publishing co., 1991.*
- [9] KRAMER, S. L., Geotechnical Earthquake Engineering, 1996.

COMMISSION INTERNATIONALE
DES GRANDS BARRAGES

VINGT-SIXIÈME CONGRÈS DES
GRANDS BARRAGES
Autriche, juillet 2018

**A METHODOLOGY FOR THE MAPPING OF TERRAIN MORPHOLOGY OF
DAM BASINS BY MEANS OF SPACEBORNE SAR IMAGES**

Giovanni NICO¹, Alfredo PITULLO², Catarina VALENTE³

¹*Researcher, CONSIGLIO NAZIONALE DELLE RICERCHE, ISTITUTO PER LE
APPLICAZIONI DEL CALCOLO*

²*Technical Officer, CONSORZIO DI BONIFICA DELLA CAPITANATA*

³*Researcher, DIAN SRL*

ITALY

Joao CATALAO

Professor, UNIVERSIDADE DE LISBOA, FACULDADE DE CIENCIAS

PORTUGAL

EXTENDED ABSTRACT

The dam basin and the area around it could be affected by important geological phenomena such as slope instability, erosion and sedimentation. Recently, a new methodology for the mapping of intertidal zone in estuarine, based on the use of Synthetic Aperture Radar (SAR) images [1]. This result makes the use of SAR images an interesting alternative for the mapping of small changes of terrain morphology due to erosion and sedimentation. The intensity variations in a SAR image are related to the surface roughness and dielectric properties as well as to the polarimetric properties and the local incidence angle of SAR acquisition. Geometrical distortions such as foreshortening, layover and shadowing strongly affect the amplitude of SAR images in mountainous regions and even in areas with a moderate topography. A water basin appears as a dark patch on a SAR image as a result of the surface

specular reflection. The exposed terrain surface behaves as a diffuse reflector due to the terrain roughness. This property of SAR image intensity allows to identify the waterline and distinguish between the dam lake and the terrain surface around it. The waterline of dam basin changes in time according to the water level. As a consequence, if the time series of water levels is known, the temporal evolution of the waterline can be observed and the land/water separation used to generate the DEM of the dam basin. The precision of terrain morphology estimation depends on the precision of water level measurements. The proposed algorithm is based on the assumption that soil moisture and roughness have different temporal scales. The idea of this work is to use the temporal changes of water level in the dam basin to map the terrain morphology of the whole area covered by water during the maximum extension of the lake. This would allow to identify areas in the dam basin where soil accumulated due to sedimentation or affected by soil depletion due to erosion and so to estimate the seasonal variation of useful water volume of the dam. Furthermore, this would also help to map the lake shoreline variations due to erosion as a function of the water level. The result depends on the spatial resolution of SAR images and the wavelength of the SAR sensor. The spatial resolution provides the precision of the waterline identification and so the spatial resolution of the DEM. The wavelength directly affects the scattering properties of terrain and water surfaces and so the capability to distinguish between water and land which at the basis of the proposed methodology. Furthermore, the application of the methodology depends also on the exposure of the dam basin with respect to the line-of-sight of current spaceborne SAR sensors which are always moving along a polar orbit. It could happen that portions of the lake cannot be observable on SAR images, especially in mountain areas, due to shadow effects. In this work we used X-band CosmoSkyMed to map the terrain morphology of the earth-filled dams of the Consorzio di Bonifica di Capitanata, located in the Apulia region, southern Italy.

REFERENCES

- [1] CATALAO J., NICO G. Multitemporal Backscattering Logistic Analysis for Intertidal Bathymetry. *IEEE Transactions on Geoscience and Remote Sensing*, 2017, Nr. 55(2), 1066.

COMMISSION INTERNATIONALE DES GRANDS BARRAGES

VINGT-SIXIÈME CONGRÈS DES GRANDS BARRAGES
Autriche, juillet 2018

DOI 10.3217/978-3-85125-620-8-230



This work licensed under a Creative Commons Attribution 4.0 International License. <https://creativecommons.org/licenses/by-nc-nd/4.0/>

MODELLING EARTH-FILLED DAMS: MERGING GBSAR AND TRADITIONAL MEASUREMENTS

Giovanni. NICO

Researcher, CONSIGLIO NAZIONALE DELLE RICERCHE, ISTITUTO PER LE APPLICAZIONI DEL CALCOLO, BARI

ITALY

Marco. CORSETTI

Technical Officer, UNIVERSITÀ DELLA SAPIENZA, FACOLTÀ DI INGEGNERIA, ROME

ITALY

Alfredo PITULLO

Technical Officer, CONSORZIO DI BONIFICA DELLA CAPITANATA, FOGGIA

ITALY

Andrea. DI PASQUALE

Researcher, DIAN SRL, MATERA

ITALY

COMMISSION INTERNATIONALE
DES GRANDS BARRAGES

VINGT-SIXIÈME CONGRÈS DES
GRANDS BARRAGES
Autriche, juillet 2018

**MODELLING EARTH-FILLED DAMS: MERGING GBSAR AND TRADITIONAL
MEASUREMENTS**

Giovanni. NICO

*Researcher, CONSIGLIO NAZIONALE DELLE RICERCHE, ISTITUTO PER LE
APPLICAZIONI DEL CALCOLO*

BARI, ITALY

Marco. CORSETTI

Technical Officer, UNIVERSITA DELLA SAPIENZA, FACOLTA DI INGEGNERIA

ROME, ITALY

Alfredo PITULLO

Technical Officer, CONSORZIO DI BONIFICA DELLA CAPITANATA

FOGGIA, ITALY

Andrea. DI PASQUALE

Researcher, DIAN SRL

MATERA, ITALY

SUMMARY

A methodology to measure displacement of earth-filled dams by means of Synthetic Aperture Radar (SAR) interferometry is described. The methodology is applied on both ground-based and spaceborne SAR data.

1. INTRODUCTION

The mechanical parameters of earth dams is one of the key issues of geotechnical problems. Parameter back-analysis using internal or external monitoring data has been proven to be an efficient way to solve this problem. In fact, based on the identified parameters, the stability and security analysis can be investigated using the finite element method (FEM). However, traditional internal or external monitoring methods have limitations in efficiency, long-term monitoring and spatial coverage. The internal monitoring methods include e.g. tension wire alignment, hydraulic overflow settlement gauges, extensometers. However, these internal monitoring methods do not meet the safety monitoring requirements of large dams in terms of efficiency and long-term observations because of their low coverage and durability, and labour-intensive monitoring needs. Traditionally, external monitoring methods include levelling or Global Position System (GPS) measurements, but they are rarely used in back-analysis because of their low coverage. Therefore, the external monitoring results from the InSAR observation can be used as a integration for traditional monitoring methods to analyse the parameters of the dam. In this work we present the results which have been obtained within the AIM-DAMS project for the monitoring of earth-filled dams. The project has been funded by the Apulia Innovation Agency. Both Ground-Based and Spaceborne SAR systems have been used. Ground-based radar interferometry has provided deformation measurements of earth-filled dams of the Consorzio di Bonifica di Capitanata, located in the Apulia region, southern Italy. Earth dams have similar scattering properties as landslides for which the Ground-Based Synthetic Aperture Radar (GBSAR) technique has been so far extensively applied to study terrain displacements [1]. In this work, SAR and Real Aperture Radar (RAR) configurations are used for the measurement of earth dam surface deformations. A methodology is described for the acquisition of SAR data and the rendering of results. The geometrical correction factor needed to transform the Line-Of-Sight (LOS) deformation measurements of GBSAR into an estimate of the horizontal deformation vector of the dam surface is derived. Furthermore, a methodology for the acquisition of RAR data and the representation of deformation temporal profiles and vibration frequency spectrum of dam concrete structures is presented. For this study, a ku-band ground-based radar equipped with horn antennas having different radiation patterns have been used. Spaceborne radar interferometry provided maps of vertical deformation of the dam crown. X-band CosmoSkyMed SAR images have

been processed using the Persistent Scatterer technique. This technique uses a time series of SAR images acquired over the the same region. Examples of application of single couples of SAR images to the measurements of vertical deformations of dams have been already published in the literature [2].

2. MONITORED DAMS

Four earth-filled dams were monitored, all located in the Apulia and Campania regions, southern Italy and managed by the Consorzio di Bonifica di Capitanata. The four dams are:

- 1) Occhito, on the Fortore river. It has been built between 1958 and 1966 and started to operate in 1972. It has one of the largest dam basins in Europe. The dam is located on the northern part of the Apulia region, in the districts of Carlantino and Celenza Valfortore, on the border between Apulia, Campania and Molise regions;
- 2) Capaccio, on the Celone river. It has been built between 1992 and 1997 and started to operate in 2000. It is located in the district of Lucera, on the northern part of the Apulia region;
- 3) Marana Capacciotti, on the Ofanto river. It has been built between 1969 and 1976, and started to operate in 1987. It is located 13.5 km south-west of the Cerignola city, on the northern part of the Apulia region, precisely;
- 4) San Pietro, on the Osento river. It has been built between 1958 and 1966, and started to operate in 1972. It is located in Aquilonia district, on the western part of the Campania region, on the border with the Basilicata region.

Figure 1 displays the Google© snapshots of the four dams with the installation sites of SAR acquisitions to derive the displacement maps of dam surfaces.

3. SYNTHETIC APERTURE RADAR INTERFEROMETRY

A Synthetic Aperture Radar (SAR) is an active microwave sensor used to produce 2D microwave images of the observed scene [1][2]. The main advantage of microwave images is their capability to observe a scene without the need of solar illumination and in any weather condition. The SAR interferometry (InSAR) technique consists in processing two SAR images of the same scene obtained either from two slightly displaced positions or from the same position. The acquisition geometry is typical of repeat-pass space SAR interferometry, while the second geometry is common in ground-based SAR interferometry.

Differencing the phase of two coherent complex-valued SAR images provides information on displacement phenomena of terrain or structures. Using data of both current and past spaceborne SAR missions, it is possible to monitor current displacement and to study displacement phenomena occurred or started in the recent past. The SAR interferometry provides only the Line-of-Sight component of the real displacement, i.e. the component along the radar line of sight. For this reason, the displacements measured by spaceborne SAR sensors are mainly related to a vertical movement of the observed scene, being the sensors looking downward with a look angle variable depending on the acquisition configuration. The technique of Ground-Based Synthetic Aperture Radar (GBSAR) interterferometry uses a frequency band 16.70–16.78 GHz. The working range distance to the study area ranges from about less than 100 m up to more than 7000 m.

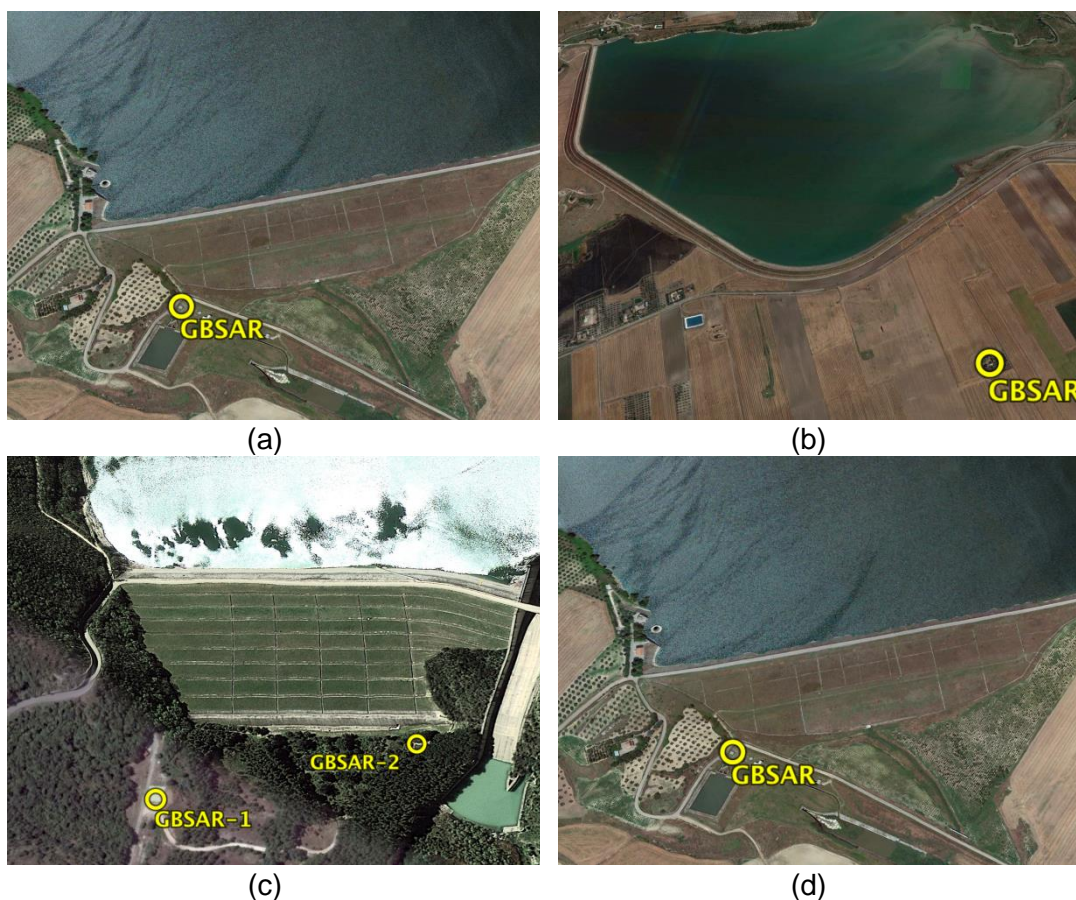


Fig. 1. From the top-left to the bottom-right, Google[®] snapshots of Marana-Capacciotti dam on the Ofanto river, Cerignola; Capaccio dam on the Celone stream, Lucera; Occhito dam on the Fortore river, Carlantino and San Pietro dam on the Osento stream, Aquilonia. The GBSAR installation sites are also shown. (after Di Pasquale et al. [1]).

The scene is mapped in terms of range and azimuth distances, where the azimuth direction is set by the orientation of the rail. The advantage of GBSAR interferometry with respect to many traditional techniques is its capability to

provide areal information on the displacement field rather than measurements of displacements in only a few points. The precision of SAR interferometry measurements of displacements are in the order of a fraction of centimeter for spaceborne SAR sensors, and of a fraction of millimeter for GBSAR interferometry, depending on the temporal coherence of the scene, depending on the landcover characteristics. The accuracy mainly depends on the correction of phase delays due to microwave propagation in atmosphere.

4. RESULTS

In this section we present a few results which were obtained by SAR interferometry, processing both spaceborne and ground-based SAR data. The use of spaceborne SAR data is an effective tool to vertical displacements due to subsidence phenomena. In this case, GBSAR sensors cannot be effectively used since the fraction (LOS component) of a vertical movement they can measure is very small. For the observation of horizontal displacements of the dam surface, spaceborne SAR sensors are most appropriate and for this reason a GBSAR system was used. For the sake of brevity, we present only the results referred to the Occhito dam. More results can be found in Di Pasquale et al. [1]. Concerning spaceborne SAR interferometry, a set of twenty Cosmo-Sky-Med X-band SAR images was processed. Images were acquired over the area around the Occhito dam. Images were acquired between 7 August 2013 and 3 March 2014. Each image was characterized by a 3m spatial resolution. Figure 2 shows a portion of the CSK amplitude image with the Occhito lake and details of the dam, which is located at the bottom of the lake image. It can be observed how the structures of the crown and down-stream surface of the dam can be easily identified.

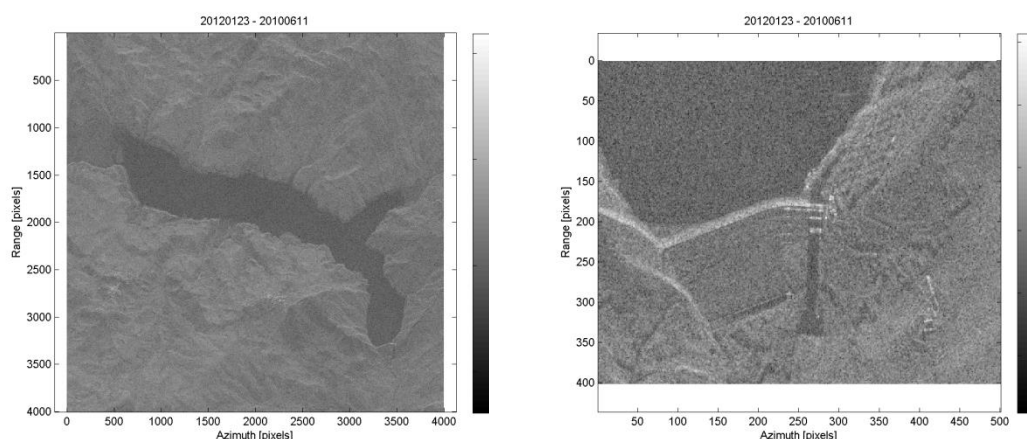


Fig. 2: Occhito lake and detail of the dam as observed by spaceborne CSK SAR image (after Mascolo et al. [3]).

A Persistent Scatterer (PS) analysis has been done to measure the mean displacement of the of both the crown and the whole down-stream surface of the

dam. Figure 3 display the maps of mean displacement velocity and the corresponding precision.

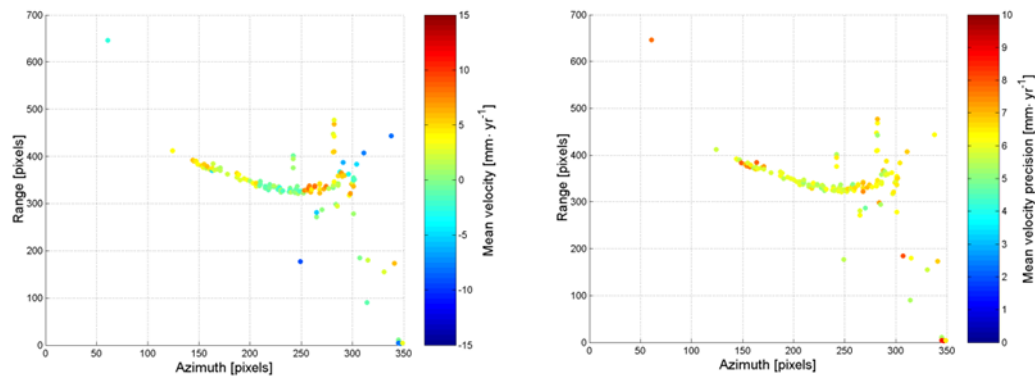


Fig. 3: Mean displacement velocity and precision. Maps are referred to the Occhito dam (see Fig. 2)

Concerning ground-based SAR interferometry, four data acquisition campaigns were carried out at the Occhito dam from 27 May 2014 to 3 March 2014. Two different acquisition sites were selected on the right and left of the downstream side of the dam. Figure 4 reports the portions of the dam observed by the two GBSAR positions and the corresponding displacement maps, obtained using a temporal baseline of about six months. The results of this work show the information that a ku-band ground-based and X-band spaceborne SAR data can provide time series of displacement maps with high spatial resolution and time sampling frequency. Besides being useful to define monitoring protocols of earth-filled dams, the information provided by SAR interferometry could be used to perform back analyses also when other monitoring data are not available, and to implement a calibration procedure to set up a reliable numerical model.

5. ACKNOWLEDGMENTS

Cosmo-Sky-Med SAR data have been provided within the project COSMO-SkyMed/RADARSAT-2 AO "Pilot project for the multifrequency and multiplatform InSAR slope stability monitoring of earth dams: merging spaceborne C and X-band and ground-based Ku-band SAR images".

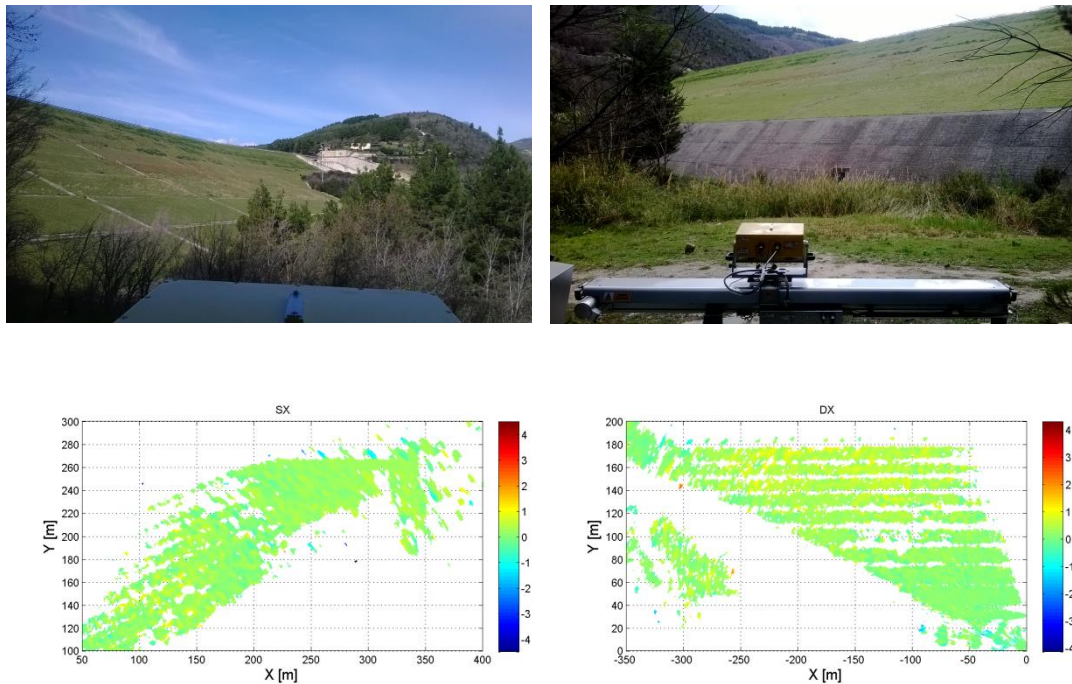


Fig. 4. Occhito dam, Carlantino. From the top to the bottom, photo of the dam as observed from the GBSAR position and displacement map. Data have collected by two GBSAR systems installed on the left (SX) and right (DX) downstream sides of the dam (see also Fig. 1). (after Di Pasquale et al. [1]).

REFERENCES

- [1] DI PASQUALE A., NICO G., PITULLO A., PREZIOSO G. Monitoring strategies of earth dams by ground-based radar interferometry: how to extract useful information for seismic risk assessment. *Sensors*, 2018, Nr. 18, 244, doi:10.3390/s18010244.
- [2] DI MARTIRE D., IGLESIAS, R., MONELLS, D., CENTOLANZA, G., SICA, S., RAMONDINI, M., PAGANO, L., MALLORQUI J.J., CALCATERRA, D., Comparison between differential SAR interferometry and ground measurements data in the displacement monitoring of the earth-dam of Conza della Campania (Italy). *Remote sensing of environment*, 2014, Nr. 148, 58–69,
- [3] MASCOLO L., NICO G., DI PASQUALE A., PITULLO A., Use of advanced SAR monitoring techniques for the assessment of the behaviour of old embankment dams, *Proc. SPIE 9245, Earth Resources and Environmental Remote Sensing/GIS Applications V*, 2014, 92450N, doi: 10.1117/12.2067363.

COMMISSION INTERNATIONALE
DES GRANDS BARRAGES

VINGT-SIXIÈME CONGRÈS DES
GRANDS BARRAGES
Autriche, juillet 2018

CRITICAL REVIEW OF DAM BREACH PARAMETERS

Ahmed H. SOLIMAN¹, Hesham BEKHIT², Alaa EL ZAWAHRY³

*¹Assistant Professor, Irrigation and Hydraulics Department, Faculty of
Engineering, CAIRO UNIVERSITY*

*²Professor of Water Resources, Irrigation and Hydraulics Department, Faculty of
Engineering, CAIRO UNIVERSITY*

*³Professor of Hydraulics, Irrigation and Hydraulics Department, Faculty of
Engineering, CAIRO UNIVERSITY*

EGYPT

ABSTRACT

The rate of dam construction has been rapidly increasing in the last two centuries especially embankment dams. This may be attributed to the increase of water scarcity all over the world. Embankment dams represent the major portion of dams in the world. It represents about 80% of dams in the United States. One of the major risks that are associated with dam construction is dam failure. Dam failure is a catastrophic event where both peak flow and volume significantly affect downstream property and could result in loss of life. The amount of the affected property and loss of life depend on the inundated area and the degree of inundation, which are in turn a function of the reservoir size and other breach parameters. Because of the high risk associated with dam failure, especially for large dams, international standards recommend performing a dam break analysis during the design stage, in which the designer should study the effect of dam failure on the downstream region. So, it is very important to accurately represent the

breach process and its final opening dimensions to mitigate flood hazards due to dam failure. Several studies were conducted to predict dam breach parameters. This paper presents a critical review of the available studies.

A comparison between the available equations for prediction of dam breach parameters is conducted to select the best equations for each breach parameter using the breach parameters of about 1400 dam failure events. The comparison between the existing equations is based on the coefficient of determination (R^2) and Root Mean Squared Error (RMSE). So, the equation which has the minimum RMSE and the maximum R^2 will be described as the best equation for this parameter. Also, the available equations is sorted from the best to the worst based on the same two evaluation factors.

Applying the comparison criteria, **Fehler! Verweisquelle konnte nicht gefunden werden.** (see fullpaper) presents the sorting of the existing prediction equations from the best to the worst equation based on R^2 and RMSE.

Based on the comparison and its results (presented in **Fehler! Verweisquelle konnte nicht gefunden werden.**- see fullpaper), it is found that Soliman 2015 equations for H_f and B_{avg} prediction are the best equations followed by Elsayed 2018 equations for the same two parameters. Regarding T_f , Elsayed 2018 is classified as the best equation based on R^2 while Von Thun & Gillette, 1990 is classified as the best equation based on RMSE and both are followed by Soliman 2015 equation.

Additionally, it is very clear from the above table that the prediction equations for T_f are uncertain as all of them have very low values for coefficient of determination (R^2). So, additional investigation and analysis should be conducted in future to find a better equation for formation time prediction.

COMMISSION INTERNATIONALE DES GRANDS BARRAGES

VINGT-SIXIÈME CONGRÈS DES GRANDS BARRAGES
Autriche, juillet 2018

DOI 10.3217/978-3-85125-620-8-232



This work licensed under a Creative Commons Attribution 4.0 International License. <https://creativecommons.org/licenses/by-nc-nd/4.0/>

SLOPES STABILITY IN THE CATCHMENT AREAS AND EFFECT OF LARGE-SCALE ROCKSLIDE DAMMING ON HYDRAULIC PROJECTS SAFETY BY EXAMPLE OF CATCHMENT AREAS OF VAKHSH AND SIANG RIVERS

Ruslan SHAKIROV

Team leader (Rogun dam), JSC "HYDROPROJECT INSITUTE"

RUSSIA

Ekaterina SHILINA

Chief expert in hydrology, JSC "HYDROPROJECT INSITUTE"

RUSSIA

Alexander STROM

*Chief expert in seismic geology, GEODYNAMICS RESEARCH CENTER –
BRANCH OF JSC "HYDROPROJECT INSTITUTE"*

RUSSIA

Anatoly ZHIRKEVICH

*Deputy Head of the Hydrological Department, JSC "HYDROPROJECT
INSTITUTE"*

RUSSIA

COMMISSION INTERNATIONALE
DES GRANDS BARRAGES

VINGT-SIXIÈME CONGRÈS DES
GRANDS BARRAGES
Autriche, juillet 2018

**SLOPES STABILITY IN THE CATCHMENT AREAS AND EFFECT OF LARGE-
SCALE ROCKSLIDE DAMMING ON HYDRAULIC PROJECTS SAFETY BY
EXAMPLE OF CATCHMENT AREAS OF VAKHSH AND SIANG RIVERS**

Ruslan SHAKIROV¹, Ekaterina SHILINA², Alexander STROM³, Anatoly
ZHIRKEVICH⁴

1 – Team leader (Rogun dam), JSC "HYDROPROJECT INSITUTE"

2 – Chief expert in hydrology, JSC "HYDROPROJECT INSITUTE"

*3 – Chief expert in seismic geology, GEODYNAMICS RESEARCH
CENTER – BRANCH OF JSC "HYDROPROJECT INSTITUTE"*

*4 – Deputy Head of the Hydrological DEPARTMENT, JSC "HYDROPROJECT
INSTITUTE"*

RUSSIA

1. INTRODUCTION

Assessment of slopes' stability is an important part of site investigations for hydraulic projects, especially in mountainous regions. Necessity of such investigation directly at the dam site is obvious. The 1963 Vajont disaster highlighted their importance at and above the reservoirs' rims to avoid collapse of large rock masses in the water body. However, quite adverse effects for hydraulic structures might be produced by powerful outburst floods caused by breach of naturally dammed lakes in the catchment area, upstream from the reservoir. While most of such floods occur due to breach of the moraine and glacier lakes, the most hazardous are associated with the breach of large rockslide dams that could create lakes comparable or exceeding reservoirs' flood-control storage.

Several examples of powerful outburst floods after breach of the historical and prehistoric rockslide dams and their effects will be presented, demonstrating what could occur downstream in the valley. Extreme level of the potential threat associated with such phenomena shows that adverse effects of the river-

damming rockslide must be taken into consideration not only if such blockage already exist in the catchment area but also if it can be anticipated there during the dam's lifetime [1]. It is exemplified by case studies from the Pamir and Himalayas, in the Vakhsh and the Siang (Brahmaputra) River basins correspondingly, where large hydraulic schemes are under construction or planned in future.

2. HISTORICAL AND PREHISTORIC OUTBURST FLOODS CAUSED BY CATASTROPHIC BREACH OF LARGE ROCKSLIDE DAMS

Breach of large rockslide-dammed lake could produce flood with peak discharge exceeding those caused by hydro-meteorological processes significantly. It can be exemplified by historical events and by prehistoric case studies, which parameters can be derived from the geomorphic observations.

2.1. HISTORICAL DISASTERS

In 1786 breach of seismically induced rockslide dam in the Dadu River in Sichuan, China, claimed about 100 000 lives, thus being the most disastrous catastrophe associated with a single slope failure [2, 3]. In 1841 and in 1885 catastrophic outburst floods affected Indus River valley at a distance exceeding 420 km where water raised up to 25 m [4, 5]. In 1914 breach of the prehistoric rockslide dam in the Rio Barrankos valley, in Argentina, and release of about 1.5 km³ of water resulted in outburst flood that devastated Rio Colorado valley for about 1000 km long passage up to Atlantic Ocean [6]. Powerful outburst flood with 100 m high surge wave just downstream from the 220 m high Bairaman landslide dam occurred in 1985 in Papua New Guinea [7]. In 2000 breach of the rockslide dam in the Yigong River valley – the left tributary of the Tsangpo-Siang-Brahmaputra River in Tibet, China and release of about 2 km³ of water stored behind the 55 m high dam (level of the artificially excavated spillway) resulted in ~120 000 m³/s peak discharge that was recorded 17 km downstream from the dam. In India, more than 400 km downstream, it was about 44,200 m³/s [8, 9].

2.2. EVIDENCE OF THE PREHISTORIC OUTBURST FLOODS

Similar catastrophic phenomena occurred in most of mountainous regions in the past as well. The disastrous potential of such events can be exemplified by the extraordinary prehistoric outburst flood with estimated peak discharge up to 400 000 – 500 000 m³/s, which traces were found in the Sarydjaz-Aksu River valley in Xingiang (China) [10]. Flood was caused by the breach of a gigantic,

300-350 m high dam formed by the rockslide about $900 \times 10^6 \text{ m}^3$ in volume (41.764° N , 79.526° E). The dammed lake was approximately 31 km long and could store up to $2.2 - 2.5 \text{ km}^3$ of water. Due to color contrast of rockslide debris and the terraces downstream, the distinct traces of the outburst flood indicate that the surge wave immediately downstream from the breached dam was up to 120 m above the riverbed and $\sim 700 \text{ m}$ wide (Fig. 1). About 16-20 km downstream, after passing a narrow gorge, this flood left the amygdaliform branching ravines on the 50-60 m high right bank terrace (Fig. 2). Farther downstream this extraordinary flood spread over the 630 km^2 older alluvial fan formed by the Sarydjaz-Aksu River at the feet of the Tien Shan Mountains [10].

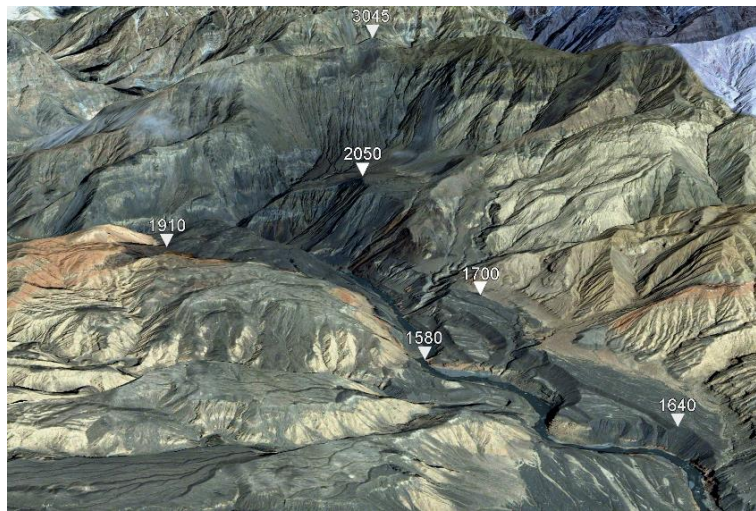


Fig. 1

Breached Sarydjaz-Aksu rockslide dam and traces of the outburst flood. 3D Google Earth view. Numbers indicate altitude in m a.s.l. After [10], with permission of Elsevier

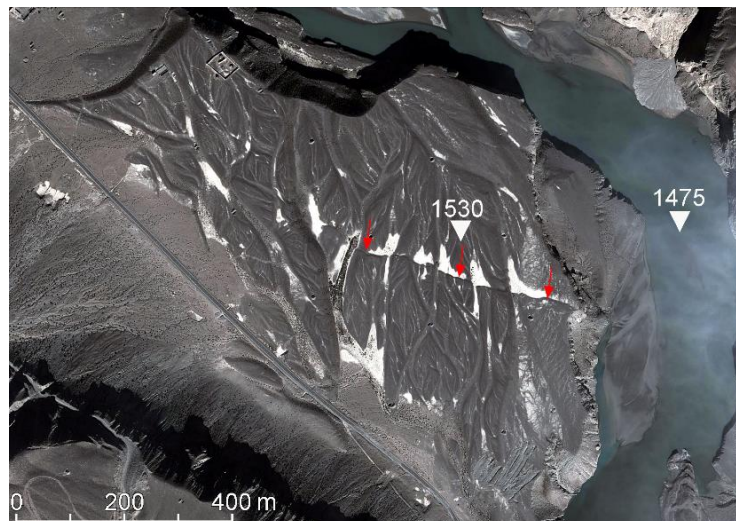


Fig. 2

Traces of the outburst flood on the 50-60 m high Aksu River terrace. Red arrows mark a small fault. Google Earth image. After [10], with permission of Elsevier

3. POTENTIAL BLOCKAGES IN THE VAKHSH CATCHMENT AREAS UPSTREAM FROM THE ROGUN RESERVOIR

Case studies described above strengthen the concern on what might occur if similar blockage would originate in the catchment areas of the existing or proposed hydraulic schemes with large reservoirs.

Several potentially hazardous sites where large lakes can be dammed either by surging glaciers or by rockslides were identified in the Muksu and the Obi-Khingou River valleys draining northern parts of the Pamir mountains, upstream from the 330 m high rock-filled Rogun dam that is under construction now, far away from its reservoir (Fig. 3). Size of the potential slope failures and of the dams that can be created were estimated according to expert judgment. Taking in mind that, due to lack of the detailed information, no quantitative assessment of slopes' and blockages' stability is possible at present, we considered the most conservative scenarios: failure of the entire slope with real evidence of instability (fractures, scarps, etc.) followed by the dammed lake impoundment up to the blockage crest level and its catastrophic breach due to overtopping.

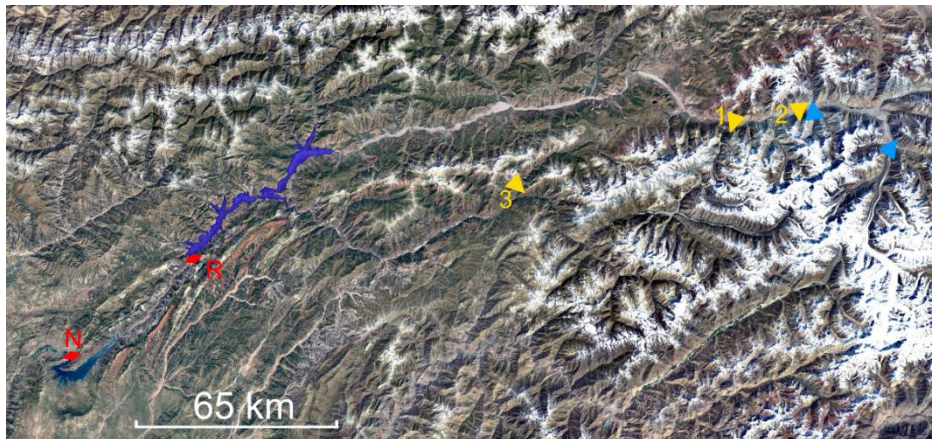


Fig. 3

Location of sites in Vakhsh River catchment where large-scale river damming is anticipated. R - Rogun dam and future reservoir at normal water level; N – Nurek dam and reservoir; blue triangles – possible glacier dams; numbered orange triangles – possible rockslide dams; Google Earth image as a background

3.1. MUKSU RIVER VALLEY

Analysis of the potential damming sites in the Muksu River valley allowed estimating potential amount of water that could be stored upstream of the anticipated blockages that could be formed by catastrophic collapse of the entire slopes affected by visible slope deformations in case of landslide damming, or by intensive and rapid glacial surges. The largest possible lake about 0.19 km³ in

volume could be formed 200 km upstream from the Rogun dam by the ca. 100 m high rockslide dam (1 on Fig. 3). According to calculations, surge wave that can originate after its breach with the initial peak discharge of ca. $13 \times 10^4 \text{ m}^3/\text{s}$ could be up to 50 m high. It will reach the tail part of the Rogun reservoir in ca. 14 hours being 10 m high with peak discharge of about $5700 \text{ m}^3/\text{s}$. Large reservoir with an area of ca. 150 km^2 at its full level will accommodate the entire outburst flood, so that reservoir level will increase less than for 1.5 m that will not produce any threat to the rock-fill dam.

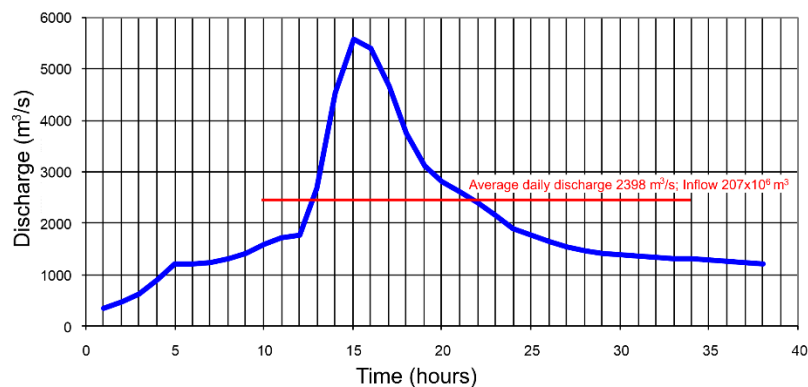


Fig. 4

The Muksu outburst flood hydrograph at the entrance of the Rogun reservoir

3.2. OBI-KHINGOU RIVER VALLEY

The largest potential river-damming landslide in the Vakhsh River catchment was found in the Obi-Khingou River basin, at the mouth of its right tributary – the Ragnow River, at 38.921° N , 70.964° E , about 140 km upstream from the Rodun dam (No 3 on Fig. 3). More than 1 km-high right bank of the valley is affected by recent landslide and by numerous downslope and upslope-facing fractures. The most distant one at 3100 m a.s.l. is about 800 m far from the crown of the recent slope failure at 2850 m a.s.l. (Fig. 5). Slope is composed of folded Upper Cretaceous sedimentary rocks (limestone, sandstone, siltstone and gypsum) with relatively low strength striking along the slope and dipping $40\text{-}45^\circ$ in the slope. Nevertheless, intensive fracturing visible on Fig. 5 allows assumption that this slope could fail in one large event forming the ~260 m high dam ca. $3 \times 10^8 \text{ m}^3$ in volume (Fig. 6). Such a dam can impound a lake up to $\sim 412 \times 10^6 \text{ m}^3$ in volume – about 2 times larger than in the Muksu River case describe above.

Its catastrophic breach caused by overtopping could result in outburst flood with the initial peak discharge up to $350\text{-}500 \times 10^3 \text{ m}^3/\text{s}$. On its' 100 km long way to the Rogun reservoir along the Obi-Khingou River valley with wider trough-like upper part and V-shape canyon in the lower reaches (see Fig. 3), flood will transform significantly and would reach the tail part of the Rogun Reservoir in ca. 1 hour being about 20-25 m high with peak discharge of ca. $30 \times 10^3 \text{ m}^3/\text{s}$ (Fig. 7). Even if the impounded dammed lake will be emptied completely, the Rogun

Reservoir level will raise for ca. 2.5 m only, less than the PMF headwater level. The most adverse effect of such flood could be the caused by waves that might originate in the reservoir. Their propagation along the reservoir and height at the dam site could be assessed by the numerical or physical modeling. However, considering that on its way such wave should split up- and downward the reservoir it is unlikely that at the dam site it would exceed the wind wave of 1% probability.



Fig. 5

Evidence of the ongoing slope deformations about 1 km above the Ragnow River. Orange arrows mark downslope-facing scarps; yellow arrows – upslope-facing scarps. Modified from [10], with permission of Elsevier

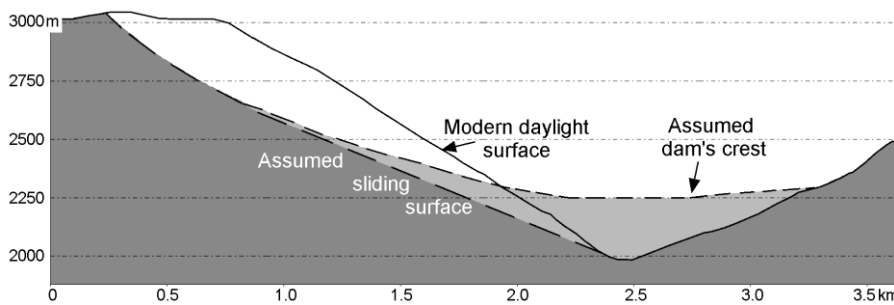


Fig. 6

Schematic cross-section of the anticipated Ragnow-mouth rockslide dam

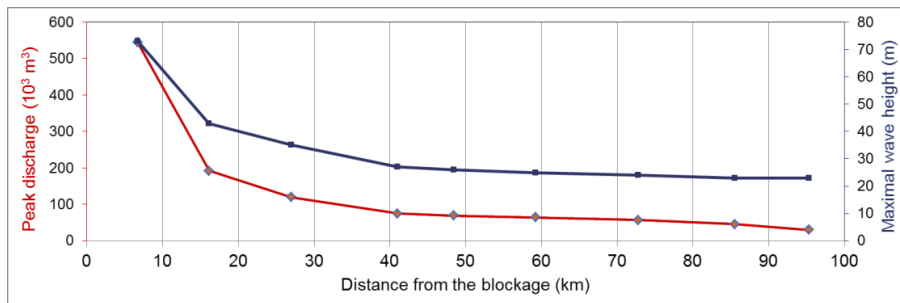


Fig. 7

Variation of peak discharge (red line) and of the maximal wave height (blue line) along the Obi-Khingou River valley from the Ragnow-mouth rockslide dam up to the entrance in the Rogun reservoir

4. POTENTIAL BLOCKAGE IN THE SIANG (BRAHMAPUTRA) RIVER BASIN

Similar analysis was performed in the Siang (Brahmaputra) River basin, whose upper part is in China and the lower one – in India. At least twice, in 1900 and in 2000 this valley was affected by the disastrous outburst floods that originated in the Yigong River valley – the large left tributary of the Brahmaputra (Fig. 8) [8, 9]. River damming was caused by rock avalanches that originated in the upper reaches of the Zhamu Creek and, after passing about 10 km, blocked the Yigong River by the dams up to 50-70 m high. As we mentioned above, in 2000 release of about 2 km³ of water resulted in 44,200 m³/s peak discharge in India, more than 400 km downstream. It can be assumed that steep walls in the Zhamu Creek head still have the potential of similar failures in future.

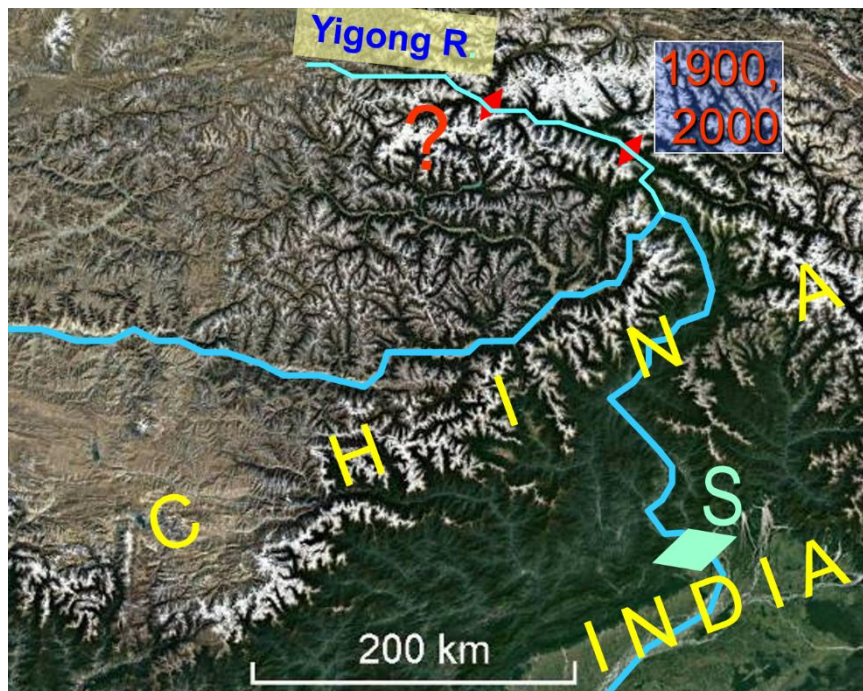


Fig. 8

Location of the potential river-damming sites in the Brahmaputra River basin (red diamond symbols): that marked by 1900, 2000 – where Zhamu Creek rock avalanches occurred; ? – the assumed rockslide site shown on Fig 9; S – location of the Siang hydraulic scheme(s) in India

However, analysis of space images revealed possibility of the, potentially, much more hazardous phenomenon that might occur in the same Yigong valley about 100 km upstream from the 1900 and 2000 dams' site at 30.448° N, 94.075° E (see Fig. 8). Here, few kilometers downstream from the Jangba village, the 1500 m high right-bank slope demonstrate distinct evidence of the ongoing large-scale instability – arcuate step on top and numerous rock falls starting at the central part of the slope and at the bounds of this slope section (Fig. 9). It differs

significantly from all surrounding slopes and looks as if the entire 600-800 m high upper part of this slope is affected by the deep-seated gravitational slope deformation. Much wider upstream section of river valley demonstrate evidence of both recent and, likely, older impoundments and could store large amount of water – up to ca. 6 km³ in case of river damming.

Possible volume of the hypothetical slope failure and of the blockage was estimated, based on expert judgment, as ca. 207-230 million m³ (volume of the blockage is slightly larger than that of the collapsed rock mass, considering its inevitable softening). Such a large failure, if it would occur as a single event, could form a dam up to 300-350 m high (Fig. 9). Similar shape of the headscarp was observed, for example, at the Lower Aral rockslide in Central Tien Shan [10].



Fig. 9

3D Google Earth view of the rockslide-prone site on the right bank of the Yigong River valley with evidence of the ongoing deformations

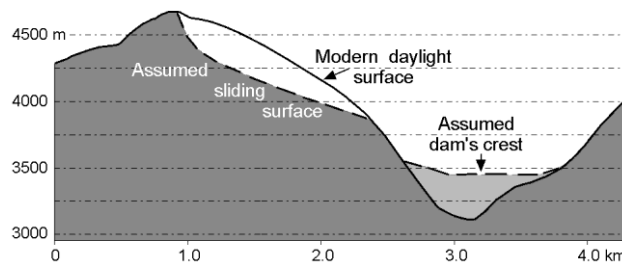


Fig. 10

Schematic cross-section of the anticipated Jangba rockslide dam

Parameters of possible outburst flood could be estimated based either on the model calculations or on the analogues some of which were presented above in Section 2. Preliminary calculations provided the assumed peak discharge of the outburst surge wave of about $600-800 \times 10^3$ m³/s. Such enormous estimate, however, seems to be reliable, considering $400-500 \times 10^3$ m³/s peak discharge of the outburst surge wave at the Sarydjaz-Aksu site (see Fig. 1) caused by the release of about 2 km³ of water only, and 120×10^3 m³/s discharge recorded 17 km downstream from the breached dam about 55 m high only (the level of the

excavated spillway canal) that had stored about 1.5 km³ of water and ca. 100 m high surge wave observed during breach of the 210 m high dam and release of 50 million m³ of water on the 1985 Bairaman case [7].

In the lower reaches of the valley, in India, after passing through the ~500 km long gorge, peak discharge of such a flood could exceed 50,000 m³/s and a flood wave could be up to 50 m high.

5. CONCLUSIONS

The extreme potential hazards provided by hypothetical outburst floods that might occur in the Vakhsh and the Siang River basins, along with the data on similar disastrous phenomena that had occurred in the past all over the world, highlights the necessity to investigate possibility of large-scale rockslide damming in the catchment areas of large hydraulic schemes in mountainous regions.

Though outburst floods anticipated in the Vakhsh River basin should not produce disastrous effects for the Rogun dam, they might cause flooding on the way and along the reservoir banks posing a threat to local communities and infrastructure. Potential hazard of river blocking in the Yigong River valley seems to be much higher.

Identification of such potentially hazardous sites based on the analysis of the remote sensing data should be followed by their more detail study and monitoring aimed not to miss occurrence of such a slope failure. Fixing of river-blocking slope failures in the catchment areas allows taking timely actions to mitigate or avoid most adverse effects of the disastrous outburst floods and to protect hydraulic structures located downstream.

REFERENCES

- [1] STROM A., ZHIRKEVICH A “Remote” landslide-related hazards and their consideration for the hydraulic schemes design. In: Genevois, R., Prestinzi, A, (eds). Proc. Int. conference on Vajont – 1963-2013. *Italian Journal of Engineering Geology and Environment*, Book series, 2013, No 6.
- [2] DAI F.C., LEE C.F., DENG J.H., THAM L.G. The 1786 earthquake-triggered landslide dam and subsequent dam-break flood on the Dadu River, southwestern China. *Geomorphology*, 2005, 65.
- [3] LEE C.F., DAI F.C. The 1786 Dadu River Landslide Dam, Sichuan, China. In: Evans SG, Hermanns R, Scarascia-Mugnozza G, Strom AL (eds.), Natural and Artificial Rockslide Dams. *Lecture Notes in Earth Sciences*, 2011, 133.
- [4] DELANEY K.B., EVANS S.G. Rockslide dams in the northwest Himalayas (Pakistan, India) and the adjacent Pamir mountains (Afghanistan,

- Tajikistan), Central Asia. In: Evans, S.G., Hermanns, R., Strom, A.L., and Scarascia-Mugnozza, G. (eds) *Natural and artificial rockslide dams. Lecture Notes in Earth Sciences*, 2011. 133. Springer, Heidelberg.
- [5] AHMED M.F., ROGERS J.D. ISMAIL E.H.. Historic Landslide Dams along the Upper Indus River, Northern Pakistan. *Natural Hazards Review*, 2014.
- [6] GONZÁLEZ DIAZ E.F., GIACCARDI A.D. AND COSTA C.H.. La avalancha de rocas del rio Barrancas (Cerro Pelan), norte del Neuquen; su relacion con la catastrofe del Rio Colorado (29/12/1914), *Revista de la Asociación Geologica Argentina*, 2001, 56.
- [7] KING J., LOVEDAY I., SCHUSTER R.L. The 1985 Bairaman landslide dam and resulting debris flow Papua New Guinea. *Q. Journal of Engineering Geology*, 1989. 22.
- [8] SHANG Y., YANG Z., LI L., LIU D., LIAO Q., WANG, Y. A super-large landslide in Tibet in 2000: background, occurrence, disaster, and origin. *Geomorphology*, 2003, 54.
- [9] DELANEY, K.B. AND EVANS, S.G. The 2000 Yigong landslide (Tibetan Plateau), rockslide-dammed lake and outburst flood: review, remote sensing analysis, and process modelling. *Geomorphology*, 2015, 246.
- [10] STROM A., ABDRAKHMATOV K. Rockslides and Rock Avalanches of Central Asia: Distribution, Morphology, and Internal Structure. In press (will be published by Elsevier in 2018).

SUMMARY

The necessity of identification of sites in the catchment areas upstream from reservoirs, where large-scale river damming rockslides following by powerful outburst floods might be anticipated, is exemplified by case studies from the Vakhsh and the Siang (Brahmaputra) River basins, where large hydraulic schemes are under construction or are planned in future.

RÉSUMÉ

Des exemples des bassins de rivières Vakhsh et Siang (Brahmapoutre), en aval de laquelle est prévue la construction de grandes ouvrages hydrauliques, on démontre la nécessité d'identifier en amont au sein du bassin d'alimentation les zones dans lesquelles peuvent se former des débris de terre et les glissements de terrain avec la formation de barrages, percée qui peut provoquer des inondations (faire face à la formation des crues).

KEYWORDS

Rockslide dam, Outburst flood, Reservoir, Remote sensing, Rogun dam, Siang HPP

COMMISSION INTERNATIONALE DES GRANDS BARRAGES

VINGT-SIXIÈME CONGRÈS DES GRANDS BARRAGES
Autriche, juillet 2018

DOI 10.3217/978-3-85125-620-8-233



This work licensed under a Creative Commons Attribution 4.0 International License. <https://creativecommons.org/licenses/by-nc-nd/4.0/>

**INFLUENCES OF WATER LEVEL CHANGES ON THE BEHAVIOUR OF A
SLOW MOVING LANDSLIDE**

Georg M. AUSWEGER

*University assistant at the Institute of Soil Mechanics, Foundation Engineering
and Computational Geotechnics, GRAZ UNIVERSITY OF TECHNOLOGY*

AUSTRIA

Helmut F. SCHWEIGER

INSTITUTE OF SOIL MECHANICS, FOUNDATION ENGINEERING AND
COMPUTATIONAL GEOTECHNICS, GRAZ UNIVERSITY OF TECHNOLOGY

AUSTRIA

Roman MARTE

INSTITUTE OF SOIL MECHANICS, FOUNDATION ENGINEERING AND
COMPUTATIONAL GEOTECHNICS, GRAZ UNIVERSITY OF TECHNOLOGY

AUSTRIA

COMMISSION INTERNATIONALE
DES GRANDS BARRAGES

VINGT-SIXIEME CONGRES DES
GRANDS BARRAGES
Autriche, juillet 2018

INFLUENCES OF WATER LEVEL CHANGES ON THE BEHAVIOUR OF A SLOW MOVING LANDSLIDE

Georg M. AUSWEGER

*University assistant at the Institute of Soil Mechanics, Foundation Engineering
and Computational Geotechnics, GRAZ UNIVERSITY OF TECHNOLOGY*

AUSTRIA

Helmut F. SCHWEIGER

Roman MARTE

1. INTRODUCTION

Slow moving landslides pose a risk to the environment and often cause severe damages to infrastructures. In this contribution, the influences of water level changes in a storage basin of a pumped-storage power plant on the movement behaviour of a slow moving landslide are investigated. After a short introduction of the site, results of pore water pressure measurements and displacement measurements are presented. The measurements showed excess pore water pressures at the slope toe. Furthermore, a clear relationship between storage operation, excess pore water pressures at the slope toe and movement rates of the landslide could be derived from the measurements. Based on numerical back-calculations, the reasons for the measured excess pore water pressures at the slope toe are discussed. The quantitative influence of the storage operation on the slope movements is estimated from the results of a fully coupled flow-deformation analysis (finite element analysis). Furthermore, the influence of other factors (creep behaviour and precipitation) on the slope movements is shown by numerical back-calculations.

2. SLOW MOVING LANDSLIDE NEXT TO WATER STORAGE BASIN

2.1. SITE DESCRIPTION

The pumped-storage power plant with the associated water storage basin is located in the Central Eastern Alps. The volume of the storage basin is roughly 300,000 m³. Due to the operation of the power plant, the water level in the storage basin changes up to three times a day with a maximum change in water level of approximately 7 m.

The dimensions of the landslide are 220 x 270 m. The main sliding surfaces in the lower part of the slope were detected by inclinometer measurements between 20 and 40 m below ground surface. The average inclination of the slope is 30°. The average movement rate of the landslide is 4-5 cm/year. Fig. 1 shows a plan view and a side view of the landslide and the storage basin. Furthermore, the positions of the installed measurement equipment are indicated in Fig. 1.

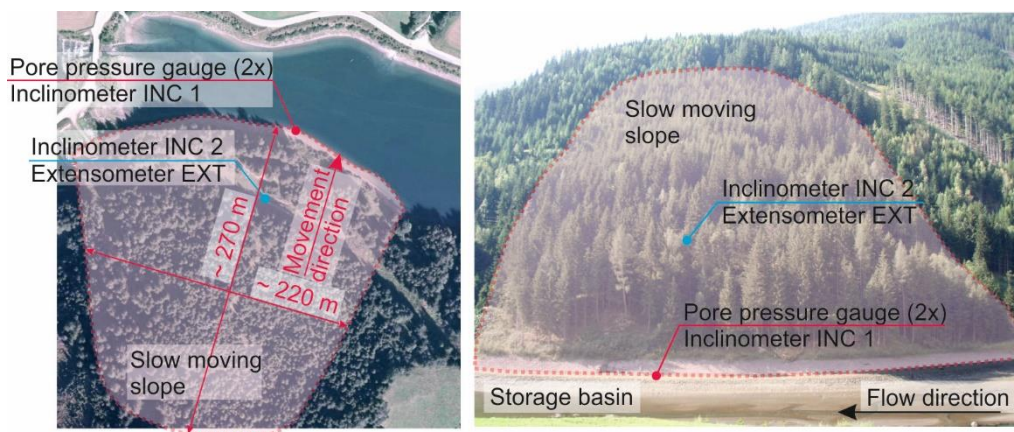


Fig. 1

Plan view and side view of water storage basin and slow moving slope [1]

The material of the slow moving landslide mainly consists of weathered and sheared rock. Beneath the slope toe and the water storage basin the subsurface explorations showed lacustrine fine sediments with an increasing fine content with depth, mainly consisting of silt.

2.2. MEASUREMENT RESULTS

To monitor the slope movements and the pore water conditions at the slope toe, a comprehensive measurement system was installed. The positions of the

measurement devices are marked in Fig. 1. In addition to the indicated devices, the entire slope is equipped with geodetic measurement points.

In the following, selected results from the on-site measurements are presented.

2.2.1. Pore water pressure measurements

Two pore water pressure gauges were installed at the slope toe of the landslide. Pore water pressure gauge PPG 1 is installed at a depth of 21 m below ground surface. PPG 2 is installed at 33 m below ground surface.

Fig. 3 shows the absolute pressure height at the position of the measurement devices and in the storage basin for one week. Furthermore, the resulting excess pore water pressures are plotted in Fig. 3. According to Fig. 3, high and fast water level changes lead to high excess pore water pressures at the slope toe as shown in the first part of the plotted period. In contrast, small water level changes, which occur in the second part of the plotted week, lead to small excess pore water pressures.

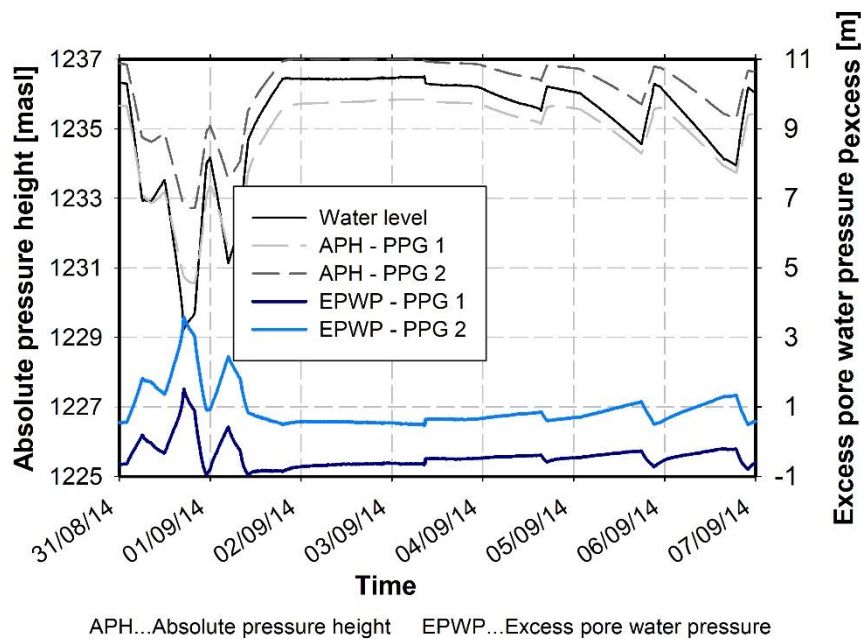


Fig. 3

Absolute pressure height and excess pore water pressures at slope toe from 31/08/2014 until 07/09/2014 [2]

Two important conclusions can be derived from the pore water pressure measurements. First, excess pore water pressures are present at the slope toe of the slow moving landslide and second, the magnitude of the excess pore water pressures depends on the storage operation.

2.2.2. Deformation measurements

In addition to the conventional inclinometer measurements, the two inclinometers were equipped with in-place inclinometers to investigate the relationship between storage operation and movement behaviour at the slope toe.

Fig. 4 and 5 show comparisons of the water level changes in the storage basin with selected deformation measurements.

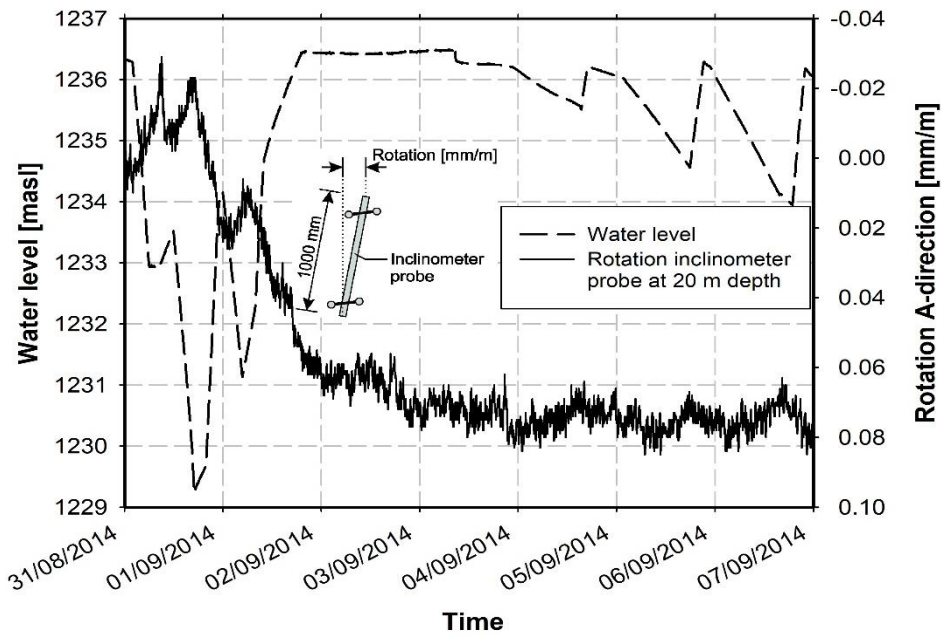


Fig. 4

Rotation of inclinometer probe at 20 m depth in inclinometer INC 1 and water level in water storage basin [2]

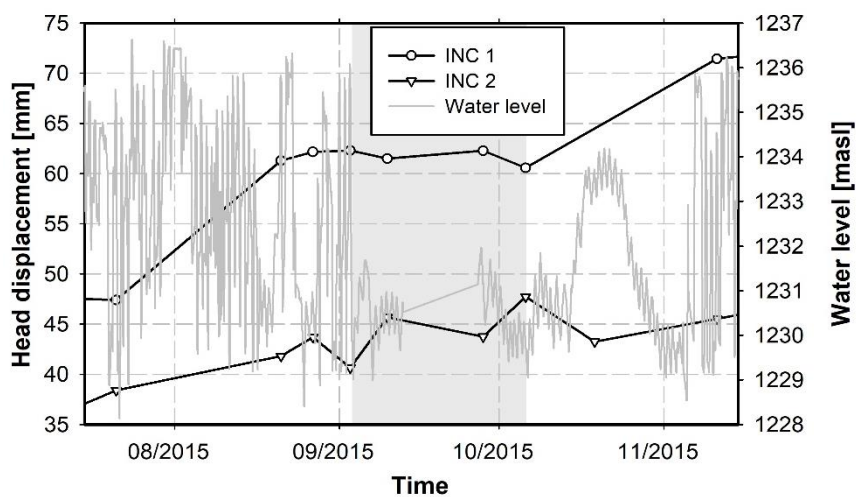


Fig. 5

Head displacements of inclinometers and water level in water storage basin [2]

In Fig. 4 the rotation of one inclinometer probe at a depth of 20 m (position of main sliding surface) at the slope toe is plotted. As shown in Fig. 4, the first high and fast water level changes lead to high deformation rates. During the days with small water level changes the deformation rate is significantly reduced. The head displacements of inclinometer INC 1 and INC 2, as plotted in Fig. 5, show almost no displacements during the period without water level changes. Based on the two presented comparisons between storage operation and deformation measurements a clear relationship between the two measurement quantities can be derived.

2.2.3. *Summary of measurement results*

In summary, the measurement results indicate a relationship between water level changes in the storage basin, excess pore water pressures at the slope toe and movement rates at the slope toe. The geodetic measurements revealed a small influence of the precipitation on the movement behaviour in the middle and upper part of the landslide. To determine the actual influence of different factors (creep behaviour, precipitation and water level changes) on the slope deformations, numerical back-calculations, which consider all these factors are performed. The results are presented in the following.

3. NUMERICAL BACK-CALCULATIONS

The numerical back-calculations concerning the pore water pressures at the slope toe and the slope deformations were performed with the FE-software Plaxis 2D 2016 [3]. The FE-model is shown in Fig. 6.

The FE-model incorporates the real water level changes from the storage basin and the precipitation and evaporation corresponding to the specific site. The precipitation was measured on site. The potential evaporation was estimated according to Thornthwaite [4]. The influences of the soil suction on the evaporation [5] and the transpiration were neglected due to the lack of measurement data. Furthermore, the lacustrine fine sediments at the slope toe (layers Fine sand, silty and Silt, fine sandy, clayey) were modelled with the Soft Soil Creep model [6] to model the creep behaviour of these soil layers.

To achieve appropriate initial conditions concerning the stress state and the hydraulic conditions, the geological history was modelled in a simplified way. Afterwards, one year with characteristic precipitation and water level changes was simulated [2].

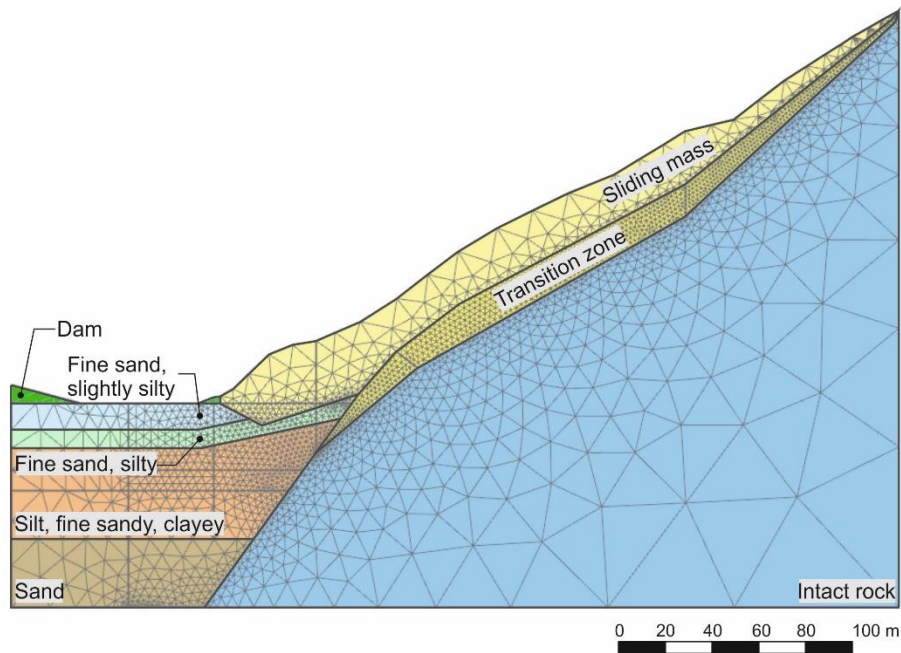


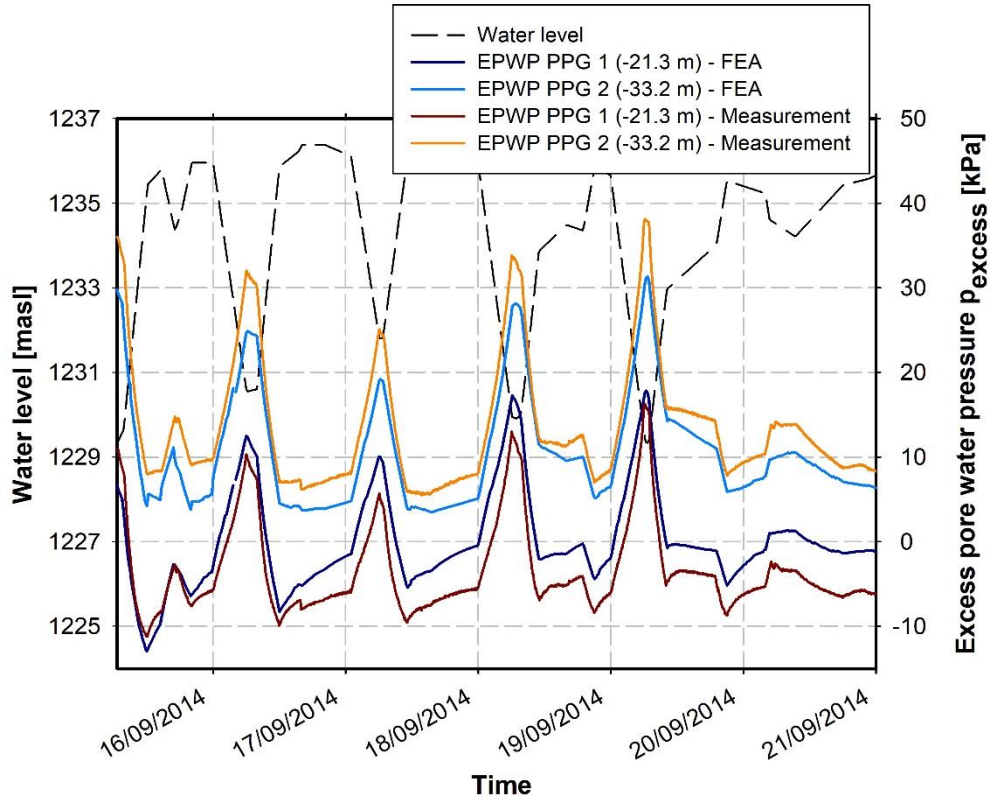
Fig. 6
FE-model for numerical back-calculations [2]

3.1. BACK-CALCULATION OF PORE WATER PRESSURES AT SLOPE TOE

The back-calculation of the pore water pressures was performed for several periods with different types of water level changes. Fig. 7 shows a comparison of the measured and calculated excess pore water pressures for the two installed pore water pressure gauges PPG 1 (21 m) and PPG 2 (33 m). Furthermore, the water level in the storage basin is plotted in the following graph.

From the comparison in Fig. 7 it can be seen that a good agreement between calculations and measurements could be achieved. Based on the numerical results, the reasons for the high excess pore water pressures at the slope toe can be investigated. For this, the groundwater head in the FE-model after the water level lowering in the storage basin on 16/09/2014 is shown in Fig. 8. As can be seen from this figure, in the majority of the subsoil the groundwater head is higher than the water level in the storage basin. I.e. positive excess pore water pressures are present in the model. In addition, the principal stresses in the area of the pore water pressure gauges are shown in Fig. 8. A rotation of the principal stresses is apparent. This clearly shows the influence of the slope on the stress state in this area. It can therefore be assumed that during the water level lowering the mechanisms, that typically occur during rapid drawdowns, lead to the excess pore water pressures in the subsoil. This is reasonable due to the high velocity of the water level changes and the low soil permeability of the lacustrine fine sediments. The mechanisms of rapid drawdowns have been discussed thoroughly in recent literature (e.g. [7], [8], [9] and [2]). Furthermore, the almost constant water level in

the slope influences the pore water pressures at the position of the measurement devices as shown by the equipotential lines turned to the left. This also leads to excess pore water pressures in the monitored area.



FEA...Finite element analysis EPWP...Excess pore water pressure PPG...Pore water pressure gauge

Fig. 7
Back-calculated excess pore water pressures [2]

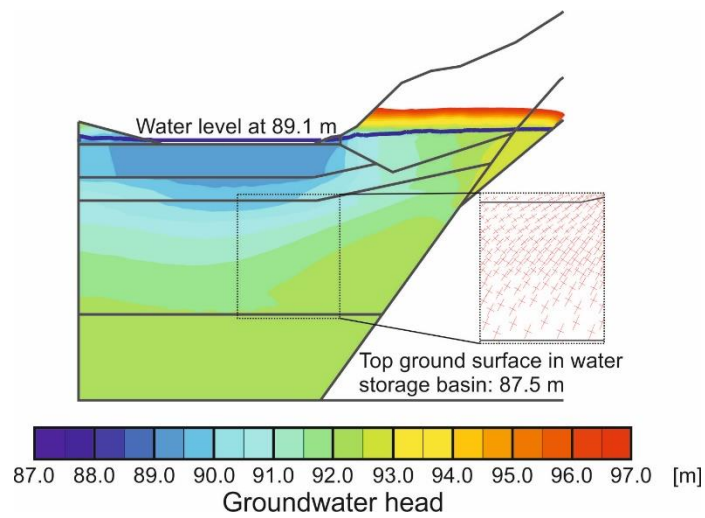


Fig. 8
Groundwater head after water level lowering on 16/09/2014 [2]

Based on the comparison of the measurement results and the calculation results and the analysis of the numerical results, it can be confirmed that the fast water level changes in the storage basin lead to excess pore water pressures at the slope toe.

3.2. BACK-CALCULATION OF SLOPE DEFORMATIONS

To estimate the quantitative contribution of the different influencing factors on the total displacements, consecutive calculation phases were performed. In each phase a new influencing factor was considered. The slope deformations due to the different influencing factors were analysed in different nodes at the slope. Fig. 9 exemplarily shows the results for node E in the middle of the slope. The difference between two time-displacement curves is the influence of each additionally considered factor as indicated by the label of the curves.

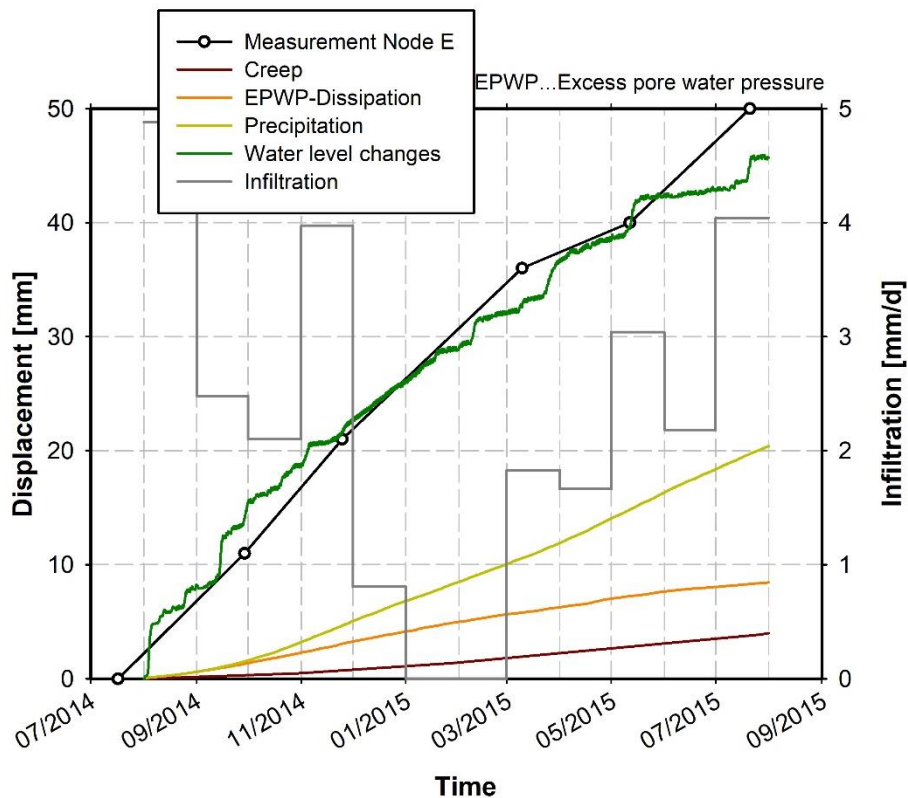


Fig. 9
Displacements at node E (in the middle of the slope) for different influencing factors [2]

A comparison between the on-site measurements in the area of node E and the total displacements from the calculation again indicate a good agreement. According to Fig. 9 the displacements are mainly due to the water level changes

in the storage basin but creep behaviour and precipitation add to the displacements. The displacements based on the dissipation of the excess pore water pressures is due to numerical reasons and can be neglected for further discussions.

The analysis as shown in Fig. 9 was performed for several nodes at the slope. This showed that the influence of the creep behaviour of the lacustrine fine sediments on the deformations decreases with the increasing distance up from the slope toe. The influence of precipitation and evaporation is increasing in the middle and upper part of the slope and the influence of the water level changes on the slope deformations is almost constant over the entire slope.

Based on the back-calculations of the slope deformations it can be stated that the water level changes are the main reason for the slope movements. However, slope movements would also occur without the storage operation but the magnitude of the deformations would be smaller.

REFERENCES

- [1] AUSWEGER G.M., SCHWEIGER H.F., MARTE R. Untersuchungen zum Einfluss von Stauspiegelschwankungen auf das Verhalten einer langsamen Massenbewegung. *Bauingenieur*, 2017, Nr. 92.
- [2] AUSWEGER G.M. Influences of water level changes on the behaviour of a slow moving landslide – In-situ measurements, model test and numerical analyses. *PhD-thesis Institute of soil mechanics, foundation engineering and computational geotechnics at Graz University of Technology*, 2017.
- [3] BINKGREVE R.B.J., KUMARSWAMY S., SWOLFS W.M. PLAXIS 2D 2016 – User Manual. 2016.
- [4] THORNTHWAITTE C.W. An approach toward a rational classification of climate. *Geographical Review*, 1948, Nr. 38/1.
- [5] FREDLUND D.G., RAHARDJO H., FREDLUND M.D. Unsaturated Soil Mechanics in Engineering Practice. 2012.
- [6] VERMEER P.A., NEHER H.P. A soft soil model that accounts for creep. *Proceedings of the International Symposium Beyond 2000 in Computational Geotechnics*, 1999.
- [7] BERILGEN M.M. Investigation of stability of slopes under drawdown conditions. *Computers and Geotechnics*, 2007, Nr. 34/7.
- [8] PINYOL N.M., ALONSO E.E., OLIVELLA S. Rapid drawdown in slopes and embankments. *Water Resources Research*, 2008, Nr. 44/1.
- [9] STELZER O., MONTENEGRO H. ODENWALD B. Consolidation analyses considering gas entrapment below the phreatic surface. *Proceedings of Numerical Methods in Geotechnical Engineering 2014*, 2014.

SUMMARY

Measurements on a slope next to a storage basin of a pumped-storage power plant indicated slope movements which are connected to the storage operation. Furthermore, excess pore water pressures were measured at the slope toe.

Based on numerical back-calculations in combination with the available on-site measurements the reasons for the excess pore water pressures at the slope toe could be identified. It could be also shown that the water level changes in the storage basin are the main reason for the slope movements. However, precipitation and creep behaviour of the lacustrine fine sediments at the slope toe also lead to deformations. I.e. without the storage operation the slope deformations would be smaller but they would be not zero.

The insights from the on-site measurements and the numerical back-calculations enable the definition of alarm values with regard to the slope deformations and an efficient design of appropriate remediation measures.

KEYWORDS

Deformation, Pore pressure, Reservoir slope, Slope stability

COMMISSION INTERNATIONALE
DES GRANDS BARRAGES

VINGT-SIXIÈME CONGRÈS DES
GRANDS BARRAGES
Autriche, juillet 2018

ESTIMATION OF LANDSLIDE INDUCED IMPULSE WAVE IN A CHANNEL TYPE RESERVOIR

Qingquan LIU

Professor, Department of Mechanics, BEIJING INSTITUTE OF TECHNOLOGY

Yi AN

*Assistant Professor, INSTITUTE OF MECHANICS, CHINESE ACADEMY OF
SCIENCES*

Jiaxiu YANG

*Head of Guiyang Engineering Corporation, POWER CONSTRUCTION
CORPORATION OF CHINA*

Ji LU

*Senior Engineer, HUANENG LANCANG RIVER HYDROPOWER CO., CHINA
HUANENG GROUP*

CHINA

1. INTRODUCTION

The landslide induced impulse wave (LIW) in reservoirs might result in tragic disasters. After the Huangtian LIW event in 2009 at the Xiaowan Reservoir, the LIW becomes a major concern to some of hydropower projects on the Lancang River, southwest of China. As most reservoirs in these projects located in narrow valleys, the estimation of LIW damage in those channel-type reservoirs is very important.

Existing theories for LIW are often generalized from wave flume and wave basin experiments, which assume that the wave generation direction is (partly) the same as the wave propagation direction. However, the LIW in channel-type reservoirs is far more complex due to its distinguishing energy transport and

dissipation mechanisms. The nearfield dissipation in the channel-type reservoir is very strong while the far field dissipation is limited because the wave propagation direction is generally the same as the channel stream direction. In this study, a novel numerical model, which characterizes both above two stages, is developed for LIW in channel-type reservoirs and applied in engineering practices.

2. METHODS

The numerical model is constituted of two parts, the nearfield model and the far field model. In the nearfield model, the water is modelled with the Navier-Stokes equation while the landslide is modelled with elasto-plastic model. The model is solved with the Smoothed Particle Hydrodynamics (SPH) method. And the far field model solves the 2D shallow water equation with adaptive mesh technique to simulate the wave propagation. These two models are connected unidirectionally using wave height matching technique.

The model is validated against several laboratory experiments and the results are promising. Both the deformation of the landslide and the initial wave could be reproduced reasonably and only a few artificial parameter is necessary.

3. RESULTS & CONCLUSION

The model is applied in the engineering design of a huge hydropower project on the upstream of the Lancang River. A slope, which locates at about ten kilometers upstream from the dam, is considered to be unstable during the attack of the extreme event. With prescribed slide surface from FEA simulation, the large deformation of the slide during both the slope failure and the impact process is well characterized.

The results show that while the initial wave generated in the impact process is huge, the wave propagated to the downstream is limited. This simulation shows the ability of the proposed model and also the unique characteristic of LIW in channel-type reservoirs.

ACKNOWLEDGEMENT

This work was financially supported by the Natural Science Foundation of China (No. 11372326, No.11432015) and the Huaneng Technology Project (NHKJ15-H13).

COMMISSION INTERNATIONALE DES GRANDS BARRAGES

VINGT-SIXIÈME CONGRÈS DES GRANDS BARRAGES
Autriche, juillet 2018

DOI 10.3217/978-3-85125-620-8-235



This work licensed under a Creative Commons Attribution 4.0 International License. <https://creativecommons.org/licenses/by-nc-nd/4.0/>

**FAILURE OF EMBANKMENT DAMS DUE TO OVERTOPPING-
EXPERIMENTAL STUDY AND HYDROGRAPH PREDICTION**

Burkhard RUEDISSER

INSTITUTE OF HYDRAULIC ENGINEERING AND WATER RESOURCES
MANAGEMENT, VIENNA UNIVERSITY OF TECHNOLOGY

AUSTRIA

Peter TSCHERNUTTER

INSTITUTE OF HYDRAULIC ENGINEERING AND WATER RESOURCES
MANAGEMENT, VIENNA UNIVERSITY OF TECHNOLOGY

AUSTRIA

COMMISSION INTERNATIONALE
DES GRANDS BARRAGES

VINGT-SIXIEME CONGRES DES
GRANDS BARRAGES
Autriche, juillet 2018

FAILURE OF EMBANKMENT DAMS DUE TO OVERTOPPING- EXPERIMENTAL STUDY AND HYDROGRAPH PREDICTION

Burkhard RUEDISSER, Peter TSCHERNUTTER

*Institute of Hydraulic Engineering and Water Resources Management, VIENNA
UNIVERSITY OF TECHNOLOGY*

AUSTRIA

1. INTRODUCTION

Despite the most careful surveillance and construction measures, the risk of failure of an embankment dam cannot be completely eliminated. The probability of failure has been quantified as $8 \cdot 10^{-5}$ for embankments with at least five years of service. The consequences of such a catastrophic event could be severe. [1]

According to ICOLD data, the two most common causes of failure are overtopping and piping. [2] According to [3] in most failure events, overtopping and piping occur in combination. Whereas piping may be the initial cause of many embankment dam failures, the worst case would be a collapse of the piping tunnel, which causes lowering of the dam crest and eventually leads to overtopping.

Existing models for hydrograph prediction display a wide range of results. The complex processes and interdependency of parameters and boundary conditions of the breaching process of overtopped embankment dams are not yet fully understood. In order to contribute to the understanding of the influence of several parameters and boundary conditions on the breach outflow hydrograph, it is necessary to conduct and analyze model test series.

2. EXPERIMENTAL METHODS

To investigate the significance of several parameters and boundary conditions on the breach outflow hydrograph of overtopped embankment dams with falling water reservoir level and no additional inflow into the reservoir, two

experimental studies were conducted in the laboratory of the Institute of Hydraulic Engineering and Water Resources Management, Vienna University of Technology [4], [5].

2.1. GENERAL SETUP

Experiments were performed as three-dimensional full models and three-dimensional half models to observe the breach processing through a transparent sidewall. Both studies refer to similar geometry values with a dam height $h_D = 0.31$ m, crest width $b_C = 0.02$ m, upstream and downstream slope $m_u = m_d = 1:2$ and a channel width at the dam $b_D = 1$ m (half model) to 2 m (full model). The depth of the triangular shaped initial breach varied from $d_B = 0.01$ to 0.05 m. The reservoir had a volume of $V_R = 1$ to 4 m^3 (referring to the full model) with the maximum water level at breach initiation $h_W = 0.30$ m. (Fig. 1) [5].

To analyze potential effects caused by the sidewall, additional full model tests were performed. [5] For the full models, the half models were mirrored at the transparent sidewall, with an initial breach in the center of the channel, $b_D = 2$ m and $V_R = 4$ m^3 .

Fig. 1 Model test rig and measurement scheme

Fig. 1 displays a scheme of the model test rig and the measurement system. All heights are defined relative to the reference datum at the top of the dam platform.

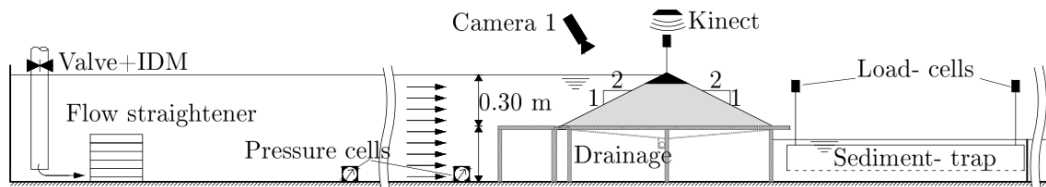


Fig. 1 Model test rig and measurement scheme

Tests were performed by constantly filling the reservoir until reaching the maximum water level h_W . The inflow was halted and simultaneously the initial breach was created by sudden pulling of a triangular shaped prism. The dam platform was pervious through a bottom drainage, which could be optionally closed for the performance of undrained tests.

Fig. 1 contains a scheme of the installed measurement devices in the test rig. Hydrograph recording as well as drainage water measurement was performed by pressure cells, according to the falling reservoir level and the reservoir characteristic by the relation $Q(t) = dV/dt$. Breach processing could be registered by three video cameras through a transparent sidewall in the breach cross section and at the upstream slope of the embankment dam. The third camera was situated

in a Microsoft Kinect module, 3 m above the dam crest. This optical device contains also an infrared sensor to capture the three-dimensional shape of the breached embankment and is described in [4] and [5] (Fig. 2).

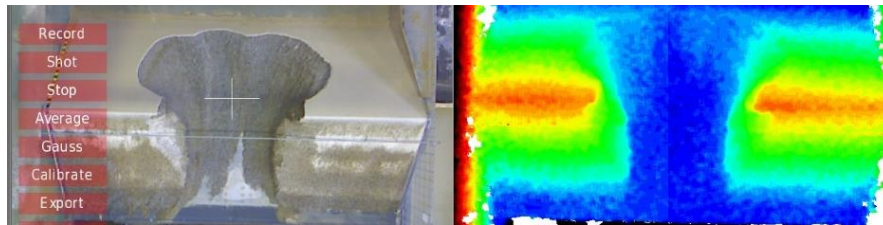


Fig. 2 Three-dimensional in situ breach recording

During breach formation shell erosion could be measured by a submerged sediment trap with load cells, which was installed downstream of the dam platform.

2.2. PARAMETERS INVESTIGATED

The first study [4] dealt with the influence of reservoir size- and shape. Therefore, the effects of three different reservoir volumes (1, 2 and 4 m³- referring to the full model) as well as a linear rectangular cross section reservoir and a nonlinear triangular cross section reservoir were investigated.

The second study [5] analyzed the effects of three different grain size distributions (nonuniform, $d_m = 1.1$ to 3.1 mm), an upstream impervious blanket, three initial breach depths (0.01, 0.03 and 0.05 m) as well as model effects due to sidewall, drainage and scalability. In order to reduce the seepage that occurred by using coarse and high permeable shell material, a membrane coating, like an upstream dam sealing blanket, was developed, which enabled impounding, by heaving no significant effect on the breaching process. In addition, a model family with a scale factor of $\lambda = 2$ was created. Most experiments were performed three times for each parameter.

3. MAIN RESULTS

3.1. SIGNIFICANCE OF THE PARAMETERS INVESTIGATED

The most significant influence on the hydrograph could be observed by varying the reservoir size, followed by the reservoir shape. By doubling the reservoir volume, an average increase of the peak hydrograph value of approx. 70% was measured. Compared to a reservoir with a rectangular shape and linear

characteristic, the nonlinear triangular shaped reservoir caused a rising of the peak hydrograph about approx. 40 to 60% [4].

Using different shell material had a significant effect on the hydrograph as well, but it was lesser and also dependent on the reservoir size. The coarse material ($d_m = 3.1$ mm) possessed the highest peak value, with a reservoir volume of 4 m³, about approx. 36% higher, than the fine grained material ($d_m = 1.1$ mm). With a reservoir volume of 2 m³, the difference was approx. 50% [5]. Regarding material properties, no cohesion or apparent cohesion is to be expected.

Steeper slopes in the breach cross section using finer materials were observed by [6] ($d_m = 0.19$ to 0.64 mm) and [7] ($d_m = 0.21$ mm). This effect can be explained by apparent cohesion. According to [6] or [8] the breaching process with material $d < 1$ mm is controlled by apparent cohesion whereas the erosion of coarser material is controlled by shear stress. However, in the current study, the slopes in the cross section were almost parallel. Just the time and the speed of the breach development differed with each material. Therefore, the nonuniform coarse material eroded faster with a higher peak erosion during the decisive phase of breaching. Yet towards the end of the breaching process, with decreasing flow intensity, the order of the erosion rates changed and subsequently the erosion of the coarse material ceased first. This could also be observed in the two-dimensional pre tests [5].

Applying an upstream impervious blanket led to higher erosion rates and therefore greater destruction of the embankment shell. The peak hydrograph increase was about approx. 30% compared to similar embankments with no impervious blanket.

The variation of the initial breach depth had no significant effect on the peak hydrograph value, but the process was delayed at the beginning. The time of peak discharge after breach initiation was increased with a smaller initial breach depth.

Model effects due to the sidewall could not be detected, undrained tests using coarse material showed a peak hydrograph increase of approx. 4% compared to fully drained tests.

3.2. SCALABILITY

The ideal Froude scaling could be affected by viscosity ν , surface tension σ or material cohesion c . To neglect the effect of viscosity and surface tension, the flow must be fully turbulent. Viscosity effects can be neglected for flow *depth* > 5 cm was stated by [9]. Concerning the shell material, the sedimentation Reynolds number $Re^* = v_c^* d / \nu$ with $v_c^* = (g R_h I_0)^{0.5}$ as the critical shear stress velocity v_c^* , the hydraulic perimeter R_h and the energy gradient I_0 , should not fall below 200 [10]. Regarding the material properties and the flow conditions in the current studies, especially in the decisive phase during peak hydrograph occurrence, scaling should be possible according to Froude's similarity law.

The test results fit very well to the scaled peak values $Q_p = Q * \lambda^{2.5}$ with a scale factor $\lambda = 2$ [5].

4. HYDROGRAPH PREDICTION MODEL

4.1. GENERAL AND IMPULSE

The processes that control breach development and eventually the outflow hydrograph depend on numerous parameters and boundary conditions. Their complex relations are not yet fully understood and are also the subject of the research studies presented in this paper.

The essential geometrical parameters are the dam height h_D , upstream and downstream slope m_u , m_d and crest width b_c . Main hydraulic factors are considered as water level h_w , reservoir volume V_R , Reservoir shape n and a potential influence of the downstream water level h_d . Geotechnical parameters are mentioned as shell material properties - represented as the medium grain size diameter d_m dam type, impervious blankets etc. x ([6], modified).

According to [11] effects of m_d are negligible as well as the influence of b_c [12].

With the assumption of a full reservoir at the start of the breach initiation (dam height $h_D \approx$ reservoir water level h_w) and no influence from a downstream water level, a global length scale $h = h_w \approx h_D$ is introduced for the normalization of the parameters displayed in this paper referring to dimensions as flow rate, volume, length and time [6]. - Eq. [1]

$$Q^* = \frac{Q}{(gh_w^5)^{0,5}} = f\left(\frac{V}{h_w^3}, \frac{d_m}{h_w}, n, x\right) \quad [1]$$

Existing hydrograph predicting models can be divided into empirical and process-based physical models. Empirical models are usually based on the analyses of historical failure events or large scale field tests. Input parameters are commonly the dam height h_D and the reservoir volume V_R , with the breach hydrograph peak Q_P as target value.

Process-based physical models are commonly based on assumed simplified breaching approaches (e.g. the enlargement of a trapezoidal or rectangular breach cross section) or calculating a breach shape by considering material parameters and slope failure mechanism. Therefore, the breach formation is predominantly controlled by erosion, calculated with standard empirical sediment transport formulae, whereas breach outflow is assessed by the assumption of a broad crested weir. However, the use of the sediment transport equations is bound to the limits of input parameters for each test series these formulae are based on. With the assumption of stationary flow conditions, the maximum permitted energy gradient is e.g. 2% (Meyer- Peter and Mueller) and 20% (Rickenmann). There is also a narrow range of input parameters regarding the sediment. For example grain size diameter is restricted from 0.2 to 2 mm (van Rijn) or 2 to 10.5 mm (Smart and Jaeggi). A large selection of empirical and physical methods was presented by [13]. Thresholds for selected commonly used sediment transport equations have been summarized by [5].

Using flood wave prediction models in engineering practice in order to fulfill government requirements related to safety issues, it is necessary to set equal standards. The application of process-based models is required to define parameter values which impact on the high complex processes is currently not fully understood. Within the possible range of feasible values, with some models it is possible to “design” a flood wave, rather than calculate it. Empirical models are strongly dependent on their often inhomogeneous and scarce database; the results of commonly used equations display a large range [5].

In order to evaluate several methods for flood routing due to embankment dam failure of reservoir basins for snowmaking, the Austrian Federal Ministry of Sustainability and Tourism initiated a workshop for the creation of guidelines. Selected empirical models as well as one-dimensional analytical and two-dimensional numerical process-based models were examined with realistic input data from prototypes. The calculations display a wide range of results, with peak hydrograph differences up to 1500%. The selection of the transport formulae as well as the variation of material parameters and hydraulic coefficients were highly significant [14].

Therefore, the model described in this paper was intended to be a simple approach for an applied hydrograph prediction model, which was initially designed for a common standard of supply reservoirs for snowmaking in Austria.

4.2. MODEL CHARACTERISTICS

From the previously described test series [4], [5], three different V_R/h_W - ratio, with each two different settings, representing the reservoir shape, the spectrum of different shell materials and an upstream impervious blanket, could be obtained. Fig. 3 shows the results of this tests as a matrix of dimensionless peak hydrograph values Q_{P^*} (Eq. [1]).

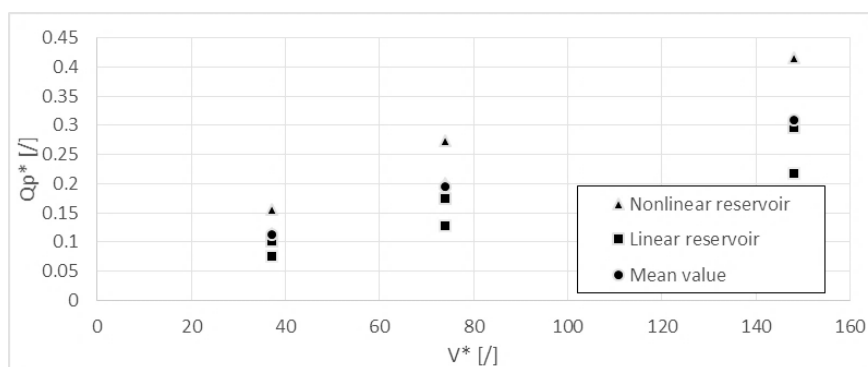


Fig. 3 Dimensionless peak hydrograph values from test series

[15] conducted model test series with numerous different reservoir sizes, simulated with reservoir inflow during the breach process. The results coincide well with the studies from Vienna University of Technology. With the calibrated equation of [15], for the calculation of the peak hydrograph using reservoir surface area and

maximum water level, the previous described spectrum of the matrix could be extended (Fig. 4).

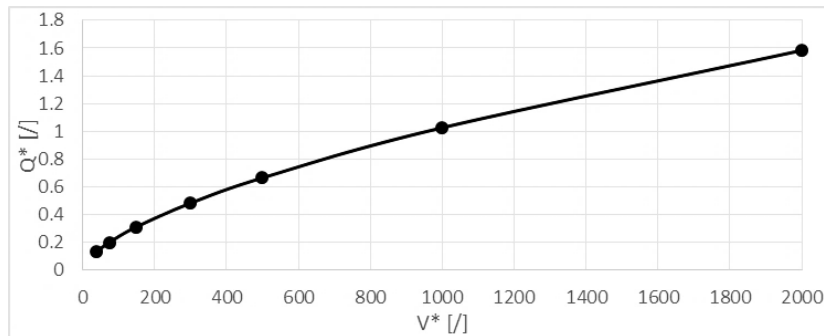


Fig. 4 Extended matrix according to [15]

Eq. [2] presents a fitting equation for the presented matrix calculating the peak outflow by using dimensional parameters based on reservoir volume V_R and maximum water level h_W .

$$Q_{max} = 0.0415 * (V_R * h_W)^{0.626} \quad [2]$$

For engineering practice and the requirement of non-steady runoff simulations, the hydrograph profile is decisive. In the first step, the peak hydrograph value was calculated as described above. The second step generates the hydrograph profile.

By analyzing the runoff hydrographs of the test series, several characteristics could be observed, despite the variation of reservoir volume, impervious blanket and shell material properties. Peak hydrograph value always occurred with approx. 80% remaining reservoir volume in linear and approx. 70% in nonlinear characteristic reservoirs. The profile shapes were quite similar as well, with a characteristic steep ascent to the peak value, followed by a less steep decent and an asymptotic approach to zero. The dam body remaining, retaining approx. 5 to 15% of the initial reservoir volume could be noted. With these assumptions and boundary conditions, the outflow hydrograph can be generated iteratively with a fixed characteristic profile, whereas the peak value occurs at 75% remaining reservoir volume and a total outflow of 90%. Defining variances, different scenarios can be generated (Fig. 5).

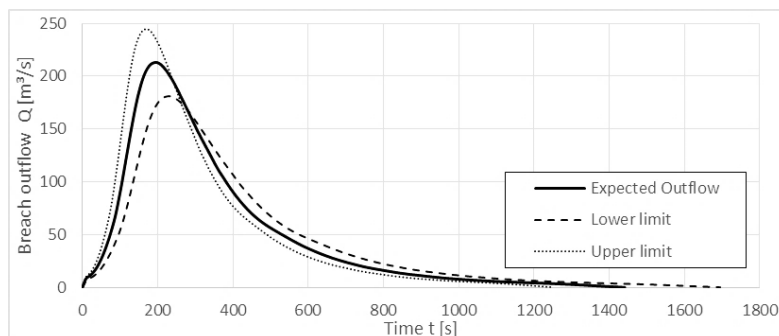


Fig. 5 Breach outflow hydrograph example - Variance + - 15%

4.3. COMPARISON WITH HISTORICAL FAILURE EVENTS

Fig. 6 presents the peak hydrograph values of different embankment dam configurations (water level h_W from 5 to 25 m, reservoir volume V_R from 5,000 to 20,000,000 m^3 and a constant, realistic grain size distribution) from selected empirical equations [16], [17], [18] and the process based model DEICH [19], compared to the model presented in this paper. The hollow circles represent the database of [18] from historical failure events.

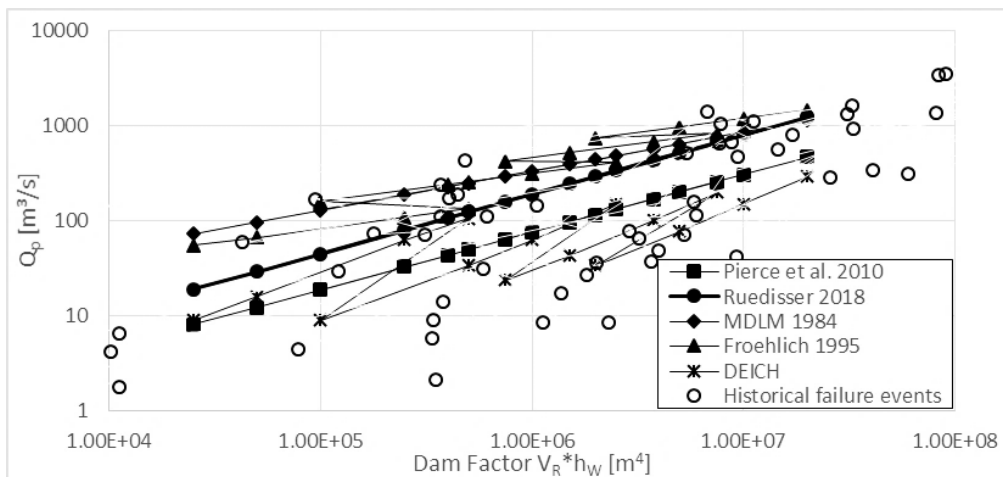


Fig. 6 Peak hydrograph prediction and historical failure events

For smaller structures with a rather small reservoir volume, the available data is quite limited. Filtering the Database of [16], for $V^* < 340$ (see Eq. 1) and a Dam Factor $V_R * h_W < 3 * 10^8$, the results are in a plausible range compared to the historical failure events (Fig. 7).

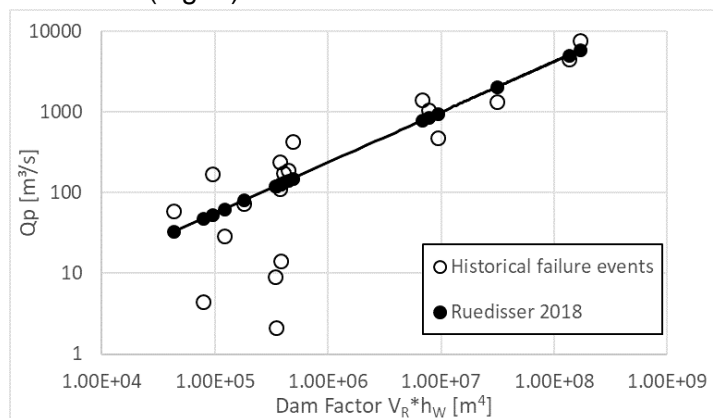


Fig. 7 Peak hydrograph and filtered database $V^* < 340$

REFERENCES

- [1] FOSTER, M.A., FELL, R., SPANNAGLE, M. Analysis of Embankment Dam Incidents. *UNICIV Report*, 1998, Nr. R-374.
- [2] FOSTER, M.A., FELL, R., SPANNAGLE, M. The statistics of embankment dam failures and accidents. *Canadian Geotechnical Journal*, 2000, Nr. 37: 1000-1024.
- [3] SINGH, V.P. Dam Breach Modeling Technology. *Kluwer*, 1996.
- [4] WALLNER, S. Influence of Reservoir Shape and Size On the Flood Wave Caused by Progressive Overtopping Dam Failure. *Ph.D. Thesis*. Institute of Hydraulic Engineering and Water Resources Management, Technical University Vienna, 2014 [published in German].
- [5] RUEDISSER, B. Effects of Shell Grain-Size Distribution and the Facing Element on Breach- Processing and Discharge Curve by Embankment Dam Failure due to Overtopping. *Ph.D. Thesis*. Institute of Hydraulic Engineering and Water Resources Management, Technical University Vienna, 2017 [published in German].
- [6] PICKERT, G., WEITBRECHT, V., BIEBERSTEIN, A. Breaching of overtopped river embankments controlled by apparent cohesion. *Journal of Hydraulic Research*, 2011, Nr. 49(2): 143-156.
- [7] WALDER, J.S., IVERSON, R.M., GODT, J.W., LOGAN, M; SOLOVITZ, S.A. Controls on the breach geometry and flood hydrograph during overtopping of non-cohesive earthen dams. *Water Resources Research*; 2015, Nr. 51(8): 6701-6724.
- [8] SCHMOCKER, L., HAGER, W.H. Modeling dike breaching due to overtopping. *Journal of Hydraulic Research*, 2009, Nr. 47(5): 585-597.
- [9] FRITZ, H.M., HAGER, W.H. Hydraulics of Embankment Weirs. *Journal of Hydraulic Engineering*, 1998, Nr. 124(9): 963-971.
- [10] ZARN, B. Lokale Gerinneaufweitung- eine Maßnahme zur Sohlenstabilisierung der Emme bei Utzenstorf. *VAW- Mitteilungen*, 1992, Nr. 118.
- [11] POWLEDGE, G.R., RALSTON, D.C., MILLER, P., CHEN, Y.H., CLOPPER, P.E., TEMPLE, D.M. Mechanics of Overflow Erosion on Embankments. I: Research Activities. *Journal of Hydraulic Engineering*, 1989, Nr. 115(8): 1040-1055.
- [12] MORRIS, M.W. and HASSAN , M.A.A.M. IMPACT, Investigation of extreme flood processes and uncertainty- a European research project. *Proc. 40th Defra Flood and Coastal Management Conference*, 2005.
- [13] WU, W. Earthen Embankment Breaching. *Journal of Hydraulic Engineering*, 2011, Nr. 137(12): 1549-1564.
- [14] BMNT, Guideline for Flood Wave Prediction of Breaching Retaining Structures, Federal Ministry of Sustainability and Tourism (BMNT), 2018 [not yet published]
- [15] FRANK, P.-J. Hydraulics of Spatial Dike Breaches. *VAW- Mitteilungen*, 2016, Nr. 236.

- [16] PIERCE, M.W., THORNTON, C.I., ABT, S.R. Prediction Peak Outflow from Breached Embankment Dams. *Colorado State University*, 2010.
- [17] MACDONALD, T.C., LANGRIDGE-MONOPOLIS, J.L. Breaching Characteristics of Dam Failures. *Journal of Hydraulic Engineering*, 1984, Nr. 110(5): 567-586.
- [18] FROEHLICH, D.C. Peak Outflow from Breached Embankment Dam. *Journal of Water Resources Planning and Management*, 1995, Nr. 121(1): 90-97.
- [19] BROICH, K. Computergestützte Analyse des Dammerosionsbruchs. *Universität der Bundeswehr München*, 1996.

SUMMARY

In order to contribute to the understanding of the significance of several parameters and boundary conditions on the breach outflow hydrograph of overtopped embankment dams under falling water level and no reservoir inflow, two studies with three-dimensional experiments have been conducted at Vienna University of Technology. The parameters investigated were the influence of reservoir size and shape, different grain size distributions of the shell material, an upstream dam blanket, the significance of the initial breach depth as well as scalability and model effects. The most influential parameters are reservoir size, followed by shape. Shell material and an upstream impervious blanket do have a clear effect on breach processing, but the effect is not dominant. Further, the results cannot be comprehended with process-based models using sediment transport formulae from river engineering. The hydraulic and geotechnical conditions are outside the thresholds of the equations. Based on the results obtained from the studies, a simple approach for breach outflow hydrograph prediction, especially for embankments with comparatively smaller reservoir volume, is presented.

KEYWORDS

DAM FAILURE, OVERTOPPING, LABORATORY TEST

COMMISSION INTERNATIONALE DES GRANDS BARRAGES

VINGT-SIXIÈME CONGRÈS DES GRANDS BARRAGES
Autriche, juillet 2018

DOI 10.3217/978-3-85125-620-8-236



This work licensed under a Creative Commons Attribution 4.0 International License. <https://creativecommons.org/licenses/by-nc-nd/4.0/>

**A RESERVOIR SYSTEM SIMULATION METHOD TO LESSEN WATER
SUPPLY DEFICIT AT DOWNSTREAM CONTROL POINTS USING A
HEURISTIC METHOD**

Sangho LEE

Professor, Civil Engineering, PUKYONG NATIONAL UNIVERSITY

KOREA, REPUBLIC OF

Youngkyu JIN

Ph.D. course, Civil Engineering, PUKYONG NATIONAL UNIVERSITY

KOREA, REPUBLIC OF

A RESERVOIR SYSTEM SIMULATION METHOD TO LESSEN WATER SUPPLY DEFICIT AT DOWNSTREAM CONTROL POINTS USING A HEURISTIC METHOD *

Sangho LEE

Professor, Civil Engineering, PUKYONG NATIONAL UNIVERSITY

Youngkyu JIN

Ph.D. course, Civil Engineering, PUKYONG NATIONAL UNIVERSITY

KOREA, REPUBLIC OF

1. INTRODUCTION

Drought is a temporary period of deficiency in precipitation relative to normal conditions that may induce insufficiency to meet the water demands of human activities. The amount of precipitation during the three months of summer is fifty to sixty percent of the annual precipitation in the central and southern parts of the Korean Peninsula. Thus, relatively small amounts of precipitation on wet periods for one or two consecutive years cause shortage of water supply. There has been a drought every five to seven years in the Nakdong River basin of the Korean Peninsula. A severe drought in 2014 led to set systematic operation rules of limited water supply from multipurpose dams in the Nakdong River basin against drought occurrence. The rules, however, have been modified to fit the actual situation of water supply, and thus alternative researches and developments have been still needed. The contents of this study on water supply operation rules of the dams include the derivation results of hedging rules for single reservoir operation and the decision results of parameters on additional water supply from upstream dams to lessen water supply shortage at downstream control points.

Korean government have constructed several multipurpose dams in the Nakdong River basin and each dam has its own purpose on water supply and flood control. A discrete hedging rule having several hedging phases can be effective method for water supply operation of a reservoir against drought periods [1]. We present briefly the derivation results of the discrete hedging rules of the five major dams for water supply operation in the section 2. The rules for independent operation of the reservoirs, however, do not always ensure a stable supply of water against different future time series of drought inflow to the dam. If the other dams may supplement the water supply shortage from a dam, overall water supply of the

* *PROCÉDÉ DE SIMULATION DE SYSTÈME DE RÉSERVOIR PERMETTANT D'ÉVITER UN DÉFICIT D'ALIMENTATION EN EAU AUX POINTS DE CONTRÔLE EN AVAL EN UTILISANT UNE MÉTHODE HEURISTIQUE*

reservoir system will be more stable. Applying the discrete hedging rules mentioned above, we made a method of reservoir system operation to lessen water supply deficit at the downstream control points. The parameters needed for the reservoir system operation are additional water supply amounts from the upstream reservoirs and minimum reserve volumes of the upstream reservoirs above the trigger volumes of the first hedging phase. We describe the formulation of the method of reservoir system operation including parameters mentioned above in the section 3. We show the heuristic search results of the parameters and reservoir system simulation results in the section 4.

2. HEDGING RULES OF INDEPENDENT OPERATION OF A RESERVOIR

Jin et al. [2] developed the discrete hedging rules of water supply for the five dams: Andong, Imha, Hapcheon, Namgang, and Miryang. The rules depend on current reservoir storage without incorporation of the future reservoir inflow. A time interval of water supply from a dam is defined as follows: the first and second periods of a month have ten days; the third period has the remaining days of the month. That time division method about ten days comes from oriental calendar. We pronounce the unit of the time interval as / sun / and name it 'sun.' A time interval has four trigger volumes of hedging phases. A hedging phase includes 36 trigger volumes that form a line for the whole year. The application of a mixed integer programming module results in four hedging rule curves of each dam. The objective function of the optimization model is Eq. [1]:

$$\text{Maximize } \sum_{t=1}^T y_{1,t} - \omega \sum_{p=1}^{12} (V_{1,p} + V_{2,p} + V_{3,p} + V_{4,p} + V_5) \quad [1]$$

where $y_{1,t} = 1$ if full demand is available during a period t or 0, otherwise; $\omega =$ a weight value; $T =$ the whole period of reservoir simulation; p is 1 to 36; $V_{1,p}$, $V_{2,p}$, $V_{3,p}$, and $V_{4,p}$, are trigger volumes of concern, caution, alert, and severe phases, respectively; and $V_{5,p} =$ the reservoir storage of low water level. Jin et al. [2] describe the twenty-five constraint equations.

Fig. 1 shows the derived hedging rule curves of four dams. Fig. 1 includes the Box-whisker plots drawn by monthly historical records of reservoir storage. The hedging rule curve values in summer are relatively larger than those of the other seasons are for Andong, Imha, and Hapcheon dams. It means that refrained release and higher storage status in summer and wet season may guarantee stable water supply until the end of dry seasons of the next year. The watershed area of Namgang dam is 2285 km² and the storage capacity is 309.2 million m³ and somewhat small. The design water supply of Namgang dam is small compared to the inflow, which results in different hedging rule curves from the other curves. The case of Miryang dam is similar to Namgang dam and is omitted here.

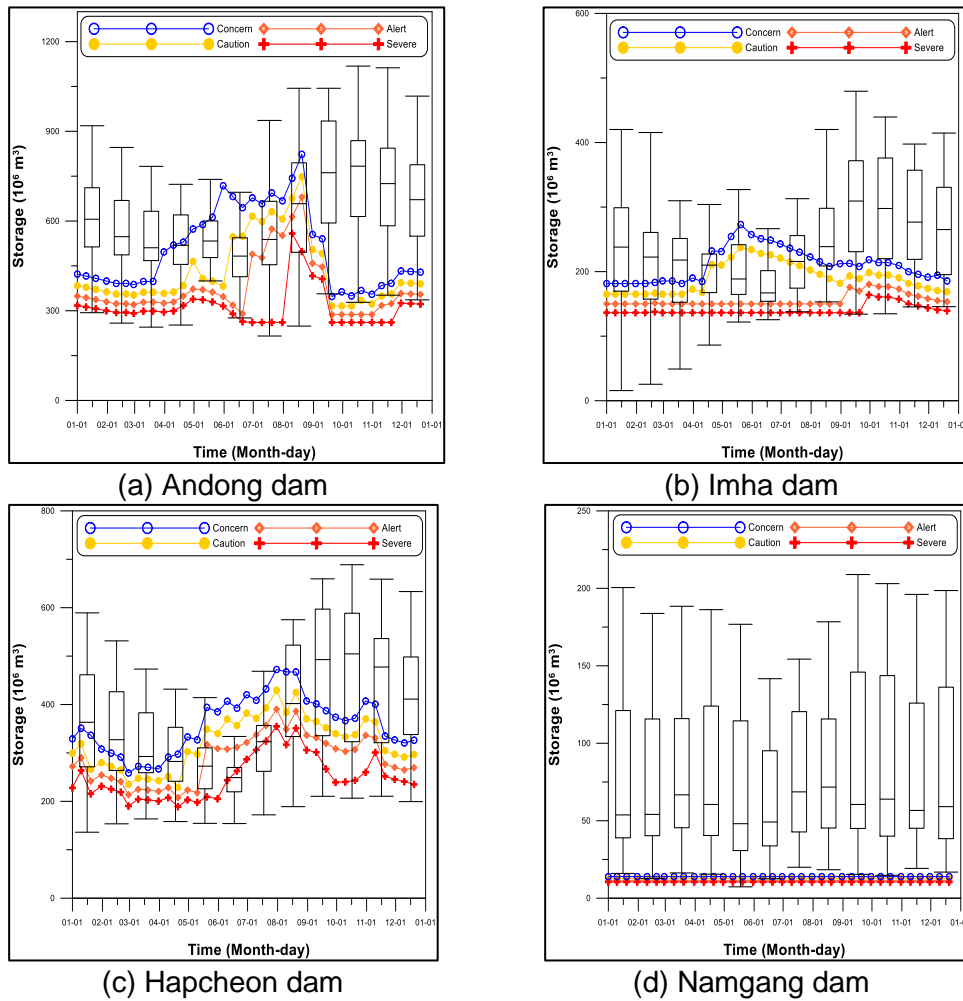


Fig. 1

Derived hedging rule curves depending on beginning storage [2]
Courbes de règles de couverture dérivées en fonction du stockage de début

3. RESERVOIR SYSTEM OPERATION METHODOLOGY

3.1. RESERVOIR SYSTEM OPERATION RULE

The five reservoirs form a system of reservoirs (Fig. 2). If the water supply shortage from a dam may be supplemented by the other dams, overall water supply of the reservoir system will be more stable. An upstream dam has water supply contracts with several demand centers near downstream control points. For example, Andong reservoir has water supply contracts with the downstream demand centers near control points 1 and 3. The rule of reservoir system operation is as follows and Fig. 3 describes it. If a water supply amount is less than the contract amount at a control point, some upstream reservoirs may supply

additional water to lessen water supply shortage at the downstream control point. Sufficient storage is the condition that upstream reservoirs provide extra water. If reservoir storage is not sufficient, the reservoir supply water independently.

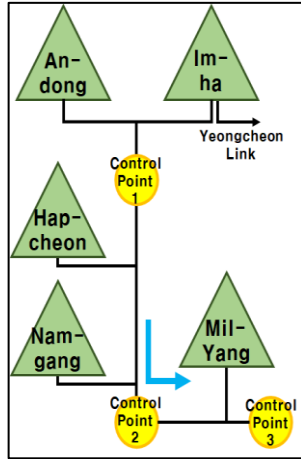


Fig. 2

Schematic diagram of the reservoir system [2]
Schéma du système de réservoir

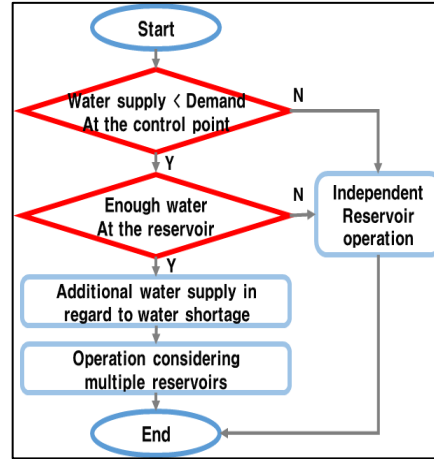


Fig. 3

Flow chart for the reservoir system operation rule to lessen water shortage at downstream control points [2]

Organigramme de la règle d'exploitation du système de réservoir pour réduire la pénurie d'eau aux points de contrôle en aval

3.2. OPTIMIZATION PROBLEM

The decision variables needed for the reservoir system operation are additional water supply amounts from the upstream reservoirs and minimum reserve volumes of the upstream reservoirs above the trigger volumes of the first hedging phase. The objective function is Eq. 2 that minimizes the total sum of water shortages at the control points over the whole simulation period and the weighted total number of times during which water supply failed at each dam:

$$\text{Minimize } Z = \left(\sum_{cp=1}^3 \sum_{t=1}^T \text{Deficit}_{cp,t} \right) + \left(\omega \sum_{r=1}^5 \sum_{t=1}^T \text{Fail}_{r,t} \right) \quad [2]$$

where cp is control point; T is the total number of periods for reservoir system optimization; t is the period; $\text{Deficit}_{cp,t}$ is water supply deficit during a period at a control point; $\text{Fail}_{r,t} = 1$ if water supply is failed during period t or 0, otherwise; ω is a weight value that is big to minimize water supply failures.

3.3. DYNAMICALLY DIMENSIONED SEARCH METHOD

The optimization problem has sixteen decision variables mentioned in the previous section. We applied a heuristic search method to decide the decision variable values. Using 2 to 80 dimensional test functions, Kang [3] evaluated three types of heuristic techniques: a genetic algorithm; shuffled complex evolution [4]; and a dynamically dimensioned search method [5]. He concluded the dynamically dimensioned search method is superior to the other two in converging performance to a global optimum. We applied a dynamically dimensioned search method to the optimization problem based on the evaluation results for the three heuristic search methods. The dynamically dimensioned search method uses search strategies that perform searches globally at the initial iteration stage and locally at the post-repeating stage, regardless of the maximum number of iterations.

4. SEARCH AND RESERVOIR SYSTEM OPERATION RESULTS

4.1. SEARCH RESULTS OF OPTIMIZATION MODEL

The total number of iterations for one search run was 0.2 million. Optimization run was carried out once more with the first answers as the initial values. Fig. 4 illustrates the convergence of the objective function in the optimization process. Although it is difficult to distinguish visually, the value of the objective function decreases slightly after the sixth search iteration.

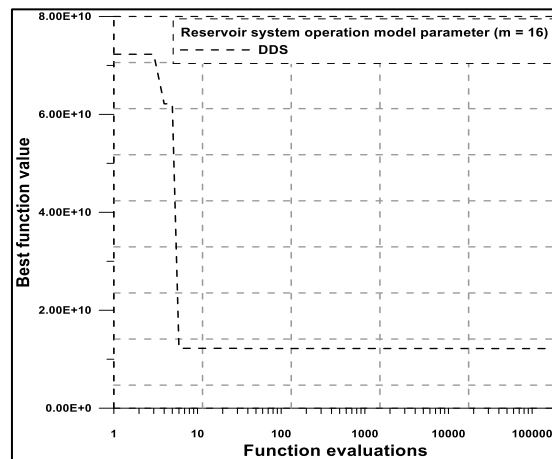


Fig. 4

Convergence of the objective function value [2]
La convergence de la valeur de la fonction objective

Tables 1 and 2 show the search results of the decision variables. Table 1 shows the priority and additional water supply proportion of the downstream water supply shortage for each dam by control point. The Andong reservoir additionally releases seven percent of the water supply shortage in the control point 1 that is

relatively small amount. Regarding the lack of water supply at the control point 2, the priority of additional release of Namgang reservoir is highest and the proportion of additional release for the lack of water supply is the largest. For the Namgang reservoir, available water is quite large due to its large basin area and high inflow. Due to these characteristics, the Namgang reservoir can be considered to have a relatively large storage margin for additional release against the shortage of downstream water supply. As the water supply volume of Hapcheon reservoir is relatively larger than the inflow and storage capacity of the reservoir, it is deemed that the proportion of additional releases was found to be small. Table 2 shows the search results for minimum water reserve above the trigger volume of concern stage to supply water additionally.

Table 1
Optimized results of additional water supply for the downstream water supply shortage [2]

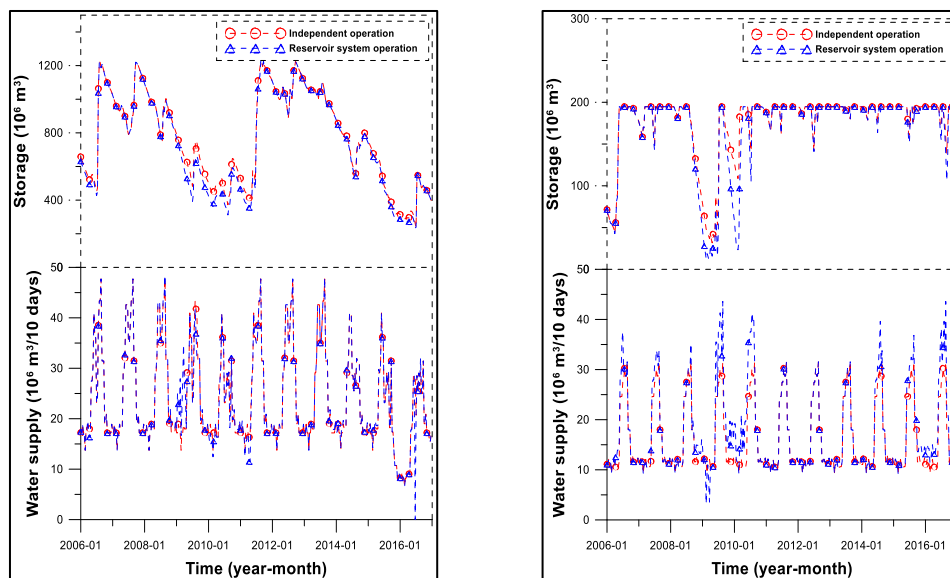
Control point	Dam	Optimization results	
		Priority	Additional water supply proportion of the downstream water supply shortage (%)
1	Andong	1	7
	Imha	2	99
2	Andong	2	85
	Imha	3	70
	Hapcheon	4	7
	Namgang	1	99
3	Andong	1	56
	Imha	2	61
	Hapcheon	3	53
	Namgang	4	99
	Milyang	5	59

Table 2
Minimum reserve volume above the trigger volume of concern stage [2]

Dam	Minimum reserve volume (m ³)
Andong	19,196,600
Imha	7,608,200
Hapcheon	8,894,950
Namgang	27,252,100
Milyang	35,588,100

4.2. RESULTS OF MITIGATION OF WATER SUPPLY SHORTAGE AT CONTROL POINTS

The results of reservoir system operation using determined variable values were compared with the results of the independent reservoir operations. The operation period of the reservoirs is 2006 to 2016. Fig. 5 shows the reservoir storages and water supply amounts excluding the spillway releases: only the results of Andong and Namgang reservoirs are shown by page limitation. The design water supply amounts are provided when the reservoir storage volumes are on the normal status beyond hedging phases. The water supply is rationed when the reservoir storage volumes are under hedging phases. Fig. 6 indicates the shortage of water supply at control points 1 and 2. Table 3 shows the total deficit of water supply, the maximum deficit of water supply, the number of rationing, and the reliability of each control point. Due to additional release of the Andong reservoir for control point 1, the reservoir water level reached low water level, resulting in a complete failure of water supply for ten days (Fig. 5(a)). As for control point 2, the total water supply deficit was reduced 91 % over the independent operation of the reservoirs due to the effects of additional releases from the Namgang reservoir (Table 3). Additional releases of upstream reservoirs into the downstream regions are considered effective in the total deficit of water supply, but may cause increased water supply deficit for short periods during a severe drought. Therefore, further research is needed to limit the search ranges of additional water supply amounts from upstream reservoirs to prevent adverse effects of reservoir system operations.



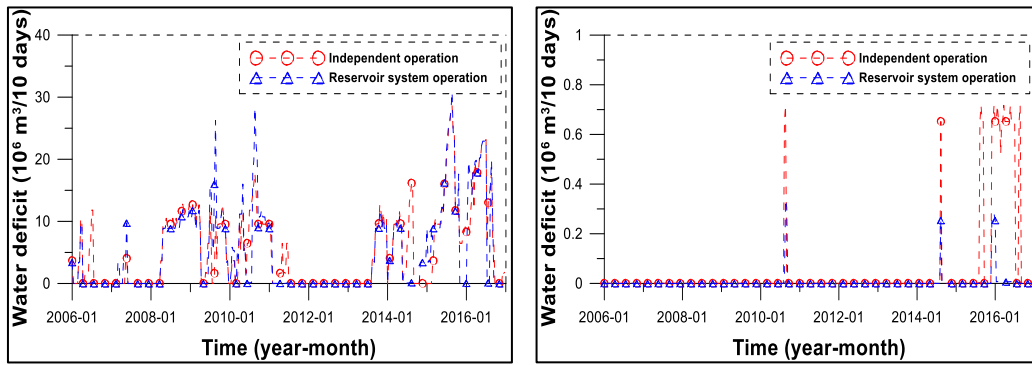
(a) Andong dam

(b) Namgang dam

Fig. 5

Comparison of results between independent reservoir operation and reservoir system operation [2]

Comparaison des résultats entre le fonctionnement indépendant du réservoir et le fonctionnement du réservoir



(a) Control point 1

(b) Control point 2

Fig. 6

Comparison of the water supply deficit at the control points between the independent and reservoir system operations [2]

Comparaison du déficit d'approvisionnement en eau aux points de contrôle entre les opérations du système indépendant et du réservoir

Table 3

Comparison of the water supply deficit at the control points between the independent and reservoir system operations [2]

Operational performance statistics	Independent operation			Reservoir system operation		
	Control point			Control point		
	1	2	3	1	2	3
Total water supply deficit ($10^6 \text{ m}^3/10 \text{ days}$)	2073	737	2	1974	67	0.2
Maximum water supply deficit ($10^6 \text{ m}^3/10 \text{ days}$)	28	12	0.7	31	11	0.3
The number of rationing	210	149	31	239	150	31
Reliability	0.47	0.62	0.92	0.40	0.62	0.92

5. CONCLUSIONS

Dynamically dimensioned search methods are excellent search techniques that can find a solution of a complex optimization problem near to a global optimum. We applied a dynamically dimensioned search method to an optimization problem of a reservoir system operation under the discrete hedging rules of independent water supply operation of the five reservoirs in the Nakdong River basin. The downstream tributaries are not included in the reservoir system. The decision variables are additional water supply amounts from the upstream reservoirs and

minimum reserve volumes of the upstream reservoirs above the trigger volumes of the first hedging phase. Results of the reservoir system operation using searched values of decision variables are as follows. Additional releases of upstream reservoirs into the downstream regions are considered effective in the total deficit of water supply, but may cause increased water supply deficit for short periods during a severe drought. Thus, further researches are needed to limit the search ranges of the additional water supply amounts from the upstream reservoirs to suppress the increase of the maximum deficits of water supply resulted from the independent operation of the reservoirs.

ACKNOWLEDGEMENTS

This work has been supported by a grant (NRF-2017R1A2B2003715) from the National Research Foundation of Korea (NRF), funded by the Korean government.

REFERENCES

- [1] SHIH J.S., REVELLE C. Water supply operations during drought: a discrete hedging rule. *European Journal of Operational Research*, 1995, Vol. 82, Issue 1, pp. 163-175.
- [2] JIN Y., LEE S., JUNG T. Reservoir operation applying discrete hedging rule curves depending on current storage to cope with droughts. *Journal of Korean Society of Hazard Mitigation*, 2017, Vol. 17, No. 1, pp. 107-115.
- [3] KANG S. Development and application of water level zone decision method for long-term reservoir operation using dynamically dimensioned search algorithm. Ph. D. thesis, Pukyong National University, 2011.
- [4] DUAN, Q., SOROOSHIAN S., GUPTA V.L. Effective and efficient global optimization for conceptual rainfall-runoff models. *Water Resources Research*, AGU, 1992, Vol. 28, No. 4, pp. 1015-1031.
- [5] Tolson B.A., Shoemaker C.A. Dynamically dimensioned search algorithm for computationally efficient watershed model calibration. *Water Resources Research*, AGU, Vol. 43, No. 1, pp. 1-16.

SUMMARY

A discrete hedging rule having several hedging phases can be effective method for water supply operation of a reservoir against drought periods. Hedging

rule curves for five multipurpose dams were determined independently by applying a mixed integer programming module in the Nakong River basin, the Republic of Korea. The derived hedging rule curves reveals the following: refrained release and higher storage status in wet season may guarantee stable water supply until the end of dry seasons of the next year; the Namgang reservoir needs little hedging operation due to the relatively large reservoir inflow and small amount of design water supply. Applying the discrete hedging rules derived above, we made a method of reservoir system operation to lessen water supply deficit at the downstream control points. The parameters needed for the reservoir system operation are additional water supply amounts from the upstream reservoirs and minimum reserve volumes of the upstream reservoirs above the trigger volumes of the first hedging phase. We decided the sixteen parameters by applying a dynamically dimensioned search method. The reservoir system operation showed that additional releases from upstream reservoirs into the downstream regions are considered effective in the total deficit of water supply, but may cause increased maximum deficit of water supply for short periods during a severe drought.

RÉSUMÉ

Une règle de couverture discrète comportant plusieurs phases de couverture peut être une méthode efficace pour l'alimentation en eau d'un réservoir contre les périodes de sécheresse. Les courbes des règles de couverture pour cinq barrages polyvalents ont été déterminées indépendamment en appliquant un module de programmation mixte dans le bassin de la rivière Nakong, en République de Corée. Les courbes dérivées de la règle de couverture révèlent ce qui suit: le rejet et le stockage plus élevé en saison humide peuvent garantir un approvisionnement en eau stable jusqu'à la fin des saisons sèches de l'année suivante; le réservoir Namgang a besoin de peu d'opérations de couverture en raison de l'afflux relativement important du réservoir et de la faible quantité d'eau de conception. En appliquant les règles de couverture discrètes dérivées ci-dessus, nous avons fait une méthode de fonctionnement du système de réservoir pour réduire le déficit d'approvisionnement en eau aux points de contrôle en aval. Les paramètres nécessaires pour le fonctionnement du système de réservoir sont des quantités d'eau supplémentaires provenant des réservoirs en amont et des volumes de réserve minimums des réservoirs en amont au-dessus des volumes de déclenchement de la première phase de couverture. Nous avons décidé les seize paramètres en appliquant une méthode de recherche dimensionnée dynamiquement. L'exploitation du système de réservoir a montré que des rejets supplémentaires provenant des réservoirs en amont dans les régions en aval sont considérés comme efficaces dans le déficit total d'approvisionnement en eau, mais peuvent causer un déficit maximal d'approvisionnement en eau pendant de courtes périodes.

COMMISSION INTERNATIONALE
DES GRANDS BARRAGES

VINGT-SIXIÈME CONGRÈS DES
GRANDS BARRAGES
Autriche, juillet 2018

LANDSLIDE DAMS - LONG KNOWN, BUT JET OVERLOOKED RARE PHENOMENON: POSSIBILITY TO PREVENT DAMAGE

Nina HUMAR¹, Klaudija SAPAČ², Mitja BRILLY, Ph.D.², Andrej
KRYŽANOWSKI, Ph.D.³

¹*Independent Professional Associate, INSTITUT FOR WATER OF THE
REPUBLIC OF SLOVENIA*

²*Research, UNIVERSITY OF LJUBLJANA, FACULTY OF CIVIL AND
GEODETIC ENGINEERING*

³*Head of the Chair of Hydraulic Engineering, UNIVERSITY OF LJUBLJANA,
FACULTY OF CIVIL AND GEODETIC ENGINEERING*

SLOVENIA

1. INTRODUCTION

Nowadays lack of space is an important factor connected to economic development and the extent of damage (magnitude) from natural disasters. According to United Nation reports, 90% of all natural disaster is somehow connected or better triggered by weather and climate changes. Floods account almost 47% of all weather related disasters. The intensity of events and disaster extent increases and the extent of damage is almost directly commensurate with intensity of settlement and land use.

Apparat from flooding, heavy rain is closely connected to another major type of natural disaster – Landslides. When the masses slide down to the bottom of the valley and block the river course – we speak of the landslide dams. Landslide dams are an old phenomenon – many glacial and other lakes are a still an existing proof. The event is quite rare. However, due climate changes and due to rapid urbanization presents a significant threat. This type of dam may not be a long lasting structure - they may last for a few hours or for thousands of years. Furthermore, it is difficult to assess the condition and predict the breaching mechanisms, since usually there is no time to make complex analysis. Flush flood or debris flow caused by brake of this type of dams is even more dangerous, than the breaching of regular dams, because the breach happens quickly and the flow is strong and destructive.

In the paper we will present several such past events in Europe and worldwide and touch the question what we could learn from historical event.

REFERENCES

- [1] Alford, D., Cunha, S.F., Ives, J.D., Lake Sarez, Pamir Mountains, Tajikistan: mountain hazards and development assistance. *Mountain Research and Development* 20, 2000 pp 20–23.
- [2] Bonnard, Ch., Technical and Human Aspects of Historic Rockslide-Dammed Lakes and Landslide Dam Breaches, *Natural and Artificial Rockslide Dams, Vol.133 of the series Lecture Notes in Earth Sciences*, 2001 pp 101-122
- [3] Duman, T.Y., The largest landslide dam in Turkey: Tortum landslide, *Engineering Geology* 104 (2009), 2009, pp 66–79
- [4] Hancox, G.T., Mc Saveney, M.J., Manville, V.R., Davies, T.R., The October 1999 Mt Adams rock avalanche and subsequent landslide dam-break flood and effects in Poerua River, Westland, New Zealand, *New Zealand Journal of Geology & Geophysics*, 2005, Vol. 48: 683–705, *The Royal Society of New Zealand*
- [5] Komac, B., Geografski vidiki nesreče (Geographical aspects of the Disaster in Log pod Mangartom), *Ujma št 14-15*, 2001, Republiški štab za civilno zaščito
- [6] Lazarević R., Jovačko klizište, *Erozija – stručno informativni bilten*, 1977, št 8
- [7] Majes, B., Analiza plazu in možnost njegove sanacije (Analysis of landslide and its Rehabilitation), *Ujma št 14-15*, 2001/2002, Republiški štab za civilno zaščito
- [8] Mankha VDC, Report on Jure Landslide, Sindhupalchowk District, Nepal Government, Ministry of Irrigation, Ministry of Irrigation Report, September 2014, <http://www.preventionweb.net/news/view/46795>
- [9] Meze, D., , Ujma 1990 v Gornji Savinjski dolini, med Lučami in Mozirsko kotlinico (Effect of Flooding in the Upper Savinja Valley Between Luče and the Mozirja Basin), *Ujma št 5*, 1991, Republiški štab za civilno zaščito
- [10] Mikoš M., Četina M. and Brilly M., Hydrologic conditions responsible for triggering the Stože landslide, Slovenia, *Engineering Geology* 73 (2004) 2004, pp 193–213
- [11] Natek, K., Plazovi v Gornji savinjski dolini, (Landslides in the Upper Savinja Valley), *Ujma št 5*, 1991, Republiški štab za civilno zaščito
- [12] Planki, J., Delovanje civile zaščite ob poplavih v Lučah, *Ujma št 5*, 1991, Republiški štab za civilno zaščito
- [13] Plaza, G. and Zevallos, O., La Josefina rockslide and rio Paute landslide dam, Ecuador. The la Josefina rockslide, *Landslide News* 8, 1994, 4–6.
- [14] Plaza, G., Zevallos, O., Cadier, E., *Natural and Artificial Rockslide Dams, Lecture Notes in Earth, Sciences* 133, 2011, Springer-Verlag Berlin Heidelberg
- [15] Schuster, R.L., 2006, Risk reduction measures for landslide dams, *Italian Journal of Engineering Geology and Environment, Special Issue 1 (2006)*, 2006
- [16] Sevilla, J., The Josefina landslide and its implications in the electrical service for the Republic of Ecuador, *Proceedings 7th International IAEG Congress*, 1994, *Balkema, Rotterdam*, pp. 1801–1810.
- [17] Witkind, I.J., Potential Geologic Hazards Near the Thistle Landslide, Utah County, Utah, *Open-File Report 86-119, United States Geological Survey*, 1986
- [18] Ušeničnik, B., Posledice in ukrepanje ob nesreči (Consequences of and response to the Disaster), *Ujma št 14-15*, 2002, Republiški štab za civilno zaščito

COMMISSION INTERNATIONALE DES GRANDS BARRAGES

VINGT-SIXIÈME CONGRÈS DES GRANDS BARRAGES
Autriche, juillet 2018

DOI 10.3217/978-3-85125-620-8-238



This work licensed under a Creative Commons Attribution 4.0 International License. <https://creativecommons.org/licenses/by-nc-nd/4.0/>

**GEOLOGY AND GEOTECHNICAL CONDITION FROM GEOLOGICAL
MAPPING, CORE DRILLING, AND GEOPHYSICAL AT MASANG II
HYDROPOWER PROJECT, WEST SUMATERA, INDONESIA**

Jodi Prakoso BASUKI

Geologist at PT. KWARSA HEXAGON. He has been involved in feasibility studies of hydropower projects in Indonesia or other geotechnical project to give the geology and geotechnical recommendation

INDONESIA

Kiki Lukman NULHAKIM

Geologist at PT. KWARSA HEXAGON. He has been involved in feasibility studies of hydropower projects in Indonesia or other geotechnical project to give the geology and geotechnical recommendation

INDONESIA

Geology and Geotechnical Condition from Geological Mapping, Core Drilling, and Geophysical at Masang II Hydropower Project, West Sumatera, Indonesia

Jodi Prakoso Basuki ¹⁾
Kiki Lukman Nulhakim ¹⁾

¹⁾ Geologist at PT. Kwarsa Hexagon. He has been involved in feasibility studies of hydropower projects in Indonesia or other geotechnical project to give the geology and geotechnical recommendation

Introduction

Masang II project is one of the hydropower projects to develop in Agam District, West Sumatra Province. To realize this project, a weir will be build on the Sianok River. Water that diverted from weir, will be used utilized for hydro power plant (hydropower) with a capacity of 2x26 MW. The Masang II hydropower project is located on the Sianok River that flows from south to north, which empties into the Masang River on the border of Agam and Pasaman districts. Seeing the area supported by the topographic condition of the region, the Sianok River has considerable potential to develop into a hydropower energy source (hydropower). The aim of this paper is to know geology and geotechnical condition at project location.

Based on the Regional Geology Map of Padang, Sumatera (Kastowo, Gerhard, Gafoer, and Amin; 1996) 1: 250.000 scale published by Geological Agency, West of Sumatera consists of 3 rock group Pre Tertiary Rock Unit, Tertiary Rock Unit, and Quaternary Rock Unit. In general, the stratigraphy of the project site is composed of tuff and metamorphic rock. The major geological structure in and around the Masang II site is the Sumatran Fault Zone (SFZ), one of the most active zones in Indonesia. It affects the condition of bearing capacity at project location.

Method

The method that used in this project is literature review of project location, field surveys include surface geological mapping, geotechnical and geophysical investigation, consisting of core drilling and seismic refraction have been performed along with soil/rock laboratory tests and analysis.

Regional Geology

Physiographically project location is belong into Mountain Barisan Block with characteiristic by a series of NW – SE Block Mountain, The Sumatran Fault Zone, locally Block Faulting and Active Volcanos.

Based on the Regional Geology Map of Padang, Sumatera (Kastowo, Gerhard, Gafoer, and Amin; 1996) project location consist of Permian Limestone Rocks (Pl), Ultrabasic Rock (Kub), Early Tertiary Andesite (Ta), Andesite of Maninjau Caldera (Qamj), and Pumiceous Tuff and Andesite (Qpt) (Fig. 1). Regional tectonic of

project location according to Barber et. Al, (2005), activities of the Sumatera Fault is continued until now. Mechanism of movement is strike slip dextral fault, is related to subduction zone from Indo-Australian Plate that subducted into under Eurasian Plate at west Sumatera Island.

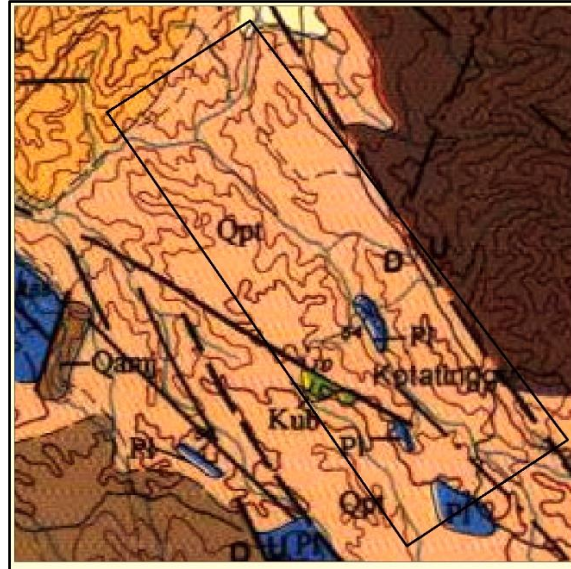


Fig. 1

Regional Geology Map of Padang, Sumatera (Kastowo, Gerhard, Gafoer, and Amin; 1996)

Investigation Result

a. Geological Mapping of Project Area

Stratigraphy of the project site from old to young: Pre Tertiary Metamorphic Polimic Fragment Rock Unit and Quaternary Pumiceous Tuff Rock Unit. Pre Tertiary Metamorphic Polimic Fragment Rock Unit consists of many types of rocks that are mixed in a matrix, it is predicted that these units are formed in the subduction zone resulting many various types of rocks. Types of rock in this unit are calcarenite, calcipulverite, metalimestone, serpentinite, schist mica, conglomerate-breccia, and diorit as fragment. Quaternary Pumiceous Tuff Rock Unit is located at the top of the hill. The outcrop was very weathered and became rice field area and plantation. The thickness of this outcrop is 1-20 meters and can be found at side of the road.

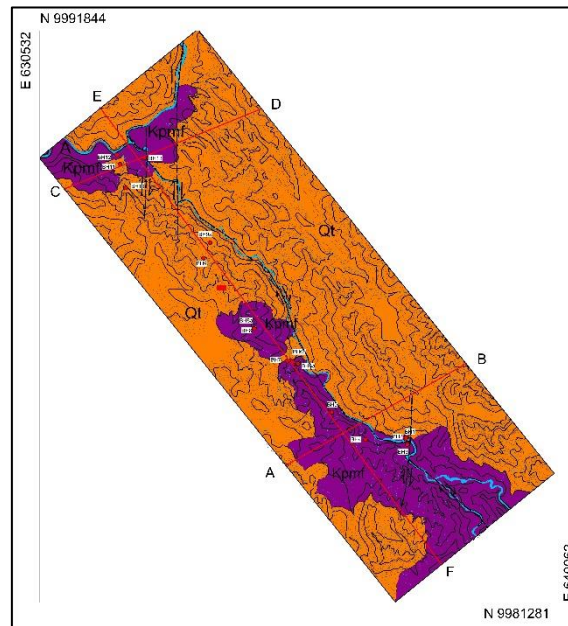


Fig. 2
Geological Map of Project Area

b. Core Drilling

There are 15 (fifteen) points of core drilling and in-situ testing from weir until power house. The result of core drilling show many various of metamorphic rocks.

Weir

Based on the geological mapping at the weir area is composed of metalimestone. At the surface metalimestone outcrop show the cracked structure and jointed. Metalimestone is predicted a part of fragment from melange zone. Meanwhile, based on the result of core drilling at weir site (BH1, BH2, and BH3), top layer (fluvial deposit) is composed by sandy clay-silty clay contain boulder. Below of top layer, generally composed by metalimestone with high fractured and cracked with thickness is about 20 meters.

Connecting Culvert

At connecting culvert there is cores drilling that is BH-4. These location core drilling at Jorong Bamban with long of the connecting culvert is 881 m. Based on the results of geological mapping of the surface can be seen that the connecting culvert composed by serpentinite and metalimestone. At the surface metalimestone outcrop show cracked structure and fractured. Serpentinite is found at Intermiten River and around the serpentinite outcrop is found polimic metamorphic rock and gneiss. But this metalimestone and serpentinite predicted part of fragment from melange zone.

Connecting Tunnel

At the connecting tunnel, there is core-drilling BH5. From geological mapping, the connecting tunnel composed by serpentinite and metalimestone. At the surface metalimestone outcrop show cracked structure and fractured. Metalimestone and serpentinite is predicted a part of mélangé. Top soil layer (sandy clay) with the thick of 0.8 meter and below of this layer is metalimestone with thick of 39.2m. The condition of metalimestone layer is fracture. That indicated at BH-05 is fault zone and it is an impact from sumateran fault.

Intermediet Pond

In the intermediate pond area, there are three (3) boreholes BH-06A (right abutment), BH-06B (as dam), and BH-07 (left abutment). Based on the results of geological mapping this area is composed by metalimestone and tuff. At the surface metalimestone outcrop show cracked structure and jointed, but this metalimestone predicted a part of fragment from melange zone.

Headrace Tunnel

At the Headrace tunnel have 3 point of core drilling (BH-8, BH-8a & BH-9). Top soil of the borehole BH-8 & BH-8a are composed by sandy clay-clayey sand with thick of 3.4 meter. Below this layer composed by Phyllite, Schist Mica, Schist & Sand (mélangé deposite) with the depth of 3.4-75 meters. Basement layer (phyllite) is found from the depth of 75-90 meters. Headrace tunnel is past of mélangé deposite and basement layer.

Around headrace tunnel found outcrop like schist and phyllite with high fractured. It indicated around headrace tunnel has affected by geological structure. Beside that, core samples at BH-08, BH-08a, and BH-09 is fractured and jointed. It can predicted that an impact of sumateran fault zone and must be aware when buikd the tunnel.

Surge Tank

At the surgetank is represented by the results of observations on the BH-10. Top soils of the borehole BH-10 are composed by soft clay sand with thick of 3.6 meter. Below this layer composed by Sand, Breccia and Serpentinite (mélangé deposite) with the depth of 3.6-78 meters. Basement layer (phyllite) is found from the depth of 78-80 meters.

Penstock

Stratigraphy at penstock is represented by the result of observation on the BH-11. Top soils of the borehole BH-11 are composed by sand and silty clay. Silty clay are dominated at the bottom of the layer. From top layer to bottom hardness of the soil rise up.

Power House

Core drilling at the Power House area is BH-12, Soil layer (silty Clay – Clayey Sand contain of Boulder) at the depth of 0 – 4.8 m. Intercalation of Metalimestone and Slate layer below the soil layer.

c. Seismic Refraction

Seismic refraction was held by using air gun as source of vibration at tunnel area. The vibration will be received by geophone with interval 10 meters. One shoot of this air gun can reach 500 meter of distance. Seismic activity is performed along the tunnel area from BH-4 until BH10 where at that bore hole are the tunnel area. Total range of distance seismic refraction is 7,5 km with 16 hole and 15 line.

The result of this seismic refraction data can interpreted layer from top to bottom with >350 meter of depth based on velocity value. This data can help to interpreted layer of the project area from velocity. However, this data must be correlation with borehole data to make interpretation correctly. Based on this seismic data, project area divided into 3 layers, that is top soil/tuff, mélange deposit, and basement. All of this layer have different characteristic from velocity in the field. Top soil have velocity 200-600 m/s, mélange deposit have velocity 600-3000 m/s, and Basement have velocity >3000 m/s.

Geology and Geotechnical Condition

From geological mapping, core drilling, and seismic refraction data can be combined to interpretation geology condition from the surface and subsurface. After combined the data can interpreted that the project area consist of three layers that are soil/tuff, melange complex, and basement.

After combined from three data (geological mapping, core drilling, and seismic refraction), can be interpreted the geological section. Soil/tuff is at the top of the layer and consist of many kind of soil result from weathering of tuff. This layer have small velocity value (v_p) that is 200-600 m/s. Melange complex is at the bottom of soil/tuff layer where at this layer consist of many rock type and mixed into a layer. Melange complex consist of diorite, basalt, andesite, metamorphic rock like mica schist, slate, gneiss, metalimestone, and phyllite. This layer have velocity value (v_p) 600-3000 m/s. Basement layer is bottom of the layer and just consist of phyllite. This layer have velocity value (v_p) >3000 m/s.

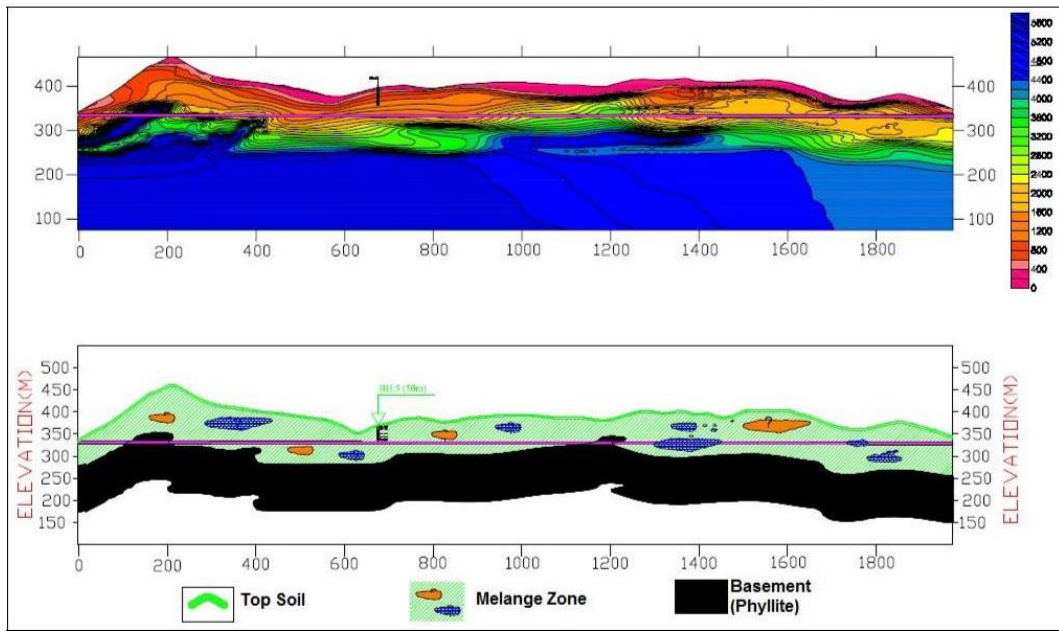


Fig. 3
Correlation between Seismic Refraction and Borehole at Connecting Tunnel

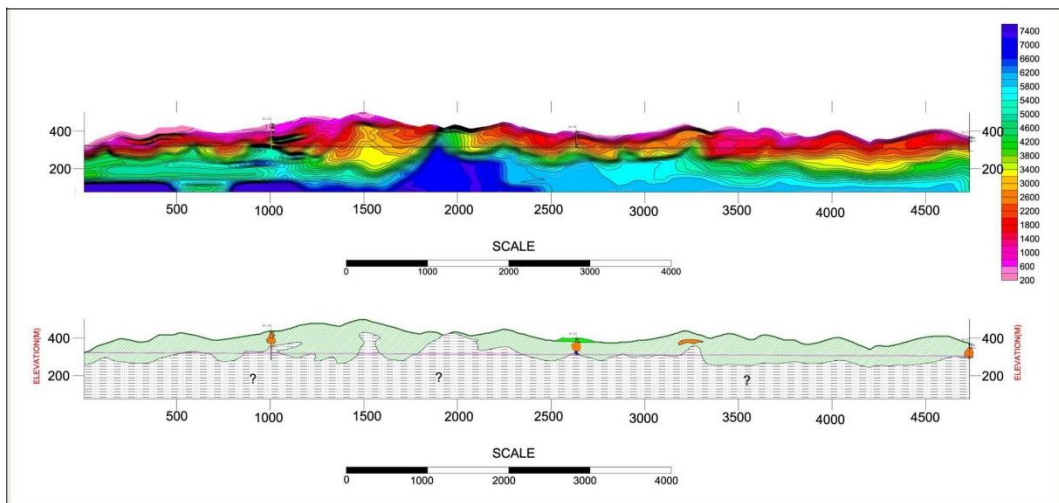


Fig. 4
Correlation between Seismic Refraction and Borehole at Headrace Tunnel

Geotechnical condition of the project area can be interpreted from core drilling and seismic refraction. Core drilling at the weir site can not be SPT test because the lithological is rock. At the depth of 5.8-15.7m is unstable based on SPT test where the SPT of the soil is 2-4 blows/feet. Meanwhile at the bottom of the weir site bearing capacity is good because bottom of the weir site is metalimestone. Although the bearing capacity of rock is high ($Q_a > 68 \text{ ton/m}^2$), but the rock conditions are fractured and cracked so it is grouting is recommended for this layer.

Due to metalimestone is fractured and cracked, possibly could be happen seepage at the weir site.

Foundation of Connecting Culvert is at the top soil and mélange deposite layer. The top soil consists of clayey sand and Sand. Bearing capacity of top soil layer with the depth of 0-12m about 6,8 – 21,8 ton/m². Melange deposite layer have bearing capacity about > 68 ton/m². Foundation of connecting culvert, where is at the top soil layer is not good, so pile foundation is recommended for it.

Foundation of dam site is at the mélange deposite layer. The mélange layer is consist of clayey sand weathered from tuff, silty clay contain diorite and metalimestone gravel, and clay contain metalimestone gravel. Based on core drilling result permeability test and bearing capacity analysis, intermediate pond no need to conducted grouting.

Foundation of headrace tunnel is at melange zone and basement. The melange layer is consist of various of rock like schist, metalimestone, breksi, and serpentinit. Bearing capacity at this layer is heterogeneous, in one place is stable but in other place is unstable. From RMR class, we can know that at melange zone is very unstable. At basement rock, bearing capacity is stable because at basement is very compact rock.

Table 1.
Corelation between Seismic Refraction and Borehole at Headrace Tunnel

Segment	Length (m)	Lithology	VP Seismic (m/sec)	Rock Mass Classificati on Terzaghi (Class)	γ (ton/m ³)		(Terzaghi , 1946) $p_v = H_p \gamma$ (ton/m ²)		Sing et al, 1995
									Pv (t/m ²)
S1	507	Metalimestone , Clayey Sand, Phyllite, Schist Mica, Schist, Sand, Breccia	600-2800	Completely crushed but chemically intact (VI)	1.53	2.3	15.2	22.32	30
S2	120	Phyllite	2800-3200	Very blocky and seamy (V)	2.26	2.3	20.3	20.98	20
S3	225	Metalimestone , Clayey Sand, Phyllite, Schist Mica, Schist, Sand, Breccia	600-2800	Completely crushed but chemically intact (VI)	1.53	2.3	15.2	22.32	30
S4	191	Phyllite	2800-3200	Very blocky and seamy (V)	2.26	2.3	20.3	20.98	20
S5	418	Metalimestone , Clayey Sand, Phyllite, Schist Mica, Schist, Sand, Breccia	600-2800	Completely crushed but chemically intact (VI)	1.53	2.3	15.2	22.32	30
S6	118	Phyllite	2800-3200	Very blocky and seamy (V)	2.26	2.3	20.3	20.98	20
S7	184	Metalimestone , Clayey Sand, Phyllite, Schist Mica, Schist, Sand, Breccia	600-2800	Completely crushed but chemically intact (VI)	1.53	2.3	15.2	22.32	30

Segment	Length (m)	Lithology	VP Seismic (m/sec)	Rock Mass Classification on Terzaghi (Class)	γ (ton/m ³)		(Terzaghi, 1946) $p_v = H_p \gamma$ (ton/m ²)		Sing et al, 1995
									Pv (t/m ²)
S8	569	Phyllite	2800-3200	Very blocky and seamy (V)	2.26	2.3	20.3	20.98	20
S9	257	etalimestone, Clayey Sand, Phyllite, Schist Mica, Schist, Sand, Breccia	600-2800	Completely crushed but chemically intact (VI)	1.53	2.3	15.2	22.32	30
S10	44	Phyllite	2800-3200	Very blocky and seamy (V)	2.26	2.3	20.3	20.98	20
S11	221	etalimestone, Clayey Sand, Phyllite, Schist Mica, Schist, Sand, Breccia	600-2800	Completely crushed but chemically intact (VI)	1.53	2.3	15.2	22.32	30
S12	27	Phyllite	2800-3200	Very blocky and seamy (V)	2.26	2.3	20.3	20.98	20
S13	297	etalimestone, Clayey Sand, Phyllite, Schist Mica, Schist, Sand, Breccia	600-2800	Completely crushed but chemically intact (VI)	1.53	2.3	15.2	22.32	30
S14	115	Phyllite	2800-3200	Very blocky and seamy (V)	2.26	2.3	20.3	20.98	20
S15	143 1	Metalimestone, Clayey Sand, Phyllite, Schist Mica, Schist, Sand, Breccia	600-2800	Completely crushed but chemically intact (VI)	1.53	2.3	15.2	22.32	30

Foundation of Penstock from BH-11 is recommended at the Hard Silty Clay – Clayey Sand layer (5-20 m depth) with the bearing capacity, $Q_{all} > 68 \text{ ton/m}^2$, which cutting the soil layer (0 – 5 m depth). From CPT's data, Dense or Cemented Sand layer at the depth between 2 – 8.2 m. Foundation of Penstock is recommended at this layer.

Foundation of Power House is recommended at the Metalimestone and Slate Intercalation layer (4.8 – 30m depth) with the bearing capacity, $Q_{all} > 68 \text{ ton/m}^2$, which cutting the soil layer (0 – 4.8m depth).

Summary

Masang project area consist of 3 layers that are soil/tuff layer, melange complex layer (consist of schist, phyllite, diorite, metalimestone, and serpentinite), and phyllite basement. This three layer have different bearing capacity value because affected to rock condition and hardness of the layer. Soil/tuff layer have small bearing capacity value because this layer is soft and easily to weathered. Melange complex is very heterogeneous condition, it can be stable but it can be stable, but the bearing capacity value is more higher than soil/tuff layer. Basement layer have high bearing capacity value is affected from the rock condition of basement rock is very compact and homogen.

Reference

Bieniawski (1974): "Engineering classification of rock masses and its application in tunneling". Proc. 3rd ISRM-Congress, Denver 1974, Vol. IIa, pp. 27-32.

Deere, D.U., Miller R.P. (1966): "Engineering classification and index properties for intact rock".

COMMISSION INTERNATIONALE DES GRANDS BARRAGES

VINGT-SIXIÈME CONGRÈS DES GRANDS BARRAGES
Autriche, juillet 2018

DOI 10.3217/978-3-85125-620-8-239



This work licensed under a Creative Commons Attribution 4.0 International License. <https://creativecommons.org/licenses/by-nc-nd/4.0/>

**NUMERICAL MODELLING OF ROCK-FALL ON THE CONCRETE ARCH-
GRAVITY DAM OF PLACE MOULIN**

Guido MAZZA'

RICERCA SUL SISTEMA ENERGETICO - RSE S.P.A.

ITALY

Antonella FRIGERIO

RICERCA SUL SISTEMA ENERGETICO - RSE S.P.A.

ITALY

Lorenzo ARTAZ

C.V.A. S.P.A. - COMPAGNIA VALDOSTANA DELLE ACQUE

ITALY

Morena COLLI

C.V.A. S.P.A. - COMPAGNIA VALDOSTANA DELLE ACQUE

ITALY

COMMISSION INTERNATIONALE
DES GRANDS BARRAGES

VINGT-SIXIÈME CONGRÈS DES
GRANDS BARRAGES
Autriche, juillet 2018

NUMERICAL MODELLING OF ROCK-FALL ON THE CONCRETE ARCH- GRAVITY DAM OF PLACE MOULIN

Guido MAZZA', Antonella FRIGERIO

RICERCA SUL SISTEMA ENERGETICO - RSE S.P.A.

ITALY

Lorenzo ARTAZ, Morena COLLI

C.V.A. S.P.A. - COMPAGNIA VALDOSTANA DELLE ACQUE

ITALY

1. INTRODUCTION

Several mountain slopes of the Alpine valleys, where many Italian large dams are located, are characterized by hazardous instability phenomena that might give rise to rock-fall that could impact on the above infrastructures. In order to plan adequate mitigation and protection works for the safety of the dams, the first step is the assessing of the consequences that potential events of rock-fall could cause on the structures.

This paper presents the numerical modeling of a massive boulder falling from the left bank of the reservoir and impacting on Place Moulin arch-gravity dam. The most hazardous instability phenomena provided by recent geological surveys were considered to characterize the volume and the trajectory of the boulder. The main consequences that the dam could suffer are described in terms of structural damage.

2. INSTABILITY PHENOMENA OF THE LEFT SLOPE OF THE RESERVOIR OF PLACE MOULIN

The dam of Place Moulin, located in the Municipality of Bionaz in Valpelline, in the Italian Region of Valle D'Aosta, is a concrete arch-gravity structure built between 1955 and 1965 (Fig. 1). The reservoir has a total volume of 105 Mm³ that feeds the power station of Valpelline.



Fig. 1
Downstream view of the dam of Place Moulin

The dam is 155 m high, with a crest length of 678 m and a thickness varying from 6,44 m at the crest and 41,94 m at the base. The dam volume is 1,51 Mm³.

The instability phenomena that occurred and might still take place on the rocky slope of the orographic left bank of the reservoir of Place Moulin were thoroughly investigated during some geological surveys [1][2]. The outcomes of these studies allowed to characterize the structural and geomorphologic setting of the left slope and to identify which potential kinematic mechanisms could directly threaten the dam.

First of all, the boulders that could detach, fall off and roll down along the left slope, will not exceed a volume of 10 m³ because of the strong fractured state of the in situ rock. The rock-fall hazard simulations highlighted that the first part of the left side of the dam crest, 30÷50 m long, has a 15÷60% probability to be threatened; the hazardous conditions progressively decrease moving towards the center of the crest and they become nearly negligible for a distance exceeding 80 m from the left abutment. The trajectories and the impact points of the main

boulders are mapped in Fig. 2 while the features of the most hazardous conditions for the dam are listed in Table 1.

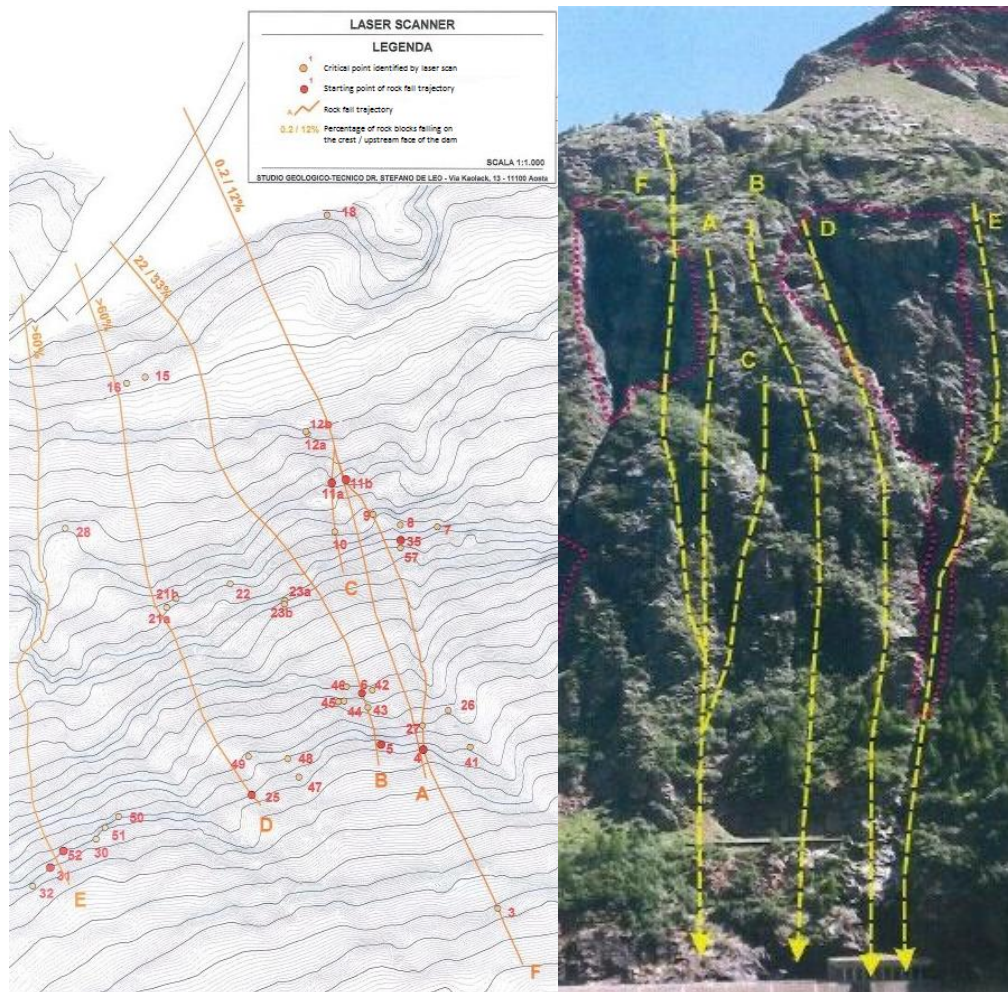


Fig. 2

Trajectories of the main boulders that could impact on the left side of the dam

Table 1

Features of the main boulder trajectories

Number of the hazardous conditions	Boulder volume [m ³]	Boulder mass [kg]	Outcrop volume [m ³]	Maximum kinetic energy [kJ]
1	9,0	24.750	483,0	24.360
2	6,9	19.000	17,2	20.500
3	8,9	24.500	34,2	23.800
4	7,1	19.500	360,0	29.972
5	5,2	14.300	12,0	24.250

Bearing in mind these results, the hazardous condition number 4 in Table 1 was selected to carry out the numerical simulations of the impact of the boulder on the dam because this situation is characterized by the highest kinetic energy and by the highest probability of occurrence.

3. THE FINITE ELEMENT MODEL

3.1. GEOMETRY AND CONTACT SURFACES

The three dimensional Finite Element model of the dam was generated on the basis of the design drawings [3]. Considering the large size of the dam with respect to both the impact zone and the boulder dimension, only half dam was modelled together with an extended part of the foundation (Fig. 3). This choice was endorsed by a preliminary analysis that modelled the whole dam with a coarse mesh; the related results have shown that the effects of the impact are restricted to the left part of the concrete structure, towards the abutment. For sake of simplicity, the numerical simulations have taken into account only a single boulder with a volume of $7,1 \text{ m}^3$, assuming a spherical shape (Fig. 3, bottom-right picture).

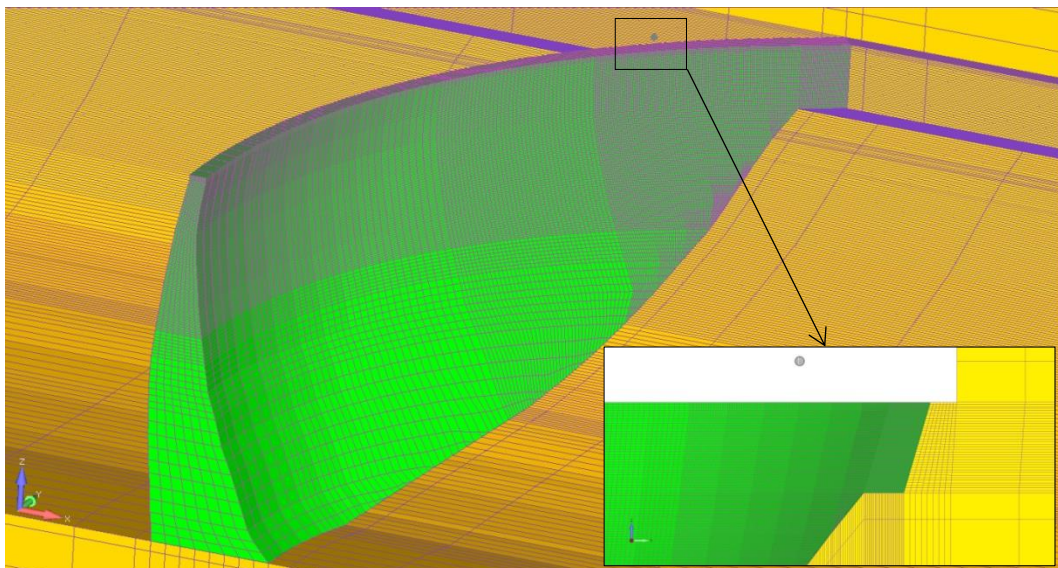


Fig. 3

Finite Element model of the half dam, the foundation and the boulder (in the bottom-right picture a zoomed downstream view of the left part of the dam with the starting position of the boulder)

In order to reduce the computational time of each simulation, the mesh was progressively refined along the following directions: starting from the main vertical

section towards the left abutment, and moving from the foundation towards the crest of the dam. The resulting model has nevertheless more than 210.000 nodes and nearly 184.000 finite elements, because the impact zone requires to be really well refined. The nodes laying on the base and vertical sides of the foundation were constrained; on the main vertical section of the dam symmetric boundary conditions were assigned to take into account the stiffness of the right part, not included in the model. The dam body was assumed monolithic, and there is also continuity between the dam and the foundation.

In order to model the interaction between the boulder and the dam, two contact surfaces were included: the former completely covers the outer surface of the boulder, the latter partially covers the crest and the upstream face of the left part of the dam.

3.2. IMPACT POINTS ON THE DAM

The numerical simulations have taken into account the following three different impact points on the dam:

- A. The upstream edge of the crest, 50 m far from the left abutment
- B. The midpoint of the crest thickness, 50 m far from the left abutment
- C. The upstream face, 50 m far from the left abutment and 10 m below the crest level

In Table 2 the impact velocity, the kinetic energy, the incidence angle from the vertical axis, and the direction cosines of the falling trajectory are listed.

Table 2
Features of the analyzed falling trajectories

Case study	Impact velocity [m/s]	Impact kinetic energy [kJ]	Incidence angle [°]	Direction cosines		
A	52,91	27.331	50°÷55°	0,259	-0,721	-0,643
B	52,91	27.331	50°÷55°	0,259	-0,721	-0,643
C	55,51	30.083	25°÷30°	0,143	-0,397	-0,906

The incidence angle in the horizontal plane was maintained constant for all the three cases.

3.3. CONSTITUTIVE MODELS AND RELATED MATERIAL PARAMETERS

In order to simulate the impact phase, non-linear constitutive models were used because the material strength is overcome both in the concrete of the dam

and into the boulder, with the exception of the foundation assumed as elastic, being rather far from the impact zone.

The parameters of all materials are summarized in Table 3 while some details of the related constitutive models, adopted to simulate their mechanical behaviour, are reported in the following paragraphs.

Table 3
Material parameters [3][4][5]

Material parameter	Foundation	Dam	Boulder
Young modulus	75.600 MPa	34.000 MPa	75.600 MPa
Poisson coefficient	0,220	0,166	0,220
Density	2.750 kg/m3	2.450 kg/m3	2.750 kg/m3
Compression strength	-	42,4 MPa	-
Tension strength	-	3,2 MPa	0,8 MPa

3.3.1. Dam

The concrete behaviour of the dam was modelled by means of the Concrete Damage Plasticity Model (CDP) provided in ABAQUS [6][7][8]. The main failure mechanisms of concrete are cracking in tension and crushing in compression. The CDP model aims to capture the effects of irreversible damage associated with these failure mechanisms, taking into account:

- different yield strengths in tension and compression, with the initial yield stress in compression being a factor of 10 than the initial yield stress in tension
- softening behavior in tension and initial hardening followed by softening in compression (Fig. 4)
- different degradation of the elastic stiffness in tension and compression, according to the following stress-strain relations under uniaxial tension and compression loading:

$$\sigma_t = (1 - d_t) E_0 (\varepsilon_t - \varepsilon_t^{pl}) \quad [1]$$

$$\sigma_c = (1 - d_c) E_0 (\varepsilon_c - \varepsilon_c^{pl}) \quad [2]$$

The unloading response of concrete from any point on the strain softening branch of the stress-strain curves is weakened being the elastic stiffness degraded. This degradation is characterized by two scalar damage variables, d_t (DAMAGE_T) and d_c (DAMAGE_C), which are assumed to be functions of the plastic strain, ε_{pl} . The damage variables can take values from 0, representing the undamaged material, to 1 which denotes total loss of strength.

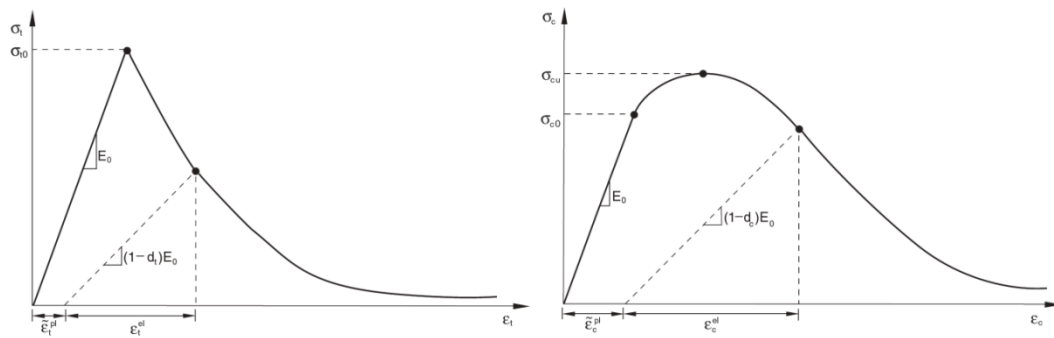


Fig. 4

Response of concrete to uniaxial loading in tension (left) and compression (right)

3.3.2. Boulder

The mechanical behaviour of the boulder was modelled by means of the Brittle Cracking (BC) Model provided in ABAQUS [6] which is designed for applications in which the tensile cracking is the dominant failure mode. A crack initiation is detected by a simple Rankine criterion which states that a crack forms when the maximum principal tensile stress exceeds the tensile strength of the brittle material. Although crack detection is purely based on Mode I fracture, post cracked behaviour includes both Mode I (opening mode) and Mode II (in plane shear/sliding mode) failures (Fig. 5). During the numerical analyses, the BC model allows removal of elements based on the Rankine criterion.

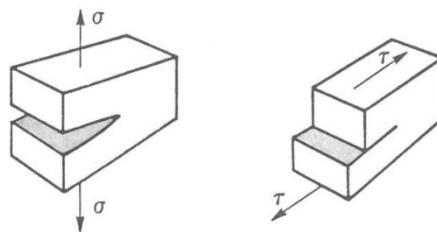


Fig. 5

Mode I – opening (left) and Mode II – in plane sliding (right) in fracture mechanics

In order to avoid mesh sensitivity into the results, the post failure stress is specified as a tabular function of displacement across the crack, u^{ck} , defining thus the energy required to open a unit area of crack in Mode I as a material parameter (Fig. 6, left).

Considering that the cracked shear modulus decreases as the crack opens, a shear retention model is adopted in which the post cracked shear modulus G_c is defined as a fraction of the uncracked shear modulus G . The shear retention factor ρ is defined as a function of the opening strain across the crack, e^{ck} (Fig. 6, right):

$$G_c = \rho(e_{nn}^{ck}) G$$

[3]

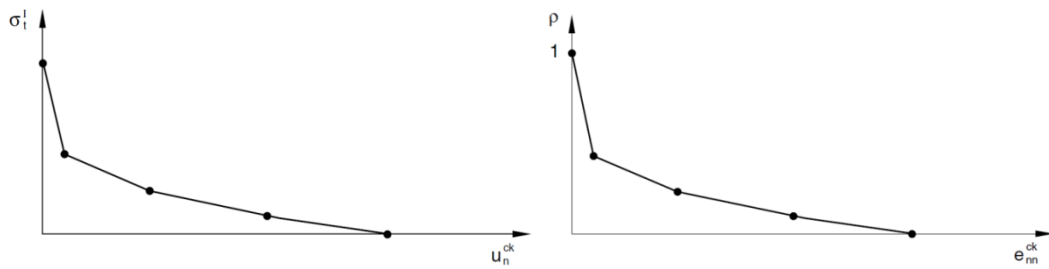


Fig. 6

Post failure stress-displacement curve (left) and shear retention model (right)

4. SENSITIVITY ANALYSES ON THE BOULDER FAILURE PARAMETERS

The boulder is composed of metamorphic rocks, characterized by marked schistosity and fracturing. The choice of the strength parameters related to this type of rock is indeed important because they define how much energy the boulder could dissipate during impact breaking into several pieces. The energy dissipated by the boulder increases with its brittle behaviour, and at the same time a major shattering of the boulder corresponds to a lower damage of the dam.

Sensitivity analyses were thus carried out to assess how the compression and tension damage varies on the dam body changing the brittle behaviour of the boulder in terms of deformation at the formation of cracks and at failure (Table 4).

Table 4

Failure parameters of the boulder used in the sensitivity analyses

Material parameter	Case 1	Case 2	Case 3
Deformation at the formation of cracks	0,0250	0,0070	0,0015
Failure deformation	0,0400	0,0090	0,0030

Making reference to the case study in which the boulder impacts against the midpoint of the crest thickness (Case B in Table 2), the results in terms of the tension damage parameter value show that the damage of the concrete is little influenced by the level of shattering of the boulder (Fig. 7). In the first case the boulder remains almost undamaged after the impact while in the last case it shatters almost completely.

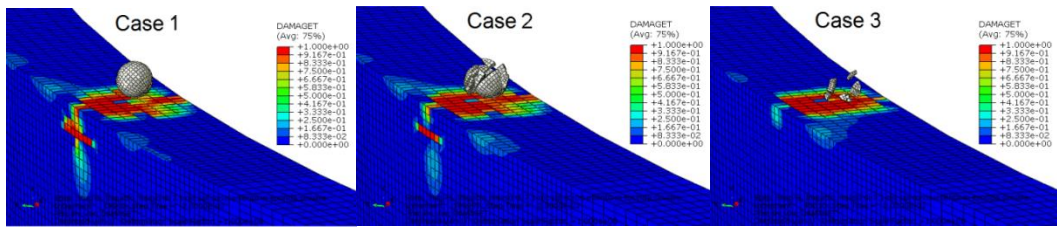


Fig. 7
Contour of the DAMAGET parameter – results of the sensitivity analyses

5. RESULTS OF THE IMPACT ANALYSES

In all the three case studies the impact analyses, carried out with ABAQUS/Explicit, shows that the compression damage on the concrete dam is limited to the impact area, and it is quite negligible for Case C as the boulder hits almost tangentially the upstream face of the dam. The tension damage is significant in the first two cases but not in the last one (Fig. 8 and Fig. 9).

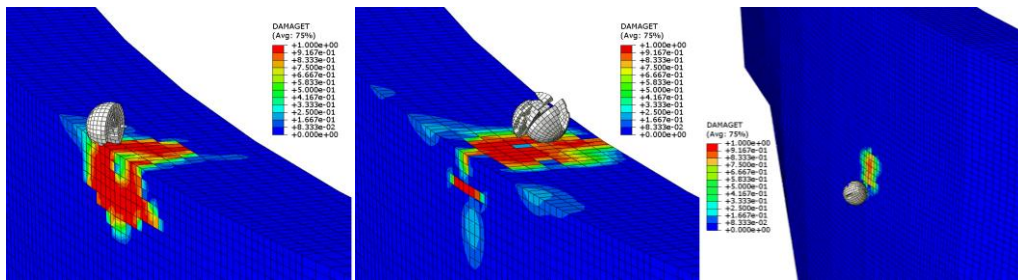


Fig. 8
Contour of the DAMAGET parameter on the crown and upstream face (Case study A - left, Case study B - centre, and Case study C - right)

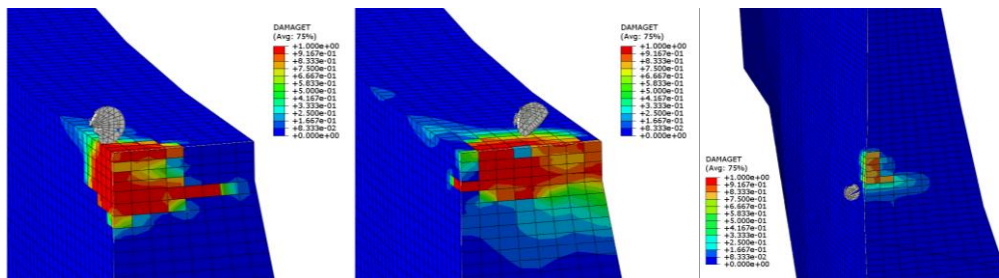


Fig. 9
Contour of the DAMAGET parameter in a vertical section of the dam (Case study A - left, Case study B - centre, and Case study C - right)

The most damaged conditions in tension are related to Case B since the formation of cracks extends down the dam nearly 2,5 m from the crest level and propagates along the whole thickness of the structure. In Case A the tension damage extends more along the vertical direction with respect to Case B, about 4,0 m from the crest level, but it does not affect the entire dam thickness.

6. CONCLUSION

The results of the impact analyses show that the boulder causes damages in tension on the concrete dam of Place Moulin because of the high kinetic energy. Being the slope rather steep, in fact, the boulder attains high velocities at the end of its falling path. The impact effects on the crest of the dam are higher than those occurring on the upstream face. Anyway, in each analysis the damaged zone in tension is quite localized.

On the contrary, in all cases the damage in compression is rather negligible being almost localised on the impact area. As expected, the static analysis, carried out after the impact simulation, has shown that the damaged zones do not affect the whole structural behaviour of the dam. These results will support the dam owner to select the most adequate mitigation works to guarantee the safety of the structure.

REFERENCES

- [1] DE LEO S. Ispezione geologica delle sponde prospicienti la diga di Place Moulin. *Studio geologico-tecnico Dr. Stefano De Leo*, 2014.
- [2] DE LEO S. Studio geologico-strutturale del versante che costituisce la spalla sinistra della diga di Place Moulin. *Studio geologico-tecnico Dr. Stefano De Leo*, 2014.
- [3] ENEL. Le dighe di ritenuta degli impianti idroelettrici italiani. Rome, Italy, 1970.
- [4] BOLDRINI A. Accoppiamento idromeccanico nella roccia di fondazione di dighe ad arco gravità. Esame di un caso reale. *PhD Thesis in Geotechnical Engineering*, University La Sapienza of Rome, 2007.
- [5] IPPOLITO I., NICOTERA P., CIVITA M., DE RISO R. Geologia tecnica. Ed. *ISED*, 1975.
- [6] DASSAULT SYSTEMES S.A. Simulia. ABAQUS Theory Manual. 2014.
- [7] LUBLINER ET AL. A Plastic-Damage Model for Concrete. *International Journal of Solids and Structures*, Vol.25, N.3, pp 229-326, 1989.
- [8] LEE J, FENVIS G.L. Plastic-Damage Model for Cyclic Loading of Concrete Structures. *Journal of Engineering Mechanics*, Vol.124, N.8, pp 892-900,1998.

COMMISSION INTERNATIONALE DES GRANDS BARRAGES

VINGT-SIXIÈME CONGRÈS DES GRANDS BARRAGES

Autriche, juillet 2018

DOI 10.3217/978-3-85125-620-8-240



This work licensed under a Creative Commons Attribution 4.0 International License.
<https://creativecommons.org/licenses/by-nc-nd/4.0/>

**EXPERIMENTAL STUDY ON OVERTOPPING BREACHING PROCESS OF
EARTH DAM AND PEAK DISCHARGE**

Duan WENGANG

ENGINEER OF HYDRAULIC DEPARTMENT, CHANGJIANG RIVER
SCIENTIFIC RESEARCH INSTITUTE

CHINA

Huang Guobing, LILI

ENGINEER OF HYDRAULIC DEPARTMENT, CHANGJIANG RIVER
SCIENTIFIC RESEARCH INSTITUTE

CHINA

COMMISSION
INTERNATIONALE DES
GRANDS BARRAGES

VINGT-SIXIÈME CONGRÈS
DES GRANDS BARRAGES
Autriche, juillet 2018

EXPERIMENTAL STUDY ON OVERTOPPING BREACHING PROCESS OF EARTH DAM AND PEAK DISCHARGE

Duan Wengang, Huang Guobing, LiLi

*Engineer of Hydraulic Department, CHANGJIANG RIVER SCIENTIFIC
RESEARCH INSTITUTE*

CHINA

1 INTRODUCTION

The pattern of dam break is important for the study of the dam failure, which decides how long the whole dam failure lasts, the level of the peak discharge and the damage to the downstream areas. The break pattern closely relates to the dam type. Generally, the sudden break happens on the concrete gravity dam and arch dam, while the gradual break mostly turns up on the earth dam. For the different way of overtopping flow, the density of fill and gradation composition of the dam's constructional material, the breaching process of earth dam is also distinctly different. Combining the indoor earth dam overtopping erosion experiment, the study tries to preliminarily explore the erosion process of earth dam, and makes further efforts to disclose the relationship between the breaching process and the peak discharge.

2 STUDY METHODS

2.1 Experimental Layout

The experimental flume is 25 meters long and 1.2 meters high with a 6-meter-wide reservoir on upstream(Figure 1). The profile of the flume on downstream is 2 meters wide. The reservoir on upstream is simulated with a certain volume of capacity which has a maximum capacity of 80m³.

The geometric profile of the experimental dam body is shown in Figure 2 with 100cm high(H), 1:1.5 slope of upstream, 1:3 slope of downstream, 20cm top width(b), 470cm bottom width(B).

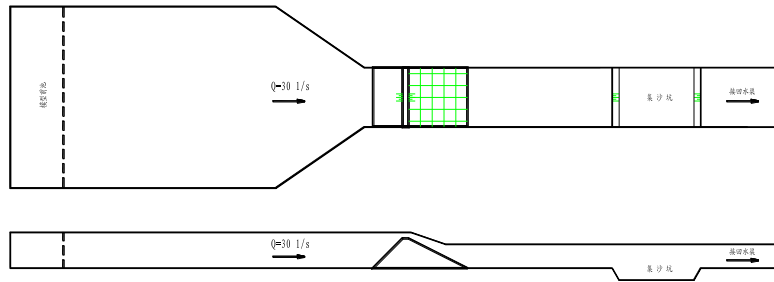


Figure 1 Sketch of experimental flume

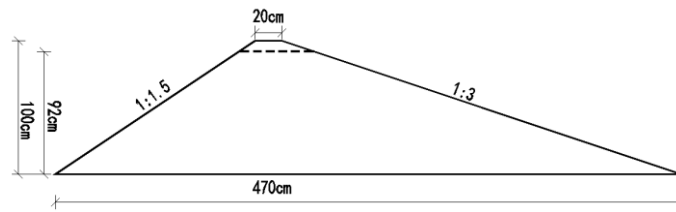


Figure 2 Sketch of experimental earth dam

2.2 Measure System

The test measure system uses many measure technology (upstream, downstream, inside and outside of the dam, multiple tools). The measured points and means are as follow: ①Real-time water level: 4 points being laid along the upstream and downstream, the dynamic process line of the water level is being recorded by the pressure sensor and DASP acquisition system;② Breach discharge: It is speculated from the the water level and reservoir capacity curve of the upsteam;③ The velocity of the breach flow: Being located on the breach part, it is dynamically measured by the electromagnetic flow velocity;④The breach shape: The vertical erosion incision is dynamically recorded by embedded light erosion catcher, while horizontal extension is observed by the grid technologies(A grid of 20cm×40cm being drawn on the downstream slope), also 2 HD cameras installed along the up and down stream of the dam to record the breach process which is analysed by the image technology.

In order to monitoring the developmental process of dam erosion process, and ensuring the layout and the size of the catchers have no impact on dam failure, 7 light erosion catchers are embedded into the dam before the experiments which is a light sphere with a diameter from 3cm to 5 cm and with different color and number on outside, so the catchers can be easily washed out by the flow and be caught. Just like in Figure 3, they are numbered from 1 to 7 according to the

elevation and profile of the embedded catchers. In the experiment, when the breach erosion goes to the location of the light erosion catcher, it is washed out by the flow that is exactly recorded by the HD camera. All above indicates that the instantaneous erosion of the dam has developed to the site and shows this method is useful and feasible and easy to operate.

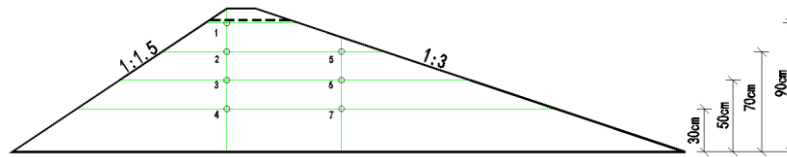


Figure 3 Sketch of embedded erosion catchers

2.3 EXPERIMENTAL PROJECT

In the experiment, flow of the upstream reservoir is constant at $Q=30\text{L/S}$. There are 2 kinds of the designed dam crest for the contrast experiment: one kind has no direct flow channel and the elevation of the crest is same (100cm); the other one has direct flow channel whose profile is designed to be trapezoid with a bottom width of 6 cm ($b=6\text{cm}$), a depth of 8cm ($h=8\text{cm}$), (that is to say the elevation of the direct flow channel is 92cm). The constructional material of the dam is cohesionless and wide gradation sandy gravel whose particle size is from 0.005mm to 40mm. The compact degree of the experimental gravel material is different. One is naturally stacked in which the gravel is in loose state; the other one is artificially tamped with water in which the gravel is close-grained.

In order to prevent the damage of the penetration before the overtopping break, one or two layers of the waterproof film are embedded around the dam. In the constraint condition of no affection on the dam break, fragment overlapping arrangement is used on the emplacement of the film.

3 RESULTS AND DISCUSSION

3.1 OVERTOPPING BREACHING PROCESS OF EARTH DAM

Depending on the way of the overtopping flow, the density of fill and gradation composition of the dam's constructional material, overtopping erosion process can be classified into 3 types such as layer-by-layer erosion, entire overtopping erosion and headcut erosion. Mostly, the entire overtopping erosion happens, when there is no direct flow channel on the crest of the dam and the elevation of the crest is the same; with a direct flow channel in the crest also the gravel of the dam's constructional material being loose, generally the layer-by-layer erosion happens; otherwise with a direct flow channel in the crest and the gravel of the dam's constructional material being compact, the headcut erosion shows up.

3.1.1 Layer-by-layer Erosion

The process of layer-by-layer erosion is shown in Fig.4 and Fig.5. Generally speaking, the erosion process of the dam is relatively even in which the erosion area gradually develops from I → II → III → IV → V. Firstly, the overtopping flow from the direct flow channel and form a distinct erosion gully. With the erosion gully continuing deeper and wider, the dam slope of the downstream is constantly slower. Then the erosion is gradually close layer-by-layer to the main area of the dam and the dam is constantly incised along with the slower the slope of the dam and the wider the extension of the breach. At last, the main dam is eroded entirely.

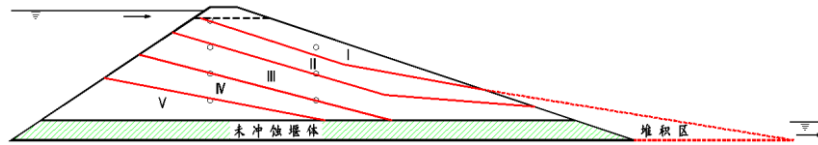


Figure 4 Sketch of layer-by-layer dam erosion



Figure 5 Test photo of layer-by-layer dam erosion

3.1.2 Entire Overtopping Erosion

The process of the entire overtopping erosion is shown in Fig.6 and Fig.7. Generally speaking, the erosion process is similar with the one of the layer-by-layer erosion in which the erosion area gradually develops from I to V. The entire overtopping flow from the crest of the dam. Firstly, the small flows just like the thin sheets whose erosion ability gradually enhances as the increasing speed of the small flows discharging along the downstream slope to erode the small particles of the dam's surface. With the erosion closing the dam's main area layer by layer, the slope of the dam becomes slower and slower until the main dam is eroded entirely at last.

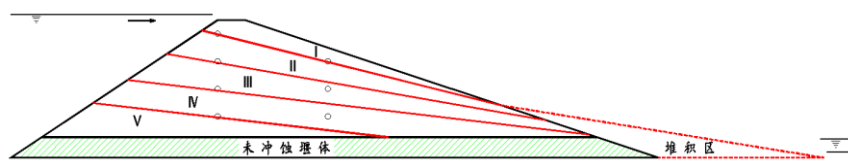


Figure 6 Sketch of entire Overtopping dam erosion



Figure 7 Test photo of entire Overtopping dam erosion

3.1.3 Headcut Erosion

The process of headcut erosion is shown in Fig.8 and Fig.9 which is very uneven. In the first half part of the dam break, the erosion mainly happens in the slope of the downstream. After the headcut waterfall flow being formed, the breach discharge is controlled by the width, the height and the shape of the breach on the dam's upstream (The entrance of the weir forms "control profile"). The breach flow increases slowly, also the water level declines slowly. The headcut becomes higher and higher for the scouring erosion with the slope on the both sides increasingly deep. The experiment finds that the scouring process can be divided into 4 stages which are as follows: ① The erosion gully formation stage in the surface of the downstream slope: the erosion of the dam occurs in the surface of the downstream slope, and the process is slowly progressive; the discharge and the speed of the breach flow are even and small, and the water level of the reservoir laying on up steam is slowly rising. ② "The multilevel drop sill" erosion stage of in the surface of the downstream slope: in this stage the erosion also mainly happens in the surface of the downstream slope, and the erosion ability of the overtopping flow is gradually enhancing; With the flow and the speed of the breach rising slowly, the water level of the reservoir laying on upstream begins to decline slowly after it reaching the maximum value. ③ "the waterfall flow" rapid erosion and break stage of the dam: in this stage, the dam break has developed to the upper edge of the dam crest, and the erosion ability is mostly powerful with a dramatic dam collapse process; rising rapidly, the discharge and the speed of the breach flow reach the peak in this stage, and the water level of the reservoir laying on up steam drops rapidly. ④ the stable stage of the dam break: the indexes of the breach flow factors (the water level of the breach on upstream, the discharge and the speed of the flow and so on) begins to drop slowly after reaching the maximum value, and the erosion ability of the flow becomes weak gradually, then erosion process of the dam slows down and eventually stabilizes, that is to say, the dam discharges the flow which comes from the upstream.

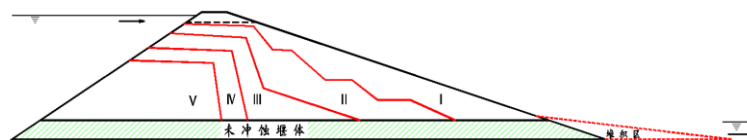


Figure 8 Sketch of headcut erosion



Figure 9 Test photo of headcut erosion

3.2 PEAK DISCHARGE OF DAM BREAK

3.2.1 Layer-by-layer erosion

The discharge change process in the layer-by-layer dam erosion is shown in Fig.10. The water level of the reservoir laying on upstream reaches the maximum value of 97.7cm after rising slowly ($t=156s$, the relevation of the bottom of the direct flow channel is 92cm), which indicates that the instantaneous discharge just reaches to 30 l/s from upstream. Then the breach flow increases rapidly to the maximum value $Q=459l/s$ at 240s which indicates that the water level drops acutely very much and the water level of the downstream reaches the maximum value later. After that, the water level of the reservoir and the breach flow decline step by step. When t within 420s, the observation is end and the water level of the reservoir declines to 35.6m along with the discharge of 41l/s just a little bit more to the flow from upstream which shows the erosion tends to be balanced.

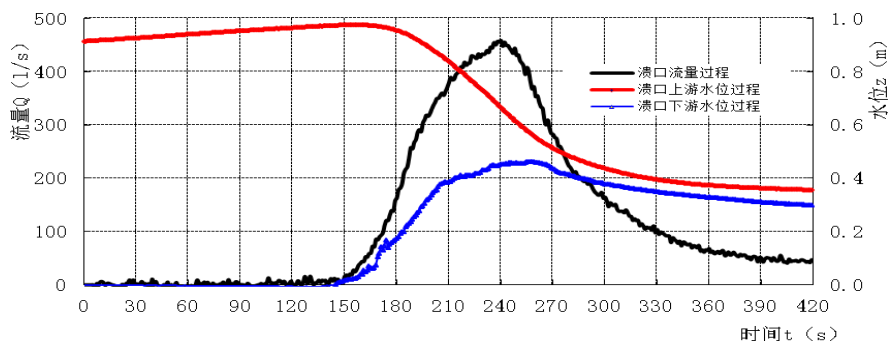


Figure 10 Water level and discharge process lines of layer-by-layer dam erosion

3.2.2 Entire overtopping erosion

The change process of the flow and the water level in the entire overtopping erosion experiment of dam break is shown in Fig.11. The water level of the reservoir laying on upstream reaches the maximum value of 102.1cm after rising slowly ($t=100s$, the relevation of the dam crest is 100cm), then the breach flow climbs up quickly which comes to the maximum value of $Q=526l/s$ when t within 165s. Later, the water level of the reservoir and the the breach flow decline step by step. When $t=360s$, the observation is over and the water level of the reservoir declines to 41.5cm along with the discharge of 39l/s just a little bit more to the flow from upstream which shows the erosion tends to be balanced.

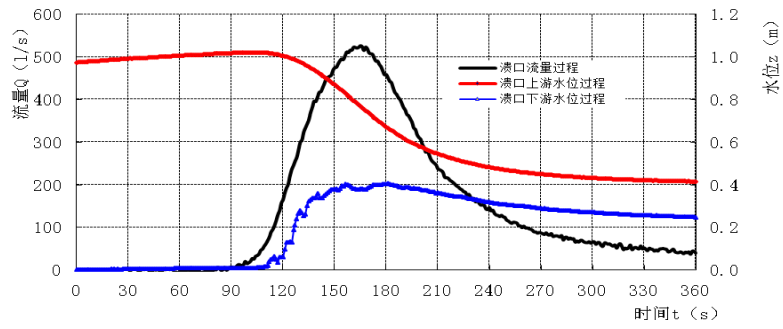


Figure 11 Water level and discharge process lines of entire overtopping erosion

3.2.3 Headcut erosion

The change process of the flow and the water level in the headcut waterfall flow erosion experiment of dam break is shown in Fig.12. The water level of the reservoir laying on upstream reaches the maximum value of 97.7cm after rising slowly($t=154s$, the relevation of the dam bottom is 92cm), then the volume of the breach flow magnifies gradually and the water level of the reservoir lying on the upstream drops slowly which falls to 89.5cm when $t=250s$. Later, the breach discharge climbs up rapidly which comes to the maximum value of $Q=654l/s$ when $t=289s$; at the same time, the water level of the reservoir drops quickly which declines to 43.2m when $t=330s$. After that, the water level of the reservoir and the breach flow decline slowly, and when $t=480s$, the observation is finished and the water level of the reservoir declines to 29.4cm along with the discharge of 40l/s just a little bit more to the flow from up stream which shows the erosion tends to be balanced.

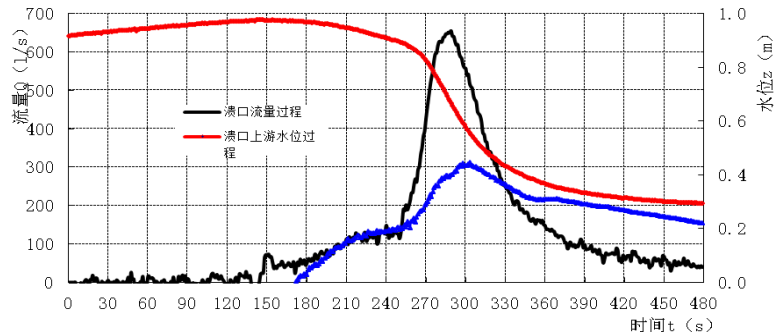


Figure 12 Water level and discharge process lines of headcut erosion

3.3 ANALYSIS AND DISCUSSION

For the comparison and the analysis, the hydraulic parameters of the above 3 kinds of the erosion process are list in the table 1.

Table 1 Hydraulic parameter peak value of different breaching process

Breaching process	upstream water level Z_{\max} (cm)	Breaching discharge Q_{\max} (L/s)	Water level maximum fall in 30s ΔZ (cm)	Main dam breaching t (s)
layer-by-layer erosion	97.7	459	17.3	90
entire overtopping erosion	102.1	526	19.9	90
headcut erosion	97.7	654	24.8	60

The table 1 shows that the breach process of the layer-by-layer erosion and the entire overtopping erosion takes more time (about 90s), in which the water level of the reservoir lying on upstream declines not so much acutely, at the maximum water level fall in 30 second, with respective drop of 17.3cm and 19.9cm and a flat peak of the process line to recording the breach discharge. Because of direct flow channel on the dam crest, in the process of entire overtopping erosion, the water level of the reservoir furthest reaches to 102.1cm and the peak discharge is measured as $Q=526\text{l/s}$, while in the process of layer-by-layer erosion, the maximum reservoir water level is 97.7cm and the peak discharge is measured as $Q=459\text{l/s}$.

The break process of the headcut erosion takes a shorter time (about 60s), the water level of the reservoir lying upstream falls dramatically with a tip and thin peak of the process line. When the headcut develops to some extent, the breach collapses suddenly both in horizontal and vertical direction with the instant increase of the discharge and the sudden drop of the upstream water level, at the maximum water level fall in 30 second, with a drop of 24.8cm. In the experiment, the maximum reservoir water level of the upstream is 97.7cm, but the peak discharge is measured as $Q=654\text{l/s}$ which is 40% more to the one measured in the type of the layer-by-layer erosion. It can be seen that even if the profile of the dam and the maximum water level of upstream are the same, the peak discharge distinctly differs because of the different erosion process of dam break.

4 CONCLUSIONS

A series of indoor flume experiments have been done on earth dam (1 meter height) constructed by wide gradation and cohesionless materials. Dam erosion process and hydraulic parameter changing process have been measured in the condition of flood overtopping. The result of the experiment indicates that depending on the way of the overtopping flow, the density of fill and gradation composition of the dam's constructional material, the overtopping erosion process can be classified into 3 types such as layer-by-layer erosion, entire overtopping erosion and headcut erosion. There is a very close relationship between the peak discharge and the breaching process. The quicker of dam-break happens, the bigger the peak discharge is. In the same situation, the peak discharge of headcut erosion increases 40% to the one of layer-by-layer erosion.

It should be noted that the experiment is operated under the specific simulation and boundary conditions, while the process and the modality of the break may be different from the reality which may lead to the difference between

the peak discharge in experiment and the one in reality.

REFERENCES

- [1] ZHANG Jian Yun, Li Yun, Xuan Guo Xiang, et al. Overtopping breaching of cohesive homogeneous earth dam with different cohesive strength. *Sci China Ser E-Tech Sci*,2009, 52(10): 3024—3029.
- [2] LI Yun, LI Jun Review of experimental study on dam—break advance in water science, 2009, 20 (2) : 304—309.
- [3] M.W.MORRIS, M.A.A.M.HASSAN, K.A.VASKINN, Breach formation: Field test and laboratory experiments (J) . *Journal of Hydraulic Research Vol.45 Extra Issue(2007)*,PP.9-17.
- [4] NIU Zhi-pan, XU Wei-lin, ZHANG Jian-min, et al.Experimenta l Investiga tion of Scour and Dam2break of Landslide Dam, *JOURNAL OF SICHUAN UN IVERSITY (ENGINEER ING SCIENCE ED ITION*, 2009, 41 (3) : 90—95.
- [5] ZHANG Jing, CAO Shu-you, YANG Feng-guang, et al.Experimental Study on Outlet and Scour of Blocked Dam, *JOURNAL OF SICHUAN UN IVERSITY (ENGINEER ING SCIENCE ED ITION*, 2010, 42 (5) : 191—196.
- [6] Duan Wengang, Yang Wenjun, Wang Siying, Li Li. Overtopping failure process of cohesionless earth dam.*Journal of Yangtze river scientific research institute* ,2012,29 (10):68-72.

SUMMARY

In order to explore the relationship between peak discharge of earth dam and breaching process, a series of indoor flume experiments have been done on earth dam (1 meter height)constructed by wide gradation and cohesionless materials. Dam erosion process and hydraulic parameter changing process have been measured in the condition of flood overtopping. The result of the experiment indicates that depending on the way of the overtopping flow, the density of fill and gradation composition of the dam's constructional material, the overtopping erosion process can be classified into 3 types such as layer-by-layer erosion, entire overtopping erosion and headcut erosion. There is a very close relationship between the peak discharge and the breaching process. The quicker of dam-break happens, the bigger the peak discharge is. In the same situation, the peak discharge of headcut erosion increases 40% to the one of layer-by-layer erosion.

KEY WORDS: Earth dam, Breaching process, Peak discharge of dam break, Overtopping erosion, Headcut erosion, Layer-by-layer erosion.

COMMISSION INTERNATIONALE DES GRANDS BARRAGES

VINGT-SIXIÈME CONGRÈS DES GRANDS BARRAGES
Autriche, juillet 2018

DOI 10.3217/978-3-85125-620-8-241



This work licensed under a Creative Commons Attribution 4.0 International License. <https://creativecommons.org/licenses/by-nc-nd/4.0/>

SETTLEMENT OF SOFT ROCKFILL MATERIALS IN MEDIUM-SCALE OEDOMETER

Ali. Komak PANAHA

*Associate Professor, faculty of civil and environmental engineering, TARBIAT
MODARES UNIVERSITY, TEHRAN*

IRAN

Hamidreza. RAHMANI

*Phd candidate, faculty of civil and environmental engineering, TARBIAT
MODARES UNIVERSITY, TEHRAN*

IRAN

SETTLEMENT OF SOFT ROCKFILL MATERIALS IN MEDIUM-SCALE OEDOMETER

Ali. Komak PANAHA

Associate Professor, faculty of civil and environmental engineering, TARBIAT MODARES UNIVERSITY, TEHRAN

IRAN

Hamidreza. RAHMANI

Phd candidate, faculty of civil and environmental engineering, TARBIAT MODARES UNIVERSITY, TEHRAN

IRAN

hr.rahmani@modares.ac.ir

Rockfill materials are used in construction projects such as dam construction, road construction and so on. Due to the increasing use of these materials, experiments and studies have also been carried out on this material and usually, these studies have been carried out on strong rockfill materials. Today, the use of soft and weak rockfill materials has expanded because of the economic and environmental issues. and still no comprehensive studies have been conducted on soft rockfill materials and need more information on the behavior of these materials in different conditions. With considering that the dimensions of the usable rockfill material may be much larger than the dimensions of the laboratory equipment. Therefore, it is always a matter of scaling and matching the results of the laboratory and the field from the important items of rockfill materials. In this research, the behavior of weak rockfill materials has been investigated in different conditions.

KEY WORDS

Particle Breakage, Weak Rockfill Material

1. PREFACE

In recent decades, hundreds of dams over 100 m high have been built in world to produce clean and renewable energy. More and more soft rocks have increasingly been used in the construction of dams because of their easy

availability and environmental considerations. These marginal materials traditionally would not be used owing to their unfavorable engineering properties that is, low strength, high compressibility, and proneness to material degradation with time. Therefore, the use of soft rocks excavated on site as rockfill materials for high rockfill dams is still a controversial issue, as weathering takes place when the rock is exposed to an environment in which variations in air, temperature, and water content are involved. Compared with conventional rockfill materials such as fragments of hard rock, soft rocks are more sensitive to weathering, with temperature and drying/wetting variations. As there are limited applications of soft rocks used in rockfill dams, the long-term behavior of the compacted soft rocks is of great concern and is not yet well understood.

2. INTRODUCTION

2.1. SOFT ROCKFILL MATERIAL

A rockfill dam is an embankment dam which relies on rockfill as its major structural element. Among the major advantages of rockfill dam construction are the following: a wide variety of sites and foundations are suitable, cheap natural construction materials can be found in local quarries since even weak rock is usable. All kinds of rock (igneous, sedimentary and metamorphic) are used for compacted rockfill [1].

The Table 1 show the strength of various rock types used in rockfill material [2].

Table 1: Strength classification of rocks [2]

Class	Description	Uniaxial Compressive Strength(MN/ m^2)
A	Very high strength	Over 200
B	High strength	100 – 200
C	Medium strength	50 – 100
D	Low strength	25 – 50
E	Very low strength	Less than 25

Rocks in class C, D, E would probably form 'weak' rockfills [2].

2.2. PARTICLE BREAKAGE

Particle breakage index that quantifies the degree of particle breakage, can reflect the degree of particle crushing of material. Particle breakage index can be divided into different categories. The methods for measuring the level of crushing

in granular materials are based on the variation of the gradation curve or the retention curve. One of the first measures was proposed by Marsal et al. [3] using the retention curve. In this case the difference between the percentages of retained mass at initial ($f_0(D)$) and final ($f_u(D)$) stages in a test is calculated for each sieve. The amount of crushing is given by the sum of positive difference values and it is equal to parameter B_g , or:

$$B_g = \frac{1}{2} \int_{D_m}^{D_M} |f_0(D) - f_f(D)| dD \quad (1)$$

The procedure is illustrated in Figure 1. The factor B_g is a simple factor describing the amount of crushed material and has been currently used by engineers in soil mechanics practice.

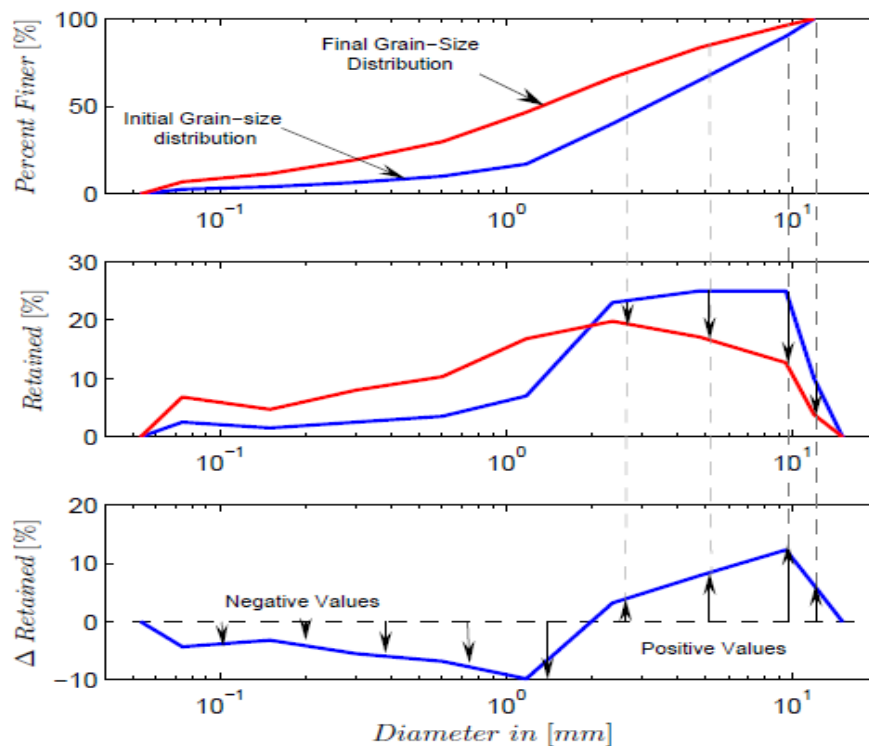


Figure 1. Calculus of Marsal's breakage index

2.3. MEDIUM-SCALE OEDOMETER APPARATUS

To carry out experiments on studied rockfill materials, a Medium-scale oedometer apparatus is used. In Figure 2 illustrate an overview of the apparatus. The specimen cell contains a stainless steel material of 15 cm in diameter and 25 cm in height [4].



Figure 2. Large-scale oedometer apparatus

2.4. NOHOB STORAGE DAM

Nohob Dam, is located on Qazvin province, 35 km southwest of Takestan city, 1 kilometer downstream the Nohob village. Nohob dam is under construction. The Nohob storage dam specification presented in Table 2 [5].

Table 2: Nohob dam specification [5]

Type of dam	Earthfill dam with clay core
Dam height	46 m
Crest length	2156 m
Crest width	10 m
Reservoir capacity	120 Mm ³
Year of construction	2012

In Figure 3, the dam site is specified.

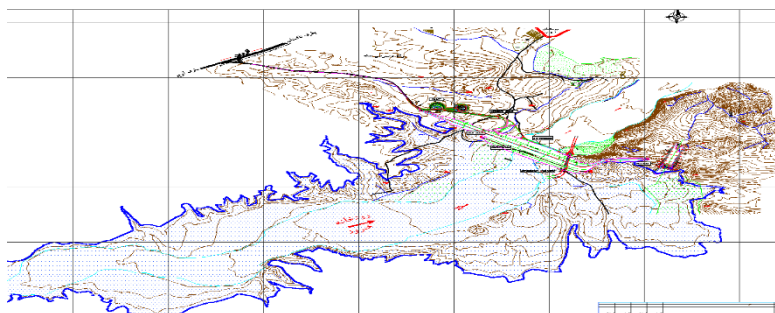


Figure 3. Nohob dam site [5]

3. METHODOLOGY AND TEST PROCEDURE

To select weak rockfill materials, Iran Water Resources Management Company was visited and information about dams in the construction stage was received and reviews were conducted on different dams. Due to the fact that most of the rockfill dams materials that in construction stage were in high strength class. Then we were visited the Nohob dam that was under construction and rockfill material in overflow excavation section that was thrown away and it was not used in the construction of the dam.

Then the rocks are sampled in different sections of the overflow excavation and uniaxial compressive strength[6] test was performed on them. The results are presented in the Table 3.

Table 3: Overflow rock specification

Sampling location	uniaxial compressive strength(MPa)
1	23.5
2	45.5
3	80.4
4	26.3

With given the strength achieved by the rock materials, sample No.1& 2 was selected which is placed in class C&D of table 1. Then materials was sampled for grading. In Figure 4 shows the sampling site.



Figure 4. Dam overflow location

Then with according the grain size distribution curves from other dam that constructed with quarried rockfill material, grain size distribution curve was selected and in Figure 4 is shown. As respects the diameter of the test cell is 15 cm and the maximum ratio is $\frac{D}{d} = 6$ that the D is the diameter of the test cell and d is the maximum grain size of sample. Modeled rockfill materials for $d_{max} = 25.4 \text{ mm}$ were obtained using parallel gradation technique that illustrated in Figure 5.

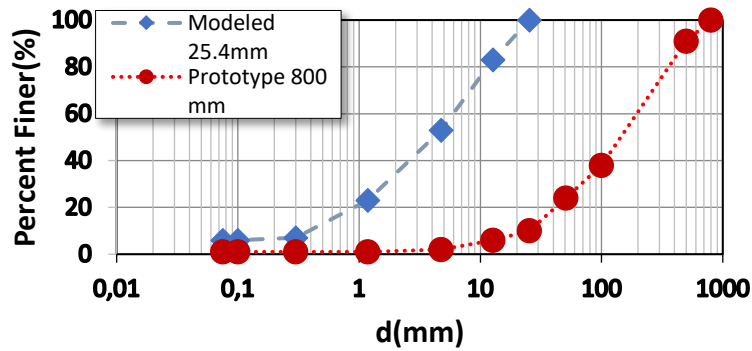


Figure 5. Grain size distribution curves

Then with according to the standard test methods for maximum index density and unit weight of soils using a vibratory table (ASTM D4253) [7] and standard test methods for minimum index density and unit weight of soils and calculation relative density (ASTM D4254) [8], these methods were used to determine γ_d . The RD mold with a volume of 14,070 mL is filled completely with a graded rockfill material Minimum dry density ($(\gamma_d)_{min}$) is determined as the ratio of total weight of the material filled in the mold to the total volume of the mold occupied by the material. To determine the maximum dry density ($(\gamma_d)_{max}$), the mold fitted to the 75 cm * 75 cm table with a motor is vibrated for 12 min and the volume change of the material in the mold is recorded. Then the $(\gamma_d)_{max}$ is determined as the ratio of total weight of the material in the mold to the total volume of the mold occupied by the material. Using $(\gamma_d)_{min}$ and $(\gamma_d)_{max}$, the specimen density is determined using Eq. (2) corresponding to RD of 87%.

$$RD = \frac{\frac{1}{(\gamma_d)_{min}} - \frac{1}{\gamma_d}}{\frac{1}{(\gamma_d)_{min}} - \frac{1}{(\gamma_d)_{max}}} * 100\% \quad (2)$$

where γ_d is the dry density in a given condition. $(\gamma_d)_{max}$ and $(\gamma_d)_{min}$ were determined and the results are presented in Table 4.

Table 4: Material unit weight

Material	γ_d (Kg/m^3)	
	Max	Min
1	1585	1470
2	2207	2055

In preparing the specimen, a lubricant was first laid on the inner side of the container to reduce side friction. The materials was compacted in five lifts in the container. The water content of the compacted specimen was less than 1% for dry

specimens and the water content of the compacted specimen was 20% for wet specimens . The maximum particle size was about the half the thickness of each lift.

Volumetric (vertical) deformations of the specimen were monitored by a linear variable differential transducer (LVDT) in all the tests. Stresses mentioned in this paper mean the vertical stress applied on the specimen.

Conventional oedometer tests were performed on the rockfill. The purpose of the tests was to quantitatively evaluate the particle breakage during compaction of specimen and in the oedometer test. After each test, a grain size distribution curve was obtained. In figure 5 shows step to do the experiment.



Figure 6. Oedometer Apparatus

4. TEST RESULTS

The oedometer tests were performed under normal stresses are presented in Table 5 for two types of materials..

Table 5: Normal stresses in specimen

Day	Stress(kpa)	
	Material 1	Material 2
425	310	425
850	620	850
1275	930	1275
1700	1240	1700
2125	1550	2125
2550	1860	2550
2975	2170	2975

4.1. MATERIAL 1

The material 1 consisted of rock fragments with sharp edges. It was prone to particle breakage induced by high levels of stress or stress concentration on the edges (Marshal, 1967)[3]. vertical strain occurred in the Oedometer test at the vertical stress owing to compression and particle breakage of the material. Fig 7 interprets the vertical strain, ϵ .

The deformation of the rockfill was considered to include a transient phase that occurred instantaneously upon applying the load and time-dependent deformation. As seen in Fig 8, the deformation developed quickly and was mostly completed within the first loading step.

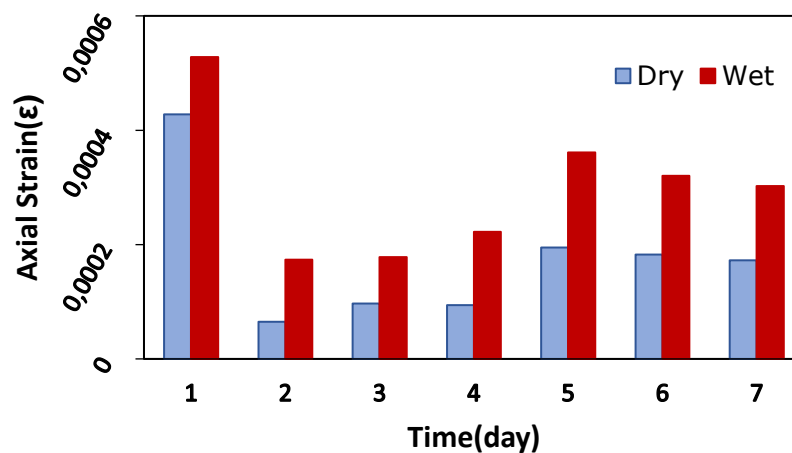


Figure 7. Axial strain in dry and wet specimens in material No.1

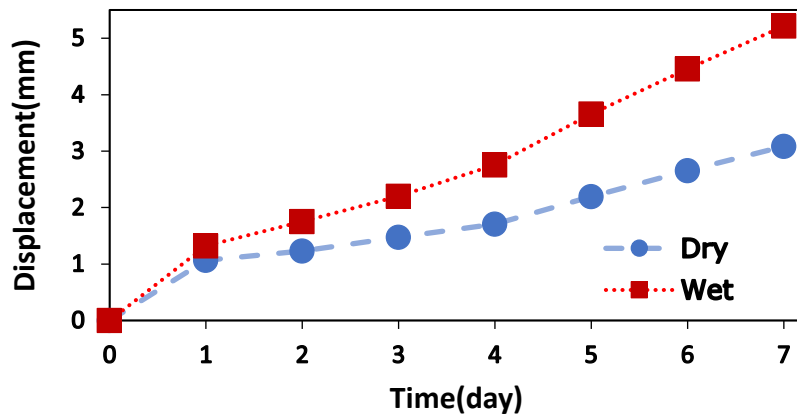


Figure 8. Total displacement in dry and wet specimens in material No.1

4.2. MATERIAL 2

The material 2 consisted of rock fragments with sharp edges. It was prone to particle breakage induced by high levels of stress or stress concentration on the edges (Marshal, 1967)[3]. vertical strain occurred in the Oedometer test at the vertical stress owing to compression and particle breakage of the material. Fig 9 interprets the vertical strain, ϵ .

The deformation of the rockfill was considered to include a transient phase that occurred instantaneously upon applying the load and time-dependent deformation. As seen in Fig 10, the deformation developed quickly and was mostly completed within the first loading step.

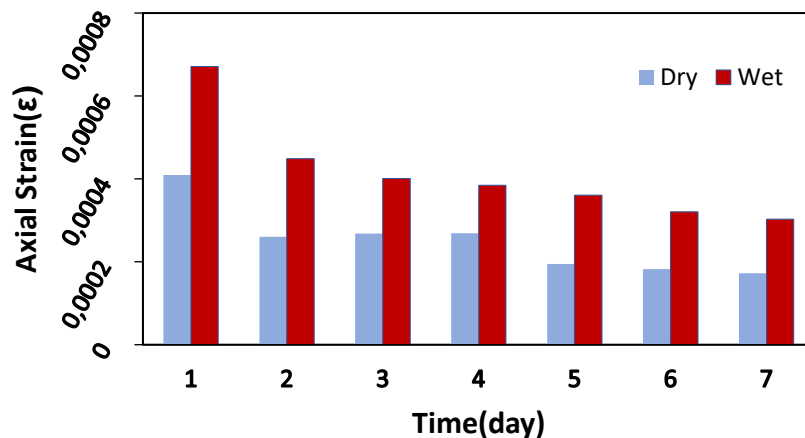


Figure 9. Axial strain in dry and wet specimens in material No.2

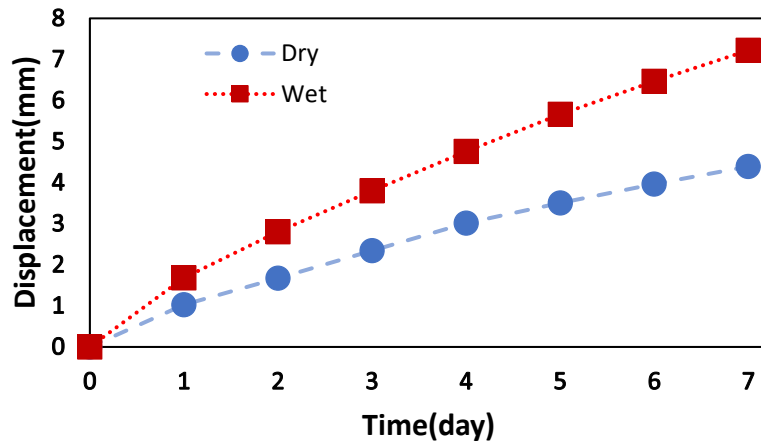


Figure 10. Total displacement in dry and wet specimens in material No.2

5. CONCLUSIONS

This paper describes a study of deformation of soft rockfill material subjected to stresses in dry and wet conditions. Based on the study, the following conclusions were drawn:

- 1) In the wet condition, the axial strain and displacement are more than dry condition.
- 2) In the initial steps of loading, the axial strain and displacement are greater than the end steps.

This research and experiment is ongoing and the more complete results will be provided in the next articles due to the experiment with other rockfill materials and variation test conditions.

ACKNOWLEDGMENT

We thank Mr. Mousavi and Mr. Keshavarz from Qazvin Regional Water Authority that provided information and cooperation on material sampling for this study.

REFERENCES

- [1] ICOLD,(1993). "Rock material for Rockfill Dams-Review and Recommendation-Bulletin92".
- [2] ICOLD, (2008). "Weak Rocks and shales in Dams-Bulletin134".
- [3] Marsal, R., (1967). "Large scale testing of rockfill material",. journal of the soil mechanics and foundation division, 93, pp.27–43.
- [4] Komak Panah, A. and Agha Majidi, M. (2011). "Creep of rockfill materials in large-scale oedometer with considering the particle breakage Los Angles test". Modares Civil Engineering Journal, '(in Persian)'.
- [5] Absaran Consulting Engineers, (2010). "Nohob Storage Dam Studies", Qazvin Regional Water Authority
- [6] ISRM, (2000). "Suggested Methods for Determining the Uniaxial Compressive Strength and Deformability of Rock Materials".
- [7] ASTM D4253, (2016), "standard test methods for maximum index density and unit weight of soils using a vibratory table"
- [8] ASTM D4254, (2016). "standard test methods for minimum index density and unit weight of soils and calculation relative density"



**Austrian Committee on Large Dams
Österreichisches Nationalkomitee für Talsperren**

Stremayrgasse 10/II, 8010 Graz

Tel: +43 316 873 8361

E-Mail: secretary@atcold.at

► <https://www.atcold.at>

Graz University of Technology

Institute of Hydraulic Engineering and Water Resources Management

Stremayrgasse 10/II, 8010 Graz, Austria

T: +43(0)316/873-8361

hydro@tugraz.at

► <https://www.hydro.tugraz.at>

ISBN 978-3-85125-620-8

DOI 10.3217/978-3-85125-620-8

© Verlag der Technischen Universität Graz 2018

